A Quantum-Mechanical Consideration of Chemical Reaction Rates

By Iwao YASUMORI and Kenji FUEKI

(Received March 22, 1955)

Introduction

As is well known, the statistical-mechanical theory of reaction rates (the absolute reaction rate theory or the ARR theory)[1] is very useful for the evaluation of reaction rates. However, apart from the knowledge of interaction potential of the reacting system, the theory also includes some imperfect points which have been often the subjects of discussion. These points are as follows: First, the motion of a mass point representing the reacting system along the reaction path is treated classical-mechanically and the concept of the "activated complex" is used even if its existence is doubtful. Second, the thermal equilibrium between the initial and activated states, or more rigorously, the reacting system in equilibrium is postulated. As a correction for these simplifications, the transmission coefficient κ is introduced, but its value cannot be determined from the theory itself.

The equilibrium postulate and then the statistical-mechanical property of κ must be discussed from the standpoint of non-equilibrium theory and several researches have been done previously[2], while the stability of the complex and the classical approximation of the motion are to be considered on the basis of quantum theory, so that the quantum-mechanical property of κ may be given.

In principle, the problem of the usual chemical reaction involving an activation energy can be treated as the quantum-mechanical transmission of a mass point representing the reacting system through an energy barrier occurring in the mutual potential field of the system[3-8].

Though this procedure has the great advantage of getting a rate equation without the concepts as stated above and of giving the definite probabilities of transitions from the initial to the final states, it has been applied only for one-dimensional problems except in a few works[5].

To examine, therefore, the validity of the ARR theory, it will be necessary to compare the ARR equation with the equation derived by this procedure for the same potential barrier which is like an actual one.

In this paper a rate equation will be derived by use of the more natural potential form than those used by others and some theoretical considerations about the quantum-mechanical property of the transmission coefficient and the validity of the ARR theory will be made on the basis of this equation.

Transmission through a Simplified Two-dimensional Potential Energy Barrier.

In this section we treat, as a typical example, the reaction between an atom A and a molecule BC in a linear configuration which involves an activation energy. Since there is scarcely any reaction for which the precise feature of the potential energy surface is known, we may assume a simple form of potential barrier from two plausible restrictions as follows:

a) When an atom A approaches to a molecule BC on a straight line (Fig. 1), the

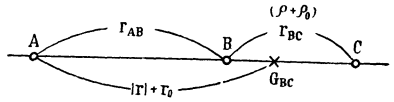

Fig. 1. Coordinate system.

minimum of the potential energy is obtained where the interatomic distance of BC is equal to its equilibrium value[9].

b) In the vicinity of the barrier the vibrational potential differs slightly from the initial one of the molecule BC.

On these bases and by taking the coordinate system r and ρ defined by

1) See, for example, S. Glasstone, K.J. Laidler and H. Eyring, "The Theory of Rate Processes", McGraw-Hill Book Co. Inc., New York, 1941, Chap. IV p. 184. The more rigorous discussion has been given by J. Horiuti, This Bulletin, **13**, 210 (1938).

2) B.J. Zwolinski and H. Eyring, *J. Am. Chem. Soc.*, **69**, 2702 (1947); I. Prigogine, *J. phys. & Colloid. Chem.*, **55**, 765 (1951).

3) E. Wigner, *Z. physik. Chem.*, B **19**, 203 (1932).

4) R.P. Bell, *Proc. Roy. Soc.*, A **139**, 466 (1933).

5) For example, J.O. Hirschfelder and E. Wigner, *J. Chem. Phys.*, **7**, 616 (1939).

6) E. Bauer and Ta-You Wu, *J. Chem. Phys.*, **21**, 726 (1953).

7) F.A. Matsen, *J. Chem. Phys.*, **22**, 165 (1954).

8) Also see, H. Eyring, J. Walter and G.E. Kimball, "Quantum Chemistry", John Wiley and Sons, Inc., New York, 1949, Chap. XVI p. 299.

9) In this case, therefore, the reaction path has no curvatures which cause the transfer of energy between several degrees of freedom. Reactions with such a straight reaction path near the barrier are known from the calculations by the semi-empirical method. See, for example, Ref. 1), Chap. V p. 202.

$$-r+r_0=r_{AB}+(m_C/(m_B+m_C))r_{BC} \quad (1)$$

and

$$\rho+\rho_0=r_{BC}, \quad (2)$$

respectively, where r_0 and ρ_0 are the coordinates of the top of the barrier (the activated state), we assume the following simple two-dimensional potential surface as shown in Fig. 2 and its analytical expression to be

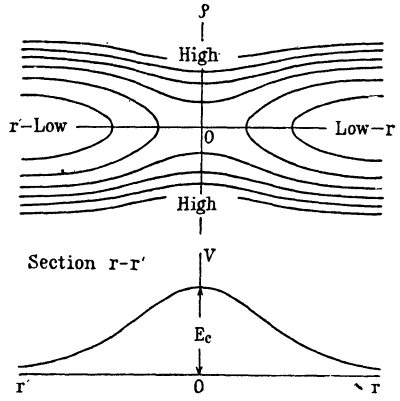

Fig. 2. Potential energy barrier.

$$V(r,\ \rho)=V_r(r)+(a_0-aV_r(r))\rho^2, \quad (3)$$

where a_0 and a are constants. Then, $aV_r(r)\rho^2$ is the deviation from the vibrational potential $a_0\rho^2$ which corresponds to that of the molecule BC, and vanishes as r becomes indefinitely large[10].

Separating the equation for the motion of the center of mass, the wave equation of the system is expressed by

$$-\frac{h^2}{8\pi^2M}\left(\frac{\partial^2}{\partial X^2}+\frac{\partial^2}{\partial Y^2}+\frac{\partial^2}{\partial Z^2}\right)\chi(X,\ Y,\ Z)=E_G\cdot\chi(X,\ Y,\ Z) \quad (4)$$

and

$$\left[-\frac{h^2}{8\pi^2\mu}\frac{\partial^2}{\partial r^2}-\frac{h^2}{8\pi^2m}\frac{\partial^2}{\partial\rho^2}+V(r,\ \rho)\right]\times\psi(r,\ \rho)=E_i\cdot\psi(r,\ \rho), \quad (5)$$

where M is the sum of m_A, m_B and m_C, masses of each atom, m and μ are the reduced masses,

$$m=m_Bm_C/(m_B+m_C)$$

and

$$\mu=m_A(m_B+m_C)/M, \quad (6)$$

respectively, X, Y and Z are the coordinates of the center of mass of the system, E_G and E_i are the energies of the translational motion of the whole system and of the internal motion of the system, respectively.

Eq. (4) can be solved immediately under some boundary conditions. To solve Eq. (5), one expands $\psi(r,\ \rho)$ in the following form

$$\psi(r,\ \rho)=\sum_n\psi_n(\rho)\cdot F_n(r) \quad (7)$$

where $\psi_n(\rho)$ is the n-th normalized eigenfunction for the harmonic oscillator and satisfies the following equation

$$\left[-\frac{h^2}{8\pi^2m}\frac{d^2}{d\rho^2}+a_0\rho^2\right]\psi_n(\rho)=E_n\psi_n(\rho). \quad (8)$$

Substituting Eq. (7) in Eq. (5) and multiplying both sides of Eq. (5) by the complex conjugate of $\psi_n(\rho)$, $\psi_n^*(\rho)$, and integrating over ρ, one obtains

$$\left[\frac{h^2}{8\pi^2\mu}\frac{d^2}{dr^2}+E_t-V_r(r)(1-a\rho_{nn}^2)\right]F_n(r)=-aV_r(r)\left[\rho_{n,n-2}^2F_{n-2}(r)+\rho_{n,n+2}^2F_{n+2}(r)\right] \quad (9)$$

$$n=0,\ 1,\ 2,\ \cdots\cdots,$$

where

$$E_t=E_i-E_n \quad (10)$$

and

$$\rho_{kl}^2=\int_{-\infty}^{+\infty}\psi_k^*(\rho)\rho^2\psi_l(\rho)d\rho. \quad (11)$$

This set of simultaneous differential equations can not be solved rigorously. However, if $a\rho_{kl}^2$ ($k=n$, $l=n$, $n\pm2$) is sufficiently small compared with unity[11], we may take, as zero-order approximation, the right-hand side of Eq. (9) to be zero. Then it is separated into the uncoupled equations and is expressed by the single term functions, $\psi_n(\rho)F_n(r)$, i.e.,

$$\left[\frac{h^2}{8\pi^2\mu}\frac{d^2}{dr^2}+E_t-V_r(r)(1-a\rho_{nn}^2)\right]F_n(r)=0, \quad (12)$$

$$n=0,\ 1,\ 2,\ \cdots\cdots.$$

Since the above equations are those for one-dimensional problems in which the potentials are given by $V_r(r)(1-a\rho_{nn}^2)$, if an analytical $V_r(r)$ with the shape like that shown in Fig. 2 is adopted, we can get its solution.

As a form of $V_r(r)$, for example, we may take the Eckart potential,

$$V_r(r)=E_c/\cosh^2(\pi r/l). \quad (13)$$

Then Eq. (12) can be solved by the manner quite analogous to Eckart's original work[12] and the approximate solutions of Eq. (5) are derived as follows:

$$\psi(r,\ \rho)=\psi_n(\rho)\cdot F_n(r),\quad n=0,\ 1,\ 2,\ \cdots\cdots \quad (14)$$

$$\psi_n(\rho)=N_nH_n(\sqrt{\beta}\cdot\rho)e^{-\frac{\beta}{2}\rho^2}, \quad (15)$$

where $\beta=(2ma_0)^{1/2}/\frac{h}{2\pi}$ and

10) Since r_{AB} is always larger than zero, a potential of this type becomes inadequate at $r>0$. But such an approximation as this is necessary to simplify the form of the solution of Eq. (5) at $r\ll0$.

11) This condition also means that $aV_r(r)$ is much smaller than a_0.

12) C. Eckart, *Phys. Rev.*, **35**, 1303 (1930). Also see Ref. 8).

$$F_n(r)=a_1F_{n1}(r)+a_2F_{n2}(r)$$
$$=a_1(-\xi)^{i\alpha_n}F\{1/2+i\zeta_n,\ -1/2-i\zeta_n,\ 1+2i\alpha_n,\ \xi/(\xi-1)\}$$
$$+a_2(-\xi/(1-\xi)^2)^{-i\alpha_n}F\{1/2+i\zeta_n-2i\alpha_n,\ -1/2-i\zeta_n-2i\alpha_n,\ 1-2i\alpha_n,\ \xi/(\xi-1)\}, \quad (16)$$

where N_n is the normalizing factor for the n-th eigenfunction for Eq. (8) and $H_n(\sqrt{\beta}\cdot\rho)$ is the Hermite polynomial of the n-th order and $F(r)$ is the hypergeometric function, in which ξ is a variable, $\xi=-\exp(2\pi r/l)$ and

$$\alpha_n=1/2(E_t/C)^{1/2}, \quad (17)$$

$$\zeta_n=[E_c(1-a\rho_{nn}^2)/C-1/4]^{1/2}, \quad (18)$$

$$C=h^2/8\mu l^2. \quad (19)$$

At $r=-\infty$, $F_{n1}(r)$ and $F_{n2}(r)$ correspond to an incident and reflected waves of unit amplitude respectively and the ratio of their coefficients a_2/a_1 is determined uniquely by giving the condition that a transmitted wave only exists at $r=+\infty$ (Appendix I). Consequently, the transmission coefficient κ_{nn} is given by

$$\kappa_{nn}=1-\left|\frac{a_2}{a_1}\right|^2=\frac{\cosh(4\pi\alpha_n)-1}{\cosh(4\pi\alpha_n)+\cosh(2\pi\zeta_n)}, \quad (20)$$

since ζ_n is real in this case. Further, when α_n and ζ_n are much larger than zero, one may take

$$\kappa_{nn}\simeq\exp(4\pi\alpha_n)/[\exp(4\pi\alpha_n)+\exp(2\pi\zeta_n)] \quad (21)$$

as an approximate formula.

Eq. (20) for κ_{nn} gives immediately its dependence on the relative momentum along the reaction path, $p_r=(2\mu E_t)^{1/2}$ and this has been discussed by Bell[4] previously.

Here we confine ourselves to its dependence on the vibrational potential. Differentiating κ_{nn} with respect to a, one can easily find

$$\frac{\partial\kappa_{nn}}{\partial a}=\frac{2\pi E_c\rho_{nn}^2\sinh^2(2\pi\alpha_n)\sinh(2\pi\delta_n)}{\delta_nC[\cosh(4\pi\alpha_n)+\cosh(2\pi\delta_n)]^2}\geqq 0. \quad (22)$$

This means that κ_{nn} increases or decreases according as the curvature of the vibrational potential at the barrier becomes smaller or larger. Also this property of κ_{nn} corresponds to the dependence of the reaction rate on the variation of the zero-point vibrational energy of the "activated complex" in the ARR theory (Fig. 3).

This relationship will be elucidated after we shall have formulated the rate equation based on κ_{nn}. If $a\rho_{k1}^2$ is not so small as assumed above, not only the transitions between the initial and final states with the same vibrational quantum number, but also the transitions between the states which differ by two quantum number become appreciable. A modified treatment for this case is shown in Appendix I.

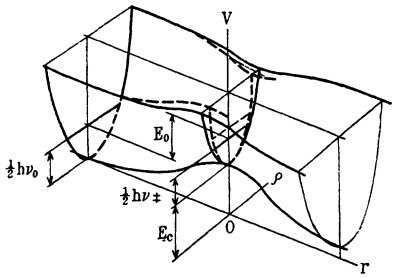

Fig. 3. Energy levels on potential surface.

Rate Equation on the Basis of the Transmission Coefficient and its Comparison with the ARR Equation for the Reaction $H+H_2\rightarrow H_2+H$

To obtain a rate equation, it is necessary to sum over the transmission of all the systems weighted by the energy distribution. Now, let $N(\boldsymbol{p}_G, p_r, n)$ be the number of the systems which exist in the volume element $d\boldsymbol{R}=dX\cdot dY\cdot dZ$ and in the width dr of the initial region far from the barrier, with the momentum of the center of mass $\boldsymbol{p}_G\sim\boldsymbol{p}_G+d\boldsymbol{p}_G$, the relative momentum along the reaction path $p_r\sim p_r+dp_r$ and the vibrational quantum number n.

$$N(\boldsymbol{p}_G, p_r, n)=N_0(\boldsymbol{p}_G, p_r, n)\frac{d\boldsymbol{p}_G d\boldsymbol{R}}{h^3}\cdot\frac{dp_r dr}{h}, \quad (23)$$

where $N_0(\boldsymbol{p}_G, p_r, n)$ is the density whose expression in thermal equilibrium is given by Appendix II Eq. (A, 13). The number of the systems moving towards the barrier in unit time is $Np_r/\mu dr$; moreover, only a fraction $\kappa_n=\sum_j\kappa_{nj}$ of them reacts and attains to the final states j. Accordingly, the reaction velocity v can be written as follows:

$$v=k(A)(BC)=\frac{1}{h^3}\iiint\sum_n\sum_j\kappa_{nj}$$
$$\times N_0(\boldsymbol{p}_G, p_r, n)\frac{p_r}{\mu h}\cdot dp_r d\boldsymbol{p}_G d\boldsymbol{R}, \quad (24)$$

where (A) and (BC) are the concentrations of the atom A and the molecule BC respectively, and k is the rate constant. Assuming the initial systems in thermal equilibrium[13], and using the approximate formula of κ_{nn} shown in Eq. (21), one can obtain the rate constant

13) The consideration about the statistical-mechanical property of κ is not given here. However the non-equilibrium effect is expected to be small. (See Ref. 2).

$$k=\frac{kT}{h}\frac{f^{+}_{+tr.}}{F_A\cdot F_{BC}}\exp\left(\frac{h\nu_0}{2kT}\right)\sum_n\left[1+2\sum_{m=1}^{\infty}\left\{(C/4\pi^2kT)^m\cdot L_{2m}(x_n)\cdot\sum_{p=1}^{\infty}\frac{(-1)^p}{p^{2m}}\right\}\right]\exp\left(-y_n^2\right), \tag{25}$$

where

$$L_{2m}(x_n)=-\left[\exp(x^2)\frac{d^{(2m)}}{dx^{(2m)}}\exp(-x^2)\right]_{x=x_n}, \tag{26}$$

$$x_n^2=\frac{1}{kT}\left[E_c-h\left(\frac{\nu_0^2-\nu_+^{+2}}{2\nu_0}\right)\cdot\left(n+\frac{1}{2}\right)-C/4\right] \tag{27}$$

and

$$y_n^2=x_n^2+\frac{h\nu_0}{kT}\left(n+\frac{1}{2}\right).$$

Derivation of Eq. (25) is shown in Appendix II. In the equation (25), $f^{+}_{+tr.}$ is the partition function per unit volume for the translational motion of the whole system and also of the "activated complex" and F_A and F_{BC} are the partition functions per unit volume of the atom A and the molecule BC defined by the usual manner of the rate theory excluding only the term for the rotational motion[1]. ν_0 and ν_+^+ are the vibrational frequencies deduced from the relations

$a_0=2\pi^2m\nu_0^2$ and $a_0-aV_r(0)=2\pi^2m\nu_+^{+2}$ (29), (30)

respectively.

The rate constant Eq. (25) formally reduces to that of the ARR theory in the case where $C/4\pi^2kT$ approaches to zero; that is, in the reaction involving heavy particles and a broad potential barrier at high temperatures, i.e.,

$$k=\frac{kT}{h}\frac{f^{+}_{+tr.}}{F_A\cdot F_{BC}}\left[1-\exp\left(-\frac{h\nu_a}{kT}\right)\right]^{-1}\times\exp\left[-\frac{1}{kT}\left(E_c+\frac{1}{2}h\nu_a-\frac{1}{2}h\nu_0\right)\right]. \tag{31}$$

It should be noted, however, that the term corresponding to the vibrational partition function of the "activated complex" in the ARR theory includes the average frequency $\nu_a=(\nu_0^2+\nu_+^{+2})/2\nu_0$ instead of ν_+^+. Here it is interesting to estimate the degree of deviation of the ARR theory from the equation derived above. Since the ARR equation for the same reaction between an atom A and a molecule BC of linear configuration, is given by Eq. (31), if ν_+^+ is adopted instead of ν_a, i.e.,

$$k_A=\frac{kT}{h}\cdot\frac{f^{+}_{+tr.}}{F_A\cdot F_{BC}}\left[1-\exp\left(-\frac{h\nu_+^+}{kT}\right)\right]^{-1}\times\exp\left[-\frac{1}{kT}\left(E_c+\frac{1}{2}h\nu_+^+-\frac{1}{2}h\nu_0\right)\right], \tag{32}$$

the ratio of k_A to k is easily given by Eqs. (25) and (32). As an example, we have calculated this deviation for the reaction $H+H_2\rightarrow H_2+H$ for which the largest quantum effect may be expected. The results are shown in Table I. In the table, $(k_A/k)_1$ are the values

TABLE I
RATIO OF CALCULATED RATES FOR THE REACTION
$H+H_2\rightarrow H_2+H$

Temp. °K	300	500	1000	2000
$(k_A/k)_1$	0.974	1.029	1.030	1.022
$(k_A/k)_2$	0.193	0.574	0.873	0.971

for the measure of width of the barrier $l=3.65\,A$, for which the curvature along the reaction path at the top of the barrier is equal to that obtained by the semi-empirical calculation[14], and $(k_A/k)_2$ are the values for $l=1.15\,A$. For other constants, $h\nu_0=12.56$, $h\nu_+^+=10.36$ and $E_c=7.63$ kcal./mol. are adopted in both calculations. The differences between both results are not very large except in the cases of small l at low temperatures.

Discussion

It seems that the result of comparison in the previous section leads to the conclusion that the ARR theory gives a fairly good approximation for usual chemical reaction rates at high temperatures. However, since our equation has been derived on several approximations and restrictions, it is necessary to examine them to confirm the conclusion. One of the approximations is that the Eckart type potential barrier which is perhaps steeper than the actual one near the top has been used. Therefore, we have calculated the rates for the two potentials with different l, so that the actual case may be between them. Though the results depend strongly on the choice of l at low temperatures, as the temperature rises, both results come to be in accord with each other and this fact suggests the behavior in the actual potential. The potential of this type seems to be the most precise form that can be used at present. Another approximation we have made is the use of the single term wave function valid when $a\rho_{kl}^2$ is very small. Since $a\rho_{nn}^2$, for in-

14) J.O. Hirschfelder, H. Eyring and B. Topley, *J. Chem. Phys.*, **4**, 170 (1936).

stance, is expressed as $a\rho_{nn}^2=h(\nu_0^2-\nu_+^{+2})(n+1/2)/2E_c\nu_0$, it increases with n, so that the condition $1\gg a\rho_{nn}^2$ loses its validity for certain large n and, then, the cross transitions between the states with n and $n\pm2$ become appreciable. For this case, the method of distorted waves is applied and the equation for the transmission coefficient κ_n including cross transitions is derived. The details are shown in Appendix I. But it is quite laborious to obtain the numerical value of κ_n because of the complicated functions F_n and $F_{n\pm2}$. However, in the case of usual reactions involving the molecule of low vibrational frequency, it may safely be said that the condition, $E_c\gg h\nu_0\gg h(\nu_0-\nu_+^+)$, holds. Then the rate constant Eq. (25), except at very high temperatures, will converge rapidly for the summation over n with the restriction $1\gg a\rho_{kl}^2$, since the concentrations of the reacting system of high energies decrease rapidly because of the Boltzmann factor. On the other hand, it is easily found from the properties of the matrix elements ρ_{kl}^2 that the set of equations (9) can be divided into two groups according as the vibrational quantum number n is even or odd. So, in the case of hydrogen atom-molecule reaction, if we put the restriction on energy, $E_{n=2}>E_i$, $\psi_0(\rho)F_0(r)$ and $\psi_1(\rho)F_1(r)$ will become good approximations for $\psi(r,\rho)$, since $E_{n=2}\gg E_c+1/2\cdot h\nu_+^+$ and $h\nu_0\gg kT$ are satisfied. In this case the summation in Eq. (25) is taken for $n=0,1$ and a correction term, $-\exp(-E_{n=2}/kT)$, is added inside the summation, assuming $\kappa_n=1$ for the systems with $E_i\geq E_{n=2}$.

By the way, it is easily shown that Eq. (25) for the rate constant includes Wigner's equation with a quantum correction[3], as a special case. Expanding the potential, $V_r(r)$, Eq. (3), in power series of r and neglecting the higher terms than r^2, one obtains

$$V_r(r)=E_c(1-(\pi r/l)^2) \tag{33}$$

and by use of this potential the vibrational frequency ν_t along the reaction path,

$$\nu_t^2=\frac{1}{4\pi^2\mu}\left(\frac{d^2V_r(r)}{dr^2}\right)_{r=0}=-\frac{E_c}{2\mu l^2}. \tag{34}$$

In Eq. (25), if one takes the term $m=1$ only, the rate constant,

$$k\simeq\frac{kT}{h}\frac{f_{tr.}^{\ddagger}}{F_A\cdot F_{BC}}\exp\left(\frac{h\nu_0}{2kT}\right)\sum_n\left[1+\frac{1}{24}\times\left(\frac{h}{kT}\right)^2\frac{E_c}{2\mu l^2}(1-\gamma_n)\right]\cdot\exp(-y_n^2) \tag{35}$$

is obtained, where

$$\gamma_n=\frac{1}{E_c}\left\{h\left(\frac{\nu_0^2-\nu_+^{+2}}{2\nu_0}\right)\left(n+\frac{1}{2}\right)+\frac{1}{4}+\frac{1}{2}kT\right\}. \tag{36}$$

Then, in the case where the conditions

$$1\gg\gamma_n \text{ and } \nu_a\simeq\nu_+^+$$

hold, the above equation (35) reduces to the ARR equation with a correction term $1/24\cdot(h\nu_t/kT)^2$, that is, Wigner's equation. Also our results are similar to those obtained by Hirschfelder and Wigner[5] in several points, for example, the dependence of the transmission coefficient κ on the relative translational energy or on the vibrational potential. Their result for the persistence of the vibrational quantum number in the reaction, even if the difference between frequencies of the initial and final states is not small, suggests that the contribution of the cross transitions to κ is not so large in our case. However because of their potential form, as well as Matsen's[7], with the abrupt change of height or of vibrational potential, the obtained κ is essentially of oscillating character with the relative momentum p_r, while in our case, it has not such a property as long as the condition $1\gg a\rho_{nn}^2$ holds.

All the considerations above have been done on the basis of the two-dimensional case. It is quite difficult to assume the behavior of reaction in the many-dimensional case concerning several vibrational and rotational motions from the results in the present case.

But when the barrier is sufficiently broad and flat, it is expected that one may conveniently suppose the energy levels of the "activated complex", for example, the vibrational levels of frequency ν_a or more roughly of ν_+^+, (Eqs. (29) and (30)), which have width occurring from the short lifetime of the complex. If the level spacings are larger than their width, it will be possible to describe the state of the "activated complex" by the quantized partition function for these levels. This approximation with an appropriate correction for the average transmission coefficient is still available as far as the levels retain their individualities. On the contrary, when the level spacing and the level width are comparable in their magnitude for several motions of the complex, for example, the lower energy states of rotational motions, such a simple approximation can not be adopted. As a step towards the many-dimensional case correlating to the above problem,

the physical scattering of atoms from diatomic molecules has been investigated only by Zener and others[15], because of mathematical difficulty. It will, therefore, be necessary for more researches in this realm to be accumulated to elucidate the nature of chemical reactions completely.

Summary

The transmission coefficient for the simplified two-dimensional potential barrier has been obtained and its property depending on the curvatures of the barrier and other factors has been discussed. On the basis of this coefficient a quantum-mechanical rate equation has been formulated, the limiting forms of which formally reduce to the ARR equation and to Wigner's equation including a quantum correction. Then the rate constants given by the equations in the present and the ARR theory have been compared for the reaction $H+H_2 \rightarrow H_2+H$.

It has been found, from the above results, that the classical approximations in the ARR theory are generally valid except the reactions involving light particles and a thin barrier at low temperatures.

The authors wish to express their hearty thanks to Professor S. Shida for his kind encouragement.

This investigation was supported by a grant in aid for fundamental scientific research.

Appendix I

Formulation of a Modified Transmission Coefficient by the Method of Distorted Waves

To solve the coupled equations (9), we have taken the right-hand side of them to be zero as zero-order approximation. A further improvement can be made by solving the equations which include the solutions $F^0_{n\pm2}(r)$, obtained from the zero-order approximate equations (12), in their right-hand side. The general solution of such a heterogeneous differential equation is easily written as follows[16]:

$$F_n(r)=F^0_n(r)+F_{n2}(r)\int_{+\infty}^{r}F_{n3}(r)W(r)dr+F_{n3}(r)\times\int_{r}^{-\infty}F_{n2}(r)W(r)dr, \qquad (A,1)$$

where

$$W(r)=-\frac{8\pi^2\mu a V_r(r)}{h^2}[\rho^2_{n,n-2}F^0_{n-2}(r)+\rho^2_{n,n+2}F^0_{n+2}(r)], \qquad (A,2)$$

considering its property at two boundaries, $r\rightarrow\pm\infty$. In Eq. (A,1), $F_{n2}(r)$ and $F_{n3}(r)$ are taken as two independent solutions of the homogeneous equation (12) and

$$F_{n3}(r)=gF^0_n(r), \qquad (A,3)$$

where $F^0_n(r)$ is also the solution of the same equation and is given by Eq. (16), i.e.,

$$F^0_n(r)=F_{n1}(r)+\frac{a_2}{a_1}F_{n2}(r). \qquad (A,4)$$

The coefficient g is determined from the condition

$$F_{n3}(r)\frac{dF_{n2}(r)}{dr}-F_{n2}(r)\frac{dF_{n3}(r)}{dr}=1. \qquad (A,5)$$

Since $F_{n1}(r)$ and $F_{n2}(r)$ approach to $\exp(2\pi ir/\lambda)$ and $\exp(-2\pi ir/\lambda)$ respectively, as $r\rightarrow-\infty$, then

$g=-\lambda/4\pi i$, where $\lambda=h/(2\mu E_t)^{1/2}$, (A,6), (A,7)

is obtained. Substituting Eqs. (A,3) and (A,6) in Eq. (A,1) and considering the asymptotic form of $F_n(r)$ as $r\rightarrow-\infty$, the modified transmission coefficient κ_n is derived as follows:

$$\kappa_n=1-\left|\frac{a_2}{a_1}+\left(\frac{\lambda}{4\pi i}\right)\int_{-\infty}^{+\infty}F^0_n(r)\cdot W(r)dr\right|^2. \qquad (A,8)$$

Introducing the detailed expression of $W(r)$, Eq. (A.2), the integral in Eq. (A,8) is written as

$$\int_{-\infty}^{+\infty}F^0_n(r)W(r)dr=-\frac{8\pi^2 a\mu E_c}{h^2}\left[\rho^2_{n,n-2}I_1+\rho^2_{n,n+2}I_2\right], \qquad (A,9)$$

where

$$I_1=\int_{-\infty}^{+\infty}F^0_n(r)\cosh^{-2}(\pi r/l)F^0_{n-2}(r)dr \qquad (A,10)$$

and

$$I_2=\int_{-\infty}^{+\infty}F^0_n(r)\cosh^{-2}(\pi r/l)F^0_{n+2}(r)dr. \qquad (A,11)$$

The analytical expressions for $F^0_{n\pm2}(r)$ are given by the equations analogous to Eq. (A,4) for $F^0_n(r)$.

Appendix II

Derivation of Equation for Rate Constant

From Eq. (24) the rate constant is expressed as follows:

$$k=\frac{1}{(A)(BC)}\times\left[\frac{1}{h^3}\iiint\sum_n\sum_j\kappa_{nj}N_0(\boldsymbol{p}_G,p_r,n)\frac{p_r}{\mu h}dp_r d\boldsymbol{p}_G d\boldsymbol{R}\right]. \qquad (A,12)$$

Assuming the initial systems in thermal equilibrium, the density function, $N_0(\boldsymbol{p}_G, p_r, n)$, is given by

$$N_0(\boldsymbol{p}_G,p_r,n)=\frac{(A)(BC)}{F_A\cdot F_{BC}}\cdot e^{\frac{h\nu_0}{2kT}}\cdot e^{-\frac{En}{kT}}\cdot e^{-\frac{p_r^2}{2\mu kT}}\cdot e^{-\frac{p_G^2}{2MkT}}. \qquad (A,13)$$

15) C. Zener, *Phys. Rev.*, **37**, 556 (1931); C.F. Curtiss and F.T. Adler, *J. Chem. Phys.*, **20**, 249 (1952).

16) See, for example, N.F. Mott and H.S.W. Massey, "The Theory of Atomic Collisions", Oxford: Clarendon Press, 1949, p. 106.

Substituting Eq. (A, 13) in Eq. (A, 12),

$$k=\frac{1}{F_A\cdot F_{BC}}\exp\left(\frac{h\nu_o}{2kT}\right)\cdot\left(\frac{1}{h^3}\iint e^{-\frac{p_G^2}{2MkT}}dp_G dR\right)$$
$$\times\left(\sum_n e^{-\frac{En}{kT}}\cdot\int_0^\infty\sum_j \kappa_{nj}e^{-\frac{f_r^2}{2\mu kT}}\cdot\frac{p_r}{\mu h}dp_r\right) \quad (A, 14)$$

is obtained. Since, in our approximation, κ_{nj} exists only for $n=j$, we obtain the following expression for the integral in Eq. (A, 14)

$$I=\int_0^\infty \kappa_{nn}(p_r, n)\cdot e^{-\frac{f_r^2}{2\mu kT}}\cdot\frac{p_r}{\mu h}dp_r$$
$$=2\frac{kT}{h}\int_0^\infty \kappa_{nn}(x, n)xe^{-x^2}dx, \quad (A, 15)$$

where $x=p_r/(2\mu kT)^{1/2}$.

Since this integral including the approximate κ_{nn}, Eq. (21), just corresponds to that occurring in the statistical-mechanical treatment of the Fermi-Dirac gas,[17] it is easily integrated in analogous way and the result is

$$I=\frac{kT}{h}\left[1+2\sum_{m=1}^{\infty}\left\{(C/4\pi^2kT)^m\cdot L_{2m}(x_n)\times\sum_{p=1}^{\infty}\frac{(-1)^p}{p^{2m}}\right\}\right]\exp(-x_n^2), \quad (A, 17)$$

17) J. E. Mayer and M. G. Mayer, "Statistical Mechanics", John Wiley & Sons, Inc., New York, 1940, p. 381.

where

$$L_{2m}(x_n)=-\left[\frac{d^{(2m)}}{dx^{(2m)}}\exp(-x_2)\right]_{x=x_n}\cdot\exp(x_n^2),$$

and

$$x_n^2=\frac{1}{kT}[E_c(1-a\rho_{n,i}^2)-C/4]. \quad (A, 19)$$

If we express $a\rho_{nn}^2$ by use of ν_0 and $\nu_+^\ddagger$ defined by Eqs. (29) and (30), then Eq. (A, 19) becomes

$$x_n^2=\frac{1}{kT}\left[E_c-h\left(\frac{\nu_0^2-\nu_+^{\ddagger 2}}{2\nu_0}\right)\left(n+\frac{1}{2}\right)-\frac{C}{4}\right], \quad (A, 20)$$

since

$$\rho_{nn}^2=\int_{-\infty}^{+\infty}\psi_n^*(\rho)\rho^2\psi_n(\rho)d\rho=\frac{h}{8\pi^2m\nu_0}(2n+1). \quad (A, 21)$$

Noting the relations

$$E_n=h\nu_0(n+1/2) \quad (A, 22)$$

and

$$f_{+\mathrm{tr.}}^+=\frac{1}{h^3}\iint e^{-\frac{p_G^2}{2MkT}}dp_G dR, \quad (A, 23)$$

in which the integration over R is carried out for unit volume, and substituting Eqs. (A, 17) and (A, 20) in Eq. (A, 14), we can get the final equation (25).

Laboratory of Physical Chemistry,
Tokyo Institute of Technology,
Tokyo

Structure of Pristimerin and Celastrol[1]

By Koji NAKANISHI, Hiroshi KAKISAWA and Yoshimasa HIRATA

(Received May 25, 1955)

Pristimerin is an antibiotic isolated by Bhatnagar and Divekar[2] from the plant *Pristimera indica* (Wild) A. C. Smith, syn. *Hippocratea indica* Wild (*Celastraceae*), which besides being active against the common gram-positive organisms, is characterized by its activity against the *Viridans* group of streptococci. It has been found to be an effective chemotherapeutic agent in the treatment of tonsilitis, inflammation of the naso-pharyngeal mucosa, etc. Celastrol is the red pigment obtained from the root bark of *Celastrus scandens*[3,4]; tripterine from *Tripterygium wilfordii* Hook f. is also reported to be identical with celastrol[5]. In the present paper we wish to present structure (I) for pristimerin and (I′) for celastrol, and also to make comments on structural studies so far undertaken[3,6,7,8] on these substances.

1) The present studies were commenced in the laboratory of Professor L.F. Fieser, Harvard University, U.S.A. A communication has appeared in *J. Am. Chem. Soc.*, **77**, 3915 (1955).

2) S.S. Bhatnagar and P.V. Divekar, *J. Sci. Industr. Res.*, **10B**, 56 (1951).

3) O. Gisvold, *J. Am. Chem. Soc.*, **28**, 449 (1939); **29**, 12 (1940); **31**, 529 (1942).

4) Chou and Mei, *Chinese J. Physiol.*, **10**, 529 (1936)

5) M.S. Schechter and H.L. Haller, *J. Am. Chem. Soc.*, **64**, 182 (1942).

6) L.F. Fieser and R.N. Jones, *J. Am. Pharm. Soc.*, **31**, 315 (1942).

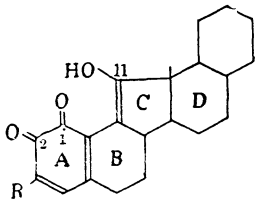

(I) R=OCH_3
(I') R=OH

One isolated nuclear double bond, probably tri- or tetra-substituted.

$-C_7H_{15}$ (Containing two C-CH_3)

Pristimerin is obtained as orange needles and possesses one methoxyl and three C-methyl groups. A molecular formula of $C_{30}H_{40}O_4$ is in better accord with analysis than the previously assigned[7] formula of $C_{28}H_{36-38}O_4$. The fact that catalytic hydrogenation gave a colorless solution which gradually regained the original coloration when exposed to air, and that the *shape* of the ultraviolet curve (Fig. 1) was similar to *o*-quinones, e.g., 3-*n*-pentadecyl-1-,2-benzoquinone[9], 4-methyl-1,2-benzoquinone[10], 3-methoxy-1,2-benzoquinone[11] (Fig. 1), etc., suggested that two of the oxygens were contained in an *o*-benzoquinonoid arrangement. Though the infrared spectrum (Fig. 2a) was compared with those of several other *o*-quinones, the bands in the 6μ region are as yet not completely interpretable; it is now understood that the conjugated enol group is evidently involved. In spite of the 3μ hydroxyl band (*vide infra*) and a positive ferric chloride test, pristimerin was recovered unchanged from rather vigorous treatment with diazomethane. Acetylation under a variety of conditions did not afford a crystalline product, but the reductive acetylation proceeded smoothly to give a colorless optical-active[12] dihydro-diacetyl derivative. However, the ultraviolet spectrum of the reductive acetate (Fig. 1) showed no conspicuous maxima, excepting a shoulder-like peak at 278 mμ (log ε 2.90), which at most could only be attributed to a benzenoid nucleus. Support of the presence of an aromatic (i.e., benzenoid) ring was obtained from the infrared bands at 1775 and 1765 cm^{-1} (enol acetate), and at 1600 and 1515 cm^{-1} (aromatic) (Fig. 2b). The disappearance of the hydroxyl band, is also to be noted.

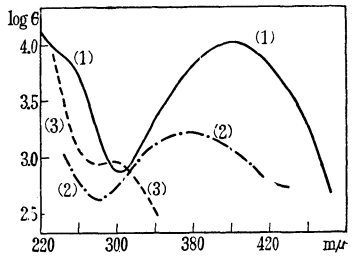

Fig. 1. ——— (1) Pristimerin
—·—· (2) 3-Methoxy-1,2-benzoquinone
---- (3) Reductive acetate

Wave numbers in cm^{-1}

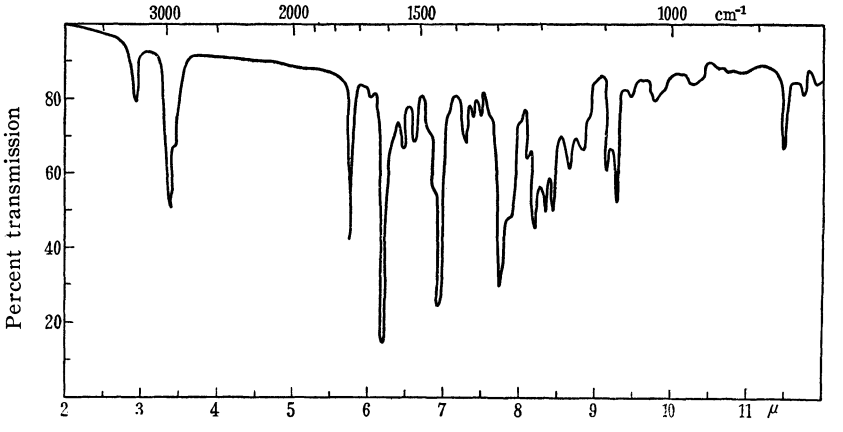

Wave length in microns

Fig. 2a. Pristimerin (CCl_4)

7) A.B.S. Kulkarni and R.C. Shah, *Nature*, **173**, 1237 (1954).
8) V.N. Kamat, F. Fernandes, and S.S. Bhatnagar, *J. Sci. Industr. Res.*, **14C**, 1 (1955).
9) H.S. Mason, *J. Am. Chem. Soc.*, **70**, 138 (1948).
10) S. Goldschmidt and F. Graef, *Ber.*, **61**, 1858 (1928).
11) Prepared according to the method of R. Willstätter and F. Müller, ibid., **44**, 2179 (1911).
12) The $[\alpha]_D$ of pristimerin could not be measured *owing to the coloration.*

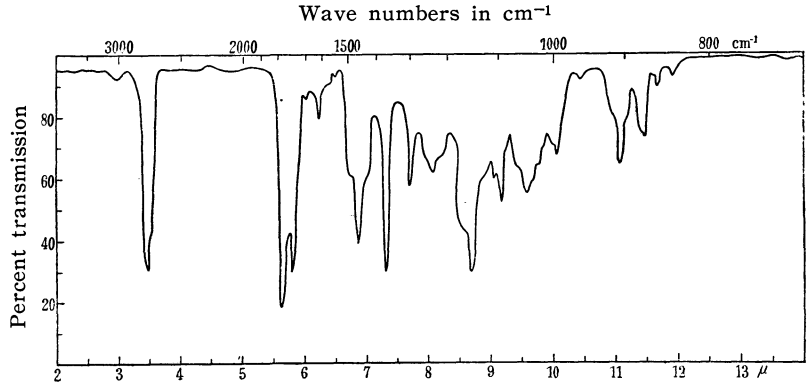

Fig. 2b. Reductive acetate (Chloroform)

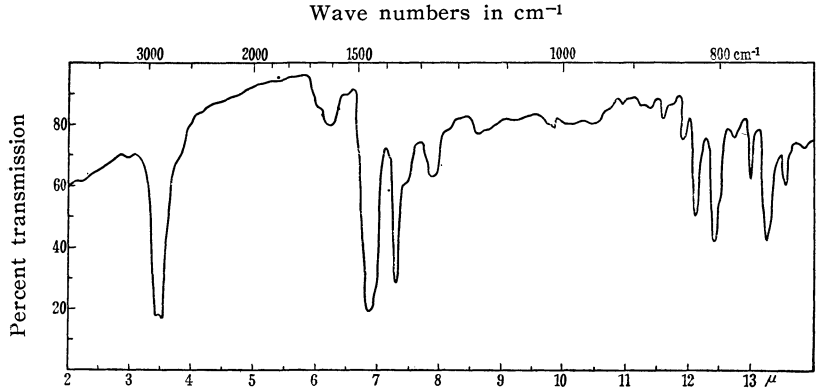

Fig. 2c. $C_{25}H_{22}$ (Nujol)

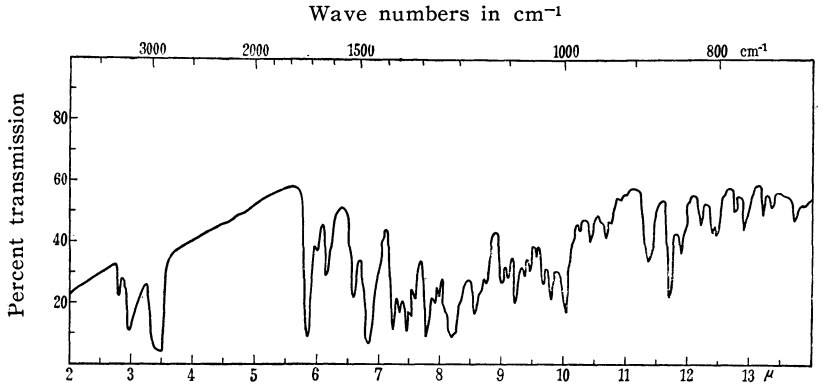

Fig. 2d. Pristimerol (Nujol)

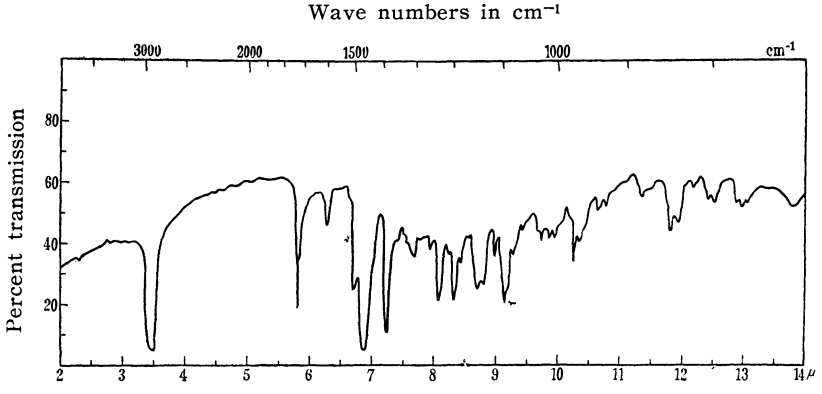

Fig. 2e. Pristimerol dimethyl ether (Nujol)

A micro zinc-dust distillation of pristimerin afforded, though in very poor yield, a strongly fluorescent crystalline product and a crude oil with an aromatic odor. The ultraviolet spectrum of the former (Fig. 3) was almost

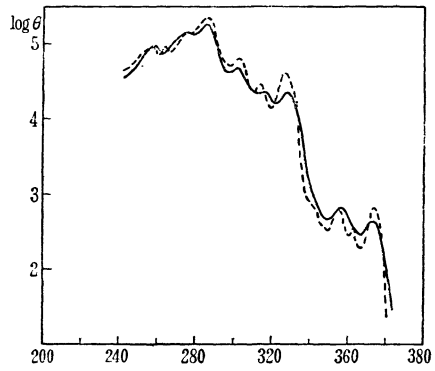

Fig. 3 ——— Zinc distliation product, $C_{25}H_{22}$
---- Picene

superimposable on that of picene except that the respective peaks were displaced slightly by 0–2 mμ towards longer wave-length; an infrared comparison clearly revealed the non-identity of the product with picene (infrared spectrum of product recorded in Fig. 2c[13]). The analysis checked with $C_{22}H_{23}$, i.e., a C_4H_9 substituted picene, and since bathochromic shifts of 5-7 mμ are observed in the ultraviolet spectra of dialkyl-substituted picenes as compared with the parent hydrocarbon[14], the product is suspected to be a monosubstituted picene with a C_4H_9-side chain. The spectrum was also comparable *in shape* with that of chrysene (and alkyl derivatives), and analysis equally agreed with a C_3H_7-substituted chrysene, $C_{21}H_{18}$, but in this case the bathochromic shifts of 6–17 mμ of the respective peaks are too high to be accounted for by three methyl groups. The crude brown oil possessed an ultraviolet spectrum somewhat similar to naphthalene derivatives. Although possibilities for ring formation during the zinc-dust distillation should not be overlooked, other evidences (*vide infra*) suggested the presence of rings A, B, and C, and also the five-membered nature of ring C; hence, a pentacyclic perhydro-1,2,7,8-dibenzofluorene skeleton with an angular methylgroup at the C/D ring junction has tentatively been assumed.

Treatment of pristimerin with sodium borohydride, or with boiling alcoholic hydrochloric acid yielded a colorless dihydro derivative, pristimerol, possessing a clear ultraviolet absorption (λ_{max}^{alc} 284 mμ, log ε 3.49, Fig. 4)

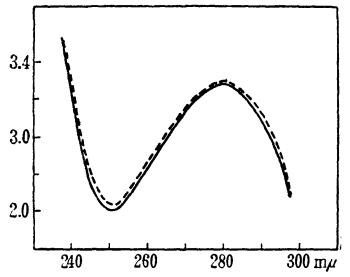

Fig. 4. ——— Pristimerol
---- 1,2,3,4-Tetrahydro-5,6,7-trimethoxy-naphthalene

which was of great value in subsequent studies. The original methoxyl group was retained, and two hydroxyl groups had been formed as evidenced by formation of a di-*p*-nitrobenzoate and a dimethyl ether (λ_{max}^{alc} 280 mμ, log ε 3.31); the infrared spectrum (Fig. 2d) showed that an hydroxylated ben-

13) The authors are indebted to Research Laboratory, Baird Associates, Cambridge, U.S.A., for running micro-infrared spectra of the zinc distillation product and related compounds.

14) L. Ruzicka, et al., *Helv. Chim. Acta*, **19**, 377 (1936); **20**, 1155 (1937).

zenoid moiety was present in pristimerol. The disposition of the hydroxyl and methoxyl groups around the benzenoid ring was inferred in the following manner: At least two carbon side-chains should be attached to this ring to account for the condensed cyclic skeleton, and on the other hand, at least one position in the benzenoid ring is unsubstituted since pristimerol coupled with *p*-diazobenzenesulfonic acid. 1,4-Dihydroxybenzene and 1,2,4-trimethoxybenzene absorbed at 294 mμ (log ε 3.49) and 286 mμ (log ε 3.56), respectively, and attachment of two side-chains would shift the maxima to a wave-length longer than that of pristimerol or its dimethyl ether[15]; accordingly, absence of these groups is apparent. Two alkyl substituents attached to pyrogallol (λ_{max}^{alc} 267 mμ) or catechol (λ_{max}^{alc} 278 mμ)[16] may be expected to shift the absorption maximum to the region of 285 mμ: this would lead to the part structures (II), (III) and (IV) for pristimerol dimethyl ether.

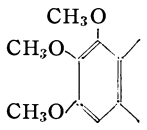

(II)

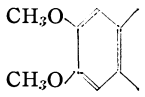

(III)

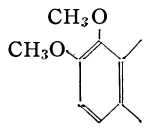

(IV)

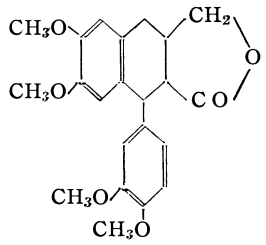

(V)

Amongst these, (III) was excluded through comparison with the absorption of (V)[17] (λ_{max}^{alc} 283 mμ), and similary, (IV) was discarded on grounds of the absorption of 1,2-dimethoxy-4-*n*-amylbenzene[18] (λ_{max}^{alc} 284 mμ), thus leaving (II) as the plausible structure. Accordingly, 1,2,3,4-tetrahydro-5,6,7-trimethoxynaphthalene[19] was synthesized, and it was found that the spectrum was superimposable on that of the pristimerol derivative (Fig. 4). This proved in a conclusive manner that in pristimerol the part structure (VI) or (VII) was

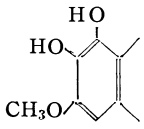

(VI)

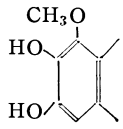

(VII)

15) (i) For the present discussion, the chromophoric power of a phenolic hydroxyl and its methyl ether is regarded as being approximately identical. (ii) Alkyl groups attached to benzenoid nuclei produce bathochromic shifts. However, when an oxygenic function is attached to the nucleus, a bathochromic shift is not necessarily the result, e.g., catechol (λ_{max} 278 mμ) and pyrogallol (λ_{max} 267 mμ). Hence, comparisons should be made only amongst compounds which are substituted by oxygenic functions in an analogous manner.

present. In agreement with these *o*-dihydroxybenzene structures, pristimerol gave a green ferric chloride test. The obvious fact that pristimerin should necessarily be the corresponding quinone received confirmation from the results of catalytic hydrogenation, i.e., pristimerin absorbed only one mole of hydrogen, and rapid processing of the colorless solution afforded the expected pristimerol. Formation of pristimerol by sodium borohyride may be presumed to proceed through the following sequences, in which only the

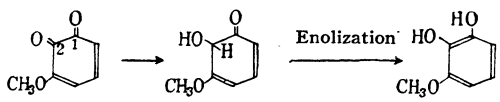

carbonyl group at position 2 is reduced since the conjugated system incorporating the other carbonyl group, $-CO-C=C-C=C-OCH_3$, may be regarded as a carbomethoxy vinylog. Formation of pristimerol with methanolic hydrochloric acid possibly proceeds through an intermolecular oxidation-reduction. (In fact, the yield of pristimerol by this latter method never exceeded 50%.)

The position and nature of the remaining oxygenic function will now be discussed. The oxygenic functions in positions 1 and 2 are hindered, as evidenced from the unreactivity of pristimerin with *o*-phenylenediamine, and recovery of pristimerol upon attempts to obtain a carbonate by treating with phosgene. Furthermore, the carbonyl group apparent in the infrared spectra of the reductive acetate, pristimerol, and its dimethyl ether (Figs. 2b, 2d, 2e) afforded no carbonyl derivatives and the dimethyl ether resisted reduction with sodium borohydride or lithium aluminum hydride. These facts may be satisfied by assuming a rather rigid structure for these functions i.e., by adopting (VI) for pristimerol and placing the carbonyl group in the steri-

16) R.A. Morton and Z. Sawires, *J. Chem. Soc.*, 1052 (1940).
17) G.N. Walker, *J. Am. Chem. Soc.*, 75, 3393 (1953).
18) R. Adams, C.K. Cain, and H. Wolff, ibid., 62, 732 (1940).
19) R.D. Haworth, B.P. Moore, and P.L. Pauson, *J. Chem. Soc.*, 3271 (1949).

cally hindered position of an angular tricyclic system as in (VIII). The bathochromic location

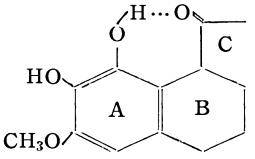

(VIII)

of the ketone band in the infrared spectrum of pristimerol (1705 cm^{-1}) as compared with the reductive acetate (1725 cm^{-1}) and pristimerol dimethyl ether (1720 cm^{-1}) may thus be satisfactorily explained by formation of the seven-membered hydrogen bond. Representation of this ketone group in a five-membered rather than in a six-membered ring C was deduced from the infrared absorption of steroidal[20] and triterpenoid[21] ketones; the fact that the analogously constructed 11-keto in the five-membered ring C of hydrojervine derivatives also absorb in the region of 1725 cm^{-1} [22] is also to be noted. However, possibilities for a six-membered ring C still remains.

The 11-oxygenic function in pristimerin has been formulated in the enol-form rather than in the alternative keto-form for the following spectroscopic reasons: (i) Contrary to the statement of Kulkarni and Shah[7], the infrared spectra of pristimerin revealed a weak but distinctive band at 3370–3380 cm^{-1} (in chloroform and carbon tetrachloride), in spite of the fact that the samples used were repeatedly recrystallized from absolute solvents and thoroughly dried. No hypsochromic shift was observed upon dilution of the solutions, thus indicating formation of an intramolecular hydrogen bond. Furthermore, the fact that the solid spectrum likewise showed an hydroxyl absorption (λ_{max}^{Nujol} 3346 cm^{-1}) excluded the possibilities of this remaining oxygenic group being involved in a keto-enol equilibrium[23]; hence, it had to be assumed that some sort of an hydroxyl was present in pristimerin. (ii) One set of isosbestic points was observed in the ultraviolet spectra of pristimerin measured in alcoholic alkali (Fig. 5). In the light of this

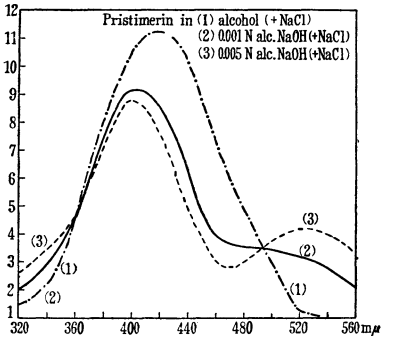

Fig. 5. Isosbestic point; 362 mμ (ε=4800), 495 mμ (ε=3300)

observation, it follows that in neutral alcohol (and presumably in other less polar solvents[24]) pristimerin exists solely in the enol-form and that an enol-enolate equilibrium is involved; if pristimerin existed in the keto-form or if a keto-enol equilibrium was involved *two* sets of isosbestic points would have been expected.

The fact that ozonolysis of pristimerin afforded no volatile carbonyl compound precluded the presence of double bonds within the side-chain. Furthermore, since pristimerol and its dimethyl ether do not absorb hydrogen upon catalytic hydrogenation it seems possible that the double bond is situated in a hindered nuclear position, i. e., either to be tri- or tetra-substituted. Though infrared bands of medium strength were observed around 840 cm^{-1} with pristimerin and derivatives, the infrared evidence alone is as yet not decisive for the presence of a tri-substituted double bond.

As already mentioned by Kulkarni and Shah[7], and by Kamat, et al. the similarity in the source and ultraviolet spectrum of celastrol to those of pristimerin demonstrated a close relationship to exist between the two substances. Though celastrol possesses no methoxyl group, it is methylated by diazomethane[3] to give a product, the analyses of which also agree with $C_{30}H_{40}O_4$ (pristimerin) as well as with the reported $C_{23}H_{32}O_3$. Professor O. Gisvold, Minnesota University, U. S. A., kindly furnished us with a sample of celastrol and its monomethyl ether, and it was found that the latter was indeed identical with pristimerin (melting point, ultraviolet and infrared spectroscopy measure-

20) R.N. Jones, P. Humphries, and K Dobriner, *J. Am. Chem. Soc.*, **71**, 241 (1949).
K. Dobriner, E.R. Katzenellenbogen and R.N. Jones. "Infrared Absorption Spectra of Steroids", Interscience, New York (1953).

21) A. Meyer, O. Jeger, V. Prelog and L. Ruzicka, *Helv. Chim. Acta*, **34**, 747 (1951).

22) O. Wintersteiner, M. Moore and B.M. Iselin, *J. Am. Chem. Soc.*, **76**, 5609 (1954).

23) The infrared spectrum of 1,1-dimethylhexanedione-1,3 in chloroform shows bands arising from both the keto- and enol-form: $\lambda_{max}^{CHCl_3}$ 2630 w, 1702 s, 1724 m, 1605 s (cf., R.S. Rasmussen, D.D. Tunnicliff and R.R. Brattain, *J. Am. Chem. Soc.*, **71**, 1069 (1949); ref. 24); H. Heymann, S.S. Bhatnager and L.F. Fieser, *J. Am. Chem. Soc.*, **76**, 3689 (1954)). However, in nujol the doublet around 1700 cm^{-1} disappeared and only the enolic bands at 2630 (m) and around 1605 cm^{-1} (s) were observed.

24) In general, the polar ketonic structure is favored in polar solvents, and the chelated enolic form in less polar solvents: cf. B. Eistert and W. Reiss, *Ber.*, **87**, 92 (1954).

ments). Accordingly, the part structure (I') may be assigned to celastrol. The oxidation-reduction potential of pristimerin, as measured by titration, gave the value of ca. +297 mV., which is exceptionally low for *o*-quinones[25]. This is probably due to the combined electron-donating nature of the methoxyl, enol, and alkyl (as ring B) groups.

Kulkarni and Shah[7] have forwarded the part structure (IX) for pristimerin. Pristimerol would then be represented by the conjugate-chelated (X), which should now possess the characteristic ultraviolet[23] and infrared[27] absorption of *o*-hydroxyacetophenones, i. e., two, λ_{max}^{alc} at ca. 250 mμ and 330 mμ, as exemplified by 2, 5-dihydroxy-acetophenone (λ_{max}^{alc} 255 mμ, log ε 3.91, and 367 mμ, log ε 3.70), and a strong infrared band around 1635 cm^{-1}, both of which, however, are contrary to facts. Moreover, structure (IX) of pristimerin leads to structure (XI) for celastrol, which would most probably exist in the *p*-quinonoid form (XII) and be methylated to give a *p*-quinone (i. e., pristimerin); the fact that pristimerin

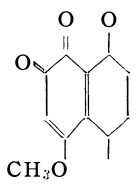

(IX)

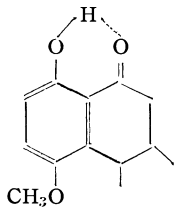

(X)

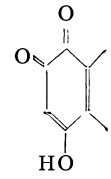

(XI)

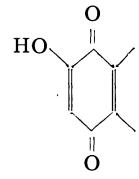

(XII)

and celastrol possess identical ultraviolet absorptions excludes the existence of an an $o \rightleftarrows p$ quinone relationship between the two. Kamat, et al.[8], have proposed a carotenoid (conjugated pentaene) structure for pristimerin, which can also be excluded on grounds of ultraviolet absorption since the chromophoric power of the group is insufficient to produce absorption as high as 423 mμ[28].

Experimental

Unless otherwise stated, melting points were determined on a micro hot-stage and are uncorrected. The ultraviolet spectra were measured on Beckman DU and Hitachi spectrophotometers in alcohol. Infrared spectra were measured on Baird, Perkin-Elmer 12C and 21 models, equipped with rock-salt prisms.

Pristimerin.—Pristimerin was recrystallized by adding petroleum ether to a concentrated acetone or benzene solution; orange needles, m.p. 219–220° (dec.). To ascertain that the 3μ infrared band was not caused by water of crystallization, samples of pristimerin were prepared by using freshly prepared absolute solvent pairs of petroleum ether and benzene, and dried over phosphorus pentoxide in vacuo at 100° for fortyeight hours; however, the crystals thus obtained still possessed the same melting point and infrared absorption (Fig. 2a): λ_{max}^{Nujol} 3350 w, 1742 s, 1736 s, 1662 w, 1595 s, 1550 m, 1519 m; $\lambda_{max}^{CCl_4}$ 3380 w, 1740 s, 1655 w, 1607 s, 1514 cm^{-1}. It is considered that the bands around 1740 cm^{-1} are associated with the *o*-quinonoid group; in celastrol, the corresponding band was shifted to 1701 cm^{-1} with a slight shoulder at 1742 cm^{-1}. Ultraviolet spectrum (Fig. 1): λ_{infl} 250–255 mμ (log ε 3.90), λ_{max} 423 mμ (log ε 4.05).

Calcd. for $C_{30}H_{40}O_4$: C, 77.55; H, 8.68; M.W., 464.62.
Found: C, 77.54, 77.84, 78.18, 77.70; H, 8.87, 8.90, 8.72, 8.67; M.W. (Rast), 394.
C–CH_3 (Kuhn-Roth): 8.08% (2.5 groups).
O–CH_3 (Zeisel): 7.69% (1.1 groups).

Attempted Acetylation.—In spite of the several conditions tested, only an amorphous white powder was obtained by regular acetylation (with combinations of acetic anhydride, pyridine, boron trifluoride, sodium acetate, sulfuric acid), repeated purifications by chromatography, and recrystallization from various solvents; m.p. 120–150°C.

Catalytic Hydrogenation of Pristimerin.—In three micro measurements conducted in acetic acid with Adams' catalyst, 1.30, 0.93, and 1.12 moles of hydrogen were absorbed to give a colorless solution, which regained the original orange color when left in contact with air for several hours (cf. Reductive acetate (ii), and pristimerol (iii)).

Reductive Acetate.—(i) A mixture of 150 mg. of pristimerin and 150 mg. of zinc dust was treated with 0.6 cc. of acetic anhydride and one drop of triethylamine, when decolorization took place in five minutes. The mixture was boiled for several minutes, extracted with 1.5 cc. of hot acetic acid, the boiling extract treated with several drops of water and the precipitate recrystallized twice by addition of methanol to a saturated acetone solution; white needless, 90 mg., m.p. 252°, $[\alpha]_D^{22°}$ +54.3° (chloroform). Ultraviolet spectrum (Fig. 1): λ_{max} 278 mμ (log ε 2.90). Infrared spectrum: Fig. 2b. It does not react with carbonyl reagents.

25) K. Wallenfels and W. Möhle, ibid., **86**, 926 (1953).
26) R.A. Morton and A.L. Stubbs, *J. Chem. Soc.*, 1347 (1940).
27) H.L. Hegert and E.F. Kurth, *J. Am. Chem. Soc.*, **75**, 1622 (1953).
28) W. Oroshnik and A.D. Mebane, ibid., **76**, 5719 (1954).

Calcd. for $C_{34}H_{46}O_6$: C, 74.15; H, 8.42.
Found: C, 73.75, 73.96; H, 8.29, 8.10.
$-OCOCH_3$ Content: 1.8 groups.

(ii) The same reductive acetate (m.p. and infrared spectrum) was obtained by hydrogenating 100 mg. of pristmerin in 6 cc. of acetic anhydride over PtO_2 catalyst, adding 1 cc. of pyridine, leaving the solution overnight, removing the catalyst, and treating as in (i).

Ozonolysis of Pristimerin.—Ozone was passed through a solution of 60 mg. of pristimerin in 5 cc. of chloroform until complete decolorization took place, and the ozonide was decomposed by boiling with water. No precipitate was formed in a solution of 2,4-dinitrophenylhydrazine connected to the top of the condenser during the refluxing; steam distillation of the ozonolysis mixture likewise afforded no 2,4-dinitrophenylhydrazone.

Zinc Distillation.—One end of a glass tubing (7×0.6 cm.) was drawn out into a capillary and the root of the capillary was stuffed loosely with some asbestos. The tubing was filled in the following order with zinc-dust, pristimerin+zinc-dust (1: 100 mixture), and zinc-dust, to make layers of 1 cm. (a), 0.5 cm. (b), and 0.5 cm. (c), respectively, and the tube was sealed outside layer c. After first heating (a) until red-hot with a microflame, the tubing was heated from (c) through (b) towards (a) during a period of three to four minutes. During the course of distillation, care should be taken to distil with heat transmitted through the zinc layer and to move the flame slowly towards new portions of the tube containing the yet undecomposed sample. Ninety of these distillations were carried out on a mixture of 600 mg. of pristimerin and 60 g. of zinc-dust. The respective capillary portions containing an oily and crystalline aromatic distillate were cut off, washed with acetone, and the solutions combined. The solvent was evaporated and the ethereal solution of the residue was passed through a column (0.5×10 cm.) of alumina (acid-washed), when a purple-red band remained sticking on the top. The eluate was passed through a column twice more and the ether was evaporated. The dark-yellow residue was submitted to a fractional dissolution using a 1: 2 mixture of acetone and petroleum ether, when a crystalline product was obtained from the fraction which was more soluble in the solvent pair. The other fraction was an orange oil with an aromatic odor and an ultraviolet spectrum resembling naphthalenoid compounds. The crystals were combined and passed through a column once more and finally recrystallized from ethanol, when 3 mg. of slight yellow flakes with a strong purple fluorescence were obtained; m.p. 299–300° (dec.) (in sealed tube, otherwise sublimation). Ultraviolet spectrum (Fig. 3); 232 mμ (log ε 4.32), 257 (4.63), 275 (4.78), 284 (4.90), 297 (shoulder, 4.40), 301 (4.39), 313 (shoulder, 4.15), 327 (4.17), 357 (2.97), 376 (2.87). Infrared spectrum: Fig. 2c.

Calcd. for $C_{25}H_{22}$: C, 93.40; H, 6.60.
Found: C, 93.43; H, 6.87. (analysis carried out on 0.975 mg.)

Pristimerol.—(i) A solution of 50 mg. of pristimerin in 2 cc. of ethanol was decolorized immediately upon addition of a small amount of sodium borohydride. After several minutes, the excess reagent was decomposed with acetic acid, and hot water was added dropwise to the boiling alcoholic solution until the solution became slightly turbid; 48 mg of white needles, m.p. 241° (ethanol-water). Acetylation of pristimerol under a variety of conditions (including procedure for preparation of reductive acetate) gave only an amorphous product. Attempts to obtain a carbonate of this *o*-dihydroxybenzene derivative by reacting with phosgene, or to prepare carbonyl derivatives resulted in recovery of starting material. Addition of *p*-diazobenzenesulfonic acid dissolved in aqueous sodium carbonate to an acetic solution of pristimerol gave rise to a red-orange coloration. Ultraviolet spectrum (Fig. 4): λ_{max} 284 mμ (log ε 3.49). Infrared spectrum: Fig. 2d.

Calcd. for $C_{30}H_{42}O_4$: C, 77.21; H, 9.07.
Found: C, 77.12, 77.08; H, 9.02, 9.22.
$O-CH_3$ (Zeisel): 5.42% (0.81 groups).

(ii) After adding 1.8 cc. of concentrated hydrochloric acid to 75 mg. of pristimerin dissolved in 10 cc. of ethanol, the solution was boiled for twenty minutes, when it was decolorized. After cooling, the solution was poured into 30 cc. of water, and the precipitates were collected, dried, and recrystallized from benzene, 25 mg., m.p. 236°.

Found: C, 77.35, 77.27; H, 9.14, 9.31.

(iii) A solution of 40 mg. of pristimerin in 2 cc. of acetic acid and 2 cc. of ethanol was reduced with PtO_2—H_2, the catalyst filtered rapidly, and the solution was worked up as mentioned in (i) to give 22 mg. of crystals, m.p. 234–5°. The samples prepared by methods (ii) and (iii) were identical with pristimerol, as ascertained by infrared spectra and identity of the di-*p*-nitrobenzoate.

Pristimerol Di-*p*-nitrobenzoate.—A mixture of 40 mg. of pristimenol, 1.5 cc. of pyridine, and 60 mg. of *p*-nitrobenzoyl chloride was heated on the bath for one hour, and poured into water after cooling. The excess reagent was dissolved by addition of sodium bicarbonate, and the precipitate was collected, dried, and recrystallized thrice from acetone, to give 30 mg. of white needles, m. p. 213°.

Calcd. for $C_{44}H_{48}O_{10}N_2$: C, 69.09; H, 6.33; N, 3.66.
Found: C, 69.02, 69.20; H, 6.65, 6.43; N, 3.72.

Pristimerol Dimethyl Ether.—To a solution of 100 mg. of pristimerol in 5 cc. of acetone, there was added 100 mg. of finely pulverized potassium carbonate and 0.1 cc. of freshly distilled dimethyl sulfate. After boiling the mixture for three hours, the same amount of potassium carbonate and dimethyl sulfate were added, and the mixture was boiled for another three hours, and filtered while hot. White crystals (70 mg.) were obtained from the filtrate. Concentration of the filtrate yielded another crop (30 mg.) of crystals; m. p. 209–10° (acetone). The substance did not react with carbonyl reagents and was not reduced with lithium aluminum hydride or sodium borohydride. Attempted enol acetylation (acetic anhydride-

pyridine) also failed. The O—CH_3 determination was unsatisfactory owing to its only slight solubility in the decomposition solvent (Zeisel method). Ultraviolet spectrum: λ_{max} 280 mμ (log ε 3.31). Infrared spectrum: Fig. 2e.

Calcd. for $C_{32}H_{47}O_4$: C, 77.69,: H, 9.37.
Found: C, 77. 28, 77.77; H, 9.20, 9 54.

Isosbestic Point of Pristimerin (Fig. 5).—A stock solution of 3.77 mg. of pristimerin in 100 cc. of alcohol was prepared. For measurement of the spectrum in neutral alcohol, one drop of 1 N sodium chloride solution was added from a hypodermic syringe to exactly 3 cc. of the stock solution in a 1 cm. Beckman cell. For measurement in the alkaline region, a solution of sodium hydroxide dissolved in 1 N sodium chloride was added instead, the alkali concentration of which was adjusted so as to give final alcoholic alkali concentrations of 0.0002 N, 0.001 N, and 0.005 N (the spectra were the same at concentrations above 0.005 N). The range 320—600 mμ was measured within two minutes, so as to avoid the effect of atomspheric carbon dioxide. The ultraviolet region, 210–340 mμ, was also measured but the curves did not cross; in this case, the initial inflection around 250 mμ ($\varepsilon=8.3\times10^3$) in neutral ethanol shifted towards longer wave-length with increase in alkali concentration, and was transformed into a well-defined peak in 0.002 N and higher solutions (e. g., 0.005 N solution: λ_{min} 250 mμ, $\varepsilon=9.2\times10^3$; λ_{max} 270 mμ, $\varepsilon=10.8\times10^3$). Apparently the somewhat weak but broad absorption around 520 mμ is responsible, in part, for the brown-red color of alkaline solutions. Acidification with acetic acid of the alkaline solutions restored the spectra to that of neutral pristimerin: however, if the alkaline solutions were left overnight, decomposition occurred.

Oxidation-Reduction Potential of Pristimerin.—A 0.001 molar alcoholic or dioxane solution (pH 1.5) of pristimerin was titrated with a $TiCl_3$—HCl solution, using saturated calomel and platinum electrodes. An accurate oxidation-reduction curve could not be obtained, owing to precipitation of a quinhydrone, but the value was around +297 mV. Polarography did not give satisfactoryresults.

Summary

Part structure (I) has been presented for pristimerin on grounds of chemical and spectroscopic evidences. Celastrol (tripterine) has been shown to be demetylated pristimerin, hence (I').

The authors are greatly indebted to Col. S. S. Bhatnagar, St. Xavier's College, Bombay, India, for his continuous support and generous supply of pristimerin used in the present studies, and to Professor L. F. Fieser, Harvard University, U. S. A., for permitting us to publish the results obtained while one of us (K. N.) was working in his laboratory on pristimerin, and for permitting us to take the problem back to Japan for continuation. The authors also wish to make grateful acknowledgements to Mr. S. Oseko, Dainippon Pharmaceutical Co., Osaka, and Mr. M. Yamaguchi, Osaka City University, for most of the infrared measurements, and to Mr. S. Senoh, Osaka City University, for microanalyses.

Chemical Institute, Nagoya University, Nagoya

The Effect of Temperature on Micelle Formation and Solubilization in Benzene

By Ayao KITAHARA

(Received April 18, 1955)

Introduction

There have been recently some reports on micelle formation[1,2,3] and solubilization[4,5,6,7] in a *non-polar solvent*. Since, however, detergents used are limited and the concentration dependence of solubilization has scarcely ever been obtained[8], more experimental data seem to be necessary in order to clarify the general behavior of detergents in a *non-polar solvent*.

The present author[9] has already discussed the micelle formation from the standpoint of the relation between the van't Hoff factor and the concentration of a detergent and

1) L. Arkin and C.R. Singleterry, *J. Am. Chem. Soc.*, **70**, 3965 (1948).
2) S. Kaufman and C.R. Singleterry, *J. Colloid Sci.*, **7**, 453 (1952).
3) M. van der Waarden, *J. Colloid Sci.*, **5**, 448 (1950).
4) L. Arkin and C.R. Singleterry, *J. Colloid Sci.*, **4**, 537 (1949).
5) M.B. Mathews and E. Hirschhorn, *J. Colloid Sci.*, **8**, 86 (1953).
6) S.R. Palit and J.W. McBain, *J. Chem. Soc. Ind.*, **66**, 3 (1947).
7) S.R. Palit and V. Venkateswarlu, *Proc. Roy. Soc.*, **A208**, 542 (1951).
8) R.C. Pink, *J. Chem. Soc.*, **1939**, 53.
9) A. Kitahara, *This Bulletin*, **28**, 234 (1955).

from the standpoint of the change of the maximum amount of water solubilized under varying concentration of detergents in benzene including a series of pure fatty acid salts of amines.

In this paper, the van't Hoff factor and the maximum amount of water solubilized are measured under varying concentrations and temperatures in benzene for the above materials. In this connection a few reports[3,7,10] on the temperature dependence of solubilization are also available, but a conclusive result has not yet been obtained.

Experimental

Materials.—Dodecylammonium propionate, butyrate, caproate, caprylate and caprate, and octadecylammonium propionate and butyrate were used as detergents. The preparation of detergents was similar to that already reported[9]. They were all white crystalline and had definite melting points within the range of ±1°C. It was suggested from their infrared spectra that their structures are ion pairs of $[RCOO^-]\,[H_3NR']^+$. Benzene and water were purified as usual.

Precedures.—Van't Hoff factors of these detergents in benzene were determined at different concentrations cryoscopically and ebullioscopically. Cryoscopy was carried out by means of the usual Beckmann's apparatus, and ebullioscopy by the revised Cottrell's apparatus[11].

A maximum amount of water solubilized in a benzene solution of a detergent was determined at various concentrations as in the preceding paper[9]. The occurrence of turbidity which determines the limit of solubilization was sharp with the change of the amount of added water for caproate, caprylate and caprate of both amines, though not relatively sharp for propionate and butyrate. The turbidity was a faintly milky state in the later cases and an assembly of very small droplets in the former cases. The measurements were carried out at 10°, 26° and 40°C in an air thermostat. The fluctuation of temperature was ±1°C.

Result and Discussion

The Effect of Temperature on Micelle Formation.—The results of cryoscopy and ebullioscopy are given in Figs. 1, 2 and 3 for dodecylammonium propionate, caproate and caprylate, respectively. The ordinate shows the van't Hoff factor (i) and the absissa the square root of the molality of detergents.

The values of van't Hoff factors were larger than 1.0 in the lower range of concentrations, and this concentration range is higher in the case of ebullioscopic result than in the case of cryoscopic one. These values, however, were not shown in these figures. This seems to show that the detergent molecule decomposes as follows:

$$[RCOO^-]\,[H_3NR']^+ \rightarrow RCOOH + R'NH_2.$$

This is also suggested from the following

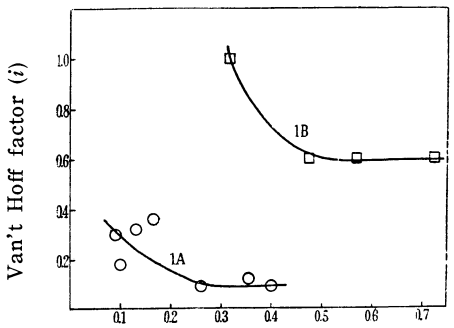

Square root of molality

Fig. 1. The relation between the van't Hoff factor and the molality of dodecylammonium propionate.
1A: at melting point
1B: at boiling point

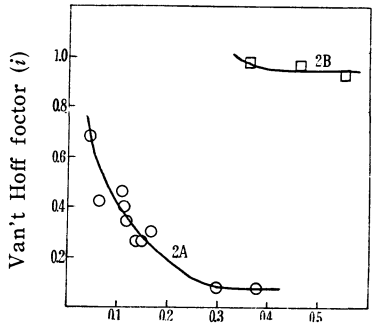

Square root of molality

Fig. 2. The relation between the van't Hoff factor and the molality of dodecylammonium caproate.
2A: at melting point
2B: at boiling point

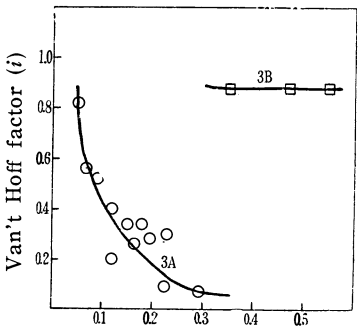

Square root of molality

Fig. 3. The relation between the van't Hoff factor and the molality of dodecylammonium caprylate.
3A: at melting point
3B: at boiling point

10) P. A. Winsor, *Trans. Faraday Soc.*, **44**, 455 (1948).
11) H. Shiba and T. Imase, *Sci. Paper Inst. Phys. Chem. Res.*, **7**, 996 (1928).

infrared spectroscopic observation. The infrared spectra of dodecylammonium caprylate in carbon tetrachloride shows an absorption peak at 1753 cm^{-1} in the concentration of 0.0046 mol./l. at room temperature. This peak is attributed to a carbonyl group of a free acid. In the concentration of 0.096 mol./l. this peak becomes very weak. It is expected that decomposition process will take place up to the relative high concentrations at a high temperature, but it will do only in the lower ones at a low temperature.

The curves of the relation between i and the concentration obtained from the cryoscopic method (1A, 2A and 3A) show a steep decrease at a certain range of concentration while at the higher concentration the values of i were markedly reduced, indicating the formation of large aggregates. On the other hand, different from the case of the melting temperature, the curves 2B and 3B which were obtained from ebullioscopy show only a very slight decrease in i over a wide range of the concentrations. The curve 1B shows apparently a moderate decrease, but since the values of i are still very much larger than those of 1A, it can be seen that the average degree of aggregation is very much smaller.

The above comparison clearly shows the effect of temperature on micelle formation, though we cannot know the precise behavior at temperatures between the melting point and the boiling point. It is evident from Figs. 1, 2 and 3 that at a low temperature (5°C), micelle formation begins to take place at a certain concentration, but at a high temperature (80°C) slight or no micelle formation takes place at least within the concentration range of the present experiment.

The Effect of Temperature on Solubilization.—The relation between the maximum amount of water solubilized (S) and the concentration of a detergent at 10°, 26° and 40°C was plotted in Figs. 4, 5 and 6, respectively. The ordinate shows the S in molality and the absissa the molality of a detergent. At 10°C the fairly slight solubility made the experiment of solubilization impossible for dodecylammonium caprate, octadecyl-

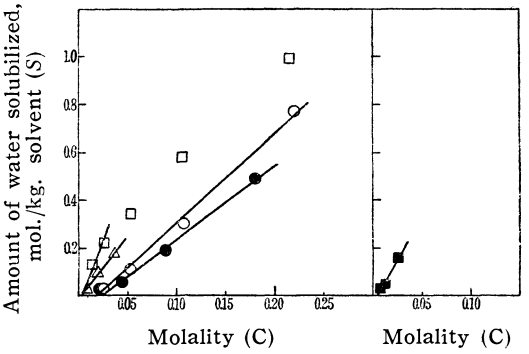

Fig. 4.
The relation between the amount of water solubilized and the molality of detergent at 10°C.
△ Dodecylammonium propionate
□ Dodecylammonium butyrate
○ Dodecylammonium caproate
● Dodecylammonium caprylate
◐ Dodecylammonium caprate
▲ Octadecylammonium propionat
■ Octadecylammonium butyrate

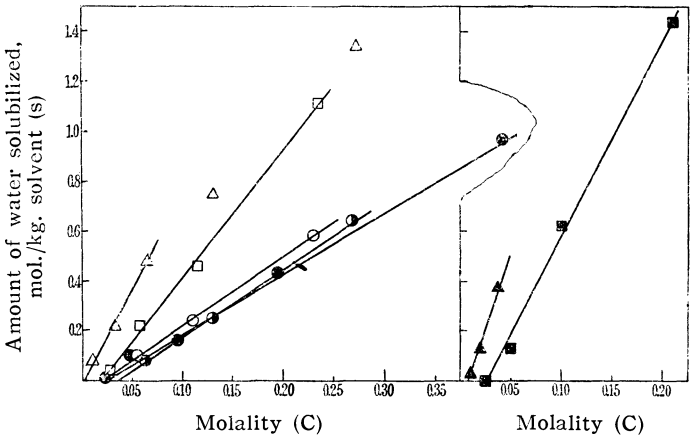

Fig. 5.
The relation between the amount of water solubilized and the molality of detergent at 26°C.
△ Dedocylammonium propionate
□ Dodecylammonium butyrate
○ Dodecylammonium caproate
● Dodecylammonium caprylate
◑ Dodecylammonium caprate
▲ Octadecylammonium propionate
■ Octadecylammonium butyrate

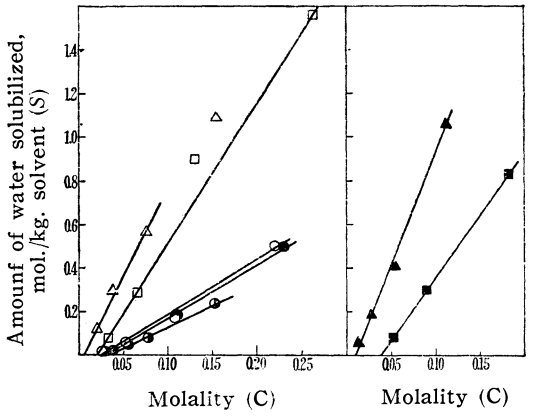

Fig. 6.
The relation between the amount of water solubilized and the molality of detergent at 40°C.
△ Dodecylammonium propionate
□ Dodecylammonium butyrate
○ Dodecylammonium caproate
● Dodecylammonium caprylate
◑ Dodecylammonium caprate
▲ Octadecylammonium propionate
■ Octadecylammonium butyrate

ammonium propionate and higher concentrations of dodecylammonium propionate. The experimental error of the S was ± 0.01 and ± 0.02 in molality at the lower and the higher S, respectively. The marks of circles, triangles and tetragons in Figs. 4, 5 and 6 were drawn somewhat larger than the range of the experimental error.

It is evident within the experimental accuracy that the S~concentration relation is linear within the concentration range of this experiment, excepting the cases of higher concentrations of dodecylammonium butyrate and probably propionate at 10°C and the cases of dodecylammonium propionate at 26°C and 40°C. That is,

$$S=\alpha(C-\beta),$$

where, C=the concentration of a detergent (molality), α, β=constants.
The value of α is referred to as the solubilizing power, and the value of β may be called the apparent critical micelle concentration obtained from solubilization.

Pink[8] has also observed this linearity, but the straight line passed the origin of the concentration. Provided that the detergent micelle is monodisperse, the value of S should be proportional to the micellar concentration. Singleterry et al.[2] have reported that the micellar concentration is proportional to the total concentration of a detergent above a critical range. Thus it will be said that the linearity, which was obtained experimentally between the S and the total concentration of a detergent, is an evidence for the monodispersity of the micellar size and shape.

However, the existence of the critical micelle concentration in a non-polar solvent may be open to discussion. Singleterry et al.[1,2] determined the critical micelle concentration of Ca-xenylstearate in benzene with use of the fluorescent dye. Since it has been found that the existence of water changes the size and shape of micelles[4], the question arises whether the critical micelle concentration is determined by the extrapolation of the relation between the amount of the solubilizate and the concentration of a detergent in a non-polar solvent as in an aqueous one. But in this experiment the effect of water on the fluidity of a solution was not qualitatively observed as in that paper[4]. Further, it is said that the effect of water on the size and shape of soap micelles disappears when the amount of water exceeds about two moles per one mole of a soap[4]. The amount of water solubilized in this experiment exceeds this value in every case, as seen from values of α of Table I. It might be, therefore, assumed that water solubilized does not affect the size and shape of micelles. Hence, the apparent critical micelle concentration was reasonably obtained by the extrapolation of the above linear relation.

The valves of α and β obtained graphically from Figs. 4, 5 and 6 are given in Table I. In the exceptional non-linear cases the formula can be applied in the lower concentration range, and the constants α and β can be similarly obtained. The values of β may not be sufficient for the quantitative discussion, considering from the standpoint of experimental accuracy. But the following qualitative conclusions are drawn from Table I.

TABLE I
CRITICAL MICELLE CONCENTRATION (c.m.c.) AND SOLUBILIZING POWER AT DIFFERENT TEMPERATURE

Temperature (°C)	β: c.m.c. (mol./kg. solvent) 10	26	40	α: Solubilizing power 10	26	40
Dodecylammonium propionate	0.002	0.002	0,005	5.7	7.2	8.0
〃 butyrate	0.003	0.018	0.020	9.4	4.6	9.2
〃 caproate	0.018	0.020	0.025	3.7	2.9	2.5
〃 caprylate	0.020	0.025	0.025	3.0	2.8	2.5
〃 caprate	—	0.035	0.032	—	2.9	2.1
Octadecylammonium propionate	—	0.008	0 010	—	12	10
〃 butyrate	0.005	0.027	0.028	8.0	9.0	5.7

At constant temperature the value of α decreases and that of β increases with the increase of the carbon number. The increase of β corresponds to the experimental result obtained by Pink et al.[12] They have reported that the number of molecules in the micelle decreases with increase in the length of the hydrocarbon chain in the case of a metal soap in toluene, though the value is an extrapolated one to infinite dilution at boiling temperature.

Rise of temperature decreases the solubilizing power except for the case of propionate and butyrate[13] and increases the critical micelle concentration. The following qualitative experiment was further carried out in order to ascertain the effect of temperature on solubilization. The value of S for benzene solutions of dodecylammonium propionate, caproate and caprylate was determined at 74°C. The amount was corrected for the solubility of water into benzene at the temperature. The corrected value was given in the 3rd column in Table II. Next, a certain amount of water was added to those solutions at 25°C, and the turbidity was observed (4th and 5th columns). Then these solutions were brought and left to stand with occasional shaking in a bath of the temperature varied in the order of 40°, 25°, 10°C and then in the reverse order. Thus the turbidity was observed at each temperature. The results were independent of the direction of temperature change, and were listed in Table II.

Relation between Micelle Formation and Solubilization. — The following facts are noticed in Table II. A benzene solution of the detergents solubilizes scarcely any water near the boiling point (74°C), though a concentrated solution of dodecylammonium propionate seems to solubilize a slight amount of water. The solution has a tendency to solubilize a certain amount of water, when the temperature is lowered. Slight or no solubilization near the boiling point and the marked increase at a lower temperature correspond to the values of higher and lower van't Hoff factors at boiling and melting temperature, respectively. It is noticeable that in the case of dodecylammonium propionate the temperature dependence is reversed between 40°C and 74°C.

Summary

Van't Hoff factors of fatty acid salts of higher aliphatic primary amines in benzene were determined cryoscopically and ebullioscopically. Slight or no micelle formation takes place at boiling temperature, though it does take place at melting temperature.

Solubilization of water into benzene by these detergents was measured at 10°, 26° and 40°C. With rise of temperature the critical micelle concentration obtained from solubilization increases and the solubilizing power decreases, though the solubilizing power of propionate and butyrate shows an anomaly. Solubilization and micelle formation determined here change parallel to each other with varying temperature.

TABLE II

THE EFFECT OE TEMPERATURE ON SOLUBILIZATION

Detergent	Concentration (molality)	Maximum amount of water solubilized at 74°C (molality)	Amount of water added at 25°C (molality)	Turbidity 25° ⇄ 40° ⇄ 25° ⇄ 10°			
Dodecylammonium propionate	0.174	0.05±0.02	0.91	+	−	+	++
	0.085	0.04±0·02	0.52	±	−	±	++
Dodecylammonium caproate	0.289	0.04±0.03	0.71	−	±	−	−
	0.140	0.00	0.31	−	++	−	−
Dodecylammonium caprylate	0.204	0.00	0.42	−	++	−	−
	0.095	0.00	0.17	++	++	++	+

++.....strongly turbid, +.....turbid, ±.....faintly turbid, −.....clear.

It is seen from Table II that the rise of temperature decreases solubilization of dodecylammonium caproate and caprylate while it promotes solubilization of dodecylammonium propionate in the range of temperature from 10° to 40°C, which are in accord with the values of the solubilizing power of Table I.

The author wishes to express his thanks to Mr. Hiroshi Tsubomura for the measurement and the discussion of the infrared spectra, and to Prof. Hideo Akamatsu for his encouragement.

Department of Chemistry, Faculty of Science, Toho University, Narashino, Chiba

12) S.M. Nelson and R.C. Pink, *J. Chem. Soc.*, **1952**, 1744.

13) Palit et al.[7] report that the solubilizing power at a definite concentration of dodecylammonium butyrate in toluene increases with rise of temperature ranging from 0° to 40°C.

Effects of Quenching and Annealing in Manufacture of Fused Iron Catalyst upon Activity for Ammonia Synthesis and Potash Distribution

By Hiroshi UCHIDA and Naoyuki TODO

(Received June 8, 1955)

Introduction

In the manufacture of an iron catalyst for the ammonia synthesis a molton oxide of the catalyst is usually allowed to cool in a vessel for melting, and the rates of cooling are mainly determined by the capacities of batches. The different rates are expected to modify grain growth as well as distribution of the promoters and to have considerable effect upon subsequent properties of the catalyst. The adequate rate is, therefore, an important factor to yield the catalyst of superior quality; but no paper, so far as we are aware, has ever been published on this subject.

In the present work, catalysts of four different promoter compositions were subjected to different rates of cooling such as quenching, annealing and normal cooling, and the subsequent activities for ammonia synthesis were measured. In connection with this, the experiment involved the measurements of surface area after reduction of the oxide, and quantities of water-soluble potash, along with the observations of microscopic structure and electronic images.

The quenched catalyst gave nearly the same activity with the normally cooled one, while the annealed catalyst a remarkably low one. The low activity has been to some extent explained in the light of information obtained from the present experiments on distribution state of the promoters in the catalysts. Moreover the present data for characteristic microscopic structures, electronic images and different quantities of water-soluble potash in the catalysts, etc. will provide us with more knowledge for better understanding of the role of the promoters.

Experimental Procedure

Preparation of Catalyst.—The catalyst employed in this work contained the following different promoters; 5% Al_2O_3, 1% K_2O, for Cat. No. 1; 4% Al_2O_3, 1% CaO, 1% K_2O for Cat. No. 2; 3% Al_2O_3, 2% SiO_2, 1% K_2O for Cat. No. 3; and 3% Al_2O_3, 2% SiO_2, 1% CaO, 1% MgO, 2.5% K_2O for Cat. No. 4*. They were prepared by burning mixtures of iron powder and promoters to fused iron oxides in oxygen within an iron container capable of holding about 1 kg. of oxides. Immediately after the fusion, the oxides were subjected to different cooling procedures such as: (1) quenching by pouring water on the container, (Cat. No. q,); (2) cooling as usually practised (normal cooling), (Cat. No. c.); (3) annealing for forty hours in an electric furnace kept at about 1000°C before cooling to room temperature, (Cat. No. an.).

Activity for Ammonia Synthesis.—The synthesis was carried out with 3 cc. of granules (1 to 2 mm. diameter) of catalyst packed in a previously described converter[1]*, under a pressure of 100 kg./cm², at temperatures ranging from 300° to 500°C, at a space velocity of 5×10^3; and the exit gas from the converter was analyzed for ammonia content to give relative activity of the catalyst for ammonia synthesis. After a series of measurements, the pressure was reduced to normal pressure, thereafter the temperature being raised to 650°C; and the catalyst was kept at this temperature for five hours, in a current of synthesis gas. Repeated series of measurements gave a measure of thermostability in terms of the decrease of activity before and after heating at 650°C.

Microscopic Structure.—A preparation of thoroughly polished catalyst was observed under a microscope in both vertical and oblique illumination, before and after etching by hydrochloric acid. In this observation, concavities produced by etching could more easily be distinguished by oblique illumination.

Potash Soluble or Insoluble in Water.—H. Kobayashi[2] et al found that part of the potash in the catalyst dissolved in water, and that the remaining quantities were closely associated with the respective activities of the catalysts. In the present work the determination was made by the following procedure: a quantity of fine powder (finer than 100 mesh size) of the catalyst was soaked in water at the room temperature for periods of time, and the aqueous extracts were analyzed for potash content by means of a Perkin-Elmer's flame photometer.

Surface Area and Potash (+Lime) Concentration in the Surface of Reduced Catalyst.—The surface area and the potash concentration in the surface of the catalyst reduced at 500°C by hydrogen at normal pressure were determined

* The compositions are expressed in the weight percentages of promoters in catalysts, on the basis of exact oxidation of iron to Fe_3O_4.

1) H. Uchida and M. Kuraishi, This Bulletin, 28, 106 (1955).

* The converter produced ammonia in somewhat higher amount than the one packed with 20 cc. of the catalyst.

2) H. Kobayashi and O. Nishijima, *J. Chem. Soc. Japan (Ind. Sect.)*, 57, 189 (1954).

from the results of measurements of carbon dioxide adsorption. The former was evaluated by the usual BET method applied to the physical adsorption isotherm at −78°C and the latter was expressed as a ratio of the amount of chemisorbed carbon dioxide to that of physically adsorbed at −78°C.

Electronic Image.—An electronic image from the polished surface of the oxide was observed at successive stages in the reduction of the oxide, by means of an emission electron microscope described in a previous paper[3]. The reduction was carried out at 450°C in the electron microscope, through which hydrogen was passed. Immediately after the observation the specimen was removed therefrom to an optical microscope to contrast the emissive regions with the optical images in oblique illumination.

Experimental Results

Activity for Ammonia Synthesis.—The results are summarized in Fig. 1, and show an outstanding common trend of activity among four

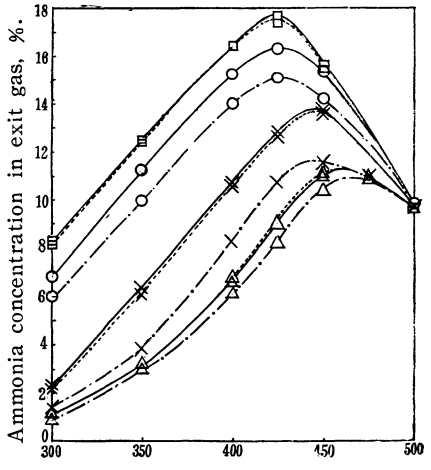

Pressure, 100 kg./cm², space velocity, $5\times10.^3$

×, Cat. No. 1, ○, Cat. No. 2.
△, Cat. No. 3, □, Cat. No. 4.
····· quenched catalyst,
——— normally cooled catalyst,
—·—· annealed catalyst.

(The activity of Cat. No. 2q coincided just with that of Cat. No. 2c.)

Fig. 1. Results of ammonia synthesis.

kinds of catalysts different in promoter composition. Generally, the annealed catalyst tended to reveal much lower activity than the normally cooled one for the ammonia synthesis, but the quenched catalyst revealed the same.

Catalyst No. 4 revealed the highest activity, while catalyst No. 3 the lowest.

The measurement of thermostability of catalysts subjected to different rates of cooling indicated that three catalysts of No. 2 series . . . No. 2q, No. 2c and No. 2an . . . were nearly the same in thermostability (Fig. 2).

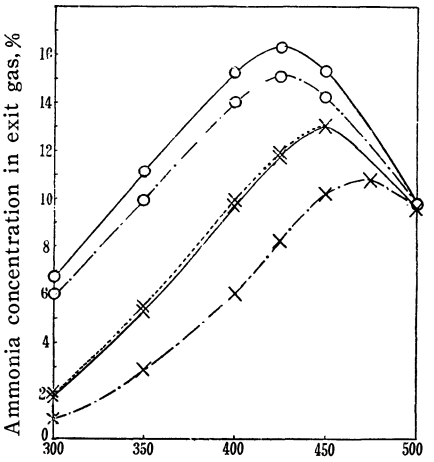

Pressure, 100 kg./cm², space velocity, 5×10^3.

○, ×, before and after heating at 650°C respectively.
····· quenched catalyst,
——— normally cooled catalyst,
—·—· annealed catalyst.

Fig. 2. Thermostability for Cat. No, 2.

Microscopic Structure.—Cleavage facets of individual grains were visible, even by the naked eye, in catalysts No. 1, No. 2 and No. 4, but scarcely any were visible in No. 3. Catalysts No. 3 and No. 4 revealed microscopic structures very different from those of catalysts No. 1 and No. 2, which might be ascribed to the presence of silica in the former.

In the case of catalysts No. 1 and No. 2, the grain growth was not markedly restrained by quenching (Phot. 1 of catalysts No. 1q), and the individual grains were locally etched to result in concavities in their interior (Phot. 2). Annealing modified the structure to develop large grains, whose diameter sometimes attained to 10 mm., and to make the oxide so resistive against etching as to be hardly ever attacked by hydrochloric acid but aqua regia causing figures seen in Phot.'s 3 and 4 of catalysts No. 1an and No. 2an. These photographs show the preservation of a comparatively homogeneous structure* over the whole grain.

As previously described[4], catalyst No. 3q containing silica with a small amount of potash revealed slag inclusions (according to Z. W. Wilchinsky[5], a potassia-silica glass) (Phot. 5), which with an increased addition of potash were apt to take a more precise crystalline outline as shown in Phot. 7 of catalyst No. 4 q. When the

3) H. Uchida and N. Todo, This Bulletin, **27**, 585 (1954).

* "Homogeneous structure" means the structure uniformly resistive against etching.

4) H. Uchida, N. Todo and K. Ogawa, *Rpt. Gvn't. Chem. Ind. Research Inst. Tokyo*, **46**, 11 (1951).

5) Z.W. Wilchinsky' *Analyt. Chem.*, **21**, 1188 (1949).

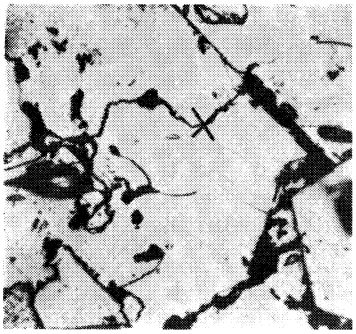

Phot. 1. Cat. No. 1q, etched by HCl. ×100

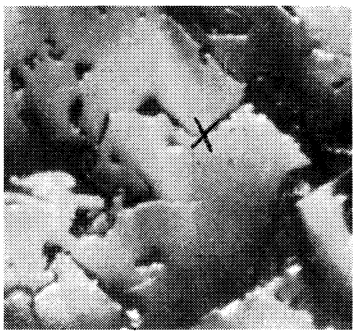

Phot. 2. Phot. 1 in oblique illumination.

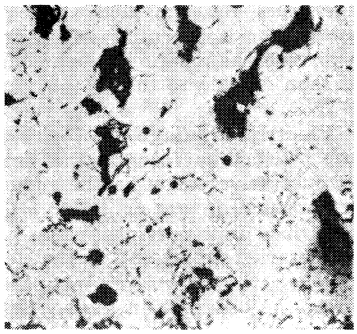

Phot. 3. Cat. No. 1an, etched by aqua regia.

Phot. 4. Cat. No. 2an, etched by aqua regia.

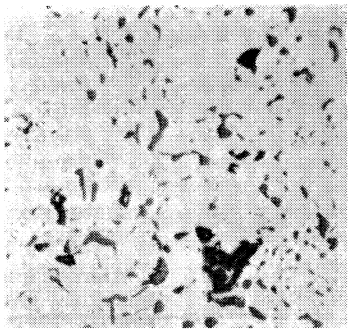

Phot. 5. Cat. No. 3q, unetched.

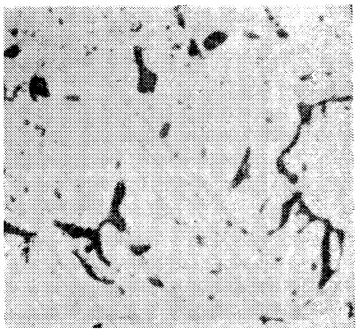

Phot. 6. Cat. No. 2an, unetched.

Phot. 7. Cat. No. 4q, unetched.

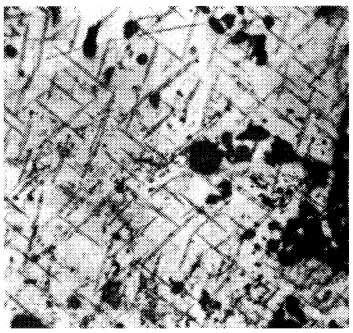

Phot. 8. Cat. No. 4an, etced by HCl.

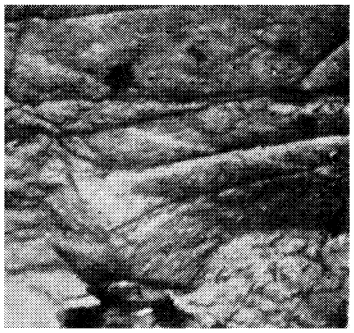

Photo. 9. Replica from surface of Phot. 4. ×5000

catalysts were annealed the inclusions tended to diminish their size and they partially disappeared, and the structure in the grain became more homogeneous. These catalysts did not, however, attain to so homogeneous a structure as those of catalysts No. 1an and No. 2an (refer to Phot.'s 6 and 8 of catalyst No. 3an and No. 4an respectively).

Potash Soluble or Insoluble in Water.—The rate of solution of soluble potash from catalyst No. 3 was found to be much slower than that from catalyst No. 2, requiring twenty hours for completion. Therefore, insoluble potash contents listed in Table I are given as ratios of the amount of potash remaining in catalyst soaked in water for twenty hours to the total amount originally contained.

TABLE I

INSOLUBLE POTASH, SURFACE AREAS, AND SURFACE CONCENTRATION OF POTASH (+LIME)

Catalyst	Total potash wt. %	Insoluble potash %[a]	Surface area m^2/g.[b]	Surface concentration of potash
No. 1q	0.91	18.8	15.6	0.64
No. 1c	0.88	56.4	15.9	0.68
No. 1an	0.89	7.8	11.7	0.42
No. 2q	0.90	30.0	17.1	0.49
No. 2c	0.93	88.9	17.5	0.53
No. 2an	0.87	17.0	12.7	0.51
No. 3q	0.94	87.0	12.0	0.36
No. 3an	0.95	63.8	7.4	0.35
No. 4q	2.43	93.2	17.4	0.54
No. 4an	2.40	68.6	14.1	0.58

a): ratio of the amount of potash remaining in catalyst soaked in water for 20 hours to the total potash.

b): surface area per g. of reduced catalyst.

Catalysts No. 1 and No. 2, when normally cooled, contained the greatest quantity of insoluble potash, whereas annealed ones the least. Similarly, in the case of catalysts No. 3 and No. 4, the quenched catalyst contained a greater quantity of insoluble potash than the annealed one. In addition, it is here worth noticing that the quantity varied remarkably according to the promoter composition, namely, it was somewhat or considerably increased by the addition of lime or silica respectively.

Soluble potash seems to come from potash existing as a separate phase[6,7] in the catalyst. The soluble potash gave no sign of dissolving as an aluminate, for no aluminium ion could be detected in the aqueous extracts. Potassium may also be present as potassium ferrite[6,7] but its dissolution as such seems to be improbable*.

Surface Area and Potash (+Lime) Concentration in the Surface of Reduced Catalyst.—The results are presented in Table I. For all kinds of catalysts, the slightly less was found on the quenched and the remarkably small on the annealed. So far as a catalyst of a definite promoter composition was concerned, the surface area as well as the activity remained nearly constant independently of the varying quantities of insoluble potash till the quantity lowered to a certain value (18.8% and 30% of the total potash with catalysts No. 1 and No. 2 respectively). but both of them diminished remarkably with the further decreasing quantity (7.8% and 17%).

Among catalysts No. 1, No. 2 and No. 3, the catalysts No. 3 gave abnormally small values of surface concentration of potash, despite their equal potash contents.

Both quenching and annealing exerted so slightly important an effect upon the surface concentration, that the concentration remained nearly unchanged by these procedures (Table I). This result may be interpreted to indicate that the soluble potash in the annealed catalysts hardly at all segregates along the grain boundaries but the greater part remains in the interior of grains, since the segregation would give rise to a decrease inpotash content in the interior and consequently the smaller surface concentration*.

How could the potash dissolve into water from the interior of such large grains as those of the annealed catalysts? To solve this problem the following observations were conducted.

Although the optical microscopic structure of the grain in the annealed catalyst seems homogeneous (Phot. 4), a replica stripped from the etched surface revealed in an electron microscope many finer grains (sub-grains) as well as narrower grain boundaries between those grains (Phot. 9). These boundaries, considering their poor resistance to acid, seemed to be rich in potash and might be considered to offer paths for potash to dissolve out from the interior of the grain. This hypothesis could be confirmed with the results given in Table II, which revealed marked increase of the surface area and simultaneously appreciable decrease of the surface concentration after dissolution of soluble potash.

TABLE II

CHANGE OF SURFACE AREA AND SURFACE CONCENTRATION OF POTASH (+LIME) AFTER DISSOLUTION OF POTASH

Catalyst	Surface area m^2/g. oxide	Surface concentration of potash
No. 1an	0.58	0.89
No. 1an after dissolution	2.02	0.06
No. 2an	0.50	0.62
No. 2an after dissolution	1.72	0.19

6) L.R. Maxwell and J.S. Smart, *J. Chem. Phys.*, **19**, 303 (1951).

7) R. Brill, "Structure and Properties of Solid Surfaces", The University of Chicago Press (1953), p. 437.

* The potash in a catalyst containing potash only (0.93%) also comprised two kinds, i.e. soluble and insoluble. The insoluble potash amounted to 70.6% of the total potash.

* As the grain interiors, not the grain boundaries, occupy the major part of the catalyst, the measured surface concentration may be chiefly dependent on the surface concentration of the individual fine particles of iron produced by reduction in the interior.

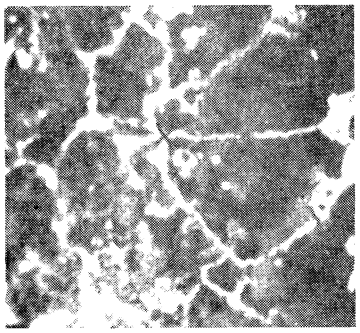

Phot. 10. Electronic image, Cat. No. 1q, oxide, 800°C. ×50

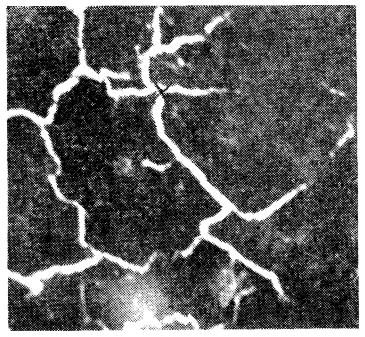

Phot. 11. Electronic image, Cat. No. 1q, after reduced for 5 min., 880°C.

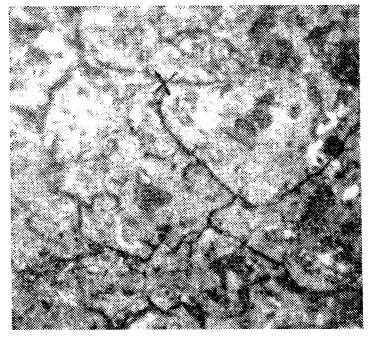

Phot. 12. Optical image, Cat. No. 1q, after electr. image observation.

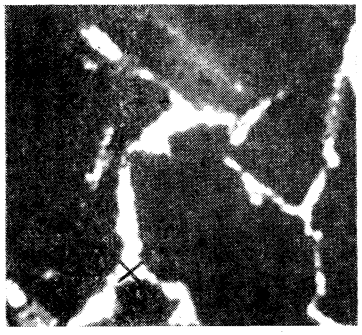

Phot. 13. Electronic image, Cat. No. 2an, oxide, 840°C.

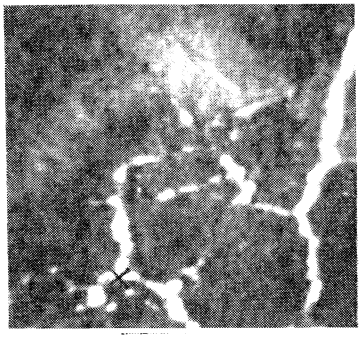

Phot. 14. Electronic image, Cat. No. 2an, after reduced for 5 min., 760°C.

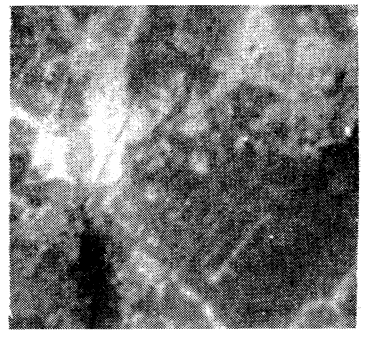

Phot. 15. Electronic image, Cat. No. 3q, oxide, 900°C.

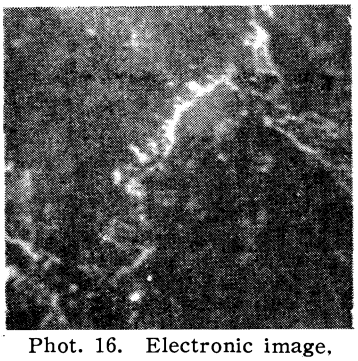

Phot. 16. Electronic image, Cat. No. 3an, oxide, 940°C.

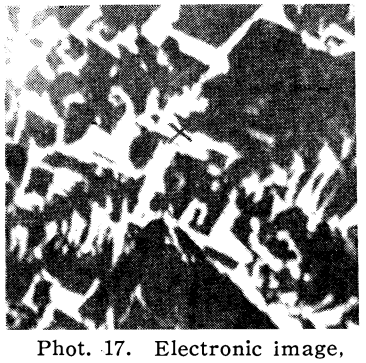

Phot. 17. Electronic image, Cat. No. 4q, oxide, 760°C.

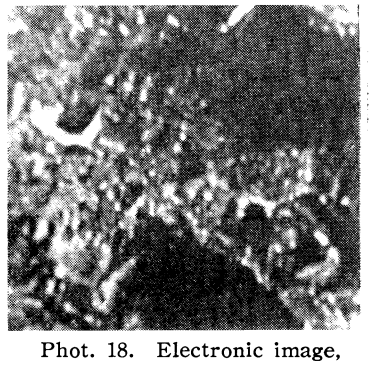

Phot. 18. Electronic image, Cat. No. 4q, after reduced for 5 min., 780°C.

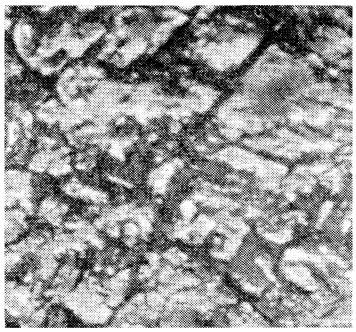

Phot. 19. Opitical image, Cat. No. 4q, after electr. image observation.

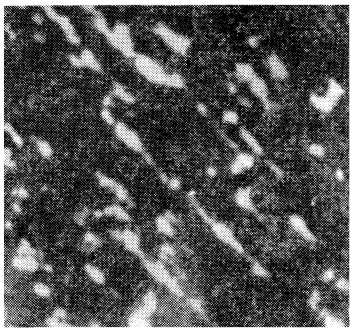

Phot. 20. Electronic image, Cat. No. 4an, oxide, 800°C. ×50

Electronic Image.—The oxide, even after comparatively prolonged heating, gave substantially unchanged electronic images. After reduction of the catalysts, the brighter images still remained without any remarkable change, but the new weaker images appeared homogeneously over wide regions on the section.

The electronic images of the normally cooled catalysts No. 1 and No. 2* were not markedly different from those of the respective quenched catalysts, but the appreciably different ones were observed with the annealed. The electronic images of the quenched catalysts of No. 1 and No. 2 are exemplified by Phot.'s 10 and 11 of catalyst of No. 1q. The images from the oxide appeared not only in regions where cracks were produced by reduction but also in the interior enclosed by the cracks (compare Phot. 10 with Phot. 12). With the progress of reduction the images from the interior tended usually to become weaker and simultaneously to impart homogeneous appearance to the grain, as is seen in Phot. 11, and exhibit strong emission coming from the cracks. In the case of annealed catalysts, the emission hardly ever took place in the interior of grains, but mainly in the grain bound aries and/or narrower grains existing between the well grown grains as shown in Phot. 13 of catalyst No. 2an. After reduction of the catalysts, the weaker homogeneous images appeared in the interior of grains (Phot. 14).

The electronic images from the catalysts containing silica were previously[3] indicated to be very different from catalysts No. 1 and No. 2. Catalysts No. 3q did not easily emit the electrons and higher temperatures were required to produce the image. The catalysts gave weaker and homogeneous images from all over the section, together with slightly stronger emissions from the slag inclusions (Phot. 15). The images from catalysts No. 3an (Phot. 16) were not very different from those from catalyst No. 3q, which would be expected from comparatively smaller difference between their microscopic structures.

Catalyst No. 4 gave the images at the temperature considerably lower than that for catalyst No. 3. The images of quenched catalyst No. 4q appeared in the crystalline inclusions seen in the microscopic structures (Phot. 17), and even after reduction they were invariably visible together with newly appearing weaker images from other regions (Phot. 18). The reduction, however, produced cracks around the inclusions (Phot. 19), which might be interpreted as indicating the grain boundaries to exist in the immediate neighbourhood of the inclusions. When the catalyst was annealed, the electronic images varied from those of the quenched, corresponding to the variation in microscopic structure, thus appearing at new etch marks of parallel orientation shown in Phot. 8 and simultaneously in the remaining inclusions (Phot. 20).

Discussion

Catalytic Activity and Surface Area.—The catalytic activity is to be directly correlated with the surface structure of the reduced catalysts. Actually, the surface area was found to be remarkably diminished by an-

TABLE III

RELATION BETWEEN DECREASE OF ACTIVITY AND DECREASE OF SURFACE AREA BY ANNEALING

Catalyst	Apparent energy of activation kcal./mol.	Aan/Aq (425°C)	San/Sq
No. 1q	50.1	0.669	0.750
No. 1an	49.8		
No. 2q	37.4	0.716	0.739
No. 2an	39.4		
No. 3q	51.1	0.803	0.616
No. 3an	49.6		
No. 4q	37.1	0.672	0.810
No. 4an	39.7		

Aan, Aq: values of A at 425°C for annealed and quenched catalysts respectively.

San, Sq: surface areas for annealed and quenched catalysts respetively.

* Refer to photographs in our preceding paper[8].

* Values of A were obtained by substituting in Arrhenius' Equation values of k calculated by Temkin-Pyzhev's Equation, and E from Arrhenius' plots of k's at 350, 400 and 425°C.

nealing, with simultaneous decrease of the activity. More quantitatively speaking, the degree of activity decrease with the diminishing surface area may be more reasonably expressed by the ratio of the frequency factors, A, of Arrhenius' Equation ($k=Ae^{-E/RT}$) than by the ratio of the rate constants, k, since the frequency factor term involves the number of active sites which is intimately correlated with the surface area of catalyst. The ratios of A's* are listed in Table III. In the case of catalyst No. 1, No. 2 and No. 4, it appeared from the table that the activity was decreased by annealing, approximately in proportion to the decrease in surface area*. Compared with these catalysts, the catalysts No. 3 also showed a decrease in activity but it was less than the decrease in surface area.

The difference in surface area between individual reduced catalysts is mainly due to the difference in size of fine particles produced by reduction in the interior of grains rather than in the grain boundaries, because the grain boundaries occupy only a part of the catalyst. Within the grains, the extent of particle growth during reduction is expected to be differently restrained by the distribution states of the promoter such as alumina and silica.

Unfortunately, details of the distribution can not be established with certainty from the available experimental results, but the observations on the electronic images from the catalysts can give some knowledge of the potash distribution, and further, when combined with the other results, may lead us to a better understanding of the different extents of particle growth between the quenched (+normally cooled) and annealed catalysts.

Potash Distribution and Surface Area.— From the fact that the oxide gives substantially unchanged electronic images after prolonged heating, it may be reasonably assumed that the insoluble potash, i. e. potash combined strongly as potassium aluminate[7,8], silicate[5] and ferrite[6,7] in the oxide, is responsible for the images. Under this assumption, it follows that the interior of grains in the quenched and normally cooled catalysts ... the interior where the images were frequently observed ... must be abundant in potash, while the same regions in the annealed catalysts, No. 1an and No. 2an must hardly contain any insoluble potash*.

To the extent that the catalysts No. 1 and No. 2 are concerned, the results obtained in the present experiment are summarised with a special regard to the insoluble potash, as follows: the catalysts comparatively rich in insoluble potash, such as the normally cooled and the quenched, reveal the inhomogeneous microscopic structure as well as the electronic images in the interior of grains; and when reduced, larger surface area. This fact may be interpreted to mean that the insoluble potash of the quenched and normally cooled catalysts, existing probably as aluminate and ferrite within the grain, prevents the formation of a perfect solid solution of Fe_3O_4 and $FeAl_2O_4$ spinel, resulting in the less homogeneous structure**, but its practical absence within the grains of annealed catalyst favours the formation. The less homogeneous structure may be considered to offer more obstacles against free migration of reduced iron atoms during reduction than the homogeneous and to restrain the particle growth, resulting in the larger surface area. However, since the structure of the mixed crystal of Fe_3O_4 and ferrite or aluminate of potassium has not yet been clarified at present, a satisfactory explanation can not be expected.

Promoting Effect of Lime and Silica.— An addition of lime has made the microscopic structure as well as electronic images of the interior of grains more heterogeneous and potash more insoluble. For the reason described in the preceding paragraph, a large surface area is what can be expected of catalyst No. 2 containing lime.

Silica exerted upon the structure of catalysts peculiar effect such as, marked decrease of surface concentration of potash, appearance of slag inclusion and a peculiar X-ray diffraction line between (333) and (440) lines on Debye-Scherrer's diagram of Fe_3O_4, and so forth. The results obtained with the catalysts containing silica gave sometimes a contradictory evidence (the higher activity of catalysts No. 4 than catalyst No. 2 of equal surface area, the comparatively small surface area of catalyst No. 3 containing a

* This does not necesarily means the nearly constant intrinsic activity, irrespective of annealing, per unit surface area. However, the surface concentration of potash and the apparent activation energy (Table II & III), remaining unchanged by annealing, are suggestive of this constant activity.

8) S. Brunauer and P.H. Emmett, *J. Am. Chem. Soc.*, **62**, 1732 (1940).

* After reduction, the two kinds of potash, soluble and insoluble, in the oxides seem no longer to behave differently in the interior of grain, both giving the stable and homogeneous images over the grain and accumulating, as described in the foregoing chapter, on the surface of fine particles of reduced iron.

** In this respect unmixed solid solution of potassium aluminate in Fe_3O_4 was pointed out by Wyckoff and Crittenden (*J. Am. Chem. Soc.*, **47**, 2866 (1925), refer to 6)).

great amount of the insoluble potash) against the phenomena that were observed with catalysts No. 1 and No. 2. From these results, promoting effects quite different from those of alumina may be expected of silica, and further they show promise for their fruitful application in the catalyst manufacturing, as realized with the highly active catalyst No. 4. However, since the experimental data so far obtained remain insufficient to permit close insight in its promoting action, further investigation is now in progress.

Summary

Catalysts of four different promoter compositions . . . 5% Al_2O_3, 1% K_2O for catalyst No. 1; 4% Al_2O_3, 1% CaO, 1% K_2O for No. 2; 3% Al_2O_3, 2% SiO_2, 1% K_2O for No. 3; and 3% Al_2O_3, 2% SiO_2, 1% CaO, 1% MgO, 2.5% K_2O for No. 4 . . . were subjected, immediately after their fusion, to different cooling rates such as quenching, annealing and normal cooling.

Among the differently cooled catalysts, the annealed catalyst tended to reveal much lower activity for ammonia synthesis than the normally cooled one, but the quenched catalyst revealed the same.

The characteristic microscopic structures of catalysts of different promoter compositions were more or less markedly modified by annealing to develop large and structually more homogeneous grains, and part of the potash in these catalysts dissolved in water more or less remarkably according to the promoter composition as well as the cooling rate. In other words, the amount of insoluble potash in the catalysts was increased somewhat or considerably by the addition of lime or silica respectively, and the greatest quantity was found in the normally cooled catalysts while the smallest was in the annealed. After the reduction of differently cooled catalysts, the largest surface area was exhibited by the normally cooled catalyst, and the smallest by the annealed, but the surface concentration of potash (+lime) was nearly the same for three differently cooled catalysts. The catalysts of different promoter composition revealed also their characteristic electronic images. After annealing, the images from the interior of grains disappeared in the case of catalysts No. 1 and No. 2. but such disappearance was less remarkably found with catalysts No. 3 and No. 4.

From the results obtained, the interpretation of the decrease due to annealing of catalytic activity has been intended on the basis of the distribution state of the promoters. Some of the effects exerted by the addition of lime can be explained on the same basis, but the peculiar effects of the addition of silica on both activity and structure remains unexplicable despite the promising effect for manufacture of the highly active catalyst.

Government Chemical Industrial Research Institute, Tokyo

Diphenylcarbazone as an Internal Indicator in Volumetric Analysis. Determination of Molybdenum by Lead Nitrate

By G. S. DESHMUKH

(Received January 6, 1955)

In quantitative analysis molybdenum is usually determined by its prior reduction to the lower valence stage and subsequent oxidation to the stable hexavalent form by a suitable powerful oxidant[1,2]. In view of the special precautions necessary in these titrimetric procedures, the precipitation of molybdenum oxinate and its weighing is considered more convenient and accurate[3]. This classical method still lacks the advantage of simplicity and rapidity so essential in routine analysis. It is known that Pb and Mo interfere in the colorimetric detection of Hg^{++} by diphenylcarbazone due to the development of an intense pink colour by these ions with the reagent[4]. Evans reported the

1) N.H. Furman and W.M. Murray, *J. Am. Chem. Soc.*, 58, 1689 (1936).
2) R. E. Oesper, "Newer Methods of Volumetric Chemical Analysis", Chapman & Hall (London), (1938) pp. 94, 148, 176.
3) A.I. Vogel, "A Text Book of Quantitative Inorganic Analysis," Longmans Green & Co., (1945), p. 523-24.
4) F. Feigl, "Qualitative Analysis by Spot Tests", Elsevier Publishing Co. Inc., New York, (1947), p. 48.

use of diphenylcarbazide in the titration of lead nitrate against molybdate[5]. The end point is arrived at by running lead nitrate into the molybdate solution. According to him, the pink colour produced by the reaction of carbazone with lead is not easily destroyed by most precipitants. It was however, interesting to note that the colour developed by the addition of diphenylcarbazone to the neutral or faintly acidic solution of lead salt is destroyed on treatment with ammonium molybdate. The precipitate thus obtained does not show any other shade excepting a light orange yellow due to the indicator itself but turns pink sharply during the slow addition of molybdate at a stage when lead is completely precipitated. Although diphenylcarbazone has been employed as an internal indicator in mercurimetric[3,7] and other[8] titrations, its use in the determination of molybdenum by lead nitrate has not been reported in the literature of this subject. This possibility was therefore investigated in some detail and the results obtained thereof are presented in this communication.

Experimental

Ammonium molybdate solutions of various concentrations were prepared by dissolving appropriate quantities of Merck's sample in water. The molybdenum content of an aliquot portion of the solution was determined by the oxinate method[2]. The standard lead nitrate solution contained an accurately weighed Merck's guaranteed reagent in 500 ml. of water to which 2–3 drops of nitric acid were added to prevent hydrolysis. The concentration of the solution was checked by the lead chromate method. A saturated alcoholic solution of diphenylcarbazone was used as the indicator.

To 10 ml. of $Pb(NO_3)_2$ about 1–2 ml. of the indicator was added followed by an equivalent volume of alcohol and the pink coloured solution was titrated slowly with constant vigorous stirring against ammonium molybdate. The pink colour was discharged during the initial stage of the titration with the formation of lead molybdate. The colour appeared momentarily with a further dropwise addition of molybdate but vanished immediately on swirling the contents. The end point was characterised by a rapid coagulation of the precipitate and the appearance of a sharp permanent pink flush. From a knowledge of the amount of Pb in the standard lead nitrate solution and that of molybdenum in the requisite volume of the titrant, the molar ratio Pb : Mo was calculated. The 1 : 1 ratio obtained indicated that the end point in the above titrimetric procedure corresponds to the quantitative formation of Pb (MoO_4). Under the specified experimental conditions it is therefore possible to determine molybdenum volumetrically by using lead nitrate as a primary standard. Data obtained over a fairly wide range of molybdenum concentration is returned in Table I.

Besides the sharp change of the indicator colour, its complete reversibility offered an additional advantage of rectifying errors due to overtitration. Compared with other classical methods of molybdenum determination, the outstanding feature of the present procedure is its simplicity, reproducibility and accuracy

The author wishes to express his sincere thanks to Professor S. S. Joshi for facilities and to the National Institute of Sciences of India for award of a research fellowship.

Summary

The use of diphenylcarbazone as an internal indicator in the volumetric determination of molybdenum by standard lead nitrate solution is suggested. The end point is characterised by the sharp appearance of a permanent pink colour when molybdate is run into the lead solution and corresponds to the formation of Pb (MoO_4). The colour change is completely reversible and errors due to overtitration are therefore eliminated.

Chemical Laboratories, Banaras Hindu University, Banaras, India

TABLE I

Expt. No.	Wt. of $Pb(NO_3)_2$ in 500 ml. g.	Vol. of Pb soln. taken ml.	Vol. of molybdate reqd. ml.	Wt. of Mo (g.) calcd. by oxinate	Wt. of Mo (g.) found by $Pb(NO_3)_2$	Diff.
1.	6.3330	5.0	4.1	0.01830	0.01834	+0.00004
2.	〃	10.0	8.2	0.03661	0.03669	+0.00008
3.	〃	20.0	16.4	0.07323	0.07338	+0.00015
4.	5.6900	10.0	3.7	0.03271	0.03212	−0.00059
5.	〃	20.0	7.4	0.0654	0.06585	+0.00045
6.	〃	40.0	14.9	0.1317	0.13168	−0.00002
7.	6.3330	20.0	17.4	0.07331	0.07338	+0.00007
8.	12.660	20.0	17.8	0.1477	0.1468	−0.0009

5) B.S. Evans, *Analyst*, **64**, 2 (1939).
6) J.V. Dubsky and J. Trtilek, *Mikrochem.*, **12**, 315 (1933).
7) J. Trtilek, *Coll. Czech. Chem. Comm.*, **10**, 242 (1938).
8) G.S. Deshmukh, *Bull. Chem. Soc.* **27**, 623 (1954).

Analytical Chemistry of Beryllium. VI. 8-Hydroxyquinaldine as a Reagent for Determination of Beryllium

By Kenji MOTOJIMA

(Received July 8, 1955)

Introduction

8-Hydroxyquinaldine, one of the derivatives of 8-hydroxyquinoline, "oxine", was found to be used as a favourable analytical reagent for the determination of beryllium. There has been reported no adaptable organic reagent to determine beryllium, and it has been desired to discover such a preferable reagent as oxine in the determination of aluminum, so the author firmly believes that the analytical method of beryllium based upon the use of this new reagent, is the most valuable. It was found possible to determine, both gravimetrically and volumetrically, 2 to 10 milligrams of beryllium. The methods to be described are simple, rapid, and accurate.

In general, 8-hydroxyquinaldine is very similar to oxine in its analytical properties, except that it does not precipitate aluminum neither in acetic acid-acetate nor in ammoniacal solutions[1]. As regards beryllium, although it has been reported that 8-hydroxyquinaldine forms no quantitative precipitate in ammoniacal solutions[2], it gives well-defined yellow crystalline precipitate, which fluoresces strongly under ultraviolet light with a green color, as shown in Fig. 1, and this precipitate dried when either in a desiccator over sulfuric acid at room temperature, or in a drying oven at 110°C, corresponds to the formula $Be(C_{10}H_8NO)_2$.

The following equation, with the beryllium compound represented as a possible chelate, best describes the reaction involved.

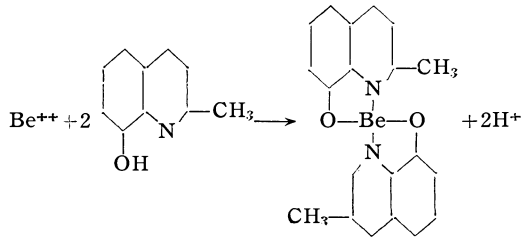

In the development of a volumetric method for the beryllium, use is made of the fact that the reagent can be quantitatively brominated in hydrochloric acid medium, such as oxine[2].

Reagents

Preparation of 8-Hydroxyquinaldine.—Crude 8-hydroxyquinaldine was prepared by a method similar to that described by Phillips and his coworkers[2], and the purification was made by the following procedure.

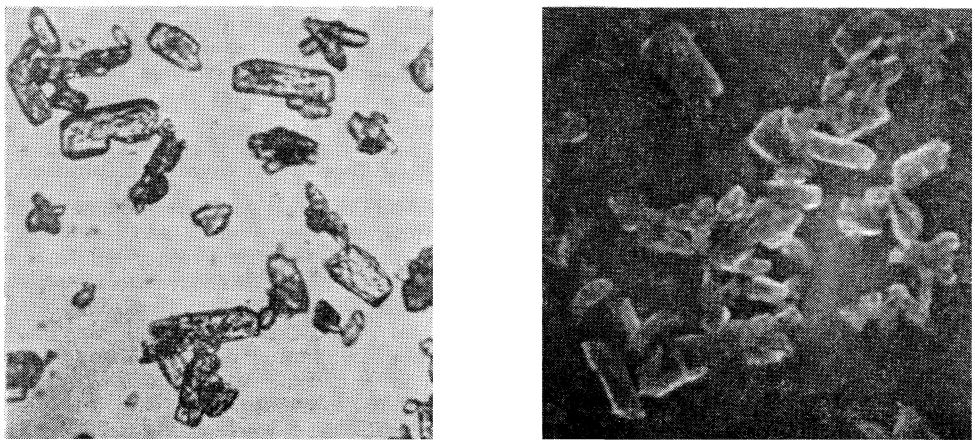

A B

Fig. 1. Microphotograph of beryllium precipitate of 8-hydroxyquinaldine (×260).
A: In ordinary light. B: In ultra-violet light.

1) L.L. Merritt, J.K. Walker, *Ind. Eng. Chem., Anal. Ed.*, **16**, 387 (1944).

2) J.P. Phillips, J.E. Emery, J.P. Price, *Anal. Chem.*, **24**, 1033 (1952).

Dissolve 20 g. of crude 8-hydroxyquinaldine in 40 ml. of glacial acetic acid by warming, dilute to 1 l. with water, and remove the insoluble materials by filtering. Heat gently this filtrate to 70°C, and add 70 ml. of 1 M cupric sulfate solution and 150 ml. of 2 N ammonium acetate solution. Allow to stand for half an hour on water bath to digest the precipitate of 8-hydroxyquinaldine complex of copper. Collect the precipitate, wash several times with hot water and then dissolve in the smallest possible quantity of hot hydrochloric acid. Then dilute to 500 ml. with water, heat to boiling, pass hydrogen sulfide into the solution to precipitate copper as sulfide, and filter. Boil the filtrate gently to remove the dissolving hydrogen sulfide, cool, nearly neutralize with concentrated sodium hydroxide solution and make slightly alkaline with sodium bicarbonate. By steam distillation of the resulting mixture, pure 8-hydroxyquinaldine comes over. More purified product for use in this investigation is obtained by recrystallization from 60% ethyl alcohol, of which melting point is 73° to 73.5°C.

The recovery of this reagent can be made by the above procedure.

8-Hydroxyquinaldine Solution.—In 4 ml. of glacial acetic acid 2 g. of the reagent was dissolved by heating, and diluted to 100 ml. with distilled water. This solution is stable for a week or longer.

Standard Beryllium Solution.—About 14 g. of beryllium basic acetate, purified by vacuum sublimation[3], was treated with 40 ml. of sulfuric acid (1:1), heated gently to remove most of acetic acid, and then the volume was brought to 250 ml. Estimation of beryllium contained in this solution was made by the ordinary beryllium oxide method. Working solution was prepared by exactly diluting 100 ml. of this solution to 1 l. with distilled water.

Standard Potassium Bromate-Bromide Solution, 0.1 N.—Exactly 2.784 g. of C. P. potassium bromate and 10 g. of C. P. potassium bromide were dissolved in distilled water and diluted to 1 l.

Standard Sodium Thiosulfate Solution, 0.1 N.—About 25 g. of reagent grade sodium thiosulfate were dissolved in 1 l. of distilled water. The standardization of this solution was made by using the above 0.1 N potassium bromate-bromide solution.

Other Reagents.—The other reagents were prepared from reagent or C. P. grade chemicals.

Properties of Beryllium Precipitate of 8-Hydroxyquinaldine

Thermal Stability.—The precipitate of beryllium 8-hydroxyquinaldine complex could be dried to constant weight in an hour at 110°C, and by further heating at this temperature for several hours, no decrease of the weight was found. Even when it was heated at 150°C for an hour, the decrease of the weight was less than 1 per cent.

Composition.—The fact that the composition of this precipitate has a formula $Be(C_{10}H_8NO)_2$, was certified by the following estimations of both amounts of beryllium and 8-hydroxyquinaldine which are present in the precipitate dried at 110°C. Beryllium was gravimetrically determined as BeO by igniting the precipitate in the platinum crucible. The results are shown in Table I.

TABLE I
AMOUNT OF BERYLLIUM IN THE PRECIPITATE

Sample	Precipitate taken, g.	BeO found, g.	Be in the precipitate, g.	Be in the precipitate, %
A	0.5117	0.0384	0.0138	2.70
B	0.5555	0.0432	0.0156	2.80
C	0.5045	0.0381	0.0137	2.72
Theoretical value for $Be(C_{10}H_8NO)_2$				2.77

The amount of 8-hydroxyquinaldine was titrated, after dissolving the precipitate in hydrochloric acid, with standard solution of potassium bromate-bromide[2]. Table II gives the results.

TABLE II
AMOUNT OF 8-HYDROXYQUINALDINE IN THE PRECIPITATE
(1 ml. of 0.1 N $KBrO_3 \equiv 0.003980$ g. of 8-Hydroxyquinaldine)

Sample	Precipitate taken, g.	0.1 N $KBrO_3$ wanted, ml.	8-Hydroxyquinaldine in the precipitate, g.	8-Hydroxyquinaldine in the precipitate, %
A	0.1912	46.76	0.1861	97.33
B	0.1867	45.54	0.1812	97.06
C	0.0922	22.78	0.0907	98.37
Theoretical value for $Be(C_{10}H_8NO)_2$				97.85

As may readily be seen from Tables I and II, the results obtained in the analysis of the precipitate very closely correspond with the theoretical values. Further proof of the validity of this structural formula is found in the fact that 0.02770, the theoretical value of the gravimetric factor for beryllium in $Be(C_{10}H_8NO)_2$, was used in all calculations with good results. In addition, the fact that this precipitate is soluble in chloroform is enough to assume that this compound has no bound water[4].

Effect of pH upon Precipitation

The optimum pH range for complete beryllium precipitation was studied, and the following experiment was performed to accomplish this.

To 10 ml. of the standard beryllium solution, containing 5.10 mg. of beryllium, 5 ml. of 4 N ammonium chloride solution, 5 ml. of 10% sodium tartrate solution and various amounts of 4 N ammonium hydroxide were added. The solution was diluted to about 50 ml. with distilled water, heated to 60°C on water bath, and then 12 ml. of 8-hydroxyquinaldine solution was added drop by drop with stirring. The precipitate was digested for about half an hour, filtered through a sintered-

3) M. Ishibashi, K. Motojima, *J. Chem. Soc. of Japan*, (Pure Chem. Sec.), **72**, 100 (1951).

4) F. Feigi (Translated by P.E. Oesper), "Chemistry of Specific, Selective and Sensitive Reactions", (1949), p. 184.

glass filter crucible (porosity No. 4), washed with dilute ammonium hydroxide (1 : 100), dried at 110°C to constant weight, and weighed, while the pH of filtrate was determined by Beckman glass electrode pH meter Model H2. The per cent precipitate was plotted against pH as shown in Fig. 2.

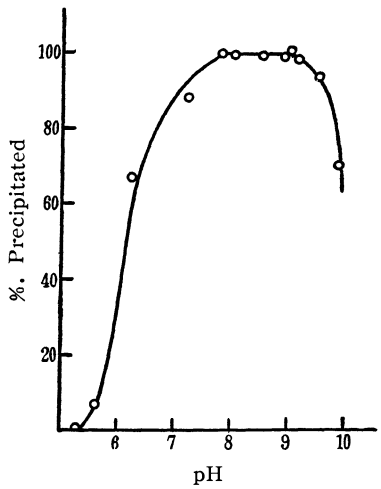

Fig. 2. Effect of pH on precipitation of beryllium 8-hydroxyquinaldine complex.

From the curve, shown in Fig. 2, it can be seen that the pH range of complete precipitation is between 7.8 and 9.2.

Gravimetric Determination

A number of beryllium determinations in which various amounts of beryllium were present, were made following gravimetric procedure.

Procedure.—To a solution containing from 2 to 10 mg. of beryllium, add 5 ml. of 4 N ammonium chloride solution and 5 ml. of 10% sodium tartrate, and then the volume is brought to about 50 ml. The solution is heated to from 60° to 70°C, and the pH is brought up to about 9 with 2 N ammonium hydroxide, thymol blue test paper being used. Then, sufficient amount of 8-hydroxyquinaldine solution is added, dropwise with stirring, so as to contain from 20 to 30 per cent in excess of the amount necessary to precipitate completely the beryllium present in solution. The resulting precipitate is digested at this temperature for about half an hour, to facilitate crystallization of the precipitate, and then, the precipitate is filtered through a weighed sintered-glass filter crucible (porosity No. 4), washed several times with small portions of dilute ammonium hydroxide (1 : 100), and dried at 110°C to constant weight, which will be obtained in about half an hour. The weight of beryllium present in the sample is calculated by multiplying the weight of precipitate by gravimetric factor 0.02770.

In the above procedure, a large amount of tartrate must not be added, because it prevents the coagulation of precipitate. On the other hand, beryllium precipitate can also be prepared without addition of sodium tartrate by following modification of procedure. To a warmed sample beryllium solution, containing ammonium chloride, firstly add 8-hydroxyquinaldine solution and then raise pH to 9 by the adding of dilute ammonium hydroxide, drop by drop with stirring. The precipitate is treated similarly as before.

Some of the results are shown in Table III.

TABLE III
GRAVIMETRIC DETERMINATION OF BERYLLIUM

Beryllium taken, mg.	Weight of precipitate, g.	Beryllium found, mg.	Error, mg.
2.55	0.0926	2.57	+0.02
2.55	0.0917	2.54	−0.01
5.10	0.1820	5.04	−0.06
5.10	0.1857	5.11	+0.01
5.10	0.1840	5.10	0.00
5.10	0.1828	5.06	−0.04
5.10	0.1825	5.06	−0.04
10.20	0.3634	10.07	−0.13
10.20	0.3723	10.31	+0.11
10.20	0.3725	10.32	+0.12

Volumetric Determination

Beryllium may be determined volumetrically, making use of the fact that 8-hydroxyquinaldine is readily and quantitatively brominated to form 5,7-dibromo-8-hydroxyquinaldine. The beryllium chelate of 8-hydroxyquinaldine is dissolved in hydrochloric acid, and treated with excess standard potassium bromate-bromide solution. The excess of bromate is determined iodometrically by back titration with standard thiosulfate. These reactions are based upon the following equations.

$$Be^{++}+2C_{10}H_8NOH \longrightarrow Be(C_{10}H_8NO)_2+2H^+ \quad (a)$$

$$Be(C_{10}H_8NO)_2+2HCl \longrightarrow Be^{++}+2C_{10}H_8NOH+2Cl^- \quad (b)$$

$$2C_{10}H_8NOH+4Br_2 \longrightarrow 2C_{10}H_5Br_2NOH+4HBr \quad (c)$$

From Equation (a) and (c), it is evident that one atom of beryllium is equivalent to 8 atoms of bromine, therefore 1 ml. of 0.1 N potassium bromate-bromide solution should correspond to 0.1127 mg. of beryllium.

Varying amounts of beryllium were determined volumetrically by the following procedure based upon above mentioned reactions.

Procedure.—The chelate, containing from 2 to 10 mg. of beryllium, after being precipitated and washed similarly as in the gravimetric procedure, is dissolved in hot 6 N hydrochloric acid, in which case 20 ml. or more is necessary in proportion to the amount of precipitate, and transferred to a glass-stoppered flask. To this solution add a few drops of 0.1% solution of methyl red as indicator, then titrate slowly with standard potassium bromate-bromide solution with constant stirring, and after the color has changed to yellow, add a few milliliters of standard potassium bromate-bromide solution. Stopper the flask, allow it to stand for a few minutes, add 1 g. of potassium iodide, and titrate 0.1 N sodium thiosulfate solution using starch as indicator. From the amount of standard potassium bromate-bromide

solution required to brominate the 8-hydroxyquinaldine, the weight of beryllium may be calculated. As before, 1 ml. of 0.1 N potassium bromate-bromide solution corresponds to 0.1127 mg. of beryllium. Some of the results are represented in Table IV.

TABLE IV
VOLUMETRIC DETERMINATION OF BERYLLIUM

Beryllium taken, mg.	0.1 N $KBrO_3$-KBr used, ml.	Beryllium found, mg.	Error, mg.
5.10	45.55	5.13	+0.03
5.10	45.19	5.09	+0.01
5.10	46.92	5.29	+0.19
5.10	45.76	5.16	+0.06
5.10	45.10	5.09	−0.01
5.10	44.78	5.05	−0.05
5.10	45.55	5.13	+0.03
2.55	22.77	2.57	+0.02
2.55	22.60	2.54	−0.01

Effect of Diverse Ions

About 1 g. of alkali and ammonium salts of chloride, nitrate, sulfate and acetate do not interfer with the determination of beryllium. The metal ions which precipitate with 8-hydroxyquinaldine in ammoniacal solutions, such as bismuth, cadmium, chromium, cobalt, copper, iron, magnesium, manganese, nickel, silver, titanium, and zinc do interfere with the procedure. When aluminum is present, though it gives no precipitation with this reagent, a large amount of tartrate must be added to prevent its hydroxide from coming down, and a relatively large amount of tartrate hinders the coagulation of beryllium chelate. So that, any excess amount of aluminum more than 0.5 mg. must be removed before the beryllium is determined.

5) A.D. Melaven, *Ind. Eng. Chem., Anal. Ed.*, 2, 180 (1930).

The separating methods of beryllium from iron and aluminum were especially studied, and the following procedure, which is based upon the fact that iron and aluminum can be removed by the extraction of their oxinate in acetic acid-acetate solutions with chloroform, was found very useful. The sample solution, containing not more than 20 mg. of iron and aluminum and having a volume about 40 ml., is treated with sufficient amounts of 5% oxine acetic acid solution to precipitate iron and aluminum, and the pH is adjusted to from 4.5 to 5 with 2 N ammonium acetate solution. Then the oxinates of iron and aluminum and the excess of oxine are extracted with five 10 ml. portions of chloroform. After the resulting solution is heated gently to expel the droplets of chloroform, beryllium is determined. By this method, these metals which can not be separated from beryllium by mercury cathod electrolysis[5], such as titanium also can be removed. But in this case titanium must be less than 10 mg.

Conclusion

The methods for determining beryllium with 8-hydroxyquinaldine, described here are fairly sensitive and the procedures are simple. The precipitate formed is well-defined insoluble crystalline, easily filtered and washed, and thermally stable. The gravimetric factor is very small, 0.02770, and the volumetric factor is low, 1 ml. of 0.1 N potassium bromate solution corresponding to 0.1127 mg. of beryllium, so that, a few milligrams of beryllium can be determined, both gravimetrically and volumetrically, with good accuracy.

The author wishes to express his sincere appreciation to Prof. Dr. M. Ishibashi for encouragement and numerous suggestions throughout this investigation.

Faculty of Science and Engineering,
Ritsumeikan University, Kyoto

Thixotropy of Alginate Gels

By Tunetaka SASAKI*, Shigeru MIYAMOTO and Yasuko MORINAGA

(Received July 9, 1955)

The various metal alginate gels are known to be formed by the reactions between metallic and alginate ions in solution. The resulting gels exhibit thixotropy which does not seem to be reported precisely in the literature of the subject. The present paper describes the details of such a thixotropy of alginate gels.

* Present address, Department of Chemistry, Faculty of Science, Tokyo Metropolitan University, Tokyo.
** Present address, Fukuoka Futaba High School, Fukuoka.

Experimental

Purification of sodium alginate was carried out by repeated precipitations by acid and dissolutions by alkali. The purified sodium alginate, whose polymerization degree was about 80[1] was dried at 80°C. Two cc. of 2% sodium alginate solution was pipetted in the test tube of an inner diameter

1) Polymerization degree of sodium alginate was determined viscometrically in the presence of sodium chloride according to K. Inokuchi. *Mem. Fac. Science, Kyûshû Univ. Series C*, **1**, 115 (1950).

being about 1.6 cm. to which 2 cc. of the electrolyte solution was added and the whole content was mixed intimately. Thixotropy was observed simply by measuring the setting time which was detected by inverting the tube. All measurements were conducted at 20°C.

Experimental Results

Thixotropic gels were obtained by adding appropriate amounts of cupric chloride, barium chloride, calcium chloride, lead nitrate, cadmium sulfate, zinc sulfate and nickel sulfate to sodium alginate solutions The setting times of resulting transparent gels are shown in Table I.

TABLE I

SETTING TIME OF THIXOTROPIC GELS FORMED BY ADDING VARIOUS ELECTROLYTES TO 2% SODIUM ALGINATE SOLUTION

(a) $CuCl_2$ addition

$CuCl_2$ added (10^{-5} mole)	Setting time: Immediately after add.	1 day after	5 days afters	10 days afters
2.08	∞	∞	∞	∞
2.34	27 min.	31 min.	1.7 hr.	48 hr.
2.60	30 sec.	2 min.	12.7 min.	6 min.
2.86	5 sec.	0 sec.	0 sec.	0 sec.
3.12	0 sec.	〃	〃	〃
3.38	〃	〃	〃	〃
3.64	〃	〃	Coag.	〃
4.16	5 sec.	Coag.	〃	〃
4.68	Coag.	〃	〃	〃

(b) $BaCl_2$ addition

$BaCl_2$ added (10^{-5} mole)	Setting time: Immediately after add.	1 day after	3 days after	8 days after
1.76	∞	∞	∞	∞
2.05	4.1 hr.	——	11 hr.	48 hr.
2.34	5 min.	1.6 hr.	2.8 hr.	〃
2.64	4 min.	〃	41 min.	〃
2.93	2 min.	5.3 hr.	48 hr.	Coag.
3.22	44 min.	Coog.	Coag.	〃
3.52	Coag.	〃	〃	〃
3.81	〃	〃	〃	〃

(c) $Pb(NO_3)_2$ addition

$Pb(NO_3)_2$ added (10^{-5} mole)	Setting time: Immediately after add.	1 day after addition
1.20	20 hr.	96 hr.
1.60	〃	〃
2.00	〃	24 hr.
2.40	8 min.	96 hr.
2.80	3 min.	〃
3.20	4 min.	〃
3.60	6.5 min.	Coag.
4.00	9 min.	〃
4.40	16 hr.	〃
4.80	Coag.	〃

(d) $CaCl_2$ addition

$CaCl_2$ added (10^{-5} mole)	Setting time: Immediately after addition	1 day after addition
1.61	∞	∞
2.42	〃	〃
3.22	17 hr.	24 hr.
4.03	26 min.	〃
4.84	2 min.	Coag.
5.64	Coag.	〃
6.45	〃	〃

(e) $CdSO_4$ and (f) $ZnSO_4$ addition

Electrolyte added (10^{-5} mole)	Setting time immediately after addition: $CdSO_4$	$ZnSO_4$
3.50	∞	∞
4.00	〃	〃
4.50	23 hr.	〃
5.00	22 hr.	20 hr.
5.50	2 min.	〃
6.00	21 hr.	Coag.
6.50	Coag.	〃

(g) $NiSO_4$ addition

$NiSO_4$ added (10^{-5} mole)	Setting time immediately after addition
3.60	∞
5.70	ca. 6 days
6.42	〃
7.13	〃
7.84	〃
8.56	〃
9.98	〃
10.7	Coag.

From these results, it is seen that the addition of neither too little amount nor too large excess of the electrolyte rendered the gel thixotropic, and we see as a whole that the thixotropic setting time decreases at first and then shows the tendency to increase with increasing amounts of electrolytes. Furthermore, it is seen that the setting time changes with the ageing of the gels. In the cases of adding other electorlytes such as hydrochloric acid, silver nitrate, manganese sulfate, aluminum sulfate and ferric chloride, the thixotropic gel was not obtained and the coagulation of the corresponding metal alginates occurred at once from the sol state. Next, the effects of the several experimental conditions on thixotropy were studied. The effect of changing volume was first studied for the systems containing the constant amount (40 mg.) of sodium alginate, as shown in Table II.

In Table II, we can see that thixotropy occurs at the intermediate alginate concentration, namely it occurs as the intermediate state between sol and coagel. This is in accord with the accepted view that the thixotropy and coagulation parallel each other[2]. The thixotropic setting time is

2) H. Freundlich und K. Söllner, *Kolloid-Z.*, **45**, 348 (1928).

TABLE II

THIXOTROPY VERS. CONCENTRATION OF GEL

Volume of the system (cc.)	Amount of $CuCl_2$ added (unit 10^{-5} mole)									
	2.72	2.94	3.10	3.30	3.64	4.04	4.36	4.72	4.96	5.18
4	T*	T	T	T	T	T	T	T	T	T
8	Sol	T	T	T	T	T	T	Coag	Coag	Coag
12	Sol	Sol	Sol	Sol	Sol	T	T	Coag	T	Coag
16	Sol	Sol	Sol	Sol	Sol	Sol	Sol	Sol	Sol	Sol

* "T" shows that the system is thixotropic.

therefore expected to depend on the polymerization degree of the alginate just as it is the case with coagulation. Table III shows these results.

TABLE III

THIXOTROPIC SETTING TIME OF COPPER ALGINATE GELS VERS. POLYMERIZATION DEGREES OF ALGINATES

$CuCl_2$ added to 2 cc. of 2% sodium alginate (10^{-5} mole)	Polymerization degree[1] of alginate			
	15	80	300	670
0.24	∞	∞	∞	∞
0.60	〃	〃	10 min.	Hard gel*
0.96	〃	〃	13 min.	〃
1.29	〃	〃	10 sec.	〃
2.34	〃	27 min.	Coag.	Coag.
2.60	〃	30 sec.	〃	〃
2.86	〃	5 sec.	〃	〃

From Table III, it can be seen that thixotropy and coagulation were easily observed for the samples of relatively high polymerization degree upon the addition of small amounts of the electrolyte. Next, the effect of pH on the thixotropy was studied. When hydrochloric acid or sodium hydroxide alone was added to sodium alginate solution, no thixotropic gel was obtained. On the contrary, the setting time was markedly influenced by pH in the presence of cupric and barium chlorides, as seen in Table IV.

TABLE IV

THIXOTROPIC SETTING TIME VERS. pH IN THE PRESENCE OF CUPRIC AND BARIUM CHLORIDES IN THE SOLUTION OF SODIUM ALGINATE

pH	$2.60 \cdot 10^{-5}$ mole $CuCl_2$	$2.93 \cdot 10^{-5}$ mole $BaCl_2$
0.5	Coagulation	Coagulation
2.5	〃	〃
3.3	〃	〃
4.1	〃	〃
4.6	10 sec.	—
6.0	—	2.5 min.
6.3	40 sec.	—
6.7	4 min.	—
7.0	3 min.	—
7.5	∞	3 min.
7.9	〃	3.5 min.
9.5	〃	〃*
11.0	〃	2.5 min.
11.7	〃	3 min.
12.3	〃	4 min.
12.6	$Cu(OH)_2$ ppt.	—

* The term "hard gel" represents such a gel as cannot be transformed into sol by hand-shaking.

* At pH values exceeding 9.5, white turbidity was seen on the addition of $BaCl_2$.

As a whole, thixotropy was observed in neither regions of strong acidity nor alkalinity. In the region of intermediate pH, the thixotropic setting time was observed which changed with pH. In the case of barium chloride addition, the setting time increased and rapidly attained a constant value. As stated before, thixotropy was caused by the addition of a suitable amount of cupric chloride to the sodium alginate solution. We compared this amount with the combining capacity of cupric ion towards sodium alginate, which was measured as follows. Two cc. of 2% sodium alginate solution was added to 10 cc. of cupric chloride solution of varying concentrations. After the equilibrium was attained, the concentrations (C) of cupric and chlorine ions in supernatant liquid were determined and they were plotted against the total concentration of Cu^{++} (C_0) as shown in Fig. 1. In this figure, it is seen that

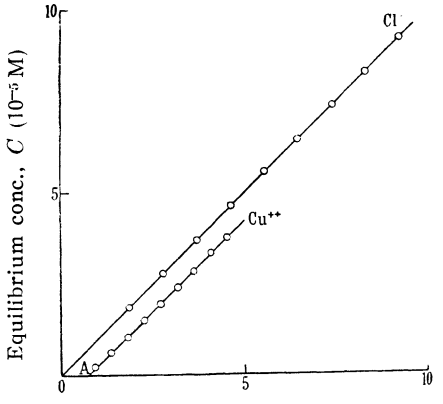

Fig. 1. Total and equilibrium concentration of cupric and chlorine ions before and after cupric chloride was added to the solution of sodium alginate.

the cupric ion combines with sodium alginate and the combining capacity of cupric ion towards sodium alginate calculated from the abcissa of the point A in Fig. 1 is $9.3 \cdot 10^{-5}$ mole per/40 mg. sodium alginate. Comparing this value with the composition of thixotropic gel formation shown in Table I (a), it is found that the thixotropy of copper alginate occurs when 25~45% of the alginate ions are combined with cupric ions, and coagulation of alginate ion occurs when more than half of the total alginate ions are combined

with cupric ions. Finally, it was found that the thixotropic gel could be obtained also from the once coagulated copper alginate by adding a suitable amount of sodium alginate. Thus, copper alginate was first precipitated by adding $7.8 \cdot 10^{-5}$ mole of cupric chloride to 4 cc. of 1% sodium alginate solution. Then more sodium alginate was added to make the total volume 16 cc., and the thixotropy was measured. The results are shown in Table V.

TABLE V

THIXOTROPY OF THE SYSTEM OBTAINED BY ADDING SODIUM ALGINATE TO COPPER ALGINATE PRECIPITATE

Sodium alginate added (mg.)	Thixotropy	
	Immediately after add.	24 hr. after add.
0	Coag.	Coag.
20	〃	〃
40	Thixotropic	Thixotropic
60	〃	〃
80	〃	〃
100	〃	〃
120	〃	Sol
140	Sol	〃
160	〃	〃

From this table, it can be confirmed that the coagulation of copper alginate ceased to persist when combined copper was decreased to less than 56% of the available alginate ion. This agreed qualitatively with the condition of the gelation mentioned above.

Summary

Thixotropy was observed on the gels formed by the addition of the suitable amounts of cupric chloride, barium chloride, lead nitrate, calcium chloride, cadmium sulfate, zinc sulfate and nickel sulfate to the solutions of sodium alginate. The setting time of the thixotropic gels was observed to change with the amount of the electrolyte added, the ageing time of the gels, the degree of polymerization of sodium alginate used and pH of the system. The thixotropic behavior was observed to change also with the volume of the system. Furthermore, it was found that thixotropy was observed when about 25–54% of the total alginate ions combine with cupric ions, whereas the combination of more than half of the total alginate ion results in non-thixotropic gelation. The thixotropic gel could be formed also by the addition of sodium alginate to the once precipitated copper alginate.

The authors wish to express their thanks to the Ministry of Education for the grant given for this research.

Department of Chemistry, Faculty of Science, Kyûshû University, Fukuoka

The State of Metal Ion in Aqueous Solutions and its Surface Chemical Effect. II. Uptake of Metal Ions from Aqueous Solutions by Stearic Acid Monolayer*

By Tunetaka SASAKI* and Mitsuo MURAMATSU***

(Received August 1, 1955)

Introduction

It has been pointed out previously[1] that the metallic ions are classified into two groups from their effects upon monolayers of fatty acid. One includes such metal ions as Co, Cu, Al and Th which make the monolayer expand and remarkably rigid, and the other includes mainly alkaline earth metals which condense it. A built-up film of stearic acid takes up many of the former ions from[2] and is wetted by[3] their solutions, while it does not show such effects with the latter ions. All these phenomena could be explained by the difference in types of the structure of metallic soap formed by the interaction between fatty acid in the film and metal ions in the solution[1-3].

In the case of the former ions, the metallic soaps seem to consist of molecules of stearic

* Part I of this series has been published recently by R. Matuura and H. Kimizuka[9].

** Present address, Department of Chemistry, Tokyo Metropolitan University.

*** Present address: Chemical Laboratory, Fukuoka Gakugei University.

1) T. Sasaki and R. Matuura, This Bulletin, 24, 274 (1951); R. Matuura, ibid., 24, 278 (1951).

2) M. Muramatsu and T. Sasaki, ibid, 25, 21, (1952).

3) M. Muramatsu and T. Sasaki, ibid., 25, 25 (1952); A. Inaba, ibid., 26, 43 (1953).

acid and polymeric and complicated aggregates of metal ions in solution, the acidity of which is adjusted to be in the region of pH where the metal hydroxide begins to precipitate[1-3]. Schulman et al.[4,5], using myristic acid monolayer, reached the similar conclusion and postulated that the polymeric nature of metallic soap is attributed to hydrogen bonding between mono- and dihydroxyl metal ions combined stoichiometrically with each acid molecule. In connection with this, it may be noteworthy that the mode of interaction between aqueous sodium alginate and octadecylamine monolayer spread on it resembles closely that between such metal ions and stearic acid monolayer[6].

In contrast with this, the latter alkaline earth ions are considered to be bound to stearate ions with simple stoichiometric relation and the metallic soaps thus formed are also considered to have no lateral binding as was postulated in the former case[1-3].

In order to obtain further knowledge about the difference between two types of metallic soap as mentioned above, it was attempted to determine the binding ratio of strontium and cobalt atoms to the acid molecules in the surface film formed by the interaction between a solution of strontium and cobaltous chlorides and monolayers of stearic acid spread on them.

Experimental

Radioactive strontium chloride was chloride of an isotopic mixture of ^{90}Sr (half-life 53 days) and ^{90}Sr (25 years) and therefore contained ^{90}Y (61 hr.) as a radioactive daughter. It was diluted isotopically to 10 mC/g. with recrystallized strontium chloride and was brought to a desired concentration and acidity with distilled water and redistilled ammonia solution. From six to twenty layers of the surface film spread on such a solution were transferred onto a metal slide coated with five layers of barium stearate under the piston pressure (30 dyn./cm.) of oleic acid. The radioactivity of this multilayer was measured with and without an aluminum disc (15 mm. diameter and 1.5 mm. thickness) placed on the center of the slide and exactly beneath the window of the GM tube. The difference between these counts was taken as the radioactivity of the part of multilayer covered by the disc, and was compared with radioactivity of the standard $SrCl_2$ mounted on cigarette papers (15 mm. diameter)[7] which were fixed on the metal slides of the same magnitude as that coated by multilayer. Identical conditions were maintained for both the disc and the papers. Number, x, of bound Sr atoms per cm^2 of monolayer was calculated from the radioactivity at transient equilibrium between ^{90}Sr and ^{90}Y which was attained after at least fifty days.

Owing to a difficulty in building up the monolayer spread on the solution of cobaltous chloride, the amount of bound cobalt atoms was determined as follows. The monolayer was collected to one side of the trough by moving the barrier and collapsed film was scooped up with a strip of filter paper. The water content of the paper was first measured by drying, from which the amount of Co atom carried merely with the solution was determined. It was then burned in a crucible and the remaining ash was treated repeatedly with 6 N hydrochloric acid. The resulting solution was transferred onto a cigarette paper, evaporated to dryness, and its radioactivity was measured by means of GM counter. The amount of Co atom bound to monolayer could be calculated from the radioactivity of this sample, taking account of the amount of cobalt mentioned above.

The surface pressure of the film was determined by the same method as used in a former report[6]. The acidity of substrate solution was adjusted by redistilled hydrochloric acid and redistilled ammonia unless otherwise mentioned.

All monolayers were kept on substrates of room temperature for from three to eight minutes after spreading, before the experiments were carried out.

Results

Interaction between Sr Ion and Monolayer.— In Table I are shown the effects of pH of substrate solution and of the number of layers in the built-up film upon x, where the concentration of strontium chloride in the substrate is maintained at 10^{-4} mol./l. According to Bikerman[8] the deposition ratio of monolayer of stearate of alkaline earth metal is always unity when it is transferred onto a solid surface. Therefore, if we assume that the cross-sectional area of stearic acid in multilayer is 20 $Å^2$, number, R, of Sr atoms bound to one molecule of stearic acid is calculated and listed in the last column. It is seen in this table that R increases with increasing pH and has little dependence upon the number of layers at each pH.

When substrate pH was greater than 9.6, the monolayers were unsuccessfully built up onto the slide. Actually it was observed that the silk thread separating the monolayer from piston oil did not move in accord with the up and down trip of the slide, and that the wettign condition as well as interference color of the surface was uneven and irregular.

Effect of concentration, c, of strontium chloride solution upon x was examined at the constant

4) J.H. Schulman, et al., *Trans. Faraday Soc.*, **46**, 475 (1950); **47**, 788 (1951); **50**, 1139 (1954).

5) J.H. Schulman and M.Z. Dogan, *Discussion, Faraday Soc.*, **16**, 158 (1954).

6) T. Sasaki and M. Muramatsu, This Bulletin, **26**, 96 (1953).

7) G. Friedlander and J.W. Kennedy, "Introduction to Radiochemistry", John Wiley and Sons, Inc., New York, N.Y. (1949), p. 231.

8) J.J. Bikerman, *Proc. Roy. Soc. London*, **A170**, 130 (1939).

pH value of 5.7, the result being shown in Table II.

TABLE I

EFFECT OF SUBSTRATE pH UPON NUMBER OF Sr ATOMS BOUND TO ONE MOLECULE OF STEARIC ACID; $SrCl_2$ 10^{-4} mol./l.

Substrate pH	No. of Built-up layers, n	Number of bound Sr atoms/cm² of monolayer, x	Number of bound Sr atoms/molecule of stearic acid, R	Mean
4.0	8	0.70×10^{13}	0.014	0.016
〃	10	$0.85\times$ 〃	0.017	
5.0	10	$6.65\times$ 〃	0.137	0.132
〃	20	$6.30\times$ 〃	0.126	
6.1	10	$10.63\times$ 〃	0.213	0.209
〃	14	$10.56\times$ 〃	0.211	
〃	20	$10.22\times$ 〃	0.204	
7.5	6	$12.11\times$ 〃	0.242	90.24
〃	10	$13.06\times$ 〃	0.261	
〃	14	$12.14\times$ 〃	0.243	
〃	20	$12.43\times$ 〃	0.249	
9.2	6	$26.33\times$ 〃	0.527	0.437
〃	10	$21.17\times$ 〃	0.423	
〃	14	$24.05\times$ 〃	0.481	
〃	20	$23.12\times$ 〃	0.462	
9.3	10	$26.68\times$ 〃	0.534	0.517
〃	20	$25.02\times$ 〃	0.500	

TABLE II

EFFECT OF CONCENTRATION OF $SrCl_2$ UPON NUMBER OF BOUND Sr ATOMS per cm² OF MONOLAYER; SUBSTRATE pH 5.7

$SrCl_2$ concentration, c, mol./l.	Number of bound Sr atoms/cm² of monolayer, x
1.0×10^{-3}	1.35×10^{14}
7.0×10^{-4}	$1.06\times$ 〃
$4.0\times$ 〃	$0.83\times$ 〃
$2.0\times$ 〃	$0.78\times$ 〃
$1.0\times$ 〃	$0.72\times$ 〃
7.0×10^{-5}	$0.49\times$ 〃
$4.0\times$ 〃	$0.31\times$ 〃
$1.0\times$ 〃	$0.28\times$ 〃
5.0×10^{-6}	$0.19\times$ 〃
$1.0\times$ 〃	$0.22\times$ 〃

Interaction between Co Ion and Monolayer.— Fig. 1 shows the effect of substrate pH upon the pressure—area curve of stearic acid spread on 10^{-4} mol./l. solution of cobaltous chloride. Generally speaking, it was seen that the monolayer condensed up to pH of about 6, while remarkable expansion and increase in compressibility of the film were observed at pH 8–9. This is similar to the result in the case of 10^{-3} mol./l. solution of the same substance, which was reported in a preceding paper[9]. pH dependence of the area per molecule at F=2 dyn./cm. is shown in Fig. 2,

9) R. Matuura and H. Kimizuka, This Bulletin, 28, 668 (1955).

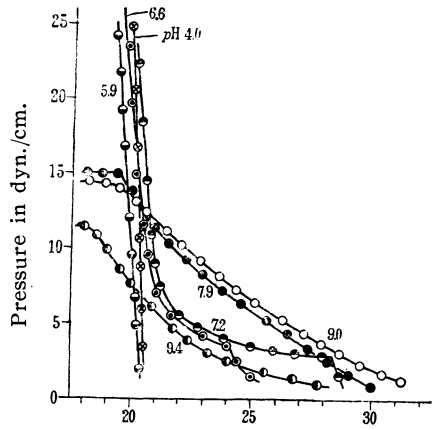

Fig. 1. Pressure—area curve of monolayer of stearic acid spread on 10^{-4} mol./l. $CoCl_2$.

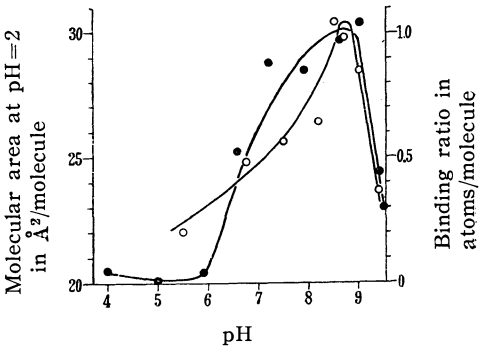

Fig. 2. Effect of pH upon molecular area at pH=2, ●, and binding ratio, R, ○, of Co atom in the film.

together with that of number, R, of bound Co atoms per one molecule of stearic acid. It is interesting that both curves changed with pH similarly, and that the maximum value of R being unity was obtained at pH 8–9, where the area reached the maximum value of 30 Å²/molecule or larger.

When sodium or potassium hydroxide was used as pH-adjusting agent instead of ammonia, we observed the less exaggerated effects of Co ion upon both area at pH=2 and compressibility, while the same result was obtained for R—pH relationship. This is represented in Table III in which the effects of pH-adjusting agent upon the nature of the film are listed.

TABLE III

EFFECT OF pH-ADJUSTING AGENT UPON MOLECULAR AREA AT pH=2, R, AND COMPRESSIBILITY OF FILM; SUBSTRATE pH 8.9

pH-adjusting agent	NH_4OH	NaOH	KOH
Molecular Area, Å²/molecule	30.5	25.7	24.8
R, atoms/molecule	1.01	0.97	0.93
Compressibility, Å²·cm./molec.·dyn.	0.76	0.49	0.43

In a region more alkaline than about pH 9.5–10, the measurement could not be performed without large accidental error, presumably due to the dissolution of monolayer or precipitation of cobalt hydroxide.

Discussion

It has been shown that[1,10] alkaline earth metals in aqueous solution exert their effects upon either pressure or mechanical properties of monolayer of fatty acid spread on it, when pH of the solution is larger than 5–6. In order to explain the phenomena, electrostatic binding was presumed between monolayer and metal ions. Experimental result in Table I supports this presumption. Since the dissolving state of Sr ion is not considered to be greatly affected by the acidity of the medium when pH<9, pH dependence of R comes mainly from an increasing ionization of stearic acid with decreasing acidity of the substrate. This consideration is also supported by a decreasing surface potential of the monolayer of stearic acid when pH of the substrate solution increases in the range of pH 3–12[11].

Such a type of binding in terms of ion—ion attraction results in formation of metal stearate in the film, the composition of which should be discussed. That R attains a maximum value of 0.5 when substrate pH is adjusted to 9.3 may favorably be explained by assuming interaction between one Sr ion and two stearate ions. Therefore it is probable that the monolayer on aqueous $SrCl_2$ of pH<9.3 consists of stearate ions, molecules of stearic acid and of Sr stearate which is formed as a result of the following reaction.

$$\underset{\text{(bulk)}}{Sr^{++}}+2\underset{\text{(surface)}}{C_{17}H_{35}COO^-}=\underset{\text{(surface)}}{(C_{17}H_{35}COO)_2Sr}$$

Ignoring the decrease of substrate concentration, c, and the surface contraction of stearate ion due to interaction, the following equation holds as far as strontium hydroxide does not precipitate,

$$\frac{K_2^2c}{K_3x}\left\{\frac{a-2x}{[H^+]+K_2}\right\}^2=\frac{K_0^2}{K_1[H^+]^2}, \qquad (1)$$

where K_0, K_1, K_2 and K_3 are dissociation constant of water, strontium hydroxide, stearic acid and strontium stearate (at the air-water interface), respectively, a the surface concentration of stearyl radical and x the surface concentration of strontium stearate. It is easy to understand the increase of x at constant c with decreasing $[H^+]$, provided that K_0^2/K_1 is much less than $[H^+]^2$.

10) I. Langmuir and V.J. Schaefer, *J. Am. Chem. Soc.*, **59**, 2400 (1937).
11) J. Glazer and M.Z. Dogan, *Trans. Faraday Soc.*, **49**, 448 (1953).

At constant acidity, Eq. (1) can be transformed into the following relation,

$$a/2-x=k\sqrt{x/c} \qquad (2)$$

where constant k denotes $\{[H^+]+K_2\}K_3/2K_2$. Fig. 3, in which $\sqrt{x/c}$ is calculated using

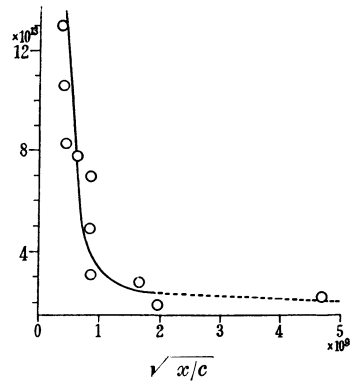

Fig. 3. Relationship between x and $\sqrt{x/c}$.

the data in Table II and is plotted against x, seems to show a partial validity of Equation (2). In the range of substrate concentration of $10^{-5}-10^{-3}$ mol./l., x decreases linearly with increasing $\sqrt{x/c}$ and this linear portion cuts the ordinate at $x=19.5\times10^{13}$ atoms/cm.^{2} of monolayer, when it is extrapolated. Thus $10^{16}/(2\times19.5\times10^{13})=26$ Å^2/molecule is obtained for the cross-sectional area of stearate ion or molecule of stearic acid in the film. This value is in fair agreement with that obtained from extrapolation of $F-A$ curves or from X-ray data. The deviation from the linearity at low concentration of solute may be due to the invalidity of the assumption that c does not change with reaction.

In the case of aqueous Co ion of pH less than 6.5, the structure of metallic soap formed in the film is considered to be the same as in the case of strontium stearate. In this pH region, the monolayers took up cobalt ions giving R less than 0.5 and did not show a remarkable expansion but rather a small condensation as pH decreased. Cobalt ions in solution are considered to be in the simple form of Co^{++} when pH of solution is maintained below 7, as seen from the measurement of self-diffusion[9]. On the other hand, decreasing surface potential[11] of stearic acid monolayer with increasing substrate pH can be accounted for by the increasing surface ionization of stearic acid. Taking account of these circumstances change of R at pH< 6.5 can be explained by the change in binding ratio of one Co^{++} ion with at most two stearate ions.

Now we should draw attention to the remarkable expansion of monolayer at pH 7–9, where R is always greater than 0.5. This fact, together with that $R_{max.}=1$, seems to be explained rather by assuming interaction betweeen one stearate ion and one monobasic cobalt ion. However, this cannot explain the extraordinarily large expansion quantitatively, so we take account of the dissolved state of monobasic cobalt ions in this pH range, which may be different from that at pH<7. Possibility of polymer formation of basic metal ions has been shown in the case of, for instance, uranyl[12] or ferric ion[13] and also in our cases[1-3]. Remarkable decrease of self-diffusion coefficient[9] of aqueous cobalt ion, when pH of it is beyond 7, is presumably due to the formation of aggregates. Actually it was observed that the colorless solution (10^{-4} mol./l.) of cobalt chloride was changed to pale blue when pH of it was increased to above 7, and that it was further changed to pale yellow after standing for 7–10 days, concentrations of Co atom in supernatant solutions being 69×10^{16} and 36×10^{16} atoms/cc. for pale blue and pale yellow solutions, respectively. These facts lead us to the conception of colloidal aggregates formed in the solution, which may consist of basic metal ions, water molecules and ammonia molecules, the latter if it is used.

The monolayer of stearic acid when spread on such a solution gives a film consisitng of widely spaced molecules, showing the large cross-sectional area as shown in Fig. 2. Low surface density of hydrocarbon chain in such a film can also be expected from the low refractive index of built-up films of Cu, Al and Th stearates[3], the behaviors of which at air-water interface are similar to those of cobalt stearate at pH 8–9. Similarly, unsuccessful building up of this film is presumably due to high compressibility and low collapsing pressure (see Fig, 1), as discussed in the case of Cu, Al or Th stearate[3]. The high compressibility of the film suggests that the interlinks between cobalt atoms in these aggregates are so loose that some cobalt atoms in them may be ejected partly from air-water interface when monolayer was compressed. There are cobalt atoms which are considered to be bound so firmly to stearate that the linkage is not destroyed by compression of monolayer, even when the other elementary ions or molecules in the aggregate are ejected from the surface. This consideration is supported by the fact that the higher compressibility was seen in the more expanded and the more brittle film. However, since we actually measured the binding ratio, R, after collapsing the film, the observed value indicates the Co atoms attached directly to stearate ions and the result of experiments is not adequate to confirm the loose structure giving rise to the anomalous expansion of the film.

This is also the reason why area—pH relation depends upon the choice of pH-adjusting agent, whilst R—pH relation does not. It is probale that the co-ordination of ammonia molecules towards Co atom has some contributions to size, shape and other nature of the aggregate, by which the cross-sectional area and compressibility of film molecules are largely affected. As is seen in Table III, this results in the increase of film expansion and compressibility. On the other hand, R is not affected by the presence of ammonia, showing that the co-ordination has no effect for direct and firm binding between the cobalt atom and stearic acid.

Many attempts[5,14,15] were made to determine the amount of metal ion bound to monolayer of fatty acid spread on it, where the ordinary microanalytical methods were used for this purpose. In our experience, however, it seems to be inevitable that these methods include an accidental error, presumably due to the long time required for collecting a few decades (or more) of monolayers. It has been pointed out in the preceding report[9] that the nature of surface film of stearic acid is changed by ageing of aqueous cobalt ion. The present radio-tracer method offers the advantage that only few times of the collection of monolayer are sufficient for the measurement and consequently it enables us to determine the binding ratio with slight accidental error.

Summary

It has been attempted to determine the binding ratio of strontium and cobalt atoms in the monolayer of stearic acid spread on aqueous strontium and cobalt solutions, respectively, containing radioactive cations.

The number of strontium atoms bound to one molecule of stearic acid increased with increasing pH of substrate solution as well as concentration of strontium ion in it. Tentative explanation was made by assuming interaction between strontium and stearate ions. A theoretical formula based on ionizations of stearic acid, strontium hydroxide,

12) K.A. Kraus and F. Nelson, *J. Am. Chem. Soc.*, **71**, 2510, 2517 (1947).

13) B.O.A. Hedström, *Arkiv för Kemi*, **6**, 1 (1952).

14) I. Langmuir and V.J. Schaefer, *J. Am. Chem. Soc.*, **58**, 284 (1936)

15) E. Havinga, *Rec. trav. chim.*, **71**, 72 (1952).

and strontium stearate proved to support the validity of this presumption.

A similar explanation was also made for interaction between monolayer of stearic acid and substrate solution containing cobaltous chloride of pH less than 6.5, where the monolayer showed no expansion but rather a small condensation, while the number of bound Co atoms per one molecule of stearic acid increased with increasing pH up to 0.5. At pH 7–9, remarkably expanded and compressible films were obtained and the binding ratio reached a maximum value of unity. Films thus formed were considered to consist of stearate ions and polymer ions of cobalt which may exist as aggregates in the solution.

Co-existing ammonia used as a pH-adjusting agent of the solution of cobaltous chloride resulted in exaggeration of these effects. It might be attributed to co-ordination of ammonia molecules towards Co atoms.

The authors wish to express their thanks to Dr. R. Matuura and Mr. H. Kimizuka for useful discussion and to the Ministry of Education for the grant given for this research.

Department of Chemistry, Faculty of Science, Kyûshû University, Fukuoka

Reaction between Iron Pentacarbonyl and Ammonia under High Pressure of Carbon Monoxide

By Hiroshi UCHIDA and Kenichiro BANDO

(Received July 13, 1955)

A recent investigation[1] showed that in the presence of iron pentacarbonyl, carbon monoxide under high pressure reacted readily with mono- and dimethylamines at 120°C to produce their formamides, but not readily with ammonia at this temperature. However the reaction with ammonia has now been found to take place at further raised temperatures, resulting in a pale yellow powdery product.

The subject matter of this paper is the reaction conditions for obtaining high yields in the powder, and also the chemical composition of the powder. Suitable conditions for the reaction has permitted us to obtain the yield so high as 90 per cent of the theoretical yield from iron pentacarbonyl used, and the powder has appeared to be a complex ferrous salt containing a complex anion of new composition consisting of CN, CO and NH_3 besides iron.

In addition, the reaction products (powder and simultaneously formed liquor) have been found capable of accelerating the formation of formamide from carbon monoxide and ammonia under high pressure.

Synthesis of Ferrous-Ammine Salt of Carbonyl-Ammine-Ferro-Cyanide

Measured amounts of iron pentacarbonyl and anhydrous ammonia were placed in a 1.1 l. shaking autoclave, and thereafter compressed carbon monoxide was admitted to a required pressure for reaction. The autoclave was kept at a certain temperature for five hours before it was allowed to cool. No reaction occurred at temperatures lower than 150°C, at which a small quantity of pale yellow powder was produced. At a high temperature of 180°C and under the certain reaction conditions nearly all of the iron pentacarbonyl could be converted into the powder and simultaneous liquor*.

The powder was practically insoluble in water, dilute acid and organic solvents such as methanol and ether, but was soluble in caustic potash solution to result in a yellow solution by developing ammoniacal odour and leaving yellowish brown precipitates of, probably, ferrous hydroxide. This solution revealed characteristic reactions of carbonyl-ferro-cyanide ion, $(Fe(CO)(CN)_5)^{3-}$ according to J. A. Müller[2], namely it produced a violet precipitate, when acidified and added a solution of ferric chloride, but formed no precipitate with lead acetate and acetic acid.

Conditions for Manufacture of the Powder.— Reactions were run first at a fixed mixing ratio of iron pentacarbonyl to ammonia, under varying pressures of carbon monoxide, secondly at different mixing ratios under a definite pressure of carbon monoxide.

1) H. Uchida and K. Bando, *J. Chem. Soc. Japan (Ind. Sect).*, 57, 941 (1954).

* With respect to the liquor a description will be made later.

2) refer to Gmelin, "Handbuch der Anorganische Chemie", 8te Aufl. Eisen Teil B, 740.

Under initial total pressures* varying from 10 to 155 kg./cm² (at room temperature), a mixture comprising 40 g. ammonia (2.35 M) and 50 g. iron pentacarbonyl (0.25 M) was brought into reaction at 175–185°C. The results are summarised in Fig. 1. At the low pressures the reaction proceeded accompanying the decomposition of iron

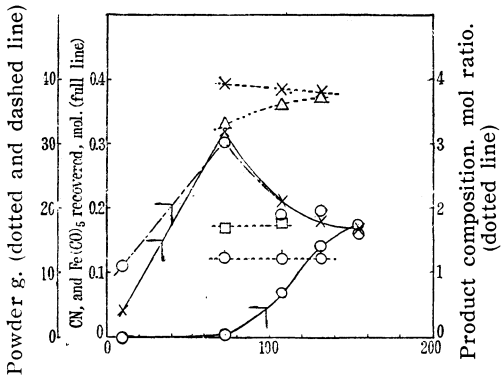

Fig. 1 Effect of total pressure upon yield and composition of product.

pentacarbonyl; however, the reaction gave only a small amount of CN, even though it gave a somewhat large amount of the powder. The greatest amount of powder as well as CN was produced at the initial pressure of 70 kg./cm², above which the powder decreased in amount but the quantity of unchanged iron pentacarbonyl increased with ascending pressures.

As shown in Fig. 1 the ratios $Fe_{ppt.}/Fe_{soln.}$, $CN/Fe_{soln.}$, and $CO/Fe_{soln.}$ . . . the first being the ratio of iron found in precipitate resulted from soaking of the powder in a caustic potash solution to that dissolved in the solution, the second the mol ratio of CN in the powder to iron dissolved, and the third the mol ratio of CO in the powder to iron dissolved . . . were kept at nearly constant levels respectively, throughout the range of pressures employed in the present experiments. On the other hand the values of $NH_3/Fe_{soln.}$, indicating the mol ratio of ammonia found in the powder to iron in the solution, were not found so constant as the above, tending to approach toward 3.75 with the increasing pressures.

* The total pressure means the sum of pressures of ammonia and the introduced gas comprising 80-81% CO, 15-16% H_2, and 4-5% N_2. After the reaction the pressure increased to 33 kg./cm² in the case of initial pressure of 10 kg./cm² (corresponding to vapour pressures of ammonia at room temperature without the presence of carbon monoxide), but decreased in the other experiments, more markedly with the increasing initial pressures. Hydrogen became richer in the gaseous product than in the initial gas.

The powder was quantitatively analyzed for CN, NH_3 and CO contents. CN content was determined by applying Liebig's method to HCN liberated by the decomposition of the powder with boiling 2-N-sulfuric acid in the presence of cuprous chloride as a catalyst. Ammonia was liberated by prolonged boiling of the powder in caustic potash solution under simultaneous aeration, and was determined by the conventional method*. CO content was determined according to the method by W. Hieber et al.[3], namely the powder was heated to 120–190°C with 70% sulfuric acid in an atmosphere of carbon dioxide, and liberated carbon monoxide was collected in an azotometer. The amount of CO originally contained in the powder could be evaluated by subtracting already determined CN content from the amount of carbon monoxide thus measured in the azotometer, since both CN and CO in the powder were to be obtained as carbon monoxide by this procedure*.

Another inquiry was made for effects of quantities of ammonia upon the yield and composition of the powder by using 50 g. of iron pentacarbonyl under approximate total pressures ranging from 105 to 113 kg./cm². The results are shown in Fig. 2. The figure reveals a tendency for the

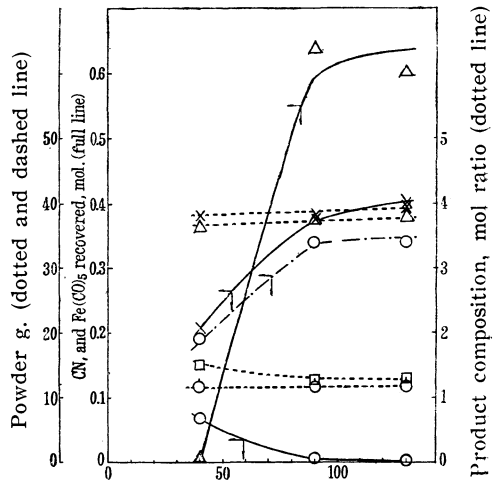

Fig. 2. Effect of amount of ammonia upon yield and composition of product.

* Total nitrogen content was, on the other hand, determined by means of Kjehldahl's method, and was found to be in agreement with the sum of nitrogen determined as CN and NH_3 respectively.

3) W. Hieber, R. Nast et al., *Z. anorg. allg. Chem.*, 272, 32 (1953).

* Similarly the usual combustion method also gave the total carbon content which agreed comparatively well with the value here obtained.

powder to increase in amount with the increasing amounts of ammonia up to a yield of 90 per cent of the theoretical yield from iron pentacarbonyl used. The larger amount of ammonia also favoured the formation of formamide.

In Fig. 2, $Fe_{ppt.}/Fe_{soln.}$, $CN/Fe_{soln.}$ and $NH_3/Fe_{soln.}$ were kept at nearly constant respective values of 1.2, 3.9 and 3.7 independently of the varying quantities of ammonia, and also $CO/Fe_{soln.}$ a value of 1.3 except for the case where a comparatively small amount of ammonia was used. The ratio of $CO/Fe_{soln.}$ attained, on the other hand, to a higher value of 1.75 as illustrated in Fig. 2 and further 2.0 when the greater amount of iron pentacarbonyl was employed*. In these cases part of iron pentacarbonyl, more or less according to the reaction condition, remained unchanged in the reaction.

Composition of the Powder.—From the results of analyses the powder seemed likely to have a practical chemical composition $Fe_2(CN)_4(CO)(NH_3)_4$, of which one half of iron, all of (CN) as well as (CO), and part of (NH_3) could be dissolved in potash solution. The crude powder itself was insoluble in most of the solvents and could not therefore be further purified by recrystallization. However, its caustic potash solution permitted recrystallization to separate out the fine crystal which was presumably a potassium salt of the complex anion.

W. Hieber et al. had described a convenient way for purification of their sodium-carbonyl-ferro-cyanide. The method, when followed in our experiment, produced a mass of fine yellow prismatic crystals. From the results of analyses for CN, CO, NH_3 and iron, conducted as described in the foregoing section, and also for K as its sulfate, the crystal appeared to have a compositon $K_2(Fe(CN)_4(CO)(NH_3))\cdot 1.5H_2O$. Considering this composition in conjunction with the composition $Fe_2((CN)_4(CO)(NH_3)_4)$ of the powder, the powder seems to consist of a complex anion $(Fe(CN)_4(CO)(NH_3))^{2-}$ and a complex cation $(Fe(NH_3)_3)^{2+}$*.

Potassium salts of the powders of two different compositions $Fe_2(CN)_4(CO)(NH_3)_4$ and $Fe_2(CN)_4(CO)_2(NH_3)_3$ (hereafter, simply denoted by A and B respectively) were recrystallised from caustic potash solutions. The powder A was the usual product of the present expertment while the powder B was produced in the particular case where iron pentacarbonyl was used in excess as compared with ammonia.

The procedure for recrystallization of potassium salt of powder A was as follows. A quantity (10 g.) of powder A was soaked in a sufficient, but not too excessive amount (38 g.) of an ice-cooled 10% caustic potash solution to replace one half of the iron (ferrous) with potassium. The yellow filtrate of this solution was then added 300 cc. of ethanol to deposit pale yellow precipitate, which was readily washed with ethanol. The precipitate was further recrystallised in the same way from the aqeous solution, and the recrystallised deposit was dissolved in the possible least amount of water for complete dissolution. The aqueous solution was subsequently allowed to stand for two days in a vacuum-dessicator containing concentrated sulfuric acid, to separate out a mass of fine prismatic crystals (6.5 g.). All the processes were conducted in a dark place in order that the decomposition due to light might be prevented.

The results of analyses of this crystal are given in mol ratios of N, CN etc. to Fe, and they are in good agreement with the composition $K_2(Fe(CN)_4(CO)(NH_3))\cdot 1.5H_2O$, as shown below.

(Total N)/Fe=4.99±0.02,
(Total C)/Fe=5.05±0.02,
CN/Fe=3.95±0.01,
NH_3/Fe=1.1±0.03, and K/Fe=1.95.

Fe	N	C	CN	NH_3	K
					wt. %
Calculated from the above formula					
18.00	22.58	19.36	33.55	5.49	25.21
Observed					
18.01	22.53	19.54	33.20	5.35	24.59
18.05	22.61	19.61	33.10	—	—

When the powder B was purified in the same way, the yield in crystalline product was somethat low (4.0 g. from 10 g. of powder B) and the product was proved to have the same composition as that of the product from powder A. The product did not involve second CO. The second CO of the powder may be less stable in the caustic potash solution, otherwise any complex compound containing two CO's, even if it were present in the solution, does not easily sparate out from the solution. No decisive conclusion has yet been given in this respect.

With regard to the complex compound of iron containing CN and CO, J. A. Muller[2] had already obtained a compound having a composition $K_3(Fe(CN)_5(CO))$ by reacting carbon monoxide on potassium ferrocyanide, and thereafter W. Hieber et al.[3] could produce a compound of this kind with a high yield of 90 per cent of the theoretical yield from $Na_3(Fe(CN)_5(OH_2))$ used as starting material. The latter[4] described also the other compound $Fe(CN)_2(CO)_2Py$, where Py represents pyridine. The complex compound obtained in the present work has a different composition from the above compounds and moreover its manufacturing procedure is characterised by the use of iron pentacarbonyl and ammonia as starting materials.

Formamide Formation in Presence of the Reaction Product

Among the results shown in Fig. 2, those

* In this case the reaction was conducted under a total pressure of 70 kg./cm², by employing 40 g. NH_3 and 200 g. iron pentacarbonyl.

According to W. Hieber and E. Fack (*Z. anorg. allg. Chem.*, **236**, 83 (1938).), the cation should theoretically be $(Fe(NH_3)_6)^{2+}$, but it easily liberates part of ammonia.

4) W. Hieber and F. Sonnekalb et al., *Ber.*, **63**, 982 (1930).

* In the reaction between carbon monoxide and ammonia at high pressure ammonium carbamate was customarily produced (refer to K.H. Meyer et al., *Ber.*, **54**, 1708 (1921)).

** Urea was determined by the amount of precipitate produced by addition of xanthydrol.

obtained with excessive amount of ammonia suggested a considerably easy formation of formamide in the presence of the reaction products (powder and liquor). This was reexamined by a succeeding reaction between ammonia and carbon monoxide, both being admitted newly in the autoclave immediately after only the gaseous products had been purged out. Actually the reaction proceeded more rapidly than it did without the presence of reaction products.

Results of the further experiments along this line are listed in Table I. The formation of formamide could be accelerated neither by the presence of the liquor-free powder nor by that of formamide (Exp. No. 1 and No. 2), but was accelerated markedly by the presence of the brown liquor of the crude reaction products (Exp. No. 3). Eighty grams of the liquor involved 41.7 g. formamide, 19.3 g. ammonium carbamate*, 1.1 g. iron and 8.9 g. urea**, among which urea was felt as promising the accelerating effect. The effect was actually realized (Exp. No. 4) and the accerelating action of the reaction product may be ascribed to urea.

TABLE I

EFFECT OF THE REACTION PRODUCT UPON FORMATION OF FORMAMIDE

Exp.*	NH_3	Additive	Initial Pres. (room temp.)	End Pres. (room temp.)	Gas after Reaction		Increase in $HCONH_2$
					CO	H_2	
	g.	g.	kg./cm²	kg./cm²	%	%	g.
No. 1	80	$HCONH_2$ 45	117	110	73.0	21.2	≒0
No. 2	80	Powder 35 $HCONH_2$ 45	130	116	69.8	21.2	≒0
No. 3	80	Liquor 80	115	77	51.8	39.6	27
No. 4	80	Urea 25 $HCONH_2$ 45	115	81	60.8	29·4	31.3

* All the experiments were conducted for five hours, at 175–185°C.

Summary

Iron pentacarbonyl has been found to react with ammonia under high pressure of carbon monoxide at temperatures higher than 150°C, to result in a stable powder usually having the practical composition $Fe_2(CN)_4(CO)(NH_3)_4$. In a particular case of the reaction the composition tends to increase in (CO) but decrease in (NH_3), till it attains the composition $Fe_2(CN)_4(CO)_2(NH_3)_3$.

The crude powder is insoluble in most of solvents, and can not therefore be further purified by recrystallisation, while a potassium salt of the complex anion has been crystallized from its caustic potash solution, in yellow fine prismatic crystals, which have appeared to have the composition $K_2(Fe(CN)_4(CO)(NH_3))\cdot 1.5H_2O$. Considering this composition in conjunction with that of the crude powder, the powder seems to consist of a complex anion $(Fe(CN)_4(CO)(NH_3))^{2-}$ and a complex cation $(Fe(NH_3)_3)^{2+}$.

Besides this compound having a different chemical composition from those found by J. A. Müller and thereafter by W. Hieber et al., its manufacturing procedure is characterized by the use of iron pentacarbonyl and ammonia as the starting materials.

The product obtained by the reaction of iron pentacarbonyl and ammonia under high pressure of carbon monoxide has been found to accelerate markedly the formation of formamide from carbon monoxide and ammonia. The product comprises powder and brown liquor, and further the liquor consists of formamide, ammonium carbamate, urea and a minute quantity of an iron salt, among which urea seems most effective for the acceleration.

Government Chemical Industrial Research Institute, Tokyo

Synthesis of 4-Methoxycarbostyril

By Yuriko TANAKA

(Received July 25, 1955)

4-Methoxycarbostyril which had not yet been synthesized by reliable methods was synthesized by the following unambiguous method, as an intermediate product for synthesizing a certain natural product.

4-Nitroquinoline 1-oxide (II), given by nitration of quinoline 1-oxide (I) with potassium nitrate, was boiled with sodium methylate to convert to 4-methoxyquinoline 1-oxide (III). The synthetical methods and the structure proofs of (II) and (III) were previously worked out by Ochiai[1]. Henze[2] had reported that treatment of quinoline 1-oxide (I) with benzoyl chloride and potassium hydroxide gave carbostyril (V). Henze's procedure was confirmed by the author, and by the application of his method to 4-methoxyquinoline 1-oxide (III), 4-methoxycarbostyril (IV) was obtained as colorless needles, m.p. 257°.

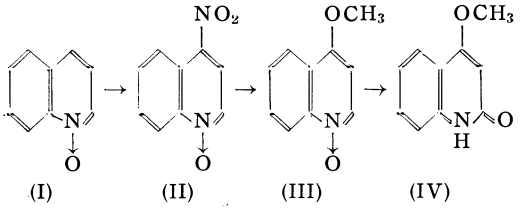

(I) (II) (III) (IV)

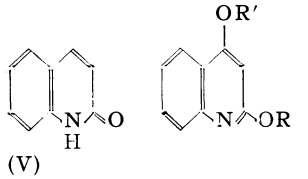

(V)

(VI) R=R′=H
(VII) R=CH_3, R′=H
(VIII) R=R′=CH_3

It was soluble in 10% aqueous sodium hydroxide and in 20% hydrochloric acid when warmed. It gave negative ferric chloride test and no reaction occurred when boiled with acetic anhydride.

There are three reports concerning the synthesis of 4-methoxycarbostyril; Meyer and Heimann[3] obtained a compound, m.p. 271°, and Naito[4], another, m.p. 174–176°. The identity of both compounds is ambiguous because of the lack of structure proof. Arndt, et al.[5] reported recently that a monomethoxy compound, m.p. 257°, was obtained from 2,4-dihydroxyquinoline (VI) by treatment with diazomethane. They deduced that this compound must be 4-methoxycarbostyril (IV) but not 4-hydroxy-2-methoxyquinoline (VII) from the fact that mild hydrolysis of 2,4-dimethoxyquinoline (VIII) gave the same monomethoxy compound, m.p. 257°, and that in this case a methoxyl group at the 2-position is hydrolysed more easily than one at the 4-position[6]. On the other hand, it leaves no doubt that the structure of the compound, m.p. 257°, obtained by the author, is (IV), considered from the synthetical course of the author. Arndt and the author made mixed melting point determination individually. Both specimens showed m.p. 257° and both were unchanged by admixture. In view of this there is no doubt about their identity.

Experimental[7]

Quinoline 1-oxide (I)[1].—To 10 g. of quinoline in 244 ml. of glacial acetic acid was added 16 ml. of 30% hydrogen peroxide. The mixture was heated at 70° in a water bath for eight hours. The solvent was removed at reduced pressure and to the residue was added saturated aqueous sodium carbonate to make the solution alkaline. This alkaline solution was extracted with chloroform. A viscous syrup was obtained by removal of the solvent and solidified on standing. It was broken up under ether, filtered, and washed with ether, m.p. 45–50°. Yield 10 g. Pure quinoline 1-oxide dihydrate; m.p. 60–62°, b.p. 171–172°/4 mm.

4-Nitroquinoline 1-oxide (II)[1].—The crude product obtained above was dissolved in 24 ml. of conc. sulfuric acid. To this solution was added 7 g. of potassium nitrate. The mixture was heated at 70° in a water bath for three hours. On cooling, the reaction mixture was poured with stirring into 500 ml. of ice water. The yellow product was collected on a filter, washed successively with water, dilute aqueous sodium carbonate and finally with water. The solid was dried to give 8 g. of material, m.p. 152°. Recrystallization from acetone gave yellow needles, m.p. 154°.

4-Methoxyquinoline 1-oxide (III)[8].—To 0.65 g. of sodium metal dissolved in 250 ml. of absolute methanol was added 5 g. of 4-nitroquinoline 1-oxide. The solution was heated for 4.5 hr. in a water bath and the solvent was removed. Water was added and the product was extracted with chloro-

1) E. Ochiai, *J. Org. Chem.*, **18**, 534 (1953).
2) M. Henze, *Ber.*, **69**, 1566 (1936).
3) A. Meyer and P. Heimann, *Compt. rend.*, **203**, 335 (1936). See also Ref. 5).
4) Naito, *J. Pharm. Soc. Japan*, **67**, 144 (1947).
5) F. Arndt, L. Ergener and O. Kutlu, *Chem. Ber.*, **86**, 951 (1953).
6) F. Arndt and L. Loewe, *Chem. Ber.*, **84**, 319 (1951).
7) All melting points were un-corrected.
8) E. Ochiai, et al., *J. Pharm. Soc. Japan*, **63**, 265 (1943).

form. The solvent was removed and the residue was poured in a dish. It soon solidified. The solid was triturated with ether to give colorless pillars, m.p. 54–55°, yield 3.5 g. (76%).

4-Methoxycarbostyril (IV).—To a solution of 4.6 g. of sodium hydroxide in 180 ml. of water was added 7 g. of 4-methoxyquinoline 1-oxide. Benzoyl chloride (7 ml.) was added dropwise with vigorous stirring. The thick white solid thus obtained was collected on a filter, washed with dilute aqueous sodium hydroxide and water. The yield of colorless solid, m.p. 251–253°, was 3 g. (43%). Three recrystallizations from methanol gave an analytical sample as colorless needles, m.p. 257°. No depression in melting point was observed on admixture with the specimen received from Prof. Arndt.

Found: C, 68.03; H, 5.06; N, 7.99. Calcd. for $C_{10}H_9NO_2$: C, 68.55; H, 5.18; N, 7.99.

The author wishes to thank Prof. F. Arndt for sending his sample and also making mixed melting point determination. This research was supported by a Grant-in-Aid from the Ministry of Education.

Department of Chemistry, Faculty of Science, Tokyo Metropolitan University, Tokyo

Studies on the Cold-Drawing of High Polymers (Part I). The Quasi-Static Drawing of Polycapramide. I. The Temperature Dependencies, the Softening Temperature and the Second-order Transition Point*

By Hirosuke YUMOTO

(Received July 20, 1955)

Introduction

The phenomenon of cold-drawing observed on polymeric substances is important for manufacturing synthetic fibres, e.g. polyamaide, polyester, polyethylene, afterchlorinated polyvinylchloride etc., because their mechanical properties are improved markedly by drawing. Even in the solidified state below the softening temperature, they can be elongated extremely beyond the yield point toward rupture. Such a phenomenon is also a very interesting problem on the chemical physics of high molecular substance. About the mechanism[1-7] of this phenomenon several opinions have been known, but their fundamental proposals are different from each other. None of them are sufficient to interpret the experimental facts, and the principal key of mechanism is considered not to have yet been grapsed. The main and ultimate objects of this study are to discover the general mechanism of cold-drawing which can interpret the experimental facts extensively and to give instructions for the manufacturing application.

The comprehensive experiments of drawing at the various conditions have been attempted about polycapramide and the elongation-stress curves of melt spun unstretched polycapramide fibre have been investigated as the first step. The following factors are concerned in the behavior of drawing, 1) the temperature, 2) the adsorbed water (also plastisizer in wider sense), 3) the rate of drawing, and 4) the microstructure (e.g. the heat-treatment or various operations at the time of spinning). It is necessary to investigate each factor separately. As the development of heat is accompanied by drawing, if the rate of drawing is large, the unevenness of temperature is caused in regard to time and space so that temperature and humidity cannot be kept constant. Then firstly the isothermal behaviors have been studied at the quasi-static deformation, where the rate of drawing is very small and further temperature and humidity are kept constant. In order to experiment at any chosen temperature and humidity below 100°C, the test materials must be completely isolated from the open atmosphere. The dependencies on temperature at completly dried state (R.H.

* Presented at the symposium on polymer science of the Chemical Society of Japan in Nagoya, November 11, 1954.

1) V. W. Broser, K. Goldstein and H. E. Krüger, *Kolloid-Z.*, **106**, 187 (1944).

2) C.W. Bunn and T.C. Alcock, *Trans. Faraday Soc.*, **41**, 317 (1945).

3) W.M.D. Bryant, *J. Polymer Sci.*, **2**, 547 (1947).

4) F.H. Müller, *Kolloid-Z.*, **115**, 118 (1949), ibid., **126**, 65 (1952).

5) F.H. Müller and K. Jäckel, *Kolloid-Z.*, **129**, 145 (1952); *Makromol. Chem.*, **9**, 97 (1953).

6) I. Marshall and A.B. Thompson. *Nature*, **171**, No. 4340, 38 (1953); *Proc. Roy. Soc.*, **221A**, 541 (1954).

7) K. Jäckel, *Kolloid-Z.*, **137**, 130 (1954).

0%), the observed singular temperatures, and the discussions about them are described in this paper.

Measurement of the Elongation-Stress Curves

The measuring apparatus for the elongation-stress curves are shown in Fig. 1. In all cases the stress was measured with a cantilever equipped with the electrical strain-gauge[8,a]; the strain of cantilever was indicated as the change of the electrical resistance of the strain-gauges. The stress subjected to lever was found through the calibration indicating the relation between the stress of cantilever and the electrical resistance of the gauges. The observational error was about ±0.5 g. (2–5%). The elongation of the test material was measured with the cathetometer.

Fig. 1 (A) is the apparatus used for the measurement below 100°C where the test material must be isolated from the open atmosphere in order to keep the water adsorption constant; the humidity in the container was controlled with phosphorus pentoxide or aqueous solution of sulphuric acid. As the uniformity of temperature between strain gauges which are fixed on both faces of the cantilever is severely demanded in order to measure the stress correctly, the container is heated through a jacket of water[b]. The outside lever, held with the cathetometer, is linked to the inside cramp of the test material with the glass rod; at the path of this rod the container is sealed with mercury or liquid paraffine in the manner shown in Fig. 1 (A).

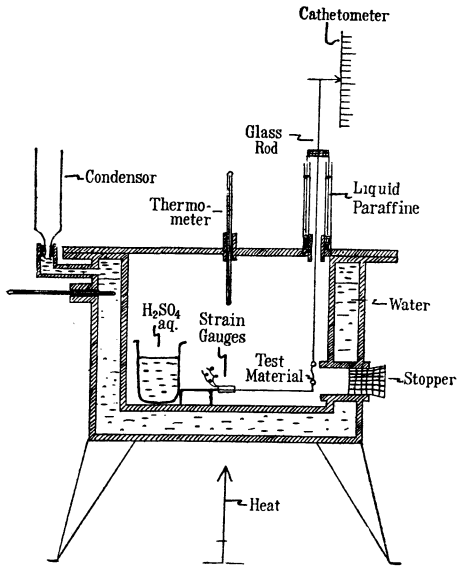

Fig. 1 (A). The apparatus for measuring the elongation-stress curves.

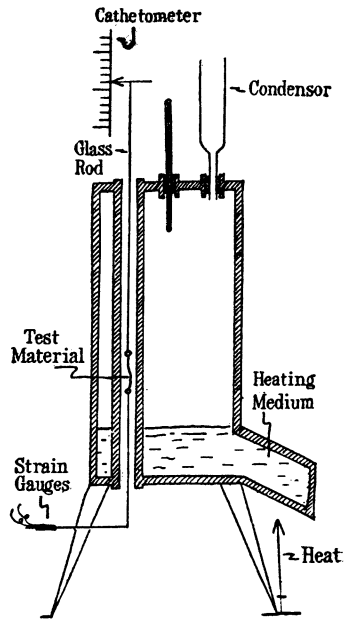

Fig. 1 (B)

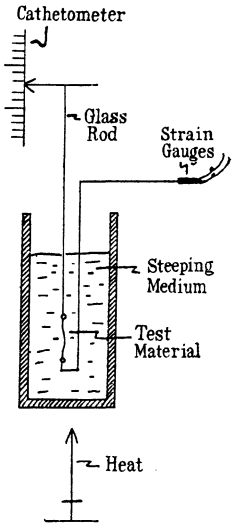

Fig. 1 (C)

Fig. 1 (B) is the apparatus used for the measurement above 100°C where sealing is not necessary because of the slight effect of the atmospheric humidity. As the effect of temperature is larger at higher temperature, the specimen is heated at a constant temperature through the medium of vapor of some appropriate boiling organic liquid.

Fig. 1 (C) is the apparatus used for the measurement in which the test material is steeped in the liquid (e.g. water)[c].

The test materials were 60.0 denier (ϕ 0.086 mm.) polycapramide (nylon 6) unstretched semi-dull mo-

8) H. Hindman and C. M. Krook, *Text. Res. J.*, **15**, 233 (1945).

a) The zero-method measuring was used.

b) For the stability of adhesion of the strain gauge, Bakelite A was used as the adhesives and baked at 120-130°C for thirty minutes.

c) This apparatus was not used for measuring in this paper (Part I), but used for measuring in following papers.

nofilament containing 1–2% caprolactam monomer and oligomers. They were spun by only chilling (without water) from the chips whose degree of polymerization was about 100. On rapid cooling from the melt, the mesomorphous state called α-form[8], which is stable at a higher temperature, is frozen at room temperature without transformation into the crystalline state called β-form which is stable at a lower temperature.

The original sample was 1.50 cm. in length and was manually stretched step by step until breaking[d]. Three minutes after each step, the stress was measured. On account of the structural elements of the much ratarded relaxation in polymer, the correctly static experiment is practically impossible. Persuing the stress relaxation curve after stretching of any extent, it was observed that after three minutes the rate of stress relaxation became much smaller: then the elapsed time of three minutes was chosen for convenience; therefore it can be conventionally considered that such measuring procedure reveals the quasi-static behavior. As the stretching rate is sufficiently small to disperse the heat generated by stretching, such a deformation is assumed to be isothermal.

When the experimental temperature is high, the effect of heat-treatment may be expected to occur. Therefore it must be considered how many minutes are spent till the start of the stretch since the temperature of the specimen has attained to the experimental temperature, where the stretch is to be excuted. The next test was made to examine such effect. Stretching was started either fifteen or sixty minutes later since the specimen is brought to the experimental temperature of 114°C, but the distinctness of behavior between both cases was not observed. In case of these experiments, stretchings were always started thirty minutes later after the setting of the specimens in the container, the temperature of which had been previously kept at the measuring temperature.

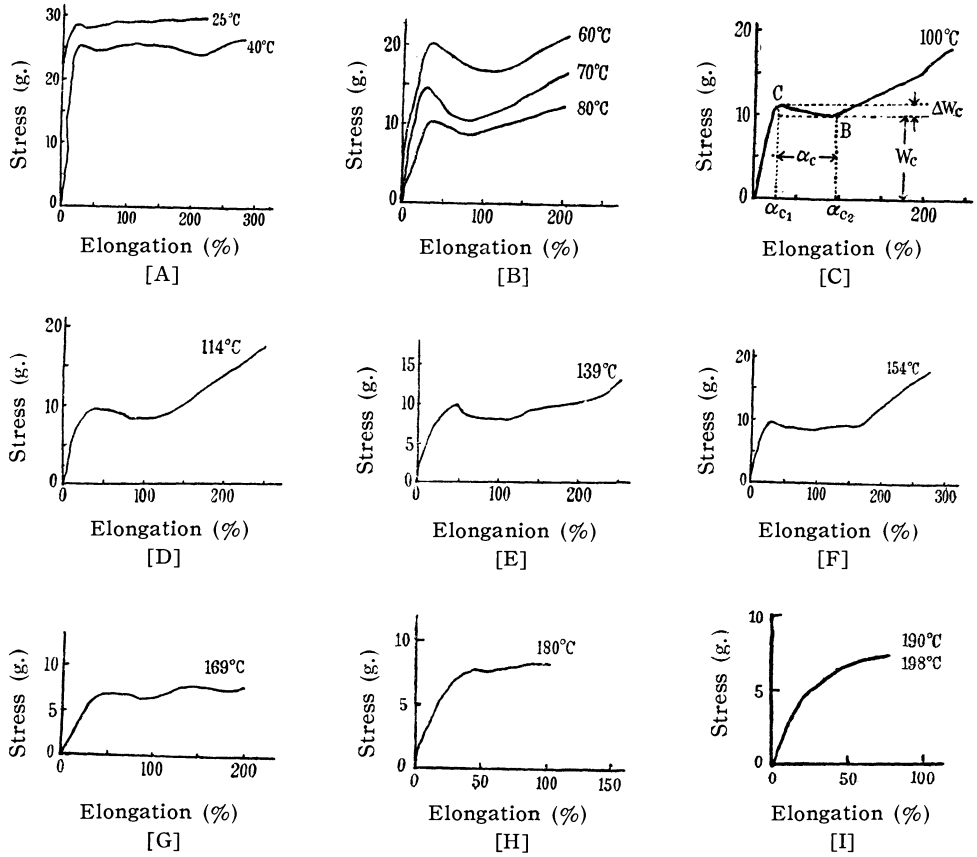

Fig. 2. [A]-[I] The elongation-stress curves of polycapramide at various temperatures in completely dried state.

9) R. Brill, *Z. Phys. Chem.*, B53, 61 (1943); *J. Prakt. Chem.*, **161**, 49 (1942); K. Fuchino and A. Okada, *Scientific Reports of Toyo Rayon Co.*, No. **13**, 163 (1949) (in Japanese).

d) When the specimen was elongated from initial (1.50 cm.) to 2.30 cm., from 2.30 cm. to 5.00 cm. or from 5.00 cm. to rupture, the extent of stretching per each step was 0.10 cm., 0.30 cm., or 0.50 cm. respectively. Shortening the stretched extent per one step, the similar curves were obtained. This procedure was adopted but only in order to save the time and investigate closely the important portion of the curve. The examples where the stress was measured at the constant rate of elongation shall be described in a subsequent paper.

The Results of Measurement

The quasi-static elongation-stress curves obtained at the R.H. of 0% and from the room temperature to 200°C are shown in Fig. (A)–(I).2 Below 40°C, the randomness in each of the measurings is large and breaking sometimes happens on the way of stretching and the curves are always zig-zag. (The zig-zag points are smoothed in Fig. 2.) Above 60°C, all curves are smooth and the reproducibilities are excellent[e].

How to define the cold-drawing is thought to have not yet been established. From the standpoint of the fiber manufacturing application the author will temporarily regard it as the process where the permanent several hundreds per cent elongation and the work hardening phenomenon with the increment of molecular orientation occur by stretching. But if one accepts such a definition the phenomenological peculiar feature of the cold-drawing should be only quantitatives, that is to say, the permanent elongation is particularly large. When stretching is carried out, the state of coexisting of two phases, stretched and unstretched, occurs in most cases; and the necking appears at the boundary of two phases. In such a case the unstretched phase transforms into the stretched one with elongation and during this state the stress stays almost constant as if the liquid solidifies at a constant temperature. But the cold-drawing is an irreversible process and is profoundly distinct from the reversible process of the solidification which can be treated with the conventional thermodynamics. F. H. Müller and K. Jäckel[5,7] have defined the cold-drawing by the coexistence of two phases discriminating it from the ordinary drawing. Stretching polycapramide in water, such a coexistent state does not appear until breaking; the whole system is uniformly elongated. (The details shall be mentioned in the next paper.) However, in spite of the permanent several hundreds per cent elongation and the orientation of molecules, such drawing is not said to be the cold-drawing from the standpoint of the Müller-Jäckel's definition. The definition can be established by determining the general mechanism[10] of drawing which shall be described in a subsequent paper. Nevertheless this coexistent state is quite a characteristic feature so that it is requisite to take close consideration upon it.

The coexistence of the two phases (necking) corresponds to the curious shape of elongation-stress curve. The relation between the necking and the shape of curve is illustrated by Fig. 2 (C) for example; it is apparently observed that from the origin to the point C only unstretched phase, from the point B to breaking only stretched phase, and between points C and B both phases are found. Once the stretched phase appears from the unstretched phase, the stress decreases a little (gradually[f] in case of polyamide). And then as far as both phases coexist, the stress si almost kept constant. Once the unstretched phase disappears, the stress begins to increase sharply again. For the present, assuming the difference of stress (ΔWc) between the points C and B as the additional stress for the formation of the necking, the stress at B (Wc) is taken as the stationary stress for the proceeding of the necking. The number of neckings is generally one or two.

Smoothing the obtained curves below 40°C, ΔWc are possibly considered to be almost zero. With the rising of the temperature, ΔWc increases to maximum 4–5 g. at 70°C, and decreases to almost constant value 1–2 g. from 80°C to about 170°C, and then decreases to zero again.

The stationary stress for the proceeding of the necking (Wc), the elongation region in which the necking exists (α_c), and the additional stress required for forming the necking (ΔWc) are respectively plotted against the temperature in Figs. 3, 4 and 5. The stress and elongation at breaking,

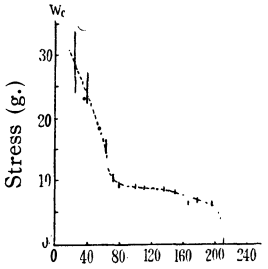

Fig. 3. The yield stresses at various temperatures.

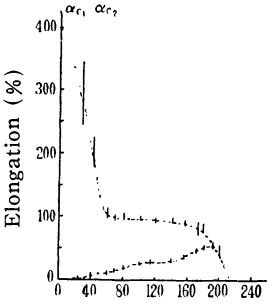

Fig. 4. The two phases coexisting regions of elongation at various temperatures.

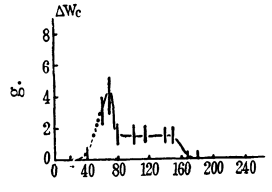

Fig. 5. The additional stresses for formation of the necking at various temperatures.

e) The times of measurement are three in the case of better reproducibility and from five to ten in the case of worse reproducibility.

10) H. Yumoto, presented at the symposium on rheology in Tokyo, June 3, 1955.

f) The stress once decreases gradually in the case of polyamide or afterchlorinated polyvinylchloride, but sharply in the case of polyethyleneterephthalate.

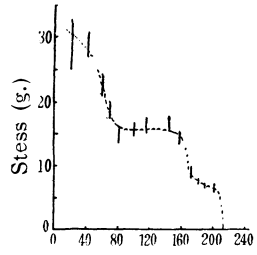

Temperature (°C)

Fig. 6. The stresses to rupture at various temperatures.

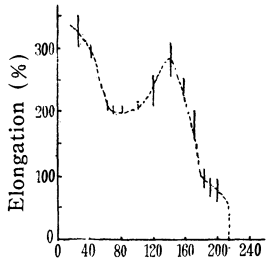

Temperature (°C)

Fig. 7. The elongations to rupture at various temperatures.

which have generally large values of randomness, are plotted aginst the temperature in Figs. 6 and 7. In these figures the length of lines at the positions of the plots indicates the magnitude of randomness.

In all these figures the singular point is explicitly found at 70–80°. Considering that the zigzag unevenness in the obtained elongation-stress curve is much smaller above this temperature than it is below this temperature as previously stated, it is probably the so-called polymer's second-order transition temperature. Because the melting point (68–70°C) of caprolactam monomer, about 1% or less of which is contained in the test materials, is near this temperature, the effect of this monomer should not be neglected. The lactam monomer free test material which was prepared by extracting it with water or benzene for seven days at room temperature, showed the same value of *Wc* with that of untreated materials. It is concluded from this result and the humidity effect which shall be described in the next paper that this singular point has no relation to the melting point of caprolactam monomer which is contained.

Another singular point, not so clear as at 70–80°C, appears in each figure at 170–180°C. Practically above this temperature no maximum or minimum is found in the elongation-stress curves. This will probably be thes oftening point, which will be discussed in the following section.

Furthermore one may find the maximum near 140°C in Figs. 6 and 7. But the singularity at this temperature does not appear in other figures; therefore this singularity is assumed to be related only to the behavior toward rupture.

Below 40°C the necking sometimes remains in the broken test material and the milky regions are always observed in the stretched phase. The milky regions are readily produced after the unstretched phase is transformed into the stretched one. Above 40°C no necking remains in the broken test material and the milky regions are not observed until just before breaking. When the milky region is observed under a microscope, for instance, the cloudy bands of 24 μ in length and the transparent bands of 20 μ in length are found alternately in stripes along the specimen of 56 μ in diameter.

Discussion

(1) **The Singularity at 170–180°.**—The singular point at 170–180°C is found in Figs. 3–7, which is conclusively regarded as the statical softening point from the results of the following experiments.

The polycapramide filaments of 0.5 mm. or 00.4 mm diameter, which had been cold-drawn to four times their original length, were steeped in a diphenyl-diphenyl ether bath which was heated with an oil bath (±1°C) and the shrinkages of them were measured with the cathetometer: the results are shown in Table I. Attaining 190°C the breaking through melting or the partial melting occurs (m. p. 220°). These phenomena are not considered to be affected with the steeping media. The experiments in air, where the uniformity of heating is rather incomplete, also showed the similar phenomena at near 190°C.

TABLE I

THE SHRINKAGES OF THE STRETCHED POLYCAPRAMIDE

$\phi = 0.5$ mm.

Temp. °C	Minute	Shrinkage %
150	15	7
170	15	12
190	30	20 (partly melted)
200	15	melted and broken

$\phi = 0.04$ mm.

Temp. °C	Minute	Shrinkage %
120	5	5
150	10	6.5
170	10	11
190	10	melted and broken

Besides, the stability of the pleats, which had been given by ironing for thirty seconds at various temperatures, were examined on polycapramide clothes: the result showed that the pleats bearable to washing with boiling water were obtained by ironing above 180°C. When clothes had been wetted on ironing, the durable pleats were obtained

above 80–100°C. (These values were the temperatures of iron.)

These results show the presence of softening temperature near 180°C, which are considered to be attributed to the macro-Brownian motion of any regions (amorphous) in the polymer[11]. This temperature may be related to the optimum temperature for crystallization, 180°C or 185–200°C, found by K. Kanamaru et al. with the dilatometry[12] or by T. Arai et al. with the electrical conductivity method[18], and the temperature where the premelting anomaly occurs, 170-180°C, found by E. Nagai et al.[13] or by S. Ueno and K. Fuchino[14] as regards the Young's modulus.

(2) **The Singularity at 70–80°C.**—It has been revealed by the measurements about various properties of polymer that a singular temperature much lower than melting point, the so-called polymer's second-order transition point, exists. The examples of the known second-order transition temperatures of polycapramide are exhibited in Table II.

TABLE II

THE SECOND-ORDER TRANSITION TEMPERATURES OF POLYCAPRAMIDE (*Tf*)

	Tf °C	The method of measuring	Reference
I	near 60	dilatometer	12)
II	near 40	ibid.	13)
III	near 30	static Young's modulus of the unstretched yarn	15)
IV	near 60	damping oscillation (dynamic viscosity and Young's modulus	19)
V	40–50	change of tension	17)
VI	50–60	electrical conductivity	18)
VII	70–80	this study	

Considerable differences are apparent in the presented values. This temperature of polycapramide descends with the adsorption of water and such effect is unexpectedly large even in R. H. 10%[11] (cf. Part II). The values from static measurements of the mechanical properties in atmosphere are lower than the value of this study obtained from measuring in completely dried state; this lowering is considered to be due to the above humidity effect. The effect of less than 1% caprolactam monomer contained in polymer is not perceptible in the result of experiments about specimens in which monomer is removed by steeping in benzene for two hundreds forty hours.

The physical interpretation about the polymer's second-order transition seems not to have been completely established. Polyethylene exhibits such transitions at −68°C and 81°C. (m. p. 115°C) The temperature −68°C is considered to be apparently the brittle point, but 81°C interpreted as the premelting anomaly[19]. According to the structural heterogeneity of polymer a few of the transition temperatures can be observed, but anyhow these may be regarded to be based on the micro-Brownian motion in the regions of less orderliness. The singular temperature on the static yield stress of polycapramide at 70–80°C seems to correspond to the higher transition temperature 81°C of polyethylene. Another transition phenomenon on the dielectric constant of polyamide has been found at −40°C[20] corresponding to the lower transition point −68°C of polyethylene. The detailed discussion of the transition phenomenon shall be described in another report.

(3) From the results of these experiments the singlar temperatures are found to be at 70–80°C and 170°–180°C.

The transformation of the crystal structure of polycapramide has been observed to take place between 100–150°C by the X-ray diffraction method[9] or near 120°C by the specific volume method[12]. It is worth noting that the static yield stress exhibits no singularity at this temperature region: it shall be the underlying experimental foundation for considering the mechanism of cold-drawing[10,11]. (cf. Part III). The Young's modulus also exhibits no singularity at this temperature region[14]. For the present, one cannot simply assume the above described maximum of the elongation to rupture near 140°C as the crystal transformation temperature. Besides the singular point at 160°C on the static viscosity measurement[21], and the development of latent heat at 168–173°C on the thermal analysis[22] have been observed. The singularity relating to the transformation of the crystal structure shall be discussed on the subject of the effect of heat-treatment in Part III.

11) H. Yumoto, presented at the 8th annual meeting of the Chemical Society of Japan in Tokyo, April 2, 1955.
12) K. Kanamaru, I. Uematsu and K. Fukuta, *J. Soc. Polymer Sci. Japan*, 7, 4 (1950) (in Japanese).
13) E. Nagai, N. Aine and Y. Konishi, ibid., 8, 407 (1951) (in Japanese).
14) S. Ueno and K. Fuchino, *J. Soc. Text. Cell. Ind. Japan*, 7, 324 (1951) (in Japanese).
15) K. Ishikawa, ibid., 9, 614 (1953) (in Japanese).
16) K. Fijino, H. Kawai and I. Nakano, presented at the symposium on rheology in Tokyo, Dec. 6, 1951.
17) E. Nagai and N. Aine, *J. Soc. Text. Cell. Ind. Japan*, 8, 429 (1952) (in Japanese).
18) T. Arai and Y. Ito, presented at the 6th annual meeting of the Chemical Society of Japan in Kyoto, April 2, 1952.
19) R.F. Boyer and R.S. Spencer, *J. Appl. Phys.*, 15, 398 (1944).
20) T. Kawaguchi, unpublished.
21) K. Fuchino, A. Okada and N. Aine, *J. Soc. Polymer Sci. Japan*, 7, 19 (1950) (in Japanese).
22) Y. Kinoshita, unpublished.

The various mechanisms about the cause of the necking formation by elongation have been supposed[1-7]. Some of them[5,6,7], in which the necking is mainly attributed to the heat generated by stretching, seem to be questionable from the fact that the necking can occur even in the isothermal stretching. The two phase coexisting state of after-chlorinated polyvinylchloride has been treated by Müller with the thermodynamic equilibrium, the van der Waals' equation being applied[4], but on polycapramide such discussion seems to be unreasonable because of the irreversible nature of the process; the stretched specimen cannot shrink to the initial length even if it is heated over the softening temperature. The cause of the necking formation shall be described in the subsequent paper[10].

Conclusion

According to the program in which the comprehensive studies on the cold-drawing of the polymer were intended, the author obtained firstly some informations concerning the effects of temperature upon the drawing of polycapramide. The test material was quasi-statically elongated under the constant temperature in completely dried state, and then the corresponding stress was measured by means of the electrical resistance strain-meter. Polycapramide can not be smoothly elongated below 40°C, but can be smoothly done above 60°C : moreover the reproducibility becomes better above 60°C. The necking appears in course of stretching under the coexistence of unstretched and stretched phases, and during such state the stress (Wc) stays almost constant which is assumed temporarily as the yield stress. For the formation of the necking an additional stress (ΔWc) besides Wc is observed. Plotting the values of Wc, the region of elongation during the state of the two phases coexisting and the stress or the elongation to rupture against temperatures, two singular points are found at 70–80°C and 170–180°C. The former is considered to be seemingly the so-called polymer's second-order transition temperature and the latter to be the softening temperature. At the temperature region where the transformation of crystal is possible, no singularity is observed.

The author wishes to thank Dr. K. Hoshino and Dr. H. Kobayashi who instructed him on studies and permitted the publication and Mr. M. Nakata who collaborated with him on experiments.

Research Department of Toyo Rayon Co. Ltd., Ohe-cho, Minato-ku, Nagoya

On the Thermal Dissociation of Organic Compounds. VIII. The Effects of the Substituents on the Thermal Dissociation of Tri-substituted Ureas

By Teruaki MUKAIYAMA[1], Shoichiro OZAKI and Yasuhiro KOBAYASHI[1]

(Received August 6, 1955)

Introduction

The kinetics of the thermal dissociation of urea and di-substituted ureas in fatty acids[2-5] and alcohols[6] have been studied and, in the present work, the kinetics of the thermal dissociation of tri-substituted ureas in fatty acids and alcohols were studied. The effects of the substituents and those of the solvents on the dissociation of these ureas compared with those of 1, 3-disubstituted ureas are discussed.

The reaction in fatty acids can be followed by measuring the rate of evolution of carbon dioxide (Eq. 3), as the reaction (1) is a rate-determining step. In the case of 1, 1-dicyclohexyl-3-*n*-propylurea in capric acid, for example, the mechanism shown by Eqs. (1)-(3) is considered.

$$(C_6H_{11})_2N-CO-NHC_3H_7 \rightleftarrows C_3H_7N=C=O+(C_6H_{11})NH \quad (1)$$

$$C_3H_7N=C=O+C_9H_{19}COOH \rightleftarrows C_9H_{19}COOCO\cdot NH\cdot C_3H_7 \quad (2)$$

1) Department of Physics and Chemistry, Gakushuin University, Mejiro, Tokyo.

2) T. Hoshino, T. Mukaiyama and H. Hoshino, *J. Am. Chem. Soc.*, **74**, 3097 (1952).

3) Idem, This Bulletin, **25**, 392 (1952).

4) T. Mukaiyama and T. Matsunaga, *J. Am. Chem. Soc.*, **75**, 6209 (1954).

5) T. Mukaiyama, S. Ozaki and T. Hoshino, This Bulletin, **27**, 578 (1954).

$$C_9H_{19}COOCO\cdot NH\cdot C_3H_7 \longrightarrow C_9H_{19}CONH\cdot C_3H_7+CO_2 \quad (3)$$

In alcohols the dissociated isocyanate reacts with the solvent to form urethane.

$$C_3H_7N=C=O+C_3H_5CH_2OH \rightleftarrows C_3H_7NHCOOCH_2C_6H_5 \quad (4)$$

The reaction in alcohols can be followed by measuring the amount of amine formed according to Eq. (1).

Tetra-substituted urea which has no mobile hydrogen atom did not dissociate under the same condition as that of ureas having more than one mobile hydrogen atom.

Experimental

Procedure—The procedure for measuring the rates of dissociation of ureas in fatty acids[2,3,5] and in alcohols[5] have been described previously. On plotting the logarithm of volume of carbon dioxide, ΔY, evolved at regular intervals of time, a straight line was obtained. This indicates a first order reaction rate. The rate constant is given by the gradient of such a plot, as shown in Fig. 1.

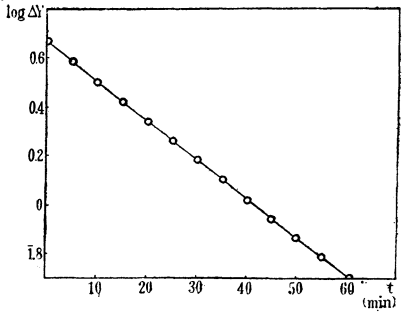

Fig. 1. Thermal dissociation of 1, 1-diisoproply-3-phenylurea in capric acid at 139.5°C.; the plot of log ΔY against time.

Preparation of materials.—*1, 1-Dicyclohexyl-3-phenylurea*: from phenyl isocyanate and dicyclohexylamine, m. p. 174–5°C, recrystallized from ligroin. Found: N, 9.22. Calcd. for $C_{19}H_{28}ON_2$: N, 9.32 %.

1, 1-Dicyclohexyl-3-n-propylurea: from *n*-propyl isocyanate and dicyclohexylamine, m. p. 146°C, recrystallized from ethanol. Found: N, 10.64. Calcd. for $C_{16}H_{30}ON_2$: N, 11.84 %. This is a very hygroscopic substance.

1, 1-Diisopropyl-3-n-propylurea: from *n*-propyl isocyanate and diisopropylamine, m. p. 54–6°C and b. p. 129°/9mm. Found: N, 14.91. Calcd. for $C_{10}H_{22}ON_2$: N, 15.02 %.

1, 1-Diisopropyl-3-phenylurea: from phenyl isocyanate and diisopropylamine, m. p. 118°C, recrystallized from ligroin.

1, 1-Dibenzyl-3-n-propylurea: from *n*-propyl isocyanate and dibenzylamine, m. p. 88°C, recrystallized from ligroin.

1, 1-Dibenzyl-3-phenylurea: from phenyl isocyanate and dibenzylamine, m. p. 124°C, recrystallized from ligroin.

1, 1, 3, 3-Tetra-n-butylurea (*I*): Phosgene was passed through a solution of 12 g. (1/10 mole) of di-*n*-butylamine and 26 g. (1/5 mole) of potassium carbonate for three hours. Then the precipitated potassium chloride was filtered and the solution was extracted with benzene. After drying over anhydrous sodium sulfate, benzene was evaporated and 4 g. of colorless liquid (I) was obtained by distillation boiling at 177–8°C/19 mm. Found: C, 71.30; H, 12.35. Calcd. for $C_{17}H_{36}ON_2$: C, 71.77; H, 12.76 %.

Solvent.—Solvents were purified by the same method as described[5,6] previously. The boiling points for fatty acids and alcohols are as follows: *n*-Capric acid b. p. 121-3°/3.2–3.5 mm.; *n*-caproic acid b. p. 104–6°/16.5–17 mm.; phenylacetic acid b. p. 117°/4.5 mm.; benzoic acid m. p. 122°; glycerol 185°/23 mm.; benzyl alcohol b. p. 114°/38 mm.; ethylene glycol b. p. 120°/20 mm.

The ratio of ureas to solvents were 1 mole: 100 moles. The rate constants of the thermal dissociation of these ureas in fatty acids and alcohols are summarized in Table I. The rates were first order with respect to ureas.

Discussion

As to the effects of the subtituents on the dissociation, it is shown by the present experiment that the rates of dissociation of six ureas decrease in the order,

1, 1-dicyclohexyl-3-phenylurea >
1, 1-dicyclohexyl-3-*n*-propylurea,
1, 1-diisopropyl-3-phenylurea >
1, 1-diisopropyl-3-*n*-propylurea ≫
1, 1-dibenzyl-3-phenylurea >
1, 1-dibenzyl-3-*n*-propylurea

As shown in the above order, as to the 1, 1-substituents, the rates of dissociation decrease in the series,

1, 1-dicyclohexyl > 1, 1-diisopropyl > 1, 1-dibenzyl

and as to the 3-substituents, the rates decrease in the series,

3-phenyl > 3-*n*-propyl

These results can be explained by the proposed mechanism[5], in which ureas dissociate by the double transfer of their proton. Accordingly, the basicity of one nitrogen atom and the acidity of the other nitrogen atom in ureas are dominant factors for the dissociation. As described in the previous report[5], the relative basicity of the nitrogen atom in ureas is represented by the basicity of the corresponding amines. Benzylamine is a weaker base than cyclohexyl and isopropyl amines and, in these six ureas studied, 1, 1-dibenzylureas are less likely to take up

6) T. Mukaiyama, ibid, 28, 253 (1955).

proton from solvent than the other four ureas.

Also, the steric strain considered in four ureas other than 1, 1-dibenzylureas will be favorable for the dissociation which forms less strained component compounds.

These two effects will explain the slower rates in 1, 1-dibenzyl ureas.

Tri-substituted ureas, except in the case of 1, 1-dibenzylureas, dissociate much faster than 1, 3-di-substituted ureas as shown in Tables I and II. In tri-substituted ureas, the basicity of one nitrogen atom corresponds to a secondary amine and the ureas have a stronger tendency to take up a proton from a solvent molecule than 1, 3-di-substituted ureas having a nitrogen atom which corresponds to a primary amine.

As mentioned in the previous reports, the ability of ureas to donate a proton to solvent is also an important factor. In these six ureas, three ureas have a phenyl group on the 3-nitrogen atom and the rest have an *n*-propyl group on the 3-nitrogen atom. The acidity of the former ureas are stronger than the latter because of the +E effect of the phenyl group. Therefore, 3-phenyl substituted ureas are easier to donate a proton to solvent than 3-*n*-propyl ureas. The slower rate in 3-*n*-propylureas than in 3-phenylureas are shown in the experiment.

Another interesting fact is that, tri-substituted ureas dissociate faster in alcohols than in fatty acids in contrast with 1,3-di-substituted ureas. In tri-substituted ureas having more basic nitrogen atoms than in 1, 3-di-substituted ureas, deprotonation by solvent may be a more dominant factor than protonation in the process of dissociation. This would be a reason for the faster rates

TABLE I

THE RATE CONSTANTS OF THE THERMAL DISSOCIATION OF TRISUBSTITUTED UREAS IN FATTY ACIDS AND ALCOHOLS

$k \times 10^3$ (min.$^{-1}$) (at t°C)

Solvents / Ureas	Fatty acids				Alcohols		
	n-Capric	*n*-Caproic	Phenyl-acetic	Benzoic	Ethylene glycol	Benzyl alcohol	Glycerol
1, 1-Dicyclohexyl-3-phenylurea	106±4.0 (139.5)	106 (139.5)	126 (139.5)	28.6 (139.5)	very fast (100)	23.7 (100)	sparingly soluble (100)
1, 1-Dicyclohexyl-3-*n*-propylurea	96.7±0.3	100	115	29.4	fast	18.8	sparingly soluble
1, 1-Diisopropyl-3-phenylurea	36.8	86.3	81	29.3	very fast	19.8	sparingly soluble
1, 1-Diisopropyl-3-*n*-propylurea	93.5±2.7	37.6	34.5	25.0	20.3	17.8	sparingly soluble
1, 1-Dibenzyl-3-phenylurea	4.58±0.08	4.33	24.5	8.0	21.6 (150)	10.4 (150)	18.4 (150)
1, 1-Dibenzyl-3-*n*-propylurea	3.06±0.46	9.9	23.3	7.9	29.9 (150)	0.54 (150)	17.0 (150)

TABLE II

THE RATE CONSTANTS OF THE THERMAL DISSOCIATION OF 1, 3-DI-SUBSTITUTED UREAS IN FATTY ACIDS[5] AND ALCOHOLS[5]

$k \times 10^3$ (min.$^{-1}$) (at t°C)

Solvents / Ureas	Fatty acids				Alcohols		
	n-Capric	*n*-Caproic	Phenyl acetic	Benzoic	Ethylene glycol	Benzyl alcohol	Glycerol
1, 3-Diethylurea	26.5 (155)	26.5 (155)	28.6 (155)	10.7 (155)			
1, 3-Di-*n*-propylurea					11.1 (174.8)	21.0 (175.1)	23.0 (175.1)
1, 3-Diisopropylurea	30.8	26.1	48.6	9.67	35.2 (175.6)	30.4 (175.2)	31.6 (175.2)
1, 3-Di-*n*-hexylurea	32.6	36.5	21.0	6.59			
1, 3-Dicyclohexylurea					26.7 (175.9)	19.8 (175.2)	sparingly soluble

for dissociation of tri-substituted ureas in alcohols than in acids which are very weak bases. However, less basic tri-substituted ureas, as in 1, 1-dibenzylureas, dissociate faster in fatty acids than in alcohols as in 1, 3-di-substituted ureas.

Tetra-substituted ureas, such as 1, 1, 3, 3-tetra-*n*-butylurea, which do not have a mobile hydrogen atom can not be formed by the addition reaction. These ureas do not react under the same condition as that of urea and mono-, di- and tri-substituted ureas which are formed by the addition of two component compounds.

By the result, the bimolecular mechanism of the direct attack of solvent on ureas as shown in Eq. (5) is denied.

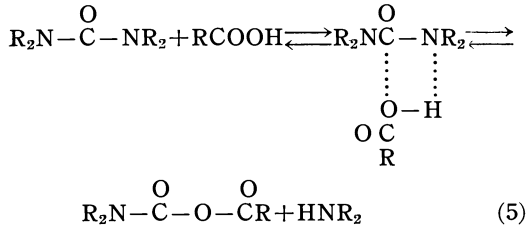

And it can be emphasized that the dissociation of ureas proceeds by the proposed mechanism in which the double transfer of their protons is involved.

Summary

The rate constants of the thermal dissociation of tri-substituted ureas in fatty acids and alcohols were determined. It was shown that tri-substituted ureas dissociate faster than 1, 3-di-substituted ureas. In tri-substituted ureas, the rates in alcohols are faster than in fatty acids in contrast with 1, 3-di-substituted ureas.

Tetra-substituted ureas which are not formed by the addition reaction do not react under the same condition with tri-substituted ureas.

The bimolecular mechanism for the dissociation of ureas involving the direct attack of one solvent molecule on urea was denied.

The authors express their hearty thanks to Professor T. Hoshino for his frequent helpful advice throughout the course of this experiment.

Laboratory of Organic Chemistry,
Tokyo Institute of Technology,
Tokyo

On the Thermal Dissociation of Organic Compounds. IX. The Urea Linkage (1,3-Di-substituted Ureas in Alcohols)

By Teruaki MUKAIYAMA and Yasuhiro FUJITA

(Received August 6, 1955)

Introduction

The kinetics of the thermal dissociation of substituted ureas in alcohols have been studied[1] and in the case of 1, 3-dibenzylurea in benzyl alcohol, for example, the mechanism shown by Eqs. (1) and (2) was suggested.

$$C_6H_5CH_2HNCONHCH_2C_6H_5 \rightleftharpoons C_6H_5CH_2N=C=O+H_2NCH_2C_6H_5 \quad (1)$$

$$C_6H_5CH_2N=C=O+HOCH_2C_6H_5 \rightleftharpoons C_6H_5CH_2HNCOOCH_2C_6H_5 \quad (2)$$

As described in the previous report, when urea is reacted in a large excess of alcohol, the equilibrium between urethane and isocyanate—alcohol in Eq. (2) is in favor of the right side of the reaction and urethane is obtained in good yields. Therefore, if the reaction (1) is the rate-determining step, one can measure the rate of dissociation of urea by determining the amount of amine formed according to Eq. (1).

In the present experiment, the rate constants of the thermal dissociation of seven 1, 3-di-substituted ureas in alcohols have been determined and the effects of the solvents and those of the substituents on the dissociation reaction are discussed.

1) T. Mukaiyama, This Bulletin, 28, 253 (1955).

Experimental

Materials.—*1,3-Di-n-propylurea* and *1,3-di-n-amylurea* were prepared from corresponding iscoyanate and water.

1,3-Di-n-heptylurea, *1,3-diisopropylurea*, *1,3-di-isobutylurea* and *1,3-dicyclohexylurea* were prepared from corresponding amines and phosgene in aqueous potassium carbonate.

1,3-Di-t-butylurea was prepared from *t*-butyl alcohol and urea.

The melting point and the solvent used for recrystallization of these ureas are summarized in Table I.

TABLE I

Ureas	m.p. (°C)	Solvent
1,3-di-*n*-propyl-	105	ligroin
1,3-di-*n*-amyl-	84	ligroin
1,3-di-*n*-heptyl-	91	ligroin
1,3-diisopropyl-	192	ligroin
1,3-diisobutyl-	135	70% aqueous ethanol
1,3-dicyclohexyl-	227	70% aqueous ethanol
1,3-di-*t*-butyl-	248	80% aqueous ethanol

The following alcohols were used: benzyl alcohol, b.p. 114°C/38 mm.; ethylene glycol, b.p. 120°C/20 mm.; glycerol, b.p. 185°C/23 mm.:

Procedure and analysis.—The experimental procedure was essentially that used in the earlier investigation[1]. The amount of amine produced in any reaction system was determined by titration with 0.1N hydrochloric acid, back-titration being carried out with 0.1 N sodium hydroxide using methyl red as indicator.

The rate constants for the thermal dissociation of ureas at temperature near 175°C were determined under the following conditions:

(a) 1,3-Di-*n*-propylurea (1 mol.) in benzyl alcohol (100 mol.), given as an example of a typical run: Fig. 1. The rate constants were obtained by Guggenheim's method[2].

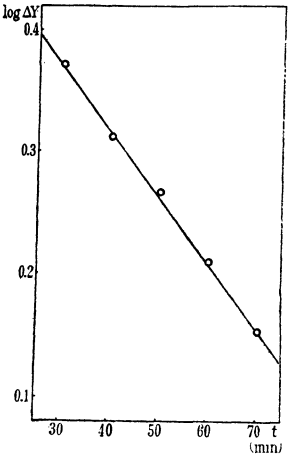

Fig. 1. Thermal dissociation of 1,3-di-*n*-propylurea in ethylene glycol at 174.8°C; the plot of log ΔY against time.

(b) Ureas (1 mol.) in alcohols (100 mol.)—The ureas were 1,3-di-*n*-propylurea, 1,3-di-*n*-amylurea 1,3-di-*n*-heptylurea, 1,3-diisopropylurea, 1,3-diisobutylurea, 1,3-dicyclohexylurea and 1,3-di-*t*-butylurea and the alcohols were benzyl alcohol, ethylene glycol and glycerol. The results are shown in Table II. The rates were first order with respect to ureas.

2) E.A. Guggenheim, *Phil. Mag.*, 2, 538 (1926).

TABLE II

THE RATE CONSTANTS OF THE THERMAL DISSOCIATION OF 1,3-DISUBSTITUTED UREAS IN ALCOHOLS

$k \times 10^2$ (min.$^{-1}$) (t°C)

Ureas \ Alcohols	Benzyl alcohol	Ethylene glycol	Glycerol
1,3-di-*n*-propyl-	2.10 (175.1)	1.11 (174.8)	2.30 (175.1)
1,3-di-*n*-amyl-		2.09 (174.5)	
1,3-di-*n*-heptyl-		1.79 (175.0)	
1,3-dicyclohexyl-	1.98 (175.2)	2.67 (175.9)	sparingly soluble
1,3-diisopropyl-	3.04 (175.2)	3.52 (175.6)	3.16 (175.2)
1,3-diisobutyl-	1.45 (175.2)	1.70 (175.0)	1.50 (175.2)
1,3-di-*t*-butyl-	sparingly soluble	very fast	sparingly soluble

Discussion

The amounts of disscociation of the seven 1,3-di-substituted ureas in these three alcohols increase in the following order,

benzyl alcohol < ethylene glycol < glycerol

However, the rate constants, as measured by the amount of amine produced, of dissociation in these three alcohols are nearly equal. As a typical run, the percentage of dissociated urea in the thermal dissociation of 1,3-diisobutylurea (1 mole) in benzyl alcohol, ethylene glycol and glycerol (100 moles) are shown against time listed in Table III.

TABLE III

THE PERCENTAGE OF DISSOCIATED 1,3-DIISOBUTYLUREA (1 mol.) IN ALCOHOLS (100 mol.) vs. TIME

Solvent	Temperature (°C)	Time (min.) 30	60	90	Rate constant
Benzyl alcohol	175.2	27	39	45	1.45
Ethylene glycol	175.0	35	53	67	1.70
Glycerol	175.2	52	75	89	1.50

A similar result was also found in the case of 1,3-dibenzylurea in these three alcohols[1].

These facts suggest that the velocities of dissociation of urea in alcohols are dependent on the concentration of the hydroxylic group in the solvent alcohols. And it can be reasonably explained by assuming an intermediate complex formed by the interaction between urea and alcoholic hydroxyl groups. The mechanism of dissociation of urea in alcohols is considered[1] as follows,

urea + alcohols $\rightleftarrows$ (urea—alcohols) (3)

$$\text{(urea—alcohols)} \overset{k_1}{\rightleftarrows} \text{isocyanate} + \text{amine} + \text{alcohols} \quad (4)$$

$$\text{isocyanate} + \text{alcohol} \rightleftarrows \text{urethane} \quad (5)$$

$$\text{urethane} + \text{alcohols} \rightleftarrows \text{(urethane—alcohols)} \quad (6)$$

The rate constants of dissociation in these three alcohols are nearly equal; however, except in the case of 1,3-di-*n*-propylurea in ethylene glycol, the rates of dissociation of six 1,3-di-substituted ureas listed in Table II increase in the following order,

benzyl alcohol < glycerol < ethylene glycol

The tendency agrees with that of 1,3-dibenzylurea in alcohols described in the previous report[1] and it may be concluded by the same consideration that, in the process of dissociation of 1,3-disubstituted ureas in alcohols, the solvent acts more effectively as a base to accept a proton from a urea molecule rather than it acts as an acid.

On the other hand, in a strong acid, as in fatty acids, the rates of dissociation of ureas generally increase as the acidity of the solvent acids increases[3]. In a strongly acidic medium, the process of protonation of urea by solvent plays an important role for the dissociation.

As shown in Table IV, the rates of dissociation of 1,3-disubstituted ureas in fatty

TABLE IV

THE RATE CONSTANTS OF THE THERMAL DISSOCIATION OF 1,3-DI-SUBSTITUTED UREAS IN FATTY ACIDS

$k \times 10^2$ (min.$^{-1}$) (at t°C)

Acids	*n*-Butyric	*n*-Caproic	*n*-Capric	Phenyl acetic
1,3-Diisopropylurea	1.79 (139.6)	2.61 (155.0)	3.08 (155.0)	4.86 (155.0)
1,3-Di-*n*-hexylurea	1.24 (139.6)	3.65 (155.0)	3.26 (155.0)	2.10 (154.9)
1,3-Di-*t*-butylurea	3.87 (139.4)	3.93 (155.0)	6.8 (155.0)	fast (155.0)

acids[4] are faster than those in alcohols and it can be concluded that, in these two kinds of solvents, the acidity of the solvent, namely the ability to donate a proton to a urea molecule is an important factor for the dissociation.

As to the effects of the substituents, the rates of dissociation of the seven 1,3-di-substituted ureas studied in this experiment increase in the series,

1,3-di-*n*-propylurea, 1,3-di-*n*-amylurea, 1,3-di-*n*-heptylurea, 1,3-diisobutylurea, 1,3-dicyclohexylurea < 1,3-diisopropylurea ≪ 1,3-di-*t*-butylurea

1,3-Di-*t*-butylurea dissociates most readily and 1,3-diisopropylurea dissociates more easily than the other ureas with *n*-alkyl or cyclohexyl groups.

Generally, the rates of dissociation of 1,3-di-substituted ureas are not so markedly affected by the substituents, but ureas with tertiary and secondary alkyl groups in which the internal strain is considered to be important dissociate more readily. In these two ureas, especially in 1,3-di-*t*-butylurea, the strained structure due to the two bulky substiutents are considered. And, when the urea is heated in alcohol, by the interaction of the solvent alcohol which facilitates the proton transfer, it dissociates very readily into less strained isocyanate and amine.

In addition to the electronic effects, namely the abilities of the two nitrogen atoms in ureas to accept or to donate a proton, mentioned in the previous reports[1,3], the structural effects are also important in determining the reactivity of ureas.

As mentioned above, the dissociation of ureas in alcohols are considered to proceed via the intermediate complex which is formed by one urea and two alcohol molecules.

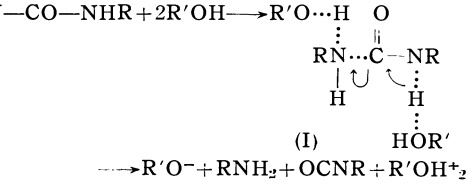

In the state(I), the one alcohol acts as a base to accept a proton and the other acts as an acid to donate a proton at the same time. By the shift of an electron pair, the state (I) dissociates to isocyanate and amine.

As shown in the above mechanism, the dissociation proceeds by the double transfer of the proton. Therefore, ureas act to solvent molecules as a base and acid at the state (I). And the effects of the substituents on the rates of the thermal dissociation of 1,3-di-substituted ureas having the same substituents in 1- and 3-nitrogen atoms are small.

Summary

The rate constants of the thermal dissociation of 1,3-di-*n*-propylurea, 1,3-di-*n*-amylurea, 1,3-di-*n*-heptylurea, 1,3-diisopropylurea, 1,3-diisobutylurea, 1,3-dicyclohexylurea and 1,3-di-*t*-butylurea in benzyl alcohol, ethylene glycol and glycerol were determined.

The effects of the substituents on the thermal dissociation of 1,3-di-substituted

3) T. Mukaiyama and T. Matsunaga, *J. Am. Chem. Soc.*, 75, 6209 (1953).
4) T. Mukaiyama, S. Ozaki and T. Hoshino, This Bulletin, 27, 478 (1954).

ureas was discussed and the effects of the solvents on the reaction was also discussed in comparison with those in fatty acids.

The authors express their hearty thanks to Professor T. Hoshino for his helpful advice throughout the course of this experiment.

Department of Physics and Chemistry, Gakushuin University, Tokyo

Ultraviolet Spectrophotometric Determination of Iron

By Masayoshi ISHIBASHI, Tsunenobu SHIGEMATSU, Yuroku YAMAMOTO, Masayuki TABUSHI and Toyokichi KITAGAWA

(Received July 18, 1955)

In the previous publications,[1,2] an ultraviolet spectrophotometric determination of iron was reported. The method was based on measuring optical densities of the absorption peak at 300 mμ, which may be due to the formation of ferric sulfate complex, and it was necessary to conduct measurement under the constant concentration of sulfuric acid, because the optical densities were affected by the concentration of sulfuric acid.

E. Rabinowitch and W. H. Stockmayer[3] have studied the absorption curves for the ferric perchlorate solutions in the presence of different amounts of OH^-, Cl^- and Br^-, and could separate the absorption curve of free (hydrated) Fe^{3+} ions from that of $Fe(OH)^{++}$ ions. It was observed by A. R. Olson and T. R. Simonson[4] and confirmed by T. H. Siddall and W. C. Vosburgh[5] that an isosbestic point exists for dilute iron (III) perchlorate solutions at about 273 mμ. Recently R. M. Milburn and W. C. Vosburgh[6] have measured optical densities in this region for 10^{-4}, 10^{-3} and 10^{-2}M iron (III) solutions. For each concentration the acidity was varied while the ionic strength was held at constant and it was observed that the isosbestic point at 273 mμ was apparent for the 10^{-4}M solutions, but not for the 10^{-2}M solutions. They took this as confirmatory evidence for the presence of polynuclear species in the 10^{-2}M solutions.

We have studied the absorption curves for the ferric perchlorate solutions (10 p. p. m.) at various acidities and confirmed that two isosbestic points exist at 271 mμ and 223 mμ, and then established a method for spectrophotometric determination of iron in which the absorbancies at this isobestic point have been measured. The proposed method is very convenient and useful, since no reagents are needed except the dilute perchloric acid to dissolve the sample, and almost no attention needs to be given to test the acidity and temperature in the solutions. Applying the proposed method, the purity of iron alloy has been determined by means of differential absorptiometry.

Apparatus

Spectrophotometric measurements were made with a Beckman Quartz Spectrophotometer, Model DU, with 1cm. silica transmission cells.

A Beckman glass electrode pH meter, Model H-2, was used for all pH measurements.

Materials

The stock solutions of iron (III) were prepared as follows.

Ferric perchlorate was formed by dissolving proper amounts of electrolytic iron in perchloric acid (about 4 N), oxidizing by hydrogen peroxide (30%) and evaporating the solution until the crystals appear. After perchloric acid was added to dissolve the deposit, the solution was evaporated again. The procedure was repeated until the solution gave negative test for chloride and iron (II) ions. The violet crystals separated on cooling were filtered with a sintered glass filter and recrystallized twice from distilled water. A stock solution of iron was prepared by dissolving the crystal of ferric perchlorate in water to the concentration of 100 p. p. m. All of the solutions for absorbance measurements were prepared by diluting the required quantity of the stock solution.

1) R. Bastian, R. Weberling and F. Palilla, *Anal. Chem.*, **25**, 284 (1953).
2) M. Ishibashi, T. Shigematsu, Y. Yamamoto, M. Tabushi and T. Kitagawa, *J. Chem. Soc. Jap. (Pure Chem. Sec.)* **76**, 758 (1955).
3) E. Rabinowitch and W. H. Stockmayer, *J. Am. Chem. Soc.*, **64**, 335 (1942).
4) A.R. Olson and T. Simonson, *J. Chem. Phys.* **17**, 1322 (1949).
5) T.H. Siddall and W.C. Vosburgh, *J. Am. Chem. Soc.* **73**, 4270 (1951).
6) R.M. Milburn and W.C. Vosburgh, *J. Am. Chem. Soc.*, **77**, 1352 (1955).

Experimental

The Isosbestic Point.—Fig. 1 shows the absorption curves of the solutions for iron (III) of 10 p. p. m. at various acidities.

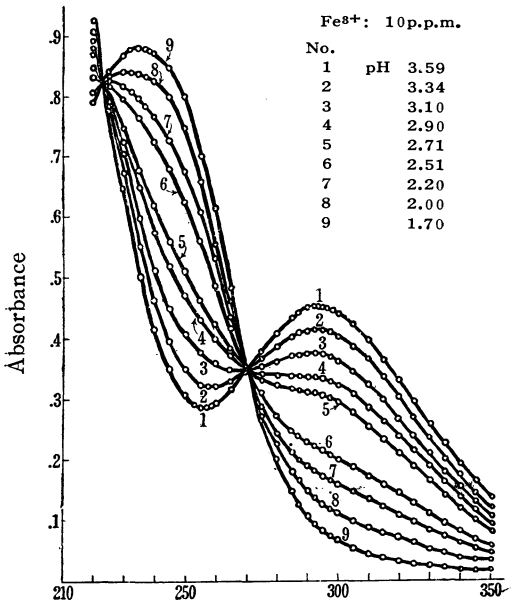

Fig. 1. Absorption curves of ferric perchlorate in aquaous solution at various acidity

Since the acidity could be adjusted by adding a few drops of perchloric acid to a larger volume of the solution, the constancy was held for both the concentration and the ionic strength in each solution. It is found that, with increasing acidity in the solution, the absorption in the region 230 mμ increased, while that of 300 mμ decreased, and there existed two isosbestic points at 223 mμ and 271 mμ.

Further measurements were conducted for the iron solutions (10 p. p. m.) varying concentration of perchloric acid from 1N to 9.5N, and it was found that the band at 238 mμ (curve 9 in Fig. 1) did not suffer any change either in the absorbance or in the position of the peak. As other workers reported, the absorption band with peak at 238 mμ can be considered as belonging exclusively to Fe^{3+}_{aq} ions, and the peak at 295 mμ must be due to $Fe(OH)^{++}$. It will be very useful to utilize this isosbestic point at 271 mμ for the determination of iron (III), since the absorbance is not affected by acidity in solutions. Although the other isosbestic point at 223 mμ is not affected by the acidity either too, it is not adequate for the iron determination, since the interferences of diverse ions and perchloric acid are great in the region of such shorter wave lengths.

Since the isosbestic position might shift by the great variation in the concentration of iron, investigation was made concerning the effects of the content of iron (III) to absorption curve in this region. Differential absorptiometry was applied and the solutions containing 10~50 p. p. m. of iron were used as references.

As shown in Table I, it is found that a variation in iron content from 10 to 40 p. p. m. gave no change in the position of the isosbestic point at 271 mμ, but in the concentrations higher than 50 p. p. m., the isosbestic point was observed to have a tendency shifting to the shorter wave length.

Temperature.—The effects of the temperature for absorbancies were investigated. The solutions

TABLE I

EFFECT OF CONCENTRATION OF IRON TO ISOSBESTIC POSITION

Concentration of ferric solution (p. p. m.)	pH	Reference	Width of slit (mm.)	Absorbancies at 267	268	269	270	271	272	273 mμ
10	2.81	water	0.3	—	0.296	.289	.283	.275	.269	.264
〃	2.61	〃	〃	—	.309	.296	.286	.275	.266	.256
〃	2.40	〃	〃	—	.319	.302	.289	.275	.265	.251
20	2.80	Fe (10 p. p. m.)	〃	—	.334	.311	.293	.274	.256	.239
〃	2.60	〃	〃	—	.361	.329	.303	.275	.253	.229
〃	2.41	〃	〃	—	.377	.341	.309	.276	.240	.220
30	2.80	Fe (20 p. p. m.)	0.4	—	.353	.325	.298	.275	.248	.226
〃	2.60	〃	〃	—	.384	.345	.308	.275	.239	.205
〃	2.40	〃	〃	—	.412	.365	.321	.276	.233	.193
40	2.82	Fe (30 p. p. m.)	0.6	0.385	.358	.328	.298	.272	.247	—
〃	2.62	〃	〃	.440	.398	.353	.310	.271	.229	—
〃	2.40	〃	〃	.496	.442	.381	.322	.271	.214	—
50	2.83	Fe (40 p. p. m.)	0.8	.410	.372	.333	.296	.265	.230	—
〃	2.54	〃	〃	.469	.413	.355	.296	.248	.196	—
〃	2.29	〃	〃	.523	.449	.370	.296	.231	.164	—
60	2.89	Fe (50 p. p. m.)	1.3	,385	.357	.328	.297	.270	.244	—
〃	2.61	〃	〃	.464	.412	.353	.296	.242	.192	—
〃	2.29	〃	〃	.550	.470	.385	.298	.220	.143	—

for measurements were of 10 p. p. m. concentration and pH value was 2.5. Tabe II shows that the

TABLE II
EFFECTS OF TEMPERATURE

Ferric solution (p. p. m.)	Temp. C°	pH	Absorbance at 271 mμ
10	32	2.5	274
〃	28	〃	275
〃	22	〃	274_5
〃	17	〃	274_5
〃	15	〃	274_5
〃	10	〃	274_5

absorbance at 271 mμ is constant at the temperatures in the range from 10° to 30°C. Furthermore it was observed that with rising temperature the absorbance in the region longer than 271 mμ increased, while that of shorter wave lengths decreases. This must be due to the expedited hydrolysis of iron at higher temperature.

Acidity.—From the above experiments, it is shown that the control of acidity in the solutions is almost needless, except when the acidity is so low as to precipitate the hydroxide. It is observed that the absorbance at 270 mμ increases remarkably in the solutions with pH value over 3.5; this may be due to the formation of the colloidal ferric hydroxide. There is no lower limit for the allowable pH value in the solution, but it is desirable to adjust the acidity in the range of pH 2.5–3.5 for more accurate measurement.

Calibration Curve.—The preparation of the standard iron solution was as follows. A 1.002 g. of electrolytic iron (purity 99.8%) was dissolved in 4N perchloric acid. The same procedures of evaporations as the stock solution were conducted until chloride and iron (II) became absent. The resulting solution was diluted to 1 *l* in a volumetric flask with distilled water. First, for the ordinary absorptiometry, the calibration curve was made by measuring the absorbance of the ferric solution in such a concentration as 5, 10, 15 and 20 p. p. m. at 271 mμ, with pure water as reference. Results are shown in Fig. 2 and Beer's law is followed in the range of 0.2–20 p. p. m. of iron. But as the sensitivity in this methods is fairly low as compared with the other spectrophotometric methods for the determination of iron, it is more useful to use in the differential absorptiometry for the determination of higher contents of iron. For this purpose, the solution with 50 p. p. m. iron was used as reference, and the calibration curve was made in such concentrations as 55, 60, 65 and 70 p. p. m. at 270 mμ. Results are also shown in Fig. 2. and Beer's law is followed in the range from 50 to 70 p. p. m. As the reference, concentration higher than 50 p. p. m. of iron can not be used, because it reduces the sensitivity of the spectrophotometer.

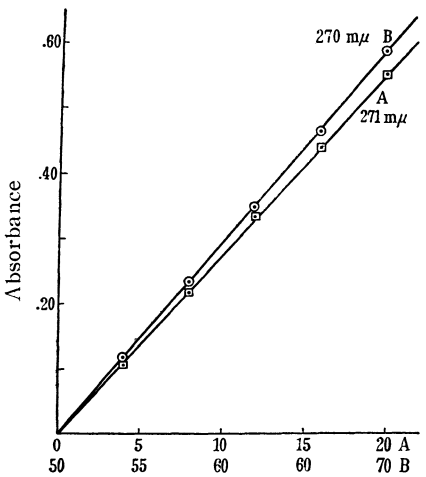

Fig. 2. Calibration curve for iron (III) in aquaous solution.

Effects of Diverse Ions.—A study was made on the effects of several cations and anions. The cations were present in solution as perchlorates and anions as sodium salts. Absorbance measurements were made for the solutions contaiving proper amounts of foreign salt with 10 p. p. m. of iron. The results are presented in Table III. It is

TABLE III
ASBORBANCIES OF DIVERSE CATION WITH 10 p. p. m. Fe^{3+}

Ion	Concentration (p. p. m.)	Absorbance at 270 mμ
Fe^{+++}	10	0.275
Ni^{++}	+1000	0.276
Co^{++}	〃	0.280
Zn^{++}	〃	0.277
Mn^{++}	〃	0.275
Al^{++}	〃	0.277

found that the presence of such cations as Na^+, Ni^{++}, Co^{++}, Zn^{++}, Mn^{++} and Al^{3+} does not interfer at the concentration of 100 p. p. m. In the previous publication,[2] it was reported that the cupric and titanic sulfates in aqueous solution have intense absorption bands in far ultraviolet regions, and considerable absorptions were also obserbed at 270 mμ. in the perchloric acid. Thus the presence of cupric and titanic ions interferes the determination of iron (III); the limit concentration of them is about 10 p. p. m. The presence of anions such as Cl^-, NO_3^-, SO_4^{--} and PO_4^{---} interferes remarkably, but chloride and nitrate ions can be easily eliminated by evaporation.

Determination of Iron in Iron Base Alloy

In order to test the reliability of the proposed method, some iron base alloys were selected as samples. The determination of iron was done by means of differential absorptiometry.

Procedure.—A 200–150 mg. of sample (weighed correctly) was dissolved in 4N perchloric acid by warming on the sand bath. After cooling several drops of H_2O_2 (30%) were added and then evaporated almost to dryness. The evaporation was repeated several times and the residue was dissolved in distilled water, then the solution was tra-

nsferred to a 500 ml. volumetric flask and diluted to the volume with distilled water. After being mixed thoroughly, an aliquot of 20 ml. was pipetted into a 100 ml. volumetric flask and then diluted to the volume with distilled water.

TABLE IV
ANALYSIS OF IRON SAMPLES

Sample	Fe Present		Fe Found	
	%	mg.	mg.	%
Haematite (J. E. S. No. 23)	61.32	4.911	4.922	61.46
			4.915	61.38
			4.915	61.38
			4.908	61.28
			av. 4.915	61.38
Iron (J. E. S. No. 7)	92.22	5.556	5.550	92.13
			5.559	92.28
			5.557	92.21
			5.550	92.13
			av. 5.554	92.20
Iron (J. E. S. No. 12) (low phosphor)	92.46	5.548	5.557	92.62
			5.547	92.44
			5.543	92.83
			5.547	92.44
			av. 5.548	92.46

The absorbance of the above solution was measured at 270 mμ, using an iron solution (50 p. p. m.) as the reference. The results are presented in Table IV, the errors in this method being 0.2–0.3%.

Summary

Absorption has been investigated for the solution of ferric perchlorate at various acidities in ultraviolet region and the existence confirmed of two isosbestic points at 223 mμ and 271 mμ. A method of spectrophotometric determination for iron has been proposed which involves the measurement of absorbance at the isosbestic point. Effects of temperature, acidity and diverse ions have been examined and the purity of iron base alloys has been determined by differential method.

The authors are grateful to Dr. R. Tsuchida for his sueful advice in the interpretation of the absorption spectra.

Department of Chemistry, Faculty of Science, Kyoto University, Kyoto

*Colloid Chemical Studies on Starching Materials. I. Structural Viscosity of Poly-Vinyl Alcohol Solution**

By Masayuki NAKAGAKI and Ayako SHIMAZAKI

(Received August 5, 1955)

As a starching material for clothes, poly-vinyl alcohol has recently been used. The colloid chemical studies interest as from both scientific and practical stand-points. As for the solution of high polymers, it has been already known that the structural viscosity is observed even for fairly dilute solutions. It has also been known that the poly-vinyl alcohol solution has structural viscosity, at least for concentrated solutions. If an anomalous viscosity named as structural viscosity is the result of the viscoelastic properities of the solution, then, it is desirable to separate the observed apparent viscosity into two parts, viscosity part and elasticity part, and to consider, e.g., intrinsic viscosity about the pure viscosity part.

* Presented before the Discussion of Rheology held by the Chemical Society of Japan on June 2, 1955 at Tokyo.

Experimental

As samples of poly-vinyl alcohol, six pure specimens provided by Nippon Gosei Kagaku Kogyo K.K. are used; that is, Gohsenol GH-20, GM-14, GL-05, NH-20, NM-14 and NL-05. In them, G means that the saponification value is 90±2%, and N means that the saponification value is 99–100%. They are white powder. The purity was 98% or better. The mean polymerization degree was determined by viscosity method using Sakurada's equation. About 0.8 g. of the specimen was warmed with 100 cc. of distilled water and dissolved in it and set alone for eight hours. 10 cc. of supernatant solution was put into the Ostwald's viscometer, and viscosity was measured at 20°C. On the other hand, 20 cc. was heated until dry, and the concentration C (g./l.) was measured. Using Sakurada's equation[1]:

1) Sakurada, *J. Chem. Soc. Japan (Engineering Sec.)*, **47**, 135 (1944).

$$[\eta]=2.303\log\eta_r/C$$

$$\log\rho=1.613\log\left(\frac{[\eta]\times10^4}{8.87}\right) \quad (1)$$

the average polymerization degree ρ was obtained. The average polymerization degree was 2,000 for H-20, 1,400 for M-14 and 500 for L-05.

Gohsenols were dried for one hour in an electrical drying oven at 110°C and cooled and kept in deisccator. It is said that four hours' warming at 40–50°C is necessary, in order to dissolve them completely in water. In this paper, however, the following method of dissolution was adopted, considering the practical method of dissolution of starching materials. A specimen weighed accurately was kneaded with a small amount of distilled water, hot water of 90°C was added under constant stirring, and the volume was made up to a nearly necessary amount. This was warmed on a water bath at 90°C for five minutes with continuous stirring. Then the volume of the solution was accurately made up, after it was kept at room temperature to cool. The concentration range measured was 0.2–5.0%.

The structural viscosity was measured with an Ostwald type over-flow viscometer, which was used before by one of authors[2]. It was a vertical type viscometer having a capillary of 21.2 cm. in length and 0.67 mm. in inner diameter. The amount of flow, Q (cc./sec.), was measured for each hydrostatic pressure difference, P (cm. H_2O). For liquids without structural viscosity, Poiseille's law has been verified for this viscometer. As stated in the previous paper, the viscosity coefficient is calculated by the equation,

$$\eta=2.57\times10^{-5}\times P/Q \text{ (g./cm./sec.)} \quad (2)$$

The range of the pressure difference measured was 4–23 cm. H_2O.

As shown in the previous paper, the viscosity coefficient obtained from Eq. (2) shows a linear relation to the reciprocal of the rate of flow, $(1/Q)$, for some solutions having structural viscosity, such as V_2O_5-sol and Hg-sulfosalicylate-sal. For the apparatus used, the linear relation is expressed:

$$\eta=\eta_N+2.57\times10^{-5}\times P_0/Q \quad (3)$$

where η_N(g./cm./sec.) and P_0 (cm.H_2O) are constants. P_0 is thought to be a pressure to destroy the net-work structure in the solution, and corresponds to a yield value. η_N corresponds to a Newtonian viscosity of distroyed structure. η_N depends pronouncedly on the history of the solution, while η_N does not depend on the history.

Results and Discussion

The same structural viscosity as cited above was observed also for poly-vinyl alcohol solution. Fig. 1 is an example of data for 2% solution of NH-20, where the variation of apparent viscosity by the history of solution is shown. For example, a solution used to measure its viscosity has been kept for some days, and again the viscosity is measured. Then a different value is obtained. In the case shown in Fig. 1, it seems that the viscosity gradually increased, but in other cases, the viscosity decreased. Curve 3 was obtained after stirring the sample of curve 2 for thirty minutes at room temperature. The distinct increase of viscosity by stirring was observed.

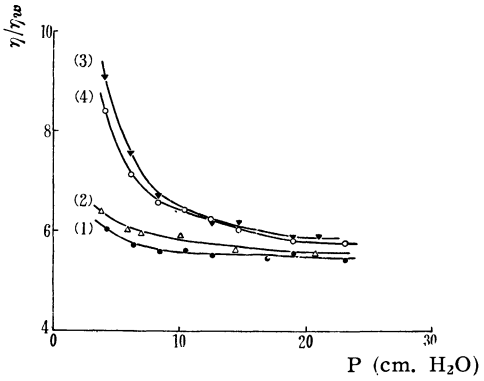

Fig. 1. The stractural viscosity of 2% Gohsenol NH-20. after the preparation of solution: (1) 1 hr (2) 72 hrs: (3) 72 hrs (stirred 30 min.): (4) 96 hrs.

These data are recalculated and plotted in Fig. 2 as a relation between (η/η_w) and and $(1/Q)$. The linear relation of Eq. (3) is certified. Moreover, Fig. 2 shows that the variation of apparent viscosity with the history of the specimen is due to the variation of the apparent yield value, P_0, while the Newtonian viscosity, η_N, does not change. The apparent yield value of the specimen of curve 2 was 0.59 cm. H_2O, which increased to 1.65 cm. H_2O by stirring for thirty minutes as shown in curve 3. This suggests the growth of net-work structure. Anyway, the treatment (e.g. stirring) is more effective than the duration of time.

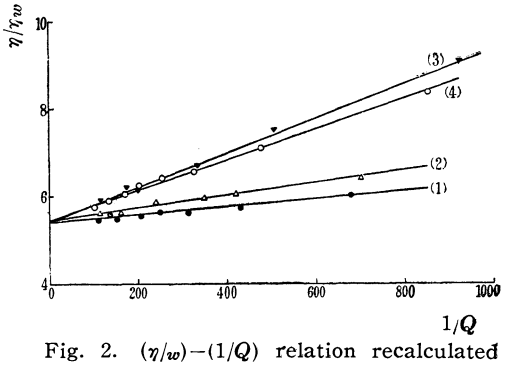

Fig. 2. $(\eta/w)-(1/Q)$ relation recalculated from Fig. 1.

For each Gohsenol specimen, structural viscosity is measured at various concentra-

2) M. Nakagaki and S. Sakata, *Bull. Chem. Soc. Japan*, 27, 548 (1954).

tions. Every data showed the linear relation of Eq. (3). Values of two constants of Eq. (3), Newtonian relative viscosity (η_N/η_w) and apparent yield value P_0, are shown in Figs. 3 and 4. (η_N/η_w) increases monotonously with the increase of concentration, while P_0 shows no definite trend for concentration. This is reasonable, since P_0 is a sensitively dependent quantity on the history of a specimen.

On the viscosity of poly-vinyl alcohol solution, E. Tsuruta and M. Takeda[3] found the following relation:

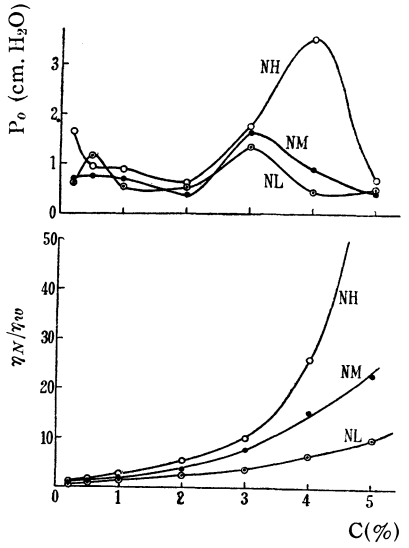

Fig. 3. (η_N/η_w) and P_0 for Gohsenol N.

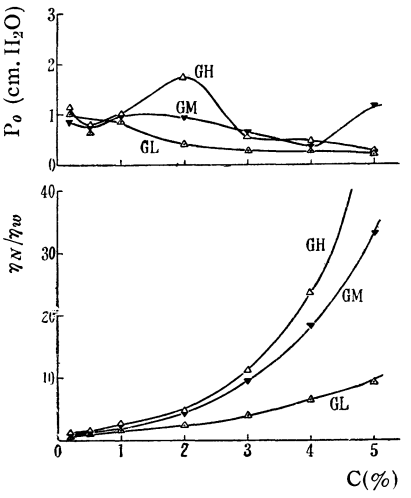

Fig. 4. (η_N/η_w) and P_0 for Gohsenol G.

$$\eta_{sp}/C=[\eta]+k'[\eta]^2C \qquad (4)$$

for the concentration range of 0.1–1%. The Present experiment, shown in Figs. 3 and 4, covers wider concentration range, and does not satisfy Eq. (4). While, the value of $[\eta_N]$ calculated by the following equation:

$$[\eta_N]=\ln(\eta_N/\eta_w)/C \qquad (5)$$

is constant in the range of 0.2–5.5%. The constancy of Eq. (5) has been already stated by Sakurada[1] and others[4]. The mean value of $[\eta_N]$ obtained is shown in Table I.

In Sakurada's Eq. (1), the concentration C is given in g./l., so it is recalculated to %, and

$$[\eta_0]=8.87\times10^{-4}\times\rho^{0.62} \qquad (6)$$

is obtained. As shown in Table I, the value of $[\eta_0]$ from this equation are greater than

TABLE I

Specimen Marks	ρ	Temp (°C)	$[\eta_N]$
NH	2000	14.0±0.9	0.828±0.010
NM	1400	14.1±1.7	0.627±0.013
NL	500	18.4±1.1	0.454±0.009
GH	2000	12.6±2.1	0.857±0.024
GM	1400	14.4±2.5	0.717±0.017
GL	500	15.8±1.3	0.456±0.014

	$[\eta_0]$	y	After 4 hr'. warming	
	Eq. (6)	(%)	$[\eta_N]$	y (%)
NH	0.985	15.9	0.838	14.9
NM	0.800	21.7	0.783	2.1
NL	0.426	~0	—	—
GH	0.985	13.0	—	—
GM	0.800	10.4	—	—
GL	0.426	~0	—	—

the values of $[\eta_N]$ cited above. It is generally accepted that the intrinsic viscosity is proportional to the volume occupied by the solute in the solution. For example, the molecular extension is greater and intrinsic viscosity is greater in a good solvent than in a poor solvent[5]. It is assumed that Sakurada's intrinsic viscosity $[\eta_0]$ of Eq. (6) corresponds to a completely dissolved state. Then, the smaller value of $[\eta_N]$ than $[\eta_0]$ means the incomplete dissolution or incomplete molecular extension; e.g. some parts of high polymer may not be dispersed to molecular dissolution but they may suspend as crystallites. In the present experiment, solution is heated only fifteen minutes at 90°C, while it is generally said that four hours warming at 40–50°C is necessary to obtain a complete dissolution[3]. Then it is assumed that y (%)

$$y=\left(\frac{[\eta_0]-[\eta_N]}{[\eta_0]}\right)\times100\,(\%) \qquad (7)$$

3) E. Tsuruta and M. Takeda, *J. Chem. Soc. Japan (Pure Chem. Sec.)*, **74**, 191 (1953).

4) For example, K. Hirabayashi, "Poval" (1952), p. 54.

5) K. Yoshioka, "Review of Recent Colloid Science", (1950) Vol. 2, p. 36.

corresponds to the fraction of incomplete dissolution. These values are also shown in Table I. It is shown that the low molecular weight specimens, NL and GL are nearly completely dissolved, but the other high molecular specimens are incompletely dissolved, as far as 10–20%. According to E. Tsuruta and M. Takeda[3], the intrinsic viscosity decreases with the increase of temperature. Considering this fact, the value of y should be somewhat greter than that cited in Table I, since Eq. (6) is derived by Sakurada at 20°C.

To discuss the effects of acetyl group, completely saponified specimens, N-series, and 90% saponified specimens, G-series, are compared. The hydration of acetyl group is weaker than the hydroxyl group, so the acetyl group left in G-series will decrease the extension of molecules, just as in a poor solvent. This expectation is not realized, since the incomplete dissolution degree, y (%), of G-series is smaller than that of N-series. To explain this, it is assumed that the existence of 10% of acetyl groups hardly change the solvation of the polymer molecule as a whole, while they decrease the mutual interaction of hydroxyl groups in a crystallite to increase the solubility and molecular extension. This assumption is also adequate to explain the difference of apparent yield values of G- and N-series. Though the apparent yield values are highly dependent on the history of the solutions, the value of P_0 for 90% saponified specimens (GH, GM, GL) are about 1 cm. H_2O, while for completely saponified specimens (NH, NM, NL) it is rather greater than that of G-series. This is also explained by the idea that the formation of intermoleular bonding of hydroxyl groups are easier and the net-work structure is stronger when the saponification is more complete and molecular weight is higher.

If the value of $[\eta_N]$ is smaller than $[\eta_0]$ by the season cited above, then the value of $[\eta_N]$ should increase by more complete dissolution. To certify it, the following procedure are tried. The solutions, made after the method cited before, are put into a flask with a rubber stopper and warmed at 45°C for four hours. The results obtained for these solutions are also cited in Table I. It is shown that the value of $[\eta_N]$ has increased by four hours warming. The fration of inccmplete dissolution, y, was about 2% for NM, therefore, it has been nearly completely dissolved. However, the dissolution of the higher molecular weight specimen, NH, was not yet complete and y was about 15%.

Summary

The structural viscosity is measured for the aqueous solutions of poly-vinyl alcohol. The relative viscosity, (η/η_w), shows linear relationship to the reciprocal of the rate of flow, Q:

$$\eta=\eta_N+2.57\times10^{-5}\times P_0/Q$$

where η_N and P_0 are constants. P_0 corresponds to the pressure to destroy a net-work structure in the solution, or an apparent yield value, and η_N corresponds to the viscosity coefficient of the destroyed structure, which is assumed to flow as Newtonian.

As for the Newtonian viscosity η_N of poly-vinyl alcohol solutions, $[\eta_N]$ defined by

$$[\eta_N]=\ln(\eta_N/\eta_w)/C$$

is independent on concentration, as far as measured. Comparing the intrinsic viscosities of specimens of the same polymerization, degree, the completely saponified specimen shows smaller value than partly saponified one. This may be explained by the decrease of molecular extension due to the strong intramolecular interaction of OH groups. The apparent yield values P_0 is 0.5~3.5 cm. H_2O and is highly dependent on the history of the solution. The completely saponified specimen shows greater P_0 value. It will also be explained by the strong intermolecular interaction of OH groups to form net-work structure.

The author appreciates to Nippon Gosei Kagaku Kogyo KK. who has kindly provided specimens.

Faculty of Living Science,
Osaka City University,
Osaka

Behavior of Surface Active Molecules at Interface. I. Statistical Mechanical Studies on Head Contact and Chain Contact

By Masayuki NAKAGAKI and Saiichi IIDA

(Received August 18, 1955)

The pressure-area curves of condensed monomolecular films are, in general classified in two types shown in Fig. 1. The one is curve a, which stands up with a steep slope at the area A_1, e.g. condensed film of saturated fatty acid on distilled water. The other is curve b, where the pressure bigins to increase gradually at the area A_2, and coincides with curve at G, e.g. the condensed film of saturated fatty acid on dilute HCl solution (N/10~N/100).

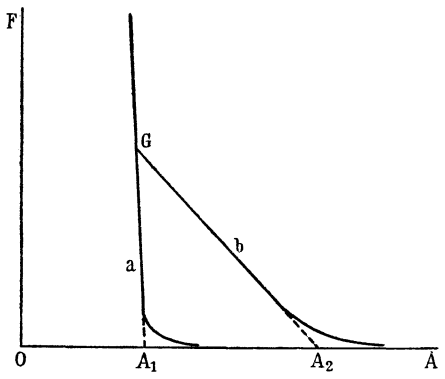

Fig. 1. Schematic diagram of pressure-area curve of condensed films.

For saturated hydrocarbon chain, the value of A_1 is 20.5 Å^2, which depends upon neither length of the chain nor the sort of end group. On the other hand, the value of A_2 depends upon the sort of end group. According to these empirical facts, Adam[1] proposed the idea of head contact and chain contact. The state of A_1 is considered to be a closs-packed chain, and 20.5 Å^2 is assumed to be the cross sectional area of the hydrocarbon chain. While, the state of A_2 is thought to be a close-packed head, and the value of A_2 is equal to the cross sectional area of end group. When the film with close-packed head is further compressed, some of the end groups are dipped into water, and the film at last reaches the state of close-packed chain at G.

Statistical Mechanical Treatment

The idea of head contact and chain contact is formulated using a model as follows. When a film with close-packed head (A_2) is compressed gradually, some of the end groups are dipped into water. Let the fraction of of dipped end group be x, and the energy required to dip one end group be w. It is assumed that the cross sectional area of hydrocarbon chain chain is A_H and that of the end group is A_P; then the average area occupied by one molecule, A_b, is

$$\left.\begin{aligned} A_b &= xA_H+(1-x)A_P = A_P-xB \\ \text{where} \quad B &= A_P-A_H \end{aligned}\right\} \tag{1}$$

Therefore, the free area per one molecule, A_f, is

$$A_f = A-A_b = A-A_P+xB \tag{2}$$

where A is the total area per one molecule.

Considering that the state of molecules in condensed film is analogous to that in a two-dimensional liquid, partition function Z may be formulated. The Gibbs free energy, G, is then calculated by

$$G = -kT \ln Z \tag{3}$$

since the Gibbs free energy is approximately equal to the Helmholtz free energy for condensed systems. As the result,

$$G/nkT = -\ln(2\pi mkT/h^2)+(\phi/kT)+(xw/kT) - \ln A_f+\{x \ln x+(1-x)\ln(1-x)\} \tag{4}$$

is obtained, where n is the number of molecules in the film, ϕ is the potential energy of a molecule on the surface referring the energy of molecules in gaseous film (zero), so that ϕ is the negative of the energy of condensation in monomolecular film, (ϕ 0), and w is the energy required to dip one end group into water as shown in Fig. 2 ($w>0$).

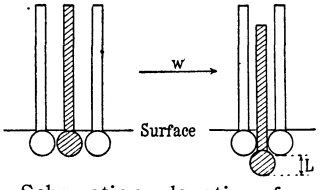

Fig. 2. Schematic explanation of energy w.

The last two terms of Eq. (4) correspond to the mixing entropy of molecules, whose polar groups are on and under the surface. The fraction of molecules dipped into water, x,

1) N.K. Adam, "Physics and Chemistry of Surfaces", Oxford (1938), p. 50.

is determined by the condition of minimum free energy:

$$(\partial G/\partial x)_{A,T}=0 \tag{5}$$

Then,

$$x/(1-x)=\{\exp.(-w/kT)\}\times\left\{\exp.\left(\frac{B}{A-A_P+xB}\right)\right\} \tag{6}$$

is obtained. From this equation, it is clear that x becomes greater when the energy required to dip molecule, w, is small, or temperature is higher or the film is compressed and A becomes smaller.

The surface pressure is obtained by

$$F=-(\partial G/\partial S)_{T,n}=-(1/n)(\partial G/\partial A)_{T,n} \tag{7}$$

where S is the area of film, that is

$$S=nA \tag{8}$$

Using Eqs. (4), (6) and (7) and assuming that w is independent to A,

$$F/kT=-(1/kT)(\partial\phi/\partial A)+(1/A_f) \tag{9}$$

is obtained. As for right side of Eq. (9), the first term shows the pressure to contract the film by the cohesional force and the second term shows the thermal pressures is equal to the surface pressure observed. The cohesional pressure and the thermal pressure are both very great compared to their difference, so it will be perhaps very difficult to calculate the absolute value of the surface pressure theoretically. The assumption will be, however, reasonable that the potential energy ϕ is a function of intermolecular distance only, and the value of $(\partial\phi/\partial A)$ is a function of A only. Then, it is possible to calculate the difference of the surface pressure of two states of the same value of A.

Imagine a state where molecules are always in chain contact. The surface pressure of this imaginary state is assumed as F_1, and the real surface pressure of a film of the same value of A is described as F. Then the difference of them is,

$$\frac{\Delta F'}{kT}=\frac{F}{kT}-\frac{F_1}{kT}=\frac{1}{A_f}-\frac{1}{A-A_H} \tag{10}$$

since the free area of the imaginary state is $(A-A_H)$. Then, using (2) and (6),

$$\frac{B}{kT}\Delta F'=(1-x)\left(\frac{w}{kT}+\ln\frac{x}{1-x}\right)^2\Big/\left\{1+(1-x)\left(\frac{w}{kT}+\ln\frac{x}{1-x}\right)\right\}$$

$$\frac{A-A_P}{B}=\left(\frac{1}{\frac{w}{kT}+\ln\frac{x}{1-x}}\right)-x \tag{11}$$

are obtained. Using these equations, the relation between $(\Delta F'B/kT)$ and $(A-A_P)/B$ is calculated for a given set of x and (w/kT).

It should be stressed here that the state assumed above as a standard state, that is the state of all chain contacts, is different from the state of $w=0$. The words close-packed chain, named by Adam for curve a in Fig. 1, may suggest that the molecules in the film are always in chain contact, but such a state can never be realized. The most compact state realizable is a state of $w=0$. In the case of $w=0$, x approaches $\frac{1}{2}$ when the film is sufficiently widened, that is $A_f\rightarrow\infty$, (see Eq. (6)). This owes to the term of mixing entropy of dipped and not dipped molecules in Eq. (4). By a sufficient compression of the film, x approaches unity when A is nearly equal to A_H. Anyway, the state of $w=0$ is the most compact state realizable, so it should correspond to the curve a in Fig. 1, and the value of $\Delta F'$ in Eqs. (10) and (11) for $w=0$ is shown as $\Delta F_0'$. While the curve b in Fig. 1 corresponds to a state where w is not equal to zero. The difference

$$\Delta F=\Delta F'-\Delta F_0' \tag{12}$$

may be calculated numerically from Eq. (11) as a function of A, for a given values of w, B and A_P. On the other hand, observed surface pressure of curve a and b in Fig. 1 are expressed as F_0 and F, respectively. Then, ΔF is obtained experimentary by

$$\Delta F=F-F_0 \tag{13}$$

and compared with the theoretical value of Eq. (12).

Comparison with Experiment

To facilitate the comparison, ΔF–A relation is recalculated and plotted as $\eta-\xi$ relation, where

$$\xi=\frac{A-A_P}{A_P-A_H}-\frac{A-A_P}{B} \tag{14}$$

$$\eta=\left(\frac{A_P-A_H}{kT}\right)\Delta F=\frac{B}{kT}\Delta F \tag{15}$$

Then, from the theoretical stand point, $\eta-\xi$ relation is determined by a parameter (w/kT), since x may be eliminated, in principle, from two equations in Eq. (11) (see Fig. 3). While, using the experimental value of ΔF and A, values of ξ and η varies with the values of B and A_P as shown in Eqs. (14) and (15). Assume that

$$A_H=20.6\quad(\text{Å}^2) \tag{16}$$

then,

$$A_P=A_H+B=20.6+B \tag{17}$$

Therefore, an experimental ΔF–A relation is recalculated to a $\eta-\xi$ relation for a given value of a parameter B. The data of Adam[2] for saturated fatty acid, is shown in Fig. 3 for some values of B. From the figure, it is seen that (w/kT) is nearly equal to 0.2, and B is nearly equal to 2.

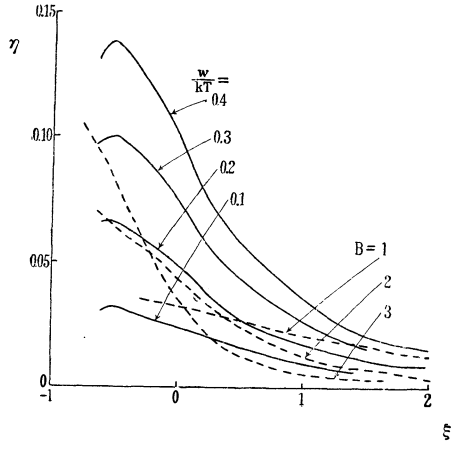

—— theor., --- exper.
Fig. 3. η–ξ Selations.

To obtain more accurate values of B and w/kT, the variation of η for a given value of ξ is studied. For a given value of ξ, and for a certain value of B, an experimental value of η is determined, and to obtain the same value of η theoretically, a value of w/kT is determined. Therefore, for a given value of ξ, a (w/kT)–B relation is obtained as shown in Fig. 4. For one value of ξ, one curve is obtained, and they cross nearly at one point P. Values of w/kT and B, corresponding to the point P, are the most convenient values, that is

$$\left.\begin{aligned} w/kT &= 0.17_5 \\ B &= 1.7_5 \end{aligned}\right\} \qquad (18)$$

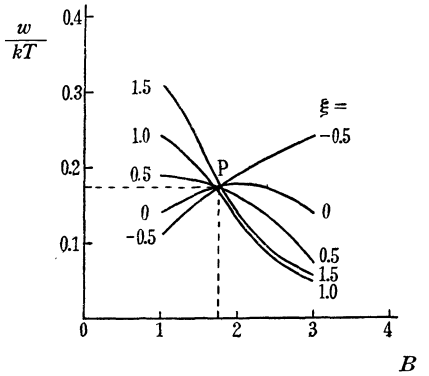

Fig. 4. (w/kT)–B relation for saturated fatty acid.

2) N.K. Adam, *Proc. Roy. Soc.*, A101, 452 (1922).

Using these values and experimental value of F_0, the value of F is calculated. The results in Fig. 5 showes a good agreement with experimental value of Adam.

The method of calculation described above is very complicated, though the results are satisfactory. The more simplified method is

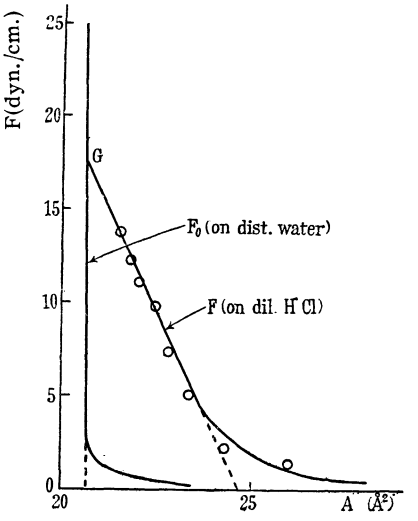

—— obsd., ○ calcd.
Fig. 5. Observed and calculated values for saturated fatty acids.

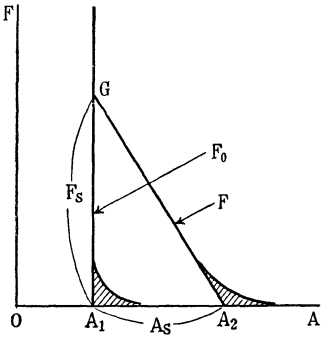

Fig. 6. Simplified F-A diagram.

desirable. The experimental relation in Fig. 1 a is simplified as Fig. 6. The low pressure tail (hatched portion) is neglected, and the curve F_0 is assumed to be zero for $A > A_H$, and it is assumed that the curve stands up vertically at $A=A_H$. In Fig. 1 b the curve F is linear from A_2 to G, where the tail at lower pressure part (hatched in Fig. 6) is also neglected. The difference of A_H and A_2 is written as A_S, and the pressure at G as F_S. Then, at $\xi=0$, or at $A=A_P=A_H+B$

$$\left.\begin{aligned} \Delta F &= (A_S-B)F_S/A_S \\ -(d\Delta F/dA) &= F_S/A_S \end{aligned}\right\} \qquad (19)$$

are obtained. On the other hand, the the-

oretical treatment is simplified as follows. From the theoretical curve in Fig. 3, the value of η and $(d\eta/d\xi)$ at $\xi=0$ are determined at a function of w/kT. Then it is seen that they are linear to w/kT, at least within the range of $w/kT=0\sim0.6$. This linear relation is, using Eqs. (14) and (15), at $A=A_H+B$,

$$\left.\begin{aligned}\frac{B}{kT}\Delta F&=0.250\frac{w}{kT}\\ -\frac{B^2}{kT}\frac{d\Delta F}{dA}&=0.190\frac{w}{kT}\end{aligned}\right\}\qquad(20)$$

Using Eqs. (19) and (20)

$$B=A_P-A_H=0.432\,A_S \qquad (21)$$

$$w/kT=0.982\,A_SF_S/kT \qquad (22)$$

are obtained. Using these equations, the values of B and w/kT are calculated. As for the saturated fatty acid shown in Fig. 5, $F_S=17.5$ dyn./cm. $A_H=20.6$ Å^2, $A_2=24.7$ Å$_2$, and therefore $A_S=4.1$ Å^2. Then, at 25°C,

$$\left.\begin{aligned}B&=1.7_7\\ w/kT&=0.17_4\end{aligned}\right\}\qquad(23)$$

are obtained from Eqs. (21) and (22). These are in good agreement with Eq. (18), obtained by a strict method.

To study more cases, data summarized by N.K. Adam[3] are used. Those and the results calculated from them using Eqs. (21) and (22) are cited in Table I, where it is assumed that $A_H=20.5$ Å^2. The value of F_S marked in Table I by * are obtained by an extrapolation, assuming that the F–A curve extends linearly to $A=20.5$ Å^2. The values of w obtained by this method are, in general, very small; that is, less than 0.5 kcal./mol. For a few molecules, w is greater than 1 kcal./mol.

The value of w corresponds to the energy required to dip an end group into water. It is, however, not the energy of solution of the whole molecule, but it is, as shown in Fig. 2, the energy to make the distribution of end group disorder. It is the energy required to dip hydrocarbon chain by the length of end group, (L in Fig. 2), if the hydration of the end group does not change before and after the dipping. Therefore, molecules of longer end group should have greater w values. Then it is acceptable that the sequence of w values in Table I is:

OH<COOH<NH·CO·CH$_3$<CH: CH·COOH<

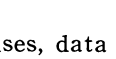

<choresterol

Compared with this, w of nitril seems too large. Interaction between end groups should be, perhaps, taken into consideration. As for the value of the cross sectional area of the end group, A_P, Anam considered that A_2 is the cross section of end group, but by Eq. (21), A_P is somewhat smaller than A_2, and the difference to A_H is not so great as that by Adrm. This is rather in agreement with molecular models. Therefore, the state at A_2 is not the close-packed head, but it is a state of looser packing.

Mixed Monolayers

Harkins and Florence[4] measured the presure-area relations for stearic acid, stearyl alcohol, and 1:1 mixture of them. The values of A_H of these three cases differ from each other, but they are 20.0~20.5 Å$_2$. For simplicity, it is assumed that A_H is 20.0 Å^2, and linear relation is extrapolated to $A=$

TABLE I

CALCULATED VALUE OF A_P w

(A_H is assumed to be 20.5 A^2)

Substances	End groups	A_2 (Å^2)	A_S (Å^2)	F_S (dyn./cm.)	B (Å^2)	A_P (Å^2)	w/kT	w (Kcal./mol.)
Alcohols	-CH_2OH	21.6	1.1	6.7	0.48	21.0	0.018	0.01
Acids	-COOH	25.1	4.6	17.3	2.0	22.5	0.193	0.12
Acetamides	-NH·CO·CH_3	24.2	3.7	25.	1.9	22.1	0.225	0.14
Isooleic acid	-CH: CH·COOH	28.7	8.2	15.2	3.5	24.0	0.303	0.18
α-Monoglycerides	-$COOCH_2$·CHOH·CH_2OH	26.3	5.8	45.3*	2.5	23.0	0.639	0.38
Nitrils	-C≡N	27.7	7.2	37.5*	3.1	23.6	0.657	0.39
p-Substituted benzene	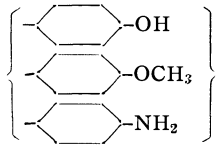	24.0	3.5	79.5*	1.5	22.0	0.677	0.41
Choresterterol	———	40.8	20.3	847. *	8.8	29.3	4.18	2.5

3) N.K. Adam, "Physics and Chemistry of Surfaces", Oxford (1938), p. 49.

4) W.D. Harkins and R'T. Florence, *J. Chem. Phys.*, 6, 847 (1938).

20.0 A^2 to obtain the value of F_N. Calculated values of A_P and w from these data by Eqs. (21) and (22) are cited in Table II, compared with that of Adam in Table I.

TABLE II
CONDENSED FILM OF FATTY ACID, ALCOHOL AND MIXTURE OF THEM

	Film	Adam	Harkins & Florence	Nakagaki & Iida
A_P (Å^2)	RCOOH	22.5	21.8	22.4
	RCOOH +R'OH	—	21.3	21.9
	R'OH	21.0	20.8	31.2
w (kcal./mol.)	RCOOH	0.12	0.15	0.18
	RCOOH +R'OH	—	0.09	0.14
	R'OH	0.02	0.04	0.09

The present autors obtained the pressure-area curves for stearic acid, cetyl alcohol and 1:1 mixed film of them. Stearic acid (m.p. 71.1°C) and cetyl alcohol (m.p. 50.2°C) used are those provided by Nippon Yushi KK. A Wilhelmy type tensiometer with torsion balance is used with grass trough and glass barrier, paraffin with Merck's paraffine (m.p. 46~48°C). The substrate was N/1000 HCl solution. Point G in Fig. 1 is observed at about $A=20$ Å^2, so that the data were treated just as those of Harkins and Florence. The results obtained are also cited in Table II. It is seen that A_P and w of 1:1 mixed monolayer are cloth to the average of both components.

Summary

The idea of head contact and chain contact proposed by Adam was formulated by statistical mechanics, introducing the energy required to dip one end group into water, w. It is concluded that the value of w is less than 1 kcal./mol. for most of molecules examined, and it is greater when the length of the group is longer. The cross sectional area of the end group, A_P, is concluded to be smaller than that estimated by Adam. As for a mixed monolayer, the value of w and A_P were almost equal to the average of components.

Faculty of Living Science,
Osaka City University,
Osaka

Spectrochemical Investigations of the Interaction between Simple Salt Anions and Transition Metal Cations. II. Association between Bisethylenediamine Cupric Complex and Several Anions

By Hayami YONEDA

(Received July 13, 1955)

Introduction

In the previous report[1] the author studied the absorption due to association between hexammine complexes of cobalt(III) and chromium(III) and anions of simple salts and concluded from the estimation of the degrees of association that the particular deforming power of the transition metal ions plays an important role in association.

In the present investigation, the author studied the absorption due to association between $[Cu\ en_2]^{2+}$ complex cation and several anions which had reducing power against cupric aquo ion. As the result, marked absorption due to association was found in the cases of iodide, sulphite and thiosulphate ions. At the same time, the author devised a new method to determine the equilibrium constant of association from the analysis of absorption data.

1) This Bulletin, 28, 125 (1955).

Experimental

Bisethylenediamine cupric complex was prepared from cupric perchlorate and an equivalent amount of ethylenediamine, and was recrystallized once from hot water.

Optical densities were measured by means of the Shimadzu spectrophotometer using tungsten and hydrogen lamps and 1 cm. quartz cells. All measurement was made at room temperature 18°C.

Results

In the preliminary experiment, the following measurement was made. The salts used were KNCS, KBr, KI, Na_2SO_3 and $Na_2S_2O_3$. Each sa was dissolved to make a solution of 1 mol./l. concentration. In each solution $[Cu\ en_2](ClO_4)_2$ was dis-

solved to 0.01 mol./l. concentration. Such solutions of the complex were measured in relation to their optical densities. In order to cancel the absorption due to the unassociated free anions, the corresponding salt solution was used as a standard. The results are shown in Fig. 1. The inspection of these curves reveals the following facts.

1) In every case the characteristic absorption band proper to the complex remained constant in its maximum position ($\nu_{max.}$: 54.8×10^{13} sec^{-1}) and height (log $\varepsilon_{max.}$: 1.82).

2) In the cases of NCS^- and Br^-, only slight enhancement of the end absorption was observed, while in the cases of I^-, SO_3^{2-} and $S_2O_3^{2-}$, marked absorption due to association was observed in the near ultraviolet. Accordingly, it was expected that we could determine the equilibrium constants of association in the latter cases by using such absorption.

In order to determine the equilibrium constant, the author made the following measurement. At first the method of continuous variations devised by Shibata[2] and Tsuchida[3] was applied to determine the composition of the association product. In the cases of SO_3^{2-} and I^-, 1/10 g.ion/l. solutions of the complex and the anion, and in the case of $S_2O_3^{2-}$, 1/40 g.ion/l. solutions were prepared respectively. Next such solutions of the complex and the anion were mixed with each other in the volume ratios (equal to the mole ratios) of 3:1, 2:1, 1:1, 1:2 and 1:3. The mixed solutions thus obtained were measured in their optical densities. As the result it was found that the absorption of the 1:1 association product was predominent under the present experimental conditions. Some parts of the results are listed in Table I. These results were used in the determination of the equilibrium constants.

TABLE I

OBSERVED OPTICAL DENSITIES

Wave-lengths / Mole ratios	350 mμ	345 mμ	340 mμ	335 mμ	330 mμ	325 mμ
[Cu en_2]$^{2+}$: SO_3^{2-}						
1:1	0.271	0.298	0.316	0.334	0.360	0.395
2:1	.255	.272	.294	.311	.335	.371
3:1	.220	.238	.254	.271	.295	.331
[Cu en_2]$^{2+}$: I^-						
1:1	0.167	0.205	0.255	0.312	0.385	0.479
2:1	.163	.197	.240	.294	.359	.449
3:1	.137	.166	.201	.245	.302	.380
[Cu en_2]$^{2+}$: $S_2O_3^{2-}$						
1:1	0.170	0.217	0.259	0.305	0.358	0.411
2:1	.153	.199	.239	.280	.325	.373
3:1	.124	.163	.191	.227	.266	.305
[Cu en_2]$^{2+}$ only (c=1/10 g.ion/l.)	0.062	0.065	0.070	0.080	0.098	0.132

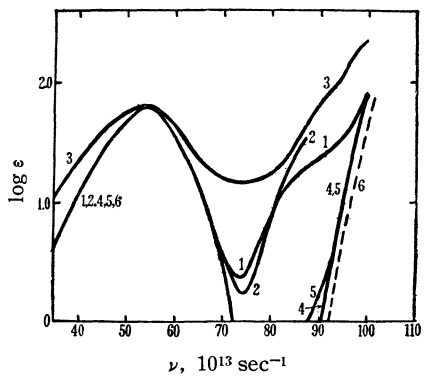

Fig. 1. Absorption Spectra of [Cu en_2] $(ClO_4)_2$
1. in Na_2SO_3 solution.
2. in KI solution.
3. in $Na_2S_2O_3$ solution.
4. in KBr solution.
5. in KNCS solution.
6. in distilled water.

(Under these mole ratios of the complex and the anion, the possibility of producing the 1:2 and 1:3 complex-anion association pairs is practically negligible. One has only to consider the 1:1 product.)

Determination of the Equilibrium Constant.— In order to determine the equilibrium constant by using the above listed values, the following method was devised.

Consider the case where [Cu en_2]$^{2+}$ and SO_3^{2-} associate in aqueous solution to form the following equilibrium

$$Cu\ en_2^{2+} + SO_3^{2-} \rightleftarrows Cu\ en_2\text{–}SO_3$$

The equilibrium constant of association is represented by

$$K = \frac{[Cu\ en_2\text{–}SO_3]}{[Cu\ en_2^{2+}][SO_3^{2-}]}$$

If we represent the total concentrations of the complex and the anion with xc and c respectively,

2) Y. Shibata, T. Inoue and Y. Nakatsuka, *J. Chem. Soc. Japan*, **42**, 983 (1921).
3) R. Tsuchida, This Bulletin, **10**, 27 (1935).

and the concentration of the association product in equilibrium with u, then the concentrations of the complex and the anion in equilibrium are represented by $xc-u$ and $c-u$ respectively. Accordingly, the equilibrium constant is represented by

$$K=\frac{u}{(xc-u)(c-u)} \tag{1}$$

Here we consider the degree of association α with the anion,

$$\alpha=\frac{u}{c} \tag{2}$$

Introducing the relation (2) into the equation (1), we obtain

$$K=\frac{x}{c(x-\alpha)(1-\alpha)} \tag{3}$$

On the other hand, the observed optical density D is represented by

$$D=\varepsilon_{\text{comp.}}(xc-u)+\varepsilon_{\text{ass.}}u \tag{4}$$

where $\varepsilon_{\text{comp.}}$ and $\varepsilon_{\text{ass.}}$ mean the extinction coefficients of the complex and the association product respectively. (In the present cases the absorption of the anion is negligible.)

Substituting the relation (2) into the equation (4), we obtain

$$\frac{D-\varepsilon_{\text{comp.}}xc}{c}=(\varepsilon_{\text{ass.}}-\varepsilon_{\text{comp.}})\alpha=\Delta\varepsilon\cdot\alpha \tag{5}$$

The left side of the equation (5) can be calculated from the observed optical density and is represented by y. The values of y are listed in Table II. The equation (5) is abbreviated to

$$y=\Delta\varepsilon\cdot\alpha \tag{6}$$

From the equation (3) and (6), we obtain

$$y^2-y\alpha\Delta\varepsilon-xy\Delta\varepsilon-(\Delta\varepsilon)^2x=0 \tag{7}$$

where $$\alpha=1+\frac{1}{ck} \tag{8}$$

The numerical values of x and y are introduced into this equation (7), then the equation of the second order about α and $\Delta\varepsilon$ is obtained. At one wave-length three such equations are obtained. From these equations we can find the most probable values of α and $\Delta\varepsilon$ by using the method of least squares. When the values of α is known, we can determine the value of K by using the relation (8). The results thus obtained are listed in Table III.

TABLE II

CALCULATED VALUES OF y

Mole ratios \ Wave-lengths	350 mμ	345 mμ	340 mμ	335 mμ	330 mμ	325 mμ
$[Cu\ en_2]^{2+}:SO_3^{2-}$						
1:1	4.80	5.30	5.63	5.89	6.22	6.58
2:1	6.42	6.88	7.41	7.76	8.10	8.49
3:1	6.92	7.58	8.08	8.44	8.84	9.30
$[Cu\ en_2]^{2+}:I^-$						
1:1		3.44	4.40	5.44	6.72	8.26
2:1		4.62	5.79	7.26	8.82	10.83
3:1		4.70	5.92	7.40	9.16	11.24
$[Cu\ en_2]^{2+}:S_2O_3^{2-}$						
1:1	12.96	16.72	20.016	23.60	27.82	31.56
2:1	17.16	22.58	27.276	32.04	37.04	42.12
3:1	17.92	24.23	28.48	33.92	39.70	44.80

TABLE III

MOST PROBABLE VALUES OF α, $\Delta\varepsilon$ AND K

Ion-pairs \ Wave-lengths	350 mμ	345 mμ	340 mμ	335 mμ	330 mμ	325 mμ
$[Cu\ en_2]^{2+}$-SO_3^{2-}						
α	1.401	1.401	1.410	1.402	1.384	1.333
$\Delta\varepsilon$	12.07	12.85	13.70	14.11	14.42	14.55
		the mean value of $\alpha=1.40$ $K=25$				
$[Cu\ en_2]^{2+}$-I^-						
α		1.094	1.098	1.095	1.100	1.107
$\Delta\varepsilon$		5.53	7.02	8.70	10.83	13.42
		the mean value of $\alpha=1.10$ $K=100$				
$[Cu\ en_2]^{2+}$-$S_2O_3^{2-}$						
α	1.160	1.180	1.217	1.118	1.298	1.244
$\Delta\varepsilon$	23.11	32.00	39.25	44.32	59.63	63.76
		the mean value of $\alpha=1.21$ $K=190$				

Discussion

As the preliminary experiment indicated, the characteristic absorption band proper to the complex remained constant in association. This fact suggests that the association is not a kind of partial substitution of the ligand by the anion, and that the association product is not a penta-coordinated complex [Cu en_2 x] like $[Cu(NH_3)_5]^{2+}$ [4]. In such cases the characteristic absorption band proper to $[Cu\ en_2]^{2+}$ must change its maximum position and height. Accordingly, the association is presumed to occur without any essential change of the structure of $[Cu\ en_2]^{2+}$. According to the results of the determination of the equilibrium constants of association, the stability of the association product increases in the order of $SO_3^{2-} < I^- < S_2O_3^{2-}$. The univalent anion I^- forms a more stable product than the bivalent anion SO_3^{2-}, and the more voluminous anion $S_2O_3^{2-}$ forms a more stable product than the less voluminous anion SO_3^{2-}. This fact indicates that the association is not caused merely by the electrostatic attraction between the complex and anion. Rather, it must be considered that, although the detailed mechanism of binding is not known, the specific polarising power of the central cupric ion acts upon the extremely polarisable anion to form the association product.

4) J. Bjerrum and C.G. Lamm, *Acta chimica Scandinavica* **4**, 997 (1950).

Conclusion

Marked absorption due to association was found between bisethylenediamine cupric complex and anions SO_3^{2-}, I^- and $S_2O_3^{2-}$ which have a strong reducing power against cupric aquo ion, and the equilibrium constants of association were determined by the newly devised method. The values of K's were 25 for SO_3^{2-}, 100 for I^- and 190 for $S_2O_3^{2-}$. This results indicates that the cause of association is not always the mere electrostatic attraction between cation and anion, rather it suggests that the association can be caused by the strong polarising effect of the central cupric ion upon the extremely polarisable anion.

The author wishes to express his heartfelt thanks to Prof. R. Tsuchida and Prof. M. Kobayashi, Osaka University for their kind advice and encouragement throughout this work. This study was supported in part by a grant from the Ministry of Education.

Chemistry Department, Wakayama University, Wakayama

Analytical Chemistry of Beryllium. VII. Spectrophotometric Determination of Micro Quantities of Beryllium with 8-Hydroxyquinaldine

By Kenji MOTOJIMA

(Received August 11, 1955)

Introduction

The colorimetric methods for the determination of micro quantities of beryllium which have been recently reported were based on the lake formation with such dyes as quinizarin-2-sulfonic acid[1], aurintricarboxylic acid[2], alkannin[3] and naphthazarin[3]. On the whole, these reactions are not specific and even small amounts of aluminum and iron interfere with the determination of beryllium. The method which has been investigated by the author and is described below, is fundamentally different from the above mentioned ones, and is more specific for beryllium.

In the previous paper[4] it was reported that beryllium forms slightly soluble chelate with 8-hydroxyquinaldine in ammoniacal medium, which has a formula $Be(C_{10}H_8NO)_2$, and that beryllium can be determined both gravimetrically and volumetrically with this reagent. The spectrophotometric method is based on the property that this chelate is soluble in chloroform and can be extracted by this solvent. The resulting chloroform

1) M. W. Cucci, W. F. Neuman and B. J. Mulryan, *Anal. Chem.*, 21, 1358 (1949).
2) G. E. Kosel and W. F. Neuman, ibid., 22, 936 (1950).
3) A. L. Underwood and W. F. Neuman, ibid., 21, 1348 (1949); T. Y. Toribara and A. L. Underwood, ibid., 21, 1352 (1949).
4) K. Motojima, This Bulletin, "Analytical Chemistry of Beryllium", VI.

solution is colored light yellow, and beryllium is determined by photometry of this extract. The method for determination of beryllium is made by the following procedure: first from the chelate of 8-hydroxyquinaldine by adding acetic acid solution of this reagent to the beryllium solution and adjusting the pH to 8.0±0.2, next extract the chelate with chloroform, and then measure the absorbancy of this extract at the wave length of 380 mμ. The reason why this wave length is chosen is that beryllium chelate of 8-hydroxyquinaldine in chloroform absorbs most strongly at this wave length, while the reagent alone in this solvent absorbs strongly below 370 mμ.

Apparatus

A Beckman Model DU spectrophotometer with 1.00 cm. glass cell was used for all absorbancy measurements. A Beckman glass electrode pH meter Model H2 was used for the pH measurements.

Reagents

Standard Beryllium Solutions.—Several standard beryllium solutions were prepared in the same way as was shown in the previous work[4], each 10 ml. of these solution contained 5.3, 10.5 and 21.0 micrograms of beryllium.

8-Hydroxyquinaldine Solution.—Dissolve 2 g. of pure 8-hydroxyquinaldine prepared by the previously described method[4], in 4 ml. of glacial acetic acid by heating and dilute to 200 ml. with distilled water.

Chloroform. — Chloroform was purified by washing several times respectively, with 6 N sulfuric acid, aqueous solution 2 N in ammonium hydroxide and in ammonium chloride and then water, drying over anhydrous calcium chloride and then distilling. The recovery of chloroform was also made by this procedure.

Other Reagents.—The other reagents were prepared from reagent grade chemicals.

Experimental

Absorption Spectra.—Absorption spectra of beryllium chelate of 8-hydroxyquinaldine in chloroform were studied. Approximately 50 ml. of solutions, containing 10.5 and 21.0 micrograms of beryllium, 5 ml. of 10% ammonium chloride solution, 3 ml. of 8-hydroxyquinaldine solution and proper amount of dilute ammonium hydroxide to attain the pH to 8.0±0.2, were extracted with each 10.0 ml. of chloroform. The resulting chloroform solutions were dried with anhydrous sodium sulfate and absorbancies were measured over a wave length range of 360 to 470 mμ. The data obtained are given in Fig. 1. From these absorption spectra, it is seen that beryllium chelate of 8-hydroxyquinaldine in chloroform has an absorption maximum at 380 mμ. Accordingly, this wave length has been chosen for the determination of beryllium.

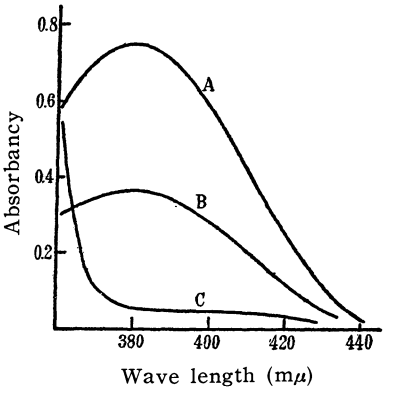

Fig. 1. Absorption spectra of beryllium chelate of 8-hydroxyquinaldine in chloroform.
A : 21.0 micrograms of Be.
B : 10.5 micrograms of Be.
C : blank.

Effect of pH on Extraction.—To determine the proper pH for the most efficient extraction of beryllium, the following series of experiments were made. Approximately 50 ml. of solutions containing 10.5 micrograms of beryllium, 3 ml. of 8-hydroxyquinaldine solution and sufficient amounts of either acetic acid and acetate or ammonium hydroxide and ammonium chloride to attain the desired pH, were extracted with each 10.0 ml. of chloroform. Measurements of pH were made on the aqueous layers after extraction. The extracts were dried with anhydrous sodium sulfate and then the absorbancies were determined at 380 mμ versus chloroform. The results obtained are shown in Fig. 2. Extraction is seen to be complete over a pH range 7.5 to 8.5. A similar experiment was made about the reagent, and it was found that the blanks were

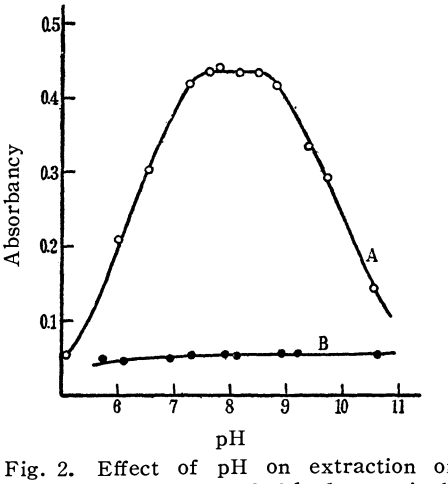

Fig. 2. Effect of pH on extraction of beryllium chelate of 8-hydroxyquinaldine.
A : 10.5 micrograms of Be.
B : blank.

reasonably constant in this pH range. So that the optimum pH range for the extraction is from 7.5 to 8.5.

Amount of Reagent.—Approximately 50 ml. of solutions containing 10.5 and 21.0 micrograms of beryllium respectively, and varying amounts of 8-hydroxyquinaldine solution, were extracted with each 10.0 ml. of chloroform at a pH 8.0±0.2. Then the measurements of the absorbancy at 380 mμ, versus chloroform, were made on these dried extracts. A similar set but with no beryllium present was also run. These results are shown in Fig. 3.

In case that more than 2.5 ml. of reagent solution is added, the rate of increase of these absorbancies is not very large, and as to the case when 10.5 micrograms of beryllium is present, the absorbancies after correction for the blank reading are almost constant. So that 3 ml. of 8-hydroxyquinaldine solution has been selected as a suitable amount of reagent.

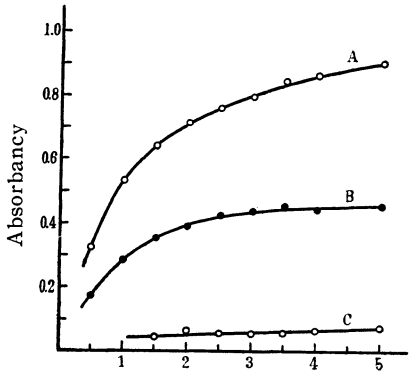

Fig. 3. Effect of reagent on absorbancy.
A : 21.0 micrograms of Be.
B : 10.5 micrograms of Be.
C : blank.

Effect of Digestion.—When extraction was made without digestion, the recovery of beryllium showed somewhat low values, but not so large an effect of digestion was observed, and it was confirmed that the digestion for from fifteen to thirty minutes at room temperature is most suitable.

Stability.—The absorbancy of the dried extract, stored in an amber glass bottle with a glass stopper, was found to remain unchanged for three days or more.

Spectrophotometric Procedure and Preparation of Calibration Curve

About 35 ml. of slightly acidic solution containing not more than 30 micrograms of beryllium, is treated with 5 ml. of 10 % ammonium chloride solution and 3 ml. of 8-hydroxyquinaldine, solution, and the pH of the resulting solution is adjusted to 8.0±0.2 with 2N ammonium hydroxide. The solution is transferred to a cone-shaped 130 ml. separatory funnel which is graduated at 50 ml., with a few milliliters of rinsed water, and the volume is brought to 50 ml. After standing for half an hour, extraction is made with 10.0 ml. of chloroform added from automatic measuring pipette[5], by vigorous shaking for a minute. The chloroform layer is drawn off into a small amber glass bottle with glass stopper, containing a gram of anhydrous sodium sulfate, and is shaken to remove droplets of water. Then the absorbancy of this extract is measured at 380 mμ using blank as a reference. Beryllium is determined by the use of a calibration curve which is prepared by similar treatment of a series of a known amount of beryllium.

The calibration curve was prepared by taking 5.3, 10.5, 15.8, 21.0, 26.3, 31.5, 36.8, and 42.0 micrograms of beryllium. The result is shown in Fig. 4. As will be seen from this curve, a close approximation to a linear relationship between beryllium concentration and the absorbancy is obtained up to 30 micrograms.

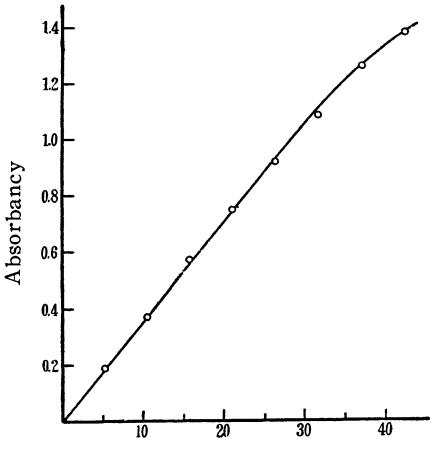

Fig. 4. Calibration curve of beryllium. (at the wave length of 380 mμ)

Interfering Substances

A few grams of sodium, potassium and ammonium salts of acetate, sulfate, chloride and nitrate do not interfere with this procedure. Less than 1 mg. of phosphate ion, 15 mg. of magnesium and 5 mg. of calcium also do not interfere with this procedure.

A small amount of aluminum, not more than 100 micrograms, does not interfere with this procedure, but when more than that exists it precipitates its hydroxide that prevents the extraction, therefore more than 100 micrograms of aluminum must not be present. Tartrate, though it is useful for the prevention of aluminum precipitation, must not be added, because it hinders the complete extraction of beryllium chelate. Bismuth, cadmium, chromium, copper, cobalt, indium, iron, nickel, tin, titanium and zinc ions do interfere with this procedure, because they form

5) K. Motojima, *J. Chem. Soc. of Japan (Pure Chem. Sec.)*, **76**, 903 (1955).

chelates of 8-hydroxybuinaldine or hydroxide, but these metals, except titanium, can be simply and rapidly removed from beryllium by mercury-cathode electrolysis[6], and such metals as copper, cadmium, iron, nickel and zinc may be masked by use of cyanide.

The separating method of beryllium from relatively large amounts of aluminum, iron and titanium, and determination method of beryllium in the presence of a minute amount of iron were especially studied.

Determination of Beryllium in Presence of Iron

Ferric iron yields a dark bluish chloroform solution under the same condition and interferes seriously with the determination of beryllium, but its absorption spectrum is entirely different from that of beryllium, and has two absorption maxima at the wave length of 470 and 580 mμ, as is shown in Fig. 5. Beer's law is obeyed at 580 and 380 mμ, respectively, as is shown in Fig. 6, while beryllium chelate has no absorption at 580 mμ. Therefore, beryllium can be determined in presence of a small amount of iron, not more than 50 micrograms, by making a correction for the amount of iron present.

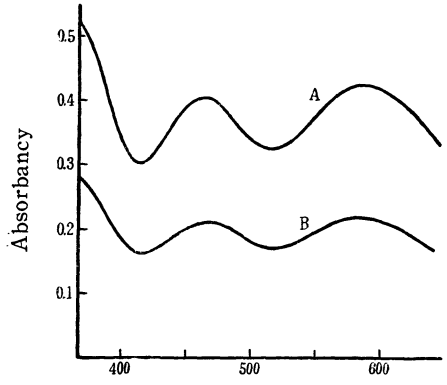

Fig. 5. Absorption spectra of ferric chelate of 8-hydroxyquinaldine in chloroform.
A : 50.0 micrograms of Fe.
B : 25.0 micrograms of Fe.

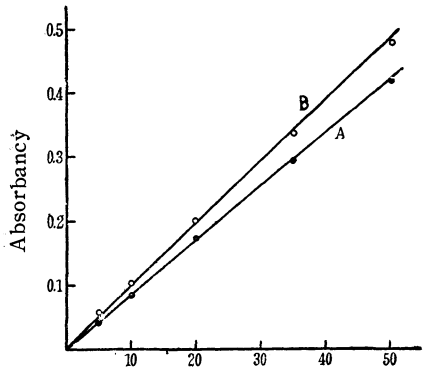

Fig. 6. Calibration curves of iron.
A : at 580 mμ.
B : at 380 mμ.

The following formula holds[7] :

$$C_{Be}=\frac{a^{Fe}_{580}A_{380}-a^{Fe}_{380}A_{580}}{a^{Be}_{380}\cdot a^{Fe}_{580}}$$

where, C_{Be}: beryllium present, A: absorbancies measured, a: absorbancy index (the absorbancy per microgram of beryllium or iron).

The values of a^{Be}_{380}, a^{Fe}_{380} and a^{Fe}_{580} are found from the calibration curves for beryllium and iron at 380 and 580 mμ, respectively. In this experiment these values are as follow:

$$a^{Fe}_{380}=0.0098,\quad a^{Fe}_{580}=0.0085,$$
$$a^{Be}_{380}=0.0352.$$

A number of mixed solutions containing known amounts of beryllium and iron in various ratios were prepared and beryllium was determined by making the above correction. Some of these results are shown in Table I, which seem to be quite satisfactory.

TABLE I
DETERMINATION OF BERYLLIUM IN PRESENCE OF IRON

Be Taken, Microgram	Fe Added, Microgram	Absorbancy, Measured 380 mμ	Absorbancy, Measured 580 mμ	Be Found, Microgram	Error, Microgram
5.3	10.0	0.283	0.085	5.1	−0.2
5.3	25.0	0.441	0.207	5.7	+0.4
10.5	10.0	0.470	0.088	10.5	0.0
10.5	25.0	0.622	0.212	10.7	+0.2
21.0	10.0	0.860	0.089	21.6	+0.6
21.0	25.0	0.990	0.216	21.1	+0.1
31.5	10.0	1.170	0.087	30.4	−1.1
31.5	25.0	1.330	0.209	30.9	−0.6

Extraction Separation Method with Oxine

Such metals as aluminum, copper, iron, nickel and titanium which precipitate chloroform-soluble oxinate from acetic acid and acetate medium can be quantitatively separated from beryllium by the following procedure. Of these metals, aluminum, iron and titanium were especially studied.

About 40 ml. of slightly acidic solution containing not more than 20 mg. of aluminum, 20 mg. of iron and 10 mg. of titanium, and a suitable amount of beryllium, is treated with a sufficient amount of 5 % oxine acetic acid solution to make oxinate of these metals, and the pH of the solution is adjusted to from 4.5 to 5.0 with 2N ammonium acetate solution. Then the oxinate of these metals and the excess of oxine are extracted with five 10 ml. portions of chloroform. The resulting solution is heated gently to expel the droplets of chloroform, and the volume is brought to about 40 ml. by evaporation. After cooling, beryllium is

6) A.D. Melaven, *Ind. Eng. Chem., Anal. Ed.*, 2, 180 (1930).

7) E.B. Sandell, "Colorimetric Determination of Traces of Metals", New York, (1950), p. 70.

determined with the above mentioned procedure. In this case it is desirable to measure the absorbancy at 580 mμ and, if necessary, make a correction for iron which seems to be accidentally mixed in the solution during the procedure. Some of the results are shown in Table II, which seem to be satisfactory.

TABLE II

THE RESULTS OF EXTRACTION SEPARATION METHOD WITH OXINE

Be Taken, Microgram	Metals Added Milligram, Fe	Al	Ti	Absorbancy Measured, 380 mμ	580 mμ	Be Found, Microgram	Error, Microgram
10.5	—	—	—	0.383	0.011	10.5	0.0
21.0	—	—	—	0.735	0.003	20.8	−0.2
0.0	20	—	—	0.016	0.010	0.1	+0.1
10.5	20	—	—	0.375	0.004	10.5	0.0
21.0	20	—	—	0.732	0.003	20.7	−0.3
0.0	—	20	—	0.012	0.002	0.4	+0.4
10.5	—	20	—	0.382	0.002	10.8	+0.3
21.0	—	20	—	0.740	0.011	20.7	−0.3
0.0	—	—	10	0.021	0.000	0.6	+0.6
10.5	—	—	10	0.361	0.001	10.2	−0.3
21.0	—	—	10	0.763	0.011	21.3	+0.3
10.5	5	5	2	0.373	0.015	10.1	−0.4
21.0	10	10	2	0.744	0.025	20.3	−0.7

Conclusion

The spectrophotometric method for determination of microquantities of beryllium with 8-hydroxyquinaldine was established. By this method from 2 to 30 micrograms of beryllium in about 40 ml. can be determined simply and accurately. Small quantities of aluminum do not interfere with this method, and even in the presence of a minute amount of iron, beryllium can be determined by making a correction for the amount of iron persent. Therefore complete separation of aluminum and iron is not necessary. Moreover, the separation method of beryllium from relatively large amounts of iron, aluminum and titanium was studied.

The author wishes to express his sincere appreciation to Prof. Dr. M. Ishibashi for his encouragement and numerous suggestion throughout the investigation.

Faculty of Science and Engineering, Ritsumeikan University, Kyoto

Analytical Chemistry of Beryllium. VIII. Fluorometric Determination of Micro Quantities of Beryllium with 8-Hydroxyquinaldine

By Kenji MOTOJIMA

(Received August 11, 1955)

Introduction

In the previous paper[1] it was reported that the beryllium chelate of 8-hydroxyquinaldine could be quantitatively extracted with chloroform and that the extract was successfully used for the spectrophotometric determination of micro quantities of beryllium. As this chloroform extract containing beryllium chelate of 8-hydroxyquinaldine shows strong yellowish green fluorescence under ultraviolet light, the following investigation was undertaken to see whether or not this fluorescence was reproducible enough for a fluorometric method for beryllium.

Beryllium chelate of 8-hydroxyquinaldine was extracted with chloroform by a way similar to that mentioned in the previous work[1], then the fluorescence of the extract was measured, and it was found possible to determine from 0.3 to 3 micrograms of beryllium in about 40 ml. of solution without

1) K. Motojima, This Bulletin, "Analytical Chemistry of Beryllium. VII."

difficulty. Therefore the sensitivity of this method is nearly equal to that of the morine method developed by Sandell[2], but is better than that of the quinizarin method established by Fletcher and others[3].

Apparatus

A fluorometric attachment for Beckman Model DU spectrophotometer with a tungsten lamp as the light source, was used for fluorescence measurement. A primary filter transmits a band of wave-lengths centering at 360 mμ, and a secondary filter which is transparent to all wave-lengths longer than about 430 mμ, were used. The reason why this secondary filter was selected, was that the wave-length band of the fluorescent light produced by the beryllium chelate of 8-hydroxyquinaldine in chloroform was approximately distributed from 450 to 625 mμ, which was observed by the visual method using a spectrometer.

All the other apparatuses were the same as were used in the previous work[1].

Reagents

Standard Beryllium Solution.—Several standard beryllium solutions were prepared by exactly diluting the standard solution used in the previous work[1]. Each 10 ml. of these solutions contained 0.53, 1.05 and 2.10 micrograms of beryllium.

Standard Quinine Sulfate Solution.—Quinine sulfate (0.100 g., reagent grade) was dissolved and diluted to 1 l. with 0.1N sulfuric acid. This solution was exactly diluted with 0.1N sulfuric acid to yield a solution containing 1 microgram of quinine sulfate per milliliter.

Other Reagents. — 8-Hydroxyquinaldine solution, chloroform and the other reagents were prepared in the same way as was mentioned in the previous work[1].

Procedure and Preparation of Calibration Curve

Approximately 35 ml. of slightly acidic solution containing from 0.3 to 3 micrograms of beryllium, is treated with 5 ml. of 10% ammonium chloride solution and 2ml. of 8-hydroxyquinaldine solution, and the pH of the solution is adjusted to 8.0±0.2 with 2N ammonium hydroxide. The solution is transferred to a separatory funnel with a few milliliters of rinsed water, and the volume is brought to 50 ml. By the same procedure mentioned in spectrophotometric method[1], extraction is made with 10.0 ml. of chloroform, and the chloroform solution is dried with unhydrous sodium sulfate. Then the fluorescence of this chloroform solution is measured with a Beckman photofluorometer setting the chloroform at 0 and the standard quinine sulfate solution to 100 (or 50 when the fluorescence of the sample solution is stronger than this standard) on the transmittancy scale with the selector switch in the 1 position. Beryllium is determined by the use of the calibration curve prepared by similarly treating a series of known amount of beryllium.

The calibration curve was prepared by taking from 0.26 to 7.35 micrograms of beryllium. The result is shown in Fig. 1. As will be seen from this curve, an approximation to a linear relationship between beryllium concentration and the intensity of fluorescence is obtained up to 3 micrograms.

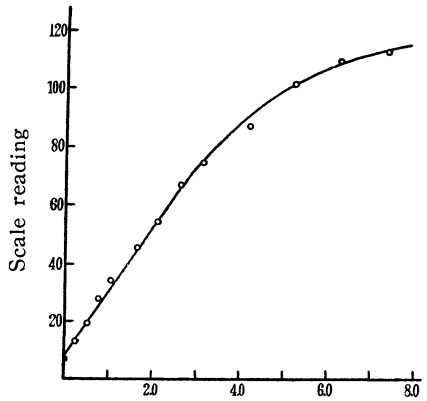

Fig. 1. Calibration curve for fluorometric determination of beryllium.

Effect of Variables

Effect of pH.—A series of several solutions each containing 2.10 micrograms of beryllium in about 35 ml. was treated with 2 ml. of 8-hydroxyquinaldine solution and suitable amounts of acetic acid and ammonium acetate or ammonium hydroxide and ammonium chloride to fall within a pH range of from 4 to 10. Then the extraction was made and the fluorescence of the extract was measured, respectively, by the above mentioned procedure. The results are shown in Fig. 2, and the approximately constant fluorescence is obtained in the pH range from 7.5 to 8.3.

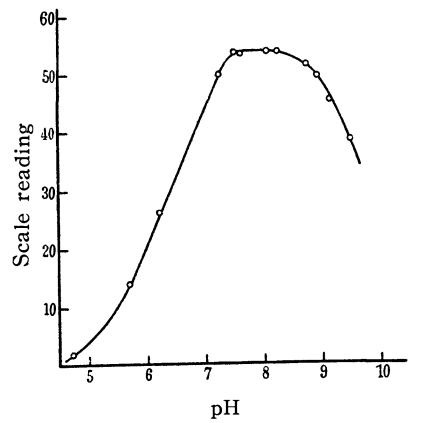

Fig. 2. Effect of pH on fluorometric determination of beryllium.

2) E.B. Sandell, *Ind. Eng. Chem., Anal. Ed.*, **12**, 674, 762 (1940); E.B. Sandell, *Anal. Chim. Acta*, **3**, 89 (1949).
3) M.H. Fletcher, C.E. White and M.S. Sheftel, *Ind. Eng. Chem., Anal. Ed.*, **18**, 179 (1946).

Ammount of Reagent.—Approximately 50 ml. of solutions each containing 2.10 micrograms of beryllium, 5 ml. of 10% ammonium chloride solution, varying amounts of 8-hydroxyquinaldine solution, and a suitable amount of dilute ammonium hydroxide, enough to adjust the pH to 8.0±0.2, were extracted with 10.0 ml. of chloroform respectively. Then, the fluorescences of these dried extracts were measured. As is shown in Fig. 3, the maximum intensity of the fluorescence is achieved by the use of 1.5 ml. of reagent solution, and as the reagent is added more and more, the intensity shows gradual decrease in proportion to its amount. For this reason 2 ml. of 1% 8-hydroxyquinaldine solution has been chosen as a suitable amount.

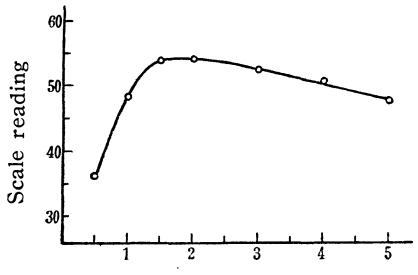

Fig. 3. Effect of amount of reagent.

Stability.—The fluorescence of the chloroform solution of beryllium chelate of 8-hydroxyquinaldine, stored in an amber glass bottle with a glass stopper and protected from sunlight was found to remain unchanged for a day, however, when the solution was left exposed to strong ultraviolet light, gradual decrease of fluorescence was observed.

Effect of Diverse Ions.—All of the ions which interfere with the spectrophotometric procedure mentioned in a previous paper[1], hinder this fluorometric method, therefore these ions should be absent. In this study, iron and aluminum were especially investigated, since they are most likely to exist together with beryllium. Their effects are shown in Table I. Though the effect of aluminum is not very great, it is desirable to remove more than 10 micrograms of aluminum.

TABLE I
EFFECTS OF IRON AND ALUMINUM
(Be taken in each case is 2.10 micrograms)

Added, Microgram		Fluorometer Scale Reading,	Be Found, Microgram
Fe	0	53.0	2.1_5
	5	47.5	1.8_7
	10	38.0	1.4_3
	15	30.5	1.0_8
	20	24.0	0.7_8
Al	5	51.9	2.0_8
	10	53.8	2.1_7
	25	58.7	2.4_0
	50	60.5	2.4_7
	100	62.0	2.5_5

The method to remove relatively large amounts of iron and aluminum from micro quantities of beryllium was made by the extraction separation method with oxine, mentioned in a previous paper[1], and then beryllium was determined fluorometrically. The results thus obtained are quite satisfactory, as shown in Table II.

TABLE II
THE FLUOROMETRIC RESULTS AFTER EXTRACTION SEPARATION WITH OXINE

Be Taken, Microgram	Metals Added, Milligram Fe	Al	Fluorometer Scale Reading,	Be Found, Microgram	Error, Microgram
0.00	20	—	7.5	0.0_0	0.0_0
0.00	—	20	13.0	0.2_6	$+0.2_6$
0.00	10	10	8.8	0.1_0	$+0.1_0$
0.53	10	10	20.0	0.6_0	$+0.0_7$
1.05	20	—	34.3	1.2_6	$+0.2_1$
1.05	—	20	32.5	1.1_8	$+0.1_3$
1.05	10	10	31.1	1.1_2	$+0.0_7$
2.10	20	—	49.7	1.9_8	-0.1_2
2.10	—	20	48.8	1.9_4	-0.1_6
2.10	10	10	52.5	2.1_0	0.0_0

Conclusion

The fluorometric method for determination of micro quantities of beryllium with 8-hydroxyquinaldine was established. By this method from 0.3 to 3 micrograms of beryllium in about 40 ml. of solution can be determined. The method of removing relatively large amounts of iron and aluminum from micro quantities of beryllium by the extraction separation method with oxine was also studied, and satisfactory results were obtained.

The author wishes to express his sincere appreciation to Prof. Dr. M. Ishibashi for his encouragement and numerous suggestions throughout the investigation.

Faculty of Science and Engineering,
Ritsumeikan University, Kyoto

On the Ion-exchange of Uranium

By Tatsujirô ISHIMORI and Hisateru OKUNO

(Received August 15, 1955)

With respect to the behavior of the uranium ion towards the ion-exchange resins, three investigations have thus far been reported: the elution of the uranium ions which have been adsorbed on cation-exchangers by the aid of oxalic acid[1]; the separation of UO_2^{+2} and NpO_2^+ with nitric acid[2]; and the adsorption of uranium ions on anion-exchangers in hydrochloric acid solution[3]. Now, the authors have studied the behavior of the uranium ion towards ion-exchangers on the basis of the distribution coefficient in solutions which contain acetate, sulfate, sulfuric acid, carbonate, and hydroxylamine, respectively. Solutions which contain oxalic acid or hydrochloric acid were also studied. Thus we have obtained some knowledge which will be useful in the separation of the uranium ion. And on this basis, we attempted the separations of uranium from thorium, iron (III), and neodymium.

In addition, we made some studies of uranyl nitrate solutions which either contained or did not contain the sulfate; and from its adsorbability we tried to get some information about the state of the uranyl ion in the solutions.

I. Method of Determination of Uranium

The uranium ion was determined colorimetrically with sodium carbonate and hydrogen peroxide[4]. Five millilitres of 10% sodium carbonate solution and 2 ml. of 3% hydrogen peroxide solution were added to a neutral sample solution, and the total volume of the solution was made 25 ml. Then, the uranium ion was determined by means of a Hitachi-photoelectric colorimeter and Tôshiba-filter VC-1. The calibration curve obtained is shown in Fig. 1. Sample solutions which were not neutral were treated similarly after being neutralized. Sample solutions which contained oxalic acid were evaporated to dryness; the residue was heated to volatilize and destroy oxalic acid, and dissolved in hydrochloric acid. Then, after volatilizing excess hydrchloric acid on a water-bath, the aqueous solutions were treated as above.

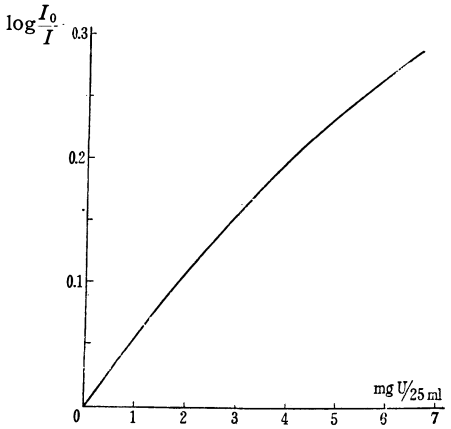

Fig. 1. Calibration curve of $Na_2CO_3.H_2O_2$ method.

II. Measurements of the Distribution Coefficient K_d

To a solution which contained a known amount of the uranyl ion and of known volume, was added a known amount of the ion-exchange resin. After the exchange-equilibrium was attained, the uranyl ions in the solution phase were determined colorimetrically, and the distribution coefficient was calculated as follows:

$$K_d = \frac{[UO_2R]}{[UO_2]_s} \quad \text{(ml./g.)},$$

where $[UO_2R]$ represents the amount of UO_2 in 1 g. of the resin, and $[UO_2]_s$, that in 1 ml. of the solution.

Most of the experiments were carried out by adding 0.2–1 g. of the resin to 25 ml. of a solution which contains 5–20 mg. of uranium. The exchange-equilibrium was attained in several hours in the case of a cation-exchanger, and in 15–20 hr. in the case of an anion-exchanger. The solutions were frequently stirred during these periods. In calculating the value of K_d, reduction in the volume of solutions due to absorption of water by the resins was neglected.

The following ion-exchangers were used. Cation-exchangers: Dowex 50, X-4; Dowex 50 (commercial). Anion-exchangers: Dowex 1, X-8.

III. Adsorption on Cation-exchange Resins

A) Uranyl Nitrate Solution.—It is reported[5] that in uranyl nitrate solutions $UO_2(NO_3)^+$ ions are present when the concentration is high, while

1) D. Dolar, Z. Draganic, *Rec. trav. inst. recherches structure matière* 2, 7783 (1953); Zd. Dizdar, *Rec. trav. inst. recherches structure matière* 2, 85 (1953).
2) G. Johansson, Sv. Kem. Tid., 65, 79 (1953).
3) K.A. Kraus. Private communication.
4) E. B. Sandell, "Colorimetric Determination of Traces of Metals" 1950, 2nd Ed., p. 601.
5) "Mukikagaku Zensho (Handbook of Inorganic Chemistry)," 251 (1953), Maruzen Co., Ltd., Tokyo.

in dilute solutions the salt dissociates to the second stage. Our experimental results on the cation exchange in uranyl nitrate solutions confirmed this fact.

The exchange equilibriums were studied by a batch method by adding a solution of $UO_2(NO_3)_2$ and $NaNO_3$ (in molar ratio, UO_2^{+2}: Na^+=1: 1.18) to Dowex 50, X-4 (NaR-form resin). The concentration range studied was 0.36 N-0.05 N. The results are plotted in Fig. 2.

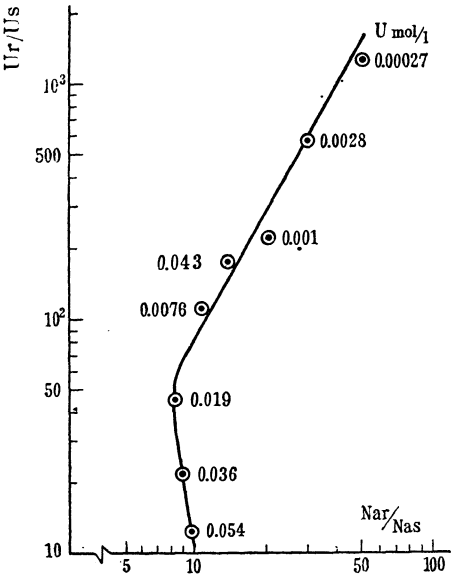

Fig. 2. Equilibrium curve of $UO_2(NO_3)_2$ in solutions.

In Fig. 2, in the concentration range where UO_2^{+2} is less than 0.007 mol./l. after equilibrium has been attained, the slope of the curve $\log \frac{[UO_2R]}{[UO_2]_s}$ vs. $\log \frac{[NaR]}{[Na]_s}$ is shown to be 2, which means that the salt is dissociated to the state of UO_2^{+2}. In the concentration range above 0.019 mol. UO_2/l., however, there can be seen no such relation; hence it is taken that the dissociation does not advance to the second stage.

In the following experiments, only the dilute uranyl solutions were dealt with; so there was no trouble with respect to the problem of dissociation of the uranyl salt. Uranyl ions may be considered to be adsorbed as di-positive ions when passed through the cation-exchanger layers.

B) Reduction of Adsorbability in Oxalic Acid, Acetate, Sulfate, Carbonate, or Hydroxylamine Solution.—The distribution coefficients in oxalic acid, acetate, or sulfate solutions are given in Table I. The adsorbability of the uranyl ion was found to decrease so considerably in the presence of acetate as well as oxalic acid that acetate solution may be utilized as an eluent for the uranyl ion. In the carbonate solution uranyl ions are not adsorbed at all. Hydroxylamine has been used for the separation of the uranyl and beryllium ions[6]. The relation between the distribution coefficient and pH in the hydroxylamine solution is given in Fig. 3.

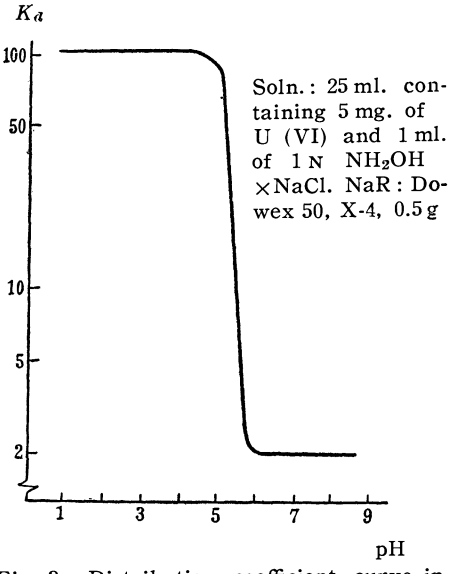

Fig. 3. Distribution coefficient curve in hyrdoxylamine solution.

TABLE I

DISTRIBUTION COEFFICIENTS OF THE URANYL IONS ON THE CATION EXCHANGER IN OXALIC ACID, ACETATE, AND SULFATE SOLUTIONS

(a)	$(COOH)_2$	$[(COOH)_2]$ %	0.05	0.2	1	2	4		
	—HR	Kd	72	25	5.7	5.6	0.5		
(b)	CH_3·COONa	[AcO] N	0	0.016	0.032	0.056	0.08	0.096	0.16
	—NaR	Kd	119	28	13	5.7	4.3	2.5	0.5
(c)	Na_2SO_4	$[SO_4]$ N	0	0.04	0.10	0.14	0.20	0.24	0.3
	—NaR	Kd	98	37	24	21	15	13	10

Solution: 25 ml.

(a) HR: Dowex 50 (commerical) 0.5 g.; 10.8 mg. U/25 ml.

(b) NaR: Dowex 50, X-4 0.5 g.; 5.4 mg. U/25 ml. CH_3COONa-$NaNO_3$ mixed soln.: conc. of the sodium ion=0.16 N

(c) NaR: Dowex 50, X-4 0.5 g.; 5.4 mg. U/25 ml. Na_2SO_4-$NaNO_3$ mixed soln.: conc. of the sodium ion=0.30 N

6) P.H. M-P Brinton, R. B. Ellestad, *J. Am. Chem. Soc.*, **45**, 395 (1923).

C) Change of Adsorbability with the Addition of Alcohol.—In the cation-exchange in an alcoholic solution, alkali metals are known to increase their adsorbabilities. In uranyl nitrate-HR form resin system, too, an increase in adsorbability was found to be produced by the addition of methyl alcohol (Fig. 4). This fact may be utilized to catch the uranyl ion which is relatively weak in adsorbability as a di-positive ion.

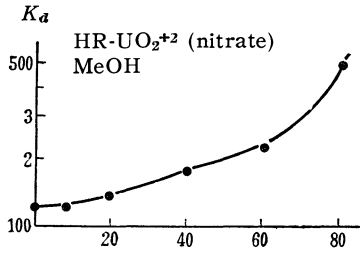

Fig. 4. Effect of alcohol.
Soln.: 25 ml. of 0.18N HNO_3, containing 20 mg. of U(VI).
HR: Dowex 50, X−4, 0.2g.

IV. Adsorption on Anion-exchange Resins

A) Adsorption in Hydrochloric Acid Solutions.—With regard to the ion-exchange of the uranyl ion in hydrochloric acid solutions, Diamond, Street, and Seaborg studied its cation-exchange[7], and Kraus studied the anion-exchange[3]. In Table II are shown our results on the adsorbability into the anion-exchanger in hydrochloric acid solutions of various concentrations. These results are found to be in agreement with those of Kraus.

B) Adsorption in Sulfuric Acid and Sulfate Solutions.—Absorption of the uranyl ion on the anion-exchanger in sulfuric acid and ammonium sulfate solutions is presented in Table II in terms of their distribution coefficients. Generally, stronger adsorption occurs in the latter solutions than in the former. This may be due to the insufficient formation of the complex anions, owing to the presence of HSO_4^- ion, in sulfuric acid solutions. In both cases adsorbability decrease as the concentration of the solution increases.

C) Adsorption in Carbonate Solutions.—In sodium carbonate solution uranyl dissolves in excess of the reagent, and the complex anion formed has a strong tendency to be adsorbed. The distribution coefficient is shown in Table II. This tendency may be used to concentrate uranium (VI) which has been extracted with excess of sodium carbonate.

An anion-exchanger was saturated with 0.2 N sodium carbonate solution and uranium (VI) solution (2 mg./ml.), then washed with dilute sodium carbonate solution. The result of measurement of the exchange capacity for the exchanger (Dowex I, X-8) showed that one mol. of uranium (VI) corresponded to 5.9 equiva lents. As one mol. of uranium corresponds to 6 equivalents, the complex anion supposed is $[UO_2(CO_3)_4]^{-6}$. The relatively small capacity is disadvantageous in concentrating and recovering uranium by this procedure.

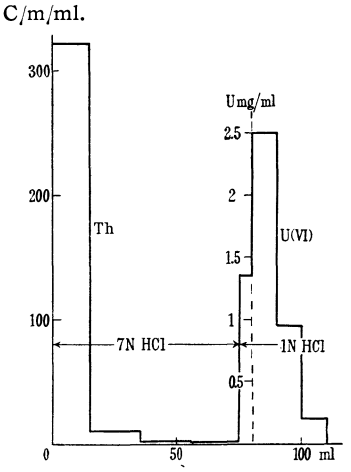

Fig. 5a. Separation from Th-234.

TABLE II

DISTRIBUTION COEFFICIENTS OF THE URANYL IONS ON ANION-EXCHANGERS IN HYDROCHLORIC ACID, SULFATE, SULFURIC ACID, AND CARBONATE SOLUTIONS

(a)	HCl-RCl	[HCl] N	2.4	3.6	4.8	6	7.2	11.5
		Kd	13	45	150	216	394	445
(b)	$(NH_4)_2SO_4$	$[(NH_4)_2SO_4]$ N	0.05	0.21	0.5	1.0	1.5	2
	$-RSO_4$	Kd	3000	1110	632	347	322	169
(c)	H_2SO_4	$[H_2SO_4]$ N	0.025	0.12	0.47	1.2	2.5	
	$-RSO_4$	Kd	590	356	69	2.6	0	
(d)	Na_2CO_3	$[Na_2CO_3]$ N	0.24	0.48	0.96	1.28	1.6	
	$-RCO_3$	Kd	3250	1230	394	261	192	

Anion exchanger: Dowex 1, X-8,
Solution: 25 ml.
(a) RCl: 0.5 g., Solution: U 20 mg.
(b) RSO_4: 0.2 g., Solution: U 10 mg.
(c) RSO_4: 0.2 g., Solution: U 10 mg.
(d) RCO_3; 0.2 g., Solution: U 11 mg.

7) R.M. Diamond, K. Street Jr., G.T. Seaborg, *J. Am. Chem. Soc.*, **76**, 1461 (1954).

V. Separations

A) Separation from Thorium.—Separation from thorium-234 was tried utilizing the adsorbability of U (VI) in hydrochloric acid solution. Dowex 50, X-8 resin was used. The elution curve is given in Fig. 5a. First, thorium was eluted with 8 N hydrochloric acid; and then U (VI), adsorbed on the exchanger, was eluted with 1 N hydrochloric acid.

The adsorption curve of the radiations of uranium here obtained was measured by means of a Lauritsen electroscope and aluminum absorbers. The results are plotted in Fig. 6.

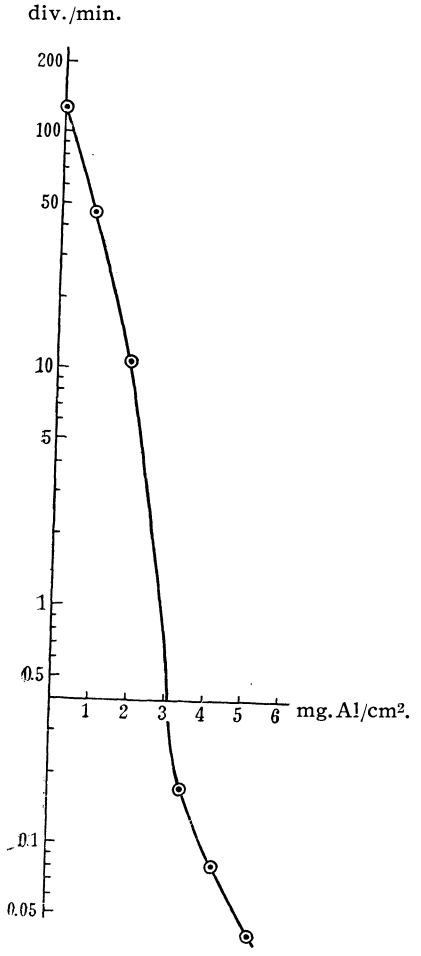

Fig. 6. Absorption curve of U-fraction.

B) Separation from Iron III.—Separation from iron (III) was carried out utilizing the adsorbability of U (VI) in sulfuric acid solution. The experimental conditions and the elution curve obtained are shown in Fig. 5b. A mixture of uranium (VI) and iron (III) in sulfuric acid solution was evaporated to dryness, then dissolved in 0.2 N H_2SO_4 and 0.6 N $(NH_4)_2SO_4$. Iron (III) was separated by passing RSO_4-form exchanging layer. Afterwards uranium (VI) was recovered by eluting with 2 N sulfuric acid.

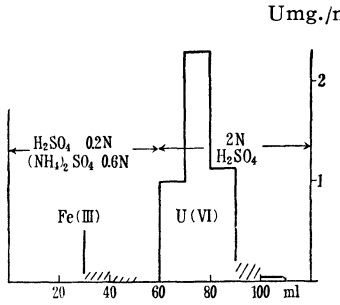

Fig. 5b. Separation from Iron (III)

C) Separation from Neodymium.—Based on the fact that neodymium is not adsorbed on an anion-exchanger in hydrochloric acid solution, the separation was carried out similarly as in the case of thorium. The same resin was used. The result is given in Fig. 5c.

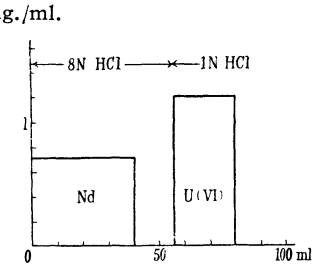

Fig. 5c. Separation from Nd.

VI. Complex Formation between Uranyl and Sulfate Ions

The state of the complex ion which is formed between uranyl and sulfate ions in solution was studied after the method suggested by J. Schu-

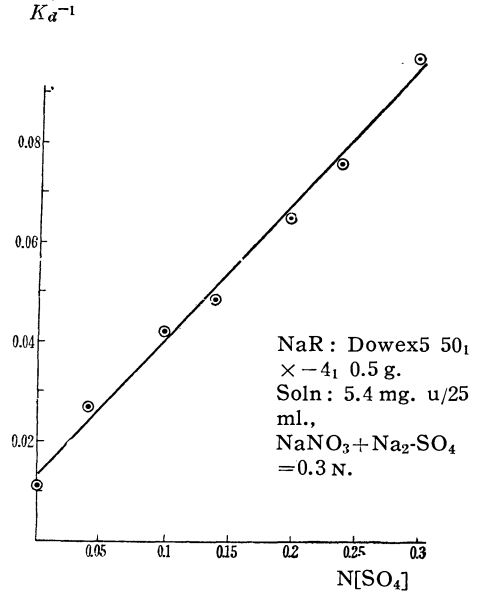

Fig. 7. The relation between K_d^{-1} and the concentration of sulfate.

bert[8], and it was found the complex present is in molar ratio UO_2^{+2}: SO_4^{-2}=1:1. A mixed solution containing sodium nitrate, sodium sulfate, and a definite amount of uranyl nitrate was added to a NaR-type resin, and the distribution coefficient was determined. The amount of uranium added was less than one-twentieth of the capacity of the ion-exchanger used. The total concentration of the $NaNO_3$-Na_2SO_4 mixed solution was 0.3 N, while the concentration of Na_2SO_4 was varied between 0 and 0.3 N. The result is given in Fig. 7.

As is seen in Fig. 7, the relation between K_d^{-1} and the concentration of sulfate ion is linear. Hence, it may be inferred that the ratio UO_2^{+2}: SO_4^{-2} is 1:1 as described above. That uranyl ions may be adsorbed on an anion-exchanger in sodium sulfate solution may be explained in terms of shifting of the equilibrium due to the formation and adsorption of the complex anion.

8) J. Schubert, *Anal. Chem.*, 22, 1359 (1950).

VII. Conclusions

From the experimetal results on the ion-exchange of uranium (VI), it was found that acetate solution is excellent for the elution in canion-exchange procedure; and that separation of uranium can be effected with sulfate solution in anion-exchange procedure.

The authors are grateful to the Ministry of Education for a Grant-in-Aid for Scientific Research.

Department of Chemistry, College of Science, Rikkyo University, Tokyo

Ultraviolet Absorption Spectra of 4-Chloro- and Bromo-pyridine N-Oxides

By Norisuke HATA

(Received August 23, 1955)

Introduction

In a previous paper[1], we have reported the ultraviolet absorption spectrum of pyridine N-oxide in solution and in vapor phase, where we observed a weak absorption system due to an n—π^* electronic transition, and discussed the effect of proton-donors on this absorption.

In the present investigation we measured the ultraviolet absorption spectra of 4-chloro- and bromo-pyridine N-oxides in various solvents.

In each of these substances we obtained a weak absorption at about 330 mμ and a strong absorption at about 290 mμ. The weak absorption is regarded as due to the n—π^* electronic transition, considering the solvent effect and the oscillator strength.

Experimental

4-Chloro- and bromo-pyridine N-oxides used in this experiment were prepared by the method described by Ochiai[2] and purified by recrystallisation from acetone several times. Melting points of 4-chloro- and bromo-pyridine N-oxides were 169.5°C and 143.5°C, respectively.

The solvents used were carbon tetrachloride, ethanol and water, which were purified by the methods described in "Organic Solvents"[3]. The spectra were measured with a Shimadzu Quartz Spectrophotometer Model QB-50, using a fused quartz cell of 1 cm. thickness. Measurements were limited to the region of wave-length shorter than 390 mμ.

Results and Discussion

Figs. 1 and 2 show the absorption curves of 4-chloro- and bromo-pyridine N-oxides, respectively, in various solvents. In the case of carbon tetrachloride solution, it appears that there are two absorption regions between 26000 cm^{-1}, and 44000 cm^{-1}, one of which is the weak absorption at about 30000 cm^{-1} (referred to as Transition I) and the other the strong absorption at about 34000 cm^{-1} (Transition II). When either ethanol or water is used as the solvent, the Transition I is not observed and the absorption maximum of the Transition II is remarkably shifted toward the shorter wave-length.

Even in water solution, however, the spectrum of 4-bromopyridine N-oxide shows a weak absorption at about 32,000 cm^{-1}. This weak absorption may be due to another transition different from the Transition I mentioned above, and the Transition I ob-

1) M. Ito and N. Hata, This Bulletin, 28, 260 (1955).
2) E. Ochiai, *J. Org. Chem.*, 18, 534 (1953).
3) A. Weissberger and E. Proskauer, "Organic Solvents", Oxford (1935).

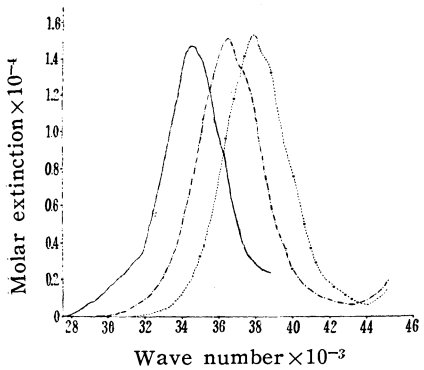

Fig. 1. Absorption curve of 4-chloropyridine N-oxide.
——— Carbon tetrachloride solution
— — — — Ethanol solution
------ Water solution

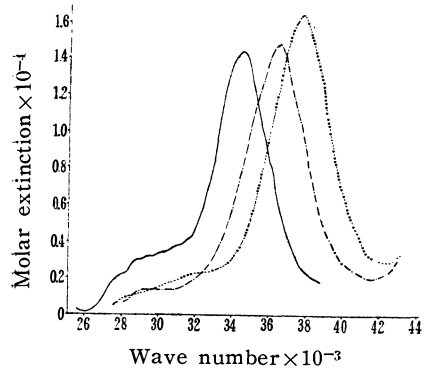

Fig. 2. Absorption curve of 4-bromopyridine N-oxide.
——— Carbon tetrachloride solution
— — — — Ethanol solution
------ Water solution

served in carbon tetrachloride solution may also overlap with this third transition.

The nature of spectra of these compounds may be explained in the same way as that of pyridine N-oxide reported by Ito and Hata[1].

4-Chloro or bromo-pyridine N-oxides molecules have two pairs of $2p$ non-bonding electrons on the oxygen atom, one of which is in conjugation with the π-electron system of the pyridine ring and the other remains as a non-bonding pair just as in the pyridine N-oxide molecule. According to our previous interpretation for pyridine N-oxide, the longer-wave weak absorption is ascribed to the transition of one of the oxygen non-bonding electrons to the lowest unoccupied orbitals (n-π^* transition), while the shorter-wave strong absorption is ascribed to the π-π^* transition, from the consideration of the solvent effect, the oscillator strength and the features in the vapor spectrum.

4-Chloro- and bromo-pyridine N-oxides may also have the weak n-π^* and the strong π-π^* transition. From the curves of Figs. 1 and 2, we see that the weak absorption (Transition I) completely disappears in ethanol or water solution.†

The disappearance of the Transition I in the ethanol and water solutions shows that it is due to the n-π^* electronic transition, since with these solvents of proton-donor character the oxygen non-bonding electron is largely stabilized in energy as a result of hydrogen bond formation.

The strong Transition II (π-π^* electronic transition) is remarkably shifted toward the shorter wave-length in ethanol and water solutions compared with carbon tetrachloride solution. These shifts are caused by the perturbation due to the hydrogen bond formation with ethanol or water. The absorption maxima and the molar extinction coefficients of Transition II of 4-chloro- and bromo-pyridine N-oxides in various solvents are given in Table I, together with that of the pyridine N-oxide.

TABLE I

ABSORPTION MAXIMA AND MOLAR EXTINCTION OF $\pi-\pi^*$ ABSORPTION (TRANSITION II)

Solvent	Carbon tetrachloride		Ethanol		Water	
Compound	$\lambda_{max.}$	$\varepsilon_{max.}\times10^{-4}$	$\lambda_{max.}$	$\varepsilon_{max.}\times10^{-4}$	$\lambda_{max.}$	$\varepsilon_{max.}\times10^{-4}$
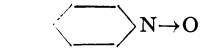	281	0.97	265	1.34	255	1.22
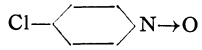	289	1.48	265	1.34	255	1.54
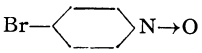	291	1.44	278	1.48	266	1.64

Next, in order to estimate the extent of contributions to the absorption by the n-π^* and π-π^* transitions respectively, peak analysis was made for carbon tetrachloride solution, and the oscillator strengths of the n-π^* and π-π^* transitions were calculated from the following equation[4], as for the pyridine N-oxide reported in our previous paper[1],

† However, 4-bromopyridine N-oxide has another absorption near 32000 cm^{-1} as previously stated, even in the water and ethanol solution.

4) H.P. Stephenson, *J. Chem. Phys.*, 22, 1077 (1954).

$$f=4.32\times10^{9}\int\epsilon dv.$$

Figs. 3 and 4 represent the peak analysis of the absorption curves of 4-chloro-and bromo-pyridine N-oxides, respectively. For 4-bromopyridine N-oxide, the π-π^* curve is extended in the exponential manner as the continuation of the normal absorption in the region where Transition I and the unknown transition mentioned above are not appreciable. The numerical results are given in Table II. As seen in this table, the ratios of oscillator strengths of n-π^* and π-π^* transitions are in the order of 10^{-2} for 4-chloro- and bromo-pyridine N-oxides, as well as for the pyridine and pyridine N-oxide. This also supports our assignment of the n-π^* and π-π^* electronic transitions assumed in this paper.

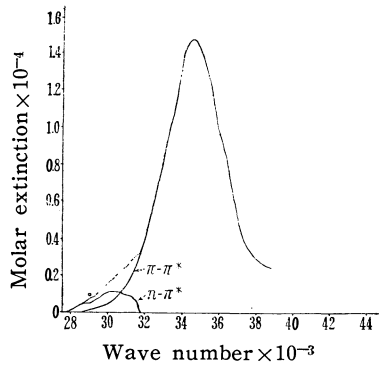

Fig. 3. Peak analysis of the absorption of 4-chloropyridine N-oxide in carbon tetrachloride solution.

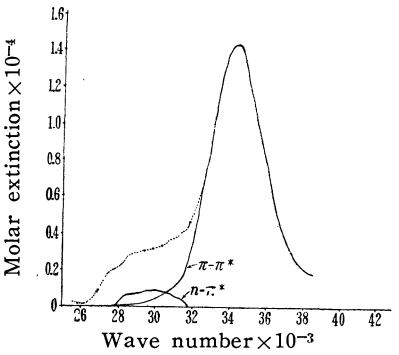

Fig. 4. Peak analysis of the absorption of 4-bromopyridine N-oxide in carbon tetrachloride solution.

TABLE II

OSCILLATOR STRENGTH OF $n-\pi^*$ AND $\pi-\pi^*$ TRANSITIONS

Compound	$f_{n-\pi^*}$	$f_{\pi-\pi^*}$	$f_{n-\pi^*}/f_{\pi-\pi^*}$
Cl— 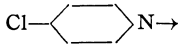 N→O	0.0059	0.205	0.029
Br— 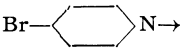 N→O	0.0063	0.249	0.025
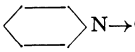 N→O[1]	0.012	0.173	0.079
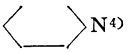 [4]	0.003	0.041	0.073

Summary

The solution spectra of 4-chloro- and bromo-pyridine N-oxides were measured in various solvents, in each of which were observed two absorption regions, one weak and the other strong.

The weak one was assigned to the transition involving the excitation of an oxygen non-bonding electron and the strong one to the transition involving the excitation of a π-electron.

In conclusion the author wishes to express his hearty thanks to Prof. S. Imanishi of Kyushu University for his kind guidance and valuable suggestions, and also to Prof. G. Kobayashi and Assistant Prof. E. Suenaga of Nagasaki University for their helpful advice. My thanks are also due to Mr. R. Tsuji and Miss. H. Yoshitomi for their assistance in the course of this work.

Faculty of Pharmacy, Nagasaki University, Nagasaki

Synthesis of Polycysteine

By Shumpei SAKAKIBARA and Hisaya TANI

(Received August 23, 1955)

Recently, poly-S-benzylcysteine has been synthesized[1,2,3] for the purpose of preparing polycysteine, which is a basic material to investigate the unique role of cysteine residues in natural proteins, but the reduction of it into polycysteine was unsuccessful because of its insolubility in liquid ammonia. So other protecting groups for sulfhydryl group were desired. Katchalski and Berger[3] published a short communication on the synthesis of polycysteine, which was prepared from poly-S-carbobenzoxycysteine by reducing it with sodium in liquid ammonia, but the details have not been reported. Jones and Lundgren[4] have prepared polycystine and their result that it was soluble in 2-mercaptoethanol in spite of its three dimensional structure suggested that polycysteine might have been formed in that solution. However, the polymerization degree of its polypeptide chain was so low that this route may not be suitable to synthesize the higher molecular weight polycysteine.

In the present paper S-thiophenyl-L-cysteine (I) was synthesized for a starting material, and polycysteine (III) was obtained by heating the solution of N-carboxyanhydride (II) of this amino acid (I) in ethyl thioglycolate, where the polymerization and the reduction occurred simultaneously; on the other hand, the reduction of poly-S-thiophenylcysteine, which was prepared quantitatively by heating the solution of the anhydride (II) in pyridine or nitrobenzene, was unsuccessful for the same reason as in the case of poly-S-benzylcysteine. The synthetic route was as follows:

The synthesis of the compound (I) from benzenesulfenyl chloride and L-cysteine was carried out at first in the cold aqueous solution under the usual condition of the Schotten-Bauman reaction, but the yield was only less than 30% because of the hydrolysis of the reagent. After several trials, it was found that absolute ethanol was an excellent solvent in this case. In the presence of sodium bicarbonate, benzenesulfenyl chloride reacted smoothly with L-cysteine hydrochloride in an alcoholic solution and the compound (I) was obtained in a very good yield. This substance (I) involved a disulfide linkage and could be reduced easily into L-cysteine by simple reactants, for example, by tin and hydrochloric acid or by excess mercaptane through the disulfide-sulfhydryl equilibrium. As the disulfide linkage in this substance was unsymmetrical unlike in cystine, it was comparatively unstable towards mineral acids or caustic alkalis; when it was dissolved in a cold aqueous solution of more than 1 N sodium hydroxide or boiling hydrochloric acid, decomposition occurred gradually and in the case of the latter L-cystine and diphenyldisulfide were formed. This phenomenon was

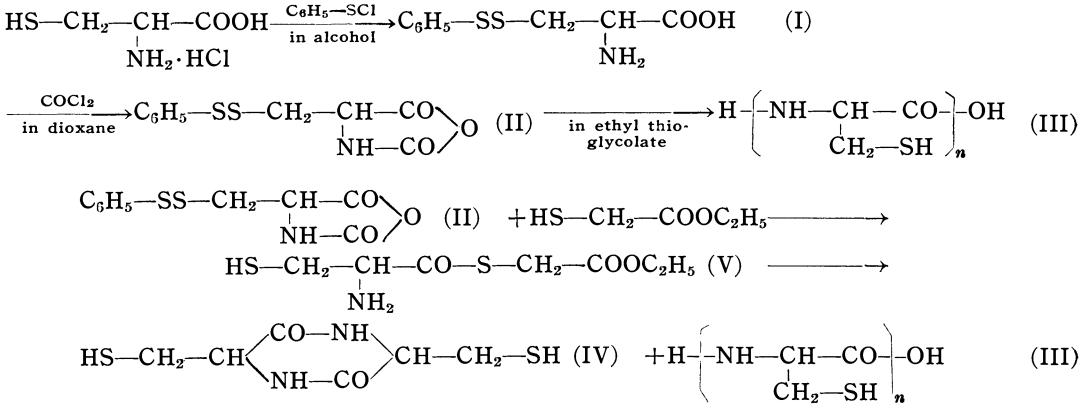

1) H. Tani, H. Yūki, and S. Sakakibara, *Seni Kagaku Kenkyusho Nenpo (Mem. Inst. Fiber Research)*, **7**, 100 (1953).
2) E.R. Blakley, A.K. Sumner, and E.Y. Spencer, *Can. J. Technol.*, **30**, 258 (1952); cf. *C.A.*, **47**, 9264 (1953).
3) E. Katchalski and A. Berger, *Bull. Research Council of Israel*, **2**, 314 (1952).
4) H.W. Jones and H.P. Lundgren, *J. Am. Chem. Soc.*, **73**, 5465 (1951).

observed also in glacial acetic acid containing dry hydrogen chloride. The specific rotation of L-cystine formed in this way was compared with that of L-cystine used as a starting material, and then it was confirmed that no racemization occurred in this synthetic route. N-Benzoyl derivative and ethyl ester hydrochloride of the compound (I) were prepared, respectively. From these results it may be expected that it will serve as a useful material for the synthesis of simple peptides containing cysteine.

N-Carboxy-S-thiophenyl-L-cysteine anhydride (II) was prepared by the usual method from the compound (I) and phosgen. By heating the anhydride (II) in ethyl thioglycolate, a white amorphous substance (IIIa) was precipitated.

The infrared spectrum of this substance had three absorption bands, 3050, 3190, and 3285 cm^{-1}, within the amide NH stretching frequency region; one of which, 3190 cm^{-1}, corresponded to the band of *cis*-hydrogen bonds formed between two amide linkages, suggesting the presence of diketopiperazine-type compounds[5]. After extraction of this substance with thioglycolic acid and methanol in order to remove any soluble matter, this band, 3190 cm^{-1}, completely vanished in the spectrum of the insoluble substance (III b), and a band at 2545 cm^{-1}, indicating the presence of the sulfhydryl-group, remained (Fig. 1). From the fact that the substance (III b) displayed two major absorption bands in the spectrum at 1520 and 1635 cm^{-1} and very small bands at 1540 and 1670 cm^{-1} within the C=O stretching and amide NH deformation frequency regions, it was suggested, according to Ambrose and Elliott[6], that the conformation of polypeptide chain in the

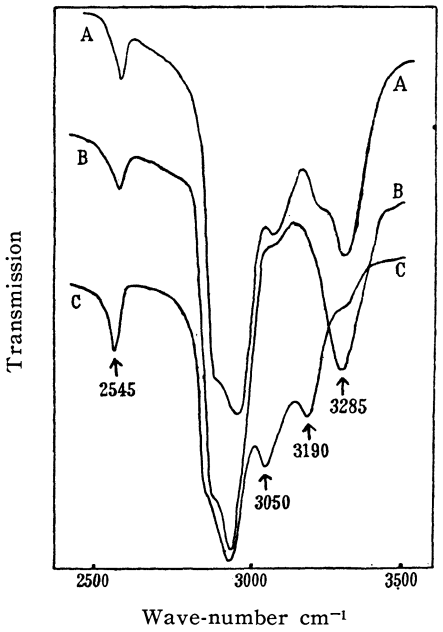

Fig. 1. Infrared spectra of IIIa(A), IIIb(B), and IV(C). Nujol suspension. Adam-Hilger H-800 double beam system.

substance (III b) was mainly in the β-keratin-type (Fig. 2). Absorption bands due to the thiophenyl group were not detected at all in this spectrum by comparison with that of poly-S-thiophenylcysteine and also no absorption bands due to ethyl thioglycolate were observed.

This substance was insoluble in usual organic solvents except ethanolamine and soluble in aqueous alkali but its alkaline solution decomposed gradually under evolution of hydrogen sulfide at room temperature. The nitroprusside test was extremely positive; the brown copper salt was formed under the condition of the biuret reaction and its mother liquor was brownish violet; the picric acid test for diketopiperazine was negative.

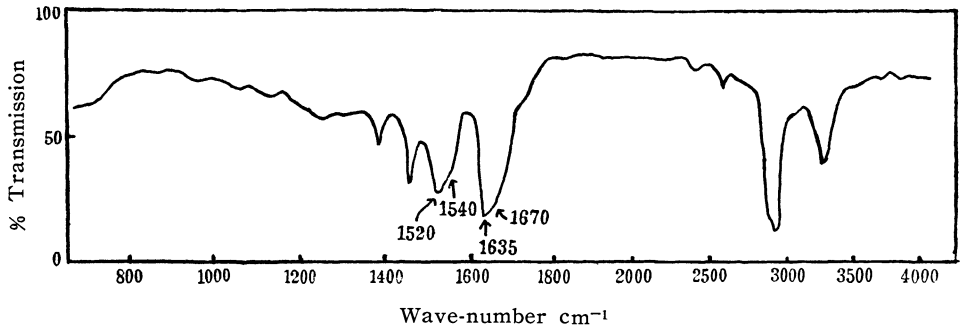

Fig. 2. Infrared spectrum of polycysteine (IIIb): Nujol suspension. Adam-Hilger H-800 double beam system.

5) M. Tsuboi, This Bulletin, 22, 255 (1949).

6) E.J. Ambrose and A. Elliott, *Proceed. Roy. Soc.*, A205, 47 (1951); cf. S. Mizushima and S. Akabori, "Chemistry of Proteins", Kyoritsu Shuppan Co. Ltd., Tokyo, Japan (1954), p 455-479.

The ammoniacal solution of this material was coagulated oxidatively to form gel on treatment with iodine. It displayed an amorphous X-ray diffraction pattern and the average polymerization degree calculated from the ratio of total nitrogen and amino nitrogen was 36.

The substance (IV) extracted from the polymer (IIIa) by thioglycolic acid and methanol was obtained as colourless fine prisms; its chemical properties have all been identified with those of cysteinyl-cysteine anhydride described by Greenstein[7] and its infrared spectrum has agreed with that of glycine anhydride, except the bands due to the presence of the mercaptomethyl group.

From these results, it may be concluded that the thioester of cysteine (V), formed from the anhydride (II) and ethyl thioglycolate, should take a part in the condensation reaction in parallel with the ordinary polymerization reaction of the anhydride (II)[8].

Experimental

S-Thiophenyl-L-cysteine (I).—Benzenesulfenyl chloride was prepared from 5 g. of thiophenol according to the method of Lecher[9], and, after removal of the reaction solvent, it was used as the solution of its residual syrup in 30 ml. of ether. A solution of 6.2 g. of L-cysteine hydrochloride in 120 ml. of absolute ethanol was cooled at 0°C, 3.8 g. of powdered sodium bicarbonate was added in one portion and into the whole mixture was dropped the chloride solution under stirring. After the complete addition of the reagent, the reaction mixture was allowed to stand at room temperature and sodium chloride was removed by filtration. After the addition of 5 ml. of pyridine into the filtrate, the fine precipitate was centrifuged, washed well with alcohol and dried; wt. 8.6 g.. After recrystallization from 0.5N hydrochloric acid, 8.1 g. (88%) of colourless plates was obtained; m.p. 192° (decomp.), $[\alpha]_D^{18}$-78.3° (c 0.38, 1N HCl). Anal. Found: C, 47.43; H, 4.64: N, 6.19; S, 27.4. Calcd. for $C_9H_{11}O_2NS_2$: C, 47.14; H, 4.84; N, 6.12; S, 27.9%. The solubility of this substance in water was about 50 mg./100 ml. at 17°C and increased about three times at 100°C. Paper chromatography showed this amino acid to have an Rf value of 0.69 in *n*-butanol: water: acetic acid (4:1:1).

Decomposition of (I) by 6N hydrochloric acid.—The solution of 0.5 g. of (I) in 20 ml. of 6N hydrochloric acid was boiled for about thirty minutes, cooled to room temperature and the crystalline diphenyldisulfide was filtered off. This was separated out as light oil and crystallized after cooling; the yield of recrystallized needles was 230mg., m.p. 60–61°, undepressed on admixture with an authentic sample. The filtrate was treated with charcoal and neutralized at pH 3 with aqueous sodium acetate; 220 mg. (84%) of L-cystine was obtained; $[\alpha]_D^{17}$-233° (c 0.85 1N HCl); cf. original L-cystine $[\alpha]_D^{17}$-233° (c 2.0 1N HCl).

Decomposition of (I) by dry hydrogen chloride in glacial acetic acid.—A suspension of 0.5g. of (I) in 50 ml. of glacial acetic acid was heated at 60 °C and dry hydrogen chloride was introduced for about thirty minutes; (I) was dissolved gradually within about ten minutes and then another crystalline precipitate was separated; this was filtered off after cooling. The filtrate was concentrated to dryness under reduced pressure, washed with petroleum ether, then some second crop was obtained. The total crop was 350 mg. in the form of L-cystine hydrochloride; $[\alpha]_D^{16.5}$-232° (c 0.85 1N HCl) (after recrystallization from 0.3 N HCl).

N-Benzopl-S-thiophenyl-L-cysteine.—A solution of 1g. of (I) in 90 ml. of 0.05N sodium hydroxide was cooled at 0°--5°C, into the solution was added 0.73 g. of benzoyl chloride, and 43.5 ml. of 0.1N sodium hydroxide was added in portions under stirring. After thirty minutes the reaction mixture was slightly acidified with hydrochloric acid, and the crystallized crude product was filtered off. This substance was dissolved in sodium bicarbonate solution, an insoluble matter, which was unchanged (I), wt. 0.5 g., was filtered off and the filtrate was extracted with ether and then slightly acidified by the addition of 6N hydrochloric acid; the N-benzoyl derivative of (I) was crystallized in fine needles, wt. 0.7 g.; m. p. 154–5° (after recrystallization from either 50% ethanol or benzene), $[\alpha]_D^{16.5}$-232° (c 1.0 ethanol). The yield based on reacted (I) was quantitative. Anal. Found: N, 4.16; S, 19.3. Calcd. for $C_{16}H_{15}O_3NS_2$: N, 4.21; S, 19.2%.

N-Carboxy-S-thiophyenyl-L-cysteine anhydride (II).—Dry phosgen was introduced into a suspension of 2 g. of finely powdered (I) in 80 ml. of dioxane at 40°C until the solid matter disappeared. After concentration to dryness under reduced pressure, the residual syrup was crystallized at 50°C in vacuo. N-carboxy anhydride was obtained as colourless plates after recrystallization from ethyl acetate and petroleum ether; wt. 1.2 g., m.p. 117–9°; a second crop was 0.7 g., total yield 85%. Anal. Found: N, 5.32. Calcd. for $C_{10}H_9O_3NS_2$: N, 5.50%.

Ethyl S-thiophenyl-L-cysteinate hydrochloride.—A solution of 0.5 g. of (II) in 50 ml. of ethanol containing 0.55 g. of dry hydrogen chloride was allowed to stand over night at room temperature. Removal of ethanol left a viscous syrup, which was crystallized by the addition of some ether; slightly coloured needles 0.57 g., m.p. 130–131.5° (after recrystallization from either ethylacetate or benzene); $[\alpha]_D^{18.5}$ −43.6°C (c 0.87 ethanol). Anal. Found: N, 4.58. Calcd. for $C_{11}H_{16}O_2NS_2Cl$: N, 4.77%.

7) J.S. Greenstein, *J. Biol. Chem.*, **118**, 321 (1937).
8) Th. Wieland und W. Schäfer, *Angew. Chem.*, **63**, 146 (1951); cf. Th. Wieland, *Angew. Chem.*, **66**, 510 (1954).
9) H. Lecher und F. Holschneider, *Ber.*, **57**, 757 (1924).

Ethyl thioglycolate.—The procedure of Fiesselmann and Schipprak[10] for methyl thioglycolate was followed. A mixture of 34 g. of thioglycolic acid, 60 ml. of ethanol, 60 ml. of chloroform, and 4 g. of conc. sulfuric acid was placed in a flask of the Soxhlet extraction apparatus and about three quarters of the thimble was filled with freshly dehydrated magnesium sulfate. After refluxing for fifteen hours, the solution was washed with water, dried over anhydrous sodium sulfate and fractionally distilled; 39 g. of ethyl thioglycolate boiling between 68°/30 mm.–64°/21 mm. was obtained.

Polymerization of N-carboxy-S-thiophenyl-L-cysteine anhydride.—A solution of 1 g. of (II) in 10 ml. of ethyl thioglycolate was sealed in a glass tube and heated for about five hours on a boiling water bath, where a white amorphous substance was precipitated spontaneously. The reaction mixture was allowed to cool; it was filtered after adding enough ethyl acetate and washed well with the same solvent, then the precipitate was suspended in 5 ml. of thioglycolic acid at 30–40°C for about thirty minutes. After adding enough methanol, the precipitate was filtered and washed well with the same solvent, 227 mg. (50% based on II) of white amorphous powder (III) was obtained after drying over phosphorus pentoxide in vacuo at room temperature for thirty minutes. Although this polymer diminished its weight 7% more by complete dryness, it was stored for any uses as it was, because after complete drying it might become insoluble, and then the weight was corrected in every analysis. Anal. Found: C, 35.1; H, 4.64; N, 13.2; S, 31.2; amino-N, 0.367; SHa, 26.9; SHb, 30.1. Calcd. for $(C_3H_5ONS)_n$: C, 34.9; H, 4.88; N, 13.6; S, 31.1; SH, 32.0%. The analytical procedures for the sulfhydryl group used here were the *p*-chloromercuribenzoate method[11] and the iodoacetic acid method[3]. In the former the sample was reacted with *p*-chloromercuri-benzoate in 0.1 N sodium hydroxide for twenty minutes, pH 5.2 acetate buffer solution was added and titrated with standardized cysteine solution (SHa). In the latter the sample was mixed with excess iodoacetic acid. and, after addition of 0.2 N sodium hydroxide, was allowed to stand at room temperature for thirty minutes, then the liberated iodide ion was titrated by the Volhard method (SHb). The filtered solution of thioglycolic acid and methanol was concentrated under reduced pressure and white powder was precipitated with ether; wt. 100 mg., m.p. 195–200° (after recrystallization from water). This substance was easily soluble in pyridine and thioglycolic acid, soluble in ethanol, methanol, and water; the nitroprusside and picric acid tests were positive respectively.

10) Fiesselmann und Schipprak, *Ber.*, **87**, 839 (1954).
11) R.E. Feeney, L.R. Mac Donnell and R.S. Silva, *Arch. Biochem. Biophys.*, **32**, 288 (1951).

Summary

The synthesis of polycysteine via S-thiophenyl-L-cysteine was described. S-thiophenyl-L-cysteine was prepared from benzenesulfenyl chloride and L-cysteine hydrochloride in absolute alcohol and its chemical properties were studied. This amino acid was polymerized by the N-carboxy anhydride method in ethyl thioglycolate containing an active sulfhydryl group, and it was confirmed by the studies of infrared spectra of these substances that the resultant polymer was polycysteine contaminated with diketopiperazine. Pure polycysteine was isolated by treating this polymer with thioglycolic acid and methanol. The benzoyl derivative and ethylester hydrochloride of S-thiophenyl-L-cysteine were prepared.

Department of Chemistry, Faculty of Science, Osaka University
Osaka

Studies on the Synthesis of Massoi-lactone and its Homologues. Part II. Synthesis of Nonyn-1-ol-4-carboxylic acid-1-lactone (Massoi-lactone)

By Shigehiro ABE and Kikumasa SATO

(Received August 23, 1955)

The main component of the essential oil of Massooi, the bark of Massoia aromatica Becc., is a lactone[1]. S. Abe named it "Massoi-lactone" and proposed its structural formula[1].

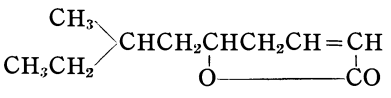

Afterwards, a part of this formula, outside the lactone ring was revised by Th. Meijer[2]

1) S. Abe, *J. Chem. Soc. Japan*, 58, 246-248 (1937); 733-738 (1937).

2) Th. Meijer, *Rec. trav. chim.*, 59, 191-201 (1940.)

to be a straight chain. S. Abe and K. Sato[3] also confirmed the new structure. Simultaneously, we undertook to synthesize Massoi-lactone and its homologues and prepared decene-1-ol-4-carboxylic acid-1-lactone[4], having one more methyene group than real Massoi-lactone has.

$$CH_3(CH_2)_5CHCH_2CH=CH$$
$$\quad\quad\quad

dissolved in 60 cc. of methanol, and after adding 2 g. of Pd-$BaSo_4$ (5% Pd). was partially hydrogenated with 0.66 l. of hydrogen (90% of the theoretical amount) at room temperature with constant shaking. After filtering off the catalyser and removing the solvent in vacuo, 50 cc. of benzene was added to the residue and the solvent was removed again in vacuo. Finally the residue was distilled in vacu. Nonene-1-ol-4-carboxylic acid-1-lactone was obtained as a colorless liquid, b. p. 147–149°/8 mm. Yield 3.4 g. (70%). $d_4^{20}=0.9787$. $n_D^{20}=1.4669$. M. R., Obs.: 47.75, Calcd.: 47.37.

Anal. Found: C, 71.18; H, 9.60. Calcd. for $C_{10}H_{16}O_2$: C, 71.39; H, 9.60%.

Summary

The Massoi-lactone (nonyn-1-ol-4-carboxylic acid-1-lactone), the main component of the essential oil of Massoi-bark was synthesized from *n*-hexanal and propargyl bromide.

A part of the cost of this study has been defrayed from the Scientific Research Expenditure of the Ministry of Education. Tue authors wish to express their sincere thanks to Mr. S. Kikuchi for his help during the course of this experiment.

Department of Chemical Industry, Faculty of Engineering, Yokohama National University, Yokohama

The Monolayer of Di- and Tri-carboxylic Fatty Acids

By Hiroshi HOTTA and Toshizo ISEMURA

(Received June 20, 1955)

Even though tremendous efforts have been devoted to the study of surface films of oily substances, since the development of surface chemistry, most investigations contributed to the study of monolayer of monocarboxylic fatty acids and their derivatives. The knowledge of the monolayer on aliphatic polycarboxylic acids is relatively insufficient at present. When we had studied the monolayer of polymethacrylic acid previously[1], we were obliged to refer to the information concerning the monolayer of monocarboxylic fatty acid to elucidate the result obtained. Now that we could fortunately get the sample of some poly-carboxylic acids, we studied their monolayer in the present investigation. Among those acids, the property of potassium alkyl malonates in aqueous solution was already reported elsewhere by Shinoda[2].

Experimental

Materials used principally in the present investigation are hexadecane-1, 1,2-tricarboxylic acid, CH_3-$(CH_2)_{13}$CH(COOH)-CH(COOH) (which is abbreviated to $C_{15}(COOH)_3$ hereafter), octadecy malonic acid (CH_3-$(CH_2)_{17}$-CH(COOH)), Japanic acid (ω, ω'-dicarboxylic acid), and stearic acid. The first two acids were kindly supplied by Mr. K. Shinoda of Yokohama National University and the others by Prof. N. Hirao of Kinki University.

The films of these acids were spread from dimethylformamide solution at the air/ and petroleum ether (b.p. 90–130°C)/aqueous phase interfaces. The substrate contained 0.01 N hydrochloric acid unless otherwise stated. Petroleum ether is called simply oil hereafter. Their interfacial pressure was measured at room temperature (about 10°C) by a hanging plate method at the air/water interface and by a ring method at the oil/water interface, respectively, as in the previous papers[1].

Results and Discussion

A. Interfacial Pressure at the Oil/Water Interface.—The interfacial pressure of $C_{15}(COOH)_3$ and octadecyl malonic acid at the oil/0.01 N hydrochloric acid aqueous phase interface is shown in Fig. 1. The observed value at the higher pressure region was somewhat varied due to partial dissolution into mediums. The result at the oil/distilled water interface was almost identical to the above result at the lower pressure region, but was more compressible under the higher pressure because the film is more soluble in this case.

When the product of interfacial pressure (π) and area per molecule (A) in Fig. 1 is plotted against π, the curves in Fig. 2 are obtained. The extrapolated values of πA to *zero pressure are almost equal to* kT. Generally, there is a fall of πA-π curve at the

1) T. Isemura, H. Hotta and S. Otsuka, This Bulletin, *27*, 93 (1954); H. Hotta, *ibid.*, *27*, 412 (1954).
2) K. Shinoda, *J. Phys. Chem.*, 59, 432 (1955).

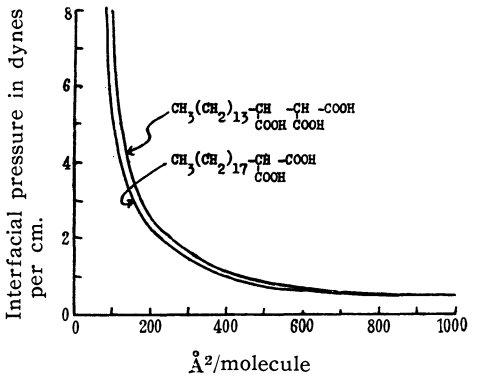

Fig. 1. The interfacial pressure at the petroleum ether/0.01 N HCl aqueous phase interface.

lower pressure region at the air/water interface due to some lateral adhesion between molecules[3]. On the other hand, there is no such fall at the oil/water interface as in the present result, since the molecules are free from such adhesion. For comparison, the curve of diethyl-ω, ω'-decane dicarboxylate, C_2H_5–OOC$(CH_2)_{10}$COO–C_2H_5 at the air/water interface by Adam and Jessop[5] is shown in Fig. 2.

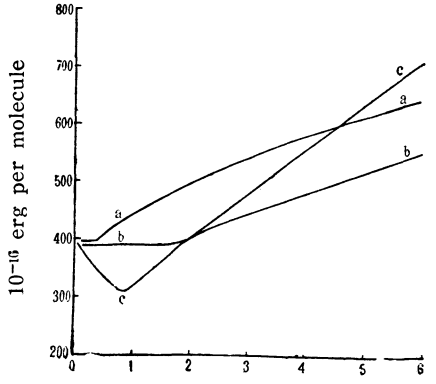

Fig. 2. The product of interfacial pressure and area per molecule plotted against interfacial pressure;
Curve a, $CH_3(CH_2)_{13}$–CH(COOH)–CH(COOH)–COOH at the oil/water interface;
Curve b, $CH_3(CH_2)_{17}$–CH(COOH)–COOH at the oil/water interface;
Curve c, C_2H_5–OOC$(CH_2)_{10}$COO–C_2H_5 at the air/water interface quoted from Ref. 5.

3) N.K. Adam, "The Physics and Chemistry of Surfaces" (1941), pp. 41.
4) H. Hotta, *J. Colloid Sci.*, 9, 504 (1954).
5) Adam and Jessop, *Proc. Roy. Soc. (London)*, A112, 376 (1926).

TABLE I

THE MEAN VALUE OF $(\pi A)_{\pi=0}$ AT THE PETROLEUM ETHER/0.01 N HCl AQUEOUS PHASE INTERFACE IN 10^{-15} ERG PER MOLECULE

Fatty acid	Spreading solvent: Dimethl-formamide	Spreading solvent: Benzene +Ether (9/1)
$CH_3(CH_2)_{13}$–CH(COOH)–CH(COOH)–COOH	395	—a)
Octadecyl malonic acid	385	380
Japanic acid	230	130
Stearic acid	80	0

a) Insoluble in this solvent.

On the other hand, Japanic acid and stearic acid could not be spread perfectly at the oil/water interface, for their extrapolated values of πA to zero pressure were varied and smaller than kT. The values of πA of the films spread from the solution in benzene and ether mixture (9/1) were notably smaller than those from dimethylformamide solution. Their mean values are also shown in Table I. This table shows that the more hydrophilic materials, spread from more polar solvent gives the value nearer to kT. The first dissociation constant of malonic acid (10^{-3}) is far greater than that of ω, ω'-dicarboxylic fatty acid (10^{-5}) due to internal hydrogen bonding[6]. The imperfect spreading of those acids has not been improved by the addition of potassium chloride or calcium chloride besides hydrochloric acid to substrate. It is concluded from these facts that the part of spreading molecules, which are dissolved as dimer in organic solvent, might be dissolved into oil phase without having access to the interface. Their spreading at the oil/distilled water interface was furthermore imperfect.

The above facts were examined with their homologues, too.

B. Surface Pressure at the Air/Water Interface.—The surface pressure of $C_{16}(COOH)_3$ and octadecyl malonic acid at the air/0.01 N hydrochloric acid aqueous phase interface is shown in Fig. 3. Here, it took a very long time to attain a constant pressure, when the film was compressed beyond a kink point. The steep rise of surface pressure was liable to occur at this region by a rapid compression. These tendencies were more remarkable in $C_{16}(COOH)_3$ than in octadecyl malonic acid. On the substrate containing 0.5 M potassium chloride in addition to hydrochloric acid, their film could better be compressed up to the higher pressure without transition than

6) L. Pauling, "The Nature of Chemical Bonds" (1938), Chapt. 9.

on the substrate without neutral salt, as shown by dotted lines in Fig. 3. Furthermore, the initial surface pressure fell down rapidly to an almost constant value beyond the kink point, although the value may still be a transient one due to the promoted reterdation of the dissolution of film into substrate by the addition of salt.

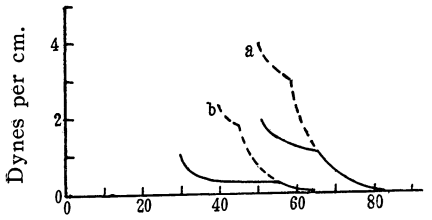

Å² per molecule

Fig. 3. Surface pressure at the air/0.01 N HCl aqueous phase interface.
The dotted lines show the result on the substrate containing 0.05 M KCl in addition to 0.01 N HCl.
Curve a, $CH_3(CH_2)_{13}-CH(COOH)-CH(COOH)-COOH$;
Curve b, $CH_3(CH_2)_{17}-CH(COOH)-COOH$.

It is concluded from these facts that the molecules at the interface would dissolve very slowly into aqueous phase without surface reorientation. It is perhaps because the non-polar tail of molecules cannot reorientate rapidly as it was compressed owing to the larger head group in comparison with its tail and therefore the irregular arrangement. We had experienced previously that the copolymers of vinyl acetate and stearate gave results which were not so reproducible owing to the difficult reorientation of heterogeneous side chains when compressed[7].

The film of octadecyl malonic acid had been already investigated by Adam and Miller[8] and discussed by Knight[9]. Their result is almost identical with the result of rapid comprission of the present investigation. Moreover, there is the study of the film of succinic acid derivatives[10]. The areas at the kink point or limiting areas in Fig. 3 are plausible in the light of the size of head group, when we take into account of these previous results. There was no essential difference between the films of dodecyl and octadecyl malonic acids.

Their films at the air/distilled water interface were more readily soluble, but not expanded, although they might be imperfectly spread.

The film of ω, ω'-hexadecadicarboxylic acid has already been reported in a previous paper[11]. The film of Japanic acid was also dissolved into substrate as it was compressed in the same way as above. Again, it is because the reorientation of non-polar parts occures with difficulty when compressed.

Conclusion

At the oil/water interface, 1, 1, 2-tricarboxylic and 1, 1-dicarboxylic fatty acids are easily spread monomolecularly, but ω, ω'-dicarboxylic and monocarboxylic fatty acids cannot be spread perfectly due to partial dissolution into oil phase. It is necessary for perfect spreading that the spreading molecule have appropriate hydrophilic nature.

At the air/water interface, monocarboxylic fatty acids generally give a perfect film as s well-known. The film of 1, 1, 2-tricarboxylic and 1, 1-dicarboxylic fatty acids is unstable and dissolves into substrate above a certain surface pressure, while the film of ω, ω'-dicarboxylic fatty acid is dissolved without any kink point as it is compressed. It is concluded from these facts that the good arrangement of the non-polar part is necessary for perfect surface transformation. If not so, because of the steric hindrance of itself or of other part, the film is dissolved into medium or collapses with out trans formation.

In conclusion, the authors express their hearty thanks to prof. N. Hirao of Kinki University and Mr. K. Shinoda of Yokohama National University who kindly supplied valuable samples to them.

The Institute of Scientific and Industrial Research, Osaka University, Sakai, Osaka

7) T. Isemura, H. Hotta and T. Miwa, This Bulletin, 26, 380 (1953).
8) Adam and Miller, *Proc. Roy. Soc.* (*London*), A142, 416 (1933).
9) Knight, *Biochem. J.*, 24, 257 (1930).
10) J.H. Schulman and W.McD. Armstrong, "Surface Chemistry" (Supplement of Research), p. 263 (1949).
11) H. Hotta and T. Isemura, This Bulletin, 25, 102 (1952).

Some Addition Compounds of Salicylaldehyde-ethylenediimine-copper. I

By Tsuguo TANAKA

(Received May, 6, 1955)

Among the addition compounds of the metal chelates of salicylaldehyde-ethylenediimine, several are well studied[1] because of their theoretical and practical importance. But most of them are the complexes of iron and cobalt which can form stable chelates not only in square but also in octahedral configurations.

Pfeiffer and others[2] observed that the green crystals of salicylaldehyde-ethylenediimine-copper gave a purple solution when dissolved in chloroform or in glacial acetic acid, and a green solution in pyridine. But they made no detailed studies about it.

The author suspected that this hypsochromic effect in the visible region must be due to the formation of the addition compounds, and succeeded in isolating some new addition compounds of salicylaldehyde-ethylenediimine-copper, of which the addition compound was hitherto unknown. Although the copper complex, crystallized from chloroform solution gives green leaflets of the original complex, an addition compound of purple needles was obtained when the saturated solution of salicylaldehyde-ethylenediimine-copper in acetic acid was concentrated under vacuum at room temperature. Further, some addition compounds with phenol were also isolated in crystalline state.

The addition compounds, salicylaldehyde-ethylenediimine-copper-acetic acid and salicylaldehyde-ethylenediimine-copper-phenol have the formulae $C_{16}H_{14}N_2O_2Cu \cdot C_2H_4O_2$ and $C_{16}H_{14}N_2O_2Cu \cdot C_6H_6O$ respectively. These compounds return to the original green complex salt, rather slowly when in contact with water and rapidly when in contact with alcohols.

The remarkable colour changes and the reversible additions and eliminations of acid and phenol must be concerned with the central metal copper, and the following three possible structures can be considered for such addition compounds.

By analogy (I) is considered to be valid in the ordinary addition compounds. But pyridine, ethyl acetate, anisole and anilline can not isolate addition compound of any stability, and in such an acidic conditions as we are now concerned with (II) and (III),.....which can be considered as the intermediates of acid degradation of the complex salt....., would be more probable and proton transfer at least would be considered to be necessary.

Among *o*-nitrophenol, *p*-nitrophenol, and picric acid, the latter two can form addition compounds, but *o*-nitrophenol can not form such an addition compound.

The addition compound with picric acid is stable and can be recrystallized from alcohol in brown crystals. This differs from the addition compounds of ordinary acids and phenols. Because of the steric hindrance of ortho substituted nitro groups, covalently linked structure (II) is not considered for the picric acid addition compound, but the ionic structure (III) is assigned to it. And consequently the structure (II) may be assigned to the ordinary purple addition compounds.

Copper complexes are known to have a square configuration[3] around copper and this configuration was justified by Pauling[4] by means of the hybridization of dsp_2 orbitals,

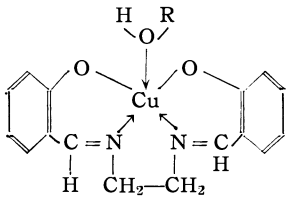

(I)

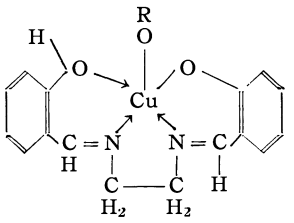

(II)

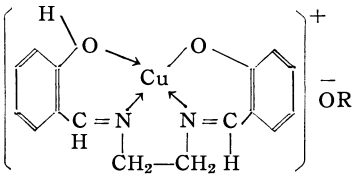

(III) R=CH_3–CO, C_6H_5

1) T. Tsumaki, *J. Chem. Soc. Japan*, 58, 1258 (1937). T. Tsumaki and Z. Endo, *J. Chem. Soc. Japan*, 64, 31 (1943). M. Calvin et al., *J. Am. Chem. Soc.*, 68, 2254, 2257, 2263 (1946).

2) P. Pfeiffer, E. Breith, E. Lübbe and T. Tsumaki, *Ann.*, 503, 85 (1933).

3) M. v. Stackelberg, *Z. anorg. Chem.*, 253, 136 (1947)

4) L. Pauling, *J. Am. Chem. Soc.*, 53, 1367 (1931).

but some complexes which have penta-covalent pyramidal structure[5,*] as in (I) and (II), are also reported.

In chloroform solution, the complex is supposed to assume such a structure as to contain intermediate weak coordinate link[**]. Anisole and anilline also produce purple coloration with the complex. 5-Nitrosalicylaldehyde-ethylenediimine-copper also forms addition compound with acetic acid or phenol, but 5-chlorosalicylaldehyde-ethylenediimine-copper does not form an addition compound with acetic acid, but forms a brick red addition compound with phenol, though this is not obtained in the pure state, because of its low solubility in any non-basic organic solvents.

Experimental

Salicylaldehyde-ethylenediimine-copper-acetic Acid

The saturated solution of salicylaldehyde-ethylenediimine-copper in glacial acetic acid is concentrated to its half volume under vacuum at room temperature. Large violet needles separate, which are filtered, and freed from acetic acid in vacuum desiccator on calcium chloride. This addition compound is unstable, and decomposed completely into the original complex on exposure to air overnight.

Water, methyl alcohol, ethyl alcohol, propyl alcohol, aniline and pyridine decompose this addition compound rapidly.

Anal. Found; C, 55.15; H, 4.56; N, 7.11; Cu, 16.45. Calcd. for $C_{18}H_{18}N_2O_4Cu$: C, 55.45; H, 4.65; N, 7.19; Cu, 16.30.

Salicylaldehyde-ethylenediimine-copper-phenol

The mixture of 1 mol. of salicylaldehyde-ethylenediimine-copper and 1.1 mol. of phenol is warmed above the melting point of the latter, immediate formation of addition compound occurs. The mass is washed with chloroform-benzene (1.10) to remove the excess of phenol.

The addition compound is stable in non-basic solvent, also in water, but is decomposed rapidly by alcohols. Fairly soluble in chloroform, sparingly soluble in benzene. m. p. 125°.

Anal. Found: C, 62.69; H, 4.77; N, 6.30; Cu, 14.50. Calcd. for $C_{22}H_{20}N_2O_3Cu$: C, 62.31; H, 4.75; N, 6.61; Cu, 14.99.

Salicylaldehyde-ethlenediimine-copper-p-nitrophenol

The mixture of 1 mol. of salicylaldehyde-ethylenediimine-copper and 1.1 mol. of *p*-nitrophenol is warmed above the melting point of the latter. Purple needles are formed immediately. The mass is dissolved in chloroform, and precipitated by the addition of benzene. The precipitates are recystallized from chloroform solution. The addition compound is obtained in purple needles. m.p. 225°.

Anal. Found: C, 55.65; H, 4.56; N, 9.16; Cu, 13.00. Calcd. for $C_{22}H_{19}N_3O_5Cu$: C, 56.34; H, 4.08; N, 8.96; Cu, 13.55.

Salicylaldehyde-ethylenediimine-copper-picric acid

A suspension of 1 mol. of salicylaldehyde-ethylenediimine-copper and 2 mol. of picric acid in chloroform is stirred for two hours at room temperature. The brown precipitates separate, which are filtered, washed with benzene and recrystallized from 80% alcohol. The brown needles, which contain 1 mol. water are stable in usual organic solvents. Stable in usual organic solvents.

Anal. Found: C, 45.62; H, 3.28; N, 12.51; Cu, 10.55. Calcd. for $C_{22}H_{17}N_5O_9Cu \cdot H_2O$: C, 45.79; H, 3.32; N, 12.14; Cu, 11.01.

The author is grateful to Prof. Dr. T. Tsumaki (Kyushu Univ.) for his kind instructions, and Mr. Mukai and Mr. Shito for the analysis.

Faculty of Liberal Arts, Saga College, Honjo, Saga

5) cf. M. Calvin and E. Martell, "Metal Chelate Compounds", Prentice-Hall (1952), pp. 113, 243, 286.

* Tetrahedral structure is also of some contribution in some cases.

cf. G. Kimball, *J. Chem. Phys.*, 8, 188 (1940); R. Hultgren, *Phys., Rev.*, 40, 891 (1932); H. Kuhn, *J. Phys.*, 16, 727 (1948); P. Pfeiffer, *Angew. Chem.*, 53, 93 (1940).

If $-O\rightarrow Cu$ coordination is weak, (II) would be irregular tetrahedral configuration and the mechanism of the addition compound formation would be bimolecular nucleophilic substitution of the protonated complex.

** This will be indicated by the special shifts of absorption bands as discussed in II of this series.

Investigation on the Molecular Structures of Titanium Tetrachloride and Zirconium Tetrachloride by Gas Electron Diffraction

By Masao KIMURA, Katsumi KIMURA, Michiro AOKI and Shuzo SHIBATA

(Received March 14, 1955)

Introduction

The structures of many metallic tetrachlorides have been studied by a number of workers and it has been proved that their configurations are regular tetrahedrons. The structures of the two chlorides dealt with in the present investigation, have already been determined by Lister and Sutton[1] as Ti−Cl =2.18 ±0.04 Å, Zr−Cl=2.33 ±0.05 Å. It is necessary, however, to obtain the data with experimental errors smaller than those disobtained by Lister and Sutton in order to cuss the structures of tetrahalide molecules more thoroughly.

The central atoms in these molecules have comparatively large atomic numbers, and the dimensions of these molecules appear to be so large that the effects of molecular vibrations cannot be ignored in a diffraction experiment. Therefore the effects can be expected to be estimated accurately from diffraction patterns.

It is well known that the physical properties have some regularities among various metallic tetrahalides. Furthermore the similarities between titanium tetrachloride and vanadium tetrachloride have been pointed out by Hildebrand[2] for boiling point, melting point, molar volume and so on. Despite their similarities, the vanadium-chlorine interatomic distance in VCl_4, 2.03 Å[3], is very different from the titanium-chlorine interatomic distance obtained by Lister and Sutton in $TiCl_4$. The present study was carried out in order to determine more accurately the structures of titanium tetrachloride and zirconium tetrachloride.

These interesting problems concerning the physical properties will not be solved until studies are made with respect to the bond character in tetrahalide molecules. In the present paper the force constants calculated on the basis of spectroscopic data are compared with the results obtained by electron diffraction and are discussed for tetrachloride molecules.

1) M.W. Lister and L.E. Sutton, *Trans. Faraday Soc.*, **37**, 393 (1941).
2) J.H. Hildebrand, *J. Chem. Phys.*, **15**, 727 (1947).
3) W.N. Lipscomb and G. Whitacker, *J. Am. Chem. Soc.*, **67**, 2019 (1945).

Experimental

The diffraction photographs were taken with the apparatus[4] which had hitherto been used. The wavelength of electron beams was about 0.06 Å. The wavelength was calibrated with a gold foil. Titanium tetrachloride was used without heating, since it is a liquid and can easily be evaporated at room temperature. Zirconium tetrachloride was evaporated by heating at about 120°C in a high temperature nozzle[5]. The diffraction photographs obtained were measured as usual by the visual method. The visual curves are drawn in Fig. 1V and Fig. 2V for $TiCl_4$ and $ZrCl_4$ respectively. The observed q values for the maxima and the minima are listed in Table I.

TABLE I
THE OBSERVED AND CALCULATED VALUES FOR $TiCl_4$

max.	min.	q_{obs}	q^0_{calc}*	$\frac{q^0_{calc}}{q_{obs}}$	$q^{0.0005}_{calc}$*	$\frac{q^{0.0005}_{calc}}{q_{obs}}$
1		7.60	7.30	(0.961)	7.30	(0.961)
	2	9.95	9.30	(0.935)	9.30	(0.935)
2		12.75	12.30	(0.965)	12.30	(0.965)
	3	15.65	15.65	1.000	15.65	1.000
3		18.65	18.90	1.013	18.85	1.010
	4	20.95	21.30	1.017	21.25	1.014
4		23.05	23.40	1.015	23.10	1.001
	5	26.60	26.40	0.992	26.40	0.993
5		29.60	29.65	1.002	29.60	1.000
	6	33.35	32.75	0.982	33.05	0.991
6		35.35	35.50	1.004	35.40	1.001
7		39.45	40.40	1.024	39.90	1.011
	8	43.60	43.55	0.999	43.60	1.000
8		47.60	46.75	0.982	47.35	0.995
	9	52.95	54.35	1.026	53.45	1.009
9		57.15	57.60	1.007	57.35	1.003
	10	61.70	60.75	0.985	61.55	0.998
10		66.05	68.40	1.035	66.65	1.009
	11	70.95	71.60	1.009	71.20	1.003
11		75.10	74.90	0.997	75.50	1.005
	12	80.60	82.40	1.022	80.40	0.998
12		84.00	85.45	1.017	84.90	1.010
	13	88.30	88.75	1.005	89.40	1.012
13		93.30	91.90	1.015	94.00	1.007
	average			1.007		1.003
	average deviation			0.013		0.005

* These values are those calculated for the model having r(Ti−Cl)=2.18 Å. The suffices 0 and 0.0005 show α values which refer to internal vibrations.

4) M. Kimura, *Chemical Researches*, **9**, 53 (1951).
5) M. Kimura and M. Aoki, This Bulletin, **26**, 429 (1953).
* See a later section.

and Table II. In these tables the values in parentheses are considered to have some uncertainties and are not used for a quantitative comparison of the observed values with theoretical ones.

TABLE II

THE OBSERVED AND CALCULATED VALUES FOR $ZrCl_4$

max.	min.	q_{obs}	q^0_{calc} *	$\frac{q^0_{calc}}{q_{obs}}$	$q^{0.0008}_{calc}$	$\frac{q^{0.0008}_{calc}}{q_{obs}}$
2		11.45	11.35	0.991	11.35	0.991
	3	14.85	14.75	0.993	14.75	0.993
3		18.35	18.20	0.992	18.20	0.992
	4	24.40	24.50	1.004	24.35	0.998
4		27.90	27.90	1.000	27.80	0.996
	5	32.00	31.10	0.972	31.60	0.987
5		37.25	37.50	1.007	37.00	0.993
	6	40.95	40.90	0.999	40.80	0.996
6		44.90	44.20	0.984	45.00	1.002
	7	50.00	50.95	1.019	49.55	0.991
7		53.80	54.00	1.004	53.95	1.003
	8	58.15	57.35	0.986	58.10	0.999
8		62.60	63.80	1.019	62.55	0.999
	9	66.60	67.20	1.009	66.80	1.003
9		70.70	70.40	1.004	71.10	1.006
	10	75.25	77.00	1.023	75.40	1.008
10		79.00	80.25	1.016	79.80	1.010
	11	83.40	83.45	1.000	84.05	1.008
11		87.80	86.80	0.989	88.35	1.006
	average			1.001		0.999
	average deviation			0.011		0.006

* These values are those calculated for the model having $r(Zr-Cl)=2.32$ Å. These suffices 0 and 0.0008 designate a values which refer to internal vibrations.

TABLE III

COMPARISON OF THE CALCULATED VALUES WITH THE OBSERVED VALUES OF $TiCl_4$

$r(Ti-Cl)=2.18$ Å

a	Curve	Average value of q_{calc}/q_{obs}	Average deviation of q_{calc}/q_{obs}
0.0000	T_0	1.007	0.013
0.0004	T_4	1.003	0.007
0.0005	T_5	1.003	0.005
0.0006	T_9	1.003	0.006

TABLE IV

COMPARISON OF THE CALCULATED VALUES WITH THE OBSERVED VALUES OF $ZrCl_4$

$r(Zr-Cl)=2.32$ Å

a	Curve	Average value of q_{calc}/q_{obs}	Average deviation of q_{calc}/q_{obs}
0.0000	T_0	1.001	0.011
0.0007	T_7	0.999	0.007
0.0008	T_8	0.999	0.006
0.0009	T_9	0.998	0.007
0.0010		0.998	0.007_5

The diffraction patterns of both $TiCl_4$ and $ZrCl_4$ show a feature with simple maxima and minima as a whole. A closer examination reveals, however, that the pattern of $TiCl_4$ is characterized by a shelf at the left side of the 7th maximum (designated in Fig. 2 by the 6th maximum) and a shelf perceptible at the right side of the 8th maximum. The pattern of $ZrCl_4$ is charaterized by a shelf at the right side of the 3rd maximum. Therefore these shelves coexistent with the maxima and minima can be expected to lead to the determination of the molecular structures with fair certainty.

(I) Radial Distribution Curve

By use of the visual curves, the radial distribution curves,

$$rD(r)=\sum_q I(q)\exp(-bq^2)\sin(\pi qr/10),$$

were calculated, where b was taken as $\exp(-bq^2_{max})=0.1$. Each curve for $TiCl_4$ and $ZrCl_4$ shows only two peaks, corresponding to the interatomic distances in the tetrahedral molecules with Ti−Cl =2.18 Å and Zr−Cl=2.32 Å. The radial distribution curves are shown in Fig. 1.

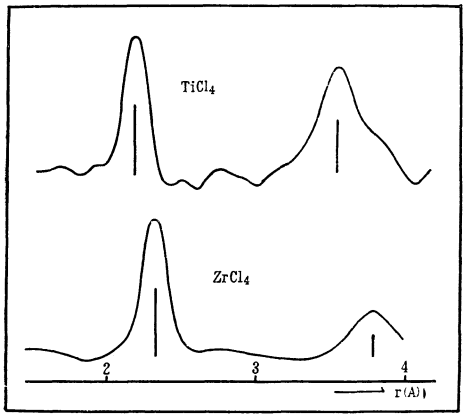

Fig. 1. The radial distribution curves for $TiCl_4$ and $ZrCl_4$.

(II) Theoretical Intensity Curve

The theoretical intensity curves

$$I(q)=\exp(-a_{MCl}q^2)\,[(4Z_MZ_{Cl}/r_{MCl})\sin(\pi qr_{MCl}/10)+6(Z_{Cl}Z_{Cl}/r_{ClCl})\exp(-aq^2)\sin(\pi qr_{ClCl}/10)],$$

were calculated for assumed models. Here M designates the central atom, $\exp(-a_{MCl}q^2)$ and $\exp(-aq^2)$ are the factors relating to the molecular vibrations and $a=a_{ClCl}-a_{MCl}$*. Since $\exp(-a_{MCl}q^2)$ is the factor relating only to the damping of curves, it was ignored by being kept constant. A regular tetrahedral form was chosen as a molecular form and the values of r(M-X) at the value obtained from the radial distribution curve were chosen.

Since these molecules have a tetrahedral form, only r(M-Cl) and a are the parameters required to calculate the theoretical intensity curves. The former is related to the position of the maxima and the minima, and the latter is related mainly to the features of the theoretical intensity curves and slightly to the positions of the maxima and

the minima.

(i) **$TiCl_4$.**—The theoretical intensity curves were calculated for the models which have the value of 2.18 Å for r(Ti−Cl) and the values ranging from 0.0000 to 0.0010 for a. Fig. 2 shows that the theoretical intensity curves for r(Ti−Cl)

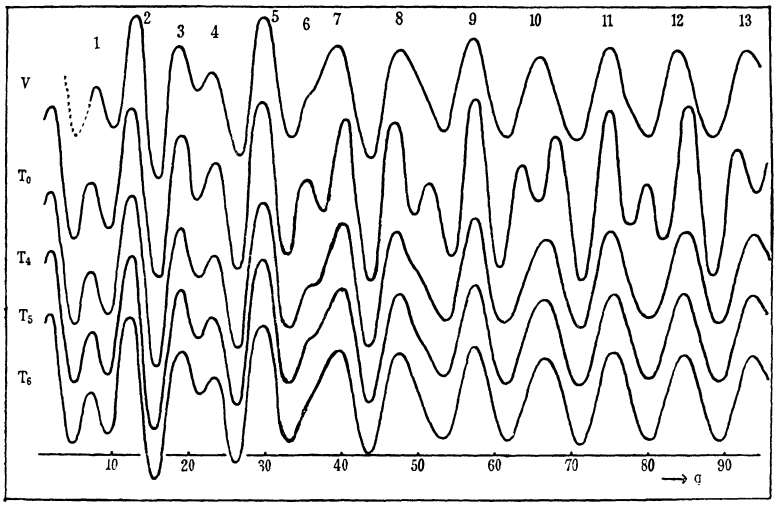

Fig. 2. Visual and theoretical intensity curves for $TiCl_4$. r(TiCl)=2.18 Å, a=0.0000, 0.0004, 0.0005 and 0.0006 for curve T_0, T_4, T_5 and T_6 respectively.

=2.18Å. The curve corresponding to a=0, i.e. a fixed model, has sharp maxima at the left side of the 7th and 10th maxima and at the right side of the 8th and 11th maxima (Fig. $2T_0$). Accordingly the curve does not agree with the visual curve at all. With the increasing value of a, the theoretical curve becomes similar to the visual curve and is in complete agreement with the visual one in the case of a=0.0005 (Fig. $2T_5$). In these curves, the shelf at the right side of the 8th maximum gives an example of noticeable change in the feature with values of a. The shelf disappears at the values of a greater than 0.0006 and is too distinct at those of a less than 0.0004. Thus a=0.0004−0.0006 are acceptable values even if experimental errors are taken into consideration. Table I and Table III show a comparison of the theoretical q values for the maxima and the minima in the case of r=2.18 Å with the observed ones. As a result, the discrepancies between the observed and the theoretical values were confirmed to be within experimental errors as long as a takes the value in the range 0.0004–0.0006. The errors in our experiments can be considered to be ±0.010 as an average deviation in ratio of the observed values and the calculated ones. Then taking into consideration the average deviations shown in Table III, those in the calculated curves having values other than r=2.18 Å and experimental errors, the molecular structure of titanium tetrachloride was obtained to be Ti−Cl=2.185 Å ±0.010 Å, a=0.0004−0.0006 and the tetrahedral form.

(ii) **$ZrCl_4$.**—The theoretical intensity curves were calculated for the models which have the value of 2.32 Å for r(Zr−Cl) and the values ranging from 0.0000 to 0.0011 for a. Fig. 3 shows the theoretical intensity curves for r=2.32 Å. The curve corresponding to a fixed model has many shelves (Fig. $3T_0$) and does not agree with the visual curve at all. With the increasing value of a, the shelves disappear except the shelf at the right side of the 3rd maximum and it also becomes indistinct. Upon comparison of these curves with the visual one, it was determined that a takes the values ranging 0.0007−0.0010 in the case of r(Zr−Cl)=2.32 Å by taking into account experimental errors. Furthermore the theoretical curves were compared quantitatively with the visual curve regarding the positions of the maxima and the minima. The results are shown in Table II and Table IV. Then the structure of zirconium tetrachloride was proved to be Zr−Cl=2.32 ±0.01 Å, a=0.0007−0.0010 and to have the tetrahedral form by means of a discussion similar to that carried out in the case of titanium tetrachloride.

Mean Amplitudes of Tetrachlorides of 4th Group Elements

The mean-square amplitudes of tetrachlorides of 4th group elements must be calculated from the normal modes of vibrations in order to compare the results obtained from electron diffraction with spectroscopic data. The method of calculation of the mean-square amplitudes of polyatomic molecules was first proposed by Karle and Karle[6]. Since then it has been improved and developed by Morino, Kuchitsu et al.[7]. If the displacements

6) J. Karle and I.L. Karle, *J. Chem. Phys.*, **18**, 957 (1950).

7) a) Y. Morino, K. Kuchitsu and T. Shimanouchi, *J. Chem. Phys.*, **20**, 726 (1952); b) Y. Morino, K. Kuchitsu, A. Takahashi and K. Maeda, *J. Chem. Phys.*, **21**, 1927 (1953).

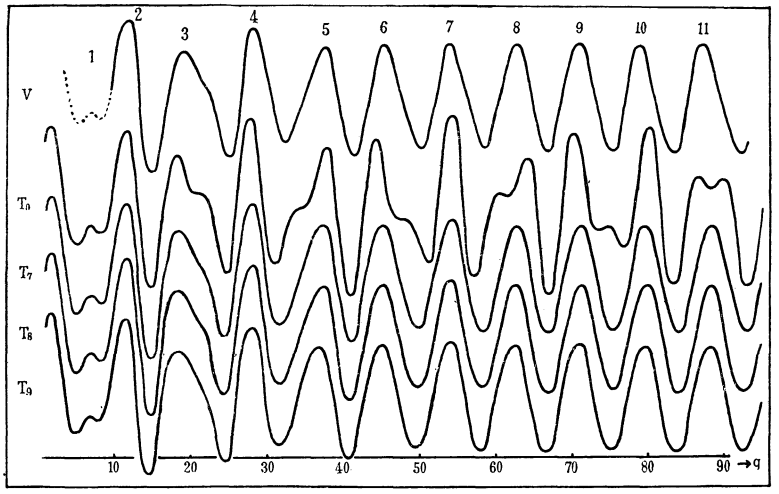

Fig. 3. Visual and theoretical intensity curves for $ZrCl_4$. $r(ZrCl)=2.32$ A, $a=0.0000$, 0.0007, 0.0008 and 0.0009 for curve T_6, T_7, T_8 and T_9 respectively.

of interatomic distances M-Cl_i and Cl_i-Cl_j are taken as the internal coordinates, and R, $\mathfrak{R}$ and Q represent the matrices of the internal coordinate, the symmetry coordinate and the normal coordinate respectively, these matrices are related to each other by the transformation matrices U' and L as follows,

$$R=U'\mathfrak{R},$$
$$\mathfrak{R}=LQ.$$

Then the mean amplitude $\langle R_i^2\rangle$ can be expressed approximately by the following equation,

$$\langle R_i^2\rangle=kT(U'F^{-1}U)_{ii}+\frac{h^2}{64\pi^2kT}(\mu+\mu').$$

Here F is the potential energy matrix subjected to the symmetry coordinate, F^{-1} is the inverse matrix of F, U' is the transposed matrix of U. The notation μ and μ' signify the reciprocal masses of two atoms associated with the displacement R_i.

The force constants giving the internal potential energy must be determined for obtaining the matrix. The method was studied systematically by Wilson[8] and full studies were reported by Shimanouchi[9] for methane and its derivatives. In the present study the same method was adopted and the potential energy was given by the equation

$$V=h_r r_0\sum_i(\Delta r_i)+(1/2)f_r\sum_i(\Delta r_i)^2$$
$$+h_q q_0\sum_{i<j}(\Delta q_{ij})+(1/2)f_q\sum_{i<j}(\Delta q_{ij})^2$$
$$+(1/2)f_\alpha r_0^2\sum_{i<j}(\Delta\alpha_{ij})^2.$$

The force constants were obtained using the frequencies of the normal modes of vibrations and F matrix was determined. Here r_0 and q_0 are the interatomic distances M-Cl and Cl-Cl in equilibrium. Table V shows the molecular structures used in the calculation, Table VI the frequencies of the normal modes of vibrations, and Table VII the results of the calculation.

TABLE V
THE MOLECULAR STRUCTURES OF TETRAHALIDES

	$SiCl_4$[10]	$TiCl_4$*	$GeCl_4$[11]	$ZrCl_4$*	$SnCl_4$[11]
M-Cl	2.01	2.18	2.08	2.32	2.30
	regular tetrahedral form				

* The values determined by the present experiment.

TABLE VI
THE FREQUENCIES OF MOLECULAR VIBRATIONS[12]

	ν_1	ν_2	ν_3	ν_4
$SiCl_4$	424	150	608	221
$TiCl_4$	386	120	495	141
$GeCl_4$	396	134	453	172
$ZrCl_4$	?	?	?	?
$SnCl_4$	366	104	403	134

No frequency of the normal modes of vibrations has yet been obtained for $ZrCl_4$. Therefore a method to be mentioned below was used. A plot of the force constant against the atomic number of the central atom yields a straight line approximately for Si, Ge, Sn (Fig. 4). It has already been pointed out[2] that if a plot is made in the same way as mentioned above for the other

8) E.B. Wilson, Jr., *J. Chem. Phys.*, 7, 1047 (1939); 9, 76 (1941).
9) T. Shimanouchi, *Sci. Papers Inst. Phys. Chem. Research* (Tokyo), 22, 958, 964 (1943); T. Shimanouchi, *J. Chem. Phys.*, 17, 245 (1949).
10) K. Yamasaki, A. Kotera, A. Tatematsu, M. Iwasaki, *J. Chem. Soc. Japan*, 69, 104 (1948).
11) L. Pauling and L.O. Brockway, *J. Am. Chem. Soc.*, 57 2684 (1936).
12) G. Herzberg, "Molecular Spectra and Molecular Structure II, Infrared and Raman Spectra of Polyatomic Molecules", 1949, p. 167.

TABLE VII

FORCE CONSTANTS AND MEAN AMPLITUDE OF MOLECULAR VIBRATIONS

	$SiCl_4$	$TiCl_4$	$GeCl_4$	$ZrCl_4$*	$SnCl_4$
f_r(×10^5dyn./cm.)	2.597	1.935	2.440	1.800	2.325
f_α(× 〃)	0.0436	0	0.0442	0	0.0237
f_q(× 〃)	0.0289	0.294	0.208	0.200	0.118
h_q(× 〃)	−0.0521	−0.0228	−0.0350	−0.010	−0.0378
$<r^2_{MCl}>$(Å)	0.045	0.049	0.044	0.050	0.045
$<r^2_{ClCl}>$(Å)	0.089	0.108	0.100	0.135	0.120
a_{calc}		0.00045**		0.00094	
a_{obs}		0.0004–0.0006		0.0007–0.0010	

* f and h were determined by the method mentioned in the present paper. a_{calc} is the value calculated using 400°K for T.

** a_{calc} is the value calculated using 300°K for T.

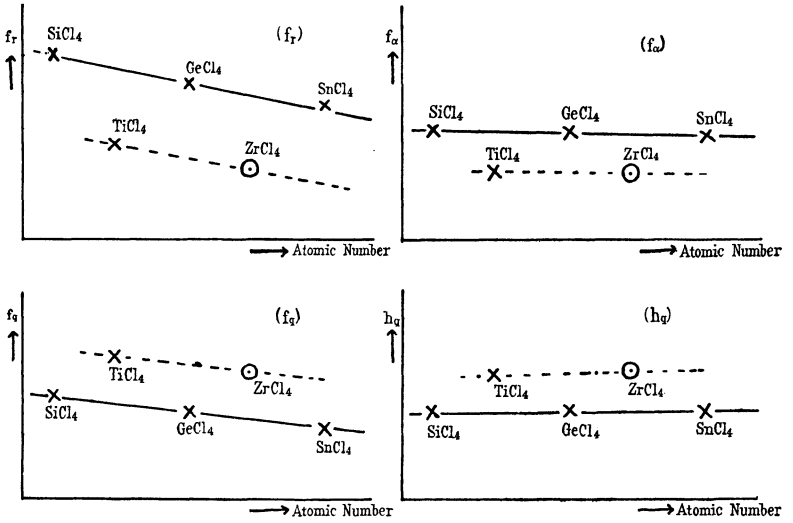

Fig. 4. Force constant of tetrachlorides plotted against the atomic number of central atom in arbitrary unit.

physical properties, the curve for Ti, Hf, Zr and Th runs parallel to that for Si, Ge, Sn and Pb. For the force constants also, a parallelism may be considered to exist between the two series. Therefore a straight line was drawn parallel to that for Si, Ge, Sn and Pb through Ti (Fig. 4). Thus the force constants for $ZrCl_4$ were obtained from the straight line as the values corresponding to atomic number 40 and are listed in Table VII. Although the force constants for a series of Si, Ge, Sn and Pb, rigorously speaking, do not lie on a straight line, f_r for $ZrCl_4$, for example, can be obtained as 1.80 ± 0.03 if the above mentioned parallelism is assumed. Since the mean amplitude depends exceedingly on f_r, such an error in f_r leads to an error of only two or three percent in the mean amplitude even if the errors of the other force constants are taken into account. Consequently the error is less than that involved in an electron diffraction experiment.

The relation between a in $\exp(-a_{ij}q^2)$ and the mean amplitude is expressed by the following equation[13],

$$a_{ij}=<r^2_{ij}>\cdot\pi^2/200.$$

Then

$$a=a_{ClCl}-a_{MCl}=[<r^2_{ClCl}>-<r^2_{MCl}>]\pi^2/200.$$

a_{calc} was calculated using this equation and is listed in Table VII. The observed values of a are in satisfactory agreement with the calculated ones.

Discussion

The interatomic distances Ti—Cl and Zr—Cl were obtained by us with smaller errors than those obtained by Lister and Sutton. Moreover detailed information was obtained for the molecular vibration from the standpoint of electron diffraction and spectroscopy.

13) e.g. P. Debye, *J. Chem. Phys.*, **9**, 55 (1941); R. W. James, *Physik. Z.*, **33**, 737 (1932).

These results can be considered to be accurate enough to be used discussing the molecular structures.

The results obtained above indicate the regular change with the atomic number of the central atom in the molecular vibrations as well as in the metal-chlorine interatomic distances of the tetrahalides of 4th group elements. At the same time the 4th group elements are classified into two groups, Si, Ge, Sn, Pb and Ti, Zr, Hf, Th. Although no detailed statement is made in the present paper, that almost all physical properties are classified into two groups may be interpreted as due to the difference of the bond character between the two groups. The difference of the bond character may be considered to be a necessary consequence arising from the difference of the valence shells between the two groups. Moreover in $TiCl_4$ and VCl_4 the similarity to one another in boiling point, melting point and molar volume, etc. is an example indicating that no physical property depends merely on the geometrical configuration of molecules.

Summary

1) The molecular structures of $TiCl_4$ and $ZrCl_4$ were determined by electron diffraction as follows: Ti—Cl = 2.185 $\pm$0.01 Å in $TiCl_4$ and Zr—Cl = 2.32 $\pm$0.01 Å in $ZrCl_4$, and both molecules have the tetrahedral form. At the same time a in exp $(-aq^2)$, the term relating to molecular vibrations, was determined. $a_{ClCl}-a_{MCl}$ is 0.0004–0.0006 for $TiCl_4$ and 0.0007–0.0010 for $ZrCl_4$.

2) The mean-square amplitudes of $SiCl_4$, $TiCl_4$, $GeCl_4$, $ZrCl_4$ and $SnCl_4$ were calculated using the frequencies of the normal modes of vibrations. $a_{ClCl}-a_{MCl}$ thus obtained is 0.00045 for $TiCl_4$ and 0.00094 for $ZrCl_4$. These values are in satisfactory agreement with those obtained by electron diffraction.

3) Almost all physical properties of tetrahalides of the 4th group elements including molecular vibrations are classified into two groups, Si, Ge, Sn and Pb tetrachlorides and Ti, Zr, Hf and Th tetrachlorides. This will be due to the difference in bond character.

We wish to express our thanks to Prof. M. Kubo for his helpful advice. Our thanks are also due to the Ministry of Education for supporting this research.

Department of Chemistry, Faculty of Science, Nagoya University, Nagoya

Studies on the Oxidation of Ferrous Sulfide

By Tsuguyasu WADA, Yutaka SHIRAISHI
and Kichizo NIWA

(Received August 12, 1955)

Itroducton

Recent investigations on the reduction of metallic oxides or oxidation of metallic sulfides have shown that the mechanism of these reactions should be discussed on the basis of the defect theory of crystal lattice. Along this line Anderson[1] and Wagner[2] have discussed the mechanisms for many cases of reactions which involve the reduction of metallic oxides with hydrogen or carbon monoxide, oxidation of metallic sulfides with oxygen, and reduction of metallic sulfides with hydrogen or other metals. Successful applications have also been carried out by Parravano[3] and Hauffe[4] on the reduction of nickel oxide with hydrogen.

When a metallic oxide is reduced with hydrogen, first the chemisorption of hydrogen on the surface of oxide takes place, being accompanied by the decrease of positive holes or the increase of free electrons. Then the reaction proceeds by filling cation vacancies or increasing excess cations until metallic nuclei appear, resulting in an appreciable change of metal/oxygen ratio. The analogous non-stoichiometric departure has been found for some cases of oxidation of metallic sulfide[1], although the change of the metal/anion ratio is opposite to that in the case of reduction of oxide. For the oxidation of sulfide, however, experimental data are very scarce up to date.

Most compounds have so small a range of deviation from the stoichiometric composition that it is difficult to observe it by means of

1) J.S. Anderson, *Discussions Faraday Soc.*, No. 4, 163 (1948).
2) C. Wagner, *J. Metals*, 4, 214 (1952).
3) G. Parravano, *J. Am. Chem. Soc.*, 74, 1194 (1952).
4) K. Hauffe and A. Rahmel, *Z. phys. Chem.* [N.F.], 1, 104 (1954).

the ordinary X-ray diffraction method. But fortunately ferrous sulfide has a relatively wide range of non-stoichiometric composition[5,6], so the X-ray diffraction method may be useful for the present purpose.

Although studies on the roasting of ferrous sulfide have been carried out by several investigators, some disagreements still remain as to those results: Schwab and Philinis[7] have measured the rate of oxidation with a precise thermobalance and have concluded that the rate is controlled by diffusion of gas, similarly to the case of pyrite. Chufarov and Averbukh[8] have found that the oxidation of ferrous sulfide proceeds as follows: Up to 250°C the oxidation takes place without evolution of gas, showing that the product is $FeSO_4$. At 350–450°C the product is a mixture of $FeSO_4$ and iron oxides, and above 450°C it is a mixture of ferric oxide and magnetite. Kameda, Yazawa, and Kurosawa[9] have investigated the kinetics of the oxidation of artificial ferrous sulfide, and have shown that the initial stage of the reaction is autocatalytic, an induction period being observed. According to Kushima and Kondo[10] who have studied the oxidation products with thermobalance, the sulfate which is produced during oxidation is presumed to be $Fe_2(SO_4)_3$, also, complete formation of oxides is observed above 600°C.

Experimental

(a) Material.—Ferrous sulfide used was prepered as follows: Two boats which had been filled with electrolytic iron and sulfur respectively were put in a quartz tube, and after evacuation up to about 10^{-4} mmHg the tube was heated to 800–900°C. After the sulfurization had been finished, which took about two days, the product was powdered and was then evacuated again at 900°C to remove excess sulfur. The final product was powdered again and its fraction between 170 and 200 mesh was collected by sieving. One-tenth grams of this fraction were used in every run.

The analysis of sample resulted as,

Fe; 61.98%, S; 38.11%.

No other line except that of ferrous sulfide was observed by X-ray powder photograph.

(b) Spring Balance.—The spring balance used is the same as that described in the writers' previous paper[11]. The rate of flow of air was fixed at 200 cc./min., because no effect on the rate of reaction was observed when the rate of flow was increased above this.

(c) X-ray Diffraction Method.—X-ray diffraction patterns were obtained by means of an ordinary powder camera with diameter of 90 mm and CoK_α radiation. Since an X-ray tube of rotating-anode-type was used, the exposure was only about ten minutes. To prepare the specimen for X-ray study, samples were quenched in nitrogen gas in a way similar to that adopted in the previous work[11].

Results

(1) Rate of Oxidation Measured with Spring Balance.—The rates of oxidation measured with spring balance over the temperature range from 504° to 700°C are shown in Fig. 1, in which the decrease of weight (%) is plotted against reaction time (min.).

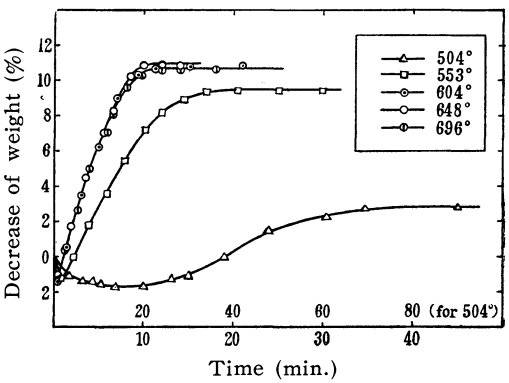

Fig. 1. Change of weight during oxidation of ferrous sulfide.

At reaction temperature of 504°C, some increase of weight appears first, and continues for about fifteen minutes until the weight begins to decrease gradually. (For this run the scale of abscissa in Fig. 1 is reduced to one half that of others.) The decrease of weight, however, is only 2.8% even after ninety minutes, which is far less than that of oxides, viz. 9.1% for ferric oxide and 12.2% for magnetite. Thus sulfate may exist. At 553°C small amounts of sulfate may also be formed; above 604°C, the product undoubtedly comprises oxides only.

Two striking phenomena are observed from Fig. 1: First, for every temperature there is an increase of weight of about 1.0–1.8% at the initial stage of reaction, and secondly above 604°C the rate of oxidation does not change with temperature. The latter fact means that the energy of activation for reaction is very small, so the rate-determining factor may be diffusion of gas.

(2) Dependence of Reaction Rate on the Amount of Sample.—Two cases of rate-controlling by diffusion can be considered: One is the diffusion of gas through the pores of the product layer formed on the surface of each particle as Schwab and Philinis have reported[7], and the

5) R. Juza, W. Biltz and K. Meisel, *Z. anorg. allgem. Chem.*, 205, 273 (1932).
6) H.S. Roberts, *J. Am. Chem. Soc.*, 57, 1034 (1935).
7) G-M. Schwab and J. Philinis, *J. Am. Chem. Soc.*, 69, 2588 (1947).
8) G.I. Chufarov and B.D. Averbukh, *Zhur. Obshei. Khim.* (*J. Gen. Chem.*), 19, 857 (1949).
9) M. Kameda, A. Yazawa and T. Kurosawa, *J. Mining Inst. Japan*, 68, 71 (1952).
10) I. Kushima and Y. Kondo, ibid., 68, 319 (1952).
11) K. Niwa and T. Wada, *J. Japan Inst. Metals*, 18, 1 (1954).

other is that in the bed of the whole sample[12]. To decide whether or not the diffusion in a particle is the only factor in rate-determination, an experiment, namely the measurement of the rate of oxidation using various amounts of the sample, was carried out. If the diffusion in a particle is the rate-determining factor, the rate should be independent of the amount of sample. If, on the other hand, the rate is controlled by diffusion in the bed of the sample, it may vary with the amount of sample. The results are shown in Fig. 2. They indicate that the rate depends on

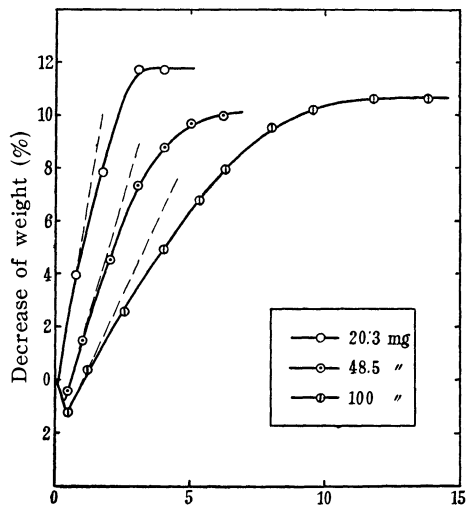

Fig. 2. Dependence of the rate of oxidation upon the amount of sample.
The broken lines indicate the relative rate of oxidation cited in Table III.

the amount of sample. Thus the observation supports the latter of the two considerations mentioned just above.

(3) X-ray Diffraction Study of Initial Stage.—Identification of oxidation products and measurements on the change of lattice parameter of ferrous sulfide in initial stage were carried out by X-ray analysis.

Since the whole data of X-ray diffraction can not be represented on account of limitation of space, only one example is shown in Table I. In this case magnetite and hematite were identified, while the existence of wüstite is not certain because the assigned line is only a very weak one. Data on identified substances are summarized in Table II.

An appreciable change of lattice parameter of ferrous sulfide was observed in this stage of reaction. This is as shown in Fig. 3b where the change of interplanar spacings of (102), (103), (004), and (202) lines may be seen in connection with change of weight which is shown in 3a. The rate of oxidation is somewhat lower than that of Fig. 1 because 200 mg. of sample was taken in this case.

12) S.E. Woods, *Discussions Faraday Soc.*, No. 4, 184 (1948).

TABLE I
AN EXAMPLE OF X-RAY POWDER PHOTOGRAPHS

Sample: No. 7, 600°C, 100 sec.

d(kX)	I	Substance
5.72	w	FeS (001) (?)*
2.97	m	FeS (100)
2.70	vw	Fe_2O_3
2.64	st	FeS (101)
2.52	w	Fe_3O_4, Fe_2O_3
2.21	vw	Fe_2O_3
2.16	vw	FeO
2.10	vw	Fe_3O_4
2.06	st	FeS (102)
1.840	vw	Fe_2O_3
1.717	st	FeS (110)
1.680	vw	Fe_2O_3
1.612	vw	Fe_3O_4
1.602	w	FeS (103)
1.483	w	FeS (200)
1.440	w	FeS (201)
1.426	w	FeS (004)
1.317	m	FeS (202)

TABLE II
PRODUCTS OF INITIAL STAGE DETECTED BY X-RAY DIFFRACTION

Reaction temperature (°C)	Time (sec.)	Detected substances (except FeS)
500	30	—
〃	75	Fe_3O_4
〃	120	Fe_3O_4
〃	180	Fe_3O_4
〃	240	Fe_3O_4, (Fe_2O_3)**
600	20	—
〃	40	Fe_3O_4
〃	60	Fe_3O_4, Fe_2O_3, (FeO)
〃	100	Fe_3O_4, Fe_2O_3, (FeO)
〃	150	Fe_3O_4, Fe_2O_3, (FeO)
700	20	Fe_3O_4, (FeO)
〃	36	Fe_3O_4, (Fe_2O_3), (FeO)
〃	60	Fe_3O_4, Fe_2O_3, (FeO)
〃	90	Fe_3O_4, Fe_2O_3, (FeO)
〃	120	Fe_2O_3, Fe_3O_4, (FeO)
〃	180	Fe_2O_3, (Fe_3O_4), (FeO)

** The existence of parenthesized substance is not certain.

It is obvious that this contraction of lattice parameter is due to the change of molar ratio of iron/sulfur. The change of lattice parameter is so rapid, that the material has become almost saturated when the increase of weight is maximum. The velocity of the change, however, depends very much on reaction temperature, which suggests a relatively high energy of activation.

* It may be open to question whether or not this weak line of 5.72 kX is assigned to (100) of ferrous sulfide, which should disappear in NiAs structure. But it is also impossible to assign it to oxide or sulfate. Thus a doubt arises as to ideal NiAs structure of pyrrhotite. Details will be discussed elsewhere. cf. F. Bertaut, *Compt. rend.*, 234, 1295 (1952).

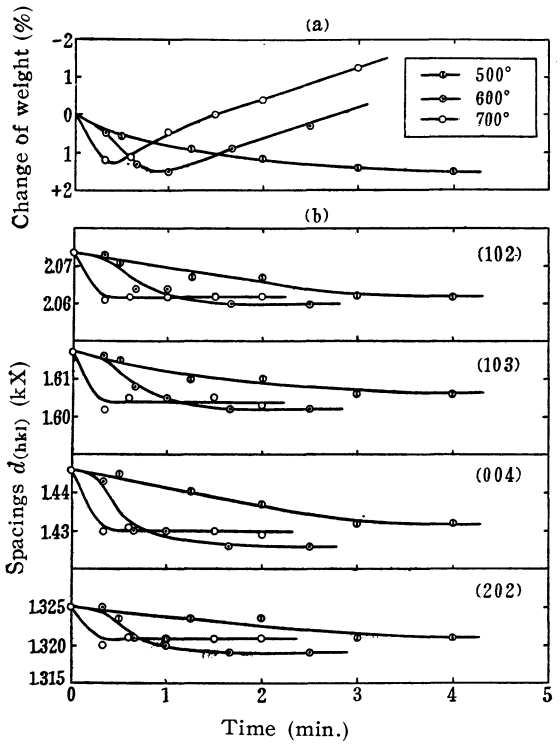

Fig. 3. Reaction of initial stage.
(a): Change of weight.
(b): Change of interplanar spacings of FeS.

The relation between lattice parameter and molar ratio of iron/sulfur has already been determined by some investigators[13,14]. According to the results of Ueda et al[14], whose measurements seem to be most reliable, these changes of lattice parameter correspond to changes of composition amounting to about 1.5–1.8, 2.1–2.4, and 1.6–1.8 atomic % of sulfur for 500°, 600°, and 700° respectively.

Discussion

The increase of weight at the initial stage of reaction is rather too great to regard its cause as merely chemisorption of oxygen. If the specific surface of the sample is of the order of 10^3 or 10^4 cm^2 per gram, about 10^2 molecular layers of adsorbed oxygen correspond to the 1–2% of weight increase. Furthermore, magnetite is found as an oxidation product at a very early stage of reaction as shown in Table II. Therefore the cause of increase of weight may be the formation of oxide on the surface rather than chemisorption.

Thus the mechanism of initial reaction can be interpreted as follows: First, oxygen is chemisorbed on the sulface, being accompanied by the formation of cation vacancies and positive holes near the surface. Then these cation vacancies diffuse into the interior of the crystal, or in other words, cations diffuse to the surface. This stage is continued until the deficiency of cation reaches the saturation where the oxide phase may already exist on the surface because the amount of chemisorbed oxygen becomes so great.

If a reaction occurs as follows,

$$FeS+\frac{2}{3}xO_2=Fe_{1-x}S+\frac{x}{3}Fe_3O_4$$

the increase of weight is expected to be 1.4–1.7%, 2.0-2.3%, and 1.5–1.7% for 500°, 600°, and 700° respectively from the values of iron/sulfur ratio. These are comparable to the experimental values which are 1.5% for 500° and 600° and 1.2% for 700°.

The rapid change of lattice parameter of ferrous sulfide indicates that the diffusion of cation vacancies or opposite diffusion of cations is relatively easy.

After this induction period, the oxidation proceeds with evolution of sulfur dioxide, and the rate is controlled by diffusion of gas at least at temperature above 600°C. Schwab and Philinis[7] have considered that the observed rate is controlled by diffusion of oxygen through the pores of the product layer formed on the surface of each particle. The diffusion coefficient thus determined from their observation, however, was of the order of 10^{-5} cm^2 sec^{-1}, which was far less than that of ordinary gas, viz., about 10^{-1} cm^2 sec^{-1}, indicating, according to their opinion, that the porosity of the product was very low.

In the present case, however, the reaction rate of oxidation depends on the amount of sample as described above. So the diffusion in the bed of the whole sample must be considered.

In Table III the relative and molar rate

TABLE III

RELATIVE AND MOLAR RATE OF OXIDATION FOR VARIOUS AMOUNTS OF SAMPLES AT 700°C

Amount of sample (mg.)	dx/dt (sec^{-1})	dm/dt (mol. sec^{-1})	A(cm^2)	$\frac{1}{A}\frac{dm}{dt}$ (mol. sec^{-1} cm^{-2})
20.3	0.76×10^{-2}	1.8×10^{-6}	0.35	0.51×10^{-7}
48.5	0.49×10^{-2}	2.7×10^{-6}	0.50	0.54×10^{-7}
100	0.30×10^{-2}	3.4×10^{-6}	0.70	0.49×10^{-7}

x: Fraction of oxidized ferrous sulfide.
m: Moles of oxidized ferrous sulfide.
A: Area of extent of sample bed in the bucket.

13) J. Hägg and I. Sucksdorff, *Z. phys. Chem.*, (B) 22, 444 (1933).
14) R. Ueda, T. Ichinokawa and T. Mitsui, *Busseiron Kenkyu* (Rescarches on Chem. Phys.), 33, 55 (1950).

of oxidation which are determined from the slopes of curves in Fig. 3, and area of extent of sample bed in bucket are recorded. As shown in the fifth column of this table, the molar rate of oxidation per unit area is almost constant. This fact offers valid evidence for the view that the diffusion in the bed contributed predominantly to the rate of oxidation.

Summary

The rate and mechanism of oxidation of ferrous sulfide was studied by means of a spring balance and X-ray diffraction analysis over the temperature range from 500°C to 700°C. The conclusion reached is as follows:

(1) Complete oxidation, in which only the formation of oxides proceeds, begins at 600°C.

(2) At the initial stage of oxidation, a slight increase of weight is found. It was observed by X-ray that the deficiency of cation in ferrous sulfide occurs in this stage. This may be due to the formation of oxide on the surface rather than to chemisorption, which is accompanied by creation of cation vacancies in ferrous sulfide crystal.

(3) Above 600°C, the rate of oxidation does not change with temperature, so the rate-determining factor is diffusion of gas. Since the observed rate of oxidation depends upon the quantity of the sample, the diffusion in the bed of sample may determine the rate.

Department of Chemistry, Faculty of Science, Hokkaido University, Sapporo

Interaction between Surface Active Agents and Proteins. I. Precipitations formed by Mixing Sodium Alkyl Sulfates and Egg Albumin

By Koichiro AOKI and Joji HORI

(Received July 13, 1955)

Introduction

Putnam and Neurath[1] studied the precipitation reaction between sodium dodecyl sulfate (SDS) and horse serum albumin by mixing solutions of SDS and serum albumin at lower pH than 4.75, the pH of the isoelectric point of this protein. They observed that white precipitate instantly formed when both solutions were mixed if there was an excess albumin, and that the precipitate was redissolved in the region of SDS excess and, further, that these two phenomena did not depend upon the protein concentration.

Pankhurst et. al.[2] studied the interaction between SDS and gelatin using that same method and Elkes et. al[3]. studied the interaction between sodium cetyl sulfate and hemoglobin. Both also found that there was a region wherein precipitation occurred when the surface active agent and the protein were mixed.

No investigation has been made of interactions between egg albumin and SDS, or its homologues. A study was made of the precipitation reaction between each one of these compounds and egg albumin at lower pH than that of the isoelectric point of egg albumin. The results obtained are reported in this paper.

1) F.W. Putnam and H. Neurath, *J. Am. Chem. Soc.*, **66**, 692 (1944).

2) K.G.A. Pankhurst and R.C.M. Smith, *Trans. Faraday Soc.*, **40**, 565 (1944).

3) J. Elkes and J.B. Finean, "Surface Chemistry", Butterworth, London (1949), p. 281.

Experimental

Materials.—SDS was prepared as follows. Purified dodecyl alcohol was sulfonated by chlorosulfonic acid; this solution was then neutralized by sodium hydroxide[4]. The crystal obtained after two recrystallizations was glossy white and scale-like. The melting point was 191–193°C and the purity was 99.8%*. The critical micelle concentration of the aqueous solution of this SDS was found to be 0.007–8 mol./l. at 25°C, by measuring the surface tension, the viscosity and the specific conductivity[6].

SOS and SBS were synthesized in the same way. The purity of these compounds was of the same degree as that of SDS.

* We took the known quantity of this crystal. We added dilute hydrochloric acid and warmed it to hydrolyze this compound. Then barium sulfafe was precipitated by adding barium chloride solution. The purity of SDS was calculated from the amount of this precipitate[5].

4) W. Kimura and H. Taniguchi, *J. Soc. Chem. Ind. Japan*, **42**, 157 (1939).

5) K. Nishizawa and T. Tomizawa, ibid., **35**, 1368 (1932).

6) K. Aoki, *Bulletin of Nagoya City University*, in press.

Egg albumin was isolated by ammonium sulfate. After several repetitions of salting out, the obtained solution was dialyzed by running water and then electro-dialyzed. This solution was evaporated to dryness to obtain solid egg albumin. This egg albumin was proved to be electrophoretically pure[7].

Procedure.—We obtained the SDS solution having the known concentration by dissolving the known amount of SDS crystal into buffer solution, the pH and the ionic strength of which were known. We dissolved the known amount of egg albumin powder into the buffer solution. Using the micro-Kjeldahl method, the concentration of egg albumin in this solution was determined by finding the amount of nitrogen in it, taking the percentage of nitrogen in egg albumin as N=15.76%. We obtained the albumin solution having the desired concentration by diluting this solution.

Known volumes of SDS solution were placed in a series of test tubes or conical flasks, and then to each test tube the calculated volume of egg albumin solution was added. They were allowed to stand over night at room temperature, and supernatants were separated from precipitates by centrifugation. Concentrations of protein in these supernatants were found by the micro-Kjeldahl analysis. Knowing both the amount of protein which originally existed and the amount of protein found in the supernatant after removing precipitate, we knew the percentage of the protein turned into precipitate. (Hereafter we call this percentage "precipitation percentage".)

The buffer solution used consisted of sodium acetate and hydrochloric acid, its pH being equal to 4.2 and ionic strength (μ) 0.34.

Precipitation reactions between SOS and egg albumin, and between SBS and egg albumin were studied in the same way as between SDS and egg albumin.

Results

Precipitation Curve.—We obtained the relation between the precipitation percentage and the mixing ratio of SDS to egg albumin at pH=4.2, μ=0.34, whereby the concentration of egg albumin was kept constant. This relation is shown in Fig. 1. Observing this curve, which is hereafter termed "precipitation curve", the precipitation percentage of protein was found to increase first with the mixing ratio, and upon reaching its maximum, the precipitation percentage then decreased. When solutions of SDS and egg albumin were mixed and the amount of SDS was sufficiently rich, precipitation did not occur even when the pH of the solution was lower than that of the isoelectric point of the protein. We observed the same phenomenon as above when the concentration of protein used was between 0.5 and 2.0%.

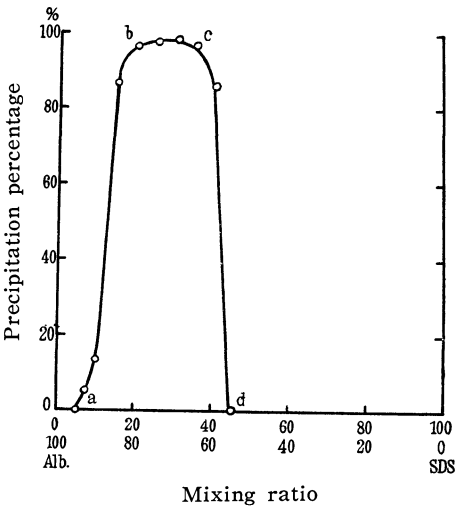

Fig. 1. Precipitation curve of the system of egg albumin and sodium dodecyl sulfate at pH 4.2 and ionic strength 0.34. Concentrations of egg albumin are follows: ⊙ 2.0%, ○ 1.0%, ● 0.5%.

In the region of albumin excess, the supernatants were not transparent, appearing slightly turbid. After these supernatants were left standing for a few days, we observed that a small quantity of precipitate had newly occurred.

Precipitate did not appear instantly when solutions of SBS and egg albumin were mixed. There was a slight daily increase in the amount of precipitate. Fig. 3 was calculated using the data obtained on mixtures left standing for ten days after mixing.

There was an instant precipitation when solutions of SOS and egg albumin were mixed. When supernatants were left standing for a few days after removing precipitate, a little precipitate appeared in the same way as in the SDS-egg albumin system. Figs. 2a and 2b show the precipitation curves of the system SOS-egg albumin. We can note in the region of SOS excess that the precipitation curves are different when the concentrations of SOS differ. In other words, when 1.0% of SOS solution is used, the precipitation percentage of protein is always near 100%; but when the concentration of SOS is over 1.5%, the precipitation curve descends, as in the SDS-egg albumin system.

Electrophoresis of Turbid Supernatant and Transparent Solution.—We electrophoretically analyzed supernatants after centrifugation and also solutions with variously different mixing ratios of SDS to egg albumin. We used Hitachi's electrophoretic apparatus and the experiments were carried

7) K. Aoki, ibid., in press.

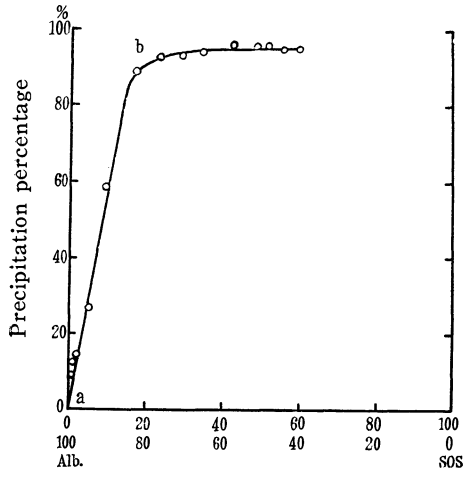

Fig. 2a. Precipitation curve of the system of egg albumin and sodium octyl sulfate at pH 4.2 and ionic strength 0.34. Concentration of egg albumin is 1.0%.

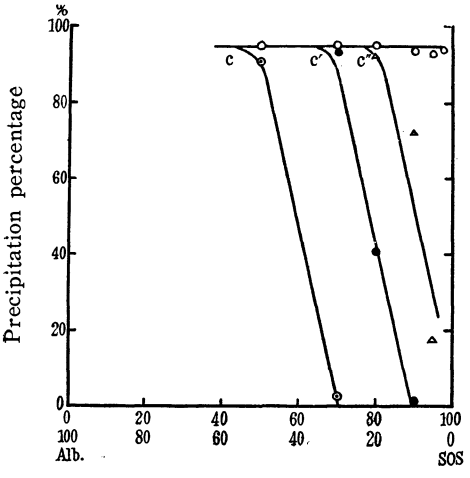

Fig. 2b. Precipitation curve of the system of egg albumin and sodium octyl sulfate at pH 4.2 and ionic strength 0.34. Concentrations of SOS are as follows: ⊙ 3.0%, ● 2.0%, △ 1.5%, ○ 1.0%.

out at 25°C, pH=3.6, and $\mu=0.1$*. Some of the results are shown in Figs. 4a and 4b. At pH=3.6, a solution which contained only egg albumin moved toward the anode and a solution which contained only SDS moved toward the cathode. In cases where the concentration of egg albumin was richer than albumin/SDS =80/20 (mixing ratio) the supernatants after centrifugation were always turbid white. In

* The experimental method of electrophoresis is described in Part II.

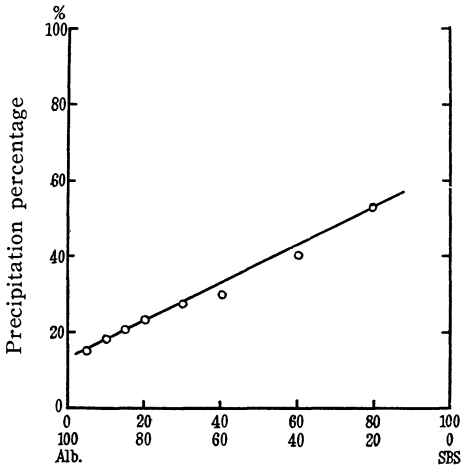

Fig. 3. Precipitation curve of the system of egg albumin and sodium butyl sulfate at pH 4.2 and ionic strength 0.34. Total concentration is 2.0%.

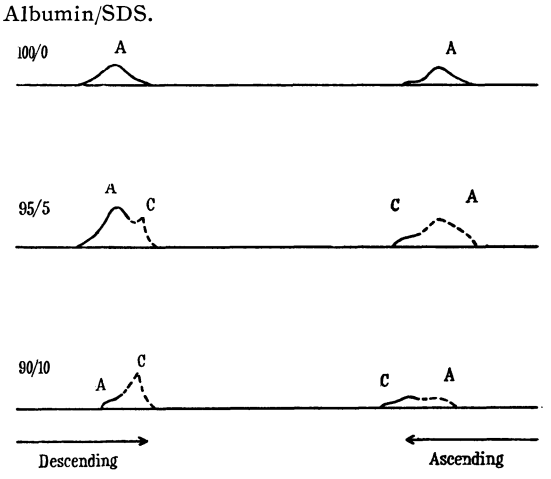

Fig. 4a. Electrophoretic pattern of the system egg albumin-sodium dodecyl sulfate at pH 3.6 and ionic strength 0.1. Both egg albumin and complex moved toward the anode. Photographs of albumin/SDS=95/5 and 90/10 were taken with larger inclination of diagonal slit. Broken line means that the light passed through the turbid phase.

electrophoretic experiments of these supernatants, we observed that all moved toward the anode and separated into two components, i. e. turbid complex and transparent egg albumin. When the ratio of albumin/SDS was less than 80/20, we observed only one complex which migrated toward the cathode. Further, when the ratio of albumin/SDS became less than 30/70 there appeared two components, i. e. SDS and complex.

Albumin/SDS.

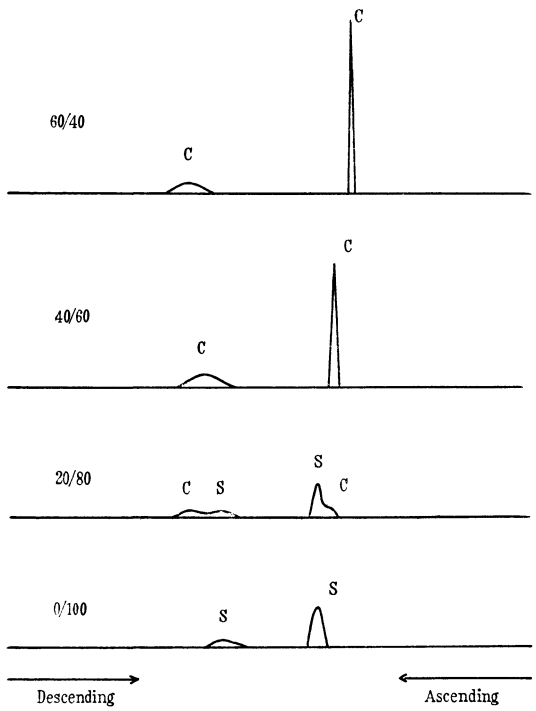

Fig. 4b. Electrophoretic pattern (continued). Both complex (C) and SDS (S) move toward the cathode.

method[8]. The dye used was Eastman's pinacyanol; the three buffer solutions used were acetate buffer solution at pH 4.2, phosphate buffer solution at pH 6.8 and carbonate buffer solution at pH 10.0*. We also studied the effect of ionic strength of sodium chloride solution on the CMC of SDS. As seen in Fig. 5a, the lowering effect of ionic strength of the three buffer solutions and sodium chloride solution upon the CMC of SDS is the same if the ionic strength of each solution is the same. Further, the curve shown in Fig. 5a coincides with the curve calculated by Corrin and Harkins[8]. This means that the lowering of the CMC does not depend upon the kinds and pH's of the buffer solutions nor upon the kinds of neutral salt solutions and that it depends only upon the ionic strength of the solution which dissolves the detergent. We can find in Figs. 5a and 5b that the CMC of SDS is 0.03% (0.0010 mol./l.) and the CMC of SOS is 1.39% (0.060 mol./l.) in the buffer solution at $\mu=0.34$.

Discussion

Number of SDS and of SOS Bound to One Molecule of Egg Albumin.—We can calculate the number of SDS bound to one molecule of egg albumin from precipitation

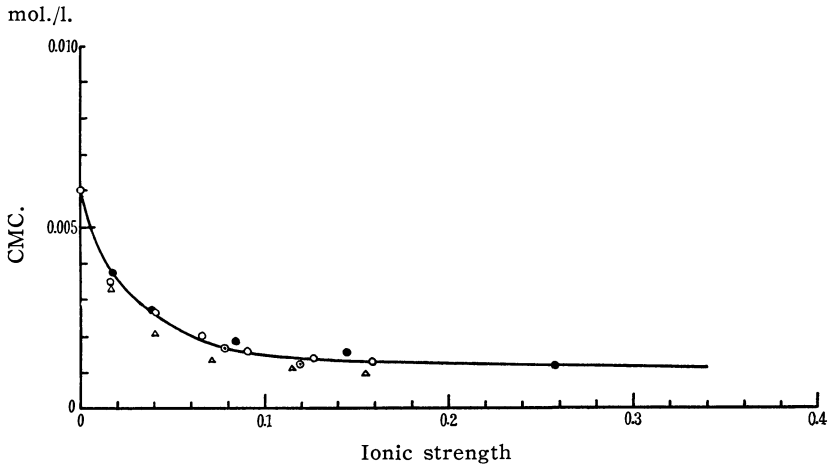

Fig. 5a. The effect of ionic strength upon the critical micelle concentration of sodium dodecyl sulfate.
● Acetate buffer solution at pH 4.2, ○ phosphate buffer solution at pH 6.8, ⊙ carbonate buffer solution at pH 10.0, △ sodium chloride solution.

Critical Micelle Concentration of SDS and of SOS in Buffer Solution.—We investigated the lowering of the critical micelle concentration (CMC) of SDS and of SOS caused by the increase in the ionic strength of buffer solution using the Corrin and Harkins, curve in Fig. 1. No precipitation occurred when barium chloride solution was added to supernatants obtained from mixtures the

8) M.L. Corrin and W.D. Harkins, *J. Am. Chem. Soc.*, 69, 683 (1947).

* This will be desdribed later.

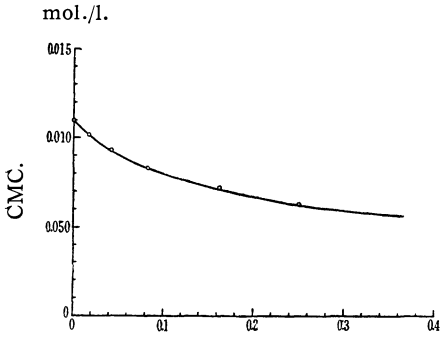

Fig. 5b. The effect of ionic strength of phosphate buffer solution at pH 6.8 upon the critical micelle concentration of sodium octyl sulfate.

compositions of which were between albumin/SDS=100/0 and 65/35, so we can assume that all of the added SDS are bound to egg albumin and form a complex, and that almost all of the complex thus formed exists in precipitate within this region of mixing ratio. White precipitate occurred when barium chloride solution was added to supernatants obtained from mixtures having the concentration of SDS over albumin/SDS=65/35, so we know that in this mixing ratio the added SDS exists both in the supernatant and in the precipitate.

We calculated the composition of precipitate, or the number of SDS bound to one molecule of egg albumin, in the region of albumin/SDS=100/0–65/35, taking the molecular weight of egg albumin as 46,000 and that of SDS as 288. The compositions of precipitate thus calculated at each mixing ratio are shown in Fig. 6a. This curve has two inflection points *a* and *b*, and the number of bound SDS at point *b* is about 40 which is considered the true number of SDS bound to one egg albumin molecule. This composition is expressed by AD_{40} (A: albumin, D: detergent). The numeral 40 is almost equal to 42 which is the number of positive charges on one egg albumin at this pH*.

In Fig. 6a, line *ab* is not horizontal. One reason is that supernatant contains not only unreacted excess albumin but also turbid complex, as seen in electrophoretic patterns of supernatants. We should not consider that the composition of the complex changes with mixing ratio in the region between points *a* and *b*, but should consider that all

* Line *a'b'* is more horizontal than line *ab*. The reason as follows: We added the amount of precipitate which was produced after standing a few days to that which was produced instantly when both solutions were mixed, and this value was used to calculate the precipitation curve.

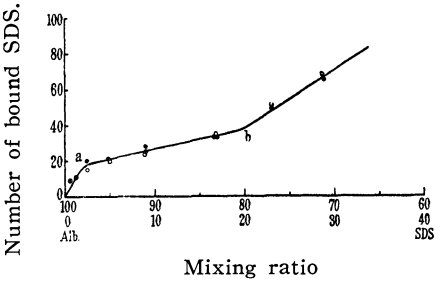

Fig. 6a. Number of SDS molecules bound to one molecule of egg albumin. Concentrations of egg albumin are as follows: ⊙ 2.0%, ○ 1.0%, ● 0.5%.

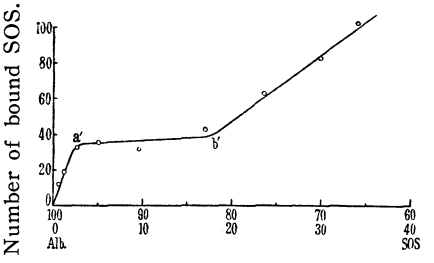

Fig. 6b. Number of SOS molecules bound to one molecule of egg albumin. Concentration of egg albumin is 1.0%.

the complex formed in this region have the same composition of AD_{40}. If we assume that all the complex formed exists in precipitate, line *ab* should be horizontal.

The curve showing the relation between the number of SOS bound to one molecule of egg albumin and the mixing ratio was calculated by using the precipitation curve of SOS shown in Fig. 2a. This curve is shown in Fig. 6b and is similar to that of the SDS-egg albumin system. The composition of precipitate calculated at point *b'* is also AD_{40}*.

We can deduce that there is no great difference in the region of albumin excess between the reactivity of SDS and that of SOS toward egg albumin.

Redissolution of Precipitate.—The precipitation curve of the SDS-egg albumin system and of the SOS-egg albumin system descends after reaching the maximum, with each position of the descending lines different. This means that the abilities of SDS and SOS to dissolve precipitate are different. As described above, at the point where only complex AD_{40} exists (point *b* in Fig. 1, albumin/SDS=80/20), 40 molecules of SDS bind to one molecule of egg albumin. Eighty molecules of SDS bind to one molecule of egg albumin at a point where the redissolution of precipitate begins (point *c* in Fig. 1,

albumin/SDS=67/33). A comparison of SDS molecules at these two points reveals that the latter is double that of the former. In the same way we can calculate the number of SOS molecules bound to one molecule of egg albumin at the point where only complex AD_{40} exists (point *b* in Fig. 2a) and at the points where redissolution of precipitate begins (points *c*, *c'*, *c''* in Fig. 2b). But here the ratio of bound SOS at two points is not double.

As previously noted, it was proved by the electrophoretic experiment that the complex was formed in supernatants and that the complex and SDS coexisted in the region where SDS was in excess. This means that the composition of the complex is limited.

Difference in Reactivity of SDS, SOS and SBS toward Egg Albumin.—As pointed out, these three compounds, viz. SDS, SOS, and SBS showed different kinds of behavior in their reactions toward egg albumin. The CMC of SDS is 0.03% and that of SOS is 1.39% in buffer solution at $\mu=0.34$. Therefore, within the concentration range of this study, SDS existed as a micellar colloidal solution, SBS behaved as a true solution, and SOS existed as a micellar colloidal solution or as a true solution according to its concentration.

There was no instant precipitation when SBS solution and egg albumin solution were mixed; but there was an instant precipitation when SDS or SOS solution and egg albumin solution were mixed. The main cause of this phenomenon is considered to be that SBS solution is a true solution and SDS and SOS solutions are colloidal.

In the SOS-egg albumin system, there are two kinds of precipitation curves depending upon the concentration of SOS; one descends and the other does not. Considering the fact that the CMC of SOS is 1.39% in a buffer solution at $\mu=0.34$, we can deduce that when the concentration of SOS is over the CMC, the curve descends, and that when the concentration of SOS is below the CMC, the curve is horizontal.

Difference in Egg Albumin and Horse Serum Albumin.—The precipitation curve of the egg albumin-SDS system begins at the original point in Fig. 1. But the precipitation curve of the horse serum albumin-SDS system begins to the right of the original point in Fig. 7. In addition Yang and Foster[9] recently found by dialysis equilibrium method that the reactivities of egg albumin and bovine serum albumin toward sodium dodecyl-benzenesulfonate were different. Thus, egg albumin and serum albumin behave in different ways toward the same detergent. That there are some differences in the structure of both proteins, may be the cause of this phenomena.

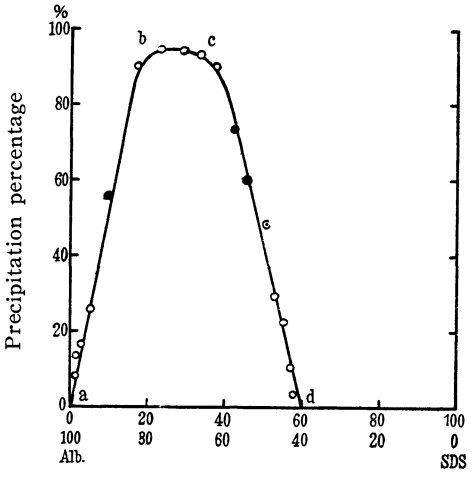

Fig. 7. Precipitation curve of the system of horse serum albumin and sodium dodecyl sulfate at pH 4.2 and ionic strength 0.34. Total concentration is 2.0%.

Summary

(1) Precipitation reactions between SDS and egg albumin, SOS and egg albumin, and SBS and egg albumin were studied. There was an instant precipitation when SDS and egg albumin solutions were mixed, and when SOS and egg albumin solutions were mixed, but not when SBS and egg albumin solutions were mixed. Comparing the precipitation curve of the SDS-egg albumin system and that of the SOS-egg albumin system, we can find that both detergents form a complex having the same formula AD_{40} (A: albumin, D: detergent) in the region of protein excess, and therefore we can conclude that there is no difference between the reactivities of SDS and SOS toward egg albumin. On the contrary, in the region where redissolution of precipitate occurs, the precipitation curves do not coincide. This means that the two detergents have different powers to dissolve precipitate. In addition, when the concentration of SOS differs, the power to dissolve precipitate differs.

(2) It was found electrophoretically that the complex is formed in turbid supernatants after centrifugation and also in transparent

9) J.T. Yang and J.F. Foster, *J. Am. Chem. Soc.*, **75**, 5560 (1953).

solutions the composition of which is in the region where no precipitation occurs.

(3) Observing the precipitation curves of the system horse serum albumin-SDS and the system egg albumin-SDS, we can see that there is a region where no precipitation occurs when a great excess of serum albumin is used; but there is not such a region when a great excess of egg albumin is used.

(4) We measured the lowering of the CMC of SDS and of SOS caused by the increase in the concentration of buffer solution. The lowering does not depend upon the kinds and pH's of buffer solutions but upon the ionic strength of buffer solution which dissolves detergent.

We are sincerely grateful to Professor Rempei Goto of the Institute for Chemical Research, Kyoto University for his kind guidance during this study.

Chemical Laboratory, Nagoya City University, Nagoya

Characteristic Absorption Bands of Vinyl Ethers

By Yukio MIKAWA

(Received March, 16, 1955)

The infrared spectra of vinyl ethers was investigated by G. D. Meakins[1], and by W. H. T. Davison and G. R. Baets[2], but the feature of the spectra associated with the presence of $-COCH=CH_2$ was not yet clear. In the present paper the infrared spectral data of a considerable number of vinyl ethers and ethyl vinylthioether are given, and the characteristic frequencies of vinyl ethers are discussed.

Experimental

a) Measurement.—A Perkin-Elmer Model 21 infrared spectrometer, with a rocksalt prism, was used. The spectrum of methyl vinyl ether is measured in its gaseous state, the others in liquid state or 10% solution of carbon tetrachloride or of carbon disulfide. In the case of solutions no bands-shift owing to solvent effect is observed.

b) Materials.—All of vinyl ethers and vinyl thioether are prepared in our Research Laboratories by applying the technique developed by W. Reppe and his co-workers. The purity of samples cannot be proved exactly, but distillations were repeated many times until all the impurity bands which had existed in the raw materials completely disappeared. The boiling point of each sample is as follows: methyl vinyl ether 5.5°C, ethyl vinyl ether 36.2°C, *n*-propyl vinyl ether 63.8°C isopropyl vinyl ether 55.0°C, *n*-butyl vinyl ether 93.8–94.1°C, 2-ethylhexyl vinyl ether 53.8–54.2°C/7 mmHg, benzyl vinyl ether 187.5–188.0°C, phenyl vinyl ether 49.5–50.0°C/13 mmHg, ethyl vinyl thioether 91.5–92°C.

1) G.D. Meakins, *J. Chem. Soc.*, **1953**, 4170.
2) W.H.T. Davison and G.R. Baets, *J. Chem. Soc.*, **1953**, 2607.

Experimental Results

The observed spectra are shown in Fig. 1 and the wave-numbers of the observed absorption maxima of methyl vinyl ether are listed in Table I.

TABLE I

THE FREQUENCIES OF THE ABSORPTION BANDS OF METHYL VINYL ETHER

Frequencies	Intensity	Type of vibration	Species
3125	M	CH str. of vinyl	
3065	M	CH str. of vinyl	
3000	M	CH str. of vinyl	
2951	M	CH str. of methyl	
2842	M	CH str. of methyl	
1655	Sh	2×817	A′
1630 P	VS		
1618 Q	Sh	CC str. of vinyl	A′
1610 R	VS		
1481	Sh	$=CH_2$ def.	A′
1462 Q	M	CH_3 def. (assym.)	A″
1390	W	CH_3 def. (sym.)	A′
1335 P	M		
1325 Q	M	$-CH=$in-plane def. of vinyl	A′
1312 R	M		
1235 P	VS		
1225 Q	Sh	CO str.	A″
1212 R	VS		
1149 P, Q ?	M	$=CH_2$ rock.	A′
1130 R	M		
1085	VW	CH_3 def.	A′
1025 P, Q	M	$-CH_2$ rocking	A″
1015 Q	W	CO str.	A′
1003 R	M		

Frequencies	Iitensity	Type of vibration	Species
965 Q	M	$-CH=$out-of-plane def.	A″
945	Sh		
902 P	M		
880 R	M		
817 Q	S	$=CH_2$ out-of-plane def.	A″

Interpretation

a) Methyl Vinyl Ether

Methyl vinyl ether has axes of internal rotation. Therefore, the determination of special configuration of this molecule is a very difficult problem. But the assumption that the molecule takes such molecular configuration as

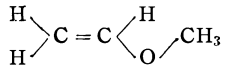

makes it possible to have a reasonable interpretation of the absorption bands.

In order to calculate the moment of inertia, further assumptions with regard to interatomic distances and bond angles are made. The CH, CO and CC distances for the molecule are assumed to be 1.07Å, 1.42Å and 1.34Å, respectively. The HCH and COC angles are taken to be 116° and 110°, respectively. The principal moments of inertia are, then, 18, 196 and 209×10^{-40} g. cm^2.

As a preliminary guide to the interpretation of the infrared spectra it is useful to consider what information may be expected from the band envelopes. The twenty-four normal vibrations of methyl vinyl ether are divided on the basis of symmetry C_s into two classes: sixteen modes in species A′ and eight modes in A″. Five CH stretching, five skeletal and six CH deformation freqencies belong to the former class and one CH stretching, one skeletal and six CH deformation frequencies belong to the latter class. Five of them (three A′ and two A″) are unlikely to be observed in the rock salt region. The envelopes of the A′ bands may be expected to have a hybrid character, each partaking in some degree of the conventional type A and type B contours. The A″ bands have type C envelopes, and Badger tell and Zumwalt's curves[3] show that the contours are characterized by very prominent Q branches. As a matter of fact, strong and clearly resolved A″ bands can be identified without hesitation. An excellent example of the type C envelope is given in 817 cm^{-1} band. This easy and definite identification of A″ bands in the spectra is a valuable aid in the subsequent vibrational analysis.

The envelopes of the bands at 1462, 965 and 817 cm^{-1} clearly indicate that their type is C. The bands at 1149 and 1025 cm^{-1} may also represent C type bands, although these overlap to the P branches of the other bands.

It is helpful to consider the spectral regions in which the fundamentals may be expected to occur. The modes associated with the CH stretching vibrations appear in the vicinity of 3000 cm^{-1}. Moreover, the bands due to $=CH_2$ or $=CRH$ group which have wave numbers higher than 3000 cm^{-1} are distinguishable from the CH_3 frequencies which appear in a longer wave-length region. The C=C and C—O frequencies occur around 1650–1600 cm^{-1} and 1250–1000 cm^{-1} respectively. The CH out-of-plane deformation frequencies of mono-substituted ethylenes are assigned by several investigators[4] to two bands near 990 and 910 cm^{-1}. In the present case, however, the corresponding bands are found in a somewhat longer wave-length. The reliability of these interpretations will be shown later.

On taking into account the preceding discussion and on comparing the spectral data on a series of other vinyl ethers and a vinyl thioether investigated in the present study, the tentative vibrational assignments are made and are given in the third column of Table I. (Weak absorptions in the overtone region are omitted from this table).

b) Other Vinyl Ether and Ethyl Vinyl-thioether

i) 3150–2800 cm^{-1} Region.—In this region there exist the CH stretching frequencies. The bands arising from the vinyl group should appear in 3200–3000 cm^{-1} and in the case of methyl vinyl ether the three bands at 3125, 3065 and 3000 cm^{-1} were assigned to them. In the case of other vinyl ethers, nearly all compounds, except phenyl and benzyl vinyl ether, have three absorption maxima above 3000 cm^{-1} (shown in Table II), which are very similar to each other. This fact shows that the CH stretching vibrations of the vinyl group remain almost constant and are not remarkably affected by the other parts of the molecule. In the case of phenyl and benzyl vinyl ether, these bands overlap CH bands arising from phenyl group. It is of interest to note the fact that phenyl vinyl ether shows no band below 3000 cm^{-1} in this region because of the absence of saturated $-CH_2-$ or $-CH_3$ group.

3) Badger and Zumwalt, *J. Chem. Phys.*, **6**, 711 (1938).

4) Sheppard and Sutherland, *Proc. Roy. Soc.*, A **196**, 195 (1949), Anderson and Seyfried, *Anal. Chem.*, 20, 998 (1948).

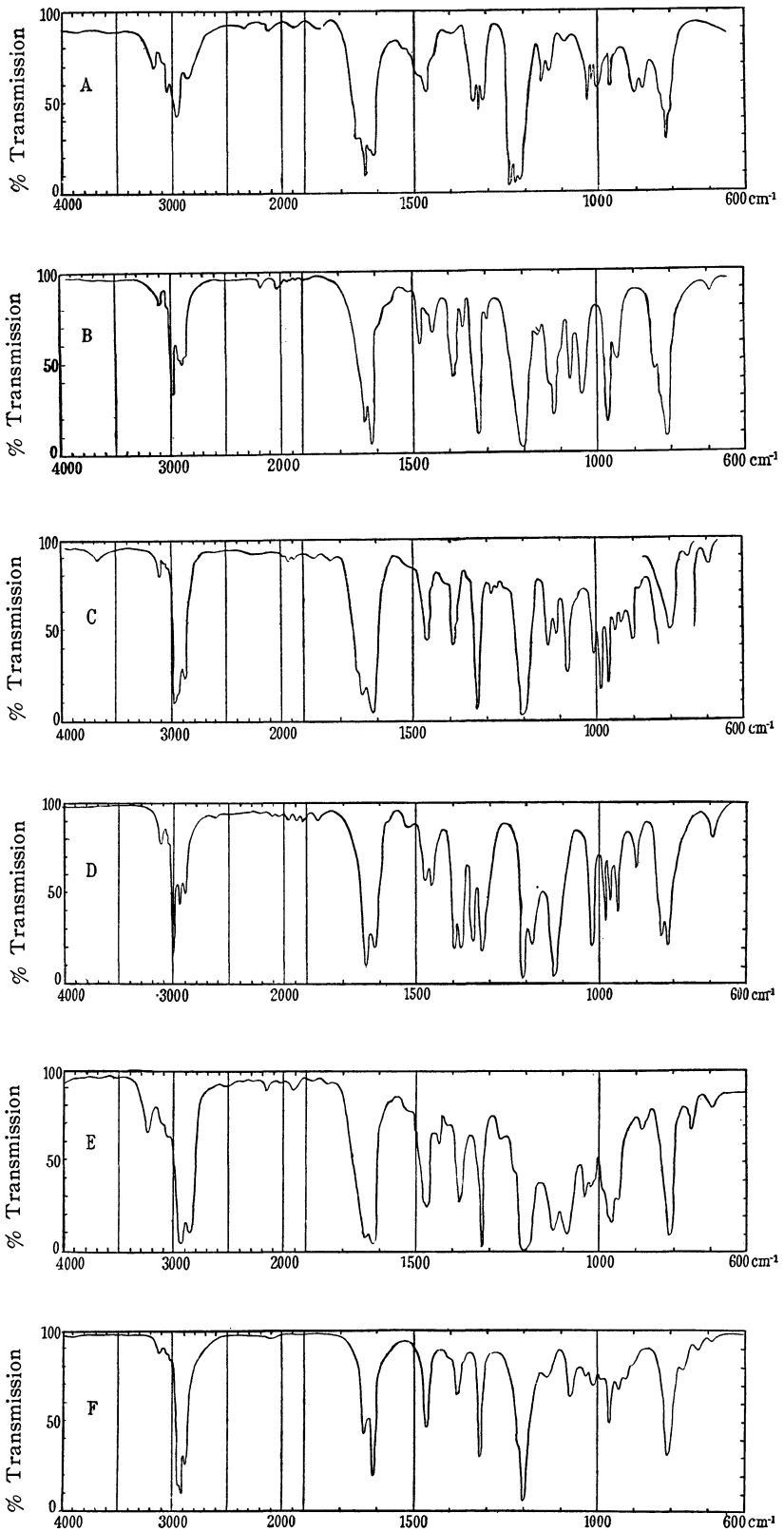
% Transmission
100
50
0
A
4000
3000
2000
1500
1000
600 cm⁻¹
B
C
D
E
F

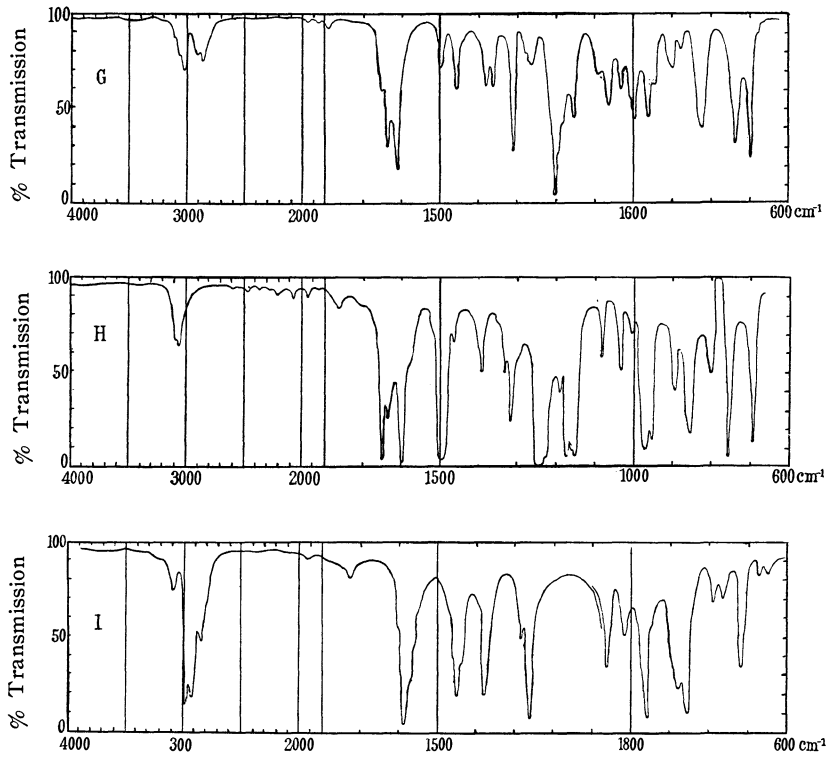

Fig. 1. Infrared spectra of vinyl ethers and ethyl vinyl thioether.

A) Methyl vinyl ether
B) Ethyl vinyl ether
C) *n*-Propyl vinyl ether
D) iso-Propyl vinyl ether
E) *n*-Butyl vinyl ether
F) 2-Ethylhexyl vinyl ether
G) Benzyl vinyl ether
H) Phenyl vinyl ether
I) Ethyl vinyl thioether

Table II

Characteristic frequencies of vinyl ethers $CH_2=CH-O-R$

R		(CH)		(C=C)	(CH)	(CO)	(CH)	(=CH_2)
CH_3—	3125,	3065,	3000	1620	1323	1223	965	817
C_2H_5—	3110,	3065,	3035	1610	1320	1205	967	810
n-C_3H_7—	3120,	3070,	3046	1615	1323	1203	968	811
iso—C_3H_7	3125,	3078,	3050	1614	1322	1203	969	812
C_4H_9—	3100,	3060,	3023	1613	1323	1200	962	810
C_8H_{17}—	3098,	—,	3015	1610	1320	1205	963	810
$C_6H_5CH_2$—		a)		1611	1320	1200	960	820
C_6H_5—		a)		1644	1313	1235	965	806
$CH_2=CH-S-Et$	3080,	—,	—	1585	1260	719b)	960	860

a) The CH stretching frequencies of vinyl group overlap with those of phenyl group.
b) This is associated with the C—S stretching mode.

ii) 1600 cm^{-1} Region.—In this region every vinyl ether shows two absorption maxima. The stronger one is assigned to the C=C stretching frequency, and the other to the overtone of a CH out-of-plane deformation frequency arising from the $=CH_2$ group. The intensity of these two bands may be explained as the Fermi resonance between the C=C stretching frequency and the overtone of 810 cm^{-1} band, because the intensities of these two bands are not greatly different from each other. In the case of ethyl vinyl thioether, however, the overtone of the CH deformation frequency appears in the vicinity of 1720 cm^{-1} and its intensity is far weaker than the C=C bands at 1585 cm^{-1}, and the Fermi resonance is excluded. In the case of ethyl β-chlorovinyl ether[5] which has no $=CH_2$ group, only one band appears in this region.

5) Cis- and trans-ethyl-β-chlorovinylether absorbed at 1649 and 1620 cm^{-1}, respectively, according to the unpublished data in our laboratories.

The frequencies assigned to C=C stretching vibration are listed in Table II. One of the characteristic frequencies of alkyl vinyl ether is 1615±5 cm^{-1}. This frequency is rather low, as compared with the corresponding frequencies of mono-substituted ethylenes which are about 1650 cm^{-1}. For explaining the shift from 1650 to 1615 cm^{-1}, the resonance between two mesomeric forms

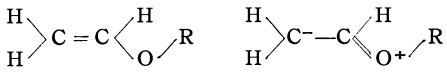

(I) (II)

is taken into consideration. The contribution of the ionic form (II) makes the double bond character weak, and the band shift to somewhat lower position may be expected. In the case of ethyl vinyl thioether the C=C stretching frequency has a frequency as low as 1585 cm^{-1}, which is explained in a similar way. In this case S atom has lower electronegativity than O atom of vinyl ethers, and the ionic structure which is similar to (II) referred to above becomes more stable.

In phenyl vinyl ether three bands occur in the vicinity of 1600 cm^{-1}; the first band at 1653 cm^{-1} is assigned to the C=C vibration of vinyl group, the second at 1635 cm^{-1} to the overtone mentioned before, and the last at 1600 cm^{-1} to the ring vibration of the phenyl group. In this case the status concerning the resonance form is somewhat different and the following five mesomeric forms are possible:

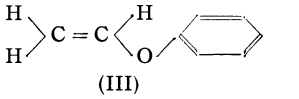

(III)

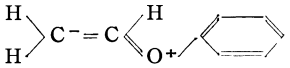

(IV)

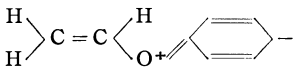

(V)

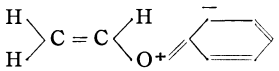

(VI)

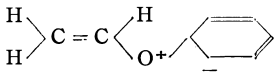

(VII)

The difference from the case of alkyl vinyl ether is that the three ionic forms (V), (VI) and (VII) in addition to (IV) contribute to the normal state.

The presence of these forms makes the contribution of structure (IV) smaller and the frequency of the C=C vibration of phenyl vinyl ether remains almost unshifted from those of usual mono-substituted ethylenes.

iii) 1320 cm^{-1} Region.—The band around 1320 cm^{-1} is the most important characteristic band to the vinyl ether, for every vinyl ether examined shows a very strong band at 1321 ±2 cm^{-1}. This band may be assigned to the CH in-plane frequency for several reasons. Stamn[6] carried out the vibrational analysis of vinyl acetylene and assigned the band at 1288 cm^{-1} to the CH in-plane rocking vibration of vinyl group. Torkington and Thompson[7] investigated a series of vinyl halides and showed that the frequencies concerned are assigned to 1306, 1280, 1262 and 1229 cm^{-1} for fluoride, chloride, bromide and iodide, respectively. It seems reasonable that the bands at 1321±2 cm^{-1} of vinyl ethers should be assigned to CH in-plane rocking frequencies. This conclusion is compatible with the assignment in the gaseous methyl vinyl ether from the consideration of band contours. Isopropyl vinyl ether has two bands at 1322 and 1340 cm^{-1}, which may be associated with the two CH groups contained in the molecule, the one in the isopropyl group and the other in the vinyl group. In the other vinyl ethers examined, no other band is observed around 1340 cm^{-1}.

Ethyl vinyl thioether shows a fairly strong absorption at 1260 cm^{-1} instead of 1340 cm^{-1}. This band is probably interpreted to the CH in-plane rocking frequency, although the reason for the band shift is uncertain. This rocking vibration may have considerable coupling effect with the C—S streching vibration.

iv) 1200 cm^{-1} Region.—In general alkyl ethers, the C-O stretching frequencies are found around 1100 cm^{-1}. In the present case, however, almost every vinyl ether shows a strong absorption at 1203±2 cm^{-1}, which is assigned to the C-O stretching frequency. The C-O bond adjacent to vinyl group has a somewhat double bond character as a result of the resonance effect referred to before. This is the reason why the frequency rises to a higher position.

The C-S stretching frequencies in mercaptans and sulphides are found in the range 700-600 cm^{-1} [8]. The corresponding frequency of ethyl vinyl thioether may be assigned to the fairly strong band at 719 cm^{-1}.

6) Stamn; *J. Chem. Phys.*, **17**, 104 (1949).
7) Torkington and Thompson, *J. Chem. Soc.*, **1944**, 303.

v) Bands around 965 and 810 cm^{-1}.—The bands around 965 and 810 cm^{-1} are also found in all vinyl ether and are useful characteristic frequencies. The vinyl type double bond gives rise to two strong bands at 995–985 cm^{-1} and 915–905 cm^{-1} [8], these being concerned with the CH out-of-plane vibration of the $-CH=CR-$ and $=CH_2$ group, respectively. The bands of vinyl ethers around 965 and 810 cm^{-1} may be assigned to the corresponding frequencies, because these two bands are similar to the two bands referred to above in their intensity and constancy in frequency, and because the contours of bands at 965 and 810 cm^{-1} in methyl vinyl ether show the C type. Both bands appear in considerably lower frequencies, as compared with the other mono-substituted ethylenes. Bellamy's suggestion that the "overtone" bands afford a useful confirmation of the presence of the $=CH_2$ groupings,[8] may give another proof for the assignment of the bands around 810 cm^{-1}.

Summary

The infrared spectra of methyl, ethyl, *n*-propyl, isopropyl, *n*-butyl, 2-ethylhexyl, benzyl and phenyl vinyl ether and also ethyl vinyl thioether were investigated over the region of 4000–650 cm^{-1}. The assignment of the spectrum of methyl vinyl ether has been made by the aid of the bands contours. The absorption bands of the other were discussed and the characteristic frequencies of vinyl ethers are concluded as follows.

(1) three bands near 3100 cm^{-1}..... CH stretching of vinyl group
(2) 1615±5 cm^{-1}.....C=C stretching
(3) 1321±2 cm^{-1}..... CH in-plane deformation
(4) 1203±2 cm^{-1}.....C-O stretching
(5) 965±5 cm^{-1}..... =CH- out-of-plane deformation
(6) 815±5 cm^{-1}..... $=CH_2$ out-of-plane deformation

The author wishes to express his sincere thanks to Prof. S. Mizushima and Dr. T. Shimanouchi of the University of Tokyo for their kind advice and encouragement and also to Mr. T. Arakawa for his earnest co-operation throughout this investigation.

The author thanks also Mr. Matsuzawa for his kindness in preparing the samples.

Research Laboratory of Mitsubishi Chemical Industries Ltd., Kawasaki-shi, Kanagawa

8) L.J. Bellamy, "The Infrared Spectra of Complex Molecules", Methuen, London (1954).

Hydrogen Bonding Effect on the Fluorescence of π-Electron System

By Noboru MATAGA, Yozo KAIFU and Masao KOIZUMI

(Received July 13, 1955)

Introduction

In recent years many interesting papers[1-5] have been published about the hydrogen bonding effect upon the visible or ultraviolet spectra of π-electron systems, and especially the beautiful work by S. Nagakura and H. Baba[1,2,3] has demonstrated that in suitable cases the quantitative studies on the equilibrium of the hydrogen bond formation is possible through such spectral investigations. There are, however, scarcely any quantitative studies for the hydrogen bonding effect upon the fluorescence of π-electron system, that is the effect of the addition of hydrogen acceptor (or donor) to the solution of fluorescent hydrogen donor (or acceptor). Such studies would be interesting from the following three points of view.

Firstly, it is expected that the fluorescence spectra would be affected by the hydrogen bond formation as was the case for absorption spectra. The shift of absorption spectra due to the hydrogen bond formation gives of course the difference of the produced energy change of π-electronic system between the ground state and excited Franck-Condon state[6], while for the fluorescence, the shift is to be attributed to the analogous difference

1) S. Nagakura, *J. Chem. Soc. Japan*, **74**, 153 (1953). S. Nagakura and H. Baba, *J. Am. Chem. Soc.*, **74**, 5693 (1952); S. Nagakura, *J. Am. Chem. Soc.*, **76**, 3070 (1954).

2) S. Nagakura, *J. Chem. Soc. Japan*, **75**, 734 (1954).

3) H. Baba, *Monograph Ser. Research Inst. Applied Electricity*, Hokkaido, No. 4, 61 (1954).

4) R. Miyasaka, *Busseiron Kenkyū*, No. 62, 94 (1951).

5) H. Tsubomura, *J. Chem. Soc. Japan*, **73**, 841, 920 (1952).

6) N.S. Bayliss and E. G. McRae, *J. Phys. Chem.*, **58**, 1002 (1954).

between the equilibrium excited state and Franck-Condon state of the ground level.

Secondly, the formation of hydrogen bond would affect the fluorescence yield of the mother substance, and this effect would give valuable information for the mechanism of fluorescence quenching or in general the mechanism of inter-or intra-molecular energy transference.

Lastly, there is a possibility that a new and different equilibrium of the hydrogen bond formation is reached during the lifetime of the excited state and this possibility would be examined through the studies of the fluorescence. The situations are probably somewhat analogous to the ionic dissociation of naphthols and other substances studied by Th. Förster and A. Weller[7,8], who confirmed that the tendency of dissociation is remarkably greater in the excited state than in the ground state.

In this paper the effects of the addition of various hydrogen acceptors to the solutions of α- and β-naphthol used as fluorescer, have been examined from the above mentioned viewpoints; particularly as to the third problem, i. e., the shift of equilibrium in the excited state. A quantitative treatment has been given with the result that β-naphthol in the excited state has a greater tendency toward hydrogen bonding, a new equilibrium being attained during its lifetime.

The main object of the present paper is to report this fact with some discussion on the interaction of the hydrogen bond and π-electron system.

Experimental

Reagent.—Chemical pure grade *n*-hexane was shaken with fuming sulfuric acid diluted with conc. sulfuric acid and distilled carefully. *n*-hexane thus purified was completely transparent throughout the whole spectral range measurable by the Beckman spectrophotometer.

Merck's analytical grade α-naphthol was used without any further purification.

β-naphthol was of commercial supply, and purified by repeated distillation in an atmosphere of dry nitrogen.

Purified β-naphthyl-methyl-ether was kindly supplied by Shionokôryô Co., Ltd.

Extra pure grade dioxane was purified according to the method of Weissberger[9].

Methylacetate was washed with the saline solution several times and fractionated after being dried over anhydrous potassium carbonate.

Ethyl and butyl acetate was dried over potassium carbonate and fractionated. Ethyl chloroacetate was kindly supplied by Mr. M. Nakazaki of this Institute. Carbon tetrachloride was purified by shaking with conc. sulfuric acid.

Apparatus.—Absorption spectra were measured by Beckman Spectrophotometer Model D. U.

Fluorescence spectra were photographed with Hilger E. 2 type quartz spectrograph. High pressure mercury lamp or copper arc filtered with 1 cm. thickness of potassium chromate 0.2 g./l. aqueous solution[10] was used as a light source. Slit width was 0.3 mm.

The relative intensity of fluorescence was measured by a fluorometer kindly constructed by S. Kato. Its circuit is almost the same as that of Beckman spectrophotometer with the usage of the ultraviolet sensitive phototube purchased as a spare for Beckman apparatus. As a light source, a high pressure mercury lamp was used and 3100 Å line was taken out as an exciting light through an aqueous solution of potassium chromate. To secure the constancy of the light source intensity, the beam in the direction oblique to that for excitation was passed through another potassium chromate solution, caught by anohter ultraviolet sensitive photocell, and a galvanometer deflection was kept constant by controlling a variable choke in the electric circuit for the mercury lamp. To eliminate 3100 Å from the fluorescence light, Matsuda colour filters VVI and UVDI were employed. Under such conditions, the phototube receives the light from ca. 3200 Å to 4000 Å, the range being enough to cover the fluorescence spectra of all the samples examined.

Experimental Results

1. Spectral Shift of Absorption and Fluorescence caused by Hydrogen Bonding

When the various proton acceptors are added gradually to the solution of naphthols in *n*-hexane, the absorption spectra show the characteristic changes due to hydrogen bonding, which are similar to those published in

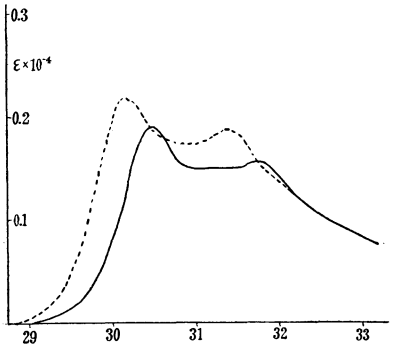

Fig. 1. Absorption spectra of β-naphthol.
——— in *n*-hexane
– – – – hydrogen bonded with butyl-acetate in *n*-hexane

7) Th. Förster, *Z. Elektrochem.*, 54, 42, 531 (1950).
8) A. Weller, *Z. Elektrochem.*, 56, 662 (1952).
9) A. Weissberger and E. Proskaner, "*Org. Solvents*" (1935), p. 110.
10) M. Kasha, *J. Opt. Soc. Am.*, 38, 929 (1948).

literature[2]; the maximum slightly shifts to the long wave length side with its extinction somewhat strengthened as shown in Figs. 1 and 2. The fluorescence spectra also show

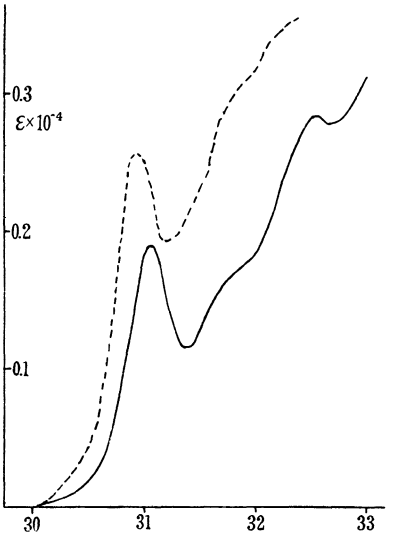

Fig. 2. Absorption spectra of α-naphthol.
——— in *n*-hexane
- - - - hydrogen bonded with butylacetate in *n*-hexane

the red shift, the magnitude of which is nearly equal or slightly larger than that of the absorption spectra. Some examples of the relative intensity curves which were obtained by the visual observation of the plates, are shown in Figs. 3 and 4. Now it

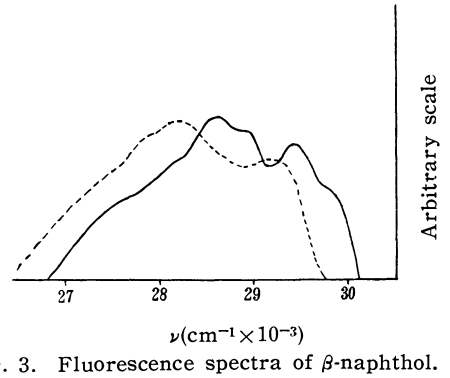

Fig. 3. Fluorescence spectra of β-naphthol.
——— in *n*-hexane
- - - - hydrogen bonded with butylacetate in *n*-hexane
(Visually observed blackening of photographic plate)

is highly plausible to attribute these spectral changes of fluorescence to the hydrogen bonding, but to confirm it further, the effects of the addition of the same proton acceptors to

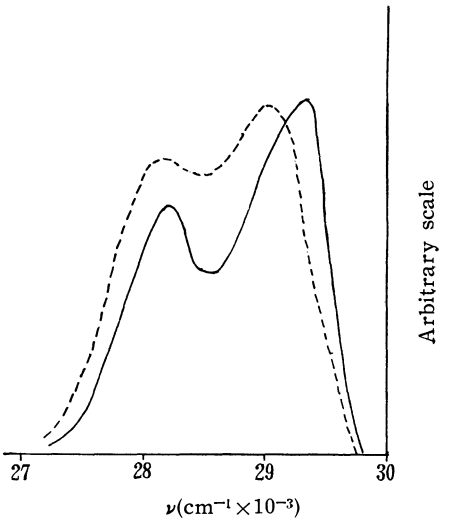

Fig. 4. Fluorescence spectra of α-naphthol.
——— in *n*-hexane
- - - - hydrogen bonded with butylacetate in *n*-hexane
(Visually observed blackening of photographic plate)

the *n*-hexane solution of β-naphthylmethylether were examined.

This substance of which the absorption and fluorescence spectra are quite similar to those of β-naphthol, is unable to form the hydrogen bond, and it was established that the addition of a large quantity of any proton acceptors cannot cause even a slight change either in fluorescence or in absorption. Hence there is no doubt that the above mentioned shifts in fluorescence spectra are due to the hydrogen bonding.

2. Hydrogen Bonding Effect on the Fluorescence Intensity

The fluorescence of both α- and β-naphthol is remarkably quenched by ethylchloroacetate, the magnitude of quenching being somewhat greater in the former case, while in the case of dioxane and acetic acid esters other than ethylchloroacetate, the intensity increases more or less in both naphthols. Some examples of these changes of fluorescence intensity by the added acceptors are shown in Fig. 5, where the ordinate is the relative intensity of fluorescence and the abscissa is the concentration of the proton acceptor. To check the fact that these intensity changes are really due to the hydrogen bond formation, the effect of the addition of similar proton acceptors to the solution of β-naphthylmethylether in *n*-hexane was examined. Again, as in the case of fluorescence spectra, there was not observed any slight change of fluorescence intensity throughout

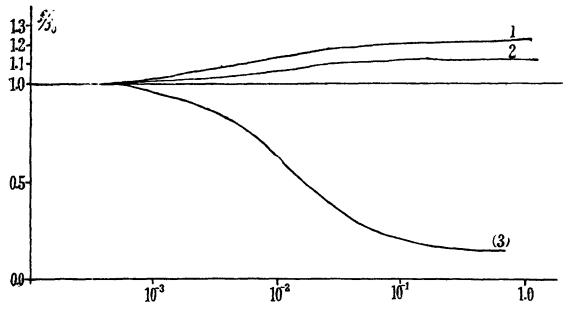

Fig. 5. Change of relative fluorescence intensity of β naphthol by various proton acceptors.
1. Butylacetate at 10°C 2. Methylacetate at 10°C
3. Cl-ethylacetate at 25°C

the whole range of acceptor concentration from ca. 10^{-3} to $\sim 5\times10^{-1}$ mol./l. Further, it was ascertained that the fluorescence of neither β-naphthol nor β-naphthylmethylether was quenched by dichloromethane. Hence the ordinary collisional quenching may be excluded in this case and it is almost certain that the change of fluorescence intensity in the case of β-naphthol is completely due to the hydrogen bond formation.

3. Interpretation of the Variation of Fluorescence Intensity on the Basis of the Hydrogen Bonding Equilibrium

It seems very plausible to attribute the observed changes of fluorescence intensity to the fact that the free naphthol and hydrogen-bonded naphthol have different efficiency of fluorescence and that the concentration of these molecular species are determined from the association equilibrium. But the question whether the situation does really correspond to such an equilibrium state, and further if it really holds, whether the equilibrium in question refers to the ground state or excited state, must be decided from the analysis of the experimental results.

Thus when the equilibrium of the ground state is maintained during the course of fluorescence, then the equilibrium constant deduced from the experimental data of fluorescence intensity must coincide with that obtained from absorption spectra. On the contrary, when the state of association approaches a new equilibrium state during the lifetime of the excited molecule, and until a new equilibrium state is almost completely reached prior to the emission, then the equilibrium constant deduced from the fluorescence data may generally be different from that obtained from absorption spectra. And lastly, if the equilibrium is only partially reached in the excited state, the quantitative relation deduced from the equilibrium consideration would fail to reproduce the experimental results.

Now let us take up first, the case in which the association equilibrium in the ground state be maintained in the excited state. Since the concentration of α- and β-naphthols employed for fluorescence measurement does not exceed 5×10^{-4} mol./l., the phenomenon of self-quenching or concentration quenching can be neglected, and the deduction about the intensity may be made according to the following scheme involving the association equilibrium in the ground state. In this scheme, D and A are respectively proton donor (fluorescer) and proton acceptor, and * denotes the excited state.

	Rate or equilibrium	
$D+A \rightleftarrows DA$	$K=[DA]/[D][A]$	(1)
$D+h\nu_a \longrightarrow D^*$	$I_{abs}[D]/[D]+[DA]$	(2)
$DA+h\nu_a' \longrightarrow DA^*$	$I_{abs}[DA]/[D]+[DA]$	(3)
$D^* \longrightarrow D+h\nu_f$	$k_f[D^*]$	(4)
$DA^* \longrightarrow DA+h\nu_f'$	$k_f'[DA^*]$	(5)
$D^* \longrightarrow D$	$k_q[D^*]$	(6)
$DA^* \longrightarrow DA$	$k_q'[DA^*]$	(7)

It must be noted that (2) and (3) can express the rate of light absorption of D and DA only under the condition that the extinction of D and DA at the wave length of exciting light are the same; this condition is practically fulfilled in the case of β-naphthol. From the above scheme, the following simple relation can be derived for the relative fluorescence intensity f of the solution in which the concentration of A is [A], f_0 being the intensity of the pure naphthol solution.

$$f/f_0=(1+\alpha K[A])/(1+K[A])$$

or

$$\frac{1-f_0/f}{[A]}=-K+\alpha K(f_0/f) \qquad (a)$$

where

$\alpha=\Phi'/\Phi$, $\Phi=k_f/k_f+k_q$, $\Phi'=k'_f/k'_f+k'_q$,

Φ and Φ' are respectively the quantum yields of fluorescence for D and DA. α, the ratio of these two quantities can easily be determined from f_0-value and the f-value of the solution to which A is amply added. To treat the problem more rigorously, it would be necessary to take into account the correction for the difference in the sensitivity of the phototube toward different wave lengths, and for this correction the second term in (a) will have to be multiplied by a certain factor. But in the present case, the spectral shift of AD against D being rather small, the above treatment may be practically exact.

In the case of α-naphthol in which the extinction of the hydrogen bonded naphthol differs to some extent from that of the free naphthol at the wave length of excitation, the relation (a) must be modified as follows.

$$\frac{1-f_0/f}{[A]}=-K+\frac{\varepsilon'}{\varepsilon}\alpha K(f_0/f) \qquad (b)$$

In this equation ε and ε' are the extinction coefficients of the free and hydrogen bonded naphthols at the wave length of excitation.

Next let us turn to the case in which a new and different equilibrium is realized during the life time of the excited state. If the extinction of D and AD are the same at the wave length of exciting light, then the sum of the rate of production D* and AD*, that is, the light absorbed per unit time is constant irrespective of the concentration of A, and the following scheme may be used to derive the relative intensity of fluorescence.

	Rate or equilibrium constant	
$\left.\begin{matrix}D+h\nu_a\rightarrow D^*\\ DA+h\nu_a'\rightarrow DA^*\end{matrix}\right\}$ total	I_{abs}	(1′)
$D^*+A \rightleftarrows DA^*$	$K'=\frac{[D^*][A]}{[DA^*]}$	(2′)
$D^*\rightarrow D+h\nu_f$	$k_f[D^*]$	(3′)
$DA^*\rightarrow DA+h\nu_f'$	$k_f'[DA^*]$	(4′)
$D^*\rightarrow D$	$k_q[D^*]$	(5′)
$DA^*\rightarrow DA$	$k_q'[DA^*]$	(6′)

The following relation (a′) analogous to (a) can easily be derived from the above scheme.

$$\frac{1-f_0/f}{[A]}=-K'+\alpha K'(f_0/f) \qquad (a')$$

In this equation K' is related to the excited state and may generally be different from K in (a).

When the extinction of D and DA is different as in the case of α-naphthol, the matter becomes somewhat complicated but it can easily be verified that the following relation must hold.

$$f/f_0=\left\{\frac{1+\alpha K'[A]}{1+K'[A]}\right\}\left\{1+\frac{K[A]\Delta\varepsilon/\varepsilon}{K[A]+1}\right\}$$

where $\Delta\varepsilon=\varepsilon'-\varepsilon$.

If the experimentally obtained f_0/f-value be multiplied by a factor $\Delta=\left\{1+\frac{K[A]\Delta\varepsilon/\varepsilon}{K[A]+1}\right\}^{-1}$,

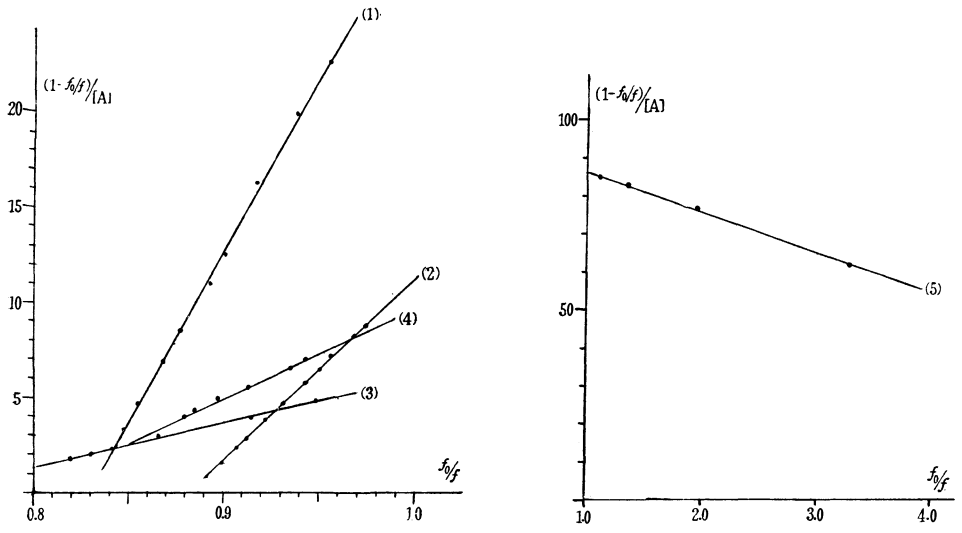

Fig. 6. $\frac{(1-f_0/f)}{[A]}\sim f_0/f$ linear relation of β-naphthol for various proton acceptors.

(1) but. acetate
(2) met. acetate
(3) dioxane
} at 10°C

(4) eth. acetate
(5) Cl-eth. acetate
} at 25°C

which is easily calculated from the experimental data, then equation analogous to (b) will hold.

$$\frac{1-(f_0/f)\Delta}{[A]} = -K' + \alpha K'(f_0/f)\Delta \qquad (b')$$

Now the experimental results in the case of β-naphthol can be reproduced very satisfactorily by (b) or (a) as seen from Fig. 6, hence it is very plausible to consider that the equilibrium condition is realized in the excited state. The question whether this equilibrium state is the same or different from that in the ground state can be settled from the comparison of K_f-value obtained from the curves in Fig. 6 and K_a-value obtained from the analysis of the absorption spectra which can simply be calculated by the method of Rosenblatt[11]. Thus if the equilibrium in the ground state is maintained during the emission process, K_f which corresponds to K must coincide with K_a, while in the alternative case K_f which corresponds to K' must be different from K_a. In Table I, the free energy changes of hydrogen bond formation ΔF^f and ΔF^a as calculated from K_f and K_a are tabulated. As seen from Table I, $|\Delta F^f|$ is greater than $|\Delta F^a|$ in the case of β-naphthol; hence it can be concluded that the equilibrium of hydrogen bonding shifts toward the association during the life time of the excited state.

TABLE I

α-Naphthol

Proton acceptor	ΔF^a_{303}	ΔF^f_{303}	$\Delta F^f_{303} - \Delta F^a_{303}$	$\delta\nu_{a,max}$ (kcal./mol.)	α
Methylacetate	−1.49	−1.8	−0.3	−0.27	1.30
Ethylacetate	−1.57	−2.0	−0.4	−0.27	1.26
Butylacetate	−1.62	−2.0	−0.4	−0.30	1.27
Ethyl-Cl-acetate	−1.08	−2.4	−1.3	−0.27	0.00

β-Naphthol

Proton acceptor	ΔF^a_{283}	ΔF^f_{283}	$\Delta F^f_{283} - \Delta F^a_{283}$	$\delta\nu_{a,max}$ (kcal./mol.)	α
Dioxane	−1.50	−1.65	−0.15	−0.65	1.33
Methyl-acetate	−1.82	−2.48	−0.66	−0.70	1.13
Butylacetate	−1.80	−2.80	−1.00	−1.00	1.20
	ΔF^a_{298}	ΔF^f_{298}	$\Delta F^f_{298} - \Delta F^a_{298}$	$\delta\nu_{a,max}$ (kcal./mol.)	α
Ethylacetate	−1.67	−2.04	−0.37	−0.95	1.29
Ethyl-Cl-acetate	−1.29	−1.85	−0.56	−0.80	0.20

As for the case of α-naphthol, we have not yet succeeded in obtaining the data which are reliable enough to test the equation (b) or (b'). The data in Table I are only provisional in nature, but scarcely any doubt remains that $|\Delta F^f|$ values are always greater than $|\Delta F^a|$ values in this case too.

Discussion

a) The Shift of Absorption and Fluorescence Spectra due to Hydrogen Bonding

For the discussion of the solvent effect on the absorption spectrum in general, it is customary to take the shift of absorption maximum as a change of the pure electronic excitation energy. But this is in general, a very crude approximation, because the former corresponds to the difference between the energy change of the Franck-Condon state of excited level and that of the equilibrium state[6] of the ground level. Thus in the case of the hydrogen bonding effect, the shift of the absorption maximum $\Delta\nu^{abs}$ (positive for the red shift) may be put as follows.

$$h\Delta\nu^{abs} = \Delta E^{abs} = (E_{of}' - E_{Hf}) - (E_{oe}'' - E_{He}'') = \Delta E_f' - \Delta E_e'' \qquad (1)$$

where $'$ and $''$ refers respectively to the excited and the ground state and the suffix o and H denote free and hydrogen-bonded state, while f and e refer to the Franck-Condon state and the equilibrium state. As for the shift of the maximum of fluorescence spectra on the other hand, the following relation must hold.

$$h\Delta\nu^{fl} = \Delta E^{fl} = (E_{oe}' - E_{He}') - (E_{of}'' - E_{Hf}'') = \Delta E_e' - \Delta E_f'' \qquad (2)$$

From (1) and (2) it is clear that $\frac{\Delta\nu^{abs}+\Delta\nu^{fl}}{2}$ is a better approximation as a change of pure electronic excitation energy; in fact if the potential diagrams are symmetrical around the equilibrium point, then this approximation will give an almost exact value.

In the present case, however, it may be permitted to take $\Delta\nu^{abs}$ as a change in a pure electronic energy, because $\Delta\nu^{fl}$ does not in general differ much from $\Delta\nu^{ab}$. Hence such a convention is followed throughout the present discussion, especially in view of such a case as ethylchloroacetate where the fluorescence is so faint that $\Delta\nu^f$ cannot be decided. $\Delta\nu^{max}$ for various proton acceptors are tabulated in Table I.

From Table I, it is seen that $|\Delta F^f| - |F^a|$ is nearly equal to $\Delta\nu^{max}$ for every acceptor added to β-naphthol. Of course it is more desirable to compare $\Delta\nu^{max}$ with the energy of the hydrogen bond, not with the free

11) D.H. Rosenblatt, *J. Phys. Chem.*, 58, 40 (1954).

energy; the evaluation of the former, however, necessitates the measurement at different temperatures, which in the present apparatus is extremely difficult. Tentatively neglecting the entropy factor, one may consider that $\Delta\nu^{max}$ is approximately equal to the difference of the energy of the hydrogen bond between the excited and the ground state.

b) The Intensity of Fluorescence affected by the Hydrogen Bond

In all the cases except ethylchloroacetate, the intensity of fluorescence is increased more or less by the hydrogen bond formation, and the quenching constant k_q may perhaps be reduced by the hydrogen bond formation. This presumption can be further confirmed by the following deduction.

Since the first and the second absorption regions are fairly well separated in the case of β-naphthol, one can easily estimate the spontaneous emission probability from the integrated absorption by the formula of Ladenburg[12]

$$k_f = 3\times 2.303\times(10^3/N)\times 8\pi cn^2\tilde{\nu}_0^2\int\varepsilon_{\tilde{\nu}}d\tilde{\nu}$$

From the k_f-value thus calculated and the α-values tabulated in Table I, the comparison of k_q and k_q' can easily be made on the basis of the following relation,

$$\alpha=\frac{\Phi'}{\Phi}=\frac{k_f'}{k_f'+k_q'}\Big/\frac{k_f}{k_f+k_q}$$

The result is that k_q' is smaller than k_q in the case of dioxane, acetic acid esters other than ethylchloroacetate, and that $\tau'=\frac{1}{k_f'+k_q'}$ does not differ from $\tau=\frac{1}{k_f+k_q}$ more than 10% in these cases.

The quenching phenomenon observed in the case of ethylchloroacetate may be a very interesting example from the standpoint of the energy transfer. In the case of β-naphthol, this quenching effect can undoubtedly be attributed to the formation of the hydrogen bond on the basis of the already mentioned facts. But in the case of α-naphthol some ambiguity remains since the theoretical relations cannot represent the experimental data so successfully as in the case of β-naphthol, and moreover, no particular experiments using α-naphthyl methyl ether was performed. The collisional quenching might possibly participate in this case making the result very complicated. Though the question still remains to be settled in future, it is quite certain that a large part of quenching in this case may also be due to the hydrogen bond formation. For the system consisting of β-naphthol and ethylchloroacetate, it was established by the above mentioned estimation that k_q' is far greater than k_q and that $\tau>\tau'\approx\frac{\tau}{5}$. In connection with the quenching action of ethylchloroacetate on β-naphthol, it may be worthy to add that we have measured the fluorescence quenching of β-naphthol and β-naphthyl methyl ether caused by the addition of carbon tetrachloride and have found that the change of relative fluorescence yield obeys the Stern-Volmer relation very well with the same quenching constant in both cases. Thus the mechanism for the quenching of fluorescence of β-naphthol by carbon tetrachloride is evidently quite different from that by ethylchloroacetate. The former may parhaps be interpreted as the ordinary collisional quenching though its microscopic mechanism is still open to question, especially in view of such facts as observed by E. J. Bowen and R. J. Cook[13] that the temperature coefficient of the fluorescence quenching of anthracene and its derivatives caused by chloroform and bromobenzene is negative. In fact, Bowen and Cook insist on the complex formation between the excited molecule and the quencher molecule and suggest that the charge transfer interaction between them induce the excited molecule to go to the triplet state.

Turning to the case of β-naphthol and ethylchloroacetate where the fluorescer and the quencher are certainly combined by the hydrogen bond, an interpretation analogous to that of Bowen and Cook may be plausible, but it is also possible to consider that the excitation energy is efficiently dissipated by Cl-atom, which in this case is closely connected with the fluorescer molecule by the hydrogen bond. At any rate it may be hoped that a key to clarify the microscopic mechanism of the quenching phenomenon in general can be got by further investigations of such systems.

c) The Mechanism of the Hydrogen Bonding Effect

According to our results, it is quite evident that the excited naphthol molecules have a greater tendency to form the hydrogen bond and that at least in the case of β-naphthol a new and different equilibrium state is reached during the lifetime of its excited state. An analogous phenomenon has also been found by Eisenbrand[14]. He reported

12) R. Ladenburg, *Z. Phys.*, **4**, 451 (1921); R.C. Tolman, *Phys. Rev.*, **23**, 693 (1924); E.J. Bowen and W.S. Metcalf, *Proc. Roy. Soc.*, A **206**, 437 (1951).

13) E.J. Bowen and R.J. Cook, *J. Chem. Soc.*, **1953**, 3059.

14) J. Eisenbrand, *Z. Elektrochem.*, **55**, 374 (1951).

that 8-quinolinesulfonic acid in the aqueous solution has a greater tendency to form the complex associate with resorcine in the excited state on the basis of the studies of the fluorescence.

The present investigation has afforded another notable example, and this example seems to be particularly valuable since it enables us to make a quite interesting interpretation about the mechanism of the hydrogen bonding effect.

As to the shift of absorption spectra due to the hydrogen bonding, the following plausible interpretation[1-5] has been given on the basis of the electron migration theory developed by Sklar and Herzfeld[15].

Taking phenol as an example, the close approach of the electronegative atom of the proton acceptor causes a decrease in the ionization potential of the non-bonding 2p electron in the OH radical by inductive or direct effect, which eventually makes easier the migration of non-bonding electrons into the vacant orbital of π-electron system. Then the rate of electron migration in the excited state will be greater than in the ground state, since one electron in the highest level of the ground state has been raised to a higher level. From this view point, the values of $\delta\nu_{a,max}$ tabulated in Table I may be interpreted as the difference of the stabilization due to the electron migration between the excited and the ground state. Now, as already stated, the difference of the hydrogen bonding energy between the excited and the ground states as revealed from $\Delta F^f - \Delta F^a$ roughly coincide with $\Delta\nu_{a,max}$. Hence it may be concluded that the extra stabilization energy of hydrogen bonding in the excited state is almost exclusively due to the increased electron migration.

The present result is noteworthy for the interpretation of the nature of the hydrogen bond in general and particularly of the interaction between the hydrogen bond and π-electron system.

15) A.L. Sklar, *J. Chem. Phys.* 7, 984 (1939); K.F. Herzfeld, *Chem. Rev.*, 41, 233 (1947).

Further studies on analogous systems are now going on.

Summary

1. The absorption and fluorescence spectra of α-, β- naphthols and related compounds were measured in various mixed solvents in connection with the hydrogen bonding phenomena. The observed spectral shifts of absorption and fluorescence spectra, which were almost the same (~30 Å), could be solely attributed to the hydrogen bonding effect.

2. It was found that the fluorescence intensity becoms stronger by hydrogen bonding when dioxane and acetic acid esters other than ethylchloroacetate are used as the proton acceptors. In the case of β-naphthol, it was established that the rate of inner quenching is decreased by hydrogen bonding. When ethylchloroacetate was used as a proton acceptor, fluorescence quenching was observed, which is also to be attributed to hydrogen bonding.

3. For β-naphthol, the measurement of the relative intensity established the fact that a new and different equilibrium state of hydrogen bonding, which shifts somewhat toward association, is reached during the life time of the excited state.

4. The mechanism of hydrogen bonding was discussed on the basis of the theory of electron migration, and it was concluded that the observed extra-stabilization of the hydrogen bond in the excited state as compared to the ground state, is mainly due to the increase of electron migration in the former state.

The authors express their cordial thanks to Mr. S. Kato for constructing the fluorometer. They also thank to Mr. M. Nakazaki and the Shionokoryo Co., Ltd. for valuable samples. Thanks are also due to the Ministry of Education for a grant in aid.

Institute of Polytechnics, Osaka City University, Osaka

The State of Metal Ion in Aqueous Solutions and its Surface Chemical Effects. III. Rheological Study for the Effect of Metal Ions on the Monolayer of Stearic Acid

By Hideo KIMIZUKA*

(Received August 26, 1955)

So far a number of investigations have been carried out on the metal ion-monolayer interaction. The remarkable effects of polyvalent or transition metal ions on the fatty acids were shown by the studies of the monolayers[1,2], built-up film[3] and wetting[4]. Although the effects are characterized by the formation of rigid film over a pH range characteristic of each ion[1,2], the quantitative measurement of viscoelasticity has not yet been carried out on the system, so the application of the rheological technique to the system may be expected to give more detailed information concerning the interaction. The present paper describes the result obtained by this technique and gives an explanation for it.

Experimental

The monolayer of stearic acid was prepared by spreading it from a benzene solution on the substrates containing 10^{-4} mol./l. salts of various kinds. The salts were used as chloride, nitrate and sulfate, which were purified by recrystallization. Of these salts, the effect of anion on the monolayer of stearic acid was found negligible[1].

The surface pressure was measured by the method already described elsewhere[5].

In Fig. 1 the rheometer is shown, in which A is a brass ring, 6 cm. in diameter, coated with paraffin, B, the platinum ring, 4 cm. in diameter C, the mirror, D, the suspension wire of phosphor bronze, 40 μ in diameter and 30 cm. in length, the torsion constant of which being 0.328 dyn. cm., and E, the torsion head. In this figure A and B are allowed to move vertically by means of a screw F and are made to touch the surface of solution, B can rotate around the wire axis while A is fixed. With this apparatus the rheological behavior of the surface film was measured as described in the preceding paper[6]. The time

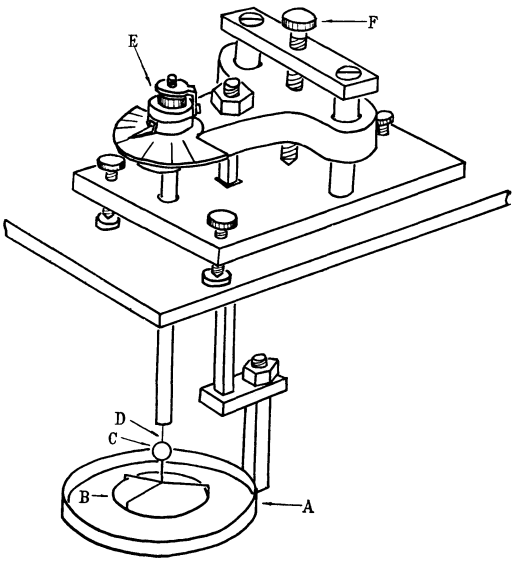

Fig. 1. Rheometer.

scale taken for rheological measurement was five minutes. The experiments were carried out at room temperature and pH was controlled using hydrochloric acid and sodium hydroxide.

Result

When the suspension wire having the torsion constant of 1.24×10^{-2} dyn.cm. was used, the monolayer of stearic acid giving the area of 20.5 Å^2/molecule on distilled water showed the rheological behavior of Voigt model at 20°C, viscosity coefficient being 0.13 g./sec. and modulus of rigidity, 8.4×10^{-3} dyn./cm., with the elastic limit (yield value) of 9.0×10^{-4} dyn./cm. This suspension wire has, however, too small torsion constant to measure the mechanical behavior of an extremely rigid film formed by the interaction with metallic ion, so the other experiments were carried out with a different suspension wire already mentioned, towards which the monolayer of stearic acid, spread on the substrates containing no metal ion, behaved as the fluid film for all the region of applied pH. The rigid film thus formed could hardly be rendered fluid when the solution of ethylene diamine tetraacetic acid (EDTA) was injected, while the formation of rigid film could not be observed when EDTA was added to the substrate containing metallic ion before stearic acid

* Present Address: Chemical Institute, Fukuoka Gakugei University.

1) R. Matsuura, This Bulletin, **24**, 274, 278 (1951).
2) G.A. Wolstenholme and J.H. Schulman, *Trans. Faraday Soc.*, **46**, 475 (1950); **47**, 787 (1951), etc.
3) M. Muramatsu and T. Sasaki, This Bulletin, **25**, 21, 25 (1952).
4) A. Inaba, Ibid., **25**, 175 (1952); **26**, 43 (1953).
5) T. Sasaki, ibid., **14**, 796 (1941); R. Matsuura and I. Hayashi, *Memoirs of the Faculty of Science, Kyusyu University*, Ser. C, **1**, 31 (1948).
6) T. Sasaki and H. Kimizuka, This Bulletin, **25**, 318 (1952); H. Kimizuka, ibid., **26**, 449 (1953).

was spread on it. This is a similar phenomenon to that reported in a preceding paper[7] and may be ascribed to be the prevention of the formation of metal stearate due to the EDTA-complex formation. Consequently the developments of visco-elastic property may be considered due to the formation of network structure of insoluble metal stearate films.

Some of the results for the interacted film are shown in Figs. 2a and 2b, in which the surface pressure, F, and the yield value, Y, of the film are plotted against the area per stearyl group, A.

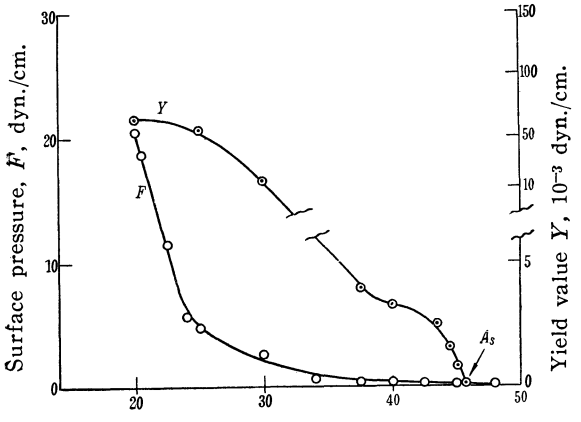

Area, Å²/molec.

Fig. 2a. Pressure-area and yield value-area curves of the monolayer of stearic acid on substrate containing aluminium ion at pH 5.2.

In this figure the area of the solidification of surface film, A_S, is indicated by that of the sudden development of the yield value. In Fig. 3 A_S–pH diagrams are shown for the various metallic ions.

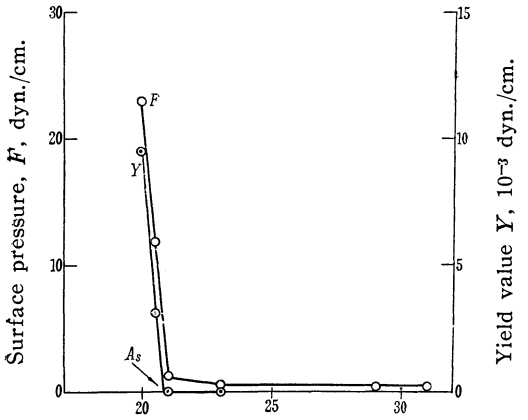

Area, Å²/molec.

Fig. 2b. Pressure-area and yield value-area curves of the monolayer of stearic acid on substrate containing calcium ion at pH 10.6.

7) R. Matsuura and H. Kimizuka, ibid., 28, 668 (1955).

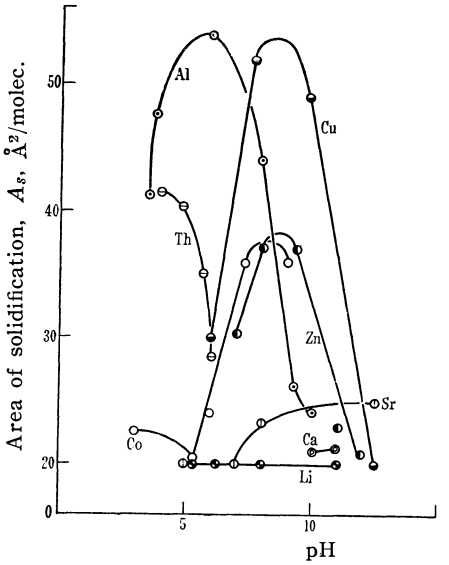

Fig. 3. Area of solidification-pH curves of the monolayer of stearic acid on substrates containing various metallic ions.

The metallic ions forming the solid film are classified into two groups based upon the mechanical behaviors of the films as in a former report[8], namely, one exhibiting Voigt model and the other, Maxwell model; they are summarized

TABLE I

MECHANICAL BEHAVIOR OF STEARATE FILM

Ions	Change of mechanical model with decreasing area
Group 1; Li, Ca, Sr and Ba	Viscous flow → Voigt model
Group 2; Th, Al, Fe, Co, Cu and Zn	Viscous flow → Maxwell model → three parameter model[8] → elastic behavior

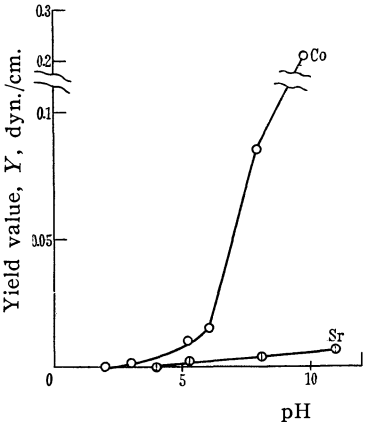

Fig. 4. Yield value-pH curves of the monolayer of stearic acid on substrates containing cobalt and strontium ion.

8) H. Kimizuka, This Bulletin, 26, 30 (1953).

in Table I. The presence of the ions, Na, K, Rb and NH_4, in the substrates yields no perceptible solid film in the present experiment.

The strength of the interacted film varies, in general, with pH. Thus, in Fig. 4 the yield values of the films at 20 Å/stearyl group on the substrates containing Sr or Co ions are plotted against pH.

The effect of colloid in the substrate was also investigated. A solution of ferric chloride was introduced into boiled water to prepare the colloidal solution of ferric hydroxide, and then the colloidal solution was dialysed with distilled water till the dialysate was no longer colored red with potassium rhodanide. Fig. 5 shows the $F-A$ and $Y-A$ diagrams for the effect of colloid and the freshly prepared solution of ferric chloride at pH 6, the former contains 5×10^{-5} mol./l. of Fe_2O_3 and the latter, 10^{-4} mol./l. of $FeCl_3$.

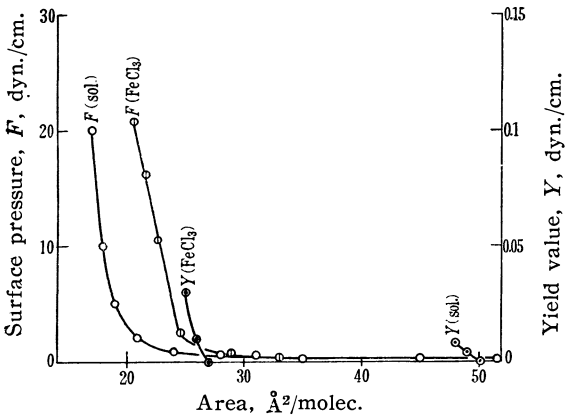

Fig. 5. Surface pressure-area and yield value-area curves of the monolayer of stearic acid on substrate containing ferric ion and ferric hydroxide sol at pH 6.

Discussion

The previous works on the effect of metallic ions on stearic acid suggested the classification of them into three groups. In conformity with this the same conclusion was also accepted in the present experiment. The results obtained are summarized in Table II together with those of the other experiments.

Here, the characteristic region of pH exhibited by a metal ion of group 2 agrees with those found in the other phenomena listed in this table. All these facts can reasonably be explained as due to the interaction between the monolayer and metallic ion in the substrate. It is interesting to note here that the mechanical behavior of the interacted monolayers with 1st and 2nd groups correspond to those of the adsorbed layer of the solutions of the micellar and the high-polymeric materials[8] respectively.

Of the group 1, the formation of simple stoichiometric compound was suggested[9,10], which may also explain our result of the formation of condensed solid film. Recently it has been shown in the preceding paper[10] and also in other report[11] that the film-bound Ca and Sr increase with pH. Fig. 4 shows the increase in the strength of strontium stearate film with the increase in pH,in which the pH of solid film formation coincides with that of appreciable amount of film-bound ion[10]. A similar correlation is recognized in this figure for the film of cobalt stearate. This fact may indicate that the rheological technique is another useful means for the study of surface film interaction. Ellis and Pankhurst[12] studied the interaction between the colllagen monolayer and tanning materials by means of the surface viscosity measurement and showed that the interaction results in a change in surface viscosity. This technique, however, would be rather inadequate to obtain the information about the structure of film, because the surface viscosity measurement may be carried out on the film which has been destroyed.

TABLE II
EFFECT OF METAL IONS ON STEARIC ACID

Groups	1	2	3
Ions	Li, Ca, Sr, Ba	Th, Fe, Al, Co, Cu	Na, K, Rb, NH_4
Region of pH	Alkaline gegion	Characteristic region of each ion	Alkaline region
Rheological behavior of stearate film	Condenced soid filim	Expanded soid filim	Fluid film
$F-A$ behavior of stearate film[1]	Insoluble condensed film	Extended film	Soluble film
Wettability of solid surface of steari cacid[4]	Non-wettable	Wettable	Wettable
Adsorption of ion on the built-up film[3]	Low constant adsorption independent of pH	Profound rdsorption	Dissolution of built-up film

9) W.D. Harkins and E. Boyed, *J. Phys. Chem.*, **45**, 20 (1941).
10) T. Sasaki and M. Muramatsu, This Bulletin, in the press.
11) E. Havinga, *Rec. trav. chim.*, **71**, 72 (1952).
12) S.C. Ellis and K.G.A. Pankhurst, *Diss. Faraday Soc.*, No. **16**, 170, (1954).

Of the second group, the rheological property of interacted film was already investigated by a somewhat different means[1]. As seen in Fig. 2a, A_S may be accounted for as the area of completion of network structure of the metal stearate and the solid film thus formed is strengthened with the successive compression of the film as shown by the increase in the yield value. Further, it may be pointed out that A_S is a characteristic point other than A_f, the limiting area estimated from the F-A diagram, since the value of A_f is frequently different from that of A_S. Further, A_S is defined more clearly than A_f as seen in Fig. 2a. Similar results were observed for the monolayer of high polymeric materials[13].

As shown in Fig. 5, the values of A_f are not so different from each other (about 25 Å^2/mol.) on the both substrates, the solution of ferric chloride and the ferric hydroxide sol, while the values of A_S are widely different namely 27 Å^2/mol. for the former and 50 Å^2/mol. for the latter. This probably means that the presence of a larger aggregate capable of interaction with the monolayer is responsible for the larger area of solidification which is also our common view as reported in the former papers[1,3,4]. In the characteristic region of pH, in which the rigid film of metal stearate are produced by the ions of 2nd group, the ions may be hydrolysed in various grade[7,14], i.e. may exist as the various forms of dispersion from the simple ion through the basic metal ion finally to the colloidal aggregate[15]. So these various forms of solute seem to have much to do with the formation of complex metal soap. Further investigations will, however, be required to obtain more detailed information on the mechanism of interaction.

Summary

The effect of metallic ions on the monolayer of stearic acid was studied by the rheological method.

(1) It was shown that the development of visco-elastic property of the film is closely correlated with the formation of metal soap. Result obtained by the rheological measurement enables us to classify the metal ions into three groups; Li, Ca, Sr and Ba belong to the 1st, showing the formation of the condensed solid film and the rheological behavior of Voigt model; Th, Fe, Al, Co, Cu and Zn, the 2nd, exhibiting the formation of the expanded solid film and the rheological behavior of Maxwell model; Na, K, Rb and NH_4, the 3rd, forming no solid film. These results were discussed in relation to the phenomena observed in the studies of the metal ion monolayer interaction, the adsorption of ion on the built-up film and the effect of ion on the wettability of a solid surface. These phenomena could be correlated with the formation of simple soap or complex metal ion-monolayer aggregate, the 1st and 3rd resulting in the former and the 2nd, in the latter.

(2) It was frequently observed for the interacted film with the ions of the 2nd group that the area of solidification is larger than the limiting area estimated from the surface pressure-area curve, while in the case of the film with the ions of 1st group the values of both area coincide with each other.

(3) It was shown that the monolayer of stearic acid, spread on the substrate containing ferric hydroxide sol, formed an expanded solid film.

(4) It was shown for Co and Sr ions that the strength of interacted film is a measure of film-bound ion.

In conclusion, the author expresses his hearty thanks to Prof. T. Sasaki of Tokyo Metropolitan Univ. for his kind guidance and encouragement throughout this study and he is also indebted to Assistant and Prof. R. Matsuura of Kyūsyū Univ. and to Mr. M. Muramatsu of Fukuoka Gakugei Univ. for suggestions and criticism.

Department of Chemistry, Faculty of Science, Kyūsyū University, Fukuoka

13) T. Tachibana and K. Inokuchi, *J. Colloid Sci.*, 8, 341 (1953).

14) N. Bjerrum, *Z. Phys. Chem.*, A 110, 656 (1924); R.E. Connick and W.H. McVey, *J. Am. Chem. Soc.*, 71, 3182 (1949); B.O.A. Hedström, *Arkiv. för kemi.* 6, 1 (1952); R.M. Milburn and W.C. Vosburgh, *J. Am. Chem. Soc.*. 77, 1352 (1955), etc.

15) H. B. Weiser, "*Inorganic Colloid Chemistry*" N. Y. (1935), Vol. II; J. D. Kurbatov and M. L. Pool, *Phys. Rev.* 65, 61 (1944); M. H. Kurbatov, H. B Webster nd J. D. Kurbatov, *J. Phys, & Colloid Chem.*, 54, 1239 (1950), etc.

Vapor Pressures of Molecular Crystals[1]. *XI. Vapor Pressures of Crystalline Urea and Diformylhydrazine. Energies of Hydrogen Bonds in these Crystals*

By Keisuke SUZUKI*, Shun-ichi ŌNISHI**, Tsutomu KOIDE*** and Syūzō SEKI

(Received September 5, 1955)

Introduction

Although reliable data about the energy of OH···O type hydrogen bond in crystals have been recently accumulated considerably[1,2,3,4], those for NH··O type are very scanty. The hydrogen bonds of the latter type, however, play an important role in the properties of synthetic polyamide fibres as well as in biological systems generally.

In order to obtain the energy of hydrogen bond with a definite meaning, it is very desirable to investigate a crystalline substance, of which the structure is completely determined and hence the mode of formation of hydrogen bond between molecules is accurately clarified. Recently, the crystal structures of these compounds given in the title have been determined very accurately[5,6], so we have undertaken to determine the energy of hydrogen bond in these materials.

Experimental

A) Apparatus and Procedures.—Vapor pressures were measured by the effusion method. The details of the apparatus and the procedures were reported previously[7].

B) Samples.—i) Urea.—The first-class-grade urea of Wako Pure Chemicals Co. was recrystallized twice from ethyl alcohol solution and then sublimated fractionally under high vacuum (ca. 10^{-5} mmHg). Melting point 132.0–132.5°C.

ii) Diformylhydrazine.—This specimen was given by Mr. Tomiie in our laboratory. It had been kindly sent him by Professor Aston through Dr. Class at the Pennsylvania State University. This material was recrystallized twice from aqueous solution and then sublimed fractionally under high vacuum (ca. 10^{-5} mmHg). Melting point 158.2–158.5°C.

Results and Discussion

Vapor pressure data of urea and diformylhydrazine are given in Tables I and II. Their vapor pressure equations derived from them by the method of least squares are also given

TABLE I

VAPOR PRESSURES OF UREA

t°C	P mmHg×10³
72.88	1.59
76.32	2.18
78.34	2.55
81.68	3.51
86.14	5.10
89.41	6.26
92.49	8.01
95.05	10.2

$$\log P = 10.44 - \frac{4579}{T}$$

TABLE II

VAPOR PRESSURES OF DIFORMYLHYDRAZINE

t°C	P mmHg×10³
97.8	2.13
100.6	2.80
103.4	3.57
106.9	4.61
112.5	7.83
113.7	8.50
120.8	11.8
124.1	14.9
126.7	22.2
129.7	28.8

$$\log P = 11.53 - \frac{5264}{T}$$

* Present Address: Department of Chemistry, Faculty of Science, Kōbe University, Mikage, Kōbe.
** Present Address: The Institute of Scientific and Industrial Research, Osaka University, Hirakata.
*** Present Address: Chemical Laboratory, Osaka Liberal Arts University, Osaka.

1) Part X of this series of investigations: I. Nitta, S. Seki and K. Suzuki, This Bulletin, **24**, 63 (1951). Present investigation was reported at the Annual Meeting of the Chemical Society of Japan in 1953.
2) I. Nitta and S. Seki, *J. Chem. Soc. Japan*, **69**, 141, 143 (1948).
3) L. Pauling, "Nature of Chemical Bond" (1941).
4) R.E. Rudin, F.E. Harris and L.K. Nash, *J. Am. Chem. Soc.*, **74**, 4654 (1952).
5) Urea: P. Vanghan and J. Donohue, *Acta Cryst.*, **5**, 530 (1952).
6) Diformylhydrazine: I. Nitta, Y. Tomiie and C.H. Koo, Presented at the Third Congress of the International Union of Crystallography in Paris (1954).
7) I. Nitta, S. Seki, M. Momotani and S. Sato, *J. Chem. Soc. Japan*, **71**, 378 (1950).

at the bottom of each table. Heats of sublimation (ΔH sub), entropies of sublimation ΔS sub) and standard free energies of sublimation at 25°C ($\Delta G^\circ_{298.16}$) calculated from the vapor pressure equations are given in Table III.

TABLE III

	ΔH(kcal./mol.)	ΔS(e.u)	$\Delta G^\circ_{298.16}$ (kcal./mol.)
Urea	20.95±0.21	34.59±0.59	10.64±0.03
Diformyl-hydrazine	24.10±0.13	39.60±0.30	12.29±0.03

In order to obtain the energy of the hydrogen bond, it is necessary to derive, first, the lattice energy from the heat of sublimation, which is given by the following equation:

$$\Delta H_{sub}=L^\circ+W_G+(E^G_{TR}+E^G_{rot}-E^S_{L.V.})+(E^G_{M.V.}-E^S_{M.V.})+n\cdot\Delta H_{ASSN}$$

where L° is the lattice energy of solid at absolute zero; W_G the work done by evaporation of the vapor ($\approx RT$); E^G_{TR} the translational energies of gas molecules ($\approx\frac{3}{2}RT$); E^G_{rot} the rotational energies ($\approx\frac{3}{2}RT$); $E^S_{L.V.}$, the energy of lattice vibration ($3RT$ for ordinary molecular crystal at ordinary temperatures); $E^G_{M.V.}$ and $E^S_{M.V.}$, the energies of intramolecular vibrations in gaseous and crystalline states, respectively; ΔH_{ASSN} the heat of association and n the fraction of associated molecule in gaseous phase, if any. In the above equation the terms in parrentheses are cancelled out with each other approximately and the second term W_G can be ignored for the first approximation. Since we measured the heat of sublimation in a region of very low pressures (10^{-2} mmHg or less), the last term may be also ignored*. Thus, we can infer that the heat of sublimation determined experimentally is nearly equal to the lattice energy. Then we may obtain the contribution of the hydrogen bond by subtracting the contribution of van der Waals' energy from the lattice energy. Practically, we may adopt one of the following three methods:

i) If the crystal structure is completely determined and some data of optical properties such as refractive indices, etc. are available, we can calculate the van der Waals' energy by use of some theoretical formulae[1].

ii) If a reference crystal, which is constituted from isoelectronic molecules with similar configuration and at the same time without appreciable permanent dipole moment and any atom or atomic group capable of forming hydrogen bond, could be found, this crystal would have nealy the same amount of contribution as the specimen in respect to the dispersion energy. For instance, we can estimate the energy of the hydrogen bond of ethyl alcohol by comparing its heat of sublimation with that of propane.

iii) By the comparison of the heat of sublimation of the specimen with that of a reference substance composed of isoelectronic molecules having similar configuration and with dipole moment with nearly the same order of magnitude as the specimen, but no ability of intermolecular hydrogen bond formation. For example; comparison of ethyl alcohol with methyl ether.

Each of these three methods of estimation has more or less different physical meaning. In the first method, we calculate the van der Waals' energies on the basis of the intermolecular distances at which the molecules are actually linked together by the hydrogen bonds. The intermolecular distances may become a little larger, however, if there would be no hydrogen bonding between the molecules. Thus, the contribution of the van der Waals' energy calculated by this method may be a little over-estimated in comparison with that of crystal in which molecules are combined together only by the van der Waals' forces.

In this paper we applied the second and the third methods. These two methods seem to be related partly with the difference of the energy of the hydrogen bond. If we define it as including the mutual interaction of molecular permanent dipoles in it, the second one may be more appropriate. On the other hand, the third may be more reasonable, if we consider the hydrogen bond as a special type of binding which does not include the energy of the dipolar interaction.

The suitable reference substances are isobutene[8] (for method ii) and acetone (for method iii) for urea, and 1, 5-hexadiene (ii) and succinic aldehyde (iii) for diformylhydrazine.

As the heats of sublimation of 1, 5-hexadiene and succinic aldehyde are not yet known, we estimated the contribution of the van der Waals' energy and the dipolar energy by

* Urea molecules would be associated with each other in the gaseous phase in a similar way as acetic acid. The calculated fraction of associated molecules, however, is found to be only 0.02% even at 1×10^{-2} mmHg, if we assume following thermodynamic functions; $\Delta H_{ASSN}=-14$ kcal./mol., and $\Delta S_{ASSN}=-36$ e.u. (These data were estimated from the experimental results of acetic acid).

8) F.D. Rossini, K.S. Pitzer, W.J. Taylor, J.P. Ebert and J. E. Kilpatrick, "Selected Values of Hydrocarbons" (1947).

TABLE IV

HEATS OF VAPORIZATION OF SOME HYDROCARBONS AT THEIR BOILING POINTS* (kcal./mol.)

	ΔH_0		ΔH_1		ΔH_2	$\Delta H_1-\Delta H_0$	$\Delta H_2-\Delta H_1$
ethane	3.517	ethene	3.237	——		−0.3	—
propane	4.487	propene	4.402	——		−0.1	—
n-butane	5.352	1-butene	5.238	butadiene	5.873[9]	−0.1	+0.6
		cis-2-butene	5.480	——		+0.1	—
		trans-2-butene	5.239	——		−0.1	—
iso-butane	5.089	*iso*-butene	5.286	——		+0.2	—
pentane	6.160	——		pentadiene	6.75[10]	—	+0.6
2-methyl-butane	5.809	——		isoprene	6.39[11]	—	+0.6

* All the data except butadiene, pentadiene and isoprene are taken from reference (8).

TABLE V

Substances			A			B		
			Diformyl-hydrazine	δ-Valero-lactam	ε-Capro-lactam	Acetamide	Oxamide	Urea
Heat of sublimation (kcal./mol.)	Observed		24.10	17.81[12]	19.86[12]	13.6[13]	27.0[14]	20.95
	Contribution from the energy of	dispersion effect*	12.0**	10.6	12.9***	7.6	10.1**	7.6
		dipolar interaction	2.2†	2.1††	2.1††	3.3†††	3.6※	3.3†††
		hydrogen bond (ii)	12.1	7.2	7.0	6.0	16.9	13.4
		hydrogen bond (iii)	9.9	5.1	4.9	2.7	13.3	10.1
Hydrogen Bond	Number of hydrogen bond per molecule		2[5]	(1)	(1)	2[22]	(4)	4[5]
	Energy of one hydrogen bond (ii) (kcal./mol.)		6.1	(7.2)	(7.0)	3.0	(4.2)	3.5
	〃	(iii)	5.0	(5.1)	(4.9)	1.4	(3.3)	2.5
	Hydrogen bond distance (Å)		2.787[6]	—	—	2.83[22] 2.99	—	2.99[5] 3.04
	Number of donated hydrogen atoms per molecule		2	(1)	(1)	2	(4)	4
	Number of hydrogen accepting atoms per molecule		2	(1)	(1)	1	(2)	1
	Hydrogen atom-Hydrogen acceptor ratio		1	(1)	(1)	2	(2)	4

* Heats of sublimation of the reference substances are obtained by adding the heats of fusion and those of vaporization near the melting point the latters of which are calculated from the vapor pressure equations. hexane (ΔH_F=3.11,[8] ΔH_v=8.31[8]) for diformylhydrazine; methylcyclohexane (ΔH_F=1.613,[15] ΔH_v=8.94[8]) for δ-valerolactam; iso-butene (ΔH_F=1.42,[8] ΔH_v=6.19[8]) for urea and acetamide; 2,3-dimethylbutane (ΔH_F=0.19,[16] ΔH_t=1.55,[16] ΔH_v=7.73[8]). For 2,3-dimethylbutane we have taken into account the heat oftransition for estimating the heat of sublimation.

** Heat of sublimation of the reference substances plus effect of conjugated π-electrons (0.6 kcal).

*** Heat of sublimation of methylcyclohexane plus increment of the heat of sublimation of CH_2 group; see ref. (17).

† Difference of the heats of sublimation of *p*-quinone (ΔH_{sub}=16.4[18]) and *p*-xylene ($\Delta H_{sub}=\Delta H_v$ (at 25°; 10.1[8])+ΔH_F(4.1[8])).

†† Difference of the heats of vaporization of cyclohexanone (ΔH_v=11.05[2]) and methylcyclohexane. (we used this difference in place of that of their heats of sublimation, since the solid phase of cyclohexanone just below the melting points belongs to the so-called plastic crystal.)

††† Difference of the heats of sublimation of acetone (ΔH_{sub}=9.5 (ΔH_v at the melting point[19])+1.36 (ΔH_F[20])) and iso-butane.

※ Difference of the heats of vaporization of glyoxal (ΔH_v=9[21]) and 2,3-dimethylbutane.

9) J.G. Aston and G.F. Szasz, *J. Am. Chem. Soc.*, **69**, 3108 (1947).

10) K. Kuchinskaya, *Chem. Abst.*, **34**, 3147 (1940).

11) Roth's data taken from Landolt-Börnstein's Physikalisch-Chemisches Tabellen (II'er Erg. Band).

12) A. Aibara, *J. Chem. Soc. Japan*, **74**, 631 (1953).

13) A. Aibara, *J. Chem. Soc. Japan*, **73**, 955 (1952).

14) R.S. Bradley and A.D. Care, *J. Chem. Soc.*, **1953**, 1681.

15) D.R. Douslin and H.M. Huffman, *J. Am. Chem. Soc.*, **68**, 173 (1946).

16) idem, ibid., **68**, 1704 (1946).

17) A. Müller, *Proc. Roy. Soc. London*, **A154**, 124 (1936).

18) I. Nitta, S. Seki, H. Chihara and K. Suzuki, *Sci. Paper Osaka Univ.*, No. 29 (1951).

19) W.A. Felsing and S.A. Durban, *J. Am. Chem. Soc.*, **48**, 2893 (1926).

20) G.S. Parks and K.K. Kelley, *J. Phys. Chem.*, **32**, 1739 (1928).

21) F. Rossini, "Selected Values of Chemical Thermodynamic Properties", (1952).

comparing the heat of sublimation of *n*-hexane with those of some other substances. In Table IV, it is seen that the heats of vaporization of *n*-paraffines and of corresponding monoolefines are nearly equal, whereas those of conjugated olefines are by ca. 0.6 kcal./mol. larger than those of corresponding paraffines. As the molecule of diformylhydrazine has conjugated π-electrons, it may be reasonable to assume that the van der Waals' energy of diformylhydrazine is larger than that of *n*-hexane by an amount of ca. 0.6 kcal./mol. For the third method, we used the difference of the heats of sublimation of *p*-benzoquinone and *p*-xylene for estimating the contribution of the dipole-dipole interaction.

All the observed heats of sublimation and the contributions from the various kinds of energies, i.e. the dispersion energy, the dipole-dipole interaction and the energy of the hydrogen bonds (derived by use of the methods (ii) and (iii)) of the present materials are given in Table V.

In this table corresponding data for δ-valero-lactam, ε-caprolactam, acetamide and oxamide are also calculated for reference.

As the number of hydrogen bonds per molecule of urea[5], diformylhydrazine[6] and acetamide[22] are already known by the X-ray methods (see the sixth row of Table V), the energies per one hydrogen bond for these substances are calculated as shown in the seventh and eighth rows. The numbers of hydrogen bonds for the other substances in this table are not yet determinede experimentally, so the energies of the hydrogen bonds are estimated by assuming appropriate number of the hydrogen bonds. (They are shown in parentheses.)

From these results, we may derive the following several conclusions:

(1) The energy of NH···O type hydrogen bond in crystal is not always so small as the value given by Davies[23] (2 kcal./mol. for aniline-benzophenone). This may be one of the reasons for the fact that almost all the substances with -NHCO- groups show rather high melting points.

(2) It is usually supposed that the shorter the distance of the hydrogen bond the larger the energies become. But, this does not always hold. For instance, if we compare urea, diformylhydrazine and acetamide with each other, then we can see that diformylhydrazine with the shortest NH···O distance have the largest hydrogen bond energy, whereas urea with the longest N-H···O distance gives larger energy of hydrogen bond than that of acetamide with a little shorter bond distance. So it seems to be rather dangerous to estimate the relative strength of the hydrogen bond only from the knowledge of the distance of the hydrogen bond, though it may be useful for a rough estate of its strength.

(3) The energies of the NH···O type hydrogen bonds show rather scattered values (7.0–3.0 kcal./mol. from the method (ii); 5.1–1.4 kcal./mol. from the method (iii)) in comparison with those of the OH···O type in which the energies are limited in the region of 4.5*–6.0** kcal./mol. (method (ii) or (i)).

As one of the reasons for such scattering as mentioned above, we may point out the varieties of the ratio of the number of donated hydrogen atoms to those of accepting oxygen atoms. In fact, we can see in Table V that for the substances of the A-class having larger energies of the hydrogen bond, i.e. for diformylhydrazine, δ-valerolactam and ε-caprolactam, this ratio is 1, whereas it is 2 or 4 for substances of the B-class with smaller energies of the hydrogen bond, i.e. acetamide, oxamide and urea. When this ratio increases, the steric hindrance between the donated hydrogen atoms surrounding the same acceptor atom will become larger. As the result, this effect may cause a considerable difference between the energies of the hydrogen bond of the classes A and B. On the other hand, in the case of the OH···O type hydrogen bond this ratio is mostly one. So, the energies of the OH···O type hydrogen bond are not so divergent as those of the NH···O type one.

The other factors, for example, the changes of electron densities of oxygen or nitrogen atoms due to the conjugations of the π-electrons, may also contribute to some extent to the energies of hydrogen bonds. This effect, however, seems less important than the effect of hydrogen atom-hydrogen acceptor ratio, at least in the crystalline state.

These conclusions mentioned above will give some contribution for the elucidation of complex structures and phenomena found in some synthetic fibers as well as in some biological systems.

Finally, the present authors wish to express their sincere thanks to Professor I. Nitta for his valuable suggestions throughout this work, and Professor J. G. Aston and Dr. J. B. Class for their kind preparation of the

22) F. Senti and D. Harker, *J. Am. Chem. Soc.*, **62**, 2008 (1940).

23) Davies, *Ann. Report*, **1946**, 5.

* Value for phenol, see ref. (2).

** Values for carboxylic acid dimer in the vapor; that is the heat of association of their dimer minus contribution of dispersion effect, see ref. (1).

sample of diformylhydrazine, and also to Mr. Y. Tomiie for his kind discussion. The expense of this research is partly defrayed from the Scientific Reseach Grant from the Ministry of Education as well as from the fund of Taniguchi Kôgyô-Shyôreikai to which the authors' thanks are due.

Department of Chemistry, Faculty of Science, Osaka University, Osaka

Semi- and Photo-conductivity of Molecular Single Crystals. Anthracene and Pyrene

By Hiroo INOKUCHI

(Received September 7, 1955)

Introduction

Recent works[1,2] in our laboratory have shown that some of the polycyclic aromatic compounds have fairly good electrical conductivity and sensitive photoconductivity in the solid state. From those and the other related properties, such as ultra-violet luminescence and xerographic phenomena, they are considered to be organic semi-conductors[3].

Since the preparation of single crystals of these compounds is generally very difficult, the measurements of electrical resistivity have been made hitherto for specimens in powdered form. In such a condition, the resistivity depends upon the compressive pressure; that is, it decreases remarkably with increasing pressure up to 80 kg./cm², however, thereafter it becomes approximately constant. Therefore in the preceding reports the electrical resistances of these organic semi-conductors were determined under compression beyond 80 kg./cm²*.

However, it is to be hoped that some single crystal could be obtained and the semi-conductivity would be measured in the single crystal state. It is difficult to obtain single crystals of compounds with larger molecular weight of this series, but in the case of smaller compounds, it is frequently possible to obtain single crystals of large size.

In this paper, the photo- and semi-conductivity of anthracene and pyrene in the single crystal state are presented.

1) H. Akamatu and H. Inokuchi, *J. Chem. Phys.*, **18**, 810 (1950), **20**, 1481 (1952).

2) H. Inokuchi, This Bulletin, **24**, 222 (1951); **25**, 28 (1952), **27**, 22 (1954).

3) H. Akamatu, "Organic Semi-conductors", Iwanami, Kagaku (1954), 282.

* The effect of hydrostatic pressure up to 8,000 kg./cm² on the semiconductivity of isoviolanthrone was reported in this Bulletin, **28**, 570 (1955).

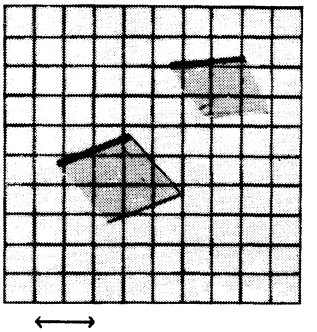

1 cm.

Fig. 1. Single crystals of pyrene.

Specimens

Since anthracene, a technical production from coal-tar, includes tetracene and carbazol, and the purification from these impurities is very difficult, pure anthracene was synthesized from anthraquinone by reduction*. This specimen was made of colourless plates, which melted at 219°C, and possessed a blue-violet luminescence. On the other hand, pyrene was recrystallized several times from aromatic solvent, and finally sublimed in a vacuum. Purified pyrene melted at 148°C, and possessed a whitish yellow colour.

Large single crystals (12 mm. × 10 mm. × 1 mm. rhomb.) of those could be grown by slow evaporation of solvent over a month in Solvesso (Standard Vac. Oil Co.). The beautiful plate-shaped single crystal obtained here was extended along [110] as shown in Fig. 1 (pyrene).

Experimental Procedure

Measurements of the electrical conductivity and the photoconductivity were made in the following manner as shown in Fig. 2. A sandwich type cell was made by coating one plane of the crystal (3) with an aluminium film (1) and the inversed plane with a half-transparent aluminium film (2).

* This anthracene was synthesized by Mr. J. Aoki in our laboratory.

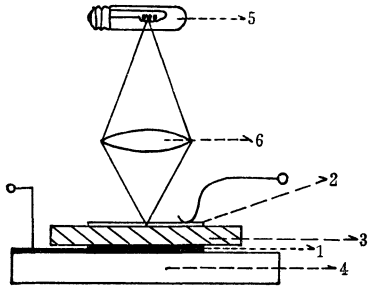

Fig. 2. The apparatus for measuring the semi- and photoconductivity.

This cell was mounted on a polystyrene plate (4), which was held in a box to control the temperature of the crystal, and it was supplied with a field of up to 11,000 volt per cm.

The electrical conductivity was measured perpendicular to the [110] plane of crystal by the potential drop method with the aid of a direct current amplifier. The light source, illuminating the crystal, was a tungsten or mercury vapour lamp (5), and a beam of light was directed on the specimen by means of a quartz lens (6).

Results and Discussion

Since the electrical resistivity of these single crystals was fairly high at room temperature, the measurements of resistance were made at the range from 50° to 150°C. Above this temperature the crystals were broken by sublimation.

The observed relation between electrical current and potential of anthracene is shown in Fig. 3. Below 2,000 volt per cm. this curve obeyed Ohm's law approximately, but above 5,000 volt per cm. employed on the crystal heated at 136°C, this linearity was highly deviated, and at 152°C when the potential was applied to 7,500 volt per cm., the current had a very large value as shown in this figure. Within this range of voltage employed here, the potential-current relation was reproducible. Then it is reasonable to assume as follows: In such a high electric field, there will be a few electrons which can gain energy from the field and remove

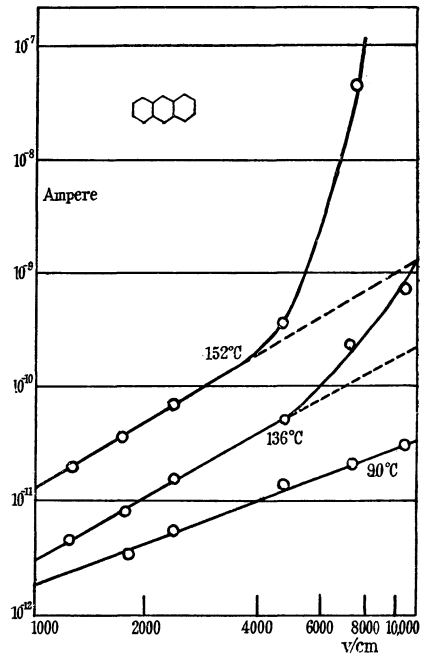

Fig. 3. The relation between electrical current and potential for anthracene.

themselves from the occupied band. The number of free electrons and hence the current will increase rapidly; i.e., this phenomenon is the preceding one of the dielectric break-down[4].

The electrical resistivity and its temperature dependency of anthracene and pyrene were measured at the applied field of 1,000 volt per cm. The temperature (T) dependency of electrical resistivity (ρ) has been expressed by the following formula,

$$\rho = \rho_0 \exp(\Delta\varepsilon/2kT)$$

where k is the Boltzmann constant and $\Delta\varepsilon$ is the activation energy. The observed values of those are tabulated on Table I and are shown in Fig. 4.

To study the correlation between the thermal activation energy and the absorption spectrum of crystal, the author has measured

TABLE I

THE VALUE OF ρ_0, $\rho_{at\ 15°C}$, $\Delta\varepsilon$ AND ENERGY GAP FROM ABSORPTION SPECTRA OF ANTHRACENE AND PYRENE

	ρ_0	$\rho_{at\ 15°C}$	$\Delta\varepsilon$	Energy gap from absorption spectra
Anthracene	$1\times10^{-2}\Omega$ cm.	$10^{22}\Omega$ cm.	2.7 eV.	3.0 eV.
	$5\times10^{-1}\Omega$ cm.[1]	$10^{17}\Omega$ cm.[1]	1.65 eV.[1]	
Pyrene	$1\times10^{-3}\Omega$ cm.	$10^{20}\Omega$ cm.	2.4 eV.	2.8 eV.

1) from H. Mette and H. Pick[5].

4) N.F. Mott and R.W. Gurney, "Electronic Processes in Ionic Crystals", Oxford Univ. Press, 2nd ed. (1948), p. 197.

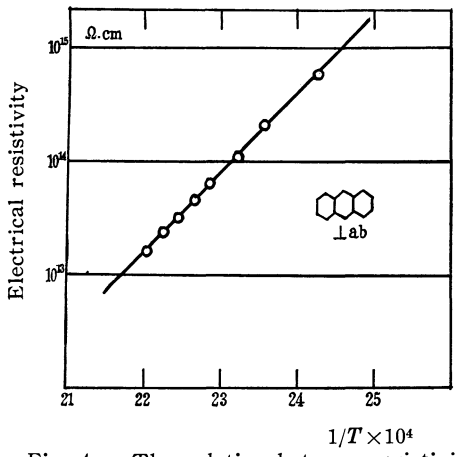

Fig. 4a. The relation between resistivity and temperature for anthracene.

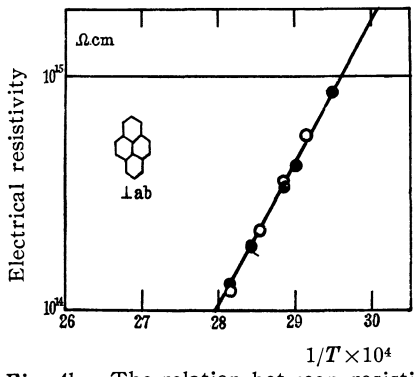

Fig. 4b. The relation between resistivity and temperature for pyrene.

the absorption spectrum of a single crystal (perpendicular to [110] plane of crystal). The longest wave edges of the absorption spectra are shown in Table I. This value and the thermal activation energy ($\Delta\varepsilon$) coincided with each other; then this will be due to the fact that molecular single crystals are intrinsic semi-conductors as in the case of the powdered form.

H. Pick and H. Mette[5] (University of Göttingen) have reported, however, that the thermal activation energy of anthracene was 1.65 eV. (a half of the value measured from the longest wave edges of absorption spectra) and their results on electrical resistivity was too small as compared with my results. But the same author has described in his next article[5] on the electrical resistivity of naphthalene single crystal, that the energy gap (3.7 eV.) observed from the temperature dependency of electrical resistivity coincided with the value of the longest wave edges of absorption spectra (3,250 Å≈3.86 eV.). It seems to the present author that his specimen was not completely pure since his anthracene was purified from a crude one.

The photoconductivity of these single crystals was detectable, and its potential dependence was as shown in Fig. 5. These results

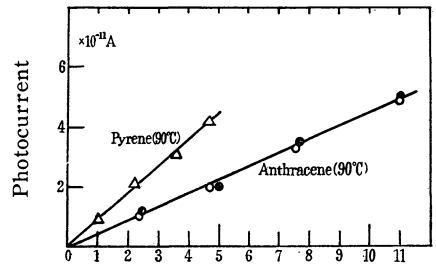

Fig. 5. Photoelectric current plotted against the voltages for single crystals.

show that the photocurrent in the single crystal is a primary current as in the case of other polycyclic aromatic compounds. It was reported that the photoconductive process in the conjugated organic compounds in powdered form is enhanced by the oxygen in the air[7,8], but my results showed that the photocurrent was not enhanced by the oxygen in the air as illustrated in Fig. 5. In this figure the points denoted as ○ show the photocurrent-voltage characteristics in the vacuum (10^{-2} mmHg) and ● the same characteristics in the air.

Summary

The electrical resistivity and photoconductivity of single crystals—anthracene and pyrene—, which could be grown by slow evaporation of a solvent over a month in Solvesso, were measured. The temperature dependency of electrical resistivity (ρ) has been expressed by the next formula, $\rho=\rho_0 \exp(\Delta\varepsilon/2kT)$, and the values of resistivity ($\rho_{at\ 15°}$) and thermal activation energy ($\Delta\varepsilon$) are $10^{22}\Omega$ cm., 2.7 eV. for anthracene and $10^{20}\Omega$ cm., 2.4 eV. for pyrene. This activation energy and the longest wave edges of absorption spectra in the solid state coincided with each other, then this phenomenon will be due to the fact that molecular single crystals are intrinsic semi-conductors as in the case of powdered form.

The author expresses his hearty thanks to Prof. H. Akamatu for his kind direction of this study and also to Mr. J. Aoki who synthesized pure anthracene. The cost of this research has been defrayed from the Scientific Research Encouragement Grant given by the Ministry of Education to which the author's thanks are due.

Department of Chemistry, Faculty of Science, The University of Tokyo, Tokyo

5) H. Mette and H. Pick, *Z. Physik*, **134**, 566 (1953).
6) H. Pick and G. Wissman, *Z. Physik*, **138**, 436 (1954).
7) A.G. Chynoweth and W.G. Schneider, *J. Chem. Phys.*, **22**, 1029 (1954).
8) A.T. Vartanyan, *Doklady Akad. Nauk, S.S.S.R.*, **71**, 641 (1950).

Theoretical Analysis of Polarographic Waves. II. Reduction of Complex Metal Ions

By Hiroaki MATSUDA and Yuzo AYABE

(Received July 6, 1955)

Introduction

In polarographic literature there are numerous papers dealing with the current-voltage curves due to the reduction of complex metal ions, but satisfactory quantitative treatments reported up to date are almost all based on the fact that the net electrode reaction takes place reversibly[1,2]. Recently, from the viewpoint of chemical kinetics, R. Tamamushi and N. Tanaka[3] attempted a theoretical analysis of the polarographic wave, especially of the irreversible type, which was obtained by the oxidation and reduction of complex metal ions. However, since they have applied the concept of Nernst's diffusion layer to the diffusion process taking place in the region very close to the surface of the dropping mercury electrode, their result cannot be quantitatively adapted to the present problem.

In the present paper, taking into account the movement of the solution caused by the expansion of the mercury drop, we shall attempt to solve the corresponding diffusion problem, which involves the electrolytic reduction of complex metal ions as the boundary condition, and then derive a general equation of the instantaneous current during the drop age for any point along the wave. Moreover, a general expression for the current-voltage curve will be given and its characteristics in several special cases will be discussed in some detail.

Formulation of the Problem

According to the pioneering investigations of N. Bjerrum and his coworkers[4], the formation of complex metal ions always occurs stepwise and the various species of complex metal ions coexist in a given solution, the stability of the individual species being characterized by a series of consecutive dissociation constants of the form:

$$K_\nu=\frac{(f_{\nu-1}C_{\nu-1})(f_XC_X)}{(f_\nu C_\nu)} \quad (\nu=1,2,\cdots\cdots,{}^{1}N) \qquad (1)$$

In this expression, C_ν and C_X denote the concentrations of the complex metal ion in the form of $MX_\nu^{(n-\nu b)+}$ and of the complexing agent X^{-b}, respectively, f's are the corresponding activity coefficients and N is the maximum number of the ligands taken up.

Now, consider the reduction to the metallic state (amalgam) of complex metal ions of a metal that is soluble in mercury. The net electrode reaction may be represented by

$$MX_\nu^{(n-\nu b)+}+ne+Hg\rightleftarrows M(Hg)+\nu X^{-b} \qquad (2)$$
$$(\nu=N, N-1, \cdots\cdots, 1, 0)$$

where M(Hg) represents the amalgam formed on the electrode surface and n is the number of electrons associated with the electrode reaction.

In this reaction, various possible types of kinetic mechanism may be considered. From the information as to the formation of complex metal ions, it seems safe to assume that the net electrode reaction described above takes place according to the following scheme:

(1) dissociation and association processes

$$MX^{(n-\nu b)+}\rightleftarrows MX_{\nu-1}^{[n-(\nu-1)b]+}+X^{-b} \quad (\nu=N, N-1,\cdots\cdots, p+1)$$
$$MX_{\mu-1}^{[n-(\mu-1)b]+}+X^{-b}\rightleftarrows MX_\mu^{(n-\mu b)+} \quad (\mu=p, p-1,\cdots\cdots, 1) \qquad (3)$$

(2) electron transfer process

$$MX_p^{(n-pb)+}+ne+Hg\rightleftarrows M(Hg)+pX^{-b} \qquad (4)$$

In this scheme, it is assumed that the complex metal ions $MX_\nu^{(n-\nu b)+}$ $(\nu=N, N-1,\cdots\cdots, p+1)$ and $MX_\mu^{(n-\mu b)+}$ $(\mu=p-1, p-2,\cdots\cdots, 1, 0)$ successively dissociate and associate up to the form $MX_p^{(n-pb)+}$ in the vicinity of the electrode surface, respectively, and the species $MX_p^{(n-pb)+}$ thus produced is electrolytically reduced to the amalgam.

If we accept the foregoing assumptions as to the kinetic mechanism of the reduction of complex metal ions, the concentration distributions of the various species of complex metal ions and of the amalgam can be determined by solving the following system of differential equations[5,6]:

1) I.M. Kolthoff and J.J. Lingane, "Polarography" (1952), vol. 1, p. 211.
2) D.D. DeFord and D.N. Hume, *J. Am. Chem. Soc.*, **73**, 5321 (1951).
3) R. Tamamushi and N. Tanaka, This Bulletin, **23**, 110 (1950).
4) J. Bjerrum, *Chem. Revs.*, **46**, 381 (1950).
5) D. MacGillavry and E.K. Rideal, *Rec. trav. chim.*, **56**, 1013 (1937).
6) J. Koutecky, *Collection Czechoslov. Chem. Communs.*, **18**, 597 (1953).

$$\frac{\partial C_N}{\partial t}=D\frac{1}{r^2}\frac{\partial}{\partial r}\left(r^2\frac{\partial C_N}{\partial r}\right)-\frac{a^3}{3r^2}\frac{\partial C_N}{\partial r}$$
$$-\rho_N(C_N-\sigma_N C_{N-1}),\ (r>r_0) \tag{5}$$

$$\frac{\partial C_\nu}{\partial t}=D\frac{1}{r^2}\frac{\partial}{\partial r}\left(r^2\frac{\partial C_\nu}{\partial r}\right)-\frac{a^3}{3r^2}\frac{\partial C_\nu}{\partial r}$$
$$+\rho_{\nu+1}(C_{\nu+1}-\sigma_{\nu+1}C_\nu)-\rho_\nu(C_\nu-\sigma_\nu C_{\nu-1}),\ (r>r_0) \tag{6}$$
$(\nu=N-1,\ N-2,\cdots\cdots,\ 2,1)$,

$$\frac{\partial C_0}{\partial t}=D\frac{1}{r^2}\frac{\partial}{\partial r}\left(r^2\frac{\partial C_0}{\partial r}\right)-\frac{a^3}{3r^2}\frac{\partial C_0}{\partial r}$$
$$+\rho_1(C_1-\sigma_1 C_0),\ (r>r_0) \tag{7}$$

$$\frac{\partial C_a}{\partial t}=D_a\frac{1}{r^2}\frac{\partial}{\partial r}\left(r^2\frac{\partial C_a}{\partial r}\right)-\frac{a^3}{3r^2}\frac{\partial C_a}{\partial r},$$
$$(r<r_0) \tag{8}$$

where

$$\rho_\nu=k_\nu f_\nu, \tag{9}$$
$$\sigma_\nu=(f_X C_X)(f_{\nu-1}/f_\nu)/K_\nu \tag{10}$$
$$(\nu=N, N-1,\cdots\cdots,\ 2,1).$$

In these equations, r is the distance from the center of the mercury drop, t is the time elapsed after the development of the drop has begun; r_0 is the radius of the mercury drop, which is given by

$$r_0=(3m/4\pi d)^{1/3}t^{1/3}=at^{1/3},$$

where m is the constant rate of flow of mercury uot of the capillary and d is the density of mercury; D and D_a are the diffusion coefficients of the complex metal ions $MX_\nu^{(n-\nu b)+}(\nu=N, N-1,\cdots\cdots,\ 1,0)$ in the solution and of the metal atoms M(Hg) in the amalgam, respectively; $C_\nu(\nu=N, N-1,\cdots\cdots,\ 1,0)$ and C_a are the concentrations of $MX_\nu^{(n-\nu b)+}(\nu=N, N-1,\cdots\cdots,\ 1,0)$ and M(Hg) at any point in the corresponding diffusion layers, respectively; C_X is the concentration of X^{-b}, which is assumed to be constant since the solution usually contains an excess of the complexing agent; f's are the corresponding activity coefficients; k_ν and $K_\nu(\nu=N, N-1,\cdots\cdots,\ 1)$ are the rate and equilibrium constants of the consecutive dissociation processes, respectively.

The initial and boundary conditions are given by

$$\left.\begin{array}{ll} t=0,\ r>r_0: & C_\nu={}^*C_\nu\ (\nu=N, N-1,\cdots\cdots,1,0) \\ t=0,\ r<r_0: & C_a=0 \end{array}\right\} \tag{11}$$

$t>0,\ r=r_0$:

$$D\frac{\partial C_p}{\partial r}=D_a\frac{\partial C_a}{\partial r}=\frac{i(t)}{nFq} \tag{12}$$

$$D\frac{\partial C_\nu}{\partial r}=0\ \left(\begin{array}{l}\nu=N, N-1,\cdots\cdots,\ p+1,\\ p-1,\cdots\cdots,\ 1,0\end{array}\right) \tag{13}$$

where ${}^*C_\nu(\nu=N, N-1,\cdots\cdots,\ 1,0)$ are the concentrations of $MX_\nu^{(n-\nu b)+}(\nu=N, N-1,\cdots\cdots,\ 1,0)$ in the bulk of the solution, which fulfill the conditions:

$${}^*C_\nu=\sigma_\nu {}^*C_{\nu-1}\ (\nu=N, N-1,\cdots\cdots,\ 1), \tag{14}$$

since the equilibrium states of the consecutive dissociation and association processes expressed by Eq. (3) are assumed to be attained in the bulk of the solution; $i(t)$ is the current flowing through the electrode surface; F is the faraday; q is the surface area of the dropping mercury electrode, which is given by $4\pi r_0^2$. The conditions expressed by Eq. (13) result from the fact that $MX_\nu^{(n-\nu b)+}$ $(\nu=N, N-1,\cdots\cdots,\ p+1,\ p-1,\cdots\cdots,\ 1,0)$ cannot participate in the electron transfer process.

It is very difficult to obtain an exact solution of the system of differential equations described above. Therefore, in the present paper our discussion will be restricted to a case when the following assumptions are satisfied.

(a) The thickness of the diffusion layer is very much less than the diameter of the mercury drop. Thus, the approximate procedure used in the previous paper[7] can be available.

(b) $\rho_\nu(1+\sigma_\nu)t\gg 1\ (\nu=N, N-1,\cdots\cdots,\ 1)$. This assumption, which is satisfied by sufficiently rapid consecutive reactions in solution, seems to be available for many cases of the reduction of complex metal ions.

Let us now introduce the substitution:

$$x=r^3-r_0^3=r^3-a^3t \tag{15}$$
$$y=t^{7/3} \tag{16}$$
$$C=\sum_{\nu=0}^{N}C_\nu \tag{17}$$
$$g_\nu=C_\nu-\sigma_\nu C_{\nu-1}\ (\nu=N, N-1,\cdots\cdots,\ 1) \tag{18}$$

Then, considering the assumptions (a) and (b), we obtain in place of Eqs. (5), (6), (7) and (8)

$$\frac{\partial C}{\partial y}=\frac{27}{7}a^4D\frac{\partial^2 C}{\partial x^2}\ (x>0) \tag{19}$$

$$0=\frac{27}{7}a^4D\frac{\partial^2 g_N}{\partial x^2}-\frac{3}{7}y^{-4/7}\rho_N(1+\sigma_N)g_N$$
$$+\frac{3}{7}y^{-4/7}\rho_{N-1}\sigma_N g_{N-1}\ (x>0) \tag{20}$$

$$0=\frac{27}{7}a^4D\frac{\partial^2 g_\nu}{\partial x^2}+\frac{3}{7}y^{-4/7}\rho_{\nu+1}g_{\nu+1}$$
$$-\frac{3}{7}y^{-4/7}\rho_\nu(1+\sigma_\nu)g_\nu+\frac{3}{7}y^{-4/7}\rho_{\nu-1}\sigma_\nu g_{\nu-1}\ (x>0) \tag{21}$$
$$(\nu=N-1,\ N-2,\cdots\cdots,\ 3,2)$$

$$0=\frac{27}{7}a^4D\frac{\partial^2 g_1}{\partial x^2}+\frac{3}{7}y^{-4/7}\rho_2 g_2$$
$$-\frac{3}{7}y^{-4/7}\rho_1(1+\sigma_1)g_1\ (x>0) \tag{22}$$

$$\frac{\partial C_a}{\partial y}=\frac{27}{7}a^4D\frac{\partial^2 C_a}{\partial x^2}\ (x<0) \tag{23}$$

The initial and boundary conditions (11), (12) and (13) can be written as follows, after being rearranged:

$$\left.\begin{array}{ll} y=0,\ x>0: & \left\{\begin{array}{l} C={}^*C \\ g_\nu=0\ (\nu=N, N-1,\cdots\cdots,\ 1)\end{array}\right. \\ y=0,\ x<0: & C_a=0 \end{array}\right\} \tag{24}$$

7) H. Matsuda and Y. Ayabe, This Bulletin, 28, 422 (1955).

$y>0,\ x=0$:

$$\begin{cases} 3a^2y^{2/7}D\dfrac{\partial C}{\partial x}=-3a^2y^{2/7}D\dfrac{1}{\sigma_{p+1}}\dfrac{\partial g_{p+1}}{\partial x} \\ =3a^2y^{2/7}D\dfrac{\partial g_p}{\partial x}=3a^2y^{2/7}D_a\dfrac{\partial C_a}{\partial x}=i(y)/nFq \end{cases} \quad (25)$$

$$\frac{\partial g_\nu}{\partial x}=0 \quad \begin{pmatrix}\nu=N, N-1,\cdots\cdots p+2,\\ p-1,\cdots\cdots, 1\end{pmatrix} \quad (26)$$

Derivation of the Equation for the Instantaneous Current

The solutions of the differential equations (19) and (23), which satisfy the initial and boundary conditions (24) and (25), have been obtained in the previous paper[7]. According to our results, the values of the functions C and C_a at the electrode surface, designated by $^\circ C$ and $^\circ C_a$ respectively, can be expressed as

$$^\circ C={}^*C-\sqrt{\frac{3}{7\pi}}\frac{1}{\sqrt{D}}\int_0^y\frac{u^{-2/7}[i/nFq]}{\sqrt{y-u}}du \quad (27)$$

$$^\circ C_a=\sqrt{\frac{3}{7\pi}}\frac{1}{\sqrt{D_a}}\int_0^y\frac{u^{-2/7}[i/nFq]}{\sqrt{y-u}}du \quad (28)$$

The system of differential equations (20) (21) and (22) can be solved by means of method similar to that used in the problem of the linear N coupled oscillators[8]. The values of the functions $g_\nu(\nu=N, N-1,\cdots\cdots, 1)$ at the electrode surface, denoted by $^\circ g_\nu$, are given by

$$^\circ g_\nu=\frac{[i/nFq]}{\sqrt{D}}G_\nu \quad (\nu=N, N-1,\cdots\cdots, 1) \quad (29)$$

where G_ν is a complicated function of σ_N, $\sigma_{N-1},\cdots\cdots$, σ_1 and $\rho_N, \rho_{N-1},\cdots\cdots$, ρ_1.

Upon using the relations expressed by Eqs. (17), (18), (27) and (29), we obtain the following expression for the concentration at the electrode surface of $MX_p^{(n-p)+}$ which participates in the electron transfer process:

$$^\circ C_p=\frac{(\overset{p}{\underset{\nu=1}{\Pi}}\sigma_\nu)}{\sigma}\left\{{}^*C-\frac{[i/nFq]}{\lambda_l\sqrt{D}}-\sqrt{\frac{3}{7\pi}}\frac{1}{\sqrt{D}}\times\int_0^y\frac{u^{-2/7}[i/nFq]}{\sqrt{y-u}}du\right\} \quad (30)$$

where

$$\sigma=1+\sum_{\nu=1}^{N}(\overset{\nu}{\underset{\mu=1}{\Pi}}\sigma_\mu)=1+\sum_{\nu=1}^{N}(f_xC_x)^\nu(f_0/f_\nu)(\overset{\nu}{\underset{\mu=1}{\Pi}}1/K_\mu) \quad (31)$$

$$(1/\lambda_l)=\sum_{\nu=p+1}^{N}\{1+\sum_{k=\nu+1}^{N}(\overset{k}{\underset{j=\nu+1}{\Pi}}\sigma_j)\}G_\nu-\sum_{\nu=1}^{p}\left\{\sum_{k=1}^{\nu}\left(\overset{\nu}{\underset{j=k}{\Pi}}\frac{1}{\sigma_j}\right)\right\}G_\nu \quad (32)$$

(λ_e is a complicated function of $\sigma_N, \sigma_{N-1},\cdots\cdots$, σ_1 and $\rho_N, \rho_{N-1},\cdots\cdots$, ρ_1, and can be related in a simple manner to the average value of the limiting current, $\bar{i}_l$, as shown later. See Eq. (48). Hence, if one gives up any discussion on the behavior of the limiting current, it is not necessary to obtain an explicit expression of the dependence of λ_l on $\sigma_N, \sigma_{N-1},\cdots\cdots$, σ_1 and $\rho_N, \rho_{N-1},\cdots\cdots$, ρ_1.)

The current flowing through the electrode surface depends on the electrode potential and the concentrations at the electrode surface of the substances which participate in the electron transfer process. According to the reaction rate theory[9], the current flowing can be expressed as

$$[i/nFq]=k_f^0(f_\mu{}^\circ C_\mu)e^{-\frac{\alpha nF}{RT}E}-k_b^0(f_a{}^\circ C_a)(f_xC_x)^pe^{\frac{(1-\alpha)nF}{RT}E} \quad (33)$$

where E is the electrode potential measured with respect to the normal hydrogen electrode; α is the transfer coefficient; k_f^0 and k_b^0 are the forward (reduction) and reverse (oxidation) rate constants of the electron transfer process at the potential of the normal hydrogen electrode, respectively.

Substituting the relations expressed by Eqs. (28) and (30) into Eq. (33) and rearranging them, we obtain Volterra's integral equation of the second kind:

$$[i/nFq]=\sqrt{D}{}^*C\lambda\times\left[1+\frac{k_b^0f_a(\overset{p}{\underset{\nu=1}{\Pi}}K_\nu)/\sqrt{D_a}}{k_f^0f_0/\sqrt{D}}\sigma e^{\frac{nF}{RT}E}\right]^{-1}-\sqrt{\frac{3}{7\pi}}\lambda\int_0^y\frac{u^{-2/7}[i/nFq]}{\sqrt{y-u}}du \quad (34)$$

where

$$\lambda=\lambda_l\frac{\frac{k_f^0f_0}{\sigma\sqrt{D}}e^{-\frac{\alpha nF}{RT}E}+\frac{k_b^0f_a}{\sqrt{D_a}}(\overset{p}{\underset{\nu=1}{\Pi}}K_\nu)e^{\frac{(1-\alpha)nF}{RT}E}}{(f_0/f_p)[\lambda_l/(\overset{p}{\underset{\nu=1}{\Pi}}\sigma_\nu)]+\frac{k_f^0f_0}{\sigma\sqrt{D}}e^{-\frac{\alpha nF}{RT}E}} \quad (35)$$

In order to obtain a description of our problem formulated by means of dimensionless parameters, we make the substitution:

$$[i/nFq]=\sqrt{D}{}^*C\lambda\times\left[1+\frac{k_b^0f_a(\overset{p}{\underset{\nu=1}{\Pi}}K_\nu)/\sqrt{D_a}}{k_f^0f_0/\sqrt{D}}\sigma e^{\frac{nF}{RT}E}\right]^{-1}\cdot\psi \quad (36)$$

8) J.C. Slater and N.H. Frank, "Introduction to Theoretical Physics" (1933), p. 107.

9) S. Glasstone, K.J. Laidler and H. Eyring, "The Theory of Rate Processes" (1941), p. 575.

$$\xi=\lambda y^{3/14} \qquad (37)$$
$$\eta=\lambda u^{3/14}$$

Then, we obtain

$$\psi(\xi)=1-2\sqrt{\frac{7}{3\pi}}\int_0^{\xi}\frac{\eta^{7/3}\psi(\eta)}{\sqrt{\xi^{14/3}-\eta^{14/3}}}d\eta \qquad (38)$$

This integral equation has already been solved in the previous paper[7], and its solution has been there expressed in the form of power series of ξ.

Hence, considering the relations expressed by Eqs. (36) and (37), replacing the surface area of the dropping mercury electrode q with $4\pi r_0^2=4\pi(3m/4\pi d)^{2/3}\,t^{2/3}$, and rearranging it, we obtain for the instantaneous current during the drop age

$$i=i_d\left[1+\frac{k_b^0 f_a(\overset{p}{\underset{\nu=1}{\Pi}}K_\nu)/\sqrt{D_a}}{k_f^0 f_0/\sqrt{D}}\sigma e^{\frac{nF}{RT}E}\right]^{-1}\cdot$$
$$\times\sqrt{\frac{3\pi}{7}}(\lambda\sqrt{t})\psi(\lambda\sqrt{t}) \qquad (39)$$

where i_d represents the Ilkovic equation for the instantaneous limiting diffusion current. The values of the function $\sqrt{3\pi/7}\times(\lambda\sqrt{t})\times\psi(\lambda\sqrt{t})$ for various values of $\lambda\sqrt{t}$ are tabulated in Table 1 of the previous paper[7].

According to DeFord and Hume[2], the half-wave potential of the reversible wave due to the reduction of complex metal ions, denoted by $E_{1/2}^r$, is given by

$$E_{1/2}^r=E^0-2.3\frac{RT}{nF}\log\frac{f_a/\sqrt{D_a}}{f_0/\sqrt{D}}-2.3\frac{RT}{nF}\cdot$$
$$\times\log\left\{1+\sum_{\nu=1}^{N}(f\mathrm{x}C\mathrm{x})^\nu(f_0/f_\nu)(\overset{\nu}{\underset{\mu=1}{\Pi}}1/K_\mu)\right\} \qquad (40)$$

where E^0 is the standard potential of the reduction of the simple metal ion M^{n+} to the amalgam state. Since the standard potential of the electron transfer process expressed by Eq. (4), which is given by $2.3\,(RT/nF)\log(k_f^0/k_b^0)$, can be related with E^0 according to

$$2.3\frac{RT}{nF}\log\frac{k_f^0}{k_b^0}=E^0+2.3\frac{RT}{nF}\log(\overset{p}{\underset{\nu=1}{\Pi}}K_\nu),$$

Eq. (40) can be rewritten as follows, by using the abbreviation expressed by Eq. (31):

$$E_{1/2}^r=2.3\frac{RT}{nF}\log\frac{k_f^0 f_0/\sqrt{D}}{k_b^0 f_a(\overset{p}{\underset{\nu=1}{\Pi}}K_\nu)/\sqrt{D_a}}$$
$$-2.3\frac{RT}{nF}\log\sigma.$$

Consequently, $\dfrac{k_b^0 f_a(\overset{p}{\underset{\nu=1}{\Pi}}K_\nu)/\sqrt{D_a}}{k_f^0 f_0/\sqrt{D}}\sigma e^{\frac{nF}{RT}E}$ and λ can be, respectively, expressed as

$$\frac{k_b^0 f_a(\overset{p}{\underset{\nu=1}{\Pi}}K_\nu)/\sqrt{D_a}}{k_f^0 f_0/\sqrt{D}}\sigma e^{\frac{nF}{RT}E}=e^{\zeta} \qquad (41)$$

$$\lambda=\frac{1+e^{\zeta}}{[(f_0/f_p)/(\overset{p}{\underset{\nu=1}{\Pi}}\sigma_\nu)]A^{-1}e^{\alpha\zeta}+\lambda_l^{-1}}, \qquad (42)$$

where

$$\zeta=(nF/RT)(E-E_{1/2}^r), \qquad (43)$$

$$A=\left\{\frac{k_f^0 f_0}{\sigma\sqrt{D}}\right\}^{1-\alpha}\left\{\frac{k_b^0 f_a}{\sqrt{D_a}}(\overset{p}{\underset{\nu=1}{\Pi}}K_\nu)\right\}^{\alpha}. \qquad (44)$$

Hence, Eq. (39) can be transformed into the form

$$i=\frac{i_d}{1+e^{\zeta}}\sqrt{\frac{3\pi}{7}}(\lambda\sqrt{t})\cdot\psi(\lambda\sqrt{t}), \qquad (45)$$

with λ defined by Eq. (42). This is the general expression showing the instantaneous current during the drop age for any point along the wave.

Derivation of the Equation for the Current-Voltage Curve

Upon integrating Eq. (45) with respect to t from zero to the drop time τ and dividing it by τ, we obtain for the average value of the current flowing

$$\bar{i}=\frac{1}{1+e^{\zeta}}\sqrt{\frac{3\pi}{7}}\frac{1}{\tau}\int_0^{\tau}i_d(\lambda\sqrt{t})\psi(\lambda\sqrt{t})dt.$$

After writting $\xi=\lambda\sqrt{t}$ and rearranging it, we obtain

$$\bar{i}=\frac{\bar{i}_d}{1+e^{\zeta}}\sqrt{\frac{3\pi}{7}}(\lambda\sqrt{\tau})^{-7/3}\int_0^{\lambda\sqrt{\tau}}\psi(\xi)\xi^{7/3}d\xi \qquad (46)$$

where $\bar{i}_d$ represents the Ilkovic equation for the average value of the limiting diffusion current.

As shown in the previous paper[7], the function $\sqrt{7\pi/3}(\lambda\sqrt{\tau})^{-7/3}\times\int_0^{\lambda\sqrt{\tau}}\psi(\xi)\xi^{7/3}d\xi$ can be, with sufficient accuracy, approximated by $(\lambda\sqrt{\tau})^{1.04}/[1.13+(\lambda\sqrt{\tau})^{1.04}]$. For the sake of simplicity, although with a little less accuracy, we replace $(\lambda\sqrt{\tau})^{1.04}/[1.13+(\lambda\sqrt{\tau})^{1.04}]$ with $(\lambda\sqrt{\tau})/[1.12+(\lambda\sqrt{\tau})]$*. Accordingly, Eq. (46) can be reduced to

* Replacing the exact function with $(\lambda\sqrt{\tau})/[1.12+(\lambda\sqrt{\tau})]$ causes an error by one unit in the second decimal. On the other hand $(\lambda\sqrt{\tau})^{1.04}/[1.13+(\lambda\sqrt{\tau})^{1.04}]$ is coincident with the exact function up to three units in the third decimal.

$$\bar{i}=\frac{\bar{i}_d}{1.12\{[(f_0/f_p)/(\prod_{\nu=1}^{p}\sigma_\nu)](\Lambda\sqrt{\tau})^{-1}e^{\alpha\zeta}+(\lambda_l\sqrt{\tau})^{-1}\}+1+e^{\zeta}} \tag{47}$$

As the electrode potential becomes sufficiently negative, i.e., $\zeta\to-\infty$, $\bar{i}$ approaches the limiting value, $\bar{i}_l$, which is given by

$$\bar{i}_l=\frac{\bar{i}_d}{1+1.12(\lambda_l\sqrt{\tau})^{-1}} \tag{48}$$

Eq. (48) shows that the limiting current, $\bar{i}_e$, is proportional to $\bar{i}_d$, (hence to $^*C$), and the proportional factor is dependent on $\lambda_l\sqrt{\tau}$.

When the relation expressed by Eq. (48) is substituted into Eq. (47), we obtain

$$\bar{i}=\frac{\bar{i}_d}{1.12[(f_0/f_p)/(\prod_{\nu=1}^{p}\sigma_\nu)](\Lambda\sqrt{\tau})^{-1}e^{\alpha\zeta}+(\bar{i}_d/\bar{i}_l)+e^{\zeta}} \tag{49}$$

This is the general equation of the current-voltage curve for the reduction of complex metal ions.

In the following, we discuss in some detail the charactetistics of the current-voltage curve in several special cases.

(A) When the Electron Transfer Process takes place reversibly.—In the first place, let us consider a case in which the value of $\Lambda\sqrt{\tau}$ is greater than $50\times[(f_0/f_p)/(\prod_{\nu=1}^{p}\sigma_\nu)]\times(\bar{i}_l/\bar{i}_d)^{1-\alpha}\alpha^{\alpha}(1-\alpha)^{1-\alpha}$. Then, since it can easily be shown that

$$(\bar{i}_d/\bar{i}_l)\exp(-\alpha\zeta)+\exp(1-\alpha)\zeta > (\bar{i}_d/\bar{i}_l)^{1-\alpha}\alpha^{-\alpha}(1-\alpha)^{-(1-\alpha)}$$

for any value of ζ, Eq. (49) can be transformed into the form

$$\bar{i}=\frac{\bar{i}_d}{(\bar{i}_d/\bar{i}_l)+e^{\zeta}}.$$

By solving the above equation with respect to E, we obtain

$$E=E^r_{1/2}-2.3\frac{RT}{nF}\log\frac{\bar{i}_l}{\bar{i}_d}-2.3\frac{RT}{nF}\log\frac{\bar{i}}{\bar{i}_l-\bar{i}}, \tag{50}$$

where $E^r_{1/2}$ is defined by Eq. (40). This is the equation of the current-voltage curve corresponding to the reversible electron transfer process. Eq. (50) shows that a plot of $-E$ versus $\log\bar{i}/\bar{i}_l-\bar{i})$ should produce a straight line with a slope equal to 2.3 RT/nF $(=59/n$ mV. at 25°C). This fact is a criterion for the reversibility of the electron transfer process.

The half-wave potential, $E_{1/2}$, is given by

$$E_{1/2}=E^r_{1/2}-2.3\frac{RT}{nF}\log\frac{\bar{i}_l}{\bar{i}_d}, \tag{51}$$

as it comes from Eq. (50).

Furthermore, consider a case when the limiting current is completely controlled by the diffusion process, i.e., $\bar{i}_l=\bar{i}_d$. Then, Eq. (50) can easily be reduced to the simple form

$$E=E^r_{1/2}-2.3\frac{RT}{nF}\log\frac{\bar{i}}{\bar{i}_d-\bar{i}}. \tag{52}$$

This is quite the same as the result obtained when the net electrode reaction takes place reversibly. Detailed discussions on this case have been set down by many workers[1,2].

(B) When the Electron Transfer Process takes place irreversibly.—In the case of $\Lambda\sqrt{\tau}<2\times10^{-2(1+\alpha)}[(f_0/f_p)/(\prod_{\nu=1}^{p}\sigma_\nu)]$ $(\bar{i}_l/\bar{i}_d)$, $\bar{i}$ is smaller than about 2 per cent of the limiting current, $\bar{i}_e$, in the range of $\zeta>-4.6$ and the appreciable value of $\bar{i}$ is observed only for the values of ζ for which the condition $\zeta<-4.6$ is satisfied. Then, since it is found that

$$\exp\zeta<10^{-2} \quad \text{for } \zeta<-4.6,$$

Eq. (49) becomes

$$\bar{i}=\frac{\bar{i}_d}{1.12[(f_0/f_p)/(\prod_{\nu=1}^{p}\sigma_\nu)](\Lambda\sqrt{\tau})^{-1}e^{\alpha\zeta}+(\bar{i}_d/\bar{i}_l)}$$

Upon solving the above equation with respect to E, we obtain

$$E=E^r_{1/2}+2.3\frac{RT}{\alpha nF}\left\{\log\left[\left(\frac{f_p}{f_0}\prod_{\nu=1}^{p}\sigma_\nu\right)\Lambda\sqrt{\tau}\right]-0.049-\log\frac{\bar{i}_l}{\bar{i}_d}-\log\frac{\bar{i}}{\bar{i}_e-\bar{i}}\right\}.$$

When the relations expressed by Eqs. (10), (31), (40) and (44) are substituted into the foregoing equation, we obtain

$$E=2.3\frac{RT}{\alpha nF}\left\{\log\frac{k^0_f f_p}{\sqrt{D}}\sqrt{\tau}-0.049-\log\frac{\bar{i}_l}{\bar{i}_d}-\log\left[\sum_{\nu=0}^{N}(f_X C_X)^{\nu-p}(f_p\prod_{\mu=1}^{p}K_\mu)/(f_\nu\prod_{\mu=0}^{\nu}K_\mu)\right]-\log\frac{\bar{i}}{\bar{i}_l-\bar{i}}\right\}, \tag{53}$$

where it is defined that $K_0=1$. This is the same equation as that obtained by neglecting the effect of the reverse (oxidation) process. It is evident from Eq. (53), that a plot of $-E$ versus $\log\bar{i}/(\bar{i}_l-\bar{i})$ is linear and the inclination of this line is found to be 2.3 $RT/\alpha nF$ $(=59/\alpha n$ mV. at 25°C). Consequently, if this plot is carried out and the tangent

of the line thus obtained is determined, the value of αn can be calculated.

From Eq. (53) the half-wave potential, $E_{1/2}$, can be obtained as

$$E_{1/2}=2.3\frac{RT}{\alpha nF}\left(\log\frac{k_f^0 f_p}{\sqrt{D}}\sqrt{\tau}-0.049-\log \tilde{i}_l/\tilde{i}_d\right)$$
$$-\log\left[\sum_{\nu=0}^{N}(f_x C_x)^{\nu-p}(f_p\prod_{\mu=1}^{p}K_\mu)/(f_\nu\prod_{\mu=0}^{\nu}K_\mu)\right]\Bigg\}. \quad (54)$$

Eq. (54) shows that if the consecutive dissociation constants K_ν ($\nu=N, N-1, \cdots\cdots, 1$) are known, the form of the complex metal ion that participates in the electron transfer process, i.e., p, can be determined from the dependence of the half-wave potential, $E_{1/2}$, on the activity of the complexing agent, and the forward rate constant of the electron transfer process, k_f^0, calculated from the measured value of the half-wave potential, $E_{1/2}$.

Let us consider a case in which only the species $MX_s^{(n-s)+}$ predominates in the bulk of the solution in the region in question of the concentration of the complexing agent, i.e., when the condition ${}^*C_s \gg {}^*C_\nu (\nu=N, N-1, \cdots\cdots, S+1, S-1, \cdots\cdots, 1, 0)$ is satisfied. Then, by considering the relations expressed by Eq. (14), Eq. (54) can be reduced to the simple form

$$E_{1/2}=2.3\frac{RT}{\alpha nF}\left\{\log\left[\frac{k_f^0 f_s}{\sqrt{D}}\frac{(\prod_{\mu=0}^{s}K_\mu)}{(\prod_{\mu=1}^{p}K_\mu)}\sqrt{\tau}\right]\right.$$
$$\left.-0.049-\log(\tilde{i}_l/\tilde{i}_d)-(S-p)\log(f_x C_x)\right\} \quad (55)$$

In this case it is evident from Eq. (55), that a plot of $-E_{1/2}-2.3(RT/\alpha nF)\log(\tilde{i}_l/\tilde{i}_d)$ versus $\log(f_x C_x)$ should produce a straight line with a slope equal to $2.3(RT/\alpha nF)(S-p)$ $(=59(S-p)/\alpha n$ mV. at 25°C).

Unfortunately, few experimental data sufficient for the testing of the validity of Eqs. (53) and (54) are at present available to the authors. As an example of the application of the theoretical results described above, only the irreversible reduction of the ammonia-nickel complex ion, which has been recently studied by K. Morinaga[10], will be treated in the present paper. K. Morinaga has shown that the reduction of the ammonia-nickel complex ion takes place irreversibly at the dropping mercury electrode and the limiting current is completely controlled by the diffusion process. He has also found that the log plot gives a good straight line, as predicted by Eq. (53), and the slope of the line thus obtained is 41.5 mV. (average), from which he has calculated the value of α resulting in 0.71. Furthermore, he has measured the half-wave potential as a function of the ammonia concentration in the range of 0.2 to 3 M. His experimental results are shown in Fig. 1 in which the circles are experimental points. The curves in this graph are theoretical ones calculated by means of Eq. (54) on the assumption that $N=6$ and $p=2$. J. Bjerrum[4] has determined the consecutive dissociation constants for the ammonia-nickel system and shown that the constants determined by direct experiment are given as $K_1=10^{-2.80}$, $K_2=10^{-2.24}$, $K_3=10^{-1.73}$, $K_4=10^{-1.19}$, $K_5=10^{-0.75}$ and $K_6=10^{-0.04}$, respectively, and those corrected on statistical grounds are $K_1=10^{-2.02}$, $K_2=10^{-1.84}$, $K_3=10^{-1.60}$, $K_4=10^{-1.32}$, $K_5=10^{-1.15}$ and $K_6=10^{-0.81}$, respectively. Theoretical curves I and II in Fig. 1 have been calculated by using

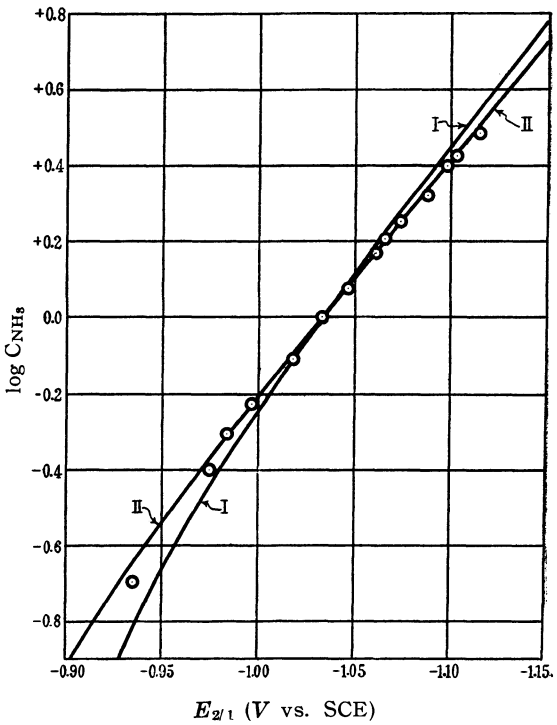

Fig. 1. Half-wave potentials of the ammonia-nickel complex ion as a function of the ammonia concentration in 0.1 M KNO_3. The curves are theoretical ones and the circles are experimental points.

the former and latter values of the consecutive dissociation constants, respectively. In these calculations, the half-wave potential at $C_{NH_3}=0.995$ N (-1.033 V vs. SCE) has been taken as the standard, and all activity coefficients which appear in Eq. (54) have been taken as if equal to unity since they are at present unavailable. The fairly good agree-

10) K. Morinaga, *J. Chem. Soc. Japan (Pure Chem. Sect.)* (in Japanese), **76**, 133 (1955).

ment of the experimental points with the theoretical curve II shows that the species $Ni(NH_3)_2^{++}$ participates in the electron transfer process, the transfer coefficient being equal to 0.71. Moreover, taking the statistically corrected values for the consecutive dissociation constants, 0.89×10^{-5} cm²/sec.* for the diffusion coefficient of the ammonia-nickel complex ion and 4–5 sec for the drop time, we have calculated the value of the forward rate constant of the electron transfer process, k_f^0, with the aid of the measured value of −1.033 V. vs. SCE (−0.787 V. vs. NHE) for the half-wave potential at the ammonia concentration equal to 0.995 N. The result obtained is

$$\log k_f^0 = -16.8 \ (k_f^0: \text{cm./sec.}).$$

For the reduction of the hydrated nickel ion, K. Morinaga has shown that the log plot produces a good straight line with a slope equal to 72 mV. and the half-wave potential is −1.047 V vs. SCE (−0.801 V. vs. NHE). Using these data, we have also calculated the forward rate constant, k_f^0, and the transfer coefficient, α, with the aid of the theory developed in the previous paper[7]. The results obtained are

$$\alpha = 0.40, \ \log k_f^0 = -13.7 \ (k_f^0: \text{cm./sec.}).$$

In this calculation we have taken 0.69×10^{-5} cm²/sec. for the diffusion coefficient of the hydrated nickel ion and 4–5 sec. for the drop time.

It is seen from the results obtained above that the complex formation of the hydrated nickel ion with ammonia decreases the forward rate constant of the electron transfer process and on the other hand increases the transfer coefficient.

Summary

Under the assumption that the electrolytic reduction of the complex metal ions at the dropping mercury electrode follows the mechanism expressed by Eqs. (3) and (4), the general expression of the current-voltage curve has been derived by solving the corresponding diffusion problem with the same accuracy as the Ilkovic equation, and the special two cases corresponding to the reversible and irreversible electron transfer process have been discussed in some detail. Moreover, as an example of the application of the present theory, the irreversible reduction of the ammonia-nickel complex ion has been analysed by the aid of the experimental data given by K. Morinaga. A fairly good agreement between the experimental data and the theoretical results has been obtained, and it has been found that the species $Ni(NH_3)_2^{++}$ participates in the electron transfer process with the forward rate constant equal to $10^{-15.8}$ cm./sec. and the transfer coefficient equal to 0.71.

Government Chemical Industrial Research Institute, Tokyo

* According to the experimental results of K. Morinaga[10], the ratio of the diffusion limiting current of the ammonia-nickel complex ion to that of the hydrated nickel ion, which is equal to the ratio of the square roots of the corresponding diffusion coefficients, is given as 2.52/2.22. Since the diffusion coefficient of the hydrated nickel ion at infinite dilution is 0.69×10^{-5} cm²/sec., the diffusion coefficient of the ammonia-nickel complex ion may be calculated as 0.89×10^{-5} cm²/sec.

Studies on the Cold-drawing of Polymers (Part II).[1] *The Quasi-Static Drawing of Polycapramide. II. The Effects of Humidity, the Heterogeneity of Polymer's Fine Structure investigated through the Moisture Adsorption and the Behavior of Deformation, and Lowering of the Second-order Transition Temperature by Adsorbed Water**

By Hirosuke YUMOTO

(Received August 8, 1955)

Introduction

The effects of temperature of the quasi-static drawing of polycapramide in the completely dried state were described in the previous paper[1]. In succession, the effect of humidity on the occasion of drawing at constant temperature of 20°C and the effects of temperature on the occasions of drawing at constant humidities of 10% and 65% or of drawing in water were investigated. In this paper the experimental information and its discussions are treated.

The procedures, with which the quasi-static isothermal elongation-stress curves were estimated, are identical with those in Part I[1]. The apparatus shown in Fig. 1 (A) and (C) of Part I were used[a]. The test materials were common with Part I; i. e. the unstretched polycapramide monofilament of 60.0 denier (ϕ 0.086 mm.), spun from the melt through chilling with air, were used.

In course of drawing, one or two neckings occur under coexisting of stretched and unstretched phases excepting the case of drawing in water. During the procession of necking, the stress was kept almost constant (Wc); but the additional stress (ΔWc) was demanded besides Wc for the formation of the necking. Wc is temporarily assumed to be the yield stress. The elongations, where the necking appears and disappears, are denoted with α_{c1} and α_{c2} respectively and ($\alpha_{c2}-\alpha_{c1}$) is denoted with α_c. These notations (Wc, ΔWc, α_{c1}, α_{c2}, and α_c) are illustrated, for example, at 20% relative humidity in Fig. 1 [B].

* Presented at the symposium on polymer science of the Chemical Society of Japan in Nagoya, November 11, 1954.

1) Contributed to This Bulletin.

a) The test material had been stored for 24-48 hr. in the humidity at which measurement was intended. Measuring was started 2-3 hr. later, than the setting of the specimen to the cramp in the measuring vessel. Especially, in case of 0% humidity, the specimen was previously dried out with phosphorous pentoxide for seven days and furthermore dried for twelve hours in the measuring vessel after setting to the cramp.

The Results of Measurements

The elongation-stress curves obtained in various humidities at 20°C are given in Fig. 1 [A]-[D]. When the relative humidity was less than 10%, stretching was not smooth and sometimes rupture happened midway of stretching, and moreover the randomness among all measurements was large; but when the relative humidity was more than 20%, the behavior was reversed. In case the stretch was not smooth the curve obtained is zigzag partially, which is smoothed in Fig. 1. In case of drawing in water, no necking was observed and the specimen seemed to be elongated homogeneously in the whole course of drawing to rupture. The values of Wc and α_{c2} are larger in lower humidities. All of the curves at various humidities have each an inclination to converge

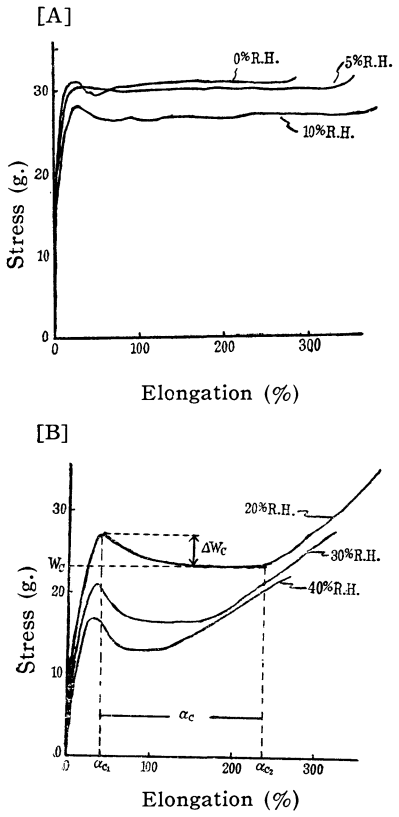

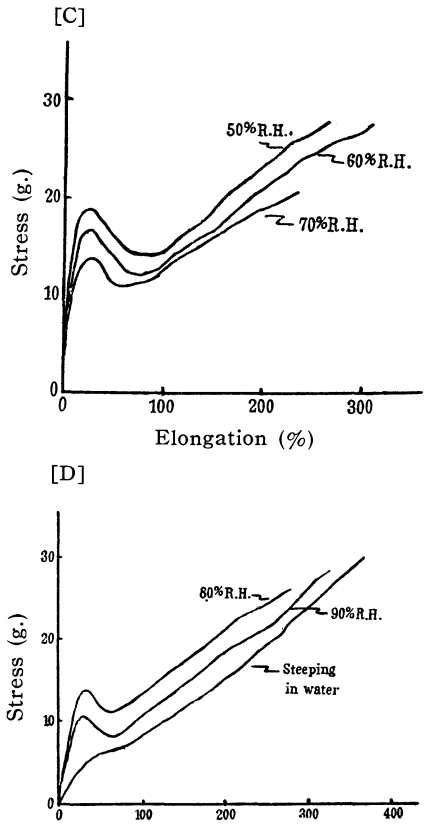

Fig. 1. The elongation-stress curves of polycapramide at various relative humidities and constant temperature of 20°C.

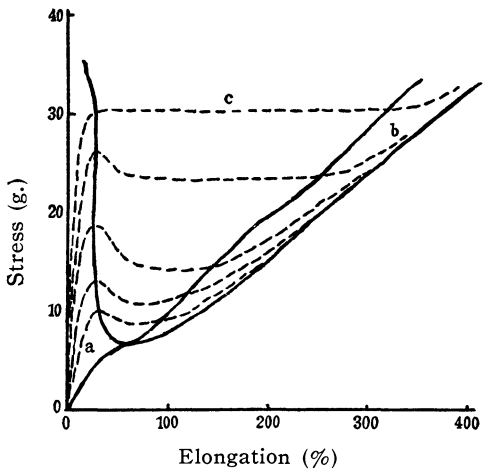

Fig. 2. Three domains schematically divided in the elongation-stress phase space at 20°C (a: Only unstretched phase existing, b: Only stretched phace existing, c: Unstretched and strectched phases coexisting).

to the curve of the sample drawn in water as schematically shown in Fig. 2. In Fig. 2 the phase space can be distinctly divided in three domains; in the first domain only the unstretched phase exists, in the second domain the unstretched and the stretched phases coexist, and in the third domain only the stretched phase exists. It is noteworthy in appearance but it is not considered to have profound physical meaning.

The additional stress (ΔWc) has a maximum at about 30% relative humidity.

The values of the stress and elongation in relation to rupture were random, so the humidity effects on them could not be studied. The values of them are always in the range of 20–25 g. stress and 200–400% elongation.

The elongation-stress curves of the samples drawn at various temperatures and a constant relative humidity of 10% or 65%, are given in Fig. 3 and Fig. 4. The curves of the samples drawn in water at various temperatures, are given in Fig. 5. In case of 10% relative humidity, smooth stretchings were possible above 40°C but not below 30°C. In other cases stretchings were always smooth.

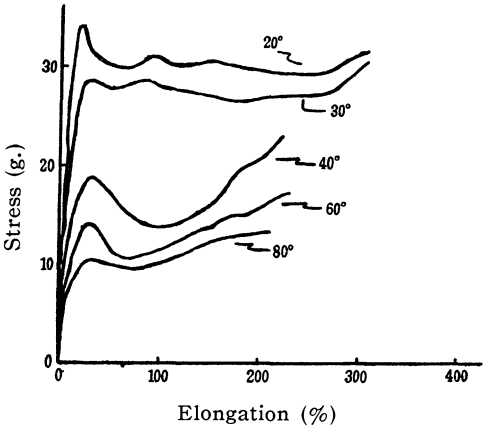

Fig. 3. The elongation-stress curves of polycapramide at various temperatures and constant relative humidity of 10%.

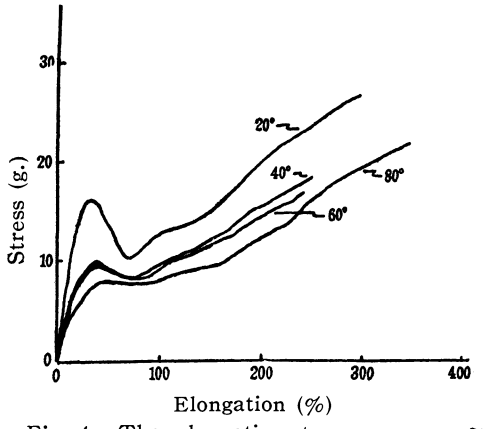

Fig. 4. The elongation-stress curves of polycapramide at various temperatures and constant relative humidity of 65%.

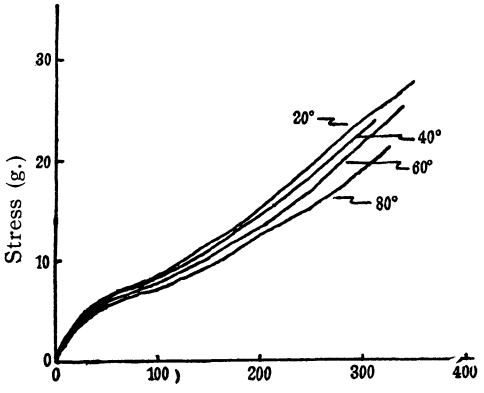

Fig. 5. The elongation-stress curves of polycapramide at steeping in water of various temperatures.

Discussion

The values of Wc and ΔWc at 20° are plotted against the relative humidities (R. H.) and against the values of weight percent of moisture adsorbed (w) in equilibrium with each of the relative humidities in Fig. 6 and Fig. 7. The values of α_{c1} and α_{c2} are similarly plotted in Fig. 8 and Fig. 9. In these figures the length of lines at the positions plotted indicates the measure of randomness. The values of w are quoted from the date[2] about the isothermal moisture adsorption of unstretched polycapramide filaments which are not heat-treated.

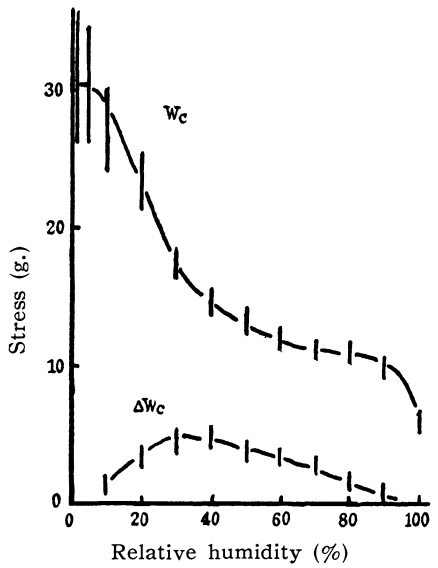

Fig. 6. The yield stresses (W_c) and the additional stresses (ΔW_c) at various relative humidities.

2) K. Hoshino and H. Yumoto, *J. Chem. Soc. Japan*, 70, 104 (1949) (in Japanese).

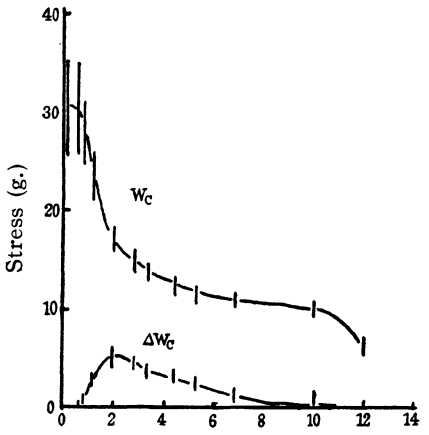

Fig. 7. The yield stresses (W_c) and the additional stresses (ΔW_c) at various amounts of moisture adsorption.

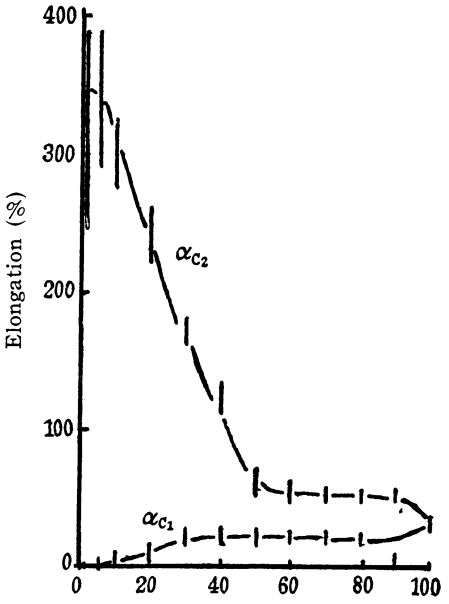

Fig. 8. The two phases coexisting regions of elongation ($\alpha_{c2}-\alpha_{c1}$) at various relative humidities.

In Fig. 6 or Fig. 7, a singular point is explicitly recognized at 10–30% R. H. or 1.0–2.0% moisture adsorption. The boundary between the smooth and the non-smooth stretching or the maximum of the additional stress lies roughly on the environs of the above limits. But in Fig. 8 or Fig. 9, the singularity is recognized at about 50% R. H. or 3.5% moisture adsorption.

Fig. 10 represents the empirical relation between the amount of water adsorbed and the isosteric differential heat of adsorption

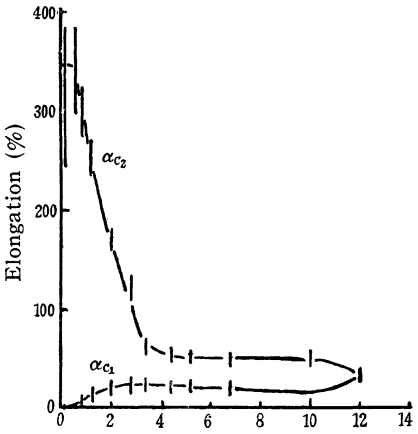

Amount of moisture adsorption (%)

Fig. 9. The two phases coexisting regions of elongation (α_{c2}–α_{c1}) at various amounts of moisture adsorption.

from liquid water ($\Delta\bar{H}$)[2]. The shape of the curve in Fig. 10 is similar to that in Fig. 6. If the values of Wc are plotted against $\Delta\bar{H}$ on trial, the nearly linear relation is obtained as shown in Fig. 11. Making use of this empirical relation, $\Delta\bar{H}$ of the initial adsorption, which is difficult to be determined from the data of isothermal adsorption, is easily evaluated by extrapolation and found to be −(3.5–4.0)kcal./mol. Besides, it is verified from this linear relation that each of the singular points found in both of the curves of Fig. 6 and Fig. 10 lies on the same value of w. Therefore the remarkable change of the mechanical property of polycapramide at 1–2% moisture adsorption is suggested to be concerned with some change in the situations of water molecules adsorbed.

On the other hand another singularity found at 50% R. H. or 3.5% moisture adsorption as seen in Fig. 8 or Fig. 9 does not appear at all in Fig. 10. But beyond this

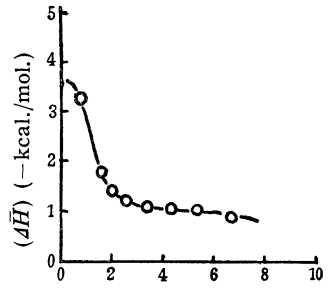

Amount of moisture adsorption (%)

Fig. 10. The isosteric differential heats of moisture adsorption to polycapramide ($\Delta\bar{H}$) at various amounts of moisture adsorption (Hoshino and Yumoto).

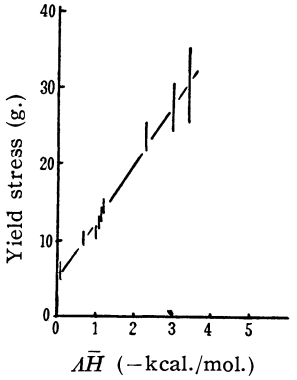

Fig. 11. The relation between the isosteric differential heats of moisture adsorption (ΔH) and the yield stresses (W_c).

humidity the amount of adsorption increases sharply and moreover begins to deviate from the values estimated semiempirically with the general equation of Brunauer, Emmett, and Teller[2].

In addition to the experiment in which fine filaments (ϕ 0.086 mm.) are used as the sample, the elongation-stress curves of unstretched polycapramide monofilament (ϕ 1.67 mm.) which was manufactured by quenching the extruded melt with water, were recorded by means of the Schopper-style tensile tester; the rate of elongation was about 5.6% per second. The test materials had been stored in the vessels, where the relative humidity was kept constant in the range from 0% to 95%, for more than three weeks in order that they can be brought sufficiently into equilibrium of moisture adsorption. Measurements were performed in atmosphere of 65% R. H. as soon as the specimens were taken out from the vessel. The result of these measurements also shows that the singularity in regard to α_{c_2} appears at 50–60% R. H. And also the necking is not observed in the whole course of drawing when the specimen has been steeped in water for twenty-two hours. It was observed that, throughout the coexistent state of unstretched and stretched phases, elongation in either of the two phases scarcely ever occurred and the stretch of the entire specimen was almost entirely attributed to the elongation through transformation from unstretched into stretched phase.

Then approximate sectional areas of each phase during the coexistent state can be tentatively calculated from the values of α_{c_1} an α_{c_2}[b]. The ratio (r) of the sectional

b) If the initial sectional area of specimen is A, the sectional area of unstretched phase is $A/(1+\alpha_{c_1}/100)$, and that of stretched phase is $A/(1+\alpha_{c_2}/100)$. The ratio (r) is $(1+\alpha_{c_2}/100)/(1+\alpha_{c_1}/100)$.

area of the stretched phase to that of the unstretched phase is larger, the lower the humidity. These ratios are plotted against the amounts of moisture adsorbed in Fig. 12, where the singularity can be found only at ca. 3.5% adsorption.

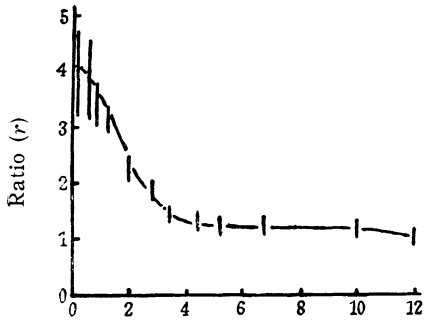

Fig. 12. The ratios of sectional area of stretched phase to that of unstretched phase at various amounts of moisture adsorption.

M. Tsuboi investigated the molecular state of water adsorbed in polycapramide by means of the infrared absorption bands[3]. The infrared spectrum was measured, the specimen being exposed to air of 76% R. H. at 11°C; therefore its moisture adsorption must be ca. 6%. His result shows that O-H band of adsorbed water is observed at 2.86 μ only. According to his consideration none of the adsorbed water molecules has any free OH groups and both of two OH groups are perturbed through O-H·····O bonding by the two peptide oxygen atoms (located near to each other). This fact may indicate that all of the adsorbed water molecules are directly linked to polycapramide molecules and then they are situated *in the adsorption of the first layer*. If this proves to be the case, the singular change of $\Delta\bar{H}$ at 1–2% moisture adsorption is conceivably due to altering of the sort of sites for adsorption. $\Delta\bar{H}$, below and above this singular point, may be assumed to be ca $-(3.5–4)$ kcal./mol. and ca -1 kcal./mol.

Consequently, the next conclusions are deducible: below 1.2% adsorption the water molecules are linked to some sites in the region, where flow cannot occur, because they can not easily affect the yield stress. Such a region may be considered to be that where the chain molecules are arranged into a lattice. The water molecules are adsorbed to the sites which are the disordered places contained in this lattice, and take comparatively stable configurations. Because the adsorbed water begins to have a large influence on the yield stress beyond 1.2% adsorption, it follows that, almost of the sites in the lattice having been already occupied by the water molecules, the sites in the region where flow can occur begin to be occupied by water molecules[c]. From 1.2% to 3.5% adsorption the effect of adsorbed water on the drawing behavior is exceedingly large, but beyond 3.5% it is a good deal smaller (Fig. 12). In the following consideration of the polymer's structure it may be possible that the former is an adsorption on the sites in the partially arranged regions which make the boundary of the arranged regions (micelles) and the latter is that on the sites in the completely amorphous regions. The author believes that the deformation of polymer can be regarded as that of the complex structure made of strong and weak networks. The former, which is tentatively called the *primary network*, is constituted from bundles of chain molecules and contains the arranged regions (micelles) together with their boundaries. The latter, which is tentatively called the *secondary network*, is constituted from the single chain molecules which are entangled with each other and fill the space among the primary networks. On deforming such a complex network, the micell behaves like a rigid body and the flow in the primary network must occur only at the boundaries of the micells. The measured yield stress is the sum of individual resistances caused against flow in the primary and the secondary networks and the stress caused in the primary network should be expected to hold the leading proportion. The behavior of the secondary network, however, has an important function in determining the deforming features of the entire complex network. The detailed discussion[4] on the mechanism of deformation shall be described in a subsequent paper. At any rate, the results obtained can give some experimental foundations to establish the fine structure of polymer and the mechanism of its deformation.

3) M. Tsuboi, This Bulletin, 25, 160 (1952).

c) If the number of sites for adsorption with $\Delta\bar{H}$ of -3.8 kcal./mol. is N_1, that with $\Delta\bar{H}$ of -1.0 kcal./mol. is N_2, and the number of sites already occupied by water molecules is N_1' or N_2' respectively, the ratio (P_2/P_1) of probabilities with which one of sites not yet occupied in either of both groups will be occupied by next water molecule is as following; $P_2/P_1=(N_2-N_2')\exp\left(\frac{1000}{RT}\right)/(N_1-N_1')\exp\left(\frac{3800}{RT}\right)\simeq(N_2-N_2')/(N_1-N_1')\ 1/100(R=2$ cal., $T=300°K$). Then division can be made fairly definitely.

4) H. Yumoto, presented at the symposium on rheology of the Chemical Society of Japan in Tokyo, June 3, 1955.

The temperature dependency on the behavior of drawing at 10% or 65% R. H. is discussed as follows. The values of *Wc* and *ΔWc* obtained from Fig. 3 and Fig. 4 are plotted against the temperature in Fig. 13 and Fig. 14.

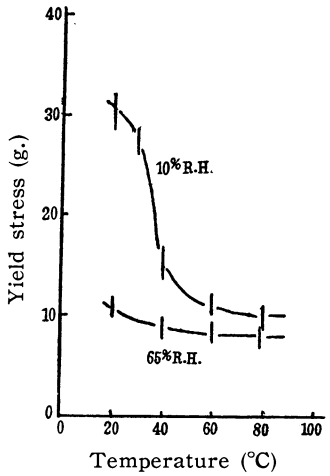

Fig. 13. The yield stresses at various temperatures and constant relative humidities of 10% and 65%.

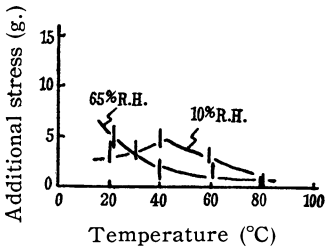

Fig. 14. The additional stresses at various temperatures and constant relative humidities of 10% and 65%.

In case of 10% R. H. a singular point is found at 30–40°C in both figures. This singularity has presumably the same physical meaning as that revealed at 70–80°C on the occasion of drawing at 0% R. H., i.e. in completely dried state. (cf. Fig. 3 in Part I[1]) In case of 65% R. H. there is no singular temperature within the observed range, but it seems likely to exist below 20°C.

The amount of adsorption is less at a higher temperature even if the relative humidity is the same; for instance, the amount of water adsorbed on the unstretched, polycapramide filaments which are not heat-treated is 0.77% at 25°C or 0.58% at 40°C in case of 10% R. H. and 4.8% at 25°C or 4.4% at 40°C in case of 65% R. H.[2] Although *Wc* should decrease with increase of water adsorbed, as a matter of fact, *Wc* becomes smaller at a higher temperature. This indicates the direct influence of temperature to be strong. Therefore this singularity must be ascribed to the fact that the micro-Brownian motion is either frozen or not in the region where flow between chain molecules can occur practically. Moreover, according to the complex network presented above, the microscopic state of the boundary region between micells gives the exceedingly great influence on the value of *Wc* and, therefore, the micro-Brownian motion under discussion will not be that in the completely amorphous region, i.e. in the secondary network, but that in the boundary region between micells.

It is proved consequently that the so-called polymer's second-order transition temperature, which is considered to be related to the microscopic state in any amorphous region, is lowered with increase of the amount of water adsorbed; e.g. it is 70–80°C at completely dried state (cf. Part I[1]), 30–40°C at less than 1% adsorption, or lower than 20°C at 4–5% adsorption. These values of the adsorption are the weight per-centage of entire amount of water adsorbed to the entire adsorbent; at present the weight per-centage of water adsorbed in regard to only the adsorption on any limited region, i.e. the boundary region between micells, cannot be estimated.

The results of drawing in water at various temperatures given in Fig. 5 exhibit no singular temperature in the observed range.

Conclusion

The effects of humidity, namely water adsorption, in case of isothermal quasi-static drawing of unstretched polycapramide filaments at constant temperature of 20°C were investigated. Interesting results, suggestive of the fine structure of polymers and the mechanism of its deformation, were obtained. Generally the necking appears under coexistence of unstretched and stretched phases in course of drawing, but the necking is not observed in case of drawing in water. During the state, in which both phases exist, the stretch of the entire specimen is almost entirely attributed to elongation through transformation of the unstretched into the stretched phase. The yield stress (*Wc*) for proceeding of necking shows sharp increase at the moisture adsorption of less than 1–2% and the additional stress (*ΔWc*) required for formation of the necking exhibits a maximum as shown in Fig. 7. The amount of water adsorbed where this singular point lies is identical with the position at which the

isosteric differential heat of adsorption ($\Delta\bar{H}$) changes markedly. $\Delta\bar{H}$ of the initial adsorption can be evaluated to be $-(3.5\text{–}4)$ kcal./mol. from the empirical relation between $\Delta\bar{H}$ and Wc. Such a result suggests that a deformation of the heterogeneous fine structure of polymer bears a close relation to moisture adsorption. The ratio (r) of sectional areas of both phases during the state of their coexistence increases sharply at the water adsorption less than 3.5% (50% R. H.) as shown in Fig. 12.

The molecular state of the water adsorbed, which has been revealed with the infrared absorption bands by M. Tsuboi, indicates that all of the adsorbed water molecules are directly bound to the polycapramide molecules; therefore the variety in the heat of adsorption should be due to the variety of adsorption sites. If water is adsorbed to the sites located in the region where flow can occur, it may facilitate the deformation of polymer. Now it may be possible to conclude as follows. Water molecules of less than 1.2% adsorption are situated at the sites in the fairly arranged regions, that is micells (U), and have no influence upon the magnitudes of Wc and r. Water molecules corresponding to the range of adsorption from 1.2% to 3.5% are situated at the sites in the partially arranged boundary regions between micells (Vab) and have a great influence upon the magnitudes of Wc and r. Water molecules corresponding to more than 3.5% adsorption lie at the sites in the completely amorphous intermiceller regions (Vc) and have little influence upon the magnitudes of Wc and r. As the magnitude of yield stress (Wc) is mainly determined by the steric resistance against flow in Vab regions, the so-called polymer's second-order transition temperature (Tf) of polycapramide seems to be the temperature, at which the micro-Brownian motion in Vab regions becomes effectual within the time of observation.

The effects of temperature on the occasions of drawing at constant humidities of 10% and 65% or of drawing in water were investigated. It is proved from this result that Tf is at 70–80°C in the completely dried state (cf. Part I), at 30–40°C if the moisture adsorption is less than 1%, and at the temperature lower than 20°C if the moisture adsorption is 4–5%.

The detailed arguments on the subject of the deformation mechanism, which can be deduced from this series of studies, shall be described in a subsequent paper.

The author wishes to thank Dr. K. Hoshino and Dr. H. Kobayashi who instructed him on his studies and permitted the publication, and Mr. M. Nakata who collaborated with him on experiments.

Nylon Laboratory, Research Department,
Toyo Rayon Co., Ltd., Minato-ku,
Nagoya

Cathodo-luminescence of Samarium as Applied to the Structural Studies of Alumina. III. On Alumina derived from Boehmite and Bayerite through Thermal Decomposition

By Eiichi IWASE, Seijiro NISHIYAMA and Toshiaki ISONO

(Received May 16, 1955)

Introduction

Both hydrargillite and bayerite are synthetic alumina-trihydrates, the latter being considered to be a metastable form, while boehmite is a synthetic alumina-monohydrate. Starting from a solution of sodium aluminate, hydrargillite is obtained by slow hydrolysis owing to seeding as in the case of Bayer process, the bayerite is yielded by rapid precipitation through introduction of carbon dioxide gas at 40°C, and the boehmite is produced by precipitation with sodium bicarbonate. The boehmite and the bayerite can also be prepared by steam digestion of the hydrargillite and by the action of water on an amalgamated aluminium respectively.

The bayerite is, on being heated, transformed into a poorly crystallised boehmite, followed by an extremely poorly crystalline and then a more completely ordered γ-modification of alumina, the latter being said to

be changed to α-modification at temperatures higher than about 1200°C.

The present authors have applied cathodo-luminescence spectrum of samarium to elucidate the thermal decomposition process of the bayerite and the boehmite.

In the present paper are shown some results of investigations on cathodo-luminescence spectra of samarium imbedded in samples of alumina, which have been produced from bayerite and boehmite.

Experimental Results and Discussion

Results of cathodo-luminescence spectra for samarium-bearing samples of alumina, which were derived from boehmite and bayerite prepared in various ways, are described separately and some discussions concerning them are also given.

1) On Aluminas derived from Boehmite, which is produced in a Solution of Sodium Aluminate.—Boehmite was precipitated from a solution of sodium aluminate by sodium bicarbonate[1]. This precipitate was washed with water as usual, dried at 110°C, soaked in a solution of samarium nitrate and then converted to anhydrous alumina by calcination, either over a blast flame of coal gas mixed with air or in a direct flame of coal gas mixed with oxygen. These samples of samarium-bearing alumina were submitted to spectrographic investigations of their cathodo-luminescences. Fig. 1, (a), (b) and (c) represent the results schematically.

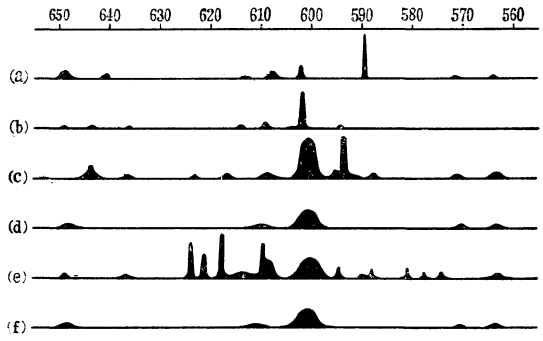

Wave-length (in mμ)

Fig. 1. Schematic representation of cathodo-luminescence spectrum of samarium-bearing alumina derived from boehmite, which was precipitated from sodium aluminate solution by sodium bicarbonate.

There appeared, as can be seen from Fig. 1 (a), D-line of sodium (589 mμ) and three luminescence bands at 602, 608 and 613 mμ, in addition to four bands of the luminescence prototype I[2], namely two bands in a spectral region of 640–650 mμ and two bands in 560–570 mμ, after the sample had been calcined over a blast flame of coal gas mixed with air. A band situated at 602 mμ may be ascribed to the luminescence prototype III[2], while bands at 608 and 613 mμ may be ascribed to either the luminescence prototype II[2] or III. The appearance of D-line of sodium in the cathodo-luminescence spectrum indicates that alkali was not removed by an ordinary washing with water from the precipitate of the boehmite prepared in a solution of sodium aluminate.

Several bands of the luminescence prototype II were perceptible and the D-line faded away in the cathodo-luminescence, as shown in Fig. 1 (b), when this sample of alumina had been heated more intensely, namely in a direct flame of coal gas and oxygen for a short time. A band was seen at 609 mμ, and another band at 602 mμ which was of a moderate intensity in Fig. 1 (a) became most intense.

After being roasted further in a flame of coal gas mixed with oxygen, this sample exhibited cathodo-luminescence bands of the prototype II at 587.5, 609, 616.5 and 623 mμ (Fig. 1, c). The facts that two bands situated at 594 and 600 mμ were very intense and only one relatively strong band at 644 mμ was seen in a spectral region of 640–650 mμ, would be characteristic of the sample of alumina under consideration, and would show that this sample was not composed of the pure α-modification. It is to be mentioned that the peak of a band near 600 mμ shifted, as the duration of heat treatment was lengthened, slightly toward a short wave-length side, namely from 602 to 600 mμ. The conclusion may thus be drawn from the above experiment that small amounts of alkali remaining in the precipitate of the boehmite washed with water as usual, exerted conspicuous influences upon the luminescence spectrum of the impregnated samarium.

Hydrochloric acid was added for the purpose of removing the tenaciously sticking alkali from the sample of the boehmite and thus the alkali was converted to sodium chloride. This sodium compound was then found to be easily eliminated by an ordinary washing with water.

The sample of the boehmite thus purified has been dried at 110°C, moistened with the solution of samarium nitrate and calcined in flames of coal gas-air and of coal gas-

1) A.S. Russell and C.N. Cochran, *Ind. Eng. Chem.*, 42, 1337 (1950).

2) E. Iwase, This Bulletin, 28, 596 (1955).

oxygen respectively. The cathodo-luminescence spectrum consists, in the former case, of prototype I (Fig. 1, d), while in the latter case almost entirely of prototype II, except that a broad luminescence band of prototype I with its intensity-maximum at 601 mμ remains still fairly intense (Fig. 1, e). Here the normal γ-α transformation of alumina is assumed to have been taking place.

It is well known that the so-called β-[3], or ζ-modification[4,5,6,7] happens to be produced, when appreciable amounts of alkali are present in the alumina. The considerable variations observed in the feature of luminescence spectrum of samarium when the alkali is present, may presumably be attributed to the formation of alumina resembling the β-, or ζ-modification.

Two intermediate anhydrous aluminas were reported in the transformation sequence from the boehmite to α-alumina, according to X-ray studies by Thibon[8], Brown[9], and Prettre[10], while three were reported according to those by Stumpf[11], Funaki[12], Day[13], Brown[9], and Prettre[10]. For instances, Stumpf et al[7]. stated that a transformation from the boehmite to anhydrous alumina proceeds in the following sequence, Boehmite→γ-alumina→δ-alumina→θ-alumina→α-alumina, and the boehmite begins to be dehydrated at 360°C and is converted to nearly anhydrous alumina at 450°C. The γ-, δ- and θ-aluminas are considered to be essentially intermediate forms having oxygen network of cubic close-packing. The plain hexagonal close-packed oxygen network of α-alumina seems not yet attained at temperatures much higher than 1200°C, as was given in Fig. 7, (c) of Stumpf's paper[7], this observation coinciding with a result of the present authors that the alumina obtained by an intense roasting in a direct flame of a mixture of coal gas and oxygen, showed a mixed cathodo-luminescence spectrum of the prototypes I and II (Fig. 1, e).

Anhydrous aluminas intermediately produced, namely γ- and δ-modifications were prepared from this purified boehmite by previous heat treatments at 550 and 1150°C respectively. These modifications of alumina were, after samarium had been added, heated at a moderately elevated temperature, namely over a blast flame of coal gas mixed with air. Their luminescence spectra caused by cathode-ray excitation were investigated, and all these were found to be of the simple prototype I, as is given in Fig. 1 (f). However, the cathodo-luminescence spectrum of the pure prototype II was obtained after these modifications of alumina had been subjected to an intense heat treatment in a coal gas-oxygen flame. Consequently, it was confirmed that confused intermediate configurations of virtually anhydrous aluminas yielded by thermal decomposition of the boehmite, have almost no effect on luminescence spectra of the resulting aluminas.

2) On Alumina derived from Boehmite, which is produced by Autoclaving of Hydrargillite.—The boehmite can also be prepared by a steam digestion of hydrargillite[14], since the hydrargillite is said to be metastable as compared with the boehmite under water at 200°C[15]. Fine crystals of the hydrargillite, namely the product of Bayer process were heated in the presence of steam at 200, 300 and 340°C for one hour under pressure of steam in an autoclave. These were washed with hydrochloric acid and then with water, and dried at 110°C. It was concluded from measurements of loss on ignition that compositions apparent were $Al_2O_3 \cdot 1.7 H_2O$, $Al_2O_3 \cdot 1.2 H_2O$ and $Al_2O_3 \cdot 1.1 H_2O$ for the samples subjected to steam treatments at 200, 300 and 340°C respectively. The dried samples thus obtained were, after samarium had been added, calcined over a blast flame of coal gas mixed with air, and their luminescence spectra caused by cathode-ray bombardments were investigated. The results are shown in Fig. 2.

A sample with its composition very near to that of the boehmite gave mainly a luminescence spectrum of prototype I (Fig. 2, c), while those prepared by steam digestion at 200 and 300°C gave mixed luminescence spectra of the prototypes I and II (Fig. 2, a and b). Bands of the prototype II were thus seen in the cathodo-luminescence spectrum, when the hydrargillite remaining undecomposed were present mixed with the newly produced boehmite, as in the cases of the

3) A. F. Wells, "Structural Inorganic Chemistry," Oxford, Clarendon Press, (1945) p. 335.
4) H.B. Barlett, *J. Amer. Ceram. Soc.*, **15**, 361 (1932).
5) E.J.W. Verwey, *Z. Krist.*, **91**, 66 (1935).
6) C.A. Beevers and S. Brohult, *Z. Krist.*, **95**, 472 (1936)
7) H.C. Stumpf, A.S. Russell, J.W. Newsome and C.M. Tucker, *Ind. Eng. Chem.*, **42**, 1401 (1950).
8) H. Thibon, J. Charrier et R. Tertian, *Bull. soc. chim. France*, [5] **18**, 386 (1951).
9) J.F. Brown, D. Clark and W.W. Elliott, *J. Chem. Soc.*, **1953**, 85.
10) M. Prettre, B. Imelik, L. Blanchin und M. Petitjean, *Angew. Chem.*, **65**, 549 (1953).
11) H.C. Stumpf, A.S. Russell, J.W. Newsome and C.M. Tucker, *Ind. Eng. Chem.*, **42**, 1398 (1950).
12) K. Funaki and Y. Shimizu, *J. Chem. Soc. Japan (Ind. Chem. Sect.)*, **56**, 53 (1953).
13) M.K.B. Day and V.J. Hill, *Nature*, **170**, 539 (1952); *J. Phys. Chem.*, **57**, 946 (1953).
14) H.C. Stumpf, A.S. Russell, J.W. Newsome and C.M. Tucker, *Ind. Eng. Chem.*, **42**, 1399 (1950).
15) "Gmelins Handbuch anorg. Chem.", **35**, Aluminium Teil B, 8 Aufl., Verlag Chemie, Berlin (1934), S. 108.

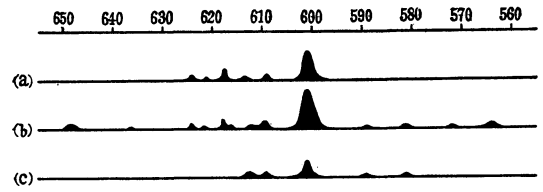

Fig. 2. Schematic representation of cathodo-luminescence spectrum of samarium-bearing alumina derived from steam-digested hydrargillite.

above two samples having apparent compositions of $Al_2O_3 \cdot 1.7\,H_2O$ and $Al_2O_3 \cdot 1.2\,H_2O$. These samples as well as that converted to the boehmite gave all the luminescence spectrum of the pure prototype II, after an intense heat treatment had been made in a direct flame of coal gas-oxygen. On the other hand, the products derived from the hydrargillite by calcination at relatively low temperatures, have shown similar results on which we will report fully in a later paper.

3) On Alumina derived from Bayerite, which is produced in a Solution of Sodium Aluminate.—Bayerite was prepared by rapid carbonation of a sodium aluminate solution at 40°C[14,16]. It was washed with water as usual, dried at 110°C and wetted by the solution of samarium nitrate. The samarium-bearing alumina derived from calcination of this bayerite at 1000°C for one hour gave, under excitation by cathode-rays, a luminescence spectrum of prototype I accompanied by the intense D-line of sodium, as is given in Fig. 3, (a).

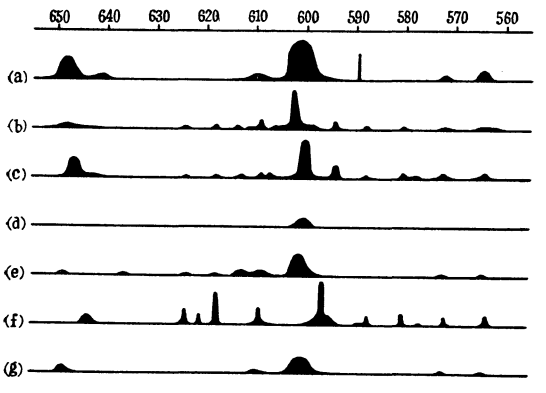

Fig. 3. Schematic representation of cathodo-luminescence spectrum of samarium-bearing alumina derived from bayerite, which was produced by carbonation of sodium aluminate solution.

16) R. Fricke and H. Severins, *Z. anorg. Chem.*, **175**, 249 (1928); ibid., **179**, 287 (1929).

A heat treatment of short duration in a coal gas-oxygen flame changed the cathodo-luminescence spectrum (Fig. 3, b); the D-line disappeared, and some bands of prototype II could then be seen, being overlapped with still remaining bands of prototype I. The most intense and sharp band situated at 602 mμ was worthy of note, which was perceptible also in the already-mentioned case of the boehmite simply washed.

The cathodo-luminescence spectrum remained, on the whole, almost unaltered even after the repeated calcination in a direct flame of a mixture of coal gas and oxygen (Fig. 3, c). Differences were, however, found in the wave-length of the peak of the most intense band near 600 mμ and in that of an intense band at 640–650 mμ. These two bands shifted toward a somewhat shorter wave-length side; the former from 602 to 600 mμ, and the latter from 648 to 646 mμ. These observations resembled those in the case of the boehmite similarly treated, which the authors already referred to.

The bayerite was made thoroughly free from alkali by immersing it at first in hydrochloric acid and then washing with water, because traces of the alkali, which could not have been removed from the bayerite by an ordinary washing with water, might be expected to cause alterations in the luminescence spectrum of the impregnated samarium. Some experiments similar to those described above were carried out with this purified bayerite. Samarium was added to this sample, which was subsequently calcined at 1000, 1100 and 1200°C respectively. Only a broad band with its intensity-maximum at 601 mμ, the most intense luminescence band of prototype I was seen in the case of the sample calcined at 1000°C (Fig. 3, d). A number of weak luminescence bands appeared, in addition to the intense band near 600 mμ, when the temperature of heat treatment had been raised, namely bands at 608, 614 and 619 mμ were seen with the sample treated at 1100°C, and bands at 608, 614, 619, 624, 637 and 648 mμ with that at 1200°C (Fig. 3, e). The sample roasted in a direct flame of coal gas mixed with oxygen gave a peculiar luminescence spectrum under cathode-ray bombardment (Fig. 3, f). This luminescence spectrum implied, besides several bands characteristic to the prototype II, three bands situated at 596.5, 643.5 and 564 mμ. The first of these was the most intense band of prototype III, but the latter two were proved to be smaller in the wave-length as compared with the corresponding bands of prototype I.

According to Stumpf et al.[7] the sequence

of thermal transformation from the bayerite to α-alumina is as follows: Bayerite→boehmite→η-alumina→θ-alumina→α-alumina. The θ-α transformation, namely a transition from a well-crystallised anhydrous alumina of cubic close-packed oxygen network to that of hexagonal one, is said to take place at 1210–1260°C, but the transition curve between θ- and α-alumina was indicated by these investigators as a dotted line in their Fig. 6 (a), which means probably a complicacy of this transition, corresponding exactly to the present authors' observation on the complicated feature of the cathodo-luminescence spectrum of samarium as mentioned above.

Stumpf and others[7,17] stated that the bayerite commences to be dehydrated at 160–200°C, is converted to the boehmite at 250–270°C and becomes nearly anhydrous alumina at 470–500°C.

Stumpf[7] as well as Thibon[8] postulated an intermediate formation of the boehmite in the way of transition from the bayerite to anhydrous alumina, while Tertian[18] concluded that the boehmite was sometimes not formed. Sato[19] arrived at the same conclusion as that of Tertian from a differential thermal analysis. According to Day[13] the formation of the boehmite is of a secondary nature in this case. Anhydrous aluminas intermediately yielded during thermal decomposition of the bayerite to the α-alumina were formerly considered exclusively as γ-modification, but they have afterwards been subdivided into two[7] (η and θ) or three phases[13] (γ, δ and θ) from the results of X-ray investigations.

The present authors have prepared the boehmite and the η-alumina by thermal decomposition of the bayerite at 230–270 and 900°C respectively. The former is a poorly crystallised form of alumina-monohydrate, and the latter is an extremely poorly crystalline γ-modification of alumina. Samarium ions imbedded in the intermediately produced boehmite and anhydrous alumina having such a low degree of crystallinity are always found to give a cathodo-luminescence spectrum of prototype I, so far as these samarium-bearing samples of boehmite and anhydrous alumina have been treated over a blast flame of coal gas mixed with air (Fig. 3, g), but the cathodo-luminescence spectrum changes clearly to prototype II, after these samples have been calcined intensely in a direct flame of coal gas-oxygen.

4) On Alumina derived from Bayerite, which is produced on Amalgamated Aluminium.—The bayerite can also be prepared in another way, namely by the action of water on an amalgamated aluminium[1]. This sample was dried at 110°C, and samarium was added to it. The samarium-bearing bayerite thus yielded was subjected to heat treatments.

The resulting alumina gave, after being heated over a blast flame of coal gas mixed with air, luminescence bands of prototype I accompanied by those of prototype II of low intensity under cathode-ray bombardment (Fig. 4, a), while that roasted much more

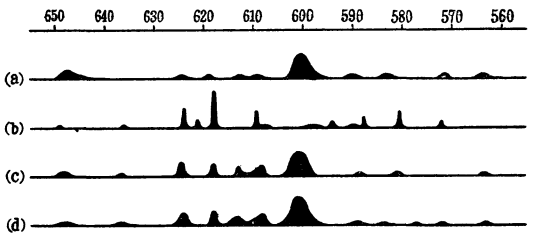

Wave-length (in mμ)

Fig. 4. Schematic representation of cathodo-luminescence spectrum of samarium-bearing alumina derived from bayerite, which was produced by action of water on amalgamated aluminium.

intensely in a direct flame of coal gas mixed with oxygen, exhibited those of the genuine prototype II (Fig. 4, b). Thermal transitions may reasonably be expected to have proceeded more simply and more readily in this case than in the before-mentioned cases of the bayerite and the boehmite, which were prepared in a solution of sodium aluminate, since the present preparation of the bayerite has been carried out free from alkali.

Partial decomposition was previously caused by submitting this sample of the bayerite to heat treatment at various temperatures; 200, 400 and 600°C. These intermediately decomposed products were soaked in the solution of samarium nitrate and then heated moderately over a blast flame of coal gas-air for 1 hour. In Fig. 4, (c) and (d) show cathodo-luminescence spectra for two of these samarium-bearing alumina, namely when heated previously at 200 and 400°C respectively. These luminescence spectra were found to be always of the prototype I overlapped by luminescence bands of the prototype II, no matter at what stages of decomposition samarium had been added.

It is to be noted that two bands are perceptible side by side at 608 and 613 mμ in an immediate vicinity of the spectral region of 610 mμ in the luminescence spectra given

17) A.S. Russell and C.N. Cochran, *Ind. Eng. Chem.*, **42**, 1339 (1950).
18) R. Tertiane et D. Papee, *Compt. rend.*, **236**, 1565 (1953).
19) T. Sato, *J. Chem. Soc. Japan (Ind. Chem. Sect.)*, **55**, 66 (1952); **56**, 478 (1953).

by the samarium-bearing γ-alumina, as shown in Fig. 4, (c) and (d), prior to the appearance of an intense luminescence band at 609 mμ belonging to the α-alumina. So far as a final heat treatment was carried out over a blast flame of coal gas mixed with air, luminescence bands of prototype II are seen much more distinctly in the cases of samples of alumina, to which samarium was added at the intermediate stages of thermal decomposition, than in the cases of those, to which samarium was added directly to the dried original bayerite. It is thus confirmed that the heating over a blast flame of coal gas-air does not convert these samples of the bayerite completely to the genuine α-alumina. A much higher temperature is needed for this transition, namely 1260 or 1300°C, as already reported by Stumpf[7] and Day[20] respectively. A cathodoluminescence spectrum of the pure prototype II was in fact given by partially decomposed products resulting from the calcination of the bayerite at 400 and 600°C, when these products had been treated in a coal gas-oxygen flame after the impregnation of samarium.

Summary

Investigations were carried out on cathodoluminescence spectra of samarium ions imbedded in alumina, which had been derived from bayerite and boehmite. The mode of thermal transformation of these alumina was concluded from the spectrographic results mentioned above.

A conversion to anhydrous alumina different from α-modification, presumably to β- or ζ-modification, occurred owing to the effect of the contaminating alkali minutely present, when this alumina was derived from calcination of either boehmite or bayerite, each of which had been produced in a solution of sodium aluminate.

The bohemite and the bayerite, purified thoroughly from the alkali, as well as those prepared in the absence of the alkali are readily converted to α- through γ-modification of alumina by thermal treatments.

The heating of the bayerite obtained through rapid carbonation of a solution of sodium aluminate is not, however, likely to result in a simple γ-α transformation of alumina even when the alkali has been removed by careful washing.

This research has been financed by the Scientific Research Encouragement Grant of the Ministry of Education, to which the authors' thanks are due.

The Scientific Research Institute Ltd.,
Komagome, Bunkyo-ku, Tokyo

20) M.K.B. Day and V.J. Hill, *J. Phys. Chem.*, **57**, 948 (1953).

Cathodo-luminescence of Samarium as Applied to the Structural Studies of Alumina. IV. On Alumina yielded by Thermal Decomposition of Hydrated Crystals of Aluminium Salts

By Eiichi IWASE and Seijiro NISHIYAMA

(Received May 16, 1955)

Introduction

Thermal decompositions of aluminium salts, such as aluminium nitrate, ammonium alum and others come frequently into consideration for the practical preparation of alumina, particularly free from silica. Crystals of hydrated aluminium nitrate, hydrated aluminium sulphate and ammonium alum are, on being heated, dissolved in their water of crystallisation; they intumesce, lose volatile constituents and produce alumina as residue, while hexahydrated crystals of aluminium chloride are decomposed to anhydrous alumina without melting.

The present authors have applied cathodo-luminescence spectrum of samarium to elucidate the thermal decomposition process of some hydrated aluminium salts.

Samarium-bearing samples of alumina have been prepared from the aluminium salts either by thermal decomposition in the presence of samarium or by the introduction of samarium into decomposition products, which were yielded through suitable thermal treatments of hydrated aluminium salts. Luminescence

spectra given by these samples of alumina have been investigated under cathode-ray excitation and the results are reported in the present paper.

Experimental results and discussions relating to them are described separately on samples of alumina, according to different combinations of the procedures for the imbedment of samarium and those for the thermal decomposition.

1) On Alumina derived from Calcination of Hydrated Crystals of Aluminium Salts, to which Samarium was previously added

Experimental Procedure

As much as 2.7, 1.7 and 2.0 ml. of a 1% aqueous solution of samarium nitrate was directly added to each 10g. of crystals of aluminium nitrate enneahydrate, aluminium sulphate octodecahydrate and aluminium chloride hexahydrate respectively, which were subsequently calcined at a certain temperature between 800 and 1000°C, or in a direct flame of coal gas mixed with oxygen. The quantity of the samarium nitrate solution to be added was so chosen that samarium calculated as oxide would amount approximately to 1% for the resulting alumina. Luminescence spectrograms of these samarium-bearing aluminas were taken under the excitation by cathode-rays and are schematically shown in Figs. 1—3. A superior quality of alumina has hitherto been prepared very often by a calcination of ammonium alum[1], since the alum can readily be purified through repeated crystallisations in an aqueous solution. A series of experiments similar to those mentioned above has been carried out on alumina derived from the ammonium alum, and the results are given in Fig. 4.

Results and Discussion

The cathodo-luminescence spectrum tends to vary from the prototype I to the prototype II, as the calcination temperature has been elevated, and the samples of alumina produced by the calcination at moderately high temperatures yield cathodo-luminescence spectra of the prototypes I and II overlapped with each other. An alumina, produced by calcining the hydrated crystals of aluminium nitrate at 800°C in the presence of samarium, gives a cathodo-luminescence spectrum of the typical prototype I, as shown schematically in Fig. 1, (a). Luminescence bands belonging to the prototype II, namely bands at 609, 618 and 624 mμ, commence to appear after the alumina was heated at about 900°C (Fig. 1, b) and become fairly intense after heated at 950°C (Fig. 1, c). Its luminescence spectrum changes almost completely to the prototype II, when the sample of alumina was

1) For example A., ℃2043743.

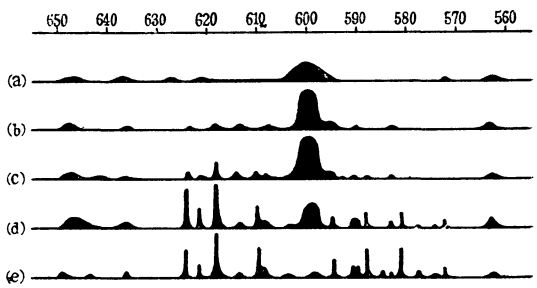

Wave-length (in mμ)

Fig. 1. Schematic representation of cathodo-luminescence spectrum given by samarium-bearing alumina, which was derived from calcination of aluminium nitrate enneahydrate in the presence of samarium.

Calcination was made at 800, 900, 950, 1000°C and in coal gas-oxygen flame for (a), (b), (c), (d) and (e) respectively.

calcined at 1000°C, but a diffuse luminescence band with the intensity-maximum at about 600 mμ, a characteristic one to the prototype I, still remains (Fig. 1, d). With the increased calcination temperature, two cathodo-luminescence bands become at first perceptible at 608 and 613 mμ, in a spectral region around 610 mμ, before a transition from the prototype I to the prototype II sets in, and a band at 609 mμ begins subsequently to appear, is increased rapidly in its intensity and at last surpasses the intensity of the above two bands (compare Fig. 1, b, c and d).

Fig. 2, (a) and (b) show schematically the cathodo-luminescence spectra given by the samarium-bearing aluminas, which were prepared in the presence of samarium through the calcination of the hydrated aluminium sulphate at 800 and 900°C respectively, while Fig. 3, (a) illustrates that of a samarium-

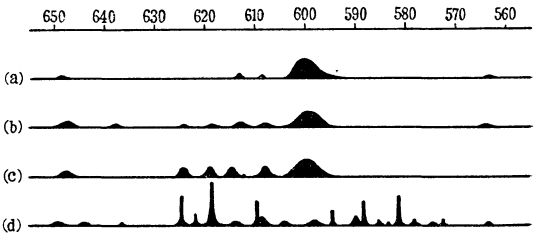

Wave-length (in mμ)

Fig. 2. Schematic representation of cathodo-luminescence spectrum given by samarium-bearing alumina, which was derived from calcination of aluminium sulphate octodecahydrate in the presence of samarium.

Calcination was made at 800, 900, 1000°C and in coal gas-oxygen flame for (a), (b), (c) and (d) respectively.

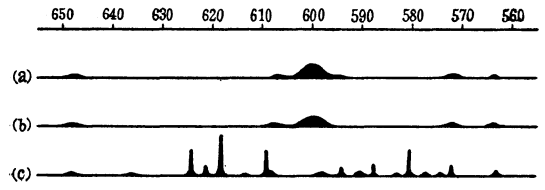

Wave-length (in mμ)

Fig. 3. Schematic representation of cathodo-luminescence spectrum given by samarium-bearing alumina, which was derived from calcination of aluminium chloride hexahydrate in the presence of samarium.
Calcination was made at 800, 1000°C and in coal gas-oxygen flame for (a), (b) and (c) respectively.

bearing alumina derived similarly by treating the hydrated aluminium chloride at 800°C.

The aluminas derived by the roasting from the hydrated aluminium sulphate and the hydrated aluminium chloride, undergo a transition toward α-modification with difficulty. To get the cathodo-luminescence spectrum of the prototype II is hardly possible, so far as the temperature of the calcination has not exceeded 1000°C (Fig. 2, c and Fig. 3, b), but it is attained through roasting in a direct flame of coal gas mixed with oxygen (Fig. 2, d and Fig. 3, c).

In the before-mentioned case of the alumina derived from the hydrated aluminium nitrate, the cathodo-luminescence spectrum of this prototype II was, however, seen in its fairly complete form, being overlapped with luminescence bands of the prototype I, after treated at 950°C (Fig. 1, c).

It might reasonably be presumed that proper structural transitions would, in some respects, be disturbed when the hydrated aluminium salts are thermally decomposed in the presence of foreign ions, namely samarium ions in the present case. This anticipation is realized by the observation that there appears an intermediate stage of alumina capable of showing luminescence bands at 608 and 613 mμ, but wanting a band at 609 mμ in its cathodo-luminescence spectrum (Fig. 1, b, Fig. 2, a, b and c).

Finally, crystals of ammonium alum were calcined over a blast flame of coal gas-air. Samarium was added to the resulting product and then the calcination was repeated over the blast flame. The cathodo-luminescence spectrum given by this sample of samarium-bearing alumina was found to consist mainly of the prototype I, accompanied by some luminescence bands of the prototype II situating at 588, 609, 618 and 624 mμ (Fig. 4, a).

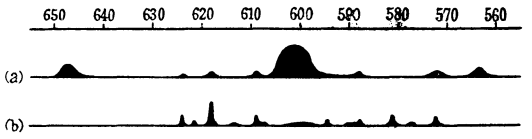

Wave-length (in mμ)

Fig. 4. Schematic representation of cathodo-luminescence spectrum given by samarium-bearing alumina, which was derived from calcination of ammonium alum in the presence of samarium.
Calcination was made in coal gas-air and coal gas-oxygen flames for (a) and (b) respectively.

According to Gorbunova[2], alumina obtained by calcination of ammonium alum at about 1100°C consists exclusively of γ-modification, and the transformation of the γ- to α-modification starts at 1150 or 1155°C, while Rinne[3] stated that the resulting alumina is composed of the γ-modification so long as the calcination temperature of ammonium alum is maintained below 1220°C. For a completion of the γ-α transformation, ammonium alum should be roasted above 1220°C according to Gorbunova[2], and it should be roasted at 1300°C according to Guseva[4]. However, the cathodo-luminescence spectrum of samarium indicates that the alumina derived from the calcination of ammonium alum is composed of the γ-modification mixed with some amounts of the α-modification, although the calcination has been made at a temperature far below that necessary for the yielding of the γ-α transformation.

The samarium-bearing alumina mentioned above gives, after being calcined strongly in a direct flame of coal gas-oxygen, a cathodo-luminescence spectrum of the genuine prototype II (Fig. 4, b), and thus the complete transformation toward the α-modification is now surely attained.

2) On the Alumina yielded in the Presence of Samarium through Calcination of Primarily Decomposed Products of Various Aluminium Salts

Experimental Procedure

Hydrated crystals of aluminium salts were heated at appropriate temperatures and the solution of samarium nitrate was added to resulting masses, which were then dried at 110°C and ignited over a blast flame of coal gas-air in order to ensure the expellation of volatile matters. Previous heat treatments prior to the introduction

2) O.E. Gorbunova and L.I. Vaganova, *Khim. Referat. Zhur.*, 2, 31 (1939); *C.A.*, 34, 2228 (1940).
3) F. Rinne, *Neues Jahrb. Mineral. Geol. Beilage Bd. A*, 58, 43 (1928).
4) P.G. Guseva and A.S. Ivanov, *Khim. Referat. Zhur.*, 2, 85 (1939); *C.A.*, 34, 3025 (1940).

of samarium, were made at 180, 500 and 700°C with crystals of aluminium nitrate enneahydrate, at 500, 700, 1100 and 1200°C with those of aluminium sulphate octodecahydrate, and at 200, 550, 1000 ond 1200°C with those of aluminium chloride hexahydrate respectively. These products were soaked with the solution of samarium nitrate and converted to anhydrous alumina by ignition over a blast flame of coal-gas mixed with air. The samples of samarium-bearing alumina thus prepared were subjected to cathode-ray bombardment, and spectrograms of the luminescence are schematically illustrated in Figs. 5–7.

Results and Discussion

It is concluded from the investigations on cathodo-luminescence spectra shown in Figs. 5–7 that, irrespective of the same final heat treatment at a comparatively low temperature, considerable distinctions are seen in the feature of the samarium-luminescence spectrum, depending upon the kinds of starting hydrated aluminium salts and the mode of their previous heat treatments. The configuration of the alumina giving rise to the luminescence prototype II, namely the α-alumina structure, seems to be much more readily produced by thermal decomposition of aluminium nitrate enneahydrate than by that of aluminium sulphate octodecahydrate and of aluminium chloride hexahydrate.

According to Parravano[5] three waters of crystallisation were, on the heating of aluminium nitrate enneahydrate, expelled at 73.5°C and the resulting hexahydrate, $Al(NO_3)_3 \cdot 6H_2O$ changed then to a basic salt, $4Al_2O_3 \cdot 3N_2O_5 \cdot 14H_2O$ at 140°C. This basic salt was decomposed to anhydrous alumina at 200°C.

The decomposition of the hydrated aluminium nitrate is now found to proceed as far as 86% by a previous heat treatment at 180°C, namely 20°C below the temperature necessary for the production of anhydrous alumina. This partially decomposed product exhibits, after being mixed with the solution of samarium nitrate and ignited over a blast flame of coal gas-air, such a cathodo-luminescence spectrum as an overlap of the prototypes I and II, in which bands of the former prototype are remarkably intense (Fig. 5, a).

A conversion to the anhydrous alumina was already completed, when a previous heat treatment had been carried out at 500°C. Samarium was introduced into this decomposed product, which was then subjected to a final heating over a blast flame of coal gas-air. The cathodo-luminescence spectrum given by this sample was almost entirely of the prototype II (Fig. 5, b).

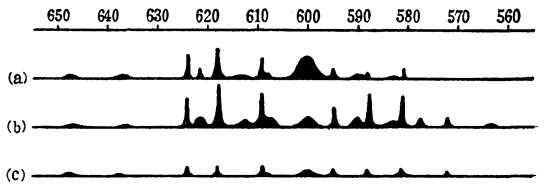

Wave-length (in mμ)

Fig. 5. Schematic representation of cathodo-luminescence spectrum given by samarium-bearing alumina, which was derived from calcination of aluminium nitrate enneahydrate.
Temperature of previous heating prior to the introduction of samarium was 180, 500 and 700°C for (a), (b) and (c) respectively. Final heat treatment was all made in a coal gas-air flame.

On heating octodecahydrated crystals of aluminium sulphate, anhydrous sulphate was formed at about 460°C[6], and this was decomposed to alumina and sulphuric oxide gas at much more elevated temperatures, for which various numerical figures were presented, namely 650~850°[6], 760°[5] and 850~900°C[7].

Samarium was added to anhydrous aluminium sulphate yielded by a previous heat treatment of the hydrated aluminium sulphate at 500°C. A samarium-bearing alumina derived by heating this product over a blast flame of coal gas-air gives a cathodo-luminescence spectrum of the typical prototype I (Fig. 6, a).

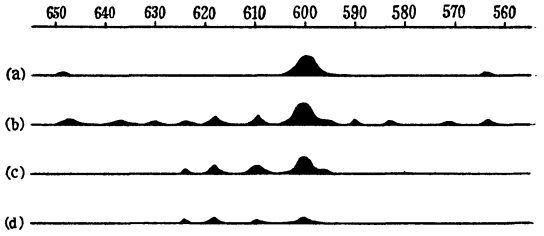

Wave-length (in mμ)

Fig. 6. Schematic representation of cathodo-luminescence spectrum given by samarium-bearing alumina, which was derived from calcination of aluminium sulphate octodecahydrate.
Temperature of previous heating prior to the introduction of samarium was 500, 700, 1100 and 1200°C for (a), (b), (c) and (d) respectively. Final heat treatment was all made in a coal gas-air flame.

5) N. Parravano and G. Malquori, *Atti II congresso naz. chim. pura applicata*, **1926**, 1131; *C.A.*, 22, 2119 (1928).

6) Y. Asada, *Bull. Inst. Phys. Chem. Reseach*, Tokyo, **17**, 1308 (1938).

7) S. Bretsznajder, *Przemyst Chem.*, 22, 285 (1938); *C.A.*, 33, 3974 (1939).

When a heat treatment prior to the introduction of samarium has been made at 700°C, a partially decomposed basic aluminium sulphate is probably produced. The samarium-bearing alumina obtained by roasting this product over a blast flame of coal gas-air, shows feeble luminescence bands of the prototype II in addition to fairly intense luminescence bands of the prototype I (Fig. 6, b). This means that the above-mentioned sample of alumina consists of a mixture of the γ- and α-modifications, although Day[8] stated that the alumina obtained by calcining the hydrated crystals of aluminium sulphate at 1000°C is wholly the pure γ-modification. It is to be mentioned that a complete disappearance of luminescence bands of the prototype I is not attained even by intense heat treatments at 1100 and 1200°C in the case of aluminium sulphate octodecahydrate (Fig. 6, c and d).

When aluminium chloride hexahydrate is heated, it decomposes without melting[9].

According to Parravano[5], the thermal decomposition curve of aluminium chloride hexahydrate showed breaks at 122° and at 180°C, the latter corresponding to a decomposition to anhydrous alumina.

The resulting samarium-bearing alumina gives always the cathodo-luminescence spectrum of the prototype I (Fig. 7, a), when

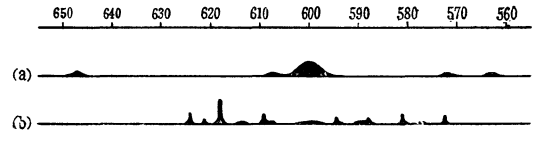

Fig. 7. Schematic representation of cathodo-luminescence spectrum given by samarium-bearing alumina, which was derived from calcination of aluminium chloride hexahydrate.
Temperature of previous heating prior to the addition of samarium was 550~1000 and 1200°C for (a) and (b) respectively. Final heat treatment was all made in a coal gas-air flame.

hexahydrated crystals of aluminium chloride was previously calcined at a temperature between 200 and 1000°C, and then soaked with the solution of samarium nitrate, followed by ignition over a blast flame of coal gas-air, while that previously calcined at 1200°C and then treated in a similar way shows the cathodo-luminescence spectrum of the pure prototype II (Fig. 7, b).

Finally, samarium was introduced into decomposed products obtained by previous thermal treatments of crystals of ammonium alum at temperatures below 1200°C. When final heat treatment on these samarium-bearing samples had been made at a comparatively low temperature, namely over a blast flame of coal gas-air, the pure prototype I of the cathodo-luminescence spectrum was always seen. However, a transition to the pure prototype II took place in the cathodo-luminescence spectrum, if the temeperature of this heat treatment had been much more raised by using a direct flame of coal gas mixed with oxygen.

The foregoing studies on the cathodo-luminescence spectrum of samarium have revealed that the thermal decomposition to the α-alumina proceeds most readily for aluminium nitrate enneahydrate, and with difficulty for aluminium sulphate octodecahydrate and ammonium alum. The cathodo-luminescence of samarium is, in general, very weak for the alumina previously heated at considerably elevated temperatures as can be seen from a comparison of Fig. 5, (b) with (c), and from that of Fig. 6, (c) with (d) respectively. From these observations a conclusion might be drawn that it is likely to be difficult for samarium to enter into the configuration of an intensely calcined alumina.

Summary

Hydrated crystals of some aluminium salts, namely nitrate, chloride, sulphate and ammonium alum were subjected to heat treatments in the presence of a small amount of samarium ions. Cathodo-luminescence spectra were investigeted on the samarium-bearing aluminas thus resulted. A conversion of the luminescence spectrum takes place, as the temperature of the heat treatment has been elevated, from the prototype I to the prototype II, which corresponds to the γ-α transformation of an alumina. It was, however, confirmed that there are some differences in the facility of this conversion according to the kinds of aluminium salts employed for the preparation of alumina.

Some alterations were, furthermore, perceived in the intensity of luminescence bands situating in the vicinity of 610 mμ, when the hydrated crystals of aluminium nitrate were submitted to the heat treatments of various elevated temperatures.

Hydrated crystals of these aluminium salts were heated previously at various temperatures between 180 and 1200°C. After the addition of samarium ions, they were roasted.

8) M.K. Day and V.J. Hill, *J. Phys. Chem.*, 57, 950 (1953).

9) J.W. Mellor, "A Comprehensive Treatise on Inorganic and Theoretical Chemistry", Longmans & Co., London (1924), 5, p. 316.

The resulting samarium-bearing aluminas give rise to cathodo-luminescence spectra, which reveal that a conversion to the genuine α-modification proceeds most readily in the case of aluminium nitrate, while it occurs with difficulty in the cases of hydrated aluminium sulphate and ammonium alum. It seems to be hard for samarium ions to enter into the configuration of alumina, when previous thermal treatments of aluminium salts have been carried out at much elevated temperatures.

This research has been financed by the Scientific Research Encouragement Grant of the Ministry of Education, to which the authors' thanks are due.

The Scientific Research Institute, Ltd,
Komagome, Bunkyo-ku
Tokyo

Cathodo-luminescence of Samarium as Applied to the Structural Studies of Alumina. V. On Alumina Derived from Hydrargillite by Thermal Treatments

By Eiichi IWASE and Seijiro NISHIYAMA

(Received June 13, 1955)

Introduction

As is well known, hydrargillite is a stable form of alumina-trihydrate and is obtained as an industrial product of Bayer process through slow hydrolysis of sodium aluminate solution. Its thermal dehydration and transformation have been studied by numbers of investigators, since these are important problems from a practical point of view.

Mechanisms regarding thermal dehydration and transformation of the hydrargillite to α-alumina are very complicated. It has, until quite recently, been presumed that the thermal decomposition of the hydrargillite occurs through a singular consecutive sequence[1]. A dual series of thermal transformation of the hydrargillite has, however, been postulated by Brown[2] and Day[3].

The present authors have applied a technique of the cathodo-luminescence spectrum of samarium to the investigations on the feature of the thermal decompositions of the hydrargillite. The results obtained and some interpretations relating to them are given in this paper.

Experimental

For the purpose of removing as much as possible of the remaining alkali, the sample of hydrargillite obtained by Bayer process was treated as follows; it was at first immersed in hydrochloric acid, washed with water, and then dried at 110°C. Experimental results are described separately in two parts, according to the degree of thermal decomposition of the purified hydrargillite prior to, and the calcination temperature after the addition of samarium, which acts as an activator for causing cathodo-luminescences.

1) On the Samarium-bearing Alumina derived from Calcination of Pydrargillite, at its dried State Samarium Being added Initially.—One ml. of 1% samarium nitrate solution was added directly to each 1 g. of the purified hydrargillite mentioned above, which was then calcined either at a temperature between 750 and 940°C or in a direct flame of coal gas mixed with oxygen. These samarium-bearing aluminas were exposed to the action of cathode-rays and the luminescence brought about was spectrographically investigated by employing a glass-prism spectrograph of Feuss.

Luminescence bands of the prototype II[4] become much more distinct, being accompanied with bands of the prototype I[4], as calcination has been made at a more elevated temperature. Variations in the feature of the cathodo-luminescence spectrum are related with the temperature of one hour's heat treatment as follows; bands of the prototype II commence to appear with a sample, which has been subjected to a heat treatment at about 750°C. and these bands become considerably more intense with that at 850°C. Luminescence bands of the prototype I remain unaltered, so far as the calcination temperature of the sample has not exceeded 940°C. The sample gives cathodo-luminescence bands of the genuine prototype II, without being accompanied by any band of the prototype I, after being heated at a greatly elevated temperature,

1) For example, H.C. Stumpf, A.S. Russell, J.W. Newsome, and C.M. Tucker, *Ind. Eng. Chem.*, **42**, 1398 (1950).

2) J.F. Brown, D. Clark and W.W. Elliott, *J. Chem. Soc.*, **1953**, 84.

3) M.K.B. Day and V.J. Hill, *Nature*, **170**, 539 (1952); *J. Phys. Chem.*, **57**, 946 (1953).

4) E. Iwase, This Bulletin, **28**, 596 (1955).

namely in a direct flame of coal gas mixed with oxygen. The structural change from an alumina giving rise to the cathodo-luminescence bands of the prototype I into that of the prototype II, corresponds to a transformation between the so-called γ- and α- modifications of alumina. A ready and gradual γ-α transformation is supposed to take place with the increasing temperature, when the dried original sample of the hydrargillite has been subjected to a calcination in the presence of samarium.

2) On the Samarium-bearing Alumina prepared from Hydrargillite by Calcination of its thermally Decomposed Products, to which Samarium was added.—The hydrargillite purified as already mentioned was previously treated at certain temperatures between 150 and 1200°C. The heating duration was one hour for the temperature range between 150 and 850°C, and fifteen minutes for that between 900 and 1200°C, unless otherwise stated. Samarium was added to each of these thermally treated samples, which was afterward ignited over a blast flame of coalgas-air for one hour to ensure the expellation of volatile constituents. Such constituents, if present, would hinderthe appearance of luminescence under the excitation by cathode rays. Cathodo-luminescence spectra given by these samples of samarium-bearing alumina are summarised schematically in Fig. 1 and reproduced in Fig. 2, in order to facilitate mutual comparisons.

It is seen from Figs. 1 and 2 that previous heat treatments of the hydrargillite bring about extremely marked effects on the cathodo-luminescence spectrum of samarium. Bands of the prototype II can be seen accompanied by bands of the prototype I in the case of the samples previously heated at certain temperatures between 150 and 230°C (Fig. 1, a). This luminescence spectrum is identical with that given by the hydrargillite treated as follows; the purified original hydrargillite was soaked with the solution of samarium nitrate and ignited over a blast flame of a mixture of coal gas and air. Luminescence bands belonging to the prototype II are, on the whole, reduced in intensity with a result of the complete lack of some bands, for example a band at 574 mμ, and a broad diffuse band of the prototype I with its peak at 600 mμ is also much weakened. when a previous heat treatment has been made at 250°C for one hour (Fig. 1, b). It is worth mentioning that an intense band at 597 mμ characteristic of the prototype III[4] becomes now extremely intense. A new band is observed at 644 mμ, very near a band at 648 mμ, and there also begin to appear two bands at 561 and 562.5 mμ in place of a diffuse band at 563 mμ.

When the duration of heat treatment at 250°C has been increased from one to five hour, the cathodo-luminescence spectrum changes markedly (Fig. 1, c): Bands situating at 561, 562.5, 612 and 644 mμ becomes much more distinct, several new bands are perceptible at 566, 568, 601.5 and 615.5 mμ, and the intensity maximum of a band lying between two bands at 618 and 624 mμ seems to be slightly shifted, namely from 621 to 620 mμ. As to a set of three bands around a spectral region of 610 mμ, a sudden reversal is brought about in the order of intensity, when the duration of heating at 250°C has been lengthened (Fig. 1, c); the weakest band at 612 mμ grows now considerably intense, and a feeble band at 610 mμ is detectable instead of a band at 609 mμ, namely the most intense band among the above three given by the sample, which was previously treated at a lower temperature. The feature of the luminescence spectrum thus obtained seeems characteristic of intermediate products of the thermal decomposition of the hydrargillite. This luminescence spectrum was already designated as the prototype III by one of the present authors[4] and was distinguished from the well-defined prototypes I and II. The luminescence prototype III is always seen with the samples of the hydrargillite, which have been subjected to a previous heat treatment at any temperature above 250 and below 900°C (Fig. 1, c). The structure of the alumina giving rise to this particular cathodo-luminescence spectrum, when once formed, is extremely persistent in the case of an intense heat treatment and remains unaltered after being heated at a temperature as high as 1200°C for fifteen minutes. However, when this samarium-bearing sample of alumina has been roasted intensely in a direct flame of coal gas mixed with oxygen, it gives distinctly the cathodo-luminescence spectrum of the prototype II owing to the corundum structure of the alumina, but a band situated at 597 mμ, namely the strongest and the most characteristic band of the prototype III, still remains intense in this spectrum.

Some changes occur in the cathodo-luminescence spectrum, if the sample of the hydrargillite has been submitted to an initial heat treatment exceeding 950°C. These changes might be ascribed to the fact that the temperature of the initial heat treatment has been higher than that of the final heating over a blast flame of coal gas mixed with air. Through heat treatments at 950 and 1000°C for fifteen minutes (Fig. 1, d), four bands at 605.5, 608, 610 and 612 mμ become almost equal in intensity, and this is also the case with two bands situated at 561 and 563 mμ.

In the case of a sample previously heated at 1050°C (Fig. 1, e), two bands at 566 and 568 mμ disappear, three bands at 618, 621 and 624 mμ may be arranged in a sequence of intensity just like in the cathodo-luminescence spectrum of the prototype II, and the same relation holds with the three bands at 607–8, 609 and 612 mμ. All the bands lying in a spectral region between 560 and 597 mμ become fairly weakened.

No remarkable differences are found in luminescence spectra given by the samples, which have been previously heated at 1050 and 1100°C respectively, except that two bands at 561 and 562.5 mμ appear jointly in the luminescence spectrum of the latter sample (Fig. 1, f).

A band situated at 597 mμ is greatly reduced in its intensity and overlaps with a diffuse band at 600 mμ in the case of a sample heated previously at 1150°C (Fig. 1, g). A band at 594 mμ begins

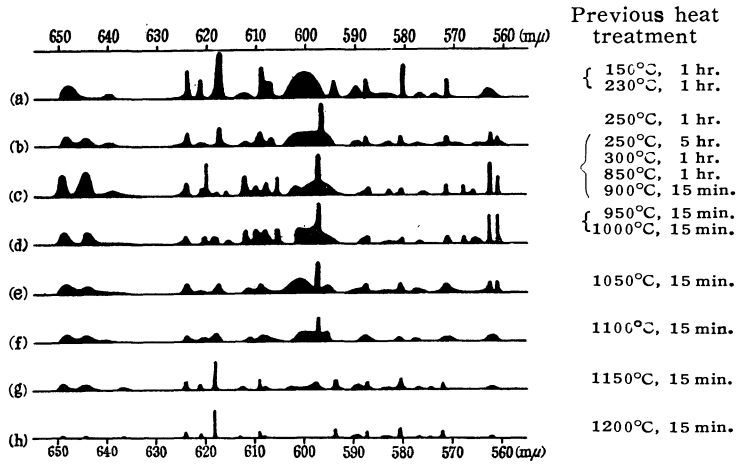

Fig. 1. Schematic representation of cathodo-luminescence spectra given by samarium bearing aluminas, which were derived from hydrargillite through previous heat treatments at various temperatures, followed by soaking with samarium nitrate solution and then roasting over blast flame of coal gas-air.

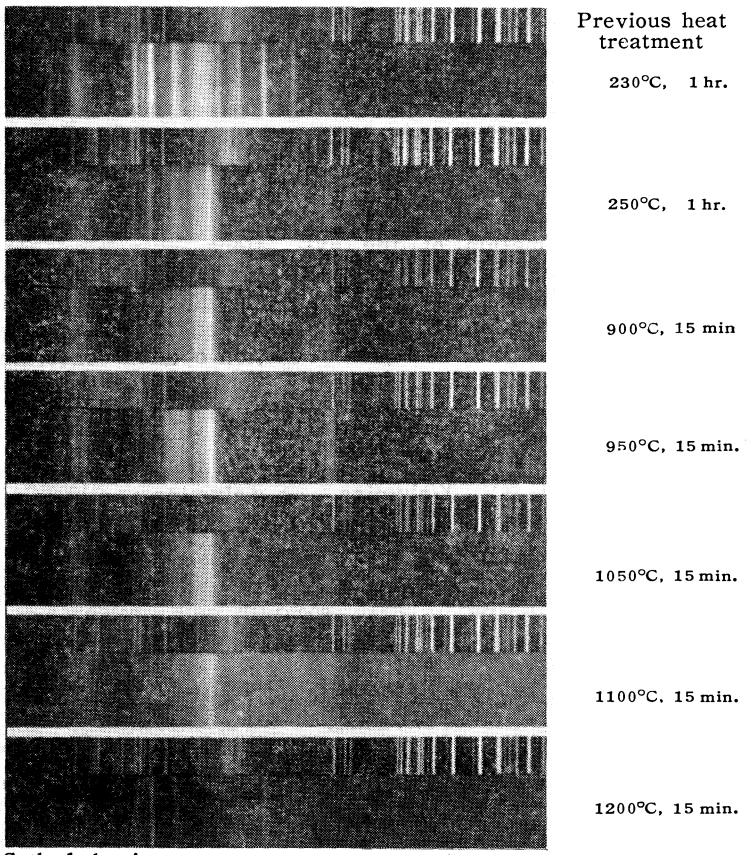

Fig. 2. Cathodo-luminescence spectrograms of samarium-bearing aluminas derived from hydrargillite by subjecting previously to various heat treatments prior to the addition of samarium, final heat treatment being made over a blast flame of coal gas-air. Spectral lines of iron-arc are taken for reference.

to appear distinctly and another band at 618 mμ becomes now the most intense one in this luminescence spectrum. Thus the luminescence spectrum is transformed entirely to the prototype II.

Finally, the circumstances are quite the same in a sample previously roasted at 1200°C (Fig. 1, h) as in that at 1150°C.

An alumina is completely transformed to α-modification through an intense initial heating at temperatures higher than 1150°C prior to the addition of samarium. This may be comfirmed by the fact that a luminescence spectrum of samarium imbedded in the above-mentioned alumina is the pure prototype II.

Discussion

First of all, the chief views hitherto set forth are briefly surveyed on thermal transformations from the hydrated to the anhydrous alumina. The view has, until quite recently, been accepted that the hydrargillite is thermally decomposed through a singular sequence of consecutive transformations. The hydrargillite dehydrates, on being heated, to boehmite, which passes on further calcination to stable α-alumina through numbers of intermediate modifications termed collectively as γ-alumina[5]. This γ-alumina was separated into two or more phases as the results of close examinations on X-ray diffraction patterns; two phases were differentiated by Tertian[6], Thibon[7], and Prettre[8], three phases by Rooksby[9], Thibon[7], and Funaki[10], and four phases by Frary[11], and Stumpf[12].

The thermal transformation of the hydrargillite to the α-alumina proceeds, according to Stumpf's studies[13] on Debye diffraction patterns, through the following singular consecutive sequence.

Hydrargillite→boehmite→χ-alumina→γ-alumina→κ-alumina→θ-alumina→α-alumina (χ-, γ-, κ-, and θ-alumina were formerly termed as γ-alumina).

However, Day and Hill[3] have recently suggested that the boehmite is produced from the hydrargillite by means of a secondary reaction; the hydrargillite is at first decomposed directly into a virtually anhydrous alumina and water vapour during its thermal decomposition, and afterwards there results the boehmite by a subsequent reaction between these two primary products.

When a fluid phase is absent, transformations from the much hydrated to the anhydrous alumina are supposed to take place, during the heat treatment, locally in inner structures of the hydrated crystals with a limited opportunity for an atomic rearrangement. Definite transformation temperatures can consequently be assigned with difficulty, and the temperatures at the start and at the finish of the transformations extend usually over somewhat wide ranges, depending on the grain-size of the hydrated crystals and the manner of the heat treatment. Mixtures of products may thus result from the thermal dehydration and the thermal transformation of the hydrargillite, joining one product with the other in this transition sequence. Roosby[9] stated that κ-modification of alumina postulated by Stumpf and others[13] was really a mixture of κ- and θ-modifications, and Day and others[14] also explained that χ-modification was in fact composed of γ- and χ-modifications.

Contrary to the above-mentioned view of singular transformation series, Brown[2] assumed for the first time a dual transformation opinion concerning the thermal decomposition of the hydrargillite as represented by the following detailed scheme:

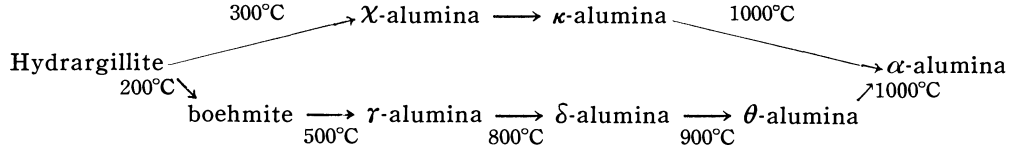

5) F. Haber, *Naturwissenschaften*, **13**, 1007 (1925); J.D. Edwards, F.C. Frary and Z. Jeffries, "Aluminum Industry, Aluminum and Its Production", New York, McGraw-Hill (1930), p. 166; R. Fricke und G.F. Huttig, "Handbuch der allgemeinen Chemie IX, Hydroxide und Oxyhydrate", Akademische Verlag, Leipzig, (1937); W. A. Lalande, W.S.W. McCarter and J. B. Sanborn, *Ind. Eng. Chem.*, **36**, 99 (1944); G. Feachem and H.T.S. Swallow, *J. Chem. Soc.*, **1948**, 267; R.J. Taylor, *J. Soc. Chem. Ind.*, **68**, 23 (1949); H. Remy, "Lehrbuch der Anorganischen Chemie", Bd. I, Akademische Verlag, Leipzig (1952), S. 308, 309; S.J. Gregg and K.S.W. Sing, *J. Phys. Chem.*, **56**, 388 (1952).

6) R. Tertian, *Compt. rend.*, **230**, 1677 (1950).

7) H. Thibon, J. Charrier et R. Tertian, *Bull. soc. chim. France*, [5], **18**, 385 (1951).

8) F. Blanchin, B. Imelik et M. Prettre, *Compt. rend.*, **236**, 1025 (1953); M. Prettre, B. Imelik, L. Blanchin und M. Petitjean, *Angew. Chem.*, **65**, 549 (1953).

9) H.D. Rooksby, "X-ray Identification and Crystal Structures of Clay Minerals", Mineralogical Society (1951), p. 244.

10) K. Funaki and Y. Shimizu, *J. Chem. Soc. Japan (Ind. Chem. Section)*, **56**, 53 (1953).

11) F.C. Frary, *Ind. Eng. Chem.*, **38**, 129 (1946).

12) H.C. Stumpf, A.S. Russell, J.W. Newsome and C.M. Tucker, *Ind Eng. Chem.*, **42**, 1398 (1950).

13) H.C. Stumpf, A.S. Russell, J.W. Newsome and C.M. Tucker, ibid, 1401, Fig. 5 (a).

14) M.K.B. Day and V.J. Hill, *J. Phys. Chem.*, **57**, 949 (1953).

15) G. Ervin, *Acta Cryst.*, **5**, 106 (1952).

The thermal dehydration and transformation of the hydrargillite occur through two series of routes before the α-alumina is produced, the one initially through the boehmite and then anhydrous aluminas, and the other directly through other anhydrous aluminas. His opinion is based mainly on the following significant facts. Firstly, the studies on X-ray diffraction patterns indicated that the disappearance of the hydrargillite agreed with the formation of the χ-alumina, and the amount of this χ-alumina remained unchanged for a while in the course of heating. Secondly, a differential thermal analysis gave a curve possessing three peaks; the first peak was due to the change from the hydrargillite to the boehmite, the second from the hydrargillite to the χ-alumina, and the third from the boehmite to γ-alumina respectively. Thirdly, the water content-ignition temperature curve for the hydrargillite showed an arrest in a range of temperature between 300 and 400°C, corresponding to the approximate composition of alumina-hemihydrate. The products in these states of decomposition consisted consequently of the monohydrated boehmite and the virtually anhydrous χ-alumina mixing in almost equal amounts.

There are some doubtful points as to whether or not each of these intermediate modifications of the alumina itself is really presumable to be a single phase[15]. According to Jellinek[16], the thermal transformation of the aulmina derived from calcination of the hydrargillite is a gradual process. This conception was expressed by Ervin[17] as a continuous transition from the disordered to ordered structure of alumina, and by Brown[2] as that from poorly crystallised to well crystallised alumina through a slow diffusion of aluminium ions into the lattice of oxygen ions.

The present authors have taken each 1 g. of the sample of the hydrargillite and heated it for five hours at certain definite temperatures respectively. The dehydration isobar thus obtained is illustrated in Fig. 3. This dehydration-isobar curve goes smoothly until a distinct arrest is observed at the composition of approximately $Al_2O_3 \cdot 0.7H_2O$. The

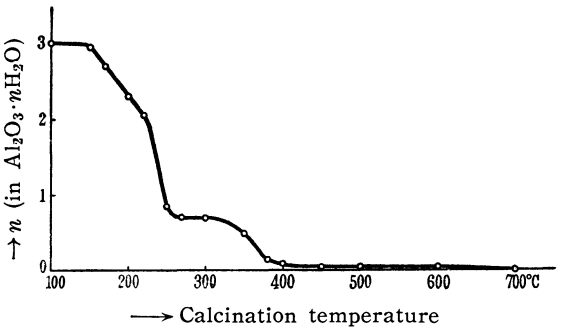

Fig. 3. Dehydration-isobar curve of hydrargillite.

composition corresponding to this arrest was, however, $Al_2O_3 \cdot 0.5H_2O$ according to Brown[18] and Milligan[19], and $Al_2O_3 \cdot 0.35H_2O$ according to Weiser and Milligan[20]. The above-mentioned observation that there is no inflection showing the existence of monohydrated alumina in the water content-calcination temperature curve of the hydrargillite, was also confirmed by Day[21]. Bentley and Feachem[22] observed, on the other hand, that the anhydrous alumina is rehydrated to the boehmite in the presence of steam. The boehmite, as is well known, is obtained when the hydrargillite has been dehydrated in a closed system. All these facts might elucidate the fact that some parts of the χ-alumina primarily yielded through a direct dehydration of the hydrargillite, are surely converted into the boehmite by reaction with the adsorbed water, which has been released from the hydrargillite during the heat treatment. Thus the practical calcination of the hydrargillite proceeds as indicated in the accompanying diagram[3].

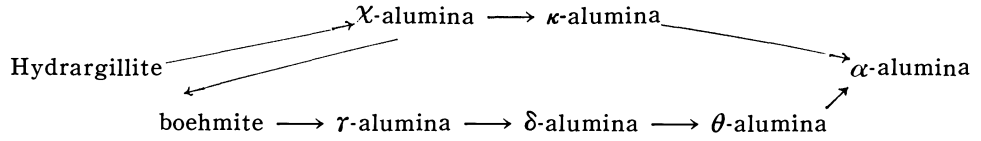

The primarily yielded χ-alumina gives rise, on subsequent calcination at higher temperatures, to mixtures of two series of anhydrous aluminas, namely $\chi \rightarrow \kappa \rightarrow \alpha$ associated with the original dehydration product, the χ-alumina, and $\gamma \rightarrow \delta \rightarrow \theta \rightarrow \alpha$ associated with the boehmite component, this component being derived from a secondary reaction between the χ-alumina and its adsorbed water.

16) M.H. Jellinek and I. Frankuchen, *Ind. Eng. Chem.*, **37**, 163 (1945).
17) G. Ervin, ibid, 108.
18) J.F. Brown, D. Clark and W.W. Elliott, ibid, 87.
19) L.H. Milligan, *J. Phys. Chem.*, **26**, 247 (1929).
20) H.B. Weiser and W.O. Milligan, ibid., **36**, 3010 (1932); **38**, 1175 (1934).
21) M.K.B. Day and V.J. Hill, *J. Phys. Chem.*, **57**, 947 (1953).
22) F.J.L. Bentley and C.G.P. Feachem, *J. Soc. Chem. Ind.*, **46**, 148 (1945).

It was also observed by the present authors, as shown in Fig. 4, that the powders of the hydrargillite is, in the course of slow heating, effluent twice over two different ranges of temperatures; namely, violent dehydration occurs apparently at two steps. This observation is likely to support the view of Day rather than that of Brown.

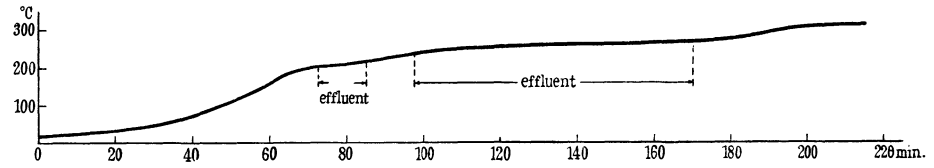

Fig. 4. Effluent phenomena observed in the course of slow heating of hydrargillite-powders.

The reason why the thermal decomposition of the hydrargillite proceeds through two different routes is indeed not easily accounted for, but some structural interpretations are given here. The χ-alumina is initially yielded from the thermal decomposition of the hydrargillite, and the γ-alumina is then derived from the boehmite, which has been produced by a subsequent reaction between the above-mentioned χ-alumina and its adsorbed water. Both of these aluminas might probably be assumed to possess structures very near to a spinel type[23]. A line situated at about 2.0 Å in the X-ray powder diffraction pattern is indexed as the (400) line for the spinel unit cell, and its intensity is supposed to be affected by the relative distribution of aluminium ions between two kinds of interstices of a cubic close-packed oxygen network; namely octahedral and tetrahedral interstices, since this line is caused by the reflection from the (400) planes passing through all the oxygen positions and the octahedral aluminium positions, but not the tetrahedral aluminium positions[15]. If its intensity is weak, the aluminium ions in the alumina under consideration would take seats in the tetrahedral interstices in preference to the octahedral interstices of the cubic close-packed oxygen network. The χ- and κ-aluminas in the transformation series associating with the original dehydration product of the hydrargillite have the weak (400) line, while the γ-, δ- and θ-aluminas in the transformation series associating with the boehmite have the intense (400) line, as can be seen from the results of X-ray investigations by Stumpf, Thibon, Brown and Day listed in Table I. It is concluded from the foregoing considerations that the occurrence of the two distinct series in the course of the thermal transformation of the hydrargillite might be ascribed to the possibility of aluminium ions in choosing one of the two different ways to enter into the interstices of the oxygen network of cubic close-packing.

The remarkable prototype III for the cathodo-luminescence spectrum of samarium ions is obtained, when these ions are imbedded in an alumina, which is presumably constituted of the aluminium ions occupying the

TABLE I
RELATIVE INTENSITY OF REFLECTIONS FROM (400) PLANES

Intermediate phase of alumina	I	II	III	IV
χ	ww(2.00 Å)	w(1.99 Å)	——	mw(2.11 Å)
κ	mw(2.00 Å)	w(2.055 Å)	mw(2.06 Å)	mw(2.06 Å)
γ	s(2.00 Å)	s(1.985 Å)	msb(1.98 Å)	s(1.982 Å)
δ	ms(2.005 Å)	s(1.985 Å)	s(1.99 Å)	s(1.985 Å)
θ	ms(2.03 Å)	s(2.01 Å)	ms(2.02 Å)	s(2.016 Å)

I) H.C. Stumpf, A.S. Russell, J.W. Newsome, and C.M. Tucker, *Ind. Eng. Chem.*, **42**, 1402 (1960).
II) H. Thibon, J. Charrier, et R. Tertian, *Bull. soc. chim. France*, **18**, 387 (1951).
III) J.F. Brown, D. Clark, and W.W. Elliott, *J. Chem. Soc.*, **1953**, 86.
IV) M.K.B. Day and V.J. Hill, *J. Phys Chem.*, **57**, 948 (1953).

Code: s —— strong; ms —— medium strong; mw —— medium weak; w —— weak; ww —— very weak; b —— broad

23) R. Brill, *Z. Krist.*, **83**, 323 (1932); H.B. Barlett, *J. Am. Ceram. Soc.*, **15**, 361 (1932); G.H. Hagg und G. Soderholm, *Z. phys. Chem.*, [B], **29**, 88 (1935); E.J.W. Verwey, *J. Chem. Phys.*, **3**, 592 (1935); G. Ervin, *Acta Cryst.*, **5**, 106 (1952).

tetrahedral interstices of cubic close-packed oxygen network.

The packing effect of the introduced samarium ions in stabilising this special configuration of alumina is considered to resemble that of sodium or others in the formation of the β- and ζ-aluminas[24], but the samarium ions in the former case serve at the same time as an activator for causing the cathodo-luminescence. The fixation, of this alumina-configuration, caused by the packing of samarium ions is so firm that the most intense band characteristic of the luminescence prototype III, namely a band situated at 597 mμ persists to be intense in the cathodo-luminescence spectrum, mixing with bands of the prototype II, although afterwards the sample has been roasted at a high temperature in a direct flame of coal gas-oxygen. This fact indicates that the tight fixation of the above-mentioned structure remains tenaciously in some local parts after an extremely intense heat treatment, which brings about a fundamental structural change of alumina into the corun dum configuration.

It is finally shown that this cathodo-luminescence spectrum of samarium may be utilised for conjecturing how an activated alumina for the chromatographic use could be prepared. The well-known sample of E. Merck's aluminium oxide, which was standardised for a chromatographic adsorption analysis according to Brockmann, is directly soaked with the solution of samarium nitrate and then ignited over a blast flame of the mixture of coal gas and air. It gives a samarium-luminescence spectrum of the pure prototype III under the excitation by the cathode-ray bombardment. This prototype of the samarium-luminescence spectrum can scarcely ever be obtained in its pure form, except the alumina derived from the hydrargillite of Bayer process. A conclusion might, therefore, be drawn that this activated alumina would possibly have been prepared by heating the purified alumina-trihydrate of Bayer process at moderately high temperatures.

Summary

Results of investigations are summarised as follows on the cathodo-luminescence spectra of samarium ions imbedded in various samples of aluminas, which were thermally derived from hydrargillite.

The transformation from γ- to α-modification of alumina takes place according as the temperature for heat treatment of the hydrargillite is elevated, at whose dried state the samarium ions have been impregnated.

After the hydrargillite was subjected to a previous heat treatment at the temperature range between 250 and 900°C, impregnated with the samarium ions and then calcined over a blast flame of coal gas mixed with air, it gives a characteristic cathodo-luminescence spectrum, which was designated by one of the present authors as the prototype III. The configuration of the alumina giving rise to luminescence bands of this prototype under the excitation by the cathode-rays is when once formed, stable and persistent for heat treatments of much elevated temperatures.

The activated alumina standardised after Brockmann can give, after being impregnated with the samarium ions, the particular cathodo-luminescence spectrum of the prototype III owing to the above-said ions. The appearance of this luminescence spectrum in its pure form is of use for choosing a material as well as for finding an activation method in the preparation of the alumina suitable for the chromatographic purpose.

The dual transformation conception postulated recently by Day on the thermal decomposition of the hydrargillite was elucidated from a structural point of view. The luminescence prototype III of samarium ions seems to be due to the special configuration of alumina, such as χ- and κ-modifications, in which the aluminium ions occupy preferably the tetrahedral rather than the octahedral interstices of oxygen network ofcubic close-packing.

This research has been financed by the Scientific Encouragement Grant of the Ministry of Education, to which the authors' thanks are due.

Scientific Research Institute, Ltd.
Komagome, Bunkyo-ku, Tokyo

24) A.F. Wells, "Structural Inorganic Chemistry", Clarendon Press, Oxford (1945), p. 335; H.B. Barlett, *J. Am. Ceram. Soc.*, **15**, 361 (1932); E.J.W. Verwey, *Z. Krist.*, **91**, 66 (1935).

Non-Newtonian Viscosity of Dilute High Polymer Solutions. I. Apparatus for Determining Shear Dependence of Viscosity over a Wide Range of Shear Rates and Measurements on Polystyrene Solution in Toluene

By Toshiaki KUROIWA

(Received September 15, 1955)

Introduction

It appears to be a conclusion reached from a number of recent investigations on the non-Newtonian viscosities of high polymer solutions[1-16] that the viscosity of a dilute solution may persistently increase with decreasing rates of shear in a linear or an exponential fashion. This dependence is, however, in marked disagreement with the theory according to which the viscosity of a dilute high polymer solution should be given by an even function of shear rate q as follows[17,18]:

$$[\eta]_q=[\eta]_0(1-aq^2+bq^4-cq^6+.....), \qquad (1)$$

where $[\eta]_q$ is the limiting viscosity number at a shear rate q, $[\eta]_0$ is the one at $q=0$, and a, b, c, etc. are constants which depend on certain molecular parameters. According to Eq. (1), the reduction of the viscosity should be a function of q^2, and the tangent of $[\eta]_q$ vs. q curve must be zero at $q=0$.

Unfortunately, it is rather difficult to determine from the data of these investigations whether the viscosities have as a function of q a finite slope or a horizontal tangent at $q=0$, since either the lower limits of the shear rates dealt with are very high or the experimental uncertainties are very large in the region of low rates of shear, and experimental verification of the theory has called much attention[19].

Recently, E. Wada[20] has extended the measurements of the viscosities of polymethylmethacrylate solutions in chloroform over a wide range of shear rates down to the very small shear rates and has shown that the change in $[\eta]_q$ of these solutions with q fits quite well to the theoretical equation (1).

The chief purpose of the present study is to check the above-mentioned theoretical prediction by measuring the non-Newtonian viscosity of dilute polymer solutions over a wide range of shear rates. The lowest limit of shear rate dealt with in this study is about 30 sec^{-1} and the highest is 2000–3000 sec^{-1}. In the succeeding paragraphs, the method and apparatus used for the experiments are briefly described and the results of the preliminary measurements on dilute solutions of polystyrene in toluene are presented.

Experimental

Method.—According to the fundamental equation for laminar flow in a capillary, the maximum shear rate at the wall of the capillary is given by the following expression[21], provided that the so-called kinetic energy contribution and the end effect are ignored:

$$q=4Q/\pi R^3 t\times(1-1/4t\times d(Pt)/dP), \qquad (2)$$

and the corresponding relative viscosity number η_r of a solution is given by

$$\eta_r=t/t_0\times(1-1/4t\times d(Pt)/dP)^{-1}, \qquad (3)$$

* Presented at the 8th Annual Meeting of the Chemical Society of Japan held in Tokyo, April, 1955.

1) R.M. Fuoss and U.P. Strauss, *Ann. N.Y. Acad. Sci.*, **51**, 836 (1949).
2) H.T. Hall and R.M. Fuoss, *J. Am. Chem. Soc.*, **73**, 265 (1951).
3) R.M. Fuoss and W.N. Maclay, *J. Polymer Sci.*, **6**, 305 (1951).
4) U.P. Strauss and R.M. Fuoss, ibid., **8**, 593 (1952).
5) G. de Wind and J.J. Hermans, *Rec. trav. chim.*, **70**, 521 (1951).
6) G. de Wind and J.J. Hermans, ibid., **70**, 615 (1951).
7) F. Akkerman, D.T.F. Pals and J.J. Hermans, ibid., **71**, 56 (1952).
8) J. Schurz and E.H. Immergut, *J. Polymer Sci.*, **9**, 279 (1952).
9) C.M. Conrad, V.W. Trip and T. Mares, *J. Phys. & Colloid Chem.*, **55**, 1474 (1951).
10) S. Newman, L. Loeb and C.M. Conrad, *J. Polymer Sci.*, **10**, 463 (1953).
11) A. Katchalsky and N. Sternberg, *J. Polymer Sci.*, **10**, 253 (1953).
12) T.G. Fox, Jr., J.C. Fox and P.J. Flory, *J. Am. Chem. Soc.*, **73**, 1901 (1951).
13) W.R. Krigbaum and P.J. Flory, *J. Polymer Sci.*, **11**, 37 (1953).
14) L.J. Sharman, R.H. Sones and L.H. Cragg, *J. Appl. Phys.*, **24**, 703 (1953).
15) T. Hotta, *Reports of Laboratory of High Polymer Research*, Nagoya University, No. **4**, 1 (1952); ibid., No. **5**, 70 (1953).
16) H. Fujita and T. Homma, *J. Polymer Sci.*, **15**, 277 (1955).
17) W. Kuhn and H. Kuhn, *Helv. Chim. Acta*, **28**, 1533 (1945); *J. Colloid Sci.*, **3**, 11 (1948); *J. Polymer Sci.*, **5**, 519 (1950).
18) N. Saito, *J. Phys. Soc. Japan*, **6**, 302 (1951).
19) A. Peterlin, *J. Polymer Sci.*, **8**, 621 (1952).
20) E. Wada, *J. Sci. Res. Inst.*, **47**, 149, 159, 168 (1953).
21) T. Hotta, *Reports of Laboratory of High Polymer Research*, Nagoya University, No. **3**, 22 (1951).

where R is the radius of the capillary, P is the driving pressure and t and t_0 are the efflux times for a given volume, Q, of the solution and the solvent, respectively. Using these equations, η_r can be calculated as a function of q if a Pt vs. P relation for the solution is derived experimentally.

For a Newtonian flow in a capillary, as the well-known Hagen-Poiseuille's law, i.e., Pt=constant, holds, the second term in the bracket of Eq. (2) vanishes and the first term can be rewritten as follows:

$$q=PR/2L\eta, \tag{4}$$

where L is the length of capillary, η is the viscosity coefficient of the liquid. From this equation it may be seen that, in order to obtain a small value of q, it is necessary to make one or more of P, R small and or to make L large for a given liquid. Difficulty arises in making R small, since a decrease in R may give erroneous efflux times due to partial plugging of the capillary by either dust or small gel particles, and also large values of L would not be desirable because of difficulty in obtaining a capillary of a uniform radius. It is inevitable, therefore, to make P small; and a high precision of pressure must be secured in order to obtain reliable results in a range of low shear rates.

In order that Eqs. (2) and (3) can be applied, it is essential that there is no change in pressure during the course of an experiment[21]. When the usual viscometer such as the Ostwald-type, whose hydrostatic head of the liquid column changes during a run, is used, these equations can be applied only when the exteranal pressure is sufficiently high as compared with the change in pressure head**.

In the present investigation, a horizontal viscometer was employed in order to minimize the pressure variation during the course of an experiment. To compensate the hydrostatic head caused by a small deviation of the viscometer from a horizontal plane, the direction of flow was alternated at a given external pressure.

Let P' be the pressure corresponding to the effective hydrostatic head*** of the horizontal viscometer during a run, and P the external pressure. It may be assumed that the efflux times of each direction t_+ and t_- correspond to the total pressure of $P+P'$ and $P-P'$, respectively. Then, for a Newtonian flow, the efflux time t at the pressure P is given by:

$$t=2t_+t_-/(t_++t_-)\fallingdotseq(t_++t_-)/2 \tag{5}$$

For a non-Newtonian flow, this relation, of course, does not hold. But fortunately, the dilute solutions of polystyrene in toluene, at least, can be regarded as the Newtonian liquids in a region of low pressures, as will be shown in the later part of this report, and so the above relation can be used without reservation. With increasing pressure, non-Newtonian behavior appears; but at the same time, the difference between t_+ and t_- decreases rapidly ($(t_--t_+)/t=2P'/P$), and Eq. (5) can be employed as a good approximation.

Apparatus.—A sketch of the manostat system is shown in Fig. 1. Water from the main flows

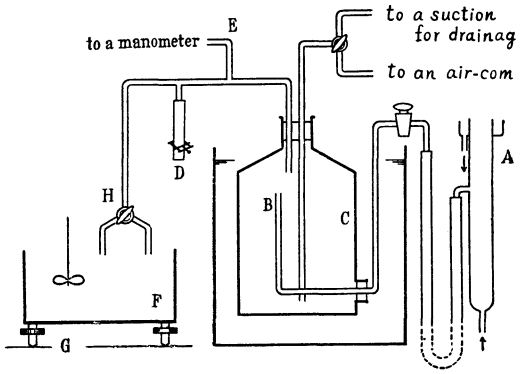

Fig. 1. Schematic diagram of the manostat system.

over the rim of the tube A. The side outlet of this tube is connected through a thick-walled rubber tube to the tube B which is inserted in the large bottle C through the hole of the lower part of the bottle. As air in C is constantly escaping through the narrow opening D; water from A flows over continuously at the upper end of B, whereby the pressure in C is kept constant at the magnitude of pressure corresponding to a difference in heights of the two overflowing surfaces, which can be adjusted by the vertical position of A.

This apparatus is similar to that described by G. de Wind and J. J. Hermans[5]; but in their apparatus, because of the lack of an air outlet, an *increasing* pressure will not be brought under any control only leading to a lowering of the water surface in the tube B. When the water surface is once lowered below the end of B, pressure in the bottle is substantially not kept under control. In other words, it is essential that water from A is always overflowing at the upper end of B in order to secure a constant pressure-regulation****. At first sight, such a marked increase of pressure with a simultaneous lowering of water surface may be inconceivable; but before the air outlet D was provided to the present manostat, a gradual increase of pressure which followed a lowering of water surface in B was often observed. This might be due to a slow recovery of the temperature in C which had previously been cooled by water flowing into C from A during the setting of the pressure.

The pressure is read on the manometer connected to E. Water is used as manometer liquid

** Fujita and Homma[16] have described an ingenious device by means of which the change of pressure head can be compensated and thus they have enabled the measurement at low rates of shear by means of the usual Ostwald viscometer. One drawback is that one who uses this device needs to have great patience in experimental manipulation.

*** This effective hydrostatic head reduces to the time average of the head during a run when the flow is Newtonian.

**** When the pressure is sufficiently high, this increase in pressure may be overcome by the decrease in pressure resulting from the travelling of the liquid in the viscometer.

for lower pressures (up to about 10 cm. in water) and mercury for higher pressures.

By means of this manostat, the driving pressure can be maintained constant throughout the course of measurement within ±0.005 cm. in water and this accuracy is comparable in magnitude to those of manometer reading.

Owing to the leakage of air in C, it is found unnecessary to regulate the temperature of the bath in which C is immersed.

The horizontal viscometer is shown in Fig. 2.

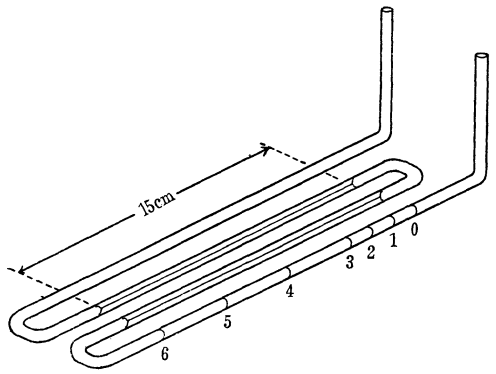

Fig. 2. The horizontal viscometer.

Uniformity of the capillary bore was checked by means of a thread of mercury, and the mean radius of the bore was determined by weighing the mercury and was found to be 0.0144_0 cm. Its length was about 30 cm. The volumes between the marks on the side arm of the viscometer (0–1, 0–2, etc. in Fig. 2) were determined by weighing the water between these marks before the viscometer was constructed. The volume between the mark 0 and 6 was about 1.1 cc.

The viscometer is mounted on a brass frame, which in turn, is fixed in a thermostatted water bath F. The bath is fitted with legs G whose lengths can be varied by screw mechanism. The inclination of the viscometer can be adjusted by varying the lengths of these legs, watching the level placed on the viscometer frame. The temperature in the bath F is controlled to 25±0.004°C. The direction of flow is altered by a specially designed three-way stop-cock H.

To check the reliability of the apparatus in the region of low pressures, the efflux times of benzene and water were measured in a range of 0.7–15 g./cm² of P. At each pressure, measurement was repeated 3–5 times for each direction of flow, and the pressure was read as often as possible during the period of each measurement. For example, at $P=0.715\pm0.004$ g./cm², t_+ and t_- were 1376±2 and 1409±3 sec., respectively, for flow volume of 0.0900 cc. (corresponds to the volume between the mark 0 and 1 in Fig. 2) of benzene. The lowest shear rate measured was about 30 sec^{-1} for both liquids. The results are shown in Table I, together with the length of the capillary calculated from these results using the relation, $\eta=\pi R^4(Pt)/8LQ$ (P being converted to the unit dyn./cm²), where t is the efflux time for 0.0900 cc. Conforming to the Newtonian behavior of these liquids, Pt of each liquid is almost independent of P within the experimental error. From these results it may be assumed that no appreciable systematic errors, such as are due to the surface tension effect, are introduced into values of P.

TABLE I

PRODUCT OF APPLIED PRESSURE AND EFFLUX TIME FOR FLOW VOLUME OF 0.0900 cc. AND RELATED DATA FOR BENZENE AND H_2O

	Average of Pt (g./cm² ×sec.)	Standard deviation, $\sqrt{\overline{\delta^2}}$	Maximum deviation, δ_{max}	η* (centipoise)	L Calc'd
Benzene	989	5	11	0.603_4	30.3_4
H_2O	1460	7	13	0.894_9	30.2_5

* K. Shiba "Tables of Physical Constants", Iwanami Shoten (1944), p. 75.

Measurement on Polystyrene Solution in Toluene.—Styrene monomer was purified by washing several times successively with 2% aqueous solution of potassium hydroxide, 3% aqueous solution of sodium bisulfite and water, by drying over calcium chloride, and by freezing twice, discarding each time some unfrozen liquid. After distillation under a reduced pressure of 30 mmHg with the flow of nitrogen gas, the monomer was placed in a thick-walled test tube and sealed after replacing air in the tube with nitrogen. The polymerization of the monomer was carried out by placing the tube in a dark temperature bath regulated at 60°C for thirty-two days. The content was then dissolved in benzene and reprecipitated in a large excess of methanol and the precipitate, after being washed with methanol, was dried under high vacuum at 60°C for ten hours. The average molecular weight $\overline{M}$ of the polymer was estimated at 32×10^5 from $[\eta]$ in toluene measured at 30°C with an Ostwald viscometer by the equation[22], $[\eta]=3.70\times10^4\ \overline{M}^{0.62}$.

Commercial toluene was washed with sulfuric acid and with pure water, dried over phosphorous pentoxide and distilled. A fraction boiling at 110.4–110.7°C was used as a solvent.

Certain experiments were carried out, in order to determine if any dependence of viscosity on the heating temperature on preparing the solutions or on the period of room temperature-storage after preparing the solutions be detcted. The results showed that viscosity neither depends on the heating temperature within the range 30–100°C nor on the period of storage, at least in the case of concentration of the solutions lower than 2%.

The solutions were filtered successively through sintered glass filter No. 2 and No. 3 immediately before measurement. In order to minimize the errors due to moisture and solvent evaporation, measurements of efflux times for each solution were carried out in a random manner with respect to pressures, and each set of measurements was repeated two or three times by recharging the

22) A.I. Goldberg, W.P. Hohenstein and H. Mark, *J. Polymer Sci.*, 2, 503 (1947).

viscometer, covering the same range of pressures by each set. At high pressures, in order to avoid too small values of t, measurements were taken for a large volume of flow: (0–2), (0–3), etc. in Fig. 2, and Pt's corresponding to (0–2), (0–3), etc. were converted to those for (0–1) by the volume ratios.

The kinetic energy contribution and the end effect estimated from the tangent of Pt vs. P curve for toluene (shown in Fig. 3) were found to be negligible even in the most unfavorable case. The drainage effect was assumed to be negligible.

Results and Discussion

Pt vs. P relations for solutions of several concentrations and for toluene are shown in Fig. 3. It is evident that each curve for solutions has a horizontal part in a region of low pressures, indicating that the shear dependences of these solutions vanish at a low pressure region.

The evaluation of the differencial quotient, $\mathrm{d}(Pt)/\mathrm{d}p$, was made graphically with a smoothed curve drawn to give the best fit to

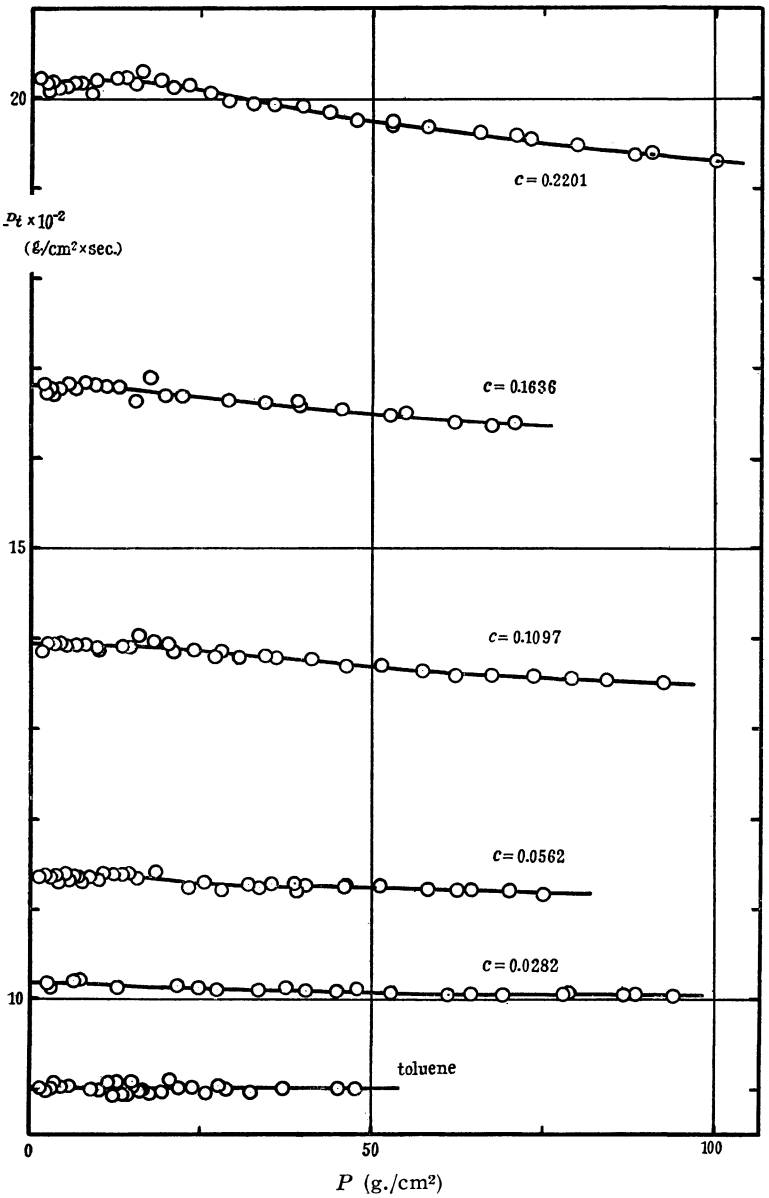

Fig. 3. Product of applied pressure and efflux time vs. applied pressure for solutions and solvent. c denotes polymer concentration in g. per 100 cc.

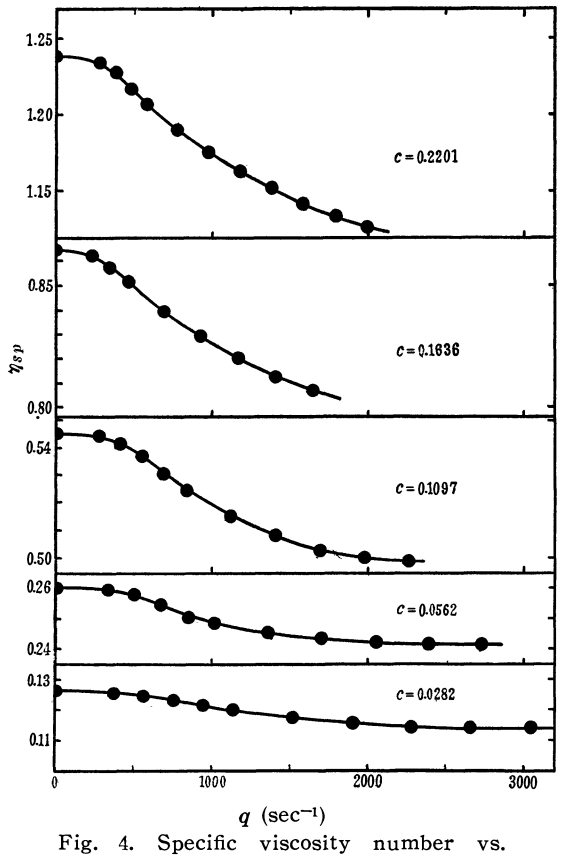

Fig. 4. Specific viscosity number vs. shear rate q.

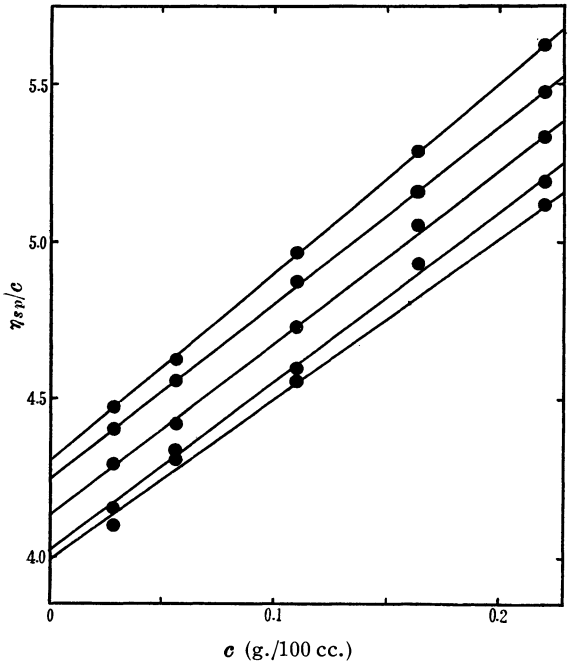

Fig. 5. η_{sp}/c vs. c curves at constant q for q=0, 600, 1000, 1600, 2000 sec^{-1} respectively, successively from the top.

the experimental points in a magnified graph of the data in Fig. 3. From these values at several pressures and the data for the dimensions of the viscometer, q and the corresponding η_r were calculated according to Eqs. (2) and (3). The relations of the resulted specific viscosity number, η_{sp}. vs. q are illustrated in Fig. 4 ($\eta_{sp}=\eta_r-1$). The η_{sp}/c vs. c plots at constant q for several values of q are shown in Fig. 5. These are almost linear within the range of concentrations studied, and fit the well-known Huggins' equation[23] well:

$$\eta_{sp}/c=[\eta]+k'[\eta]^2c. \qquad (6)$$

The $[\eta]_q$ obtained by extrapolating the curve at constant q to $c=0$ and Huggins' constant k' are plotted in Fig. 6 as functions of q.

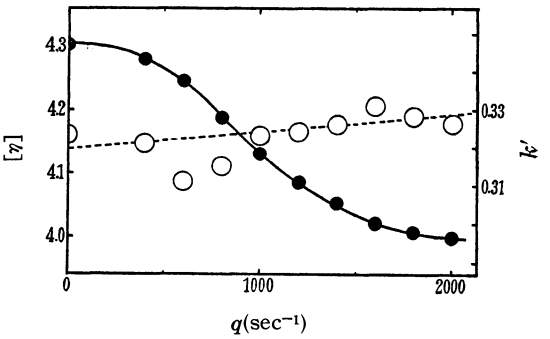

Fig. 6. Influence of rate of shear on the limiting viscosity number, (●), and Huggins' constant k', (○).

Although the values of $[\eta]_q$ at higher rates of shear are less reliable in view of the rather large scattering of points at high values of q shown in Fig. 5, it is apparent from Fig. 6 that the influence of rate of shear on the limiting viscosity number of the solution may be described adequately by an even function of q conforming, qualitatively at least, with the theoretical equation (1). A precise comparison of these data with the theory which takes into account the numerical values of a, b, etc. in Eq. (1) was not made since $\overline{M}$ of this sample was estimated roughly.

The k' vs. q relation in Fig. 6 seems to show that the dependence of k' on the magnitude of q is, if any, relatively small for the present case. This does not mean, however, that the usual viscometry such as made with an Ostwald viscometer always gives k' which is not very much different from k' at $q=0$: because, in the Ostwald viscometer,

23) M.L. Huggins, *J. Am. Chem. Soc.*, **64**, 2716 (1942).

***** τ-values were calculated by the relation $\tau=PR/2L$, P being converted to the unit dyn./cm^2.

measurements are made at a constant shearing *stress* rather than at a constant q by keeping the average driving pressure constant, the smaller the polymer concentration, the greater is the mean shear rate in the capillary as may be seen from the relation, τ (shearing stress)$=\eta \times q$. Moreover, it is customary to evaluate the relative viscosity number of a solution by the ratio t/t_0, which is merely the apparent η_r rather than the true η_r because of discarding the second term in the bracket of Eq. (3). Under these circumstances, a very marked difference appears between η_{sp}/c vs. c relation at constant q and apparent η_{sp}/c vs. c relation given by the usual viscometry to the extent that the shear rate effect of solution is appreciable.

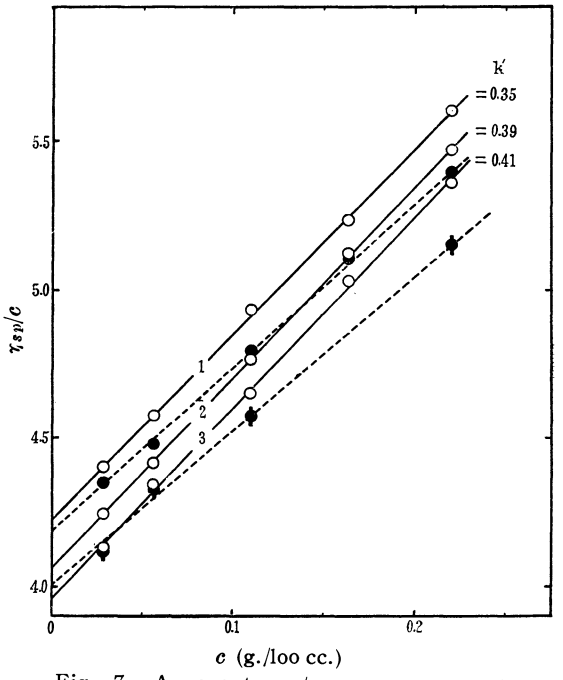

Fig. 7. Apparent η_{sp}/c v. c curves at constant τ for τ=4.7 (1), 9.4 (2) and 14.1 dyn./cm^2 (3); η_{sp}/c vs. c curves at constant q for q=800 (●) and 1800 sec.$^{-1}$ (●).

The apparent η_{sp}/c at constant τ calculated from the present data are plotted in Fig. 7 as functions of c for τ=4.7, 9.4 and 14.1 dyn./cm^2*****. For comparison, true η_{sp}/c vs. c plot at constant q for q=800 and 1800 sec^{-1} are inserted in the same figure. The k' derived from these apparent η_{sp}/c vs. c plots are also inserted in Fig. 7. It appears that apparent k' at constant τ is strongly dependent on τ in contrast with the relatively small variation in true k' with q.

The author wishes to express his hearty thanks to professor S. Murahashi for his guidance and to professor S. Akabori for his encouragement throughout the course of this study.

He is much indebted to Mr. T. Nakagawa of Tokyo University for his valuable advice and to Mr. E. Wada of the Scientific Research Institute for his kind encouragement and also to Mr. K. Kawahara for his cooperation in preparing the sample. This study was financed by the Technical Research Fund of the Tekkôsha Company.

Department of Chemistry, Faculty of Science, Osaka University, Osaka

*The Cyclic Oligomers of ε-Caprolactam**

By Osamu FUKUMOTO

(Received July 2, 1955)

Introduction

The cyclic oligomers of ε-caprolactam, extractable from polycapramide with boiling water or methanol are here studied.

One of the cyclic dimers was found by K. Hoshino[1] from the sublimate which was obtained during the polymerisation of ε-caprolactam. The brief notes of the cyclic oligomers were also described by German investigators[2].

In addition to the cyclic dimer which was found by K. Hoshino, there are also the dimeric isomer and the cyclic trimer in the extracts of polycapramide. Recently H. Hermans reported the isomers of the cyclic dimers of ε-caprolactam independently[3].

* This work was presented at the Symposium of Polymer Science at Nagoya, Nobember 11, 1954.

** Research Department of Toyo Rayon Co., Ltd.

1) K. Hoshino, This Bulletin, **19**, 171 (1944).

2) PB. 44806.

3) H. Hermans, *Rec. Trav. Chim. Pays-Bas*, **72**, 798 (1953).

Experiments

(1) Separation of Cyclic Oligomers

The greater part of ε-caprolactam is removed by vacuum distillation from the hot water extracts of polycapramide, then the residue is extracted with acetone to remove the still remaining monomer and other extractable impurities. The residue can be fractionated in three parts by the difference of the solubility of oligomers in water (cold or hot). The following results are finally obtained.

	m. p.	yield from the residue
[I]	234~236°C	32.8 %
[II]	343~345°C	30.4 %
[III]	231.4~237.2°C	30.1 %

The solubility in water increases in the series [I]<[II]<[III]. No carboxyl group is contained in them.

(2) Identification of the Cyclic Dimer (α-Dimer)

It is confirmed by the mixed examination of melting point that [II] is the cyclic dimer which was found by K. Hoshino.

(3) Confirmation of the Isomer of Cyclic Dimer (β-Dimer)

It is confirmed that [III] is the isomer of the cyclic dimer from the following results.

Mol. Wt. (Rast's method) Found: 225. Calcd. for $(C_6H_{11}N_1O_1)_2$: 226.

When [III] is hydrolysed in boiling concentrated hydrochloric acid and then dried up, the weight increase is 47.6 %. (Calculated for the conversion from $[NH(CH_2)_5CO]_n$ to $n[HCl.NH_2(CH_2)_5COOH]$: 48.2 %). ε-Benzoylaminocaproic acid is obtained from the hydrolysed [III] by the reaction with benzoyl chloride.

Since [III] is different from [II] in regard to the water solubility and melting point, it seems that [III] is an isomer of the cyclic dimer which was found by K. Hoshino.

(4) Confirmation of the Cyclic Trimer

It is confirmed that [I] is the cyclic trimer of ε-caprolactam from the following results.

Mol. Wt. (Rast's Method) Found: 339. Calculated for $(C_6H_{11}N_1O_1)_3$: 339.

Anal. Found: C, 63.45; H, 10.15; N, 12.59; O, 13.81. Calcd. for $(C_6H_{11}N_1O_1)_3$: C, 63.65: H, 9.81; N, 12.38; O, 14.15.

This can be hydrolysed quantitatively in boiling concentrated hydrochloric acid to ε-aminocaproic acid, which is identified by conversion to the benzoyl derivative (m.p. 76.5~78.0°C). Its melting point agrees with that of ε-benzoylaminocaproic acid (78~80°C).

Discussion

K. Hoshino gave the following constitutional formula [IV] (cyclic dimer of ε-caprolactam) for the sublimate which was obtained during the polymerisation of ε-caprolactam.

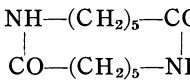

[IV]

3,6-Dioxopiperazine [V] which has a comparatively high melting point (311°C), has a similar constitutional formula and considerable high sublimation pressure.

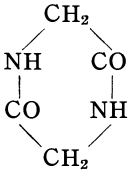

[V]

The structure of [V] is *cis* form for adjacent

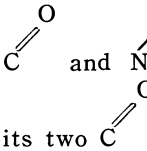

and of each amide[4] and also its two

are symmetrical to the plane which is perpendicular to the line between two carbonyl C atoms and contains the median of its line. Studying the cyclic dimers with the molecular structural model, there must be at least two geometrical isomers. The one is composed of the special arrangement of carbon atoms by which the intramolecular free rotation is hindered, such as by double bond. (Fig. 1).

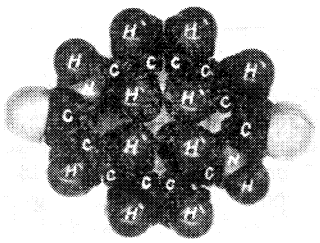

Fig. 1. α-Dimer.

It has probably the same structure as 3,6-dioxopiperazine, which has two methylene groups instead of two pentamethylene groups. It seems that the crystal structure of [III] is also the same as that of 3,6-dioxopiperazine, which has been already known.

Rearranging these carbon atoms of pentamethylene groups, another structural model

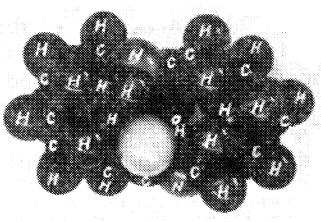

Fig. 2. β-Dimer.

4) M. Tsuboi, This Bulletin, 22, 255 (1949).

can be obtained which is able to rotate freely, for instance, as Fig. 2.

Conversion between these two configurations which are derived from the study of the molecular structural model, will require a considerable amount of energy and really the mixture of [II] and [III] cannot be obtained by the fusion of [II].

Since the melting point of cyclic hexamethylene adipamide [VI] is similar to that of the β-dimer of ε-caprolactam, and besides the isomer of [VI] has not been found, the α-dimer of ε-caprolactam which has an unusually high melting point should be composed of the special arrangement of atoms.

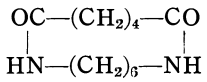

(VI)

E. Fischer reported that 3, 6-dioxo-2, 5-diethylpiperazine [VII] had two isomers[5]. But unlike the cyclic dimer of ε-caprolactam these isomers may exist because of the asymmetric carbon atoms at 2 and 5 position. 3, 6-Dioxo-2, 2, 5, 5-tetraethylpiperazine [VIII] which was found by Freytag[6] is the constitutional isomer of caprolactam dimer and it melts at 346~346.5°C and dissolves 0.11 g. in 100 cc. of water at 26°C. These physical properties of [VIII] are exactly similar to those of the α-dimer of ε-caprolactam.

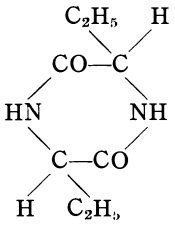

[VII]

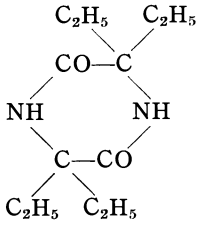

[VIII]

In the case of [VIII], owing to the tension of the dioxopiperazine ring, hydrogen bonds

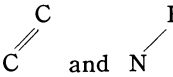

formed by C and N should be intermolecular. Then the hydrogen bonds of the α-dimer may be also intermolecular. ε-Caprolactam trimer has a 21-membered ring and considering the idea of closely packed atom groups in molecular lattices and its lower melting point, the structure of the trimer may be a type such as its three hydrogen bonds are all intramolecular. Regarding a benzene ring as one atom, the cyclic trimer of polyethylene terephthalate which has recently been discovered (m. p. 325~327°C)[7] has also a 21-membered ring, and in this case, owing to the steric hindrance of benzene rings, the probability of the cyclic dimer formation may be less than that of the trimer formation.

W. H. Stockmayer gave the following formula[8] for the configulation of the cyclic polymer, which is obtained during the polymerisation of ω-hydroxyundecanoic acid type monomer.

$$R_n = BVn^{-\frac{5}{2}}x^n$$

$$B = \left(\frac{3}{2\pi r}\right)^{\frac{3}{2}}/b^3$$

R_n: The number of n mer rings.
V: The volume of the system.
r: The number of chain atoms per molecular unit.
b: The effective link length.
x: The fraction of reacted end-groups in the chain fraction.

For the case of oligomers the following expression is derived.

$$R_1 : R_2 : R_3 = x : \frac{2^{-\frac{5}{2}}x^2}{8} : \frac{3^{-\frac{5}{2}}x^3}{27},$$

where V, r are constant.

For $x=0.99$, the weight ratios of the cyclic oligomers are as follows.

$$R_1 : 2R_2 : 3R_3 = 1 : 0.35 : 0.19$$

Since the weight ratios of the oligomers actually measured are 1 : 0.17 : 0.08, the calculated value agrees with that observed for the ratio of the dimer (α-type+β-type) to the trimer. Then Stockmayer's equation which is reasonable when ring molecules are long enough (15 skeltal atoms and up) so that short-range steric effects are not dominant, is applicable in this case. The hot water or methanol extracts from polycapramide having an average polymerisation degree of about 100~150, mostly consist of the cyclic monomer and oligomers. There are very few linear oligomers in such high polymers.

Conclusion

From the extracts of polycapramide, two kinds of cyclic dimers and one trimer are obtained. One of the dimers which was found by K. Hoshino may be the diketopiperazine type. The ratio of the dimer to the trimer which is experimentally observed, agrees with the calculated value by Stockmayer's equation.

The author wishes to thank Dr. K. Hoshino and Dr. H. Kobayashi who directed his studies and permitted this publication.

Nylon Laboratory, Toyo Rayon Co. Ltd., Nagoya

5) E. Fischer, *Ber.*, **39**, 3985 (1906).
6) Freytag, *Ber.*, **48**, 651 (1915).
7) Sidney D. Ross, *J. Polymer Sci.*, **13**, 406 (1954).
8) W.H. Stockmayer, *J. Chem. Phys.*, **18**, 1600 (1950).

The Structure of Surface-denatured Protein. VII. The Activity and the Shape of the Surface-denatured Pepsin Molecule

By Kazutomo IMAHORI

(Received July 14, 1955)

The author was able to show that the serum albumin molecule which expanded on the extremely acid solution had an elongated shape, but the albumin molecule which expanded on the solution of its isoelectric point was rather round[1]. This observation indicated that many of the bonds of the albumin molecule which expanded on the acid solution were destroyed and the molecule showed the elongated shape but on the solution at the pH of its isoelectric point many of the intramolecular secondary bonds were still retained and the molecule could not take the elongated shape.

If this indication is correct, it would be possible to expect that the most part of the activity of the protein molecule will be lost when expanded on the extremely acid solution, but some part of the activity of the molecule on the solution at the pH of its isoelectric point will be reserved. The following experiments were planned with this expectation. The protein selected was pepsin.

Experimentals

(a) **Sample.**—The pepsin was purchased from The Armour Chem. Lab. of U. S. A. and it was the two times recrystallized enzyme of the salt free state. The serum albumin was purified by Dr. S. Nakamura and was the same sample as the author had used in the previous experiments.

(b) **Solution and Apparatus.**—Three acetate buffered solutions of pH=2, 3 and 5 were used as the underlying solutions. A Wilhelmy balance registered the film pressure.

(c) **Size and Shape Determination.**—The methods and techniques used for the determination of the size and shape of pepsin molecules on the solutions of various pH were quite the same as those used in the previous paper[1].

(d) **Activity Determination.**—The activity of the surface denatured pepsin molecule was determined by the following three methods.

(1) One of them used the time needed for the clotting of a standard skim milk solution into which the pepsin had been introduced. The milk solution containing 16.7 % of dry produced skim milk in 0.1 M acetate buffer adjusted to pH 5 was used. The pepsin unit can ordinarily be defined as the amount which causes the clotting of 6 cc. of this solution at 37°, or it can be expressed by the equation

$$U = V/6t,$$

where V is the volume of the used milk solution in cc., and t is the clotting time in minutes. V and t were measured by the following method. Pepsin was at first spread on the surface of solutions of various pH. The spread film was transfered onto a stainless-steel plate covered with a double layer of barium stearate, using the method of Blodgett. Then the thickness of the film was measured by an ellipsometer[2]. This plate was immersed for two minutes in 6 cc. of standard milk solution, during which time the milk was agitated continuously by gently shaking and rotating the tube. The plate was then removed and the time needed for the clotting was measured.

(2) *Hemoglobin Method.* This method is quite analogous to that of Northrop[3]. Four cc, of 2.5 per cent pure hemoglobin solution was added with pipette to a test tube and then 1 cc. of 0.3 N hydrochloric acid was added from a pipette. The final pH was 1.6. Thus the substrate solution was obtained. The built up film which was obtained by the method similar to that of (1), was put in 5 cc. of the substrate solution and the solution was mixed by whirling the plate. After ten minutes 10 cc. of 0.3 N trichloracetic acid was added, the tube was shaken vigorously, and the suspension was filtered.

To 5 cc. of the digestion filtrate were added 10 cc. of 0.5 N sodium hydroxide and 3 cc. of phenol reagent of Folin. The color was read against the standard after two to ten minutes. The number of activity unit corresponding to the colour value of the digestion products in 5 cc. of digestion filtrate was read from the curve shown in Northrop's book[3].

(3) *Mixed Film Method.* A given volume of 0.05 per cent pepsin solution was mixed well with the equal volume of 0.05 per cent serum albumin solution. A part of the mixed solution was put promptly on the surface of the solutions of various hydrogen ion concentrations. The mixed film of pepsin and serum albumin was obtained. If the film was kept under a constant surface area, the surface film pressure would increase gradually, as pepsin splits an albumin molecule into smaller ones. The more active the pepsin is, the more intensely would the surface pressure increase, and so if we plot the surface pressure against the time, the slope of the curve would indicate the activity of the pepsin. The relative activity of the pepsin could be obtained by this method.

1) K. Imahori, This Bulletin, 27, 146 (1954).

2) Y. Yoneyama and K. Imahori, *Sci. Pap. College Gen. Educ. Univ. Tokyo*, 3, 145 (1953).

3) J.H. Northrop "Crystalline Enzyme", Columbia Univ. Press (1948), p. 303.

Results and Discussion

The molecular weight of pepsin which was expanded on the solution of pH=1, 3 and 5 was determined by the method of Bull and Guastalla[4]. The molecular weight thus obtained was 35,000 in all cases.

The limiting area per molecule and the shape of each molecule on pH=1, 2 and 3 are listed in the Table I.

TABLE I

pH	*Am*	f/f_0	*a*/*b*	*a*	*b*
1.0	5250 Å²	—	—	—	—
2.0	6100 Å²	1.5	15	342 Å	23 Å
3.0	5370 Å²	1.2	5.5	205 Å	37 Å
5.0	—	—	—	—	—

In the table, *Am* is the limiting area of one molecule in Å², f/f_0 the frictional ratio, *a*/*b* the axial ratio and *a* and *b* are the length of the longer and the shorter axes respectively. The data of pH=1 are lacking as the film on the substrate of pH=1 is hydrolyzed easily and the diffusion constant cannot be determined. The film on the substrate of pH=5 is not spread well and its data are also lacking. The result indicates that the pepsin molecule on pH=2 is more perfectly expanded and has a more elongated shape than that on pH=3.

The activities of pepsin expanded on pH=2 and 3 and measured by the earlier two methods are listed as Table II.

TABLE II

pH	Activity: Displacement method	Activity: Hemoglobin method
Native	9,000	0.27
2.0	3,900	0.15
3.0	7,900	0.24

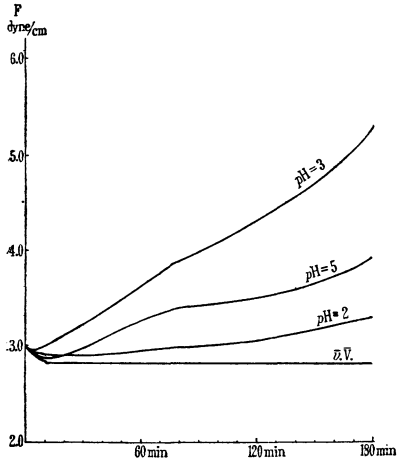

Fig. 1.

Table II shows that the pepsin film which has been built up from the solution of pH=3 is far more active than the film from pH=2. The result of the mixed film method, which is shown in Fig. 1 is quite in accordance with the above results. But as is obvious from the previous report of this series, the serum albumin on the substrate of pH 3 can be denatured more completely than that on the substrate of pH 5, so that the former will be digested more easily by pepsin than the latter. This would make also the mixed film on the substrate of pH 3 to have higher surface pressure than that on pH 5. Accordingly it cannot be concluded that the pepsin on the substrate of pH 3 is more active than that on pH 5. On the other hand, the albumin film on the substrate of pH 2 is denatured most perfectly and will be digested most easily and this fact verifies the fact that pepsin on the substrate of pH 3 is more active than that on pH 2. The curve U. V. in Fig. 1 which means that the mixed film is irradiated with the ultraviolet light from a mercury lamp shows that pepsin is completely inactivated by the ultraviolet light.

The above results show that the pepsin expanded on the solution of pH 2, which is more completely surface-denatured and has a more elongated shape has lost the larger part of its activity, while the pepsin expanded on the solution of its isoelectric point retains its activity to some extent. This result is in accord with the author's expectation. Yet, this activity disappears when the pepsin molecule is irradiated with the ultraviolet light. At any rate, it is quite interesting that pepsin monolayer retains its activity even on the solution of pH 2.

Summary

(1) The molecular weight, the size and the shape of the pepsin molecule on the substrates of pH 2 and 3 were determined. The molecule on the substrate of pH 3 (its isoelectric point) was of rather a round shape, but the molecule on pH 2 had a far more elongated shape.

(2) The enzymatic activity of the surface-denatured pepsin molecule on the solutions of various pHs was determined. The round-shaped molecule on the substrate of pH 3 was the most active, but the elongated molecule on pH 2 retained less activity.

The author owes much to Prof. Bun-ichi Tamamushi for his encouragement throughout this study. This work is supported by the Scientific Research Grant from the Ministry of Education.

Chemical Institute, College of General Education, The University of Tokyo, Tokyo

4) H. B. Bull, "Adv. in Protein Chem." Vol. III, p. 97.

Study on ZnO-Cr_2O_3 Catalyst. I. Electrical Conductivity of Zinc Oxide in Oxygen and Hydrogen

By Hiroshi UCHIDA and Yoshisada OGINO

(Received December 15, 1954)

Introduction

Since the electrical conductivity of a sintered material is determined mainly by the specific boundary material existing between the grains, it is greatly affected by gases chemisorbed on the boundary surface. Therefore, the mechanism of adsorption of gases and consequently the nature of catalytic activity can be discussed from the results of measurement of the conductivity, so far as the measurement is undertaken on a working catalyst at a working temperature.

Zinc oxide is a typical *n*-type semiconductor and has been widely investigated by many workers[1~3]. Most of the investigations, except a few, have been conducted on highly sintered zinc oxides at high temperatures. Though these few investigations were indeed of considerable merit, they seemed, from the view point of electrical conductivity, to be not sufficient for a perfect understanding of ZnO-Cr_2O_3 catalyst, i.e. a catalyst for the synthesis of methanol, etc.

The measurement of conductivity in conjunction with chemisorption of oxygen and hydrogen has been conducted here, as a supplement to the investigations described above, at temperatures below 500°C on zinc oxide sintered at 600°C. Some of the present results are rather different from those reported previously and some of them are unknown. These results may be interpreted in terms of the interstitial zinc atom pair or the zinc molecule suggested by P. H. Miller.

Experimental Procedure

At varying temperatures from 45° to 500C° the conductivity of a zinc oxide pressed into a bar was measured in vacuo, and subsequently, in an atmosphere of oxygen as well as hydrogen in a range of pressure from 10^{-3} to 10^{-1} mmHg. The conductivity measurement was supplemented by the direct measurement on a separate specimen of the identical bar of both the rate of adsorption and equilibrium amount of adsorbed oxygen and hydrogen in another apparatus.

A commercial zinc oxide (chem. pure) was pressed into a bar of 8×8 mm. square and 81 mm. in length, then sintered at 600°C for two hours and allowed to cool in air. Part of the bar was subjected to theelectrical measurement by direct current, and the rest was crushed into granules of 1–2 mm. diameter for the measurement of adsorption of oxygen and hydrogen.

The general technique of conductivity measurement was similar to that used by R. H. Grifith et al[4]. The specimen was placed between Pt electrodes, the upper one of which was weighted with a perforated iron cylinder. The measurement was made in vacuo and at a constant pressure of oxygen as well as hydrogen, by using a Wheatstone bridge. With capillary leaks connected to a gas reservoir it was possible to expose the specimen for prolonged periods to oxygen as well as hydrogen of well difined and reproducible pressures ranging from 10^{-3} to 10^{-1} mmHg.

The adsorption measurement was conducted in an apparatus similar to that used by R. T. D. Frankenburg[5]. The amount of adsorbed oxygen or hydrogen was evaluated from the pressure decrease in an adsorption chamber of a constant volume. The pressure was measured by means of a Pirani gauge.

Experimental Results

Electrical Conductivity for Evacuated Oxide.—The oxide sintered at 600°C in air was a poor conductor, unless it was de-oxygenated. The conductivity was, however, gradually increased by prolonged heating of the oxide in vacuo (10^{-5} mmHg) at 500°C, and then came to attain a steady value.

The temperature-dependence of resistivity at the steady state in a temperature range from 100° to 500°C was given by the usual equation,

$$R = A \cdot \exp(\varepsilon/kT) \qquad (1)$$

where R is resistivity, A, a constant, k, Boltzmann's constant, T, absolute temperature, and ϵ, activation energy of conductivity. The Arrhenius line for the above equation gave an apparent activation energy of about 0.025 eV. (Fig. 1). The value was nearly equal to that obtained by P. H. Miller[1] (0.02 eV.) at temperatures below room temperature. The constant A was evaluated to be approximately 2.24×10^2.

1) P.H. Miller, *Phys. Rev.*, **60**, 890 (1941).
2) H. Fritsche, *Z. Phys.*, **133**, 422 (1952).
3) E. Scharowsky, ibid., **135**, 318 (1953).
4) R.H. Grifith, P.R. Chapman et al., *Disc. Faraday Soc.*, 8, 258 (1950).
5) R.T.D. Frankenburg, *J. Am. Chem. Soc.*, **66**, 1827 (1944).

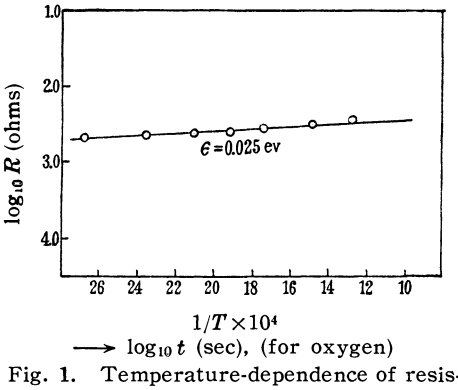

Fig. 1. Temperature-dependence of resistivity of zinc oxide in vacuo.

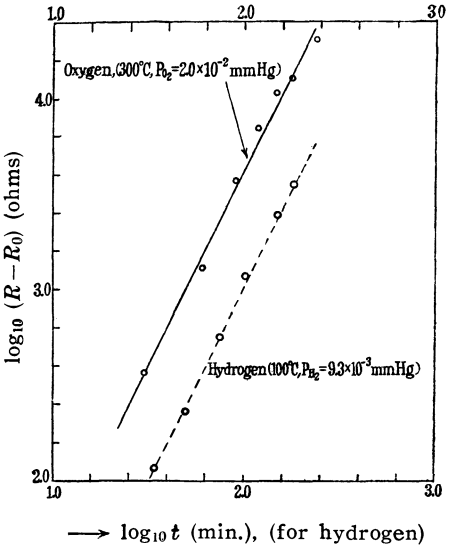

Fig. 2. Relation between resistivity and time, at the earlier stage of adsorption.

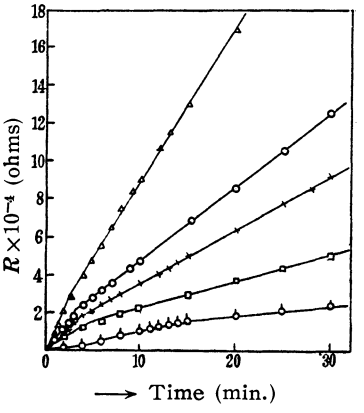

Fig. 3a. Relation between resistivity at 300°C and time, at various pressures; △, $p_{O_2}=5.8\times10^{-2}$ mmHg, ○, $p_{O_2}=2.8\times10^{-2}$ mmHg, ×, $p_{O_2}=2.0\times10^{-2}$ mmHg, □, $p_{O_2}=9.3\times10^{-3}$ mmHg, ◎, $p_{O_2}=3.6\times10^{-3}$ mmHg.

Electrical Conductivity in Oxygen Atmosphere.—Fig. 2 and 3 show the adsorption

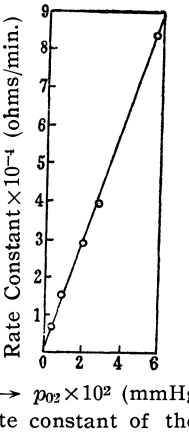

Fig. 3b. Rate constant of the change of resistivity as a function of oxygen pressure at 300°C.

kinetics as the rate of change in resistivity of the oxide under a series of oxygen pressures at 300°C. The resistivity increased with time at an earlier stage of the adsorption, according to the relation

$$R-R_0=k'\cdot p_{O_2}\cdot t^2 \quad (2),$$
$$k'\simeq2.5\times10^5 \text{ (ohm/min. mmHg)}$$

where R_0 is the resistivity for the evacuated oxide, and then the increase was solwed down being represented by another relation, as

$$R=k''\cdot p_{O_2}\cdot t+\text{Const.} \quad (3),$$
$$k''\simeq1.5\times10^5 \text{ (ohm/min. mmHg)}$$

With prolonged period of further adsorption, it tended to increase always more slowly until an equilibrium was established between resistivity and oxygen pressure. The relationship of the resistivity in equilibrium with the oxygen pressure (Fig. 4) was given by Eq. (4)

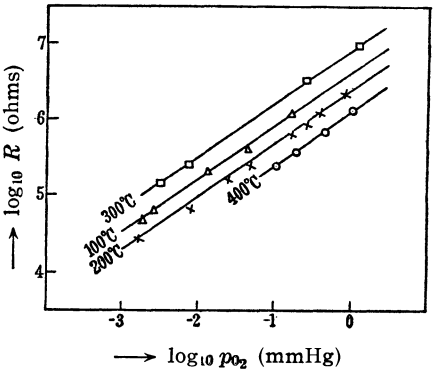

Fig. 4. Ralation between resistivity of zinc oxide and oxygen pressure at various temperatures.

$$R=\alpha\cdot p_{O_2}^{n},\quad n\simeq 2/3 \qquad (4)$$

This differs somewhat from that of $R=\alpha'\cdot p_{O_2}^{1/4}$.....(5), which was usual at the higher temperature.

A rapid elevation of temperature, after an equilibrium between resistivity and oxygen pressure had been established at a certain temperature, produced an instantaneous fall of resistivity followed by a slower rise towards a new equilibrium value corresponding to a higher temperature (Fig. 5). The equilibrium value of the resistivity is exemplified in Fig. 6

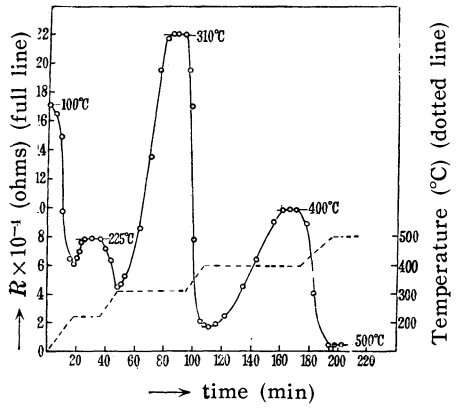

Fig. 5. Change of resistivity with rises of temperature, at an oxygen pressure of 6.9×10^{-3} mmHg.

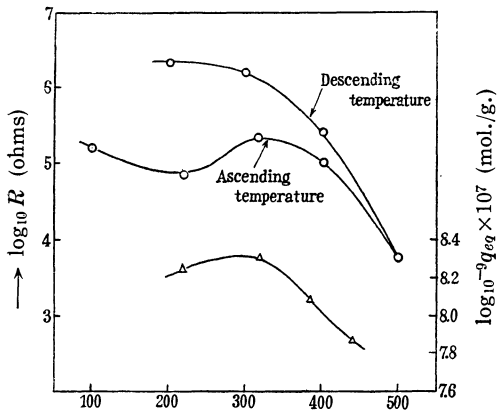

Fig. 6. Temperature-dependence of resistivity of zinc oxide at oxygen pressure of about 6.9×10^{-3} mmHg (-○-), and isobar of oxygen adsorption at the pressure of 3.0×10^{-2} mmHg (-△-).

as a function of temperature at an isobaric oxygen pressure of 6.9×10^{-3} mmHg. In this figure, a minimum as well as a maximum of resistivity is observed at about 220° and 300°C respectively with ascending temperature, while resistivity increases rather monotonously with descending temperature from 500°C.

Adsorption of Oxygen.—The evacuated oxide could adsorb oxygen at a measureable rate at temperatures above 200°C. The equilibrium amount of the adsorbed oxygen at a range of temperature from 220° to 440°C was plotted against oxygen pressures in Fig. 7

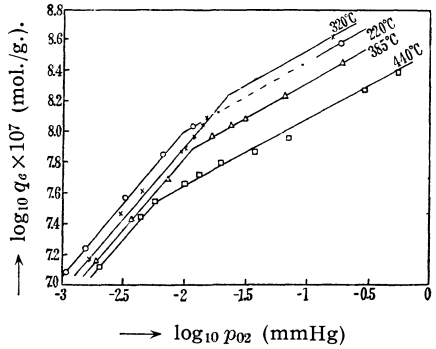

Fig. 7. Adsorption isotherms of oxygen on zinc oxide at various temperatures.

The adsorption isotherm comprised two straight lines, the one being expressed by Eq. (6) and the other by Eq. (7)

$$q_{eq}=a\cdot p_{O_2}^{n},\quad n\simeq 1.0\sim1.2 \qquad (6)$$

$$q_{eq}=b\cdot p_{O_2}^{n},\quad n\simeq 0.5 \qquad (7)$$

in a respective range of small and large adsorbed amount q_{eq}. The differential heats of the adsorption are evaluated by means of the Clausius-Clapeyron's equation to give a nearly constant value of 1.1 kcal./mol. at $p_{eq}=1.2\sim4.0\times10^{-7}$ mol./g. and 24 kcal./mol. at $q_{eq}=1.0\sim2.6\times10^{-6}$ mol./g. for Eq. (6) and Eq. (7) respectively.

The rate of decrease of the pressure is represented by Eq. (8)

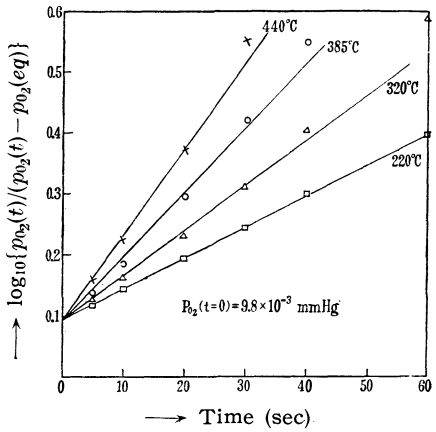

Fig. 8. Relation between $\log_{10}\{p_{O_2}(t)/(p_{O_2}(t)-p_{O_2}(eq))\}$ and time at various temperatures.

$$\log_{10} p_{O_2}(t)/\{p_{O_2}(t)-p_{O_2}(eq)\}=k'''\cdot t+\text{Const.} \quad (8)$$

at the earlier stage and becomes gradually more slow with the increasing amounts, as illustrated in Fig. 8. The activation energy of the adsorption at the earlier stage was found to be 3.6 kcal./mol.

Electrical Conductivity in Hydrogen Atmosphere.—An initial steady state of conductivity was required for a series of repeated measurements in hydrogen atmosphere. On the exposure of the evacuated oxide to hydrogen, the conductivity increased more or less rapidly at temperatures above 200°C (Fig. 9a), but recovered very slowly in prolonged

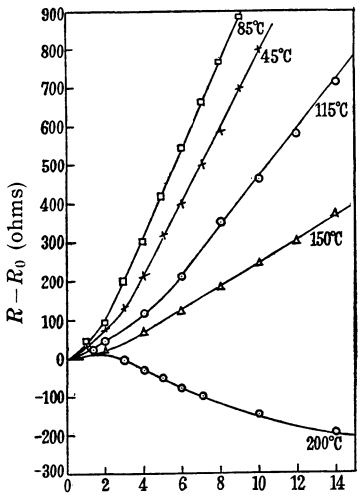

Fig. 9a. Relation between resistivity and time at a ahydrogen pressure of 9.3×10^{-3} mmHg, at various temperatures.

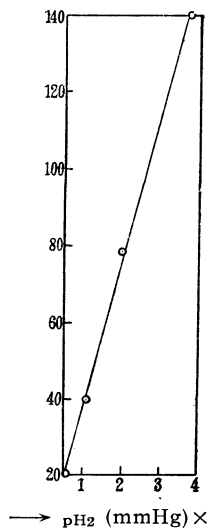

Fig. 9b. Rate constant of the change of resistivity as a function of hydrogen pressure at 150°C.

duration of evaquation at 500°C. This might probably be due to the slow evaporation of zinc metal* which was confirmed by the deposit on the cold wall of the vessel. In this respect, a steady state could be readily established by the oxidation of a specimen, which had been employed in hydrogen atmosphere, in oxygen at 500°C followed by a subsequent evacuation at the same temperature.

The decrease of conductivity accompanied by the adsorption of hydrogen took place on zinc oxide at temperatures below 200°C (Fig. 9a, 10); the matter being just the converse

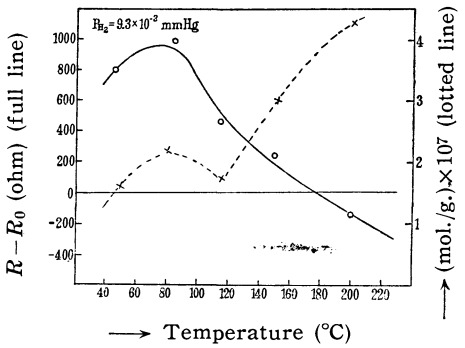

Fig. 10. Increase and decrease of resistivity (full line) accompanied by hydrogen adsorption (dotted line, indicating the amount adsorbed in 10 minutes) at various temperatures.

of the above**. The adsorption at lower temperatures was recognizable only when the specimen had been subjected to evacuation at. 500°C, but scarcely so when the specimen had been oxygenated. The resistivity at a constant time interval after the beginning of adsorption being plotted against the temperature (Fig. 10, full line), a maximum appears at about 80–90°C above which it decreases monotonously with increasing temperatures, while the adsorbed amounts of hydrogen show a maximum at 80–90°C as well as a minimum at about 110°C (Fig. 10, dotted line). In contrast to two maxima expected in the adsorption*** of oxygen, no other maximum has been found in the R-T curve for the hydrogen adsorption. Whether another maximum would be present or not below 45°C could not be confirmed. The conductivity nearly paralleled the adsorbed amount of hydrogen at 45–110°C.

* The appearance of zinc metal had already been reported by L. Yang (*J. Amer. Electrochem. Soc.*, **97**, 910 (1950).

** Y. Kubokawa and O. Toyama (*Bull. Naniwa Univ.*, 2, 103 (1954)) have recently observed the decrease at 45°C, but the increases at temperatures higher than 80°C. Their results are somewhat different from the ours.

** In the R-T curve of oxygen adsorption at an atomos- pheric pressure, two maxima were found at 150° and 350°C respectively.

The adsorption on hydrogen on oxide at temperatures below 200°C is similar in rate to the oxygen adsorption. The rate of increase of resistivity could be again represented by Eq. (2) at the earlier stage and by Eq. (3) at the subsequent stage respectively (Figs. 2 and 9).

Discussion

Zinc Atom Pair and its Ionized State.—The straight line relation between log R and $1/T$ as well as the small activation energy of the conductivity (0.02 eV.), which for the case below room temperature had already been reported by P. H. Miller, was also found in the intermediate range between 100° and 500°C. The value of the activation energy which was considerably lesser than that (0.5 eV.) obtainable normally above 500°C, was attributed by P. H. Miller to the presence of interstitial zinc atom pairs, while the greater value was generally believed to be due to interstitial zinc atoms.

With respect to ionization of the interstitial zinc atoms, Zn^{++} was estimated by C. Wagner et al[6] and K. Hauffe et al[7] and Zn^{+} by F. Seitz[8] and E. Scharowsky[9]. E. Scharowsky conducted his experiments at temperatures nearly the same as that of the present experiments, and suggested the presence of Zn^{+} from his experimental results. It seems to be reasonable to assume that Zn^{+}, consequently, $Zn^{+}\cdot Zn^{+}$ or $Zn^{+}\cdot Zn$ in conjunction with the atom pairs, may confer the conductivity at temperatures below 500°C.

Equilibrium of Conductivity and Rate of Conductivity Change in Oxygen.—The observed isotherms of oxygen adsorption given by Eqs. (6) and (7) are suggestive of a molecular adsorption and an adsorption with dissociation occurring at a small and a large q_{eq} respectively. According to T. Iijima[10], the rate equation given by Eq. (8) can be derived from the postulate of a molecular adsorption. However, even the adsorption at the earlier stage has been shown to be always associated with change of the conductivity, and any adsorption with dissociation may therefore take place consecutively at a stage where the molecular adsorption may be predominant. In this respect, an interpretation of the results will be given in terms of the zinc atom pair under the following assumptions.

1. A molecular adsorption takes place between oxygen in gas phase and S′ site on the oxide surface according to expression (1),

$$S'+O_2 \rightleftarrows S'O_2 \qquad (1)$$

S′ may be any one of the sites, Zn, Zn·Zn, cation Zn^{++}, and anion O^{--} of the surface of the stoichiometric crystal.

2. An activated complex $S'O_2^{\mp}$ is produced by a reaction of quasi-free electrons on the surface with $S'O_2$, and the reaction rate determines the rate of the conductivity change.

$$S'O_2+2e \rightleftarrows S'O_2^{\mp} \qquad (2)$$

3. S′O reacts with other site S″ to produce $S''O^{-}$ and S′

$$S'O_2^{\mp}+2S'' \rightleftarrows 2S''O^{-}+S' \qquad (3)$$

Interaction between the oxygen molecule and the electron may take place in either of the following, $O_2+2e \rightleftarrows 2O^{-}$ or $O_2+e \rightleftarrows O^{-}+O$. In this respect, the latter proves, however, inadequate for teh interpretation of the results. S″ may be any one of the sites, $Zn^{+}\cdot Zn$, and $Zn^{+}\cdot Zn^{+}$. Oxygen is adsorbed on either of the sites in two different manners, say, on $Zn^{+}\cdot Zn^{+}$

$$2O^{-}+Zn^{+}\cdot Zn^{+} \rightleftarrows \overset{O^{-}\quad O^{-}}{\diagdown\ \diagup}\ Zn^{+}\cdot Zn^{+} \qquad (a),$$

$$2O^{-}+2(Zn^{+}\cdot Zn^{+}) \rightleftarrows 2(Zn^{+}\cdot \overset{O^{-}}{\diagup}Zn^{+}) \qquad (b)$$

Among the above, (a) proves inadequate for the interpretation of the results.

(A) *Rate at the Later Stage of Adsoption.* The rate of adsorption is given by Eq. (4), the equilibrium being established in (1)

$$V_{ads}=[S'O_2]_{eq}\cdot[e]^2\frac{kT}{h}\cdot\frac{f_{\mp}}{f_{S'O_2}\cdot f_e^2}\cdot \exp(-\epsilon_1/kT) \qquad (4)$$

where f is a partition function with respect to the subscripts. As the rate of the disappearance of the electron is equal to tiwice the above rate, one obtaines

$$-\frac{d[e]}{dt}=k_1\cdot[S'O_2]_{eq}\cdot[e]^2 \qquad (5),$$

$$k_1\equiv 2\frac{kT}{h}\cdot\frac{f_{\mp}}{f_{S'O_2}\cdot f_e^2}\cdot\exp(-\epsilon_1/kT).$$

From (1), in equilibrium, $[S'O_2]_{eq}=K_1\cdot p_{O_2}\cdot[S']_{eq}$, is obtained, where K_1 is the equilibrium constant at a constant temperature. The substitution of this relation in Eq. (5) gives

6) H.H. von Baumbach and C. Wagner, *Z. Phys. Chem.*, **22**, 199 (1933).
7) H.J. Engell and K. Hauffe. *Z. Elektrochem.*, **56**, 366 (1952).
8) F. Seitz, "Modern Theory of Solids", p. 466 (1940).
9) E. Scharowsky, *Z. Phys.*, **135**, 318 (1953).
10) T. Iijima, *Riken Iho* (*Bull. Phys. Chem. Res. Inst.*, Tokyo), **17**, 286 (1937) (in Japanese).

$$-\frac{d[e]}{dt}=k_1\cdot K_1\cdot[S']_{eq}\cdot p_{O_2}\cdot[e]^2 \quad (6).$$

Integrating Eq. (6), one obtaines

$$[e]^{-1}=A\cdot p_{O_2}\cdot t+\text{const.},\ A\equiv k_1\cdot K_1\cdot[S']_{eq} \quad (7)$$

When combined with the relation $[e]=B\kappa=BR^{-1}$, where κ is electrical conductivity, B, a constant, Eq. (7) results in Eq. (8)

$$R=A\cdot B\cdot P_{O_2}\cdot t+\text{const.} \quad (8)$$

which agrees well with the experimental equation (2) in the preceding chapter.

(B) *Rate at the Earlier Stage of Absorption.* At the sarlier stage of the adsorption before the equilibrium in (1) is established, the rate of disappearance of $S'O_2$ according to Eq. (2) $\left(\text{denoted by } -\frac{d[S'O_2]_{(2)}}{dt}\right)$ depends upon the rate of appearance of $S'O_2$ according to (1) $\left(\text{denoted by } \frac{d[S'O_2]_{(1)}}{dt}\right)$. The respective rate is given by the following equation (9) and (10).

$$\frac{d[S'O_2]_{(1)}}{dt}=k_2\cdot p_{O_2}\cdot\{[S']_0-[S'O_2]_{(1)}\} \quad (9)$$

$[S']_0$, concentration of S' on the surface of the evacuated oxide.

$$-\frac{d[S'O_2]_{(2)}}{dt}=\frac{k_1}{2}\cdot\{[S'O_2]_{(1)}-[S'O_2]_2\}\cdot[e]^2 \quad (10)$$

Combining $-\frac{d[e]}{dt}=-2\frac{d[S'O_2]_{(2)}}{dt}$ with Eq. (10) and rearranging, one obtaines

$$-\frac{d[e]}{dt}=k_1\cdot[S'O_2]_{(1)}\cdot\left\{1-\frac{[S'O_2]_{(2)}}{[S'O_2]_{(1)}}\right\}\cdot[e]^2 \quad (11)$$

At the earlier stage there may be $\frac{[S'O_2]_{(2)}}{[S'O_2]_{(1)}}\ll 1$, and therefore

$$-\frac{d[e]}{dt}=k_1\cdot[S'O_2]_{(1)}\cdot[e]^2 \quad (12)$$

By integrating Eq. (9) and substituting the integrated equation (13) in Eq. (12), Eq. (14) is obtained.

$$[S'O_2]_{(1)}=[S']_0\cdot\{1-\exp(-k_2\cdot p_{O_2}\cdot t\} \quad (13)$$

$$-\frac{d[e]}{dt}=k_1\cdot[S']_0\cdot\{1-\exp(-k_2\cdot p_{O_2}\cdot t)\}\cdot[e]^2 \quad (14)$$

The second term in the bracket can be simplified by neglecting the terms including higher powers of t in the expanded series of $\exp(-k_2p_{O_2}\cdot t)$ and Eq. (15) results

$$-\frac{d[e]}{dt}=k_1\cdot[S']_0\cdot(-k_2\cdot p_{O_2}\cdot t)\cdot[e]^2 \quad (15)$$

Integration of Eq. (15) gives Eq. (16)

$$[e]^{-1}-[e]_0^{-1}=k_1\cdot k_2\cdot[S']_0\cdot p_{O_2}\cdot t^2 \quad (16)$$

where $[e]_0$ is concentration of quasi-free electrons on the evacuated oxide. Eq. (16) may be expressed in terms of resistivity as follows.

$$R-R_0=B\cdot k_1\cdot k_2\cdot[S']_0\cdot p_{O_2}\cdot t^2 \quad (17)$$

Eq. (17) is consistent with the experimental equation (2) at the earlier stage of the adsorption*.

(C) *Equilibrium Conductivity in Varying Pressures of Oxygen.* The rate of desorption is expressed by Eq. (18) according to (2).

$$V_{des}=\frac{[S''O^-]^2\cdot[S']}{[S'']^2}\cdot\frac{kT}{h}\cdot\frac{f_{\mp}\cdot f_{S''}^2}{f_{S''O^-}^2\cdot f_{S'}}\exp(-\epsilon_2/kT) \quad (18)$$

By taking into account the relation, $\frac{d[e]}{dt}=2V_{des}$, Eq. (18) may be rearrnaged to Eq. (19)

$$\frac{d[e]}{dt}=k_3\cdot\frac{[S''O^-]^2\cdot[S']}{[S'']^2} \quad (19),$$

$$k_3\equiv 2\frac{kT}{h}\cdot\frac{f_{\mp}\cdot f_{S''}^2}{f_{S''O^-}^2\cdot f_{S'}}\cdot\exp(-\epsilon_2/kT)$$

When the adsorption equilibrium is reached, the net rate of adsorption becomes zero, which results in Eq. (20)

$$\frac{[S'']_{eq}^2[e]_{eq}^2}{[S''O^-]_{eq}^2}=\frac{k_3}{k_1\cdot K_1}\cdot p_{O_2}^{-1}\equiv D\cdot p_{O_2}^{-1} \quad (20)$$

On the other hand, $[e]_{eq}$ is given by $[e]_{eq}=[e]_0-[e]'_{eq}$, where $[e]'_{eq}$ is concentration of quasi-free electrons occupied by oxygen atoms at equilibrium. By combining Eq. (20) with the following relation, Eq. (21) can be obtained

$$[S'']_{eq}=[S'']_0-[S''O]_{eq}=[S'']_0-[e]'_{eq}=[S'']_0-[e]_0+[e]_{eq}$$

$$\{[S'']_0-[e]_0+[e]_{eq}\}^2\cdot[e]_{eq}^2/\{[e]_0-[e]_{eq}\}^2=D\cdot p_{O_2}^{-1} \quad (21)$$

When $[S'']_0/[e]_0\ll 1$, and $[e]_{eq}/[e]_0\ll 1$, Eq. (21) reduces to Eq. (22).

$$[e]_{eq}^2\simeq D\cdot p_{O_2}^{-1} \quad (22)$$

$$\text{i.e. } \kappa\propto p_{O_2}^{-1/2} \text{ or } R\propto p_{O_2}^{1/2}$$

The relation is approximate to the experimental relation of $R\propto p_{O_2}^{2/3}$, but does not attain to a complete agreement.

Temperature-dependence of Conductivity in Oxygen Atmosphere.—The temperature-

* Without simplification, Eq. (14) results in the following equation.

$R-R_0=B\cdot k_1\cdot[S']_0\cdot t+B\cdot k_1\cdot k_2\ [S']_0\cdot p_{O_2}\cdot\exp(-k_2\cdot p_{O_2}\cdot t)$

The equation is rather inconvenient for comparison with the experiments.

dependence of conductivity at a constant pressure of oxygen (the shape of the isobar as well as the change caused by a rapid rise of temperature) is similar to that obtained by H. S. Taylor with the adsorption of hydrogen on zinc oxide. H. S. Taylor[11] explained his results in terms of the heterogeneity of active sites on the surface. A similar consideration being employed, two kinds of impurity centers associating with the conductivity should be assumed. In this respect, the heat of adsorption would probably be different, irrespective of the nearly equal activation energy of adsorption, for the adsorption on either the $Zn^{+}\cdot Zn^{+}$ or the $Zn^{+}\cdot Zn$ site suggested in the foregoing chapter, but no decisive explanation is available at this time.

Adsorption of Hydrogen.—H. S. Taylor[12] as well as E. Wicke[13] has already found two maximum amounts of the adsorbed hydrogen, the one at a temperature below 100°C and the other at a temperature between 250·300°C respectively. H. S. Taylor explained his results as was described, but gave no concept of the structure of the sites. E. Wicke attributed the adsorption predominant at temperatures below 100°C to the adsorption with dissociation on the oxide cation Zn^{++} of the surface of stoichiometric crystal of zinc oxide, and the other at higher temperatures to the formation of surface hydroxides.

In the light of the present results, the adsorption at the lower temperature may be estimated to take place predominantly on zinc atom pairs of the surface. The evidence is given by the facts that the adsorption at the lower temperature can take place on the evacuated oxide with relatively high conductivity, but not on the oxygenated one with negligibly small conductivity, and that the rate of the adsorption is closely relevant to the change of the conductivity. Zn^{++} in the normal lattice of zinc oxide suggested by E. Wicke seems not to participate in the adsorption, as it can hardly confer the conductivity. The parallel relation observed between the conductivity and the adsorbed amount in the range of temperature is also an evidence in favour of the above estimation.

The expression for the rate of hydrogen adsorption at lower temperatures similar to that for the oxygen adsorption is suggestive of a molecular adsorption taking place predominantly at the earlier stage of adsorption as well as the adsorption with dissociation at the subsequent stage.

The hydroxyl formation between the adsorbed hydrogen and O^{--} in the oxide above 200°C as is suggested by E. Wicke may probably be expected from the view point of the facts for the higher temperatures, that the conductivity increases markedly on the exposure of the oxide to hydrogen and that the specimen subjected to the hydrogen treatment evaporates zinc metal which may be produced as the result of loss of OH radical combined previously with zinc metal.

11) H. S. Taylor, "Advances in Catalysis and Related Subjects", Academic Press Inc., New York (1948), **1**, 1.
12) H. S. Taylor, *J. Am. Chem. Soc.*, **49**, 2468 (1927).
13) E. Wicke, *Z. Elektrochem.*, **53**, 279 (1949).

Summary

With the evacuated zinc oxide, there has been found, in an intermediate range of temperatures from 100° to 500°C, a linear relation between log R and $1/T$, from which an activation energy of 0.025 eV. has been evaluated.

From the results of the measurement of adsorption a molecular adsorption and an adsorption with dissociation seemed to take place on the evacuated oxide at an earlier and a subsequent stage of oxygen adsorption respectively. The more detailed results from the conductivity measurements revealed that the adsorption with dissociation took place consecutively in the earlier stage in which the molecular adsorption was predominant.

At temperatures below 200°C, the conductivity decreases accompanied by hydrogen adsorption, while it increases at higher temperatures. The adsorption kinetics as the rate of change of the conductivity is given by expressions similar to those in the oxygen adsorption.

The adsorption of oxygen as well as hydrogen accompanied by the conductivity decrease may be explained in terms of two different kinds of sites, on which the molecular adsorption and the adsorption with dissociation take place respectively. The interstitial zinc atom pair suggested by P. H. Miller being employed for the site of the latter adsorption, a quantitative interpretation is available for the rate and the equilibrium of the adsorption associating with the conductivity.

Government Chemical Industrial Research Institute, Tokyo

Study on Fused Iron Catalyst for Alcohol Synthesis from Water-gas. IV. Reaction Rate and Composition of Product in the Synthesis with Catalyst Promoted by Copper

By Hiroshi UCHIDA, Michio KURAISHI, Hideo ICHINOKAWA and Kiyoshi OGAWA

(Received February 15, 1955)

Introduction

In a previous investigation[1] with a small convertor a catalyst containing copper as a promoter gave a high yield of oxygenates from water-gas. However, the rate equation of reaction for the case was not derived, as the quantitative measurements of the rate at widely varying flow rates of synthesis gas were difficult.

The present investigation has been made to confirm the high yield of oxygenates with a synthesis under similar conditions of flow rate and temperature in a larger convertor of the same diameter and ten fold the previous catalyst content, and also to determine the equation of rate by means of a differential reactor procedure. The procedure had already been employed by R. B. Anderson et al[2] as well as H. Tramm[3] for the syntheses with a cobalt catalyst at normal pressure and an iron catalyst at high pressure respectively. According to their procedure the synthesis gas had been withdrawn from different heights of a catalyst bed during the synthesis to be analyzed for the reactants and products.

From the results obtained here, it appears that the synthesis product (solid and oil) contains a large amount of oxygenates, though slightly less than the previously reported yield, attaining to half the total yield, and that the reaction rate is similarly expressed by equations of two types for the rate controlled by the desorption of the adsorbed product and by the reaction on the surface respectively.

With respect to the lateral temperature gradient across the catalyst bed W. Broetz[4] made a brief description for the case of synthesis with an iron catalyst at high pressure. His differential equation of heat transfer has been analytically solved, with simplification and by combining with one of the rate equations obtained, to give the lateral temperature gradient of the catalyst bed.

1) H. Uchida, H. Ichinokawa et al., This Bulletin, 28, 68 (1955).
2) R.B. Anderson, A. Krieg et al., *Ind. Eng. Chem.*, **41**, 2189 (1949).
3) H. Tramm, *Brennstoff Chem.*, 33, 21 (1952).
4) W. Broetz and W. Rottig, *Z. Elektrochem.*, **56**, 896 (1952).

Experimental Procedure

Apparatus.—The convertor was 16 mm. I. D. and 30 mm. O. D. by 3.5 m. high and cooled by an external oil (S.K. oil supplied by Yawata Iron Factory) circulation (refer to Fig. 1)*1, and was

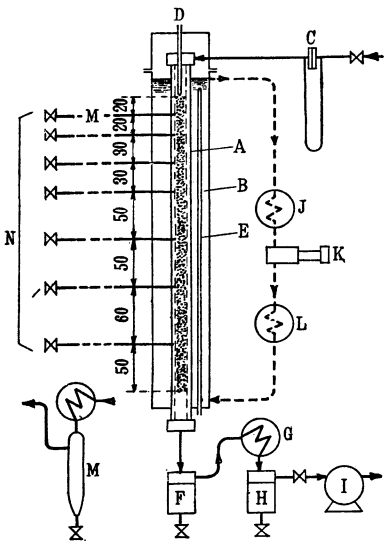

Fig. 1. Flow diagramm of synthesis.
A: Convertor B: Oil bath
C: Flow meter
D and E: Thermocouple well
F: Hot-separator G: Cooler
H: Cold-separator I: Gas meter
J: Coolor
K: Pump } for oil
L: Preheater
M: Water-cooler and separator
N: Sampling port

packed with 620 cc. (1.4 kg.) of granules (1 to 2 mm. diameter) of the catalyst which had been exhaustively reduced at 500°C by hydrogen under normal pressure in a separate vessel. The catalyst contained the following promoters such as 3% Al_2O_3, 1% CaO, 1% MgO, 1% WO_3, 0.25%

*1 Since a pump capable of circulating hot oil was not available, the oil was cooled before entering the pump.

CuO, 0.5% K_2O in wt. % and gave a high yield of oxygenates in the small convertor as described previously. The catalyst bed was 3.1 m. high, and from successive seven ports at various intervals along the bed (refer to Fig. 1) quantities of gases, each not exceeding 7 vol. % of the entering gas, were alternatively led during the synthesis to a water-cooled separator, to be freed of oil and water. The gas from the exit of the convertor was also passed through a hot separator for removal of wax and then through a sequence of three cold separators for removal of oil. The gases, after the reduction of their pressure through respective reducing valves, were analysed for the reaction products, such as carbon dioxide, methane and gaseous olefin, as well as for the residual reactants, such as carbon monoxide and hydrogen. Their volumes were measured by gasmeters without removal of gasol and carbon dioxide.

The temperature was measured by a thermocouple placed in the catalyst bed near the entrance of convertor as well as by another inserted in the oil bath.

Synthesis.—The synthesis was conducted under a pressure of 25 kg./cm², at a flow rate of about 280 l./hr. (S.V., 450) of synthesis gas containing hydrogen and carbon monoxide in a ratio of 1; 1, and at temperatures maintaining the synthesis at a desired apparent contraction*2. The steady state of synthesis was required for measurements and it was attained as follows: After an induction of 50 hr., during which the flow rate and the apparent contraction were kept considerably low (S.V., 250; the contraction less than 20%), the temperature was gradually raised until the contraction was about 45% at S.V. of 450; thereafter an additional operation of 30 hr. established the constant yield of solid plus liquid for a definite duration of synthesis. After the measurements at the contraction of about 45% (test No. 1) the temperature was adjusted to lower the contraction to about 35% (test No. 2) at the same S.V. for repeating series of measurements.

Composition of the Product.—The oily product was distilled into fractions of a temperature difference of 20°C under the atmospheric pressure and then a reduced pressure of 5 mmHg, until the final distillation temperature attained to 200°C and 190°C respectively. The fractions were then analyzed for alcohol, ester, cabonyl compound, olefin and paraffin*3. The aqueous product was first subjected to the determination of acid content, and then distilled into fractions for the determination of the content of alcohols (C_1—C_4). The products separated from the gases withdrawn through the ports were, however, too small in amount to be fractionated, and hence the average alcohol content in the aqueous products was estimated only as an equivalent of C_2-alcohol.

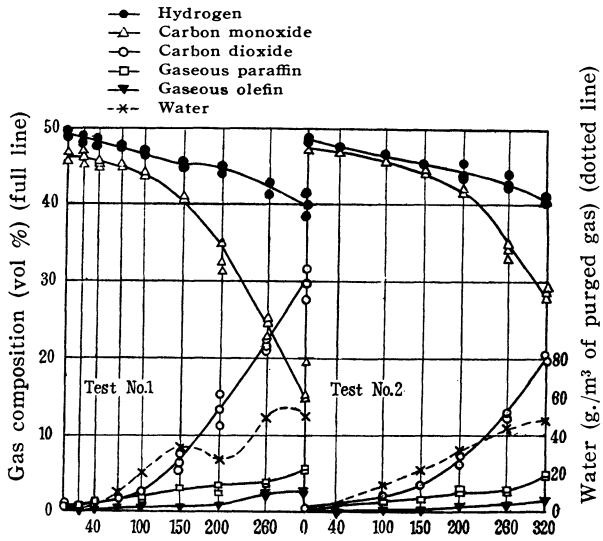

Fig. 2. Results of analyses for reactants and products in gases taken from bed and amounts of water obtained per m³. of purged gases.

*2 The apparent contraction is defined as $1-E/F$, where E is the volume of exit gas containing gasol and CO_2, and F is the volume of feed gas at standard temperature and pressure.

*3 The hydroxyl number, from which alcohol content in the fraction was estimated, was determined by acetylation at 100°C with acetic anhydride in pyridine. The saponification number was determined in the usual way with alcoholic potassium hydroxide. The carbonyl number was determined by reaction with hydroxylamine in alcoholic solution and titration with aqueous hydrochloric acid. Olefin contents were calculated from bromine number determined as usually (refer to H.L. Johnson et al., *Anal. Chem.*, 23, 869 (1951)), and paraffin contents were given as residues obtained by dissolving the fraction in a mixture of phosphoric anhydride and concentrated sulfuric acid (A.S.T.M. Standards (1953), Part 5, p. 1040).

Results and Computation

Results.—Results obtained from syntheses at apparent contractions of 46.3% and 36.1% are shown in Fig. 2 and Table I. In Fig. 2

TABLE I
FLOW RATE AND CHARACTER OF EXIT GAS AND YIELD OF PRODUCTS

	Test No. 1	Test No. 2
Flow rate of entering gas g./h.	192	192
Flow rate of exit gas g./h.	151	162
Composition g./h.		
H_2	5	6
CO	27	62
CO_2	93	70
N_2	14	15
gaseous paraffin (CH_4)	6	5
gaseous olefin (C_3H_6)	6	4
Product obtained (aqueous)	7	9
in separator g./h. (oil+solid)	21	14
Difference between entering and exit gas g./h.	13	7
Use ratio (H_2 : CO)	1 : 1.25	1 : 1.34
(oil+wax+spirits)/m^3. ($CO+H_2$), g.	103	98
(C_3H_6)/m^3. ($CO+H_2$), g.	30	29
(CH_4)/m^3. ($CO+H_2$), g.	28	32

the dotted curve indicates the amount, per 1 m^3 of purged gas, and of water given by the subtraction of amount of alcohol from that of aqueous product in the cold separator. The alcohol content tended to increase with the extent of conversion, as is shown in Table II. Table II shows use ratios of hydrogen to carbon monoxide for increasing conversion.

TABLE II
USE RATIO AND ALCOHOL CONTENT VARYING WITH LENGTH OF CATALYSET BED

	Distance from entrance, cm.							
	20	40	70	100	150	200	260	310
Use ratio Test No. 1	1.00	1.11	1.08	1.04	0.93	0.74	0.75	0.80
Test No. 2		1.80		1.10	1.04	0.92	0.81	0.75
Alcohol in ,, No. 1	0	1.6	2.4	3.3	4.7	3.3	8.2	10.5
aq. product ,, No. 2					3.0	4.6	4.0	12.1

(wt %)

In the present experiment, as the method used for the analysis of the residual gases has been incapable of providing the details in composition of the gaseous hydrocarbon ($C<5$), the gaseous paraffin and olefin are roughly assumed to consist of methane and propylene respectively, as shown in Table I. This table shows that the flow rate of the entering gas differs slightly from that of the exit gas. The greater part of this difference might probably be due to the escape of lower alcohol and liquid hydrocarbon included by the purged gas through the separator.

The composition of the oil from test No. 1 is shown in Fig. 3. In this case the aqueous

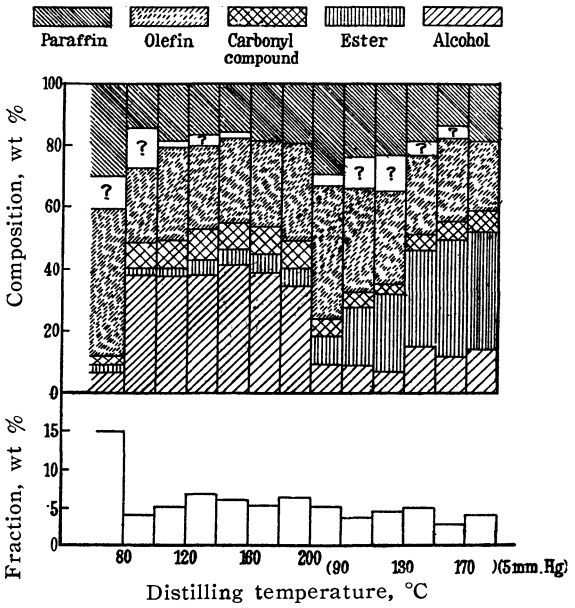

Fig. 3. Results of analyses for liquid product in test No. 1.

product amounted to about one third of the amount of oil plus solid, and contained 0.6% C_1–, 6%, C_2–, 1% C_3– and 3% C_4–alcohols with 2.4% acid equivalent in amount to acetic acid. The oil and aqueous product from test No. 2 contained a somewhat smaller amount of oxygenates than that from test No. 1, whereas the amount of aqueous product from test No. 2 was greater than from test No. 1. Though the amount of oxygenates produced in the larger convertor was slightly less than that in the previous small convertor, the catalyst produced invariably the oxygenates attaining to half the total yield even under the conditions less suitable for oxygenates formation than those in the Synol process.

Computation of Partial Pressure of the Components in the Catalyst Bed.—The apparent contraction and the partial pressure of any component of synthesis gas entering the convertor at any point in the bed are computed from the results shown in Fig. 2.

Since the amount of oxygen appearing as oxygenates (but not water) in the separator of the exit attained to only a few per cent of the amount of oxygen supplied as carbon monoxide, the following oxygen balance is permissible.

$$Vf_{CO}=V'(f'_{CO}+2f'_{CO_2})+v_{H_2O}$$

where V is the volume of entering gas and V' the estimated volume of gases at different heights of the bed, both corresponding to normal temperature and pressure; f and f', the mole fractions referred to subscript in the entering gas and residual gas from the separator; v_{H_2O}, the volume of vapour at N.T.P. of the water obtained in the separator per V' of the residual gas. V' and hence the apparent contraction ($C=1-V'/V$) at any point in the bed may be evaluated from this oxygen balance in conjunction with the measured values of f, f' and v_{H_2O}.

TABLE III

COMPOSITION, FLOW RATE, AND PHYSICAL CHARACTERISTICS OF ENTERING AND EXIT GASES

	Entering gas		Exit gas	
	Test No. 1	Test No. 2	Test No. 1	Test No. 2
Composition				
H_2	49.3	48.0	36.0	37.6
CO	46.2	47.2	13.9	26.0
CO_2	0.4	0.5	29.3	18.6
N_2	4.1	4.3	6.9	6.2
H_2O			5.2	6.0
C_2H_5			5.3	3.9
C_6H_{12}			2.5	1.4
C_4H_9OH			0.7	0.3
Flow rate kg./h.	192	192	185	185
; l./h. at N.T.P.	283	277	174	196
C_p kcal./kg. °C	0.468	0.456	0.414	0.434
μ kg./m. h.	0.0851	0.0853	0.0813	0.0830
λ kcal./m. h. °C	0.1003	0.0990	0.0698	0.0765
C_pGS kcal./h. °C	0.0899	0.0876	0.0766	0.0803
U kcal./m². h. °C	58.1	57.7	51.5	52.5

The flow rate of gas and vapour in the convertor is, however, not directly related to V' because part of the oily product exists as a vapour. In this respect the amount of product from the hot separator predicted the amount of the liquid in the catalyst bed, since the separator was maintained at a temperature similar to that of the convertor. As for the mean molecular weight of the product (hydrocarbon and alcohol) in gaseous and vapour state at the exit the results in Fig. 3 and in Table I are available for the estimation when the fraction and composition of a product distilling below the lowest distillation temperature (140°C at 5 mmHg) of the total product in the hot separator are taken into account. The results are shown in Table III. Since the flow rates of the gases plus vapourized products at the exit of the convertor are available from the results in Table III, the flow rate and partial pressure of the components at any point of the bed are computed when the flow rate is assumed to vary proportionally with the change of V' (Fig. 4).

Consumption of Carbon Monoxide and its Rate.—The principal primary reaction of the synthesis with iron catalysts may be represented by the equation*4

$$\left.\begin{aligned} H_2+CO &\rightarrow -CHOH \\ -CHOH+H_2 &\rightarrow -CH_2-+H_2O \end{aligned}\right\} \quad (1)$$

Alcohols or hydrocarbons may be formed as the results of the stepwise addition of methylene radicals to one end of a growing chain terminated by a hydroxymethylene radical or a methylene radical[5,6]. The water-gas shift-reaction (2) between carbon monoxide and water formed primarily by (1) may be the source of carbon dioxide[7,8]

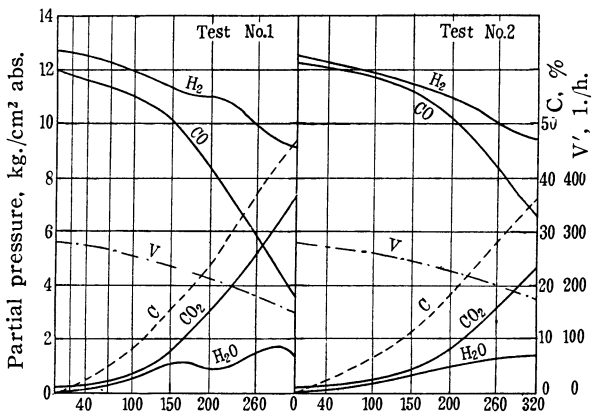

Fig. 4. Change of partial pressure of components, apparent contraction C, and volume of residual gas V', with length of catalyst bed.

*4 In the synthesis the reaction represented by the equation $H_2+2CO \rightarrow -CH_2- +CO_2$ would also take place. The previous investigation (*J. Chem. Soc. Japan, (Ind. Chem. Sect.)* **57**, 100 (1954)) revealed that the reaction took place actually in the synthesis with the catalyst containing silica as a promoter but not with the catalyst described in this paper.

5) E.J. Gibson and C.C. Gall, *J. Appl. Chem.*, **4**, 49 (1954).
6) A.W. Weitkamp and C.G. Fuge, *Ind. Eng. Chem.*, **45**, 363 (1953).
7) H. Koelbel and F. Engelhardt, *Chem. Ing. Tech.*, **22**, 27 (1950).
8) R. B. Anderson, B. Seligman et al., *Ind. Eng Chem.*, **44**, 391 (1952).

$$CO+H_2O \rightarrow H_2+CO_2 \quad (2)$$

The consumed amounts of carbon monoxide observed at different heights of the catalyst bed can be attributed to the sum of the amount of two kinds, the one from (1) and the other from (2), without conflict of evidence in the observed use ratios of hydrogen to carbon monoxide as well as the amount of water formed. When the evaluated amounts of carbon monoxide consumed according to either Eq. (1) or (2) are plotted against the quantity of the catalyst packed in the bed, Fig. 5

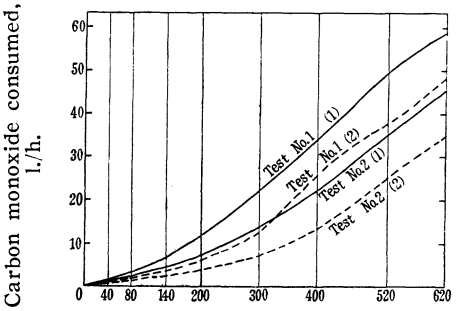

Fig. 5. Consumption of carbon monoxide by reaction (1) or (2) with increasing volume of catalyst.

results. The curves in this figure may then be graphically differentiated to give the rates of the carbon monoxide consumption, cc. $CO_{conv.}$/hr. cc. catalyst.

Computation of Temperature Gradient in Catalyst Bed.—In the present experiment the temperature was measured in the oil bath along the wall of the convertor, but not in the catalyst bed except at the top. The temperature gradient thus measured might relate to the longitudinal distribution in the bed by the usual computation as follows.

Although S. Kodame et al.[9] already pointed out that the true temperature gradient in the catalyst bed where the heat of reaction was great and simultaneously the flow rate was small could not be given unless a three dimensional mathematical treatment of the problem should be employed, the treatment was so difficult in this case, where no rate equation had yet been given, that the calculation was conducted conventionally under the assumption of uniform temperature in the lateral direction of the bed. Under this assumption the rise of temperature due to the heat of synthesis in the longitudinal direction of the bed might be usually given by Eq. (3) or (4).

$$C_pGS\frac{dt}{dx}=S\sum_i\phi_iq_i-2\pi RU(t-t_w) \quad (3)$$

$$C_pGS\Delta t=Q-2\pi RU\Delta x(t-t_w) \quad (4)$$

In Eqs. (3) and (4), C_p is specific heat at a constant pressure, kcal./kg. °C; G, mass velocity of the fluid kg./m² hr.; S, cross sectional area of the convertor, m²; x, height of the bed from the top, m; t, mean temperature of the bed at x from the top, °C; t_w, temperature measured in the oil, °C; ϕ_i, rate of ith reaction, cc. CO/hr. cc. catalyst; q_i, heat of ith reaction, kcal./cc. CO; U, overall coefficient of heat transfer kcal./m². hr. °C; R, radius of the bed, m; and Q is heat evolved by reaction in a volume $S\Delta x$, kcal./hr. The values of C_pGS and U at the entrance and the end of the bed are computed to give the results as shown in Table III*5. C_pGS and U are expressed as functions of the bed length as shown in Fig. 6, when they are again assumed to vary proportionally with the change of V'.

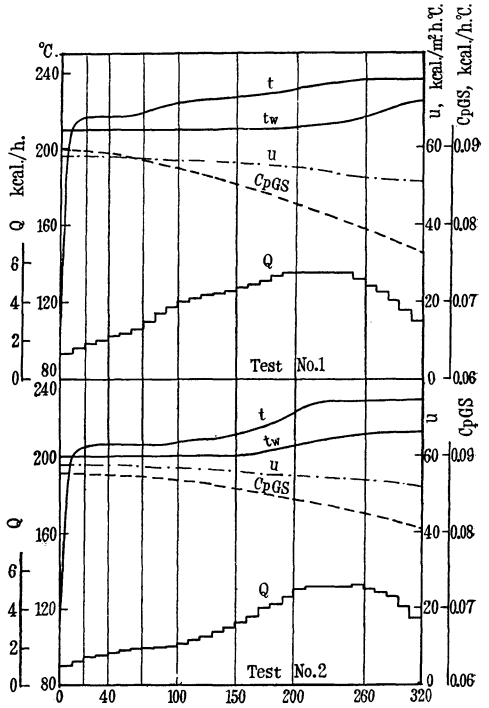

Fig. 6. Temperature measured in oil bath (t_w), C_pGS, and heat of synthesis (Q) related to bed length, and temperature gradient in bed.

9) S. Kodama and K. Fukui, *Kagaku Kikai* (*Chem. Eng.*), 12, 72 (1948) (in Japanese).

*5 The computations were conducted as follows: The values of C_p were obtained from the additive property with the corrections upon pressure by Hougen-Watson of the components. The viscosity and the thermal conductivity were evaluated by the application of the Wilke's method (*J. Chem Phys.*, 18, 517 (1950)) and the Lindsay-Bromley's (*Ind. Eng. Chem.*, 42, 1508 (1950)) respectively, with which the theorem of corresponding state being used. The values obtained are listed in Table III. The heat transfer coefficient between S.K. oil and the wall of the convertor was computed by means of the equation in annular spaces for the case of laminar flow by C.Y. Chen et al (*Trans. A.S.M.E.*, 68, 99 (1946)), and attained to the value of 44.4 kcal./m²hr.°C. The heat transfer coefficient based upon the average temperature of the packed bed for the entering and exit gases was computed by use of the equation by S. Hatta et al. (*Kagaku Kikai*, 12, 58 (1948); 13, 79 (1949) (in Japanese)) which was applicable to the present experiment (R_e<100) and resulted in a respective value of 198 and 136 kcal./m²hr.°C, from which the respective overall heat transfer coefficient was consequently given (Table III).

The heat evolved in the synthesis is also expressed as a function of the bed length, as shown in Fig. 6, from the amount of carbon monoxide consumed according to either (1) or (2), by employing 620 kcal./m³ (H_2+CO) and 9.0 kcal./mol. CO for the heats of reaction by (1) and (2) respectively. From these distributions together with the temperature gradient in the oil bath the temperature is expressed as a function of the bed length when a numerical stepwise computation by trial and error method is employed for Eq. (4) by starting the process from a bed length of 10 cm. from the entrance.

Discussion

Rate Equation of the Synthesis.—Data available for kinetic interpretation are generally obtained from the measurement in an isothermic convertor with a small amount of catalyst, however, in the synthesis such as described in this paper the yield in products such as oil and water is usually too small to permit a detailed treatment of the rate. Although the present experiment was conducted in the convertor with a temperature gradient in the bed, the results were available for the interpretation, as two portions nearly isothermic over a relatively wide range of the catalyst bed were fortunately present.

Rate equations for the synthesis, based on different steps as the rate determining step in terms of the Hougen-Watson's classification, are listed in Table IV together with the equations once proposed by R. B. Anderson et al[10] and H. Tramm[3]. The equation (h) by the former was based on the desorption of adsorbed product as the rate determining step, while that by the latter was not obvious about the rate-determining step in terms of the above classification. S. Kodama[11] proposed the rate equation given by $\phi=d[CH_2]/dt=kC_{carbide}C_H^2$, where C_H is the concentration of hydrogen adsorbed with dissociation no the catalyst surface. The equation resulted in Eq. (c) when $C_{carbide}$ could be assumed equivalent to CO_{ad}, however, the mechanism seemed somewhat improbable[12]. With respect to the components adsorbed on the surface, only one component among the reactants and products was taken into consideration, since the two components made the equation too complicated to be used for the interpretation of the experimental results, whereas an equation without consideration of the adsorbed component, such as Eq. (f) by R. B. Anderson et al for the synthesis with an iron catalyst, proved too simplified to permit the interpretation.

The Equations may be generalized to Eq. (5) which is then rearranged to Eq. (6)

$$\phi=k\overset{i}{\Pi}p_i/(1+k'\overset{j}{\Pi}p_j)^n \tag{5}$$

$$\sqrt[n]{\overset{i}{\Pi}p_i/\phi}=\sqrt[n]{1/k}+\sqrt[n]{k'^n/k}\overset{j}{\Pi}p_j \tag{6}$$

The correct assumption gives a straight line with a positive value of slope and intercept when values of $\sqrt[n]{\overset{i}{\Pi}p_i/\phi}$ are plotted against $\overset{i}{\Pi}p_i$. In Fig. 7, some of the rate equations are shown, being thus plotted, and the Eq. (a), (b), and (h) appear to be more adequate expressions of the rate. The values of k and k' at the temperatures of 229 and 237°C are hence computable and then the apparent activation energy is obtained by the Arrhenius' equation to give the values shown in Table V. From these values here obtained, the rates of synthesis at different temperatures are computed by the respective equations and compared, as shown in Table VI,

TABLE IV
RATE EQUATION

Surface reaction controlling		
$CO_{ad}+H_{ad}\longrightarrow COH_{ad}$	$\phi=kp_{H_2}^{1/2}p_{CO}/(1+k'p_{CO})^2$	(a)
$COH_{ad}+H_{ad}\longrightarrow CHOH_{ad}$	$\phi=kp_{H_2}p_{CO}/(1+k'p_{CO})^2$	(b)
$CO_{ad}+2H_{ad}\longrightarrow CHOH_{ad}$	$\phi=kp_{H_2}p_{CO}/(1+k'p_{CO})^3$	(c)
Adsorption controlling		
$H_2\longrightarrow 2H_{ad}$	$\phi=kp_{H_2}^{1/2}/(1+k'p_{CO})$	(d)
$CO\longrightarrow CO_{ad}$	$\phi=kp_{CO}/(1+k'p_{H_2}^{1/2})$	(e)
By Anderson (Fe-catalyst)	$\phi=kp_{H_2}$	(f)
Desorption controlling		
$Product_{ad}\longrightarrow Product$	$\phi=(kk'p_{H_2}^2p_{CO}/p_{H_2O})/(1+k'p_{H_2}^2p_{CO}/p_{H_2O})$	(g)
By Anderson (Co-catalyst)	$\phi=kk'p_{H_2}^2p_{CO}/(1+k'p_{H^2}^2p_{CO})$	(h)
By Tramm	$\phi=(kp_{H_2}^2/p_{CO})/[1+k'(p_{CO_2}+p_{H_2O})^5]$	(i)

10) H.H. Storch, N. Golumbic et al, "Fischer-Tropsch and Related Syntheses", (1951), pp. 529, 554.
11) S. Kodama, *J. Chem. Soc. Japan*, **62**, 1185 (1941) (in Japanese).
12) O. A. Hougen and K. M. Watson, "Chemical Process Principles", (1950), p. 924.

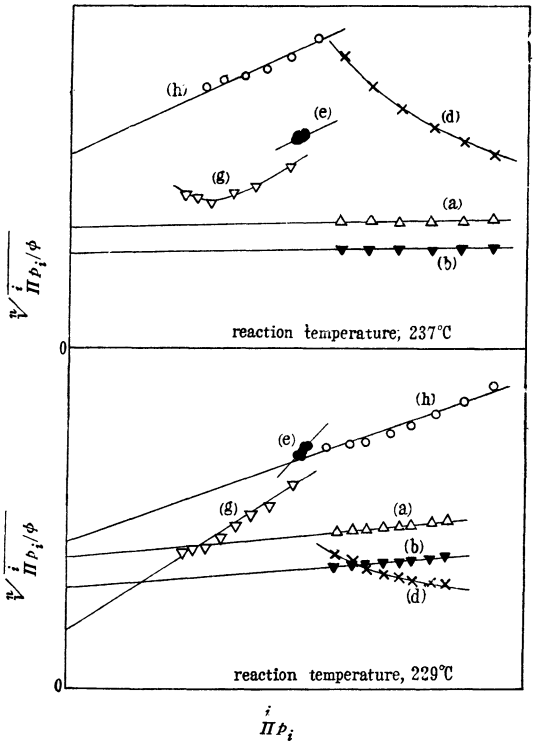

Fig. 7. Experimental rate plotted by various rate equations in Table IV.

with the experimental rate obtained from Fig. 5. Table VI shows good agreement with three rate equations and the agreement is incontestable among them.

With respect to the water-gas shift reaction accompanying the reaction (1), the following rate equation by Padovani-Lotteri[13] is employed

$$\phi = k(p_{H_2O}p_{CO} - Kp_{H_2}p_{CO_2}) \quad (7)$$

and the rate constant as well as the apparent activation energy is similarly evaluated to give the values of 13.45, 9.14 cc. CO/cc. Cat. hr. atm^2 for the former in test No. 1 and No. 2 respectively, and 24.5 kcal./M for the latter. The agreement between the rates computed from the values thus obtained and the experimental is, however, less satisfactory than that attained in the reaction (1).

Lateral Temperature-distribution of Catalyst Bed.—W. Broetz et al[4] gave a following differential equation (Eq. (8)) of lateral heat transfer across the catalyst bed, provided that the temperature were uniform in the direction of gas flow and, at the same time, the concentrations uniform across the bed

$$d^2\theta/dr^2 + (1/r)(d\theta/dr) + \sum_i \dot{n}_{i,w} Q_i e^{B_i\theta}/\lambda = 0 \quad (8)$$

In the equation, r is a lateral distance from center, m; θ, temperature difference between

TABLE V

VALUES OF k, k', AND APPARENT ACTIVATION ENERGY OBTAINED FROM Eqs. (h), (b) and (a)

Equation	Temperature °C	k	k'		Energy of activation
	237	347	0.918×10^{-3}		
Eq. (h)			cc. CO/cc. cat. hr.	atm^{-3}	22.3
	229	244	0.902×10^{-3}		
	237	2.81	2.58×10^{-2}		
Eq. (b)			cc. CO/cc. cat. hr. atm^2	atm^{-1}	25.8
	229	1.88	2.70×10^{-2}		
	237	2.88	1.23×10^{-2}		
Eq. (a)			cc. CO/cc. cat. hr. $atm^{1.5}$	atm^{-1}	25.9
	229	1.91	1.27×10^{-2}		

TABLE VI

COMPARISON OF EXPERIMENTAL RATE WITH RATES COMPUTED FROM Eqs. (h), (b) and (a)

Temperature °C	Test No.	Distance from Entrance cm.	Rate obtained from Fig. 5 cc. CO/h. cc. cat.	Rate computed from Eq. (h)	Eq. (b)	Eq. (a)
237	1	260	119	119.8	122.3	119.2
	1	300	85	85.0	88.2	85.2
229	2	250	109	110.5	110.2	113.0
	2	290	96	92.6	93.1	94.2
222	1	90	105	109.9	102.9	103.2
	2	198	99	98.0	88.6	90.3
217	1	30	63	85.5	81.9	82.1
207	2	90	50	51.8	44.2	45.6

13) C. Padovani and A. Lotteri, *J. Soc. Chem. Ind.*, **56**, 391T (1937).

catalyst bed and oil bath, °C; $\dot{n}_{iw}$, rate of ith reaction corresponding to the temperature of oil bath, mol. CO/m³ cat.; Q_i, heat evolved by ith reaction, kcal./mol. CO; λ, effective thermal conductivity of packed bed, kcal./m. hr. °C; B_i is given by $B_i=E_i/\mathbb{R}T_w^{2*6}$, where E_i is apparent activation energy of ith reaction, T_w, temperature of oil bath, °K; $\mathbb{R}$, gas constant. On the basis of this equation, he derived a relation between $\dot{n}_{iw}$ and $\bar{\dot{n}}_i$, the rate averaged over a cross section in the bed. In the derivation, he gave graphically or numerically the lateral temperature distribution as a function of $R\sqrt{\frac{B\bar{\dot{n}}_iQ_i}{\lambda}}$, but not analytically[14].

Attempts are made here of an analytical solution with simplification of the Broetz's equation and also of its application to the experimental results. The boundary conditions for Eq. (8) are given by

$$-\lambda(d\theta/dr)=U'\theta \quad \text{at } r=R$$

and θ has a finite value at $r=0$

U' is overall heat transfer coefficient, kcal./m² hr. °C, and R, radius of the bed. The equation can neither be analytically solved nor numerically integrated without tedious computation, but reduces to an equation similar to that obtained by R.H. Wilhelm et al[15]. when the terms higher than the third in the expanded series of $e^{B\theta}$ are neglected, and then it is solved to give Eq. (9)

$$\left.\begin{aligned}\theta&=\frac{C}{A}\left[\frac{J_0(r\sqrt{A})}{D}-1\right]\\ A&\equiv\sum_i \dot{n}_{iw}Q_iB_i/\lambda, \qquad C\equiv\sum_i \dot{n}_{iw}Q_i/\lambda\\ D&\equiv U'J_0(R\sqrt{A})-\lambda\sqrt{A}J_1(R\sqrt{A})\end{aligned}\right\} \tag{9}$$

where J_0, J_1 are the Bessel functions of first kind, zeroth and first order respectively. From the equation in conjunction with the observed data, such as the composition of gaseous product, t_w (temperature of oil bath, °C) and the rate equation, the temperature difference θ in the portions of convertor with relatively uniform temperature in the direction of gas flow is given as a function of lateral distance r in Fig. 8. In the computation, B_i is evaluated from the observed t_w and the apparent activation energy (25.8 and 24.5 kcal./mol. for the reaction (1) and (2) respectively), and also $\dot{n}_{iw}$ from the rate equation (h) (Table IV) and Eq. (7) employing the values of k, k' and the partial pressures in gaseous product and hence A and C are consequently determined. D is computable from the values of U' (83.5 and 81.4 kcal./m². hr. °C. at points 90 and 260 cm. apart from the entrance respectively) and λ (0.636 and 0.443 kcal./m. hr. °C.) which are similarly obtained as previously described.

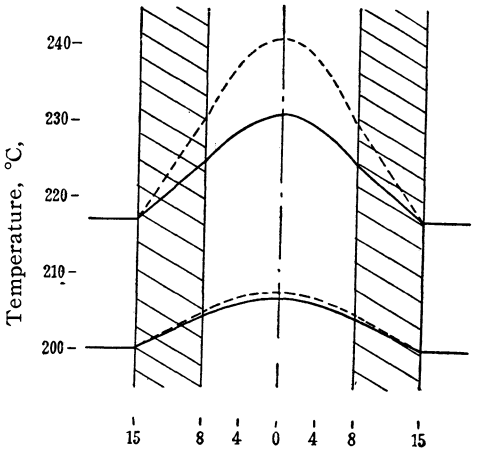

Fig. 8. Lateral temperature gradient in bed computed by Eq. (8). above; Test No. 1, 260 cm. apart from entrance. below; Test No. 2, 90 cm. apart from entrance. full line, analytical solution with simplification. dotted line, numerical computation.

In this figure, it appears that the higher terms may no longer be ignored when θ is larger than 10°C. This is conceivable from the value of B of about 0.05 and illustrated in the temperature-diameter curve at the point 260 cm. apart from the entrance.

Summary

The catalyst containing copper as a promoter has produced a good yield of the oxygenates in the small convertor (volume of the catalyst, 60 cc.) as well as in the larger convertor (620 cc.). Although the syntheses have been conducted at relatively low space velocity of the synthesis gas as compared with the Synol synthesis, the oxygenates amount to so high a value as half the liquid

*6 W. Broetz introduced a relation between the reaction rate ($\dot{n}_i$) at T°K in the catalyst bed and the one ($\dot{n}_{iw}$) corresponding to the temperature in the oil bath, which was given by

$$\dot{n}_i=\dot{n}_{iw}\cdot\exp\left(-\frac{E_i}{\mathbb{R}\cdot T\cdot T_w}(T_w-T)\right)$$

He assumed the following relation when T differed not so much from T_w

$$E_i/\mathbb{R}\cdot T\cdot T_w=E_i/\mathbb{R}\cdot Tw^2=B_i,$$

and attained to

$$\dot{n}_i=\dot{n}_{iw}e^{B_i\theta}.$$

14) W. Broetz, *Z. Elektrochem.*, 57, 470 (1953).

15) R. H. Wilhelm, W. C. Johnson et al., *Ind. Eng. Chem.*, 35, 582 (1943).

and solid products and the result may promise the higher yield of oxygenates at the working conditions analogous to those with the Synol synthesis.

From the results of analyses for the reactants and products in the gases withdrawn from seven different heights of the catalyst bed together with the results of the composition of the product at the exit and also with special attention paid to the temperature gradient and flow rate through the catalyst bed, two types of the rate equation have been presented as shown by Eq. (A) and Eq. (B), both of which are similarly applicable to the observed rate.

$$\phi = kk' p_{H_2}^2 p_{CO}/(1+k' p_{H_2}^2 p_{CO}) \qquad (A)$$

$$\phi = k p_{H_2} p_{CO}/(1+k' p_{CO})^2,$$

$$\phi = k p_{H_2}^{1/2} p_{CO}/(1+k' p_{CO})^2 \qquad (B)$$

The equation (A) was once proposed by R. B. Anderson et al. for the synthesis with a cobalt catalyst.

The lateral temperature distribution in the catalyst bed is given by a simplified analytical solution of the W. Broetz's equation of the heat transfer only when the temperature difference between the wall of the convertor and the catalyst bed is considerably small.

The authors wish to acknowledge the participation of Mr. Tadasuke Hosoya in a part of the experiment and to thank him for his assistance.

Government Chemical Industrial Research Institute, Tokyo

Atomic Weight of Oxygen in Quartz of Contrasted Geologic Origin

By Taneki TOKUDA

(Received July 26, 1955)

It is obvious that the study of the oxygen isotope abundances in silicate rocks, which form about 99% of the outer shell of the earth, may yield valuable information on the origin of the rocks. Therefore, the atomic weight of oxygen combined in silicate minerals and in silica stones of contrasted geological origin was investigated. And some new knowledge on silica stones in Japan has been obtained.

Experimental

Some reactions have been known for decomposition of silicate minerals and rocks:

(a) $SiO_2+2C+2Cl_2 \xrightarrow{>1200^\circ C} SiCl_4+2CO$[1]

(b) $SiO_2+2CCl_4 \xrightarrow{1000^\circ C} SiCl_4+2CO+2Cl_2$[2,3,4,5]

(c) $SiO_2+2C \xrightarrow{2000^\circ C} Si+2CO$[6,7]

(d) $SiO_2+4M^+ \rightarrow Si+2M^+{}_2O \xrightarrow[300\sim310^\circ C]{Cl_2} \uparrow SiCl_4$
$+2M_2O \xrightarrow[400\sim500^\circ C]{HCl} 2M^+{}_2Cl_2+2H_2O$[8,9]

(e) $SiO_2+4KHF_2 \xrightarrow{230^\circ C} K_2SiF_6+2KF+2H_2O$[8,10]

(f) $3M^{++}{}_2SiO_4+8ClF_3 \xrightarrow[Pt,\ HF]{430^\circ C} 6M^{++}F_2+3SiF_4$
$+4Cl_2+6O_2$[11,12]

(g) $M^{++}{}_2SiO_4+4F_2 \xrightarrow[HF]{420^\circ C} 2M^{++}F_2SiF_4+2O_2$[12]

The reaction (e) was used for this investigation. The obtained water and also standard water (tap water of Osaka city[13]) were decomposed electrolytically, and the obtained oxygen was recombined respectively with the hydrogen gas in the same bomb. And the density difference between these two kinds of water was determined by the froat method.

The obtained results are shown in the Table I.

1) F. Ullmann, "Enzyklopädie der technischen Chemie", 2 Aufl. Urban & Schwarzenberg, Berlin, **9**, 504 (1932).
2) S.H. Manian, H.C. Urey and W. Bleakney, *J. Am. Chem. Soc.*, **56**, 2601 (1934).
3) E. Demarcay, *Compt. rend.*, **104**, 111 (1887).
4) Quantin, ibid., **104**, 223 (1887); **106**, 1074 (1888).
5) P. Camboulives, ibid., **150**, 175 (1910).
6) A.P. Vinogradov and E.I. Dontsova, *Doklad. Akad. Nauk S.S.S.R.*, 58, 83 (1947); *C.A.*, **46**, 4442a (1952).
7) M.L. Keith, M.A. Tuve, G.L. Davis and J.B. Doak, *Am. Min.*, **38**, 346 (1953).
8) T. Tokuda and T. Kashida, *Sci. Pap. Osaka Univ.*, No. **6**, 1 (1949).
9) L. Gattermann, *Ber.*, **22**, 186 (1889); L. Gattermann u. K. Weinlig, ibid., **27**, 1943 (1894).
10) T. Titani, *Ann. Rept. Sci. Works Fac. Sci. Osaka Univ.*, **1**, 39 (1952) (Publ. 1953).
11) P. Baertschi, *Helv. Phys. Acta*, **23**, 536 (1950).
12) P. Baertschi, and Sol R. Silverman, *Geochimica et Cosmochimica Acta*, **1**, 317 (1951).
13) I. Kirschenbaum, "Physical Properties and Analysis of Heavy Water", McGraw-Hill Book Co., N.Y. (1951), pp. 378, 417, 422.

TABLE I

THE DENSITY DIFFERENCES BETWEEN THE OXYGEN IN ROCK SAMPLES AND THAT IN STANDARD WATER DETERMINED IN THE FORM OF WATER

No.	Rocks and Minerals	Excess Density of Water (γ)	Locarity
	Sedimentary rocks		
1	Quartz schist	5.8	Mikawa (Okuyama), Japan
2	,,	4.4	,, (Yagen), ,,
3	Vein quartz (Sedimentary?)	4.1	Wakasa, ,,
4	,, (,,)	3.8	Tamba, ,,
5	Recrystallized chert	4.7	,, ,,
6	,,	3.8	,, ,,
7	Radiolarian chert	3.0	Kuroda, Shiga, ,,
8	Diatomite	3.4	(Commercial) ,,
9	,,	5.0	,, ,,
	Igneous minerals		
10	Microcline	2.0	Yamanashi, ,,
11	Augite	1.5	Fukushima, ,,
12	Tourmaline	2.0	Hyōgo, ,,
	Sedimentary rocks		
13	Cheshire orthoquartzite	3.4	Vermont
14	Arkose	3.2	Connecticut
15	Dover flint	6.1	England
16	Moquoketa shale	4.3	Iowa
	Igneous rocks		
17	Gneissic granite	2.8	South Dakota
18	Greenland basalt	1.8	
19	Basalt	2.4	Columbia River, oregon
20	Lavas	2.7	Paricutin

(No. 1~No. 12). Those by P. Baertschi[14] obtained using the massspectrometer are also shown in the same Table (No. 13~No. 20). Excess density of oxygen in these silica stones, namely Mikawa quartz schist, chert, vein quartz, and diatomite was $+3.0\sim+5.8\gamma$, and that in the igneous minerals, namely microcline, augite and tourmaline was $+1.5\sim+2.0\gamma$. According to P. Baertschi, excess density of oxygen in sedimentary rocks was $+3.2\sim+6.1\gamma$, and that in igneous rocks is $+1.8\sim+2.8\gamma$. Therefore, the results of the author by the froat method is in good agreement with those of P. Baertschi by the massspectrometer, in spite of the fact that chemical procedure of decomposition of rocks and method of determination of oxygen abundance ratio of the present author is based on an entirely different principle from that of P. Baertschi.

Discussion

It has been known that chert and diatomite are sedimentary rocks. Therefore, the obtained value; $+5.0\sim+3.0\gamma$, is recognizable. From the results on Mikawa quartz schists; $+5.8\sim+4.4\gamma$, It is recognized that Mikawa silica stone is a metamorphic rock of sedimentary origin. And the stone has been grown, may be, from chert[15]. It is noteworthy that the vein quartz in the Tamba silica stone and in the Wakasa silica stone has the value, $+4.1\sim+3.8\gamma$, as high as the recrystallized chert, $+4.7\sim+3.8\gamma$. They clearly, belong to a group of sedimentary rock, and not to that of igneous one. Accordingly, these kinds of vein quartz are presumed

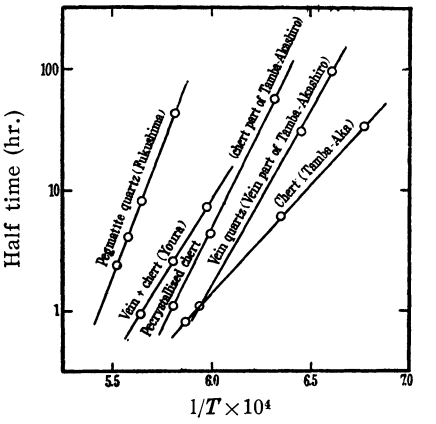

Fig. 1. Half time (hr.) of sluggish inversion from quartz to cristobalite (This inversion is a reaction of first order) when heated at a constant temperature (T °K) in an electric furnace. The firing atmosphere is air.

14) P. Beartschi, *Nature*, **166**, 112 (1950).

15) H. Yamada, "Petrographical Studies on Refractory Materials" Gihodo, Tokyo, (in Japanese), p. 1 (1926).

not to be igneous rock, but to be segregation product[16,17,18].

According to the experimental results of the author[19], sluggish inversion of silica stone from quartz to cristobalite is a reaction of first order. Half times of silica stones are compared with each other in the Fig. 1. As is shown in the Figure, half time of vein quartz is closer to that of chert than to that of pegmatote quartz, in spite of the fact that its chemical composition, density (Table II, Fig. 2), and degree of crystal growth (Fig. 3) are closer to that of pegmatite than to that of chert.

According to O. F. Tuttle[20] and M. L. Keith[21], vein quartz is presumed to be grown at far lower temperature than the quartz in igneous rocks such as pegmatite, granite, and rhyolite; namely at a similar temperature to that of the cryptocrystalline quartz, found in limestone. This result does not contradict our results. According to Keith, Davis, Tuve, and Dork[7,22], the samples of quartz known to have been formed at low temperature have higher content of O^{18} than do the samples that have been formed at high temperatures. The atomic weight of oxygen in silicate minerals and rocks is useful for the investigation of their geological origin, and will be used as a geological thermometer[23].

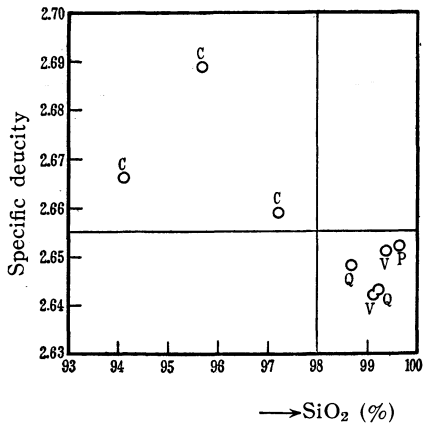

Fig. 2. Relation between specific density and silica content of silica stone.
C: Chert Q: Quartzite
V: Vein quartz P: Pegmatite quartz

TABLE II
CHEMICAL ANALYSIS AND SPECIFIC DENSITY OF SILICA STONE

Classification	Pegmatite quartz	Vein quartz	Vein quartz	Quartzite	Quartzite	Vein and chert	Recrystallized chert	Chert	Radiolarian chert
Common name	Fukushima silica stone	Vein part of Wakasa-Aoshiro silica stone	Vein part of Tamba-Akashiro silica stone	Mikawa silica stone (Yagen)	Mikawa silica stone (Okuyama)	Youra silica stone	Chert part of Tamba-Akashiro silica stone	Tamba-Aka silica stone	Kuroda silica stone
SiO_2	99.72	99.40	99.13	99.25	98.69	98.35	97.23	95.68	94.12
Al_2O_3	0.00	0.12	0.01	tr.	0.38	0.52	0.20	2.87	1.87
Fe_2O_3	0.14	0.15	0.63	0.09	0.20	0.43	2.12		1.89
CaO	0.10	tr.	0.09	—	0.07	0.05	0.09	0.81	0.25
MgO	0.00	—	0.01	0.07	0.29	0.28	0.03	0.24	0.66
MnO	—	—	—	0.65	—	—	—	—	0.24
Alkalis	—	0.10	0.11	—	0.17	—	0.18	—	—
Ig. loss	0.00	0.05	0.10	0.24	0.10	0.35	0.09	0.19	0.77
Total	99.96	99.82	100.08	100.68	99.95	99.98	99.99	99.79	99.80
Specific density	2.652	2.651	2.642	2.643	2.648	2.666	2.659	2.689	2.667

16) S. Iwao, T. Anzai and T. Okabe, *Bull. Geol. Survey Japan*, 2, 10 (1951).
17) H. Koide, *J. Geol. Soc. Japan*, 56, 351 (1950).
18) M. Watanabe, ibid., 57, 6 (1951).
19) T. Tokuda, This Bulletin, 28, 435 (1955).
20) O.F. Tuttle, *Am. Min.*, 34, 723 (1949).
21) M.L. Keith and O.F. Tuttle, *Am. J. Sci. Bowen Volume*, 203 (1952).
22) M.L. Keith, M.A. Tuve, G.L. Davis and J.B. Doak, *Carnegie Institution of Washington Year Book*, No. 49, 36 (1950).
23) Sol R. Silverman, *Geochimica et Cosmochimica Acta*, 2, 26 (1951).

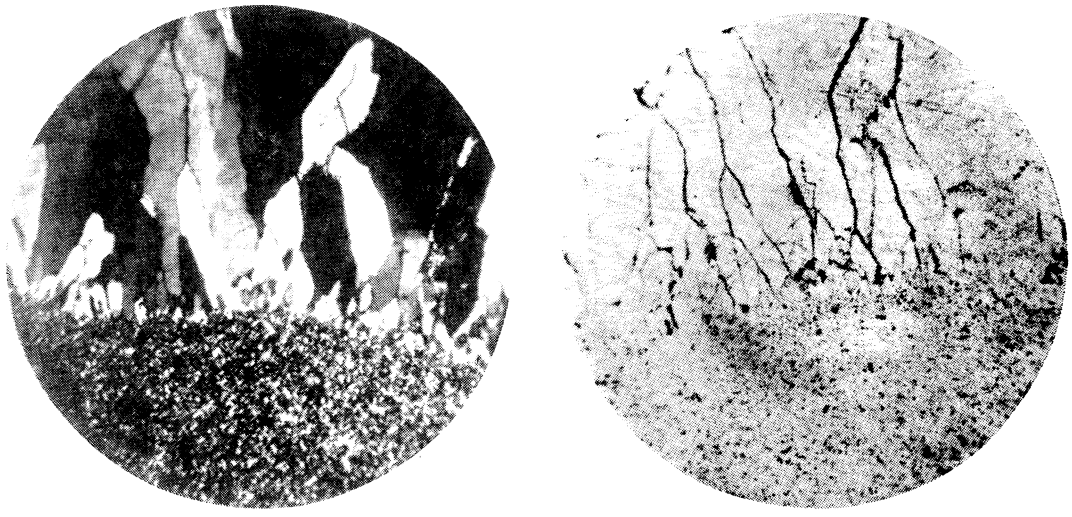

(Crossed nicol.) (Opened nicol.)

Fig. 3. Photomicrographs of vein quartz with recrystallized chert. (×40, Wakasa silica stone, Japan) Upper part of the photographs show vein quartz, and lower part show recrystallized chert.

Grateful acknowledgement is made to Prof. T. Ao of Osaka University and Prof. S. Matsushita of Kyoto University, for their guidance, and to Master K. Kurita for his cooperation. Thanks are also due to the Education Ministry for a Scientific Research Grant.

The Institute of Scientific & Industrial Research, Osaka University
Osaka

Purification of Graphite. I. Removal of Vanadium by Chlorine Gas Treatment

By Akiya KOZAWA and Kumazo SASAKI

(Received August 1, 1955)

Many kinds of industrial uses require high purity graphite. Particularly anode graphite electrode for the chlorinecaustic electrolysis must be especially freed from vanadium[1] among other metal impurities. In the following study the writers tried to remove a small amount of vanadium from carbon materials using chlorine gas, as Y. Kato and R. Yazima[2] did in removing silicon, aluminum and iron from coke samples.

1) Removal of Vanadium from Powdered Samples

The powder of a graphite or coke sample (0.5 g.) which can pass through a 100 mesh sieve is taken in a porcelain boat (50×8 ×8 mm.) and placed in an electric furnace as shown in Fig 1. It is heated for one to two hours in the current of chlorine gas, the current velocity of which is adjusted at about 20 cc. per minute. Then the sample with the addition of sodium carbonate powder is ashed and the vanadium is determined according

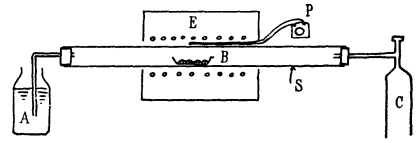

A. 5N–NaOH sol. E. Electric furnace.
B. Porcelain boat. P. Pyrometer.
C. Cylinder chlorine. S. Silica tube.
Fig. 1. Apparatus for Cl_2 treatment.

1) G. Angel, T. Lundén, S. Dahlerus and R. Brännland, *J. Electrochem. Soc.*, **102**, 124, 246 (1955).
2) Y. Kato and R. Yazima, *J. Electrochem. Soc. Japan*, **6**, 168 (1938).

to the colorimetric method proposed by the present writer[3].

The results given in Table I show that vanadium removal is nearly complete at 400°C for the graphite sample, while for coke, amorphous carbon, it is incomplete even at 600°C. It is highly probable that the different behavior between graphite and coke is due to their difference in crystal structure.

central) was determind. The results given in Table II show that the vanadium content does not differ much between these two portions. This fact makes it probable that vanadium escapes as some volatile chloride such as VCl_4, b.p. 154°C or $VOCl_3$, b.p. 127.2°C.

Further, the state of vanadium in the original sample is beyond our present knowledge and the only thing that can definitely

TABLE I

REMOVAL OF VANADIUM FROM POWDERED SAMPLE

No.	Sample	Temp. (°C)	Time treated (hr.)	Vanadium content (γ/0.5 g.) original	after Cl_2 treatment
1	Anode graphite	400	1	136	9
2	Anode graphite	400	2	136	7
3	Coke	400	1	230	190
4	Coke	500	1	230	190
5	Coke	600	1	230	200

TABLE II

REMOVAL OF VANADIUM FROM GRAPHITE RODS

No.	Temp. (°C)	Time (hr.)	Vanadium content* after Cl_2 treatment Central part (γ/0.5 g.)	Outer part (γ/0.5 g.)	Removal (%)
1	100	1	100	105	33
2	220	1	92	95	39
3	340	1	21	20	86
4	400	1	11	12	93
5	520	1	9	8	94
6	620	1	6	5	96

* original vanadium content: 140–170 γ/0.5 g., mean 150 γ/0.5 g.

2) Removal of Vanadium from Graphite Rods

A number of rods (10×10×35 mm.) were cut from a sample of anode graphite for mercury cell process, a product of graphitization at a temperature above 2200°C. The rods were treated with chlorine gas in a similar way as in experiment (1). After this treatment, the vanadium content of two separate portions of the rods (outer and

be said is that the element can not occur as carbide because vanadium carbide is attacked by chlorine gas only when it is heated red[4].

Studies concerning other impurities will be published shortly.

Department of Applied Chemistry, Faculty Engincering, Nagoya University, Nagoya

3) K. Sugawara, M. Tanaka and A. Kozawa, This Bulletin, 28, 492 (1955).

4) H.J Emeléus and J.S. Anderson, "Modern Aspects of Inorganic Chemistry", (1952), p. 475.

Studies on the Reduction Rate of Aromatic Nitrocompounds by Bechamp's Method

By Sakae YAGI, Terukatsu MIYAUCHI and Chia You YEH

(Received August 2, 1955)

I. Introduction

Since 1854, the year in which Béchamp reduced aromatic nitrocompounds to corresponding primary amino-compounds using iron particles and acetic acid, many investigations into Bechamp's reduction have been carried out by various authors[1] from the scientific and technical standpoints. The curious catalytic action of hydrochloric acid which came into use later was investigated by Witt[2], Whol[3], Raikow[4] and others.

Effective catalysts for the reaction were greatly extended in their scope by Lyons and Smith[5], and recently the reaction mechanism has been discussed by Luder and Zuffanti[6] from the electronic point of view.

Technical preparations of primary amines by this method are now generally performed by batchwise operation.

Some investigations[7] into a continuous process have been reported in the literature, but their industrial success is yet uncertain. With the same purpose as mentioned above, we have studied the technical reaction rate of this reduction as a fundamental approach to an industrially feasible continuous operation. No systematic data on the reaction rate seem to have been published yet.

First, we investigated a batchwise process using an agitated vessel and later a continuous process by means of a fluidized bed reactor proposed by one of the authors[8]. Studies reported here only cover the former.

II. Experimental Procedures

Fig. 1 illustrates the assembly of the reactor. The reaction vessel is composed of double cylindrical tanks, both made of mild steel. The dimensions of the inner part are 100 mm. dia. × 114 mm. height (about one liter in volume). The annular space between the tanks is filled with a boiling

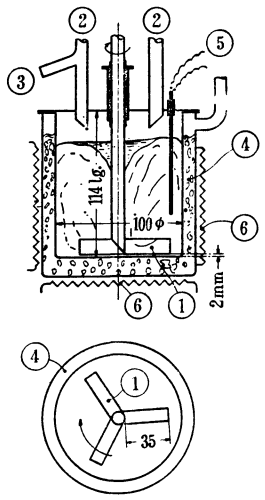

Fig. 1. Experimental apparatus.
1. Three-blades impeller.
2. Reflux condenser.
3. Sampling tube for condensate.
4. Constant-temperature bath.
5. Thermocouple.
6. Electric heatee.

liquid as a heat-transfer medium, choice being made among water, methanol, ethanol and a mixture of water and ethanol, each for its own reaction temperature.

Two reflux condensers at the upper part of the reactor and a sampling tube, to obtain samples of refluxing condensate for analysis, are arranged as shown in the figure.

An impeller composed of three brass blades and a mild steel shaft (blade length 35 mm., blade width 13 mm., blade inclination to the horizontal plane 30° and diameter of the shaft 10 mm.) is rotated in the inner vessel at the axial position, with variable speed.

After the temperature is raised to the desired point, weighed aqueous hydrochloric acid solution of known concentration and weighed iron particles are introduced into the reaction vessel and agitated. When evolution of hydrogen gas ceases about three or four minutes later, the weighed nitrocompound preheated to the reaction temperature is introduced as fast as possible within about 20 sec. The lapse of time from the completion of the introduction to the sampling is regarded as the reaction time. Prior to the runs, the iron particles are pretreated as follows. To remove oily matter, the particles are kept in a loosely closed glass flask and exposed to the

1) P.H. Groggins, "Unit process in Organic Synthesis", McGraw-Hill Pub. Co., 4th ed., (1952).
2) O.N. Witt, *Chemische Ind.*, **10**, 218 (1887).
3) A. Wohl, *Ber.*, **27**, 1432, 1815 (1894).
4) P.N. Raikow, *Zeit. für Angew. Chem.*, **26**, 196, 239 (1916).
5) R.E. Lyons and L.T. Smith, *Ber.*, **60**, 173 (1927).
6) W.F. Luder and S. Zuffanti, refer to 1), p. 89.
7) A.G. Kalle, (I.G.), *Ind. Eng. Chem.*, **40**, 1574 (1948); Vikman and Mukhanova, Russian p. 52006 (1937).
8) Sakae Yagi, Japanese pat. 204, 536 (1954).

temperature of 450°C for ninety minutes. They are cooled and then etched with dilute hydrochloric acid. Nitrobenzene and hydrochloric acid are respectively of "extra-pure grade" and the other nitrocompounds are of "chemically-pure grade".

III. Analytical Methods

Liquid mixtures such as $PhNO_2$–$PhNH_2$–H_2O or *o*-nitrotoluene-*o*-toluidine-water are analysed under ordinary temperature as follows:

Provided the value of Φ, the molar ratio of the residual nitrocompound to its initial quantity, is higher than about 0.1, a fairly good linearlity holds between amine mole fraction, in an equilibrium mixture of three components, and its refractive index, as shown in Fig. 2. Then with

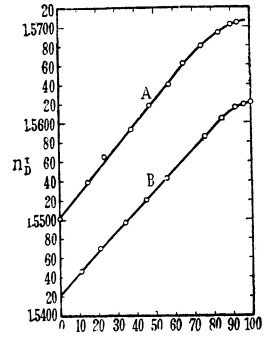

Fig. 2. Refractive index vs. Φ.
(a) Ph. NO_2–Ph. NH_2–H_2O System at 42.5°C.
(b) ortho. $CH_3C_6H_4NO_2$ –ortho. $CH_3C_6H_4NH_2$–H_2O at 25.0°C.

a small quantity of refluxing condensate taken at intervals, its refractive index is measured with an Abbe Refractometer after separating the sample into two liquid layers by a centrifuge. The true value of Φ can then be determined from the equilibrium relationship between composition of the refluxing condensate and that of the bulk.

A polarographic determination[9] is made when Φ is smaller than 0.05 because the linearlity does not hold in this range. Samples are taken from liquid bulk in this case.

p-nitrotoluene and *α*-nitronaphthalene are determined by volumetric analysis since their reaction mixtures remain in solid state under ordinary temperatures.

During reduction, a few ml. of the oil layer is taken from the liquid bulk, neutralized with a saturated aqueous solution of sodium carbonate and diluted with a known quantity of ethanol.

Analysing this filtrate, total amine and nitrocompound are determined respectively. The former is back-titrated[10] with 0.1 N sulfanilic acid solution after an excess of 0.1 N sodium nitrite solution is added. The reduction method[11] with $TiCl_3$ is employed to determine the content of nitro-compound.

IV. Expression of the Reaction Rate

As will be later described, it is experimentally found out that the reaction rate is proportional to the surface area of iron, provided the iron particles are fully fluidized into the reaction mixture.

The overall reaction rate, R is expressed as the rate of nitrocompound consumption per unit surface area of active iron, as

$$R=-\frac{1}{A_T}\frac{dN_N}{d\theta}=-\frac{1}{a_T}\frac{d\Phi}{d\theta}$$

$$=-\frac{1}{a_p+a_w}\frac{d\Phi}{d\theta} \quad (1)$$

where R=Overall reaction rate (mol./cm²min.)
θ=Reaction time (min.).
$A_T=(A_p+A_w)$, the total surface area of reacting iron after the lapse of time θ (cm²).
A_p=Surface area of iron particles after θ (cm²).
A_w=Inside wall area of the reaction vessel plus the surface area of mild steel shaft both of which keep contact with the reaction mixture (cm²).
N_{N_0}=Initial molal quantity of nitrocompound (mol.).
N_N=Residual molal quantity of θ nitrocompound after θ (mol.).

$\Phi=N_N/N_{N_0}$, $a_T=A_T/N_{N_0}=a_p+a_w$,
$a_p=A_p/N_{N_0}$, $a_w=A_w/N_{N_0}$

From the material balance between reactants, N_F, the residual atomic quantity of iron particles after θ, is given by Eq. (2), with an assumption that the overall stoichiometric chemical equation is as follows since hydrochloric acid behaves ultimately as a catalyst

$$R\cdot NO_2+H_2O+\frac{9}{4}Fe=R\cdot NH_2+\frac{3}{4}Fe_3O_4$$

$$N_F=N_{F_0}-\frac{9}{4}\left\{(N_{N_0}-N_N)-\int_0^\theta A_w R d\theta\right\} \quad (2)$$

where N_{F_0} is the initial atomic quantity of iron particles (atms).

On the other hand, F_p, the weight of iron particles after θ, and A_p are assumed to be expressed by Eqs. (3) and (4) respectively

$$F_p=\psi\rho_F d_p^3 n=N_F M_F \quad (3)$$

9) T. Takeuchi and M. Kasaki, *J. Soc. Chem. Ind. Japan*, 52, 69 (1949).
10) J. Phillips and A. Lowy, *Ind. Eng. Chem., Anal. Ed.*, 9, 381 (1937).
11) F.L. English, *Ind. Eng. Chem.*, 12, 994 (1920).

$$A_p = \phi d_p^2 n \tag{4}$$

where M_F = Atomic weight of Fe (g./mol.).
ρ_F = True density of iron (g./cm³).
d_p = Mean representative diameter of iron particles after θ (cm.).
n = Total number of iron particles (−).
ψ = Volumetric shape factor (−).
ϕ = Surface shape factor (−).

From the Eqs. (2), (3) and (4), a_p or A_p/N_{N0} is finally transformed into Eq. (5), provided the ratio of ϕ to ψ remains fairly constant or its mean value maintained throughout the progress of the reaction.

$$a_p = \frac{\phi}{\psi \rho_F} \cdot \frac{M_F \beta}{d_{p0}} \left[1 - \frac{9}{4\beta}\left\{(1-\Phi) - \int_0^\theta a_w R \mathrm{d}\theta\right\}\right]^{2/3} \tag{5}$$

where $\beta = N_{F0}/N_{N0}$
d_{p0} = Mean representative diameter of iron particles at the beginning (cm.).

By means of Eqs. (1) and (5), we are able to express the experimental data in terms of R.

For practical calculations, however, the term $\int_0^\theta a_w R \mathrm{d}\theta$ is inconvenient to use. Therefore, from equation (1) we obtain

$$R \mathrm{d}\theta = -\mathrm{d}\Phi/(a_p + a_w)$$

and which enables us to transform the above integral into:

$$\int_0^\theta a_w R \mathrm{d}\theta = \int_\Phi^{1.0} \frac{\mathrm{d}\Phi}{1 + a_p/a_w}$$

This final form is used to correct the surface effect of iron vessel and agitator shaft.

In order to calculate a_p, by Eq. (5), based on the experimental data, the integral in the parentheses is neglected at first, as the first approximation, and R is calculated based on this approximation. With this approximate value of R, a_p is recalculated by Eq. (5) as the second approximation. Such recalculations are repeated until the final value of R is obtained.

In our experiments, the value of A_w is 210 cm² and the ratio of a_w/a_p, in one of our runs, is 2.72% at the initial stage of reaction and 10.1% at the final stage, provided the β- value is 2.50. The mean representative diameter of the iron particles is defined as the geometrical mean value of the upper and lower sizes of mesh, and the ratio of the shape factors is determined by microscopic observation.

V. Reduction of Nitrobenzene by Bechamp's Method

Because of the fundamental importance of nitrobenzene among various nitrocompounds, basic studies are mainly centered on the reduction of this compound.

V-1. Effects of Various Physical Factors. —In this reaction, the system is composed of a mixture of four heterogeneous phases of solid iron particles, oxide sludge, an acidic aqueous layer and an oil layer. Experiments are made to determine in which phase or phase boundary the reaction proceeds mainly.

a. Effect of Rotation Speed of the Impeller. —Rotation speed of the mixing impeller mainly has influences on fluidization of iron particles into liquid bulk (settling of iron particles results in decrease in effective reaction surface), diffusional rate of reactants to the surface of iron particles, dispersion of heterogeneous liquid phases, mass transfer rate between these phases, removal and control of reaction heat and equalization of reaction temperature within the reaction mixture.

Under a standard reaction condition (refer to V-3), the rotation speed of the impeller is set at 550, 1100 and 2200 r.p.m. Between 800 and 900 r.p.m., there is a critical rotation speed where the total iron particles are fully fluidized into the liquid bulk.

The reaction rate at Φ-value of 0.5 (the rate around this Φ-value is apparently expressed by zeroth-order reaction) is illustrated in Fig. 3.

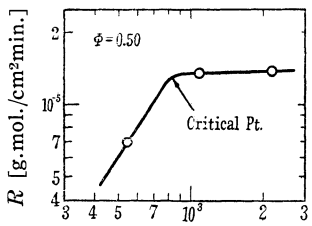

Fig. 3. R vs. r. p. m.

As obvious from the figure, the effect due to the rotation speed of the stirrer on the reaction rate is negligible when the iron particles are fully fluidized into the liquid bulk or the total surface area of iron particles is all effectively used.

For this reason, all the subsequent runs are performed at the rotation speed of 1100 r.p.m.

b. Effect of Surface Area of Iron Particles on the Reaction Rate.—Under the standard reaction conditions, experiments are made to

trace the effect of surface area of iron particles on the reaction rate. A method of varying β with constant mesh size of iron particles and another of varying particle size with constant β are taken in turn to determine the surface effect.

Results obtained are illustrated in Fig. 4. The solid lines in this figure are derived from the integral form of Eq. (1), that is

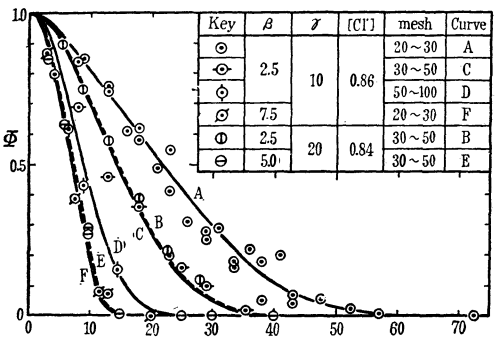

Fig. 4. Effect of the surface area of iron particles on the reaction rate.

$$\theta = -\int_{1.0}^{\Phi} \frac{d\Phi}{(a_p + a_w)R} \qquad (6)$$

where R is the standard reaction rate given as line A in Fig. 11. Agreement between the experimental results and the calculated lines seems to verify that the reaction rate is proportional to the surface area of iron particles.

Provided γ-value, the molal ratio of water to nitrocompound, is less than 6~7, the rate decreases steadily as the reaction proceeds.

The experimental results, however, verify the above conclusion as obvious from the lines B and C in Fig. 11.

c. Effect of Liquid Volume on the Reaction Rate.—Fig. 5 illustrates the effect of γ on the reaction rate under Φ-value of 0.5. If γ is

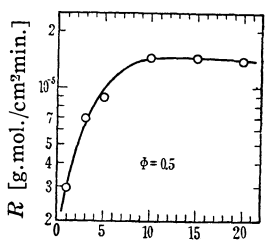

Fig. 5. Effect of the liquid bulk volume on the reaction rate.

larger than 6~7, the reaction proceeds smoothly and the rate is fairly constant, independent of changing γ.

This is supposed to mean that the reaction does not occur in the aqueous phase.

An increase in the volume of the oil layer also fails to improve the rate; in this case local reaction proceeds violently due to local overheating when the aqueous layer is decreased in volume compared with the oil layer.

In such an extreme case as when a theoretically required amount of water is used, even generation of ammonia vapor is observed.

This local phenomenon is supposed to be ascribed to insufficient removal of evolving reaction heat as a result of difficulty in vaporization of the co-existing water.

d. Reduction of Nitrobenzene with a Rotating Circular Iron Disk.—Nitrobenzene containing aniline in various proportions is reduced with a circular iron disk, made of mild steel, (80 mm. in dia., 6~7 mm. thick), with a center shaft, in order to determine whether the reaction proceeds mainly on the iron surface contacting with the aqueous phase or on that contacting with the oil layer.

This disk is rotated in any desired phase of oil or aqueous layer.

A reactor composed of flat-bottomed double glass cylinders of similar form is used and the annular space is filled with water boiling under atmospheric pressure. The inner cylinder has dimensions of 100 mm. dia., 250 mm. height, a capacity of about two liters.

Temperature of the reactants is maintained at 98°C. Prior to a run, the same volume of aqueous layer (1N-$FeCl_2$ solution) and that of oil layer (ratio of $Ph.NO_2$ to $Ph.NH_2$ is varied) are both preheated and charged to the height of 200 mm.

A circular iron disk etched with aqueous hydrochloric acid and washed with water is then placed in the axial position in a desired layer.

A low agitation speed of 550 r.p.m. is used to prevent intermixing of the separated aqueous and oil layers.

The reduction rate is expressed as the weight decrease of the disk, per unit surface area of the disk, per unit time. Fig. 6 illustrates the mean curves obtained from various runs when the disk is rotated in oil or in aqueous layer.

It is obvious from the figure that the overall rate of the reaction on the aqueous layer-iron interface is initially higher than that on the oil-iron interface, but there is no appreciable difference between the two in the final reduction stage.

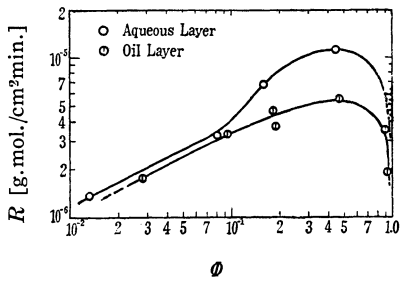

Fig. 6. R vs. Φ with the rotating disk.

In the initial reduction stage, an interesting phenomenon is observed when the disk is rotated in the oil layer, especially when the nitrobenzene content is much higher than the aniline content.

In this case, a hard black crust of Fe_3O_4 covers the disk uniformly and the progress of the reaction is retarded. This would probably be attributed to rapid oxidation of the surface oxide film of lower grade into a final form of ferroso-ferric oxide as a result of insufficient supply of water to the reaction interface due to low solubility of water into the nitrobenzene-rich oil layer. Such retardation due to crust formation is not observed in the water phase under the same conditions or in the final stage of the reduction.

The surface of the smoothly oxidized iron disk is composed of three layers-a thin surface oxide layer of loose structure, a middle thin layer consisting of very fine silvery iron grains and a ground iron layer beneath it.

These layers can easily be recognized by washing the disk with a gentle stream of water.

The existence of the layer of fine iron crystal grains seems to suggest that the reaction of the ground iron surface is liable to proceed along the intergranular zone between iron crystal grains.

In order to calculate R, the residual weight of the iron disk is weighed, for convenience, sake, after the oxide crusts or the fine iron grains are all removed.

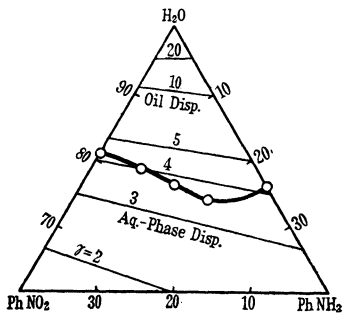

Fig. 7. Phase inversion

R given in Fig. 6 is therefore fairly overestimated in comparison with the value obtained from the batch reduction with iron particles.

e. *Effect of Phase Inversion.*—Fig. 7 illustrates the phase inversion caused by changing the compositions of the three component liquid mixture, Ph. NO_2–Ph. NH_2–1 N $FeCl_2$ aqueous, under the temperature of 100°C. If γ is larger than about four, the oil layer disperses into the aqueous layer to form stable droplets, when the reaction mixture is agitated.

This γ-value roughly corresponds to the critical condition determining the mechanical properties of the oxide sludge obtained from the oxidation of iron particles. If γ is larger than 4–5, an iron oxide sludge which has good filtering property is obtained, but even under the same condition, if the reaction does not proceed to completion, the iron oxide sludge has poor filtering property. Thus, the filtering properties of the oxide sludge seems to depend on the degree of completion of the reaction and the progress of the reaction seems to relate to the phase inversion. One probable explanation for this is that the volumetric ratio of oil to aqueous layer in the above case is much higher than that in the range where γ-value is lower than 4–5 (the equivolumetric point corresponds roughly to γ-value of 6–7) and that such phenomenon as crust formation on the iron particles retards the completion of the reaction.

f) *Some Considerations on the Reaction Zone.*—As obovious from the above-mentioned experiments, the reaction rate seems to be controlled by an overall process going on over the iron surface, because the reaction rate is in proportion to the surface area of iron particles. As illustrated in Fig. 3, no appreciable influence of rotation speed of the agitator is observed, provided the iron particles are fully fluidized into the liquid bulk.

If the rate of mass transfer between heterogeneous liquid phases has some influences on the reaction rate under such fluidized state, the rate should vary with (rotation speed)$^{2\sim5}$ [12]. Similarly, if the diffusion process of reactants through the liquid film formed on the surface of iron particles to the iron surface is the rate-determining step, the rate should vary with (rotation speed)$^{0.8}$ [13].

12) A.W. Hixon and M.I. Smith, *Ind. Eng. Chem.*, **41**, 973 (1949): S. Yagi, T. Miyauchi and K. Kogure, *Chem. Eng. Japan*, **15**, 65 (1950).

13) S. Nagata, *Chem. Eng. Japan*, **13**, 41 (1948). The exponent, 0.8 is determined by extraporation of Nagata's experimental correlation.

Thus, it seems to be reasonable to assume that the overall chemical (or may be physico-chemical) process on the iron surface is the rate-determining step.

From the experimental results obtained with a rotating disk, it is also pointed out that the overall rate of the reaction on the water-iron interface is higher than the rate on the oil-iron interface in the initial stage of the reduction, but that there is no appreciable difference between the two in the final stage.

V-2. Effect of Some Physico-chemical Factors.—a. *Reaction Temperature.*—Fig. 8 illustrates the effect of varying reaction temperature under the following conditions

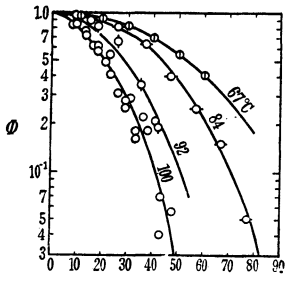

Fig. 8. Φ vs. θ under various temperature.

$\beta = 2.5$ [Cl′]=0.84 N
$\gamma = 10$ r. p. m.=1100
Size of iron particles=20-30 mesh.

Plotting of R vs. $1/T$ is shown in Fig. 9 under Φ of 0.3, because, in this range of Φ, the reaction proceeds, almost independent of the concentration of nitrocompound, that is, according to pseudo-zeroth-order.

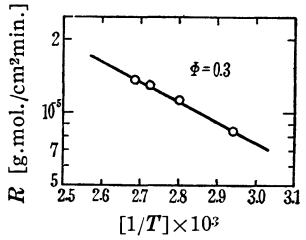

Fig. 9. R vs. $1/T$ (T in °K).

Apparent activation energy calculated is 3.66×10^3 cal./mol. which is unexpectedly small for the large exothermic reaction heat.

The color of oxide sludge also changes with reaction temperature as follows:

React. Temp. °C	60–67	75–84	85–95	100
Color of oxide sludge	pale yellow	reddish yellow	reddish brown	black

b. *Chlorine Iron Concentration.*—According to Lyons and Smith (5), 0.98 N of chlorine ion concentration (0.035 g. of Cl′ as $FeCl_3$ per ml.) gave the best result. Fig. 10 illustrates an example of our experiments with varying chlorine ion concentration under the following conditions:

$\beta = 2.5$ r. p. m.=1100
$\gamma = 10$ Reaction temp.=100°C
Size of iron particles=30-50 mesh.

It is observed that no appreciable improvement can be brought about if the chlorine ion concentration is greater than 0.8 N and that a rapid decrease in the reaction rate

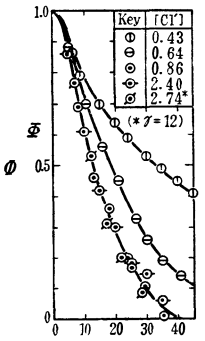

Fig. 10. Φ vs. θ under various chlorine ion concentrations.

occurs for chlorine ion concentration when it is less than 0.8 N.

V-3. Standard Reaction Rate.—On the above mentioned studies is established, for convenience' sake, a standard reaction rate at the boiling point of the reaction mixture under atomospheric pressure, the usual condition industrially applied. This is because the rate is proportional only to the surface area of iron particles employed, provided γ is larger than about 8 and [Cl′] is larger than 0.8 N. With experimental accuracy taken into consideration, the selected experimental condition will be,

$\beta = 2.5$ [Cl′]=0.86 N
$\gamma = 10$ Temp.=100°C
r. p. m.=1100
Size of iron particles=20-30 mesh.

Plotting of Φ vs. θ is illustrated as curve D in Fig. 12, and R, calculated by Eqs. (1) and (5) based on these data, is plotted in Fig. 11 as a function of Φ. The reaction rate is traced up to Φ of 10^{-4}, because aniline of this purity is usually employed both in industry and commerce. The curve is characterized as follows: the initial induction period is followed by zeroth-order behavior up to

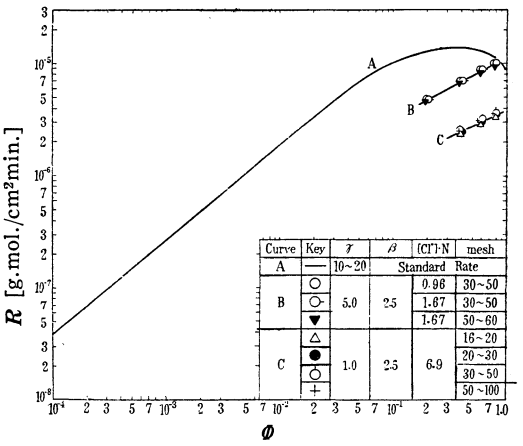

Fig. 11. Typical R vs. ϕ.

ϕ of 0.1, and then, in the final reaction stage, the slope of the reaction rate curve drops, roughly corresponding to that of the apparent first order reaction. These behaviors have also been confirmed experimentally with the continuous flow reactor. As mentioned above, this curve is employed to calculate θ in Eq. (6) and good agreement is obtained between calculated lines and experimental results as already illustrated in Fig. 4.

VI. Preparation of Various Primary Amines

The effects of surface area, chlorine ion concentration and molal ratio of water to nitrocompound are respectively examined using *o*-nitrotoluene.

The results indicate that the reaction proceeds in a similar manner to those of nitrabenzene.

Fig. 12 illustrates the reduction rates of various mononitrocompounds under the conditions given in the figure. The rate curve of *p*-nitroaniline is assumed because the reaction proceeds too fast for us to measure the rate accurately.

Comparisons between the reaction rates of examined nitrocompounds by these curves lead us to conclude that there is a parallel relation between the overall reactivity and the mutual solubility of water and oil layers, although the latter is not yet accurately made clear. Moreover, there may be some influence of the chemical reactivity of each nitrocompound itself. More investigations are needed to solve these problems.

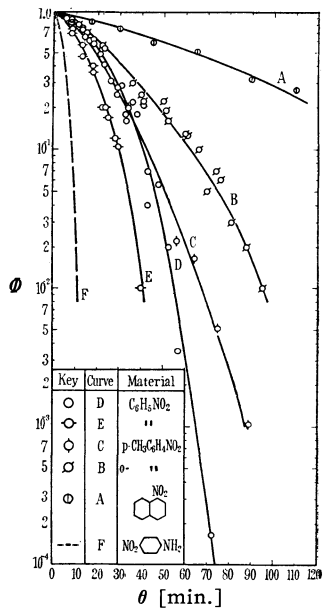

Fig. 12. Reduction rates of various mononitrocompounds $\beta=2.5$, $\gamma=10\sim15$, [Cl'] $=0.84\sim0.88$N, reduction temp.$=100°C$, r.p.m.$=1100$, size of iron particles$=30\sim50$ mesh (Curve D: 20~30 mesh).

VII. General Conclusions

(1) As a fundamental approach to the continuous operation, the technical reaction rates of Bechamp's reduction have been studied, and it has become clear that the continuous process is industrially feasible.

(2) This reaction proceeds mainly according to the surface reaction mechanism on the iron surface, provided the iron particles are fully fluidized into the reaction mixture.

(3) Under the standard reaction conditions, the reduction of nitrobenzene largely proceeds according to the zeroth-order behavior after the initial induction period and according to the first-order in the final stage. In the stage of the zeroth-order behavior, the reaction occurs mainly on the aqueous layer-iron interface, but in the final stage reaction proceeds simultaneously on both water-iron interface and oil-iron interface.

(4) γ whose values are larger than 6–7 is suitable for smooth progress of the reaction.

(5) Apparent activation energy of the reduction of nitrobenzene is determined as 3.66×10^3 cal./mol. in the zeroth-order range.

(6) No appreciable difference in the reaction rate is observed when [Cl'] is 0.8–2.7 N, but rapid decrease in the reaction rate is obserbed when [Cl'] is smaller than 0.8 N.

(7) Various mono-nitrocompounds are also reduced under similar conditions. The reaction rate of each compound seems to have some parallel relationship with its own solubility in addition to its chemical reactivity.

Chemical Engineering Laboratoty, Faculty of Engineering, The University of Tokyo, Tokyo

*Physico-Chemical Studies on Dyeing Process. I. Theory of Dyeing Equilibrium and Half Dyeing Time of Direct Cotton Dyes on Viscose Rayon**

By Masayuki NAKAGAKI

(Received August 3, 1955)

The rate of dyeing is subjected to the slow diffusion of dye into the fibre. Neale et. al. measured this rate under the condition that the liquid yarn ratio is infinite. In this case, the outer surface of yarn spontaneously adsorbs the dye corresponding to the dyeing equilibrium. At the same time, the slow diffusion begins to penetrate the yarn, but the dye concentration of the outer surface is constant, the dye diffused into the yarn being supplied at once from the bath. The rate determing process of dyeing is the slow diffusion into the inner part of a fibre. Meanwhile the slow diffusion is affected by the adsorption amount at the outer surface. To study the rate of dyeing, the dyeing equilibrium should be, therefore, known. As for the latter, Vickerstaff et al.[1] studied it both theoretically and experimentally for the case of the liquid yarn ratio is assumed to be infinite.

Boulton et al.[2] defined the "half dyeing time" to compare the rate of dyeing. That is the time required to absorb one half of the equilibrium amount. The experimental determination of the half dyeing time is done under a rather small liquid yarn ratio of 40 : 1, and the results are dependent on the equilibrium exhaustion ratio. The theoretical justification on the half dyeing time has not yet been done.

Theory of Dyeing Equilibrium in Finite Liquid Yarn Ratio

In this paper, the dyeing equilibrium of direct cotton dye on viscose rayon is mainly studied. In this case, dye may be assumed to migrate into the capillary gap or miceller interspace. The volume of dye bath per 1 g. of yarn is assumed to be v (l./g.), and the volume of capillary gap per 1 g. of yarn to be V (l./g.). The liquid yarn ratio v was 40 (cc./g.) in Boulton's experiment, and usually much more larger, that is,

$$v \geq 40 \times 10^{-3} \text{ (l./g.)}. \tag{1}$$

The volume of capillary gap is according to Marshall and Peters[3], for viscose rayon,

$$V = 0.27 \times 10^{-3} \sim 0.46 \times 10^{-3} \text{ (l./g.)}. \tag{2}$$

The dye molecule discussed here contains z Na atoms and dissociates in solution as follows:

$$DNa_z \rightleftarrows zNa^+ + D^{z-} \tag{3}$$

where D^{z-} is dye anion. In the dye bath, NaCl may be added. The concentration of dye ion, Na^+ ion and Cl^- ion is expressed as [D], [Na], and [Cl] (mol./l.) for solution, and [Dφ], [Naφ], and [Clφ] for fibre phase, respectively. Assuming the absorption amount of dye per 1 g. of fibre as x (g./g. fibre),

$$[D\phi] = x/MV \tag{4}$$

where M is the molecular weight of dye. The standard chemical potentials of all ions are expressed as $\mu_0(D)$, $\mu_0(Na)$, $\mu_0(Cl)$, $\mu_0(D\phi)$, $\mu_0(Na\phi)$, $\mu_0(Cl\phi)$, and activity coefficients as f_D, f_+, f_-, f_D^ϕ, f_+^ϕ, and f_-^ϕ. Then the free energy of the total system, F, is

$$\begin{aligned} F = {} & v[D]\mu_0(D) + v[D]RT \ln f_D[D] \\ & + v[Na]\mu_0(Na) + v[Na]RT \ln f_+[Na] \\ & + v[Cl]\mu_0(Cl) + v[Cl]RT \ln f_-[Cl] \\ & + V[D\phi]\mu_0(D\phi) + V[D\phi]\,RT \ln f_D^\phi[D\phi] \\ & + V[Na\phi]\mu_0(Na\phi) + V[Na\phi]\,RT \ln f_+^\phi[Na\phi] \\ & + V[Cl\phi]\mu_0(Cl\phi) + V[Cl\phi]\,RT \ln f_-^\phi[Cl\phi]. \end{aligned} \tag{5}$$

As for the electrical interaction of fibre surface and dye ion, Gilbert and Rideal[4] introduced the electrical potential difference ψ at the surface, to explain the combination of protein and inorganic acid. But this is less important to discuss than the interaction of direct cotton dye with cellulose. Assuming that the change of electrical potential during the dyeing process may be rather small, it is included in the term μ_0, in this paper.

* A part of this paper was presented before the Discussion of Colloid Chemistry held by this Society at Nov. 1954.

1) Vickerstaff, "The Physical Chemistry of Dyeing", 2nd. rev. ed. (1954), p. 191-256.

2) J. Boulton and B. Reading, *J. Soc. Dyers and Colourists*, **50**, 381 (1934); J. Boulton, ibid., **54**, 268 (1938); **60**, 5 (1944).

3) W.J. Marshall and R.H. Peters, *J. Soc. Dyers and Colourists*, **63**, 446 (1947).

4) G.A. Gilbert and E.K. Rideal, *Proc. Roy. Soc.*, **A 182**, 335 (1944).

Since the total amount of dye ion is constant,

$$vN_o = v[D] + V[D^\phi] \quad (6)$$

where N_o is the initial concentration of dye in the bath. Then, this gives, with Eq. (4), the formula to calculate the adsorption amount:

$$x = MV[D^\phi] = Mv(N_o - [D]). \quad (7)$$

From the constancy of Na and Cl,

$$vN_s + zvN_o = v[Na] + V[Na^\phi] \quad (8)$$

and

$$vN_s = v[Cl] + V[Cl^\phi] \quad (9)$$

where N_s is the initial concentration of NaCl in the bath. From the condition of electrical neutrality for dye bath and for the fibre phase,

$$z[D] + [Cl] = [Na] \quad (10)$$

and

$$z[D^\phi] + [Cl^\phi] = [Na^\phi] \quad (11)$$

are obtained.

With these equations and Eq. (5), the free energy may be expressed as a function of [Na] and [D]. Then, using the equilibrium condition that the partial differentiation of F by [Na] and [D] are respectively equal to zero, the dyeing equilibrium is formulated. Using the further assumption that

$$\mu_0(Na^\phi) - \mu_0(Na) = \Delta\mu(Na) = 0 \quad (12)$$

$$\mu_0(Cl^\phi) - \mu_0(Cl) = \Delta\mu(Cl) = 0 \quad (13)$$

that is Na^+ and Cl^- do not have any especial affinity to the fibre, Donnan's equation for membrane equilibrium:

$$f_+ f_-[Na][Cl] = f_+^\phi f_-^\phi [Na^\phi][Cl^\phi] \quad (14)$$

is obtained from one of the equilibrium conditions

$$\partial F/\partial[Na] = 0. \quad (15)$$

Nearly every theoretical study ever proposed is assuming Eq. (14) a priori. It should be, however, emphasized that this equation is correct merely when Na^+ and Cl^- have no affinity to the fibre.

Then, from the other equilibrium condition

$$\partial F/\partial[D] = 0 \quad (16)$$

and Eq. (13) and Eq. (14),

$$\Delta\mu(D) = \mu_0(D^\phi) - \mu_0(D) = RT \ln\left\{\frac{f_D[D]\{f_+[Na]\}^z}{f_D^\phi[D^\phi]\{f_+^\phi[Na^\phi]\}^z}\right\} \quad (17)$$

is obtained. On the other hand, from Eqs. (11) and (14),

$$[Na^\phi] = (z/2)[D^\phi] + \sqrt{(z^2/4)[D^\phi]^2 + [Na][Cl]} \quad (18)$$

is obtained, if $f = 1$.

At the infinite liquid yarn ratio,

$$[Na] = N_s + zN_o \quad (19)$$

and

$$[Cl] = N_s. \quad (20)$$

Marshall and Peters[3] and Peters and Vickerstaff[5] used these equations in Eq. (18) to calculate the value $[Na^\phi]$, and showed that Eq. (17) is supported by experimental data. Vickerstaff[1] also showed that the equation of Willis, Warwicker, Standing and Urquhart[6] and that of Hanson, Neale and Stringfellow[7] are, respectively, derived as special cases of Eqs. (17) and (18).

In the case of finite liquid yarn ratio, [Na] and [Cl] both depend on $[Na^\phi]$, so that Eqs. (19) and (20) can not be used. Using Eqs. (7)–(11) and (14), $[Na^\phi]$ is strictly calculated as a function of $[D^\phi]$, N_s, and N_o. Even when the liquid yarn ratio is finite,

$$f^2 \equiv f_+^\phi f_-^\phi / f_+ f_- \gg (V/v)^2 \quad (21)$$

$$(V/v)N_o \ll f^2[D^\phi] \equiv f^2(v/V)(N_o - [D]) \quad (22)$$

and

$$z[D^\phi]/2 \gg (V/v)N_s/f^2 \quad (23)$$

are satisfied, referring to Eqs. (1) and (2). Under these approximations,

$$[Na^\phi] \fallingdotseq (z/2)[D^\phi] + \sqrt{(z^2/4)[D^\phi]^2 + N_s(N_s + zN_o)/f^2} \quad (24)$$

is obtained. This equation for finite liquid yarn ratio is coincident with Eq. (18), using Eqs. (19) and (20) for infinite ratio. Under the approximation of Eqs. (21)–(23), the value [Na] for finite liquid yarn ratio is, however,

$$[Na] \fallingdotseq N_s + zN_o - (z/2)(V/v)[D^\phi] - (V/v)\sqrt{(z^2/4)[D^\phi]^2 + N_s(N_s + zN_o)/f^2} \quad (25)$$

which does not coincide with Eq. (19) for infinite ratio.

In a special case where

$$(z/2)[D^\phi] \gg N_s/f \quad (26)$$

Eq. (25) becomes

$$[Na] \fallingdotseq N_s + z[D] \quad (27)$$

which also does not coincide with Eq. (19). from Eqs. (27), (7) and (8),

$$[Na^\phi] \fallingdotseq z[D^\phi] \quad (28)$$

is obtained. Let the eqilibrium adsorption amount be x_∞ and the concentration of dye in the bath be N_∞, then under the condition of Eq. (26),

$$\left.\begin{aligned} \log x_\infty &= \alpha + \left(\frac{1}{z+1}\right)X \\ X &= \log N_\infty + z\log(N_s + zN_\infty) \\ \alpha &= -\frac{0.4343}{z+1}\frac{\Delta\mu(D)}{RT} - \log h \\ &\quad + \log MV - \frac{z}{z+1}\log z \end{aligned}\right\} \quad (29)$$

5) R.H. Peters and T. Vickerstaff, *Proc. Roy. Soc.*, A 192, 292 (1948).

6) H.F. Willis, J.O. Warwicker, H.A. Standing and A.R. Urquhart, *Trans. Faraday Soc.*, **41**, 506 (1945).

7) J. Hanson, S.M. Neale and W.A. Stringfellow, ibid., **31**, 1718 (1935).

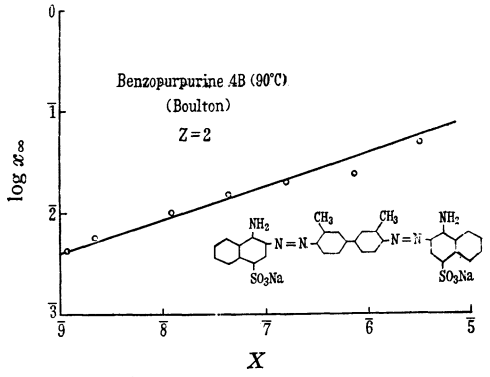

Fig. 1. Absorption of Benzopurpurine 4B on viscose rayon yarn in finite liquid yarn ratio (by Boulton).

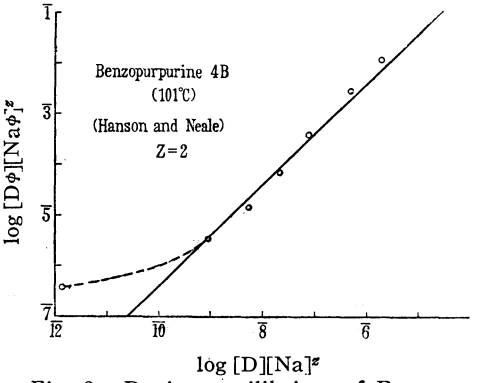

Fig. 2. Dyeing equilibrium of Benzopurpurine 4B on cellophane in infinite liquid yarn ratio (by Hanson and Neale).

is obtained. Fig. 1 shows the varification of Eq. (29). Plots in the figure are calculated by the present author from the Boulton's data[2] for the dyeing of Cautould's 150/27 viscose rayon yarn by Benzoperpurine 4B in finite liquid yarn ratio (40 : 1). The straight line in the figure is drawn so as to satisfy the theoretical inclination, $1/(z+1)=1/3$. The agreement with the experimental value is good. From this straight line,

$$\alpha=0.60 \tag{30}$$

is obtained. Assuming

$$h\equiv\left(\frac{f_D^{\phi}(f_+^{\phi})^z}{f_D(f_+)^z}\right)^{\frac{1}{z+1}}\fallingdotseq 1 \tag{31}$$

and, for viscose rayon[3],

$$V=0.45\times10^{-3}\ (\text{l./g.}) \tag{32}$$

the following is obtained:

$$-\Delta\mu(\text{Benzoperpurine 4B})=6.4_5\ \text{kcal./mol. (at 90°C)} \tag{33}$$

Hanson and Neale[8] measured the dyeing equilibrium of the same Benzoperpurine 4B on viscose rayon (cellophane film, in this case), at infinite liquid yarn ratio. In this case, however, the ratio (NaCl/dye) was much greater than in the case of Boulton, so that the assumption (26) and Eq. (29) cannot be used. In this case, [Na] and [Naφ] should be calculated from Eqs. (19) and (24), and inserted into Eq. (17). The latter may be rewritten as

$$\left.\begin{aligned}&\log[D\phi][Na\phi]^z=\beta+\log[D][Na]^z\\&\beta=-0.4343\Delta\mu/RT-(z+1)\log h\end{aligned}\right\} \tag{34}$$

under the assumption of

$$f=1. \tag{35}$$

The result of calculation is shown in Fig. 2, where the straight line is drawn so as to satisfy the theoretical gradient in Eq. (34). From this straight line,

$$\beta=3.59 \tag{36}$$

is obtained. Using the second equations of (34) and Eq. (31), Eq. (36) is recalculated to

$$-\Delta\mu(\text{Benzoperpurine 4B})=6.2\ \text{kcal./mol. (at 101°C)} \tag{37}$$

which is in good agreement with Eq. (33).

The dyeing equilibrium of Sky Blue FF (Chicago Blue 6B) on viscose rayon measured by Boulton[2] at finite liquid yarn ratio, and by Hanson and Neale[8] and Marshall and Peters[3] at infinite liquid yarn ratio are plotted in Fig. 3. Eqs. (24), (25) are used for

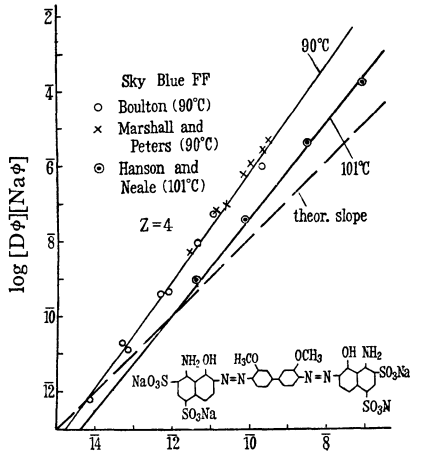

Fig. 3. Dyeing equilibrium of Sky Blue FF on viscose rayon.

finite liquid yarn ratio, and Eqs. (18), (19) and (20) are used for infinite ratio. V is assumed to be 0.45×10^{-3} (l./g.). As shown in the figure, $\log[D\phi][Na\phi]^z$ shows linear relationship to $\log[D][Na]^z$, but the slope of the line is greater than the theoretical value,

8) J. Hanson and S.M. Neale, *Trans. Faraday Soc.*, **30**, 386 (1934).

unity, shown in Eq. (34). The straight lines are:

$$\log [D\Phi][Na\Phi]^4 = 7.92 + 1.42 \log [D][Na]^4 \quad \text{for } 90°C \tag{38}$$

and

$$\log [D\Phi][Na\Phi]^4 = 4.97 + 1.24 \log [D][Na]^4 \quad \text{for } 101°C. \tag{39}$$

It is noticeable that both data for infinite and finite liquid yarn ratio are on the same straight line of Eq. (38) for 90°C, as shown in Fig. 3.

Marshall and Peters[3] attributed the deviation of the slope of the straight lines from the theoretical value to the aggregation of dye ions. They thought that the standard chemical potential $\Delta\mu(D)$ is dependent on the concentration, assuming the activity coefficients always equal to unity. This is, however, not correct, since the activity coefficients largely deviate from unity when the aggregation sets up. While, the standard chemical potential of adsorption may be assumed unchanged, considering that the adsorbed dye is in equilibrium with monomolecularly dispersed dye, and that the effective concentration of the latter should be properly expressed using the activity coefficient. Details of the concentration dependence of the activity coefficient of dye is not known, yet but it is known for soaps. Soap belongs to the same colloidal electrolyte as dye. Curves such as in Fig. 4 are obtained for the osmotic coefficient, g. If the concentration C is smaller

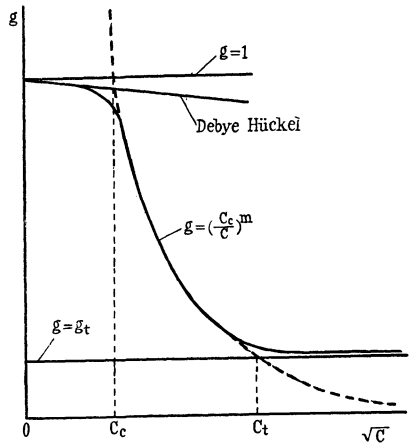

Fig. 4. Schematic explanation of osmotic coefficient-concentration relation for micelle colloids.

than C_c, the activity coefficient of soap follows the Debye-Hückel equation, and is nearly equal to unity. C_c is the critical micelle concentration. When the concentration is greater than C_c, the micelle is formed and the osmotic coefficient decreases rapidly. When the concentration is greater than C_t, the osmotic coefficient becomes constant, or increases gradually. Data on some soaps are shown in Fig. 5[9], where $\log g$-$\log C$ relation

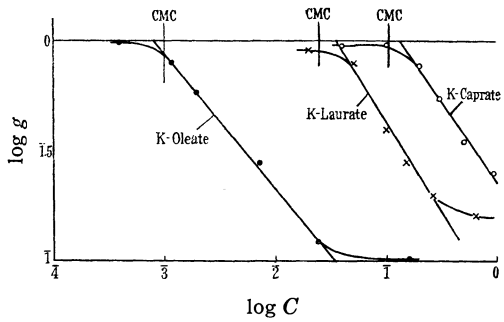

Fig. 5. $\log g$-$\log C$ relation for some soap solutions.

is nearly linear at the concentration range from C_c to C_t.

The osmotic coefficient g is nearly equal to the mean activity coefficient, $\bar{f}$,

$$\bar{f} = (\prod_i f_i^{\nu_i})^{\frac{1}{\sum \nu_i}} \tag{40}$$

In the case of dye shown in Eq. (3), the mean activity coefficient is written as

$$\bar{f} = (f_D \cdot f_+^z)^{\frac{1}{z+1}} \tag{41}$$

Then, it is assumed that the activity coefficient of dye may be assumed to be the same as that of soap, that is:

$$\bar{f} = \begin{cases} 1 & (C < C_c) \\ (C_c/C)^m & (C_c < C < C_t) \\ f_t & (C_t < C) \end{cases} \tag{42}$$

where f_t is a constant. It is generally accepted that the micelle is seldom formed at 90°C or so, and the micelle forming tendency of dye is not so conspicuous as that of soap. Then,

$$\bar{f} \simeq 1. \tag{43}$$

On the other hand, the concentration of dye in fibre phase, $[D\Phi]$, is usually 50–2000 times greater than that in solution, $[D]$. Therefore, it may correspond to the case of $C > C_t$, so

$$\bar{f}^\Phi = \{f_D^\Phi \cdot (f_+^\Phi)^z\}^{\frac{1}{z+1}} = f_t \tag{44}$$

and

$$h = \bar{f}^\Phi / \bar{f} = f_t = \text{const.} \tag{45}$$

Then the slope of the linear relation in $\log [D\Phi][Na\Phi]^z \sim \log [D][Na]^z$ diagram is equal to the theoretical value, unity, but the value of $\Delta\mu(D)$ cannot be obtained without knowing the value of f_t, Benzoperpurine 4B (Fig. 1 and 2) will be the case, and the values of $\Delta\mu(D)$ of Eqs. (33) and (37) are apparent values.

9) J.W. Mc Bain, "Colloid Science" (1950), p. 245-253.

On the other hand, Sky Blue FF has 4 sulphonic groups and it may be more difficult for it to form micelle than Benzoperpurine 4B having 2 sulphonic groups. Then, the concentration of Sky Blue FF in fibre phase may correspond to the concentration range of $C_c < C < C_t$. Then,

$$h=(C_c/C^{\phi})^m \tag{46}$$

where C_c is a constant and C^{ϕ} is

$$C^{\phi}=\{[D^{\phi}][Na^{\phi}]^z\}^{\frac{1}{z+1}}. \tag{47}$$

Eq. (34) should be rewritten as

$$\log [D^{\phi}][Na^{\phi}]^z=\gamma+\left(\frac{1}{1-m}\right)\log [D][Na]^z$$

$$\gamma=-\frac{0.4343}{1-m}\frac{RT}{\Delta\mu}-\frac{m}{1-m}(z+1)\log C_c. \tag{48}$$

To satisfy the observed relations, Eqs. (38) and (39), the following values

$$m=\begin{cases} 0.30 & \text{for } 90^{\circ}\text{C} \\ 0.19 & \text{for } 101^{\circ}\text{C} \end{cases} \tag{49}$$

should be adopted. For soap solutions, $m=0.6$–0.8 is obtained from Fig. 5, while the value for dye may be smaller than these values, since dye forms micelle with more difficulty. Therefore, the values cited in Eq. (49) are acceptable.

Theory on the Rate of Dyeing

The rate of dyeing of Benzoperpurine 4B and Sky Blue FF on viscose rayon yarn (Coutauld's 150/27) was measured by Boulton[2] at 90°C using purified dyes. The liquid yarn ratio was 40. The exhaustion ratio E was measured as a function of time t (min.). The exhaustion ratio was defined by

$$E=(C_0-C)/C_0=(N_0-N)/N_0 \tag{50}$$

where C_0 (g./l.) or N_0 (mol./l.) is the initial dye concentration and C or N is the dye concentration after t (min.) The exhaustion ratio after sixteen hours was assumed as the equilibrium exhaustion ratio, E_∞, and the time required to reach $E=E_\infty/2$ is named as half dyeing time, T. The half dyeing time was measured by Boulton for many dyes but theoretical treatment was not tried.

To find a simple empirical relationship, the ratio of adsorption amount ξ, that is

$$\xi=E/E_\infty=x/x_\infty \tag{51}$$

is plotted against the ratio of time to the half dyeing time, that is,

$$\tau=t/T. \tag{52}$$

In Fig. 6, ξ-τ relationship from Boulton's data is shown. For the dyeing of Benzoperpurine 4B on viscose rayon, dye concentration varied

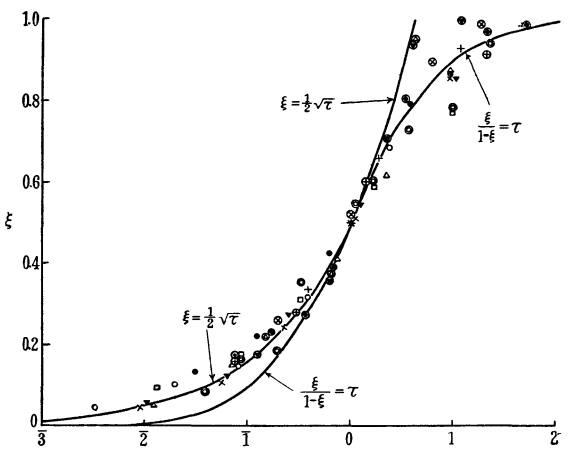

Fig. 6. ξ-τ relationship.

0.02–2.6 millimole, NaCl concentration 1.1–40 millimole, and equilibrium adsorption amount 4.2–25 mg./g. yarn, and for Sky Blue FF on the same yarn, dye concentration varied 0.005–0.14 millimole/l., NaCl concentration 4–43 millimole/l., and equilibrium adsorption amount 0.2–7.4 mg./g. yarn. All plots fall on a single curve, irrespective of the sorts of dyes and the dyeing conditions were very widely different. The simple empirical equations obtained are,

$$\xi=\tfrac{1}{2}\sqrt{\tau} \quad \text{for } \tau<1 \tag{53}$$

and

$$\xi/(1-\xi)=\tau \quad \text{for } \tau>1 \tag{54}$$

Then, suppose that fibre has many capillary gaps and the total volume of them is V (l./g. yarn). The shape of the gap is assumed for the simplicity as a capillary of uniform diameter. At the opening of the capillary, the dyeing equilibrium is immediately established, and the dye diffused into the inner part of the capillary is readily supplied from the dye bath, so that the concentration at the opening N_0^{ϕ} (mol./l.) is a function of the dye bath composition only. At the initial stage of the diffusion, N_0^{ϕ} is approximately constant, and the depth of the penetration of dye is smaller than the depth of the capillary, L. Then, the equation of Fürth[10] is used:

$$\left.\begin{aligned} y^2/t&=D/\varphi(q) \\ q&=N_0^{\phi}/N^{\phi} \end{aligned}\right\} \tag{55}$$

where the concentration of dye ion at the distance y (cm.) from the opening is N^{ϕ} and diffusion coefficient is D, and time is t. $\varphi(q)$ is the function of q only and

10) R. Fürth, *Phys. Z.*, **26**, 719 (1925); *Kolloid-Z.*, **41**, 300 (1927).

$$1/q=1-\frac{2}{\sqrt{\pi}}\int_0^{\frac{1}{2\sqrt{\varphi}}} e^{-\xi^2}\mathrm{d}\xi \qquad (56)$$

Using these, the concentration gradient at time t and location y becomes,

$$\frac{\mathrm{d}N^{\phi}}{\mathrm{d}y}=-\frac{N_0^{\phi}}{\sqrt{\pi}\sqrt{D}}\frac{1}{\sqrt{t}}e^{-\frac{1}{4\varphi}}. \qquad (57)$$

Then, using the relation[11] that,
when $y\to 0$, and therefore $q\to 1$,
then $\varphi\longrightarrow\infty$ (58)
the concentration gradient at the opening is

$$\left(\frac{\mathrm{d}N^{\phi}}{\mathrm{d}y}\right)_0=-\frac{1}{\sqrt{\pi}\sqrt{D}}\frac{N_0^{\phi}}{\sqrt{t}}. \qquad (59)$$

The rate of dyeing $\mathrm{d}x/\mathrm{d}t$ is,

$$\frac{\mathrm{d}x}{\mathrm{d}t}=-\frac{DAM}{1000}\left(\frac{\mathrm{d}N^{\phi}}{\mathrm{d}y}\right)_0$$

$$=\frac{A\sqrt{D}}{\sqrt{\pi}}\cdot\frac{MN_0^{\phi}}{1000}\frac{1}{\sqrt{t}} \qquad (60)$$

where A is the sum of the cross section of capillary (cm^2/g. yarn) and adsorption amout x is expressed in g. dye/g. yarn, and the factor 1000 is used to rewrite the N_0^{ϕ} in mol./l. to mol./cc.

At the initial stage of diffusion, N_0^{ϕ}=constant, so that

$$x=\frac{2A\sqrt{D}MN_0^{\phi}}{1000\sqrt{\pi}}\sqrt{t} \qquad (61)$$

is obtained. Then the definition of the half dyeing time,

$$x=x_\infty/2 \quad \text{when } t=T \qquad (62)$$

is used with Eq. (61) and

$$\xi=x/x_\infty=\tfrac{1}{2}\sqrt{\tau} \quad \text{where } \tau=t/T \qquad (63)$$

is obtained. This is equal to Eq. (53). Then,

$$N_0^{\phi}=x_t/MV \qquad (64)$$

where x_t is the equilibrium adsorption amount (g./g.) when an infinitesimal amount of fibre (that means the surface only of the fibre) is dipped into the dye bath, whose composition is that at time t. Moreover, V (l./g.) is

$$V=AL\times 10^{-3}. \qquad (65)$$

Using these equations, the half dyeing time is,

$$T=\frac{\pi L^2}{16D}Q^2$$

$$Q=x_\infty/x_t \qquad (66)$$

At the infinite liquid yarn ratio,

$$x_t=x_\infty \qquad (67)$$

so that the value of Q is equal to unity, and from Eq. (66),

$$T=0.197\ L^2/D \qquad (68)$$

is obtained. On the other hand, Neale, Stringfellow, Hanson, Andrew and Johnston[12] used the equation by Hill[13]

$$\left.\begin{aligned}\xi=1-\frac{8}{\pi^2}\Big\{&e^{-\frac{\pi^2 D}{4b^2}t}+\frac{1}{9}e^{-\frac{9\pi^2 D}{4b^2}t}\\&+\frac{1}{25}e^{-\frac{25\pi^2 D}{4b^2}t}+\cdots\cdots\Big\}\end{aligned}\right\} \qquad (69)$$

where b is a half of the thickness of a cellophane film. The relation between ξ and Dt/b^2 calculated from Eq. (69) is shown in the first two columns of Table I. Since the time at which $\xi=0.5$ is the half dyeing time, T, so from Table I,

$$DT/b^2=0.197$$

that is

$$T=0.197\ b^2/D \qquad (70)$$

is obtained. If it is assumed that the value of L corresponds to b, Eq. (70) is equal to Eq. (68). Then,(Dt/b^2) is recalculated to τ, by the equation

$$\tau=t/T=\frac{Dt}{0.197\,b^2} \qquad (71)$$

as shown in the third column of Table I, and ξ is calculated by Eq. (63), as shown in the fourth column of the table. The results are in good agreement with that by Hill, as far as $\xi\leq 0.7$. Therefore, the complicated Hill's equation is replaced by a simpler equation (63) without any loss of accuracy as far as $\xi\leq 0.7$.

TABLE I

Dt/b^2	ξ Eq. (69)	τ Eq. (71)	ξ Eq. (63)
0.0085	0.1	0.0432	0.104
0.0315	0.2	0.160	0.200
0.049	0.25	0.249	0.250
0.0725	0.3	0.369	0.303
0.125	0.4	0.635	0.398
0.197	0.5	1.000	0.500
0.286	0.6	1.452	0.602
0.404	0.7	2.05	0.715
0.472	0.75	2.40	(0.775)
0.570	0.8	2.90	(0.850)
0.843	0.9	4.28	(1.03)
1.13	0.949	5.74	—
1.35	0.971	6.85	—
1.80	0.990	9.13	—
2.25	0.997	11.42	—

11) M. Nakagaki, *Bull. Chem. Soc. Japan*, **23**, 104 (1950).

12) S.M. Neale and W.A. Strigngfellow, *Trans. Faraday Soc.*, **29**, 1167 (1933); J. Hanson and S.M. Neale, ibid., **30**, 386 (1934); D.H. Andrew and J. Johnston, *J. Am. Chem. Soc.*, **46**, 640 (1924).

13) A.V. Hill, *Proc. Roy. Soc.*, B **104**, 39 (1928).

At the finite liquid yarn ratio, Q is not equal to unity. When the equilibrium exhausion is greater, and equilibrium dye bath concentration is smaller, then, x_∞ becomes smaller and Q becomes smaller. Therefore, T becomes smaller when the E_∞ is greater, as shown by Boulton. As shown before, the dyeing equilibrium of Benzoperpurine 4B on viscose rayon yarn is expressed by Eq. (29). The dye concentration of dye bath N should be used in place of N_∞, for x_t. Then, replacing N and N_∞ by E and E_∞ using Eq. (50),

$$Q=\frac{x^\infty}{x_t}=\frac{(1-E_\infty)^{\frac{1}{z+1}}\left(\frac{N_s}{N_0}+z-zE_\infty\right)^{\frac{z}{z+1}}}{(1-E)^{\frac{1}{z+1}}\left(\frac{N_s}{N_0}+z-zE\right)^{\frac{z}{z+1}}} \quad (72)$$

is obtained. At the initial stage of dyeing, E is nearly equal to zero, so the value of Q is

$$Q\fallingdotseq(1-E_\infty)^{\frac{1}{z+1}}\left(\frac{N_s}{N_0}+z-zE_\infty\right)^{\frac{z}{z+1}}\Big/\left(\frac{N_s}{N_0}+z\right)^{\frac{z}{z+1}} \quad (73)$$

The relation between Boulton's half dyeing time and the Q value, calculated from Eq. (73), is shown in Fig. 7. As a rough approximation T is proportional to Q^2, though the plot for $T=24.9$ min. deviates from the linearity. The results of Hanson and Neale[8] showed that the apparent diffusion coefficient becomes smaller when the salt concentration is smaller. The case of $T=24.9$ corresponds to this case, so that the deviation from the linearity will be explained from the decrease of apparent diffusion coefficient, which is often attributed to the variation of the surface potential at the fibre-water interface. From the inclination of the straight line in Fig. 7,

$$L^2/16D=16.6\ (\text{min.}) \quad (74)$$

is obtained. As already said about Eq. (70), L should be approximately equal to the radius of the single fibre. The latter is

$$r=1.1\times10^{-3}\ \text{cm.} \quad (75)$$

for 150/27 yarn, (a single yarn is 5.5 deniers), assuming that the density of fibre is about 1.5. Using this value in L of Eq. (74), diffusion coefficient is,

$$D=1.4\times10^{-8}\ (\text{cm}^2/\text{min.}) \quad (76)$$

This is approximately equal to the value by Hanson and Neale[8].

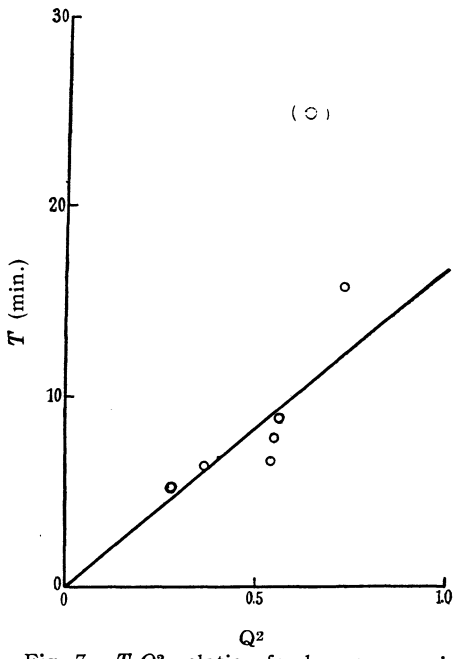

Fig. 7. T-Q^2 relation for benzopurpurine 4B.

Summary

The theory of dyeing equilibrium is treated generally. On the way of derivation, it is emphasized that the Donnan's equation,

$$f_+f_-[\text{Na}][\text{Cl}]=f_\pm^\phi f_\pm^\phi[\text{Na}^\phi][\text{Cl}^\phi]$$

is correct only when Na^+ and Cl^- have no affinity to the fibre. An equation expressing dyeing equilibrium is obtained for finite liquid yarn ratio, and compared to the equation by Vickerstaff for infinite liquid yarn ratio. Moreover, data for both finite and infinite liquid yarn ratio could be plotted on the same straight line according to the newly derived equation. The deviation of the inclination of the straight line from the theoretical value is attributed to the deviation of the activity coefficient from unity. The latter was assumed as analogous to that of soap, and a reasonable conclusion could be obtained.

On the theory of dyeing rate, all data from widely different dyeing conditions are brought into a simple relation

$$x/x_\infty=\frac{1}{2}\sqrt{t/T} \quad \text{when} \quad t<T$$

using the half dyeing time T proposed by Boulton. This equation was justified theoretically, and it was shown that Hill's complicated equation is replaced by this simple equation, without loss of accuracy, as far as $x/x_\infty\leq0.7$. Then, Boulton's relation, that

the half dyeing time becomes longer when the equilibrium exhaustion ratio is smaller, is justified theoretically. The apparent diffusion coefficient in fibre agrees with that of Hanson and Neale.

The author wishes to express his hearty thanks to Dr. Hachiro Hiyama for his kind guidance and encouragement.

Faculty of Living Science,
Osaka City University,
Osaka

SHORT COMMUNICATIONS

On the Crystal Structure of 2,3-Dichloro-2, 3-dimethylbutane

By Tsutomu ODA and Tsutomu KOIDE

(Received July 25, 1955)

Hexachloroethane and hexamethylethane are characterized by relatively high melting points, 185°C and 100.6°C respectively, by polymorphism in the solid state, the transition points being 43°C and 71°C for haxachloroethane[1] and −125°C for hexamethylethane[2], and by high symmetrys of the high temperature modification as shown by optical isotropy and confirmed by X-ray studies[3,4]. Recently, it has been reported[5] that hexabromoethane is also isotrimorphous with hexachloroethane. In order to examine what occurs in the high temperature modifications by symmetrical replacement of methyl group pair or pairs by Cl pair or pairs (resulting in substances such as $(CH_3)_2ClCCCl(CH_3)_2$ and $(CH_3)Cl_2CCCl_2(CH_3)$), we have carried out an X-ray diffraction study of 2, 3-dichloro-2, 3-dimethylbutane crystal, which has been also reported to have relatively high melting point, 161°C, in a sealed tube[6].

This compound was perpared by treating[6] pinacol with phosphorus trichloride and was subjected to sublimation under about 30 mm Hg. The solid is very volatile and plastic, its vapour having a camphoric odour. A melting point of 158°C was observed in a sealed tube. The crystals were found to be optically isotropic at room temperatures. Using Cu K_α radiation and samples in thin-walled capillary tubes, we prepared X-ray powder photographs, in which seven lines appeared. The reflections were indexed with a body-centered cubic lattice, the edge length being 7.58 Å. By suspension in an aqueous solution of sodium chloride, the density of the solid was measured as 1.14 g./cc. at 30°C. Hence, it was found that the unit cell contains two molecules, yielding the calculated density of 1.18 g./cc. Since the lattice is body-centered and the unit contains two molecules, we may place the two centers of them at the lattice points 000 and $\frac{1}{2}\frac{1}{2}\frac{1}{2}$, of which the symmetry should be at least T–23. On the other hand, as the symmetry of the rigid molecule of $(CH_3)_2ClCCCl(CH_3)_2$ can be at highest $C_{2h}-2/m$[7], it becomes necessary to consider some statistical explanation of the structure, as is always the case in plastic crystals[3,4,8]. In order that the statistical symmetry of the molecule be higher than T–23 at 000 and $\frac{1}{2}\frac{1}{2}\frac{1}{2}$, the molecule of the symmetry $C_{2h}-2/m$ should orientate its axis C–C parallel to one of the four body-diagonals statistically equally, and at the same time with its two-fold axis oriented parallel to one of the three similar azimuthal directions also equally so that the axis C–C acquires three-fold symmetry statistically. Such statistical high symmetry is similarly gained with a model of molecule of the "*gauche*" form[7], the other rotational isomer having the symmetry C_2-2, or with another model of molecule which is in free rotation about the C–C axis. Which one is the case of the present statistical structure seems, almost entirely undiscriminable from the presents intensity data, since the lines are so few as mentioned above. However, it may be said that this structure is statistically isomorphous with cubic hexamethylethane at room temperatures and hexachloroethane above 71°C. The edge length of 7.58 Å is between those[3] of 7.69 Å and 7.43 Å for $C_2(CH_3)_6$ and C_2Cl_6 at 80°C respectively. In the diffraction of X-rays by the present crystal, we have observed, similarly to the hexa-substituted ethanes stated above, a very rapid decrease of intensity with increasing angles of scattering, which is evidently in close relationship with the disordered orientation of the molecule in intense thermal motion.

It will be expected that such a "rotational" mode of the molecules in the crystal will change at lower temperatures. We have undertaken a differential thermal analysis, and observed, on its heating curve from low temperatures, anomalous heat effect at about −112°C. Therefore, X-ray studies of single crystals of the probably ordered phase below the transition point must await techniques for the growth of single crystals below the temperature.

In conclusion, we should express our hearty appreciation to Professor I. Nitta, Professor T. Watanabé and Dr. S. Seki, Faculty of Science, Osaka University, for their gracious interest during the work. We also wish to thank Mr. H. Suga for his kind aid. The cost of this research was defrayed from the Scientific Research Grant from the Ministry of Education, to which our thanks are due.

Chemical Laboratory, Osaka University of Liberal Arts and Education, Tennoji, Osaka

1) O. Lehman, *Z. Krist.*, **1**, 106 (1877); ibid., 6, 584 (1882); I. Nitta and S. Seki, *J. Chem. Soc. Japan*, **62**, 581 (1941); K.J. Ivin and F.S. Dainton, *Trans. Faraday Soc.*, **43**, 32 (1947); S. Seki and M. Momotani, This Bulletin, **23**, 30 (1950).

2) G.S. Parks, H.M. Huffman and B. Thomas, *J. Am. Chem. Soc.*, **52**, 1032 (1930).

3) C.D. West, *Z. Krist.*, **88**, 195 (1934).

4) C. Finbak, *Tids. Kjem. Bergvesen*, **17**, No. 9, 2 (1937); M. Atoji, T. Oda and T. Watanabe, *Acta Cryst.*, **6**, 868 (1953).

5) G.J. Snaauw and E.H. Wiebenga, *Rec. Trav. Chim. Pays-Bas*, **61**, 253 (1942). See also B. Goszner, *Z. Krist.*, **38**, 151 (1904); K. Yardley, *Proc. Roy. Soc., London (A)*, **118**, 449, 485 (1928).

6) F. Couturier, *Ann. Chim. Phys.*, **26**, 433 (1892).

7) Y. Morino, I. Miyagawa, T. Haga and S. Mizushima, This Bulletin, **28**, 165 (1955).

8) J. Timmermans, *J. Chim. Phys.*, **35**, 331 (1938); I. Nitta and T. Watanabe, This Bulletin, **13**, 28 (1938); T. Oda and T. Watanabe, *J. Chem. Soc. Japan*, **65**, 154 (1944); T. Oda and I. Nitta, ibid., **65**, 621 (1944); R.S. Schwartz, B. Post and I. Fankuchen, *J. Am. Chem. Soc.*, **73**, 4490, 5113 (1951); T.B. Reed and W.N. Lipscomb, *Acta Cryst.*, **6**, 108 (1953).

On the Phenolic Hydroxyl Group of Lignosulfonic Acid and the Existence of Carboxyl Group in Lignosulfonic Acid

By Hiroshi MIKAWA, Koichiro SATO, Chizuko TAKASAKI and Kiyo EBISAWA

(Received August 26, 1955)

The amount of the phenolic hydroxyl group of lignin in situ was estimated from the difference of the phenolic hydroxyl group content of the lignothioglycolic acid prepared from untreated wood and methylated wood. The amount was found to be about one OH* per 5.3 CH_3O. Wood powder sulfonated at neutral pH contains lignosulfonic acid, called solid lignosulfonic acid, which has sulfonic acid group only at X and Z groups of lignin[1]. The phenolic hydroxyl group content of the soild lignosulfonic acid was also measured in the same way with the wood power sulfonated at neutral pH, and was found to be the same as that of the lignin in situ. It was, therefore, found that the sulfonation of lignin at neutral pH causes no increase of the phenolic hydroxyl group of lignin. The "low sulfonated lignosulfonic acid" prepared from the sulfonated wood by Kullgren process was also found to have nearly the same amount of the phenolic hydroxyl group as the lignin in situ. The phenolic hydroxyl group of the low sulfonated lignosulfonic acid is, therefore, the one already present in the lignin in situ. The amount of the phenolic hydroxyl group of these lignin preparations was estimated spectroscopically according to the method of Aulin-Erdtman[2].

The nature of the conductometrically observed weakly acidic group of α-lignosulfonic acid was not definitely known, being thought to be phenolic or carboxylic in nature[3]. It was reported recently[4] that this group consisted of nearly equal amounts of carboxyl and phenolic hydroxyl groups. It was also reported, that only about 30 % of the total phenolic hydroxyl group of α-lignosulfonic acid, was ionized before the second "break", i. e. conductometrically titratable, the remaining 70 % being too weak to be titrated. From the following experimental findings it was concluded that the former conductometrically titratable group is of simple guaiacol (type I) and the latter untitrable one is of type II.

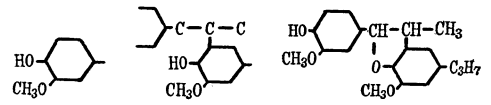

type I type II (2)

Conductometric titrations of many model compounds showed that the phenolic hydroxyl group of type I was without exception titratable. For example, phenolic hydroxyl group of vanillyl sulphonic acid and one of the phenolic hydroxyl groups of compound (1), which belongs to type I were titratable (cf. Fig.), while the other belonging to type II was not. As the existence of these two types of phenolic hydroxyl groups in lignosulfonic acid is quite probable, it may reasonably be concluded that the conductometrically un-

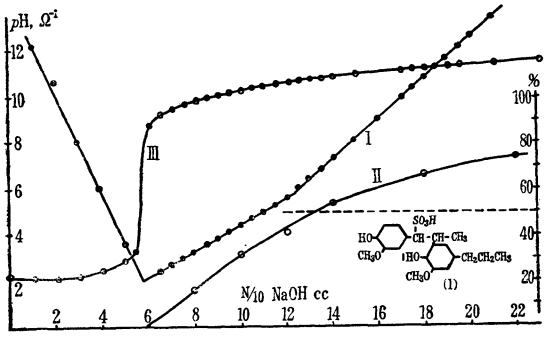

Fig. 1. Trtrations of model compound (I). I conductometric titration, III potentiometric titration, II percentage of the ionized phenolic hydroxyl groups of the compound.

titratable phenolic hydroxyl group of lignosulfonic acid belongs to type II.

Coductometric titration of the so-called low sulfonated lignosulfonic acid revealed that the ratio of the phenolic hydroxyl groups of type I and II was about 1 : 1. As stated previously the phenolic hydroxyl group of this acid is the same as that of the lignin originally present in wood. For this reason the phenolic hydroxyl group of lignin in wood may contain these two types in approximately equal amounts. The content of type I is higher in heach α-lignosulphonic acid than in spruce α-acid, the ratio of type I and II being about 1 : 1.

Synthesis of sulfonic acid (1)

Dihydro-dehydrodiisoeugenol (2) (4.7 g.) was dissolved in 50 ml. of 50 % aqueous alcohol containing NaOH (0.85 g.) and SO_2 (2.5 g.), kept at 140° for twenty hours. The sulfonic acid (1) was separated as benzylthiuroniumsalt. Repeated recrystallization raised the m.p. to 136–138°, 0.8 g. After being kept at 80° in vacuo with P_2O_5 for two days the m.p. was 145–147°.

Anal. Found: C, 58.43; H, 6.17; N, 4.98; CH_3O, 11.6. Calcd. for $C_{28}H_{36}O_7N_2S_2$ (benzylthiuronium salt of (1)): C, 58.3; H, 6.24; N, 4.86; CH_3O, 10.75 %

Research Laboratory of the Kokusaku Pulp Ind. Co. Ltd., 184, 1-chome, Kamiochiai, Shinjuku-ku, Tokyo

1) H. Mikawa, K. Sato, C. Takasaki and H. Okada, *J. Chem. Soc. Japan Ind. Chem. Sec.*, **54**, 229 (1951).
2) Aulin-Erdtman, *Svensk Papperstidn.*, **56**, 287 (1953).
3) Y. Hachihama, H. Shinra and Y. Kyogoku, *J. Chem. Soc. Japan Ind. Chem. Sec.*, **47**, 212 (1944); S. Regestad and O. Samuelson, *Svensk Kem. Tid.*, **61**, 9 (1949).
4) H. Mikawa, K. Sato, C. Takasaki and K. Ebisawa, This Bulletin, 28, 653 (1955).

Disordered Structure in Crystalline Cyclohexanoxime

By Yoshiharu OKAYA*, Akira SHIMADA** and Isamu NITTA

(Received September 3, 1955)

Since cyclohexanoxime $C_6H_{10}NOH$ is peculiar in that it dissolves readily not only in polar but also in non-polar solvents, and its molecular weight estimates in solution suggest that more than two molecules are associated, this substance in crystalline state was put under X-ray study. It was found that the crystal belongs to the hexagonal system with $a=12.18$, $c=8.10$ Å, and space group C_6^6-$P6_3$, the number of chemical units in the unit cell being six.

Projection of structure on (0001) was obtained as usual using Patterson Projection and trial-and error methods. It is evident from this projection that three molecules of cyclohexanoxime associate to form a trimeric molecule through three OH . . . N hydrogen bonds of the length about 2.75 Å around the threefold axis, and that such trimeric molecules arrange themselves in a hexagonal closepacked structure (Fig. 1). These results might well be compared with those of the structure of acetoxime as analysed by Bierlein and Lingafelter[1]. Anomalies in the molecular weight in solution will thus be accounted for by the existence of the trimeric form in solution.

It is quite remarkable that, while the (*hki* 0)-reflexions are regular, the general (*hkil*)-reflexions with non-zero l show diffuse scattering which corresponds to non-integral h and k values, l being strictly limited to integral numbers. Such diffuse scattering is undoubtedly due to some disordering in the packing of molecules in the crystal. In order to explain such anomaly there are many possible ways, which it is difficult to deal with rigorously case by case. However, in view of chemical and structural considerations, the following explanation seems to be quite reasonable and probable.

On the assumption of the more stable chair-form configuration of the ring, the cyclohexanoxime molecules can be expected to exist in the enantiomorphic forms as shown in Fig. 2. They are equally stable and are supposed to be in solution in equal numbers. Let us call one "A" and the other "B". In forming the trimers, four types of combination are conceivable: AAA, BBB, ABA

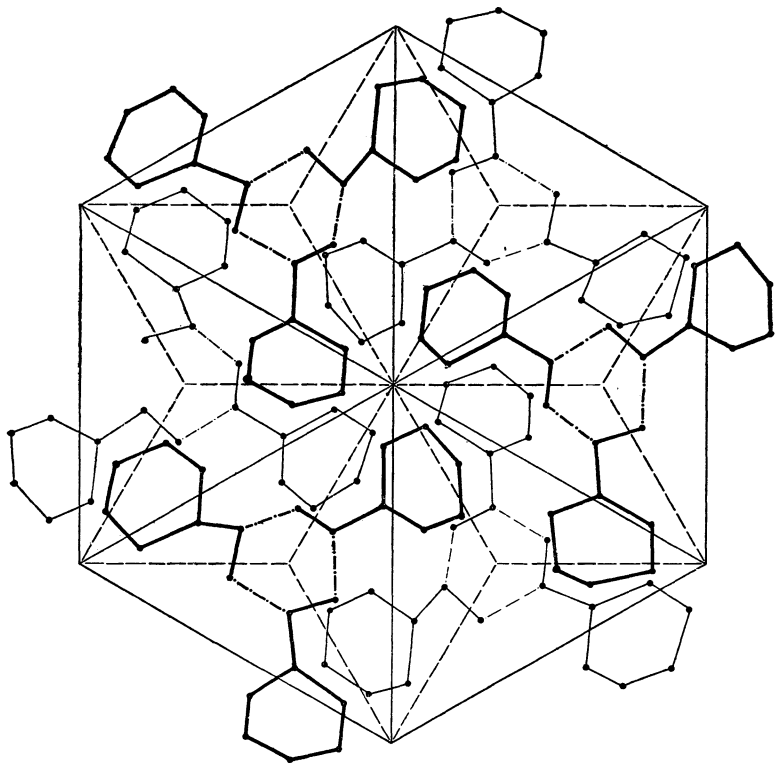

Fig. 1

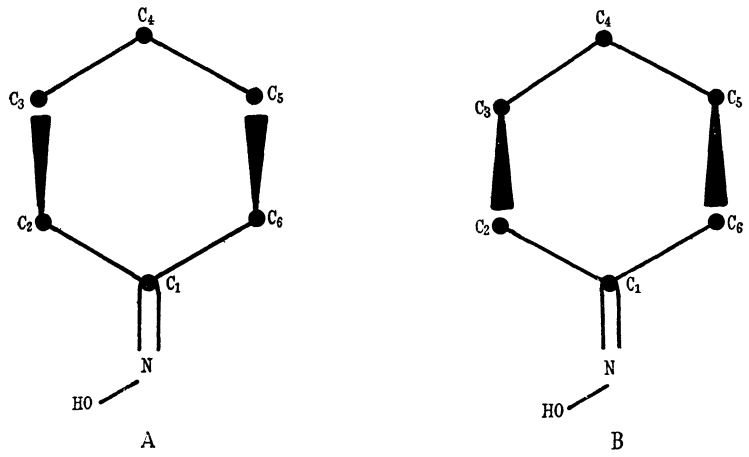

Fig. 2

and ABB. These four types can be arranged in the crystal with the same atomic x- and y- coordinates, but with partly different z-values, so that the (hki 0)-reflexions are unaffected and regular, the projection of the structure on (0001) being the same. Further it seems to be required, from the consideration of the steric hindrance between adjacent cyclohexane rings, that each 6_3-axis should be always surrounded by the same kind of molecule, A or B. Such a condition can be fulfilled with the four types of trimers in many ways resulting in the two-dimensionally random distribution of the 6_3-(A) and 6_3-(B)-axes. One example of how such a structure can be reallized is illustrated by Fig. 3. Thus the situation very well explains the characteristics mentioned

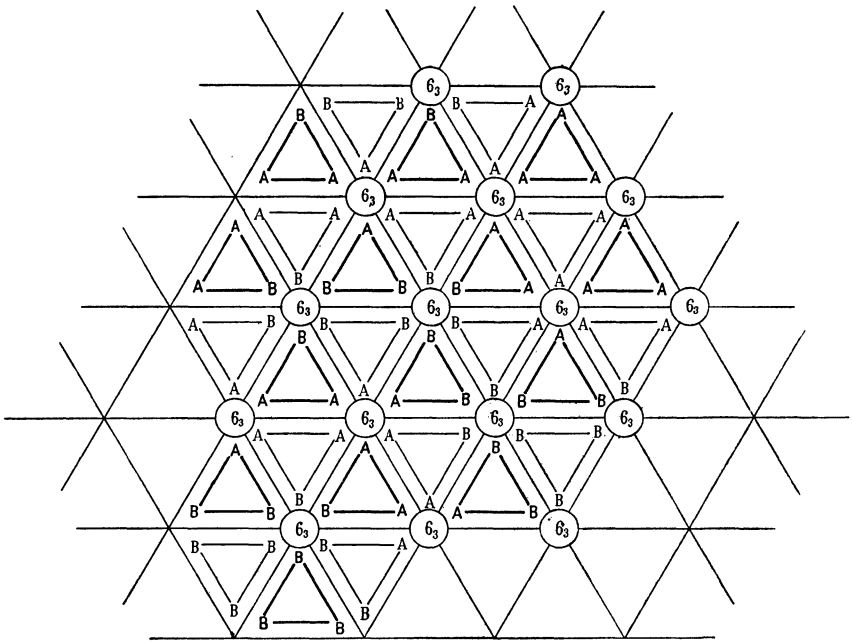

Fig. 3

before of the diffuse scattering observed in this crystal, because the crystal should have a quite constant repetition period in the z-direction, the only condition disturbing the periodicity being the random distribution of the two kinds of the 6_3-axes.

Department of Chemistry, Faculty of Science, Osaka University, Osaka

* Present address: Department of Physics, The Pennsylvania State University, State College, Pa., U.S.A.

** Present address: Department of Chemistry, Konan University, Kobe, Japan.

1) T.K. Bierlein and E.C. Lingafelter, *Acta Cryst.*, 4, 450 (1951).

Organic Semiconductors with High Conductivity. I. Complexes between Polycyclic Aromatic Hydrocarbons and Halogens

By Hideo AKAMATU, Hiroo INOKUCHI and Yoshio MATSUNAGA

(Received July 7, 1955)

Introduction

Some of the polycyclic aromatic compounds have a pretty good electrical conductivity in the solid state, and from this and other properties they are considered to be organic semiconductors[1]. However, their electrical resistivity at room temperature is of the order of 10^7–10^{12} ohm-cm., even for the most favourable compounds. Hence, it is hoped to learn whether there are any simple organic substances having higher electrical conductivity.

As reported in a preceding paper[2], we have found that some complexes formed between polycyclic aromatic hydrocarbons and halogens have a very good electrical conductivity in the solid state. It is rather surprising to know that such simple organic substances have electrical resistivity as low as 1–10^3 ohm-cm.. Therefore, studies on the electrical properties as well as the structures of these complexes should give us information about the necessary conditions for electrical conduction in organic materials.

Complexes between Polycyclic Aromatic Compounds and Halogens

Brass and Clar[3] have reported that from a benzene solution of perylene, by the addition of bromine, a black coloured precipitate is obtained. Zinke and Pongratz[4] have also found that perylene absorbs bromine vapour directly and changes to a black substance. These authors were in agreement in considering this black substance as a complex or an additive compound formed between perylene and bromine, but there was a little controversy between them over the composition of this substance.

We have found that not only perylene but also most polycyclic aromatic hydrocarbons may form molecular complexes with bromine or iodine, by a method similar to that of Brass and Clar or Zinke.

When we applied Brass and Clar's method, a known quantity of sample was dissolved or suspended in benzene, and an excess amount of bromine or iodine was added to it while boiling the solution. After cooling the solution by itself, the precipitate so obtained was filtered through a glass filter and washed with benzene.

Zinke's method was applied solely to the formation of bromine complex. In this case, a known quantity of sample was taken on a glass filter and put in contact with bromine vapour in a closed glass vessel. The absorption of bromine is completed generally within about ten minutes. After the excess bromine adsorbed is removed by aspiration and dried under reduced pressure, the increased weight of the sample is measured, from which the bromine content of the complex is known.

In the case of bromine complex formation by either method, there occurs a substitution reaction of bromine in the aromatic rings, with simultaneous liberation of hydrogen bromide. This substitution reaction proceeds with a moderate velocity while the complex is forming and continues after the complex is fully formed. This is the reason for confusion about the composition of the complex. Consequently, the apparent bromine content is not fixed but fluctuates in a small range according to the conditions of preparation, even in the case when excess bromine is added to the solution in Brass and Clar's method or when the absorption is completed in Zinke's method. This will be discussed in a later section.

In the preliminary experiments, the following substances were found to form complexes with bromine by Zinke's method. The complex formation is made obvious by the strong colour change and the increment in mass. Benzanthrone (reddish brown), perylene (black), dibromoperylene (black), dibenzoylperylene (brown), distearylperylene (brown), 1,2-benzperylenequinone (dark brown), anthanthrene (black), mesonaphtho-dianthrone (black), pyranthrene (black), violanthrene

1) H. Akamatu and H. Inokuchi, *J. Chem. Phys.*, **18**, 810 (1950); **20**, 1481 (1952), H. Inokuchi, This Bulletin, **24**, 222 (1951); **25**, 28 (1952); **27**, 22 (1954), D.D. Eley, G. Parfitt, M. Perry and D. Taysum, *Trans. Faraday Soc.*, **49**, 79 (1953).

2) H. Akamatu, H. Inokuchi and Y. Matsunaga, *Nature*, **173**, 168 (1954).

3) K. Brass and E. Clar, *Ber.*, **65**, 1660 (1932); **69**, 1977 (1936).

4) A. Zinke and A. Pongratz, *Ber.*, **69**, 1591 (1936); **70**, 214 (1937).

(black), violanthrone (dark violet), dibenzpyrene (black), dibenzcoronene (black), and ovalene (black).

The following compounds were found to make complexes with iodine by Brass and Clar's method: perylene (black), violanthrene (black), and dinaphthylene oxide (black).

It was concluded that most of the hydrocarbons can readily form complexes with bromine or iodine and darken their colours nearly to black. Whilst, in the case of quinones, iso-dibenzpyrenequinone could not form a complex with bromine nor iodine, violanthrone formed a complex with bromine but not with iodine. It seems less easy to make them complexes with halogens and even though they form complexes the colour does not change as much as in the case of the hydrocarbons.

The Electrical Conductivity Measurement

The conductance measurement was made by the potential drop method in the following conditions. The sample powder was packed in an ebonite cylinder and attaching to each end a silver coated metallic cap, compressed under about 200 kg. per cm^2 pressure.

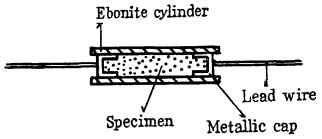

Fig. 1. Specimen cell for the conductance measurement.

It was found that most of the black complexes cited above show good conductance. The values of resistivity lie between about 5 ohm-cm of dibromoperylene-bromine complex and about 900 ohm-cm of dinaphthylene oxide-iodine complex. However, the resistivity is not stable and increases rapidly at first and then gradually over a period of days. The values cited above are that of the freshly prepared specimens, as the resistivity increases to kilo ohm-cm after several weeks even in the case of dibromoperylene-bromine complex. The features are shown in Fig. 2. The reason for this instability of resistivity will be considered in detail in the following section.

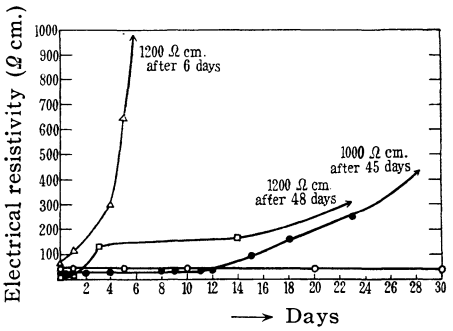

Fig. 2. Change of resistivity with time.
- ● Perylene-bromine
- ○ Violanthrene-iodine.
- □ Dibromoperylene-bromine
- △ Violanthrene-bromine.

There is one further problem to be considered concerning the observed conductance, that is the question whether it is an intrinsically electronic conductance or not.

It was found, during the measurement of resistivity, that after application of the potential through the specimen cell, the cell itself developes a small electromotive force of a few millivolts in a direction opposite to the applied potential. Therefore, a part of the conductance at least must be attributed to ionic conductance. The resistivity due to the ionic conductance (R_i) and that due to the electronic conductance (R_e) can be separately estimated by the following way. Assuming the total resistivity (R) which is measured in the usual way, to be made up of R_e and R_i in parallel, then $1/R=1/R_e+1/R_i$, where R_i can be estimated from the current which results from the electromotive force of the specimen cell itself, without any applied potential from outside, measured by reference to a standard resistor. In most cases, the conductance due to ionic ($1/R_i$) is 10-20 per cent of the total conductance for fresh specimens and thereafter decreases to 5 per cent or less. The remainder is assumed to be electronic conductance ($1/R_e$). If we take the value of R_e, they were found to be more stable than R itself. In Fig. 2, the R_e is plotted as a function of time (days).

Furthermore, it was soon found that if moisture is carefully excluded and the specimen is made from a thoroughly dried sample, the ionic conductance part decreases to an almost undetectable value. Therefore the larger part of the observed conduction may be considered as due to the electronic conductance. All values cited in the present paper, however, are those R_e calibrated in the above way.

Further evidence against ionic conduction can be obtained by the following consideration. A specimen of violanthrene-iodine complex, as an example, contained 150 mg. of iodine as its component. If the observed current is wholly due to electrolytic conduction, it must drop within sixteen minutes after the current of 120 mA has passed

through the cell. It did not do so, however, and the stable current was observed as long as five hours or more, excepting a small drop in resistance which is due to the thermal effect of the current. This latter drop in resistance recovered to the initial value after the current was ceased.

The Conductivity of Perylene-Bromine Complex

The resistivity of perylene-bromine complex is several ohm-cm at the freshly prepared state, but it changes over a period of days and increases to 10^3 ohm-cm. or more after several weeks. Therefore, it must be ascertained whether the nature of conduction itself is so unstable or the complex itself is unstable and changes its structure. Concerning the latter possibility, in the case of the bromine complex the liberation of hydrogen bromide is observed as mentioned above. This is due to the substitution reaction of bromine. Therefore, the specimen is in a dynamic state in which a part of bromine combined as the molecular compound at the beginning takes place substitution reaction to make bromoperylene and at the same time the equivalent bromine is liberated as hydrogen bromide. Moreover, decomposition is caused in the specimen cell at the place of contact of the metallic electrodes.

Hence, the electrical resistivity as a function of the composition was investigated in the following way. A set of samples of perylene-bromine complex was made by Zinke's method. Their composition was one perylene molecule to nearly four bromine atoms in the fresh state. Specimen cells for the conductivity measurement were made using parts of these samples, and the resistivity was measured in as fresh a state as possible. The resistivity and the bromine content of these specimens are shown by the points of 1, 2, and 3 in Fig. 3. The remaining parts of the samples were preserved in a desiccator over potassium hydroxide. At an appropriate period of days, the decrease in mass of the preserved samples was measured. From this the bromine content was determined, and at the same time the resistivity was measured, using a part of the sample. The resistivities thus obtained as the function of the bromine content are shown in Fig. 3 by the points of 4, 5, etc.

When the sample in which the bromine content had decreased was put into bromine vapour, it absorbed bromine again and its conductivity recovered to a certain degree. This is shown in Fig. 3 by the points of 4′, 5′, etc., (concerning these points, the bromine content on the abscissa has no meaning).

From this investigation, it is understood that the instability of the conductivity of the complex is due to the change of the bromine content of the complex itself.

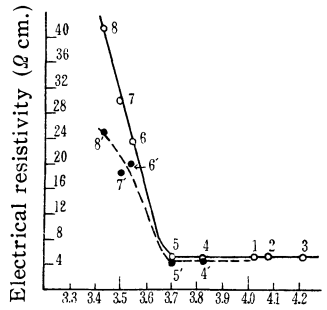

Fig. 3. Electrical resistivity of perylene-bromine complex as the function of total bromine content.

Perylene-bromine complex decomposes spontaneously as mentioned above. The change of the total apparent bromine content through a period of days, for an example, is shown in Fig. 4. If it is assumed that the decomposition is solely due to the substitution reaction to make dibromoperylene, the reaction is

$$(C_{20}H_{12}\text{-}4Br) \longrightarrow C_{20}H_{10}Br_2+2HBr.$$

Hence, the complex of which the apparent composition is one perylene molecule to n bromine atoms is in fact made of dibromoperylene-bromine complex and perylene-bromine complex. This is expressed by

$$(C_{20}H_{12}\text{-}nBr) \simeq \alpha C_{20}H_{10}Br_2+(1-\alpha)C_{20}H_{12}+(n-2\alpha)Br.$$

The amount of the additively combined bromine can be estimated, and distinguished from substituted bromine, by titration with sodium thiosulphate solution. In the case shown in Fig. 4, n was 4.03 in the fresh complex and it changed to 3.30 at a final

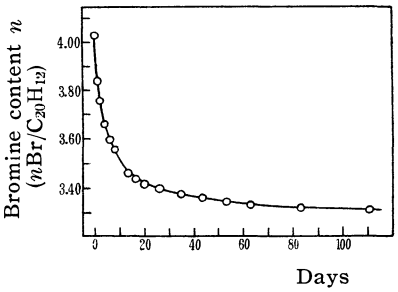

Fig. 4. Change of total bromine content following the decomposition of perylene-bromine complex.

state after the decomposition had proceeded. In this final complex, the content of the free bromine was found to be 0.97 atoms per one perylene molecule, consequently 2.33 atoms were substituted bromine. During this decomposition process, 0.73 bromine atoms per one perylene molecule were lost and the equivalent amount had been substituted, therefore, the content of bromine as dibromoperylene contained in the initial fresh complex was 1.60 (=2.33−0.73) atoms per one perylene molecule. This means $\alpha=0.8$ in the above scheme.

The complex of which the apparent composition is one perylene molecule to 4 bromine atoms was in fact a mixture of 80 per cent of dibromoperylene dibromide and 20 per cent of perylene tetrabromide, even in the initial fresh state. From this it is understood that the substitution reaction of bromine is relatively rapid at least at the beginning, and a large part of the perylene changes to dibromoperylene during complex formation. The resistivity of the "perylene-bromine (1 : 4) complex" agrees well with that of dibromoperylene-bromine (1 : 2) complex, both in the fresh state, and is about 5 ohm-cm.

Dibromoperylene dibromide, further changes to tetrabromoperylene with simultaneous liberation of hydrogen bromide,

$$2(C_{20}H_{10}Br_2-2Br) \rightarrow C_{20}H_8Br_4 + C_{20}H_{10}Br_2+2HBr.$$

With the progress of this reaction, the content of the additively combined bromine is progressively lost. Hence, passing the point 5 in Fig. 3, all perylene molecules have changed to dibromoperylene and thereafter only the above reaction takes place, at the same time the conductivity of the complex begins to decrease rapidly. In this stage, the reabsorption of bromine leads to a recovery of the conductivity in a certain limited degree, but not completely. This is due to the formation of the additive compound between dibromoperylene and bromine, but it is supposed that tetrabromoperylene can scarcely form a complex.

It is concluded that the instability or decrease in the conductivity of the complex is due to the loss of bromine which combines to form the additive compound. In other words, the origin of the conductivity is attributed to the interaction between a molecule of perylene or its bromine derivative and additively combined bromine molecules.

Violanthrene-Iodine Complex

If there is any system in which the substitution reaction of halogen does not take place, such a complex will be stable of itself as well as of electrical property. It was found that the violanthrene-iodine complex is such a case.

This complex was made by Brass and Clar's method. About 600 mg. of violanthrene were suspended in 50 cc. of benzene, and boiled with 5 g. of iodine. The suspension was precipitated, forming the complex. Since the solubility of violanthrene in benzene is negligibly small, the increased weight of the precipitate was assumed to be due to the iodine content of the complex formed, from which the composition was determined as one violanthrene molecule to 4 iodine atoms. However, the composition can be varied by controlling the ratio of violanthrene to iodine, adding more or less.

The mass of this complex did not change when it was kept in a desiccator, therefore it was concluded that no decomposition takes place. Furthermore, it is quite stable up to 60°C. When it is heated beyond this temperature in a sealed glass tube, it is observed that iodine vapour is liberated. However, the recombination of iodine takes place spontaneously when it is cooled down.

The conductivity of violanthrene-iodine complex is quite stable and does not show any change over a period of weeks. The resistivity as the function of the composition is shown in Fig. 5. In this figure, it is seen that the maximum conductivity is attained at the composition of $n=4$, beyond this composition the conductivity again begins to decrease. It is assumed that in the range of the composition up to $n=4$, iodine content is insufficient to make up the additive compound with all molecules of violanthrene, whilst beyond $n=4$ excess iodine molecules are present, in some other state than the above additive compound, they fail to contribute to the conduction, giving rise to an insulating effect. Hence, 4 iodine atoms per

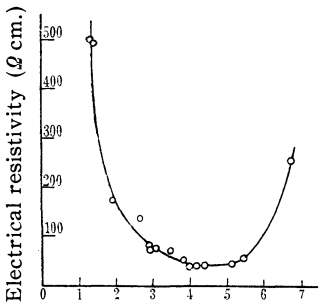

Iodine content n ($nI/C_{34}H_{18}$)

Fig. 5. Electrical resistivity of violanthrene-iodine complex as the function of the composition.

one violanthrene molecule is the saturation value of the composition of this additive compound and its resistivity is about 40 ohm-cm. at room temperature.

The Temperature Coefficient of the Resistivity

The temperature dependence of the resistivity was measured, for some complexes, in the range from room temperature down to the temperature of liquid air. The resistivity increases with decreasing temperature and a good linear relationship was observed between the logarithm of the resistivity and the reciprocal of temperature, as expressed in $\rho=\rho_0 \exp(\Delta\varepsilon/2kT)$ where ρ is the resistivity and $\Delta\varepsilon$ is the energy gap for conductivity. An example of the results is shown in Fig. 6, for violanthrene-iodine complex. The behaviour is as found with typical semiconductors. In Table I the values of $\Delta\varepsilon$ of the complexes are shown referring to $\Delta\varepsilon^*$ of the corresponding hydrocarbons. The decrement in the energy gap for conductivity is remarkable when the mole cular complex is formed.

Discussion

Among simple organic substances, excepting graphite or carbons, no substance has ever been known with so high an electrical conductivity as in the present case. Violanthrene itself is assumed to be an intrinsic semiconductor, but its resistivity is still 2×10^{14} ohm-cm., and the resistivity of perylene is presumably more than 10^{22} ohm-cm. It is concluded that the high conductivity of the complexes between polycyclic aromatic hydrocarbons and halogens is due to an appropriate electronic state following the formation of the additive compound. Hence, in such a state, it must be assumed that there are strongly labile electrons and they can transfer from molecule to molecule under the influence of an electric field.

TABLE I
SEMICONDUCTIVITY DATA OF COMPLEXES

Complex	Resistivity at room temp. (ohm-cm.)	Temp. range (°C.)	$\Delta\varepsilon$ (eV.)	$\Delta\varepsilon^*$ (eV.)
Perylene-bromine (1 : 4. 4)*	7. 8	−20～−170	0. 13	—
Pyranthrene-bromine (1 : 3. 3)	220	〃	0. 20	1. 07
Violanthrene-bromine (1 : 4. 5)	66	〃	0. 20	0. 85
Violanthrene-iodine (1 : 4. 0)	45	〃	0. 15	〃
Violanthrene-iodine (1 : 4. 0)	45	10～60	0. 14	〃

* The composition is an apparent one, expressed in one hydrocarbon molecule to halogen atoms.

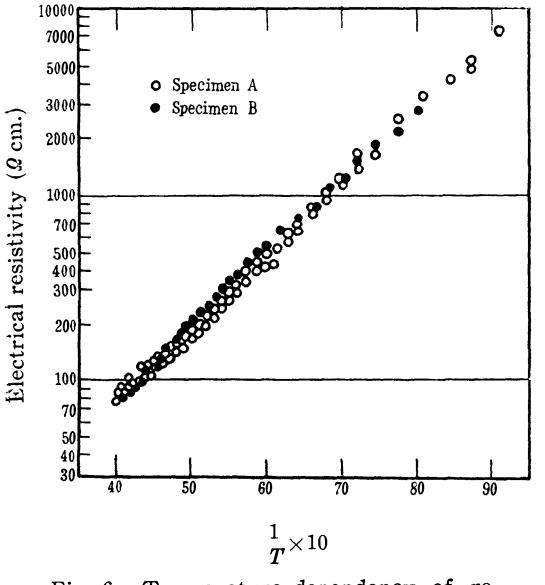

Fig. 6. Temperature dependency of resistivity of violanthrene-iodine complex.

It is known that in benzene solution of iodine, a complex formation takes place between a benzene molecule and an iodine molecule. Mulliken[5] pointed out the possibility of the intermolecular charge transfer force between them, from the presence of the corresponding spectrum, that is to say, an electron transfer takes place from a benzene molecule toward an iodine molecule accompanied by an overlapping of the molecular orbitals. The formation of the present complexes can be assumed to be due to the similar force as in the case of benzene-iodine complex. However, there is a noteworthy difference between these two cases.

In a benzene solution of iodine, a stoichiometric one to one molecular complex is formed in a state isolated from each other. On the other hand, in the present case the complexes are formed in the crystalline state, in which the molecular orbital for any one

5) R. S. Mulliken, *J. Am. Chem. Soc.*, **74**, 811 (1952); *J. Phys. Chem.*, **56**, 801 (1952).

molecule might overlap, if possible, with those of more than one of its neighbours. Moreover, the stoichiometric relationship is not necessarily fulfilled. In the case of violanthrene-iodine complex, the relative composition is 1:4 in the saturated state. Nevertheless, in fact, in the range where the iodine content is far less than this ratio, the complex still has a pretty good conductance. Hence, in this range of composition, it would not be a mechanical mixture of violanthrene tetraiodide and violanthrene, but it would be a non-stoichiometric molecular compound as a whole, in which iodine molecules are distributed among violanthrene molecules or vice versa. In such a state, there is not a one to one correspondence between violanthrene molecules and iodine molecules.

In the present complexes, the bond character between a hydrocarbon molecule and a halogen molecule is presumably far from an ionic one, and even from a dative covalent bond, and it might be shifted to the more metallic-like bond with delocalized electrons. Such a bond character might be attributed to an appropriate balance between the low ionization potential of a hydrocarbon molecule, which decreases with an increasing number of aromatic rings, and the high electron affinity of the halogen molecule.

Results from magnetic susceptibility measurements show that the presumable diamagnetism decreases and the paramagnetism increases, from which the presence of non-paired electrons is predicted. The details of the magnetic measurements has been presented by one of us[3].

When examined by X-rays, violanthrene-iodine complex gives merely a very diffused amorphous pattern. This agrees with the discussion mentioned above. On the other hand, in the case of perylene-bromine complex, the X-ray diffraction pattern is made of sharp lines, of which the features are varied according to the relative composition of the complex. Hence, the non-stoichiometric or amorphous state is not necessary for conductance.

Recently, Holmes-Walker and Ubbelohde[7] have reported that complexes formed between anthracene and alkali metals show semiconductor behaviour with electrical conductivity ranging 10^{-8}–10^{-12} (ohm-cm.)$^{-1}$. It was suggested that the complexes are formed by a non-stoichiometric electron transfer between alkali metal atoms and hydrocarbon molecules.

Besides these molecular complexes, even the polycyclic aromatic compounds themselves show semiconductor behaviour, and their resistivity decreases with an increase in the number of aromatic rings. In this case, it can be assumed, analogous to the complexes, that each molecule behaves as an electron-donor or electron-acceptor, one by one, and a sort of inner complex is formed between the same kind of molecules in the crystalline state.

All of these cases suggest strongly that there takes place an intermolecular overlapping of the molecular orbitals stretching throughout the crystal, whilst the molecular crystals are commonly considered as being held together merely by the force of van der Waals type between the molecules.

Summary

It was found that most polycyclic aromatic hydrocarbons form molecular complexes with bromine or iodine. Those complexes which are black behave as typical semiconductors with energy gaps for conductivity of 0.1–0.2 eV., as well as with low electrical resistivity ranging from 10^{0} to 10^{3} ohm-cm. The complexes are unstable and a substitution reaction of halogen takes place; when this is not the case, e. g. the violanthrene-iodine complex, and the complex itself is quite stable, so also is the electrical property. It is concluded that the origin of the high conductivity is due to the interaction between hydrocarbon molecules and halogen molecules, and this is presumably due to the overlapping of molecular orbitals stretching throughout the crystal.

The cost of this research has been defrayed from the Grant in Aid for Fundamental Scientific Research from the Ministry of Education, to which the authors' thanks are due.

Department of Chemistry, Faculty of Science, The University of Tokyo, Tokyo

6) Y. Matsunaga, This Bulletin, 28, 475 (1955).
7) W.A. Holmes-Walker and A.R. Ubbelohde, *J. Chem. Soc.*, 1954, 720.

Paper Chromatography of Radioactive Substances. (Radiochemical Studies on "Bikini Ashes" (March 1, 1954), Part III). (Studies of the Analytical Chemistry on Filter Paper XVI)

By Shoichi NAKANO

(Received August 4, 1955)

Since Consden, Gordon and Martin[1] found in 1944 that filter paper sheets can be used as support of a stationary phase in partition chromatography, radioactive tracer techniques are applied to the identification of the substances developed on paper without the aid of reagents. For example, Wieland et al.[2] determined amino-acids by chromatographing their Cu salts containing radioactive Cu.

The methods for the separation of radioactive substances by means of ion exchange resins developed very rapidly by the studies carried out in connection with the work on atomic energy in the U. S. A.[3-13]. Tompkins, Khym and Cohn[14] found that a mixture of fission products which passed through a column of Amberlite IR-I (HR-form) to separate anions could be further separated into three groups by washing the column with oxalic acid to remove Zr and Hf, then with citrate at pH 3 to remove rare earths, and then with citrate at pH 5 to remove alkaline earths.

On the other hand, the separation of radioactive substances by paper chromatography has also been studied by several workers, but not so fully as ion exchange resins. For example, radioactive ^{42}K and ^{24}Na were separated by Frierson and Jones[15]. Bouissieres and Lederer[16] separated Ra and Ba using ethanol- water (80 : 20) as solvent, ^{22}Na and Mg with ethanol-20% water. By paper electromigration, Sato, Norris and Strain[17] obtained a good separation of many radioactive elements with 0.1 M lactic acid. In Japan, the separation of the radioactive substances adhering on the surface of tunny was also studied with the aid of paper chromatography by Kiba et al[18].

As above mentioned, the separation of radioactive substances by paper chromatography has not been investigated in detail, therefore many problems remain to be solved in a fundamental field. The important variables which have influence on the degree of separation, R_f values, purity and spot shape are: (I) carrier and its quantity; (2) other inactive substances (such as scavenger, analogous element, impurities in paper and solvent); (3) filter paper; (4) solvent; (5) self-absorption of radiation in paper (thickness of paper)[19]; (6) quantity spotted on original point; (7) temperature.

The author studied paper chromatography of radioactive substances in connection with ion-exchange resins so as to examine these effects in detail.

Experimental and Results

Separation by Ion-exchange Resins into four Groups.—According to Tompkins, Khym and Cohn[14], a mixture of fission products are separated into about four groups, and the nuclides in each group are further separated by ion exchange resins. The author tried the separation of nuclides in each group, which had been previously separated by ion exchange resins as shown in Fig. 1, with the aid of paper chromatography. The author treated the nuclides which are described in each group in Fig. 1. The obtained result is as follows.

Filter Paper.—Sheets of the Toyo filter paper

1) R. Consden, A. H. Gordon and A. J. P. Martin, *Biochem. J.*, 38, 224 (1944).
2) T. Wieland, K. Schmeiser, E. Fischer and H. Maier-Laibnitz, *Naturwissenschaften*, 36, 280 (1949).
3) B.H. Ketelle and G.E. Boyd, *J. Am. Chem. Soc.*, 69, 2800 (1947).
4) F. H. Spedding, *Discuss. Faraday Soc.*, 7, 214 (1949).
5) L.B. Werner and I. Perlman, *USAECD*, 1898.
6) S.G. Thompson, R. A. James and L. O. Morgar, *USAECD*, 1907.
7) K. Street Jr. and G.T. Seaborg, *J. Am. Chem. Soc.*, 72, 2790 (1950).
8) S.G. Thompson, B.B. Cunningham and G.T. Seaborg, ibid., 72, 2798 (1950).
9) K. Street Jr., S.G. Thompson and G.T. Seaborg, ibid., 72, 4832 (1950).
10) L.B. Magnusson, S.G. Thompson and G.T. Seaborg, *Phys. Rev.*, 78, 363 (1950).
11) R. Bouchez and G. Kayas, *Compt. rend.*, 228, 1222 (1949).
12) G. Kayas, *J. Chim. Phys.*, 47, 408 (1950).
13) E.R. Tompkins, ibid., 70, 3520 (1948).
14) E.R. Tompkins, J.X. Khym and W.E. Cohn, *J. Am. Chem. Soc.*, 69, 2769 (1947).
15) W.J. Frierson and J.W. Jones, *Anal. Chem.*, 23, 1447 (1951).
16) G. Bouissieres and M. Lederer, E. Lederer, M. Lederer and A.T. James, "Chromatography", Elsevier Publishing Co., Amsterdam, (1954), p. 331.
17) T.R. Sato, W.P. Norris and H.H. Strain, *Anal. Chem.*, 26, 267 (1954).
18) T. Kiba, S. Ohashi, M. Sibata and T. Mizube, *Japan Analyst*, 3, 361 (1954).
19) F. P. W. Winteringham, A. Harrison and R.G. Bridges, *Analyst*, 77, 19 (1952).

No. 5A or No. 5B (40×32 cm., with up to 8 samples on one sheet) are commonly used so as to prevent the influence of paper. When the development is completed (25 cm.), the sheet is hung for drying andc ut into strips (4×32 cm.) for measurement.

mm. in width and trailing the paper strip 10 mm. to every five minutes. Furthermore, the determination of each nuclide is done by the use of Nuclear Type 183, G. M. Counter having a mica window with a thickness of 1.4 mg./cm².

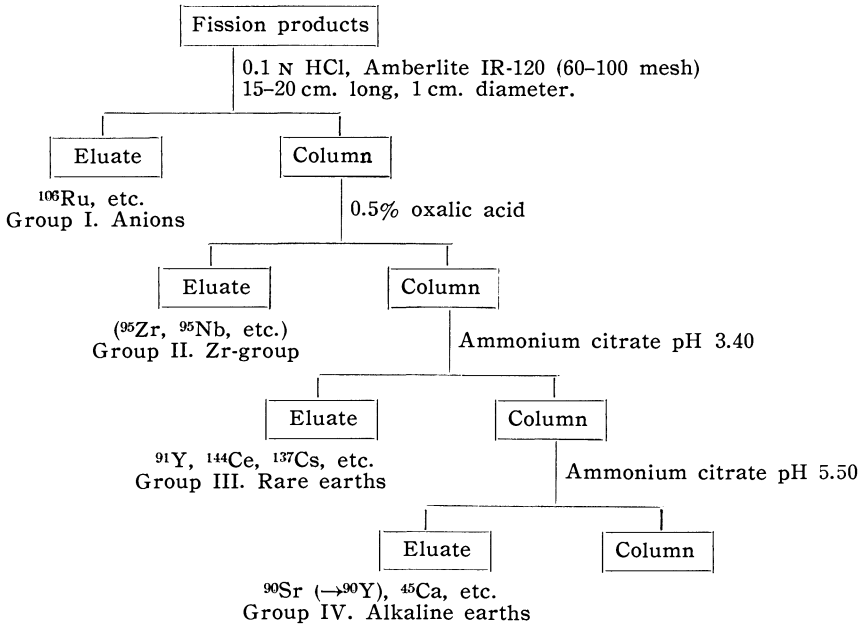

Fig. 1. Separation by ion exchange resins into four groups.

Test Solution.—The test solution separated from ion exchange resins or by distillation are concentrated to 3–10 cc. on the water bath, therefore, those solutions contain ammonium citrate, etc. (pH about 2–6).

Measurement of Radioactivity.—The distribution of radioactive substances on filter paper is measured by the Lauritzen electroscope with the author's continuous scanning device as shown in Fig. 2. It consists of lead plate (3 g./cm²) with paper holder and a slit which can be regulated by a screw. It is inserted into the gutter of the ionization chamber, and a filter paper strip is moved between the slit and the holder.

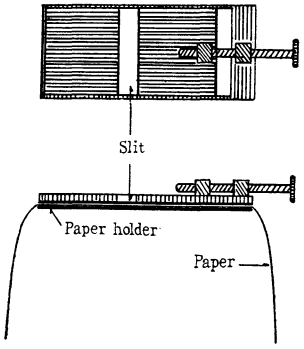

Fig. 2. Scanning slit of lead plate.

As shown in Fig. 3, it was observed that the best result is obtained by keeping the slit to 10

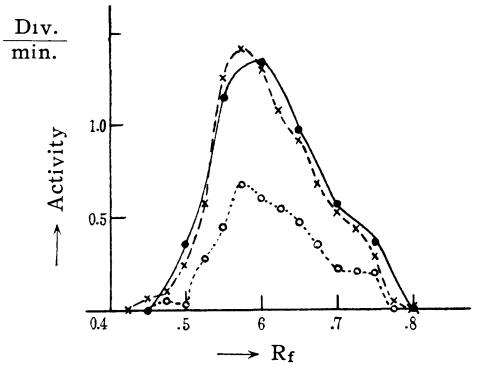

Methanol 9, c. NHO_3 1, Toyo filter paper No. 5B 15°–16°C, 4 hr./25 cm.

Fig. 3. Measurement of radioactivity using Lauritzenelectroscope.

•—•—• Slit: 10 mm. in width, trailing; 10 mm./5 min.

o···o···o Slit: 10 mm. in width, trailing; 5 mm./5min.

×···×···× Slit: 10 mm. in width, trailing: 5 mm./5 min.

(1) Separation of Group I (Anions).—At first, the author tried the separation of anions by using a sample solution separated with the aid of ion exchange resins from "Bikini Ashes" by the above mentioned method on May 24, 1954 (Fig. 4). Iso-amylalcohol-HCl (74 : 26) was used

as solvent. But the radioactivity was so low that nuclides could not be determined thoroughly. ^{35}S was reported on June 25, 1954 by the Tokyo University later.

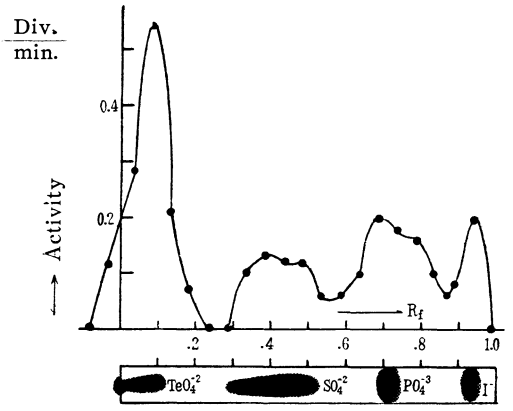

Fig. 4. Radio-chromatogram of anions (Group I).

{iso-Amylalcohol 74
{conc. HCl 26

Toyo filter paper No. 5A; 22°C.; 22 hr. /25 cm. (SO_4^{-2} and PO_4^{-3} could be detected by chemical reactions.)

Fig. 5 is the radio-chromatogram of carrier-free ^{106}Ru separated from "Bikini Ashes" and ^{235}U-fission products by ion exchange resins. It is interesting that ^{106}Ru appears at two separated spots. As shown in Fig. 6, however, ^{106}Ru is detected as a spot extending over the whole paper with methanol-HNO_3 (9:1). This figure contains the radio-chromatograms of carrier-free ^{106}Ru derived from ion exchange resins and the distil lation method.

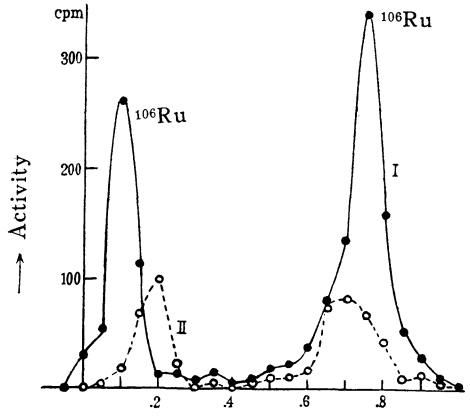

Fig. 5. Radio-chromatograms of ^{106}Ru (Group I).

{iso-Amylalcohol 74
{conc. HCl 26

From "Bikini Ashes". Quantity spotted on O. P.:
I: Large amounts.
II: Small amounts.
The same result was obtained in respect of a sample from ^{235}U-fission products.

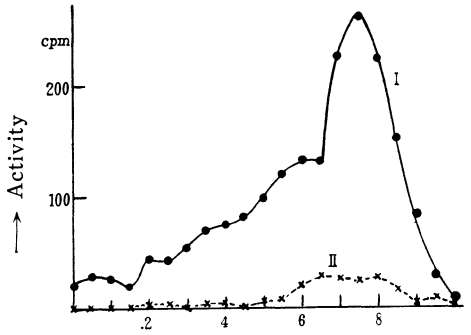

Fig. 6. Radio-chromatograms of ^{106}Ru.

{Methanol 9
{conc. HNO_3 1

Toyo filter paper No. 5B.
Sample solution: I: From ion exchange resins: II: From distillation.

(2) Separation of Group II(Zr-group).—The author has not obtained results to report here about this group yet, because the test solution was used for an other experiment by another student.

(3) Separation of Group III(Rate Earths).—A sample solution separated with the aid of ion exchanger from ^{235}U-fission products by the above mentioned method was developed with methanol-HNO_3(9:1). It is observed clearly in Fig. 7 that ^{137}Cs (alkali metal) is contained within this portion of eluates from the ion exchanger, and that ^{144}Ce and ^{137}Cs are separated completely. But also that ^{137}Cs was not found in the "Bikini Ashes" by this method.

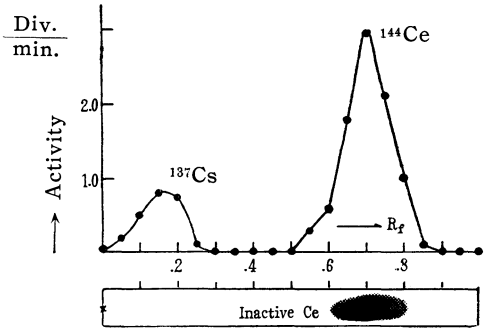

Fig. 7. Radio-chromatogram of rare earths (Group III).

{Methanol 9
{conc. HNO_3 1

Toyo filter paper No. 5B; 15°–16°C.; 4 hr./25 cm.
From ^{235}U-fission products.

A radio-chromatogram of ^{91}Y obtained from "Bikini Ashes" using ion exchange resins is shown in Fig. 8.

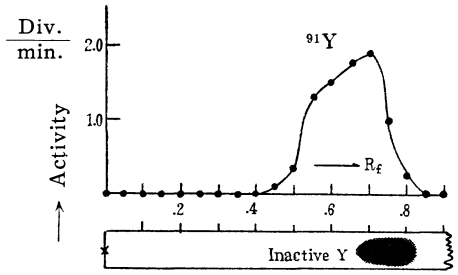

Fig. 8. Radio-chromatogram of rare earths (Group III).
{Methanol 9
{conc. NHO_3 1
Toyo filter paper No. 5B; 15°–16°C; 4 hr. /25 cm. From "Bikini Ashes".

In both chromatograms developed with methanol-HNO_3 (9:1), R_f values of carrier-free ^{144}Ce and ^{91}Y agree with R_f values of inactive Ce and Y nitrates (spot on paper strip in figure, $R_f=0.70$ and 0.75 respectively). When 1% oxine in glacial acetic acid is used as solvent, however, R_f values of carrier-free radioactive ^{144}Ce and ^{91}Y are not in agreement with R_f values of inactive Ce and Y respectively. In Figs. 9 and 10, ^{144}Ce containing ^{137}Cs and ^{91}Y are developed with 1% oxine in glacial acetic acid. In Fig. 9, inactive Ce separates to two spots ($R_f=0.00$ and 0.86),but carrier-free radioactive ^{144}Ce travels to $R_f=0.85$ only. The behavior of ^{144}Ce containing inactive Ce as carrier has also a different appearance as shown later. The peak of $R_f=0.5$–0.65 may be due to ^{137}Cs. In Fig. 10, the peak of ^{91}Y is found at $R_f=0.30$, but inactive Y has an $R_f=0.48$.

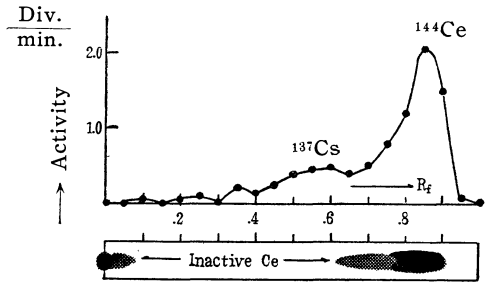

Fig. 9. Radio-chromatogram of rare earths (Group III).
1% oxine in gl. acetic acid. Toyo filter paper No. 5A; 15°–16°C; 5 hr./25 cm. From ^{235}U-fission products.

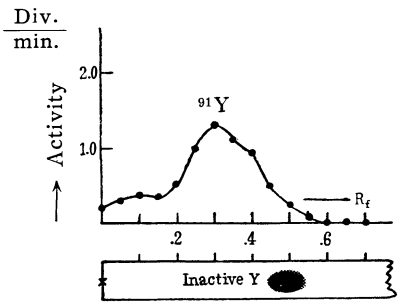

Fig. 10. Ralio-chromatogram of rare earths (Group III).
1% oxine in gl. acetic acid. Toyo filter paper No. 5A; 15°–16°C; 5 hr./25 cm. From "Bikini Ashes".

(4) Separation of Group IV(Alkaline Earths).—The typical results of separation of alkaline earths using methanol-HNO_3 (9:1) or 1% oxine in glacial acetic acid as solvent are shown in Figs. 11, 12, 13 and 14. A sample solution of carrier-free ^{90}Sr (containing ^{90}Y as its daughter) was separated by means of ion exchange resins from ^{235}U-fission products by the above mentioned method. A solution of ^{45}Ca was obtained from the liver of a tunny and separated using ion exchanger. It may contain inactive Ca. But the radioactivity was so low that ^{45}Ca could not be determined thoroughly (whether 0.7–0.8 or 0.0–0.4). In case of methanol-HNO_3 (9:1), R_f values of radioactive carrier-free ^{90}Sr, ^{90}Y and pure ^{90}Y separated from ^{90}Sr nearly agree with R_f values of inactive Sr and Y. In case of 1% oxine in glacial acetic acid, however, R_f values of radio-

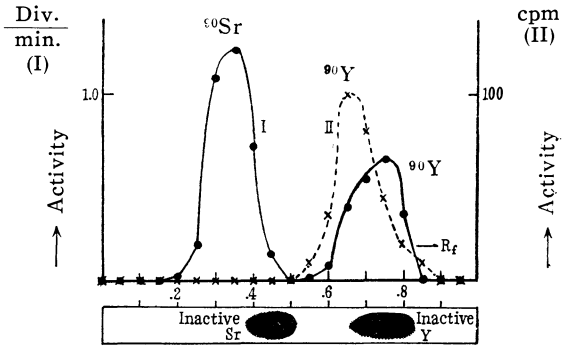

Fig. 11. Radio-chromatogram of alkaline earths (Group IV).
{Methanol 9
{conc. HNO_3 1
Toyo filter paper No. 5B; 15°–16°C; 4 hr. /25 cm. From ^{235}U-fission products.
I: ^{90}Sr containing ^{90}Y. II; Pure ^{90}Y.

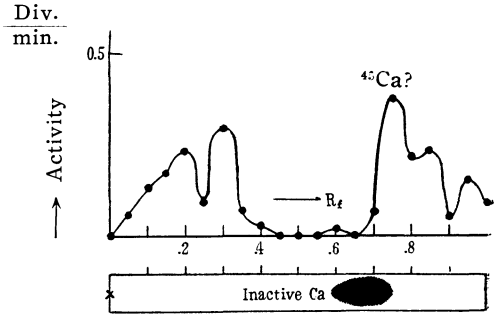

Fig. 12. Radio-chromatogram of alkaline earths (Group IV).
Toyo filter paper No. 5B; 4 hr./25 cm. From liver of tunny.
{Methanol 9
{conc. HNO_3 1

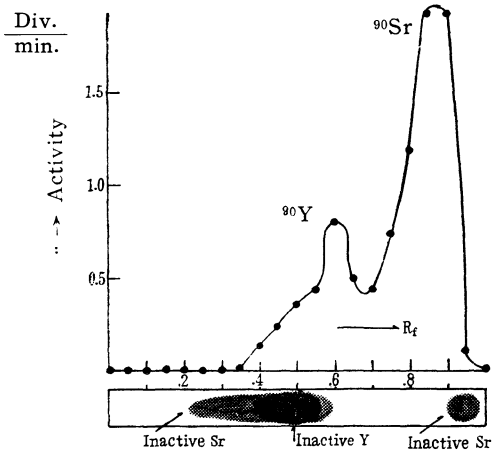

Fig. 13. Radio-chromatogram of alkaline earths (Group IV).
1% oxine in gl. acetic acid. Toyo filter paper No. 5A; 15°–16°C; 5 hr./25 cm.
From ^{235}U-fission products.

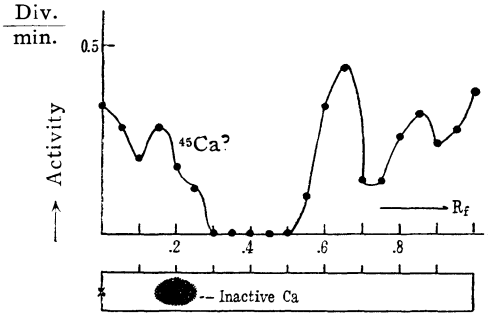

Fig. 14. Radio-chromatogram of alkaline earths (Group IV).
1% oxine in gl. acetic acid. Toyo filter paper No. 5A; 15°–16°C; 5 hr./25 cm.
From liver of tunny.

active and inactive elements are different from those shown in Fig. 13. That is, ^{90}Sr travels to R_f=0.87 which corresponds to one of the spots of inactive Sr (R_f=0.40 and 0.95), and R_f values of radioactive ^{90}Y and inactive Y are 0.60 and 0.45 respectively. The position of ^{45}Ca could not be determined as low counts in both of the solvents. In addition, as shown in Figs. 10 and 13 with 1% oxine in glacial acetic acid, it is interesting that R_f values of radioactive ^{91}Y, ^{90}Y and inactive Y are 0.30, 0.60 and 0.45 respectively.

(5) Influence of Carrier or other Elements.— As above shown, in 1% oxine in glacial acetic acid, the behavior of radioactive elements differs from that of the inactive elements. Therefore, it is very clear that the existence of carrier or other elements have some influence upon R_f value of a radioactive element. The qualitative results obtained are shown in Fig. 15. In this experiment, 1% oxine in glacial acetic acid is used as solvent. The strips ,a, b and c in Fig. 15 represent the movements of inactive Ce, ^{144}Ce (containing

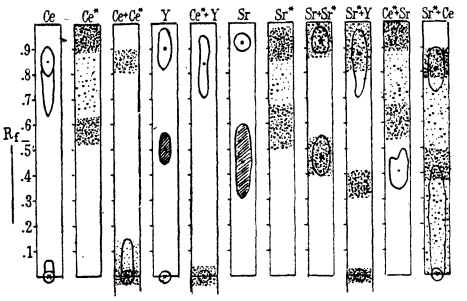

Fig. 15. Influence of carrier or other elements.
1% oxine in gl. acetic acid. Toyo filter paper No. 5A; 15°–16°C. 5hr./25 cm.
Ce* contains Cs*. Sr* contains ^{90}Y.

: Represents inactive element (Ce, Y and Sr).
: Represents position of a large part of ion.
* : Represents radioactive elements.
: Represents radioactivity

^{137}Cs), and ^{144}Ce with inactive Ce as carrier respectively. These strips show the influence of the carrier on ^{144}Ce containing ^{137}Cs (radioactivity of an R_f of 0.00). From the strips, b, d and e, it is clear that an addition of inactive Y to ^{144}Ce alters the R_f of ^{144}Ce remarkably. The results with respect to Sr and ^{90}Sr (containing ^{90}Y) are shown in the strips, f, g and h. The influence of inactive Y and Ce upon radioactive ^{90}Sr are remarkable as shown in the strips, i and k. This phenomenon may be due to ^{90}Y in ^{90}Sr. There is no influence of inactive Sr on ^{144}Ce (containing ^{137}Cs), and the former is not detected at R_f=0.92 (the strip, j). But a limit of detection of inactive Sr, as above inactive Ce and Y, is a question.

Discussion

The present author studied the paper chromatography of radioactive substances in connection with ion exchange resins, and obtained the results that nuclides can rapidly be determined by applying the paper chromatography to the separation of radioactive elements of the four groups eluated from ion exchange resins. In particular, the author knew that the factors influencing on R_f value and degree of separation of radioactive substances are (I) carrier or analogous element; (2) quantity spotted on original point of filter paper. These effects are shown in Figs. 15 and 5. Furtheremore, the R_f values of inactive and active elements are generally ^{144}Ce≦Ce (inactive) (Fig. 7); ^{90}Sr<Sr (inactive), ^{90}Y<Y (inactive) (Fig. 11) in methanol-HNO_3, and are ^{144}Ce≦Ce (Fig. 9); ^{91}Y<Y (Fig. 10); ^{90}Sr<Sr, ^{90}Y>Y (may be due to ^{90}Sr, Fig. 13) in 1% oxine in glacial acetic acid. That is, as shown in the reports with respect to

the influence of cations on the R_f values of anions (Cl^-, NO_3^- and SO_4^{2-})[20], the R_f values of the element of a large mass are smaller than those of the element of a small mass. But it can not be concluded in these experiments that the difference of an R_f of inactive and active element is due to a mass number. Because a difference of quantity spotted on the original point of paper between inactive and active solutions, a different complex formation in very dilute solution and the existence of some other substance in an active sample solution (ammonium citrate) in place of nitrate of inactive sample solution. It is the author's wish to study these questions quantitatively.

The author wishes to express his heartfelt thanks to Prof. Takanobu Siokawa, Sizuoka University, for his kind advice and encouragement.

Institute of Chemistry, Sizuoka Women's College, Sizuoka

20) S. Nakano, *J. Chem. Soc. Japan*, **75**, 150 (1954).

Über den Mechanismus von Goldsensibilisierung der Photographischen Emulsion. II. Die Einflüsse von Gold bzw. Goldverbindungen auf die Lichtelektrische Leitfähigkeit des Silberbromides. I

Von Keiichi YAMADA, Shumpei OKA und Takashi MUKAIBO

(Eingegangen am 27, September, 1955)

Einleitung

Der erste Teil dieser Untersuchungen[1] zeigt, daß der Ersatz durch Gold von den in od. auf dem Silberbromid sich befindenden Silberkeimen auch von dem Gesichtspunkt der Elektronenbeugung höchst wahrscheinlich ist.

Der zweite Teil hat also die Rolle dieser Goldkeimen beim Lichtempfindungsprozeß klar in stellen.

Es ist vorher behauptet worden, daß diese Goldkeime als Elektronen- od. Elektronendefektstellen-Fallen stärker als Silberkeime wirken. Wenn diese Vermutung zu recht besteht, muss die Veränderung an der Bewegung von Elektronen bzw. Ionen auf die elektrische Leitfähigkeit des Kristalls irgendeinen Einfluß ausüben. Der Zweck dieser Untersuchung ist folglich, durch die Messung von lichtelektrischer Leitfähigkeit vor und nach dem Zusatz von Goldkeimen, einige Kenntnisse davon zu erlangen.

Experimentelles

(1) Herstellung der Präparate. — Das auf 500–520°C geschmolzene Silberbromid wurde in die Spalte zwischen zwei Glasplättchen (25 mm. × 75 mm.) eingegoßen. Nach langsamer Abkühlung wurde das entstandene Polykristall im Wasser von den Glasplättchen abgezogen. Aus dem so hergestellten Polykristall wurden 6–7 Stücke von Proben genommen.

(2) Apparatur und Messmethodik. — Die Messung von dem lichtelektrischen Strom wurde mit einen Röhrenverstärker von Du Bridge und Brown[2], den Herr Suzuki hergestellt hatte, durchgefürt.

Die Probe wurde auf einem Ebonitplättchen zwischen die zwei Silberelektroden geschraubt. (Elektrodenabstand rund 7 mm.)

Man bemerkte eine Schwingung des Galvanometers, gleichbeim Anfang der Lichtstrahlung mit einer 100 W Wolframlampe.

(3) Ergebnisse.—a. Die Proben wurden in die Lösung folgender Zusammensetzungen bei Zimmertemperatur für dreißig Minuten eingeweicht.

1. in Wasser.
2. in Goldchloridlösung (0.01% Gew. Au).
3. in Goldrhodanidlösung (0.01% Gew. Au), die aus Goldchlorid und 50-fach überschüssigem Ammoniumrhodanid hergestellt wurde.

Die lichtelektrische Leitfähigkeit dieser Proben nimmt durch solche Behandlungen ab. Der Effekt sit beim 3. Fall stärker als beim 2. Fall. (Fig. 1)

Dieser Einfluß scheint sich mit der Zeit zu verkleinern, wenn man die Proben länger im Dunkeln hält.

b. Man setzt erstens die Proben in gesättigtes Bromwasser, das 10% Kaliumbromid ent-

* Ein Teil von dem Vortrage bei der achten Versammlung dieser Gesellschaft (1955).

1) K. Yamada, S. Oka und T. Mukaibo, *Bull. Soc. Sci. Photo. Japan*, No. 4—5, 1 (1955).

2) Du Bridge und Brown, *Rev. Sci. Instr.*, **4**, 532 (1933).

3) S. Suzuki, *J. Ind. Chem. Japan*, **52**, 77 (1949).

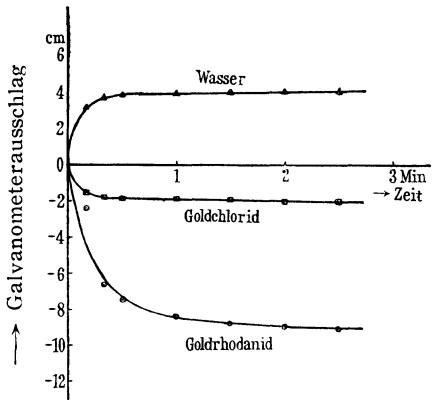

Fig. 1. Der Einfluß von Goldverbindugen.

hält. Diese Proben wurden danach, um das überschüssige Brom abzuscheiden, in die Lösung von 5% Semicarbazid-Chlorwasserstoff, der 10% Kaliumbromid enthält, eingeweicht. Nach wiederholtem Waschen mit distilliertem Wasser, wurde die Behandlung mit Goldrhodanid (a-3) durchgeführt.

Dieses Mal konnte man keine bemerkenswerte Veränderung an der lichtelektrischen Leitfähigkeit herausfinden.

c. Eine sehr kleine Menge von Gold wurde, durch Verdampfung in Vakuum (10^{-3} mmHg), auf die Oberfläche des Kristalls hinzugesetzt[4].

Die lichtelekrische Leitfähigkeit dieser Proben nimmt aber dadurch sehr stark ab. (Fig. 2)

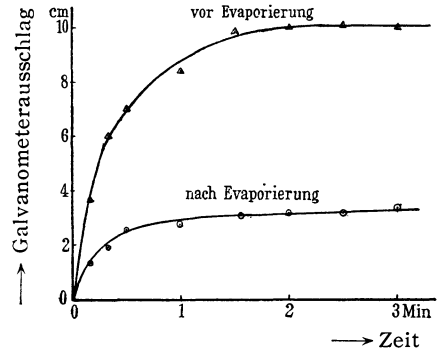

Fig. 2. Der Einfluß von evaporiertem Gold.

d. Statt Gold, wurde eine kleine Menge von Silber auf die Proben hinzugesetzt. Diese Proben wurden dann in die Lösung von Goldrhodanid eingeweicht.

In diesem Fall, war der Einfluß von der Goldverbindung nicht gross.

e. Die beiden nach d. hergestellten Proben wurden wie b mit Bromwasser behandelt.

Dadurch war die Wiederherstellung von der lichtelektrischen Leitfähigkeit bei solchen Proben, welche keine Wirkung von Goldrhodanid erlitten, bemerkenswerter. Die lichtelektrische Leitfähigkeit erniedrigende Wirkung von Silber wurde dagegen durch Bromierung fast vollkommen vernichtet. (Fig. 3)

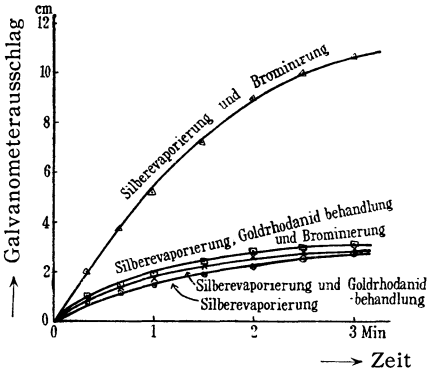

Fig. 3. Der Einfluß von Evaporierung des Silbers, Goldrhodanidbehandlung, und Bromierung.

f. Nach Bromierung wurden die Proben für 2-3 Wochen im Dunkeln gehalten und dann in die Lösung von Goldrhodanid eingesetzt.

In diesem Falle, geschieht, die Verminderung von lichtelektrischer Leitfähigkeit wieder. (Fig. 4)

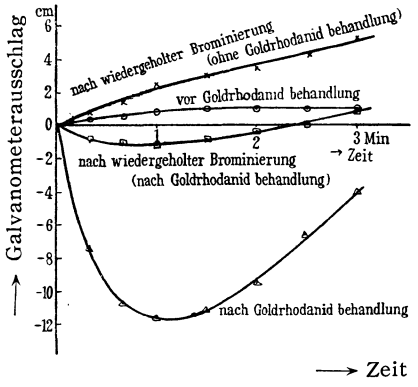

Fig. 4. Der Einfluß von Goldrhodanid auf die Proben, die nach Bromierung in Dunkel gehalten wurden.

g. Durch Einweichung in die Lösung von Ammoniumrhodanid, dessen Konzentration dieselbe wie von a. ist, beobachtete man keinen so großen Einfluß auf die lichtelektrische Leitfähigkeit, obwohl die Oberfläche dieses Kristalls davon starken Schaden erlitt.

Diskussion

(1) Zur Deutung der Ergebnisse. — Ein Kristall von Silberbromid, der in dem nicht luftdicht verschlossenen Ofen hergestellt wird, ist wegen der Verdampfung von Brom nicht stöchiometrisch, sondern enthält überschüssiges Silber. Es ist also wahrscheinlich, daß dieses Silber nahe an der Oberfläche od. in den vielerlei Unvollkommenheiten sehr kleine Silberkeime bildet und durch Gold

4) Die auf das Silberbromid hinzugesetzten Körnchen von einigen Metallen u. s. w. üben auf die lichtelektrische Leitfähigkeit einen bemerkenswerten Einfluss aus (z. B. Cadmiun; heftige Vergrösserung). Untersuchung darüber wird nächstens veröffentlicht).

substituiert wird. Würden unter den Umständen diese Silberkörnchen durch Bromierung verloren gehen, so hätte die Goldvervindung folglich keine ausgezeichnete Wirkung auf die Proben.

Diese Ergebnisse sind also einer der Beweise, daß die Goldsensibilisierung ihre Ursache von diesem Ersatz hat. Auch die Tatsache, daß auf das Silberbromid die zugefügten Goldkörnchen die lichtelektrische Leitfähigkeit erniedrigende Wirkung hat, unterstützt diese Meinung.

Der kleinere Einfluß von dem Ersatz der verdampften Silberkeime durch Gold sollte aus diesem Grund, daß die Wirkung dieser Keime sich nur auf die makroskopische Oberfläche beschränkt, erklärt werden.

Die Proben, die nach Bromierung lange im Dunkeln gehalten wurden, hatten weniger lichtelektrische Leitfähigkeit und zeigten endlich negativen Effekt; Diese Erniedrigung der Leitfähigkeit erlosch durch zweimalige Brominierung. Es ist möglich, daß durch langsame Zersetzung Silberkörnchen verursacht werden, wenn diese Vermutung zutrifft, kann die Wiederholung von Goldeffekt bei solchen Proben leicht verständlich gemacht werden.

Die Reihenfolge von dem Vermögen verschiedener Goldverbindungen stimmt mit dem Sensibilisierungsvermögen überein.

(2) **Mechanismus.**—Die ohenerwähnte lichtelektrische Leitfähigkeit erniedrigende Wirkung von Goldkeimen kann ohne ausführlichere Aufklärung des Lichtempfindungsprozesses nicht ganz klar werden. Aber sie würde nach der bisherigen Lichtempfindungstheorie auf diese Weise erklärt.

Die Austrittsarbeit von Gold bzw. Silber ist;

	optisch	thermisch
Silber	4.73 eV.	4.06
Gold	4.76	4.23

Das Fermische Energieniveau von Silber liegt bei ca. 1 eV. tiefer als das Leitungsband von Silverbromid und Gold befindet sich noch tiefer. Deswegen werden die Goldkeime, wie Hörlin und Müller in ihrem älteren Bericht behaupten[5], stärkere Elektronenfallen als diejenigen aus Silber (Fig. 5). Diese negative Ladung tragenden Keime ziehen Silberionen in Zwischengitterstellen, welche den Hauptteil von Ionenleitung in Silberbromid innehaben aw sich. Die dadurch hervorgerufene heftigere Verminderung an Silberionen, neben der Verminderung an Elektronen, erzeugt eine Abnahme an der lichtelektrischen

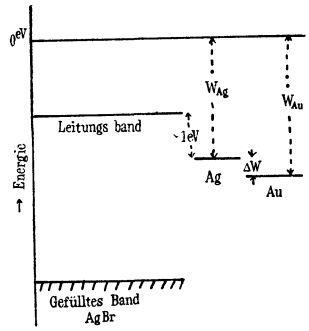

Fig. 5. Energiediagramme.

Leitfähigkeit in dem Falle von Goldzusatz.

Nach der Lichtempfindungstheorie von Mitchell[6], im Gegensatze zu der Theorie von Mott und Gurney[7], sollten diese Goldkeime sich als stärkere Fänger von Elektronendefektstellen beweisen. Aber diese Meßergebnisse können auch nach dieser Theorie verständlich sein, weil bei diesen Umständen eine Aufnahme an den Fänger von Elektronendefektstellen die Entstehung von Silber aus Silberionen dringend verlangen könnte. Die ausführlicheren Gründe, warum diese Goldkeime dabei wirksamer sind, sind noch nicht klar. Aber das stärkere Widerstandsvermögen von Goldkeimen gegen Bromierung kann ihre Haltbarkeit als der Fänger von Elektronendefektstellen zeigen.

Für die Entscheidung dieses Gegenstandes sollten mehrere Untersuchungen erforderlich sein.

Zusammenfassung

1. Die Einflüsse von Goldsensibilisierung auf den elektronischen sowie ionischen Prozeß der Photographischen Lichtempfindung wurden durch die Messung von lichtelektrischer Leitfähigkeit untersucht.

2. Der Zusatz von Gold bzw. Goldverbindungen wurde in den folgenden Weisen durchgeführt;

a. Die Evaporierung von metallischem Gold.

b. Die Einweichung in die Lösung von Goldchlorid bzw. Goldrhodanid.

3. Diese Untersuchung ergab die folgenden Tatsachen;

a. Goldverbindungen sind wirksam nur wenn die Probe Silberkeim enthält.

b. Die Behandlungen mit Goldverbindungen lassen die lichtelektrische Leitfähigkeit des Silberbromides heftig vermindern und rufen oftmals den negativen Effekt hervor.

5) H. Hoerlin und F.W.H. Müller, *J. Opt. Soc. Amer.*, 40, No. 5, 246 (1950).

6) J.W. Mitchell, *J. Photo. Sci.*, Vol. 1,110 (1953).

7) N.F. Mott und R.W. Gurney, "Electronic Processes in Ionic Crystals", Oxford Clarendon Press, (1940).

4. Die Verfasser dieses Berichtes sind der Ansicht, daß die Silberkeime in od. auf dem Silberbromid durch Gold substituiert wird und diese Goldkeime als die Fänger von Elektronen od. Elektronendefektstellen stärkere Wirkung haben.

Herrn Dozent S. Suzuki in unserem Laboratorium möchten wir für seine Ratschläge unseren herzlichen Dank aussprechen.

Institut für Angewandte Elektrochemie und Photochemie, Technische Fakultät, Universität Tokio, Tokio

Photonitrosation of Cycloalkanes with Nitrosyl Chloride. I. Synthesis of Cyclohexanone Oxime*

By Yoshikazu Ito

(Received August 29, 1955)

Introduction

It has been reported[1] that nitrosyl chloride reacts with most of the organic compounds and may cause various types of reactions such as nitrosation, chlorination, chloronitrosation, oxydation and diazotization. Of these reactions, nitrosation of hydrocarbons under the influence of light is particularly interesting. This reaction was first investigated by Lynn[2] and Hilton[3] and later by Mitchell and Carson[4]. From their work it was found that aliphatic hydrocarbons, for example, *n*-heptane or *n*-hexane, may be nitrosated by nitrosyl chloride under the influence of light and subsequently isomerized to the corresponding ketoximes. If ketoximes are obtainable from cycloalkanes in this way, this procedure will probably present a new route to prepare cycloalkanone oximes which are important intermediates of polyamide from lactam.

From this point of view, the author has investigated the nitrosation of cycloalkanes with nitrosyl chloride, and, first of all, cyclohexane was used as cycloalkane. From the results of preliminary experiments it was found that cyclohexane is unable to react with nitrosyl chloride at room temperature in the dark, but reacts immediately in the presence of sunlight, forming cyclohexanone oxime. However, this photonitrosation is generally accompanied by various side reactions corresponding to the reaction conditions. Therefore, for the purpose of obtaining cyclohexanone oxime in a good yield, it is necessary to find the optimum conditions under which the side reactions are reduced as far as possible and the rate of photonitrosation is favorably rapid.

Naylor and Anderson[5] reported a similar photonitrosation of cyclohexane, and according to their work, cyclohexanone oxime was obtained in a good yield (at least 71%) by adding nitrosyl chloride slowly and continuously into cyclohexane so that only a slight trace of color was present at any instant, maintaining the reaction liquid at low temperature (−30∼0°C). According to the author's results, it seems that such low temperature (−30∼0°C) and such low concentrations of nitrosyl chloride in cyclohexane, which Naylor proposed for the optimum conditions, may not always be necessary.

The present paper deals with the photonitrosation of cyclohexane with nitrosyl chloride and shows the effects of reaction conditions on the yield of cyclohexanone oxime.

Experimental

Reagents.—Crude cyclohexane obtained by the hydrogenation of pure benzene was purified by treating it with mixed acid (a ratio of sulphuric acid to nitric acid is 1.5 : 1) and washing it thoroughly with water followed by distillation. Physical constants of such purified cyclohexane are:

b. p. 80.2°C, n_D^{15} 1.4290, d_4^{15} 0.7991.

Nitrosyl chloride was prepared by adding a solution of nitrosyl sulfuric acid in conc. sulfuric acid to dried sodium chloride at 80°C. Pure

* This work was presented in the 6th annual meeting of the Chemical Society of Japan in April, 1953, in Kyoto.

1) L. J. Beckham, W. A. Fessler and M. Kise, *Chem. Rev.*, **48**, 320-96 (1951).

2) E. V. Lynn, *J. Am. Chem. Soc.*, **41**, 368 (1919).

3) E. V. Lynn and Hilton, ibid., **44**, 645 (1922).

4) S. Mitchell and S. C. Carson, *J. Chem. Soc.*, **1936**, 1005.

5) M. A Naylor and A. W. Anderson, *J. Org. Chem.*, **18**, 115-20 (1953).

nitrosyl sulfuric acid was prepared following the method described in a piece of literature[6]. Pure nitrosyl chloride (b. p. −5.5°C) was obtained by condensing crude nitrosyl chloride gas and then rectifing it repeatedly.

Apparatus.—A photoreactor employed for continuous reaction is shown in Fig. 1. One of the most effective and convenient light sources for this reaction was the high vapor pressure mercury lamp of [ca. 2 atm. of which the spectrum is shown in Fig. 3. Another type of photoreactor which is shown in Fig. 2 was also employed for the investigations of reaction conditions.

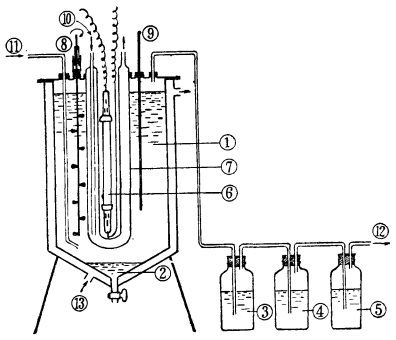

Fig. 1. Photoreactor for continuous reaction.

1. Cyclohexane
2. Oily products
3. Sulphuric acid
4. Aqueous caustic soda
5. Liquid paraffin
6. Mercury lamp
7. Cooling glass tube
8. Stirrer
9. Thermometer
10. Cooling water
11. Gas inlet
12. Gas outlet
13. Brine inlet

Procedure.—**(1) Batch Reaction.**—100 ml. of cyclohexane were charged into a reactor (Fig. 2) and nitrosyl chloride was blown into cyclohexane under irradiation. The color of the reaction liquid changed from colorless to cloudy yellow and oily substances began to separate from the

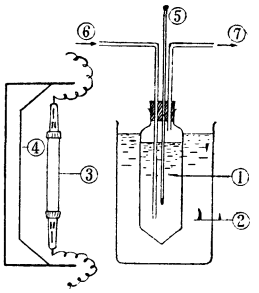

Fig. 2. Photoreactor for batch reaction.

1. Glass reactor
2. Cooling bath
3. Mercury lamp
4. Reflector
5. Thermometer
6. Gas inlet
7. Gas out let

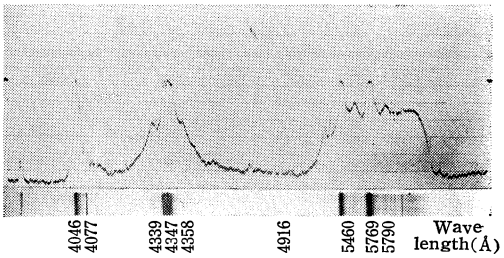

Fig. 3. Spectrum of high vapor pressure mercury lamp.

reaction liquid. After completion of the addition of nitrosyl chloride, the reaction product was separated from unreacted cyclohexane, dissolved in cold water and then neutralized with 20% aqueous caustic soda until it had pH 6.5. Crystals of precipitated oxime were separated from the mother liquor and dried. Additional amounts of crude oximes were obtained by extracting the latter with cyclohexane. Crude oximes were purified by recrystallization with methanol.

(2) Continuous Reaction.—4.7 l. of cyclohexane were charged into a reaction vessel (Fig. 1) and irradiation was applied with sufficient stirring. A gaseous mixture of nitrosyl chloride

TABLE I

EFFECT OF TEMPERATURE

Temperature* °C	Reaction time hr.	Nitrosyl sulfuric*** acid used g.	Color of reaction liquid	Pure oxime g.	Yield**** %
0**	5	14.1	Yellow	5.36	63.3
5**	5	15.3	Yellow	5.38	63.5
10	5	14.6	Yellow	5.89	65.4
15	5	13.2	Yellow	5.41	63.9
20	5	14.6	Yellow	4.48	52.8
25	5	15.6	Greenish yellow	2.93	37.6
30	5	14.3	Greenish yellow	3.57	44.5

* Temperature was controlled within a range of ±1°C.
** A mixture of cyclohexane and benzene (80 : 20, by volume) was used.
*** Nitrosyl sulfuric acid was used as a solution in conc. sulfuric acid (1 : 1, by weight).
**** The yield is that based on the consumed cyclohexane.

6) Coleman, Lillis and Gohen, "Inorganic Syntheses", (1939), I, p. 55.

and hydrogen chloride was continuously bubbled into cyclohexane at a definite rate. After about thirty minutes, the oily products were withdrawn from the bottom of the vessel and, at the same time, cyclohexane was added through the top inlet. The gases drawn off from the reactor were led in sequence-conc. sulfuric acid, aqueous caustic soda and liquid paraffin. Nitrosyl chloride was caught by sulfuric acid to form nitrosyl sulfuric acid, hydrogen chloride by caustic soda, and cyclohexane by liquid paraffin.

(3) The Identification of Reaction Product.— 100 ml. of cyclohexane was placed in a photoreactor (Fig. 2) and irradiated with a mercury lamp. Five grams of nitrosyl chloride together with 2.8 g. of hydrogen chloride were blown into cyclohexane over a period of three hours at 10°C. After about twenty minutes, oily substances began to deposit at the bottom of the reactor, which increased gradually as reaction proceeded. 6.2 g. of this oily produdt was obtained. After treating the product following the method described above, 3.4 g. of purified crystals were obtained, m.p. 88–89°C, which did not depress the melting point of pure cyclohexanone oxime (m.p. 89°C).

TABLE II
EFFECT OF HYDROGEN CHLORIDE

Mol. ratio NOCl : HCl	Oily product obtained	Color of reaction liquid	Pure oxime obtained	Yield of oxime based on added NOCl
	g.		g.	%
1 : 0	4.0	Greenish yellow	2.17	20.9
1 : 0.9	7.1	Yellow	4.16	39.6
1 : 2.7	6.2	Yellow	3.69	35.2
1 : 4.5	8.2	Yellow	3.86	36.8
1 : 6.3	6.9	Yellow	3.79	36.1

(4) Effect of Temperature.— : Consult Table I.

(5) Effect of Hydrogen Chloride.— : Consult Table II.

Note: A 270 W. mercury lamp was used for light source. 6.2 g. of nitrosyl chloride and various amounts of hydrogen chloride were continuously blown into 150 ml. of cyclohexane at 10°C during a period of five hours.

From these results it may be said that hydrogen chloride added to nitrosyl chloride may act not only as a diluent for nitrosyl chloride but also as an accelerator for the formation of oxime hydrochloride.

(6) Flow Rate of Nitrosyl Chloride.— : Consult Table III.

It seemed that side reactions are mainly affected by the concentrations of nitrosyl chloride in the system. The addition rate of nitrosyl chloride should thus be controlled according to the concentration of nitrosyl chloride at every instance. However, it is practically difficult to measure the concentration of nitrosyl chloride quantitatively by analysing the reaction liquid, because of the very low concentration of nitrosyl chloride which favours the yields of the oxime. Since the solution of nitrosyl chloride in cyclohexane has a characteristic color–reddish brown at high concentrations, and yellow or pale yellow at low concentrations–and since the by-products formed in the system are characterized by blue or green color, the concentration of nitrosyl chloride can be inferred conveniently by this change of color.

The addition rate of nitrosyl chloride must be controlled so as to maintain the yellow or pale yellow color for the purpose of the good yield.

(7) The Influence of Water present in Reaction Mixtures.—Here, crude cyclohexane containing small amounts of water was used in order

TABLE III
EFFECT OF FLOW RATE OF NYTROSYL CHLORIDE

Flow rate of NOCl*	Oily product obtained after 5 hr.	Color of reaction liquid	Pure oxime obtained	Yield of oxime based on added NOCl	Yield of oxime based on consumed cyclohexane
g./hr.	g.		g.	%	%
0.63	4.50	Pale yellow	2.22	40.8	53.0
0.97	5.30	Yellow	2.86	34.2	54.0
1.21	7.55	Yellow	4.33	41.2	69.0
1.90	8.40	Deep yellow	4.46	30.9	70.9
3.64	13.60	Brown	6.16	19.8	49.1

* Hydrogen chloride was added to nitrosyl chloride in a mol. ratio of 1 : 1.

TABLE IV
THE INFLUENCE OF WATER PRESENT IN REACTION MIXTURES

Addition of water	NOCl added for 5 hr.	Temperature	Oily product obtained	Color of reaction liquid	Pure oxime	Yield based on added NOCl
	g.	°C	g.		g.	%
None	6.2	10	9.3	Yellow	5.04	48.5
1%	6.2	10	10.0	Yellow	5.70	53.2
None	8.0	25	6.6	Greenish yellow	2.93	21.3
1%	6.7	25	4.0	Greenish yellow	1.10	10.5

to examine the influence of water on the photonitrosation. The results obtained are listed in Table IV. These results show that the photonitrosation is scarcely influenced by the presence of water at 10°C, but much more influenced at 25°C. It may be reasonable to consider that, on account of its very hygroscopic nature, the oxime hydrochloride formed in reaction mixture absorbs even a trace of water present and forms an oily substance which is insoluble in cyclohexane and is fairly stable below 10°C. At 25°C, oxime hydrochloride present in an oily substance, seems to be gradually hydrolized to cyclohexanone oxime and hydroxylamine.

(8) Continuous Reaction.—A continuous reaction was carried out under the favorable conditions which were established for batch reaction (consult Table V).

TABLE V

CONTINUOUS REACTION

Conditions:—	
Temperature	10±1°C
Mol. ratio of NOCl : HCl	1 : 2
Flow rate of NOCl	51.6 g./hr.
Reaction time	10 hr.
Light source	1 kW. high vapor pressure mercury lamp.
Results:—	
Oily product	914 g.
Pure oxime obtained	463 g.
Consumed cyclohexane	520 g.
Unreacted NOCl	124 g.
Yield based on consumed cyclohexane	72.4%
Yield based on reacted NOCl	74.0%

The yields of oxime based on consumed cyclohexane and reacted nitrosyl chloride were 72.4% and 74.0% respectively. Moreover, these yields may be raised considerably by minimizing the loss of cyclohexane and nitrosyl chloride during operation.

Summary

The photonitrosation of cyclohexane with nitrosyl chloride was investigated. It was established that cyclohexanone oxime may be easily produced in good yield (72%) under suitable conditions. The dilution of nitrosyl chloride with hydrogen chloride was most effective for preventing the side reactions, and the photonitrosation of cyclohexane was carried out successsfully at a temperature of 10°C.

The color of the reaction liquid played the role of indicator for a successful photonitrosation; the side reactions seemed not to occur practically so long as the color of the reaction liquid is yellow, and hence, the addition rate of nitrosyl chloride into cyclohexane should be controlled following the color change of reaction liquid.

The author wishes to thank Dr. K. Hoshino and Dr. H. Kobayashi who instructed him in these studies and permitted this publication.

Research Department of Toyo Rayon Co. Ltd., Nagoya

Dependence of the Exchange Reaction Rate in Catalyst Bed upon the Rate of Feed Gases and the Length of the Bed

By Sadahiro SAKATA and Noriyoshi MORITA

(Received September 12, 1955)

In a recent paper[1] we published a preliminary report of this article. In the present paper other series of experiments concerning chromic oxide catalyst are included and the reexamination of the relation under consideration is made.

Many papers concerning the kinetics of gaseous reactions in flow systems have appeared since the time of Bodenstein[2]. A brief summary of these papers is made by Harris[3]. In addition to these kinetic studies of chemical reactions, transport phenomena occurring in the flow systems have been treated from an engineering standpoint. Colburn and Chilton[4] discussed the mass- and heat-transfer phenomena at the gas-liquid

1) S. Sakata and N. Morita, *Chem, Eng. (Japan)*, **19**, 64 (1955).

2) M. Bodenstein and K. Wolgast, *Z. physik. Chem.*, **61**, 422 (1908).

3) G.M. Harris, *J. Phys. & Colloid Chem.*, **51**, 505 (1947).

4) A.P. Colburn, *Ind. Eng. Chem.*, **22**, 967 (1930); **23**, 910 (1931); T.H. Chilton and A.P. Colburn, ibid., **23**, 913 (1931); A.P. Colburn and W.J. King, ibid., **23**, 919 (1931); T.H. Chilton and A.P. Colburn, ibid., **26**, 1183 (1934); **27**, 255 (1935).

and the gas-solid boundaries, and introduced the concept of the height of a transfer unit, H.T.U. Hurt[5] applied this concept to catalytic reaction and introduced concepts of the height of a reaction unit, H.R.U., and the height of a catalytic unit, H.C.U. For an unpoisoned catalyst surface and for reaction with no volume change, the relation: H.R.U.=H.T.U.+H.C.U., is established. H.T.U. is independent of the nature of catalyst and is slightly influenced by the change of temperature and pressure; it can be calculated by the condition of gas flow. The method of the calculation of this quantity, or the film resistance, and the degree of contribution to H.R.U., or the over-all resistance, have been considered by Hougen[6], and the minimizing methods of film resistance due to transfer of mass have been indicated.

Contrary to the general complexity of kinetics of reactions conducted in flow systems, exchange reaction has very simple properties even when the reaction is conducted in a flow system. The most prominent property of exchange reaction is that during the course of the reaction the chemical concentrations of all components of the system do not change and, therefore, the reaction rate is independent of the progress of the reaction and can be defined only by the mechanism of the reaction. Consider an *exchange reaction*:

$$AX+BX' \longrightarrow AX'+BX, \qquad (1)$$

where X and X′ are the same chemical species (atom or atomic group) and differ only in the fact that X is originally combined with a chemical species A, and X′ is combined with another species B. Assume that for the detection of this exchange reaction, we used, as usual, an isotope of X, i.e. X*, then the *isotopic exchange reaction*:

$$AX+BX^* \longrightarrow AX^*+BX, \qquad (2)$$

is a fraction of the reaction (1), and the fractional percentage is easily seen from a probability calculation, in so far as the isotopic effect is negligible. Now we denote the rate of reaction (1) by R, number of exchange per sec. per cc. of reactor. Then this exchange reaction rate, R, which is differential in its nature but which can be measured by integral conversion of the isotopic exchange reaction (2), is independent not only of the duration of the reaction, but also of the volume or the shape of the catalyst bed so long as the over-all resistance of the reaction remains constant. In other words, when R changes with any one of the following variations: the feed rate F cc. (S.C.)/sec., reactor diameter D cm., height of the bed Z cm., and the volume of the catalyst $(1/4)\pi D^2 Z$, while the temperature remains constant, then the change shows that any one of the steps of the reaction has been influenced by that variation. When the reaction is catalytic, then so long as the intrinsic catalytic activity remains constant, the change in R indicates some change in mass-transfer steps.

In addition to this prominent feature of exchange reaction, isotopic exchange reaction has two other characteristics. The one is that the heat of reaction is nearly zero, and the other is that the integral rate is expressed by the first order equation. These characteristics are amenable to the kinetic study of chemical reaction.

Anticipating these characteristics, we have studied the catalytic exchange reaction of oxygen atoms between gaseous oxygen and water vapor by use of heavy oxygen. By using chromic oxide catalyst, values of R were measured at varying temperatures by varying the feed rate of reacting gases and the length of the catalyst bed.

Rate Equation

One of the authors in an earlier paper[7] introduced a mathematical relation between the percentage exchange and the gas flow rate, as concerned with the catalytic exchange reaction of oxygen atoms between gaseous oxygen and water vapor on the surface of solid catalyst. There it was ascertained that the exchange reaction rate was related by a simple probability relation to the rate of isotopic exchange reaction regardless of which step of the reaction (viz. adsorption, desorption, surface reaction, or any mass-transfer process) was rate controlling, so long as isotopic effect was negligible, and the following relation was obtained,

$$R'=\{N_A N_B/(N_A+N_B)\}(1/t)\{-\ln(1-x)\} \qquad (3)$$

Here, N_A and N_B are the total numbers of molecules of chemical species AX+AX* and BX+BX* in a unit volume of feed gases at S.C. and remain constant during the exchange reaction, x is the conversion represented by the net fraction of isotopic exchange to equilibrium, and t is the contact time in sec. R' denotes the rate of the exchange reaction concerning per unit volume of the reacting gases at S.C. and is related

5) D.M. Hurt, ibid., 35, 522 (1943).

6) B.W. Gamson, G. Thodos and O.A. Hougen, *Trans. Am. Inst. Chem. Eng.*, 39, 1 (1943); O.A. Hougen and K.M. Watson, *Ind. Eng. Chem.*, 35, 529 (1943); K.H. Young and O.A. Hougen, *Chem. Eng, Progr.*, 46, 146 (1950); O.A. Hougen, *Z. Electrochem.*, 59, 479 (1953).

7) N. Morita, This Bulletin, 15, 166 (1940).

with R by the relation: $R=R'F_e(273/T)$ $(p/760)$, where F_e is the void fraction of the catalyst bed and T and p are the temperatures in °K and pressure in mmHg. The time of contact can be expressed by: $t=\{\pi D^2 Z F_e/4F\}$ $(237/T)$ $(p/760)$, and therefore Eq. (3) becomes:

$$R=(4F/\pi D^2 Z)\{N_A N_B/(N_A+N_B)\}\{-\ln(1-x)\}. \quad (4)$$

Norris[8] contemplated the rate equation deduced by Duffield and Calvin[9] as identical with Eq. (3), and set forth his opinion concerning the application of the equation for heterogeneous reactions. Harris[10] also introduced the same kind of equation for isotopic exchange reactions and deduced equations dealing with the kinetic implication of isotopic effect. For oxygen isotopes, isotopic effect is not large and we will not consider it in this paper.

In addition to the rate equation deduced above, we can point out the following interesting relation:

$$\text{N. R. U.}=\int_{u_A}^{u_{Ao}}\frac{du_A}{u_A-u_{Ae}}=\ln\left(\frac{u_{Ao}-u_{Ae}}{u_A-u_{Ae}}\right)$$
$$=-\ln(1-x) \quad (5)$$

or, $$\text{H. R. U.}=Z/(\text{N. R. U})=Z/\{-\ln(1-x)\}, \quad (6)$$

where u_A is the fraction of AX* in N_A, and u_{Ao} and u_{Ae} denote the original and equilibrium values of u_A, respectively. By this relation we can calculate H. R. U. from the conversion x. H. T. U. can be calculated from the conditions of the flow of reacting gases in the reactor by Hougen's method or introduced others, and then we can find the percentage contribution of mass-transfer process for the over-all reaction velocity.

Experimental Procedure

Four kinds of quartz tubes were used as the reactor, of which two were vertical and two were horizontal. We call these tubes V–I, V–II, H–I and H–II, respectively, whose dimensions are shown in Tables I–IV. Centered in thereact or is a thin tube of quartz for thermocouple. Pelleted catalyst is poured into the reactor to a fixed height and both ends are filled with granular quartz. The reactor is heated in a properly fitted electrical oven.

Oxygen in cylinder is used as the reacting gaseous oxygen; the content in heavy oxygen was analyzed in advance. The oxygen passes through pressure regulator, flow rate regulator, flow meter, and preheater, and then flows into mixer with water vapor. Heavy oxygen water prepared by fractional distillation of water is placed in a glass cylinder with graduation and pressed with the same pressure used for gaseous oxygen. The water flows at a known speed through the flow rate regulator and flows into evaporator. The evaporator is made of quartz and heated by three small gas burners. The vapor mixes with gaseous oxygen, passes through another preheator, and flows into the reactor. The gaseous mixture from the reactor is passed through condenser. The condensed water is refined as usual[11] and its heavy oxygen content is determined from its excess density as compared with normal water. Comparing the heavy oxygen content with original concentration the conver sion x is determined.

Chromium oxide is prepared from recrystallized chromium alum. The precipitated hydroxide of chromium with ammonia is repeatedly washed with water until no sulphuric acid ion is detectable. The hydroxide is dried in an electrical air oven and then powdered. One part of this powder is throughly mixed with three parts of the "Naegi" kaolin and a small quantity of water is added. The paste is pressed out of a press made of brass, having several pores of 2 mm. dia. in the bottom, and then cut into 2 mm. lengths. The pellete are first air-dried and then placed in an electrical oven at 110°C, and finally dried at 500°C for 7 hr. under oxygen gas stream. Before each experiment, a reacting gas mixture is passed through the catalyst for several ten-minute periods after which we can expect the steady state of the exchange reaction.

Results obtained

Tables I–IV show the results obtained under various conditions of experiments. In these tables A is the cross sectional area of the reactor and α is the volume ratio of gaseous oxygen to water vapor. Experimental number show the order of experiments. Throughout all the experiments the

TABLE I

DATA OBTAINED BY V–I (RUN 600)

$D=1.6$ cm., $A=2.01$ cm², $Z=24.0$ cm. (No. 1–19): 23.5 cm. (No. 29–36); 23.8 cm. (No. 37–51)

Exp. No.	Temp. °C	F/A cc./sec.·cm²	α	x	$R\times10^{-18}$ atoms/sec.·cc.	H. R. U. cm.
632	542	16.5	2.28	.789	7.34	15.1
611	538	15.0	2.14	.823	7.49	13.9
636	522	16.4	2.38	.605	4.10	25.3
629	501	17.3	2.06	.432	2.96	41.5
602	489	15.2	2.05	.405	2.32	46.3
633	488	17.1	2.07	.375	2.42	50.0
631	541	23.0	2.19	.652	7.13	22.3
613	540	22.3	2.18	.729	8.35	18.3
635	522	22.8	2.18	.490	4.51	34.9
630	500	23.6	2.01	.312	2.70	62.9
614	492	22.6	2.11	.321	2.54	62.1
634	487	23.8	1.99	.233	1.93	88.8
645	563	32.0	2.08	.895	21.29	10.6

8) T.H. Norris, *J. Phys. & Colloid Chem.*, **54**, 777 (1950).

9) R.B. Duffield and M. Calvin, *J. Am., Chem. Soc.*, **68**, 557 (1946).

10) G.M. Harris, *Trans. Faraday Soc.*, **57**, 716 (1951).

11) T. Titani and N. Morita, This Bulletin, **13**, 409 (1938).

Exp. No.	Temp. °C	F/A cc./sec.·cm²	α	x	$R\times10^{-18}$ atoms/sec.·cc.	H.R.U. cm.
640	542	32.1	2.02	.717	12.15	18.9
610	537	35.2	2.21	.653	10.60	22.7
651	522	33.7	1.81	.381	5.09	49.7
648	501	32.0	2.33	.339	3.69	57.5
601	494	34.7	2.20	.366	4.49	52.9
642	561	37.7	2.61	.844	18.39	12.8
646	560	40.7	2.21	.856	22.62	12.3
639	539	39.2	2.18	.590	10.08	26.7
650	533	42.6	2.00	.506	9.03	33.8
643	523	38.7	2.37	.581	9.31	27.3
638	503	38.1	2.42	.286	3.51	70.7
604	598	64.8	2.49	.931	46.53	8.9
617	580	47.5	2.28	.890	29.36	10.9
619	556	49.4	2.03	.634	14.72	23.9
612	554	60.7	2.08	.558	14.51	29.4
616	500	48.9	2.22	.227	3.57	93.5
603	492	67.7	2.30	.183	3.81	119

TABLE II

DATA OBTAINED BY V-II (RUN 700)

$D=2.5$ cm., $A=4.9$ cm², $Z=6.0$ cm.

Exp. No.	Temp. °C	F/A cc./sec.·cm²	α	x	$R\times10^{-18}$ atoms/sec.·cc.	H.R.U. cm.
702	475	0.43	2.00	.652	0.539	5.7
704	425	〃	〃	.197	.112	27.4
703	400	〃	〃	.145	.080	38.2
712	475	0.46	2.00	.555	0.444	7.4
707	450	〃	〃	.450	.328	10.0
714	425	〃	〃	.210	.129	25.5
713	400	〃	〃	.161	.096	34.3
710	500	1.50	2.00	.524	1.327	8.1
708	475	〃	〃	.278	0.581	18.5
716	475	〃	〃	.231	.470	22.9
715	450	〃	〃	.111	.210	51.3

TABLE III

DATA OBTAINED BY H-I (RUNS 100–500)

$D=1.6$ cm., $A=2.01$ cm², $Z=30.0$ cm.

Exp. No.	Temp. °C	F/A cc./sec.·cm²	α	x	$R\times10^{-18}$ atoms/sec.·cc.	H.R.U. cm.
107	590	34.7	2.27	.894	17.61	13.3
503	580	43.9	1.92	.945	31.00	10.3
105	540	44.2	2.06	.670	11.54	27.1
210	535	33.4	2.57	.729	9.09	23.0
109	520	35.8	2.21	.404	4.25	57.9
405	520	42.1	2.10	.442	5.73	51.5
207	495	44.1	2.03	.374	4.89	64.2
110	480	35.4	2.11	.185	1.69	141
301	470	34.9	1.92	.196	1.86	137
111	445	35.7	2.05	.085	0.76	333
205	438	44.6	1.94	.099	1.12	289
103	580	62.0	1.95	.924	38.50	11.6
106	580	47.8	1.82	.845	22.21	16.1
504	570	57.0	2.23	.959	41.34	9.4
502	530	52.5	2.79	.643	10.68	29.2
108	520	49.5	1.56	.596	11.90	33.1
208	506	63.0	1.81	.409	8.26	57.1
508	505	55.2	2.40	.460	7.37	48.6
507	500	45.3	1.72	.398	5.85	59.1
201	480	52.2	3.06	.189	4.32	69.0
505	450	57.8	2.06	.261	8.36	50.0

TABLE IV

DATA OBTAINED BY H-II (RUN 000)

$D=1.7$ cm., $A=2.27$ cm², $Z=3.0$ cm. (No. 002–013); 2.1 cm. (No. 0.17–021)

Exp. No.	Temp. °C	F/A cc./sec.·cm²	α	x	$R\times10^{-13}$ atoms/sec.·cc.	H.R.T. cm.
013	500	0.44	2.00	.791	1.649	1.9
004	475	〃	〃	.535	0.807	3.9
003	450	〃	〃	.346	0.446	7.1
005	425	〃	〃	.271	0.332	9.5
002	400	〃	〃	.113	0.126	25.0
021	724	46.1	1.68	.624	166.1	1.5
020	693	46.5	1.64	.446	111.8	2.0
018	653	45.9	1.70	.234	57.7	3.9
017	598	45.9	1.70	.068	20.1	13.5

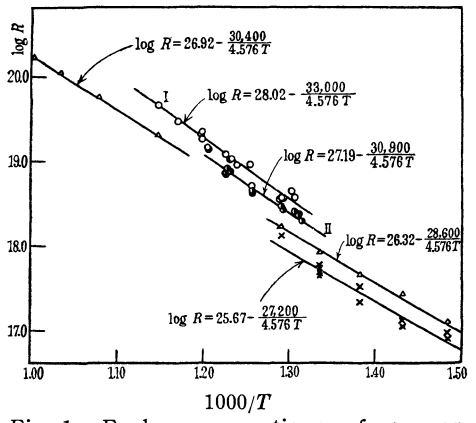

Fig. 1. Exchange reactions of oxygen atoms.

△ Run 000

◑ Run 600 $F/A\leq23.8$ cc.(s.c.)/sec.·cm².

○ 〃 〃 ≥32.0

× Run 700

same catalyst was used repeatedly, having been only treated with oxygen gas at 500°C before each run. During these runs the catalytic activity had remained almost constant, as will be shown later.

In Fig. 1 the points indicated by circles are the relations of $\log R$ vs. $1/T$ obtained by run 600. The fluctuation of each experimental point is rather large and the effect of the differences in linear velocity of reacting gas mixture F/A on the rate R can not be confirmed point-by-point. But, generally speaking, these points show a tendency toward a smaller R with decreasing gas velocity. When, for convenience, we classify these points into two groups, one with a feed rate larger than 32.0 and the other with one smaller than 23.8 cc. (S. C.)/sec.·cm², then we can draw the two lines I and II in Fig. 1. The ratio in R for the two lines ranges from 1.3 to 1.5. These differences can be attributed only to the differences in the flow

velocities of reacting gases. The mean value of α is 2.18, most of the values deviating not more than $\pm 5\%$, although the maximum deviation is about 20%. The effect of α on R was examined in an other run of experiments not included in this paper, and it was ascertained that these deviations in α had no effect on the rate R.

The results obtained by runs 000 and 700 are represented by triangles and crosses, resp. (Fig. 1), where the shorter catalyst beds and smaller feed rates were applied. The decreases in R are more conspicuous than those in line-II, and at run 700 the values of R are about one-fourth the values in line-I.

The runs 100–500 are conducted in a horizontal reactor and differ slightly from run 600 in the length of the catalyst bed. Deviation from linearity of the experimental results (not shown in Fig. 1) is more marked than in run 600. As runs 100–500 were the preliminary experiments done at high feed rates, and, in addition, as the reactor was horizontal and channeling was conceivable, thus a larger experimental error may have resulted. Taking this fact into consideration, the coincid ence with run 600 is considerable, indicating that during all the runs the catalytic activity remained almost constant.

Discussion

As noted in Fig. 1, the activation energy of the exchange reaction ranges from 33.3 to 27.2 kcal./equiv. These high values of activation energy indicate that the mass-transfer processes can not be the main controlling factor of the reaction. The values of the frequency factor also show that the internal surface of the catalyst plays a dominant role. The value ranges from 1×10^{28} to 5×10^{25}. The outer-surface area a_v of the catalyst pellets is 21.6 cm²/cc. and the collision frequency of the water molecules on this surface is 1.26×10^{24} molecules/sec.·cc. under the operating conditions of 500°C and 1/3.2 atm. The frequency factor is about 8,000–40 times greater than this collision frequency.

Although the mass-transter can not be the rate-controlling step, the decrease in linear velocity of reacting gas mixture and the shortening of the bed length retard the over-all rate R to a significant extent. Decrease in R accompanies the decrease in both activation energy and frequency factor. This fact clearly indicates that the mass-transfer processes have influence on the over-all rate to some extent.

The relative importance of film resistance to the rate R can be seen by calculating H. T. U. From the observed values of the pellet density of the catalyst 1.02 g./cc. and the bulk density of the catalyst bed 0.735 g./cc., and from the data cited in preceeding sections, we have calculated H. T. U. by Hougen's method. In Table V, the mass

TABLE V

CONTRIBUTION OF MASS-TRANSFER

Exp. No.	Temp. °C	$G\times10^2$ g./sec.·cm²	$\mu_m\times10^4$ g./sec.·cm.	D_m cm²/sec.	H. T. U. cm.	H. T. U. / H. R. U. ×100
021	724	5.51	4.28	1.265	.151	10.33
017	598	5.49	3.83	1.033	.155	1.15
013	500	0.054	3.61	0.864	.015	0.79
002	400	0.054	3.27	0.702	.015	0.06
103	580	7.54	3.87	1.000	.182	1.57
210	535	4.18	3.73	0.922	.134	0.58
507	500	5.43	3.56	0.864	.158	0.27
604	598	8.11	4.00	1.032	.185	2.07
645	563	3.93	3.84	0.972	.131	1.24
632	542	2.04	3.80	0.933	.094	0.62
648	501	3.97	3.67	0.864	.133	0.23
603	492	8.39	3.63	0.850	.194	0.16
710	500	0.183	3.61	0.864	.028	0.34
702	475	0.052	3.51	0.820	.015	0.24
715	450	0.183	3.43	0.780	.028	0.05
703	400	0.052	3.27	0.702	.015	0.04

velocity G, mean diffusivity D_m and mean viscosity μ_m are calculated from the temperature, volume velocity and mixing ratio of the gas mixture. From these values the j_d factors are calculated by $j_d=1.82(D_pG/\mu_m)^{-0.51}$, and then H. T. U. by H. T. U. $=(1/a_vj_d)(\mu_m/\rho D_m)^{2/3}$, where D_p is the effective diameter of the catalyst pellet and is equal to $0.2\sqrt{1.5}=0.245$ cm., and ρ is the density of the reacting gas mixture. From Table V it can be seen that even at the highest temperature in the experiments H. T. U. is 10% of H. R. U., in most cases only one percent or a fraction. The correctness of these calculations is not certified for such flow systems with small Reynolds numbers, but film resistance seems insufficient to explain the retardation of the rate caused by the slowing down of the gas flow.

As long as the intrinsic catalytic activity remains constant, uniform packing of catalyst and piston-like flow of reacting gases will give the largest value of R and any deviation from these conditions always reduces the rate R. Thus non-uniform gas flow, channeling, local eddy motion, convective circulation, longitudinal diffusion of isotopic components, and other disturbances always have retarding effects on R. If we assume that the reaction was conducted under complete mixing of the reacting gases as if it were in a tank reactor, then the observed rate R for high conversion and small flow

rate would be as small as one-third compared with the rate when the reaction was conducted under piston flow.

Hitherto we did not consider the effect of pressure drop through the reactor. Eq. (4) does not contain pressure p. This is due to the fact that the calculations of N_A+N_B and of F are made at the same pressure (i.e. 1 atm). However, the change in pressure will affect the state of adsorption, collision frequency and other stages, and may ultimately affect the intrinsic catalytic activity or other factors governing the rate. Though this is the case, yet the highest value of the pressure drop is about 120 mmHg and the mean pressure throughout the reactor, 760+60 mmHg, is only 8% greater than the normal value. This small deviation will not cause any serious error in the results.

For comparison with our results, we have calculated the rate of exchange reaction between hydrogen and deuterium catalyzed by zins oxide by using Holm and Blue's data[12]. In this case R can be calculated by the equation, again neglecting isotopic effect: $R=(N/2)(S.V.)\cdot\{-\ln(1-x)\}$, where N is the total number of molecules of hydrogen and deuterium in a unit volume. Applying this equation to the data of Table V of Holm and Blue's paper, we have obtained the relation of $\log R$ vs. $1/T$ as shown in Fig. 2.

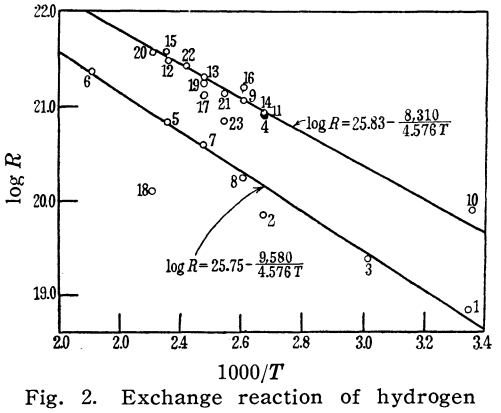

Fig. 2. Exchange reaction of hydrogen atoms (Holm, Blue).

Here the numbers affixed to the experimental points are the order of their data in the mentioned Table. From Fig. 2 we can observe that all the points except Nos. 4, 9, 18 and 23 are almost in linear relation with $1/T$ and that there is no speciality as indicated by the signs b and c in their table. The fact that the points can be divided in two groups: one with lower $S.V.$ and the other with higher $S.V.$ is in qualitative coincidence with our results. But the difference in R in their two groups is about ten and this difference is greater than ours. For hydrogen, isotopic effect may contribute a large effect on the velocity of isotopic exchange reaction and the calculated values of R may be incorrect in absolute value, but the error will not change greatly the mutual relation of these values. As they used a very small quantity of catalyst, the turbulence of reacting gases at the inlet and outlet may have contributed a considerable percentage. In addition, it is not certain to what extent the intrinsic catalytic activity remains constant during the run. These facts make any quantitative comparison difficult.

12) V.C.F. Holm and R.W. Blue, *Ind. Eng. Chem.*, **44**, 107 (1952).

Summary

(1) Exchange reaction has the prominent feature that the rate does not change with the progress of the reaction and can be determined only by the mechanism of the reaction. Therefore we can immediately detect the effect of variation in any one of the reacting conditions by the observed conversion of the isotopic exchange reaction.

(2) The relation between exchange reaction and isotopic exchange reaction is considered and an equation which gives the exchange reaction rate (R) using the integral conversion of the isotopic exchange reaction (x) is introduced.

(3) The method is applied to the exchange reaction of oxygen atoms between gaseous oxygen and water vapor catalyzed by chromic oxide, and examination is made of the effect of the variation in the rate of feed gases and in the length of the catalyst bed.

(4) At feed rates higher than 32.0 cc. (S.C.)/sec. cm^2 the value R remains almost constant, but by the lowering of the feed rate more than this and by the shortening of the bed length, R is decreased. This decrease accompanied decreases both in activation energy and in frequency factor.

(5) The results are explained by the effects of mass-transfer through the gas film, of eddy or diffusional mixing of the reacting gases and of other kinds of disturbances. Mass-transfer resistance of the gas film is a small fraction of the retardation. Mixing of the reacting gases may contribute a higher percent.

(6) The results are compared with the rate of exchange between hydrogen and deuterium measured by Holm and Blue.

Department of Chemical Engineering
Faculty of Engineering, Nagoya
University, Nagoya

On the Lower Boiling Product of Silicon-methylchloride Reaction

By Rokuro ŌKAWARA and Minoru SAKIYAMA

(Received September 13, 1955)

Among the products obtained from the reaction of silicon and methylchloride, methyltrichlorosilane, dimethyldichlorosilane and trimethylchlorosilane were well known since the finding of the "direct method of synthesis" by Rochow. These three main chlorosilanes have a close boiling point centering around 65°C and have been used for the starting materials of "silicones".

Now we wish to report on the presence of tetramethylsilane $(CH_3)_4Si$ (I′), dimethylchlorosilane $(CH_3)_2SiHCl$ (II′) and methyldichlorosilane CH_3SiHCl_2 (III′) and a small amount of trichlorosilane $HSiCl_3$ (IV′) in the lower boiling product centering around 35°C of the direct synthesis. The compounds (I′)[1,2], (III′)[3] and (IV′)[4,5] have already been characterized, but on the compound (II′) only the boiling point has been assumed by calculation to be 35.5°C[6] and 39.1°C[7].

To obtain pure (II′), the starting material was twice distilled through a modified large Stedman column of about 15 theoretical plates and divided into many fractions. These fractions may be roughly included into three main fractions A (b. p. 26°–34°C), B (b. p. 34°–36°C) and C (b. p. 36°–41°C). As the fraction B was supposed to be a plateau of impure (II′), B was repeatedly fractionated through a more efficient column. Finally a constant boiling fraction was obtained, but its chlorine content was found to be lower than the calculated value. The reason may be explained by assuming the contamination of a hydrocarbon by-product having the boiling point close to (II′). In fact, the presence of such a hydrocarbon in the starting material has been found by hydrolysis. Referring to the case of trimethylchlorosilane[8], it may be considered that an azeotrope of (II′) and the hydrocarbon is formed at the constant boiling plateau at 34.5°–35°C, but it could not be verified in this experiment.

As it was difficult to separate (II′) from the contaminating hydrocarbon by distillation, B was ethanolyzed in excess ethanol and dimethylaniline, and the dimethylethoxysilane thus formed was reacted in a bomb with benzoylchloride. From the product the freaction boiling at 36°C was confirmed to be (II′).

Ethanolysis of the fraction B in excess dimethylaniline and ethanol, liberated dimethylethoxysilane, methyldiethoxysilane and a small amount of dimethyldiethoxysilane and ill-defined triethoxysilane. It was supposed that dimethyldiethoxysilane was produced by the fission of Si-H during the course of ethanolysis. The presence of triethoxysilane reveals the presence of (IV′) in the redistilled product, this assumption was further supported by the fact that on repeated fractionation of B, the fraction B′ having a higher chlorine content was found in front of the plateau B″ as shown in Fig. 1.

By hydrolysis, methylhydropolysiloxanes were obtained as the main product. In this paper, to denote various methylpolysiloxanes, shorthand notation is used which is based on that of Wilcock[9], in which **M**, **D** and **T** represent mono-, di- and tri- functional units. Prime is used to indicate the hydrogen atom directly attached to silicon atom.

Unit	Formula
M′	$(CH_3)_2HSiO_{1/2}$
D′	CH_3HSiO
D	$(CH_3)_2SiO$
T	$CH_3SiO_{3/2}$

The following compounds were made by hydrolyzing the starting material and rigorously distilling the resultant oil.

$\mathbf{M'D'_nM'}$	$(n=0\text{–}6)$
$\mathbf{M'D}_n\mathbf{M'}$	$(n=1\text{–}2)$
$\mathbf{D'_n}$	$(n=4\text{–}\ )$
M′D′DM′	

The main components of the resultant oil were a series of linear copolymers $\mathbf{M'D'_nM'}$,

1) J.G. Aston, R.M. Kennedy and G.H. Messerly, *J. Am. Chem. Soc.*, 63, 2343 (1941).
2) A.P. Mills and C.A. MacKenzie, ibid., 76, 2672 (1954).
3) R.O. Sauer, W.J. Scheiber and S.D. Brewer, ibid., 68, 962 (1946).
4) H.S. Booth and W.D. Stillwell, ibid., 56, 1529 (1934).
5) A. Stock and F. Zeidler, *Ber.*, 56 B, 986 (1923).
6) C.A. MacKenzie, A.P. Mills and J.M. Scott, *J. Am. Chem. Soc.*, 72, 2032 (1950).
7) R.N. Lewis and A.E. Newkirk, ibid., 69, 701 (1947).
8) R.O. Sauer, W.J. Scheiber and E.M. Hadsell, ibid., 70, 4254 (1948).
9) D.F. Wilcock, ibid., 69, 477 (1947).

which were formed from (II′) and (III′). A small amount of $\mathbf{M'D_nM'}$, in which only **M′DM′** was accurately characterized, may be assumed to be formed by the fission of Si-H bond during the hydrolysis in the concentrated hydrogen chloride solution.

$$3H(CH_3)_2SiCl+2H_2O = H(CH_3)_2SiOSi(CH_3)_2OSi(CH_3)_2H+3HCl+H_2$$

(**M′DM′**)

Such a reaction may occur also with Si-H of methyldichlorosilane to form $\mathbf{M'_3T}$, an isomer of **M′D′DM′**. But in this experiment, the presence of this compound could not be detected accurately. The presence of $\mathbf{D'_n}$, which has already been characterized by Sauer[3] by hydrolyzing (III′), was found between the plateaus of $\mathbf{M'D'_nM'}$.

The distribution of these polymers, tetramethylsilane (I′) and hydrocarbon by-product in the hydrolyzates with regard to the chlorine content of the redistilled chlorosilane, is shown in Fig. 2. The properties of these polymers are given in Table II.

Experimental

Starting Materials.—The industrial low boiling methylchlorosilane, having the boiling point between 26°C to 40°C (hydrolyzable chlorine, 40%) obtained from the reaction of silicon and methylchloride was supplied from the Shin-etsu Chem. Ind. Co.

A. Chlorosilane and Its Ethanolysis

Distillation.—The starting material (4 Kg.) was fractionated through a modified Stedman column of about 15 theoretical plates (38 mm. inner diameter, packed length 30 cm.). From the boiling point and the chlorine content, the distillates were roughly separated into three main fractions as follows.

Main fraction	Boiling point (°C)	Hydrolyzable chlorine (%)	Weight (%)
A	26–34	–36	25
B	34–36	36–43	25
C	36–41	43–60	50

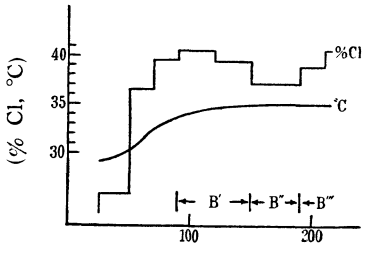

Fig. 1. Redistillation of fraction B through a 30 plates column.

As the fraction B was supposed to be an incomplete plateau, a part of which was fractionated through a Stedman column of about 30 theoretical plates (inner diameter 18 mm. and packed length 40 cm.). The result are shown in Fig. 1.

The distillation curve obtained was similar to that of the starting material, but the chlorine content of the distillate was somewhat different. The fraction B″ having a slightly lower chlorine content than the neighbouring fractions, B′ and B‴, was found. The higher values in B′ and B‴ were supposed to be caused by the contamination of a asmall amount of trichlorosilane (IV′) (b.p. 31.5°C[4], 31.8°C[5] Calcd. Cl, 78.5%) and methyldichlorosilane (III′) (b.p. 41.0°C[3] Calcd. Cl, 61.5%), respectively. The fraction B″ (Found Cl, 37.1%) was distilled through the same column and the constant boiling frection of 34.5° to 35°C was obtained, but the chlorine contents of 39.4, 35.1 and 36.4% were found with the amount of each 10 cc. of the distillate. If the fraction B″ was (II′) contaminated only by a small amount of (IV′) and (III′), the redistilled fraction having the minimum chlorine content would become closer to the chlorine content calculated for (II′) (37.4%). In this experiment, the second fraction having the minimum chlorine content (35.1%) did not close to the calculated value, but too small a value resulted.

Ethanolysis.—A fraction of B (150 g., b.p. 35°–36°C, Anal. Cl, 42.5%) was added to the mixture of excess of ethanol (120 g.) and dimethylaniline (250 g.) in a three-necked flask equipped with an efficient stirrer, a dropping funnel and a condenser with a calcium chloride tube. During the reaction, the mixture was cooled with an ice-bath below 5°C. After the addition of the chlorosilane, the reaction mixture was refluxed over a period of two hours with vigorous stirring, followed by the separation of dimethylanilinehydrochloride through a separating funnel and the fractional distillation of the organic layer. The fraction boiling at 53°–57°C (39 g.) thus obtained, was rigorously fractionated by a Stedman column of about 50 theoretical plates. The fraction boiling at 54°C was found to be dimethylethoxysilane $H(CH_3)_2SiOC_2H_5$ from the analysis of H(-Si). n_D^{20} 1.3683, d_4^{20} 0.7572, MR_D Found: 31.00, Calcd.[10]: 31.30.

Anal. Found: H(-Si), 0.94%. Calcd. for $H(CH_3)_2SiOC_2H_5$: H(-Si), 0.97%.

This compound contained a trace of chlorine compound detectable by the Beilstein test and gradually decomposed by evolving a gas from the bottom of the receiver. Even after repeated distillation, the chlorine compound and evolution of the gas did not completely disappear.

The higher boiling fraction collected from several ethanolysis reactions, was fractionally distilled through a Stedman column of about 30 plates. The following three ethoxysilanes were obtained.

Methyldiethoxysilane, $HCH_3Si(OC_2H_5)_2$.

b.p. 97.5°C, n_D^{20} 1.3772

10) Calculated from bond refractivities by E.L. Warrick, *J. Am. Chem. Soc.*, **68**, 2455 (1946).

Reported[11]: b.p. 97.5°C, n_D^{25} 1.3738, d_{25}^{25} 0.8295

Dimethyldiethoxysilane, $(CH_3)_2Si(OC_2H_5)_2$.

b.p. 112°C, n_D^{20} 1.3821, d_4^{20} 0.8398

MR_D Found: 41.09, Calcd.[10]: 41.06

Reported[12]: b.p. 114°C, n_D^{20} 1.3805, d_4^{20} 0.8395

Triethoxysilane, $HSi(OC_2H_5)_3$.

b. p. 134°–5°C, n_D^{20} 1.3840

Anal. Found: H(-Si), 0.43%, Calcd. 0.61%

Reported[6]: b.p. 131.5°C, n_D^{20} 1.3767

The data of triethoxysilane did not accord well with the reported value. On account of the small amount (1 cc.) of this fraction, the satisfactory separation from the neighbouring compounds could not be achieved. By the alcoholysis reaction carried out as above, cyclocompound $\mathbf{D}_4'$ (Reported[3]: b.p. 134.5°C, n_D^{20} 1.3873) having the boiling point close to that of triethoxysilane might not be formed. The active hydrogen content of this fraction lower than the calculated value also reveals the absence of $\mathbf{D}_4'$ (Calcd. H(-Si), 1.68%).

Chlorination of Dimethylethoxysilane.—Dimethylethoxysilane (28 g., 0.27 mol.) was reacted with benzoylchloride (38 g., 0.27 mol.) in an iron bomb at 200°C over a period of four hours. The reaction mixture was rigorously fractionated through a Stedman column of about 50 theoretiplates. The constant boiling fraction at 36°C (2 cc.) was obtained. From its chlorine content, it was found to be dimethylchlorosilane (II'). n_D^{20} 1.3820

Anal. Found: Cl, 37.6%. Calcd. for (II'): Cl. 37.4%.

B. Hydrlyzates

Hydrolysis.—Hydrolysis was carried out by adding a sufficient amount of cracked ice to the ice-cooled chlorosilane. The oily layer was vigorously shaken with fresh ice-water repeatedly, but it was found to be difficult to complete the hydrolysis, for the red color of methylorange, which was added as an indicator, appeared gradually on standing. To complete the hydrolysis the hydrolyzate and water were vigorously stirred at room temperature with an efficient stirrer. When the red color of methylorange appeared, the mixture was titrated back to the orange color with a dilute sodium bicarbonate solution until the orange color remained unchanged. Then useing chlorophenolred (pH 5.0–6.6) as an indicator, the same treatment was repeated. The hydrolysis reaction was very slow and it required twenty to thirty hours' stirring with 200 to 250 g. of the hydrolyzate. The hydrolyzates of the starting material and fraction A, which contain volatile tetramethylsilane (I'), were twice washed with fresh ice-water, followed by the dehydration on sodium sulfate and the fractionation to distil off (I'). And the residue was neutralized as above.

In spite of these careful treatments, a trace of chlorine compound was sometimes found in the distillate. Accordingly, on each fractionation, the distillate and the residue were tested by the Beilstein test and a trace of chlorine compound was again hydrolyzed off.

Composition of the Hydrolyzate.—As it was very difficult to separate the starting material into its components through distillation, the hydrolysis was carried out with the representative fractions which were obtained by redistillation through the 15 plate large Stedman column. The results are given in Table I (Expt. 1 to 8).

TABLE I

HYDROLYSIS OF REDISTILLED AND STARTING MATERIAL

	Sample				Hydrolyzate
Expt. No.	Boiling range	Hydrolyzable chlorine	Classed to the Main fraction	Weight	Yield
	°C	%		g.	%
1	28.5–29.0	22.9	A	30	78
2	30.1	28.7	A	195	68
3	30.1–33.5	34.6	A	250	71
4	34.0–34.5	39.8	B	135	69
5	34.8–35.4	40.0	B	210	77
6	35.4–35.9	42.7	B	140	81
7	36.0–37.0	46.7	C	120	73
8	37.5–38.1	49.5	C	100	68
9*	38.8–	53.7	C	290	76
10**	26 –40	40	—	870	79

* Residue of the distillation of Expt. 1 to 8.
** Starting material.

The results obtained with the residue of redistillation and the starting material are also given in Expt. 9 and 10, respectively. By the hydrolysis, the formation of gelatinous mass was found in Expt. 3 and 4 which may be contaminated by (IV'). In Expt. 9 some gelatinous mass and viscous oil resulted.

Throughout this experiment, the distillation of the hydrolyzate was carried out through a semimicro Stedman column of about 50 theretical plates. By distillation, tetramethylsilane (I') distilled out at first, then a small amount of hydrocarbon boiling at 33°–37°C and the succeeding plateaus of $\mathbf{M}_2'$, $\mathbf{M'D'M'}$, $\mathbf{M'DM'}$, $\mathbf{D}_4'$ and $\mathbf{M'D_2'M'}$ were obtained at 70°, 117°, 128°, 133° and 154°C, respectively. The small plateau $\mathbf{M'DM'}$ appeared in the fraction A and B and its amount was found to be about 5% of $\mathbf{M}_2'$. The presence of $\mathbf{D}_4'$ was assumed by its higher refractive index at its boiling point in the hydrolyzates of the fraction C, while in Expt. 8 and 9 the small plateau of $\mathbf{D}_4'$ was found.

In calculating the percentage composition, $\mathbf{M'DM'}$ and $\mathbf{D}_4'$ were included into the trimer

11) Dow-corning Silicone Notes.
12) H. J. Fletcher and M. J. Hunter, *J. Am. Chem. Soc.*, **71**. 2918 (1949).

fraction and the intermittent fraction between the succeeding plateaus was assigned to both sides fractions by cutting on the distillation curve. The percentage composition of the hydrolyzate plotted against the chlorine content of the samples (Expt. 1-9) is shown in Fig. 2.

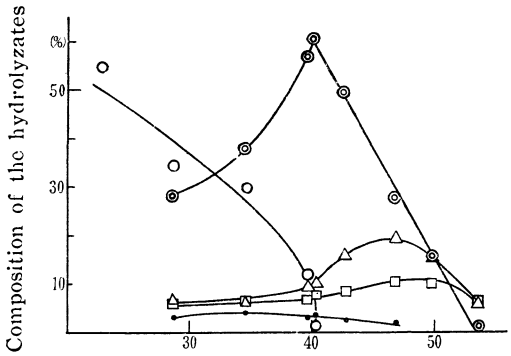

Fig. 2. Composition of the hydrolyzates with regard to the chlorine content of the redistillates.
● Hydrocarbon by-product
○ Tetramethylsilane ◎ Disiloxane
△ Trisiloxane □ Tetrasiloxane

From Fig. 2, the distribution of the components of the starting materials will be assumed.

Tetramethylsilane and Hydrocarbon By-product.—Crude tetramethylsilane (I′) was shaken with a dilute sodium hydroxide solution and redistilled. A small amount of fore-run and then the constant boiling fraction having the constant refractive index was obtained.

b.p. 26.5°–26.6°C, n_D^{10} 1.3649, d_4^{10} 0.6495.

MR_D Found: 30.34, Calcd.[10] for (I′): 30.28.

(Reported: n_D^{20} 1.3588[2], d_4^{20} 0.6399[2] and 0.6461[1] b.p. 26.64°[1] and 25.5°C[2])

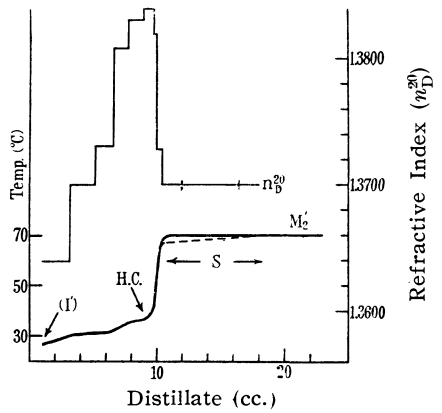

Fig. 3. An example of the redistillation curve of the hydrocarbon by-product (H. C.) and disiloxane ($\mathbf{M}_2'$).
Dotted line ---- shows the curve when the silanol is present.

As described above, a small plateau was found at 33°–37°C by the distillation of A and B. In some experiments, the fractionation was carefully carried out at the reflux ratio of 40–50 and the distillate was divided into many small fractions. The stepwise rise of the refractive index was observed as shown in Fig. 3.

The qualitative test, by taking a sample in a capillary and burning it slowly on a flame, gave a whit silicious smoke or white residue stuck at the end of the capillary with the samples of lower refractive index, but with the samples of higher refractive index this characteristic of the silicon compound was not found. The analysis for the fraction (n_D^{20} 1.3785) gave a high carbon content (Found: C, 80.96%; H. 14.18%).

From these data, the rigorous separation from the contaminating silicon compound, probably (I′), may be questionable and the determination by what kind of hydrocarbon the hydrolyzate is contaminated was not successful.

Isolation and Characterization of the Methylhydropolysiloxanes

Disiloxane ($\mathbf{M}_2'$).—As shown by the dotted line on Fig. 3, the gradually rising plateau (S) at 68°–70.5°C was obtained after the hydrocarbon by-product had distilled out. It was found usually that the refractive index of (S) decreased gradually from n_D^{20} 1.3715 to that of $\mathbf{M}_2'$ (n_D^{20} 1.3700). During the course of distillation in this temperature range, droplets of water were observed to accumulate gradually in the outlet tube of the column. The formation of water may be assumed to be caused by the condensation of unstable silanol to disiloxane.

$$2H(CH_3)_2SiOH = H(CH_3)_2SiOSi(CH_3)_2H + H_2O$$

By redistillation, the formation of water and the range indicated in the dotted line rapidly decreased. On repeated distillation three or four times, the formation of water has not been observed and the rigorously constant plateau of $\mathbf{M}_2'$ at 70.5°C, which was indicated by full line in Fig. 3, resulted.

Trisiloxanes ($\mathbf{M'D'M'}$ and $\mathbf{M'DM'}$).—Redistilled trisiloxanes having the constant boiling point and refractive index are given in Table II.

Tetrasiloxanes ($\mathbf{M'D_2'M'}$, $\mathbf{M'D'DM'}$ and $\mathbf{M'D_2M'}$).—The residues of the hydrolyzates of main fractions A and B, and starting material from which $\mathbf{M'D_2'M'}$ has been distilled out, were gathered and rigorously fractionated under reduced pressure. Between the plateaus of $\mathbf{M'D_2'M'}$ and $\mathbf{M'D_3'M'}$, two small plateaus appeared. The refractive index and the hydrogen evolved by aqueous sodium hydroxide were determined throughout the distillation and the results are shown in Fig. 4.

TABLE II
METHYLHYDROPOLYSILOXANES

Polysiloxane	Boiling point °C/mmHg	Refractive index n_D^{20}	Density d_4^{20}	Molecular weight Found** (Calcd.)	Molar Refraction Found (Calcd.)[10]	% H(-Si) Found*** Found**** (Calcd.)
$\mathbf{M}'_2$	70.5/760	1.3700	0.7545	133 (134.33)	40.26 (40.18)	— 1.45 (1.50)
$\mathbf{M}'\mathbf{D}'\mathbf{M}'$*	117/760	1.3774	0.8245	192 (194.46)	54.37 (54.45)	— 1.54 (1.56)
$\mathbf{M}'\mathbf{D}'_2\mathbf{M}'$	154/760	1.3830	0.8613	254 (254.60)	68.89 (68.72)	— 1.57 (1.58)
$\mathbf{M}'\mathbf{D}'_3\mathbf{M}'$	82.5/21	1.3860	0.8897	309 (314.73)	83.06 (82.99)	1.60 1.58 (1.60)
$\mathbf{M}'\mathbf{D}'_4\mathbf{M}'$	104/21	1.3882	0.9081	368 (374.86)	97.46 (97.26)	1.58 1.54 (1.61)
$\mathbf{M}'\mathbf{D}'_5\mathbf{M}'$	122/21	1.3900	0.9218	425 (434.99)	111.84 (111.53)	1.61 1.51 (1.62)
$\mathbf{M}'\mathbf{D}\mathbf{M}'$	128/760	1.3811	0.8222	208 (208.49)	58.89 (58.82)	— 0.95 (0.97)

* $\mathbf{M}'=H(CH_3)_2SiO_{1/2}$, $\mathbf{D}'=H(CH_3)SiO$, $\mathbf{D}=(CH_3)_2SiO$.
** Cryoscopic measurements in benzene.
*** The sample in ethanol was reacted with aqueous sodium hydroxide.
**** The sample was reacted with butanol saturated with sodium hydroxide.

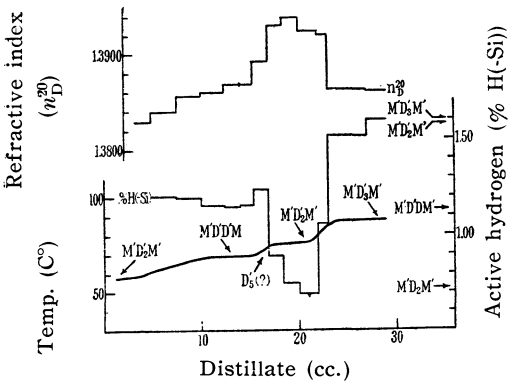

Fig. 4. Distillation curve of the intermittent fraction between $\mathbf{M}'\mathbf{D}'_2\mathbf{M}'$ and $\mathbf{M}'\mathbf{D}'_3\mathbf{M}'$ under reduced pressure (26 mm.).
Active hydrogen content was determined by adding aqueous sodium hydroxide to the sample in ethanol.

From the active hydrogen content, these two small plateaus were supposed to be those of $\mathbf{M}'\mathbf{D}'\mathbf{D}\mathbf{M}'$ and $\mathbf{M}'\mathbf{D}_2\mathbf{M}'$. As the amounts of these compounds were small, it may be questionable whether or not the physical constants acquired here may be taken for those of pure compounds. Further, there is a possiblity of the appearance of isomeric $\mathbf{M}'_3\mathbf{T}$ in front of the plateau of $\mathbf{M}'\mathbf{D}'\mathbf{D}\mathbf{M}'$. This is because the branched chain polymer ($\mathbf{M}_3\mathbf{T}$: b.p. 190°C) has been reported[13] to have a slightly lower boiling point than the isomeric linear polymer ($\mathbf{M}\mathbf{D}_2\mathbf{M}$: b.p. 194°C). Cyclopentamer $\mathbf{D}'_5$ (b.p. 168.7°C, n_D^{20} 1.3912)[3] will be expected to appear between the plateaus of $\mathbf{M}'\mathbf{D}'_2\mathbf{M}'$ and $\mathbf{M}'\mathbf{D}'_3\mathbf{M}'$. In this experiment, no proofs were found as to its presence except the higher active hydrogen content at the back part of the plateau of $\mathbf{M}'\mathbf{D}'\mathbf{D}\mathbf{M}'$.

Polysiloxanes Higher than Tetrasiloxane.—Distillation was further continued and the succeeding plateaus of $\mathbf{M}'\mathbf{D}'_3\mathbf{M}'$, $\mathbf{M}'\mathbf{D}'_4\mathbf{M}'$, $\mathbf{M}'\mathbf{D}'_5\mathbf{M}'$ and $\mathbf{M}'\mathbf{D}'_6\mathbf{M}'$ were obtained at the temperature of 82.5°C/21 mm., 104°C/21 mm., 122°C/21 mm. and 87°C/2 mm. The portions having the refractive index higher than the neighbouring plateaus, a relation similar to that which is shown in Fig. 4, were found between the succeeding plateaus. The differences between the boiling points of the neighbouring plateaus became less with the distillate and it became difficult to differentiate the complete plateau from the intermittent fractions above $\mathbf{M}'\mathbf{D}'_6\mathbf{M}'$. Judging from the active hydrogen content and the increment of the refrcative index of the succeeding plateaus, the plateau of 87°C/2mm. (n_D^{20} 1.3940. Found: H(-Si), 1.53%. Calcd. for $\mathbf{M}'\mathbf{D}'_6\mathbf{M}'$: H(-Si), 1.63%.) was considered to be contaminated by the neighbouring compounds.

The properties of the polysiloxanes until $\mathbf{M}'\mathbf{D}'_5\mathbf{M}'$ are given in Table II.

Analysis of Active Hydrogen.—The determination of % H(-Si) was carried out by using Zerewitinoff apparatus. The values in the data obtained by adding butanol saturated with sodium hydroxide to the sample or its butanolic solution, were smaler than the calculated value with $\mathbf{M}'\mathbf{B}'_4\mathbf{M}'$ and $\mathbf{M}'\mathbf{D}'_5\mathbf{M}'$, the causes of which may be related to the formation of gelatinous mass[14] in the reaction mixture. Accordingly, aqueous sod-

13) W.I. Patnode and D.F. Wilcock, ibid., 68, 358 (1946).

14) U. Takahashi, This Bulletin, 28, 443 (1955).

ium hydroxide was added to the sample in ethanol, as described by Sauer[3], and the satisfactory results were obtained with the higher polymers without formation of gelatinous mass. Because of the closed value of % H(-Si) as the polymer size increased, it was necessary to characterize each compound practically by means of both % H(-Si) and molecular weight.

Summary

(1) Tetramethylsilane, dimethylchlorosilane and methyldichlorosilane and a small amounts of trichlorosilane and hydrocarbon by-product were found in the lower boiling product (b. p. 26°–40°C) of silicon methylchloride reaction.

(2) Dimethylethoxysilane and methyldiethoxysilane besides small amounts of dimethyldiethoxysilane and triethoxysilane were found in the ethanolysis product.

(3) Owing to the contamination of the hydrocarbon by-product, dimethylchlorosilane could not be isolated by repeated distillation. To characterize this substance, it was synthesized from dimethylethoxysilane and benzoylchloride.

(4) By hydrolysis, linear copolymers $\mathbf{M'D'_nM'}$ and $\mathbf{M'D_nM'}$ were found. Of these, copolymers $\mathbf{M'D'_nM'}$ having two to eight silicon atoms and $\mathbf{M'DM'}$ have been characterized.

The authors wish to express their hearty thanks to the Shin-etsu Chem. Ind. Co. for giving them valuable samples.

Department of Applied Chemistry
Faculty of Engineering, Osaka
University, Osaka

Some Considerations of Suspension Polymerization of Minute Droplets

By Shōzō KAICHI

(Received September 2, 1955)

Introduction

By the study of Hohenstein and Mark[1] on suspension polymerization, it has been established that such a polymerization is equal to a summation of individual bulk processes of many droplets of monomer which are suspended in water. But more critically Haward[2] has published his study on the effect of volume change of the monomer droplet on active centre concentration, where it is assumed that the formation of an active centre is always in pairs and it is concluded that subdividion of the system, i. e., the decrease in the volume of droplets, causes the stationary value of active centre concentration to decrease.

In this discussion, we shall reconsider the subject, introducing a new quantity which represents the yield of polymer radicals from initiator fragments which are formed by the decomposition of initiator and may produce free polymer radicals.

Stationary State

We can recognize suspension polymerization processes as probability processes concerned with the appearance and disappearance of active centres, and the following probabilities are taken into consideration:

probability of appearance of one new active centre in a droplet during a time interval Δt which is very short ····· λ_1,

probability of appearance of two new active centres in a droplet during Δt ····· λ_2,

probability of disappearance of two active centres during Δt by mutual termination within a droplet which has n active centres ····· $\mu n(n-1)$, where μ is a constant,

probability that an arbitrarily chosen droplet has n active centres at time t ····· $P_n(t)$,

and (1) is given,

$$P_n(t+\Delta t)=\{1-\lambda_1\Delta t-\lambda_2\Delta t-\mu n(n-1)\Delta t\}P_n(t)+\lambda_1\Delta tP_{n-1}(t)+\lambda_2\Delta tP_{n-2}(t)+\mu(n+2)(n+1)\Delta tP_{n+2}(t)+o(\Delta t) \quad (1)$$

where $o(\Delta t)$ represents a higher order term of Δt. Formula (1) gives the differential equation (2).

$$dP_n/dt=-\{\lambda_1+\lambda_2+\mu n(n-1)\}P_n+\lambda_1P_{n-1}+\lambda_2P_{n-2}+\mu(n+2)(n+1)P_{n+2} \quad (2)$$

In order to solve (2), we introduce a generating function B, i. e.,

$$B=\sum_{n=0}^{\infty}P_nS^n$$

1) W. P. Hohenstein and H. Mark, *J. Polymer Sci.*, **1**, 127 (1946).

2) R. N. Haward, *J. Polymer Sci.*, **4**, 273 (1949).

and (3) is given.

$$\partial B/\partial t=\mu(1-s^2)\partial^2 B/\partial s^2 -\{(\lambda_1+\lambda_2)-\lambda_1 s-\lambda_2 s^2\}B \quad (3)$$

Using a new quantity f, which is the yield of polymer radicals from initiator fragments, λ_1 and λ_2 are represented as follows, provided that Δt is sufficiengly short,

$$\lambda_1=2\varphi Vf(1-f),\quad \lambda_2=\varphi Vf^2 \quad (4)$$

where φ is the rate of formation of initiator fragments and V is the average volume of droplets. μ is proportional to $1/V$ and represented by (6), where k_t is the chain termination reaction constant.

$$\mu=k_t/V \quad (5)$$

(3), (4) and (5) give (6).

$$\partial B/\partial t=k_t(1-s^2)\partial^2 B/\partial s^2/V -\varphi Vf(1-s)\{2-f(1-s)\}B \quad (6)$$

It is difficult to obtain the solution of (6) generally, and we shall discuss the stationary state only.

In the stationary state, $\partial B/\partial t=0$, and (7) is given,

$$(1-s^2)\partial^2 B/\partial s^2=\varphi V^2 f(1-s)\{2-f(1-s)\}B/k_t \quad (7)$$

which can be solved approximately.

Now we wish to estimate active centre concentration R. There exists a relationship (8) between R and M, where M is the average number of active centres per droplet, as represented by (9).

$$R=M/V \quad (8)$$

$$M=\sum_{n=1}^{\infty} nP_n \quad (9)$$

Using (7), (8) and (9), we can estimate the approximate numerical values of R (Appendix). Variations in f and V alter the values of R. These are shown in Table I. When

TABLE I

$f\sim V\sim R$ RELATIONSHIPS

f	V	m	P_0	P_1	P_2	M	R	R : $1/2V$
1	$\sqrt{k_t/\varphi}\times 1/3.16$	0.1	0.909	0	0.091	0.182	$\sqrt{\varphi/k_t}\times 0.575$	0.364
	〃 1/10	0.01	0.990	0	0.010	0.020	〃 0.200	0.040
	〃 1/31.6	0.001	0.999	0	0.001	0.002	〃 0.063	0.004
	〃 1/100	0.0001	1.000	0	0.000	0.000	〃 0.000	0.000
0.99	〃 1/3.16	0.1	0.476	0.492	0.024	0.540	〃 1.71	1.080
	〃 1/10	0.01	0.498	0.499	0.003	0.504	〃 5.04	1.008
	〃 1/31.6	0.001	0.500	0.500	0.000	0.500	〃 15.8	1.000
	〃 1/100	0.0001	0.500	0.500	0.000	0.500	〃 50.0	1.000
0.75	〃 1/3.16	0.1	0.478	0.493	0.022	0.538	〃 1.70	1.076
	〃 1/10	0.01	0.499	0.500	0.000	0.500	〃 5.00	1.000
	〃 1/31.6	0.001	0.500	0.500	0.000	0.500	〃 15.8	1.000
	〃 1/100	0.0001	0.500	0.500	0.000	0.500	〃 50.0	1.000
0.50	〃 1/3.16	0.1	0.482	0.494	0.018	0.530	〃 1.67	1.060
	〃 1/10	0.01	0.499	0.500	0.000	0.500	〃 5.00	1.000
	〃 1/31.6	0.001	0.500	0.500	0.000	0.500	〃 15.8	1.000
	〃 1/100	0.0001	0.500	0.500	0.000	0.500	〃 50.0	1.000
0.25	〃 1/3.16	0.1	0.490	0.496	0.011	0.517	〃 1.63	1.034
	〃 1/10	0.01	0.499	0.500	0.000	0.500	〃 5.00	1.000
	〃 1/31.6	0.001	0.500	0.500	0.000	0.500	〃 15.8	1.000
	〃 1/100	0.0001	0.500	0.500	0.000	0.500	〃 50.0	1.000
0.01	〃 1/3.16	0.1	0.500	0.500	0.000	0.500	〃 1.58	1.000
	〃 1/10	0.01	0.500	0.500	0.000	0.500	〃 5.00	1.000
	〃 1/31.6	0.001	0.500	0.500	0.000	0.500	〃 15.8	1.000
	〃 1/100	0.0001	0.500	0.500	0.000	0.500	〃 50.0	1.000
0	no reaction					0	〃 0	0

It is shown in this table that R, regarded as a function of f, changes discontinuously at two points, i.e., $f=0$ and $f=1$. This is a reasonable result from the difference between two boundary conditions which have been used in the course of solving (7), and completely right so far as stationary states are discussed ($t\longrightarrow\infty$). At a stationary state which has been attained after a long enough period of reaction, there exist significant differences of active centre distributions between $f=1$ and $f=0.99$ or $f=0$ and $f=0.01$.

On the other hand, it is naturally thought that at the beginning of a reaction there should be little differences of active centre distributions between $f=1$ and 0.99 or $f=0$ and 0.01. Therefore, R ought to change continuously in the whole range of $0\leqq f\leqq 1$ if t takes some finite value, sometimes taking a stationary value and sometimes an unstationary one, as f varies. Actually, such a $R\sim f$ relationship at a constant finite t is the matter to be discussed. A general discussion of this would require a general solution of (6), which will not be touched on in this paper. Only the case when V is extremely small will be discussed in the next section.

f is zero, R equals zero and polymerization does not occur. When f is unity, the decrease in V causes R to decrease. When f is between zero and unity and equals neither of them, the decrease in V increases R to a maximum, $1/2V$, which is approached more and more as V decreases. The greater values of R, in this case, mean not only higher rates of polymerization reaction, but also higher degrees of polymerization of products, since the greater values of R at the same initiation rate are caused only by longer lives of molecular chains. We can know, therefore, that the subdivision of the system makes both the rate and degree of polymerization lower when $f=1$, and higher when $0<f<1$.

Of course, the above discussion is based on the assumption of a stationary state, and the length of time it takes for R to reach the stationary value is not given here.

Initial Stages of Polymerization

The usual suspension polymerization should show a very similar figure at its initial stage to bulk polymerization, if it is true that suspension polymerization is a summation of bulk polymerizations of dispersed monomer droplets. The time necessary for R to reach half of the stationary value is $(k_t\varphi f)^{-1/2}$ which is independent of V[3], provided that V is very great as compared with $1/R_\infty$[4]*.

In the case of suspension polymerization of minute droplets, on the other hand, it has been established in this paper that the stationary value of R approximately equals $1/2V$ when $0<f<1$ is satisfied. In this case the probabilities that a droplet contains no active centre and one are both 1/2. And an active centre freshly created in a droplet which contains another active centre previously created, quickly terminates together with the old one, and the probability of coexistence of two or more growing active centres in one droplet is very small as compared with unity. In this case we can make the following approximate expression,

$$v_t=4\varphi f(1-f)VR$$

where v_t is the disappearance rate of active centre (rate of chain termination reaction), and $0<f<1$ is assumed. It gives

$$dR/dt=(\lambda_1/V)-v_t=2\varphi f(1-f)(1-2VR),$$

which being integrated, gives (10).

$$R=[1-\exp\{-4f(1-f)\varphi Vt\}]/2V \qquad (10)$$

When t goes to infinity, R goes to $1/2V=R_\infty$. The time necessary to reach the half value of R_∞, or the measure of quickness with which R approaches to stationary value, is expressed by τ in (11).

$$\tau=\ln 2/4f(1-f)\varphi V \qquad (11)$$

This relationship is shown in Fig. 1.

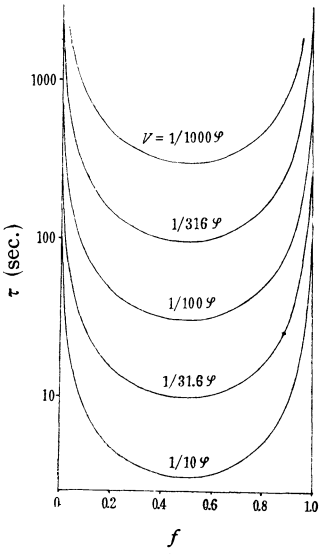

Fig. 1. Relations between τ, f and V.

If we estimate the numerical values of φ, f, and V, the numerical value of τ is known. Nozaki and Bartlett[5] have shown that the decomposition rate of benzoyl peroxide in methyl methacrylate at 60°C is 0.36×10^{-5}/sec., which means that φ is 0.72×10^{-5} (BPO) mol./l. sec. If V is smaller than $\ln 2/4f(1-f)\times0.72\times10^{-5}$ (BPO), τ is greater than one second, and the decrease in V proportionally increases τ. If V is much smaller than this, τ is much greater than unity and the decrease in V ultimately increases τ so much that the stationary state would not be reached at any late stage of reaction.

Nevertheless, R in the case of the smaller V is always greater than R in the case of the greater V at the same reaction time. This is shown in Fig. 2. The greater values of R in such cases mean not only the higher reaction rates, but also the higher degrees of polymerization of products as indicated in the previous section.

We can know, therefore, that the suspension polymerization of minute droplets should show high values in both rate and degree of polymerization than usual suspension process in either initial (unstationary) or stationary stages of reaction. In other words, a system of suspension polymerization, subdivided to smaller and smaller droplets should

3) W.H. Stockmeyer, *J. Chem. Phys.*, **12**, 143 (1944).

4) This is satisfied in the case of usual suspension polymerization. Ref. 2).

* R_∞ is the stationary value of R. See the latter part of this section.

5. K. Nozaki and P.D. Bartlett, *J. Am. Chem. Soc.*, **68**, 2377 (1946).

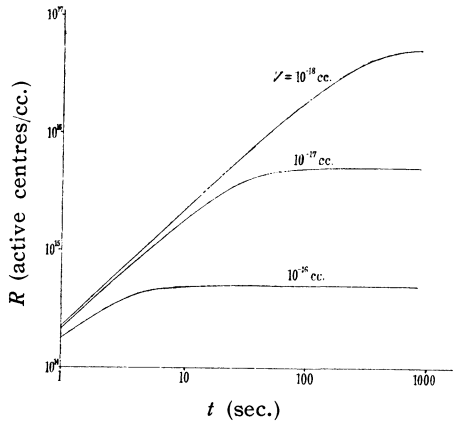

Fig. 2. $R \sim t$ relationships as for (BPO)= 0.1 mol./l.

ultimately shift to a system where both rate and degree of polymerization are greater than when undivided, provided that $0<f<1$ is satisfied. This agrees with the observation by Hohenstein and Mark[1] that the rate is increased in suspension polymerization, when agitation is done vigorously.

Emulsion Polymerization Accelerated by Oil-soluble Initiator

Following the practice that the polymerization of monomer emulsion by water-soluble initiator is called emulsion polymerization, we usually name the polymerization of monomer emulsion by oil-soluble initiator also as emulsion polymerization. These two are, indeed, common in that rate accelerating and molecular weight increasing effects are observed as compared with bulk or suspension polymerization in the same condition. But the two emulsion polymerizations cannot be the very same ones because of the difference in the modes of free radical appearance into polymerization loci, viz., one by one in the former and two at once in the latter.

There coexist in monomer emulsion two sorts of monomer dispersions, i. e., emulsified droplets and solubilized monomer in soap micelles[8]. In the case of emulsion polymerization accelerated by oil-soluble initiator, polymerization should occur in both of them. A study on BPO-initiated emulsion polymerization of methyl methacrylate, worked by Kagawa and the author[7], showed, in addition to the above mentioned rate and molecular weight increasing effects, that the turbidity decreased as reaction proceeded, which suggested that the polymerization in micelle is preferential.

The preceding authors[8] imagined some mechanisms agreeable with the characteristic figures of emulsion polymerization, accelerated by oil-soluble initiator, i. e., capture of free radicals by aqueous phase, and pre-existing of free radicals in reaction system etc. But now, these are unnecessarily essential to illustrate the characteristic figures of emulsion polymerization accelerated by oil-soluble initiator. We can do it by assuming only $0<f<1$, as follows.

Solubillzed monomer in micelles are very small crowds of monomers and can be recognized as extremely small monomer droplets. If $f=1$, the value of R should be very near to zero in micelles because of their smallness and micelles should not contribute to the reaction practically. So the reaction should proceed only in the emulsion droplets. On the other hand, when $0<f<1$, R in the micelles should be very great because of their smallness and reaction in the micelles should surpass that in droplets which in this case serve almost only as reservers of monomers, and decrease in turbidity is expected. Therefore, the above-mentioned experimental results by Kagawa and Kaichi are simply illustrated by assuming $0<f<1$. This condition ($0<f<1$) is perhaps satisfied in all oil-soluble initiators because the mutual reaction between two decomposition fragments can always be considered[9].

Thus we can understand suspension polymerization and emulsion polymerization accelerated by oil-soluble initiator on a simple common basis that there is no essential difference in mechanisms and only volume difference of reaction loci between these two.

Conclusion

Systems of suspension polymerization, subdivided into smaller and smaller droplets, should shift ultimately to those where both the rate of reaction and the degree of polymerisation are greater than the initial, provided that the yield of polymer radicals from initiator fragments equals neither zero nor unity. The characteristic figure of emulsion polymerization accelerated by oil-soluble initiator can be understood on this basis.

Appendix

Estimation of R from Formulae (7), (8) and (9)

The stationary state assumption gives (i), when we represent the numbers of droplets which contain odd and even numbers of active centres by N_o and N_e, respectively,

$$dN_o/dt=\lambda_i(N_e-N_o), \quad dN_e/dt=\lambda_i(N_o-N_e) \quad \text{(i)}$$

6) W.d. Harkins, *J. Am. Chem. Soc.*, **69**, 1428 (1947).
7) S. Kaichi and I. Kagawa, *J. Chem. Soc., Japan* (Ind. Chem. Section), **58**, 509 (1955).
8) Ref. 2); Ref. 7).
9) M.S. Matheson, *J. Chem. Phys.*, **13**, 584 (1945).

which gives (ii).

$$(N_e-N_o)/(N_e+N_o)=\exp(-2\lambda_1 t) \qquad \text{(ii)}$$

(A) $\lambda_1=0$

This means $f=0$, or $f=1$.

a) $f=0$ No reaction.

b) $f=1$ This means the formation of active centers exclusively in pairs.

(ii) gives (iii).

$$\left.\begin{array}{l} N_o=0 \\ \quad\therefore\ \sum P_{2i+1}=0 \\ N_e=N_e+N_o \\ \quad\therefore\ \sum P_{2i}=1 \\ N_e+N_o=\text{const.} \\ \quad\therefore\ \sum P_n=1 \end{array}\right\} \quad \therefore\ B_{s=-1}=1 \quad \therefore\ B_{s=1}=1 \qquad \text{(iii)}$$

Using (iii) as boundary conditions, we obtain (iv) from (7), (8) and (9), which gives the approximate numerical values of R, neglecting higher order terms of m, where m is the abbreviation of $\varphi V^2/k_t$. (iv) is applicable to small values of V.

$$\left.\begin{array}{l} P_0=1/1+m, \quad P_1=0, \\ P_2=m/1+m, \quad P_3=0,\cdots\cdots. \\ R=2m/(1+m)V. \end{array}\right\} \qquad \text{(iv)}$$

(B) $\lambda_1\neq 0$

The means $0<f<1$.

(v) is given by (ii).

$$\left.\begin{array}{l} N_e=N_o \\ \quad\therefore\ \sum P_{2i}=\sum_{2i+1} \quad\therefore\ B_{s=-1}=0 \\ N_e+N_o=\text{const.} \\ \quad\therefore\ \sum P_n=1 \quad\therefore\ B_{s=1}=1 \end{array}\right\} \qquad \text{(v)}$$

Using (v) as boundary conditions, we obtain (vi) from (7), (8) and (9), neglecting higher order terms of m, which is applicable to small values of V.

$$\left.\begin{array}{l} P_0=1/2[1+mf(2-f)/2-0.032\,mf(1-f)] \\ P_1=1/2[1+mf(2-f)/6-0.010\,mf(1-f)] \\ P_2=mf(2-f)/4[1+mf(2-f)/2-0.032\,mf(1-f)] \\ R=(P_1+2P_2)/V \end{array}\right\} \qquad \text{(vi)}$$

Above P_3 are not given because of their extreme smallness. Fig. 1 is the result of the abovementioned numerical estimations of P_0, P_1, P_2 and R by inserting several values of m and f into (iv) and (vi).

The author wishes to express his sincere thanks to Prof. Ikumi Kagawa, Nagoya Univ., for introducing him to this field of work.

Department of Industrial Chemistry
Faculty of Engineering, Shizuoka University, Hamamatsu

Studies on the Cooking Mechanism of Wood. XIII[1]. *On the Phenolic Hydroxyl Group of Lignosulphonic Acid*

By Hiroshi MIKAWA, Koichiro SATO, Chizuko TAKASAKI and Kiyo EBISAWA

(Received September 6, 1955)

That the lignin in situ contains phenolic hydroxyl group was definitely established by the recent investigations of Richtzenhain[2]. By methylation of wood with diazomethane followed by permanganate oxidation, he could obtain veratric acid and isohemipinic acid. This fact proves that the lignin contains two types of phenolic hydroxyl groups, (I) and (II), already in wood. As it seems to be quite improbable that some destruction of the phenolic hydroxyl group occurs during the sulphonation, the phenolic hydroxyl groups already existed in wood must exist in lignosulphonic acid too.

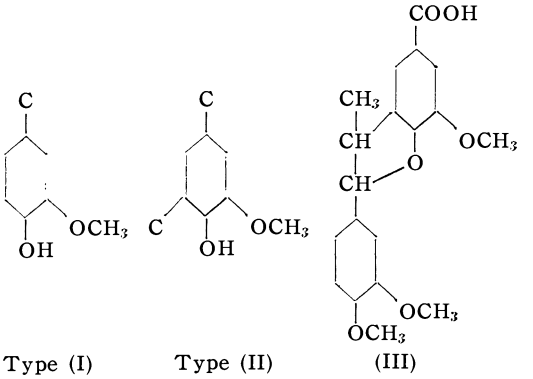

Type (I) Type (II) (III)

A method to estimate the amount of the phenolic hydroxyl group of the lignin in wood was worked out, and the amount was estimated

1) Part XII, This Bulletin, 28, 653 (1955); cf. also short communication, ibid., 29, 209 (1956).
2) H. Richtzenhain, *Chem. Ber.*, 83, 488 (1950).

as 0.15–0.18/CH_3O. The amount of the phenolic hydroxyl group of the solid lignosulphonic acid, i.e. sulphonated lignin contained in the wood sulphonated at neutral pH, was also measured, and it was confirmed that the content was exactly the same as that of the lignin in situ. This fact proves that no new formation of phenolic hydroxyl group occurs during the sulphonation at neutral pH.

No definite conclusion has been obtained as yet, as to whether the sulphonation reaction accompanies the formation of phenolic hydroxyl group or not. Hägglund and Carlsson observed a new formation of hydroxyl group[3], and the nature of this hydroxyl group was thought by Freudenberg to be phenolic, formed by the opening of benzopyran or fran rings[4]. Hachihama, Shinra and Kyogoku recognized a quantitative relationship between the amount of sulphur introduced and the phenolic hydroxyl group formed[5]. Freudenberg, Lautsch and Piazolo, however, could not recognize any appreciable increase of phenolic hydroxyl group by sulphonation at low temperature, although the decrease of the amount of the ether oxygen was quite appreciable[6]. One of the reasons for such discrepancies may be due to the difference of the methods used for the estimation of the phenolic hydroxyl group.

The amount of the phenolic hydroxyl group of lignin itself depends also on the methods of estimation used. By two different methods, Freudenberg estimated the amount as one/3.9CH_3O[7] and one/1.7–3.3CH_3O[8]. Aulin-Erdtman introduced a spectroscopic method, and by the method she estimated the amount of phenolic hydroxyl group of lignosulphonic acid as one/4–6CH_3O. In our present communication, her spectroscopic method was used.

Low sulphonated lignosulphonic acid, obtained from the sulphonated wood by the Kullgren process[9], has according to Aulin-Erdtman 0.13 phenolic hydroxyl group per methoxyl group[10]. Our samples showed slightly greater values, but the difference was very little. This fact proves that no new formation of phenolic hydroxyl group occurs during the Kullgren process, either. It will also be concluded, from this fact that wood seems to contain no easily hydrolizable linkages, which can produce phenolic hydroxyl group. As the lignin in wood contains two types of phenolic hydroxyl groups, (I) and (II), phenolic hydroxyl groups of low sulphonated lignosulphonic acid belong also to these two types.

According to Aulin-Erdtman[10], ordinary lignosulphonic acid contains 0.17 phenolic hydroxyl group, 0.04 more than that of low sulphonated acid. As will be stated later, a slight increase of phenolic hydroxyl group was also recognized in the acidic further sulphonation of low sulphonated lignosulphonic acid, i.e. in the sulphonation of B-group region. Freudenberg showed previously, that the so-called Erdtman's acid (III) was sulphonatable by acidic sulphite solution, accompanying the formation of phenolic hydroxyl group by opening its coumaran structure[11]. This acid contains, however, carboxyl group in the para position to its benzyl-aryl ether bond belonging to phenyl-coumaran structure, which may affect the reactivity of the aryl ether bond. As will be stated later, dihydro-dehydro-diisoeugenol (XIV) was also found to be sulphonatable by acidic sulphite solution. Lindgren and Mikawa[12] confirmed that such structure reacts with thioglycolic acid very easily, whereby the phenyl-coumaran structure is split accompanying the new formation of phenolic hydroxyl group. Lignothioglycolic acid prepared from the completely methylated wood has about 0.16–0.2 phenolic hydroxyl group per methoxyl. This fact provides a possibility that the lignin in wood contains at most about this amount of phenyl-coumaran structure with benzyl-aryl ether linkage. From these experimental findings, it will reasonably be assumed, that such phenyl-coumaran structure exists in lignin, and a part of the B group must have such structure.

As stated previously, low sulphonated lignosulphonic acid contains two types of phenolic hydroxyl group, that of type (I) and (II). The sulphonation of B group accompanies the new formation of phenolic hydroxyl group, which is expected to belong to type (II), since a part of the B group may have phenyl-coumaran structure having benzyl-aryl ether bond. It will, therefore, be very interesting to know the amount of both these phenolic hydroxyl groups belonging to different types, in various lignin preparations. Conductometric titrations of many model compounds

3) E. Hägglund and G. Carlsson, *Biochem. Z.*, **257**, 467 (1933).
4) K. Freudenberg, *Annual Rev. Biochem.*, **8**, 81 (1939).
5) Y. Hachihama, H. Shinra and Y. Kyogoku, *J. Soc. Chem. Ind. Japan*, **47**, 212 (1944).
6) K. Freudenberg, W. Lautsch and G. Piazolo, *Cellulosechem.*, **22**, 97 (1944).
7) K. Freudenberg and H. Walch, *Ber.*, **76**, 305 (1943).
8) K. Freudenberg, *Das Papier*, **1**, 209 (1947); K. Freudenberg and D. Rasenack, *Ber.*, **86**, 755 (1953).
9) C. Kullgren, *Svensk Kem. Tid.*, **44**, 15 (1932).
10) G. Aulin-Erdtman, *Svensk Papperstidn.*, **55**, 745 (1952); **56**, 91 (1953).
11) K. Freudenberg, M. Meister and E. Flickinger, *Ber.*, **70**, 500 (1937).
12) B. Lindgren and H. Mikawa, *Acta Chem. Scand.*, **8**, 954 (1954).

showed that the phenolic hydroxyl group of type (I), i.e. that of the simple guaiacol type, was without exception titratable, that of type (II), however, was found to be conductometrically untitratable, even a slight change of inclination not being observed in the titration curve. This fact provides a very sharp method to measure tne frequency of both types of phenolic hydroxyl group in lignin. Aulin-Erdtman[10] reports that the model compounds having the phenolic hydroxyl group of type (II) are not neutralized completely even at about pH 12. She supposes the existence of some amount of such phenolic hydroxyl group (termed "hindered" phenolic hydroxyl group by Coggeshall[13].) in lignosulphonic acid.

By this method, it was found that low sulphonated lignosulphonic acid contains both types in approximately equal amounts. As the phenolic hydroxyl group of this acid is the same with that of the lignin in situ, the phenolic hydroxyl group of the lignin in wood may consist of about equal amounts of both phenolic hydroxyl groups. α-Lignosulphonic acid contains type (II) much more than type (I), the ratio being 7: 3 in this acid. As a part of the B group is expected to be phenyl-coumaran structure, it is quite understandable, that type (II) increased very much after the sulphonation of the B group. The content of the type (I) is higher in birch α-lignosulphonic acid than in spruce α-acid, the ratio of type (I) and (II) being about 1: 1. This fact will easily be understood, as the titrations of model compounds show that the phenolic hydroxyl group belonging to syringyl nucleus is conductometrically titratable, which can not form phenyl-coumaran structure.

On the Amount of Phenolic Hydroxyl Group and Phenyl-coumaran Structure of Lignin in Wood

As stated previously, Richtzenhain proved definitely that the lignin in situ contains already phenolic hydroxyl group. The amount, however, was not known. Based on the yield of veratric and isohemipinic acid, the frequency of the phenolic hydroxyl group is calculated to be one per 15.4 methoxyl group. This value is, however, only the lower limit of the frequency of the phenolic hydroxyl group, as one can not estimate the loss of these acids during the oxidation.

During the preparation of lignothioglycolic acid, the most reactive groups, i.e. X, Z and B, combine with thioglycolic acid[14,15] very quickly under comparatively mild conditions, thus protecting the reactive groups and preventing secondary reaction. It will, therefore, reasonably be assumed, that the phenolic hydroxyl group of lignothioglycolic acid is the sum of the phenolic hydroxyl group of lignin already existing in wood, and of that formed during the reaction with thioglycolic acid. The latter hydroxyl group may at least partly be formed from the phenyl-coumaran structure. It is, therefore, expected that the frequency of the phenolic hydroxyl group of lignothioglycolic acid, prepared from completely methylated wood, gives the upper limit of the frequency of the phenyl-coumaran structure of the lignin in situ. The difference of the amount of the phenolic hydroxyl group of the lignothioglycolic acid, prepared from untreated wood, and that prepared from the

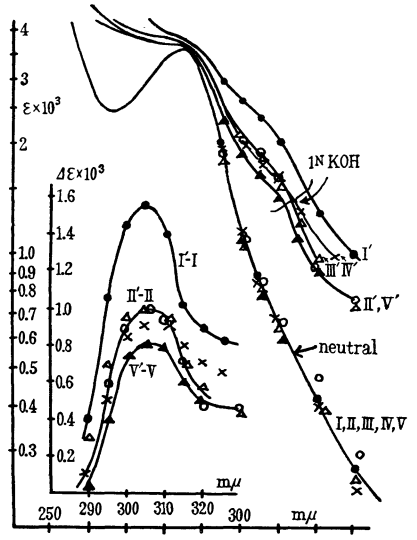

Fig. 1. UV-absorption spectra and $\Delta\varepsilon$-curves of lignothioglycolic acids prepared from various wood powders.

wood powders	CH_3O% of wood	CH_3O% of lignothioglycolic acid
(I) ● Spruce wood powder (s.)	—	11.81
(II) ○ CH_2N_2 methylated s.	11.91	13.88
(III) △ S. Sulphonated at neutral pH and then methylated with CH_2N_2	14.90	14.25
(IV) × S. methylated with Me_2SO_4	15.80	15.30
(V) ▲ 〃	22.10	16.15

13) N. Coggeshall, *J. Am. Chem. Soc.*, **69**, 1620 (1947); N. Coggeshall and A. Gtessner, ibid., **71**, 3150 (1949); **72**, 2275 (1950). cf. also Kirk-Othmer, Encyclopedia of Chem. Tech., Vol. 10, 301 (1953).

14) H. Mikawa and K. Sato, *J. Chem. Soc. Japan Ind. Chem. Sec.*, **57**, 605 (1954).

15) Part XI of this series. This Bulletin, **28**, 649 (1955).

methylated wood is expected to be the same as the amount of the phenolic hydroxyl group of the lignin in situ.

Curves (I) and (I') of Fig. 1 are the neutral and alkaline (1 N KOH) absorption spectra of the lignothioglycolic acid prepared from untreated wood powder, (II), (IV), (V) and (II'), (IV'), (V') are those of the lignothioglycolic acids prepared from the methylated wood powder taken in neutral and alkaline media, respectively. In (I) and (I') the molar extinction was calculated on the methoxyl basis, the positions of the curves (II)-(V) were, however, settled by shifting them so as to give the same extinction with the Curve (I) at 282 mμ maximum. By fixing the positions of the Curves (II)-(V) in this way, the positions of the other Curves (II')-(V') are also fixed. Curves (I)-(V) superpose each other almost completely over the whole range of wave-lengths. So-called $\Delta\varepsilon$-curves obtained from these neutral and alkaline spectra are shown in the same figure. (I')-(I) is the value obtained for the lignothioglycolic acid prepared from the untreated wood powder, (II')-(II) is from the diazomethylated wood powder (CH_3O 11.9%). In order to comfirm, whether the methylation with diazomethane is complete or not, wood powders methylated with dimethyl sulphate up to CH_3O 15.80 and 22.10% were also investigated. The curve obtained for the latter is (V')-(V). The difference of (I')-(I)=1550 and (V')-(V)=800, i.e. 750 corresponds to the amount of the phenolic hydroxyl group of the lignin in wood, the amount being 0.18-0.15/CH_3O by assuming the $\Delta\varepsilon$ value for monophenols as 4000-5000, according to Aulin Erdtman.

As seen in the figure, the amount of the phenolic hydroxyl group of the lignothioglycolic acid prepared from diazomethylated wood and from the wood sulphonated at neutral pH followed by diazomethylation (Curves (III) and (III')) is approximately the same, which fact proves that no new phenolic hydroxyl group was formed during the sulphonation at neutral pH. The phenolic hydroxyl group corresponding to (V')-(V), i.e. $\Delta\varepsilon$=800 or one per 5-6.3 CH_3O=0.16-0.2/CH_3O, is that formed during the reaction with thioglycolic acid, and this amount is expected to be the upper limit of the amount of the phenyl-coumaran structure in lignin.

On the Increase of Phenolic Hydroxyl Group of Low Sulphonated Lignosulphonic Acid by its Further Sulphonation

In a previous communication[15], further sulphonation of low sulphonated lignosulphonic acid was studied. The amount of the phenolic hydroxyl group of many sulphonic acids prepared at that time was measured by spectroscopic method, and the values thus obtained were plotted against the time of the sulphonation (Fig. 2). In this figure,

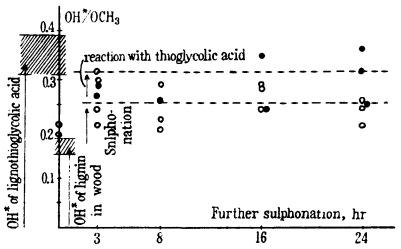

Fig. 2. Amount of the phenolic hydroxyl group of low sulphonated lignosulphonic acid (LSLSA) (○), LSA obtained by acidic further sulphonation of LSLSA (○) and of these acids after the reaction with thioglycolic acid (●). $\Delta\varepsilon$ value of monophenols was assumed to be 4000.

lignosulphonic acid corresponding to time zero is the low sulphonated lignosulphonic acid used. As stated previously, the amount of the phenolic hydroxyl group of this acid is approximately the same as that of the lignin in situ.

As can be seen in the figure, the content of the phenolic hydroxyl group increases about 0.1/CH_3O by further sulphonation. As stated previously, this newly formed phenolic hydroxyl group may be of type (II) formed by the opening of the phenyl-coumaran structure. As low sulphonated lignosulphonic acid contains phenolic hydroxyl groups belonging to type (I) and type (II) in equal ratio with the lignin in situ, the content of the type (II) must be higher in α-lignosulphonic acid. It will, therefore, be very interesting to measure the ratio quantitatively.

Conductometric Titrations of Model Compounds and the Method of the Estimation of Both Type (I) and Type (II) Phenolic Hydroxyl Group

In a previous communication[15], it was shown that the conductometrically observable so-called weakly acidic group of lignosulphonic acid consists of weak carboxyl group and the "conductometrically titratable" phenolic hydroxyl group. As an example, the curves of the conductometric titration of low sulphonated lignosulphonic acid are shown in Fig. 3. With extremely thin cell, UV-absorption spectra were taken at points A, B, C, D and E of the conductivity curve by using the

16) Part XII of this series, *loc. cit.*

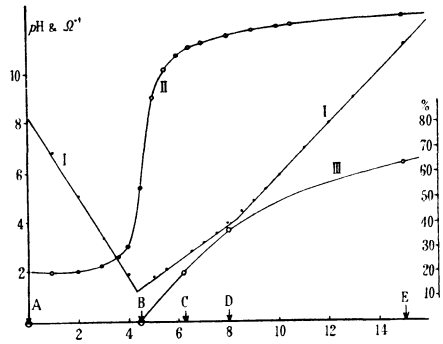

Fig. 3. Conductometric titration (I) and potentiometric titration (II) of low sulphonated lignosulphonic acid, and the percentage of the ionized phenolic hydroxyl group measured during the titration (III).

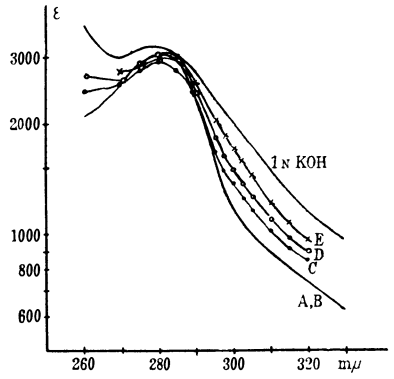

Fig. 4. UV-absorption spectra taken at points A-E of Fig. 3.

same technique as mentioned in the previous communication. (Fig. 4). The differences of the spectra taken at B-E, and in 1 N KOH, and the spectrum taken at A were indicated in Fig. 5. The percentage of the ionized

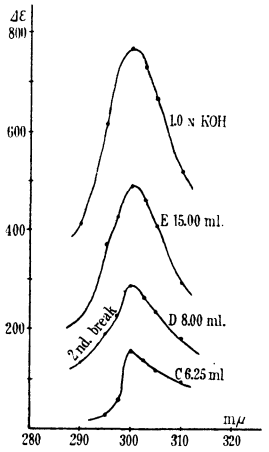

Fig. 5. $\Delta\varepsilon$-curves obtained at points C~E of the conductometric titration curve of the low sulphonated lignosulphonic acid shown in Fig. 3.

phenolic hydroxyl group at various stages of the titration calculated from Fig. 5 is shown by Curve (III) of Fig. 3. As can be seen, the phenolic hydroxyl group, which remains unionized before the second break, amounts to approximately 55% of the total phenolic hydroxyl group.

As discussed in the previous papers, simple

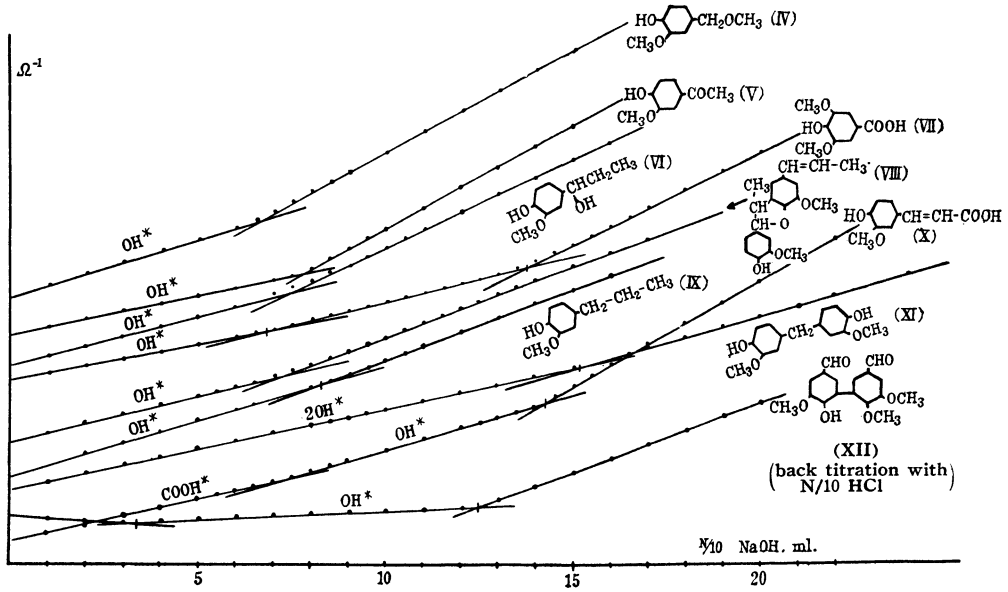

Fig. 6. Conductometric titrations of various model compounds in 30~50% aqueous alcohol. (Almost quantitative values are obtained in every case)

guaiacol type phenolic hydroxyl group was expected to be titratable. In order to confirm it, many model compounds were titrated conductometrically in aqueous alcohol (30–50%). As can be seen in Fig. 6, all these compound were titrated quantitatively without exception. As it is known that pK values of phenols are larger in alcohol than in water[17], guaiacol type phenolic hydroxyl group must be titratable in aqueous solution too, as they are titrable in aqueous alcohol. As an example of a water soluble model, vanillyl sulphonic acid was titrated in the previous communication. Another water soluble compond. guaiacyl glycerol (XVII) was titrated (Fig. 7),

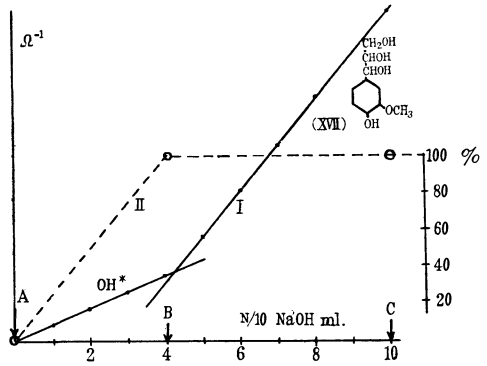

Fig. 7. Conductometric titration (I) of guaiacyl glycerol and the percentage of the ionized phenolic hydroxyl group measured at points A~C (II).

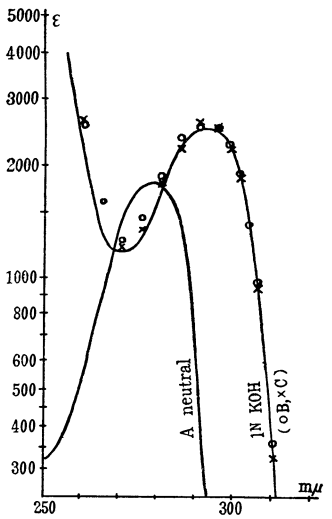

Fig. 8. Change of the UV-absorption spectrum during the titration of guaiacyl glycerol shown in Fig. 7.

As the titration proceeds along the Curve (I), the phenolic hydroxyl group ionized along the Curve II and at point B, i.e. at the end point of the titration, the ionization of the phenolic hydroxyl group was spectroscopically complete (Fig. 8). Based on these experimental findings, it will reasonably be concluded, that at the end point of the conductometric titration of the "conductometrically titratable" phenolic hydroxyl group, this group must be completely in phenolate form, i.e. that the conductometric titration and the ionization of the phenolic hydroxyl group proceeds pararell in equal amounts.

As an example of the phenol belonging to type (II), a model compound (XIII) was titrated.

This compound was synthesized by sulphonating racemic dihydro-dehydro-diisoeugenol (XIV) or its thioglycolic acid adduct (XV) with acidic sulphite solution. (XIII) was obtained in crystalline form as its benzylthiuronium salt having a sharp melting point. The structure of this compound was concluded from the analyses and its UV-absorption spectra, taken in acidic and in alkaline media shown in Fig. 10. As dihydro-dehydro-diisoeugenol contains two asymmetric carbon atoms, the product is expected to be a mixture of two different racemic modifications, provided that the racemization at the α-carbon atom is involved in the reaction. As the product was obtained, however, in crystalline form, having a sharp melting point, it appears that the compound isolated may be one of the two expected racemic modifications, if the reaction involves racemization at the α-carbon atom. It may, however, also be possible that the reaction proceeds under complete retention or complete inversion of the benzylaryl ether bond resulting in a formation of only one racemic modification. In connection with this problem, it may be remarked that Hart[18] reports that the configuration of α-phenoxy ethylbenzene (XVI) is not altered when its benzylaryl ether bond is split by hydrogen chloride.

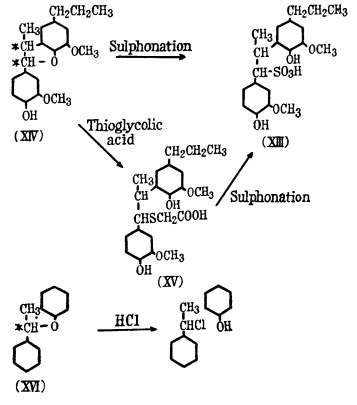

As can be seen from the Curve (I) of Fig. 9, the amount of the conductometrically titratable

17) W. Treadwell and G. Schwarzenbach, *Helv. Chim. Acta*, **11**, 386 (1928).

18) H. Hart and H. Eleuterio, *J. Am. Chem. Soc.*, **76**, 1379 (1954).

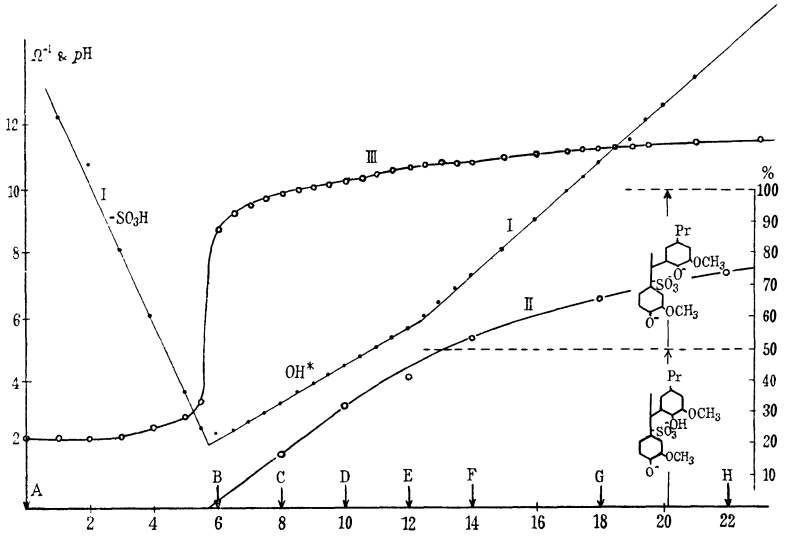

Fig. 9. Conductometric (I) and potentiometric (III) titrations of the model compound (XIII) and the percentage of the phenolic hydroxyl group ionized during the titration.

phenolic hydroxyl group is equivalent to the amount of the sulphonic acid group, i.e. only one phenolic hydroxyl group is conductometrically titrable, which is expected to be a simple guaiacol type. Curve (II), which indicates the ionization of the phenolic hydroxyl group during the titration, shows that only 50% of the total phenolic hydroxyl group is ionized at the second break of the titration curve. Even after the second break, the ionization of the remaining phenolic hydroxyl group proceeds only gradually; no quantitative relation exists, however, between the added alkali and the increase of the ionization, the phenolic hydroxyl group titrated in this region being too weak and the hydrolysis of the phenolate ion being consequently too great. Even a slight change of inclination was not observed in the titration Curve (I) around the expected third break, 18 ml. region. UV-absorption curves measured at A-H and the corresponding $\Delta\varepsilon$ curves are shown in Fig. 10 and 11 respectively.

From these experimental findings, it will be possible to conclude as follows. Potentiometric titration cannot differentiate the phenolic hydroxyl group of type (I) and (II). The curve of the spectroscopically determined percentage of the ionized phenolic hydroxyl group against the volume of the alkali added, i.e. for example Curve (II) of Fig. 9, does not show any distinct break between the two types of the phenolic hydroxyl groups. Although type (I) is conductometrically titratable and type (II) untitratable, it is impossible to determine the amount of both types by conductometric titration alone, as the phenolic

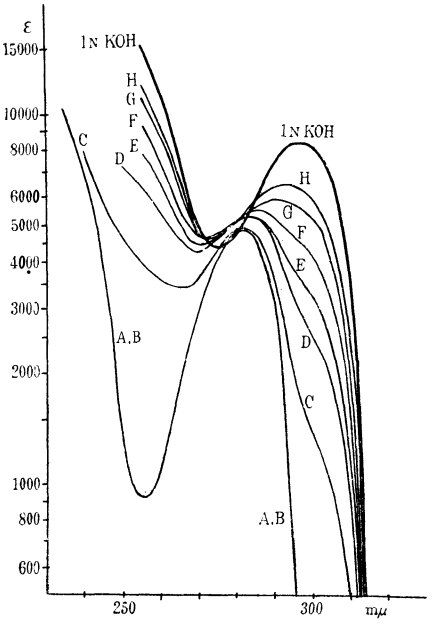

Fig. 10. Change of the UV-absorption spectrum observed during the titration of the compound (XIII) shown in Fig .9.

hydroxyl group of type (I) can not be distinguished by conductometric titration from the weak carboxyl group present in lignosulphonic acid. By combining conductometric titration (Curve I) and the curve of the percentage of the ionized phenolic hydroxyl group (Curve II), one can determine very clearly the amount of both types separately, the amount of the phenolic hydroxyl group ionized before the second break being equal

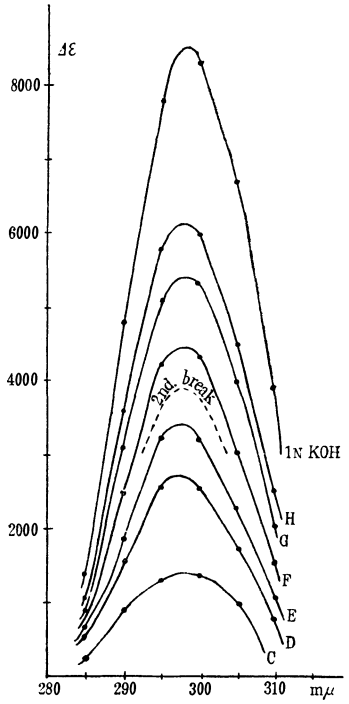

Fig. 11. Δε-curves obtained at points C~H of the conductometric titration curve of the compound (XIII) shown in Fig. 9 and 10.

to that of type (I) and the remaining one being that of type (II).

Ratio of the Phenolic Hydroxyl Group belonging to Type (I) and Type (II) in various Lignosulphonic Acid Preparations

Fig. 3 shows the conductometric titration of the low sulphonated lignosulphonic acid and, as stated previously, about 40–50% of the total phenolic hydroxyl group was found to be conductometrically titratable and 60–50% remained untitrated in this case. The former may be of type (I) and the latter type (II). As the phenolic hydroxyl group of the lignin in wood may be the same as that of the low sulphonated lignosulphonic acid, it appears that the ratio of the phenolic hydroxyl group of the lignin in wood belonging to type (I) and (II) may be the same as that of the low sulphonated lignosulphonic acid, i.e. the amounts of these two types are thought to be about the same in this case, too.

Titration curves of an α-lignosulphonic acid was shown by Fig. 3 of the previous communication (Part XII). Only about 30% of the total phenolic hydroxyl group was conductometrically titratable. The amount of the phenolic hydroxyl group of type (II) must be, therefore, much higher in this acid than in low sulphonated lignosulphonic acid or the lignin in situ. As stated previously, the increase of the amount of type (II) may be attributed to the sulphonation of phenyl-coumaran structure in the sulphonation of B-group region.

Conductometric titration and the change of the UV-spectrum of the birch α-lignosulphonic acid are shown in Fig. 12 and 13.

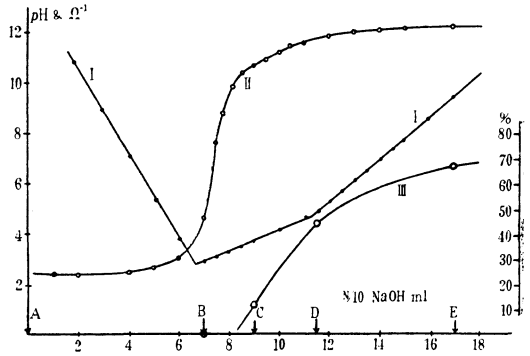

Fig. 12. Conductometric (I) and potentiometric titrations (II) of birch α-lignosulphonic acid, and the percentage of the phenolic hydroxyl group ionized during the titration (III).

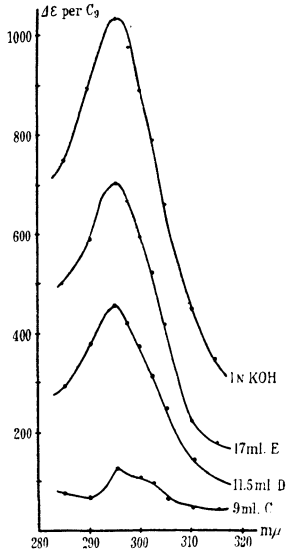

Fig. 13. Δε-curves at points C~E of the titration curve of birch α-lignosulphonic acid shown in Fig. 12.

Conductometrically titratable phenolic hydroxyl group is about 50% of the total group in this case. The comparatively higher content of type (I) in this acid may be attributed to the existence of syringyl nucleus, which cannot form phenyl-coumaran structure. That the phenolic hydroxyl group belonging to syringyl.

nucleus is conductometrically titratable was confirmed by the titration of syringic acid shown in Fig. 6.

Experimental

Methylation of various Wood Powders.—Methylation of wood powder with dimethyl sulphate was performed as usual with concentrated alkali at room temperature. Methylation with diazomethane was performed by simply keeping wood powder in etherial diazometane solution for about a week, changing the solution several times with a fresh one. Sulphonated wood powder was prepared by sulphonating at pH 6 for ten hours at 135°. Analyses of the methylated wood powders are shown in Fig. 1.

Preparation of Lignothioglycolic Acid from These Methylated Wood Powders.—To the methylated wood powder (5 g.) were added fresh distilled thioglycolic acid (25 g.) and 2N HCl (2.5 ml.), and the mixture was heated at 100° for two hours. A large amount of water was added, and the precipitate separated and washed with water by centrifuge. The residue was kept in 0.5N NaOH (50 ml.) over-night, the carbohydrate which remained insoluble was separated, and the lignothioglycolic acid was precipitated by dilute hydrochloric acid and centrifuged, washed with water, dissolved in a little amount of acetone, centrifuged and a mixture of alcohol and ether was added to the clear acetone solution of the lignothioglycolic acid. The reprecipitated lignin was washed with alcohol-ether, ether and petroleum ether successively. The yield of the cream colored powder thus obtained was 0.5–0.7 g. in every case. Analytical values are shown in Fig. 1.

Measurement of the UV-Absorption Spectra of Various Lignothioglycolic Acids.—Lignothioglycolic acid (ca. 10 mg.) was dissolved in dioxane (0.5 ml.) containing several drops of water. The solution was made up to 30 ml. with absolute alcohol purified with NaOH and zinc dust. When the spectrum in neutral medium is to be measured, 4 ml. of this solution was diluted with the same purified alcohol to 30 ml., and the alkaline spectrum was measured with the solution made by diluting 4 ml. of the solution with 60% aqueous alcohol and 3 ml. of 10 N KOH, to 30 ml. The results were shown in Fig. 1.

Conductometric Titrations of Lignosulphonic Acids.—The method was the same as in the preceding papers, Part (XI) and (XII). 500 mg. of barium lignosulphonate was dissolved in 20 ml. of water, passed through cation exchanger IR 120 and the eluate was made up to 50 ml. The solution was titrated conductometrically with 0.1N sodium hydroxide solution.

Syntheses of Known Model Compounds.—Vanillyl methyl ether (IV): B. Leopold, *Svensk Papperstid.*, **55**, 816 (1952); acetovanillone (V): K. Nakazawa, *J. Pharm. Soc. Japan*, **74**, 836 (1954); α-guaiacyl propanol (VI): $LiAlH_4$ reduction of propioguaiacone acetate synthesized according to Nakazawa, loc. cit.; syringic acid (VII): M. Bogert and B. Coyen, *J. Am. Chem. Soc.*, **51** 569 (1929); Dehydro-diisoeugenol (VIII): B. Leopold, *Acta Chem. Scand.*, **4** 1523 (1950); coeruligno! (IX): hydrogenation of isoeugenol with Pd-C; ferulic acid (X); Adams, Organic Reactions Vol. I, p. 250; 3, 3′-dimethoxy-4, 4′-dihydroxy-diphenyl methane (XI): H. Mikawa, *Bull. Chem. Soc. Japan*, **27**, 53 (1954); guaiacyl glycerol (XVII): E. Adler and S. Yllner, *Acta Chem. Scand.*, **7**, 570 (1953).

Synthesis of Dehydro-divanillin Monomethyl Ether (XII).—Dehydro-divanillin[19] (25 g.) was dissolved in a sodium hydroxide solution, dimethyl sulphate (30 g.) added and the methylation was performed at room temperature. Dimethyl ether separated was filtered and the filtrate was acidified with carbon dioxide. A mixture of monomethyl ether and the starting material was washed with methanol and extracted with hot benzene. The monomethyl ether thus extracted was recrystallized from benzene, m.p. 196.5–197°, yield 4.5 g.

Anal. Found: C, 64.44; H, 5.30; CH_3O, 29.5. Calcd. for $C_{17}H_{18}O_6$: C, 64.55; H, 5.10; CH_3O, 29.4%.

Synthesis and Conductometric Titration of α-(3-Methoxy-4-hydroxyphenyl)-β-(2-hydroxy-3-methoxy-5-propylphenyl)-*n*-propane Sulphonic Acid (XIII).—*Method I:* Dehydro-diisoeugenol (racemate) was hydrogenated with Pd-C to dihydro-dehydro-diisoeugenol. To 4.7 g. of Di-De-Di was added 50 ml. of cooking acid (17 g. of NaOH and 50 g. of SO_2 in one liter of 50% alcohol) and the mixture was heated in a quickly rotating autoklave at 140° for twenty hours. A slight excess of sulphuric acid was added, SO_2 expelled in vacuo, and the solution was neutralized with $BaCO_3$, centrifuged, and concentrated to about 30 ml. Benzylthiuronium salt of the sulphonic acid was precipitated by adding conc. solution of benzylthiuronium hydrochloride, washed well with water, dissolved in a small amount of alcohol, filtered and reprecipitated with water. The precipitate separated at first as oil, solidified over-night. This was purified in the same way until constant m.p. was reached. M.p. 136–138°, 0.8 g. After being kept at 80° in vacuo with P_2O_5 for two days the m.p. was 145–147°.

Anal. Found: C, 58.43; H, 6.17; N, 4.98; CH_3O, 11.6. Calcd. for $C_{28}H_{33}O_7N_2S_2$ (benzylthiuronium salt of XIII): C, 58.3; H, 6.24; N, 4.86; CH_3O, 10.75%.

99.6% of the sulphonic acid group of this compound was titrated conductometrically.

Method II: 4 g. of Di-De-Di was reacted with thioglycolic acid[12] and the product XV was treated as in method I. Treating the product in the same way as above, 0.5 g. of the benzylthiuronium salt melting at 145–147° was obtained. Mixed with the product obtained by Method I, no melting point depression was observed. 0.8 g. of dihydro-dehydro-diisoeugenol was recovered, which fact shows that a part of the thioglycolic acid adduct splits off its thioglycolic acid residue, regenerating the phenyl-coumaran ring.

Conductometric titration of (XIII): 400 mg. of the benzylthiuronium salt was dissolved in 10 ml. of alcohol, 20 ml. of water added and warmed. The warm solution was passed through a column

19) K. Elbs and H. Lerch, *J. prak. Chem.*, 93, 1 (1916).

of ion exchange resin IR 120, washed with warm aqueous alcohol until neutral pH. Alcohol was boiled off in vacuo and the solution was diluted with water to 50 ml. and conductometrically titrated.

Summary

The amount of the phenolic hydroxyl group of the lignin in situ was estimated to be about one per 5–6 methoxyl. Phenolic hydroxyl group of low sulphonated lignosulphonic acid is the same as that of the lignin in situ. There exist two types of phenolic hydroxyl groups (I) and (II) in lignin and lignosulphonic acid, the former being conductometrically titratable and the latter untitratable. With several lignosulphonic acid preparations, the ratios of these two types of phenolic hydroxyl groups were measured, the ratio being 1 : 1 with lignin in wood, low sulphonated lignosulphonic acid, and birch α-lignosulphonic acid and about 3 : 7 with α-acid of gymnosperm origin. The structures of these two types of phenolic hydroxyl groups were suggested.

The anthors are indebted to Dr. H. Okada, the head of the laboratory, and to Miss. S. Suehiro for ther encouragement. They wish to express their appreciation also to Prof. Y. Hachihama Assist. Prof. Y. Kyogoku for helpful advice and during the course of the investigation.

Research Laboratory of the Kokusaku Pulp Co. 184 1-chome, Kamiochiai Shinjuku-ku, Tokyo

Studies on the Cooking Mechanism of Wood. XIV.[1] *On the UV-Absorption Spectrum, Phenolic Hydroxyl Group and Carboxyl Group of Thiolignin*

By Hiroshi MIKAWA, Koichiro SATO, Chizuko TAKASAKI and Kiyo EBISAWA

(Received September 22, 1955)

UV-Absorption Spectrum

UV-absorption spectrum of lignosulphonic acid is not so different from that of the lignin in wood[2], the minimum at about 260 mμ being rather deep and the maximum at 280 mμ comparatively sharp. This fact suggests that the structure of the building unit of lignosulphonic acid is at least optically almost uniform. UV-absorption spectrum of thiolignin has been investigated by Enkvist in order to estimate the amount of the phenolic hydroxyl group[3]. The spectra were very different from that of lignosulphonic acid and were very diffuse.

Curve (I) of Fig. 1 is the absorption spectrum of thiolignin, prepared by an experimental cook under the condition similar to that of the industrial cooking. The spectrum is very diffuse, indicating that the structure of the building units is not very uniform. The absorption around 280 mμ, calculated on methoxyl basis, is high in comparison with that of lignin or lignosulphonic acid. As the methoxyl content of thiolignin is in general not so low, except those prepared under very drastic condition or the fraction suffered an intense disintegration, the comparatively high absorbancy at this wave-length region must not be due to demethoxylation.

As will be reported later[4], benzyl alcoholic group, i. e. X group and Z group of lignin, must be exposed to high temperature alkali during the kraft cooking. Model experiments done by Leopold[5] in connection with nitrobenzene oxidation of lignin show that models with benzyl alcoholic groups (I) and (II) were split by hot alkali, resulting in a formation of carboxyl group and double bond conjugated to benzene nucleus.

Merewether recognized the existence of some amount of carbonyl group in Eucalyptus regnans thiolignin[6]. As will be reported

1) Part XIII, This Bulletin, **29**, 245 (1956).
2) P. Lange, *Svensk Papperstidn.*, **47**, 262 (1944); **48**, 241 (1945); **50**, No. **11** B, 130 (1947); G. Aulin-Erdtman, *Tappi.*, **32**, 160 (1949).
3) T. Enkvist and B. Alfredsson, *Svensk Papperstidn.*, **54**, 185 (1951).
4) Part XVI, to be published in this Bulletin.
5) B. Leopold, *Acta Chem. Scand.*, **4**, 1523 (1950).
6) J. Merewether, *Aust. J. Sci. Res., Ser.* A, **1**, 241 (1948).

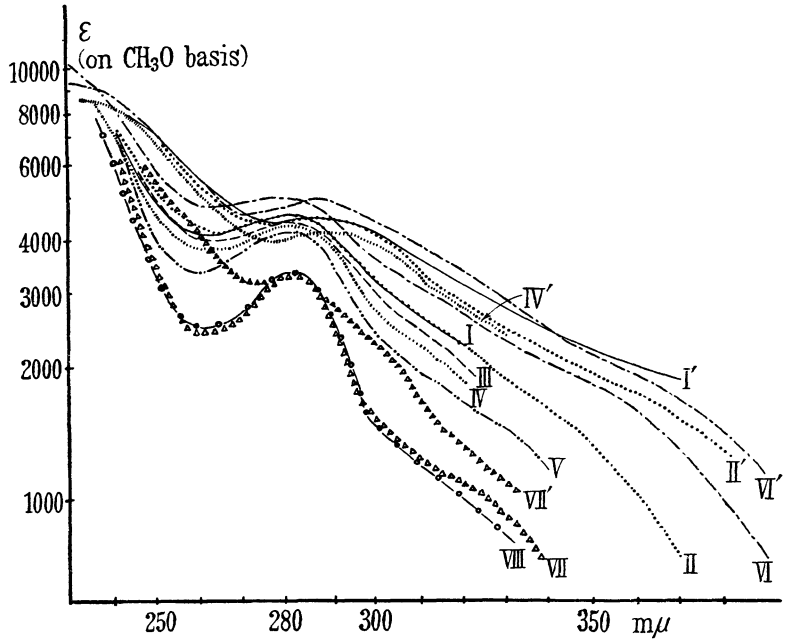

Fig. 1. UV-absorption spectrum of thiolignin, thiolignin treated in various ways, native lignin and dioxane lignin in neutral medium and in 1 N KOH.

neutral	1 N KOH	curves	lignin
I alcohol	I′ 80% alcohol	———	thiolignin
II water	II′ water	. . . . .	after sulfonation
III alcohol		— — — — —	after reduction with $NaBH_4$
IV 〃	IV′ 80% alcohol	.....	after reduction with Raney alloy
V 〃		—··—··—··	IV after reduction with Pd-H_2
VI 〃	VI′ 〃	—·—·—·—	thiolignin prepd. from dioxane lignin
VII 〃	VII′ 〃	△△△△△△	dioxane lignin
VIII 〃		—O—O—O—	native lignin

later[4], the carbonyl group contained in thiolignin is expected, at least partly, to be conjugated with benzene nucleus, being formed at the same position, where the sulphur atom is situated, after it was split off by alkali. It is reported also that acetovanillone with such a carbonyl group is obtained from the kraft waste liquor but not from that of the soda cooking[7].

Experiments done by Leopold[5] include also reactions between high temperature alkali and model compounds with such conjugated carbonyl as those of group (III) and (IV). Formation of the carboxyl group directly connected with of benzene nucleus was observed. Not much attention has been paid to the existence of carboxyl group in thiolignin. Merewether showed, however, the existence

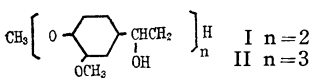

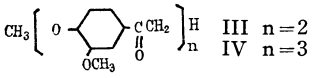

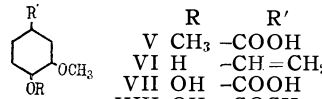

I or II $\xrightarrow[180°C]{2N\ NaOH}$ V+VI

III or IV $\xrightarrow{〃}$ V+VII+VIII

of carboxyl groups in a fraction containing no sulphur, separated from Eucalyptus regnans thiolignin by solvent fractionation[8].

7) T. Enkvist, M. Moilanen and B. Alfredsson, *Svensk Papperstidn.*, 52, 53 (1949); D. Brink, R. Hossfeld and W. Standstrom, *J. Am. Chem. Soc.*, 71, 2275 (1949).

8) J. Merewether, *Aust. J. Sci. Res., Ser.* A, 2. 117 (1949).

Based on the model experiments discussed above and on the mechanism of the kraft cooking which will be reported later[4], the existence of the carbonyl group and the double bond conjugated with benzene nucleus and the carboxyl group directly connected to the nucleus seems to be quite probable, and it is conceived that such structures in the side chain influence the absorption spectrum of thiolignin, making it diffuse and the absorption deep. It appears, therefore, to be very interesting to investigate the influence of such treatment on the absorption spectrum of thiolignin, that the carbonyl group or double bond is expected to be eliminated.

Curve (II) is the absorption of thiolignin prepared by sulphonating (I) according to the Enkvist's method[9]. No appreciable change of the absorption was observed. (III) is the absorption of (I), measured after the reduction with sodium boronhydride, a reduction which is reported to be sufficient to reduce the carbonyl group to the hydroxyl group. The change of the absorption was not very appreciable. (IV) is the absorption of the lignin prepared from (I) by reducing it with Raney alloy and alkali. This reduction is reported to be sufficient to reduce the carbonyl group conjugated with benzene nucleus to methylene[10].

As seen in the figure, this reduction lowers the absorption at about 300 mμ very much, probably because of the complete elimination of the carbonyl group. As this lignin is expected to be completely desulphurized, one can reduce this lignin with palladium black, a catalyst which is very sensitive to sulphur. (V) represents the spectrum of thiolignin (I) reduced with Raney alloy and palladium successively. Here, the spectrum is very similar to that of native or dioxane (curves (VII) and (VIII)) lignin, all of the sulphur atom, carbonyl group and double bond in the thiolignin being eliminated by these treatments. Native lignin was isolated according to Brauns[11] and dioxane lignin according to Freudenberg[12].

These experimental results suggest to us that the absorption spectrum of thiolignin is diffuse and the absorption is higher in thiolignin than that of lignin in situ due to the presence of the carbonyl group and the double bond conjugated with benzene nucleus in thiolignin. Absorbancy shown by curve (V) around 280 mμ region is as yet higher than that of native lignin, probably because carboxyl group exists in lignin (V) as yet. As shown in Fig. 2, vanillic acid has very large absorption around 260–290 mμ region.

As stated previously, thiolignin (I) was prepared from wood powder and the thiolignin investigated by Enkvist was also prepared from wood. Absorption spectrum of thiolignin prepared from lignin without the existence of carbohydrate is not reported as yet. It is known that especially hemicellulose suffers a severe degradation during the alkaline cooking of wood. As such compounds, Sohn isolated reductic acid (V)[13] and Enkvist identified methylcyclopentenolone VI[14].

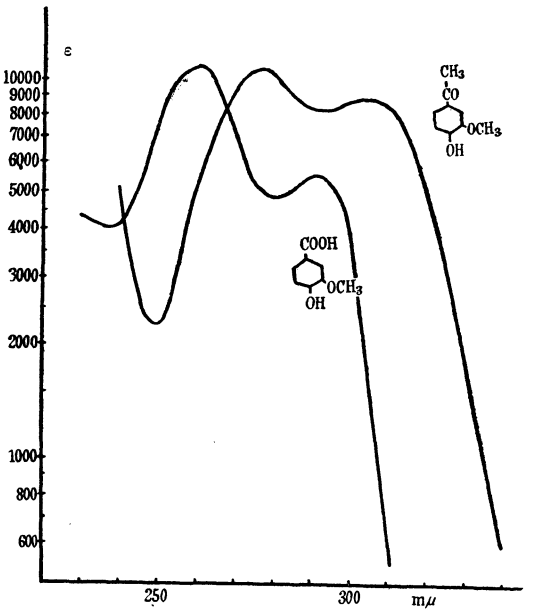

Fig. 2. UV-Absorption spectrum of vanillic acid and acetovanillone (in alcohol).

Migita and Kanda report that the color of kraft pulp is due not only to lignin but also to substances originating from hemicellulose[15]. Richtzehain assumed the condensation of lignin with some substances originating from carbohydrate during the kraft cooking in order to explain his results, that thiolignin gives a comparatively high yield of isohemipinic acid, when it is methylated with dimethyl sulphate and oxidized with permanganate[16]. It will, therefore, be con-

9) T. Enkvist, B. Alfredsson and E. Hägglund, *Svensk Papperstidn.*, **55**, 588 (1952).
10) D. Papa, E. Schwenk and B. Whitman, *J. Org. Chem.*, **7**, 587 (1942).
11) F. Brauns, *J. Am. Chem. Soc.*, **61**, 2120 (1939).
12) W. Stumpf and K. Freudenberg, *Angew. Chem.*, **62**, 537 (1951).
13) A. Sohn, *Das Papier*, **4**, 379 (1950).
14) T. Enkvist, B. Alfredsson, M. Merikallio, P. Paakbonen and O. Jarvela, *Acta Chem. Scand.*, **8**, 51 (1954).
15) N. Migita, T. Kanda, S. Mochizuki and H. Nishimura, *Japanese Tappi.*, **8**, 277 (1954).
16) H. Richtzenhain, *Svensk Papperstidn.*, **53**, 644 (1950).

ceivable that the absorption spectrum of thiolignin differs from that of the lignin in situ, because of the condensation of the substances originating from wood carbohydrate with lignin. Thiolignin was prepared, therefore, from Freudenberg's dioxane lignin under the ordinary kraft cooking condition and its spectrum was measured. The spectrum (VI) represents, however, a typical thiolignin spectrum, thus indicating that the influence of wood carbohydrate on thiolignin spectrum may not be very large and the spectrum of thiolignin must be explained by the structure of the thiolignin itself alone.

Summarizing the results, it was shown that the UV-absorption spectrum of thiolignin must be explained by assuming the existence of the carbonyl group, the double bond conjugated with the nucleus and the carboxyl group attached directly to the nucleus in thiolignin.

Estimation of the Amount of the Phenolic Hydroxyl Group and the Carboxyl Group of Thiolignin

Enkvist measured the amount of the phenolic hydroxyl group of thiolignin spectroscopically[17]. His method was, however, the old method of Aulin-Erdtman, which is not sensitive enough even when applied to simple model compounds[18].

Absorption spectra of thiolignin (I), shown in Fig. 1, which were taken in neutral and alkaline media, indicate that this lignin contains only 0.22–0.18 phenolic hydroxyl group per methoxyl group when calculated by the Aulin-Erdtman's new method[19].

The content of the phenolic hydroxyl group of thiolignin has been estimated by several different methods, and the values obtained are much greater. Enkvist titrated with sodium ethylate in ethylenediamine solution or with hydrochloric acid after addition of barium chloride to the sodium hydroxide solution of the lignin[20]. According to these methods, equivalent weight was about 200–300. Methylation with diazomethane is also used. Values measured by this method, hitherto reported, are shown in the table. The amount 0.55–0.9 per methoxyl group, being about the same as those obtained by titration methods.

As stated previously, the UV-absorption spectrum of thiolignin is rather complex,

	MeO %	After CH_2N_2 methylation MeO %	After CH_2N_2 methylation followed by hydrolysis MeO %	COOH+OH* per MeO	OH* per MeO	OH* per MeO spectroscopically measured	Literature
Alkali lignin A (spruce)	14.9	22.2		0.55			21)
Alkali lignin B (spruce)	14.0	24.8		0.87			21)
Thiolignin (spruce)	14.6	24.8		0.79			22)
Thiolignin (spruce)	12.9	23.1		0.89			3)
Alkali lignin (oat straw)	14.8 14.7	23.5 22.4					23)
Thiolignin (Eucalyptus)	21.1	27.1					24)
Native lignin (spruce)	14.8	21.4		0.49		0.4 −0.32	25)
Dixane lignin (Picea jezoensis)	15.56	17.98	17.23	0.16	0.12	0.2 −0.16	
Thiolignin I (Picea jezoensis)	15.31	23.3	20.81	0.58	0.40	0.225 −0.18	
Thiolignin prepd. from dioxane lignin	14.55						

17) T. Enkvist, B. Alfredsson, *Svensk Papperstidn.*, **54**, 185 (1951).
18) G. Aulin-Erdtman, *Tappi.*, **32**, 160 (1949).
19) G. Aulin-Erdtman, *Svensk Papperstidn.*, **55**, 745 (1952).
20) T. Enkvist, *Svensk Papperstidn.*, **51**, 225 (1948).
21) H. Marshall, F. Brauns and H. Hibbert, *Can. J. Res.*, **13B**, 103 (1935).
22) C. Ahlm, *Paper Trade J.*, **113**, No. 13, 115 (1941).
23) M. Phillips and M. Goss, *J. Biol. Chem.*, **114**, 557 (1936).
24) F. Lahey and J. Merewether, *Austr. J. Sci. Res.*, **A 1**, 112 (1948).
25) F. Brauns, *J. Am. Chem. Soc.*, **61**, 2120 (1939).

and the building unit seems to be not very uniform. It is, therefore, as yet open to question, whether it is justifiable or not to estimate spectroscopically the amount of the phenolic hydroxyl group of such ununiform substance as thiolignin. Diazomethylation method seems to be much more reliable in such cases.

Since thiolignin is expected to contain some amount of carboxyl group as mentioned before, one can not expect, to obtain exact values simply from the increase of the methoxyl group by diazometylation. The content of the phenolic hydroxyl group must be calculated from the difference between the methoxyl group content of the thiolignin, methylated with diazomethane followed by alkaline hydrolysis, and that of the original untreated thiolignin, the difference of the content of the methoxyl group before and after the hydrolysis being expected to show the amount of the carboxyl group in the thiolignin. The content of the phenolic hydroxyl group of thiolignin (I) estimated according to this method is 0.4 per methoxyl group, and the amount of the carboxyl group is 0.18 per methoxyl group.

As reported previously, lignin in wood contains only about 0.14 phenolic hydroxyl group per methoxyl group; the phenolic hydroxyl group increases, therefore, very much during the kraft cooking. Because of the presence of this phenolic hydroxyl group and the carboxyl group, thiolignin is very easily soluble in alkali.

Added in proof. According to the recent investigation by J. Lindberg and T. Enkvist (*Suomen Kemistilehti*, **B 28**, 23 (1955)) the spectroscopic method of the detection of the phenolic groups due to G. Aulin-Erdtman could not be used in the case of orthovanillic acid, salicylic acid, 5-carboxyvanillin and 5-carboxyvanillic acid. As it might not be improbable that thiolignin contains some amount of pherolic hydroxyl groups with a carboxyl group in its ortho position, their findings might provide us one of the reasons why herspectroscopic method of the estimation of phenolic hydroxyl groups in lignin was not suitable in the case of thiolignin preparations.

Experimental

Preparation of Thiolignin I.—Extractives free Picea jezoensis wood powder (550 g.) was cooked with 3.5 l. of white liquor of 20% sulphidity with 4% active alkali. Temperature was raised to 165° within two hours and kept at this temperature for one hour. The black liquor was acidified, filtered and the crude thiolignin obtained was dissolved in a mixture of acetone (200 ml.) and alcohol (40 ml.) and precipitated with ether. After repeated reprecipitation, the yield was 38 g.

Anal. C, 61.33; H, 5.64; S, 2.42; CH_3O, 15.31%.

Sulphonation of Thiolignin I at Neutral pH.—To 3 g. of thiolignin I was added sulphite cooking acid of pH 8 (80 ml.) and the whole was heated at 105° for two hours in a quickly rotating autoklave. Thiolignin went into solution almost completely. Sulphonic acid was separated as Ba salt as usual and analyzed. CH_3O, 14.05; SO_3H/CH_3O, 0.119.

Reduction of Thiolignin I with Sodium Borohydride.—Five grams of thiolignin was dissolved in 100 ml. of phosphate buffer, which can dissolve lignin but has as low pH as possible. 1.5 g. of $NaBH_4$ was added and kept at room temperature over-night. CH_3O, 15.08%.

Reduction of Thiolignin with Raney Alloy and Alkali.—Three grams of thiolignin was dissolved in 20 ml. of 10% alkali and was reduced with 12 g. of fine Raney alloy powder at 80–90°. CH_3O, 15.10%.

Reduction with Palladium and Hydrogen.—0.1 g. of palladium chloride was dissolved in 20 ml. of water slightly acidified with hydrochloric acid, 500 mg. of thiolignin reduced with Raney nickel added, and the lignin was dispersed by agitation. Palladium was reduced with hydrogen and precipitated on lignin, which was separated and washed by centrifuge. The precipitate thus obtained was hydrogenated in 100 ml. of alcohol for two hours at room temperature.

Hydrolysis of the Thiolignin methylated with Diazomethane.—The lignin wasl gently refluxed with 1 N alcoholic KOH for two hours.

Kraft Cooking of Dioxane Lignin.—Three hundred milligrams of dioxane lignin was dissolved in white liquor of 20% sulphidity with 4% active alkali (5 ml.) and was heated as in the case of wood powder. CH_3O, 14.55%.

Summary

It was shown that the UV-absorption spectrum of thiolignin must be explained by assuming the existence of the carbonyl group, the double bond conjugated with the nucleus and the carboxyl group attached directly to the nucleus. The amount of the phenolic hydroxyl group and the carboxyl group of thiolignin were estimated by methylating with diazomethane and subsequently hydrolyzing the methylated lignin with alkali.

The avthors wish to express their gratitude to Dr. H. Okada, the head of the laboratory, and to Miss. S. Suehiro for their encouragement.

Research Laboratory of the Kokusaku Pulp Ind. Co., 184, 1-Chome, Kamiochiai, Shinjuku-ku, Tokyo

Studies on the Cooking Mechanism of Wood. XV[1]. *Mannich Reaction on Lignin Model Compounds and the Estimation of the Amount of the Simple Guaiacyl Nucleus in Thiolignin*

By Hiroshi MIKAWA, Koichiro SATO, Chizuko TAKASAKI and Kiyo EBISAWA

(Received September 29, 1955)

Introduction

Our knowledge on the side chain and nuclear structure of thiolignin is very unsatisfactory. The elucidation of this problem is of fundamental importance to find out a valuable utilization of thiolignin, which is now burned in order to recover sodium. According to the investigation of Richtzenhain[2], the yield of isohemipinic acid by permanganate oxidation of the methylated lignin preparations is higher in the case of thiolignin, than in the case of the lignin in wood or other lignin preparations. In order to explain this fact, it was assumed that a condensation of substances of carbohydrate origin occurred at the 5th position of the nucleus during the digestion, resulting in the increase of the frequency of the nucleus of type II. According to Csellak[3], the yield of vanillin from thiolignin by nitrobenzene oxidation is lower, when compared to that from the lignin in wood or the other types of lignin preparations. The yield of vanillin and syringaldehyde from Meadol by cupric oxide oxidation or oxidation with Fehling solution is also lower, when compared to that from lignosulphonic acid[4]. According to Leopold, model compounds having such nucleus as ((I) (R=H)), except those belonging to diphenyl methane type (III) or to pinoresinol type (IV), give vanillin in very high yield on oxidation with nitrobenzene[5]. The fact, that the yield of vanillin is lower in thiolignin in spite of its rather high content of phenolic hydroxyl group, suggests us, to together with the results of Richtzenhain, that thiolignin contains nuclei of type ((II) (R=H)) in rather high frequency.

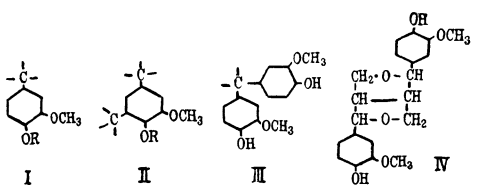

I II III IV

As the yield of veratric acid and isohemipinic acid from the methylated lignin preparations by permanganate oxidation is supposed to be far from quantitative, and the yield of vanillin from thiolignin is expected to be very much influenced by the presence of carbonyl group[6] or of carboxyl group directly connected to benzene nucleus, it seems to be very interesting to estimate the frequency of the nucleus of type I (R=H) and II (R=H) by a quite different method. As will be stated later, Mannich reaction was used to differentiate both types of phenolic hydroxyl groups and the ratio of the amount of the phenolic hydroxyl groups belonging to these two types were found to be 25-40% and 75-60% respectively. If one can assume, according to Leopold[5], the ratio of (I) and (II) of the lignin in wood as 50 to 50%, one must probably admit the slight increase of (II) during the kraft cooking. It seems, however, incorrect to explain the low yield of vanillin from thiolignin by nitrobenzene oxidation by the increase of the condensed nucleus alone. It seems also to be important that thiolignin contains a carbon atom of higher oxidation stage directly connected to the nucleus, i.e. carbonyl group and carboxyl group, as was reported in the previous communication[1].

Estimation of the Amount of the Non-etherified Simple Guaiacyl Nucleus in Thiolignin

Mannich reaction on phenols, especially with dimethylamine, has been investigated rather much and the investigations done until 1942 are summarized by Blicke[7]. Among them, however, there is only guaiacol as phenols having a close connection to lignin, i.e. with guaiacyl nucleus. In general,

1) Part XIV, This Bulletin, 29, 254 (1956).
2) H. Richtzenhain, *Svensk Papperstidn.*, 53, 644 (1950).
3) W. Csellak, *Tappi.*, 34, 472 (1951).
4) I. Pearl, *J. Am. Chem. Soc.*, 64, 1429 (1942).
5) B. Leopold, *Svensk Kem. Tid.*, 64, 18 (1952).
6) A. Wacek and K. Kratzl, *Cellulosechem.*, 20, 108 (1942), *Ber.*, 76, 891 (1943), *Ber.*, 77, 516 (1944).
7) F. Blicke, "Organic Reactions", John Wiley & Sons, Inc., New York, Vol. I (1942), p. 303.

dimethylaminomethyl radical is introduced by Mannich reaction to ortho and para positions of the phenolic hydroxyl group.

As the phenolic hydroxyl groups of lignin belong mainly to type (I) and (II), it seems to be possible to estimate the amount of the former type with Mannich reaction, if it is confirmed by many model phenols that only those having the former nucleus react with formalin and dimethylamine under the condition of Mannich reaction. As will be stated later, experiments with model compounds revealed that 1) model compounds of type (I) give, without exception, Mannich base with substituent at 5th position in very high yield, 2) those of type (II) do not react, 3) carboxyl group having phenolic hydroxyl group in its para position is split off as carbon dioxide and dimethylaminomethyl group is introduced to the same position, 4) methylol group having phenolic hydroxyl group in its para position reacts with dimethylamine resulting in a formation of dimethylaminomethyl group at the same position, 5) other groups remain intact even when phenolic hydroxyl group exists in the para position, and 6) no reaction occurs when the phenolic hydroxyl group is etherified.

Since it is possible to estimate the amount of the carboxyl group, as reported previously[1], and the benzyl alcoholic group can be sulphonated at neutral pH to the sulphonic acid group, a group which does not react under the condition of Mannich reaction, it seems possible to estimate the amount of the phenolic hydroxyl groups belonging to type (I) and (II) (R=H) by Mannich reaction with dimethylamine.

When treated with formaldehyde and dimethylamine, the N/OCH_3 values of the thiolignin, which was used in the previous communication[1], increase along the curve I of Fig. 1. Saturation of the reaction is very good and about 0.35 atom nitrogen was introduced per methoxyl group after one to two days nitrogen content remaining constant even after prolonged reaction. Detailed analytical values are listed in the table.

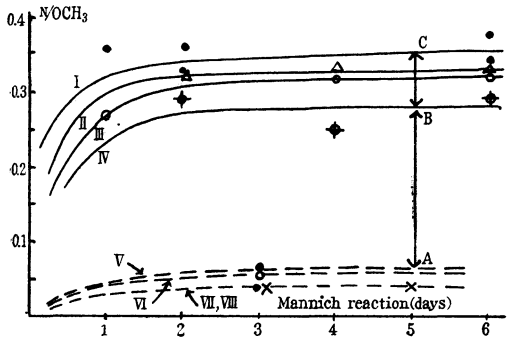

Fig. 1. N/OCH_3 values of thiolignin preparations after Mannich reaction with dimethylamine (D) or with piperidine (P). I Thiolignin (D), II Raney-Ni (D), III $NaBH_4$ (D), IV Sulphonation (D), V CH_2N_2 (D), VI $NaBH_4$, CH_2N_2 (P), VII CH_2N_2 (P), VIII Dioxanelignin CH_2N_2 (P).

Analytical Values of the Thiolignin Treated with Mannich Reaction.
(Analyzed in perchlorate form)

Reaction (days)	0	1	2	6
C%	61.33	55.12	56.36	56.51
H%	5.64	5.44	6.21	6.24
MeO%	15.31	12.56	13.05	12.95
S%	2.42			
N%	0.0	2.02	1.91	2.02
			2.10	2.22
N/MeO%	0.0	0.356	0.323	0.345
			0.356	0.379

Curves II and III, which show the N/MeO values of the thiolignin reduced with Raney alloy or with sodium borohydride respectively, followed by the treatment with Mannich reaction, are almost the same as Curve I. Curve IV is for the thiolignin sulphonated at neutral pH. This curve is lower than the Curves I, II or III. The difference BC seems to be due to the sulphonation of benzyl alcoholic group with phenolic hydroxyl group in its para position.

When thiolignin is once methylated with diazomethane, nitrogen must not be introduced by Mannich reaction. Curve V is for thiolignin methylated with diazomethane. Curves VI, VII and VIII are the N/MeO values of the thiolignin, thiolignin reduced with sodium borohydride and of the dioxane lignin used in the preceeding communication, after treating them with Mannich reaction using piperidine instead of dimethylamine. AB, obtained by subtracting this, so to say, blank value from the N/MeO value for the sulphonated thiolignin, corresponds to the amount of the nitrogen introduced to the unsubstituted fifth position and to the first position by displacing the carboxyl group.

As can be seem from the Fig. 2, the content of the phenolic hydroxyl group and the carboxyl group of the thiolignin used in these experiments are 0.4 and 0.18 per methoxyl group. Although it is unknown, how much of the carboxyl group has phenolic hydroxyl group in its para position, we may be allowed to assume, that about a half of the total carboxyl group has phenolic hydroxyl group in the para position, as the

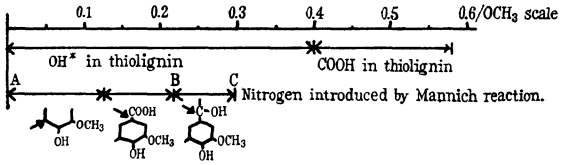

Fig. 2. Relation between the content of OH* and COOH groups thiolignin and the amount of nitrogen introduced by Mannich reaction.

thiolignin contains 0.4 phenolic hydroxyl group per methoxyl group, i.e. about one phenolic hydroxyl group per every two building units. If so, about one half of the total carboxyl group, i.e. 0.09 carboxyl group, may be displaced with dimethylaminomethyl group with Mannich reaction. Subtracting this amount from AB=0.22, the amount of the guaiacyl nucleus having no C–C bond at the fifth position may be obtained, the amount being calculated as 0.13 per methoxyl group. Admitting some uncertainty concerning the amount of the carboxyl group having free phenolic hydroxyl group in its para positon, it will be concluded that about 25–40% of the phenolic hydroxyl group of the thiolignin belongs to the simple guaiacol nucleus having no C–C bond at its fifth position.

Mannich Reaction on Lignin Model Compounds

Vanillin gives 5-dimethylaminomethyl vanillin (V) almost quantitatively by Mannich reaction with dimethylamine after one day. With piperidine, 5-piperidinomethyl vanillin (VI) was obtained in good yield. The structure of (V) was confirmed by synthesizing from it 5-formylvanillin (VII). At first, we attempted to lead (V) to (VII) with Thesing's method[8], i.e. to convert (V) to its methiodide (VIII) and then to oxidize the methiodide with nitrobenzene and phenylhydroxylamine to (VII). Although the methiodide was obtained in very good yield, the subsequent oxidation was unsuccessful. Snyder's method[9] was then attempted and found to be successful. 5-dimethylaminomethyl vanillin was reacted with hexamine in acetic acid and the product was hydrolyzed with water. 5-formylvanillin was obatined in the yield of 20%, which gave 5-carboxyvanillin with silver oxide oxidation, according to Pearl[10]. 5-Formylvanillin has been synthesized, according to Pearl, by nitrobenzene oxidation of 5-propenylvanillin, but the method was not so simple. Our method seems to be very convenient to synthesize 5-formylvanillin.

8) J. Thesing, *Ber.*, 87, 507 (1954).
9) H. Snyder, S. Swaminathan and H. Sims, *J. Am. Chem. Soc.*, 74, 5110 (1952).
10) I. Pearl, ibid., 74, 4263 (1952).

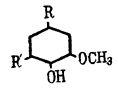

R	R′
V –CHO	$-CH_2N(CH_3)_2$
VI –CHO	$-CHN(CH_2)_5$
VII –CHO	–CHO
VIII –CHO	$-CH_2N(CH_3)_3I$
IX $-COCH_3$	H
X $-COCH_2CH_3$	H
XI $-COCH_3$	$-CH_2N(CH_3)_2$
XII $-COCH_2CH_3$	$-CH_2N(CH_3)_2$
XIII $-CH_2CH_2CH_2$	H
XIV $-CH_2CH_2CH_2$	$-CH_2N(CH_3)_2$
XV $-CH_2SO_3\,\frac{1}{2}\,Ba$	H
XVI $-CH_2SO_3\,\frac{1}{2}\,Ba$	$-CH_2N(CH_3)_2$
XXI $-CH_2N(CH_3)_2$	$-OCH_3$
XXII $-CH_2N(CH_3)_2$	$-CH_2N(CH_3)_2$
XXIII $-CH_2OH$	$-CHN(CH_2)_5$
XXIV $-CHN(CH_2)_5$	$-CHN(CH_2)_5$

Acetovanillone (IX) and propiovanillone (X) gave 5-dimethylaminomethyl derivatives (XI) and (XII) respectively. Although it is known that some methylene group adjacent to carbonyl group reacts under some condition of Mannich reaction, Mannich base derived from acetovanillone (XI) was iodoform test positive (existence of -COMe) and Millon reaction negative (nonexistence of phenolic hydroxyl group with unsubstituted ortho position) and the Mannich base derived from propiovanillone (XII) was Millon reaction negative. As the iodoform tests of (V) and (XII) were negative and Millon reaction of (V) was negative and those of vanillyl sulphonic acid (XV) and guaiacol were positive, these color reactions seem to be effective for Mannich bases, too. The side chains of acetovanillone and propiovanillone may, therefore, remain intact during the Mannich reaction.

Propylguaiacol (XIII) and vanillyl sulphonic acid (XV) gave also 5-dimethylaminomethyl derivatives (XIV) and (XVI) in good yield under the same condition. Divanillyl monosulphide (XVII) gave Mannich base (XVIII) with two dimethylaminomethyl groups at its two unsubstituted fifth positions.

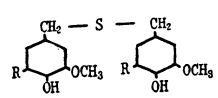

XVII R=H
XVIII R=$CH_2N(CH_3)_2$

Mannich base (XX) derived from dihydro-dehydro-diisoeugenol (XIX) could not be obtained in crystalline form, but the analytical values of the perchlorate, obtained as a glassy substance, revealed that one dimethylaminomethyl group was introduced to the substance. As can be seen from the Fig. 3,

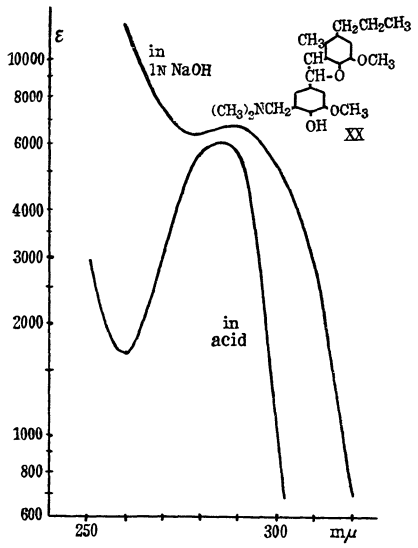

Fig. 3. UV-absorption spectra of the Mannich base obtained from Dihydro-dehydro-diisoengenol in acidic and alkaline media.

the UV-absorption spectrum of the Mannich base is very similar to that of the starting material and it is concluded, from the difference of its alkaline spectrum and acidic spectrum, that the base is a monovalent phenol. For that reason, it may be concluded, that the phenyl-coumaran structure remains intact during the reaction and the dimethylaminomethyl is introduced only to the unsubstituted fifth position.

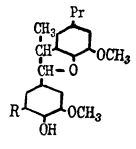

XIX R=H
XX R=$CH_2N(CH_3)_2$

Syringic acid gave Mannich base (XXI) with simultaneous decarboxylation of the carboxyl group. This base was converted to syringaldehyde by the Snyder's method, which was mentioned before. The yield of the syringaldehyde was rather low, but if it is possible to increase the yield by changing the reaction condition, this method may provide a very convenient way to synthesize syringaldehyde from gallic acid.

Mannich reaction with dimethylamine on vanillyl alcohol gave, after one day, picrate of Mannich base melting at 164-5°, with dimethylamino groups both at the fifth position and at the position of the methylol group (XXII). With piperidine, only the fifth position reacted even after four days, the picrate having the m. p. 153–4° (XXIII) being obtained. The yield was good in both cases.

With dimethylamine, vanillic acid gave Mannich base (XXII) having the m. p. of the picrate 164–5° after six days, which was found to be the same with the picrate obtained from vanillyl alcohol. The reaction must, therefore, involve the substitution under replacement of the carboxyl group, as well as the substitution at the fifth position. After only one day a picrate having the m. p. 175.5–176.5° was obtaind. No structural formula having the same analytical values with this compound was however found.

Mannich reaction with piperidine on vanillic acid during four days gave mannich base (XXIV) with simultaneous decarboxylation and substitutions at the fifth position and the position of the carboxyl group, the m. p. of the picrate being 204.5–5.5°. Mannich reaction during one day gave this picrate and that having the m. p. 209–210°. No structural formula for the latter picrate corresponding to the analytical values was however found. The structure of this unknown picrate seems to be analogous with that having the m. p. 175.5–176.5° obtained with dimethylamine.

Experimental

Mannich Reaction on Vanillin with Dimethylamine.—A mixture of vanillin (18.3 g.), 25% dimethylamine (64.8 ml.) and 30% formaldehyde (30 ml.) was set aside overnight, concentrated repeatedly in order to expel dimethylamine by adding water and then concentrated nearly to dryness. The separated yellowish-colored crystal was recrystallized from normal butanol. Product from the first recrystallization gave correct m.p. 138–139°, 15 g.

Anal. Found: C, 63.28; H, 7.14. Calcd. for $C_{11}H_{15}O_3N$ (V): C, 63.14; H, 7.23%.

The yield of the melting point pure picrate, obtained by adding picric acid to the reaction mixture obtained in the same reaction condition as above, was 95%, m.p. of the picrate 190.5–192°.

Anal. Found: C, 46.5; H, 4.18; N, 13.0; MeO, 7.32. Calcd. for $C_{17}H_{18}O_{10}N_4$ (picrate of V): C, 46.6; H, 4.12; N, 12.8; MeO, 7.08%.

Perchlorate, m.p. 207–208°.

Anal. Found: C, 42.81; H, 5.11; N, 4.47; Cl, 11.52. Calcd. for $C_{11}H_{16}O_7ClN$ (perchlorate of V): C, 42.8; H, 5.18 N, 4.53; Cl, 11.3%.

Mannich Reaction on Vanillin with Piperidine.—Vanillin (18.3 g.), acetic acid (200 ml.), piperidine (30 ml.) and 30% formalin (30 ml.) were mixed and allowed to stand at room temperature overnight. Acetic acid was distilled off in vacuo, sulphuric acid (20 g.) diluted with water added, and the acetic acid was expelled as completely as possible. An appropriate amount of a dilute sodium hydroxide solution was added to make piperidine and the reaction product free, and the mixture was concentrated. The separated reaction product, which is contaminated by inorganic salt, was filtered, extracted with hot benzene, the benzene solution dried, and the product was crystallized from the benzene solution by adding ligroin and keeping in a refrigerator. After reprecipitation from its benzene solution by ligroin, the slightly brownish-colored 5-piperidinomethyl vanillin melted at 127–128.5°, 16.2 g.

Anal. Found: C, 67.30; H, 7.50. Calcd. for $C_{14}H_{20}O_3N$ (VI): C, 67.44; H, 7.68%.

Perchlorate, m.p. 212–213.5°C.

Anal. Found: C, 48.26; H, 5.58; N, 4.02; Cl 10.15; MeO, 9.28. Calcd. for $C_{14}H_{20}O_7NCl$ (perchlorate of VI): C, 48.2; H, 5.73; N, 4.02; Cl 10.0; MeO, 8.94%.

Picrate, m.p. 163–164°.

Anal. Found: C, 50.2; H, 4.60; N, 11.7. Calcd. for $C_{20}H_{22}O_{10}N_4$ (picrate of VI): C, 50.2; H, 4.60; N, 11.7%.

5-Dimethylaminomethyl Vanillin Methiodide.—5-Dimethylaminomethyl vanillin was shaken with methyl iodide, set aside over-night, petroleum ether added and the product was filtered. The iodide, m.p. 188–192° decomp., which was obtained nearly quantitatively, was dissolved in ethanol, which contained a little water, precipitated with ether, the m.p. being raised to 200–201° (decomp.).

Anal. Found: C, 40.97; H, 5.04; N, 3.76. Calcd. for $C_{12}H_{18}O_3NI$ (VIII): C, 41.0; H, 5.12; N, 3.99%.

Synthesis of 5-Formylvanillin from 5-Dimethylaminomethyl Vanillin.—A mixture of 5-dimethylaminomethyl vanillin (4.3 g.), hexamethylenetetramine (3.0 g.) and acetic acid (13 ml.) was boiled for five minutes, poured into water (130 ml.) and extracted repeatedly with ether. The etherial extract was shaken with dil. NaOH and the alkaline extract was acidified with dil. acid and kept in a refrigerator overnight. The separated crystal (0.8 g.), which melted at 115–118°, was filtered and recrystallized from xylol-ligroin, the m.p. being raised to 120–122° after one recrystallization

Anal. Found: C, 60.0; H, 4.35. Calcd. for $C_9H_8O_4$ (VII): C, 60.0; H, 4.4%.

5-Formylvanillin thus obtained gave 5-carboxyvanillic acid, m.p. 176–177°, by silver oxide oxidation according to Pearl[10].

Anal. Found: C, 50.66; H, 3.85. Calcd. for $C_9H_8O_6$: C, 50.9; H, 3.8%.

Mannich Reaction on Acetovanillone with Dimethylamine.—One gram of acetovanillone was dissolved in 25% dimethylamine (8 ml.), and 35% formalin (4 ml.) was added and the mixture was kept at room temperature overnight. Water was added and the picrate was precipitated by adding an alcoholic solution of picric acid. 3.3 g. of crude picrate, m.p. 166–170°, thus obtained, was recrystallized from 70% alcohol to give 2.0 g. of the pure picrate melting at 175–176°, yield 73.5%.

Anal. Found: C, 48.17; H, 4.63; N, 12.1. Calcd. or $C_{18}H_{20}O_{10}N_4$ (picrate of XI): C, 47.8; H, 4.43; N, 12.4%.

Mannich Reaction on Propioguaiacone with Dimethylamine.—Propioguaiacone (1 g.), synthesized according to Nakazawa[11], was dissolved in 25% dimethylamine (4 ml.), and 35% formalin (2 ml.) was added and the mixture was kept at room temp. overnight. Water was added and the picrate was precipitated by adding an alcoholic solution of picric acid. 3.3 g. of crude picrate, m.p. 155–157°, thus obtained, was recrystallized from 70% alcohol to give 2.2 g. of pure picrate melting at 160.5–161.5°, yield 85%.

Anal. Found: C, 49.33; H, 4.99; N, 11.8. Calcd. for $C_{19}H_{22}O_{10}N_4$ (picrate of XII): C, 49.0; H, 4.72; N, 12.0%.

Mannich Reaction on Cörulignol with Dimethylamine.—Cörulignol (XIII) (1 g.) was dissolved in 25% dimethylamine (4 ml.), and 35% formalin (2 ml.) was added and the mixture was kept at room temperature overnight. Water was added and the solution was acidified with dilute hydrochloric acid and extracted with ether. An alcoholic solution of picric acid was added in excess to the aqueous solution and the picrate, which separated as an oil was rubbed with a little amount of toluene to give 2.5 g. of crude picrate, m.p. 116–119°. 2.0 g. of the pure picrate was obtained from propyl alcohol, m.p. 120–121° yield, 74%.

Anal. Found: C, 50.7; H, 5.44; N, 12.6. Calcd. for $C_{19}H_{24}O_9N_4$ (picrate of XIV): C, 50.5; H, 5.31; N, 12.4%.

Mannich Reaction on Vanillyl Sulphonic Acid with Dimethylamine.—Barium salt of vanillyl sulphonic acid (0.5 g.) was dissolved in a mixture of 25% dimethylamine (2 ml.) and 35% formalin (1 ml.), and the mixture was kept at room temperature overnight, poured into alcohol and the precipitated barium salt was washed well with alcohol and analyzed.

Anal. Found: C, 37.40; H, 5.02; N, 3.87; S, 9.6; Ba, 20.7, Calcd. for $C_{11}H_{16}O_5NS\frac{1}{2}Ba$ (XVI): C, 38.55; H, 4.67; N, 4.08; S, 9.32; Ba, 19.9%.

Mannich Reaction on Divanillyl Monosulphide (XVII) with Dimethylamine.—Divanillyl monosulphide synthesized previously[12] (1.0 g.) was dissolved in a mixture of 25% dimethylamine (8 ml.) and 35% formalin (4 ml.), and kept at room temperature for four days. The solution was diluted with water, acidified with dilute hydrochloric acid and the separated starting material (0.3 g.) was recovered by filtration. Alcoholic solution of picric acid was added to the filtrate, and the picrate precipitated as an oil was washed with water and crystallized with alcohol to give 1.4 g. of pure picrate, melting at 179–180°.

11) K. Nakazawa, *J. Pharm. Soc. Japan*, **74**, 836 (1954).

12) H. Mikawa, This Bulletin, **27**, 50 (1954).

0.3 g. of the melting point pure picrate was recovered from the mother liquor, total yield 1.7 g.

Anal. Found: C, 46.63; H, 4.69. Calcd. for $C_{34}H_{36}O_{18}SN_{10}$ (picrate of XVIII): C, 46.5, H, 4.35%.

Mannich Reaction on Dihydro-dehydro-diisoeugenol (XIX) with Dimethylamine.—Dihydro-dehydro-diisoeugenol (0.2 g.) was dissolved in a mixture of 25% dimethylamine (0.4 ml.), 35% formalin (0.2 ml.) and 70% alcohol (1 ml.) and kept at room temperature overnight. On adding water to the solution, white precipitate separated, and this dissolved completely when dilute hydrochloric acid was added. Perchlorate was separated by perchloric acid, which did not crystallize.

Anal. Found: C, 57.99; H, 7.14; N, 3.06. Calcd. for $C_{23}H_{31}O_4N \cdot HClO_4$ (perchlorate of XX): C, 56.9; H, 6.59; N, 2.88%.

Mannich Reaction on Syringic Acid with Dimethylamine.—Syringic acid (1.5 g.) was dissolved in a mixture of 25% dimethylamine (6 ml.) and 35% formalin (3 ml.), was kept for four days at room temperature, diluted with water (100 ml.), and acidified with 2N hydrochloric acid; then an alcoholic solution of picric acid was added. The alcohol was distilled off in vacuo, and the separated picrate was filtered and washed with water. The crude picrate (3.2 g.) was recrystallized from aqueous alcohol to give 2.0 g. of melting point pure picrate, yield 60%.

Anal. Found: C, 46.55; H, 4.56; N, 12.60. Calcd. for $C_{17}H_{20}O_{10}N_4$ (picrate of XXI): C, 46.36; H, 4.58; N, 12.72%.

Syringaldehyde from 5-Dimethylaminomethyl-1, 3-Dimethylpyrogallol (XXI).—One gram of the picrate was dissolved in 50% aqueous acetone, passed through a column of an ion exchange resin IR 400 in bicarbonate form, acetone and water were distilled off in vacuo and the free base thus obtained was dissolved in the mixture of acetic acid (1.5 ml.) and hexamethylenetetramine (0.32 g.). The mixture was heated in an oil bath (115°) for five minutes, water was added and the mixture was extracted with ether. From the ether extract 50 mg. of melting point pure syringaldehyde was obtained by sublimation, yield 13%.

Mannich Reaction on Vanillyl Alcohol with Dimethylamine.—A mixture of vanillyl alcohol (1 g.), 25% dimethylamine (12 ml.) and 35% formalin (6 ml.) was kept at room temperature overnight, diluted with water, acidified and the picrate was precipitated with an alcoholic solution of picric acid. The precipitate was washed with water and recrystallized from aqueous alcohol to give 0.9 g. of pure dipicrate, melting at 164–165°.

Anal. Found: C, 42.26; H, 4.47; N, 16.2, 16.0. Calcd. for $C_{25}H_{29}O_{16}N_8$ (picrate of XXII): C, 42.1; H, 4.16; N, 16.1%.

Mannich Reaction on Vanillyl Alcohol with Piperidine.—Vanillyl alcohol (0.5 g.) was dissolved in a mixture of piperidine (0.8 ml.), 35% formalin (1 ml.) and alcohol (2 ml.), and the solution was kept at room temperature for four days, diluted with water, and acidified with dilute hydrochloric acid; alcoholic solution of picric acid was added and concentrated in vacuo. The separated crystalline picrate was recrystallized from aqueous alcohol to give 1.0 g. of pure picrate melting at 153–154°.

Anal. Found: C, 49.60; H, 5.12; N, 11.60. Calcd. for $C_{20}H_{24}O_{10}N_4$ (picrate of XXIII): C, 50.0; H, 5.0; N, 11.65%.

Mannich Reaction on Vanillic Acid with Dimethylamine.—Vanillic acid (1.1 g.) was dissolved in a mixture of 25% dimethylamine (4 ml.) and 35% formalin (2 ml.), and kept at room temperature for six days. The solution was poured into 10 ml. of water and acidified with dil. hydrochloric acid. Alcoholic solution of picric acid was added and the alcohol was evaporated in vacuo. The separated picrate was recrystallized from aqueous alcohol, m.p. 165.5–167°. No melting point depression was observed on admixture with the picrate XXII, m.p. 164–166°, obtained from vanyllyl alcohol. Marked melting point depression was observed, however, on admixture with the picrate, m.p. 175.5–176.5°, which was obtained by Mannich reaction on vanillic acid during only one day. Yield 2.7 g.

The crude picrate obtained at the same reaction conditions but after only one day gave a picrate, m.p. 175.5–176.5°, after recrystallization from dilute alcohol. From the mother liquor 0.2 g. of the same substance was further recovered. Total 0.95 g. No other substances were obtained. (Found: C, 45.21; H, 4.48; N, 11.73%). No structural formula corresponding to these analytical values was found.

Mannich Reaction on Vanillic Acid with Piperidine.—Vanillic acid (1.1 g.) was dissolved in a mixture of piperidine (1.7 ml.), 35% formalin (2 ml.), water (3.3 ml.) and alcohol (4 ml.), and kept at room temperature overnight, poured into water and an alcoholic solution of picric acid was added. On recrystallization of the crude picrate from dilute alcohol, two different picrates having m.p. 204.5–205.5° and 209–210° were obtained. The former one, 1 g., which is comparatively sparingly soluble needles, was analyzed as follows.

Anal. Found: C, 47.5; H, 4.57; N, 14.1. Calcd. for $C_{31}H_{36}O_{16}N_8$ (picrate of XXIV): C, 47.9; H, 4.64; N, 14.4%.

The latter picrate, 1 g., which is comparatively easily soluble, showed the following analytical values, but no structural formula having these values were found

(Found: C, 43.11, 43.88, 43.72; H, 3.51, 3.49, 3.74; N, 13.65, 12.83; MeO, 4.5%).

This picrate with unknown structure disappeared when the Mannich reaction was performed four days at the same condition, picrate having the m.p. 204.5–205.5°, XXIV, being the only product obtained. Yield, 1.6 g.

Mannich Reaction on Thiolignins.—Various thiolignin preparations used in this communication are the same with those prepared in the previous communication[1]. When dimethylamine was used, 0.5 g. of lignin was dissolved almost completely in a mixture of 25% dimethylamine (4 ml.) and 35% formalin (2 ml.), and set aside at room temperature. When piperidine was used, 0.2 g. of lignin was dissolved in 2 ml. of piperidine solution (a mixture of piperidine (5 ml.), 35% formalin (6 ml.) and alcohol (12 ml.)), and the solution was

kept at room temperature. After the reaction, the solution was poured into an excess of 2N hydrochloric acid, and the coagulated lignin was filtered and washed with water. The lignin was then dissolved in a little amount of acetone, poured into a dilute solution of perchloric acid and the precipitated lignin was filtered and washed with perchloric acid. The precipitate was redissolved in acetone and reprecipitated with perchloric acid in the same manner. After the lignin was washed well with perchloric acid, it was washed with water, ether-alcohol 1: 1, ether and then with petroleumether.

Summary

Mannich reactions on many lignin model compounds revealed that 1) model compounds of type (I) give without exception Mannich base with substituent at fifth position in very high yield, 2) those of type (II) do not react, 3) carboxyl group having phenolic hydroxyl group to its para position is split off as carbon dioxide and dimethylaminomethyl group is introduced to the same position, 4) methylol group having phenolic hydroxyl group to its para position reacts with dimethylamine resulting in the formation of dimethylaminomethyl group at the same position, 5) other groups remain intact even when phenolic hydroxyl group exists in para position, and 6) no reaction occurs when the phenolic hydroxyl group is etherified.

By applying the Mannich reaction with dimethylamine on thiolignin, it has been concluded that about 25–40% of the phenolic hydroxyl group of thiolignin belongs to the simple guaiacol nucleus of type (I) having no C–C bond at its fifth position, admitting some uncertainty concerning the amount of carboxyl group having free phenolic hydroxyl group in its para position.

The authors are indebted to Dr. H. Okada, the head of the laboratory and to Miss. S. Suehiro for their encouragement.

Research Laboratory of the Kokusaku Pulp Co., 184, 1-chome, Kamiochiai, Shinjuku-ku Tokyo

Studies on the Cooking Mechanism of Wood. XVI[1]. *On the Mechanism of Kraft Cooking*

By Hiroshi MIKAWA, Koichiro SATO, Chizuko TAKASAKI and Kiyo EBISAWA

(Received October 5, 1955)

Hydrogen Sulphide Cooking of α-Guaiacyl Propanol

Hägglund and Enkvist found that the lignin in wood combines with sulphur, when the wood is cooked by a neutral aqueous solution of hydrogen sulphide at 100°[2]. This so-called hydrogen sulphide cooking was thought by them to represent the initial reaction of the ordinary kraft cooking. It was shown by us, that the sulphur, introduced to lignin by the hydrogen sulphide cooking, combined with the so-called X group of the lignin[3], a group which was most easily sulphonatable by a neutral sulphite solution. The structure of this group is now believed to be benzyl alcohol or benzyl ether group with free phenolic hydroxyl group in its para position[3,4]. It is, therefore, very important for the elucidation of the mechanism of the kraft cooking reaction, to investigate the behavior of the model compounds for the X group toward hydrogen sulphide cooking. Among others[5], only vanillyl alcohol (I), *p*-hydroxybenzyl alcohol (II) and its ethers are investigated in some detail by Enkvist[6] and ourselves[7]. It has been shown, that they gave the corresponding monosulphide (III, IV) and disulphide (V), while recently Zentner[8] reported that α-guaiacyl propanol (VI) gave only its dehydrated product, isoeugenol, under the condition of the ordinary

1) Part XV, This Bulletin, **29**, 259 (1956).
2) a) E. Hägglund, *Svensk Papperstidn.*, **44**, 183 (1941); b) T. Enkvist, M. Moilanen and B. Alfredsson, *Svensk Papperstidn.*, **52**, 517 (1949).
3) H. Mikawa, K. Sato, C. Takasaki and H. Okada, *J. Chem. Soc. Japan* (*Ind. Sect.*), **54**, 299 (1951); H. Mikawa, ibid., 651.
4) B. Lindgren, *Acta Chem. Scand.*, **5**, 603 (1951).
5) T. Enkvist and M. Moilanen, *Svensk Papperstidn.*, **55**, 668 (1952).
6) T. Enkvist and M. Moilanen, *Svensk Papperstidn.*, **52**, 183 (1949).
7) H. Mikawa, This Bulletin **27**, 50. 53 (1954).
8) T. Zentner, *Tappi.*, **36**, 517 (1953)

hydrogen sulphide cooking. It seemed, therefore, to be quite important to reinvestigate the propanol with special attention to the sulphur containing reaction products, if any.

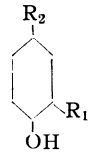

	R_1	R_2
I	OCH_3	$-CH_2OH$
II	H	$-CH_2OH$
VI	OCH_3	$-CH(OH)C_2H_5$
IX	OCH_3	$-CHO$
X	OCH_3	$-CH_2SH$
XI	OCH_2	$-CHS$

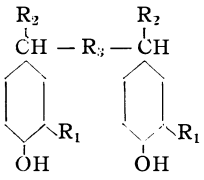

	R_1	R_2	R_3
III	OCH_3	H	$-S-$
IV	H	H	$-S-$
V	OCH_3	H	$-S-S-$
VII	OCH_3	$-C_2H_5$	$-S-S-$
VIII	OCH_3	$-C_2H_5$	$-S-$

Reaction products obtained from the α-guaiacyl propanol by the hydrogen sulphide cooking at 100° during six hours, gave four spots by paper chromatography, those of unreacted propanol, bis-(1-(4-hydroxy-3-methoxyphenyl)-1-propyl) disulphide (VII), bis-(1-(4-hydroxy-3-methoxyphenyl)-1-propyl) monosulphide (VIII) and some unknown compound. The separation of these compounds in larger scale was performed by developing the product adsorbed on a Florizil column with benzene. The disulphide, thus separated, showed no melting point depression on admixture with the product synthesized according to Zentner[8]. The monosulphide was separated as dibenzoate and its structure was determined from the analytical values and the molecular weight measured according to Rast's method.

Thus confirming the formation of mono- and disulphide also from α-guaiacyl propanol, the mechanism of the formation of monosulphide and disulphide from *p*-hydroxybenzyl alcohols by hydrogen sulphide cooking discussed in the previous communication[7] seems to be applicable in general.

Alkaline Decomposition of Vanillyl Monosulphide (III)

The sulphur introduced to lignin by hydrogen sulphide cooking was partly split off by the treatment with alkali at 160°[2b,9], resulting in a formation of thiolignin with rather low content of sulphur, thus explaining why the sulphur content of the thiolignin isolated from the black liquor of the industrial cooking was comparatively low.

Enkvist investigated the behavior of vanillyl disulphide (V) against alkali, as the model for the "hydrogen sulphide lignin". He confirmed the fact that the disulphide sulphur was split as hydrogen sulphide, resulting in a formation of vanillin[2b]. The stability of the disulphide sulphur of this model compound was, however, much lower than the sulphur contained in the hydrogen sulphide lignin. The alkaline decomposition of 4,4'-dihydroxydibenzyl monosulphide (IV) and of vanillyl monosulphide (III), synthesized by us, was investigated previously very briefly[7]. The latter compound was investigated also by Enkvist spectroscopically[10]. These monosulphides were found to be much more stable against hot alkali than the disulphide, although they also split sulphur as hydrogen sulphide just as in the case of vanillyl disulphide and hydrogen sulphide lignin. As it seems to be very important to know the decomposition products of the vanillyl monosulphide against hot alkali, the behaviour of this compound was investigated rather precisely in the present communication.

Vanillyl monosulphide was decomposed with 5% alkali and the products were examined by paper chromatography. A spot for the starting monosulphide was too strong even after heating for six hours at 120° as yet and the decomposition condition of three hours at 130° was found to be suitable for the investigation of the products. The chromatogram was not so simple, and the materials which were isolated as crystals and identified by mixed melting point determinations, were unreacted starting monosulphide, vanillin and vanillyl alcohol. By comparing the chromatogram with that of the products of the alkaline decomposition of vanillyl alcohol alone, however, almost all of the unidentified spots were found to be due to the secondary reaction products of vanillyl alcohol. Only one spot remained

9) T. Enkvist, *Svensk Papperstidn.*, **51**, 225 (1948); T. Enkvist and E. Hägglund, *Festskr. J. A. Hedvall*, 149 (1948).

10) J. Lindberg and T. Envist, *Societas Scientiarum Fennica Commentationes Physico-Mathematicae* (1953), XVII, 4.

unidentified, which corresponded to the direct decomposition product of the vanillyl monosulphide. The decomposition proceeds, therefore, as follows: $III \rightarrow IX + I + (I)_x + SH^-$.

As stated above, Enkvist investigated spectroscopically the decomposition of vanillyl monosulphide at 100°. Comparing the UV-absorption spectrum of vanillyl monosulphide and its decomposition products and from the vanillin odor of the product, he assumed that some amount of vanillin may be formed by the alkaline decomposition of the monosulphide. From the fact that the adsorption maximum of the monosulphide at 284 mμ shifts 4 mμ to the shorter wave-length side after the alkaline decomposition, he pointed out also the possibility that the monosulphide was degraded to smaller molecules, possibly to vanillyl alcohol or to vanyllyl mercaptan. From these considerations he assumed the mechanism of the decomposition of the monosulphide as follows: $2III \rightarrow X + I + XI$, $XI \rightarrow IX + SH^-$.

In so far as the reaction products are concerned, the mechanism agrees rather well with our findings. The fact that both monosulphide and disulphide, the products of the hydrogen sulphide cooking of the model compounds for the X-group, gave vanillin when decomposed with hot alkali, suggests to us that thiolignin contains carbonyl group at the same position, where the X-group was situated before the cooking.

On the Mechanism of the Kraft Cooking and the Structure of the Thiolignin

It was pointed out at first by Kullgren[11], that the combination of sulphur and lignin was the main reason why wood was delignified much more easily by the kraft cooking process than by the soda process. At the beginning of the ninteen forties, Hanson, Brauns and Ahlm investigated the sulphur atoms contained in the ordinary thiolignin, recovered from the black liquor[12]. All of them though that it was in the form of mercaptan. Hägglund and Enkvist, however, made clear that thiolignin contained mainly only monosulphide (thioether) sulphur[2]. They also showed that the sulphur contained in the hydrogen sulphide lignin was in monosulphide and disulphide form[2] and that this sulphur was partly split off by alkali at 160° resulting in the formation of the ordinary thiolignin.

As stated previously, it was shown by us that the sulphur introduced to lignin by the hydrogen sulphide cooking combined with the X-group of lignin[3] and the hydrogen sulphide cooking of the model compounds for the X-group were investigated in the present paper and by Enkvist[5,6] and ourselves[7]. They gave monosulphide and disulphide just as in the case of the hydrogen sulphide cooking of lignin. The alkaline decomposition of these compounds was also investigated not only in this paper but also by them[6,7,10] and it was found that the monosulphide sulphur was much more stable than the disulphide sulphur, although both of them were split as hydrogen sulphide. The behaviour of the hydrogen sulphide lignin against alkali was thus confirmed with the model compound.

The second important reaction involved in the kraft cooking process is the alkaline cleavage of the arylether linkages in the lignin. The content of the phenolic hydroxyl group of alkali lignin and thiolignin has been investigated by Marshall et al.[13], Brauns[14], Enkvist[15] and ourselves[16]. According to our data, the phenolic hydroxyl group of the lignin in situ, 0.14/CH_3O as was reported in Part XIII of this series, increased to 0.4/CH_3O[16] after the kraft cooking, thus confirming the marked increase of the phenolic hydroxyl group during the digestion.

The cleavage of the ether linkage of lignin accompanies the degradation of its molecular size. The molecular weight of alkali lignin and thiolignin has been measured by a number of authors[17]. Almost all values are less than 1000 and some of them are so small as 400–500. The molecular weight determination of alkali lignin and thiolignin by the Rast method was investigated by us and it was concluded that the measurement must be made with the methylated or acetylated samples[18]. By this method, molecular weight distribution curves for alkali lignin and thiolignin were obtained and it was found that the molecular weight concentrated mainly around 1000 and 1500[19]. Enkvist reports also that the molecular weight lies

11) C. Kullgren, *Papierfabrikant*, **24**, 20 (1926).

12) F. Hanson, *Paper Trade J.*, **112**, No. 2, 32 (1941); F. Brauns, ibid., **111**, No. 14, 33 (1940); C. Ahlm, ibid., **113**, No. 13, 115 (1941).

13) H. Marshall, F, Brauns and H. Hibbert, *Can. J. Res.*, **13** B, 103 (1935).

14) F. Brauns and W. Grimes, *Paper Trade J.*, **108**, No. 11, 40 (1939).

15) T. Enkvist and B. Alfredsson, *Svensk Papperstidn.*, **54**, 185 (1951).

16) H. Mikawa, K. Sato, C. Takasaki and K. Ebisawa, This Bulletin, **29**, 254 (1956).

17) Y. Hachihama and S. Jodai, "Chemistry of Lignin", Nihonhyronsha, Tokyo (1946), p. 270; R. Glover and J. Bain, *Can. J. Res.*, **14** B, 65 (1936); Y. Hachihama and S. Jodai, *J. Soc. Chem. Ind. Japan*, **52**, 306 (1949); F. Lahey and J. Merewether, *Australian J. Sci. Res. Ser. A.*, **1**, 112 (1948).

18) H. Mikawa and H. Okada, *J. Chem. Soc. Japan, (Ind. Sec.,)* **54**, 239 (1951).

19) H. Mikawa, ibid., 150, 152.

mainly between 1000–1500[9].

The structure of the side chain of thiolignin has not been much investigated, especially in connection with the mechanism of the sulphidation of lignin and the subsequent splitting of the sulphur once introduced at the beginning of the kraft cooking by alkali. This problem was discussed rather precisely in the previous communication[16], and the existence of the carbonyl group and the double bond conjugated

Summarizing these findings mentioned above, one may be allowed to formulate the mechanism of the kraft cooking as follows (cf. Fig. 1): (1) At the beginning of the cooking, the X-group of the lignin in wood (XIV) reacts with sodium sulphide to give mercaptan (XV). The mercaptan reacts rapidly with the other hydroxyl group of the lignin to give monosulphide (XVI), while it is partly oxidized with some group of the lignin to the disulphide group (XVII). The

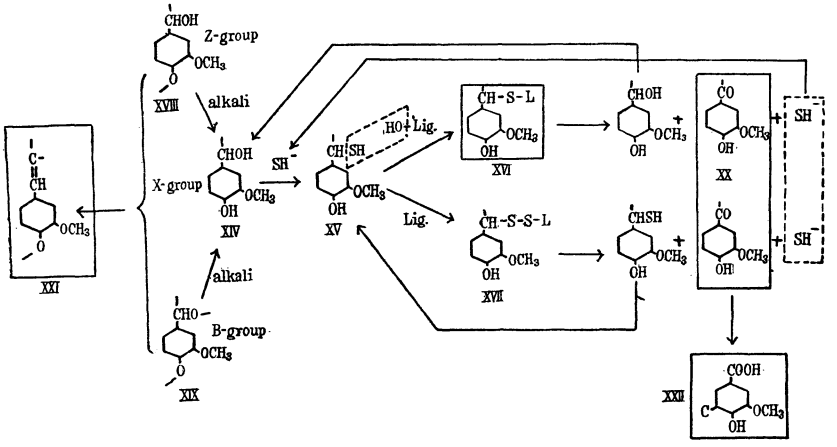

Fig. 1. Reactions of lignin during the kraft cooking.

with the benzene nucleus and the carboxyl group directly attached to the nucleus was concluded, and the mechanism involved in the formation of these group was also discussed.

The nuclear structure of thiolignin was investigated rather precisely by Richtzenhain[20] and also by us in the previous communication[1]. Richtzenhain proved the existence of the nuclei of type XII and XIII and showed the increase of the proportion of the latter nucleus during the kraft cooking. We showed that the proportion of XII(R_2=H) and XIII(R_2=H) was about 25–40% and 75–

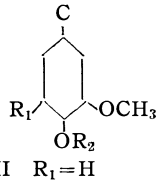

XII R_1=H
XIII R_1=–C

60%, indicating that the nuclei belonging to the latter type increase a little during the cooking. This problem has been thoroughly discussed in the previous communication[1].

lignin isolated at this stage is the hydrogen sulphide lignin obtained by the hydrogen sulphide cooking of wood. Until this stage, only the X-group enters into reaction and the sulphur contained in the hydrogen sulphide lignin is in both monosulphide and disulphide form.

(2) Next, the temperature rises in the presence of alkali and the cleavage of the ether linkage occurs. This cleavage of the ether linkage occurs also at the Z-group (XVIII) and B-group (XIX), resulting in a formation of the X-group, which reacts further to give monosulphide and disulphide just as in the case of (1). This cleavage of the ether linkage causes the splitting of the lignin molecule and the increase of the content of the phenolic hydroxyl group.

(3) At the same time, the disulphide group (XVII) is decomposed very easily with hot alkali to give the mercaptan, regenerating SH^- ion. A certain amount of carbonyl group conjugated with the nucleus (XX) is also formed. Monosulphide group (XVI) is much more stable than the disulphide group, but it is also partly decomposed with hot alkali to give carbonyl group (XX) at its position, while partly regenerating the X-

20) H. Richtzenhain, *Svensk Papperstidn.*, 53, 644 (1950).

group and the SH^- ion.

(4) X, Z (XVIII) and B-groups (XIX), which are taking part in such complex reactions mentioned above, are on the other hand partly dehydrated by hot alkali to give double bond conjugated with the nucleus (XXI). The carbonyl group (XX) thus formed is converted partly to the carboxyl group (XXII) directly connected to the nucleus. Condensation reaction occurs to some extent at the same time resulting in an increase of the amount of the nuclei having C–C bond at the fifth position adjacent to the phenolic hydroxyl group.

(5) During these complicated reactions most of the very reactive X, Z and B-groups are kept in combination with sulphur, especially in the most stable monosulphide form. These groups are thus protected from the undesired condensation reason tion during the cooking. This is the main reason why the delignification is easier in kraft cooking than in the soda cooking. Thus, ultimately, thiolignin with a small amount of sulphur mainly in the form of the stable monosulphide having the molecular weight of about 1000–1500 dissolves out in alkali due to its carboxyl group and phenolic hydroxyl group.

Experimental

Hydrogen Sulphide Cooking of α-Guaiacyl Propanol (VI).—Hydrogen sulphide was bubbled through a Clark-Lubs buffer solution (100 ml.) (50 g. of KH_2PO_4 and NaOH in one liter of water, pH 7) until the concentration of hydrogen sulphide reaches 0.36 N, α-guaiacyl propanol (3 g.) added and the mixture was rotated in a stainless autoklave (150 ml.) for six hours at 100° in an oil bath.

The solution was extracted exhaustively with ether, ether was expelled, and the residue (3 g.) was tested chromatographically on a strip of the Toyo filter paper No. 50 buffered with Clark-Lubs buffer solution at pH 7 using benzene-petroleum ether 1:1 as a mobile phase. Four spots were observed by diazotized sulphanilic acid at Rf 1.0, 0.90, 0.79 and 0.52, of which the weak spot at Rf 0.52 was of the unreacted α-guaiacyl propanol.

The residue was kept in a refrigerator for two weeks and the separated crystal was filtered, washed with a mixture of benzene and petroleum ether and recrystallized from the same solvent mixture, m.p. 112–114.5°, 100 mg., Rf=0.79. This crystal did not show any melting point depression on admixture with the bis(1-(4-hydroxy-3-methoxyphenyl)-1-propyl) disulphide (VII), m.p. 115–116°, synthesized according to the method of Zentner[8].

Anal. Found: C, 61.58; H, 6.77; S, 16.32. Calc. for $C_{20}H_{26}O_4S_2$ (VII): C, 61.0; H, 6.59; S, 16.21%.

The filtrate from the crystal was concentrated, dissolved in benzene, adsorbed on a Florizil column (diameter 17 mm., length 270 mm.), developed at first with benzene, and the eluate was tested by paper chromatography. After the first fraction with Rf=1.0, 0.61 g., the second fraction, a mixture of two substances with Rf=0.90 and 0.79, 2.1 g., was obtained by eluting the column with a mixture of benzene and alcohol 9:1. The column was then washed with alcohol and a small amount of the third fraction consisting of only unreacted α-guaiacyl propanol was obtained.

The first fraction was crystallized as a benzoate having m.p. 154–155° from alcohol, 0.25 g. The analyses and the molecular weight obtained by the Rast method agree with the corresponding valueus of the dibenzoate of bis(1-(4-hydroxy-3-methoxyphenyl)-1-propyl) monosulphide (VIII).

Anal. Found: C, 71.4; H, 6.13; S, 5.7; OCH_3, 11.2; molecular weight (Rast), 630. Calc. for $C_{34}H_{34}O_6S$ (dibenzoate of VIII): C, 71.2; H, 5.93; S, 5.6; OCH_3, 10.8%; molecular weight, 574.6.

The second fraction containing the disulphide and an unknown compound with Rf=0.90 was not investigated further. The sulphur content of the fraction, 10.37%, was rather high.

Decomposition of Vanillyl Monosulphide (III) with Hot Sodium Hydroxide Solution.—Vanillyl monosulphide (1.5 g.) was dissolved in 5% sodium hydroxide (75 ml.), kept at 130° for three hours in an autoklave with nitrogen atmosphere, acidified with sulphur dioxide and extracted with ether. From the aqeous solution 2,4-dinitrophenyl hydrazone having m.p. 255–257° was obtained, 0.24 g. After recrystallization from dioxane the hydrazone did not show any melting point depression on admixture with the authentic vanillin 2,4-dinitrophenyl hydrazone.

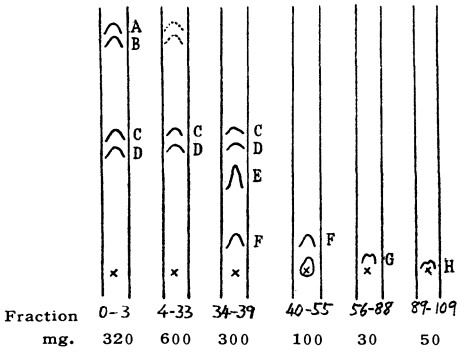

Fig. 2. Paper chromatograms of the products of alkaline decomposition of vanillyl monosulphide separated into 109 fractions by Al_2O_3 adsorption chromatograph, B: Vanillyl monosulphide, H; Vanillyl alcohol, D: ?, A, C, E, F, G: Secondary products of vanillyl alcohol.

The ether extract was concentrated, dissolved in benzene, adsorbed on a column of alumina (a mixture of 330 g. of active alumina and 33 g. of cellite, diameter 30 mm., length 580 mm.), developed with benzene and separated into 109 fractions. Paper chromatograms of these fractions are shown in Fig. 2. From the fractions O-3 vanillyl monosulphide was separated and identified

by mixed melting point determination, 100 mg. Fractions 89–109 contain only vanillyl alcohol, 50 mg. These chromatograms were compared with that of the product obtained by treating the vanillyl alcohol with sodium hydroxide just in the same condition as in the case of the vanillyl monosulphide and it was found that the spots A, C, E, F and G were those of the secondary products produced from the vanillyl alcohol by alkali. Although the substance corresponding to the spot D seemed to be the direct fission product of the vanillyl monosulphide, it was impossible to isolate it, as the intensity of C was very strong. Yield; recovered monosulphide 7%, vanillin 8%, vanillyl alcohol 4%. Almost all of the remaining part consisted of secondary products from vanillyl alcohol.

Summary

1. Hydrogen sulphide cooking of α-guaiacyl propanol (VI) gave bis(1-(4-hydroxy-3-methoxyphenyl)-1-propyl) monosulphide (VIII) and disulphide (VII).

2. Vanillyl monosulphide was decomposed with alkali at 130°. Vanillin, vanillyl alcohol and the secondary products from vanillyl alcohol were identified.

3. The mechanism of the kraft cooking process was discussed and a new mechanism was proposed.

The authors wish to express their gratitude to Dr. H. Okada, the head of the laboratory, and to Miss S. Suehiro for their encouragement.

Research Laboratory of the
Kokusaku Pulp Ind. Co., Ltd.
184, 1-Chome, Kamiochiai
Shinjuku-ku, Tokyo

Heats of Dilution of Polystyrene Solutions. I

By Kazuo AMAYA and Ryoichi FUJISHIRO

(Received September, 19, 1955)

Introduction

It is well known that entropy plays an important role in defining thermodynamical behaviours of high polymer solutions. Enthalpy has also a great significane as an interaction parameter between polymer and solvent.

Enthalpy can be obtained from the temperature dependence of osmotic pressure or vapor pressure of polymer solutions, and such experiments were reported by various authors[1,2,3,4,5], but the data calculated from their results are not accurate. Direct measurements of heat of dilution of polymer solutions were reported by a few authors[6,7,8] but their results had a considerable error in the range of concentrations where the heat changes are small.

It is thought that a more accurate measurement of heat of dilution of various polymer solutions has a great significance in explaining the thermodynamical behaviours of polymer solutions.

We constructed a calorimeter using thermister capable of measuring temperature change down to 0.5×10^{-4}°C (0.003 cal.) and measured the heats of dilution of three polystyrene solutions, using toluene, ethylbenzene and chloroform as solvents.

Experimental

Apparatus and Procedure.—The calorimeter. The calorimeter, similar to those described by Gee[9] and Meares[7], but different from them in using a thermister, was constructed and is shown in Fig. 1.

A is an unsilvered Dewar vessel 21 cm. long and 3.5 cm. in inner diameter. A double bulb, consisting of the inner bulb B and the outer bulb C, is the mixing bulb. The polymer solution S to be diluted was introduced into the outer bulb C from a pipette with a long delivery tube which reached to the bottom through the inner bulb B, and was separated by a pool of mercury F from the solvent S′ which is in the inner bulb B. To minimize the evaporation loss of the solvent from the outer bulb a rubber ring D which was fixed to the inner bulb was fitted tightly with the

1) G. Gee and W.J.C. Orr, *Trans. Faraday Soc.*, **42**, 507 (1946).
2) M.J. Newing, ibid., **46**, 613 (1950).
3) C.E.H. Bawn, R.F.J. Freeman and A.R. Kamaliddin, ibid., **46**, 677 (1950).
4) M.J. Schick, P. Doty and B.H. Zimm, *J. Am. Chem. Sec.*, **72**, 531 (1950).
5) C.E.H. Bawn and M.A. Wajid, *J. Polymer Sci.*, **12**, 109 (1954).
6) J. Ferry, G. Gee and L.R.G. Treloar, *Trans. Faraday Soc.*, **41**, 340 (1945).
7) P. Meares, ibid., **47**, 699 (1951).
8) H. Tompa, *J. Polymer Sci.*, **8**, 51 (1953).

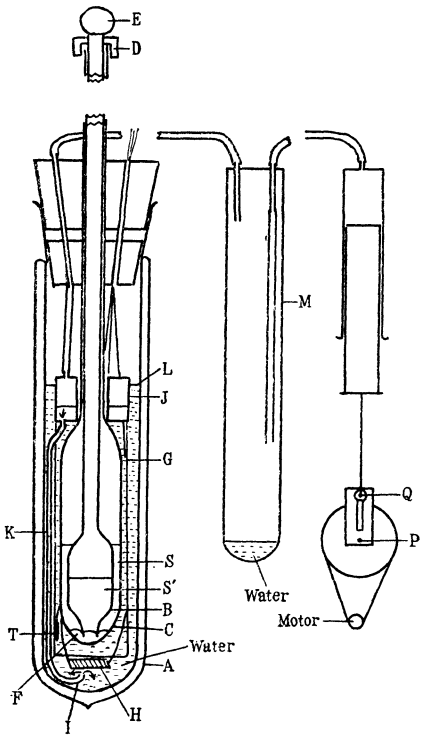

Fig. 1.

outer bulb. The inner bulb was closed by a rubber cap E at the top.

By raising the inner bulb and then moving it up and down in the solution, the solution was moved up and down through the aperture between the inner bulb and the outer bulb, and the mixing was performed. The polymer solution was fairly viscous, and sufficient mixing could not be achieved by only rotating the inner bulb.

The mixing bulb fitted centrally through a rubber bung into the Dewar vessel A filled with water up to the level L indicated in the diagram. A stirrer fitted with an injector was devised. The piston of the injector was connected to a rod R at Q which was rotated around the pivot P at a speed 20 r.p.m.. The volume of the air pumped in and out of the injector during a cycle was controlled by adjusting the distance between P and Q.

The exit of the injector was connected, through the water vapor saturator M, 270 cc. in volume, acting also as a temperature moderator, to a copper tube J in the Dewar vessel. J is a coaxial copper tube the inner tube of which was fitted loosely to C having holes at the upper and the bottom. To the hole at the bottom was connected a rubber tube K, the other end I of which reaches to the bottom of the Dewar vessel. By the motion of the piston of the injector the water in J going in and out through the rubber tube K and the water in the Dewar vessel was stirred.

To ensure immediate attainment of the thermal equilibrium, a piece of copper plate G, which almost covers the outer bulb C was connected to J. The calorimeter and the saturator were immersed in the water thermostat at 25°C kept constant to $\pm 1\times10^{-4}$°C.

The temperature changes were measured with a thermister T having about 400 KΩ in resistance and a temperature coefficient of −5.5 percent at 25°C. The heat capacity of the calorimeter was determined by introducing measured amounts of electrical energy through the constantan heater H having resistance of about 37 Ω. An electrical current passing through the heater was measured by a precision type m.A. meter, and the time during which the electrical current was passed was measured with a stop watch.

Various kinds of thermometer systems employing a thermister were tried. The most simple one, combining a low resistance thermister and a galvanometer was proved to be unsatisfactory because of the effect of self-heating of the thermister. The one employing a.c. Wheatstone bridge with a high resistance thermister and a.c. vacuum tube amplifier was quite satisfactory to eliminate the self-heating, but the adjustment of 2 components, namely resistance and capacitance was very cumbersome in the actual operation. The following was finally adopted.

The block diagram of the resistance measuring unit adopted is shown in Fig. 2. Unbalanced d.c. voltage across the Wheatstone bridge was converted to 30 c/s a.c. voltage by a converter driven by 30 c/s oscillator. The converter was made of a permanent dynamic speaker and was shown in Fig. 3. Converted signals were fed to a narrow band amplifier and to a phase sensitive detector. The output was detected by a μA meter

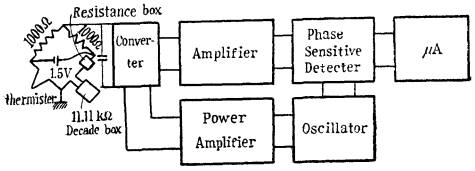

Fig. 2

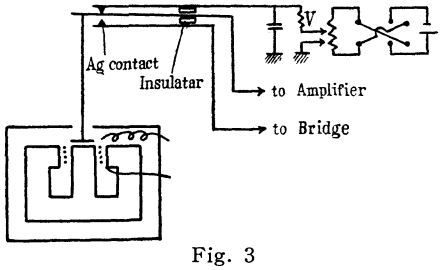

Fig. 3

and the resistance reading was performed by adjusting the resistance of the Wheatstone bridge so that the meter deflection returns to its zero point. The arms of the Wheatstone bridge were immersed in the thermostat except the 11.11 KΩ decade box.

The electrical circuits of the narrow band amplifier employing two twin-T. bridge is shown in Fig. 4. The phase sensitive detector is the same as that described by Schuster[9]. The oscillator and the driver of the converter are shown in Fig. 5 and Fig. 6 respectively.

1 Ω change in resistance can be detected. The resistance of the thermister is about 400 KΩ and

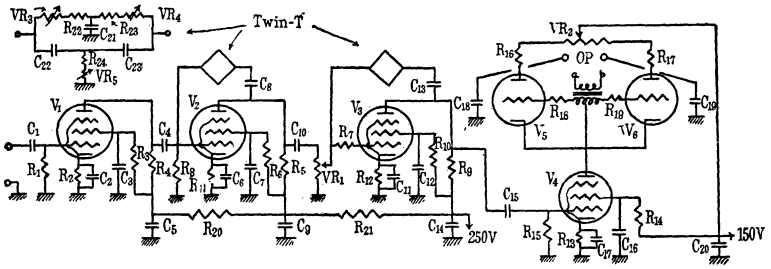

Fig. 4

R_1	100 KΩ	R_{16}	20 KΩ	C_2	100 μF	C_{16}	10 μF
R_2	2 KΩ	R_{17}	20 KΩ	C_3	2 μF (oil)	C_{17}	100 μF
R_3	1 MΩ	R_{18}	30 KΩ	C_4	0.1 μF	C_{18}	20 μF
R_4	500 KΩ	R_{19}	30 KΩ	C_5	20 μF	C_{19}	20 μF
R_5	500 KΩ	R_{20}	100 KΩ	C_6	100 μF	C_{20}	20 μF
R_6	1 MΩ	R_{21}	100 KΩ	C_7	3 μF	C_{21}	0.04 μF
R_7	2 MΩ	R_{22}	250 KΩ	C_8	0.1 μF	C_{22}	0.02 μF
R_8	2 MΩ	R_{23}	250 KΩ	C_9	20 μF	C_{23}	0.02 μF
R_9	500 KΩ	R_{24}	125 KΩ	C_{10}	0.1 μF	V_1	6SH7
R_{10}	1 MΩ	VR_1	1 MΩ	C_{11}	100 μF	V_2	6SH7
R_{11}	2 KΩ	VR_2	10 KΩ	C_{12}	3 μF	V_3	6SH7
R_{12}	2 KΩ	VR_3	100 KΩ	C_{13}	0.1 μF	V_4	6SH7
R_{13}	150 Ω	VR_4	100 KΩ	C_{14}	20 μF	V_5	1/2 6SN7
R_{14}	50 KΩ	VR_5	50 KΩ	C_{15}	0.1 μF	V_6	1/2 6SN7
R_{15}	500 KΩ	C_1	0.1 μF				

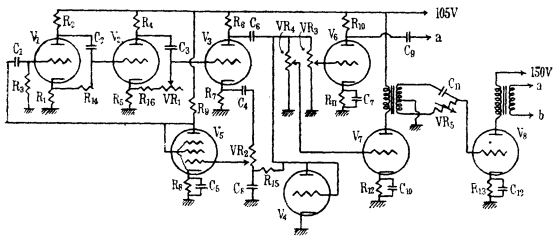

Fig. 5

R_1	1 KΩ	C_1	0.1 μF
R_2	1 KΩ	C_2	0.05 μF
R_3	1 MΩ	C_3	0.05 μF
R_4	2 KΩ	C_4	0.1 μF
R_5	2 KΩ	C_5	100 μF
R_6	20 KΩ	C_6	0.1 μF
R_7	4 KΩ	C_7	100 μF
R_8	300 Ω	C_8	2 μF
R_9	100 KΩ	C_9	0.1 μF
R_{10}	50 KΩ	C_{10}	100 μF
R_{11}	1 KΩ	C_{11}	0.02 μF
R_{12}	1 KΩ	C_{12}	100 μF
R_{13}	1 KΩ	V_1	1/2 6SL7
R_{14}	130 KΩ	V_2	1/2 6SL7
R_{15}	1 MΩ	V_3	1/2 6SL7
R_{16}	100 KΩ	V_4	1/2 6SL7
VR_1	50 KΩ	V_5	6BD6
VR_2	1 MΩ	V_6	1/2 6SN7
VR_3	500 KΩ	V_7	1/2 6SN7
VR_4	500 KΩ	V_8	6J5
VR_5	500 KΩ		

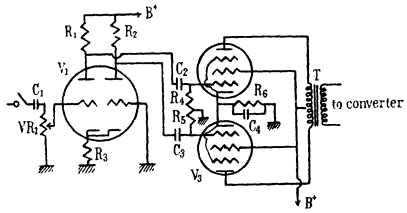

Fig. 6

R_1	100 KΩ	C_1	0.1 μF
R_2	100 KΩ	C_2	0.1 μF
R_3	1 KΩ	C_3	0.1 μF
R_4	250 KΩ	C_4	100 μF
R_5	250 KΩ	V_1	6SL7
R_6	210 Ω	V_2	UZ42
VR_1	500 KΩ	V_3	UZ42

the temperature coefficient is about −5.5 percent at 25°C and thus it corresponds to about $1/2\times10^{-4}$ degree.

Very little amounts of polarization in the thermister, probably due to the ions present, were observed. But the experiments were not affected, for the measurements were carried out after the polarization had been saturated. Thermoelectromotive force in the bridge circuit was cancelled by adjusting a variable resistor V in Fig. 3. Methods of Operation. After setting the calorimeter in the thermostat regulated at $25\pm1\times10^{-4}$°C, temperature of the calorimeter was adjusted

9) N.A. Schuster, *Rev. Sci. Inst.*, 22, 254 (1951).

almost equal to that of the thermostat by heating. It was then left for three to five hours in order to establish the thermal equilibrium.

The resistance reading was started after the calorimeter had reached thermal equilibrium. After mixing the solution and the solvent, the resistance reading was taken at an interval of one minute for about twenty minutes and a cooling curve was constructed. The heat change was always complete in two or three minutes. The heat capacity was determined for each run by introducing a certain amount of electrical energy which produces approximately equal resistance change to that in the mixing. The mixed solution was stirred manually by moving the inner bulb up and down from 10 times to 30 times according to the viscousness of the mixed solution until no inhomogeneity of the solution was observed. A stirring correction for the mixing was obtained by stirring the already mixed solution by the same standard technique as that employed in the mixing.

During the stirring, heat was developed and was quite reproducible in the cases of toluene and ethylbenzene, both having fairly low vapor pressure at 25°C. In the case of chloroform, however, reproducibility was not so satisfactory. This may be as-cribed to the fact the latter solvent has a fairly high vapor pressure at 25°C, and evaporates during the stirring and its amount is irregular because of the manual operation.

Materials.—A sample of Polystyrene* was prepared by polymerizing the monomer in carbon tetrachloride. This sample was purified by dissolving in benzene and precipitating with methanol. The same procedure was repeated twice and dried for about a week under the pressure of 1 mmHg.

The solvents used were purified according to the method described in the literature and finally distilled. Toluene, ethylbenzene** and chloroform used were fractions having boiling point 110.8–111.2°C, 135.5–136.0°C and 61.1–61.2°C respectively.

Results and Discussion

The heat of dilution was measured by adding 5 or 10 cc. of solvent successively to the solution of a definite concentration. The results obtained are shown in Table I.

Assuming that the heat of mixing is represented by the van Laar form, the heat of mixing H_m of solvent of volume V_0 and polystyrene of volume V_r can be represented as:

$$H_m=\alpha V_0V_r/(V_0+V_r), \quad (1)$$

where α is a constant describing the interaction between solute and solvent. Accordingly, when the solvent of volume dV_0 is added to this solution, its heat of dilution is given by:

$$dH_d=(\partial H_m/\partial V_0)_p dV_0=[\alpha V_r^2/(V_0+V_r)^2]\cdot dV_0. \quad (2)$$

Thus, the integral heat of dilution ΔH_0 obtained when the solvent of the volume ΔV_0 is added to this solution is given by:

$$\Delta H_0=\int dH_d=\int_{V_0}^{V_0+\Delta V_0}[\alpha V_r^2/(V_0+V_r)^2]dV_0. \quad (3)$$

Assuming that α is constant within a small

TABLE I

HEAT OF DILUTION OF POLYMER SOLUTION

	Before dilution V cc.	v_r	After dilution V' cc.	v_r'	Heat evolved cal.	$-\alpha_d$	$-\alpha_{av}$	$-\mu$
1. Polystyrene-toluene system.								
1	4.70	0.189	9.70	0.092	0.099	1.14		
	9.70	0.092	14.70	0.060	0.035	1.26	1.37	0.24
	14.70	0.660	19.70	0.045	0.025	1.82		
2	4.70	0.170	9.70	0.083	0.106	1.51		
	9.70	0.083	14.70	0.055	0.037	1.64	1.51	0.27
	14.70	0.055	19.70	0.041	0.014	1.29		
3	9.70	0.083	14.70	0.055	0.037	1.64	1.51	0.27
	14.70	0.055	19.70	0.041	0.016	1.41		
2. Polystyrene-chloroform system.								
1	4.75	0.275	9.75	0.134	0.234	1.28		
	9.75	0.134	14.75	0.088	0.122	1.29	1.36	0.17
	14.75	0.088	19.75	0.066	0.046	1.58		
2	4.70	0.171	9.70	0.083	0.081	1.11	1.13	0.14
	9.70	0.083	14.70	0.055	0.028	1.25		
3. Polystyrene-ethylbenzene system.								
	4.75	0.194	9.75	0.081	0.002	0.02	0.00	0.00
	9.75	0.081	14.75	0.053	−0.002	−0.07		

* We are indebted to Prof. T. Matsumoto of the Faculty of Technology of our University for this sample.

** We wish to thanks Dr. H. Yoshida of the Government Industrial Research Institute, Osaka, for supplying purified ethylbenzene.

concentration range (of course it is generally concentration dependent), we can express (3) as follows:

$$\Delta H_0 = -\alpha[V_r^2/(V_0+\Delta V_0+V_r) - V_r^2/(V_0+V_r)] \quad (4)$$

If we introduce the quantities V, V', v_r and v_r' defined as:

$V_0+V_r=V$ (Total volume of solution before dilution),
$V_0+\Delta V_0+V_r=V'$ (Total volume of solution after dilution),
$v_r=V_r/(V_0+V_r)$ (Volume fraction of polymer before dilution),
$v_r'=V_r/(V_0+\Delta V_0+V_r)$ (Volume fraction of polymer after dilution),
the above expression can be written as follows:

$$\Delta H_0 = \alpha(Vv_r^2 - V'v_r'^2). \quad (5)$$

The amount of polystyrene in the solution is the same before and after the dilution. Then (5) can be written as:

$$\Delta H_0 = \alpha V_r(v_r - v_r'). \quad (6)$$

Plotting ΔH_0 obtained from the experiment as ordinate and v_r as abscissa for each of three systems, we obtain a straight line in each case in the concentration range from 0.2 to 0.05 volume fractions. As an example, H_0-v_r diagram of the polystyrene-toluene system is shown in Fig. 7.

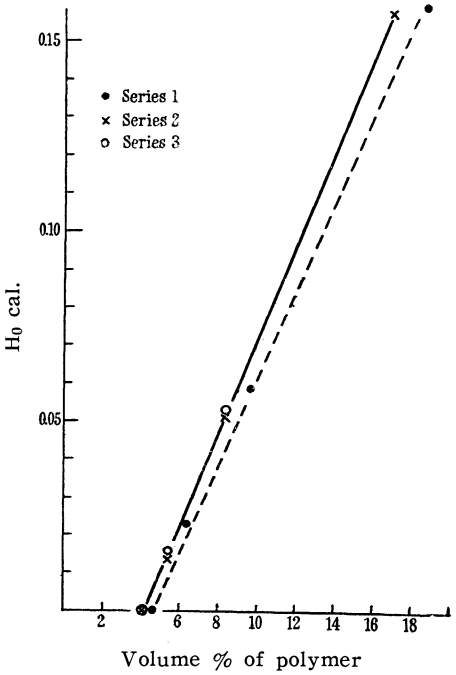

Fig. 7. Polystyrene—Toluene Solution.

α can be obtained from the tangent of the straight line in the diagram and its value for each system is given in Table I as $\alpha_{av.}$ Using (5), α at each concentration can be evaluated and the values thus obtained are represented as α_d. From these α values, μ can be derived by the equation, $\mu=\overline{V}\alpha/RT$, where $\overline{V}$ is the partial molal volume of the solvent, and shown in Table I.

For the sake of comparison with these data, the heat of mixing and the heat of dilution of ethylbenzene, which may be regarded as a monomer unit of polystyrene, with toluene and chloroform were also measured and the results are shown in Table II. From these

TABLE II
HEAT OF DILUTION OF MONOMER-UNIT (ETHYLBENZENE) SOLUTION

	Before dilution V cc.	v_r	After dilution V' cc.	v_r'	Heat evolved	$-\alpha_m$	$-\alpha_d$
1. Ethylbenzene-toluene system.							
1	5	1.000	10	0.500	0.206	0.08	
	10	0.500	15	0.333	0.098	0.09	0.20
	15	0.333	20	0.250	0.070	0.10	0.17
2	3	1.000	6	0.500	0.124	0.08	
	6	0.500	9	0.333	0.074	0.10	0.15
2. Ethylbenzene-chloroform system.							
	2	1.000	4	0.500	5.619	5.62	
	4	0.500	6	0.333	2.030	5.74	6.09
	6	0.333	8	0.250	1.135	5.86	6.81
	8	0.250	10	0.200	0.653	5.90	6.53
	10	0.200	12	0.167	0.243	5.81	3.65
	12	0.167	17	0.116	0.343	5.68	3.47

data α values were calculated by the same procedure as in the polystyrene under the assumption that the equations (1) and (5) can also be applied. These values are shown in Table II as α_m and α_d respectively.

It is interesting that the interaction parameters between polymer and solvents have the same signs as those between monomer unit of polymer (ethylbenzene) and that the polymer-monomer unit system is athermal. That the polymermonomer unit system is athermal was confirmed by Meares[7] in the polyvinylacetateethylacetate system.

It is expected that α or μ for the polymer-solvent system is smaller in magnitude than that for the monomer unit-solvent system owing to the self-contact between polymer segments. But for the polystyrene-toluene system the reverse was observed. From this fact it is expected that there are some anomalous phenomena which might be explained by measuring the volume change or the changes of other physical properties on mixing for this system.

TABLE III

COMPARISON WITH THE DATA OBTAINED BY VARIOUS METHOD

1. Polystyrene-toluene system.

Observer	Method	$-\mu$	Temperature °C	Volume fraction	D.P.
Tompa[8]	a	0.10–0.17	25	0.25–0.40	17–30
Bawn et al[3]	b	0–0.01	25–55	0.003–0.009	$(1.5–3)\times10^3$
Doty et al[4]	b	0.17–0.04	27–69	0.01–0.08	540
Schulz[10]	b	0.09–0.05	15–40	0.01–0.03	90
Schulz et al[11]	b	0.03–0.04	20–42	0.03	$(2.3–5.8)\times10^3$
This experiment	a	0.24–0.27	25	0.04–0.19	275
2. Polystyrene-chloroform system.					
Bawn et al[3]	b	0	25–55	0.2–0.6	$(1.5–3)\times10^3$
Schulz et al[11]	b	0.02	20–42	0.03	$(2.3–5.8)\times10^3$
This experiment	a	0.14–0.17	25	0.05–0.27	275

Method a: Direct measurement.
b: From the temperature dependence of osmotic pressure or vapor pressure.

Our results are compared with the previous data obtained by various methods, and shown in Table III. For the chloroform-polystyrene system, it is found that the μ value is negative and large. This is consistent with the fact that chloroform is a good solvent for polystyrene. That the μ value obtained by Bawn and Wajid[5] from the temperature dependence of vapor pressure was zero, is in marked contrast to our result.

A direct measurement of heat of dilution for the toluene-polystyrene system was carried out by Tompa[8]. His value was the same in sign but different in magnitude. The degree of polymerization of the sample used by him was from 17 to 30, but our sample had a degree of polymerization of about 275. From the μ values obtained for various samples of different polymerization degree, ($\mu=-0.27$ for D.P.$=275$, -0.17 for 17 to 30, -0.03 for 1) it seems that an apparent correlation exists between the μ value and the polymerization degree. But for a definite conclusion, further investigation will be needed.

Summary

A calorimeter equipped with a thermister capable of measuring the temperature change down to 0.5×10^{-4}°C was constructed. By this apparatus the heats of dilution of three polystyrene solutions were measured and the values of interaction parameters were derived. The μ values for toluene solution and chloroform solution were both negative and large, but that for ethylbenzene solution was zero.

In order to compare with the polymer solution, the heat of mixing of ethylbenzene, which may be regarded as the monomer-unit of polystyrene, with same solvents were also measured and it was found that the interaction parameters of polymer solutions have the same signs as that of the corresponding monomer-unit solutions.

We should like to express our gratitude to Professor Y. Morino of Tokyo University and Professor A. Kotera of Tokyo University of Education for there kind encouragement and discussions throughout the work. We are also greateful to Mr. K. Suzuki for his helpful discussions.

Department of Chemistry, Faculty of Science, Kobe University, Kobe

10) G.V. Schulz, *Z. physikal. Chem.*, A 180, 1 (1937).
11) G.V. Schulz und H. Hellfritz, *Z. Elektrochem.*, 57, 835 (1953).

Studies on the Supplementary Reduction in Oscillographic Polarography

By Hideo IMAI

(Received August 8, 1955)

A supplementary kink was found in the oscillographic potential-time curve of the metal ion such as Cd^{++} which exists in a neutral solution containing the dissolved oxygen. Vogel[1] was the first who reported the phenomenon, which was more recently assigned to a sudden decomposition of a metal hydroxide by Behr and Chodkowski[2].

In this paper are presented the results of detailed studies of the phenomenon by means of a current-potential oscillographic polarograph and a proposal of a new mechanism of the effect.

Experimental

The technique of the oscillographic current-potential curve introduced by Ševčik[3] was used with some modifications[4]. The arrangement is illustrated in Fig. 1. The cell used was a H-cell with double partitions made with sintered glass disks, and a supporting electrolyte solution was instilled in a compartment between a test solution and a saturated calomel electrode. Thus, the contamination of a test solution by chloride ion was avoided.

To prepare all test solutions reagent grade chemicals were recrystallized twice from their aqueous solutions.

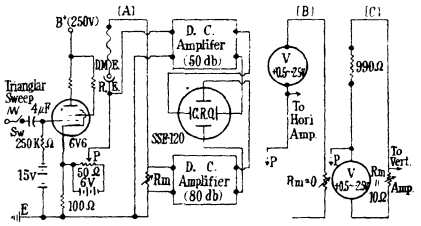

Fig. 1. Schematic diagram of measuring apparatus. (A) polarographic circuit, (B) and (C) calibrating circuit for horizontal and vertical deflection, respectively.

In the solution of Pb^{++}, Zn^{++}, Bi^{+++}, Al^{+++}, or Fe^{+++} no reproducible current was observed, owing to the irregular fluctuation of the lifetime of the D. M. E. (Sometimes it amounts to a variation as large as 10% of the mean life time.). Accordingly, Cd^{++} in N KCl was used for the quantitative measurements. The possible experimental error in measuring the polarographic current amounts to ±3%[5].

Results

1. Influence of the Dissolved Oxygen.— In an ordinary polarography the reduction of the metal ion such as Cd^{++} in a neutral

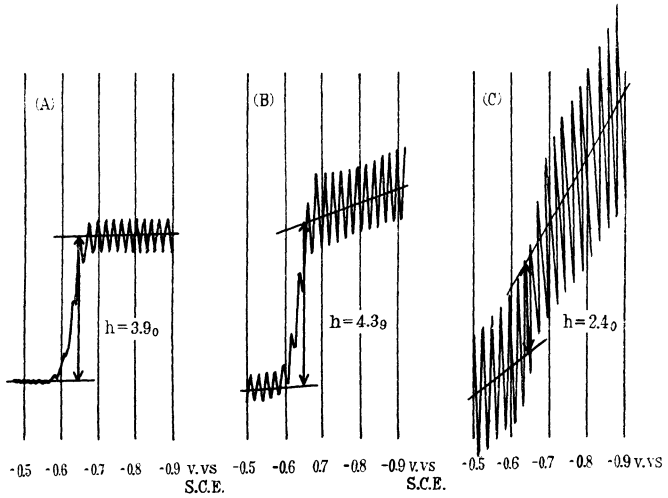

Fig. 2. Ordinary polarogram of $5 \cdot 3 \cdot 10^{-4}$ M/l. Cd^{++} in 0.5 N KCl (s=1/20, 24.6° C). (A) deaerated soln., (B) test soln. contg. atm. oxygen, (C) test soln. contg. conc. oxygen.

1) J. Vogel, Proc. 1st Intern. Polarog. Congr., Part III, 731 (1951); *C.A.*, **47**, 11030 (1953).
2) B. Behr and J. Chodkowski, *Rozniki Chem.*, **26**, 650 (1950); *C.A.*, **48**, 3816 (1954).
3) A. Sevcik, *Collection Czechoslov. Chem. Communn.*, **13**, 349 (1948).
4) M. Shinagawa, H. Imai and S. Chaki, *J. Electrochem. Soc. Japan*, **23**, 132, 187 (1955).
5) H. Imai, *J. Electrochem. Soc, Japan*, **23**, 530 (1955).

medium gives the current-potential curve irreversible to some degree. The limiting current increases as the concentration of oxygen increases. However, the presence of oxygen in its high concentration results in the reduction of the diffusion controlled current. The typical polarograms of these cases are illustrated in Fig. 2.

In the oscillographic current-potential polarogram a reduction peak and a reoxidation peak can be observed in the cathodic and anodic branches, respectively. Dissolved oxygen being present in a neutral Cd^{++} solution, the normal reduction peak, i. e. the reduction peak of an aquo cadmium ion, is lowered and it accompanies a supplementary reduction peak, while no remarkable change is observed in the anodic branch as is illustrated in Fig. 3.

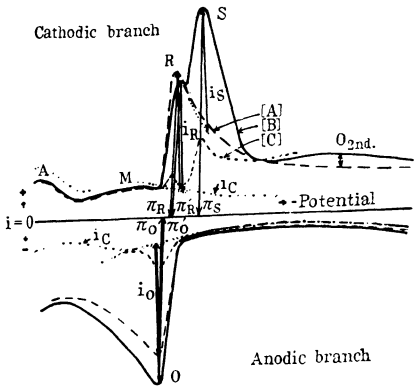

Fig. 3. Oscillographic polarogram of 1.10^{-3} M/l Cd^{++} in N KCl (20 c.p.s., v= 50 v/s): Full curve, interrupted curve and dotted curve correspond to (A), (B) and (C) of Fig. 2, respectively.

This effect can be observed not only in a multi-sweep method, but also in a single sweep method. As the concentration of the dissolved oxygen increases, at first the normal reduction peak lowers and, on the contrary, the supplementary reduction peak increases attaining a maximum value, then all peaks begin to decrease simultaneously, being extinguished ultimately.

Since, the shift of the initial sweep voltage toward more positive potential elongates the duration of the first oxygen reduction, the influence of the dissolved oxygen can be best realized by changing the initial sweep voltage.

The plot of the relation between the peak height and the initial sweep voltage is illustrated in Fig. 4. When the initial sweep voltage is shifted toward more positive potentials, at first the supplementary reduction peak remarkably increases and it amounts to a limiting value at −0.05 volts vs. S. C. E., which coincides with the half wave patential of the first oxygen reduction in N KCl*.

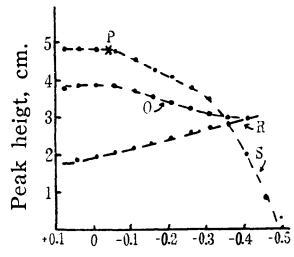

Fig. 4. Variation of the peak height with the initial sweep voltage. 20 c.p.s., v= 50 v/s, $2.0 \cdot 10^{-4}$ M/l Cd^{++}.

It must be recalled here that in the oscillographic technique the applied voltage sweeps during a single lifetime of the D.M.E., therefore, the electrode suffers from the hysteresis of a prior reduction (namely, the first reduction of the dissolved oxygen in this case.). Since the supplementary reduction does not affect the second oxygen reduction, it may be assumed that the hydroxide ion formed in the course of the first oxygen reduction plays a role in the supplementary reduction.

2. Influence of the Concentration of a Metal Ion.—The plot of the relation between the wave height and the concentration of Cd^{++} is illustrated in Fig. 5, where the full curve and the interrupted curve represent the plot in the cases of the deäerated and the undeäerated solutions, respectively. In the former case a good linearity is obtained by the ordinary polarograph concurring with Ilkovič's equation, while in the latter case the linearity deviates slightly. Likewise, in the deäerated solution a linear plot is obtained by the oscillographic technique, while in the undeäerated solution the supplementary reduction peak steeply increases at first as the Cd^{++} concentration increases, and it amounts to a limiting value at a certain Cd^{++} concentration (i. e., about 0.5 mM/l, which is

* Behr and Chodkowski[2] coined the term "latent limiting current" for the first oxygen reduction in an potential-time oscillographic method. The present author has assigned the effect to its irreversible process and also to the fact that the cathodic current has probably been likely misjudged for a large charging current. The peak current of the dissolved oxygen was observed in the surfaceinactive supporting electrolyte such as nitrate, perchlorate or sulfate. while it was not observed in the solution containing halogen ion. The electrode reaction proceeds as follows:

1st reduction: $O_2+2H_2O+2e=H_2O_2+2OH^-$

2nd reduction: $H_2O_2+2e=2OH^-$

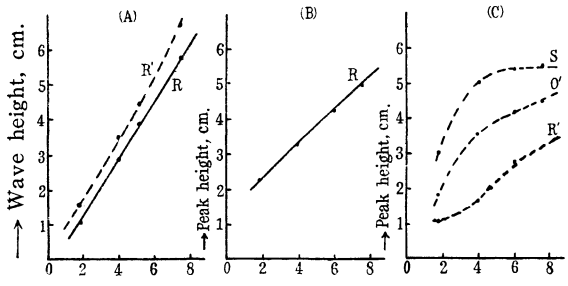

Fig. 5. Variation of the wave height with the conc. of Cd^{++}: (A); ordinary polarograph (s=1/20), (B) and (C): oscillographic polarograph (20 c.p.s., v=36 v/s): full curve; deäerated soln., interrupted curve; test soln. contg. atm. oxygen.

greater than the equivalent concentration of the dissolved oxygen (0.3_3 mM/l.)).

These results seem to indicate that the simultaneous reduction of Cd^{++} and oxygen does not affect the diffusion controlled current of Cd^{++} as the case is an ordinary polarograph, but in the oscillographic polarograph the hydroxide ion formed in the course of the first oxygen reduction changes an aquo Cd^{++} into cadmium hydroxide which pertains to the increment of the supplementary reduction.

3. Variation of the Peak Height with the Rate of Potential Change.—The peak height of Cd^{++} is linearly proportional to the square root of the rate of potential change in the range of 20–60 volts per second. The supplementary reduction behaves similarly, however, the gradient of the plot is about two and a half times greater than that of the normal reduction as is illustrated in Fig. 6. This effect is assigned to the fact that not only the reduction of Cd^{++} but also that of the dissolved oxygen increase with the increase of the rate of potential change,

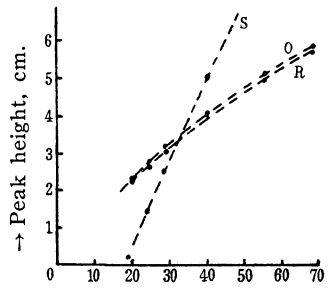

Fig. 6. Variation of the peak height with the rate of potential change, v. (20 c.p.s., $V_i = -0.30$ v. vs. S.C.E., $1 \cdot 10^{-3}$ M/l. Cd^{++}).

therefore, the increase of the supplementary reduction results from the conjoined effect of two reducible species, i.e. Cd^{++} and oxygen.

4. Influence of the Concentration of Hydrogen Ion.—The supplementary reduction can be observed in the neutral solution of bromide, chloride, rhodanate, nitrate or sulfate. However, there is a limit in an acidic or in an alkaline solution. The influence of pH on the supplementary reduction was persued in non-buffered media, and the results are illustrated in Fig. 7.

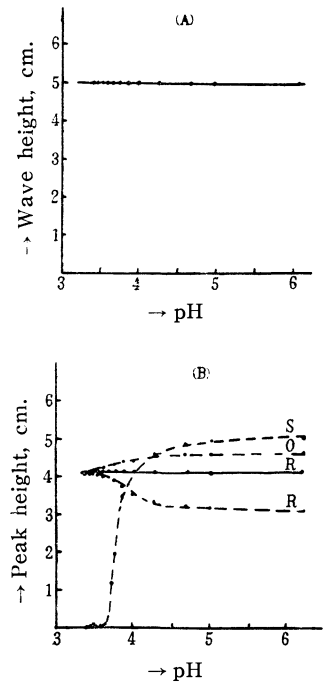

Fig. 7. Variation of the wave height with pH: (A) ordinary polarograph (s=1/20), (B) oscillographicp olarograph: full curve; deäerated soln., interrupted curve; test soln. contg. atm. oxygen.

In the ordinary polarography pH does not affect the diffusion controlled current of Cd^{++}. Also in the oscillographic work the normal reduction in the case of the deäerated solution is independent of pH. On the contrary, the effect is remarkable in the undeäerated solution. When pH of the test solution is less than 3.53 the supplementary reduction was not observed. In the pH range from 3.53 to 3.67 the supplementary reduction gradually increases as the D. M. E. drops repeatedly. Hence, the peak height recorded during the first single drop was taken into account. In Fig. 7 the supplementary reduction increases as pH increases, while the normal reduction varies vice versa. The supplementary reduction was not observed in

the buffered solution containing N acetic acid and N sodium acetate.

As a result, it may be assumed that the variation of the solubility of a metal hydroxide in an acidic solution results in the variation of the supplementary reduction. This effect corresponds to the fact that the metal ion which gives rise to the supplementary reduction in a neutral medium is confined to its ability to form the sparingly soluble hydroxide. Only Cd^{++}, Pb^{++}, Zn^{++}, Bi^{+++}, Fe^{+++} or Al^{+++} was found to give the supplementary reduction.

From these results it is evident that the supplementary reduction results from the sparingly soluble metal hydroxide. It can not be elucidated, however, that not only the normal reduction but also the supplementary reduction decrease by the presence of oxygen in its high concentration. The following experiment was pursued to clarify this point.

5. Variation of the Peak Height with the Mercury Head.—In an ordirnary polarography, the variation of the limiting current is linearly proportional to the square root of the mercury head as is illustrated in Fig. 8 Aa. However, in an oscillographic polarograph the peak height is practically independent of the mercury head (Fig. 8 Ba). These relations deviate in the case of the undeäerated solution (Figs. 8 Ab, 8 Bb), especially by the presence of oxygen in its high concentration (Figs. 8 Ac, 8 Bc).

The presence of oxygen in its high concentration results in the depletion of a reducible metal ion by the formation of a metal hydroxide at the electrode surface. When the mercury head is raised, the rate of the drop growth of the D. M. E. increases in proportion to the mercury head, and accordingly, the expanding electrode surface can encounter the reducible metal ion which locates a little apart from the electrode surface.

From the fact that not only the normal reduction but also the supplementary reduction increase as the mercury head is raised, it is reasoned that the supplementary reduction is originated from an intermediate, i. e. a colloidal metal hydroxide, between an aquo metal ion and a metal hydroxide.

6. The Microscopic Observation of the D. M. E.—When the supplementary reduction arises, a smoky cloud is observed microscopically as the case is Pb^{++} or Fe^{+++}. The smoky cloud is formed at the vicinity of the

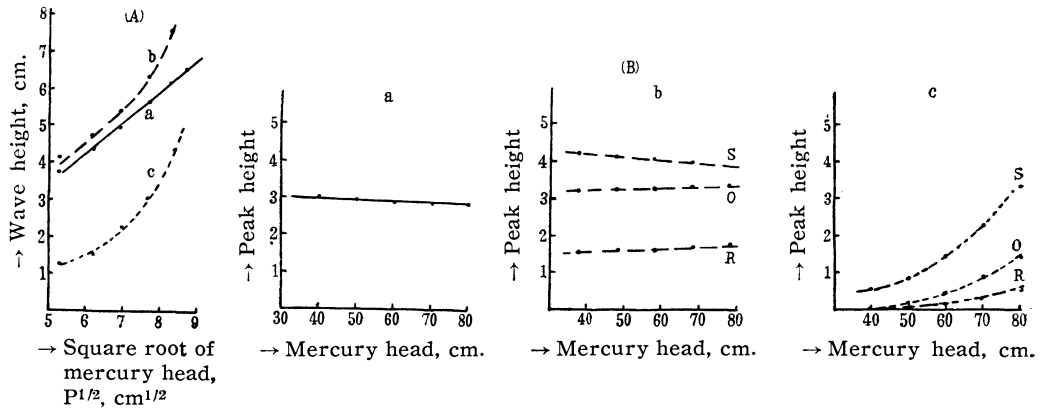

Fig. 8. Variation of the wave height with the mercury head: ($5.3 \cdot 10^{-4}$ M/l Cd^{++} in 0.5 N KCl), (A) ordinary polarograph, (B) oscillographic polarograph: full curve; deäerated soln., interrupted curve; test soln. contg. atm. oxygen, dotted curve; test soln. contg. conc. oxygen.

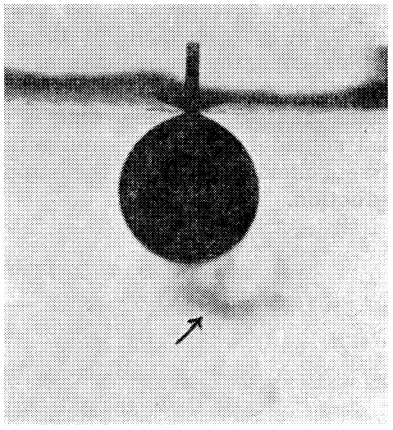

Fig. 9. Photomicrograph of metal hydroxide colloids repulsed from the surface of the D.M.E.

D. M. E. at an early stage of the lifetime, and some time after it is suddenly repulsed from the electrode surface prior to the drop of the D. M. E. The photomicrograph is illustrated in Fig. 9.

It may be assumed that a colloidal metal hydroxide is formed by the reaction of a metal ion with a hydroxide ion, and being deprived of the stabilizing ion as the result of the supplementary reduction, the metal hydroxide is repulsed by the negatively charged electrode. This assumption will be supported by the following experiment.

7. Influence of the Surface Active Reagent.—The variation of the peak height with the concentration of gelatine is illustrated in Table I.

Both Triton X 100 and dodecyl-trimethyl ammonium chloride give the same results as that of gelatine.

Conclusion

From the above mentioned results the mechanism of the supplementary reduction can be given as follows.

At first the dissolved oxygen is reduced at the vicinity of the electrode surface to form a colloidal metal hydroxide with an aquo metal ion. When the cathodically produced hydroxide ion is not as much as the equivalent concentration of the metal ion, the excess metal ion is adsorbed around the colloidal metal hydroxide as the inner ion (i. e. the potential determining ion) of the colloid.

TABLE I

VARIATION OF THE WAVE HEIGHT WITH THE GELATINE CONCENTRATION

A. Ordinary Polarograph: sensibility=1/20						
Gelatine conc., %		0	0.005	0.01	0.05	0.1
Wave height of Cd^{++} in deaerated soln., cm.		5.85	5.85	5.85	5.65	5.50
In the test soln. containing oxygen, cm.		6.43	5.92	5.92	5.78	5.78
B. Oscillographic Polarograph: v=50 v/s, 20 c.p.s.						
Gelatine conc., %		0	0.005	0.01	0.05	0.1
Peak ht. of Cd^{++} in deaerated soln., cm.	R	3.86	3.80	3.71	2.40	2.40
	O	3.87	3.90	3.90	3.80	2.80
In the test soln. contg. oxygen, cm.	R	3.11	3.76	3.80	3.21	2.99
	S	4.04	2.75	2.70	0	0
	O	4.39	3.92	3.74	2.83	2.62

In Table I, A the reduction of Cd^{++} is not hindered by the presence of 0.01% gelatine in the case of the deaerated solution, however, in the undeaerated solution the reduction is hindered even by the presence of 0.005% gelatine. In Table I, B the normal reduction is retarded only a little by the presence of gelatine. However, the supplementary reduction remarkably decreases as the concentration of gelatine increases, and by the presence of 0.05% gelatine the supplementary reduction is perfectly extinguished.

It seems that a gelatine film is formed around a colloidal hydroxide, and acting as a protective colloid it retards the supplementary reduction. This inner ion will give rise to the supplementary reduction. The potential required for the reduction of the inner ion will be greater than the aquo metal ion on account of its Coulombic attraction to the metal hydroxide. Thus, the supplementary reduction is observed at the more negative potential than the normal reduction.

The author wishes to express his hearty gratitude to Prof. Mutsuaki Shinagawa for his valuable advice and encouragement. Also the author thanks Mr. Shōkichi Chaki who assisted in a part of this experiment.

Department of Chemistry, Minami College,
University of Hiroshima,
Hiroshima

Studies on Electrocapillarity with Respect to the Supplementary Reduction in Oscillographic Polarography

By Hideo IMAI

(Received August 8, 1955)

The mechanism of a supplementary reduction has been proposed in a previous report[1], where the supplementary reduction was assigned to the reduction of the inner metal ion (the potential determining ion which establishes the electrical double layer of a colloidal metal hydroxide with the counter ion (anion)). Hence, the difference between the peak potential of the normal reduction (i.e. the reduction of an aquo metal ion) and that of the supplementary reduction may be the measure of Coulombic attraction between the inner ion and the colloidal metal hydroxide. In this paper are presented the estimation of the Coulombic attraction in various supporting electrolytes and some related phenomena.

Experimental

The multi-sweep oscillographic technique of a current potential curve was employed[1]. The rate of potential change, 70 v./s. (20 c. p. s.), was used throughout the measurments. Waves were recorded during the lifetime of a single drop, but for the sake of clarity, only the pattern corresponding to the maximum size of the mercury drop is shown in Figs. 1–4. In general it is observed that the cathodic peak potential is shifted toward more negative values as the drop grows. This shift is caused by an increase in the ohmic drop in the cell and the measuring circuit. Likewise, the anodic peak potential is shifted toward more positive potentials as the drop grows. The shift in the peak potential is indicated in Figs. 1–3 by a straight line. In order to obtain correct peak-potentials it suffices to extrapolate the potential to zero current as is indicated in Figs. 1–3. The possible error in measuring the peak potential amounts to ± 0.005 volt.

The test solution contains about 1 mM/l. Cd^{++}, Pb^{++} or Zn^{++} in N KI, KBr, KCl, KNO_3, $NaNO_3$, Na_2SO_4 or sat. K_2SO_4 and about 0.37 mM/l. oxygen equilibrated with atmospheric oxygen at 25°C. In the preparation of these solutions, reagent grade chemicals were recrystallized twice from their aqueous solutions.

The temperature was 25 ± 0.1°C.

Results

The current-potential curves are illustrated in Figs. 1–3, where full curves and dotted curves denote those of the deäerated solutions and of the undeaerated solutions, respectively. The charging current, i_c, in each solution is also appended.

From these polarograms, peak potentials were estimated by the method described in the preceding section, and are illustrated in Tables I–III. It was confirmed that the peak potential of a metal ion in the presence of the dissolved oxygen approximately coincides with that of a metal ion in the deäerated solution within the experimental error.

TABLE I

$1 \cdot 10^{-3}$ M/l. Cd^{++} IN N KnX

X^{n-}	π_R	π_S	π_0	$(\pi_R+\pi_0)/_2$	$\pi_R-\pi_S$
I^-	-0.75_5	—	-0.73_0	-0.74_3	—
Br^-	-0.68_0	-0.81_0	-0.63_5	-0.65_8	0.13_0
Cl^-	-0.67_0	-0.80_5	-0.61_0	-0.64_0	0.13_5
OS_4^{--}	-0.63_0	-0.79_0	-0.56_5	-0.59_7	0.16_0
NO_3^-	-0.62_0	-0.79_0	-0.56_0	-0.59_0	0.17_0

TABLE II

$1 \cdot 10^{-3}$ M/l. Pb^{++} IN N KnX. [( ); ILL-DEFINED DATA]

X^{n-}	π_{R1}	π_{R2}	π_{S1}	π_{S2}	π_{01}	π_{02}	$(\pi_{R2}+\pi_{02})/_2$	$\pi_{R2}-\pi_{S1}$
I^-	-0.59_5	-0.67_5	—	—	(-0.80_0)	-0.59_0	-0.63_3	—
Br^-	-0.47_5	-0.52_5	-0.60_8	(-1.00_0)	(-0.66^0)	-0.48_0	-0.50_3	R1 : 0.13_3 R2 : 0.08_3
Cl^-	—	-0.48_0	-0.61_0	(-1.04_0)	(-0.51_0)	-0.40_5	-0.44_3	0.13_0
NO_3^-	—	-0.45_0	-0.62_7	(-1.05_0)	(-0.45_7)	-0.35_0	-0.40_0	0.17_7
OH^-	—	-0.80_0	—	—	—	-0.70_0	-0.75_0	—

1) H. Imai, This Bulletin, 29, 276 (1956).

TABLE III

$1 \cdot 10^{-3}$ M/l. Zn^{++} IN N KnX. [( ); ILL-DEFINED DATA]

X^{n-}	π_{R1}	π_{R2}	π_{S1}	π_{S2}	π_{01}	π_{02}	$(\pi_{R2}+\pi_{02})/2$	$\pi_{R22}-\pi_{S1}$
I^-	(-1.01_8)	-1.20_0	-1.38_2	(-1.59_3)	(-1.12_5)	-0.93_8	-1.06_9	-0.18_2
Br^-	(-1.00_0)	-1.20_0	-1.39_0	—	(-1.12_0)	-0.90_2	-1.05_1	-0.19_0
Cl^-	(-0.90_0)	-1.20_0	-1.39_5	—	(-1.11_8)	-0.88_0	-1.04_0	-0.19_5
SO_4^{--}	(-1.10_0)	-1.22_0	-1.42_0	(-1.56_0)	(-1.11_0)	-0.88_0	-1.05_0	-0.20_0
NO_3^-	(-1.10_0)	-1.20_2	-1.40_5	(-1.55_0)	$(-1.11'_0)$	-0.87_5	-1.03_8	-0.20_3
OH^-	—	-1.71_0	—	—	-1.50_0	-1.00_5	-1.36_7	—

Fig. 1. Oscillographic polarogram of $1 \cdot 10^{-3}$ M/l. Cd^{++} in N KnX (X=negative ion).

Fig. 2. Oscillographic polarogram of $1 \cdot 10^{-3}$ M/l. Pb^{++} in N KnX.

Fig. 3. Oscillographic polarogram of $1 \cdot 10^{-3}$ M/l. Zn^{++} in N KnX.

Fig. 4. Oscillographic polarogram of N KnX (X=negative constituent of supporting electrolyte.).

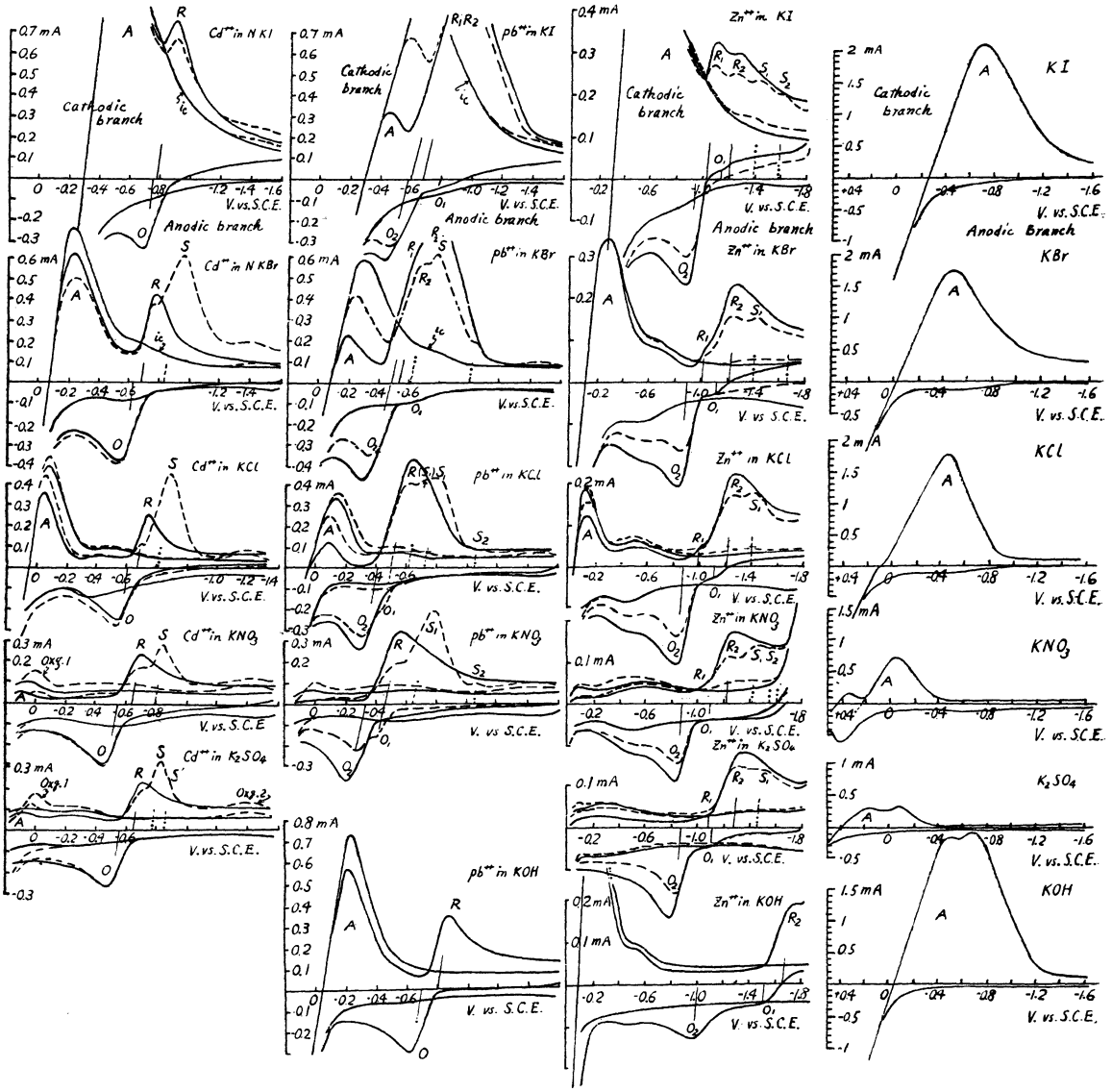

In the current-potential oscillogram of Cd^{++} in N KBr or in N KCl the second supplementary reduction is perceptible by a judicious choice of the initial sweep voltage. Also in the oscillogram of Cd^{++} in K_2SO_4 the supplementary reduction consists of double peaks regardless of any control of the applied sweep. All these auxiliary peaks are ill-defined and are omitted.

In the solutions containing Zn^{++}, the normal reduction waves consist of two peaks in the cathodic branch and in the anodic branch, respectively. This characteristic shape has been discussed by Delahay[2]. However, the remarkable consecutive peaks shown in the case of Zn^{++} in N KBr or KI can not be elucidated by Delahay's concept. The problem remains for the future[3].

The second supplementary reduction, S_2, observed in the case of Pb^{++} or Zn^{++} is that of the hydroxide complex such as $HPbO_2^-$, $HZnO_2^-$. These hydroxide complexes result from their amphoteric nature.

Among these complicated results, the following features hold in common:

(1) Both the peak potential of the normal cathodic process, π_R, and that of the anodic process, π_0, are shifted toward more negative potentials in the solutions of NO_3^-, SO_4^{--}, Cl^-, Br^-, I^- in the order given. The mean potential, $(\pi_R+\pi_0)/2$, behaves likewise.

(2) The values of $\pi_R-\pi_S$ (π_S; the peak potential of the supplementary reduction) increase in the solutions of I^-, Br^-, Cl^-, (SO_4^{--}, NO_3^-) in the order given.

These common features seem to correlate intimately with the electrocapillary behaviors of anions as shown in the following.

The current-potential oscillograms of deäerated supporting electrolytes are shown in Fig. 4.

In every solution an enormously large charging current passes through the cell in the cathodic branch. Every charging current attains a maximum at an appreciably positive or a less negative potential (The potential of the maximum charging current is always positive with respect to the potential referred to the electrocapillary maximum.), then decreases gradually as the applied potential sweeps toward more negative potentials. It is interesting that such a large charging current is not observable in the anodic branch. Moreover, such a current can not be observed by an ordinary polarograph. This irreversible current can be assigned to the variation of a differential capacity as is shown in the following.

The charging current consists of two components, one is the charging current, i_{c_1}, due to the increase in capacity of the electrical double layer and another is the charging current, i_{c_2}, due to the differential capacity. Since the complete current-potential curve is recorded in a small fraction of the drop life, i.e. 1/20 seconds in this experiment, i_{c_1} is very small.

The charging current, i_{c_2}, is equal to the rate of flow of charge due to the variation of the differential opacity, c, i.e.

$$i_{c_2}=\frac{dQ}{dt}=c\frac{dE}{dt} \tag{1}$$

Under the condition of the experiment where a linearly increasing and decreasing potential sweep is applied to the D.M.E. the rate of potential change with respect to time, t, is equal to a constant, v.[4] Hence,

$$\frac{dE}{dt}=v \qquad \therefore \quad i_{c_2}=c\cdot v \tag{2}$$

The linear relation between i_{c_2} and v has been verified experimentally by the present author[5]. Since v is as large as 70 v./s. in this experiment, i_{c_2} is enormously large and i_{c_1} is negligible.

Integration of equation (1) leads to an equation for the charge flowed (Q):

$$Q=\int_{E_1}^{E_2} c\ dE+k \tag{3}$$

Substituting Eq. 2 into Eq. 3, one has:

$$Q=\frac{1}{v}\int_{E_1}^{E_2} i_{c_2}dE+k \tag{4}$$

where E_1 is the potential of the D.M.E. and E_2 is that of an electrocapillary maximum.

Supposing the surface area of the D.M.E. is kept constant, the area surrounded by the charging current curve means the surface charge density.

The surface area of the D.M.E. is proportional to $m^{2/3}\ t^{2/3}$ (m; the flow rate of mercury, t; the lifetime of the D.M.E.). In this experiment m is constant and t decreases in the solutions of (NO_3^-, SO_4^{--}), Cl^-, Br^-, I^- in the order given. Hence, the surface area of the D.M.E. under a given applied sweep increases in the solutions of I^-, Br^-, Cl^-, (SO_4^{--}, NO_3^-) in the order given, while from Fig. 4 Q increases vice versa. Hence, the surface charge density at a given applied potential decreases in the solutions of I^-, Br^-, Cl^-, (NO_3^-, SO_4^{--}) in the order given.

2) P. Delahay, *J. Am. Chem. Soc.*, 75, 1190 (1953).

3) H. Imai and H. Sunahara, Symposium on presented at the Polarography, Hiroshima (1955).

4) Strictly speaking, the assumption is not valid, because iR drop affects v. This assumption holds approximately[5].

5) H. Imai, *J. Electrochem. Soc. Japan*, 23, 530 (1955)

From the above mentioned results it is reasoned that the surface charge density of is the D. M. E. inversely proportional to the value of $\pi_R - \pi_S$. Here, $\pi_R - \pi_S$ was assumed to be the measure of Coulombic attraction of a metal ion to its colloidal hydroxide. Since a metal ion is attracted both to its hydroxide and to the anion which exists in the electrode surface, it is reasoned that the former attractive force is becoming weaker as the surface charge density of the electrode increases.

In this connection, it was suggested by Heyrovský[6,7] that a halogen ion suffers from a polarization by the negative charge of the electrode. Hence, the electric field exerted on the metal ion results from the polarization of an anion as is illustrated in Fig. 5. Thus, the more polarizable is the anion, the larger is the negative charge represented by $G-G'$. The existence of such a space charge requires an extra applied potential for an electron transfer. (This is best realized by comparing the function of $G-G'$ with that of the grid of a triode vacuum tube.). Thus, the shift of the peak potential listed in Tables I, II and III can be explained. In the same manner, it can be expressed

Polarized anion, Adsorbed metal ion

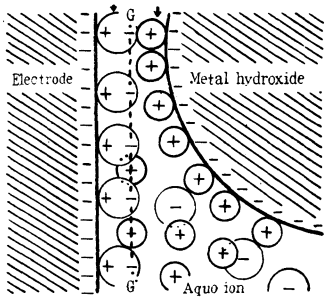

Fig. 5. Schematic representation of the electrode surface.

that the more polarizable is the adsorptive anion layer, the less is the attractive force between the inner metal ion and the colloidal metal hydroxide.

The author wishes to express his hearty gratitude to Prof. Mutsuaki Shinagawa for his valuable advice and encouragement.

The work is partially supported by a Subsidy for Scientific Research given by the Ministry of Education.

Department of Chemistry, Minami College, Hiroshima of University, Hiroshima

6) J. Heyrovsky, *Discs. Faraday Soc.*, **1**, 212 (1947).
7) J. Heyrovsky, *Wien. Chem. Ztg.*, **48**, 24 (1947).

SHORT COMMUNICATIONS

On the Relative Volatility of Heavy- and Light-oxygen Water

By Sadahiro SAKATA and Noriyoshi MORITA

(Received October 3, 1955)

As concerns the relative volatility of heavy- and light-oxygen water at 100°C, M. H. Wahl and H. C. Urey[1] obtained a value of 1.003 by extrapolating their experimental values measured at four temperatures between 11.25 and 46.35°C, and this value has been accepted. Recently, H. E. Watson[2] analysed the results of his experiments on the concentration of light oxygen water and concluded that a value of 1.0056 is the most probable one for the relative volatility of H_2O^{16} and H_2O^{18}. He quoted for comparison the values between 1.0046 and 1.0062 which were obtained by several other authors. During our experiments on the concentration of heavy oxygen by the fractional distillation of water, we became aware of the fact that the degree of enrichment of the heavy oxygen was excessive as compared with that of the deuterium, so far as the value of 1.003 was used as the single plate fractionation factor for heavy oxygen. Therefore we attempted to verify the relative volatility by the following experiments.

A packed column is operated at total reflux under atmspheric pressure. Distillation is started with 4l of normal water in the pot. As distillation is continued, the same volume of normal water as that of distillate is refluxed at the top of the column. Thus, at intervals small quantities of water sample (about 30 cc. each time) are taken out of the pot and their contents in heavy oxygen and deuterium are measured separately. Assum-

ing that the plate efficiencies are equal for isotopes of oxygen and hydrogen, and that the fractionation factor for H_2O/HDO is 1.0260, we can obtain the apparent fractionation factors each time of sampling for heavy oxygen water by applying Fenske equation. Some of the results obtained are tabulated in the accompanying table.

Duration of operation days	Excess density due to deuterium r	Excess density due to heavy oxygen r	Number of plates in Fenske eq. based on deuterium	Apparent fractionation factor for heavy oxygen
24	14.9	36.2	25.9	1.0058
38	24.4	46.2	36.4	1.0052
46	25.9	49.4	37.8	1.0053
55	29.5	54.2	41.0	1.0053
63	32.2	56.1	43.3	1.0052
80	39.5	59.0	48.8	1.0048
88	41.3	59.4	50.0	1.0047
95	43.7	59.5	51.8	1.0045

As will be seen in the table, the apparent fractionation factor for oxygen isotope diminishes gradually as the fractionation proceeds toward equilibrium. This fact may indicate that the concentrations of heavy oxygen and deuterium in water do not proceed at the same rate, but that heavy oxygen reaches equilibrium earlier than deuterium. Time (t) necessary for equilibration can be calculated by the equation advanced by H. C. Urey, et. al.[3]:

$$t=\frac{H\left\{(1-N)\ln\frac{1-N}{1-N_0}+N\ln\frac{N}{N_0}\right\}}{wN(\alpha-1)k\ln\alpha}+\frac{h(N_0-N)}{wN(\alpha-1)}$$

Here, N and N_0 denote the mole fraction of the less-volatile component at the top and the bottom, H and h are the hold-up in the column and the pot, w is the through-put, α is the single plate fractionation factor, and k is the number of theoretical plates. Under our experimental conditions t's are calculated to be about 39 days for heavy oxygen and about 78 days for deuterium, i. e. the former reaches equilibrium twice as rapidly as the latter. The experimental results show a longer time than that mentioned for equilibration but their tendency is in accord with the prediction.

In conclusion, it is quite clear that the value of 1.003 obtained by Wahl and Urey is too low. However, the value of 1.0056 obtained by Watson seems too high because his calculation might be based on an incorrect plate number which was determined by the non-equilibrated concentration of deuterium.

Recently the following relation for the relative volatility and the temperature T in °K is presented[4]:

$$\log(p_{H_2O^{16}}/p_{H_2O^{18}})=3.20/T-0.00680$$

According to this equation, the relative volatility is 1.0041 for 100°C. Extrapolating our experimental results, we can also conclude that the correct value may lie between 1.0043 and 1.0040. In another experiment done under a larger through-put, we obtained a value of 1.0043.

Department of Chemical Engineering,
Faculty of Engineering,
Nagoya University,
Nagoya

1) M. H. Wahl and H. C. Urey, *J. Chem. Soc.*, 3, 411 (1935).
2) H. E. Watson, *J. Appl. Chem.*, 3, 556 (1953).
3) H. C. Urey, J. R. Huffman, H. C. Thode, and M. Fox, *J, Chem. Phys.*. 5, 856 (1937).
4) I. Kirschenbaum, "Physical Properties and Analysis of Heavy Water", McGraw-Hill Book Co. Inc., New York, N. Y. (1951), p. 29.

Über die unmittelbare Messung von den Zuständen in die Ionenaustauschharzphase adsorbierter Komplexionen mit den Harzmembranen

Von Masatoshi FUJIMOTO

(Eingegangen am 6. Oktober, 1955)

Whnn die gefärbten Komplexionen ins farblosen Ionenaustauschharz adsorbiert werden, färbt sich das Harz häufig ganz verschieden von der Farbe der wässerigen Lösungen. Diese Verschiedenheit der Färbung beruht vermutlich auf den besonderen Zuständen in die Harzphase adsorbierter Komplexionen.

Sehr interessantes Beispiel dafür bietet eine charakteristische himmelblaue Färbung, die die wässerige Lösung der Kobalt(II)rhodanide in Berührung mit einer farblosen starkbasischen Anionenaustauschharz liefert. Diese himmelblaue Färbung ist derjenigen von den Komplexsalzen ganz ähnlich, die mit dem organischen Lösungsmittel, z. B. einem Gemisch des Äthyläthers und Isoamylalkohols, ausgezogen werden, und diese Färbung ist auch zum Nachweis geringer Menge des Kobaltes anwendbar[1].

Um diese charakteristische Färbung direkt und quantitativ zu bestimmen, hat der Verfasser erstens mit einer Suspension[2]

starkbasisches Anionenaustauschharzes, Dowex 1-X4, einfacheV ergleichung von der Extinktion, mit Komplexionen ausgetauschter Harzsuspension und von derjenigen der Harzsuspension von Chloridform durchgeführt. Abb. I. stellt ein Resultat dar, worin eine gewisse Ähnlichkeit zwischen den Zuständen in die Harzphase adsorbierter Kobalt(II)-rhodanidkomplexe und denjenigen mit organischem Lösungsmittel ausgezogener Komplexe deutlich gezeigt wird. Jedoch, durch diese Methode konnte man nicht immer ein konstantes Ergebnis erhalten, weil es sehr schwierig ist, Suspension des Harzes von gleicher und sehr feinster Korngrösse herzustellen.

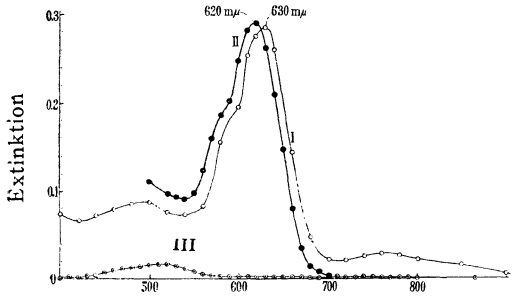

Abb. I. Lichtabsorption der Harzsuspension.

I.-Kurve. Harzsuspension: (1 ccm Harzsuspension(A) + Probelösung + Wasser → 10 ccm)-Lösung verglichen mit (1 ccm Harzsuspension(A) + Wasser → 10 ccm)-Lösung.

Harzsuspension(A):—

Man zerreibt 0.2 g Dowex 1-X4 mit geringer Menge destilliertes Wassers völlig, verdünnt das Gemisch mit destilliertem Wasser genau zu 10.0 ccm, schüttelt danach um, und lässt sie 10 Min lang stehen.

Probelösung:—$CoCl_2$ 0.0039 M, NH_4SCN 0.023 M, HCl 0.0020 M, pH 3.81. ($CoCl_2$ ≒ 195 γ).

Spektrophotometer:—Beckman DU Typus Spektrophotometer.

II.-Kurve. Die mit organischem Lösungsmittel extrahierte Lösung:

Lösungsmittel:—Äthyläther 1.00 Vol.+ Isoamylalkohol 3.00 Vol. ·····(B)

Probelösung:—$CoCl_2$ (114 γ Co/ccm)-Lösung 1 ccm + {20% H_3PO_4 2 ccm; 70% CH_3COONH_4 0.5 ccm; 60% NH_4SCN 2.0 ccm} + H_2O → 10 ccm ·····(C)

Mit (B) extrahiert man (C) und verdünnt es genau zu 10.0 ccm mit (B).

III.-Kurve. Dieselbe Probelösung für I.-Kurve, aber nur verdünnt mit Wasser:

Kürzlich, stellte der Verfasser ein Paar einfacher Küvette mit einer hellgelben und halbdurchsichtigen starkbasischen Anionenaustauschharzmembran[3] zur Lichtabsorptionsmessung auf (Abb. II.), um die Extinktion von den in die Harzphase adsorbierten Komplexionen genauer und ohne obenerwähnte Schwierigkeit zu bestimmen. Die Resultate der Messungen werden in Abb. III. zusammen dargestellt.

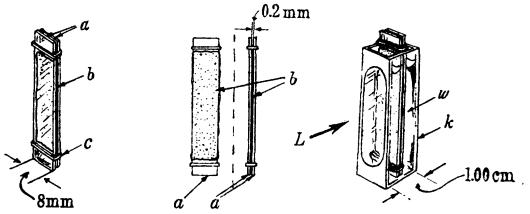

Abb. II. Harzmembranküvette zur Lichtabsorptionsmessung.

a: Mikroskopsobjektglas; *b*: Harzmembran; *c*: Kautschukband; *k*: Küvette für Spektrophotometrie; *w*: destilliertes Wasser; →*L*: Richtung des monochromatischen Lichtes.

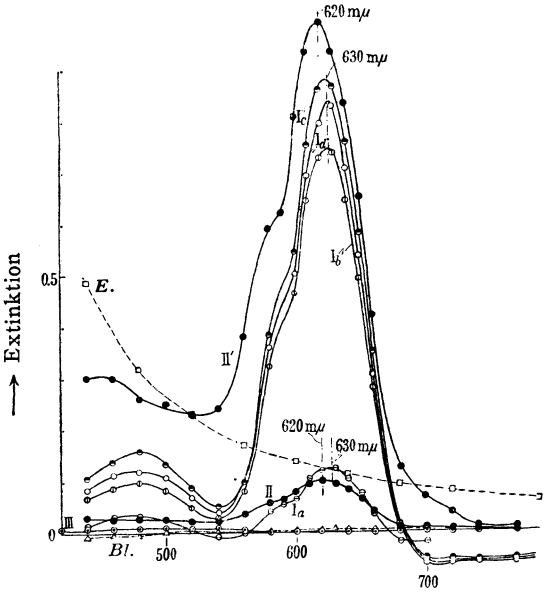

Abb. III. Absorptionsspektra der ins Harzmembran adsorbierten Komplexionen.

I.-Kurve. Absorptionsspektra mit den Kobaltrhodanidkomplexe ausgetauschter Harzmembran verglichen mit Harzmembran von Chloridform:[3]

a: ⊖ 30 Min
b: ◐ 18 Std
c: ◓ 66 Std
d: ○ 164 Std

nach dem Eintauchen der Harzmembran in die Probelösung.

II.-Kurve. Absorptionsspektra der Probelösung, die in Gegenwart überschüssiges Ammoniumrhodanides mit organi-

schem Lösungsmittel (vgl. (B) über II.-Kurve von Abb. I.) ausgezogen wird:

II'.-Kurve. II.-Kurve zehnfach vergrössert:

III.-Kurve. (⊙) Absorptionskurve der Probelösung:

Bl. Absorption für Probe benutzter Harzmembran (RCl) verglichen mit der für Wasser benutzten Membran (RCl):

E. Absorption für Probe benutzter Harzmembran (RCl) verglichen mit destilliertem Wasser:

Probelösung:—Co^{2+} 0.00025 M, SCN^- 0.1045 M, pH 2.18. (Co ≒ 150 γ).

Harzmembran:—10mm×38mm×0.2mm; Mit Kaliumchloridlösung wird sie in die Chloridform übergeführt.

Wie man in Abb. I. und III. leicht sieht, ist es sehr interessant, dass die Gestalt der Lichtabsorptionskurve der in die Harzphase adsorbierten Komplexionen derjenigen ins organische Lösungsmittel ausgezogener Komplexe bedeutend ähnlich ist, und dass die erste Kurve immer „red shift" von etwa 10 mμ gegen die zweite hat[4].

Diese unmittelbare Messung der Lichtabsorption von der Ionenaustauschharzphase mit Hilfe farbloser Harzmembrane[3] wird eine neue und sehr geeignete Methode zur Bestimmung von den Zuständen ins Ionenaustauschharz adsorbierter verschiedenartiger Komplexionen bieten.

Für die Harzmembran ist der Verfasser Herrn Prof. Dr. T. Kuwada zu grossem Dank verpflichtet.

Laboratorium der analytischen Chemie,
Chemisches Institut der wissenschaftlichen Fakultät, Tokyo
Universität, Tokyo

1) M. Fujimoto, Dieses Bulletin, 27, 48 (1954).

2) Durch völliges Zerreiben der mit geringer Menge destilliertes Wassers angefeuchteten Harzkörnchen kann man diese Harzsuspension verhältnismässig leicht herstellen.

3) Eine aus künstlicher Kautschukmembran dargestellte starkbasische Anionenaustauschharzmembran von quartärem Ammoniumtypus: (Nach der Privatmitteilung von Herrn S. Yoshikawa). Als der Kontrast von der Absorptionsmessung wird die obengenannte Harzmembran angewendet, die nur mit Kaliumchloridlösung in die Chloridform übergeführt wird. Zur Zeit führt der Verfasser noch eingehende Untersuchung über die Einflüsse verschiedener Bedingungen, darauf die Veränderung der Quellung und der Durchsichtigkeit von Harzmembran beruht, sowie die der Neigung der Membranfläche gegen die Richtung des Lichtes durch.

4) Man könnte vermuten, dass diese Wellenlängendifferenz der Absorptionsbäuder hauptsächlich auf irgendeiner Wirkung zwischen den Rhodanidionen und den Harzkationen beruht, worüber doch man später eingehende Untersuchungen durchführen müsse.

Copolymerization of Optically Active Ethyl 2-Methyl-2-ethyl-2-butenoate with Vinyl Acetate

By Matsuji TAKEBAYASHI and Yasumasa ITO

(Received November 19, 1955)

In order to investigate the steric effect on the radical polymerization of vinyl compounds, we have prepared ethyl 2-methyl-2-ethyl-2-butenoate (Et-MEB)* which has an optical center nearest to the vinyl group, and studied the polymerization of the ester at 60°C. in the presence of benzoyl peroxide. The ester polymerized only slightly by itself, while it polymerized to a certain extent with vinyl acetate (VAc) under the experimental conditions. A sample of (+)-Et-MEB, the optical purity of which was 75%, was resolved by using brucine from (±)-Et-MEB, and the monomer reactivity ratios, r_1 and r_2, in the copolymerization of (+)-Et-MEB with VAc were compared with those in the same reaction of (±)-Et-MEB with VAc. The results obtained are given in the following table.

Monomer Reactivity Ratio within the Limits of [VAc]/[Et-MEB]=1–3

In the case of	Monomer reactivity ratio
(±)-Et-MEB and VAc	$r_1=k_1/k_2=3.2\pm0.5$, $r_2=k_3/k_4=0.3\pm0.2$
(+)-Et-MEB and VAc	$r_1=k_1/k_2=2.2\pm0.4$, $r_2=k_3/k_4=0.1\pm0.1$

where k_1, k_2, k_3 and k_4 indicate the rate constant of the reactions (1), (2), (3) and (4), respectively.

$$\cdots\cdots VAc\cdot + VAc \xrightarrow{k_1} \cdots\cdots VAc\cdot \quad (1)$$

$$\cdots\cdots VAc\cdot + Et\text{-}MEB \xrightarrow{k_2} \cdots\cdots Et\text{-}MEB\cdot \quad (2)$$

$$\cdots\cdots Et\text{-}MEB\cdot + Et\text{-}MEB \xrightarrow{k_3} \cdots\cdots Et\text{-}MEB\cdot \quad (3)$$

$$\cdots\cdots Et\text{-}MEB\cdot + VAc \xrightarrow{k_4} \cdots\cdots VAc\cdot \quad (4)$$

The data in the table suggest that the reactivity of (+)-Et-MEB on the radical of VAc-type may be about 1.5 times as large as that of (±)-Et-MEB in the reaction (2), because no steric effect will appear on the rate of reactions (1) and (4).

Assuming that the acetyl group of polyvinyl acetate is arranged over five to six units of vinyl acetate at least in such an orientation as has been recognized in that of hydroxyl group of polyvinyl alcohol, a similar orientation will also be given to the acetyl group of the growing copolymeric radicals.

Then it may be possible that the reactivity of (+)-Et-MEB on the growing radical of VAc-type is different from that of (±)-Et-MEB.

The details of this study will be reported in a separate paper.

We express our hearty thanks to Prof. S. Murahashi and Prof. S. Okamura for their kind advice and to the Ministry of Education for a Grant-in-Aid for Scientific Research.

Chemical Institute, South College, Osaka University, Osaka

* The physical properties of the ester were found as follows: b.p.$_{50}$ 82.0°C., d_4^{20} 0.89423, n_D^{20} 1.4290.

Spectrochemical Study of Microscopic Crystals. X.[1] *The Absorption Spectra and Configuration of Bis(ethylenediamine)-copper(II) Complexes*

By Shoichiro YAMADA and Ryutaro TSUCHIDA

(Received October 13, 1955)

It is known that copper usually forms squareplanar complexes with ammonia and amines. Complexes of square-bipyramidal configuration, however, are also formed in some compounds involving water molecules of crystallization. For example, two molecules of water in the crystal of bis(ethylenediamine)-copper(II) nitrate dihydrate occupy positions comparatively close to the copper atom in the direction normal to the plane formed by one copper and four nitrogen atoms[2]. On the other hand, bis(ethylenediamine)-copper (II) perchlorate, which involves no water of crystallization, apparently has separate ions, $[Cu(en)_2]^{2+}$ [3], of planar configuration in the crystalline state. When molecules of ions approach the copper atom in the planar $[Cu(en)_2]$-group along the direction normal to the complex plane, the light absorption and its anisotropy usually undergo more or less distinct changes. Thus the measurement of the absorption spectra is expected to be of use to the elucidation of the problems on the configuration of the planar copper(II)-complexes. In the present paper polarized absorption spectra of bis(ethylenediamine)-copper(II) perchlorate, nitrate dihydrate, and tetrathiocyanato-mercurate have been determined in the crystalline state, and the above problems discussed using the results of the measurements.

Experimental

Materials.—Bis(ethylenediamine)-copper(II) perchlorate, $Cu(en)_2(ClO_4)_2$, was prepared in violet needles according to the method of Pfeiffer et al[4]. The crystal shows a striking dichroism on the prism face, that is, reddish purple and bluish purple. The measurement of polarized absorption spectra was made on the above face in the directions of extinction. The A- and B-absorption refer to the directions A and B as shown in the figure.

Bis(ethylenediamine)-copper(II) nitrate dihydrate, $Cu(en)_2(NO_3)_2 2H_2O$, was obtained in violet plates by the method of Grossmann et al[5]. The monoclinic crystals thus obtained show a marked dichroism on the well-developed (001)-face; it appears light purple with the electric vector along the b-axis and purplish blue with the electric vector along the a-axis. The dichroism measurement was made on the c-plane with polarized light vibrating along the a-axis and along the b-axis. The a- and b-absorption denote absorption with the electric vector along the a- and b-axis, respectively.

Bis(ethylenediamine)-copper(II) tetrathiocyanato-mercurate(II), $[Cu(en)_2][Hg(SCN)_4]$, was prepared in monoclinic plate-like crystals from aqueous solutions of $Cu(en)_2(NO_3)_2$ and of $K_2Hg(SCN)_4$. The crystals are deep purple, with the (010)-plane dominating. Dichroism is observed on the (010)[6]. The measurements of the absorption spectra were made on this plane with polarized light along α- and along β-direction of the crystal[7]. The a- and b-absorption refer to the absorption with the electric vector along the α- and β-direction, respectively.

Measurements.—Quantitative dichroism measurements of the crystals were made by Tsuchida-Kobayashi's microscopic method[8] with polarized light in the regions covering 7500 to 2400 Å. The notations used are the same as those in the previous papers of this series[1].

Results and Discussion

Dichroism of Bis(ethylenediamine)-copper (II) Perchlorate.—The results of the measurements are given in Fig. 1 and Table I. The crystal structure is unknown at present. But since the crystal has no water of crystallization, the perchlorate in the crystalline state involves the separate ions of $[Cu(en)_2]^{2+}$. Therefore, the absorption spectra obtained with this crystal are considered to represent the absorption of the separate planar complex ion, $[Cu(en)_2]^{2+}$, under rather small effect from external perchlorate ions. It is seen

1) Part IX of this series, S. Yamada and R. Tsuchida, This Bulletin, 28, 664 (1955).

2) T. Watanabe and M. Atoji, *Kagaku*, 21, 301 (1951) (in Japanese); read before the meeting of the Chemical Society of Japan, Osaka, May, 1950.

3) The notation, en, denotes a molecule of ethylenediamine.

4) P. Pfeiffer and H. Glaser, *J. Prakt. Chem.*, 151, 134 (1938).

5) H. Grossmann and B. Schück, *Z. anorg. allgem. Chem.*, 50, 1 (1906).

6) H. Scouloudi, *Nature*, 166, 357 (1950); *Acta Cryst.*, 6, 651 (1953).

7) The notations, α, β and γ, represent conventional symbols for optic elasticity axes of the crystal. The γ-direction corresponds with the b-axis. See ref. (6).

8) R. Tsuchida and M. Kobayashi, This Bulletin, 13, 619 (1938); "The Colours and the Structures of Metallic Compounds," Zoshindo, Osaka (1944), p. 180.

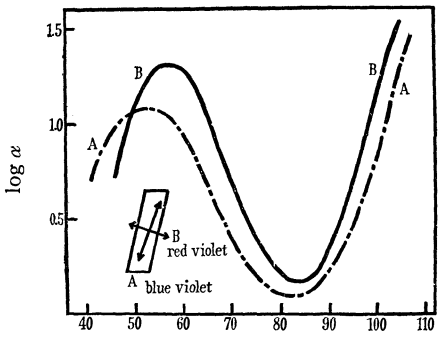

Frequency, ν, 10^{13}/sec.

Fig. 1. Absorption spectra of $[Cu(en)_2](ClO_4)_2$.

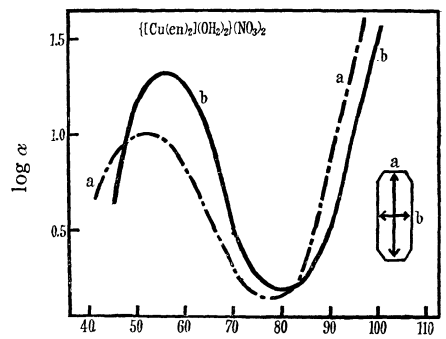

Frequency, ν, 10^{13}/sec.

Fig. 2. Absorption spectra of $\{[Cu(en)_2](OH_2)_2\}(NO_3)_2$.

TABLE I

ABSORPTION MAXIMA OF BIS(ETHYLENEDIAMINE)-COPPER(II) PERCHLORATE IN THE CRYSTALLINE STATE

	ν, 10^{13}/sec.	log α	Half width
A-abs.	57.2	1.31	16.9
B-abs.	53.0	1.08	21.7

TABLE II

ABSORPTION MAXIMA OF BIS(ETHYLENEDIAMINE)-COPPER(II) NITRATE DIHYDRATE IN THE CRYSTALLINE STATE

	ν, 10^{13}/sec.	log α	Half width
b-abs.	56.0	1.33	16.5
a-abs.	52.2	1.00	21.5

from the measurements that the crystal of the perchlorate shows absorption at about 50×10^{13}/sec. (band A) and at a wave-length shorter than 110×10^{13}/sec. (band B). The band at the longer wave-length is supposed to be due to the copper atom in combination with ligands. The absorption at the shorter wave-length may be considered as originating from the electron transfer between the copper atom and the ligand molecules, as will be discussed in the later part of this paper.

It was formerly established with planar complexes of copper(II)[9] that for the band A, absorption with the electric vector along the complex-plane, $\parallel$-absorption, has a larger absorption coefficient than $\perp$-absorption, absorption with the electric vector normal to the above. Therefore, it may be reasonable to suppose that the A- and B-absorption represent characteristics of the $\parallel$-absorption and those of the $\perp$-absorption, respectively. Thus the following relation on the dichroism may be derived. For the band A, the $\parallel$-absorption shows its maximum at a shorter wave-length than the $\perp$-absorption, and the absorption is much stronger with the $\parallel$-absorption than with the $\perp$-absorption. For the band B, the $\parallel$-absorption is bathochromic to the $\perp$-absorption.

Dichroism of Bis(ethylenediamine)-copper (II) Nitrate Dihydrate.—The results of the measurements are shown in Fig. 2 and Table II. According to the X-ray study of crystal structure, the copper atom is bound with four nitrogen atoms of ethylenediamine molecules in planar configuration, with the neighbouring oxygen atoms of water molecules at a slightly greater distance in the direction normal to the plane formed by the copper and four nitrogen atoms. The planes of the complexes are inclined to the bc-plane at a small angle. Referring to absorption with the electric vector along the a-axis as a-absorption and absorption with the electric vector along the b-axis as b-absorption, then the crystal analysis indicates that the a-absorption corresponds roughly with the $\perp$-absorption of the planar complex ions and the b-absorption corresponds with the $\parallel$-absorption[2].

The crystals of bis(ethylenediamine)-copper (II) nitrate dihydrate exhibit in the region of the present measurement two bands at $50\text{–}60\times10^{13}$/sec. (band A), and at the wave-length shorter than 110×10^{13}/sec. (band B), both bands corresponding to the absorption bands of the perchlorate.

The band A of this crystal is seen to be slightly displaced bathochromically as compared with the crystal of the perchlorate. This seems to indicate that the complexes, in the crystal of the nitrate dihydrate undergo an effect from the two water molecules in the direction normal to the complex-plane.

From the present measurement are obtained the following relations on the dichroism of the complex ion. *For the band A, the $\parallel$-absorption has much greater intensity than the $\perp$-absorption, and the former is hypsochromic*

9) R. Tsuchida and S. Yamada, Read before the sixth annual meeting of the Chemical Society of Japan, Kyoto, April, 1953.

to the latter. The above rule about the intensity is the same as that formerly derived with other planar complexes of copper(II) as well as with the perchlorate[9]. For the absorption bands of planar complexes of platinum(II) and palladium(II) which are considered as due mainly to co-ordinate linkages, the ∥-absorption was found to have much greater oscillator strength than the ⊥-absorption[10]. The above relation with the cupric complexes seems to be in good agreement with the general rule for planar complexes of palladium(II) and platinum(II).

The second rule that the ∥-absorption is hypsochromic to the ⊥-absorption seems to indicate that the band A consists of two components having opposite polarization properties. This may be discussed later with reference to the absorption of the complex ion, $[Cu(en)_2]^{2+}$, in solution.

The present measurement also shows that, *for the band B, the ⊥-absorption is bathochromic to the ∥-absorption.* The fact that the nitrate dihydrate shows with the band A polarization property essentially similar to the perchlorate seems to indicate that the effect of the two water molecules on the band A is small and, at the same time, that the energy level associated with the band A is disturbed very little. On the contrary, their marked effect is observed with the absorption at the shorter wave-length. Thus the polarization property for the band B of the nitrate dihydrate is found to be reversed, as compared with the perchlorate. This reversal, which is ascribed to the effect of the two water molecules close to the copper atom, will be discussed in the later part of this paper.

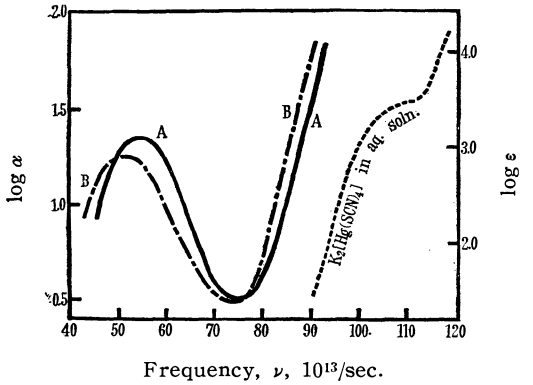

Fig. 3. Absorption spectra of $[Cu(en)_2][Hg(SCN)_4]$. The spectrum of the solution (dotted curve) is taken from ref. 1.

10) S. Yamada, H. Yoneda and R. Tsuchida, *J. Chem. Soc. Japan*, **69**, 145 (1948); S. Yamada, *J. Am. Chem. Soc.*, **73**, 1182 (1951); S. Yamada and R. Tsuchida, This Bulletin, **26**, 489 (1953).

Bis(ethylenediamine)-copper(II) Tetrathiocyanato-mercurate(II).—The results of the present measurement are shown in Fig. 3 and Table III. According to the result of the

TABLE III

ABSORPTION MAXIMA OF BIS(ETHYLENEDIAMINE)-COPPER(II) TETRATHIOCYANATOMERCURATE(II) IN THE CRYSTALLINE STATE

	ν, 10^{13}/sec.	log α	Half width
A-abs.	54.8	1.18	15.0
B-abs.	51.5	1.05	17.3

crystal analysis[5], it is seen that the B-absorption involves more ⊥-absorption of the $[Cu(en)_2]^{2+}$-ion than the ∥-absorption, and that the A-absorption involves more ∥-absorption. The crystal is found to show absorption bands at about 50×10^{13}/sec. and at a shorter wave-length than about 90×10^{13}/sec. The band at 50×10^{13}/sec. of the crystal clearly corresponds to the band A of the $[Cu(en)_2]^{2+}$-group, since the $[Hg(SCN)_4]^{2+}$-ion is expected to absorb at a much shorter wave-length region[1] (Fig. 3). For the $[Cu(en)_2]^{2+}$-ion in the crystal of $[Cu(en)_2][Hg(SCN)_4]$, the following relation is found on the dichroism. *For the band A, the ∥-absorption is hypsochromic to the ⊥-absorption the intensity being greater with the ∥-absorption than with the ⊥-absorption.* This relation is essentially similar to that with the crystal of $\{[Cu(en)_2](OH_2)_2\}(No_3)_2$.

The X-ray investigation showed that "two N atoms of the SCN-groups in the crystal of $[Cu(en)_2][Hg(SCN)_4]$ are co-ordinated to each copper atom at a distance of 2.58 Å in the direction perpendicular to the complex-plane, giving the copper atom a total of six-fold co-ordination"[5]. In the same report a value of 2.07 Å was obtained for the co-ordinate bond distance between the copper and nitrogen atoms in the plane formed from a copper and four nitrogen atoms of ethylenediamine molecules. The Cu-N distance of 2.58 Å seems to be too great for the ordinary co-ordinate linkage to be expected between the copper atom and the nitrogen atoms of the NCS-groups. The band A of $[Cu(en)_2][Hg(SCN)_4]$, however, is seen to be displaced slightly bathochromically, as compared with that of $[Cu(en)_2](ClO_4)_2$. This may be regarded as one effect by the interaction between copper and nirtogen atoms. The dichroism for the band A is the same as that with the perchlorate, as was found to be the case with the nitrate dihydrate.

Another absorption band in the ultra-violet may be considered as superposition of the

absorption bands of complex ions, $[Cu(en)_2]^{2+}$ and $[Hg(SCN)_4]^{2-}$. In any case, the absorption is seen to lie in the far longer wave-length regions than would be expected from the corresponding bands of either of the component complexes in solution. This bathochromic shift also may be taken as indicating that the complexes are subjected to the effect caused by the interaction between a copper and two nitrogen atoms of the NCS-groups. Judging from the absorption curves of the separate component complexes, the ascending curve at about $80-90\times10^{13}$/sec. may most probably be considered as due to the $[Cu(en)_2]^{2+}$-ion. *It is found for this band that the* $\parallel$*-absorption is hypsochromic to the* $\perp$*-absorption.* This dichroism, reverse to that of the $[Cu(en)_2](ClO_4)_2$, shows the effect of NCS^- ions on the $[Cu(en)_2]^{2+}$ group.

General Discussion

Inspecting the results presented above, we find the following rules about the effects on the absorption spectrum of the complex ion caused by the outer groups which come comparatively close to the copper atom. (1) *The band A is displaced bathochromically, its polarization property being unchanged.* (2) *The band B undergoes a large bathochromic shift, its polarization property being reversed.*

These changes, above all the reversal of the polarization property, are so definite that they may be used for determining whether or how close such molecules as water and ammonia in the crystalline state approach the copper atom in the direction normal to the square-planar complex.

The results stated above clearly indicate that water molecules in the nitrate dihydrate or thiocyanate ions in the tetrathiocyanato-mercurate(II) have considerable effects on the copper atom. But judging from the distance between the copper atom and the approaching groups, as revealed by the X-ray analysis[2,6], the effect may be mostly electrostatic, and the linkage between them may be different from the linkage between the copper atom and ethylenediamine molecules in the complex-plane. Furthermore, the typical sexa-co-ordinate copper(II) complex of octahedral configuration would show its absorption in the much longer wave-length region, as may be readily realized from the absorption maximum at $40–45\times10^{13}$/sec. for the $[Cu(en)_3]^{2+}$ in aqueous solution against about $52–57\times10^{13}$/sec. for the $[Cu(en)_2]^{2+}$ in the crystalline state[11]. This also seems to support the above conclusion.

The magnitude of the bathochromic change for the band A and band B may be supposed to depend upon the strength of the effect of the approaching groups on the copper atom. Thus, inspecting the results, we obtain with both the bands the decreasing order of the effect on the copper atom: tetrathiocyanato-mercurate(II) > nitrate dihydrate > perchlorate.

Formerly, one of the present authors (R. T.)[11] reported that the band A of planar quadri-co-ordinate complexes of copper(II) suffers large bathochromic change when taking up two more ligands to complete the sexa-co-ordination. This would indicate that the approach of the fifth or sixth group to the copper atom may cause bathochromic shift of the band. The general rule (1) seems to be in good agreement with it. This is also in qualitative agreement with the result obtained by Ballhausen[12] through quantum-theoretical treatment on the basis of the crystal field theory. It is to be noted that the polarization property for the band A is not changed on the approach of the fifth and sixth groups. This fact seems to show that the band A may originate from an electronic transition of the comparatively deeper part of the complex ion, favouring the interpretation that the absorption band A of copper (II)-complexes is due to transition of the *d*-electrons of the copper atom which is under the effect of the surrounding ligands.

The general rule (2) indicates that the effect of the approaching outer groups on the band B is seen to be quite large. One explanation for the general rule (2) may be that the same transition in the shorter wave-length that exist in the separate $[Cu(en)_2]^{2+}$-ion may have their polarization properties reversed due to the approach of the outer groups to the copper atom. But an alternative explanation may be that, as the groups come closer to the copper atom in a complex ion, a new transition polarized in the X-Cu-X direction, X being the approaching groups, is given rise to in the wave-length region slightly longer than the original transition. Assuming the latter interpretation, this new transition would most probably be due to the electron transfer from the copper atom to the ligands, as was assumed between the copper and ethylenediamine for the absorption band B of the separate complex ion without any specific effect from outside. Based on the electron transfer model on the supposed new band, we may consider that, when the outer groups come close enough to the copper atom, the electronic clouds on

11) R. Tsuchida and H. Ito, Read before the symposium on co-ordination compounds, Nagoya, November, 1953.

12) C.J. Ballhausen, *Kgl. Danske Videnskab. Selskab, Mat.-fys. Medd.*, **29**, No. 4 (1954).

the copper atom move to increase the electronic density toward the approaching groups, making the electron transfer easier with the electric vector along the L-Cu-L direction.

This mechanism of electron transfer provides the possibility of explaining the association band of planar complexes[13]. Thus when some anions in solution come very close to the metal atom in the centre of the planar complex ion, there would be electron transfer between the metal atom and the anions.

Now the absorption spectrum of $[Cu(en)_2]^{2+}$ in aqueous solution may be discussed using the above results. In aqueous solution, water molecules are considered to be located so close to the copper atom in the square-planar complex that the interaction of the above type may be expected between the copper atom and water molecules. In fact, the absorption maximum of $Cu(en)_2(NO_3)_2$ in aqueous solution lies at about 54×10^{13}/sec.[11], a much longer wave-length than the maximum of the perchlorate, and even longer than the nitrate dihydrate in the crystalline state. In consequence, the effect of water molecules on the $[Cu(en)_2]^{2+}$ ion may be greater in aqueous solution than in the crystals of the nitrate dihydrate. But, as is discussed in the preceding section of this paper, the approaching water molecules are not supposed to form strongly covalent bonds with the copper atom, since the supposed octahedral complex formed by strong bonds would show its absorption at a far longer wave-length.

It seems unusual that the absorption band A of the solution is quite symmetrical, since the simple superposition of the $\parallel$- and $\perp$-absorption, as obtained with the crystal, would yield unsymmetrical curve for the band A. It must be concluded, therefore, that the band A, which has only one component in the solution, is split in the crystalline state into two components having opposite polarization properties. The splitting of the band A in the crystal may be ascribed to the perturbation by the surrounding ions, and might be a kind of Davydov splitting[14].

A similar consideration applies to the absorption spectrum of $[Cu(en)_2]^{2+}$ in ammoniac solution, which exhibits the band A at about 48×10^{13}/sec.[15]. The bathochromic shift of the band A is seen to be much greater in ammoniac solution than in aqueous solution, and even than in the tetrathiocyanato-mercurate(II), suggesting that the effect of ammonia on the copper atom is greater than that of water molecules in the aqueous solution or that of thiocyanate ions in the latter. Judging from the remarkable, bathochromic shift, it may be reasonable to suppose that the linkage between ammonia molecules and the copper atom should have considerable covalent bond character.

Summary

Polarized absorption spectra of bis (ethylenediamine)-copper(II) perchlorate, nitrate dihydrate and tetrathiocyanato-mercurate(II) in the crystalline state have been determined by Tsuchida-Kobayashi's microscopic method in the region between 2400 and 7000Å. These compounds all show a band at about 50×10^{13}/sec. (band A) and another absorption at a wave-length shorter than 90×10^{13}/sec. (band B).

The band A of the latter two compounds suffers bathochromic effect, and the polarization property for the band B is reversed, as compared with the former. From these differences, it has been concluded that in the former two compounds, OH_2 or NCS^- causes a considerable effect upon the copper atom.

Using the results of the measurements, the nature of the absorption bands and absorption spectra of the complex ion in aqueous solution has been discussed.

The present author wish to thanks Mr. M. Atoji for his interest in this work and the Ministry of Education for a grant.

Department of Chemistry, Faculty of Science, Osaka University, Osaka

13) H. Yoneda, to be published soon.

14) A.S. Davydov, *Zhur. eksp. teor. Fiz.*, **18**, 210 (1948); *Akad. Nauk S.S.S.R., Pamyati S. I. Varilov*, **1952**, 197; *C.A.*, **43**, 4575 (1949).

15) F. Rosenblatt, *Z. anorg. Chem.*, **204**, 351 (1932).

Vapor Pressure of Germanium Monosulfide

By Ei-ichi SHIMAZAKI and Tsuguyasu WADA

(Received October 6, 1955)

Germanium monosulfide has a relatively high volatility, and hence it can be removed from germanite or other minerals containing germanium sulfide by vaporizing it in reducing atmosphere[1]. However, the quantitative value of vapor pressure has not yet been reported.

In the present work, the vapor pressure of germanium monosulfide is determined by means of Knudsen's effusion method over the temperature range from 338°C to 399°C, and the heat, free energy, and entropy of sublimation are calculated from the experimental results obtained.

As Kundsen has first derived[2], the weight of vapor G effusing in a time τ through an area A is related to the pressure p by

$$p=\sqrt{\frac{2\pi RT}{M}}\cdot\frac{G}{\tau}\cdot\frac{1}{A}, \qquad (1)$$

where R is the gas constant, T is the absolute temperature and M is the molecular weight of effusing vapor. The method based on the above relation is the most reliable one when the vapor pressure to be measured is lower than 10^{-2} mmHg.

It has been already confirmed that the dissociation of germanium monosulfide such as

$$GeS(s) \rightleftarrows Ge(s)+\frac{1}{2}S_2(g), \qquad (2)$$

does not practically occur at the temperature of this experiment. According to the recent study of Ono and Sudo[3], the dissociation pressure P_{S_2} of the above reaction is only 10^{-13} atm. even at 415°C.

The molecular association in effusing vapor is not considered, regarding the molecular formula as GeS. Although there is no direct evidence, this assumption is supported by the measurement on the density of vapor at 1100°C and 1500°C[4], and by the spectroscopic information on the gaseous germanium monosulfide[5].

Experimental

Apparatus and Procedure.—The apparatus used for determination of vapor pressure is the same as that used by Niwa in the studies on the vapor pressure of alkali halides[6]. It is essentially composed of a quartz cell having a small orifice from which the vapor is effused, and a microbalance by which the weight of effused vapor is determined. Details have been described in Niwa's original paper.

The original experimental procedure is modified in some respect: In the present work the decrease of weight during a certain time is measured by the microbalance which is calibrated in advance, whereas in the original paper the time required to effuse a certain quantity of a sample, a quantity corresponding to the rider, was measured. There is no essential difference, however, between these two procedures.

The accuracy of experiment is not greatly different from Niwa's, in which the maximum error is estimated as 2.6% at most.

Material.—Germanium monosulfide used was prepared by treating metallic germanium with hydrogen sulfide. Metallic germanium was obtained by reduction of germanium dioxide having a purity of 99.999% with hydrogen. The powder

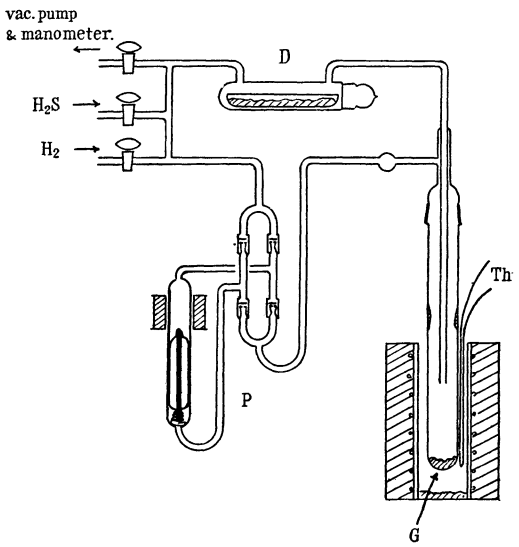

Fig. 1. Apparatus for preparation of GeS.
D; Phosphorous pentoxide.
P; Circulation pump.
Th; Pt-PtRh thermocouple.
G; Powder of germanium metal.

1) W.C. Johnson, L.S. Foster and C.A. Kraus, *J. Am. Chem. Soc.*, **57**, 1828 (1935).
2) M. Knudsen, *Ann. Phys.*, **28**, 75, 999 (1909); **29**, 179 (1909).
3) K. Ono and K. Sudo, *Bull. Res. Inst. Mineral Dressing and Metallurgy*, Tohoku Univ., **10**, 181 (1954).
4) L.F. Nilson and O. Pettersson, *Z. phys. Chem.*, **1**, 27 (1887).
5) V. Shapiro, R.C. Gibbs and A.W. Laubengayer, *Phys. Rev.*, **40**, 354 (1932).
6) K. Niwa, *J. Fac. Sci. Hokkaido Imp. Univ.*, Ser. III, **2**, 202 (1938).

of germanium thus obtained was taken in a reaction tube of Telex glass with 2 cm. diameter and 20 cm. long, which is connected to vacuum pump, circulation pump, and storage bulbs of hydrogen sulfide and hydrogen, as shown in Fig. 1. Then, after the treatment with hydrogen at 600°C to remove completely the rest of oxygen, hydrogen sulfide was introduced up to about 100 mmHg and was circulated gently at 550°C. As reaction proceeded, germanium monosulfide was condensed on the cold part of reaction tube.

Germanium monosulfide thus prepared has the appearance of dark grey with metallic lustre, whereas it becomes reddish brown when it is finely powdered[7]. The X-ray powder pattern is consistent with the crystal structure of germanium monosulfide which is proposed by Zachariasen[8] such as orthorhombic with lattice parameters of a=4.29, b=10.42, and c=3.64 Å, as shown in Table I. The lines of metallic germanium, germanium

TABLE I

X-RAY DIFFRACTION PATTERN OF GERMANIUM MONOSULFIDE

obs.		(hkl)	d (calc.)	Intensity observed by Zachariasen[8].
d (A)	Intensity.			
5.26	vvw	(020)	5.21	vvw
4.00	vw	(110)	3.97	vw
3.34	st	(120)	3.32	m
3.00	mw	(012)	2.97	m
2.79	mw	(101)	2.77	—
2.70	st	(111)	2.68	st
2.63	vst	(040)	2.61	vvst
2.18	m	(131)	2.17	st
2.11	w	(210)	2.10	mst
1.910	mw	(141)	1.899	st
1.888	vw	(150)	1.876	m⁻
1.824	m	(230)	1.826	m
1.746	vw	(060)	1.737	vw
1.669	m	(151)	1.689	st
1.639	vw	(231)	1.632	w
1.618	vw	(160)	1.610	m
1.598	vw	(122)	1.590	m
1.578	vw	(061)	1.568	m
1.497	w	(250)	1.496	m
1.386	w dif.			
1.311	w			

dioxide, or germanium disulfide are not observed. Germanium disulfide may be the only possible impurity. But its vapor pressure is far less than that of monosulfide[9], so it does not markedly affect the results even if it is present.

Ono and Sudo[3] have shown that the decomposition of germanium monosulfide to form disulfide and metal such as

$$2GeS(s) \rightleftarrows GeS_2(s)+Ge(s), \qquad (3)$$

is possible at the temperature below 388°C. After the measurement, however, the residue remaining in the cell was reexamined by X-ray diffraction, and it was confirmed that the decomposition like the above had not occurred.

Results

Vapor pressure.—The experimental results on G and τ for various temperatures, and vapor pressures calculated according to equation (1) are recorded in Table II.

TABLE II

RESULTS OF EXPERIMENTS AND VAPOR PRESSURE OF GERMANIUM MONOSULFIDE

Temp. °C	Decrease of weight, G, (mg.)	Duration, τ, (sec.)	Vapor pressure p, (mmHg)
399	5.48_0	3780	12.73×10^{-3}
387	2.73_5	3600	6.61 〃
382	3.38_4	5400	5.44 〃
378	1.88_0	3720	4.37 〃
375	1.95_2	5300	3.18 〃
368	0.95_4	3630	2.26 〃
364	1.76_4	7200	2.10 〃
361	0.63_6	3000	1.82 〃
356	0.54_9	3600	1.30 〃
348	0.65_1	6600	0.83 〃
338	0.34_7	6300	0.46 〃

The area of orifice is 4.94×10^{-3} cm.

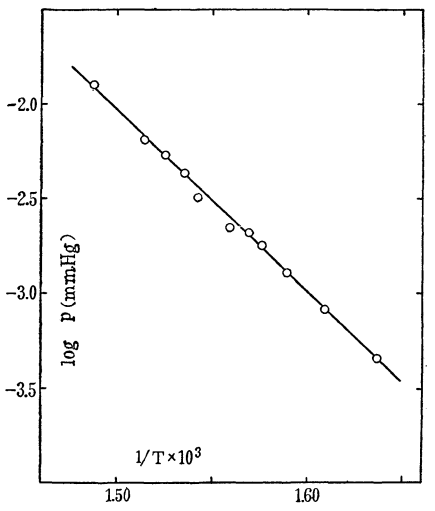

Fig. 2. Logarithms of vapor pressures of GeS, plotted against $1/T$.

As shown in Fig. 2, the logarithms of vapor pressures are linearly related against the reciprocals of the absolute temperature. This straight line is represented by the following equation;

$$\log p_{(mmHg)} = -\frac{9591}{T}+12.357. \qquad (4)$$

7) W.C. Johnson and A.C. Wheatley, *Z. anorg. allgem. Chem.*, **216**, 273 (1932).
8) W.H. Zachariasen, *Phys. Rev.*, **40**, 917 (1932).
9) N. Matsumoto and E. Shimazaki, *J. Chem. Soc. Japan (Pure Chem. Sect.)* (to be published).

Calculation of Thermodynamic Values.— The heat of sublimation ΔH_T, free energy change of sublimation ΔG_T, and entropy change of sublimation ΔS_T are calculated according to well-known thermodynamic relations:

From Clausius-Clapeyron's equation,

$$\Delta H_T = -R\frac{\mathrm{d}\ln p}{\mathrm{d}(1/T)}. \quad (5)$$

As to free energy change of sublimation,

$$\Delta G_T = -RT\ln p_{(\mathrm{atm.})}, \quad (6)$$

and as to entropy change of sublimation,

$$\Delta S = \frac{\Delta H_T - \Delta G_T}{T}. \quad (7)$$

The values of these thermodynamic functions are obtained as shown in Table III.

TABLE III

HEAT, FREE ENERGY, AND ENTROPY OF SUBLIMATION OF GERMANIUM MONOSULFIDE AT THE TEMPERATURE FROM 338° TO 399°C

ΔH_T, kcal./mol.	ΔG_T, cal./mol.	ΔS_T, cal./deg.mol.
43.9	43869–43.343T	43.3

The authors wish to express their thanks to Professor K. Niwa for his encouragement, and Professor Kenji Ono and Mr. Hideo Baba for the supply of germanium dioxide.

Department of Chemistry, Faculty of Science, Hokkaido University
Sapporo

*Studies on Dimethylglyoximato-cobalt (III) Complexes. IV. Intramolecular O-H-O Hydrogen Bonds in Bis-(dimethylglyoximato)-cobalt (III)-complexes**)

By Akitsugu NAKAHARA, Junnosuke FUJITA and Ryutaro TSUCHIDA

(Received October 6, 1955)

Introduction

It has been well-known for the last two decades that two dimethylglyoximate ions usually tend to coördinate to a metal atom with planar configuration[1,2]. The origin of this tendency, however, remained unclarified till last year[3]. In the former papers of this series[3,4], one of the present authors elucidated the tendency by taking intramolecular O-H-O hydrogen bonds into consideration. As far as the dimethylglyoximato-cobalt (III)-complexes are concerned, there has never been found any paper which dealt with direct confirmations of such hydrogen bonds. Although the first description of the subject was already published in the preceding paper[5], it seems to be desirable to perform further investigations in order to clear up some ambiguity which was concerned with the assignment of the infrared absorption band at 1725 cm^{-1}. In this work, we have measured infrared absorption spectra of hydrogen dichloro-bis-(dimethylglyoximato)-cobaltate (III) preparing with both normal and deuterated dimethylglyoxime and of several other dimethylglyoximato-cobalt (III)-complexes. Consequently, we have succeeded not only in justifying our previous conclusion but also in finding out a series of very short and symmetric O-H-O hydrogen bonds.

Experimental

Materials. Normal and Deuterated Dimethylglyoxime.—A convenient method was applied to prepare the deuterated dimethylglyoxime, dgD_2.

First of all, normal dimethylglyoxime was converted into dipotassium salt, dgK_2, by the action of an excessive amount of potassium hydroxide. 5g of dipotassium dimethylglyoximate which was perfectly free from moisture was mixed with 10 ml. of heavy water, and to this 10 ml. of concentrated deuterium chloride was added. After vigorous shaking of the mixture the insoluble

* Although in the former papers of this series the symbols, DH_2 and DH, were used for dimethylglyoxime and its ion, respectively, in the present paper the symbols, dgH_2 and dgH, are preferably chosen for the convenience of discrimination from deuterated dimethylglyoxime, dgD_2, and its ion, dgD.

1) L. Cambi and C. Coriselli, *Gazz. chim. ital.*, **66**, 91 (1936).

2) Y. Nakatsuka and H. Iinuma, This Bulletin, **11**, 48 (1936).

3) A. Nakahara, ibid., **27**, 560 (1954).

4) A. Nakahara, ibid., **28**, 207 (1955).

5) A. Nakahara, ibid., **28**, 473 (1955).

deuterated dimethylglyoxime was separated from liquor. It was heated to 110° in order to remove the moisture and adsorbed deuterium chloride. Pure normal dimethylglyoxime, dgH_2, was purified by the same procedure using normal water and hydrochloric acid instead of heavy water and deuterium chloride.

Normal and Deuterated Hydrogen Dichloro-bis-(dimethylglyoximato)-cobaltate (III).—The normal complex, $H[Co(dgH)_2Cl_2]$, was prepared by the method of Cambi et al.[6] as described in the former paper[4]. Deuterated complex, $D[Co(dgD)_2Cl_2]$, was prepared according to the following direction: 0.6 g of cobalt (II) chloride hexahydrate which was perfectly free from nickel (II) ion was dehydrated by heating until the color changed from red to blue. Instantly, it was dissolved in 10 ml. of heavy water and to this 0.6 g of deuterated dimethylglyoxime was added. The mixture was heated on a water bath and oxidized by a few drops of hydrogen peroxide. Then, the reaction mixture was filtered by suction. Dark green microscopic crystals of deuterated complex were precipitated from the filtrate by adding excess of concentrated deuterium chloride. On the other hand, partly deuterated complex, $H[Co(dgD)_2Cl_2]$, was obtained from the aqueous solution of the residual by adding excess of concentrated hydrochloric acid.

Concentrated solution of deuterium chloride was obtained by passing hydrogen chloride through **heavy water**, (specific weight $d_4^{20}=1.1049$) which was produced by Norsk Hydro Elektrisk Kvaelstofaktieselskab.

Hydrogen Dibromo-bis-(dimethylglyoximato)-cobaltate (III), $H[Co(dgH)_2Br_2]$; Hydrogen Dinitro-bis-(dimethylglyoximato)-cobaltate (III), $H[Co(dgH)_2(NO_2)_2]$; Sodium Dinitro-bis-(dimethylglyoximato)-cobaltate (III), $Na[Co(dgH)_2(NO_2)_2]$; Nitro-bis-(dimethylglyoximato)-aquo-cobalt (III), $[Co(OH_2)(dgH)_2(NO_2)]$; Nitro-bis-(dimethylglyoximato)-ammine-cobalt (III), $[Co(NH_3)(dgH)_2(NO)_2]$; Chloro-bis-(dimethylglyoximato)-ammine-cobalt (III), $[Co(NH_3)(dgH)_2Cl]$; Bis-(dimethylglyoximato)-diammine-cobalt (III) Chloride, $[Co(NH_3)_2(dgH)_2]Cl$; Hydrogen dinitro-bis-(mono-O-methyl-dimethylglyoximato)-cobaltate (III), $H[Co(dgCH_3{}^*)_2(NO_2)_2]$; Tris-(dimethylglyoximato)-cobalt (III), $[Co(dgH)_3]$.—These complexes were prepared by the direction described in the former paper[4].

Bis-(dimethylglyoximato)-nickel (II), $[Ni(dgH)_2]$.—This was recrystallized from chloroform solution as long acicular crystals.

Measurements. The spectra were obtained with a Perkin-Elmer Model 21 spectrophotometer using sodium chloride prisms and Nujol suspensions of the compounds. For optical measurements all the samples were freed from accompanying moisture including their own water of crystallization.

Results and Discussion

The Infrared Absorption Spectra of Normal and Deuterated Dimethylglyoxime.—The results of the measurements are shown in Fig. 1. Among many differences between the two curves, the one in the region from 3300 to 2300 cm^{-1} is the most significant, so far as this study is concerned.

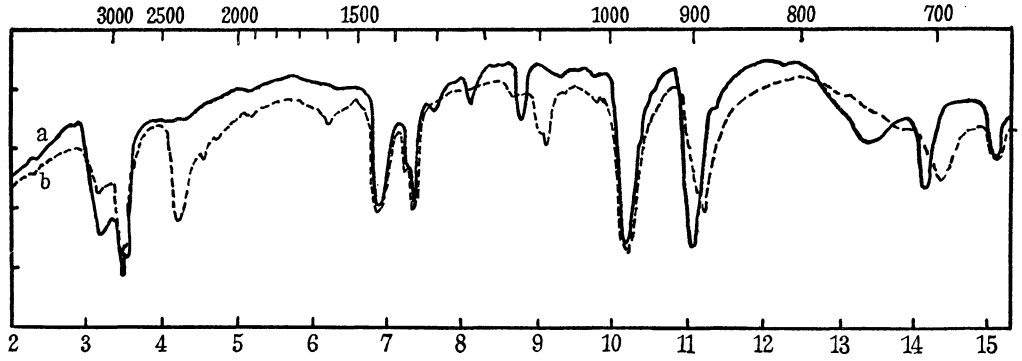

Fig. 1. Infrared absorption spectra of dimethylglyoxime: dgH_2, (a); dgD_2, (b).

In that region normal dimethylglyoxime, (a), has a strong absorption band at about 3170 cm^{-1}, which corresponds to the O-H fundamental stretching vibration frequencies. On the other hand, the curve of deuterated dimethlyglyoxime, (b), shows a rather weak band at the same wave-length in compensation for a new strong band at about 2360cm^{-1}, which is characteristic of O-D stretching vibration. This is the clear evidence for the success in substituting deuterium for hydrogen atom. Rundle et al.[7] obtained the deuterated dimethylglyoxime by recrystallizing the parent compound from heavy water. But the present method may be more effective than theirs.

The Spectra of Normal and Deuterated Hydrogen Dichloro-bis-(dimethylglyoximato)-cobaltate (III).—The spectra of normal

6) L. Cambi and C. Coriselli, *Gazz. chim. ital.*, **66**, 81 (1936).

7) L.E. Godycki, R.E. Rundle, R.C. Voter and C.V. Banks, *J. Chem. Phys.*, **19**, 1205 (1951).

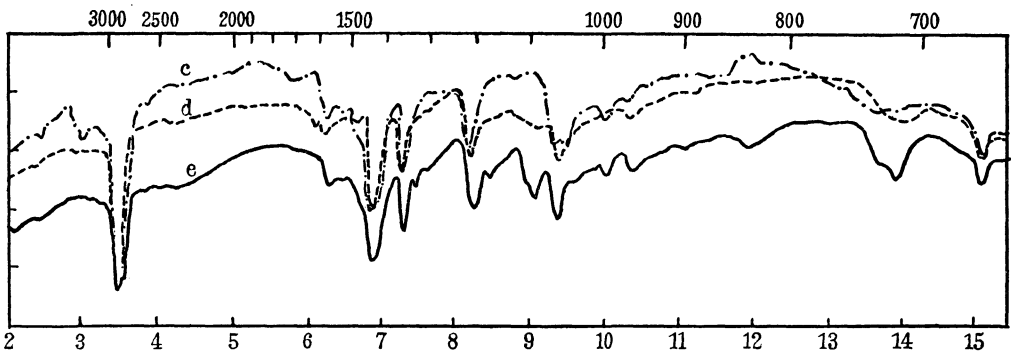

Fig. 2. Infrared absorption spectra of: (c), $H[Co(dgH)_2Cl_2]$; (d), $H[Co(dgD)_2Cl_2]$; (e), $D[Co(dgD)_2Cl_2]$.

complex, (c), partly deuterated complex, (d), and completely deuterated complex, (e), are shown in Fig. 2. In the former paper[5] the band at 1725 cm^{-1} on the curve of normal complex, $H[Co(dgH)_2Cl_2]$, was assigned to the O-H stretching frequency under the formation of strong intramolecular O-H-O hydrogen bond. (See, Fig. 3.) But the assignment

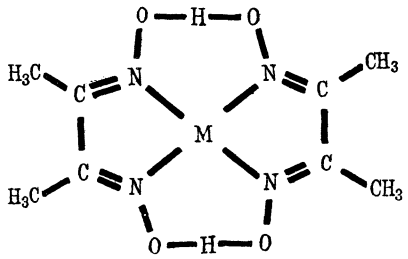

Fig. 3. Planar configuration of two dimethylglyoximate ions in bis-(dimethylglyoximato)-cobalt (III)-complexes.

was less reliable on account of the lack of decisive evidence. Now this ambiguity is perfectly swept off by the fact that the concerned band at about 1700 cm^{-1} have not been recognized on the curve of corresponding deuterated complexes, (b) and (e), as is clear from Fig. 2.

Thus, there is nodoubt in the conclusion that the absorption band at 1725 cm^{-1} of hydrogen dichloro-bis-(dimethylglyoximato)-cobaltate (III) is attributable to the O-H stretching frequency under the formation of intramolecular O-H-O hydrogen bonds.

Furthermore, it is also of interest to compare the curve of partly deuterated complex, $H[Co(dgD)_2Cl_2]$, with that of completely deuterated complex, $D[Co(dgD)_2Cl_2]$. The former complex was prepared, as described in the experimental part, through a procedure in which deuterated complex was dissolved in ordinary water. Nevertheless, there cannot be recognized on the curve, (d), any indication of such O-H stretching band as can be seen in the normal complex, (c). It is, therefore, clear that the deuterium atom in the complex is hardly affected by hyrogen atom of the solvent. It may be supposed that the deuterium atom situated between the two oxygen atoms is as hard to replace as that of hydrogen.

Spectra of Other Bis-(dimethylglyoximato)-cobalt (III)-complexes.—The infrared absorption spectra of several other complexes are shown in Fig. 4, not about the whole aspect

Fig. 4. Infrared absorption spectra of: (f), $H[Co(dgH)_2Br_2]$; (g), $H[Co(dgH)_2(NO_2)_2]$; (h), $Na[Co(dgH)_2(NO_2)_2]$; (i), $[Co(OH_2)(dgH)_2(NO_2)]$; (j), $[Co(NH_3)(dgH)_2(NO_2)]$; (k), $[Co(NH_3)(dgH)_2Cl]$; (l), $[Co(NH_3)_2(dgH)_2]Cl$.

but only about the concerned region.

All the bis-(dimethylglyoximato)-cobalt(III)-complexes show their respective O-H stretching band at about 1700 cm^{-1}. While in some

* $dgCH_3 = H_3C \cdot C(NOCH_3) \cdot C(NO) \cdot CH_3$

complexes the stretching bands are rather high in frequency and comparatively distinct in appearance, in other complexes they are the opposite. (Table I).

TABLE I

O-H STRETCHING FREQUENCIES OF BIS-(DIMETHYLGLYOXIMATO)-COBALT (III)-COMPLEXES

Complexes	O-H stretching frequencies cm^{-1}
$H[Co(dgH)_2Cl_2]$	1725
$H[Co(dgH)_2Br_2]$	1686
$H[Co(dgH)_2(NO_2)_2]$	1725
$Na[CO(dgH)_2(NO_2)_2]$	1740
$[Co(dgH)_2(NH_3)_2]Cl$	1695
$[Co(OH_2)(dgH)_2(NO_2)]$	1770
$[Co(NH_3)(dgH)_2Cl]$	1760
$[Co(NH_3)(dgH)_2(NO_2)]$	1766

hydrogen bonds in the series of above bis-(dimethylglyoximato)-cobalt (III)-complexes.

The Spectra of Hydrogen Dinitro-bis-(mono-O-methyl-dimethylglyoximato)-cobaltate(III), $H[Co(dgCH_3)_2(NO_2)_2]$, Tris-(dimethylglyoximato)-cobalt (III), $[Co(dgH)_3]$, and bis-(dimethylglyoximato)-nickel (II), $[Ni(dgH)_2]$. —The results of the measurements are shown in Fig. 5. The above described O-H stretching band at about 1700 cm^{-1} can be recognized neither on the curve of the first complex, (m), nor on that of the second complex, (n).

This fact may certify the previous conclusion[5] that the band at about 1700 cm^{-1} is characteristic of the bis-(dimethylglyoximato)-metal-complexes in which the two dimethylglyoximate ions coördinate to a metal atom with planar configuration. The infrared absorption spectrum of bis-(dimethylglyoximato)-nickel (II), (o), which was newly measured in the present work shows the characteristic band at 1775 cm^{-1}, agreeing with the results of the measurement by Rundle et al.

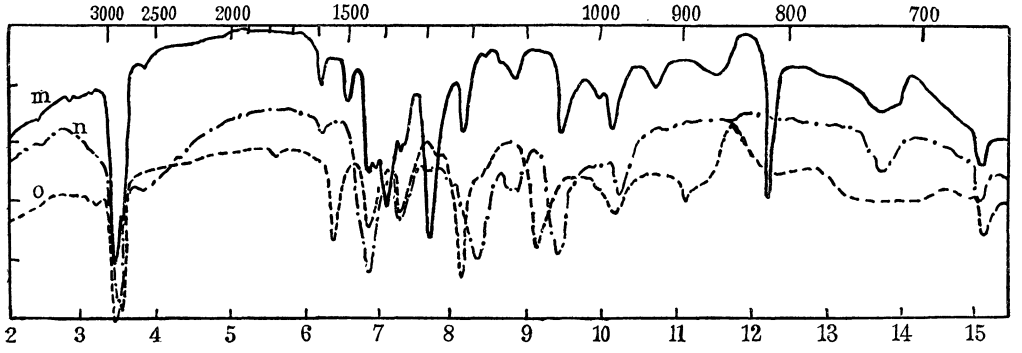

Fig. 5. Infrared absorption spectra of: (m), $H[Co(dgCH_3)_2(NO_2)_2]$, (n), $[Co(dgH)_3]$; (o), $[Ni(dgH)_2]$.

But the relations between those absorption bands and the chemical structures are probably complicated matters. At any rate, those data shown in Fig. 4 and Table I are a series of the same examples of O-H-O hydrogen bond as those of hydrogen dichloro-bis-(dimethylglyoximato)-cobaltate (III) and Bis-(dimethylglyoximato)-nickel (II). There are some reports of both theoretical and experimental investigations concerning the relation between the oxygen-oxygen distance and the fundamental optical vibration frequency of the hydrogen atom of an O-H-O hydrogen bond[7,8,9,10]. According to Rundle et al., the O-H-O hydrogen bond in bis-(dimethylglyoximato)-nickel (II) is a kind of very short and symmetric hydrogen bond. If it be the case, *there might be expected the same kind of examples of very short O-H-O*

Summary

Infrared absorption spectra of hydrogen dichloro-bis-(dimethylglyoximato)-cobaltate (III) prepared from both normal and deuterated dimethylglyoxime and of several other dimethylglyoximato-cobalt (III)-complexes were measured. It has been ascertained through the data of deuterated complexes that the absorption band at 1725 cm^{-1} of hydrogen dichloro-bis-(dimethylglyoximato)-cobaltate (III) is attributable to the O-H stretching frequency under the formation of intramolecular O-H-O hydrogen bonds.

All the bis-(dimethylglyoximato)-cobalt (III)-complexes show similar O-H stretching bands in the same region. It has been forecast that a series of examples of the very short and symmetric O-H-O hydrogen bond may be expected in the bis-(dimethylglyoximato)-cobalt (III)-complexes.

8) R.E. Rundle and M. Parasol, *J. Chem. Phys.*, **20**, 1487 (1952); L.E. Godycki and R.E. Rundle, *Acta Cryst.*, **6**, 487 (1953).

9) R.C. Lord and R.E. Merrifield, *J. Chem. Phys.*, **21**, 166 (1953).

10) A.N. Baker, Jr., ibid., **22**, 1625 (1954).

The authors are indebted to Mr. Naofumi Ooi of the Sumitomo Chemical Co. for obtaining most of the spectra. We also wish to thank the Ministry of Education for a grant which enabled us to carry out this investigation.

Department of Chemistry, Faculty of Science
Osaka University, Osaka

The Crystal Structure of Potassium Tetranitro-diammine-cobaltiate (III), $K[Co(NH_3)_2(NO_2)_4]$

By Yoshimichi KOMIYAMA (formerly, Y. TANITO)

(Received October, 12, 1955)

Introduction

Various attempts[1] have been made to determine the configuration of a complex anion, $[Co(NH_3)_2(NO_2)_4]^-$, because such a di-substituted complex should be capable of existing in two geometrically isomeric forms on the octahedral theory. In 1936, Wells[2] determined the crystal structure of the silver salt, $Ag[Co(NH_3)_2(NO_2)_4]$, and found that the two ammonia groups were co-ordinated to the central cobalt atom in *trans*-positions with respect to each other. On the other hand, in 1949 Kuroya and Yamasaki[3] examined very closely the oxalato-dinitrodiammine complex derived from the NH_4-salt or "Erdmann's salt". Namely they repeated fractional crystallizations and attempted to resolve each fraction into optical isomers. Finally they came to the conclusion that in the aqueous solution of the Erdmann's salt at room temperatures the *cis*- and *trans*-isomers should possibly coexist as an equilibrium mixture. It would be of interest to determine the configuration of the complex anion in the crystals of the Erdmann's salt itself, $NH_4[Co(NH_3)_2(NO_2)_4]$ and also the potassium salt. Since these two salts are isomorphous, their structures have been determined at the same time. In this paper the crystal structure of the potassium salt will be given; that of the Erdmann's salt will be treated in the next paper.

1) Y. Shibata and T. Maruki, *J. Chem. Soc. Japan*, 37, 1142 (1916); E.H. Riesenfeld and R. Klement, *Z. anorg. Chem.*, 124, 1 (1922). W. Thomas, *J.C.S.*, 123, 617 (1923); I.E. Knaggs, *J. C. S.* 121, 2074 (1922); B.C. Ray, *J. Indian Chem. Soc.*, 440 (1937); H. Sueda, *J. Chem. Soc. Japan*, 57, 406 (1936); E.A. Gilinskaya, *Ser. Fiz-Mat. i Estestven. Nauk*, 3, 133 (1953).

2) A.F. Wells, *Z. Krist.*, (A)., 95. 74 (1936).

3) Read at the annual meeting of Chem. Soc. Japan, (1949).

Experimental

Potassium tetranitro-diammine-cobaltiate (III) was prepared according to the method described by Jörgensen[4] and was recrystallized from water not exceeding 60°C. They belong to the orthorhombic bipyramidal class and are usually thin needles elongated along the *c*-crystal axis. Three crystal rods less than 0.2 mm. in diameter parallel to each principal axis were prepared. All the equatorial reflections were recorded by using Fe $K\alpha$ radiation (λ=1.937 Å). Usual multiple film technique was employed and the intensity of reflections were visually estimated by comparison with a standard scale. The usual correction factors were applied by means of the chart given by Cochran[5]. No correction for absorption was applied. A temperature factor and a scale factor for converting the observed values of $|F_{rel}|$ approximately to the absolute scale were calculated by Wilson's method[6]. The unit cell dimensions were obtained from high order reflections of the equatorial lines of the oscillation photographs.

The results are: a=11.38±0.02 Å, b=12.95±0.02 Å and c=6.76±0.01 Å, giving the axial ratio $a:b:c$=0.879: 1: 0.522, in agreement with those obtained morphologically, i.e., 0.8783: 1: 0.5192. From the density 2.107 g./cc. measured by the pyknometer method at 25.0°C, it was found that the unit cell contains four formula units of $K[Co(NH_3)_2(NO_2)_4]$, the calculated value being 2.106 g./cc. The space group is D_2^4-$P\ 2_12_12_1$. All the atoms are on the general positions: x, y, z; $\frac{1}{2}-x, \frac{1}{2}+y, \frac{1}{2}-z$; $\frac{1}{2}+x, \frac{1}{2}-y, \bar{z}$; $\bar{x}, \bar{y}, \frac{1}{2}+z$.

Determination of the Structure

Firstly the Patterson projections $P(X, Y)$ $P(Y, Z)$ and $P(X, Z)$ were evaluated.

Comparing these results with the corresponding Patterson maps of the Erdmann's salt, whose analysis has been carried out at

4) S.M. Jörgensen, *Z. anorg. Chem.*, 17, 477 (1898).

5) W. Cochran, *J. Sci., Inst.*, 25, 253 (1949).

6) A.J.C. Wilson, *Acta Cryst.*, 2, 318 (1949).

the same time, it was confirmed that these two crystals are isomorphous as expected, and moreover it was possible to identify Co–Co, K–K and K–Co vectors on each projection. Hence the positions of cobalt and potassium were fixed at once.

Preliminary Fourier projections of electron density upon the planes perpendicular to each principal axis were synthesized using observed F-values, whose sign was calculated from the parameter values of cobalt and potassium. From these projections it was possible to assign approximate parameters for nitrogen atoms which are co-ordinated nearly octahedrally around each cobalt atom. These were in good accord with the conclusion drawn from each Patterson projection. Though the Fourier prejections showed faint outlines of oxygen atoms they could not be located unequivocally. The c-crystal axis is as short as 6.76 Å, and it should be possible to obtain a clear projection of the whole structure in this direction, as any interleaving of the complex anion within this periodicity is probably ruled out. An attempt was made to determine the signs of $F(hk0)$ directly by taking the difference of the corresponding F-values observed for the ammonium and potassium salt, since both are isomorphous and the positions of potassium atoms are already known. The signs of 46 out of 120 observed reflections could be determined successfully. The projection thus obtained showed the outlines of the oxygen atoms more clearly than the previous one. A vector convergence map[7] was also made for this projection, by using the positions of cobalt atoms. Closer examination of this projection and vector convergence map enabled one to deduce the x- and y-parameters of all the atoms in the unit cell. $F(hk0)$ were then calculated. The agreement was reasonably good and enabled a start to be made with the process of refinement by means of Fourier syntheses. At this stage, all the z-parameter values of oxygen atoms were assumed using the data of interatomic distances and bond angles. Calculation of $F(0kl)$ and $F(h0l)$ values eliminated at once the possibility of the *cis*-configuration. Finally only one set of parameter values corresponding to the *trans*-configuration remained which could account for $F(0kl)$ and $F(h0l)$s. Then all the projections were refined by successive approximations as usual. The final parameters are listed in Table I. A final electron density projection along the c-crystal axis is shown in Fig. 1.

7) C.A. Beevers and J.H. Robertson, *Acta Cryst.*, 3, 164 (1950).

TABLE I

FINAL PARAMETERS

	x/a	y/b	z/c
Co	0.1690	0.1915	0.2500
K	0.117	0.473	0.695
$NH_3(1)$	0.278	0.265	0.064
$NH_3(2)$	0.062	0.118	0.436
N(1)	0.250	0.264	0.466
N(2)	0.056	0.305	0.234
N(3)	0.088	0.119	0.034
N(4)	0.281	0.078	0.266
O(1)	0.264	0.226	0.632
O(2)	0.293	0.350	0.442
O(3)	0.040	0.353	0.083
O(4)	−0.003	0.332	0.383
O(5)	−0.018	0.112	0.017
O(6)	0.150	0.072	−0.078
O(7)	0.257	0.005	0.376
O(8)	0.367	0.080	0.163

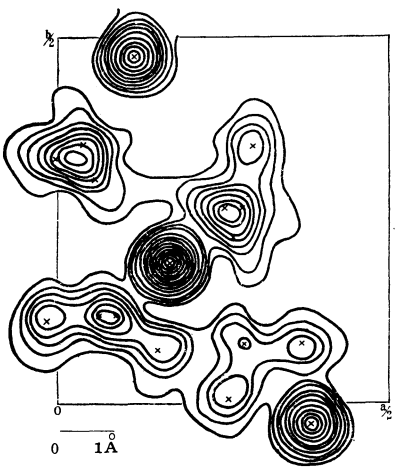

Fig. 1. Electron densities along the c-axis of $K[Co(NH_3)_2(NO_2)_4]$. Contours are at intervals of 2 e. A^{-2}.

The comparison of the observed structure factors with those calculated is given in Table II. The atomic scattering factors used for the calculation of the structure factors were those listed in the International Tables. A temperature factor of the form $\exp -B\left(\frac{\sin\theta}{\lambda}\right)^2$ was used, where B was given the value 2.5 Å^2. The value of B and the scale factor were estimated by plotting the values of $\log F_c/F_o$ versus $(\sin\theta)^2$ at the final stage. The reliability factor $R=\sum||F_o|-|F_c||/\sum|F_o|$ are 0.165, 0.185 and 0.235 for $(hk0)$, $(0kl)$ and $(h0l)$ respectively. The weighted mean value of R is 0.179, for which only observed reflections up to $\frac{\sin\theta}{\lambda}=0.501$ have been used.

TABLE II

OBSERVED AND CALCULATED STRUCTURE AMPLITUDES

ORIGIN OF CO-ORDINATE IS TAKEN AT A CENTER OF SYMMETRY ON EACH PROJECTION

hkl	$F_{obs.}$	$F_{cal.}$	*hkl*	$F_{obs.}$	$F_{cal.}$	*hkl*	$F_{obs.}$	$F_{cal.}$	*hkl*	$F_{obs.}$	$F_{cal.}$
200	17.8	−19.8	510	13.2	10.9	011	2.0	− 1.6	0121	12.2	13.0
400	1.8	3.8	520	16.3	15.5	012	12.9	13.1	0122	2.1	2.1
600	9.0	4.5	530	1.5	− 0.2	013	8.3	5.6			
800	4.0	7.1	540	16.5	−14.9	014	5.4	− 5.5	101	26.8	27.4
1000	3.6	− 4.6	550	11.7	11.3	015	2.0	1.4	102	4.8	− 0.1
020	12.3	−12.2	560	10.3	6.1	016	3.8	3.7	103	7.4	5.9
040	2.7	0.8	570	2.5	− 2.1				104	4.2	− 3.9
060	9.2	9.5	580	5.2	− 5.6	021	15.1	−16.2	105	17.2	16.6
080	6.5	− 4.4	590	—	0.1	022	1.8	1.5	106	6.0	− 7.1
0100	7.5	11.0	5100	9.1	− 8.9	023	19.5	21.7			
0120	—	− 1.0	5110	4.0	− 1.8	024	9.0	9.0	201	2.2	− 2.6
						025	6.5	− 6.0	202	6.8	11.6
110	4.8	− 4.9	610	3.2	4.2	026	8.6	− 9.3	203	16.2	13.2
120	19.3	−19.9	620	12.3	− 8.5				204	4.6	3.5
130	13.5	−13.9	630	5.8	3.8	031	7.0	−14.4	205	8.4	8.8
140	5.5	4.7	640	9.3	− 9.6	032	13.0	−18.0	206	5.0	4.8
150	13.5	−12.1	650	8.7	9.2	033	8.0	− 4.5			
160	7.1	− 7.7	660	6.6	6.8	034	—	4.7	301	8.2	9.5
170	6.3	− 5.3	670	3.9	3.1	035	—	2.2	302	6.0	0.4
180	10.5	14.1	680	16.5	−16.0	036	—	− 2.7	303	2.6	3.6
190	7.2	6.7	690	6.3	7.0				304	7.2	− 6.0
1100	13.0	11.3	6100	5.0	5.0	041	6.3	8.1	305	—	2.0
1110	3.6	1.9	6110	3.0	1.9	042	14.0	−16.3	306	1.4	− 1.3
1120	6.0	− 4.4				043	12.6	13.7			
1130	5.0	− 4.8	710	2.0	− 1.7	044	—	− 2.7	401	—	− 5.3
			720	2.4	− 2.3	045	8.1	− 8.8	402	23.0	−22.4
210	24.9	−24.4	730	6.0	− 1.9	046	2.2	2.1	403	—	− 0.2
220	11.1	11.0	740	5.8	4.3				404	8.0	− 7.8
230	—	− 3.2	750	4.2	3.0	051	—	− 0.5	405	3.2	− 0.2
240	27.0	−26.4	760	14.9	−14.0	052	6.3	4.6	406	2.6	1.1
250	1.8	0.1	770	9.0	− 7.8	053	4.7	4.1			
260	8.2	6.0	780	2.6	− 2.9	054	7.0	− 7.2	501	1.4	0.4
270	18.9	−18.5	790	—	0	055	7.4	− 7.2	502	8.6	5.6
280	5.2	4.0	7100	—	0.1	056	4.7	3.5	503	20.0	−16.4
290	2.5	1.3							504	6.0	5.8
2100	4.3	− 2.3	810	13.5	−13.8	061	15.7	−15.9	505	4.0	1.2
2110	12.3	−11.8	820	15.0	11.7	062	13.5	13.5	506	2.6	1.2
2120	2.9	− 3.6	830	4.0	6.3	063	16.2	16.4			
			840	6.2	9.3	064	7.3	− 2.3	601	3.2	− 5.4
310	1.2	− 0.9	850	4.5	0.9	065	2.2	− 2.6	602	15.0	−11.1
320	1.5	− 1.0	860	3.0	− 3.3	066	2.7	4.5	603	14.1	−13.4
330	36.0	35.3	870	6.3	− 5.2				604	8.0	− 8.0
340	5.0	1.2	880	6.6	5.6	071	9.0	8.8	605	7.8	− 4.6
350	20.5	−20.2	890	7.0	6.2	072	6.8	− 5.9			
360	14.2	13.7				073	1.8	− 4.0	701	17.6	−18.1
370	4.2	4.6	910	12.4	−11.8	074	4.3	5.4	702	4.8	− 4.4
380	10.8	7.1	920	4.0	2.1	075	4.0	4.6	703	15.2	−13.6
390	10.9	9.4	930	—	0.5				704	4.8	2.1
3100	3.0	1.9	940	1.2	− 1.4	081	2.9	1.9	705	5.2	− 5.5
3110	10.6	− 5.4	950	10.8	− 9.7	082	21.0	21.1			
3120	6.0	5.0	960	1.9	− 1.7	083	3.1	− 2.9	801	—	− 0.9
			970	4.0	4.1	084	9.0	− 8.0	802	2.5	− 2.4
410	—	− 3.8	1010	12.2	12.4	085	2.4	− 3.4	803	—	2.1
420	16.2	−19.7	1020	5.0	4.1	091	7.2	− 5.9	804	3.6	− 8.0
430	11.8	− 9.7	1030	2.1	− 2.8	092	2.5	2.1	805	—	− 1.7
440	6.7	− 1.7	1040	2.0	− 2.4	093	4.5	6.6			
450	3.9	1.4	1050	2.7	− 2.8	094	2.7	− 0.5	901	—	− 2.7
460	4.9	− 2.1	1060	3.7	1.8				902	5.0	− 1.6
470	8.1	9.4	1110	6.0	5.5	0101	—	0.7	903	—	− 2.8
480	10.2	10.7	1120	7.9	8.5	0102	10.3	10.3	904	3.6	− 2.9
490	13.4	−12.6	1130	3.3	− 3.2	0103	6.7	− 4.8	1001	2.4	2.0
4100	6.4	− 3.9	1140	1.4	− 1.6	0104	7.0	− 7.2	1002	2.6	1.1
4110	2.5	3.1	002	8.8	−12.5				1003	2.1	1.6
4120	4.2	4.5	004	13.7	11.6	0111	2.3	1.1			
			006	5.6	− 9.9	0112	—	0.2	1101	11.0	9.3
						0113	2.9	− 6.4	1102	—	0.4

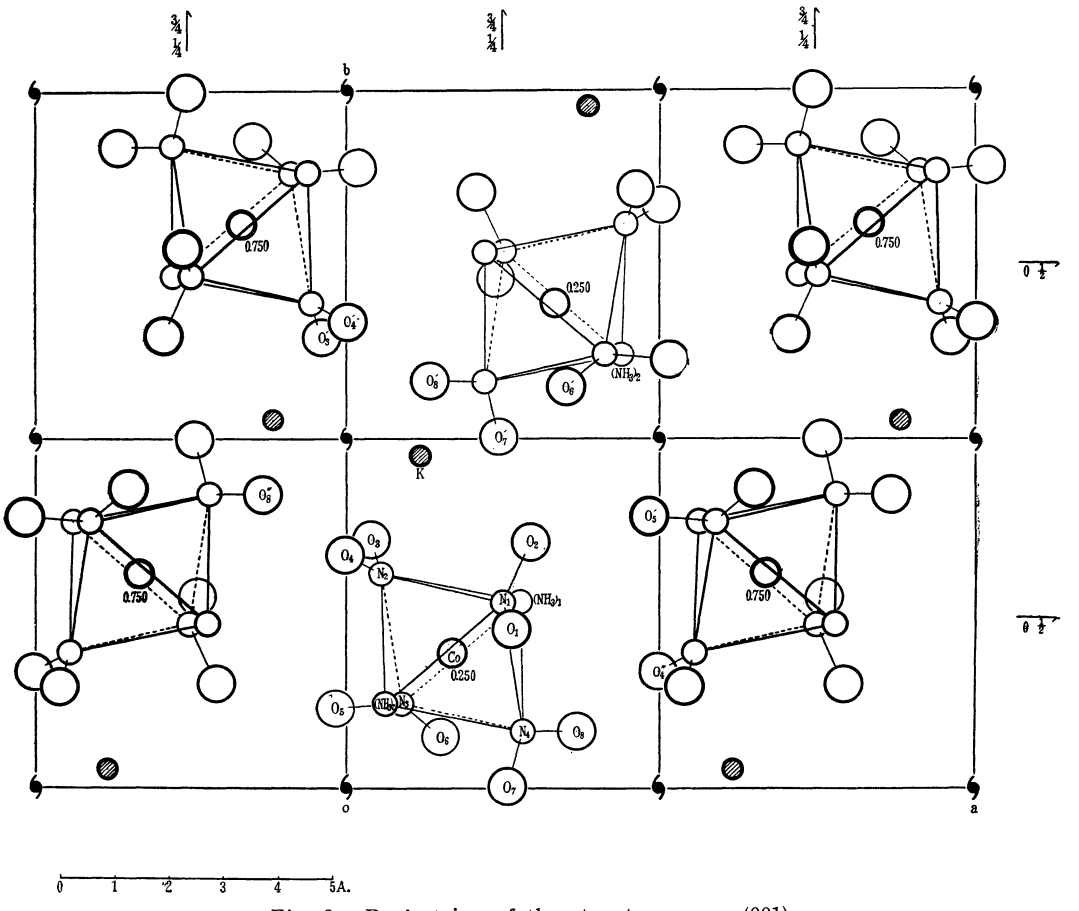

Fig. 2. Projectcion of the structure upon (001).

Description of the Structure

The structure projected upon a plane normal to the *c*-crystal axis is shown in Fig. 2, which corresponds to Fig. 1. The structure is built from potassium ions and complex anions $[Co(NH_3)_2(NO_2)_4]^-$, thus being essentially ionic.

Interatomic distances and bond angles calculated on the basis of the atomic parameters in Table I are listed in Table III. A perspective drawing of the complex anion is shown in Fig. 3.

TABLE III

INTERATOMIC DISTANCES AND INTERBOND ANGLES

Co.....NH_3(1)	2.00 Å	K	O(2)	3.08 Å	
.....NH_3(2)	2.00 Å		O(3)	3.17 Å	
.....N(1)	1.96 Å		O(4)	3.11 Å	
.....N(2)	1.96 Å		O(3′)	2.97 Å	
.....N(3)	1.96 Å		O(4′)	3.11 Å	
.....N(4)	1.96 Å		O(7′)	3.26 Å	
			O(8′)	2.79 Å	
N(1).....O(1)	1.24 Å		O(8″)	3.08 Å	
.....O(2)	1.23 Å				
O(1) O(2)	2.08 Å	(NH_3)(1)	O(1)(−)	2.97 Å	
∠O(1)N(1)O(2)	115°		O(5′)	2.87 Å	
N(2).....O(3)	1.21 Å	(NH_3)(2′)	O(5′)	3.07 Å	
.....O(4)	1.26 Å				
O(3) O(4)	2.10 Å	O(1)	O(4″)	2.76 Å	
∠O(3)N(2)O(4)	116°	O(2)	O(6′)	3.09 Å	
		O(2)	O(7′)	2.99 Å	
N(3).....O(5)	1.22 Å	O(3)	O(7′)	3.05 Å	
.....O(6)	1.20 Å	O(3)	O(8″)	2.72 Å	
O(5) O(6)	2.08 Å				
∠O(5)N(3)O(6)	118°				
N(4).....O(7)	1.23 Å				
.....O(8)	1.20 Å				
O(7) O(8)	2.14 Å				
∠O(7)N(4)O(8)	124°				

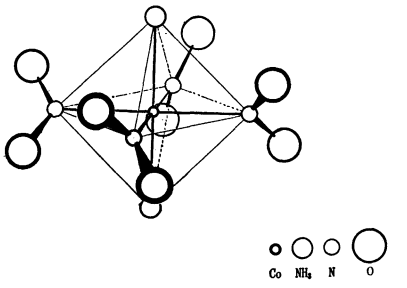

Fig. 3. A perspective drawing of a complex anion.

Two ammonia molecules are co-ordinated to a cobalt atom in *trans*-positions with respect to each other at a distance of 2.00 Å. Four nitrogen atoms of the nitro groups form a square around the cobalt atom within experimental errors, being 1.96 Å apart from it. Thus an octahedral co-ordination is completed around a cobalt atom. These interatomic distances are in good agreement with those found in the structures of various complex compounds of tervalent cobalt[8,9,10,11].

The size and shape of the nitro groups are also in agreement with our previous results.

The planes containing each nitro group are inclined at angles 58°, 56°, 42° and 86° respectively with the plane of four nitrogen atoms of the nitro groups in the same sense. Hence, the configuration of the complex anion is essentially similar to that found in crystals of the silver salt, $Ag[Co(NH_3)_2(NO_2)_4]$[2].

The distances of approach between N atom of ammonia molecule and O atom of nitro group of adjascent complex anion are found to be 2.87 Å, and 2.97 Å. They may be compared with those found in crystals of trinitro-triammine-cobalt (III). These short distances suggest hydrogen bonding between them. By these NH·····O bonds the complex anions are held together, forming a network perpendicular to the *b*-crystal axis. Between these layers exist potassium ions.

A potassium ion is surrounded by eight oxygen atoms of the nitro groups with distances ranging from 2.79 Å to 3.26 Å. The co-ordination polyhedron around a potassium atom is rather distorted.

8) Y. Tanito, Y. Saito and H. Kuroya, This Bulletin, 25, 188 (1952).
9) Y. Tanito, Y. Saito and H. Kuroya, This Bulletin, 25, 328 (1952).
10) A. Nakahara, Y. Saito and H. Kuroya, This Bulletin, 25, 331 (1952).
11) Y. Tanito, Y. Saito and H. Kuroya, This Bulletin, 26, 420 (1953).

Summary

The crystal structure of potassium tetranitrodiammine-cobaltiate (III), $K[Co(NH_3)_2(NO_2)_4]$, prepared according to the method of Jörgensen, has been determined by two-dimensional Fourier method. The orthorhombic unit cell has the dimensions $a=11.38\pm0.02$ Å, $b=12.95\pm0.02$ Å and $c=6.76\pm0.01$ Å containing four formula units in it (Fe K_α, $\lambda=1.937$ Å), and the space group is D_2^4-$P2_12_12_1$. The shape and size of a complex ion was found to be similar to the one found in crystals of silver salt, $Ag[Co(NH_3)_2(NO_2)_4]$. Two ammonia molecules are co-ordinated to the central cobalt atom in *trans*-positions, with Co–N distance 2.00 Å.

The average dimensions of the nitro groups were: N–O=1.22 Å and $\angle ONO=118°$, in agreement with the results obtained for other nitro-complex compounds of cobalt. Each potassium atom is surrounded by eight oxygen atoms of the nitro-groups with distances ranging from 2.79 Å to 3.26 Å.

The author expresses his hearty thanks to Professor H. Kuroya and Dr. Y. Saito of this university for encouragement and invaluable discussions. Part of the cost of this study has been defrayed by a Grant of the Ministry of Education.

Institute of Polytechnics, Osaka City University, Osaka

*The Magnetic Susceptibility of Iodine in Various Solvents**

By Michio KONDO, Michihiko KISHITA, Masao KIMURA and Masaji KUBO

(Received October 25, 1955)

According to studies made by Bhatnagar and Lakra[1], iodine dissolved in cyclohexane has a much smaller diamagnetism than it has in other solvents, such as benzene. It seems rather peculiar that cyclohexane is abnormal as a solvent for iodine in view of the fact that both cyclic and aliphatic saturated hydrocarbons are quite normal in their general behavior as solvents. On the other hand, benzene is surely not an indifferent solvent for iodine. As Mulliken[2] has already clearly pointed out, iodine forms a molecular complex with benzene, the latter playing a role of a π donor ($b\pi$) while the former that of a halogenoid σ acceptor ($x\sigma$). By this conception, he could explain the finite electric moment of iodine in benzene and the charge-transfer spectra observed for a number of cases of similar complex formation.

The present writers have therefore undertaken to carry out the measurements of the magnetic susceptibility of iodine in various solvents in order to examine whether it depends upon the kinds of solvents to any appreciable degree, and if so, in what solvents iodine has an abnormal diamagnetism. The diamagnetism of differently colored solutions of iodine has already been studied by Courty[3], who believed that the magnetic susceptibilities of violet and brown solutions of iodine obey the additivity rule, while red and red-brown solutions do not. His results will be discussed critically in the present paper.

Apparatus and Experimental Procedure

A simple Gouy magnetic balance was employed for the determination of magnetic susceptibility at room temperature. The sample tube made of hard glass was symmetrical in form. It was 22 cm. long with a partition in the middle forming two compartments. The one compartment was filled with the solvent, while the solution under investigation was placed in the other compartment. The cross-sectional area of the liquid column amounted to 0.22 cm^2. The cell was suspended between the poles of a magnet from a semi-microbalance capable of determining weight changes as small as 0.01 mg. The electromagnet could be supplied with a direct current of up to 17 amp. taken from selenium rectifiers, ripples having been removed by means of a system of condensers. The rectifiers were fed from a 200-volt, three-phase alternating current source stabilized with an appropriate voltage stabilizer and led through suitable transformers before it was applied to the rectifiers. The total resistance of the coil of the electromagnet was less than 3 ohms. Each tip of the pole pieces separated by 1.2 cm. had a circular surface plane of 3 cm. in diameter. The resulting magnetic field could be raised up to about 24,000 oersteds.

The magnitude of the downward force f acting on the tube along its length is given by the expression,

$$f=\frac{1}{2}(\kappa-\kappa_a)AH^2=g\Delta w,$$

where κ and κ_a denote respectively the volume susceptibility of the liquid in one compartment and that of the air in the other compartment of the tube. A is the cross-sectional area of the liquid column, g the gravitational constant, and Δw the apparent increase in weight of the tube on application of the magnetic field. The magnetic balance was calibrated with distilled water and its magnetic susceptibility per cubic centimeter, which is practically identical with that per gram, was set equal to -0.720×10^{-6}. The susceptibility κ per unit volume of the solution under investigation was calculated from

$$\frac{\kappa-\kappa_a}{\kappa_o-\kappa_a}=\frac{\Delta w}{\Delta w_o},$$

where the suffix o refers to water used as the standard, and the volume susceptibility of air κ_a was put equal to $+0.0295\times10^{-6}$. For greater accuracy, a differential method was employed, viz., actual measurements were made of $\kappa-\kappa_o$ rather than $\kappa-\kappa_a$. Due correction was made of the force acting on the glass container because of its possible asymmetry by a blank test with the empty tube. The density of each solution was measured in order to convert the susceptibility per unit volume κ into that per unit weight $\chi=\kappa/\rho$.

Materials

Iodine was purified twice by sublimation. Hexane, benzene, toluene, ethyl alcohol, and carbon disulfide used as solvent were prepared according

* Read before a meeting of the Chemical Society of Japan held on October 14, 1955.

1) S.S. Bhatnagar and C.L. Lakra, *Indian J. Phys.*, 8, 43 (1933). See also P.W. Selwood, "*Magnetochemistry*," Interscience Publishers, Inc., New York, 1943, p. 66.

2) R.S. Mulliken, *J. Am. Chem. Soc.*, **72**, 600 (1950); **74**, 811 (1952); *J. Phys. Chem.*, **56**, 801 (1952).

3) C. Courty, *Compt. rend.*, **204**, 1248 (1937); *Bull. soc. chim. France*, **5**, 84 (1938).

to the procedure given by Weissberger[4]. Special precaution was taken against the possible contamination of ferromagnetic impurities in the experimental materials.

Results

The diamagnetic susceptibilities of the solutions of iodine in various solvents are plotted against the weight fraction w of the solute in Fig. 1. It will be seen that the

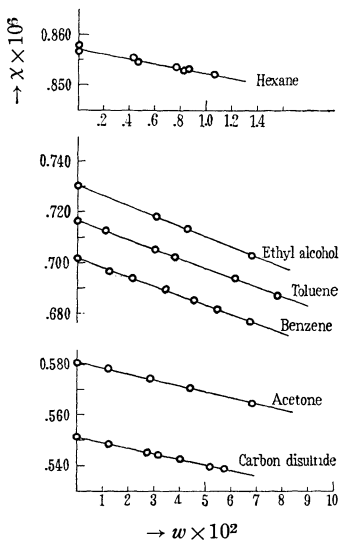

Fig. 1. Dependence of the diamagnetic susceptibilities per gram of solutions of iodine in various solvents upon the weight fraction of the solute.

experimental points lie on a straight line for each solvent over the whole range of concentrations investigated. In other words, the susceptibility of the solutions χ_{12} obeys a simple formula,

$$\chi_{12}=\chi_1(1-w)+\chi_2 w,$$

where suffixes 1 and 2 refer to the solvent and the solute respectively. The susceptibility of iodine in various solvents could be evaluated from the slope of the straight lines and are given in Table I.

TABLE I

MAGNETIC SUSCEPTIBILITY PER GRAM OF IODINE IN VARIOUS SOLVENTS

Solvent	$\chi\times10^6$	Bhatnagar	Color
Hexane	−0.363		violet
Cyclohexane		−0.35	violet
Carbon disulfide	−0.337	−0.50	violet
Benzene	−0.334	−0.51	red
Toluene	−0.341		red
Ethyl alcohol	−0.329		brown
Acetone	−0.344		brown
(Iodine crystal)	−0.350∼0.36		

4) A. Weissberger and E. Proskauer, "Organic Solvents", Oxford at the Clarendon Press, 1935.

The accuracy of the magnetic susceptibility of a solute depends upon the precision of the measurement of magnetic susceptibilities of the solutions as well as on the concentration range available. The probable error of the present data is estimated to be less than a few percent except that in hexane which may amount to several percent owing to the small solubility. The solubility of iodine in cyclohexane is almost as small as in hexane.

The susceptibility* of iodine in crystalline state is reported to be −0.36[5] or −0.350[6] at room temperature.

Discussion

The present authors have found no such remarkable dependence of the susceptibility upon solvents as has been reported by Bhatnagar and Lakra and by Courty. And yet a slightly lower value of susceptibility was observed for all employed solvents other than hexane in which iodine assumes a susceptibility value practically identical with that in a crystal.

Bhatnagar and Lakra[1] using a modified Quincke's method obtained the susceptibility values given in the third column of Table I. The striking difference between their results and the present writers' is that Bhatnagar and Lakra found a very high diamagnetism in benzene and in carbon disulfide while the present writers did not. As is mentioned later, one has good reason to believe it is unlikely that the diamagnetism of iodine in solutions is greater than that in pure phase.

Courty[2] used the following solvents for dissolving iodine: carbon tetrachloride, chloroform, and carbon disulfide (violet solutions), ethyl ether (brown solution), and benzene and toluene (red solutions). He found an increasing deviation from the additivity rule as the color changed from violet into red. The additivity of magnetic susceptibility implies two points, first the linear dependence of the susceptibility per unit weight of the solution upon the weight fraction of the solute and second the identity of the susceptibility of the solute in solutions with that of the pure phase. As regards the first, the present writers' data are in conformity for all the solvents employed. Courty's experimental points, on the other hand, are scattered about the respective straight lines to such a great extent that his conclusions concerning the additivity rule seem difficult to be accepted. As to the second point, the

* Susceptibility values are given in unit 10^{-6}.

5) International Critical Tables, VI.

6) S.R. Rao and H.S. Venkataramiah, *Current Sci.*, (India), **14**, 195 (1945); *Chem. Abstr.*, **40**, 258 (1946).

diamagnetism of iodine which was found by the present writers in solutions other than hexane solution is slightly smaller than that in hexane or in pure phase. Even a violet-colored carbon disulfide solution gave a result nearly identical with that in benzene solution. The deviations found by Courty for brown and red solutions are of the same sign as in the present investigation but much greater in magnitude, whereas the deviations found by Bhatnagar and Lakra for benzene and carbon disulfide are of the opposite sign. They are also great, as has already been mentioned. In order to lend support to the present writers' results, the following theoretical calculation was carried out of the change of diamagnetism of iodine on dissolution in benzene.

Benesi and Hildebrand[7], using spectroscopic methods, have shown definitely that benzene and iodine form a 1:1 complex of considerable stability. They found that 60 percent of iodine dissolved in benzene is present in the complex. On the other hand, the close agreement in form and intensity between the spectrum of iodine in the vapor state and in violet solutions indicates that complexes are not formed in these.

Mulliken[2] developed a theory of molecular complexes based on the concept of charge-transfer. He discussed the structure of the complex of iodine with benzene (Bz) in terms of resonance between a predominant no-bond structure (Bz, I_2) and a small admixture of the type (Bz^+–I_2^-). From Fairbrother's[8] data of the moment of iodine in benzene and the overlap integral estimated for the most probable model of the complex, Mulliken calculated the ionic character of the complex in the ground state to be approximately 2.8 percent. The susceptibility of the complex in the hypothetical no-bond state may be assumed to be equal to the sum of the susceptibilities of its component parts. The diamagnetism of the dative structure was estimated in the following way. The principal susceptibility of benzene normal to the plane of the ring ($K_3=-91.2$) is more than twice that in the plane ($K_1=K_2=-37.3$)[9]. The loss of one out of six π-electrons of benzene to form Bz^+ will lead to the decrease of molal diamagnetism of the order of magnitude $(1/3)(1/6)\Delta K=3.0$, where the factor 1/3 was introduced to take into account all the possible orientations of the plane of the benzene ring in space. It would be more desirable to calculate the diamagnetic contribution of an electron in the highest occupied orbital of a benzene molecule by means of molecular orbital treatment. However, noticeable improvement is not to be expected in view of the uncertainty of other data[10]. The increase of diamagnetism of I_2 due to the gain of an electron to form I_2^- may be approximated by the difference between the diamagnetism of I^- and Pascal's constant for I, $50.6-44.6=6.0$*. Therefore with due regard to the constitutive correction constant (+4.1*) for C–I bond formation, the increase of molal susceptibility of the complex (Bz^+–I_2^-) over that of (Bz, I_2), i.e., the decrease of diamagnetism was calculated as $3.0-6.0+4.1=1.1$. It is doubtful whether this figure is really significant in view of the accumulated errors for a small difference. However, it would seem that the decrease of diamagnetism of iodine on dissolution in benzene should be very small, if at all, because the contribution of the dative structure is only 2.8 percent and in addition only 60 percent of iodine is present in the complex.

Summary

The diamagnetic susceptibility per gram of iodine in solutions of various solvents was measured with a Gouy magnetic balance at room temperature. The value -0.363×10^{-6} in hexane solution was practically identical with that of iodine in pure phase. The values of diamagnetism of iodine in carbon disulfide, benzene, toluene, ethyl alcohol, and acetone ranging from -0.329 to -0.341 are only slightly smaller than the value in hexane, in disagreement with the data found in literatures. A qualitative support for the present writers' result was afforded by theoretical considerations based on Mulliken's theory of complexes formed in accordance with the mechanism of electron transfer from a donor molecule to an acceptor.

We express our appreciation to the Ministry of Education for the financial support of this research.

Chemical Department, Faculty of Science
Nagoya University, Nagoya

7) H.A. Benesi and J.H. Hildebrand, *J. Am. Chem. Soc.*, **70**, 2382 (1948); **71**, 2703 (1949).
8) F. Fairbrother, *Nature*, **160**, 87 (1947); *J. Chem. Soc.*, **1948**, 1051.
9) K. Lonsdale and K.S. Krishnan, *Proc. Roy. Soc. London*, A **156**, 597 (1936).
10) S. Fujii and S. Shida, This Bulletin, **24**, 242 (1951).
* These numerical data were taken from Selwood. loc. cit.

Magnetochemical Study of Hydroxyazobenzenes

By Yoshio MATSUNAGA

(Received October 21, 1955)

Introduction

Zincke[1] showed in 1884 that the product of the condensation of phenylhydrazine with α-naphthoquinone is identical with 4-benzeneazo-1-naphthol which is prepared by the coupling of diazotized aniline with 1-naphthol, so that the problem of structure immediately presented itself. Although the physical and chemical properties of 4-hydroxyazobenzenes indicate that they exist in the azophenol form, Borsche[2] succeeded to show that "2'-nitro-4-hydroxyazobenzene" (I or II) can be prepared by the following distinct methods similarly.

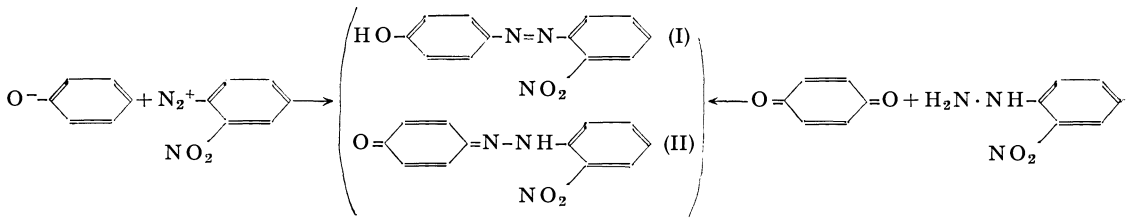

Furthermore, evidence of the quinonoid character of 2', 4'-dinitro-4-hydroxyazobenzene was provided by its ability to undergo the Diels-Alder reaction[3]. In spite of many researches, the investigators came to the different conclusions in regard to the structure of 2-hydroxyazobenzene; e. g. Kuhn and Bär[4] believed that the spectroscopic evidence favors the benzenoid structure, but on the other hand, Burawoy and Markowitsch[5] suggested that the same evidence favors the quinonoid structure.

These studies are merely concerned with the dissolved state of hydroxyazobenzenes. We can not decide conclusively the structure in the solid state. Diamagnetic susceptibility measurements seem to be of great service in deciding the forms of these compounds, as the azophenol form is made of the benzenoid structures, while the quinonehydrazone form contains the quinonoid structure. In such a case, a large difference between the susceptibilities of these two forms is expected. From this point of view, Pascal[6] examined the molar susceptibilities of some compounds, and compared them with the ones calculated from his own empirical constants. But his results quoted in Table I seem to be unplausible, as they are not consistent with the other evidences, and allowed the equilibrium between two forms in the solid state, and the migration of alkyl groups. Namely he concluded that 4-hydroxyazobenzene is quinonehydrazone form, and 4-methoxyazobenzene and 1-benzeneazo-2-naphthol are mixture of tautomers.

TABLE I

MOLAR SUSCEPTIBILITIES OF HYDROXYAZOBENZENES AND THEIR RELATED COMPOUNDS GIVEN BY PASCAL

Substance	Molar Suscept. ($-\chi_M$)*		
	obs.	calcd. (a)**	calcd. (b)**
4-Hydroxyazobenzene	99.6	117.3	95.0
4-Methoxyazobenzene	118.8	129.1	107.6
1-Benzeneazo-2-naphthol	140.7	153.7	124.8
4, 4'-Dimethoxyazobenzene	147.5	146.9	117.8
4, 4'-Diethoxyazobenzene	171.4	170.6	141.3
4-Aminoazobenzene	118.4	118.8	103.7

* Susceptibility values have been multiplied by 10^6 throughout this paper.

** (a) Azophenol form, (b) Quinonehydrazone form.

For the determination of the structures of hydroxyazobenzenes from the susceptibility measurement, it is necessary to reexamine the molar susceptibilities of azobenzene and its derivatives which have no tautomeric forms, and establish the empirical method to estimate them correctly.

1) T. Zincke and H. Bindewald, *Ber.*, **17**, 3026 (1884).
2) W. Borsche, *Ann.*, **357**, 171 (1907).
3) W.M. Lauer and S.E. Miller, *J. Am. Chem. Soc.*, **57**, 180 (1933).
4) R. Kuhn and F. Bär, *Ann.*, **516**, 143 (1935).
5) A. Burawoy and I. Markowitsch, ibid., **503**, 180 (1933).
6) P. Pascal, *Compt. rend.*, **150**, 1167 (1910), *Bull. soc. chim. France*, **9**, 868 (1911), *Ann. chim. phys.*, **25**, 289 (1912).

Experimental

Materials.—No. 1–10, 19 and 30 were kindly provided by Drs. F. Iimura and M. Kobayashi. No. 11–18 and 20–27 were prepared by the coupling of diazotized aniline or its substituted derivatives with phenol or *p*-cresol, and purified by recrystallization from aqueous ethanol or benzene, and finally by distillation or sublimation in vacuo. No. 28 and 29 were synthesized by the alkali fusion of nitrophenol[7] and recrystallized from aqueous ethanol. No. 28 was sublimed finally in vacuo. Their melting points are presented in Tables II and III.

Magnetic Measurement.—The susceptibilities were measured using a Gouy balance as previously described[8].

Results and Discussion

The results are shown in Table II for azobenzene and its derivatives which have unquestionable form and in Table III for hydroxyazobenzenes. The molar susceptibility of azobenzene has been found to be −111.3 by Pascal[9], while it is −105.0 by Banerjee[10]. Our result supports the latter value, so that Pascal's constitutive correction constant for azo-group 1.8 is not appropriate for the estimation of molar susceptibilities of the other compounds of which the structures will be discussed in this paper. We assumed that the molar susceptibilities are given by the sum of those of constitutional fragments of the molecules. For instance, we assumed that the azophenol form of 4-hydroxyazobenzene is built up from benzene, phenol, and azo-group by the loss of two atoms of hydrogen, and the molar susceptibility is given by the same relation too. Similar computations have been done for the compounds shown in Table II, and the mean value −0.4 has been obtained for the contribution of azo-group. Then the calculated values in Tables II and III have been estimated by the combination of this constant for azo-group and the molar susceptibilities of benzene and its derivatives; the following values were used, benzene −55.2[11], toluene −65.8[12], anisol −72.6[13], dimethylaniline −85.0[13], chlorobenzene −70.0[14], acetophenone −71.6[13], ethyl benzoate −93.3[15], nitrobenzene −61.8[12], phenol −60.8[13], *p*-cresol −71.4[16], resorcinol −67.9[17]. The accordance between the observed and the calculated molar susceptibilities is satisfactorily good within the limit of experimental errors. As the effect of substituents to single benzene nucleus is taken into consideration in our estimations, our calculated values are more compromising for these compounds than the ones obtained by the direct summation of Pascal's constants. For instance, Angus[15] and Trew[18] showed that methyl substitution in the aromatic nucleus gives a diamagnetic increment about one unit lower than the normal CH_2 increment of −11.7; furthermore, French[17] deduced that the isomerides of disubstituted benzenes possess different susceptibilities respectively. Even in our case, the interaction of substituents through an azo-group is not considered, so the results in Table show that the method is not adequate in a few cases.

TABLE II

SUSCEPTIBILITIES OF AZOBENZENE AND ITS DERIVATIVES

No.	Substance	M. p.	Suscept. $(-\chi)$	Molar Suscept. $(-\chi_M)$ obs.	calcd.
1	Azobenzene	67.5–68.5	0.578	105.3	104.9
2	4-Methyl-	69–69.5	0.590	115.8	115.5
3	2-Methoxy-	39–40	0.574	121.9	122.3
4	4-Methoxy-	55	0.575	122.0	122.3
5	4-Dimethylamino-	115–115.5	0.594	133.8	134.7
6	4-Chloro-	87	0.551	119.4	119.7
7	4-Acetyl-	113–114	0.535	122.1	121.3
8	4-Carboethoxy-	86	0.568	144.4	143.0
9	4-Nitro-	133–134	0.492	111.7	111.5
10	4,4'-Dimethoxy-	162	0.574	139.0	139.7

For the quinonehydrazone form of 4-hydroxyazobenzene, the molar susceptibility

7) R. Willstätter and M. Benz, *Ber.*, 39, 3492 (1906).
8) H. Akamatu and Y. Matsunaga, This Bulletin, 26, 364 (1953).
9) P. Pascal, *Bull. soc. chim. France*, 9, 79 (1911).
10) S. Banerjee, *Z. Krist.*, A 100, 316 (1939).
11) B.C. Eggleston et al., *J. Chem. Soc.*, 1954, 941.
12) F.G. Baddar and S. Sugden, ibid., 1950, 308.
13) "International Critical Tables", Vol. 6, McGraw-Hill Book Co. Inc., New York, 1929, p. 362.
14) C.M. French and V.C.G. Trew, *Trans. Faraday Soc.*, 41, 439 (1945).
15) W.R. Angus, *Bull. soc. chim. France*. 1949, D 483.
16) estimated. = 65.8 (toluene) − 60.8 (phenol) + 55.2 (benzene).
17) C.M. French, *Trans. Faraday Soc.*, 41, 676 (1945).
18) V. C. G. Trew, ibid., 49, 604 (1953). See also, C.M. French, ibid., 50, 1320 (1954).

is estimated as −102.2 by the following schematic chemical equation,

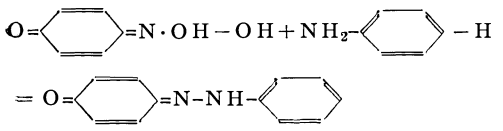

The values used in the above equation are −50.3 for *p*-benzoquinonemonoxime[13], −62.4 for aniline[12], and Pascal's constants for hydrogen and oxygen in alcohol. Consequently the difference of susceptibility between these two forms is expected to be 8.3 in 4-hydroxyazobenzene. Our calculated difference is remarkably smaller than that expected from the calculated molar susceptibilities for two isomeric forms given by Pascal. Although there is no experimental result which can compare with these two expected differences, comparison will be drawn in the later paper on the azo-derivatives of naphthols. For the other compounds, the data on substituted anilines and quinonemonoximes required by the estimation of molar susceptibility for the quinonehydrazone form are not always available, but the susceptibility difference between these two forms may be nearly constant.

The observed molar susceptibilities of all compounds in Table III are in accordance with the calculated values for the azophenol form, so that there can be no doubt that these hydroxyazobenzenes are in the azophenol form in the solid state. At first glance, the discrepancy in 2,2′-dihydroxyazobenzene is seriously large, but molar susceptibility of this compound is only 3.3 units higher than that of 4,4′-dihydroxyazobenzene. In the isomerides of dihydroxybenzene, molar susceptibility of catechol is 2.3 units more diamagnetic than the value for hydroquinone, so the difference between these two dihydroxyazobenzenes may be of probable magnitude, and the calculated values seem to be too small in these cases.

In the *ortho*-compounds, hydrogen bond undoubtedly exists between the nitrogen and oxygen atoms, but the effect of hydrogen bond to the molar susceptibility is not detectable in these compounds either[19]. Furthermore, the position of the proton between the nitrogen and oxygen atoms may not be the same in the tautomeric forms[20], because the observed susceptibility does not deviate so much from the value calculated for azophenol form.

TABLE III

SUSCEPTIBILITIES OF HYDROXYAZOBENZENES

No.	Substance	M. p.	Suscept.	Molar Suscept. ($-\chi_M$)	
			($-\chi$)	obs.	calcd.
11	4-Hydroxy-	152	0.555	110.0	110.5
12	4′-Methyl-4-hydroxy-	150	0.569	120.8	121.1
13	2′-Methoxy-4-hydroxy-	145–146	0.558	127.4	127.9
14	4′-Methoxy-4-hydroxy-	137–139	0.559	127.6	127.9
15	4′-Chloro-4-hydroxy-	153–155	0.537	125.0	125.3
16	2′-Nitro-4-hydroxy-	160–161	0.478	116.2	117.1
17	3′-Nitro-4-hydroxy-	157.5–158.5	0.483	117.4	117.1
18	4′-Nitro-4-hydroxy-	213	0.477	116.0	117.1
19	2-Hydroxy-	81–82	0.559	110.8	110.5
20	5-Methyl-2-hydroxy-	105–107	0.569	120.8	121.1
21	2′,5-Dimethyl-2-hydroxy-	97–98	0.594	134.4	131.7
22	4′,5-Dimethyl-2-hydroxy-	111–112	0.582	131.7	131.7
23	2′-Methoxy-5-methyl-2-hydroxy-	119	0.577	139.8	138.5
24	4′-Methoxy-5-methyl-2-hydroxy-	94–95	0.577	139.8	138.5
25	4′-Chloro-5-methyl-2-hydroxy-	152	0.551	135.9	135.9
26	3′-Nitro-5-methyl-2-hydroxy-	162–163	0.496	127.6	127.7
27	4′-Nitro-5-methyl-2-hydroxy-	181–183	0.503	129.4	127.7
28	2.2′-Dihydroxy-	165–167	0.568	121.7	116.1
29	4,4′-Dihydroxy-	decomp.	*	118.4**	116.1
30	2,2′,4,4′-Tetrahydroxy-	decomp.	0.537	132.2	130.3

* Monohydrate 0.566.

** 131.4 (Monohydrate) − 13.0 (water).

19) P. Rumpf and M. Séguin, *Bull. soc. chim. France*, 1949, D 366, 1950, 177, 542.

20) G.W. Wheland, "Advanced Organic Chemistry" John Wiley & Sons, Inc., New York, 1949, p. 628.

The observed molar susceptibilities of azo-derivatives of phenol are smaller than the calculated values in many cases. This decrease of diamagnetism will be interpreted by the resonance effect indicated in the structure (III).

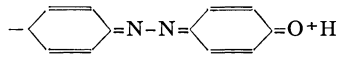

(III)

Such an effect will be strengthened by the electron withdrawing substituents, and 2′- and 4′-nitro-derivatives are examples of this. In the azo-derivatives of *p*-cresol, methyl group will perturb such an effect to some extent, so that in some cases the observed values are more diamagnetic than the calculated ones. But we will not discuss in detail these apparent discrepancies on accounts of the complicated influence of substituents and the rather large experimental errors.

Summary

The magnetic susceptibilities of azobenzene and its nine derivatives were measured by the Gouy method. The procedure to estimate the molar susceptibility from the values observed for constitutional fragments of the molecule was applied to these compounds, and the empirical constant for azo-group −0.4 was determined. Twenty hydroxyazobenzenes, mainly derivatives of phenol and *p*-cresol, were also measured, and their molar susceptibilities were compared with the calculated values for the azophenol form and the quinonehydrazone one. The author concluded that they are all in the azophenol form in the solid state.

The author expresses his hearty thanks to Prof. H. Akamatu for his interest and to Drs. F. Iimura and M. Kobayashi for samples of many substances investigated. The cost of this research has been defrayed by the Grant in Aid for Scientific Research from the Ministry of Education, to which the author's thanks are due.

Department of Chemistry, Faculty of Science, The University of Tokyo
Tokyo

Absorption Spectra of Co(III) Complexes. II. Redetermination of the Spectrochemical Series

By Yoichi SHIMURA and Ryutaro TSUCHIDA

(Received October 27, 1955)

In the course of our studies on thec urve analyses of absorption spectra[1], the absorption curves of many Co(III) complexes have been determined. In the present paper, experimental details will be given for the cobaltic ammine, oxalato, carbonato and amino-acido complexes. Moreover, the "spectrochemical series" will be redetermined on the basis of the new data.

Experimental

Absorption measurements were made in aqueous solutions by a Beckman DU spectrophotometer, or by a spectrograph with a sector photometer. The concentration of the solutions varied from 1.0×10^{-2} to 3.3×10^{-5} gram complex-ion per litre. All measurements were made at room temperature. The complex perchlorates were used to minimize interaction between the complex ion and anions. The complexes were analyzed for water of crystallization and for perchlorate ion[2]. The results of the measurements are shown in

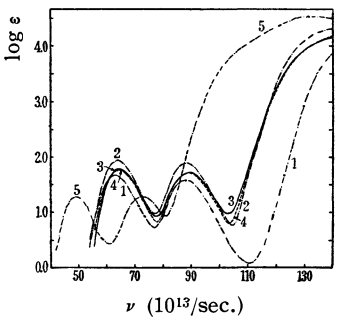

Fig. 1. Absorption curves of:
1, $[Co(NH_3)_6](ClO_4)_3$;
2, $[Co\ en_3](ClO_4)_3$;
3, *cis*-$[Co\ en_2(NH_3)_2](ClO_4)_3\cdot H_2O$;
4, *trans*-$[Co\ en_2(NH_3)_2](ClO_4)_3\cdot H_2O$;
5, $[Co(O_6Mo_6O_{18}H_6)](NH_4)_3\cdot 7H_2O$.

1) Part I of this series: Y. Shimura and R. Tsuchida, This Bulletin, 28, 572 (1955).

2) M. Linhard and G. Stirn, *Z. anorg. Chem.*, 268, 105 (1952).

Figs. 1–5. The numerical data for the first and the second absorption bands were previously reported[1].

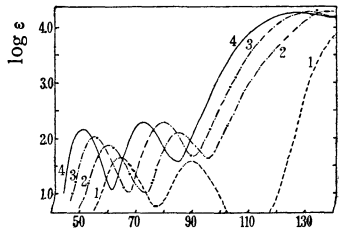

Fig. 2. Absorption curves of Co (III) ammine-oxalato series:
1, [Co $(NH_3)_3$] $(ClO_4)_3$;
2, [Co $(NH_3)_4$ ox] $ClO_4 \cdot H_2O$;
3, [Co $(NH_3)_2$ ox_2] $NH_4 \cdot H_2O$;
4, [Co ox_3] $K_3 \cdot 3H_2O$.

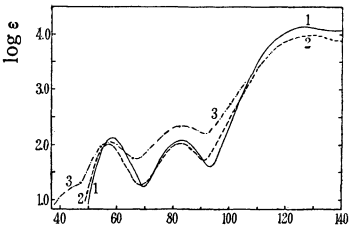

Fig. 3. Absorption curves of Co(III) carbonato complexes:
1, [Co en_2 CO_3] ClO_4;
2, [Co $(NH_3)_4$ CO_3] ClO_4;
3, [Co $(NH_3)_4$ CO_3] ClO_4 (solution after standing three hours at room temperature).

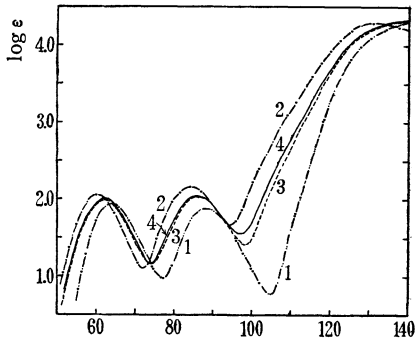

Fig. 4. Absorption curves of:
1, [Co en_3] $(ClO_4)_3$;
2, [Co en_2 ox] $Cl \cdot 3H_3O$;
3, [Co en_2 glycine'] $(ClO_4)_2$;
4, [Co en_2 leucine'] $(ClO_4)_2$.

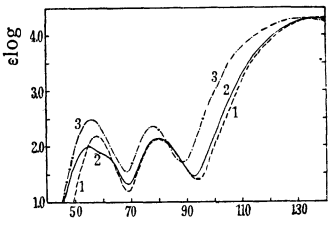

Fig. 5. Absorption curves of amino-acido complexes of Co(III);
1, β-[Co glycine'$_3$]·H_2O;
2, α-[Co glycine'$_3$]·$2H_2O$;
3, [Co edta] $Na \cdot 4H_2O$.

Description of the Individual Complexes

α-[Co(glycine')$_3$]·$2H_2O$ and β-[Co(glycine')$_3$]·H_2O.—For the preparations, the method of Ley and Winkler[3] was followed. The α-form has purple color and the β-form red. These two forms correspond to geometric isomers, *cis-cis* and *cis-trans* forms. The β-isomer was insoluble in water and the spectrum of the isomer was measured in 60% $HClO_4$. As will be seen in Fig. 5, the main difference between the curves of the two isomers occurred in the region of the first band: the first band of the β-form is normal but the α-form shows distinct indication of splitting of the first band. This splitting may be considered as a proof for the *cis-trans* structure of the α-form, since the similar splitting was reported for the first band of *trans*-[$Co(NH_3)_4(OCOCH_3)_2$] ClO_4 and not for the first band of the corresponding *cis* isomer[4].

[Co en_2glycine'] $(ClO_4)_2$ and [Co en_2 leucine'] $(ClO_4)_2$.—These perchlorates were prepared by adding concentrated aqueous solution of $NaClO_4$ and alcohol to the solutions of the corresponding chlorides[5]. They were twice recrystallized from water-alcohol mixture, and washed by alcohol and dried in air. The absorption curves of the two complexes have almost the same features.

[Co$(NH_3)_4CO_3$]ClO_4[6].—The tetrammine complex was unstable in aqueous solutions. The decomposition intermediates have more hyperchromic and more diffuse bands than the original tetrammine complex (see Fig. 3). The bisethylenedaimine complex was very stable in aqueous solutions

cis- and trans- [Co $en_2(NH_3)_2$] $(ClO_4)_3 \cdot H_2O$.—These were precipitated from the concentrated

3) H. Ley and H. Winkler, *Ber.*, **42**, 3894 (1909); H.F. Holtzclaw, Jr. and D.P. Sheetz, *J. Am. Chem. Soc.*, **75**, 3053 (1953).
4) M. Linhard and M. Weigel, *Z. anorg. Chem.*, **264**, 321 (1951).
5) J. Meisenheimer, L. Angermann and H. Holsten, *Ann.*, **438**, 261 (1924); I. Lifschitz, *Rec. trav. chim.*, **58**, 785 (1939).
6) M. Linhard and M. Weigel, *Z. anorg. Chem.*, **260**, 65 (1949).

solutions of the corresponding chlorides[7] by addition of 60% $HClO_4$, and were recrystallized twice from water and dried in air. The freshly dried crystals were analyzed since they effloresced on exposure to the air.

[Co $(NH_3)_6$]$(ClO_4)_3$, [Co en_3]$(ClO_4)_3$, [Co en_2 CO_3] ClO_4 [Co en_2 ox] $Cl \cdot 3H_2O$, NH_4[Co ox_2 $(NH_3)_2$]$\cdot H_2O$, K_3[Co ox_3]$\cdot 3H_2O$ and Na [Co edta]$\cdot 4H_2O$ were prepared essentially by the method described in literature.

Spectrochemical Series for the Ligands of Co (III) Complexes

The spectrochemical series represents the order of hypsochromic effects of ligands on the first or second absorption band of metallic complexes. During about the two decades which have elapsed since the first determination of the series by Tsuchida[8], a great deal of new measurement has been made by many authors. Examining the data found in literature as well as in the author's measurements, revision of the series for the ligands of Co(III) complexes has been attempted.

In Table I to VI, the ligands have been arranged in the order of frequencies of the first bands of their comlexes.

Abbreviations and Conventions i) An unidentate ligand is designated by the full formula. The atom which is attached directly to the central cobalt atom takes precedence of the other atoms; for example, chromate ion, $OCrO_3^=$; unidentate oxalate ion, $OCOCO_2^=$.

TABLE I

PENTAMMINE SERIES, [Co $(NH_3)_5$ A]

Ligand, A	First band ν (log ε)	Second band ν (log ε)	Ref.	Supplementary refs.
NO_2^-	65.5 (2.00)	(( ))	Linhard (1951)[9]	10, 11, 16)
$SO_3^=$	63.6 (2.15)	(( ))	Kiss (1938)[10]	17)
NH_3	62.9 (1.68)	88.3 (1.60)	12)	10, 11, 13, 14, 15)
OH_2	61.6 (1.62)	87.5 (1.62)	Kuroya (1950)[11]	10, 15)
ONO^-	61.1 (1.86)	(( ))	Linhard (1955)[18]	11, 16)
NCS^-	60.5 (2.24)	(( ))	19)	10, 18, 20, 21)
ONO_2^-	60.0 (1.77)	86.6 (1.77)	19)	10)
$OSO_3^=$	60.0 (1.70)		8)	
$OCHO^-$	59.7 (1.77)	85.3 (1.65)	Linhard (1951)[4]	
OH^-	59.6 (1.80)	81.1 (1.85)	Kiss (1938)[10]	
$OCOCH_3^-$	59.6 (1.82)	85.2 (1.70)	Linhard (1951)[4]	
$OCONH_2^-$	59.4 (1.85)	84.9 (1.70)	Linhard (1951)[4,22]	
$OCOCO_2^=$	59.2 (1.87)	(( ))	8)	17)
$OCO_2^=$	59.2 (1.92)	(( ))	Kiss (1938)[10]	17)
$SSO_3^=$	58.8 (1.82)	(( ))	19)	10, 23)
F^-	58.4 (1.70)	84.8 (1.63)	Linhard (1951)[22]	
N_3^-	57.8 (2.41)	(( ))	Linhard (1951)[24]	
Cl^-	56.2 (1.71)	82.5 (1.72)	Linhard (1951)[22]	10, 11, 14, 15)
$OCrO_3^-$	55.6 (2.14)	(( ))	8, 25)	17)
Br^-	54.7 (1.77)	(( ))	Linhard (1951)[22]	
I^-	51.8 (1.90)	(( ))	Linhard (1951)[22]	

7) A. Werner, *Ann.*, **386**, 1 (1912); A. Werner, F. Bräunlich, E. Rogowina and C. Kreutzer, ibid., **351**, 65 (1907).
8) R. Tsuchida, This Bulletin, **13**, 388, 436 (1938).
9) M. Linhard and M. Weigel, *Z. anorg. Chem.*, **267**, 113 (1951).
10) A. Kiss and D. Czeglédy, *Z. anorg. Chem.*, **235**, 407 (1938).
11) H. Kuroya, *J. Inst. Polytech. Osaka City Uuiv.*, C **1**, No. 1, 29 (1950).
12) This paper.
13) M. Linhard, *Z. Elektrochem.*, **50**, 224 (1944).
14) H. Kuroya and R. Tsuchida, This Bulletin, **15**, 427 (1940).
15) R. Tsuchida, *J. Chem. Soc. Japan*, **59**, 731 (1938).
16) B. Adell, *Z. anorg. Chem.*, **271**, 49 (1952).
17) H. Yoneda and M. Kobayashi, *J. Chem. Soc. Japan*, **75**, 1192 (1954).
18) M. Linhard, H. Siebert and M. Weigel, *Z. anorg. Chem.*, **278**, 287 (1955).
19) Y. Shimura, unpublished data.
20) R. Tsuchida, *J. Chem. Soc. Japan*, **59**, 586 (1938).
21) Y. Shimura, *J. Am. Chem. Soc.*, **73**, 5079 (1951).
22) M. Linhard and M. Weigel, *Z. anorg. Chem.*, **266**, 49 (1951).
23) A. Kiss, G. Auer and E. Major, *Z. anorg. Chem.*, **246**, 28 (1941).
24) M. Linhard and M. Weigel, *Z. anorg. Chem.*, **267**, 121 (1951).
25) R. Tsuchida and M. Kobayashi, This Bulletin, **13**, 471 (1938).

TABLE II

Cis SERIES OF TETRAMMINE COMPLEXES

Ligand	First band ν (log ε)	Second band ν (log ε)	Ref.	Supplementary refs.
NO_2^-	67.5 (2.20)	(( ))	Linhard (1951)[9]	11, 14, 26)
$SO_3^=$	65.9 (2.26)	(( ))	27)	
NH_3	62.9 (1.68)	88.3 (1.60)	12)	
OH_2	60.0 (1.40)	84.0 (1.49)	28)	10)
ONO^-	58.8	(( ))	Yalman[53]	
ox	58.7 (1.91)	84.0 (2.11)	12)	10, 11, 14, 17)
ONO_2^-	58.5 (1.7)	85 (1.6)	19)	
$OCHO^-$	58.2 (1.94)	82.5 (1.69)	Linhard (1951)[4]	
carb	57.4 (2.01)	82.6 (2.02)	12)	10, 11, 14)
$OCOCH_3^-$	57.3 (2.01)	82.0 (1.77)	Linhard (1951)[4]	
F^-	57.3 (1.74)	81.9 (1.51)	Linhard (1952)[29]	
N_3^-	55.7 (2.42)	(( ))	Linhard (1951)[24]	

TABLE III

Cis SERIES OF BISETHYLENEDIAMINE COMPLEXES

Ligand	First band ν (log ε)	Second band ν (log ε)	Ref.	Supplementary refs.
NO_2^-	69.0 (2.26)	(( ))	Adell (1951)[30]	14, 26)
$SO_3^=$	67.1 (2.35)	(( ))	19)	
ONO^-	65.9 (2.13)	(( ))	Adell (1951)[30]	
NH_3	64.4 (1.79)	89.4 (1.74)	12)	26)
en	63.9 (1.94)	88.4 (1.90)	12)	
gly	61.3 (2.00)	86.4 (2.04)	12)	
NCS^-	61.1 (2.53)	(( ))	19)	21, 26)
OH_2	60.6 (1.85)	84.5 (1.82)	Basolo (1950)[26]	32)
ox	60.1 (2.05)	84.3 (2.16)	12)	11, 14, 31)
$OCOC_2H_5^-$	59.4 (2.16)	82.7 (1.91)	Linhard (1951)[4]	
carb	58.4 (2.13)	83.0 (2.09)	12)	14)
OH^-	58* (1.97)*	81* (2.01)*	Bjerrum (1952)[32]	
Cl^-	55.9 (1.95)	76.6 (1.84)	Linhard (1952)[29]	26)
Br^-	54.3 (2.04)	(( ))	Linhard (1952)[29]	

TABLE IV

Trans SERIES OF TETRAMMINE COMPLEYXES

Ligand	First band Ia ν (log ε)	First band Ib ν (log ε)	Second band ν (log ε)	Ref.	Supplementary refs.
NO_2^-	68.2 (2.37)		(( ))	Linhard (1951)[9]	11, 14, 26, 43)
$SO_3^=$	66.6 (2.32)		(( ))	27)	
NH_3	62.9 (1.68)		88.3 (1.60)	12)	
OH_2	58.6		84.0	Yalman[53]	
$OCOCH_3^-$	54.4 (1.76)	64* (1.37)*	82.1 (1.76)	Linhard (1951)[4]	
N_3^-	52.8 (2.57)		(( ))	Linhard (1951)[24]	
Cl^-	47.7 (1.63)	63.0 (1.38)	74.8 (1.54)	Linhard (1952)[29]	28)

26) F. Basolo, *J. Am. Chem. Soc.*, **72**, 4393 (1950).
27) Y. Shimura, This Bulletin, **25**, 46 (1952).
28) R. Tsuchida, This Bulletin, **11**, 721 (1936).
29) M. Linhard and M. Weigel, *Z. anorg. Chem.*, **271**, 101 (1952).
30) B. Adell, *Acta Chem. Scand.*, **5**, 54 (1951).
31) A. Mead, *Trans. Farad. Soc.*, **30**, 1052 (1934).
32) J. Bjerrum and S. E. Rasmussen, *Acta Chem. Scand.*, **6**, 1265 (1952).

TABLE V

Trans SERIES OF BISETHYLENEDIAMINE COMPLEXES

Ligand	First band Ia ν (log ε)	First band Ib ν (log ε)	Second band ν (log ε)	Ref.	Supplementary refs.
NO_2^-	69.8 (2.27)		(( ))	Adell (1951)[33]	
NH_3	64.2 (1.77)		89.2 (1.73)	12)	11, 14, 26)
NCS^-	59.4 (2.44)		(( ))	19)	21, 26)
ONO^-	58.3 (1.72)		(( ))	Adell (1951)[33]	
$ONO_2^=$	58 (1.8)	66 (1.6)	85 (1.9)	19)	
OH^-	57* (1.72)*		79* (1.73)*	Bjerrum (1952)[32]	
$OCOC_2H_5^-$	55.7 (1.73)	67* (1.40)*	84.1 (1.80)	Linhard (1951[4])	
OH_2	55* (1.52)*	68* (1.57)*	86* (1.73)*	Bjerrum (1952)[32]	26)
$SSO_3^=$	54.9 (1.93)		(( ))	19)	23)
F^-	51.6 (1.35)	67.9 (1.49)	82.8 (1.67)	Linhard (1952)[29]	
Cl^-	48.8 (1.58)	64.9 (1.41)	77.5 (1.68)	1)	26, 29)
Br^-	45.6 (1.73)	(( ))	(( ))	Linhard (1952)[29]	
I^-	44.8	(( ))	(( ))	Ernsberger (1934)[34]	

TABLE VI

COMPLEXES CONTAINING ONLY ONE SPECIES OF LIGAND

Complex Ion	First band ν (log ε)	Second band ν (log ε)	Ref.	Supplementary refs.
$[Co(CN)_6]^{3-}$	?	?		10, 23, 26)
$[Co(C_5H_5)_2]^+$	74* (2.38)*	99* (3.04)*	Wilkinson (1952)[37]	
$[Co\ dg_3]$	(( ))	(( ))	Nakahara (1954)[38]	
$[Co\ dip_3]^{3+}$	66.7	(( ))	Yamasaki (1940)[39]	
$[Co\ phen_3]^{3+}$	66.5 (2.49)	(( ))	Yamasaki (1953)[40]	
$[Co\ pn_3]^{3+}$	64.5 (1.95)		Mathieu (1936)[41]	
$[Co\ dien_2]^{3+}$	64.2	88.0	Brigando (1953)[42]	
$[Co\ en_3]^{3+}$	63.9 (1.94)	88.4 (1.90)	12)	10, 11, 13, 14, 31)
$[Co(NH_3)_6]^{3+}$	62.9 (1.68)	88.3 (1.60)	12)	10, 11, 13, 15)
$[Co(ONO)_6]^{3-}$	62.8 (2.41)	(( ))	Kuroya (1950)[11]	10, 43)
β-$[Co\ gly_3]$	57.7 (2.20)	80.2 (2.14)	12)	
$[Co\ edta]^-$	55.9 (2.51)	78.1 (2.36)	12)	
$[Co\ acac_3]$	51.0 (2.04)	74.0 (2.47)	Sone (1948)[44]	45)
$[Co\ ox_3]^{3-}$	49.7 (2.17)	70.9 (2.30)	12)	10, 31, 46, 47)
$[Co(O_3Mo_6O_{18}H_6)]^{3-}$	49.2 (1.29)	72.8 (1.30)	1, 12, 35)	
$[Co(OH_2)_6]^{3+}$	49 (1.6)	75 (1.7)	Topp (1928)[48]	
$[Co(S_2COC_2H_5)_3]$	48.5 (2.43)	62.5 (2.56)	Kida (1955)[52]	
$[Co(S_2CNH_2)_3]$	47.2 (2.45)	62.0 (2.80)	Kida (1955)[52]	
$[Co\ carb_3]^{3-}$	46.5 (2.19)	68.2 (2.22)	Mori (1954)[47]	

33) B. Adell, *Acta Chem. Scand.*, **5**, 941 (1951).
34) M.L. Ernsberger and W.R. Brode, *J. Am. Chem. Soc.*, **56**, 1842 (1934).
35) Y. Shimura, H. Ito and R. Tsuchida, *J. Chem. Soc. Japan*, **75**, 560 (1954).
36) H. Kuroya and R. Tsuchida, *J. Chem. Soc. Japan*, **61**, 597 (1940).
37) G. Wilkinson, *J. Am. Chem. Soc.*, **74**, 6148 (1952).
38) A. Nakahara, This Bulletin, **27**, 260 (1954).
39) K. Yamasaki, This Bulletin, **15**, 130 (1940).
40) K. Yamasaki, T. Hara and M. Yasuda, *Proc. Japan Acad.*, **29**, 337 (1953).
41) J.-P. Mathieu, *Bull. soc.chim.* [5] **3**, 463 (1936).
42) J. Brigando, *Compt. rend.*, **236**, 708 (1953).
43) R. Tsuchida and S. Kashimoto, This Bulletin, **11**, 785 (1936).
44) K. Sone, I. Miyake, H. Kuroya and K. Yamasaki, *J. Chem. Soc. Japan*, **69**, 70 (1948).
45) I. Lifschitz, *Rec. trav. chim.*, **69**, 1495 (1950).
46) S. Kashimoto and M. Kobayashi, This Bulletin, **12**, 350 (1937).
47) M. Mori and M. Shibata, *J. Chem. Soc. Japan*, **75**, 1044 (1954).
48) J. Topp, Dissertation, Münster (1928): quoted in "Handbuch der Physik" XXI, p. 59 (1929).
49) K. Nakamoto, M. Kobayashi and R. Tsuchida, *J. Chem. Phys.*, **22**, 957 (1954).
50) F. Basolo, *J. Am. Chem. Soc.*, **75**, 227 (1953).
51) M. Martinette and J.C. Bailar, Jr., *J. Am. Chem. Soc.*, **74**, 1054 (1952).
52) S. Kida and H. Yoneda, *J. Chem. Soc. Japan*, **76**, 1059 (1955).
53) R.G. Yalman and T. Kuwana, *J. Phys. Chem.*, **59**, 298 (1955).

ii) Chelate and polydentate ligands are abbreviated as follows: acac, acetylacetonate ion; carb, chelate carbonate ion; dg, univalent ion of dimethylglyoxime; dien, diethylenetriamine; dip, 2,2'-dipyridyl; edta, ethylenediaminetetraacetate ion (quadrivalent); en, ethylenediamine; gly, glycinate ion; ox, chelate oxalate ion; phen, 1,10-phenanthroline; pn, propylenediamine.

iii) Frequency values are given by the unit of 10^{13}/sec.

iv) The bands hidden under the specific absorption bands of the ligands are indicated as (( )).

v) The data asterisked were roughly estimated from the figures of absorption curves in literature.

vi) The references collected under the column, "Supplementary Refs.", are not exhaustive or complete but may provide some information for the details.

Conclusion

From the Tables I–VI, the following series are obtained for the simple ligands:

NO_2^- $SO_3^=$ en NH_3 (ONO^-, NCS^-, OH_2) ox (ONO_2^-, $OSO_3^=$) ($OCHO^-$, OH^-, carb, $OCOR^-$) ($OCOCO_2^=$, $OCO_2^=$) $SSO_3^=$ F^- N_3^- Cl^- $OCrO_3^=$ Br^- I^- (1)

where the ligands in parentheses stand in almost the same positions. For more complicated ligands, the following series are obtained:

CN^- $C_5H_5^-$ dg (dip, phen) (dien, pn, en) NH_3 gly edta acac ox polymolybdate-ion $S_2COC_2H_5$ S_2CNH_2 carb. (2)

Miscellaneous notes

(A) **Cyanate Ion.**—Two broad absorption bands were reported for $K_3[Co(CN)_6]$ at 97.2 ($\log \varepsilon_{max}=2.37$) and at 117.0 ($\log \varepsilon_{max}=2.08$). Kiss and Czeglédy[10] assigned the two bands to the first and the second bands, but later Kuroya and Tsuchida[36] to the second and the third bands. More recently, Nakamoto, Kobayashi and Tsuchida[49] interpreted the effects of polar solvents no these two bands assuming that the bands are equally the specific bands due to the coordinated cyanate radicals. In view of the above condition, $[Co(CN)_6]^{3-}$ was marked by a question mark in Table VI. But it is very likely that the cyanate ion has an extraordinary high position on the spectrochemical series.

(B) **Carbonate and Oxalate Ions.**—The unidentate carbonate ion has a lower position on the spectrochemical series than the chelate carbonate ion. This is also true for oxalate radical. In accordance with this fact, carbonato- or oxalato- pentammine Co(III) salts are more unstable than the corresponding tetrammine salts.

(C) **Methylamine.**—Brigando[42] reported the following data:

	First band	Second band
$[Co(NH_3)_4(NH_2CH_3)_2]Cl_3$	61.9	86.7
$[Co(NH_3)_5]Cl_3$	62.5	88.2

The data show that methylamine stands immediately behind NH_3.

(D) **Substituted Ethylenediamines.**—Basolo[50] measured the absorption spectra of *trans*-dichlorobis(N- or C-alkylethylenediamine)-cobalt(III) chlorides. From the curves reported by him, it is shown that the first bands of these complexes are displaced towards the longer wave-lengths in the order of

en (C-dimethyl)-en (C,C'-tetramethyl)-en (N-methyl)-en (N-ethyl)-en (N-*n*-propyl)-en. (3)

The absorption data reported for some of the propylenediamine complexes[41,25,51] show that propylenediamine has almost the same position in relation to ethylenediamine.

(E) **Pyridin.**—Few data published for absorption spectra of Co(III) pyridin complexes. But judging from the data on [Co py_4 NH_3 Cl] Cl_2[14], it is certain that pyridin comes behind NH_3.

(F) **Organic Acids.**—Linhard[4] reported that many organic mono-acid-radicals have almost the same positions on the spectrochemical series, but that in the case of mono-, di- or tri-chloro acetic acid some blue shifts occurred in the first and second bands of the acido-pentammine or *cis*-diacido-tetrammine complexes. From the order of the blue shifts, the spectrochemical series of $OCOR^-$ is determined as follows:

$OCOR^-$: R=CCl_3, $CHCl_2$, CH_2Cl, CH_3 and others. (4)

Summary

The visible and ultra-violet absorption spectra of many cobaltic ammine, oxalato, carbonato and amino-acido complexes have been determined in solution.

The spectrochemical series for the ligands of Co(III) complexes has been redetermined.

Department of Chemistry, Faculty of Science, Osaka University
Nakanoshima, Osaka

Sterols and Other Unsaponifiable Substances in the Lipids of Shell Fishes, Crustacea and Echinoderms. XVII. Mono-unsaturated Sterol Components of the Starfish, Asterina Pectinifera

By Yoshiyuki TOYAMA and Toru TAKAGI

(Received November 15, 1955)

In the 16th report[1] of this series, hitodesterol, which was first separated from *Asterina pectinifera* by Matsumoto and Toyama[2], was re-examined with the result that this sterol was found to be identical with α-spinasterol. It was further indicated that a di-unsaturated C_{28}-sterol, possibly of the $\Delta^{7,22}$-type, is also present in a lesser amount in this starfish.

The present study is concerned with mono-unsaturated sterol components of this starfish. As described in the 16th report, the steryl acetate mixture of this starfish was subjected to repeated recrystallizations by which hitodesteryl acetate was eventually separated as the highest melting fraction. In the present study, the steryl acetate mixture recovered from mother liquors of these recrystallizations was fractionally crystallized, and two fractions, the fraction I of m.p. 157–158°C and the fraction II of m.p. 118–119°C, were separated. The acetate fraction I and its free sterol and benzoate were found to agree with the corresponding derivatives of Δ^7-spinastenol in their properties. Also the properties of the $\Delta^{8(14)}$-and Δ^{14}-isomers prepared from the fraction I were found to accord with those of the corresponding isomers of Δ^7-spinastenyl acetate. Accordingly the sterol of the fraction I was recognized as Δ^7-spinastenol. Regarding the sterol of the fraction II, the results of our examination of the properties of the acetate, free sterol, benzoate and two isomers ($\Delta^{8(14)}$- and Δ^{14}-isomers) showed its identity with Δ^7-cholestenol, which was previously found in *Asterias amurensis*[3]. Thus it is indicated that Δ^7-spinastenol and Δ^7-cholestenol are present in the mono- unsaturated sterol components of *Asterina pectinifera*. It should, however, be noted that the possibility of the presence of Δ^7-sterols of the C_{28}-series is not excluded, though such sterols of the C_{28}-series could not be separated in the present study. Although Δ^7-spinastenol has recently been found in oats[4] and wheat[5], the present study is the first instance in which the occurrence of this sterol in the animal kingdom is demonstrated.

It was reported in previous studies by the authors that sterols of *Coscinasterias acutespina*[6] as well as of *Luidia quinaria*[7] consist mainly of mono-unsaturated Δ^7-sterols of the C_{28}- or C_{29}-series. A steryl acetate fraction,

TABLE I

PROPERTIES OF Δ^7-SPINASTENOL

	Fraction from *Asterina pect.*		Fraction from *Luidia quinaria*		Δ^7-Spinastenol[8]	
	m.p. (°C)	$[\alpha]_D^\circ$	m.p. (°C)	$[\alpha]_D^\circ$	m.p. (°C)	$[\alpha]_D^\circ$
Free sterol	145–147	+8.4	145–147	+9	144–145	+11
Acetate	157–158	+6.1	157	+6	156–157	+ 8
Benzoate	178–180	+15	177	——	180.5	+13
$\Delta^{8(14)}$-Isomer	112–113	+20	115	——	112–113	+23
Acetate of $\Delta^{8(14)}$-Isomer	113–114	+14	111–112	+18	116–117	+12
Δ^{14}-Isomer	123–124	——	——	——	127.5	+36.5
Acetate of Δ^{14}-Isomer	86– 87	+26	——	——	86.5	+24.3

1) Y. Toyama and T. Takagi, This Bulletin, **28**, 469 (1955).
2) T. Matsumoto and Y. Toyama, *J. Chem. Soc. Japan*, **64**, 1069 (1943).
3) T. Matsumoto and T. Wainai, *J. Chem. Soc. Japan, Pure Chem. Sect.*, **75**, 756 (1954); Y. Toyama and T. Takagi, This Bulletin, **27**, 421 (1954).
4) D.R. Idler et al., *J. Am. Chem. Soc.*, **75**, 1712 (1953).
5) D.R. Idler, A.A. Kandutsch and C.A. Baumann, *J. Am. Chem. Soc.*, **75**, 4325 (1953).
6) Y. Toyama and T. Takagi, *J. Chem. Soc. Japan, Pure Chem. Sect.*, **76**, 243 (1955).
7) Y. Toyama and T. Takagi, This Bulletin, **27**, 39 (1954).
8) D. Larsen and F.W. Heyl, *J. Am. Chem. Soc.*, **56**, 2663 (1934); D.H.R. Barton and J.D. Cox, *J. Chem. Soc.*, **1948**, 783.

m.p. 157°C, obtained in the previous study on *Luidia quinaria* was not closely studied at that time due to the scarcity of the material, but this fraction is very likely to consist mainly of Δ^7-spinastenyl acetate. In Table I, the melting points and specific rotations of the free sterol and its derivatives of the Δ^7-spinastenol fractions from *Asterina pectinifera* and *Luidia quinaria* are compared with those reported for Δ^7-spinastenol by previous authors.

Experimental

1. Δ^7-Spinastenyl Acetate Fraction.—As described in the 16th report, the solid material (49 g.) separated from the unsaponifiable matter of the acetone-soluble oil extracted from the starfish, *Asterina pectinifera*, was refluxed with acetic anhydride. The acetylated product was then recrystallized from 200 cc. of acetone-ether, yielding 26.5 g. of crystalline solid (crude steryl acetate). This was subjected to repeated recrystallizations from acetone until eventually a crude hitodesteryl acetate fraction (2.2 g.) of m.p. 182–183°C was obtained after thirteen recrystallizations. In the present study, a steryl acetate fraction (4.8 g.), m.p. 153–156°C, recovered from the mother liquors of the 5th–9th recrystallizations was fractionally crystallized from acetone, and the main fraction obtained was fractionated further. After several repetitions of fractionation, a fraction (1.6 g.) of m.p. 157–158°C was obtained. The melting point of this fraction was unaltered by further recrystallizations, and all fractions obtained by a further fractionation had the same melting point.

The fraction, m.p. 157–158°C, had $[\alpha]_D^{22}=+6.1°$, saponification value 123.9 and iodine value by the perbenzoic acid method 58.7 (calcd. for $C_{71}H_{52}O_2$: saponification value 122.8; iodine value 55.6). The change of color developed in the Liebermann-Burchard reaction for this fraction with the period of reaction is shown by the curve A in Fig. 1 in which the absorption at 620 mμ is plotted against the period of reaction. The curve A is quite similar to the curve for a typical Δ^7-sterol. Saponification of this fraction gave free sterol which had m.p. 145–147°C and $[\alpha]_D^{22}=+8.4°$ after recrystallization from acetone. Benzoate prepared from the free sterol had m.p. 178–180°C, $[\alpha]_D^{24}=+15°$ and saponification value 108.9 (calcd. for $C_{36}H_{54}O_2$: 108.1).

The acetate fraction of m.p. 157–158°C was dissolved in glacial acetic acid, palladium catalyst was added to the solution, and the mixture was shaken in an atmosphere of hydrogen for seven hours. Absorption of hydrogen did not occur, but an isomerization product was obtained, which showed m.p. 113–114°C and $[\alpha]_D^{24}=+14°$ after recrystallization from methanol. The change of color vs. the period of reaction in the L. B. reaction for this product is shown by the curve B in Fig. 1 which closely resembles the curve for a $\Delta^{8(14)}$-sterol. Saponification of this product gave free sterol which had m.p. 112–113°C and $[\alpha]_D^{25}=+20°$ after recrystallizations from methanol and acetone.

The $\Delta^{8(14)}$-isomer (acetate) obtained above was dissolved in chloroform, and dry hydrogen chloride was passed through the solution for two hours. The product obtained had m.p. 86–87°C and $[\alpha]_D^{27}=+26°$ after recrystallization from ethanol. Saponification of this product gave free sterol which, recrystallized from methanol, had m.p. 123–124°C. The change of color vs. the period of reaction in the L. B. reaction for this sterol is shown by the curve C in Fig. 1 which is similar to the curve for a typical Δ^{14}-sterol.

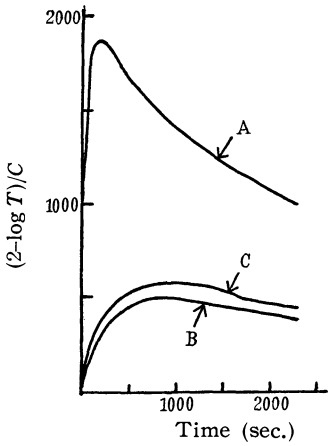

Fig. 1. Liebermann-Burchard reaction for Δ^7-spinastenyl acetate fraction.
T: Transmittance, C: Concentration (10^{-3} mol.)
Curve A for Δ^7-spinastenyl acetate fraction.
Curve B for $\Delta^{8(14)}$-isomer (acetate)
Curve C for Δ^{14}-isomer (free sterol)

2. Δ^7-Cholestenyl Acetate Fraction.—The acetone-ether filtrate separated from the crude steryl acetate (26.5 g.) was concentrated, and a further quantity (2.5 g.) of crude steryl acetate fraction was obtained. This fraction and the fractions recovered from the mother liquors of the 1st and 2nd recrystallizations of the crude steryl acetate (26.5 g.) were united. The united material (9.3 g.), m.p. 105–126°C, was fractionally crystallized from methanol, yielding the 1st crop (1.3 g.) of m.p. 130–132°C and the 2nd crop (6.0 g.) of m.p. 119–123°C. The 2nd crop was separated further into the following fractions by fractional crystallization from methanol: the 1st fraction (0.9 g.) of m.p. 125–127°C; the 2nd fraction (0.5 g.) of m.p. 123–124°C; the 3rd fraction (0.6 g.) of m. p. 120–121°C; the 4th fraction (0.8 g.) of m.p. 119–120°C; the 5th fraction (0.6 g.) of m.p. 119–120°C; the 6th fraction (2.6 g., recovered from the final filtrate) of m.p. 118–119°C. A further fractional crystallization of the 6th fraction gave fractions of the same melting point, 118–119°C. This frac-

tion had $[\alpha]_D^{28} = -2.0°$, saponification value 130.0 and iodine value by the perbenzoic acid method 62.0 (calcd. for $C_{29}H_{48}O_2$: saponification value 130.8; iodine value 59.2). The L. B. reaction for this fraction is shown by the curve A in Fig. 2. Free sterol obtained by saponification of this fraction had m.p. 122–123°C and $[\alpha]_D^{19} = \pm 0$ after recrystallization from methanol. Benzoate prepared from the free sterol had m.p. 153–155°C,

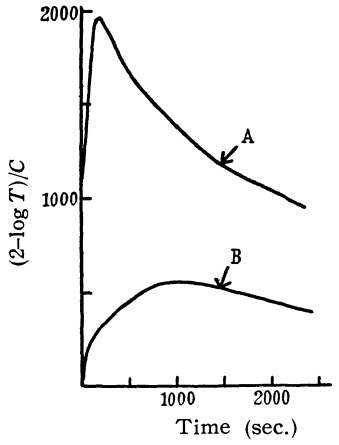

Fig. 2. Liebermann-Burchard reaction for Δ^7-cholestenyl acetate fraction.
T: Transmittance, C: Concentration (10^{-3} mol.)
Curve A for Δ^7-cholestenyl acetate fraction.
Curve B for $\Delta^{8(14)}$-isomer (acetate)

$[\alpha]_D^{19} = +4°$ and saponification value 112.6 (calcd. for $C_{34}H_{50}O_2$; 114.3) after recrystallization from acetone.

The isomerization product obtained by shaking a solution of this fraction (acetate) in an atmosphere of hydrogen for five hours in the presence of palladium catalyst showed m.p. 77–78°C and $[\alpha]_D^{21} = +9°$ after recrystallization from methanol. The L. B. reaction for this product is shown by the curve B in Fig. 2. Saponification of this product gave free sterol of m.p. 119–120°C and $[\alpha]_D^{21} = +20°$ after recrystallization from methanol.

Summary

In a continuation of the study on sterol components of *Asterina pectinifera*, the present study is concerned with mono-unsaturated sterol components. The steryl acetate fraction recovered from the mother liquors of the recrystallizations, which were carried out for the separation of hitodesteryl (α-spinasteryl) acetate in a previous study, was subjected to fractional crystallizations by which two fractions, Δ^7-spinastenyl acetate fraction and Δ^7-cholestenyl acetate fraction, were eventually separated. Accordingly it has been found that the sterol mixture of *Asterina pectinifera* contains Δ^7-spinastenol and Δ^7-cholestenol besides hitodesterol.

Department of Applied Chemistry
Faculty of Engineering
Nagoya University, Nagoya

Spectrochemical Investigations of the Interaction between Simple Salt Anions and Transition Metal Cations. III. Association between Cupric Alaninate Complex and Sulphite Anion

By Hayami YONEDA

(Received October 25, 1955)

Introduction

In the previous report[1] the author studied the absorption due to association between bisethylenediamine cupric complex and several anions, which had strong reducing power against cupric aquo ion, and concluded from comparison of the equilibrium constants of association that the special polarising power of the central cupric ion and the large polarisability of anions played an important role in association. If such a conclusion is appropriate, we can expect that there should exist the similar absorption due to association between the electrically neutral complex and the very easily polarisable anion and that we could determine the equilibrium constant of association by analyzing the absorption data.

In the present investigation, marked absorption due to association was found between cupric alaninate complex and sulphite and thiosulphate anions, and the estimation of the equilibrium constant was performed in the case of sulphite anion.

1) This Bulletin, **29**, 68 (1956).

Experimental

Cupric alaninate $Cu(CH_3CHNH_2\cdot COO)_2\cdot H_2O$ was prepared by dissolving freshly precipitated cupric hydroxide into the boiling solution containing an equivalent amount of alanine and was recrystallized twice from hot water.

Optical densities were measured by means of Shimadzu the spectrophotometer using tungsten and hydrogen lamps and 1 cm. quartz cells. All measurement was done at room temperature 20°C.

Results

In the preliminary experiment the following measurement was made. Na_2SO_3 and $Na_2S_2O_3$, were dissolved to make 1 M solutions. In each solution cupric alaninate complex was dissolved to the concentration of 0.01 M. Such solutions of the complex were measured in their optical densities. In order to cancel the absorption due to the unassociated free anions, the corresponding salt solution was used as a standard. The results are shown in Fig. 1 with the results obtained in the

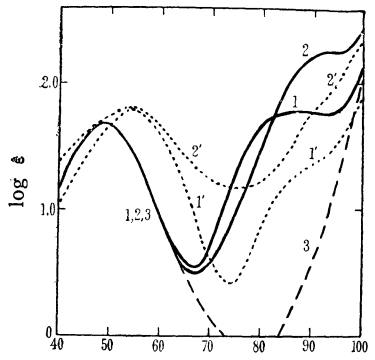

ν, 10^{13} sec^{-1}

Fig. 1.

1. ——— [Cu alanine$_2$] in 1 mol./l. Na_2SO_3
2. ——— [Cu alanine$_2$] in 1 mol./l. $Na_2S_2O_3$
3. - - - - [Cu alanine$_2$] in water
1'. ----- [Cu en$_2$]$(ClO_4)_2$ in 1 mol./l. Na_2SO_3
2'. ----- [Cu en$_2$]$(ClO_4)_2$ in 1 mol./l. $Na_2S_2O_2$

(Curves 1' and 2' were cited from the previous work.)

ethylenediamine complex. It is interesting to find that the absorption due to association appears more distinctly here than in the case of the cupric ethylenediamine complex. In the present case too, the characteristic absorption band proper to the complex remains constant.

In addition, it is noteworthy that the solution was photosensitive in the case of thiosulphate and that the reduction of cupric ion to cuprous ion proceeded at a measurable rate during measurment, and that the characteristic blue color of the complex faded gradually. In the sulphite solution such reduction was not observed during measurement. Accordingly, the determination of the equilibrium constant was done only in the case of sulphite. In order to estimate the equilibrium constant, optical densities of the following solutions were measured in the wavelength regions 400–320 mμ.

1) The solution which contains both [Cu alanine$_2$] and Na_2SO_3 at 0.01 M concentration.

2) The solution which contains both the complex and sulphite at 0.0075 M concentration.

3) The solution which contains both the complex and sulphite at 0.0050 M concentration.

4) The solution which contains only the complex at 0.01 M concentration.

The slight absorption which originated from Na_2SO_3 was canceled by taking the sulphite solutions of the corresponding concentration as a standard in the measurement. The results are shown in Fig. 2. In the figure, the full

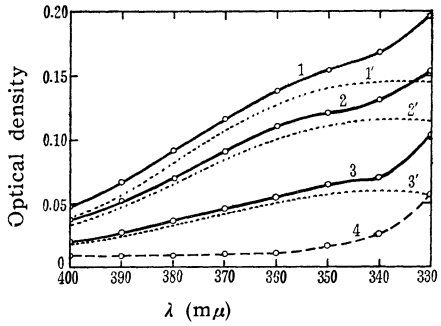

Fig. 2.

lines 1, 2, 3 correspond to the absorption of 0.01, 0.0075, 0.0050 M solutions and a broken line 4 to that of the complex only solution. The dotted lines 1', 2', 3' are the results of subtraction from the absorption 1, 2, 3 by the absorption of the complex of the corresponding concentrations.

Determination of the Equilibrium Constant.—In the following equilibrium

$$Cu\ alanine_2 + SO^2{}_3 \rightleftarrows (Cu\ alanine_2\cdot SO_3)$$

the equilibrium constant of association is represented by

$$K=\frac{[(Cu\ alanine_2\cdot SO_3)]}{[Cu\ alanine_2]\cdot[SO_3{}^{2-}]}$$

As the total concentrations of the complex and the anion in the solution are always the same in the present case, we put them as u. If we represent the concentration of the association product in equilibrium with x, then the concentrations of the complex and the anion in equilibrium are both represented with $u-x$, and the equilibrium constant K is expressed by

$$K=\frac{x}{(u-x)^2} \quad (1)$$

where u takes the values of 0.01, 0.0075, and 0.0050. If we represent x corresponding to $u=0.01$, 0.0075, 0.0050 with x_1, x_2, x_3, and then these x_1, x_2, and x_3 take the definite values against the definite value of K. Consequently, x_2/x_1 and x_3/x_1 are also definite against the definite value of K. The values of x_2/x_1 and x_3/x_1 against K were calculated and plotted in Fig. 3.

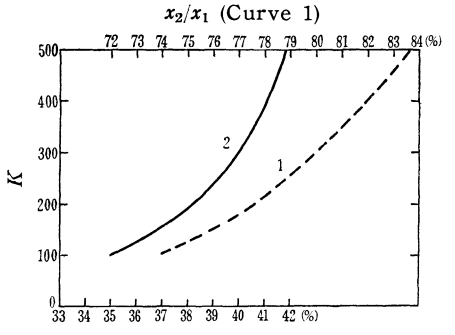

Fig. 3.

On the other hand, the measured optical density D is represented by

$$D=\varepsilon_c(u-x)+\varepsilon_a x \quad (2)$$

This relation is modified to

$$D-\varepsilon_c u=(\varepsilon_a-\varepsilon_c)x=y \quad (3)$$

where ϵ_c and ϵ_a are the molar extinction coefficients of the complex and the association product, and y represents the absorption due to association. If we represent y in the cases of x_1, x_2, x_3 with y_1, y_2, y_3 respectively, then $x_2/x_1=y_2/y_1$ and $x_3/x_1=y_3/y_1$. The values of y_2/y_1 and y_3/y_1 in each wave-length were calculated from the observed values of D, and the corresponding values of K were read from the graph. The results thus obtained are listed in Table I.

Discussion

We have obtained $K=240$ as the value of the equilibrium constant of association between [Cu alanine$_2$] and SO_3^{2-}. This value is almost ten times as large as that between [Cu en$_2$]$^{2+}$ and SO_3^{2-}($K=25$). This surprising fact can be interpreted only by assuming that the electronic configuration of the central cupric ion plays an important role in association. In other words, in the ethylenediamine complex the charge of the central cupric ion is considerably neutralized by the lone pair electrons of the coordinating N atoms of the ethylenediamine molecules and as the result it has only the small polarising power against the outer anion. In contrast to this, in the alanine complex, though the charge neutralization as a whole complex radical is complete, the charge of the cupric ion is incompletely canceled, so that the cupric ion has enough polarising power against the outer anion.

As reported previously, $S_2O_3^{2-}$ associates much more firmly with [Cu en$_2$]$^{2+}$ than SO_3^{2-}. This fact suggests the much greater polarisation of $S_2O_3^{2-}$. Such polarisation is to be strengthened in the association with [Cu alanine$_2$]. As the result $S_2O_3^{2-}$ excited by a photon easily transfers its electron to the central cupric ion. The photochemical reduction of [Cu alanine$_2$] in the thiosulphate solution can be thus explained.

Conclusion

Marked association absorption was found between electrically neutral [Cu alanine$_2$] and SO_3^{2-}, and $S_2O_3^{2-}$ and the equilibrium constant of association was determined spectrophotometrically in the case of [Cu alanine$_2$] and SO_3^{2-}. The value of K was found to be 240. This value is much larger than that obtained in the corresponding case of [Cu en$_2$]$^{2+}$ and SO_3^{2-} ($K=25$). This result can be explained by assuming that the central

TABLE I
VALUES OF y AND K

λ(mμ)	y_1	y_2	y_3	y_2/y_1	K	y_3/y_1	K
390	0.058	0.045	0.023	77.5%	200	39.7%	285
380	.084	.065	.033	77.4%	195	39.8%	290
370	.106	.083	.042	78.5%	235	39.6%	280
360	.127	.099	.049	77.8%	210	39.0%	245
350	.141	.109	.057	77.7%	205	39.0%	245
340	.145	.113	.057	78.0%	215	39.3%	260
330	.143	.112	.056	78.7%	245	39.2%	255
320	.145	.114	.056	78.6%	240	39.0%	245
				Mean	218	Mean	263

Probable value of $K=240$

cupric ion in [Cu alanine$_2$] has much stronger polarising power than in [Cu en$_2$]$^{2+}$. The assumption of such strong polarising power can explain the photochemical reduction of Cu alanine$_2$·S_2O_3 system.

The author wishes to express his sincere thanks to Prof. R. Tsuchida and Prof. M. Kobayashi, Osaka University for their kind advice and encouragement during this work.

Chemistry Department, Wakayama University, Wakayama

Cyanoethylation of Trichlorosilane. I. β-Addition.[1]

By Shunichi NOZAKURA and Shiro KONOTSUNE

(Received October 20, 1955)

Since Sommer and coworkers[2] discovered the peroxide-catalyzed addition of trichlorosilane to 1-octene in 1947, a number of olefins have been found to react in the following manner[3]:

$$HSiCl_3 + CH_2=CHR \longrightarrow Cl_3SiCH_2CH_2R$$

Wagner and Strother[4] also reported the preparation of vinyltrichlorosilane from acetylene and trichlorosilane in the presence of catalysts such as peroxide and platinized asbestos. Thus the method gained its importance in the industrial production of vinyltrichlorosilane.

However, the olefins which have hitherto been used were generally simple olefins, and only a few reactive vinyl compounds were tried. In an attempt to effect the addition of trichlorosilane with styrene, Burkhark[3] was only able to isolate a nonvolatile telomeric product. Quite recently, in the midst of our experiments, butadiene[5] and vinyltrimethylsilane[6] were reported to react with trichlorosilane.

In this paper we describe the addition reaction of trichlorosilane and acryronitrile. Acrylonitrile among the various vinyl compounds was tried first, as we expected that the addition might take place readily and the identification of its products might also be easy.

TABLE I

CYANOETHYLATION OF TRICHLOROSILANE IN THE PRESENCE OF BENZOYLPEROXIDE AND PLATINIZED ASBESTOS

No.	Trichlorosilane, g.	Acrylonitrile, g.	Catalyst, g.	Reaction[a] temp. °C	Reaction time, hr.	Yield,[b] %
1	19.1	7.6	—	160	5.0	9.7
2	19.9	7.8	—	180	5.0	10
3	18.5	8.0	benzoylperoxide, 0.05	160	5.0	46[c]
4	19.9	7.8	〃 0.05	130	5.0	0[d]
5	19.9	7.8	〃 0.05	100	5.0	0[e]
6	19.6	7.8	benzoic acid 0.05	160	5.0	0
7	19.7	7.8	platinized asbestos 0.1	160	5.5	11
8	19.3	7.6	〃 0.1	180–200	5.8	61

a) Reaction temperatures fluctuated within ±3°C.
b) The yields are based on trichlorosilane used.
c) A pale yellow precipitate weighed 3.2 g. (Si, 5.3%)
d) Precipitate, 1.1 g. (Si, 4.01%)
e) Precipitate, 2.8 g. (Si, 1.69%)

1) Paper IV in a series on the study of organosilicon compound.
2) L.H. Sommer, et. al., *J. Am. Chem. Soc.*, 69, 188 (1947).
3) C.A. Burkhard and R.H. Krieble, ibid., 69, 2687 (1947); W. Pietrusza, et. al.; ibid., 70, 484 (1948); C.L. Agre, ibid., 71, 300 (1949); C.A. Burkhard, ibid., 72, 1402 (1950).
4) G.H. Wagner and C.O. Strother, *Brit.*, 670, 617, Apr. 23, 1952; C.A. 46, 8894c.
5) D.L. Bailey and A.N. Pines, *Ind. Eng. Chem.*, 46, 2363 (1954).
6) D. Seyferth and E.G. Rochow, *J. Org. Chem.*, 20, 250 (1955).

Cyanoethylation of Trichlorosilane in the Presence of Benzoylperoxide and Platinized Asbestos

Table I shows the catalytic effects of benzoylperoxide and platinized asbestos. Benzoylperoxide was effective at above 160°C., and it produced simultaneously a considerable amount of an insoluble pale yellow precipitate which appeared to be either polyacrylonitrile or tellomeric product. Although such an insoluble precipitate was also produced at 130°C or at lower temperatures, no addition product, except the polymer, was obtained. Experiment with benzoic acid alone, which is a possible decomposition product of benzoylperoxide, had no catalytic action at all. On the other hand, platinized asbestos, which has been known to be effective in the addition of trichlorosilan to acetylene, catalyzed effectively and gave cyanoethylation product without accompanying the precipitate.

Cyanoethylation of Trichlorosilane in the Presence of Organic Bases

Organic and inorganic bases are known to be effective catalysts in the usual case of cyanoethylation. However, in our cases inorganic bases such as metal hydroxides were inadequate because of their strong reactivity towards trichlorosilane, and this led us to turn our attention to tertiary organic bases. The results obtained with the addition of organic bases are given in Table II. The reaction mixtures were clear in almost all the cases and colored from a light yellow to a light orange. The addition product obtained here was the same as that from peroxidecatalysed. In contrast to the latter case, there occurred no precipitate. Pyridine was also effective at a temperature as low as 130°. Catalytic activities of the bases increased in the order, dimethylaniline$\ll$quinoline$<$pyridine, piperidine$<$triethylamine.

It is also of interest to note that pyridine hydrochloride, benzyltriethylammonium chloride, and piperidine have shown a moderate catalytic activity. Since piperidine has an active hydrogen, it may react with trichlorosilane to form piperidylsilicon bonds and piperidine hydrochloride. The catalytic activity of piperidine may possibly be due to the effect of the latter two compounds.

It must be taken into consideration that tertiary amine may have also changed to its hydrochloride to a certain extent prior to heating by a small amount of moisture which inevitably adhered to the sealed tube and the resulting hydrochloride acted as a catalyst. However, this is not very serious in view of the fact that the catalytic activity of pyridine was found to be higher than its hydrochloride as clearly demonstrated in the experiment No. 8 and 9 (Table II).

Structural Proof of Addition Products

The addition product was proved to consist almost exclusively of β-cyanoethyltrichlorosilane, which was identified by the process described below. Cyanoethyltrichlorosilane was converted to the corresponding trimethylsilylpropionic amide (IV), m.p. 95–6°C.

TABLE II

CYANOETHYLATION OF TRICHLOROSILANE IN THE PRESENCE OF ORGANIC BASES

No.	Trichlorosilane, g.	Acrylonitrile, g.	Catalyst, g.	Reaction temp. °C	Reaction time, hr.	Yield,[b] %
1	19.9	8.7	pyridine, 0.1	185	5.0	67
2	27.8	13.0	〃 0.1	160	5.0	69
3	19.9	8.7	〃 0.1	130	6.0	14
4	18.6	8.0	triethylamine, 0.1	160	5.0	76
5	20.1	8.7	piperidine, 0.1	160	5.0	69
6	20.2	8.7	quinoline, 0.1	160	5.0	40
7	20.5	7.9	dimethylaniline, 0.1	160	5.0	0
8	20.0	7.8	pyridine, 0.05	160	5.0	59
9	19.8	7.8	pyridine hydrochloride[a]	160	5.0	35
10	20.5	8.9	benzyltriethylammonium chloride, 0.1	160	5.0	70

a) The pyridine hydrochloride was prepared in the reaction tube by interacting 0.05 g. of pyridine and an excess of concd. hydrochloric acid and by drying in vacuo.

b) The yields are based on trichlorosilane used.

The structure of the latter compound was already proved by Sommer[7] through a series of reactions. Mixed melting point test of our addition product with that synthesized showed no depression. Therefore, the compound (I) was assigned to be β-cyanoethyltrichlorosilane.

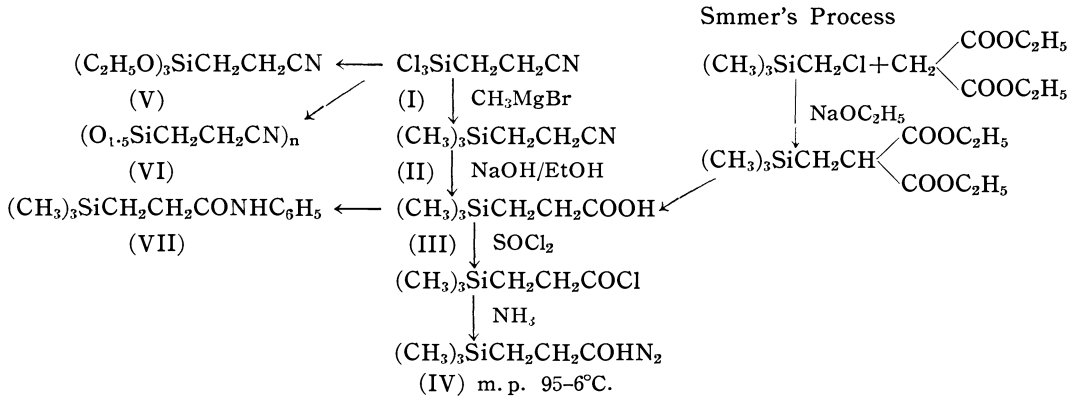

The examination of the compound (II) by infra red spectrum proved it to be identical with that derived from β-trimethylsilylpropionic amide according to Sommer's method.

The following new compounds were prepared and characterized; β-cyanoethyltriethoxysilane (V), β-cyanoethylpolysiloxane (VI), and β-trimethylsilylpropionic anilide (VII).

The Effect of Solvent on the Base-catalyzed Cyanoethylation of Trichlorosilane

Although a more accurate measurement of reaction rate must be done for a detailed discussion, we carried out here an approximate comparison of three solvents, acetonitrile, chlorobenzene, and benzene, dielectric constants of which being 37.5, 5.61, and 2.29 respectively. The effect of the solvents on the base-catalyzed addition reaction are summarized in Table III. When the reactions were carried out in the presence of the strongest catalyst such as triethylamine, there were no detectable differences among the solvents studied. However, when a weaker base catalyst such as pyridine was used, a marked difference was observed among them.

Discussion of Reaction Mechanisms

The peroxide-catalyzed cyanoethylation may be regarded as a radical chain reaction as Sommer and others have suggested in the case of other olefins. Tne base-catalyzed cyanoethylation of trichlorosilane does not seem to be a radical reaction. Although there

TABLE III

CYANOETHYLATION OF TRICHOLOROSILANE IN VARIOUS SOLVENTS AT 160°C

No.	Trichlorosilane, g.	Acrylonitrile, g.	Catalyst, g.	Solvent, ml.	Reaction time, hr.	Yield[b] %
1	22.2	9.6	triethylamine, 0.1	acetonitrile, 26	5.0	64
2	21.8	9.4	〃, 0.1	benzene, 45	5.0	59
3	20.4	8.8	pyridine, 0.1	acetonitrile, 40	1.0	39
4	16.8	7.3	〃, 0.07	〃 34	2.0	59
5	20.4	8.8	〃, 0.1	benzene, 40	1.0	0
6	17.1	7.5	〃, 0.07	〃, 34	2.0	0
7	18.8	8.1	〃, 0.1	〃, 38	5.0	0
8	20.0	8.7	〃, 0.1	chlorobenzene, 40	5.0	0
9	16.8	7.3	〃, 0.07	nitrobenzene, 34	2.0	—[a]

a) The colour of the reaction mixture was brownish black and its distillation was difficult due to decomposition.

b) The yields are based on trichlorosilane used.

7) L.H. Sommer, et. al., *J. Am. Chem. Soc.*, 73, 5130 (1951); 76, 1609 (1954).

has not yet been reported an example in which the fission of silicon-hydrogen bond and addition of it to a double bond may be explained in terms of ionic mechanism, we believe that ionic mechanism involved in our case. The following three pieces of evidence may support such an ionic mechanism. First, base catalysts are effective. Second, no appreciable amount of precipitates of polyacrylonitrile is produced in the base-catalyzed reactions in contrast to the case of peroxide-catalyzed. Third, solvents give a considerable effect in some cases as mentioned above. The deficiency of the influence of the solvents in the case of triethylamine catalyst is probably due to the much higher catalytic activity of triethylamine than that of pyridine.

In view of these facts we may suggest the following reaction mechanism, which is similar to the ordinary cyanoethylation:

$$Cl_3SiH + B \longrightarrow Cl_3Si^- + HB^+$$
$$Cl_3Si^- + CH_2=CHCN \longrightarrow Cl_3SiCH_2CH^-CN$$
$$Cl_3SiCH_2CH^-CN + HB^+ \longrightarrow Cl_3SiCH_2CH_2CN + B$$

where B represents organic bases.

Organic salts, such as pyridine hydrochloride and benzyltriethylammonium chloride, are soluble in the reaction mixture and we considered that their catalytic effect is probably due to a salt effect.

Experimental

General Procedure for Cyanoethylation of Trichlorosilane.—Trichlorosilane (b.p. 31.5–32.0°C) and freshly distilled acrylonitrile) b.p. 76.5–77°C) were charged into a hard glass reaction ampule of about a 100 ml. capacity and cooled in an ice-salt bath, and the open end of the ampoule was sealed after the air had been replaced by dry nitrogen. Heating was carried out in an electric furnace equipped with an automatic controller. After cooling, the reaction tube was opened and the precipitate if any was filtered. The precipitate was washed with dry benzene and absolute alcohol, dried in a desiccater, and analyzed for silicon.

A mixture of the solvent and the unreacted starting material of the filtrate was distilled under atmospheric pressure, and then the product was distilled from a Claisen flask under reduced pressure.

Catalyst.—Platinized asbestos was prepared according to the following directions. Three grams of purified asbestos was mixed with 0.06 g. of chloroplatinic acid, H_2PtCl_3, and an appropriate quantity of water. After being dried on the water bath, the mixed asbestos was heated in a glass tube at 200°C in a stream of air for one hour and then reduced with dry hydrogen at 200°C for three hours.

β-Cyanoethyltrichlorosilane (I).—After the purification by redistillation, the physical constants of β-cyanoethyltrichlorosilane were determined. B.p. 109° (30 mmHg), m.p. 34.6–35.1°C.

Anal. Found: Cl, 56.25. Calcd. for $C_3H_4NSiCl_3$: Cl, 56.43%.

β-Cyanoethylpolysiloxane (VI).—β-cyanoethyltrichlorosilane (I) was poured into a large quantity of water to give a homogeneous solution. When the solution was neutralized with 6N aqueous ammonia, β-cyanoethylpolysiloxane (VI) precipitated as a white amorphous powder. After filtration and washing with water the precipitate was dried at 100°C over phosphorous pentoxide.

Anal. Found: Si, 26.38; N, 13.22. Calcd. for $C_3H_4NO_{1.5}Si$: Si, 26.42; N, 13.21%.

β-Cyanoethyltriethoxysilane (V).—In a 200 ml. three-necked flask equipped with a mercury-sealed stirrer, a dropping funnel, and a calcium chloride tube, a mixture of 9.8 g. of absolute ethanol and 9.8 g. of dry benzene was placed. A solution of 12 g. of β-cyanoethyltrichlorosilane in an equal quantity of dry benzene was added dropwise through the dropping funnel under vigorous stirring. The temperature of the reaction mixture was kept below 0°C by the external cooling with ice-salt bath. After the addition was completed stirring was continued for one and a half hours. Then a slight excess of dry ammonia was introduced into the reaction mixture under cooling. An excess amount of ammonia was driven off by dry air, and the resulting ammonium chloride was filtered off. Vacuum distillation of the filtrate gave 9.0 g. of the crude β-cyanoethyltriethoxysilane (V), b.p. 121–130°C (20 mmHg) (65%). Redistillation yielded the pure compound, b.p. 111.5–112.5° (10 mmHg), d_4^{25}, 0.9699; n_D^{25}, 1.4103.

Anal. Found: Si, 12.58; N, 5.8; MR_D, 55.55. Calcd. for $C_9H_{19}NO_3Si$: Si, 12.92; N, 6.4%; MR_D, 55.26.

β-Cyanoethyltrimethylsilane (II).—Eleven gram (0.058 Mol.) of β-cyanoethyltrichlorosilane (I) was methylated in the usual manner with the ether solution of methylmagnesiumbromide prepared from 6.2 g. (0.25 Atom) of magnesium and the reaction gave 5.8 g. of β-cyanoethyltrimethylsilane (II)., b.p. 98.5–101.8° (75 mmHg) (78%).

In order to remove a possible impurity of β-trimethylsilylmethylketone, the crude product was shaken with a saturated solution of sodium bisulfite. After washing with the water and drying over calcium chloride, it was subjected again to vacuum distillation, b.p. 98°–97.5° (65–64 mmHg), d_4^{20}, 0.8226; n_D^{25}, 1.4202.

The infra red spectrum of the compound (II) was identical with that of the standard sample prepared according to the method described by Sommer[7].

Anal. Found: Si, 21.67; N, 10.7; Mol. Wt. (in benzene), 127; MR_D, 39.09. Calcd. for $C_6H_{13}NSi$; Si, 21.92; N, 11.0%; Mol. Wt., 127; MR_D, 39.07.

β-Trimethylsilylpropionic Acid (III).—A mixture of 3.0 g. of β-cyanoethyltrimethylsilane, 10 ml. of 50% aqueous sodium hydroxide and 10 ml. of alcohol was refluxed for three and half hours until the evolution of ammonia ceased. The reac-

tion mixture was concentrated by an aspirator on a water bath to a slushy state. It was dissolved in a small portion of water and extracted with ether in order to remove the unreacted nitrile. The water layer was acidified with concentrated hydrochloric acid and the separating oil was extracted again with ether. The ether solution was dried with sodium sulfate, filtered, and distilled under vacuum to yield 1.0 g. of β-trimethylsilylpropionic acid. (III), b.p. 114–6° (20 mmHg) (49%). n_D^{25}, 1.4257 (in literature[7]); n_D^{20}, 1.4282).

Anal. Found: Si, 18.85; Mol. Wt., (from titration), 142. Calcd. for $C_6H_{14}O_2Si$: Si, 19.19%; Mol. Wt., 145.

β-Trimethylsilylpropionic Amide (IV) and Anilide (VII).—When 0.9 g. of thionylchloride was added to 0.2 g. of β-trimethylsilylpropionic acid (III), a vigorous reaction took place instantly. After refluxing for a half hour, an excess of thionylchloride was evaporated in vacuo. To the ice-cold residual oil 20 ml. of ether saturted with dry ammonia was poured in. After standing for about a half hour, an excess ammonia was driven off with a stream of dry air. The precipitating ammonium chloride was separated by filtration and the filtrate was evaporated to yield 0.2 g. of β-trimethylsilylpropionic amide (IV), m.p. 95–6°C (recrystallised from petroleum benzine).

Anal. Found: Si, 19.23. Calcd. for $C_6H_{15}NOSi$: Si, 19.34%.

The mixed melting point test of the compound (IV) with the standard sample prepared according to Sommer[7] showed no depression.

β-Trimethylsilylpropionic anilide (VII) was prepared by heating in a sealed tube the mixture of 0.1 g. of the acid (III) and 0.2 g. of aniline at 180°C for eight hours. The reaction mixture was digested with 4 ml. of 2N hydrochloric acid and the insoluble oil crystallised in large needles after standing for a long time, m.p. 87–8°C. (recrystallised from alcohol)

Anal. Found: Si, 12.99. Calcd. for $C_{12}H_{19}NOSi$: Si, 12.68%.

Summary

1. Cyanoethylation of trichlorosilane was found to be catalysed by organic bases, benzoylperoxide, or platinized asbestos at about 160°C. The catalytic activities of organic bases increased in the order, dimethylaniline ≪ quinoline < pyridine, piperidine < triethylamine. Pyridine hydrochloride and benzyltriethylammonium chloride has also catatytic effects.

2. The orientation of the addition reaction was found to be almost exclusively of the β-position.

3. An ionic mechanism was suggested for the organic base-catalysed addition reaction.

The authors are much indebted to Profs. S. Murahashi and H. Tani for their many helpful suggestions. Appreciation is also expressed to Nihon Silicon Resin Co. for their kindness of supplying the trichlorosilane.

Department of Chemistry, Faculty of Science, Osaka University, Osaka

Cyanoethylation of Trichlorosilane. II. α-Addition[1]

By Shunichi NOZAKURA and Shiro KONOTSUNE

(Received October 20, 1955)

In the previous paper[2] the authors reported the cyanoethylation of trichlorosilane in the presence of organic bases, benzoyl peroxide, or of platinized asbestos. These addition reactions which were carried out in sealed glass tubes gave exclusively the β-adduct, β-cyanoethyltrichlorosilane.

In an attempt to bring about this reaction in a large scale with an autoclave made from 18–8 stainless steel in the presence of pyridine or platinized asbestos, there was obtained, curiously enough, an α-addition product instead of the expected β-adduct:

$$Cl_3SiH + CH_2=CHCN \begin{cases} \xrightarrow{\beta\text{-addition}} Cl_3SiCH_2CH_2CN \quad \text{b.p. } 117\text{–}8^\circ \text{ (41 mmHg)} \\ \xrightarrow{\alpha\text{-addition}} Cl_3SiCHCN \quad \text{b.p. } 96\text{–}8^\circ \text{ (41.5 mmHg)} \\ \qquad\qquad\quad | \\ \qquad\qquad\quad CH_3 \end{cases}$$

1) Paper V in a series on the study of organosilicon compound.

2) S. Nozakura and S. Konotsune, This Bulletin **29**, 322, (1956).

Since this is a new example where trichlorosilane reacted with olefin according to the Markownikow's rule, we performed a more detailed research concerning this unusual reaction. In this paper, we describe the details of the characteristic features of the above reaction, the structural proof of the product, and some discussions on the reaction mechanisms.

Cyanoethylation of Trichlorosilane in an Autoclave

The typical experiment of the cyanoethylation which was carried out in an autoclave is shown in Fig. 1. The reaction started at a temperature ranging from 150 to 170°C. As the reaction was exothermic, the pressure rose rapidly with the simultaneous elevation of the temperature, and dropped also very quickly, and at last settled on a constant value in the course of about ten minutes.

In the absence of the catalyst, the initiation of a reaction could be observed at a somewhat higher temperature than that of the reaction using catalyst, but no distillable product was obtained.

Another feature was a yield of a considerable amount of nonvolatile distillation residue. It was also noticeable that any fraction which distilled in the range of boiling point of the β-isomer was not obtained at all.

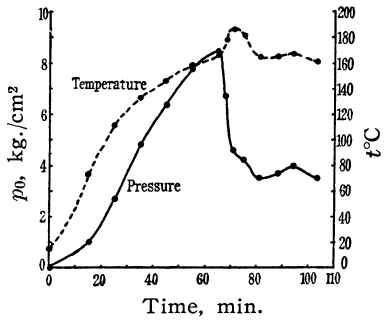

Fig. 1. An example of the cyanoethylation of trichlorosilane in an autoclave. (Trichlorosilane, 32.5 g., acrylonitrile, 19.1 g., and pyridine, 0.2 g.)

The Structural Proof of the Product obtained in an Autoclave

Several derivatives of the addition product was prepared, and their chemical and physical properties were compared with those of the derivatives of the known β-cyanoethyltrichlorosilane. The reactions involved are as follows:

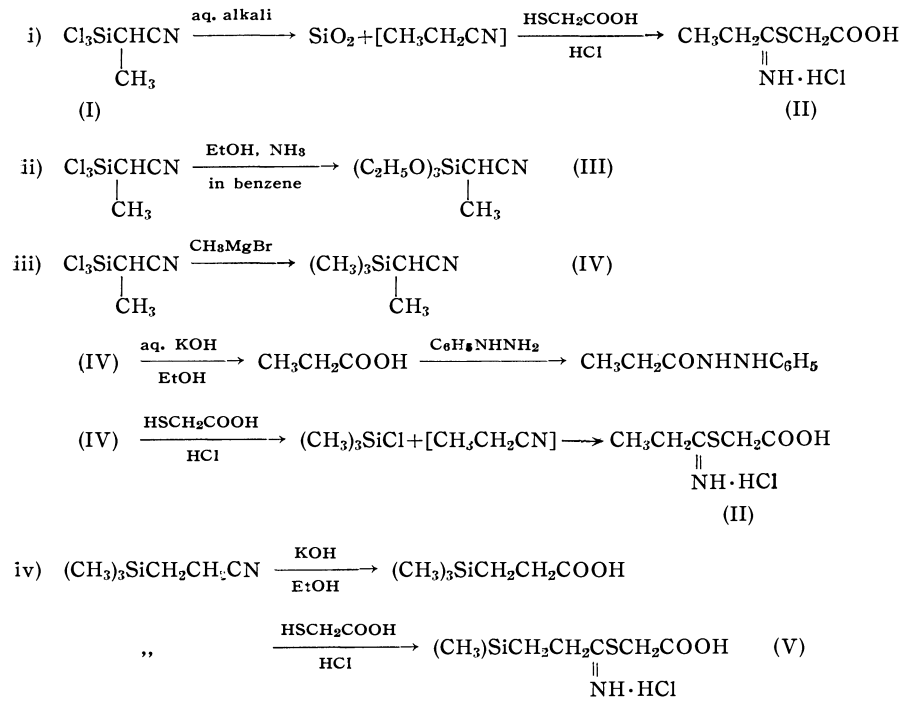

i) When the product (I) was hydrolyzed in a large excess of water and neutralized with an aqueous solution of ammonia, there was precipitated an amorphous silica as the result of the cleavage of the silicon-carbon bond. The organic fragment, propionitrile, was separated out and identified as the

thioglycolic acid adduct (II). In contrast with this, the β-isomer did not result in the cleavage of the silicon-carbon bond but gave the corresponding β-cyanoethylpolysiloxane.

ii) The alcoholysis of the compound (I) was carried out according to an usual manner which contains the treatment with absolute alcohol in benzene and with dry ammonia. The low yield (37%) of the alcoholysis may be partly due to the cleavage of the silicon-carbon bond during the reaction. The physical constants of the compound (III) were also quite different from that of the β-isomer.

iii) The hydrolysis of α-cyanoethyltrimethylsilane (IV) by an aqueous solution of alkali resulted in the cleavage of the silicon-carbon bond. The fission product, propionic acid, was identified as its phenylhydrazide. The reaction of the compound (IV) with thioglycolic acid in the presence of dry hydrogen chloride also gave the fission product (II).

iv) On the other hand, the hydrolysis and the reaction with thioglycolic acid of the β-cyanoethyltrimethylsilane yielded β-trimethylsilylpropionic acid and silicon-containing thioglycolic acid adduct (V), respectively. This is the marked difference from the case of the α-isomer.

The fission of the silicon-carbon bonds shown in these reactions is reasonably explainable by assigning α-cyanoethyltrichlorosilane to the structure of this addition product. Sommer and Marans[3] also reported the fission of ethyltrimethylsilylacetate by acid or alkali:

$$(CH_3)_3SiCH_2COOC_2H_5 \xrightarrow{HCl} (CH_3)_3SiCl + CH_3COOC_2H_5$$
$$(CH_3)_3SiCH_2COOC_2H_5 \xrightarrow{OH^-} (CH_3)_3SiOH + CH_3COOC_2H_5$$

The ease of fission of α-cyanoethylsilyl derivatives may be interpreted by the similar situation of its electronic configuration to that of ethyltrimethylsilylacetate, that is, in both cases an electronically negative atom

TABLE I

α-CYANOETHYLATION OF TRICHLOROSILANE IN SEALED TUBES AT 160°C[a]

No.	Catalysts, g.		Reaction time, hr.	Yield of α-adduct, %[b]	Appearance after heating
1	$AlCl_3$,	0.1	5.0	0	light brown
2	$FeCl_3$,	0.1	5.0	0	light yellow
3	stainless foil, pyridine	2.0 0.1	5.0	0	characteristic deep brownish black
4	Fe powder pyridine,	1.5 0.1	5.0	trace	light brown
5	Ni powder pyridine,	2.0 0.1	5.0	7	characteristic deep brownish black
6	Cr powder pyridine,	2.0 0.1	5.0	12	brown, mainly β-addition[c]
7[d]	stainless foil, pyridine,	2.0 0.1	3.0	0	light yellow
8[e]	stainless foil, pyridine,	2.0 0.1	5.0	31	characteristic deep brownish black
9	$NiCl_2$,	0.2	5.0	trace	colorless
10	$NiCl_2 \cdot C_5H_5N \cdot HCl$,	0.2	5.0	22	characteristic deep brownish black[f]
11	$NiCl_2 \cdot C_5H_5N$,	0.1	2.0	17	,, [g]
12	$NiCl_2 \cdot 4C_5H_5N$,	0.1	5.0	7	,, [h]

a) About 20 g. of trichlorosilane and 1.1 times equivalents of acrylonitrile were used.
b) Considering from their boiling points, the contamination by β-adduct if any is probably very small. The yields are based on trichlorosilane.
c) b.p. 97–101° (30 mmHg).
d) Benzene (40 ml.) was used as solvent.
e) Acetonitrile (40 ml.) was used as solvent.
f) Distillation residue, 5 g.
g) Residue, 7 g.
h) Reaction temp., 160–70°C. Residue, 8 g. Hydrolyzable Cl, 32.1 %.

3) L.H. Sommer and N.S. Marans, *J. Am. Chem. Soc.*, 72, 1935 (1950).

(oxygen or nitrogen) having the unshared electrons is situated at the β-position to silicon by an unsaturated bond.

$$\equiv Si-CH_2-\underset{|}{\overset{OC_2H_5}{C}}=\ddot{O}: \qquad \equiv Si-\underset{|}{\overset{CH_3}{CH}}-C\equiv N:$$

Cyanoethylation of Trichlorosilane in sealed Tubes

In order to find out what catalysed the α-cyanoethylation in an autoclave, we carried out the reaction in a sealed glass tube in the presence of one of several possible catalysts taking it into consideration that the wall of the autoclave might have some catalytic influences. Experimental results are given in Table I. The Friedel-Crafts type catalyst, anhydrous ferric chloride and aluminum chloride, showed no effect. Only nickel metal among the constituent metals of 18–8 stainless steel of the autoclave seemed te be responsible for a catalytic effect for the α-addition in the presence of pyridine, but in this case the yield of the product was very low and the distillation residue amounted to a considerable quantity. Anhydrous nickel (II) chloride also showed only a poor catalytic activity. Mono- and tetrapyridine nickel (II) chloride, $NiCl_2 \cdot C_5H_5N$, $NiCl_2 \cdot 4C_5H_5N$, and nickel chloride pyridine hydrochloride complex compound, $NiCl_2 \cdot C_5H_5N \cdot HCl$, were found to show the marked catalytic effect for the α-addition.

In all the α-addition reactions, as we mentioned above, the comparatively large amount of distillation residue was observed. This may have a close correlation with the fact that α-cyanoethyltrichlorosilane was found to be easily decomposed by heating in the presence of tetrapyridine nickel chloride. When α-cyanoethyltrichlorosilane was heated along with a catalytic amount of tetrapyridine nickel chloride in a sealed tube at 160°C., only 43% of the starting chlorosilane was recovered from the deep brownish black reaction mixture by distillation in vauco. The distillation residue was about 19% of the starting material, and therefore the total weight loss during the procedure amounted to about 38% of the starting material. Thus, the large weight loss and the considerable amount of the residue suggest us the decomposition of the α-adduct. Therefore, it seems to be probable that the low yield of the α-cyanoethyltrichlorosilane is partly due to the secondary degradation reaction, and the yield of the primary addition product may be much higher than the observed value.

Reaction Mechanism

In view of the above results it appears to be that either nickel chloride pyridine hydrochloride complex, mono- or tetrapyridine nickel chloride is one of the probable catalyst for the reaction in an autoclave. The mechanism of the catalytic action of these compounds still remains to be ambiguous.

As both the peroxide- and base-catalyzed additions are known to lead to the β-addition, one of the possible interpretations of the α-addition is the intermediate ionization of a silicon-hydrogen bond to a siliconium cation and a hydride anion.

$$Cl_3Si-H+\overset{\delta+}{C}H_2=\overset{\delta-}{C}HCN \cdots\cdots\rightarrow CH_2\underset{|}{\overset{SiCl_3}{C}}HCN$$

These ionic mechanism is supported in part by the effect of solvents, which is shown in experiment No. 7 and 8 in Table I.

Experimental

Catalysts.—The preparation of the platinized asbestos was described in the preceding paper[2].

Mono- and tetra-pyridine nickel chlorides and nickel chloride pyridine hydrochloride complex were prepared according to the method of Reizenstein[4].

Iron powder was the commercial product, and nickel and chrom powder were prepared from the electrolyzed metals.

The Reaction of Trichlorosilane and Acrylonitrile.—A mixture of trichlorosilane, acrylonitrile, and a catalyst was charged into a 18–8 stainless steel autoclave of 100 ml. capacity. The air in the autoclave was replaced by nitrogen, and then the gradual heating was applied. (Fig. 1). A sudden exothermic reaction started at a temperature between 150 and 170°C in the presence of either pyridine or platinized asbestos. The heating was stopped in about thirty minutes after the rapid decrease of the pressure had ceased. The color of the reaction mixture was always a deep brownish black which was characteristic to the α-cyanoethylation of trichlorosilane. The reaction mixture was then washed out by benzene, and after the removal of benzene by distillation at an atmospheric pressure, the remaining product was distilled in vacuo. The yield of α-cyanoethyltrichlorosilane was 21–39% (to trichlorosilane used) and approximately equal volume of nonvolatile distillation residue was produced.

Without catalyst, the reaction started at about 190°C, the yield of addition product was null, and a resin-like distillation residue of about 30 weight % was obtained.

The purified α-cyanoethyltrichlorosilane boils at 96–8° (41.5 mmHg).

Anal. Found: Hydrolyzable Cl, 56.3. Calcd. for $C_3H_4NSiCl_3$: Cl, 56.5%.

4) F. Reizenstein, *Z. anorg. Chem.*, **11**, 254 (1896); **18**, 264 (1898).

The procedure for the reaction of trichlorosilane and acrylonitrile in sealed glass tubes was similar to that of the preceding paper.

Degradation of α-Cyanoethyltrichlorosilane.—A mixture of 27 g. of α-cyanoethyltrichlorosilane (b.p. 99–102° (50 mmHg)) and 0.1 g. of tetrapyridine nickelchloride sealed in glass reaction tube was heated at 160°C. for six hours. The reaction mixture was colored to a deep brownish-black. Distillation gave 11.6 g. (43%) of the recovered chlorosilane (b.p. 101–5° (51 mmHg)), and 5.0 g. of a resin-like distillation residue (hydrolyzable Cl, 32.3%).

Hydrolysis of α-Cyanoethyltrichlorosilane (I).—When a small portion of α-cyanoethyltrichlorosilane was poured onto a large amount of water, it dissolved clearly with the evolution of heat. By neutralizing the acidic solution with an excess of 6 N aqueous solution of ammonia, the gellation took place. The gelled silica was filtered, washed with water, and dried in vacuo at 100°C.

Anal. A qualitative test for N was negative. Found: Si, 44.15. Calcd. for SiO_2: Si, 46.65%.

When 2.5 g. of trichlorosilane (I) was added dropwise to 10 ml. of 6 N aqueous sodium hydroxide, the once precipitated silica dissolved clearly into the solution. The alkaline solution was extracted twice with 20 ml. of ether. The ether layer was dried with calcium chloride, filtered, 1.0 g. of thioglycolic acid was added, and it was saturated with dry hydrogen chloride under the ice-cooling. After standing over night in ice-water, the thioglycolic acid adduct of propionitrile (II) crystallised in fine needles. The crystal was filtered, washed with ether, and dried in desiccater over phosphorous pentoxide, the yield was 0.5 g. (20%), m.p. 124°.

Anal. Found: Cl, 19.38. Calc. for $C_5H_{10}NO_2SCl$: Cl, 19.33%.

α-Cyanoethyltriethoxysilane (III).—The reaction procedure was analogous to that of β-cyanoethyltriethoxysilane in the preceding paper. From 16.6 g. (0.088 mol.) of α-cyanoethyltrichlorosilane and 13.0 g. (0.28 mol.) of absolute alcohol, 1.4 g. of ethylorthosilicate (b.p. 76–8° (26 mmHg)) and 7.1 g. of the crude α-cyanoethyltriethoxysilane (III) (b.p. 115–9° (26 mmHg)) was obtained. (37%). The compound (III) was purified by redistillation, b.p. 119–120° (26.5 mmHg) d_4^{25}, 0.9630; n_D^{25}, 1.4070.

Anal. Found: N, 6.45; Si, 12.73. MR_D, 55.46. Calcd. for $C_9H_{19}NO_3Si$: N, 6.45; Si, 12.91%. MR_D, 55.26.

α-Cyanoethyltrimethylsilane (IV).—When 19g. (0.10 mol.) of α-cyanoethyltrichlorosilane (I) was methylated in a usual manner with the ether solution of methylmagnesium bromide prepared from 10.7 g (0.44 Atom) of magnesium, 6.4 g. of crude α-cyanoethyltrimethylsilane (IV) was obtained, b.p. 95–9° (66 mmHg) (50%). In order to remove the possible impurity of α-trimethylsilylethylmethylketone, the crude product was shaken with the saturated solution of sodium bisulfite, washed with water, dried with sodium sulfate, and distilled again in vacuo, yielding 4.1 g. of pure α-cyanoethyltrimethylsilane (IV), b.p. 91.5–92.5° (58 mmHg); d_4^{25}, 0.8254; n_D^{25}, 1.4232.

Anal. Found: N, 10.50; Si, 21.09. MR_D, 39.19. Calcd. for $C_6H_{13}NSi$: N, 11.02; Si, 22.05%. MR_D, 39.09.

Reactions of β- and α-Cyanoethyltrimethylsilane (IV) with Thioglycolic Acid.—When a mixture of 0.2 g. of α-cyanoethyltrimethylsilane (IV), 0.3 g. of thioglycolic acid, and 1 ml. of dry ether, was saturated with dry hydrogenchloride under the cooling with ice water, a needlelike crystal began to appear within a half hour. After standing for one hour, the crystal was filtered and washed with ether, dried in desiccater. The yield of the thioglycolic acid adduct of propionitrile was 0.1 g., m.p. 119–120°.

Anal. Found: Cl, 19.23; Si, 0.00. Calcd. for $C_5H_{10}NO_2SCl$: Cl, 19.33; Si, 0.00%.

A mixture of 0.2 g. of β-cyanoethyltrimethylsilane, 0.3 g. of thioglycolic acid, and 1 ml. of ether was similarly treated with dry hydrogen chloride. The crystallization was completed in half an hour and 0.2 g. of the needle-like adduct was obtained, m.p. 143°.

Anal. Found: Cl, 13.98; Si, 11.03. Calcd. for $C_8H_{18}NO_2SClSi$: Cl, 13.87; Si, 10.95.

Alkaline Hydrolysis of α-Cyanoethyltrimethylsilane (IV).—When a solution of 4.0 g. of potassium hydroxide in 4 ml. of water was added to 3.1 g. of α-cyanoethyltrimethylsilane, a vigorous reaction took place. Then 10 ml. of alcohol was added to the solution and it was refluxed for five hours until the evolution of ammonia ceased. To the reaction mass 40 ml. of water was added after cooling, and extracted with 10 ml. of ether to remove the unreacted nitrile. The aqueous layer was acidified with hydrochloric acid and extracted again with ether. The ether layer, which contained the produced carboxylic acid, was dried with sodium sulfate, filtered, and distilled. The carboxylic acid thus obtained was identified as its phenylhydrazide as follows; the distillate (b.p. 65–145°, 1.3 g.) and 2.0 g. of phenylhydrazine were refluxed for a half hour on a free flame. After cooling, the crystalline mass was filtered and washed thoroughly with benzene to yield 1.0 g. of propionic phenylhydrazide as a scaly crystal, m.p. 154–5°. After recrystallization from benzene, it melted at 155–6°C (157° in literature).

Summary

Contrary to the case of β-cyanoethylation, α-cyanoethylation of trichlorosilane was found to take place in an autoclave in the presence of either pyridine or platinized asbestos.

In the reactions in sealed glass tubes, on the other hand, stainless steel and pyridine, mono- and tetrapyridine nickel chloride, and nickel chloride pyridine hydrochloride complex were effective for the α-addition. An ionic mechanism was suggested for the α-cyanoethylation.

The structural proof of α-cyanoethyltrichlorosilane was given from the comparison

of the physical constants and chemical behaviour of it to those of the β-isomer. α-Cyanoethyl-triethoxysilane and -trimethylsilane were prepared from α-cyanoethyltrichlorosilane and characterised.

The authors are much indebted to Profs. S. Murahashi and H. Tani for their many helpful suggestions. Appreciation is also expressed to Nihon Silicon Resin Co. for their kindness of supplying the trichlorosilane.

Department of Chemistry
Faculty of Science
Osaka University, Osaka

Electronic States of the C_2 Radical

By Kenji FUEKI and Jiro HIGUCHI

(Received October 25, 1955)

Introduction

The investigation of the electronic properties for the carbon-carbon bond have generally been performed on the interactions between the π-electrons. For the precise study of charge distribution, hyperconjugation and so on, it is very desirable to take into consideration the mutual interactions between all the electrons, at least between all the valence electrons. Nevertheless, only a few investigations have been carried out in such a way, because of the complicated procedure required, in comparison with that for the π-electrons only. Moreover, it is very difficult to appraise the effect of the errors accompanying the calculation for the σ-electrons, since there are, in general, few experimental data except for the π-orbitals. From this point of view, the C_2 radical is one of the most suitable examples, because it is the simplest molecule and there are abundant experimental data on it.

The Swan bands and the Mulliken bands of the C_2 radical have been detected in flames, explosions and electric discharges of hydrocarbons, and recently also in flash photolysis; the other bands have also been observed by spectroscopic technique. On the other hand, theoretical investigations were qualitatively made by Mulliken[1], who predicted many unobserved states. A quantitative calculation was carried out by Araki, Tutihasi and Watari[2] using the AO method, but the results were not sufficiently satisfying to explain the observed electronic states. In the present work, therefore, the LCAO-SCF method was adopted and the interactions between all the electrons were included.

Outline of Calculation

The calculation was carried out by taking ten atomic orbitals c, s, σ, π_+, π_-, c', s', σ', π_+' and π_-' into consideration, which mean $1s$, $2s$, $2p\sigma$, $2p\pi_+$, $2p\pi_-$ orbitals of each carbon atom. The $1s$ AO's were regarded as the inner shells, since the overlap integrals between c or c' and the other AO's are fairly small in comparison with the others[3]. The internuclear distance was taken as 1.33 Å, nearly equal to the equilibrium internuclear distance of the observed lowest state $^3\Pi_u$, i.e., 1.31 Å[4].

The atomic orbitals used were the Hartree SCF AO's for the s^2p^2 configuration of carbon atom[5] as in the case of the CH radical[6], assuming that they satisfy the following Fock equations for the valence state $V_2(\sigma\pi)$ in the s^2p^2 configuration.

$$(I+2J_c-K_c+2J_s-K_s+J_\sigma-\frac{1}{2}K_\sigma+J_\pi-\frac{1}{2}K_\pi)s$$
$$=(I_s+2J_{cs}-K_{cs}+J_{ss}+J_{s\sigma}-\frac{1}{2}K_{s\sigma}+J_{s\pi}-\frac{1}{2}K_{s\pi})s, \quad (1)$$

$$(I+2J_c-K_c+2J_s-K_s+J_\pi-\frac{1}{2}K_\pi)\sigma$$
$$=(I_\sigma+2J_{c\sigma}-K_{c\sigma}+2J_{s\sigma}-K_{s\sigma}+J_{\sigma\pi}-\frac{1}{2}K_{\sigma\pi})\sigma, \quad (2)$$

1) R.S. Mulliken, *Phys. Rev.*, **41**, 751 (1932); **56**, 778 (1939).

2) G. Araki, S. Tutihashi and W. Watari, *Prog. Theor. Phys.*, **6**. 135 (1951); G. Araki and W. Watari, *Prog. Theor. Phys.*, **6**, 945 (1951).

3) $S_{cc'}=0.00005$, $S_{sc'}=0.05086$, $S_{\sigma c'}=0.08619$, while $S_{ss'}=0.45626$, $S_{s\sigma'}=0.44413$.

4) G. Herzberg, "Molecular Spectra and Molecular Structure", D. Van Nostrand Company, Inc., New York (1950), Second Edition, Vol. 1, p. 518.

5) C.C. Torrance, *Phys. Rev.*, **46**, 388 (1934). The Hartree-Fock SCF AO's for the V_2 ($\sigma\pi$) have not yet been obtained, and therefore the Hartree SCF AO's were used.

6) J. Higuchi, *J. Chem. Phys.*, **22**, 1339 (1954).

$$(I+2J_c-K_c+2J_s-K_s+J_\sigma-\frac{1}{2}K_\sigma)\pi_\pm$$
$$=(I_{\pi_\pm}+2J_{c\pi_\pm}-K_{c\pi_\pm}+2J_{s\pi_\pm}-K_{s\pi_\pm}+J_{\sigma\pi_\pm}$$
$$-\frac{1}{2}K_{\sigma\pi_\pm})\pi_\pm. \quad (3)$$

Here

$$I=-\frac{1}{2}\Delta_\nu-\frac{6}{r_{c\nu}}, \quad (4)$$

$$J_i{}^\nu\phi^\nu=\left(\int\bar{\phi}_i{}^\mu\frac{1}{r^{\mu\nu}}\phi_i{}^\mu d\tau^\mu\right)\phi^\nu, \quad (5)$$

$$K_i{}^\nu\phi^\nu=\left(\int\bar{\phi}_i{}^\mu\frac{1}{r^{\mu\nu}}\phi^\mu d\tau^\mu\right)\phi_i{}^\nu, \quad (6)$$

and

$$I_i=\int\bar{\phi}_i{}^\nu\left(-\frac{1}{2}\Delta_\nu-\frac{6}{r_{c\nu}}\right)\phi_i{}^\nu d\tau^\nu, \quad (7)$$

$$J_{ij}=\int\bar{\phi}_i{}^\mu\bar{\phi}_j{}^\nu\frac{1}{r^{\mu\nu}}\phi_i{}^\mu\phi_j{}^\nu d\tau^{\mu\nu}, \quad (8)$$

$$K_{ij}=\int\bar{\phi}_i{}^\mu\bar{\phi}_j{}^\nu\frac{1}{r^{\mu\nu}}\phi_j{}^\mu\phi_i{}^\nu d\tau^{\mu\nu}. \quad (9)$$

Consequently, one-center integrals calculated by Ufford[7] were used. It is very difficult, however, to calculate the majority of the two-center integrals and it is assumed that the use of the Slater AO's[8] instead of the SCF AO's gives good approximations of these integrals, and they were taken from the table by Kotani et al[9]. The core-field energies were obtained from the above Fock equations (1)–(3).

From the eight available AO's, the symmetry orbitals for the C_2 radical were obtained as follows:

$$\begin{array}{ll}\sigma_1=2^{-1/2}(s+s'), & \sigma_2=2^{-1/2}(\sigma+\sigma')\\ \sigma_3=2^{-1/2}(s-s'), & \sigma_4=2^{-1/2}(\sigma-\sigma')\\ \sigma_5=2^{-1/2}(\pi_+ +\pi_+'), & \sigma_6=2^{-1/2}(\pi_- +\pi_-')\\ \sigma_7=2^{-1/2}(\pi_+ -\pi_+'), & \sigma_8=2^{-1/2}(\pi_- -\pi_-').\end{array} \quad (10)$$

By taking linear combinations of these, a like number of MO's of the same symmetry was formed as follows:

$$\begin{array}{ll}K=c, & K'=c'\\ 1\sigma_g=a_{11}\sigma_1+a_{12}\sigma_2, & 1\sigma_u=a_{33}\sigma_3+a_{34}\sigma_4\\ 2\sigma_g=a_{21}\sigma_1+a_{22}\sigma_2, & 2\sigma_u=a_{43}\sigma_3+a_{44}\sigma_4\\ 1\pi_g^+=a_{77}\sigma_7, & 1\pi_u^+=a_{55}\sigma_5\\ 1\pi_g^-=a_{88}\sigma_8, & 1\pi_u^-=a_{66}\sigma_6.\end{array} \quad (11)$$

7) C.W. Ufford, *Phys. Rev.*, 53, 568 (1938).

8) $c=(\delta'^3/\pi)^{1/2}\exp(-\delta' r)$, $s=(\delta^5/3\pi)^{1/2}r\exp(-\delta r)$, $\sigma=(\delta^5/\pi)^{1/2}r\exp(-\delta r)\cos\theta$, $\pi_\pm=(\delta^5/2\pi)^{1/2}r\exp(-\delta r)\sin\theta\exp(\pm i\varphi)$.
In the present calculation δ and δ' are chosen as 1.59 and 5.6875, respectively.

The prescripts 1, 2 are in the order of increasing energy within each symmetry. The coefficients of a_{ip}'s of the symmetry orbitals were chosen to satisfy the orthogonality conditions:

$$\int\bar{\phi}_i{}^\nu\phi_j{}^\nu d\tau^\nu=\sum_{p,q}\bar{a}_{ip}S_{pq}a_{jq}=\delta_{ij}, \quad (12)$$

where the overlap integrals S_{pq}'s are defined by

$$S_{pq}=\bar{S}_{qp}=\int\bar{\sigma}_p\sigma_q d\tau. \quad (13)$$

In the first place, the SCF calculation[10] was carried out for the lowest ${}^3\sum_g^-$ state $KK'(1\sigma_g)^2(1\sigma_u)^2(1\pi_u)^2(2\sigma_g)^2$, which has been considered to be close above the lowest ${}^3\Pi_u$ state or to be the ground state.

Next the SCF calculation was also carried out for the state ${}^1\sum_g^+$ $KK'(1\sigma_g)^2(1\sigma_u)^2(1\pi_u)^4$, which has been supposed to be the lowest singlet state. However, the energy for the lowest ${}^3\Pi_u$ state $KK'(1\sigma_g)^2(1\sigma_u)^2(1\pi_u)^3(2\sigma_g)^1$, was not minimized, because the properties of the state can readily be inferred from the results of the ${}^3\sum_g^-$ and ${}^1\sum_g^+$ states.

LCAO MO's

The LCAO MO's obtained by the SCF procedure are given in Table I, and the SCF solutions are given in Table II. The ${}^3\sum_g^-$

TABLE I

LCAO SCF MO's FOR $\left\{\begin{matrix}{}^3\sum_g^-\\ {}^1\sum_g^+\end{matrix}\right\}$ STATE

$K=c$,	$K'=c'$
$1\sigma_g=\left\{\begin{matrix}0.628\\ 0.693\end{matrix}\right\}\sigma_1+\left\{\begin{matrix}0.395\\ 0.298\end{matrix}\right\}\sigma_2$	
$2\sigma_g=\left\{\begin{matrix}0.609\\ 0.534\end{matrix}\right\}\sigma_1-\left\{\begin{matrix}0.830\\ 0.870\end{matrix}\right\}\sigma_2$	
$1\sigma_u=\left\{\begin{matrix}1.089\\ 1.085\end{matrix}\right\}\sigma_3-\left\{\begin{matrix}0.303\\ 0.307\end{matrix}\right\}\sigma_4$	
$2\sigma_u=\left\{\begin{matrix}1.658\\ 1.660\end{matrix}\right\}\sigma_3+\left\{\begin{matrix}1.746\\ 1.745\end{matrix}\right\}\sigma_4$	
$1\pi_u^\pm=0.888\underset{6}{\sigma}$,	$1\pi_g^\pm=1.193\underset{8}{\sigma}$.

9) M. Kotani, A. Amemiya, T. Shimose, *Proc. Phys-Math. Soc. Japan*, 20, Extra No. 1 (1938); M. Kotani, E. Ishiguro, K. Hijikata, T. Nakamura and A. Amemiya, *J. Phys. Soc. Japan*, 8, 463 (1953).

10) In the present calculation, the following approximation was used

$$\int\bar{p}^\nu\left(-\frac{6}{r_{\nu c}}\right)q'^\nu d\tau^\nu+2(pq':cc)-(pc:cq')$$
$$\sim\int\bar{p}^\nu\left(-\frac{4}{r_{c\nu}}\right)q'^\nu d\tau^\nu,$$

where the c, p orbitals and the q' orbital belong to different atoms. In the calculation of $\int\frac{4}{r_{c\nu}}s^\nu q'^\nu d\tau^\nu$, the orthogonalized $2s$ function was used for s, because the error due to the nonorthogonal $2s$ function is very significant near the C nucleus.

TABLE II

SELF-CONSISTENT SOLUTIONS*

		state	$^3\sum_g^-$	$^1\sum_g^+$
$S_{\sigma_1\sigma_1}$	1.45626	$G_{\sigma_1\sigma_1}$	4.2347	4.3051
$S_{\sigma_1\sigma_2}$	0.44413	$G_{\sigma_1\sigma_2}$	1.7262	1.7115
$S_{\sigma_2\sigma_2}$	1.31869	$G_{\sigma_2\sigma_2}$	4.1287	4.5383
$S_{\sigma_3\sigma_3}$	0.54374	$G_{\sigma_3\sigma_3}$	1.4686	1.5006
$S_{\sigma_3\sigma_4}$	−0.44413	$G_{\sigma_3\sigma_4}$	−1.1376	−1.1632
$S_{\sigma_4\sigma_4}$	0.68131	$G_{\sigma_4\sigma_4}$	1.7847	1.8224
$S_{\sigma_5\sigma_5}$	1.28695	$G_{\sigma_5\sigma_5}$	3.6731	3.7450
$H'_{\sigma_1\sigma_1}$	−5.7954	$\varepsilon_{1\sigma_g}$	−1.1922	−1.1196
$H'_{\sigma_1\sigma_2}$	−2.5345	$\varepsilon_{2\sigma_g}$	−0.5395	−0.2044
$H'_{\sigma_2\sigma_2}$	−5.2574	$\varepsilon_{1\sigma_u}$	−0.6375	−0.5793
$H'_{\sigma_3\sigma_3}$	−1.8011	$\varepsilon_{2\sigma_u}$	+0.2559	+0.3103
$H'_{\sigma_3\sigma_4}$	+1.4718	$\varepsilon_{1\pi_u}$	−0.5448	−0.4851
$H'_{\sigma_4\sigma_4}$	−2.0356	$\varepsilon_{1\pi_g}$	+0.0699	+0.0854
$H'_{\sigma_5\sigma_5}$	−4.3742			

* S_{pq}'s are the overlap integrals, H'_{pq}'s the core-field energy matrix elements, G_{pq}'s the electronic interaction matrix elements, ε_t's the LCAO SCF orbital energies.

state MO's also satisfy the conditions which minimize the energy of the $^1\Delta_g$ state $KK'(1\sigma_g)^2(1\sigma_u)^2(1\pi_u)^2(2\sigma_g)^2$ and the $^1\sum_g^+$ state $KK'(1\sigma_g)^2(1\sigma_u)^2(1\pi_u)^2(2\sigma_g)^2$, because the energy differences between these states are only proportional to the energy $K_{1\pi_u{}^+1\pi_u{}^-}$ which is independent of the LCAO-SCF procedure. These LCAO MO'S are, therefore, also the $^1\Delta_g$ state MO's and the $^1\sum_g^+$ MO's as well as the $^3\sum_g^-$ state MO's.

The coefficients of the AO's in these LCAO MO's are in good agreement with those predicted by Mulliken, and the LCAO MO's for the $^3\sum_g^-$ and $^1\sum_g^+$ states in Table I resemble each other. The special similarity for the weakly antibonding $1\sigma_u$ MO is due to the fact that the MO hardly effects the bonding property of the radical. In the strongly bonding $1\sigma_g$ MO, however, the coefficient of σ_1 for the $^1\sum_g^+$ state MO is rather large, but in the weakly bonding $2\sigma_g$ MO this relation is reversed, since the $2\sigma_g$ MO is vacant in the $^1\sum_g^+$ state while it is occupied in the $^3\sum_g^-$ state.

The coefficients of the AO's in the $^{1,3}\Pi_u$ MO's are generally considered to have the values between those of the $^3\sum_g^-$ state MO's and the $^1\sum_g^+$ stane MO's from the numbers of the occupied electrons in each MO's. In the total energies of the $^{1,3}\Pi_u$ states, however, the coefficients of the $K_{2\sigma_g1\pi_u}$ are not the same and consequently the forms of the MO's will be somewhat different from each other. However, the $^3\Pi_u$ state MO's may be rather close to the $^3\sum_g^-$ state MO's (while the $^1\Pi_u$ state MO's may somewhat resemble to the $^1\sum_g^+$ state MO's), on account of the same coefficient of the $K_{2\sigma_g1\pi_u}$. These MO's also rather resemble the N_2 ground state MO's by Scherr[11]. This is mainly due to the fact that the values of δR, R being the internuclear distance, are nearly equal and so the overlap integrals are very close in both cases.

In the $^3\sum_g^-$ state MO's, the orbital energy of $1\pi_u$ MO is very close to that of the $2\sigma_g$ MO. However, the result of the N_2 molecule by Scherr showed that the incomplete treatment gave the very close orbital energies for these MO's, while the $2\sigma_g$ MO energy is 0.96 eV. higher than the $1\pi_u$ MO enegy in the complete treatment. In consideration of these facts, the energy difference between these MO's will be increased by taking into account the inner-shell-outer-shell-mixing. The orbital energy of the $2\sigma_g$ MO in the $^1\sum_g^+$ state MO's is very high as compared with that in the $^3\sum_g^-$ state MO's, because the MO is vacant in the $^1\sum_g^+$ state and this value is the SCF orbital energy but not the orbital energy by Mulliken[12].

Electronic States

By using the LCAO MO's given in Table I, the energies of the lower electronic states were calculated without configuration interaction[13], and are shown in Fig. 1. The electronic configurations of these states are given in Table III. The energy levels calculated by both the LCAO MO's considerably resemble each other; therefore the energy levels which are to be obtained by the other state MO's than the $^3\sum_g^-$ and $^1\sum_g^+$ state MO's will be very similar to those in Fig. 1, as in the case of the CH radical.

The calculated value (2.5 eV.) of the $^3\Pi_g$ (a)—$^3\Pi_u$ (a) transition and that (5.4–5.5 eV.) of the $^3\Pi_g$ (b)—$^3\Pi_u$ (a) transition are in good

11) C.W. Scherr, *J. Chem. Phys.*, **23**, 569 (1955).
12) R.S. Mulliken, *J. chim. phys.*, **46**, 497 (1949).
13) The interactions between the wave functions arising from rotation operation were taken into consideration.

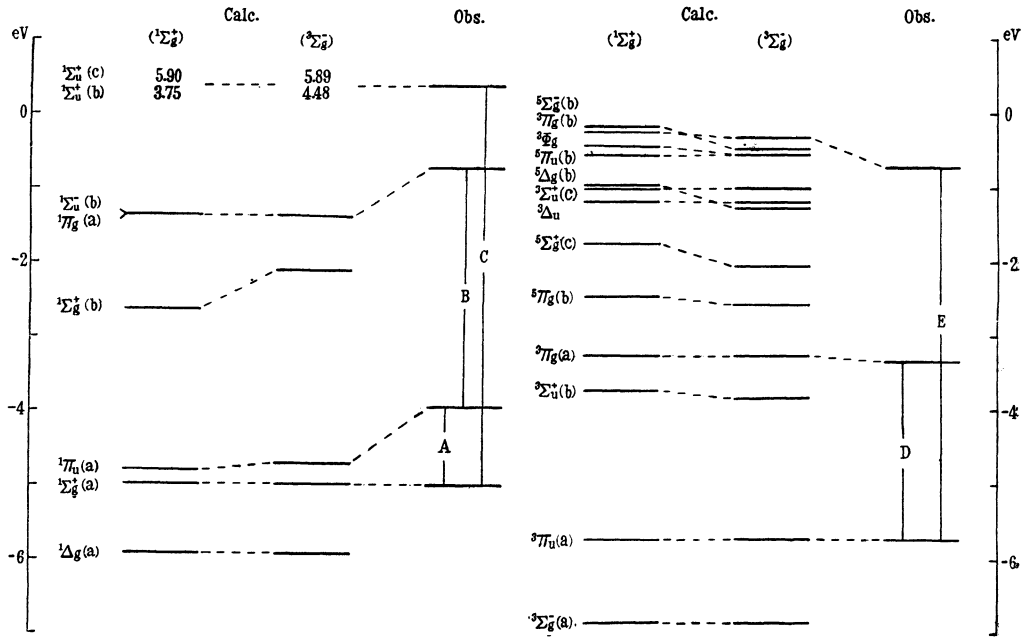

Fig. 1. Lower electronic states of the C_2 radical.
(A) The Phillips bands (B) The Deslandres-d'Azambuja bands (C) The Mulliken bands (D) The Swan bands (E) The Fox-Herzberg bands. The origin of energy is chosen to be $C(^3P)+C(^3P)$ without configuration interaction.

TABLE III

ELECTRON CONFIGURATIONS OF THE LOWER ELECTRONIC STATES

Configuration	State
$KK'(1\sigma_g)^2(1\sigma_u)^2(1\pi_u^{\pm})^2(2\sigma_g)^2$	$^1\Delta_g$(a)
〃 $(1\sigma_g)^2(1\sigma_u)^2(1\pi_u^{+})^1(1\pi_u^{-})^1(2\sigma_g)^2$	$^1\Sigma_g^+$(a), $^3\Sigma_g^-$(a)
〃 $(1\sigma_g)^2(1\sigma_u)^2(1\pi_u^{\pm})^2(1\pi_u^{\mp})^1(2\sigma_g)^1$	$^{1,3}\Pi_u$(a)
〃 $(1\sigma_g)^2(1\sigma_u)^1(1\pi_u^{\pm})^2(1\pi_u^{\mp})^1(2\sigma_g)^2$	$^{1,3}\Pi_g$(a)
〃 $(1\sigma_g)^2(1\sigma_u)^2(1\pi_u^{\pm})^2(1\pi_u^{\mp})^1(1\pi_g^{\mp})^1$	$^{1,3}\Sigma_u^+$(a), $^{1,3}\Sigma_u^-$(a)
〃 $(1\sigma_g)^2(1\sigma_u)^2(1\pi_u^{\pm})^1(2\sigma_g)^2(1\pi_g^{\pm})^1$	$^{1,3}\Delta_u$
〃 $(1\sigma_g)^2(1\sigma_u)^2(1\pi_u^{\pm})^2(2\sigma_g)^1(1\pi_g^{\pm})^1$	$^{1,3}\Phi_g$
〃 $(1\sigma_g)^2(1\sigma_u)^2(1\pi_u^{+})^2(1\pi_u^{-})^2$	$^1\Sigma_g^+$(b)
〃 $(1\sigma_g)^2(1\sigma_u)^1(1\pi_u^{+})^2(1\pi_u^{-})^2(2\sigma_g)^1$	$^{1,3}\Sigma_u^+$(b)
〃 $(1\sigma_g)^2(1\sigma_u)^2(1\pi_u^{\pm})^1(2\sigma_g)^2(1\pi_g^{\mp})^1$	$^{1,3}\Sigma_u^-$(b), $^{1,3}\Sigma_u^+$(c)
〃 $(1\sigma_g)^2(1\sigma_u)^2(1\pi_u^{+})^1(1\pi_u^{-})^1(2\sigma_g)^1(1\pi_g^{\pm})^1$	$^{1,1,3,3,3,5}\Pi_g$(b)
〃 $(1\sigma_g)^2(1\sigma_u)^1(1\pi_u^{\pm})^2(1\pi_u^{\mp})^1(2\sigma_g)^1(1\pi_g^{\pm})^1$	$^{1,1,3,3,3,5}\Delta_g$(b)
〃 $(1\sigma_g)^2(1\sigma_u)^1(1\pi_u^{+})^1(1\pi_u^{-})^1(2\sigma_g)^2(1\pi_g^{\pm})^1$	$^{1,1,3,3,3,5}\Pi_u$(b)
〃 $(1\sigma_g)^2(1\sigma_u)^1(1\pi_u^{\pm})^2(1\pi_u^{\mp})^1(2\sigma_g)^1(1\pi_g^{\mp})^1$	$^{1,1,3,3,3,5}\Sigma_g^-$(b), $^{1,1,3,3,3,5}\Sigma_g^+$(c)

agreement with the observed value (5179 Å)[14] of the Swan bands and that (2495 Å) of the Fox-Herzberg bands, respectively. The $^1\Pi_g$ (a) $-{}^1\Pi_u$ (a) interval (3.4–3.5 eV.) in this calculation is also in good agreement with the observed value (3865 Å) of the Deslandres-d'Azambuja bands. The experimentally known Phillips bands and Mulliken bands

14) All the observed values are taken from reference (4).

correspond to the $^1\Pi_u$ (a)—$^1\Sigma_g^+$ (a) (or $^1\Pi_u$ (a)—$^1\Sigma_g^+$ (b)) and $^1\Sigma_u^+$ (c)—$^1\Sigma_g^+$ (a) (or $^1\Sigma_u^+$ (b)—$^1\Sigma_g^+$ (b)) transitions, respectively, but the calculated transition of the latter bands is considerably larger than the experimental one. This is mainly due to the facts that the present calculation ignores configuration interaction and that the SCF procedure is carried out for the $^3\Sigma_g^-$ (a) and $^1\Sigma_g^+$ (b) states only. The calculated ground state is the $^3\Sigma_g^-$, while the lowest state observed is the $^3\Pi_u$. As pointed out by Mulliken[1], the ground state of the C_2 radical has not yet been conclusively decided from the experiment. But the $^1\Sigma_g^+$ state is most unlikely from the standpoint of spin multiplicity. On the other hand, Norrish, Porter and Thrush[15] pointed out that the separation between the $^1\Sigma_g^+$ and $^3\Pi_u$ states of 0.69 eV., as predicted by Herzberg and Sutton[16], is quite possible. In the present calculation, this separation is 0.76 eV. in good agreement with their prediction. The ground state may, therefore, be likely to be the $^3\Sigma_g^-$. In the complete treatment with the inner-shell-outer-shell-mixing, however, the $1\pi_u$ MO energy is expected to be somewhat lowered as compared with the $2\sigma_g$ MO energy, as supposed from the result of N_2 by Scherr; then the $^3\Pi_u$ (a) state may be calculated as the ground state in accord with the experiment. In a similar way, the $^1\Sigma_g^+$ (b) state will be very close to the $^1\Sigma_g^+$ (a) state, consequently the Phillips bands will be satisfactorily explained, if consideration is made of the configuration interaction between the above two $^1\Sigma_g^+$ states.

The dissociation energy of C_2 has not definitely been known. Herzberg gave the value of 3.6 eV. from spectroscopic evidence. Gaydon[17], however, pointed out that an extrapolation of the vibrational levels leads to 4–7 eV. Brewer, Gilles and Jenkins[18] have measured the variation in intensity with temperature of the Swan bands and deduced 4.95±0.3 eV., which has been accepted by Gaydon. The value of about 6.2 eV.[19] has been suggested from the temperature dependence of the rate of evaporation of C_2 and graphite. Glockler[20] has given 5.9 eV. from bond energy-bond length relationships. In the present calculation, the dissociation energy obtained is 5.7 eV.[21] for the $^3\Pi_u$ state, which is rather close to the value by Gaydon, although the value will be decreased by the atomic configuration interaction.

Discussion

The results in the present calculation are qualitatively correct and also are semi-quantitatively satisfying. This is mainly due to the fact that the one-center integrals used are obtained by the SCF AO's. The two-center integrals are, however, still somewhat unsatisfying, because most of them are calculated by using the simple Slater AO's. In fact the errors due to the use of the simple $2s$ AO are not small, but the strong influence near the nucleus is modified by the approximation given in reference (10). Further, the use of the Slater AO's reduces the electronic interaction, especially between the σ-electrons, and consequently the form of the LCAO MO's will be somewhat changed by use of the two-center integrals of the SCF AO's.

The use of the fixed internuclear distance of 1.33 Å is not completely satisfactory to explain the experiment, because the equilibrium distances of the various states do not generally coincide with the value of 1.33 Å; for example, the state such as the $^1\Sigma_g^+$(b) has a rather small internuclear distance. Moreover, the interpretation of multiple bond must include the change of bond distance. Considering these facts, it is desirable to carry out the calculations for various internuclear separations. The treatment with the inner-shell-outer-shell-mixing is also desirable in a precise discussion. But the approximations in the present calculation may be fairly useful for larger molecules, if the problem is restricted to the subjects such as the order of the orbital energies, the one-electron excitation levels and so on. In the light of these facts, it is very hopeful to investigate the electronic properties of hydrocarbons with considerable accuracy by means of such a treatment.

15) R. G. W. Norrish, G. Porter and B.A. Thrush, *Nature*, **169**, 582 (1952).
16) G. Herzberg and R.B. Sutton, *Can. J. Res.*, A 18, 74 (1940).
17) A.G. Gaydon, "Dissociation Energies and Spectra of Diatomic Molecules", Chapman and Hall Ltd., London (1953), Second Edition.
18) L. Brewer, P.W. Gilles and F.A. Jenkins, *J. Chem. Phys.*, **16**, 797 (1948).
19) T.L. Cottrell, "The Strength of Chemical Bonds", Butterworths Scientifiic Publications, London (1954), p. 199.
20) G. Glockler, *J. Chem. Phys.*, **19**, 124 (1951).
21) The zero-point energy is not included.

Summary

LCAO MO's and ionization energies have been calculated for the $^3\sum_g^- KK'\ (1\sigma_g)^2(1\sigma_u)^2(1\pi_u)^2(2\sigma_g)^2$ and $^1\sum_g^+ KK'(1\sigma_g)^2(1\sigma_u)^2(1\pi_u)^4$ states of the C_2 radical at the internuclear distance of 1.33 Å using the LCAO-SCF method. The interactions of all the electrons have been taken into consideration, but the orthogonality relationship between the 1*s* and the other orbitals was assumed. The LCAO MO's obtained are in good agreement with those predicted by Mulliken. Using these LCAO MO's, the lower electronic states have been investigated without configuration interaction. The calculated levels are generally in good agreement with the experimental. The ground state obtained is the $^3\sum_g^-$ state, while the observed is the $^3\Pi_u$, but the result is not conclusive because of the ignorance of the inner-shell-outer-shell-mixing.

The authors wish to thank Professor S. Shida for his continued interest and kind advice.

Laboratory of Physical Chemistry, Tokyo Institute of Technology, Ookayama Meguro-ku, Tokyo

*Densities and Optical Properties of Organic Compounds in the Liquid State. VI. The Refractive Indices of Paraffin Hydrocarbons and Some of Their Derivatives**

By Maurice L. HUGGINS**

(Received November 8, 1955)

Introduction

The purpose of this paper is to relate the refractive indices, n_D, of various liquid aliphatic organic compounds at 20°C to their composition. This relationship is best shown with the aid of molal refractions (R, R' or R''), defined by the equations

$$R = V(n_D - 1), \tag{1}$$

$$R' = V(n_D^2 - 1), \tag{2}$$

and

$$R'' = V\frac{n_D^2 - 1}{n_D^2 + 2}. \tag{3}$$

V is the molal volume. These molal refractions are approximately additively calculable from contributions of the atoms, atomic groups, or bonds composing the molecule.

Although Eq. (3) has the soundest theoretical basis for simple gaseous system, for condensed systems it seems necessary to choose between these relationships on a purely empirical basis[2]. Fairly extensive calculations by the writer, both for liquid organic compounds and for glasses[3] indicate that R, R', and R'' exhibit about the same degree of additivity. For the present purpose, we choose the simplest: R.

The molal volume is the molecular weight divided by the density. If experimental density values are not available or are insufficiently accurate, the molal volume can, in many cases, be computed by simple empirical relationships.[1,4,5,6,7].

A considerable amount of accurate density and refractive-index data for organic compounds is now conveniently available[8,9].

* Communication No. 1757 from the Research Laboratories of the Eastman Kodak Company, Rochester 4, New York, U. S. A.

This paper is a revision of parts of a previously published paper[1] and of an unpublished paper, entitled "Refractive Indices of Liquid Aliphatic Organic Compounds," presented October 3, 1940 at a meeting of the Optical Society of America in Rochester, New York, U. S. A.

** Fulbright Exchange Professor, Osaka and Kyoto Universities, 1955-1956, on leave from the Research Laboratories of the Eastman Kodak Company, Rochester, 4, New York, U. S. A.

1) M.L. Huggins, *J. Am. Chem. Soc.*, **63**, 116 (1941).

2) S.S. Kurtz, Jr. and A.L. Ward, *J. Franklin Inst.*, **222**, 563 (1936); **224**, 583 (1937).

3) M.L. Huggins, *J. Opt. Soc. Am.*, **30**, 495 (1940).

4) M.L. Huggins, *J. Am. Chem. Soc.*, **63**, 916 (1941).

5) M.L. Huggins, *J. Am. Chem. Soc.*, **76**, 843 (1954).

6) M.L. Huggins, *J. Am. Chem. Soc.*, **76**, 845 (1954).

7) M.L. Huggins, *J. Am. Chem. Soc.*, **76**, 847 (1954).

8) "Selected Values of Properties of Hydrocarbons," Circular of the National Bureua of standerds C461, U.S. Government Printing Office, Washington, D.C., (1947).

9) J. Timmermans, "Physico-Chemical Constants of Pure Organic Compounds", Elsevier Publishing Co., Inc., Amsterdam (1950).

These data form the basis for the results reported here.

Hydrocarbons

The additivity relationships may be described in terms of contributions from the different types of atoms (C, H), atomic groups (CH_3, CH_2, CH, C), or bonds (C-C, C-H). For example, for normal paraffins, C_nH_{2n+2}, the best data lead to

$$R_n=7.821n+2.064, \tag{4}$$

which is equivalent to

$$R_n=5.757N_C+1.032N_H \tag{5}$$

or

$$R_n=7.821N_{CH_2}+8.853N_{CH_3}. \tag{6}$$

No similar equation, involving a uniform contribution of each C-C bond and each C-H bond, fits the data, for either normal paraffins or those of other types. By differentiating between different types of C-C and C-H bonds, however, one can deduce satisfactory additivity equations and constants.

To do this, use is made of data for several other series of saturated aliphatic hydrocarbons. These data are well satisfied by equations of the form of Eq. (4), but with different values of the constant term. Putting

$$R=R_n+k=7.821n+2.064+k, \tag{7}$$

the following values of k have been found:

2-Methyl alkanes $k_1=+0.014$ (8)

3-Methyl alkanes and 4-methyl alkanes $k_2=-0.137$ (9)

2, 2-Dimethyl alkanes $k_3=+0.005$ (10)

3, 3-Dimethyl alkanes and 4, 4-dimethyl alkanes $k_4=-0.278$ (11)

As previously shown, these can be used to obtain relative bond refraction contributions, α_{ij}. The appropriate equations* are:

$$\alpha_{21}=(b-a)/2+2k_1-2k_2+k_3-k_4/2+5\delta=3.325+5\delta \tag{12}$$

$$\alpha_{31}=\alpha_{22}=(b-a)/2+2k_1-2k_2+k_3-k_4/2+4\delta=3.325+4\delta \tag{13}$$

$$\alpha_{41}=\alpha_{32}=(b-a)/2+k_1-k_2+k_3-k_4/2+3\delta=3.174+3\delta \tag{14}$$

$$\alpha_{42}=\alpha_{33}=(b-a)/2+k_1-k_2+k_4/2+2\delta=2.891+2\delta \tag{15}$$

$$\alpha_{43}=2.5+\delta \tag{16}$$

$$\alpha_{44}=2.0 \tag{17}$$

$$\alpha_{1H}=(b+a)/4-k_1/3+k_2/2-k_3/6+k_4/12-\delta=2.397-\delta \tag{18}$$

$$\alpha_{2H}=(b+a)/4-k_1+k_2-k_3/2+k_4/4-2\delta=2.248-2\delta \tag{19}$$

$$\alpha_{3H}=(b+a)/4-k_1+2k_2-3k_3/2+3k_4/4-3\delta=1.967-3\delta. \tag{20}$$

The subscript 21 refers to a bond between a methylene carbon atom and a methyl carbon atom; the subscript 1H refers to a bond between a methyl carbon atom and a hydrogen atom; etc. The δ is an arbitrary constant, which need not be evaluated.

The molal refraction of saturated aliphatic hydrocarbons can also be represented by the equivalent relation

$$R_s=\sum_i N_i\alpha_i+\sum_{ij} N_{ij}\alpha'_{ij} \tag{21}$$

with the α_i and α'_{ij} values given in Table I.

TABLE I
REFRACTION CONTRIBUTIONS FOR SUBSTITUTION INTO EQ. (21)

i	α_i	ij	α'_{ij}
CH_3	8.853	CH-CH_3	+0.151
CH_2	7.821	C-CH_3	+ .283
CH	6.500	CH-CH	− .132
C	4.912	CH-C	− .088
		C-C	− .456

If either i or j is CH_2, the bond contribution α'_{ij} is zero. In other words, the α_i contributions given are those for i groups attached only to CH_2 groups.

Refractive indices computed with these relationships agree with the more precise experimental values to within a few units in the fourth decimal place. Since the results of extensive comparisons were summarized in Ref. 1, further comparisons need not be given here.

Derivatives

Molal refractions of a large number of α-substituted normal paraffin have been compared with those of the parent hydrocarbons. For each homologous series, the difference is found to be quite constant. Addition of $\alpha_{CH_3}-\alpha_{CH_2}$ to these differences gives the values (α_X) of the refraction contributions of the substituents (X), for compounds in which they are attached to CH_2. The same contribution can be used for derivatives of branched-chain paraffins, provided the attachment is to a methylene carbon. Application to derivatives in which the attachment is to a carbon bonded to only one hydrogen or to none has not been adequately tested.

The contributions of 12 X substituents are listed in Table II.

The normal nitriles (X=CN) have been very carefully studied and will serve to illustrate the measure of agreement with

* The corresponding equations in Reference (1) were in error with regard to the coefficients of the k_1 and k_3 terms. Since these constants were then taken as zero, the relationships derived from these equations were not affected.

TABLE II

GROUP REFRACTION CONTRIBUTIONS FOR R-X AND R-Y-R′ COMPOUNDS

-X	α_X	-Y-	α_Y
-F	0.8	-O-	3.0
-Cl	9.6	-NH-	6.3
-Br	15.0	-S-	14.9
-I	24.6	-CO-	8.22
-OH	4.1	-CO-O-	10.6
-SH	15.1	-CO-O-CO-	19.8
-CN	8.88	-CO-NH-	14.4
$-NH_2$	7.2	$-CH(CH_3)-$	15.50
-CHO	9.7	$-C(CH_3)_2-$	23.18
$-CO_2H$	12.1		
$-NO_2$	11.2		
-ONO	11.7		

the assuption of constancy of the α contributions. (Table III)

7.897, respectively. For $m>6$, the average departure of the average R-R_m values from constancy is less than the average difference between the experimental values.

The reasons for the deviations from constancy of R-R_m, indicating deviations from additivity of the α-contributions, for the smaller values of m, will not be discussed at this time. It should be noted, however, that because of these deviation, in this and other series, refractive indices computed from the constants given here are much less accurate for the lower-molecular-weight compounds than for the higher members of the series.

The n_D (calc) values in Table III were from the experimental densities and an assumed constant value of $\alpha_{CN}=8.880$; hence R-$R_m=7.848$ and R_m is given by Eq. (4). For

TABLE III

REFRACTIONS OF n-ALKYL NITRILES, $C_mH_{2m+1}CN$

m	Ref.	d_4^{20}	R(exp)–R_m(calcd.)	n_D(expt.)	n_D(calcd.)
1	10	0.78212	8.176	1.34409	1.338
	11	.78204	8.167	1.34389	1.338
2	10	.78184	8.077	1.36600	1.363
	11	.78171	8.071	1.36585	1.363
	12	.78169	8.071	1.36585	1.363
3	10	.79090	8.031	1.38408	1.382
	11	.79085	8.027	1.38402	1.382
	12	.79085	8.010	1.38385	1.382
4	10	.79929	7.988	1.39745	1.3961
	11	.79919	7.960	1.39713	1.3960
	12	.79919	7.958	1.39711	1.3960
5	11, 12	.80531	7.925	1.40694	1.4063
6	11, 12	.80958	7.891	1.41419	1.4139
7	11	.81355	7.855	1.42018	1.42013
	12	.81362	7.850	1.42018	1.42016
	13	.81344	7.888	1.20344	1.42007
8	11	.81690	7.842	1.42522	1.42525
	12	.81684	7.847	1.42522	1.42522
9	11	.81967	7.846	1.42946	1.42947
	12	.81967	7.834	1.42940	1.42947
10	11, 12	.82180	7.838	1.43286	1.43290
11	11	.82390	7.844	1.43596	1.43597
	12	.82390	7.842	1.43595	1.43597
12	11	.82586	7.840	1.43867	1.43870
	12	.82574	7.845	1.43867	1.43864
13	12	.82792	7.848	1.44126	1.44126

The paraffin refractions R_m, were computed from Eq. (4), replacing n by m. For m greater than 5, these differ insignificantly from the best experimental values. (Cf. Ref. 1.) For m less than 5, experimental values are unobtainable. For $m=5$, the R-R_m values obtained using the *experimental* data for the paraffins from Refs. 8 and 10, are 7.912 and

$m>6$, the calculated and experimental indices agree, on the average, within three units in the fifth decimal place.

Table II also lists α_Y-values, for compounds containing Y substituents bonded to two CH_2 groups. These contributions were obtained by substracting from the molal refraction of the compound R-Y-R′ that of the

hydrocarbon RR′. For comparison and for future reference, the contributions of two hydrocarbon Y groups, computed from the equations of the preceding section, are included.

Summary and Conclusion

For the saturated hydrocarbons, the more accurate data, published since the first paper of this series[1] was written, have been found to agree well with the previous additivity postulates. Revised values of the constants have been computed.

Refraction-contribution constants for various atoms and atomic groups, attached to CH_2 groups, have been deduced. Good additivity has been found, except for the compounds of lowest molecular weight in each series.

Pending further testing, caution should be observed in using the constants and additivity assumptions presented here in compounds containing C=C and C≡C bonds and in compounds in which the X and Y are attached to groups other than CH_2.

Discussion of the theoretical interpretation of the relative magnitudes of the group contributions will be postponed until a later time.

The Research Laboratory of the Eastman Kodak Company, Rochester 4, New York, U. S. A.

Studies on the Chemical Constitution of Agar-agar. XVIII[1]. *Isolation of a New Crystalline Disaccharide by Enzymatic Hydrolysis of Agar-agar*

By Choji ARAKI and Kiyoshi ARAI

(Received November 16, 1955)

The partial depolymerization of agar-agar by chemical methods, such as acid-hydrolysis[2], methanolysis[1], and mercaptolysis[3], has led to the isolation of agarobiose (4-O-β-D-galactopyranosyl-3,6-anhydro-L-galactose) (XI) or its derivatives as the chief oligosaccharide constituent so far identified. The enzymatic hydrolysis would be of great service to examine the structure of the polysaccharide, since the method might bring about oligosaccharide fragments different from those produced by chemical methods. This has been proved to be the case as reported herein.

The enzymatic hydrolysis of agar was first studied by Gran[4], who assigned the name gelase to the agar-hydrolysing enzymes of a microorganism isolated from sea water. Oshima[5] found gelase in the viscela of *Haliotus giganteus* Gm. (ear-shell), and Mori[6] also found it in the viscela, especially in hepatopancreas, of *Turbocornutus* (top-shell) and of other gastropodes. Kadota[7] prepared the enzyme solution capable of hydrolysing agar from a microorganism isolated from sea water. Fukumoto and Ishimatsu[8] gave the name agarase to the agar-hydrolysing enzymes of a microorganism isolated from putrid *tokoroten* (agar-gel). But little has been studied concerning the isolation and the structure of the hydrolysis product, until Ishimatsu and his co-workers[9] recently reported the characterization of a disaccharide, produced by the action of agarase upon agar, as its phenylosazone (m.p. 197°).

The enzyme extract used in this study has been prepared from *Pseudomonas kyotoensis*, an agar-digesting bacterium, isolated from putrid *tokoroten* by these authors[10]. An aqueous solution of agar was hydrolysed with this enzyme extract under the optimum condition until the reducing power of the solution reached a maximum value. From the resulting solution, there was obtained a mixture of reducing sugars, which were

1) Part XVII: C. Araki and S. Hirase, This Bulletin, **27**, 109 (1954).
2) C. Araki, *J. Chem. Soc. Japan*, **65**, 533, 627 (1944).
3) S. Hirase and C. Araki, This Bulletin, **27**, 105 (1954).
4) H.H. Gran, *Centralbl. Bakt. Abt.*, II, **9**, 562 (1902).
5) K. Oshima, *J. Agr. Chem. Soc. Japan*, **17**, 328 (1941).
6) T. Mori, *J. Agr. Chem. Soc. Japan*, **15**, 1070 (1939); **16**, 886 (1940).
7) H. Kadota, *Mem. Coll. Agr. Kyoto Univ.*, **59**, 54 (1954).
8) J. Fukumoto and K. Ishimatsu, *Bull. of the Osaka Municipal Technical Research Institute*, **13**, 1 (1951); K. Ishimatsu, ibid., **14**, 1 (1953).
9) K. Ishimatsu, Y. Kibesaki and S. Maitani, *Science and Industry (Japanese)*, **28**, 100 (1954).
10) C. Araki and K. Arai, *Memoirs of the Faculty of Industrial Arts, Kyoto Technical Univ.*, **3B**, 7 (1954).

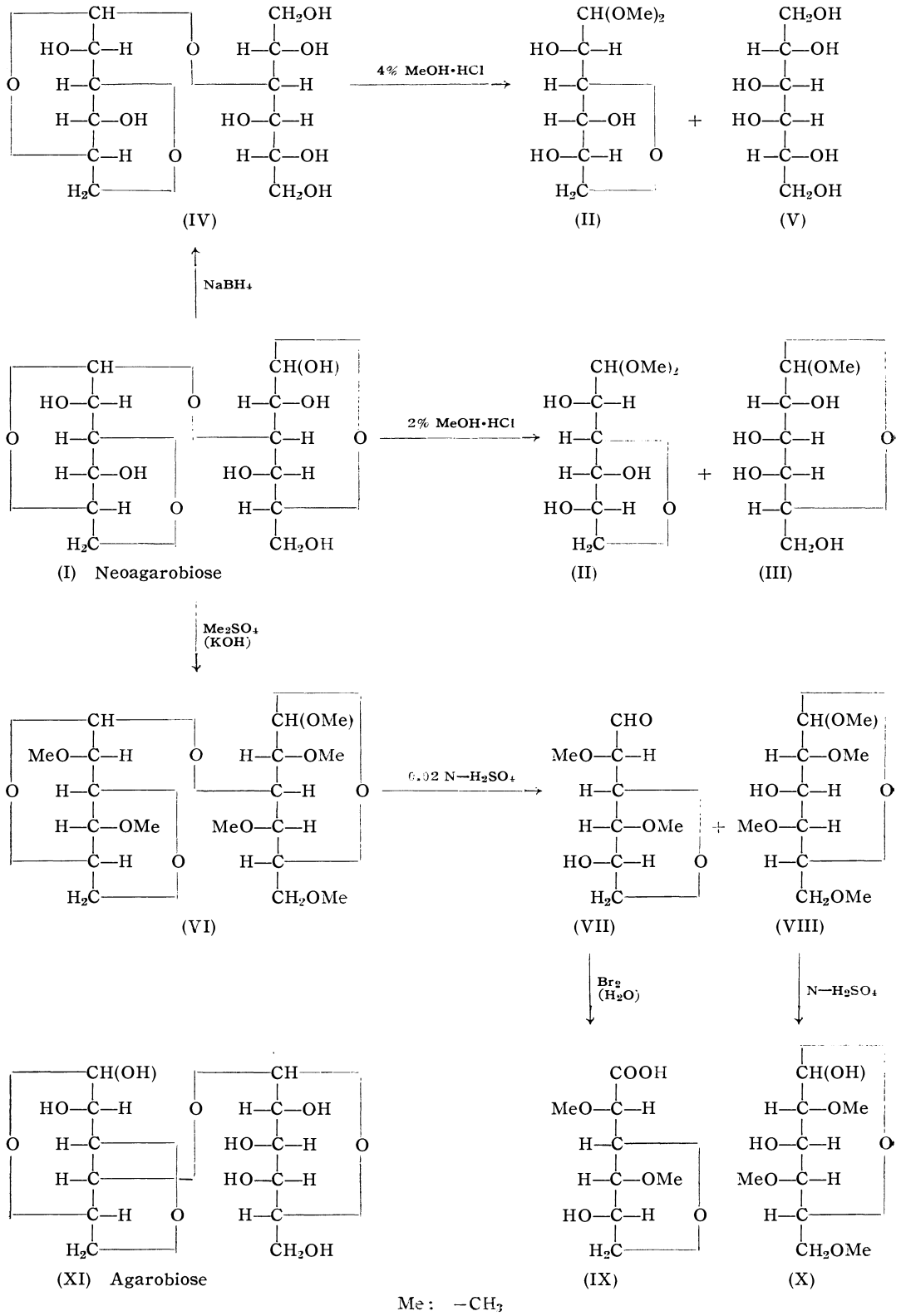
4% MeOH·HCl
NaBH4
2% MeOH·HCl
Me2SO4 (KOH)
0.02 N—H2SO4
Br2 (H2O)
N—H2SO4
(IV)
(II)
(V)
(I) Neoagarobiose
(II)
(III)
(VI)
(VII)
(VIII)
(XI) Agarobiose
(IX)
(X)

Me: $-CH_3$

shown by paper chromatography to be four oligosaccharides. The separation was possible by the charcoal chromatography of Whistler and Durso[11]. An aqueous solution of the mixture was placed on a charcoal column and developed with water and then with successive higher concentrations of ethanol in water. The four oligosaccharides were desorbed from the column on elution with 7.5, 17.5, 30 and 40% aqueous ethanol, respectively.

From the 7.5% ethanol eluate, there has been isolated a new crystalline disaccharide (I) having the composition $C_{12}H_{20}O_{10}$. Its hexaacetate and phenylosazone were also obtained in a crystalline state. The phenylosazone seems to be identical with that obtained by Ishimatsu and his co-workers[9]. The glycoside linkage of the disaccharide is so weak that it was hydrolysed to give D-galactose and 3, 6-anhydro-L-galactose, when heated in a 0.02N-oxalic acid solution for two hours. Methanolysis of the disaccharide afforded 3, 6-anhydro-L-galactose dimethylacetal (II) and methyl D-galactoside (III). These facts indicate that the disaccharide is composed of 3, 6-anhydro-L-galactose and D-galactose residues. When the disaccharide was reduced to the corresponding glycitol (IV) with sodium borohydride and was subsequently methanolysed, 3, 6-anhydro-L-galactose dimethylacetal (II) and dulcitol (V) were produced. This proves that the disaccharide is shown to be 3, 6-anhydro-L-galactosyl-D-galactose, and hence that it is an isomer of agarobiose (XI) previously obtained. So the disaccharide has been named neoagarobiose.

In order to elucidate further the structure of neoagarobiose (I), it was methylated with dimethylsulfate and a potassium hydroxide solution and subsequently with Purdie's reagents. The resulting methyl penta-O-methyl-β-neoagarobioside (VI) was obtained in a crystalline state. On hydrolysis with .002 N-sulfuric acid the methylated neoagarobioside yielded a mixture of methyl 2, 4, 6-tri-O-methyl-β-D-galactoside (VIII) and 2, 4-di-O-methyl-3, 6-anhydro-L-galactose (VII). The former was separated from the latter by solvent extraction, and was obtained as crystals. On hydrolysis it gave crystalline 2, 4, 6-tri-O-methyl-D-galactose (X), the anilide of which was also obtained as crystals. This trimethyl-galactose and its anilide coincided in all respects with the corresponding authentic specimens. 2, 4-di-O-methyl-3, 6-anhydro-L-galactose (VII) was oxidised with bromine water to give crystalline 2, 4-di-O-methyl-3, 6-anhydro-L-galactonic acid (IX), which was further converted into the crystalline amide. These crystals were also in good agreement with the corresponding authentic specimens. The identification of VIII and VII as cleavage fragments establishes the structure of methyl penta-O-methyl-β-neoagarobioside (VI) as methyl 3-O-2', 4'-di-O-methyl-3', 6'-anhydro-L-galactopyranosyl-2,4,6-tri-O-methyl-β-D-galactopyranoside, and hence the structure of neoagarobiose (I) as 3-O-3', 6'-anhydro-L-galactopyranosyl-D-galactose.

The glycoside linkage has been suggested to be of the α'-type on the following basis. The specific rotations of α- and β-forms of methyl 3,6-anhydro-L-galactopyranoside would be in the neighborhood of $-80°$ and $+115°$, respectively, in water, the inference being drawn from the values recorded for their enantiomorphs[12]. If the 3, 6-anhydro-L-galactopyranosyl group is combined through a β-type likage with D-galactose, which proper has a positive optical rotation, the resulting disaccharide would have a highly positive optical rotation. Meanwhile, if they are combined with each other through an α-type linkage, the resulting disaccharide would have a relatively low value of optical rotation, as a result of the compensation between positive and negative rotatory values of the components. The specific rotation of neoagarobiose ($[\alpha]_D +34.4° \rightarrow +20.3°$) seems to fall in with the latter instance. The specific rotation of neoagarobitol (IV) ($[\alpha]_D$ ca. $-20.0°$) also supports the α'-configuration on a similar consideration. In addition, the downward mutarotation observed when neoagarobiose is dissolved in water indicates that it crystallizes with the α-configuration.

Experimental

Evaporation and concentration were carried out under reduced pressure below 40°. All the melting points are uncorrected. The optical rotations are determined in aqueous solutions unless otherwise stated.

Preparation of Enzyme Extract.—A small amount of *P. kyotoensis* was inoculated to sterized media (50 cc.) having the following composition: sodium chloride 0.1 %, dipotassium phosphate 0.1 %, potassium nitrate 0.1 %, magnesium sulfate heptahydrate 0.05 %, and agar 0.5 %; pH 7, adjusted with a 0.1 N-sodium hydroxide solution. The inoculated media were incubated at 30° for three days, and were diluted with the same media (400 cc.), the pH being again adjusted to 7 with a 0.1 N-sodium hydroxide solution. After incubation at 30° for a week, toluene (3 cc.) was added, and the mixture was digested at 30° for

11) R.L. Whistler and D.F. Durso, *J. Am. Chem. Soc.*, 72, 667 (1950).

12) W.N. Haworth, J. Jackson and F. Smith, *J. Chem. Soc.*, 1940, 620.

TABLE I

CHROMATOGRAPHIC SEPARATION OF ENZYMATIC HYDROLYSATES OF AGAR-AGAR

Ethanol	%	0	5	7.5	10	15	17.5	22	30	40	50
	l.	2.5	1.2	3.3	1.8	1.1	4.2	2.8	3.0	1.5	2.7
Yield	g.	0.67	0.1	3.7	0.15	0.15	5.3	0.6	1.63	0.65	0.40
$[\alpha]_D^{\circ}$ (H_2O)		—	+2.8	+17.7	+6.6	+6.8	+1.1	−9.1	−7.9	−16.9	−15.5

sixteen hours with occasional shaking. It was then filtered through an asbestos-bed, concentrated to 50 cc. below 35°, and was dialysed in a fish skin sack against running water until chlorine ions and reducing sugars were diffused (thirteen hours). The dialysed contents (110~130 cc.) were used as the enzyme extract to hydrolyse agar.

Enzymatic Hydrolysis of Agar.—Agar powder (5.5 g., or 5.27 g. as dry material), which had been defatted with acetone, was dissolved in hot water (1400 cc.) and sterized in steam, the pH of the solution being 5.2. After cooling, the enzyme extract (110–130 cc.) and three drops of toluene were added, and the mixture was kept at 40° in an incubator for about seventy two hours, when the reducing power reached a maximum value. After being heated in steam for fifteen minutes, it was filtered through double filter papers and concentrated to a sirup, to which methanol was added so that the concentration became 85 %. Insoluble precipitates were removed by filtration and washing with 85 % methanol, and the filtrate and washings were concentrated to a sirup (about 5 g.). The sirup was combined with three similar batches and extracted with hot 95 % methanol. Evaporation of the extract gave a mixture of reducing sugars as a pale brown sirup; yield 18–19 g. (moisture 10.6 %), or 71–81 % of agar in weight; $[\alpha]_D$+5.3° (*c* 1); reducing power, 26.1 % of galactose; aldose value, 43.0 % of hexose.

Paper Chromatography of Hydrolysates.—An aliquote of the above sirup was analysed on paper chromatograms (Tōyō Filter Paper No. 52) by the usual ascending method. *n*-Butanol-acetic acid-water (4:1:2 v/v) was used as an irrigating solvent and an ethanolic solution of O-aminophenol phosphate was sprayed[13]. Four yellowish brown spots were revealed: I (R_{gal} 1.30), II (R_{gal} 0.62), III (R_{gal} 0.34) and IV (R_{gal} 0.15), where R_{gal} is the rate of movement relative to that of galactose. The color of the spots presumably indicates the presence of 3,6-anhydro-galactose component.

Column Chromatography of Hydrolysates. A 10 % aqueous solution of the hydrolysates (13.4 g) obtained above was placed on a column (6.0×19.0 cm.) of active carbon Shirasagi[14] (Celite was not mixed with it), and the column was eluted with water, 5, 7.5, 10, 15, 17.5, 22, 30, 40 and 50 % aqueous ethanol in succession. Aliquotes of every 100 cc. portion of the eluates were withdrawn for examination of reducing power, and the next higher developer was added, after several continuous portions were recognized to be non-reducing. Each eluate was separately evaporated to dryness to recover the material. The result is quoted in Table I.

The water eluate left inorganic substances on evaporation. The 7.5, 17.5 and 30% ethanol eluates were chromatographically pure fractions, showing R_{gal} values 1.30, 0.62 and 0.34, respectively. Both 40 and 50% ethanol eluates were shown by paper chromatography to be mixtures of two components, whose R_{gal} values were 0.34 and 0.15. Solely the 7.5% ethanol fraction is treated in this communication.

Isolation of Neoagarobiose(I).—The 7.5% ethanol fraction was a colorless amorphous powder, which amounted to 28% of the hydrolysates. One gram of it was dissolved in a few drops of hot water, methanol was added while heating, and insoluble precipitates were removed by filtration. Crystallization of neoagarobiose was facilitated by addition of further methanol to the filtrate while heating. After standing overnight in a refrigerator, crystals were filtered, washed with methanol and ether, and dried; yield 0.85 g.; m.p. 197–198°. Recrystallization was repeated several times by dissolving it in a small amount of water and adding ethanol, until no more change of the physical constants was recognized; m.p. 207–208°; $[\alpha]_D^9$+34.4° (initial)→+20.3° (after twenty fuor hours, *c* 2.0); reducing power, 40.6% of galactose.

Anal. Found: C, 44.46; H, 6.20%; aldose equiv., 325., Calcd. for $C_{12}H_{20}O_{10}$: C, 44.44; H, 6.22%; aldose equiv., 324.

Neoagarobiose Phenylosazone.—A mixture of neoagarobiose (0.5 g.), phenylhydrazine (0.75 g.) and 50% acetic acid (0.75 cc.) in water (25 cc.) was heated at 90° for two hours. After cooling, crystals of the osazone were filtered, washed successively with water, ethanol, and ether, and dried; yield 0.35 g. The pure osazone was obtained as yellow needles on recrystallization from ethanol; m.p. 199–200°; $[\alpha]_D^9$+59.8° (initial)→+56.1° (after twenty four hours, *c* 0.82) in pyridine-methanol (2:3).

Anal. Found: C, 57.25; H, 6.12; N, 11.37. Calcd. for $C_{24}H_{30}O_8N_4$: C, 57.36; H, 6.02; N, 11.15%.

Hydrolysis of Neoagarobiose with 0.02N-Oxalic Acid Solution.—Neoagarobiose (0.60 g.) in a 0.02 N-oxalic acid solution (30 cc.) was heated in a boiling water bath. The progress of the reaction was followed by determination of the optical rotation of the solution; $[\alpha]_D$+17.5° (initial), +15.0° (15 min.), +14.5° (30 min.), +12.5° (1 hr.), +8.0° (2 hr.), +6.0° (2.5 and 3 hr., constant). After three hours, the solution was neutralized with calcium carbonate, filtered, and

13) S. Hirase, C. Araki and S. Nakanishi, This Bulletin, **26**, 183 (1953).

14) Product of Takeda Pharmaceutical Industries, Ltd., Osaka.

concentrated to a sirup (0.55 g.). Paper chromatographic examination revealed a distinct spot of galactose together with a diffused tailing presumably of 3,6-anhydro-galactose. This indicative evidence was made conclusive by their isolations. A 10% aqueous solution of the sirup was placed on a charcoal column and developed with water. Every 30 cc. of the eluate was determined for the optical rotation, and fractions with positive and negative rotations were separately combined and concentrated to dryness.

a) D-Galactose.—From the first eight fractions with positive rotations, there was obtained a sirup (0.35 g.), from which D-galactose was crystallized; yield 0.25 g.; m.p. and mixed m.p. with an authentic specimen 166–167°; $[\alpha]_D^{26}$+81.5° (after twenty fourhours *c* 1.5). Nitric acid oxidation afforded mucic acid (m.p. 213°).

b) 3,6-Anhydro-L-galactose.—Next, eleven fractions with negative rotations gave on evaporation a sirupy 3,6-anhydro-L-galactose (0.18 g.). It reduced Fehling's solution at room temperature, and showed a strong Seliwanoff's reaction. Treatment with phenylhydrazine and acetic acid in the usual manner afforded 3,6-anhydro-L-galactose phenylosazone; m.p. and mixed m.p. with an authentic specimen[15] 217–218°.

Anal. Found: N, 16.23. Calcd. for $C_{18}H_{20}O_3N_4$: N, 16.46%.

Methanolysis of Neoagarobiose.—Neoagarobiose (1.0 g.) in 2% methanolic hydrogen chloride (50 cc) was boiled until the optical rotation became constant: $[\alpha]_D$+16.0° (initial), −38.0° (15 min.), −41.0° (30 min.), −35.0° (1 hr.), −30.0° (1.5 and 2 hr.). The solution was neutralized with silver carbonate, filtered, and concentrated to a sirup (1.1 g.). Paper chromatographic examination indicated that it was a mixture of 3,6-anhydrogalactose dimethylacetal and methyl galactoside. The mixture was chromatographed on a starch column exactly in the same way as described by Araki and Hirase[1]. 3,6-Anhydro-galactose dimethylacetal was eluted with *n*-butanol saturated with water, and then methyl galactoside was eluted with 80% aqueous methanol.

a) 3,6-Anhydro-L-galactose Dimethylacetal (II).—Evaporation of butanolic eluate gave 3,6-anhydro-L-galactose dimethylacetal as a colorless sirup; yield 0.50 g.; $[\alpha]_D^{12}$−24.6° (*c* 1.05); OCH_3, found 26.2 (calculated for $C_6H_{10}O_4(OCH_3)_2$ 29.8%). Identification was carried out by hydrolysing it to the free sugar, which was then converted into the diphenylhydrazone in the usual manner[15], m.p. and mixed m.p. with and authentic specimen 153°; $[\alpha]_D^{22}$−34.6° (initial, methanol, *c* 1.21).

Anal. Found: N, 8.67. Calcd for a $C_{18}H_{20}O_4N_2$: N, 8.53%.

b) Methyl D-Galactoside.—Evaporation of the 80% methanal eluate gave a sirup (0.54 g.), which on crystallization from acetone-methanol (2:1) afforded crystals of methyl α-D-galactoside monohydrate; yield 0.35 g.; m.p. 109°, not depressed on admixture with an authentic specimen; $[\alpha]_D^{28}$+174.1° (*c* 1.1).

Anal. Found: C, 39.25; H, 7.59; OCH_3, 14.60. Calcd. for $C_7H_{14}O_6 \cdot H_2O$: C, 39.60; H, 7.60; OCH_3, 14.62%.

Hydrolysis with N-sulfuric acid gave D-galactose, m.p. and mixed m.p. 168°; $[\alpha]_D^{27}$+81.5° (after twenty four hours, *c* 1.5).

Reduction and Methanolysis of Neoagarobiose.—Neoagarobiose (1.0 g.) in water (20 cc.) was mixed with an aqueous solution (10 cc.) of sodium borohydride (0.15 g.). The mixture was kept at room temperature (10–13°) with occasional shaking for two hours, when it showed no longer the reducing power. The solution was then ice-cooled, carefully neutralized with an 1.5% aqueous acetic acid, and concentrated to dryness. Crude neoagarobitol (IV) was obtained as an amorphous solid; yield 1.2 g.; $[\alpha]_D^{16}$−20.0° (*c* 1.25).

The glycitol (1.15 g.) was heated in boiling 4% methanolic hydrogen chloride (50 cc.) until a constant optical rotation was observed: $[\alpha]_D$−28.3° (initial), −22.6° (15 min.), −21.7° (30 min.), −20.9° (45 min.), −20.4° (1 hr.), −21.3° (2 and 3 hr.). The solution was neutralized with silver carbonate, filtered, and concentrated to give a semi-crystalline residue.

a) Dulcitol (V).—The above residue was triturated with methanol. Crystals of dulcitol (0.35 g.), separated by filtration, were recrystallized from ethanol-water (1:1); m.p. and mixed m.p. with an authentic specimen 187–188°; $[\alpha]_D^{19}$±0° (*c* 1.37).

Anal. Found: C, 39.66; H, 8.06. Calcd. for $C_6H_{14}O_6$: C, 39.56; H, 7.75%.

b) 3,6-Anhydro-L-galactose Dimethylacetal (II).—The filtrate separated from crystals of dulcitol was concentrated, and chromatographed on a starch column in the same manner as described before. 3,6-Anhydro-L-galactose dimethylacetal was obtained as a colorless sirup; yield 0.48 g.; $[\alpha]_D^{17}$−25.3° (*c* 1.2); OCH_3, found 28.4% (calcd. for $C_8H_{14}O_6$ 29.8%).

An additional specimen of dulcitol (0.12 g.) was also recovered from the column.

Hexa-O-acetyl-neoagarobiose. — Neoagarobiose (1.0 g.) was acetylated with pyridine (25 cc.) and acetic anhydride (7.0 g.) for seventy two hours in the usual manner. The reaction mixture was poured into ice-water (100 cc.) with stirring, neutralized with sodium bicarbonate, and extracted with chloroform. The extract was washed twice with water, dried with sodium sulfate, and evaporated. The hexaacetate (0.70 g.) obtained was recrystallized from ethanol; yield 0.46 g.; m.p. 112°; $[\alpha]_D^{27}$+1.57° (chloroform, *c* 1.27); $[\alpha]_D^{29}$+0.82° (methanol, *c* 1.22).

Anal. Found: C, 49.75; H, 5.80; CH_3CO, 45.01. Calcd. for $C_{12}H_{14}O_{10}(CH_3CO)_6$: C, 50.00; H, 5.60; CH_3CO, 44.80%.

Methyl Penta-O-methyl-β-neoagarobioside

15) C. Araki, *J. Chem. Soc. Japan*, **65**, 725 (1944).

(VI).—A 32% potassium hydroxide solution (38 cc.) and dimethylsulfate (16 cc.) were alternatively dropped during eight hours into an ice-cooled and vigorously stirred solution of neoagarobiose (2.0 g.) in water (7 cc.), care being taken to keep the medium alkaline. More potassium hydroxide solution (5 cc.) was added, and the solution was cooled and stirred for two hours. After standing overnight, the potassium hydroxide solution (106 cc.) and dimethylsulfate (47 cc.) were run in during twenty hours at room temperature (23–25°), the same care being taken. After the addition, the solution was stirred for ten additional hours, and then extracted with four 50 cc. portions of chloroform. The extracts were dried with sodium sulfate, evaporated, redissolved in ether, and again evaporated, when a crystalline mass was obtained; yield 2.16 g.; OCH_3 42.8%. This was twice methylated with methyl iodide (25 g.) and silver oxide (15 g.) in the usual manner. The final product was isolated as a crystalline mass by extraction with ether and evaporation; yield 2.20 g., OCH_3 46.0%. Recrystallization from petroleum ether (b.p. 38–43°) gave a pure sample of methyl penta-O-methyl-β-neoagarobioside; m.p. 127–128°; $[\alpha]_D^{30}$ −19.6° (methanol, *c* 1.28); $[\alpha]_D^{30}$ −22.0° (chloroform, *c* 1.28).

Anal. Found: C, 52.89; H, 8.12; OCH_3, 45.45%; M.W. (Rast's), 408. Calcd. for $C_{12}H_{14}O_4(OCH_3)_6$: C, 52.93; H, 7.90; OCH_3, 45.62%; M.W., 408.

Hydrolysis of Methyl Penta-O-methyl-β-neoagarobioside.—The sample (2.0 g.) in 0.02N-sulfuric acid (100 cc.) was heated in a boiling water bath until the optical rotation reached a constant value: $[\alpha]_D$ −18.0° (initial), −16.0° (15 min.), −15.0° (30 min.), −13.5° (45 min.), −12.5° (1 hr.), −3.5° (1.5 hr.), −1.5° (2 hr.), +1.0° (2.5 hr.). +2.0° (3 and 4 hr., constant). It was neutralized with barium carbonate, filtered, concentrated, redissolved in ether, and again evaporated, when a mixture of methyl 2,4,6-tri-O-methyl-β-D-galactoside and 2,4-di-O-methyl-3,6,-anhydro-L-galactose was obtained as a semi-crystalline residue (1.68 g.).

Methyl 2,4,6-Tri-O-methyl-β-D-galactoside (VIII).—The above mixture was extracted several times with boiling petroleum ether, an insoluble sirup (0.5 g.) being set aside. Evaporation of the extracts afforded methyl 2,4,6-tri-*O*-methyl-β-D-galactoside as a crystalline mass (1.10 g., OCH_3 47.1%). Recrystallization twice from petroleum ether gave pure silky needles (0.37 g.); m.p. 110–112°; $[\alpha]_D^{14}$ +2.90° (*c* 1.71). Araki[15] recorded m.p. 110–112° and $[\alpha]_D^{22}$ +6.38°.

Anal. Found: C, 50.61; H, 8.56; OCH_3, 51.97. Calcd. for $C_6H_8O_2(OCH_3)_4$: C, 50.85: H, 8.47; OCH_3, 52.54%.

An additional crop (0.50 g., OCH_3 50.2%) was recovered by evaporating the mother liquor of the recrystallization and extracting again with boiling petroleum ether. A petroleum ether-insoluble sirup (0.22 g.) was also obtained.

2,4,6-Tri-O-methyl-D-galactose (X).—The recovered crystals of methyl 2,4,6-tri-O-methyl-β-D-galactoside (0.50 g.) were hydrolysed with N-sulfuric acid for three hours in the usual manner. 2,4,6-Tri-O-methyl-α-D-galactose (0.45g.) was obtained as crystals, and recrystallized from ether; m.p. 113–114°, not depressed on admixture with an authentic specimen[16]; $[\alpha]_D^{24}$ +112.6° (initial)→+90.9° (after twenty four hours, *c* 1.2).

Anal. Found: C, 48.90; H, 8.04 OCH_3, 42.00. Calc for $C_6H_9O_3(OCH_3)_3$: C, 48.65; H, 8.11; OCH_3, 41.89%.

Anilide: m.p. 172–173°. not depressed on admixture with an authentic specimen[13]; $[\alpha]_D^{24}$ −84.0° (initial)→−44.8° (after twenty four hours)→+2.8° (after fourty eight hours, *c* 0.45) in acetone.

Anal. Found: N, 4.80; OCH_3, 30.20. Calcd. for $C_{15}H_{23}O_5N$: N, 4.71; OCH_3, 31.31%.

2,4-Di-O-methyl-3,6-anhydro-L-galactose (VII).—Petroleum ether-insoluble residue, separated from methyl 2,4,6-tri-O-methyl-β-D-galactoside, was proved to be 2,4-di-O-methyl-3,6-anhydro-L-galoctose[17]; a pale yellow sirup; yield 0.72 g., n_D^{25} 1.4871; $[\alpha]_D^{23}$ −6.9° (*c* 0.88); OCH_3 31.1% (Calcd. for $C_6H_8O_3(OCH_3)_2$ 32.64%). It reduced a Fehling's solution at room temperature, decolorized a neutral permanganate solution, showed a strong Seliwanoff's reaction, and restored the color to a Schiff's reagent.

2,4-Di-O-methyl-3,6-anhydro-L-galactonic Acid (IX).—Bromine (0.75 cc.) was dropped during five hours into an ice-cooled and vigorously stirred aqueous solution (30 cc.) of 2,4-di-O-methyl-3,6-anhydro-L-galactose (0.50 g.), in the presence of barium carbonate (6 g.). The stirring and cooling were continued for three more hours. After standing overnight, the non-reducing reaction mixture was aerated to remove excess bromine, filtered, and concentrated to a sirup, which was extracted with boiling chloroform. The residual barium salt was dissolved in water, and passed through a column of a cation exchange resin Amberlite IR-120, the column being then washed thoroughly with water. The acidic percolate and washings were combined, neutralized with silver carbonate, filtered before and after treatment with hydrogen sulfide, and concentrated to a sirup. Extraction with ethanol-benzene (1: 1) followed by evaporation afforded a semi-crystalline residue (0.30 g.), from which crystals of 2,4-di-O-methyl-3,6-anhydro-L-galactonic acid were separated by use of a porous plate; yield 0.22 g. The pure acid was obtained by recrystallization from ethanol-benzene (1: 1); m.p. 150°, not depressed on admixture with an authentic specimen[12,17]; $[\alpha]_D^{24}$ −60.8° (*c* 1.94).

Anal. Found: C, 46.47; H, 7.02; OCH_3, 29.8. Calcd. for $C_6H_8O_4(OCH_3)_2$: C, 46.58; H, 6.85; OCH_3, 30.12%.

Amide: The above acid was esterified with methanolic hydrogen chloride in the usual manner. The methyl ester obtained was converted into the amide in the usual manner; m.p. 150°, not

16) C. Araki, *J. Chem. Soc. Japan*, **58**, 1362 (1937).

17) C. Araki, *J. Chem. Soc. Japan*, **61**, 503 (1940).

18) I.A. Forbes and E.G.V. Percival, *J. Chem. Soc.*, **1939**, 1844.

depressed on admixture with an authentic specimen[17,18]; $[\alpha]_D^{24}-74.0°$ (c 0.94).

Anal. Found: N, 7.00; OCH_3, 30.12. Calcd. for $C_8H_{15}O_5N$: N, 6.83; OCH_3, 30.25%.

Summary

1. A new crystalline disaccharide has been isolated from enzymatic hydrolysates of agar. Its hexaacetate and phenylosazone have been prepared in crystalline states.

2. The name neoagarobiose has been assigned to the disaccharide isolated.

3. The structure of neoagarobiose has been shown beyond doubt to be 3-O-3′,6′-anhydro-L-galactopyranosyl-D-galactose. It has been suggested that the glycoside linkage is of α'-configuration.

The authors are indebted to Mr. N. Nakata for assistance in study, and to Mr. S. Hirase for help in description. This study has been aided by the Grant for the Fundamental Scientific Research from the Ministry of Education, for which thanks are also expressed.

Institute of Chemistry, Faculty of Industrial Arts, Kyoto Technical University, Matsugasaki, Kyoto

*Electrophoretic Studies of Tobacco Mosaic Virus**

By Itaru WATANABE and Nobuo UI

(Received November 7, 1955)

Since the early study of Eriksson-Quensel and Svedberg[1], the electrophoretic mobility of tobacco mosaic virus (TMV) has been measured by several investigators. However, the various recorded values of its mobility show some discrepancy (see Table I) and there have been few systematic studies under different conditions.

TABLE I

THE DATA OF ELECTROPHORETIC MOBILITY OF TOBACCO MOSAIC VIRUS

Buffer	Ionic Strength	pH	Temp. (°C)	Mobility $\left(\frac{-u\times10^5}{\text{cm}^2/\text{sec. volt}}\right)$	Investigator
Acetate	0.02	4.01	20	7.5	Ericksson-Quensel et al. (1936)[1]
〃	〃	4.35	〃	10.5	〃
〃	〃	4.65	〃	13.9	〃
〃	0.04	4.95	〃	18.9	〃
Phosphate	0.1	6.91	0–0.5	9.3	Pfankuch et al. (1940)[2]
Phosphate-KCl	〃	7.3	——	8.5	Miller et al (1941)[3]
Veronal-NaCl	〃	6.72	0	5.5	Cohen (1941)[4]
Phosphate	(0.05 M)	7.1	〃	8.8 (Des)	Knight et al. (1942)[5]
〃	(0.1 M)	7.5	——	39 (Des)	Frampton et al. (1946)[6]
〃	0.2	7.00	1	7.2	Fischer et al. (1949)[7]
〃	〃	7.7	0	7.5 (Des)	Watanabe et al. (1950)[8]
Acetate	〃	4.2	3.2	4.2	Kahler (1951)[9]
〃	〃	4.9	〃	8.0	〃

* Part of this paper was read before the 4th Annual Meeting of the Chemical Society of Japan held in Tokyo, April, 1951.

1) I.-B. Eriksson-Quensel and T. Svedberg, *J. Am. Chem. Soc.*, **58**, 1863 (1936).

2) E. Pfankuch, G.A. Kausche and H. Stuble, *Biochem. Z.*, **304**, 238 (1940).

3) G.L. Miller and W.M. Stanly, *J. Biol. Chem.*, **141**, 905 (1941).

4) S.S. Cohen, *Proc. Soc. Exptl. Biol. Med.*, **48**, 163 (1941).

5) C.A. Knight and M.A. Lauffer, *J. Biol. Chem.*, **144**, 411 (1942).

6) V.L. Frampton and W.N. Takahashi, *Phytopathology*, **36**, 129 (1946).

7) M.A. Fischer and M.A. Lauffer, *J. Am. Chem. Soc.*, **71**, 3800 (1949).

8) I. Watanabe, Y. Otsuka and S. Mizushima, *Repts. Radiation Chemistry Research Institute, Tokyo Univ.*, No. 5, 10(1950).

9) H. Kahler, private communication (1951).

In the present investigation the variations of the mobility of TMV with changes in concentration and ionic strength have been measured. The charge on the virus particle has been calculated from the mobility data, using Gorin's equation for long cylinders. It also seems to be interesting from the electrophoretic point of view to study such an elongated rod-shaped particle as TMV.

Experimental

Materials.—Of the several TMV preparations obtained, the most homogeneous preparation, TMV-9, was used in these studies. The virus was extracted from frozen and ground young White Burley tobacco leaves three weeks after the inoculation with common TMV and purified by differential centrifugation in a manner essentially similar to that described by Stanley[10], using a vacuum-type air-driven ultracentrifuge[11,12]. The details of the purification procedure have been reported in previous paper[12] with the results of several chemical and physical measurements of purified virus.

The homogeneity of TMV-9 was proved to be excellent by electrophoresis, sedimentation, and electron microscope measurements[12].

The final purified virus solution was stored in 0.01 M phosphate buffer at pH 7.0 in a refrigerator, and subjected to electrophoresis experiments.

Measurements.—Prior to electrophoresis, the virus solution in 0.01 M phosphate buffer was diluted to desired concentrations with a phosphate buffer of ionic strength 0.2 at pH 7.7, and dialyzed against a large quantity of the same buffer at least two days in a cold room. In the study of the variation of mobility with ionic strength, the ionic strength was varied by diluting the phosphate buffer of ionic strength 0.2 at pH 7.7 with water; no apparent change in pH was found even after ten-fold dilution.

Electrophoretic measurements were carried out at 0°C in a Tiselius-type apparatus[13] equipped with a Svensson optical system[14]. The electrolytic current was automatically controlled by a constant-current regulator[15].

The movements of the boundaries were recorded photographically at appropriate intervals and the electrophoretic mobilities were calculated by the method of Longsworth[16] from the centroidal ordinates, or the first moments, of the curves of concentration gradient versus distances. Mobility values corresponding to a temperature of 0°C were obtained by using specific conductivities of solutions measured at 0°C.

Virus concentrations were determined by micro-Kjeldahl nitrogen analysis* assuming that TMV nucleoprotein contains 16.6–16.7% nitrogen[12].

Results

This preparation of TMV, TMV-9, was found to be electrophoretically homogeneous under all conditions examined and single boundaries remained sharp during the course of electrophoresis (for example, see Fig. 1).

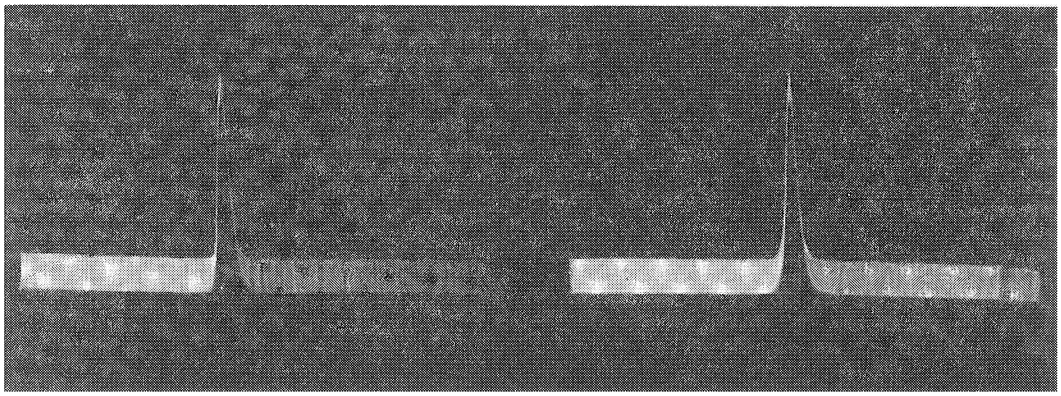

Ascending ⟵ ⟶ Descending

Fig. 1. Electrophoretic pattern of TMV in the phospate buffer (pH 7.7, $\mu=0.2$).

A. The Variation of Mobility with Concentration of TMV.—The variation of electrophoretic mobility with concentration of TMV was examined over the concentration range 0.17–1.08% in the same phosphate buffer, pH 7.7, at a constant ionic strength of 0.2. These results are given in Table II together with the relative viscosity of solutions[17]. It can be easily seen, from Table II, that the mobility is essentially independent of the concentration although the relative viscosity of the

10) W.M. Stanley, *J. Am. Chem. Soc.*, **64**, 1804 (1942).
11) S. Sasaki and O Taniguchi, *J. Japan Soc. Mech. Eng.*, **54**, 255 (1951).
12) I. Watanabe and Y. Kawade, This Bulletin, **26**, 294 (1953).
13) A. Tiselius, *Trans. Faraday Soc.*, **33**, 524 (1937).
14) H. Svensson, *Kolloid-Z.*, **87**, 181 (1939).
15) H. Noda and N. Ui, *Kagaku*, **20**, 179 (1950).
16) L.G. Longsworth, *J. Am. Chem. Soc.*, **65**, 1755 (1943).
* The nitrogen determinations were made by Miss T. Kitamura in our laboratory.
17) Y. Kawade, *Repts. Institute of Science and Technology, Univ. of Tokyo*, **8**, 115 (1954).

TABLE II

THE VARIATION OF MOBILITY WITH CONCENTRATION OF TMV AT 0°C

(In Phosphate Buffer of Ionic Strength 0.2 and pH 7.7)

Conc. (%)	Field strength* (volt/cm.)	Mobility ($-u\times10^5$cm²/sec. volt)		Relative viscosity of solution (η_r)
		Descending	Ascending	
0.17	3.60	7.1_5	7.2_5	1.11
0.24	3.57	7.1_5	7.3_0	1.17
0.44	3.62	6.9_5	7.1_0	1.36
0.65	3.65	7.0_0	7.1_0	1.59
1.08	3.72	7.0_0	7.1_0	2.24
Average.....		7.0_5	7.1_5	

* In our preliminary test, it was confirmed that the mobility is essentially independent of the field strength.

solutions increases by more than twofold. Similar phenomena were also observed in the electrophoretic studies of deoxypentose nucleic acid[18–20]. In this connection, it is very interesting to recall the fact that the sedimentation rates of both TMV[21–23] and deoxypentose nucleic acid[24–26] strongly depend upon their concentration and that, especially in the case of TMV, this concentration dependency of sedimentation coefficient is directly related to the viscosity of the solution[21]. This difference in dependence of sedimentation coefficient and electrophoretic mobility upon concentration is of considerable interest and, as yet, no reasonable explanations have been proposed.

The average value of descending mobilities in the phosphate buffer of ionic strength 0.2 and pH 7.7 was calculated to be $-7.0_5\times10^{-5}$cm²/sec. volt and is in close agreement with that reported by Fischer and Lauffer[7].

B. The Dependence of Mobility on Ionic Strength.—The ionic strength was varied over the range 0.02–0.2 at constant pH. The results obtained are given in Table III and Fig. 2, in which mobilities are plotted against the square roots of ionic strengths. It is evident from Fig. 2 that the mobility increases greatly with the reduction of ionic strength.

TABLE III

THE VARIATION OF MOBILITY OF TMV WITH IONIC STRENGTH AT 0°C

(In Phosphate Buffer at pH 7.7)

Ionic Strength	Conc. (%)	Field Strength (volt/cm.)	Mobility ($-u\times10^5$cm²/sec. volt)	
			Descending	Ascending
0.02	0.49	3.24	15.7	17.5
0.05	0.37	3.79	11.6	11.9
0.1	0.52	3.47	9.0_5	9.2_5
0.2	.....	.....	7.0_5*	7.1_5*

* Average value given in Table II.

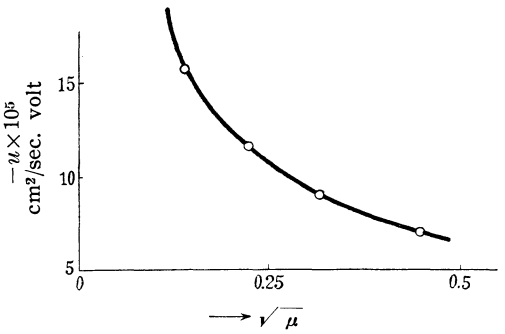

Fig. 2. The variation of descending mobility of TMV with ionic strength at 0°C (in phosphate buffer at pH 7.7).

Discussion

A. The Net Charge on TMV Molecule.—The single particles of TMV were found to be rod-shaped, of about 280 mμ to 300 mμ in length and 15 mμ in diameter, and have molecular weight of about 4×10^7 to 5×10^7 [22,27,28]. Similar molecular size and shape have also been observed for the virus preparation (TMV-9) used in these studies[12], by sedimentation, diffusion, viscosity, and electron microscopic measurements. In the following calculations TMV particles were regarded as long cylinders, 300 mμ in length and 15.2 mμ in diameter: these values correspond to a molecular weight of 4.5×10^7 [12].

The net charge, Q, on such a long cylinder as TMV can be related to the experimentally measured mobility, u, by the following equation developed by Gorin[29]:

$$Z|e|=Q=\pi\eta\cdot F'(\kappa a)\cdot(l+2a)\cdot u\Big/2\left[\frac{K_0(\kappa a+\kappa r_i)}{(\kappa a+\kappa r_i)\cdot K_1(\kappa a+\kappa r_i)}+\ln\left(\frac{a+r_i}{a}\right)\right] \qquad (1)$$

18) E. Stenhagen and T. Teorell, *Trans. Faraday Soc.*, **35**, 743 (1939).
19) J.M. Creeth, D.O. Jordan and J.M. Gulland, *J. Chem. Soc.*, **1949**, 1406.
20) N. Ui and I. Watanabe, *Repts. Radiation Chem. Research Institute, Tokyo Univ.*, No. 5, 17 (1950).
21) M.A. Lauffer, *J. Am. Chem. Soc.*, **66**, 1195 (1944).
22) G. Schramm and G. Bergold, *Z. Naturforsch.*, 2b, 108 (1947).
23) H.K. Schachman and W.J. Kauzmann, *J. Phys. & Colloid. Chem.*, **53**, 150 (1949).
24) H. Kahler, *J. Phys. & Colloid Chem.*, **52**, 676 (1948).
25) R. Cecil and A.G. Ogston, *J. Chem. Soc.*, 1948, 1382.
26) Y. Kawade and I. Watanabe, *Biochem. et Biophys. Acta*, in press.
27) M.A. Lauffer, *J. Am. Chem. Soc.*, **66**, 1188 (1944).
28) R.C. Williams, R.C. Backus and R.L. Steere, *J. Am. Chem. Soc.*, **73**, 2062 (1951).
29) H.A. Abramson, L.S. Moyer and M.H. Gorin, "Electrophoresis of Proteins," Reinhold, New York (1942).

Here, Z is the valency of ion, $|e|$ is the electronic charge, l and a are the length and the radius of the cylinder, respectively, r_i is the average radius of the ions in the ionic atmosphere, κ is the Debye-Hückel function, i. e., the inverse of the thickness of the double layer, and η is the viscosity coefficient of the solvent. $F'(\kappa a)$ is the function developed by Gorin to account for the random orientation of cylinders, and K_0 and K_1 are Bessel functions, values of which have been given by Abramson, Moyer, and Groin[29] together with the values of $F'(\kappa a)$.

The valency at ionic strength 0.02 can be calculated directly from the equation (1) and is given in Table IV A. In this calculation the valeus of l and a were taken as 3000 Å and 76 Å respectively, and the value of r_i was assumed to be 2.5 Å. The value of κ at 0° C is $3.24\times10^8\sqrt{\mu}$, where μ is the ionic strength. In the calculations of the valencies at higher ionic strengths, however, an alternative indirect method was adopted by using Gorin's calculation of the ratio (R) of the mobility of the cylinder to that of the sphere of the same molecular volume and charge[29]. After obtaining the mobility as the sphere, the charge can be calculated from the following equation:

$$u(\text{sphere})=\frac{Z|e|(1+\kappa r_i)\cdot f(\kappa r)}{4\pi\eta a(1+\kappa r+\kappa r_i)} \qquad (2)$$

Here, r is the radius of the equivalent sphere above-mentioned, which was calculated to be 240 Å, and $f(\kappa r)$ is a function of κr given by Henry[30] (often called the Henry factor). These results were shown in Table IV B. From Table IV it is clearly shown that the valency of TMV is independent of the change in ionic strength within the error of calculation and is about $-1,800$.

In the above calculation, it was assumed that no change in the molecular state occurred with the variation of ionic strength, although the concentration of buffer was reported to have some effect on the degree of aggregation of TMV[23]. There are, moreover, many assumptions and limitations in Gorin's equation* and the meaning of the value obtained is not yet so self-evident.

This electrophoretic valency of TMV, $-1,800$, seems to be too small, compared with its very high molecular weight. Our calculations based upon the amino acid analyses of Knight[32] and the amide nitrogen analyses of Ross[33] indicate a valency of about $-800\sim-900$ at pH 7.7. In this calculation, the molecular weight of TMV was taken to be 4.5×10^7 and any contribution of nucleic acid was neglected. Although this figure appears to be in the same order of magnitude as that obtained from the mobility, the presence of the nucleic acid should be taken into consideration to obtain a correct theoretical value.

Considering the contribution made by pentose nucleic acid as free acid, the theoretical valency of TMV was calculated to be about $-9,000$. This value is very large, when compared with the surface charge calculated from the electrophoretic mobility, but is in fairly good agreement with that obtained from the titration experiments by Fischer

TABLE IV
THE NET CHARGE ON TMV PARTICLE*

A. THE VALUE CALCULATED FROM EQ. (1)

μ	$u\times10^5$ (cm²/sec. volt)	κ	$\kappa a+\kappa r_i$	$\frac{K_0(\kappa a+\kappa r_i)}{(\kappa a+\kappa r_i)K_1(\kappa a+\kappa r_i)}$	$F'(\kappa a)$	η (poise)	Z
0.02	−15.7	0.46×10^7	3.6	0.24	5.3	1.80×10^{-2}	−1.720

B. THE VALUE CALCULATED FROM EQ. (2)

μ	$u\times10^5$	R**	u(sphere) $\times10^5$	κ $\times10^{-7}$	κr	κr_i	$f(\kappa r)$	η (poise)	Z
0.02	−15.7	0.39	−40.3	0.46	11.0	0.1	0.84	1.80×10^{-2}	−1.800
0.05	−11.6	0.38	−30.5	0.72	17.3	0.2	0.88	1.81×10^{-2}	−1,800
0.1	− 9.0_5	0.38	−23.8	1.02	24.5	0.3	0.91	1.83×10^{-2}	−1,800
0.2	− 7.0_5	0.38	−18.5	1.45	34.8	0.4	0.93	1.87×10^{-2}	−1,800

* $r_i=2.5$Å; $R=2.4\times10^2$Å.
** $R=u$(cylinder)/u(sphere). To calculate these values, asymmetry$=S_r=l/2a$ was taken as 19.7.

* The limitations of Gorin's equation were discussed in detail by Abramson, Moyer, and Gorin[29] and Overbeek[31].

30) D.C. Henry, *Proc. Roy. Soc. London*, **133A**, 106 (1931).

31) J.Th.G. Overbeek, *Advances in Colloid Sci.*, **3**, 97 (1950).

32) C.A. Knight, *J. Biol. Chem.*, **171**, 297 (1947).

33) A.F. Ross, *J. Biol. Chem.*, **143**, 685 (1942).

and Lauffer[7]*.

It is very interesting to investigate the reason why the surface charge obtained from the electrophoretic experiments is much smaller than the calculated or the titration value. In this respect, it seems not inadequate to point out that the charge of horse serum albumin derived from the mobility agrees very well with the titration value[35].

B. The Dilution Factor in a Three-Ion System Containing TMV.—Strong "boundary anomalies"[36] are usually observed in electrophoretic experiments of proteins such as albumin, globulin, etc. It was found in our studies, however, that these "boundary anomalies" were greatly diminished in TMV solutions. First, the ascending mobility is not so different from descending mobility (see Table II); second, both the δ- and ε-boundaries are very small and hardly recognized (see Fig. 1); and third, the descending boundary is also as sharp as the acending one**.

All these characteristic phenomena of TMV in electrophoresis may be interpreted by the fact that the charge density of TMV is very small. Now we are trying to calculate a dilution factor[37], ξ, which is a measure of the divergence of real systems from the ideal behaviour and becomes unity at sufficiently low protein concentrations. In a three-ion system, ξ is given by the following equation[37]:

$$\xi=1+\left(\frac{r_S-r_R}{r_S}\cdot\frac{r_A}{r_A-r_R}-\frac{1}{2}\right)\frac{C_S^{\alpha}}{C_A^{\gamma}} \qquad (3)$$

Notations are the same as in the paper of Longsworth[37]. The subscript A, R, and S refer to Na^+, HPO_4^{--}***, and the negatively charged protein ion; and the superscripts γ and α mean buffer and protein solutions respectively. r is the mobility of ion relative to that of Na^+ ion (22.7×10^{-5} cm²/sec. volt) taken as unity and C is the equivalent concentration of ion.

In Table V are shown the results of the

TABLE V

THE DILUTION FACTOR AND BUFFER-CONCENTRATION BOUNDARY IN A THREE-ION SYSTEM

1% Protein Solutions in Sodium Phosphate Buffer (pH 7.7, Ionic Strength 0.2)

A: Na^+; R: HPO_4^{--}; S: Protein Ion; $r_A=1,000$ (unity); $r_R=-1.101$; $C_A^{\gamma}=0.14$; $K_{AR}=0.0148$

Protein	TMV	Horse serum albumin B
M (molecular weight)	4.5×10^7	67,100
Z (valency)	−1,800	−15.7
u (mobility)	$-7.0_0\times10^{-5}$	$-5.8_4\times10^{-5}$
r_S (relative mobility)*	−0.308	−0.257
C_S^{α} (euivalent per liter)	−0.00040	−0.00234
ξ (dilution factor)	1.005	1.035
Δn (ε-boundary)	0.000010	0.000072

* Taken the mobility of sodium ion as unity.

calculations on one per cent solutions of TMV and horse serum albumin B (according to Kekwick[38]) in sodium phosphate buffer of ionic strength 0.2 and pH 7.7. It is clear from Table V that ξ is very close to unity in the case of TMV. This low value of $\xi-1$ in TMV solution is in good accord with the fact that no marked divergence from an ideal electrophoretic behaviour can be observed. Since ξ is equal to the ratio of ascending mobility to decending one as a first approximation[37], the small differences between ascending and descending mobilities of TMV can qualitatively be explained.

The change in refractive index across the buffer-concentration boundary, so-called "ε-boundary", in the descending side can be expressed as follows[37]:

$$\Delta n=K_{AR}(\xi-1)C_A^{\gamma}$$

$$=K_{AR}\left(\frac{r_S-r_R}{r_S}\cdot\frac{r_A}{r_A-r_R}-\frac{1}{2}\right)C_S^{\alpha} \qquad (4)$$

Here, Δn is the difference in refractive index and K_{AR} is the increment of refrective index per equivalent of AR or Na_2HPO_4. Δn is also found to be very small in the case of TMV (see Table V) and small areas of both δ- and ε-boundaries may be expected from this fact.

When ξ becomes close to unity, the change in the conductivities across the boundary is also largely reduced and the boundary pattern, therefore, becomes independent of the

* Fischer and Lauffer[7] obtained a value of—6,900for the valency at pH 7 by titration studies. They reported, in their original paper, a value of—8,300 for the theoretical valency, but they re-examined their calculation and have found that the correct theoretical value should be about—1,000 instead of—8,300[34]. In their calculations, they neglected the presence of nucleic acid and assumed a molecular weight of 3.4×10^7.

34) M.A. Lauffer, private communication.

35) I. Watanabe, N. Ui and M. Nakamura, *J. Phys. & Colloid Chem.*, **54**, 1366 (1950).

36) L.G. Longsworth and D.A. MacInnes, *J. Am. Chem. Soc.*, **62**, 705 (1940); *Chem. Revs.*, **24**, 271 (1939).

** In Fig. 1 the descending boundary seems to be slightly sharper, but it is due to the difference in the sharpness of the initial boundaries.

37) L.G. Longsworth, *J. Phys. & Colloid Chem.*, **51**, 171 (1947).

*** To simplify the problem, buffer solution was assumed to consist of only Na^+ and HPO_4^{--} ions.

38) R.A. Kekwick, *Biochem. J.*, **32**, 552 (1938).

direction of the current. In this limiting case, the ascending pattern should be the mirror image of the descending one. Thus the reason why the descending boundary of TMV solution moves as sharply as the ascending one may be easily understood.

In the solution of serum albumin, on the contrary, the ascending boundary moves more rapidly than the descending one and, moreover, the later becomes more diffuse. In addition, the areas of the δ- and ε-boundaries become very significant. The values of ξ and Δn in Table V also explain these considerable "boundary anomalies" in the case of horse serum albumin.

At any rate, it may be conculded that a condition which is closer to the ideal case for electrophoresis can be easily attained in TMV solution even though its concentration is relatively high.

Summary

The variations of the mobility of tobacco mosaic virus (TMV) in phosphate buffer at pH 7.7 with changes in concentration and ionic strength have been investigated. The mobility is essentially independent of the concentration and has an average value of $-7.0_5 \times 10^{-5}$ cm^2/sec. volt in the phosphate buffer of ionic strength 0.2. On the other hand, the mobility increases greatly with the decrease of ionic strength. The net charge on the TMV particle, calculated from the mobility data by the aid of Gorin's equation, was found to be constant (about $-1,800$) all over the range of ionic strength examined. Although it is considerablly lower than the theoretical valency calculated from the analytical data, this low value of the valency from the mobility is quite reasonable to explain the observation that there is no serious divergence from the ideal behaviour in the electrophoresis of TMV solution.

The authors are indebted to Dr. J. Hitaka, Tobacco Experimental Station at Hatano, Kanagawa Prefecture, for tobacco leaves. Part of the expense of this investigation was defrayed by the Grant in Aid of the Ministry of Edcation for the Scientific Research.

Institute of Science and Technology,
The University of Tokyo,
Tokyo

Kinetics of the Oxydation of Red Phosphorus by Potassium Bromate

By M. VENUGOPALAN and K. J. GEORGE

(Received September 20, 1955)

Potassium bromate is a powerful oxidising agent in acid solution. Reducing agents convert it smoothly into the bromide:

$$BrO_3^- + 6H^+ + 6\epsilon = Br^- + 3H_2O.$$

At the end of the reaction free bromine appears:

$$BrO_3^- + 5Br^- + 6H^+ = 3Br_2 + 3H_2O.$$

Numerous quantitative oxidation processes involving the use of potassium bromate show that its oxidising property is almost equivalent to that of potassium iodate[1-5].

Many quantitative oxidation reactions with potassium bromate[6], iodate[7], periodate[8], ceric sulphate[9], and iodine[10] as powerful oxidising agents for the oxidation of red phosphorus have been studied by earlier workers.

The use of potassium bromate in the volumetric determination of elementary red phosphorus has been investigated by Deshmukh and Sant[6]. They have observed that the addition of acidified potassium bromate solution to phosphorus leads to its gradual disappearance accompanied with a rapid evolution of bromine. The method is based on the oxidation and subsequent conversion of phosphorus into phosphoric acid. Bromine liberated during the process or the unreacted bromate after the completion of the reaction is estimated iodometrically and the amount of phosphorus is calculated from the following reaction mechanism:

$$2P + 2KBrO_3 + H_2SO_4 + 2H_2O \longrightarrow 2H_3PO_4 + Br_2 + K_2SO_4.$$

1) S. Györy, *Z. anal. Chem.*, 32, 415 (1893).
2) A. Kurtenacker and J. Wagner, *Z. anorg. allgem. Chem.*, 120, 261 (1922).
3) R. Lang, *Z. anal. Chem.*, 106, 12 (1935).
4) R. Lang, *Z. anorg. allgem. Chem.*, 142, 229 (1925).
5) E. Rimini, *Gazz. chim. ital.*, 29, 265 (1899).
6) G.S. Deshmukh and B.R. Sant, *Anal. chem.*, 24, 901 (1952).
7) T.F. Büehrer and O.E. Schupp, *J. Am. Chem. Soc.*, 49, 9-15 (1927).
8) G.S. Deshmukh and M. Venugopalan, *J. Ind. Chem. Soc.*, 32, 309-312, (1955).
9) G.S. Deshmukh, *Analyst*, 76, 604, (1951).
10) G.S. Deshmukh and M. Venugopalan, *J. Ind. Chem. Soc.*, 30, 747-750 (1953); 32, 305-308 (1955).

Experience, however, has shown that the rate of the above oxidation process is measurably slow at ordinary temperatures. Hence, it was of interest to study the kinetics of this oxidation process in some detail.

Experimental

Red phosphorus of British Drug House laboratory reagent grade quality was purified by Buehrer and Schupp's method[7] and subsequently by the copper phosphide process[8]. Its purity was checked by the magnesium pyrophosphate and bromate procedures.

An accurately weighed quantity of the sample was introduced in a ground-glass stoppered Erlenmeyer flask to which a known excess of standard potassium bromate solution was added, followed by 5 to 10 ml. of carbontetrachloride. Acidified with about 5 to 10 ml. of 4N sulphuric acid so that the overall acidity of the system was maintained at or about 0.5N sulphuric acid. The flask was maintained at a desired constant temperature for thirty minutes prior to the addition of potassium bromate and also during the course of subsequent observations in an electrically heated thermostat fitted with an accurately calibrated automatic thermoregulator. The contents of the flask were swirled from time to time and an aliquot portion (5 ml.) of the clear supernatent aqueous layer was pipetted out carefully at different time intervals and titrated iodometrically by standard thiosulphate[11]. Series of experiments were carried out at different temperatures, viz., 30°, 35°, 40°, 45°, 50° atd 55°C using the same conditions for concentrations and also by varying the concentrations of potassium bromate and the weight of red phosphorus over a fairly wide range.

Results and Discussion

From the initial titre value of bromate and that obtained at various time intervals during the course of the oxidation, the order of the reaction was calculated by the integration method. Under the given operative conditions the value of K was found to be constant and within limits of experimental error according to the following equation:

$$K=\frac{2.303}{tC_\infty}\log_{10}\frac{C_t(C_0-C_\infty)}{C_0(C_t-C_\infty)}$$

where C_0—initial concentration of potassium bromate;
C_t—concentration of potassium bromate at time t;
C_∞—concentration of potassium bromate at time ∞;
and t—time in minutes.

A representive group of results is shown in Table I.

11) A.I. Vogel, "Text Book of Quantitative Inorganic Analysis," London, Longmans, Green and Co., 1945, p. 451.

TABLE I

Temperature: 45°C Weight of phosphorus: 0.02 g.
Reaction mixture: 5 ml. Concentration of $KBrO_3$: 40 ml. N/5 solution.

Time	N/10 Thiosulphate	$\log_{10}\frac{C_t(C_0-C_\infty)}{C_0(C_t-C_\infty)}$	$K\times10^{-3}$
0 min.	8.5 ml.	—	—
5	8.2	0.0174	1.8
15	7.85	0.0405	1.4
30	7.3	0.0774	1.4
50	6.7	0.1438	1.5
85	6.05	0.2477	1.5
∞	4.4	—	—

Mean $K=1.5\times10^{-3}$

The results in Table I therefore show that the oxidation of red phosphorus by potassium bromate is an overall second order reaction.

A reaction of the second order depends principally on the initial concentration of the reactants, the half value period and the temperature at which the reaction is carried out. The variation of the velocity constant K with temperature for the same initial concentrations of the reactants is represented in Table II.

TABLE II

Weight of Phosphorus taken: 0.02 g.
Concentration of bromate: 40 ml. N/5 solution.
Normality of thiosulphate: 0.1 N.

Temperature (t)	Mean $K\times10^{-3}$
30°C	0.35
35	1.00
40	1.40
45	1.50
50	1.90
55	4.85

From the results, it can be inferred that the velocity constant K increases as the temperature increases; the values of $\log_{10}\frac{C_t(C_0-C_\infty)}{C_0(C_t-C_\infty)}$ plotted against time t for different temperatures, at which the reaction has been studied, are represented graphically in Fig. 1.

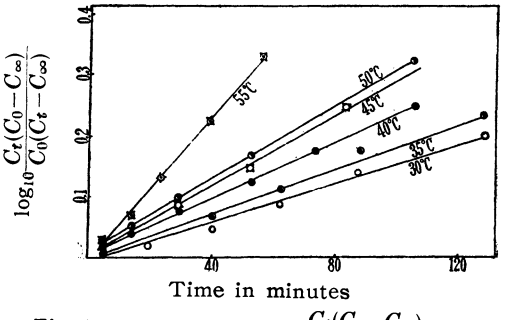

Fig. 1. Variation of $\log_{10}\frac{C_t(C_0-C_\infty)}{C_0(C_t-C_\infty)}$ with temperaure.
Wt. of P=0.02 g.
Conc. of $KBrO_3$=40 cc. N/5 soln.

The variation of the velocity constant K for different initial concentrations of the reactants has been studied by varying the concentration of bromate solution and keeping the weight of phosphorus constant in all the experiments. A typical set of results is returned in Table III.

TABLE III

Temperature: 30°C.
Weight of phosphorus taken: 0.02 g.
Normality of thiosulphate: 0.1 N.

Expt. No.	Concentration of $KBrO_3$ added	Mean $K\times10^{-3}$
1.	40 ml. N/5 solution	0.35
2.	〃 N/6 〃	0.52
3.	〃 N/9 〃	0.94

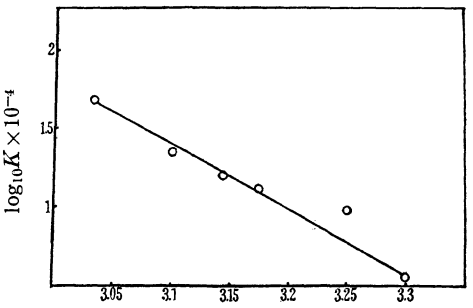

Fig. 3. Variation of $\log_{10}K$ with $1/T$.

equation[12] which expresses the influence of temperature on reaction velocity.

TABLE IV

Temp. absolute T_1-T_2	$K_1\times10^{-3}$	$K_2\times10^{-3}$	Temp. coeff. K_2/K_1	Energy of activation $E=\frac{2.303\log_{10}K_2/K_1\times R\times T_1\times T_2}{T_2-T_1}$
303–313°	0.35	1.40	4.00	26290 g. cals.
308–318	1.00	1.50	1.50	7942
313–323	1.40	1.90	1.36	6215
318–328	1.50	4.85	3.23	24450

Fig. 2 represents graphically the variation of $\log_{10}\frac{C_t(C_0-C_\infty)}{C_0(C_t-C_\infty)}$ with time for different initial concentrations of bromate at the same temperature.

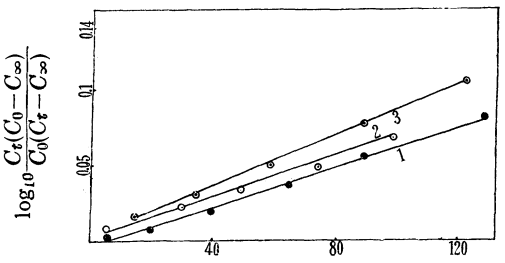

Fig. 2. Variation of $\log_{10}\frac{C_t(C_0-C_\infty)}{C_0(C_t-C_\infty)}$ with time for different concentration of potassium bromate.
Wt. of P=0.02 g. Conc. of $KBrO_3$
1. 40 ml. N/5 soln.
2. 〃 N/6 〃
3. 〃 N/9 〃

The energy of activation and the temperature coefficient were calculated from the values obtained for K at different temperatures T_1 and T_2 as indicated in Table IV.

The variation of log K with $1/T$ is shown in Table V; the results are plotted in Fig. 3. The linear relationship between log K and $1/T$ (Fig. 3) is in accord with the Arrhenius

TABLE V

Temp. absolute	$1/T\times10^{-3}$	$K\times10^{-4}$	$\log_{10}K\times10^{-4}$
303	3.30	3.5	0.5441
308	3.25	10.0	1.0000
313	3.17	14.0	1.1461
318	3.14	15.0	1.1761
323	3.10	19.0	1.2788
328	3.05	48.5	1.6857

The essential bimolecularity of the overall oxidation process shows that the molecular ratio of P to $KBrO_3$ is 1:1 which is in agreement with the earlier observation of Deshmukh and Sant[6].

Nature of the Reactions involved

The reactions involved in the oxidation of phosphorus by $KBrO_3$ have been found to take place as follows:

$$5P+3BrO_3^-+3H^++6H_2O = 3/2Br_2+5H_3PO_3 \quad \text{(i)}$$

This reaction is slow and goes partially to phosphoric acid.

$$2P+3Br_2+6H_2O=6H^++6Br^-+2H_3PO_3 \quad \text{(ii)}$$

This reaction is quite rapid.

$$5H_3PO_3+2BrO_3 = Br_2+3H^++5H_2PO_4^-+H_2O \quad \text{(iii)}$$

This reaction is very slow as is strikingly shown by adding $KBrO_3$ to a phosphorus

12) Arrhenius, *Z. phys. Chem.*, 4, 226 (1889); *Trans. Farad. Soc.*, 33, 72 (1937).

acid solution. Very little bromine is liberated even on refluxing the solution for some time.

$$H_3PO_3+Br_2+H_2O=3H^++2Br^-+H_2PO_4^- \quad \text{(iv)}$$

This reaction has been shown by a number of authors to be slow, and to depend in large measure upon the acid concentration. It appears that the oxidation of phosphorus acid by bromine determines the rate of reaction as a whole.

$$5Br^-+BrO_3^-+6H^+=3Br_2+3H_2O \quad \text{(v)}$$

This latter reaction is instantaneous and complete. The possibility of adopting this reaction for a quantitative oxidation of red phosphorus to phosphoric acid bromometrically is being investigated.

Summary

Kinetics of the oxidation of Red Phosphorus by Potassium Bromate in acid solution has been studied. Using varying concentrations of potassium bromate and the quantity of red phosphorus between 0.01 g. and 0.02 g., the reaction has been found to be bimolecular with respect to potassium bromate over a temperature range of 30–55°C. The energy of activation and temperature coefficient of the reaction have been calculated. Further work on the oxidation of red phosphorus by bromide-bromate mixture in acid solution is suggested.

Grateful thanks of the authors are due to Professor S. S. Joshi for facilities and kind interest in the work.

Chemistry Department, Banaras Hindu University, Banaras, India

Studies on the Cold-drawing of Polymers (Part III).[1] *The Quasi-static Drawing of Polycapramide. III.** *The Effects of Heat-treatments and the Temperature Dependencies of the Heterogeneous Structure in Polymers*

By Hirosuke YUMOTO

(Received October 3, 1955)

Introduction

In the development of the investigation on the cold-drawing of polymers (for example, polycapramide), the influences of temperature and humidity (the moisture adsorption) on the quasi-static drawing have been reported in Part I[2] and Part II[1]. In succession the effects of heat-treatment were investigated.

In addition to drawing behaviors, densities were chosen for the measure of the structure change through heat-treatment. Each of various singular temperatures obtained is considered as the transition temperature of each micro-region in the heterogeneous structure. Then the temperature dependencies of polycapramide are brought to light and some experimental foundations for conjecturing the drawing mechanism are established. Such experimental results and the discussion on them are the subject of this paper.

1) H. Yumoto, This Bulletin, **29**, 141 (1956).

* H. Yumoto, presented at the 8th annual meeting of the Chemical Society of Japan in Tokyo, April 2, 1955.

2) H. Yumoto, This Bulletin, **29**, 45 (1956).

Experiments

(1) The Specimens.—60 denier (ϕ 0.086 mm.) polycapramide semidull unstretched monofilament was used which was spun from the melt through chilling by air and contained about 2% of caprolactam monomer and oilgomers.

(2) The Methods of Heat-Treatments.—For the heat-treatment in the dry state, the above specimen had been inserted in a glass tube, which was sealed after substituting air with carbon dioxide, and was heated at a constant temperature ($\pm$1°C) from 50° to 200°C in a bath of an appropriate boiling organic liquid or in an electric thermostat. For the heat-treatment in water or in the saturated water vapor, water was let into a tube together with the specimen before sealing; in case of the former the specimen was entirely steeped in water and in case of the latter the specimen was placed apart above the water in the tube. The heating procedure of the sealed tube was the same as in the case of the treatment in the dry state. The specimens in the tube were always tensionless.

After the heating, the tubes were always cooled in room temperature without particular means for rapid or slow cooling.

(3) The measurements of Isothermal Quasi-static Elongation-Stress Curves.—The methods were the same as those described in Part I. Measuring was performed on the drawing at 80°C in completely dried state or at 20°C in water.

(4) The Measurements of Densities.—The densities in dried state were measured at 25± 0.005°C by the floatation method using ethylene chloride: xylene mixtures[a] as media. Specimens were previously cut into about 0.5 mm. of length and dried completely with phosphorous pentoxide in a desiccator. The mixture was poured on to pieces so finely cut and dried under the vacuum as to avoid bubbles remaining on the pieces and the equilibrium between floatation and precipitation was brought about by controlling the mixture ratio of medium at 25°C. The densities of media at the equilibrium were measured with an Ostwald picnometer. The error of measurement was about ±0.0005 g./cc.

Results of Measurement

(1) Density

The densities (25°) of specimens subjected to various heat-treatments are shown in Table I. The specimens treated in air give slightly larger densities than those treated in carbon dioxide; this fact may be attributed to the increase of molecular weight owing to the combination of oxygen, because polycapramide kept in air at high temperature suffers oxidation. When the temperature and the medium for treatment are the same, the density seems to converge to a certain level; i.e. even if the time of treatment is prolonged, the density does not increase apparently beyond a certain value. Such limiting values are shown in Fig. 1.

TABLE I

DENSITIES OF POLYCAPRAMIDE SUBJECTED TO VARIOUS HEAT-TREATMENTS AT 25°C

Heat-Treatment			Density at 25°C (g./cc.)
Temp. (°C)	Time (hr.)	Medium	
	Untreated		1.1340
115	10	air	1.1375
〃	5.0	CO_2	1.1355
138	2.0	air	1.1410
139	1.0	CO_2	1.1410
〃	3.0	〃	1.1420
150	2.0	air	1.1450
158	2.0	air	1.1465
〃	3.0	CO_2	1.1425
〃	5.0	〃	1.1420
168	1.0	CO_2	1.1430
171	3.0	〃	1.1465
183	1.0	〃	1.1505
〃	3.0	〃	1.1505
190	1.0	〃	1.1590
〃	3.0	〃	1.1580
203	1.0	〃	1.1705
205	3.0	〃	1.1720
ca. 20	240	benzene	1.134
〃	240	H_2O liquid	1.135
40	30	〃	1.137
60	2.0	〃	1.140
80	20	〃	1.143
100	2.0	〃	1.148
120	2.0	〃	1.157
140	2.0	〃	1.168
60	2.0	H_2O vapor	1.137
80	2.0	〃	1.141
100	2.0	〃	1.142
120	2.0	〃	1.156
140	2.0	〃	1.170
50	168	air	1.1355
60	50	〃	1.1350
〃	〃	CO_2	1.1355
80	20	air	1.1355
〃	20	CO_2	1.1345
〃	50	〃	1.1350
〃	100	〃	1.1350
100	50	air	1.1375
〃	0.5	CO_2	1.1345
〃	1.0	〃	1.1345
〃	5.0	〃	1.1355
〃	10	〃	1.1350
〃	20	〃	1.1345
〃	30	〃	1.1350
〃	40	〃	1.1355

a) Using carbon tetrachloride: xylene mixture, the same values were obtained. Using benzene: nitrobenzene mixture slightly lower values were obtained.

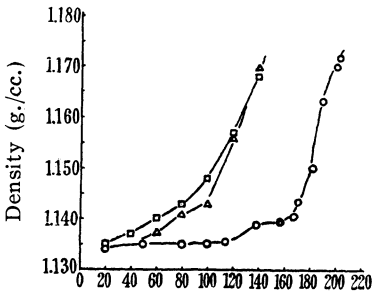

Fig. 1. Densities at 25°C limitted with varicus treatment-temperatures.
○ Treatment in dried state
□ Treatment in liquid water
△ Treatment in saturated vapor of water

The heat-treatment is the process where some of the distortions in substances diminish through the thermal Brownian motion of structural elements; therefore the time of treatment is an important factor. In polymers some microscopic movements cannot come into effect before exceedingly long elapse of time. Nevertheless the

transfiguration due to the movements, which will be caused after times of treatment have elapsed, can be considered to be negligibly small because of the limit of density increment as above described.

Fig. 1 indicates the following facts. In case of the treatment in dried state, the increase of density is not apparent at the temperature below ca. 100°C, but becomes apparent beyond ca. 120°C, and is remarkable at 180–200°C. In case of the treatment in water (liquid), the specimen treated even at room temperature gives somewhat greater density than the untreated one. The increase of density with rise of the treatment temperature, is just noticed from 40°C and is remarkable beyond ca. 100°C. In case of the treatment in water vapor the increase of density is similar to that in case of the treatment in liquid water; the densities in both cases at the same treatment-temperature are the same above 120°C, but the former is somewhat less than the latter below 100°C.

Under the apprehension that the increase of density through steeping in water for 240 hrs. might be attributed to the removal of caprolactam monomer through extraction, the density of specimen which had been freed from monomer by steeping in benzene for 240 hrs. was measured on trial; but the increase of density was not noticeable. Therefore, the increase of density through steeping in water is caused in conclusion not by the removal of monomer but by the transfiguration of fine structure.

(2) Drawing Behaviors

Only the specimens, which had attained to the limit of density increment by heat-treatment at each of the temperatures, were subjected to the drawing experiment. The elongation-stress curves at 80°C in dried state and at 20°C in water are given in Figs. 2, 3 and Figs. 4, 5. Polycapramide, even if heat-treated, can be easily stretched in these conditions; but below 80°C in dried state it is quite difficult to stretch it and breaking happens mostly before 20–30% elongation. The obtained curve takes the similar shape with that of the untreated specimen, which gives the steep rise of stress from the environs of 100% elongation at any case. When the temperature of treatment is higher, the stress at the same elongation and the Young's modulus are higher. It is noteworthy that, in spite of exhibiting maximum and minimum of stress in case of drawing at 80°C in

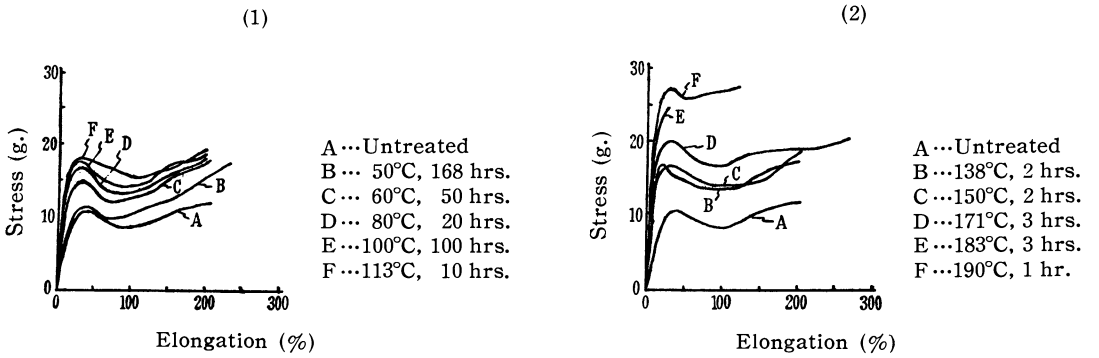

Fig. 2. The quasi-static elongation-stress curves of polycapramide subjected to heat-treatments in dried state at various temperatures on drawing at 80°C in completely dried state.

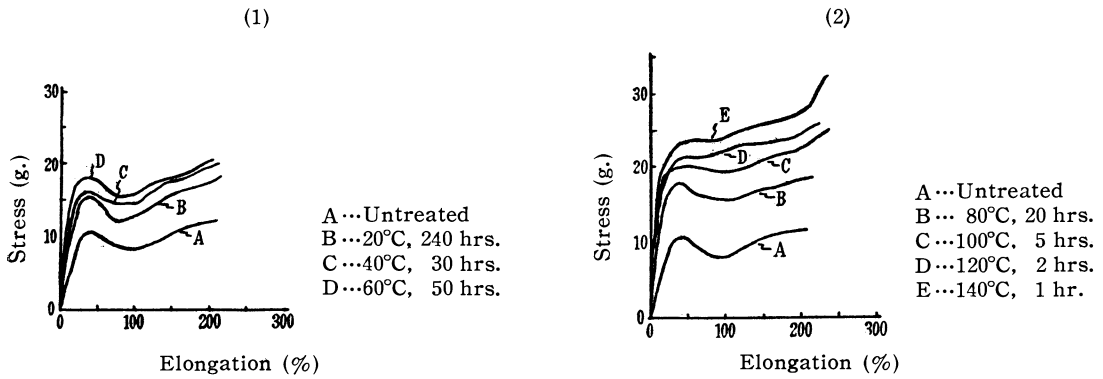

Fig. 3. The quasi-static elongation-stress curves of polycapramide subjected to heat-treatments in liquid water at various temperatures on drawing at 80°C in completely dried state.

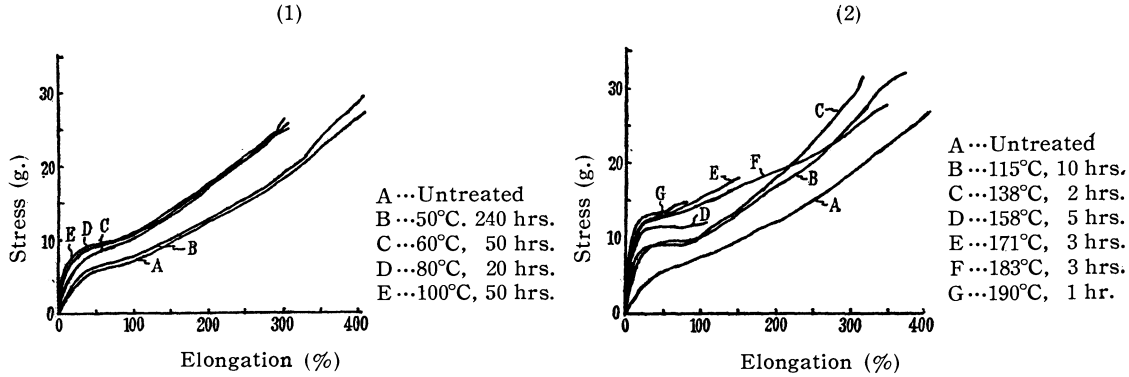

Fig. 4. The quasi-static elongation-stress curves of polycapramide subjected to heat-treatments in dried state at various temperatures on drawing at 20°C in water.

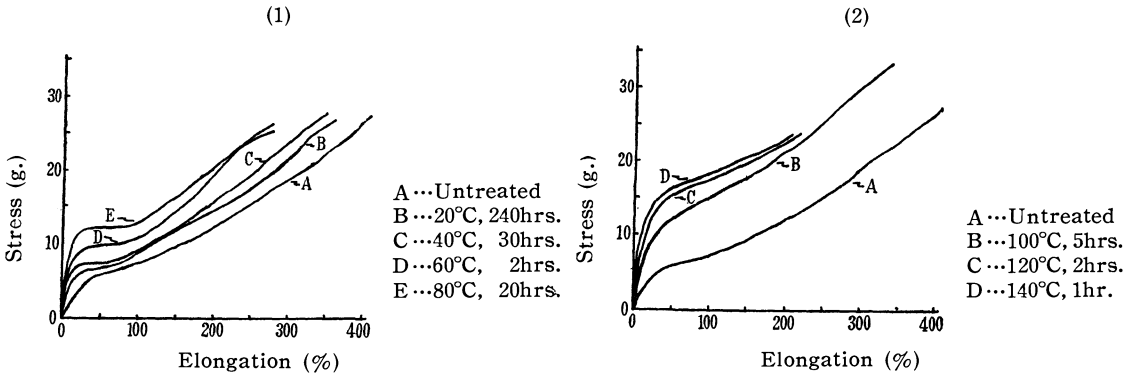

Fig. 5. The quasi-static elongation-stress curves of polycapramide subjected to heat-treatments in liquid water at various temperatures on drawing at 20°C in water.

dried state, most[b] of the heat-treated specimens are stretched homogeneously, without necking, towards rupture. In case of the drawing at 20°C in water, all are stretched homogeneously, and neither maximum nor minimum of stress are found in the curves. But an inflection part is found as shown in Fig. 4; the part following after the inflection lies on the identical line in every case of dry treatment below 140°.

(i) Drawing at 80°C in Dried State.—The tentative yield stresses (*Wc*), which are the minimum stresses in curves as explained in Part I or II, are plotted against the temperatures of heat-treatment in Fig. 6.

Fig. 6 indicates the following facts. In case of the treatment in dried state, *Wc* increases with temperature below ca. 120°C, especially at ca. 60°C, and is almost invariable from ca. 120°C to ca. 170°C; but the great increase of *Wc* is noticed between 170–180°C. In case of the treatment in liquid water, even if merely being steeped for a long time in water at room temperature, *Wc* is somewhat higher. *Wc* increases peculiarly at ca. 40°C and 80–100°C, but scarcely alters in the other temperature ranges.

Consequently it is found that the increase of yield stress is not parallel with the increase of density (cf. Fig. 8).

(ii) Drawing at 20°C in Water.—The stress at the inflection part, which is well assumed as the tentative yield stress (*Wc*), increases with rise of the treatment-temperature as shown in Fig. 7.

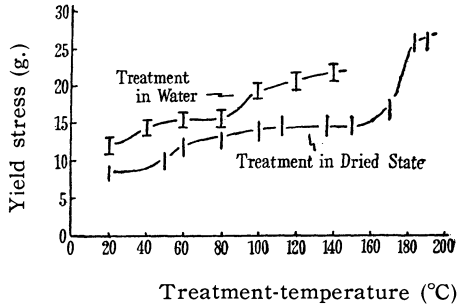

Fig. 6. The relations between yield stresses at 80°C in completely dried state and treatment-temperatures.

b) No specimens treated in water above 40°C or in dried state at higher temperature gave necking in this drawing condition. If treatment was executed in dried state at lower temperatures (the limit of temperature could not be determined), the necking appeared. On the other hand the untreated specimen showed the necking distinctly, even if drawing was carried out at 160°C. Although appearance of necking depends on the rate of drawing, it is evident that the appearance of max. and min. in the curves is not always attended with the appearance of the necking.

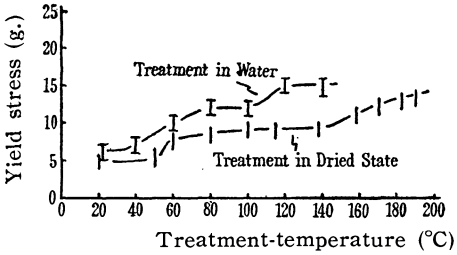

Fig. 7. The relations between yield stresses at 20°C in water and treatment-temperatures.

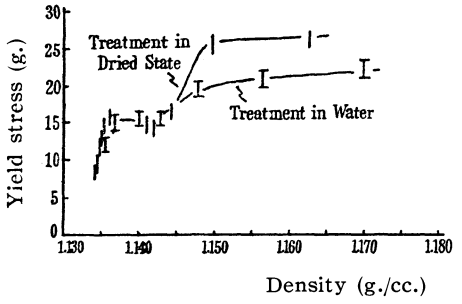

Fig. 8. The relations between yield stresses at 80°C in completely dried state and densities at 25°C.

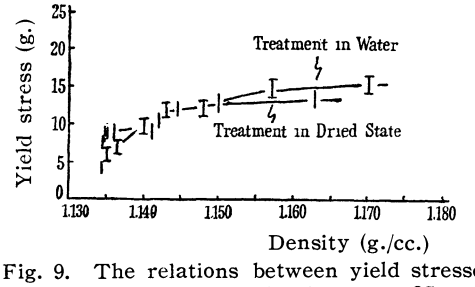

Fig. 9. The relations between yield stresses at 20°C in water and densities at 25°C.

Discussion

(1) The Dry Heat-Treatment

The singular temperatures in respect to the treatment in dried state exist at near 60°, 120°, and 180°C; those at 120° and 180°C are noticed on both of density and yield stress but at 60°C on the yield stress alone. (Fig. 10, where maxima of stress in Fig. 2 are plotted against treatment-temperature, gives singularities more clearly than Fig. 6.) Any of them is thought to be a sort of transition temperature. The temperature near 180°C is assumed as the softening temperature explained in Part I[2], at which the macro-Brownian motion in any micro-region begins to be effectual. Hence there will be tow transition temperatures, 60°C and 120°C, in which the micro-Brownian motion participates. This indicates the coexistence of two micro-regions; the one where the micro-Brownian motion comes into effect easily, and the other where it is relatively difficult for it to do so. Presumably the former can be assumed as the amorphous region [Am.], but the latter cannot be simply assumed as the crystalline region. The sharp increase of density by heat-treatment above 120°C suggests the latter to be assumed as the intermediate state between amorphous and crystalline, i.e. the mesomorphous state [Qcr.]. Therefore the complete crystalline region [Cry.] (containing a little disorder) must exist as the another region. The thermal behaviors of these three hypothetical regions may be taken into account under the experimental facts, setting aside the question how such regions are distributed.

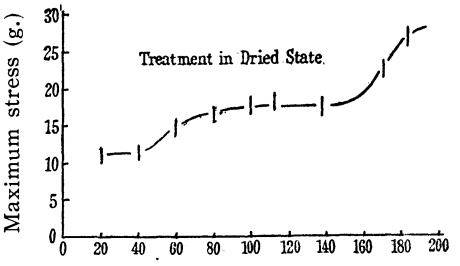

Fig. 10. The relation between maximum stresses at 80°C in completely dried state and treatment-temperatures.

The peculiar temperature at which the micro-Brownian motion becomes effectual[c] is denoted by Tf. The heat-treatment relaxes the frozen distortion and brings about the thermal equilibrium. The treatment at above Tf of [Am.] makes part of [Am.] transformed into [Qcr.] or [Cry.] (1st.-transformation), and still that at above Tf of [Qcr.] makes [Qcr.] transformed into [Cry.] (2nd.-transformation). Hence it can be said from Figs. 1, 4, 6, and 10, that through the 1st.-transformation the stress at deformation is increased but the density is scarcely altered, and on the other hand through the 2nd.-transformation the increase of stress is little but the increase of density is large. The relation is recognized more explicitly in Fig. 8 where *Wc* are plotted against densities. Therefore it is proved that, by drawing, the large flow between the chain molecules is caused only in the amorphous regions [Am.] and is not done in more or less orderly regions [Cry.], [Qcr.]. If this prove to be the case, the crystallization[3] brought about

c) The meaning of "effectual," is that the effects of elementary transfiguration, owing to the movement within ordinary time of observation or heat-treatment, become observable.

3) K. Fuchino and A. Okada, *Scientific Reports of Toyo Rayon Co.*, No. 13, 1 (1949) (in Japanese). J. Fankuchen and H. Mark, *J. Appl. Phys.*, 15, 364 (1944).

by drawing must be attributed to the transformation of [Qcr.] into [Cry.] resulting from the slip of small extent in [Qcr.] caused by the stress; the elongation due to this slip is negligibly small in comparision to the entire elongation. Tf is lowered under the large stress[4] (about the motion only parallel to the stress) and the transformation becomes possible at the temperature where it is impossible in the ordinary state.

The reason, why the increase of density is not apparent through the 1st.-transformation, is probably due to the little difference between densities of [Am.] and [Qcr.][d].

By treatment at the temperature above the softening temperature (ca. 180°C), both the yield stress and the density are markedly increased. In polymer there are distortions which cannot be removed by the micro-Brownian motion of each individual element (segment) but can removed by the simultaneous co-operative movement of some individual elements. The simultaneous co-operative movement of many elements means the macro-Brownian motion, and the temperature at which such a movement becomes effectual is denoted by Tm. The experimental facts show that the distortions are markedly removed through heating at the temperature above the softening temperature, which is considered to be Tm of the amorphous region. (Tm of the orderly region can be assumed as the melting point 220°C).

(2) The Heat-Treatment in Water

The singular temperatures in respect of the treatment in water exist at about 100°C and 40–50°C. The latter is obscure; but taking into account the fact that, when lactam monomer and oligomers are removed from the chip of polycapramide by scouring with water, the rate of extraction is very much smaller below 40°C than from 60°C to 100°C, it is also supposed to be a certain singular temperature. It is found in Figs. 1, 6, and 8 that singularities at 100°C and 40°C in water resemble those at 180°C and 120°C in dried state, respectively; this indicates Tf of [Qcr.] in water to be ca. 40°C and Tm of [Am.] in water to be ca. 100°C. Tm and Tf are much largely lowered in water than in dried state.

The specimens of the same density give generally the same yield stress, but the density being beyond 1.15 g./cc. the dry treatment gives larger yield stress than the wet treatment as shown in Fig. 8. Such distinction of properties among specimens of the same density also appears on the elongation to rupture; namely the dry treatment gives apparently small value as shown in Figs. 2 and 3. Besides it has been observed qualitatively that the wet treatment gives the lower water adsorption and higher dyeability than the dry treatment. Even if the mean value of density is the same, the variation of density distribution in the structure of polymers will probably cause such distinction of properties.

(3) The Effects of Water

The effects of water on the heat-treatment is very remarkable. If water molecules coexist with polyamide molecules, it is expected that the resistance against flow between chain molecules decreases, Tf is lowered, and the internal pressure is generated by swelling. Some of these effects are revealed on experiment as described already. That Tf of [Qcr.] is lowered by steeping the samples in water, indicates the penetratability of water molecules into [Qcr.] regions.

It is noteworthy that the effects of heat-treatment are much smaller in the case of the drawing in water at 20°C than in the case of the drawing in dried state at 80°C; especially such tendency is large in the case of the dry treatment. For example, the specimens subjected to the dry treatment between 60–138° give the same elongation-stress curve beyond 100% elongation (Fig. 4). This fact suggests that the drawing in water can bring about the similar effect with some of the effects caused by heat-treatment.

(4) Further Considerations of Each Micro-Region

The above description has been deduced on assuming the coexistence of [Am.], [Qcr.], and [Cry.] micro-regions and the transformation among them, but the aspect, how these regions are mixed, has not yet been mentioned. Such aspect cannot be ascertained only by this experiment, nevertheless it can be discussed under consideration of the facts formerly known.

The spherulites are observed in various polymers under the microscope[7,10]. The spherulite is an aggregate of crystallites which is thought to be the inevitable form

4) R.F. Boyer and R.S. Spencer, *J. Appl. Phys.*, **16**, 594 (1945).

d) The density of [Am.] at 25°C is presumed to be about 1.1 by extrapolating densities of the melt at the various temperatures[5]. The density of [Qcr.], which is well assumed as the defective crystallite of frozen α-form as described later, is presumed to be about 1.13 from X-ray data[3,6]. The density of [Cry.] is presumed to be 1.21 from X-ray data[8,6]. Then the difference of density between [Am.] and [Qcr.] is very smaller than that between [Qcr.] and [Cry.].

5) H. Yumoto, *Scientific Reports of Toyo Rayon Co.*, No. **25**, 6 (1953) (in Japanese). Y. Kinoshita, ibid. No. **27**, 1 (1954) (in Japanese).

6) R.Z. Brill, *Z. Phys. Chem.*, B **53**, 61 (1943); *C.A.*, **37**, 4576 (1943); *J. Prakt. Chem.*, **161**, 49 (1942); *C.A.*, **37**, 4608 (1943).

7) C.W. Bryant, *J. Polymer Sci.*, 2, 547 (1947).

in the crystallization of linear polymers. Concerning polycapramide, although spherulites have been observed practically in the case of the specimens crystallized by slow cooling of the melt or by evaporation of the solution, spherulites which are too small to be observable are generally be expected to be formed. It has been known that spherulites are deformed in proportion with the deformation of specimen[8] and the rupture occurs only along the boundaries between spherulites or along the radii of them[10]. Then [Am.] regions, where flow can occur, must exist in both the boundary and the interior of spherulites. Consequently a spherulite is constituted from [Am.], [Qcr.], and [Cry.] micro-regions, and [Qcr.] or [Cry.] is assumed as a sort of crystallite.

It was already reported in 1925[11] that the crystal structure of paraffine (C_{20}—C_{30}) transforms at much lower temperature than the melting point, and also on polyethylene[12], polyamide[12,3,6] such phenomena were observed. The structure stable at lower or higher temperature has been called by β- or α-form. The transition temperature of polycapramide, although uncertainly, a has been found to be about 150°C[3,6] by means of X-ray. α-Form does not take the stable configuration as the ordinary crystal and is rather assumed as the state where chain molecules arrange in parallel lines into a bundle, having lower entropy-than the amorphous state; i. e. all of the elements of chain molecule do not take the *trans*-configuration of rotational isomers. (All of the structural elements take the *trans*-configurations in β-form.) The micro-Brownian motion in α-form always alters the configuration but it does so only partially so as not to lose the whole arrangement. It is most reasonable to suppose that [Cry.] is the crystallite of β-form and [Qcr.] is that of α-form frozen at lower temperature by rapid cooling. If the transition temperature as regard the α, β-transformation is said to be about 150°C[e], it should be Tf of [Cry.]. In the course of the treatment at a higher temperature than Tf of [Cry.], [Cry.] (β-form) can transform into α-form while it is heated, but it can retransform, if not rapid, into β-form on cooling. Then, as far as the effect of heat-treatment is concerned, the singularity can not be observable at about 150°C.

Now let us consider the relations to the micro-regions, U, Vab, and Vc described in Part II[1]. U region, i. e. the micell, where chain molecules are fairly arranged, corresponds to [Cry.] or [Qcr.], and Vab region, i. e. the boundary region between micells, where molecules are partially arranged, and Vc region, i. e. the intermiceller region, where each of the molecules is completely entangled, both correspond to [Am.]. Therefore [Am.] is divided into two sorts which are different in the order. Taking all things together, Tf of [Am.] in this paper will correspond to Tf (70–80°C) of Vab in the previous paper. Then another Tf of [Am.] corresponding to Tf of Vc must be found; the singularity found at about −40°C on polycapramide[13] will be probably due to Tf of Vc.

Summary

The obtained results are summarized in Tables II and III.

The values in these tables are not precise because of the methods of evaluation, and the shift of ca. ±10°C will be admitted.

All of these temperatures is not always observed in any experiment. The revelation of this singularity is dependent on the character measured and the state of the specimen.

TABLE III

THE EFFECTS OF HEAT-TREATMENT

	Temp. °C	Increase of Density	Increase of Yield Stress	Change in Structure
Treatment in Dry State	below ca. 60	none	none	none
	ca. (60–120)	small	large	Am.→Cry. or Qcr.
	ca. (120–180)	large	small	Qcr.→Cry.
	above ca. 180	very large	very large	Am.→Cry.
Treatment in Water	below ca. 50	small	large	Am.→Cry. or Qcr.
	ca. (50–100)	large	small	Qcr.→Cry.
	above ca. 100	very large	very large	Am.→Cry.

8) C.M. Langkammer and W.E. Catlin, *J. Polymer Sci.*, **3**, 305 (1948).
9) C.W. Bunn, "Fibres from Synthetic Polymers", R. Hill, Elsevier Publ. Co. (1953), pp. 251-6.
10) F.P. Reding and A. Brown, *Ind. Eng. Chem.*, **46**, 1962 (1954).
11) Müller and Saville, *J. Chem. Soc.*, **127**, 599 (1925).
12) W.O. Baker, "Advancing Fronts in Chemistry", S.B. Twiss. Reinhold Publ. Corp. (1945), p. 145.
13) T. Kawaguchi. Unpublished.

TABLE II
THE MICRO-REGIONS IN POLYCAPRAMIDE AND THEIR TRANSITION TEMPERATURES

(1) At Lower Temperature

	Micro-Region	Temp. at which the micro-Brownian motion becomes effectual in relaxed state (Tf), °C	
		Dry State	In Water
Am.	Completely amorphous region (Vc)	ca. −40[13]	*
Am.	Partially arranged region (Vab)	ca. 60, 70~80	below 20
Qcr.	Defective crystallite (U) of frozen α-form	ca. 120	ca. 40–50
Cry.	Crystallite (U) of β-form	ca. (150)[e]	*

(2) At Higher Temperature

	Micro-Region	Temp. at which the macro-Brownian motion becomes effectual (Tm), °C	
		Dry State	In Water
Am.	Vc	—	—
Am.	Vab	ca. 180 (softening pt.)	ca. 100
Qcr. (Cry.)	Mesomorphous state of α-form (U)	215–220 (melting pt.)	*

Conclusions

The densities and drawing behaviors of polycapramide subjected to various heat-treatments give the useful facts in fiber manufacturing applications. And the reasonable considerations on them suggest the coexistence of some micro-regions, i. e. the heterogeneity of polymer structure. In connection with the results described in Part II, where influences of humidity are considered, the following are concluded. Polymers are constituted from micells (U), boundaries between micells (Vab), and intermiceller regions (Vc). The crystallites of β-form [Cry.] and the defective crystallites of frozen α-form [Qcr.] are U regions. Both of Vab and Vc are amorphous regions [Am.]; Vab indicates a partial arrangement and Vc is completely amorphous. Various singular temperatures can be assigned as the following. At dried state Tf (the temperature at which the micro-Brownian motion becomes effectual) of Vc, Vab, [Qcr.] and [Cry.] are about −40°C[13], 70°C, 120°C and (150°C)[e] respectively. In case when the sample is steeped in water Tf of Vab is lower than 20°C and that of [Qcr.] is about 40°C. (Water molecules can penetrate into [Qcr.]). At dried state Tm (the temperature at which the macro-Brownian motion becomes effectual) of Vab and [Qcr.] are about 180°C (softening point) and 220°C (melting point). (Above Tf of [Cry.] discrimination of [Cry.] and [Qcr.] is lost.) At the state of the sample steeped in water Tm of Vab is about 100°C. The effects of various heat-treatments are compatible with the characters above described.

The other important conclusion is that, by drawing, flow between chain molecules can occur in [Am.] alone; but only a slip of some extent, negligibly small in comparision with the entire elongation, can be caused in [Qcr.].

The density is largely increased by the transformation of [Qcr.] into [Cry.], and the yield stress is largely increased by that of [Am.] into [Cry.] or [Qcr.].

Such precise definitions of micro-regions may be unaccountable, but considerable definite divisions among them can be suggested from the experimental facts. Later, it is hoped that the theoretical interpretation on it can be given.

The author wishes to thank Dr. K. Hoshino and Dr. H. Kobayashi, who instructed him and approved this publication, and M. Nakata who assisted him on experiments.

Nylon Laboratory, Research Department
Toyo Rayon Co. Ltd., Ohe-cho
Minato-ku, Nagoya

e) The value of 150°C is quoted from the X-ray diffraction data of Dr. Fuchino[8], but the thermal analysis[14] gives no singularity at this temperature and gives development of a slight latent heat at 168-173°C. Whether this latent heat is due to the beginning of macro-Brownian motion in [Am.] or to transformation of β to α owing to the beginning of micro-Brownian motion in [Cry.], and then 150°C is still uncertain.

14) Y. Kinoshita, Unpublished.

Heats of Dilution of Polyvinylalcohol Solution. I

By Kazuo AMAYA and Ryoichi FUJISHIRO

(Received October 10, 1955)

Introduction

The measurement of heats of dilution of polymer solutions is important for investigating the thermodynamical behavior of polymer solutions as well as for industrial purposes. Previously we reported the heats of dilution of several polystyrene solutions. In this paper we shall report the heats of dilution of polyvinylalcohol solutions using water as a solvent.

Experimental

Apparatus and Procedures.—The apparatus used was an older type though an improved one had been already described in the previous paper[1]. The former is different from the latter in two points, (1) using A.C. bridge instead of D.C. bridge combined with the converter, and (2) introducing the solution directly into the Dewar vessel as shown in Fig. 1. The thermister has resistance of about 33 KΩ at 30°C, and its temperature

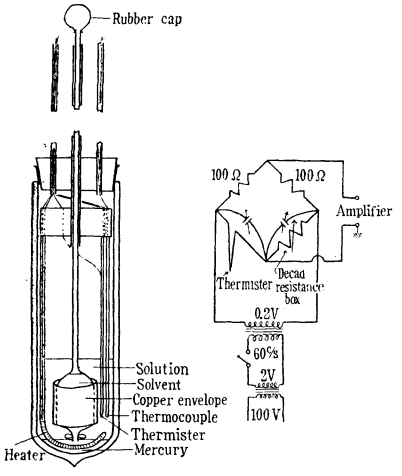

Fig. 1.

coefficient is about 5%. The resistance change of 0.1 Ω can be detected and this corresponds to about 0.005 cal. Fifteen or 20 cc. of solution was introduced with a pipet in the Dewar vessel and 5 or 10 cc. of water was taken into the solvent container. By raising the solvent container and pushing the rubber cap, mixing was performed. Stirring of the mixed solution was operated manually after mixing. Other procedures were the same as those described in the previous paper[1].

1) K. Amaya and R. Fujishiro, This Bulletin 29, 270 (1956).

Samples*.—The degree of polymerization of polyvinylalcohol used in this experiment was 450 and 600. The content of acetyl radical of the latter sample was less than 0.3 mol. %, but that of the former one was 1.7 mol. %.

Results and Discussion

The heats evolved $-\Delta H$ when the polyvinylalcohol solutions are diluted successively with water at 30°C, are shown in Table I.

TABLE I

HEATS OF DILUTION OF P.V.A. SOLUTIONS

Exp. series	V* cc.	v_r*	v* cc.	v'_r*	$-\Delta H$* cal.	α	T_p* °C.
	System I. Solution of P.V.A. of D.P. 450.						
	15	0.155	5	0.115	0.312	−4.3	30
	20	0.115	5	0.092	0.252		
	25	0.092	5	0.077	0.172		
	System II. Solution of P.V.A. of D.P. 600.						
1	15	0.100	5	0.075	0.112	−3.2	70
	20	0.075	5	0.059	0.074		
	25	0.059	5	0.049	0.046		
	30	0.049	5	0.042	0.010		
2	20	0.143	5	0.114	0.192	−2.3	100
	25	0.114	5	0.094	(0.119)**		
	20	0.094	5	0.075	0.069		
	25	0.075	5	0.062	0.050		
	30	0.062	10	0.046	0.063		
	40	0.046	10	0.037	0.044		
3	25	0.114	5	0.094	0.120	−2.3	100
	30	0.094	5	0.081	0.090		
	35	0.081	5	0.071	0.078		
	40	0.071	5	0.063	0.046		
	45	0.063	5	0.056	0.037		

* These notations are as follows: V: Volume of solution before dilution. v_r: Volume fraction of polymer before dilution. v: Volume of water added. v'_r: Volume fraction of polymer after dilution. $-\Delta H$: Heat evolved. T_p: Pre-heating temperature.

** This value in the brace is the expected one owing to the failure of the experiment.

Both systems, solutions of P. V. A. of D. P. 450 and 600, proved to be exothermic.

Assuming that the heat of mixing is represented by the van Laar form, we find

* We are indebted to Dr. S. Matsumoto of the Kurashiki Rayon Company and Mr. H. Inagaki of Kyoto University for these samples.

easily that the integral heat of dilution ΔH_o from the volume fraction of polymer v_r to v_r' is given by

$$\Delta H_o = aV_r(v_r - v_r')$$

where α is a constant describing the interaction between polymer and solvent and V_r is the volume of polymer in the solution.

Plotting ΔH_o or $\Delta H_o/V_r$ as ordinate and V_r as abscissa for each series, we obtain straight lines as shown in Fig. 2 and this

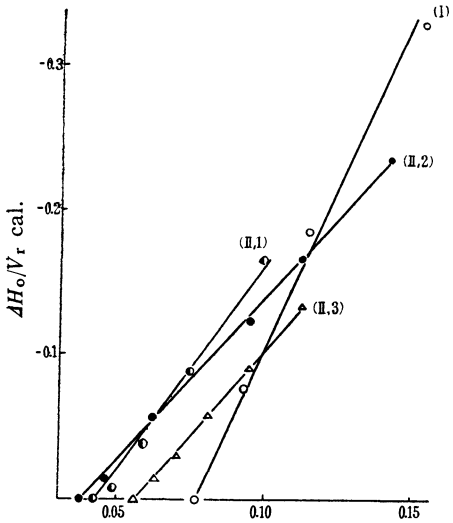

Fig. 2.

result suggests that the assumption mentioned above is satisfied. In the figure we adopt the integral heat of dilution per unit volume of polymer $\Delta H_o/V_r$, as ordinate for the sake of convenience. The values of α can be derived from the tangent of the straight lines in the figure and these values from each series are given in Table I.

As ethanol may be regarded as a monomer-unit of P. V. A., the value of α obtained from the heat of mixing of ethanol solution may be compared with that of P. V. A. solution. Using the data in the literature[2], we find that the value of α for the ethanol-water system is about $-40 \sim -20$ cal./cc. in the equal concentration range. This value is the same in sign as that of our experiment, but its magnitude is remarkably larger. According to G. Gee[3] and P. Meares[4], the value of α for the polymer solution is said to be 70–80% of that of the corresponding monomer-unit solution, owing to the increase of polymer-polymer contacts in the polymer solution. But the value of α for the P. V. A.-water system is only 10% of that of the ethanol-water system. This suggests that the strong intersegmental hydrogen bonds in P. V. A. exist and the apparent interaction between P. V. A. and water decreases considerably.

In the system I the solution was introduced into the Dewar vessel after warming to about 30°C. But in the system II before being introduced into the calorimeter, solutions were warmed to about 70°C or 100°C respectively, corresponding to series 1 or 2 and 3. From the values of α of both systems the effects of pre-heating was observed. In other words the absolute magnitude of α is in the inverse relation to the temperature of pre-heating.

It may be considered that the P. V. A.-water system being exothermic the polymer-water contact is energetically more stable than the polymer-polymer contact and therefore, by raising the temperature, the number of polymer-polymer contacts having higher energy increases owing to intersegmental associations of P. V. A.. This state produced by heating is expected to be maintained to some extent even after cooling the solution to 30°C. The higher the temperature of heating, the more the number of polymer-polymer contacts increases and the more that of polymer-water contacts decreases. Thus the number of polymer-water contacts is the most in the system I, next in the series 1 of the system II and the least in the series 2 and 3 of the same system. Consequently on dilution the change in these numbers may be in the same order.

The fact that high degree of intersegmental association by hydrogen bonding is present is more confirmed by other experimental facts. The one is the heats of solvation for lower polyalcohol homologues which were measured by S. Seki and K. Suzuki[5]. They showed that the more the number of hydroxyl radicals in a molecule, the stronger the intramolecular hydrogen bonds are and the apparent interaction between solute and solvent per unit hydroxyl radical decreases considerably even for lower alcohols. Their results seem to be consistent with our ones that the values of α for the polymer solutions are remarkably lower than that for the ethanol solution. Secondly, according to our unpublished data[6], the value of α increases by substituting a fraction of hydroxyl radicals with acetyl. This may be due to the hindrance of intersegmental hydrogen bonds

2) E. Bose, *Z. physik. Chem.*, **58**, 585 (1907).
3) G. Gee and W.J.C. Orr, *Trans. Faraday Soc.*, **42**, 507 (1946).
4) P. Meares, *Trans. Faraday Soc.*, **47**, 699 (1951).
5) S. Seki and K. Suzuki, This Bulletin, **26**, 63 (1953).
6) To be published in the forthcoming paper.

by acetyl radicals and seems to support our interpretation.

Summary

The heats of dilution of P. V. A. solutions were measured and the interaction parameter α between P. V. A. and water was found to be in the range of $-2\sim-4$ cal./cc. That these values are remarkably lower than that of ethanol solution suggests the presence of strong intersegmental hydrogen bonds of P. V. A.. The effect of pre-heating was also observed. It may be attributed to the increase of intersegmental associations by heating.

We would like to express our gratitude to Professor Y. Morino of Tokyo University and Professor A. Kotera of Tokyo University of Education for their encouragements and discussions.

Department of Chemistry, Faculty of Science, Kobe University, Mikage Kobe

The Relationship between Longifolic and Isolongifolic Acids

By Isao OGURA

(Received March 4, 1955)

Naffa and Ourisson[1] and later Zeiss and Arakawa[2] observed that the longifolic acids are monobasic with formula $C_{15}H_{24}O_2$ and not $C_{14}H_{22}O_2$. The present author obtained the same results, and furthermore confirmed the fact that the logifolic and isolongifolic acids are isomers in endo- and exo-forms.

Simonsen[3] and others[4] reported that the oxidation of longifolene with chromic acid in acetic acid or with potassium dichromate in sulfuric-acetic acid furnishes isolongifolic and α-longifolic acids besides longifolic acid, that longifolic and isolongifolic acids are isomers having formula $C_{14}H_{22}O_2$, that longifolic acid isomerizes to isolongifolic acid on treatment with mineral acid, and that longifolic acid is considered to be one of the C_{14}-acid varieties.

Zeiss and Arakawa obtained these acids by the oxidation of longifolene with potassium dichromate and reduced them as well as their esters with lithium-aluminum hydride. Namely, when isolongifolic acid and methyl isolongifolate were reduced with the reagent, they were converted into isolongifolol ($C_{15}H_{26}O$), m. p. 112°C. Longifolic acid was converted mainly into isolongifolol and partly into longifolol, m. p. 78.5–80.5°C. α-Longifolic acid gave isolongifolol and impure alcohols rich in isolongifolol. From these results it is obvious that longifolic and α-longifolic acids are mixtures consisting chiefly of isolongifolic acid.

Further, oxidation of isolongifolol with potassium dichromate in sulfuric-acetic acid regenerated isolongifolic acid. On treatment with phosphorus pentachloride in ether at room temperature, it gave an olefin which proved to be longifolene on the basis of optical rotation and infrared spectrum. From these results Zeiss and Arakawa presumed that longifolic and α-longifolic acids are probably epimeric mixtures, and determined that they are monobasic acids of formula $C_{15}H_{24}O_2$.

Longifolene used in the present experiments was regenerated from longifolene hydrochloride (m. p. 59–60°C). The former was oxidized with chromic acid in acetic acid under the same conditions as used by Simonsen[5] and others. Longifolic acid obtained by this treatment was esterified with dimethyl sulfate in the usual manner, and the ester was separated by distillation to give methyl longifolate and methyl isolongifolate, m. p. 54–55°C, which on saponification with alcoholic potash gave longifolic acid, m. p. 152–153°C, and isolongifolic acid, m. p. 136–137°C, respectively. These melting points agreed with other workers' results. Analyses and experiments described below gave values for C_{15}-acid. When dihydrolongifolene, obtained by the catalytic hydrogenation of longifolene, was oxidized similarly, isolongifolic acid was produced. When methyl longifolate and methyl isolongifolate were treated with phenyl magnesium bromide, a crystalline carbinol,

1) P. Naffa and G. Ourisson, *Chem. and Ind.*, **1953**, 917.
2) H.H. Zeiss and M. Arakawa, *J. Am. Chem. Soc.*, **76**, 1653 (1954).
3) J. L. Simonsen, *J. Chem. Soc.*, **1920**, 117, 578; ibid., **1923**, 125, 2624.
4) A.E. Bradfield, E.M. Francis and J.L. Simonsen, *J. Chem. Soc.*, **1934**, 118.
5) J.L. Simonsen, loc. cit.

m. p. 120.5–121.5°C, was obtained from the former, and another carbinol, m. p. 117–118°C, from the latter. On trating it with formic acid, or with potassium bisulfate, or on distilling under diminished pressure, the two carbinols gave the same dehydration product, m. p. 109–110°C, the carbinol of m. p. 117–118°C being dehydrated more easily. These results assumptively show that the two carbinols differ in the steric arrangments of the diphenyl carbinol group and the hydrogen atom ttached to the ring carbon atom which originally possessed the carboxyl group in the longifolic acids. Thus, longifolic and isolongifolic acids are stereo-isomers as regards the carboxyl group and the hydrogen atom. This relationship is imaginable from the results of Zeiss and Arakawa. Just as the endo form (I) and the theoretically possible exo form (II) in dihydrocamphene[6], longifolic and isolongifolic acids may be considered to be in a similar relation.

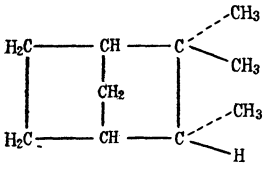

(I)

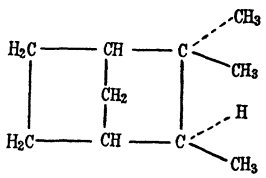

(II)

According to the structural formula presented by Naffa and Ourisson, the relationship is represented as forms (III) and (IV).

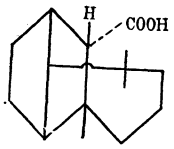

(III)

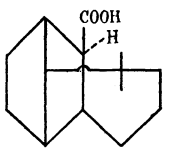

(IV)

The infrared spectra of longifolic and isolongifolic acids showed absorptions at 5.93 μ and 5.90 μ respectively in the solid state, and both at 5.87 μ in carbon tetrachloride solution. All these data proved that longifolic and isolongifolic acids are endo and exo isomers, and it was concluded from the infrared spectra that isolongifolic acid is the endo form.

Experimental

1. Longifolene.—Terpentine oil obtained from oleo-resin was distilled under diminished pressure, and the fraction boiling at 149–152°/36 mmHg or 122–125°/10 mmHg was collected. The longifolene fraction was refluxed with metallic sodium for one hour, and then hydrogen chloride was passed for five to eight hours with cooling in ice-water.

6) H. Alder and G. Stein, *Ann.*, 525, 236 (1936).

Longifolene hydrochloride thus obtained in needles melting at 59–60°C was treated with acetic anhydride and sodium acetate under reflux for three hours to give longifolene. 180.5 g. of this longfolene was dried with calcium chloride, and fractionated under a pressure of 10 mmHg as follows:

Fraction	b.p., °C	Yield, g.	d_4^{25}	n_D^{25}
1	–123	0.9	—	—
2	123–124	157.0	0.9300	1.5025
3	124–125	19.3	0.9303	1.5026
4	125–126	2.1	0.9303	1.5028
5	126–	1.2	0.9351	1.5051

Mol. Refract. (Fraction 2); 64.53. Calcd. for $C_{15}H_{24}(F_1)$: 64.40.

Fraction 2 was used in the following experiments.

2. Methylation.—Longifolene was oxidized according to the procedures of Simonsen and others. The acids obtained were dried and esterified with dimethyl sulfate in the usual way. 51.7 g. of the ester were subjected to fractional distillation:

Fraction	b.p. °C (8.5 mmHg)	Yield, g.	d_4^{25}	n_D^{25}
1	139.5–140.5	16	1.0378	1.5012
2	140.5–142	13	1.0278	1.5012
3	142 –143.5	7	1.0382	1.5016
4	143.5–145	2.5	crystals	
5	145 –147	7	〃	
6	147 –150	3	〃	
7	150 –	2	〃	

Recrystallization of the crystalline fractions from alcohol gave a substance melting at 54–55°C, which agreed with methyl isolongifolate obtained by Simonsen and others.

Anal. Found: C, 76.42; H, 10.16. Calcd. for $C_{16}H_{24}O_2$: C, 76.75; H, 10.4%.

Hydrolysis of the crystalline fractions with alcoholic potash gave an acid which melted at 136–137°C which agreed with isolongifolic acid.

Anal. Found: C, 76.16: H, 10.25. Calcd. for $C_{15}H_{24}O_2$: C, 76.22; H, 10.23%.

On the other hand, the acid obtained from fractions 1–3 by similar treatment was identified with longifolic acid, m.p. 152–153°C.

Anal. Found: C, 76.41; H, 9.75. Calcd. for $C_{15}H_{24}O_2$: C, 76.22; H, 10.23%.

Thus, fractions 1–3 were methyl longifolate (yellowish oil) and other fractions were rich in methyl isolongifolate.

3. Grignard Reaction.—Methyl longifolate (30 g.) was treated with a Grignard reagent prepared from brombenzene (47.1 g.) and magnesium (7.2 g.) in ether solution. The ethereal solution was dried, and evaporated left to stand for two or three days, the residue gave the crystalline carbinol melting at 120.5–121.5°C.

Anal. Found: C, 86.29; H, 9.41. Calcd. for $C_{27}H_{34}O_2$:C, 86.58; H, 9.15%. A similar treatment of methyl isolongifolate gave the carbinol melting at 117–118°C, (Found C, 86.49; H, 9.14). The presence of hydroxyl group in these molecules was

indicated by the Deniges reagent and by the analysis described above.

4. Dehydration of Carbinols.—The product from methyl longifolate and the Grignard reagent were immediately distilled before the crystals separated out, to give the following results:

Fraction	b.p., °C (10 mmHg)	Yield (g.)	d_4^{25}	n_D^{25}
1	–120	1.5	1.0775	1.5140
2	120–142	2.5	1.0475	1.5240
3	142–146	2.0	1.0413	1.4998
4	146–148	3.0	1.0264	1.5030
5	148–	5.0	crystals	

The residual crystalline substance obtained in the above fractional distillation had a melting point of 109–110°C after recrystallized from alcohol. The presence of a double bond and a phenyl group was inferred from the infrared absorptions at 6.27 μ and 6.70 μ, respectively. Analysis showed it was a hydrocarbon, $C_{27}H_{32}$.

Anal. Found: C, 90.55; H, 9.17. Calcd. for $C_{27}H_{32}$: C, 90.95; H, 9.05%. Another crystalline hydrocarbon, m.p. 67–68°C was obtained from fraction 2. Found: (C, 93.60; H, 6.71). It was not investigated further.

When the carbinols from methyl longifolate and methyl isolongifolate were treated with formic acid or potassium bisulfate under reflux for 1.5 hours, they gave the same hydrocarbon $C_{27}H_{32}$ melting at 109–110°C.

The author is indebted to Prof. T. Kubota, Osaka City University, for his advice and direction, and to Mr. M. Yamaguchi, Osaka City University, for the measurement of the infrared absorption.

Kinki University, Fuse City, Osaka

*The Kinetic Study of Surface-chemical Reactions at Extremely Low Pressures. I. The Thermal Reaction between Water Vapor and a Tungsten Filament. Part I**

By Nobuji SASAKI** and Takuya HAMAMURA

(Received February 28, 1955)

Introduction

For the kinetic study of a series of chemical reactions on the solid surface, the reaction between water vapor and a tungsten filament at high temperatures was first chosen, because the filament can readily provide an extremely clean surface by merely flashing it at a high temperature. The equilibrium study of the system of W, O_2, and H_2 has been reported by some investigaters. Chaudron[1] studied the equilibrium by starting from tungsten trioxide and hydrogen at temperatures ranging from 600 to 1100°C. Wöhler[2] and Gulbransen[3] started from water vapor and tungsten at temperatures below 1000°C. Alterthum[4] extrapolated Wöhler's results to obtain the equilibrium constant at 3000°C where vapors of tungsten oxides also must be taken into consideration and concluded that water vapor in equilibrium must almost completely be decomposed.

From these reports, however, nothing can be guessed about the reaction-kinetic behaviour of water molecules impinging upon the heated surface of tungsten.

The Principle of the Experiment

A tungsten filament is heated inside a cold glass vessel through which a reacting gas is rapidly flowing at a sufficiently low pressure. In this way some unnecessary complications can be avoided, namely, the rate of diffusion of the reacting gas has no influence on the rate of reaction, and the reaction products diffuse away to the cold wall of the reaction vessel to escape any secondary reaction in the gas phase. The collision frequency of gas molecules with the reacting surface can be calculated easily, so that the reaction probability per collision of the reacting gas molecule can be evaluated provided that the over-all rate of the reaction can be determined separately. The surface area of the filament can be determined from

* Read before the Sixth Annual Meeting of the Chemical Society of Japan, held on April 1953.

** Department of Chemistry, Faculty of Science, Kyoto University.

1) M.G. Chaudron, *Compt. Rend.*, **170**, 1056 (1920).

2) L. Wöhler and R. Gunther, *Z. Elektrochem.*, **29**, 276 (1923).

3) E.A. Gulbransen, *J. Phys. Colloid. Chem.*, **53**, 690 (1949).

4) H. Alterthum and F. Koref, *Z. Elektrochem.*, **31**, 508 (1925).

the apparent area by multiplying a certain factor correcting for the roughness[5]. The method of obtaining a high temperature for a chemical reaction by heating a filament electrically has the advantage of dispensing with a special refractory material and heating devices.

The flow method is preferred to the static one to avoid the effect of the adsorption of water vapor on the wall, which is inevitable in the static method at very low pressures.

Apparatus.—The apparatus of all soda-glass is shown schematically in Fig. 1. Reservoir 1 containing about 3 cc. of purified water can be connected directly to the reaction vessel by breaking a thin glass bulb 2 by means of a glass rod containing an iron core and disconnected from it by chipping constriction 3 when the experiment is finished.

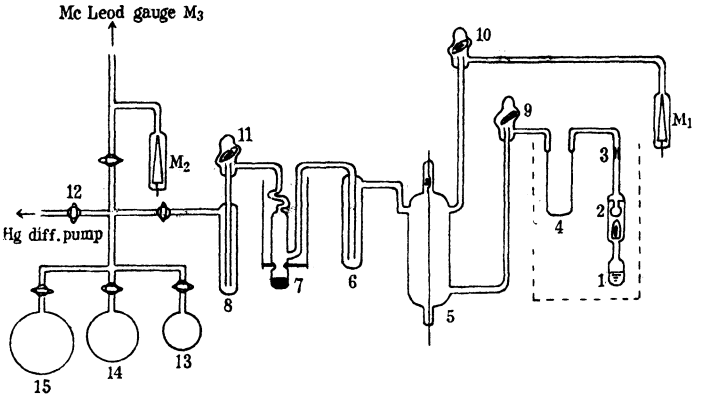

Fig. 1.

Water was purified by repeating sublimation in a high vacuum, dry ice being used for condensation. Capillary tube 4 controls the flow of water vapor. The reservoir and the capillary are immersed in a thermostat. Reaction vessel 5 is 3.5 cm. in diameter and 12 cm. long, so that the pressure gradient along the vessel may be negligibly small. Manometer M_1 used to measure the pressure of condensible water vapor is a 70 mm. long hair pin of 0.3 mm. diameter quartz fibre. It was calibrated against a McLeod gauge using oxygen and hydrogen. The vapor pressure within the reaction vessel can be changed by the change of temperature of the thermostat. A tungsten filament 0.114 mm. in diameter and 120 mm. long was cleaned by dipping in the boiling 40 percent caustic soda solution for five minutes followed by wiping off aqua dag with filter paper, and then it was stretched along the axis of the vessel by means of a tungsten spring. Trap 6 cooled in liquid nitrogen freezes out undecomposed water vapor coming from the reaction vessel. Permanent gasses untrapped are compressed by mercury diffusion pump 7 into glass balloons 13, 14, 15 of different volume from 634 to 6543 cc. connected in a desired combination by means of stop cocks. To determine the composition of the permanent gasses consisting of hydrogen and possibly a small amount of oxygen, the pressure is measured with McLeod gauge M_3 and quartz fibre manometer M_2 at the same time. From the measurement the apparent molecular weight and therefore the composition of the gas can be determined. One percent oxygen added to pure hydrogen reduces by about 7 seconds the interval of time (195 seconds at 50×10^{-4} mmHg.) required for the amplitude to decrease to half value. Trap 8 cooled with dry ice is to prevent grease vapor from entering into the reaction vessel. Particular precautions have been taken to keep the filament from grease vapor contamination by using greaseless stop cock 9, 10, 11, which can be operated with a magnet.

The Procedure.—Prior to the proper experiment, all the apparatus is evacuated for several days by a mercury diffusion pump with a liquid nitrogen trap before it. The reaction vessel is heated at 300°C for ten hours in an electric furnace, and the other tubes are baked out by a hand burner. After thorough evacuation of the cooled vessel the filament is heated at 2400°K for twelve hours.

After the degassing schedule is over, trap 6 is dipped into liquid nitrogen, and glass bulb 2 is broken, the thermostat being kept at a desired temperature. Water vapor flows into the reaction vessel through the capillary tube to be frozen out in trap 6. Pressure measurements with quartz fibre manometer M_1 will show the moment when the flow has become stationary. The filament is now heated, and the temperature is measured with an optical pyrometer. As the reaction proceeds the pressure in the glass balloons increases gradually and this increase is measured with McLeod gauge M_3 at suitable intervals for about eight minutes. The filament is then cooled and the balloons are evacuated through cock 12.

Experimental Result

The pressure of the balloons increases linearly with the time of heating. Some

5) L. Tonks, *Phys. Rev.*, 38, 1030 (1931).

typical examples are shown in Fig. 2. The

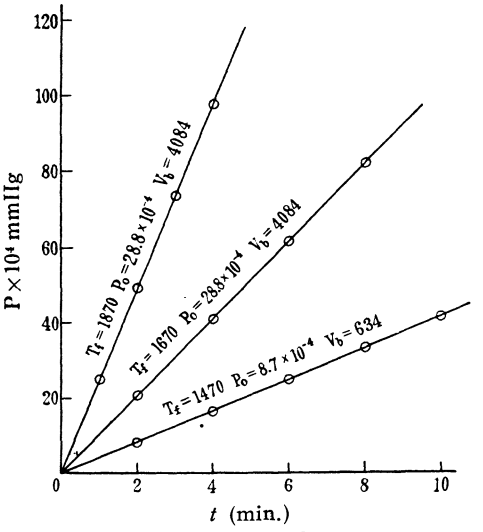

T_f=temp. of filament (°K)
P_0=press of H_2O (mmHg)
V_b=vol of balloons (cc.)

Fig. 2. The pressure change of the glass balloons with the time of heating.

linearity can be observed for more than thirty minutes. This shows the stability both of the flow of water vapor and the surface condition of the filament. The rate of increase of the pressure gives the rate of reaction which is shown in Fig. 3 as a

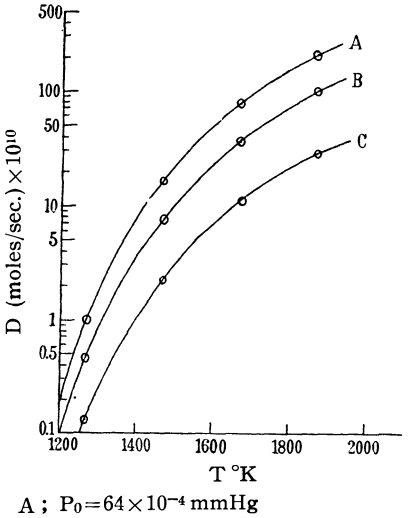

A ; $P_0=64\times10^{-4}$ mmHg
B ; $P_0=28.8\times10^{-4}$ mmHg
C ; $P_0=8.7\times10^{-4}$ mmHg

Fig. 3. Rate of reaction at various filament temperature.

function of the filament temperature. The gas analysis carried out as mentioned above shows the gas produced to be pure hydrogen for varied conditions of the reaction. The temperature increase of the reaction vessel is negligibly small when the filament is heated.

Discussion

From the reaction rates thus obtained, it is possible to evaluate the probability of reaction of a water molecule with the surface of tungsten when a molecule impinges upon it. If the pressure of water vapor is low and the mean free path is comparable with the diameter of the vessel and the length of the vessel is not too long, the following conditions are satisfied.

1. The composition and the pressure of the gas are uniform throughout the vessel.
2. The temperature of water molecules inside the vessel is equal to that of the wall.
3. The flow of gas molecules through the outlet tube obeys Knudsen's law of molecular flow.

Now, if the filament is heated, and water vapor is introduced into the vessel, a part of the water molecules reacts with the filament and leaves the vessel together with the unchanged molecules which are caught in the trap. The quantity in moles of water vapor thus trapped per second is

$$\frac{8\pi r^3}{3l}\times\frac{P}{\sqrt{2\pi MRT}} \qquad (1)$$

where r and l are respectively the radius and the length of the outlet tube in cm, P the partial pressure of water vapor inside the vessel in dyne/cm², M the molecular weight of water, and R the molar gas constant.

Putting $\frac{8\pi r^3}{3l}=A$ and $\frac{1}{\sqrt{2\pi MRT}}=B$ in (1)

it becomes $ABP.$ (1′)

The quantity in moles of water vapor which reacts per second with the filament is

$$kSBP \qquad (2)$$

where k is the probability of reaction of the water molecule with the filament for a single collision, and S the surface area in cm² of the filament. The quantity of water vapor G which enters into the vessel through the inlet tube per second is equal to the sum of (1′) and (2),

thus $$G=ABP+kSBP. \qquad (3)$$

On the other hand

$$G=ABP_0 \qquad (4)$$

if P_0 is the pressure of water vapor inside the reaction vessel when the filament is cold.

The stationary state being assumed, the quantity in moles of the permanent gas produced in the vessel per second is equal to that of the gas D carried into the balloons per second by mercury pump 7 so that

$$D=kSBP \tag{5}$$

provided that one mole of hydrogen alone is produced from one mole of water. From Eqs. (3) and (5), P which is difficult to measure directly is given by

$$P=\frac{G-D}{AB}. \tag{6}$$

Eliminating P and G from Eq. (3), we get

$$k=\frac{AD}{S(ABP_0-D)}. \tag{7}$$

Thus k, the probability of reaction of the water molecule with the filament for a single collision, may be evaluated from all measurable quantities for various filament temperatures and water vapor pressures.

For the conductance A of the outlet tube the value of 0.047 cm^2 is used which has been obtained by actually passing carbon dioxide, (the calculated value is 0.055 cm^2) and for the roughness factor of the filament the value of 1.225 is used according to the result of Tonks[5].

Results

The probabilities of reaction for a single collision of the water molecule with the heated tungsten surface thus evaluated are shown in Table I.

The conclusion therefrom is that the major part of water molecules which hit the hot surface rebound without reacting with it even at the high temperatures employed, and the reaction is of the first order with regard to the pressure of water vapor. The relation between the reaction probability and the temperature of the filament is given in Fig. 4. The mechanism of the reaction will be discussed in the succeeding paper.

6) Roughness factor of the tungsten filament.

TABLE I

Temp. of filament (°K)	Probability of reaction ($k\times1.225$[6])	Press. of water P_0 (mmHg)	Press. of water P (mmHg)
1270	4.5×10^{-5}	8.7×10^{-4}	8.7×10^{-4}
	4.8×10^{-5}	29×10^{-4}	29×10^{-4}
	4.6×10^{-5}	64×10^{-4}	64×10^{-4}
1470	7.9×10^{-4}	8.7×10^{-4}	8.7×10^{-4}
	8.2×10^{-4}	29×10^{-4}	29×10^{-4}
	8.0×10^{-4}	64×10^{-4}	64×10^{-4}
1670	4.2×10^{-3}	8.7×10^{-4}	8.4×10^{-4}
	3.9×10^{-3}	29×10^{-4}	28×10^{-4}
	3.8×10^{-3}	64×10^{-4}	62×10^{-4}
1870	1.1×10^{-2}	8.7×10^{-4}	7.9×10^{-4}
	1.2×10^{-2}	29×10^{-4}	26×10^{-4}
	1.1×10^{-2}	64×10^{-4}	58×10^{-4}

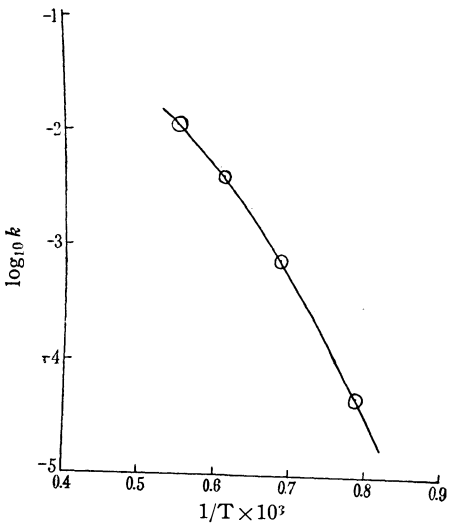

Fig. 4. Effect of the filament temperature on the reaction probability.

We wish to express our sincere thanks to Professor K. Kodera of Kyoto Technical University for his kind discussion and encouragement.

Department of Chemistry, Faculty of Industrial Art, Kyoto Technical University, Kyoto

Interaction between Surface Active Agents and Proteins. II. Electrophoretic Investigation of the System Sodium Dodecyl Sulfate and Egg Albumin

By Koichiro AOKI*

(Received August 12, 1955)

Introduction

Precipitation occurs when the anionic detergent and the protein are mixed at a lower pH than that of the isoelectric point of the protein, and no precipitation occurs when they are mixed at a higher pH than that of the isoelectric point of the protein. In the latter case a transparent solution is obtained, so we cannot confirm whether or not they react, merely from the appearance of the solution when mixed. It is known by the electrophoretic investigation, however, that the complex is formed in the solution. Lundgren et al.[1] proved the existence of the complex in the system alkylbenzenesulfonate-egg albumin, and Putnam and Neurath[2] proved the existence of the complex in the system sodium dodecyl sulfate-horse serum albumin. Further, Yang and Foster[3] studied the interaction between sodium dodecylbenzenesulfonate and egg albumin, and also between this detergent and bovine serum albumin by both the electrophoretic method and the dialysis equilibrium method, holding a different opinion on the behavoir of serum albumin toward detergent from that of Putnam and Neurath.

We discussed in Part I[4] the precipitation reaction which occurred when sodium dodecyl sulfate and egg albumin were mixed at a lower pH than that of the isoelectric point of the protein. No electrophoretic investigation has yet been made on the interaction between sodium dodecyl sulfate (SDS) and egg albumin on the alkaline side of the isoelectric point of the protein. For this reason we investigated this interaction electrophoretically at various pH's and the results obtained are discussed.

* Present temporary address: Department of chemistry, Purdue University, Lafayette, Indiana, U.S.A.

1) H.P. Lundgren, D.W. Elam and R. A. O'Connell, *J. Biol. Chem.*, **149**, 183 (1943); H.P. Lundgren and R.A. O'Connell, *Ind. Eng. Chem. Ind. Ed.*, **36**, 370 (1944).

2) F.W. Putnam and H. Neurath, *J. Biol. Chem.*, **159**, 195 (1945).

3) J.T. Yang and J.F. Foster, *J. Am. Chem. Soc.*, **75**, 5560 (1953).

4) K. Aoki and J. Hori, This bulletin, **29**, 104 (1956).

Experimental

SDS and egg albumin used were prepared by the same method as described in Part I.

We used Hitachi's electrophoretic apparatus equipped with the Schlieren diagonal system. The size of the cell for electrophoresis is $2\times15\times40$ mm. All experiments were carried out in a thermostat at 25 ± 0.01°C.

We prepared and electrophoretically analyzed a series of samples, the weight mixing ratio of which varied, while the sum of the concentration of SDS and that of egg albumin was kept constant at 1.0%. In the same way an electrophoretic study was made on samples the total concentration of which was 0.5%. The ionic strength (μ) of all the buffer solutions used was 0.1. The value of pH and composition of buffer solutions are as follows. No dialysis of the sample was

pH	Composition
5.4	sodium acetate and hydrochloric acid
6.8	sodium monohydrogenphosphate and sodium dihydrogenphosphate
7.6	〃 〃
9.6	〃 〃
9.9	sodium carbonate and sodium bicarbonate
10.8	〃 〃 〃 〃

carried out before electrophoresis, because we found that a small quantity of SDS was dialysed through the membrane into the outer solution and that the composition of egg albumin to SDS was slightly changed during the dialysis.

Results

Fig. 1 shows typical electrophoretic patterns. Fig. 2 shows the mobilities of components calculated from the distance of migration on the descending side. We can decide from this figure that the two components existing in the region of albumin excess are egg albumin and complex, and that the two components in the region of SDS excess are complex and SDS.

We can calculate the number of positive and negative charges on one egg albumin molecule. Curve A in Fig. 4 shows the numbers of positive charges on one egg albumin molecule at each pH.

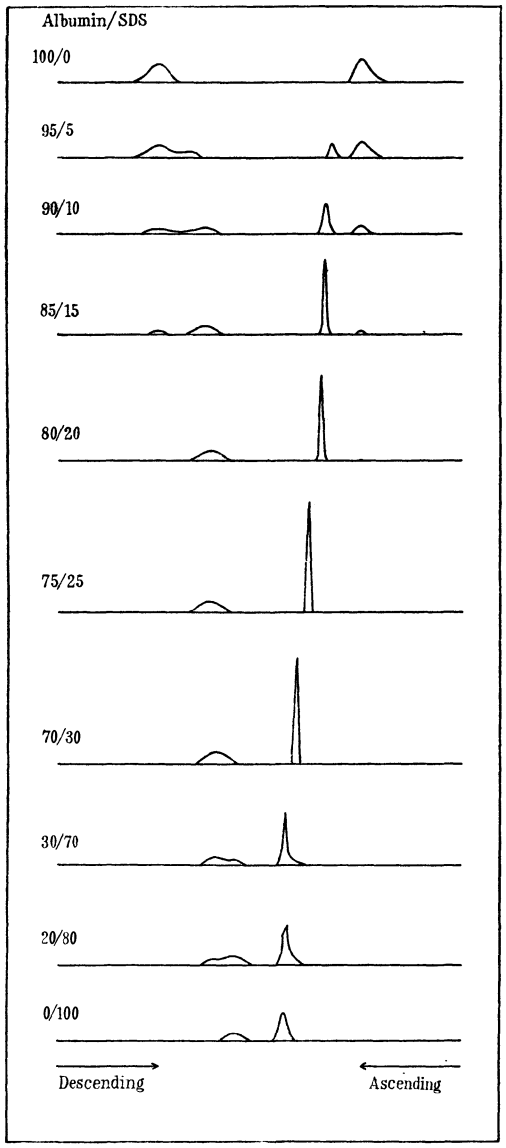

Fig. 1. Electrophoretic patterns of the system sodium dodecyl sulfate–egg albumin at pH 6.8 and ionic strength 0.1. Total concentration is 1.0%.

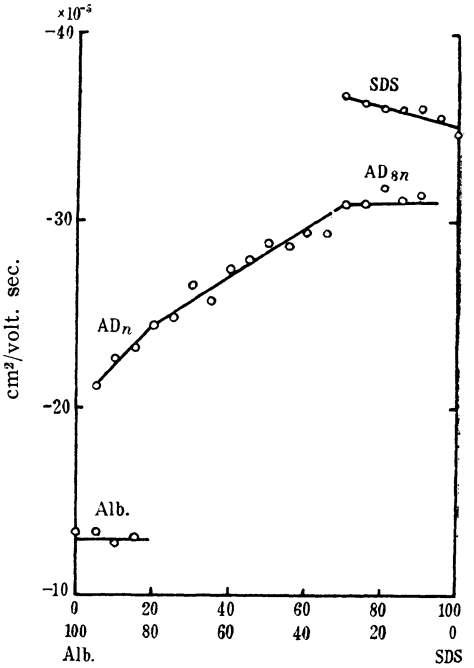

Fig. 2. Electrophoretic mobilities of components in the sodium dodecyl sulfate–egg albumin system.

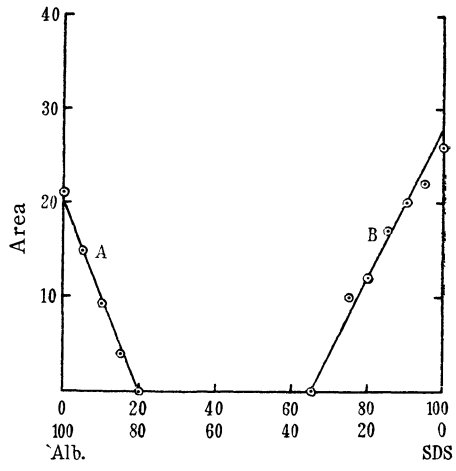

Fig. 3. A: Relation between the area of egg albumin boundary (in arbitrary unit) and the mixing ratio. B: Relation between the area of SDS boundary (in arbitrary unit) and the mixing ratio.

Discussion

Electrophoretic Patterns at pH 6.8.—Electrophoretic patterns obtained can be divided into the following three groups.

The first group comprises the patterns obtained when the mixing ratio albumin/SDS is between 100/0 and 80/20, each pattern having two components, i.e., albumin and complex. With the change of the mixing ratio albumin/SDS, the area of the complex boundary in the pattern increases and that of egg albumin boundary decreases. The electrophoretic pattern on the mixture of albumin/SDS ratio of 80/20 shows merely a trace of the albumin boundary. In Fig. 3, the relation between the composition and the area of albumin boundary is shown. From the slope of the straight line A and the value of 46000 and 288 for the molecular weight of egg albumin and SDS respectively, we can calculate and confirm the fact that about 40 molecules of SDS are bound to one

molecule of egg albumin. In other words, when the mixing ratio albumin/SDS is between 100/0 and 80/20, the composition of the complex is constant and has the formula AD_{40} (A: albumin, D: detergent). We can find that 46 detergent molecules are bound to one egg albumin molecule at pH 6.5, if we use the data given by Lundgren et al. for the electrophoretic experiment on the system alkylbenzenesulfonate-egg albumin[1]. Yang and Foster[3] studied the interaction between sodium dodecylbenzenesulfonate and egg albumin, and found that 43 detergent molecules were bound to one egg albumin molecule at pH 7.6. Further, as described before, we found that about 40 molecules of SDS were bound to one egg albumin molecule at pH 4.2, a lower pH than that of the isoelectric point of egg albumin. Thus, the number of detergent molecules which are bound to one egg albumin molecule seems to be nearly the same for all cases.

As seen in curve A in Fig. 4, the number of positive charges of one egg albumin molecule at pH 6.8 is 38. We found that the composition of the complex first formed was AD_{40}, and this number 40 is almost equal to the number of positive charges on one egg albumin molecule at pH 6.8. Therefore we can assume that the complex is formed through the electrostatic attraction between one negative charge of dodecyl sulfate ion and one of the positive charges on egg albumin molecule.

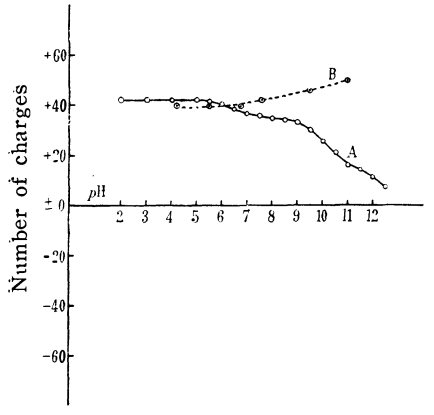

Fig. 4. A: Number of positive charges on one egg albumin molecule at each pH. B: Number of SDS bound to one molecule of egg albumin.

The second group of patterns are obtained when the mixing ratio albumin/SDS is between 80/20 and 35/65. All patterns of this group have only one complex. The mobility of the complex changes continuously with the mixing ratio, so we can assume that the composition of this complex changes continuously with the mixing ratio. As pointed out before, the composition of the complex at the point albumin/SDS=80/20 is AD_n (n=40). The composition of the complex formed at the point albumin/SDS=35/65 is AD_{8n}. It is our opinion that the composition of the complex changes continuously after the formation of AD_n to the completion of AD_{8n}.

The thired group of patterns are obtained when the mixing ratio albumin/SDS is between 35/65 and 0/100. In this region, the patterns have two components, i. e., complex and SDS, and the mobilities of both components are constant, independent of the mixing ratio. Thus, in the region of SDS excess, the mobility of the complex is constant and an unreacted SDS boundary appears. This means that the range of composition of the complex is limited. The line B in Fig. 3 shows the relation between the area of SDS boundary and the mixing ratio. The composition of the complex coexisting with unreacted SDS is found to be AD_{8n} in the same manner as described in the preceding section.

It may be added that our division of the electrophoretic patterns of the syetem SDS-egg albumin is not the same as that presented by Putnam and Neurath for the system SDS-horse serum albumin.

In the case of solutions in which the total concentration was 0.5%, the electrophoretic results were almost the same as those obtained with solutions of total concentration 1.0%.

Curve A in Fig. 5 shows the relation between the relative viscosity (value compared

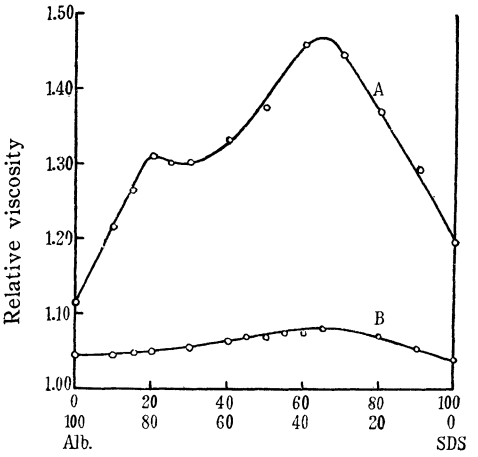

Fig. 5. Relative viscosity, compared to the buffer solution, of the system egg albumin-SDS at pH 6.8 and ionic strength 0.1. A: Total concentration 4.0%. B: Total concentration 1.0%. 25±0.01°C.

with that of the buffer solution) and the mixing ratio, the total concentration being kept at 4.0%. We can see that there are two maxima at points where albumin/SDS=80/20 and 35/65.

The compositions at these maxima are equal to those which divide the electrophoretic results into three groups.

Electrophoretic Patterns at Various pH's.—Similar experiments as above were carried out at a total concentration 1.0%, and at pH 5.4, 7.6, 9.6, 9.9 and 10.8.

At each pH the electrophoretic patterns change with the mixing ratio in a similar manner as when pH is 6.8, but in the region of albumin excess, there is a slight change in values of the mixing ratio at which the albumin boundary disappears. The number of SDS molecule bound to one molecule of egg albumin at this mixing ratio increases from 40 to about 50 with the increase of pH. Curve B in Fig. 4 shows the relation between pH and the number of bound SDS to one egg albumin molecule.

Comparing curves A and B in Fig. 4, we can see that below pH 7 the number of positive charges of one egg albumin is almost equal to the number of SDS molecules which are bound to one egg albumin molecule. In this region it is possible to assume that one positive charge on egg albumin and one negative detergent ion combine electrostatically as described above, but when pH is above 7 this relation cannot hold. The cause of this is not made clear in this study alone. In the experiment at different pH from 6.8, in the region of SDS excess, SDS boundary disappears when the mixing ratio albumin/SDS is between 35/65 and 30/70.

Mechanism of the Combination of Egg Albumin and SDS.—Now we compare the next two electrophoretic patterns with each other: the one obtained on the sample pH 6.8, μ 0.1, albumin/SDS=95/5 and the total concentration 1.0%, and the other pH 6.8, μ 0.1, albumin/SDS=95/5 and the total concentration 0.5%. We can find that the shapes of the patterns are identical, although the areas covered by the corresponding boundaries are unequal. In addition, as seen in Fig. 5a in Part I[4], the CMC of SDS is 0.04% (0.0013 mol./1.) when the ionic strength is 0.1, so that in the first sample the micellar SDS exists, but in the second sample SDS exists as a single ion not forming a micelle. Considering these facts we can find in the reaction between egg albumin and SDS that it is not reasonable to assume that SDS reacts only in a micellar form, and that it is reasonable to assume that a single ion, not forming a micelle, can react.

Summary

We studied electrophoretically the interaction of SDS and egg albumin in the pH range between 5.4 and 10.8, higher pH's than that of the isoelectric point of egg albumin. Results obtained are as follows.

(1) The electrophoretic patterns of the system egg albumin-SDS can be divided into three groups. This method of division is different from that in the system SDS-horse serum albumin by Putnam and Neurath. The first group of the division contains the patterns obtained when the mixing ratio albumin/SDS is between 100/0 and 80/20, and here the complex AD_n (n=40, A: albumin, D: detergent) and egg albumin coexist. The second group contains the patterns obtained when the mixing ratio albumin/SDS is between 80/20 and 35/65 and in this region the composition of the complex changes continuously from AD_n to AD_{8n}. The third region appears when the mixing ratio albumin/SDS is between 35/65 and 0/100 and here the complex AD_{8n} and SDS coexist. The above mixing ratio values are obtained at pH 6.8, and they change somewhat as a function of pH.

(2) Below pH 7, a number n of the first complex AD_n equals the number of positive charges on one egg albumin, but above pH 7, this relation cannot hold.

(3) In the reaction between egg albumin and SDS, it is not assumed that SDS reacts only in a micellar form but that SDS existing as a single ion can react.

The author is sincerely greateful to Professor Rempei Goto of the Institute for Chemical Research, Kyoto University for his kind guidance during this study.

Chemical Laboratory, Nagoya City University, Nagoya

On the Base Strength of Some Nitrogen Heterocycles in the Excited State

By Noboru MATAGA, Yozo KAIFU and Masao KOIZUMI

(Received October 27, 1955)

Introduction

Some properties of a molecule such as basicity and acidity or its ability of dydrogen bonding etc., depend in general upon its electronic structure. Therefore, it may be expected that the above-mentioned properties in the excited electronic state are different as compared with the ground electronic state, and we really have such examples.

Th. Förster and A. Weller[1,2] have investigated the ionization tendency of naphthols, aminopyrene derivatives, etc. in their excited electronic states by measuring the fluorescene spectra and fluorescene intensities and confirmed that the degree of dissociation in the excited state is far greater than that in the ground state. Hence these compounds can be said to have a greater acidity in the excited state than in the ground state. As for hydrogen bonding, the present authors[3] have measured the absorption and fluorescence spectra and fluorescene intensities of *n*-hexane solutions of naphthols with addition of various proton acceptors, and found that the excited naphthols have a greater tendency to form hydrogen bond and that a new equilibrium is reached during the lifetime of the excited state.

Now in order to compare the basicity of a molecule in the ground and excited state, same nitrogen heterocycles such as quinoline, acridine and 2,8-diaminoacridine were chosen and their fluorescene and absorption spectra were measured over a wide pH range. In addition their spectra and fluorescene intensities in various organic solvents were compared. The present paper reports the results obtained with some discussions about the electronic structures of these molecules.

Experimental

Apparatus.—Fluorescene spectra were taken with Hilger E_2 type quartz spectrograph and small type glass prism spectrograph. For the excitation of fluorescene spectra, a high-pressure mercury lamp was used with appropriate filters for each samples.

Filters: for quinoline, K_2CrO_3 aq. solution (0.2 g./l.) which takes out 310 mμ line.

for acridine, Matsuda color filter UV-DI which takes out 360 mμ line.

for 2,8-diaminoacridine, Matsuda color filter UV-DI, which takes out 360 mμ or VC-I and IR-OI which together take out 405 and 435 mμ lines.

For the measurement of absorption spectra in solution, Beckman spectrophotometer model DU was used.

The apparatus used for the measurement of fluorescence intensity was the same as described elsewhere.* In the case of quinoline, the filters used were the same as before*, and in the case of acridine, Matsuda color filter UV-DI was used for exciting light and the solution of acridine in *n*-hexane, ca. 10^{-3} mol./l., was used as a filter for the fluorescent light.

Reagent.—Extra pure grade quinoline was dried over K_2CO_3 and distilled under the atmosphere of dry nitrogen before use.

Chemical pure grade acridine was recrystallized from alcohol.

A synthesized and purified sample of 2,8-diaminoacridine was kindly supplied by Mr. T. Tokuyama of this institute.

For the pH control of aqueous solution, citrate-phosphate-borate buffer was used. The reagents were of extra pure grade, and were used without further purification.

n-Hexane, CH_3CO_2Bu and CCl_4 were the same samples as described elswhere*. Extra pure grade benzene was recrystallized and distilled. Ethanol used was 99% in purity.

Extra pure grade *n*-butanol and pyridine were used without further purification.

Experimental Results

a) Dependence of the Absorption and Fluorescence on the Hydrogen Ion Concentration in Aqueous Solution

The absorption spectra of quinoline in aqueous solution of various pH values are shown in Fig. 2.

Quinoline being isoelectronic with naphthalene, its absorption spectrum is similar to that of the latter, with three absorption regions in the near ultraviolet; 295–320 mμ (band I), 250–295 mμ (band II) and the region

1) Th. Förster, *Z. Elektrochem.*, **54**, 42, 531 (1950).
2) A. Weller, *Z. Elektrochem.*, **56**, 662 (1952); *Z. physikal. Chem. N.F.*, 3, 238 (1955).
3) N. Mataga, Y. Kaifu and M. Koizumi; *Nature*, **175**, 731 (1955).

* N. Mataga, Y. Kaifu and M. Koizumi; to be published in this Bulletin.

near 220 mμ (band III). The absorption spectra in the pH range <1.4 and >8 coincide with the curve (1) and (6) respectively, and between ca. pH=7 and 2, they gradually change with isosbestic point at ca. 290 mμ. Therefore this spectral change can be attributed to the change of the concentration of free quinoline (A) and quinolinium ion (AH^+), according to the equilibrium relation $A+H^+ \rightleftarrows AH^+$. pK value is easily obtained from the inspection of these changes, and is depicted in Fig. 1 as a pH value at which $[A]=[AH^+]$.

It is seen from Fig. 2 that in A the intensity of band I is rather smaller than that of band II, while in AH^+, the former becomes far greater, and the latter is diminished. It is noteworthy that λ_{max} of band I remains constant throughout the whole change, though in AH^+ there appears a slight hump in the neighbourhood of 330 mμ. The fluorescene spectrum shifts from 305–350 mμ band of A to 340–440 mμ band of AH^+ as indicated in Table I, but the change occurs at larger pH value compared with that of absorption spectrum. The line depicted in Fig. 1 is the pH value at about the middle point of the region in which the spectral change occurs.

TABLE I

RANGE OF FLUORESCENCE SPECTRA OF A, AH^+, AH_2^{++} AND AH_3^{+++} (in mμ)

	A	AH^+	AH_2^{++}	AH^{3+++}
Quinoline	305–350	340–440	——	——
Acridine	390–500	390–600	——	——
2,8-Diaminoacridine	——	450–610	505–610	420–610

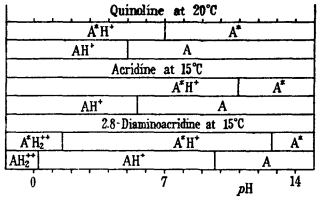

Fig. 1. Shift of the equilibrium in the excited state as revealed by the change of fluorescence and absorption spectra.

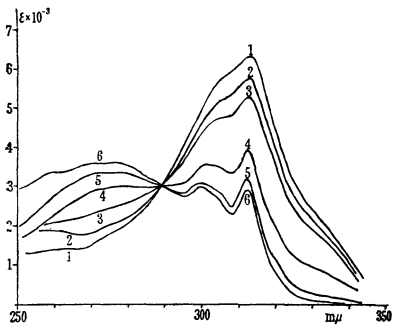

Fig. 2. pH Dependence of the absorption spectrum of quinoline in aqueous solution. at ca. 20°C
concentration of quinoline, 1.08 ×10⁻⁴ mol./l.
pH: 1. 1.42
2. 4.45
3. 4.89
4. 5.59
5. 6.47
6. 8.04

ii) Acridine.—The absorption spectrum of acridine is similar to that of isoelectronic anthracene, and there are 300–400 mμ band (Band I) and the band near 250 mμ (band II)*.

pK value or pH value at which $[A]=[AH^+]$ is ca. 5 as shown in Fig. 3. The intensity of band I is stronger in AH^+ than in A and the position of maximum remains constant throughout the whole pH range. In the acidic solution, a new broad band appears in the region 380–440 mμ, and two isosbestic points are seen at 360 mμ and 377 mμ. λ_{max} of band II (249 mμ) in A shifts to 254 mμ in AH^+ with the intensity somewhat decreased.

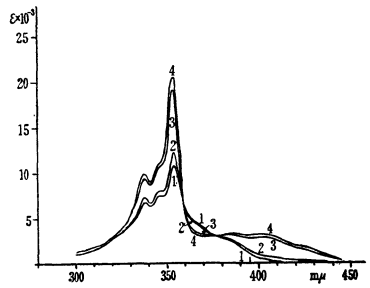

Fig. 3. pH Dependence of the absorption spectrum of acridine in aqueous solution. at ca. 15°C
concentration of acridine, 5.78 ×10⁻⁵ mol./l.
pH: 1. <8.04
2. 6.47
3. 4.88
4. >3.69

The fluorescence spectrum are shown in Fig. 4. At first sight, it appears as if there are two steps of change, i.e. at pH=ca. 10

* The nomenclature in this case is rather conventional.

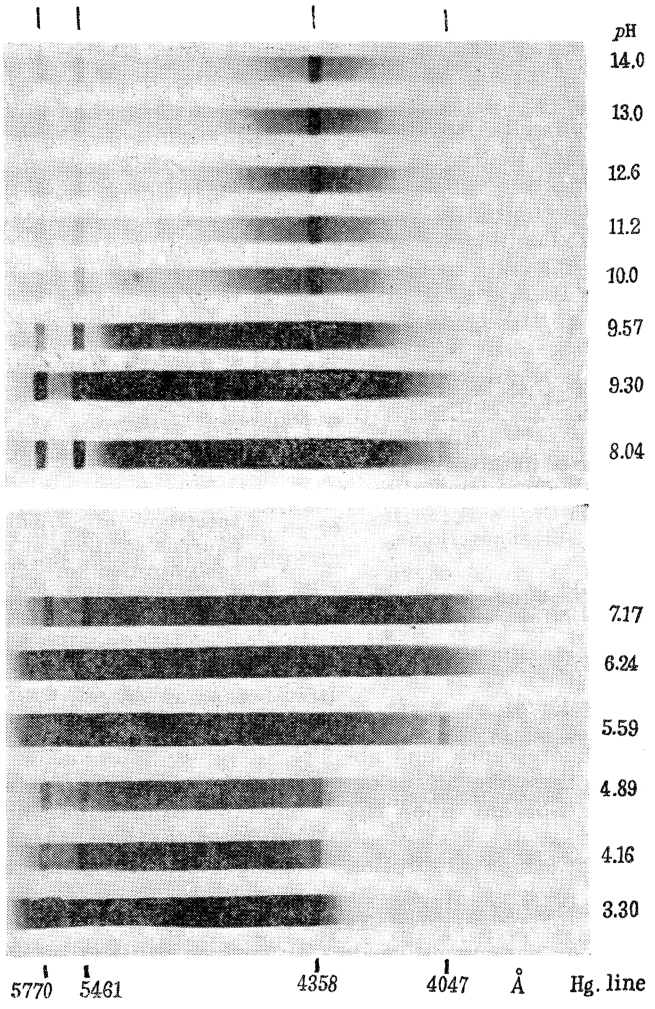

Fig. 4. pH Dependence of the fluorescence spectrum of acridine in aqueous solution, at ca. 15°C.

and pH=ca. 5. But the latter change is most probably attributed to the reabsorption of fluorescence by 380–440 mμ band, which is prominent when pH<5. It seems that the change of colour in the fluorescence of acridine cited in Pringsheims' book[4] corresponds to this apparent change. There scarcely remains any doubt that the real change of fluorescence spectrum occurs at far greater pH value compared with that of absorption spectrum.

iii) 2, 8-Diaminoacridine.—This molecule has three nitrogen atoms each of which may act as a proton acceptor. Accordingly, the spectral changes seem to occur in three stages. As indicated by Craig et al.[5], the first proton may attach to the ring nitrogen. In this first stage, the spectrum shows a marked change as shown in Fig. 5a. The spectrum shifts to longer wave length from λ_{max}=395 mμ to λ_{max}=443 mμ with the isosbestic point at 410 mμ, and the absorption intensity increase remarkably.

The change of fluorescence spectrum in the first stage occurs at far greater pH value than that of absorption spectrum as shown in Fig. 1. The two succeeding stages are not so clear-cut as the first one, but the following features may be observed from Fig. 5b. In the second stage, there appear two peaks at 455 mμ and 360 mμ with two isosbestic points at 470 mμ and 370 mμ, and the change of fluorescence spectrum occurs at larger pH value. In the third stage the band at 360 mμ and 455 mμ decline and a new band appears at 350 mμ. In this case,

4) P. Pringsheim, "Fluorescence and Phosphorescence" Interscience Publishers Inc., 1949, p. 416.

5) D.P. Craig and L.N. Short, *J. Chem. Soc.*, **1945**, 419.

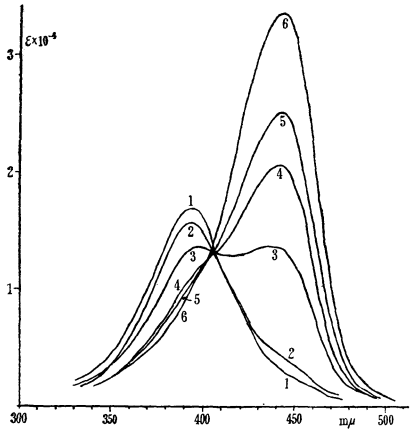

Fig 5a. pH Dependence of the absorption spectrum of 2, 8-diaminoacridine in aqueous solution, at 15°C
concentration of 2, 8-diaminoacridine, 1.28×10^{-5} mol./l.
pH: 1. 13~12
2. 11.24
3. 10.06
4. 9.57
5. 9.30
6. 4.89~1.92

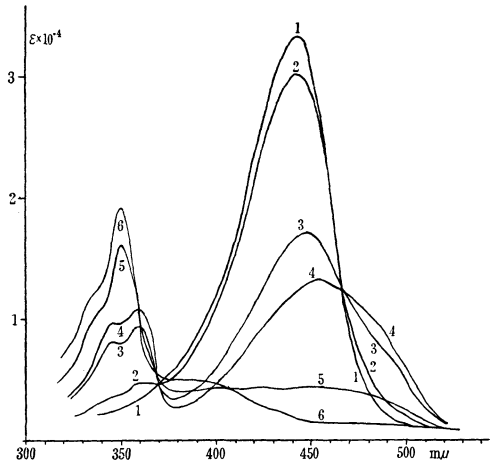

Fig. 5b. pH Dependence of the absorption spectrum of 2, 8-diaminoacridine in aqueous solution, at ca. 15°C
concentration of 2, 8 diaminoacridine, 1.28×10^{-5} mol./l.
1. pH 1.925
2. pH 1.038
3. pH O.
4. 3.6 N H_2SO_4
5. 12.6 N H_2SO_4
6. 18 N H_2SO_4

the spectral change of fluorescence and absorption occur almost at the same pH value.

b) Effect of Organic Solvent upon the Spectrum

In Table II the variations of absorption spectra in several solvents are indicated. When the solvent molecule increases in its proton-donating power from *n*-hexane to ethanol, band I grows and band II declines regularly in the case of quinoline, and in the case of acridine 373 mμ band becomes broader and the band edge shifts to longer wave length also in a regular manner. These changes conform completely to the already mentioned changes induced by the proton addition. Thus the parallelism exists between the spectral change induced by proton addition and that induced by the hydrogen bonding.

TABLE II

CHANGE OF ABSORPTION SPECTRA IN SEVERAL ORGANIC SOLVENTS

Quinoline

Solvent		*n*-Hexane	CCl_4	CH_3CO_2Bu	BuOH	EtOH
Extinction coeff. of abs. max. ($\times10^3$)	band I	2.1	2.3	2.1	2.8	3.0
	band II	3.6	4.1	3.6	3.4	3.3

Acridine

Solvent	*n*-Hexane	Benzene	Pyridine	BuOH	EtOH
Edge of the longest wave length band	392	393	395 (in mμ)	397	402

TABLE III

EFFECT OF SOLVENT ON THE FLUORESCENCE INTENSITY

Solvent	*n*-Hexane	Benzene	BuOH	EtOH	H_2O
Quinoline	$\lesssim10^{-3}$	$\sim10^{-3}$	$\sim3\times10^{-2}$	$\sim3\times10^{-2}$	~1.0 (pH 4.79)*
Acridine	——§	$\sim10^{-3}$	$\sim2\times10^{-2}$	$\sim3\times10^{-2}$	~1.0 (pH 6.30)*

* pH was not controlled by buffer, and measured by glass electrode pH meter.
§ Fluorescence was not detectable with our apparatus.

c) Effect of Solvent upon the Fluorescence Intensity

In Table III the relative yield of fluorescence in quinoline and acridine are given. The data in this Table were determined in the following way. When the concentration of a fluorescer is very small, the relation $I_f=\varepsilon c\Phi I_0$ must hold, where,

I_f ; Fluorescence intensity
Φ ; Quantum yield of fluorescence
ε ; Extinction coefficient at the exciting wave length
c ; Concentration of fluorescer
I_0 ; Intensity of exciting light

Hence when I_0 is constant, the relative yield is easily calculated from $\Phi'/\Phi=I'_f\varepsilon c/I_f\varepsilon' c'$.

As seen from Table III, the fluorescence yields in the solvents such as *n*-hexane and benzene which are not able to make hydrogen bond with nitrogen heterocycles, are only 10% or smaller compared with those in the solvents such as BuOH or EtOH.

The fluorescence intensity of AH^+ in aqueous solution can not be compared with those data, because the spectral range of fluorescence is considerably different (For quinoline, in *n*-hexane; 305–350 mμ, in EtOH; 305–370 mμ against 340–440 mμ of AH^+. For acridine in EtOH; 360–480 mμ against 450–610 mμ of AH^+) and the exact calibration of the wave length sensitivity of the phototube was not undertaken. It is certain, however that the sensitivity falls with the increase of wave length*, and if one takes this into account, the fluorescence yield of AH^+ is expected to be far greater than the fluorescence yield of A in organic solvents. In the case of 2, 8-diaminoacridine, however, fairly strong fluorescence is observed even in the non-polar solvent such as benzene, and the hydrogen bond formation or proton addition is not necessarily indispensable for the fluorescent transition.

Discussion

I. The Increase of the Basicity in the Excited State

It can be concluded from the experimental results, that in these nitrogen heterocycles the excited electronic structure is more liable to proton addition than the ground state electronic structure. Thus the stabilization energy by proton addition is larger in the excited state than in the ground state. As Förster and his collaborators have confirmed, naphthols and some other compounds have greater acidity in the excited state, while in the present investigation, it has been confirmed that N-heterocycles have larger basicity in the excited state. Both effects will most certainly be attributed to the increase of polarity in the excited state. In the case of naphthol, for example, the migration of lone pair electrons of oxygen atom to the ring is larger in the excited state, the result of which makes the oxygen atom more repulsive toward proton. Nitrogen atom in the heterocycles on the contrary, will become more negative in the excited state and this makes the excited state more attractive toward proton.

The increase of electronegativity of N atom in the latter case will be interpreted in various ways but here the problem will be discussed on the basis of the electronic structures of cata-condensed hydrocarbons which are isoelectronic to their aza derivatives.

The so-called cata-condensed hydrocarbons generally exhibit three main band systems in the near ultraviolet or visible region of the spectrum. The prototypes of all these systems are to be found in benzene, which shows a weak band system in the 2500 Å region, exhibits absorption of moderate intensity around 2000 Å, and absorbs strongly near 1750 Å. Band systems of a similar type also occur for the higher homologs. According to Moffitt's notation[6], these are N→V, N→U and N→Y transitions, respectively. Among these, N→Y transition corresponds to the so-called "intramolecular charge transfer spectrum" of Mulliken[7]. From the standpoint of VB method, Y state is mainly contributed by ionic structures.

Now in the case of inductive substitution such as the replacement of —CH= by —N=, the effect of this perturbation is to mix the unperturbed V state to which transition from the ground state is virtually forbidden, with some contribution from Y state to which transition is strongly allowed. The result is that the partial transfer of intensity from N→Y transition to N→V transition occurs as is actually confirmed by the comparison of the absorption spectra of N-heterocycles and of their isoelectronic cata-condensed hydrocarbons. V state thus acquires considerable ionic character with negative charge at nitrogen atom, and this is the reason why the interaction energy with proton is larger in the excited state than in the ground state.

The intensification of the spectrum in the acidic region as observed in acridine, may

* The phototube used is ultraviolet sensitive one.

6) W. Moffitt, *J. Chem. Phys.*, 22, 320 (1954).
7) R. S. Mulliken, *J. Chem. Phys.*, 7, 20, 353 (1939).

be attributed to the further increase of such a polar structure since the electronegativity of N becomes larger by the attachment of a proton. But the conspicuous change of spectra in the case of quinoline and 2,8-diaminoacridine can not yet be interpreted.*

II. Solvent Effect on Fluorescence Intensity

It is almost certain that in the case of acridine and quinoline, the settlement of non-bonding electrons by proton addition or hydrogen bonding increases the fluorescence efficiency. The mechanism may presumably be interpreted in the following way.

In these compounds, $^1\Gamma_{\pi\to\pi^*}$ which is produced directly by the illumination has probably a large tendency of transfer to $^1\Gamma_{n\to\pi^*}$, because the authors have newly found the spectra of quinoline due to $n\to\pi^*$ transition and moreover, their positions are in the neighbourhood of $\pi\to\pi^*$ band (see Appendix).

If $^1\Gamma_{n\to\pi^*}\to{}^1\Gamma_{n\to\pi^*}$ transfer occurs, then it is followed by $^1\Gamma_{n\to\pi^*}\to{}^3\Gamma_{n\to\pi^*}$ with considerable ease[8]. Then owing to the long life of $^3\Gamma_{n\to\pi^*}$ state, emission is scarcely to be expected. This may be the reason why the fluorescence is not observed in non polar solvents. By proton addition or hydrogen bonding, however, the non-bonding character is lost almost completely or to some extent and the level of $^1\Gamma_{n\to\pi^*}$ state is raised remarkably. Accordingly, it becomes quite difficult for $^1\Gamma_{n\to\pi^*}\to{}^1\Gamma_{n\to\pi^*}$ transition to occur and the result is that the molecule emits more easily.

In the case of 2,8-diaminoacridine, the reasonance interaction between π-electron system and substituent-NH_2, makes $n\to\pi^*$ transition shift to blue, while $\pi\to\pi^*$ transition to red[9]. As the result of this perturbation, $^1\Gamma_{\pi\to^*}\to{}^1\Gamma_{n\to\pi^*}$ transition becomes energetically difficult. This will be the reason why the fluorescence of 2,8-diaminoacridine can be observed even in the non-polar solvent.

Appendix

$n\to\pi^*$ Spectrum of Quinoline Vapor

The absorption spectrum of quinoline vapor was photographed by Hilger E_2 type quartz spectrograph. The quartz absorption cell was 50 cm. in length with a side tube for reserving sample. As a light source an A. C. high voltage hydrogen discharge tube with water cooling was used. The temperature of bath was 90°C and that of absorption cell was 95°C. The slit width was 0.05 mm. and the time of exposure was about 2 min.

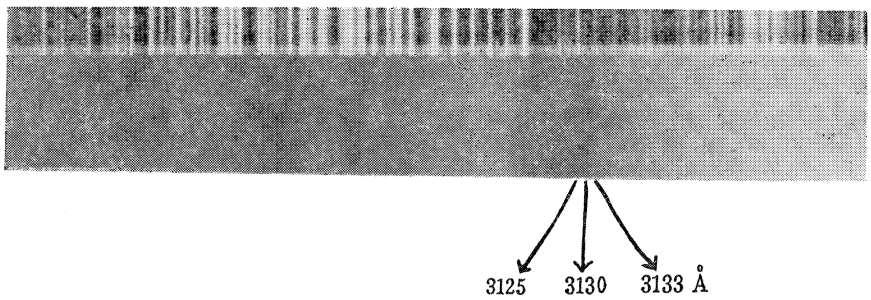

Fig. 6. Absorption spectrum of quinoline vapor.

As seen from Fig. 6, the line spectra at 3125, 3130 and 3133 Å are clearly observed, and these line spectra may most certainly be interpreted as due to the $n\to\pi^*$ transition.

In general, when molecule becomes larger, $\pi\to\pi^*$ transition becomes superposed by strong $\pi\to\pi^*$ transition[10], and moreover the oscillator strength of $n\to\pi$ transition becomes smaller[9]. Hence the observation of $n\to\pi^*$ transition is difficult in larger molecules. In fact the $n\to\pi^*$ transition of pyridine has been reported in literature, while that of quinoline has not been observed as yet, and we really had much difficulty in taking the line spectra in question.

In solution, the $n\to\pi^*$ spectra can never be observed even in n-hexane. It is certain from these line spectra, that $n\to\pi^*$ state of quinoline is nearly at the same energy level with $\pi\to\pi^*$ state.

* Note added in prof:
An alternative interpretations of these spectral changes are as follows. We divide the 300-400 mμ band of acridine into two parts, i.e., 300-370 mμ band (band I) and 370-400 mμ band (band II), and regard these bands as corresponding ones to N→V and N→U band, resqectively. In quinoline, the assignment is; band I←→N→V, band II←→N→U. By proton addition, band II of acridine shifts to red and somewhat strengthened, whereas band I does not shift although it is enhanced. The spectral changes of quinoline are similar to those of acridine, but in the case of quinoline, the shift of band II is very great, and the slight hump near 330 mμ may be attributable to this shifted band II. Moreover, the longest wave length band of 2,8-diaminoacridine may plausibly correspond to N→U transition, shifted to red by resonance interaction with substituent amino groups.

8) M. Kasha, *Discuss. Farad. Soc.*, No. 9, 14 (1950).

9) L. Goodman and H. Shull, *J. Chem. Phys.*, **22**, 1138 (1954).

10) J.R. Platt, *J. Chem. Phys.*, **19**, 101 (1951).

Summary

1. The fluorescence and absorption spectra of aqueous solutions of quinoline, acridine and 2, 8-diaminoacridine were observed at various pH values, and it became clear that the stabilization energy by proton addition is larger in the excited state than in the ground state.

2. The effects of hydrogen bonding and proton addition upon the spectra were confirmed to be the same in tendency.

3. On the basis of the fluorescence intensities in various organic solvents, some discussions were made about the contribution of non-bonding electron to the inner quenching of fluorescence.

4. The vapor spectrum of quinoline was taken and line spectra were observed, which are most certainly attributable to $n \rightarrow \pi^*$ transition.

The Institute of Polytechnics
Osaka City University
Osaka

Geochemical Investigations of Volcanoes in Japan. XXXII. Residual Magmatic Waters in Cavities of Trachyandesitic Basalt in Imari District, Saga Prefecture, Japan*

By Iwaji IWASAKI, Nobuhide KOKUBU and Takashi KATSURA

(Received September 16, 1955)

Introduction

It is of high importance to understand the nature of water and other volatile components in magmas for the study of many important phenomena such as the nature of the primary hot springs, the primary atmosphere, the primary hydrosphere, magmatic differentiation, ore deposits, etc. But our knowledge of the nature of the magmatic substances is very scanty. Although many reports[1] related to the magmatic water have been published, the most part of these works is only the survey of the nature of the magmatic waters and gases. There have been only a few reports[2] on the relation between the real magmatic waters and these geochemical phenomena from the geochemical point of view.

In the previous paper[3] one of the present authors (Iwasaki) has given the definition of the real magmatic state that we can see on the surface of the Earth's crust, and in the present paper this definition described in the following paragraph was also adopted.

The real magmatic state near the surface of the Earth's crust can be defined as natural molten state of the rock-forming material such as molten lavas at lava lake of Volcano Kilauea in Hawaii and Volcano Mihara, Oo-sima, Idu in Japan[3]. Substances derived directly from these rock-forming materials in the real magmatic state can be called the magmetic substances, and the waters derived directly from these magmatic substances can be also called the magmatic waters. By this definition, the waters contained in these natural rock-forming minerals of igneous rocks are no doubt magmatic, but all of them are not always juvenile, because the molten rock-forming material may come from the resulting substances, some of which can be already solidified on the surface of the Earth before the introduction of them into the magmatic chemical system by remelting, assimilation or migmatization.

According to the theory of the magmatic

* XXXI; *J. Chem. Soc. Japan*, **76**, 1116 (1955).

1) H. Davy, *Phil. Trans.*, II, 367 (1822); *Ann, Chim. et Phys.*, **21**, 132 (1822); D. Brewster, *Trans. Roy. Soc. Edinburgh*, **10**, 1 (1826); R.T. Simmler, Pogg. *Ann.*, **105**, 460 (1858); H.C. Sorby, *Geol. Soc. London Quart. Journ.*, **14**, 453 (1858); A.W. Wright, *Am. J. Sci.*, **21**, 209 (1881); W. Ramsay, *Proc. Roy. Soc.*, **58**, 65 (1895); A. Gautier, *Compt. rend.*, **132**, 58, 189 (1901); *Econ. Geol.*, **1**, 688 (1906); R.T. Chemberlin, "The Gases in Rocks", (1908); A. Brun, "Recherches sur L'Exhalaison Volcanique", (1911); A. L. Day and E. S. Shepherd, *Bull. Geol. Soc. Am.*, **24**, 573 (1913); E.S. Shepherd, *Am. J. Sci.*, **35** A, 311 (1938); J. Jaggar, ibid., **238**, 313 (1940); E.F. Holden, *Am. Mineralogist*, **10**, 203 (1925); W.H. Newhous, *Econ. Geol.*, **27**, 419 (1932); **28**, 744 (1933); S.T. Yuster, *Am. J. Sci.*, 5 ser. **31**, 363 (1936); E. Ingerson, *Am. Mineralogist*, **32**, 375 (1947); P.A. Peach, ibid., **34**, 413 (1949); H.S. Scott, *Econ. Geol.*, **43**, 637 (1948).

2) S. Tsuboi, K. Sugawara and S. Oana, *Science* (*Kagaku*), **14**, 102 (1944); K. Sugawara, S. Oana and T. Koyama, *Proc. Imp. Acad. Tokyo*, **20**, No. 10, 721 (1944); *Proc. Japan Acad.*, **25**, No. 3, 103 (1949).

3) I. Iwasaki, *Journ. of Geography* (Japan), **60**, 140 (1951).

differentiation by N. L. Bowen[4] and V. M. Goldschmidt[5], along with lowering of temperature fractional crystallizations of magmas take place with a separation of solids and mother liquors or residual magmas, and the aqueous magmatic solutions derived from the volatile components of magmas will remain when most of the parts of rock-forming silicate minerals have crystallized out from the magmas and the temperature of the residual magmas is lowered below the critical point of water (374.3°C, 217.7 atm.). These aqueous magmatic solutions which remained in the cavities of igneous rocks and rock-forming minerals as liquid inclusions, etc. can be called the residual magmatic water.

From these points of view the present authors have distinguished the magmatic waters obtained directly from the molten magmatic substances such as molten lavas from the residual magmatic waters which remained in the cavities of their mother *igneous rocks and minerals. In the present* paper some of the results obtained on the residual magmatic waters from trachyandesitic basalt in Imari district which has been found by K. Muta, Geological Institute, Faculty of Engineering, Kyushu University, in 1948, and the related problems are reported.

line, Kuhara, Saga Prefecture as shown in Fig. 1. These rocks have higher alkali contents than the volcanic rocks in the Fuji Volcanic Zone as will be seen in Table I, and lots of amygdaloidal cavities, some of which are filled with mineral substances mainly carbonate and silicate minerals; some are empty and some have mineral substances and aqueous solutions.

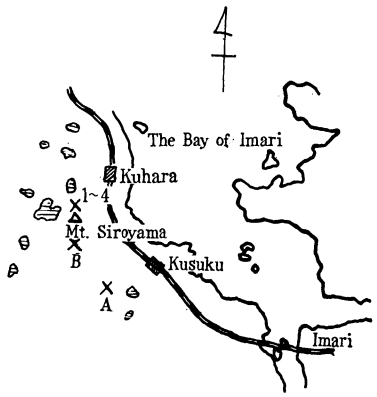

Fig. 1. Locality map.

TABLE I

CHEMICAL COMPOSITION OF VOLCANIC ROCKS FROM IMARI DISTRICT, NAGAHAMA, HAMADA-SI, SIMANE PREFECTURE AND THE FUJI VOLCANIC ZONE

	Imari District				Hamada Nephline-basalt	Fuji Volcanic Zone	
	No. 1	No. 2	No. 3	No. 4			
SiO_2	48.87	50.46	54.90	56.17	34.98	49.60	54.66
TiO_2	1.24	2.12	1.94	1.00	2.39	1.40	1.10
Al_2O_3	16.00	18.41	17.38	16.83	11.18	16.96	17.91
Fe_2O_3	5.52	2.10	1.35	1.62	5.99	5.40	1.92
FeO	5.16	7.08	5.66	5.43	8.83	6.65	6.26
MnO	0.21	0.29	0.15	0.14	0.26	0.21	0.18
MgO	8.66	4.03	4.46	2.83	8.36	5.92	5.45
CaO	8.97	7.11	7.25	6.98	13.52	10.03	8.42
Na_2O	2.75	3.35	3.04	4.18	4.22	2.48	2.89
K_2O	0.86	1.28	0.84	1.17	3.99	0.58	0.42
H_2O	2.04	3.70	2.63	4.55	3.63	0.62	1.04
P_2O_5	n.d.	n.d.	n.d.	n.d.	2.53	0.20	0.10
S	n.d.	n.d.	n.d.	n.d.	0.10	n.d.	n.d.
Cl	0.015	n.d.	0.012	0.029	0.013	n.d.	0.010
Total	100.29	99.93	99.71	100.93	100.01	100.05	100.49

Occurrence and the Nature of Mother Rocks and their Cavities

The trachyandesitic basalts in question are distributed in hill country running close to the south of a railway-station of the Matuura-

According to Dr. H. Kuno, Geological Institute, Faculty of Science, Tokyo University, these trachyandesitic basalts have intergranular texture and holocrystalline structure, and a relatively small amount of phenocrysts (olivine, titaniferous augite, etc.) in the groundmass, in which labradorite, potash-andesine, olivine and augite are seen. And also in the druses of these rocks, calcite, aragonite, siderite and ankerite are seen.

These rocks show a remarkably heterogeneous appearance; for instance in some

4) N.L. Bowen., "The Evolution of the Igneous Rocks", (1928).

5) V.M. Goldschmidt, *Z. Elektrochem.*, 28, 411 (1922).

parts of the mother rocks many cavities are clustered, but few cavities in the other parts. The size of these cavities varies from extremely small to about 10 cm. long, and these cavities are irregularly distributed in their mother rocks. There seems to be no remarkable regularity among their distribution of their sizes, number and inclusions (minerals, solutions and gases). The nature of these cavities in their mother rocks from Imari district closely resembles that of nepheline-basalts from Nagahama, Hamada-si Simane Prefecture, but there are some distinct differences between the properties of these two volcanic rocks. The cavities of nepheline-basalt are lined by zeolite (often bearing a smaller amount of calcite crystals), and the great part of larger cavities have irregularly angular form. On the other hand the forms of the cavities in trachyandesitic basalts are smoothly amygdaloidal, and in them the carbonate minerals such as calcite, aragonite and siderite are remarkably abundant. From the facts mentioned above, it seems that the rocks in Imari district have not been subjected to so large a pressure that their amygdaloidal cavities had changed their forms during their solidification as in the case of nepheline-basalt from Nagahama district, and are, therefore, more suitable to be used in the study of the nature of the magmatic substances.

The locations from which the samples for the chemical analysis were collected, are also shown in Fig. 1. The chemical compositions of the minerals co-existing with magmatic waters in the cavities are also shown in Table II. For example, one of the modes of occurence of these minerals is shown in Fig. 2. The number in Fig. 2. is the same as Table II.

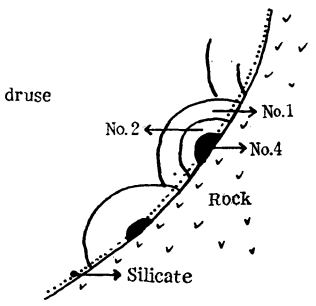

Fig. 2. The mode of occurrence of these minerals in the cavities of rocks.

Chemical Composition of the Residual Magmatic Solutions

Although it has already been found by Sugawara et al.[2] that each chemical composition of the inclusion waters from various cavities in nepheline-basalt in Hamada district varies remarkably each others, we are obliged to study the mixed sample from several cavities, because we cannot collect a sufficient amount of waters from only a single cavity for the complete chemical analysis on account of the nature of their occurrence. But some of the ingredients of these solutions, such as pH, Cl^-, NO_3^-, NO_2^-, NH_4^+, are determined for each cavity as shown in Table III.

As pH values in Table III were measured by pH test paper (B. T. B.), these values are not exact as already mentioned in the previous papers[6], but we can guess the outline of the properties of the waters and their variation from these so-called pH values.

TABLE II

CHEMICAL COMPOSITIONS OF THE MINERALS IN THESE CAVITIES

	Calcite ⟷ Siderite				Silicate		
CO_2	42.57	41.82	26.43	38.88	35.63	—	—
CaO	50.47	49.58	33.84	14.58	1.28	1.82	1.33
MgO	1.17	1.71	2.57	5.84	1.43	11.18	14.15
FeO	2.56	3.83	22.28	36.23	58.19	1.88	2.39
Fe_2O_3	0.31	1.44	2.33	3.06	1.41	14.93	13.26
MnO	1.68	1.47	7.05	0.73	0.76	0.32	0.62
SiO_2	—	—	2.52	—	—	41.02	44.13
Al_2O_3	—	—	1.76	0.38	0.51	2.89	0.60
H_2O (−)	—	—	—	—	—	20.53	18.04
H_2O (+)	—	—	—	—	—	6.19	5.63
P_2O_5	—	—	—	—	—	0.12	0.06
Cl	—	—	—	—	—	0.002	0.002
Total	98.76	99.85	98.78	99.70	99.21	100.88	100.21

6) I. Iwasaki, "Geochemistry", in "Chemical Experiments", (1941) II, Vol. 12, 1; I. Iwasaki, M. Ieyosi, *J. Chem. Soc. Japan*, 64, 1456 (1943); I. Iwasaki, *Japan Analyst*, 1, 175 (1952).

TABLE III

CHEMICAL COMPOSITION OF THE RESIDUAL MAGMATIC WATER IN THE CAVITIES OF TRACHYANDESITIC BASALT FROM IMARI DISTRICT

Sample	Date of sampling	Location	Amount collected (g.)	pH	Cl (mg./l.)	NH_4 (mg./l.)	NO_2 (mg./l.)	NO_3 (mg./l.)
M	Aug. 1948	Kusuku	0.4594	—	76	71.2	—	—
A1	Mar. 1949	〃	—	7.0	—	—	—	—
A2	〃 〃	〃	—	6.6	—	—	—	—
A3	〃 〃	〃	0.4789	6.9	7.2	40.5	0.8	0.2
A4	〃 〃	〃	0.4135	6.7	5.8	61.6	0.4	0.4
A6	〃 〃	〃	—	6.4	—	—	—	—
A8	〃 〃	〃	—	6.6	—	—	—	—
1	Oct. 1949	Kuhara	—	6.6	—	—	—	—
2	〃 〃	〃	—	6.8	—	—	—	—
3	〃 〃	〃	0.3934	6.8	9.0	66.7	0.3	0.3
4	〃 〃	〃		6.8				
B1a	〃 〃	Kusuku	0.8209	6.0	29.2	11.4	0.4	0.2
B1b	〃 〃	〃	1.1465	〃	12.5	15.9	0.2	0.6
B1c	〃 〃	〃	0.1896	〃	4.0	72.2	0.3	1.7
B2	〃 〃	〃	0.5834	〃	6.2	10.0	0.2	0.7
B3a	〃 〃	〃	0.9982	〃	7.2	10.1	0.7	0.2
B3b	〃 〃	〃	0.9455	〃	6.6	17.1	0.3	0.3
B3c	〃 〃	〃	1.4472	〃	9.8	4.7	0.04	0.2
River water	〃 〃	〃	—	6.8	3.7	0.8	0.8	—
K	Nov. 1950	〃	100 cc.	7.0	10.1	0.63	0.005	0.033
River water	〃 〃	〃	—	6.7	9.1	0.096	0.000	0.030

TABLE IV

CHEMICAL COMPOSITION OF NATURAL WATERS FROM VARIOUS ORIGINS

	Residual magmatic waters			River water	Sea water+
	Imari (mg./l.) (K)	Hamada (mg./l.) (1)	Hamada (mg./l.) (2)	Imari (mg./l.)	(mg./kg.)
pH	7.0	5.6	3.6	6.7	7.5–8.8
Evaporation residue	280	—	—	—	35,500
Na	30.2	139	491	48.4	10,600
K	29.0	—	120	9.0	380
Ca	126	76	112	10.2	400
Mg	0.0	22	11	0.0	1,300
Fe	0.67	4.1	2.3	0.64	0.002
Al	<0.6	11.	16	<0.6	0.1
NH_4	0.8	0.08	14	0.096	—
Cl	10.1	170	732	9.1	19,000
SO_4	4.2	173	326	3.0	2,600++
NO_3	0.033	4.4	97	0.030	—
NO_2	0.005	21	0.54	0.000	—
SiO_3	—	35	28	—	—

\+ V.M. Goldschmidt, "Geochemistry", (1954) p. 49.

++ Calculated from S=880 mg./kg.

pH values vary from about 6.0 to about 7.2, and the tendency of going to the alkaline side of these values after collection of samples from the mother rocks for location B is perhaps due to the fact that dissolved carbon dioxide escapes from the sample waters when they are exposed to the atmosphere, in which carbon dioxide content is very small as 0.03% (vol.), by crushing the mother rocks. This fact indicates that the waters in the cavities are almost neutral or slightly acidic and absence of the extremely acidic and basic substances, so far as the data tell. And also this fact will easily be understood if they have already reacted completely with the substance around the cavities and have

already attained nearly completely to the equilibrium between them. This nature is quite different from that of the residual magmatic waters in rocks from Hamada district where acidic (pH 3.6; 5.6) and alkaline (pH 8.1) waters were found.

Chlorine content of these waters (4.0–29.2 mg./l.) is very small compared with that (25–1220 mg./l.) of the waters from Hamada district and comparable with that of the river waters near the mother rocks in this district as will be seen in Table IV.

On the contrary, NH_4^+ content of the waters in this district ranging from 0.63 to 66.7 mg./l. seems as a whole to be remarkably higher than that of the waters in Hamada district and the river waters described above.

NO_3^- and NO_2^- content of these waters ranging from 0.005 to 0.8 mg./l. and 0.033 to 1.7 mg./l. respectively are very small compared with that (4.4–97; 0.54–21 mg./l.) of the waters in Hamada district as the case of chlorine content.

As will be seen in Table IV, the concentrations of the other components such as Na, K, Mg, Fe, Al, SO_4, in these waters are remarkably lower than that of the waters from Hamada district. But only the calcium content of these waters is very high compared with that of the other components, and comparable with that of the waters from Hamada district. This nature is also quite different from that of the waters from Hamada district and sea water. It seems to be the corresponding nature that calcium carbonate minerals are very abundant in the cavities of the mother rocks in Imari district.

As will be seen in Tables III and IV, the variation in the chemical compositions of the inclusion waters from each cavity is quite remarkable like that recognized in Hamada district. Consequently we can conclude that these volatile components of magmas are not always collected uniformly in each cavity during the fractional crystallization of magmas depending on their geological environments and the nature of magmas and volatile components. This fact is also recognized from the irregular distribution of the cavities; their inclusions and minerals in their cavities as described above.

Discussion

a) Real Magmatic Waters.—The real magmatic waters defined above have already been obtained from lava lake at Volcano Kilauea in Hawaii by A. L. Day and E. S. Shepherd[1], and at Volcano Mihara, Oo-sima, Idu in Japan by the present authors[3]. In the magmatic waters from lava lake at Volcano Kilauea, a large amounts of many volatile components, such as Na, K, Ca, Fe, Al, Cl, F, Ti, S, are determined together with many volcanic gases such as CO_2, CO, H_2, SO_2. Afterward these results have been confirmed by Shepherd[1] and J. Jaggar[1] in lava lake at Volcano Kilauea and Mauna Loa in Hawaii. From these results we can conclude that all these magmatic waters obtained from lava lakes in Hawaii are of acidic nature. The magmatic waters obtained from lava lake at Volcano Mihara are also strongly acidic as will be seen in Table V.

TABLE V

CHEMICAL COMPOSITION OF THE MAGMATIC WATER OBTAINED FROM LAVA LAKE AT VOLCANO MIHARA, OO-SIMA, IDU, JAPAN

Sample: April 1, 1950.

Acidity	1.4 N
Cl	67.6 g./l.
Total S	0.16 〃
Si	0. 〃
Fe	69.8* 〃
Ca	0. 〃
Mg	0. 〃
Ti	0. 〃
Al	(trace) ?

* Mixed with iron chloride derived from iron tube.

As the temperature of molten lavas in these active lava lakes mentioned above is as high as about 1100°C, a remarkable distillation of the volatile matters in lavas is thought to take place. As a result, many volatile components of magmas (volcanic sublimates) issued in the volcanic gases are dissolved in distillates, magmatic waters, and some of them are hydrolyzed, and these magmatic waters acquire an acidic nature. These facts are already demonstrated by laboratory experiments. For example, when the mixture of sodium chloride and quartz powder is heated with water at about 1000°C, a large amount of hydrogen chloride is distillated with water[7]. Thus, we can understand easily that these magmatic waters have acidic nature, but the chemical composition of these real magmatic waters from different volcanoes, and the same volcano at different times and also different parts of the same lava lake of one volcano at the same time are evidently very dissimilar in appearance depending on the nature of the magmas, especially the surface of the magmas as that volcanic gases in lava lake at Volcano

7) For example, R. Kiyoura and Y. Ito, *J. Ceram. Assoc. Japan*, 60, 325 (1952).

Kilauea[1] and Volcano Mihara[3,8].

When these magmatic waters spring out directly on the surface of the Earth's crust, they form the primary hot springs, which are consequently of acidic nature, and are thought to be distributed usually in the vicinity of volcanic active centers. On the other hand, when these magmatic gases and waters remain in the cavities of the mother rocks, the acidity of these solutions is decreased gradually by the reactions, with their country rocks either before or after the condensation of these volatile magmatic components into aqueous solutions. Consequently it will easily be understood that all these residual magmatic solutions in the cavities of their mother rocks as found in Hamada and Imari districts are almost all neutral or slightly acidic or slightly alkaline in nature as described above. And when these reactions with their country rocks proceed still more, these waters must gradually become alkaline in nature depending on their nature. And also it will easily be understood that there are many kinds of chemical compositions of magmatic waters depending on time elapsed after separation from their magmas, and the nature of their mother magmas and volatile components and chemical reactions with their country rocks after separation from their magmas.

b) Primary Hot Springs.—The primary hot springs distributed in the vicinity of active volcanic craters as described above are usually of acidic nature. But, needless to say, there are many acidic hot and cold (mineral) springs in the world which are distributed in various places where no relations with volcanic activity can be seen, or in the special places where oxidation process by oxygen in the atmosphere easily takes place owing to the special geological conditions. These acidic mineral springs have usually a characteristically large amount of sulphate ion compared with the other hot springs as already shown in the hot springs of Japan by the present authors[9], and their acidity is thought to be due to the existence of a large quantity of sulphuric acid formed by the oxidation of sulphur compounds in these springs by the atmospheric oxygen near the surface of the Earth's crust (Table VII). Considering these facts, these acidic mineral springs are thought to be of secondary origin[10]. Thus, the primary hot springs of acidic nature are distinguished from these cold acidic mineral springs of secondary origin. Some of these primary hot springs formed by condensation of the volatile components of magmas after the separation from their magmas are easily distinguished from the other hot springs by means of determination of distribution of radioactive components such as radon and thoron between a gas phase and an aqueous phase as already reported in the previous papers[11]. In these primary hot springs Rn and Tn are distributed in a gas phase in excess of the equilibrium content which is calculated on the basis of partition law between a gas phase and an aqueous phase. On the contrary, in the ordinary hot springs Rn or Tn are distributed usually in an aqueous phase in excess.

When these primary acidic hot springs react for a long time with their country rocks and the other substances around their ways to the surface of the Earth's crust the properties of these hot springs will gradually change, and in the end become of alkaline nature as the residual magmatic solutions in the cavities of volcanic rocks in Hamada and Imari district. If all alkaline hot springs are thus formed from these primary acidic hot springs, the alkaline hot springs are of course of secondary nature. But on the other hand, it is well known that alkaline aqueous solutions can be derived directly from the residual magmatic solutions as in the cavities of volcanic rocks in Hamada and Imari district. When these alkaline aqueous solutions spring out directly on the surface of the Earth's crust, they also form the primary alkaline hot springs. Consequently, it will easily be understood that there are two kinds of alkaline hot springs (primary and secondary in this sense), but they cannot yet be distinguished from each other by observations. When the springs which contain the magmatic substances are genetically called hot springs as is done by Allen and Day[12,10] the hot springs must have various kinds of chemical compositions and temperature depending on the nature of their geological environments, and the chemical compositions of the magmatic and meteoric substance introduced into the chemical system of hot springs. On the other hand it has been found by T. Terada[13] that hot springs which have no relations to volcanic activities are

8) I. Iwasaki, H. Shimojima and M. Tsuda, *Mass Spectroscopy*, No. 1, 52 (1953); No. 4, 39 (1955).

9) I. Iwasaki, *J. Chem. Soc. Japan*, 56, 1427 (1935); *J. Balneol., Soc. Japan*, Vol. I, No. 3 and 4, 106 (1942).

10) E.T. Allen and A.L. Day, "Hot Springs of the Yellowstone National Park", (1935) p. 39.

11) I. Iwasaki, T. Katsura, H. Shimojima and M. Kamada, "Radioactivity of volcanic gases in Japan", Bull. Volcanologique, in press.

12) E.T. Allen, *Econ. Geol.*, 30, 1 (1935); A.L. Day, *Bull. Geol. Soc. Am.*, 50, 317 (1939).

13) T. Terada, *Bull. Earthq. Res. Ins.*, 8, 377 (1930).

formed by the heat produced by crustal movements. Considering these facts, we cannot distinguish the hot springs of magmatic origin from the other mineral springs only by their chemical compositions and temperature of their waters, because we have no method to distinguish the magmatic substances from the others. These facts give the basis to the genetical definition of hot springs reported in the previous papers[14] that hot springs can be defined genetically as the springs which contain more or less magmatic substances regardless of their chemical compositions and temperatures.

c) Primary Hydrosphere and Primary Atmosphere.—The nature of the primary hydrosphere and the primary atmosphere are largely conditioned by the mode of origin of the Earth. There have been many reports on the origin and formation of the Earth, but up to the present, we cannot understand completely yet the chemical processes of the formation of the Earth without any serious objection. The formation of the hydrosphere starts with the condensation of water vapour. On the geochemical processes of the formation of the primary atmosphere and the primary hydrosphere, there are distinct differences between Goldschmidt's theory[15] and the accretion theory[16] developed recently. According to Goldschmidt, the primary atmosphere and the primary hydrosphere are mainly formed by the condensation of the original atmosphere, which was formed at the first stage of the geochemical distribution of the chemical elements in the Earth, and they have increased unceasingly by addition of volcanic gases during the long geologic time. On the other hand, according to the accretion theory the primary atmosphere and the primary hydrosphere are thought to be mainly formed gradually from the volcanic gases expelled by heating from the cold original Earth material.

But in all cases, it has been shown that the volcanic gases occupy the important part of the formation of both the atmosphere and the hydrosphere. From these points of view, it seems to be able to estimate the nature of the primary hydrosphere and the primary hydrosphere from the properties of the volatile magmatic substances, especially the magmatic waters and volcanic gases. As already reported in the previous paper[17], water, nitrogen and carbon dioxide expelled from volcanic rocks by heating have larger contents in the gases expelled at relatively lower temperature (up to about 500°C) than in that expelled at high temperature (800–1200°C). And also we can detect many halogen and sulphur compounds in the volcanic gases from lava lakes and fumaroles of high temperature, but cannot detect any halogen compounds in the volcanic gases from fumaroles of low temperature. Although sulphur compounds such as hydrogen sulphide are detected in many fumarolic gases of low temperature, the main components of these fumaroles are usually nitrogen, carbon dioxide and water vapour. From these model experiments descibed above[17] and the nature of the volcanic gases, by accretion theory we can guess that during the period of relatively low temperature up to about 500°C the contents of sulphur and halogen compounds in atomsophere and hydrosphere should be very small, but when the temperature reached above about 800°C, sulphur and halogen compounds are abundantly expelled from the original Earth material, and consequently the hydrosphere condensed from these volcanic gases will have more sulphur and halogen compounds. In the initial stage of the formation of the hydrosphere, its acidity would increase by the addition of hot acidic rain waters[18] condensed from the volcanic gases of high temperature until active chemical reactions with country rocks which occurred in hydrosphere used up these acids supplied by these volcanic gases. Then the acidity of the hydrosphere would decrease gradually to that of the present hydrosphere (Table IV). The chemical nature of the hot acidic rain waters will be able to be estimated from magmatic waters as will be seen in Table V, and the waters condensed from fumaloric gases. And the chemical properties

TABLE VI

CHEMICAL COMPOSITION OF THE RESIDUAL MAGMATIC GASES IN THE NEPHELINE-BASALT IN HAMADA DISTRICT

Dissolved gases in the inclusion.

	No. 13	No. 19
O_2	0.00 cc./l.	0.00 cc./l.
N_2	6.32 〃	13.54 〃
CO_2	2.25 〃	1.23 〃
H_2	0.00 〃	0.00 〃
CH_4	0.00 〃	0.00 〃
Tension of nitrogen gas	0.366 atm.	0.795 atm.

14) I. Iwasaki, *J. Chem. Soc. Japan*, **56**, 252 (1935).
15) V. M. Goldschmidt, *Z. Elektrochem.*, **28**, 411 (1922); "Geochemistry", (1954) p. 11.
16) H. O. Urey, *Geochim. et Cosmochim. Acta*, **1**, 209 (1951); 263 (1952).
17) I. Iwasaki, T. Katsura and N. Sakato, *J. Chem. Soc. Japan*, **76**, 778 (1955).
18) I. Iwasaki, "Introduction to Geochemistry", (1953) p. 206; I. Iwasaki, T. Nitta and T. Tarutani, *J. Chem. Soc. Japan*, **74**, 1003 (1953).

of the primary atmosphere will also be able to be estimated from the chemical compositions of the residual magmatic gases and volcanic gases from various volcanoes[1,3,8] and various kinds of volcanic rocks[1,17,19]. Chemical compositions of the residual magmatic gases in the nepheline-basalt in Hamada district reported by Sugawara et al[2] are shown in Table VI.

From these volcanic gases we can completely understand that there is no free oxygen in the primary atmosphere. This fact is in good aggreement with the nature of the original atmosphere by Goldschmidt[15].

The primary hydrosphere formed by condensation of the original atmosphere by Goldschmidt must also be acidic nature owing to the dissolution of volcanic exhalation by the violent volcanic action as in the case of the accretion theory. In all cases, the acidic nature of the primary hydrosphere is derived from volcanic exhalations and by unceasing reactions with the country rocks, its acidity would decrease until it became equal that of the present hydrosphere. The chemical nature of the primary hydrosphere at the initial stage, especially primary ocean, seems to be able to be estimated from the chemical composition of hot river waters which are formed by the condensation of the volcanic gases and by running on the hot volcanic rocks erupted recently[18]. After violent chemical reactions with country rocks the nature of the hydrosphere seems to resemble that of the residual magmatic waters and the hot springs. The average contents of main components, such as Cl, SO_4, HCO_3, Na, Ca, Mg, of the hot springs in Japan calculated by the present author[9] are shown in Table VII.

From these points of view, it seems that the content of carbon dioxide in the primary atmosphere is larger than that of the present atmosphere, and the salt content of the primary ocean is about one-tenth that of the present hydrosphere.

d) Magmatic Substances in the Cavities.— As already shown in the description of the nature of the mother rocks and their cavities in this paper, these rocks and the distribution of cavities show remarkably heterogeneous appearance from one part to another. There seem to be no remarkable regularities among their distribution and the nature of their cavities (sizes, inclusions, such as minerals, solutions and gases). Some of the cavities are empty (only filled with gases); on the other hand, some of them are completely filled with mineral substances, mainly carbonates and silica and silicate minerals, and some of them hold mineral substances and aqueous solution in addition to the residual gases. From the nature of these cavities it might be safely concluded that these mineral materials, waters and gases, are easily mobile in the mother rocks at the stage of the formation of these cavities. If these characteristics are excluded, it seems to be impossible to understand the fact that some of these cavities are completely filled with the mineral substances or are empty. From this point of view, the computation of the concentration of the inclusion water before the minerals, lining the cavity-wall, separated was carried out by K. Sugawara et al.[2], and they showed that the concentration is very high (280.88 g./l.); that is, 3.65 times higher than the Japanese record of hot spring salinity, 77.1 g./l. of Arima-shin-onsen.

TABLE VII

AVERAGE CONTENTS OF MAIN COMPONENTS OF THE HOT SPRINGS IN JAPAN

	Number of sample	Salt content (g./kg.)	Na (g./kg.)	Ca (g./kg.)	Mg (g./kg.)	Cl (g./kg.)	SO_4 (g./kg.)	HCO_3 (g./kg.)
Acidic "hot spring" (>25°C)	63	2.21	0.305	0.195	0.0537	0.787	1.51	0.257
Acidic mineral spring (<25°C)	162	6.09	0.692	0.210	0.0833	1.07	4.51	0.547
Neutral "hot spring" (>25°C)	25	2.76	0.631	0.247	0.0199	1.01	0.472	0.321
Neutral mineral spring (<25°C)	23	4.08	0.873	0.438	0.0829	1.98	0.471	0.532
Alkaline "hot spring" (>25°C)	331	2.19	0.534	0.192	0.0198	0.847	0.349	0.246
Alkaline mineral spring (<25°C)	108	6.78	2.06	0.300	0.107	3.20	0.337	1.34
Total hot spring	712	3.86	0.768	0.221	0.0557	1.25	1.70	0.491

19) E.S. Shepherd, *J. Geol.*, **33**, 289 (1925); E.S. Shepherd and H.E. Merwin, *J. Geol.*, **35**, 97 (1927).

Conclusion

From the definition of the real magmatic state, many kinds of the magmatic waters should be formed even from the same magma depending on their geological environments. The residual magmatic water described above can be distinguished from the magmatic waters derived directly from the molten lavas. The magmatic waters are acidic on account of dissolution of volatile magmatic components, but the residual magmatic waters must be usually neutral, slightly alkaline or acidic owing to the chemical reactions with their country rocks. These magmatic waters are not always juvenile, and their temperature, salt contents and chemical composition must cover a wide range. Consequently these magmatic waters cannot be distinguished distinctly from the ordinary natural waters by means of their temperature and chemical compositions.

When the hot springs are defined as the springs which contain the magmatic waters, many kinds of springs should be formed owing to the mechanism of the formation of hot springs. Even the primary hot springs derived directly from the magmatic waters have also a wide variety. For example, the acidic primary hot springs formed directly from the magmatic waters can be changed gradually into the alkaline hot springs by the reactions with their country rocks and the introduction of the other substances. On the other hand, the primary alkaline hot springs can also be formed directly from the residual magmatic waters.

From the nature of the magmatic waters and volcanic gases, the chemical nature of the primary hydrosphere and the primary atmosphere in their initial stage can be estimated. The primary hydrosphere must be acidic on account of the hot acidic rain waters at first, and change gradually into alkaline nature by the reactions with their country rocks and the other substances introduced by river waters. The primary atmosphere has no free oxygen, but has larger carbon dioxide content than the present atmosphere.

From these facts that all the cavities of the mother rocks in question have a quite distinct boundary and the distribution of the magmatic substances in these cavities are quite dissimilar, it also might be safely concluded that these mineral substances must be easily mobile in the initial stage of the formation of these cavities. The problems on the mechanism of this surprising concentration of these mineral materials into the small cavities will be answered by the geochemical investigations in future.

Summary

1) The nature of the residual magmatic waters in the cavities of the trachyandesitic basalt in Imari district is described with the nature of their mother rocks and druse minerals.

2) From the definition of the real magmatic state, temperature, and chemical properties of many kinds of magmatic waters are discussed, and the residual magmatic waters are distinguished from the magmatic waters derived directly from lava lakes. It is concluded that the magmatic waters are not always juvenile.

3) The formation of the various kinds of the primary hot springs are discussed from the definition of hot springs and the various kinds of the magmatic waters.

4) Chemical nature of the primary hydrosphere and the primary atmosphere in the initial stage of their formation are discussed from the chemical properties of the magmatic waters and volcanic gases.

5) The important properties of the magmatic substances in the cavities of the volcanic rocks are discussed from the standpoint of the distribution of the magmatic substances in the cavities.

The authors wish to express their hearty thanks to Professor H. Kuno of Tokyo University, Assistant Professor N. Saito, T. Ishimori and S. Taneda, Mr. H. Yamamoto of Kyushu University for their kind advice and help. The cost of this research was defrayed from the Scientific Research Grant from Ministry of Education, to which the writers' thanks are due.

Laboratory of Analytical Chemistry and Geochemistry, Tokyo Institute of Technology, Tokyo
and
Chemical Institute, Faculty of Science, Kyushu University, Fukuoka

On the Attribution of the Super Oxidation-resistance of Cemented Chromium Carbide

By Kazuhiko OGAWA and Tamotsu FUKATSU

(Received October 25, 1955)

Introduction

At present, the various kinds of the titanium carbide, TiC, or chromium carbide, Cr_3C_2, base sintered products have been successfully investigated as a superior heat-resistant material. Among them, the cemented chromium carbide, "CR", gives promise of many useful practices of chemical engineering because of its supper oxidation- and corrosion-resistance.

On the method of manufacture of the "CR" product and its properties, some valuable studies have been published[1]. Recently, the effect of the added chromium carbide on the oxidation-resistance of the other cemented carbide products was studied by J. Hinnüber and co-workers[2], yet much remains to be investigated on the cause of this remarkable oxidation-resistance.

Therefore the experimental work of this report has been to investigate the relationship between the structure of the surface oxidized film and the oxidation-resistance. Namely, the crystal structural change of the surface oxidized film at various temperatures was examined mainly by the electron diffraction method, and, at the same time, its microstructural change was also observed by electron microscope.

Experimental Method

The "CR" alloy was produced by sintering a compacted body of Cr_3C_2 powder mixed with 15 weight per cent of pure Ni powder with the same process reported by Y. Matsuyama, S. Kasahara and H. Hase[3]. The specimens of "CR" used here were given by Tungaloy Co.. Their characters were as shown in Table I.

Specimens for electron diffraction were prepared by the following procedures: making a bar with 4 mm. of diameter and about 10 mm. of length from this "CR" alloy, polishing the one end of the bar and then cleaning it with 10% HCl solution, distilled water, methyl alcohol and benzen in this order.

1) J.D. Kennedy, *Steel*, **131**, 92 (1952); P. Schwarzkopf and R. Kieffer, "Refractory Hard Metals", (1953) p. 122.
2) J. Hinnüber and O. Rüdiger, *Archv. für Eisenhüttenwesen*, **24**, 267 (1953).
3) Y. Matsuyama, S. Kasahara and M. Hase, Reported in the annual meeting of Japan-Kinzoku-Gakkai (1954).

TABLE I
THE PROPERTIES OF THE "CR" ALLOY

Properties \ Alloy	CR
Density	~6.9 g./cm³
Hardness	at Room Temp. 84–88 Hr A.
	at 500°C 83–36
	at 900°C 73–31
Trans. Rupt. St.	70 kg./mm²
Ther. Expans.	at 30–750°C 11.5×10^{-4}
Elect. Resist.	$\sim4.3\times10^{-4}\Omega$ cm.
Magnetic Prop.	(non-magnetic)

CR: Cemented chrome-carbide, Cr_3C_2, contained 15% Ni.

This was oxidized in air up to 1000°C at every 100°C in a ceramic crucible to prevent contamination. These oxidized specimens were at once mounted on the spcimen holder of electron diffraction camera and surface film of them was examined by the reflection method. The diffraction unit used was attached to on the Simazu SM-C2 electron microscope, the camera length 15.9 cm. and acceleration voltage 50 kV.

At the same time, a micro structural change of the surface oxidized film at various temperatures was observed by electron microscope with the polysthylene-Al replica method. On the other hand, the process of oxidizing of the carbide powder itself was also observed by means of X-ray analysis and electron microscopy.

Moreover, the structure of the sintered product as determined with a special X-ray diffraction method and at the same time the Curie point of this specimen was also measured with magnetic balance.

Experimental Results

I. On the Oxidation Resistance of "CR" at High Temperature

According to J. Hinnüber's results, the "CR" alloy increased in weight by being heated in air at each temperature of 500, 600, 700, 800, 900 and 1000°C for one hour. As shown in Table II, the weight-gain was so small that the advancing of oxidation was not confirmed below 800°C. Though the weight-increase was small, it came to be measurable at 1000°C. In our results, the lustre of the polished surface changed little at 300°C, then faded gradually with the rise of temperature and vanished completely at

TABLE II

WEIGHT INCREASES OF "CR" BY OXIDATION AT VARIOUS TEMPERATURES FOR TWO HRS. IN AIR, FROM J. HINNUBER AND CO-WORKER'S RESULTS

Temperature °C	Weight increase g./m², hr.
500	<0,1
600	<0,1
700	0,2
800	0,2
900	0,75
1000	1,2

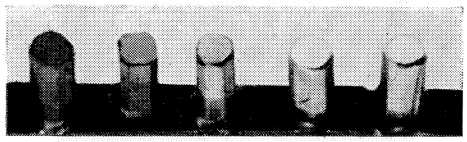

1000°C 800°C 500°C 300°C Polished surface

Photo. I. The lustre change of the polished surface by oxidation at various temperatures for 1 hr. in air.

From these results, it shoult be concluded that the "CR" alloy is useful for practical purposes of long time operation at such high temperature as 800°C in air. It must be studied whether such an excellent oxidation-resistance is based on these starting materials themselves or any characteristic structure of these oxidized films. Firstly, oxidizing the chrome carbide powder, Cr_3C_2, itself at various temperatures, the weight-increase was measured as shown in Table IV, and also, the crystal structural change of its powder was observed by the X-ray method such as illustrated in Photo II. This indicated that Cr_3C_2 had begun to change into Cr_2O_3 at 500°C already, and then the weight-gain step by step increased with rising temperature. On the other hand, the oxidation-resistance of nickel, which was the binder of "CR", was checked: Ni plate was heated in air and the structure of surface was examined by the electron diffraction. The patterns obtained were shown in Photo. III. It also indicated that the formation of NiO are faintly observed at 300°C and clearly at 500°C. It is worth being discussed that, as understood from these above results, though each component of "CR" alloy, Cr_3C_2 and Ni becomes unstable at even lower temperature than 500°C, the sintered products were stable for oxidizing for a long time at such a high temperature as about 800°C. This result suggests that the oxidation-resistance of "CR" alloys is attributed to the formation of some desirable protective film.

TABLE III

THE CHANGES OF THE COLOR, THE STRUCTURE AND THE COMPOSITION OF THE OXIDE FILM DURING OXIDATION

Temperature °C	Color	The composition of the oxide-film	Remarks
100	Metallic lustre	Imperfect Cr_2O_3	
200	Metallic lustre	Imperfect Cr_2O_3	
300	Metallic lustre, Very faint bronze-like color	Cr_2O_3	Little oriented crystals
350	Metallic lustre, Faint bronze-like color	Cr_2O_3	Little oriented crystals
500	Lustre, Bronze-like color	Cr_2O_3	At random orientation
800	Faded lustre, Green black color	Cr_2O_3	〃
1000	Non-lustre Green and gray	Cr_2O_3 and NiO–Cr_2O_3	〃

TABLE IV

WEIGHT INCREASES OF Cr_3C_2 POWDER BY HEATING AT VARIOUS TFMPERATURES FOR ONE HOUR IN AIR

Temperature °C	Weight increase	By X-ray※ diffraction
300	−5 mg./g. hr.	—
500	5 〃	3%
800	150 〃	60%
1000	——	90%

※ The estimation was measured by comparing the observed intensities of oxide lines with the standards.

1000°C or up (Photo. I), while a faint color appeared first at 300°C for two hours, then changed with the rise of temperature. These results were described in Table III. These changes of lustre and color corresponded with the above weight-increase.

II. The Structure of Oxide Film

Therefore, to confirm the formation of such protecting surface film, the variations of the surface structure with oxidizing at various conditions were examined by the electron diffraction.

The abstract of the main results from these observations were enumerated in Table III.

Phot. II. The shape and structural change of chrome-carbide powder during oxidation process.

(a)

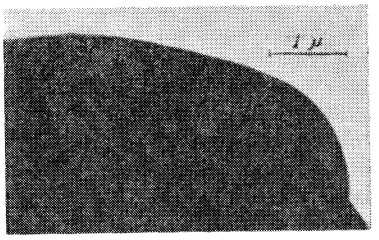

at 300°C for 1 hr.

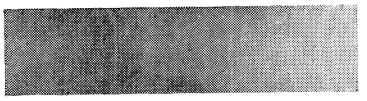

Cr_3C_2

(b)

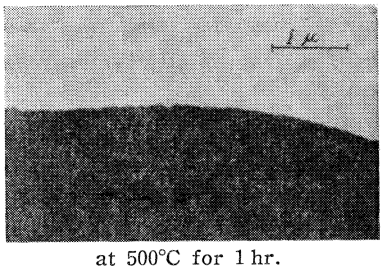

at 500°C for 1 hr.

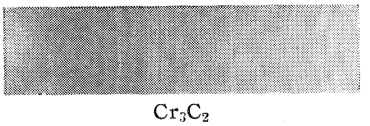

Cr_3C_2

(c)

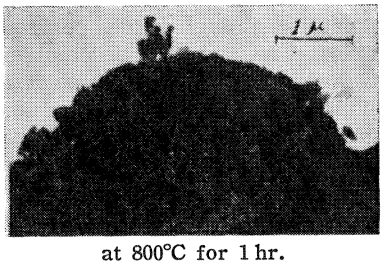

at 800°C for 1 hr.

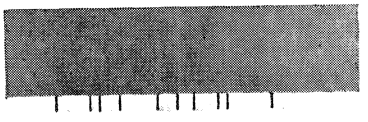

Cr_2O_3

(d)

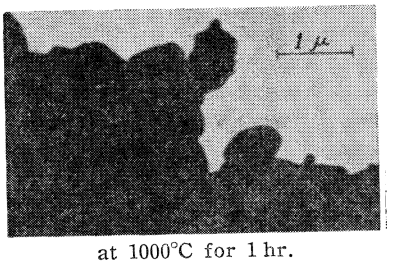

at 1000°C for 1 hr.

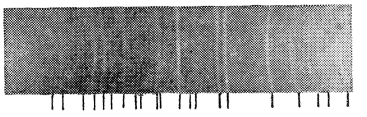

Cr_2O_3

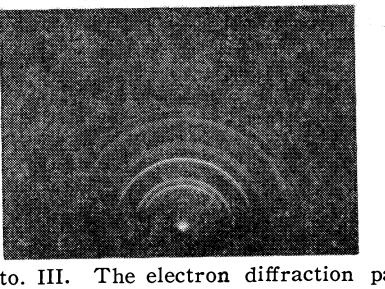

Photo. III. The electron diffraction pattern of the oxidized Ni plate at 500°C for 1 hr. in air.

Among them, the interesting results would be reviewed as follows.

i) The surface film consisted of one kind of chromic oxide, Cr_2O_3, only and not of other chromium oxide or nickel oxide below 800°C. When at such higher temperature as about 1000°C, remarkable oxidation was observed by weight-increasing, then both Cr_2O_3 and the chromium-nickel spinel, $NiO \cdot Cr_2O_3$, were first observed in the oxide film.

ii) Concerning the chromic oxide filme below 800°C, the variation of its structure corresponding to the rise of temperature was so remarkable as not to be expected previously. Namely, the surface films heated from the room temperature to 250°C for one hour consisted of very fine and imperfect crystallites of Cr_2O_3 and, moreover, were very flat. Heating it at 300°C in air continuously, the imperfect crystallites of Cr_2O_3 in the oxide film altered into perfect ones and tended to be oriented, their basal planes being parallel to the surface. This tendency was observed up to 500°C. However, in the oxidized film at higher temperature than 500°C, such orientation became at random and, the surface, also, became rough step by step. On these problems, the further sufficient explanations must be supplied as follows.

a) The confirmation that the oxide film at lower temperature was composed of imperfect and minute crystallites was based on the experimental evidences of the diffraction patterns. The diffraction patterns as Photo. IV (1) and Fig 1, are interpreted to be two-dimensional-like patterns diffracted by imperfect crystallites of Cr_2O_3 with the crystal basal planes slipped at random as observed in the polished graphite pattern[4]. At the same time, the diffuse ring patterns indicated that the crystallites were very minute. In the sample, oxidized at higher temperature,

Photo. IV. The electron diffraction patterns of oxide film formed on the surface of "CR" by oxidation at various temperatures for 1 hr. in air.

(1)

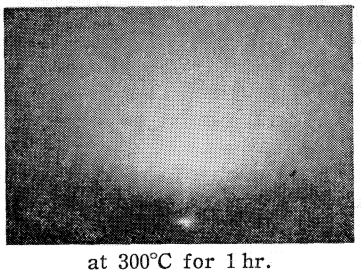

at 300°C for 1 hr.

(2)

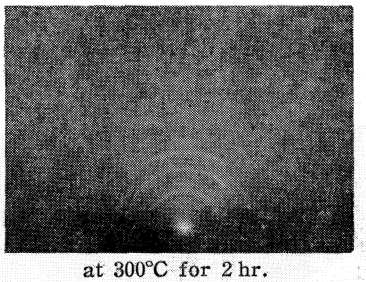

at 300°C for 2 hr.

(3)

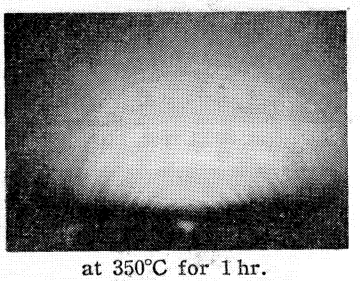

at 350°C for 1 hr.

(4)

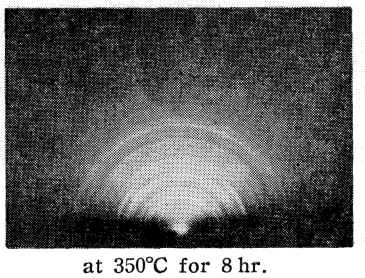

at 350°C for 8 hr.

(5)

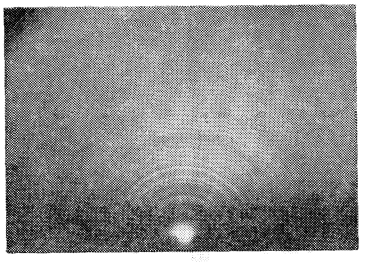

at 500°C for 1 hr.

(6)

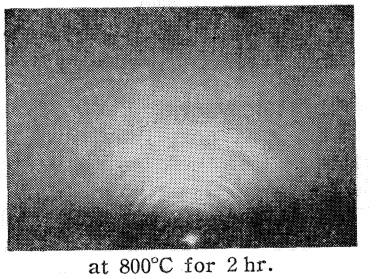

at 800°C for 2 hr.

(7)

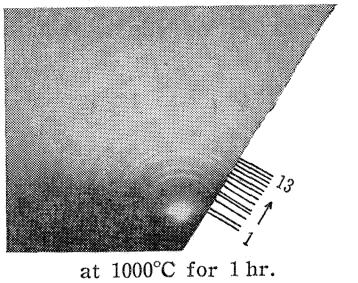

at 1000°C for 1 hr.

Comparison between observed spacing and the spacing of spinel oxide, Cr_2O_3NiO

	Observed	Spinel
1	4.75 A	4.79 A
2	4.26	4.15
3	2.96	2.94
4	2.52	2.50
5	2.40	2.40
6	2.12	2.10
7	1.92	1.91
8	1.73	1.77
9	1.64	1.63
10	1.50	1.50
11	1.44	1.445
12	1.347	1.345
13	1.299	1.297

(8)

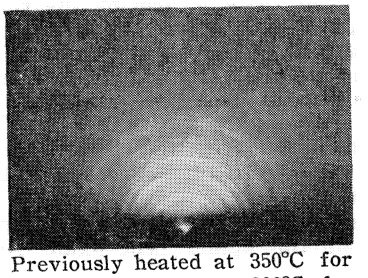

Previously heated at 350°C for 1 hr. and again at 800°C for 1 hr.

Fig. 1. The sketch of the electron diffraction pattern of the polished surface.

the diffraction patterns Photo. IV, (6) were *more remarkably sharp than* those at lower temperature. However, both patterns always coincided with Cr_2O_3 patterns.

b) The appearence of arcing in Photo. IV (2) must suggest that these chromic oxide crystallites were oriented. Orientation was determined by the ordinary method, using the reciprocal lattice as illustrated in Fig. 2.

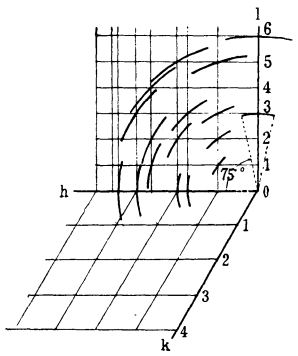

Fig. 2. The schematic diagram of the diffraction pattern of oriented chromic oxide crystals with their C-axis inclined 75°C to the matrix surface, in reciprocal lattice.

This figure shows the diffraction pattern of oriented Cr_2O_3 crystals with their C-axis inclined at the angle of 75° to the matrix surface.

c) Film-thickness or flatness can be estimated from the electron-microscopic photographs substantially, also by the ring width or diffusing behavior of the electron diffraction pattern. The arcs of the diffraction patterns obtained from the specimens below 500°C, diffused toward the centre of the ring. This diffused ring was different from the usual halo pattern and interpreted to be originated from a refraction of electrons because of the very flat surface.

d) In the oxidized film at 1000°C, the existence of the spinel type oxide, $NiO \cdot Cr_2O_3$ was confirmed with the result of Photo. IV (7). This pattern and spacing showed a good agreement with the spinel type oxide observed previously on the surface oxide film of Ni–Cr alloy. It has been reported by several workers[5,6] that the oxidation-resistance of this alloy at high temperature took place because of the formation of the densed and flexible oxide film of $NiO \cdot Cr_2O_3$.

However, in this experimental result, the oxide film composed of this spinel oxide did no longer act the most effective part in preventing the oxidation. Though it is interesting to consider why this spinel oxide was formed on the surface of this product, this will be discussed in the later.

From the above-mentioned results, it will be suggested that the tendency of the oxidation-resistance declines with the increasing roughness of the surface film, because of the crystal-growth of Cr_2O_3 crystallites. To study this problem, the micro-structural change of surface must be observed sufficiently.

III. Observation of the Microstructure of the Surface

The microstructure of each surface film treated at various conditions were illustrated in Photo. V. It was proved from these figures

Photo. V. The electron-microscopic structure of each surfaces of "CR" in various stages in oxidation.

(1)

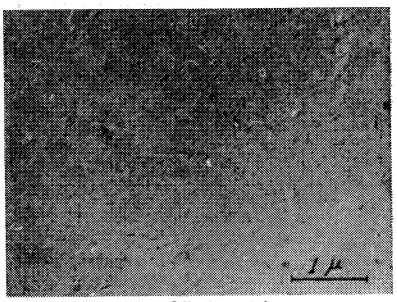

at 300°C for 1 hr.

(2)

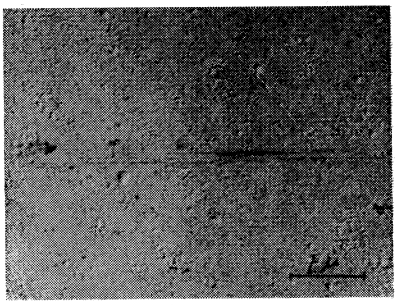

at 500°C for 1 hr.

4) G.P. Thomson and W. Cochrane, "Theory and Practice of electron diffraction", (1939) p. 185.

5) J. Iidaka and S. Miyake, *Nature* **137**, 457 (1935).

6) A. Gulbransen and W. R. McMillan, *Ind. Eng. Chem.*, **45**. 1734 (1953).

(3)

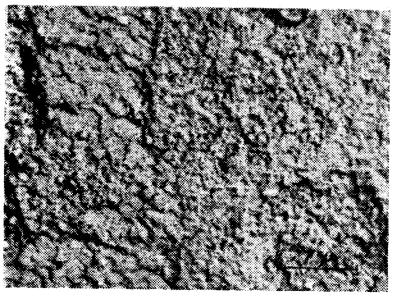

at 800°C for 1 hr.

(4)

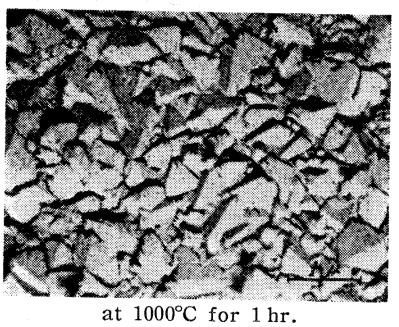

at 1000°C for 1 hr.

(5)

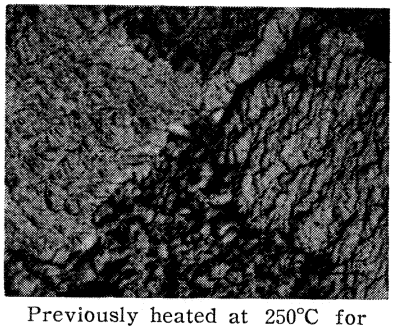

Previously heated at 250°C for 1 hr. and again at 1000°C for 1 hr.

that the appearance of the surface up to 500°C was very flat, and the grain size was too small to be measurable as already suggested. However, the oxidized surface above 800°C, became more rouge consequently, and, in this film, the coarse chromic oxide crystals were observed as showed in Photo. V (4).

Moreover, in the oxidized film at 1000°C, the grains became so coarse that their diffraction pattern rings were spotty as shown in Photo IV, (7). Sometimes, as appeared in Photo. V (4), piramid-like large grains of one micron order were observed and the surface began to break out into small cracks.

From such a result, it will be confirmed that the increasing roughness of the surface may be caused by the coarsening of the minute chromic oxide crystals.

It is a valuable new result to discover that the stability of protective film may be more responsible for the structure of film, than the kinds of oxide.

IV. The Inner Structure of "CR" Tip

Lastly, it must be studied why the oxidized film below 800°C consisted of one kind of the chromic oxide, Cr_2O_3, though the nickel binder metal was oxidized already into NiO at 500°C.

Concerning this problem, though it was recently suggested by J. Hinnüber that the binder phase would exist in the alloying state, yet it has not been confirmed experimentally.

Therefore, the inner structure was examined by X-ray and magnetic balance. The method of the X-ray diffraction of "CR" tip was outlined in Fig. 3 and its photographs were illustrated in Photo. VI in which were observed the ortho rhombic structure, Cr_3C_2 and a face centered cubic structure.

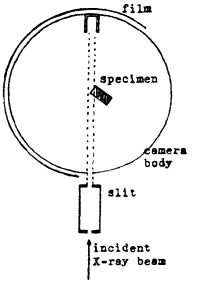

Fig. 3. The method of mounting specimen in this X-ray diffraction.

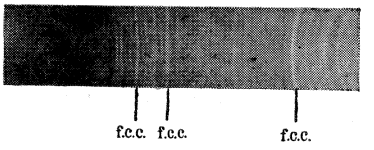

Photo. VI. The X-ray diffraction pattern of "CR" showing some f.c.c. structure.

Though the difference between the lattice constants of this f. c. c. and Ni was almost never observed, it seemed that this f. c. c. was perhaps not the pure Ni. This f. c. c. did not appear in the specimen sintered at such a lower temperature as 500°C, but appeared first clearly at the higher temperature at which the reaction between Cr_3C_2 and Ni occurred. However, the reason was not yet clear that the pure Ni was not observed by X-ray diffraction patterns in the specimen sintered at the lower temperature.

Therefore, when the magnetic properties of these specimens were measured, the intensity of saturation magnetization of the specimen sintered at the temperature which the f. c. c. appeared, was more remarkably small than that of the sintered one at the lower tem-

perature. On the other hand, the Curie temperature of the specimen was measured by magnetic balance. One of these results was shown in Fig. 4.

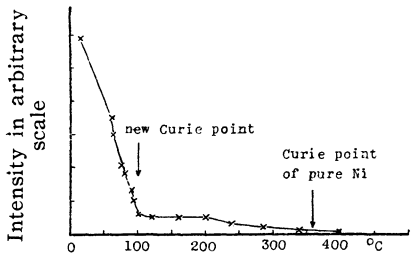

Fig. 4. Magnetization curve of "CR".

This indicated a Curie temperature of 100°C differing from the usual one, 358°C of the pure Ni. Curie points lay below 150°C, and the amount of these materials which have these Curie points are more numerous than pure Ni, as they can be estimated from Fig. 4.

If this alloy is assumed to be Ni-Cr solid solution, it will be expected that the quantity of Cr dissolved in Nickel binder phase is 5 per cent or more by weight. Therefore, it can be confirmed that the binder phase no longer exists as pure Ni, but as some Ni-Cr alloy or some intermetallic compound of double carbide of Cr_3C_2-NiC. If this assumption is true, then the appearing of nickel chrome spinel at 1000°C coincides with the previous works.

General Discussion

From these experimental results, two subjects to be discussed more sufficiently were as follows.

a) The oxidation of "CR" was nothing but the complicated process combined with the following to processes: the decarburization and oxidation of the Cr_3C_2 grain, and the oxidation of some Ni-Cr alloy in the part of binder.

b) The dense and flat oxidized film composed of the chromic oxide crystallites very suitable for oxidation-resistance. In such film, these minute crystallites tend to have a orientation.

With the coarsening of these crystallities, the surface became rough gradually, and broke out into small cracks. Such film was not sutiable to prevent oxidation. Generally speaking, it was confirmed that the tendency of oxidation-resistance depended not only on the kind of oxide but on the chracteristic structure of the surface film.

Firstly, from the above mentioned experimental confirmation that "CR" consisted of both Cr_3C_2 and some Ni-Cr alloy, the consideration in the item a) was concluded.

From the previous experimental results, the reason was easily understood why the formation of the spinel oxide, $NiO \cdot Cr_2O_3$, was observed in the oxidized film at 1000°C or up. However, to our regret, the reason of the nickel oxide not being found in the oxidized film below 800°C has not yet been revealed.

According to the information of the oxidation process of Ni-Cr alloy by J. Gulbransen, the nickel mono-oxide was observed at such a low temperature at 500°C, and its tendency depended considerably on the composition of such alloy.

Though this difference between our result and Gulbransen's might have been due to small amounts of Ni-Cr alloy in "CR", further studies were necessary.

Secondly, as described in the item b), the oxidation-resistance depended also on the structural change of the surface film. Therefore, it was necessary to understand a mechanism of the decarburization and oxidation of Cr_3C_2, during which process the structure of the oxide film changed with rise of temperature. To understand it easily, some models of oxidation process were sketched schematically in Fig. 5. This film consisted of small

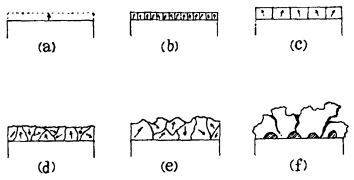

Fig. 5. The models of the oxide film at various stages of oxidation.

bricks, which were the chromic oxide crystallites, and the noted arrow in the bricks was the direction of C-axis. The brick pictured with the broken line was the imperfect crystal. The shaded one was the spinel-type oxide. As shown in these figures (a) (b) (c), the surface film was the aggregation of the chromic oxide crystallites. With the rise of temperature, these changed in size as well as in the crystal structure. In the figure (c), the oxide film composed of these oriented crystals carried out the effective role in preventing the oxidation. These models were devised from the above-mentioned experimental results by the electron diffraction. In the figures (d, e), the surface became more rough corresponding to the crystal growth of these crystallites. In this stage, these crystals grew remarkably at random and the rate of oxidation increased rapidly. This model was devised from the

experimental results concerning the surface micro-structural change of "CR" and the shape-change of Cr_3C_2 powder in oxidation. During the oxidation of the chrome carbide (Cr_3C_2) powder at various temperatures the irregularities were formed on the surface of powder, and increased with the rise of temperature. This result was shown in Photo. II (2).

Lastly, a little more description of the oriented film was added.

When the specimen already heated to have the oriented film was heated again at higher temperature with the virgin one, the latter tended to be more remarkable in the crystal growth and the increasing roughness of surface than the former. Such tendency was observed from the comparison in Photo. V (4, 5).

From this experimental result, it was confirmed that the oriented film was more suitable for oxidation-resistance than the non-oriented one, yet much remained to be investigated.

The authors wish to express their great indebtedness to Professor Keizo Iwase for helpfull advice, and Professor Ryoji Uyeda for useful discussions in the part of the electron diffraction pattern. Thanks are due to Mr. Kazuichi Sugiura for aid in the electron microscope work, and also Tungaloy Products Co. which kindly offered them the specimens.

Chemical Department, Faculty of Science
Kyoto University, Kyoto
and
Tungaloy Products Co.

Detection of ^{103m}Rh in the "Bikini Ashes"

By Kenjiro KIMURA, Nagao IKEDA* and Kenji YOSHIHARA**

(Received December, 1, 1955)

Introduction

The radiochemical analysis of the so-called "Bikini Ashes" which fell on a Japanese fishing boat, the No. 5 Fukuryu Maru on March 1, 1954, was carried out in our laboratory[1] and in several other university laboratories[2]. In the course of their studies, scientists detected ^{103}Ru (half-life: 39.8 d.) in the ashes together with ^{106}Ru (half-life: 1.0 y.) and its daughter ^{106}Rh (half-life: 30 s.). As is well known, ^{103}Ru decays into ^{103m}Rh (half-life: 57 m.) which successively disintegrates into stable ^{103}Rh by isomeric transition. The half-life of ^{103m}Rh is rather short and the energy of the converison electron of ^{103m} Rh is so low (0.034 Mev) that it has been still remained undetected in the ashes. The present authors tried to separate ^{103m}Rh from its parent ^{103}Ru in the carrier-free form by the ion exchange resin method in a short time and to detect the weak radioactivity by the use of the windowless gas flow counter.

* Department of Chemistry, Faculty of Science, Tokyo University of Education, Koishikawa, Tokyo, Japan.

** Electrotechnical Laboratory, Agency of Industrial Science and Technology, Ministry of International Trade and Commerce, Tanashi, Tokyo, Japan.

1) K. Kimura, E. Minami et al. *Japan Analyst*, 3, 335 (1954). (in Japanese).

2) T. Shiokawa, et al, ibid., 349; H. Yamatera, et al., ibid., 356.

Experimental

1. Materials and Apparatus

Materials.—The sample ashes are so-called "Bikini Ashes" which fell on board No. 5 Fukuryu Maru sailing near the Bikini Atoll on March 1, 1954. The chemical and radiochemical compositions of the ashes were already reported in the previous paper[1]. The ashes used in this experiment were collected on board the boat and contained fairly large amounts of dust.

Apparatus for Activity Measurements.—The Geiger-Müller counter model TGC-2 made by Tracerlab Inc. was used for the general activity counting. The thickness of the mica window of the counter tube is 1.4 mg./cm^2 and counting efficiency is about 10%. For the measurement of the weak activity of rhodium fraction, 2π Q-gas flow counter model D42A made by Nuclar Instrument and Chemical Corporation was used.

2. Separation of Ruthenium from "Bikini Ashes"

At first, ruthenium fraction was separated from the ashes by the procedure written below. The sample of some ten million cpm. was taken and ignited to burn away all combustible substances. Then, it was dissolved with 6 N hydrochloric acid, and the insolubles were filtered off. The activity of a small aliquot of the filtrate was measured on the second shelf of the Geiger-Müller counter. Total activity was estimated about 10^6 cpm., 10 mg. of ruthenium was added to the filtrate as a carrier, the acidity of the solution was adjusted

to 2 N, and then hydrogen sulfide was passed through to precipitate ruthenium as sulfide. The precipitate was dissolved with nitric acid. The solution thus obtained was then treated according to the D. N. Hume's procedure[3]; to the ruthenium solution were added an appropriate amount of water, potassium permanganate and concentrated sulfric acid, then ruthenium was distilled off as ruthenium tetroxide. The distillate was caught in a small volume of water containing a small amount of hydrogen proxide.

The appropriate aliquot portion of the distillate was taken in a counting dish, evaporated up to dryness and the activity was measured under the same measuring condition as in the case of the starting sample solution. The total activity of the distillate was considered to be 1.5×10^5cpm.

The absorption curve of the distillate for aluminum foil was also investigated. The result is shown in Fig. 1. The activity is considered to

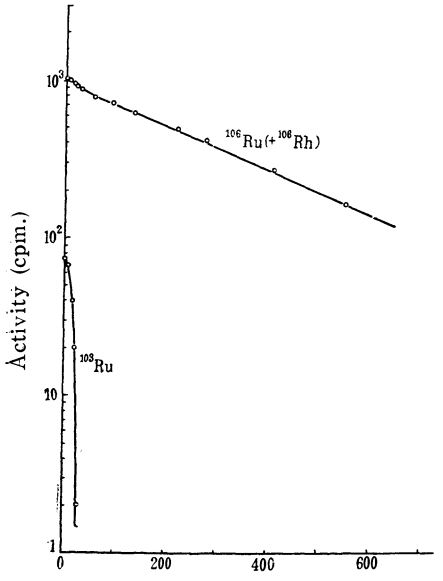

Fig. 1. Absorption curve of Ru*+Rh* fraction (Apr. 5, 1955).

be composed of two parts; rather high energy β-ray of some 3.9 MeV and low energy β-ray of less than 0.3 MeV. The former is considered to correspond to that of ^{106}Rh (3.55 MeV), the daughter of ^{106}Ru, and the latter to that of ^{103}Ru (0.22 MeV).

3. Separation of Rhodium from Ruthenium and Detection of ^{103m}Rh

The separation of rhodium from ruthenium for the purpose of detecting ^{103m}Rh includes two essential problems; (1) the half-life of ^{103m}Rh is very short (57 m.), so that the separation must be finished in a short time, (2) the energy of internal conversion electron of ^{103m}Rh is very low (0.034 MeV). Therefore, it is desirable for it to be separated in as high a specific activity as possible to minimize the effect of self-absorption.

3) D.N. Hume, *NNES-PPR*, **9**, 1557 (1951).

P. C. Stevenson, et al.[4] reported that rhodium adhers to the cation exchange resin, Dowex-50, and it is easily eluted out by passing 2 N hydrochloric acid. The workers thus succeeded in the separation of rhodium from such platinum group elements as platinum, palladium and iridium. On the other hand, it is known that ruthenium in 0.2 N hydrochloric acid solution passes through Dowex-50 resin without adhering. The procedure for the separation of rhodium and ruthenium which the present authors used in this experiment is based in principle on this difference of the properties of these elements against resin.

The resin used in this experiment was a cation exchange resin, Dowex-50 in HR-type, 50–100 mesh, ane 1.0 cm. $\phi\times6.0$ cm. in dimension. The flow rate of the solution was 1 ml./min.

The appropriate aliquot of the above mentioned ruthenium distillate was evaporated up to dryness and the residue was dissolved in a small amount of hydrochloric acid. The evaporation and dissolution processes were repeated several times; then, the acidity and total volume of the hydrochloric acid solution were adjusted to 0.2 N and 10 ml., respectively. The solution thus obtained was allowed to flow through the resin bed. After the resin bed was washed with a small quantity of 0.2 N hydrochloric acid, 2 N hydrochloric acid was passed through as the elutriant for rhodium. The effluent was collected and evaporated up to dryness in a counting dish. The activity of the residue was then measured with the 2π Q-gas flow counter, and its decay curve was observed.

The result is shown graphically in Fig. 2-I

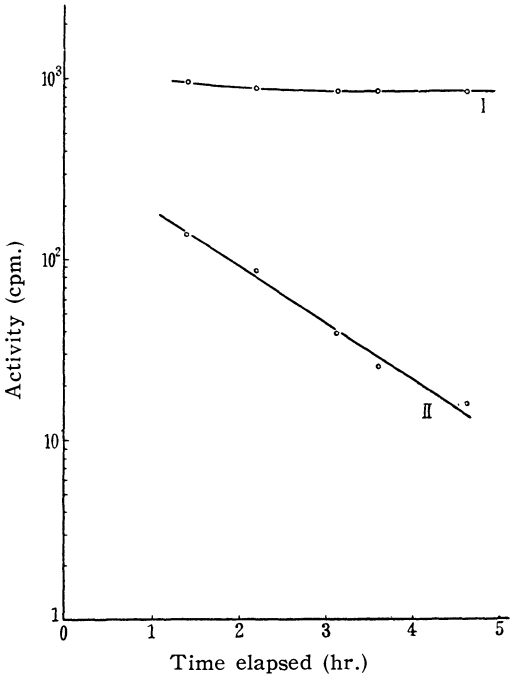

Fig. 2. Decay curve of Rh-fraction (Apr. 14, 1955).

4) P.C. Stevenson, et al., *J. Am. Chem. Soc.*, **75**, 4876 (1953).

representing the logarithm of the radioactivity against the time which has elapsed. The activity decreases rather considerably for the first several hours[5], and then it becomes approximately constant. In order to analyse this decay curve, the above-mentioned approximately constant value of the later period was subtracted from the activity values for the earlier period, and the differences were again plotted against time. Then, a virtually straight line is obtained as shown in Fig. 2-II. As its inclination coincides with that corresponding to the half-life fifty-seven minutes, the activity can be attributed to that of ^{103m}Rh. Judging from its absorption curve for aluminum foil, the radioactivity which still remains after the decay of ^{103m}Rh is attributed to the radioactivites of ^{103}Ru and ^{105}Ru+^{105}Rh. It is shown that rhodium separated by the above-mentioned method is still accompanied with considerable amounts of radioactive ruthenium.

The ruthenium fraction which passed through the resin bed was set aside and let stand over several hours to allow the growth of its daughter ^{103m}Rh and used for the next separation of ^{103m}Rh. Thus, the separation experiment of ^{103m}Rh was repeated three times in the above-mentioned way, and always observed the radioactivity which should be assigned to ^{103m}Rh.

As to the energy of the internal conversion electron of ^{103m}Rh, it was rather difficult to measure directly in the 2π Q-gas flow counter for its short half-life and low activity. Therefore, the authors applied the following conventional method; after the rhodium fraction was separated and collected in the counting dish in the way mentioned above, the dish was wrapped with the aluminum foil of 4.75 mg./cm^2 thickness[6] and its activity decay was measured. The result is shown in Fig, 3, indicating no decrease in activity. It

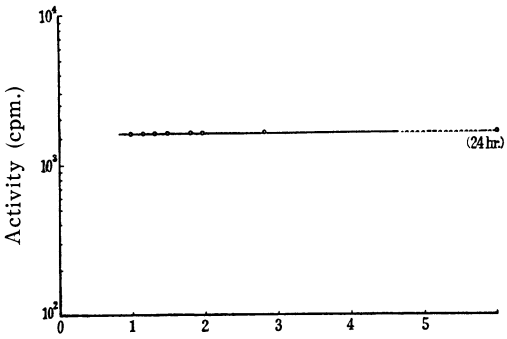

Fig. 3. Masking of ^{103m}Rh decay by 4.75 mg./cm^2 Al-foil (Apr. 21, 1955).

seems to be concluded deservedly that the radioactivity of the shorter half-life observed in this fraction in the former experiments is perfectly absorbed by the alumium foil of 4.75 mg./cm^2 thickness, and this low energy activity shoud be attributed to the internal conversion electron of ^{103m}Rh whose energy is described 0.034 MeV.

Conclusion

It can be now concluded that ^{103m}Rh is directly detected in the "Bikini Ashes" in the above mentioned way.

As the separation of rhodium must be done in as short a time as possible because of the short half-life of ^{103m}Rh, the efficiency of separation of rhodium from ruthenium in this experiment is by no means satisfactory from the analytical point of view. The rapid and clean-cut separation of ruthenium and rhodium from each other is the problem still remaining to be solved.

The radionuclides detected in the ashes are summarized in Table I including newly

TABLE I

RADIONUCLIDES DETECTED IN THE "BIKINI ASHES"

Nuclides detected	Half-life	Activity percentage of each nuclide (on March 26, 1954) (%)
^{32}P	14.30 d	—
^{35}S	87.1 d	0.1±0.05
^{45}Ca	152 d	0.2±0.1
^{89}Sr	53 d	1±0.5
^{90}Sr	19.9 y	0.02±0.01
^{90}Y	61 h	0.02±0.01
^{91}Y	61 d	8±3
^{95}Zr	65 d	5±2
^{95m}Nb	90 h	—
^{95}Nb	35 d	3±1
^{103}Ru	39.8 d	8±5
^{103m}Rh	57 m	
^{106}Ru	1.0 y	0.9±0.2
^{106}Rh	30 s	
^{125}Sb	2.7 y	—
^{129m}Te	33.5 d	—
^{129}Te	72 m	—
^{132}Te	77.7 h	—
^{131}I	8.141 d	—
^{132}I	2.4 h	—
^{137}Cs	33 y	—
^{140}Ba	12.80 d	5±1
^{140}La	40.0 h	6±1
^{141}Ce	33.1 d	7±5
^{144}Ce	282 d	2±1
^{143}Pr	13.7 d	16±5
^{144}Pr	17.5 m	2±1
^{147}Nd	11.3 d	9±4
^{147}Pm	2.6 y	—
^{237}U	6.75 d	20±10
^{239}Pu	24360 y	α: $(4\pm2)\times10^{-4}$

5) The initial time ($t=0$) corresponds to the middle time when the sample solution starts and finishes passing through the resin bed.

6) The aluminum foil of 4.75 mg/cm^2 thickness corresponds to the maximum range of β-ray of 0.05 MeV energy.

detected ^{103m}Rh as well as ^{35}S[7], ^{125}Sb[8] and ^{137}Cs[8] which are also detected after the issue of the previous paper. In addition, the contribution of each nuclide to the total activity is tabulated in Table I. These numerical values are all expressed by the percentage contribution of activity on March 26, 1954 —twenty-five days after detonation of the Bikini bomb—when the quantitative measurements of activity of the ashes were started.

7) K. Kimura, N. Ikeda and M. Inarida, Read before the Annual Meeting of the Japan Society for Analytical Chemistry, Oct. 1954 Osaka.

8) M. Honda, Y. Sasaki, Read before the Annual Meeting of the Chemical Society of Japan, Apr. 1955, Tokyo.

Summary

^{103m}Rh having very short half-life (57 m) and very low energy in electron conversion (0.034 MeV) was searched for and detected in the "Bikini Ashes". It was separated from the ashes by the method using the cation exchange resin, Dowex-50, and its activity was measured by the 2π Q-gas flow counter.

The radionuclides detected in the ashes are briefly summarized in a table.

Department of Chemistry, Faculty of Science, The University of Tokyo, Tokyo

Studies on the Infrared Spectra of Ephedrine and Related Compounds. I. On the Discrimination between Diastereoisomeric Ephedrines

By Tokunosuke KANZAWA

(Received November 29, 1955)

The discrimination whether a compound like ephedrine, which has two asymmetric carbons, belongs to the erythro or threo series has been tried by various physical or chemical methods. For example, it was reported that a large difference in the rate of N→O acyl migration in N-acyl ephedrine and in N-acyl Ψ-ephedrine was available for the discrimination between diastereoisomeric ephedrines, N-methylephedrines and 1, 2-diphenyl-2-methylaminoethanols-(1)[1]. On the other hand, the fact that pKa of Ψ-ephedrine is larger than that of ephedrine was applied to the determination of the relative configuration of 8- and 9-carbon atoms in quinine and quinidine[2]. It was also reported that from the observations of the infrared absorption spectra no general relationship was obtained for the discrimination between diastereoisomers of β-oxyamino-acids[3] and chloramphenicols[4], although it had been postulated that in their spectra finger print region should show marked differences.

Many chemical evidences revealed that spatial configuration of erythro compound like ephedrine differed from that of Ψ-ephedrine[5] and that hydroxyl and methylamino groups were placed near each other in Ψ-ephedrine and far apart in ephedrine. However, recent investigations of crystal structure of ephedrine hydrochloride[6] and of reaction mechanism of ephedrine[7] confirmed spatial approach of the two polar groups also in ephedrine. Accordingly there seems to be a contradiction between these results and the old conclusions. If the earlier view of spatial configurations of diastereoisomeric ephedrines be correct, there should be hydrogen bond between the hydroxyl and methylamino groups only in Ψ-ephedrine. Then it will be expected reasonably that the existence of this hydrogen bonding should cause some characteristic difference in the infrared spectra of diastereoisomers.

One of the purposes of the present investigation is to find some correlation, if any, useful for the discrimination between diastereoisomers in the infrared spectra of ephedrines and related compounds.

Experimental

Materials.—All compounds used in the present experiments were prepared by Dr. K. Tanaka

1) G. Fodor, V. Bruckner, J. Kiss and G. Ohegi, *J. Org. Chem.*, **14**, 337 (1949).
2) V. Prelog and O. Haefliger, *Helv. Chim. Acta*, **33**, 2021 (1950).
3) H.E. Carter, J.B. Harrison and D. Shapiro, *J. Am. Chem. Soc.*, **75**, 4705 (1953); E.D. Bergmann, H. Bendas and E. Resnick, *J. Chem. Soc.*, **1953**, 2564; W.A. Bolhofer, *J. Am. Chem. Soc.*, **71**, 1322 (1954).
4) R.A. Cutler, C.M. Martini and F.C. Nachod, *J. Am. Pharm. Assoc. Sci. Ed.*, **43**, 697 (1954).
5) L.H. Welsh, *J. Am. Chem. Soc.*, **71**, 3500 (1949); W.J. Close, *J. Org. Chem.*, **15**, 1131 (1950); K. Tanaka, *J. Pharm. Soc. Japan*, **70**, 212, 216, 220 (1950).
6) G.D. Phillips, *Acta Cryst.*, **7**, 159 (1954).
7) M. Murakami and T. Fukumoto, *J. Chem. Soc. Japan (Pure Chem. Sect.)*, **76**, 270 (1955).

and Mr. S. Sugawa and their m.p.'s and $[\alpha]_D$'s were consistent with the already reported values.

Solvents.—*Chloroform.*—Washed with dilute NaOH solution, and water, distilled after drying with anhydrous sodium sulfate and before use, dried with phosphorous pentoxide for two hours.

Carbon tetrachloride.—Washed with conc. sulfuric acid, dilute NaOH solution and water. After drying with anhydrous sodium sulfate, distilled over phosphorous pentoxide through a 40 cm., glass helix-packed column. Used after confirmation of the elimination of water by the absence of OH absorption at 2.70 μ in a 2 cm. cell.

Infrared Measurement.—A Perkin-Elmer double beam infrared spectrophotometer Model 21 was used. Spectra of solid materials were taken in Nujol mull with NaCl optics. The thickness of cell spacer was 0.01 mm. Concentration of chloroform solution was about 20 mg./cc. and a sealed cell of 0.056 cm. thickness with NaCl windows was used. The absorption of the solvent was compensated by placing a variable thickness cell filled with the solvent in the reference beam. The spectra in the case of NaCl optics were taken under the following conditions; gain 5, response 1, suppression 4, resolution 3. The spectra of carbon tetrachloride solution were taken with LiF prism in a 2 cm. glass cell having calcium fluoride windows. Ammonia-treated casein paste was used to attach the windows to the glass cell. The absorption curves were obtained by subtraction of optical densities of solvent from that of solution. The following operating conditions were used (LiF); gain 7, response 2, slit 30 μ, suppression 0, scanning speed 10–15 min./μ. Under these conditions the absorption spectra of ethylene glycol and N-methyl acetamide in the dilute carbon tetrachloride solutions were in good agreement with those reported by other authors[8].

Experimental Results and Discussion

A. Absorption Spectra of Solid Materials 3600–1800 cm^{-1} Region.—In this region the appearance of absorption bands due to OH and NH stretching vibrations are expected. As shown in Table I, most of the compounds examined show only one band near 3300 cm^{-1}, but exceptions are diastereoisomers of 1-chloro substituted ephedrine hydrochlorides and of O-benzoyl ephedrine hydrochloride, which have no OH group and no absorption band near 3300 cm^{-1}. These two compounds, however, show a well-defined band near 2400 cm^{-1}, which is observed also in the

TABLE I

ABSORPTION BANDS OF SOLID MATERIALS IN 3 μ REGION

Substance	Absorption bands (cm^{-1})		
dl-ephedrine hydrochloride	3333 (3333)*	2740	2460
l- 〃	3328 (3330)	2740	2460
dl-Ψ-ephedrine hydrochloride	3260 (3247)	2710	2455, 2425
d-Ψ- 〃	3250 (3230)	2710	2465, 2425
dl-ephedrine	3300 (3300)		2340 (?)
l-ephedrine (liquid)	3290	2786	
〃 (solid)**			2330 (?)
dl-Ψ-ephedrine	3300 (3290)		2350
d-Ψ- 〃	3200 (3216)		
dl- and *l*-1-chloro-1-phenyl-1-2-methyl-aminopropan hydrochloride		2670	2460
dl- and *d*-Ψ-1-chloro-1-phenyl-2-methyl-aminopropan hydrochloride		2670	2470, 2430
dl-N-benzoyl ephedrine	3310	2660	
dl-N-benzoyl Ψ-ephedrine	3240	2660	
dl-O-benzoyl ephedrine hydrochloride		2700	2450
dl-O-benzoyl Ψ-ephedrine hydrochloride		2700	2415
l-N-methylephedrine	***		2350 (?)
d-Ψ-N-methylephedrine (liquid)	3330	2780	
dl-N-methylephedrine hydrochloride	3215	2674	2494, 2421
dl-erythro-1, 2-diphenyl-2-methylamino-ethanol-(1) hydrochloride	3280		2421, 2300
dl-threo-1, 2-diphenyl-2-methylamino-ethanol-(1) hydrochloride	3290	2667	2494, 2353

* Values in parentheses were taken with LiF prism in perfluorocarbon mull.
** Monohydrate.
*** A broad band superposed on CH absorption.

8) a) L.P. Kuhn, *J. Am. Chem. Soc.*, **74**, 2492 (1952); b) M. Tsuboi, *Bull. Chem. Soc. Japan*, **22**, 215 (1948).

spectra of ephedrine hydrochlorides, not so marked in those of ephedrines and absent in those of N-benzoyl compound having no NH group. Since a band near 3300 cm^{-1} of N-methyl ephedrine and N-benzoyl ephedrines is undoubtedly due to OH group, it seems to be reasonable to assign ν (OH) to the band near 3300 cm^{-1}.

Following the above-mentioned assignment of ν (OH), it may be said that absorption due to free NH vibration, for which Randall et al.[9] quote an overall range of 3480–3050 cm^{-1}, is absent near 3300 cm^{-1}. Therefore, either a band near 2700 cm^{-1} or one near 2400 cm^{-1} may be due to perturbed NH vibration. The latter band seems to be due to the ionic form like $>NH_2^+$, at least in the case of hydrochlorides, because the evidences for the existence of such a band were found in the cases of bydrochlorides of triethylamine (2540 cm^{-1})[10], pyridine (2425 cm^{-1})[10], myosmine and nicotine (2560–2360 cm^{-1})[11], and in the fact that N-benzoyl ephedrine without NH group shows no absorption near 2400 cm^{-1}. As to the absorption band near 2700 cm^{-1} it seems to be related not to NH group, but to N-CH_3 group as will be seen in chloroform solution, since this band is observed forN-methylephedrine and N-benzoyl ephedrine, having no NH group.

Three absorption bands in the 1950–1800 cm^{-1} region can be ascribed to a monosubstituted benzene ring from their position and intensity relationship[12].

It will be noticed that there are systematic differences in ν (OH) of hydrochlorides of diastereoisomeric ephedrines near 3300 cm^{-1}. That is, Ψ-ephedrine hydrochloried shows an absorption of frequency about 100 cm^{-1} lower than that of ephedrine hydrochloride and the corresponding racemic modifications. The same is the case for N-benzoyl compounds, but not so marked in the cases of ephedrines and 1, 2-diphenyl-2-methylamino-ethanols-(1). From these observations and the generally accepted explanation that formation of hydrogen bond in a crystal causes a lowering of the OH absorption frequency from its normal position and that the magnitude of the shift is related to the strength of the hydrogen bond, it will be said that the hydrogen bond is formed in crystals of both of the corresponding diastereoisomers, it being only stronger in Ψ-ephedrine than in the normal one. Although such a tendency cannot be said to be general for all of the test compounds in crystalline state, it is worth noticing that a difference in the OH absorption frequency is found between diastereoisomers and between optically active, *d*- or *l*-compound and the corresponding recemic modification.

1800–1600 cm^{-1} Region.—From Figs. 1 and 2 it is seen that a band common to all compounds appears at 1600 cm^{-1}. Absorption bands which are expected to appear in this region are those due to a benzene ring and NH deformation vibration. Since the latter band is generally very weak, the 1600 cm^{-1} band may be assigned to C-C vibration of benzene ring in conjunction with 1500 cm^{-1} band observed[12].

N-benzoyl compounds show a strong band near 1600 cm^{-1}, which may be due to C=O vibration of the benzoyl group (Fig. 2). For

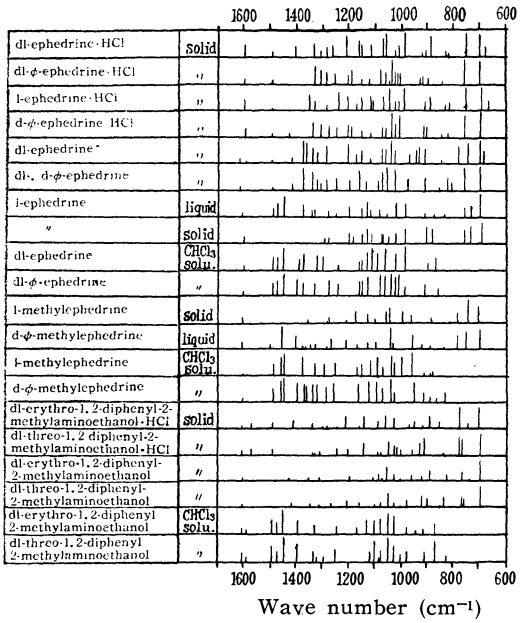

Fig. 1. Absorption spectra of ephedrine and related compounds in Nujol mull and in chloroform solution: 1600–600 cm^{-1}.

it can be considered that hydrogen bonding may lower the C=O frequency from 1670–1630 cm^{-1}, which is normal absorption frequency range for C=O group in disubstituted amide[12], to 1590–1613 cm^{-1}. Here again, pseudo compounds give a lower C=O frequency than that of the normal ones. On the other hand, O-benzoyl compounds also show a C=O band of slightly lower frequency (1715 cm^{-1}) than that for the C=O group in

9) H.M. Randall, R.G. Fowler, N. Fuson and J.R. Dangle, "Infrared Determination of organic structures", Van Nostrand (1949).
10) R.C. Lord and R.E. Merrifield, *J. Chem. Phys.*, **21**, 166 (1953).
11) B. Witkop, *J. Am. Chem. Soc.*, **76**, 5597 (1954).
12) L.J. Bellamy, "The infrared spectra of complex molecules", Methuen & Co. London (1954).

methyl benzoate (1754 cm^{-1})[13].

Finger Print Region.—From a survey of the spectra of all the compounds examined in the finger print region, it is noticed that there is a marked difference between the spectra of diastereoisomer for both optically active and corresponding racemic pairs. If there is any systematic difference in band position, this will be available for the discrimination between diastereoisomers. Bolhofer[3] attributed the erythro structure to the substituted β-phenyl-serines showing a band at 11.90–11.95 μ (840 cm^{-1}). However, his assignment stands in contradiction with observation by Cutler et al.[4] on the substituted chloramphenicols and that on the present series of compounds.

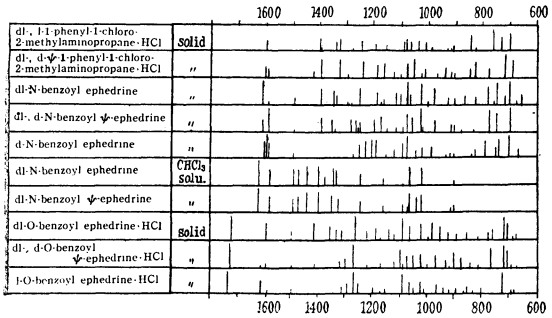

Fig. 2. Absorption spectra of ephedrine derivatives: 1800–600 cm^{-1}.

pending on compounds. It will be noticed that the pseudo-compounds give a lower frequency absorption than that of the normal ones, except ephedrine and ψ-ephedrine. This fact may be used to discriminate diastereoisomers in conjunction with the absorption in other region such as 3 μ region.

Besides these, the following observation may be added that ψ-ephedrine, N-benzoyl ψ-ephedrine, O-benzoyl ψ-ephedrine hydrochloride and both diastereoisomers of 1-chloro-substituted ephedrine give the same spectra for both the optically active compound and its racemic modification. These facts may suggest that some factors like steric configuration of molecule and the existence of a polar group capable of forming hydrogen bond affect the formation of crystal of racemic compounds as Sensi and Fagioli[14] observed on chloramphenicols.

B. Absorption Spectra in Chloroform Solution

In Fig. 3 absorption spectra in 3 μ region of chloroform solutions of ephedrines, N-methylephedrines, 1, 2-diphenyl-2-methylaminoethanols-(1) and N-benzoyl ephedrines are shown. There is a remarkable similarty among these spectra; that is, all of the compounds examined show two bands in a region 2.7–3.2 μ, one of which is sharp (the higher frequency) and the other is broad (the lower frequency). The higher frequency band near 2.7 μ may

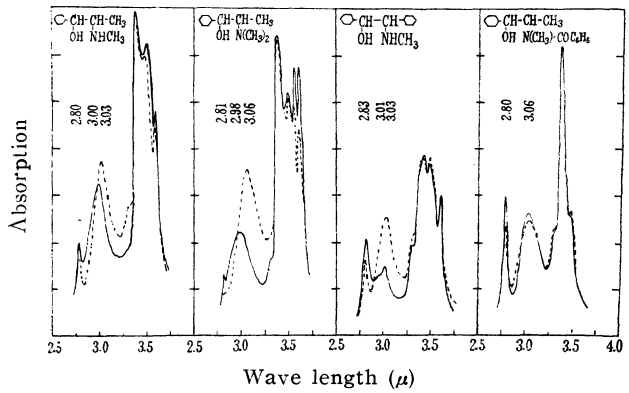

Fig. 3. Absorption of ephedrine and related compounds in chloroform solution (~0.1 mol./l.) near 3 micron.
——— erythro (normal), ----- threo (pseudo). NaCl prism.

It is usually accepted that the absorption due to secondary alcohol occurs near 1100 cm^{-1} and 1300 cm^{-1} [12], the former being fairly strong. As seen in Figs. 1 and 2, there appears a strong band within a range of 1030–1060 cm^{-1}, the position of which varies de-

be due to free OH vibration, but the lower one near 3.1 μ will be due to hydrogen-bonded OH vibration, free NH vibration or superposition of these. Since in N-methylephedrine the lower frequency absorption can be ascribed undoubtedly to the bonded OH vibration, the

13) E.J. Hartell, R.E. Richards and H.W. Thompson, *J. Chem. Soc.*, **1948**, 1436.

14) P. Sensi and O. Fagioli, *Gaz. Chim. Italiana*, **83**, 73 (1953).

same assignment seems to be reasonable for the other compounds. Moreover, the frequency difference between the sharp band and the broad one seems to be larger for pseudo-compounds than for normal ones, except in the case of N-benzoyl ephedrines.

The absorption bands near 3.4 μ are assigned to CH stretching vibration of methyl and $-CH_2-$ groups. 3.59 μ band of ephedrine, 3.56 μ band of 1,2-diphenyl-2-methylaminoethanol-(1) and 3.56 μ and 3.62 μ bands of N-methyl ephedrine, which are lower than any of CH vibration frequency of saturated hydrocarbon, could be regarded as due to CH_3-N group.

The absorption due to monosubstituted benzene derivatives in 2000–1800 cm^{-1} region appear very clearly in the spectra of chloroform solution. Absorption spectra with frequency lower than 1600 cm^{-1} are shown in Figs. 1 and 2. The spectra of the diastereoisomers show closer similarity than those in solid state. A strong band near 1000–1100 cm^{-1} has the same position for both isomers, except for ephedrines.

C. Absorption Spectra of Dilute Carbon Tetrachloride Solution[15]

As mentioned above a molecule like ephedrine may have an intramolecular hydrogen bond and this should be proved by spectra taken in a dilute carbon tetrachloride solution within the concentration range causing no intermolecular association. To ascertain more precisely the results of chloroform solution, spectra of diastereoisomers in 3 μ region were taken in carbon tetrachloride solution under a concentration of about 0.005 mol./l., by using LiF prism. The results are shown in Fig. 4.

In this case also, all compounds give very similar spectra, consisting of a higher frequency sharp band (3615–3621 cm^{-1}) and a lower frequency broad band (3329–3466 cm^{-1}). However, it is worthy of notice that only exceptionally erythro 1,2-diphenyl-2-methylaminoethanol-(1) shows two sharp bands near 3600 cm^{-1}. The difference in the frequency of the sharp and the broad band is always greater in a pseudo compound ($\Delta\nu$=ca. 200 cm^{-1}) than in the corresponding normal one ($\Delta\nu$=ca. 150 cm^{-1}). Thus, the results obtained in chloroform solutions were fully confirmed. According to the generally accepted explanation the sharp bands (3615–3621 cm^{-1}) may be attributed to free OH vibration and the broad ones (3329–3466 cm^{-1}) to the hydrogen-bonded OH vibration. Since the concentration dependence of the ratio of the optical densities of the two bands was not appreciable and also since it was reported from the result of molecular weight determination in benzene solution that the association of the alkamines did not occure over the concentration range such as in the present experiments[16], it might be said that in a sense the hydrogen bond is that of an intramolecular type. Then, it will be concluded that a hydrogen bond exists in molecules of both of corresponding diastereoisomers, only strong in Ψ-ephedrine than in a normal one. This conclusion confirms the above-mentioned suggestion based on results of the experiments in the solid state and chloroform solution, and the discrimination between diastereoisomers of ephedrine and its derivatives can be carried out simply and clearly by comparing the magnitude of the frequency difference between the free and the hydrogen-bonded OH vibrations.

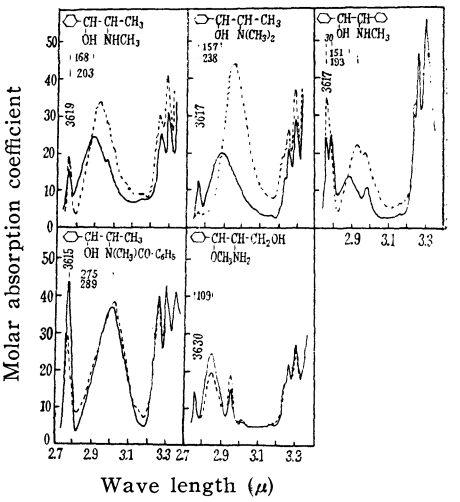

Fig. 4. Absorption of ephedrine and related compounds in carbon tetrachloride solution (~0.005 mol./l.) near 3 micron.
——— erythro (normal),
----- threo (pseudo). LiF prism.

On applying this method of discrimination between diastereoisomers to other compounds, it should be noted that the method is only applicable to compounds having two polar groups directly attached to the two adjacent asymmetric carbon atoms like ephedrines and forming a five-membered hydrogen bond ring. For example, N-benzoyl ephedrine isomers show almost the same frequency difference, because of the formation of a six-membered hydrogen bond ring, probably formed between OH and C=O group in the benzoyl radical (Fig. 4). Another example is shown in Fig. 4. 1-Phenyl-1-methoxy-2-aminopropanol-(3)

15) Partly reported as communication. T. Kanzawa, *Pharm. Bull.*, 3, 71 (1955).

16) E.D. Bergmann, E. Gil-Av and S. Pinchas, *J. Am. Chem. Soc.*, 75, 68 (1953).

which may form hydrogen bond between the amino group attached to asymmetric carbon and the OH group in the terminal CH_2OH, shows almost identical band position for diastereoisomers.

The author wishes to express his sincere thanks to Professor I. Nitta of Osaka University for his kind guidance and to Dr. K. Tanaka and Mr. T. Sugawa in this Laboratory for the kind supply of many materials. The author's thanks are also due to Dr. S. Kuwada, head of this Laboratory, and to Dr. A. Watanabe, head of the department, for their continued encouragement.

Research Laboratory, Takeda Pharmaceutical Industries Ltd., Osaka

*Ultraviolet Spectrophotometric Determination of Nickel with α-Benzildioxime**

By Yasumitsu UZUMASA and Shigenari WASHIZUKA**

(Received November 4, 1955)

α-Benzildioxime was first used by Tschugaeff[1] for the detection of nickel. The reagent was further studied by Atack and others for its estimation[2,3]. Though this reagent is superior to dimethylglyoxime as a precipitant of nickel, very few methods have been hitherto proposed for the colorimetric as well as spectrophotometric determination of microgram quantities of the element, the dimethylglyoxime method being thus still widely utilized[4].

In the present paper a sensitive spectrophotometric method for determining nickel with α-benzildioxime is proposed. This method comprises extraction of the nickel (II) chelate compound with chloroform and subsequent photometric measurement in the ultraviolet region. Recently, Ni (II)-α-furildioxime in 1, 2-dichlorobenzene[5] and also Ni (II)-dimethylglyoxime in chloroform[6] have been recommended as colored complexes suitable for the direct determination of nickel. However, because of the higher sensitivity of its colored system, the present procedure seems to have some advantage over these two methods.

The absorbance readings for the determination have been carried out at the wave lengths of 275, 358, and 406 mμ. The characteristic absorption maximum at 275 mμ is more sensitively measured than those at 358 and 406 mμ. On account of intense spectral absorption of α-benzildioxime itself in the ultraviolet region, the absorbance reading at 275 mμ can not be performed unless the excessive reagent is completely eliminated from the solvent. The present method is available for the determination of nickel in the presence of copper.

Reagent and Apparatus

The stock solution of nickel was prepared by dissolving 4.805 g. of nickel sulfate heptahydrate in 0.1 N sulfuric acid and diluted with the same to 1 liter. An aliquot of this solution was again diluted with 0.1 N sulfuric acid and the resultant solution containing 2 μg. of nickel per ml. served as standard.

The α-benzildioxime 0.02% solution was prepared by dissolving 0.02 g. of the reagent in 100 ml. of a mixture of ethyl alcohol and concentrated ammonia (95 to 5 by volume).

Redistilled chloroform was used for extraction and sodium tartrate or citrate 10% solution for preventing the precipitation of ferric hydroxide.

Glass stoppered test tubes (20 mm. × 150 mm.) and a shaking apparatus (200 cycles per minute) were most conveniently utilized for extraction and washing.

All absorbance readings were made with a Beckman Model DU spectrophotometer equipped with 1 cm. quartz cells.

---

* On October 31, 1954, part of this paper was read before the 3rd Annual Meeting of the Japan Society for Analytical Chemistry.

** Present address, Laboratory of Chemistry, Hokkaido Gakugei University, Asahigawa.

1) L. Tschugaeff, *Z. anorg. Chem.*, **46**, 144 (1905).

2) F.W. Atack, *Analyst*, **38**, 316 (1913); *C.A.*, **7**, (1913); *J. Chem. Soc.*, **1913**, 103 1317.

3, 7) Frank J. Welcher, "Organic Analytical Reagents", Vol. III., D. Van Nostland Company, Inc. New York, 1947, pp. 224-7; W.F. Hillebrand, G.E.F. Lundell, H.A. Bright, J.I. Hoffman, "Applied Inorganic Analysis", 2nd Ed., John Wiley & Sons, Inc., New York, 1953, pp. 411-2.

4, 9) E.B. Sandell, "Colorimetric Determination of Traces of Metals", 2nd, Ed., Interscience Publishers, Inc., New York, (1950) pp. 469-74.

5) A.R. Gahler, and A.M. Mitchell with M.G. Mellon, *Anal. Chem.*, **23**, 500 1951.

6) W. Nielsch, *Z. anal. Chem.*, **140**, 267 (1953).

Absorption Spectra of α-Benzildioxime and its Nickel Chelate in Chloroform

Nickel compound was precipitated according to the procedure described to the ordinary analytical method[7] and recrystallized from chloroform. It was dissolved in chloroform and subjected to the spectral measurements at the wave lengths between 250 and 500 mμ. Three distinct absorption bands of the chelate appeared at $\lambda=275$, 358, and 406 mμ, among which the band at 275 mμ was most pronounced in intensity[8].

In Fig. 1, curve 1 shows the absorption spectrum of nickel chelate obtained by the extraction process. In the region shorter than 300 mμ there appears a continuous absorption. This is obviously due to the intense absorption of the excessive reagent transferred to the chloroform layer during the extraction. However, the absorption curve showed a maximum at 275 mμ when the chloroform solution was washed with a dilute sodium hydroxide solution (curve 2). Curves 3 and 4 represent the absorption spectra of α- benzildioxime before and after being washed with sodium hydrodroxide. From these observations it was made clear that the excessive reagent transferred frkm the aqueous solution into the chloroform layer can be almost entirely removed by washing.

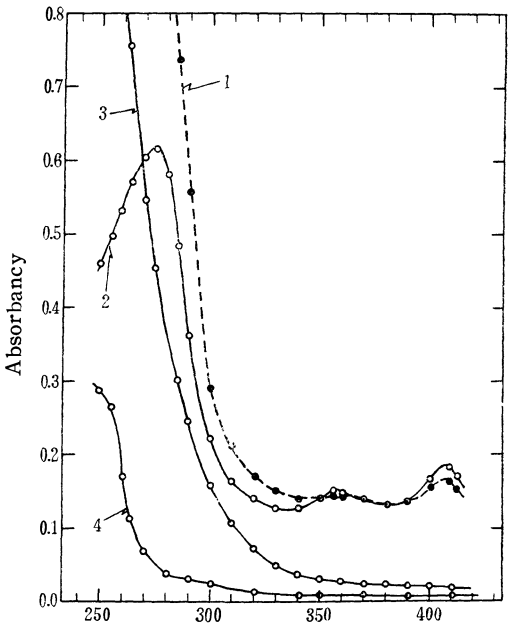

Fig. 1. Absorption spectra of α-benzildioxime and its nickel (II) chelate in chloroform.
1: Ni chelate, 0.8 p.p.m. as nickel, 2: Ni chelate washed with dil. NaOH, 0.8 p.p.m. as nickel, 3: α-benzildioxime, 4: α-benzildioxime washed with dil. NaOH.

Absorption Spectra of Copper (II) and Cobalt (II) combined with α-Benzildioxime

Copper was found to be also transferred to the chloroform phase to a great extent in the said extraction process which certainly caused an interference in the estimation of nickel. This interference was nearly obviated, however, since a striking color change from brown to yellow took place when the liquid was shaken with a dilute sodium hydroxide solution. Further elimination of the copper from the chloroform phase could be made if the chloroform phase was shaken with dilute ammonia. In case of the dimethylglyoxime method[9] copper may be entirely removed from the chloroform extract when shaken with dilute ammonia. However, the removal of copper α-benzildioxime from the chloroform phase is not satisfactory if the extract is washed only with ammonia.

Cobalt is also transferred to the chloroform phase in the extraction process, and the interference of this metal could not be simply eliminated by washing with sodium hydroxide solution and ammonia. These effects are shown in Fig. 2 and are summarized as follows:

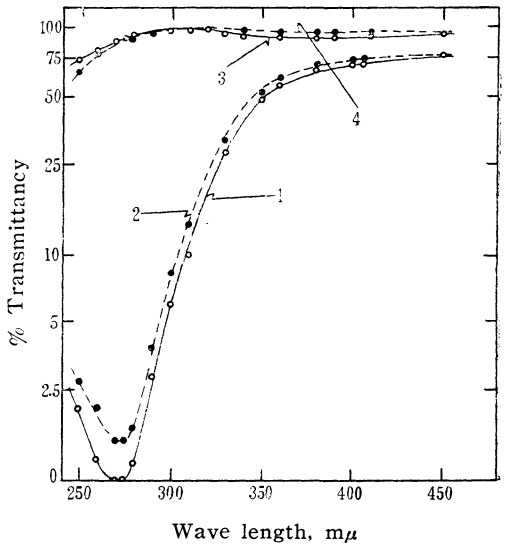

Fig. 2. Absorption spectra of copper with α-benzildioxime in chloroform.
1: copper in original extract, 2: washed with dil. ammonia, 3: washed with dil. NaOH, 4: washed with dil. NaOH, then with dil. ammonia.

8) K. Sone, *J. Am. Chem. Soc.*, 75, 5207 (1953).

Metal,	Color in chloroform,	Color after washing with NH_4OH,	with NaOH,	with NaOH then NH_4OH
Ni–complex	yellow	yellow	yellow	yellow
Cu–complex	brown	brown	yellow	colorless
Co–complex	yellow	yellow	yellow	yellow

From these experimental results it was confirmed that the positive error due to the presence of copper is most effectively minimized by washing the chloroform extract first with a dilute sodium hydroxide solution and then with dilute ammonia.

Fig. 3 indicates that by this treatment the absorption of the copper compound becomes almost negligible in the region longer than 300 mμ whereas the band due to cobalt whose maximum is 260 mμ still predominates. This fact suggests to us that the present procedure allows us to estimate nickel in the solution which contains a certain amount of copper but no cobalt.

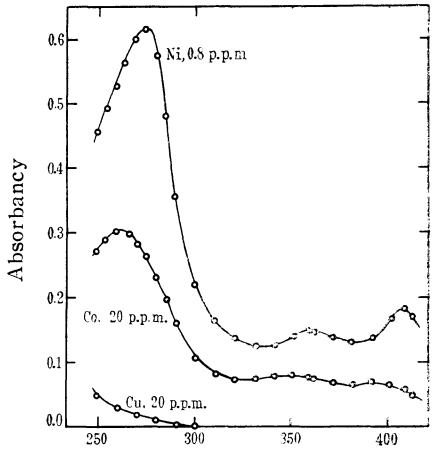

Fig. 3. Absorption curves of nickel, cobalt, and copper.

Conditions for Color Development and Extractions

Effect of pH.—Completeness of precipitation and extractability with chloroform using buffer solutions with pH ranging from 6.0 to 11.4. The optimum pH for the extractions was found to be 8.8 or above. When pH of the solution exceeds 8.8 the nickel complex precipitates immediately, allowing the extraction to be carried out rapidly. This fact shows that the strict adjustment of pH is not necessary, thus eliminating the use of a buffer.

Duration and Number of Extractions.—In order to determine the duration of extraction a series of solutions containing a definite amount of nickel were extracted by shaking the containers mechanically with a shaking apparatus (200 cycles per min.) for some time. Data in Table I show that the duration of two minutes is sufficient for removing the complex from the aqueous solution provided that 5 ml. of chloroform is used. Complete removal was confirmed by the absence of the spectral absorption due to the nickel chelate in the second chloroform extract. When the volume of the aqueous solution was 5 to 50 ml., complete extraction was established by shaking with 5 ml. of chloroform for two minutes.

Table I

Effect of duration on extraction

Duration, min.	Absorbancy 358 mμ	406 mμ
2	0.666	0.740
5	0.668	0.744
10	0.666	0.744
15	0.666	0.744

Aqueous volume, 15 ml. Nickel taken, 20 μg. Organic solvent, 5 ml. of chloroform at a time.

Amount of Reagent. — The solubility of α-benzildioxime in ethyl alcohol is about 0.2 g. per liter, which increases to some extent in ammoniacal medium. In the present method the reagent solution of 0.02% was prepared, 2 ml. of which was required to extract 20 μg. of nickel (theor. mole ratio of the reagent for nickel was 1 : 2.5) this was the maximum concentration (4 p. p. m. in chloroform) available in this determination. Although up to 4 ml. the reagent was found to give no effect on the absorbancy of the nickel chelate in the measurements at 358 and 406 mμ, 2 ml. was used lest the reagent should make any disturbance. Since the absorption, especially at 275 mμ, due to α-benzildioxime itself, was intense the use of more of the reagent must be avoided.

General Procedure

Isolation of Nickel.—To about 15 ml. of slightly acidic sample solution in a glass stoppered test tube, containing up to 20 μg. of nickel, add 2 ml. or more of 10% sodium tartrate or citrate solution to prevent the precipitation of hydroxide of ferric iron. Make the solution ammoniacal by adding 2 ml. of 10% ammonia or a few drops of concentrated ammonia in excess, add 2 ml. of 0.02% α-benzildioxime solution, and shake the tube for ten seconds by hand. As red precipitate appears immediately, add exactly 5 ml. of chloroform with a pipet. Shake the tube for two minutes horizontally with a shaking apparatus (200 cycles per min.), and extract the precipitate.

Washing. — Draw off the aqueous layer by suction, introduce 10 ml. of 1% sodium hydroxide solution into the tube, and shake the tube for one minute as before. Draw off the alkaline layer by suction, and wash the chloroform layer once with 10 ml. of 0.5% ammonia, then with two 10 ml. portions of 1% sodium hydroxide solution for one minute successively.

Photometric Determination of Nickel.—After the last washing liquid is nearly completely removed, the chloroform solution is taken up with

a dry pipet and filtered into a 1 cm. quartz cell using dry filter paper of small size. Prepare a blank reagent solution by introducing about 15 ml. of distilled water into the tube and treating the water by the same procedure. The standard nickel solutions prepared for setting up the calibration curves should be also treated by the same procedure as the sample solution. Make the absorbance measurements for the chloroform solutions of the sample, standard, and reagent blank at 275, 358, or 406 mμ respectively, pure chloroform being put in the reference cell. Subtract the absorbancy of the reagent blank from that of the sample as well as the standard, and determine the amount of nickel in the given sample. Fig. 4 gives the calibration curves for nickel at 275, 358, and 406 mμ. As shown in Fig. 4 and Table II, the maximum sensitivity on the present spectrophotometric method is attained when the absorbance readings at 275 mμ are used. The sensitivity is superior to that of he classical dioxime method.

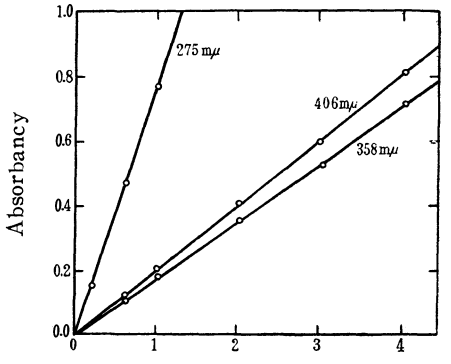

Fig. 4. Calibration curves for nickel. Beckman Model DU spectrophotometer, with 1 cm. quartz cells.

TABLE II

SENSITIVITY FOR α-BENZILDIOXIME METHOD (Solvent, chloroform)

Ni taken,	Ni, p. p. m./($A_s \times 10^3$)(b)		
p. p. m.(a)	275 mμ	358 mμ	406 mμ
0.2	1.31×10^{-3}	5.56×10^{-3}	4.76×10^{-3}
0.4	1.33 〃	5.55 〃	4.88 〃
0.6	1.29 〃	5.56 〃	4.92 〃
1.0	1.31 〃	5.59 〃	4.74 〃
2.0		5.62 〃	4.95 〃
4.0		5.59 〃	4.95 〃
Average	1.31 〃	5.59 〃	4.94 〃

(a) Microgram of nickel per ml. of chloroform.

(b) Sensitivity, by Sandell's definition[10]. A_s, absorbancy.

10) E. B. Sandell, "Colorimetric Determination of Traces of Metals", 2nd Ed., Intersince Publishes, Inc. New York, 1953, p. 49.

Influence of Foreign Ions

By observing the conditions prescribed above better extractability and stability of the complex are attained thusall owing much more satisfactory separation of nickel from ferric iron, aluminum, zinc, chromate, vanadate, and molybdate ions. In Table III the results for the determination of nickel in the presence of ferric iron and other interfering elements such as copper and cobalt are shown. This table shows that when as much as 5 μg. of nickel is to be determined the allowable concentration for copper is as high as 0.1 mg. and for cobalt 0.01 mg.

As already discussed copper is readily extracted into the chloroform phase from which it is eliminated by washing with sodium hydroxide solution and ammonia. In case where its concentration is higher than 0.1 mg., however, copper may hinder nickel from reacting with the reagent (expt. Nos. 4 and 5 in Table III). Therefore, if the concentration of copper should be much higher than that of nickel, the amounts of the reagent as well as chloroform must be increased.

TABLE III

EFFECT OF COPPER, COBALT, AND IRON ON THE DETERMINATION OF NICKEL

No.	Foreign ion added, mg.		Ni found, μg. 275 mμ	358 mμ	406 mμ
1	0.01	Cu	5.0	5.0	5.0
2	0.05	〃	5.1	5.1	5.0
3	0.1	〃	5.4	5.1	5.2
4	0.5	〃	1.0	1.0	0.7
5	1.0	〃	1.2	1.2	0.8
6	0.005	Co	4.9	5.0	5.0
7	0.01	〃	5.1	4.9	5.0
8	0.05	〃	5.5	5.5	5.6
9	5.5	Fe (III)	5.1	5.0	5.0
10	11.0	〃	5.1	5.0	5.0

Ni taken in 10 ml. of aqueous solution, 5.0 μg. 10 % sodium citrate solution added, 4 ml. Reagent solution added, 2 ml. Chloroform, 5 ml.

TABLE IV

REPRODUCIBILITY OF DETERMINATION OF NICKEL IN SYNTHETIC SOLUTION

Ni found, absorbancy,			Deviation from Av. absorbancy		
275 mμ	358 mμ	406 mμ	275 mμ	358 mμ	406 mμ
0.755	0.181	0.212	0.019	0.003	0.004
0.783	0.184	0.216	0.009	0.000	0.000
0.780	0.178	0.217	0.006	0.006	0.001
0.775	0.180	0.216	0.001	0.004	0.000
0.785	0.189	0.217	0.011	0.005	0.001
0.770	0.188	0.214	0.004	0.004	0.002
0.768	0.187	0.218	0.006	0.003	0.002
Av. 0.774	0.184	0.216			
Av. deviation			0.0080	0.0036	0.0014
Max. deviation			0.019	0.006	0.004
Av. relative deviation			1.03%	1.96%	0.65%
Max. relative deviation			2.45%	3.26%	1.85%

Composition of the synthetic solution, Fe (III) 54.5%, Cu (II) 1.0%, Cr (VI) 1.1%, Al 32.7%, Mo (VI) 4.4%, V (V) 0.7%, Zn 5.5%, Ni 0.1%. Total amount of elements, 5.0 mg. in 10 ml.

In order to test the precision of the method, the determination was made with the synthetic solution which contained ferric iron, aluminum, zinc, chromate, vanadate, molybdate, copper, and nickel ions whose total amount was 5.0 mg. The absorbance readings of seven determinations showed average and maximum relative errors to be 1.03 and 2.45% at 275 mμ, 1.96 and 3.26% at 358 mμ, and 0.65 and 1.85% at 406 mμ respectively. These are shown in Table IV.

Summary

A new method described here involves the extraction of nickel (II)-benzildioxime with chloroform and the spectrophotometric measurements of the colored system in the same solvent. The wide pH range for the extraction eliminates the use of a buffer, and nickel is readily separated from ferric iron, aluminum, zinc, chromate, vanadate, and molybdate ions. By obviating the excessive benzildioxime with dilute alkali, the most sensitive absorbance readings are achieved, and the sensitivity at 275 mμ is 0.0013. Beer's law holds up to 1 p. p. m. of nickel at 275 mμ, and up to 4 p. p. m. at 358 and 406 mμ. The nature and degree of interference of copper and cobalt on the color development are also discussed, and their allowable amounts are determined.

Department of Chemistry, Faculty of Science, Hokkaido University
Sapporo

On the Dielectric Constant of Polar Liquid

By Masasi YASUMI and Hitoshi KOMOOKA

(Received November 15, 1955)

Introduction

The Debye's theory for the dielectric constant of polar fluids seems to be inadequate to explain quantitatively most of the experimental results for the polar liquids.

The origin of the failure of the theory has been discussed by many authors[1]. It is concluded that the inadequacy of the assumption concerning the local field adopted by Debye[2] plays the most important role.

Assuming an simplified model for the polar liquid, Onsager has obtained a quite different expreession for the local field and succeeded in deriving a formula for the dielectric constant of polar liquid[1]. In spite of the rather over-simplified model, the Onsager's formula seemed to be able to eliminate the difficulties appearing in Debye's theory[1]. Although the Onsager's theory succeeded in explaining the experimental results (at least semiquantitatively), the problem of the local field in polar liquid seems not to have been solved completely.

1) L. Onsager, *J. Am. Chem. Soc.*, 58, 1486 (1936). J.H. Van Vleck, *Ann. N.Y. Acad. Sci.*, 40, 289 (1940). S. Oka, "Theory of Dielectrics", Iwanami-shoten, (in Japanese) (1954).

2) The local field adopted by Debye is sometimes called Lorentz field. However, Lorentz applied this field only to the case of induced polarization. As shown below, the Lorentz field is correct when applied within this limitation.

In the present work, we have obtained an expreession for the local field, from the point of view of the classical electrodynamics in the continuous medium. Using this expersion for the local field we have obtained also an expression for the dielectric constant. [section 2–A]

The result is as follows: a Wyman type relation between dielectric constant ε and absolute temperature T exists, i.e. $\varepsilon \sim 1/T$.

If we take into account the fluctuation of the internal field, a slightly different expression is obtained. [section 2–B]

The Internal Field and the Dielectric Constant

We assume that polar fluid is continuous and that its dipolar density $\vec{p}$ is expressed as follows:

$$\vec{p} = \vec{\mu}/v \tag{1}$$

where v is the volume element in the polar liquid and $\vec{\mu}$ is the dipole moment of this volume element. If we assume that the shape of the molecule of which the dipolar substance consists is the sphere of the radius a, we may choose $\frac{4}{3}\pi a^3$ as volume element v, and μ may be considered as the dipole mo-

ment of the molecule i. e.

$$v=\frac{4}{3}\pi a^3 . \quad (2)$$

[A] The case when we do not take into account the fluctuation of the internal field.

The electric field, the external field, the internal field and the self-field of the volume element v are denoted by $\vec{E}$, $\vec{E}_0$, $\vec{F}$, $\vec{E}_S$, respectively. The expression of the $\vec{E}_S$ is determined when we know the type of the self-field (i. e. dipolar, quadrupolar, etc.).

On the other hand the expression of the internal field, which is the vector sum of the external force and the forces of all other volume elements in the dielectric medium, may have a complicated form.

However, in the continuous medium, the expression of the internal field may be obtained as follows.

In the continuous medium the electric field $\vec{E}$ is resolved into the internal field and the self-field, i. e.[3,4]

$$\vec{E}=\vec{F}+\vec{E}_S . \quad (3)$$

If the self-field $\vec{E}_S$ is assumed to be dipolar and if the Eq. (2) is valid, $\vec{E}_S$ is represented as[4]:

$$\vec{E}_S=-\frac{4\pi}{3}\vec{p}=-\frac{\vec{\mu}}{a^3} . \quad (4)$$

The dipole moment of a molecule consists of two parts i. e. the permanent dipole moment $\vec{\mu}_0$ and the induced dipole moment $\alpha\vec{F}$,

$$\vec{\mu}=\vec{\mu}_0+\alpha\vec{F} \quad (5)$$

where α is the polarizability of the molecule.

The case when the molecule has not a permanent moment (non-polar molecule), the following equation holds

$$(n^2-1)\vec{E}=4\pi\vec{p} \quad (6)$$

where n is the refractive index.

In this case

$$\vec{E}_S=-\frac{(n^2-1)}{3}\vec{E} . \quad (7)$$

From the Eqs. (3), (4) (6) and (7) $\vec{F}$ is represented as:

$$\vec{F}=\vec{E}+\frac{n^2-1}{3}\vec{E}=\frac{n^2+2}{3}\vec{E} . \quad (8)$$

This is the Lorentz-Lorenz internal field.

On the other hand from the Eqs. (7), (1) and (2) (taking $\mu_0=0$)

$$\vec{p}=\frac{\alpha\vec{F}}{(4/3)\pi a^3} . \quad (9)$$

From the Eqs. (5) and (9)

$$\frac{\alpha}{a^3}=\frac{n^2-1}{n^2+2} . \quad (10)$$

Eq. (10) is the well-known Lorentz-Lorenz formula.

For the case of the polar liquid, the internal field $\vec{F}$ is expressed as: (Eqs. (3), (4) and (5) being used)

$$\vec{F}=\frac{1}{(1-\alpha/a^3)}\left[\frac{\vec{\mu}_0}{a^3}+\vec{E}\right] . \quad (11)$$

Putting (10) into (11), we obtain

$$\vec{F}=\frac{n^2+2}{3}\left[\frac{\vec{\mu}_0}{a^3}+\vec{E}\right] . \quad (12)$$

Using this equation and the Eq. (5) we have,

$$\vec{\mu}=\frac{n^2+2}{3}(\vec{\mu}_0+\alpha\vec{E}) . \quad (13)$$

The component of $\vec{\mu}$ along the direction of $\vec{E}$ is denoted by μ_E, and the mean value of μ_E is denoted by $<\mu_E>$.

Assuming Boltzman statistics, we have the following equation,

$$<\mu_E>=\int\mu_E\cdot e^{-\frac{U}{kT}}d\Omega\Big/\int e^{-\frac{U}{kT}}d\Omega \quad (14)$$

where U is the potential energy of the dipole $\vec{\mu}$ in the electric field and $d\Omega$ is an elementary solid angle. U has the following expression.

$$U=-\left\{\frac{1}{2}\alpha F^2+(\vec{\mu}_0\cdot\vec{F})\right\} . \quad (15)$$

Let the angle between $\vec{E}$ and $\vec{\mu}_0$ be θ,

$$\mu_E=\frac{n^2+2}{3}(\mu_0\cos\theta+\alpha E) . \quad (16)$$

Inserting (15) and (16) in (14) and making a simple calculation we have the following expression for $<\mu_E>$,

$$<\mu_E>=\frac{n^2+2}{3}\alpha E+\left(\frac{n^2+2}{3}\right)^3\frac{\mu_0^2}{3kT} . \quad (17)$$

In this calculation $e^{-\frac{U}{kT}}$ is expanded in the power series of E, and only the terms proportional to E are retained.

The dielectric constant is related to $<\mu_E>$ by the following equation.

$$(\varepsilon-1)E=\frac{4\pi N}{V}<\mu_E> , \quad (18)$$

where N is Avogadro's number and V is

3) J.H. Van. Vleck, "Theory of Electric and Magnetic Susceptibilities".

4) H. Fröhlich, "Theory of Dielectrics". Oxford (1949).

molecular volume. In our model of the dipolar molecule,

$$\frac{N}{V}=\frac{1}{(4\pi/3)a^3} . \tag{19}$$

Using the Eqs. (18), (17), (19) and (10), we have

$$\varepsilon-n^2=\frac{4\pi N}{V}\left(\frac{n^2+2}{3}\right)^3\frac{\mu_0^2}{3kT} . \tag{20}$$

J. Wyman proposed the following simple experimental formula for the dielectric constant of polar liquids[5],

$$\varepsilon+1=K_w\bar{p} , \tag{21}$$

where

$$\bar{p}=\frac{4\pi}{3}\cdot\frac{N}{V}\cdot\frac{\mu_0^2}{3kT} . \tag{22}$$

K_w represents a constant and amounts to about 8.5 for most of normal polar liquids.

In the case when ε is much greater than n^2, the form of the Eq. (20) is similar to that of the Eq. (21), i. e.

$$\varepsilon\simeq 3\left(\frac{n^2+2}{3}\right)^3\bar{p} . \tag{23}$$

Moreover if $n=1.5$ the factor of $\bar{p}$ $\left(\text{i. e } 3\left(\frac{n^2+2}{3}\right)^3\right)$ amounts to about 8.5. Since the refractive index of most of the liquid is about 1.5 the validity of the Wyman's relation is explained by our theory.

[B] The case when the fluctuation is taken into account.

In the above-mentioned treatment, we have assumed that the local field is expressed by means of the self-field and the electric field. However, actually the form of the local field may be very complicated, since it is the sum of the external field and the fields of all other molecules. It is beyond our ability to treat this problem rigorously.

We attempt to solve this problem making an assumption for the form of the fluctuating local field $\vec{F}_f$, when it is slightly different from its mean value $\vec{F}_m$.

Consider at first the static equilibrium. In this case, $\vec{F}_m=\vec{F}$. Next we imagine that the molecule considered changes its orientation by some action. In this case we assume that the arrangement of the sorrounding molecules does not change. That is to say, the magnitude of F_f is equal to that of F_m, but its orientation is not the same as in the static equilibrium.

5) J. Wyman, *J. Am. Chem. Soc.*, 58, 1482 (1936).

In other words, the direction of $\vec{F}_f$ can take any direction independent of the direction of $\vec{\mu}_0$. Moreover we assume that the probability of orientation is regulated by Boltzmann's factor.

The expression for $\vec{F}_f$ and $\vec{\mu}$ may have the following forms:

$$\vec{F}_f=\left(\frac{n^2+2}{3}\right)\left(\vec{E}+\frac{\mu_0}{a^3}\vec{u}_1\right) \tag{24}$$

$$\vec{\mu}=\alpha\vec{F}_f+\mu_0\vec{u}_2 , \tag{25}$$

where $\vec{u}_2$ is the unit vector along the direction of $\vec{\mu}_0$, and $\vec{u}_1$ represents the unit vector along the direction of the fluctuating local field. In this case, the electric field (denoted by $\vec{E}_f$) also fluctuates about the direction of $\vec{E}$.

$$\vec{E}^f=\vec{F}_f+\vec{E}_S=\vec{E}+\frac{\mu_0}{a^3}(\vec{u}_1-\vec{u}_2) . \tag{26}$$

In the case of absence of the fluctuation $u_1=u_2$, then $\vec{E}_f$ coincides with $\vec{E}$.

The potential energy of a molecule assumes the following form:

$$U=-\left\{\frac{1}{2}\alpha F_f^2+\mu_0(\vec{u}_2,\vec{F}_f)\right\} . \tag{27}$$

In this case $<\mu_E>$ is expresses as:

$$<\mu_E>=\iint(\vec{\mu},\vec{\mu}_0)e^{-\frac{U}{kT}}d\Omega_1 d\Omega_2\Big/\iint e^{-\frac{U}{kT}}d\Omega_1 d\Omega_2 \tag{28}$$

where $\vec{u}_0$ denotes the unit vector along $\vec{E}$. $d\Omega_1$ and $d\Omega_2$ represent the elementary solid angles the around directions of $\vec{u}_1$ and $\vec{u}_2$ respectively.

A calculation transforms the Eq. (28) to the following expression:

$$<\mu_E>=E\left[\frac{n^2+2}{3}\alpha+\frac{\mu_0^2}{3kT}\left(\frac{n^2+2}{3}\right)\times\left\{1+\left(\frac{n^2-1}{3}\right)^2\right\}+\frac{2\mu_0^2}{3kT}\left(\frac{n^2-1}{3}\right)\left(\frac{n^2+2}{3}\right)L(y)\right] \tag{29}$$

$$y=\frac{n^2+2}{3}\frac{\mu_0^2}{a^3kT} , \tag{30}$$

where $L(y)$ denotes Langevin function. As in the previous case, $e^{-\frac{U}{kT}}$ is expanded in the power series of E and only the terms proportional to E are retained.

Inserting this expression for $<\mu_E>$ to the Eq. (18) we have this expression for ε,

$$\varepsilon-n^2=\frac{4\pi N}{V}\frac{\mu_0^2}{3kT}\left(\frac{n^2+2}{3}\right)\left\{1+\left(\frac{n^2-1}{3}\right)^2\right\}$$

$$+\frac{4\pi N}{V}\frac{2\mu_0^2}{3kT}\left(\frac{n^2+2}{3}\right)\left(\frac{n^2-1}{3}\right)\mathrm{L}(y). \quad (31)$$

For the large value of y, $\mathrm{L}(y)$ is approximately equal to 1. Then the Eq. (31) coincides with the Eq. (20).

For the value of y greater than 3, $\mathrm{L}(y)\fallingdotseq 1-1/y$. In this case the Eq. (31) is approximated as follows:

$$\varepsilon-\frac{n^2+2}{3}=\frac{4\pi N}{V}\frac{\mu_0^2}{3kT}\left(\frac{n^2+2}{3}\right)^3. \quad (32)$$

For most of polar liquids, the approximate Eq. (32) is sufficient, because the values of y are greater than 3 for them.

Comparison of Our Formula with Experiments

The coefficient K_w in the Wyman's formula, takes the value 8.5 for most of the normal polar liquids but fluctuates from 6.2 to 11. K_w corresponds to $3\left(\frac{n^2+2}{3}\right)^3$ in our formula (32). $3\left(\frac{n^2+2}{3}\right)^3$ takes the value 6.2 when $n=1.34$, and 11 when $n=1.62$.

For example, we calculate the dielectric constant of some of the polar liquids referred to in Wyman's paper[5], by means of our formula (32).

In Table I, the dielectric constants of esters, chlorides and nitro-compounds calculated with the Eq. (32) are given, and compared with those calculated with the Wyman's formula (21). The observed values are also given. The values of $\bar{p}$ are taken from the Wyman's paper[5].

The values of refractive indices for sodium D line n are taken from "International Critical Tables" and are also given in Table I.

TABLE I

THE DIELECTRIC CONSTANTS OF ESTERS, CHLORIDES AND NITROCOMPOUNDS

Name	n	$3\left(\frac{n^2+2}{3}\right)^3$	$\bar{p}$	$\varepsilon(Y-K)$	$\varepsilon(W)$	ε(obs.)*
Ethyl formate	1.358	6.35	1.21	9.2	9.3	8.6
Isobutyl formate	1.386	6.67	0.93	7.5	6.9	8.0
Methyl acetate	1.359	6.35	1.03	7.8	7.8	7.3
Isobutyl acetate	1.391	6.76	0.81	6.7	5.8	5.6
Ethyl salysilate	1.525	8.85	1.55	15.2	12.2	8.6
Ethyl cinnamate	1.544	9.20	0.95	10.2	7.1	6.6
Methyl benzoate	1.518	8.73	0.87	9.0	6.7	6.9
Ethyl nitrate	1.385	6.68	2.4	17.3	19.4	19.7
Acethyl chloride	1.390	6.75	2.38	17.5	19.2	15.9
Ethylidene chloride	1.417	7.15	1.15	9.5	8.8	10.9
Allyl chloride	1.415	7.10	1.27	10.3	9.8	8.2
p-Chlorotoluene	1.519	8.75	0.89	9.2	6.6	6.2
tert-Amyl chloride	1.408	6.98	1.04	8.5	7.9	9.5
Nitromethane	1.381	6.60	3.82 5.81	26.5 39.7	31.5 43.4	39.4
Nitroethane	1.390	6.75	3.26 4.76	23.3 33.3	26.7 39.5	30.0?
Nitrobenzene	1.553	9.40	3.05 3.74	30.1 36.6	24.9 30.8	36.1
o-Nitrotoluene	1.547	9.32	2.78	27.4	22.6	27.4

* $\varepsilon(Y-K)$ is the value calculated with our formula.
$\varepsilon(W)$ is the value calculated with the formula of Wyman.
ε(obs.) is the observed value.

As Wyman has stated[5], the values of $\bar{p}$ are not satisfactorily reliable. Accordingly, we cannot bring up detailed discussion with the above-described comparison. We can only say that from the experimental point ot view, our formula (32) has applicability comparable to that of Wyman.

Next we calculate the dielectric constants of benzonitrile, nitrobenzene, ethyl bromide, ethyl iodide and chlorobenzene.

For these substances the dielectric constants in the liquid state have been measured over a considerably wide range of temperature[6]. The values are given in Table II. The densities are calculated with the equa-

6) R.J.W. Le Fevre, *Trans. Faraday Soc.*, **34**, 1127 (1938).

tion referred to in "International Critical Tables".

The refractive indices are calculated from the value of molecular refraction[7] according to the Lorentz-Lorenz formula.

a) Benzonitrile.—The values of ε are calculated with the Eq. (32).

TABLE II-1

THE DIELECTRIC CONSTANTS OF BENSONITRILE

$\mu_0=4.39$ D[8]

t(°C)	d	n	$3\left(\frac{n^2+2}{3}\right)^3$	$\overline{p}$	ε(calcd.)	ε(obs.)
0	1.0228	1.539	9.26	4.23	40.7	27.6
18	1.0070	1.529	9.07	3.94	37.3	25.85
25	1.0018	1.526	9.02	3.83	36.0	25.2
40	0.9874	1.517	8.85	3.60	33.2	24.0
50.3	0.9782	1.511	8.74	3.45	31.5	23.28
60	0.9697	1.506	8.64	3.32	30.2	22.7
70	0.9607	1.501	8.55	3.19	28.7	22.1

b) Nitrobenzene.—The values of ε are calulated with the Eq. (32).

TABLE II-2[9]

THE DIELECTRIC CONSTANTS OF NITROBENZENE

$\mu_0=4.19$ D[10]

t	d	n	$3\left(\frac{n^2+2}{3}\right)^3$	$\overline{p}$	ε(calcd.)	ε(obs.)
10	1.222	1.563	9.75	3.98	40.3	37.9
25	1.168	1.550	9.48	3.76	37.1	34.9
30	1.193	1.547	6.42	3.68	36.2	34.0
40	1.183	1.542	9.32	3.53	34.3	32.3
60	1.163	1.531	9.12	3.26	31.2	29.1

c) Ethyl Bromide.—The values of ε are calculated with the Eq. (32).

TABLE II-3

Ethyl bromide

$\mu_0=2.01$ D[11]

t	d	n	$3\left(\frac{n^2+2}{3}\right)^3$	$\overline{p}$	ε(calcd.)	ε(obs.)
−30	1.564	1.461	5.70	1.463	9.57	11.69
−20	1.543	1.454	5.64	1.359	8.97	11.20
−10	1.5215	1.446	5.58	1.290	8.56	10.68
0	1.5014	1.439	5.52	1.226	8.09	10.19
10	1.4813	1.433	5.47	1.166	7.73	9.71
25	1.4500	1.422	5.40	1.087	7.21	9.01

d) Ethyl Iodide.—The values of ε are calculated with the Eq. (32).

TABLE II-4

Ethyl iodide

$\mu_0=1.87$ D[31]

t	d	n	$3\left(\frac{n^2+2}{3}\right)^3$	$\overline{p}$	ε(calcd.)	ε(obs.)
0	1.980	1.528	9.03	0.995	10.42	8.33
10	1.958	1.521	8.88	0.950	9.86	8.00
25	1.924	1.510	8.70	0.887	9.15	7.64
35	1.902	1.503	8.55	0.848	8.68	7.37
45	1.880	1.496	8.44	0.812	8.29	7.11
55	1.859	1.490	8.32	0.779	7.88	6.90
65	1.839	1.483	8.23	0.746	7.54	6.66

7) "International Critical Tables", Vol. VII, p. 32.

8) L.G. Groves and S. Sugden, *J. Chem. Soc.*, **1934**, 1094.

9) The values of n and d are calculated as in the previous cases.

10) K.B. McAlpine and C.P. Smyth, *J. Chem. Phys.*, **3**, 55 (1934).

11) L.G. Groves and S. Sugden, *J. Chem. Soc.*, 158 (1937).

e) **Chlorobenzene.**—The values of ε are calculated with the Eq. (29).

TABLE II-5

Chlorobenzene
$\mu_0=1.70$ D[10]

t	d	n	ε(calcd.)	ε(obs.)
21	1.1053	1.524	6.05	5.67
25	1.1014	1.522	5.98	5.61
40	1.0847	1.512	5.69	5.37
48	1.0761	1.508	5.46	5.23
70	1.0520	1.495	5.10	4.89

Conclusions and Remarks

It is suprising that our theory can fairly explain the experimental data. For our theory is based upon the above-described over-simplified assumption.

As in the case of the Wyman's equation, our theory cannot be applied to the so-called abnormal liquids.

It seems that our Eqs. (31) and (32) become in better agreement with the experimental data near the boiling point than near the melting point.

The degree of coincidence of our theory with the experimental data seems to depend on the chemical structure of the molecule forming the liquid considered.

As stated by Wyman[5], if a linear relation between ε and $\bar{p}$ exists, the critical frequency ν_c will be represented as

$$2\pi\nu_c\tau=1\,, \tag{33}$$

where τ denotes the relaxation time, because the value of $<\mu_E>$ in the case of an alternating field may be represented as:

$$<\mu_E>=\left\{\frac{1}{1+i\omega\tau}\frac{\mu_0^2}{3kT}\left(\frac{n^2+2}{3}\right)+\left(\frac{n^2+2}{3}\right)\alpha\right\}E, \tag{34}$$

where ω denotes the angular frequency.

Inserting Eq. (34) into Eq. (18), ε (complex quantity) is obtained, and Eq. (33) is readily obtained.

We are grateful to Prof. San-ichiro Mizushima for his kind advice and encouragement throughout this work. Our thanks are also due to the Ministry of Education for a grant in aid of this research.

Summary

An equation for the dielectric constant of polar fluids is obtained from the point of view of the classical theory of electricity in the continuous medium.

The obtained equation has a close relationship to the empirical equation of Wyman.

The comparison with the experimental data are represented.

Institute of Science and Technology, The University of Tokyo, Tokyo

Polar Structures in the VB-Theory of Conjugated Molecules

By Hiroshi KOKADO and Yuji MORI

(Received Nobember 29, 1955)

Introduction

The parameters appearing in the semi-empirical valence bond (VB) calculation of the electronic structure of molecules, have been estimated on the basis of thermochemical data of molecules. For instance, the value of the exchange integral for π-electrons between adjacent atoms r and s,

$$\alpha = \int \cdots r(i)s(j) \cdots H \cdots s(i)r(j) \cdots d\tau$$
$$= -1.92 \text{ eV.}, \qquad (1)$$

was determined from the heat of hydrogenation of unsaturated hydrocarbons by Sklar[1]. However, two improprieties are inevitable in his procedure; one is the underestimation of the ionic contribution and the other is the disregard of the compression energy resulting from bond compression in molecules. Recently Craig[2], adopting this value for α, evaluated three more quantities which enter in a rather detailed theory including polar structures,

$$\eta = \int \cdots r(i)r(j) \cdots H \cdots r(i)s(j) \cdots d\tau \qquad (2)$$

$$\xi = \int \cdots r(i)r(j) \cdots H \cdots r(i)r(j) \cdots d\tau$$
$$- \int \cdots r(i)s(j) \cdots H \cdots r(i)s(j) \cdots d\tau \qquad (3)^*$$

$$\zeta = \int \cdots r(i)r(j) \cdots H \cdots s(i)s(j) \cdots d\tau \qquad (1')$$

1) A.L. Sklar, *J. Chem. Phys.*, 5, 669 (1937).

2) D.P. Craig, *Proc. Roy. Soc.*, A 200, 390 (1950).

* This is recognized to be the difference between Coulomb integral of polar structure Q′ and that of non-polar one Q.

as —0.54, 4.28 and —0.48 eV. respectively, from the consideration of the spectrum of ethylene. On the other hand inconsistent with Craig's evaluation, Mulliken's approximation formula[3] claims that

$$\alpha=\int r(i)s(j)Hs(i)r(j)d\tau_{ij}$$

$$=S_{rs}\int r(i)r(j)Hr(i)s(j)d\tau_{ij}=S_{rs}\eta\ , \qquad (4)$$

where S_{rs} is the overlap integral between atomic orbitals of atoms r and s. This great discrepancy occurs clearly from the adoption of the above large value of α without any criticism. Keeping this fact in mind, we shall attain a new set of the semi-empirical values of integrals, making use only of spectroscopically observed results of ethylene, and examine the applicability of them to the calculation of *trans*-butadiene. In the last part of this paper, the role of η and α will be discussed in connection with the importance of the ionic character of conjugated molecules.

Evaluation of Integrals

First, the wave functions of ethylene as following are used;

$$^1A_g\,(\text{ground})\quad \Psi_0=a\psi_a+\frac{b}{\sqrt{2}}(\psi_b+\psi_{b'}), \qquad (5)$$

with a relation between the coefficients $a^2+b^2=1$, and

$$^1B_{1u}\,(\text{excited})\quad \Psi_1=\frac{1}{\sqrt{2}}(\psi_b-\psi_{b'}), \qquad (6)$$

in which ψ_a is written for the non-polar structure and ψ_b, $\psi_{b'}$ for the two polar ones (see Fig. 1). Then ignoring overlap, these

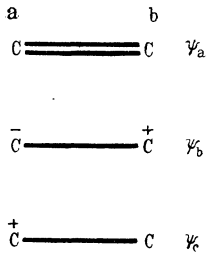

Fig. 1.

lead to a formula for the $^1A_g-{}^1B_{1u}$ excitation energy ΔE,

$$\Delta E=-2\alpha+\frac{\xi}{2}+\sqrt{\xi^2/4+4\eta^2}\,. \qquad (7)$$

Another representation of this is

$$\Delta E=\xi-2b^2\xi-2\alpha-4\sqrt{2}\,ab\eta-2b^2\alpha. \qquad (7')$$

3) R.S. Mulliken, *J. Chem. Phys.*, **46**, 497 (1949).

In order to determine the numerical values for a and b, the oscillator strength,

$$f=1.085\times10^{11}\omega(\int\Psi_0\vec{r}\,\Psi_1\,d\tau)^2 \qquad (8)$$

$$=1.085\times10^{11}\omega(R^2\times10^{-16}b^2)$$

may be turned to use, where ω is the frequency of the transition in cm^{-1}, $\vec{r}$ is the sum of the position vectors of π-electrons and R is the C=C bond distance in ethylene of ground state. Information on experimental results (ΔE=7.6 eV., f=0.25, bond length =1.35Å) makes it possible to calculate a, b, and with a further assumption of the relation (4), α, ξ and η numerically. If 0.28 is employed for S in equation (4), then we have

$$\left.\begin{aligned}a&=0.889\\b&=0.498\end{aligned}\right\} \qquad (9)$$

$$\left.\begin{aligned}\eta&=-2.15\ \text{eV.}\\\xi&=3.51\ \text{eV.}\\\alpha&=-0.60\ \text{eV.}\end{aligned}\right\} \qquad (10)$$

Much attention must be paid to the comparison of the present set of η, ξ and α with that given by Craig[2,*]. Moreover, a striking fact is that the values attained here allow the VB calculation to come very near the semi-empirical molecular orbital (MO) method which was developed quite successfully by Pariser and Parr[5] in recent years. η has a comparable numerical value as the resonance integral β (=2.75 eV.) in the semi-empirical MO calculation. This is owing to the fact that these are quite similar quantities by nature. That is, if overlap is put equal to zero,

$$\eta=\int r(i)r(j)Hr(i)s(j)d\tau_{ij}\fallingdotseq\int r(j)H's(j)d\tau_j=\beta.$$

On the other hand, ξ can be approximated as

$$\xi=(aa:aa)-(aa:bb) \qquad (11)$$

where,

$$(rr:ss)=\int r(i)s(j)\frac{e^2}{r_{ij}}r(i)s(j)d\tau_{ij}. \qquad (12)$$

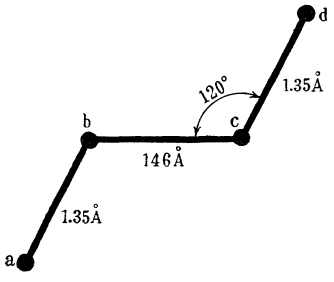

Fig. 2.

* ζ is set equal to α, like the treatment by Sklar (reference 1).

5) R. Pariser and R.G. Parr, *J. Chem. Phys.*, **21**, 466, 766 (1953)

According to the reference 5, this difference is predicted to be 10.53−7.38=3.15 eV. being close to the present value.

Another set of parameters which can be determined from the consideration of the singlet-triplet separation of ethylene, is not useful, because of the small value of ξ*.

Application to *trans*-Butadiene

In order to examine the applicability of the new set of η, ξ and α to other molecules, *trans*-butadiene is chosen. All the polar and non-polar structures are taken into account, but a simplification of considering only single exchange integrals between adjacent atoms is allowed. Corrections for η, ξ, α should be made, corresponding to the change of the internuclear distances (Fig. 3). These are done according to the following procedures**.

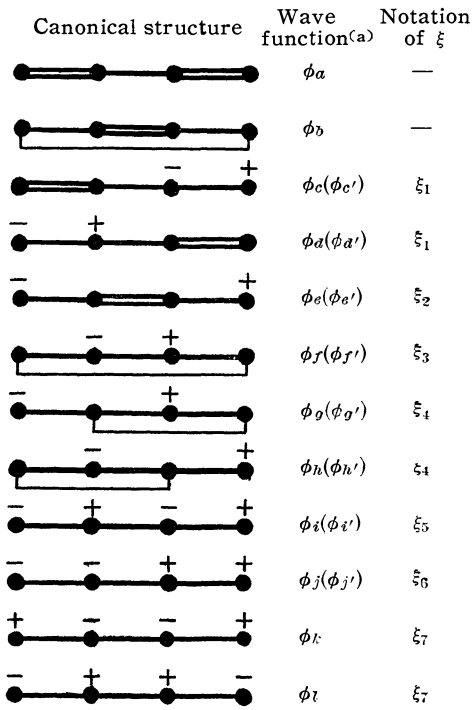

Fig. 3.

(a) $\phi_{c'}$'s are given by inversion respect to the center of molecule from ϕ_c's.

$$\left.\begin{aligned}\eta_{rs}&=\int\cdots r(i)r(j)\cdots H\cdots r(i)s(j)\cdots d\tau=S=_{rs}\eta_0\\ \alpha_{rs}&=S_{rs}\eta_{rs}=S_{rs}^2\eta_0.\end{aligned}\right\}\quad(13)$$

where η_0 is a constant to be determined by insertions of η_{rs} and S_{rs} for ethylene into (13). So, if $S_{ab}=0.27$ and $S_{bc}=0.23$ are used*,

$$\eta_{ab}=-2.07,\ \eta_{bc}=-1.77\text{ eV.};\ \alpha_{ab}=-0.56,\ \alpha_{bc}=-0.41\text{ eV.}\quad(14)$$

Moreover as to ξ next relation holds;

$$\xi=Q'-Q=(\Sigma I+\Sigma K)_{Q'}-(\Sigma I+\Sigma K)_{Qi}\quad(15)$$

where I and K are respectively core and Coulomb type repulsion integrals,

$$I=\int r(i)\sum_{p\neq r}U_p(i)r(i)d\tau_i$$

$$K=\int r(i)r(i)\frac{e^2}{r_{ij}}s(j)s(j)d\tau_{ij}=(rr:ss).$$

$U_p(i)$ signifies the potential of electron i in the field of the p-th carbon atom less its $2p\pi$-electron. Being used the Sklar type potential,

$$U_p(i)=U_p^0(i)-\int s(j)^2\frac{e^2}{r_{ij}}d\tau_{ij}$$

and zero $U_p^0(i)$(i.e., the potential of electron i in the field of the neutral p-th carbon atom) asumed, the problem is reduced to an estimation of Coulomb type repulsion integrals (rr : ss) only. In the case of $r=s$, i.e., (rr : rr), by a simple approximation it can be set equal to the difference between the ionization potential and the electron affinity of carbon atom (=10.53 eV.)[5]. When this is accepted, (rr : ss) corresponding to 1.34Å ($r-s$ separation for ethylene) is obtainable to be 10.53−3.51=7.02 eV., from the value of ξ. Repulsion integrals at arbitrary separations, may then be easily found supposing a linear relation to Pariser and Parr's result. Seven ξ's required are estimated by this procedure as follows (see Fig. 3).

$$\left.\begin{aligned}\xi_1&=(aa:aa)-(aa:bb)=3.53\text{ eV.}\\ \xi_2&=(aa:aa)-(aa:dd)=6.97\text{ eV.}\\ \xi_3&=(aa:aa)-(bb:cc)=3.74\text{ eV.}\\ \xi_4&=(aa:aa)-(aa:cc)=5.45\text{ eV.}\\ \xi_5&=2\xi_1+2(aa:cc)-(aa:dd)\\ &\quad-(bb:cc)=6.87\text{ eV.}\\ \xi_6&=2\xi_4+2(aa:bb)-(aa:dd)\\ &\quad-(bb:cc)=14.63\text{ eV.}\\ \xi_7&=2\xi_1-2(aa:cc)+(aa:dd)\\ &\quad+(bb:cc)=7.25\text{ eV.}\end{aligned}\right\}\quad(17)$$

The calculated energy diagram is shown in Fig. 4 together with results by several other methods.

* See reference 2.

** These formulae which contain S explicitly, never mean the inclusion of S in the actual calculation. Here, S should be recognized as a parameter defining the integrals in a function of internuclear distances.

* These values are obtained conveniently using the calculated bond orders p by the simple LCAO method, according to

$$S=0.080p+0.115$$

(N. Müller et al., *J. Am. Chem. Soc.*, **76**, 4770 (1954)).

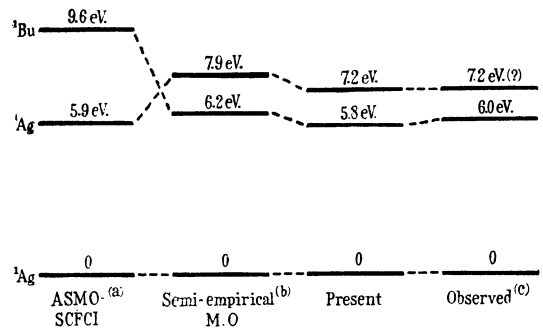

Fig. 4. Energy diagrams

(a) Y. Mori, This Bulletin, **28**, 291 (1955).
(b) Reference 5.
(c) R. S. Mulliken, Rev. Mod. Phys., **14**, 265 (1942).

The wave functions of the ground state and the first excited singlet state are

$$\left.\begin{aligned}
(^1A_g)\quad \Phi_0 &= 0.671\phi_a+0.062\phi_b+0.305(\phi_c+\phi_{c'})\\
&\quad +0.337(\phi_d+\phi_{d'})+0.044(\phi_e+\phi_{e'})\\
&\quad +0.103(\phi_f+\phi_{f'})+0.074(\phi_g+\phi_{g'})\\
&\quad +0.070(\phi_h+\phi_{h'})+0.153(\phi_i+\phi_{i'})\\
&\quad +0.009(\phi_j+\phi_{j'})+0.131\,\phi_k\\
&\quad +0.153\,\phi_l,\\
(^1B_u)\quad \Phi_1 &= 0.366(\phi_c-\phi_{c'})+0.376(\phi_d-\phi_{d'})\\
&\quad +0.204(\phi_e-\phi_{e'}+0.131(\phi_f-\phi_{f'})\\
&\quad +0.176(\phi_g-\phi_{g'})+0.173(\phi_h-\phi_{h'})\\
&\quad +0.323(\phi_i-\phi_{i'})+0.034(\phi_j-\phi_{j'}).
\end{aligned}\right\}(17)$$

Finally the oscillator strength of the transition $^1A_g-{}^1B_u$ is calculated to be 0.62 (observed 0.53).

These agreements with experimental observations are sufficient to confirm the conclusion that our first evaluation of quantities η, ξ, α is not at all an irresponsible one. The resemblance to the semi-empirical MO is a natural consequence of our arrangement of the integral values.

Discussion

The most marked point in our method exists, of course, in an estimation of a great deal of ionic contribution to electronic structures. On the contrary, the semi-empirical VB-method heretofore in use, estimates little about this but a great amount of the interaction between non-polar configurations. Now, it will be worth while to study the signification of our evaluation of the quantities η and α. If the Mulliken's approximation is allowable, the extent of contribution of interaction between polar and non-polar structures may be measured by the degree of overlapping. A large overlap suggests much contribution of polar structures and vice versa. So, we shall try a VB calculation of ethylene, studying the influence of the overlap integral. The wave function are

$$\left.\begin{aligned}
&^1A_g(\text{ground})\\
&\Psi_0=\alpha\Psi_a+\frac{b}{\sqrt{2(1+S^2)}}(\psi_b+\psi_{b'})\\
&^1B_{1u}(\text{excited})\quad \Psi_1=\frac{1}{\sqrt{2(1-S^2)}}(\psi_b-\psi_{b'}).
\end{aligned}\right\}(18)$$

where ψ_a, ψ_b and $\psi_{c'}$ are normalized.

The secular equation for $_1A_g$ state is

$$\begin{vmatrix}
\frac{1}{1+S^2}(Q+\alpha)-E_1 & \frac{2}{1+S^2}(\eta-SE^1)\\
\frac{2}{1+S^2}(\eta-SE_1) & \frac{1}{1+S^2}(Q+\xi+\alpha)-E_1
\end{vmatrix}=0 \quad (19)$$

$$\frac{1}{1-S^2}(Q+\xi-\alpha)-E_2=0. \quad (20)$$

Here, we shall try to express η and α in functions of S. Coulomb integral Q is given by direct integration.

$$\begin{aligned}
Q&=2W_{2p\pi}+2(U_a:\text{bb})+(\text{aa}:\text{bb})\\
&=2W_{2p\pi}+(U_a:\text{bb})+(U_a^0:\text{bb})
\end{aligned}$$

where, $W_{2p\pi}$ is the energy of $2_{p\pi}$ electron of carbon atom. Consequently

$$QS=2W_{2p\pi}S+(U_a:\text{bb})S+(U_a^0:\text{bb})S \quad (22)$$

while η is

$$\begin{aligned}
\eta&=2W_{2p\pi}S+(U_a:\text{bb})S+(U_a:\text{ab})+(\text{aa}:\text{ab})\\
&=2W_{2p\pi}S+(U_a:\text{bb})S+(U_a^0:\text{ab}). \quad (22)
\end{aligned}$$

Then from equations (21) and (22) it is seen that

$$QS=\eta-(U_a^0:\text{ab})+(U_a^0:\text{bb})S. \quad (23)$$

Furthermore, $(U_a^0:\text{ab})$ is approximated by the method of Sklar, thus*

$$(U_a^0:\text{ab})=S(U_a^0:\text{b}'\text{b}'). \quad (24)$$

Numerical values of the penetration integrals $(U_a^0:\text{b}'\text{b}')$ and $(U_a^0:\text{bb})$, i.e., -8.739 and -1.091 eV.** respectively, give

$$\left.\begin{aligned}
&\eta=SQ-7.648S\\
&\text{and}\\
&\alpha=S^2Q-7.648S^2.
\end{aligned}\right\}(25)$$

Inserting Eqs. (25) and an adequate numerical value of ξ into Eqs. (19) and (20), one can calculate the excitation energy ΔE in function of S. Fig. 5 shows the results of calculations in the cases of $\xi=3.51$ and 7.69 eV. The latter is true in the non-empirical calculation. The amount of ionic contribution is accounted for by the ratio b/a, and also by the ratio of the calculated stabilization

* b′ is a $2p\pi$ function located midway between a and b atoms.

** Calculated from the paper of R.G. Parr and B.L. Crawford, *J. Chem. Phys.*, **18**, 1049 (1948).

energy of the ground state including polar structures to that excluding them. These ratios are seen in Fig. 5. The experimental

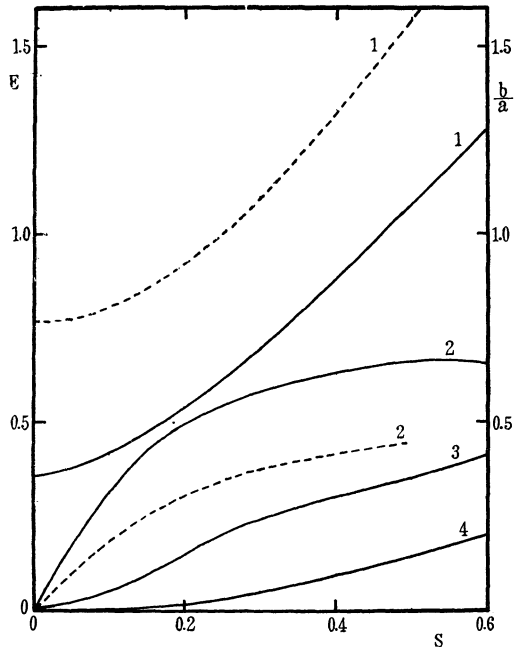

Fig. 5. Ionic Character of Ethylene.
1. Excitation energy ΔE
2. Ratio of b to a
3. Binding energy calculated from (18)
4. Binding energy calculated using ϕ_a only
Broken lines show results of using $\xi=7.69$ eV.

excitation energy is attainable at the value of the overlap integral by 0.3, consistent with our first assumption ($S=0.28$). When the overlap integral is small like this, η causes the most part of the stabilization energy and as S becomes large, the importance of polar structures of the molecule, consequently the contribution of η, decreases to the ground state.

Conjugated molecules, so far as we are dealing only with the π-electron system, have small S in general. Concerning this fact, one may understand that the simple MO method, which ignores the exchange and overlap integrals and includes a large amount of polar structures, is reliable in the calculation of π-electron systems and the good agreement with experiments of the results obtained by Pariser and Parr[5] may not be accidental. In the present calculation of *trans*-butadiene, the small value of α does not cause the contravention to the experiments and furthermore the disregard of the exchange integrals will cause the results of the calculation to come near those by the method of Pariser and Parr.

However, in the treatment of σ-bond, say like a hydrogen molecule, in which the overlap of atomic orbitals is large that it can never be excluded from the calculation, the approximation we have used here will not fit. In such cases, non-polar configurations will play an important role.

Conclusion

The usual VB-method, in spite of its theoretical infirmity that all or at least the large part of ionic influence is entirely ignored, has been served for predications and interpretations of electronic phenomena. But from a different point of view, we have described another direction of the VB-theory, and applying that to butadiene, we have shown that excellent agreements with experiments can be realized. A further study on the polar character of conjugated molecules could give an assurance to the propriety of our procedure. Our method was found to be very near the semi-empirical MO-method, but a large complication accompanies the practical calculation*. In this point, VB-method must fall below the MO-method.

Finally, from the present study, it was pointed out that the old VB-method in the semi-empirical theory of conjugated molecules, although it sometimes could lead to a good result, never represents the essential figure of a molecule and also that its agreement with experimental facts was accidental.

Laboratory of Physical Chemistry
Tokyo Institute of Technology
Tokyo

* Benzene is a rather simple and important object in the discussion of the propriety of a theory of electronic structures. But it is almost impossible to represent the wave function of benzene by VB-theory, since in order to expect a statisfactory result it requires inclusion of all kind polar structures, even triply-polar ones.

Synthetic Studies on Oxirane Compounds. I. Ammonolysis of 2,3-Epoxyl-3-pheny-1-propanol

By Tetsuo SUAMI, Ichiro UCHIDA and Sumio UMEZAWA

(Received December 20, 1955)

The study described in the present communication was a part of a program involving synthetic studies on chloramphenicol which is an important antibiotic found by the scientists of Parke, Davis and Co.. An attractive synthetic path to chloramphenicol involves the opening of the oxide ring of 1-phenylglycidol with ammonia. Although it has been shown recently by Fusco and Trave[1] that 1-*p*-nitrophenyl-1-amino-2, 3-propanediol is obtained by the action of ammonia on 1-*p*-nitrophenylglycidol, the substituent exerts often a profound effect on the direction of opening of the oxide ring, an example apparently being found in the reaction of nitrostyrene oxide[2] with hydrogen chloride. The direction of opening is opposite to that observed with styrene oxide[3]. This possibility made it desirable to attempt the ammonolysis of 1-phenylglycidol. The experiments described here established, however, the fact that 1-phenyl-1-amino-2, 3-propanediol (II) is obtained by the action of methanolic ammonia on 1-phenylglycidol, the direction of opening being much the same as that observed with 1-*p*-nitrophenylglycidol.

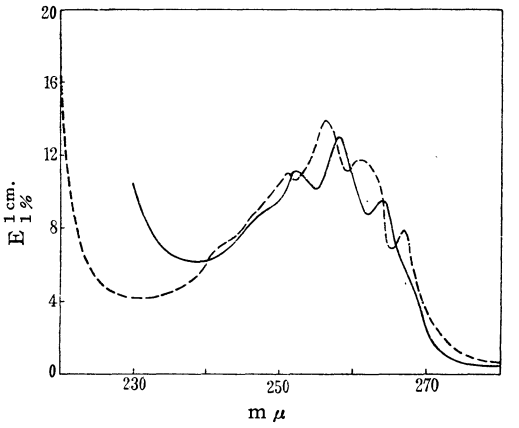

Fig. 1. Ultraviolet spectra of 1-phenyl-1-amino-2, 3-propanediol.
(----- : in 1 N hydrochloric acid;
——— : in ethanol)

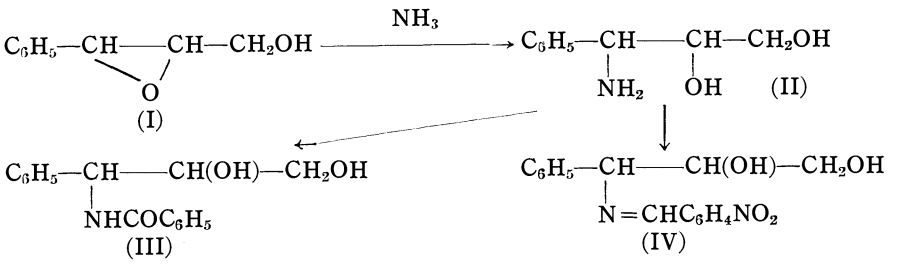

1-Phenylglycidol was prepared from cinnamyl alcohol and perbenzoic acid and had essentially the same boiling point with that reported by Platt and Hibbert[4]. By treatment with an excess of ammonia in absolute methanol in an autoclave, the epoxide ring of 1-phenylglycidol was split with the formation of 1-phenyl-1-amino-2, 3-propanediol (II), m. p. 90–91°, which depressed the melting point of the authentic sample of DL-threo-1-phenyl-2-amino-1, 3-propanediol, m. p. 87–88°. Treatment of II with *p*-nitrobenzaldehyde gave a Schiff base (IV), m. p. 149–150°, which also depressed the melting point of the corresponding Schiff base (V), m. p. 143–145°, prepared similarly from DL-threo-1-phenyl-2-amino-1, 3-propanediol.

To establish the identity of 1-phenyl-1-amino-2, 3-propanediol (II) the known 1-phenyl-1-benzamido-2, 3-propanediol was synthesized by the method of Lott[5] from cinnamyl benzoate bromohydrin and ammonia and did not depress the melting point of the benzoyl

1) R. Fusco and R. Trave, *Gazz. chim. ital.*, 80, 366 (1950).
2) F. Arndt, B. Eistert and W. Partale, *Ber.*, 61 B, 1107 (1928).
3) C. Golumbic and D.L. Cottle, *J. Am. Chem. Soc.*, 61, 996 (1939).
4) M.E. Platt and H. Hibbert, *Can. J. Research*, 7, 629 (1932); *C.A.*, 27, 1334.
5) Lott, U.S. patent 2,103,266. The structure was elucidated by Controulis et al., who found that the migration of benzoyl group from O to N takes place during ammonolysis. *J. Am. Chem. Soc.*, 71, 2463 (1949).

derivative (III) of the product (II) from the cleavage of 1-phenyl-glycidol (I). Ultraviolet absorption (Fig. 1) agreed in every respect with that obtained by Controulis et al..

On treatment of II with hot acetone an *iso*-propylidene derivative was produced which regenerated II readily by hydrolysis with hydrochloric acid at room temperature.

Experimental

1-Phenylglycidol (I) (2, 3-Epoxy-3-phenyl-1-propanol).—To a solution of 8.8 g. of perbenzoic acid in 100 cc. of chloroform was added 8.0 g. of cinnamyl alcohol. The solution was kept at 0° for about twenty-four hours and was shaken frequently during the first hour. The benzoic acid was removed from the chloroform solution by shaking with an excess of 10% sodium hydroxide solution, the alkali was removed by washing with water, and the chloroform solution was dried with sodium sulfate. It was then fractionated. Removal of the chloroform left a practically colorless liquid which distilled at 117–118°/1.5 mm. The yield was 4.5 g. (45% of the theoretical amount). Platt and Hibbert[4] described already the b. p. 136–137°/5 mm.

1-Phenyl-1-amino-2, 3-propanediol (II) (Cleavage of I with Ammonia).—The phenylglycidol (I) (13.6 g.) was heated with 350 cc. of a saturated solution (at 0°) of ammonia in absolute methanol at 80–90° for five hours in a stainless-steel autoclave. The solution was concentrated to a dark brown gum under reduced pressure which crystallized on trituration with ether. The ether-mixture was kept in a stoppered flask for about twenty hours. The crystals formed 9 g. and were collected on a filter. Three times of recrystallization from chloroform-ethylacetate (1: 1) gave colorless needless melting at 90–91°. (Found: N, 8.22. Calcd. for $C_9H_{13}O_2N$: N, 8.38%.)

This depressed the melting point of an authentic sample of DL-threo-1-phenyl-2-amino-1, 3-propanediol, m. p. 87–88°.

1-Phenyl-1-benzamido-2, 3-propanediol (III).—0.5 g. Sample of the above described product (II) was treated with a small excess of benzoyl chloride in 1 N sodium hydroxide. The precipitate was recrystallized from water, colorless needles, m. p. 163–164°. This did not depress the melting point of 1-phenyl-1-benzamido-2, 3-propanediol, m. p. 163–164°, prepared by the method of Lott[5] from cinnamyl benzoate bromohydrin and ammonia.

1-Phenyl-1-(*p*-nitrobenzylidene)-amino-2, 3-propanediol (IV).—1.0 g. Sample of (II), m. p. 89–90° was mixed with 0.9 g. of *p*-nitrobenzaldehyde in 5.0 cc. of ethylacetate and warmed. Soon the resulting clear solution began to precipitate pale-yellow crystals. After standing overnight at room temperature the crystals were collected on a filter, washed with ethylacetate and ether, m. p. 140–143°. The yield was 1.0 g. Further recrystallization from methanol gave pale-yellow needles, m. p. 149–150°. (Found: N, 9.23. Calcd. for $C_{15}H_{15}O_4N_2$: N, 9.33%.)

1-Phenyl-2-(*p*-nitrobenzylidene)-amino-1, 3-propanediol.—The condensation of *p*-nitrobenzaldehyde with DL-threo-1-phenyl-2-amino-1, 3-propanediol was carried out exactly as described above and led to 1-phenyl-2-(*p*-nitrobenzylidene)-amino-1, 3-propanediol, pale-yellow needles, m. p. 137–140°, 1.0 g. Recrystallization from acetone gave pale-yellow needles, m. p. 143–145°. (Found: N, 9.44. Calcd. for $C_{16}H_{16}O_4N_2$: N, 9.33%.)

This depressed the melting point of a sample of IV.

***iso*-Propylidene Derivative of II.**—A portion of 0.5 g. of the dark brown gum from which 1-phenyl-1-amino-2, 3-propanediol (II) described above was isolated, was dissolved in acetone by warming on a steam-bath. After standing at room temperature a colorless crystalline precipitate 0.3 g. was obtained, m. p. 93–96°. After recrystallization from acetone, the *iso*-propylidene derivative melted at 102.5–103°. (Found: N, 6.47. Calcd. for $C_{12}H_{17}O_2N$: N, 6.76%).

A sample of 0.2 g. of the *iso*-propylidene derivative was hydrolyzed with 1 cc. of 2 N hydrochloric acid at room temperature in a few minutes. The hydrolysate was neutralized with potassium carbonate and evaporated to dryness under reduced pressure. The colorless residue was dissolved in 1 cc. of water, made alkaline to pH 10 and extracted with ethylacetate. The ethylacetate solution was dried over sodium sulfate and evaporated to a syrupy residue, 0.1 g., which crystallized from ether. Recrystallization from ethylacetate-chloroform (1: 1) gave colorless needles, 0.05 g., m. p. 89.5–90°. The mixed melting point with an authentic sample of II showed no depression.

An attempt was made to prepare *iso*-propylidene derivative from DL-threo-1-phenyl-2-amino-1, 3-propanediol by the same procedure described above. However, only a syrup was obtained.

Summary

1-Phenyl-1-amino-2, 3-propanediol, m. p. 90–91°, was obtained by ammonolysis of 2, 3-epoxy-3-phenyl-1-propanol. Several derivatives of this compound were described.

A part of the cost of the present research has been defrayed from the Scientific Research Encouragement Grant from the Ministry of Education, to which the authors' thanks are due.

Department of Applied Chemistry, Engineering Faculty of Keio University, Tokyo

The Synthesis and the Estrogenic Activity of Bis-2, 4-dihydroxyphenyl Disulfide and the Related Thiophenol

By Yoshiyuki URUSHIBARA and Gen KOGA

(Received December 28, 1955)

One of the authors (Y. U.) and T. Takahashi[1] reported the synthesis and the estrogenic activity of 2, 4, 2′, 4′-tetrahydroxyazobenzene. It produced full estrus in 100% animals (mice) at a dosage of 20 γ injected subcutaneously in two portions. The estrogenic activity of 4, 4′-dihydroxyazobenzene being very small (active in 80% at 1 mg.), the 2, 2′-hydroxyl groups of 2, 4, 2′, 4′-tetrahydroxyazobenzene were considered to form a double chelation, thus effecting a rigid, chrysene-shaped structure favorable for the development of a strong estrogenic activity. The infrared absorption spectrum of the crystals in Nujol showed the presence of hydrogen bonding between the azo nitrogen atom and the phenolic hydroxyl group. The insolubility of the tetrahydroxyazobenzene defied the measurement of its infrared absorption in solution, but 2-hydroxyazobenzene, a reference compound, in carbon tetrachloride solution showed a broad absorption at 3.4–3.5 μ due to an intramolecular hydrogen bonding[2], and thus gave an indirect evidence for the presence of chelation in the tetrahydroxyazobenzene at least in dilute state as when administered to the animal. If the supposed double chelation exists in the tetrahydroxyazobenzene, it is necessarily connected with a coplanar structure of the molecule, which was supposed to be one of the reasons why the substance is less active than the most potent synthetic estrogens[3].

The present authors expected bis-2, 4-dihydroxyphenyl disulfide (IV) might be a compound with a structure similar to that of 2, 4, 2′, 4′-tetrahydroxyazobenzene but not coplanar and thus a stronger estrogen, because of the presence of two unshared pairs of electrons in the valence shell of the covalent-bonded sulfur atom.

C. Lefevre and Ch. Desgrez[4] reported in 1934 that they prepared phenol disulfides by heating several phenols with sulfur and sodium carbonate in glycerol solution at 120°, and that from the ordinary phenol they obtained a disulfide melting at 116°, and from resorcinol a disulfide decomposing without fusion. They assigned the constitutions of bis-4-hydroxyphenyl disulfide and bis-2, 4-dihydroxyphenyl disulfide, respectively, without stating any detailed investigation of their structures. In 1890 R. Leuckart[5] already described bis-4-hydroxyphenyl disulfide melting at 150–151°, and in 1947 S. Magnusson, J. E. Christian, and G. L. Jenkins[6] prepared the same disulfide melting at 151–152°. Hence, the structures of the disulfides of Lefevre and Desgrez were probably different from the supposed. The present authors synthesized bis-2, 4-dihydroxyphenyl disulfide in the following way:

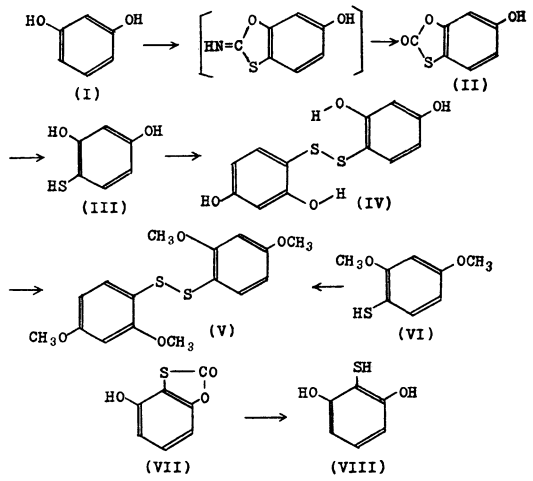

6-Hydroxy-1, 3-benzoxathiolone-(2) (II), m. p. 154.5–155°, was prepared from resorcinol (I), copper sulfate, and ammonium thiocyanate, by a method similar to that described by M. Pantlitschko and H. Benger[7] but without using sodium carbonate. It was hydrolyzed to 2, 4-dihydroxythiophenol (III), m. p. 110–111° by treatment with caustic soda. Oxidation of the thiophenol with hydrogen peroxide gave bis-2, 4-dihydroxyphenyl disulfide (IV), m. p. 170–171°, in white crystalline powder.

Pantlitschko and Benger observed that the product (m. p. 160°) from the reaction of

1) This Bulletin, **26**, 162 (1953).
2) T. Takahashi, *J. Chem. Soc. Japan*, **74**, 673 (1953).
3) Cf. M. Ōki and Y. Urushibara, This Bulletin, **25**, 109 (1952).
4) *Compt. rend.*, **198**, 1791 (1934).
5) *J. prakt. Chem.*, **41**, 179 (1890).
6) *J. Am. Pharm. Assoc. Sci. Ed.*, **36**, 257 (1947).
7) *Monatsh.*, **81**, 293 (1950); *Chem. Abstr.*, **45**, 2471 (1951).

resorcinol, copper sulfate, and ammonium thiocyanate, was 4-hydroxy-1, 3-benzoxathiolone-(2) (VII), from which they obtained 2, 6-dihydroxythiophenol (VIII), m. p. 83–84°. G. Werner[8] claimed a preparation of the same or isomeric compound melting at 158°, and, although the Chemical Abstracts, Vol. 38, gives the name 6-hydroxy-1, 3-benzoxathiolone-(2) for the substance in the Index, it is not shown in either the Chemical Abstracts or the original patent comment how its constitution was determined. It is also unknown whether the substance of G. Werner is identical with the substance melting at 154.5–155° obtained by the present authors or not. The following facts, however, support the structures assigned to the substances described in this paper.

Namely, the methylation of the disulfide, m. p. 170–171°, gave a product identical with the bis-2, 4-dimethoxyphenyl disulfide (V) prepared from the known 2, 4-dimethoxythiophenol (VI). The latter compound (VI) was prepared, and the constitution was determined, by C. M. Suter and H. L. Hansen[9]. The estrogenic activity of the disulfide (IV) and the thiophenol (III) is also a strong evidence for their structures.

Bis-2, 4-dihydroxyphenyl disulfide (IV) produced full estrus in 100% animals (mice) at a dosage of 10 γ by a single subcutaneous injection in oil solution, while 2, 4-dihydroxythiophenol (III) was fully active in 60–70% animals at the same dosage and in 100% at 20 γ. 2, 4-Dihydroxythiophenol appears to be an estrogen of the least molecular weight ever known, but it must be considered that it is oxidized in vivo to bis-2, 4-dihydroxyphenyl disulfide and acts as such.

Bis-4-hydroxyphenyl disulfide, $4\text{-}HOC_6H_4\cdot SSC_6H_4OH\text{-}4$, prepared by the method described by Magnusson et al., showed much less activity. Namely, it was totally inactive at 50 γ, but produced estrus in 20–40% animals at 100 γ and in 80% at 500–1000 γ. The structure of this compound may be non-coplanar contrary to those of 4, 4'-dihydroxyazobenzene and 4, 4'-dihydroxystilbene, considering the possible repulsion of the unshared pairs of electrons of the two sulfur atoms, and considering certain results from the investigations on the molecular structure of sulfur monochloride S_2Cl_2 by means of electron diffraction[10] and on the dipole moments of diphenyl disulfides[11]. Bis-4-hydroxyphenyl disulfide and bis-2, 4-dihydroxyphenyl disulfide may possibly possess the same or very similar twisted conformation of the hydrogen peroxide type, and then it may facilitate a chelation in the latter compound because one of the two unshared pairs of electrons of each sulfur atom is oriented towards the ortho hydroxyl group of the farther ring, but the distance between the two para hydroxyl groups may be shorter than the optimum for estrogenic potency[3].

At any rate, it has been demonstrated that the introduction of an ortho hydroxyl group into each ring of bis-4-hydroxyphenyl disulfide to form bis-2, 4-dihydroxyphenyl disulfide (IV) increases the estrogenic potency to a great extent, but it has not yet been determined in any other way whether a chelation really exists.

Experimental Part[12]

6-Hydroxy-1, 3-benzoxathiolone-(2) (II).—To a solution of 22 g. of resorcinol and 100 g. of crystalline copper sulfate in 500 ml. of water, 62 g. of ammonium thiocyanate dissolved in 100 ml. of water were added with stirring. A black precipitate appeared and turned gray in color. After standing for one hour with occasional stirring, the precipitate was removed, and the orange-red filtrate was heated on a waterbath and left to stand to complete the precipitation of a yellow substance. The yellow precipitate was collected on a filter and recrystallized three times from water-alcohol. Pale yellow needles, m. p. 154.5–155°. Yield, 12 g. (36% of the theory).

Anal. Found: C, 49.83; H, 2.36; S, 18.90. Calcd. for $C_7H_4O_3S$: C, 49.99; H, 2.40; S, 19.07%.

2, 4-Dihydroxythiophenol (III).—In the stream of nitrogen 100 ml. of 2 N caustic soda was added gradually to 10 g. of 6-hydroxy-1, 3-benzoxathiolone-(2) (II) contained in an Erlenmeyer flask. The mixture was gently heated to complete dissolution, left to cool down to the room temperature, acidified to acid reaction to Congo Red with 2 N hydrochloric acid, and extracted with ether. The white residue from the ethereal extract was recrystallized twice from benzene. A white crystalline powder, m. p. 110–111°. Yield, 6.5 g. (79% of the theory).

Anal. Found: C, 50.90; H, 4.37; S, 22.49. Calcd. for $C_6H_6O_2S$: C, 50.68; H, 4.25; S, 22.55%.

Bis-2, 4-dihydroxyphenyl Disulfide (IV).—A solution of 6 g. of the thiophenol (III) in 40–60 ml. (as little as possible) of water was cooled below 10°, about 4 ml. of 35% hydrogen peroxide was added gradually with stirring at a temperature not exceeding 15°, and the mixture was left to stand with cooling. The white crystalline substance was collected on a filter and recrystallized twice from water. A white crystalline powder,

8) U.S. Patent, 2,332,418; *Chem. Abstr.*, 38, 1889 (1944).

9) *J. Am. Chem. Soc.*, 55, 2080 (1933).

10) E. Hirota and Y. Morino, private communication. Cf. also S. Mizushima, "Structure of Molecules and Internal Rotation," Academic Press, New York (1954), p. 93.

11) E. Bergmann and M. Tschudnowsky, *Z. physik. Chem.*, B, 17, 107 (1932).

12) Melting points uncorrected.

m.p. 170–171°, Yield, 4 g. (67% of the theory).

Anal. Found: C, 51.14; H, 3.42; S, 22.27. Calcd. for $C_{12}H_{10}O_4S_2$: C, 51.05; H, 3.57; S, 22.72%.

Bis-2, 4-dimethoxyphenyl Disulfide (V).—2, 4-Dimethoxythiophenol, prepared by the method of C. M. Suter and H. L. Hansen[9], was treated with a slight excess of iodine in alcoholic solution. The precipitate was recrystallized from alcohol. Colorless needles, m.p. 113–115°. Yield, quantitative.

Anal. Found: C, 56.59; H, 5.19; S, 18.79. Calcd. for $C_{16}H_{18}O_4S_2$: C, 56.78; H, 5.36; S, 18.91%.

Bis-2, 4-dihydroxyphenyl disulfide (IV), dissolved in caustic soda, and dimethyl sulfate gave a white crystalline product. Recrystallized from alcohol, it showed a melting point 109.5–112.5° and no depression of the melting point was observed in admixture with the bis-2, 4-dimethoxyphenyl disulfide described above.

Attempted methylation of 2, 4-dihydroxythiophenol (III) to the known methyl 2, 4-dimethoxyphenyl sulfide, $C_6H_3(SCH_3)(OCH_3)_2$ (1, 2, 4), was accompanied by oxidation and resulted in the formation of 2, 4-dimethoxyphenyl disulfide (V).

Department of Chemistry, Faculty of Science, The University of Tokyo
Tokyo

Spectrochemical Study of Microscopic Crystals. XI.[1] *The Structure and Polarized Absorption Spectra of Some Metallic Compounds with Remarkable Interaction between Metal Atoms through Anions*

By Shoichiro YAMADA and Ryutaro TSUCHIDA

(Received January 9, 1956)

These several years the present authors have been particularly interested in those inorganic compounds which display in the crystalline state much deeper colours than would be expected from the colours of their components in solution. In one type of the compounds, the metal-to-metal interaction was concluded to exist, causing the unusual deepening of the colour[2]. In the compounds of another type, there was supposed to be interaction between metal atoms through anions[3]. In the study of the above compounds, the measurement of polarized absorption spectra has proved to be a feasible means, since the interaction was found to cause enormous changes in the direction along which the interaction was known to exist between the metal atoms. We have taken up those compounds in which there would be expected to be infinite chains of metal atoms connected with anions as bridging groups. In the present work, polarized absorption spectra of $Pd(NH_3)_2Cl_3$, Pt (en)Cl_3[4] and $(NH_4)_3AgAuCl_7$ have been quantitatively determined and the results have been discussed with relation to the structure of the compounds.

Experimental

Materials.—Trans-$[Pd(NH_3)_2Cl_2]$ was prepared in orange crystals of moderate size by spontaneous evaporation of an aqueous solution of $[Pd(NH_3)_4]Cl_2$[5]. The crystals show a straight extinction. They appear yellow with the electric vector along the *c*-axis, and orange with the electric vector normal to the *c*-axis. The measurement was made along the two directions. The X-ray study of the crystal structure[5] indicates that the *c*- and *a*-absorption denote absorption with the electric vector along and normal to the complex molecules, respectively.

$[Pd(NH_3)_2Cl_2][Pd(NH_3)_2Cl_4]$ was prepared according to the method of Cohen et al.[6] The crystals obtained in black needles belong to the orthorhombic system, showing a straight extinction and a remarkable dichroism. They appear quite dark with the electric vector along the *c*-axis, and yellow with the electric vector normal to the *c*-axis. There were sometimes grown crystals with a different habit, which exhibited a dichroism different from the above. The dichroism measurement was made with the crystals of the former type.

$[Pt(en)Cl_2]$ was prepared in yellow powder according to the method of Basolo[7]. Crystals of

1) Part X of this series, S. Yamada and R. Tsuchida, This Bulletin, **29**, 289 (1956).

2) S. Yamada and R. Tsuchida, *J. Chem. Soc. Japan*, **70**, 142 (1949); S. Yamada, *J. Am. Chem. Soc.*, **73**, 1579 (1951); This Bulletin, **24**, 125 (1951); S. Yamada and R. Tsuchida, *J. Am. Chem. Soc.*, **75**, 6351 (1953); This Bulletin, **27**, 156 (1954).

3) S. Yamada, Y. Shimura and R. Tsuchida, This Bulletin, **26**, 72 (1953); R. Tsuchida and S. Yamada, *Nature*, **174**, 1064 (1954).

4) The notation, en, denotes a molecule of ethylenediamine.

5) F.G. Mann, D. Crowfoot, D.C. Gattiker and N. Wooster, *J. Chem. Soc.*, **1935**, 1642.

6) A.J. Cohen and N. Davidson, *J. Am. Chem. Soc.*, **73**, 1955 (1951).

7) F. Basolo, ibid., **72**, 2433 (1950).

a moderate size suitable for the absorption measurement could not be obtained. Its absorption spectrum was determined in the aqueous solution with a Beckman DU spectrophotometer.

$[Pt(en)Cl_4]$ was prepared in pale yellow powder by the method of Basolo[7]. The measurement of the polarized absorption spectra with the crystals could not be made, since the crystals large enough for the measurement were not available. Its absorption spectrum was determined using the aqueous solution.

$Pt(en)Cl_3$ was prepared by oxidizing $[Pt(en)Cl_2]$ with ammonium persulphate according to the method of Tschugaeff et al.[8] or by allowing to cool a hot, mixed solution of $[Pt(en)Cl_2]$ and $[Pt(en)Cl_4]$. Red, plate-like crystals thus obtained were strongly dichroic; purplish-red and pale yellow with the electric vector along and normal to the *c*-axis, respectively. The measurement of the polarized absorption spectra was performed along the above two directions. The *a*- and *c*-absorption have the same meaning as the above.

$Cs[AuCl_4]$ was prepared in yellow prisms from tetrachloro-auric acid and caesium chloride, which were purified by repeated recrystallization from water. A slight dichroism was observed with the crystals under the microscope. The measurement of the dichroism was made along the directions parallel and normal to the prism axis. The C- and A- absorption denote absorption with the electric vector along and normal to the prism axis, respectively. Measurement of absorption spectra was also made with the aqueous solution containing CsCl.

$Cs_2AgAuCl_6$ was obtained in black microcrystals by the method of Wells[9]. To an aqueous solution of tetrachloro-auric acid acidified with hydrochloric acid was added silver nitrate and caesium chloride, followed by warming on a water bath. The precipitate of silver chloride, which was formed at first, again entered into solution, from which the black crystals sparated out. The crystals of a larger size suitable for the absorption measurement could not be obtained. The visual observation, however, could be made with some of them under the microscope. The crystals showing a straight extinction were strongly dichroic. They appear almost black with the electric vector along the *c*-axis, and yellow with the electric vector normal to the *c*-axis.

$(NH_4)_3AgAuCl_7$ was prepared in very dark crystals follwing the same procedure as that with the above caesium compound, except that ammonium chloride was used instead of caesium chloride[10]. The reaction also proceeded in a way very similar to the case of the corresponding caesium compound. The needles of the compound, which belong to the orthorhombic system, showed a marked dichroism. They appeared quite dark along the *c*-axis, and yellow in the direction normal to the *c*-axis. The dichroism measurement was made with reference to the above two directions.

Measurement.—Quantitative dichroism measurements were made by Tsuchida-Kobayashi's microscopic method[11] with polarized light in the regions covering 2400 to 8000 Å. The notations used are the same as those in the previous papers of this series[1].

Results and Discussion

In 1948, Brosset[12] studied the crystal structure of $Pt(NH_3)_2Br_3$. The crystal analysis indicates that the crystal of the compound, which should be formulated as $[Pt(NH_3)_2Br_2][Pt(NH_3)_2Br_4]$, consists of infinite chains, each containing alternate planes of $[Pt(NH_3)_2Br_2]$ and octahedra of $[Pt(NH_3)_2Br_4]$, as illustrated in Fig. 1. From visual observation of the crystals under the microscope and examination of their magnetic property, Cohen et al.[5] supposed that the crystal of $Pd(NH_3)_2Cl_3$, which could be represented by $[Pd(NH_3)_2Cl_2][Pd(NH_3)_2Cl_4]$, would possess the same structure as that of $[Pt(NH_3)_2Br_2][Pt(NH_3)_2Br_4]$. This was confirmed later by the X-ray analysis of the crystal[13].

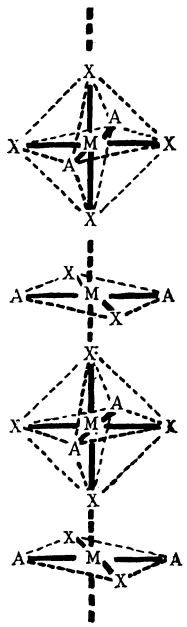

M: Pd or Pt A: ammonia or amine
X: halide or hydroxyl group

Fig. 1. Chain structure in the crystals of the compounds having the empirical formula, MA_2X_3.

8) L. Tschugaeff and J. Tschernyaeff, *Z. anorg. allgem. Chem.*, **182**, 159 (1929).
9) H. L. Wells, *Amer. J. Sci. Silliman*, (5) **3**, 257 (1920); *Chem. Zentr.*, **1922**, 239.
10) W. B. Pollard, *J. Chem. Soc.*, **117**. 99 (1920).
11) R. Tsuchida and M. Kobayashi, This Bulletin, **13**, 619 (1938); "The Colours and the Structures of Metallic Compounds", Zoshindo, Osaka, Japan (1944), p. 180.
12) C. Brosset, *Arkiv Kemi Mineral. Geol.*, **25 A**, No. 19 (1948).
13) E. W. Hughes, unpublished; private communication from Dr. A. J. Cohen; C. S. Adams, M. S. thesis, University of Sydney, 1952.

The result of the present measurement is shown in Fig. 2. Polarized absorption spectra of one component, *trans*-$[Pd(NH_3)_2Cl_2]$, are also given in Fig. 2. The other component,

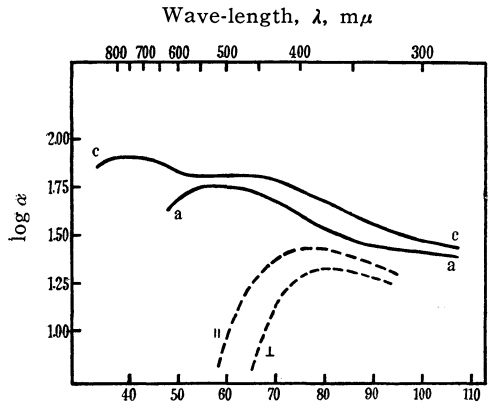

Fig. 2. Absorption spectra of $[Pd(NH_3)_2Cl_2][Pd(NH_3)_2Cl_4]$ (——) and *trans*-$[Pd(NH_3)_2Cl_2][Pd(NH_3)_2Cl_4]$ (- - - -), both in crystalline state.

$[Pd(NH_3)_2Cl_4]$, is too unstable to be isolated in crystals. Its solution, however, is orange in colour. The crystal of $[Pd(NH_3)_2Cl_2][Pd(NH_3)_2Cl_4]$, therefore, is seen to show its absorption at much longer wavelength than would be expected from the absorption spectra of the components. This suggests that the component complexes would undergo specific effects in the crystal of $[Pd(NH_3)_2Cl_2][Pd(NH_3)_2Cl_4]$. Moreover, the present measurement shows that absorption is much more bathochromic with the electric vector along the chains, - - -Cl—Pd^{IV}—Cl- - - Pd^{II}- - -Cl—Pd^{IV}—Cl- - -, than that normal to the chain. This relation is seen to be reverse to that with the crystal of *trans*-$[Pd(NH_3)_2Cl_2]$. *It may be presumed from the above relations that in the crystals of* $[Pd(NH_3)_2Cl_2][Pd(NH_3)_2Cl_4]$ *there would be strong interaction between the metal atoms in different oxidation states through the anions.* Thus with the electric vector along the chain, absorption was observed at $30\text{–}45\times10^{13}$/sec., whereas the absorption in this region was not observed with the electric vector normal to the above chain. This absorption might be assumed to be a charge-transfer band[14] due to the chain, - - -Cl—Pd^{IV}—Cl- - -Pd^{II}- - -Cl—Pd^{IV}—Cl- - -.

The compound, $Pt(en)Cl_3$, may be considered as a compound of a similar type. Thus the compound can be prepared from a mixed aqueous solution of $[Pt(en)Cl_2]$ and $[Pt(en)Cl_4]$. Further, magnetic examination[15] indicates that this compound is diamagnetic, involving no platinum in tervalent state. The above facts seem to show that the compound should be formulated as $[Pt(en)Cl_2][Pt(en)Cl_4]$.

The compound, $[Pt(en)Cl_2][Pt(en)Cl_4]$, in the crystalline state has much deeper colour than either of the component complexes; $[Pt(en)Cl_2]$ is pale yellow, and $[Pt(en)Cl_4]$ is also yellow. Thus the compound, $[Pt(en)Cl_2][Pt(en)Cl_4]$ dissolves in hot water to give a yellow solution, from which its red crystals separated. As may be expected from the colours, $[Pt(en)Cl_2][Pt(en)Cl_4]$ in the crystalline state is found to show its absorption at far longer wave-length than either of the component complexes (Fig. 3). This shows

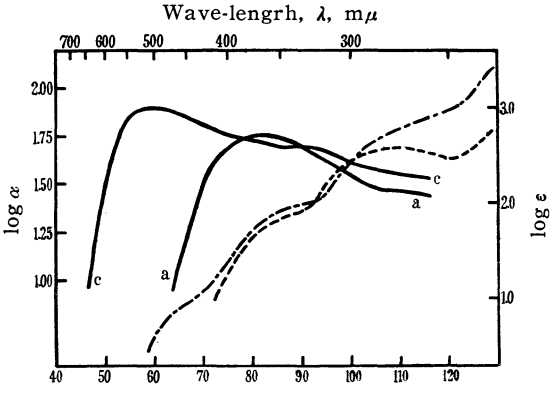

Fig. 3. Absorption spectra of $[Pt(en)Cl_2][Pt(en)Cl_4]$ (——), $[Pt(en)Cl_2]$ (- - - -) and $[Pt(en)Cl_4]$ (—·—·—).

that the complexes are under remarkable effect in the crystalline state. The nature of the effect may be judged from the results of the dichroism measurement. The dichroism of the above compound, as given in Fig. 3, may be well understood, assuming that the red compound involves infinite chains similar to those in the crystal of $[Pd(NH_3)_2Cl_2][Pd(NH_3)_2Cl_4]$. That is, assuming the *c*-absorption to be the absorption along the infinite chains, - - -Cl—Pt^{IV}—Cl- - -Pt^{II}- - -Cl—Pt^{IV}—Cl - - -, and the *a*-absorption to be the absorption normal to the chain, then the absorption is seen to be much more bathochromic with the electric vector along the above chains than the absorption normal to the chains. This relation on the dichroism is found to be quite similar to that of $[Pd(NH_3)_2Cl_2][Pd(NH_3)_2Cl_4]$, and may be best understood in the same way as with the above palladium compound. *It is most likely that the crystal of* $[Pt(en)Cl_2][Pt(en)Cl_4]$ *involves the infinite chains along the c-axis, as assumed above.* The absorption at $50\text{-}65\times10^{13}$/sec.,

14) See, for example, R.S. Mulliken, *J. Am. Chem. Soc.*, **72**, 605 (1950), etc.

15) Y.K. Syrkin and V.I. Belova, *Zhur. Fiz. Khim.*, **23**, 664 (1949); *C.A.*, **43** 7277 (1949).

which is not observed with the electric vector normal to the chains, is observed with the electric vector along the chains. This absorption may be a charge transfer band due to the chains, ---Cl—Pt^{IV}—Cl---Pt^{II}---Cl—Pt^{IV}—Cl---.

Besides the compounds described above, another type of compounds is known in which similar interaction may be found between metal atoms through anions. One of the compounds may be $Cs_2AgAuCl_6$. This crystal is very dark, almost black in colour. Elliott et al.[16] studied the crystal structure of the above compound, showing that the crystal of this compound involves infinite chains along the *c*-axis, each containing alternate planes of $[AuCl_4]^-$ and linear ions of $[Cl–Ag–Cl]^-$. The crystals of $Cs_2AgAuCl_6$ which we obtained were too small to be used for the dichroism measurement. We, however, could observe visually some of the crystals under the microscope. The observation showed that the crystals appeared almost black with the electric vector along the *c*-axis, and yellow with the electric vector normal to the *c*-axis. This fact seems to suggest that absorption with the electric vector along the infinite chains lies at much longer wave-length than that with the electric vector normal to the chains. Thus, it may be supposed that the crystal of $Cs_2AgAuCl_6$ exhibits dichroism of a type similar to that of $[Pd(NH_3)_2Cl_2]$ $[Pd(NH_3)_2Cl_4]$. The absorption at the longer wave-length, which would be allowed only with the electric vector along the infinite chains, ---$Au^{III}(Cl_4)$---Cl—Ag^{I}—Cl---Au^{III} (Cl_4)---, may be a charge transfer band, characteristic of the above chains. This may be considered as showing that there would be a strong interaction between the metal atoms through the chlorine atoms.

By following the same procedure as in the preparation of $Cs_2AgAuCl_6$ except that ammonium chloride was used instead of caesium chloride, a dark-coloured compound, $(NH_4)_3AgAuCl_7$, was obtained. The reaction proceeded in quite the same way as in the caesium compound. The crystal structure of $(NH_4)_3AgAuCl_7$ has not been determined as yet. But similarity to the corresponding caesium compound in the method of preparation and in the reaction of its formation seems to indicate that the crystals of $(NH_4)_3AgAuCl_7$ involve components similar to those of the corresponding caesium compound; that is, $[Cl–Ag–Cl]^-$ and $[AuCl_4]^-$ ions. The crystals of this compound are found to absorb in much longer wave-length than would be expected for the component complexes (Figs. 4 and 5). This indicates

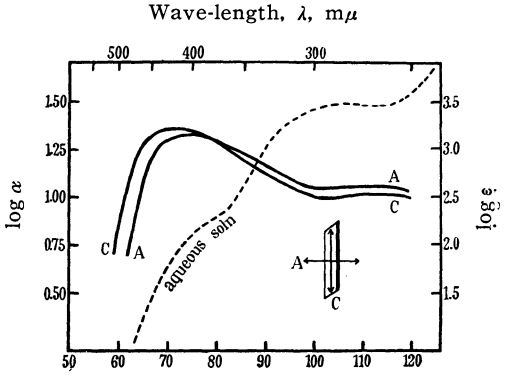

Fig. 4. Absorption spectra of $Cs[AuCl_4]$.

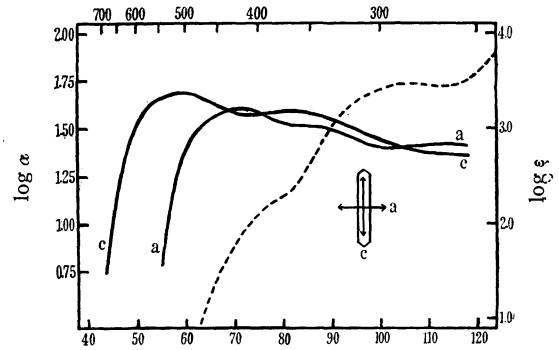

Fig. 5. Absorption spectra of $(NH_4)_3$ $AgAuCl_7$ (——) and $Cs[AuCl_4]$ (- - - -).

that the component complexes undergo some effects in the crystalline state.

It has also been found that the *c*-absorption is much more bathochromic and somewhat more hyperchromic than the *a*-absorption. These relations, which are similar to those with the crystals of $Pd(NH_3)_2Cl_2$, $Pt(en)Cl_2$ and $Cs_2AgAuCl_6$, seem to agree with the assumption that *the crystals of* $(NH_4)_3AgAuCl_7$ *may contain infinite chains of* ---$Au^{III}(Cl_4)$---*Cl*—Ag^{I}—*Cl*---$Au^{III}(Cl_4)$--- *along the c-axis.* Thus the absorption at 55×10^{13}/sec. for the *c*-absorption, which is not observed for the *a*-absorption, may be assigned to a kind of charge transfer band due to the above chains.

General Discussion

Surveying the above results, the following generalization may be induced. *Those compounds having infinite chains such as* ---*X*—M^m—*X*---M^n---*X*—M^m—*X*---, *M and X being metal and halogen atoms, show at the*

16) N. Elliott and L. Pauling, *J. Am. Chem. Soc.*, 60, 1846 (1938).

longer wave-length a new absorption band, characteristic of the infinite chains and polarized along the chains. The new band may be interpreted as due to a charge transfer between the two components.

This may be taken as showing that *in those crystals there would exist some interaction between metal atoms through anions.* In the above instances, the halogen atoms are supposed to act as bridges, facilitating the electron transfer between the metal atoms. Assuming the picture of the electron transfer between metal atoms, the interaction would be stronger between atoms in different oxidation states of the same or similar elements than between atoms of different elements. The interaction between the metal atoms in the above compounds, however, seems to be slightly different from the interaction between metal atoms in μ-peroxo-dicobalt-compounds, magnetite or prussian blue[17]. That is, in the groups of the latter compounds all the metal atoms are almost or completely equivalent and undistinguishable, while in the former there are involved two kinds of the metal atoms which are clearly unequivalent. The electronic migration between the two metal atoms would occur much more readily in the compounds of the latter type than in those of the former.

It is to be noted that the complex, $[Pd(NH_3)_2Cl_4]$, is rather stable in the crystal of $[Pd(NH_3)_2Cl_2][Pd(NH_3)_2Cl_4]$, although the former has never been isolated in solid under any ordinary condition. In the same way, the $[Cl\text{–}Ag\text{–}Cl]^-$ anion seems to be much more stable in the crystal of $Cs_2AgAuCl_6$ and $(NH_4)_3AgAuCl_7$ than in other compounds of an ordinary type involving the anions. The remarkably enhanced stability of the above complexes in the present compounds may be closely associated with the interaction between the metal atoms through the anions.

It is suggested that a number of compounds having platinum or palladium in apparently tervalent state would involve similar chains. Thus, in the crystals of $Pt(NH_3)_2(OH)Cl_2$ there would be similar chains, in which the atom of bivalent platinum would be connected with the atoms of quadrivalent platinum through OH^- or Cl^- ions. In fact, according to Bokii et al., the crystals of $Pt(NH_3)_2(OH)Cl_2$ appears black with polarized light having its electric vector along the needle axis, and very pale with the electric vector normal to the needle axis[18]. This seems to indicate that the compound in the crystalline state displays in the visible region an absorption band which would be polarized in the direction of the needle axis. It is most probable that the band at the longer wave-length may be a charge transfer band due to the possible chains, $\cdots X\text{—}Pt^{IV}\text{—}X\cdots Pt^{II}\cdots X\text{—}Pt^{IV}\text{—}X\cdots$, indicating the interaction between the bivalent and quadrivalent platinum atoms through negative ions such as OH^- or Cl^- ions (Fig. 1).

The so-called copper-coloured oxalato-platinum compounds[19] and the Wolffram's compound[20], $Pt(NH_2\cdot C_2H_5)_4Cl_3\cdot 2H_2O$, also are believed to belong to the same type of compounds involving similar chains. Polarized absorption spectra which were determined lately[21,22] are found to support the above presumption. The detailed reports on those compounds will be submitted later.

Summary

Polarized absorption spectra of $[Pd(NH_3)_2Cl_2]$ $[Pd(NH_3)_2Cl_4]$, $Pt(en)Cl_3$ and $(NH_4)_3AgAuCl_7$ in the crystalline state have been determined by Tsuchida-Kobayashi's microscopic method in the regions betwen 2400 and 8000 Å.

The crystals of the above compounds which are supposed to involve infinite chains of a type, $\cdots X\text{—}M^m\text{—}X\cdots M^n\cdots X\text{—}M^m\text{—}X\cdots$, have been found to display absorption at longer wave-length than any of the respective component complexes. This absorption at the longer wave-length has been shown to be completely polarized along the direction of the supposed chains in the crystals.

The above results show that in these crystals there would be rather strong interaction between the metal atoms through the anions along the infinite chains.

The work reported here was supported by the grant in aid of the Ministry of Education.

Department of Chemistry, Facutly of Science, Osaka University, Osaka

17) S. Yamada, Y. Shimura and R. Tsuchida, This Bulletin, 26, 72 (1953); P.E. Fielding and D.P. Mellor, *J. Chem. Physics*, 22, 1155 (1954), etc.

18) G.B. Bokii and G.I. Distler, *Doklady Akad. Nauk S.S.S.R.*, 56, 923 (1947).

19) A. Werner and E. Grebe, *Z. anorg. Chem.*, 21, 381, 387 (1899), etc.

20) H. Wolffram, Dissertation, Königsberg, 1900.

21) R. Tsuchida and S. Yamada, read before the annual meeting of the Chemical Society of Japan, Kyoto, April, 1953.

22) To be submitted later.

*Studies on Phosphonitrile Chlorides by their Pure Quadrupole Spectra**

By Hisao NEGITA and Sumio SATOU

(Received December 20, 1955)

A group of phosphonitrile chlorides $(PNCl_2)_n$ have been known so far[1], where n is the degree of polymerization and is three or above. Of these, the trimer is the most ordinary compound and has been thought to form a plane ring[2], composing of nitrogen and phosphorus atoms alternatively. On the contrary, the tetramer has been shown to have a puckered ring and two kinds of chlorine atoms attached to the same phosphorus atom[3].

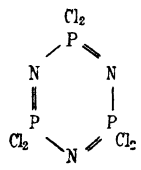

Trimer

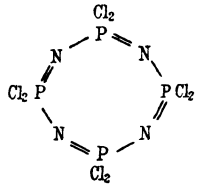

Tetramer

We therefore examined the pure quadrupole spectra due to Cl^{35} of these two compounds and considered the states of their chlorine atoms, comparing the resonance absorption frequencies or absorption lines with each other.

Experimental

Preparation of Samples.—Phosphonitril chlorides were prepared by heating phosphorus pentachloride and ammonium chloride in *sym*-tetrachloroethane[4]. After the product was freed from ammonium chloride, solvent, and rubber-like residue, it was fractionally distilled at about 13 mmHg. The most part of the product was distilled off at about 127°C and this fraction was used as the sample of the trimer (m.p. 114°C). The fraction at 185–190°C was about one-tenth of the trimer, showing m.p. of 121–124°C. Thus it was used as the tetramer (m.p. 123.5°C), for a small content of impurities does not affect the absorption frequency, though they make the line width broader.

Apparatus.—To measure the absorption frequencies, we used the spectrometer reported in the previous paper[5], which was improved on a few points. For instance, a variable condenser of small capacity was connected parallel to the tank circuit of the main oscillator for the purpose of band spread, and its graduations were corrected every time by the crystal oscillator. By this method, the absorption frequency of potassium chlorate $KClO_3$ was found to be 28.147 Mc. at 14°C, which was in good agreement with the value of Wang et al.[6], taking the temperature effect into consideration.

Results and Considerations

The absorption frequencies of phosphonitrile chlorides were found at room temperature as shown in Table I. The experimental error was assumed to be several kc. in each case.

TABLE I

THE RESONANCE ABSORPTION FREQUENCIES DUE TO Cl^{35} IN PHOSPHONITRILE CHLORIDES $(PNCl_2)_n$ (287°K)

Compound	$(PNCl_2)_3$	$(PNCl_2)_4$
Frequency (Mc./sec.)	27.630	27.265
	27.704	28.124
	27.834	28.182
	27.903	28.616

It is noticed that both compounds show four kinds of frequencies. This fact seems to be curious in the case of the trimer $(PNCl_2)_3$, for six chlorine atoms of this molecule might be equivalent in the solid as well as in the vapor phase[2], and only one absorption frequency is to be expected. Otherwise, two or six kinds of frequencies may reasonably be expected, assuming slight distortion of P-Cl bonds or of the ring.

In the same way, two, four, and eight kinds may be probable in the case of the tetramer $(PNCl_2)_4$, for there are at least two kinds of chlorine atoms; that is, two chlorine atoms attached to the same phosphorus atom are at distances of 1.97 Å and 2.01 Å, respectively, according to the X-ray analysis[3].

The patterns of the spectra are illustrated in Fig. 1, where the intensity of each line is estimated roughly from the ratio of signal to noise. It is seen from this figure that

* A part of this research was reported at the 8th meeting of the Chemical Society of Japan, on April 2, 1955.

1) L.F. Audrieth, R.S. Steinman and A.D.F. Toy, *Chem. Rev.*, **32**, 109 (1943).

2) L.O. Brockway and W.M. Bright, *J. Am. Chem. Soc.*, **65**, 1551 (1943).

3) J.A.A. Ketelaar and T.A. de Vries, *Rec. trav. chim.*, **58**, 1081 (1939).

4) R. Schneck and G. Römer, *Ber.*, **57**, 1343 (1924).

5) H. Negita, H. Yamamura and H. Shiba, This Bulletin, **28**, 271 (1955).

6) T.C. Wang, C.H. Townes, A.L. Schawlow and A.N. Holder, *Phys. Rev.*, **86**, 810 (1952).

four lines of the trimer are characterized by two kinds, the stronger and the weaker, whereas those of the tetramer are all of the same order. Consequently, it may be concluded that the stronger of the trimer and all of the tetramer are caused by two equivalent chlorine atoms in their molecules, and the weaker by only one. Thus, the four lines in each spectrum are concerned with the numbers of chlorine atoms in the corresponding molecules as 2+1+1+2=6 and 2+2+2+2=8, respectively.

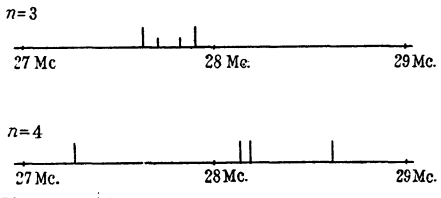

Fig. 1. The relative intensities of the absorption lines in $(PNCl_2)_n$.

However, it must be borne in mind that the intensity of the line in the pure quadrupole spectra is not always proportional to the amounts of the corresponding atoms, because it is affected also by the spin-lattice relaxation time and other factors[7].

The ionic character α of P-Cl bond may be assumed[8] by the relation $\alpha=1-\nu/\nu_0$, where ν is the measured absorption frequency of the compound and ν_0 is the absolute value of the coupling constant of atomic chlorine[9], 54.87 Mc.. Accordingly, the smaller is the frequency, the larger is the ionicity of the bond.

Several compounds which have P-Cl bonds and whose absorption frequences have been known are listed in Table II. From this table and Table I, it is seen easily that the ionicity of P-Cl bonds in phosphonitrile chlorides are closest to those of phosphorus oxychloride, taking account of frequancy increases, which presumably amount to several hundreds kc. at 77°K.

TABLE II
THE RESONANCE ABSORPTION FREQUENCIES OF SEVERAL COMPOUNDS WHICH HAVE P-Cl BONDS (77°K)

Compound	m. p. (°C)	Frequency (Mc./sec.)
PCl_3	−92	26.202[10]
		26.107
$POCl_3$	1.4	28.9378[11]
		28.9835
PCl_5	163	32.282[12]
		32.384
		32.63

Furthermore, two chlorine atoms in the trimer, corresponing to the absorption frequenty 27.630 Mc., are regarded as the most ionic of the six chlorine atoms, and they are to be replaced together to yield disubstituted compounds in place of monosubstituted compounds. In this way, the fact can be explained without difficulty that hydrolysis of the trimer gives triphosphonitrile dihydroxytetrachloride $P_3N_3(OH)_2Cl_4$ as a main product[13]. Trimeric phosphonitrilic acid $P_3N_2(OH)_6$ is unstable, whereas tetrameric phosphonitrilic acid $P_4N_4(OH)_8\cdot 2H_2O$ is so stable that various hydrolytic intermediates have not been obtained[1]. However, these are likely to be isolated by controlled hydrolysis, for the absorption lines of the tetramer are widely spaced. Studies on the chemical behaviour of the phosphonitrile chlorides and their derivatives are now in progress, in connection with the results of the pure quadrupole spectra.

In conclusion, the authors wish to express their sincere thanks to Prof. T. Ichikawa and Dr. H. Yamamura for their encouragement and useful discussions throughout this research, and also to Messers. M. Miyashita and Z. Hirano for their able assistance of this work. This research was supported by the research grant from the Ministry of Education.

Chemical Department, Faculty of Science, Hiroshima University, Hiroshima
and
Chemical Laboratory, Faculty of Education, Kagawa University, Kagawa

7) J. Hatton and B.V. Rollin, *Trans. Faraday Soc.*, 50, 398 (1954).
8) W. Gordy, W. V. Smith and R. F. Trambarulo, "Microwave Spectroscopy", John Wiley & Sons Inc., New York (1953) p. 284.
9) V. Jaccarino and J.G. King, *Phys. Rev.*, 83, 471 (1951).
10) R. Livingston, *J. Phys. Chem.*, 57, 496 (1953).
11) R. Livingston, *Phys. Rev.*, 82, 289 (1951).
12) D.W. McCall and H.S. Guttowsky, *J. Chem. Phys.*, 21, 1300 (1953).
13) H.N. Stokes, *Am. Chem. J.*, 17, 275 (1895); *Ber.*, 28, 437 (1895).

Studies on Crystals of Metallic Tris-ethylenediamine-complexes. I. The Crystal Structure of DL-*Tris-ethylenediamine-cobalt (III) Chloride Trihydrate,* $[Co\ en_3]Cl_3 \cdot 3H_2O$

By Kazumi NAKATSU, Yoshihiko SAITO and Hisao KUROYA

(Received January 1, 1956)

Introduction

No complete structure determination of a complex salt containing the $[Co\ en_3]^{3+}$ ion has yet been reported, although determination of a complex salt containing the $[Ni\ en_3]^{2+}$ ion has been carried out by Watanabé and Atoji[1].

The present work on the familiar crystals of the complex salt $[Co\ en_3]Cl_3 \cdot 3H_2O$ was undertaken mainly to determine the shape and size of the complex ion in the course of our studies on metallic tris-ethylenediamine complex compounds. Ter Berg[2] has reported the unit cell dimensions, space group and other crystallographic data of this substance together with several related compounds. In this work his results were indeed verified.

Experimental

Tris-ethylenediamine-cobalt (III) chloride trihydrate was prepared according to the method described by Jörgensen[3]. Jaeger[4] reported that the crystals belong to ditrigonal scalenohedral class with $a:c=1:0.6667$. Crystals grown for this work by slow evaporation of saturated aqueous solution at room temperatures were hexagonal prisma. Cylindrical specimens of about 0.3 mm. in diameter parallel to all principal axes were prepared. All the equatorial reflections were recorded by using Fe K radiation ($K\alpha$, $\lambda=1.937$ Å).

The unit cell dimensions were obtained from high order $(hki0)$ and $(h0\bar{h}l)$ reflections on the equatorial lines of oscillation photographs. The results are: $a=11.50\pm0.02$, $c=15.52\pm0.04$ Å, giving the axial ratio $2a:c=1:0.668$, in agreement with that reported by Jaeger.

From the density 1.504 g./cc. obtained by the pyknometer method at 17°C, one finds that the unit cell contains four formula units of $[Co\ en_3]Cl_3 \cdot 3H_2O$. Laue symmetry was found to be D_{3d}-$\bar{3}m$. The systematic absences are: $(000l)$ present only with $l=$even, and $(h0\bar{h}l)$ present only with $l=$even. Hence the space group is either C_{3v}^3-$P3c1$ or D_{3d}^4-$P\bar{3}c1$. No piezoelectric effect was observed*, so that the space group is probably $D_{\bar{d}3}^4$-$P\bar{3}c1$. This space group has 12-fold general positions; accordingly the four cobalt atoms have to be placed in some special positions**.

Usual multiple film technique was used and the intensities of reflections were obtained visually by comparison with a calibrated standard. The usual correction factors were applied by means of the chart given by Cochran[5]. No correction for absorption was made. Observed structure amplitudes were later placed on an absolute scale by comparison with the calculated values.

Determination of the Structure

At the outset of the analysis it was found that reflections $(hki0)$ are generally rather strong when $h-k=3n$ and, moreover, odd-layer lines of oscillation photographs about the c-crystal axis are weaker than even-layer lines. These characteristics of reflections, combined with the results of Patterson projections $P(U, V)$ and $P(U, W)$, suggested that the cobalt atoms are on the 4-fold special positions; 4 d, 1/3, 2/3, z, etc. with $z \fallingdotseq 1/8$.

All the large peaks in $P(U, V)$ except those due to Co–Co interatomic vectors were mainly interpreted in terms of Co–Cl and Co–N vectors. The Co–N peaks were readily identified, if an approximate octahedral coordination of six nitrogen atoms of ethylenediamine molecules was assumed. First an electron-density projection $\rho(X, Y)$ was prepared using all the observed $F(hki0)$ values, whose signs were calculated from the arrangement of Co, Cl and N atoms only. The resulting distribution showed heavy cobalt and

TABLE I

FRACTIONAL ATOMIC COORDINATES

atom	x	y	z
Co	1/3	2/3	0.125
Cl	0.097	0.493	0.372
O	0.087	0.225	0.873
C_1	0.180	0.397	0.077
C_2	0.215	0.397	0.173
N_1	0.192	0.525	0.050
N_2	0.333	0.525	0.200

1) T. Watanabé and M. Atoji, *Kagaku*, **21**, 301 (1951).
2) J. Ter Berg, *Diss. Univ. Groningen*, (1937).
3) S.M. Jörgensen, *J. pr. Ch.*, **2**, **39**, 546 (1898).
4) F.M. Jaeger, *Z. Krist.*, **38**, 546 (1904).

* We are grateful to Mr. Y. Iidaka of the Mineralogical Institute, University of Tokyo, for piezoelectric test of the crystals.

** The unit cell, space group and the assignment of the positions of the cobalt atoms are in agreement with the results obtained by Ter Berg.

5) W. Cochran, *J. Sci. Instruments*, **25**, 253 (1949).

chlorine atoms clearly resolved, together with faint outlines of the remaining atoms. Successive refinements with $(Fo-Fc)$ syntheses[6] led to the final projection shown in Fig. 1, which can be interpreted with the aid of Fig. 2. From this electron-density map x- and y-parameters of all the atoms were fixed. The z-parameters of each atom were deduced from $P(U, W)$, taking of complex ions and Cl^- ions into consideration. Successive Fourier syntheses, $\rho(X, Z)$ were carried out and the final electron-density map is shown

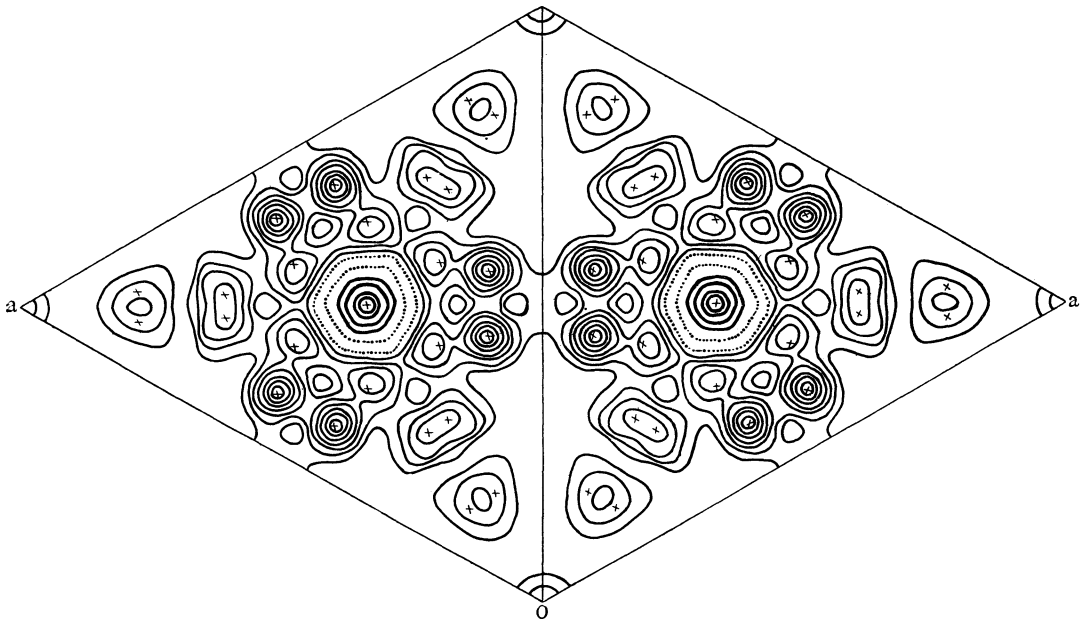

Fig. 1. Electron-density map of $[Co\ en_3]Cl_3 \cdot 3H_2O$ projected on (0001) (Contours are drawn at intervals of 4 e. Å^{-2}, the zero contour line being broken. The heavy lines of the Co peak are drawn at intervals of 20 e. Å^{-2}).

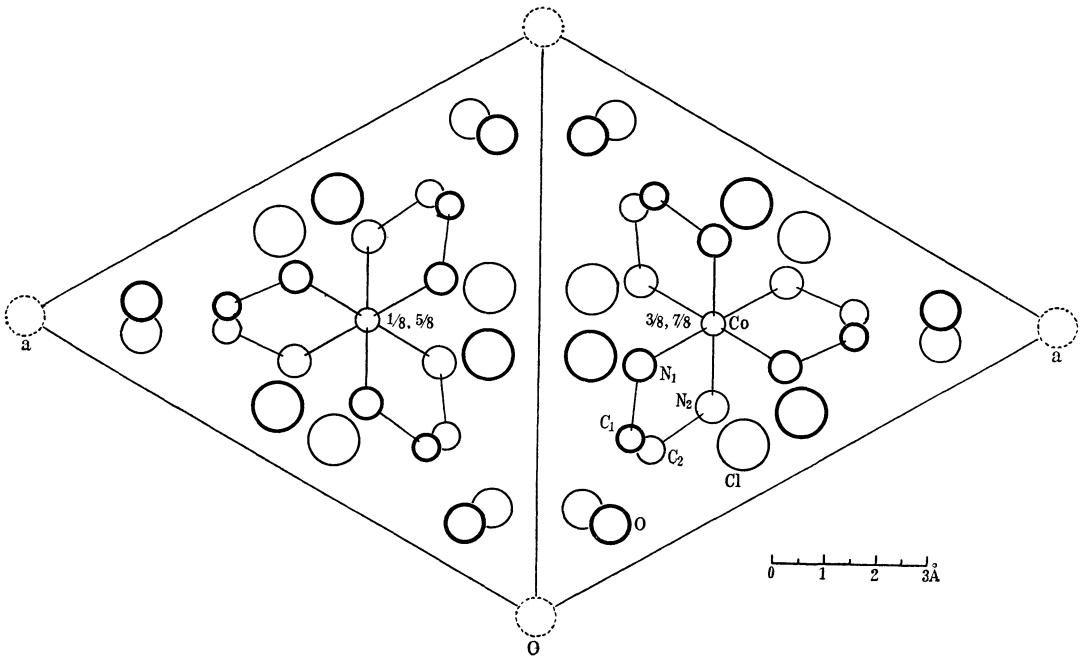

Fig. 2. Projection of the structure upon (0001).

6) W. Cochran, *Acta Cryst.*, **4**, 408 (1951).

TABLE II

OBSERVED AND CALCULATED STRUCTURE AMPLITUDES

*h*0.0	*Fo*	*Fc*	10.*l*	*Fo*	*Fc*	40.*l*	*Fo*	*Fc*
1	134	−134	2	104	−104	$\bar{6}$	41	−44
2	11	−26	4	55	35	$\bar{8}$	44	−50
3	51	−55	6	62	−57	$\bar{10}$	34	32
4	69	−71	8	—	−8	$\bar{12}$	22	25
5	44	−33	10	24	11	$\bar{14}$	1	−13
6	66	58	12	40	28	50.*l*		
7	84	−93	14	12	14	2	43	32
8	12	1	2	97	102	4	59	49
9	15	20	4	60	45	6	26	−21
10	40	42	$\bar{6}$	70	54	8	60	−68
			8	—	−19	10	6	20
*h*1.0			10	17	−6	12	54	52
1	84	95	12	46	40	$\bar{2}$	35	−29
2	17	−28	14	25	−19	$\bar{4}$	51	46
3	—	−13				$\bar{6}$	24	14
4	91	94	20.*l*			$\bar{8}$	60	−68
5	18	−23	2	39	74	$\bar{10}$	9	−12
6	35	−34	4	13	−16	$\bar{12}$	61	50
7	85	74	6	82	−77	61.*l*		
8	30	−26	8	45	34	2	—	−15
9	31	−38	10	71	72	4	13	−6
			12	25	−20	6	23	1
*h*2.0			14	32	−35	8	—	−4
2	72	62	2	80	−53	12	—	7
3	20	−20	4	8	−13	14	18	−24
4	56	−52	6	92	85	$\bar{2}$	—	17
5	48	33	8	52	30	$\bar{4}$	17	−5
6	32	−28	10	82	−85	$\bar{6}$	18	−6
7	19	−21	12	20	−16	$\bar{8}$	—	−5
8	50	51	14	33	47	$\bar{10}$	1	−1
9	—	−11				$\bar{12}$	16	−24
			30.*l*			70.*l*		
*h*3.0			2	177	178	2	129	−125
3	105	110	4	25	−14	4	48	52
4	50	47	6	66	−92	6	54	51
5	49	−53	8	48	42	8	29	−27
6	71	51	10	42	44	$\bar{10}$	50	−38
7	54	−41	12	—	−20	$\bar{2}$	124	127
8	14	−4	14	29	−34	$\bar{4}$	42	44
			$\bar{2}$	174	−172	$\bar{6}$	41	−57
*h*5.0			4	20	2	$\bar{8}$	21	−16
4	—	−22	6	72	82	$\bar{10}$	35	45
5	10	−8	$\bar{8}$	54	21	80.*l*		
6	13	−20	$\bar{10}$	46	−34	2	46	62
7	27	30	$\bar{12}$	—	−7	4	16	−20
			$\bar{14}$	23	25	6	8	−8
*h*5.0						8	19	25
5	19	15	40.*l*			$\bar{2}$	46	−64
6	—	2	2	27	6	$\bar{4}$	16	−19
			4	84	64	$\bar{6}$	—	15
00.*l*			6	40	38	$\bar{8}$	17	24
2	—	−11	8	32	−45	90.*l*		
4	315	−313	10	41	−25	2	15	22
6	—	18	12	22	21	4	19	−9
8	84	103	14	1	8	6	11	29
10	19	−19	2	17	−4	$\bar{2}$	12	22
12	109	−121	$\bar{4}$	74	68	$\bar{4}$	15	13
14	25	15				$\bar{6}$	11	−25
						100.*l*		
						$\bar{2}$	19	−22
						$\bar{2}$	15	19

Fig. 3. Electron-density map projected on a plane perpendicular to the *a*-axis (Contours are drawn in the same manner as Fig. 1.

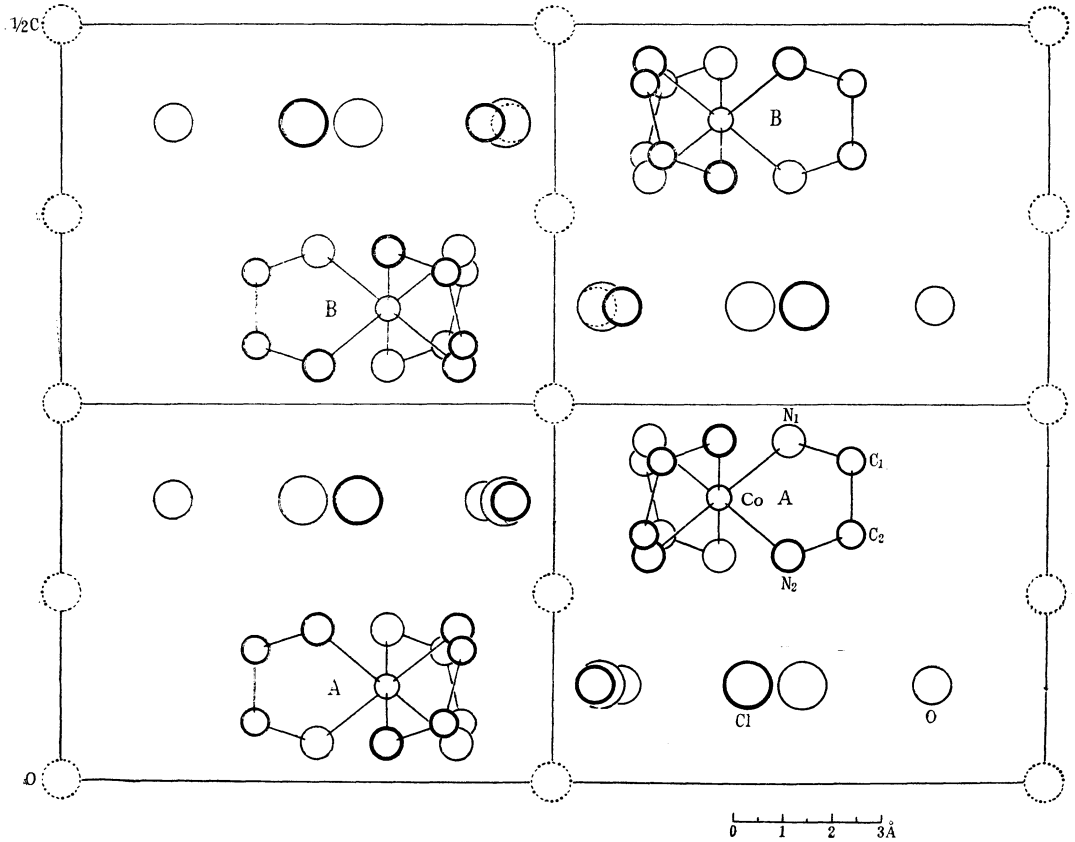

Fig. 4. Projection of the structure upon a plane perpendicular to the *a*-axis (The figure represents an elevation of the structure shown in Fig. 2, and does not correspond to $\rho(X, Z)$ in Fig.3.)

in Fig. 3. Since the resolution of the atoms on $\rho(X, Z)$ was not very good, the z-parameters deduced from $\rho(X, Z)$ were further refined by the method of least squares. The final set of coordinates thus obtained is shown in Table I, and the observed and calculated structure amplitudes are given in Table II. The atomic scattering factors used for the calculation of the structure factors were those listed in the International Tables. Temperature corrections of the form exp $-B(\sin\theta/\lambda)^2$ were used, where B was given the value 2.5 Å^2 for ($hki0$) zone and 3.0 Å^2 for ($h0\bar{h}l$) zone respectively. The values of B and the scale factor were estimated by plotting the values of log Fc/Fo versus $(\sin\theta)^2$ at the final stage. The discrepancy factors $R=\sum||Fo|-|Fc||/\sum|Fo|$, are 0.140 for ($hki0$) reflections and 0.202 for ($h0\bar{h}l$) reflections respectively, with a weighted mean value of 0.186, where all the observed reflections up to $\sin\theta=0.98$ are included. The calculated interatomic distances and bond angles are recorded in Table III.

TABLE III

CALCULATED INTERATOMIC DISTANCES AND BOND ANGLES

Co–N_1	2.00 Å	Cl···N_1	3.13 Å
N_2	2.00		3.26
N_1–C_1	1.47	Cl···N_2	3.18
C_1–C_2	1.54		3.41
C_2–N_2	1.47	Cl···O	3.34
		Cl···C_1	3.30
Co–N_1–C_1	105.4°	C_2	3.67
N_1–C_1–C_2	112.6°	O···C_1	3.36
N_2–C_2–C_1	112.6°	C_2	3.12
Co–N_2–C_2	105.4°		

Description of the Structure

The final electron-density map shown in Fig. 3 gives the arrangement of atoms shown in Fig. 4, which represents an elevation of the structure in Fig. 2. The shape and size of a complex ion [Co en_3]$^{3+}$ as it exists in the crystal is illustrated in Fig. 5. This figure shows one of the two stereo-isomeric ions, which are present in equal numbers in the structure. The complex ion is required by the space group to have trigonal symmetry. However, within the errors of experiment it possesses the symmetry D_3–32. Six nitrogen atoms of three ethylenediamine molecules form a slightly distorted octahedron around the central cobalt atom. The five-membered ethylenediamine cobalt rings are not planar, that is, the ethylenediamine ligands take so-called "gauche" forms. Arrangement of atoms about C_1-C_2 bond is illustrated in Fig. 6.

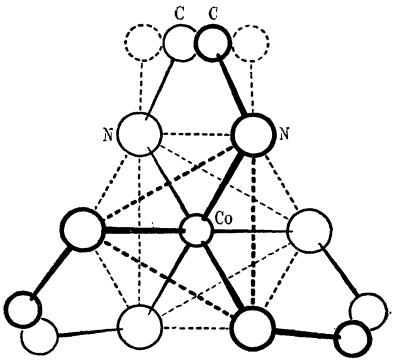

Fig. 5. The complex ion [Co en_3]$^{3+}$.

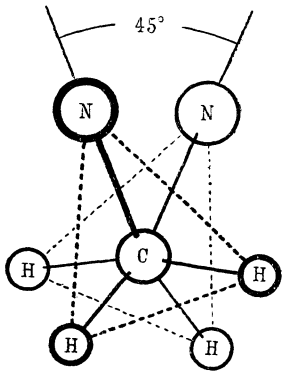

Fig. 6. Arrangement of atoms around C_1–C_2 bond.

The Co–N distances of 2.00 Å as well as the shape and size of the ethylene diamine molecules may be compared with those perviously described by Nakahara and two of us[7] for the complex ion [Co en_2Cl_2]$^+$.

The gauche configuration of ethylenediamine has a mirror image non-superposable, which we shall denote as d and l. Then ethylenediamine molecules may enter into combination with a cobalt atom in its d- or l-form. The possibilities of isomerism are, therefore, greatly increased and the following cases should arise:[8,9]

Dddd, Dddl, Ddll, Dlll,
Llll, Llld, Lldd, Lddd,

where D or L indicates the configuration of the whole complex ion, i.e. the way in which the three ligands coordinate to a central cobalt atom. Nevertheless, our X-ray evidence showed that the complex ion possesses trigonal symmetry. Thus the representation for the

7) A. Nakahara, Y. Saito and H. Kuroya, This Bulletin, 25, 331 (1952).
8) M. Kobayashi, *J. Chem. Soc. Japan*, 64, 652 (1943).
9) J.V. Quagliano and S. Mizushima, *J. Am. Chem. Soc.*, 75, 6084 (1953).

complex ion in the crystal should be one of the following sets: (*Dddd*, *Llll*) and (*Dlll*, *Lddd*). The projections of the carbon atoms in Fig. 4 will change as indicated by dotted circles, if the other antipode of the ethylenediamine ligands coodinates to the central cobalt atom, keeping the configuration of the whole complex ion as before. However, final electron-density projection $\rho(X, Y)$ excludes this latter possibility, so that only one definite configuration is possible for each stereoisomeric complex ion in the crystal. By no means, should the presence of various stereoisomers in solution be excluded by our *X*-ray evidence. At this stage, however, it is impossible to decide whether the complex ion illustrated in Fig. 4 corresponds to dextro or laevo rotatory. Recently the determination of the absolute configuration of this complex ion has been carried out in our laboratory and a brief account has been published already[10].

The way in which the complex ions form bonds in the structure is best described by referring to Figs. 1 and 4. A complex ion is surrounded by nine Cl ions. Six of them are at the apices of a distorted trigonal prism, being 3.18 Å and 3.26 Å apart form N atoms. The other three form an equilateral triangle, being nearly on the same level as a cobalt atom. These N···Cl distances are 3.13 Å and 3.41 Å. The former distance of 3.13 Å suggests a hydrogen bond of the type N–H···Cl between N_1 and Cl. All these N···Cl distances are in good agreement with those reported by various authors[11,12,13,14,15]. Fig. 4 also indicates the packing of the formula units in the structure. Starting with any complex ion denoted by A, another complex ion denoted by B follows by the operation of the glide plane "*c*" or center of symmetry.

Remarks on the Water of Crystallization

Together with Cl^- ions the complex ions form structure with hollow channels along the *c*-crystal axis, in which water molecules are enclosed. They are on a set of general positions 12 *g*. A water molecule is associated to Cl^- ions with a distance of 3.34 Å. Other environmets of an oxygen atom are as follows: O···C_1=3.36 Å, O···C_2=3.12 Å, O···O=3.90 Å, 4.19 Å and 4.54 Å.

It seems to be an unlikely occurrance that water molecules are held together with such long O···O distances in the hollow channel. On the other hand, it was found that small peaks on electron-density maps, corresponding to the sets of 2-fold positions 2 *a* (000); (00$\frac{1}{2}$) and 2 *b* (00$\frac{1}{4}$); (00$\frac{3}{4}$), could by no means be eliminated even at the final stage of refinement. These positions are indicated by dotted circles in Figs. 2 and 4. This fact led us to assume that water molecules are randomly distributed on these positions as well as the above-mentioned general positions. Such a random arrangement of water molecules gives rise to a sequence of oxygen atoms with reasonable distances of 2.96 Å and 3.00 Å in the channel. Calculation of the structure amplitudes based on this model gave a lower value of *R* by about 0.02. From this fact only, one cannot decide whether such random distribution of water molecules is realized or not in the crystal.

It is to be noted here that water content of the crystal varies appreciably according to its history. Careful measurements of the density and analyses of the water of crystallization revealed that the crystal contains about 3.5 mol. of water of crystallization, when freshly prepared, and it gradually loses part of its water of crystallization on standing in the air, and the chemical formula tends to [Co en_3] $Cl_3 \cdot 3H_2O$. These excessive water molecules may be randomly distributed on the sets of special positions 2 *a* and 2 *b*. It was observed that a single crystal can be completely dehydrated by gently heating at 120°C, without bringing about any remarkable change in its appearance except a loss of transparency. A single crystal oscillation photograph was obtained even after complete dehydration, and furthermore, practically no change was found in its cell dimensions. These observations seem to support such a weak bonding of water molecules in the crystal. Further studies on the behaviour of this water of crystallization, including thermal analysis, are now going on. The results will be published soon.

Summary

The crystal structure of [Co en_3]$Cl_3 \cdot 3H_2O$ has been determined by *X*-ray methods. It is trigonal D_{3d}^4–$P\bar{3}c1$ with four formula units in a cell of dimensions: a=11.50±0.02, c=15.52±0.04 Å. The configuration of the two stereoisomeric complex ions [Co en_3]$^{3+}$ is described. The three ethylenediamine molecules in a complex ion assume "gauche" forms; their nitrogen atoms form a slightly distorted

10) Y. Saito, K. Nakatsu, M. Shiro and H. Kuroya, *Acta Cryst.*, 8, 729 (1955).
11) W.P. Binnie and J.M. Robertson, *Acta Cryst.*, 2, 180 (1949).
12) J.M. Bloomhead, *Acta Cryst.*, 1, 324 (1948).
13) W. Cochran, *Acta Cryst.*, 4, 81 (1951).
14) D.C. Phillips, *Acta Cryst.*, 7, 159 (1954).
15) J. Trommel and J. M. Bijvoet, *Acta Cryst.*, 7, 703 (1954).

octahedron around a central cobalt atom. It is shown that ionic bonds essentially link the complex ions in the structure. The water molecules are weakly associated to chlorine ions. It is found that a single crystal can be completely dehydrated by gently heating at 120°C, without bringing about any remarkable change in its appearance, except a loss of transparency. A single crystal oscillation photograph was obtained even after complete dehydration.

The authors wish to thank Professors I. Nitta, T. Watanabé and R. Tsuchida of the Osaka University for their kind advice and encouragement throughout this work. This research was aided by a fund from the Scientific Research Expenditure of the Ministry of Education to which the authors' thanks are due.

Institute of Polytechnics, Osaka City University, Osaka

Infrared Spectra of Charoninsulfuric Acid, Chondroitinsulfuric Acid, and Some Related Polysaccharides

By Koji NAKANISHI, Noriko TAKAHASHI and Fujio EGAMI

(Received January 1, 1956)

As reported in a recent publication[1], charoninsulfuric acid isolated from the mucus of *Charonia lampas*, has been fractionated into F-1, F-3, F-A, and F-B, and the respective fractions identified as shown in Chart 1; it was also shown that the anomeric cellulose and amylose structures were not contained merely as mixtures, but that they constituted a compound charonin, which was decomposed by the action of Schweitzer's reagent.

Chart 1. Fractionation of charoninsulfuric acid.

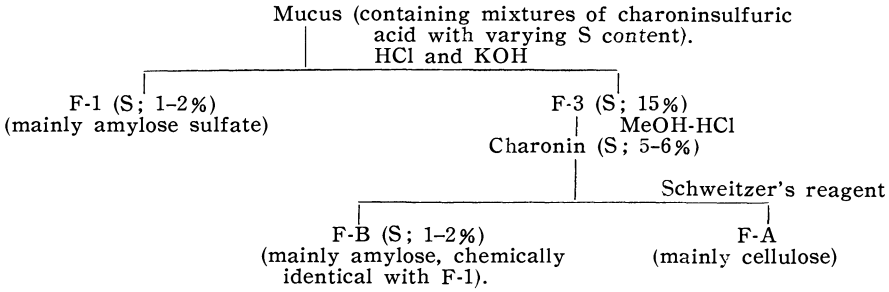

Barker, et al.[2,3] have analysed the complicated infrared spectra of D-pyranoses and its derivatives (O-methyl, O-acetyl) in the 730–960 cm^{-1} region, and have shown that the method renders possible the assignment of the derivatives to either the α- or the β-series, no matter whether they are reducing sugars, acetates, or polysaccharides; α-anomers absorb at 844 ± 8 and β-anomers at 891 ± 7 cm^{-1} (type 2a and 2b band). The method has been applied to the present series of fractions from *Charonia lampas* and extended to several related sulfates. The data fully substantiate the chemical findings; in addition, an assumption, though tentative, as regards the distribution of sulfate groups in the glucose units is forwarded. The results are summarised in Table I. The spectrum of chondroitinsulfuric acid from shark cartilage has also been measured and has been shown to be identical with "chondroitinsulfuric acid B" obtained from bovine nuclei pulpose[4].

Experimental

Materials.—The various fractions of charoninsulfuric acid are those reported in a previous communication[1]. The other materials were obtained as follows.

1) F. Egami, T. Asahi, N. Takahashi, S. Suzuki, S. Shikata and K. Nisizawa, This Builetin, 28, 685 (1955).
2) S.A. Barker, E.J. Bourne, M. Stacey and D.H. Whiffen, *J. Chem. Soc.*, **1954**, 171.
3) S.A. Barker, E.J. Bourne, R. Stephens and D.H. Whiffen, ibid., **1954**, 3468.
4) S. F. D. Orr, *Biochim. Biophys. Acta*, **14**, 173 (1954).

Cellulose: Whatman, ashless powder for chromatography.

Amylose: Potato amylose prepared through Schoch's butanol precipitation method. An aqueous solution of the precipitate was filtered through a glass filter and dried-frozen.

Dextran: From *Leuconostoc mesenteroides*.

Cellulose sulfate (Na): Prepared from filter paper.

Potato starch sulfate (Na), and Dextran sulfate (Na): Prepared according to conventional methods.

Chondroitinsulfuric acid: Prepared from shark cartilage and freed from protein by kaolin adsorption and by Sevag's chloroform-gel method. $[\alpha]_D^{11°}$ of Na-salt, $-15.4°$.

Infrared Spectra.—These were measured with a Hilger H 800 spectrometer, sodium chloride optics, by the Nujol mull method. The wavelength was callibrated against a polystyrene film. The sulfates easily gave satisfactory mulls, but for the free polysaccharides thorough grinding in ether and subsequent drying was necessary. Absorptions arising from Nujol are marked with small circles in Figs. 1-5.

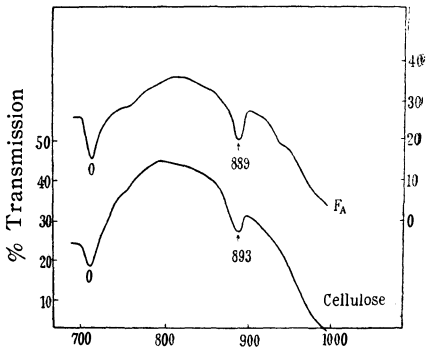

Fig. 1. F-A and cellulose.

TABLE I

INFRARED ABSORPTION OF SOME POLYSACCHARIDES

Compounds	Principal type of glycosidic linkage	Type 1[2] (ring vibr.)	Type 2[2] (C-H Deform.) 2a	Type 2[2] (C-H Deform.) 2b	Type 3[2] (ring-breathing)	Sulfate[4]	Others
α-D-Glucopyranose		912 s	835 s		765 s		
Cellobiose	β 1 : 4			896, 889 s			835, 738 m***
Dextran	α 1 : 6, α 1 : 4 branches	912 s	848 m		758 m		
Fig. 1 Cellulose	β 1 : 4	**		893 m	**		
Fig. 1 F-A	β 1 : 4			899 m			
Fig. 2 Amylose	α 1 : 4	932 m	860, 846 m	893* vw	758 m		
Fig. 2 F-1	α 1 : 4	931 m	856, 847 m	888 vw	759 m	803 w	
F-B	α 1 : 4	929 m	854, 841 m	896 vw	755 m	802 w	781 w
Fig. 3 Charonin (F_3)	Compd. of F-A & F-B	935, 919 m**	855 w	900 w	769 m	812 m	
Sulfate of Dextran (Na-salt)	α 1 : 6, α 1 : 4 branches	939 w	845 w		740 m	809, 826 w	
Fig. 4 Cellulose (Na-salt)	β 1 : 4	937 m		895 vw	767 m, 731 vw	800, 815 w	
Fig. 4 Potato starch (Na-salt)	α 1 : 4, α 1 : 6 branches	937 m			740 vw	823 m br	
Fig. 4 F-3 (K-salt)	Compd. of F-A & F-B	935 m		887 vw	760, 730 vw	806 m br	

Remark: Abbreviations, s (strong), m (medium), w (weak), vw (very weak), br (broad).

* Since the possibility that this small but evident band which is not seen in the spectrum given by Barker, et al.[2] could have arisen from contaminating cellulose (filter paper), glass filters were used throughout the purification procedure. However, the 893 cm^{-1} band became even more evident with the disolved, filtered, and dried-frozen samples. Hence, this 893 cm^{-1} band seems to be inherent to amylose, rather than being due to an impurity.

** Barker, et al.[2] give 914 w br, 933 w br (type 1), 894 w (type 2b), 766 vw (type 3) for cellulose, and the bands of charonin (935, 919) may corespond to the first set of bands, which, however, was not observed by us.

*** Also observed in Sadtler's curve (# 1020).

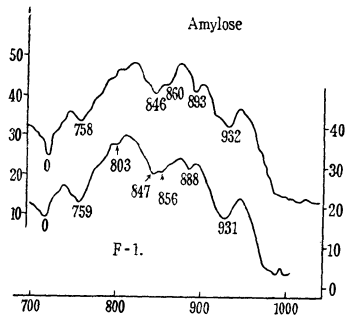

Fig. 2. F-1 and amylose.

Discussion

Charoninsulfuric Acid.—The closes similarity of the absorptions displayed by cellulose and F-A (Fig. 1), and by amylose, F-1, and F-B (Fig. 2; F-B not shown in figure), provide convincing evidence of the results obtained chemically. Since F-1 is presumed as being a slightly sulfated compound of amylose and cellulose, in which the former is predominant, the weak type 2b band (β-anomers) at 888 cm^{-1} and sulfate band[4] at 803 cm^{-1} is not unexpected. F-B shows no difference with F-1 in its chemical behavior[1] and this is also supported from infrared data; the presence of minor cellulose* (type 2b band at 896 cm^{-1}) and sulfate structures (band at 802 cm^{-1}) may be explained by the incomplete desulfation and decomposition by HCl-MeOH and Schweitzer's reagent, respectively. The curve of

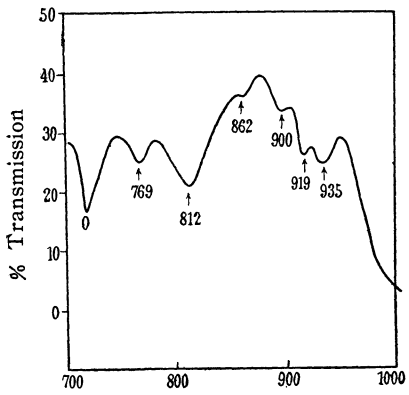

Fig. 3. Charonin.

charonin (Fig. 3) may not precisely be compared with the composite of F-A and F-B owing to the still relatively high sulfur content (5–6%; also evidenced by distinct sulfate band at 812 cm^{-1}); however, as might be expected, both type 2a and 2b bands may be observed. At present, differentiation between a compound and a mere mixture is probably not possible in this case, owing to the high molecular weight of the two constituents; chemical evidences point to a compound formation[1].

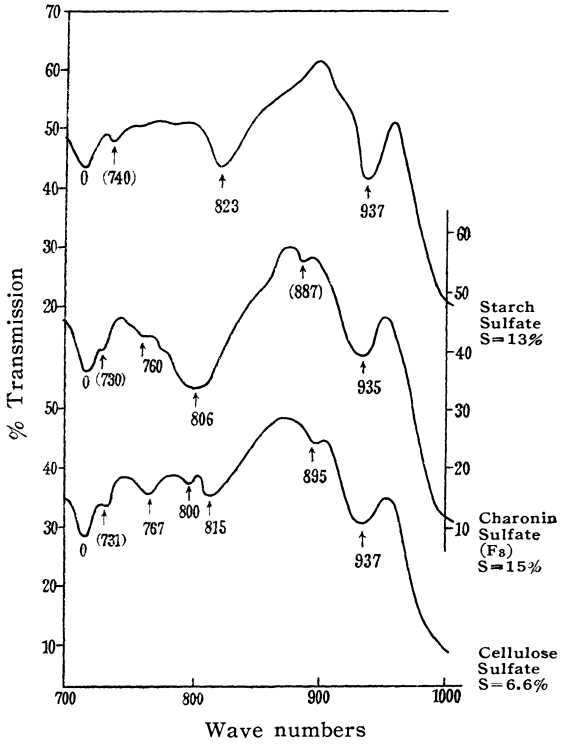

Fig. 4. Typical sulfates (Na-salt).

The spectra of the sulfates may be summarised as follows. Type 1 band appeared at 937–939 cm^{-1} with no difference between α- and β-series. Type 2 bands were generally weak or overlaid by the stronger nearby sulfate absorption at 810 cm^{-1} and though the results of Barker, et al. seem to be equally applicable for diagnosing anomeric polysaccharide sulfates, more data are necessary. As noted by Barker, et al.[3] the bathochromic shift of type 3 bands acompanying conversion of glucose to its tetra- or penta-acetate, i. e., 770→740 cm^{-1}, may be satisfactorily correlated with its assignment to a ring breathing frequency of the tetrahydropyran nuclei, the extra weight of the substituents being responsible for the shift (for tetrahydropyran, the corresponding band is at 813 cm^{-1},[8]). It may be seen (Fig. 4 and Table I) that two sets of bands, i) 765 cm^{-1} ii) 735 cm^{-1},[8]), falling in the range of type 3 bands are present in the polysaccharide sulfates, and it may also be noted that cellulose sulfate having the

* cf. Foot note *) of Table I.

8) S.C. Burket and R.M. Badger, *J. Am. Chem. Soc.*, 72, 4397 (1950).

lowest sulfur content, shows the strongest relative intensity of the 3-i band. It would be tempting to assign 3-i and 3-ii bands to the ring breathing frequencies of the unsulfated and heavily sulfated glucose residues, respectively. And from this, the assumption that the sulfate groups have a tendency to be crowed into certain glucose units rather than to be evenly distributed may be made. However, the assumption is based on a very limited amount of data, and furteer work in this line is certainly necessary to test its validity.

Chondroitinsulfuric Acid.—Orr[4] has been able to characterize two isomers of chondroitinsulfuric acid, designated A and B, from the infrared absorption and has discussed the hexuronic acid to hexosamine ratio and the stereochemistry of the sulfate groups (i. e., axial or equatorial). The B isomer has been found alone in samples from bovine nuclei pulposi, but both isomers have been found together in samples from bovine articular cartilage and trachea. The spectrum of Fig. 5 the present sample from shark cartilage

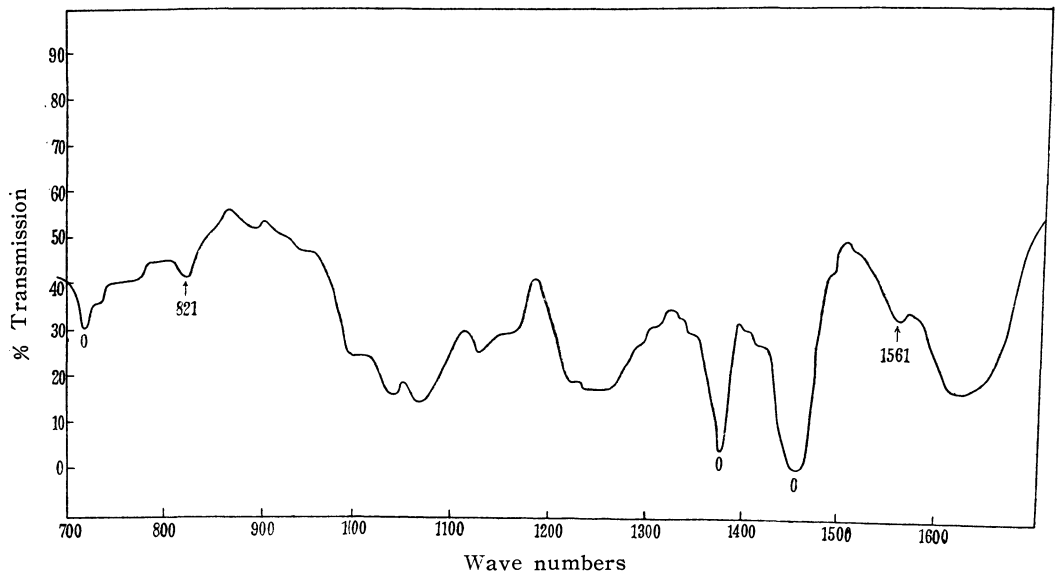

Fig. 5. Chondroitinsulfuric acid-Na (Nujol).
~1615 (carboxylate and amide I band, 1561 (amide II band), ~1240 (sulfate), ~1050 (O-H and C-O-C), 821 cm^{-1} (sulfate)

shown in Fig. 5 is identical with the B isomer and not with the A ismer. Hence, if the conclusions brought forth by Orr be accepted, the same apply to the present sample. Namely, the ratio of hexuronic acid residue to hexosamine residue is 25% less than that in hyaluronic acid, and the sulfate groups are attached to equatorial hydroxyl groups. Orr's conculusions were based on i) assigning a 820 cm^{-1} band observed in sulfates to "vibrational modes involving stretching within the C-O-S system" similar to the 1240 cm^{-1} acetate band, and ii) extending the stereochemical correlation between the acetate band and its conformation (splitting of 1240 cm^{-1} acetate band occurs in axial acetates[5]) to the sulfate band of polysaccharides. Assignment of the band at 820 cm^{-1} seems to warrant further investigation, especially since the frequency remains unaltered when passing from the free form to the salt form of polysulfated hyaluronic acid. In this connection, it may be mentioned that the 1250 cm^{-1} band in trichloroacetic acid assigned to a C-O stretching vibration (coupled with the OH bending vibration) is shifted to 1350 cm^{-1} upon conversion into the salt[6]. In addition, notwithstanding several known instances of the splitting of the C-O stretching frequency[7], in which the phenomena were correlated with stereochemistry after the conformations had been established via chemical methods, the origin of this splitting is still not clarified. Accordingly, it appears that the interesting deductions of Orr should be accepted with some reserve.

5) R.N. Jones, P. Humphries, F. Herling and K. Dopriner, *J. Am. Chem. Soc.*, **73**, 3215 (1951). A.R.H. Cole, R.N. Jones and K. Dobriner, ibid., **74**, 5571 (1952).

6) K. Kuratani, *J. Chem. Soc. Japan*, **73**, 758 (1952).

7) A.R.H. Cole, *J. Chem. Soc.*, **1952**, 4969. W.G. Dauben and N.K. Freeman, *J. Am. Chem. Soc.*, **74**, 5206 (1952). A. Stoll, Th. Petrizilka, J. Rutschmann, A. Hofmann and Hs. H. Günthard, *Helv.*, **37**, 2039 (1954). J.R. Lewis and C.W.S. Shoppee, *J. Chem. Soc.*, **1955**, 1375. C. R. Eddy, M. Barnes and F.S. Fenske, *Anal. Chem.*, **27**, 1067 (1955).

Summary

The infrared spectra of charoninsulfuric acid and related carbohydrates have been measured and the results support previous chemical evidences. The work has been extended to a few polysaccharide sulfates, and a tentative assumption as to the distribution of the sulfate groups within the polysaccharide chain is presented.

Chondroitinsulfuric acid from shark cartilage has been shown to be identical with the chondroitinsulfuric acid from bovine nucleus pulposi; a comment on the 820 cm^{-1} sulfate band is made.

Chemical Institute, Faculty of Science
Nagoya University, Nagaya

SHORT COMMUNICATION

Synthesis of Ethylenediamine labeled with Carbon-14

By Kunihiko KIGOSHI and Shizuko OKAMOTO

(Received December 15, 1955)

Studies on the isotopic exchange of ethylenediamine with ethylenediamine complex have been initiated in this laboratory. In these studies, the synthesis of ethylenediamine labeled with isotopic carbon is required. Since radiocarbon is available in the form of barium carbonate, it is necessary to examine the procedures of preparation of ethylenediamine starting with the carbonate. The procedure which is employed in this laboratory is based on the following scheme.

$$Ba\overset{*}{C}O_3 \rightarrow K\overset{*}{C}N \rightarrow CH_3\overset{*}{C}N \rightarrow CH_3\overset{*}{C}H_2NH_2 \rightarrow$$
$$CH_3\overset{*}{C}H_2OH \rightarrow CH_2\overset{*}{C}H_2 \rightarrow CH_2Br\overset{*}{C}H_2\,Br \rightarrow$$
$$NH_2CH_2\overset{*}{C}H_2NH_2$$

By these steps the overall yield was about 20% of the theoretical value, based on barium carbonate.

Experimental

The methods of preparation of alkali cyanide from radioactive barium carbonate have been described by a number of authors; among those we adopted the method proposed by O. Simamura et al.[1] by which these authors obtained the highest yield up to 100%. Also, in our experiments the yield of the cyanide above 90% of the theory was confirmed. Radioactive silver cyanide was precipitated by adding the calculated amount of silver nitrate to the alkali cyanide solution which was obtained by the distillation of crude potassium cyanide in sufuric acid solution as usual.

About 200 mg. of radioactive silver cyanide was dissolved in a solution of 7.8 g. of inactive sodium cyanide in 12 ml. water. The solution was shaken at room temperature with 25 g. of methyl iodide in order to prepare acetonitrile. After about twenty to thirty hours' shaking the solution became homogeneous, and then the solution was slowly distilled, of which a fraction of 76–100°C was collected as crude acetonitrile. Hydrogenation was carried out at room temperature and atmospheric pressure with 50 ml. solution containing crude acetonitrile and 8 g. of Raney's nickel. The process adopted here to obtain ethylamine from sodium cyanide is similar to that performed by Kilmer and duVigneaud[2]. The filtered solution containing ethylamine was acidified and the yield of ethylamine was estimated by titrating with acid. Ethyl alcohol was obtained by the action of the calculated amount of sodium nitrite on the acid solution.

The dilute ethyl alcohol obtained by distillation of this solution was redistilled with calcium oxide by which ethyl alcohol was concentrated 80–90%. The yield of ethyl alcohol from sodium cyanide was about 60% of the theory.

The procedure of catalytic dehydration of ethyl alcohol consists in passing the vaporized alcohol through a tube which is packed with granules of alumina and maintained at the temperature of 360°C in an electric furnace. The reaction products were condensed in a trap cooled with liquid oxygen, and the whole system was evacuated to a few mmHg. After the dehydration process the trap containing ethylene was connected to a bromination apparatus. The bromination and the purification of the resulting ethylene dibromide were carried out in the usual way. The preparation of ethylenediamine from ethylene dibromide was made by the action of ammonia in a sealed tube. Five grams of the ethylene dibromide and 40 g. of concentrated ammonia (containing 35% NH_3 in weight) was sealed in the glass tube. By shaking the tube at the temperature of 50°C for seven hours the solution was made homogeneous, and then it was kept at the temperature of 50°C for twenty hours. The content of the tube was evaporated to dryness and distilled with alkali as usual to obtain ethylenediamine hydrate. Because of the scarcity

of the product, we cannot make an accurate measurement on the physical properties of the ethylenediamine monohydrate. However the obtained product was roughly identified by chlorine analysis on nhe ethylenediamine hydrochloride precipitated from the alcoholic solution.

Anal. Found: Cl, 54. Calcd. for $NH_2CH_2CH_2NH_2 \cdot 2HCl$: Cl, 53.4%.

The purity of the product was also certified by cation exchange resin, using 0.1 f. caustic soda eluant. The elution curve taken from the activity of the product just correspounds to the curve for the ordinary reagent of ethylenediamine. The yield of ethylenediamine from ethyl alcohol was 30% of the theory.

Department of Physics and Chemistry
Gakushuin University, Mejiro
Tokyo

1) M. Hasegawa, N. Inamoto and O. Simamura, This Bulletin, 28, 445 (1955).
2) G.W. Kilmer and V. duVigneaud, *J. Biol. Chem.*, 154, 247 (1944).

N-Dialkylaniline as a Solvent of Polyvinyl Chloride

By Teiji TSURUTA and Junji FURUKAWA

(Received December 28, 1955)

It has been found that polyvinyl chloride (PVC) is soluble in N-dialkylaniline, but is practically insoluble in unsubstituted aniline. In this paper, some properties of the dialkylaniline solution of PVC are reported.

Materials.—Geon 101 ($\bar{P} \fallingdotseq 1400$) was washed with methanol and hot water and dried at 60°C in an air oven for twenty hours. N-Dimethylaniline was treated with acetic anhydride, distilled at reduced pressure; the distillate was washed with water, dried on anhydrous sodium sulfate and was distilled under nitrogen at reduced pressure. N-Diethylaniline was purified in a similar way. C. P. aniline and nitrobenzene were purified by distillation.

Solubility.—A mixture of PVC and 50 ml. of the aniline was heated at 95°C in a steam bath under a reflux condenser for four hours. The solution was filtered by sintered glass at 15°C. To 10 ml. of the filtrate, methanol (about 100 ml.) was added and powdery precipitates separated from the solution were collected, washed with methanol, dried at 60°C, and were weighed. The results are shown in Table I.

TABLE I

SOLUBILITY OF GEON 101 ($\bar{P} \fallingdotseq 1400$) IN THREE ANILINES AT 15°C

Solvent	Solubility (g./100 ml.)
Aniline	0.00
Dimethylaniline	2.25
Diethylaniline	0.68

Viscosity.—The viscosity of PVC in the N-alkylaniline and in nitrobenzene was measured by the Ostwald viscometer at 30°C. The results are shown in Fig. 1.

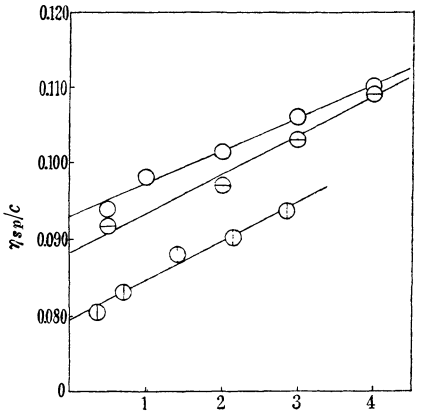

Concentration c (g./l.)

Fig. 1. Viscosity of polyvinyl chloride in three solvents: ○, in nitrobenzene; ⊖, in dimethylaniline; ⓛ, in diethylaniline.

From the table and the figure, it is seen that dimethylaniline is a better solvent for PVC than the other two anilines are. The property of the N-dimethyl derivative may be noted in connection with that of dimethylformamide as a unique solvent for polyacrylonitrile. The lack in the dissolving power in unsubstituted aniline seems to be partly interpreted in terms of the hydrogen bonding between aniline molecules themselves.

The authors are grateful to Dr. M.L. Huggins for advice and to the Japanese Geon Co. Ltd. for donating the sample.

Institute for Chemical Research
Kyoto University, Takatsuki
Osaka

A Theoretical Relation between Bond-order and Bond-length in Conjugated Systems using Morse-type Potential Function

By Toshinobu Anno, Mitsuo Ito,
Ryoichi Shimada, Akira Sadô
and Wataru Mizushima

(Received December 12, 1955)

It has been well known that there exists a definite relation between bond-order and bond-length in conjugated systems[1]. For C-C bonds Coulson[2] derived a theoretical formula explaining the relation between bond-lengths and bond-orders calculated by MO approximation. Anno and Sado[3] showed that a similar formula applies also to C-Cl bonds in conjugated systems. In deriving their formula, they used a method originally due to Lennard-Jones[4], who used Hooke-type stretching potential functions of bonds in reference molecules. For this reason, their formulae combined with the empirical values of parameters do not explain completely the order-length relationships for C-C and C-N bonds, where the bond-orders and bond-lengths change widely from molecule to molecule. One way of removing this difficulty may be to use the Morse-type function instead of the Hooke-type one. This idea was first suggested by Lennard-Jones[4] and used by Coulson[2] in qualitative explanation of the correction to the empirical parameters for fitting the theoretical order-length curve to an empirical one. However, the quantitative study of the theoretical order-length relationship using Morse-type function has not been undertaken.

In the present communication, a theoretical equation for order-length relation will be proposed taking this idea into account. The results for applications to C-C and C-N bonds will also be given.

The energy difference between pure single and triple bonds may be considered to be mainly due to π-electrons. Then the following equation holds:

$$4\beta = E_t^0 - E_s^0 + V_t(x-x_t) - V_s(x-x_s) \qquad (1)$$

where β is the resonance integral, and E_s^0 and E_t^0 denote the bond energy in pure single and triple bonds at their equilibrium values x_s and x_t, respectively. $V_s(x-x_s)$ and $V_t(x-x_t)$ are the potential energies of single and triple bonds when the internuclear distances are x. Instead of assuming the Hooke-type function, the following forms of the Morse-type function may be assumed:

$$\begin{aligned} V_s(x-x_s) &= D_s[1-\exp\{-a_s(x-x_s)\}]^2 \\ V_t(x-x_t) &= D_t[1-\exp\{-a_t(x-x_t)\}]^2 \end{aligned} \qquad (2)$$

where D is the bond strength and a is given by

$$a = \sqrt{\frac{k}{2D}}$$

in which k is the bond stretching force constant.

On the other hand, the total bond energy F which allows for the compression of the σ-bond is given by

$$F = V_s(x-x_s) + 2p\beta \qquad (3)$$

where p is the mobile bond-order. By a method similar to that used by Coulson[2], and using Eqs. (1), (2) and (3), it follows that

$$p = \frac{2}{1 - \frac{a_t D_t}{a_s D_s}\left[\frac{\exp\{-a_t(x-x_t)\} - \exp\{-2a_t(x-x_t)\}}{\exp\{-a_s(x-x_s)\} - \exp\{-2a_s(x-x_s)\}}\right]}. \qquad (4)$$

Taking reasonable values of constants, which will be discussed in subsequent articles, curves shown in Figs. 1 and 2 are obtained. Figs. 1 and 2 refer to C-C and C-N bonds, respectively. As can be seen in these figures

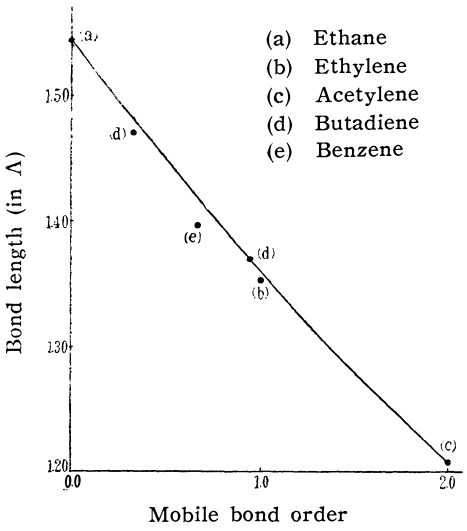

Fig. 1. The relation between bond-order and bond-length for C-C bonds

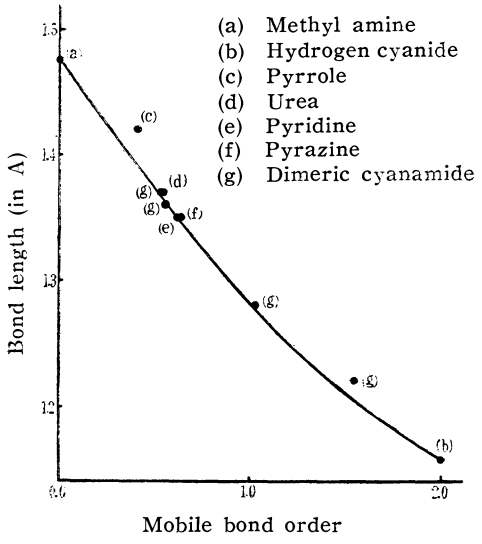

Fig. 2. The relation between bond-order and bond-length for C-N bonds.

the theoretical curves explain the empirical data in fair approximation.

The equation (4) can also be used to calculate the force canstants if it is combined with the considerations similar to those due to Coulson and Longuet-Higgins[5].

Full account of this communication will be published in the near future.

The authors express their hearty thanks to Professor S. Imanishi for his encouragement throughout this work and for reading this manuscript.

Department of Chemistry, Faculty of Science
Kyushu University, Fukuoka

1) See, for example, E.G. Cox and G.A. Jeffery, *Proc. Roy. Soc.* (London), A **207**, 110 (1951).
2) C.A. Coulson, *Proc. Roy. Soc.* (London), A **169**, 413 (1939).
3) T. Anno and A. Sado, This Bulletin, **28**, 350 (1955).
4) J. E. Lennard-Jones, *Proc. Roy. Soc.* (London), A **158**, 280 (1937).
5) C.A. Coulson and H.C. Longuet-Higgins, *Proc. Roy. Soc.* (London), A **193**, 456 (1948).

On the Geochemical Study of Carbon 14. I. The Ozegahara Peat

By Makoto SHIMA

(Received November 9, 1955)

Introduction

It is well known that ^{14}C is continuously produced in the atomsphere by the action of neutrons produced by cosmic-rays, involving the reaction $^{14}N(n, p) \rightarrow {}^{14}C$. Libby[1], with a number of associates, for the first time recognized that atmospheric carbon dioxide, including those present in hydrosphere and biosphere, showed radio-activity of the order of 15.3 dpm. per g, (about $1.5 \times 10^{-10}\%$). He also found that the age of substances containing carbon can be calculated from the half-life of ^{14}C (5568±30 years). Since these pioneering experiments[2,3], Libby and Arnold measured and published the ages of more than 100 specimens, including neary every conceivable kind of relic of the past. In Japan, T. Hamada and F. Yamazaki set up a counter of Libby's type and mainly measured the amount of ^{14}C in the biological and archaeological substances[4].

The present author took up this method to determine the age of peat in Ozegahara in his study of geochemistry with special reference to the sedimentation of coal. It was found that the layer of 2 m. beneath the surface is about 1000 years old and that of 3 to 4 m. is about 5000 years old. The rate of sedimentation is about 1.6 mm. per year at present and appears to have been 1 mm. and 0.25 mm. per year when the layers 2 m. and 3–4 m. beneath the surfaces were formed, respectively. This fact suggests that the apparent volume of the peat has been changed to such an extent in the course of the years concerned.

Sample Occurrence

Ozegahara exists on the boundary of Tochigi, Fukushima, Niigata and Gumma prefectures. It is a famous subtundra. The peat of Ozegahara had been formed upon the lake sediments of the old Ozegahara lake. The samples at Nakatashiro (P11) are illustrated in the column section (Fig. 1). At

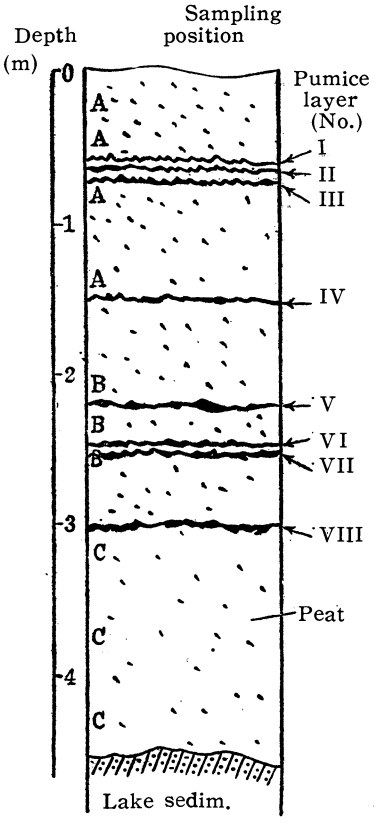

Fig. 1. The column section of peat occurence.

480 cm. depth there are sand and clay layers of the old Ozegahara lake sediments. During the peat sedimentation, volcanic action occurred several times and then layers of volcanic ash and pumice were formed as shown in Fig. 1. The peat is found in two different types of texture in the layers, and the two types are mixed with each other. One is fibrous and maintains the original plant organ; the other is so-called sedimentary peat and the texture has been destroyed by volcanic sediments. The volcanic sediments has 8 layers; among them, No. 2, No. 3 (both Ikaho pumice), No. 6 and No. 7 (Nantai pumice) predominate. The sampling position is shown in Fig. 1. "A" represents the

1) W.F. Libby et al., *Science*, **109**, 227 (1949); ibid, **110**, 678 (1949); *Phys. Rev.*, **81**, 64 (1951); *R. S. I.*, **22**, 225 (1951).
2) W. F. Libby, "Radiocarbon Dating", Univ. of Chicago Press (1952).
3) T.P. Kohman and N. Saito, *Ann. Review of Nuclear Sci.*, **4**, 401 (1954).
4) T. Hamada, *Nuclear Study*, **1**, No. 3, 187 (1954) (in Japanese).

samples of the first unit, "B" those of the second and "C" those of the third.

Chemical Procedure

Chemical processing was almost the same as Libby's[2], except several points as shown below.

a) Chemical Procedure.—The apparatus, in which the main part of the chemical procedure was conducted, is shown in Fig. 2. The combustion of the sample (40-50 g. dry peat) is carried

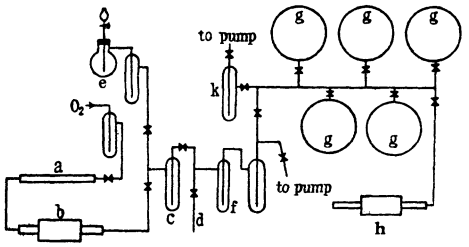

Fig. 2. Chemical preparation apparatus.

out in the quartz tube (a). Oxygen is slowly passed over the sample, which is ignited at its one end. The combustion gas is passed through the copper oxide wire, heated at about 600°C (quartz tube b) to complete the oxidation, is dried in the dry-ice trap (c) and introduced into ammonium hydroxide solution.

In this method, the final product consists only of carbon dioxide, contaminated by oxides of nitrogen and sulfur, resulting from combustion of minor constituents of the peat. It is necessary to carry out a chemical purification before carbon dioxide is submitted to reduction. Therefore the combustion gas is taken out through (d).

A 1 l. flask containing 500 ml. of 6 N ammonium hydroxide is attached to the end of (d). In this vessel, carbon dioxide is absorbed by ammonia and is converted into $(NH_4)_2CO_3$. A rapid absorption of the gas is effected. During this reaction the flask is shaken to insure the absorption until the sample is burnt off. A second solution, containing 180 g. of calcium chloride in 180 ml. of water, is heated nearly to boiling. The flask is removed from the line, and the hot calcium chloride solution is added slowly with stirring. A rapid precipitation of calcium carbonate takes place. The precipitate is filtered and washed with water on a Buechner funnel. At this point, all of the oxides of nitrogen and sulfur have been left behind in the form of soluble salts. After washing, the precipitate is dried in an air bath. This calcium carbonate (about 130 g.) precipitate is transferred to flask (e). Carbon dioxide is now recovered from the precipitate, using the same system employed in the combustion by adding concentrated hydrochloric acid. The stopcock leading to the flask is opened, and acid is added from a separatory funnel (about 200 ml.).

The chemical purification procedure is thus completed. The recovered gas is passed through the dry-ice trap (c) into two successive liquid air traps (f) in which the carbon dioxide is condensed. The Dewars are removed and the solid carbon dioxide is evolved. The gas is passed into the system of reserver (g) (total volume, 25 l.) which has been already evacuated, and then the gas is ready for the reduction step. Reduction is carried out in a seamless stainless steel tube (h) which is filled with 80 g. of magnesium turning together with a little of cadmium turning as a catalyst. An electric furnace, capable of reaching about 800°C, is placed around the tube. One end of the tube is sealed with a rubber stopper and wax, and the reduction system is evacuated and tested for freedom from leaks. Carbon dioxide is now admitted to the tube up to a pressure approaching one atmosphere, and external heat is applied to the magnesium filling. When it gets the melting point of magnesium (660°C), the reaction begins violently and produces sufficient heat to maintain itself, provided that the gas is admitted at a moderate rate from the bulbs. Since the reaction "$2Mg+CO_2=2MgO+C$" yields no gaseous products, no circulation is required. It is the practice to run the gas from the bulb until the pressure is reduced to about 200 mmHg, when the next bulb is cut in. In this way the gas can be reacted smoothly before the other end of the magnesium filling is reached. To complete the reduction, it is necessary to apply external heat using the furnace. The remaining gas is condensed in the trap (k) and may either be expanded into a single bulb or allowed to react directly. After this method, has been used the remaining gas is no more than 50 mmHg. The reduction tube is allowed to cool, and the carbon, magnesium oxide and unreacted magnesium are removed from the tube using an iron rod. These products are transferred to a 5 l. beaker. Concentrated hydrochloric acid is cautiously added (total, of about 800 ml.); violent evolution of gas takes place. The mixture is allowed to stand overnight. It is then brought to boiling point on a large hot plate. One litre of water is added and it is again boiled for about fifteen minutes. The supernatant is then removed by filtration, using a sintered glass filter stick operating directly into a water aspirator; 300 ml. of nitric acid is added to the residue. The nitric acid solution is again nearly boiled for fifteen minutes and filtered. It is recognized that this method eliminates the carbon ash at least down to a fraction of a percent. One and a half litres of water are added; the solution is once again boiled for fifteen minutes and filtered. This cycle is repeated three times more. After the carbon is washed into a small beaker, the water is removed using the filter stick. This beaker is transferred into an air-bath and the carbon is thoroughly dried. The carbon thus obtained weighs about 12–15 g. It is now ready for mounting and measurement. The overall yield of the chemical processing sequence, described above, is in the neighborhood of 80% of the carbon content of the peat. One of the problems in producing a final product free from intrusive radioactivity is, of course, the purity of the reagent used. After burning, the peat ash was analysed by the common plant analytical method. Water content of peat was measured in

a water stop trap. The carbon ash was analysed by the combustion method and the total impurity (mainly Fe, Mg, Ca, etc.) was measured.

b) Mounting Procedure.—At the carbon corrected by the above methods is coarse, it is fully ground by an agate motor. About 8 g. of carbon are weighed into a 150 ml. beaker. Water (total volume, about 50 ml.) is added little by little continuously with stirring, until the well-stirred slurry maintains just the proper consistency. This can be judged by the rate of flow on tipping the beaker. The slimy mass is transferred to the one of the pair of a split cylinder which can be connected together, (for details of counter construction see below), using a long glass rod.

The cylinder is continuously rolled with a moter driven rotator throughout the mounting. A small portion of the slime is placed on the one end of the cylinder and spread with the aid of a long glass rod so that a uniform layer is formed on the inner surface of the cylinder. Care must be taken to make the slurry just slimy enough to keep itself on the surface. Then a hot stream of air is blown over the inside of the rotating cylinder with a hair dryer. After about five minutes, sufficient water will be thus removed and the carbon layer is fixed on the surface so firmly that no appreciable amount falls down during the further procedure. The pair of the cylinders are connected together and inserted into the screen-wall counter through the free end. When the layer is too dry, it may be torn off forming a crack on the surface. Therefore the drying must be given up before it gets too dry. The end cap is put on and attached to a vacuum system and the remaining water is generally pumped off through a dry ice trap. This operations must be carried out rapidly and with special attention not to touch the cylinder or the sample by hand. After two days when no leakage is observed, ethylene (6 mmHg) and argon (100 mmHg) are introduced into the cylinder. After one night the whole is transferred into a shielding box and submitted to measurement.

After each run, the sample is removed from the cylinder with a spatula. The final cleaning of the cylinder (before mounting a new sample) is achieved by carefully wiping it with a powder-paper.

Instrument

The author has used the counter that was made by Yamazaki's group. The instrument is illustrated by Mr. T. Hamada in detail[4].

a) Screen-wall Counter. — The screen-wall counter has the grid wire between the anode and the cathode of an ordinary cylindrical Geiger-Müller tube. The counter, presently in use, is illustrated in Fig. 3. The main part is almost the same as the Libby's counter, but is not so in some material used. The counts of the sample and background can be directly compared by sliding the cylinder from one end to the other.

b) Anticoindence Counter.—It is a common cosmic-ray counter shown in Fig. 4. The necessary reduction in background can be achieved by connecting the screen-wall counter and the eleven shielding counters placed around it in anticointences. These counters are filled with ethylformate (7 mmHg) and argon (100 mmHg).

c) Shiled.—A shiled is constructed of steel plates (1 inch thick; contributed by the Yahata Iron Company); the arrangement is shown in Fig. 5. The total thickness is 7 inches and the total weight amouts to 4.3 tons. The door is made of the same steel plates, and can be moved forward on the rail by hand.

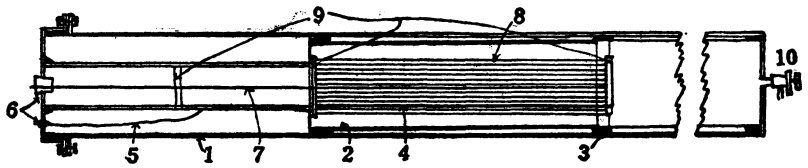

Fig. 3. The screen-wall counter.

1. Screen-wall counter body, brass-made. Inside diameter 75 mm., length 614 mm., thickness 1 mm.
2. Sample tube, copper-made. Inside diameter 67 mm., length 200 mm., two unit.
3. Joinband of above two copper tubes.
4. Grid support 5 drillrod.
5. Lead wire of grid.
6. Stupakoff seal.
7. Center wire. #28 Dumet wire.
8. Grid wire #30 Dumet wire 33 wires.
9. Methacryl-resin.
10. Bellows value.

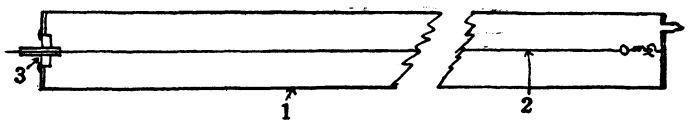

Fig. 4. The anticoindence counter.

1. 2″ Copper tube. thickness 2 mm., length 784 mm.
2. Center wire 0.1 mm. W wire.
3. Stupakoff seal.

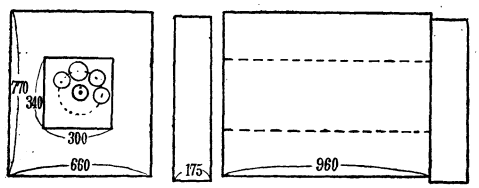

Fig. 5. The shielding.

High voltage and plate supply voltage are stabilized in the usual way.

Result

Sample A represents the upper part, sample B the mean part and sample C the lower part of the peat sediments. Chemical components of these ashes are analysed and shown in Table I.

TABLE I

CHEMICAL COMPONENT

Sample No.	Total Ash (%)	H_2O (%)	HCl (%) Insoluble	Si (%)	Al (%)	Fe (%)	Ca (%)	Mg (%)	Na (%)	K (%)
A	10	40	11.4	—	0.62	0.25	0.75	0.51	0.03	0.07
B	11	36	9.8	tr.	1.09	0.18	0.66	0.28	0.02	0.05
C	10	40	10.4	—	0.36	0.35	1.28	0.47	0.01	0.06

d) Electronic Circuit.—The circuit is shown in Fig. 6 in block diagram. High voltage regulator is shown it Fig. 7; this circuit is an automatic control of high voltage. Univibrator has

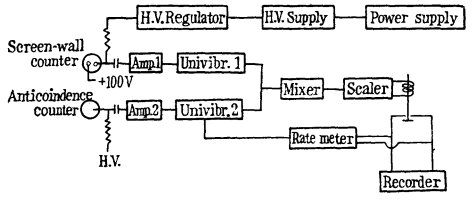

Fig. 6. Blockdiagram of circuits.

a dead time of 15 mμ seconds to prevent multiple pulses of the screen-wall counter. The mixer consists of the resistance network. The scaler is a scale of 16 using for 12AU7'S. The output of the scaler is fed to a thyratron. Each 16 counts of the screen-wall counter mark a knick on the recording paper, writing the background counting rate of the anticoindence counters, which is about 1400 cpm. During very long unattended runs which have to be made, there is the possibility of accidents. For this reason the automatic recording device was used.

The variation of chemical components indicates that sample B has more clay part than the others. It can be explained in two ways: the pumice layer was dispersed into the peat layer or the chemical component migrated into the peat layer.

A chemical study has also been carefully made by Dr Yamagata[5]. Age determination of peat, carried out by the above method, requires about forty hours, for the background measurment twenty hours, and for the sample twenty hours. The two measurement can be carried out by changing the position of the cylinder. These results are shown in Table II. Background of the instrument used, was about 4.5–5.5 cpm.

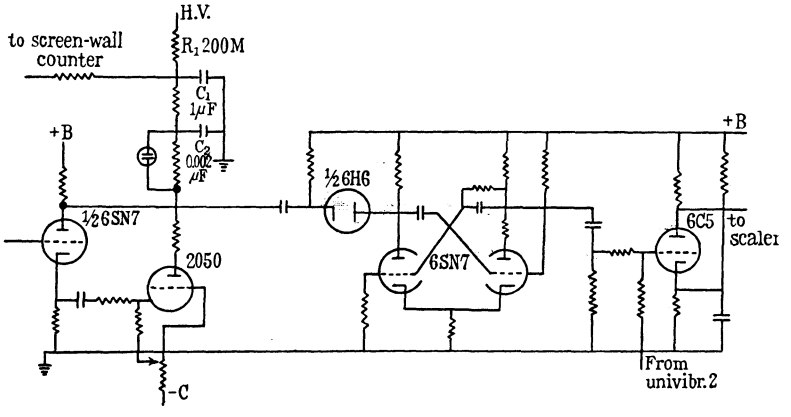

Fig. 7. High voltage regulater.

Conclusion

Several examples of the counts of the biological substances were shown by Yamazaki's[4] group and found to come between 5.5–6.3 cpm. Then the author considers that

5) N. Yamagata, Read before 1954's Geochemical Meeting of Chem. Soc. of Japan.

sample A can be regarded in the same way as the recent ones.

If so, sample B must be about 1000 years old and sample C 5000 years. The data are shown in Table II.

Dating by means of natural radio-carbon has some problems: constancy of ^{14}C specific activity, contamination by ^{14}C from different sources, constancy of cosmic ray flux, accuracy of measurement etc..

TABLE II

THE COUNTS OF NATURAL RADIO CARBON

Sample No.	Background			Sample counts			C^{14} c. pm.	Dating (y)	Carbon Ash (%)
	Time (min.)	Counts	c. p. m.	Time (min.)	Counts	c. p. m.			
A	1145.5	5856	5.11±0.067	1429.5	15296	10.7 ±0.086	5.59±0.10	0	4.79
B	1350.5	5856	4.34±0.056	1469.0	14584	9.25±0.084	4.91±0.10	1000±250	2.42
C	1161.5	5344	4.61±0.063	1095.5	8320	7.59±0.083	2.98±0.10	5000±400	2.40

The rate of sedimentation of peat is considered to be 1.6 mm. per year for sample A, 1.0 mm. per year for sample B, and 0.25 mm. per year for sample C.

If the rate of sedimentation has been the same as at present, sample C might have decreased its volume to about 1/6. During the 5000 years, sample C could have been pressed on the upper part or have lost some of its components by dissolution to descrease the volume to such an extend.

The volume of sample B has been also slightly decreased during the 1000 years. During the 5000 years, sedimentation of the total depth of this column region as thick as 480 cm. has been accumulated.

In other words the apparent mean rate of sedimentation is 0.7–0.9 mm. per year.

The author is of the opinion, however, that the present study is not interfered with by such factors, so far as the samples obtained from different depths at one position are studied. Further development is expected by fundamental experiments and by geochemical studies.

The author wishes to acknowledge the contributions of Dr. F. Yamazaki and Mr. T. Hamada in the counting equipment, and of Professor Dr. K. Kimura in giving valuable suggestions. The author is also grateful to Mrs. M. Shima (nèe Asada) and to Dr. N. Yamagata, for their kind supply of the samples.

Scientific Research Institute Ltd. Tokyo

Untersuchungen über die photochemischen Additionsreaktionen. III. Die Additionsreaktion von Mercaptanen an Propargylalkohol

Von Kazuo YAMAGISHI, Toyosuke TANAKA[1] und Toshio HOSHINO

(Eingegangen am 17. Januar 1956)

In der vorgehenden Mitteilung[2] konnte über die in besserer Ausbeute erfolgten photochemischen Additionsreaktionen einiger Mercaptane durch Belichtung mit ultravioletten Strahlen von etwa 3660 Å an die Doppelbindung solcher ungesättigten Verbindungen wie Vinylacetat, Vinylchlorid und Allylalkohol berichtet werden. Wir haben nun festgestellt, dass auch Mercaptane unter fast gleichen Bedingungen an die Dreifachbindung des Propargylalkohols addieren können, und dass die gesättigten Verbindungen, anders als bei Anlagerungen an Doppelbindungen, unter Umständen durch die zweifache Addition von Mercaptanen gewonnen werden.

Die Additionsreaktion von Methylmercaptan an Propargylalkohol liess sich herbeiführen beizweistündiger Belichtung mit ultravioletten Strahlen unter Verwendung von Methylmercapto-quecksilber, Merkuriacetaten oder Azo-iso-buttersäurenitril als Katalysatoren in Stickstoffatmosphäre. Es ergab sich ein katalytischer Effekt des Sauerstoffs, wenn die Reaktion in Sauerstoffatmosphäre ausgeführt

1) Institut für Chemie der Saitama Universität, Urawa.
2) T. Hoshino, K. Yamagishi und Y. Ichikawa, *J. Chem. Soc. Japan*, (*Reiner Chem. Teil*), **74**, 510 (1953). K. Yamagishi und N. Nakajima, ibid., **75**, 1086 (1954).

wurde. Die Ausbeute unter diesen Bedingungen betrug bis zu 50–60%. Ohne diese Katalysatoren oder Belichtung mit ultravioletten Strahlen kam es zu keiner Additionsreaktion. Die Temperaturerhöhung des Reaktionsgemisches bei der Additionsreaktion sind in Fig. 1 dargestellt.

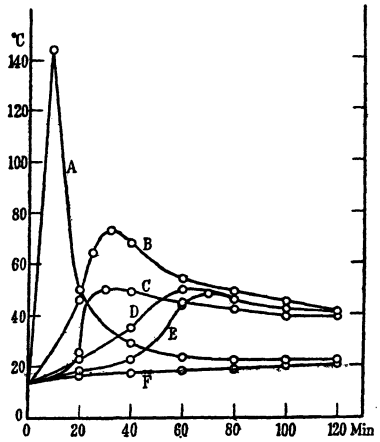

Fig. 1. Schema für die Temperaturerhöhung des Reaktionsgemisches.

A: Azo-iso-buttersäurenitril—N_2
B: Methylmercapto-quecksilber—O_2
C: Methylmercapto-quecksilber—N_2
D: Ohne Katalysator—O_2
E: Merkuriacetaten—N_2
F: Ohne Katalysator—N_2

Bei der Fortsetzung der Belichtung bis zu sechs Stunden steigerte sich die Ausbeute auf etwa 65–80%. Es ergab sich ferner: Die Additionsreaktionen von *n*-Butyl-, Phenyl- und Benzylmercaptan an Propargylalkohol unter Verwendung von Merkuriacetaten als Katalysator bei vierstündiger Belichtung verliefen unter geringer Temperaturerhöhung des Reaktionsgemisches mit langsamer Reaktionsgeschwindigkeit. Die Ausbeute hierbei betrug bis zu 50% beziehungsweise 40% und 30%.

2,3-Dimethylmercapto-propanol wurde durch Additionsreaktion von Methylmercaptan an Propargylalkohol gewonnen, 2,3-Di-*n*-butylmecrapto-propanol durch Additionsreaktion von *n*-Butylmercaptan und 2,3-Dibenzylmercapto-propanol durch Reaktion von Benzylmercaptan. Diese Produkte sind neue Verbindungen ausserhalb 2,3-Dimethylmercapto-propanol[3,4]. Das Additionsprodukt von Methylmercaptan an Propargylalkohol erwies sich auf Grund der physikalischen Konstanten und der Elementaranalyse als identisch mit dem authentischen Produkt 2,3-Dimethylmercapto-propanol, das von A. De Barbieri und S. Tricerri[3] aus Natriummethylsulfid und Allylalkoholdibromid dargestellt wurde. Darum darf man von den Konstitutionen anderer Produkte dasselbe annehmen.

3) A. De Barbieri und S. Tricerri, *Boll. soc. ital. biol. sper.*, **25**, 522 (1949); *C.A.*, **44**, 8862 (1950).
4) R.M. Evans, J.B. Fraser und L.N. Owen, *J. Chem. Soc.*, **1949**, 248.

Beschreibung der Versuche

Käuflicher Propargylalkohol wurde einmal fraktioniert, dann mit Kupfersulfat getrocknet, schliesslich innerhalb der Siedegrenzen von 113° rektifiziert und der Additionsreaktion unterworfen. Die Mercaptane wurden auf die übliche Weise dargestellt. Die photochemische Reaktion wurde, wie bei den früher mitgeteilten Versuchen, meist auf die folgenden Weise herbeigeführt:

Eine Mischung von 0.1 Mol Propargylalkohol und 0.22 Mol Mercaptan wurde in einem Reaktionsrohr von 80 ccm Inhalt auf −40° gekühlt. Nach Ersetzung der Rohratmosphäre durch Stickstoff wurde sie mittels einer Quecksilberlampe von 200 Watt (SHL-200, Japan Akkumulator A. G., Kyoto) ultravioletter Belichtung ausgesetzt. Das nach dem Verdampfen des unveränderten Materials zurückgebliebene Produkt wurde im Vakuum destilliert.

Einige Eigenschaften der Additionsprodukte werden im folgenden beschrieben.

1) 2,3-Dimethylmercapto-propanol: Sdp. 88° (1 mm); $d_4^{19}=1.144$; $n_D^{19}=1.5431$.

Anal. Gef.: C, 39.60; H, 7.82; S, 42.25. Ber. für $C_5H_{12}OS_2$: C, 39.44; H, 7.94; S, 42.11%.

Die farblose und viskose Substanz riecht nach Methionol[5], dem wichtigsten Riechstoff in der japanischen Sojasauce, löst sich leicht in Äther, Methanol, Äthanol, Aceton und Benzol, aber schwer in Petroläther und Wasser. Das aus dieser Substanz und Quecksilberchlorid dargestellte Doppelsalz schmilzt bei 92°.

2) 2,3-Di-n-butylmercapto-propanol: Sdp. 132–133° (1 mm); $d_4^{15}=0.997$; $n_D^{15}=1.5089$.

Anal. Gef.: C, 55.71; H, 10.03; S, 26.98. Ber. für $C_{11}H_{24}OS_2$: C, 55.88; H, 10.23; S, 27.12%.

3) 2,3-Diphenylmercapto-propanol: Sdp. 119–122° (10^{-2} mm); $d_4^{21}=1.178$; $n_D^{21}=1.6301$.

Anal. Gef.: C, 64.93; H, 6.05; S, 23.42. Ber. für $C_{15}H_{16}OS_2$: C, 65.18; H, 5.84; S, 23.20%.

4) 2,3-Dibenzylmercapto-propanol: Sdp. 120–130° (5×10^{-4} mm); $d_4^{24}=1.155$; $n_D^{24}=1.6085$.

Anal. Gef.: C, 66.91; H, 6.61; S, 21.36. Ber. für $C_{17}H_{20}OS_2$: C, 67.06; H, 6.62; S, 21.06%.

Wir möchten hier dem Unterrichtsministrium für die Gewährung einer Unterstützung zur Anregung wissenschaftlicher Forschung Dank sagen, ebenso auch Herrn Asaji Kondoh für die Ausführung der Mikroanalysen.

Das Institut für organische Chemie der Technischen Hochschule Tokyo, Tokyo

5) S. Akabori uud T. Kaneko, *J. Chem. Soc. Japan (Reiner Chem. Teil)*, **57**, 832 (1936).

Diphenylcarbazone as an Internal Indicator in Volumetric Analysis. III. Volumetric Determination of Thorium by Ammonium Molybdate

By G. S. DESHMUKH and Indumati BOKIL

(Received September 19, 1955)

The growing interest in the chemistry of thorium and its compounds has necessitated the development of new and rapid methods of analysis. Of the large number of procedures which have appeared in the literature, practically all are based on the precipitation of thorium in some form from its solution and subsequent gravimetric determination as ThO_2[1,2]. Comparatively few titrimetric methods have been reported for estimating thorium. Among these the iodate method of Chernikhov and Uspenskaya[3] as modified by Moeller and Fritz[4] and the oxidimetric oxalate method of Gooch and Kobayashi[5] are noteworthy. The possibility of precipitating thorium oxinate and titrating the equiv alent of iodine as suggested by Berg[6] has been extensively studied. Iodometric titration of selenious acid liberated from a quantitatively precipitated thorium selenite has been reported from these laboratories[7]. The molybdate procedure of Metzger and Zones[8] which has been modified by Banks and Diehl[9] is found to be applicable to pure thorium or the mixed thorium uranium solution.

Amperometric titration of thorium with ammonium molybdate has recently been studied by Gordon[10], and it is claimed that under the specified conditions, this procedure may be adopted for the estimation of thorium in presence of rare earths and other congeners. Recent observations in these laboratories on the use of diphenylcarbazone as an internal indicator in volumetric analysis showed that on treatment with ammonium molybdate this indicator develops an intense pink colour which is destroyed by the addition of a lead salt solution. The colour change was found to be reversible and formed therefore the basis of the titrimetric determination of molybdenum by using Pb $(NO_3)_2$ as the primary standard[11]. Extension of these observations to the estimation of metals forming stable molybdates suggested itself and a series of experiments were carried out to study the possibility of using the above indicator in the titration of ammonium molybdate with a thorium salt solution. A systematic study of the operative conditions led to the development of a simple and rapid titrimetric method for the estimation of thorium. This has now been described in the present communication.

Experimental

Thorium nitrate (or chloride) solution was obtained by dissolving the pure salt in water; the ThO_2 content of an aliquot portion of the solution was determined by the *m*-nitrobenzoic acid method.

To a known volume of the aqueous thorium solution containing 50–60% alcohol, one ml. of saturated alcoholic solution of diphenylcarbazone was added and the yellow or orange yellow solution was titrated slowly with constant swirling against standard ammonium molybdate. The end point was characterised by a sharp pink flush in the precipitated thorium molybdate. At this point the precipitate tended to coagulate rapidly and the supernatent solution also assumed a pink shade. Since the colour change from pale yellow to pink is completely reversible, any error due to overtitration is rectified easily by running in a known volume of thorium solution and continuing the titration as usual. The accuracy and sharpness of the end point was, however, found to enhance by adopting the following modified procedure: To an aliquot of the thorium solution a measured volume of standard aqueous Pb $(NO_3)_2$ was added followed by an equal volume of ethanol and 0.5 ml. of the indicator. The pink coloured solution was titrated slowly against ammonium molybdate. The colour faded during the initial addition of the molybdate with the simultaneous appearance of a white precipitate. The titration was continued till a sharp pink flush was observed in the precipitate. A blank titration of $Pb(NO_3)_2$ against molybdate using the indicator was carried out under identical experimental conditions. This titre value when subtracted from the total volume

1) B. Justel, *Die Chemie.*, **56**, 157 (1943).
2) T. Moeller, G.K. Schweitzer and D.D. Starr, *Chem. Rev.*, **42**, 64 (1948).
3) Y.A. Chernikhov and T.A. Uspenskaya, *Zavodskaya Lab.*, **9**, 276 (1940).
4) T. Moeller and N.D. Fritz, *Anal. Chem.*, **20**, 1055, (1948).
5) F.A. Gooch and M. Kobayashi, *Amer. J. Sci.*, **45**, 227 (1918).
6) R. Berg, *J. Prakt. Chem.*, **115** (ii), 178 (1925).
7) G.S. Deshmukh and L.K. Swamy, *Anal. Chem.*, **24**, 218 (1952).
8) F.J. Metzger and F.W. Zones, *J. Ind. Eng. Chem.*, **4**, 493 (1912).
9) C.V. Banks and H. Diehl, *Anal. chem.*, **19**, 222 (1947).
10) L. Gordon and C.R. Stine, ibid., **25**, 192 (1953).
11) G.S. Deshmukh, *Bull. Chem. Soc. Japan*, **27**, 623 (1954).

of molybdate required for the mixed thorium and lead nitrate solution, gave the quantity of molybdate required for the precipitation of thorium as molybdate. Varying quantities of the thorium solution were thus titrated against standard ammonium molybdate. From a knowledge of the ThO_2 content of the solution taken for titration and the molybdenum content of the titrant, the molar ratio Th: Mo corresponding to the end point was calculated. Series of trial experiments showed that within limits of 100–200 mg. of thorium the molar ratio corresponded on the average to 1 : 1.99. It may therefore be inferred that within the specified limits of the above experimental procedure, the titrimetric estimation of thorium may be carried out with reasonable accuracy. This date are returned in Table I.

It has been observed that the sharpness of the end point depends on the quantity of alcohol added initially to the thorium solution. While in the presence of too large a quantity exceeding 70–80% the end point appears prematurely; an excess of molybdate is consumed if the titration is carried out in a purely aqueous media. The overall alcohol content (50–60%) has been determined by a series of trial experiments. For a permanent and sharp end point it is also not desirable to dilute the contents during and/or towards the end of the titration.

The molar ratio Th: Mo=1: 1.99 as observed in the above series of experiments (cf. Table I) is in close agreement with that reported by Gordon.

The amperometric titration method developed by him offers however, a distinct advantage of being applicable to the determination of thorium in presence of other rare earths. This procedure, however, necessitates a rigid control of operative conditions and a special type of apparatus. On the other hand the titrimetric method of Metzger and Zones involves the use of acetic acid- sodium acetate buffer and diphenyl-carbazide as an *external* indicator. It may therefore be pointed out that the present procedure is more rapid, simple and accurate than other titrimetric methods adopted for the determination of thorium.

TABLE I

10 ml. of $Pb(NO_3)_2 \equiv 0.07550$ gm. Pb

Expt. No.	Vol. of Th Cl_4 in ml. (a)	Vol. of Am. Molybdate required in ml. (b)	Wt. of Th in (a)	Wt. of Mo in (b)	Molar Ratio Th: Mo
1.	10.0	9.40	.06489	.05249	1: 1.955
2.	20.0	19.05	.1297	.1064	1: 1.984
3.	42.5	40.60	.1378	.1133	1: 1.987
4.	22.5	21.50	.1460	.1200	1: 1.987
5.	47.5	45.45	.1541	.1269	1: 1.991
6.	25.0	23.95	.1622	.1338	1: 1.995
7.	52.5	50.55	.1703	.1411	1: 2.004
8.	27.5	26.55	.1784	.1483	1: 2.010
9.	57.5	55.50	.1865	.1550	1: 2.009

Summary

A simple volumetric method for the quantitative estimation of thorium as molybdate is described. This is based on the titration of aqueous thorium nitrate (or chloride) solution against standard ammonium molybdate in presence of ethanol by using diphenylcarbazone as the internal indicator. Under specified operative conditions, normal thorium molybdate is precipitated. The indicator behaves reversibly and the accuracy of the method is comparable with those obtained by classical procedures.

Our grateful thanks are due to Professor S. S. Joshi for kind interest in the work.

Department of Chemistry, Banaras Hindu University

By-products of Acrylonitrile Synthesis from Acetylene and Hydrocyanic Acid. I. Neutral Constituents

By Shiro MORIMOTO

(Received October 10, 1955)

For several years the present author has been studing the vapor phase synthesis of acrylonitrile from acetylene and hydrocyanic acid. It is very likely that many reaction products are produced in this process because the starting materials are very reactive. It seems to be very important from the scientific as well as from the industrial standpoint to detect the byproducts which are produced by this process.

No report seems to have been made on this detection, although some reports have been made on that in the liquid phase synthesis using the so-called Nieuwland's cat-

alyst[1]. According to these reports, what was considered to be a reaction products of acetylene and hydrocyanic acid was only cyanobutadiene: no separation has been carried out between 1- and 2-cyanobutadiene. No report has been made on the formation of higher nitriles. The following substances have been known as the polymerization products of acetylene alone using Nieuwland's catalyst: (Nieuwland[2], Georgieff[3]).

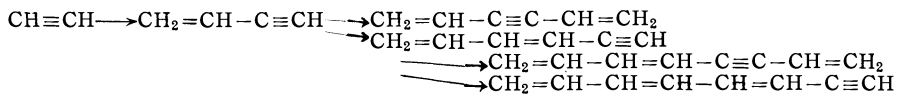

In the case of the reaction between acetylene and hydrocyanic acid, formation of olefinic nitriles is considered possible because hydrocyanic acid may be added to the above mentioned polymerization products of acetylene as follows:

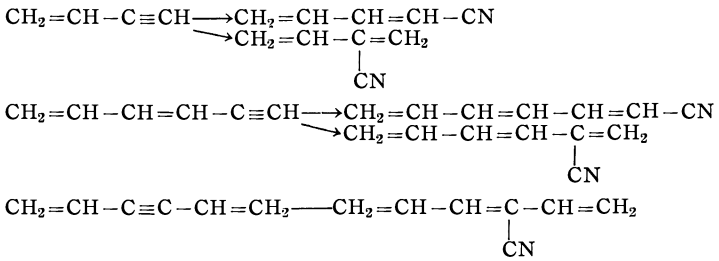

Results and Discussion

A. Reaction Conditions and By-products.—A carrier, reaction temperature, and composition of the feed gas mixture are factors responsible for kinds and amounts of the by-products in the acrylonitrile synthesis from acetylene and hydrocyanic acid using zinc oxide as catalyst.

The author's studies have revealed that the use of some kinds of carrier seems to result in the formation of acetonitrile and basic by-products in a greater amount.

In the present experiment, pumice stone has been used as carrier and the reaction has been carried out at around 400°C[4].

TABLE I

BOILING POINTS AND INFRARED SPECTRA OF CONSTANT BOILING FRACTIONS

Fraction No.	Boiling point °C/mmHg	Distillate cc.	Infrared absorption spectra (μ) C≡N a*	C≡N b*	C=C c*	d*	CH_2 e*	C=O f*	OH g*	**
A-2	95.8–97.0	6.5								(1)
A-4	121.5–120	5.5	++	+	++	±	+	−	+	(2)
B-4	73–75/75	12.5	++	+	++	+	+	−	±	(3)
D-3	80–82/33	5.0	+		+	±	+	+	−	
D-5	85–86/33	4.7	+		+	±	+	++	+	
D-10	93/33	3.3	++		+	+	+	+	−	(4)
E-3	69/7									(5)

* Wave length (μ) a, 4.48–4.51 (conj.); b, 4.44 (nonconj.); c, 6.07–6.11; d, 6.68–6.70, 6.21–6.25; e, 3.4; 6.8; f, 5.8; g, 2.83–2.89.

** The substances which may be expected to exist in the above mentioned fractions are listed below with their literature values of boiling points °C/mmHg.

(1) Propionitrile (identified).
(2) 2-Cyanobutadiene, 24–31/30, 30–40/40; *n*-octane 124.
(3) *p*-Xylene 136; *m*-xylene 139; *o*-xylene 141; ethylbenzene 136; styrene 146; 1-cyanobutadiene 140, 135–8.
(4) Benzonitrile (identified) 190.6, 103.9/50; 1-cyanohexatrine, 56–57/2–3.
(5) Naphthalene (identified).

1) A. Cambron, P.B. 19678; B.L. Hasche and J.G. McNally, P.B. 34813; P.B. 81283; P.B. 47715.
2) J.A. Nieuwland, W.S. Calcott, F.B. Downing and A.C. Carter, *J. Am. Chem. Soc.*, **53**, 4197 (1931); J.A. Nieuwland, U.S. Patent, 1811, 959 (1931).
3) K.K. Georgieff, W.J. Cave and K.G. Blaikie, *J. Am. Chem. Soc.*, **76**, 5494 (1954).
4) Considerable variation of temperature by local heating in the reaction tube was observed.

B. Separation of Neutral Substances.—The intermediate distillation fraction between the two main reaction-products, acrylonitrile and succinodinitrile, was divided into three parts, i. e., neutral, basic and acidic.

The neutral part was fractionally distilled through a Stedmantype column (plate number, 20). And the constant boiling fractions were obtained, i. e., A-2(liq.), A-4(liq.), B-4 (liq.), D-3(liq.), D-5(liq.), D-10(liq.), E-3(sol.) (Table I).

A-2 was treated with thioglycolic acid and hydrogen chloride, resulting in the formation of crystals which melted at 123–124°C (decomp.). The melting point corresponded with that of α-iminopropylmercaptoacetic acid hydrochloride $CH_3 \cdot CH_2 \cdot C(SCH_2COOH) : NH \cdot HCl$ in literature[5].

D-10 was hydrolyzed by a 75% sulfuric acid solution to form benzoic acid with a yield of 50–70%. So it was confirmed that D-10 contained benzonitrile in the above mentioned ratio.

E-3 solidified to crystals melting at 80°C and was identified to be naphthalene by a mixed melting test.

The principal infrared absorption bands of A-4, B-4, D-3, D-5, and D-10 are also shown in Table I.

The most marked and common to all samples has been found to be the characteristic absorption of the nitrile radical (ν-C≡N). The absorption bands are observed at two kinds of wave length, 4.44 μ and 4.48–4.51 μ. According to Kitson et al.[6] nitriles nonconjugated with an olefinic bond give an absorption band at 4.44±0.02 μ; nitriles conjugated with an olefinic bond give an absorption band at 4.49±0.02 μ. Each sample indicates a marked absorption of the conjugated nitrile, but A-4 and B-4 are accompanied by a weak nonconjugated nitrile absorption.

Another common absorption observed is that of the olefinic bond. The absorption bands are observed at 3.24–3.29 μ (ν C-H), 6.07–6.11 μ (ν-C=C-).

D-10 demonstrates the absorption of the benzene nucleus more markedly than that of the olefinic bond.

The absorption bands of the acetylenic bond at 3.0 μ (ν≡C-H) and 4.71–4.78 μ (ν-C≡C-) are absent. (Acetylenic compounds seem to have disappeared in these samples during purification, especially during fractional distillation.)

Qualitatively the absorption of D-10 may be regarded as a superposition of absorption of both benzonitrile and 1-cyanohexatriene.

The above mentioned results suggest the existence of 2-cyanobutadiene (cyanoprene) in A-4, 1-cyanobutadiene in B-4, 3-cyanohexatriene in D-3, 2-cyanohexatriene in D-5, and 1-cyanohexatriene besides benzonitrile in D-10.

There also exist absorption bands at 3.4 μ, and 6.8 μ which are considered to be absorption of the methyl or methylene radical. This fact may be explained, considering the existence of nitriles obtained through partial reduction of the above-mentioned unsaturated nitriles, since the existence of propionitrile has been confirmed. Weak absorption of benzene nucleus is somewhat observed in fractions other than D-10. This may be due to the presence of substances having nothing to do with the nitriles.

Formation of benzonitrile seems due to a ring formation of cyanohexatrienes, and especially 1-cyanohexatriene seems easily to aromatize at higher temperature.

$$CH_2=CH-CH=CH-CH=CH-CN \longrightarrow$$

$$[CH_2=CH-CH=CH-CH=\overset{(-)}{C}-CN] \longrightarrow \langle\bigcirc\rangle\text{-CN}$$

Other experimental results supporting these suggestions will be reported in following papers.

Experimental

(A) Reaction of Acetylene and Hydrocyanic Acid.—*1) Reaction Tube.*—A stainless steel tube with inner diameter of 6 cm., length of heated part 100 cm. (heated directly without bath), length of part packed with catalyst 60 cm.

2) Catalyst.—A carrier of pumicestone of 8–10 mm. diameter was surmounted with zinc hydroxyde (precipitated) which was burnt in the reaction tube at the reaction temperature to form zinc oxide.

3) Reaction Conditions and Results.—These are shown in Table II.

(B) Chemical Separation of the Intermediate Fraction.—The above-mentioned intermediate fraction (242.5 g.) was dissolved in the same amount of ether and treated with a 25% aq. sodium hydroxide solution and then with a 2% aq. hydrochloric acid solution, resulting in the separation of 5 g. (containing water) of the acidic part, 15 g. (containing water) of the basic part, and 229 g. (containing water) of the neutral part.

(C) Fractional Distillation of the Neutral Part.—The neutral part (liquid, 229 g.) was roughly fractionated into A, B, C, D and E by distillation using a Claeisen-flask under reduced pressure. By further fractionating the respective fractions using a Stedman-Type distillation column (with a brass net, plate number 20) under proper pressure, the results shown in Fig. 1–4 were obtained.

5) F.E, Condo, E.T. Hinkel, A. Fassero and R.L. Shriner, *J. Am. Chem. Soc.*, **59**, 230 (1937).

6) R.E. Kitson and N.E. Griffith, *Anal. Chem.*, **24**, 334 (1952).

TABLE II

REACTION OF ACETYLENE AND HYDROCYANIC ACID

Expt. No.	Heating temp. °C	Temp. in reaction tube °C	reaction time hrs.	C_2H_2 /HCN	Charg. HCN g.	Consum. HCN g.	Acrylo-nitrile g.	Inter-mediate fraction g.	Succi-nodini-trile g.
1	300–340	330–480	36.5	3.3	716	447	495	30	50
2	300–360	370–510	32	3.2	637	396	376	28.5	53
3	310–390	370–560	32	4.4	529	220	306	103	47
4	350–380	380–560	32	3.9	561	255	294	81	50

Total amounts:
(a) Acrylonitrile 1471 g.
(b) Intermediate fraction 242.5 g.
(c) Succinodinitrile 160 g.

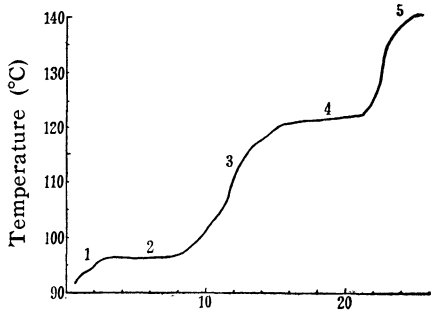

Fig. 1. Distillation curve of fraction A (atm. press.).

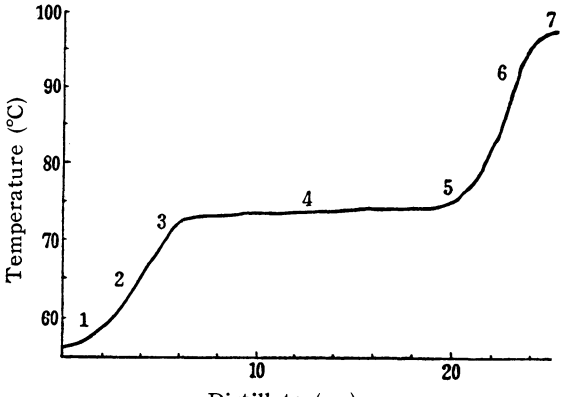

Fig. 2. Distillation curve of fraction B, C (75 mmHg).

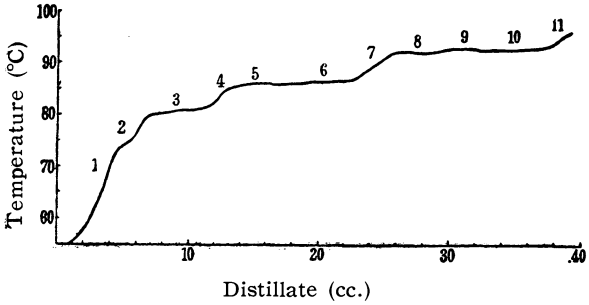

Fig. 3. Distillation curve of fraction D (33 mmHg).

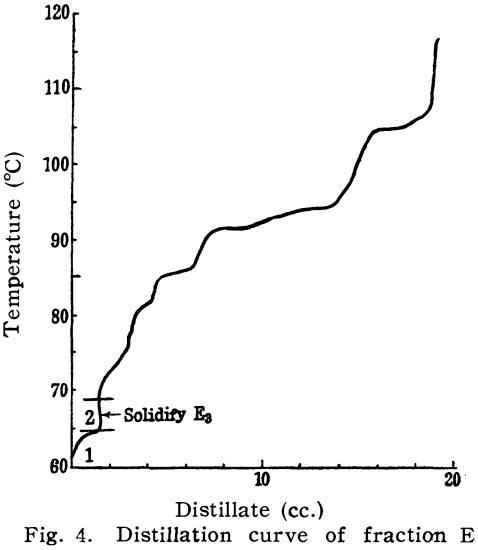

Fig. 4. Distillation curve of fraction E (7 mmHg).

(D) Preparations of Crystalline Derivatives.—*1) Propionitrile.*—A-2 fraction (1 g.) and thioglycolic acid (2 g.) were dissolved in dry ether and tnen treated with dry hydrogen chloride gas under cooling with ice from outside. It was then allowed to stand in a refrigerator for half an hour to form white crystals. It was filtered and dried in a desiccator to form 0.5 g. of crystals melting at 123–124°C (decomp.). The melting point (decomposition) of α-iminopropylmercatoacetic acid hydrochloride so far reported is 124°C.

2) Benzonitrile.—The mixture of D-10 fraction (1.0 g.) and a 75% aq. sulfuric acid solution (5 cc.) together with sodium chloride (0.2 g.) was heated at 160°C and then at 190°C for half an hour. each. After cooling the reaction product was added to 20 g. of ice. The precipitate was filtered. It was dissolved in aq. potassium carbonate solution and the insoluble substances were filtered off. One gram of black insoluble solid was obtained after drying in a disiccator. The filtrate was made acidic with sulfuric acid and then allowed to stand over night. The precipitate was filtered and dried in a desiccator to form 0.85 g. of crystals which melted at 121–121.5°C. The crystals were recrystallized from 20 cc. of water. It was dried in a desiccator to form 0.65 g.

of crystals which melted at 121–121.5°C. These crystals mixed with benzoic acid melted at 121.2–121.7°C, showing no melting point depression.

Anal. Found: C. 68.69; H, 4.97. Calcd. for $C_7H_5O_2$: C, 68.84; H, 4.95%.

3) *Naphthalene.*—A solid separated in E-3 fraction melted at 80.2°C. It melted at 81.8°C after recrystallization from methanol. It melted at 81.8°C when mixed with naphthalene showing no melting point depression.

Anal. Found: C, 93.63; H, 6.28. Calcd for $C_{10}H_8$: C, 93.71; H, 6.29%.

(E) Infrared Absorption Spectra.—Fig. 5–9 show infrared absorption spectra of A-4, B-4, D-3, D-5, D-10 fractions (Perkin Elmer C12).

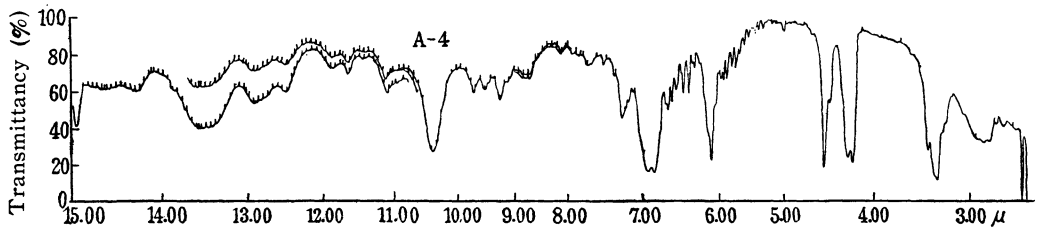

Fig. 5. Infrared absorption spectra of A-4.

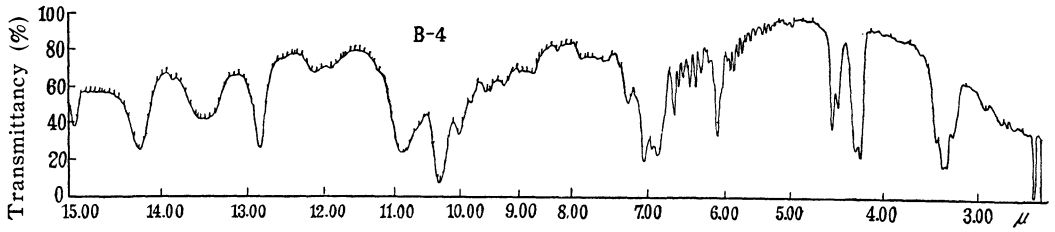

Fig. 6. Infrared absorption spectra of B-4.

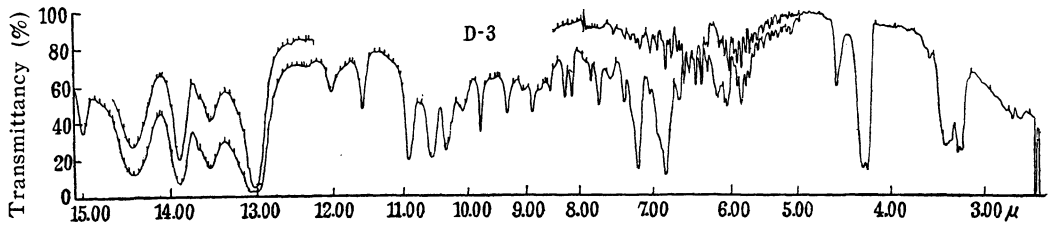

Fig. 7. Infrared absorption spectra of D-3.

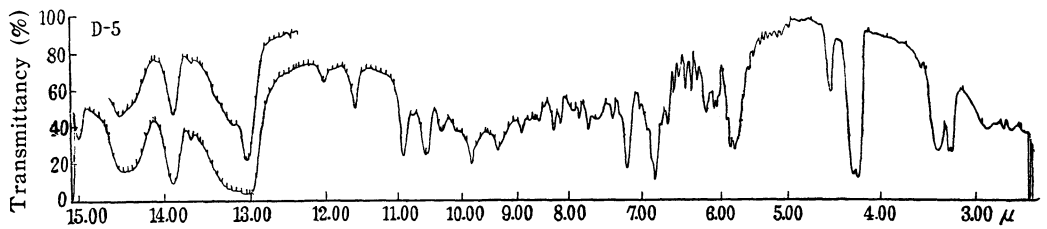

Fig. 8. Infrared absorption spectra of D-5.

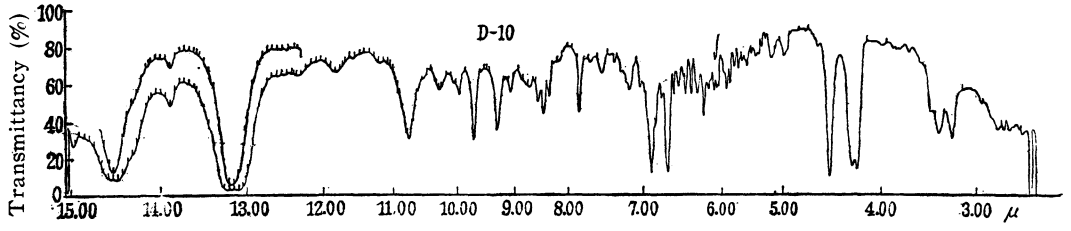

Fig. 9. Infrared absorption spectra of D-10

Summary

By distilling the reaction products of the vapor phase acrylonitrile synthesis from acetylene and hydrocyanic acid an intermediate fraction was obtained between two main fractions, acrylonitrile and succinodinitrile. The neutral portion of the intermediate fraction was carefully distilled through an efficient column and separated into constant boiling fractions. From these fractions propionitrile, benzonitrile naphthalene were isolated and identified as the byproducts. On the basis of the boiling points and the infrared spectra of other fractions, the presence of unsaturated nitriles such as 1-cyanobutadiene, 2-cyanobutadiene, 1-cyanohexatriene, 2-cyanohexatriene, 3-cyanohexatriene as the constituents of the neutral portion was suggested.

Heartfelt thanks are to be returned to Professors Shiro Akabori and Shunsuke Murahashi of Osaka University for their kind instruction and suggestions, to Kazuo Adachi, Masamichi Miura, Tadamichi Fukunaga, Tatsuo Takaya, Yasumasa Kiyokawa, Shinpei Hamada, Sumihiko Mori, Tohoru Okuda and Noriyuki Yamamoto for their helpful technical assistance, and to Yoshiki Matsui for taking infrared absorption spectra.

Part of the expenditure required for this study has been kindly subsidized by the Scientific Fund of the Education Ministry, Textile Research Institute, and Tekkosha, Inc.

Department of Chemistry, Faculty of Science, Osaka University, Osaka

Spectrophotometric Determination of Micro Quantities of Titanium with 8-Hydroxyquinaldine

By Kenji MOTOJIMA

(Received November 21, 1955)

Introduction

Titanium forms slightly soluble chelate with oxine and this chelate can be extracted with chloroform, giving a yellow colored solution which has an absorption maximum at 385 mμ. This property can be used for the photometric determination of a small amount of this metal[1]. On the other hand, Gardner[2] has described a method based on a measurement of the color intensity of a chloroform solution of peroxidised titanium oxinate extracted from the solution containing hydrogen peroxide. These two methods are very sensitive, but the reactions are not very selective and, especially, the former method is affected seriously by small amounts of the aluminum and iron which are most likely to accompany titanium. In the method to be described below, 8-hydroxyquinaldine, one of the derivatives of oxine, is used as a reagent, and the method employed by the author for the spectrophotometric determination of beryllium with this reagent[3] is applied to this metal. By this method from 3 to 50 micrograms of titanium in about 35 ml. of solution can be determined without being affected by a few milligrams of aluminum. Moreover, small amounts of iron and titanium can be determined simultaneously in the similar way used for the simultaneous spectrophotometric determination of iron and aluminum with oxine[4].

1) K. Motojima, Unpublished work.
2) K. Gardner, *Analyst*, **76**, 485 (1951).
3) K. Motojima, This Bulletin, **29**, 71 (1956).

Apparatus

A Beckman Model DU type spectrophotometer (Shimadzu, QB-50) with 1 cm. glass cell was used for all absorbancy measurements. A glass electrode pH meter (Horiba, Model M) was used for pH measurement. Separatory funnel, automatic measuring pipette and all other glass wares were the same ones used in the previous investigations[3,4].

Reagents

Standard Titanium Solution.—In 30 ml. of hot concentrated sulfuric acid, 3 g. of meta-titanic-acid (about 75% TiO_2) purified by reprecipitation, was dissolved and, after cooling, it was diluted to 1 liter. After suspended insoluble titanium

4) K. Motojima, *J. Chem. Soc. Japan (Pure Chem. Sect.)*, **76**, 903 (1955).

oxide was filtered off with a fine filter paper, the titanium content was determined gravimetrically as the oxide. Working solutions were prepared by exactly diluting this solution with 0.5 N sulfuric acid. Each 10 ml. of these solutions contained 10.8 and 21.6 micrograms of titanium.

Standard Ferric Iron Solution.—Several ferric iron standard solutions were prepared by dissolving pure ammonium iron alum in 0.1 N sulfuric acid.

8-Hydroxyquinaldine Solution.—1% 8-hydroxyquinaldine acetic acid solution was prepared[3].

Chloroform.—Purified chloroform[3] was used.

Other Reagents.—The other reagents were prepared from reagent grade chemicals.

Experimental

Absorption Spectra.—Absorption spectra of titanium chelate of 8-hydroxyquinaldine extracted with chloroform were studied. The data obtained are shown in Fig. 1. From these curves, it is seen that this chelate in chloroform has an absorption maximum at the wave length of 370 mμ, and at the same time, the reagent alone in this solvent has a considerable absorption at this wave length. Accordingly, the wave length of 380 mμ has been chosen for the analytical purpose.

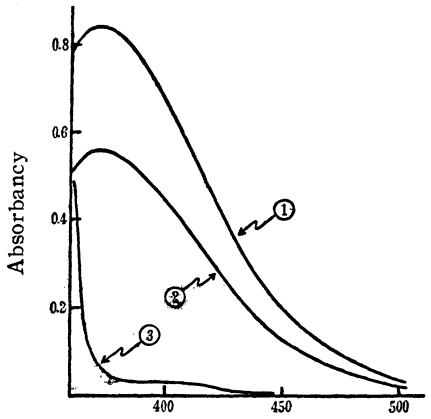

Fig. 1. Absorption spectra of titanium chelate of 8-hydroxyquinaldine in chloroform.
①: 32.4 micrograms of Ti,
②: 21.6 micrograms of Ti,
③: blank.

Effect of pH upon Extraction.—The proper pH for the efficient extraction of titanium was determined. A series of several solutions each containing 21.6 micrograms of titanium in about 35 ml. was treated with 3 ml. of 8-hydroxyquinaldine solution and suitable amount of ammonium acetate or ammonium hydroxide enough to fall within a pH range from 2 to 11. After the volume of the solution was brought to 50 ml., extraction was made with exactly 10 ml. of chloroform. Then, the absorbancy of the extract dried with anhydrous sodium sulfate, was measured at 380 mμ versus chloroform. On the other hand, measurement of pH was made on the aqueous layer after extraction. The results obtained are shown in Fig. 2. Extraction is seen to be almost complete over a pH range from 5.0 to 9.0, and the approximately constant absorbancies are obtained in the pH range from 5.0 to 6.0. A similar experiment was made about the reagent, and it was found that the blanks were reasonably constant in the pH range from 4.0 to 10.0. So that the pH range from 5.0 to 6.0 has been chosen as the optimum range for this method.

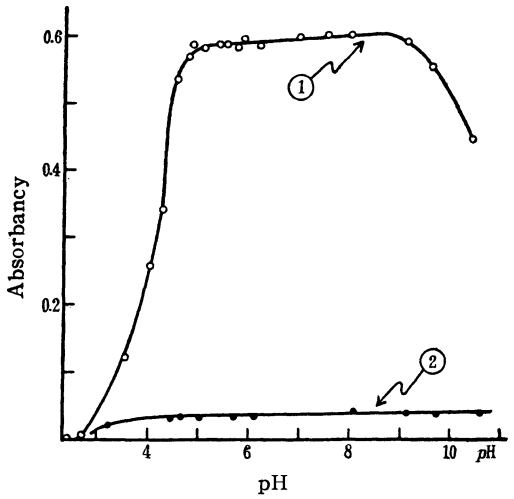

Fig. 2. Effect of pH upon extraction.
①: 21.6 micrograms of Ti,
②: blank.

Amount of Reagent.—Approximately 50 ml. of solutions each containing 43.2 micrograms of titanium and varying amounts of 8-hydroxyquinaldine solution, were extracted with exactly 10 ml. of chloroform respectively, at a pH of 5.3±0.2, and the absorbancies of these dried extracts were measured at 380 mμ, versus chloroform. A similar set but with no titanium present was also done. The results are shown in Table I.

TABLE I
EFFECT OF AMOUNT OF REAGENT

8-Hydroxyquinaldine Added, ml.	Absorbancy Measured: Ti is present	Absorbancy Measured: Blank	Correct for Blank
0.5	0.404	0.017	0.387
1.0	0.855	0.017	0.838
1.5	0.980	0.015	0.965
2.0	1.100	0.027	1.073
2.5	1.130	0.031	1.099
3.0	1.135	0.033	1.102
3.5	1.150	0.039	1.111
4.0	1.135	0.046	1.089
5.0	1.155	0.047	1.108

When more than 2.5 ml. of reagent solution is added, the absorbancies, after correction for the blank reading are reasonably constant. Therefore, 3 ml. of 8-hydroxyquinaldine solution has been selected as a sufficient amount of reagent.

Effect of Temperature and Digestion.—After five, fifteen, thirty and sixty minutes of digestion

at various temperatures, from 10° to 80°C, extractions were made respectively, in case of high temperature, solution being cooled to room temperature before extraction. And it was found that since the absorbancies of their dried extracts were reasonably constant, no digestion was necessary.

Shaking Period.—The complete extraction of titanium chelate of 8-hydroxyquinadline with chloroform seems to be attained by vigorous shaking for thirty seconds.

Stability.—The absorbancy of the dried chloroform extract of titanium chelate, stored in a glass bottle with a glass stopper and protected from sunlight, was found to remain unchanged for a week.

Spectrophotometric Procedure and Preparation of Calibration Curve

About 35 ml. of acidic solution containing not more than 50 micrograms of titanium, is treated with 3 ml. of 8-hydroxyquinaldine solution and suitable amounts of 2 N ammonium hydroxide and 2 N ammonium acetate solution enough to attain the pH to 5.3±0.2. The solution is transferred to a separatory funnel with a few milliliters of rinsed water and the volume is brought to 50 ml. Then extraction is made with exactly 10 ml. of chloroform by vigorous shaking for a minute. The chloroform layer is drawn off into a small glass bottle with a glass stopper, containing 1 g. of anhydrous sodium sulfate, and is shaken to remove droplets of water. The absorbancy of this extract is measured at 380 mμ using blank as a reference. Titanium is determined by the use of the calibration curve prepared by the same treatment of a series of known amount of this metal.

The calibration curve obtained is shown in Fig. 3. As will be seen from this curve, a close approximation to a linear relationship between titanium concentration and the absorbancy is obtained up to 50 micrograms or more.

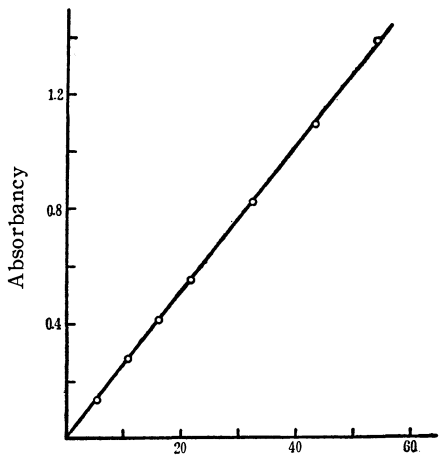

Fig. 3. Calibration curve of titanium (at the wave length of 380 mμ).

Interfering Substances

Relatively large amounts of alkali, ammonium, calcium and magnesium salts of acetate, chloride, nitrate and sulfate, and less than about 10 mg. of aluminum do not interfere with this procedure. Tartrate produces a serious effect and gives a low result. Such metals as bithmus, cobalt, copper, iron, nickel, vanadium and zirconium which form chloroform soluble chelate with 8-hydroxyquinaldine in acetic acid and acetate medium interfere with this method, and these metals, except a small amount of ferric iron, should be absent.

Ferric iron yields a dark blue chloroform solution under the same condition and interferes seriously with this method, but when its amount is less than about 100 micrograms, titanium and iron can be determined simultaneously by a method similar to that presented by the author[3,4].

Simultaneous Spectrophotometric Determination of Titanium and Iron

Ferric chelate of 8-hydroxyquinaldine in chloroform has two absorbancy maxima at 470 and 580 mμ, and Beer's law is obeyed at both 380 and 580 mμ, respectively. On the other hand titanium chelate has no absorption at 580 mμ. Therefore, both titanium and iron can be determined simultaneously, by the very same treatment mentioned above, and by measuring the absorbancies at 380 and 580 mμ and applying the following formulas[5].

$$C_{Fe}=\frac{A_{580}}{a^{Fe}_{580}}$$

$$C_{Ti}=\frac{a^{Fe}_{580}\cdot A_{380}-a^{Fe}_{380}\cdot A_{580}}{a^{Ti}_{380}\cdot a^{Fe}_{580}}$$

Where, C_{Fe}, C_{Ti}: iron and titanium present, in microgram,

A_{380}, A_{580}: absorbancies measured at 380 and 580 mμ,

a^{Ti}_{380}, a^{Fe}_{380}, a^{Fe}_{580}: absorbancy indexes of titanium and iron at 380 and 580 mμ (the absorbancy per microgram of these metals).

In this experiment the values of these absorbancy indexes obtained are as follows:

$$a^{Fe}_{380}=0.0088 \qquad a^{Fe}_{580}=0.0077$$

$$a^{Ti}_{380}=0.0254$$

the values of a^{Fe}_{380} and a^{Fe}_{580} are slightly lower than that when extraction is made in ammoniacal medium[3], because these values slightly increase in proportion to the pH at which extraction is made. Nevertheless, their changes are negligible when extraction is made at the pH range from 5 to 6.

5) E. B. Sandell, "Colorimetric Determination of Traces of Metals", 2nd Ed., Interscience Publisher Inc., New York (1950) p. 70.

Several mixed solutions containing known amounts of titanium and iron in various ratios were prepared and these two metals were determined. Some of the results are shown in Table II, which seem to be quite satisfactory.

TABLE II
SIMULTANEOUS DETERMINATION OF TITANIUM AND IRON

Taken Microgram		Absorbancy Measured		Calculated Microgram	
Ti	Fe	380 mμ	580 mμ	Ti	Fe
5.4	20.0	0.324	0.161	5.5	20.9
5.4	40.0	0.481	0.308	5.1	40.1
5.4	60.0	0.657	0.466	5.3	60.6
5.4	80.0	0.830	0.623	4.6	81.0
5.4	100.0	0.990	0.774	4.2	100.7
10.8	20.0	0.450	0.160	10.6	20.8
10.8	40.0	0.626	0.311	10.7	40.5
10.8	60.0	0.810	0.476	10.5	61.9
10.8	80.0	0.975	0.614	10.9	79.9
10.8	100.0	1.125	0.765	9.9	99.5
21.6	20.0	0.724	0.164	21.1	21.3
21.6	40.0	0.875	0.312	20.5	40.6
21.6	60.0	1.090	0.473	21.8	61.6
21.6	80.0	1.270	0.627	22.0	81.5
32.4	20.0	1.025	0.164	33.1	21.3
32.4	40.0	1.160	0.315	31.5	41.0
32.4	60.0	1.350	0.471	32.0	61.3

Conclusion

The spectrophotometric method for determination of micro quantities of titanium with 8-hydroxyquinaldine was established. By this method from 3 to 50 micrograms of titanium in about 35 ml. of solution can be determined; therefore the sensitivity of this method is almost equal to that of the tiron method established by Yoe and his coworker[6], but is much better than that of the ordinary hydrogen peroxide method[7]. A few milligrams of aluminum do not interferes with this method. Moreover, the method for simultaneous determination of micro quantities of titanium and iron was studied.

The author wishes to express his sincere appreciation to Prof. Dr. M. Ishibashi, Kyoto University, for his encouragement and Mr. H. Hashitani for his frequent assistance throughout the investigation.

Faculty of Science and Engineering
Ritsumeikan University, Kyoto

6) J.H. Yoe and A.R. Armstrong, *Anal. Chem.*, **19**, 100 (1947),
7) E. B. Sandell, "Colorimetric Determination of Traces of Metals", 2nd Ed. (1950), p. 572.

Spectrophotometric Determinatoin of Micro Quantities of Iron, Titanium and Aluminum when They accompany Each Other. Use of 8-Hydroxyquinaldine and Oxine

By Kenji MOTOJIMA and Hiroshi HASHITANI

(Received November 21, 1955)

Introduction

In general, iron, titanium and aluminum accompany each other, and the methods for separation and determination of these three metals are very essential. By the method described below, micro quantities of these three metals can be separated and determined by the use of 8-hydroxyquinaldine and oxine as reagents.

In the previous paper[1] presented by one of the authors, it has been reported that small amounts of iron and titanium can be extracted with chloroform as their chelate of 8-hydroxyquinaldine, and that by measuring the absorbancies of the extract at 380 and 580 mμ, these two metals can be determined simultaneously. At the same time iron and titanium are quantitatively extracted off and aluminum is perfectly left in aqueous phase. Therefore, after the above extraction aluminum can be determined photometrically without being effected by iron and titanium. using oxine as a reagent[2,3].

Apparatus and Reagents

All the apparatus and the reagents except for the following ones were the same as those had been used in the previous work[1].

Standard Aluminum Solution.—Several stand-

1) K. Motojima, This Bulletin, **29**, 455 (1956).

2) E. B. Sandell, "Colorimetric Determination of Metals", 2nd Ed. (1950), p. 152.

3) K. Motojima, *J. Chem. Soc. Japan (Pure Chem. Sect.)* **76**, 903 (1955).

ard aluminum solutions were prepared from pure potassium aluminum alum.

Oxine Solution (1% acetic acid solution).—In 5 ml. of glacial acetic acid 2 grams of pure oxine were dissolved by warming, and the volume was brought to 200 ml. with distilled water.

Procedure

Approximately 50 ml. of acidic solution containing not more than 50 micrograms of iron, titanium and aluminum respectively, 3 ml. of 8-hydroxyquinaldine solution and suitable amounts of ammonium hydroxide and ammonium acetate enough to adjust the pH to 5.3±0.2, is extracted with exactly 10 ml. of chloroform. Then, the measurements of two absorbancies at 380 and 580 mμ of the dry extract are made using blank as a reference, and iron and titanium are determined by the method mentioned in the previous paper[1]).

The aqueous layer is washed three times with 10 ml. of chloroform by shaking for about thirty seconds respectively. By this treatment iron, titanium and 8-hydroxyquinaldine will be quantitatively removed from the aqueous phase. Then the aqueous solution is transferred into a 100 ml. beaker with a few milliliters of rinsed water, treated with 3 ml. of 2 N sulfuric acid and heated on water bath to expel the chloroform which comes into the solution, and the volume is brought to about 35 ml. by evaporation.

After cooling, the solution thus resulting is treated with 3 ml. of oxine solution and a suitable amount of 2 N ammonium acetate enough to adjust the pH to 5.0±0.2, and transferred in a separatory funnel with a few milliliters of rinsed water, and the volume is brought to 50 ml. Then the extraction is made by vigorous shaking for a minute with exactly 10 ml. of chloroform. The chloroform layer is dried with a gram of anhydrous sodium sulfate and the absorbancy at 390 mμ is measured using blank as a reference. Aluminum is determined by the use of the calibration curve[3]).

Discussion and Results

If 8-hydroxyquinaldine extraction is made with 20 or 30 ml. of chloroform, double or triple amounts of iron and titanium can be determined respectively. When the amount of aluminum is more than 50 micrograms, the acidified solution from which iron and titanium have been removed by 8-hydroxyquinaldine extraction, is exactly diluted to suitable volume with distilled water using a volumetric flask, and an aliquot is taken for determination of aluminum. By this method up to a milligram of aluminum can be determined accurately.

TABLE

DETERMINATION OF IRON, TITANIUM AND ALUMINUM

Taken Microgram			Absorbancy Measured: 8-Hydroxyquinaldine Extraction		Absorbancy Measured: Oxine Extraction		Found Microgram		
Fe	Ti	Al	380 mμ	580 mμ	390 mμ	470 mμ	Fe	Ti	Al
0.0	5.4	25.0	0.124	0.004	0.656	0.011	0.1	4.7	25.4
0.0	10.8	25.0	0.275	0.011	0.678	0.012	0.1	10.3	26.2
0.0	21.6	25.0	0.549	0.000	0.674	0.014	0.0	21.6	26.0
40.0	0.0	25.0	0.338	0.291	0.617	0.014	37.9	0.2	23.8
40.0	5.4	25.0	0.486	0.308	0.612	0.004	40.0	5.3	23.9
40.0	10.8	0.0	0.605	0.303	0.005	0.007	39.4	10.2	0.0
40.0	10.8	10.0	0.633	0.318	0.279	0.008	41.4	10.6	10.7
40.0	10.8	25.0	0.629	0.311	0.640	0.001	40.5	10.8	25.0
40.0	10.8	50.0	0.638	0.319	1.210	0.011	41.5	10.8	47.1
40.0	21.6	0.0	0.905	0.311	0.004	0.006	40.5	21.7	0.0
40.0	21.6	10.0	0.910	0.305	0.284	0.008	39.7	22.2	10.9
40.0	21.6	25.0	0.910	0.302	0.665	0.018	39.3	22.3	25.5
40.0	21.6	50.0	0.900	0.312	1.240	0.021	40.6	21.4	48.0
40.0	32.4	0.0	1.160	0.308	0.010	0.014	40.0	31.8	0.0
40.0	32.4	10.0	1.190	0.306	0.280	0.009	39.8	33.1	10.7
40.0	32.4	25.0	1.190	0.322	0.651	0.005	41.9	32.4	25.4
40.0	32.4	50.0	1.200	0.319	1.210	0.005	41.5	33.0	47.2
0.0	5.4	200.	0.126	0.005	*1.270	0.017	0.1	4.8	197.
0.0	10.8	200.	0.277	0.012	*1.250	0.015	0.2	10.4	194.
0.0	21.6	100.	0.573	0.003	*0.631	0.018	0.0	22.4	97.
0.0	21.6	200.	0.549	0.000	*1.225	0.016	0.0	21.6	190.
40.0	5.4	200.	0.472	0.300	*1.235	0.016	39.0	5.1	190.
40.0	10.8	100.	0.639	0.313	*0.629	0.013	40.7	11.1	97.
40.0	10.8	200.	0.635	0.318	*1.255	0.030	41.4	10.7	194.
40.0	21.6	100.	0.915	0.305	*0.645	0.012	39.7	22.3	100.
40.0	21.6	200.	0.910	0.299	*1.220	0.016	38.9	22.4	189.

* Measurement was made for 25 ml. portion of the solution diluted to 100 ml.

The pH of the solution, after 8-hydroxyquinaldine extraction, is about 5.3 and at this pH aluminum tends to form hydroxide and give low analytical result; for this reason the solution should be acidified with sulfuric or hydrochloric acid before the determination of aluminum is carried out.

When the measurement of absorbancy of aluminum oxinate extract is made, it is desirable to measure the absorbancy of the extract at 470 mμ which is caused by iron oxinate, and, if necessary, make a correction for iron which seems to come accidentally into the solution during the procedure, by the method mentioned by one of the authors[3].

Relatively large amounts of alkali, ammonium, calcium and magnesium salts of acetate, chloride, nitrate and sulfate do not interfere with this procedure. Tartrate, fluoride and metal ions which form chloroform soluble chelate with 8-hydroxyquinaldine and oxine in acetic acid and acetate medium interfere with this method, and they should be absent.

A number of mixed solutions containing known amounts of iron, titanium and aluminum were prepared and these three metals were determined. Some of the results are shown in the following table, which seems to be quite satisfactory.

Conclusion

The method for separation and spectrophotometric determination of micro quantities of iron, titanium and aluminum with 8-hydroxyquinaldine and oxine was established. By this method, from 3 to 50 micrograms of iron, titanium and aluminium mixed in about 35 ml. of solution, are determined, rapidly and accurately.

The authors wish to express their sincere appreciation to Prof. Dr. M. Ishibashi, Kyoto University, for his encouragement and numerous suggestions throughout the investigation.

Faculty of Science and Engineering
Ritsumeikan University, Kyoto

The Electronic Structures of Azine Compounds. I. The Molecular Structures and the Electronic States of Fluoflavine and Fluorubine

By Yûmi AKIMOTO

(Received July 29, 1955)

The recent development of the organic chemistry concerning azine compounds has made it possible to offer us some various theoretically interesting problems. This series includes as its purpose the semi-empirical discussions on such problems, in terms of the simple LCAO molecular orbital theory, which would permit us to take a bird's-eye view of the electronic structures of the azine compounds.

As the first venture, fluoflavine (dihydro-5, 6, 11, 12-tetraaza-naphtacene) and fluorubine (dihydro-5, 6, 7, 12, 13, 14-hexaaza-pentacene) were chosen for consideration here. The electronic absorption spectra were observed and discussed. Attention was also paid to the position of *meso*-H atoms of the molecules.

Experimental

Difficulty arises in the selection of a good solvent of fluoflavine and fluorubine, as none of the non-polar solvents dissolve these compounds or do not dissolve them completely. As a result of the solvent test extended to ten odd solvents and their mixtures*, slight solubility was observed on several alcoholic solvents, where the solubility slightly increased as the size of the alkyl group increased**. Here, considering the absorption ranges of the solvents, *n*-propylalcohol was used. Fluoflavine saturates up to 1/20,000 mol, and fluorubine to 1/150,000 mol. already, so the confidence regarding the absolute intensity of the absorption is slight.

For the observation, a Beckman quartz DU-type spectrophotometer was used. Samples used were synthesized by the members of Kawai Laboratory of Tokyo University of Education. Observed curves were shown in Fig. 1.

---

* Methyl- to octyl-alcohol, benzene, toluene, $CHCl_4$, CCl_4, dioxane, etc., and their mixtures.

** These samples are slightly soluble in dioxane and in mixtures of CCl_4 and alcohols. But in the former case, the formation of the hydrogen bonds is apprehended, and in the latter, the tendency of deepening of color shows the possibility of the formation of some intermolecular compounds.

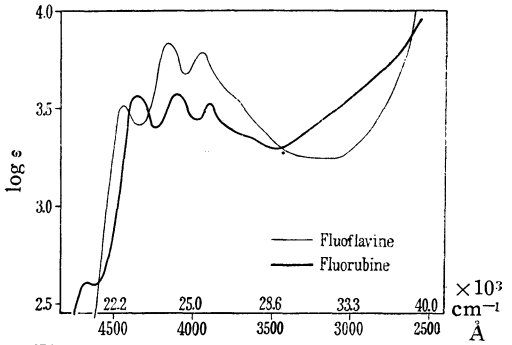

Fig. 1. The absorption curves of fluoflavine and fluorubine.

Interpretation of Spectra

Platt[1] presumed that a weak absorption tail near 24,000 cm^{-1} of phenazine is to be the transition of *n*-type. If we admit his postulate that, with increasing size of the parent conjugated systems, n-π transition moves to the red only about half as far as the longest wave-length π-π transition, we may anticipate that the n-π transition will be hidden when the molecule becomes larger and larger. Moreover, in the case of dihydro-azine as fluoflavine, *n*-electron of the hydrogenated N atoms (N_H atoms) conjugates with the π-electron system increasing the number of the filled orbitals, and so the n-π transition will move farther to the blue side. Because of these aspects, and also from the standpoint of the transition intensity, the longest strong wave-length absorption of fluoflavine may be assumed to be the π-π transition.

In fluorubine, the increase of the number of non-hydrogenated N atoms two to four, will produce some interaction to shift the *n*-band to red, just as the increase of the number of N atom one to two, produced the absorption tail on phenazine which was not present in acridine. Actually, fluorubine has a weak absorption near 21,000 cm^{-1}. If we assume this absorption to be of *n*-type, fluorubine has come to have three absorption maxima in the longest wave-length π-π band just as in the case of fluoflavine.

Such a way of thinking does not conflict with the spectral results of hemofluorindine (dihydro-5, 7, 12, 14-tetraaza pentacene) which was reported by Badger et al.[2] Hemofluorindine has only two nonconjugated *n*-electrons, so n-π transition does not show the independent maximum.

Concerning these dihydro-azine compounds, many isomers are possible in regard to the positions of *meso*-H atoms (N_H atoms). Up to the present, no report has been presented about the isolation of these isomer, and the deduction will be drawn that either there is only the most stable isomer or the tautomerism between these isomers. The resemblance of these spectra to that of the corresponding polyacene compounds, seems to favor the former assumption[3]. But according to Badger et al.[4], the absorption curves of azine compounds generally lack the detailed structures as compared to that of polyacene. The measurement of the oscillator strengths will give the information about this problem, while we simply assume the former hypothesis, namely the presence of only one isomer to each dihydro-azine compound, leaving out further detailed discussion.

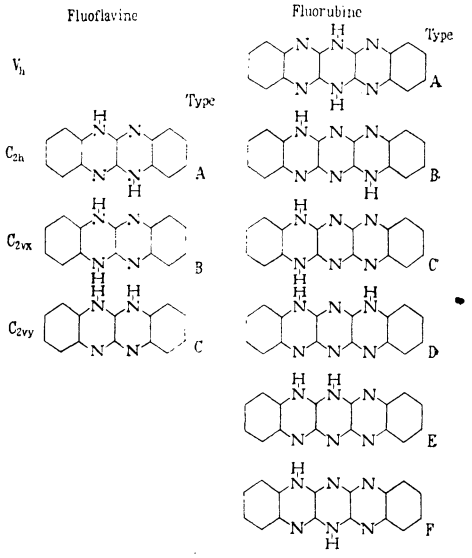

Fig. 2. The quoted isomers of fluoflavine and fluorubine.

MO Calculation

Simple molecular orbital calculations are applied to the various isomers of fluoflavine and fluorbine, as well as to the azine compounds which have the same skeleton with the above dihydro-azine compounds. (see Fig. 2)

The π-orbital energies of the azine compounds: 5, 6, 11, 12-tetraaza-naphtacene and 5, 6, 7, 12, 13, 14-hexaaza-pentacene, are calculated usng the ordinary simple variation method. For each isomer of fluoflavine and fluorubine, the second-order perturbation method is used, taking the changes of Coulomb integral values affected by the introduction of *meso*-H atoms on some N atoms of the former azine molecules, as the pertur-

1) J.R. Platt, *J. Chem. Phys.*, **19**, 101 (1951).
2) G.M. Badger and R. Pettit, *J. Chem. Soc.*, 3211 (1951).
3) A. Buraway, *J. Chem. Soc.*, 1177 (1939).
4) G.M. Badger and R. Pettit., *J. Chem. Soc.*, **1951**, 3211.

bation terms. The adoption of the perturbation method offers us the following advantages:

(1) The labor of calculation is reduced.

(2) The Coulomb integral value of N_H atoms is taken to be changeable easily, as the change of the value of perturbation.

All overlap integrals are neglected.

(1) Variation Method Calculation.—In 1951, P. O. Löwdin discussed the dipole moments of some aza-compounds to determine the most profitable Coulomb integral value α_r, for heterocyclic N atom, which was found to be $\alpha_N=\alpha_C+0.6\beta$[5]. A year later, H. H. Jaffé obtained the same conclusion from facts concerning the reactivity of some aza-compounds[6].

In this calculation we adopt the above value for α_r of every N atom. Inductive effect is assumed on the adjacents of N atoms to be 1/8 of 0.6β. After all concerns about the tolerable changes of the π-electron energies, which may be yielded by the choice of exchange integral values the privation of any reliable data compeles us to take the values as 1β indiscriminately, leaving the detailed discussion hereafter[7]. The results of the calculations are shown in Fig. 3.

(2) Perturbation Method Calculation.—P. O. Löwdin has developed this theory, making it applicable on any changes of Coulomb or exchange integral values of the molecules[8].

In general, when some Coulomb terms are perturbed by V, the π-orbital energy changes as follows:

$$\varepsilon^j=\varepsilon^{j(0)}+\sum_\mu V_\mu d_\mu^{jj(0)}+1/2\sum_{\mu\nu} V_\mu V_\nu \pi_{\mu\nu}^{jj(0)}$$

where upper indices $j, \alpha, \ldots\ldots$indicate the molecular orbitals, lower indices $\mu, \nu, \ldots\ldots$the atomic orbitals, and (o) the quantities, belonging to the original system. π is known by the name of mutability, defined as follows:

$$\pi_{\mu\nu}^{jj}=\sum_{\alpha\neq j}\frac{2d_\mu^{j\alpha}d_\nu^{j\alpha}}{(j\alpha)}$$

$$d_\mu^{j\alpha}=C_\mu^j C_\mu^\alpha$$

where C is the orbital coefficient, and $(j\alpha)$ indicates the energy difference between j-th and α-th orbitals.

For the perturbation terms, the differences of the Coulomb integral magnitudes, $\alpha_{NH}-\alpha_N=\Delta\alpha_N$, (conventionally taken to be 0.3, 0.6, and 1.2β) and the induction effects (assumed to be 1/8 for all adjacents of the perturbed atoms) are taken. In Fig. 3, the π-orbital energies of all isomers are shown in regard to the case of 0.6β perturbation. In Table II, the relations between the reduced representations of the π-orbitals and the symmetry properties of the perturbed molecules are shown.

TABLE I
THE ORBITAL ENERGIES OF 5,6,11,12-TETRAAZA-NAPHTACENE (X) AND 5,6,7,12,13,14-HEXAAZA-PENTACENE (Y)
(Calculated by the simple variation method)
$x=(\alpha-\varepsilon)/\beta$
$\beta=1$, $\alpha_N=\alpha_C+0.6\beta$, $S=0$

(X)		(Y)	
B_{3g}	−2.2752	B_{3g}	−2.2706
A_{1u}	−2.1147	A_{1u}	−2.1752
B_{3g}	−1.6657	B_{3g}	−1.8704
B_{1u}	−1.2267	A_{1u}	−1.4739
A_{1u}	−1.2056	B_{1u}	−1.2144
B_{2g}	−1.1037	B_{2g}	−1.1491
B_{3g}	−0.9373	B_{3g}	−1.1266
B_{1u}	−0.5886	A_{1u}	−0.9204
B_{2g}	0.0686	B_{1u}	−0.8050
		B_{2g}	−0.3349
A_{1u}	0.6104	B_{1u}	0.2028
B_{3g}	0.8747		
B_{1u}	1.0581	B_{3g}	0.6086
A_{1u}	1.3849	A_{1u}	0.7969
B_{2g}	1.4018	B_{2g}	1.0721
B_{3g}	1.8285	B_{3g}	1.1902
B_{1u}	1.8609	B_{1u}	1.3382
B_{2g}	2.3082	A_{1u}	1.5972
B_{1u}	2.7212	B_{2g}	1.7437
		B_{3g}	1.8939
		B_{1u}	2.1190
		B_{2g}	2.4935
		B_{1u}	2.7842

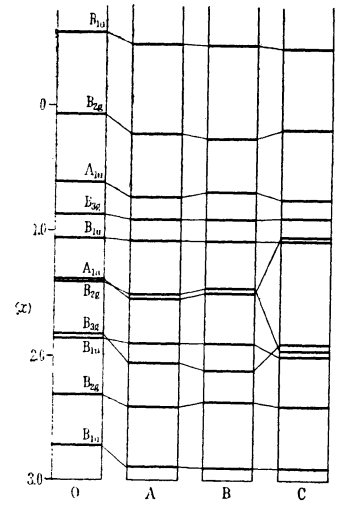

Fig. 3A. The orbital energies of each isomer of fluoflavine. (0 indicates 5, 6, 11, 12-tetraaza-naphtacene (0 was calcalculated by the variation method and the others by the perturbation method)

5) Per-Olov Löwdin, *J. Chem. Phys.*, **19**, 1323 (1951).
6) H.H. Jaffé, *J. Chem. Phys.*, **20**, 1554 (1952).
7) C.A. Coulson and J. der Heer, *J. Chem. Soc.*, **1952**, 482.
8) Per-Olov Löwdin, *J. Chem. Phys.*, **21**, 496 (1953).

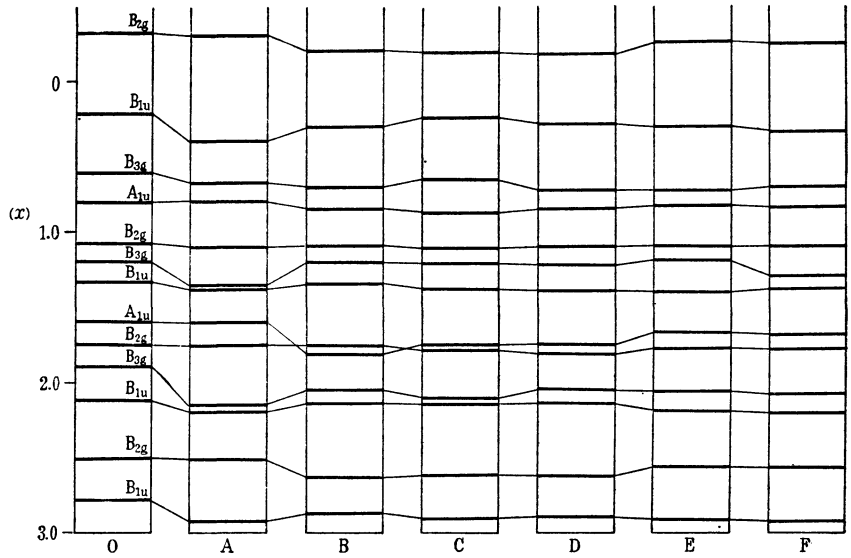

Fig. 3B. The orbtial energies of each isomer of fluorubine. (0 indicates 5: 6: 7: 12: 13: 14-hexaaza-pentacene) 0 was calculated by the variation method, and the others by the perturbation method.

TABLE II

THE RELATION BETWEEN THE REDUCED ORBITAL REPRESENTATION AND THE SYMMETRY PROPERTY OF THE MOLECULE

Symmetry property	V_h	C_{2h}	C_{2vx}	C_{2vy}
Reduced representation	A_{1u}	A_u	A_2	A_2
	B_{1u}	A_u	B_2	B_2
	B_{2g}	B_g	B_2	A_2
	B_{3g}	B_g	A_2	B_2

Discussion

1) Delocalization Energy.—The comparison of the stability are performed between the isomers using the terms of the vertical delocalization energy, defined as follows[9]:

$$\Delta\varepsilon=\varepsilon(L)-\varepsilon(D)$$

In spite of habitual suspicions which are entertained on the propriety of making it the criterion of the molecular stability, the identity of the skeletons such as between the isomers, is observed to offer us the considerable confidence in it. In Fig. 4, the delocalization energies are compared with the changes of $\Delta\alpha_N$.

In the case of fluoflavine, A-type isomer retains invariably the highest stability, but in fluorubine, the stability of A-type isomer is surpassed by B-type isomer over the $\Delta\alpha_N$ of 0.75β.

9) C.A. Coulson and Altmann, *Trans. Faraday Soc.*, 48, 293 (1952).

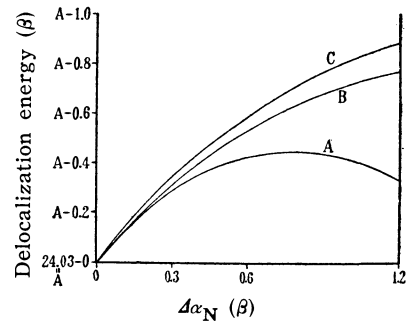

Fig. 4A. The delocalization energy of each isomer of fluoflavine.

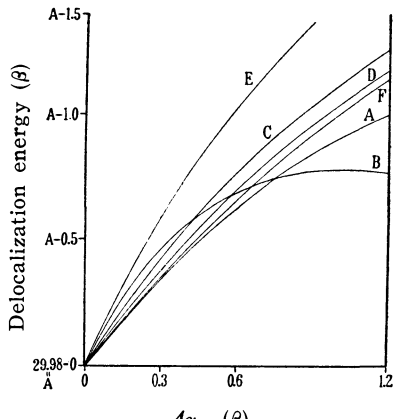

Fig. 4B. The delocalization energy of each isomer of fluorubine.

2) The Correspondency with the Absorption Curve.—The above results are examined from the aspect of correspondency with the

conclusion deduced from the positions of absorptions of absorption maxima. On the conversions of the π-electron transition energies of polyacene molecules (in β unit) into the positions of the longest wave-length absorptions (in wave number unit), good agreements are obtained in taking the exchange rates increasing with the size of molecular skeletons. Here, the rates are taken to agree with the transition energies of naphtacene and pentacene (polyacene molecules which have the same skeletons with fluoflavine and fluorubine respectively) calculated by the simplest MO calculations, with the observed positions of the longest wave-length absorptions: naphtacene 35,500 cm^{-1}/β, and pentacene 39,000 cm^{-1}/β. In Fig. 5, calculated positions of the longest wave-length absorption of each isomer is shown with the magnitude of $\Delta\alpha_N$.

We saw in Fig. 1, the so called blue shift with increase of molecular size: fluoflavine to fluoflavine. In Fig. 4, the curve of the most stable isomer of fluorubine A-type, rises up rapidly with the increase of $\Delta\alpha_N$ to cross to that of fluoflavine A-type about the position of $\Delta\alpha_N=0.4\beta$. Consequently, so long as the $\Delta\alpha_N$ is larger than 0.4β, a satisfactory explanation is obtained on the observed blue shift. (Fluorubine B-type does not explain the blue shift, in removing to further red side with increase of the perturbation.)

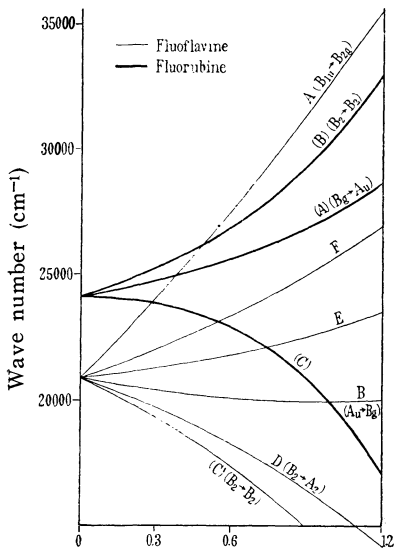

Fig. 5. The calculated longest-wave π-π transition energies of fluoflavine and fluorubine.

3) **Conclusion.**—As the result of the above discussions, unless we assume the existence of only one isomer, only A-types of both molecules satisfy all the conditions quoted here, and in this case, $\Delta\alpha_N$ must be larger than 0.4β and smaller than 0.75β.

If we set on Fig. 5, the calculated difference between the absorption positions of both molecules, 500 cm^{-1}, the perturbation is concluded by 0.45β. The observed values, 33,500 cm^{-1} for fluoflavine, and 23,000 cm^{-1} for fluorubine, are somewhat smaller than the calculated values corresponding to the perturbation of 0.45β, but within the permissible ranges.

Summary and Conclusion

1) The absorption spectra of fluoflavine and fluorubine were observed in *n*-propyl alcohol solution.

2) The longest wave-length π-π transitions were observed in 22,500 cm^{-1} for fluoflavine, and in 23,000 cm^{-1} for fluorubine.

3) The n-π transition was observed near 21,000 cm^{-1} in fluorubine, while no independent n-π absorption was observed in fluoflavine.

4) The simple MO calculations were applied to 5, 6, 11, 12-tetraaza-naphtacene and 5, 6, 7, 12, 13, 14-hexaaza-pentacene.

5) The π-orbital energies of all isomers of fluoflavine and fluorubine were calculated using the second- order perturbation-method.

6) Supposing that only one isomer exists on each molecule, the blue shift, appearing in fluoflavine to fluorubine, was explained by setting the following structures: 5, 11-dihydro-5, 6, 11, 12-tetraaza-naphtacene for fluoflavine, and 6, 13-dihydro-5, 6, 7, 12, 13, 14-hexaaza-pentacene for fluorubine.

7) The above conclusion was consistant with the conclusion from the comparisons of the vertical delocalization energies.

8) To satisfy the conclusions 6) and 7), the Coulomb integral value of N_H atom must be between $\alpha_C+1.0\beta$ and $\alpha_C+1.35\beta$. Consequently, twice the Coulomb integral value as large as that of N atom will be the most appropriate.

We are deeply indebted to Prof. A. Kotera and Assist. Prof. K. Suzuki for their continued encouragement and valuable advice for this study. The kindness of Prof. S. Kawai who gave us the samples is gratefully acknowledged. Thanks are also due to Mr. S. Noguchi and Mr. K. Ihaya for their helpful discussions.

The cost of this research has been defrayed by the Scientific Research Encouragement Grant from the Ministry of Education to which the author's thanks are due.

Chemical Laboratory, Tokyo Bunrika University, Tokyo
**Hosokura Smelter & Refinery, Mitsubishi Metal Mining Co., Ltd., Miyagi-Prefecture*

* Author's present address.

*Solvent Effects upon Fluorescence Spectra and the Dipolemoments of Excited Molecules**

By Noboru MATAGA, Yozo KAIFU and Masao KOIZUMI

(Received October 19, 1955)

Introduction

Although solvent effects upon the absorption spectra have been studied extensively, there are rather few investigations of the solvent effects upon the fluorescence spectra.

These two are generally different from each other, and from the study of this difference one may expect to derive some information as to the nature of the excited state in contrast to the ground state. To accomplish this program, however, it is necessary to have a general and reliable theory upon the interaction between solute and solvent molecules. Now in 1954 Ooshika[1] published a general theory concerning the solvent effect upon the absorption spectra and the objective of the present communication is to apply his theory to the solvent effect upon the fluorescence spectra, and to compare the two effects.

An important piece of information obtained from this comparison is that one can estimate the dipolemoment of the excited state. An independent and analogous work has already been published by Lippert[2] employing the substances of quite a different type from ours.

Theoretical Consideration

Generally speaking, the difference of the solvent shifts between the absorption and fluorescence spectra is due to the following circumstances.

As to the absorption spectra which correspond to the energy difference between excited state and the ground state, the interaction energies between solute molecule and the solvent molecules sorrounding it are different in the ground and excited state, and this difference produces the solvent shift. Now, according to the Franck-Condon principle, the configuration of the solvent molecules around the the solute molecule does not change during the light absorption, and the above mentioned difference of the interaction energy refers to this Franck-Condon excited state[3] and the equilibrium ground state. But the Franck-Condon excited state is in general not the most stable equilibrium state appropriate to the excited solute molecule. The equilibrium excited configuration is only reached, for example, by reorientation of the solvent molecules, which requires at least a time of the order of 10^{-11} sec., the relaxation time of molecular rotation. The life-time of the excited state, on the other hand, is known to be of the order of 10^{-8} sec., which is ample for the equilibrium configuration to be realized prior to the emission. Hence, for the fluorescence spectrum, the initial state is the equilibrium excited state. During the emission, the solvent configuration does not change, and the momentary ground state in the Franck-Condon ground state which is different from the ground equilibrium state. Thus, when the stabilization energies due to solvent effects are represented as $\langle \Delta E \rangle_e^g$, $\langle \Delta E \rangle_f^g$, $\langle \Delta E \rangle_e^e$ and $\langle \Delta E \rangle_f^e$ for the ground equiribrium and Franck-Condon state and for the excited equilibrium and Franck-Condon state, respectively, the solvent shift of absorption and fluorescence spectrum may be written as follows:

$$hc\Delta\sigma_a = \langle \Delta E \rangle_f^e - \langle \Delta E \rangle_e^g$$

$$hc\Delta\sigma_f = \langle \Delta E \rangle_e^e - \Delta E \; {}_f^g$$

which are different from each other in general.

In the case when these interaction energies are mainly contributed by dipolar interaction, it is expected that a quantitative theory will enable us to estimate the difference of the dipolemoment between the excited state and the ground state, from the data of the two solvent shifts. As such, one may use Ooshika's theory[1] on the light absorption in solution which treats only the long range dipolar interaction between solute and solvent molecules surrounding it without taking into consideration the short range interactions such as higher polar interactions, charge transfer, hydrogen bonding, etc.

Applying the Ooshika's theory to the case where the solvent molecules surrounding the

* A preliminary short communication was published in This Bulletin, 28, 690 (1955).

1) Y. Ooshika, *J. Phys. Soc. Japan*, 9, 594 (1954).

2) E. Lippert, *Z. Naturforsch.*, 10a, 541 (1955).

3) N.S. Bayliss and E.G. McRae, *J. Phys. Chem.*, 58, 1002 (1954).

solute molecule are in the equilibrium configuration appropriate to the dipolemoment $\vec{\mu}_e$ of the excited solute molecule, one obtains the stabilization energy of solute molecule in its m state, $<\Delta E>^m$.

$$<\Delta E>^m=-\left\{\frac{2(D-1)}{2D+1}-\frac{2(n^2-1)}{2n^2+1}\right\}\left\{\frac{\vec{\mu}_e\cdot\vec{\mu}_m}{a^3}\right.$$
$$+\frac{2(D-1)}{2D+1}\frac{2}{a^3}\sum_{m'\neq e}$$
$$\left.\times\frac{\{\vec{\mu}_e(e|\vec{\mu}_0|m')\}\{\vec{\mu}_m(e\vec{\mu}_0|m')\}}{\varepsilon_{m'}-\varepsilon_e}\right\}$$
$$-\frac{1}{2}\frac{2(n^2-1)}{2n^2+1}\frac{\mu_m^2}{a^3}+\frac{2(D+1)(D-n^2)}{3(2D+n^2)D}\frac{kT}{a^3}$$
$$\times\sum_{m'\neq m}\frac{(m\cdot\vec{\mu}_0|m')^2}{\varepsilon_m-\varepsilon_{m'}}+\left\{\frac{2(D-1)}{2D+1}\right\}^2\frac{1}{a^3}$$
$$\times\sum_{m'\neq m}\frac{\{\vec{\mu}_e(m\vec{\mu}_0|m')\}^2}{\varepsilon_m-\varepsilon_{m'}}-\frac{1}{2}\frac{2(n^2-1)}{2n^2+1}\frac{1}{a^3}$$
$$\times\sum_{m'\neq m}(m|\mu_0|m')^2\left\{1-\frac{\varepsilon_m-\varepsilon_{m'}}{E_g-E_n}\right\}\qquad(1)$$

Where, D, n: dielectric constant and refractive index of the solvent, ε_m: electronic energy of solute molecule in its m state, E_n: electronic energy of solvent molecule in its n state, a: cavity radius in Onsager's theory of reaction field[4], $\vec{\mu}_m$, $\vec{\mu}_0$: dipolemoment in the m state and dipole operator of solute molecule.

The meaning of each term appearing in eq. (1) is as follows: The first term is due to the orientation effect between permanent dipole of solute molecule and those of solvent molecules, the second term represents the interaction of permanent dipole of solute with induced dipoles of solvent molecules (induced by solute permanent dipole), the third term arises from the fact that the average field of the solvent due to interaction between the permanent dipoles and induced dipoles of solvent molecules (induced by solvent permanent dipoles) polarizes the solute molecule, the fourth term is attributable to the interaction between the reaction field due to the mutual orientation of the solvent molecules and the dipole induced on the solute molecule by it, and the fifth term comes from the contribution of dispersion force.

Now the formula for $<\Delta E>_e^e$ and $<\Delta E>_f^g$ can be obtained easily from (1); the solvent shift of fluorescence spectrum $hc\Delta\sigma_f$ is represented as follows:

$$hc\Delta\sigma_f=<\Delta E>_e^e-<\Delta E>_f^g=\frac{2(D-1)}{2D+1}$$
$$\times\frac{\vec{\mu}_e\vec{\mu}_g-\vec{\mu}_e^2}{a^3}+\frac{2(n^2-1)}{2n^2+1}\frac{(\vec{\mu}_e-\vec{\mu}_g)^2}{2a^3}$$
$$+\frac{2(D+1)(D-n^2)}{3(2D+n^2)D}\frac{kT}{a^3}\left\{\sum_{m\neq e}\frac{(e\vec{\mu}_0|m)^2}{\varepsilon_e-\varepsilon_m}\right.$$
$$\left.-\sum_{m\neq g}\frac{(g|\vec{\mu}_0m)^2}{\varepsilon_g-\varepsilon_m}\right\}+\left\{\frac{2(D-1)}{2D+1}\right\}^2\frac{1}{a^3}$$
$$\times\left[3\sum_{m\neq e}\frac{\{\vec{\mu}_e(e|\vec{\mu}_0|m)\}^2}{\varepsilon_e-\varepsilon_m}-\sum_{m\neq g}\frac{\{\vec{\mu}_e(g|\vec{\mu}_0m)^2\}}{\varepsilon_g-\varepsilon_m}\right.$$
$$\left.-2\sum_{m\neq e}\frac{\{\vec{\mu}_e(e\vec{\mu}_0m)\}\{\vec{\mu}_g(e|\vec{\mu}_0|m)\}}{\varepsilon_e-\varepsilon_m}\right]$$
$$+\frac{1}{2}\frac{2(n^2-1)}{2n^2+1}\frac{1}{a^3}\left[\sum_{m\neq g}(g|\vec{\mu}_0m)^2\right.$$
$$\times\left\{1-\frac{\varepsilon_g-\varepsilon_m}{E_g-E_n}\right\}-\sum(e|\vec{\mu}_0|m)^2$$
$$\left.\times\left\{1-\frac{\varepsilon_e-\varepsilon_m}{E_g-E_n}\right\}\right].\qquad(2)$$

On the other hand, the solvent shift of absorption spectrum is[1].

$$hc\Delta\sigma_a=<\Delta E>_f^e-<\Delta E>_e^g=\frac{2(D-1)}{2D+1}$$
$$\times\frac{\mu_g^2-\vec{\mu}_g\vec{\mu}_e}{a^3}-\frac{2(n^2-1)}{2n^2+1}\frac{(\vec{\mu}_e-\vec{\mu}_g)^2}{a^3}$$
$$+\frac{2(D+1)(D-n^2)}{3(2D+n^2)D}\frac{kT}{a^3}\left\{\sum_{m\neq e}\frac{(e\vec{\mu}_0m)}{\varepsilon_e-\varepsilon^m}\right.$$
$$\left.-\sum_{m\neq g}\frac{(g|\vec{\mu}_0|m)^2}{\varepsilon_g-\varepsilon_m}\right\}+\left\{\frac{2(D-1)}{2D+1}\right\}^2\frac{1}{a^3}$$
$$\times\left[3\sum_{m\neq g}\frac{\{\mu_g(g|\mu_0|m)\}^2}{\varepsilon_m-\varepsilon_g}-\sum_{m\neq e}\frac{\{\vec{\mu}_g(e|\vec{\mu}_0m)\}^2}{\varepsilon_m-\varepsilon_e}\right.$$
$$\left.-2\sum_{m\neq g}\frac{\{\vec{\mu}_g(g|\vec{\mu}_0|m)\}\{\vec{\mu}_e(g|\vec{\mu}_0|m)\}}{\varepsilon_m-\varepsilon_g}\right]$$
$$+\frac{1}{2}\frac{2(n^2-1)}{2n^2+1}\frac{1}{a^3}\left[\sum_{m\neq g}(g|\vec{\mu}_0m)^2\right.$$
$$\times\left\{1-\frac{\varepsilon_m-\varepsilon_g}{E_n-E_g}\right\}+\sum_{m\neq e}(e|\vec{\mu}_0|m)^2$$
$$\left.\times\left\{1-\frac{\varepsilon_m-\varepsilon_e}{E_n-E_g}\right\}\right].\qquad(3)$$

From (2) and (3) we obtain:

$$hc(\Delta\sigma_f-\Delta\sigma_a)=-\left[\frac{2(D-1)}{2D+1}-\frac{2(n^2-1)}{2n^2+1}\right]$$

4) L. Onsager, *J. Am. Chem. Soc.*, 58, 1486 (1936).

$$\times\frac{(\vec{\mu}_e-\vec{\mu}_g)^2}{a^3}+\left\{\frac{2(D-1)}{2D+1}\right\}^2\frac{1}{a^3}$$
$$\times\Bigg[3\sum_{m\neq e}\frac{\{\vec{\mu}_e(e|\vec{\mu}_a|m)\}^2}{\varepsilon_e-\varepsilon_m}+3\sum_{m\neq g}\frac{\{\vec{\mu}_g(g|\vec{\mu}_0|m)\}^2}{\varepsilon_g-\varepsilon_m}$$
$$-\sum_{m\neq g}\frac{\{\vec{\mu}_g(g|\vec{\mu}_0|m)\}^2}{\varepsilon_g-\varepsilon_m}-\sum_{m\neq e}\frac{\{\vec{\mu}_g(e|\vec{\mu}_0|m)\}^2}{\varepsilon_e-\varepsilon_m}$$
$$-2\sum_{m\neq e}\frac{\{\vec{\mu}_e(e|\vec{\mu}_0|m)\}\{\mu_g(e\ \vec{\mu}_0\ m)\}}{\varepsilon_g-\varepsilon_m}$$
$$-2\sum_{m\neq g}\frac{\{\vec{\mu}_g(g(\vec{\mu}_0\ m)\}\{\vec{\mu}_e(g\ \vec{\mu}_0|m)\}}{\varepsilon_g-\varepsilon_m}\Bigg]. \quad (4)$$

All the discussions given above are on the basis of long range dipolar interaction between solute and solvent molecules. The theory, therefore, is not appropriate to the system with the specific short range interactions. For the consideration of such short range interactions, it may be necessary to compute the quantum mechanical interaction energy for each special pair of solute and solvent molecules, and, in fact, the general treatment as shown above may not be allowed. Even in the limit of the approximation of dipolar interaction, it is practically a very complicated and difficult problem to apply to this case Kirkwood's theory[5] which is a higher approximation than Onsager's[4], taking into consideration the correlation of nearest neighbour dipoles.

Now, consider the case of solutes such as naphtholes in the solvents such as acetic acid esters, where hydrogen bond is formed between solute and solvent molecules but for solvent molecules Onsager's approximation may be fairly well applicable. Put a hydrogen bonded solute molecule in the cavity in dielectric continuum, and apply to this system the Onsager's approximation.

Then one may be able to separate approximately the interaction energy of solute molecule with solvent molecules surrounding it as follows:

$$<\Delta E>^m_{f\cdot e}=<\Delta E(s)>^m_{f\cdot e}+<\Delta E(l)>^m_{f\cdot e} \quad (5)$$

Where, s and l indicate the terms arising from short range interaction due to hydrogen bonding and long range dipolar interaction, respectively. The superscript m represents that $<\Delta E>_m$ is the interaction energy in the m state of solute molecule, and subscript f or e means the Franck-Condon or equilibrium state.

From (5), the solvent shifts of fluorescence and absorption spectra can be written as follows:

$$\left.\begin{aligned} hc\Delta\sigma_f&=(<\Delta E(s)>^e_e+<\Delta E(l)>^e_e)\\ &\quad-(<\Delta E(s)>^g_f+<\Delta E(l)>^g_f)\\ hc\Delta\sigma_a&=(<\Delta E(s)>^e_f+<\Delta E(l)>^e_f)\\ &\quad-(<\Delta E(s)^g_e+<\Delta E(l)>^g_e)\end{aligned}\right\} \quad (6)$$

From (6) we obtain:

$$\begin{aligned} hc(\Delta\sigma_f-\Delta\sigma_a)&=[(<\Delta E(l)>^e_e+<\Delta E(l)>^g_e)\\ &\quad-(<\Delta E(l)>^e_f+<\Delta E(l)>^g_f)]\\ &\quad+[(<\Delta E(s)>^e_e+<\Delta E(s)>^g_e)\\ &\quad-(<\Delta E(s)>^g_f+<\Delta E(s)>^g_f)] \end{aligned} \quad (7)$$

The first term in square bracket in (7) is formally equated to the right hand side of (4), where, however, all the quantities associated with solute molecule must be replaced by those of hydrogen bonded solute. The second term is unknown but we may estimate this experimentally as will be mentioned later.

When the associating liquids such as alcohols are used as solvents, owing to the short range interactions between solvent molecules themselves, applicability of Onsager's theory, becomes much doubtful.

Experimental

According to the idea mentioned above, we have examined the fluorescence and absorption spectra of β-methylnaphthalene, β-naphthyl methyl ether, and α-, β-naphthols in various organic solvents. Fluorescence spectra were photographed with Hilger E_2 type spectrograph and the peaks of fluorescence spectra were visually observed. Absorption spectra were measured with Beckman Quartz spectrophotometer, and also photographed with Hilger E_2 type spectrograph. The solvents used were *n*-hexane, benzene, toluene, acetic acid esters, and alcohols.

α-, β-naphthols and β-naphthyl methyl ethers were the same samples as used before[6], methylnaphthalene was kindly supplied by Shionogi & Co., Ltd. and distilled under the atmosphere of dry nitrogen before use.

n-hexane and acetic acid esters were the same samples as described before[6], benzene, toluene and butanol were extra pure grade and used without further purification. Ethanol was 99% in purity.

Experimental Results and Discussions

The experimental results are shown in Table I, where σ^m_a is the position of the longest wave length peak of absorption spectra which is most prominent in all cases,

5) J.G. Kirkwood, *J. Chem. Phys.*, **7**, 911 (1939).

6) N. Mataga, Y. Kaifu and M. Koizumi, This Bulletin, **29**, 115 (1956).

TABLE I

σ_f^m AND σ_a^m VALUES FOR NAPHTHALENE DERIVATIVES (σ IN cm^{-1})

Solvent	$\left[\frac{2(D-1)}{2D+1}-\frac{2(n^2-1)}{2n^2+1}\right]$	β-Methylnaphthalene			β-Naphthyl methyl ether			α-Naphthol			β-Naphthol		
		σ_f^m	σ_a^m	$(\sigma_a^m-\sigma_f^m)$	σ_f^m	σ_a^m	$(\sigma_a^m-\sigma_f^m)$	σ_f^m	σ_a^m	$(\sigma_a^m-\sigma_f^m)$	σ_f^m	σ_a^m	$(\sigma_a^m-\sigma_f^m)$
n-Hexane	~0	29810	31340	1530	29070	30550	1480	30710	31090	380	29800	30460	660
Benzene	~0	29690	31270	1580	28930	30420	1490	30600	30980	380	29550	30290	740
Toluene	0.026	29670	31280	1610	28910	30430	1520	30540	30990	450	29510	30280	770
Butyl acetate	0.345	29810	31330	1520	28930	30520	1590	30460	30950	490	29220	30130	910
Ethyl acetate	0.398	—	—	—	28930	30540	1610	30460	30980	520	29210	30160	950
Methyl acetate	0.444	—	—	—	28950	30550	1600	30420	30980	560	29200	30180	980
Butanol	0.540	29760	31350	1590	28900	30530	1630	30330	30920	590	29110	30180	1070
Ethanol	0.582	29760	31350	1590	28880	30550	1670	30370	30950	580	29120	30220	1100
Methanol	0.616	—	—	—	28840	30560	1720	30380	30960	580	29110	30270	1160

while σ_f^m is that of the strongest or the most clearly observable peaks of fluorescence spectra, and are shown schematically in Fig. 1.

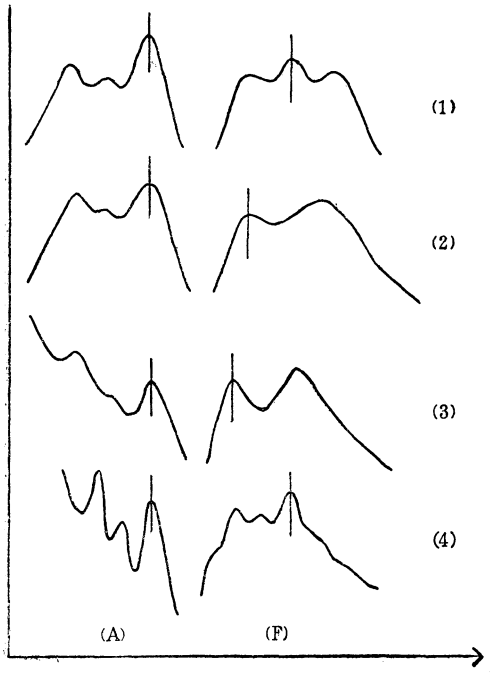

Fig. 1. Schematic diagrams of absorption and fluorescence spectra, the vertical lines showing the chosen peaks. (A), absorption (F), fluorescence; (1), β naphthylmethylether; (2), β naphthol; (3), β naphthol; (4), β methylnaphthalene.

For the comparison of the theory developed in II with the experimental results, the shifts of O–O bands should be employed, but it is very difficult to determine them exactly especially for such large molecules as naphthols. Hence it is necessary at first to consider the difference between O–O band on one hand and σ_a^m, σ_f^m on the other.

When σ_f^m and σ_a^m are used instead of O–O bands, equation (4) can easily be rewritten as follows.

$-hc(\sigma_f^m-\sigma_a^m)=hc(\delta\sigma_f+\delta\sigma_a)+\{$right hand side of (4)$\}$ (8) where $\delta\sigma_f$ and $\delta\sigma_a$ are the wave number differences between O–O bands and the peaks in the fluorescence and absorption spectra, respectively. Now the experimental results show that the solvent shifts of spectra take place as a whole; in other words, both the fluorescence and absorption spectra have respectively the same shape with the same interval between peaks irrespective of the solvents employed. Hence it may be allowed to put $(\delta\sigma_f+\delta\sigma_a)=$const. for one solute molecule.

Next, the theoretical formula (4) can be made much simpler for naphthalene derivatives, because the first term is far greater than the remaining terms in the order of magnitude. Thus a rough estimation for the given solvents mentioned in III, gives,

first term $\lesssim 10^{-13}-10^{-14}$ erg.

second term $\lesssim 10^{-17}-18^{-18}$ erg.

Therefore eq. (8) becomes

$$-hc(\sigma_f^m-\sigma_f^m)\cong\text{Const.}+\left[\frac{2(D-1)}{2D+1}-\frac{2(n^2-1)}{2n^2+1}\right]\times\frac{(\vec{\mu}_e-\vec{\mu}_g)^2}{a^3} \quad (9)$$

Lastly the second term of (7) must be estimated when the hydrogen bond is formed between solute and solvent molecules. As reported already[6], we have compared the

fluorescence and absorption spectra of α-, β-naphthols in pure n-hexane on one hand and in n-hexane added with acetic acid esters on the other and confirmed that $\Delta\sigma_f$ and $\Delta\sigma_a$ due to hydrogen bonding is nearly equal. Hence second term in (7) in the present case may be neglected in comparison with the first term.

After all, the theory can be tested by (9) using the data tabulated in Table I. The result is that (9) is fairly well satisfied by all the experimental data as shown in Fig. 2.

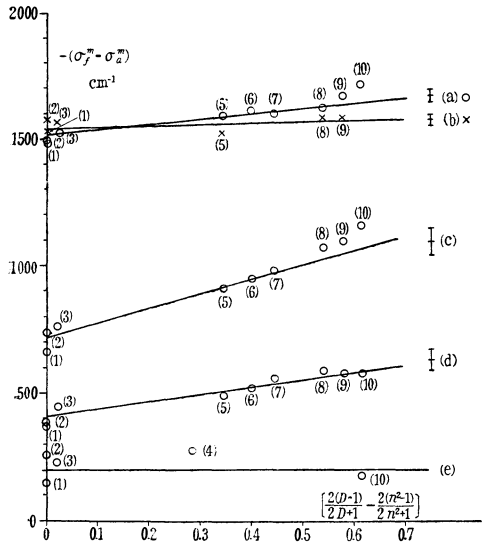

Fig. 2. $(\sigma_f^m-\sigma_a^m)\sim\left[\frac{2(D-1)}{2D+1}-\frac{2(n^2-1)}{2n^2+1}\right]$

relation for naphthalene derivatives and anthracene*.

Solutes: (a), β-naphthylmethylether; (b), β-methylnaphthalene; (c), β-naphthol; α-naphthol; (e) anthracene.

Solvents; (1), n-hexane; (2), benzene; (3), toluene; (4) chlorobenzene; (5), butylacetate; (6), ethylacetate; (7), methylacetate; (8), butanol; (9), ethanol; (10), methanol.

The veitical lines in the right hand of figure indicate the ranges of probable errors,

* Data from Ref. (9).

Thus it can be concluded that the orientation polarization is in fact the most prominent factor for the difference of solvent shifts of fluorescence and absorption.

The values for alcohols seem to show some systematic deviations, but the experimental errors are too large for us to say definitely.

From the inclination of these lines, $\frac{(\vec{\mu}_e-\vec{\mu}_g)^2}{a^3}$ can be calculated as follows:

β-naphthol: $\sim 9\times10^{-14}$ erg.
α-naphthol: $\sim 5\times10^{-14}$ erg.
β-naphthyl methyl ether: $\sim 3\times10^{-14}$ erg.
β-methylnaphthalene: $\lesssim 4\times10^{-15}$ erg.

If one puts $\vec{\mu}_e-\vec{\mu}_g\sim 0.5$ and a$\sim$3 Å, then $\frac{(\vec{\mu}_e-\vec{\mu}_g)^2}{a^3}$ becomes ca. 10^{-14} erg, which is near the value for β-naphthyl methyl ether. Thus for this compound the dipolemoment in the excited state is about 0.5 D. larger than in the ground state.

Of course such an evaluation would be valuable only for the estimation of the order of magnitude.

Next some discussions will be given about the value of $\vec{\mu}_e-\vec{\mu}_g$. No doubt this difference originates from π electron systems and most certainly the electron migration from substituent may be predominant in determing this value. Hence it may be reasonable to put in the first approximation,

$$\vec{\mu}_e-\vec{\mu}_g\simeq\vec{\mu}_e^{mig}-\vec{\mu}_g^{mig}$$

The effect of hydrogen bonding in the case of α-, β-naphthols would not alter the relative order,

$$(\vec{\mu}_e-\vec{\mu}_g)^{mig}_{\beta\text{-naphthol}}>(\vec{\mu}_e-\vec{\mu}_g)^{mig}_{\alpha\text{-naphthol}}$$

Thus the increments of dipolemoments in the excited state due to the enhanced electron migration are in the order of magnitude, 0.5–1 D. for β-naphthyl methyl ether and α-, β-naphthols.

It is to be noted here that a theoretical computation of migration dipole in the ground and excited state of phenol was done by Baba[7] using the theory of Sklar[8]. The increment $(\mu_e^{mig}-\mu_g^{mig})$ which he obtained is 0.3 D., which shows that the contribution of electron migration to the dipole increase in the excited state can be fairly large.

The value for β-methylnaphthalene, $\lesssim 4\times10^{-15}$ erg. given above is only provisional as an upper limit, and it is certain that this compound has much smaller dipole increment in the excited state as compared with those of naphthols and β-naphthyl methyl ether.

It may be expected from the present theory, that a nonpolar molecule with high symmetry such as anthracene does not show any effect as shown above.

In fact, the data reported by Sambursky and Wolfsohn[9], as plotted in Fig. 2, do not show any such effect. They interpreted the

7) H. Baba, *Monograph Ser. Research Inst. Applied Electricity Hokkaido Univ.*, No. 4, 61 (1954).
8) A.L. Sklar, *J. Chem. Phys.*, 7, 984 (1939).
9) S. Sambursky and Wolfsohn, *Trans. Far. Soc.*, **36**, 427 (1940).

difference of solvent shifts in fluorescence and absorption spectra as due to the dipole-moment produced in the excited anthracene molecule, but it is quite certain from the present analysis that their conclusion is wrong.

As to somewhat larger deviations from the straight line, they may perhaps be due to some short range interaction specific to each solvent molecule. An anthracene molecule is larger than a naphthalene molecule, and for larger molecules even when they have symmetrical structure with a uniform charge distribution for the entire molecule, some short range interaction may arise from the local charge unbalance which may be produced in the excited state.

The results obtained by Lippert[2] for 4-dimethylamino-4′-nitrostilbene, 4-dimethylamino-4′-cyanostilbene and dimethylnaphthenrhodine, show some deviations, rather larger than ours, from the theoretical line. He has recently made a quite different attack on the problem and confirmed that his results are quite reasonable[10].

One of the authors (N. M.) wishes to express his thanks to Mr. T. Yamaguchi of Osaka University for his discussions.

10) E. Lippert, *Z. physiked Chem.*, N.F., 6, 125, (1956).

Summary

A general formula for the difference of solvent shifts of fluorescence and absorption spectra in the approximation of long range dipolar interaction was derived using Ooshika's theory of light absorption in solution.

Measurements of fluorescence and absorption spectra of some naphthalene derivatives in various organic solvents were undertaken, and the data were analysed by the theoretical formula. The formula reproduces the experimental data satisfactorily, and from this fact it was concluded that the most predominant factor which determines the difference of solvent shifts of fluorescence and absorption spectra of these molecules is the interaction energy between solute and solvent molecules due to orientation polarization. The incremental values of dipolemoments in the excited state were estimated, and those for α-, β-naphthols and β-naphthyl methyl ether were interpreted as due to the increase of electron migration from the substituent in the excited state.

Institute of Polytechnics, Osaka City University, Osaka

The Synthesis of o,o'-Dihydroxydiphenyldiacetylene

By Yoshinobu ODAIRA

(Received October 13, 1955)

The synthesis of *o,o*-dihydroxydiphenyldiacetylene has been carried out along the following schema.

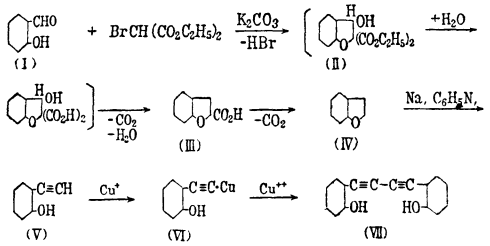

Coumarone (IV) was prepared by a similar method to Tanaka's[1]. Diethyl 3-hydroxycoumarone-2, 2'-dicarboxylate (II), obtained by condensing salicylaldehyde with diethyl bromomalonate in the presence of potassium carbonate, was saponified to coumarylic acid (III). The treatment of this acid (III) with a small amount of copper-chromite in quinoline gave coumarone (IV) with good yield.

Although *o*-hydroxyphenylacetylene (V) was prepared by Reichstein[2] previously from 3-bromocoumarone with Grignard's reagent, the yield was not good. Then Grey's method[3] has been applied to this reaction and the compound (V) has been obtained with good yield. The cleavage of its ether ring with sodium-pyridine under slow current of nitrogen gas gave a compound, having guaiacol-like odour. This has been identified with *o*-hydroxyphenylacetylene by its refractive index and its 3, 5-dinitro-benzoate.

The oxidative condensation of hydroxy-

1) S. Tanaka, *J. Chem. Soc. Japan*, 72, 307 (1951).

2) Reichstein, *Helv. Chim. Acta.*, 20, 892 (1951).

3) Grey, *Monatsch.*, 80, 790 (1949).

phenylacetylene, as described in the experimental part, gave *o,o'*-dihydroxydiphenyldiacetylene (VII), the identity of which was established by elementary analysis and infrared absorption spectra measurement. (see Figs. 1 and 2)

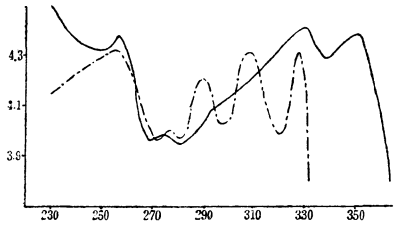

Fig. 1. Ultra-violet absorption spectra of *o,o*-dihydroxydiphenyldiacetylene (—) and diphenyldiacetylene (—·—)[4], all in ethanol solution.

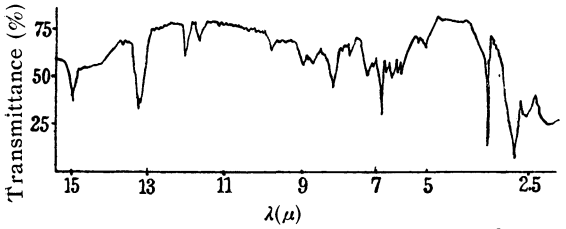

Fig. 2. Infra-red absorption spectrum of *o,o'*-dihydroxydiphenyldiacetylene.

Since the compound (VII) has remained unchanged for several months at room temperature, it seems to be fairly stable.

Experimental

o-Hydroxyphenylacetylene (V).—A mixture of coumarone (5.9 g.), metallic sodium (3.5 g.) and pyridine (5.4 g.) was heated under reflux in an atmosphere of nitrogen gas at 190°C for four hours. After cooling, pyridine (20 cc.) and water (30 cc.) were added slowly with stirring. The reaction mixture was extracted with ether, weakly acidified with dilute hydrochloric acid under cooling with ice, extracted with ether again and then the extract was washed with water. After evaporation, the red residual oil was twice distilled under reduced pressure with a stream of dry nitrogen gas, giving *o*-hydroxyphenylacetylene (V) as a colorless oil (3.2 g, 54.2%), b.p. 82–84°C/20 mm., n_D^{20} 1.5818. The 3,5-dinitrobenzoate had m.p. 169°C. V. Grey[3] cites m.p. 169°C for this compound.

o-Hydroxyphenylacetylene-cuprous salt (VI).—*o*-Hydroxyphenylacetylene (1.8 g.) in ethanol (140 cc.) was added with stirring to a solution of Ilosvay's reagent prepared from hydroxylamine hydrochloride (22.5 g.), copper sulfate (7.5 g.) and aqueous ammonia (28%, 30 cc.). After being allowed to stand overnight, the yellow precipitate was filtered and washed with ethanol (30 cc.).

o, o'-Dihydroxydiphenyldiacetylene (VII).—The cuprous acetylide (VI), prepared from the compound (V) (1.8 g.), was suspended in water (115 cc.), and then cupric chloride (115 cc.) was added gradually to the suspension with stirring for six hours. The reaction mixture was filtered and the filtrate was extracted with ether. The extract was washed with water and finally dried over anhydrous sodium sulfate. After evaporation, a crystalline solid was isolated. By recrystallisation from acetic acid (75%) with charcoal, white needle crystals, which melted at 143°C, were obtained, and weighed 324 mg. (18%).

Anal. Found: C, 81.65; H, 4.41. Calcd. for $C_{16}H_{12}O_2$: C, 82.6; H, 4.43%. Molecular weight Found: 227; Calcd.: 234.

I am greatly indebted to Professor Munio Kotake for his constant attention to my work.

Department of Applied Chemistry,
Faculty of Engineering,
Osaka University, Osaka

4) M. Nakagawa, *J. Chem. Soc. Japan*, **72**, 561 (1951).

*Rheological Properties of Some Polymerized Oils**

By Tsurutaro NAKAGAWA and Manabu SENŌ

(Received December 9, 1955)

Introduction

It has long been known that some colloidal or polymeric solutions exhibit the structural viscosity, the thread-forming property or the Weissenberg effect, and various authors have attributed these properties to some "elastic" nature of the liquid.

Some drying oils, e.g., tung oil or linseed oil get rapidly polymerized when heated to about 250°C and become not only viscous but also elastic; they actually turn back elastically when stirred in a vessel; they show a marked thread-forming ability and the liquid-thread springs back elastically when it snaps. These elasto-viscous liquids are

still more peculiar in that they show obviously the Weissenberg effect; they "climb up" to a rotating rod which is dipped in them to several centimeters or more. When they undergo still more heating, polymerization proceeds to leave a rubber-like brittle solid.

It is intended, in this study, to obtain some relation between these rheological properties by measuring the dynamic visco-elasticity.

Experimental Procedure

Torsional Oscillation.—**(I)**[1,2,3].—If a cylinder (moment of inertia I g.·cm^2) is suspended from a wire coaxially in the other fixed cylinder which is filled with a visco-elastic liquid (whose resistance R, elastance E), and a torsional oscillation of the amplitude Θ_0

$$\Theta=\Theta_0 e^{i\omega t} \tag{1}$$

is applied at the top of the suspension wire whose torsion constant is k dyn.·cm., the complex amplitude ratio $\boldsymbol{m}$ is given by

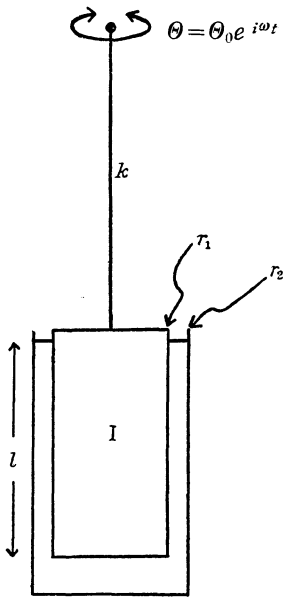

Fig. 1. Top-drive coaxial rheometer.

$$\boldsymbol{m}=\frac{\boldsymbol{A}}{\Theta_0}=\frac{k}{(k+E-\omega^2 I)+i\omega R},$$

$$\theta=\boldsymbol{A}e^{i\omega t}=Ae^{i(\omega t-\phi)} \tag{2}$$

where l, r_1, and r_2 are the length of the immersed portion of the internal cylinder, the radii of the

So that if the amplitude ratio $m=|\boldsymbol{A}/\Theta_0|=A/\Theta_0$ which is the ratio of the amplitude of the motion θ of the inner cylinder to that of the top end of the suspension wire, and the phase angle $\phi=-\mathrm{Arg}(\boldsymbol{A}/\Theta_0)$ by which the inner cylinder lags the top end of the wire are experimentally observed, the complex quantity $\boldsymbol{m}$ is determined as $\boldsymbol{m}=me^{-i\phi}$, and R and E are known from (2) or from

$$\begin{cases} R=\dfrac{kT\sin\phi}{2\pi m} \\ E=k\left(\dfrac{\cos\phi}{m}-1\right)+\dfrac{4\pi^2 I}{T^2} \end{cases} \tag{3}$$

where T is the period of oscillation ($\omega=2\pi\nu=2\pi/T$). The dynamic viscosity η and the dynamic rigidity G are calculated by the conventional formula

$$\begin{cases} \eta=\dfrac{R}{4\pi l}\left(\dfrac{1}{r_1^2}-\dfrac{1}{r_2^2}\right) \text{ poises} \\ G=\dfrac{E}{4\pi l}\left(\dfrac{1}{r_1^2}-\dfrac{1}{r_2^2}\right) \text{ dyn./cm}^2 \end{cases} \tag{4}$$

internal and the external cylinder respectively.

(II).—The scheme of analysing the visco-elasticity of liquid outlined above is inexact from the theoretical point of view. Recently several authors[4,5,6] have developed the rigorous treatment of this type rheometer. Among them S. Oka[6] proposed a rigorous method of determining the visco-elastic constants by the same top-drive oscillatory device as that described here. According to the theory the complex dynamic rigidity G^* of the liquid studied is obtained as a root of a quadratic equation

$$(B_0+B_1)G^{*2}-\{\mu B_1-(B_2+B_3)\rho\omega^2 r_1^2\}G^* -B_3\mu\rho\omega^2 r_1^2=0 \tag{5}$$

where ρ is the density and μ is a quantity which involves the observable amplitude ratio and the phase difference

$$\mu=\frac{1}{2\pi l r_1^2}\left(I\omega^2-k+\frac{k}{\boldsymbol{m}}\right), \qquad \boldsymbol{m}=me^{-i\phi} \tag{6}$$

and the coefficients B_0, B_1, B_2,.....are the quantities relating only to the geometry of the vessel, viz. $x=(r_2-r_1)/r_1$ (which must be less than 1)

$$\begin{cases} B_0=\dfrac{1+(1+x)^2}{2(1+x)} \\ B_1=\dfrac{x(2+x)}{2(1+x)} \\ B_2=\dfrac{1}{16}\left\{-4(1+x)\ln(1+x)+4x-6x^2+2x^3-\dfrac{3x^4}{1+x}\right\} \\ B_3=\dfrac{1}{16}\left\{4(1+x)\ln(1+x)-4x-2x^2-2x^3+\dfrac{x^4}{1+x}\right\} \end{cases} \tag{7}$$

If G^* is known from Eq. (5), its real and imaginary

* Part of this paper was read before the Third Rheological Meeting at Kyoto, Japan, Nov., 1953.

1) T. Nakagawa, *J. Chem. Soc. Japan* (in Japanese), **72**, 759 (1951).

2) T. Nakagawa, This Bulletin, **24**, 191 (1951).

3) T. Nakagawa, ibid., **25**, 93 (1952).

4) J.G. Oldroyd et al., *Proc. Phys. Soc.* B, **64**, 44 (1951); *Quart. Journ. Mech. and Applied Math.*, **4**, 271 (1951).

5) H. Markovitz et al., *Rev. Sci. Instr.*, **23**, 430 (1952); *J. Appl. Phys.*, **23**, 1070 (1952).

6) S. Oka et al., *Bull. Kobayashi Inst. Phys. Res.*, **3**, 9, 17 (1953) (in Japanese).

* In our unpublished work on the concentrated carbon-black suspensions, a distorted ellipse which had without doubt resulted from the non-linearity of the material itself was obtained (cf. Fig. 6).

parts give the usual dynamic rigidity G and the dynamic viscosity η by the relation

$$G^*=G+i\omega\eta \tag{8}$$

It goes without saying that the rigorous scheme (II) involves the scheme (I) as the limiting case when $\omega\to 0$.

Lissajous' Figure Method for the Determination of m and ϕ.—Whether the approximate analysis (I) or the rigorous treatment (II) is applied, two experimentally determined quantities m and ϕ need to be measured.

When two simple harmonic motions whose directions of oscillation are at right angles to one another are composed, the resulting Lissajous' figure is an ellipse as long as they are of the equal period (cf. Fig. 2). Let the area of the ellipse be

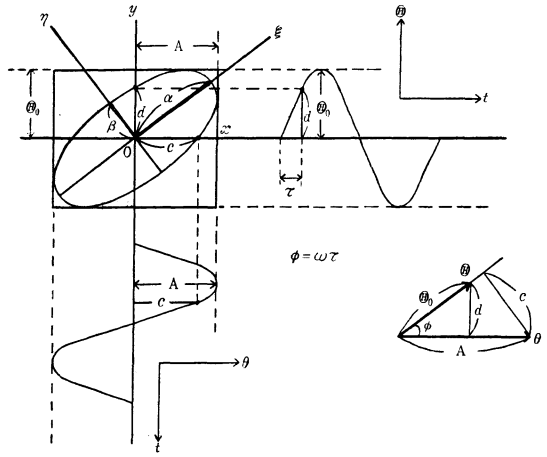

Fig. 2. Lissajous' figure.

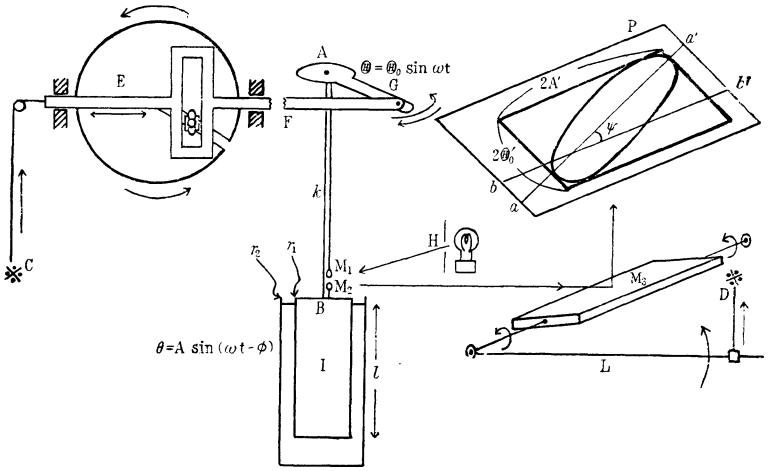

Fig. 3. General assembly of the apparatus.

(S) and that of the rectangle tangent to the ellipse be $[S]$. Then the next relation is known to hold.

$$\sin\phi=\frac{4}{\pi}\cdot\frac{(S)}{[S]}=1.273\times\frac{(S)}{[S]} \tag{9}$$

Eq. (9) gives a means of computing the phase angle ϕ by the planimetry. Since ϕ is an angle which satisfies

$$0\leqq\phi\leqq\pi,$$

two values of ϕ are generally obtained from Eq. (9), and they are discriminated as follows from the simple consideration.

1°. When the major axis of the ellipse finds itself in the first quadrant of the θ-Θ plane as in Fig. 2, ϕ is an angle of the first quadrant, that is

$$0\leqq\phi\leqq\frac{\pi}{2}$$

2°. When the major axis is in the second quadrant, ϕ is

$$\frac{\pi}{2}\leqq\phi\leqq\pi$$

and if ϕ' satisfying Eq. (9) and being smaller than $\pi/2$ is determined, the true phase angle ϕ is obtained from $\phi=\pi-\phi'$. From 1° and 2° it is possible to determine to what quadrant the angle ϕ belongs by inspecting the direction of the Lissajous' ellipse.

As is known from Fig. 2, it is also possible to determine ϕ from

$$\sin\phi=c/A=d/\Theta_0$$

The apparatus for practising the above-stated is sketched in Fig. 3. The whole apparatus consists of (1) the driving device and (2) the measuring system.

(1) A driving motor (1/16–1/20 HP, 1500 rpm) and a reduction gear train can produce several low speed rotations ranging from 20 rpm to 0.05 rpm by changing the combination of the gears. Use of a friction table and a movable friction wheel makes it possible to change the motion speed continuously. Rotational motion from the friction desk is changed into the oscillatory motion at the top A of the suspension wire by the eccentric coupling mechanism E and levers F (33 cm.) and G (28.5 cm.). Eccentricity on E is adjustable along its radius between 0 and 5 cm. It is thus possible to obtain the driving oscillation whose period can be changed continuously from about 0.5 seconds to about thirty minutes and whose

amplitude Θ_0 is changeable between 0–10 degrees. It was, of course, confirmed beforehand that the motion is harmonic. The observed Θ-t curve is correctly sinusoidal. (The oscillation of the internal cylinder, on the other hand, is not always harmonic. In the case of Fig. 6, it is known from the Fourier analysis that the contribution from the over-tones reaches several per cent.)

(2) The measuring system is constructed as follows. In order to observe the motion of the internal cylinder, a small galvanometer mirror M_2 is attached to a chuck B by which the lower end of the suspension wire is connected to the inner cylinder; and in front of the mirror M_2 a strip mirror M_3 (3 cm. × 15 cm. × 3 mm.) is placed at the angle 45° to the beam of light from M_2, and is oscillated in phase of the driving motion $\Theta=\Theta_0 \sin \omega t$ by a lever L (10–40 cm., adjustable) which is connected to the oscillation mechanism E by a cord C-D. A Lissajous' figure is thus traced on a photographic plate or paper P; a proper lens system should be used in order to focus the image of a pin-hole H onto the plate P.

Experimental determination of the amplitude ratio m is a little complicated. It is incorrect to compute m directly as A'/Θ_0' from the observed Lissajous' figure, because the transverse deflection A' and the vertical deflection Θ_0' on the plate are of different scale by reason of the different paths as is plain from Fig. 3. One way for evaluating m is to use another mirror M_1 which is attached to the lower end of a long rod connected to the upper end of the suspension wire. As M_1 moves in phase of the driving oscillation $\Theta_0 \sin \omega t$, the Lissajous' figure obtained from M_1 is an oblique line aa'. If then the strip mirror M_3 is kept in position, a horizontal line bb' is obtained and m is determined as follows

$$m=\frac{A}{\Theta_0}=\frac{A'}{\Theta_0' \cdot f}=\frac{A'}{\Theta_0'} \cdot \tan \psi \qquad (11)$$

$$f=\cot \psi \qquad (12)$$

where A', Θ_0', and ψ are the quantities illustrated in Fig. 3. A' and Θ_0' are respectively side lengths of the rectangle in contact with the ellipse which is easily drawn if the base line bb' is obtained.

It goes without saying that the determination of ϕ is not influenced by the difference of the scale unit of the two axes of coordinates as is understood from Eqs. (9) and (10) and Fig. 2. This is the same in the case of the discrimination 1° and 2°.

Torsion constant k and the moment of inertia I are determined from the observation of the period of the free torsional oscillation[1,2,3]. It should of course be kept in mind that k changes with the length of a wire.

The experimental condition is as follows.

Internal cylinder (made of brass): $r_1=2.02$ cm., Height: 15.0 cm., $I=3.28\times10^3$ g.·cm.^{2} (mass: 1608.6 g.)

External cylinder: $r_2=2.51$ cm., Height: 18.14 cm.

Immersion depth l: 14.5–15.0 cm. (to be observed in each run of measurement). End-effect of the internal cylinder was neglected.

Torsion constant k: one wire is properly selected from the piano wires or drill rods tabulated below (Table I) according to the consistency of the liquid being tested. Wire length A-B (about 67 cm, cf. Fig. 3) is measured in each run of the experiment and k is calibrated.

TABLE I

SUSPENSION WIRES USED AND THEIR TORSION CONSTANT

Wire or rod	Length (cm.)	k (dyn.· cm.)
0.30 mm. dia. piano-wire	67.40	9.96×10^2
0.44 mm. dia. piano-wire	67.53	4.44×10^3
0.60 mm. dia. piano-wire	67.29	1.475×10^4
0.80 mm. dia. piano-wire	67.11	4.745×10^4
1.0 mm. dia. drill-rod	67.27	1.258×10^5

Θ_0, amplitude of the driving oscillation: 4–6 degrees of angle. A, amplitude of the forced oscillation of the internal cylinder is designed to be less than 2 degrees of angle, so that the maximum angle of shear γ (cf. Fig. 4) of the sample itself at the

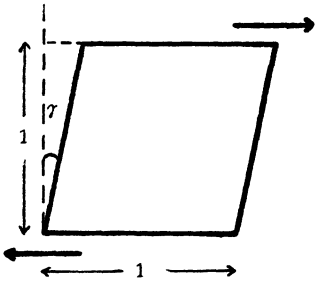

Fig. 4. Shear straining of a unit cube.

wall of the internal cylinder is known to be less than about 11 degrees (cf. Eq. (23)). It may therefore be possible to say that the measurement is done under the condition of small deformation. Temperature control is made by a water thermostat in which the external cup is immersed. For the sake of securing the uniform temperature of the whole measuring vessel, the thermostat is covered by a plate from which only the suspen-

TABLE II

SAMPLES TESTED AND THEIR GENERAL PROPERTIES

Sample	Remark
No. 0	The most highly polymerized, sticky, visco-elastic matter with strong thread-forming ability.
No. 1	Moderately polymerized, thread forming, highly viscous liquid.
No. 2	〃
No. 3	Less thread-forming liquid of lower viscosity without elastic nature

sion wire and the mirror M_2 are led outwards. Measurement was done by changing temperature and frequency as follows.

Temperature: 20°–60°C

Period of oscillation: 10–300 seconds

Samples.—Four sample oils listed below (Table II) were made from the thermal polymerization (above 200°C) of linseed oil, and subjected to test.

Results and Discussion

The rigorous scheme of analysis (II) of the observed results, of which description was made in the previous section, was compared with the simple method (I) which has since been used by the author, and it proved that, in such low frequencies as were used here, the difference between the two methods was negligible. In the present study all the data were therefore analysed along the simple scheme (I).

Amplitude Effect.—Our whole procedure of analysing the observed quantities, including the scheme (I) and (II), is based on the assumption that the shear stress S and the shear strain γ satisfy the generalized Hooke's law

$$S=G^*\gamma \qquad (13)$$

in which complex rigidity G^* should not depend upon S and γ, while it is a function of frequency. If the linearity relation (13) does not hold, various non-linear behaviors are expected to be observed; e.g., Lissajous' figure will probably deviate from ellipse, or the amplitude dependence of the dynamic visco-elasticity will be notable.

In all the Lissajous' figures obtained, deviation from ellipticity was not perceptible (cf. Fig. 5)*.

Moreover, it is possible to test experimentally the influence of amplitude on the dynamic properties by keeping the period T constant and by changing the eccentricity at the cam E. As to the amplitude effect the experimental result is summarized in Fig. 7 and Fig. 8, in which $\gamma_{\max.r=r_1}$ is the amplitude of the shear strain at the wall of the internal cylinder[7] (cf. Fig. 4)

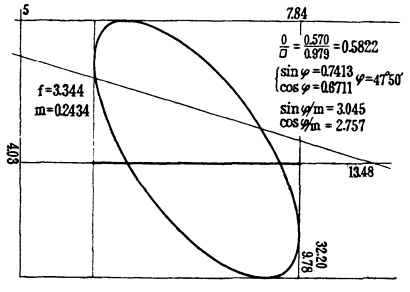

Fig. 5. A sample photograph of the observed Lissajous' figure. (linear visco-elasticity)

7) Th. Schwedoff, *J. de Phys.*, [2], 8, 341 (1889).

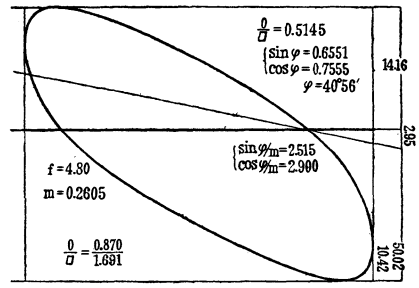

Fig. 6. A sample photograph of the distorted Lissajous' figure. (non-linear visco-elasticity)

$$\gamma_{\max.r=r_1}=\left[\frac{2Ar_1^2r_2^2}{(r_2^2-r_1^2)r^2}\right]_{r=r_1}=\frac{2Ar_2^2}{(r_2^2-r_1^2)}. \qquad (14)$$

A is the amplitude of the oscillation of the internal cylinder, and in the present case $\gamma_{\max.r=r_1}=5.67\cdot A$ ($r_1=2.02$ cm., $r_2=2.51$ cm.). $\sin\phi/m$ and $\cos\phi/m$ are the quantities corresponding to viscosity and elasticity respectively, if the period T is kept constant (cf. Eqs. (5), (6)). Three series I, II and III were tested under the following condition using the most sticky varnish No. 0 whose rheological details are shown in Fig 9 (cf. Table III).

TABLE III

EXPERIMENTAL CONDITION ADOPTED FOR THE TEST OF THE AMPLITUDE EFFECT

Oil	Series	Temperature (°C)	Period of oscillation (sec.)
No. 0	I	20	50
	II	30	20
	III	20	20

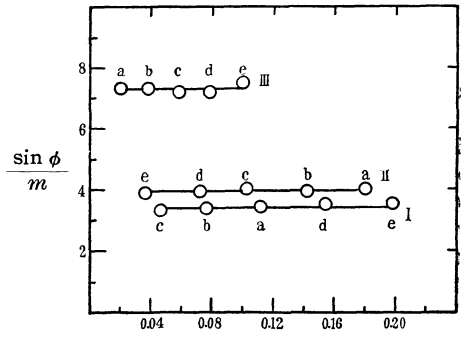

Fig. 7. Amplitude dependence of dynamic viscosity. (No. 0 varnish)

In each series, measurement was done in the order $a\rightarrow b\rightarrow c\rightarrow d\rightarrow e$ in about six hours, that is, in II the sample first undergoes the largest straining and the other measurements are all carried out within a smaller shear strain; in III, on the other hand, the sample is subjected to a new and larger deformation in each run.

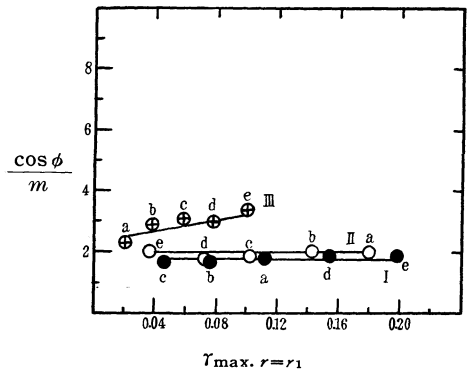

Fig. 8. Amplitude dependence of dynamic elasticity. (No. 0 varnish)

As is known from Figs. 7 and 8, effect of the amplitude on the dynamic viscosity and elasticity is null or slight within the amplitude region tested.

Since the dynamic viscosity is independent on the strain amplitude, it again ought to be independent on the amplitude of the strain velocity from the relations $\theta = Ae^{i\omega t}$, $\dot{\theta} = i\omega Ae^{i\omega t}$, and

$$\dot{\gamma}_{\max.r=r_1} = \frac{2\omega A r_2^2}{(r_2^2 - r_2^2)}. \qquad (15)$$

Visco-elasticity of these varnishes is therefore supposed to be nearly linear.

Series III shows a slight non-linearity, especially in the elastic property. Measurement is, in this series, started from the smallest strain, and the sample suffers a new larger deformation in each run of measurement. No. 0 varnish has, as will be seen later, a viscosity of 10^3 poises and an elastic constant of 10^2 dyn./cm^2 at 20°C of temperature. And such a sticky sol as this generally has a tendency to solidify into a gel-like structure in the course of settling. It will be attributed to this gel-like nature that the elastic constant d(stress)/d(strain) increases with the increase of strain. Since it is expected that this structure breaks down by agitation or straining, the non-linear property will be reduced when the measurement is done in the opposite direction (cf. Series II).

Frequency Dependence.—Frequency dependence of the dynamic viscosity and rigidity was tested under various conditions. The results are summarized in Figs. 9–12. Since it is confirmed in the previous section that no amplitude effect is observed, it will hereafter be possible to consider these data as those of Newtonian and Hookean nature.

Oil No. 0 (Fig. 9) is typically visco-elastic. Dynamic property-frequency curves show a marked dispersion; the dynamic viscosity decreases with the increase of frequency, and the dynamic rigidity increases markedly on the other hand. The lower the temperature, the stronger is the dispersion effect. These materials appear as if they are an elastic mass when handled by a sudden shock; they contract and turn back when freed after being agitated. The external work can, in spite of their fluid nature, be stored up as the elastic potential for a short time. This elastic potential energy gradually dissipates away as a viscous loss; they behave like a viscous fluid when they are treated gently. Varnish No. 0 actually exhibits this property, and Fig. 9 reflects this situation.

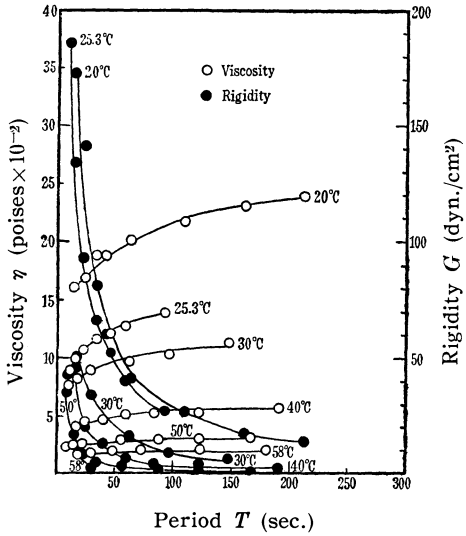

Fig. 9. Dynamic properties of varnish No. 0.

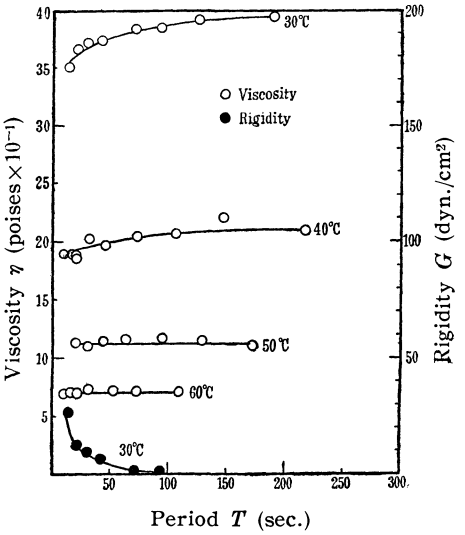

Fig. 10. Dynamic properties of varnish No. 1.

The varnish No. 0 is used as an adding agent in the printing ink manufacturing industry in order to control and improve the "printability" of inks. The peculiar rheological property of the oil No. 0 is supposed to have some influence upon printability.

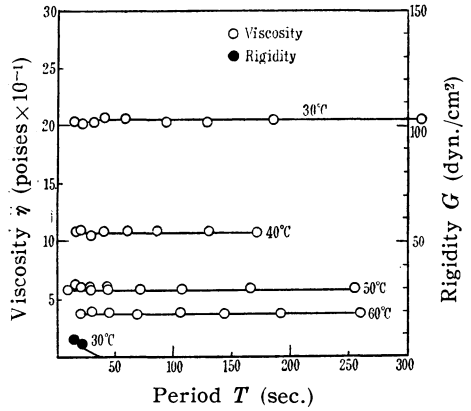

Fig. 11. Dynamic properties of varnish No. 2.

Varnishes No. 1 (Fig. 10) and No. 2 (Fig. 11) are viscous liquids, showing a slight elastic nature at a low temperature and high frequency; towards a very gentle handling they behave as simply viscous liquids. The oil No. 3 (Fig. 12) is a purely viscous liquid and shows no elasticity at any temperature and frequency tested. It is of course possible for this varnish to appear as elastic at a lower temperature and higher frequency than this. In fact, it may occur that these oils act not as simply viscous matter but as a visco-elastic medium between the rollers of a high-speed printing machine when they are used as a vehicle.

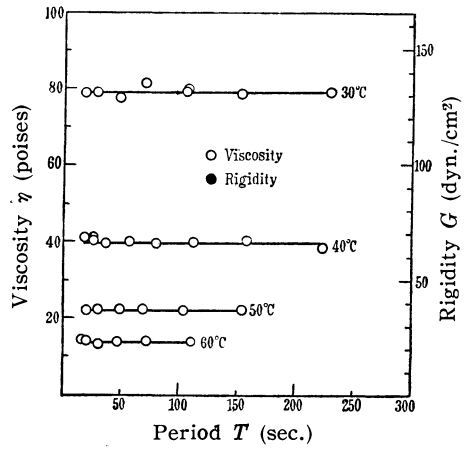

Fig. 12. Dynamic properties of varnish No. 3.

Returning to the varnish No. 0 (Fig. 9), the visco-elastic behavior at 25°C is a little peculiar. The elasticity at 25°C has a value nearly equal to that at 20°C, though the viscosity at 25°C is decreased in an ordinary manner. The fact is that the measurement at 25°C was carried out on the sample which was left and settled in the measuring vessel (between the inner and the external cylinder) for about a month. It is therefore possible for the oil to cause a gel-formation as was stated above, and this gel-formation may be ascribed to a weak network structure of the solute molecules formed in the sol by the secondary forces. On account of the elasticity from this network, the observed dynamic rigidity does not so markedly decrease by raising temperature from 20°C to 25°C. The dynamic viscosity, on the other hand, is supposed to come, in its considerable part, from the flow of the low molecular weight solvent molecules spread in such structure, and therefore it decreases considerably when temperature is raised.

Temperature Dependence.—When the frequency independent viscosities of the varnishes No. 1—No. 3 are plotted against the reciprocal absolute temperature, Fig. 13 is

$$\eta = Ae^{B/T} = Ae^{\Delta E/RT} \qquad (16)$$

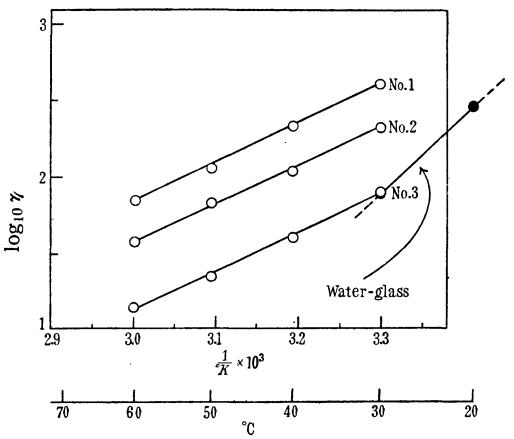

Fig. 13. Temperature dependence of viscosity.

obtained. These curves conform to the Andrade formula T is here the absolute temperature (not the period), and R the gas constant. The constants A and B or the apparent activation energy ΔE are calculated and tabulated in Table IV.

TABLE IV

CONSTANTS OF THE ANDRADE FORMULA

$\eta = Ae^{B/T} = Ae^{\Delta E/RT}$

Oil	A	$B\times10^{-3}$	ΔE (kcal.)
No. 1	2.33×10^{-6}	5.72	11.4
No. 2	1.03×10^{-6}	5.78	11.5
No. 3	2.12×10^{-7}	5.94	11.8

The value of B (or ΔE) is, when compared with those of the other materials[2], larger than those of the low molecular weight liquids (mercury, toluene, water), smaller than those of the highly associated liquids (glass, rosin, tar-pitch, glucose melt), and of the same order as those of asphalts and the glucose-melt at higher temperature. This is possible from the fact that these oils are polymerized to a certain degree.

It is noted that the apparent activation energy ΔE for the viscous flow has almost the same value as that of others in spite of the great difference of the absolute value of viscosity. One of the possible interpretations may be that at a certain stage of the thermal polymerization the growth of the polymer molecule itself does not occur, but the number of polymers simply increases.

Weissenberg Effect

In 1946–1948 K. Weissenberg[8,9,10] noted that some elastic liquids show a peculiar property to climb up to a rotating rod or ascend in a rotating pipe, and the various authors[8–14] have since developed the theoretical and experimental study of this phenomenon.

Our varnishes No. 0–No. 2, as seen in Figs. 9–11, show evidently an elastic property even in the very low frequencies like 0.1 cycles per second. It is therefore expected that the Weissenberg effect may appear even when a rod is slowly rotated in these oils. The result is illustrated in Fig. 14. A rod of 10 mm. dia., sunk to about 3 cm. depth, is rotated at the rate of two and three rotations per second, and the behavior of the liquids was observed. The experiment was made at the room temperature of about 20°C; the visco-elastic constants of the varnishes at 20°C can be estimated from Figs. 9–13.

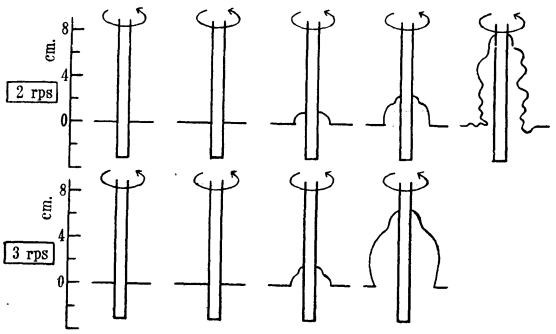

Fig. 14. Weissenberg effect.

In the varnish No. 3 no effect was observed at this temperature and revolution rate, and this situation corresponds to Fig. 12 where no elastic property is shown. The oils No. 2 and No. 1 evidently exhibit the Weissenberg effect, and the varnish No. 1 which is more sticky than No. 2 climbs up higher than No. 2. The effect is stronger when the rotation rate is increased; this is natural from the fact that the Weissenberg effect is concerned with the relaxation phenomena of liquid. In the oil No. 0 which is the most sticky and elastic of all, the effect is so strong that even at 2 rps the oil climbs up to 8 cm. or more in a very irregular manner like a towel which is squeezed.

For the sake of comparison, we tested a water-glass sample, which was previously confirmed to lack an elastic nature in these low frequencies[3]; and no effect was observed. From the falling-sphere method, its viscosity was estimated to be 290 poises at 20°C and it is the similar value to that of No. 3 or No. 2 at 20°C. It is therefore argued that the liquid is too fluid to climb up and that if the viscosity were increased the Weissenberg effect might appear. Water-glass was then cooled to 5°C of temperature in order to make it be more than 1000 poises of viscosity which is the same order of that of No. 1 varnish. The effect was still nothing. As has been discussed above, viscosity alone is not enough to cause the Weissenberg effect however viscous a liquid may be.

Summary

(1) A method for measuring the dynamic visco-elasticity of liquid by the torsional oscillation is described.

(2) The visco-elastic oils produced by the thermal polymerization of linseed oil to various degrees were studied by this rheometer.

(3) The amplitude effect of the dynamic properties was negligible; so that these materials are supposed to be linear in their visco-elastic behavior.

(4) The dynamic visco-elasticity of these oils was measured in the very low frequency region (period: 10 seconds–5 minutes).

(5) The temperature dependence of the dynamic viscosity was discussed.

(6) Weissenberg effect of these oils was tested in a qualitative way.

8) K. Weissenberg, *Nature*, **159**, 310 (1947).
9) S.M. Freeman and K. Weissenberg, *Nature*, **161**, 324 (1948).
10) S.M. Freeman and K. Weissenberg, *Nature*, **162**, 320 (1948).
11) M. Reiner, "Deformation and Flow", H.K. Lewis, London (1949).
12) M. Mooney, *J. Appl. Phys.*, **24**, 675 (1953).
13) F.J. Padden and T.W. DeWitt, *J. Appl. Phys.*, **25**, 1086 (1954).
14) M. Yamamoto, *Busseiron Kenkyu*, No. 78, 51 (1954) (in Japanese).

The authors hereby express their thanks to Prof. H. Akamatu for his interest and leadership in this investigation. All the samples of the polymerized oils used in this program were furnished through the kindness of Mr. T. Enya and Mr. I. Ishizu of the Dainippon Printing Ink Manufacturing Co. It is also a pleasure to acknowledge the assistance of Mr. S. Kojima who built the apparatus. This work was supported in part by the Scientific Research Grant from the Ministry of Education.

Department of Chemistry, Faculty of Science, The University of Tokyo
Hongo, Tokyo

Studies on the Infrared Spectra of Ephedrine and Related Compounds. II. Infrared Spectra of Diastereoisomeric Ephedrines in 3 Micron Region

By Tokunosuke KANZAWA

(Received January 11, 1956)

In the preceding paper[1] the present author showed that the infrared spectra of dilute carbon tetrachloride solutions of ephedrines and related compounds in 3 μ region were useful for the discrimination between diastereoisomers. However, there remain some problems unsolved. For example, the questions why there appear always two bands, sharp and broad, and which of OH and NH groups participates in hydrogen bond formation should be answered. Moreover, the reasons why the frequency difference ($\Delta\nu$) between the sharp band and the broad one (150–238 cm.$^{-1}$) is much larger than that found for 2,3-butanediol[2] (meso-form, 39 cm.$^{-1}$, *d*-form, 45 cm.$^{-1}$) and why $\Delta\nu$'s of pseudo compounds are always larger than those of normal ones also need explanation. In order to obtain information about these problems, the present experiments have been carried out on concentration dependence of ephedrines in carbon tetrachloride solution, solvent effect and the interaction with triethylamine. In connection with these, spectra of ethanolamine and 3-amino-2-butanol and the interaction between benzyl alcohol and triethylamine have been observed.

Experimental

Infrared Measurement.—The spectrophotometer used and its operating conditions were the same as described previously[1]. The spectra were taken with LiF prism at a room temperature adjusted at 25°C±2°. The accuracy of the measurement of wave numbers was ±2 cm^{-1}. Absorption cells of 0.056 cm. (NaCl windows), 0.3, 2.0 cm. (CaF_2 windows), 5 and 10 cm. (silica windows) in length were used. Since the silica cell absorbs 2.75 μ ray by 10–20% in transmission, it is unsuitable for the quantitative measurement of the free OH absorption at 2.76 μ.

Materials and Solvents.—Ephedrine and Ψ-ephedrine were of ther ecemic modification. The spectra of *dl*-ephedrine were quite in agreement with those of *l*-ephedrine. Ethanolamine, diethylamine and triethylamine were carefully distilled through a 40 cm., glass helix-packed column and dried over NaOH. 3-Amino-2-butanol was prepared after the method reported by Vanderbilt et al.[3] The product was liquid and did not crystallize after repeated distillation. Dickey et al.[4] reported that the product obtained by Vanderbilt's method was of erythro series and slightly impure. Benzyl alcohol was washed with sodium hydroxide solution, sodium bisulfite solution and water, dried over potassium carbonate and distilled under a reduced pressure.

Chloroform and carbon tetrachloride were purified as described previously. Benzene was purified by the usual method. Carbon disulfide was shaken with potassium permanganate solution, mercury, mercuric sulfate solution and water, dried over calcium chloride and distilled.

Preparation of Solutions.—On the preparation of solutions care was taken to avoid the contact with atomospheric moisture. It is worth noticing that fine crystallites happen to precipitate gradually in the carbon tetrachloride solution of ephedrines. It was feasible that the precipitation should occur as the concentration increased. Melting points of the precipitates were consistent with hydrochlorides of ephedrines. Although the reason why such precipitation occurred was not clarified, a slow chemical reaction might proceed

1) T. Kanzawa, This Bulletin, **29**, 398.
2) L.P. Kuhn, *J. Am. Chem. Soc.*, **74**, 2492 (1952).
3) B.H. Vanderbilt and H.B. Hans, *Ind. Eng. Chem.*, **32**, 34 (1940).
4) F.H. Dickey, W. Fickett and H.J. Lucas, *J. Am. Chem. Soc.*, **74**, 944 (1952).

in the carbon tetrachloride solution. The similar precipitation occurred in CS_2 solution of ephedrine already at a concentration of 0.03 M, but the precipitates were not identified. The spectra when precipitation occurred were omitted.

Experimental Results

A. Concentration Dependence of the Spectra in 3 μ Region

Ephedrine.—Concentration dependence of the absorption spectrum of ephedrine in 3 μ region is shown in Fig. 1-a. Over a concentration range from 0.001 to 0.01 M, the spectrum of the carbon tetrachloride solution remains almost unchanged in the relative intensities and positions of bands. On raising the concentration of ephedrine up to 0.21 M it is observed that the intensity of the sharp band component at 3619 cm.$^{-1}$ decreases, that of the broad band component at 3451 cm.$^{-1}$ increases, and besides a new band appears at 3321 cm.$^{-1}$. Such behavior of the concentration dependence will be explained as follows. As long as the concentration remains dilute, the bands due to hydrogen bonding are only from the intramolecular origin. It may be added that from the molecular

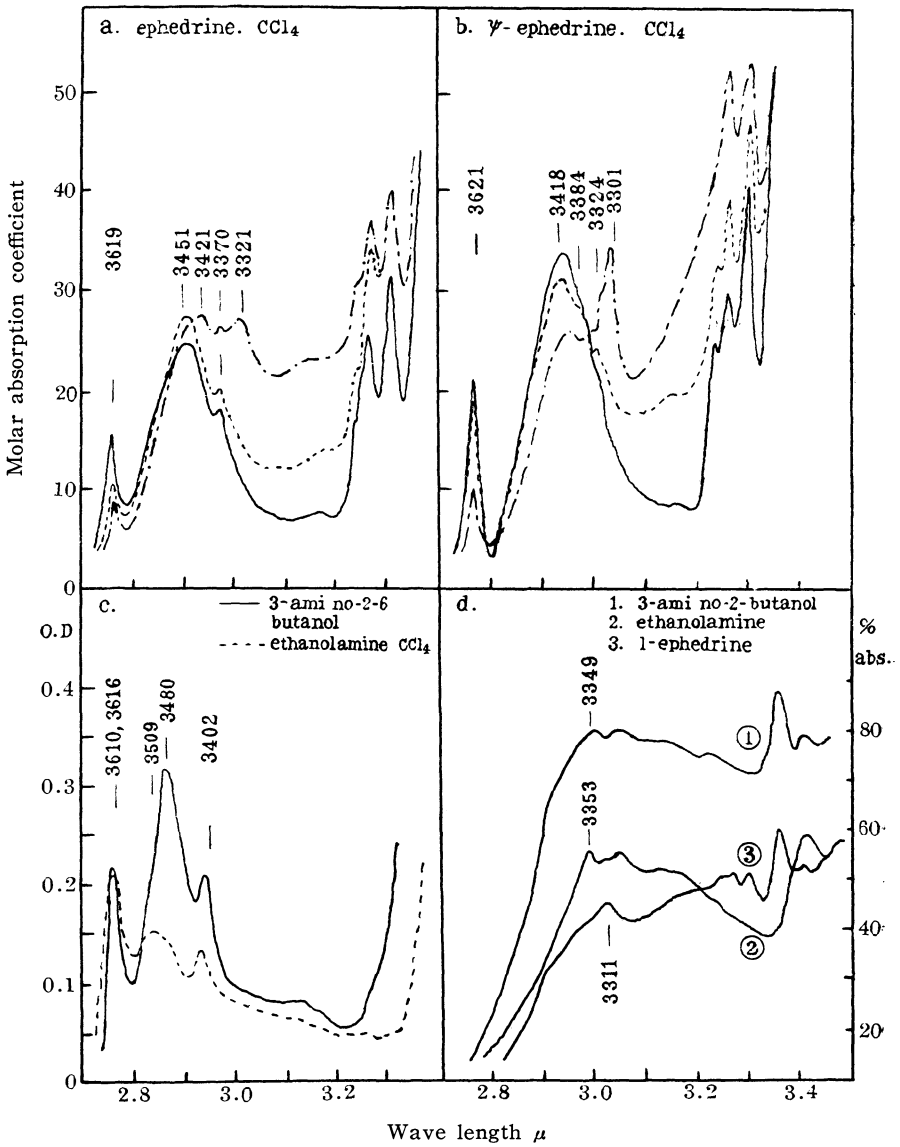

Fig. 1. Spectra of ephedrines, ethanolamine and 3-amino-2-butanol in 3 μ region.
a) ——— 0.0054 M/l.×2 cm., - - - - 0.075 M/l.×0.3 cm., —·— 0.21 M/l.×0.056 cm.
b) ——— 0.003 M/l.×2 cm., - - - - 0.05 M/l.×0.3 cm., —·— 0.11 M/l.×0.056 cm.
c) ——— ca. 0.005 M/l. d) liquid state. 0.01 mm. thick.

weight determination[5] the formation of ring dimer may be improbable in the dilute solution. However, the change observed at the concentration 0.21 M may be due to the formation of hydrogen bond between molecules.

In the spectra of the solution at lower concentrations the sharp band (3619 cm.$^{-1}$) is clearly due to free OH stretching vibration. The broad band can be ascribed to the intramolecularly hydrogen-bonded OH vibration. Then, a band due to NH vibration may be either covered by the broad band or assigned to a small peak at 3370 cm.$^{-1}$. In this respect the results obtained by Russell and Thompson[6] for carbon tetrachloride solutions of many disubstituted amines will be helpful. According to their results, the absorption of ν (NH) appears in a range 3311–3350 cm.$^{-1}$ for dialkylamines and in 3430–3490 cm.$^{-1}$ for arylalkylamine, diarylamine and heterocyclic compounds. As to the intensity the absorption of dialkylamines is usually very weak compared with that of the other amines. From these results it may be reasonable to assign the band at 3370 cm.$^{-1}$ to free ν (NH), since NH group in ephedrine is very similar in structure to that in dialkylamine. However, whether this ν (NH) band is due to nitrogen atom bridged by a neighboring OH group or not is not certain. Russell and Thompson described that there is some suspicion that the intensity of the NH absorption, so low as almost to disappear, for dialkylamine is connected with a slow chemical reaction of amines with carbon tetrachloride. This description is consistent with the observation in the present experiments that the precipitation of hydrochloride occurs. Therefore the spectra of the alkamine in carbon tetrachloride solution may represent a sort of metastable state of molecule.

At 3.14 μ appears a weak band, which seems to be independent on the change of concentration. The bands at 3.3 μ are due to CH vibration of benzene ring and have no relation with hydrogen bonding.

In connection with the spectra of ephedrines, those of ethanolamine and 3-amino-2-butanol in carbon tetrachloride solution at a concentration of about 0.005 M are recorded and shown in Fig. 1-c., of which the structure is similar to that of ephedrine in 2.7–3.1 μ range. The sharp bands with higher frequency are due to free OH vibration and a band at 3509 or 3490 cm.$^{-1}$ may be due to either free NH vibration or the bonded OH vibration overlapping with free NH vibration. If the bands near 3500 cm^{-1} are due to the intramolecularly hydrogen-bonded OH vibration, the values 101 cm.$^{-1}$ for ethanolamine and 126 cm.$^{-1}$ for 3-amino-2-butanol of the frequency difference between the free and the bonded OH absorption are much less than that for ephedrine (168 cm.$^{-1}$).

The spectrum of the solution at 0.21 M seems to show co-existence of free molecules having intramolecular hydrogen bond and associated molecules. As absorption at a higher concentration than 0.21 M could not be observed because of rapid precipitation of crystallites, a spectrum of *l*-ephedrine in liquid state was taken (Fig. 1-d). It shows a band at 3311 cm.$^{-1}$ with a very weak shoulder near 2.9 μ and continuous absorption over 3.1–3.3 μ. In the previous paper[1], it was reported that in crystalline state *dl*-ephedrine shows only one band at 3300 cm^{-1}, assigned to the perturbed OH vibration. Then, the 3311 cm.$^{-1}$ band for ephedrine in liquid state can be considered to be due to this OH vibration. The weak shoulder near 2.9 μ may be due to the intramolecularly hydrogen-bonded OH absorption still remaining in the liquid state.

From these observations and the assignment of the spectrum at a concentration of 0.0054 M the spectral change accompanied with the changes from dilute solution → concentrated solution → liquid state → solid state may be explained as follows. As the concentration of ephedrine increases from a dilute solution a free molecule having an intramolecular OH···N hydrogen bond (3451 cm.$^{-1}$) gradually associates with a neighboring molecule having free OH group, forming OH···O intermolecular hydrogen bond, which gives rise to a new band at 3321 cm.$^{-1}$*. At the same time the band at 3451 cm.$^{-1}$ shifts to 3421 cm.$^{-1}$ by a reinforcing effect of the intermolecular hydrogen bond formation on the intramolecular one, as is known to occur for the frequency shift during the formation of dimer and polymers of alcohols[2]. In the condensed phase the free OH absorption disappears and only the intense OH absorption (3311 cm.$^{-1}$) relating to the intermolecular hydrogen bond remains.

As to whether NH in the $NHCH_3$ group play a part in hydrogen bond formation, the following fact will be helpful for interpretation; that is, the band at 3370 cm.$^{-1}$ assigned to free NH absorption remains even at a higher concentration (0.21 M), at which the association is appreciable. Thus, it may be concluded that NH group plays almost no rôle in the hydrogen bond formation.

Ψ-Ephedrine.—The spectrum of Ψ-ephedrine in dilute carbon tetrachloride solution is much like that of ephedrine (Fig. 1-b). A sharp band at 3621 cm^{-1} is due to free OH vibration, a broad band at 3418 cm.$^{-1}$ may be due to the intramolecularly hydrogen-bonded OH vibration. However, in this case $\Delta\nu$ (203 cm.$^{-1}$) between the sharp and broad band is larger than that in ephedrine (168 cm.$^{-1}$) and the free NH absorption almost disappears. Although the NH band may be masked by the overlapping of the broad band, a weak band appearing at 3324 cm.$^{-1}$ or a very weak shoulder at 3350 cm.$^{-1}$ may be due to NH vibration.

The spectral change on raising the concentrataion of Ψ-ephedrine proceeds just as in the case of ephedrine; that is, the intensity of the free OH absorption decreases and the broad OH absorption (OH···N) shifts by about 30 cm.$^{-1}$ towarde the lower frequency, accompanied by the appearance of a new band at 3301 cm.$^{-1}$, which is due to intermolecular OH···O hydrogen bonding. As

5) E.D. Bergmann, E. Gil-Av and S. Pincas, *J. Am. Chem. Soc.*, 75, 68 (1953).

6) R.A. Russell and H.W. Thompson, *J. Chem. Soc.*, 1955, 483.

* OH absorption for alcohol polymer appears over a range 3338-3384 cm^{-1} [2].

concentration increases, the intensity of the hydrogen-bonded OH absorption (3418 cm.$^{-1}$) rapidly decreases in contrast to the case of ephedrine.

B. Temperature Dependence

In order to observe the temperature dependence of the relative intensities of the free and bonded OH absorption bands, the spectra of ephedrines at about 0.005 M in carbon tetrachloride were taken at about 10° and 55°C. Comparing the spectrum at 10° with that at 25°C, it was found that the intensity of the free OH absorption in the latter increased as usually observed for the intermolecular hydrogen bonding[7]. However, at 55°C the intensities of both free and bonded OH absorptions were lower than those at 25°C for either diastereoisomers. This may be caused by the above-mentioned specific interaction of ephedrines with solvent molecules. A rough estimamation of energy of hydrogen bonding for ephedrine and Ψ-ephedrine from the data at 10° and 25°C give the values of about 5 kcal./mol.

C. Solvent Effect

In Fig. 2 are shown the spectra of solutions of ephedrine and Ψ-ephedrine in various solvents, together with that of carbon tetrachloride solutions at a concentration where association is appreciable.

Chloroform.—The free OH absorption shifted slightly towards the lower frequency in chloroform solution (3603 cm.$^{-1}$) more than in carbon tetrachloride solution (3619 cm.$^{-1}$). The bonded OH absorption also shifted by 30–40 cm.$^{-1}$ towards the lower frequency. The band ascribed to ν (NH) in the spectrum of carbon tetrachloride solution appears at almost the same frequency (3360 cm.$^{-1}$) for ephedrine, whereas for Ψ-ephedrine no band corresponding to ν (NH) appears. From the figure it seems that the intermolecular association does not occur at such concentration.

Benzene.—The shift of the free OH absorption towards the lower frequency is large and amounts to 50 cm.$^{-1}$ for both diastereoisomers, compared with that in carbon tetrachloride. The bonded OH absorptions also shift towards the lower frequency. The well-defined band at 3356 cm^{-1} for ephedrine may be due to ν (NH), which remains unchanged on adding triethylamine three times more concentrated as ephedrine, whereas the 3436 cm.$^{-1}$ band shifts to 3401 cm.$^{-1}$. Also a 3311 cm.$^{-1}$ band for Ψ-ephedrine may be due to the NH group. There is no indication that marked association occurs in benzene solution at 0.16 M.

Carbon Disulfide.—The absorption of ephedrines is stronger in carbon disulfide solution, than in other solution. The solution was yellow and unstable, especially for ephedrine.

The free OH absorptions appear at 3597 cm.$^{-1}$ for ephedrine and at 3590 cm.$^{-1}$ for Ψ-ephedrine, which are the frequencies between those in chloroform and benzene solutions. For ephedrine the intensity of the band is greater than for carbon tetrachloride solution of about the same concentration, but for Ψ-ephedrine it is remarkably small and almost zero at 0.16 M.

For ephedrine an intense band appears at 3279 cm.$^{-1}$, which is the lowest value of the bonded

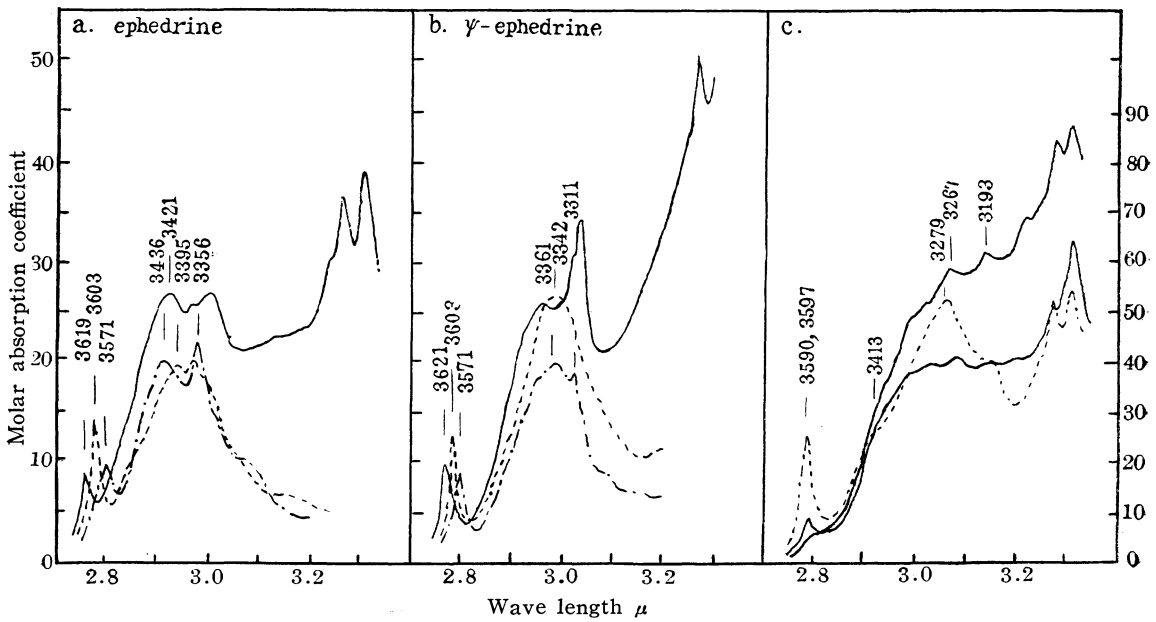

Fig. 2. Solvent effect on spectra of ephedrines. a), b) ——— CCl_4 (ca. 0.1 M/l.), ---- $CHCl_3$ (0.16 M/l.), —·— benzene (0.16 M/l.), cell 0.056 cm. c) CS_2, ---- ephedrine (0.0045 M/l.×2 cm), ——— φ-ephedrine, 1) 0.0045 M/l.×2 cm., 2) 0.16 M/l. ×0.056 cm.

7) e.g. M. Tsuboi, *J. Chem. Soc. Japan (Pure Chem. Sect.)*, **76**, 376 (1955).

OH vibration observed in the present experiments, if this band be ascribed to the bonded OH vibration. A weak shoulder is observed at about 3410 cm.$^{-1}$, corresponding to the band (3451 cm.$^{-1}$) due to the intramolecularly hydrogen-bonded OH vibration in the carbon tetrachloride solution. It is to be added that the spectrum of ephedrine in carbon disulfide solution is very much like that taken in carbon tetrachloride solution with a small amount of crystalline precipitates, both showing a weak shoulder at 3430 cm.$^{-1}$ and an intense peak at 3280 cm.$^{-1}$. Therefore, such spectra may be due to a metastable state of ephedrine molecule.

It is also remarkable that the absorption of *Ψ*-ephedrine in such a small concentration as 0.0045 M shows a spectrum like that when an intermolecular interaction occurs.

As is well known a relationship exists between dielectric constant of a solvent and the frequency difference in the OH or NH absorption of a substance in vapor state and in the solution[8]. This relationship is satisfied for the free OH absorption in the present experiments. Thus, the dif-

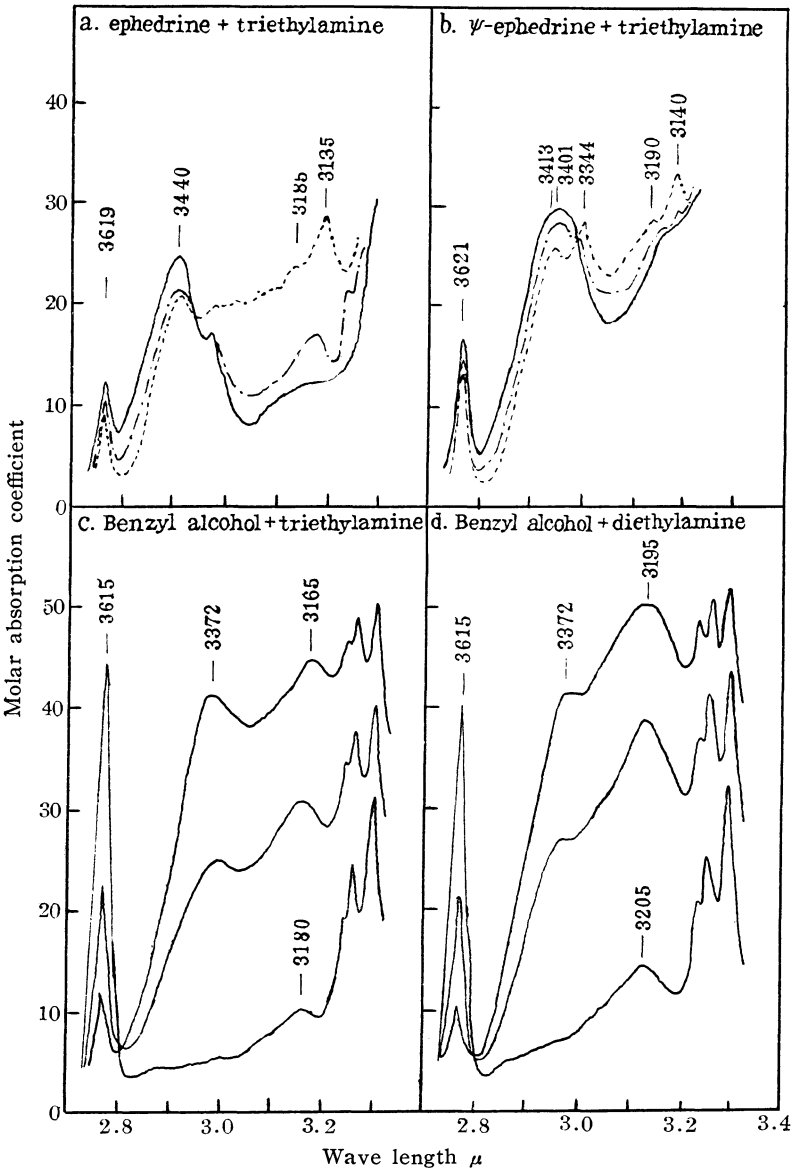

Fig. 3. The interaction of ephedrines and benzyl alcohol with proton acceptor in CCl_4 soln. a), b), ephedrines. 0.03 M/l. + triethylamine, ——— 0.072, —·— 0.27, ···· 0.50 M/l. c), d) 1 : 1 mixture in mol. 0.51, 0.179, 0.003 M/l.

8) E. Bauer and M. Magat, *J. phys. radium.*, **9**, 319 (1938).

ferences in frequency of the free OH absorption in the respective solvents and that of alcohol vapor (3680 cm^{-1}) increases in the order of carbon tetrachloride, chloroform, carbon disulfide and benzene*.

On the other hand, it is also known that the degree of the intermolecular association of phenol in solutions increases in the order of benzene, chloroform and carbon disulfide[9]. From Fig. 2 it will be seen that if the frequency difference in the free and bonded OH absorption means the strength of hydrogen bonding, the above-mentioned relation holds also for the intramolecular hydrogen bonding in the case of ephedrines. In almost the same concentration (about 0.1 M) association seems to occur only in carbon tetrachloride and carbon disulfide solutions, especially strong in the latter.

D. The Interaction with a Proton Acceptor

When a proton acceptor like ethyl ether, ethyl benzoate or pyridine is added to a 0.006 M solution of ephedrine in corbon tetrachloride, no appreciable interaction occurs between ephedrine and the proton acceptor, unless the molar ratio of the latter to the former exceeds 10 : 1. In the case of a molar ratio of 40 : 1 for pyridine to ephedrine new bands due to the intermolecular interaction appear.

In Fig. 3-a and -b are shown the interaction between ephedrines and triethylamine, which is a strong proton acceptor. As seen from the figure the intensity of the free OH band decreases already at the concentration of 0.072 M of triethylamine. As the concentration of triethylamine increases, the intensities of the free and bonded OH vibrations of both isomers decrease, at the same time the bonded OH band shifts towards lower wave number and a new band appears at about 3140 $cm.^{-1}$. Ψ-Ephedrine mixed with higher concentration of triethylamine shows splitting of the band near 3400 $cm.^{-1}$ into two bands at 3413 and 3344 $cm.^{-1}$.

These facts may be explained as follows. At first, a molecule which forms no intramolecular hydrogen bond may interact with triethylamine molecule through either OH or $NHCH_3$ group of the ephedrines. In connection with this assumption, an 1 : 1 mixture in mole of benzyl alcohol and triethylamine or diethylamine was examined. The results are shown in Fig. 3-c and -d. A free OH band of benzyl alcohol at 3615 $cm.^{-1}$ increases its intensity with decreasing concentration of the mixture, while a band at 3372 $cm.^{-1}$ disappears, which seems to be due to the interaction between benzyl alcohol molecules themselves, and the intensity of a band at 3165 cm^{-1} (triethylamine) or 3195 $cm.^{-1}$ (diethylamine) decreases. The band at 3165 or 3195 $cm.^{-1}$, which is due to OH···N intermolecular hydrogen bonding, shifts to 3180 or 3205 $cm.^{-1}$ at a lower concentration.

From these results, it will be evident that the band at 3140 $cm.^{-1}$ observed for ephedrines (Figs. 3-a and -b) can be assigned to OH vibration perturbed by OH···N intermolecular hydrogen bond. Although $NHCH_3$ group may also participate in the hydrogen bond formation of the type NH. . .N, this seems to be rather weak because of the weaker proton donating power of $NHCH_3$ group than OH group[10]. However, the appearance of very weak absorption at 3190 $cm.^{-1}$ and the shift of the bonded OH absorption may suggest that the NH group also takes part in the intermolecular hydrogen bond formation. The splitting of the bonded OH absorption into 3413 and 3344 $cm.^{-1}$ in Ψ-ephedrine may be explained as follows. The lower frequency component is due to OH···N intramolecular hydrogen bond strengthened by the increase of proton accepting power of the N atom because of forming an intermolecular hydrogen bond (NH···N) with triethylamine. A band due to NH···N intermolecular hydrogen bond may be assigned to the absorption at 3185 $cm.^{-1}$, but this assignment is not so conclusive because of the lack of data about the interaction between NH group of amine and N atom of another proton acceptor.

As Ψ-ephedrine shows stronger continuous absorption in 3.0–3.2 μ region than ephedrine at the same concentration, it may be suggested that Ψ-ephedrine interacts more easily with the proton acceptors examined than ephedrine.

Discussion

Although the existence of the intramolecular hydrogen bond in the molecules of both diastereoisomers of ephedrine was verified in various solvents, the appearance of the free OH absorption remained unexplained. This may be accounted for as follows. The conformations of ephedrine and ψ-ephedrine capable of forming the intramolecular hydrogen bond may be illustrated as in Fig. 4.

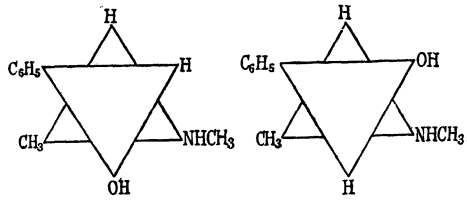

ephedrine Ψ-ephedrine

Fig. 4.

One of them (ephedrine) is different from that hitherto accepted commonly on the chemical ground[11]. However, the present conformation of ephedrine is in agreement with that suggested recently by Murakami and Fukumoto[12] from consideration of reac-

* The results of the same kind have been obtained for pyrrole, phenol and methanol (M. Josien and N. Fuson, *J. Chem. Phys.*, 22, 1169 (1954).

9) R.A. Friedel, *J. Am. Chem. Soc.*, 73, 2881 (1951).

10) S. Mizushima, "Structure of molecules and internal rotation." Academic Press Inc. Publishers, New York (1954), p. 133.

11) e.g. W.J. Close, *J. Org. Chem.*, 15, 1131 (1950).

12) M. Murakami and T. Fukumoto, *J. Chem. Soc. Japan (Pure Chem. Sect.)*, 76, 270 (1955).

tion mechanism and that found by X-ray crystal analysis for ephedrine hydrochloride[13]. The appearance of the free OH absorption suggests that a part of the molecules have a conformation in which OH and $NHCH_3$ groups are trans. Moreover, it is also possible that in a gauche type molecule the OH group may take an orientation not to form hydrogen bond with $NHCH_3$ group. These two possibilities have actually been observed in the case of ethylene chlorhydrine[14].

The above suggestion that the ephedrine and ψ-ephedrine molecules consist of the mixture of the rotational isomers may be supported by the appearance of one or two more bands in the finger print region spectra in $CHCl_3$ solution than those observed in solid state[1] (970–1190 cm^{-1}).

As to whether there are differences in the equilibrium ratio of the rotational isomers between diastereoisomers, only a qualitative discussion may be given. As seen in Fig. 4, it is conceivable that if we assume the repulsion between the phenyl and methyl groups it will give the effects that the OH and $NHCH_3$ groups are more apart for ephedrine than for ψ-ephedrine and thus the hydrogen-bonded conformation of ψ-ephedrine will be relatively more stable, when compared with its trans form, than in the case of ephedrine.

Such a consideration may also explain the difference of $\Delta\nu$ between the present diastereoisomers. In general it is accepted that the magnitude of $\Delta\nu$ is related to the energy of the hydrogen bonding[15] and in solid state related to the distance between a proton donor and an acceptor[16]. Thus, because of the repulsion assumed above, the OH group is to some extent nearer to the $NHCH_3$ group in the gauche type isomer of ψ-ephedrine and the $\Delta\nu$ will be accordingly larger than that for ephedrine. The observed values of $\Delta\nu$ are, as already given, 203 $cm.^{-1}$ for ψ-ephedrine and 168 $cm.^{-1}$ for ephedrine. It is to be remarked that these values are much larger than those found for OH···O intramolecular hydrogen bonds in diols (30–60 cm^{-1})[2]. This may be attributed partly to the difference in the proton affinity of the proton acceptor.

In Table I the values of $\Delta\nu$ of the inter- and intramolecular OH···N hydrogen bonds are summarized. From the Table it is seen that $\Delta\nu$ due to OH···N intermolecular hydrogen bond is very large except that in the case of benzyl alcohol-azobenzene and $\Delta\nu$ due to the intramolecular OH···N hydrogen bond adjucent to a conjugate system like pyridoine is larger than that of intermolecular bond between corresponding pair, phenol-pyridine. It may be said that compared with these $\Delta\nu$ values, those of ephedrines are rather small.

TABLE I

$\Delta\nu$ OF OH. . .N HYDROGEN BOND

Intermolecular	Phenol-pyridine	770*
	Phenol-N-methylpiperidine	820*
	Benzyl alcohol-azobenzene	170**
	〃 -triethylamine	450
	〃 -diethylamine	420
	Acetaldoxime	470***
Intramolecular	α-Pyridoin	880*
	Ephedrine	168
	Ψ-Ephedrine	203

* W. Luettke and H. Marsen, *Z. Electrochem.*, 57, 680 (1953).

** M.S.C. Flett, *J. Soc. Dyers and Colourist*, 68, 59 (1952).

*** S. Califano and W. Luettke, *Z. Physik. Chem.*, 5, 240 (1955).

The author wishes to express his sincere thanks to Professor I. Nitta of Osaka University for his kind guidance and to Dr. T. Shimanouchi of Tokyo University for helpful discussions. The author's thanks are also due to Dr. S. Kuwada and Dr. A, Watanabe of this laboratory for their continued encouragement.

Research Laboratory Takeda Pharmaceutical Industries, Ltd. Osaka

13) G.D. Phillips, *Acta Cryst.*, 7, 159 (1954).
14) S. Mizushima, loc. cit, p. 86.
15) R.M. Badger, *J. Chem. Phys.*, 8, 288 (1940).
16) R.C. Lord and R.E. Merrifield, *J. Chem. Phys.*, 21, 166 (1953).

Studies on Serine Peptides. I. Optical Resolution of O-Benzyl-DL-serine and Synthesis of DL-Serine Peptides

By Kenzi OKAWA

(Received January 1, 1956)

The serine peptides are important in organic and biological chemistry. For example, these peptides readily undergo hydrolysis with dilute acids or alkalis and acyl migration occurs in the acidic condition. Some of these peptides have been considered to have growth-promoting effect or enzymatic activity. However, there have been few papers available concerning the synthesis of the serine peptides[1], mainly because this amino acid has a free hydroxyl group which induces side reaction in the peptide synthesis.

The author tried in the present work to synthesize the serine peptide from the O-benzyl-serine[2] in which the hydroxyl group was protected with a benzyl rest. An optically active O-benzyl-L-serine was prepared by the enzymatic resolution of the N-acetyl derivative with the takadiastase. The O-benzyl-L-serine was easily obtained in 78% yield from the reaction mixture, since this amino acid was slightly soluble in water.

Price reported in his paper that the optical active L-serine was obtained from the N-acetyl-DL-serine in 40% yield[3].

The O-benzyl-L-serine showed a specific rotation of +5.86 in 1 N-hydrochloric acid solution at 15°C, and the L-serine which was prepared quantitatively by the acid hydrolysis of the benzyl derivative, showed a rotation of +14.6 in 1N-hydrochloric acid solution at the same temperature.

At the preliminary experiment, the O-benzyl-L-serine peptides have been synthesized by the N-carboxylic acid anhydride method (N. C. A. method) of Bailey[4], but satisfactory results were not obtained except in the case of a seryl-glycine peptide.

With O-benzyl-DL-seryl-L-glutamic acid, O-benzyl-DL-seryl-L-leucine, and O-benzyl-DL-seryl-L-phenylalanine, so many by-products were formed during the reaction period that the purification of the products was very difficult.

1) A. Miekely and J. Fruton, *J. Biol. Chem.*, **146**, 463 (1942); D. Wooley, *J. Biol. Chem.*, **159**, 753 (1948); R.F. Fischer and R.R. Whetson, *J. Am. Chem. Soc.*, **76**, 5076 (1954); M. Botunik, *Zhur. Obschcliei, Khim*, **23**, 1716-19 (1953).

2) K. Okawa and H. Tani, *J. Chem. Soc. Japan*, **75**, 1199 (1954).

3) V. Price, *J. Biol. Chem.*, **179**, 1169 (1949).

4) J. Bailey, *J. Chem. Soc.*, **1950**, 3461.

O-Benzyl-DL-seryl-L-leucine ethyl ester and DL-seryl-L-leucine have been synthesized by the Fischer's acid chloride method.

It has been found from the above experiments that the O-benzyl-serine can be utilized as the starting material in the peptide synthesis.

Experimental

Enzymatic Resolution of O-benzyl-DL-serine. —O-Benzyl-N-acethyl-DL-serine.—Into a mixture of 33 g. of O-benzyl-DL-serine and 83 cc. of 2N-sodium hydroxide solution were added separately 25 cc. of acetic anhydride and 163 cc. of 2N-sodium hydroxide solution under cooling. The reaction mixture was neutralized with 1 N-hydrochloric acid solution, when white crystals precipitated. Recrystallization from hot water gave 37 g. of the crystals in 80% yield, m.p. 139-140°C.

Anal. Found: C, 60.59; H, 6.67. Calcd. for $C_{12}H_{15}O_4N_1$: C, 60.76; H, 6.38%.

Carboxypeptidase Preparation.—Twenty six grams of Takadiastase were extracted with distilled water at 0°C. The mixture was filtered using Celite. This extracted solution was used directly in the enzymatic resolution. The acetyl derivative (33 g.) was dissolved in 24 cc. of 6N-sodium hydroxide solution. To this solution were added the above enzymatic extract and 60 cc. of phosphate buffer which brought the total mixture to pH 6.8. In order to insure complete hydrolysis, the digests were usually set up in the late afternoon and allowed to stand at 37°C. until early next morning. The L-amino acid crystallized in high yield and usually filled the digestion flask. The mixture is brought to pH 5.0 by the addition of glacial acetic acid. The L-amino acid was filtered by suction, and washed with cold water. The mother liquor was combined with washings and concentrated in vacuo to a low bulk. A small amount of the L-amino acid appeared during this concentration. The crystals were combined with the main product and recrystallized from hot water with the aid of Celite. Optically active 11 g. of crystals were obtained in 78% yield, $[\alpha]_D^{15} = +5.86$. (in 1N-hydrochloric acid) The residual concentrated solution was brought to pH 2.0 with conc. hydrochloric acid. The acetyl derivative was extracted several times into ethylacetate. The extracts were combined, dried for a few minute over anhydrous sodium sulfate, and finally filtered. The ethylacetate was removed in vacuo. To the oily residue was added twice their volume of petroleum ether and it was allowed

to stand over night in an ice bath, then white precipitate was obatined. After recrystallization from hot water, 13.6 g. of N-acetyl-D-derivative was prepared in fine crystals. in 80% yield, m.p. 103°C.

D- and L-Serine.—D- and L-Serine were obtained by acid hydrolysis of benzyl derivatives with 5N-hydrochloric acid for half an hour. The D- and L-form exhibit $[\alpha]_D^{15}$ of -14.6 and $+14.6$ in 1N-hydrochloric acid solution, respectively.

O-Benzyl-DL-serine N.C.A.—This was prepared by the reaction of carbonylchloride with O-benzyl-DL-serine in dioxane at 40°–50°C by the method of Leuchs[5,6]. Several times recrystallization from ethylacetate-petroleum ether gave white crystals, m.p. 76°-77°C, in 82% yield.

Preparation of Serine Peptides.—The peptide coupling experiments were carried out under anhydrous conditions. All solvents were stored over suitable dry reagents.

O-Benzyl-DL-seryl-glycine.—Glycine ethylester hydrochloride (0.7 g.) was treated with 3.3 cc. of 1.66N-ammonium-chloroform solution and the reaction mixture filtered from the precipitated ammonium-chloride. After removal of a slight excess of ammonia by the concentration of the solvent in vacuo, 6.6 cc. of ethylacetate were added and the solution was cooled to 65°C in solid carbondioxide-aceton bath. After addition of triethylamine (0.5 cc.) to the ester solution, a solution of DL-serine N. C. A. (0.9 g.) in 6.6 cc. of ethylacetate was precooled to 65°C and slowly run into the mixture. The reaction mixture was allowed to stand at this temperature for six hours, the mixture was then warmed to room temperature and the solvent removed in vacuo. The O-benzyl-DL-seryl-glycine ethylester was hydrolized with 11.1 cc. of 0.37 N-barium hydroxide, neutralized with 11.1 cc. of 0.37 N-sulfuric acid and concentrated in vacuo. White crystals were obtained. Recrystallization gave 0.15 g. of O-benzyl-DL-seryl-glycine, m.p. 202°C, in 65% yield.

Anal. Found: N, 10.95. Calcld. for $C_{12}H_{15}O_4N_2$: N, 11.10%.

DL-Seryl-glycine.—O-Benzyl-DL-seryl-glycine (0.3 g.) was suspended in 30 cc. of methyl alcohol. After addition of palladium oxide (0.3 g.) and 0.2 cc. of hydrochloric acid, the mixture was reduced for six hours. Then palladium oxide was removed and the reaction mixture was concentrated in vacuo. Recrystallization of residual precipitate gave 0.23 g. of seryl-glycine hydrochloride, m.p. 195°C, with decomposition, in 95% yield.

Anal. Found: N, 14.24. Calcd. for $C_5H_{11}O_4N_2Cl$: N, 14.16%.

O-Benzyl-DL-seryl-L-glutamic acid.—Glutamic acid ethylester was prepared from 1.5 g. of the hydrochloride. The free ester was treated with 1.1 g. of O-benzyl-DL-serine N. C. A. and 0.1 cc. of triethylamine under the same conditions. White precipitate was obtained in 50% yield.

Anal. Found: N, 8.36. Calcld. for $C_{15}H_{20}O_6N_2$: N, 8.60%.

O-Benzyl-DL-seryl-L-leucine.—Under the same conditions, 0.37 g. of crystals were obtained in 10% yield from 2.5 g. of leucine ethylester hydrochloride and 2.2 g. of O-benzyl-DL-serine N. C. A.

Anal. Found: N, 9.48. Calcd. for $C_{16}H_{24}O_4N_2$: N, 9.10%.

O-Benzyl-DL-seryl-L-phenylalanine.—Under the same conditions, 0.17 g. of crystals were obtained in 10% yield, from 1.4 g. of phenylalanine ethylester and 1.1 g. of O-benzyl-DL-serine N. C. A.

Anal. Found: N, 8.19. Calcld. for $C_{19}H_{22}O_4N_2$: N, 8.18%.

O-Benzyl-N-carbobenzyloxy-DL-serine.—O-Benzyl-N-carbobenzyloxy-DL-serine was prepared in the previous experiments by the author[7]. The carbobenzyloxy derivative (2.8 g.) was synthesized in 80% yield from 2 g. of O-benzyl-DL-serine and 2.68 g. carbobenzyloxychloride.

O-Benzyl-O-carbobenzyloxy-DL-seryl-L-leucine ethylester.—N-Carbobenzyloxy derivative was treated with 2.5 g. of phosphorus pentachloride in 30 cc. of absolute ether. After dissolution of N-carbobenzyloxy derivative, excessive phosphorus pentachloride was filtered off and the filtrate was concentrated in vacuo at 0°C. The concentrated syrup was extracted twice with petroleum ether in order to remove phosphate oxychloride, and the residual syrup was dissolved in 20 cc. of ethylacetate. To the 20 cc. of ethylacetate solution of L-leucine ethylester which was prepared from 3.3 g. of the hydrochloride, was added the acid chloride solution. After removal of the leucine ethylester hydrochloride, the reaction mixture was washed twice with petroleum ether, and then allowed to stand over night in an ice box. White precipitate was obtained. Recrystallization from ethylacetate-petroleum ether gave 2.7 g. of peptide, in 70% yield, m.p. 78°C.

Anal. Found: N, 5.80. Calcld. for $C_{26}H_{34}O_6N_2$: N, 5.95%.

O-Benzyl-N-carbobenzyloxy-DL-seryl-L-leucine.—The peptide ester (2.6 g.) was hydrolized with mixed reagent (4 cc. of 1N-sodium hydroxide and 5 cc. of aceton). The reaction mixture was neutralized with 1N-hydrochloric acid being obtained in white crystals. Recrystallization from ethylacetate-petroleum ether gave 1.0 g. of peptide, m.p. 92°C, in 72% yield.

DL-Seryl-L-leucine.—N-Carbobenzyloxy peptide was suspended in 30 cc. of methyl alcohol. Into the methyl alcohol solution were added 0.1 cc. of acetic acid and 0.3 g. of palladium oxide. The mixture was reduced under the ordinary pressure in the hydrogen atmosphere at room temperature. After removal of palladium oxide, the reaction mixture was concentrated in vacuo; then white crystals were obtained. Recrystallization gave 0.12 g. of seryl-L-leucine, m.p. 189°C., in 71% yield.

Anal. Found: N, 12.63. Calcld. for $C_9H_{18}O_4N_2$: N, 12.80%.

---

5) H. Leuchs, *Ber.*, **39**, 857 (1906).
6) K. Okawa and H. Tani, *J. Chem. Soc. Japan*, **75**, 1199 (1950).
7) K. Okawa and H. Tani, *J. Chem. Soc. Japan*, **75**, 1199 (1954).

Summary

The optically active O-Benzyl-L-serine was prepared in 78% yield by the enzymatic resolution of the N-acetyl derivative with Takadiastase.

DL-Seryl-glycine was prepared by the N. C. A. method of Bailey and DL-seryl-L-leucine was synthesized by the Fischer's acid chloride method respectively.

As was expected, it was found that O-benzyl-serine can be utilized as the starting material in the peptide syntheses.

The author wishes to express his appreciation to Prof. S. Akabori for his kind guidance during the course of this work and also to thank Asst. Prof. H. Tani for his frequent advice.

Department of Chemistry, Faculty of Science, Osaka University, Osaka

Studies on Serine Peptides. II. Synthesis of Optically Active Serine Peptide Derivatives

By Kenzi OKAWA

(Received January 1, 1956)

Although a number of peptides containing several kinds of the simpler amino acids have been prepared, little is known about the preparation of peptides which include more than one of trifunctional amino acids. This is especially true for peptides of L-serine and L-histidine.

In the previous paper[1], the author reported on the DL-serine peptides which include monofunctional amino acids.

In the present work, some derivatives of optically active peptides containing L-serine have been synthesized by means of the Sheehan's dicyclohexylcarbodiimide method[2], with O-benzyl-L-serine as starting material.

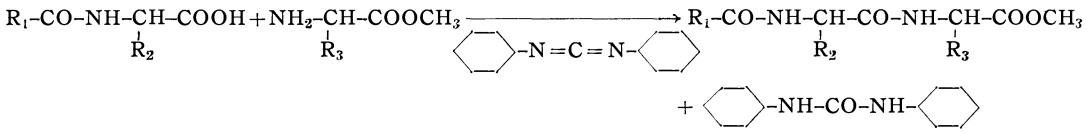

O-Benzyl-N-carbobenzyloxy-L-seryl-L-histidine methyl ester, O-benzyl-N-carbobenzyloxy-L-seryl-L-tyrosine methyl ester and bis-(O-benzyl-N-carbobenzyloxy-L-seryl)-L-cystine dimethyl ester have been synthesized in good yield.

Sheehan reported in his paper that the hydroxyl group of the serine was not affected by this coupling reagent, and L-seryl peptide was synthesized in 59% yield. But the relatively lower yield of the peptide shows that some side reactions may take place in the coupling procedure.

In the present experiments, a tyrosine peptide has been prepared in 76% yield. It seems that the free hydroxyl group of tyrosine is less reactive than that of serine.

It has been found from the above experiments that this coupling reagent is useful for peptide syntheses.

Experimental

N-N'-Dicyclohexyl Thiourea[3].—Into the solution of 100 g. of cyclohexylamine and 250 cc. of ethylalcohol was added 100 g. of carbondisulfide through the reflux condenser at the presence of two or three pieces of sodium hydroxide, and the mixture was refluxed for twenty-four hours on a waterbath. After cooling the reaction mixture, precipitated yellowish crystals were filtered. Recrystallization of the crystals from hot alcohol gave 100 g. of the pure material, m. p. 180–181°C.

Dicyclohexylcarbodiimide[4].—The intimate mixture of 100 g. of freshly pulverized mercuric oxide and 40 g. of dicyclohexylthiourea were placed in a suitable bottle of 500 cc. After adding 200 cc. of freshly distilled carbondisulfide, the mixture was shaken on a shuttle machine for 1.25 hrs. The precipitate was filtered and the

1) K. Okawa, Part I. This Balletin, 29, 486.
2) J.C. Sheehan and G.P. Hess, *J. Am. Chem. Soc.*, 77, 1067 (1955).
3) A. Skita und H. Rolfes, *Ber.*, 53, 1242 (1955).
4) R. Herbeck and M. Pezzati, *Ber.*, 71, 1933 (1938).

solvent was removed. The residual syrup was dissolved in petroleum ether and an insoluble precipitate was filtered. After removal of petroleum ether the residual gelatinous mass was distilled under reduced pressure. Colourless crystals (b. p. 132°C/4 mmHg) were obtained in 80% yield. Dicyclohexylcarbodiimide was stored in a sealed tube at 5°C.

O-Benzyl-N-carbobenzyloxy-L-serine[5].—Five grams of O-benzyl-N-carbobenzyloxy-L-serine were prepared from the 3.5 g. of O-benzyl-L-serine and 3.8 g. of carbobenzyloxychloride by the method as with O-benzyl-N-carbobengyloy-DL-serine, m. p. 98°C.

Syntheses of L-serine peptide derivatives.—All the condensation reactions carried out under anhydrous conditions.

O-Benzyl-N-carbobenzyloxy-L-seryl-L-tyrosine Methyl ester.—L-Tyrosine methyl ester hydrochloride (1.51 g.) was treated with 0.9 cc. of triethylamine in 10 cc. of tetrahydrofuran. After removal of triethylamine hydrochloride, the filtrate was mixed with 1.34 g. of carbodiimide and 1.65 g. of carbobenzyloxy derivative in 10 cc. of tetrahydrofuran at room temperature. Immediately, N-N'-dicyclohexylurea was precipitated from the above reaction mixture; then the coupling solution was kept for four hours in room temperature. To remove unchanged carbodiimide 0.15 cc. of acetic acid was added and the mixture was allowed to stand at this temperature for one hour, and filtered from the precipitate. Then, tetrahydrdofuran as the solvent was replaced with ethylacetate. Since a small amount of precipitate was formed in the ethylacetate solution, the precipitate was filtered off and petroleum ether was added to the solution until crystals of the peptide ester appeared. Recrystallization from ethylacetate-petroleum ether gave 1.8 g. of peptide, m. p. 111-112°C, in 72% yield. $[\alpha]_D^{15}=+15.5$ (28.4 mg./cc. in 99% EtOH).

Anal. Found: N, 5.74. Calcd. for $C_{28}H_{30}O_7N_2$: N, 5.53%.

O-Benzyl-N-carbobenzyloxy-L-seryl-L-histidine Methyl ester.—The free ester of histidine was obtained by the Fischer's method[6]. A methyl alcohol solution of histidine methyl ester dihydrochloride was treated with 13 cc. of 2 N-CH_3ONa solution and the reaction mixture filtered from the precipitated sodium hydrochloride. After removal of methyl alcohol, the free ester was dissolved in 15 cc. of tetrahydrofuran. The tetrahydrofuran solution was coupled with 3.3 g. of carbobenzyloxy derivative and 2.1 g. of carbodiimide in tetrahydrofuran. Under the same conditions as those of the above experiments, 4.2 g. of peptide ester were prepared in 87% yield, m. p. 110°C. $[\alpha]_D^{15}=+7.21$ (49.2 mg./cc. in 99% EtOH).

Anal. Found: N, 12.04. Calcd. for $C_{25}H_{33}O_6N_4$: N, 11.7%.

Bis-(O-benzyl-N-carbobenzyloxy-L-seryl)-L-cystine Dimethyl ester.—Into 20 cc. of the solution of cystine dimethyl ester in the tetrahydrofuran which was prepared from 2.2 g. of the dimethyl ester dihydrochloride and 1.8 cc. of triethylamine, were added 3.3 of carbobenzyloxy derivative and 2.6 g. of carbodiimide in 20 cc. of tetrahydrofuran. From the coupling mixture, 2.5 g. of crystals were obtained, m. p. 101-102°C, in 57% yield. $[\alpha]_D^{15}=+22.17$ (26.6 mg./cc. in ethylacetate.

Anal. Found: N, 6.33. Calcd. for $C_{44}H_{50}O_{12}N_4S_2$: N, 6.29%.

Summary

The derivatives of optically active L-seryl peptides containing trifunctional amino acids have been synthesized by the Sheehan's method in good yield.

In this method, the free hydroxyl group of the serine must have been substituted by a suitable protecting group, fx. benzyl rest, in order to obtain good results.

The present author wishes to express his appreciation to Prof. S. Akabori for his kind guidance throughout this work.

Department of Chemistry, Faculty of Science, Osaka University, Osaka

5) K. Okawa and H. Tani, *J. Chem. Soc. Japan*, **75**, 1197 (1950).

6) E. Fischer and L.H. Cone, *Ann.*, 363, 107 (1908).

Rheology of Surface Films. V. Mechanical Behaviours and Structures of 6-Nylon at Air/Water Interface

By Kiyoshi INOKUCHI*1

(Received January 24, 1956)

Introduction

In the preceding paper[1], detailed description was made on the rheological characteristics of 6-nylon at air/water interface. It is desirable to investigate the film structure, which is responsible for the development of the rheological properties of the film. For this purpose, electron microscopic examination was carried out at various areas, together with the simultaneous determination of surface pressure and potential. Microfibrillar structures were thus revealed, and the change of the mechanical properties of the film, accompanied by the compression process, was discussed in terms of such structures.

Experimental

Materials and the experimental conditions were just the same as described in the preceding paper[1]. Unless otherwise stated, the sample was spread on distilled water from the mixed solution of benzene/phenol (3: 1 in volume) at the initial spreading area of about 90 A^2/residue. About twenty minutes were allowed to stand before the determination of the isotherms under the compression of constant speed 9.6 cm²/min. For the determination of surface pressure-area curve (π-A curve), the surface balance of a float type was used, which was constructed by the present author[2]. Surface potential was measured by means of a vibrating electrode apparatus. For the electron microscopic examination, the films were transferred onto the collodion support with use of the following technique. The collodion supports were held and touched parallel to the surface film on the substrate water and then immersed into the water. After the film was swept off, these supports were picked up through the clean surface of water, and dried. In order to avoid heterogeneity of the film near the enclosing barriers, all the film specimens were taken from the middle part of the enclosing area of the surface films. Hitachi HS-II type electron microscope was used.

Results

(I) Surface Pressure

(1) Force-Area Curve. — The general trend of the form of the π-A curve was shown in Fig. 1. Surface pressure at large

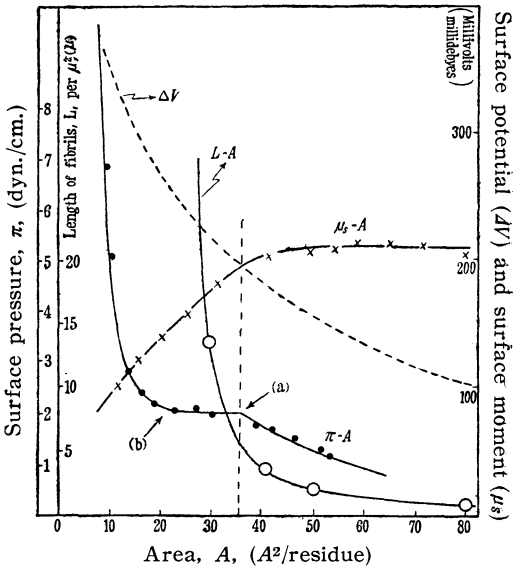

Fig. 1. Relationships of surface pressure versus area (π-A, full circles), surface electric moment versus area (μ_s-A, crosses), and amounts of fibrils versus area L-A, open circles). Broken line represents the surface potential versus area curve.

areas gradually increased as the film was compressed until a distinct kink point (a) appeared at the area of about 37 A^2/residue. Below the area of the kink point, however, the pressure ceased to increase upon compression forming a high compressibility region— a plateau—, whereas the pressure again rose, on further reducing area below about 20 A^2/residue, more steeply up to the pressure of 40 dyn./cm. The end of the plateau is denoted as point (b) hereafter. The pressure relaxation after compression was sudden and pronounced below the kink point, and hence, the more the plateau became distinct, the slower the compression rate was.

In view of our experience, it was likely that the Wilhelmy dipping slide method registered a more distinct kink point (a) than the case in which the float balance was used. This may be due to the considerable change

*1 Present adress: The 2nd Surgical clinic, Medical School, Kyushu University, Fukuoka, Japan.

1) K. Inokuchi, This Bulletin, 28, 453 (1955).
2) K. Inokuchi, This Bulletin, 26, 471 (1953).

of the wetting condition of the slide. In any case, it is evident that there occurred a sudden change in the film structure at the point (a).

(2) **Effect of the Composition of the Substrate Water.**—It has been emphasized that coherent films generally badly spread at air/water interface. So, it seemed necessary to examine the extent of the spreading under various conditions. The results were summarized in Table I, in which the areas of

TABLE I

EFFECT OF THE SUBSTRATE WATER UPON THE π-A CURVE

Substrate water	a	b	c	Pressure at point (a)	Temperature
	A^2/residue			dyn./cm.	C°
Distilled water	37	20	7.5	2.2	21.5
3 N H_2SO_4	37	21	7.5	5.4	21.3
3% Urea	38	24	7.6	2.1	21.2
20% Urea	—	—	7.6	—	20.0

point (a), (b), and the limiting area (c), obtained by extrapolating the straight portion of the high pressure region*2 (15 to 40 dyn./cm.) to zero pressure, were tabulated together with the pressure at the kink point. It was found that these characteristic areas were not appreciably influenced by the composition of the substrate solution, yielding identical values of (a)=37 A^2/residue, (b)=20 A^2/residue, and (c)=8.5 A^2/residue, respectively. On the other hand, the pressure was appreciably raised when spreading was made on the acidic solution (3 N sulfuric acid solution). That is, the film became expanded, as reported by Crisp[3] with nylon [-$(CH_2)_4$-CO-NH-]$_n$.

(3) **Effect of the Composition of the Dropping Solution.**—Spreading was also tested in relation to the composition of the dropping solution. Mixtures of benzene-phenol as a solvent, whose proportions vary from 2.5/7.5 to 9.2/0.8 (in volume), gave practically identical values of the characteristic area (a, b, and c), whereas the solution, whose benzene/phenol proportions exceeded 9.5/0.5, yielded far smaller areas than that above (Table II). The solvent of too large proportions of phenol made the experiment impossible, since the solvent was solidified at room temperature. Since 6-nylon does not dissolve, either in pure benzene or in pure phenol, this fact may indicate that the poor solvent caused bad spreading. when the sample was spread from the mixed solution of sulfuric

TABLE II

EFFECT OF THE SOLVENT OF THE DROPPING SOLUTION UPON THE π-A CURVE

Solvent proportion in volume	a	b	c	Pressure at point (a)	Temperature
Benzene/Phenol	Area in A^2/residue			dyn./cm.	°C
2.5/7.5	—	—	8.5	—	19.4
7.5/2.5	37	20	8.5	2.4	19.5
9.2/0.8	36	20	8.4	2.4	19.4
9.5/0.5	20	11	5.7	2.4	20.3
9.8/0.2	—	—	—	—	21.6
H_2SO_4/Isopropanol 1/10	28	19	7.0	1.6	19.4

acid and isopropyl alcohol (1/10 in volume), somewhat smaller characteristic areas were obtained than that from benzene-phenol solution. Since partial hydrolysis of the sample cannot be denied in strong sulfuric acid solution, reduced values of the characteristic points may partly be attributed to this. From the facts that the spreading areas were not appreciably influenced by the hydrogen bond breaking agents, and that the change of the composition of the dropping solution does not practically affect the extent of spreading except for the extreme case, it may be considered that spreading attains to saturation even on the distilled water.

(4) **Molecular Weight Variations.**—As shown in Table III, it was found that the

TABLE III

EFFECT OF MOLECULAR WEIGHT OF 6-NYLON UPON THE π-A CURVE

Molecula weight	a	b	c	Present at point (a)	Temperature
	Area in A^2/residue			dyn./cm.	°C
17,300	37	20	8.5	2.2	21.5
4,600	37	—	7.8	2.5	30.0
2,800	38	—	7.5	2.5	20.0
1,000	31	18	4.8	2.4	20.5
Caplolactam	—	—	4.8	—	20.5

form of the π-A curve was not affected by the molecular weight of the sample so far as the molecular weight changed from 2800 to 17300. This phenomenon is similar to the case with the surface films of cellulose acetates reported by Borgin[4]. With the fraction of extremely low molecular weight 1000, however, a slightly small value of the point (a) was produced, and the plateau in the π-A curve was less distinct. When caprolactum, a monomer of 6-nylon, was spread on a sat-

*2 The high pressure region used for obtaining the point (c) did not appear in Fig. 1.

3) D.J. Crisp, *J. Colloid Sci.*, **1**, 161 (1946).

4) K. Borgin, *Trans. Far. Soc.*, **49**, 956 (1953).

urated ammonium sulfate solution, a comparatively stable surface film was produced, having no plateau and showing less value of point (c) in the π-A curve, and exhibiting no elasticity covering the whole range of compression.

(5) **Compression-Expansion Hysteresis.**—Hysteresis of the π-A curve was also tested at various areas by exercising the compression and re-expansion at constant speed. Fig. 2 shows an example of the results thus obtained, in which the arrows represented a

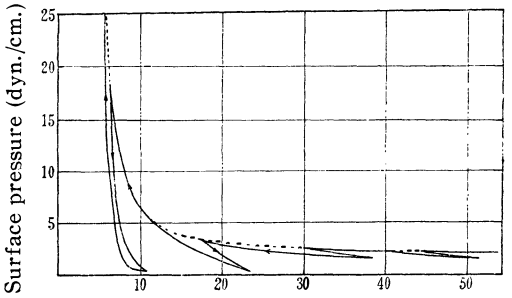

Fig. 2. Compression-expansion hysteresis curve. Temperature, 16°C. rate of expansion, 9.6 cm²/min.

series of the hysteresis loop. In general, the pressure, when the film was re-expanded, became lower than that of the foregoing compression, such a trend was found to be slight at larger areas than the point (a), whereas it became appreciable at the areas below the plateau region. Marked hysteresis occurred below the areas of about 20 A^2/residue, where the steep increase in pressure took place. In this region, the pressure dropped down to almost zero only when the film was slightly re-expanded. Such a phenomenon may reasonably be related to the coherent nature of the film.

(6) **Anisotropy of Surface Pressure.**—It was observed that one drop of castor oil, the form of which was perfectly circular when dropped down onto the surface film of 6-nylon, became deformed to an ellipsoid as the film was compressed, the longer axis being at right angles to the direction of compression. This is schematically illustrated in Fig. 3. It was also observed that the deformation of the oil drop which thus occurred became relaxed as the time elapsed after compression. It was also found that two blades of the Wilhelmy dipping slide for measuring the surface pressure, which were so hung that one was parallel to the direction of compression, the other at right angles to it, respectively, registered different pressures

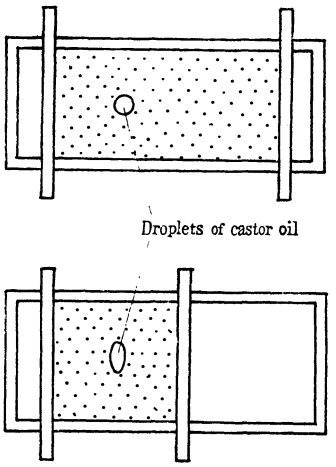

Fig. 3. Schematic illustrations of the anisotropy of surface pressure set up after compression of the films.

below the area of about 40 A^2/residue, somewhat larger values being obtained with the latter slide. These facts readily show that the surface pressure became anisotropic under compression.

(7) **Effect of Temperature on Surface Pressure.**—Temperature dependence of the surface pressure at a fixed area was examined at various areas. Temperature change was performed at a rate of 10 minutes/temperature degree, and the results were listed in Fig. 4. The pressure decreased with the

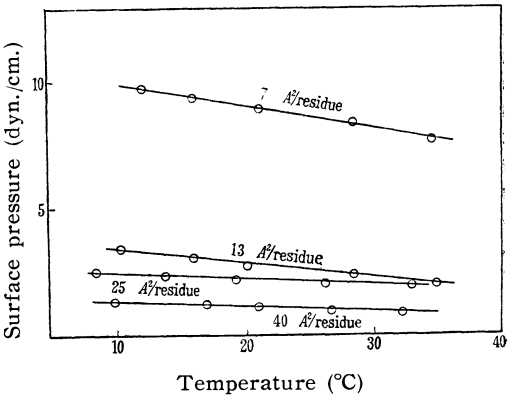

Fig. 4. Temperature dependence of surface pressures at various areas.

rise of temperature at all areas. Such a temperature effect is similar to that on the films of synthetic polypeptides[5]. Buna-N[6], and of the long chain Ureas[7].

5) T. Isemura and K. Hamaguchi, This Bulletin, **25**, 40 (1952).
6) K. Suzuki, *Kōshitsugaku-ronso* (Discussions of Colloid Science), **1**, 63 (1947).
7) J. Glazer and A.E. Alexander, *Trans. Far. Soc.*, **47**, 401 (1951).

(II) Surface Potential-Area Curve

The surface potential versus area curve was shown together with the π-A curve in Fig. 1. The surface moment (μ_s), which persisted almost constant value about 230 millidebyes at large areas, began to decrease below the area of about 40 A^2/residue which was fairly consistent with the point (a) in the π-A curve.

(III) Electron Microscopic Examinations

It is of importance to inquire what structural change of the film corresponds to the

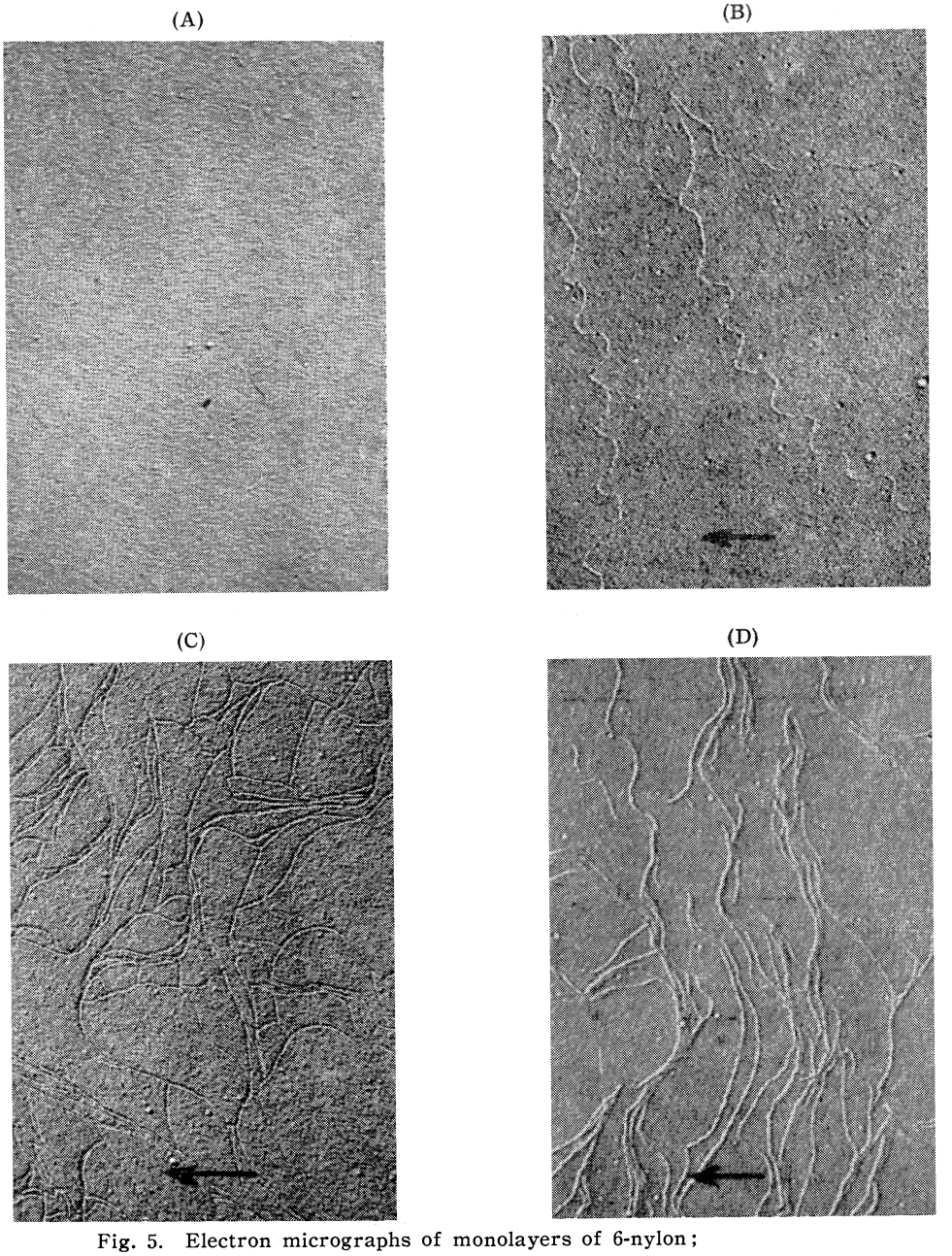

Fig. 5. Electron micrographs of monolayers of 6-nylon;
A, Blank, no film, magnification 13500;
B, Uncompressed films at 80 A²/residue, magnification, 13500
C, Compressed films at 50 A²/residue, magnification 13500
D, Compressed films at 40 A²/residue, magnification 13500

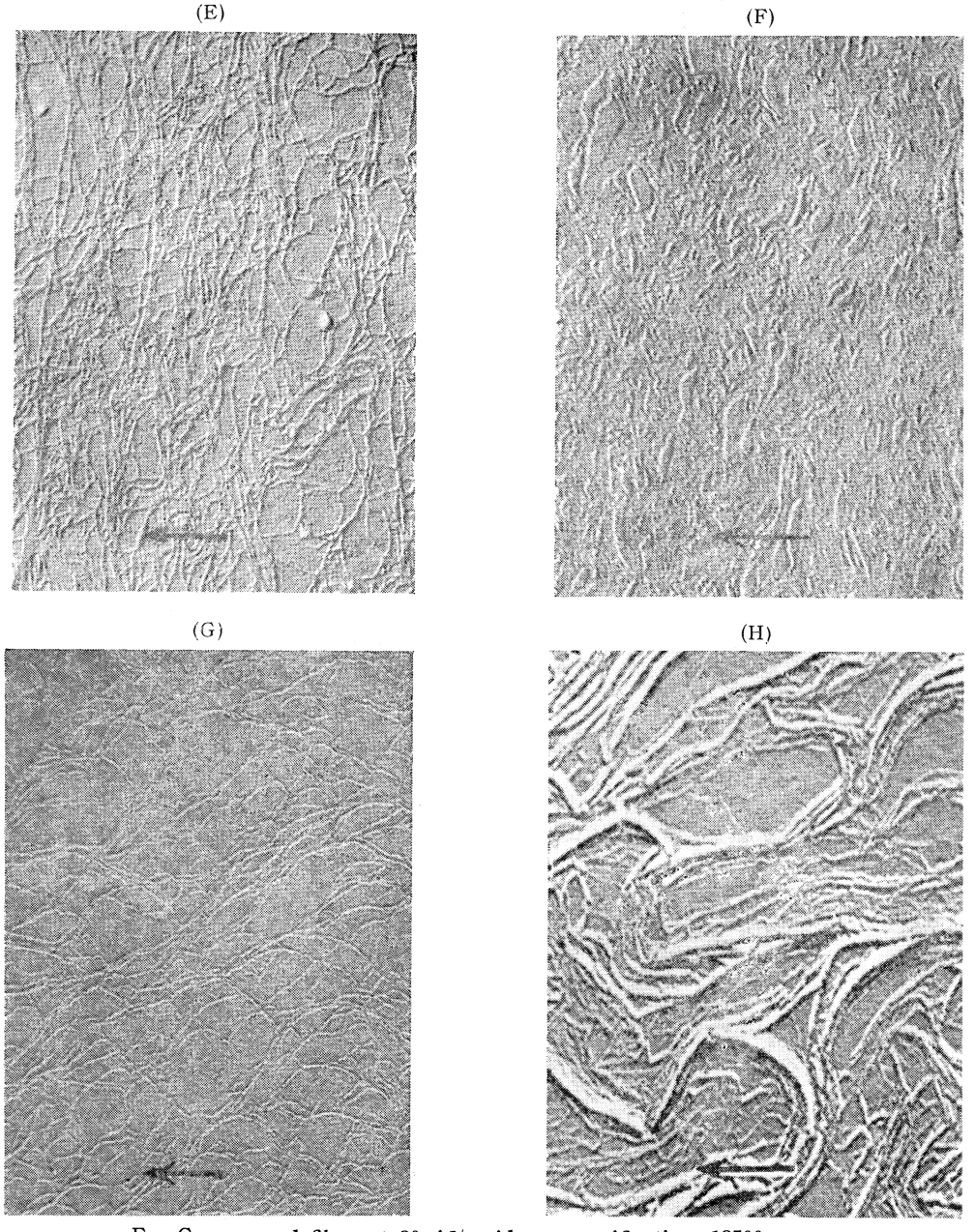

E, Compressed films at 30 A²/residue, magnification, 13500
F, Compressed films at 18 A²/residue, magnification, 13500
G, Uncompressed films at 18 A²/residue, magnification, 13500
H, Uncompressed films of low molecular fraction at 18 A²/residue, magnification, 135000
Arrows indicate the direction of compression.

characteristic areas (a) and (b). For this purpose, electron microscopic examination of the film[8], developed in our laboratory, have proved considerable merits.

A blank water sample is shown in Fig. 5A. Fig. 5B shows the film, taken at 80 A^2/residue at which the film was initially spread. There exist unspread materials which appeared as several fibrils running windingly. This film was compressed to various areas, at which the film specimens for electron microscopy were taken. Figs. 5C, 5D and 5E

8) T. Tachibana, K. Inokuchi and T. Inokuchi, *Nature* **176**, 1117 (1955).

are the films compressed to 50 A^2/residue, 40 A^2/residue, and 30 A^2/residue, respectively. It is shown that as the reducing area, more fibrils appeared than those which were expected to increase by the compression of the films, and came to link together forming a network structure. It is to be noted that at 30 A^2/residue, fibrils oriented normal to the direction of compression. Such an orientation, which could hardly be seen above 40 A^2/residue, was more and more pronounced as the compression advanced. Fig. 5F is an appearance of the film, which was compressed to 18 A^2/residue. Bare portions inside the network of fibrils disappeared, the whole area of the film being covered by the skinlike texture. Fig. 5G shows the uncompressed film which was initially spread at 18 A^2/residue. In contrast with the compressed film, it was noted that uncompressed films have fewer fibrils, and showed no sign of orientation of microfibrils. The effect of the degree of polymerisation on the structure of surface films has also been revealed by electron microscope. In Fig. 5H is shown the structure of uncompressed films (M. W. 1000) spread at 18 A^2/residue. Comparison of Fig. 5G, and Fig. 5H shows that the low molecular weight fraction produced thicker microfibrils than the high molecular one.

The relationship between amounts of microfibrils and area were roughly evaluated from the micrographs at various areas. In Fig. 1, the avarage total sum of the length of the microfibrils per sq. micron was plotted against the area together with the π-A curve and the potential curves. It is seen in this figure that increase in microfibrils, which was relatively slight at large areas, became pronounced below about 40 A^2/residue. It is suggestive that this area is fairly consistent with the point (a) in the π-A curve as well as with the point of the levelling off in the surface moment-area curve.

Discussion

Microfibrillar Structure of Surface Films. —It is first noticed that electron micrographs exhibit microfibrils, the size of which is almost constant at all compression, being estimated close to 40 Å from the width of the shadow. Although it is not clear at the present stage why the molecular association is stable with this size, it is very interesting to refer the Ribbi's experiment[9] that demonstrated the submicroscopic fibrils of forming the structural unit in the fibre of 6-nylon. Since, as the film was compressed, more fibrils appeared than the increase which is to occur as the result of the compression alone, it is clear that the bare portions of the micrographs, at which the microfibrils are absent, also possess film molecules. Although it is difficult to inquire in detail the film structure of this bare portion, it is readily known from the simple calculation*3 that the fraction of the molecules participating to form the microfibrils against the total amount of the spreading molecules is comparatively small at large areas, being about 10% at the point (a), and the remainder forms the bare portions of the films. Moreover, the co-area of the molecular residue at the bare portions of the area of point (a) is roughly estimated by counting the increase of about 10% to the value of the mean co-area of the point (a) (37 A^2/residue), and it is noticed that this value obtained is approximately consistent with the co-area of a residue of flat configuration calculated from the molecular model (40 A^2/residue). Hence, it may be assumed that the bare portions of the surface film at the point (a) possess close-packed molecules with their chains flat on water surface.

It was found from the rheological measurement that the film manifested a distinct elasticity below the areas of about 80 A^2/residue (gelation-area), which is about twice the area of the close-packed area. From the molecular weight dependence of the gelation-area, it was shown in the preceding paper that the film molecules took configuration which was considerably stretched and of less flexibility. Such a molecular configuration may be favorable for the alignment of adjacent molecular chains to form two-dimensional micellar structure. Such film molecules may come into contact with each other under compression to form a two-dimensional network at the gelation-area, at which a distinct elasticity begins to manifest itself. Thus, there must be a two-dimensional network covering the bare portion of the electron micrograph at 80 A^2/residue. Further compression would make

9) Cf. E. Ribbi, *Nature*, **168**, 1082 (1951).

*3 Percentage of molecules of forming the microfibrils against the total molecules (P) at the area of point (a) (mean co-area, 37 A^2/residure) is given as

$$\left\{\left(\frac{L}{m}\right)\times n \Big/ \frac{1}{37\times10^{-8}}\right\}\times 100,$$

where L is the mean total sum of the length of the microfibrils per μ^2, expressed in μ, the value of which at the point (a) is obtained as about 5 μ from Fig. 1, and m, the length of the residue which is 8.5 A with 6-nylon, and n, the number of molecules within the cross section of the microfibril. Assuming that a microfibril is made of the molecular chains, closely packed against each other and running parallel to the length of it, it follows that the cross section of the fibrils consists of about 64 molecules, since the cross sectional area of a molecular chain is calculated as about 20 A^2 from the molecular model. Hence, P is obtained as about 10%.

the network denser until a monomolecular layer of the close-packed molecules is formed at the point (a), though a few of the molecules happen to associate with each other to form microfibrils. Below the area of point (a), all the molecules at the monolayer portions are no longer allowed to stand flat on water surface, and the film may fall into collapse. This is indicated by the surface moment-area curve, which shows sudden decrease in electric moment below about 40 A^2/residue. It is likely that this collapsing process actually involves fibril formation of molecules in the monolayer, since it is visualized from Fig. 1 that a steep increase in the amount of microfibrils appears below the areas 35 to 40 A^2/residue, fairly coincident with the point (a). Thus, the onset of the plateau in the π-A curve is accounted for by the sudden increase in association of molecules to the three-dimensional direction (formation of microfibrils), in which the lateral pressure might relax on further compression. As visualized in Fig. 5E and F, with the advancing compression, the microfibrils become denser and denser until they cover the whole area at about 20 A^2/residue, below which the pressure again rises steeply, and the micrographs fail to exhibit any fibrillar structure, showing. a skinlike texture. At 18 A^2/residue (Fig. 5F), there exsist a number of islands of about 50 A thick upon the back texture. From these findings, it may be considered that the plateau region in the π-A curve corresponds to the stage of formation of monofibrillar layer, and that the compression below the plateau region results in bifibrillar layer which transforms to polyfibrillar layer on further compression. In brief, it was evidently proved that the surface film of 6-nylon possesses microfibrillar structures, which presumably develop from monomolecular network, and transform to polyfibrillar layer under compression process.

Rheological Characteristics of Surface Films.—As shown in the electron micrographs, surface concentration of microfibrils at larger areas than the point (a) is so small that they fail to link together. So it is considered that the microfibrils are not primarily concerned with the film elasticity, but the portions of the monolayer network (bare portions of the micrographs) are chiefly responsible for the development of the elasticity. On the contrary, it was found that the microfibrils link together at areas below about 40 A^2/residue, forming a network of microfibrils. This time, it is easily understood that the microfibrils play an important role in the development of the film elasticity. This trend may be pronounced as the film is compressed, since the network of the microfibrils become more and more dense. In short, two types of surface films are presented; a monomolecular network at larger areas, and a network of the microfibrils at smaller areas.

In the preceding paper[1], it was reported in detail that the film at areas larger than about 40 A^2/residue behaves as a purely elastic body which is hardly seen in the ordinary materials at bulk, whereas it became viscoelastic as is often the case with the ordinary materials at bulk when the film was compressed to small areas. It is readily noticed that the ideal elastic film corresponds to the monomolecular network, and the viscoelastic film, to the network structure of microfibrils. Fibrillar structure is essentially the same as that of the bulk materials, and it is rather natural that the film of fibrillar structure shows viscoelasticity.

It is also suggested that, with the films of ideal elasticity, the cross-linkings of the molecular chains are necessarily homogeneous. As is indicated from Fig. 2, showing that the expansion hysteresis of the π-A curve is only slight at areas larger than the point (a) (the portion of the monomolecular network), it is easy to accept the thought that orientation and alignment of molecules at the monomolecular network may be relatively easy compared with the films at smaller areas, and the relatively homogeneous network may result. Ideal elasticity of the monomolecular film of 6-nylon may thus be explained.

Correspondence between Surface Pressure and Surface Elasticity.—There are many evidences which support the view that the apparent surface pressure exerted here is intimately related to the surface elasticity. It has been observed that the characteristic form of the force-area curve, involving the plateau, bears considerable resemblance to that of the rigidity-area curve. The sign of the temperature dependence on the surface pressure was found to be negative, being just the same with the case of surface rigidity as reported in the preceding paper[1]. Moreover, surface compressibility $\left(-\frac{1}{A}\frac{dA}{d\pi}\right)$ was obtained from the π-A curve, and according to Bateman[10], the surface modulus of rigidity was calculated under the assumption that the film is isotropic and the poisson ratio 0.4. The calculated values were compared with the observed ones obtained with our direct measurement of the surface rigidity. The result is given in Fig. 6, in which

10) J.B. Bateman and J.A. Chambers, *J. Phys. Chem.*, 45, 209 (1941).

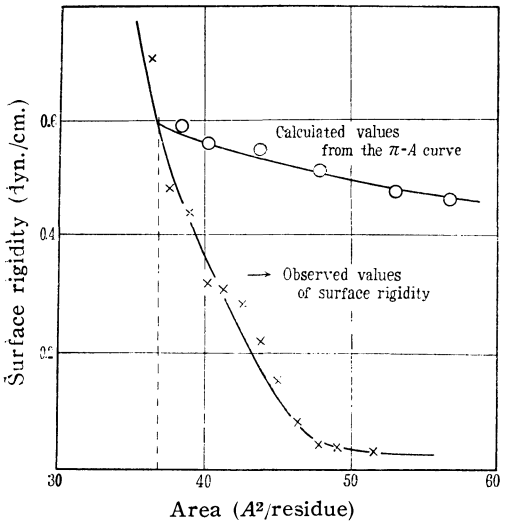

Fig. 6. Correspondence between surface pressure and surface rigidity.

considerable departure between the observed values and the calculated ones at larger areas became less serious as the reducing areas, and finally coincide with each other at the vicinity of 37 A^2/residue. Discrepancy of these values at larger areas may be plausible, since, at larger areas than the point (a), the observed pressures involve osmotic natures of the film molecules which do not participate in the formation of network. Coincidence of these values at the close-packed monolayer may possibly indicate that the surface pressure from the close-packed monolayer is wholly due to the internal stress of the solid film. These facts strongly suggest that the pressure exerted from the compressed films is not likely to have osmotic pressure of entropy nature as commonly considered, but is intimately related to the elasticity of solids.

Orientation of Microfibrils during Compression.—It is worth noticing that below about 40 A^2/residue, the microfibrils came to orient at right angles to the direction of compression. Extremely high compression of surface film gave rise to tiny visible striations running across the width of the through and finally produced fibrous threads which can be picked up from the water surface. It was observed that the structure of such films exhibited an array of microfibrils developed in straight lines orienting in a parallel manner to the striation or to the fibre. On the other hand, as shown in Fig. 5G, the uncompressed film initially spread at small area, e. g., 18 A^2/residue, gave winding microfibrils which had no sign of orientation.

It was demonstrated above that the compression process makes the surface pressure anisotropic, the pressure against the right angles to the direction of compression being larger than that parallel to it. This is not surprising, because it is considered that the film under investigation is not fluid, but probably solid. It is easily surmised that the orientation effect of the film molecules is brought about from this anisotropic nature of the surface pressure, which may probably orient the molecules with their long axis to the right angles to the direction of compression, in order to relax the pressure difference set up readily after compression.

The author believes that these interesting results provide a new line of evidence for the information of surface films of crystalline polymers.

Summary

(1) Surface films of 6-nylon at air/water interface were investigated by means of electron microscopic observation together with the study of the surface pressure and potential.

(2) An unique structure involving the microfibrils of about 40 A thick were revealed which are formed from the monomolecular network at large areas, and are transformed to polyfibrillar layer during the compression process.

(3) Network structures of the film were divided into two types: a monomolecular network at large areas, and a network of the microfibrillar structure at small areas. Rheological characteristics of 6-nylon film were explained in terms of such structures.

(4) Many evidences were provided which support the view that the surface pressure measured with this film is not likely to have the osmotic pressure as commonly considered, but is intimately related to the surface elasticity of the film.

(5) It was observed that the compression process orients the microfibrils at right angles to the direction of compression. This phenomenon was explained by the anisotropy of surface pressure set up by the compression of the film.

The present author wishes to express his hearty thanks to Prof. T. Tachibana for his helpful advice and encouragement throughout this study, and to Mrs. T. Inokuchi for her elaborate technique of the electron micrography.

Department of Chemistry, Faculty of Science, Ochanomizu University
Tokyo

*Effect of Surface Active Reagents on Electrode Process in Oscillographic Polarography**

By Hideo IMAI and Shōkichi CHAKI

(Received February 7, 1956)

The effect of a surface active reagent on a polarographic reduction has been investigated from two points of view, one of which is the suppression of a maximum wave and the other is the retardation of an electron transfer process. Delahay[1], Randles[2], Gierst and Juliard[3], Heyrovský[4], and others studied the latter phenomenon, and from their experimental results Frumkin[5] proposed the "sieve" theory and Heyrovský suggested a mechanism with respect to the dismutation or disproportionation process of polyvalent cations. On the other hand, Loshkarev and Kryukova[6] observed that in solutions of 6 N-H_2SO_4 containing Ag^+ or Tl^+ ions their electrodeposition was hindered by surface active materials. More recently, Tamamushi[7] pointed out the similar effect on monovalent Tl^+.

An investigation of the same phenomenon has been carried out by one of the present authors[8]. The result of the more detailed investigation is presented in this report.

Experimental

A Ševčik type oscillographic polarograph was employed. The apparatus and the method of measurement were described in the previous report[9]. The details of the experimental conditions are as follows: the rate of variation of the applied voltage (v) = 40 V./s. (in the case of gelatine solution), 50 V./s. (in the case of methyl cellulose solution); sweep frequency = 20 c.p.s.; mercury head = 40 cm.; the rate of mercury flow = 1.94 mg./s.; the life time of the dropping mercury electrode (D.M.E.) = 3.1-3.8 ± 0.02 sec.; the current measuring resistor (Rm) = 30-70 Ω; temp. = 30 ± 0.1°C.

From reagent grade chemicals was prepared the test solution of a constant concentration of 0.5 mol./l. Tl^+, Cd^{++} or Zn^{++}, and each test solution contained 1 mol./l. KBr, KCl, KNO_3 or Na_2SO_4 as the supporting electrolyte and 0.002-0.01% gelatine (G.) or methyl cellulose (M.C.), respectively.

Purified nitrogen was used to remove the dissolved oxigen of the test solution prior to taking a polarogram.

Results and Discussion

The current-potential oscillograms are exemplified in Figs. 1 and 2 in the cases of Tl^+ in mol./l. KCl and Na_2SO_4 containing 0-0.01% M.C., respectively. From these polarograms the maximal peak current, i.e. the current at the maximum life time of the D.M.E., is plotted against the concentration of G. or M.C. as illustrated in Figs. 3, 4 and 5.

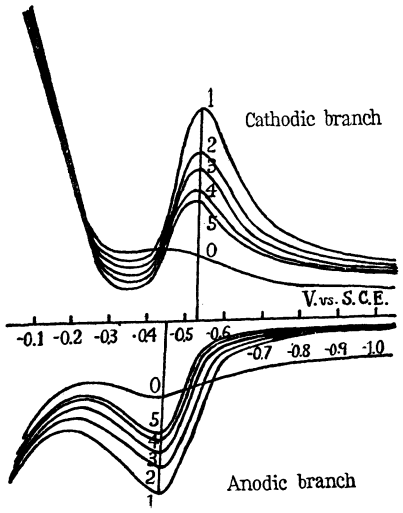

Fig. 1. Maximal peak current-potential oscillogram of 0.5 mM/l. Tl^+ in M KCl: Curve 1; 0% M.C., Curve 2; 0.002%, Curve 3; 0.005%, Curve 4; 0.008%, Curve 5; 0.01%, Curve 0; charging current. $R_m = 40\ \Omega$, $t = 3.1_4$ sec.

* Presented at the discussion on polarography held by the Chemical Society of Japan, the Electrochemical Society or Japan and the Japan Society for Analytical Chemistry in November, 1955.

1) P. Delahay, *J. Phys. Colloid Chem.*, **53**, 1279 (1949).

2) J.E.B. Randles, *Discs. Faraday Soc.*, **1**, 11 (1947).

3) R. Gierst and A.L. Juliard, *J. Phys. Chem.*, **57**, 70 (1953).

4) J. Heyrovský, *Collection Czechoslov. Chem. Communs.*, **19**, S. 58 (1954).

5) A.H. Frumkin, *Discs. Faraday Soc.*, **1**, 224 (1947), *Dokl. Akad. Nauk S.S.S.R.*, **85**, 373 (1952).

6) M.A. Loshkarev and A.A. Kryukova, *Dokl. Akad. Nauk S.S.S.R.*, **62**, 97 (1948).

7) R. Tamamushi, *Polarography*, **3**, 56 (1955); R. Tamamushi and T. Yamanaka, This Bulletin, **28**, 673 (1955).

8) M. Shinagawa and H. Imai, *J. Electrochem. Soc. Japan*, **23**, 187 (1955). Presented at the discussion on analytical chemistry held by the Chemical Society of Japan in November, 1953.

9) H. Imai, This Bulletin, **29**, 276 (1956).

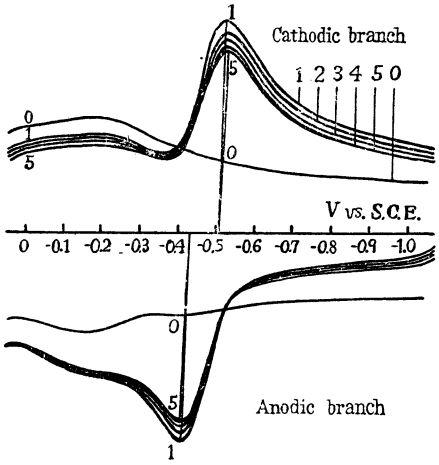

Fig. 2. Maximal peak current-potential oscillogram of 0.5 mM/l. Tl^+ in M Na_2SO_4: The curve numbers correspond to those of Fig. 1. $R_m=70\,\Omega$, $t=3.3_0$ sec.

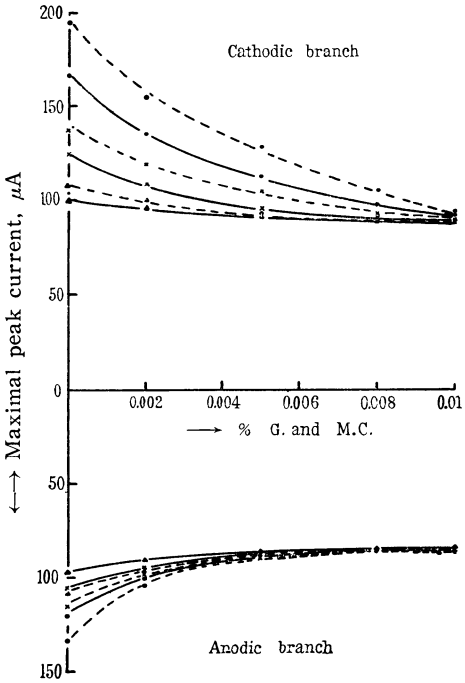

Fig. 3. Variation of the maximal peak current of 0.5 mM/l. Tl^+ with the concentration of G. or M. C.: G.; full curve, M. C.; interrupted curve. G: full curve, M.C: interrupted curve, -●- Cl^-, -×- NO_3^- -▲- SO_4^{--}.

In Fig. 4 it is evident that the cathodic peak current of the solution containing no surface active reagent increases in the solution of SO_4^{--}, NO_3^-, Cl^-, Br^- in the order given. This trend is emphasized in the case of Tl^+ (Fig. 3) and is weakened in the case of Zn^{++} (Fig. 5). Since the peak potential of Tl^+ is more positive than that of Cd^{++} and the

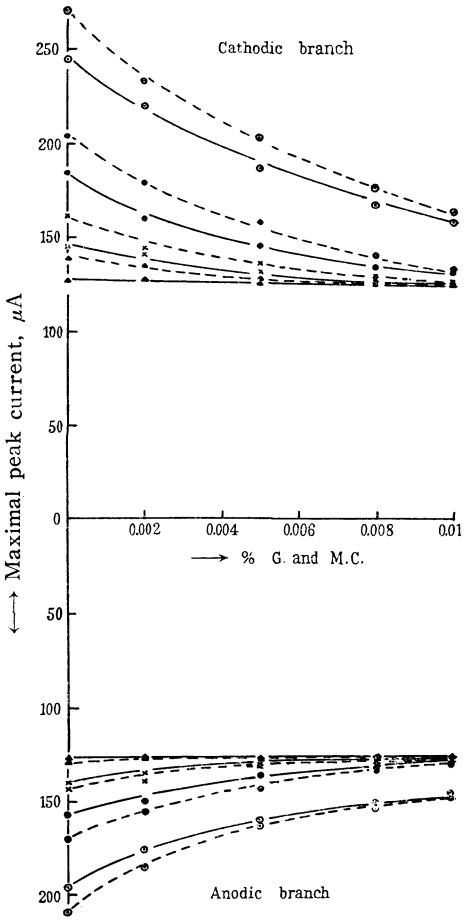

Fig. 4. Variation of the maximal peak current of 0.5 mM/l. Cd^{++} with the concentration of G. or M. C.: G: full curve, M. C.: interrupted curve, -⊙- Br^-, -●- Cl^-, -×-NO_3^-, -▲- SO_4^{--}.

peak potential of Zn^{++} is more negative than that of Cd^{++}, it is assumed that the above mentioned trend becomes weaker as the reduction potential shifts toward more negative potentials. In the anodic branch the same trend is also observed, although the net variation of the peak current is in any case less than the cathodic one.

The above mentioned effect of anions has already been reported by Heyrovský[10], Randles[2], Doss and Agarwal[11], and others[5,12]. One of the present authors[13] has pointed out the parallelism between the catalytic

10) J. Heyrovský, *Discs. Faraday Soc.*, **1**, 212 (1947).
11) K.S.G. Doss and H.P. Agarwal, *J. Phys. Col.oid Chem.*, **54**, 804 (1950).
12) P. Lukovtsev, S. Levina and A.H. Frumkin, *Acta Physicochim. U.R.S.S.*, **11**, 21 (1939). J'OM. Bockris, *Chem. Revs.*, **43**, 525 (1948). R. Pointelli, Int. Comm. Electrochem. Therm. Kin., Proc. 2nd meeting, Tamburini, Milan, 1950, p. 185.
13) H. Imai, Presented at the discussion on polarography held by the Chemical Society of Japan etc. in November, 1955.

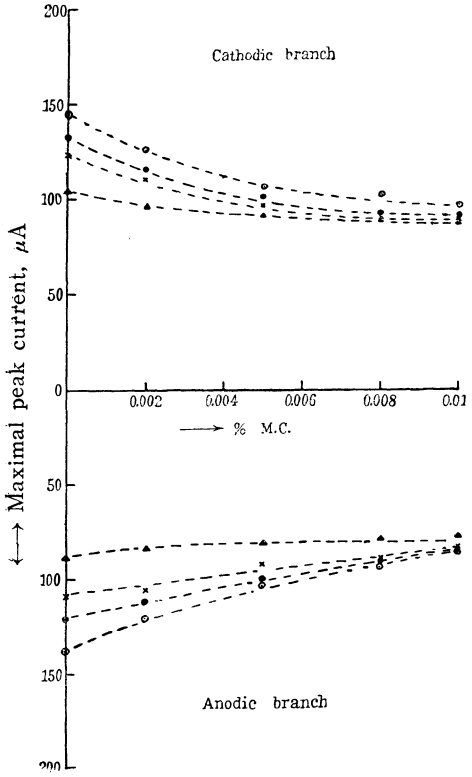

Fig. 5. Variation of the maximal peak current of 0.5 mM/l. Zn^{++} with the concentration of M.C.: -⊙- Br^-, -●- Cl^-, -×- NO_3^-, -△- SO_4^{--}.

effect of an anion and the charging current[14] resulting from anions adsorbed on the surface of the D. M. E.; namely, the charging current becomes more pronounced in the solution containing SO_4^{--}, NO_3^-, Cl^-, Br^-, I^- in the order given and it decreases as the applied potential shifts toward more nagative potentials in the cathodic branch. In the anodic branch a less charging current than the cathodic current is observed in every supporting electrolyte solution. Assuming that the adsorptive density of an anion is proportional to the charging current, one can conclude that the catalytic effect originates from the establishment of the combination such as Hg (electrode)—Adsorbed Anion—Depolarizer Ion, through which the electrone transfer is facilitated.

In the presence of G. or M. C. the catalytic process of an anion is retarded as is illustrated in Figs. 3, 4 and 5. Namely, the effect of G. or M. C. becomes more pronounced in the test solution of the same depolarizer (Tl^+, Cd^{++} or Zn^{++}) containing SO_4^{--}, NO_3^-, Cl^-, Br^- in the order given, and also in the solution of the same supporting electrolyte containing Zn^{++}, Cd^{++}, Tl^+ in the order given. In the anodic process the effect is less than the cathodic one. The parallelism between the catalytic effect and the retarding effect is best realized in the solution containing 0.01% G. or M. C.; that is, in this solution the catalytic effect of an anion is almost perfectly reduced, and accordingly, the cathodic current is nearly equal to the anodic current regardless of the anion constituent.

In the test solution containing Tl^+ no appreciable shifts of the peak potential owing to the presence of G. or M. C. was observed either in the cathodic branch or in the anodic branch. $E_p - E_{p1/2}$ (E_p; the peak potential, $E_{p1/2}$; the half peak potential), however, slightly increases within a few millivolts as the concentration of G. or M. C. increases. The increase of $E_p - E_{p1/2}$ results from the retardation of the rate of the electrode process as is indicated theoretically by Matsuda and Ayabe[15].

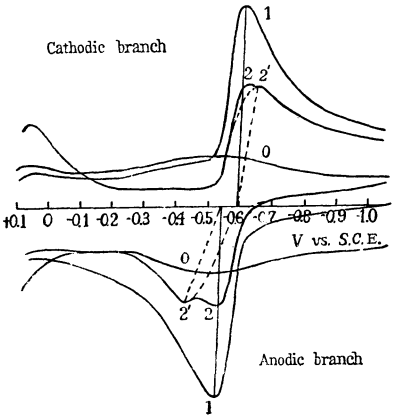

Fig. 6. Maximal peak current-potential oscillogram of 0.5 mM/l. Cd^{++} in M KNO_3: Curve 1; no M.C., Curve 2; 3/4 life time of D.M.E. (0.008% M.C.), Curve 2'; just before the drop falls. (0.008% M.C.)

In the case of Cd^{++} in KNO_3 solution containing more than 0.008% M. C. the peak remarkably shifts toward more negative or more positive potentials in the cathodic or the anodic branch, respectively, as the mercury drop grows ripe. The current-potential oscillogram is illustrated in Fig. 6. Zn^{++} behaves likewise. It is assumed that the phenomenon results from the steric hindrance by the film formation of surface active molecules.

Finally the molecules of a surface active reagent, the concentration of which is as low as 0.002–0.01%, exchange with the anions

14) H. Imai, This Bulletin, 29, 281 (1956).

15) H. Matsuda and Y. Ayabe, *Z. Elektrochem.*, 59, 494 (1955).

existing in the electrode surface (Helmholtz layer) and result in the retardation of the catalytic process displayed by the anions. Hereupon, not only a polyvalent cation but also a monovalent cation (Tl^+) suffer from the catalytic effect of the anion and the retarding effect of the surface active reagent. In this conncetion Heyrovský[4] observed that the electrodeposition of Tl^+ is reversible and is not hindered by the presence of gelatine. From Matsuda and Ayabe's theory[15] it is reasoned that the electrode process of Tl^+ is quasi-reversible and is controlled not only by the diffusion of Tl^+ but also by the rate of the electrode process as far as the rate constant, k_G, of the electrode process does not exceed 2 cm./sec. This value is estimated by substituting the numerical values of n and v in $0.3\sqrt{nv}$, where n is the number of electrons transferred per ion and v is the rate of variation of the applied voltage. By the way, the value of k_G of Tl^+ in mol./l. KNO_3 solution is given as great as >1 cm./sec. by Randles and Somerton[16]. Since the electrode process of Tl^+ suffered from the catalytic action of anions in this experiment, it seems that the value of k_G will not be greater than 2.

The phenomenon occurring in the concentration region greater than 0.008% of the surface active reagent is mentioned above, and in the region from 0.008% to 0.04% the diffusion controlled current of an ordinary polarograph is scarcelly retarded, but the peak potential in the oscillographic polarograph shifts remarkably. This effect can be assigned to the film formation of the surface active reagent. The retardation of the diffusion controlled current of an ordinary polarograph in the concentration region of the surface active reagent more than 0.04% is probably explicable on the basis of the "sieve" effect.

Randles[2] observed that the rate constant of the electrode process of Cd^{++} in mol./l. KCl solution is reduced in two steps as the concentration of gelatine increases, and the first step appears in the concentration region from 0 to 0.01% of gelatine and the second step appears in the concentration region of more than 0.04% gelatine. Since these results coincide with those of the present authors, the mechanisms of Randles's results are reasonably explicable by adopting the above mentioned conclusion.

The authors wish to express their hearty gratitude to Dr. Takeshi Taketa and Dr. Mutsuaki Shinagawa for their encouragement throughout this study.

Laboratory of Chemistry, Minami College
Hiroshima University, Hiroshima

16) C.W. Conway, "Electrochemical Data", Elsevier Publ. Co., Amsterdam (1952), p. 356.

Ionization Potentials of Some Organic Molecules. I. Apparatus

By Itiro OMURA, Keniti HIGASI and Hiroaki BABA

(Received February 7, 1956)

With the rapid progress in the theories of molecular orbitals the study of ionization potentials of molecules has gained much theoretical importance. Besides being used to determine which electron is the most loosely bound[1], they can provide data for the calculation of electronic wave functions[2]. And recently these data have been employed even in interpreting the mechanism of organic reactivity[3]. In spite of these facts there are available comparatively few data for only a small number of molecules. In the series of the present reports some results of our measurement will be given which have recently been carried out by the use of a mass spectrometer constructed in the laboratory of the present writers.

1) R.S. Mulliken, *Phys. Rev.*, **46**, 549 (1934); *J. Chem. Phys.*, **3**, 514 (1935).
2) G.G. Hall and J.E. Lennard-Jones, *Proc. Roy. Soc.* (London), A **202**, 155 (1950); A **205**, 541 (1951).
3) S. Nagakura and J. Tanaka, *J. Chem. Phys.*, **22**, 563 (1954).

Instrumental Details and Experimental Method

The apparatus constructed and employed by the present writers belongs to a Hagstrum type mass spectrometer[4]. Its main part of the electron and ion gun circuits is shown schematically in Fig. 1. Electrons emitted from the hot tungsten

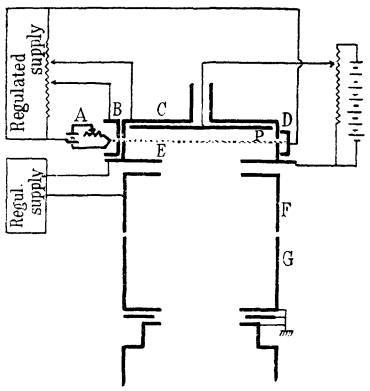

Fig. 1. Schematic diagram of electron and ion gun circuits of a mass spectrometer. A filament, B, C electron accelerating plates, C ionization chamber, D electron trap, P pusher electrode, E electron beam, F, G ion accelerating plates.

filament A are collimated into a beam by the systems of electrodes, B, C, enter the ionization chamber and finally are collected into the trap, D. The energy of the electrons causing ionization is largely determined by the potential difference between C and A, which can be varied. Ions formed in this chamber are acted on by a cross-field of up to one volt, which is applied between the pusher electrode P and the ionization chamber, and then they pass into the F—G lens in which they focus upon the input slit of the magnetic analyzer[4]. In order to make the collimation of the electron beam easier, a magnetic field of 200 oersted is applied, the lines of force of which are parallel to the axis of the electron beam.

Finally, ion currents to the collector plate are measured and their dependence on the potential difference between C and A is recorded. The

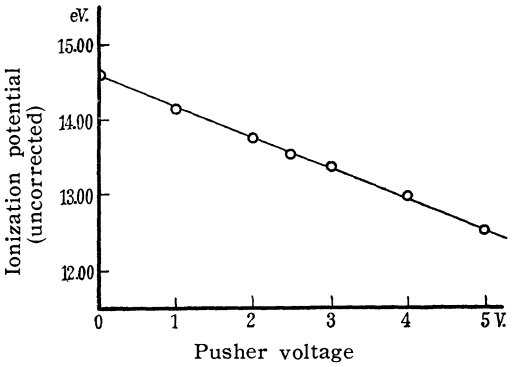

Fig. 2. Variation of the uncorrected ionization potential of argon with the potential of the cross field.

latter quantity is not to be simply put as equal to the energy of the ionizing electron beam. That is, there are many complicating factors which influence the energy of the ionizing electron[5]. From among the factors examined in the present work, two will be mentioned; viz., the effects of the pusher voltage and the intensity of ion current. First, the effect arising from the pusher voltage is shown in Fig. 2. The linear relationship exists between the ionization potential and the pusher voltage which is in accord with the calculation of Jordan et al[6]. Second, Fig. 3 shows

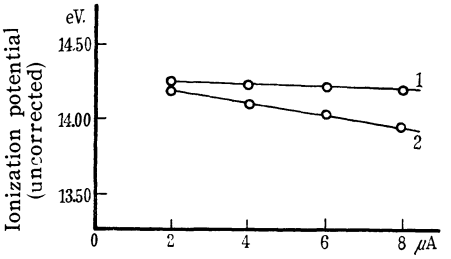

Fig. 3. Variation of the uncorrected ionization potential of argon with the intensity of the electron current.
1 critical slope method; 2 extrapolation method.

the effect due to the intensity of the electron current. The variation of the ionization potential is less pronounced in the critical slope method[7] than in the usual extrapolation method.

The ionization potentials recorded in the present work were determined in comparison with the spectroscopic value of argon, 15.76 eV. This standard gas is introduced and measured, immediately before and after the ion being studied. The fluctuations in this correction in a day were usually less than ±0.02 eV.

Measurements of the ionization potentials were made with the following conditions;

i) Electron currents trapped at D 5 μA,
ii) Electron accelerating voltage 0∼+20 V.,
iii) Trap potential at D+100 V.,
iv) Potential at the pusher electrode 0∼+1 V.,

The slits employed in the ion lenses are wider than usual, the slit in ionization chamber 4×10 mm., and the final slit 0.25×10 mm.

Accuracy of the Experimental Results

Two methods have been frequently employed in determining the ionization potentials[5]: (1) the method of linear extrapolation and (2) Honig's[7] critical slope method. Both of them were examined in the present work (see Table I). Values obtained by critical slope method were in better agreement with spectroscopic values. Generally the critical slope method gave reproduceable values. Therefore, this method was employed throughout in the present work.

In Table II representative values of ionization

4) H. D. Hagstrum, *Revs. Modern Phys.*, 23, 185 (1951).
5) See, for example, G.P. Barnard, "Modern Mass Spectrometry", London (1953).
6) E.B. Jordan and N.D, Coggeshall, *J. Appl. Phys.*, 13, 539 (1942).
7) R.E. Honig, *J. Chem. Phys.*, 16, 105 (1948).

TABLE I

APPEARANCE POTENTIALS MEASURED BY VARIOUS METHODS, eV.

Substance	Linear extrapolation	Critical slope	Spectroscopic
Argon	(15.76)	(15.76)	15.76[a]
Neon	21.68	21.62	21.58[5]
Nitrogen	15.67	15.56	15.58[5]
Hydrogen disulfide	10.62	10.54	10.47[b]

a) Moore's value cited by D.P. Stevenson (*Trans. Faraday Soc.* **49,** 867 (1953)).
b) W.C. Price, *Chem. Rev.*, **41,** 257 (1947).

there is no need of perfect agreement among the values of the two methods[5], if the impact value of argon is taken from its spectroscopic value.

In conclusion, it may be said that the use of a single standard gas is justfied and also that ionization potentials of molecules are satisfactorily obtained by the apparatus of this experiment for the samples treated so far.

Summary

Instrumental details of electron impact method for determining ionization potentials are recorded. Further, it is shown that the potential values obtained by the present method are in good agreement with the data reported by the previous workers.

TABLE II

FIRST IONIZATION POTENTIALS OF MOLECULES, eV.

Substance	Present work (Electron impact)	Values in literature (Electron impact)	(Spectroscopic)
Argon	15.76[a]	15.76[a] (15.77)[5]	15.76[a] (15.77)[5]
Neon	21.62±0.05	21.53[b] (21.61; 21.24; 21.42; 21.57)[5]	21.58[5]
Hydrogen	15.51±0.10	15.40[c]	15.42[d]
Nitrogen	15.56±0.10	15.66[b] (15.60; 15.57)[5]	15.50[e]
Oxygen	12.45±0.10	12.50[b] (12.20; 12.39)[5]	12.26[5]
Methyl alcohol	10.97±0.05	10.95[b]	10.80[f]
Ethyl alcohol	10.65±0.05	10.60[b]	10.70[f]
Methyl amine	9.41±0.02	9.41[b]	9.80[f]
Benzene	9.52±0.10	9.52[b]	9.24[f]
Toluene	9.20±0.05	9.23[b]	8.82[f]
Pyridine	9.76±0.05	9.8[h]	
Furan	9.00±0.10	9.05[b]	9.01[g]

a) Moore, loc. cit.
b) J.D. Morrison and A.J.C. Nicholson, *J. Chem. Phys.*, **20,** 1021 (1952).
c) W. Bleakney, *Phys. Rev.*, **35,** 1180 (1930).
d) H. Beutler und H.-O. Jünger, *Z. Physik.*, **100,** 80 (1936).
e) R.E. Worley and F.A. Jenkins, *Phys. Rev.*, **54,** 305 (1938).
f) W.C. Price, *Chem. Rev.*, **41,** 257 (1947).
g) W.C. Price and A.D. Walsh, *Proc. Roy. Soc.* (London), **A179,** 210 (1941).
h) A. Hastrulid, P. Kusch and J.T. Tate, *Phys. Rev.*, **54,** 1037 (1938).

potentials determined in the present studies are compared with those of previous workers. They include five inorganic gases and seven organic vapours. Observed potentials lie in the range between 9 and 22 eV. In all these examples there is general agreement with the values of the previous workers obtained by electron impact method.

On the comparison with spectroscopic values there exists some divergence in values. But

8) J.D. Morrison and A.J.C. Nicholson, *J. Chem. Phys.*, 20, 1021 (1952).

The authors wish to express their gratitude to Prof. K. Hirota for initiating the present work, and also to the Ministry of Education for a Grant in Aid.

Research Institute of Applied Electricity
Hokkaido University, Sapporo

Ionization Potentials of Some Organic Molecules. II. Aliphatic Compounds

By Itiro OMURA, Keniti HIGASI and Hiroaki BABA

(Received February 7, 1956)

Introduction

There are numbers of molecules the ionization potentials of which are largely determined by non-bonding electrons. When dealing with these molecules it was often assumed that there is some relation between the dipole moment and the ionization potential[1]. First, in the present article, the appearance potentials obtained for seven aliphatic alcohols and three aliphatic amines will be reported. Contrary to the majority of the homologous series the polarity of homologous alcohols remains constant or even decreases with the increase in the carbon number[2,3].

Second, the appearance potentials of two unsaturated aldehydes and two ketones will be treated. From the studies on the dipole moment[4] it is known that there are two factors which affect the electron migration in these molecules, viz., hyperconjugation and inductive effect. For instance, it was inferred that the molecule of acrolein facilitates the transmission of charge to the negative oxygen by means of contribution from structures such as

$$^{+}CH_2-CH=CH-O:^{-} \quad H^{+}\ddot{C}H-CH=CH-O:^{-}$$

If the ionization potential of acrolein is determined by the lone pair of electrons on the oxygen atom, the effect of hyperconjugation will appear in the observed values of potentials.

Lastly, discussion will be presented on the ionization potentials of the molecules, $CH_3CO\cdot X$ (X=OH, NH_2, H and CH_3).

Experimental Materials

Alcohols (Kanto Chem. Co., Inc.) were distilled and their purity was checked by measuring the refractive index for D-line at room temperature. Methyl alcohol b. p. 64.5°C, $n^{20}=1.3310$; ethyl alcohol b. p. 78°C, $n^{20}=1.3623$; *n*-propyl alcohol b. p. 97°C, $n^{20}=1.3846$; isopropyl alcohol b. p. 82.4°C, $n^{25}=1.3764$; *n*-butyl alcohol b.p. 117.0°C, $n^{20}=1.3962$; isobutyl alcohol b. p. 107.0°C, $n^{15}=1.3975$; *tert*-butyl alcohol b. p. 82.4°C, $n^{25}=1.3847$.

Amines (Kanto Chem. Co., Inc.) were prepared by distilling off their 25% water; and the degree of purity was examined by a mass spectrometer.

The sample of mesityl oxide in the pure form was very kindly provided by Dr. Nagakura of Tokyo University. Crotonaldehyde was kindly provided by Mr. Maekawa; b. p. 95–110°C, $n^{20}=1.4394$. The remaining samples were obtained from Kanto Chem. Co., Inc. Acrolein b. p. 52–53°C, $n^{20}=1.4005$; acetone b. p. 56.2–56.5°C, $n^{20}=1.3592$; acetic acid b. p. 117–118°C, $n^{20}=1.3723$; ethyl mercaptan b. p. 36–37°C, $n^{20}=1.4307$; acetamide m. p. 79.5°C.

Experimental Method and Result

The measurement of the first appearance potentials was made by the use of an apparatus described in a previous report[5]. Honig's critical slope method was employed throughout, and examples of this application to butyl alcohols are shown in Fig. 1. It is to be noted in this connection that Morrison and Nicholson[3] reported that

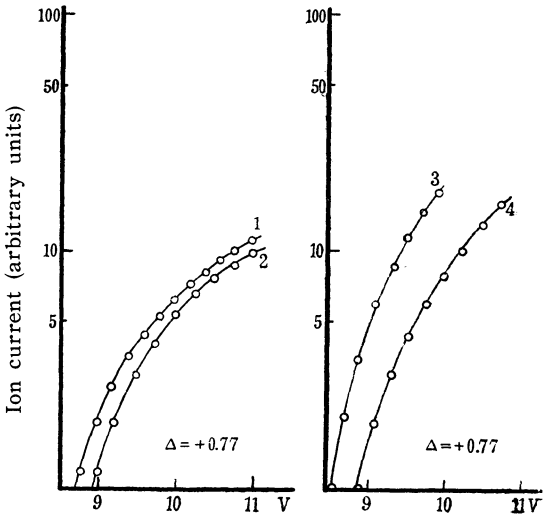

Fig. 1. Relative ionization efficiency curves for alcohols. 1 *tert*-butyl alcohol; 2 isopropyl alcohol; 3 isobutyl alcohol; 4 *n*-butyl alcohol.

1) C.A. Coulson, "Valence", Oxford (1952), p. 186.
2) M. Kubo, *Sci. Pap. Inst. Phys. Chem. Res.* (Tokyo), **26**, 242 (1953); **27**, 65 (1935).
3) K. Higasi, ibid., **31**, 311 (1937).
4) C.P. Smyth, "Dielectric Behavior and Structure", McGraw-Hill Book Co., New York (1955).
5) I. Omura, K. Higasi and H. Baba, This Bulletin, **29**, 501 (1956).
6) J. D. Morrison and A. J. C. Nicholson. *J. Chem. Phys.*, **20**, 1021 (1952).

no measurement on *n*-butyl alcohol was possible for them on account of the small quantity of molecular ion. Further, Franklin[7] appears to have also failed in measuring the appearance potential of *tert*-butyl alcohol. The reason why such difficulty could be overcome in the present work is probably due to the use of the cylindrical ion lenses[5].

In Table I the results of the present work are collected and compared with the data available. It will be seen that the agreement is satisfactory throughout.

TABLE I

FIRST IONIZATION POTENTIALS, eV.

Substance	Present work	Previous workers	
Methyl alcohol	10.97±0.05	10.95[5]	(10.80[9])
Ethyl alcohol	10.65±0.05	10.60[5]	(10.70[9])
n-Propyl alcohol	10.42±0.10	10.46[5]	(10.70[9])
Isopropyl alcohol	10.27±0.10		
n-Butyl alcohol	10.30±0.10		
Isobutyl alcohol	10.17±0.10		
tert-Butyl alcohol	9.92±0.10		
Methyl amine	9.41±0.02	9.41[5]	(9.80[9])
Dimethyl amine	9.21±0.05		(9.60[9])
Trimethyl amine	9.02±0.05		(9.40[9])
Ethyl mercaptan	9.21±0.05		(9.70[9])
Acetone	9.89±0.05	9.92[5]	
Acetic acid	10.66±0.05	10.70[11]	
Acetamide	10.39±0.05		
Acrolein	10.25±0.05	10.34[5]	
Crotonaldehyde	9.81±0.05		
Mesityl oxide	8.89±0.05		

Values in parentheses refer to spectroscopic potentials.

Discussion

As reported in a previous note[8] the general lowering of the ionization potential with the increase in carbon number is found in the observed values of aliphatic alcohols. When one hydrogen atom is replaced by one methyl radical at α carbon atom, the decrease 0.3–0.4 eV. is found, while such decrease amounts to only 0.2 eV., if the same occurs at β carbon atom (see Table II).

Three kinds of explanation can be offered for the observed change of the potential. The first may result from the following assumptions; (1) the ionization potentials of alcohols are solely determined by the non-bonding electrons on the oxygen atom[9]; and (2) alkyl radicals have the property of electron repulsion, the latter being increased along the series[10]

$$-CH_3 < -CH_2(CH_3) < -CH(CH_3)_2 < -C(CH_3)_3.$$

By the so-called inductive effect electrons tend to move from the alkyl group to the oxygen atom, thus reducing the electronegativity of the oxygen atom. Consequently, it would result in the lowering of potentials which is in qualitative agreement with the results shown in Table II.

TABLE II

BRANCH EFFECT OF ALIPHATIC ALCOHOLS ON POTENTIALS (eV.) AND MOMENTS (DEBYE)

Substance	Potential (obs.)	Potential (calcd.)	Moment[3] (gas)	Moment[3] (solution)
CH_3OH	10.97	[10.95]	1.69	1.62
	(0.32)			
$CH_2(CH_3)OH$	10.65	10.54	1.69	1.66
	(0.38)			
$CH(CH_3)_2OH$	10.27	10.07	1.63	1.66
	(0.35)			
$C(CH_3)_3OH$	9.92	9.69	——	1.66
CH_3CH_2OH	10.65	10.54	1.69	1.66
	(0.23)			
$CH_2(CH_3)\cdot CH_2OH$	10.42	10.36	1.66	1.66
	(0,25)			
$CH(CH_3)_2\cdot CH_2OH$	10.17	9.97	1.63	1.65

Potential value in brackets was taken as the standard in calculations.

To argue against the above view, one may point out the fact that the electric moment of alcohols does not increase with the increase in the carbon number[2,4]. But this evidence may not be convincing. There are two dipoles in the molecule: one along the O–H linkage, the other along the C–O linkage and they make an angle with each other. Although the C–O bond moment may increase with the electron transmission toward the oxygen atom, the larger O–H moment will not increase but possibly decrease. Consequently, it is likely that no appreciable increase in the whole moment would result, if such electron displacement actually occurs. One is to note instead that the above series of the electron repelling property have been derived from chemical reactivities and they rest on no sound physical evidence*. If this mechanism of the electron displacement be true, it is highly doubtful whether it is significant enough to produce the observed effect.

The second explanation comes from the application of group orbitals[11]. As is well known this method requires the solution of the secular equation

$$|e_{ij} - E\delta_{ij}| = 0$$

7) J.L. Franklin, Private communications.
8) I. Omura, H. Baba and K. Higasi, This Bulletin, 28, 147 (1955).
9) W.C. Price, *Chem. Rev.*, 41, 257 (1947).
10) C. K. Ingold, "Structure and Mechanism in Organic Chemistry", Cornell Univ. Press (1951); Table 7-2, p. 71.

* One of the present writers discussed this problem in other place (cf. K. Higasi and K. Hirota, "Theory of Organic Chemistry", Asakura Book Co., Tokyo (1951), Chap. V).
11) J.L. Franklin, *J. Chem. Phys.*, 22, 1304 (1954).

where i and j refer to various groups in the molecule. The roots of secular equation represent the ionization potentials of the molecule, the lowest root being the first ionization potential measured.

Calculation of ionization potentials according to this method has been done by Franklin[11] for methyl, ethyl and *n*-propyl alcohols. In the present work, further calculations are carried out for remaining alcohols, assuming the same values for the constants, *e*, *b*, *g*, and *c* with those of Franklin. Calculated results are given in the third column of Table II. In view of the fact that this calculation is based on many bold assumptions, it is surprising that the calculated values are in fair accord with those observed.

Both of the views stated above are based on the assumption that the ionization potential is concerned solely with the normal state of neutral molecule before electron impact. Therefore, the third explanation comes from the view that this assumption is not always valid. For instance, Price[9] argues that the effect of alkyl substitution on the ionization potential is due mainly to preferential stabilization of the ionic or excited state. Indeed, his explanation for the ionization potential of RX is in good accord with our results on alcohols. The only regret in regard to this view is that no estimation is possible as to the effect of such a mechanism.

In Table III the measured potentials of

TABLE III

POTENTIALS IN eV. AND MOMENTS IN DEBYE OF ALIPHATIC AMINES

Substance	Potential (obs.)	Potential[11] (calcd.)	Moment[2,3] (gas)
Methyl amine	9.41	[9.41]	1.28
Dimethyl amine	9.21	8.67	1.02
Trimethyl amine	9.02	8.06	0.8

aliphatic amines are recorded. The calculated values based on group orbital method by Franklin[11] are shown in the same table together with the dipole moment values. It will be seen that both potentials and moments decrease with the increase in the number of methyl groups. Agreement with the calculated values is not good. Possibly, this is a case when the effect of molecular ion stabilization is important.

Before discussing the ionization potentials of unsaturated aldehydes and ketones, attention will be drawn to those of saturated compounds in which the lone-pair electrons of the O-atom play a dominant role in the ionization potential[1] (Table IV). Upon the alkyl substitution the decrease in the potential which is accompanied by the increase

TABLE IV

IONIZATION POTENTIALS (eV.) AND DIPOLE MOMENTS (DEBYE) OF KETONES AND ALDEHYDES

Substance	Potential (obs.)	Potential (calcd.)	Moment[3] (gas)
HCHO	10.88[9]	[10.88]	2.27
CH_3CHO	10.28[5]	[10.28]	2.72
CH_3COCH_3	9.89	9.84	2.85
$CH_2=CHCHO$	10.25	——	3.04
$CH_3\cdot CH=CHCHO$	9.81	9.74	3.67
$(CH_3)_2C=CHCOCH_3$	8.89	8.75	2.84*

* Moment obtained in solution.

in moment occurs in these molecules. This is in accord with the simple view that the effect of hyperconjugation as well as the inductive effect of the alkyl group cooperate to concentrate the electrons more towards the oxygen atom, thus resulting in a higher CO bond moment and a lower ionization potential.

The situation in acrolein and crotonaldehyde is somewhat complicated, since there are π-electrons in the C=C bond. The potential decrease on the introduction of one methyl group into the β carbon atom of acrolein amounts to 0.44 eV. If this large decrease be attributable to the change in the electron concentration on the oxygen atom*, this would indicate that the electron transfer is greatly facilitated along the π-bonds. The potential value of mesityl oxide $(CH_3)_2C=C\cdot COCH_3$ is of special interest. It shows a further decrease of 0.92 eV. over the value of crotonaldehyde $CH_3\cdot CH=CHCHO$. For comparison's sake, the results of calculation based on the group orbital method are included in Table IV. The calculated values are in accord with the observed.

Lastly, the potential values of $CH_3CO\cdot X$ will be considered. According to the present measurement (Tables I and IV), $CH_3CO\cdot OH$ 10.66, $CH_3CO\cdot NH_2$ 10.39, CH_3CHO 10.28 and $CH_3CO\cdot CH_3$ 9.89 eV. If the ionization potential is largely determined by the non-bonding electrons at the O-atom, the sequence of $OH>NH_2>H>CH_3$ would indicate that the groups attract electrons more strongly along this series from the oxygen atom. Indeed, this expectation may be fulfilled, if only the inductive mechanism[10] be taken into consideration. But this is a problem which needs further investigation, because there are complicating factors including another mechanism of the electron displacement.

* A support for this view may be found in McMurry's work (*J. Chem. Phys.*, 9, 231, 241 (1941)). According to him, in ketones and aldehydes including acrolein and croton aldehyde, one of the non-bonding electrons corresponds to the most loosely bound electron.

Summary

Ionization potentials of seven alcohols, three amines and nine other aliphatic compounds were determined by a mass spectrometer of Hagstrum type. In view of the fact that no reliable explanation of the ionization potentials of molecules has been given an examination of the possible interpretations of the results was presented. The relation of ionization potentials to the dipole moments, non-bonding electrons and the group orbital method are briefly discussed.

The authors wish to express their gratitude to Dr. S. Nagakura for valuable criticisms and suggestions, and also to the Ministry of Education for a Grant in Aid.

Research Institute of Applied Electricity
Hokkaido University, Sapporo

*Hydrazinolysis of Peptides and Proteins. II. Fundamental Studies on the Determination of the Carboxyl-ends of Proteins**

By Shiro AKABORI, Ko OHNO, Tokuji IKENAKA, Yoshimi OKADA, Hidesaburo HANAFUSA, Ichiro HARUNA, Akira TSUGITA, Kin-ichi SUGAE and Taijiro MATSUSHIMA

(Received January 17, 1956)

Since it was first proposed by Akabori, Ohno and Narita in 1952[1] the hydrazinolysis method has been applied by the same authors and others for the characterization of carboxyl-terminal amino acids in various proteins. On heating the protein in anhydrous hydrazine, peptide bonds are split with the formation of amino acid hydrazides, while the C-terminal residues only are liberated as free amino acids. In earlier works[1,2] hydrazides were removed by condensing with benzaldehyde to give insoluble dibenzal derivatives and the remaining amino acids were identified by paper chromatography. Although it has been applied to several proteins and peptides[1–6], this procedure was rather troublesome, and some less soluble amino acids might be lost in the treatment. Later we have improved the method in the following way: dinitrophenylating the hydrazinolysates and separating the C-terminal DNP-amino acids from di-DNP-amino acid hydrazides, the former thus extracted were characterized and estimated quantitatively by silica gel chromatography[7,8]. Further a method of pre-treatment with isovaleraldehyde followed by dinitrophenylation was also reported briefly[7]. These improved methods were applied to lysozyme[7,8], Taka-amylase A[7], ovalbumin[7], α-chymotrypsinogen[9], α-chymotrypsin[9], tobacco mosaic virus[10,11], and protease hydrolysates of lysozyme[12]. Another application of this method to characterize the mode of linkage of acidic amino acids in the protein was also reported[13].

Another technique to separate C-terminal amino acids from hydrazides using ion-exchangers was also proposed[14].

On the other hand, criticism on the hydrazinolysis method (chiefly on the hydrazinolysis-benzaldehyde method) was proposed in which it was said that the results obtained

* The present paper was written before the Symposium on Protein Structure held on November 15, 1954 at Osaka University.

1) S. Akabori, K. Ohno and K. Narita, This Bulletin, 25, 214 (1952).

2) S. Akabori and K. Ohno, IIe Congres Internationale de Biochimie, Paris, 1952, Resume des communications, p. 47.

3) K. Schlögl and E. Wawersich, *Naturwiss.*, 41, 38 (1954).

4) R.H. Locker, *Biochim. Biophys. Acta*, 14, 533 (1954).

5) K. Satake, K. Kusama and H. Ozawa, Symposium on Protein Structure, Osaka, 1954.

5a) N. Ohta and M. Yamasaki, Symposium on Protein Structure, Osaka, 1954.

6) K. Narita, *J. Chem. Soc. Japan*, 75, 487 (1954).

7) S. Akabori, K. Ohno. T. Ikenaka, A. Nagata and I. Haruna. *Proc. Japan Acad.*, 29, 561 (1953).

8) K. Ohno, *J. Biochem.*, 40, 621 (1953).

9) N. Sakota, S. Kubo, Y. Okada and S. Akabori, *Symposia on Enzyme Chemistry*, 10, 155 (1954).

10) G. Braunitzer, *Z. Naturforsch.*, 9b, 675 (1954).

11) C.I. Niu and H. Fraenkel-Conrat, *Biochim. Biophys. Acta*, 16, 597 (1955).

12) K. Okunuki, B. Hagihara and H. Matsubara, Symposium on Protein Structure, Osaka, 1954.

13) K. Ohno, *J. Biochem.*, 41, 345 (1954).

14) A.J. Ultée, Personal communication.

by this procedure were not in line with those obtained by carboxypeptidase method[15,16] and that the hydrazine is not an entirely satisfactory reagent for this purpose[16].

The present investigation was designed to reinspect this method according to the results obtained by various fundamental experiments, to establish the best method applicable to various proteins, and to consider the scope of it. Experiments reported in this paper include those on (a) the decomposition of free amino acids, (b) the hydrolysis of amino acid hydrazides to amino acids during the treatment, (c) the separation procedure of amino acids from hydrazides, and (d) the rate of hydrazinolysis of peptide bonds. From the results obtained here it can be concluded that the hydrazinolysis-DNP method gives mostly correct results with the exception of the case where tyrosine, cystine, histidine and tryptophan are situated at the C-terminal. These amino acids can be characterized by adopting the modified method described below.

Materials

Anhydrous hydrazine. — Anhydrous hydrazine was prepared by the method of Stähler[17]. Fifty grams of 80 per cent hydrazine hydrate and 175 g. of calcium oxide were mixed in a copper flask and gently heated in an oil bath. The distillate was led through a glass tube and a cooler and collected into a flask, which was attached by a calcium chloride tube. All cork fittings were covered with tin foil. After a few ml. of forerun were discarded, the main distillate was run at a bath-temperature range of 130–160°C. This was immediately kept in sealed tubes, each containing a 1 ml. portion. Yield 15–18 g. Purity was more than 99 per cent.

Amino acid hydrazides.—Leucine hydrazide dihydrochloride is the same one as reported previously[1]. Glycine-, alanine- and serine-hydrazides were prepared as follows: amino acids were esterified as usual, and hydrochlorides of amino acid esters were treated with computed amounts of dry chloroform saturated with dry ammonia. After filteration, the solution was concentrated under diminished pressure to give a syrup. The computed amount of anhydrous hydrazine was added to the syrup under cooling, and after standing overnight at room temperature, the reaction mixture was concentrated in vacuo. In all the treatments care was taken to avoid moisture. Thus glycine- and serine-hydrazides were obtained as crystals, but alanine hydrazide was crystallized as hydrochloride by adding dry alcohol saturated with HCl gas to the syrup of hydrazide until the pH of the solution reached to pH 6 and was concentrated in vacuo. The former two hydrazides were recrystallized three to five times from ethanol-ether, and the latter hydrazide hydrochloride from hot methanol.

Glycine hydrazide. m.p. 84–85°C (Found: N, 47.16. Calcd: 46.91%)

Serine hydrazide. m.p. 99-100°C (Found: N, 35.28. Calcd: 35.25%)

Alanine hydrazide dihydrochloride. m.p. 222–223°C (Found: N, 23.84. Calcd.: 23.87%)

15) A.C. Chibnall, "Les protéines", (1953) p. 126.
16) A. C. Chibnall and J.L. Bailey, "CIBA Symposium" (1952) p. 148, 149.
17) A. Stähler, *Ber.*, 42, 3018 (1909).

Experiments and Results

(1) Decomposition of Amino Acids during Hydrazinolysis

It has been observed that C-terminal amino acids liberated during hydrazinolysis are partly decomposed. Locker[4] reported that common amino acids were recoverable in amounts exceeding 85 per cent with the exception of glutamic and aspartic acids, tryptaphan, arginine, cystine, cysteine and asparagine after heating them for eight hours at 100°C in a sealed tube. We have, therefore, estimated recoveries of about fifteen amino acids during hydrazinolysis, and we have studied briefly the decomposition products.

(a) Recoveries.—About 1 mg. of each amino acid was heated at 100°C with 0.5 ml. anhydrous hydrazine for five and ten hours. After excess hydrazine was evaporated in vacuo over sulphuric acid, the residue was dinitrophenylated, extracted, chromatographed and the recoveries of DNP-amino acids were estimated in the same way as in the case of proteins[7]. The procedure is similar to that shown in Table VIc. On the other hand, free amino acids were treated, without heating with hydrazine, in the same way to find control values of this procedure. The control values were mostly found to be more than 85 per cent. The recoveries cited in Table I are corrected by these control values. Histidine is dinitrophenylated not quantitatively—to an extent of only 30 per cent of theory—and was estimated, therefore, as the free amino acid by column chromatography using Dowex-50. Cystine and proline were also not fully dinitrophenylated. As DNP-derivatives of tyrosine and tryptophan are extracted by sodium bicarbonate solution not completely from ethyl acetate solution but completely from ether solution.

Table I indicates that the recoveries of amino acids during the hydrazinolysis of ten hours range from 90 per cent (leucine) to 27 per cent (cystine) and most of them are 50 to 70 per cent. Arginine decomposes completely in ten hours' hydrazinolysis, but is recoverable as ornithine. Contrary to the report of Locker[4], methionine does not change to sulfoxide, but remains about 80 per cent unchanged in ten hours. The reason of discrepancies between the results of Locker and ours is not clear. Some experiments were done in a dark room, but the effect of light was not remarkable.

It is not known whether C-terminal amino acid residues in protein decompose or not in the same way as free amino acids in the course of hydrazi-

TABLE I
RECOVERY OF AMINO ACIDS

Amino acid	Blank	After heating with anhydrous hydrazine for 5 hr.	10 hr.	Locker[4]
Glycine	87%	85%	52, 53**%	85
Alanine	84	81	48, 55**	85
Valine	100*		85**	85
Leucine	100*		90	85
Serine	86	75	57	85
Proline	71		65	
Tyrosine	100	92	74	85
Tryptophan	94**	57**	47**	40
Histidine	89	73	62	85
Arginine	83	36	0	0
(Ornithine)	85*	39	45	
Aspartic acid	85*		50**	20
Glutamic acid	85*		46**	40
Cystine	60	38	27	—
Methionine	91		80	sulphoxide

* Assumed values.
** Treated under shutting from direct light.

nolysis, but, being recovered 80 to 90 per cent of theory in the case of protein[7,13], C-terminal amino acid seems to be recoverable not less than free amino acids (Table I) as discussed later.

(b) Decomposition Product.—It is not yet known how amino acids decompose by the treatment with hydrazine. They did not change to hydrazides principally. Decomposition products gave no DNP-compounds which might be apprehensive for confusion with DNP-amino acids with the exception of cystine. Cystine changes partially to three sorts of by-products, two of which, on dinitrophenylating, changes to DNP-compounds which have nearly the same R values of DNP-glycine and -alanine, respectively, but on treating with isovaleraldehyde before dinitrophenylation, these compounds disappear almost completely.

In the case of arginine, a trace of DNP-compounds other than DNP-ornithine was detectable on silica gel columns, but on dissolving in acetic acid the yellow colour disappeared.

The degree of decomposition of amino acids in hot hydrazine seems to depend on the purity of anhydrous hydrazine. Anhydrous hydrazine of lower concentration (about 95 per cent) might cause more decomposition and undersirable by-products as reported previously[8].

(2) Hydrolysis of Hydrazides

Amino acid hydrazides which are produced in the course of hydrazinolysis might partially change to other substances by side-reactions. If free amino acids were produced during hydrazinolysis and/or after-treatment, they might be mistaken for C-terminals. Therefore the degrees of hydrolysis of hydrazides in aqueous solution and in hot hydrazine were determined.

(a) Estimation Method of Hydrolysis.—(i) Estimation as DNP-derivatives of Amino Acids produced by Hydrolysis.—The mixture of amino acid hydrazides and free amino acids, the latter resulting from the former by treating with hydrazine, were together dinitrophenylated, and DNP-amino acids were extracted fractionally by the same procedure as in the case of C-terminal, chromatographed on silica gel and estimated colorimetrically.

(ii) Estimation of Hydrazine liberated by Hydrolysis.—Preliminary experiments indicated that the hydrazine reacted with piperonal quantitatively to give a condensation product and that the product in acidic solutions showed a specific absorption curve which is distinctly different from those of amino acid hydrazides with the aldehyde in the range of the wave lengths of 365–380 mμ as shown in Fig. 1. The optical density

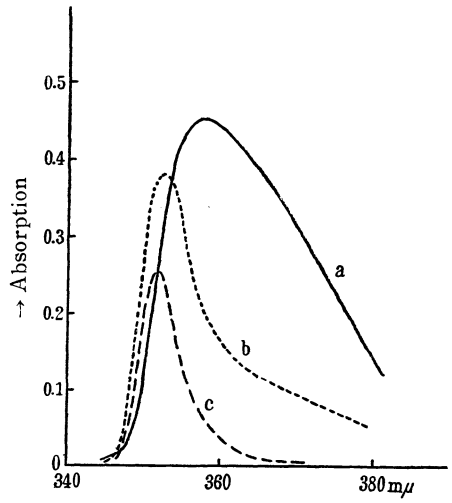

Fig. 1. Absorption spectra of condensation products of piperonal with hydrazine and amino acid hydrazides.
(a) Condensation product of piperonal with hydrazine (0.08 μM).
(b) Condensation product of piperonal with leucine hydrazide (4.36 μM).
(c) Condensation product of piperonal with serine hydrazide (4.87 μM).

reached a constant value within thirty minutes and was stable at least one to two hours. The colour intensity obeyed Beer's law. Basing on the results the following standard method to estimate microgram quantities of hydrazine was devised: to one ml. of sample solution containing about 5 to 10 μg. of hydrazine 2 ml. of propanol containing 34 mg. piperonal and 1 ml. of glacial acetic acid were added. After standing one hour at room temperature, the reaction mixture was subjected to colorimetric estimation by Beckman's spectrophotometer at the wave lengths of 363–375 mμ.

(b) Hydrolysis of Hydrazides in Aqueous Solution.—Serine hydrazide was kept at room temperature for various times in aqueous solution, in dilute acetic acid (pH 4) and in 1% sodium bicarbonate solution. The degrees of hydrolysis under these conditions were estimated by the method **(ii)**. As shown in Fig. 2 serine hydrazide

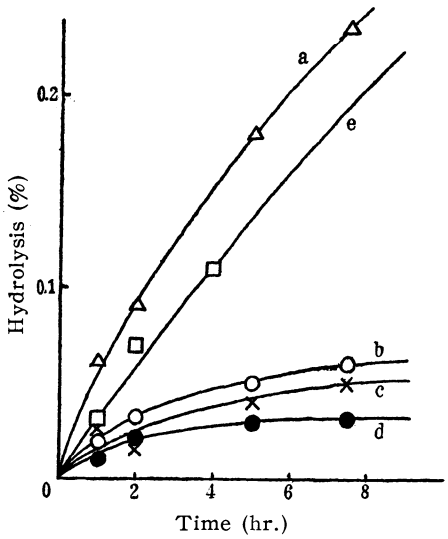

Fig. 2. Hydrolysis of amino acid hydrazides in aqueous solutions at room temperature
(a) Serine hydrazide in 1% sodium bicarbonate solution.
(b) Serine hydrazide in 66% alcoholic solution of sodium bicarbonate (medium for dinitrophenylation).
(c) Serine hydrazide in water.
(d) Serine hydrazide in dilute acetic acid (pH 4).
(e) Leucine hydrazide in 1% sodium bicarbonate solution.

is hydrolysed 0.05% in 7.5 hours in aqueous solution, 0.03% in acetic acid solution of pH 4, and 0.25% in 1% sodium bicarbonate solution. Further results obtained by the method (i) with glycine-, alanine- and leucine-hydrazides (Table II) indicate that the extent of hydrolysis of these hydrazides in neutral solution is less than 0.1 per cent in eighteen hours at room temperature.

From these results it is concluded that the amino acid hydrazides are stable in neutral and slight acidic media but somewhat unstable in alkaline medium. Therefore, one must avoid standing the hydrazides in solutions, especially in alkaline, for a long time. Consequently, it might be better to avoid treating the hydrazinolysates with strong basic and acidic ion-exchange resins.

The extent of hydrolysis of hydrazides by dinitrophenylation are shown in Table II, that is, 0.1 to 0.5 per cent of hydrazides are hydrolysed by the dinitrophenylation for two hours. The longer the time of dinitrophenylation, the greater the extent of hydrolysis.

To examine the hydrolysis during the extraction of C-terminal amino acids according to the above-mentioned procedure ethyl acetate solution of di-DNP-serine hydrazide was shaken with 2% sodium bicarbonate solution for three and five hours and the extent of hydrolysis of the DNP-hydrazide was estimated, the results of which are shown in Table II.

From these results, it can be concluded that the hydrazinolysates must be given a preliminary treatment with aldehyde to remove the bulk of the hydrazides, and all the treatment must be carried out as rapidly as possible.

(c) Hydrolysis of Hydrazides during Hydrazinolysis.—Amino acid hydrazides, such as serine-, glycine-, alanine- and leucine-hydrazides, were heated with anhydrous hydrazine in the same conditions as in the case of proteins, and free amino acids liberated by this treatment were estimated. The results shown in Table II indicate that serine-, glycine-, alanine- and leucine-hydrazides are hydrolysed by 1.2, 1.7, 0.4 and 0.5 per cent, respectively, which are considerably higher than in aqueous solutions. Of course, these data do not indicate directly the percentage of free amino acids of non-C-terminal liberated during hydrazinolyses of proteins, as discussed later, and it might be preferable to compare results of hydrazinolysis of various reaction time, when C-terminal amino acids of proteins are intended to be characterized.

(3) Hydrazinolyses of Peptides

It is desirable to know the rates of hydrazinolysis of various peptides and to have some informations about the extent of hydrolysis of non-C-terminal peptide bonds during the hydrazinolysis. Experiments have been carried out on three peptides, L-leucyl-L-alanine, glycyl-L-alanine and glycyl-L-leucine. The results are cited in Table III, in which it is remarkable that as much as 30 percent of leucyl-alanine remains intact by hydrazinolysis for ten hours.

TABLE II
HYDROLYSIS OF AMINO ACID HYDRAZIDES IN VARIOUS CONDITIONS

	Serine hydrazide	Glycine hydrazide	Alanine hydrazide	Leucine hydrazide
Dinitrophenylation in 2 hr.	0.1%	0.5%	0.1%	0.2%
Dinitrophenylation in 7 hr.	0.7			
Shaking for 3 hr.*	0.15			
Shaking for 5 hr.*	0.3			
Heating with N_2H_4 for 5 hr.	0.5	0.7	0.2	0.2
Heating with N_2H_4 for 10 hr.	1.1	1.2	0.3	0.3
Standing in solution (pH 7.2) for 18 hr. at room temp.	0.06	0.02	0.04	0.08

* Hydrazides were dissolved in ethyl acetate and shaken with 2% sodium bicarbonate solution (to test the hydrolysis in extractive process).

TABLE III

HYDRAZINOLYSIS OF PEPTIDES

Peptide	Time of hydrazinolysis	Residual peptide	C-terminal liberated	Free amino acid non-C-terminal
L-Leucyl-L-alanine	5 hr.	60%	33%	
	10	30	45	
Glycyl-L-alanine	10	0	60	
Glycyl-L-leucine	3	10	83	
	5	Trace	87	Trace
	10	0	90	Trace

(4) Separation between Amino Acids and their Hydrazides

(a) Treatment with Aldehydes.—From the data cited in Table III, it is preferable to treat hydrazinolysates with aldehyde prior to the dinitrophenylation in order to remove the bulk of the hydrazides. We in our earlier works[1,2] and other investigators[3,4] used benzaldehyde, but it must be used as a freshly distilled preparation because it is apt to produce peroxide, which might oxidize hydrazides to form free amino acids. Thus we used piperonal and isovaleraldehyde in place of benzaldehyde. As the former did not give very good results, the latter was employed throughout this investigation. The procedure, which is nearly the same as reported before[7], is shown in Table VIa. Care was taken to avoid the hydrolysis of hydrazides by treating in shorter time under mild conditions.

(b) Fractional Extraction of C-terminal Amino Acids as DNP-derivatives.—The solution obtained by the above treatment contains C-terminal amino acids and residual hydrazides which could not be removed. After dinitrophenylation, the C-terminal DNP-amino acids must be separated from di-DNP-amino acid hydrazides. To separate the DNP-amino acids we have used the procedure cited in Table VIa, in which ethyl acetate was employed as organic solvent. Although nearly all sorts of DNP-amino acids were extracted quantitatively by dilute sodium bicarbonate solution from ethyl acetate solution while di-DNP-hydrazides remained in the latter, all of the di-DNP-tyrosine, and a part of the di-DNP-histidine and DNP-tryptophan were found to remain in the organic phase. Accordingly, if these amino acids are situated at C-terminal, they are fully or partly lost and cannot be characterized as DNP-derivatives.

This is the reason why contrary to the result by carboxypeptidase method, tyrosine has not been found as C-terminal of chymotrypsin by our earlier method.

To take measures on this problem, ethyl acetate was replaced by ethyl ether or isopropyl ether, or using ethyl acetate as organic solvent a special treatment for the three amino acids was established. These procedures are shown in Table VIb.

Of these procedures the ethyl acetate method gives the most clear-cut separation between DNP-amino acids and di-DNP-hydrazides. By the other methods, di-DNP-hydrazides contaminate the C-terminal fraction, so that it is necessary to treat hydrazinolysate with aldehyde prior to the dinitrophenylation. Applying these methods to lysozyme hydrazinolysates plus tyrosine, results shown in Table IV were obtained, i.e. about 90 per cent of leucine (C-terminal of lysozyme) and tyrosine added were recovered.

TABLE IV

RESULTS OBTAINED BY STANDARD METHODS WITH LYSOZYME PLUS TYROSINE

Sample	Method	Results
Lysozyme* tyrosine**	I	Leucine, 88%; tyrosine 90%
Lysozyme* tyrosine**	II (ether)	Leucine, 94%; tyrosine 88%
Lysozyme* tyrosine**	II (isopropyl ether)	Leucine, 90%; tyrosine 86%
Lysozyme*	III	Leucine, 90%

* Lysozyme was hydrazinolysed for ten hours at 100°C.
** Tyrosine was added to the hydrazinolysate of lysozyme.

Being not dinitrophenylated quantitatively histidine might be better estimated by other methods, such as ion-exchanger chromatography etc., after treating the hydrazinolysates with aldehyde.

(5) Characterization of Aspartyl and Glutamyl Residues in Chain and C-terminal Asparagine and Glutamine

Contrary to the case of determination of N-terminal by DNP method, in which lysine residue in chain is also detected as DNP-derivative, by the hydrazinolysis method aspartic and glutamic acid residues bearing free carboxyl group in the chain and C-terminal asparagine and glutamine are extracted into acidic fraction together with other C-terminals. The possible products throughout this method are shown in Table V.

TABLE V

POSSIBLE PRODUCTS OF HYDRAZINOLYSIS AND DINITROPHENYLATION DERIVED FROM ASPARTIC AND GLUTAMIC RESIDUES

Dicarboxylic acid residue	Products of hydrazinolysis	Corresponding DNP-derivatives
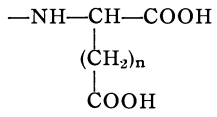 (Ia)	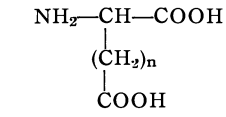 (Ib)	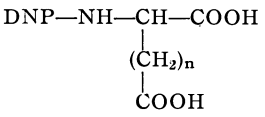 (Ic)
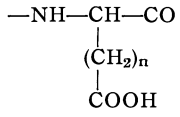 (IIa)	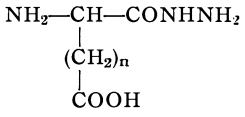 (IIb)	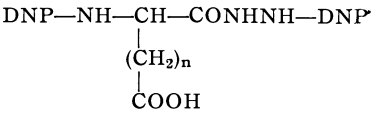 (IIc)
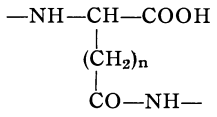 (IIIa)	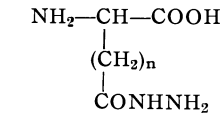 (IIIb)	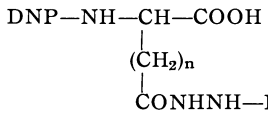 (IIIc)
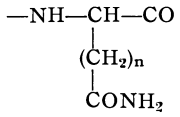 (IVa)	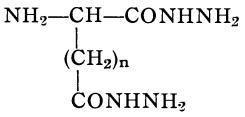 (IVb)	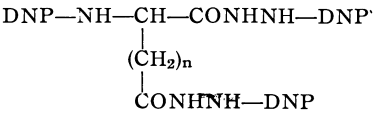 (IVc)

By the treatment with isovaleraldehyde followed by dinitrophenylation, other derivative such as (V) and/or (VI) might be formed from dicarboxylic acids bearing one free carboxyl group.

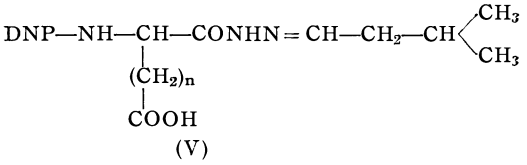

(V)

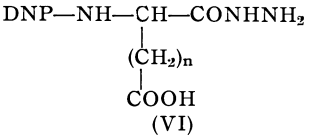

(VI)

In the fractional extractions by the procedure of Table VIa, (I) and (IV) are distributed as sharply as other DNP-amino acids and di-DNP-hydrazides, respectively, and (II) and (III) are distributed less sharply but finaly all extracted to alkaline solution from ethyl acetate, but (V) and (VI) behave somewhat irregularly and are distributed to all the fractions by the procedure. These facts seem to disturb the characterization of C-terminal amino acids of proteins, although no appreciable difficulties were experienced in the case of the proteins which we have investigated. For the quantitative estimation of C-terminal amino acids, however, it is convenient to estimate DNP-aspartic and/or DNP-glutamic acids, if they exist, and then to estimate other DNP-amino acids after hydrolysing the C-terminal fraction with 6 N hydrochloric acid at 100°C for several hours, whereby (II), (III) or (V), (VI) are hydrolysed to DNP-aspartic and glutamic acids. Thus a clear-cut estimation of all the C-terminal amino acids and aspartyl and glutamyl residues in chain are attained.

In spite of the complexity of these dicarboxylic acid derivatives, we can make use of the fact described above, to characterize the mode of linkage of these acidic amino acids in peptide chain and also to determine the C-terminal glutamine and asparagine. This advantage can not be achieved by the original benzaldehyde method. Thus lysozyme was proved to have one aspartyl, 12 asparaginyl and 4 glutaminyl residues in the molecule[13]. The characterization of a free carboxyl group in peptide chain have been reported by Jollès and Fromageot[18] and the characterization of the amide group was reported by Chibnall and Rees[19].

Preliminary experiments to distinguish four types of derivatives of dicarboxylic acids were done as described hereinafter.

Di-DNP-aspartic acid-α-hydrazide was prepared as follows: Hydantoin acetic acid was hydrazinolysed for ten hours at 100°C, whereby it converted partly to aspartic acid-α-hydrazide, which was purified as di-DNP-derivative through silica gel chromatography. Di-DNP-glutamic acid-α-hydrazide was prepared in the same manner from hydantoin propionic acid, which was identical with that obtained by the hydrazinolysis of poly-α-glutamic acid*. The syntheses through hydantoin

18) T. Jollès and C. Fromageot, *Biochim. Biophys. Acta*, 9, 287, 416 (1952).

19) A.C. Chibnall and M.W. Rees, *Biochem. J.*, 48, xlvii 1951); ibid., 52, iii (1952).

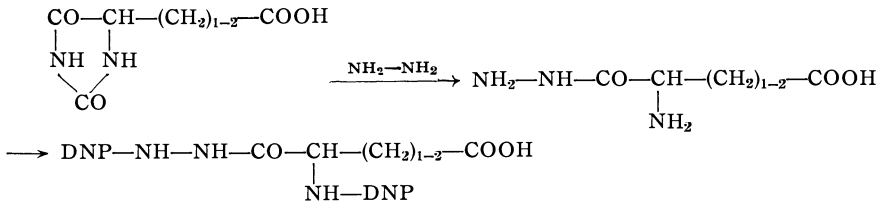

derivatives were rather poor in yields and many other by-products were also detected as DNP-derivatives. Di-DNP-glutamic acid-γ-hydrazide was obtained by dinitrophenylating the hydrazide*.

These four DNP-derivatives can be detected together with other DNP-amino acids, on suitable silica gel columns. Fig. 3 is an example indicating that all the DNP-derivatives can be separated distinctly. Moreover, di-DNP-aspartic and glutamic acid monohydrazides can be distinguished easily from DNP-amino acids as they develop brown red colour on dissolving in dilute bicarbonate solution.

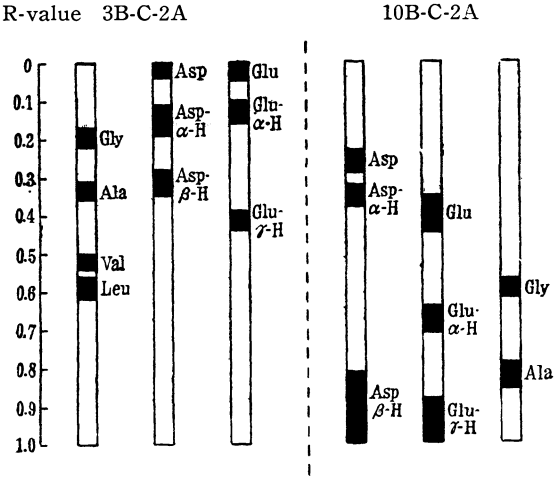

Fig. 3. Chromatograms of DNP-derivatives of aspartic and glutamic acid monohydrazides and DNP-amino acids on silica gel chromatograms.
Solvent: 3B-C-2A: n-BuOH: $CHCl_3$: 2% acetic acid=3: 97: 100
10B-C-2A: n-BuOH: $CHCl_3$: 2% acetic acid=10: 90: 100

Standard Methods

Considering the results mentioned above, three standard methods shown in Table VIa, VIb and VIc are established to characterize C-terminal amino acids and aspartyl and glutamyl residues in chain. In most cases all methods are available to give correct results, but differ in some points described below, so that the suitable method(s) may be chosen for the protein investigated.

The methods described here were applied succesfully to the proteins, but the volumes or weights of reagents described in Table VI may be modified according to the proteins investigated. As the C-terminal fraction is contaminated with DNP-derivatives of acidic amino acid monohydrazides and some C-terminal peptides, each component separated on chromatograms is better to be identified after hydrolysis with hydrochloric acid. Hydrazinolysis must be done twice or more varying the time of hydrazinolysis to estimate the amount of C-terminals, where the time of hydrazinolysis must not be longer than fifteen hours, as non-C-terminal amino acids appear and C-terminal amino acids decompose considerably for the longer hydrazinolysis.

By the three methods described below almost all amino acids can be characterized almost entirely quantitatively, but care must be taken when tyrosine, tryptophan, arginine, histidine, cystine, glutamine and asparagine are at the C-ends, among which histidine, cystine and amides may be characterized less quantitatively. The mode of linkage of acidic amino acids in peptide chain may be characterized, too, but less quantitatively.

Standard Method I.—This is a slightly modified method reported previously[7] and may be applied for general protein except the case where histidine and tryptophan are at C-ends and when one desires to seek terminal glutamine and asparagine or glutamyl and aspartyl residues in chain. If tyrosine is situated at C-terminal, the ethyl acetate fraction asterisked of Table VIa must be treated further, where all DNP-tyrosine and a part of DNP-histidine and DNP-tryptophan which are not included in the C-terminal fraction are detected.

Standard Method II.—While method I gives very clear-cut separation of DNP-amino acids from di-DNP-amino acid hydrazides, method II, in which ethyl ether or isopropyl ether is used in place of ethyl acetate, has more advantages than the method I in the case where tyrosine, histidine and tryptophan are at C-terminals. However, separation of DNP-amino acids from di-DNP-hydrazides is rather dull, so that the pretreatment of the hydrazinolysates with isovaleraldehyde is necessary.

Standard Method III.—This method which is nearly the same as reported previously[7,8] is established for the purpose of determining C-terminal glutamine and asparagine or glutamyl or aspartyl residues in chain. Of course other C-terminal amino acids can be characterized as in the case of method I, but small amounts of non-C-terminal amino acids would also be detected, though they would be almost negligible. Ethyl-

* Poly-α-glutamic acid was available through the kindness of Mr. H. Yuki, Laboratory of Fibre Research of this University, to whom the authors' thanks are due.
* Glutamic acid-γ and α-hydrazides and aspartic acid-β-hydrazide were also supplied by Mr. K. Narita, to whom we are grateful.

TABLE VIa

STANDARD METHOD I

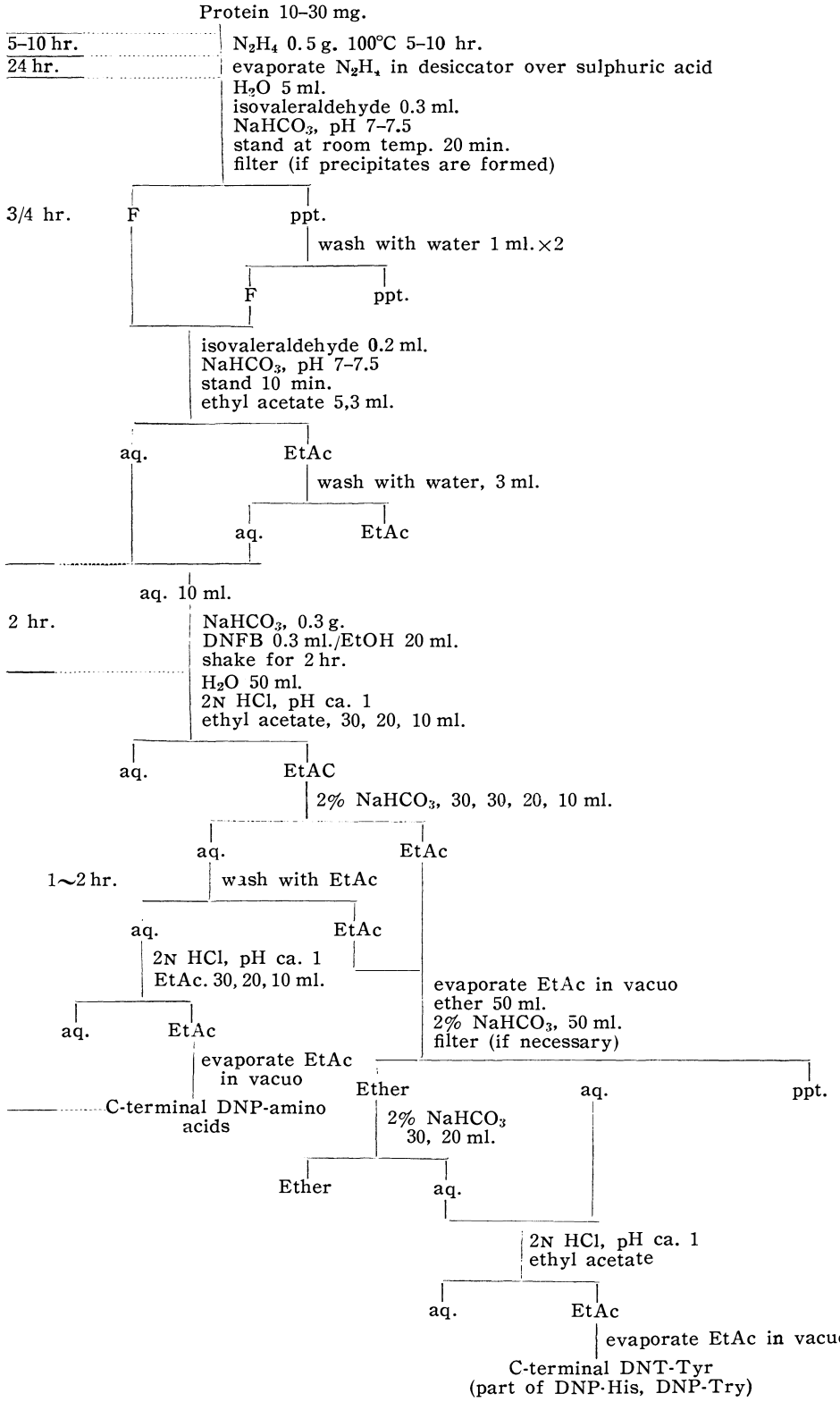

TABLE VIb

STANDARD METHOD II

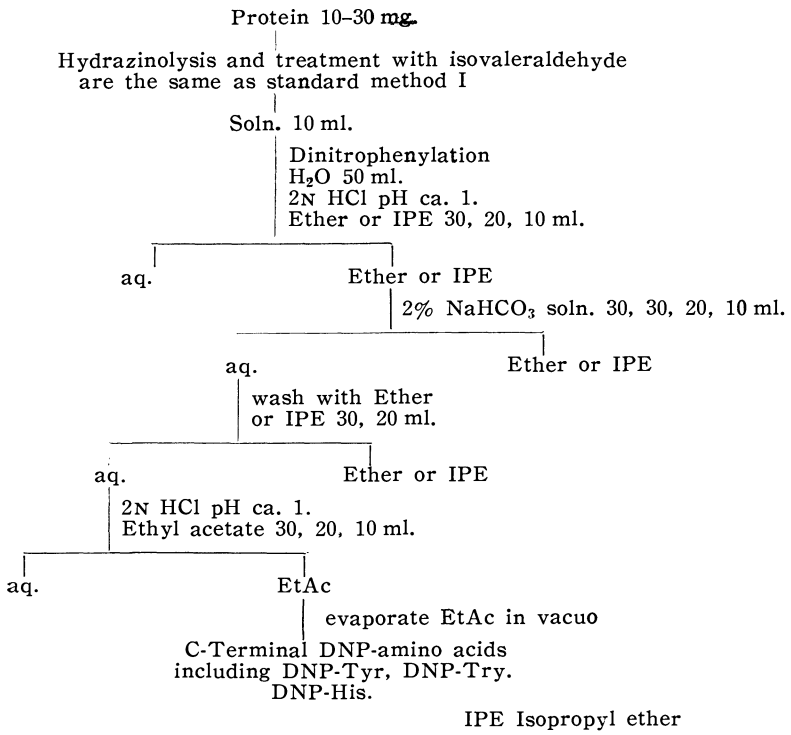

IPE Isopropyl ether

TABLE VIc

STANDARD METHOD III

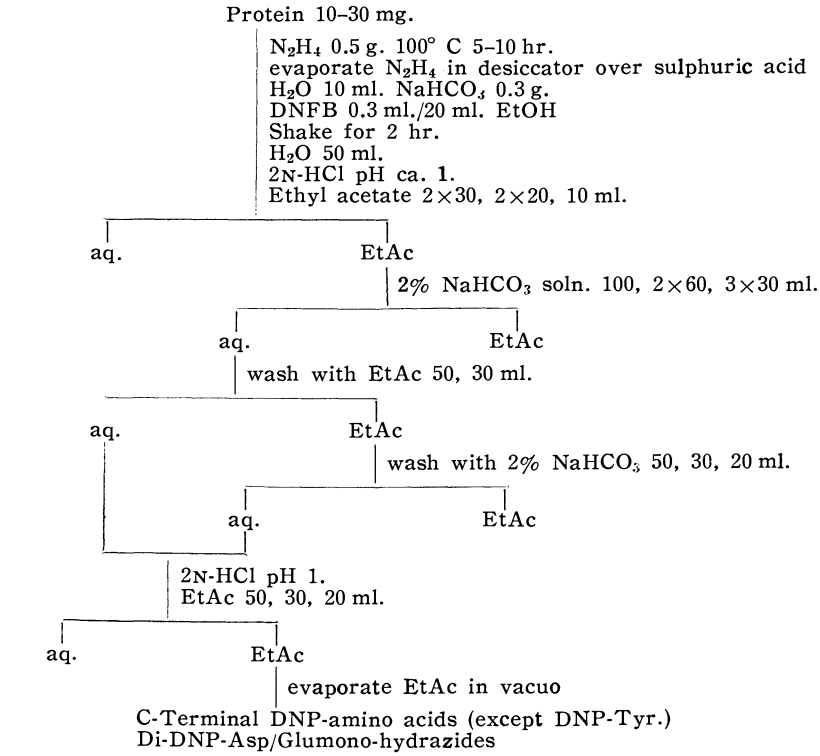

acetate cannot be replaced by ethyl ether or isopropyl ether in this case.

Discussion

As a matter of course, various data obtained by the present fundamental experiments cannot be applicable directly in the case of proteins; for example, it was really confirmed that about one per cent of amino acids were liberated during the ten hours' "hydrazinolysis" of amino acid hydrazides, but in the case of proteins, it takes several hours to produce amino acid hydrazides which, in turn, were subjected to hydrolysis partially, thus the percentages obtained in fundamental experiments indicate only the maximum values. About the decomposition of amino acids during the "hydrazinolysis", too, it is uncertain whether the amino acids bound at the C-end decompose similarly to the results cited in Table II. Therefore, we shall discuss below how to interpret the results obtained in the hydrazinolysis of real proteins.

First of all, let us consider all possible reactions involved in the hydrazinolysis. These may be expressed by the following scheme. The principal reaction is, of course,

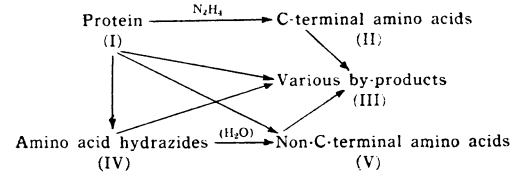

the splitting of the peptide bonds with formation of amino acid hydrazides (I → IV) and the liberation of C-terminal residues as free amino acids (I → II). Yet the hydrazides thus formed liberate, though very slightly, free amino acids (IV → V), and free amino acids are also partly decomposed to unknown by-products (II → III, V → III). Being not yet comfirmed directly, following other side reactions might be possible: splitting of peptide bond under formation of free amino acids (I → V); decomposition of amino acid residues in peptide and at C-terminal before their liberation by hydrazinolysis (I → III); and decomposition of amino acid hydrazides directly to some by-products (IV → III).

On applying the hydrazinolysis to a protein, participations of all side reactions depend on the sorts of C-terminal amino acids and compositions and sequences of amino acids in the protein, so that it cannot be decided summarily which is predominant among these reactions. However, we have estimated almost one mole of each C-terminal, but no appreciable other amino acids applying this method to two proteins (lysozyme, and Taka-amylase A). If we are allowed to generalize the results from these few examples, we might be able to consider that results really obtained on proteins are mainly due to the desired principal reaction, no matter how many side reactions are possible theoretically. It can be admitted, at least, to speak generally, that if more than 0.5 mol. of free amino acids are obtained by the hydrazinolysis of ten hours, they can be regarded as C-terminals, but if only less than 0.2 mol. of them are detected they may be artifact, and it needs further study if 0.2 to 0.5 mol. appears.

The supposition described above was justified also by some calculations from the fundamental data obtained. We shall calculate for example, the amount of non-C-terminal amino acid formed through the reactions $I \xrightarrow{k_1} IV \xrightarrow{k_2} V$.

Assuming that the each step of the reactions is the first order reaction and the step of V → III is negligible, the concentration of V at time t is given by equation (1).

$$[V]_t = [I]_0 + \frac{[I]_0}{k_1 - k_2}(k_2 e^{-k_1 t} - k_1 e^{-k_2 t}) \qquad (1)$$

where $[I]_0$ and $[V]_t$ are the concentration of I and V at time 0 and t respectively, k_1 and k_2 are the rate constants of each step.

If the conversion of I → IV is 90 per cent in eight hours' hydrazinolysis and IV → V is one per cent in ten hours, the amount of V at ten hours is calculated as only 0.67 per cent.

The similar calculation can be applied to the reactions $I \xrightarrow{k_3} II \xrightarrow{k_4} III$. Assuming that, here again, each step of the reactions is the first order, the concentration of II at time t is

$$[II]_t = \frac{k_3[I]_0}{k_3 - k_4}(e^{-k_4 t} - e^{-k_3 t}) \qquad (2)$$

where $[I]_0$ is the initial concentration of I and $[II]_t$ is the concentrations of II at time t, k_3 and k_4 are the rate constants of each step.

If the conversion I → II is 90 per cent in ten hours and II → III is 10 per cent in ten hours the following result is obtained.

Time (hr.)	2	5	10	14
Mol. of II from 1 mol. of I	0.37	0.74	0.84	0.87 (max.)

This value is rather coincident with the observed value in the case of liberation of leucine from lysozyme[7].

Further if the conversion of I → II is 90 per cent in twenty hours and II → III is 45 per cent in ten hours (decomposition of alanine, Table I), the calculated value of II is as follows:

Time (hr.)	5	10	12
Mol. of II from 1 mol. of I	0.37	0.49	0.50 (max.)
Mol. of alanine from 1 mol. of leucyl-alanine (observed)	0.33	0.45	

Since these calculations involve some assumption and simplification of complex reactions, one must avoid attaching too much importance to the result derived from these calculations. However, it is obvious from these considerations that liberation of C-terminal is a function of time, which has one maximum value, so that it may be necessary to determine C-terminal at various time intervals.

On Taka-amylase A, we have other data not mentioned before. Even if the amylase solution in hydrazine was brought to dryness in vacuo at room temperature directly after the addition of hydrazine 0.3 mol. of serine and 0.1 mol. of glycine were detected as C-terminals. On the other hand, 8.955 mg. (47.7 μM.) of glycyl-L-leucine, the content of glycine of which is about the same as that of Taka-amylase[20], were added to 51.5 mg. (1.1 μM,) of Taka-amylase A followed by hydrazinolysis, whereby 0.068 mg. (0.9 μM.) and 0.082 mg. (1.1 μM.) of glycine were found, respectively, by the hydrazinolysis of five and ten hours. These results indicate that only 0.4 per cent of glycyl residue was liberated as free amino acid from added glycyl-leucine in ten hours' hydrazinolysis. From these two facts it can be concluded that glycine and serine are really C-terminals of this protein. On another terminal, alanine, there might be some doubt because of its slow liberation by hydrazinolysis[7], but on considering that the rate of hydrazinolysis of L-leucyl-L-alanine is slow as in case of this protein (see Table IV), it is more probable that alanine is bound at a C-terminal by some hard-hydrazinolysable bond.

On the C-terminal of ovalbumin, Steinberg[21] reported the liberation of alanine by carboxypeptidase but later[22] found this due to a DFP-sensitive, contaminated enzyme. Locker[4] also reported that the protein was not attacked by DFP-treated carboxypeptidase. Turner and Schmerzler[23], however, have found alanine to be a C-terminal by the thiohydantoin method. Although some of us[7] also reported the presence of one alanine at the C-terminal, Dr. Fraenkel-Conrat[24] informed us recently that the C-terminal of this protein is valyl-seryl-proline. Thus we reinvestigated on the protein and found that we had taken proline for alanine. The DNP-derivative of the C-terminal amino acid was proved to be proline and not alanine by variety of chromatography and its absorption curve. The detail of this account shall be published later by one of the authors.

Although carboxypeptidase method has been applied successfully to many proteins, it has several distinct restrictions by nature. For example, it is not applicable to insoluble proteins such as wool keratin[14] and silk fibroin[5]; its action depends not only on the nature of the C-terminal but also on the adjacent amino acid residues; when a protein has more than two C-terminals, it is difficult to characterize it distinctly; and so on. The hydrazinolysis method has, at least, the advantages in these cases. The result on ovalbumin might be the best example of the success of the hydrazinolysis method, becauce proline situated at C-terminal is liberated neither by carboxypeptidase nor by the thiohydantoin method.

Summary

1. Fundamental experiments on the hydrazinolysis method, a method for characterization of C-terminal amino acids of proteins, were carried out.

2. Amino acids were found to decompose to various extents by heating with anhydrous hydrazine.

3. Amino acid hydrazides were hydrolysed about 1% or less by heating with anhydrous hydrazine (ca. 99%) for ten hours. Hydrolyses of them in neutral and slightly acidic solutions at room temperature are negligible, but in alkaline solution the extent of hydrolyses are somewhat greater though less than 0.2% in five hours in 1% bicarbonate solution.

4. Procedures for separating free amino acids from amino acid hydrazides as DNP-derivatives with or without treatment of iso-valeraldehyde prior to dinitrophenylation were reinvestigated thoroughly.

5. Some experiments on the hydrazinolyses of peptides were done.

6. Fundamental investigations of the characterization of the mode of linkage

20) S. Akabori, T. Ikenaka, H. Hanafusa and Y. Okada, *J. Biochem.*, **41**, 803 (1954).
21) D. Steinberg, *J. Am. Chem. Soc.*, **74**, 4217 (1952).
22) D. Steinberg, *J. Am. Chem. Soc.*, **75**, 4875 (1953).
23) R.A. Turner and G. Schmerzler, *Biochim. Biophys. Acta*, **11**, 586 (1953).
24) H. Fraenkel-Conrat, Personal communication. The authors are grateful to him for his information prior to his publication, *J. Am. Chem. Soc.*, **77**, 5882 (1955).

of monoaminodicarboxylic acids in peptide chains by the hydrazinolysis method indicate its availability.

7. Standard methods for quantitative estimation of C-terminal amino acids or proteins are established based upon the results obtained by the present investigation.

8. Brief consideration on the mechanism of the hydrazinolysis was described and the scope of this method was discussed in connection with that of the carboxypeptidase method.

Laboratory of Biochemistry, Faculty of Science, Osaka University. Osaka

Dielectric Polarization of Some Aliphatic Amines in the Liquid State

By Michio SHIRAI

(Received February 14, 1956)

Introduction

The relation between the dielectric constant of a liquid and the properties of its individual molecule is a complicated problem. Debye[1] derived the well-known formula,

$$\frac{M}{d}\frac{\varepsilon-1}{\varepsilon+2}=\frac{4\pi N}{3}\left(\alpha+\frac{\mu^2}{3kT}\right),$$

based on Mosotti's hypothesis, where M is the molecular weight, d the density, ε the dielectric constant, N Avogadro's number, α the polarizability, μ the dipole moment, k Boltzmann's constant, and T the absolute temperature. Debye's formula was found to be in agreement with the experimental results for gases and dilute solutions in non-polar solvents. In this formula the intermolecular interactions are neglected. But, when any effect of interactions between polar molecules exists, some modifications of this theory are required.

Onsager[2] worked out this problem by taking into account the so-called reaction field as well as the cavity field. The formula derived by him is as follows:

$$\frac{M}{d}\frac{(\varepsilon-n)^2(2\varepsilon+n^2)}{\varepsilon(n^2+2)^2}=\frac{4\pi N}{3}\frac{\mu^2}{3kT}$$

where n is the refractive index for optical region. Onsager's formula accounts for the dielectric constants of all substances except a few highly associated liquids, and can be used to calculate dipole moments from the dielectric constants of several polar liquids.

Previously, Estermann[3] found that in pure liquids of diethyl ether, diphenyl ether, and ethylamyl ether, the molecular polarization calculated from the dielectric constant of the pure liquid by means of Debye's formula was in good agreement with that measured with the dilute solution in non-polar solvent, in spite of the considerable polarity of its molecule. Recently, the author has found that the same rule also holds for some aliphatic amines.

Experimental

Method of Measurement.—The measurement of dielectric constant was carried out at a frequency of 2 Mc./sec. by means of resonance method, the details of which were described elsewhere[4]. The density was measured with a pycnometer.

Materials.—Diethylamine was purified from a commercial sample by drying over caustic soda and distillation. b. p. 55.5°C.

Triethylamine was purified from a commercial sample by the method given for diethylamine. b. p. 88.8°C.

i-Propylamine was purified from a commercial sample by distillation. b. p. 33.0–33.5°C.

n-Heptane was purified from a commercial sample by shaking with sulfuric acid, washing with water, drying over metallic sodium, and fractional distillation. b. p. 97.5°C.

Cyclohexane was purified from a commercial sample by the method given for *n*-heptane. b. p. 81.0°C.

Results and Discussion

Dipole Moment.—The mole fraction of the solute x, the dielectric constant ε, and the density d are indicated in Table I, together with the molecular polarization P_2, calculated from them. The molecular polarization was calculated by the following formula;

1) P. Debye, "Polare Molekeln", S. Hirzel Press, Leipzig (1929), p. 33.
2) L. Onsager, *J. Am. Chem. Soc.*, 58, 1486 (1936).
3) I. Estermann, *Z. physik. Chem.* B 1, 134 (1928).
4) M. Yasumi and M. Shirai, This Bulletin, 28, 193 (1955).

$$P_2=P_1+\frac{P_{12}-P_1}{x}$$

where P_1, P_2, P_{12} are the molecular polarization of the solvent, solute, and solution, respectively.

The molecular polarization at infinite dilution $P_{2\infty}$ and the dipole moment μ calculated from it are also shown in Table I. The dipole moment is given by

$$\mu=0.0128\sqrt{(P_2-P_E-P_A)T}=0.0128\sqrt{P_0T}$$

where P_E, P_A, and P_0 are the electronic, atomic, and orientation polarization, respectively. P_E+P_A for diethylamine and that for triethylamine were taken to be 25.7 cc. and 33.0 cc., respectively. These were determined by the temperature dependence of their molecular polarization in the gaseous state[5]. For *i*-propylamine, P_E was taken to be equal to the molar refraction for sodium D line, and P_A was assumed to be 5% of the electronic polarization.

The dipole moment of diethylamine and that of triethylamine measured in different solvents are nearly the same, but they are a little greater than those in the gaseous state. This fact is interpreted in terms of solvent effect[6].

TABLE I
DIELECTRIC CONSTANT, DENSITY, MOLECULAR POLARIZATION, AND DIPOLE MOMENT

Diethylamine ($P_E+P_A=25.7$ cc.)

n-Heptane Solution (−25°C)

x	ε	d	P_2 (cc.)
0.00000	2.0167	0.7229	(58.0)
0.03235	2.0590	0.7233	58.0
0.05199	2.0855	0.7235	57.9
0.07101	2.1123	0.7238	58.2
0.09068	2.1399	0.7241	58.0

$P_{2\infty}=58.0$ cc. $P_0=32.3$ cc. $\mu=1.14$ D

(25°C)

0.00000	1.9529	0.6824	(50.0)
0.03235	1.9816	0.6826	49.9
0.05199	1.9997	0.6827	50.1
0.07101	2.0178	0.6828	50.3
0.09068	2.0361	0.6829	50.2

$P_{2\infty}=50.0$ cc. $P_0=24.3$ cc. $\mu=1.09$ D

Cyclohexane Solution (25°C)

0.00000	2.0309	0.7735	(50.6)
0.03079	2.0672	0.7710	50.6
0.05106	2.0905	0.7691	50.4
0.07069	2.1153	0.7675	50.6
0.09052	2.1391	0.7655	50.7

$P_{2\infty}=50.6$ cc. $P_0=24.9$ cc. $\mu=1.10$ D

i-Propylamine ($P_E+P_A=20.6$ cc.)

n-Heptane Solution (−25°C)

x	ε	d	P_2 (cc.)
0.00000	2.0167	0.7229	(56.3)
0.03214	2.0624	0.7229	56.3
0.05110	2.0907	0.7229	56.5
0.07577	2.1292	0.7230	56.5
0.09341	2.1564	0.7220	56.4

$P_{2\infty}=56.3$ cc. $P_0=35.7$ cc. $\mu=1.20$ D

(25°C)

0.00000	1.9529	0.6824	(50.0)
0.03214	1.9863	0.6820	50.1
0.05110	2.0067	0.6818	50.0
0.07577	2.0337	0.6815	50.1
0.09341	2.0531	0.6813	49.8

$P_{2\infty}=50.0$ cc. $P_0=29.4$ cc. $\mu=1.20$ D

Triethylamine ($P_E+P_A=33.0$ cc.)

n-Heptane Solution (−25°C)

x	ε	d	P_2 (cc.)
0.00000	2.0167	0.7229	(47.8)
0.03179	2.0344	0.7240	48.0
0.05113	2.0459	0.7247	48.3
0.07319	2.0584	0.7252	48.4
0.09115	2.0690	0.7258	48.4

$P_{2\infty}=47.8$ cc. $P_0=14.8$ cc. $\mu=0.78$ D

(25°C)

0.00000	1.9529	0.6824	(45.8)
0.03179	1.9665	0.6836	45.9
0.05113	1.9745	0.6840	46.0
0.07319	1.9852	0.6849	46.2
0.09115	1.9921	0.6853	46.0

$P_{2\infty}=45.8$ cc. $P_0=12.8$ cc. $\mu=0.79$ D

Cyclohexane Solution (25°C)

0.00000	2.0309	0.7735	(46.5)
0.03090	2.0473	0.7716	46.5
0.05119	2.0578	0.7700	46.6
0.07103	2.0676	0.7687	46.5
0.09195	2.0778	0.7672	46.4

$P_{2\infty}=46.5$ cc. $P_0=13.5$ cc. $\mu=0.81$ D

Dielectric Polarization in Pure Liquid State.—Dielectric constant and density measured at different temperatures are shown in Table II. The molecular polarization and the dipole moment calculated from them according to Debye's formula and Onsager's formula, respectively, are also listed there. The refractive index which is to be inserted into Onsager's formula should contain the atomic polarization, so that it was calculated by the following formula:

$$\frac{M}{d}\frac{n^2-1}{n^2-2}=P_E+P_A$$

assuming that Lorentz field is valid for the electronic and atomic polarization.

5) G.A. Barcley. R.J.W. Le Fèvre and B.M. Smyth, *Trans. Faraday Soc.*, **46**, 812 (1950).
6) K. Higashi, *Sci. Pap. I.P.C.R.*, **31**, 311 (1937).

TABLE II

DIELECTRIC CONSTANT, DENSITY, MOLECULAR POLARIZATION, AND DIPOLE MOMENT IN THE LIQUID STATE

Diethylamine ($P_E+P_A=25.7$ cc.)

Temp. (°C)	ε	d	Debye P_0 (cc.)	Debye μ (D)	Onsager P_0 (cc.)	Onsager μ (D)
−45	7.2301	0.7684	38.5	1.20	66.0	1.57
−40	6.8079	0.7665	37.2	1.19	61.5	1.53
−30	6.1119	0.7534	35.5	1.19	55.0	1.48
−25	5.8220	0.7508	34.3	1.18	51.8	1.45
−20	5.5797	0.7484	33.3	1.18	49.1	1.43
−10	5.1246	0.7382	31.6	1.17	44.5	1.38
0	4.7734	0.7286	30.2	1.16	41.0	1.36
10	4.4575	0.7183	28.8	1.16	37.9	1.34
20	4.1823	0.7070	27.5	1.15	35.2	1.30
25	4.0656	0.7016	27.0	1.15	32.8	1.28
30	3.9639	0.6964	26.5	1.15	33.1	1.27
40	3.7615	0.6856	25.4	1.14	31.0	1.25
50	3.6063	0.6754	24.6	1.14	29.7	1.25

i-Propylamine ($P_E+P_A=20.6$ cc.)

Temp. (°C)	ε	d	Debye P_0 (cc.)	Debye μ (D)	Onsager P_0 (cc.)	Onsager μ (D)
−60	9.5531	0.7732	37.0	1.14	75.0	1.61
−50	8.8388	0.7630	36.4	1.15	70.1	1.60
−40	8.1835	0.7497	36.0	1.17	65.9	1.58
−30	7.5819	0.7401	35.2	1.18	61.5	1.56
−25	7.2929	0.7354	34.8	1.19	59.2	1.55
−20	7.0448	0.7308	34.4	1.19	57.4	1.54
−10	6.5882	0.7216	33.7	1.20	53.9	1.52
0	6.2176	0.7098	33.3	1.22	51.5	1.52
10	5.9490	0.7012	32.9	1.23	49.6	1.51
20	5.6268	0.6900	32.4	1.24	47.4	1.51
25	5.4656	0.6843	32.1	1.25	46.2	1.50

Triethylamine ($P_E+P_A=33.0$ cc.)

Temp. (°C)	ε	d	Debye P_0 (cc.)	Debye μ (D)	Onsager P_0 (cc.)	Onsager μ (D)
−60	3.0238	0.7923	18.4	0.80	21.7	0.87
−50	2.9387	0.7812	17.8	0.80	19.0	0.83
−40	2.8552	0.7739	16.9	0.80	18.1	0.83
−30	2.7795	0.7678	16.0	0.80	17.4	0.83
−25	2.7470	0.7651	15.6	0.80	16.9	0.82
−20	2.7161	0.7626	15.3	0.80	15.9	0.82
−10	2.6550	0.7549	14.6	0.79	15.7	0.82
0	2.5922	0.7472	13.9	0.79	14.9	0.82
10	2.5348	0.7379	13.4	0.79	14.2	0.82
20	2.4886	0.7280	13.1	0.79	13.8	0.82
25	2.4651	0.7229	13.0	0.80	13.6	0.82
30	2.4492	0.7181	12.9	0.80	13.6	0.82
40	2.3910	0.7097	12.1	0.79	12.7	0.81
50	2.3161	0.7007	11.0	0.76	11.5	0.78

As shown in Tables I and II, both for diethylamine and for *i*-propylamine the dielectric polarization calculated from the dielectric constant and the density of a pure liquid by Debye's formula is in fairly good agreement with that measured in solution at 25°C and −25°C. And, the dipole moment measured by the solution method agrees well with that calculated from the dielectric constant and the density of a pure liquid by Debye's formula throughout the range of temperature −50°C–50°C at which the measurement was performed. On the other hand, the molecular polarization and the dipole moment calculated by Onsager's formula are considerably greater than those in dilute solutions both for diethylamine and *i*-propylamine. Of course, ambiguity about the estimation of the atomic polarization exists, but the contribution of the atomic polarization to the dielectric constant is so small that it has little effect on the value of molecular polarization or dipole moment. For triethylamine, it is impossible to determine whether Debye's formula or any other formula holds, on account of its low dielectric constant. Dielectric polarizations of some other aliphatic amines such as ethylamine, *n*-propylamine, *n*-butylamine, etc. have been measured both in dilute solutions and in pure liquids by Barcley et al[5]. All of them show a considerable departure from Debye's formula and are rather consistent with Onsager's formula.

The difference between the derivation of Debye's formula and that of Onsager's formula may be described as follows: in deriving the former formula, the polarizing effect of the molecule on the surrounding medium is assumed to have average rather than its instantaneous value whereas the latter formula is derived for the instantaneous orientation of each molecule. In other words, in Onsager's field it is taken into account that the field due to the permanent moment polarizes the surrounding medium and produces a reaction field to the dipole. Accordingly, whether Debye's formula or Onsager's formula is valid, depends upon the existence of dipolar interaction.

In this way, it is reasonable to say that the reason why Debye's formula is valid in these pure liquids is the absence of a dipolar interaction. In fact, for these molecules the permanent dipole is screened by non-polar groups and has little effect on the surrounding medium. The result obtained in this work will be useful for the discussion of dipolar interaction in the liquid state, such as micelle formation in organic solvent. The latter problem will be discussed later.

Summary

For diethylamine, *i*-propylamine, and triethylamine, Debye's formula holds as the relation between dielectric constant and dipole moment over a wide range of temperature. This fact can be attributed to the absence of the dipolar interaction on account of the screening of the permanent dipole by non-polar alkyl groups.

The author wishes to express his sincere thanks to Prof. B. Tamamushi for his guidance and encouragement.

College of General Education
The University of Tokyo
Tokyo

Ionization Potentials of Some Organic Molecules. III. Aromatic and Conjugated Compounds

By Hiroaki BABA, Itiro OMURA and Keniti HIGASI

(Received February 7, 1956)

Introduction

There are available considerable numbers of reports dealing with the characteristic properties of aromatic and conjugated molecules. Resonance energy, bond length, dipole moment, absorption spectrum and directive power in substitution reactions have been extensively investigated. But unfortunately little information exists in the literature about the ionization potentials.

In the present article some results of the measurement on the appearance potentials of conjugated molecules will be reported. And an interpretation of the results will be given with special reference to its relation to the ultraviolet data of the same compounds.

Experimental Materials

The samples with a few exceptions were obtained from Kanto Chem. Co., Inc. and purified by distillation whenever possible. The refractive index was measured by D-line at 20°C if not recorded.

Benzene b. p. 80°C, $n^{25}=1.4974$; toluene b. p. 109.2°C; thiophenol $n^{23.5}=1.5882$; aniline b. p. 182.8°C, $n=1.5867$; *o*-xylene b. p. 143°C, $n^{21.5}=1.5031$; *m*-xylene b. p. 138°C, $n^{15.7}=1.4994$; *p*-xylene b. p. 137°C, $n^{16}=1.4970$; pyridine b. p. 115.9°C, $n^{21}=1.5087$; α-picoline b. p. 128–9°C, $n^{16.7}=1.5023$; β-picoline b. p. 142.8–143.0°C, $n^{24}=1.5038$; γ-picoline b. p. 144–144.5°C, $n^{17}=1.5057$; pyrrole b. p. 130.7°C, $n=1.5098$; furan b. p. 32.5°C, $n=1.4212$ and thiophene b. p. 83.8°C, $n^{19.7}=1.5267$.

The samples of phenol, anisole and mesitylene were kindly provided by Dr. S. Nagakura of Tokyo University in the pure form. For the pure sample of cyclo-octatetraene we are indebted to Dr. I. Tanaka, Tokyo Institute of Technology.

TABLE I

FIRST IONIZATION POTENTIALS, eV.

Substance	Present work	Previous workers
Benzene	9.52±0.10	9.52[a] (9.24)[b]
Toluene	9.20±0.05	9.23[a] (8.82)[c]
Phenol	9.01±0.05	9.03[a]
Thiophenol	8.56±0.02	
Aniline	8.23±0.02	
Anisole	8.56±0.05	
o-Xylene	8.96±0.02	8.97[d] (8.58)[c]
m-Xylene	9.01±0.02	9.02[d] (8.58)[c]
p-Xylene	8.86±0.02	8.88[d] (8.48)[c]
Mesitylene	8.76±0.05	8.79[d]
Pyridine	9.76±0.05	9.80[e]
α-Picoline	9.66±0.05	
β-Picoline	9.71±0.05	
γ-Picoline	9.56±0.05	
Pyrrole	8.97±0.05	(8.90)[f]
Furan	9.00±0.10	9.05[g] (9.01)[f]
Thiophene	9.10±0.20	(8.91)[f]
Cyclo-octatetraene	8.63±0.15	

Values in parentheses refer to spectroscopic potentials.

a) J.D. Morrison and A.J.C. Nicholson, *J. Chem. Phys.*, **20**, 1021 (1952).
b) W.C. Price and R.W. Wood, *J. Chem. Phys.*, **3**, 439 (1935); W.C. Price, *Chem. Rev.*, **41**, 257 (1947).
c) V.J. Hammond, W.C. Price, J.P. Teegan and A.D. Walsh, *Discuss. Faraday Soc.*, **9**, 53 (1940).
d) F.H. Field and J.L. Franklin, *J. Chem. Phys.* **22**, 1895 (1954).
e) A. Hustrulid, P. Kusch and J.T. Tate, *Phys. Rev.* **54**, 1037 (1938).
f) W.C. Price and A.D. Walsh, *Proc. Roc. Soc.* (London), **A179**, 201 (1941).
g) J.D. Morrison, *J. Chem. Phys.*, **19**, 1395 1951).

Experimental Method and Results

The measurement of the appearance potential was made by an apparatus described in a previous report[1]. The evaluation of the ionization potentials was made by Honig's critical slope method. Argon was employed as the reference standard.

The results of this experiment are recorded in Table I. Agreement with the data by previous workers is seen to be satisfactory.

Discussion

With the progress in the molecular orbital theory, various calculations of electronic properties have been made for a wide range of molecules. It appears not possible, however, for accurate prediction to be made as to the exact values of ionization potentials when dealing with such complicated molecules as are treated in the present work. In the following, only qualitative discussion will be undertaken in regard to some experimental results of this work.

As mentioned in the previous paper[2], the first ionization potential is related to the most loosely bound electron, which, in the majority of conjugated molecules, will be an electron belonging to the highest occupied π-orbital. However, in a heterocyclic molecule containing a nitrogen atom, which has a pair of non-bonding electrons, the ionizing electron may possibly be due to one of the non-bonding electrons. This point is important when discussing the potentials of pyridine and picolines.

Substituted Benzenes.—The effect of substitution on the absorption spectrum of benzene has been investigated by Sklar[3], Herzfeld[4], Nagakura and Baba[5] from the viewpoint of electron migration; and the red shift of the near ultraviolet absorption, caused by an ortho-para directing substituent, has been interpreted as due to the following facts. (1) The migration of electrons from the substituent into the unoccupied ring π-orbitals gives rise to an extra stabilization energy. (2) This extra stabilization energy is greater in the excited state than in the ground state. Later, it was shown by Matsen[6] that the electron migration theory is equivalent to the usual perturbation treatment.

The method of electron migration may be used to explain the ionization potentials of substituted benzenes. When one π-electron belonging to the aromatic ring is ionized, a substituent electron will be allowed to migrate into the previously filled π-orbital. As a result of this migration, the extra stabilization energy of the molecular ion will become great compared with that of the neutral molecule. Then the energy difference between the ionized and neutral states will be less for the substituted molecule than for the unsubstituted one. Thus we can expect that the ionization potential will decrease by the introduction of a substituent into the benzene ring. Actually, the potentials of all the substituted benzenes listed in Table I are lower than that of benzene.

The degree of electron migration, hence, the amount of the extra stabilization energy is dependent on the sort of substituent. It is largely determined by ionization energy of the substituent X: the smaller the ionization energy, the greater is the stabilization energy. However, it depends also upon the magnitude of overlapping between X and the neighbouring carbon atom in the ring. Thus, as Robertson and Matsen[7] concluded from ultraviolet absorption data, the stabilization energy will increase in the sequence

$$CH_3 < OH < SH < NH_2;$$

while the ionization energies of the groups X, estimated from those for HX or CH_3X molecules, are in the order $CH_3 > OH > NH_2 > SH$[6]. We may then expect that the ionization potentials of the substituted benzenes will be in the order

benzene > toluene > phenol > thiophenol > aniline.

This expectation is fulfilled by our experimental results shown in Table I.

Next, we shall turn to the ionization potentials of polymethyl benzenes. Herzfeld[4] showed for polysubstituted benzenes that the red shift of absorption spectrum is nearly additive. In fact, it is seen from Table II that this rule of additivity holds for polymethyl benzenes. Taking into account the electron migration theory, a similar additivity rule may be expected for the change in ionization potential with methyl substitution. The ionizatioh potential data given in Table II and also the plot of potential values versus the number of methyl substituents in Fig. 1 are all in fair accord with the above view.

1) I. Omura, K. Higasi and H. Baba, This Bulletin, **29**, 501 (1956).

2) I. Omura, K. Higasi and H. Baba, This Bulletin, **29**, 504 (1956).

3) A.L. Sklar, *J. Chem. Phys.*, **7**, 984 (1939); *Revs. Modern Phys.*, **14**, 232 (1942).

4) K.F. Herzfeld, *Chem Rev.*, **41**, 233 (1947).

5) H. Baba and S. Nagakura, *J. Chem. Soc. Japan*, **72**, 72 (1951); S. Nagakura and H. Baba, *J. Am. Chem. Soc.*, **74**, 5693 (1952).

6) F.A. Matsen, *J. Am. Chem. Soc.*, **72**, 5243 (1950).

7) W.W. Robertson and F.A. Matsen, *J. Am. Chem. Soc.*, **72**, 5248 (1950).

TABLE II

ULTRAVIOLET ABSORPTIONS[a] and IONIZATION POTENTIALS OF POLYMETHYL BENZENES

Substance	$\nu(0\text{-}0)$[b] (cm^{-1})	$\Delta\nu$ (cm^{-1})	I[c] (eV.)	ΔI (eV.)	
Benzene	38089		9.52		
Toluene	37484	−605	9.20	−0.32	
o-Xylene			8.96	−0.56	Average −0.58
m-Xylene			9.01	−0.51	
p-Xylene			8.86	−0.66	
Mesitylene	36488	−1601	8.76	−0.76	

a) The data on the ultraviolet absorptions were taken from Table III (in ref. 4).

b) $\nu(0\text{-}0)$ represents the wave-number of the 0–0 transition in the vapor state.

c) I represents the first ionization potential.

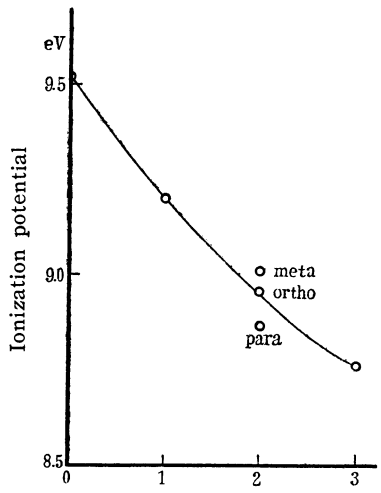

Fig. 1. Variation of ionization potential with the number of methyl radicals in polymethyl benzenes.

Pyridine and Picolines.—According to Table I, the differences of the potential values between pyridine and three isomeric monomethyl pyridines, viz., α-, β-, γ-picolines, are −0.10 eV., −0.05 eV., −0.20 eV., respectively. That is, the lowering of ionization potential caused by the methyl substitution is seen to be less pronounced in pyridine than in benzene (cf. Table II). On the contrary, the red shift of the $\pi\rightarrow\pi^*$ transitions in picolines appears to be not very different from that in toluene[8,9], so that the perturbation effect of methyl radical on the ring π-orbitals will be almost the same for pyridine and benzene rings. Therefore, if the ionizing electron in question were the one belonging to the π-orbital, the lowering in the ionization potential would not be so small as observed in this experiment. Consequently, it seems very likely that the first ionization potentials of pyridine and its methyl derivatives are primarily determined by the nonbonding $sp^2\sigma$-electron of the N atom.

Indeed, the above view seems to have support from the studies of ultraviolet absorption spectra[8,9,10,11]. Both in pyridine and picolines, there appear two absorptions of markedly different intensities. The weaker one has been assigned to the transition from the non-bonding orbital of the N atom to the lowest vacant π-orbital ($n\rightarrow\pi^*$ transition), and the stronger one to the transition from the highest occupied π-orbital to the lowest vacant π-orbital ($\pi\rightarrow\pi^*$ transition). The $n\rightarrow\pi^*$ transitions of all these substance occur at the longer wave-lengths, indicating that there is a non-bonding level of the N atom situated above the highest occupied π-level. Therefore, one electron in this non-bonding orbital must be inferred to be responsible for the first ionization*.

Lastly, we shall try to explain the slight decrease in ionization potential upon the methyl substitution. As a result of the resonance among various structures including those of Fig. 2 the methyl group in toluene

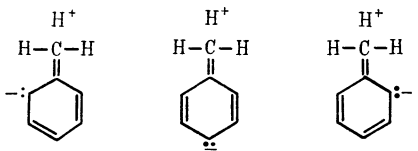

Fig. 2.

sends partial negative charge to the carbon atoms of the ortho and para positions. The situation in isomeric picolines may be deduced from this. That is, extra negative charges will appear at the N atoms of α- and γ-picolines, but not at the N atom of β-picoline. Therefore the ionization potentials of the former two substances will become smaller on account of the increased electron density at the N atom, while the potential of β-picoline will remain almost the same as pyridine (cf. Table I).

Summary

First ionization potentials of 18 aromatic and conjugated compounds were measured by the electron impact method. Seven out of

8) J.H. Rush and H. Sponer, *J. Chem. Phys.*, 20, 1847 (1952).

9) H.P. Stephenson, *J. Chem. Phys.*, 22, 1077 (1954).

10) M. Kasha, *Discuss. Faraday Soc.*, 9, 14 (1950).

11) F. Halverson and R.C. Hirt, *J. Chem. Phys.*, 19, 711 (1951).

* There is still some uncertainty about the above assignment. Next, we are intending to measure the ionization potentials of the isomers of diazines and triazines. And then we shall be able fo present more complete and fuller discussion on this problem.

these were newly determined in the present work. Discussion of the results was given with special reference to their relation to the ultraviolet data.

It was suggested that the ionization potentials in benzene derivatives are primarily determined by π-electrons, while those in pyridine and picolines are largely by one of the non-bonding electrons belonging to the N atom in the ring.

The authors with to express their gratitude to Dr. S. Nagakura for valuable criticisms and suggestions, and also to the Ministry of Education for a Grant in Aid.

Research Institute of Applied Electricity
Hokkaido University, Sapporo

Studies on the Intramolecular Hydrogen Bond in Conjugated Systems by the Measurements of Dipole Moments. I. o-Nitrophenol

By Bunzo EDA and Kazuo ITO

(Received February 9, 1956)

Introduction

When a molecule having conjugated double bonds forms an intramolecular hydrogen bond, it is expected that the charge migration is caused by the bonding in the molecule. But the magnitude and direction of the migration have not been determined experimentally as yet. For the purpose of obtaining these, we measured the dipole moments of several compounds. In this paper we report the results obtained on *o*-nitrophenol.

From the infrared absorption spectrum it has been found that *o*-nitrophenol has no free hydroxyl group and consequently all the molecules form the intramolecular hydrogen bond[1]. In order to get information on the charge migration caused by the hydrogen bond in the molecule, it is necessary to compare the dipole moment of *o*-nitrophenol with the moment of a hypothetical *o*-nitrophenol molecule having no intramolecular hydrogen bond in regard to the directions of moments as well as their absolute values. The components of the dipole moment of *o*-nitrophenol can be obtained from the measurements of the dipole moments of *o*-nitrophenol, 4-chloro-2-nitrophenol and 4-methyl-2-nitrophenol, while the components of the dipole moment of the hypothetical *o*-nitrophenol having no hydrogen bond can be obtained from the sum of the respective components of the dipole moments of phenol and nitrobenzene. The order of magnitude of errors due to the assumption that the dipole moment of a molecule can be expressed by the vector sum of bond moments was estimated with the aid of the dipole moments of anisole and its derivatives.

1) L. Pauling, "The Nature of the Chemical Bond", Cornell University Press, Ithaca, New York (1940), p. 318.

Experimental

Materials.—All the materials were prepared in our laboratory except *o*-nitrophenol and 4-chloro-2-nitroanisole which were purchased and purified by recrystallization. 4-Chloro-2-nitrophenol and 4-methyl-2-nitrophenol were purified by steam distillation followed by recrystallization, while *o*-nitroanisole was purified by vacuum distillation.

Measurements.—All the measurements were made in benzene solutions at 25°C. The dielectric constants were measured by heterodyne beat method. A modified Hedestrand method was employed for obtaining the specific polarization at infinite dilution. The method was similar to that introduced by Halverstadt and Kumler[2], differing in that densities were used rather than the specific volumes. The sum of electronic polarization and atomic polarization was assumed to be equal to the molecular refraction for D-line calculated additively from the atomic refractions of the constituent atoms.

Results.—The results are shown in Table I and II, where μ is the dipole moment in Debye unit. All the notations have the same significances as those used by Kurita et al.[3]. The data found in literatures to be compared with the present results are those of Jenkins on *o*-nitrophenol[4] and of Cowley and Partington on *o*-nitroanisole[5].

2) I.F. Halverstadt and W.D. Kumler, *J. Am. Chem. Soc.*, **64**, 2988 (1942).

3) Y. Kurita, T. Nozoe and M. Kubo, This Bulletin, **26**, 242 (1953).

4) H.O. Jenkins, *J. Chem. Soc.*, **1936**, 1049.

5) E.G. Cowley and J.R. Partington, *J. Chem. Soc.*, **1933**, 1257.

TABLE I

DIELECTRIC CONSTANTS AND DENSITIES IN BENZENE SOLUTIONS OF *o*-NITROPHENOL, *o*-NITROANISOLE AND THEIR DERIVATIVES AT 25°C

Compounds	$w\times10^5$	ε	d
o-Nitrophenol	138	2.2825	0.87169
(m.p. 45°)	777	2.3328	0.87372
	1681	2.4050	0.87642
	3019	2.5110	0.88040
4-Chloro-2-nitrophenol	295	2.2836	0.87211
(m.p. 86°)	594	2.2943	0.87331
	1172	2.3144	0.87516
	2741	2.3717	0.88096
4-Methyl-2-nitrophenol	214	2.2928	0.87192
(m.p. 32°)	778	2.3401	0.87329
	1664	2.4183	0.87565
	2913	2.5272	0.87904
o-Nitroanisole	152	2.2971	0.87130
(b.p. 165° at 39 mmHg)	331	2.3271	0.87182
	520	2.3598	0.87239
	765	2.3991	0.87307
4-Chloro-2-nitroanisole	302	2.3117	0.87344
(m.p. 98°)	496	2.3360	0.87413
	824	2.3761	0.87503

Let it be assumed that the methoxy group is in the plane of an anisole molecule as illustrated in Fig. 1 (a). The components of dipole moment in x- and y-directions are

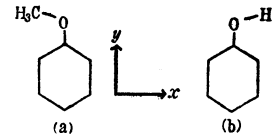

Fig. 1.

denoted by μ_x and μ_y, respectively. Since the observed moment of anisole in benzene solution is 1.28 D[8] we have

$$\mu_x^2+\mu_y^2=1.28^2 \qquad (1)$$

The mesomeric moment from the methoxy group to benzene ring is, of course, included in these two components. The dipole moment of hydroquinone dimethylether $C_6H_4(OCH_3)_2$ would have the same value[9], which is equal to $\sqrt{2}\mu_x$, whether (i) the methoxy groups rotate freely, (ii) they are fixed in equally probable *cis*- and *trans*-forms, (iii) the groups in these *cis*- and *trans*-forms rotate freely within certain limits of angle, or (iv) the oscillation, not being free, is such that the probability of any angle, of swing is some function of that angle, the same function applying to each group. The observed moment in benzene solution is 1.73 D[8], hence μ_x is ±1.2 D. As it is most probable that the direction is $H_3{}^+C\text{–}O^-$, we prefer $\mu_x=+1.2$ D. Putting it in (1), we get $\mu_y=\pm0.4$ D. If we use the components $\mu_x=+1.2$ D and $\mu_y=-0.4$ D, the calculated moments of anisole, its *ortho*- and *para*-derivatives and 4-chloro-2-nitroanisole agree with the observed ones to within less than 0.1 D as shown in Table III. Therefore, the moments of anisole, its *ortho*- and *para*-derivatives and the *para*-derivative of *o*-nitroanisole can be expressed by the vector sum to within less than 0.1 D including the difference in mesomeric effect and solvent effect unless they are compelled to be in the other particular configuration by

TABLE II

MOLECULAR POLARIZATIONS AND DIPOLE MOMENTS OF *o*-NITROPHENOL, *o*-NITROANISOLE AND THEIR DERIVATIVES IN BENZENE SOLUTIONS AT 25°C

Compounds	ε_1	d_1	α	β	$P_{2\infty}$	MR_D	μ
o-Nitrophenol	2.2714	0.87132	7.94	0.301	239.4	34.4	3.16
4-Chloro-2-nitrophenol	2.2727	0.87106	3.60	0.360	152.8	39.3	2.35
4-Methyl-2-nitrophenol	2.2734	0.87129	8.71	0.265	287.8	39.2	3.49
o-Nitroanisole	2.2720	0.87086	16.68	0.290	517.2	39.2	4.83
4-Chloro-2-nitroanisole	2.2746	0.87248	12.33	0.314	476.3	44.0	4.60

Their values of 3.11 D and 4.83 D respectively are in good agreement with ours.

Discussion

The near-ultraviolet absorption spectra of phenol and anisole in cyclohexane solutions[6] agree with each other to a high degree of precision both in the wavelengths of maximum absorption and in intensities. Moreover, the resonance energy of phenol is almost the same as that of anisole[7]. Accordingly, if the observed moments of anisole, its *ortho*- and *para*-derivatives and the *para*-derivative of *o*-nitroanisole are fairly consistent with those calculated by vector addition, it will be reasonable to suppose that the method of vector sum of bond moments can also be used with nearly the same accuracy in the corresponding phenol derivatives.

6) R.A. Friedel and M. Orchin, "Ultraviolet Spectra of Aromatic Compounds", John Wiley & Sons, Inc., New York (1951); Fig. 31 and Fig. 55.

7) G.W. Wheland, "The Theory of Resonance", John Wiley and Sons, Inc., New York (1944), p. 69.

8) K.B. Everard and L.E. Sutton, *J. Chem. Soc.*, **1949**, 2312.

9) K.B. Everard and L.E. Sutton, *J. Chem. Soc.*, **1951**, 19.

TABLE III
DIPOLE MOMENTS OF ANISOLE DERIVATIVES IN BENZENE SOLUTIONS

Substituents	$\mu_{calcd.}$ (D)[a,b]	$\mu_{obs.}$(D)[c]
p-CH_3	1.20	1.20
p-Br	2.31	2.23
p-Cl	2.33	2.24
o-F	2.50*	2.31
o-Cl	2.60	2.50
o-Br	2.58	2.47
o-CH_3	1.05	1.0
o-NO_2	4.92	4.83
4-Cl-2-NO_2	4.66	4.60

a) The bond moments of the substituents are based on the following data[10], bromobenzene 1.57 D, chlorobenzene 1.60 D, fluorobenzene 1.48 D, toluene 0.4 D and nitrobenzene 4.0 D in benzene solutions.

b) In *ortho*-derivatives it is assumed that the methoxy group is fixed in the molecular plane and the methyl carbon is in the side opposite to *ortho*-substituent.

c) The observed values were taken from "Tables of Electric Dipole Moments"[11] except those of *o*-nitroanisole and 4-chloro-2-nitroanisole.

* The difference for *o*-fluoroanisole is greater because the small size of the fluorine atom makes the *cis*-configuration less improbable for this compound than for the other *ortho*-substituted anisoles.

steric hindrance, etc. Likewise, were it not for the hydrogen bond or a remarkable change of configuration, it should be possible to express the dipole moments of phenol, its *para*-derivatives and *ortho, para*-disubstituted derivatives by the vector sum to within less than 0.1 D.

The x- and y-components of dipole moment of phenol, Fig. 1 (b), can be obtained from the moment of phenol and its *para*-derivatives. If it is assumed that $\mu_x=1.55$ D and

TABLE IV
DIPOLE MOMENTS OF PHENOL AND ITS *para*-DERIVATIVES IN BENZENE SOLUTIONS

Compounds	$\mu_{calcd.}$(D)	$\mu_{obs.}$(D)[a]	$\Delta\mu$(D)[b]
Phenol	1.55	1.56	+0.01
p-Bromophenol	2.21	2.13	−0.08
p-Chlorophenol	2.23	2.22	−0.01
p-Methylphenol	1.59	1.57	−0.02
p-Fluorophenol	2.14	2.10	−0.04

a) The observed values for all compounds were taken from "Tables of Electric Dipole Moments[11]" except *p*-fluorophenol, the value of which is due to Leonard and Sutton[12].

b) $\Delta\mu$ denotes the difference between $\mu_{obs.}$ and $\mu_{calc.}$.

10) K.B. Everard, L. Kumar and L.E. Sutton, *J. Chem. Soc.*, **1951**, 2814.
11) L.G. Wesson, "Tables of Electric Dipole Moments", The Technology Press, M.I.T. (1948).
12) N.J. Leonard and L.E. Sutton, *J. Am. Chem. Soc.*, **70**, 1566 (1948).

$\mu_y=0.0$ D, the observed moments agree with the calculated ones as shown in Table IV. On the contrary, the calculated moments of *o*-nitrophenol, 4-chloro-2-nitrophenol and 4-methyl-2-nitrophenol do not agree with the observed ones by the order of 0.4 D as shown in Table V. These discrepancies are definitely greater than those in Table III and IV. Since all the compounds given in Table V

TABLE V
DIPOLE MOMENTS OF *o*-NITROPHENOL AND ITS DERIVATIVES IN BENZENE SOLUTIONS

Compounds	$\mu_{calcd.}$(D)	$\mu_{obs.}$(D)	$\Delta\mu$(D)
o-Nitrophenol	2.77	3.16	0.39
4-Chloro-2-nitrophenol	1.95	2.35	0.40
4-Methyl-2-nitrophenol	3.07	3.49	0.42

are supposed to have an intramolecular hydrogen bond between the hydroxyl group and the nitro group, this abnormality may be due mainly to the hydrogen bond. The components of *o*-nitrophenol that satisfy the observed moments of *o*-nitrophenol, 4-chloro-2-nitrophenol and 4-methyl-2-nitrophenol are $\mu_x=$ 2.2–2.3 D and $\mu_y=2.2$–2.35 D, respectively. The calculated components based on the aforementioned components of phenol and the dipole moment of nitrobenzene are $\mu_{x\,calcd.}=$ 1.9 D and $\mu_{y\,calcd.}=2.0$ D, respectively. Hence we have $\Delta\mu_x=0.3$–0.4 D and $\Delta\mu_y=0.2$–0.35 D as the abnormal values.

In *o*-nitrophenol, therefore, the formation of intramolecular hydrogen bond causes the charge migration of the order of 0.3–0.4 D in x-direction and 0.2–0.35 D in y-direction. Such charge migration may be explained, for instance, by two main charge migrations illustrated in Fig. 2. Further studies are required, however, of other compounds similar to *o*-nitrophenol in order to see whether or not such charge migrations are common in the molecule having an intramolecular hydrogen bond.

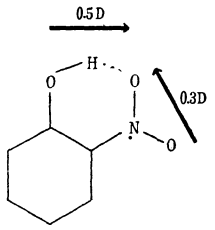

Fig. 2.

Summary

Dipole moments of *o*-nitrophenol, 4-chloro-2-nitrophenol, 4-methyl-2-nitrophenol, *o*-nitroanisole and 4-chloro-2-nitroanisole were meas-

ured in benzene solutions. Their values are 3.16, 2.35, 3.49, 4.83 and 4.60 D respectively. Instead of obtaining the directions of the dipole moments of phenol and anisole, μ_x and μ_y, the two components in x- and y-directions in the molecular plane, were evaluated from the moments of their derivatives. When the dipole moments of *o*-nitrophenol, *o*-nitroanisole and their derivatives were calculated according to the vector addition using these components, the calculated moments for *o*-nitrophenol and its derivatives do not agree with the observed ones whereas fairly good agreement was found between the observed and calculated ones for *o*-nitroanisole and its derivative. The order of the discrepancy is 0.3–0.4 D in x-direction and 0.2–0.35 D in y-direction. The authors suggest that the cause of this discrepancy is due mainly to the formation of an intramolecular hydrogen bond.

The authors wish to express their sincere thanks to Prof. M. Kubo and Dr. Y. Kurita for their kind discussions. A part of the expense for the experiment has been defrayed from a grant given by the Ministry of Education, to which the authors' thanks are due.

Department of Chemistry, Faculty of Science, Nagoya University
Nagoya

A Theoretical Treatment of Activity Coefficients in Resin Phase

By Hiroshi SOBUE and Yoneho TABATA

(Received July 25, 1955)

Introduction

The phenomena of ionic exchange have been studied from the statistical point of view by several investigators. Hamada[1] and Davis[2] independently applied a statistical model to the ion exchange equilibria. Hamada derived the equation of the simple mass action type by assuming a lattice model as ion exchange equilibria, while Davis dealt with ion exchange equilibria, assuming a regular model for ionic exchange, by a modification of a statistical theory of a localized monolayers derived from Fowler and Guggenheim[3]. The latter author first applied the theory to an uni-uni-valent exchange and showed that the resultant equation is of the simple mass action type, ignoring the interaction energy between ion pairs in the exchanger phase. Afterwards he studied two types of irregular models of ionic exchange systems. Seiyama, Sakaki and Nagamatsu[4] developed the statistical theory of Hamada and Davis, by applying "a quasi-chemical method" of Guggenheim[5], and they discussed in detail the ion exchange equilibria involving uni-uni-valent and uni-di-valent exchange.

According to the experimental results of Argersinger, Davidson[6] as well as the present authors[7], it can be expected that the activity coefficients in any exchange ratio will be affected markedly by the interaction energy of each ion pair in the solid phase. Generally the interaction of each pair presumably involves the following forces: ion-dipole, van der Waals and covalent bond forces as short range forces, and electrostatic forces (Coulomb force) as long range forces.

Accordingly ion exchange phenomena should be investigated under consideration of all these forces. Above all, the anomaly in the activity coefficients in the resin phase will principally depend on the interaction forces described above.

Davis[2] and Hamada[1] ignored the interaction energy between ion pairs in the exchanger phase, while Seiyama, Sakai and Nagamatsu[4] gave a statistical explanation of the ion exchange equilibrium constants under consideration of the interaction energy between ion pairs in the resin phase. But they did not treat the activities in the exchanger phase extensively. The authors

1) H. Hamada, *The Journal of Japanese Chemistry* (*Kagaku-no-ryoiki*), **1**, 83 (1946).
2) L.E. Davis, *J. Colloid Sci.*, **5**, 71, 107 (1959).
3) R.H. Fowler and E.A. Guggenheim, "Statistical Thermodynamics" (1938).
4) T. Seiyama, M. Nagamatsu and W. Sakai *Electro. Chem.*, **21**, 218, 393 (1953).
5) E.A. Guggenheim, *Trans. Faraday Soc.*, **44**, 1007 (1948).
6) W.J. Argersinger, Jr. and A.W. Davidson, *J. Phys. Chem.* **56**, 92 (1952).
7) H. Sobue and Y. Tabata *J. Chem. Soc. Japan* (*Ind. Chem. Sect.*) **56**, 938 (1653); ibid. **57**, 469 (1954).

present here a theoretical treatment under several assumptions, in which it will be shown that the energy of mutual ionic-interaction has an important significance in the activity determination in the solid phase.

Theoretical

The following discussions are based on Guggenheim's theory which deals with "A Generalization of the Quasi-Chemical Method". In this treatment, the following conditions are assumed.

1) Ionic exchange systems have no empty sites.

2) A polyvalent ion will occupy a set of r adjacent sites, r being the number of sites occupied by an ion.

3) We may neglect interaction between pairs of ions that are not nearest neighbours, so that the total interaction energy of the ions can be expressed as the sum of contributions from each pair of nearest neighbours.

4) We treat ion exchange resins as slightly swollen gels so that the volume change of the system due to the exchange process is small.

5) It is assumed that the electrolyte solution involving the exchangeable ions is able to diffuse freely through the network of the exchange resin, so that there is no mechanical resistance associated with ionic size in the exchange process.

6) We also considered the case where the ionic concentration of the electrolyte solution in the exchange system is comparatively small, so that the effect of the presence of the free electrolytes (non-fixed electrolytes at the exchanging lattice points) in the resin phase at equilibrium will be small.

Let us consider a lattice model which has regular N sites as the ion exchange resin phase and in which one site has one negative charge.

Let N_A: Number of ions of any type of A.
r_A: Number of sites occupied by one ion of type A.
z: Number of sites which are nearest neighbours of any given site in regular array.
q_A: A function of z and r_A which determines the frequency with which a valence element of an ion of type A will occupy a site adjacent to another occupied site.

In a specific state having any exchange ratio, we have

$$N=r_AN_A+r_BN_B$$

Parameters q_A, q_B are defined by

$$z(r_A-q_A)=2(r_A-1)$$

$$z(r_B-q_B)=2(r_B-1)$$

zq_A is the so-called corrected co-ordination number, i.e., the number of sites, neighbours of the r_A sites occupied by an ion A, excluding those neighbours of each site occupied by the next element of the same ion. The physical meaning of q_B is similar to q_A. It is assumed that in any given configurations of the system, inter-ionic (inter-ionic of hydrogen ion and metallic ions) potential energy consists of a sum of the following terms ϕ_{AA}, ϕ_{BB} and ϕ_{AB}. ϕ_{AA}, ϕ_{BB} and ϕ_{AB} denote the contribution to the internal energy by a pair of sites occupied both by A ions, botn by B ions, and one occupied by A and the other occupied by B respectively.

Let the number of pairs of neighbouring sites in which one site is occupied by an ion A and the other by an ion B be denoted by zX. The partition function Q of the system is written in the form

$$Q=\sum_x g(N_A, N_B, X) \exp(zX\phi/2kT),$$

where $\phi=\phi_{AA}+\phi_{BB}-2\phi_{AB}$ and $g(N_A, N_B, X)$ denotes the number of distinguishable configurations of all the N_A ions of A and N_B ions of B for a given value of X. This combinatory factor $g(N_A, N_B, X)$ is expressible as an explicit function of N_A, N_B, X, involving z, r_A, r_B, q_A, q_B as parameters. In a real exchange system, each ion in an exchangeable point (lattice point) will exist in a hydrated state according to the size of the framework and the kinds of the exchangeable ions.

The total free energy F' can be represented by the following equation,

$$F'=N_A\mu_A^{0'}+N_B\mu_B^{0'}+\Delta F_1+\Delta F_2,$$

where ΔF_1 and ΔF_2 are the free energies of mixing, which contain the configurational term and the term due to the interaction energy respectively.

The terms of $\mu_A^{0'}$ and $\mu_B^{0'}$ in the total free energy F' should be expressed by the following equations.

$$\mu_A^{0'}=-\frac{q_Az}{2}\phi_{AA}+u_A^0-kT\log v_{f_A}-kT\times\log\left(\frac{2\pi m_AkT}{h^2}\right)^{3/2}$$

$$\mu_B^{0'}=-\frac{q_Bz}{2}\phi_{BB}+u_B^0-kT\log v_{f_B}-kT\times\log\left(\frac{2\pi m_BkT}{h^2}\right)^{3/2}$$

In these expressions, u_A^0 and u_B^0 are the potential energies of ions A and B in an equilibrium state respectively. v_{f_A}, v_{f_B} are the free volumes and m_A, m_B the masses of

the respective ions in the exchangeable point at constant temperature. If we consider free energy due to configuration only, the free energy F can be expressed by the following equation,

$$F=N_A\mu_A^0+N_B\mu_B^0+\Delta F_1+\Delta F_2=kT\log Q.$$

In this expression, μ_A^0 and μ_B^0 are respectively the chemical potentials of each pure resin. The quantity which has the most important meaning in the problem treated here is free energy of mixing $\Delta F=\Delta F_1+\Delta F_2$. If we use Flory's approximation for ΔF_1,

$$\Delta F_1/kT=\left(1-\frac{1}{2}z\right)r_AN_A\log r_AN_A$$
$$+\left(1-\frac{1}{2}z\right)r_BN_B\log r_BN_B-\left(1-\frac{1}{2}z\right)$$
$$\times(r_AN_A+r_BN_B)\log(r_AN_A+r_BN_B)$$
$$+\frac{1}{2}z\{q_AN_A\log q_AN_A+q_BN_B\log q_BN_B$$
$$-(q_AN_A+q_BN_B)\log(q_AN_A+q_BN_B)\}.$$

ΔF_2 which contains the term of the interaction energy can be expressed as,

$$\Delta F_2/kT=\frac{1}{2}z(q_AN_A+q_BN_B)\left\{\theta\log\frac{\beta-1+2\theta}{\theta(\beta+1)}\right.$$
$$\left.+(1-\theta)\log\frac{\beta+1-2\theta}{(1-\theta)(\beta+1)}\right\}.$$

In this expression β and θ are represented as follows,

$$\beta=\left\{(1-2\theta)^2+4\theta(1-\theta)e^{\frac{\phi}{kT}}\right\}^{1/2}$$

$$\theta=\frac{q_AN_A}{q_AN_A+q_BN_B},\quad 1-\theta=\frac{q_BN_B}{q_AN_A+q_BN_B}.$$

Therefore by using the above equations the chemical potentials of ions A and B are given as the differential forms of the corresponding free energies:

$$\mu_A=\frac{\delta F}{\delta N_A}=\mu_A^0+kT\left\{(1-\frac{1}{2}z)r_A\right.$$
$$\log\frac{r_AN_A}{r_AN_A+r_BN_B}+\frac{1}{2}zq_A\log\frac{q_AN_A}{q_AN_A+q_AN_B}$$
$$\left.+\frac{1}{2}zq_A\log\frac{\beta-1+2\theta}{(\beta+1)\theta}\right\}$$

$$\mu_B=\frac{\delta F}{\delta N_B}=\mu_B^0+kT\left\{(1-\frac{1}{2}z)r_B\log\right.$$
$$\times\frac{r_BN_B}{r_AN_A+q_BN_B}+\frac{1}{2}zq_B\log\frac{q_BN_B}{q_AN_A+q_BN_B}$$
$$\left.+\frac{1}{2}zq_B\log\frac{\beta+1-2\theta}{(\beta+1)(1-\theta)}\right\}$$

The relation between the activity and the chemical potential is expressed by the following equations,

$$\mu_A=\mu_A^0+kT\log a_A$$
$$\mu_B=\mu_B^0+kT\log a_B$$

where a_A, a_B are activities of A and B ions in the resin phase respectively, therefore the activity coefficients are given by the following expressions,

$$\frac{N_A}{N_A+N_B}f_A=e^{\frac{\mu_A-\mu_A^0}{kT}}$$

$$\frac{N_B}{N_A+N_B}f_B=e^{\frac{\mu_B-\mu_B^0}{kT}}$$

Then we can calculate the activity coefficients in the ion exchange resin phase from the above equations. The results obtained by calculation using the above equations are shown in Figs. 1, 2 and 3.

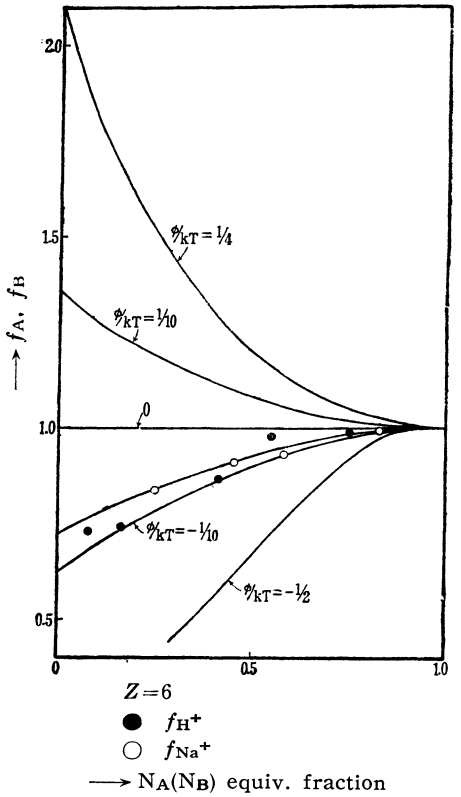

Fig. 1. Relationship between activity coefficients and exchange ratios in the resin phase of uni-uni-valent exchange system. (The dots show the experimental values).

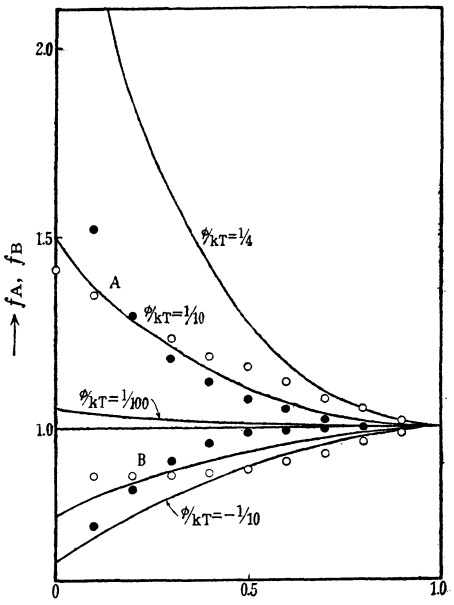

Fig. 2. Relationship between activity coefficients and exchange ratios in the resin phase of uni-uni-valent exchange system. (The dots show the experimental values of Argersinger and Davidson).

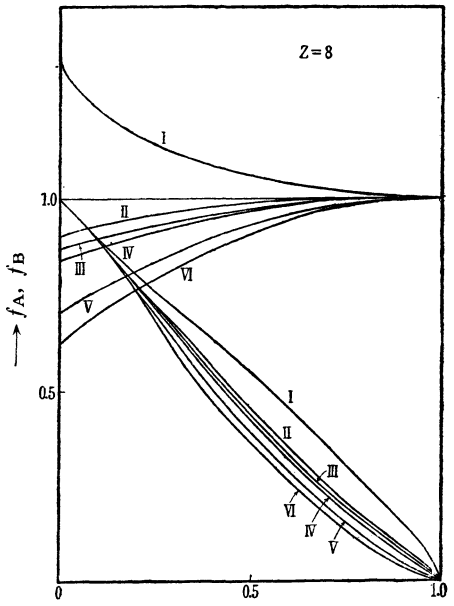

Fig. 3. Relationship between activity coefficients and exchange ratios in the resin phase of uni-di-valent system.

I. ..... $\frac{\phi}{kT}=1/10$
II. I/100
III. 0
IV. ..... -1/100
V. ..... -2/100
VI. ..... -1/10

Experimental

A film of carboxymethylcellulose (ion exchange capacity 3.29 meq./g. for dry sample) was used as the cation exchanger. The film (acid form), which was about 2.5×2.5 cm^2 and about10 μ thick, was used as the sample. Equilibrium studies of the H-Na, H-NH_4 and H-Ca exchanges were made while maintaining Na, NH_4 and Ca concentrations constant at various hydrogen ion concentrations in the solution phase.

In each exchange experiment, the sample was placed in a ground glass stopperd flask in contact with an aqueous solution of the appropiate salts of the cations. The volume of the electrolyte solution was 100 ml. Initial and equilibrium concentrations of hydrogen ions were determined by the glass electrode in the solution phase. The films, which reached equilibrium, were washed with sufficient 70% alcoholic solution in the uni-uni-valent case (H-Na exchange), and with distilled water in the uni-di-valent case (H-Ca exchange). The equilibrium temperature was maintained at 15 ± 1°C. The infrared spectra of the exchanger film were measured with a double beam system spectrometer of Baird Co. with a rock salt prism*.

As described in the previous paper[7], several precautions were necessary to minimize errer in measurements of the infrared spectra. The apparent equilibrium constants were calculated by the following equation, using the spectrophotometric method,

$$pKa = r_B \log \varepsilon_a - r_A \log k\varepsilon_b - (r_B - r_A)\log(\varepsilon_a + k\varepsilon_b) + r_A \log B^{+r_B} - r_B \log A^{+r_A} + \log \frac{r_B{}^{r_A}}{r_A{}^{r_B}}$$

where A and B are the concentrations of the two exchangeable ions respectively, r_A is the valence of the A ion, γ_A is the activity coefficient of the A ion in the electrolyte solution, ε_a is the absorption intensity of carbonyl band (5.6 μ or 6.3 μ) of carboxyradical fixing the A ion in an exchanger, when the C-H stretching vibration in 3.4 μ was selected as the reference band, and k is a constant. In the calculation of pKa, the mean activity coefficients of the electrolyte from "Lewis, Table" were used.

Evaluation of the Activity Coefficients

For an ion exchange system we could consider the true equilibrium constant K as

$$K = Ka\frac{f_B{}^{r_A}}{f_A{}^{r_B}}$$

In the above equation, f expresses the activity coefficient of resin component on mole fraction basis, with pure resin as the standard state. The following equation is given from the Gibbs-Duhem relation,

$$m_A d\mu_A + m_B d\mu_B = (n_A/r_A)d\mu_A + (n_B/r_B)d\mu_B = 0,$$

where m and n represent a mole fraction and an equivalent fraction of the respective ion in the solid exchanger phase respectively, and μ the chemical potential of the exchangeable ions in the resin phase. We can obtain the differential form of the logarithmic relation between K and Ka from the Gibbs-Duhem equation at constant temperature and pressure for the solid solution phase.

$$\left(\frac{n_A}{r_A}\right) d \log f_A + \left(\frac{n_B}{r_B}\right) d \log f_B = 0$$

On the other hand, the following equation is obtained from the above equation.

$$r_A \, d \log f_B - r_B \, d \log f_A = -d \log Ka$$

Now, we calculate the activity coefficient f from these equations. We carried out the calculation of the activity coefficients of salts in the three exchange systems of Na-H, NH_4-H and Ca-H at 0.02 N ionic concentration. The results are shown in Fig. 1. and Table I.

TABLE I

ACTIVITY COEFFICIENTS IN RESIN PHASE

Activity coefficients of Na^+ and H^+ in Na-H exchange system

n Equivalent fraction of Na^+	pKa Apparent equil. const.	f_A Activity coeff. of Na^+	f_B Activity coeff. of H^+
1.0	2.72*	1.000	0.79*
0.9	2.71	0.998	0.790
0.8	2.70	0.995	0.795
0.7	2.69	0.990	0.800
0.6	2.66	0.987	0.818
0.5	2.62	0.948	0.860
0.4	2.57	0.860	0.926
0.3	2.53	0.796	0.968
0.2	2.48	0.757	0.988
0.1	2.46	0.737	0.933
0	2.44*	0.72*	1.000

Activity coefficients of Ca^{++} and H^+ in Ca-H exchange system

n Equivalent fraction of Ca^{++}	pKa Apparent equil. const.	f_A Activity coeff. of Na^+	f_B Activity coeff. of H^+
1.0	2.97*	1.000	0.69*
0.9	2.96	1.000	0.697
0.8	2.95	0.988	0.705
0.7	2.93		0.719
0.6	2.88	0.953	0.747
0.5	2.80	0.871	0.783
0.4	2.66	0.731	0.842
0.3	2.50	0.582	0.904
0.2	2.30	0.412	0.957
0.1	2.10	0.278	0.990
0	1.88*	0.13*	1.000

* After the samples were dried at 70-80°C for ten hours under reduced pressure, the measurements of the infrared spectra were carried out in the room of approximately constant relative humidity (35-40%) and constant temperature (20°C) during twenty minutes. Under such experimental rircumstances, the authors confirmed that the quantity of water contained in the film was quite small and the relative optical density of ν(CO) was affected to an extremely small extent by the contained water.

Extrapolated Values

These experimental results obtained by the authors and the results obtained by Argersinger and Davidson have been compared with the theoretical values.

Discussion

Activity coefficients vary with the exchange ratio (fraction n in the resin phase) for constant co-ordination number z and inter-ionic interaction energy ϕ. In case of an uni-uni-valent system, both activity coefficients vary symmetrically, but in the case of an uni-di-valent system the activity coefficient of the di-valent ion varies more intensively than the uni-valent ion, with the increase of the exchange ratio.

In this derivation, the authors wish to emphasize that the activity coefficients are predominantly affected by the interaction energy.

In the uni-uni-valent case, corresponding to $\phi<0$, $\phi=0$, or $\phi<0$, the activity ceofficients are found to be smaller than unity, equal to unity, or greater than unity, respectively. According to the experimental results obtained by the authors and Argersinger and Davidson, the resin activity coefficients in Na-H and NH_4-H systems were found to be smaller than unity, therefore $\phi<0$. But in the Ag-H exchange system, both activity coefficients were found to be larger than unity.

Argersinger and Davidson[6] have explained that the difference in both cases may be due to the greater dissimilarity between the silver and hydrogen resins, as compared with the sodium and hydrogen resins. According to the theory derived here, this difference may be explained as due to the inter-ionic interaction in the resin phase, which plays an extremely important role.

From the above statements, it is evident that an activity coefficient larger than unity corresponds to one case only, that is $\phi>0$. Accordingly the activity coefficients generally may be explained as a function of the ionic interaction energy between each ion pair. In Na-H and NH_4-H exchange systems of carboxymethylcellulose the interaction energies ϕ/kT of each system are about -0.1 and -0.7–0.8 respectively.

In the case of the uni-di-valent exchange, when $\phi=0$, the activity coefficients are not unity owing to the contribution due to the configurational term. The activity coefficients of the di-valent ion, as compared with those of the uni-valent ion, vary extremely depending on the exchange ratio, but are always

smaller than unity. On the other hand, the coefficients of the uni-valent ion in the uni-di-valent system have a trend similar to the uni-uni-valent case.

According to the experimental results by Argersinger and Davidson, the activity coefficients in the solid phase are affected only to an extremely small extent by the concentration of the electrolyt solutions. On the other hand, the activity coefficients are shown to be independent of the concentration of the electrolyte solutions and are denoted only as a function of n (equivalent fraction) in the resin phase. Thus the results obtained by the theoretical consideration coincide with experimental ones.

In real exchange phenomena, the experimental results would deviate more of less from the theory due to the following reasons:

1) The effect of the free ions which exist in the resin phase.

2) The swelling of the ion exchange resin actually does vary the exchange ratio, although it was assumed that the resin maintained a constant structure, independent of the exchange ratio.

3) The hydrated ions of Na and Ca have approximately the same volume under the same conditions. The ions of Na and Ca exist in the hydrated state in the resin phase. Therefore the size of each hydrated ion will also be nearly equal in the resin phase. Then the di-valent ion such as Ca would not be able to occupy the two ajacent sites completely, as was assumed in this theory.

In future work, it will be possible to predict and analyse the phenomena of both the "relative selectivity" of the ions in the exchanger and the separation efficiency, from the concept of the inter-ionic interraction involving ϕ. Of course, the size of the ions and the degree of hydration must be taken into consideration.

Conclusion

A theoretical treatment of activity coefficients in the resin phase of cation exchangers is given by using Guggenheim's theory which deals with "A Generalization of the Quasi-Chemical Method".

The results indicate that the activities in the resin phase are markedly affected by the interaction energy ϕ between ion pairs and they are expressed as a function of ϕ, z, r and n.

Experimental evidence indicates that this conclusion is useful in several cases to explain the activity behavior of ions in the resin phase.

As a result, it is pointed out that the activity behavior in the resin phase of cation exchanger would be generally explained fairly well by considerations of the concept of the interaction energy.

Department of Applied Chemistry
Faculty of Engineering
The University of Tokyo
Hongo, Tokyo

Distribution of Boron in Natural Waters

By Satoru MUTO

(Received November 2, 1955)

Introduction

The distribution of boron in natural waters was reported on some mineral springs[1], thermal springs[2], and irrigation waters[3]. The amounts of boron in the ground waters[4], rains and snows[5] were also reported by several authors. But the discussion on the distribution of boron in these waters has never been made in detail.

The author has reported on the boron content of mineral springs[6], thermal springs[7], river waters[8,9], rains[10], snows[11] and plant

1) T. Tagaya, et al., *Bull. Inst. Phys. Chem. Research* (Tokyo), **21**, 165 (1942).
2) T. Tagaya, et al., *Bull. Inst. Phys. Chem. Research* (Tokyo), **21**, 188 (1942).
3) L.V. Wilcox, *U.S. Dept. Agr. Tech. Bull.* No. **962**, 40 (1948).
4) K. Sugihara, *J. Chem. Soc. Japan* (*Pure Chem. Sect.*), **73**, 359 (1952).
5) K. Sugawara, *Science* (in Japanese), **18**, 485 (1948).
6) S. Muto, *J. Chem. Soc. Japan* (*Pure Chem. Sect.*), **73**, 108 (1952).
7) S. Muto, ibid, **75**, 407 (1954).
8) S. Muto, ibid. **74**, 576 (1953).
9) S. Muto, ibid, **74**, 640 (1953).
10) S. Muto, ibid, **73**, 446 (1952).
11) S. Muto, ibid, **74**, 420 (1953).

ashes[12]. Although, the analyses were performed mainly with the samples from Kantô District, the author is of the opinion that the following discussion could be extended to the samples from various districts.

As an average content of boron in rains and snows, a value of 0.1 mg. B/l. was obtained. The Watarase River and the Kiriu River in Kantô District are supposed to have no supply of boron from mineral or thermal springs in the upper stream region, and the element seems to be supplied only by rains and snows. The average content of boron in these river waters is as much as 0.20 mg. B/l. Therefore, it is likely that rain and snow play an important role as the supplying source of boron to the rivers. Biological matters and soils are considered to be another supplying source of boron. The present author made the analyses of some plant ashes and obtained a value of 10–1000 p. p. m. B as the average content of the element, while some authors obtained the values of 0.1–1.2 p. p. m. B as the content of boron which exists in water-soluble form in soils[13]. In the main stream of the Tone River, the average content is 0.36 mg. B/l. This value is higher than those of the Watarase River and the Kiriu River. This high value may be due to the supply of boron by mineral and thermal springs, rich in boron, which issue in the upper stream region. The higher boron content is obtained among the mineral springs. For example, Isobe Mineral Spring has an average value of 123.3 mg. B/l. The thermal springs in Gunma Prefecture have an average value of about 10 mg. B/l.; they are supplying a large quantity of water in the upper stream region of the Agatsuma River. The Agatsuma River, which originates from the thermal spring region contains more than 1 mg. B/l. of the element. Numerous springs such as Kawarayu, Shima and Manza Springs etc. are located along the stream of this river.

Boron in Rain and Snow Waters

On the basis of chemical analyses of rain and snow waters which were reported by K. Sugawara and I. Iwasaki, the former author explained that boron was condensed remarkably in rain waters and the gravimetric ratios of boron to chlorine are 4000 times that of sea water[5]. Similar phenomena are for the ratios Ca/Cl and SO_4/Cl in rains and snows. K. Sugawara pointed out that the inorganic constituent of rain water originates from sea water and the rain of the hinterland has the greater value on the ratios Ca/Cl and SO_4/Cl. And he explained that this fact is based on the selective dissolution of the element to the rain.

In this study the present author collected 5 kinds of rain at Kiriu City. The boron content of the samples analysed by L. V. Wilcox's electrometric titration method[14] is summarised in Table I.

TABLE I

BORON CONTENT OF RAIN WATER

No.	Sampling station	Date	Cl mg./l.	B mg./l.	B/Cl
RKM–1	Kiriu	IX '51	2.9	0.03	0.011
RKM–2	Kiriu	VI '52	5.9	0.13	0.020
RKM–3	Kiriu	VI '52	1.3	0.11	0.084
RKM–4	Kiriu	VI '52	1.8	0.11	0.060
RKM–5	Kiriu	VI '52	0.3	0.11	0.367
Average value			2.44	0.098	0.0403
RAM–1*	8°34′ S 156°53′ E	II '52	176.7	0.13	0.001
Sea water (Western Pacific Ocean)[15]			18760.	4.73	0.00025

The gravimetric ratio of boron to chlorine in rain water is about 200 times that of sea water, but it is not clear whether or not the fact is due to the selective dissolution of boron in rain water. The average value of the element in rain water in Table I is about 0.1 mg. B/l. However, there is a possibility that the value tends to fluctuate according to the sampling station. Still more, the boron content of fresh snow is shown in Table II.

TABLE II

BORON CONTENT OF FRESH SNOW

No.	Sampling station	Date	Cl mg./l.	B mg./l.	B/Cl
SKM–1	Kiriu	II '52	2.7	0.04	0.015
SKM–2	Kiriu	II '52	2.2	0.13	0.059
SKM–3	Kiriu	III '52	2.7	0.15	0.056
Average value			2.53	0.107	0.0436
SNY–1	Norikura	VII '52	—	0.002	—
SSM–1	Sennokura	I '55	0.43	0.002	0.004
SAM–1*	64°18′ S 163°16′ E	XI '51	351.9	0.36	0.001

Although there were only a few samples, the boron content in fresh snow was found to be about 0.1 mg. B/l. The gravimetric ratio of boron to chlorine is approximately 0.04. In

12) S. Muto, *J. Chem. Soc. Japan (Pure Chem. Sect.)*, **75**, 1028 (1954).

13) J.A. Naftel, *Ind. Eng. Chem. Anal. Ed.*, **11**, 407 (1939).

14) L.V. Wilcox, *Ind. Eng. Chem. Anal. Ed.*, **4**, 38 (1932).

15) Y. Miyake, This Bulletin, **14**, 56 (1939).

* RAM-1 and SAM-1 were given for the reference of boron content of falling waters at the heart of the ocean. They were collected through the kindness of Taiyô Fisheries Co. while on duty, and the author offers his thanks for it.

other words, the boron content in fresh snow is almost equal to the rain water. It is notable that such lower values were obtained for the snow in a mountainous area (SNY-1, SSM-1).

Table III shows the boron content of a series of rains which were collected at different times from the begining of a rainfall.

TABLE III
BORON CONTENT OF RAIN PARTITIONS

Sample No.	Part	pH	Cl mg./l.	B mg./l.	B/Cl
KR-2	1	5.6	2.91	0.03	0.011
	2	—	—	0.03	—
	3	—	0.38	0.02	0.063
KR-5	1	6.7	5.86	0.13	0.022
	2	6.7	4.85	0.12	0.026
	3	6.7	0.50	0.11	0.210
KR-9	1	6.6	6.41	0.06	0.010
	2	6.6	1.95	0.08	0.041

The inorganic constituents of rain water are condensed in the initial stage of rain fall and as was shown in Table III. But when the table is more carefully observed, it is discovered that the rate of decrease in boron content is lower than that of chlorine. Consequently, the ratio of boron to chlorine in the later stage of rain fall is larger than in the initial stage.

Boron in River Waters

According to the above experiments, the water of rain and snow contains about 0.1 mg. B/l. Rains and snows are considered to be the main supplying source of water to the rivers and their tributaries. The boron content of the main stream of the Tone River in Kantô District is shown in Table IV.

TABLE IV
BORON CONTENT OF THE TONE RIVER

Sampling station No.	pH	Cl mg./l.	B mg./l.	B/Cl
St-1	—	6.48	0.38	0.059
St-2	—	6.89	0.40	0.058
St-3	6.9	7.16	0.40	0.056
St-4	6.8	6.89	0.36	0.052
St-5	6.9	6.21	0.40	0.066
St-6	6.9	5.54	0.45	0.081
St-7	6.8	5.27	0.45	0.081
St-8	6.9	5.67	0.28	0.049
St-9	6.8	5.67	0.16	0.028
St-10	6.9	5.94	0.13	0.022
Average		6.162	0.345	0.0560

According to Table IV, the boron content of the Tone River is approximately 3 times those of rain and snow, while the chlorine content is approximately 2.5 times larger than those of rain and snow. Therefore the gravimetric ratio of boron to chlorine is larger than those of rain and snow. As for the chlorine content of river water, for example, about 4 mg. Cl/l. is given by J. Kobayashi, et al.[16] for the Kôryô River at Hiroshima Prefecture, and 5.67 mg. Cl/l. by Clarke[17] as the average content of river waters. Compared to those values, the chlorine content of the Tone River gives rather high value. The social effect of human beings could be considered as one of the important supplying sources of chlorine, but the thermal and mineral springs in the upper stream region seem to be a more important source. The Watarase River and the Kiriu River, the tributaries of the Tone River have no springs in their upper stream region. The composition of those river waters is given in Table V, while the composition of the Agatsuma River and the Okuresawa River to which the spring waters are supplied in the upper stream are given in Table VI.

TABLE V
BORON CONTENT OF THE WATARASE RIVER AND THE KIRIU RIVER

(a) Watarase

Sample no.	pH	Cl mg./l.	B mg./l.	B/Cl
1	7.0	10.1	0.24	0.024
2	7.1	9.4	0.14	0.015
3	7.0	11.7	0.21	0.018
Average value		10.40	0.197	0.0190

(b) Kiriu

Sample no.	pH	Cl mg./l.	B mg./l.	B/Cl
1	6.6	0.16	0.30	1.879
2	6.9	0.17	0.15	0.879
3	7.2	0.11	0.20	1.818
4	7.2	0.14	0.25	1.799
5	7.2	0.16	0.17	1.063
6	7.1	0.21	0.17	0.810
Average value		0.158	0.207	1.310

TABLE VI
BORON CONTENT OF THE AGATSUMA AND THE OKURESAWA

(a) Agatsuma

Sample no.	pH	Cl mg./l.	B mg./l.	B/Cl
1	2.3	167.5	2.25	0.013
2	2.3	140.4	2.25	0.016
3	5.5	18.0	1.88	0.105
4	5.7	10.8	1.50	0.139
Average value		84.2	1.97	0.0234

16) J. Kobayashi, et al., *J. Chem. Soc. Japan (Pure Chem. Sect.)*, **72**, 567 (1951).
17) F.W. Clarke, "Data of Geochemistry", **63**, 119 (1924).

(b) Okuresawa

Sample no.	pH	Cl mg./l.	B mg./l.	B/Cl
1	2.4	3.5	0.75	0.214
2	2.9	0.7	1.88	2.689
3	2.9	1.4	1.23	0.985
4	3.0	3.5	1.25	0.357
Average value		2.28	1.305	0.5724

High boron content is observed for the Agatsuma River and the Okuresawa River which run through the thermal spring region, and have a minimum value of boron content for such rivers are about 1 mg. B/l. But as much as 0.2 mg./l. of boron content is observed for the Watarase River and the Kiriu River which have no supplying source of boron, like thermal springs. This value is almost equal to those of rain and snow. As the result of the social effect on its drainage, the Watarase River has high value of chlorine content, whereas the Kiriu River has no such drainage and the chlorine content is found to be very much lower than that of the former river. Therefore, the gravimetric ratio of boron to chlorine for the former is low, but the corresponding value for the latter is approximately 1. The Agatsuma River contains the larger amounts of boron and chlorine as the water of many thermal springs flows into the river directly. The values of boron and chlorine content of this river are about 2 mg. B/l., and 10–170 mg. Cl/l. respectively. Accordingly the ratio of lower value is observed for the upper stream and the value decreases for the lower stream which has no supplying source of boron, like springs. However, the value for the lower stream is higher than that of the main stream of the Tone River. The Okuresawa River contains no spring in its drainage so that the chlorine content of the river is almost 1–3 mg. Cl/l. It is slightly higher than those of rain and snow. But the boron content of the Okuresawa River is high and some supplying source of boron might be considered beside the spring.

Boron in Spring Waters

In the foregoing chapter, the author discussed one of the supplying sources of boron in river water. However, before we draw a definite conclusion about the source which supplies boron to river waters, the following three facts should be considered. Mineral and thermal springs, geological erosion and communities of human beings will have some effects on the boron content of river waters. And the effect of mineral and thermal springs will be discussed in this chapter.

The author has stated that the water of the Tone River has higher value of boron content owing to the existence of springs in its upper stream region. The springs which have highest boron content are among the alkaline common salt springs such as Isobe and Yashio Mineral Springs, etc. In Table VII some data on the boron content of the mineral springs are shown.

TABLE VII

BORON CONTENT OF ALKALINE COMMON SALT SPRINGS

Name	pH	Cl mg./l.	B mg./l.	B/Cl
Isobe No. 1	8.2	11926.	124.7	0.0105
Isobe No. 2	8.6	12658.	136.9	0.0108
Isobe No. 3	8.4	13642.	156.7	0.0115
Yashio No. 1	7.3	11004.	105.8	0.0096
Yashio No. 2	7.5	8262.	92.8	0.0112
Yashio No. 3	7.6	12989.	122.7	0.0084
Average Value		11747.3	123.33	0.01052

The gravimetric ratio of boron to chlorine for the samples in Table VII is about 0.01, which is lower than that of the Tone River, although the spring water shows the high value of boron and chlorine content. These spring waters are considered to be the petrified marine water similarly to the petroleum salt water. In these springs, the amount of flowings is not very large.

The neutral springs in Table VIII and acid springs in Table IX have large flowing amounts, but these give low boron and chlorine content.

TABLE VIII

BORON CONTENT OF NEUTRAL SPRINGS

Name	pH	Cl mg./l.	B mg./l.	B/Cl
Yunohana	7.3	361.3	5.98	0.0166
Yunokoya	7.5	122.6	4.35	0.0355
Kawarayu	5.8	322.3	8.75	0.0371
Kirizumi	7.1	48.9	0.59	0.0121
Hatonoyu	7.9	683.4	7.01	0.0103
Takaragawa	7.6	246.3	4.44	0.0180
Minakami	7.6	145.9	4.94	0.0340
Sarugakyo	7.4	342.5	14.81	0.0433

TABLE IX

BORON CONTENT OF ACID SPRINGS

Name	pH	Cl mg./l.	B mg./l.	B/Cl
Kusatsu No. 1	2.0	470.5	9.84	0.0210
Kusatsu No. 2	2.0	645.4	3.92	0.0069
Manza No. 1	—	501.8	9.97	0.0199
Manza No. 2	—	123.9	3.98	0.0321
Average value of neutral and acid sprins.		334.61	6.547	0.01964

Generally, the boron and chlorine content of the neutral and acid springs are almost the same and considerably lower than that of the alkaline common salt springs. The

gravimetric ratio of boron to chlorine of the former springs has the higher value than the latter springs. But the average ratio for all springs is lower than that of the main stream of the Tone River.

Summary

On the basis of the data and discussions in the preceding chapters, the distribution and migration of boron in natural waters are summarized in Figure 1. And the data in the figure were confirmed mainly with the samples from Kanto District, whereas the author is of the opinion that the distribution of boron and chlorine in natural waters is generally illustrated as here shown.

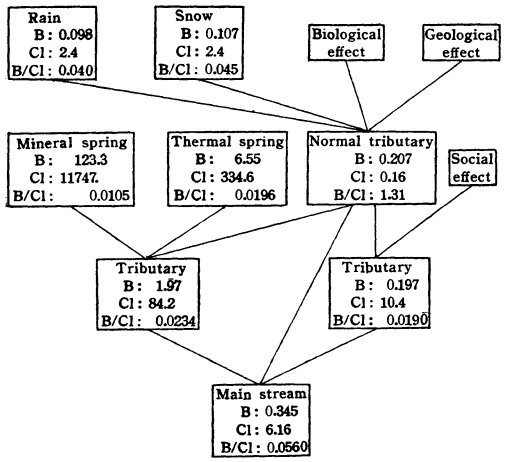

Fig. 1. Boron in natural waters (mg./l.).

The water of rain and snow at Kiriu District contain 0.1 mg. B/l., and 2.4 mg. Cl/l., and the ratio of boron to chlorine is 0.04. (these values might be lower at high mountainous area) Being affected by the biological and geological influences of the drainage, the original water becomes to contain 0.2 mg. B/l. and 0.16 mg. Cl/l. The ratio of boron to chlorine amounts to 1.31 as in the Kiriu River. At this stage, the increase of boron content or decrease of chlorine content are remarkable. When these branches of tributaries are affected by the mineral springs (123.3 mg. B/l., 11747 mg. Cl/l. and 0.0105 of B/Cl) and the thermal springs (6.55 mg. B/l., 334.6 mg. Cl/l. and 0.0196 of B/Cl) the boron and chlorine contont change their value to 1.97 mg. B/l., 84.2 mg. Cl/l. as well as the ratio of boron to chlorine 0.0234 as respectively in the Okuresawa River and the Agatsuma River. And the values of 0.197 mg. B/l., 10.4 mg. Cl/l. and boron to chlorine 0.0190 are obtained for the Watarase River which is affected by communities. Of course the actual condition will not be so simple and many complicated factors may exist before they join the river water. The main stream collects various kinds of tributaries and comes to have the value of 0.345 mg. B/l., 6.16 mg. Cl/l. and the ratio of boron to chlorine 0.0560. Then the stream flows down to the ocean while it is affected by many kinds of things during the way.

The auther's best thanks are due to Dr. S. Matsuura and Dr. N. Yamagata for their continued interest and advice.

Kiriu College of Technology
Gunma University
Kiriu

Study on the Electric Conductivity of Sodium Silicate Aqueous Solution. I.

By Hiroshi UKIHASHI

(Received November 14, 1955)

Introduction

The electric conductivity of sodium silicate solution has been only rarely reported, since Harman[1] measured it in 1925 in one of his consecutive experiments attempted for the electrochemical investigation of this solution. Though his experiment exceeds far beyond that previously reported by Kohlrausch[2], with repect to the range of molar ratio and concentration of solutions measured, it still lacks satisfactory abundance of data, especially for higher concentration. In the present study the measurement was made for the solution of molar ratio (SiO_2/Na_2O) 1.00, 1.52, 2.15, 3.02. and 3.95 at the concentration ranging from 0.001 N up to that, over which the solution hardly flows due to high viscosity, with reasonable numbers of measured points between both extreme concentrations. Where the ratio and concentration of the hereby measured silicate solutions corresponds to those measured by Harman, the two values were in good accordance.

The equivalent conductivity was derived from the specific conductivity, using the molecular weight as indicated by a formula. Thus far no theoretical treatment has been given for the conductivity of sodium silicate solution. Herein theoretical calculation was attempted for the equivalent conductivity of the molar ratio 3.95 silicate solution, and the results were found to be in good agreement with experimental data, if some supposition was admitted. In lower ratio solution, as hydrolysis takes place considerably, the results could not be dealt with theoretically, due to the complicated state of ions in solution.

Experimental

Materials.—Two methods were used for the preparation of pure sodium silicate solution. (1) First, sodium metasilicate crystal $Na_2(H_2SiO_4)\cdot 8H_2O$ was prepared by the following method from the original solution of molar ratio 3.0 and Na_2O concentration of 9%, then it was electrolyzed with mercury cathode to obtain the desired molar ratio. The original solution, of commerical grade produced by Asahi Glass Co., was diluted by the same volume of water, adding 2 volumes of NaOH solution of sp. gr. 1.26 and 2 volumes of ethyl alcohol. A small number of crystals were used as nuclei in order to hasten the crystallization which otherwise would have taken several days. After the crystals developed, they were filtered off by Buchner funnel, washed by 50% alcohol, drained off thoroughly, then resolved again into pure water. To the solution, containing about 20% sodium metasilicate, was added one tenth volume of NaOH solution (sp. gr. = 1.26), ethyl alcohol and a bit of nuclei. The solution was kept cool in ice water under stirring. Then sodium metasilicate recrystallized out in a few hours. This was filtered off, washed, drained and dried completely in a vacuum desiccator. The stock solution was prepared by dissolving these crystals. In order to make higher molar ratio silicate solution, this stock solution, usually containing 20% metasilicates was electrolyzed with mercury cathode and rotating platinum plate anode. An electrolytic cell is shown in Fig. 1.

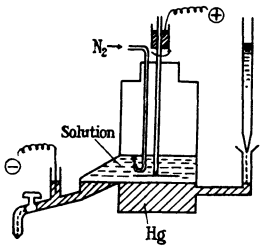

Fig. 1. Electrolytic cell.

The anode, a disk of 5 cm. diameter, was rotated with a velocity of 200 r. p. m. keeping 5 mm. away from the surface of mercury. The Na-amalgam produced was pushed out towards the outlet owing to the increased surface level caused by constantly supplied fresh mercury. During the electrolysis CO_2-free nitrogen gas was bubbled through the solution. In a run 150 cc. of solution was treated. The current density was kept at 0.8 amp. per sq. cm. Electrolysis was conducted for the time necessary for removing the definite amount of Na_2O to reach the degired molar ratio. (2) As it was time-consuming to make a concentrated solution of high molar ratio by the foregoing method, the following method of purification was substituted for it. The original various solutions, of commercial grade, were diluted to the concentration of about 3% Na_2O. After being filtered twice through hardened, alkali-proof filter paper, they were concentrated by vacuum evaporation. The

1) R.W. Harman, *J. Phys. Chem.*, **29**, 1155 (1925).
2) F.W. Kohlrausch, *Z. Physik. Chem.*, **12**, 773 (1893).

products were quite transparent, though retaining their original yellowish colour. The silicate solutions of ratio 2 prepared by the two methods were compared with each other as to their conductivity. The results showed no significant differences between the two series of data. The stock solutions thus prepared were analysed respecting their SiO_2 and Na_2O content and the molar ratio was decided strictly. Besides, the CO_2 content was analysed for check because of its deleterious effects. The more dilute solutions were prepared by diluting the stock solution with pure water which was distilled twice using quartz apparatus. It has the conductivity of $1\sim2\times10^{-6}$ Ω^{-1} cm^{-1}. Every solution was stored in a polyethylene bottle free from the atmosphere. All chemicals used were of reagent grade.

Apparatus for the Conductivity Measurement.—Conductivity was measured by Wheatstone bridge, using cathode ray oscillograph as detector. The bridge consisted of shielded variable resistance boxes, of which two had 10,000 Ω, and one 100,000 Ω. A variable condenser was set up parallel with the latter one. The measurement was made at 1000 cycles. A variable audio-frequency oscillator served as current source. The constants of four conductivity cells used were 1.242, 1.380, 0.4850 and 0.6568. The former two had platinized electrodes and they were used for the concentrated silicate solutions, the latter two, used for the dilute solution had non-platinized electrodes. The inner surface of the cell was coated with epoxy resin film to protect the glass wall from corrosion by the alkaline solution. The temperature was controlled to $\pm0.01°$ at 25°C, employing a double thermostat with sensitive regulator operated by electronics circuit.

Measurement.—Measurement was made at twenty-four hours after new dilute solution had been prepared, except for a very dilute solution, where it was made at thirty minutes after the preparation. The variation of conductivity with time was small enough to allow the later theoretical consideration without correction, even with very dilute solutions. The data were reproduced within $\pm0.2\%$ except for a very dilute solution. The cell constant was checked frequently with 0.01 N or 0.1 N KCl standard solution. Even after the most concentrated silicate solution was measured, the constant did not change appreciably, if washed carefully.

Results

The specific conductivity λ for various molar ratio sodium silicate solutions is shown in Fig. 2 and Fig. 3. The concentration is indicated by Na_2O weight percent. The conductivity increases with increasing concentration until it attains its maximum, then begins to decrease. This tendency of conductivity curve is not very different from what is seen with common low molecular electrolyte solution. As shown here, all the curves seem to have much the same form regardless of molar

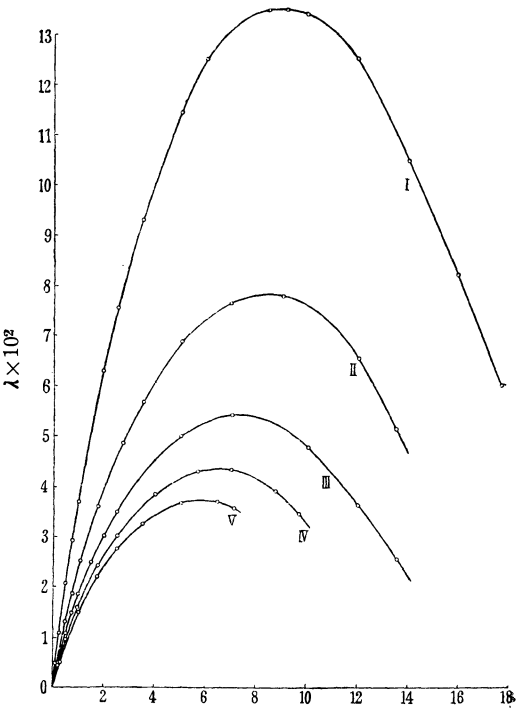

Fig. 2. Variation of specific conductivity of sodium silicate solutions with concentration at 25°C.

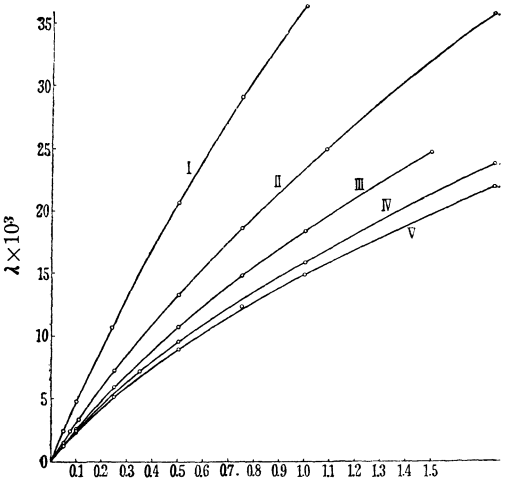

Fig. 3. Specific conductivity of sodium silicate solutions for lower concentration range at 25°C. Molar ratio, I 1.00; II 1.52; III 2.15; IV 3.02; V 3.95.

ratio of sodium silicate solution, although the change of conductivity becomes greater as the molar ratio of solution decreases. It is noteworthy that the form of conductivity curves, having similarity among different molar solutions, appears to have little dependence on

their viscosity. For instance the solution of molar ratio 3.95 has the maximum specific conductivity at the concentration of 6%, and at 7% it has a slightly lower, but still high conductivity. However, viscosity increases surprisingly between the two concentrations (0.25 poise at 6%, more than 1000 poise at 7%). On the other hand, for the solution of molar ratio 2.15, viscosity changes slowly from 0.032 poise at the concentration where maximum conductivity is shown, to 1.03 poise at as high as 13%. Also there is only a little increase of viscosity for the metasilicate solution over the measured concentration range, though specific conductivity varies very widely.

Fig. 4 shows the change of specific conductivity with molar ratio of silicate solution

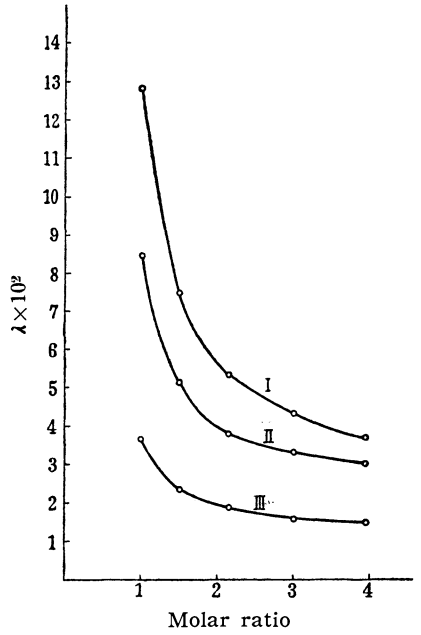

Fig. 4. Relationship between specific conductivity and molar ratio. Na_2O wt. %, I 6.50; II 3.00; III 1.00.

of the definite Na_2O content. The variation of conductivity with the ratio appears to be sharp around molar ratio 2. This would be explained by the fact that hydrolysis increases rapidly as the molar ratio of solution falls below 2, and OH ion with exceptionally high mobility comes to contribute to the conductivity.

Equivalent conductivity Λ was calculated from the following equation.

$$\Lambda = 1000\,\lambda \cdot N/A \cdot d = 1000\,\lambda/C$$

A represents the solid content (g.) per 1000 g. solution, d, the density of solution, N, normal weight, and C, normality. For the estimation of normality, expressed with regard to Na gram equivalent per 1000 cc. of solution, molecular composition such as Na_2SiO_3, $Na_2O \cdot 2SiO_2$, $Na_2O \cdot 3SiO_2$, etc. was employed. Thus, for example, 1 N solution of 2.15 molar solution contains 1/2 ($Na_2O \cdot 2.15\,SiO_2$) expressed in grams, in 1000 cc. solution. Fig. 5 shows Λ vs. C curves for various

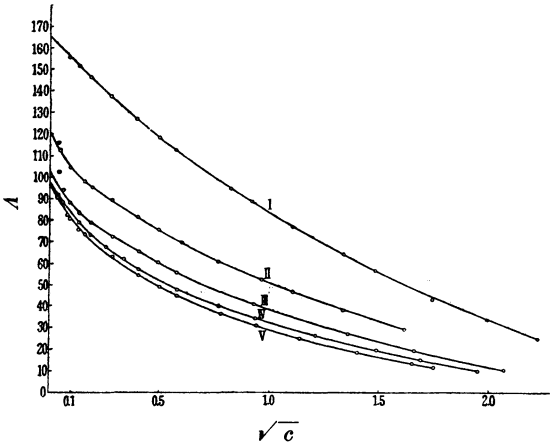

Fig. 5. Variation of the equivalent conductivity of various sodium silicate solutions with square root of concentration. Molar ratio, I 1.00; II 1.52; III 2.15; IV 3.02; V 3.95.

silicate solutions. The fact that curves in Fig. 5 show no breaking point would evict any idea of discontinuous change of molecular constitution, e. g. micelle formation, over the whole range of concentration. At the extreme dilution it appear that equivalent conductivity tends to go up irregularly high, so that it is difficult to extrapolate them to zero concentration. It may have been caused partly by hydrolysis effect[3].

Nevertheless, limiting equivalent conductivity was estimated by the extrapolation of curves on Fig. 5. The extrapolation would have eliminated the effect of hydrolysis which increased rapidly below the concentration of 0.005 N. Thus obtained values for silicate solution of molar ratio 1.00, 1.52, 2.15, 3.02 and 3.95 were 165, 120, 103, 98, and 96 respectively. Since the limiting equivalent conductivity of sodium ion is 50.1, that of silicate ion seems to be fairly high, almost comparable with that of sodium ion, taking into consideration the fact that the contribution of OH ion is very small for the higher molar ratio solution[4].

3) Harman[5] calculated hydrolysis percentage for various molar ratio solutions from the pH values, showing that it increases rapidly in the extreme dilution for the lower ratio solution.

4) According to Harman's data hydrolysis % of $Na_2O \cdot 4SiO_2$ solution at 0.01N is 1.5% which contributes only 2 to its limiting equivalent conductivity.

Discussion

It is well accepted that a molecule of sodium metasilicate[5,7] consists of $Na_2(H_2SiO_4)$ which dissociates in solution into four kinds of ion, i.e. Na^+, $H_3SiO_4^-$, $H_2SiO_4^{--}$ and OH^-. Here OH^- ion is brought about by hydrolysis which takes place in two steps,

$$H_2SiO_4^{--} + H_2O \rightleftarrows H_3SiO_4^- + OH^-$$
$$H_3SiO_4^- + H_2O \rightleftarrows H_4SiO_4 + OH^-$$

As for the silicate solutions having other molar ratio than 1, there is not yet a definite theory as to the kinds and behaviors of ions present in solution. However, the light scattering experiments[8] revealed that in these solutions molecules were still not of large size as with organic high molecular compound, but at most, of several hundreds in molecular weight. This fact was also well explained by viscometric study[8,9]. Furthermore there are other indications[7,10] showing that the existence of molecular-type compounds such as expressed by $Na_2O \cdot 2SiO_2$, $Na_2O \cdot 3SiO_2$, etc.[11] in solution may not be highly inadequate. First of all, assuming this is the case, it was attempted to see whether the equivalent conductance could be explained by theory. For this purpose the silicate solution of molar ratio 3.95 was sampled, because its negligible hydrolysis made it possible to consider the existence of only two kinds of ion, i.e. two sodium ions and one silicate ion. Secondly it was assumed that the silicate ion possessed two minus charges as a result of dissociation of two sodium ion. The theoretical treatment was based on Falkenhagen's equation which was the recent theoretical extension of the theory of Onsager to include the effect of definite ionic size and has been proved to show excellent agreement with experimental data for 1:1 type electrolyte solution[12].

Wishow and Stokes[13] showed furthermore, that Falkenhagen's equation stands good for 1:1 electrolyte solution up to surprisingly high concentration if applied with the correction for bulk viscosity. For unsymmetrical electrolytes, the apparent defect of the theory, caused by the unsatisfactory convergence of electrophoretic terms may be eliminated, if a large effective ionic diameter can be assigned to them. With these facts, it would be interesting to attempt here the comparison of the experimental data with those derived from the theory, though electrolyte was assumed hereby to be 1:2 type instead of 1:1.

Falkenhagen's expression for the equivalent conductivity of single electrolyte solution is written as follows:

$$\Lambda = \left\{\Lambda^0 - \frac{1.546\times10^{-7}}{6\pi\eta}(|z_1|+|z_2|)\frac{\kappa}{1+\kappa a}\right\} \times\left(1+\frac{\Delta X}{X}\right)$$

$$\kappa = \left(\frac{8\pi N e^2}{1000\varepsilon KT}\right)^{1/2}\sqrt{I}$$

e: electronic charge
N: Avogadro's number
η: viscosity of solvent
z_1, z_2: valencies of cations and anions respectively
I: ionic strength
K: Boltzmann's constant
T: absolute temperature
ε: dielectric constant of solvent
a: mean ionic diameter

The second term on the right hand expresses the electrophoretic effect on conductivity. The last term $\Delta X/X$ expresses the relaxation field and is shown as[14]

$$\frac{\Delta X}{X} = \frac{z_1 z_2 e^2}{3\varepsilon KT}\cdot\frac{q}{1-q}\cdot\frac{\kappa}{\kappa a(1+\kappa a)}[e^{\kappa a(1-\sqrt{q})}-1]$$

q is defined by

$$q = \frac{|z_1 z_2|}{|z_1|+|z_2|}\cdot\frac{\lambda_1^0+\lambda_2^0}{z_2\,\lambda_1^0+|z_1|\lambda_2^0} = \frac{|z_1 z_2|}{(|z_1|+|z_2|)(|z_2|t_1^0+|z_1|t_2^0)}$$

t_1, t_2 and λ_1^0, λ_2^0 denote transport number and equivalent conductivity of cation and anion respectively at infinite dilution. Here the Eigen and Wicke distribution function was replaced by the Boltzmann distribution function.

Inserting the values of constants the equation reduces to

$$\Lambda = \left(\Lambda^0 - \frac{156.5}{1+0.568\mathring{a}\sqrt{c}}\right)\times\left(1-\frac{0.721\sqrt{c}}{1+0.568\mathring{a}\sqrt{c}}\cdot F\right)$$

5) R.W. Harman, *J. Phys. Chem.*, **30**, 1100 (1926).
6) E. Thilo and W. Miedreich, *Z. anorg. allgem. Chem.*, **267**, 76 (1951).
7) P.P. Roller and G. Erwin, *J. Am. Chem. Soc.*, **62**, 461 (1940).
8) P. Debye and P.V. Nauman, *J. Phys. Chem.*, **55**, 1 (1951).
9) H. Ukihashi, *Reports of the Research Laboratory, Asahi Glass Co.*, Vol. II, No. 1, 48 (1952).
10) R.W. Harman, *J. Phys. Chem.*, **30**, 359 (1926).
11) The foregoing molecular formulae are stoichiometrically satisfied by writing as $Na_2O \cdot 2SiO_2 \cdot 2H_2O$, $Na_2O \cdot 3SiO_2 \cdot 3H_2O$, etc.
12) R.A. Robinson and R.H. Stokes, *J. Am. Chem. Soc.*, **76**, 1991 (1954).
13) B.F. Wishaw and R.H. Stokes, *J. Am. Chem. Soc.*, **76**, 2065 (1954).
14) R.H. Stokes, *J. Am. Chem, Soc.*, **76**, 1988 (1954).

$$F=(e^{\kappa a(1-\sqrt{q})}-1)/\kappa a(1-\sqrt{q}),$$
$$\kappa a=0.568\mathring{a}\sqrt{c}$$

$\mathring{a}$: mean ionic diameter expressed in Ångstrom

In order to calculate the equivalent conductivity of sodium silicate solution according to this equation it is important to assign the most probable value to $\mathring{a}$ and q. Here, t_1 was assumed to be equal to t_2, thus $t_1=t_2=0.5$. This assumption would not be so far away from the truth, as judged from the value of limiting equivalent conductivity and also the result obtained by Harman[10] regarding the transport number of sodium silicate solution[15]. For evaluating $\mathring{a}$, calculations were made on the equation by inserting to it various values of $\mathring{a}$, and the results were plotted on Fig. 6. It seems that the use of the value 7 Å. of $\mathring{a}$ on the calculation fits best for the agreement between experimental and theoretical curve. This value appears rather small. However, if attention is turned to the fact that at the concentration where the viscosity of sodium silicate solution abruptly increases to a remarkable degree, the distance between solute molecules was approximately 10 Å.[8,9], it would be allowable value, considering the hydration effect in the above case, along with such a discrepancy between the value of $\mathring{a}$ required theoretically and estimated from ionic radii, as usually encountered in the case of unsymmetrical electrolyte solution.

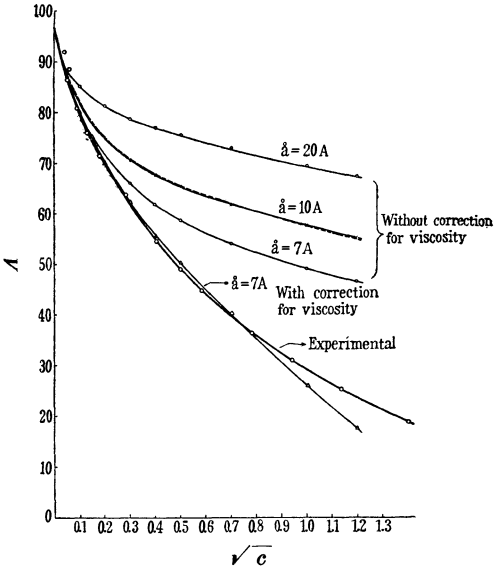

Fig. 6. Comparison of the equivalent conductivity of sodium silicate solution of molar ratio 3.95 with those calculated from the theoretical equation.

Since sodium silicate solution bears high viscosity owing to its hydration as with lithium chloride solution[13], the correction for the bulk viscosity would be necessary. For this purpose, Falkenhagen's equation has to be divided by relative viscosity of solution. After this was done, the agreement was further improved up to the higher concentration, about 0.8 N (2% of Na_2O concentration). Above that, the viscosity correction increases rapidly so that the theoretical line fall increasingly below the experimental values.

Thus, it is possible to explain the conductivity of sodium silicate solution, within the moderate concentration range, on the basis that its molecule essentially be small, and silica ion be polymerized to such an extent as expressed by its formula, even if it might be supposed to contain some aggregated molecules in the higher concentration. This fact is well consistent with the results obtained by both viscometric and light-scattering investigation.

The author wishes to express his sincere thanks to Dr. Tadashi Yawataya for his inspiring support and kind interest in this work.

Research Laboratory, Asahi Glass Co., Ltd., Bentencho, Tsurumi-ku Yokohama

15) A little difference in this value does not affect sensitively on the result of calculation. In Fig. 6 a curve is drawn which was obtained by using the values $t_1=0.6$, $t_2=0.4$ as a comparison.

SHORT COMMUNICATIONS

Ion Dissociation in a Parabola Mass-spectrogram

By Yosaburo Yoshikawa and
Kozo Hirota

If we ionize some molecules by the electron-impact method, instead of the usual glow-discharge method, in a Thomson's parabola mass-spectrograph, several spots will appear, all of which correspond to the ions deflected to the same degree by the electric field. However, Henglein and Ewald[1] found that secondary spots also appear lying on parabolas and taking the positions of the lower energy side, i.e., on the right side of the vertical line x_0 formed by the primary spots, as shown in Fig. 1. They ascribed the secondary spots to the ion fragments which cracked, flinging themselves between the ionizing and analyzing field, and

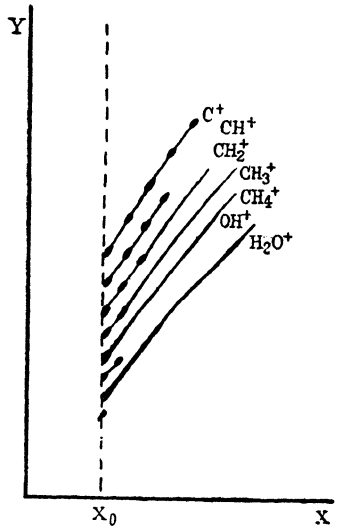

Fig. 1. Ion dissociation; mass-spectrogram of illuminating gas taken by Henglein and Ewald[1].

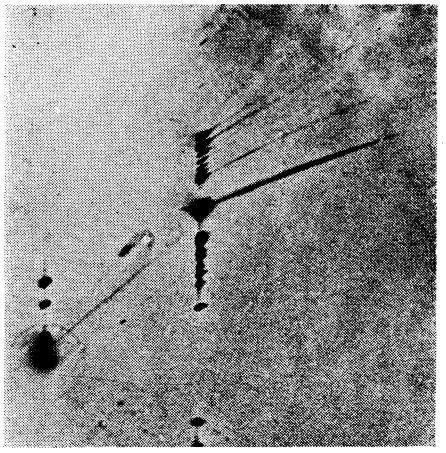

Fig. 3. Acetylene:
Impact electron voltage 200 V,
Ion accelating valtage 7500 V.

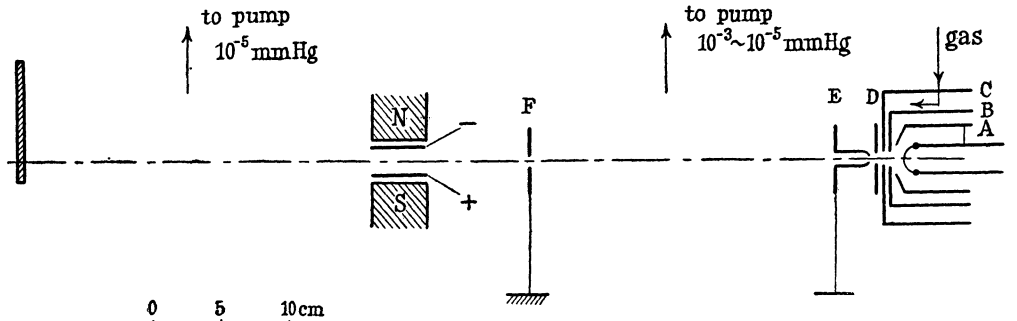

S_A	4 mmϕ	A ~ B (+)	50 ~ 200 V
S_B	2 〃	B ~ C (−)	4.5 V
S_C	3 〃		
S_D	1 〃	C ~ D (−)	4.5 V
S_E	0.3 〃	D ~ E (−)	0.5 ~ 20 KV
S_F	0.1 〃		

Fig. 2. Scheme of the apparatus.

their energy thus became smaller than that of the primary ions, while their velocity was kept constant.

The authors repeated their experiment, but found slightly different results as will be described.

The ionizing chamber and scheme of the apparatus are shown in Fig. 2, while two examples of the mass-spectrograms taken are shown in Fig. 3 (acetylene) and Fig. 4

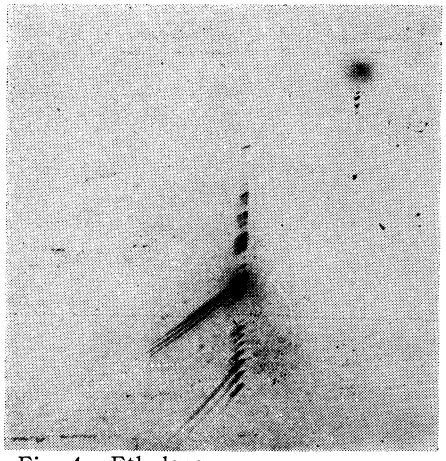

Fig. 4. Ethylene:
Impact electron voltage 100 V,
Ion accelating voltage 7500 V.

ethylene). It will be seen clearly that several spots of secondary ions really appear together with some secondary lines, and that the secondary spots have more prolonged tails than those of Henglein and Ewald. Moreover, our secondary "spots" do not appear in the parabolas whose m/e is 12-15, but the intense ones correspond to m/e=26 ($C_2H_2^+$) in Fig. 3 and to m/e=28 ($C_2H_4^+$) in Fig. 4; they are calculated to be the dissociation fragments of the polymerized acetylene and ethylene ($(C_2H_2)_3^{++} \rightarrow C_2H_2^+$ and $(C_2H_4)_3^{++} \rightarrow C_2H_4^+$, etc.), respectively. Such a result may be due to the difference of the apparatus and, even more, of the experimental conditions. To our regret, owing to the brief description given by Henglein and Ewald, we cannot discuss the real cause of the present discrepancy in detail.

The time of the ions flinging themselves between the ionizing and analyzing field is calculated to be the order of 10^{-7} second, the secondary "spots" being thus produced by the ions cracked within that time. It is smaller by one order of magnitude than the mean life of the metastable ions found by Hipple and others[2].

Detailed studies are going on.

The authors are greatly indebted to Dr. K. Ogata and his laboratory members for affording various kinds of conveniences to their work, and express their thanks to Mr. T. Nakatsuka for preparing Schumann plates.

Chemical Department, Science Faculty
Osaka University, Osaka

1) A. Henglein and H. Ewald, "Mass Spectroscopy in Physics Research" (1953), p. 205.
2) J.A. Hipple and E.U. Condon, *Phys. Rev.*, 68, 54 (1945).

Structure of the Agarose Constituent of Agar-agar

By Choji ARAKI

(Received February 7, 1956)

The latest communication[1] together with the previous ones contributed from this laboratory has enabled me to come to the following conclusion concerning the composition and the structure of agar.

Agar is composed of two polysaccharides, agarose and agaropectin, a composition similar to starch, which is composed of amylose and amylopectin. Agarose, a main constituent of agar, exhibits a composition $[C_{12}H_{14}O_5(OH)_4]_n$; whereas agaropectin is a more complicated polysaccharide with sulfuric and uronic acid residues. This view is supported by the actual separation of the acetylated agar into two different constituents; agarose acetate and agaropectin acetate, most of the sulfuric acid and uronic acid present in agar being accumulated in the latter constituent[2]. The former constituent, having the formula $[C_{12}H_{14}O_5(OCOCH_3)_4]_n$, is converted into the corresponding methyl ether $[C_{12}H_{14}O_5(OCH_3)_4]_n$ being treated with dimethylsulfate and sodium hydroxide[3].

Now, it is possible to propose that agarose consists of alternatively repeated residues of 1, 3-linked β-D-galactopyranose and 1, 4-linked 3, 6-anhydro-α-L-galactopyranose as shown in Fig. 1, the chain being terminated by D-galactose and 3, 6-anhydro-L-galactose residues at the reducing and non-reducing ends, respectively.

The above structure, which is in agreement with the composition $[C_{12}H_{14}O_5(OH)_4]_n$, accounts for all the experimental facts reported previously. Since the 3, 6-anhydro-L-galactoside linkages appearing every second unit in the molecule are extremely susceptible to acid-cleavage, even very mild methano

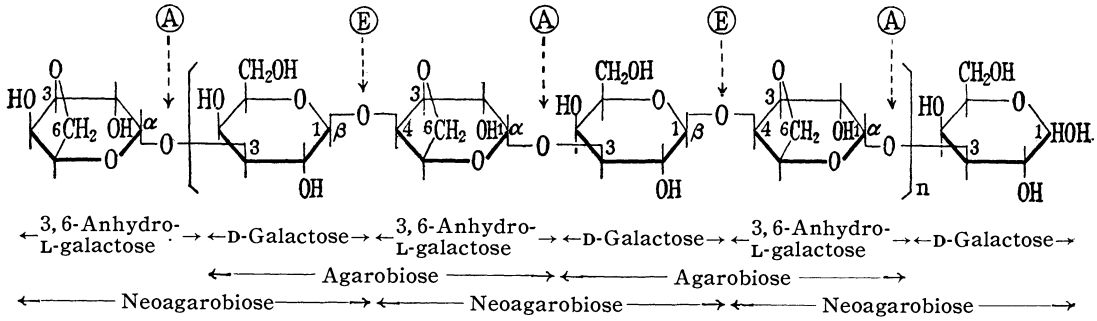

Fig. 1. Possible structure of agarose.
Ⓐ: the position cleaved by acid.
Ⓔ: the position cleaved by enzymes.

lysis led to the isolation of agarobiose dimethylacetal in an excellent yield, together with small amounts of methyl D-galactoside and 3, 6-anhydro-L-galactose dimethylacetal[4]. The last two products are inferred to have arisen chiefly from the reducing and non-reducing ends of the molecule, respectively. The partial acid-hydrolysis[5] and mercaptolysis[6] also afforded agarobiose (4-*O*-*β*-D-galactopyranosyl-3, 6-anhydro-L-galactose) and its diethylmercaptal, respectively, supporting the structure proposed. On the other hand, when agar was subjected to the enzymatic hydrolysis[1], neither D-galactose nor 3, 6-anhydro-L-galactose was detected in the hydrolysate, but neoagarobiose (3-*O*-3, 6-anhydro-*α*-L-galactopyranosyl-D-galactose) was isolated as the lowest cleavage fragment. This fact is also explained by the structure, if the enzymes are capable of splitting only the *β*-D-galactoside linkages. Moreover, the structure is in accordance with the fact that scission of the methylated agarose yielded 2, 4, 6-tri-*O*-methyl-D-galactose[7], 2-*O*-methyl-3, 6-anhydro-L-galactose[8], and none of tetra-*O*-methyl-D-galactose. In addition, the absence of adjacent hydroxyl groups in the molecule of the polysaccharide is corroborated by the observation of Barry and Dillon[9] that agar consumed no periodate at all.

In conclusion, all the experimental results are compatible with only one structure (Fig. 1) for agarose, which constitutes the greatest part of agar. The sole problem to be solved is whether it is a linear polysaccharide or a branched one.

Faculty of Industrial Arts
Kyoto Technical University
Matsugasaki, Kyoto

1) C. Araki and K. Arai, This Bulletin, **29**, 339 (1956).
2) C. Araki, *J. Chem. Soc. Japan*, **58**, 1338 (1937).
3) C. Araki, *J. Chem. Soc. Japan*, **58**, 1351 (1937).
4) C. Araki and S. Hirase, This Bulletin, **27**, 109 (1954).
5) C. Araki, *J. Chem. Soc. Japan*, **65**, 533, 627 (1944).
6) S. Hirase and C. Araki, This Bulletin, **27**, 105 (1954).
7) C. Araki, *J. Chem. Soc. Japan*, **58**, 1362 (1937); E.G.V. Percival and J.C. Sommerville, *J. Chem. Soc.*, **1937**, 1615.
8) C. Araki, *J. Chem. Soc. Japan*, **61**, 775 (1940).
9) V.C. Barry and T. Dillon, *Chemistry & Industry*, **1944**, 167.

*On the Dismutation Process of Zinc Ion**

By Hideo IMAI and Hiroshi SUNAHARA

(Received February 7, 1956)

In the current-potential curve of the Ševčik type oscillographic polarograph a quantitative relation between the cathodic and anodic currents of zinc ion was found.

Under the high rate of variation of the applied voltage (20 c. p. s., 50 v./s) the cathodic branch of zinc ion consists of two peaks in the solution containing iodide ions or bromide ions. On the contrary, a single peak can be observed in the anodic branch, as is illustrated in Figs. 1 and 2. Since the first cathodic peak is symmetrical with the anodic one, the first reduction is assumed to be reversible, and the second reduction to be irreversible. In this case the cathodic currents superposed on each other were estimated by the modified method developed by the present authors[1] (cf. Breyer et al.[2]).

The cathodic currents and the anodic currents thus estimated are plotted against the concentration of KI and KBr in Fig. 3 or 4, respectively. In this case the ionic strength of the supporting electrolyte is maintained at a constant value as much as 4 mol./l. by adding KNO_3 solution. In Fig. 3 it is easy to see that the value of $R_1+1/2\,R_2$ is, in any case, equal to the anodic current. This rela-

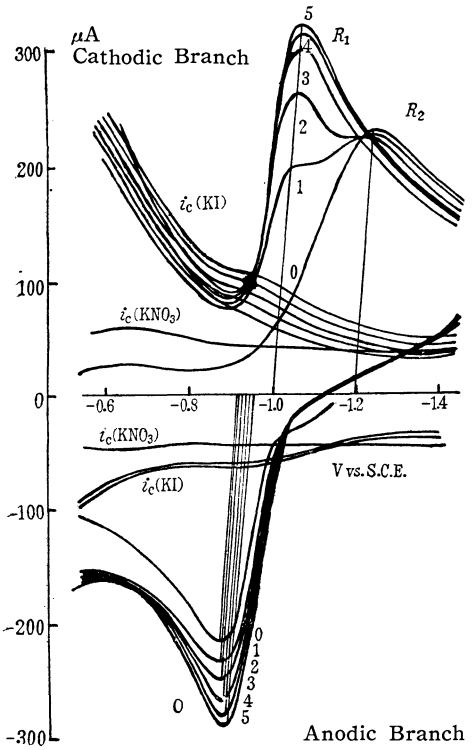

Fig. 1. Current-potential oscillograms of 0.37 mM Zn^{++} in various concentrations of KI (0-0M KI, 1-0.45 M KI, 2-0.9 M KI, 3-1.8 M KI, 4-2.7 M KI, 5-3.6 M KI, i_c-charging current).

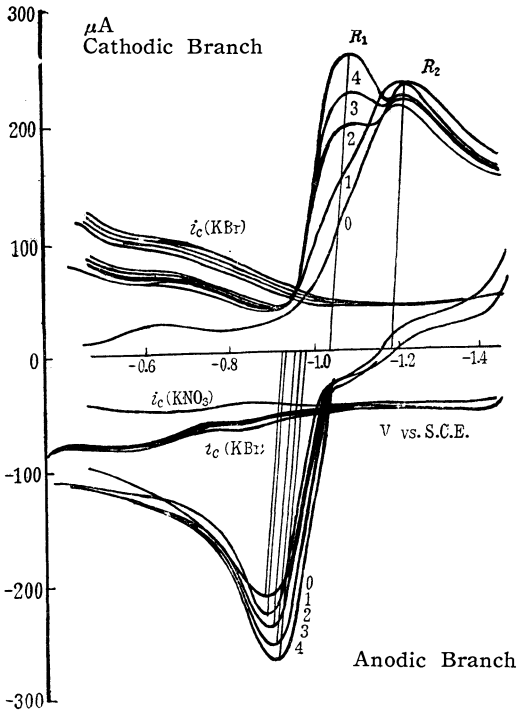

Fig. 2. Current-potential oscillograms of 0.73 mM Zn^{++} in various concentrations of KBr (0-0M KBr, 1-0.59 M KBr, 2-1.77 M KBr, 3-2.95 M KBr, 4-4.0 M KBr, i_c-charing current).

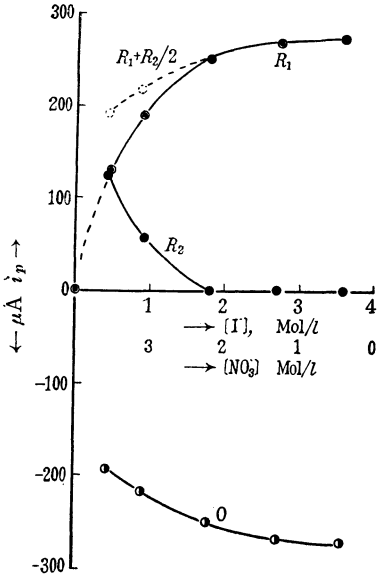

Fig. 3. Variation of the peak current with the concentration of KI.

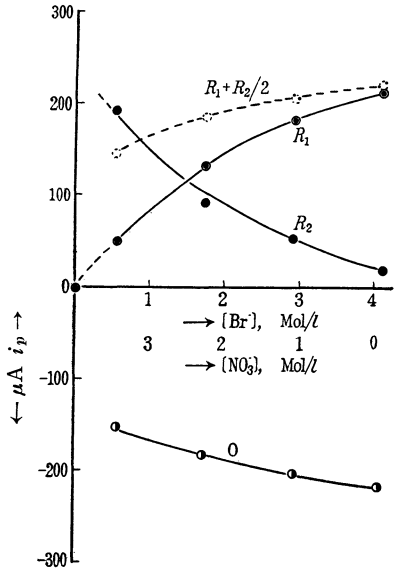

Fig. 4. Variation of the peak current with the concentration of KBr.

tion is better realized in Fig. 4.

From these results it can be reasoned that a half of the irreversible peak current corresponds to the reversible one in yielding

the anodic current. Supposing that the dismutation process proposed by Heyrovský[3] is the case mentioned above, the reversible process, in which the electron transfer is facilitated by the catalytic action of anions such as iodide or bromide ions, results from the repetition of a cycile process, $2Zn^{++}+2e \rightleftarrows 2Zn^{+} \rightarrow Zn^{++}+Zn$, and yields the reduced metal the concentration of which is equivalent to that of the oxidant. Virtually this process is party limited except in the case of the solution containing more than 2 mol./l. I^-, and the residual oxidant is reduced in the second reduction when the applied potential shifts toward the more negative potential.

The irreversible process (R_2), however, is limited in the reaction, $2Zn^{++}+2e \rightarrow 2Zn^{+} \rightarrow Zn^{++}+Zn$. In this case the concentration of the reduced metal will be invariably as much as a half of the concentration of the oxidant. Since the peak current is linearly proportional to the concentration of a depolarizer, it is now easy to see why we obtain the above-mentioned characteristic relation between two cathodic peak currents (R_1, R_2) and the anodic peak current (0). In other words, these results seem to endorse the validity of the dismutation process assumed by Heyrovský. A more detailed investigation is now in progress.

Laboratory of Chemisry, Minami College, Hiroshima University, Hiroshima

* Presented at the discussion on polarography held by the Chemical Society of Japan in November, 1955.

1) M. Shinagawa, H. Imai and H. Sunahara, *J. Chem. Soc. Japan* (in press).
2) B. Breyer, F. Gutman and S. Hacabian, *Australian J. Sci. Resear.*, **3**, 567 (1950).
3) J. Heyrovsky, *Z. Elektrochem.*, **59**, 820 (1955).

Methylhydropolysiloxanes from Cohydrolysis of Methylhydrochlorosilanes and Methylchlorosilanes

By Rokuro ŌKAWARA and Minoru SAKIYAMA

(Received January 23, 1956)

Recently, we reported[1] on the presence of tetramethylsilane (I′) (b. p. 26.5°C), dimethylchlorosilane (II′) (b. p. 36°C), hydrocarbon by-product (b. p. 33°–37°C) and methyldichlorosilane (III′) (b. p. 41°C) in the low boiling product of silicon-methylchloride reaction. We wish now to report on the lower members of copolymer which were obtained by hydrolyzing these two methylhydrochlorosilanes with three kinds of methylchlorosilane.

In this experiment, for the source of **M′***, industrial low boiling fraction (b. p. 35°–36°C) was used without further purification. Because of the result of the preceding paper, it was considered to be difficult to obtain pure (II′) by conventional fractionation through an ordinary laboratory column. Also the hydrolyzate of the low boiling fraction used in this experiment was found to be composed of mainly methylhydropolysiloxanes and a small amount of (I′) and the hydrocarbon by-product. The percentage composition of the lower members of the methylhydropolysiloxanes based on the amount of the hydrolyzate is given in Table I (Expt. 1). It was considered that $\mathbf{M}_2'$ was formed from (II′) and the succeeding linear polymers, $\mathbf{M'D}_n'\mathbf{M'}$ from (II′) and (III′).

In the preceding paper, a small amount of linear polysiloxanes, **M′DM′**, **M′D′DM′** and $\mathbf{M'D}_2\mathbf{M'}$, were found to be present in the hydrolyzate of the low boiling product, but among them only **M′DM′** could be characterized. In that case, **D** unit was supposed to be formed from (II′) by the fission of Si-H bond during the hydrolysis reaction. In order to obtain sufficient amounts of **M′D′DM′** and $\mathbf{M'D}_2\mathbf{M'}$, various amounts of dimethyldichlorosilane (II), as a source of **D** unit, were added to the low boiling fraction. It succeeded to characterize these two compounds from the hydrolyzate which were obtained by mixing a relatively small amount of (II).

The polysiloxane which could be accurately characterized from the cohydrolyzate of trimethylchlorosilane (I) with the low boiling fraction was **MM′**.

The trisiloxanes which were supposed to be formed, such as **M′DM′**, **M′D′M**, **M′DM** and **MD′M** could not be separated.

Since the linear polysiloxanes were formed from the low boiling fraction itself, it was not easy to separate the branched chain polysiloxanes from the isomeric linear polymers when the low boiling fraction was cohydrolyzed with methyltrichlorosilane (III). Two branched chain polymers, $\mathbf{M}_3'\mathbf{T}$ and $\mathbf{M}_2'\mathbf{TD'M'}$, could be characterized in this experiment.

Further, a series of copolymer $\mathbf{MD}_n'\mathbf{M}$ ($n=1-6$), some of which have already been characterized by Sauer[2], were obtained by cohydrolysis of (I) and (III′).

Properties of copolymers obtained in this experiment are summarized in Table II.

Experimental

Starting Materials.—The low boiling fraction (b. p. 35°–36°C, specific gravity : 0.873, chlorine content : 38.5%) and methylchlorosilanes used in this experiment were supplied from Shin-etsu Chem. Ind. Co. Methyltrichlorosilane and methyldichlorosilane were redistilled through a Stedman column of about 30 theoretical plates and the fraction having the calculated chlorine content was used for the experiments.

Cohydrolysis.—In all cases, cohydrolysis was performed by the same method described in the preceding paper. The fractionation of the hydrolyzate was carried out by a semi-micro Stedman column of about 50 theoretical plates throughout this experiment.

Analysis of Active Hydrogen.—Active hydrogen content was measured by decomposing the sample with aqueous ethanolic sodium hydroxide in a Zerewitinoff's apparatus.

Cohydrolyzate with Dimethyldichlorosilane (II), (Expt. 2–5).—The results of the cohydrolysis are given in Table I. In Expt. 2, 3 and 4, the amounts of (II) mixed were 90, 65 and 51% of the low boiling fraction respectively. In each case, the distribution of the fraction boiling below 150°C was determined. Then the residues of

1) R. Ōkawara and M. Sakiyama, This Bulletin, **29**, 236 (1956).

* In this paper, the shorthand notation will be used which was indicated in the preceding paper[1].

$\mathbf{M'}=H(CH_3)_2SiO_{1/2}$ $\mathbf{M}=(CH_3)_3SiO_{1/2}$

$\mathbf{D'}=HCH_3SiO$ $\mathbf{D}=(CH_3)_2SiO$

$\mathbf{T}=CH_3SiO_{3/2}$

2) R. O. Sauer, W. J. Scheiber and S. D. Brewer, *J. Am. Chem. Soc.*, **68**, 962 (1946).

TABLE I

Expt. No.	Mixture of chlorosilanes		Hydrolyzate yield		Composition of the hydrolyzate (%) Disiloxanes			Trisiloxanes			Tetrasiloxanes	Higher siloxanes
		(g.)	(g.)	(%)theory**	M_2'	MM′	M_2	M′D′M′	M′DM′	MD′M		
1	(L)*	2200	1120	73	44	—	—	15	1	—	10	19
2	(L)	95	86	74	5	—	—	5	17	—	(69)	
	(II)	86										
3	(L)	113	88	71	7	—	—	5	17	—	(68)	
	(II)	77										
4	(L)	113	84	75	10	—	—	7	21	—	(60)	
	(II)	58										
5	(L)	435	250	72	21	—	—	9	19	—	10	28
	(II)	75										
6	(L)	350	390	65	4	24	38	3	(5)		(19)	
	(I)	400										
7	(L)	380	224	75	12	—	—	7	2	—	26	37
	(III)	75										
8	(III′)	200	345	89	—	—	46	—	—	10	8	30
	(I)											

* (L): The low boiling fraction, (I): $(CH_3)_3SiCl$, (II): $(CH_3)_2SiCl_2$, (III): CH_3SiCl_3, (III′): CH_3SiHCl_2

** Calculated from the chlorine content of the mixture of chlorosilanes.

TABLE II

METHYLHYDROPOLYSILOXANES

Polysiloxanes	Boiling point °C/mmHg	Refractive index n_D^{20}	Density d_4^{20}	Molar refraction	Molecular weight	%H(-Si)
	((Reported))[2]	Found ((Reported))	Found ((Reported))	Found (Calcd.)*	Found** (Calcd.)	Found (Calcd.)
MD′M	141.5/760	1.3818	0.8193	63.18	—	0.45
		((1.3818))	((0.8194))	(63.19)	(222.52)	(0.45)
MD$_2'$M	81/28	1.3862	0.8556	77.63	—	0.70
		((1.3854))	((0.8559))	(77.46)	(282.66)	(0.71)
MD$_3'$M	105/28	1.3880	0.8798	91.94	—	0.87
	((85.6/10))	((1.3878))	((0.8806))	(91.73)	(342.79)	(0.88)
MD$_4'$M	77/2	1.3904	0.8966	106.6	—	1.00
	((107/10))	((1.3895))	((0.8991))	(106.0)	(402.92)	(1.00)
MD$_5'$M	94/2	1.3920	0.9136	120.7	—	1.08
				(120.3)	(463.06)	(1.09)
MD$_6'$M	104/2	1.3925	—	—	—	1.11
					(523.19)	(1.16)
MM′	85/760	1.3740	0.7578	44.71	145	0.68
				(44.55)	(148.36)	(0.68)
M′D′DM′	71/26	1.3862	0.8623	73.21	272	1.13
				(73.09)	(268.63)	(1.13)
M′D$_2$M′	77/25	1.3875	0.8632	77.18	285	0.72
				(77.46)	(282.66)	(0.71)
M$_3'$T	60/19	1.3852	0.8612	73.13	270	1.14
				(73.09)	(268.63)	(1.13)
M$_2'$TD′M′	100/38	1.3882	0.8891	87.29	329	1.22
				(87.36)	(328.76)	(1.23)

* Calculated from bond refractivities by E.L. Warrick, *J. Am. Chem. Soc.*, **68**, 2455 (1946).

** Cryoscopic measurements in benzene.

these three runs were gathered and rigorously fractionated. A small plateau (ca. 10 cc.) of **M′D′DM′**, though not so pure (Found: H(−Si), 1.15. Calcd. for **M′D′DM′**: H(−Si), 1.13%.) and a succeeding large plateau (ca. 45 cc.) of gradually rising temperature (80°–85°C/31 mm.) were obtained.

As the refractive index (n_D^{20}) of this incomplete plateau changed from 1.3911 to 1.3935 and the active hydrogen content of the distillate showed a lower value than that of $M'D_2M'$, it may be natural to suppose that $M'D_2M'$ was contaminated with cyclic polysiloxanes having **D** (reported[3]: D_4, n_D^{20} 1.3968), or **D** and **D'** units in this plateau.

In Expt. 5, the low boiling fraction was cohydrolyzed with a relatively small amount (17% of the low boiling fraction) of (II) to avoid the formation of cyclic polysiloxanes as far as possible. By redistillation, **M'D'DM'** and $M'D_2M'$ were obtained as the complete plateaus and were accurately characterized.

Cohydrolyzate with Trimethylchlorosilane (I), (Expt. 6).—The low boiling fraction was cohydrolyzed with (I). The succeeding plateaus of M_2' (b. p. 70.5°C), **MM'** (b. p. 85°C) and M_2 (b. p. 100°C) were obtained. Above **M'D'M'** (b. p. 117°C), two main plateaus having a gradually changing refractive index were observed until 141°C. One centering around 130°C was supposed to contain a pair of isomers **M'DM'** and **M'D'M** (Found: H(−Si), 0.95. Calcd. for **M'DM'** or **M'D'M**: H(−Si), 0.97%.), the other from 137° to 141°C, **M'DM** and **MD'M** (Found: H(−Si), 0.53. Calcd. for **M'DM** or **MD'M**: H(−Si), 0.45%.). Owing to the close boiling points of isomers in a pair, neither was accurately separated. The distribution of the components in the hydrolyzate is given in Table I.

Cohydrolyzate with Methyltrichlorosilane (III), (Expt. 7).—After $M'D_2'M'$ has been distilled out, a large plateau (ca. 50 cc.) was obtained between 73°C to 77°C at 38 mm. The first 30 cc. of this plateau had the value of refractive index (n_D^{20}) of 1.3850 to 1.3853 and then it gradually increased to 1.3860. Since the branched chain polysiloxane (M_3T) has been reported[3] to have a slightly lower boiling point and refractive index than the isomeric linear polysiloxane (MD_2M), it was supposed naturally in this experiment that the fore part of this plateau is that of $M_3'T$ and at the back part of the plateau, $M_3'T$ is gradually contaminated with accompanying isomeric linear **M'D'DM'** (n_D^{20} 1.3862) which was produced inevitably from the hydrolysis of the starting material. By redistilling the portion having the refractive index 1.3850 to 1.3853, the plateau having the constant refractive index was obtained, and this was assigned to $M_3'T$.

3) W. Patnode and D. Wilcock, *J. Am. Chem. Soc.*, **68**, 358 (1946).

The succeeding five small plateaus were obtained until 115°C/0.4 mm. Among them only the plateau (100°C/38 mm., n_D^{20} 1.3882), which was found next to the linear $M'D_3'M'$, had its active hydrogen content and molecular weight consistent with the calculated value for the branched chain pentasiloxane, $M_2'TD'M'$. But the purity of this compound would not be insisted upon merely because of its hydrogen content and molecular weight, for there is a possibility of contamination of a small amount, if any, of isomeric linear pentasiloxane.

Cohydrolyzate of Methyldichlorosilane (III') and Trimethylchlorosilane (I), (Expt. 8).—A series of methylhydropolysiloxanes indicated by $MD_n'M$ ($n=1-4$) was first synthesized by Sauer[2], but the boiling points of trisiloxane and tetrasiloxane were not reported. We synthesized a series of these compounds by cohydrolysis of (I) and (III'). As no equilibration by concentrated sulfuric acid was performed to avoid the fission of Si-H by this reagent, trisiloxane was much contaminated with cyclic tetrasiloxane, D_4' (b.p. 134.5°C) and it was necessary to repeat rigorous fractionation until the distillate gave a satisfactory active hydrogen content. Tetrasiloxane and pentasiloxane were also redistilled once. Octasiloxane was supposed to be not so pure as other compounds referring to its active hydrogen content.

Summary

1) The low boiling fraction of silicon-methylchloride reaction was cohydrolyzed with the three kinds of methylchlorosilane and the methylhydropolysiloxanes, **MM'**, **M'D'DM'**, $M'D_2M'$, $M_3'T$ and $M_2'TD'M'$, have been prepared and characterized.

2) A complete series of linear methylhydropolysiloxanes, $MD_n'M$ having three to eight silicon atoms have been prepared and characterized from the cohydrolyzate of methyldichlorosilane and trimethylchlorosilane.

We wish to express our hearty thanks to Shin-etsu Chem. Ind. Co. for giving us precious samples.

Department of Applied Chemistry
Faculty of Engineering, Osaka University, Osaka

Über die heterogene Acetylierung der ebenen Cellulose

Von Toshikazu FUJIMURA

(Eingegangen am 9. Januar 1956)

Einleitung

Um die Grundlage der chemischen Veredlung der Kunstseide und der Zellwolle aufzuklären, ist es interessant, die Reaktionsgeschwindigkeit der heterogenen Acetylierung der Cellulose, den Reaktionsmechanismus und die Beziehung mit der inneren Struktur zu untersuchen. Darüber hat der Autor die verkürzten Formel auf der zyliderischen Form unter der Annahme des quasistationären Zustandes vorgestellt[1]. Diesmal wird die Methode auf die unendliche Ebene angewandt und wird die Gültigkeit über mehreren aufeinandergestellten Schichten der Cellophane geprüft, die ungeachtet der inneren heterogenen Struktur im ganzen als einheitlich betrachtet werden kann. Der Haufen wurde mit dem Gemisch, das aus Benzol, Essigsäureanhydrid und Sulfoessigsäure besteht, von einer Seite ab durchgesetzt und die acetylierten Schichten wurden mittels der Anfärbung unterschieden. Dabei wurde der Einfluss der Zusammensetzung des Gemisches, des Verhältnisses des Gemisches zur Folien (nämlich des statischen Druks), der Temperatur und der Weise der Vorbehandlung untersucht.

Ableitung der theoretischen Gleichung

Wird der quasi-stationäre Zustand und die gleichen Hinüberwanderngeschwindigkeiten des Acetylierungsmittels an allen Orten angenommen, so ergibt die Differentialgleichung:

$$dm'/dt = dm/dt = dm''/dt = a(dX/dt) \quad (1)$$

Wenn die Reaktion der ersten Ordnung gilt, so ergibt man die Gleichung:

$$dm''/dt = k''(C''-C''') \quad (2)$$

Für das Stoffüberwndern an der Oberfläche erhält man;

$$dm'/dt = k'(C^*-C') \quad (3)$$

Als Zusammenhang der innen Diffusion ergibt die Ficksche Gesetze:

$$dm/dt = D(dC/dx) \quad (4)$$

Hierbei:

C^*, C', C, C'', C''': Konzentration des Acetylierungsmittels im aussen Acetylierungsmittel, an der Oberfläche, in acetylierten Schicht, an der Reaktionsgrenze unter Gleichgewicht.

dm'/dt: Stoffübergangsgeschwindigkeit an der Oberfläche.

dm/dt: Diffusionsgeschwindigkeit in der acetylierten Schicht.

dm''/dt: Reaktionsgeschwindigkeit.

X: Dicke der acetylierten Schicht.

a: Die Gewicht des ein Längseinheit der Cellophane von einer Flächenraumeinheit acetylierenden Acetylierungsmittels.

D: Diffusionskonstante.

k': Stoffübergangskonstante an der Oberfläche.

k'': Reaktionskonstante.

Durch Einsetzen von (1) in (4) ergibt sich:

$$Ddc = a(dX/dt)dx.$$

Mit der Integration auf x von 0 bis X gewinnt man:

$$D(C'-C'') = aX(dX/dt). \quad (5)$$

Aus (1) und (2) folgt:

$$C'' = C''' + a(dX/dt)/k''. \quad (6)$$

Aus (1) und (3) erhält man:

$$C' = C^* - a(dX/dt)/k'. \quad (7)$$

Durch Elimination von C' und C'' ergeben (5), (6) und (7):

$$D\{C^*-C'''-a(dX/dt)/k'-a(dX/dt)/k''\} = aX(dX/dt). \quad (8)$$

Für das Integral auf t von 0 bis t und auf X von 0 bis X folgt:

$$(C^*-C'')t = a(X^2/2D+X/k'+X/k''). \quad (9)$$

(a) Für den mit der Diffusion bestimmten Fall:

$$D \ll k',\ k'';\ X^2 = 2D(C^*-C'')t/a. \quad (10)$$

(b) Für den mit dem Oberflächewiederstand bestimmten Fall:

$$k' \ll D,\ k'';\ X = k'(C^*-C'')t/a. \quad (11)$$

(c) Für den mit der chemischen Reaktion bestimmten Fall:

$$k'' \ll D,\ k';\ X = k''(C^*-C'')t/a. \quad (12)$$

Material und Methode

Cellophane (0.02 mm dick, 2–3 mg/cm²) wurde in 2 cm×23 cm geschnitten und in 10 Schichten gefaltet und diese 6–10 Haufen wurde aufeinandergesetzt. Falls keine besondere Bemerkung, wurden diese Haufen zwei Tage lang in Wasser getaucht, auf dem Verhältnis des Gewichts von 1:2.4 abgepresst, und dann in zwölffachen Teile Essigsäure zu Cellophane eingesetzt. Diese Vorbehandlung wurde zehnmal wiederholt. Dann wurde die Folien zwischen der Flanschen der in

1) T. Fujimura, Dieses Bulletin, 28, 248 (1955).

Abb. 1 gezeigten Apparat geklemmt und in den

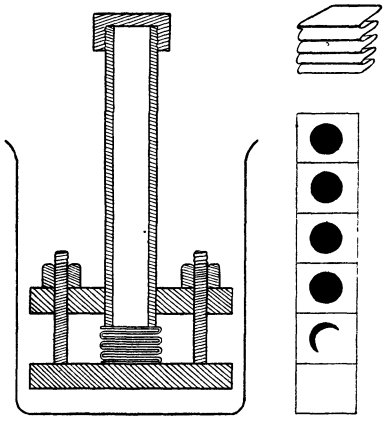

Abb. 1. Acetylierungsapparat.

Vorbehandlungsmittel enthaltenden Becherglas eingetaucht und der Gemisch, der zwei Stunden lang bei 75°C zwecks der Umwandlung der Schwefelsäure in die Sulfoessigsäure erwärmt geworden war, wurde in der oberen Röhre eingegossen.

Nach bestimmten Dauer wurde die Folien weggenommen, dann mit Alkohol und Wasser nacheinander gewäscht und mit dem Gemisch von Celliton-Farbstoff und Substantiv-Farbstoff anfärbt, um die Zahl der acetylierten Schichten zu erkennen. Die Fraktion einer Schicht wurde auf den Flächenraum des angefärbten Teils bezogen.

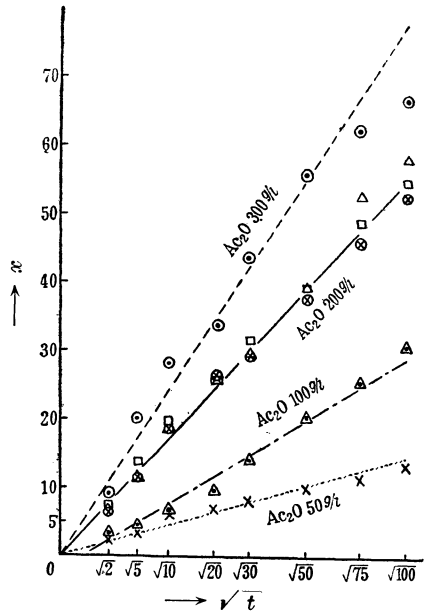

H_2SO_4 6.75 g/l H_2SO_4 4.5 g/l
H_2SO_4 2.25 g/l

Abb. 2. Der Einfluss von der Zusammensetzung des Acetylierungsmittels.
t: Zeit (Stunden),
x: Anzahl der acetylierten Schichten.

Ergebnisse und Diskussion

Zusammensetzung des Acetylierungsmittels.—Wie aus Abb. 2 hervorgeht, ist die Zahl der acetylierten Schichten ungefähr in Verhältnis zur Quadratwurzel der Zeit, so dass die von der innen Diffusion abhängige Gleichung (10) gelten muss. Aber, nach der langen Reaktionszeit eintritt die Abweichung aus der Gleichung. Es kann davon herrühren, dass die acetylierte Schicht allmählich quillt, dass der kleinere Durchmesser des acetylierten Teils in der tieferen Schichten mit der Annahme der Diffusion in einen Richtung im Widerspruch steht und dass der Verbrauch der Essigsäureanhydrid zufolge der Reaktion die Konzentration um 10% abnimmt.

Am ersten geraden Teil der Kurve wird die Regression-Analyse nach der Gleichung:

$$X=a+bt^{1/2} \tag{13}$$

ausgeführt und die Ergebnisse in der Tabelle I wiedergegeben.

TABELLE I
REGRESSION-ANALYSE
(EINFLUSS DER KONZENTRATION VON ESSIGSÄUREANHYDRID)

Essigsäureanhydrid (g/l)	50	100	200	300
Konstant b	1.39	2.97	5.43	7.65
Konstant a	0.66	−2.13	1.01	1.28
Streung der a: S_a	2.62	27.2	6.12	9.85
Streung der Fehler: S_f	0.40	1.26	1.22	5.18
$F_o=S_a/S_f$	6.5	21.6	5.0	1.9

Hierbei: $S_a=n(a-0)^2$
$S_f\sum(X-a-bt)^2/(n-2)$
n: Anzahl der Punkte.

Abgesehen von der Konzentration 100 g/l, kann die Annahme nicht aufgegeben wurden, dass die Konstant a als Null betrachtet wird. Daraus ergibt sich:

$$X=bt^{1/2} \tag{14}$$

Daher passiert die gerade Linie durch die Anfangspunkt. Aus (10) und (14) folgt:

$$b^2=2D(C^*-C''')/a \tag{15}$$

Wie aus Abb. 3 ersichtlich, ist die Beziehung zwischen b^2 und C^* zwar in Hauptteil geradlinig, aber an der Bereich der niedrigen Konzentration gebogen. Es kann auf die Veränderung der Quellungszustandes beruhen.

Da die Konzentration der Sulfoessigsäure wenigen Einfluss ausübt, kann die Hinüberwanderngeschwindigkeit nicht von der Reaktion, auf die die Sulfoessigsäure katalytisch auswirkt, sondern von Diffusion bestimmt werden.

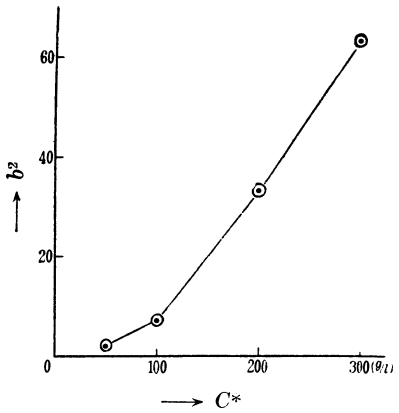

Abb. 3. Die Beziehung zwischen der Regression-Koefizient (b) und der Konzentration von Essigsäureanhydrid (C).

Volumenverhältnis.—Das Verhältnis der Acetylierungsmittels zur Folien, d.h. die Höhe des Acetylierungsmittels in der Röhre, ist von kleine Bedeutung auf der Zahl der acetylierten Schichten, wie in Abb. 4 gezeigt. Deshalb muss das hydrodynamischen Fliessen zufolge des statischen Drucks keine Rolle spielen.

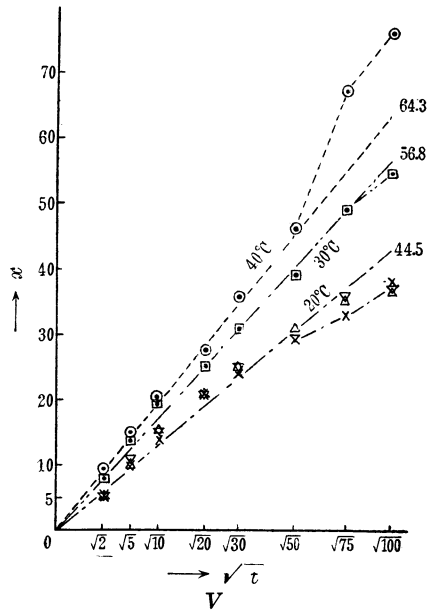

△ 5 ccm ▽ 10 ccm × 15 ccm

Abb. 4. Der Einfluss von Temperatur und von Volumen des Acetylierungsmittels (V).
t: Zeit (Stunden),
x: Anzahl der acetylierten Schichten.

Temperatur der Reaktion.—Es ist in Abb. 4 dargestellt. Bei 20°C und 30°C, gilt ungefähr die geradlinige Beziehung von der Gleichung (10), bei 40°C nicht. Es kann davon herrühren, dass die Folien verdorben werden und die Diffusion gefördert wird.

Die gemäss der Gleichung (15) berechnete Diffusionskonstant nimmt bei höher Temperatur zu, aber die Veränderung ist so klein dass die Vorgang nicht von der chemischen Reaktion sondern von der Diffusion entschieden werden mag.

Vorbehandlungsweise.—Der Einfluss der Vorbehandlung wurde in Abb. 5 verglichen. Je grösser die Quellung nach der Vorbe-

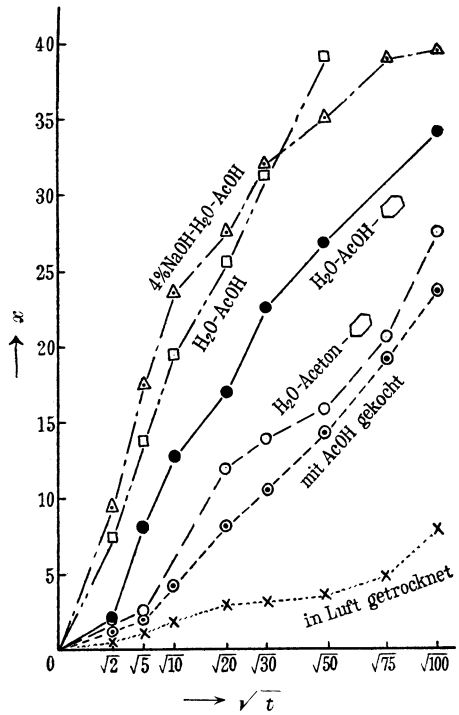

Abb. 5. Der Einfluss von Vorbehandlungsweise.
t: Zeit (Stunden),
x: Anzahl der acetylierten Schichten.

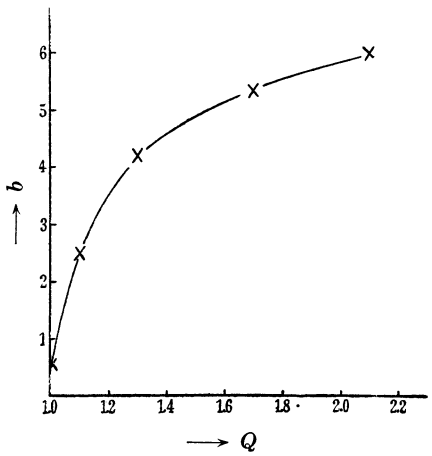

Abb. 6. Die Beziehung zwischen der Regression-Koeffizient (b) und des Quellungs grads (Q).

handlung, desto schneller die Acetylierung, wie in Abb. 6 ersichtlich. Die Beziehung von der Gleichung (10) besteht nicht mehr bei der geringen Quellung, abgesehen vom nicht vorbehandelten Fall. Es kann darauf beruhen, dass der stationäre Zustand nicht in Anfang erreicht wird. Die mit der Alkali-Lauge vorbehandelten Folien ist so schwach, dass die Zahl zufolge Verderben nicht sicher gezählt wird.

Zusammenfassung

Um den Mechanismus der heterogen Acetylierung der Cellulose in eine Dimmension aufzuklären, wurde mehreren aufeinandergesetzten Schichten der Cellophane von einer Seite mit Acetylierungsmittel aus Essigsäureanhydrid—Benzol—Sulfoessigsäure behandelt und der acetylierte Teil wurde mit Anfärbung unterschieden. Das Ergebnis wurde mit der Gleichung verglichen, die unter der Annahme des quasi-stationären Zustand abgeleitet wird.

1. Die Beziehung zwischen der Anzahl der acetylierten Schichten und der Zeit entspricht ungefähr von Diffusion bestimmten Gleichung, nach welcher die Zahl in Verhältnis zum Quadratwurzel der Zeit ist.
2. Je höher die Konzentration der Essigsäureanhydrid, desto schneller das Hinüberwandern der acetylierten Grenze.
3. Da die Konzentration der Sulfossigsäure oder der statische Druck wenigen Einfluss hat und die Abhängigkeit von der Temperatur nicht bedeutend ist, kann der von Diffusion bestimmte Mechanismus unterstützt werden.
4. Die die höhere Quellung ergebende Vorbehandlungsweise übt den grösseren Einfluss aus.

Kokoku Reyon und Zellstoff G.m.b.H.,
Yatsushiro-Fabrik, Yatsushiro-shi,
Kumamoto-ken

The Electronic Structures of Azine Compounds. II. The General Considerations on the Electronic Structures of Azine and Dihydroazine Compounds

By Yûmi Akimoto

(Received January 28, 1956)

Introduction

In the preceding paper[1], the semi-empirical LCAO molecular orbital calculations were made on some azine and dihydroazine compounds. In this paper, for the purpose of generalizing the above conclusions, the scope of the discussions is extended to ten odd azine, dihydroazine, and aza compounds. The results are arranged and investigated systematically from several viewpoints: electronic states, molecular structures, stabilities, etc.

Experimental

With the object of replenishing the spectra data for the sphere of azine compounds, the electronic absorption spectrum was taken on quinoxaline (1, 4-diaza-naphthalene). The sample used was synthesized by the members of Kawai Laboratory of Tokyo University of Education. For the solvent, anhydrous methanol was always employed. The other experimental conditions were similar to that previously described. The result is shown in Fig. 1.

From the standpoint of the transition intensity and the correspondency with the absorption curves of phenazine or quinoline, the strong absorption maximum near 32000 cm^{-1}, may be considered as the π–π transition.

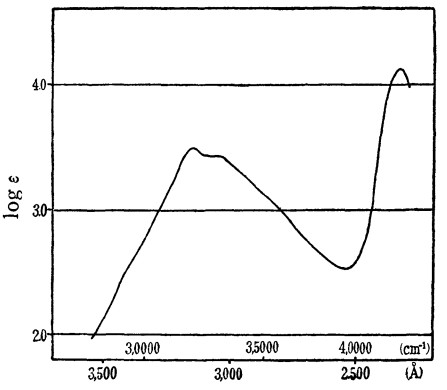

Fig. 1. The absorption spectrum of 1:4-diaza-naphthalene (quinoxaline) (in anhydrous methanol).

1) Y. Akimoto, This Bulletin 29, 460 (1956).

MO Calculation

MO calculations have been carried out for all the molecules shown in Fig. 2. The same calculations were extended to several aza compounds. The π-electron energies of the molecules in the heavy line frames, were calculated by the simplest variation method, and the others by the second order perturbation method, taking as the parent molecules the corresponding molecules which are in the heavy line frames, and for the perturbation term the changes of Coulomb integral values affected by the replacements by N atoms or the introductions of meso-H atoms[2]. According to the conclusions of the previous paper[1], Coulomb integral values are taken as follows:

for every N atom, $\alpha_c+0.6\beta$
for every N_H atom, $\alpha_c+1.2\beta$
for every adjacent atom of
N or N_H atoms (r), $\alpha_c+\frac{1}{8}\sum(\alpha_r-\alpha_c)$

Regarding the other conditions and the detailed explanations of the calculations, the previous paper[1] is to be quoted.

The results of the calculations are summarized in Table I-II, and Fig. 3. Table I shows the results of the variation method calculations applied to the "parent molecules" of the following perturbation calculations. Fig. 3 indicates the π-electron energy states of all molecules referred to above. The underlined column shows the results obtained by the variation method calculations, and the others by the perturbation calculations. In Table II, two calculation methods: variation and perturbation methods, are compared in regard to the numerical results. The first column indicates the electron energies cal-

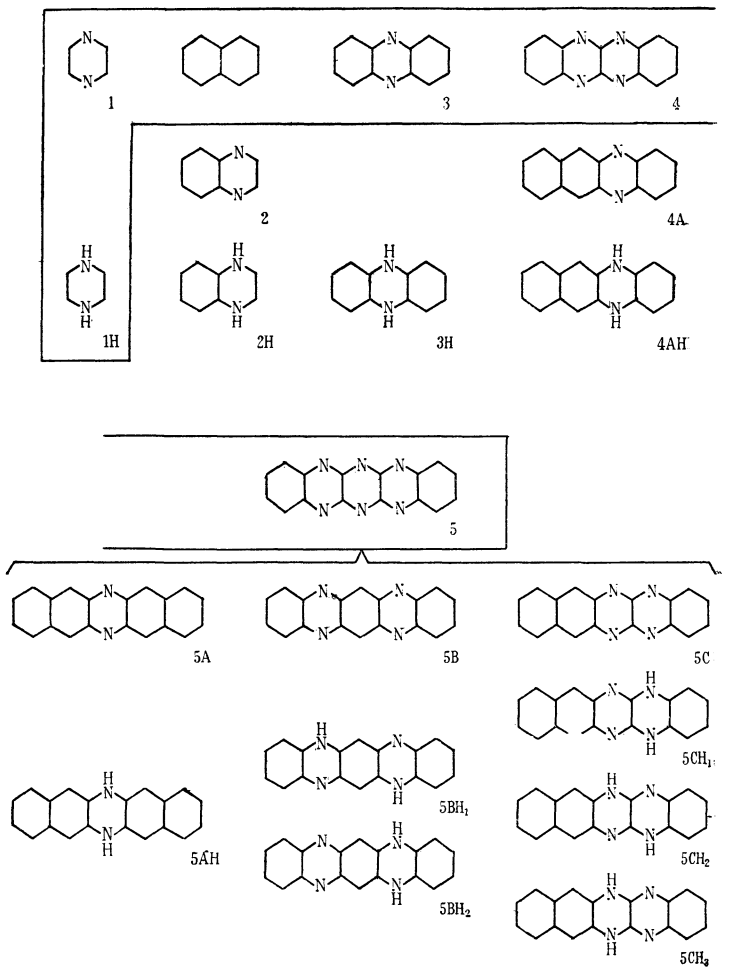

Fig. 2. The model numbers of azine and dihydroazine compounds quoted for the calculations.

2) Per-Olov Löwdin, *J. Chem. Phys.*, **21**, 496 (1953).

culated by the second order perturbation method taking anthracene as the parent molecule, and the second column by the simplest variation method. The result is in a satisfactory agreement.

TABLE I

THE ORBITAL ENERGIES OF "PARENT MOLECULES" CALCULATED BY THE SIMPLE VARIATION METHOD

$x=(\varepsilon-\alpha)/\beta$

Pyrazine (x)		Naphthalene (x)		Phenazine (x)	
				B_{3g}	-2.2834
				A_{1u}	-1.9760
		B_{3g}	-2.0000	B_{3g}	-1.3384
		B_{1u}	-1.6180	B_{1u}	-1.2493
B_{3g}	-1.5716	A_{1u}	-1.6180	B_{2g}	-0.9878
A_{1u}	-0.8500	B_{3g}	-0.6180	A_{1u}	-0.9618
B_{1u}	-0.2394	B_{2g}	-0.6180	B_{1u}	-0.1565
B_{2g}	1.1500	A_{1u}	0.6180	B_{3g}	0.6132
B_{3g}	1.9216	B_{1u}	0.6180	A_{1u}	1.0129
B_{1u}	2.5894	B_{2g}	1.6180	B_{2g}	1.0368
		B_{3g}	1.6180	B_{1u}	1.4908
		B_{1u}	2.0000	B_{3g}	1.6836
				B_{2g}	2.0261
				B_{1u}	2.5900

On 5,6,11,12-tetraaza-naphtacene, and 5,6,7,12,13,14-hexaaza-pentacene, cf. ref. (1).

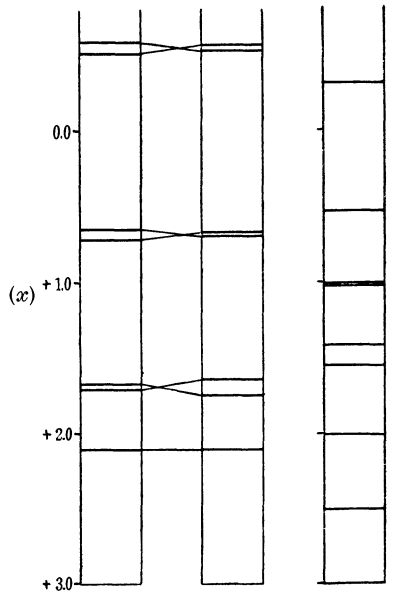

Fig. 3a. The electronic states of some aza compounds.

$x=\frac{\varepsilon-\alpha}{\beta}$ (Calculated by the perturbation method).

TABLE II

THE COMPARISON OF TWO CALCULATION METHODS ON THE ORBITAL ENERGIES OF ANTHRACENE

	Calculated by perturbation method (A)	Calculated by variation method (B)	Differences (A)-(B)
B_{3g}	0.415	0.414	+0.01
A_{1u}	1.000	1.000	0
B_{2g}	1.000	1.000	0
B_{1u}	1.414	1.414	0
B_{3g}	1.412	1.414	−0.02
B_{2g}	2.000	2.000	0
B_{1u}	2.416	2.414	−0.02

Discussion

1) **Delocalization Energy.**—In consideration of the previous paper's results[1], the positions of meso-N atoms are determined in comparing the vertical delocalization energy values (vertical delocalization energy $\Delta\varepsilon$ is defined as follows:

$$\Delta\varepsilon=\varepsilon(L)-\varepsilon(D)$$

cf. ref. (1))

over all isomers of each compound (see Table III). Underlined isomers are the most stable ones.

Through the considerations continued from the preceeding paper[1], as far as dihydroazines are concerned, the following practical principle may be established. *The stabilities of dihydroazine isomers increase according to the following order of molecular symmetry:* $C_{2vx}\rightarrow C_{2h}\rightarrow V_h$. In Table IV, the vertical delocalization energy of the most stable isomer of each dihydroazine compound is compared with that of its parent azine compound.

In general, the reactivities and the stabilities of meso dihydro derivatives increase rapidly with the increase of the number of rings of azine compounds[3]: It is impossible to oxidize fluoflavine to parent azine compound[4], while quinoxaline has not any stable dihydroazine derivatives. Table IV shows that delocalization energies of all dihydroazine compounds are smaller than those of the corresponding azine compounds, nevertheless on account of the differences which the number of atoms or π-electrons make, the direct comparisons can not provide the conclusion that all dihydroazine compounds are less stable than the corresponding azine compounds. However, the tendency to contract the difference of both energies according to the increase of molecular sizes, enables

3) G.M. Badger and R. Pettit, *J. Chem. Soc.*, **1951**, 3211.

4) S. Kawai and S. Noguchi, private communication.

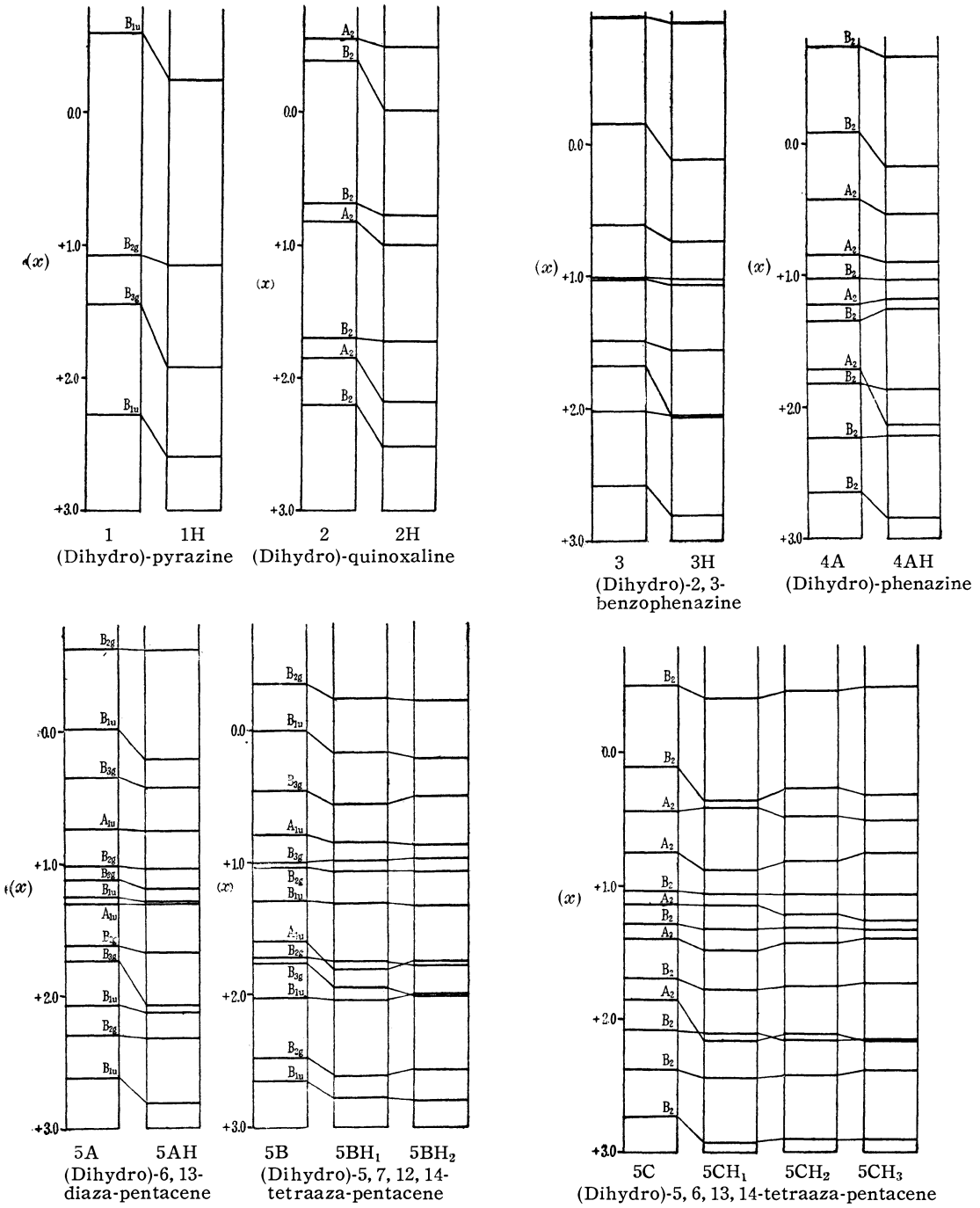

Fig. 3b. The electronic states of some azine and dihydroazine compounds.

$$x = \frac{\varepsilon - \alpha}{\beta}$$

us to predict the stabilities from the ground of the vertical delocalization energies. The reduction rates of the energies, shown in the last column of Table IV, seem to give us some criteria. None of the molecules which have the reduction rates over 17% have any stable dihydroazine derivatives, and less than 6% of any azine compounds. About 9% of the rate seems to correspond to the equal stability between azine and dihydroazine compounds.

In 1926, Dutt reported on his accomplishment of synthesis of 5, 7, 12, 14-tetraza-pentacene[5]. But the result of the re-examination which was followed by Badger et al.[3] was negative. On 5, 6, 11, 12-tetraza-naphtacene, since Hinsberg had reported on his success of the syntheses in 1896[6], no report has been presented, while, the recent result of the re-examination performed by Kawai and Noguchi is negative[4]. Such being the case, the prediction of the stability based on the reduction rates of the delocalization energies, may, though it has not any close theoretical backing, be put to the practical uses.

TABLE III
THE COMPARISONS OF THE DELOCALIZATION ENERGIES ON DIHYDROAZINE ISOMERS

Compounds	Position of meso-H atoms (Model number)	Delocalization energy (β)
Dihydro-5, 7, 12, 14-tetraaza-pentacene	5, 14 ($5BH_2$)	28.920
	5, 12 ($5BH_1$)	28.979
Dihydro-5, 6, 13, 14-tetraaza-pentacene	5, 14 ($5CH_1$)	29.296
	5, 13 ($5CH_2$)	29.205
	6, 13 ($5CH_3$)	29.201

2) The position of the Longest Wave-length Absorption.—Supposing that only the most stable isomer exists on each molecule, the longest wave-length π-π absorption is calculated. In Table V, these values are compared with the observed ones. The conversion rates are chosen so that the calculated transition energies of the corresponding polyacene molecules, agree with the observed absorptions[7] (see ref. (1)). In Fig. 4, these

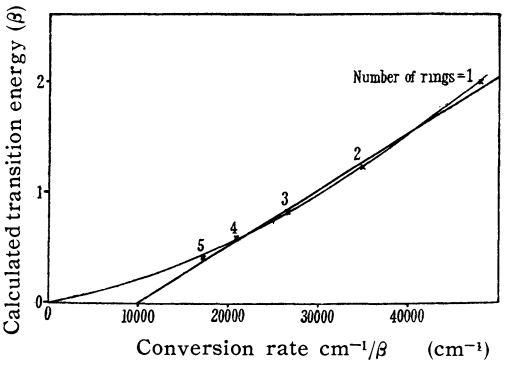

Fig. 4. The conversion rates for the absorption wave number calculations.

TABLE IV
THE DELOCALIZATION ENERGIES OF AZINE AND DIHYDROAZINE COMPOUNDS

Group model number	Molecular structure	Delocalization energy (β) Azine (A)	Dihydroazine (B)	A–B	$\frac{A-B}{A}$
1		8.081	(5.743)	2.338	28.9
2	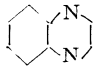	13.060	(10.807)	2.253	17.25
3	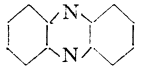	19.407 >	17.482	1.924	9.91
4A	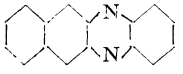	25.084 <	23.103	1.981	7.89
4	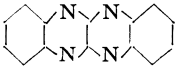	/25.097/	23.614	1.483	5.91
5A	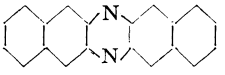	(30.808)	29.126	1.682	5.46
5B	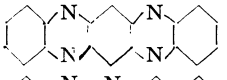	/30.677/	28.979	1.698	5.54
5C	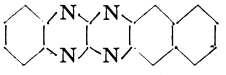	(30.723)	29.296	1.427	4.64
5	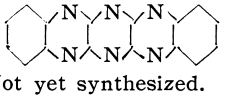	(30.775)	29.353	1.422	4.62

( ) Not yet synthesized.
/ / Accomplishment of synthesis was reported, but negotiated by the re-examination.
> The stability tendency.

5) O. Dutt, *J. Chem. Soc.*, **1926**, 1178.
6) O. Hinsberg and J. Pollak, *Ber.*, **29**, 784 (1896).
7) E. Clar, *Ber.*, **69**, 607 (1936).

rates are shown: The smooth relations are observed between them.

The lack of the spectra data in this sphere, obstructs the overall examinations, while the presented observed values show almost perfect agreements with the calculated ones.

TABLE V

THE COMPARISONS OF THE CALCULATED LONGEST WAVE-LENGTH ABSORPTION POSITIONS WITH THE OBSERVED ONES

Group model number	Molecular skeleton	Conversion rate	Azine compounds				Dihydroazine compound				Reference
			calcd.		obs.	calcd. −obs.	calcd.		obs.	calcd. −obs.	
		(cm^{-1}/β)	(β)	(cm^{-1})	(cm^{-1})	(cm^{-1})	(β)	(cm^{-1})	(cm^{-1})	(cm^{-1})	
1	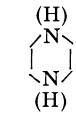	24,000	1.672	40100	38000	+2100	0.511	12300			(8)
		28,500	1.156	32900	31900	+1000	—	—			(9)
		28,500	1.198	34100	31300	+3000	—	—			(9)
2	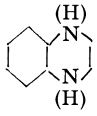	28,500	1.070	30500	31700	−1200	0.490	14000			Present paper
	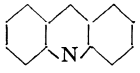	32,500	0.840	27300	28000	− 700	—	—			(10)
3	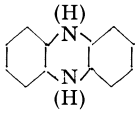	32,500	0.770	25000	27800	−2800	1.047	34000			(10)
4A	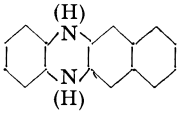	35,500	0.520	18500			0.825	29300			
4	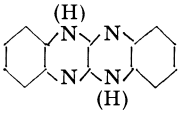	35,500	0.542	19200			0.723	25700	22500	+3200	(1)
5A	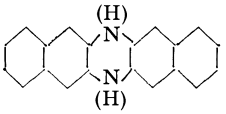	39,000	0.377	14700			0.826	32200			
5B	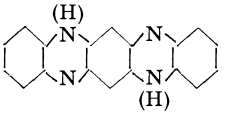	39,000	0.409	16000			0.409	16000	17700	−1700	(3)
5C	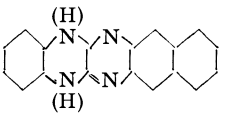	39,000	0.542	21100			0.706	27500			
5	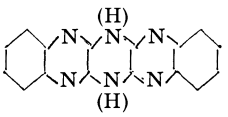	39,000	0.406	15800			0.707	27600	23000	+4600	(1)

8) W.K. Miller, S.B. Knight and A. Roe, *J. Am. Chem. Soc.*, **72**, 1629 (1950).

9) G.W. Ewing and E.A. Steck, *J. Am. Chem. Soc.*, **68**, 2181 (1946).

10) G.M. Badger, R.S. Pearce and R. Pettit, *J. Chem. Soc.*, **1951** 3198.

3) Molecular Diagram.—On several molecules, the charge densities and the bond orders are calculated (see Fig. 5). Except 6, 13-dihydro-5, 6, 7, 12, 13, 14-hexaaza-pentacene, all diagrams are calculated by the simplest variation method. On the former molecule, perturbation method is used in applying the following relations[1,2].

$$q_\mu^j = q_\mu^{j(0)} + \sum_\kappa V_\kappa \pi_{\mu\mu,\kappa}^{jj(0)}$$

$$p_{\mu\nu}^j = p_{\mu\nu}^{j(0)} + \sum_\kappa V_\kappa \pi_{\mu\nu,\kappa}^{jj(0)}$$

$$\pi_{\mu\nu,\kappa}^{jj} = \sum_{j \neq \alpha} \frac{d_{\mu\nu}^{j\alpha} d_{\kappa\kappa}^{\alpha j} + d_{\kappa\kappa}^{j\alpha} d_{\mu\nu}^{\alpha j}}{(j\alpha)}$$

$$d_{\mu\nu}^{j\alpha} = C_\mu^j C_\nu^\alpha$$

where q indicates the charge density, p, bond order, V, perturbation terms, C, orbital coefficient, and π, mutability. Upper indices j, α,……indicate the molecular orbitals, lower indices μ, ν, κ,……the atomic orbitals, (0) the quantities belonging to the original system, and $(j\alpha)$ the energy difference between j-th and α-th orbitals.

The unification of the exchange integral to 1β, takes away the significance of bond order considerably[11], while the tendency to prejudicing the orders according to the increase of azine molecule size, and to compensate the prejudice in introducing the meso-H atoms explains the above mentioned tendency which is observed on the reactivities or the stabilities of azine compound series. This tendency will support the conclusions deduced from the former vertical delocalization energy discussions. In any way, the MO recalculation based on the above diagrams, will make more reliable the conclusions stated above.

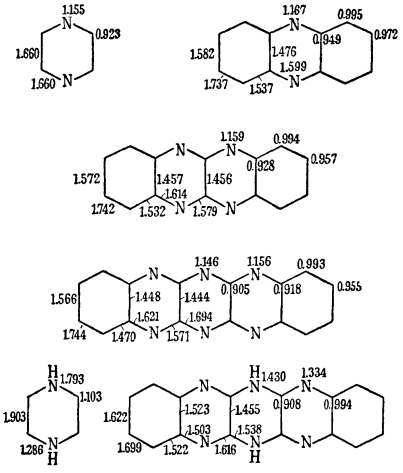

Fig. 5. The molecular diagrams of several azine and dihydroazine compounds.

11) C. A. Coulson, J. de Heer, *J. Chem. Soc.*, **1952** 482.

Summary and Conclusions

1) The absorption spectrum of quinoxaline was observed in anhydrous methanol solution.

2) The longest wave-length π-π transition was observed near 31000–33000 cm^{-1}.

3) The MO calculations were made on ten odd aza, azine, and dihydroazine compounds.

4) Comparing the vertical delocalization energies, the most stable isomer was decided as follows.

molecules	positions of meso-H atoms
dihydro-5, 7, 12, 14-tetraaza-pentacene	5, 14
dihydro-5, 6, 12, 13-tetraaza-pentacene	5, 12.

5) Concerning the stabilities of each dihydroazine isomers, the following tendency was observed. *The stabilities of dihydroazine isomers, increase according to the certain order of molecular symmetry:* $C_{2vx} \rightarrow C_{2h} \rightarrow V_h$.

6) The reduction rates of the delocalization energies, azine to dihydroazine compounds, could be a criterion to predict the stabilities of dihydroazine compound as compared with the corresponding azine compounds. When the rate was less than 6%, only the dihydroazine form could exist steadily; more than 17%, the only stable form was the azine form; and between 6–17%, both forms could exist, while the stability of the azine form was surpassed by that of the dihydroazine form near the rate of 9%.

7) The positions of the longest wave-length absorption were predicted or compared with the observed ones. Agreements were satisfactory in the permissible ranges.

8) The molecular diagrams were drawn on several azine and dihydroazine molecules, which could possibly explain the higher stabilities of dihydroazines, the larger skeletons of molecules.

The author wishes to express his sincere thanks to Prof. A. Kotera and Assist. Prof. K. Suzuki for their continued encouragement and valuable advice for this study. The kindness of Prof. S. Kawai who gave us the sample is gratefully acknowledged. Thanks are also due to Mr. S. Noguchi and Mr. K. Ihaya for their helpful discussions.

A part of the cost of this research has been defrayed from the Scientific Research Encouragement Grant from the Ministry of Education, to which the author's thanks are due.

*Chemical Laboratory Tokyo Bunrika University, Tokyo**

* Author's present adress: *Hosokura Smelter and Refinery, Mitsubishi Metal Mining Co. Ltd., Miyagi-ken.*

The Effect of the Segment Size upon Thermodynamic Properties of Polymer Solutions

By Tōru KAWAI

(Received February 16, 1956)

Introduction

The statistical mechanical theories of polymer solutions currently in use do not entirely conform with observed thermodynamic data. Recently it has become apparent from the extensive measurements on the polymer-solvent systems, that the entropy of dilution differs widely for a given polymer in different solvents, and that, moreover, these entropy values are many times lower than can be accounted for by current theories[1,2].

The crucial point in all these theories lies in the expression for the second virial coefficient A_2. Various theories based on the idealized lattice model are essentially equivalent[3], and may be written uniquely as

$$A_2=(1/V_1\rho^2)\left\{\frac{1}{2}-\left(\frac{1}{Z}\right)\left(1-\frac{1}{m}\right)\right\} \qquad (1)$$

where V_1 is the molar volume of the solvent, ρ, density of the polymer, Z, the coordination number of the lattice sites, and m, the number of submolecules in a polymer molecule. (Hereafter we shall designate the degree of the approximation in these theories as the first order approximation.) A number of osmotic measurements, however, give evidence that the observed values of A_2, in general, are much less than is predicted by Eq. (1).

Various attempts have been made to eliminate this lack of conformity; however, none of them seems to have successfully removed it. Accounting for the influence of a bending back of the polymer chain on to itself (long-range interference), Flory and Krigbaum[4] derived an expression for the second virial coefficient. When the polymer is homogeneous, their expression may be written

$$A_2=(1/V_1\rho^2)\,(\varphi_1-\kappa_1)F(\chi) \qquad (2)$$

$$\chi=2(\alpha^2-1) \qquad (3)$$

where φ_1 and κ_1 are the entropy and energy parameters respectively. The function $F(\chi)$ is a definite integral the evaluation of which is discussed in reference (4). The quantity α is a factor by which the spatial distribution of segments is expanded due to the long-range interference. Thus, the effect of the long-range interference (designated, for convenience, as the "long-range excluded volume effect") upon A_2 appears only through the function $F(\chi)$. Actually, Eq. (2), in combinaton with Eq. (3), well interprets the dependency of the molecular weight of the polymer on A_2, which has been borne out by experiments. As an example, the A_2 values were cited in Table I from the osmotic data

TABLE I

EXAMINATION OF THE DEPENDENCY OF A^2 UPON MOLECULAR WEIGHTS (M: NUMBER AVERAGE MOLECULAR WEIGHT) BY THE THEORY OF FLORY ET AL. (POLYSTYRENE-TOLUENE)

				At 25°C
$M\times10^{-4}$	$A_2\times10^4$ g^{-2} cc	α	$F(\chi)$	$A_2/F(\chi)$
158	2.89	1.52	0.82	3.52
87	3.01	1.44	0.87	3.46
32	3.28	1.32	0.89_5	3.66
28.8	3.09	1.31	0.90	3.43
24.8	3.32	1.30	0.90_5	3.67
16.2	3.36	1.25	0.91_5	3.67
9.4	3.89	1.21	0.93_5	4.16

of Bawn et al. for various molecular weights of polystyrene in toluene[5]. The values of $F(\chi)$ are calculated for the corresponding molecular weights, employing the α values evaluated from the data of intrinsic viscosities[2,6]. The ratio $A_2/F(\chi)$ may be regarded as constant in a wide range of molecular weights (M).

However, the question how the abnormally low values of $(\varphi_1-\kappa_1)$ should be explained remains unsolved; since the value of $F(\chi)$ is seldom far from unity (the α values are smaller than 2 apparently including all practical cases for any polymer-solvent pair so far investigated), the "long-range excluded

1) M.J. Schick, P. Doty and B.H. Zimm, *J. Am. Chem. Soc.*, **72**, 530 (1950).
2) T.G. Fox, Jr., and P.J. Flory, *J. Am. Chem. Soc.*, **73**. 1909; 1915 (1951).
3) T. Kawai, This Bulletin, **26**, 409 (1953); **25**, 336 (1952).
4) P.J. Flory and W.R. Krigbaum, *J. Chem. Phys.*, **18**, 1086 (1950).
5) C.E.H. Bawn and M.A. Wajid, *J. Polymer Sci.*, **12**, 109 (1954).
6) P.J. Flory and T.G. Fox, Jr., *J. Am. Chem. Soc.*, **73**, 1904 (1951).

volume effect" cannot eliminate the above lack of conformity between theory and experiment. Moreover, the definition of the parameters φ_1 and κ_1 still lacks precision; a more careful analysis of the meaning of these parameters is desirable.

At first, we must consider the problem of the preferential ordering induced in the solution by difference in the interaction energies, when the heat of dilution is not zero. However, it was shown that Eq. (I) did not conform with observed thermodynamic data for several systems which can be regarded as more or less athermal[7].

Another possible reason for this nonconformity may exist in neglecting the excluded volume effect in a short range scale, which will be discussed in the next section together with the segment size effect; the excluded volume for a segment in a polymer chain (not for a polymer molecule as the whole) would have to be taken into account, beside the effect in a long-range scale mentioned above.

It may be remarked here that existing theories of polymer solutions fail to take into account the specific geometrical character of the solvent in relation to the polymer segment. Considering the widely different entropies of dilution exhibited by different solutions of the same polymer at the same concentration, it is obvious that this is a serious deficiency which must be made up. In order to establish a unique explanation of these thermodynamic data in terms of molecular concept, an attempt will be made in this paper by proceeding with the idea of the segment size effect, which was already discussed briefly in the previous paper[3].

Athermal Solutions

Most of the existing theories involve an over-simplified assumption which usually has escaped notice; it was assumed that the solvent molecule and segment are the same in size and shape. Some investigators arrived within crude approximations, at the conclusion that the choice of any length of the submolecule along the polymer chain as a segment has no appreciable effect on the resultant formula for the entropy of dilution[8,9]. However, no one has taken into account the dependence of the entropy of dilution and of other related quantities on the relative dimensions of the solvent molecules and the solute molecule cross sections. As was shown in the treatment of rod-like molecules[10], this might play an important role on the explanation of unreasonably low values of φ_1. Zimm[11] also has shown an analogous effect for athermal solutions of various infinite chains in an artificial cubic lattice.

Here, the modification of the entropy expression by Flory[12], who first introduced the effect of the segment size, may be recalled, although his definition of the segment was somewhat ambiguous. In our treatment the segment in a thermodynamical sense will be redefined as a purely stereometric one in character. The essential feature of it is that it has to satisfy the condition that it is isotropic and spherical. The effect of anisotropy in the force fields around the segment can be ignored in athermal solutions; however, the geometrical anisotropy, i. e. its shape factor, must be taken into account. If the segment is assumed as a section of the polymer chain which occupies a volume equal to that of the solvent molecule, the resultant expression of the entropy must fail its validity, since it is quite different from the solvent molecule in shape when the dimensions of the polymer cross sections differ extremely from those of the solvent molecule. Therefore, we must construct a more realistic model with regard to the molecular constructions of the solvent and solute. The restriction of the lattice model, which arise from its artificiality, may possibly be removed by choosing a suitable size and shape of the segment as well as by introducing the coordination number characterizing the type of the lattice.

Let us consider four cases; (a) both the polymer and solvent are "aliphatic" (The term "aliphatic" used here means, for convenience, the "effectively" small dimensions of the solvent molecule and the polymer molecule cross sections. The solutions of the polymer consisting of a linear sequence of carbon atoms without any bulky side chains or branches in the open chain solvents belong to this case.) (b) the polymer consists of a sequence of rings[13] (the polymers in

7) H. Stuart, "Das Makromolekül in Lösungen", Berlin (1953).
8) M.L. Huggins, *Ann. N.Y. Acad. Sci.*, **43**, 1 (1942).
9) B.H. Zimm, *J. Chem. Phys.*, **14**, 164 (1946).
10) Exactly the same expression was derived for the solutions of large rigid rod-like molecules as Eq. (1). Even for these solutions, where both the excluded volume effect and ordering effect mentioned above need not be considered, Eq. (1) does not coincide with the formula obtained by methods using molecular distribution function, without considering the segment size effect (This Bulletin, **24**, 269 (1951)).
11) B.H. Zimm, ref. (20), p. 364.
12) P.J. Flory, *J. Chem. Phys.*, **10**, 51 (1942).
13) These rings may be contained not only in the main chain but in the side chains; the bulky nature of the effective cross sections of such polymer chain is speculated here.

this class are designated by "aromatic polymer"), and the solvent is "aliphatic". (c) the polymer is "aliphatic", and the solvent is "aromatic" (of course, all rigid cyclic compounds such as cyclohexane or dioxane are also involved). (d) both the polymer and solvent are "aromatic". These are hypothetically illustrated in Fig. 1.

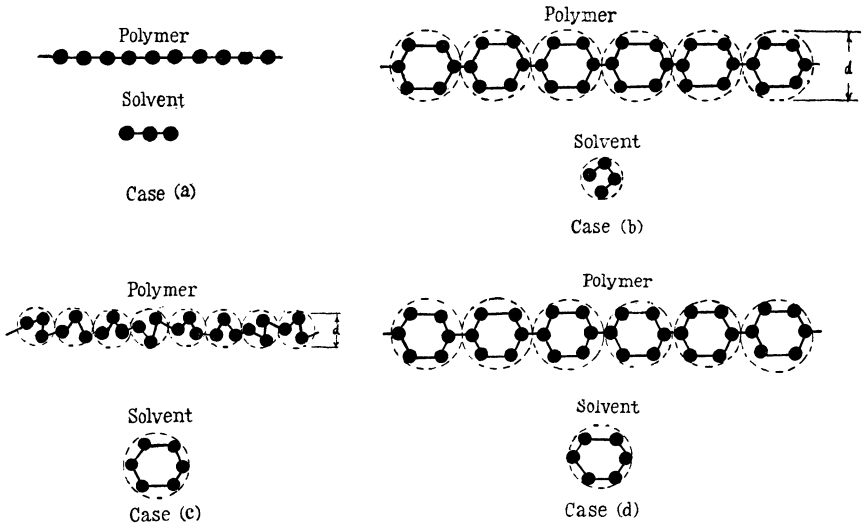

Fig. 1. Hypothetical models of polymer and solvent molecules.

For the case (a) Guggenheim obtained, within a crude approximation, an expression of entropy of dilution, which does not much differ from the results (for instance, Eq. (1)) deduced from the usual assumption that the solvent molecule and segment are the same in size and shape[14]. Here, considering the effect of the flexibility of the polymer chain[15,16], it would be preferable to write

$$A_2=(1/V_1\rho^2)\varphi_1^*. \qquad (4)$$

The parameter φ_1^* is characteristic to the polymer chain, irrespective of the solvent, and the effect of flexibility of the chain, if it gives rise to some alteration in the expression of A_2, may be involved into this parameter[15,16].

For the case (b) the author derived[3]

$$A_2=(1/V_1\rho^2)(V_1/V_2)\varphi_1^* \qquad (5)$$

which is formally analogous to the Flory's formula in reference (12). In our derivation of Eq. (5), however, the segment was assumed to be a sphere of radius $d/2$ (d is the diameter of the cross section of the polymer chain), the "molar" volume of which is V_2. Thus, the segment is defined by the steric factor only, and is characteristic of the polymer without regard to the type of the solvent.

To the case (c) our equation derived previously[3] is also applicable;

$$A_2=(1/V_1\rho^2)\{1/2-(V_1/V_2)(1/2-\varphi_1^*)\}. \qquad (6)$$

In arriving at this equation, the probability that V_1/V_2 sites must be in one group was calculated to an approximation which corresponds to that employed usually for the mixing of substances of low molecular weight[3], leading to the expression of the entropy of mixing;

$$\Delta S=-R[N_1\ln v_1+N_2\ln v_2]$$

(the N's are the numbers of the molecules and the v's, the volume fractions of the two components).

To the case (d) Eqs. (5) and (6) may be applicable again, according to the respective cases when $V_1>V_2$ and when $V_1<V_2$.

The above simplified models would not be able to provide the comprehensive picture of actual polymer solutions. It seems difficult, however, to take into account the molecular structure of the two components in more detail, because of the complicated character including the effect of the side chains, the non-uniformity of the cross sections along the polymer chain, and the spatial factors of the solvent molecule (our treatment of copolymer solutions may be suggestive in this point[17]).

Therefore, it seems to be rather preferable

14) E. A. Guggenheim, "Mixture", Oxford Univ. Press, London (1952), p. 197.
15) M. Kurata, M. Tamura and T. Watari, *J. Chem. Phys.*, **23**, 991 (1955).
16) M.L. Huggins, *J. Polymer Sci.*, **16**, 209 (1955).
17) T. Kawai, Meeting of Soc. of High Polymer, Japan, IIth Dec., 1954.

to introduce effective volumes of the solvent molecule and segment, V_1^* and V_2^*, involving all the complicated factors mentioned above, instead of V_1 and V_2, and use Eq. (5) when $V_1^* < V_2^*$ and Eq. (6) when $V_1^* > V_2^*$.

Furthermore, as was pointed out by Rushbrook et al.[18], even small molecules such as trimer or tetramer (in their terms) provide some difference in the entropy of mixing between rigid and flexible chains. This difference may be considered to arise from such effect of the excluded volume in a short-range scale as was mentioned previously. Zimm[9] showed an analogous effect on polymer solutions in somewhat different way; in his expression of A_2, the higher segment interaction integrals cannot be ignored in some cases. These integrals describe the effect of the interaction of the neighbouring segments on the probability of a meeting between a segment of one polymer molecule and that of the other molecule at a particular place. Thus, this effect depends on the local structure of the chain molecule and is more or less appreciable, except in the case where the segments are many times longer than their width (such long segments may be inadequate from our viewpoint in this treatment).

Here, the effect of the higher segment interaction, in Zimm's term, upon A_2 has been separated into two factors; the segment size effect (represented by V_1^*/V_2^*) and the effect of the chain flexibility (expressed by the parameter φ_1^*). The flexibility parameter φ_1^*, in other words, represents the just mentioned excluded volume effect in a short-range scale, and, if necessary, the expression of Kurata et al.[15] for A_2 may be utilized:

$$\varphi_1^* = 1/3 - (1/24)\{6\gamma + (1-\gamma)^2\} \qquad (7)$$

where γ is a parameter adjustable between zero and one, which increases with increasing flexibility of the polymer chain and reaches unity when polymer chains coil up tightly.

Taking account of the "long-range excluded volume effect", the final formulas may be written:

when $V_1^* < V_2^*$

$$A_2 = (1/V_1\rho^2)(V_1^*/V_2^*)\varphi_1^* F(\chi) \qquad (8)$$

when $V_1 > {}^*V_2^*$

$$A_2 = (1/V_1\rho^2)\{1/2 - (V_1^*/V_2^*)(1/2 - \varphi_1^*)\}F(\chi). \qquad (9)$$

Since the segment in this treatment is characteristic of the polymer chain regardless of the solvent, Eqs. (8) and (9) would be very useful especially when we inquire into the effect of the solvent type on the thermodynamic properties of polymer solutions[3]. However, unless the spatial character of the solvent molecule (including the average configurations of its flexible carbon chains) may be represented by the "effective sphere" of volume V_1^*, the validity of this treatment fails[19]. The theoretical limitations for further analysis of this spatial factor would be apparent.

Solutions not Athermal

In this section, we shall consider the segments and solvent molecules of different sizes, each being approximated by an effective sphere in shape as was considered in the previous section, and we shall discuss the case when mixing of them is not athermal. Let us assume Z_{11} unit sites around the solvent molecule, and similarly Z_{22} unit sites around the segment; i.e., Z_{11} or Z_{22} corresponds to the surface area of each molecule and approximately, to its volume (in the latter case, this procedure is analogous to the usual treatment employing the cohesive energy density[20]). In their pure state, both the solvent molecule and segment may be assumed to have Z nearest neighbor contacts, and then, each one contact occupies Z_{11}/Z and Z_{22}/Z unit sites, respectively (Z is determined by the steric character of the segment and solvent molecule. When both

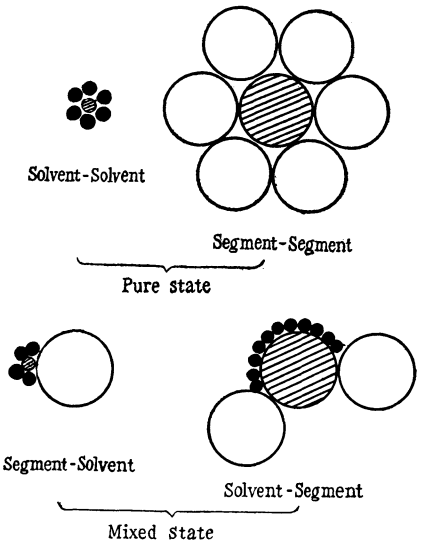

Fig. 2. Illustration of kinds of contacts.

18) G.S. Rushbrook, H.I. Scoins and A.J. Wakefield, *Trans. Faraday Soc., Discussion*, **15**, 57 (1953).

19) The value of V_1^* is to be determined by the spatial character of the solvent. When the solvent molecule consists of a long flexible carbon chain, "the flexibility entropy" of the solvent molecule contributes to the partial molal entropy of the solvent (see reference (16)).

20) J.H. Hildebrand and R.L. Scott, "The Solubility of Nonelectrolyes", 3rd edition, Reinhold Publ. Co., New York (1950).

are effectively spherical, we can assume $Z=12$ for the closely compacted state).

When the two kinds of elements are mixed, we can suppose that, of the $Z_{11}n_1/2$ sites around the solvent molecule, X'_{12} sites come from the segments (n_1: the total number of the solvent molecules), and that, similarly, of the $Z_{22}n_2/2$ sites around the segment, X'_{12} sites come from the solvent molecules (n_2: the total number of the segments). (see Fig. 2).

One solvent molecule occupies Z_{11}/Z unit sites both around the solvent molecule and segment, and, similarly, one segment occupies Z_{22}/Z unit sites. Therefore the number of each contact in the mixture may be written as follows:

kinds of contacts	number of contacts expressed by that of the unit sites	actual number of contacts
solvent-solvent	$\frac{Z_{11}n_1}{2}-X'_{12}$	$X_{11}=a\left(\frac{Z_{11}n_1}{2}-X'_{12}\right)$
solvent-segment	X'_{12}	aX'_{12}
segment-solvent	X'_{12}	bX'_{12}
segment-segment	$\frac{Z_{22}n_2}{2}-X'_{12}$	$X_{22}=b\left(\frac{Z_{22}n_2}{2}-X'_{12}\right)$

$(a=Z/Z_{11}, \quad b=Z/Z_{22}).$

Here, we have distinguished between the solvent-segment contacts (solvent molecules around a segment) and the segment-solvent contacts (segments around a solvent molecule).

Introducing the combinatory method developed by Guggenheim[14], the above assumptions lead to

$$g=g^*\times\frac{X_{11}^*!\,(aX'^*_{12})!\,(bX'^*_{12})!\,X_{22}^*!}{X_{11}!\,(aX'_{12})!\,(bX'_{12})!\,X_{22}!} \tag{10}$$

where g^* is the number of configurations for the athermal mixing of the two kinds of the elements, which was discussed in the previous section, and g, that for specified n_1, n_2 and X'_{12} (the asterisk means the athermal mixing).

For a given value of X'_{12} the configurational energy is given by

$$E_c=X_{11}w_{11}+X_{22}w_{22}+(a+b)X'_{12}w_{12} \tag{11}$$

where the w's denote the energies of the respective contacts. Consequently the configurational partition function Ω may be written

$$\Omega=\sum_{X'_{12}} g(n_1, n_2, X'_{12})\exp\{E_c(n_1, n_2, X'_{12})\}. \tag{12}$$

By replacing the sum of g on all X'_{12} values by its maximum term,

$$\Omega=g(n_1, n_2, X'_{12})\exp\{X_{11}w_{11}+X_{22}w_{22}+(a+b)X'_{12}w_{12}\}. \tag{13}$$

Now, X'_{12} should have the value determined by

$$\partial \ln \Omega/\partial X'_{12}=0.$$

From this condition the following relationship is obtained;

$$(u-y)^a(v-y)^b=Ay^{(a+b)} \tag{14}$$

where $A=e^{W/\kappa T}$,

with $W=(a+b)w_{12}-aw_{11}-bw_{22}$.

In arriving at Eq. (14) we have introduced such abbreviations as Guggenheim[14] did:

$$u=\frac{Z_{11}n_1}{Z_{11}n_1+Z_{22}n_2}, \qquad v=\frac{Z_{22}n_2}{Z_{11}n_1+Z_{22}n_2}$$

$$y=\frac{X'_{12}}{Z_{11}n_1+Z_{22}n_2}. \tag{15}$$

Similarly, since X'^*_{12} denotes the values of X'_{12} which maximizes the expression, $X_{11}!\,(aX'_{12})!\,(bX'_{12})!\,X_{22}!$, there is obtained

$$(u-y^*)^a(v-y^*)^b=y^{*(a+b)} \left(y^*=\frac{X'^*_{12}}{Z_{11}n_1+Z_{22}n_2}\right). \tag{16}$$

Eqs. (14) and (16) cannot be solved straightforwardly; however, writing $y=y^*+\Delta y$, we can evaluate y in spite of the crude approximation involved in its calculation[21]. The resultant equation is given by

$$y\fallingdotseq Kuv+(1-A^{1/b})(v-Kuv). \tag{17}$$[21]

We thus obtain the energy of mixing ΔE:

21) Expanding Eq. (14) into the binomial series with respect to Δy, we may write

$$\frac{1}{A^{\frac{1}{b}}}\left\{y^{*\frac{a+b}{b}}(u-y^*)^{-\frac{a}{b}}+\left[\left(\frac{a+b}{b}\right)y^{*}\left(\frac{a+b}{b}\right)-1\right]\right.$$

$$\left.\times(u-y^*)^{-\frac{a}{b}}-\left(\frac{a}{b}\right)y^{*\frac{a+b}{b}}(u-y^*)^{-\left(\frac{a+b}{b}\right)}\right]\Delta y+\cdots\Big\}$$

$$=v-y^*-\Delta y.$$

Since we can neglect safely the coefficient of Δy in the left hand side of this equation in comparison to that in the right (i.e. $(-1)\times\Delta y$) when $y^*<v\ll 1$ (for dilute solutions), except the case when $a\ll b$, the relation, $y=y^*+(1-A^{1/b})(v-y^*)$ is obtained to a satisfactory approximation provided that $\Delta y<y^*$. Next, Eq. (16) can be solved approximately as follows: when $a=b$, $y^*=uv$, and at infinite dilution, $y^*=uv$ when $a\gg b$ aud $y^*=uv/2$ when $a\ll b$. So long as the extremely dilute region (say, 0-2% polymer) is concerned, it is possible to show that y^* may be written approximately as Kuv, where K is about unity when $a>b$ and decreases with the decreasing values of a/b when $a<b$.

$$\Delta E=(Z_{11}n_1+Z_{22}n_2)Wy=(Z_{11}n_1+Z_{22}n_2)W\{Kuv+(1-A^{1/b})(v-Kuv)\}. \quad (18)$$

From this we may obtain the Helmholtz free energy of mixing, ΔF, by integration, assuming W independent of temperature T;

$$-\frac{\Delta F}{T}=\int\frac{\Delta E}{T^2}dT+C. \quad (19)$$

The temperature independent term C is of course the athermal entropy of mixing (ΔS^*). The integration yields ΔF, and the partial molal quantities may be written as follows;

$$\Delta\bar{F}_1=\Delta\bar{S}_1^*+KZ_{11}W[1+(1/2)\{W/(bkT)\}+(1/6)\{W/(bkT)\}^2+\cdots\cdots]v^2+\cdots\cdots \quad (20)$$

$$\Delta\bar{E}_1=KZ_{11}W[1+W/(bkT)+(1/2)\{W/(bkT)\}^2+\cdots\cdots]v^2+\cdots\cdots \quad (21)$$

$$\Delta\bar{S}_1=\Delta\bar{S}_1^*+KZ_{11}W[(1/2)\{W/(bkT)\}+(1/3)\{W/(bkT)\}^2+\cdots\cdots]v^2+\cdots\cdots. \quad (22)$$

In the above treatment the connection between the segments in the chain molecule is not essentially taken into account. So far as the second virial coefficient is concerned, however, it was shown[4,9] that the neglect of it does not bring out any serious difference in the resultant formula. Evidently from the theory of Flory and Krigbaum[4], only interaction between pairs of the segments belonging to two different polymer molecules was considered in the introduction of the parameters φ_1 and κ_1. Therefore, the treatment in this section may be available to discuss the parameters φ_1 and κ_1, and the second virial coefficient may be written

$$A_2=(1/V_1\rho^2)(\varphi_1-\kappa_1)F(\chi),$$

with

$$\varphi_1=\varphi_1^{**}+KZ_{11}(V_1Z_{22}/V_2Z_{11})^2W[(1/2)\times\{W/(bkT)\}+(1/3)\{W/(bkT)\}^2+\cdots\cdots] \quad (23)$$

where $\varphi_1^{**}=(V_1^*/V_2^*)\varphi_1^*$ when $V_1^*<V_2^*$, and $\varphi_1^{**}=1/2-(V_1^*/V_2^*)(1/2-\varphi_1^*)$ when $V_1^*>V_2^*$.

22) T. Kawai and R. Kashiwagi, Annual Meeting of Chem. Soc. Japan, April 1955.

And

$$\kappa_1=KZ_{11}(V_1Z_{22}/V_2Z_{11})^2W[1+W/(bkT)+(1/2)\{W/(bkT)\}^2+\cdots\cdots] \quad (24)$$

Comparison with Experiment

Unfortunately, there are very few polymer-solvent systems which have been investigated accurately enough either with respect to the temperature dependency of osmotic pressure or to (the direct measurements of) the heat of dilution to permit anything but a rough estimate of the adequacy of the treatment developed here for calculating $\Delta\bar{S}_1$ (or φ_1) and $\Delta\bar{E}_1$ (or κ_1). The treatment of intrinsic viscosities presented by Flory and Fox[6] affords very good agreement with the experiment as was pointed out elsewhere[22], and fortunately, the ($\varphi_1-\kappa_1$) values deduced from intrinsic viscosity measurements[2] well coincide with those from osmotic data[1,5,23], at least for the polymer solutions investigated here. This is illustrated in Table II (for polyisobutyrene solutions) and in Table III (for polystyrene solutions). These values of φ_1 and κ_1 may be available for the present purpose.

TABLE II

COMPARISON BETWEEN THEORY AND EXPERIMENT FOR POLYISOBUTYRENE SOLUTIONS

At 25°C

Solvent	($\varphi_1-\kappa_1$) from $[\eta]$[2]	($\varphi_1-\kappa_1$) from osmotic data	$(\varphi_1)_{exp.}$	κ_1	φ_1**	V_1 cc.
Benzene	0	0[23]	0.15	0.15	0.21_8	89.4_7
Cyclohexane	0.081	0.074_2[23]	0.14	0.059	0.15_7	108.7
Toluene	0.02		0.14	0.12	0.16_3	106.8
Ethylbenzene	0.023		0.14	0.117	0.11_4	122.4
75:25 E. B.: P. E.	0		0.17	0.17	(0.10_1)	126.3
50:50 E. B.: P. E.	−0.03		0.21	0.24	(0.07_7)	133.9_5
Diisobutyrene	0.040		0.056	0.016	0.04_7	156.9
n-Hexadecane	0.039		0.094	0.055	(−0.42)	291.9_2
n-Heptane	0.035		0.035	0	0.03_5	147.3_2
Triptane	0.047		0.047	0	—	—

TABLE III

COMPARISON BETWEEN THEORY AND EXPERIMENT FOR POLYSTYRENE SOLUTIONS

At 25°C

Solvent	($\varphi_1-\kappa_1$) From $[\eta]$[2]	($\varphi_1-\kappa_1$) From osmotic data	$(\varphi_1)_{exp.}$	κ_1	V_1 cc
Cyclohexane	0	0.003_7[1]	0.13	0.13	108.7
Toluene	0.05	0.050_2[1]	0.11	0.06	106.8
Benzene	0.06	—	0.09	0.03	89.4_7
Dichloroethane	0.022	—	0.06	0.038	84.3
Methyl ethyl ketone	0.006	0.005_8[5]	0.006	0	90.1_2

23) P. J. Flory, *J. Am. Chem. Soc.*, 65, 372 (1943).

All these φ_1 values are much smaller than those predicted from Eq. (1). Furthermore, it has become apparent that the entropy of dilution differs widely for a given polymer in different solvents. For athermal mixing, the φ_1 values are predicted from Eqs. (8) and (9) to decrease with the increasing V_1^* values when $V_1^* > V_2^*$ and with the decreasing V_1^* when $V_1^* < V_2^*$.

To polyisobutyrene solutions Eq. (9) may be applicable, since it seems reasonable to choose the isobutene unit as the segment, which is considered to be smaller than the solvents used. Assuming $\varphi_1^* = 0.2$[24], for convenience, the ratio V_1^*/V_2^* has been calculated from the $(\varphi_1)_{exp.}$ value (experimental values of φ_1) for heptane solution, which can be regarded as athermal. This ratio is 1.55 for heptane and then, assuming $V_1^* = V_1$, $V_2^* = 95$ cc. This value of the segment volume V_2^* corresponds approximately to the isobutene unit. Regardless of these values of V_2^* and φ_1^*, we can evaluate the φ_1^{**} values for the solvents used from Eq. (9), regarding the heptane solution as a standard. Also these values are given in Table II (by employing the approximation, $V_1^* = V_1$ again), together with the molar volumes of the solvents. Except the two mixed solvents (ethylbenzene (E. B.)-phenyl ether (P. E.)) and *n*-hexadecane, the agreement between the $(\varphi_1)_{exp.}$ and φ_1^{**} values is rather satisfactory, considering the crudity of the assumptions on the one hand and the uncertainty of absolute magnitude of $(\varphi_1)_{exp.}$ on the other[25]. There appears to be no correlation between $(\varphi)_{exp.}$ and κ_1. In the systems having great κ_1 values such as the two mixed solvent solutions, however, there might be some contribution of the heat of mixing to φ_1. For *n*-hexadecane, the long asymmetrical solvent capable of assuming a number of different configurations, the assumption $V_1^* = V_1$ could no longer hold its validity[19].

The situation is entirely different for polystyrene solutions. For methyl ethyl ketone, in which $\kappa_1 = 0$, the $(\varphi_1)_{exp.}$ value is unexpectedly small. Considering the bulky nature of the aromatic side chain of polysyrene, we are inclined to apply Eq. (8) to these solutions. However, Eq. (8) leads us to an unreasonably large value of V_2^*; from this φ_1^{**} value we obtain $V_1^*/V_2^* = 0.02$ and $V_2^* = 7370$ cc. (assuming $\varphi_1^* = 0.3$ and $V_1^* = V_1$)[26]. The reason for this is not known, and probably, this might be partly due to the same reason as was mentioned in reference (25). Nevertheless, it may be easily supposed from the chemical structure of the polystyrene chain that the value of V_2^* is fairly great, and the values of φ_1^{**} would not exceed, at the greatest, 0.1 for all the solvents cited in Table III (see the V_1 values given in the same table)[27]. The apparent discrepancy between thus estimated value of φ_1^{**} and the $(\varphi_1)_{exp.}$ values cannot be interpreted until Eq. (23) is introduced for the expression of φ_1. We can find semiqantitatively good correspondence between $(\varphi)_{exp.}$ and κ_1 values in Table III. This, of course, may be expected from Eqs. (23) and (24).

It must be emphasized that the preferential ordering induced by the difference in the interaction energies gives rise to a notable contribution to φ_1 for polystyrene solutions, whereas it does not appear to bring out so much influence for polyisobutyrene solutions. This result is in good agreement with Eq. (23), since the value of $(1/b)$ may be supposed to be much larger for polystyrene than for polyisobutyrene. It is an important conclusion in our theory that the above ordering effect is governed to a large extent by the size of the segment (strictly speaking, by its surface area, and approximately by V_2^*) as well as by the value of κ_1. At this point it is of interest to note that in an osmotic investigation of dilute polyvinylchloride solutions the highest entropy values were obtained in the solvents capable of the least specific interaction with the polymer[28].

In view of the simplicity of the concepts involved and of the paucity of available data, the good agreement between our theory and the experiments such as mentioned above may be to some extent fortuitous, and further improvement of the present theory and more extensive measurements would be necessary to establish the unique explanation of experimental data in terms of more detailed molecular concept. It may be said, however,

24) According to Eq. (7) the value of φ_1^* decreases from 0.292 to 0.083 with increasing flexibility (γ) of the chain. Here, for convenience, we adopt $\varphi_1^* = 0.2$, obtained with $\gamma = 0.5$ for polyisobutyrene.

25) The free energy is fairly insensitive to the errors introduced in any over-simplified treatment, but the entropy and heat are not. Therefore, even if the $(\varphi_1 - \kappa_1)$ values coincide with those obtained from osmotic data, we cannot conclude that the precise values of φ_1 and κ_1 have been obtained. Especially in the case of the good solvent, estimated uncertainties in φ_1 and κ_1 amount to 20-30%, whereas they are very little (0-5%) for the bad solvent.

26) We have assumed $\varphi_1^* = 0.3$, with $\gamma = 0$ for polystyrene (see Eq. (7)).

27) It may be remarked that the $(\varphi_1)_{exp.}$ value is larger for the polyisobutyrene-*n*-heptane system (a fairly flexible chain) than for the polystyrene-methyl ethyl ketone (a less flexible chain). This is approved by our treatment, but is in contradiction with the theories in which only the flexibility of the chain was taken into account.

28) P. Doty and E. Mishuck. *J. Am. Chem. Soc.*, **69**, 1631 (1947).

that the widely different entropies of dilution exhibited by different solutions of the same polymer and abnormally low values of them have been semiquantitatively interpreted by the above treatment.

This paper was read at the Special Symposium on Polymer Solutions, held by Chem. Soc., Japan, Phys. Soc., Japan, and the Soc. of High Polymer, Japan, in Tokyo, on 9th Oct., 1955.

Laboratory of Textile Chemistry,
Tokyo Institute of Technology, Tokyo

Mikroanalyse mit Hilfe von Ionenaustauschharzen. III. Über den Nachweis geringer Menge des Sulfides mit p-Aminodimethylanilin oder p-Phenylendiamin*[1]

Von Masatoshi FUJIMOTO

(Eingegangen am 27. Januar 1956)

Einleitung

Durch mikroanalytische Anwendung der Ionenaustauschharze zur Tüpfelmethode wird die Empfindlichkeit oder die Selektivität der Nachweisreaktionen häufig auffallend erhöht[1,2,3,4]. Diese Erhöhung der Empfindlichkeit oder Selektivität beruht hauptsächlich auf dem selektiven Austausch sowie der bemerkenswerten Konzentrierung der Ionen in die Harzphase und manchmal auf besonderen Zuständen von den in sie adsorbierten Ionen[1,2,5]. Um diese Bedingungen befriedigend zu realisieren, untersucht man spezifische Reaktionen mit bemerkenswürdigen Zustandsänderung der Probe, z. B. Färbung, Entfärbung, Gasenentwicklung, Niederschlagbildung usw. Als ein Beispiel von diesen Reaktionen hat der Verfasser die Bildung von kationischen[6] Thiazinfarbstoffe wie Methylenblau oder Lauthschem Violett (Thionin), die in die farblosen starksauren Kationenaustauschharze stark adsorbiert werden und diese entschieden deutlich grün bzw. blau färben, zum Nachweis des Sulfides angewendet[7].

Wenn *p*-Aminodimethylanilin (I) oder *p*-Phenylendiamin (III) bei Gegenwart von Salzsäure und Eisen(III)chlorid mit Schwefelwasserstoffsäure oder Sulfide reagiert, entsteht Methylenblau (II) oder Lauthsches Violett (IV) gemäss den folgenden Reaktionen:

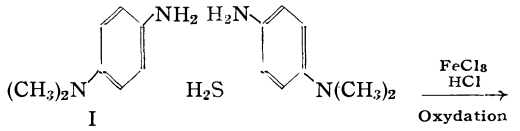

I
farblos

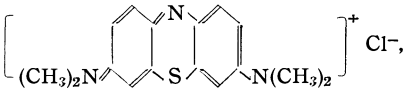

II
blau

oder

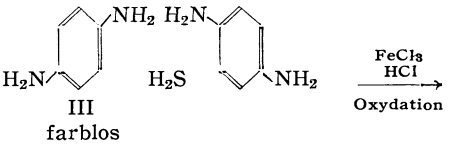

III
farblos

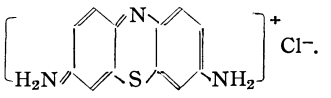

IV
violett

* Statt des Ausdrucks „ionenaustauschendes Harz." der in den vorhergehenden Mitteilungen als geeignete Übersetzung vom Englisch „ion-exchange resin" gebraucht wurde, wird hier die gegenwärtige Terminologie „Ionenaustauschharz," die heute gewöhnlicher angewendet wird, folgerichtig angewendet.

1) Zweite Mitteilung: M. Fujimoto, Dieses Bulletin 27, 347 (1954).

2) M. Fujimoto, Dieses Bulletin 27, 48 (1954).

3) H. Kakihana und T. Murase, *J. Chem. Soc. Japan (Pure Chem. Sect.)*, 75, 907 (1954).

4) H. Kakihana, Y. Mori und K. Yamasaki, *ibid.* 76, 215 (1955).

5) M. Fujimoto, Dieses Bulletin 29, 285 (1956).

6) Die freie Base von diesen Farbstoffen sind sehr starkbasisch; d. h. pK_0 (negativer gemeiner Logarithmus von Dissoziationskonstante als die freie Base, K_0) sind weniger als 1 (Methylenblau) und 2.73 (Lauthsches Violett): Vgl. O. Tomiček, „Chemical Indicators", übersetzt von A.R. Weir, 1. Aufl., London (1951), S. 150.

7) Vgl. E. Fischer, *Ber.* 16, 2234 (1883), sowie F. Feigl, „Spot Tests. I. Inorganic Applications," übersetzt von R. E. Oesper, 4. engl. Aufl., Amsterdam (1954), S. 283.

Die so gebildeten chinoiden Farbstoffkationen werden ins hellgelbe starksaure Kationenaustauschharz adsorbiert, und geben der Harzphase eine grüne oder blaue Färbung, die entschieden deutlicher im Vergleich mit der von Lösungsphase ist. Z. B.:

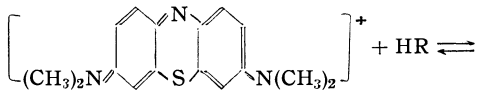

blau hellgelb

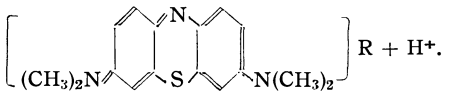

grün bzw. blaugrün

HR bedeutet ein starksaures Kationenaustauschharz von freier Säureform.

Dass das obige Ionenaustauschgleichgewicht wegen des grösseren Ionengewichts des Farbstoffkations beträchtlich auf der rechten Seite liege, trotzdem dieses Gleichgewicht verhältnismässig langsam erreicht werde, ist vor allem für den Nachweis des Sulfides sehr günstig[8].

Das in dieser Untersuchung benutzte Kationenaustauschharz

Dowex 50W-X8[9]: Ein farbloses aus Styrol und Divinylbenzol dargestelltes starksaures Harz von Sulfonsäuretypus, das vor dem Gebrauch durch zweimaliges Durchlaufen der 2 N Salzsäure oder 2 N Lösung von Natriumchlorid und destilliertes Wassers in die HR- oder NaR-Form übergeführt wurde. Die Korngrösse ist 50 bis 100 Maschen von Tylerschem Normalsieb.

Versuchsanordnung

Auf einer weissen Tüpfelplatte[2] versetzt man zuerst kleinste Menge vom festen Reagens mit einem Tropfen (0.04 ccm[10] mit Kapillarpipette) der Salzsäurelösung des Eisen(III)chlorides. Nach einige Minuten lang stehen gelassen, fügt man dazu einige Körnchen von Kationenaustauschharz, schüttelt danach um, und versetzt man mit einem Tropfen der Probelösung. Von einigen Minuten bis einer Stunde nach, je nach der Sulfidmenge der Probelösung, entsteht am Rande oder über das Ganze der Harzkörnchen eine grüne bzw. blaugrüne Färbung, welche mit einer Lupe von etwa zwanzigfacher Vergrösserung wohl nachweisbar ist.

Bestimmung der Bedingungen höchster Empfindlichkeit

1. Massflüssigkeit.—Eine Reihe der Massflüssigkeiten wurde aus der wässerigen Lösung des extrareinen Natriumsulfides dargestellt, deren 1 ccm 7.85 mg von Sulfide (als S^{2-}) enthielt[11]. Alle folgende Vergleichungen der Experimentalbedingungen wurden mit einer Lösung ausgeführt, deren ein Tropfen (0.04 ccm) 3.14 γ von Sulfide enthielt.

2. Schematische Darstellung von der scheinbaren Intensität der Färbung[1].—Um die Versuchsergebnisse halbquantitativ zu bestimmen, stellte der Verfasser die scheinbare Intensität der Färbung durch eine Reihe der Zahlen, d. h., die Zeichen, −, ±, (+), + usw.[12] durch 0, 1, 1.5, 2 usw. dar, und betrachtete die Gesamtsumme dieser Zahlen an allen für die Reaktion benutzten Vertiefungen von der Platte, die durch die Zahl der Vertiefungen geteilt wurde, als die scheinbare Durchschnittsintensität der Färbung. Nach diesem Verfahren kann man beispielsweise die Erfassungsgrenze der Reaktion durch die Durchschnittszahl „2" deutlich bezeichnen.

3. Die Bedingungen höchster Empfindlichkeit.—Die Resultate der Vergleichung der Empfindlichkeiten unter verschiedenen Bedingungen ausgeführter Reaktionen werden in Abb. I und Tabelle I kurz gefasst:

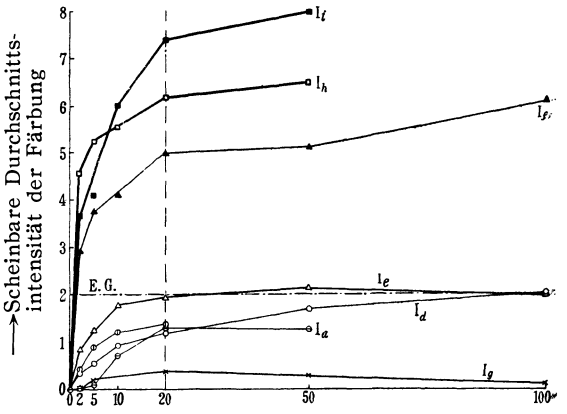

Abb. 1. Vergleichung verschiedener Bedingungen.

8) Vgl. z. B. R. W. Richardson, *Nature*, **164**, 916 (1949) sowie M. Honda, „Ionenaustausch (Ion-kôkan)" 1. Aufl. (japanisch), Tokyo (1954), S. 59.

9) Dowex 50 von verschiedenem Divinylbenzolgehalt, sowie Amberlite IR-120 und IR-112, die durch gelindes Erwärmen mit verdünnter Natronlauge und ungefähr zehnprozentiger Lösung des Wasserstoffperoxyds fast völlig entfärbt werden, wurden gleichfalls benutzt, wobei befriedigende Ergebnisse erhalten wurden. In Bezug auf die Entfärbung der gefärbten starksauren Kationenaustauschharze, vergleiche M. Honda, H. Kakihana und Y. Yoshino, „Ionenaustauschharze (Ion-kôkan Jushi)" 1. Aufl. (japanisch), Tokyo (1955), S. 48.

10) Da 0.02 ccm, der in den vorhergehenden Mitteilungen als ein Tropfen der Mikropipette verwendet wurde, für gewöhnliches mikroanalytisches Verfahren allzu klein ist, wählt der Verfasser von nun an „0.04 ccm" als ein Tropfenmenge der Mikropipette aus.

11) Die Menge von Sulfide wurde folgenderweise einfach bestimmt: Nach der Oxydation der Probelösung mit bestimmtem Überschusse der 0.1 N Massflüssigkeit des Jodes, wurde deren Überschuss mit einer Massflüssigkeit des 0.1 N Natriumthiosulfats umgekehrt titriert.

12) In Bezug auf die Zeichen, −, ±, (+) ±, ∓, ∓ usw., vergleiche Tabelle II von Fussnote 1).

TABELLE I

VERSCHIEDENE REAKTIONSBEDINGUNGEN VON ABB. I

Nr. des Expts.	Zeichen	Ordnung der Versetzung von Reagenzien und Probelösung 1.	2.	3.	4.	Anmerkungen über die Resultate*
I_a	⊖	Probelsg.**	1proz. Lsg. (3 N HCl) des *p*-Phenylendiamins	0.05 M Lsg. (6 N HCl) des Eisen-(III)chlorids	NaR	*a*
I_b	◫	Probelsg.	ungefähr 2 mg vom festen *p*-Phenylendiamin	0.05 M Lsg. (6 N HCl) des Eisen-(III)chlorids	NaR	*a*
I_d	○	Probelsg.	ungefähr 1 mg vom festen *p*-Phenylendiamin	0.1 M Lsg. (12 N HCl) des Eisen-(III)chlorids	NaR	*a*
I_e***	△	ungefähr 1 mg vom festen *p*-Phenylendiamin	0.1 M Lsg. (12 N HCl) des Eisen(III)chlorids	NaR	Probelsg.	*a*
I_f***	▲	Nadelspitzmenge**** vom festen *p*-Phenylendiamin	0.1 M Lsg. (12 N HCl) des Eisen(III)chlorids	NaR	Probelsg.	*b*
I_g***	×	Nadelspitzmenge vom festen *p*-Phenylendiamin	0.03 M Lsg. (12 N HCl) des Eisen(III)chlorids	NaR	Probelsg.	—
I_h***	□	Nadelspitzmenge vom festen *p*-Phenylendiamin	0.1 M Lsg. (12 N HCl) des Eisen(III)chlorids	HR	Probelsg.	*b*
I_i***	■	Nadelspitzmenge vom festen *p*-Aminodimethylanilin	0.1 M Lsg. (12 N HCl) des Eisen(III)chlorids	HR	Probelsg.	*c*

a: mit sehr merklichem Unterschied
b: mit grösserem Unterschied
c: ohne Unterschied
} der Färbungsintensität zwischen den verschiedenen Vertiefungen der Platte.

** Die hier benutzte Probelösung enthält 3.14 γ Sulfid (78.5 γ/ccm).
*** Etwa 5 Min nach dem Zusatz von NaR oder HR wird die Probelösung vorsichtig beigefügt.
**** Ungefähr 30 γ.

TABELLE II

EINFLÜSSE DER BEGLEITIONEN

Begleitionen	benutzter Verbindungstypus	Menge der Begleitionen	Nachweisbare Sulfidmenge	Grenzverhältnis	Anmerkungen
SO_3^{2-}	Na_2SO_3	Völlig hemmt die Reaktion.		——	Die oben erörterte Trennungsmethode ist gar nicht anwendbar
$S_2O_4^{2-}$	$Na_2S_2O_4$	〃	〃	——	〃 〃 〃
$S_2O_3^{2-}$	$Na_2S_2O_3$	〃	〃	——	〃 〃 〃
F^-*	KF	130 γ	0.16 γ	$1:4.2\times10^2$	Nur wenn die Konzentration des Fluorides weniger ist, ist dieses Verhältnis nutzbar.
$PO_4^{3-}(H_2PO_4^-)$*	H_3PO_4	1.0 mg	1.6 γ	$1:6.5\times10^2$	——
〃*	〃	8.0 mg	0.31 γ	$1:2.6\times10^5$	Nach der Trennung von S^{2-} als H_2S.
NO_3^-	KNO_3	2.1 mg	0.25 γ	$1:8.3\times10^4$	——
Fe^{2+}	Mohrsches Salz	Völlig hemmt die Reaktion.		——	Die obige Trennungsmethode ist wohl anwendbar.
〃	〃 〃	2.3 mg	0.31 γ	$1:7.4\times10^4$	Nach der Trennung von S^{2-} als H_2S.

* Zwei bzw. drei Tropfen der Eisen(III)chloridlösung werden angewendet.

Betrachtet man von diesen Ergebnissen und sorgsamen Beobachtungen der Färbungen aus, wird das folgende Verfahren als ein am besten geeignetes festgestellt:

„Man versetzt auf einer Tüpfelplatte eine Nadelspitzmenge vom festen *p*-Aminodimethylanilin mit einem Tropfen in die 12 N Salzsäure gelöster 0.1 M Lösung des Eisen(III)chlorids, und lässt sie etwa fünf Minuten lang stehen. Man fügt dann dazu einige Körnchen vom starksauren Kationenaustauschharz von HR-Form, rührt sie völlig mit einem kleinen Glasstab um. Nach einigen Minuten, versetzt man mit einem Tropfen der Probelösung, und beobachtet man die Grünfärbung, die die Harzphase nach zwanzig Minuten beinahe vollends liefert."

Hier muss man besonders das entbehrende Überschuss des *p*-Aminodimethylanilins (ebenso wie des *p*-Phenylendiamins) und die niedrige Konzentration der Salzsäure sowie des Eisen(III)-chlorids vermeiden, da diese beide die Reaktionsempfindlichkeit beträchtlich beschädigen.

Wie man aus der obigen Abbildung und dem folgenden Abschnitt ersieht, ist das *p*-Aminodimethylanilin als das Reagens für den Nachweis des Sulfides in mancher Hinsicht, z. B. grösserer Empfindlichkeit und bedeutend grösserer Sicherheit der Reaktionen, dem *p*-Phenylendiamin entschieden überlegen.

Bestimmung der Erfassungsgrenze[13]

Die Resultate der Experimente werden nach gleichem Verfahren mit dem vorhergehendes Abschnitts in Abb. 2 kurz zusammengestellt:

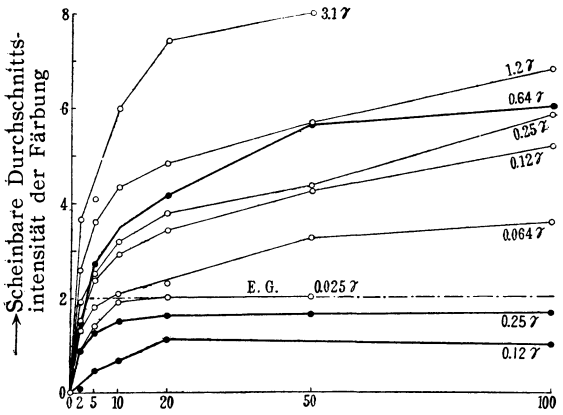

Abb. 2. Bestimmung der Erfassungsgrenze.
—○—: mit p-Aminodimethylanilin,
—●—: mit p-Phenylendiamin.

An diesen Reaktionen für den Nachweis des Sulfides (S^{2-}) wurden die Erfassungsgrenze 0.05 γ unter Grenzkonzentration $1:0.8\times10^6$, wenn man als Reagens *p*-Aminodimethylanilin verwendet, sowie dieselbe 0.3 γ unter Grenzkonzentration $1:1.3\times10^5$, wenn man *p*-Phenylendiamin verwendet, festgestellt.

13) Hinsichtlich der Bedeutung der Erfassungsgrenze, vergleiche Fussnote 2).

Trennung des Sulfides als Schwefelwasserstoff von den Begleitstoffen

Wenn die Probelösung fremde Ionen, die die Reaktion stören, enthält, ist es oft nötig die Sulfide in der Form von Schwefelwasserstoff von diesen Begleitionen zu trennen. Zu diesem Zwecke, stellte der Verfasser einen einfachen Apparat (Abb. 3) auf[14], worin Schwefelwasserstoff, der durch gelindes Erhitzen der Probelösung mit verdünnter (1 bis 4 N) Schwefelsäure über Mikrobrenner[15] sich entwickelt, in 0.01 bis 0.02 ccm von 1 N Natronlauge aufgesogen, und danach in gleicher Weise wie die obige ohne Störung der Begleitstoffe geprüft wird.

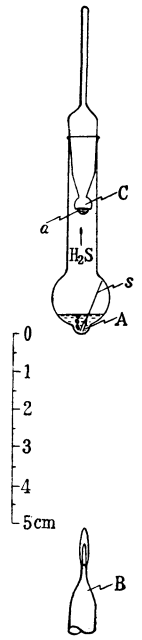

A: Gefäss von der Probelösung und verdünnter Schwefelsäure.
B: Mikrobrenner.
C: Glasknopf mit dem Absorptionsmittel (a), d. h., 0.01 bis 0.02 ccm von 1 N Natronlauge.
s: Mikrosiedestein.

Abb. 3. Apparat zur Trennung und aufsaugung des Schwefelwasserstoffs.

Die kleinste Sulfidmenge, die auf solche Weise deutlich nachgewiesen wird, ist doch 0.3 γ unter Grenzkonzentration $1:1.3\times10^5$, wenn man als Reagens *p*-Aminodimethylanilin verwendet.

Einflüsse der Begleitionen

Die Resultate der mit *p*-Aminodimethylanilin als der Vertreter dieser Art der Reagenzien ausgeführten Versuche werden in Tabelle II (S. 569) kurz gefasst:

Zusammenfassung

1. Durch einfache Anwendung von der farblosen starksauren Kationenaustauschharze wird die Empfindlichkeit der Nach-

14) Vgl. F. Feigl, „Spot Tests. I. Inorganic Applications," übersetzt von R. E. Oesper, 4. engl. Aufl., Amsterdam (1954), S. 46.

15) A. A. Benedetti-Pichler, „Introduction to the Microtechnique of Inorganic Analysis," 1. Aufl., New York (1942), S. 8.

weisreaktion von Sulfide mit *p*-Aminodimethylanilin oder *p*-Phenylendiamin bemerkenswerterweise erhöht, wobei als Reagens *p*-Aminodimethylanilin in vieler Hinsicht weit überlegen ist.

2. Die Bedingungen höchster Empfindlichkeit werden durch genaue Untersuchungen vollkommen festgestellt, und die Einflüsse der Begleitionen werden ausführlich untersucht.

3. Durch schematische Darstellung von der scheinbaren Intensität der Färbung wird eine neue halbquantitative Methode zur Bestimmung der Erfassungsgrenze sowie der Experimentalbedingungen vorgeschlagen und erfolgreich angewendet.

Zum Schluss möchte der Verfasser Herrn Prof. Dr. E. Minami für seine wertvolle Ratschläge über diese Untersuchung seinen herzlichen Dank aussprechen.

Laboratorium der analytischen Chemie,
Chemisches Institut der
wissenschaftlichen Fakultät,
Tokyo Universität, Tokyo

Mikroanalyse mit Hilfe von Ionenaustauschharzen. IV. Über den Nachweis geringer Menge des Bromides mit Schiffschem Reagens[1]

Von Masatoshi FUJIMOTO

(Eingegangen am 17. Februar 1956)

Einleitung

Wegen der bedeutend selektiven Austauschbarkeit der Farbstoffionen in die Harzphase sowie der charakteristischen starken Färbung dieser Phase, bietet die mikroanalytische Anwendung der Farbstoffionenbildungsreaktionen zur Tüpfelanalyse mit Ionenaustauschharzen eine sehr geeignte Nachweismethode[1]. Bei gegenwärtigem Versuche, wurde eine violette Färbung[2], die bei Anwesenheit von Brom mit Schiffschem Reagens in der farblosen Kationenaustauschharzphase entsteht, auf den Nachweis geringer Menge des Bromides sowie Broms wohl angewandt.

Die in dieser Untersuchung benutzten Ionenaustauschharze

Dowex 50 W-X8: Ein farbloses aus Styrol und Divinylbenzol dargestelltes starksaures Kationenaustauschharz von Sulfonsäuretypus, das vor Gebrauch durch zweimaliges Durchlaufen der 2 N Salzsäure oder 2 N Lösung von Natriumchlorid und destilliertes Wassers in die HR- oder NaR-Form übergeführt wurde. Die Korngrösse ist 50 bis 100 Maschen von Tylerschem Normalsieb.

Amberlite IR-112: Ein ebenso starksaures Harz wie Dowex 50W-X8 mit kleinerem Divinylbenzolgehalt. Dieses Harz wurde durch gelindes Erwärmen mit verdünnter Natronlauge und ungefähr zehnprozentiger Lösung des Wasserstoffperoxyds fast völlig entfärbt[3]. HR- sowie NaR-Form wurden benutzt. Die Korngrösse ist 20 bis 40 Maschen.

Überdies wurden ein farbloses starkbasisches Anionenaustauschharz, Dowex 1-X2 (Korngrösse: 50 bis 100 Maschen) sowie ein hellgelbes mittelstarkbasisches Harz, Amberlite XE-114 (Korngrösse: ungefähr 30 Maschen) auch gebraucht. Diese beide wurden vorher mit 2 N Salzsäure in die RCl-Form übergeführt.

Versuchsanordnung

Auf einer weissen Tüpfelplatte versetzt man einen Tropfen Schiffsches Reagens mit einigen Kationenaustauschharzkörnchen, rührt danach mit einem kleinen Glasstab um, und lässt sie einige Minuten stehen. Dann wäscht man die Harzkörnchen mit je drei Tropfen destilliertes Wassers zwei- bzw. dreimal aus, und dazu fügt man einen Tropfen der Probelösung, worin die Anwesenheit von freiem Brom erwartet wird. Einige Minuten nach der Mischung, entsteht, je nach der Brommenge in der Probelösung, vom Rande nach innen der Harzkörnchen allmählich eine klare violette Färbung, die man unter Beleuchtung mit einer Tischlampe und durch eine Zwanzigfachvergrösserungslupe wohl nachweisbar ist.

Bestimmung der Bedingungen höchster Empfindlichkeit

1. Massflüssigkeit.—Eine Reihe der Massflüssigkeiten des Broms wurde aus dem Brom-

1) Die dritte Mitteilung: M. Fujimoto, Dieses Bulletin 29, 567 (1956).

2) Von I. Guareschi (*Z. anal. Chem.* 52, 451 (1913)) wurde die Zusammensetzung dieses tief blauvioletten Farbstoffes als $C_{20}H_{17}Br_4N_8O$ bestimmt.

3) Vgl. M. Honda, H. Kakihana und Y. Yoshino „Ionenaustauschharze (Ion-kôkan Jushi)", 1. Aufl. (japanisch), Tokyo (1955), Zweites Kapitel, S. 48.

wasser dargestellt, dessen 1 ccm ungefähr 8 mg von Brom enthielt[4]. Alle folgende Vergleichungen der Experimentalbedingungen wurden mit einer Lösung ausgeführt, die durch genau einhundertfache Verdünnung des obigen Bromwassers mit destilliertem Wasser hergestellt wurde.

2. Schiffsches Reagens (Wässerige Lösung der fuchsinschwefligen Säure).—Nach der sorgsamen Vergleichung verschiedener Darstellungsweisen des Reagens, wurde folgenden Verfahren als das günstigste angewandt:

Man versetzt erstens 1 ccm der 0.2prozentigen Lösung vom Fuchsin („Merck" zur Analyse) mit 0.3 ccm der 6 N Salzsäure, verdünnt sie mit destilliertem Wasser bis zum ungefähr 5 ccm, und fügt man dazu unter Erschüttelung tropfenweise eine 30prozentige wässerige Lösung des Natriumbisulfites bis zur vollkommenen Entfärbung. Die so erhaltene farblose Lösung wird, nach dem Zusatz noch 0.1 ccm von 6 N Salzsäure, mit Wasser bis zum 10 ccm verdünnt, und in einem wohl verstöpselten Gefäss im Dunkeln aufbewahrt.

3. Die Bedingungen höchster Empfindlichkeit.—Die Ergebnisse unter verschiedenen Experimentalbedingungen ausgeführter Versuche stehen in Abb. 1 und Tabelle I. Dabei wurde zum Vergleich die schematische Darstellungsweise der scheinbaren Durchschnittsintensität der Färbung, die in der vorhergehenden Mitteilung[1] genau beschrieben ist, erfolgreich angewandt:

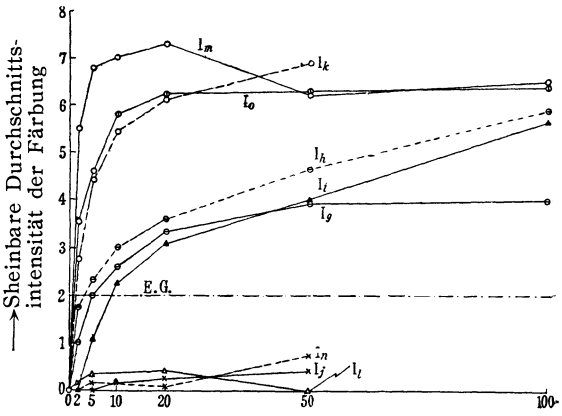

Abb. 1. Vergleichung verschiedener Bedingungen.

TABELLE I

VERSCHIEDENE REAKTIONSBEDINGUNGEN VON ABB. 1

Nr. des Experiments	Zeichen der Kurve	Inhaltsangabe des Verfahrens	Bemerkungen über Verfahren und Resultate*
I_g	—⊖—	Reagens+Dowex 50 W-X8 → (5∼6 Min**) → +Probelsg.*** (HR)	*a*
I_h	--⊖--	Reagens+Amberlite IR- → (5∼6 Min) → +Probelsg. 112 W****(HR)	*a*, *a'*
I_i	—▲—	Reagens+Dowex 1-X2 → (5∼6 Min) → +Probelsg. (RCl)	*a*, *b*
I_j	—×—	Reagens+Amberlite XE- → (10 Min) → +Probelsg. 114 (RCl in 10^{-3} N HCl)	*a*
I_k	--○--	Reagens+Amberlite IR- → (1 Std) ----→ +Probelsg. 112 W (HR)	*c*
I_l	--△--	Reagens+Dowex 1-X2 → (1 Std) ----→ +Probelsg. (RCl)	*c*
I_m	—○—	Reagens+Dowex 50 W- X8 (HR) → (1 Std) ----→ +Probelsg.	*c*
I_n	--×--	Reagens+Amberlite XE- → (1 Std) ----→ +Probelsg. 114 (RCl in 10^{-3} N HCl)	*c*
I_o	—⊘—	Reagens+Dowex 50 W- X8 (HR) → (10 Min) --→ +Probelsg.	*c*

**a*: Ohne Auswäschung der Harzkörnchen mit Wasser wird die Probelösung direkt hinzugefügt.

a': Von dem Färbungszustand der Harzphase, könnte man vermuten, dass in diesem Falle eine Art des Farbstoffsniederschlages am Rande des Harzkörnchens gebildet wird.

b: Eine violettrote Färbung, die sehr langsam in der Harzphase entsteht.

c: Die Probelösung wird in die Harzkörnchen eingetropft, die mit je drei Tropfen destilliertes Wassers dreimal ausgewaschen werden, um die Störung überschüssiges Bisulfites, das entbehren ist, völlig zu beseitigen, —— und, die dabei sehr hell himmelblau sich färben.

** Zeitdauer von Eintauchen der Harzkörnchen im Reagens.

*** Die hier benutzte Probelösung enthält 3.15 γ Brom (78.8 γ/ccm).

**** IR-112 W bedeutet „weisse" Amberlite IR-112, die vorher entfärbt wird[3].

4) Die Brommenge der Probelösung wurde jedesmals kurz vor Gebrauch folgenderweise genau bestimmt: Man versetzt ungefähr 1 g vom festen Kaliumjodid mit 2 ccm von 6 N Salzsäure in einem mit Glasstopfen versehenen Erlenmeyerkolben, und verdünnt sie mit ungefähr 30 ccm von destilliertem Wasser. Dann fügt man dazu ein bestimmtes Volumen vom Bromwasser, schüttelt sie um, und titriert das hier gebildete Jod mit einer 0.1 N. Massflüssigkeit des Natriumthiosulfates.

In Betracht dieser Resultate, wurde das Verfahren „I_m" als das am besten geeignete ausgewählt; d.h., „Etwa eine Stunde[5]) nach dem Eintauchen einiger Körnchen des Kationenaustauschharzes, Dowex 50 W-X8, von HR-Form ins Reagens, wäscht man diese mit je drei Tropfen destilliertes Wassers dreimal aus, und fügt dazu einen Tropfen der Probelösung, u.s.w."

Hier ist es vor allem bemerkenswert, dass man durch dieses Verfahren die Hinderung des im Reagens enthaltenen überschüssigen Bisulfites vollständig beseitigen kann.

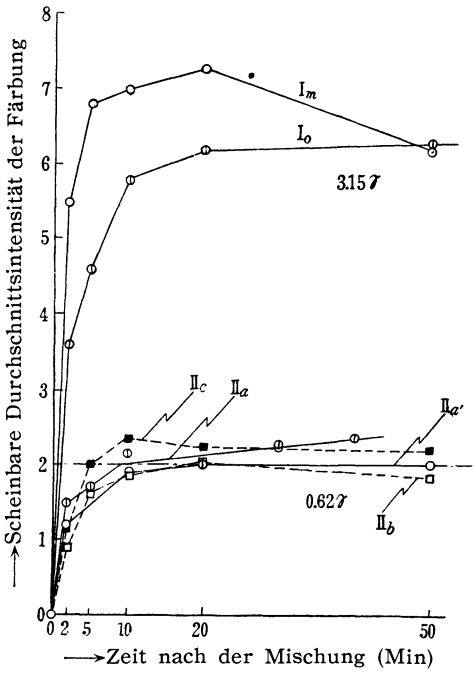

Abb. 2. Bestimmung der Erfassungsgrenze.
Kurve-II_a —◯— Reagens+HR→(10 Min) - - -→(Auswaschen)- - -→+Probelsg.,
Kurve-$II_{a'}$ —○— Reagens+HR- - -→(1 Std) - - -→(Auswaschen)- - -→+Probelsg.,
Kurve-II_b - -□- - Reagens+HR-→(5-6 Min) - - -→(Auswaschen)- - -→+Probelsg., und
Kurve-II_c - -■- - Reagens+NaR-→(5 Min) - - -→(Auswaschen)- - -→+Probelsg..

Bestimmung der Erfassungsgrenze

Vom in Abb. 2 dargestellten Resultate aus betrachtet, wurde die Erfassungsgrenze an dieser Reaktion für Brom als 0.62γ unter Grenzkonzentration $1:6.4\times10^4$ festgestellt, wobei das Harz von NaR-Form dem von HR-Form ein wenig überlegen ist, und zwar das Eintauchen des Harzes im Reagens nur um etwa fünf Minuten wünschenswerter ist (Vgl. Fussnote 5)).

5) Wie im Falle der Erfassungsgrenzbestimmung, ist es dann noch günstiger, etwa fünf Minuten nach dem Eintauchen ins Reagens die Harzkörnchen mit Wasser auszuwaschen, falls die Bromgehalt der Versuchslösung so gering ist, dass selbst die hellhimmelblaue Färbung der Harzphase die Unterscheidung der hellviolette Färbung des Farbstoffs beträchtlich schwierig macht.

Bestimmung der Erfassungsgrenze für Bromid nach der Oxydation des Bromides zum Brom

1. Massflüssigkeit des Bromides wurde aus der wässerigen Lösung des extrareinen Kaliumbromides, deren 1 ccm 10.24 mg von Bromid (als Br) enthielt[6]), vorbereitet.

2. Entwicklung des Broms und seiner Prüfung.—Um die Bromide durch gegenwärtige Tüpfelmethode nachzuweisen, wurde ein einfacher Apparat (Abb. 3) aufgestellt:

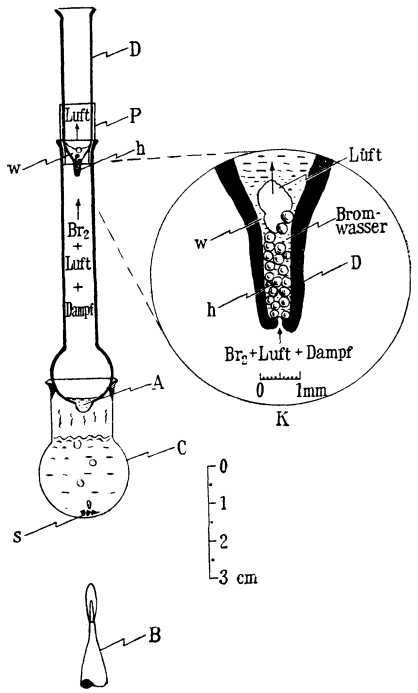

Abb. 3. Apparat zur Entwicklung und Prüfung des Broms.
A: Gefäss zur Oxydation der Probe, B: Mikrobrenner, C: Mikrowasserbad, D: Gefäss zur Aufsaugung und Prüfung des Broms, P: Vinylschlauch, h: das Reagens adsorbierte Kationenaustauschharz, w: destilliertes Wasser, s: Mikrosiedestein (Glassplitter); und K: Vergrössertes Bild des wesentlichen Teils des Apparates.

In einem Mikrokolben (A) werden alle Bromide in der Probelösung in weniger als 20 Sekunden durch Erwärmen mit einigen Tropfen eines Gemisches von 1 Teil gesättigter wässeriger Lösung des Kaliumbichromates und 1 Teil konzentrierter Schwefelsäure zu freiem Brom sehr glatt oxydiert, und hierbei erzeugter Bromdampf wird

6) Die Menge des Bromides wurde mit 0.1 N Massflüssigkeit des Silbernitrates nach Mohrschem Verfahren genau bestimmt.

7) Hierbei ist es empfehlenswert, die Entwicklungsgeschwindigkeit des durch Harzschicht durchgelassenen Dampfs bis auf alle Sekunden eine Blase einzuschränken, da sonst wegen der Temperatursteigerung des in D enthaltenen destillierten Wassers die Harzkörnchen schnell dunkelblau gefärbt werden.

mit Luft und Dampf zusammen durch die Spitze von Gefäss D in die Schicht von den in einigen Tropfen destilliertes Wassers (w) eingetauchten Harzkörnchen (h) eingeleitet[7]. Nach dem Erwärmen muss man das Gefäss D vom Mikrokolben schnell wie möglichst wegnehmen, weil anderfalls wegen Temperaturerniedrigung des Apparates destilliertes Wasser (w) in den Mikrokolben (A) rasch zurück eingezogen wird. Nach etwa 10 Min, beobachtet man die Färbung der Harzkörnchen (h) mit einer Lupe.

Die kleinste Menge auf solche Weise nachweisbares Bromides war jedoch 1.2 γ unter Grenzkonzentration $1:1\times10^5$.

Einflüsse fremder Anionen

Die Resultate der durch Oxydation mit Chromsäuregemisch ausgeführten Untersuchungen werden in Tabelle II kurz gefasst:

TABELLE II

EINFÜLSSE DER BEGLEITIONEN

Begleitionen	benutzter Verbindungstypus	Menge der Begleitionen	Nachweisbare Bromidmenge	Grenzverhältnis
F^-	KF	1.4 mg	4 γ	$1:3.5\times10^2$
Cl^-	KCl	14.2 mg	1.6 γ	$1:8.9\times10^3$
J^-	KJ	102 mg	2.4 γ	$1:4.3\times10^4$
SCN^-	NH_4SCN	2.3 mg	12 γ	$1:1.9\times10^2$
S^{2-}	Na_2S	314 γ	4 γ	$1:7.9\times10$
NO_2^-	$NaNO_2$	266 γ	12 γ	$1:2.2\times10$

Zusammenfassung

1. Durch mikroanalytische Anwendung der mit Schiffschem Reagens aufgesogenen farblosen starksauren Kationenaustauschharze wird eine empfindliche und selektive Nachweismethode für geringe Menge des Broms sowie Bromides festgestellt, wobei durch völliges Auswaschen der Harzkörnchen mit destilliertem Wasser die Reaktionsstörung von entbehrendem Überschusse im Reagens enthaltenes Bisulfites glücklicherweise vollständig beseitigt wird.

2. Zur Oxydation des Bromides zu freiem Brom wird ein einfacher Apparat aufgestellt, damit man alle Bromide in der Probelösung in der Form von Bromwasser beinahe quantitativ ansammeln und auf der Stelle mit der obengenannten Harzkörnchen direkt prüfen kann, und die Einflüsse fremder Anionen werden auch mit Hilfe dieses Apparates ausführlich untersucht.

Zum Schluss möchte der Verfasser Herrn Prof. Dr. E. Minami für seine vielen wertvollen Ratschläge bei dieser Untersuchung seinen herzlichen Dank aussprechen.

Laboratorium der analytischen Chemie,
Chemisches Institut der
wissenschaftlichen Fakultät, Tokyo
Universität, Tokyo

*Studies on the Graphitization. I. Changes of Crystallinity, Diamagnetic Susceptibility and Electrical Conductivity in the Process of Graphitization**

By Hideo AKAMATU, Hiroo INOKUCHI, Hiroshi TAKAHASHI and Yoshio MATSUNAGA

(Received February 21, 1956)

Introduction

Graphites are made by heat treatments of carbonaceous materials such as soots or cokes. It is widely known, however, that even under the similar conditions of heat treatment the degree of graphitization varies according to the sort of starting materials. In an extreme case, "non-graphitizable" carbons are known[1]. It is frequently said in the manufacturing process, that soots are less easy to be graphitized than pitch cokes, and among the cokes, petroleum-cokes are more facile than coal-tar-cokes. On the other hand, some questions arise when we intend to define the degree of graphitization. This is due to the fact that the graphitized materials are in multi-crystalline states and their physico-chemical properties can not be determined by their crystallinity alone, but depend upon functions of the system as a whole.

In this paper, the degree of graphitization has been studied from the viewpoints of crystallinity, magnetic susceptibility and

* The principal part of this paper was presented at the 7th annual meeting of the Chemical Society of Japan on April 1954 at Tokyo, excepting the data by X-ray. The photographic measurements were revised by a Geiger counter X-ray spectrometer.

1) R.E. Franklin, *Compt. rend.*, 232, 232 (1951).

electrical conductivity, and comparison will be made among various starting materials concerning their tendency to graphitization.

Materials and Heat Treatments

The following substances were selected as the starting materials of graphitization; they are classified into three groups.

I. Pitch cokes:
  I-1. Petroleum-coke (Great Lake Co. U.S.A.)
  I-2. Coal-tar-coke (Yahata Seitetsu Co. Japan)
II. Carbon blacks:
  II-1. "Thermax" (Thermatomic Carbon Co. U.S.A.)
  II-2. "Kosmos-15A" (United Carbon Co. U.S.A.)
  II-3. "Tokyo Gas" (Tokyo Gas Co. Japan)
III. Simple organic compounds:
  III-1. Violanthrone ($C_{34}H_{16}O_2$)
  III-2. Polyvinyl chloride

All the commercial carbonaceous products (from I-1 to II-3) were heated in vacuum at several temperatures from 1000 to 2000°C in an electric furnace of Arsem type. The duration at a peak temperature was about ten minutes. Violanthrone and polyvinyl chloride were treated preliminarily at 600°C in the ordinary atmosphere and thereafter the carbonaceous substances obtained were heated in the same way as mentioned above. The heat treatments at 2500 and 3000°C were made in an electric furnace of which the principle nearly resembles that of the industrial graphitizing furnace excepting the fact that the dimension was a laboratory scale[2]. The duration at a peak temperature was about five minutes. This procedure was made in Ohmachi manufactory of Showadenko Co., to whom our thanks are due.

X-Ray Measurements

Changes in the inter-layer spacings, $d(002)$, as the function of the heat treatment, were carefully observed. A Geiger counter X-ray spectrometer (Norelco) with copper anticathode was used. The diffraction maxima were estimated by referring to that of lead nitrate. For this purpose, (220), (211), (210) and (200) spacings of lead nitrate were used, the corresponding values of 2θ were 32.211°, 27.849°, 25.390° and 22.670° for CuK_α radiation respectively. These values had been calibrated referring to a standard quartz specimen. It has been known that in the case of low graphitized carbons, the diffraction maxima do not give directly the true inter-layer spacings[3]. Further corrections are necessary for the transformation of recorded diffraction curve into $|F^2|$ curve. This procedure was made by using the correction factors given by Ruston[4]. In the present case, however, these correction factors did not become large even in the specimens treated at lower temperatures, and they were negligibly small for the specimens treated at higher temperatures.

Following Franklin[5], in the graphitic carbons the graphite-like layers are grouped in parallel packets within which there is a random distribution of orientated and disorientated layers. In the orientated layers the inter-layer spacing is constant and equal to that of graphite 3.354 Å; in the disorientated layers the inter-layer spacing is equal to that in the non-graphitic carbons 3.44 Å, and there is a spacing of intermediate value among the first disorientated layers on either side of each orientated group.

By this formula, the apparent inter-layer spacing is in reality a mean value which depends upon the proportion of the number of disorientated layers to the total number of layers. Franklin has proposed an empirical equation which is expressed as

$$d = 3.440 - 0.086(1 - p^2),$$

where d is the mean inter-layer spacing observed and p is the fraction of the randomly disorientated layers. A similar formula has been concluded from a more theoretical point of view by Houska and Warren[6]. The value of p can be interpreted as a measure of the degree of non-graphitization, from the above point of view. The observed values of the inter-layer spacings and the p-values are shown in Table I.

Table I

Inter-layer spacings and corresponding p-values of graphitic carbons

Starting material	Heat-treatment temperature (°C)	Inter-layer spacing (Å)	p-value	$\frac{I(112)}{I(110)}$
Petroleum-coke	1550	3.413	0.828	0
	2040	3.385	0.600	0.40
	2500	3.365	0.358	0.62
	3000	3.351	0.000	0.73
Coal-tar-coke	1900	3.426	0.915	0.47
	2500	3.361	0.285	0.69
	3000	3.353	0.000	0.75
Thermax	1740	3.433	0.957	
	1960	3.423	0.896	
	2500	3.379	0.535	0.39
	3000	3.376	0.507	0.39
Kosmos	1960	3.428	0.900	0
	2500	3.422	0.890	0.12
	3000	3.422	0.890	0.18
		3.356	0.167	
Violanthrone	1520	3.436	0.976	
	1720	3.423	0.896	
	1960	3.420	0.876	
	2500	3.402	0.749	0.33
	3000	3.389	0.640	0.34
Polyvinyl chloride	1680	3.440	1.000	
	2020	3.428	0.925	0
	2500	3.384	0.586	0.40
	3000	3.371	0.441	0.45

2) S. Yamaguchi, T. Noguchi, S. Hatta and M. Hino, *Carbon*, 2, 239 (1952).
3) R.E. Franklin, *Acta Cryst.*, 3, 107 (1950).
4) W.R. Ruston, *Fuel*, 31, 52 (1952).
5) R.E. Franklin, *Acta Cryst.*, 4, 253 (1951).
6) C.R. Houska and B.E. Warren, *J. Appl. Phys.*, 25, 1503 (1954).

The crystallite size determination was made from the broadening of X-ray diffraction. The X-ray spectrometer profiles were used for this purpose. In order to get the broadening β of the line due to the finite size of the crystallites, the experimentally observed width B was corrected for the instrument width b. The instrument width was obtained from the lines of reference quartz powder (10–20 micron), and the correction curve of β/B against b/B for the X-ray spectrometer line breadths was used[7].

The crystallite dimensions were calculated by the formula,

$$L=K\lambda/\beta\cos\theta,$$

where L is the mean dimension of the crystallite perpendicular to the set of planes giving rise to the line at the glancing angle θ, λ is the wave length of the X-ray and K is a shape factor. K is nearly 0.9 for ordinary three-dimensional lattice, provided β is defined as the half-maximum line breadth, while 1.84 for two-dimensional lattice[8].

The L_c-dimension, the thickness of the parallel packets of layers, was obtained from (002) line using $K=0.9$, while the L_a-dimension, the width of the graphite-like layers was obtained from (hk0) lines. Because the low graphitized carbons have the tarbostratic structure, they give nearly the two-dimensional reflections. In such a case, the L_a-dimension was obtained from (10) line using $K=1.84$. However, when the graphitization proceeded there appears the cross lattice (101) reflection, overlapping with the (100) line on the large angle side of the latter. This makes it difficult to estimate the half-width value of (100). Therefore, for highly graphitized specimens, (110) reflection was used for the determination of the L_a-dimension. Furthermore, there occurs some question concerning the value of the shape factor.

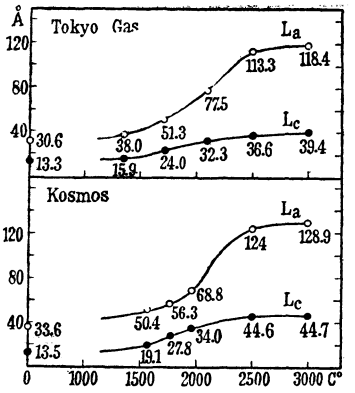

Fig. 1a. Growth of crystallites in graphitized carbon blacks.

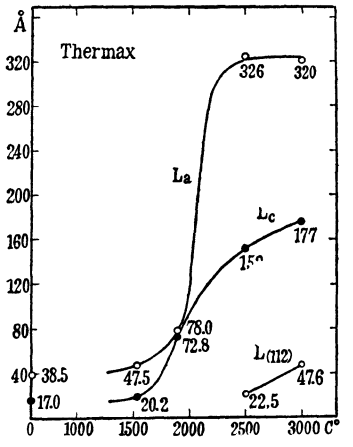

Fig. 1b. Growth of crystallites in graphitized carbon blacks.

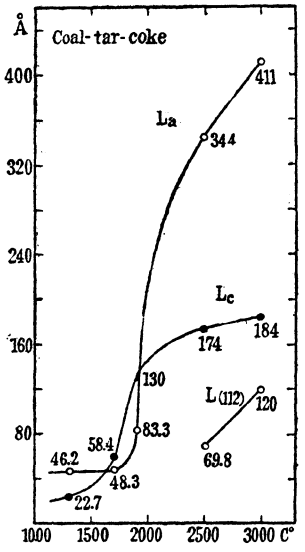

Fig. 2a. Growth of crystallites in graphitized pitch-cokes.

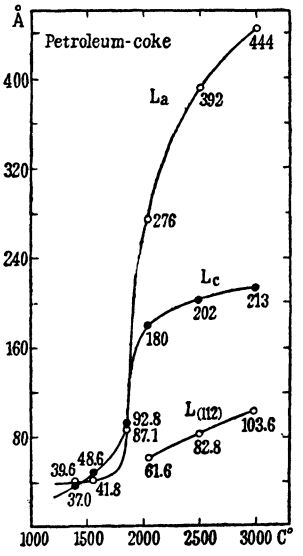

Fig. 2b. Growth of crystallites in graphitized pitch-cockes.

7) H.P. Klug and L.E. Alexander, "X-Ray Diffraction Procedures" (1954), p. 509.

8) B.E. Warren, *Phys. Rev.*, **59**, 693 (1941).

When the graphitization has proceeded, and the cross lattice reflection (101) and (112) has appeared, the structure of a crystallite consists of a stack of parallel planes composed of a random mixture of groups of perfectly orientated planes and groups of completely disorientated planes; the former gives the three-dimensional reflection while the latter gives the two-dimensional reflection. In such a case, K must be some average value between 0.9 and 1.84. Concerning the shape factor, we refer the p-value in the preceding section, and used $K=0.9+(1.84-0.9)p$. Another method is obtained by referring the intensity of (112) and (110) reflection. When the graphitization has been completed, the ratio of intensity of (112) to that of (110) is 1.61. Therefore in an intermediate state,

$$K=1.84-(1.84-0.9)\left(\frac{I(112)/I(110)}{1.61}\right),$$

can be used. The values of I(112)/I(110) are shown in Table I. The observed values of the crystallite dimensions are shown in Fig. 1, Fig. 2 and Fig. 3 as the function of the temperature of heat treatment.

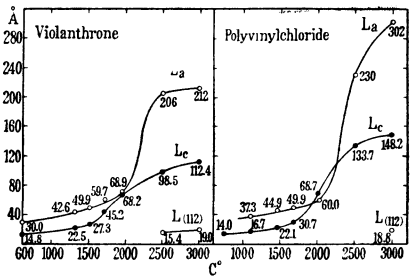

Fig. 3. Growth of crystallites in graphitized violanthrone- and polyvinyl chloride-base carbons.

Magnetic Measurements

The magnetic susceptibility at the room temperature has been measured by the Gouy method. The details of the method have been presented in a preceding paper from our laboratory[9].

To remove ash impurities which might have some effect on the magnetic susceptibility, each specimen was subjected to heating with hydrofluoric acid in a platinum crucible until the latter was evaporated up, then boiled with hydrochloric acid and finally washed with water throughly. Even after the purification, it was found in several specimens that a trace of ferromagnetic impurity still persisted, as a result the apparent susceptibility varied,depending on the magnetic field strength applied. In such a case, the ferromagnetic effect was calibrated by the formula,

$$\chi^*=\chi_\infty+2\sigma/H,$$

where χ^* is the apparent susceptibility observed, H is the field strength applied, σ is the saturation intensity of the ferromagnetic impurity, and χ_∞ is the susceptibility proper to the sample itself.

9) H. Akamatu and Y. Matsunaga, This Bulletin, 26, 364 (1953).

When we plot the mass susceptibility against the temperature of heat treatment, we find that the features vary widely according to the sort of starting materials, especially of the groups. However, when we plot them as a function of the L_a-dimension, it is found that all points mount on nearly one curve, irrespectively of the sort of starting materials. This is shown in Fig. 4.

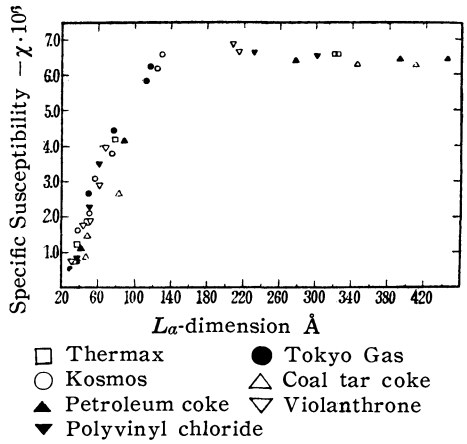

Fig. 4. Magnetic susceptibilites of graphitic carbons.

For comparison with the graphitized carbon, the magnetic susceptibility of natural graphite has been measured. Concerning the latter, there are many reports in the literature of the subject; however, they have given rather various values. The reason is presumably due to some contaminations in the graphite. In the present investigation, the purification procedure was made of two steps, e.g., in the first step specimens were subjected to alkali fusion with potassium hydroxide and carbonate at 300–400°C, and then accompanied by boiling with hydrochloric acid; in the second step the specimens which had been subjected to the above treatment were further treated with hydrofluoric acid and hydrochloric acid consecutively in the same manner as mentioned above.

The results are shown in the fourth column of Table II. The observed values are unexpectedly small; furthermore, the values for flake graphites are rather lower than those of amorphous graphites. This is due to the fact that when a graphite specimen is packed into the sample tube for magnetic measurement, the plate-like crystals take a preferred orientation with planes perpendicular to the axis of the sample tube; as a result, the measured value of susceptibility decreases, since in this direction the susceptibility has the least value. To avoid the orientation effect, the graphite powder diluted with γ-alumina was used. As an example, the mean gram susceptibility of the mixture of Korea flake graphite and alumina as a function of weight per-centage of graphite is shown in Fig. 5. A good linearity is found in the range of the lower concentration. This shows that the orientation effect of graphite crystals was almost cancelled.

The values in the last column in Table II are those which were obtained by using the mixture of graphite and alumina. Comparing those values to that in the preceding column, the difference, consequently the orientation effect, is large in the case of flake graphite, whilst in the case of amorphous graphite the effect is negligible.

TABLE II

GRAM SUSCEPTIBILITY OF NATURAL GRAPHITE

Sample	State of purification*	Ash content (%)	Gram-susceptibility in $-\chi\cdot10^6$. From graphite alone	From mixture with alumina
Korea (flake)	Raw material	1.72		
	I-Step	0.02	5.07	6.22
	II-Step	0.07	5.38	
Korea (amorph.)	Raw material	5.47		
	I-Step	0.30	5.90	
	II-Step	0.28	5.95	6.12
	Without alkali fusion	0.36	5.77	
Ceylon (flake)	Raw material	0.74		
	I-Step	0.05	5.14	6.10
	II-Step	0.01	5.51	6.34
	Heated up to 3000°C			6.08
Madagascar (flake)	Raw material	19.85		
	I-Step	0.18	4.97	6.54
	II-Step	0.08		6.69
Mexico (amorph.)	Raw material	5.85		
	I-Step	0.14	5.57	
	II-Step	0.14	5.64	5.65

* Raw materials are commercial products which have been purified in the commercial sense.

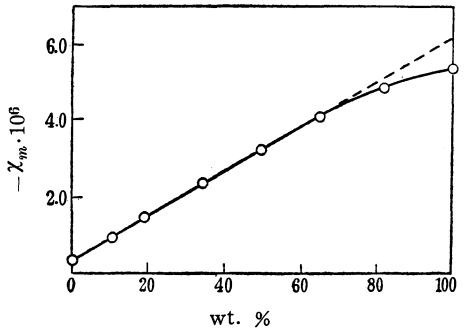

Fig. 5. The gram susceptibility of the mixture of graphite (Korea, flake) and alumina, against weight percentage of graphite.

It is seen in Table II that further purification makes increase of the diamagnetic susceptibility in every case; however, the difference is rather small. From this and the smallness of ash content, the observed value is presumably near the limiting value of the susceptibility of each specimen. In conclusion, the susceptibility of natural graphite can be assumed -6.4×10^{-6} in its good crystal form, and this agrees with the limiting values of the graphitized carbons.

Electrical Resistivity Measurements

The electrical resistivity at the room temperature has been measured by the usual potential drop method. Since the specimens are in powder form, the measurements were made under compressed states up to 200 kg/cm² in a bakelite cylinder. A nearly linear relationship was obtained between the resistivity and the reciprocal of the pressure, from which, by extrapolation, the value at the infinite compression was read as the resistivity of each specimen. The observed values are shown in Fig. 6 as the function of the L_α-dimension.

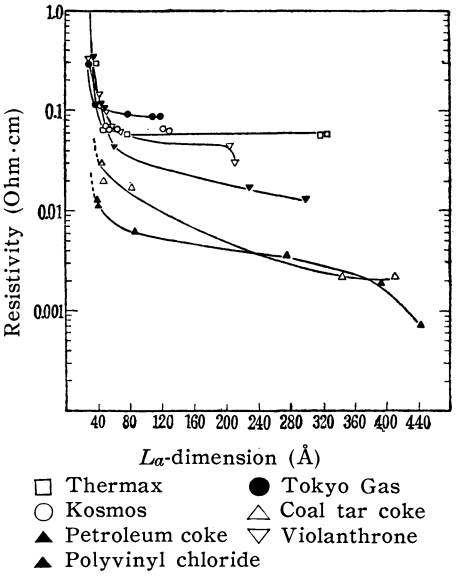

Fig. 6. Electrical resistivities of graphitic carbons.

Discussion

From the results of X-ray measurements, it has been found that the development of crystallinity by heat-treatment varies remarkably among the groups of the starting materials. This is seen from the growth of crystallites as well as the change of the inter-layer spacing or p-value.

The growth of crystallites proceeds with the most facility in pitch-cokes, and so far as this point is concerned, a large difference can not be found between petroleum-coke and coal-tar-coke. In both specimens, p-values tend to zero when they have been treated at 3000°C. This means that in this state disorientated layers have been almost entirely transformed to orientated layers. However, the intensity ratio I(112)/I(110) was yet 0.75; therefore, the perfect graphite lattice has not been completed.

In the case of carbon blacks, the growth of crystallites is slow and limited. This is due to the fact that carbon black is made

of individual particles and in each particle the growth of crystallites is limited by its particle size. The final diameters of crystallites are 118 Å, 129 Å and 320 Å in "Tokyo Gas", "Kosmos" and "Thermax" respectively, while their particle sizes estimated by electron microscopy are 400 Å, 400–500 Å and 2000-4000 Å respectively. Furthermore, the crystallinity is low; hence, the p-values were still large even in the state which was subjected to the heat-treatment at 3000°C. This might be partly due to the fact that for promoting the transformation of disorientated layers to orientated layers, the growth of crystallites in advance to a certain large size is needed. But even in the case of "Thermax" which has a pretty large dimension, the p-value is still large compared with pitch-cokes.

In the case of "Kosmos" treated at 3000°C, it was found that the (002) diffraction maximum was divided into two peaks. This is shown in Table I. It might be assumed that this carbon is made of two parts in itself in a heterogeneous manner; one is completely graphitizable and the other is less graphitizable and the graphitization proceeded suddenly in the former at this temperature.

Violanthrone is a typical polycyclic aromatic compound and polyvinyl chloride is made of linear chain molecules. No remarkable difference could be found between those materials in the general feature of graphitization. However, in the violanthrone-base carbon the growth of crystallites seems to have been attained to a saturation value already at 2500°C, while in the polyvinyl chloride-base carbon the growth is proceeding even after the heat-treatment at 3000°C. So far as this point is concerned, the former is rather like carbon black and the latter is like pitch-coke. In the case of violanthrone, all molecules themselves are stable and might become as nuclei for the aromatic condensation, and so many graphite-like layers would arise from the outset, but the development of them by the expense of nonorganized carbons, which are less in number in this case, would be rather obstructed. In order to develop each crystallite to a large one, it is desirable that there occur a small number of nuclei and a large number of nonorganized carbon atoms. This is presumably the case of polyvinyl chloride and pitch-cokes.

Since graphite is a substance having a large value of diamagnetic susceptibility, it is of interest to see how it changes the magnetic property during the process of the graphitization. The diamagnetic susceptibility increases with the size of crystallites, and this is most impressive when we plot the gram susceptibilities against the L_a-dimensions as shown in Fig. 4.

It is a noteworthy fact that all the values obtained lie on a curve irrespective of the sort of starting materials. This result agrees with the conclusion of Pinnick[10] who studied two types of carbons, while it disagrees with the result of Wynne-Jones, Blayden and Iley[11], whose curves for three types of carbons do not overlap but are shifted somewhat relative to one another along the horizontal axis. On the other hand, when we plot the gram susceptibilities against the L_c-dimensions we obtain the various curves, which do not overlap with each other, according to the sort of materials. Consequently, the present result shows that the gram susceptibility is principally determined by the value of L_a alone, and does not depend upon any other second-ordered structures in polycrystalline states. This is rather a natural conclusion when we remember the origin of the magnetism.

This result is useful to understand that the crystallite sizes obtained by the X-ray method are self-consistent with each other. The crystallite sizes estimated by the X-ray method are not necessarily in agreement with each other among the investigators. This is perhaps due to the difference in the method of calibration, apparatus and other factors. The characteristic feature of the curve of the magnetic susceptibility will be useful to make the adjustment for the differences in crystallite sizes among the investigators. Thus, in our result the rapid increment of the susceptibility begins at 30 Å and attains to the saturation value at about 130 Å, whilst in the work of Pinnick the corresponding range is 50—150 Å. Therefore, our crystallite sizes are shifted to somewhat lower values than that of Pinnick.

In a previous work[9], we have studied the diamagnetic susceptibility of polycyclic aromatic hydrocarbons. The large values of the diamagnetism of those compounds are due to the anisotropic components which are due to the closed-shell diamagnetism of the London type. This diamagnetic anisotropy increases with increasing the number of benzene rings. However, their magnetic properties are rather structure-sensitive, and even the paramagnetic contributions are found[12]. In such a case, the diamagnetic susceptibility becomes smaller than the ex-

10) H.T. Pinnick, *Phys. Rev.*, **94**, 319 (1954).
11) W.F.K. Wynne-Jones, H.E. Blayden and R. Iley. *Brennstoff-Chem.*, **33**, 268 (1952).
12) Y. Yokozawa and I. Tatsuzaki, *J. Chem. Phys.*, **22**, 2087 (1954).

pected value. Thus, $n\Delta K_b$ gives the upper limit of the molar anisotropy, where n is the number of aromatic rings and ΔK_b is the diamagnetic anisotropy of benzene (-54×10^{-6}). However, as pointed out by Mrozowski[13], the large values of graphitized carbons can not be explained by this London-type diamagnetism alone, because the susceptibility converges to -1.0×10^{-6}, when the molecule becomes a large one, and when it is expressed in the mass susceptibility per gram*.

Marchand[14] has observed the temperature dependence of the magnetism of graphitized carbons in the range of $-200-1000$°C. He found that the gram susceptibility χ, is nearly constant when the L_a-dimension is small such as 36 Å, but it becomes dependent upon the temperature when L_a becomes larger than 45 Å and when χ at the room temperature becomes above -2×10^{-6}. The susceptibility increases with decreasing the temperature and tends asymptotically to a limiting value, which is characteristic for each carbon and becomes larger with the increment in L_a. The whole behaviour is similar to that of graphite which was found by Ganguli and Krishnan[15] and interpreted as Landau diamagnetism due to the two-dimensional free electron gas having a low degeneracy temperature. The result of Marchand may be understood when we suppose the degeneracy temperatures of carbons are higher than that of graphite.

Our result, Fig. 4, corresponds to the points on Marchand's curves at the room temperature. They are in good agreement with each other. In conclusion, the large values of diamagnetic susceptibility of graphitized carbons are due to the anisotropic components, which are partly contributed from the closed-shell diamagnetism of London-type and mainly from the free electron gas diamagnetism of Landau-type. The former is related to the ground states and the latter is due to the exited states of electrons. However, a question is left how in the relatively small range of 30—130 Å of L_a the Landau diamagnetism rapidly takes place. It is of interest, at least, to see the rapid change in electronic states of graphitized carbons in this range of L_a.

However, the values of the gram susceptibility itself can not be used for the reference of the graphitization degree, as they converge so rapidly to a saturation value of graphite.

Whilst the magnetic property is determined solely by the size of the molecular plane regardless of the sort of carbon, the apparent electrical resistivity remarkably depends on the starting materials. This can be see in Fig. 6.

The general feature of the electrical resistivity of carbon at room temperature as a function of the heat-treatment has been well illustrated and discussed by Mrozowski[13]. The resistivity decreases very rapidly with increasing the temperature of heat-treatment up to about 1000°C, but above this temperature the decreasing stops and a flat plateau is generally observed. So in the present investigation, the resistivity decreases rapidly with increasing L_a in the region where L_a is small, but it comes to have a nearly constant value when L_a becomes above 40 Å. It is noteworthy that the plateau is formed at the L_a-demension where the Landau diamagnetism begins to take place. The values of resistivity at the plateau vary among the sorts of carbons. The graphitized pitch-cokes have less resistivity than the graphitized carbon blacks, and violanthrone- and polyvinyl chloride-base carbons have intermediate values. In the case of carbon blacks, each plateau is a completely flat one, while in the case of pitch cokes the resistivity gradually decreases as increase in L_a even in the range of the plateau formation. Concerning this behaviour, the polyvinyl chloride-base carbon is like pitch coke, and the violanthrone-base carbon is rather like carbon black again, as mentioned in the above discussion on the X-ray analysis. So far as the crystallite dimension is concerned, the graphitized "Thermax" at 3000°C is not different from the graphitized pitch-coke "Yahata" at 2500°C concerning both L_a and L_c, and the resitivity of the former is still twenty-five times as high as the latter.

All of those facts suggest that not only the crystallites dimension but also the higher-ordered structures of multi-crystalline states are reflected on the resistivity. Carbon black is made of particles, furthermore, in each particle the crystallite micelles aggregate in such a manner that they are independent of each other. On the other hand, pitch cokes are made of a continuous massive material in which the crystallite micelles are bridged with cross-linkages, such as C-C valence bonds, to neighbors. The difference in the mode of the aggregation between those two

13) S. Mrozowski, *Phys. Rev.*, 85, 609 (1952).

* When a molecule becomes large, the increment in number of carbon atoms is two per ring, and the limiting value of gram susceptibility is
$-\chi\cdot10^6=n(2\times3.36+\Delta K_b/3)\div n(2\times12)=1.0$ (cf. (9)).

14) M.A. Marchand, *Compt. rend.*, 238, 1645; 239, 1609 (1954).

15) N. Ganguli and K.S. Krishnan, *Proc. Roy. Soc.*, A177, 168 (1941).

groups has been well illustrated in the rate of wet oxidation of them[16]. This difference will persist or even be exaggerated in the graphitized state. In consequence, conserning the resistivity, the contact resistance or boundary scattering will be high in the case of carbon black, but it will be less in the case of pitch coke because of the transparent linkages between crystallites.

To explain the formation of the plateau, Mrozowski has assumed that the expected decrease of the resistivity due to growth of crystallites is compensated by a decrease in concentration of excess electrons or holes, which are responsible for the rapid decrease in the resistivity before the formation of a plateau, and the presence of which is due to the peripheral atoms which happen not to be bonded to neighbouring crystallites. This explanation may be applicable to the case of pitch cokes, in which the recombination among atoms at the peripheries of plane molecules will continue as long as the linkages remain, and the chance of occurrence of excess electrons or holes will persist. The decrease in the resistivity in a gradual manner in the region of a plateau may be understandable. But, such a flat plateau as observed in the graphitized carbon black is rather incomprehensible.

It has been found from the small angle scattering of X-ray that the fine structures are different between the graphitized carbon blacks and pitch cokes. In the graphitized carbon blacks, microporous parts arose and developed following graphitization. We are inclined to suppose that the expected decrease of the resistivity due to growth of crystallites is compensated by decrease in the number of contact points between crystallites due to the development of microporous parts. Further studies on the fine structures will be presented in the second part of this work.

16) H. Akamatu, H. Takahashi and K. Tamaru, This Bulletin, **21**, 27 (1951).

Summary

Three sorts of carbon black, two sorts of pitch coke, violanthrone, and polyvinyl chloride have been subjected to heat treatment up to 3000°C. Changes in crystallinity during the graphitization have been studied by X-ray referring to inter-layer spacings and growth of crystallites. It was found that pitch cokes are graphitized with more facility than carbon blacks, and the other two substances are intermediate.

The magnetic susceptibility is determined solely by the size of plane molecules (L_a) irrespective of the sort of carbons, and tends to a limiting value -6.5×10^{-6} per gram which is coincident with the value of natural graphite, when L_a grows above 130 Å.

The electrical resistivity decreases as growth of crystallites, but there is a region when L_a becomes above 40 Å, where it tends to a nearly constant value for each carbon. Those values are different among the groups of carbons, and graphitized pitch cokes have less resistivity than graphitized carbon blacks. It was discussed that fine structures of multi-crystalline states are reflected on the resistivity.

This work is a part of the research project for carbon supported by the 117 committee in Nippon Gakujutsu Shinkokai, and the expense has been defrayed in part from a grant given by the Ministry of Education, for which the authors' thanks are due.

Department of Chemistry, Faculty of Science, The University of Tokyo
Hongo, Tokyo

Magnetochemical Study of Dianthraquinone and its Thermochromism in the Solid State

By Yoshio MATSUNAGA

(Received February 23, 1956)

Introduction

Harnik and Schmidt[1] analysed the crystal structure of dianthraquinone, and established the fact that steric limitations prevent the molecule from being planar, and the distortions within the molecule are distributed over several bonds. In the first place, with the intention of ascertaining the effect of non-coplanarity of aromatic net plane on the delocalization of π-electrons, we examined the diamagnetic susceptibility of dianthraquinone and compared it with those of some related compounds.

The reversible color change on heating (thermochromism) of a solution of dianthraquinone has been of great interest, since Meyer[2] synthesized this compound about fifty years ago. He also reported that this compound turns from lemon yellow to green, if it is heated to about 170°C in the solid state. But in this case, recrystallization or boiling with alcohol was necessary to the perfect recovery of the original color. Grubb and Kistiakowsky[3], and Theilacker and his associates[4] performed spectroscopic investigations, and concluded that the thermochromism in solution is due to the transition between isomeric forms which are in a thermal equilibrium with each other. The same absorption spectrum was also found by Hirshberg and Fischer[5], when a solution was irradiated with ultraviolet light at low temperatures. As to the nature of the colored form, Schönberg proposed a betaine-like structure[6] and in the later paper an increase of planarity of the molecule[7], while many other investigators[3,4,8,9] suggested a biradical or long-life triplet state. Only magnetic measurements will make it possible to decide whether or not the colored excited form represents a biradical. But two reports which have already appeared are unfortunately in disagreement with each other. Nielsen and Fraenkel[9] reported that paramagnetic resonance absorption can be detected in the green colored solution and solid specimen heated above 265°C; nevertheless, Theilacker[10] could not find the anticipated decrease of diamagnetism by the direct susceptibility measurements. Thus, the thermochromic phenomenon in solution has been studied by many investigators, but we have few knowledge of it in the solid state. Considerable differences are found even in the temperature at which color change occurs; the values recorded include 170°C[2], 240°C[11], and 265°C[9]. To throw further light on the thermochromism in the solid state, we examined the changes of some properties accompanying the color change on heating of crystalline powder of this compound.

Experimental

Materials.—Anthracene and dianthryl were provided by Mr. T. Handa. They were sublimed in vacuo before being used for measurements. Anthrone was prepared by reduction of commercial anthraquinone with hydrochloric acid and tin, and recrystallized from the mixture of benzene and ligroin[12]. It was oxidized again to anthraquinone with chromic acid, and a repeatedly sublimed specimen was used for the magnetic measurement. Dianthrone (or dianthronyl) was prepared by oxidation of anthrone with ferric chloride in glacial acetic acid[13], and recrystallized from Solvesso-100 which was obtained from Standard Vacuum Oil Co.. It was isomerized to dianthranol by boiling with alcohol containing potassium hydroxide, and repeatedly recrystallized from ethanol, and its pyridine compound was obtained by the recrystallization of dianthrone from pyridine as described by Schönberg and Ismail[14]. Dianthrone was dissolved in pyridine

1) E. Harnik and G.M.J. Schmidt, *J. Chem. Soc.*, **1954**, 3295.
2) H. Meyer, *Monatsh. Chem.*, **30**, 165 (1909).
3) W.T. Grubb and G.B. Kistiakowsky, *J. Am. Chem. Soc.*, **72**, 419 (1950).
4) W. Theilacker, G. Kortüm and G. Friedheim, *Ber.*, **83**, 508 (1950).
5) Y. Hirshberg and E. Fischer, *J. Chem. Soc.*, **1953**, 629.
6) A. Schönberg, A. Ismail and W. Asker, ibid., **1946**, 442.
7) A. Schönberg, A. Mustafa and W. Asker, *J. Am. Chem. Soc.*, **76**. 4134 (1954).
8) S.L. Matlow, *J. Chem. Phys.*, **23**, 152 (1955).
9) W.G. Nielsen and G.K. Fraenkel, ibid., **21**, 1619 (1953).
10) W. Theilacker, G. Kortüm and H. Elliehausen, *Z. Naturforsch.*, **9**, 167 (1954).
11) R. Padova, *Ann. chim. phys.*, (8) **19**, 408 (1910).
12) "Organic Syntheses", Coll. Vol., **1** (1948) p. 60.
13) O. Dimroth, *Ber.*, **34**, 219 (1901).
14) A. Schönberg and A. Ismail, *J. Chem. Soc.*, **1944**, 307.

and oxidized with bromine to dianthraquinone[15]; it was recrystallized three times from Solvesso-100.

Heat Treatment.—About 1 g. of dianthraquinone which was put in a test tube with a thermometer inserted in it was placed in vacuo and heated by an electric furnace. The temperature of the specimen was measured from time to time, and controlled to ±3°C by means of regulating the applied voltage to the furnace. After the heat treatment, the specimen was cooled down in vacuo as quickly as possible.

Magnetic Measurement.—The susceptibility was measured using a Gouy balance as previously described[16].

X-Ray Measurement.—It was made on a North American Philips recording X-ray diffractometer, using filtered copper radiation.

TABLE I

DIAMAGNETIC SUSCEPTIBILITIES OF DIANTHRAQUINONE AND ITS RELATED COMPOUNDS

Substance	Formula	Suscept. ($-\chi$)	Molar Suscept. ($-\chi_M$) obs.	calcd.	lit.
Anthracene	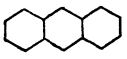	0.731	130	—	129.4[17], 134.2[18]
Dianthryl	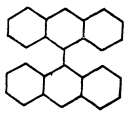	0.707	250	254	—
Anthrone	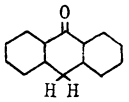	0.609	118	—	125.6[20]
Dianthrone	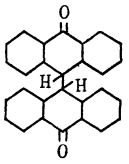	0.592	229	230	—
Anthraquinone	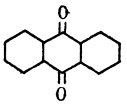	0.548	114	—	119.6[19], 113[20] 116.9[21]
Dianthraquinone	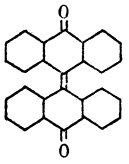	0.573	220	226	218[20]
Dianthranol	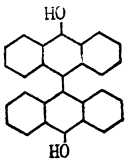	0.679	262	266	—
Dianthranol+2 pyridine	——	0.664	361	363	(pyridine 48.4[22])

15) E.B. Barnett and M.A. Matthews, ibid., **123**, 380 (1923).
16) H. Akamatu and Y. Matsunaga, This Bulletin, **26**, 364 (1953).
17) P. Pascal, *Bull. soc. chim. France*, **9**, 79 (1911).
18) A. Pacault, ibid., **1949**, D 40.
19) P. Pascal, ibid., **9**, 177 (1911).
20) E. D. Bergmann et al., *J. chim. phys.*, **49**, 474 (1952).
21) S. Banerjee, *Z. Krist.*, **A 100**, 316 (1939).
22) C. M. French, *Trans. Faraday Soc.*, **47**, 1056 (1951).

Results

The diamagnetic susceptibilities of dianthraquinone and the other compounds under consideration are given in Table I[23]. The molar susceptibilities of dianthryl, dianthrone, dianthranol and dianthraquinone have been estimated from measurements on anthracene, anthrone, and anthraquinone respectively with the aid of the Pascal's constants[24], and they also are given in Table I. In these cases, the observed values of molar susceptibility are less diamagnetic than the calculated values except dianthrone the value of which is in agreememt with the calculated one within accuracy of measurements.

The susceptibilities of dianthraquinone heated at various temperatures are given in Table II with the condition of treatment, its color, and the type of X-ray diagram. The sublimed specimen is pale green, but it possesses the identical susceptibility with the original one, and we can not find any difference in the X-ray diagram. On heating to 220°C, its color changes to deep green, susceptibility falls off to some extent, and X-ray diffraction patterns lose sharpness. (Fig. 1, curve B) On further heating to 240°C or above it, diamagnetism decreases still more, and diffraction patterns vanish almost completely (Fig. 1, Curve C). The assignment of indices in Fig. 1, curve A based on the crystallographic constants given by Harnik and Schmidt.

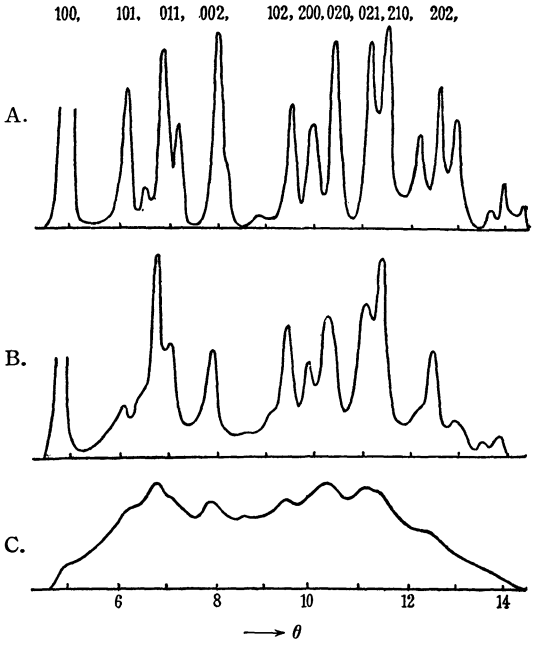

Fig. 1. Change of X-ray diagram of dianthraquinone on heating.
A. Recrystd. B. Heated to 220°C.
C. Heated to 244°C.

TABLE II
CHANGES OF SOME PROPERTIES OF DIANTHRAQUINONE ON HEATING

Conditions	Color	Suscept. ($-\chi$)	X-Ray diagram
recrystd.	yellow	0.573	cryst. (Fig. 1, Curve A)
sublimed (ca. 220°C)	pale green	0.572	cryst.
194°C, 60 min.	yellow	0.570	cryst.
220°C, 60 min.	green	0.538	cryst.+amorph. (Fig. 1, Curve B)
244°C, 60 min.	dark green	0.478	amorph. (Fig. 1, Curve C)
255°C, 80 min.	dark green	0.472	amorph.
266°C, 60 min.	dark green	0.467	amorph.
282°C, 40 min.	dark green	0.446	amorph.
297°C, 60 min.	dark green	0.418	amorph.

Discussion

Diamagnetism of Dianthraquinone.— Aromatic compounds, especially those containing large numbers of rings conjugated or condensed with each other, show the diamagnetic anisotropies which depend strikingly upon the molecular shape[25]. For such cases, it is difficult to estimate the molar susceptibilities by the direct application of the Pascal's additivity law, and we need many constitutive correction constants which are characteristic for each type of condensation of nuclei[25]. In the previous paper[27], we suggested as a compromise to assume that the molar susceptibility of an

23) Susceptibility values have been multiplied by 10^6 throughout this paper.

24) Atomic constants, −2.93 for hydrogen, −4.61 for oxygen in hydroxyl group, and +1.73 for oxygen in carbonyl group. Constitutional correction constants, +5.5 for carbon-carbon double bond and −1.29 for tertiary carbon atom in the position α to hydroxyl group.

25) Ref. (16) and references cited there.

26) A. Pacault, *Ann. chim.*, (12) **1**, 527 (1946). *Rev. sci.*, **86**, 38 (1948).

27) Y. Matsunaga, This Bulletin, **29**, 308 (1956).

aromatic compound containing conjugated rings is equal to the sum of those observed for the constitutional fragments of the molecule, and showed that this procedure gives nearly correct values for hydroxyazobenzenes. But in a few cases, the calculated values were also in serious disagreement with the experimental ones, because the effect of conjugation between the fragments of the molecule on the molar susceptibility was left out of consideration. Therefore, our calculated values in Table I by the above-mentioned procedure are nothing but the values for the imaginary cases in which the conjugations between the conjugated nuclei are absent. Then the effect of conjugation will be considered qualitatively with the aid of theoretical results given by London's method. If the theory predicts that conjugation brings about a reduction of diamagnetic anisotropy, our calculated molar susceptibilities will be the upper limits, and if the reverse effect is predicted, they will be the lower limits. McWeeny[28] established the theory that addition of rings, joined to the original system by single links, gives an increase in anisotropy less than that which will be expected in the absence of any conjugation across the bonds, so that dianthryl and dianthranol must belong to the former case. The steric hindrance completely prevents the conjugation between two anthracene nuclei, or their susceptibilities will be less than the calculated values. The observed decrease of diamagnetism suggests the imcomplete prevention of conjugation, although the planar structures of molecules as a whole are not plausible in both cases. As to dianthrone, a new conjugation does not occur by the joining of two anthrones; consequently the agreement between the observed and the calculated susceptibilities is quite natural.

For anthraquinone and dianthraquinone themselves, theoretical investigations have not yet been performed, and it seems that they would be fruitless[29]. For their isoelectronic hydrocarbons, i.e. 9. 10-anthraquinodimethane and dianthraquinodimethane, theoretical values of anisotropies were already presented by Pullman and his associates. Their results are as follows.

anthraquinodimethane, 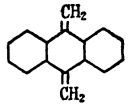 $1.941\ \Delta K_{benzene}$[30]

dianthraquinodimethane, 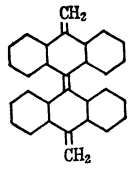 $4.033\ \Delta K_{benzene}$[20]

By analogy, it is plausible to assume that the calculated molar susceptibility for dianthraquinone is the lower limit, as the increase of anisotropy by the conjugation between two nuclei is expected in the reference compound. Theoretically, a similar relation was also predicted for *p*-benzoquinodimethane and *p*-diphenoquinodimethane[30], so that the compound containing two or more ring systems, joined to each other by double bonds, probably gives an anisotropy more than the sum of those of the original systems. Therefore the disagreement between the observed and the calculated susceptibilities for dianthraquinone must be attributed to the other cause. According to the model given by Harnik and Schmidt (Fig. 2), the length of the central ethylene linkage is 1.31 Å., owing to the angle of 40° between the planes of this double bond and the benzene rings, and the absence of the conjugation between the central double bond and four phenyl groups. In such a case, the π-electron system in dianthraquinone may be divided into three parts, namely an isolated central ethylene linkage and two identical conjugated systems. If we substitute the conjugated system of anthrone for each of the latter two, the molar susceptibility—219 will be expected from this model. The magnitude of susceptibility is consistent with the model presented by X-ray analysis. If we assume that the carbonyl groups are also completely localized, owing to the distortions distributed over the conjugated systems, further smaller value for molar susceptibility—212 will be expected. Therefore, it may be concluded that deviations of several degrees from planarity scarcely affect the delocalization of π-electrons.

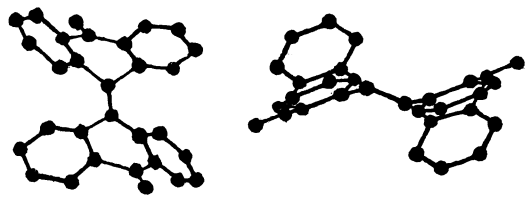

Fig. 2. Perspective view of molecular model (after Harnik and Schmidt).

Thermochromism of Dianthraquinone.—Our results show that the color change from

28) R. McWeeny, *Proc. Phys. Soc.* A 66, 714 (1953).
29) M.G. Evans, J. de Heer and J. Gergely, ibid., A62, 505 (1949).
30) G. Berthier, M. Mayot and B. Pullman, *J. phys. radium*, 12, 717 (1951).

yellow to dark green is accompanied by the decrease of diamagnetic susceptibility and the complete vanishing of sharp diffraction patterns in the X-ray diagram. This structural change does not occur suddenly at a definite temperature, but takes place gradually at an elevated temperature. The color of a specimen heated to 220°C for one hour was green; however, its change was imcomplete judging from its susceptibility and its X-ray diagram. At 240°C, the change finished within one hour. Hence, the temperature at which we can find the apparent color change must depend on the speed of elevating its temperature. The higher values recorded by Padova[11], and Nielsen and Fraenkel[9] will be due to the rapid heating of the specimen. On the other hand, Meyer's observations[2] cannot be interpreted in the same manner, since we could not succeed in recovering its color by boiling with alcohol, and their recrystallization was practically impossible, as our green specimen was scarcely dissolved in the solvent. We cannot but conclude that Meyer's green specimen is not quite the same as the other authors' including also our own. It is supposed that Meyer said green for the specimen slightly colored, so that the structural change barely occurred in his specimen. This suggestion is supported by his description; namely, he stated that the solution of dianthraquinone turns on heating to deep green and then to blackish green, but for the color of the heated solid specimen, he wrote only green.

Kortüm and his associates[31] discovered that when the deep red sulfuric acid solution of dianthraquinone is added to cold water, dianthraquinone precipitates as a dark green mass for a short period of time, and changes spontaneously to the original yellow form. The solution of the green specimen in concentrated sulfuric acid was also deep red, and we obtained a dark green precipitate similarly, when the solution was poured into water. But in this case, the precipitate did not show such a characteristic color change, and darkened somewhat on standing. For these reasons, the net change occurring in the so-called thermochromism of solid dianthraquinone from yellow to dark green may be concluded as an irreversible chemical reaction, although in its process, the same green form with that which appeared in the reversible thermochromism of solution may be supposed to be an intermediate. The large decrease of diamagnetism accompanying the color change suggests the occurrence of a paramagnetic state, and this expectation is consistent with the result given by Nielsen and Fraenkel, but we cannot discuss further its nature from our measurements.

31) G. Kortüm, W. Theilacker, H. Zeininger and H. Elliehausen, *Ber.*, 86, 294 (1953).

Summary

The magnetic susceptibilities of dianthraquinone and its seven related compounds were measured by the Gouy method. The effect of conjugation between the constitutional fragments of the molecule was discussed with the aid of theoretical values of diamagnetic anisotropies. The depression of molar susceptibility of dianthraquinone was attributed to the localization of π-electrons in the central ethylene linkage, owing to the large distortion of the molecule. The remarkable decrease of susceptibility and the complete vanishing of sharp diffraction patterns in X-ray diagram accompanying the color change on heating of dianthraquinone were shown. The author concluded that the net change occurring in the so-called thermochromism of solid dianthraquinone is an irreversible chemical reaction.

The author wishes to express his hearty thanks to Prof. H. Akamatu for his kind direction, to Dr. M. Kobayashi for a sample of dianthraquinone used in the beginning of this study, and to Mr. T. Handa for samples of anthracene and dianthryl. The cost of this study has been defrayed from the Grant in Aid for Fundamental Scientific Research from the Ministry of Education, to which the author's thanks are also due.

Department of Chemistry, Faculty of Science, The University of Tokyo
Hongo, Tokyo

Study on Zinc Oxide-Chromium Oxide Catalyst. II. Variation of Catalytic Activity for Methanol Decomposition with Addition of Chromia and Structural Dependence of Activity

By Hiroshi UCHIDA and Yoshisada OGINO

(Received February 28, 1956)

Introduction

Zinc oxide-chromium oxide, used as a catalyst for the methanol synthesis, has been the object of intense studies made by a number of investigators since about thirty years ago. Nevertheless, most of the works have been made only on the catalytic activity of the substance in the methanol synthesis as well as in the methanol decomposition, and a knowledge sufficient for understanding the activity in relation to the structure of the catalyst is still lacking.

The present study has been made in an attempt to see as correct and comprehensive a picture of such catalysts as possible, and deals with the electrical conductivity, the surface area, the crystal structure, and the excess oxygen content, of catalysts of different chromia contents, along with their catalytic activity for methanol decomposition.

The results of the activity may be explained, to some extent, from the structural point of view.

Experimental Procedure

Catalyst Preparation.—Two series of catalysts were prepared. The catalysts of the one series, each denoted by catalyst I, were produced by the impregnation of commercial zinc oxide powder (c. p.) in chromium nitrate solutions of varied concentrations and the catalysts of the other series, each denoted by catalyst P, were by the co-precipitation of the hydroxides of zinc and chromium from solutions of zinc and chromium nitrates of different relative concentrations with aqueous ammonia. The powder of catalyst thus formed was heated at 400°C for a few hours and then pressed into a bar of 8×8 mm. square. The bar was sintered at 600°C in air for two hours and then allowed to cool to room temperature. Part of the bar was crushed into granules of 1–2 mm. diameter, to be used for the determination of activity in methanol decomposition and the surface area.

Catalytic Activity for Methanol Decomposition.—The experimental method consisted of passing methanol vapour at a constant rate of 1.98 m. mol./min. through a bed of granular catalyst in a vertical glass tube heated to temperatures from 350° to 430°C in an electric furnace. The apparatus was similar to the one described by J. R. Huffman et al.[1], but was different from it in that the constant rate was maintained, as performal by M. R. Fenske et al.[2], by immersing the methanol reservoir in a water bath at a constant temperature.

A bed of catalyst (1 g.) was reduced at 450°C in a current of hydrogen for six hours, and then methanol vapour was passed through the bed at the reaction temperature. About two hours were required for the catalyst to establish the stationary activity, and measurements were commenced thereafter. The products, gaseous and liquid, were collected and their amounts were determined. The gaseous product was analyzed, as is usually done, for carbon dioxide, carbon monoxide, and hydrogen, and the liquid product was analyzed both for methyl formate by saponification and for formaldehyde by the iodine method.

Electrical Conductivity.—As described in a previous paper[3], electrical conductivity was measured according to the method of R. H. Griffith et al.[4], by using a cube of catalyst (8×8×8 mm.) as a sample. Measurements were made first in vacuo both after the oxidation of the catalyst in oxygen at 450°C and after the reduction in hydrogen at 450°C, and second in an atmosphere of hydrogen after the measurement on the reduced catalyst.

Crystal Structure.—Information on crystal structure was furnished by the Debye-Scherrer's X-ray diagram obtained by using chromium as an anode. It was supplemented by the electron diffraction pattern of powdered catalyst.

Surface Area.—Surface area was determined from the nitrogen adsorption data plotted according to the BET theory.

Quantity of Excess Oxygen in Catalyst.—The excess oxygen content was determined according to the procedure by S. W. Weller[5]. One mole of iodine liberated from an aqueous solution of potassium iodide by the addition of a quantity of catalyst was estimated to be equivalent to 0.5 mol. excess oxygen in the catalyst. A powder of catalyst under 100 mesh was used for the determination.

1) J.R. Huffman and B.F. Dodge, *Ind. Eng. Chem.*, **21**, 1056 (1929).
2) M.R. Fenske and P.K. Frolich, ibid., **21**, 1052 (1929)
3) H. Uchida and Y. Ogino, This Bulletin, **29**, 174 (1956).
4) R.H. Grifith, P.R. Chapman et al., *Disc. Faraday Soc.*, **8**, 258 (1950).
5) S.W. Weller and S.F. Voltz, *J. Am. Chem. Soc.* **76**, 4695 (1954).

Results

Catalytic Activity for Methanol Decomposition.—Among the results of the measurement of activities of catalysts in methanol decomposition at temperatures from 350° to 430°C, the results for catalysts I at 350° and 400°C are shown in Fig. 1 and Fig. 2. In

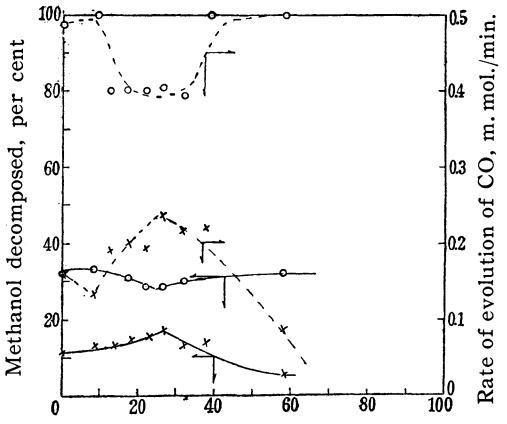

Composition of catalyst, mol. per cent Cr_2O_3

Fig. 1. Total decomposition ratio (full line) and rate of evolution of carbon monoxide (dotted line) as a function of ZnO–Cr_2O_3 composition of catalysts I.
—×—, at 350°C. ··×··, at 400°C
—○—, at 350°C. ··○··, at 400°C

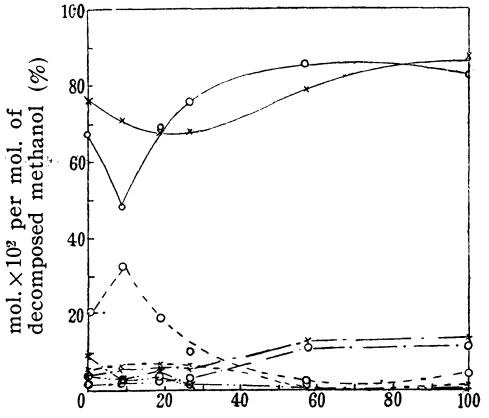

Composition of catalyst, mol. per cent Cr_2O_3

Fig. 2. Products of methanol decomposition as a function of ZnO–Cr_2O_3 composition of catalysts I.
—○— CO, at 350°C. —×— CO, at 400°C
··○·· $HCOOCH_3$, at 350°C
··×·· 〃 , at 400°C
—··—○··— HCHO, at 350°C
—··×—··— 〃 , at 400°C
—·○—·— CO_2, at 350°C
—·×—·— 〃 , at 400°C

Fig. 1, the total decomposition ratio of methanol ($CH_3OH_{decomp.}/CH_3OH_{introd.}$) and the rate of evolution of carbon monoxide (mole CO/min.) are illustrated by the full and dotted lines respectively, as functions of catalyst composition. In Fig. 2, the composition of decomposition product is plotted also as such. The results for catalysts P are presented in similar manner in Figs. 3 and 4.

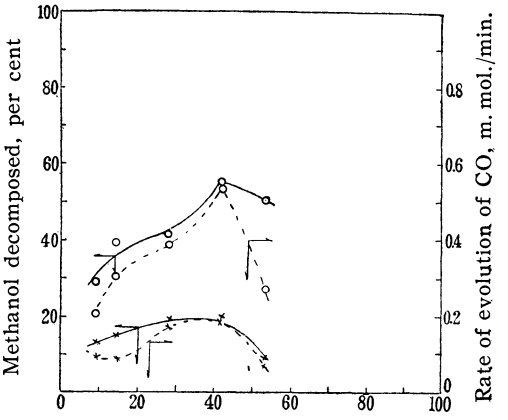

Composition of catalyst, mol. per cent Cr_2O_3

Fig. 3. Total decomposition ratio (full line) and rate of evolution of carbon monoxide (dotted line) as a function of ZnO–Cr_2O_3 composition of catalysts P.
—×—, at 350°C. ··×··, at 400°C
—○—, at 350°C. ··○··, at 400°C

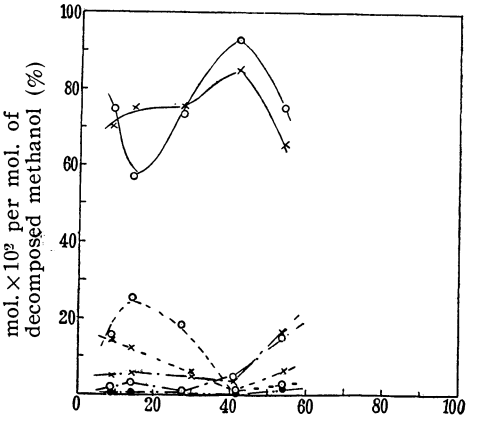

Composition of catalyst, mol. per cent Cr_2O_3

Fig. 4. Products of methanol decomposition as a function of ZnO–Cr_2O_3 composition of catalysts P.
—○— CO, at 350°C. —×— CO, at 400°C
··○·· $HCOOCH_3$, at 350°C
··○·· , at 400°C
—··●—·· HCHO, at 350°C
, at 400°C
—·—○—· CO_2, at 350°C
—·—×—· , at 400°C

It can be seen from Figs. 1 and 3 that at 350°C a catalyst containing, for example, 26 mol.% chromia gives the highest values of the total decomposition ratio and the rate of evolution of carbon monoxide, whereas at

400°C it gives rather lower values. Fig. 5

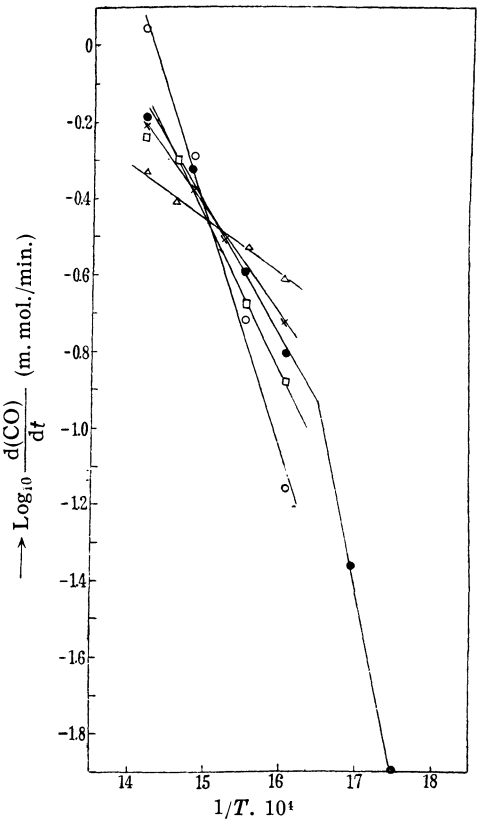

Fig. 5. Temperature dependence of rate of evolution of carbon monoxide.
—●—, zinc oxide.
—○—, catalyst I containing 58.6 mol.% chromia within.
—△—, 〃 26.3 mol.%
—□—, 〃 9.5 mol.%
—×—, 〃 14.3 mol.%

is a detailed representation of the data on the decomposition. This figure shows that the rates increase logarithmically with reciprocal absolute temperature but differently depending on the compositions of the catalysts. Therefore, catalytic activity can not be evaluated correctly unless measurements are made over a wide range of temperature.

There is a good similarity in tendency between the full line and the dotted line, both in Fig. 1 and in Fig. 3, except for the case of a catalyst containing 10 mol.% chromia. This catalyst yielded a greater amount of methyl formate particularly at a low temperature of 350°C (refer to Figs. 2 and 4)*1, but gave a lower rate of evolution of carbon monoxide despite the greater decomposition ratio.

On the basis of H. Dohse's view that the methanol decomposition follows a zeroth order reaction, the apparent activation energy of methanol decomposition by the catalysts I was given by the slope of the straight line in Fig. 5. The activation energy thus determined is lowest at a chromia content of 26 mol.%, whereas it rises with decreasing chromia content on the one side and also with increasing chromia on the other side (refer to Fig. 10 also). The more active a catalyst is at lower temperatures, the smaller is the activation energy, whereas the more active a catalyst is at a higher temperature, the greater is the activation energy.

H. Dohse[7] described that the plot of log v vs. $1/T$ for zinc oxide has a bend. Such a bend appears also at 330°C on the line constructed from the present data of experiments, and is of particular interest in view of the fact that a bend, as will be described later, appears also on the plot of electrical conductivity vs. $1/T$ for zinc oxide at the same temperature. The bend in the conductivity curve, however, shifts, with the increasing chromia content, towards so low a temperature that the corresponding bend in the activity curve can scarcely be determined accurately (refer to Fig. 7).

A comparison of the activation energy of the catalysts I with that of the catalysts P indicates that within the range of chromia content of up to 30 mol.% the energy for the latter is greater than that for the former and beyond this content the situation is reversed (refer to Fig. 10).

Electrical Conductivity.—The results of the measurements of electrical conductivity on evacuated catalysts at 350°C, which were made both after the oxidation and after the reduction of catalysts at 450°C, are shown as functions of catalyst composition in Fig. 6*2. The electrical conductivity of the oxidized, evacuated catalysts is the higher for the increasing chromia contents, whereas that of the reduced, evacuated catalysts is the lower for the increasing chromia content. In Fig. 6, the conductivity curve for oxidized, evacuated catalysts intersects that for reduced evacuated catalysts, at a certain chromia content, which is 26 mol.% for the catalysts I, and 13 mol.% for the catalysts P.

The catalyst has naturally the conductivity centres of two types, the one is the zinc

*1 This may perhaps have a close relation to the highly selective catalyst that was used in the methanol synthesis by G. Natta[6] and which contained 11 mol. % of chromia.

6) G. Natta, "Catalysis (edited by P.H. Emmett)", Rheinhold Publishing Corporation, (1955), III, P. 349.

7) H. Dohse, *Z. Physik. Chem.*, **B 8**, 159 (1930).

*2 The conductivity of the oxidized catalysts in oxygen atmosphere differed little from that of the oxidized, evacuated ones.

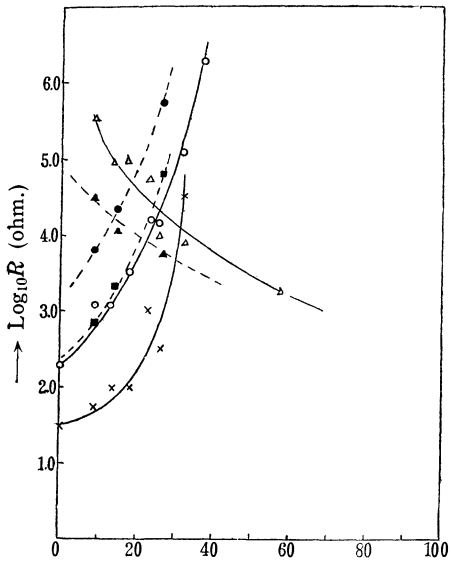

Composition of catalyst, mol. per cent Cr_2O_3

Fig. 6. Electrical conductivity of catalysts I (full line) and catalysts P (dotted line) at 350°C as a function of ZnO–Cr_2O_3 composition.
×, ■, in hydrogen after reduction
○, ●, in vacuo after reduction
△, ▲, in vacuo after oxidation

atoms (n-type) due to zinc oxide and the other the excess oxygen atoms (p-type) due to chromia. This fact implies that the n-type semi-conductivity becomes predominant in the catalysts of reduced state whereas the p-type becomes so in the catalysts of oxidized state, and that the greater amount of chromia favour the production of a larger number of p-type centres.

Logarithms of electrical resistivity determined on the catalysts in vacuo both after the oxidation and after the reduction of catalysts at 450°C, and those of catalysts in the hydrogen atmosphere after the reduction at the same temperature, are plotted against reciprocal temperatures in Fig. 7*3. As for the catalysts I in the hydrogen atmosphere, the plots for every catalyst form a pair of straight lines intersecting at a certain temperature that shifts to lower values with increasing contents. The change of the electrical conductivity with the lowering temperature was not reversible by the subsequent raise of temperature, and showed a pronounced drift.

The slope of the straight line in the high temperature range should give the activation energy of electrical conductivity in this

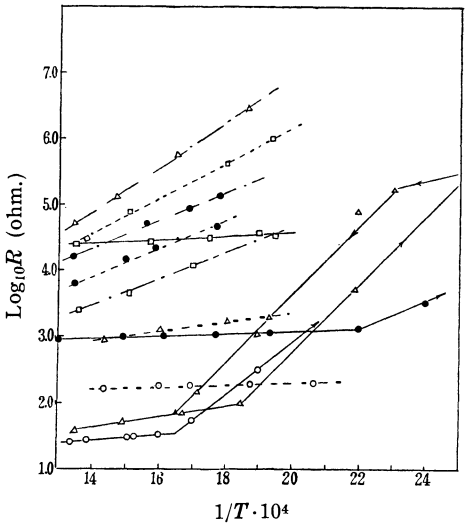

Fig. 7. Temperature dependence of electrical conductivity of catalysts I in hydrogen (full line), in vacuo after reduction (dotted line), and in vacuo after oxidation (dotted and dashed line).
○, zinc oxide. △, catalyst with 9.5 mol. % Cr_2O_3. ●, , , , 23.3 mol. %. □, , , , 33.2 mol.%

range*4. The energy thus determined for catalysts in hydrogen depends on the chromia content of catalysts. Within the range of low chromia content (less than about 26 mol.%), the energy rises slightly with the increase of chromia content and soon reaches a maximum at about 10 mol.% chromia and thereafter takes a downward course to a minimum at 26 mol.% chromia, and this decrease is followed by a rapid rise with the further increasing chromia content (refer to Fig. 10).

In contrast, the activation energy of conductivity for catalysts evacuated after their reduction rises monotonously with increasing chromia content, whereas the energy for the catalysts evacuated after their oxidation persists almost unaffected by the increase of chromia content.

Catalyst Structure Revealed by Debye-Scherrer's X-ray Diagram and Electron Diffraction Pattern.—The catalysts I and catalysts P gave Debye-Scherr's X-ray diagrams that did not show any line corresponding to Cr_2O_3, even though the catalysts were heated at 600°C for two hours and their chromia contents were as high as 59%, but showed the lines corresponding to zinc oxide.

The diffraction lines for zinc oxide, however, become weaker with increasing chromia content. Besides these lines, the lines cor-

*3 The electrical conductivity of catalysts P at temperatures below 300°C was not determined.

*4 Considering the performance of catalysts at the practical working temperature, the energy in the low temperature range is of minor significance.

responding to neither zinc oxide nor Cr_2O_3 but to $ZnCr_2O_4$ spinel were observed. The lines due to the spinel appeared even at so small a chromia content as of 9.5 mol.% and their number increased with the chromia content increasing up to 25–30 mol.%, but above this content the lines became gradually diffused till it was difficult to distinguish the lines.

The electron diffraction patterns for catalysts I and catalyst P reveal also the lines due to the spinel. The number of these lines is far greater than the number of the diffraction lines in the X-ray diffraction diagram. The electron diffraction lines remained sharp while the chromia content increased even up to the value where the X-ray diffraction lines became rather diffused.

The results described above reveal that the catalyst comprises the oxides of zinc and chromium and the spinel of zinc chromite presumably produced by the reaction $ZnO+Cr_2O_3 \rightarrow ZnCr_2O_4$, and that the spinel in the catalyst of high chromia content exists as crystallites too small to be detected by the X-ray analysis. Accordingly, the quantity of chromia in excess of the proper amount for combination with zinc oxide seems to prevent the growth of the crystallites.

Surface Area and Quantity of Excess Oxygen in Catalyst.—The surface area of and the quantity of excess oxygen in 1 g. of catalysts are illustrated by the full and the dotted lines respectively, as functions of chromia content, in Fig. 8 for catalysts I,

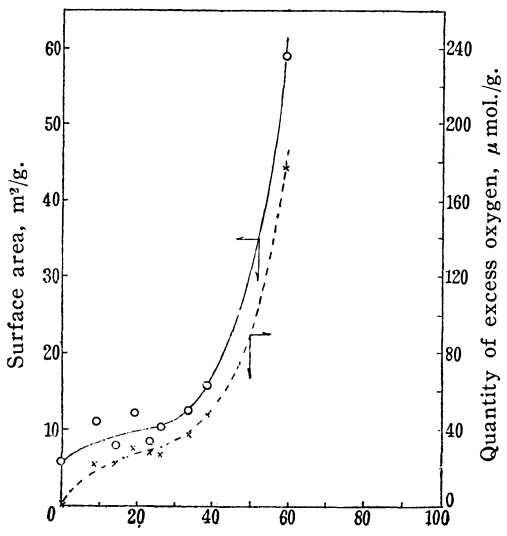

Composition of catalyst, mol. per cent Cr_2O_3

Fig. 8. Surface area (full line) of and quantity of excess oxygen (dotted line) in 1 g. of catalysts I as a function of $ZnO–Cr_2O_3$ composition.

and in Fig. 9 for catalysts P. As is seen in

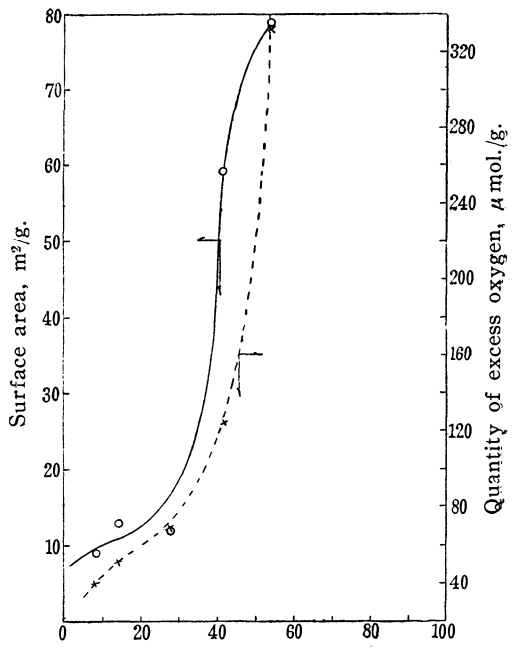

Composition of catalyst, mol. per cent Cr_2O_3

Fig. 9. Surface area (full line) of and quantity of excess oxygen (dotted line) in 1 g. of catalysts P as a function of $ZnO–Cr_2O_3$ composition.

these figures, every curve has a sigmoid shape and rises with increasing chromia content. The initial part (over very low chromia contents), an almost rectilinear line, shows a rather rapid rise, the middle part a very dull rise, and the last part a rise becoming very sharp. The last part begins when the chromia content attains to 35 mol.% for catalysts I, and 30 mol.% for catalysts P.

The results described above may bring out the following picture of the surface structure of catalysts. As revealed by the trend of the surface area change, the size of the larger particles having composed granules of zinc oxide changes a little even though the chromia content attained to 30 mol.%, and any further addition of chromia results in the abrupt creation of numerous fine particles as to catalysts I, whereas it results in the sudden reduction of the particle size as to catalysts P.

For the reason that excess oxygen can exist only in the presence of the chromia which fails to combine with zinc oxide, the steep rise of the excess oxygen curve in the range of high chromia content indicates that the quantity of uncombined chromia is increasing rapidly on the surface of the catalyst. On the other hand, the deviation

of the curve from the expected rectilinear line with increasing chromia content is suggestive of the formation of crystallites between the oxides of zinc and chromium*5. From the results seen in the diffraction patterns, the crystallite may be the one of zinc chromite spinel. The highest concentration of the spinel crystallites in the surface, therefore, is to be found with catalysts whose excess oxygen content deviates most greatly from the quantity expressed by the expected rectilinear line*6.

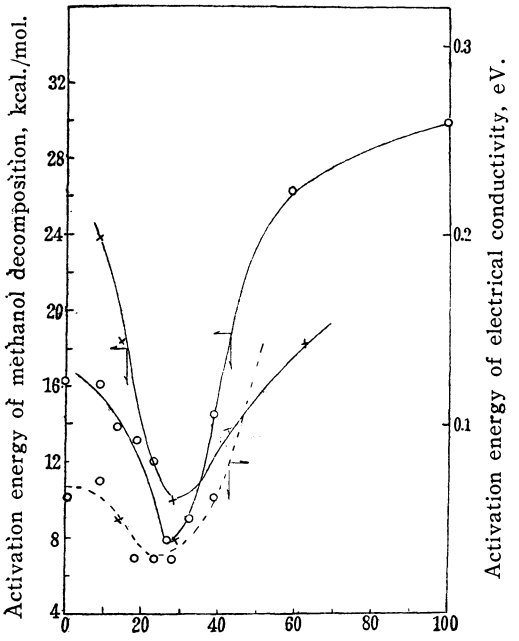

Fig. 10. Variation of activation energies for methanol decomposition (full line) and electrical conductivity (dotted line) with catalyst compositions.
○, catalysts I. ×, catalysts P.

Discussion

Methanol Decomposition.—By assuming that the rate of methanol decomposition follows the zeroth order reaction given by

$$v = Ae^{-E/kT} \quad (1)$$

where v is the rate per unit surface area of the catalyst, the logarithms of frequency factor (log A) are plotted against activation energy (E) in Fig. 11 for catalysts I and catalysts P. The lines for the two kinds of catalysts are straight and approximately identical. The linear relation between log A and E has already been described by E. Cremer[8], for the rate of methanol decomposition with neodium oxides, and by G-M. Schwab[9], for the rate of the decomposition of formic acid with alloy catalysts, and some others.

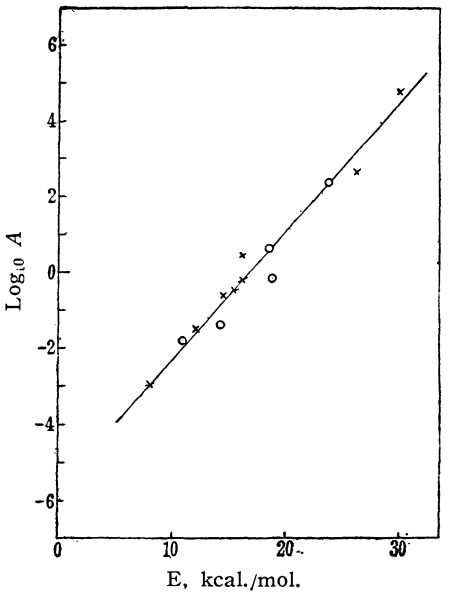

Fig. 11. Plot of logarithm of frequency factor in the rate of evolution of carbon monoxide vs. activation energy.
—×—, catalysts I. —○—, catalysts P.

The straight line can be represented by an equation,

$$A = ae^{\alpha E} \quad (2)$$

where log a is the intercept on the ordinate and α is the slope of the line. This equation is explained by assuming that active centres with high activation energy in the catalyst surface are more frequent than the ones with low activation energy[9].

The combination of Eq. (2) with Eq. (1) gives

$$v = a \cdot e^{\alpha E} \cdot e^{-E/kT} \quad (3)$$

When v is expressed in the number of moles of carbon monoxide evolved per unit surface (cm^2) per second the substitution of the values of a and α obtained from Fig. 10 in Eq. (3) results in

$$v = 1.24 \times 10^{-7} \cdot e^{0.81E} \cdot e^{-E/kT} \quad (4)$$

Eq. (4) indicates that the rate at a certain temperature, so far as the rate per unit

*5 The slow increase within the range of very low chromia content can not readily be explained. The increase is probably due to the condition that chromia is too dispersed to build up the spinel crystallite, though it is combined with zinc oxide.

*6 A greater amount of the crystallites may be produced in 1 g. of the catalyst by the further addition of chromia, but since the amount considered is based on the unit surface area it becomes rather less owing to the steep rise of surface area.

8) E. Cremer, *Z. Elektrochem.*, **53**, 269 (1949).
9) G-M. Schwab, *Disc. Faraday Soc.*, 8, 166 (1950).

surface area is considered, is determined solely by the activation energy inherent to a catalyst, but not by any other factors.

Catalytic Activity and Electrical Conductivity.—At first sight, one may be inclined to expect the relation of the activation energy of methanol decomposition to the concentration of either the *n*-type or the *p*-type conductivity centres in the catalyst. Namely, the concentration of *n*-type conductivity centres need be only adequately low to permit electrons to transfer more readily from methanol to catalyst, and the transfer thus taking place causes the catalyst to adsorb methanol and cosequently to decompose methanol with less activation energy, if the rate of adsorption determines the rate of decomposition of methanol. However, there is a minimum of the activation energy at a catalyst (26 mol.% chromia) of *n*-type semiconductor in I series, whereas at a catalyst (30 mol.% chromia) of *p*-type semi-conductor in P series*[7]. Thus, no direct relation of the activation energy of methanol decomposition to the types of semiconductor can easily be found at all*[8].

When both the activation energy of methanol decomposition and the activation energy of electrical conductivity are plotted as functions of the composition of catalysts I (Fig. 10), the line for the activation energy of methanol decomposition runs parallel to the line for the activation energy of electrical conductivity. Moreover, both the bend in the plot $\log R$ (in hydrogen) and the bend in the plot of $\log v$ vs. $1/T$ for zinc oxide appear at the same temperature (compare Fig. 5 with Fig. 7). A couple of these results serve as a favourable evidence for corroborating the rather direct relation between the activation energies of methanol decomposition and electrical conductivity.

In a previous paper[3] it is stated that the decrease of electrical conductivity of zinc oxide in hydrogen with the rise of temperature in the low temperature range was caused by the adsorption of hydrogen on zinc atom-pairs whereas the increase of electrical conductivity in the high temperature range was due to the adsorption on oxygen atoms. This fact in connection with the evidence just described for the relation between activation energies of methanol decomposition and electrical conductivity may lead us to expect that the rate of adsorption of a reactant (methanol or something intermediate in the decomposition) on oxygen atoms (or the electron transfer between the reactant and oxygen atoms) is determining the rate of the methanol decomposition.

Promoting Action of Chromia.—In the methanol decomposition the increase in exponential terms of the rate equation (1) is always compensated by the decrease in the frequency term. According to a recent paper by E. Cremer[10], this compensation effect may be expected at multicomponent catalysts of the same type, if different kinds of active centres act simultaneously as sites of the catalytic reaction and if the proportions of these different active centres (involving different energies) are shifted by changes in its composition. An illustration is given by E. Cremer on a reaction that takes place on two kinds (1 and 2) of active centres involving the activation energies E_1 and E_2 and frequency factor terms A_1 and A_2, respectively. In this case the overall rate constant k (or the rate v of a zeroth order reaction) becomes

$$k=A_1\exp(-E_1/kT)+A_2\exp(-E_2/kT),$$

and the Arrhenius plots of k for the greater values of A_2, the values of E_1, E_2 and A_1 being kept at the same, give the straight lines of decreasing slope, i.e. the decreasing activation energy, and of a common intersection point, provided that A_1 is greater than A_2 and E_1 greater than E_2.

A comparison of Fig. 10 with Fig. 8 or 9 indicates that the greater the spinel concentration in the catalyst surface the smaller is the activation energy of methanol decomposition. The fact may be explained as follows from E. Cremer's point of view. In the surface of the catalysts within the range of chromia content up to 26 per cent, zinc oxide and zinc chromite (or the oxygen atoms in zinc oxide and zinc chromite) are the two kinds (1 and 2) of the active centres for the methanol decomposition, while chromia and zinc chromite are such in the surface of the catalyst of higher chromia content. Accordingly, the catalyst with the greater concentration of zinc chromite spinel in the surface can give the smaller activation for the methanol decomposition than both the zinc oxide and chromia alone, if the activation energy of the spinel is assumed to be smaller than that of zinc oxide and of chromia.

No direct relation between the extent of the surface area and the activity for meth-

*7 According to D. J. Bevan et al. (*J. Chem. Soc.*, 1948, 1729), zinc chromite is a *p*-type semi-conductor.

*8 The influence of the concentration of *n*-type semiconductor on the catalytic activity can not completely be denied, particularly at low temperatures where the adsorption of a reactant, as will be described later, takes place on zinc atom pairs.

10) E. Cremer, "Advances in Catalysis", VII((1955), p. 85.

anol decomposition can be found. The activity at, for example, 350°C rose at first with the slow increase of surface area, but thereafter fell off despite the rapid further increase of surface area (compare Fig. 8 with Fig. 10). This result can be explained from the fact that while the surface area increases slowly the activation energy decreases, but once the surface area has begun to increase rapidly the energy turns to increase steeply. The greater amount of the chromia disintegrates the crystallites of the spinel into so extremely fine ones that it may cause the steep increase of surface area and also cover the surface to such an extent that the activation energy approaches a value as high as 30 kcal./mol. for chromia alone.

The favourable effect of chromia is thus to increase the specific activity of catalyst surface rather than to provide and stabilize the larger accessible area. This is quite contrary to G. Natta's statement[6] that the activation energy of methanol synthesis is independent of the chromia content and the promoting action of chromia is solely due to its hindering effect upon the recrystallization of zinc oxide. No decisive conclusion can as yet be made between these two different promoting actions revealed in the synthesis and in the decomposition.

Summary

From the results on the rates of methanol decomposition by the catalysts of different zinc oxide-chromium oxide compositions the rate (v) of evolution of carbon monoxide per unit surface area of catalyst has appeared to be represented by the following equation

$$v = ae^{\alpha E} \cdot e^{-E/kT}$$

where a and α are constants applicable throughout the two series of catalysts produced by different methods. The activation energy (E) of the methanol decomposition attains to a minimum value when the catalyst has a certain chromia content. It is directly related with the activation energy of electrical conductivity of the catalyst in hydrogen at high temperature but neither with the concentration of n-type conductivity centres nor with that of p-type conductivity centres. At such temperatures, the adsorption of hydrogen on the oxygen atoms in the surface was considered to participate in the electrical conductivity.

Moreover, the results on determinations of the surface area and the excess oxygen content, together with the information about the structure obtained from diffraction patterns, reveal that there is a similarity in tendency between the increase of concentration of zinc chromite spinels in the catalyst surface and the decrease of activation energy of the decomposition. This relation can be explained from the view of E. Cremer on the compensation effect.

The quantity of chromia added in excess of the proper amount for combination with zinc oxide causes both the surface area and the activation energy to increase towards those of chromia alone.

The addition of chromia has therefore a considerable influence upon the activation energy of methanol decomposition, which is quite contrary to what G. Natta described on the methanol synthesis.

Government Chemical Industrial Research Institute, Tokyo

Mikroanalyse mit Hilfe von Ionenaustauschharzen. V. Über den Nachweis spurweise vorhandenes Molybdäns mit Ammoniumrhodanid und Zinn(II)chlorid [1]

Von Masatoshi FUJIMOTO

(Eingegangen am 20. Februar 1956)

Einleitung

Wohl bekannt ist von früher her, dass eine scharlach- bzw. orangerote Färbung, die die Molybdate bei Anwesenheit von Zinn(II)-chlorid durch Einwirkung von Ammonium- oder Kaliumrhodanid liefern, als eine sehr ausgezeichnete Methode für den Nachweis sowie die Bestimmung des Molybdäns weit benutzt wird[2]. Diese rote Färbung beruht auf der Bildung von Komplexrhodanide fünfwertiges Molybdäns wie $[Mo(SCN)_5]$, $[Mo(SCN)_6]^-$ [3]. Der Nichtelektrolytkomplex ist für kolorimetrische Bestimmung des Molybdäns besonders geeignet, da dieser nicht nur mit organischem Lösungsmittel leicht ausgezogen wird, sondern auch sehr starke rote Färbung liefert. Nach Babko[3], ist es für die Bestimmung des Molybdäns nicht wünschenswert, unter den zur Bildung von Komplexanion $[Mo(SCN)_6]^-$ geeigneten Bedingungen[4] Kolorimetrie auszuführen, da dieses Anion verhältnismässig schwächer als der Nichtelektrolytkomplex gefärbt wird. Trotz diesem Nachteil wird dieses Komplexanion ins Anionenaustauschharz stark adsorbiert, und die Harzphase sich dabei deutliche und merklich beständige Orange- bzw. Orangerotfärbung liefert, welche infolgedessen als eine Tüpfelmethode mit Ionenaustauschharzen anwendbar ist. Bei gegenwärtigem Versuche, hat der Verfasser, um diese lebhaft orangerote Färbung zur Nachweismethode mit Ionenaustauschharz am zweckmässigsten zu benutzen, ausführliche Untersuchung über verschiedene Bedingungen der Färbung von der Harzphase durchgeführt, und es gelang ihm, eine neue und sehr empfindliche sowie spezifische Nachweismethode für Molybdän vollkommen festzustellen.

1) Die vierte Mitteilung: M. Fujimoto, Dieses Bulletin 29, 571 (1956).

2) Vgl., z. B., E. B. Sandell, „Colorimetric Determination of Traces of Metals", 2. Aufl., London (1950), S. 455ff.

3) A. K. Babko, *J. Gen. Chem.* (U.S.S.R.), 17, 642 (1947); *Chem. Abstr.*, 42, 476*g* (1948).

4) Nach optischen Messungen Babkos wird diese Färbung dann infolge der Bildung des Komplexanions $[Mo(SCN)_6]^-$ verhältnismässig geschwächt, wenn die Konzentration der Rhodanidionen grösser als 0.2- bzw. 0.4 M ist (vgl. letztgenannte Fussnote).

Die in dieser Untersuchung benutzten Ionenaustauschharze

Dowex 1-X1: Ein aus Styrol und Divinylbenzol dargestelltes starkbasisches farbloses Anionenaustauschharz von quartärem Ammoniumtypus, dessen Divinylbenzolgehalt etwa einprozentig ist. Die Korngrösse ist ungefähr 50 Maschen von Tylerschem Normalsieb.

Dowex 1-X4: Ein ebenso starkbasisches farbloses Harz wie Dowex 1-X1, dessen Divinylbenzolgehalt jedoch etwa vierprozentig ist. Die Korngrösse ist 50 bis 100 Maschen.

Amberlite XE-114: Ein hellgelbes mittelstarkbasisches Harz. Die Korngrösse ist ungefähr 30 Maschen.

Amberlite IR-45: Ein hellbraunweisses sowie undurchsichtiges schwachbasisches Harz. Die Korngrösse ist ungefähr 30 Maschen.

Überdies wurde ein starksaures Kationenaustauschharz, Dowex 50-X8, um die fremden Matallionen, die den Nachweis stören, zu beseitigen, als eine Mikroharzsäule von NH_4R-Form angewandt. Die Korngrösse ist ungefähr 100 Maschen.

Versuchsanordnung

Auf einer weissen Tüpfelplatte versetzt man einen Tropfen der Probelösung mit einigen Körnchen des starkbasischen Anionenaustauschharzes von RCl-Form, rührt danach mit einem kleinen Glasstab völlig um, und lässt sie etwa drei Minuten stehen. Dann fügt man dazu einen Tropfen verdünnter wässeriger Lösung des Ammoniumrhodanides, und nach weiteren drei Minuten, einen Tropfen der in die Salzsäure gelösten verdünnten Lösung des Zinn(II)chlorides. Nach einigen Minuten, je nach dem Molybdängehalt von der Probelösung, entsteht über das Ganze der Harzkörnchen eine orangerote bzw. hellorange Färbung, die unter Beleuchtung mit einer Tischlampe und durch etwa zwanzigfache Vergrösserung mit einer Lupe wohl erkennbar ist.

Bestimmung der Bedingungen höchster Empfindlichkeit

1. Massflüssigkeit.—Eine Reihe der Massflüssigkeiten des Molybdäns wurde aus der gering ammoniakalischen wässerigen Lösung des extrareinen Ammoniumparamolybdates, deren 1 ccm 1.22 ± 0.003 mg von Molybdän enthielt[5], vorbereitet.

5) Die Menge des Molybdäns wurde folgenderweise einfacher bestimmt: Nach dem Verdampfen zum Trocknen bestimmtes Volumens der Probelösung, wurde der Rückstand durch Erhitzen bei ungefähr 500°C etwa eine Stunde lang ins Molybdänsäureanhydrid, MoO_3, vollkommen übergeführt und danach genau gewogen.

2. Reagenzien.—Als die Stocklösungen der Reagenzien wurden die folgenden Lösungen vorbereitet:

(1) 20prozentige wässerige Lösung des extrareinen Ammoniumrhodanids.

(2) Lösung des in die 6 N Salzsäure gelösten Zinn(II)chlorides wird in einer besonders wohl verstöpselten Flasche aufbewahrt. Diese Flasche wird gewöhnlich zur Bestimmung von ins Naturwasser gelöstem Sauerstoff nach Winklerschem Verfahren benutzt.

(3) Destillierte Salzsäure: ungefähr 6 N.

3. Bedingungen höchster Empfindlichkeit.—Die Ergebnisse unter verschiedenen Experimentalbedingungen ausgeführter Versuche werden mittels schematischer Darstellungsweise von der scheinbaren Durchschnittsintensität der Färbung, die in der dritten Mitteilung[6] genau beschrieben wurde, in Abb. 1 und Tabelle I zusammen dargestellt:

TABELLE I

VERSCHIEDENE REAKTIONSBEDINGUNGEN VON ABB. 1

Nr. des Experiments	Zeichen der Kurve	Ordnung der Versetzung von Reagenzien und Probelösung 1.	2.	3.	4.	Bemerkungen über die Resultate*
I_a	—△—	Probelsg.**	20proz. Lsg. des NH_4SCN	10proz. Lsg. (6 N HCl) des $SnCl_2$	Dowex 1-X4 (RCl)	*a*
I_b	—▽—	Dowex 1-X4 (RCl)	10proz. Lsg. (6 N HCl) des $SnCl_2$	20proz. Lsg. des NH_4SCN	Probelsg.	*a*
I_c	--○--	Dowex 1-X4 (RCl)	Probelsg.	1proz. Lsg. des NH_4SCN	0.5proz. Lsg. (6 N HCl) des $SnCl_2$	*b*
I_d	-·-○-·-	Dowex 1-X4 (RCl)	Probelsg.	20proz. Lsg. des NH_4SCN	0.5proz. Lsg. (6 N HCl) des $SnCl_2$	*c*
I_e	—○—	Dowex 1-X4 (RCl)	Probelsg.	0.2proz. Lsg. des NH_4SCN	0.5proz. Lsg. (6 N HCl) des $SnCl_2$	*b*
I_f	--△--	Probelsg.	0.2proz. Lsg. des NH_4SCN	0.5proz. Lsg. (6 N HCl) des $SnCl_2$	Dowex 1-X4 (RCl)	*d*
I_g	—□—	Dowex 1-X1 (RCl)	Probelsg.	0.2proz. Lsg. des NH_4SCN	0.5proz. Lsg. (6 N HCl) des $SnCl_2$	*b*
I_h	—×—	Amberlite XE-114 (RCl in 10^{-3} N HCl)	Probelsg.	0.2proz. Lsg. des NH_4SCN	0.5proz. Lsg. (6 N HCl) des $SnCl_2$	*b*
I_i	--×--	Amberlite IR-45 (RCl in 10^{-3} N HCl)	Probelsg.	0.2proz. Lsg. des NH_4SCN	0.5proz. Lsg. (6 N HCl) des $SnCl_2$	*b*, *e*
I_j	--▨--	Dowex 1-X1 (RCl)	Probelsg.	0.2proz. Lsg. des NH_4SCN	0.5proz. Lsg. (3 N HCl) des $SnCl_2$	*b*
I_k	-·-◪-·-	Dowex 1-X1 (RCl)	Probelsg.	0.2proz. Lsg. des NH_4SCN	10proz. Lsg. (6 N HCl) des $SnCl_2$	*b*
I_l	—◪—	Dowex 1-X1 (RCl)	Probelsg.	0.2proz. Lsg. des NH_4SCN	0.5proz. Lsg. (1 N HCl) des $SnCl_2$	*b*
I_m	—●—	Dowex 1-X1 (RCl)	Probelsg.	0.5proz. Lsg. (6 N HCl) des $SnCl_2$	0.2proz. Lsg. des NH_4SCN	*f*

**a*: Die Färbung der Harzkörnchen ist sehr schwach und unbeständig.

b: Die Harzkörnchen färben sich sehr deutlich schon nach weniger als eine Sekunde.

c: Die Harzkörnchen färben sich allmählich stärker, wobei es um die höhere Konzentration der Rhodanidionen händelt. (vgl. Abb. 3 sowie den Abschnitt „Diskussion.")

d: Die Harzkörnchen werden sehr langsam gefärbt.

e: Wegen der Undurchsichtigkeit der Harzkörnchen wird die scheinbare Intensität der Färbung beträchtlich geschwächt.

f: Die Harzkörnchen färben sich erst etwa 5 Sekunden nach der Mischung.

** Die hier benutzte Probelösung enthält 0.49 γ Molybdän (16.2 γ/ccm als MoO_3).

6) M. Fujimoto, Dieses Bulletin 29, 567 (1956).

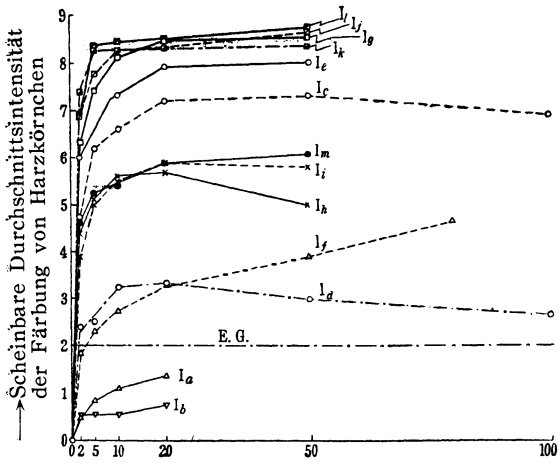

Abb. 1. Vergleichung verschiedener Experimentalbedingungen.

Von diesen Ergebnissen aus betrachtet, wurde das folgende Verfahren als das best geeignete vollkommen festgestellt:

„Man versetzt auf einer weissen Tüpfelplatte einen Tropfen der neutralen oder schwach alkalischen[7] Probelösung mit einigen Körnchen von Dowex 1-X1 (RCl-Form), rührt sie mit einem kleinen Glasstab völlig um, und lässt sie etwa drei Minuten lang stehen. Dann fügt man dazu einen Tropfen 0.2 prozentiger wässeriger Lösung des Ammoniumrhodanids, und nach weiteren drei Minuten, einen Tropfen der 0.5- bzw. 10prozentigen Lösung des in 1- bzw. 6 N Salzsäure gelösten Zinn(II)chlorides. Nach einige Minuten, beobachtet man die orange bzw. orangerote Färbung der Harzkörnchen."

Bestimmung der Erfassungsgrenze[8]

Abb. 2 stellt die Resultate durch Verfahren „I_g" von Abb. 1 durchgeführter Experimente dar:

Wie man von diesen Kurven aus klar ersieht, wurde die Erfassungsgrenze an dieser Reaktion für Molybdän, 0.024 γ unter Grenzkonzentration $1:1.6\times10^6$ festgestellt.

Einfluss der Anionenkonzentration der Probelösung auf die Empfindlichkeit der Reaktion

Gibt es eine grosse Menge von fremden Salzen in der Probelösung, wird die Empfindlichkeit der Färbungsreaktion beträchtlich beschädigt. Die Resultate der Vergleichungen der Empfindlichkeitsveränderung, die mit Natriumchlorid als ein Vertreter dieser Art von Salzen durchgeführt wurden, stehen in Abb. 3:

Wie man aus der Vergleichung dieser Kurven leicht erkennt, sinkt die Empfindlichkeit der

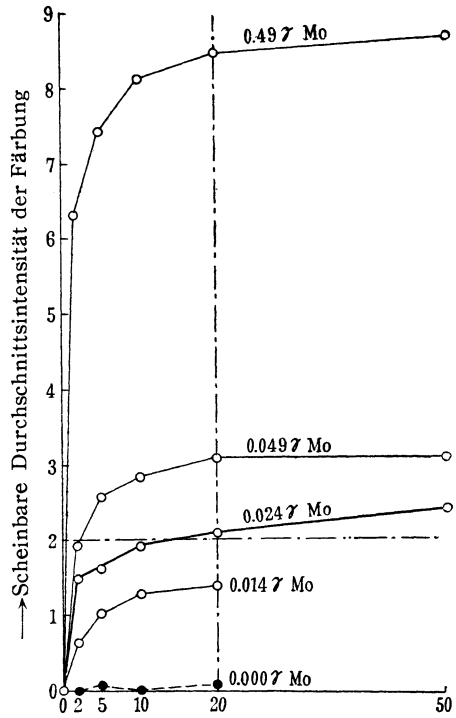

Abb. 2. Bestimmung der Erfassungsgrenze.

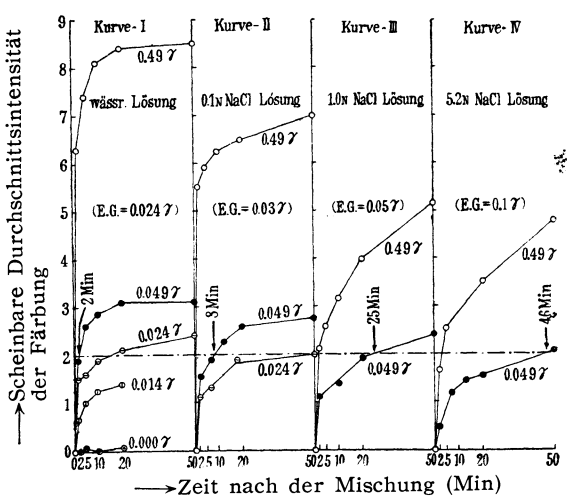

Abb. 3. Einfluss der Anionenkonzentration auf die scheinbare Färbungsintensität.

Farbenreaktion mit dem steigenden Konzentration der Chloridionen in der Probelösung allmählich herab; d.h. die Erfassungsgrenze der Nachweisreaktion verändert sich von der Menge 0.024 γ bei Abwesenheit fremder Anionen bis zu 0.05 γ im Falle der ins 1.0 N Natriumchlorid gelöster Probelösung, und noch zu 0.1 γ, wenn die Probelösung als 5.2 N Natriumchloridlösung angewandt wird. Die Ursache dieser Empfindlichkeitsabnahme wird später genau diskutiert werden[6].

7) Vgl. den Abschnitt „Diskussion" (S. 598).

8) In bezug auf die Erfassungsgrenze, vergleiche die erste Mitteilung: M. Fujimoto, Dieses Bulletin 27, 48 (1954).

Einfluss der Wasserstoffionenkonzentration der Probelösung auf die Empfindlichkeit der Reaktion

Wenn die Probelösung sauer ist, wird die Färbungsintensität der Harzphase sowieso beträchtlich schwächer, wenn auch die Konzentration fremder Anionen verhältnismässig niedrig ist.

Abb. 4 zeigt ein typisches Beispiel dafür; d. h. die Empfindlichkeitsveränderung der Reaktion,

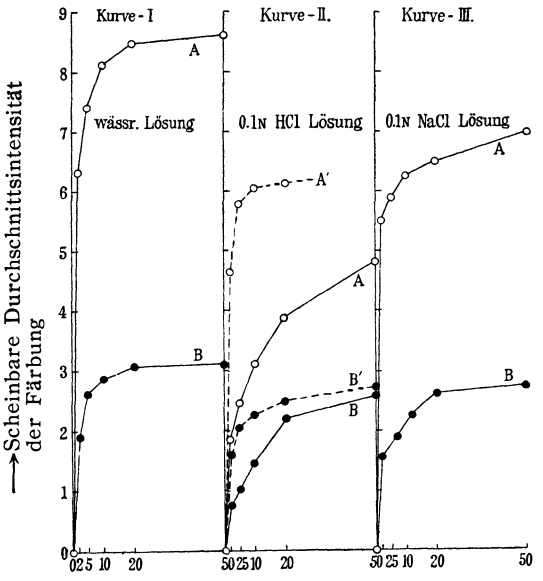

Abb. 4. Einfluss der Acidität der Probelösung auf die scheinbare Färbungsintensität.
—○—, --○-- 0.49 γ Mo in der Probelösung (0.04 ccm)
—●—, --●-- 0.049 γ Mo in der Probelösung (0.04 ccm)

wenn die Probelösung als 0.1 N-salzsaure Lösung verwandt wird. Die gestrichelten Linien stellen die Empfindlichkeitssteigerung durch gelindes Erwärmen mit ein wenig überschüssigem verdünntem Ammoniakwasser dar. Durch dieses Verfahren kann man die Reaktionsempfindlichkeit einfach zum beinahe gleichen Grade mit dieselbe des Falls, wenn die Probelösung als 0.1 N Natriumchloridlösung verwandt wird, steigern. Über diesen Verlauf der Reaktion wird der Verfasser im folgenden Abschnitt kurz erörtern.

Diskussion

Obgleich man darüber nur halbquantitativ diskutieren kann, ist der Verlauf der in Abb. III dargestellten Kurven besonders interessant. Da in der wässerigen Lösung, deren pH-Wert zwischen 14 und 6.8 liegt, die Molybdationen grösstenteils als einfache Orthomolybdationen, MoO_4^{2-}, vorhanden sind[9], könnte man vermuten, dass das Anionenaustauschgleichgewicht zwischen Chloridionen in der Harzphase und Molybdationen in der Probelösung verhältnismässig geschwind erreicht wird. Daher beruht die etwa zwei Minuten nach der Mischung beobachtete scheinbare Intensität der Färbung von der Harzphase vielleicht hauptsächlich auf die durch Reaktion der Orthomolybdationen in der Harzphase mit Rhodanidionen und Reduktionsmittel gebildeten Komplexanionen, $[Mo(SCN)_6]^-$, deren Menge, wie man in Abb. 3 deutlich ersieht, mit steigenden Chloridionenkonzentration deutlich abnimmt. Ausserdem ist es auch sehr interessant, dass, je höher die Konzentration der in der Probelösung enthaltenen Chloridionen, desto grösser ist die Zunahme der später als zwei Minuten nach der Mischung mit der Zeit entwickelten Färbung der Harzphase. Diese Steigerung der Färbungsintensität kann man als die langsame Adsorption der in der Lösungsphase gebildeten gefärbten Rhodanidkomplexanionen halbquantitativ betrachten (vgl. den Unterschied zwischen den Kurven-I_d, I_c und I_e von Abb. 1).

Abb. 4 erzeigt auch ein sehr interessantes Verhalten der in der sauren Lösung vorhandenen Molybdationen gegen das Anionenaustauschharz, wobei die Menge vorher in die Harzphase adsorbierter Molybdationen ausserordentlich kleiner als dieselbe der

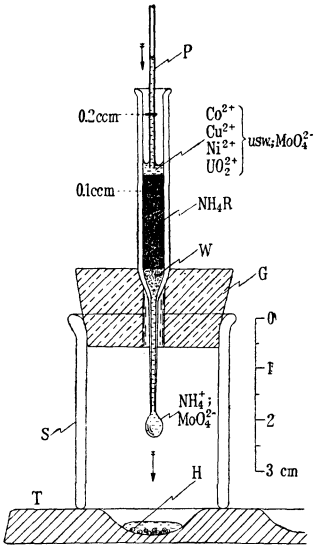

Abb. 5. Mikroharzsäule zur Trennung von Metallionen.
NH_4R: Mikrosäule des Kationenaustauschharzes von NH_4R-Form, P: Kapillarpipette (1 Tropfen = 0.02 ccm), G: Gummistopfen, S: Glasrohr (3×3.7 cm), T: Tüpfelplatte, H: Anionenaustauschharz von RCl-Form, W: Glaswolleschicht.

9) G. Jander, K.F. Jahr und W. Heuckeshoven, *Z. anorg. u. allgem. Chem.*, **194**, 383 (1930).

neutralen Probelösung mit gleicher Anionenkonzentration. Da dieser Nachteil, der von der Acidität der Probelösung herrührt, durch Neutralisation mit Ammoniakwasser beinahe vollends beseitigt wird (vgl. die bemerkenswürdige Ähnlichkeit zwischen der Gestalt von Kurve-IIA′ sowie IIB′ und der von Kurve-IIIA sowie IIIB), ist es wahrscheinlich, dass diese ungewöhnlich niedrige Färbungsintensität der Harzphase auf die Aggregation[9] der Molybdationen in der Lösung zu Riesenanionen beruht, die selbst mit Dowex 1–X1 schwierig sich adsorbieren lassen.

Einflüsse der Begleitstoffe

Wie man in Tabelle II klar ersieht, wurden die Einflüsse verschiedenartiger Begleitstoffe auf die Nachweisreaktion besonders ausführlich untersucht, und dabei wurde die Störung solcher Kationen wie Kupfer(II), Kobalt(II), Nickel(II), Uranyl(II) usw. durch einfache Anwendung einer Mikrosäule des starksauren Kationenaustauschharz von NH_4R-Form (Abb. V)[10] sehr leicht und völlig beseitigt.

TABELLE II

EINFLÜSSE DER BEGLEITSTOFFE

Begleitstoffe	benutzter Verbindungstypus	Menge von Begleitstoffen	Nachweisbare Molybdänmenge	Grenzverhältnis	Bemerkungen
Cr(VI)	K_2CrO_4	Stört völlig den Nachweis.		——	——
〃 〃	$K_2Cr_2O_7$	180 γ	0.054 γ	$1:3.3\times10^3$	*a*
W(VI)	Na_2WO_4	Stört völlig den Nachweis.		——	——
〃 〃	〃 〃	220 γ	0.12 γ	$1:1.8\times10^3$	*b*
U(VI)	$UO_2(CH_3COO)_2$	112 γ	0.098 γ	$1:1.15\times10^3$	U(VI)≦0.3proz.
〃 〃	〃 〃 〃 〃	4 mg	0.049 γ	$1:8.2\times10^4$	*c*
Mn(II)	$MnSO_4$	1.6 mg	0.049 γ	$1:3.3\times10^4$	——
Fe(III)*	$FeCl_3$	830 γ	0.098 γ	$1:8.5\times10^3$	——
Co(II)**	$CoCl_2$	230 γ	0.24 γ	$1:9.6\times10^2$	Co(II)≦0.5proz.
〃 〃	〃 〃	2.3 mg	0.12 γ	$1:1.9\times10^4$	*c*
Ni(II)	$NiCl_2$	1 mg	0.24 γ	$1:4.1\times10^3$	——
Cu(II)	$CuSO_4$	20 γ	0.24 γ	$1:8.3\times10$	Cu(II)≦0.05proz.
〃 〃	〃 〃	1.6 mg	0.06 γ	$1:2.7\times10^4$	*c*
Zn(II)	$ZnSO_4$	280 γ	0.036 γ	$1:7.8\times10^3$	——
Cd(II)	$CdCl_2$	380 γ	0.098 γ	$1:3.9\times10^3$	——
Hg(II)	$HgCl_2$	740 γ	0.024 γ	$1:3.1\times10^4$	——
$PO_4^{3-}(H_2PO_4^-)$	H_3PO_4	7.2 mg	0.048 γ	$1:1.5\times10^5$	——
NO_2^-	$NaNO_2$	44 γ	0.20 γ	$1:2.2\times10^2$	NO_2^-≦0.1proz.
NO_3^-	NH_4NO_3	7.4 mg	0.12 γ	$1:6.2\times10^4$	——
Oxalsäure	Oxalsäure	2.3 mg	0.041 γ	$1:5.6\times10^4$	——
Weinsäure	Weinsäure	3.7 mg	0.054 γ	$1:6.7\times10^4$	——
Zitronensäure	Zitronensäure	3.6 mg	0.028 γ	$1:1.3\times10^5$	——

* 10prozentige Lösung (6N HCl) des $SnCl_2$ wurde angewandt.

** Drei Tropfen der 1proz. Lösung des NH_4SCN wurde angewandt.

a: Nach der Reduktion des Chromates zum Chrom(III)salze durch gelindes Erhitzen auf einem Wasserbad mit einem Tropfen der 3proz. Lösung (1N H_2SO_4) des Wasserstoffperoxydes:

b: Nach der Trennung des Wolframates als Wolframsäureniederschlag durch Zusatz von einem Tropfen der 6- bzw. 12N Salzsäure: Es ist wahrscheinlich, dass es hier um eine Art der Siebeffekt von der Harzphase für Polymolybdate und Polywolframate sich händelt.

c: Nach der Trennung des Kations durch eine Mikroharzsäule von NH_4R-Form (Abb. 5):

10) Trennung von Metallionen mit Hilfe dieser Mikroharzsäule wird folgenderweise durchgeführt: Mit einer kleinster Mikropipette (P: ein Tropfen=0.02 ccm) fügt man zu dieser Mikrosäule einen Tropfen der Probelösung, worin verschiedenartige fremde Metallionen, die die Nachweisreaktion stören, enthalten sind, und wäscht die Säule danach mit zwei bzw. drei Tropfen destilliertes Wassers aus (1 Tropfen/Min). Man kann mit hier erhaltener metallionenfreier Lösung von Ammoniummolybdat und in der Vertiefung der Tüpfelplatte vorher vorbereiteten Anionenaustauschharzkörnchen in gewöhnlicher Weise den Nachweis des Molybdäns durchführen. Die gebrauchte Harzsäule wird durch dreimaliges Durchlaufen je dreissig Tropfen der 2 N Salzsäure, 6 N Ammoniakwassers und destilliertes Wassers leicht in die NH_4R-Form zurückgeführt.

Zusammenfassung

1. Durch einfache Anwendung farbloser starkbasischer Anionenaustauschharze zur Farbenreaktion der Molybdate mit Rhodanid und Zinn(II)chlorid wird eine neue sehr empfindliche und spezifische Methode zum Nachweis kleinster Menge des Molybdäns vollkommen festgestellt, und dabei wird das best geeignete Verfahren durch Vergleichungen verschiedener Experimentalbedingungen ausführlich untersucht.

2. Die Einflüsse der Anionen- sowie Wasserstoffionenkonzentration von der Probelösung auf die Empfindlichkeit der Nachweisreaktion werden genau untersucht, und durch genügende Überlegung über das Anionenaustauschgleichgewicht zwischen Chlorid- und Molybdationen und über die Aggregation der Molybdationen werden diese Beziehungen halbquantitativ genau diskutiert.

3. Die Einflüsse verschiedenartiger Begleitstoffe wird vollkommen studiert, wobei eine einfache Mikrosäule des Kationenaustauschharzes von NH_4R-Form zur Trennung fremder Kationen, die die Reaktion beträchtlich stören, erfolgreich angewandt wird.

Zum Schluss möchte der Verfasser Herrn Prof. Dr. E. Minami für seine vielen wertvollen Ratschläge sowie freundliche Anregungen über diese Untersuchung seinen herzlichsten Dank aussprechen.

Laboratorium der analytischen Chemie,
Chemisches Institut der
wissenschaftlichen Fakultät,
Tokyo Universität, Tokyo

Mikroanalyse mit Hilfe von Ionenaustauschharzen. VI. Über den Nachweis kleinster Menge des Nitrites mit m-Phenylendiamin[1]

Von Masatoshi FUJIMOTO

(Eingegangen am 24. März 1956)

Einleitung

Aus einer sauren wässerigen Lösung wird das *m*-Phenylendiamin in der Form von Ammoniumion in starksaures Kationenaustauschharz von HR-Form stark adsorbiert. Wirkt die salpetrige Säure oder das Nitrit bei Anwesenheit der Säuren auf das in der Lösungsphase vorhandene *m*-Phenylendiamin ein, so bildet sich intermediär ein Gemisch der Diazoniumsalze gemäss den folgenden stufenweisen Reaktionsgleichungen:

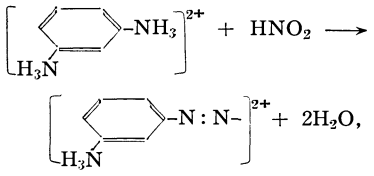

I

oder weiter

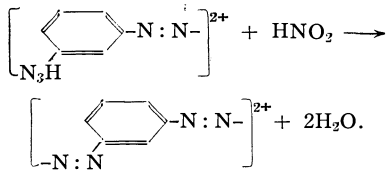

II

Sobald die letztgenannten Reaktionen stattfinden, werden die hier gebildeten Diazoniumionen (I und II) gleichfalls in obengenanntes Harz stark adsorbiert, worin diese beiden sogleich mit dem bereits in die Harzphase etwas adsorbierten *m*-Phenylendiamin koppeln und durch intramolekulare Umlagerung in ein Gemisch kationischer Azofarbstoffe (III und IV), sogenanntes Bismarckbraun[2], übergeführt werden:

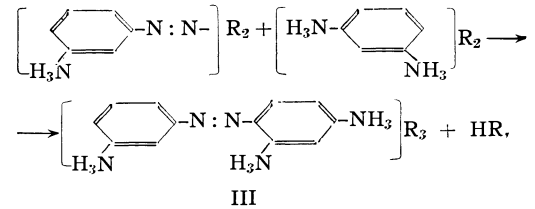

III

und auch

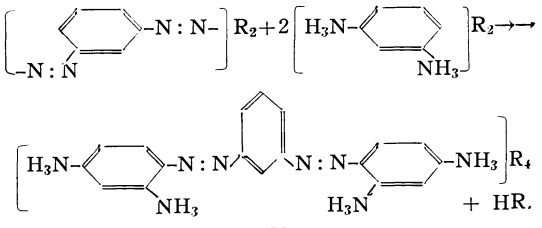

IV

1) Die fünfte Mitteilung: M. Fujimoto, Dieses Bulletin **29**, 595 (1956).

Hierbei bedeutet R einwertiges Anion vom Kationenaustauschharze.

Wegen sehr beschränktes Rauminhalts[3] der Harzkörnchen, worin die obenerwähnten Farbstoffionen unmittelbar gebildet werden, nimmt die Konzentration dieser sich färbenden Kationen durch Adsorption in die Harzphase merklich zu, und demnach verstärkt sich die Färbung der Harzphase auffallend. Auf solche Weise konnte man eine neue und sehr empfindliche sowie spezifische Nachweismethode für die Spurmenge des Nitrites mit dem Kationenaustauschharze[4] folgendermassen feststellen.

Die in dieser Untersuchung benutzten Kationenaustauschharze

Zum gegenwärtigen Zwecke wurde ein aus Styrol und Divinylbenzol dargestelltes starksaures sowie farbloses Harz von Sulfonsäuretypus hauptsächlich angewandt, dessen Divinylbenzolgehalt einprozentig ist[5]. Die Korngrösse ist ungefähr 30 Maschen von Tylerschem Normalsieb. In der vorliegenden Mitteilung wird dieses Harz als „1proz. DVB" kurz beschrieben.

Überdies wurden folgende Harze auch angewandt:

„20proz. DVB": Ein ebenso starksaures und gelbes Kationenaustauschharz wie das letztgenannte Harz, dessen Divinylbenzolgehalt jedoch zwanzigprozentig ist.[5] Die Korngrösse ist ungefähr 50 Maschen.

Dowex 50W-X8: Ein käufliches farbloses und starksaures Harz von Sulfonsäuretypus, dessen Divinylbenzolgehalt etwa achtprozentig ist. Die Korngrösse ist 50 bis 100 Maschen.

Duolite C-60: Ein hellgelbes mittelstarksaures Kationenaustauschharz von Phosphonsäuretypus, dessen Korngrösse ungefähr 20 Maschen ist.

Alle diese Harze wurden vor dem Gebrauch durch zweimaliges Durchlaufen der 2 N Salzsäure sowie destilliertes Wassers völlig in die HR-Form übergeführt.

Versuchsanordnung

Man bringt auf eine weisse Tüpfelplatte einige Körnchen des Kationenaustauschharzes und einen Tropfen verdünnter Reagenslösung, rührt danach mit einem kleinen Glasstab völlig um, und lässt sie einige Minuten lang stehen. Dann fügt man einen Tropfen der Probelösung, und nach einigen Minuten, beobachtet man unter Beleuchtung einer Tischlampe mit einer Lupe eine in der Harzphase entstandene Orange- bzw. Braunfärbung.

Bestimmung der Bedingungen höchster Empfindlichkeit

1. Massflüssigkeit.—Zum vorliegenden Zwecke wurde eine Reihe der Massflüssigkeiten des Nitrites aus der wässerigen Lösung des extrareinen Natriumnitrites vorbereitet, deren 1 ccm 9.75 mg von Nitrite (als NO_2) enthielt[6].

2. Reagenslösung.—Als die Stocklösungen des *m*-Phenylendiamins wurden folgende zwei Arten der Lösungen vorbereitet:

(1) Eine in die 0.3 N Salzsäure gelöste 0.5-prozentige Lösung.

(2) Eine in die 10prozentige Essigsäure gelöste 0.5prozentige Lösung.

3. Einfluss der Harzart[7].—Betrachtet man aus der Vergleichung verschiedenartiger Harze,

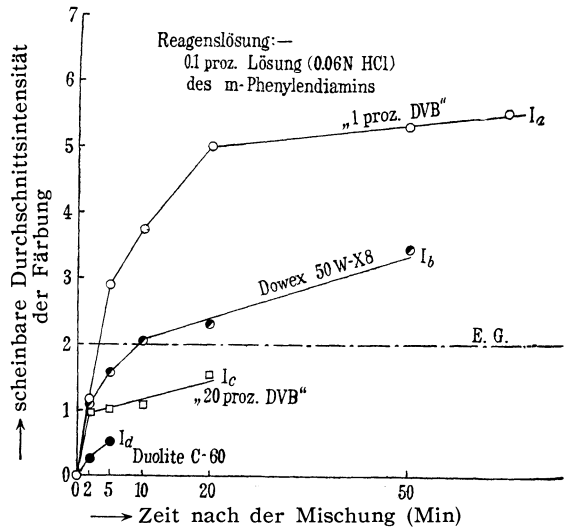

Abb. 1. Einfluss der Harzart.

2) Nur dann, wenn die obengenannten Azofarbstoffe innerhalb der Harzphase unmittelbar sich bilden, ist die gegenwärtige Nachweismethode wirksam, da die bereits in der Lösungsphase völlig gebildeten Farbstoffe wegen ihrer geringen Löslichkeit in Wasser sowie ihrer grösseren Ionenvolumen nur langsam in die Harzphase adsorbiert werden und die Färbung der Harzphase infolgedessen an ihrer Intensität geringfügig sich verstärkt (vgl. den Verlauf der Kurve-I_f von Abb. II).

3) Angenommen, dass bei der Reaktion zehn Körnchen des Harzes, dessen Korngrösse beim Eintauchen in der Lösung sechzig Maschen sei, benutzt werden, so beträgt das Volumenverhältnis zwischen der Harzphase und der Lösungsphase (0.08 ccm) etwa 1:520.

4) Starkbasisches Anionenaustauschharz adsorbiert auch diese Farbstoffe, obgleich die Ursache dafür gegenwärtig unverständlich sei. Aber die Anionenaustauschharze wurden diesmal nicht benutzt, da diese im Vergleich mit den Kationenaustauschharzen bedeutend schwächer sich färben.

5) Diese beiden Harzproben wurden von Herrn Prof. Dr. A. Kawamura an der Landwirtschaftlichen und Technischen Universität zu Tokyo nach dem Verfahren K.W. Peppers kürzlich dargestellt.

6) Die Menge in der Massflüssigkeit vorhandener Nitritionen wurde folgenderweise titrimetrisch bestimmt: 20 Min nach dem Zusatze bestimmter Menge der Massflüssigkeit des Nitrites zu einem Gemisch bestimmtes Überschusses von 0.1 N Kaliumpermanganatmassflüssigkeit und verdünnter Schwefelsäure, fügt man dazu etwa 1 g festes Kaliumjodides und titriert das hier gebildete freie Jod mit 0.1 N Massflüssigkeit des Natriumthiosulfates (vgl. S. Takagi „Teiryo-Bunseki no Jikken to Keisan (Experimente und Rechnung der quantitativen Analyse)," Band II., 5. Aufl., 1952, (japanisch), Tokyo, S. 363.

7) In bezug auf die in Abbildungen gegenwärtiger Mitteilung angewandte halbquantitative Darstellungsweise der scheinbaren Durchschnittsintensität der Färbung von der Harzphase, vergleiche III. Mitteilung: M. Fujimoto, Dieses Bulletin 29, 567 (1956).

die in Abb. 1 steht, wird das Harz, „1proz. DVB", als das best geeignete ausgewählt.

4. Vergleichung verschiedener Versuchsbedingungen.—Abb. 2 stellt die Resultate der Vergleichungen von den in Tabelle I kurzgefassten verschiedenen Experimentalbedingungen dar.

Aus der obigen Weise, werden hier zwei Verfahren, d. h., „I_n" und „I_a" als die insbesondere ausgezeichneten festgestellt; nämlich:

„Auf eine weisse Tüpfelplatte bringt man einige Körnchen des Kationenaustauschharzes, „1proz. DVB", von HR-Form sowie einen Tropfen der in die 0.06 N Salzsäure oder in die 10prozentige Essigsäure gelösten 0.1prozentigen Lösung des *m*-Phenylendiamins, rührt mit einem kleinen Glasstab um, und lässt sie etwa 10 Min stehen. Dann fügt man dazu einen Tropfen der Probelösung, und nach einigen Minuten, beobachtet man eine Braunorange- bzw. Rotorangefärbung, die über dem Ganzen der Harzkörnchen entsteht".

Hier muss man darauf besonders beachten, dass man die Salzsäure nicht im Überschuss anwendet.

TABELLE I

VERSCHIEDENE EXPERIMENTALBEDINGUNGEN VON ABB. 2

Nr. des Experiments	Zeichen der Kurve	Ordnung der Versetzung von Reagenzien und Probelösung 1.	2.	3.	4.	Bemerkungen über die Resultate*
I_a	—○—	HR**	0.1proz. Lsg.—(10 Min)***→Probelsg.**** (0.06 N HCl) des *m*-Phenylendiamins	——		*a*
I_e	—◐—	HR	0.5proz. Lsg.—(10 Min)→Probelsg. (0.3 N HCl) des *m*-Phenylendiamins	——		*a*
I_f	—△—	0.5proz. Lsg. (0.3 N HCl) des *m*-Phenylendiamins	Probelsg.—(10 Min)→HR	——		*b*
I_g	—×—	HR	6 N HCl	0.5proz. Lsg-—(10 Min)→Probelsg. (0.3 N HCl) des *m*-Phenylendiamins		*a*
I_k	—□—	HR	Probelsg.	0.1proz. Lsg. (0.06 N HCl) des *m*-Phenylendiamins	——	*a, c*
I_h	—⊞—	HR	Probelsg.	0.5proz. Lsg. (0.3 N HCl) des *m*-Phenylendiamins	——	*a, c*
I_j	—◇—	HR	0.1proz. Lsg.—(5 Min)→Probelsg. (0.06 N HCl) des *m*-Phenylendiamins	——		*d, e*
I_i	—◈—	HR	0.5proz. Lsg.—(5 Min)→Probelsg. (0.3 N HCl) des *m*-Phenylendiamins	——		*a, d*
I_l	—■—	HR	0.5proz. Lsg.—(5 Min)→Probelsg. (0.3 N HCl) des *m*-Phenylendiamins	6 N HCl		*a, d*
I_m	- -×- -	HR	0.5proz. Lsg.—(5 Min)→Probelsg. (0.3 N HCl) des *m*-Phenylendiamins	6 N HCl		*f*
I_n	—⊙—	HR	0.1proz. Lsg.—(10 Min)→Probelsg. (10proz. CH_3COOH) des *m*-Phenylendiamins	——		*e*

**a*: Enthält die Probelösung kein Nitrit, so färben sich die Harzkörnchen nur schwach Purpur.

b: Die Harzkörnchen färben sich sehr langsam an ihren Rändern[2].

c: Gerade nach dem Zusatze von der Probelösung, wird die Lösung des *m*-Phenylendiamins hinzugefügt.

d: Etwa fünf Minuten nach dem Zusatze der Lösung des *m*-Phenylendiamins, werden die Harzkörnchen mit je drei Tropfen destilliertes Wassers dreimal ausgewaschen.

e: Wenn kein Nitrit in der Probelösung vorhanden ist, werden die Harzkörnchen kaum gefärbt.

f: Die Harzkörnchen sind beinahe farblos.

** HR bedeutet bei der vorliegenden Tabelle „1proz. DVB" von HR-Form.

*** Zeitdauer nach dem Eintauchen der Harzkörnchen in die Reagenslösung.

**** Die hier benutzte Probelösung enthält 0.39 γ Nitrit (9.75 γ/ccm).

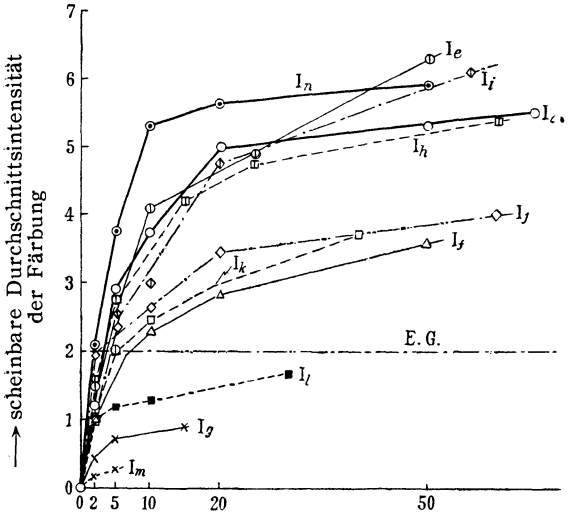

Abb. 2. Einflüsse verschiedener Experimentalbedingungen.

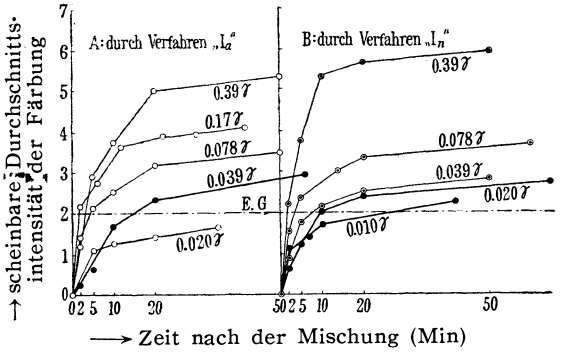

Abb. 3. Bestimmung der Erfassungsgrenze.

Bestimmung der Erfassungsgrenze

Die Ergebnisse durch Verfahren „I_n" sowie „I_a" durchgeführter Experimente werden in Abb. 3A sowie 3B zusammengestellt:

Die so bestimmte Erfassungsgrenze und die Grenzkonzentration an dieser Reaktion für Nitrit stehen in nachfolgender Tabelle:

	Durch Verfahren „I_a":	Durch Verfahren „I_n":
Erfassungsgrenze	0.039 γ NO_2	0.015 γ NO_2
Grenzkonzentration	$1:1.0\times10^6$	$1:2.7\times10^6$

Einflüsse der Begleitionen

Die Resultate durch Verfahren „I_n" durchgeführter Untersuchungen stehen in Tabelle II:

Nachweis des Nitrates nach der Reduktion zum Nitrite mit Zinkstaub

Durch Zusatz von Zinkstaub werden die Nitrate sehr glatt zu den Nitrite reduziert, und demnach werden diese mit Hilfe obengenannter Verfahren leicht nachgewiesen.

Hier wurde eine wässerige Lösung des Kaliumnitrates, deren 1 ccm 10 mg von Nitrat (als NO_3) enthielt, als die Massflüssigkeit des Nitrates vorbereitet.

Der käufliche Zinkstaub, so wie er ist, reagiert mit Nitrationen nur langsam. Daher wurde dieser, um dessen Reduktionsaktivität beträchtlich zu vergrössern, mit 1 N Essigsäure auf einem Wasserbade etwa ein Stunde lang erwärmt,

TABELLE II

EINFLÜSSE DER BEGLEITIONEN

Begleitionen	benutzter Verbindungstypus	Menge der Belgleitionen	Nachweisbare Nitritmenge	Grenzverhältnis	Bemerkungen*
F^-**	KF	Stört völlig den Nachweis.		—	*a*
Cl^-	NaCl	7.1 mg	0.03 γ	$1:2.4\times10^5$	—
Br^-	KBr	7.7 mg	0.02 γ	$1:3.8\times10^5$	—
J^-	KJ	9.2 mg	0.02 γ	$1:4.6\times10^5$	—
SCN^-	NH_4SCN	4.1 mg	0.015 γ	$1:2.7\times10^5$	—
S^{2-}	Na_2S	180 γ	0.017 γ	$1:1.1\times10^4$	*b*
SO_4^{2-}	Na_2SO_4	850 γ	0.14 γ	$1:6.1\times10^3$	—
〃	〃	2.2 mg	0.04 γ	$1:5.7\times10^4$	*c*
$Cr_2O_7^{2-}$	$K_2Cr_2O_7$	Stört völlig den Nachweis.		—	*d*
NO_3^-	KNO_3	10 mg	0.08 γ	$1:1.3\times10^5$	—
PO_4^{3-}	Na_2HPO_4	8.6 mg	0.04 γ	$1:2.2\times10^5$	—

*a: Die Lösungsphase färbt sich orangebraun und die Harzphase hellrot.

b: Infolge der Bildung von weissem Niederschlag wird die Färbung der Harzphase verhältnismässig schwierig erkennbar.

c: Nach dem Zusatze von zwei Tropfen 10 prozentiger Lösung von Bariumchlorid, wird der Nachweis durchgeführt.

d: Ein dunkelbrauner Farbstoff wird gebildet, der die Harzphase intensiv dunkelbraun färbt.

** Noch ein Tropfen 33prozentiger Essigsäure wird angewandt.

dekantiert, mit Wasser dreimal umgewaschen, und in einem Vekuumexsikkator völlig getrocknet[8]).

Die kleinste Nitratmenge, die nach der Reduktion mit der Nadelspitzmenge[9]) des oben behandelten Zinkstaubs nachgewiesen wurde, war jedoch 0.08 γ durch Verfahren „I_n" und 0.4 γ durch „I_a".

Zusammenfassung

1. Durch Anwendung starksaurer Kationenaustauschharze zu einem der Diazoreaktionssysteme gelingt es, starkgefärbte Azofarbstoffkationen, Bismarckbraun, unmittelbar in dem sehr beschränkten Raum-inhalt des Harzkörnchens fest bilden zu lassen, und dadurch wird eine neue und sehr empfindliche Nachweismethode für kleinste Menge des Nitrites mit *m*-Phenylendiamin festgestellt.

2. Zwei Arten der Verfahren höchster Empfindlichkeit werden durch ausführliche Erforschung über verschiedene Experimentalbedingungen einwandfrei festgestellt, und durch deren Anwendung werden die Einflüsse verschiedenartiger fremder Anionen vollständig untersucht.

3. Weiterhin wird geringe Menge des Nitrates auch nach der Reduktion mit der Nadelspitzmenge des Zinkstaubs gleichermassen wie beim Nitrit nachgewiesen.

Zum Schluss möchte der Verfasser Herrn Prof. Dr. E. Minami für seine freundlichen Anregungen bei vorliegender Untersuchung seinen herzlichsten Dank aussprechen.

Für die Kationenaustauschharze, „1proz. DVB" sowie „20proz. DVB",[5]) ist der Verfasser Herrn Prof. Dr. A. Kawamura an der Landwirtschaftlichen und Technischen Universität zu Tokyo zu verbindlichstem Dank verpflichtet.

Laboratorium der analytischen Chemie,
Chemisches Institut der
wissenschaftlichen Fakultät,
Tokyo Universität, Tokyo

8) Vgl. F. Feigl, „Spot Tests. I. Inorganic Applications," übersetzt von R.E. Oesper, 4. engl. Aufl., 1954, Amsterdam, S. 302.

9) Sie entspricht etwa 200 γ.

Studies on the Infrared Spectra of Ephedrine and Related Compounds. III. Infrared Spectra of Diastereoisomeric N-Methylephedrines and 1, 2-Diphenyl-2-methylaminoethanols-(1) in 3 micron Region

By Tokunosuke KANZAWA

(Received February 13, 1956)

The spectra of the diastereoisomeric N-methylephedrines and 1, 2-diphenyl-2-methylaminoethanols-(1) in 3 micron region are very like those of ephedrines as shown in the previous paper[1], but their $\Delta\nu$ values, which are differences in wave numbers of the free and the bonded OH absorption band, are somewhat different from those of ephedrines. Thus, the difference in $\Delta\nu$ values between N-methylephedrine isomers ($238-157=81\ cm^{-1}$) is much larger than that between ephedrines ($203-168=35\ cm^{-1}$). On the other hand, the two isomers of 1, 2-diphenyl-2-methylaminoethanol-(1) give smaller $\Delta\nu$ values (151 and $193\ cm^{-1}$) than those of ephedrines, and the erythro isomer exceptionally shows an absorption near $3600\ cm^{-1}$ consisting of two bands by $30\ cm^{-1}$ apart from each other, whereas the other compounds examined show only one band. Although these two pairs of compounds are similar in chemical behavior to ephedrines, the appreciable changes in $\Delta\nu$ seem to be related to the change of steric structure caused by substitution of the groups. The object of the present experiments is to obtain information on the molecular structure of these compounds and to discuss their conformations in connection with that of ephedrines as proposed previously[2].

Experimental

The spectrophotometer used, its operating conditions and the procedure for the purification of the solvents are the same as described previously[2]. N-methylephedrines were in optically active forms and 1, 2-diphenyl-2-methylaminoethanols-(1) were racemic modifications. They were supplied by Dr. K. Tanaka and Mr. T. Sugawa in this Laboratory.

1) T. Kanzawa, This Bulletin, 29, 398 (1956).

2) T. Kanzawa, This Bulletin, 29, 479 (1956).

Experimental Results

A. N-Methylephedrines.—In Fig. 1. the concentration dependence of the absorption for N-methylephedrines is shown. Over a concentration range of 0.001–0.01 mol./l. the spectra of both isomers show no appreciable change in the position and intensity of the absorption bands. On raising the concentration up to a few tenth mol./l. spectral changes are observed for both isomers, although not so marked as in the cases of ephedrines. Thus, for N-methylephedrine the intensity of a sharp band at 3617 cm^{-1} decreases and that of a broad band at 3460 cm^{-1} increases with concentration. For Ψ-N-methylephedrine a band at 3613 cm^{-1} disappears already at 0.045 mol./l. (not shown in Fig. 1b) and the intensity of a broad band at 3375 cm^{-1} decreases. The shift of the broad band towards lower frequency for the concentration change from ~0.005 to ~0.1 mol./l. is about 10 cm^{-1} for both isomers.

Since N-methylephedrines have no NH group, it will be reasonable to assign the higher-frequency band to free OH stretching vibration and the lower-frequency one to bonded OH vibration (OH -N). From a behavior in concentration dependence it may be said that as long as the concentration remains small the hydrogen bond is of an intramolecular type. The possibility of the formation of the ring dimer seems to be difficult to consider from cryoscopic data for alkamines[3]. In the spectra of the dilute solution shown in Fig. 1a and 1b, it will be noticed that, when

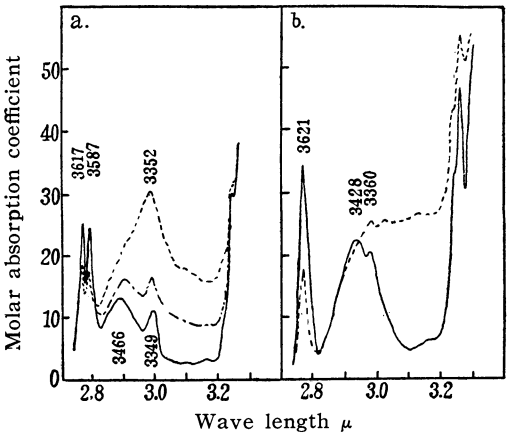

Fig. 1. Concentration dependence. N-Methylephedrine. CCl_4 solns.
a) normal. ——— 0.0046 (2 cm.), —·—· 0.097 (0.056 cm.), - - - - 0.19 mol./l. (〃).
b) pseudo. ——— 0.0053 (2 cm.), - - - - 0.45 mol./l. (0.0195 cm.).

compared with the corresponding diastereoisomers of ephedrine, N-methylephedrine shows a smaller $\Delta\nu$ value (157 cm^{-1}) and a comparable intensity of the free OH absorption, while Ψ-N-methylephedrine shows a much larger $\Delta\nu$ value (238 cm^{-1}) and a much smaller intensity.

3) E.D. Bergmann, E. Gil-Av. and S. Pincas, *J. Am. Chem. Soc.*, 75, 68 (1953).

The shifts of the bonded OH absorptions with increasing concentration for N-methylephedrines are smaller than those for ephedrines (30 cm^{-1}) and no band appears near 3300 cm^{-1} as seen in the cases of ephedrines, where the band was assumed to be due to OH- - -O intermolecular hydrogen bond. For N-methylephedrine, this absence may be due to the lack of appreciable association at a concentration of 0.19 mol./l. The spectrum at a concentration higher than 0.19 mol./l. could not be taken because of the precipitation of crystallites. For Ψ-N-methylephedrine the spectrum at a concentration of 0.45 mol./l. (Fig. 1b) may show one in a state containing associated molecules, because in the spectrum of liquid state only one broad band appears at 3347 cm^{-1}.

B. 1, 2-Diphenyl-2-methylaminoethanol-(1).—1) Concentration-Dependence.—In Fig. 2a the concentration dependence of the absorption of erythro (normal) 1, 2-diphenyl-2-methylaminoethanol-(1) is shown. Since this compound has the hydroxyl and methylamino groups like ephedrine, it is expected that spectra similar to that of ephedrine should be obtained. However, as seen in Fig. 2a the spectra are quite different. Thus, the absorption near 3600 cm^{-1} is a doublet composed of two sharp bands (3617 and 3587 cm^{-1}) of about the same intensity, and a broad absorption at 3466 cm^{-1} is weaker than the bands near 3600 cm^{-1} and also a well-defined band appears at 3349 cm^{-1}.

On raising the concentration, the intensities of the two bands near 3600 cm^{-1} decrease in the same degree and at a concentration of 0.063 mol./l. a single absorption appears at 3352 cm^{-1}. Since, as in the cases of ephedrines and N-methylephedrines, the intensities and the positions of the absorption bands remain unchanged in a concentration range 0.001–0.01 mol./l., the presence of the intramolecular hydrogen bond will be expected in a dilute

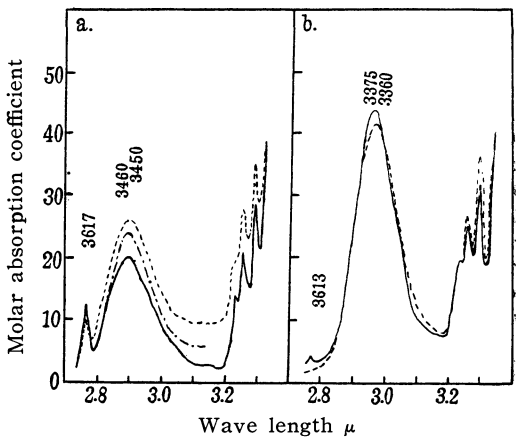

Fig. 2. Concentration dependence. 1,2-Diphenyl-2-methylamino-ethanol-(1). CCl_4 solns.
a) erythro (normal). ——— 0.0062 (2 cm.), —·—· 0.046 (0.3 cm.), - - - - 0.068 mol./l. (〃).
b) threo (pseudo). ——— 0.0031 (2 cm.), - - - - 0.068 mol./l. (0.3 cm.).

solution. The spectrum at 0.063 mol/l. shows an interaction between molecules and thus the association occurs at a lower concentration than in the cases of ephedrines (0.1–0.2 mol./l.). As for the doublet structure of the bands near 3600 cm^{-1}, it seems that some kind of resonance splitting occurs as will be discussed later.

The band at 3466 cm^{-1}, which becomes stronger and shifts to 3448 cm^{-1} with concentration increase may be due to OH vibration perturbed by an intramolecular OH---N hydrogen bond in the same way as in the cases of ephedrines. The band at 3349 cm^{-1}, which may be assigned to NH vibration, is more intense than the NH absorption for ephedrines. This increase in the intensity of the NH absorption may be attributed to a change of structure from methylethylamine type of ephedrines to methylbenzylamine type*.

An intense peak at 3352 cm^{-1} at a higher concentration may be the superposition of the bonded OH absorption shifted by an intermolecular OH---O hydrogen bond and the NH absorption. It will be noticed that $\Delta\nu$ (151 cm^{-1}) between the higher-frequency component of the free OH vibration and the broad band at 3466 cm^{-1} is smaller than that of ephedrine (168 cm^{-1}) and the intensity ratio of the sharp component to the broad one is much larger than that for ephedrine and N-methylephedrine.

Threo 1, 2-diphenyl-2-methylaminoethanol-(1) (Fig. 2b) shows only one band near 3600 cm^{-1} unlike erythro isomer and a similar absorption in a range 2.7–3.3 μ to that of Ψ-ephedrine and Ψ-N-methylephedrine. The change in the absorption with concentration proceeds in the same manner as the other compounds. Therefore, a band at 3621 cm^{-1} can be assigned to free OH vibration, and a band at 3428 cm^{-1} to bonded OH vibration and further a peak at 3360 cm^{-1} to NH vibration. Here again, the NH absorption is more intense than that of Ψ-ephedrine. At a concentration of 0.068 mol./l. association is appreciable. As in the case of the erythro isomer, at the lower concentration, the free OH absorption is stronger than the bonded one and, at the higher concentration, the bonded OH absorption at 3428 cm^{-1} is covered by a slope of a peak at 3348 cm^{-1}. In this case a continuous absorption over a range 3.0–3.2 μ appears unlike the erythro isomer.

2) Solvent Effect and Interaction with Triethylamine.—The solvent effect and the interaction with triethylamine were studied in order to obtain information on the nature of the doublet band shown by erythro 1, 2-diphenyl-2-methylaminoethanol-(1) (Fig. 3).

In carbon disulfide solution the doublet bands shift towards lower frequency, compared with those in carbon tetrachloride solution, and the lower frequency component (3571 cm^{-1}) is much more intense than the higher-frequency one (3592 cm^{-1}). At a lower concentration, the bonded OH absorption (3442 cm^{-1}) and NH absorption (3338 cm^{-1}) are well-defined. At a higher concentration, association seems to occur and the NH absorption still remains. The tendency of association of the erythro compound in carbon disulfide solution is weaker than that of ephedrine.

In chloroform solution the shift of the doublet is to about the same degree as in carbon disulfide solution and the intensities of the components are about the same. The NH absorption at 3344 cm^{-1} is stronger than the bonded OH absorption. A weak absorption seems to appear in the region with longer wave length than NH absorption, but no appreciable association occurs.

In benzene solution the free OH absorption is not a doublet, but a single band at 3571 cm^{-1}. The bonded OH absorption is weak and the NH absorption is well-defined.

In Fig. 3b the interaction of the erythro compound with triethylamine in carbon tetrachloride solution is shown. By addition of triethylamine, the higher-frequency component of the doublet becomes weaker than the lower-frequency one and a continuous absorption appears in 3.1–3.3 μ region. At a concentration of 0.5 mol./l. of triethylamine the bonded OH absorption still remains and the NH absorption at 3345 cm^{-1} shifts to 3339 cm^{-1} and new bands appear at 3185 and 3143 cm^{-1}. These spectral bahaviors may be explained as in the cases of ephedrines[2]. By the interaction of free molecules with triethylamine an intermolecular OH---N hydrogen bond is formed and gives rise to an absorption at 3143 cm^{-1}. At the same time $NHCH_3$ group bridged by an intramolecular OH---N bond may interact with triethylamine and causes an absorption (NH---N) at 3185 cm^{-1}. It is seen that the intramolecularly bonded OH absorption and the NH absorption still remains at higher concentrations of triethylamine.

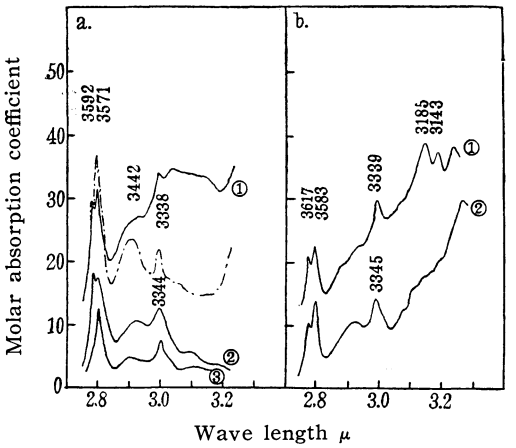

Fig. 3. Solvent effect and interation with triethylamine. Erythro 1, 2-diphenyl-2-methylaminoethanol-(1).

a). 1. CS_2 ——— 0.03 (2 cm.), —·— 0.0044 mol./l. (0.3 cm.) 2. $CHCl_3$, 0.16 mol./l. (0.056 cm.) 3. Benzene, 0.16 mol./l. (〃).

b). 1. 0.02 mol./l. + $(C_2H_5)_3N$ 0.26 mol./l. 2. +0.5 mol./l. (0.3 cm.) in CCl_4.

* According to the results obtained by Russell and Thompson (*J. Chem. Soc.*, **1955**, 483) absorption of ν(NH) in dibenzylamine is stronger than that in dialkylamine.

Discussion

The above results may be explained in the same manner as described for ephedrines[2]. The conformations capable of forming an intramolecular OH---N hydrogen bond are illustrated in Fig. 4 for diastereoisomers of N-methylephedrine and 1, 2-diphenyl-2-methylaminoethanol-(1). The appearance of the free OH absorption in the spectra for these two diastereoisomers will mean that all the compounds examined may be mixtures of rotational isomers, in one of which the OH and NR_1CH_3 groups are *trans* and in the others of which they are *gauche*.

$\Delta\nu$ of N-methylephedrine (151 cm^{-1}) is somewhat smaller than that of ephedrine (168 cm^{-1}). This may be explained qualitatively as follows. $N(CH_3)_2$ group will exert a stronger repulsive force from its bulkiness and, on the other hand, in a favorable steric position, a stronger attraction because of the stronger proton accepting power than $NHCH_3$ group in ephedrine. Since a repulsion between the methyl and phenyl groups may be the same in both compounds, the repulsion between the OH and $N(CH_3)_2$ groups may contribute more to the $\Delta\nu$ value of N-methylephedrine than the attraction between them. The equilibrium ratio of the rotational isomers may be about the same as that for ephedrine.

On the other hand, for ψ-N-methylephedrine $\Delta\nu$ (238 cm^{-1}) is much larger than that for N-methylephedrine and ψ-ephedrine (203cm^{-1}). In this case the repulsion between the methyl and phenyl groups will give rise to a closer approach and accordingly a smaller $\Delta\nu$ than that of N-methylephedrine. However, considering the above-mentioned repulsion between the OH and $N(CH_3)_2$ groups $\Delta\nu$ of ψ-N-methylephedrine should be about the same as or smaller than that of ψ-ephedrine. Accordingly, the observed larger value of ψ-N-methylephedrine may be explained by the predominance of the other gauche type isomer than that shown in Fig. 4, in which the repulsion between the phenyl and $N(CH_3)_2$ groups will be larger than that between the phenyl and $NHCH_3$ groups in ephedrine. A possible explanation as regards the very weak intensity of the free OH vibration will be that the trans isomer may be fairly unstable because of the repulsion between bulky groups crowded together.

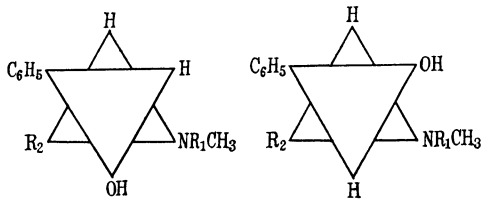

erythro (normal) threo (pseudo)

Fig. 4.

R_1	R_2	
H	CH_3	Ephedrine
CH_3	CH_3	N-Methylephedrine
H	C_6H_5	1, 2-Diphenyl-2-methylaminoethanol-(1)

For 1, 2-diphenyl-2-methylaminoethanol-(1) the origin of the doublet bands near 3600 cm^{-1} found for the erythro isomer should be discussed first. From the behavior of the doublet under various conditions described hitherto it will be noticed that the solvent effect seems to be different for each component. Such a tendency would suggest that the lower-frequency component might be caused by a sort of bonding of the OH group. Considering the smallness of $\Delta\nu$ (30 cm^{-1}) between the components, this bonding is not so strong as the ordinary OH---N hydrogen bonding. From this point of view proton acceptor other than $NHCH_3$ group should be considered. As an acceptor as such, the phenyl group attached to the asymmetric carbon atom adjacent to the other one having OH group might be considered. To confirm such an assumption a spectrum of benzylphenyl carbinol was taken in a dilute carbon tetrachloride solution. Only one sharp band was observed at 3610 cm^{-1} and therefore it may be said that the doublet is not caused by such an interaction. On the other hand, a spectrum of erythro 1, 2-diphenyl-2-aminoethanol-(1) showed also a doublet composed of bands at 3617 and 3590 cm^{-1}, a broad band at 3482 cm^{-1}, NH absorption at 3399 cm^{-1} and one more band near 3μ. The wave numbers of all the absorptions except one at 3617 cm^{-1} are larger than those of corresponding bands of erythro 1, 2-diphenyl-2-methylaminoethanol-(1). Those shifts are probably caused by a difference in nature of amino and methylamino groups. From these observations, it will be more reasonable to consider that the doublet is caused by some resonance effect or other.

It will be noticed from the spectra that the intensity of the free OH absorption at 3617 cm^{-1} for the threo isomer is stronger than the bonded OH absorption, and the intensities of the doublet for the erythro isomer are also stronger than that of the bonded one. Moreover, assuming the sum of the intensities of the components of the doublet as that of the free OH absorption subjected to no perturbation, an intensity ratio of the free OH absorption to the

bonded one is much larger for the erythro isomer than for the threo isomer. Accordingly this will mean that a rotational isomer having the OH and $NHCH_3$ groups in trans position is more stable in the erythro isomer than in the threo one. In addition it may be said from the comparison of the intensity ratios that the trans isomer is more aboundant in 1,2-diphenyl-2-methylaminoethanols than in ephedrines. These considerations on the equilibrium ratio of the rotational isomers can also be obtained by taking account of the repulsion between the larger phenyl groups in the conformation of the erythro compound shown in Fig. 4, although the presence of the stable trans isomer in the threo compound seems to be difficult to explain.

$\Delta\nu$ for the erythro isomer (151 cm^{-1}) and the threo isomer (193 cm^{-1}) are smaller than the corresponding isomers of ephedrine (168 and 203 cm^{-1}) and N-methylephedrine (157 and 238 cm^{-1}). This may be explained as follows. For the erythro isomer a larger repulsion between the phenyl groups of the gauche type molecule (Fig. 4) than that between the methyl and phenyl groups in ephedrine will give rise to a longer O–N distance and a smaller $\Delta\nu$ value than those in ephedrine. For the threo isomer, it can be expected that the repulsion between the phenyl groups will make $\Delta\nu$ larger than that of ephedrine. However, the experimental result is the reverse. Considering this fact another gauche isomer which has two phenyl groups in trans position may be more stable than that shown in Fig. 4 and show the smaller $\Delta\nu$ value as observed.

From the results obtained through this series of experiments, it can be concluded that the values of $\Delta\nu$ due to OH---N intramolecular hydrogen bond are more or less dependent on the kind and the nature of substituents attached to the asymmetric carbon atoms in ephedrine-like molecules. It has been observed, however, that $\Delta\nu$'s of the erythro (normal) isomers are always smaller than those of the threo (pseudo) isomers. The present finding of the presence of the intramolecular OH---N hydrogen bond in the erythro isomers as well as in the threo isomers may be related to the chemical fact that a crystalline ephedrine-copper complex can be prepared, although it is much less stable than ψ-ephedrine complex in aqueous organic solvent[4].

The author wishes to express his sincere thanks to Professor I. Nitta of Osaka University for his kind guidance and Dr. T. Shimanouchi of Tokyo University for his valuable advice. The Author's thanks are also due to Dr. S. Kuwada and Dr. A. Watanabe in this Laboratory for their continued encouragement.

Research Laboratory Takeda Pharmaceutical Industries, Ltd., Osaka

4) *Z.* Földi, T. Földi and A. Földi, *Chemistry and Industry*, 1297 (1955).

Introduction of Side Chains into Polyglycine Dispersed on Solid Surface. I

By Shiro AKABORI, KENJI OKAWA and Mikio SATO

(Received February 22, 1956)

In 1953, Snell[1] reported a reversible catalytic cleavage of β-hydroxy amino acids in the presence of pyridoxal and certain metal ions in aqueous solutions of pH 3–12. Th. Wieland[2] observed recently, the conversion of glycyl-residue into seryl- or threonyl residue by Snell's method.

$$\underset{\substack{|\\OH}}{R\text{-}CH}\text{-}\underset{\substack{|\\NH_2}}{CH}\text{-}COOH \rightleftarrows R\text{-}CHO + \underset{\substack{|\\NH_2}}{CH_2}\text{-}COOH$$

In 1954, one of the authors (S. Akabori) postulated[3] a hypothesis that the "fore-proteine" should have been produced by the following reactions in three steps.

1. Formation of amino-acetonitrile from formaldehyde, ammonia and hydrogen cyanide.

$$CH_2O + NH_3 + HCN \longrightarrow H_2N\text{-}CH_2\text{-}CN + H_2O$$

2. Polymerization of amino-acetonitrile on a solid surface, followed by the hydrolysis to polyglycine and ammonia.

1) E. Snell, D. Metzler and J. Longenecker, *J. Am. Chem. Soc.*, 75, 2786 (1953).

2) Th. Wieland and K. Dose, *Angew. Chem.*, 66, 781 (1954).

3) S. Akabori, *Science* (Japan), Vol. 25, 54 (1955).

$$x(NH_2\text{-}CH_2\text{-}CN) \longrightarrow \text{-(-NH-}CH_2\text{-}\underset{\underset{NH}{\|}}{C}\text{-)}_x\text{-} \xrightarrow{H_2O}$$

$$\text{-(-NH-}CH_2\text{-CO-)}_x\text{-} + x\cdot NH_3$$

3. Introduction of side chains into polyglycine.

Akabori pointed out, further, that the asymmetric formation of amino acid residues could be explained, at least in one single peptide chain, by his hypothesis, assuming that the configuration of polyglycine absorbed on the solid surface is *cis*-form, as shown in the following scheme.

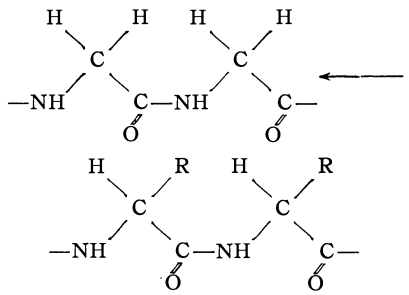

Experimental studies on the first and second reactions are now in progress in the author's laboratory. The present work deals with studies in regard to the reaction of the last step.

By the treatment of polyglycine spread on kaolinite with formaldehyde or acetaldehyde in the presence of a basic catalyst, glycyl residues are partly converted to seryl- or threonyl residues. By treating powdered polyglycine without solid bearer, with formaldehyde or acetaldehyde in the same way, practically no introduction of side chains was observed.

Experimental

Outline of Experiments.—Polyglycine was prepared, on one hand, through glycine N-carboxylic anhydride (G. C. A.) according to Leuchs[4] and on the other hand, by the polycondensation of glycine ester according to Kurtius[5]. Bulk preparations of polyglycine were obtained from G. C. A. by keeping its solution in dioxane, with a small quantity of pyridine, at room temperature for several days.

Materials.—Glycine N-Carboxylic Anhydride.[6]—Five grams of carbobenzyloxy glycine and 2.3 ml. of thionylchloride were dissolved in 5 ml. of acetic anhydride and heated to boiling for five minutes. On cooling the solution, fine crystals of G. C. A. were deposited. Yield 1.9 g.

Polyglycine in Bulk (without Bearer).—Two grams of G. C. A. were dissolved in 20 ml. of dry dioxane, 4 ml. of dry pyridine was added to it and the solution was kept in a sealed tube at room temperature. After four to five days, a mixture of ether and petroleumether was added to the reaction mixture, polyglycine precipitated in amorphous state was filtered, washed with ether and dried. The yield was 0.8 g. Polyglycine thus obtained was soluble in water with great difficulty, and gave positive biulet reaction.

Polyglycine Dispersed on Kaolinite.—a) From G. C. A.—Two grams of G. C. A. were dissolved, in 20 ml. of dry dioxane with 4 ml. of dry pyridine 15 g. of kaolinite were added to it and the whole mixture was placed in a sealed tube and allowed to stand at room temperature for eighteen hours under occasional shaking. The gelatinized reaction mixture was finally heated to 70°C for two hours. After cooling, the mixture was taken out from the tube and washed with ether, then with water. The dried polyglycine kaolinite weighed 16.5 g.

b) From Glycine Ester.—Glycine ethyl ester dissolved in ether was mixed with kaolinite, ether was distilled off and the remaining mixture was heated to 130°C for five hours. The product was washed with ether, then three times with hot water, and dried.

Several preparation of polyglycine kaolinite prepared in almost the same ways were analysed for their N contents. The results are shown in Table I.

Table I

Sample	Material Glycine ester	Kaolinite	Reaction Temp.	Reaction Time	N Contents %
P. G. K. 1	5.9 g.	20.0 g.	130°C	5.0 hrs.	1.58
P. G. K. 2	4.9	15.0	130	5.0	1.26
P. G. K. 3	4.9	15.0	130	5.9	1.38
P. G. K. 4	4.9	15.0	130	5.9	1.34

Degree of Polymerization of Polyglycine Kaolinite.—One hundred and fifty mg. of polyglycine kaolinite (Sample P. G. K. 3) were suspended in 10 ml. of 4% aq. sodium bicarbonate solution mixed with 0.3 ml. of dinitrofluorobenzene dissolved in 10 ml. of ethyl alcohol and shaken for seven hours at room temperature. After the alcohol was distilled off, 10 ml. of 12 N hydrochloric acid were added and boiled for three hours. Dinitrophenyl-glycine formed was extracted with ether, purified by a silica gel column and determined by a photoelectric colorimeter. Terminal-N % 0.0098. Degree of polymerization; Total.N %/Term.-N % =140.

A determination of terminal. N% by van Slyke's method gave 0.008%, Total-N %/Term.-N % =172.

4) H. Leuchs, *Ber.*, **39**, 857 (1906).
5) T. Kurtius, *Ber.*, **16**, 755 (1833).
6) A. Farthing, *J. Chem. Soc.*, **1950**, 3213.

Condensation of Formaldehyde or Acetaldehyde with Polyglycine Kaolinite.—Powdered polyglycine kaolinite was mixed with aq. formaldehyde or acetaldehyde and small quantity of various basic catalysts and kept at 60°C–100°C. After various reaction times, the solid matter was filtered, washed with alcohol and dried. An aliquot of the reaction products was boiled with 6 N hydrochloric acid for five hours. Kaolinite was filtered and filtrate was concentrated in vacuo. A small quantity of alcohol was added to the residue and evaporated again to removed hydrochloric acid. The remaining solution was diluted with water, neutralized to pH 7 and brought to 10 or 20 ml. A measured volume of the solution was pipetted out, dinitrophenylated by the usual method and the resulted DNP-amino acids were separated by a silica gel chromatography as shown in Fig. 1-2. The yellow bands corresponding to DNP-

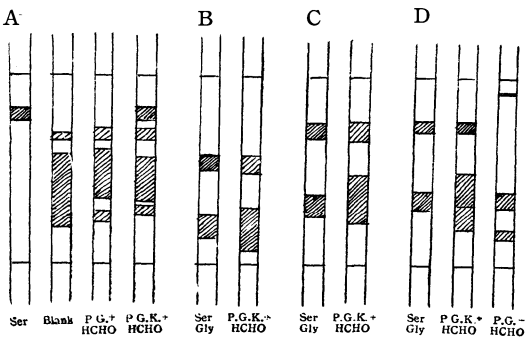

Fig. 1. D.N.P.-amino acids' column chromatograph of P.G.K.+HCHO.

	Column.	Solvent
A.	Silica Gel-W.	AcOH−6.5 Phosph. Etp. Buff.
B.	Silica Gel-I.	20 ml. BuOH+80 ml. $CHCl_3$ −20% AcOH.
C.	Silica Gel-10	20 ml. BuOH+80 ml. $CHCl_3$ −20% AcOH.
D.	Celite	50 ml BuOH+100 ml. $CHCl_3$ −pH. 4.6 Acetate Buff.

glycine and DNP-serine or DNP-threonine were cut out, eluted by methyl alcohol and determined by a photoelectric colorimeter. The results of experiments under various conditions are listed in Table II.

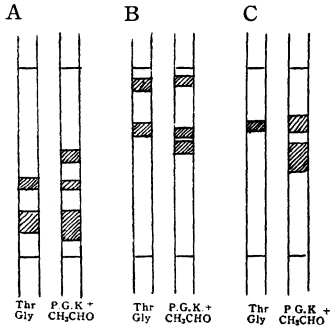

Fig. 2. D.N.P.-amino acids' column chromatograph of P.G.K.+CH_3CHO.

	Column	Solvent
A.	Silica Gel-I.	20 ml. BuOH+80 ml. $CHCl_3$ −20% AcOH.
B.	Silica Gel-I.	5 ml. sec. BuOH+95 ml. $CHCl_3$ −2% AcOH.
C.	Silica Gel-X.	50 ml. BuOH+100 ml. $CHCl_3$ −pH. 4.6 Acet. Buff.

Discussion

From the results described above, it could be concluded that the methylene group of polyglycine adsorbed on kaolinite is quite susceptible as compared with polyglycine without bearer, to the condensation reaction with aldehyde giving rise to β-hydroxy amino acids residues. It is also clear from the results of end group determination of the polyglycine and molar ratio of serine/glycine in the reaction products, that the condensation occurred not only at amino terminal glycyl residues but also at methylene groups of non-terminal glycyl residues.

Summary

1) Polyglycine dispersed on the surface of kaolinite was prepared by the polycondensation of N-carboxylic anhydride or glycine ester on kaolinite.

2) It was concluded that a part of glycyl residues in polyglycine dispersed on kaolinite

TABLE II

Sample	Weight	Catalyst	Aldehyde	Solutions	Reaction Temp.	Reaction Time	Mol. ratio of Oxy amino acids/Gly.
PGK*	1.0 g.	K_2CO_3	HCHO	10 ml.	80°C	7 hrs.	0.031
PGK*	1.0	$NaHCO_3$	HCHO	10	80	7	0.030
PGK*	1.0	T. E. A.	HCHO	10	100	2.5	0.004
PGK3	1.0	K_2CO_3	HCHO	10	80	7	0.02–0.03
PGK*	0.5	K_2CO_3	CH_3CHO	10	60	50	0.015
PGK*	0.5	$NaHCO_3$	CH_3CHO	10	60	50	0.014
PG	25 mg.	T. E. A.	HCHO	3	100	3	—
PG	100 mg.	K_2CO_3	HCHO	10	80	7	+

PGK*, Polyglycine kaolinite which was prepared by N carboxylic anhydride method.
PG, Polyglycine without kaolinite. T. E. A., Triethylamine.
HCHO, 35% aq. solution. CH_3CHO, 20% aq. solution.

was easily converted to seryl or threonyl residues by the condensation with formaldehyde or acetaldehyde.

3) The condensation occurred not only at amino terminal glycyl residues but also at non-terminal glycyl residues.

Department of Chemistry, Faculty of Science, Osaka University, Osaka

*Kinetic Studies on Hydrogenation of Fat. An Effect of Poison Formed in Catalysis on the Rate of Hydrogenation**

By Ryoichi MIYAKE and Yoshizo SHIMAMURA

(Received January 10, 1956)

Despite the considerable experimental studies conducted during these fifty years, there is still much remaining to be cleared up as to the facts regarding the hydrogenation rate, and no satisfactory method has been obtained so far of analyzing the reaction rate mathematically, since hydrogenation has several peculiarities which render mathematical analysis of it difficult. For instance, even the reaction order[1] of an unsaturated molecule, a fundamental problem in kinetics has not yet been clarified. The present discussion is based upon the results of experiments using copper catalysts and whale oil. The conclusions obtained in this study are applicable not only to a specific catalyst and oil, but also to the common reaction of hydrogenation of fat. Further reports confirming these points in greater detail will be issued in the near future. Throughout this experiment, the pressure of hydrogen is kept constant, so the kinetic behavior of the hydrogen molecule is left out of consideration.

Experimental and Results

The hydrogenation of finback whale oil was carried out throughout this series of experiments under atmospheric pressure of hydrogen and at 180°C by using somewhat modified H. Adkin's[2] Cu-Cr-O catalysts.

The experimental technique is outlined here which is practically identical with those employed previously[3]. A static method was employed. The whole glass apparatus was used, which consists of a reaction bulb (a 25 mm. height and a 45 mm. in diameter) connected through a flexible spiral glass tube to a gas burett. The reaction bulb was immersed in an oil bath and was given a horizontal rotation of R.P.M. 200 by a piston of 3 cm. in diameter. The reaction periods from start to end of the motion were recorded.

Two types of slightly modified H. Adkin's Cu-Cr-O catalyst[4] were used.

Type (a): Without barium chromate. Copper content amounting to 43% as a metal on an average.

Type (b): With barium chromate. The amount of barium chromate was adjusted so as to contain 10% of metallic copper in the catalyst.

The activity of those catalysts is satisfactorily uniform when the decomposition temperature of copper ammonium chromate is strictly controlled at about 350°C. Their characteristic features will be briefly described.

The Cu-Cr-O catalyst readily reduced accompanying initial induction period to an active metallic copper and to chromium oxide (Cr_2O_3) at above 120°C consuming about 18 cc. (N.T.P.) of hydrogen per 0.1 g. of type (a) catalyst about 8 cc. per 0.1 g. of the type (b) catalyst in hydrogen atmosphere, and somewhat less volume of hydrogen is consumed in the wet reducing process at the same temperature in each case. In hydrogenation of whale oil with this catalyst under low pressure of hydrogen, highly unsaturated acids are partly saturated while those of oleic acid series are not hydrogenated. The selection is perfect[3,5]. The catalyst is usually added to oil after it is reduced, but sometimes it may be used without reduction. In the latter case reduction of the catalyst takes place within thirty minutes at 180°C accompanying simultaneous hydrogenation of oil.

The results[6] of the analysis using finback whale oil indicate that when selective hydrogenation goes on completely, unsaturated acids ($|\overline{\overline{3}}$-acids) higher than acids of linoleic acid series ($|\overline{\overline{2}}$-acid) are converted to those of linoleic acid series ($|\overline{\overline{2}}$-acid) at iodine value (I.V. in short) 90, and that acids of linoleic acid series which are unsaturated

* A principal part of the present work was presented at the Monthly Meeting of the Pharmaceutical Society of Japan held on March 17th, 1951 in Tokyo Univ.

1) F.L. Morritz, E. Lieber and R.B. Bernstein, *J. Am. Chem. Soc.*, **75**, 3116 (1953).

2) H. Adkins, R. Connor and K. Folkers, *J. Am. Chem. Soc.*, **54**, 1138 (1932).

3) R. Miyake, *J. Pharm. Soc. Japan*, **68**, 9 (1948).

4) ibid., **68**, 18-31 (1948).

5) Mr. T. Namba kindly informed us about the result of his observation several years ago, that in the hydrogenation of soybean oil by a hydrogen bubbling method some acids in oleic acid series are saturated in the presence of Cu-Cr-O catalyst under the same conditions as in this experiment.

6) R. Miyake, *J. Pharm. Soc. Japan*, **68**, 2 (1948).

in middle grade are reduced to those of oleic acids series at I. V. 70.

Experiment No. 1.—A case in which velocity of hydrogenation apparently obeys unimolecular law.

In the run V. 317 a sintered catalyst reduced at rather high temperature was used. 0.1252 g. of catalyst (a) was completely reduced in the reaction bulb in hydrogen at 270°C for twenty minutes absorbing 14.9 cc. of hydrogen (N. T. P.); then the reduced catalyst was covered by 0.9572 g. of whale oil (I. V. 98.6) to avoid exposure to the air before it was used for hydrogenation. The I. V. of hydrogenated oil was 74.4. The hydrogen adsorption rate is shown in Fig. 1 and the experimental formula obtained by the method of least square from the data of Fig. 2 is as follows:

$$2.303 \log (23.07 - x) = -0.008475t + 3.914.$$

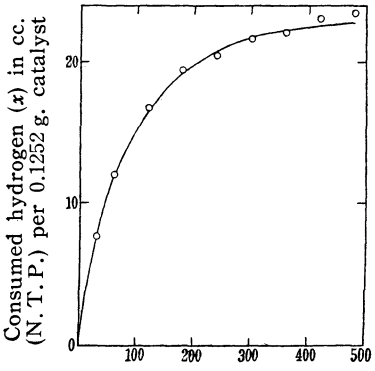

Fig. 1. Run V 317. 0.1252 g. of catalyst was used after reduction at 270°C. The curve is the calculated one from the formula V 317.3 and V 317.4.

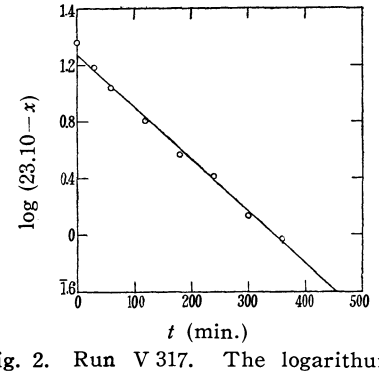

Fig. 2. Run V 317. The logarithum of concentration of highly unsaturated compounds in cc. is plotted against time. The reaction is seemingly of the first order.

Experiment No. 2.—This experiment was carried out to show that the velocity of hydrogenation was independent of the concentrations of highly unsaturated acids in oil. The unreduced catalyst (a) was used. Within the range of the experiment the velocity may be regarded as equal regardless of the change of the concentration. Results are summarized in Table I and in Fig. 3.

TABLE I

Run no.	Catalyst (g.)	Whale oil (g.)	Refined hydrogenated whale oil (g.)	Highly unsaturated compounds (%)
V 321	0.1023	0.8894	1.9570	4.5
V 322	0.1200	1.0759	3.006	3.8
V 323	0.1040	0.8970	—	14.3

Whale oil: I. V. 110, n_d^{40} 1.4655; content of highly unsaturated compounds, weight % 14.3. Refined hydrogenated whale oil: I. V. 70.6, n_d^{40} 1.4603.

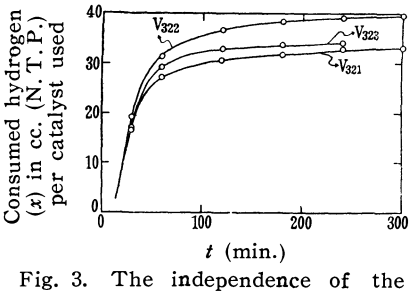

Fig. 3. The independence of the rate upon the concentration of acceptor. In run V 323 whale oil and in run V 321 and V 322 mixtures if whale oil and refined hydrogenated whale oil are hydrogenated with unreduced catalysts listed in Table I.

Experiment No. 3.—An experiment was undertaken to discover the cause of the fall of catalyst activity. With 0.1 g. of unreduced catalyst 1 g. of whale oil was hydrogenated (V 283 (1)). Then 1 g. of whale oil was added and hydrogenated (V 283 (2)), and once again 1 g. of whale oil was added and hydrogenated (V 283 (3)). The catalyst thus deactivated was thoroughly washed with ether in Soxhlet apparatus and then used again as a catalyst of hydrogenation of fresh whale oil (V 285). In experiments V 283 (2) and (3), catalyst was evidently in reduced state. In V 285 catalyst was slightly oxidized due to exposure to the air during washing by either. The data are shown in Table II and in Fig. 4. In Fig. 5 to show more clearly the reactivation of catalyst, the net amount of hydrogen absorbed per one g. of whale oil, i. e. a corrected value obtained by substrating from the total absorbed hydrogen the volume of hydrogen consumed for the reduction of catalyst which are calculated from the drop of iodine value, are plotted against the reaction time.

TABLE II

Run no.	Catalyst (g.)	Whale oil (g.)	Iodine value of hydrogenated oil
283 (1)	0.1192	1.0265	69.2 (calculated)
283 (2)	0.1192	0.1192	
283 (3)	0.1192	0.9826	
285	0.0508	0.5099	70.2 (experimental)

Iodine value of whale oil: 107

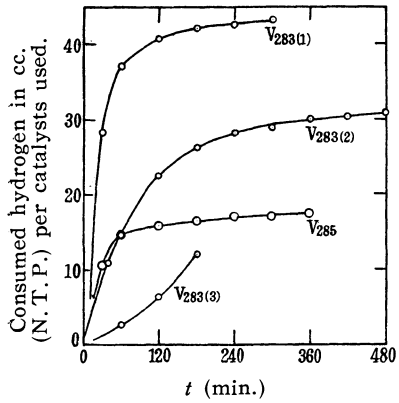

Fig. 4. The deactivation feature of catalyst in hydrogenation with succesive addition of 1 g. oil and reactivation of waste catalyst by washing with ether.

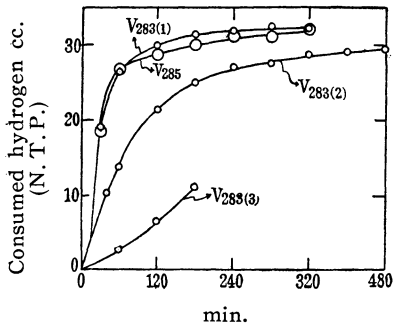

Fig. 5. The net amount of hydrogen absorbed per one g. of oil, calculated from Fig. 4 and Table II.

Experiment No. 4.—The fact that the reaction rate was increased when the amount of catalyst increased in a certain range is illustrated here using the unreduced catalyst type (a). The hydrogenation conditions were similar to those of the foregoing experiments. 1–2 g. of whale oil was used. The results are summarized in Fig. 6., in which the maximum rate (cc./min.) of hydrogenation of the higher unsaturated acids ($|\overline{\overline{3}}$-acid) are plotted against the amounts of catalyst used. The rate is proportional to the amounts of catalysts used, when too much catalyst is not applied. If sufficient catalyst is used, the rate of reaction becomes nearly constant, being independent of the amount of catalyst. This fact might induce an opinion that the diffusion rate of hydrogen into an oil phase may be the limiting factor[7] in this case. Discussion on this follows. The diffusion theory, however, is not tenable in this case, because faster consumption of hydrogen can be observed in the same apparatus by using a more effective catalyst such as nickel. A study on this phenomenon is now being undertaken by Yajima. It will suffice here to state that oil is saturated with hydrogen under the conditions of this experiment.

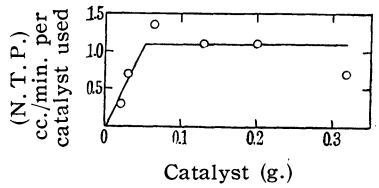

Fig. 6. The dependance of rate upon the amount of catalyst. Differing from the circumstance employing the dry-reduced catalyst, the wet-reduced catalyst becomes partially inactivated by the irreversible poisonous substances, presumably formed from the fat by the accompanying oxidizing action of the oxide catalyst in the reduction period. The injurious effect, however, do not become pronounced until not too much unreduced catalyst (about 0.2 g. in this case) is used.

Kinetic Consideration

The consideration are principally inferred from the behavior of unsaturated oil molecules in the reaction system, quite apart from the behaviour of hydrogen molecule, since the hydrogen pressure was maintained constant throughout this series of experiments, and further, as mentioned in Experiment No. 4, the oil was evidently saturated with hydrogen. The fact that hydrogenation rate is independent of the concentration of the highly unsaturated molecules indicates the rate determining step is the hydrogenation process on the surface of catalyst, that the diffusion of oil molecules to the catalyst surface is fast enough to establish the adsorption equilibrium of oil molecules between the catalyst and the liquid phase, and that the highly unsaturated molecules are strongly adsorbed, although the reaction is sometimes apparently first-order kinetics as shown in Experiment 1.

The decrease in rate of reaction with time is necessarily ascribed to successive deactivation of catalyst, by possible two principal factors, poisoning and sintering. The results of Experiment No. 3 indicate that the effect of the latter can be ignored.

In conclusion, as the equilibrium in the reaction system is established, the rate of hydrogenation is directly proportional to the amount of catalyst, i.e., the decrease in the rate is directly corresponding to the decrease in the number of active centers caused by a catalytic poison in a first approximation.

In order to interpret the change in rate in view of this conclusion, an assumption is made induced from the suggestive results obtained in Experiment No. 1 that the num-

7) V.I. Gol'danski and S.Yu. Elovich, *C.A.*, **41**, 2973 (1948).

ber of active centers is reduced by the quantity of poison formed in the process of catalysis in proportion to the amount of hydrogenated molecules. Thus, if x cc. of hydrogen reacts at time t min. the rate is assumed

$$dx/dt = K_1(N_0 - K_2x),$$

where

K_1 = the hydrogenation rate constant (cc./min.) per unit active center,

N_0 = the original number of active centers, which is supposed here to be capable of combining an unsaturated compound and hydrogen together,

K_2 = this term consists principally of the proportional constant of catalytic poison formation reaction, absorption coefficient of poison and proportionality constant so as to make K_2x correspond to the number of active centers deactivated.

This equation, however, has a linear expression with respect to x similar to the first order formula; it involves two reaction rate constants, K_1 and K_2. Although N_0/K_2 corresponds to the initial concentration of reactant in the first order kinetics, it can be determined only from experimental data.

The analysis of Run No. V 317 with the applification of this equation is shown in Fig. 7, wherein an abrupt change in rate at point (b). Hence it is expressed by the following two equations.

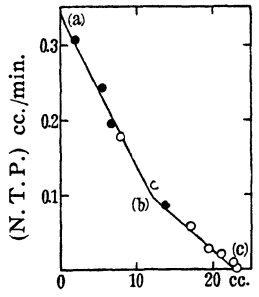

Fig. 7. $dx/dt - x$ relation from V 317.
○ experimental
● interpolated

$$dx/dt = 0.3430 - 0.02021x \quad \text{(V 317.1)}$$

$$dx/dt = 0.2047 - 0.00889x \quad \text{(V 317.2)}$$

These equations are dissolved and calculated integral constants by adopting suitable experimental points on Fig. 7. The result is

$$2.303 \log (16.97 - x) = -0.0202t + 2.826 \quad \text{(V 317.3)}$$

$$2.303 \log (23.06 - x) = -0.00889t + 2.935 \quad \text{(V 317.4)}$$

From these four equations, the following figures for the point (b) are obtained: 0.0967 cc./min., 12.18 cc. and sixty two minutes respectively for dx/dt, x and t. The iodine value at (b) is estimated as 88. This is in good agreement with the calculated iodine value 90, at which $\overline{\overline{3}}\sim$-acids will disappear. Thus, the equation (V 317.3) can be used for the former stage of hydrogenation of $\overline{\overline{3}}\sim$-acids before sixty-two minutes and thereafter the equation (V 317.4). Therefore K_1N_0 for $\overline{\overline{2}}$-acids must be taken 0.0967 cc./min. (at point b). The slopes of the pair of straight lines in Fig. 7 are shown respectively in terms of K_1K_2 for $\overline{\overline{3}}\sim$-acids and K_1K_2 for $\overline{\overline{2}}$-acids in the equations (V 317.3 and V 317.4) and the ratio of these $K_1(\overline{\overline{3}}\sim)/K_1(\overline{\overline{2}})$ can be calculated from the ratio of the value of these slopes if the value of $K_2(\overline{\overline{3}}\sim)/K_2(\overline{\overline{2}})$ is known. If an assumption is made that $K_2(\overline{\overline{3}}\sim)/K_2(\overline{\overline{2}})$ is unity, then $K_1(\overline{\overline{3}}\sim)/K_1(\overline{\overline{2}}) = 0.0202/0.00899 = 2.25$, which is comparably consistent with the value obtained from instances in which $K_2(\overline{\overline{3}}\sim)$ and $K_2(\overline{\overline{2}})$ happen to be negligible compared with the change in K_1 terms as will be reported in the next work. The appearance of the breaking point (b) in Fig. 7 indicates the occurrence of good selectivity which is also consistent with being indifferent to the reaction rate with the concentration of the highly unsaturated molecules.

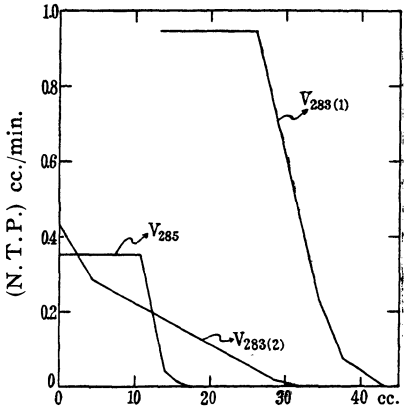

Fig. 8. $dx/dt - x$ relation from Experiment No. 3 (Fig. 4). The graph of V 283 (1) will proceed same in shape from this position to the left through decreasing values of 9.9 cc. to x, provided correction is made on it by substracting the required hydrogen for the reduction of catalyst in Fig. 4.

Reviewing Fig. 8, it deserves special notice here for the arising of different types of active center in the hydrogenation range of $\overline{\overline{2}}$-acids, their slopes being respectively 0.0861 and 0.0476. An assumption being made

of the equality of both K_2 again here concerning both types of active center, the ratio of slope is nearly 2** which corresponds to the ratio of K_1 term in two types of active center, catalyzing the same substance in this case.

The reaction rate after passing over the point of about I. V. 75 changes to the very slow one in this catalyst indicating the possibility of the appearanse of some special constitution of fatty molecule ($\overline{|\overline{2}}'$) (Table III).

is not expressed in explicit form for the present.

The features under the above consideration, however, are shown in very few instances; they hold true also for many examples we have tested. On the other hand, the occurrence of induction period incidentally which appeared in Experiment No. V 283 (3) in the reduced state catalyst is not so rare but is not reproducible, and of course quite different from that which was experienced with the unreduced catalyst as noticed before.

TABLE III

THE STRAIGHT LINES IN FIG. 8 ARE EXPRESSED BY TWO TYPES OF FORMULAS EITHER $dx/dt=a$ OR $2.303\log(b-x)=-ct+d$. THE ESTIMATED VALUE OF THESE TERMS ARE TABULATED. $(dx/dt)_i$, $(x)_i$ AND (I. V.)$_i$ ARE THE RESPECTIVELY THE CALCULATED VALUES AT THE POINT OF INTERSECTION OF CROSSING TWO LINES

Run no.	a	b	c	d	$(dx/dt)_i$	$(x)_i$	(I. V.)$_i$	Acids range being hydrogenated
V 283 (1)	0.944							$\overline{\overline{3}\sim}$-acids
					0.944	26.2	89	
		37.1	0.0861	4.76				$\overline{\overline{2}}$-acids
					0.229	34.5	79	
		39.2	0.0476	3.66				$\overline{\overline{2}}$-acids
					0.080	37.6	76	
		43.4	0.0138	2.64				$\overline{\overline{2}}'$-acids
V 283 (2)		13.0	0.0331	2.56				$\overline{\overline{3}\sim}$-acids
					0.288	4.32	103	
		30.3	0.0111	3.42				$\overline{\overline{3}\sim}$, $\overline{\overline{2}}$-acids
					0.0195	28.6	77	
		31.6	0.00641	2.78				$\overline{\overline{2}}'$-acids
V 285	0.3505							$\overline{\overline{3}\sim}$-acids
					0.350	10.6	85	
		14.4	0.0946	4.355				$\overline{\overline{2}}$-acids
					0.0425	13.9	78	
		16.8	0.0159	1.881				$\overline{\overline{2}}'$-acids
					0.0162	15.7	74	
		17.5	0.00921	1.653				$\overline{\overline{2}}'$-acids

The occurrence of linear sector of rate in the early stage is evidently the direct proof of zero order reaction with unsaturated molecules, but it is of interest in view of the point of poison formation. It is suggested that the solubility of poison must be taken into account. In fact, the hydrogenated whale oil contains poisonous substance in it, so hydrogenized oil must be re-refined by alkali and bleaching clay before applying it in Experiment No. 2. Some reactivation of activity accompanied by adding a fresh oil as will be seen in V 283 (2) and (3) might be attributed to, apart from the change in constitution of oil by adding new whale oil, the desorption of poison from catalyst and this concept is introduced into K_2, although it

Some other criteria will be afforded here as regards to the phenomena which are encountered in the hydrogenation of fat aside from the one as discussed above. The inherent impurities present in oil are irreversible poison, leading to permanent inactivation of the catalyst, and bearlittle relation to the change in rate under the condition wherein the absorption equilibrium is established.

The gaseous poisons which happen to occur as impurities in hydrogen may damage a catalyst in the very similar manner proportional to the consumed hydrogen. There is evidence, however, against this in the experiments using the same hydrogen in a gas bubbling hydrogenation method, in which the extent of volume of hydrogen passed had no effect on the activity of catalyst. Another

** This figure will be shown as a characteristic one of this catalyst in the next report.

effect might be raised from the pyrolysis of oil. It can be left out of consideration in view of kinetics also because time effects were not observed in the above analytical treatments. All these factors can be left out of consideration in the first approximation.

The present criterion appears to be in general accord with the view originally set forth by Armstrong and Hilditch[8], which unfortunately has not been developed to further kinetic treatments. The present authors in writing this report are feeling utmost reverence toward their foresight. In addition it will be pertinent here to recall the Ubbelohde's observations[9], whose data are seemingly all responsible for the present conception, although he did not interpret his results from the viewpoint of catalytic poison.

Summary

Estimation of the volume of hydrogen consumed by a static method with Cu-Cr-O under atmospheric pressure of hydrogen at 180°C by hydrogenation of whale oil was studied kinetically.

It was observed that the reaction is zero order to the concentration of the molecule to be hydrogenized, and, in spite of it, the reaction velocity gradually decreases due to the reversible poisoning of catalyst. An assumption was made that a poisonous substance is formed in the process of catalysis, and that its amount is proportional to the degree of hydrogenation. The following formula is presented.

$$dx/dt = K_1(N_0 - K_2x)$$

The authors wish to express their condial thanks to Dr. G. Fujinaga, Ex-Director, and Dr. H. Fujii, Director, of Nippon Marine Company for their kind offer of aid.

A part of the expense of this research has been defrayed from the Scientific Research Grant of the Ministry of Education.

The Pharmaceutical Institute of Chiba University, Chiba

8) E. F. Armstrong and T. P. Hilditch, *Proc. Roy. Soc. London*, A **96**, 137 (1919).
9) L. Ubbelohde and R. Schönfeld, *Z. angew. Chem.*, **44**, 184 (1931).

*Studies on the Oxy-acid Phosphors. V. Stannate Phosphors (Part I)**

By Yoshihide KOTERA, Tadao SEKINE and Michiko YONEMURA

(Received January 7, 1956)

Introduction

The stannate phosphors were investigated for the first time by E. Tiede and E. Villain, who reported magnesium stannate activated by manganese showing green emission under cathode rays excitation[1]. F. A. Kroeger[2] studied the alkali-earth and zinc stannates activated by titanium and calcium stannate activated by manganese, but the details of their preparation, characteristics, etc. are yet unknown. We have prepared various stannate phosphors and found some remarkable results.

Experimental and its Results

(1) Purification of Sodium Stannate and Metallic Salts.—In the preparation of stannate phosphors, a commercially available chemically pure grade of stannic chloride was used as one of the starting materials and purified as follows. The stannic chloride was dissolved in water and filtered. The sodium stannate solution was obtained by the reaction of the stannic chloride solution with solution of caustic soda in excess and by filtering off the resulting sediment. The precipitate, which was obtained by neutralization of this solution with conc. hydrochloric acid was filtered and dissolved again by addition of caustic soda solution. The filtrate was used as the purified sodium stannate solution.

The other starting materials were respective metallic salts, which were purified by the process described in a previous paper[3].

Each metallic salt solution was added to the sodium stannate solution, and respective metastannate salts were precipitated, their purity being established spectrographically.

(2) Mixing and Firing.—Each metastannate salt, respective metallic oxide or carbonate, flux

* Read before the Sixth Annual Meeting of the Chemical Society of Japan 1953. Report IV was published in This Bulletin, 28, 132 (1955).

1) E. Tiede and E. Villain, *Ber.*, 73, 274 (1940).

2) F.A. Kroeger, "Some Aspects of the Luminescence of Solids", Elsevier Publishing Co. (1948), p. 158.

3) Y. Kotera and T. Sekine, This Bulletin, 27, 13 (1948).

TABLE I

THE COLOURS OF EMISSIONS OF STANNATE PHOSPHORS

Host Lattice	Activator	3650Å		2537Å		Cathode Rays	
Mg_2SnO_4	Mn	none		green	ff	green	m
〃	Mn*1	none		none		blue	m
〃	Ti	none		bluish white	s	bluish white	s
〃	Ti*1	none		blue	s	blue	s
〃	Bi	blue	m	blue	ff	bluish violet	f
〃	Pb	none		green	ff	bluish violet	f
Ca_2SnO_4	Mn	none		none		orange	m
〃	Ti	none		blue	s	blue	s
〃	Bi	violet	m	violet	ff	bluish violet	m
〃	Pb	yellowish orange	m	none		yellow	m
〃	Ce	bluish white	f	red	ff	blue	m
Sr_2SnO_4	Ti	none		blue	m	blue	m
〃	Pb	none		orange	ff	orange	f
〃	Bi	none		none		yellowish orange	f
〃	Bi*2	none		none		red	f
Ba_2SnO_4	Ti	yellow	ff	yellowish orange	m	blue	m
〃	Pb	none		yellow	m	yellow	m
Zn_2SnO_4	Mn	yellowish white	f	none		yellowish white	f

s: strong, m: medium, f: faint, ff: very faint

*1. $Na_2B_4O_7 \cdot 10H_2O$ as a flux, other, NaF.

*2. SrO: SnO_2=1:1, others, see Table II.

TABLE II

THE OPTIMUM MIXING RATIO FOR THE PREPARATION OF STANNATE PHOSPHORS

Host Littice	SnO_2: MO or MCO_3	Flux	Activator
Mg_2SnO_4	1: 2.2 (MgO)	NaF or $Na_2B_4O_7 \cdot 10H_2O$ 0.1 mol.	Mn 1 mol. %
Ca_2SnO_4	1: 2-3* (CaO)		Ti 1–10 mol. %
Sr_2SnO_4	1: 2 ($SrCO_3$)		Bi 1 mol. %
Ba_2SnO_4	1: 2 ($BaCO_3$)		Pb 5 mol. %
Zn_2SnO_4	1: 6 (ZnO)		Ce 1 mol. %

* There is a difference between the optimum ratio for ultraviolet excitation and that for cathode rays.

and activator were mixed in an agate mortar. Sodium fluoride, borax or some other salt was used as a flux. The solution of flux salt was purified by the addition of ammonium sulfide and, after filtration, the filtrate was added to the batch. As for activator, commercially available chemically pure manganese sulfate, ceric oxide, lead oxide, bismuth nitrate or titanium oxides were used. If necessary, they were purified by the process previously reported[3].

The batch was fired for two hours at 1100°C in air by an electric furnace.

(3) Properties.—The properties of some stannate phosphors and the optimum mixing ratios for their preparation were shown in Tables I and II respectively.

In the case of magnesium stannate activated by titanium, the change of flux caused the spectral shift of emission, as shown in Figs. 1 and 2 for 2537Å and cathode rays excitations respectively. In Fig. 1, the radiant energy curves were drawn in the same energy scale by arbitrary adjustment of the heights of the individual curves, to show relative spectral locations, while, in Fig. 2, the full lines were drawn relative to the value

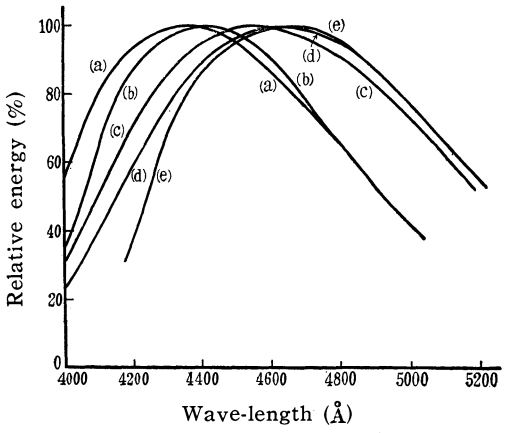

Fig. 1. The variation of emission spectra with different fluxes in Mg_2SnO_4: Ti (ultraviolet light).
(a) $Na_2B_4O_7$ (b) H_3BO_3 (c) $Na_2B_4O_7$ (Ti 1%) (d) NaF, MgF_2 or Al_2O_3 (e) KH_2PO_4 (Ti 10 mol.% (except (c)), 1100°C ×2 hrs, MgO: SnO_2=2.2)

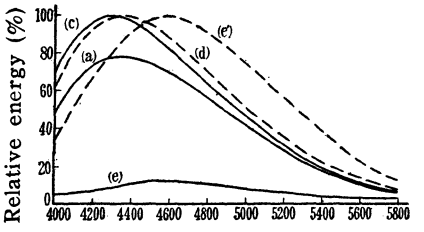

Fig. 2. The variation of emission spectra with different fluxes in Mg_2SnO_4: Ti (cathode rays)
(a) $Na_2B_4O_7$ (c) $Na_2B_4O_7$ (Ti 1%) (e) KH_2PO_4 (8 kV, 200 μA)

of 100 for the highest energy of sample (a) and the dotted lines were drawn in the manner analogous to Fig. 2. Both flux and activator amounted to 0.1 mol. per 1 mol. of the host crystal, and the other conditions were the same as the previous ones. Although lithium, sodium or potassium halides was used as a flux, the emission spectrum was found to be identical with that of sodium fluoride. Magnesium stannate showed itself to be a weak bluish emission when borax was employed as a flux, but it was difficult to determine the emission spectrum.

The emission spectra and the brightness of calcium stannate activated by titanium under cathode rays excitation were shown in Fig. 3 and Table III. In these measurements, the ratio of

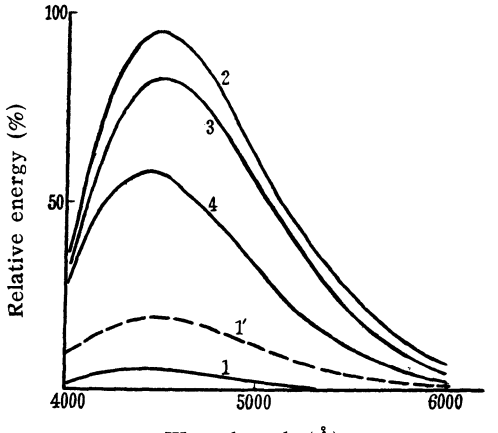

Fig. 3. The variation of emission spectra with CaO : SnO_2 in Ca_2SnO_4: Ti (5 kV, 50 μA, current density, $5\cdot10^{-5}$A/cm^2, 1': measured with higher sensitivity for sample 1. See Table III).

TABLE III

THE BRIGHTNESS OF Ca_2SnO_4: Ti

No. of samples	CaO : SnO_2	Brightness
1	1 : 1	4.8
2	2 : 1	24.1
3	3 : 1	16.7
4	6 : 1	14.7

CaO to SnO_2 was varied from 1 : 1 to 6 : 1, and the generation of cathode rays was made at 5 kV., 50 μamp., the current density being $5\cdot10^{-5}$amp./cm^2. Taking a zinc silicate activated by manganese as the standard sample for the measurements of brightness, commercial calcium magnesium silicate activated by titanium had the value of 35.0. The same measurements were carried out on calcium stannate activated by cerium, in which case the amount of cerium was varied from 0.001 to 0.05 mol. per mol. of the host crystal. The results were shown in Fig. 4 and Table IV,

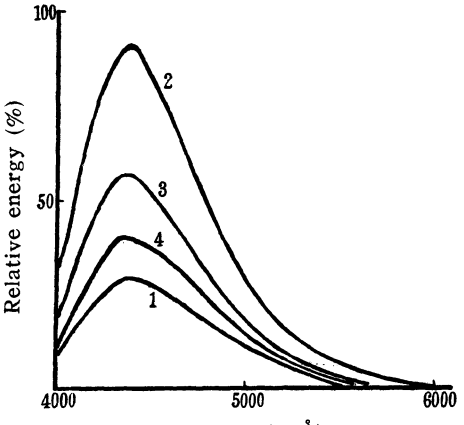

Fig. 4. The variation of emission spectra with Ce concentration in Ca_2SnO_4: Ce (5kV, 50 μA, current density 10^{-5}A/cm^2. See Table IV)

TABLE IV

THE BRIGHTNESS AND RADIANT ENERGY AT 4350Å OF Ca_2SnO_4: Ce

No of Samples	Ce Concentration mol./1 mol. Ca_2SnO_4	Brightness	Relative energy
1	0.001	4.4	30
2	0.01	8.8	90
3	0.02	7.7	58.5
4	0.05	4.4	39

See Fig. 4.

the fourth column of the latter expressing the relative value of radiant energy at the wavelength 4350Å.

These measurements were carried out by means of an automatic recording spectroradiometer[4].

Discussion

The stannate phosphors activated by titanium were investigated by F. A. Kroeger[2]. He studied the function of titanium as an activator in the matrix of silicate, stannate or zirconate, and discussed the properties of stannate phosphors activated by titanium in detail. He found that titanium acts in the above-mentioned matrixes as an activator

4) Y. Kotera, *Rept. Gov. Chem. Ind. Research Institute, Tokyo*, 50, 398 (1955),

only when the preparation was made under oxidizing condition and it does not act as an activator in compounds of aluminium, phosphorus, or boron. From these facts he concluded that the luminescence effect correlated with titanium is attributed to tetravalent Ti^{4+} ions and the activator is built in isomorphously. Further he found that the amounts of titanium are considerably higher than is usual for activation; there is a certain relation between the spectral distributions of absorption and emission due to titanium and orthostannates and metastannates of Ca, Sr, and Ba present examples of the systematic change of the temperature quenching.

We found that some stannates, particularly orthostannates, show considerably strong emission when activated by several heavy metals including titanium. As may be seen in Table I, manganese acts as an activator in the matrix of zinc stannate, in addition to magnesium and calcium stannates[1,2] and the emission is also ascertained when activated by cerium, bismuth and lead. The optimum mixing ratio in Table II corresponds roughly to the highest value of brightness. It is remarkable that zinc stannate shows the strongest emission when prepared by employing zinc oxide in much excess, such result not being obtained in other matrixes. Probably this matrix is not composed of the compound which contains zinc oxide in much excess, but the formation of the matrix would proceed rather slowly and incompletely. Further it is noteworthy that the various emissions are observed for the preparations of magnesium stannate activated by titanium or manganese with different fluxes. In the case of magnesium stannates activated by titanium the emission changes are confirmed from the results shown in Fig. 1. These might be explained by an assumption that there are two kinds of centers, one is that of tin and the other that of titanium, each emission being intensified by different fluxes. It is expected that a longer wave-length emission might be caused by tin and a shorter one by titanium from the comparison of emission spectra of (a) and (c), but it is difficult to draw an accurate conclusion. Hoffmann[5] found that SnO_2 or glass containing SnO_2 luminesceses under excitation of ultraviolet light, but the colors of their emissions are mostly brown, and probably tin does not always act as an activator; it seems to be difficult to compare his results with ours. In the case of manganese activation, the blue emission is found under excitation of cathode rays when borax is used as a flux, and this result supports the above explanation. Kroeger[2] found that two different emissions occur, depending on the wave-length of the exciting radiation, and this fact might be explained by assuming the existence of two kinds of luminescence centers. The emission spectra under excitation of cathode rays for magnesium stannates with different fluxes look somewhat varied (Fig. 2), and such a phenomenon has not yet been observed.

From the practical viewpoint, it is important that calcium stannate activated by titanium with flux of borax shows the emission, the intensity of which is about 75% of that of $CaWO_4$. Furthermore, calcium stannate activated by titanium or cerium shows emission as indicated in Figs. 3, 4, Tables III and IV, and might be used as a blue component of color television.

5) J. Hoffman, *Sprechsaal*, **65**, I, 82 (1932).

Summary

Various stannate phosphors were prepared and some of their emissions were determined. Stannate phosphors emit green, blue or yellowish white light when activated by manganese, blue, violet or red by bismuth, orange, green or blue by lead, while those activated by cerium show blue or red emission. It is expected that the activation by tin also occurs in some cases. This is supported by the fact that the emission of magnesium stannate activated by titanium changes by the variation of flux. For different specimens of calcium stannate activated by titanium or cerium, emission spectra under excitation of cathode rays were measured.

The authors wish to thank Mr. Masami Yamada and Mr. Koji Mitsuhashi for the measurements of spectral distribution of cathode rays emission, and Dr. Shoji Makishima and Mr. Kenji Tanaka for the general discussion on the subject and the experimental work they have done.

Government Chemical Industrial Research Institute, Tokyo

*A Method for Determination of Thermodynamic Dissociation Constants from Absorption Spectra with Applications to ortho- and para-Phenylenediamines**

By Tosinobu ANNO and Akira SADÔ

(Received January 18, 1956)

Introduction

The dissociation constants of the mono-acidic bases or the mono-basic acids can be determined fairly well from the absorption curves of the substances in solution at different pH values[1], while with the dibasic acids and diacidic bases the spectroscopic determination of dissociation constants becomes more complicated[2]. Thamer and Voigt[2] have described a method for determining the dissociation constants in these cases. They measured the optical density of solutions of constant ionic strength at different pH values for a fixed wave length. The apparent dissociation constants are determined from these optical density data, and corrected to the true ones, using the Debye-Hückel equation.

We present here another method using the optical density data of solutions at only five different pH values. As an application of the present method, *ortho-* and *para-*phenylenediamines are chosen. There are a good many prior determinations of dissociation constants for the latter compound while the value of the second dissociation constant of the former compound is not found in the literature on the subject. The advantages and the disadvantages of the present method will also be discussed.

Method

We shall describe the method only for the diacidic bases, the application to acids or amphoteric electrolytes being obvious. The following equation can be shown to hold[2]:

$$D=\frac{Lc\left[\epsilon_1+\frac{k_{1b}}{a_{OH}}\epsilon_2+\frac{k_{1b}k_{2b}}{a^2_{OH}}\epsilon_3\right]}{1+\frac{k_{1b}}{a_{OH}}+\frac{k_{1b}k_{2b}}{a^2_{OH}}} \quad (1)$$

where ϵ_1, ϵ_2, and ϵ_3 represent the molar extinction coefficients of undissociated diacidic base B, its singly and doubly dissociated ions BH^+ and BH_2^{++}, respectively. D denotes the optical density of the solution of hydroxyl-ion activity a_{OH} and of analytical concentration c of the base in all its forms measured with an absorption cell of the length L. k_{1b} and k_{2b} are the apparent basic dissociation constants defined by

$$k_{1b}=\frac{a_{OH}[BH^+]}{[B]}, \qquad k_{2b}=\frac{a_{OH}[BH_2^{++}]}{[BH^+]}, \quad (1a)$$

where brackets indicate concentrations. According to Thamer and Voigt "If k_1 and k_2 overlap and k_1/k_2 is therefore small, one can use optical density data and pH data with equation 4 (our equation 1) to obtain ϵ_2, k_1, and k_2 by successive approximations. However, the calculations are very laborious". It is the purpose of this paper to show that using Eq. (1) the dissociation constants can be calculated *without* successive approximations. From Eq. (1) the following equation can easily be derived:

$$D'x-y+(D'-\epsilon_3)z/a_{OH}=(\epsilon_1-D')a_{OH}, \quad (2)$$

where $D'=D/Lc$, $x=k_{1b}$, $y=k_{1b}\epsilon_2$, and $z=k_{1b}k_{2b}$. ϵ_1 and ϵ_3 are measurable as D' in alkaline ($pOH \ll pk_{1b}$) and acidic ($pOH \gg pk_{2b}$) solution, respectively. If the measurements are made of D' at three different medium pH values and constant ionic strength, Eq. (2) gives a set of linear simultaneous equations, in which x, y and z are unknowns, for a fixed wave length. No iterative process is involved in solving these equations for x, y and z, from which k_{1b}, k_{2b}, and ϵ_2 can be determined. Although what values of pH are appropriate as "three different medium pH values" depends on the substance, the following general rule may be given:

If $k_{1b}/k_{2b} \gg 1$, (usually >10), these pH values are chosen such that $a_{OH} \cong \sqrt{k_{1b}k_{2b}}$, $a_{OH} \cong k_{1b}$ and $a_{OH} \cong k_{2b}$.

If $k_{1b}/k_{2b} \cong 1$, they are all chosen such that $p_{OH} \simeq pk_{1b}$ ($\cong pk_{2b}$), usually with intervals of 0.3–0.5 pH units.

* Presented at the Meeting of the Kyushu Branch of the Chemical Society of Japan, Fukuoka, November 7, 1953.

1) For example see, Hughes, Jellinek, and Ambrose, *J. Phys. Colloid Chem.*, **53**, 410 (1949).

2) B.J. Thamer and A.F. Voigt, *J. Phys. Chem.*, **56**, 225 (1952).

Experimental Results

The samples of *o*- and *p*-phenylenediamines used were commercial ones. Absorption curves were determined with a Beckman DU spectrophotometer with a fixed slit-width for each substance at a given wavelength. Values of pH were determined using a pH-meter supplied by Shimadzu Seisakusho with a Beckman glass electrode. They were converted into the hydroxyl-ion activity using the ionization constant of water K_w[3]. The optical density data are listed in Tables I and II for *o*- and *p*-phenylenediamines, respectively. They are limited to those corresponding to 10–90 percent transmittance. Since it is impossible to obtain the optical density data satisfying the above criterion with one concentration value of the solution, we must use two different concentration values for each substance and for each pH value. In acidic and alkaline extremes dilution by the solvent does not bring about the change of the hydrogen-ion concentration, since in such cases the buffer action of the solvent is strong. For intermediate pH values McIlvaine's[4] Na_2HPO_4-citric acid buffer solutions with appropriate pH values were first prepared and then diluted to low ionic strength so that the Debye-Hückel equation can be applied. In this way, the buffer action was weakened and the pH value of the solution came to depend slightly upon the analytial concentration of the substance. Therefore, the optical density data of solutions with different concentrations are listed separately in the table. This supplied additional equations for the calculation of the dissociation constants and, as far as possible, two sets of equations were selected and used for calculation for a fixed wave length. The agreement between the values of the dissociation constants calculated from different sets of equations for a fixed wave length represents a measure of the experimental accuracy, particularly, of pH measurements. A preliminary investigation shows the dissociation constants of these substances to be: *o*-, $k_{1b} \cong 10^{-10}$, $k_{2b} = 10^{-14}$; *p*-, $k_{1b} \cong 10^{-8}$, $k_{2b} \cong 10^{-11}$. From these figures appropriate values of pH are selected according to the criterion stated above. All measurements were made at room temperature. The control of the ionic strength was made with KCl. In the case of *o*-compound, where the relatively high ionic strength was necessary, dilution of the buffer solutions as prepared according to the indication in the literature was unnecessary. In this case the pH value does not depend on the concentration of the substance, since the buffer action of the solvent is strong. This is the reason why Table I for *o*-compound contains only one column for each intermediate pH value. The extinction coefficient ϵ_2 of singly charged ion BH^+ can in principle be calculated, but the error included will be great compared with k_{1b} and k_{2b}, because, contrary to them, ϵ_2 cannot be determined as an average value, since ϵ_2 assumes, in

3) The values used for calculations are obtained by interpolation of the values reported by Harned and Hamer, *J. Am. Chem. Soc.*, 55, 2194 (1933).

4) T.C. McIlvaine, *J. Biol. Chem.*, 49, 183 (1921).

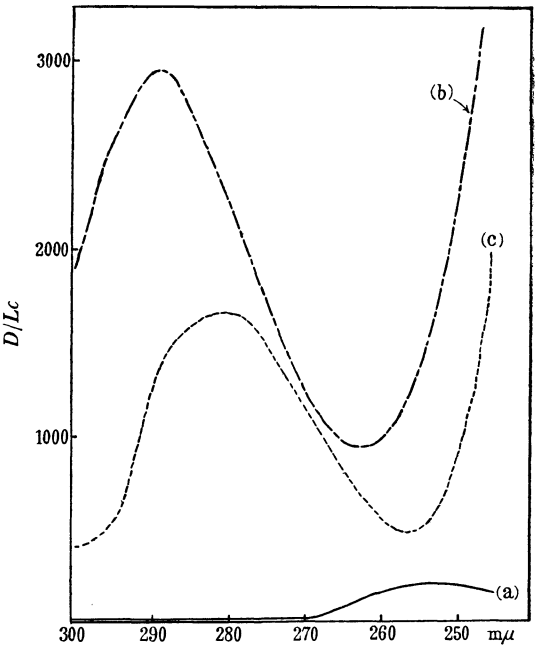

Fig. 1. Absorption curves of *o*-phenylenediamine in 6 N-HCl (a), 0.2 N-Na_2CO_3 (b), and pH 2.10 (c) solutions.

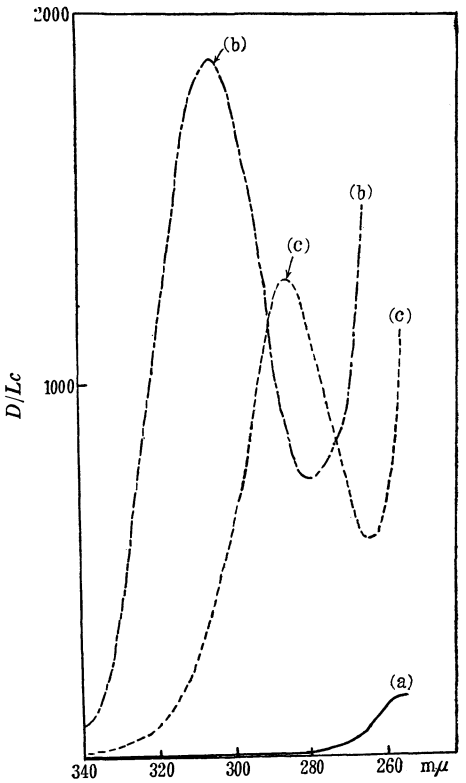

Fig. 2. Absorption curves of *p*-phenylenediamine in 1 N-HCl (a), 0.2 N-Na_2CO_3 (b), and pH 4.95 (c) solutions.

TABLE I

THE VALUES OF D', AND DISSOCIATION CONSTANTS OF *o*-PHENYLENEDIAMINE

Temp.: 14°C, μ: 1.0 mol./l.

Wavelength in mμ	D' Values					k_{1b} ×10¹⁰	k_{2b} ×10¹⁴
	6 N HCl	1.00 N HCl pH 0.00[a]	Na_2HPO_4-citric acid buffer solutions pH 2.10	Na_2HPO_4-citric acid buffer solutions pH 4.60	0.2 N Na_2CO_3		
290	9.5	125	1210	1640	2930	4.77	4.43
285	9.2	162	1550	1940	2800	4.11	4.21
280	12.0	175	1650	1940	2280	2.80	4.22
275	12.0	160	1490	1710	1690		5.44
270	16.0	131	1170	1340	1230		4.21
265	61.2	131	840	1000	970		4.78
260	130	166	560	710	950	2.84	5.20
255	172	192	475	700	1280	4.01	6.88
250	160	216	810	1200	2100	3.54	4.99
				Mean		3.68 ±0.32	4.93 ±0.30

a) The value of the mean activity coefficient of 1.00 N-HCl is given in B. E. Conway, Electrochemical Data (Elsevier Publishing Company, Amsterdam, 1952), p. 75, to be 0.809 at 25°C which amounts to pH=0.10.

TABLE II

THE VALUES OF D', AND DISSOCIATION CONSTANTS OF *p*-PHENYLENEDIAMINE

Temp.: 14.5°C, μ: 0.049 mol./l.

Wavelength in mμ	D' Values								k_{1b} ×10⁸	k_{2b} ×10¹²	Columns[a] used for calc.	k_{1b} ×10⁸	k_{2b} ×10¹²	Columns[a] used for calc.
	1 N HCl	Na_2HPO_4-citric acid buffer solutions pH 3.13	pH 3.00	pH 5.20	pH 4.95	pH 6.75	pH 6.70	0.2 N Na_2CO_3						
340	3	4		7		61	60	87	1.10		3, 5, 7	1.02		3, 5, 8
335	3	4		14		127	122	180	1.08		3, 5, 7	1.09		3, 5, 8
330	3.3	6		21		248	247	355	1.07		3, 5, 7	0.97		3, 5, 8
325	3.7	7		43		447	454	645	1.06		3, 5, 7	0.93		3, 5, 8
320	4.0	16		82		721	714	1034	1.12		3, 5, 7	1.03		3, 5, 8
315	4.3	34		144	109		1000	1432	1.02		3, 5, 8	1.12		3, 6, 8
310	4.7	71		250	213		1240	1760	1.07	7.56	3, 5, 8	1.08	8.19	3, 6, 8
305	5.0	130		407	375		1390	1880	1.02	8.67	3, 5, 8	1.02	9.38	3, 6, 8
300	5.3	217	170		606		1430	1820	0.99	10.05	3, 6, 8	0.95	10.86	4, 6, 8
295	5.6	335	280		906		1395	1590	0.89	10.50	3, 6, 8	0.87	9.60	4, 6, 8
290	6.1	437	378		1177		1292	1300		10.50	3, 6, 8		10.15	4, 6, 8
285	6.6	480	408		1283		1137	1015	1.46	10.68	3, 6, 8	1.47	10.13	4, 6, 8
280	7.4	455	388		1200		961	815	1.15	10.22	3, 6, 8	1.16	10.59	4, 6, 8
275	8.3	381	316		989		827	773	0.63	10.45	3, 6, 8	0.65	10.28	4, 6, 8
270	13.5	297	237		767		814	1035		10.37	3, 6, 8		10.93	4, 6, 8
265	53	256	199		592		1058	1600	2.49	11.34	3, 6, 8	2.57	12.01	4, 6, 8
260	114	297	243		628		1738	2620	1.73	9.87	3, 6, 8	1.73	12.37	4, 6, 8
255	150	490	443		1138		3120	4400	1.46	8.95	3, 6, 8	1.45	9.56	4, 6, 8
						Mean			1.21 ±0.11	9.93 ±0.30		1.19 ±0.11	10.34 ±0.33	

a) The set of numbers in column 12 shows that for each wave length the set of D' values corresponding to the column indicated by these numbers is substituted in Eq. (2) and the values of k_{1b} and k_{2b} found in column 10 and 11, respectively, are calculated from the resulting set of three equations. Column 15 relates to columns 13 and 14 as column 12 does to columns 10 and 11.

general, different values at different wave lengths. For this reason, the calculated ϵ_2 values are not given in the tables. The observed D'-values of a solution whose pH value lies in the middle of pk_{1b} and pk_{2b} is a fairly good measure of the absorption by the species BH^+ only, provided pk_{1b} and pk_{2b} are separated with each other by 3 or 4 as in phenylenediamines. The influence of the other species can be neglected at this value of pH. Figs. 1 and 2 show the absorption curves of *o*- and *p*-phenylenediamines, respectively, in acidic (a), alkaline (b), and medium pH (c) solutions. As was mentioned above, the curves (a), (b) and (c) are mainly due to species BH_2^{++}, B and BH^+, respectively. If at a given wave length the extinction coefficients of species B and BH^+ are alike, the calculated value of k_{1b} at this wave length is prboably in error. In the same way, if the extinction coefficients of species BH^+ and BH_2^{++} are alike, k_{2b} calculated at this wave length is probably in error. Furthermore, the D' values corresponding to too high transmittance are likely to be in error. In fact, anomalous values are obtained from these data and these values are not given in the tables.

Thus the mean values of the apparent dissociation constants are:

o-, $k_{1b}=(3.68\pm0.32)\times10^{-10}$, $k_{2b}=(4.93\pm0.30)\times10^{-14}$:

p-, $k_{1b}=(1.20\pm0.08)\times10^{-8}$, $k_{2b}=(1.01\pm0.03)\times10^{-11}$.

For the apparent dissociation constants obtained above, activity corrections were made, using the Debye-Hückel equation of the following form[5]:

$$-\log\gamma_i=\frac{Az_i^2\sqrt{\mu}}{1+Ba_i\sqrt{\mu}},$$

$$A=\frac{1}{2.303}\frac{N^2e^3}{(DRT)^{3/2}}\left(\frac{2\pi}{1000}\right)^{1/2},$$

$$B=\left(\frac{8\pi N^2e^2}{1000DRT}\right)^{1/2}$$

where e is the electronic charge, R is the gas constants, D is the dielectric constant of water at the absolute temperasure T, N is the Avogadro's number, and μ is the ionic strength of the solution[6]. z_i and a_i are the charge and the radius of ion i. a_i is assumed to be 5 Å for both phenylenediamines in all their forms. The activity coefficients thus calculated for each experimental condition are collected in Table III.

TABLE III

ACTIVITY COEFFICIENTS OF *o*- AND *p*-PHENYLENEDIAMINES CALCULATED BY DEBYE-HÜCKEL EQUATION

Isomers	*ortho*	*para*
Temp., °C	14	14.5
μ (mol./l)	1.0	0.049
γ_B	1.00	1.00
γ_{BH^+}	0.646	0.830
$\gamma_{BH_2^{++}}$	0.174	0.474

Then the final dissociation constants are calculated to be:

o-, $K_{1b}=(2.4\pm0.3)\times10^{-10}$,
$K_{2b}=(1.3\pm0.1)\times10^{-14}$ at 14°C;

p-, $K_{1b}=(1.0\pm0.1)\times10^{-8}$,
$K_{2b}=(5.8\pm0.1)\times10^{-12}$ at 14.5°C,

where the errors due to the Debye-Hückel equation are neglected. It is interesting to compare these results with the values obtained by other methods. They are listed in Table IV taken from Landolt-Börnstein Tables[7]. It can be seen that the present method yields reasonable values of dissociation constants. Moreover, the present work adds the value of the second dissociation constants of *o*-phenylenediamine to the literature. Of course the precise value of K_{2b} of this compound is still uncertain since we were forced to make this determination at rather high ionic strength.

TABLE IV

DISSOCIATION CONSTANTS OF PHENYLENEDIAMINES[a]

Isomers	Step	Temp., °C	Constant	Method	Author
o-	1st	21	$2.3_5\times10^{-10}$	Potentiometric	Kuhn & Wassermann Kuhn & Zumstein
o-	1st	25	3.3×10^{-10}	Hydrolysis, partial extraction	Farmer & Warth
p-	1st	18	1.3×10^{-8}	Conductmetric	Walden & Ulich
p-	1st	18	1.1×10^{-8}	Potentiometric	Kolthoff & Bosch
p-	1st	ca. 20	1.0×10^{-9}	Potentiometric & colorimetric	Pring
p-	1st	21	9.5×10^{-9}	Potentiometric	Kuhn & Wassermann
p-	2nd	18	3.5×10^{-12}	Potentiometric	Kolthoff & Bosch
p-	2nd	21	1.5×10^{-11}	Potentiometric	Kuhn & Zumstein

a) Taken from ref. (7) in text.

5) For example see, D. A. McInnes, "The Principles of the Electrochemistry", Reinhold, New York (1939), Chap. 7.

6) The values of physical constants used in the calculation are taken from DuMond and Cohen, *Revs. Modern Phys.*, **25**, 691 (1953), except for the dielectric constant of water, for which the values are obtained by the interpolation of the values listed in S. Kaneko, *J. Electrochem. Soc. Japan*, **20**, 273 (1952).

7) Landolt-Börnstein, "Physikalisch-Chemische Tabellen" Springer, Berlin (1931), 2te Ergänzungsband, p. 1094.

Comparison with Thamer-Voigt's Method[8,9]

As an application of the present method to the case where k_1 and k_2 are not separate from each other as for phenylenediamines, and also as a comparison of the present method with Thamer-Voigt's we have calculated the dissociation constants for isophthalic acid from the data presented by these authors[2]. The results are given in Table V. The mean values of the dissociation constants calculated by both methods agree very well.

TABLE V

OPTICAL DENSITIES[a] AND DISSOCIATION CONSTANTS OF ISOPHTHALIC ACID

Wave length in Å	Optical densities (pH)					$k_1 \times 10^4$	$k_2 \times 10^5$
	1.58	3.56	4.18	5.095	8.72		
2476.0	0.987	1.134	1.152	1.036	0.982	3.21	3.62
2460.0	1.298	1.435	1.421	1.233	1.146	3.45	3.29
Wave length in Å	Optical densities (pH)					$k_1 \times 10^4$	$k_2 \times 10^5$
	1.58	3.37	3.96	4.91	8.72		
2476.0	0.987	1.109	1.164	1.056	0.982	3.02	3.96
2460.0	1.298	1.410	1.446	1.256	1.146	2.71	4.52
					Mean[b]	3.10	3.85
					Mean (Thamer-Voigt)[c]	2.78	4.00

a) Optical density data are taken from ref. (2) in text.
b) Mean over four calculated values using the present method.
c) See ref. (2) in text.

In Thamer-Voigt's method it is ture that the optical density measurements of many kinds of solution of different pH values reduce the errors due to optical density or pH measurements included in the final values of k_1 and k_2, but the preparation of many kinds of solution is laborious especially for substances unstable in solution. Besides, it is necessary in their method that the optical density versus pH curve should show a decided maximum or minimum. In most cases a suitable wave length may be chosen so that the curve has a maximum or minimum. In the present method, the number of solutions to be prepared is considerably reduced. In addition, the above mentioned maximum or minimum are unnecessary. These are the advantages of the present method. While the error due to the optical density measurement becomes less by taking the mean over many values determined at different wave lengths, the error due to pH measurement cannot be reduced, which is the disadvantage of the present method.

In conclusion, the present method is experimentally easier to carry out especially for substances unstable in solution. For stable substances, the dissociation constants

8) It should be noted that k_1 and k_2 used in this section should be read as k_{1b} and k_{2b}, respectively, for diacidic bases such as phenylenediamines. For dibasic acids such as isophthalic acid k_1 and k_2 should be read as k_{1a} and k_{2a}, respectively, and defined by

$$k_{1a}=\frac{a_H[AH^-]}{[AH_2]},\quad k_{2a}=\frac{a_H[A^{--}]}{[AH^-]}$$

where a_H is the H-ion activity and AH_2, AH^- and A^{--} denote undissociated, singly and doubly dissociated dibasic acid, respectively.

9) After the preparation of this manuscript had been completed, a paper by B.J. Thamer (*J. Phys. Chem.*, 59, 450 (1955)) came to our attention. This method is essentially identical with ours excepting that ε_1 and ε_3 (in our notation) are not assumed to be the molar extinction coefficient at alkaline and acidic extremes. In diacidic bases (for example) having very small values of dissociation constants, his method may be particularly useful, since the direct determination of ε_3 necessitates the high value of ionic strength of the solution. If the optical density of the solution as acidic as possible (comforming to the requirement of low ionic strength) is practically equal to ε_3, Thamer's method has no advantages because in his method a set of five equations containing five unknowns must be solved for a fixed wave length instead of a set of three equations in our method. If the optical density of the solution as acidic as possible is considerably different from ε_3, his method may not give the precise value of the k_{2b}, because in such a solution rather a small fraction of the base exists in the form BH_2^{++} and even a small error in the optical density measurement results in a rather considerable error in k_{2b}. Therefore, for most practical purposes, our method involving the solution of a set of three equations for a fixed wave length may be sufficient.

may be determined by Thamer-Voigt's method a little more accurately.

The extension, of our method to polyelectrolytes appears possible, provided that each dissociated species has a different extinction coefficient in a proper wave-length region, although the number of simultaneous equations to be solved increases. For example, a tribasic acid requires a set of five equations.

The authors express their hearty thanks to Professor S. Imanishi who read the manuscript and made many suggestions. Thanks are also due to Professor R. Matuura for permission to use a pH meter and for making valuable suggestions.

Departments of Chemistry, Faculty of Science, Kyushu University, Fukuoka

The Action of Hydrogen Bromide and Oxygen on Various Ethenoid Compounds. I

By Makoto TAKAHASI*

(Received January 12, 1956)

The mechanism of the hydrocarbon oxidation by means of molecular oxygen at room or higher temperature is very complicated and its study has been an object of many investigations for many years. Although the mechanism has not yet been completely elucidated, the recent progress of the free radical chemistry has made clear that the oxidation by molecular oxygen involves free radical intermediates in the course of the reaction. The research of the oxidation at room temperature is very interesting and important, but the relatively slow velocity of the reaction at room temperature makes difficult such an investigation. It has been found that many materials such as catechol and hydroquinone which can serve as hydrogen donors retard the oxidation. However, hydrogen bromide which is also one of the hydrogen donors is known to be a distinguished accelerator of the oxidation of hydrocarbons by molecular oxygen, as described by F.F. Rust and W.E. Vaughan[1]. They carried out an extensive investigation of the oxidation of aliphatic and aromatic hydrocarbons catalysed by hydrogen bromide, and they proposed the following mechanism for the reaction,

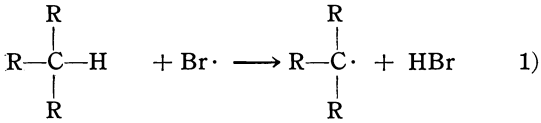

1)

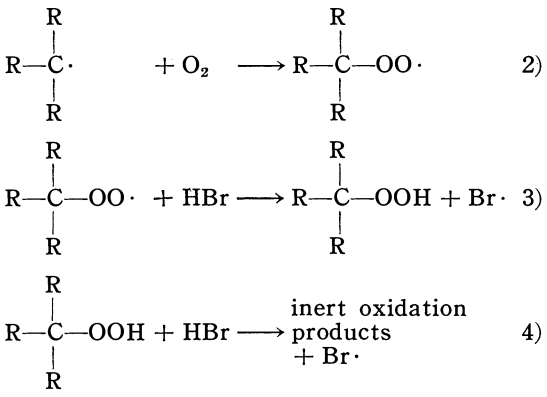

2)

3)

4)

Y. Urushibara and O. Simamura[2] extended their study of oxygen effect in the addition of hydrogen bromide to ethenoid compounds to the action of the mixture of oxygen and hydrogen bromide on allyl bromide, crotonic acid, and several other compounds. O. Simamura and the present author[3] studied the joint action of hydrogen bromide and oxygen on cinnamic acid and determined the orientation of the bromine atom when it adds to the double bond of cinnamic acid. Namely,

the free radical 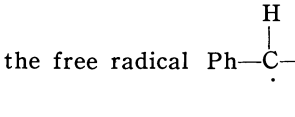 is more likely formed as the intermediate rather than

* Present address: Department of Chemistry, College of General Education, The University of Tokyo.

1) F.F. Rust and W.E. Vaughan, *Ind. Eng. Chem.*, **41**, 2595 (1949).

2) Y. Urushibara and O. Simamura, This Bulletin, **14**, 323 (1939).

3) O. Simamura and M. Takahasi, ibid., **22**, 60 (1949).

the alternative 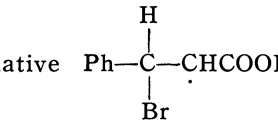 , because

ω-bromoacetophenone and carbon dioxide are obtained as the oxidation products and it can be supposed that they are derived from

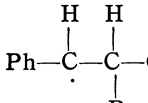

through the hydroperoxide

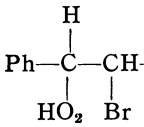

In order to compare the relative stability of these radicals theoretically, the author carried out a computation of the delocalization energies of the odd electron of the free radicals, Ph—$\dot{C}H_2$ and $\dot{C}H_2$—COOH, according to the same method as that which was adopted by G. W. Wheland[4], and obtained 15.3 kcal./mol. for the former and 16.7 kcal./mol. for the latter, assuming $S=0.25$, $\delta=0.8$, $\delta'=0$ and $\eta=0.8$. It may be impossible to conclude from these values that the latter is more stable than the former, for the calculation is of the zeroth order approximation. The values of bond dissociation energies of benzyl bromide and bromoacetic acid measured by the pyrolytic method of M. Szwarc[5] or that of toluene by the substitution reaction of bromine according to E. R. VanArtsdalen[6] will supply useful knowledge concerning this problem.

In this series of our papers the general scheme of the oxidation of various olefinic compounds in the presence of hydrogen bromide is discussed on the ground of the experimental data. This first paper deals with α,β-disubstituted ethenoid compounds, such as cinnamic acid, *m*-nitrocinnamic acid, *p*-methoxycinnamic acid, maleic acid, citraconic acid, crotonic acid, stilbene, and ω-nitrostyrene. The two substituted cinnamic acids, *p*-methoxycinnamic acid with an electron donative methoxyl group, and *m*-nitrocinnamic acid with an electron attractive nitro group, are both unreactive to the mixture of hydrogen bromide and oxygen at room temperature. The former has been found to have an antioxidant action by itself. When *p*-methoxycinnamic acid was added to the solution of cinnamic acid in carbon tetrachloride, it suppressed the reaction of cinnamic acid with the mixture of hydrogen bromide and oxygen to some extent. This may be attributed to the fact that the substitution reaction of *p*-methoxycinnamic acid with bromine atom may take place rapidly, stopping the chain reaction by bromine atom.

The general scheme of the action of hydrogen bromide and oxygen on ethenoid compounds has been discussed by Y. Urushibara[7a] and O. Simamura[7b] and by F. F. Rust and W. E. Vaughan[8], and is supposed to be as follows.

1) olefin + oxygen + hydrogen bromide $\longrightarrow$ Br· (initiations)

2) 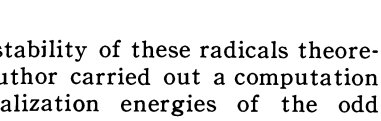 (propagation)

3) 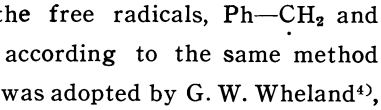 (propagation)

4) 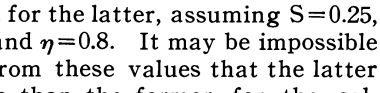 (propagation)

5) 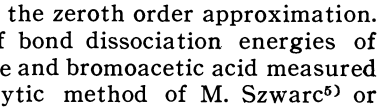 $+H_2O$ (overall reaction for the formation of bromohydrin)

6) 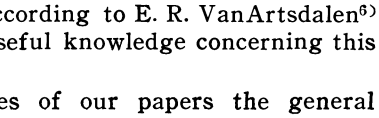 (formation of bromoketone)

7) 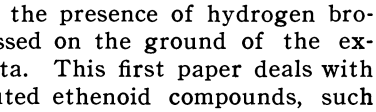 (formation of dibromide, termination)

8) 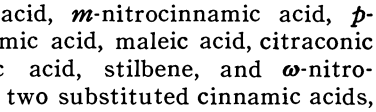 (formation of dibromide, propagation)

9) $Br\cdot + Br\cdot \longrightarrow Br_2$ (termination)

However, this scheme, applied to the reaction of cinnamic acid with hydrogen bromide and oxygen, may not give a satisfactory explanation of our experimental results. If it is assumed that all cinnamic acid dibromide is produced as a chain termination product

4) G. W. Wheland, *J. Am. Chem. Soc.*, **64**, 900 (1942).
5) M. Szwarc, *Chem. Revs.*, **47**, 75 (1950).
6) M. R. Anderson, Jr., H. A. Scheraga and Erwin R. VanArtsdalen, *J. Chem. Phys.* **21**, 1258 (1953).
7a) Y. Urushibara, *Kagakusoho*, Vol. **6**, (1944).
7b) O. Simamura, This Bulletin, **17**, 326 (1942).
8) F. F. Rust and W. E. Vaughan, *J. Org. Chem.*, **7**, 491 (1942).

as in the above mechanism, one mole of bromine would be required to produce one mole of cinnamic acid dibromide, and in order to obtain one mole of bromine, at least one mole of cinnamic acid would be consumed by the reaction with one mole of oxygen molecule giving some oxidized product of cinnamic acid. That is, according to the above mechanism, one cycle of propagation reaction would involve only the reaction of one mole of cinnamic acid with one mole of oxygen molecule giving one mole of bromine as cinnamic acid bibromide or as free bromine molecule. Furthermore, in order to obtain one mole of ω-bromoacetophenone, one mole of cinnamic acid and one mole of oxygen molecule would be consumed giving no excess bromine.

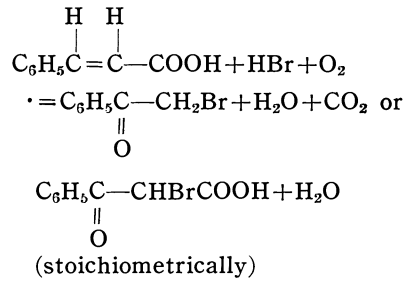

Our semi-quantitative experiment on the reaction of cinnamic acid with the mixture of hydrogen bromide and oxygen gives some evidence suggesting that the above scheme is not sufficient. The amount of cinnamic acid dibromide produced from 0.0187 mol. of cinnamic acid was 0.0101 mol. (53.4 mol. percent) and that of ω-bromoacetophenone was 0.0048 mol. (25.6 mol. percent for cinnamic acid used). The amount of carbon dioxide evolved was 0.0006 mol. It is noted that the amount of carbon dioxide in mole was not the same as that of ω-bromoacetophenone. This fact suggests the presence of the unstable compound $C_6H_5CCHBrCOOH$ in the

reaction product. Although the fate of the residual cinnamic acid of about 20% is not ascertained now, neither bromohydroxycinnamic acid nor dihydrocinnamic acid were found in any detectable amount in the reaction products. These compounds, if they existed, would suggest some other process of the formation of bromine from hydrogen bromide. Here, in order to give a reasonable explanation on the experimental result that cinnamic acid dibromide is produced in the yield of more than fifty percent, the following process is proposed in addition to the above ones:

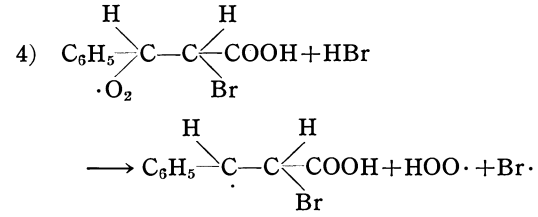

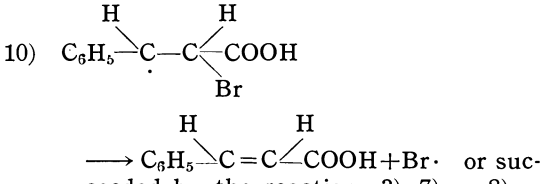

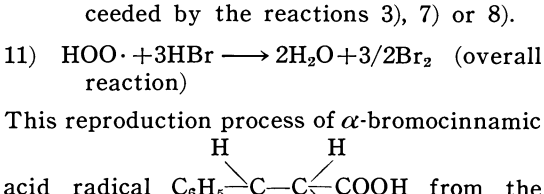

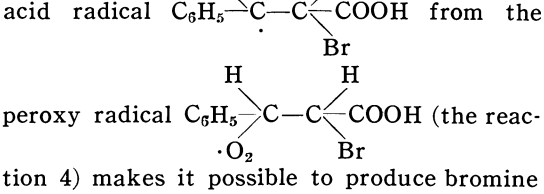

11) $HOO\cdot + 3HBr \longrightarrow 2H_2O + 3/2Br_2$ (overall reaction)

This reproduction process of α-bromocinnamic acid radical

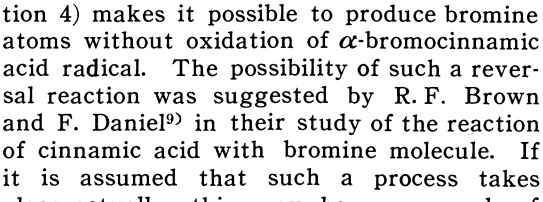

from the peroxy radical

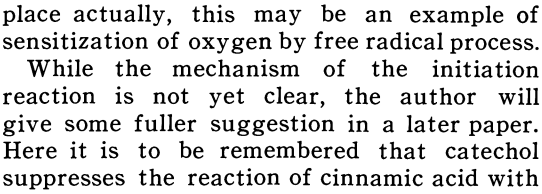

(the reaction 4) makes it possible to produce bromine atoms without oxidation of α-bromocinnamic acid radical. The possibility of such a reversal reaction was suggested by R. F. Brown and F. Daniel[9] in their study of the reaction of cinnamic acid with bromine molecule. If it is assumed that such a process takes place actually, this may be an example of sensitization of oxygen by free radical process.

While the mechanism of the initiation reaction is not yet clear, the author will give some fuller suggestion in a later paper. Here it is to be remembered that catechol suppresses the reaction of cinnamic acid with oxygen and hydrogen bromide incompletely. This incompleteness of the antioxidant action of catechol in the presence of an excess of oxygen suggests that catechol cannot inhibit the initiation reaction. Nitrobenzene was found to have no action as an antioxidant in the reaction of cinnamic acid with hydrogen bromide and oxygen, while it is known that it has an inhibiting action in the polymerization reaction. This may be explained by the fact that nitrobenzene does not react with bromine atoms very rapidly.

In the reaction products of crotonic acid with the mixture of hydrogen bromide and oxygen, carbon dioxide and an irritating aldehyde are found in addition to β-bromobutyric acid, α,β-dibromobutyric acid, α-

9) R. F. Brown and F. Daniels, *J. Am. Chem. Soc.*, **62**, 2820 (1940).

hydroxy-β-bromobutyric acid which were already described by O. Simamura[1]. The aldehyde gave 2,4-dinitrophenylhydrazone containing bromine and was not identified with the supposedly probable aldehyde, α-bromopropionaldehyde, which gave a 2,4-dinitrophenylhydrazine derivative containing no bromine. At present, the quantitative estimation of these compounds is difficult, so that the material balance in the reaction is not discussed here.

The reaction of maleic acid with hydrogen bromide and oxygen was confusing. The reaction gave a small amount of carbon dioxide. The author at first considered that carbon dioxide was an oxidation product of maleic acid produced in nearly the same way as from cinnamic acid. However, the acid gave carbon dioxide in the reaction with hydrogen bromide in the absence of oxygen, so that it is considered that the acid was decarboxylated through the ionic or any molecular process. It is known that maleic acid adds almost no bromine molecule at room temperature. Citraconic acid gave no reaction product except citraconic anhydride with the mixture of hydrogen bromide and oxygen. These experiments with maleic acid and citraconic acid show that ethenoid α,β-dicarboxylic acids do not react with the mixture of hydrogen bromide and oxygen, due to the stabilization of the ethylenoid double bond by two carboxyl groups.

The reaction of hydrogen bromide and oxygen with stilbene was already studied by O. Simamura[2], and he decribed the formation of stilbene dibromide and an oily product. The present author found a bromophenol and a carbonyl compound in the oily product in addition to a very small amount of carbon dioxide, but the identification of the phenol and the carbonyl compound has not yet been successful. The yield of stilbene dibromide was about 25 mol. percent of the stilbene used. The mechanism of the formation of a phenol from stilbene will be discussed in a later paper concerning the mechanism of the reaction of diphenylethylene with the mixture of hydrogen bromide and oxygen.

The reaction of ω-nitrostyrene with hydrogen bromide appears to be remarkably different from those of the other olefinic compounds. It gave a bromine atom by the action of hydrogen bromide in the absence of oxygen. No influence of oxygen was observed here. M. Takebayashi[10] described a similar action of nitroethylene on hydrogen bromide. ω-Nitrostyrene gave hydroxylamine, ammonia, ω-nitrostyrene dibromide, and an oily substance which was not identified until the present. The reaction mechanism will be discussed in future, when the reaction products have been analysed completely.

10) M. Takebayashi, *J. Chem. Soc. Japan*, **64**. 192 (1942).

Experimental

Materials.—Hydrogen bromide was prepared by the three following methods. a) Bromine was dropped from a dropping funnel into tetralin with gentle heating, and the produced hydrogen bromide was passed through tetralin, anthracene, and phosphorus pentoxide. This method was adopted at first, but hydrogen bromide thus prepared was found to contain a small amount of carbon dioxide, which was presumably produced by the decomposition of some impurities such as tetralin hydroperoxide. b) Bromine was dropped on wet red phosphorus, and the produced hydrogen bromide was purified as in (a). The hydrogen bromide thus produced contained no carbon dioxide, but the production of hydrogen bromide was not smooth enough and the yield was small. c) Hydrogen and bromine were combined directly according to "Org. Synth"[11]. The tank hydrogen dried with phosphorus pentoxide was mixed with bromine, and the mixture was heated by a gentle flame. The hydrogen bromide was passed through copper turnings under a slightly reduced pressure applied to the outlet of the reaction vessel by a Mariot bottle.

Oxygen was obtained from a tank, and passed through aqueous alkali and over phosphorus pentoxide.

Benzene and carbon tetrachloride were purified and dried according to "Org. Solvents,"[12] and distilled.

Cinnamic acid obtained from a commercial source was recrystallized from ethyl alcohol, and kept for a time in an evacuated desiccator, m.p. 133°C.

p-Methoxycinnamic acid was synthesized from anisaldehyde and malonic acid in the presence of ammonia, m.p. 173–4°C.

m-Nitrocinnamic acid was synthesized from *m*-nitrobenzaldehyde according to "Org. Synth."[13], m.p. 196–7°C. Crotonic acid and maleic acid were commerical products. Maleic acid was recrystallized from a mixture of ether and acetone, m.p. 130°C.

Citraconic acid was obtained by pyrolytic distillation of citric acid through citraconic anhydride. ω-Nitrostyrene was synthesized from benzaldehyde and nitromethane, m.p. 58°C.

Stilbene was synthesized by the reduction of benzoin according to "Org. Synth."[14] and recrystallized from ethyl alcohol, m.p. 120°C.

Reactions.—Reaction of Cinnamic Acid with Hydrogen Bromide and Oxygen.—Cinnamic

11) "Organic Syntheses", Collective Vol. 2, John Wiley & Sons, Inc., p. 339.

12) A. Weissberger and E. Proskauer, "Organic Solvents", Oxford University Press, pp. 105, 156.

13) "Organic Syntheses", Collective Vol. 1, John Wiley & Sons, Inc., p. 398.

14) ibid., Vol. 23, p. 86.

acid (0.0187 mol.) was weighed and put together with 30 ml. of carbon tetrachloride, and the dry mixed gas of hydrogen bromide and oxygen was passed through the suspension at room temperature for about 230 minutes. The reaction gas was passed through a calcium chloride tube, over water to absorb hydrogen bromide, and through a barium hydroxide solution. The precipitated barium carbonate was collected on a glass filter, and weighed. About 0.0006 mol. of carbon dioxide was produced from 0.0187 mol. of cinnamic acid. In the reaction vessel about 2.953 g. of a solid matter were deposited, and this matter was proved to be almost pure cinnamic acid dibromide by melting point measurement and analysis of bromine. The carbon tetrachloride solution gave 3.8 g. of a mixture of oil and solid mattter on evaporation at atmospheric pressure. The oil and solid matter were separated on a glass filter. The solid, weighing 0.146 g., melted at 195°C. without recrystallization and was identified with cinnamic acid dibromide. The light-greenish oil weighed 2.23 g. and had an irritating smell. 0.318 g. of the oil was added to a solution of 0.4 g. of 2, 4-dinitrophenylhydrazine prepared according to R. L. Shriner[15]. Rapid formation of a dinitrophenylhydrazone was observed but the mixture was left overnight. The collected 2, 4-dinitrophenylhydrazone weighed 0.257 g., which corresponded to 1.8 g. (0.0048 mol.) of the hydrazone to the total amount of the oil. The 2, 4-dinitrophenylhydrazone melted at 214-6°C and contained 21.1% of bromine (Calcd. for $C_{14}H_{11}O_4N_4Br_2$: Br, 21.1 %). It was identified with the 2, 4-dinitrophenylhydrazone of ω-bromoacetophenone by a mixed melting point with an authentic specimen. In addition to cinnamic acid dibromide and ω-bromoacetophenone, a small amount of an unidentified substance was obtained, but no dihydrocinnamic acid (m.p. 47°C), bromohydroxycinnamic acid (m.p. 120°, 156°, 164°C) nor any other acidic substance were found in the reaction mixture. The total amount of cinnamic acid dibromide was 3.099 g. (0.0101 mol.) which corresponded to 53.4 mol. percent of cinnamic acid used. The substance was dried in a desiccator to constant weight. Two more experiments on the reaction of cinnamic acid with hydrogen bromide and oxygen under the same conditions gave similar results. The amounts of cinnamic acid dibromide produced did not differ by more than 0.3 g.

The Reaction of Cinnamic Acid with Hydrogen Bromide and Oxygen in the Presence of Catechol.—Two solutions of cinnamic acid (3.0 g.) in 40 ml. of carbon tetrachloride were prepared, 0.1 g. of catechol being added to one. Both the solutions were subjected to the action of hydrogen bromide and oxygen at the same time. For the solution containing catechol, carbon dioxide was not evolved, and cinnamic acid was recovered, and no 2, 4-dinitrophenylhydrazone was precipitated with the 2, 4-dinitrophenylhydrazine. From the other solution, carbon dioxide was evolved, and cinnamic acid dibromide was obtained.

15) R.L. Schriner and R.C. Fuson, "The Systematic Identification of Organic Compounds", John Wiley & Sons, Inc., p. 171.

Effect of Nitrobenzene.—In 40 ml. of carbon tetrachloride containing 1 ml. of nitrobenzene, 2.01 g. of cinnamic acid were added and the mixture of hydrogen bromide and oxygen was passed through the solution for 535 minutes. Carbon dioxide and cinnamic acid dibromide were obtained and no antioxidant effect of nitrobenzene was observed.

Reactions of *p*-Methoxycinnamic Acid and of *m*-Nitrocinnamic Acid with Hydrogen Bromide and Oxygen.—Hydrogen bromide and oxygen were pased through a solution of *p*-methoxycinnamic acid (3.0 g.) in 40 ml of carbon tetrachloride for 310 minutes. Evolution of carbon dioxide did not take place, and *p*-methoxycinnamic acid was recovered. When hydrogen bromide and oxygen were passed through a solution of 2 g. cinnamic acid and 0.021 g. of *p*-methoxycinnamic acid in 30 ml. of carbon tetrachloride for 265 minutes, a small amount of carbon dioxide was produced, and the reaction product consisted mainly of cinnamic acid dibromide. When 2 g. of cinnamic acid and 2 g. of *p*-methoxycinnamic acid dissolved in 30 ml. of carbon tetrachloride were subjected to the action of hydrogen bromide and oxygen for 405 minutes, a very small amount of carbon dioxide was produced during the passage of the mixed gas, but almost all cinnamic acid and *p*-methoxycinnamic acid were recovered from the carbon tetrachloride solution as a mixture.

Hydrogen bromide and oxygen were passed through a suspension of 2.0 g. of *m*-nitrocinnamic acid in 30 ml. of benzen for 310 minutes at room temperature. *m*-Nitrocinnamic acid was recovered completely without evolution of carbon dioxide.

Reaction of Crotonic Acid with Hydrogen Bromide and Oxygen.—In 50 ml. of carbon tetrachloride 10 g. of crotonic acid was added and the mixture of hydrogen bromide and oxygen was passed through the solution at room temperature for 265 minutes. The carbon dioxide formed was caught as barium carbonate, which weighed 0.215 g. (0.001 mol.). On the bottom of the vessel an oily product deposited from the carbon tetrachloride solution, and, on being kept in a refrigerator, gave a crystalline mass which melted at 95°C. and was identified with α-hydroxy-β-bromobutyric acid. The oil separated from the crystalline mass reduced Fehling's solution at room temperature and gave a small amount of 2, 4-dinitrophenylhydrazone, m.p. 180–200°C. The purification of the hydrazone by either recrystallization or chromatography was unsuccessful. The carbon tetrachloride solution gave about 15 g. of an oil on evaporation. The oil was distilled under a reduced pressure of 20 mmHg. The first fraction which boiled at 48–100°C under that pressure was crotonic acid, the second fraction (1.5 g.) which boiled at 125–130°C was β-bromobutyric acid, and the third fraction (6.5 g.) which passed over at 135–148°C solidified for the most part and the solid melted at 86–88°C. In the flask remained some residue, which melted at 86–88°C. It was identified with crotonic acid dibromide. The velocity of hydrolysis of the second fraction was compared with those of α-bromo- and β-bromobutyric acids. Each compound was weighed into

a flask, and 2.0 ml. of a 5.9 N NaOH solution was added. After standing for one hour at room temperature the mixture was neutralized with nitric acid, silver nitrate was added, and the precipitated silver bromide was weighed. α-Bromo- and β-bromobutyric acids liberated 2.6 and 70% of bromine, respectively. The second fraction of the distillation was hydrolysed under the same condition to the extent of 68% and was thus proved to be composed of β-bromobutyric acid. Every fraction gave a positive reaction with Fehling's reagents, and gave a small amount of a 2,4-dinitrophenylhydrazone suggesting a contamination with some aldehyde, the identification of which was not successful.

Reaction of Maleic Acid with Hydrogen bromide and Oxygen.—Hydrogen bromide and oxygen were passed through a solution of 3.000 g. (0.026 mol.) of maleic acid in 50 ml. of carbon tetrachloride for 315 minutes at room temperature, and 0.0008 mol. of carbon dioxide and 3.199 g. of a precipitate were obtained. The carbon tetrachloride solution gave almost no residue on evaporation. The precipitate showed a large range of melting points. From the precipitate 1.00 g. was sampled and 20 ml. of distilled water was added to it. The water-insoluble part was very small in quantity and it was found to be fumaric acid by a melting point measurement. The water-soluble part was extracted with 20 ml. of ether twice, but both the ethereal extract and the aqueous solution contained maleic acid contaminated with some unidentified compound containing bromine. Formerly the author considered that the carbon dioxide was produced by the free radical mechanism, but, the recent experiment on the reaction of maleic acid with hydrogen bromide in the absence of oxygen showed that carbon dioxide was formed in nearly the same order of amount as in the presence of oxygen. Namely a carbon tetrachloride solution containing 3.00 g. of maleic acid gave about 0.0004 mol. of carbon dioxide on passing hydrogen bromide for 270 minutes at room temperature. Furthermore, when 3 g. of maleic acid with 0.05 g. of catechol was dissolved in 40 ml. of benzene, and hydrogen bromide and oxygen were passed for 165 minutes, 0.0005 mol. of carbon dioxide as barium carbonate was formed.

Reaction of Citraconic Acid with Hydrogen Bromide and Oxygen.—In 60 ml. of benzene 5.0 g. of citraconic acid was dissolved, and the mixture of hydrogen bromide and oxygen was passed through the solution for 360 minutes at room temperature. During the reaction no evolution of carbon dioxide was observed. After evaporation of the reaction mixture, the residual oil was distilled under a reduced pressure of 18 mmHg. and nearly the whole distilled at 98–100°C. The distillate contained no bromine and was identified with citraconic anhydride.

Reaction of Stilbene with Hydrogen Bromide and Oxygen.—To 70 ml. of carbon tetrachloride 5.0 g. (0.028 mol.) of stilbene was added and the mixture of hydrogen bromide and oxygen was passed through the solution for 330 minutes at 19.0°C. Carbon dioxide produced from stilbene was caught in the form of barium carbonate which weighed 0.092 g. (0.00047 mol.). In the reaction vessel a colorless precipitate was deposited from the carbon tetrachloride solution of red color. The deposit weighed 2.73 g. and was found to be composed of stilbene dibromide, m.p. 237°C. It corresponds to 25 mol. percent of the stibene used. The carbon tetrachloride solution was divided into two parts, 44 ml. and 20 ml. The former was shaken with 50 ml. of a 1 N sodium hydroxide solution twice. The sodium hydroxide solution was saturated with carbon dioxide and the separated oil was extracted with ether. The ethereal extract gave a small amount of a phenolic substance on evaporation which gave a positive test for a phenol with ceric ammonium nitrate, the color being brown. It melted at 75°C, and contained bromine, although its amount was very small and its analysis was not successful. It was presumed to be crude tribromophenol, m.p. 96°C. The aqueous solution, saturated with carbon dioxide and shaken with ether, was acidified with sulfuric acid and extracted with ether, but the extract gave practically no appreciable amount of a residue on evaporation. From the carbon tetrachloride solution, shaken with aqueous sodium hydroxide, an oily matter was obtained on evaporation and was distilled under a reduced pressure. A fraction boiling at 112–118°C under 0.9 mmHg gave a crystalline matter. It was separated from the oily part, and recrystallized from alcohol. The substance melted at about 100°C and contained only 8.6% of bromine. Probably it was not pure enough, but the amount was so small that no further recrystallization was attempted. It was supposedly unchanged stilbene, b.p. 166–7°C under 12 mmHg, m.p. 124°C.

Summary

(1) The reaction of α,β-substituted ethenoid compounds with the mixture of hydrogen bromide and oxygen were studied. In the case of cinnamic acid, a reaction mechanism has been tentatively proposed on the basis of the identfied products and their semi-quantitative estimation. The quantitative study of the reaction of cinnamic acid suggests the possibility that oxygen is sensitized by the presence of some free radical if it is relatively stable.

(2) Some experimental data with crotonic acid, sitlbene, and other compounds were presented. Unfortunately, the analysis of the reaction products has not yet been completed up to the present, so that no detailed discussion on these compounds was attempted. A general discussion on the reactions of ethenoid compounds with the mixture of hydrogen bromide and oxygen will be made in a later paper.

The author wishes to express his hearty thanks to Prof. Y. Urushibara and Prof. O. Simamura for their kind guidance and encouragement throughout this work.

Department of Chemistry,
Faculty of Science,
The University of Tokyo,
Komaba, Tokyo

Studies on Seven-membered Heterocyclic Compounds Containing Nitrogen. I. Synthesis of 1-Azacycloheptan-4-one Hydrochloride

By Akira YOKOO and Shiro MOROSAWA

(Received March 28, 1956)

As to azacycloheptanones, syntheses of 1-methyl-1-azacycloheptan-3-one[1], 1-methyl-2-ethyl-1-azacycloheptan-3-one[2], 1,2-dimethyl-1-azacycloheptan-3-one[3], and 1-alkyl-5-phenyl-1-azacycloheptan-4-ones[4] have been reported, but no such compound as one that has no side-chain is obtained except a lactam-type 1-azacycloheptan-2-one.

The present authors obtained 1-benzyl-1-azacycloheptan-4-one (II) (b.p. 137–139°C/2 mmHg.; hydrochloride, m.p. 186–187°C (decomp.); 2,4-dinitrophenylhydrazone hydrochloride, m.p. 206°C (decomp.)) by the Dieckmann condensation of ethyl N-benzyl-γ-(β-carbethoxyethylamino) butyrate[5] (I), using the methods of Prill and McElvain[1], and of Leonard and Barthel[2]. Reduction of II hydrochloride by palladous oxide as a catalyst afforded 1-azacycloheptan-4-one hydrochloride (III), m.p. 171°C (decomp.). 2,4-Dinitrophenylhydrazone hydrocholoride of III was formed in two kinds of crystal; one melted at 155°C (decomp.) and the other at 211°C (decomp.). The formed could be converted into the latter.

The action of diazomethane on 1-benzoyl-1-azacyclohexan-4-one yielded an oil, b.p. 172–179°C/0.01 mmHg. likely to be 1-benzoyl-1-azacycloheptan-4-one from the analytical value and also from that of 2,4-dinitrophenylhydrazone, m.p. 175–6°C. An attempt was made to obtain III by hydrolysis of the oil with hydrochloric acid, but the resultant oily substance did not crystallize. 2,4-Dinitrophenylhydrazone derived from the oily substance, however, was, though in poor yield, found to be identical with the one, m.p. 155°C (decomp.) from III by mixed fusion. Further detailed study on these experiments will be described in subsequent papers.

The Dieckmann condensation of ethyl N-benzoyl-γ-(β-carbethoxyethylamino) butyrate[5] was unsuccessful.

The present study was carried out as a part of the general research on the azulenoid compounds (the representative, Prof. Tetsuo Nozoe). The authors take this opportunity to extend their deep gratitude to the members of the Department of Organic Chemistry of Tokyo Institute of Technology for their carrying out the carbon and hydrogen microanalyses and also to Mr. Kameji Yamane (this laboratory) for his cooperation in the present experiments.

Experimental

1-Benzyl-1-azacycloheptan-4-one (II).—In a 1 l. three-necked, round-bottomed flask fitted with a Hershberg stirrer, a dropping funnel and a fractionating column which had a thermometer on its head and a side arm attached to a condenser set for downward distillation, were placed sodium ethoxide, prepared from 2.3 g. of sodium[6] and 400 cc. of dry xylene. The reaction flask was heated under stirring in an oil-bath sufficiently to cause gentle refluxing from the column, and a solution of 32.1 g. of ethyl N-benzyl-γ-(β-carbethoxyethylamino) butyrate in 200 cc. of dry xylene was added dropwise during sixteen hours. The heating was then continued until the mixture of alcohol and xylene distilled out and the thermometer registered the boiling point of xylene. The reaction mixture was extracted with four 30 cc. portions of water and three 40 cc. portions 2N hydrochloric acid. The extracts were united and refluxed with 240 cc. of concentrated hydrochloric acid for five hours. The hydrochloric acid was expelled by heating on a water-bath under reduced pressure as completely as possible and 50% potassium hydroxide solution was added to the residue to make pH 8 and extracted with five 50 cc. portions of ether. The aqueous solution was then made strongly alkaline and further extracted with seven 30 cc. portions of ether. These ether extracts were all combined and dried over magnesium sulfate. Dry hydrogen chloride was passed through to give hydrochloride of II as a precipitate. The precipitate was dried in a desiccator and dissolved in 12 cc. of methanol

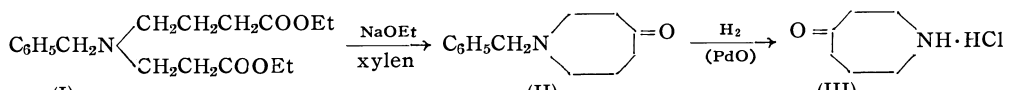

(I) (II) (III)

1) E.A. Prill and S.M. McElvain, *J. Am. Chem. Soc.*, 55, 1233 (1933).
2) N.J. Leonard and E. Barthel, ibid., 71, 3098 (1949).
3) N.J. Leonard and S. Gelfand, ibid., 77, 3269 (1955).
4) R.E. Lyle and G.G. Lyle, *C.A.*, 49, 9047 (1955).
5) A. Yokoo and S. Morosawa, *J. Chem. Soc. Japan*, 77, 599 (1956).
6) "Organic Reaction", Vol. I, p. 278.

and crystallized by adding ether. This crystal was recrystallized from methanol-ether solution as white needles, m.p. 186–187°C (decomp.), yield 5.2 g. (Found: N, 5.74. Calcd. for $C_{13}H_{17}ON \cdot HCl$: N, 5.85%).

2, 4-Dinitrophenylhydrazone Hydrochloride.—The mixture of II hydrochloride (0.1 g.), 2, 4-dinitrophenylhydrazine (0.2 g.), alcohol (10 cc.) and concentrated hydrochloric acid (0.2 cc.) was heated for two minutes. The crystals formed were recrystallized from water to yield 0.2 g. of yellow crystals, m.p. 206°C (decomp.). (Found: N, 16.87. Calcd. for $C_{19}H_{21}O_4N_5 \cdot HCl$: N, 16.65%).

The above-mentioned hydrochloride was made alkaline by adding 50% potassium hydroxide solution and taken up in ether. After drying over magnesium sulfate, the ether was removed and vacuum distillation of the residue gave II, b.p. 115–118°C/0.01 mm. (Found: N, 7.17. Calcd. for $C_{13}H_{17}ON$: N, 6.89%).

1-Azacycloheptan-4-one Hydrochloride (III).—A solution of 4 g. of II hydrochloride in 150 cc. water was shaken with 0.3 g. of PdO under hydrogen atomosphere at room temperature until the theoretical amount of hydrogen had been absorbed. After separation of the catalyst by filteration, water was removed under reduced pressure and the residue was crystallized from alcohol and ether to yield 2.1 g. (84%) of colorless needles, m.p. 171°C (decomp.).

Anal. Found: C, 48.51; H, 7.98; N, 9.29. Calcd. for $C_6H_{11}ON \cdot HCl$: C, 48.83; H, 8.08; N, 9.36%.

2, 4-Dinitrophenylhydrazone hydrochloride was obtained in yellow needles, m.p. 212°C (decomp.) (Found: N, 21.61. Calcd. for $C_{12}H_{15}O_4N_5 \cdot HCl$: N, 21.24%). Another kind of crystal was also obtained in orange scales, m.p. 152–155°C (decomp.), which was not depressed on admixture with the specimen derived from 1-benzoyl-1-azacycloheptan-4-one by hydrolysis and was also able to be converted into the modification in yellow needles by boiling with hydrochloric acid in methanol.

Chemical Institute, Faculty of Science, Okayama University

Raman Spectrum of Hinokitiol (m-Isopropyltropolone)

By Sunao IMANISHI and Mitsuo ITO

(Received April 6, 1956)

Introduction

In a previous paper[1] the Raman spectrum of tropolone in benzene solution was studied, and the more important vibrational frequencies there found were compared with infrared and vapor ultra-violet absorption data[2], together with known facts about benzene, and the types of vibrational modes in the tropolone molecule having these frequencies were discussed qualitatively. Up to the present no complete theoretical calculation of normal vibrational modes of any cycloheptatriene derivatives has been attempted, preventing unambiguous interpretation of all the vibrational frequencies found in the Raman spectrum to be given. In this paper the Raman effect for hinokitiol was studied in order to obtain further experimental information regarding the characteristic frequencies common to "tropolonoid" molecules.

Experimental

The hinokitiol sample used in this experiment was prepared in the Medical Department of Kumamoto University, and was kindly placed at our disposal by Prof. K. Sebe. The sample was expected to be sufficiently pure, so no further purification was attempted. Five grams of the sample was dissolved in 20 cc. of pure benzene, and with this solution a Wood's tube of 1 cm. bore and 15 cm. length was filled. The Wood's tube has an outer jacket through which a saturated solution of sodium nitrite was circulated to cut off ultra-violet radiations of wave-lengths below 4047Å completely, and the Hg 4047Å line partially.

Filtering the mercury radiations with sodium nitrite solution appeared to help suppress photochemical coloring of hinokitiol markedly. However, after a prolonged irradiation with two quartz mercury lamps, burning at 10 amp. each, the sample ultimately turned red-brown as in the case of tropolone, and the effective time of exposure must have been much shorter than the twenty hours' used in the experiment.

The spectrograph employed had two dense flint glass prisms each of 13 cm. height and 22 cm. side length. The camera lens was of 60 cm. focal length, giving an effective aperture of F/5 and a linear dispersion of about 20Å/mm. at 4359Å. Kodak "Plus X" panchromatic film was used to record the scattered spectrum. The microphotometer trace of the spectrum is reproduced in Fig. 1, together with those of tropolone and the solvent (benzene). The Raman lines due to benzene are marked with arrows. The original

1) S. Imanishi and M. Ito, This Bulletin, 28, 75 (1955).
2) S. Imanishi and M. Ito, to appear in *J. Chem. Phys.*, 1956.

traces were made with a recording microphotometer supplied by the former Institute of Physical and Chemical Research, Tokyo. It is seen in this figure that in the hinokitiol spectrum the long wave end is superposed by a strong background, making eye observation of weak Raman lines not

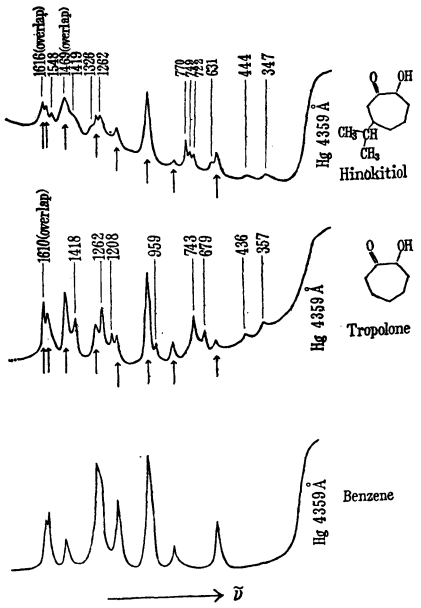

easy. Wave-lengths of Raman lines were determined against those of Fe comparison lines. Their wave-number shifts from the exciting Hg line 4359Å, as well as estimates of their relative intensities, are given in Table I.

TABLE I

VIBRATIONAL FREQUENCIES IN HINOKITIOL (cm^{-1})

Hinokitiol Raman C_6H_6 Solution	Infra-red Absorption* Liquid	Tropolone[1] Raman C_6H_6 Solution
347 (2)		357 (2)
444 (1)		436 (1)
631 (2)		679 (2)
722 (2)	730 (m)	
749 (2)		
770 (3)	770 (w)	743 (3)
	820 (m)	
	890 (w)=2×444	
	910 (w)	
	940 (m)	959 (1)
	990 (w)=347+631	
	1050 (w)=347+722	
	1100 (w)=347+749	
		1208 (2)
1264 (4)	1250 (s)	1262 (4)
1326 (3)	1350 (w)	
1419 (4)	1410 (m)	1418 (5)
1469 (5)	1470 (s)	
1548 (4)	1560 (m)	
1616 (5)	1600 (s)	1610 (5)

* The frequencies and intensities in this column are those estimated from the published absorption curve of ref. (3).

Discussion

The only data pertaining to the vibrational spectrum of hinokitiol so far published and available for comparison are those we owe to Shimanouchi et al[3] which deal with the infra-red absorption. Approximate positions and relative intensities of absorption maxima observed by these authors are listed in column 2 of Table I. In the Raman spectrum of hinokitiol three new bands are found in the low frequency region below 650 cm^{-1}, which were not found infra-red absorption. In the high frequency region above 1200 cm^{-1} agreement with infra-red data is very good. As any Raman frequency associated with a considerable intensity must be regarded as a fundamental, all of the twelve Raman shifts given in the Table are here taken as such. On the basis of this assumption, in fact, many of the weak maxima measured in the infra-red in the intermediate frequency region can be interpreted as overtones and combinations as indicated in the Table.

The two low frequencies 357 cm^{-1} (2) and 436 cm^{-1} (1) in tropolone (Table I) are preserved in hinokitiol [347 cm^{-1} (2) and 447 cm^{-1} (1)], almost unaffected by the substitution with the isopropyl group. From their magnitudes these frequencies are very probably of out-plane torsional vibrations of the tropolone ring. The strong Raman shifts of 1262, 1419 and 1616 cm^{-1} in hinokitiol coincide exactly with the 1262, 1418 and 1610 cm^{-1} shifts in tropolone, allowing for errors in measurement. As absorption bands of almost the same frequencies as these three are invariably found in infrared absorption of many tropolone derivatives it is apparent that these also belong to vibrations characteristic of the tropolone skeleton. Among them the strongest 1616 cm^{-1} is attributed to the C=O stretching vibration[4], although the value is considerably lowered from that of the ordinary C=O frequency ($\gtrsim$1700 cm^{-1}). On the other hand the frequencies between 1262 and 1548 cm^{-1}, which are considered to be of C—C stretching vibrations of the ring, are as a whole higher than the corresponding frequencies in benzene compounds. These facts support Koch's[5] view that in molecules with the heptatriene ring C=O bond forces are weaker and C—C bond forces are stronger than those in benzenoids. These changes in bond forces may have been

3) K. Kuratani, M. Tsuboi and T. Shimanouchi, This Bulletin, 25. 250 (1952).

4) Scot and Tarbel, *J. Am. Chem. Soc.*, 72, 240 (1950). Doering and Knox, ibid., 73, 828 (1951).

5) Koch, ibid., 73, 512 (1951); Bellamy, "The Infra-red Spectra of Complex Molecules", Methuen, London (1954), p. 75.

caused on the one hand by resonance, or what amounts to the same thing, by the electron migration from the carbonyl O atom into the ring, and on the other by the formation of intramolecular hydrogen bonding between the two O atoms of the tropolone molecule. Furthermore these facts seem to suggest that the heptatriene ring in tropolone owes its stability to the attachment of the carbonyl group.

The comparatively strongly observed Raman shift 770 cm^{-1} corresponds to the strong 743 cm^{-1} in tropolone. This frequency is also found in infra-red absorption, but there it was found as a shoulder to the strong absorption peak at 730 cm^{-1}. By analogy with tropolone the vibrational mode with this frequency is assumed to be the totally symmetric breathing vibration of the molecule, to which in-plane ring deformation contributes considerably. This conclusion is supported by the hinokitiol vapor ultra-violet absorption[6], in which three strong and board bands form a progression with $\sim$600 cm^{-1} interval, starting from the O, O band on its shorter wave side. Then this $\sim$600 cm^{-1} frequency must represent the excited (electonic) state value of the 770 cm^{-1} fundamental of the ground state. In tropolone the excited state value of the corresponding 743 cm^{-1} breathing vibration is 643 cm^{-1}. Apart from the above evidence from ultra-violet absorption, we have calculated the two totally symmetric vibration frequencies of the cycloheptatrienyl (tropylium) ion $(CH)_7^+$ with D_{7h} symmetry, using force constants borrowed from benzene, in order to check the magnitudes of these vibration frequencies in a seven-membered ring compound. They came out to be 863 cm^{-1} (C and H in phase) and 3038 cm^{-1} (C and H in reversed phase), showing that the in-plane breathing frequency is considerably lowered from 992 cm^{-1} in benzene (D_{6h}). These vibrations should be strictly infra-red inactive and the most Raman-active. In fact, in the infra-red data reported by Doering and Knox[7] there is no absorption near the calculated 863 cm^{-1} region, just as expected.

Now, it can be seen in analogy with benzenoids that this type of vibration will gain intensity in infra-red absorption with still lowered frequency by the substitution of H atoms with heavy radicals as in tropolonoids, with the consequent loss of the D_{7h} symmetry. These arguments also support our assignment regarding the breathing vibrations in tropolone and hinokitiol, and make understandable their intensity relation in infra-red and Raman spectra.

The ramaining Raman frequencies 722 and 749 cm^{-1} in hinokitiol have no corresponding shifts in tropolone, so that they may be attributed to internal vibrations of the isopropyl radical.

The authors thank Professor K. Sebe of Kumamoto University for the supply of the hinokitiol samples. The cost of the experiment was defrayed from the Science Research Expenditures of the Education Board.

Chemical Laboratory, Faculty of Science, Kyushu University, Fukuoka

6) S. Imanishi and M. Ito, Orally communicated to the Chem. Soc. Japan Meetings, 1952.

7) Doering and Knox, *J. Am. Chem. Soc.*, **76**, 3203 (1954).

Studies on Organic Reagents for the Colorimetric Analysis of Germanium. I. Reactions between Germanium and Some Organic Compounds

By Kenjiro KIMURA, Kazuo SAITO and Masako ASADA

(Received January 24, 1956)

Recently germanium, one of the less-common elements, found its special usefulness in electronics. This fact makes it very important for scientist to explore even the very poor resource of germanium in nature. The study on the distribution and migration of germanium in the earth's crust is also important from the standpoint of geochemistry.

For these reasons an excellent method for the quantitative analysis of germanium is urgently needed. Up to the present time a variety of analytical methods for germanium have been proposed, which covered gravimetric, volumetric, colorimetric, spectrographic and polarographic methods[1]. For a trace amount of germanium, however, the colorimetric method seems to be most excellent. In the colorimetric analysis choice of a reagent is always important. So far the use of many reagents such as ammonium molybdate[2], oxidized hematoxyline[3], phenylfluorone[4] quercetin[5], and quinalizarine acetate[6] has been proposed. But none of them was found to be entirely satisfactory. The difficulty lies in the complicated procedure required to remove interfering ions, as well as in the adjustment of hydrogen ion concentration within a narrow range. Moreover, for some reagents, the reagent itself or the compound between the reagent and germanium is not stable. Some other reagents form sparingly soluble precipitates with germanium. In such a case the colorimetric measurement has to be made on a colloidal solution.

In this report the authors tried to confirm the functional groups which combine with germanium. Special attention was paid to correlate the structure of the reagent to its reactivity with germanium. A search was made for a reagent which combines with germanium in a strongly acidic solution without forming any precipitates, its absorption spectrum being changed. In addition, the reaction should not be interfered with by foreign ions. A. Tchakirian and P. Bevillard studied the functional groups* which are supposed to combine with germanium. In their earlier studies[7a-e] they concluded as follows. (1) In order to react with germanium the organic molecule under consideration must have two hydroxyl groups on ortho positions and also a carbonyl- or quinoimine-group; the latter is able to bring about a tautomery between hydroxyl- and carbonyl-groups. (2) *Ortho* diamine groups, that are analogous to ortho dihydroxyl groups fail to react with germanium. (3) The larger the molecule, the more sensitive the reaction with germanium. A larger molecule reacts with germanium even at a low pH. Reaction at such a low pH excludes the interference by other elements. On the other hand, the molecule tends to be sparingly soluble in solvents. To increase the solubility of such a compound it is desirable to introduce an acidic group such as sulphonate into the compound. In their late studies[7f-g], they stated that the function of the carbonyl group was not clear and that a salt was formed by the combination of the quinoimine group with the dihydroxyl germanic acid which was preliminarily formed. They also stated that the ortho dihydroxyl groups react with germanium even in a compound without carbonyl- or quinoimine group. In order to confirm their results, the present authors examined the reaction between germanium and flurone-, naphthoquinone-, and cumarin derivatives. This study appears to give an orientaion to find a new reagent for the colorimetric analysis of germanium.

1) H.H. Krause and O.H. Johnson, *Anal. Chem.*, **25**, 134 (1953).

2) N.A. Filippona and L.I. Kusentzowa, *Zavodskaya Lab.*, **16**, 536 (1950) (C.Z., **2**, 2503 (1951)). E.B. Sandell, "Colorimetric Determination of Trace of Metals", New York (1953), pp. 134, 333. L. Erday and E. Boder, *Z. Anal. Chem.*, **134**, 81 (1951).

3) H. Newcombe, W.A.E. Mcbryde, J. Bortlett and F.W. Beamish, *Anal. Chem.*, **23**, 1023 (1951).

4) H.J. Cluley, *Analyst*, **76**, 523 (1951). Y, Oka, T. Kanno and K. Shiba. *Japan Analyst*, **3**, 389 (1954).

5) Y. Oka and S. Matsuo, *J. Chem. Soc. Japan*, **76**, 610 (1955).

6) C.K.N. Nair and J. Gupta, *J. Sci. Ind. Research*, **10** B, 300 (1951); ibid., 11 B, 274 (1952).

* On the nomenclature of functional group, A. Tchakirian et al. had used "phenol-" and "quinon-". In the present paper, they are called "hydroxyl-" and "carbonyl-", respectively.

7) A. Tchakirian and P. Bevillard, a) *Compt. rend.*, **233**, 256 (1951); b) ibid., 1003; c) ibid., 1112; d) P. Bevillard, ibid., **234**, 216 (1952); e) *Mikrochem.*, **39**, 209 (1952). f) *Compt. rend.*, **235**, 880 (1952). g) *Bull., Soc. Chim. France*, **1954**, 304.

Experiment

The following experiments were carried out to examine whether or not the presence of hydroxyl groups on ortho positions be essential for the compound to react with germanium.

The Reaction between Fluorone Derivatives and Germanium

The following compounds were used in this experiment.

2, 6, 7-Trihydroxy-9-methylfluorone[8]

6-Hydroxy-2, 7-dimethoxy-9-phenylfluorone[9]

2, 6, 7-Trimethoxy-9-phenylfluorone[10]

4, 5, 6-Trihydroxy-9-phenylfluorone[11]

In the first place, the authors synthesized these compounds by conventional method. After the syntheses, the absorption spectra, the reactivity with germanium and the shift of the maximum of the absorption band, resulting from the addition of germanium, were examined for each compound. For the measurement of absorption spectrum the solution was prepared in the following way. A 10^{-4}mol. of each compound was dissolved in a mixture of about 80 ml. of ethanol (94%) and 5 ml. of 6 N sulphuric acid. The resulting solution was transferred into a measuring flask and its volume adjusted to 100 ml. A 2 ml. portion was diluted to 50 ml. with either pure water or water containing 13 ml. of ethanol and 10 ml. of 6 N hydrochloric acid. The concentration of each compound in the solution was 4×10^{-5} mol. per ml. The reactivity of these compounds with germanium was studied over a wide range of pH. The results are summarized in Table I; the absorption curves are shown in Fig. 1.

TABLE I

PROPERTIES OF FLUORONE DERIVATIVES

Name	Structure	M. p.	Colour of crystals	Colour of aq. and/or ethanolic soln.	Change in colour of an acidic soln. on the addition of germanium solution
(1) 2,6,7-Trihydroxy-9-phenylfluorone	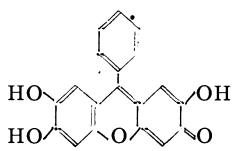	350°C	Reddish orange	Dark red (b.) Orange (n.) Yellow (a.)	Change to reddish (similar to that in a neutral solution) Precipitate formed
(2) 2,6,7-Trihydroxy-9-methylfluorone	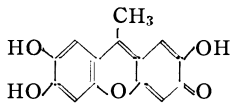	Decomp. at 279°C	Yellowish orange	Dark red (b.) Orange (n.) Yellow (a.)	Change to reddish (similar to that in a neutral solution) Precipitate formed
(3) 6-Hydroxy-2,7-dimethoxy-9-phenylfluorone	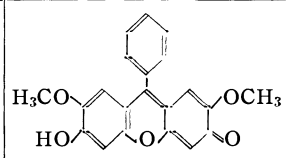	282°C	Dark red	Light orange (n.) Yellow (a.)	None
(4) 2,6,7-Trimethoxy-9-phenylfluorone	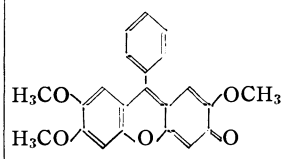	174°C	Orangish yellow	Insoluble (b.) Light orange (n.) Yellow (a.)	None
(5) 4,5,6-Trihydroxy-9-phenylfluorone	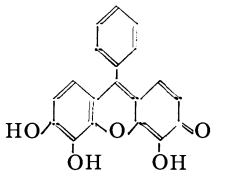	Decomp. at ca. 200°C	Dark purple	Violet blue (b.) Dark purple (n.) From red to yellow (a.)	Change to more reddish (similar to that in a neutral solution) Precipitate appeared after one day

b.: basic solution n.: neutral solution a.: acidic solution

8) C. Lieberman and S. Lindenbaum, *Ber.*, **37**, 1171 (1904); ibid., 2728.

9) F. Kehrmann and M. Gunther, *Ber.*, **45**, 2884 (1923).

10) F. Kehrmann and M. Gunther, *Ber.*, **45**, 2884 (1923).

11) W.R. Orndorff and C. Wang, *J. Amer. Chem. Soc.*, **47**, 290 (1925); ibid., **49**, 1284 (1927); R.N. Sen and N.N. Sarkar, ibid., **47**, 1079 (1925).

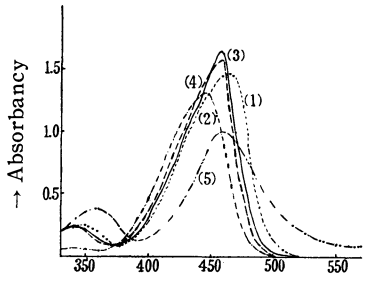

Fig. 1–(1). Absorption curve of fluorone derivatives.
(1) 2, 6, 7-trihydroxy-9-phenylfluorone
(2) 2, 6, 7-trihydroxy-9-methylfluorone
(3) 6-hydroxy-2, 7-methoxy-9-phenylfluorone
(4) 2, 6, 7-trimethoxy-9-phenylfluorone
(5) 4, 5, 6-trihydroxy-9-phenylfluorone

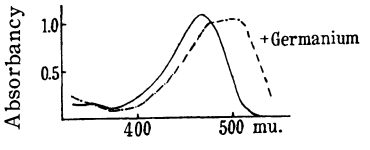

Fig. 1–(2). The absorption curve of 2,6,7-trihydroxy-9-phenylfluorone, (3×10^{-8} mol. per ml.) in acetone and that of the solution containing both germanium (6.94 μg. per ml.) and the reagent. (These are true solutions almost without water.)

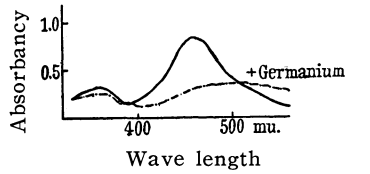

Fig. 1–(3). The absorption curve of 4,5,6-trihydroxy-9-phenylflourone (4×10^{-8} mol. per ml.) in ethanol and that of the soln. containing both germanium (13.9 μg. per ml.) and the reagent.

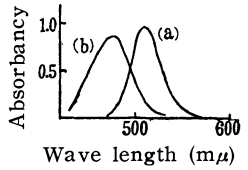

Fig. 1–(4). Absorption curves of complexes between germanium and 2, 6, 7-trihydroxy-9-phenylfluorone[a] and 2, 6, 7-trihydroxy-9-methylfluorone[b]. These solutions contain germanium (8.33 μg. per ml.) and a large amount of reagent. Here reference soln. is an ethanolic solution of the reagent.

The synthesis of a new compound, 2-hydroxy-6, 7-dimethoxy-9-phenylflurone, was tried in vain by methylation of 2, 6, 7 trihydroxy-9-phenylfluorone with diazomethane. If this compound could have been synthesized, it would have been possible to decide whether the functional group which directly combines with germanium is only hydroxyl group. Since it is possible that not only hydroxyl but also carbonyl-group can combine with germanium such an experiment would be very important.

The Reaction between Naphthoquinone Derivatives and Germanium

In order to examine the relation between two hydroxyl groups and a carbonyl group with respect to the reaction with germanium, naphthoquinone derivatives were chosen. For these derivatives the reactivity and the change in the absorption band resulting from the complex formation were studied. The compounds used in the experiment are summarized in Table II.

About 5 mg. of each compound were dissolved in 10 ml. of ethanol (94%). To 1 ml. of this solution was added 1 ml. of ethanol and the volume adjusted to 10 ml. with water. One ml. of first solution was added to the mixture of 1 ml. of ethanol and 4 ml. of germanium standard solution (6.9 μg. per ml.). This solution was made up to 10 ml. with water and its absorption measured. The results are shown in Fig. 2. As was expected, neither the compounds without two hydroxyl groups (e. g. the compound No. 1.) nor those in which two hydroxyl groups are not located on ortho positions (e. g. the compounds No. 2 and 3) showed any significant reaction with germanium.

The reactions between germanium and those compounds which have a carbonyl group adjacent to a hydroxyl group were also negative. According to these results it was clear that one hydroxyl group is not one of the functional groups which directly combine with germanium.

The solutions of these compounds were true solutions and did not show any appreciable precipitate on the addition of germanium. The reaction of these compounds with germanium brings about a change in colour of the solution, from orange or red to purple or dark red. The extinction of the solution was slightly increased, whilst the absorption spectrum remained almost unchanged in each case. Since it is possible that they have a low tendency to react with germanium, further experiments were carried out by use of a larger quantity of germanium (70 μg. per ml.). As shown in Fig. 2–(4), however, the absorption spctra changed only very slightly.

The Reaction between Cumarin Derivatives and Germanium

Compared with naphthoquinone derivatives, fluorone derivatives have many advantages in their reactivity with germanium. The syntheses of these compounds are easier; they react not only with a trace amount of germanium but also selectively in an acidic solution. Apart from the

TABLE II
NAPHTHOQUINONE DERIVATIVES

	Conventional Name	Structure	Reaction with Germanium
(1)	2-Hydroxynaphthoquinone	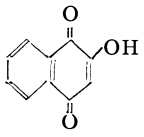	Negative
(2)	2-Hydroxynaphthazarine	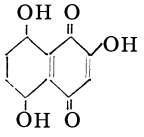	Nagative
(3)	Shikonin	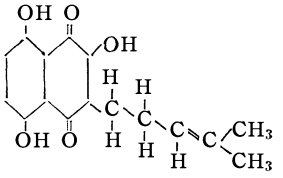	Negative
(4)	Spinazarin	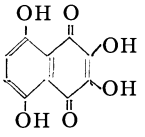	The colour of ethanolic solution changes from orange to reddish orange
(5)	Spinochrome Bl	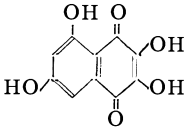	The colour of ethanolic solution changes from yellow to yellowish orange
(6)	Spinochrome F	?	The colour of ethanolic solution changes from red to purple
(7)	Spinochrome Aka	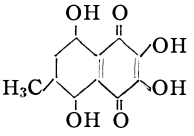	The colour of ethanolic solution changes from pale red to dark red
(8)	Spinochrome Ml	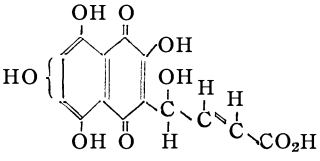	The colour of ethanolic solution changes from pale red to dark red

number of benzene rings, the greatest difference in the structure of these two kinds of compound lies in the fact that the fluorone derivatives are heterocyclic and contain an oxygen atom in the ring, whilst the naphthoquinone derivatives are not. In order to find whether the difference in the structure of those compounds has any effect upon the reactivity with germanium, the reaction between germanium and the following two cumarin derivatives was similarly studied.

cumarin diol[12] 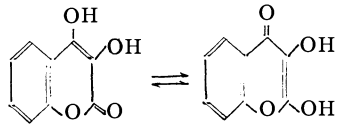

4-methyl-esculetin[13] 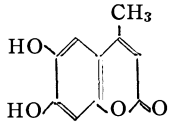

12) F. Arndt, L. Löwe, R. Un and E. Ayca, *Ber.*, 84. 319 (1951).

13) "Organic Syntheses", Collective Volume I, New York (1932), p. 352.

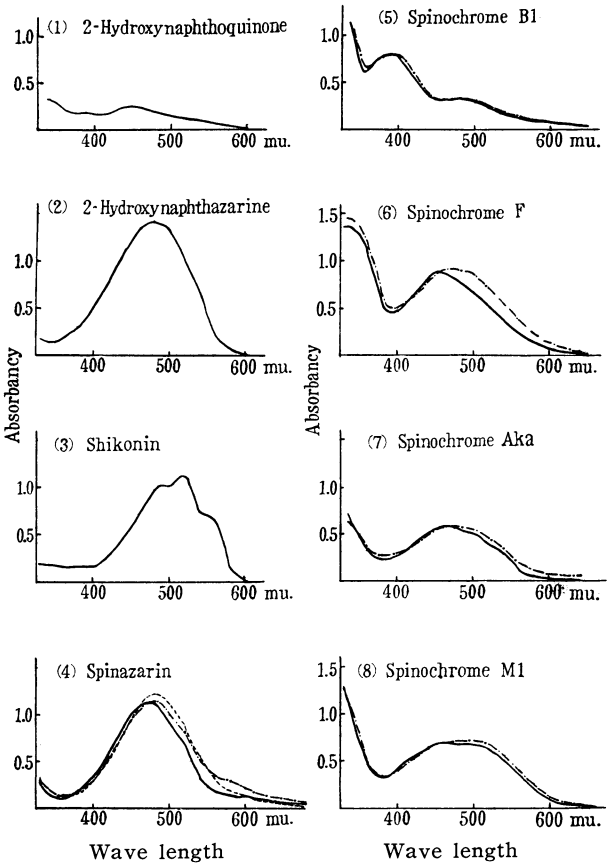

Fig. 2. Absorption curves of naphthoquinone derivatives contaning 5.5 μg. of germanium per ml.
(1) (2) and (3) do not change by the addition of germanium.

The compounds were synthesized by the conventional methods. Their colour ranges from colorless to yellow. The absorption spectrum of the solution of each compound as well as of a mixed solution with germanium was studied, both in neutral and 1 N-hydrochloric acid solutions. It was disclosed that cumarindiol fails to react with germanium, whereas 4-methyl esculetin shifts the absorption band from ultra violet to visible. This seems to arise from the formation of germano-complex in a neutral solution. The red shift was more remarkable than in the cases of naphthoquinone derivatives. The results are shown in Fig. 3.

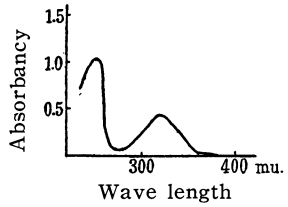

Fig. 3-(1). Absorption curve of cumarindiol. This curve does not change by the addition of germanium.

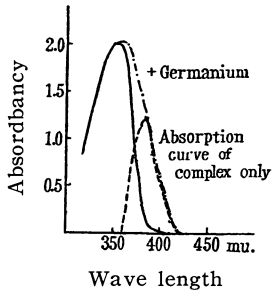

Fig. 3-(2). Absorption curve of 4-methyl-esculetin.

This compound appears, however, not very suitable for the colorimeteric analysis of germanium. In the presence of sodium- or ammonium chloride, the above-mentioned red shift does not take place. Moreover, these compounds are less sensitive for the detection than fluorone derivatives. The wave length of the absorption maximum lies in the boundary between ultraviolet and visible regions.

Conclusion

In order to find an organic compound which is suitable for the colorimetric analysis of germanium, several compounds including fluorone-, naphthoquinone- and cumarin derivatives were studied. The relation between the structure of these compounds and the reactivity with germanium, as well as the shift of the maximum of the absorption spectrum on reaction with germanium, were closely studied. The results confirmed one of the conclusions previously presented by A. Tchakirian and his co-loborators. That is, the presence of two hydroxyl groups on ortho positions is essential for the reaction with germanium. The larger the molecule, the more marked the reaction with germanium. The reactivity with germanium at a low pH is increased with increase in moleculer weight. A compound such as spinazarine, shikonin and 2-hydroxy-naphthoquinone in which one of the two hydroxyl groups on ortho positions is replaced by a carbonyl oxygen, fails to show any reaction with germanium. Cumarindiol has two hydroxyl groups on ortho positions, but in this compound there is a tautomery between the hydroxyl group and the carbonyl oxygen. This could be the reason why this compound does not show any appreciable reaction with germanium, although it has two hydroxyl groups on ortho positions. Accordingly, it is clear that the functional groups which combine directly with germanium are ortho hydroxyl groups. Carbonyl group provides negative results even when it is situated ortho to the hydroxyl group. Present results also indicate that heterocyclic compounds such as fluorone- and cumarin derivatives are more advantageous than homocyclic ones such as naphthoquinons as a reagent which selectively combines with germanium at a low pH. The former compounds are also superior in the fact that their absorption spectra are much more affected by the addition of germanium. Concerning the structures of the compound between germanium and these organic compounds, no diffinite conclusion can be drawn from this study. Further studies are in progress.

The authors wish to express their sincere thanks to Dr. Chika Kuroda for supplying precious samples of naphthoquinone derivatives, and to the late Dr. Fujiro Iimura of Tokyo University for helpful advice in this study. The expenses were defrayed from a grant given by the Ministry of Education to which the authors' thanks are due.

Department of Chemistry, Faculty of Science, The University of Tokyo, Hongo, Tokyo

Studies on Organic Reagents for the Colorimetric Analysis of Germanium. II. Synthesis of a New Reagent and its Reaction with Germanium

By Kenjiro KIMURA, Hirotoshi SANO and Masako ASADA

(Received January 24, 1956)

In the previous report[1] it was observed that the absorption band of the solution of heterocyclic compounds such as fluorone and cumarine derivatives shows red shift in the presence of germanium. The authors examined many organic reagents for germanium which have been reported so far by other workers[2,3,4,5]. The results of the experiments showed that among these reagents phenylfluorone is the best because it has high sensitivity for germanium. In addition, the analytical procedure using this reagent is simple, and the reaction is obstructed by few ions. On the other hand, it forms slightly soluble compound with germanium. This makes colorimetric determination very difficult. Moreover, the absorbancy of the colored solution varies with the time elapsed since the solution was prepared. In this study, therefore, the present authors tried

1) K. Kimura, K. Saito and M. Asada, This Bulletin **29**, 635 (1956).

2) Hanna Newcombe, W.A.E. McBryde, John Borthlett and F.E. Beamish, *Anal. Chem.*, **23**, 1023 (1951).

3) H.J. Cluley, *Analyst*, **76**, 523 (1951).

4) C.K.N. Nair and J. Gupta, *J. Sci. Ind. Research*, **10** B, 300 (1951); ibid., **11** B, 274 (1952).

5) Y. Oka and S. Matsuo, *J. Chem. Soc. Japan*, **74**, 931 (1953).

to synthesize a new reagent which is similar to phenylflurone but has none of such defects as described above.

Since it is very difficult to find out a specific reagent for germanium, germanium has to be separated from other elements before it is subjected to quantitative determination. The best procedure for the separation of a trace of germanium seems to be the distillation of germanium tetrachloride from a fairly concentrated hydrochloric acid solution. If we could determine germanium in the distillate with or without simple pretreatment, the procedure would be very convenient for analysis. For this reason it is desirable to find out a new reagent which reacts specifically with germanium, forming a soluble complex in a strongly hydrochloric acid solution. The authors considered that one of the phenylfluorone derivatives, 2, 6, 7-trihydroxy-9-(4'-dimethylaminophenyl)-fluorone, is a reagent suitable for such purpose. Hereafter we call this reagent dimethylaminophenyl-fluorone. Since such a compound has never been described in the literature of the subject, the authors tried to synthesize this reagent by similar procedure which was widely used for the synthesis of phenylfluorone and its analogous compounds[6].

Experiment

The Synthesis of the New Compound

Reagents Used.—*p-Dimethylaminobenzaldehyde*: First-grade reagent prepared by Tokyo Kasei Ind., Co. Japan, was used without any purification.

Hydroxyhydroquinone triacetate: The reagent was synthesized[7] from commercial *p*-benzoquinone, anhydrous acetic acid and concentrated sulfuric acid. Recrystallized twice from 95% ethanol solution.

Ethanol: Commercial 95% ethanol.

The Procedure for Synthesis.—To a mixture of 160 ml. of ethanol, 160 ml. of water and 16 ml. of concentrated sulfuric acid in a round-bottomed flask was added 37 g. of hydroxyhydroquinone triacetate and 11 g. of dimethylaminobenzaldehyde*. Under a reflux condenser the solution was heated in a water bath for twenty hours. Then the solution was allowed to cool until the precipitation of orange crystalline substance was completed. The precipitate was filtered and washed with water until the red color of the washing solution almost disappeared. The crystals seemed to be hydrolyzed easily and the colour of crystals was changed after washing. The precipitate on the filter paper was mixed with a larger amount of water and the system was heated until the hydrolysis was complete. The hydrolyzed precipitate was filtered under suction, washed thoroughly with water and dried in a vacuum desiccator. To 1 to 2 g. of the product was added a mixture of 50 ml. of ethanol, 50 ml. of water and 5 ml. of concentrated sulfuric acid. The resulting system was heated on a water bath to dissolve the precipitate. The small amount of active charcoal was added to the resulting solution. The charcoal adsorbed a dark-reddish brown substance which was supposed to be a polimerized product. The suprenatant solution was filtered through a hot funnel. The cooling of filtrate resulted in the formation of yellowish orange crystalline precipitate. The precipitate was filtered, washed thoroughly with a small amount of the mixture of ethanol and water. And then it was mixed with a large amount of water. The hydrolysis of the precipitate was performed by heating. The filtration, washing and drying up of the precipitate was repeated several times for the purpose of recrystallization. The authors are of the opinion that the followtng reactions occurred in this procedure.

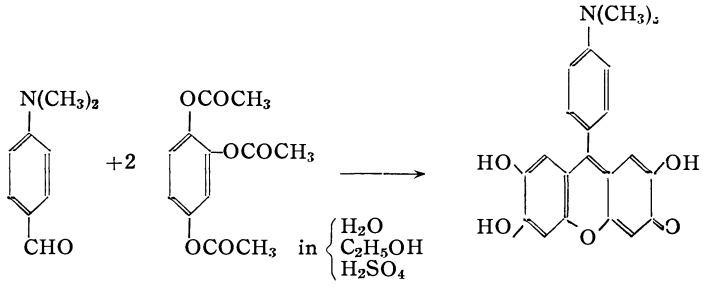

Anal. Found: C, 68.10; H, 4.75; N, 4.07. Calcd.: C, 69.30; H, 4.69; N, 3.83%.

Properties of the Product.—M. p. >250°C. Colour: Red, Green fluorecence. Form: While the sulfate forms plate-like crystals, its hydrolyzed product is powder. Solubility: Insoluble in water. Slightly soluble in ethanol, giving an orange solution.

6) C. Lieberman and S. Lindenbarum, *Ber.*, **37**, 1171 (1904); ibid., 2728; F. Kehrmann and M. Gunther, *Ber.*, **45**, 2884 (1923); W.R. Orndorff and C. Wang, *J. Am. Chem. Soc.*, **47**, 290 (1925); ibid., **49**, 1284 (1927); Rajendra Nath Sen and Nripendra Nath Sarkar, ibid., **45**, 2984 (1923); ibid., **47**, 1079 (1925).

7) "Organic Syntheses, Collective Volume I", John Wiley & Sons Inc., New York (1948), p. 317.

* Two mol. of hydroxyhydroquinone triacetate and one mol. of dimethylaminobenzaldehyde are used to prepare the reagent. A mixture of ethanol, water and concentrated sulfuric acid in the proportion of 10:10:1 was used as a solvent to dissolve the above compounds. The proportion of each compound in the solvent and the amount of the solvent are fixed at such values that the compounds were completely dissolved and the yield of the resulting product was maximum.

The addition of acid to the ethanol solution of the compound increased its solubility and the colour of solution became deep red. When the addition of acid was continued further, the red colour of solution was diminished and changed from orange to yellow. At the same time, the solubility was decreased. The concentration of acid which was necessary to change the colour of the solution was dependent on the amount of the reagent in the solution.

Absorption Curves of the Reagent Solution.—The following samples were used to measure absorption curves. The original solution was prepared by dissolving 1 mg. of new compound in 50 ml. of ethanol.

Sample 1: 5 ml. of the original solution was diluted with ethanol to 25 ml.

Sample 2: The original solution was mixed with 2 ml. of 0.2 N -HCl and diluted with ethanol to 25 ml. The concentration of acid in the resultant solution was 0.016 N.

Sample 3: The original solution was mixed with 2 ml. of 2 N-HCl and diluted with ethanol to 25 ml. The final acid concentration was 0.16 N.

Sample 4: The original solution was mixed with 2 ml. of 6 N HCl and diluted with ethanol to 25 ml. The final acid concentration was 0.48 N.

Sample 5: The original solution was mixed with 5 ml. of 6 N-HCl and diluted with ethanol to 25 ml. The final acid concentration was 1.2 N. The results are shown in Fig. 1.

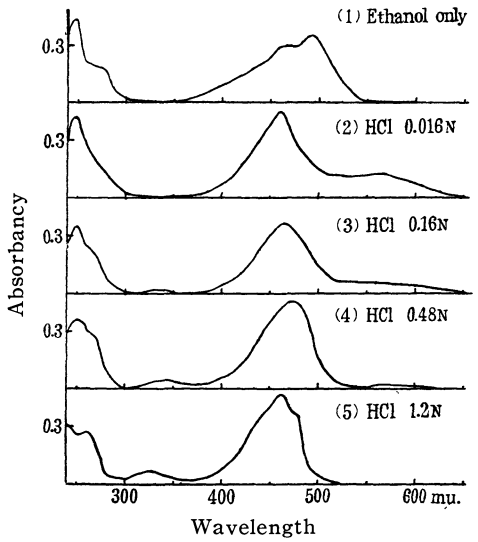

Fig. 1. Absorption curves of dimethylaminophenylfluorone.

In strongly acidic solution in which the effect of amino group is almost negligible, the absorption curve of this compound is very similar to that of phenylfluorone. Considering the above-mentioned properties as well as the procedure for synthesis, there is little doubt that the compound is a reagent suitable for our purpose. For the measurement of absorption spectra, the commerical 95% ethanol was purified until the substance such as aldehyde showing the absorption bands at the near ultraviolet region was completely eliminated.

Reaction of the New Compound with Germanium

Reagents Used.—Germanium standard solution: The germanium dioxide used in this experiment was prepared by Tokyo Gas Co.. The standard solution was made by dissolving 1.00 g. of water-soluble powder (99.9% GeO_2) in hot water. Then the volume of the resulting solution was adjusted to 1 liter.

Two ml. of this solution was taken in 200 ml. volumetric flask and diluted up to 200 ml. The final solution contained 10.0 μg. of GeO_2 [6.94 μg. of Ge) per ml. The solution could not be preserved for a long time without the change of concentration.

0.05% solution of dimethylaminophenylfluorone: 0.050 g. of dimethylaminophenylfluorone was dissolved by heating in a mixture of approximately 80 ml. of ethanol and 5 ml. of 6 N-hydrochloric acid. After cooling, the solution was diluted with ethanol until the volume of solution became 100 ml. The final solution was deep red and contained 0.05 per cent of dimethylaminophenylfluorone by weight.

Hydrochloric acid: Commercial first-grade reagent (sp. gr. 1.2) was diluted with water.

Procedure.—Two ml. aliquots of standard GeO_2 solution were taken in four 25 ml. volumetric flasks. Then 1.3 ml., 6.3 ml. and 12.5 ml. of 2 N-HCl were added to the first three volumetric

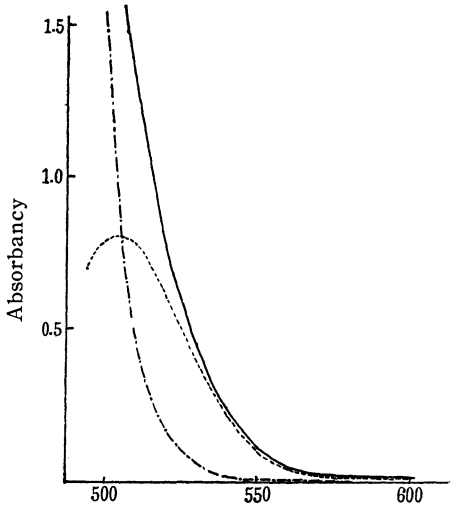

—·—·— 0.01% Dimethylaminophylfluorone soln. only (reference soln.: distilled water)

———— Germanium added (〃)

------ Complex between Ge and dimethylaminophenylfluorone (reference soln.: 0.01% dimethylaminophenylfluorone soln)

Fig. 2. Absorption curves of the complex between germanium and dimethylaminophenylfluorone.

flasks respectively and 8.3 ml. of 6 N-HCl was added to the last volumetric flask. The volume of each solution was made up to approximately 15 ml. To the resulting solutions were added 5 ml. aliquots of 0.05% dimethylaminophenylfluorone solution and the final volume of the solutions were adjusted to 25 ml. The final concentration of hydrochloric acid in the solutions obtained are 0.1 N, 0.5 N, 1 N and 2 N, respectively. Four reference solutions were prepared without adding germanium. These solutions were compared with those containing germaium. The results are summarized in Table I.

TABLE I

Concentration of HCl	Reaction with Germanium
0.1 N	Red orange colour appeared immediately after the addition of reagent.
0.5 N	Same as above.
1 N	Orange colour appeared 5 minutes after the addition of reagent.
2 N	No change was observed.

After the addition of reagent, the solution contained 0.01% dimethylaminophenylfluorone by weight and 0.56 μg. of germanium per ml. Even when these solutions were kept standing for about fifty hours, no precipitate appeared. The absorption spectrum of the obtained complex is shown in Fig. 2. The figure shows the absorption spectrum of the complex in 0.5 N-HCl.

Conclusion

An attempt was made to synthesize a new colorimetric reagent for germanium which has no such defects as was observed in the other reagents. Using a comparatively simple procedure, a crystalline substance was obtained, which was found to be suitable for our purpose. The authors call this reagent dimethylaminophenylfluorone. The compound reacts with germanium in an acid solution and forms a soluble complex. The present experiments led us to the conclusion that this compound is an excellent reagent for the colorimetric analysis of germanium.

Department of Chemistry, Faculty of Science, The University of Tokyo
Hongo, Tokyo

SHORT COMMUNICATION

Splitting of the First Band of [Co^{III}(X) (edtaH)]-type Complexes

By Yoichi SHIMURA and Ryutaro TSUCHIDA

(Received March 20, 1956)

Recently it was reported[1] that the absorption band of rare-earth cation split into several bands by interacting with EDTA in solution. The main purpose of the present communication is to report that somewhat similar splitting occurred with a cobaltic EDTA complex anion.

The visible and ultraviolet absorption spectra of [Co^{III}(edta)]Na·4H$_2$O, [Co^{III}(NO$_2$)(edtaH)] Na·H$_2$O and [Co^{III}(Br)(edtaH)]Na·3H$_2$O* were examined. The salts were prepared by the method of Schwarzenbach[2]. Measurements were made by a Beckman DU spectrophotometer. The spectra of the bromo complex was measured in 60% perchloric acid solutions to prevent its aquation, and the other two salts in aqueous solutions. The absorption curves obtained and their analyses are shown in Figs. 1 and 2. The curve analyses were made by use of the same method as described in a previous paper[3].

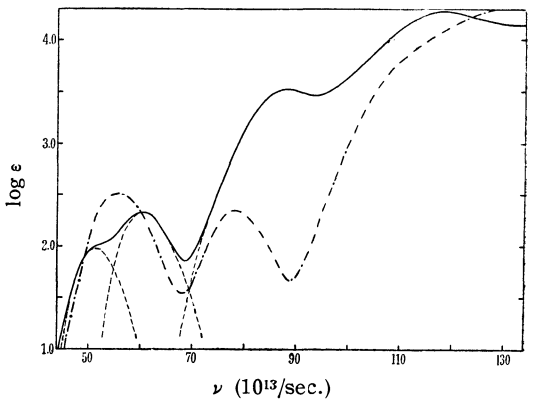

Fig. 1. Absorption curve of the nitro complex.
——— [Co^{III}(NO$_2$) (edtaH)] Na·H$_2$O: Ia band, ν_{max}=60.4 (log ε_{max}=2.32); Ib band, 51.4 (1.97); nitro specific band, 88.6 (3.52); third band, 118.5 (4.27).
–·–·– [Co^{III}(edta)]Na·4H$_2$O: first band, 55.9 (2.51); second band, 78.1 (2.36).

As is seen in Fig. 1, the first absorption band of [Co(NO$_2$)(edtaH)]$^-$ distinctly split

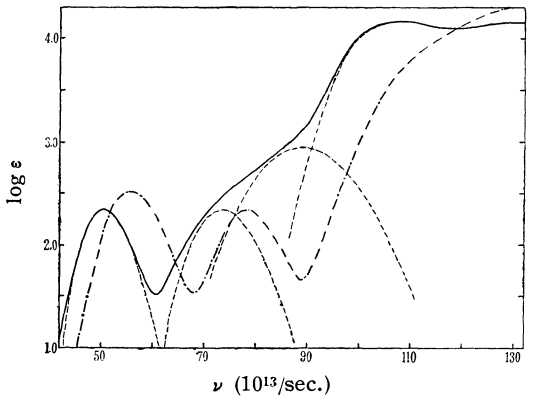

Fig. 2. Absorption curve of the bromo complex.
——— [Co^{III}(Br)(edtaH)]Na·3H$_2$O: first band, ν_{max}=50.6 (log ε_{max}=2.34); second band, ca. 73.5** (ca. 2.34); bromo specific band, 89.0 (2.95); third band, ca. 108 (4.16).
-·-·-·- [Co^{III}(edta)]Na·4H$_2$O.

into two components. This is the first example of such splitting in connection with the complexes containing one or more nitro ligands. The Ia-component is in the region of shorter wave lengths as compared with the first band of [Co(edta)]$^-$. This is in agreement with what is expected from the higher position of the nitro-group on the spectro-chemical series. The sub-component Ib is in the long wave length side of the first band of [Co(edta)]$^-$. Contrary to the nitro complex, no splitting is observed in [Co(Br)(edtaH)]$^-$ (Fig. 2). Since distinct splittings were reported[4,5] for [Co(NH$_3$)$_5$(Br)]$^{2+}$ and *trans*-[Co(en)$_2$(Br)$_2$]$^+$, the present result is rather unexpected. The reason for this is unknown. To solve the problem it will be necessary to collect more extensive data for the spectra of the complexes belonging to several different structural types.

The occurrence of a nitro or bromo specific band in these nitro or bromo complexes confirms the opinion that these complexes contain the EDTA anion as quinquedentate ligand. The third absorption bands due to co-ordination of the nitro and bromo anions are also observed. The specific and the third bands are equally shifted towards longer wave lengths than those of the corresponding nitro- or bromo-pentammine cobaltic complexes, as follows:

	Specific band	Third band
[Co(NO$_2$)(edtaH)]$^-$	88.6×10^{13}/sec.	118.5×10^{13}/sec.
[Co(NO$_2$)(NH$_3$)$_5$]$^{2+}$	92.4[6]	125.7[6]
[Co(Br)(edtaH)]$^-$	89.0	ca 108
[Co(Br)(NH$_3$)$_5$]$^{2+}$	95.4[4]	118.4[4]

Further work is in progress on the analogous EDTA complexs of Cr(III) and V(III).

Department of Chemistry, Faculty of Science, Osaka University, Osaka

* edta represents a quadrivalent ethylenediaminetetraacetate anion $C_{10}H_{12}N_2O_8^{4-}$ and edtaH a tervalent anion $C_{10}H_{18}N_2O_8^{3-}$.

** This value was estimated by Sone's formula, ν_2= 1.189 ν_1+13.31 (see ref. (3)).

1) a) T. Moeller and J.C. Brantley, *J. Am. Chem. Soc.*, **72**, 5447 (1950). b) R.C. Vickery, *J. Chem. Soc.*, **1952**, 421. c) L. Holleck and D. Eckhardt, *Naturwiss.*, **40**, 409 (1953); *Z. Naturforsch.*, 8 a, 660 (1953); ibid., 9 a, 347 (1954); ibid., 9 b, 274 (1954).
2) G. Schwarzenbach, *Helv. Chim. Acta*, **32**, 839 (1949).
3) Y. Shimura and R. Tsuchida, This Bulletin, **28**, 572 (1955).
4) M. Linhard and M. Weigel, *Z. anorg. Chem.*, **266**, 49 (1951).
5) M. Linhard and M. Weigel, ibid., **271**, 101 (1952).
6) M. Linhard and M. Weigel, ibid., **267**, 113 (1951).

An X-ray Diffraction Line Observed in Acid-treated Carbonized Coals and Paramagnetic Absorption

By Katsuya INOUYE

(Received April 18, 1956)

During our extensive examinations of carbonization mechanism of various coals by means of X-ray diffraction[1], it has been experienced for several samples that a new diffraction line appears other than the usually observed carbon patterns which are indexed as (002) and (100). The characteristics of the line and its occurence are as follows:

(1) The lattice constant is 4.18 ±0.10Å, the line existing just inside (002) band. The line is fairly intense and sharp. (See Fig. 1).

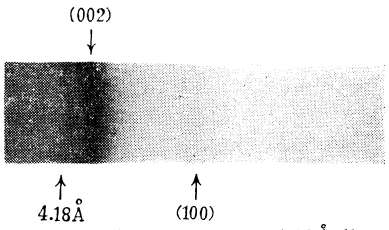

Fig. 1. The position of 4.18Å line

No other pattern than this and carbon patterns has been observed on the film, using Kodak No-screen X-ray film in 45 mm. radius powder camera covering 5–80° Bragg angle and Ni-filtered CuKα ray operated at 35 kV. and 20 mA. No low-angle band was recognized by a Geiger-counter goniometer recording up to 1° of Bragg angle.

(2) The line has been observed in the samples produced from the following bituminous coals (single or blended) and carbonized up to the following maximum temperatures: American coking coal, 520 and 620°C; Yatake coking coal, 500°C; blended coal slack of 25 parts American coking coal and 75 parts Yubari weakly coking coal, 600°C; blended coal slack of 6 kinds of bituminous coals in order to obtain a coherent coke, 200, 300 and 400°C. The volatile matter content (dry ash-free basis) of the single or blended coals prior to carbonization was approximately 34 to 43%. The carbonization was carried out in an experimental electric furnace at a rate of elevation of temperature of 3.3°C/min. in nitrogen atmosphere. At other carbonization temperatures, the similar coals did not show the line by similar treatments.

(3) The line appears only after the carbonized samples are boiled with 20% HCl for approximately forty hours or more, with reflux and frequent renewing, followed by alternative wetting and gentle evaporating with 40% HF in Pt crucible over fifteen times.

(4) The line is stable at room temperature for over one year, but disappears by heating the sample at 600°C for ten minutes in nitrogen atmosphere.

The probable mistakes in X-ray techniques, e.g., diffraction by CuKβ ray or WLα_2 ray, diffraction caused by camera body or sample amount, etc. have all been denied by careful experiments. The cause of the line is unlikely in the inorganic impurities, because the treatments with acids result naturally in gradual diminishing of inorganic components and, in particular, because no accompanying lines exist and the line disappears by heating the sample at 600°C. The lattice parameter is not consistent with any carbon halide patterns so far reported.

This phenomenon may be at fault but is interesting if it is remembered that the distinct paramagnetic resonance absorption has been reported recently for coals carbonized especially up to 500–600°C[2], and the absorption has been ascribed to the existence of some broken carbon bonds. The paramagnetic resonance absorption of one of the series which showed the line (cf. Table I) was measured by Mr. I Miyashita using a microwave of 3.2 cm. wave-length[3].

These results may imply that a correlation is expected to be found between the appearance of the 4.18Å line and the structural disturbance during a certain stage of carbonization before the carbon cluster commences to grow up to more rigid hexagonal lamellae in coke. To show a rather sharp

TABLE I

PARAMAGNETIC RESONANCE ABSORPTION OF CARBONIZED COALS

Coal slack carbonized: 25 American coking coal and 75 Yubari weakly coking coal.

Sample No.	Carbonization Temperature °C	4.18Å Line	χ_g
1	400	−	2.6×10^{-8}
2	600	−	$10.\times10^{-8}$
3*	600	+	8.5×10^{-8}
4	800	−	No absorption

* Sample 3, which shows the 4.18Å line, was prepared by treating Sample 2 with acids as described above.

diffraction pattern, the formation of a crystallographic lattice by means of acid treatments is expected, for example in the peripheries of cluster. The pre-existence of some broken bonds may be advantageous for further lattice development. According to Miyashita[4], the decrease of the absorption from 10×10^{-8} to 8.5×10^{-8} in accordance with the appearance of the line after acid treatments coincides with the general rule that the value of absorption decreases with the development of crystalline state, though he holds the view that the absorption may be due to a state of triplet and not necessarily to the broken bonds.

The author's thanks are due to M. Abiko and A. Roppongi, with whose assistance in the X-ray studies of carbonization of coals this fact has been revealed and to Mr. I. Miyashita (Hokkaido Univ.) for measuring the paramagnetic resonance absorption. Financial support has been provided by the Hirohata Iron Works of Fuji Iron and Steel Ind. Co. Ltd.

Resources Research Institute
Saitama-Kawaguchi

1) K. Inouye, H. Tani and M. Abiko, *J. Fuel Soc. Japan*, **32**, 292 (1953); K. Inouye and M. Abiko, ibid., **32**, 386 (1953); K. Inouye and M. Abiko, *J. Chem. Soc. Japan* (*Ind. Chem. Sect.*), **59**, 37 (1956).

2) J. Uebersfeld, A. Etienne and J. Combrisson, *Nature*, **174**, 614 (1954); A. Etienne and J. Uebersfeld, *J. Chim. Phys.*, **51**, 328 (1954); D.J.E. Ingram, J.G. Tapley, R. Jackson, R.L. Bond and A.R. Murnachan, *Nature*, **174**, 740 (1954); J.E. Bennett, D.J.E. Ingram and J.G. Tapley, *J. Chem. Phys.*, **23**, 215 (1955).

3) Y. Yokozawa, I. Miyashita, M. Kugo and K. Higashi, This Bulletin, **28**, 536 (1955).

4) Private communication.

Über die Erhöhung der Empfindlichkeit von den Niederschlagbildungsreaktionen durch Anwendung der Ionenaustauschharze

Von Masatoshi FUJIMOTO

(Eingegangen am 17. Februar, 1956)

In einer Reihe der Untersuchungen über die mikroanalytischen Anwendungen der Ionenaustauschharze zum Nachweis geringer Substanzmenge[1] werden lediglich solche Reaktionen, die die in die Harzphase selektiv adsorbierenden und stark sich färbenden der Harzkörnchen mit Silberionen in der Lösung gemäss den Gleichungen

$$[RCl] + NO_3^- \rightleftarrows [RNO_3] + Cl^-, \quad \text{und}$$

$$Cl^- + Ag^+ \longrightarrow [AgCl]\downarrow \text{ (weisse Niederschlagmembran)}$$

reagieren. Der so gebildete Silberchloridniederschlag wird als eine weisse dichte Schicht an der Oberfläche der Harzkörnchen angesammelt, und gegen schwarzen Hintergrund deutlich nachgewiesen.

Die Ergebnisse mit einem durchsichtigen[3] und farblosen starkbasischen Anionenaustauschharze, Dowex 1-Xl (RCl-Form) unter verschiedenen Bedingungen ausgeführter Untersuchung stehen in Tabelle I:

TABELLE I

VERGLEICHUNG VERSCHIEDENER BEDINGUNGEN VON NIEDERSCHLAGBILDUNG

		Zeit nach der Mischung (Min)															
		2				5				10				20			
Mit 4.3γ Ag^+ (108 γ/ccm)	A:	+	+	+	+	(+)	(+)	(+)	(+)	(+)	(+)	(+)	(+)	(+)	(+)	(+)	(+)
	B:	+	+	±	∓	+	±	±	∓	+	±	∓	∓	+	±	±	±
	C:	±	±	±	±	±	±	±	±	±	±	±	±	∓	∓	∓	∓
Mit 0.43γ Ag^+ (10.8 γ/ccm)	A:	−	−	−	−	−	−	−	−	−	−	−	−	−	−	−	−
	B:	±	(+)	±	±	±	(+)	±	(+)	±	(+)	±	(+)	(+)	(+)	(+)	(+)
	C:	+	+	+	+	+	+	+	+	+	+	+	+	+	+	+	+

−: kein Niederschlag; ±: unsicher, (+): schwach, +: sicher, und ±, ∓, usw.: intensiv getrübt.

Inhaltsangabe des Verfahrens:—

A: 2N NaCl (1 Tropfen) + $AgNO_3$ (1 Tropfen) + H_2O (1 Tropfen),
B: RCl (einige Körnchen) + $AgNO_3$ (1 Tropfen) + H_2O (1 Tropfen),
C: RCl (einige Körnchen) + $AgNO_3$ (1 Tropfen) + 4M NH_4NO_3 (1 Tropfen).

Ionenaustauschharz: Dowex 1-Xl (RCl-Form).

Ionen bilden, deshalb gern verwandt, weil die Färbung dieser Ionen, die sich hauptsächlich in den *beschränkten Rauminhalt* der Harzkörnchen adsorbieren lassen, bemerkenswerterweise verstärkt wird.

Dagegen wurde hier eine Art der Niederschlagbildungsreaktionen zur Tüpfelanalyse mit Ionenaustauschharze angewandt, wobei die Empfindlichkeit von der Reaktion durch Beschränkung der Fällungsstelle an der *Grenzfläche* zwischen Harz-und Lösungsphase beträchtlich vergrössert wurde.

Als ein geeignetes Beispiel dafür wurde folgende Reaktion ausgewählt:

$$Ag^+ + Cl^- \longrightarrow [AgCl]\downarrow$$[2] (weisser Niederschlag).

Wenn eine Lösung von Silbernitrat mit einem Anionenaustauschharze von RCl-Form sich berührt, werden die Nitrationen in der Lösung zuerst mit den Chloridionen von Harzphase ausgetauscht, welche sofort an der Oberfläche

Abb. 1 ist eine Skizze des Zustandes von den mit 4.3γ Silberionen 20 Min nach der Mischung erhaltenen Harzkörnchen (nach Verfahren „B"), worin man eine am Rande der Harzkörnchen sich entstehende weisse Trübung gegen schwarzen Hintergrund der Tüpfelplatte entschieden deutlich erkennen kann.

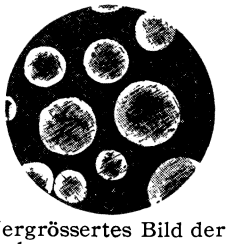

Abb. 1. Vergrössertes Bild der getrübten Harzkörnchen.

Wie man im obengenannten Beispiel klar ersieht, lässt sich diese Methode zur Niederschlagbildung durch Ionenaustausch an der Grenzfläche zweier Phasen künftig als eine sehr geeignete empfindliche Tüpfelmethode auf die verschiedenartigen Niederschlagbildungsreaktionen umfangreich erweitern.

Laboratorium der analytischen Chemie, Chemisches Institut der wissenschaftlichen Fakultät, Tokyo Universität, Tokyo

1) Vgl. M. Fujimoto, „Mikroanalyse mit Hilfe von Ionenaustauschharzen. I, II, III, IV, V und VI", Dieses Bulletin, 27, 48, 347 (1954) sowie 29, 567, 571, 595, 600 (1956).

2) Das Zeichen, [ ], bedeutet die feste Phase, und, ↓, die Niederschlagbildung.

3) Obwohl hinsichtlich der Löslichkeit schlechthin die Anwendung des Harzes von RJ-Form günstiger als die des Harzes von RCl-Form ist, ist es nicht zweckmässig, das Harz von RJ-Form zu hier erwähntem Zweck zu verwenden, da dieses beträchtlich undurchsichtig ist.

Polymerization of Vinyl Acetate by High Energy Radiation

By Seizo OKAMURA, Takao YAMASHITA and
Toshinobu HIGASHIMURA

(Received February 22, 1956)

Introduction

While extensive work has been carried out on the radiation polymerization of vinyl compounds, there has been comparatively little attention paid to that of vinyl acetate. One of the reasons for this seems to be that in the case of vinyl acetate the reproducibility was very poor as shown by the work of Chapiro[1]. It is, however, even more attractive for us to study the radiation polymerization of vinyl acetate, because the considerations on the degree of polymerization are done more easily from two sides as polyvinyl acetate and also as polyvinyl alcohol. Manowitz et al.[2] had recognized that the degree of polymerization increased during polymerization and this could be explained by the branching or the cross-linking of polymers. Attempts have now been made to clarify the chain transfer mechanism of polymer molecules in the radiation polymerization of vinyl acetate. This leads to some preliminary conclusion that the increase of the molecular weight during polymerization is coming from the branching at the acetyl side chain of polyvinyl acetate. The degree of polymerization of polyvinyl alcohol was found to be comparatively higher than that in the thermal polymerization. This reason, however, has not yet been clarified in this paper.

Experimental

Vinyl acetate (VAc), methyl acrylate (MA) and methyl methacrylate (MMA) were polymerized in sealed tubes, in which gas phase was replaced by vacuum and thereafter by nitrogen. Sources of gamma-rays were 20 and 0.5 curies of Cobalt-60, and its doses were measured by the method of Weiss[3]. X-ray from a 180 kV.–20 mA. apparatus were filtered by 0.3 mm. Cu and 0.5 mm. Al, and the dose rate at 12.5 cm. distance from target, that is at the middle point of reaction vessel, was 977 r/min. The average degrees of polymerization were calculated by the following equations,

PVAc in acetone: $\bar{P}_{AC}=(\text{antilog}\ \frac{[\eta]}{0.28}-1)\cdot 2000$

PMMA in chloroform: $[\eta]=2.52\cdot 10^{-3}\bar{P}^{0.80}$

PVA in water: $\log \bar{P}_A=1.613\log \frac{[\eta]\times 10^4}{8.87}$

Results

The rates of polymerization were shown in Figs 1 and 2. In both cases of gamma- and X-rays, the polymerization of MMA showed

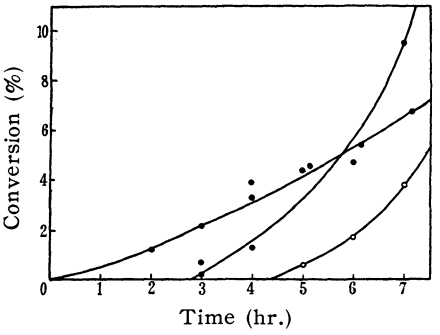

Fig. 1. Gamma-ray polymerization of VAc (●), MMA (⊙) and MA (○).
2 cm from 20 curie Co-60., 10±2°C, dose rate; about 15×10^3 r/hr.

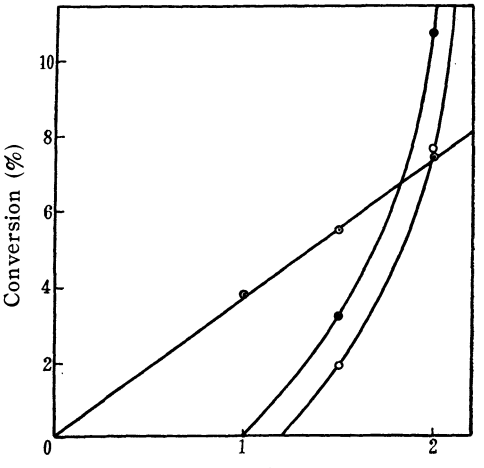

Fig. 2. X-ray polymerization of VAc (○ and ●) and MMA (⊙).
18±2°C, dose rate; 977 r/min.

no induction period, that of VAc showed a moderate one and that of MA a long one. The order of the rates of polymerization was VAc>MA>MMA, in accordance with the results obtained by Chapiro[1]. Table I repre-

1) A. Chapiro, *J. chim. phys.*, **47**, 764 (1950).
2) D.S. Ballantine, P. Colombo, A. Glines and B. Manowitz, *Chem. Eng. Prog. Symp.*, **50**, No. 11, 267 (1954).
3) J. Weiss, *Nucleonics*, **10**, (7), 28 (1952).

TABLE I
THE DEGREES OF POLYMERIZATION OF POLYVINYL ACETATE

Expt. No.	Condition of Irradiation	Polym. Time (hr.)	Polym. Yields (%)	Viscosity [η]	$\bar{P}_{AC}$	Huggins Constants k'
gamma-4	2 cm. from 20 curies Co-60	4	3.35	0.232	11480	0.28
gamma-5	〃 〃 〃	5	4.41	0.248	13370	0.31
gamma-7	〃 〃 〃	7	9.53	0.290	19710	0.37
X-1	X-rays	1.5	3.20	0.158	5330	0.30
X-2	〃	2	10.70	0.187	7190	0.32

sents the degrees of polymerization of polyvinyl acetate obtained by gamma- and X-rays.

As shown in Table I, the degrees of polymerization were found to increase rapidly during polymerization. In the case of MA, the intrinsic viscosities were measured as 0.38 and 0.73 at the polymerization yields of 1.7 and 3.9 respectively. The degrees of polymerization of PMMA were 6000–7000 independent of the polymerization yields in the range of 1–7. Table II shows the degrees of polymerization of polyvinyl alcohol obtained by the saponification of PVAc.

The degrees of polymerization of the polyvinyl alcohol were found to be very high compared with those obtained by the thermal polymerization. The content of 1,2 glycol bond in PVA, measured by the comsumption of periodic acid[4] was found to be 1.23% in the sample S-1.

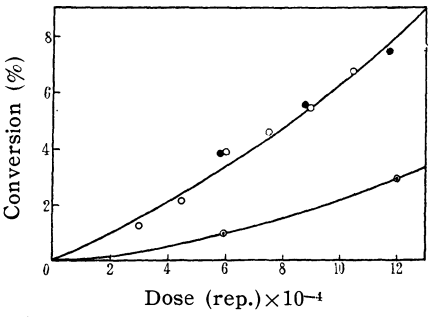

Fig. 3. The relationship between dose and conversion of gamma- and X-ray polymerization of MMA.
○; gamma-ray polym. (15000 r/hr. 10°C)
●; X-ray polym. (58600 r/hr. 18°C)
⊙; gamma-ray polym. (Manowitz et al.[2] 250000 r/hr. room temperature).

TABLE II
THE DEGREES OF POLYMERIZATION OF POLYVINYL ALCOHOL

Expt. No.	Condition of Irradiation	Polym. Time (hr.)	Polym. Yields (%)	Polym. Temp. (°C)	Viscosity [η]	$\bar{P}_A$	k'
gamma-7'	Same as gamma-7 in Table I	7	9.53	10	0.223	7440	0.77
gamma-15*	〃	15	95	〃	0.219	6710	0.75
gamma-24*	〃	24	100	〃	0.195	5990	0.63
X-2'	Same as X-2 in Table I	2	10.70	18	0.155	4140	0.90
S-1	at 3.5 cm. from 0.5 curies Co-60,	ca. 8 days	27	0–5	0.269	10070	0.82
S-2	〃	ca. 9 days	92	〃	0.234	7980	0.75
H-1*	Same as gamma-7	7	95.6	51	0.144	3680	0.80
L-III*	Upper	15	Average		0.255	9230	—
L-M*	Middle of test tube at 1–6.4 cm. from 20 curies Co-60	〃	75	10	0.232	7950	—
L-d*	Under	〃			0.202	6420	—

* Marks indicate that PVAc forms gel in acetone.

Discussion

The relationships between the rates of polymerization and the total doses of radiation are shown in Fig. 3. In these conditions, that was 15,000 r/hr., 10°C at gamma-rays and 58,600 r/hr. 18°C at X-rays respectively, just the same rates were obtained in both cases of gamma- and X-rays. The results of Manowitz[2] were considerably low, as shown in Fig. 3. It has been reported that the lower rates of polymerization were obtained at a higher dose rate in the same total doses[5].

4) I. Sakurada and G. Takahashi, Private communications. Sep., 10, 1955.

5) I.A. Berstein, E.C. Farmer, W.G. Rothschild and F.F. Spalding, *J. Chem. Phys.*, 21, 1303 (1953).

These situations were just the same as those shown in Fig. 3.

The degrees of polymerization of PVAc increase during polymerization, and the extrapolated values of degrees of polymerization to zero yields coincide well with that of PVA. This relation is just the same as in thermal or catalysed polymerization.

From the following equation[6], we could obtain the branching reactivity of polymer (k'_b/k_b) and that of monomer (k''_b/k_b).

$$\left(\frac{1}{\bar{P}_A}-\frac{1}{\bar{P}_{AC}}\right) = -\frac{k'_b}{k_b}\left\{1+\frac{1}{X}\ln(1-X)\right\}+\frac{k''_b}{k_b}$$

where X was the polymerization yield, k'_b and k''_b were the branching velocity constants of polymer and of monomer respectively, and k_b was the propagating velocity constant.

As shown in Table III, the branching reaction by monomer is of the same order as the normal one ($k''_b/k_b \fallingdotseq 0.5\times10^{-4}$), but the branching by polymer (k'_b/k_b) occurs more rapidly than in the thermal or catalyzed polymerization ($k'_b/k_b \fallingdotseq 2.5\times10^{-4}$).

TABLE III

VELOSITY CONSTANTS RATIOS OF SECONDARY POLYMERIZATION BY GAMMA- AND X-RAYS

Conditions of polymerization	k'_b/k_b	k''_b/k_b
gamma-rays	$12.0\cdot10^{-4}$	$0.33\cdot10^{-4}$
X-rays	$13.9\cdot10^{-4}$	$0.36\cdot10^{-4}$

One of the observed complexities, hitherto reported in the case of styrene, methyl acrylate and so on, was found to be related to the branching reactions, which occurred during the radiation polymerization. Much further work, however, is of course necessary in these important points.

The authors wish to express their heartfelt thanks to Prof. Ichiro Sakurada and also to Prof. Tadashi Fukuda for kind advice and encouragement.

Department of Textile-chemistry, Faculty of Engineering, Kyoto University, Kyoto

6) S. Okamura and T. Yamashita, *Bull. of the Institute for Chemical Research*, Kyoto University, **18**, 46 (1949).

*The Oxygen Equilibrium of Denatured Hemoglobin and the Mechanism of Denaturation**

By Masaji KUBO

(Received April 5, 1956)

Hemoglobin is perhaps one of the most interesting compounds known to biochemists. The development of the physico-chemical methods, such as x-ray analysis[1] and magneto-chemical investigation[2], has led to a considerable increase of knowledge in regard to the structure of the molecule of this important compound. The problem of the structure could also be tackled with the aid of chemical equilibria involving hemoglobin molecules capable of undergoing a great variety of reactions with other molecules and ions. Since, however, the normal physiological function of hemolobin is the transport of oxygen, the combination thereof with hemoglobin has been studied in the most extensive way. From the analysis of the oxygen equilibrium curve, it has been concluded that the four hemes in a hemoglobin molecule are located at the corners of a square (or a rectangle) and that stabilizing interaction exists between the hemes along the sides of the square[3,4,5]. The effect of pH on the oxygen equilibrium, i.e., Bohr effect, has clarified the existence of oxygen-linked acid groups[6].

* The substance of this paper was presented in a lecture delivered before the annual meeting of the Chemical Society of Japan on April 4, 1956.

1) M.F. Perutz, *Nature*, **143**, 731 (1939); ibid., **149**, 491 (1942). J. Boyes-Watson and M.F. Perutz, ibid., **151**, 714 (1943). J. Boyes-Watson, E. Davidson and M.F. Perutz, *Proc. Roy. Soc. London*, A **191**, 83 (1947).

2) L. Pauling and C.D. Coryell, *Proc. Natl. Acad. Sci. U. S.*, **22**, 159, 210 (1936).

3) L. Pauling, *Proc. Natl. Acad. Sci. U. S.*, **21**, 186 (1936).

4) J. Wyman, *Adv. Protein Chem.*, **4**, 407 (1948).

5) D. Allen, K.F. Guthe and J. Wyman, *J. Biol. Chem.*, **187**, 393 (1950).

6) B. German and J. Wyman, *J. Biol. Chem.*, **117**, 533 (1937).

From the temperature dependence of the oxygen equilibrium[7], the heat of oxygenation has been evaluated.

The effect of denaturation has attracted little attention[8], probably because the oxygen equilibrium curve of denatured homoglobin can be less easily interpreted than that of a fresh preparation. Although denaturation is a property common to a large group of proteins, it is doubtful whether a general theory can be worked out which would be universally applicable to all proteins. In view of this point, any theory of denaturation for a particular protein, if the theory is definite and detailed, will lead to a better understanding of this important phenomenon. The present investigations has been undertaken in order to infer the mechanism of denaturation of hemoglobin from its oxygen equilibrium curve.

Experimental Method and Results

Experiments were carried out at the Biological Laboratories of Harvard University. The experimental procedure was essentially the same as that used by Wyman and his collaborators[5]. Hemoglobin solutions were prepared from cow blood and were buffered with a phosphate mixture, pH being equal to 6.8. Slight denaturation took place while the preparations were left to stand in an ice-box for a few days or more. The degree of partial saturation with oxygen was determined at 20°C by the spectrophotometric method described in a previous paper[9].

The oxygen equilibrium curve depends upon the degree of denaturation. A typical example in the case of slight denaturation is shown in Fig. 1, in which Y, the degree of partial saturation with oxygen, is plotted against log p, the logarithm of the partial pressure of oxygen in equilibrium with the hemoglobin solution. It will be seen that the curve is not exactly symmetric across the center at $Y=1/2$ and $\log p=\log p_0$, where p_0 denotes the partial pressure of oxygen corresponding to 50% saturation. Therefore the data cannot be fitted by any symmetric curve of whatever shape. If a symmetric curve is drawn through the center in accordance with Hill's empirical equation described below, both sets of data lie above the curve for large as well as small values of saturation. This feature of the curve is characteristic of the denatured hemoglobin irrespective of the degree of denaturation. The deviation from symmetry seems to lie within the fringe of experimental errors in the case of a fresh preparation, but increases with increasing degree of denaturation, until it becomes apparent and indubitable in view of the accuracy of measurements.

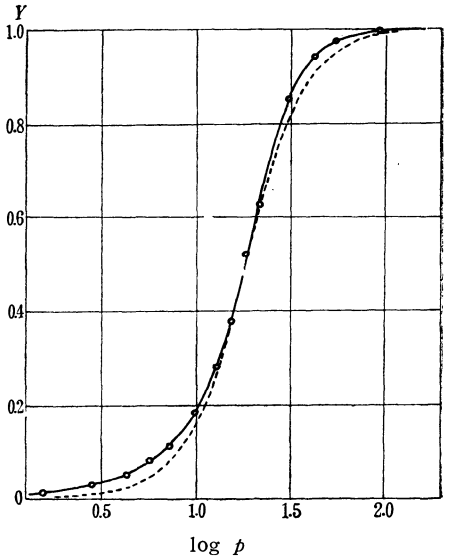

Fig. 1. The degree of partial saturation with oxygen of a slightly denatured cow hemoglobin plotted against the logarithm of the partial pressure of oxygen. The dotted curve depicts the symmetric equilibrium curve of Equation (2), which is applicable to a fresh preparation.

It should be mentioned in this connection that the same trend of asymmetry can also be seen in the oxygen equilibrium curves obtained by Forbes and Roughton[10] on sheep hemoglobin and by Courtice and Douglas[11] on human hemoglobin. Both employed a gasometric method. Their data were considered to be most accurate before the advent of the spectrophotometric method, which shortened the time required for measurements and thus minimized the effect of denaturation.

Discussion

The oxygen equilibrium of a fresh preparation of hemoglobin accords, to a fair degree of accuracy, with Hill's empirical equation[12].

$$Y=Kp^n/(1+Kp^n), \qquad (1)$$

where K and n are constants. The present writer[13] proposed an equation of the following form.

$$Y=\frac{1}{2}+\frac{1}{2}\tanh\left(\frac{n}{2}\ln\frac{p}{p_0}\right). \qquad (2)$$

The relation between the two sets of constants is $K=p_0^{-n}$. Eq. (2) is mathematically equivalent to Hill's original equation but expresses the property of symmetry with greater clearness. The hyperbolic tangent curve has

7) J. Wyman, *J. Biol. Chem.*, **127**, 581 (1939).

8) A.E. Mirsky and L. Pauling, *Proc. Natl. Acad. Sci. U. S.*, **22**, 439 (1936).

9) M. Kubo, This Bulletin, **26**. 189 (1953).

10) W.H. Forbes and F.J.W. Roughton, *J. Physiol.*, **71**, 229 (1931).

11) F.C. Courtice and C.G. Douglas, *J. Physiol.*, **105**, 345 (1947).

12) A.V. Hill, *Biochem. J.*, **7**, 471 (1913).

13) M. Kubo, *Proc. Japan Acad.*, **29**, 156 (1953).

a center of symmetry, the existence of which has been confirmed very carefully by the experimental data of Wyman et al.[5]. From Eq. (2), the following relation can be derived.

$$\ln[Y/(1-Y)]=n(\ln p-\ln p_0). \quad (3)$$

Therefore a plot of $\ln[Y/(1-Y)]$ against $\ln p$ yields a straight line, the inclination of which gives the value of n. In the case of denatured hemoglobin a similar plot gives a slightly curved line, which is convex towards the abscissa.

Obviously the experimental points can never be fitted by an empirical equation having two constants. One must resort to the more general expression for Y of the following form first proposed by Adair[14].

$$Y=\frac{L_1p+2L_2p^2+3L_3p^3+4L_4p^4}{4(1+L_1p+L_2p^2+L_3p^3+L_4p^4)}. \quad (4)$$

The meaning of this equation becomes clear from the following considerations. At any given partial pressure of oxygen, hemoglobin will be present in five different forms distinguished by i, the number of molecules of oxygen combined with each molecule of hemoglobin. The different forms may be referred to by Hb, HbO_2, $Hb(O_2)_2$, $Hb(O)_3$, and $Hb(O_2)_4$, which are present in relative amounts, $1:L_1p:L_2p^2:L_3p^3:L_4p^4$. Obviously L_i is the equilibrium constant of the formation of $Hb(O_2)_i$ from Hb and i molecules of oxygen. Accordingly the equilibrium constant of oxygenation,

$$Hb(O_2)_{i-1}+O_2=Hb(O_2)_i,$$

is given by $K_i=L_i/L_{i-1}$. By definition, $L_0=1$.

Although Eq. (4) is general and theoretically sound, it is difficult to determine the four constants uniquely from a rather smooth curve, because the equation contains too many constants. Let the discussion be opened with a consideration of symmetry, which is realized, at least approximately, even in the case of slightly denatured hemoglobin.

If the relation (4) is plotted in a Y versus $\ln p$ diagram and if the origin of the coordinates is shifted to the center of symmetry at $Y=1/2$ and $\ln p=\ln p_0$ according to the relations,

$$y=Y-1/2,\ x=\ln p-\ln p_0,$$

one has

$$\begin{aligned} y&=\frac{-2-L_1p+L_3p^3+2L_4p^4}{4(1+L_1p+L_2p^2+L_3p^3+L_4p^4)}\\ &=\frac{-2-L_1p_0e^x+L_3p_0^3e^{3x}+2L_4p_0^4e^{4x}}{4(1+L_1p_0e^x+L_2p_0^2e^{2x}+L_3p_0^3e^{3x}+L_4p_0^4e^{4x})}\\ &=\frac{-2e^{-2x}-L_1p_0e^{-x}+L_3p_0^3e^x+2L_4p_0^4e^{2x}}{4(e^{-2x}+L_1p_0e^{-x}+L_2p_0^2+L_3p_0^3e^x+L_4p_0^4e^{2x})}. \end{aligned} \quad (5)$$

The condition of symmetry implies that y is an odd function of x.

$$y=\frac{2L_4p_0^4e^{-2x}+L_3p_0^3e^{-x}-L_1p_0e^x-2e^{2x}}{4(L_4p_0^4e^{-2x}+L_3p_0^3e^{-x}+L_2p_0^2+L_1p^0e^x+e^{2x})}. \quad (6)$$

The right hand sides of Eqs. (5) and (6) are identically equal to each other, irrespective of the value of x. Hence

$$1=L_4p_0^4,\ L_1p_0=L_3p_0^3,$$

or

$$\Delta\equiv L_3^2-L_1^2L_4=0. \quad (7)$$

Eq. (7) embodies the necessary and sufficient condition of symmetry of the equilibrium curve[4].

The same relation can be obtained in a different way, which is more instructive. The oxygenation of hemoglobin is analogous to acid-base titration in that the former represents progressive saturation of hemoglobin with oxygen while the latter is nothing but a process in which the negative charges of a base are successively neutralized with protons. The analogy is complete if one considers the reverse process of the dissociation of a polybasic acid, H_2R, and compares it with oxygenation in the following way:

$$R^{--}+2H^+=HR^-+H^+=H_2R,$$

$$Hb+4O_2=HbO_2+3O_2=\cdots=Hb(O_2)_4.$$

Just as pK_1 (or pK_2) of the polybasic acid is the value of pH at which the amounts of H_2R and HR^- (or HR^- and R^{--}) are equal to each other, one may define pO_i** as the value of $\ln p$ at which the amount of $Hb(O_2)_{i-1}$ is equal to that of $Hb(O_2)_i$. Since the equilibrium constant of oxygenation of $Hb(O_2)_{i-1}$ is $K_i=L_i/L_{i-1}$ as mentioned above, it follows that

$$pO_i=-\ln K_i=\ln(L_{i-1}/L_i). \quad (8)$$

If pO_i increases with increasing i and the four values of pO_i are far apart from each other, the oxygen equilibrium curve would show seven inflection points at each of the pO_i's and also between the neighboring pO_i's. Then it would bear striking resemblance to a titration curve. If the pO_i's approach towards each other or if their order is reversed, a number of inflection points disappear leaving only one, as is actually found in the oxygen equilibrium curve of hemoglobin.

The condition of symmetry of the curve is that the middle point of pO_1 and pO_4 coincides with that of pO_2 and pO_3. In other words, pO_4-pO_3 is equal to pO_2-pO_1. This, in terms of the constants L in Eq. (8), is the following:

14) G.S. Adair, *Proc. Roy. Soc. London*, A 109, 292 (1925); *J. Biol. Chem.*, 63, 529 (1925).

** This p should not be confused with p denoting the partial pressure of oxygen.

$$\frac{L_3}{L_4}\Big/\frac{L_2}{L_3}=\frac{L_1}{L_2}\Big/\frac{1}{L_1} \quad \text{or} \quad L_3^2=L_1^2L_4, \quad (9)$$

which is identical with the relation (7). It will be seen that the constant L_2 has nothing to do with the symmetry property, although it affects the slope of the curve at the center, or at $Y=1/2$.

If, on the other hand, $L_3^2-L_1^2L_4$ is not equal to zero, the Y-ln p curve of Eq. (4) loses its symmetry. If the difference is positive, pO_4-pO_3 is greater than pO_2-pO_1 and the whole curve, except the point at $Y=1/2$, lies below the curve of Eq. (2) with the suitable choice of the constant n. Conversely if the difference is negative, the curve of Eq. (4) is above the symmetric curve of Eq. (2), as was actually found for denatured hemoglobin in the present experiment. How can the condition:

$$\Delta\equiv L_3^2-L_1^2L_4<0 \quad (10)$$

be realized? One must look for the solution of this inequality.

Pauling[3] has given an analysis of the oxygen equilibrium curve obtained by Ferry and Green[15] on horse hemoglobin, assuming the four hemes to interact in pairs as if located at the corners of a square with interactions between adjacent hemes along the sides of the square but with no interactions along diagonals. His formula for the degree of oxygenation is as follows.

$$Y=\frac{kp+(2\alpha+1)k^2p^2+3\alpha^2k^3p^3+\alpha^4k^4p^4}{1+4kp+(4\alpha+2)k^2p^2+4\alpha^2k^3p^3+\alpha^4k^4p^4}. \quad (11)$$

Here k is the equilibrium constant of oxygenation of a single heme unaffected by the reaction of its neighbors, that is to say, RT ln k is the decrease in free energy accompanying the combination of a heme with oxygen. Since there are four hemes in a hemoglobin molecule, $K_1=L_1=4k$. The constant α has the following significance. The equilibrium constant of the combination of two oxygen molecules with a hemoglobin molecule would be k^2 provided that no interaction exists between the hemes, but it is αk^2 if the two hemes are adjacent, because the equilibrium constant of the second heme is increased by the factor α as a result of the reaction of the first. In other words, RT ln α is the additional free energy stabilizing two interacting oxygen-combining centers. The factors 2 and 4 in Eq. (11) result from the symmetry numbers. Pauling's model involves only two constants, and it is remarkable that with a suitable choice of these constants ($k=0.033$ and $\alpha=12$) it may be made to fit the data of the fresh preparation of hemoglobin apparently within the allowable limit of errors of observation.

From the comparison of Eq. (11) with Eq. (4), one has for Pauling's model,

$$L_1=4k,\ L_3=4\alpha^2k^3,\ L_4=\alpha^4k^4. \quad (12)$$

Inasmuch as $\Delta=0$, Pauling's formula satisfies the symmetry condition (7). Therefore his formula cannot be applied to denatured hemoglobin. When denaturation takes place, the oxygen equilibrium curve changes its shape. There are two conceivable causes bearing on this matter. One involves the effect of the change of the equilibrium constant k, the other the effect of the interaction constant α, on the form of the oxygen equilibrium curve. Therefore a number of conceivable cases will be subjected to critical examination to see what change in k or α leads to the required condition (10) of asymmetry actually found.

(1) Let it be assumed that k's, the equilibrium constants of the four hemes, are equivalent to each other, while the interactions between different pairs of hemes are not mutually equivalent. In other words, supposing interactions to be represented by distances, Pauling's model may be depicted by a square, while this more general model having different interaction constants, α_1, α_2, α_3, and α_4, between the successive pairs of oxygen-combining centers would be represented by a quadrilateral having unequal sides. A case in which one of the stabilizing interactions of Pauling's model is annihilated would be a special case of this general model. For this model, the equilibrium constants L_i are given by the following equations.

$$L_1=4k,\ L_3=(\alpha_1\alpha_2+\alpha_2\alpha_3+\alpha_3\alpha_4+\alpha_4\alpha_1)k^3,$$
$$L_4=\alpha_1\alpha_2\alpha_3\alpha_4k^4. \quad (13)$$

Accordingly,

$$\Delta=[(\alpha_1\alpha_2+\alpha_2\alpha_3+\alpha_3\alpha_4+\alpha_4\alpha_1)^2-16\alpha_1\alpha_2\alpha_3\alpha_4]k^6$$
$$=[(\alpha_1\alpha_2+\alpha_2\alpha_3-\alpha_3\alpha_4-\alpha_4\alpha_1)^2+4\alpha_2\alpha_4(\alpha_1-\alpha_3)^2]k^6. \quad (14)$$

The right hand side of Eq. (14) is either zero (when $\alpha_1=\alpha_3$ and $\alpha_2=\alpha_4$) or positive (otherwise). In the former case, Y-ln p curve would be symmetric. In the latter case, although the curve is asymmetric it would lie below the symmetric curve of Eq. (2). In any way, this model does not satisfy the required condition (10). It is worth mentioning that even if interactions are assumed to exist along diagonals, Δ always turns out to be either positive or zero.

(2) Having seen that the changes in α do not lead to the required condition provided that k remains unchanged, one must inquire

15) R. M. Ferry and A. A. Green, *J. Biol. Chem.*, **81**, 175 (1929).

into the effect of change in k. The next case taken up is that in which each of the k's, the equilibrium constants of the four hemes, is slightly altered by an amount δk_i independently of others, while the interaction constant is tentatively assumed to be unchanged. The equilibrium constants L_i are given by

$L_1=(k+\delta k_1)+$three similar terms,

$L_3=\alpha^2(k+\delta k_1)(k+\delta k_2)(k+\delta k_3)+$three similar terms,

$L_4=\alpha^4(k+\delta k_1)(k+\delta k_2)(k+\delta k_3)(k+\delta k_4)$.

Disregarding higher powers in δk, one has

$$L_1=4k(1+\sum \delta k_i/4k),$$
$$L_3=4\alpha^2k^3(1+3\sum \delta k_i/4k),$$
$$L_4=\alpha^4k^4(1+\sum \delta k_i/k). \quad (15)$$

Accordingly $\Delta=0$, which is the condition (7) of symmetry. That is to say, small changes in k do not affect the symmetry property of Pauling's curve in any appreciable manner.

(3) Pauling's model was modified in such a way that the equilibrium constant of one of the four hemes is increased (or decreased) to βk. Then the constants L_i are given by

$L_1=k(\beta+3)$, $L_3=\alpha^2k^3(3\beta+1)$, $L_4=\alpha^4k^4\beta$. (16)

Therefore

$$\Delta=\alpha^4k^6[(3\beta+1)^2-(\beta+3)^2\beta]=\alpha^4k^6(1-\beta)^3.$$

If $\beta>1$, this expression is negative, satisfying the required condition (10). At first sight, it may appear rather surprising that the oxygen affinity of a heme increases as a result of denaturation. It is, however, a remarkable fact that in almost every case in which hemes are separated, there appears to be an increase of oxygen affinity, i.e., the decrease of p_0. For example, the data of Altschul and Hogness[16] on hemoglobin in dilute solutions, where the molecules may be expected to dissociate, show a decrease in p_0. The same effect is seen in the results of Hill and Wolvekamp[17] on diluted hemoglobin and of Taylor and Hastings[18] on spilt hemoglobin. The latter authors found that p_0 is considerably less for horse hemoglobin split in urea solution than for native hemoglogin.

(4) If two of the four hemes have an increased equilibrium constant βk relative to the remaining two, one has

$L_1=k(2\beta+2)$, $L_3=\alpha^2k^3(2\beta^2+2\beta)$, $L_4=\alpha^4k^4\beta^2$. (17)

Hence

$$\Delta=\alpha^4k^6[(2\beta^2+2\beta)^2-(2\beta+2)^2\beta^2]=0.$$

Again a symmetric Y-ln p curve would result.

(5) Finally let the case be considered, in which one of the four oxygen-combining centers has lost its ability to combine with oxygen. In this case,

$L_1=3k$, $L_2=(2\alpha+1)k^2$, $L_3=\alpha^2k^3$, $L_4=0$. (18)

Since $L_4=0$, the condition of symmetry of the equilibrium curve must be altered, which in terms of the constants L_i, is

$$\frac{L_2}{L_3}\Big/\frac{L_1}{L_2}=\frac{L_1}{L_2}\Big/\frac{1}{L_1} \text{ or } L_2^3-L_1^3L_3=0, \quad (19)$$

rather than Eq. (9), and the condition of asymmetry in conformity with experiment is

$$L_2^3-L_1^3L_3<0,$$

in place of Eq. (10). Introducing the values given by (18) into the left hand side of this equation, one is led to

$$L_2^3-L_1^3L_3=[(2\alpha+1)^3-3^3\alpha^2]k^6$$
$$=(8\alpha+1)(\alpha-1)^2k^6.$$

The right hand side of this equation is positive inasmuch as $\alpha>1$ for stabilizing interaction. Here again the required condition is not fulfilled. It is of course possible that the changes of molecules due of denaturation take place only partly, leaving unchanged molecules. However, a mixture of two kinds of such molecules, one giving a symmetric oxygen equilibrium curve, the other an asymmetric one having a trend contrary to experimental observations, would never yield a curve even in qualitative agreement with experiments.

So far a numbers of conceivable cases have been examined for the change of k as well as of α. Although they cover by no means all the possible combinations of changes in k and α, yet relatively simple changes appropriate for the first stage of denaturation seem to have been taken into account. It was found that the condition of asymmetry (10) is so severe that it can rule out almost all except case (3). Therefore one may conclude that the increase in the equilibrium constant of the combination with oxygen of one of the four hemes takes place in the first stage of the denaturation of hemoglobin.

Summary

The oxygen equilibrium curve of a slightly denatured preparation of hemoglobin solution was determined by the spectrophotometric method. The plot of Y, the degree of partial saturation with oxygen, against log p, the logarithm of the partial pressure of oxygen, was not symmetric across the point at 50% saturation. The trend of asymmetry was

16) A. M. Altschul and T. R. Hogness, *J. Biol. Chem.*, **139**, 315 (1939).

17) R. Hill and H. R. Wolvekamp, *Proc. Roy. Soc. London*, **B107**, 286 (1930).

18) J. F. Taylor and A. B. Hastings, *J. Biol. Chem.*, **144**, 1 (1942).

such that if the lower left portion of the curve was rotated through 180° about the point at $Y=1/2$, it lay below the upper right portion of the original curve. The condition of this trend of asymmetry was derived from the theory of chemical equilibrium. This condition was tested with various conceivable changes in k, the equilibrium constant of oxygenation of a single heme, as well as in α, the constant of interaction stabilizing the combination of each of two adjacent hemes with an oxygen molecule. It was found that the deviation from the equivalence of α, of whetever kind and degree, can never satisfy the required condition, provided that the k's of the four hemes remain equivalent to each other. A number of other conceivable cases were subjected to critical examination. The condition of asymmetry was so severe that it could rule out almost all except the case in which one of the four hemes increases its affinity towards an oxygen molecule compared with the other three. This conclusion is in conformity with the results on hemoglobin dissociated in a dilute solution or split in a urea solution.

Chemical Department, Faculty of Science
Nagoya University, Nagoya

Synthetic Amphoteric Polypeptide. I. Syntheses and Some Properties of Linear Amphoteric Polypeptides

By Heimei YUKI, Shumpei SAKAKIBARA and Hisaya TANI

(Received February 27, 1956)

Introduction

The behavior of synthetic amphoteric polypeptides is of great interest, because of their relationship to those of proteins. With this in mind, Akabori, Tani and Noguchi[1] have synthesized copoly-1 : 1-(L-glutamic acid, DL-lysine), the first synthetic amphoteric polypeptide. This substance, unfortunately, had some unfavorable properties as a "model protein". Its solubility in water was too great, due to its relatively low molecular weight; also it differed from proteins in that all of the component amino acid residues had the ionisable side chain groups.

It would be desirable to obtain a high molecular weight polypeptide having acidic, basic and neutral amino acid residues in proportions nearly equal to those in protein. Therefore, copoly-1 : 1 : 3-(DL-glutamic acid, DL-lysine, DL-phenylalanine) (A) and copoly-1 : 1 : 1.9-(L-glutamic acid, L-lysine, L-leucine) (B) have been synthesized and some properties of their solutions investigated.

Preparations

The copolymerizations were carried out with mixtures of N-carboxy anhydrides of γ-benzyl DL-glutamate, ε-N-carbobenzoxy-DL-lysine and DL-phenylalanine (I, II, III respectively) and of γ-benzyl L-glutamate, ε-N-carbobenzoxy-L-lysine and L-leucine (IV, V, VI respectively). To obtain a homogeneous high molecular polypeptide, a suitable solvent must be used for the polymerization. The results obtained with several solvents tried in these experiments are shown in Table I. It was found that chlorobenzene was the most suitable solvent, giving the polymers having the highest specific viscosities. In nitrobenzene and in ethyl phenylacetate, the reaction mixtures formed transparent gels or highly viscous solutions. The polymer produced in benzene and its reduction product were found to be heterogeneous in their solubility behavior. In dioxane and tetrahydrofuran the polymerization could not proceed; after evaporating the solvents in vacuo the crystalline masses, supposedly mixtures of the N-carboxy anhydrides, were recovered. These could now be polymerized in any of the suitable solvents mentioned above, the polymerization proceeding apparently in the same manner as when fresh monomer mixtures were used. It has been observed previously[2] that N-carboxy-α-amino acid anhydride was very stable in purified acetone. The dioxane and tetrahydrofuran used in these experiments contained traces of an aldehydic substance, which might have some stabilizing effect on the monomers.

The polymers were reduced with phosphonium iodide and converted into the hydriodides of corresponding amphoteric polypeptides. The hydriodides gave the free polypeptides quantitatively on treatment with triethylamine. Dialyses of these hydriodides were also carried out to remove

1) S. Akabori, H. Tani and J. Noguchi, *Nature*, **167**, 159 (1951); H. Tani and J. Noguchi, *Chem. High Polymers, Japan*, 8, 57 (1951).

2) H. Tani and H. Yuki, *Chem. High Polymers. Japan*, 8, 62 (1951).

TABLE I

Monomers	Solvents	Results	Yield (%)	η_{sp} *3)
(A) I, II, III*1)	Nitrobenzene	Transparent gel	100	
(1 : 1 : 3)	Ethyl Phenylacetate	Opalescent gel	100	
	Benzene	Gel particles in viscous soln.	94	
	Dioxane	No change		
(B) IV, V, VI*2)	Chlorobenzene	Clear viscous soln.	94	0.48
(1 : 1 : 2)	Nitrobenzene	Viscous soln., partially gelling	70	0.15
	Ethyl Phenylacetate	Transparent gel	95	0.31
	Chloroform	Soln. of low viscosity		
	Tetrahydrofuran	No change		

*1) The polymerizations were carried out by heating at 70°C for 60 hr.
*2) The polymerizations were carried out with about 8% solution at 60°C for 8 hr. and then at room temperature for ten days.
*3) The specific viscosities of 0.1% solution of the polymers in chloroform at 30°C.

hydriodic acid, but the polypeptides obtained here still contained a small amount of hydrogen iodide and about half of the polypeptides were lost. Such fractionation caused during dialysis may produce changes in the ratios of the amino acid residues composing the polypeptides, if, in each case, the compositions of the individual molecules are not the same. However, the elementary analyses and the amounts of lysine residues estimated from van Slyke's amino-nitrogen determinations indicated that these polypeptides contained the amino acid residues in the same molar ratios as those of the starting monomer mixtures.

Titration curves (see Fig. 1) of these polypeptides in aqueous solutions showed typical amphoteric properties and the carboxyl group contents calculated from the hydrogen ion combining capacities corresponded to the values obtained from analytical data. These polypeptides were soluble in dilute mineral acids and in dilute alkalis, but were insoluble in water over a rather wide range of pH, i.e., 4.0–10.8 for polypeptide A and 4.5–10.2 for polypeptide B, respectively.

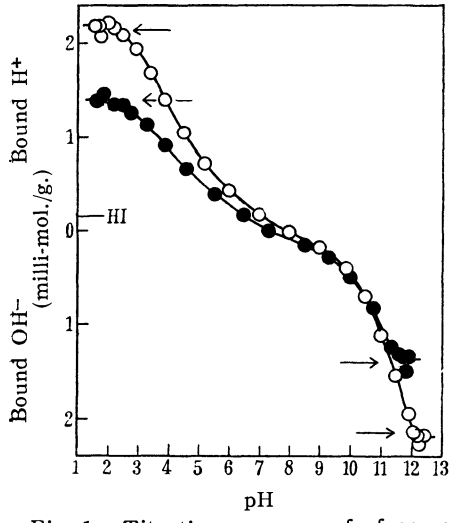

Fig. 1. Titration curves of free amphoteric polypeptides.
●: Copoly-1 : 1 : 3-(DL-glutamic acid, DL-lysine, DL-phenylalanine).
○: Copoly-1 : 1 : 1.9-(L-glutamic acid, L-lysine, L-leucine).
Arrows represent the theoretical end points respectively.

Properties of the Solution

The properties of the aqueous solution of polypeptide B were studied, using the dialysed solution of the hydriodide. The dialysed solution had

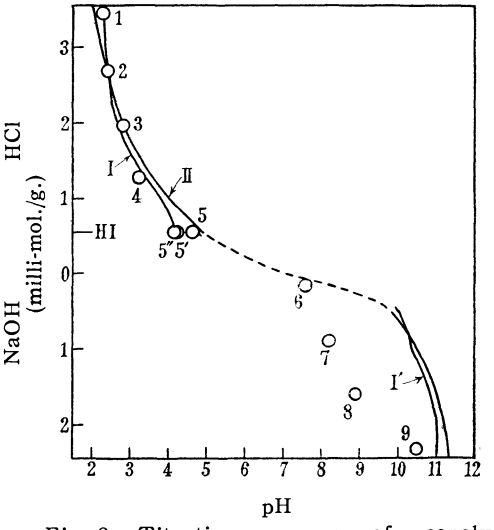

Fig. 2. Titration curves of copoly-1 : 1 : 1.9-(L-glutamic acid, L-lysine, L-leucine).
Curves I and I': Titration of the dialysed solution by 0.1 N HCl and 0.1 N NaOH respectively. Curve II: Titration of a solution of the dry sample in hydrochloric acid with 0.1 N NaOH. The dotted line indicates the insoluble region. The numbered circles represent the pH of the solutions for viscosity measurements, 400 hr. after the preparation of solutions.

a pH value of 4.3. It contained 0.27 mol. of hydriodic acid per lysine residue of the polypeptide. The resulting polypeptide had an isoelectric point at about pH 7.3 as shown in the titration curve in Fig. 2.

The relation of the reduced viscosity to the concentration of the polypeptide was linear in the concentration below about 1%. The intrinsic viscosity was 0.70 (see Fig. 3).

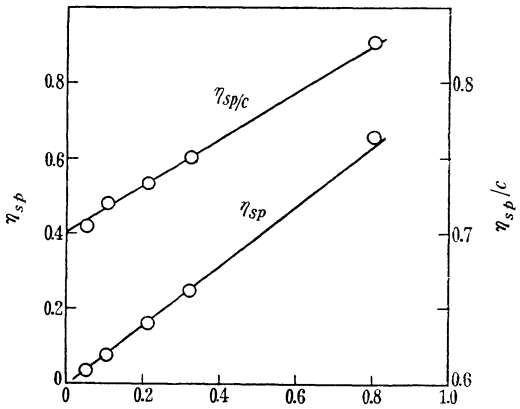

Fig. 3. Relationship between viscosity and concentration.

Because of the insolubility of this polypeptide in the pH range near its isoelectric point, the pH-dependence of viscosity could be measured only outside of this insoluble region. The results (see Fig. 4) showed that the viscosity increased gradually towards its isoelectric point from both sides and that it was considerably higher in the acidic than in the alkaline region.

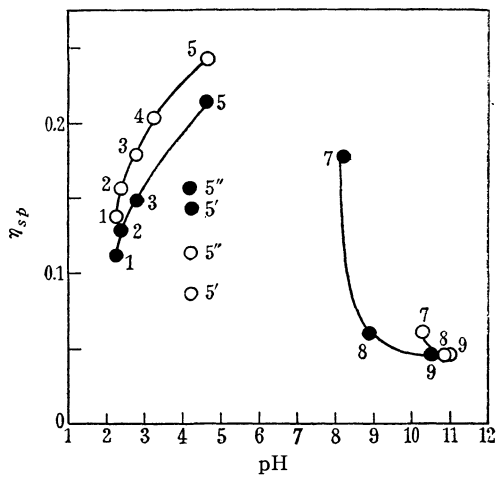

Fig. 4. Relationship between specific viscosity and pH: ○, at 17–52 hr.; ●, at 305–355 hr., after the preparation of the solutions.

The viscosities of solutions of this polypeptide changed gradually with time. In acidic solution the growth of mould was found occasionally, but it is not certain whether or not such bacterial decomposition of the polypeptide caused this decrease in viscosity (see Fig. 5). In alkaline solu-

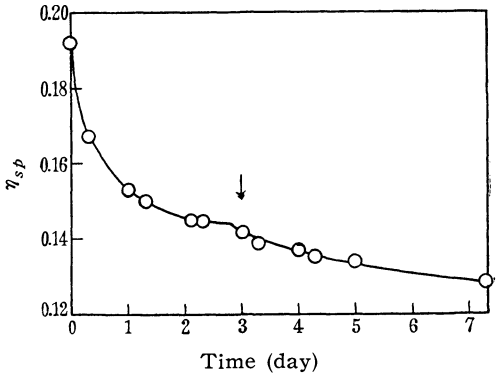

Fig. 5. Change of specific viscosity of solution No. 1. The arrow represents the appearance of mould.

tion the viscosity remained constant for a rather long period and then suddenly began to increase linearly with time. The final solution exhibited thixotropy (see Fig. 6). It was observed also

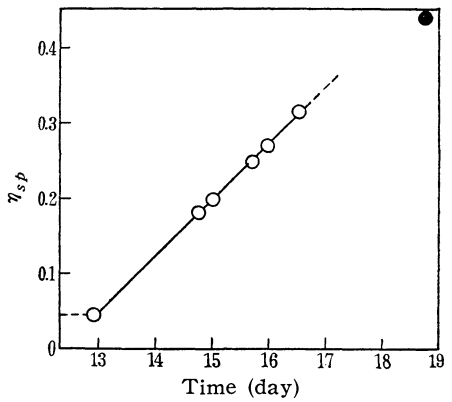

Fig. 6. Change of specific viscosity of solution No. 7.
●: Thixotropy.

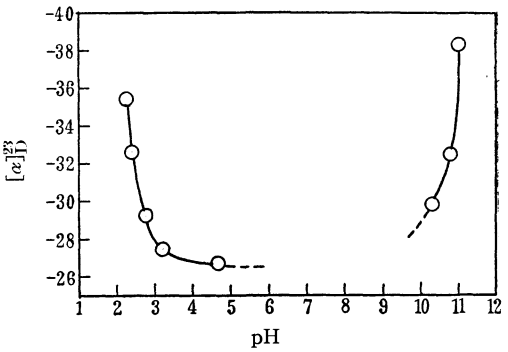

Fig. 7. Relationship between optical rotation and pH.

that at the beginning of this increase in viscosity the solution began to show opalescence, which became gradually strong with time, and that the

pH of the solution shifted toward neutrality, as a result of absorption of atmospheric carbon dioxide.

The pH dependence of optical rotatory power of this polypeptide was observed in the soluble region. All of the observed values were laevo-rotatory, the absolute magnitudes decreasing toward the isoelectric region (see Fig. 7).

Discussion

From the results of studies[3] on synthetic vinyl polymers, it has been stated that poly-ampholytes are insoluble in water in any pH range, if the dissociation constant of either the acidic or the basic group is very small, or if the number of one of these groups is much less than that of the other. In the polypeptides obtained in this research, the acidic and basic groups have pK′ values of 4.3 and 10.5 respectively[4], and hence have sufficient dissociation constants to form dipolar ions in their isoelectric regions; moreover, the numbers of these groups are equal. Although the insolubility of these polypeptides in the isoelectric regions may be presumed to be due to the large contribution of the hydrophobic side chain groups of leucine or phenylalanine residues, which are contained in relatively high proportions, high molecular weight copoly-1 : 1-(L-glutamic acid, L-lysine)[5], which contains no such hydrophobic side chain group, also had a wide insoluble region around its isoelectric point.

For solutions of synthetic amphoteric vinyl polymers[3,6,7] and of some of natural proteins[8], it has been reported that viscosity exhibits a minimum at the isoelectric point and a maximum on each side. This viscometric behavior has been interpreted as due to the coiling and stretching of long chain molecules caused by the electrostatic attraction and repulsion between positive and/or negative charges of ionized groups distributed along the molecular chains.

In these experiments the viscosity could be measured only on the outsides of both maxima, because of the insolubility of polypeptide in the neutral region. The lower viscosity in an alkaline region than that of an acidic region may be due to sodium iodide, which was present as extra-salt in the alkaline solutions. It has been shown that a small amount of neutral salt caused a considerable decrease in the viscosity of vinyl polyelectrolyte solutions[3].

The change of viscosity on ageing has been observed in cases of the solution of proteins, such as gelatin[9], but the cause remains obscure.

The increase in viscosity as the pH approaches that of the insoluble region from either side and the appearance of turbidity in the alkaline solution, together with the shift of pH of the solution caused by ageing, suggest that the aggregation of the solute polypeptide becomes greater as the solution approaches to its isoelectric point. Likewise, the insolubility of these amphoteric polypeptides in the neutral region may be due to this aggregation.

As one of the factors causing such an inter-molecular association, the formation of inter-molecular salt-linkages, such as have been assumed by Isemura and Hamaguchi[10] on the basis of their studies of the surface viscosity of these polypeptides, might be considered. Further, the role of hydrogen bonds formed between large numbers of carbonyl and imino groups distributed in the polypeptide chains can not be ignored, since these amphoteric polypeptides differ essentially from the vinyl polyampholytes only in having peptide bonds in their skeletal molecular chains. The large intrinsic viscosity of the polypeptide suggests that it had a more-or-less rigid and highly extended structure in solution.

The behavior of the solution of the polypeptide with regard to optical rotation is quite similar to that of natural proteins[11].

All of these properties of the polypeptides in solution, together with their surface chemical properties reported by Isemura and Hamaguchi[10] and by Davies and Llopis[12] show that they are interesting substances, similar in many respects to polypeptides of natural proteins.

Experimental

γ-Benzyl DL-Glutamate.—A mixture of 30 ml. of conc. hydrochloric acid, 12 ml. of water, 30 g. of powdered DL-glutamic acid and 300 ml. of benzyl alcohol was heated to 95°C for 1/2 hr. with stirring.

3) T. Alfrey, Jr. and H. Morawetz, *J. Am. Chem. Soc.*, **74**, 436 (1952); T. Alfrey. Jr., R.M. Fuoss, H. Morawetz and H. Pinner, ibid., **74**, 438 (1954).

4) E.J. Cohn and J.T. Edsall, "Proteins, Amino Acids, and Peptides as Ions and Dipolar Ions", Reinhold, New York (1943), p. 84.

5) H. Yuki and H. Tani, Unpublished.

6) T. Matsumoto, *Chem. High Polymers, Japan*, **8**, 412 (1951).

7) A. Katchalsky and I.R. Miller, *J. Polymer Sci.*, **13**, 57 (1954).

8) S. Akabori and S. Mizushima, "Protein Chemistry", Vol. 2, Kyoritsushuppan, Tokyo (1954), p. 390.

9) S. Akabori, "Amino Acids and Proteins", Kyoritsushuppan, Tokyo (1944), p. 463.

10) T. Isemura and K. Hamaguchi, This Bulletin, **27**, 339 (1954); K. Hamaguchi and T. Isemura, ibid., **28**, 9 (1955).

11) W. Pauli and E. Valko, "Kolloidchemie der Proteine", T. Steinkopff, Dresden (1933).

12) J.T. Davies, *Biochem. J.*, **56**, 509 (1954); J.T. Davies and J. Llopis, *Proc. Roy. Soc.*, A **227**, 537 (1955).

The resultant clear solution gave no phase-separation on cooling. The cooled solution was neutralized by an aqueous solution of 30 g. of sodium bicarbonate, and 500 ml. of ether was added with stirring. The precipitated crystals were filtered and washed with a small amount of water, ethanol, and ether. Plates, m.p. 163–163.5°C; no change in m.p. was observed by recrystallization from 520 ml. of water. Yield 26 g. (54% of the theor.)

Anal. Found: N, 5.97. Calcd. for $C_{12}H_{15}NO_4$: N, 5.91%.

γ-Benzyl L-Glutamate[13].—A mixture of 14.5 g. of powdered L-glutamic acid, 24 ml. of conc. hydrochloric acid and 150 ml. of benzyl alcohol was treated as above, and the product was recrystallized from 370 ml. of water to give 12.6 g. (53% of the theor.). Plates, m.p. 173°C, $[\alpha]_D^{17}$ 20.7° (glacial acetic acid, *c* 6.76).

Anal. Found: N, 5.85. Calcd. for $C_{12}H_{15}NO_4$: N, 5.91%.

γ-Benzyl N-Carboxy-DL-glutamate Anhydride (I).—Phosgene was passed for one hour into a suspension of 13 g. of powdered γ-benzyl DL-glutamate in 260 ml. of anhydrous dioxane with stirring at room temperature. After excess phosgene was removed by passing dry air through the solution, it was concentrated to a syrup in vacuo at 40°C and finally at 50°C. The ethyl acetate solution of this syrup gave colorless needles on the addition of petroleum ether. Yield 12 g. (77% of the theor.), m.p. 70–83°C.

Recrystallization from ethyl acetate and petroleum ether gave 8.5 g. of crystals (Ia) of m.p. 70–71°C, and the concentrated mother liquor gave 2 g. of crystals (Ib) of m.p. 83–85°C by adding petroleum ether. Ia and Ib are supposed to be different crystallographic modifications of the same substance, because neither of them showed optical rotation in ethyl acetate solution and both gave the same infra-red absorption spectra.

Anal. Found: N, (Ia) 5.35; (Ib) 5.39. Calcd. for $C_{13}H_{13}NO_5$: N, 5.32%.

γ-Benzyl N-Carboxy-L-glutamate Anhydride (IV).—A suspension of 10 g. of powdered γ-benzyl L-glutamate in 300 ml. of dry dioxane was treated with phosgene as described above. The crystalline product was recrystallized from ethyl acetate and petroleum ether to give 10.5 g. (95% of the theor.) of needles, m.p. 91–92.5°C. Further recrystallization from ethyl acetate raised the m.p. to 93.5–94.5°C. $[\alpha]_D^{29}$ −17.0° (ethyl acetate, *c* 3.65).

Anal. Found: N, 5.28. Calcd. for $C_{13}H_{13}NO_5$: N, 5.32%.

α-N-Carboxy-ε-N-carbobenzoxy-DL-lysine Anhydride[14] **(II).**—This compound was prepared from 12 g. of N, N′-dicarbobenzoxy-DL-lysine and 20 ml. of thionyl chloride and recrystallized several times from ethyl acetate and petroleum ether. Yield 2.4 g. (27% of the theor.), m.p. 103°C.

α-N-Carboxy-ε-N-carbobenzoxy-L-lysine Anhydride[14] **(V).**—A solution of 15 g. of crystalline N, N′-dicarbobenzoxy-L-lysine in 20 ml. of dry dioxane and 30 ml. of dry ether was cooled to 0°C and 8.8 g. of phosphorus pentachloride was added. After shaking for 1/2 hr., the supernatant liquid was decanted and concentrated in vacuo at 40°C. The resultant crystalline mass was decolorized by washing with a small amount of dry ether. Yield 10 g. (80% of the theor.). Recrystallization from ethyl acetate and petroleum ether gave crystals of m.p. 100°C, $[\alpha]_D^9$ −24.1° (ethyl acetate, *c* 6.22).

N-Carboxy-DL-phenylalanine Anhydride[15] **(III).**—This compound was prepared from 14 g. of N-carbobenzoxy-DL-phenylalanine and 20 ml. of thionyl chloride, and repeatedly recrystallized from ethyl acetate and petroleum ether. Yield 6 g. (72% of the theor.), m.p. 123°C.

N-Carboxy-L-leucine Anhydride[16] **(VI).**—Phosgene was passed for two hours into a suspension of 5 g. of powdered L-leucine in 200 ml. of dry dioxane at 40°C. The crystals, which were obtained in the same manner as described above, were recrystallized from ethyl acetate and petroleum ether. Yield 4.8 g. (80% of the theor.), m.p. 76.5–77.5°C. $[\alpha]_D^{11}$ −42.2° (benzene, *c* 0.95).

Anal. Found: N, 8.83, Calcd. for $C_7H_{11}NO_3$: N, 8.91%.

The Effect of Solvent on the Copolymerization.—All the solvents were purified by distillation, and benzene, dioxane and tetrahydrofuran were further dried over metallic sodium. Dioxane and tetrahydrofuran were colored by Schiff's reagent.

The mixtures of N-carboxy anhydrides in the ratio shown in Table I were dissolved in each solvent in a sealed glass tube, and heated to polymerize them.

The solutions of dioxane and tetrahydrofuran showed no change, and on evaporating the solvents in vacuo the crystalline residues were obtained. These residues were dissolved in nitrobenzene or chlorobenzene and heated in sealed tubes. They polymerized rapidly and formed transparent gels or viscous solutions.

The polymers (B) listed in Table I were precipitated by adding ether and petroleum ether to each reaction mixture and reprecipitated from chloroform solutions by petroleum ether. The viscosities of 0.1% chloroform solutions were determined at 30±0.1°C using an Ostwald viscometer.

Copolymer of I, II and III (VII).—The copolymerization was carried out for the mixture of 0.413 g. (1.57 m mol.) of I, 0.480 g. (1.57 m mol.) of II, and 0.900 g. (4.71 m mol.) of III in 20 ml. of each of the solvents listed in Table I, (A). The dioxane solution was evaporated off, and the residual crystals were polymerized in nitrobenzene. Each polymer was precipitated by adding petroleum ether and reprecipitated from tetrahydrofuran by petroleum ether and ether. All the polymers, excepting that from benzene solution, were collected and dried; white powder, 4.35 g.

13) W.E. Hanby et al. (*J. Chem. Soc.*, **1950**, 3239) obtained this compound with a considerably lower yield, using hydriodic acid instead of hydrochloric acid.

14) M. Bergmann, L. Zervas and W.F. Ross, *J. Biol. Chem.*, **111**, 245 (1935).

15) H. Leuchs and W. Geiger, *Ber.*, **41**, 1721 (1908).

16) A.C. Farthing, *J. Chem. Soc.*, **1950**, 3213; D. Coleman, ibid., **1950**, 3222.

(100% of the theor.), soluble in dioxane, tetrahydrofuran, hot glacial acetic acid, and hot chloroform.

Anal. Found: C, 68.71; H, 5.99; N, 9.07. Calcd. for $[(C_{12}H_{13}NO_3), (C_{14}H_{18}N_2O_3), 3(C_9H_9NO)]_n$: C, 68.94; H, 6.34; N, 9.11%.

The polymer obtained from benzene solution (N, 9.16%) contained a small amount of material which was insoluble in the above solvents.

Copoly-1: 1: 3-(DL-glutamic acid, DL-lysine, DL-phenylalanine) (VIII).—A mixture of 4 g. of VII and 100 ml. of glacial acetic acid was heated until a complete solution was obtained. Six grams of phosphonium iodide was then added in portions during 4.5 hr. at 60–70°C with passing through dry hydrogen. After cooling, the precipitate formed was separated by decantation and washed with dry ether. Repeated reprecipitation from absolute ethanol and dry ether gave 3.3 g. (95% of the theor.) of polypeptide hydriodide as white powder. This was hygroscopic and was soluble in ethanol, methanol, water, wet dioxane and wet tetrahydrofuran.

This hydriodide was dissolved in 100 ml. of water and dialysed against distilled water. The solution obtained had a pH of 5.5 and an osmotic pressure of about 30 mm-H_2O (*c*, 6 g./l.); it coagulated to a white gelatinous precipitate on warming to 30°C. After evaporating the solution in an evacuated desiccator at room temperature, 1.6 g. (53% based on the polymer) of pale yellow glassy solid was obtained. This was soluble in dilute mineral acids and in dilute alkalis, but insoluble in water and conc. hydrochloric acid. It was also insoluble in methanol, ethanol and dioxane, but readily soluble in any of these containing hydrochloric acid. It was also soluble in hot, but not in cold, aqueous pyridine. It gave a positive biuret reaction in aqueous solution and foamed even in dilute solution.

Anal. Found*: C, 62.38; H, 6.62; N, 11.12; amino-N, 1.87; I, 3.70. Calcd. for $[(C_5H_7NO_3), (C_6H_{12}N_2O), 3(C_9H_9NO), 0.21\ HI]_n$: C, 62.90; H, 6.40; N, 11.59; amino-N, 1.93; I, 3.68%.

The polymer obtained from benzene solution was reduced and treated in the same manner as described above, but the product contained a small amount of matter which was insoluble in dilute alkali.

Copolymer of IV, V and VI (IX).—A solution of 2.63 g. (0.01 mol.) of IV, 3.06 g. (0.01 mol.) of V and 2.98 g. (0.019 mol.) of VI in 100 ml. of chlorobenzene was sealed in a glass tube and heated for several hours at 80°C and then for 135 hr. at 60°C. The polymer was precipitated from the clear viscous solution by ether and petroleum ether and then reprecipitated from acetone and petroleum ether. The dried white powder weighed 6.90 g. (99% of the theor.). This polymer was easily soluble in chloroform and dioxane, and soluble in tetrahydrofuran, ethyl acetate, acetone and hot glacial acetic acid.

Anal. Found: C, 64.24; H, 7.18; N, 9.96. Calcd. for $[(C_{12}H_{13}NO_3), (C_{14}H_{18}N_2O_3), 1.9(C_6H_{11}NO)]_n$; C, 64.51; H, 7.52; N, 9.86%.

Copoly-1: 1: 1.9-(L-glutamic acid, L-lysine, L-leucine) Hydriodide (X).—As described for the preparation of VIII the solution of 2 g. of IX in 75 ml. of glacial acetic acid was treated with 4.2 g. of phosphonium iodide (with stirring), and the resultant precipitate was repeatedly reprecipitated from absolute ethanol and ether, and dried. The polypeptide hydriodide was obtained as a pale yellow powder. Yield 1.66 g. (96% of the theor.). Its solubility was similar to that of the hydriodide of VIII described above.

Anal. Found*: C, 43.56; H, 6.55; N, 10.62; amino-N, 2.32; I, 22.7. Calcd. for $[(C_5H_5NO_3), (C_6H_{12}N_2O \cdot HI), 1.9(C_6H_{11}NO)]_n$: C, 44.80; H, 6.87; N, 11.43; amino-N, 2.33; I, 21.2%.

Copoly-1: 1: 1.9-(L-glutamic acid, L-lysine, L-leucine) (XI).—To the solution of 1.4 g. of X in 15 ml. of methanol, 0.75 g. of triethylamine was added. The precipitated polypeptide was washed with methanol repeatedly until no halogen was detectable, then washed with ether and dried. The white powder weighed 1.04 g. (94% of the theor.). It was slightly soluble in water and methanol, and considerably soluble in hot water. In dilute mineral acids and in dilute alkalis, it gave a very foamy and viscous solution and gave a positive biuret reaction.

Anal. Found*: C, 56.16; H, 8.03; N, 14.42; amino-N, 3.03. Calcd. for $[(C_5H_7NO_3), (C_6H_{12}N_2O), 1.9(C_6H_{11}NO)]_n$: C, 56.94; H, 8.52; N, 14.53; amino-N, 2.97%.

Dialysis of the Solution of X.—A solution of 1.3 g. of X in 50 ml. of water was dialysed against distilled water for four days. This was concentrated in an evacuated desiccator at room temperature to 65 ml. and used in the following experiments as the "original solution". The concentration of this solution was determined using 5 ml.; making the correction of the content of hydrogen iodide, the concentration of free polypeptide was 8.07 mg./ml. and its yield was 51% of the theoretical value. The dried substance was transparent glassy solid, soluble in dilute mineral acids or in dilute alkalis, but not in water.

Anal. Found*: C, 52.96; H, 8.11; N, 13.69; amino-N, 2.78; I, 6.8. Calcd. for $[(C_5H_7NO_?), (C_6H_{12}N_2O), 1.9(C_6H_{11}NO), 0.27\ HI]_n$: C, 53.05; H, 7.99; N, 13.54; amino-N, 2.76; I, 6.79%.

Electrometric Titrations.—Titrations were made on solutions containing a known weight of the sample (*c*, ca. 10 mg./ml.) dissolved in a known amount of hydrochloric acid with 0.1 N NaOH using a Beckman G pH meter. During the titrations, insoluble precipitates appeared at pH 4.0–10.8 and 4.5–10.2 for VIII and XI. Blank titrations were made under the same conditions. The hydrogen ion and hydroxyl ion combining capacities were estimated from the differences between the measurements for the unknowns (VIII and XI) and those for the blanks[17] (Fig. 1). Curve II in Fig. 2 represents the titration of a dry sample obtained from the "original solution," and curves I and I′ in Fig. 2 are the titration curves.

* The analytical samples were dried over phosphorus pentoxide for several hours at 108°/3 mmHg.

17) T.V. Parke and W.W. Davis, *Anal. Chem*, 26, 642 (1954).

of the "original solution" with 0.1 N HCl and 0.1 N NaOH respectively.

The Solution Used for Measurements.—Twenty ml. of the "original solution" was diluted to 50 ml.; this was designated as "solution-N". Each 0.25 m mol. of hydrochloric acid and sodium hydroxide were added to each 10 ml. of the "original solution" and these were diluted with water to 25 ml., giving "solution-A" and "solution-B", respectively. By mixing these solutions the following eleven solutions were made. The numbers inserted in Figs. 2, 4, and 7 represent these solution numbers.

Solution No.	1,	2,	3,	4,	5,	5′,	5″,	6,	7,	8,	9
Solution A (ml.)	11	6	5	3	0	3	2	0	0	0	0
Solution N (〃)	0	2	5	9	10	0	4	9	5	2	0
Solution B (〃)	0	0	0	0	0	3	2	3	5	6	11

In solution No. 6, precipitation occurred.

Measurement of Viscosity.—The measurements were carried out at 25±0.01°C using an Ostwald viscometer. As viscosity changes with time, the time intervals between the measurements and the preparation of the solution were noted.

(1) The effect of concentration.—The measurements were carried out on the "original solution," solution No. 5, and its diluted solution 17–24 hr. after their preparation.

(2) The effect of the time.—Solutions No. 1 and 9 were placed, respectively, in the viscometers held in a thermostat, and the measurements were made at appropriate intervals.

(3) The effect of pH.—The measurements were carried out twice on solutions No. 1–9 at 17–52 hr. and at 305–355 hr.

In Fig. 2 the points numbered 1–9 represent the pH of each solution about 400 hr. after their preparations.

Measurement of Optical Rotation.—The measurements were made 43–48 hr. after the preparation of solution.

Measurement of Osmotic Pressure.—The measurement was carried out on solution No. 5 (c, 3.23 mg./ml.) using a Bull and Currie type osmometer at 25±0.01°C. The observed osmotic pressure was 22.8 mm-H_2O**.

Summary

1. Two linear highmolecular amphoteric polypeptides were synthesized.

2. The pH-dependences of viscosity and optical rotation were measured. Some of these properties resembled that of vinyl polyampholytes and some proteins.

The authors express their hearty thanks to Prof. S. Akabori and Prof. S. Murahashi for their interest and encouragement throughout the work, to Dr M. L. Huggins for reading the manuscript, and to Mr. C. Oizumi for a part of the experimental work. This research was financially supported by the Institute for Fiber Research.

Department of Chemistry, Faculty of Science, Osaka University, Osaka

** Using van't Hoff's equation and neglecting the presence of hydrogen iodide, this corresponds to a molecular weight of about 3.6×10^4. Davies et al.[12] reported the molecular weight of this substance being 35,000 from their measurements of the surface pressure.

Addition of Trichlorosilane to Acetylene and to Vinyltrichlorosilane[1]

By Shunichi NOZAKURA

(Received March 29, 1956)

The addition of trichlorosilane to acetylene is one of the well-known methods for the preparation of organosilicon compounds, and is known to be accelerated in the presence of peroxides or platin catalyst[2].

$$HSiCl_3 + CH \equiv CH \longrightarrow CH_2 = CHSiCl_3$$

$$CH_2 = CHSiCl_3 + HSiCl_3 \longrightarrow Cl_3SiCH_2CH_2SiCl_3$$

In the course of our study on the additional reactions of trichlorosilane to various vinyl compounds, it was observed in the previous paper[3] that cyanoethylation of trichlorosilane took place easily in the presence of organic bases as well as platin or benzoylperoxide. All these catalysts resulted in the formation of β-cyanoethyltrichlorosilane. On the contrary, when the reactions were carried out either in the presence of pyridine in an autoclave, or in the presence of tetrapyridine nickel (II) chloride in sealed glass tubes, the reversal of the orientation of addition was observed[4].

1) Paper VI in a series on the study of organosilicon compounds.

2) G.H. Wagner and C.O. Strother, Brit. Pat. 670, 617, Apr. 23, 1952; *C.A.*, **46**, 8894c.

3) S. Nozakura and S. Konotsune, This Bulletin, **29**, 322 (1956).

4) S. Nozakura and S. Konotsune, ibid., **29**, 326 (1956).

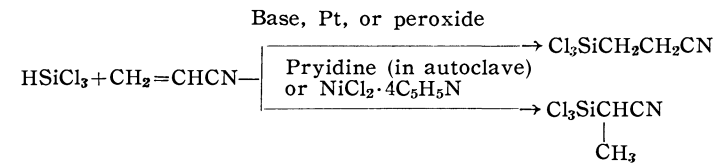

The present work was undertaken to see if the same base catalyst could hold its effect in the above reaction, i.e., the reaction between acetylene and trichlorosilane, and to see if the reverse orientation of addition would also take place in this case. In fact, the reverse addition took place, and there obtained 1,1-di(trimethylsilyl) ethane which otherwise would not be obtainable.

Addition of Trichlorosilane to Acetylene.—For the comparison of the reactions, the reaction in an autoclave was carried out in the first place according to the procedure described by Wagner and Strother[2]. Thus, in the presence of platinized asbestos, the reaction started at about 170°C. When an excess amount of trichlorosilane over acetylene was used, the principal product was found to be di(trichlorosilyl) ethane. On the other hand, when a sufficient amount of acetylene was supplied to the reaction system, the main product was vinyltrichlorosilane. These results confirmed the description of Wagner and Strother.

In the presence of a catalytic amount of pyridine, on the contrary, the reaction was observed to be initiated at temperatures as high as 180–185°C. Since it was rather tedious to handle the reaction mixture directly, the chlorine atoms attached to silicon atoms were replaced by methyl groups and the mixture of silico-hydrocarbons thus obtained were fractionally distilled through the fractionating column of the Stedman type. Two main fractions were obtained being accompanied with a considerable amount of distillation residue. The physical properties of these main fractions were listed in Table I. Although the data for the first main fraction of molecular weight, analysis, and molar refraction were in good agreement with that of di(trimethylsilyl)ethane, those of boiling point, density, and refractive index showed marked differences from that of 1,2-di(trimethylsilyl)ethane (151–2°C, 0.7565, and 1.4199, respectively[5]). This discrepancy is thought to be due to the presence of the isomeric mixture, which will be shown later on in this paper. The second main fraction was considered to be di(trimethylsilyl)butene, but the structural proof was not undertaken. In any way, the occurrence of this compound might be explained to be due to the presence of vinylacetylene which might be produced under the reaction condition.

Addition of Trichlorosilane to Vinyltrichlorosilane.—In the course of the addition of trichlorosilane to acetylene leading to the formation of di(trichlorosilyl)ethane, vinyltrichlorosilane may be considered to be an indispensable intermediate. To make the situation simpler, vinyltrichlorosilane was used as the starting material instead of using acetylene and the reaction was carried out in glass tubes according to the following consideration: in the case of cyanoethylation of trichlorosilane published preceedingly, the reaction in an autoclave in the presence of pyridine could be well reproduced in glass tubes in the presence of tetrapyridine nickel chloride. Therefore, the analogous phenomenon was expected to occur here in the reaction of trichlorosilane and acetylene. In fact, that was the case. The typical examples of the experiments were summarized in Table II. This reaction did not take place in the presence of pyridine alone, but in the presence of a catalytic amount of tetrapyridine nickel

TABLE I

PRODUCTS OBTAINED FROM THE REACTION OF ACETYLENE AND TRICHLOROSILANE IN AN AUTOCLAVE IN THE PRESENCE OF PYRIDINE

	Fraction No. 1	Calcd. for $[(CH_3)_3Si]_2C_2H_4$	Fraction No. 3	Calcd. for $[(CH_3)_3Si]_2C_4H_6$
B. p. °C[a]	71–2 (43 mmHg), 155–6		82–5 (24 mmHg)	
d_4^{20}	0.7699		0.7933	
n_D^{20}	1.4280		1.4440	
Mol. Wt.	175	174.4	195	200.4
C %	55.30	55.05	59.53	56.92
H %	12.57	12.72	11.89	12.07
Double bond per mol.	0	0	1	1
MR_D	58.26	58.43	67.10	67.22

a) All temperature are uncorrected.

5) M. Kumada and A. Habuchi, *J. Inst. Polytech., Osaka City Univ.*, 3, Ser. C, 65 (1952).

TABLE II

ADDITION OF TRICHLOROSILINE TO VINYLTRICHLOROSILANE AT 180–5°C

	Run 1	Run 2	Run 3	Run 4
$HSiCl_3$, g.	17.3	21.6	32.7	22.8
$CH_2=CHSiCl_3$, g.	22.6	24.0	38.0	25.8
Catalyst, g.	$NiCl_2 \cdot C_5H_5N \cdot HCl$, 0.2	C_5H_5N 0.1	$NiCl_2 \cdot C_5H_5N$ 0.1	$NiCl_2 \cdot 4C_5H_5N$ 0.1
Reaction time, hr.	8.0	5.4	7.3	7.5
B. p. of product, °C (mmHg)	110–5 (54)	—	111–5 (51)	111–4 (49)
Yield, %[a]	8.5	0	13	55[b]

a) The yields are based on the vinyltrichlorosilane used.

b) The chlorine content of the product was 70.4. (Calcd. for $C_2H_4Si_2Cl_6$, 71.7%).

chloride, the addition was realized to the extent of about 50 percent. The reaction product was then methylated by treating with methylmagnesium bromide and subjected to fractional distillation (Fig. 1). The physical data of two main fractions (fractions No. 3 and 9) were listed in Table III. As the lower boiling fraction (No. 3) shows physical constants which correspond closely to that described by Kumada[5], this fraction can probably be assigned as 1, 2-di(trimethylsilyl)ethane. The higher boiling fraction, which has a similar composition, may be assigned as 1, 1-di(trimethylsilyl)ethane. However, as it was generally unusual that the branched isomer has a higher boiling point than the normal one, the normal compound was synthesized according to the processes of Frisch and Young[6] as follows, and thus the structure of the lower boiling isomer was established conclusively:

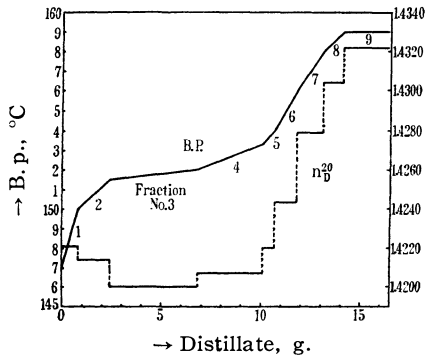

Fig. 1. Fractional distillation curve of the methylated product obtained from trichlorosilane and vinyltrichlorosilane.

TABLE III

PHYSICAL CONSTANTS AND ANALITICAL DATA OF DI(TRIMETHYLSILYL)ETHANE OBTAINED BY VARIOUS METHODS

	C[c] Fraction No. 3	C[c] Fraction No. 9	A[a]	B[b]
B. p. °C	151.5–2.0	159	150.0–0.5	150.5–1.0
d_4^{20}	0.7539	0.7808	0.7542	0.7532
n_D^{20}	1.4200	1.4322	1.4196	1.4194
Mol. Wt. in benzene	177	176	—	—
C %	55.53	54.66	54.55	55.68
H %	12.60	12.41	12.30	12.74
MR_D	58.54	57.95	58.46	58.51

a) A is the product of the reaction between acetylene and trichlorosilane in the presence of platinized asbestos.

b) B is the product obtained from acetylene via di-Grignard reagent of acetylene.

c) C is the product obtained from the reaction of trichlorosilane and vinyltrichlorosilane in the presence of tetrapyridine nickel chloride.

$$2\ C_2H_5MgBr \xrightarrow{CH\equiv CH} BrMgC\equiv CMgBr \xrightarrow{(CH_3)_3SiCl} (CH_3)_3SiC\equiv CSi(CH_3)_3 \xrightarrow{H_2,\ Pt} (CH_3)_3SiCH_2CH_2Si(CH_3)_3 \quad \text{(Table III, B)}$$

From the comparison of these physical data, the structure of the lower boiling fraction (No. 3) is established to be 1, 2-di(trimethylsilyl)ethane. Further evidence for the identity of these compounds was obtained from the comparison of infrared spectra. Although the higher boiling compound could not be compared with the authentic sample because of the difficulty of synthesis, it may be reasonably considered to be the branched isomer. For the sake of comparison, the di(trimethylsilyl)ethane which is derived from the reaction of acetylene and trichlorosilane in the presence of platinized asbestos is also listed in Table III (A).

The author refers again to the aforementioned di(trimethylsilyl)ethane which was obtained from acetylene in the autoclave in the presence of pyridine. This compound proved to be a mixture of these two isomers through comparison of physical constants and infrared spectra. But at that time it could not be fractionated into the components, owing to its small amount.

As the results of the above experiments, the author is led to the conclusion that the main reaction in this condition may be represented as follows:

$$CH\equiv CH + HSiCl_3 \longrightarrow CH_2=CHSiCl_3$$

$$CH_2=CHSiCl_3 + HSiCl_3 \longrightarrow Cl_3SiCH_2CH_2SiCl_3 + Cl_3SiCHSiCl_3 \quad (CH_3)$$

Experimental

Reaction of Trichlorosilane and Acetylene in an Autoclave.—The procedure described by Wagner and Strother[2] was followed by the author. One and a half grams of platinized asbestos[3] and 28 g. of trichlorosilane were charged into an autoclave of 100 ml. capacity. The air in the autoclave was replaced several times by acetylene, and then gradual heating was applied.

6) K.C. Frisch and R.B. Young, U.S. Pat. 2,671,099, Mar. 2 (1954); *C.A.* **49**, 2498g.

The initial pressure of acetylene was 12 kg./cm² at room temperature. The reaction started at 168°C, and the pressure at that time was 27.5 kg./cm² and decreased smoothly to the constant value of 3.2 kg./cm² at 174°C within three hours. After cooling, the contents of the autoclave was washed out by dry ether, filtered, and distilled, yielding 11.5 g. of 1,2-di(trichlorosilyl)ethane, b.p. 197–8.5°C.

In the other run, the pressure was maintained at above 15 kg./cm² throughout the operation by charging the acetylene intermittently, and the heating was stopped when the decrement of the pressure had amounted to 28 kg./cm² as a total. Distillation yielded 12.4 g. of vinyltrichlorosilane (b.p. 89.5–91.0°C) and 5.2 g. of higher boiling product.

Reaction of Trichlorosilane and Acetylene in an Autoclave in the Presence of Pyridine.—A half gram of pyridine and 55.8 g. of trichlorosilane (0.41 mol.) were charged into an autoclave of 240 ml. capacity, and treated in a similar manner as mentioned above. The reaction started at 184C° and 0.21 mol. of acetylene was consumed within 8.3 hr. Upon distilling the unreacted trichlorosilane, there remained 46 g. of a higher boiling product (Cl, 58.6%). The product was methylated in the usual manner with methyl magnesium bromide prepared from 23 g. of magnesium, and fractionally distilled through a Stedman column of about thirty theoretical plates, giving the following fractions: (1) b.p. 72°(70 mm.)–63°(27 mm.), 3.5 g.; (2) b.p. 59–76°C(23 mm.), 1.3 g.; (3) b.p. 76–88°C(23 mm.), 1.3 g.; (4) residue, 3.5 g. The first main fraction (No. 1) was purified by shaking it with concentrated sulfuric acid to remove the higher boiling unsaturated compound and by redistilling. The physical data of the purified compound are listed in Table I. The second main fraction (No. 3) was redistilled and its physical constants are also given in Table I.

Reaction of Trichlorosilane and Vinyltrichlorosilane.—Vinyltrichlorosilane was the product of Linde Air Products Co. and distilled at 89–90°C.

The reactions were carried out in sealed glass tubes and its procedure was as follows: trichlorosilane (b.p. 31.5–32.0°C), a vinylcompound, and catalyst were charged into a hard glass reaction ampoule of about 100 ml. capacity and cooled in an ice salt bath, and then the open end of the ampoule was sealed after the air had been replaced by dry nitrogen. Heating was carried out in an electric furnace equipped with an automatic controller. After cooling, the reaction tube was opened, the content was washed out with dry benzene, and the precipitate, if any, was filtered. The unreacted starting material and the solvent in the filtrate was distilled under atmospheric pressure, and then the product was distilled from a Claisen fiask under reduced pressure. The results are summarized in Table II.

The product of several runs are combined (35.4 g.) and methylated in the usual manner with methylmagnesium bromide prepared from 20.0 g. of magnesium, yielding 14.5 g. of di(trimethylsilyl)-ethane, b.p. 150–8°C (70%). It (19.2 g.) was then distilled fractionally through a Stedman column (Fig. 1). The physical data of two main fractions (No. 3 and 9) are given in Table III.

Di(trimethylsilyl)ethyne.—This compound was synthesized according to the description of Frisch and Young[6]. Into the ethereal solution of ethylmagnesium bromide prepared from 30 g. of magnesium, dry acetylene was bubbled slowly for about six hours at room temperature. After boiling for a short time and then cooling, 1 g. of cuprous chloride was added, and stirred until the gas evolution settled down. Then, 30 g. of trimethylchlorosilane was added, stirred for half an hour, and refluxed for two and a half hours. After cooling, the reaction mixture was treated with ice and diluted hydrochloric acid, and the ether layer was separated, washed with water, and dried with calcium chloride. After filtration the ether solution was distilled through a Stedman column, yielding 2.1 g. of di(trimethylsilyl)ethyne, b.p. 136.0°C; d_4^{25}, 0.7578; n_D^{25}, 1.4231; MR_D, 57.25 (calcd. 56.82).

1,2-Di(trimethylsilyl)ethane.—A solution of 2.84 g. of di(trimethylsilyl)ethyne in 10 ml. of alcohol was reduced catalytically in the presence of palladium charcoal. The amount of hydrogen absorbed was quantitative. After the removal of the catalyst by filtration, 50 ml. of water was added, and the separating oily layer was extracted with ether. The ether extract was washed with a small amout of water and dried over calcium chloride. Distillation of the ether solution yielded 1.8 g. of the crude product. The crude product was shaken twice with about equal volume of concentrated sulfuric acid and then distilled, yielding 1.0 g. of the pure 1,2-di(trimethylsilyl)ethane, b.p. 150.5–151.0°C. The physical constants and analytical data are shown in Table III (B).

Summary

The addition reactions of trichlorosilane and acetylene in an autoclave were carried out in the presence of platinized asbestos or of pyridine. In the case of the former catalyst, 1,2-di(trichlorosilyl)ethane was obtained exclusively. In the case of the latter, on the other hand, the principal product proved to be a mixture of 1,2- and 1,1-di(trichlorosilyl)-ethane.

The addition of trichlorosilane to vinyltrichlorosilane in the presence of tetrapyridine nickel(II) chloride in glass tubes also led to the formation of a mixture of two isomers. Therefore, it might be considered that the reaction processes in the autoclave in the presence of pyridine was reproduced by the reactions in glass tubes. This situation seems to be analogous to that in the case of cyanoethylation of trichlorosilane which was previously reported.

The author is much indebted to Profs. S. Murahashi and N. Hagiwara for their many helpful suggestions, and to Mr. S. Konotsune for his help in the experiments. Appreciation is also expressed to Nihon Silicon Resin Co. for their kindness in supplying the trichlorosilane.

Department of Chemistry, Faculty of Science, Osaka University, Osaka

*Synthetic Amphoteric Polypeptide. II. Synthesis and Some Properties of a Reversibly Contractile Amphoteric Polypeptide**

By Heimei YUKI, Shumpei SAKAKIBARA, Toshio TAKI and Hisaya TANI

(Received February 27, 1956)

K. H. Meyer[1] has suggested that the contraction and relaxation of muscle may be attributed to the electrostatic attraction and repulsion of ionised ammonium and/or carboxyl groups in the molecule of myosin. Recently W. Kuhn and A. Katchalsky et al.[2] have synthesized vinyl-type polyanions as such mechanochemical systems. Studies concerning these substances are, of course, very useful and instructive, but a study of polypeptide-type polyampholyte would be more desirable. In this paper the synthesis of a three-dimensional amphoteric polypeptide network composed of L-glutamic acid, L-lysine and DL-cystine residues, and some properties concerning its reversible contractility are described.

Preparation

A mixture of N-carboxy anhydrides of ε-N-carbobenzoxy-L-lysine, γ-benzyl L-glutamate and DL-cystine, the molar ratio of which was 26 : 26 : 1, was polymerized in dry chlorobenzene-pyridine mixture. Reduction of the polymer by phosphonium iodide gave the hydriodide of a linear polypeptide consisting of L-glutamic acid, L-lysine and DL-cysteine residues. The amino acid composition of this polypeptide was approximately the same as that derived from the starting monomer mixture. This linear polypeptide hydriodide was soluble in water, methanol and ethanol, and gave positive biuret and nitroprusside reactions. The free polypeptide had an isoelectric point at pH 7.4 and was insoluble in the pH range between about 5.0 and 10.0.

When the foil, made on a glass plate from the methanol solution of this linear polypeptide hydriodide, was soaked in commercial (not purified) ether overnight, it turned insoluble in water and yellowish-brown in color, due to the liberation of iodine; this color vanished by soaking in dilute alkali. This insoluble foil may be considered to be a network polypeptide, in which cysteine residues were converted into cystine ones.

Measurements of the Contractility

A piece of this foil, which was swollen in distilled water, became greatly extended in dilute acids and in dilute alkalis, and then contracted to its initial length in pure water (see Table I).

TABLE I

Immersion medium*	Parallel to the orientation: Length (×55, cm.)	Parallel to the orientation: Ratio	Perpendicular to the orientation: Length (×55, cm.)	Perpendicular to the orientation: Ratio
dry sample	1.77	1.00	4.00	1.00
in water	2.07	1.17	4.70	1.18
in 0.01 N NaOH	2.99	1.69	6.80	1.70
in water	2.30	1.30	5.42	1.36
in 0.01 N HCl	2.75	1.55	6.42	1.61
in water	2.10	1.19	4.78	1.20

* The foil was immersed in the media in descending order.

An attempt was made to give an orientation to the foil by allowing the methanol solution to flow in one direction when casting it on a glass plate, but practically no effect on the swelling was observed.

A strip, cut from the foil, was fastened at one end and a load attached to the other end. It was then immersed in various media and its length measured as a function of time.

The elongation of the strip in dilute hydrochloric acid and in dilute aqueous sodium hydroxide and its contraction in a neutral medium are shown in Fig. 1. The strip was elongated more in the alkaline than in the acidic medium, and the time required for contraction by neutralising from the alkaline solution was longer than that from the acidic solution. This time of contracting from the alkaline solution was shortened by using dilute aqueous sodium chloride as a neutral medium instead of pure water and by slightly agitating the medium. This behavior suggests that sodium ions were more strongly adsorbed on the strip than chloride ions. When the strip, which was elongated in alkaline (or acidic) medium, was soaked in an acidic (or alkaline) one, it contracted strongly momentarily and then elongated in the usual manner in the latter medium.

The lengths of the strip at various pH values from 2 to 11 are shown in Fig. 2. The minimum length was at pH 3–4 in Clark-Lubs' buffer and at pH 5 in acetate buffer. It is noticeable that the strip contracted more strongly in phthalate

* A preliminary report of the part of this paper was published in *J. Am. Chem. Soc.*, **75**, 3042 (1953).

1) K.H. Meyer, *Biochem. Z.*, **214**, 253 (1929); *Experientia* **7**, 361 (1951).

2) W. Kuhn, B. Hargitay, A. Katchalsky and H. Eisenberg, *Nature*, **165**, 514 (1950); A. Katchalsky and H. Eisenberg, ibid., **166**. 267 (1950); W. Kuhn and B. Hargitay, *Experientia*, **7**, 1 (1951); A. Katchalsky, *J. Polymer Sci.*, **7**, 392 (1951).

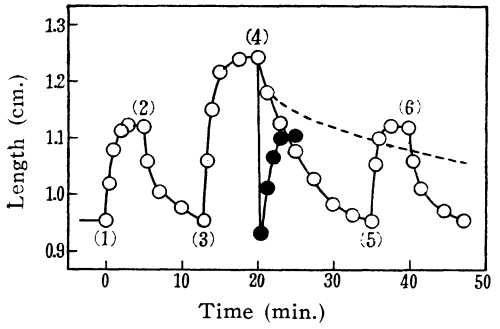

Fig. 1. Reversible lifting and lowering of a load by a strip.

Dry strip: $0.764\times0.038\times0.003$ cm^3, 0.065 mg. Load: 5.07 mg. Medium: (1) and (5), 0.005 N NaCl (15 ml.)+0.01 N HCl (3 ml.); (2) and (6), 0.005 N NaCl (18 ml.); (3), 0.005 N NaCl (15 ml.)+0.01 N NaOH (3 ml.); (4) ○, 0.005 N NaCl (slight agitation); (4) ●, 0.005 N NaCl (15 ml.)+0.01 N HCl (3 ml.); (4) dotted line, H_2O.

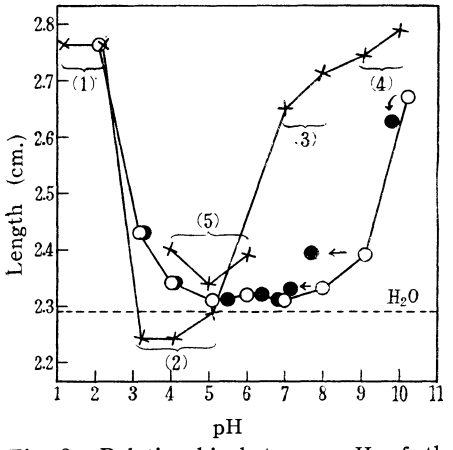

Fig. 2. Relationship between pH of the medium and length of a strip.

Dry strip: length, 1.974 cm.; weight, 0.4 mg. Load: 18 mg. Medium (70 ml.): ×, buffer solutions —— (1), HCl-KCl; (2), potassium biphthalate-NaOH; (3), KH_2PO_4-NaOH; (4), H_3BO_4-KCl-NaOH; (5), AcOH-AcONa. ○, NaOH-HCl mixtures (ionic strength 0.01). ●, After immersion of the strip.

buffer than in pure water. This behavior is supposed to be attributable to the large bulk of the bivalent phthalate ions.

In the solutions made by mixing various proportions of 0.01 N hydrochloric acid and 0.01 N sodium hydroxide, the length of the strip was a minimum at pH from 5 to 7 and the pH of the media shifted towards pH 6.5 after immersion of the strip. These results demonstrate the adsorption of sodium and chloride ions on the strip, i.e., the ion-exchange ability of the strip. The maximum pH shift was found in solution of pH 9, in which the excess of the number of sodium ions over the number of chloride ions was approximately equal to the number of carboxyl groups in the strip used, and the length of the strip reached the equilibrium value only after a very long time.

The elongation of the strip was constant in the media so acidic (i.e., pH below 2) that no dissociation of the carboxyl groups in the strip could take place.

The elongation of the strip by a load up to about two thousand times the dry weight of the strip per 1 cm. of length was measured in 0.01 N hydrochloric acid and in 0.01 N aqueous sodium chloride. The results are shown in Fig. 3. In

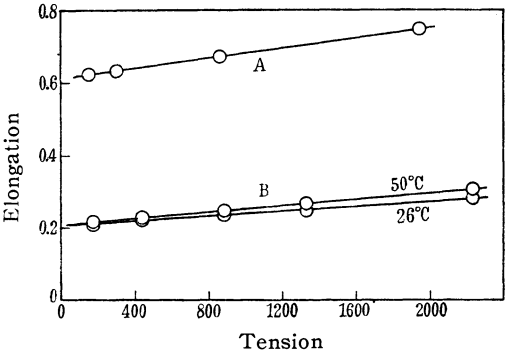

Fig. 3. Relationship between tension and elongation of a strip.

Elongation: $(l-l_0)/l_0$, where l and l_0 are the lengths of the immersed and the dry strip respectively. Tension: $W/(w_0/l_0)$, where W and w_0 are the weights of load and the dry strip respectively. A: In 0.01 N HCl at room temperature; l_0= 1.46 cm., w_0=0.30 mg. B: In 0.01 N NaCl at 26°C and 50°C; l_0=1.985 cm., w_0=0.23 mg.

these media the elongation was proportional to the weight of load; but after removing the load a slight hysteresis was observed, which vanished on prolonged standing.

The length of the strip increased slightly on raising the temperature. The relation of temperature *versus* tension, for a constant length of the strip, is shown in Fig. 4. This figure was ob-

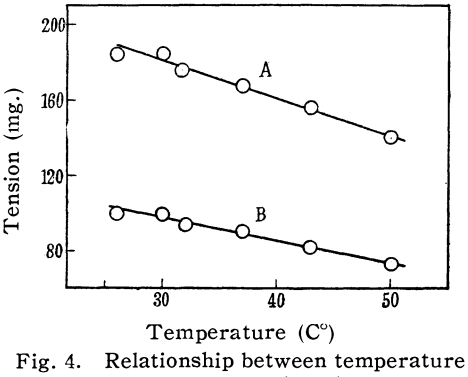

Fig. 4. Relationship between temperature and tension at constant lengths of a strip.

Dry strip: length, 1.985 cm.; weight, 0.23 mg. A: length=2.500 cm. B: length =2.450 cm.

tained graphically from the data of the measurements of load-elongation relationships at various temperatures from 20 to 50°C. It was found that the strip tends to decrease its tensile strength with increasing temperature.

It is interesting to study the effects of inorganic salts on the contractility of this strip compared with that of actomyosin.

The strip, immersed in water, was elongated by the addition of sodium chloride; the higher its concentration, the greater the elongation. The sodium chloride concentration was increased stepwise from 0.1 to 4 N and then decreased reversely. As shown in Fig. 5, the elongation

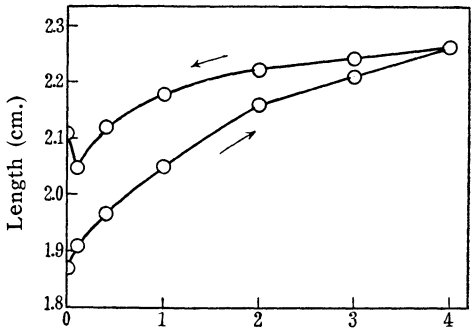

Fig. 5. Effect of concentration of NaCl on length of a strip.
Dry strip: length, 1.594 cm.; weight, 0.3 mg. Load: 18 mg.

of the strip was not reversible and its length could not return completely to its initial value. Upon immersing this strip in distilled water it was elongated. Subsequent immersion in dilute hydrochloric acid then caused it to contract rapidly, suggesting that the adsorption of sodium ions in the strip is rather strong.

The behavior of the strip in concentrated sodium chloride solution was somewhat complicated. When it was transferred directly into 4 N aqueous sodium chloride from distilled water, its length increased instantly; this was followed by a slow additional elongation proportional to the time, until the equilibrium length was approached. This elongated strip contracted now reversely by replacing it in distilled water; the rate of contraction was rapid at first and then slow (see Fig. 6).

Very striking and interesting phenomena were observed in the following series of experiments (see Fig. 6). The strip, which was elongated previously in 4 N aqueous sodium chloride as described above, contracted sharply on the addition of a small amount of dilute hydrochloric acid to the medium, and regained its original length in distilled water. When it was soaked again in 4 N aqueous sodium chloride, no change in length was observed, but on subsequent immersion in distilled water an instantaneous strong elongation and contraction was observed. On insertion of the strip into 4 N aqueous sodium chloride, it was lengthened in a manner similar to that when first immersed in this medium.

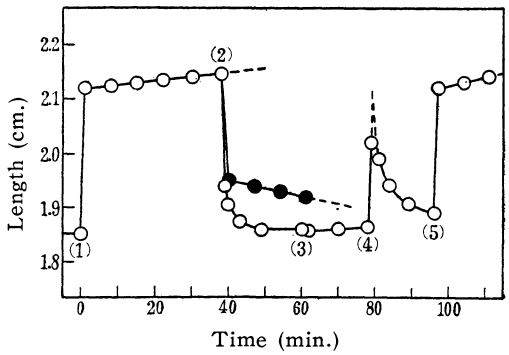

Fig. 6. Contractility of a strip in concentrated NaCl solution. I.
Dry strip: length, 1.594 cm.; weight, 0.30 mg. Load: 18.0 mg. Medium: (1), (3) and (5), 4 N NaCl; (4), H_2O; (2) ○, 4 N NaCl (15 ml.) +0.01 N HCl (3 ml.); (2) ●, H_2O.

This series of experiments was repeated by using 2 N aqueous sodium chloride (see Fig. 7).

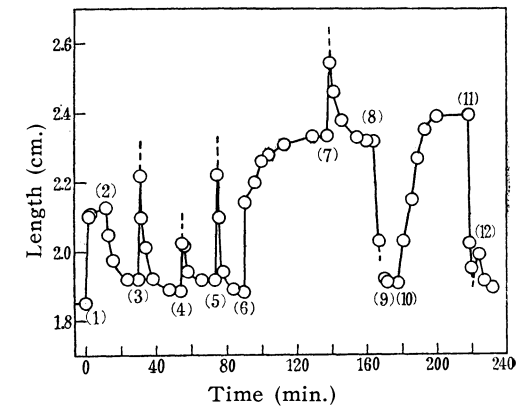

Fig. 7. Contractility of a strip in concentrated NaCl solution. II.
Dry strip: length, 1.594 cm.; weight, 0.30 mg. Load: 18.0 mg. Medium: (1), 2 N NaCl; (2) and (4), 2 N NaCl (16.5 ml.) +0.01 N HCl (1.5 ml.); (3), (5), (7), (9) and (12), H_2O; (6), 2 N NaCl (16.5 ml.)+0.01 N NaOH (1.5 ml.); (8) and (11), H_2O (16.5 ml.) +0.01 N HCl (1.5 ml.); (10), H_2O (16.5 ml.) +0.01 N NaOH (1.5 ml.).

When the strip was transferred from distilled water into 2 N aqueous sodium chloride solution containing a small amount of hydrochloric acid, an instantaneous elongation and contraction was observed. This phenomenon appeared to be an overlap of the elongation by the sodium chloride and the following contraction by the acidic sodium chloride solution.

The effect of the addition of a small amount of sodium hydroxide to aqueous sodium chloride was contrary to that of hydrochloric acid. The strip was elongated further stronger in the alkaline sodium chloride solution than was elongated in 2 N aqueous sodium chloride. Then, on soaking in distilled water, a strong elongation and

contraction was observed; but the final length of the strip was the same as that in the preceeding medium. Soaking the strip in dilute hydrochloric acid then caused it to return to the original length which it had had in distilled water. This process was similar to the contraction observed on the transfer of the strip into dilute hydrochloric acid from dilute aqueous sodium hydroxide (see Fig. 7).

A series of immersion media was prepared by dissolving various amounts of sodium chloride in 0.005 N hydrochloric acid, and the length of the strip was measured in these media (see Fig. 8). Though at the lower concentration (i.e., below 0.1 N) of sodium chloride the length of the strip was somewhat longer than that in hydrochloric acid alone, the strip contracted with an increase in the concentration of salt, and at the higher concentration (i.e., above 0.1 N) the extent of contraction was proportional to the logarithm of the concentration. This behavior is contrary to that in neutral sodium chloride solution.

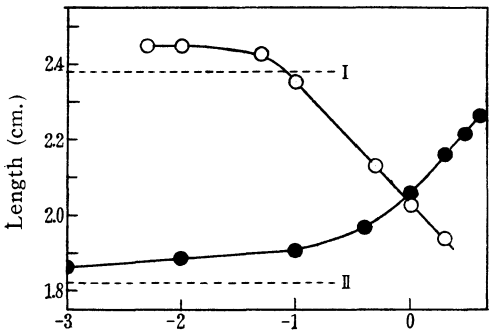

Fig. 8. Length of a strip in acidic and neutral NaCl solution.
Dry strip: length, 1.594 cm.; weight, 0.30 mg. Load: 18.0 mg. ○, Solution of NaCl in 0.005 N HCl. ●, Aqueous solution of NaCl. Dotted lines I and II represent the lengths of the strip in 0.005 N HCl and water, respectively.

The effects of neutral inorganic salts containing bivalent ions are shown in Fig. 9. The length-concentration relationships were similar for $CaCl_2$, $MgCl_2$, Na_2SO_4 and $(NH_4)_2SO_4$ solutions to that for aqueous sodium chloride. On the contrary, the strip contracted in aqueous $CuSO_4$ and in aqueous $ZnCl_2$ at the concentrations below and above 0.1 N respectively, and very strongly in aqueous $HgCl_2$ at the whole concentration tested. Since it has been known that these metal ions (Hg^{++}, Cu^{++} and Zn^{++}) are capable of forming complexes with amino groups and particularly that Hg^{++} ion can combine strongly with sulfur atoms, the contraction of the strip in these solutions appears to be due to the formation of cross-linkages of these complexes. In aqueous $KHCO_3$ the strip was elongated strongly as a result of its alkalinity. The strip was also slightly elongated with increasing temperature in all these salt solutions.

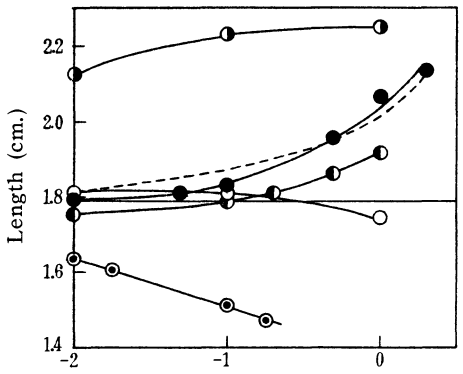

Fig. 9. Effects of various salts on length of a strip.
Dry strip: length, 1.47 cm.; weight, 0.30 mg. Load: 19.5 mg. ●, $CaCl_2$; ○, $ZnCl_2$; ◐, $CuSO_4$; ⊙, $HgCl_2$; ◑, $KHCO_3$; dotted line, NaCl. $MgCl_2$, Na_2SO_4, $(NH_4)_2SO_4$ gave curves similar to that for $CaCl_2$.

Discussion

W. Kuhn and A. Katchalsky et al.[2] reported with their three-dimensional polyanion network that a statistical consideration concerning the entropy of a three-dimensional network and considerations concerning the electrostatic energy of the ionised system are required for the theoretical treatment of the elongation and contraction phenomena. S. Asakura[3] and H. Noguchi[4] stated that the entropy force of counter-ions bound by the system plays a predominant role, tending to expand the system against the rubber-like elastic force.

In this experiment the phenomena shown by the strip-form polyampholyte system was, as expected, more complicated than that shown by the polyanion system. Contrary to the polyanion system, the strip of this amphoteric polypeptide decreased its restoring force with increasing temperature. This fact shows that at a given temperature the internal energy and the entropy increase with the elongation of the strip: that is,

$$(\partial E/\partial l)_T > 0 \quad \text{and} \quad (\partial S/\partial l)_T > 0$$

in the relation

$$K=(\partial E/\partial l)_T-T(\partial S/\partial l)_T$$
$$=(\partial E/\partial l)_T+T(\partial K/\partial T)_l$$

in which K, E, S, l, and T represent restoring force, internal energy, entropy, length and absolute temperature respectively.

It appears that there are some cross-linkages in the foil in addition to the cystine -S-S- linkages and that the number of the

3) S. Asakura, *Busseiron Kenkyu*, **62**, 39 (1953).
4) H. Noguchi, ibid., **62**, 30 (1953).

former changes with the increase and decrease of temperature by their rupture and reformation. Such linkages might include the salt linkages between carboxyl and ammonium ions and the hydrogen bonds between two amide linkages. This consideration is supported also by the strong elongation of this strip in concentrated salt solutions and by both the viscosity increase and the insolubility of synthetic linear polypeptide, reported in the preceeding paper[5], in neutral region. Furthermore, it was found that synthetic high molecular copoly-1 : 1-(L-glutamic acid, L-lysine)[5], which was insoluble in distilled water, could be dissolved in concentrated sodium chloride solution. The solubility and the viscosity behavior of these linear amphoteric polypeptides is closely related to the contractility of this strip and qualitatively coincide with it.

As found in most instances, the strip adsorbed cations more strongly than anions. This difference in adsorption appears to be caused by reasons such as the decrease in the number of amino groups during the formation of the foil, but the true reason remained unknown. The difference in the hydrations of cations and anions is also considered to be concerned with the above behavior of the foil. Although no satisfactory conclusion could be obtained, since the phenomena are too complicated, the contractility of this foil, e. g. the rapid elongation and contraction of the strip found in some instances, is very interesting as compared with the behavior of actomyosin.

Experimental

N, N'-Dicarbobenzoxy-cystine.—This was synthesized from L-cystine according to the Bergmann's method[7], but showed no optical rotation in acetic acid probably due to the racemisation during the reaction. Recrystallized from acetone-chloroform, it combined 1/4 mol. of chloroform m.p. 101–103° (sintered from 80°C).

Anal. Found: C, 49.83; H, 4.71; N, 5.14; SO_4 and Cl, 40.53. Calcd. for $C_{22}H_{24}N_2O_8S_2 \cdot 1/4\ CHCl_3$: C, 49.63; H, 4.54; N, 5.20; SO_4 and Cl, 40.63% (S and Cl were measured by Stragand's method[8] and obtained as the sum of converted SO_4 and Cl).

DL-Cystine Bis-(N-carboxy-anhydride). — To the solution of 2 g. of dicarbobenzoxy-cystine in 12 ml. of dry dioxane 4.4 g. of phosphorus pentachloride was added. After shaking for 15 min. at 10°C, the mixture was filtered and heated for one hour at 40°C. The crystallized anhydride was filtered and washed with ethyl acetate. Yield 1.0 g., colorless needles. m.p. 134° (decomp.). It contained 1 mol. of combined dioxane.

Anal. Found: C, 38.04; H, 4.18; N, 7.31; S, 16.65. Calcd. for $C_8H_8N_2O_2S_2 \cdot C_4H_8O_2$: C, 37.90; H, 4.24; N, 7.37; S, 16.84%.

Copolymerization.—A mixture of 2.104 g. (8.0 m mol.) of γ-benzyl N-carboxy-L-glutamate anhydride[5], 2,448 g. (8.0 m mol.) of ε-N-carbobenzoxy-L-lysine anhydride[5] and 0.117 g. (0.308 m mol.) of DL-cystine bis-(N-carboxy-anhydride) in 42 ml. of chlorobenzene and 3 ml. of dry pyridine was heated rapidly to 100°C in a sealed glass tube until in solution, and then kept for ninety hours at 50°C and for ten days at room temperature. The solution gradually increased in viscosity and finally became an opalescent gel. The polymer, precipitated by adding petroleum ether, was allowed to swell in acetone, and after reprecipitating by petroleum ether, it was obtained as a white powder. Yield 3.890 g. (99% of the theor.).

Anal. Found*: C, 63.86; H, 6.54; N, 8.70. Calcd. for $[26(C_{12}H_{13}NO_3), 26(C_{14}H_{18}N_2O_3), (C_3H_8N_2O_2S_2)]_n$: C, 64.37; H, 6.45; N, 8.81%.

The polymer swelled in chloroform, acetone, pyridine, dioxane, tetrahydrofuran, and hot glacial acetic acid, but could not be dissolved.

Reduction of the Polymer.—After 0.7 g. of the polymer was swelled by heating in 50 ml. of glacial acetic acid, 1.7 g. of phosphonium iodide was added in portions during five hours at 55°C, with dry hydrogen bubbling through the solution. The supernatant liquid was separated from the resultant precipitate by decantation, and a small amount of absolute alcohol was added. This dissolved the major part of the precipitate, but some swollen material remained. The polymer was reprecipitated from the solution by freshly distilled ether and was then extracted repeatedly with water. The extracts were combined and were concentrated in vacuo at 40°C. The polypeptide hydriodide was precipitated from the residual syrup by adding ethanol and ether, washed with ether and dried. White powder; yield 0.27 g. (48% of the theor.). It was soluble in water, methanol, and ethanol, and gave positive biuret and nitroprusside test.

Anal. Found: C, 33.77; H, 5.25; N, 10.83; I, 32.1; amino-N, 3.46. Calcd. for $[26(C_5H_7NO_3), 26C_3H_{12}N_2O \cdot HI), 2(C_3H_5NOS)]_n$: C, 34.25; H, 5.23; N, 10.96; I, 32.3; amino-N, 3.56%.

Preparation of the Foil.—The foil was made on a parraffin-treated glass plate by casting a 2 % methanol solution of the above polypeptide hydriodide. After immersing overnight in commercial ether, the foil became orange-yellow in color and turned insoluble, but swelled in water. This foil gave no nitroprusside test, and was quite flexible and strongly elastic in water. It was decolorised by soaking in dilute alkali, and, after washing with dilute hydrochloric acid and water, it was contracted easily by alcohol and ether, and dried.

The powdered polypeptide hydriodide was treated with commercial ether as before and then

5) H. Yuki, S. Sakakibara and H. Tani, This Bulletin, 29, 654 (1956).
6) H. Yuki and H. Tani, Unpublished.
7) M. Bergmann and L. Zervas, *Ber.*, 65, 1192 (1932).
8) G.L. Stragand and H.W. Safford, *Anal. Chem.*, 21, 625 (1949).

with 0.001 N sodium hydroxide, washed with water, ethanol and ether, and dried. This substance contained a small amount of combined sodium.

Anal. Found: C, 49.99; H, 7.12; N, 14.77; Na, 3.92. Calcd. for $[16(C_5H_7NO_3), 10(C_5H_8NO_3 \cdot Na), 26(C_9H_{12}N_2O), (C_8H_8N_2O_2S_2)]_n$: C, 49.28; H, 6.98; N, 15.75; Na, 3.24%.

Swelling of the Foil (Table I).—A piece of the foil was immersed in the media and its length was measured by photographs (magnification 55×), taken after one hour of immersion.

Elongation and Contraction of the Strip.—The strips used for measurements were 1.5–2 cm. in length, 0.04–0.07 cm. in width, and 0.2–0.5 mg. in weight. Assuming the specific gravity to be approximately equal to unity its thickness was about 0.003 cm.

Glass clips were attached to the two ends of the strip. The upper clip was fastened to the hook of a glass rod. The lower clip was used itself as a load, and, if necessary, also used for hanging platinum rings, varied according to the desired additional load. The strip was immersed in the medium in a large test tube, held in a thermostat. The upper end of the strip was fixed and the change of the length was followed with a microscope.

To obtain the reproducibility the measurements were made after training the strip to elongate and contract, using successively dilute aqueous NaOH, water, dilute HCl and water. By this training the strip came to a constant length in a given medium. In most cases either the length of the strip in distilled water or that in dilute aqueous sodium chloride was used as a standard, from which each experiment was started. The strip was used in each experiment after recovering its standard length by washing it with dilute hydrochloric acid and then with water in order to remove any of the rather strongly adsorbed cations. The measurements were made at 25°C unless otherwise stated.

Summary

1. A reversibly contractile amphoteric polypeptide, copoly-26 : 26 : 1-(L-glutamic acid, L-lysine, DL-cystine), was synthesised.

2. The foil of this polypeptide contracted at its isoelectric region and extended in both acidic and basic media. This extension and contraction was pH-dependent and fully reversible.

3. The load-elongation relation of the strip of this foil was measured in aqueous media using the load up to about 2,000 times the dry weight per 1 cm. of length of the strip. This relation was linear in this range.

4. The temperature-elongation relation was measured in aqueous media at 20–50°C. From the data it was concluded that, at a given temperature, the internal energy and entropy increased with the elongation of the strip.

5. The change of length of the strip in aqueous media, containing hydrochloric acid, sodium hydroxide, sodium chloride and some other neutral salts individually or in pairs, was measured. Some peculiar and interesting phenomena were observed.

The authors express their hearty thanks to Prof. S. Akabori and Prof. S. Murahashi for their interest and encouragement throughout the work, to Dr. M. L. Huggins for reading the manuscript, and to Mr. Y. Hozumi and Miss S. Mori for a part of the experimental work. This research was financially supported by the Institute for Fibre Research and The Asahi Press.

Department of Chemistry, Faculty of Science, Osaka University, Osaka

Spectrophotometric Microdetermination of Arsenic in Natural Waters and its Application to Silicate and Biological Materials

By Ken SUGAWARA, Motoharu TANAKA and Satoru KANAMORI

(Received February 20, 1956)

Introduction

Ordinary natural waters are usually very poor in arsenic. As shown later, well water on the Higashiyama campus of Nagoya University contains only 0.4 μg./l. of this element and the sea water off Sugashima Island in Ise Bay contains 1.8 μg./l. For determining arsenic in such dilution, various methods[1,2,3] already proposed are not satisfactory. Some are liable to be contaminated, thus causing a considerable error while others are of low sensitivity. The neutron activation method by Smales and Pate[4] which boasts the highest sensitivity is usable only to those to whom a nuclear reactor is accessible.

After considering these points and closely examining the merits and defects of the current methods, the writers finally succeeded in establishing the following time-saving method fulfilling every requirement for water analysis with fair accuracy.

Our method consists of five steps; (a) coprecipitation with ferric hydroxide, (b) mineralization of the filtered precipitate, (c) extraction of arsenic xanthate by carbon tetrachloride, (d) oxidation of the xanthate into quinque-valent arsenic followed by extraction by water, and (e) final spectrophotometry of the extracted element as molybdenum blue.

Thus, usually using 3 l. of the sample, 2 μg. of arsenic can be safely determined with an error of only 5%. With appropriate pretreatment, the method is also applicable to silicate and biological materials.

Experimental

Reagents.—*Ferric Chloride.*—4.84 g. of arsenic-free ferric chloride ($FeCl_3 \cdot 6aq.$) is dissolved in 25 ml. of sulfuric acid and diluted to 100 ml. This solution contains 10 mg. of iron per ml.

Bromcresol Purple.—0.1% W/V solution.

Ammonia (1 : 3).—Reagent quality.

Nitric acid.—Reagent quality, freshly distilled.

Sulfuric acid.—Reagent quality, arsenic free.

Potassium iodide.—25% W/V solution.

Sodium thiosulfate.—5% W/V solution.

Carbon tetrachloride.—Reagent quality.

Potassium xanthate.—0.1% W/V solution, reagent quality.

Carbon tetrachloride containing bromine (1 : 25).—One part of bromine is mixed with 25 parts of carbon tetrachloride.

Sulfuric acid (1 : 9).

Ammonium molybdate.—2% W/V solution, reagent quality.

Hydrazine sulfate.—0.1% W/V solution, reagent quality.

Arsenic standard solution.—0.132 g. of arsenous oxide is dissolved in 2 ml. of 1 N sodium hydroxide solution, slightly acidified with dilute sulfuric acid, and diluted to 100 ml. This solution contains 1.00 mg. of arsenic per ml. A working standard solution is prepared by adequately diluting this solution.

Apparata.—Automatic Filtering Apparatus (Fig. 1).—This apparatus consists of three parts: a funnel (A), its receptacle (B), and a siphon (C).

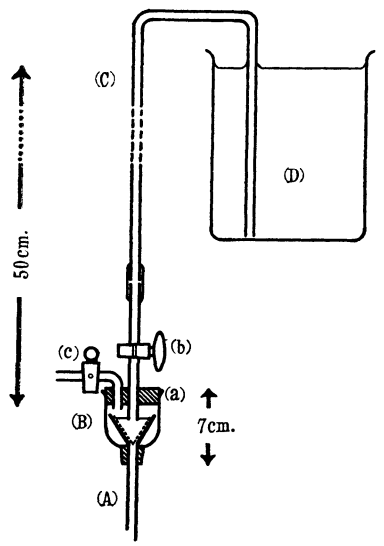

Fig. 1. Automatic filtering apparatus.

The funnel with a filter paper is fixed in the receptacle. A rubber stopper (a) with two leading tubes (b and c) is then tightly fixed into the mouth of the receptacle and the upper end of tube (b) is connected to the end of one of the arms of the siphon. Filteration is carried out as follows: Cocks (b and c) are opend and lips are placed to the end of tube (c) to gently suck,

1) R. Pieruccini, *Spectrochim. Acta*, 4, 189-99 (1950).
2) M. Ishibashi, T. Shigematsu, Y. Nakagawa and Y. Ishibashi, *Bull. Inst. Chem. Research Kyoto Univ.*, 24, 68 (1951).
3) A.K. Klein and F.A. Vorhes, Jr., *Assoc. Offic. Agr. Chemists*, 23, 121-30 (1939).
4) A.A. Smales and B.D. Pate, *Analyst*, 77, 188-95 (1952).

while the stem-end of the funnel is closed with a finger. When the liquid in vessel (D) flows down to the end of tube (b), both cocks are closed. Then the cock (b) is opend and the liquid is allowed to drop down into the funnel. Filtration continues under automatic control by the pressure change in the closed receptacle. Thus when the water level difference is kept at 50 cm., liquid continues to filter at a rate of about 500 ml. per hr.

Digestion Apparatus[5] (Fig. 2).—This apparatus

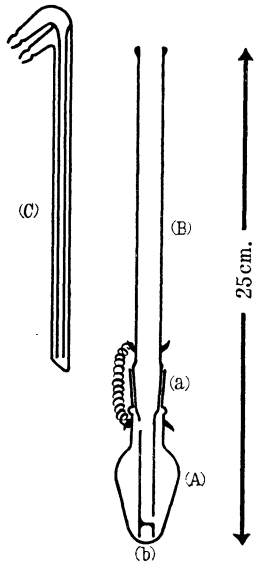

Fig. 2. Digestion apparatus.

consists of three parts: a digestion flask (A), a chimney (B), and a Schirm's[6] condenser (C). The chimney is so designed as to fit into the mouth of the digestion flask with ground joint (a). The small elongation of the chimney extending into the flask has a septum near its opening (b) bearing a small air space. When the chimney is fixed and the liquid in the flask is heated to boiling the open space immersed in the liquid continuously supplies air bubbles whereby bumping is avoided so that boiling continues smoothly. The chimney elongation has two openings, one near the mouth of the flask and the other just above the septum, through which the vapour evolving in the flask is led into the chimney where it is cooled and condensed by the previously inserted Schirm's condenser.

Procedure.—Co-precipitation.—To a suitable amount of the sample containing 1–5 μg. of arsenic, 1 ml. of ferric chloride solution is added per liter. After warming to 70–80°C, the solution is neutralized with ammonia (1 : 3) using bromcresol purple as indicator. While stirring vigorously, 1 ml. of the same reagent is added in excess per liter of the solution. When the solution is sufficiently cooled, the ferric hydroxide precipitate is filtered off through the automatic filtering apparatus just described.

5) M. Tanaka and S. Kanamori, *Anal. chim. Acta* **14**, 263 (1956).

6) E. Schirm, *Z. anorg. Chem.*, **25**, 1225 (1912).

Mineralization—The filter paper with precipitate is placed in the digestion flask and the chimney with Schirm's condenser is fixed in the flask. Gradually 2 ml. of nitric acid and 5 ml. of sulfuric acid are successively added through the chimney. A violent reaction occurs. When the reaction slows down, the contents of the flask are digested for 1–3 hr. During this digestion period repeated additions of nitric acid in small portions are necessary to avoid carbonization. After completion of mineralization, the contents of the flask are transferred into a quartz evaporating dish and heated on a water bath to drive off the excess nitric acid.

Extraction.—The residual solution in the dish is transferred into a 100 ml. beaker. After dilution with 25 ml. of water, it is warmed on a water bath and 2 ml. of potassium iodide solution added. After the solution is left to cool sufficiently for about thirty min., sodium thiosulfate solution is added with care in order to remove the liberated iodine. Any excess addition of the reagent must be avoided. Then the solution is transferred into a 100 ml. separatory funnel to which 5 ml. of potassium xanthate solution and 3 ml. of carbon tetrachloride were previously added. The funnel is vigorously shaken for two min. When carbon tetrachloride layer separates on the bottom, it is drawn out into a 25 ml. separatory funnel. The carbon tetrachloride extraction is repeated with 5 ml. of potassium xanthate solution and 3 ml. of carbon tetrachloride, and this second extract is joined to the first.

It is often the case that a part of the carbon tetrachloride is emulsified into numberless small droplets, their unification being difficult. This difficulty, however, is easily solved by filtering through a cotton plug 1 mm. thick placed at the bottom of the funnel. The droplets are united by passing through the plug and running down to form larger drops associated with some considerable amount of water. This water can be completely removed by repeated separatory funnel treatment.

To the joined carbon tetrachloride extract, are added 1.2 ml. of sulfuric acid (1 : 9), 2 ml. of water and one or more of carbon tetrachloride containing bromine (1 : 25), to give a deep red color to the organic layer. After thorough shaking, the funnel is left to stand until two perfectly separate layers form. A greater part of the oxidized arsenic has gone into the acid layer. The bottom carbon tetrachloride layer is separated into another 25 ml. separatory funnel and shaken with 3 ml. of water to remove the last trace of arsenic in carbon tetrachloride by the water. The acid extract and the water extract are united and washed with two portions of 3 ml. of carbon tetrachloride to remove the remaining bromine. Then the joined extract is transferred into a 10 ml. measuring flask. The separatory funnels are washed with 3 ml. of water and this washing is also added to the flask.

Determination.—After first adding 0.4 ml. of ammonium molybdate solution and 0.4 ml. of hydrazine sulfate solution and then making it up

to 10 ml., the flask is kept in boiling water for thirty min. and then cooled with tap water. Now the extinction measurement is made using a wave length greater than 700 mμ, preferably 840 mμ. The value obtained is corrected by referring to the value of a blank test which was conducted, omitting no step of the procedure. Finally the amount of arsenic is determined by referring to a standard curve constructed by using various known amounts of arsenic.

Discussion

In the analysis of minute quantities of arsenic, special care must be paid to avoid the slightest contamination. Glass and enamel vessels are sources of considerable contamination, particularly when they are warmed in the process of evaporation or co-precipitation. The following experiment proved this: 100 ml. of 1 N suluric acid was put in each of three beakers, glass, enamel, and porcelain, of equal size. They were heated on an electric plate for thirty min. Then the arsenic from each beaker was determined with the result that 2 μg., 50 μg., and below 0.1 μg. were the arsenic values for glass, enamel, and porcelain beakers respectively. Thus a porcelain vessel is recommended as the best for our purpose.

The reason why co-precipitation with ferric hydroxide was adopted is that it suffers the least from contamination and also saves considerable time when compared with evaporation.

Ferric hydroxide, however, co-precipitates not only dissolved arsenic but also other suspended particulates which might contain combined arsenic. Therefore the obtained arsenic value indicates the total amount of arsenic.

The recovery of tri-valent and quinquevalent arsenic in the co-precipitation process was separately examined as follows: Various quantities of each arsenic species were dissolved in 1 l. of water and co-precipitated with 10 mg. of ferric hydroxide. The precipitate filtered off through a fine glass filter was dissolved in dilute sulfuric acid and determined according to the prescribed procedure. The results given in Table I show that the recovery is between 98 and 100%. The experiment also proved that 10 mg. of ferric hydroxide is sufficient to complete co-precipitation of arsenic in ordinary waters even if they contain other substances susceptible to ferric hydroxide co-precipitation.

The optimum pH for the co-precipitation is around 9 and in order to bring the pH of the solution up to this value, approximately 1 ml. of ammonia (1: 3) must be added in excess beyond the neutral point for bromcresol purple. The addition must be made with vigorous stirring so that a uniform shifting of pH is ensured.

TABLE I

CO-PRECIPITATION OF ARSENIC WITH FERRIC HYDROXIDE

Fe used mg.	As^{III} added μg.	As^{III} co-pptd. μg.
10	2	1.9
10	5	5.2
10	100	97
10	1000	990
Fe used mg.	As^{V} added μg.	As^{V} co-pptd. μg.
10	2	2.1
10	5	4.8
10	100	98
10	1000	990

As for extraction of tri-valent arsenic, it is complete even with an acidity of 1 N sulfuric acid so long as co-existing elements are poor. With an increase of such elements, the pH range for a complete extraction is narrowed, a fact by the consideration of which the writers adopted an acidity of 6 N sulfuric acid in the present procedure.

Fig. 3 shows interferences with the extraction of arsenic xanthate by various elements.

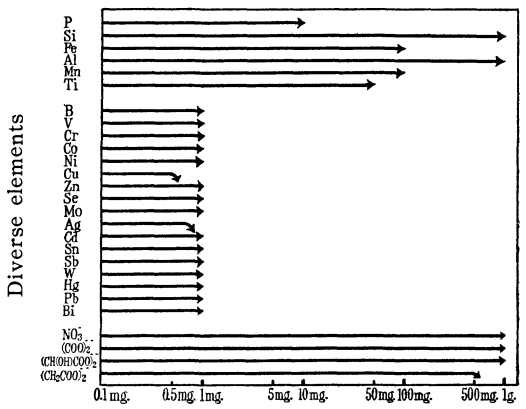

Fig. 3. Interferences of diverse elements.

Straight arrows indicate interference ranges no greater than 3%. A greater interference is first visible at the points where arrows begin to bend. Downward bending indicates a negative interference greater than 3%.

It is remarkable to find that phosphorus and silicon show no considerable interference despite the fact that they are likely to develop the same molybdenum blue as arsenic.

The interferences by alkalis, alkaline earths, aluminum, manganese, zinc, cadmium, vanadium, and boron cause no greater error than the minor unavoidable error straying in through mechanical treatment.

If selenium is in the original sample, it is reduced into metal partly during the course of potassium iodide treatment and in part in the hydrazine sulfate treatment. The first selenium metal can be easily removed by filtering off through a cotton plug similar to that used in the treatment of carbon tetrachloride droplets, while the second metallic selenium can be removed by adding a small amount of carbon tetrachloride and shaking.

The results of application of the method are given in Table II. They show the quantitative recoveries of arsenic which was previously added to the original sample.

TABLE II
EXAMPLES OF APPLICATION

Description	Sample taken	As added	As found
Ground water from a well on the campus of Nagoya Univ.	5 l.		2.1 μg.
	5 l.	10 μg.	12.0 μg.
Sea water at Sugashima Is., Mie pref.	2 l.		3.3 μg.
	2 l.	10 μg.	13.6 μg.
Serpentine (Sugashima Is., Mie pref.)	1 g.		0.4 μg.
	1 g.	5 μg.	5.6 μg.
Bottom deposit of Aburagafuchi, a brackish lake, Aichi pref.	1 g.		7.7 μg.
	1 g.	5 μg.	12.5 μg.
York	4.6 g.		0.6 μg.
	4.6 g.	5 μg.	5.4 μg.

Application to Silicate and Biological Materials

Silicate Materials.—To 0.5–1 g. of powdered silicate material weighed in a nickel crucible, 0.5 g. of sodium hydroxide and 1 ml. of water are added and placed on a water bath. When completely dried out, 0.5 g. of sodium peroxide and 2 g. of fused sodium hydroxide are successively added and the crucible is quickly covered with a lid. A violent reaction occurs. When the reaction is over, the crucible is heated to dull-red for 0.5–1 hr. until decomposition is supposed to be complete. The melt is digested with 20 ml. of water and then neutralized with 9 ml. of sulfuric acid (1 : 1). Disregarding any separation of silica, the solution is acidified with 5 ml. of sulfuric acid and processed according to the prescribed procedure.

Biological Materials.—A suitable amount of a biological material is first decomposed in the digestion apparatus. Then the digest is processed to the prescribed procedure.

Results of application of the method to silicate and biological materials are also given in Table II.

Chemical Institute, Faculty of Science
Nagoya University, Nagoya

On the Transport Number for Ion-exchange Resin Membranes

By Yoshio Oda and Tadashi Yawataya

(Received February 24, 1956)

Introduction

The ionic permselectivity of ion-exchange resin membrane has been expressed quantitatively by means of a transport number defined as the fraction of current carried by either cations or anions through it. The transport number for a membrane is generally computed from the membrane potential measurement which arises at a membrane separating two solutions of different concentrations. In this case, the Nernst's equation is generally used for correlating the membrane potentials with the transport number.

$$n_+ = \frac{1}{2}\left(1+\frac{E_{obs}}{E_{th}}\right) \quad (1)$$

$$E_{th} = \frac{RT}{nF} \ln \frac{a_2}{a_1} \quad (2)$$

n_+: transport number (*t. n.*) of cations

E_{obs}: observed value of membrane potential

E_{th}: calculated value of membrane potential by use of Eq. (2)

a_1, a_2: activities of the solutions separated by the membrane. R, T, n, and F have their usual significances.

If an ion-exchange membrane is subjected to an electric field in an electrolyte solution, movement of a definite amount of solvent occurs simultaneously with ion transference[1]. Since the Nernst's equation holds in the case where only ion transference is considered, a correction should be made for the transport number in Eq. (1). This is identical with the "Hittorf transport number", which is calculated from the changes in concentra-

1) Y. Oda and T. Yawataya, This Bulletin, 28, 263 (1955).

tion of solution after the passage of the current, without taking account of transport of solvent molecules, and consequently expressed in terms of ionic velocities relative to an imaginary plane moving with the same speed as the solvent.

The errors arising from neglecting the solvent transference were already remarked by A. J. Staverman[2], and G. Scatchard[3], but experimental proof has not yet been reported.

As for the case of ion-exchange resin membranes, the difference between the Hittorf- and true-transport number is comparatively large and plays a very important role for practical applications.

In the present report, the Hittorf- and true-transport numbers of the various cation-exchange resin membranes were determined in sodium chloride solutions and the differences between them were discussed in view of electro-osmotic water transfer.

Experimental

Membranes.—Strong acid cation-exchange resin membranes of sulfonated type, the thickness being about 0.5 and 1.0 mm., and the water contents ranging from 30 to 60%. Prior to the measurement, membranes were thoroughly equilibrated with the solutions to be used. When a membrane is required to be interposed between two solutions of different concentration, as is the case with the membrane potential measurement, it had been equilibrated with the more dilute solution of the two. In such a case at least thirty minutes were needed to attain a stationary state after setting the membrane in the cell.

Hittorf Transport Number.—The potential was measured for a cell shown in Fig. 1, consisting of two glass half cells, a sample membrane, and calomel electrodes. Temperature was regulated at 25±0.2°C.

Calomel electrode	Satd. KCl soln.	NaCl soln. (m_1)	Membrane	NaCl soln. (m_2)	Satd. KCl soln.	Calomel electrode

Fig. 1.

The membrane potential was obtained by making a correction for the liquid junction potential at the boundaries, KCl (satd.) | NaCl (m_1) and NaCl (m_2) | KCl (satd.). This correction amounted to several millivolts under the conditions prevailing in the present experiments. From the membrane potential thus measured, the Hittorf $t.n.$ was computed by the Eq. (1).

Although it is desirable to correlate the $t.n.$ with the concentration of a solution, the measurement above described has to be made for a membrane placed between two solutions of different concentration. In order to obtain the $t.n.$ as a function of a single concentration, an interpolating method was employed as follows. At first, fixing the concentration of a solution in one side of the cell constant, which being a parameter, membrane potentials were measured employing solutions of various concentrations in another side. And, as shown in Fig. 2 the $t.n.$ computed therefrom

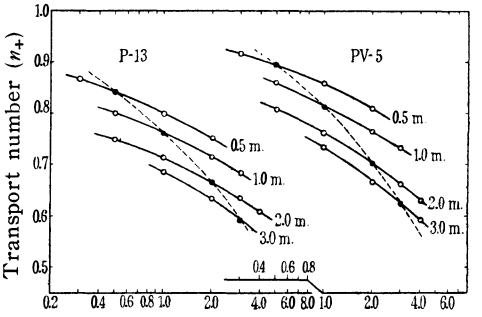

Conc. of NaCl-soln. (molality)

Fig. 2. Transport numbers for cation-exchange resin membranes, determined from membrane potential measurements.

were plotted on a diagram against the varied concentrations respectively for each parameter. Then the $t.n.$ corresponding to a single concentration can be obtained by interpolating the curve to a point where the reading of the parameter and the abscissa coincides. In Fig. 2, these points are shown by black solid circles connected with a dotted line.

True Transport Number.—A cell made of methyl metacrylate resin was used (Fig. 3). The effective area of a membrane was 4.0 cm². A stirrer was provided in each compartment to keep the solutions as uniform as possible.

Prior to an experiment, the sodium chloride solution was filled in the cell to equilibrate the membrane with it. After the solution was taken out, the remaining solution on the cell wall was wiped out clean with filter paper. A weighed amount of the sodium chloride solution (W_S g.; NaCl: m_S mol.) of the same concentration as previously used, was put in the cell, and silver-silver chloride electrodes (weight of the cathode being W_E) were inserted. Then the circuit was closed, iodine coulometer being connected in series. After a certain amount of electricity (Q coulomb) passed, the solution in the cathode compartment and the cathode itself were taken out separately in dried weighing bottles and their weights were measured rapidly. Let the weight of cathode in wet state be W_E', and that of the solution W_S'. Next, the solution remaining on the cell wall and the membrane inside the cathode cell was blotted rapidly but cautiously with filter paper, and was titrated for chloride ion with silver nitrate standard solution (NaCl: m_S''). Sodium chloride in

2) A. J. Staverman, *Trans. Faraday Soc.*, **48**, 176 (1952).
3) G. Scatchard, *J. Am. Chem. Soc.*, **75**, 2883 (1955).

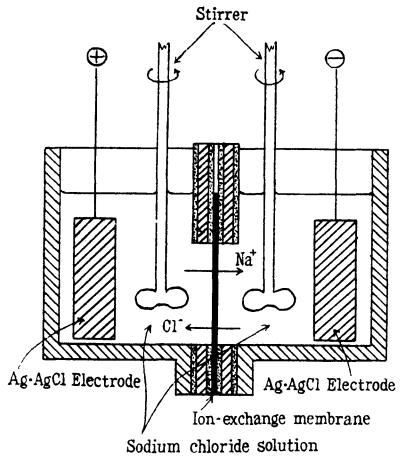

Fig. 3. Apparatus for measuring true transport number.

the main solution taken out from the cathode compartment (m_S') and that imbibed in the cathode material (m_E') were also determined by titration.

Then the material balance in the cathode cell is shown as follows.

NaCl increase $(\Delta m)=(m_S'+m_E'+m_S'')-m_S$

Total weight increase $(\Delta W)=(W_S'+W_E'+W_S'')-(W_S+W_E)$, where, $W_S''=W_S'\cdot\frac{m_S''}{m_S'}$.

From these, the true transport number and the amount of transferred water are computed by the next equations.

$$n_+'=\frac{\Delta m}{Q/F} \tag{3}$$

$$\beta_W=[\Delta W-\Delta m\times M_{Na}+(Q/F-\Delta m)\times M_{Cl}]/Q \tag{4}$$

M_{Na}, M_{Cl}: atomic weight of sodium-and chloride ion

The electrolysis was carried out for about thirty to sixty minutes with the current density of 5 A/dm². By preliminary experiments it was ascertained that the *t. n.* was scarcely dependent on current density over the range from 1 to 6 A/dm².

Since the surface of the solution was inevitably exposed to the atmosphere during the experiment, the amount of water that might be lost by evaporation was not negligible. For this correction, the rate of water evaporation was measured for the same solution in an other vessel.

The β_W computed from the Eq. (4) is the amount of water transferred by one coulomb, i.e. the electro-osmotic water exclusive of solute. In the following part of this report, there will be discussed the relation between β_W and β, volume of transferred solution per unit coulomb, which was determined volumetrically in the previous report[1].

Water Content, Fixed Ion Concentration and the Donnan Absorption.—For the discussion on the transport numbers, measurements were made on water content, fixed ion concentration, along with the concentration of non-exchangeable ions absorbed in membrane due to the Donnan equilibrium, for each membrane in the similar manner to those reported by G. Manecke or W. Juda et al.[4,5].

Results

Transport Numbers.—In Figs. 4 and 5, are shown Hittorf *t. n.* (n_+) and true *t. n.* (n_+')

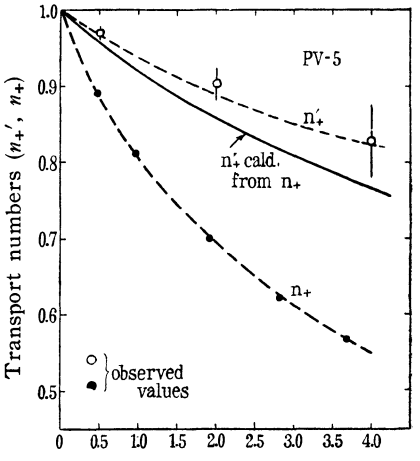

Fig. 4. Transport numbers for cation-exchange resin membrane PV-5.

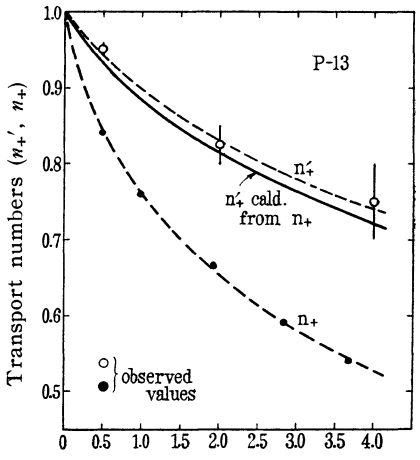

Fig. 5. Transport numbers for cation-exchange resin membrane P-13.

determined by the procedures above described for two typical cation-exchange resin membranes against the concentration of outer solutions. Both *t. n.* show the similar tendency that they decrease with increase in outer concentration, but remarkable differences exist between their absolute values. True *t. n.*, the "dynamic transport number" so to speak, is much higher than Hittorf *t. n.* computed from nearly static thermodynamic membrane potentials.

4) G. Manecke, *Z. phys. Chem.* 201, 193 (1952).
5) W. Juda et al., *J. Am. Chem. Soc.*, 74, 3736 (1952).

Electro-osmotic Water Transference.—Measured values of β_W are plotted on Fig. 6 against the concentrations of outer solution. For the purpose of comparison, β are shown in Fig. 7.

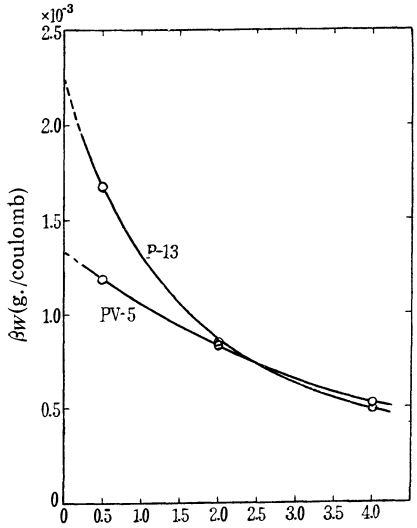

Fig. 6. Electro-osmotic water transference of cation-exchange resin membranes.

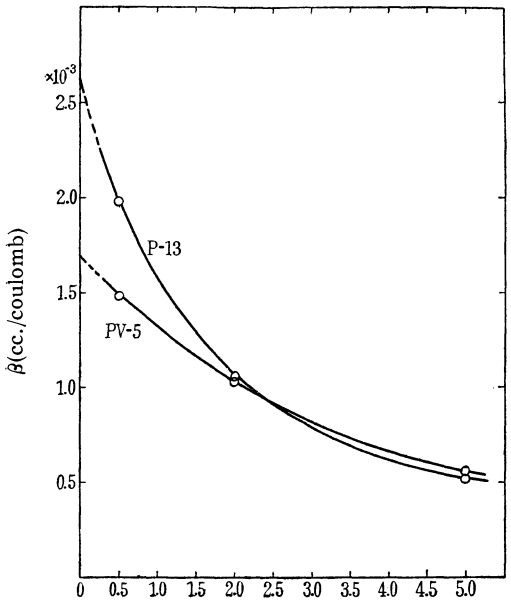

Fig. 7. Electro-osmosing solution transference of cation-exchange resin membranes.

When the concentration of the outer solution was raised from zero concentration upward, β_W and β, irrespective of membrane difference, tend to decrease rather sharply and converge to nearly constant values respectively.

Water Content, Fixed Ion Concentration and the Donnan Absorption.—These are shown in Figs. 8, 9 and 10. Here the Donnan

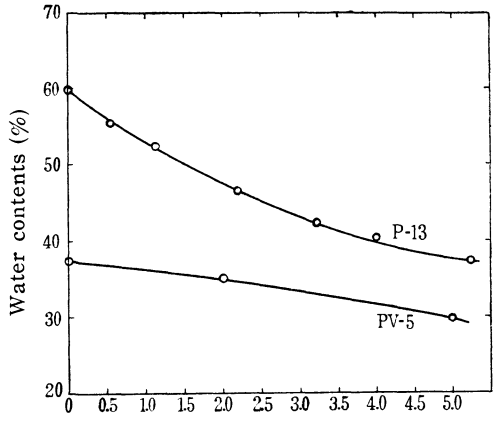

Fig. 8. Water contents of cation-exchange resin membranes.

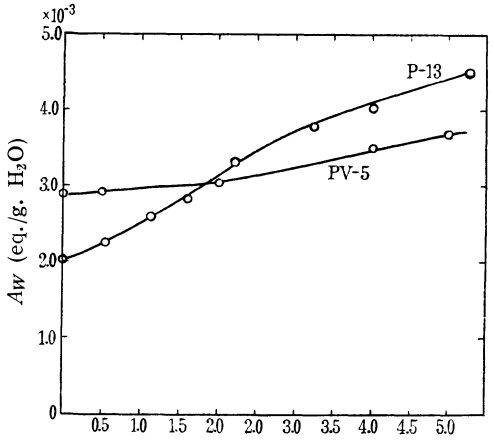

Fig. 9. Fixed ion concentration of cation-exchange resin membranes.

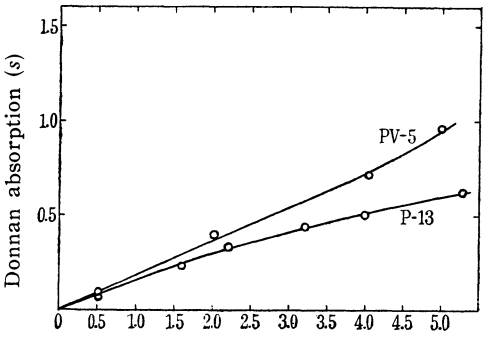

Fig. 10. Donnan absorption of cation-exchange resin membranes.

absorption (s) is expressed by the ratio of the concentration of absorbed chloride ion to that of fixed ion of the resin, both concentrations being computed in relation either to the weight of water taken up in the resin, or to the swollen volume of the resin.

$$s=[Cl^-]/[-SO_3^-]$$

Then, if the fixed ion concentration is expressed by A, which is the content of fixed ion per unit volume of swollen resin, $A(1+s)$ indicates the concentration of Na^+, and $A\cdot s$ that of Cl^-.

Discussion

Transport Numbers.—When a membrane is interposed between two solutions of different concentration, flow of materials takes place across it. Namely, solute molecules diffuse through the membrane from the more concentrated side to the dilute side, and at the same time solvent molecules in the reverse direction. As the membrane potential has to be measured under such a situation, the $t.n.$ derived therefrom may cause the erroneous result due to this material transference.

But, the error would be minimized by the application of the "interpolation method" as mentioned above. In fact, R. Schlögl[6] has shown that the $t.n.$ computed from membrane potential measurement* stands in good agreement with that derived from the rate of self-diffusion within a membrane, the latter being determined for the membrane placed between two solutions which are only differentiated with radioactive Na^{24} or Br^{82} on one side.

On the other hand, the water transport due to the current passage across the membrane is so large that its effect on the $t.n.$ can never be overlooked.

In order to consider the contribution of electro-osmosis to the passage of the current within a resin membrane, it will be assumed that ions are present in completely dissociated state in the resin. The assumption seems to be not so far from reality because of the strong acidic nature of the sulfonate type cation-exchange resin.

As G. Schmid has already reported[7], electric conduction within micro-porous membrane consists of electrolytic and convective conduction. If we denote the mobilities of cation and anion relative to the pore wall by u'_+ and u'_-, they are written as,

$$u'_+=u_+ + u_s,\quad u'_-=u_- - u_s \tag{6}$$

where u_+ and u_- are the mobilities relative to the solution, and u_s that of the solution.

In this way, ions seem to move in a similar manner to "a walking man on a running vehicle". In cation-exchange resin membranes, the velocity of cation is accelerated, that of anion retarded.

On this basis, the conductivity of a membrane, k', is derived as,

$$\begin{aligned} k' &= F[A(1+s)u'_+ + A\cdot s\cdot u'_-] \\ &= FA[(1+s)u_+ + s\cdot u_- + u_s]. \end{aligned} \tag{7}$$

On the other hand, the conductivity of a membrane, if without any electro-osmosis, is,

$$k=F\cdot A[(1+s)u_+ + s\cdot u_-]. \tag{8}$$

Therefore, the conductivity rise due to electro-osmosis is,

$$k'-k=F\cdot A\cdot u_s \tag{9}$$

On the basis of a similar concept, the transport numbers may be expressed as,

$$n'_+=\frac{(1+s)u'_+}{(1+s)u'_+ + su'_-} \tag{10}$$

$$n_+=\frac{(1+s)u_+}{(1+s)u_+ + su_-}. \tag{11}$$

Thus,

$$n'_+ - n_+ = (n_-+s)\frac{k'-k}{k'}. \tag{12}$$

Now, if we denote by β_E the volume of electro-osmosing solution under unit potential gradient applied to a membrane,

$$\beta_E=\beta\cdot k'=u_s S \tag{13}$$

where S is the total cross sectional area of pores of membrane resin. In this case, the spaces occupied by the hydration water of sulfonate group should be excluded from the pore volume, if it is considered as immobile even under electric field.

Hence, from Eqs. (9), (12) and (13),

$$\begin{aligned} n'_+ - n_+ &= (n_-+s)\cdot FAu_s/k' \\ &= (n_-+s)\cdot(A/S)\cdot\beta\cdot F \\ &= (n_-+s)\cdot A_S\cdot\beta\cdot F \end{aligned} \tag{14}$$

where A_S is the content of fixed ion per unit volume of electro-osmosing solution, i.e. mobile solution in the resin.

In Eq. (14), the term $(n_-+s)\cdot A_S$ expresses the sodium chloride concentration of electro-osmosing solutions. This expression does eventually coincide with "strömende Konzentration"* by G. Schmid[8], which has been

6) R. Schlögl, *Z. Elektrochem.*, 57, 199 (1953).

* He applied the interpolation method on the membrane potential vs. activity of outer solution curves.

7) G. Schmid, *Z. Elektrochem.*, 56, 181 (1952).

* $C_s=(C_k-n_k\cdot A)=(C_A+n_A\cdot A)=[A(1+s)-n_k\cdot A]$
$=A(1+s-n_k)=A(n_-+s)$

G. Schmid used the notation A as the content of fixed ions per unit volume of solution within resin phase.

8) G. Schmid, *Z. Elektrochem.*, 56, 35 (1952).

derived for the salt concentration of solution flowing out of a membrane when hydrostatic pressure is applied on one side.

Since it is difficult to determine A_S, a volumetric quantity, experimentally, one had better reform the expression (14) into Eq. (15) by use of gravimetric quantities,

$$n'_+ - n_+ = (n_- + s)A'_W \cdot \beta_W \cdot F \qquad (15)$$

where A'_W is the content of fixed ion per unit weight of the water contained in electro-osmosing solution. The transformation from Eq. (14) to Eq. (15) would be justified when it is considered that the term $A_S \cdot \beta \cdot F$ is a dimensionless quantity.

Here, let us examine the implication of A'_W in a little more detail. There are three kinds of water within ion-exchange resin, (1) hydration water of sulfonate ion, (2) that of free cations and anions, and (3) solvent water. The latter two are "mobile water"[1], and (1) is considered as immobile even under electric field. According to R. H. Stokes and R. A. Robinson[9], the former two have been called "bound water" and (3) "free water".

Basing on this concept, A'_W may be expressed in terms of (2)+(3), since the hydration water of sulfonate ion is considered to be almost indifferent to electro-osmosis. It follows, therefore, that the water which contributes to the "convective conduction" is the mobile water, i. e. (2)+(3).

For these reasons, in order to exactly compute the right-hand term of Eq. (15), it is necessary to know the distribution of water within the exchanger. But, since no satisfactory knowledge on the water distribution is available at present, Eq. (15) is approximately computed by substituting A_W for A'_W, the concentration of fixed ion in the total water within the resin.

In Figs. 4 and 5, the solid line shows the results of computation on n'_+ from observed values of n_+, A_W, β_W and s. The concordance of observed and computed values of n'_+ seems fairly good.

Since the water distribution in ion-exchanger, though neglected in the above treatment, seems very important to account for the nature of ion-exchange resin, it will be examined in more detail in the succeeding paper.

Electro-osmotic Transference of Water, β_W and β.—In the preceding paper the present authors reported on the electro-osmotic water transference through cation-exchange resin membranes. There, employing a volumetric procedure, observed data were expressed by β (cc./coulomb), volume of electro-osmotically transferred solution per unit coulomb.

During current passage, a solution containing excess sodium ion flows into a cathode cell across the membrane, and it is neutralized with chloride ion formed by the cathode reaction with the result that a certain amount of concentrated sodium chloride solution is added to the cathode solution. In this case, although the volume change occurs due to dilution, it may readily be seen that that is negligible for the sensitivity of the present electro-osmotic measurement. Also, the volume change due to the cathode reaction, $AgCl + e \longrightarrow Ag + Cl^-$, may be neglected.

Then, the relation between β_W and β is written as,

$$\beta = \frac{1}{d}(\beta_W + n'_+ \cdot M/F) \qquad (16)$$

where d is the density of the concentrated sodium chloride solution which is added to cathode cell due to electro-osmosis and electrode reaction combined, and M is molecular weight of NaCl.

A difficulty arises to know d, when the electro-osmosing solution is so concentrated in sodium ion that it, combined with chloride ion from cathode, is to form supersaturated solution. In such cases, the values of d were approximately calculated by use of the partial molal volume of sodium chloride at saturation.

In Fig. 11, the value of β calculated from β_W and n'_+ is shown by the solid line in com-

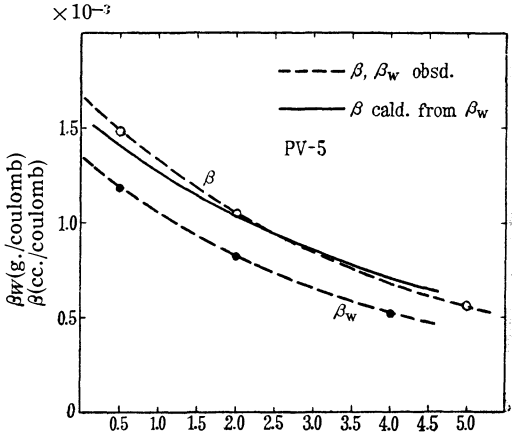

Fig. 11. Relation between β and β_W of a cation-exchange resin membrane.

9) *Annual Review of phys. Chem.*, **1954**, p. 420.

parison with the experimentally observed values.

Conclusion

The cation transport numbers through cation-exchange resin membranes were determined experimentally by two methods, first, computation from membrane potential measurement, and second from analytical tracing of the concentration change which takes place, on current passage, in the solution separated by the membrane. The former, which is considered as "Hittorf transport number", is found to be far smaller than the latter, the true transport number. The difference between the two sorts of transport number was accounted for on the basis of the concept of convective conduction within the pores of ion-exchange resin.

The electro-osmotic water transference through the membrane was discussed on comparing the results of its volumetric- and gravimetric measurements.

The authors are grateful to Dr. M. Sekino, Dr. S. Uemura and Mr. M. Funaoka for their encouragement in this work.

Research Laboratory Asahi Glass Co. Ltd. Benten-cho Tsurumi-ku Yokohama

Flame Photometric Determination of Alkali and Alkaline Earth Elements in Waters. I. Sodium and Potassium

By Ken SUGAWARA, Tadashiro KOYAMA and Nobuko KAWASAKI

(Received March 20, 1956)

Introduction

It is our usual experience in a flame photometric determination of an element that when other elements and compounds co-exist they often interfere with that element, sometimes positively and other times negatively. The present investigation was commenced to develop sensitive methods for determining alkali and alkaline earth elements by making use of the positive interference phenomena toward one element in such a way that the determinable amount of that element is greatly lessened.

Thus the writers succeeded in establishing a more satisfactory method of determining sodium and potassium in which the minimum determinable amount is lowered to one-tenth for both these two elements in any comparison with the most sensitive methods hitherto proposed. A method for the simultaneous determination of calcium and strontium was also achieved in which the minimum determinable amount of strontium was lowered to one-tenth.

Determination of Sodium and Potassium

Preliminary Experiments.—Previous investigators have proved that the addition of methyl alcohol, ethyl alcohol or propyl alcohol to the solutions of gelatine and cane sugar increases the detectability of sodium and potassium in these solutions probably by intensifying the emissions of the two elements[1,2].

Based upon this information, and taking into consideration physical properties, the writers chose a number of alcohols, aldehydes and ketones. The same volume of one of these substances was added to a series of a solution containing sodium chloride or potassium chloride. Then the intensities of emissions of sodium and potassium in these solutions were determined with a Perkin-Elmer type flame photometer.

The results listed in Table I show that acetone, methyl ethyl ketone, propyl alcohol and ethyl alcohol are particularly effective and that the effectiveness decreases successively.

The next test was to compare the effectiveness by changing the added amount of these substances. It is evident from Fig. 1 that acetone is the most effective with the least amount added and that there is a particular range of concentration for each substance in which the effectiveness is the greatest.

The results also show that, as expected, the physical properties of the individual

1) J.W. Berry, D.G. Chppel and R.B. Barnes, *Ind. Eng. Chem., Anal. Ed.*, 18, 19 (1946).
2) R.D. Catom, Jr. and R.W. Bremer, *Anal. Chem.*, 26, 805 (1954).

TABLE I

EMISSION INTENSITIES OF Na AND K IN NaCl SOLUTIONS (0.05 ppm FOR Na) AND IN KCL SOLUTIONS (0.4 ppm FOR K) IN THE ADDITION OF OTHER SOLVENTS IN SINGLE OR IN COMBINATION. BRACKETED VALUES ARE FOR Na. INTENSITY OF THE ORIGINAL SOLUTION IS 8–9 FOR Na AND 6–7 FOR K.

	Acetone	Ethyl alcohol	Propyl alcohol	Methyl ethyl ketone	Butyl alcohol	Formal-dehyde	Acetic acid	Isooctyl phenol	Lauryl amine hydro-chloride
Acetone	13 (20)								
Ethyl alcohol	13	9 (10)							
Propyl alcohol	35	18	9 (15)						
Methyl ethyl ketone	35	7	27	10 (20)					
Butyl alcohol	10	20	16	15	—				
Formaldehyde	10	5	11	—	—	7 (9)			
Acetic acid	18	15	14	12	10	25	8 (9)		
Isooctyl phenol	20	15	13	14	12	10	20	10 (−)	
Lauryl amine hydrochloride	20	12	10	15	18	—	10	8	14 (16)

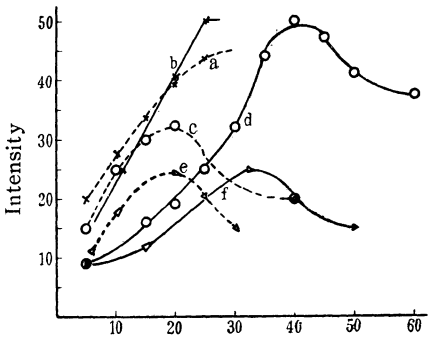

Added amount by volume %

Fig. 1. Effectiveness of acetone, propyl alcohol and ethyl alcohol on the emissions of Na and K.

a Acetone Na b Acetone K
c Propyl alcohol Na d Propyl alcohol K
e Ethyl alcohol Na f Ethyl alcohol K

substances are closely connected with the intensifying effect.

As shown in Table II, acetone which has the greatest interference is the greatest in heat of combustion, small in heat of vaporization as well as in sulface tension, and exceedingly small in viscosity.

TABLE II

PHYSICAL CONSTANTS OF THE SOLVENTS RECOMMENDED

	Surface tension dyn./cm.	Viscosity	Heat of combustion cal./g.	Heat of vaporization cal./g.
Acetone	22.5	2.9×10^{-3}	7400	132.1
Methyl ethyl ketone	18.1	3.9×10^{-3}	5831	124.1
Propyl alcohol	23.8	17.2×10^{-3}	4821	159.0
Ethyl alcohol	22.3	12.0×10^{-3}	7090	224.6

The circumstances are interpreted as follows: Its smallness in surface tension and in viscosity makes it easy for a large amount to pass into the flame as finely atomized. The small heat of vaporization makes easy the vaporization whereby the emission intensity is increased. And its large heat of combustion contributes considerably to raising the flame temperature.

A further test was made on the effect produced by the binary combination of the most effective substances. By Table I it is shown that the best results are obtained in two combinations, one of the acetone-methyl ethyl ketone and the other of acetone-propyl alcohol.

The next test was carried out by changing the amounts of the components in the system of acetone-propyl alcohol. The results in Table III show that the intensity is halved

TABLE III

EMISSION INTENSITIES AT DIFFERENT COMPOSITIONS IN THE ACETONE-PROPYL ALCOHOL SYSTEM

Na ppm	K ppm	Acetone %	Pyropyl alcohol %	Intensity
0.05		20	40	40
0.05		10	40	32
0.05		20	30	20
0.05		0	0	8
	0.4	20	40	100
	0.4	10	40	65
	0.4	20	30	50
	0.4	0	0	6–7

for propyl alcohol when the amount is reduced by one-quarter, while a 35% drop in intensity is first seen for acetone when the amount drops to one-half. This finding points to the

fact that propyl alcohol is more essential to the intensifying action than acetone to the acetone-propyl alcohol system.

One point which must not be overlooked when acetone is applied to the flame photometry is that its relatively large amount might cause an incomplete combustion. As a matter of course the writers examined whether or not a part of the acetone in the acetone-propyl alcohol system could be replaced by ethyl alcohol. The examination shows that in order to keep the original degree of intensity, a large amount of ethyl alcohol is required (see Table IV).

TABLE IV

EMISSION INTENSITY FOR THE COMBINATION SYSTEM OF ACETON, PROPYL ALCOHOL AND ETHYL ALCOHOL

K ppm	Acetone %	Propyl alcohol %	Ethyl alcohol %	Intensity
0.4	15	40	20	100
0.4	15	40	25	100
0.4	0	0	0	6–7

Another approach to the positive interference is the addition of surface active agents. Two kinds of such agents, isooctyl phenol and lauryl amine hydrochloride, accidentally at hand, were tested.

The result (Table V) shows that at surface tension minimum, isooctyl phenol is more active than lauryl amine hydrochloride. However, the background of isooctyl phenol is considerably great. For this reason isooctyl phenol was rejected and the addition of lauryl amine hydrochloride at a concentration of 0.25% was recommended where it can give an intensifying effect with the least background comparable to isooctyl phenol.

TABLE V

EFFECTIVENESS OF SURFACE ACTIVE AGENTS

Agent	Concentration %	K ppm	Intensity	Background
Isooctyl phenol	0.5	0.4	32	20
Lauryl amine hydrochloride	0.25	0.4	16	1–2

The final experiment was to ascertain in the presence of this amount of lauryl amine hydrochloride to what extent the amount of propyl alcohol could be reduced with no heavy decrease in intensity. The answer was, as listed in Table VI, that the amount of propyl alcohol can be decreased to a concentration about 10% by an intensity decrease of 40% for sodium and 34% for potassium of the original values for the respective elements.

Hereupon arose another question: Can butyl alcohol replace at least in part the propyl alcohol? Primarily, butyl alcohol is more effective than propyl alcohol but because of its low solubility in water it has not been recommended by the writers. This situation was changed when lauryl amine hydrochloride was introduced. The introduction of this substance promises a great solubility of butyl alcohol in the system whereby the effectiveness of the system is considerably

TABLE VI

EFFECTIVENESS OF THE COMBINATION SYSTEM OF ACETONE, PROPYL ALCOHOL, BUTYL ALCOHOL, METHYL ETHYL KETONE AND LAURYL AMINE HYDROCHLORIDE

Na ppm	K ppm	Acetone %	Propyl alcohol %	Butyl alcohol %	Lauryl amine HCl %	Methyl ethyl ketone %	Intensity	gain
0.05		5	40	0	0.25	0	80	
0.05		5	30	0	0.25	0	70	
0.05		5	20	0	0.25	0	56	
0.05		5	10	0	0.25	0	48	
0.05		5	0	10	0.25	0	110	18:10
0.05		5	0	5	0.25	0	100	18:30
0.05		0	0	5	0.25	5	100	18: 8
0.05		0	0	0	0	0	10–11	18: 8
	0.4	5	40	0	0.25	0	80	
	0.4	5	30	0	0.25	0	75	
	0.4	5	20	0	0.25	0	60	
	0.4	5	10	0	0.25	0	55	
	0.2	5	0	10	0	0	60	
	0.2	5	0	5	0	0	45	
	0.4	5	0	5	0.25	0	100	20: 6
	0.4	0	0	5	0.25	5	100	20: 0
	0.4	0	0	0	0	0	6–7	

increased. The result of the examination actually evidenced that a system, 5% of acetone, 5% of butyl alcohol and 0.25% of lauryl amine hydrochloride, gives an intensity comparable to the highest value ever obtained among many combinations. Thus was established the system upon which the following analytical method of sodium and potassium determination is constructed.

Temperature Regulation in the Environment.—Table VII shows that the emission intensity drops by 17–23% when the thermometer, inserted in the space between the atomizer and the photometer cover, drops from 30°C to 10°C.

TABLE VII
INTENSITY OF EMISSION AND ENVIRONMENTAL TEMPERATURE

Na ppm	K ppm	10°C		30°C	
		Intensity	Gain	Intensity	Gain
20		100	12:68	100	11:25
10		100	13:27	100	13:47
2		100	17:28	100	17:68
0.1		100	21: 9	100	21:20
0.1		22±1	18:36	22±1	18:51
	2.0	60	21: 0	97	21: 0
	1.0	35	21: 0	50	21: 0
	0.4	12	21: 0	28	21: 0

Thus it is advisable in winter to heat the atomizer by placing an adjustable electric plate at the bottom whereby the constancy and consequently the accuracy of the meter reading are secured.

Stock Solutions.—Stock solutions are prepared different in concentration for sodium and potassium and different in their proportions. Here the maximum concentration is 10 ppm. for both sodium and potassium. The solutions are kept in polyethylene bottles with a cap.

Calibration Curves.—From the stock solutions several series of standard solutions are prepared as follorwed: To a suitable amount of the stock solution, 25 ml. of acetone, 25 ml. of butyl alcohol and 1.25 g. of lauryl amine hydrochloride are added. After shaking thoroughly, the solution is made up to 500 ml. Each series consists of solutions different in dilution but definite in the ratio Na/K. Then a calibration curve is made for each of these series (see Figs. 2 and 3).

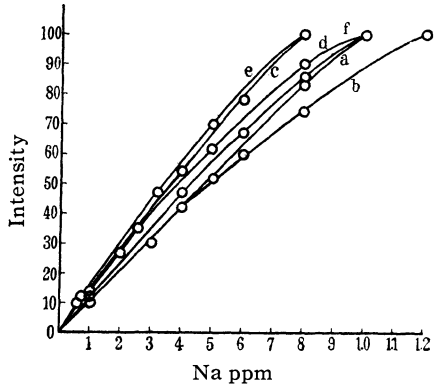

Fig. 2. Calibration curves for sodium at different Na/K. Ratios on the map are Na/K values for the individual curves.
a 1:1 b 3:1 c 4:1
d 5:1 e 8:1 f 10:1

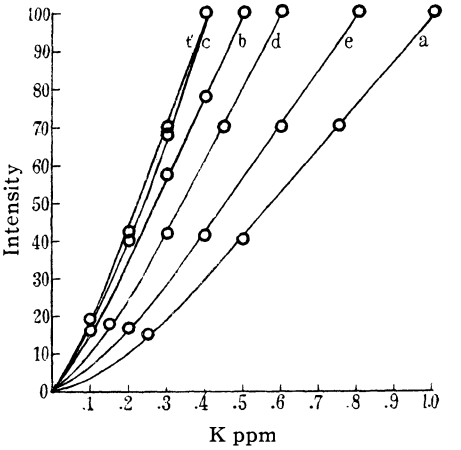

Fig. 3. Calibration curves for potassium at different Na/K. Ratios on the map are Na/K values for the individual curves.
a 1:1 b 3:1 c 4:1
d 5:1 e 8:1 f 10:1

Method of Processing Samples.—Originally the writers' attempt was to afford a method to meet the requirements for determining minor amounts of sodium and potassium as found in rain and other terrestrial waters in which both sodium and potassium are often found in quantities of 0.1 ppm or below. Thus the method of processing will be described so that it can easily be applied to such materials.

From a rain sample previously filtered through absorbent cotton and freed from all contamination such as soot and other dusts, an accurately measured amount (at least 40 ml.) is transferred to a 50 ml. measuring flask. To this are successively added 2.5 ml. of acetone 2.5 ml. of butyl alcohol and 2.5 ml. of a 5% aqueous solution of lauryl amine hydrochloride. After thorough shaking, the solution is made up to 50 ml., put to the flame photometer and the intensities of sodium and potassium are read.

Accuracy of Method.—The accuracy of the method was tested as follows: To rain water samples, the sodium and potassium contents of which were previously determined, a certain amount of sodium or potassium is added and sample content is determined.

As shown in Tabe VIII, for sodium the deviation of the observed value from the theoretical is from 0 to −8.6% with an average error −4.7%, while for potassium the deviation is from −1.9 to +7.5% with an average error +3.6%.

Interferences by Other Elements.—Among the interferences by other elements, those by

TABLE VIII

APPLICATION TO RAIN WATER AND ACCURACY OF DATA

Collected on	Fraction	Original content Na ppm	Original content K ppm	Added Na ppm	Added K ppm	Theoretical Na ppm	Theoretical K ppm	Found Na ppm	Found K ppm	Error in % Na	Error in % K
July 23, '55	1	0.35	0.10	0.30	0.30	0.65	0.40	0.60	0.43	−7.7	+7.5
	2	0.45	0.11	0.30	0.30	0.75	0.41	0.75	0.41	0.0	0.0
	3	0.65	0.18	0.30	0.30	0.95	0.48	0.90	0.49	−5.2	+2.1
	4	0.50	0.10	0.30	0.30	0.80	0.40	0.78	0.43	−2.5	+7.5
	5	0.30	0.10	0.30	0.30	0.60	0.40	0.55	0.42	−8.3	+5.0
	6	0.23	0.075	0.30	0.30	0.52	0.375	0.50	0.38	−5.8	+1.4
	7	0.28	0..63	0.30	0.30	0.58	0.363	0.53	0.38	−8.6	+2.8
	8	0.30	0.081	0.30	0.30	0.60	0.38	0.58	0.38	−3.3	+0.26
Aug. 27, '55	2	0.35	0.24	0.30	0.30	0.65	0.54	0.63	0.53	−3.1	−1.9
	3	0.24	0.11	0.30	0.30	0.54	0.44	0.51	0.45	−5.6	+9.1
	4	0.20	0.18	0.30	0.30	0.50	0.48	0.51	0.49	−2.0	+2.1
								Average		−4.7	+3.6

TABLE IX

APPLICATION TO ONTOLOGICAL MATERIAL

Lymph of Animal	Sample taken mg.	Na ppm	K ppm
Internal ear Guineapig	0.59	85.5×10^3	13.5×10^4
External ear Guineapig	0.31	13.7×10^3	14.5×10^3
Internal ear Corpse (Labyrinthin fluids)	0.96	1.99×10^3	7.99×10^3
External ear Calf	1.22	2.05×10^3	3.98×10^3
External ear Shark	0.02	37.5×10^3	11.2×10^3

calcium and magnesium are particularly notable. The presence of 20 ppm. of calcium causes an error −2% to sodium and −1% to potassium, wile 25 ppm of magnesium causes an error −2% to sodium and −1% to potassium. Consequently, the method can be direetly applied to ordinary fresh waters in which the portions of calcium or magnesium to sodium or potassium are not large. Other elements in the ordinary fresh waters show no interference.

Chemical Institute, Faculty of Science
Nagoya University, Nagoya

Flame Photometric Determination of Alkali and Alkaline Earth Elements in Waters. II. Calcium and Strontium

By Ken SUGAWARA, Tadashiro KOYAMA and Nobuko KAWASAKI

(Received March 20, 1956)

Preliminary Experiments

It is known that sodium, potassium and calcium intensify the emission of strontium while strontium has no interference with calcium[1,2,3]. In making use of this fact the writers started to elaborate a method of simultaneous determination of calcium and strontium in a solution sufficiently free from sodium and potassium in which the boundary concentration of the determinable amount, at least for strontium, is considerably lowered.

As the first step in this investigation, the writers examined in vain the possible effectiveness of additional solvents, i. e. acetone, butyl alcohol and lauryl amine hydrochloride which have proved to be very effective for

1) O.N. Hinsvark, S.H. Wittwer and H.M. Sell, *Anal. Chem.*, 25, 320 (1953).
2) T.J. Chow and T.G. Thompson, *Anal. Chem.*, 27, 18 (1955).
3) T.J. Chow and T.G. Thompson, *Anal. Chem.*, 27, 910 (1955).

the determination of sodium and potassium as reported above.

On the contrary, we found quite unexpectedly great effectiveness in oxalic acid which is used as a precipitant for separating calcium and strontium from a solution containing sodium and potassium. As suggested by these findings, other substances belonging to the same category were tested with the result that among them formic acid, acetic acid and propionic acid are found to be particularly effective. (See Table I).

TABLE I
EFFECTIVENESS OF ORGANIC ACID ON STRONTIUM EMISSION

Agent	Added amount in volume %	Intensity
Formic acid	5.0	60
	10	46
Tartaric acid	0.5	60–70
	1.0	30–35
Propionic acid	5.0	25
	10	40

Further, a comparative study of these three substances at different concentrations showed that tartaric acid especially in a 0.5% solution is the most effective of all and finally a one % solution was recommended as the best because of its greater constancy in meter reading.

On the other hand, the dependence of the intensifying effectiveness of calcium toward strontium was explored on calcium concentration with the result that strontium emission was found to increase uniformly with calcium increase (see Fig. 1).

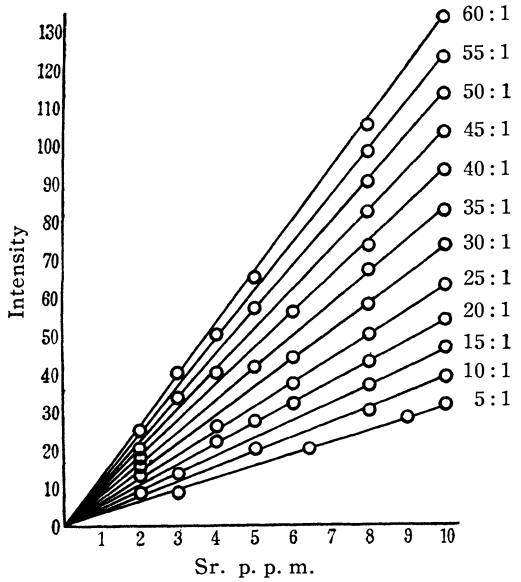

Fig. 1. Calibration curves at different Ca/Sr. Ratios on the map are Ca/Sr values for the individual curves.

Based upon these results the fundamentals of the anticipated procedure for the simultaneous determination of calcium and strontium were determined as follows: By using a precipitated mixture of oxalates of calcium and strontium with the addition of a suitable amount of tartaric acid, calcium is first determined and then after the addition of a quantity of calcium, (if necessary), the emission of strontium is determined.

Stock Solutions.—There are prepared stock solutions which contain 10% of tartaric acid, various amounts of chlorides of calcium and strontium in various proportions. Each solution is preserved in a polyethylene bottle with a cap.

Calibration Curves.—From stock solutions there are prepared several series of standard solutions as follows: A suitable amount of the stock solution is taken into a measuring flask. Suitable amounts of oxalic acid, tartaric acid and hydrochloric acid are added and the solution is made up to 500 ml. so that the final solution contains 10 ml. of hydrochloric acid (1 ; 1) and 5 g. of tartaric acid with a quantity of oxalic acid equivalent to the total of calcium and strontium. Each series of the standard solutions consists of members different in dilution but with a definite ratio Ca/Sr. For each series a calibration curve is constructed at a constant gain because of the fact that the emission of calcium itself is never influenced by the change in the amount of strontium (see Fig. 1).

Preparation of Samples.—For its lower concentration, rain water usually needs a previous concentration especially for strontium. Measured amounts, usually from 100 to 500 ml. for calcium and 1.5 to 2 liters for strontium, of the collected rain water which has passed through the pretreatment mentioned in Part I of the present paper are, if necessary, evaporated down to a volume of about 100 ml.

The next step is to prepare separate samples for determining calcium and strontium by using these condensed rain waters or any river or lake water.

To a measured amount of such a water, 2 ml. of hydrochloric acid (1 : 1), 20 ml. of a saturated solution of ammonium oxalate, 10 g. of urea and 2 drops of a methyl red solution are added successively. The solution is warmed on an electric plate until its color changes to orange-yellow.

After cooling at room temperature, the precipitate consisting of the oxalates of calcium and strontium is filtered off through a filter paper and washed five times with 10 ml. of an ammoniacal ammonium oxalate solution. With distilled water it is rinsed out into a beaker. After the addition of 2 ml. of hydrochloric acid (1 : 1), the contents of the beaker including the filter paper are warmed until thr precipitate completely dissolves. Then the solution is filtered. To the combined filtrate 2.5 ml. of a 20% tartaric acid solution is added.

TABLE II

APPLICATION TO THE SOLUTIONS WITH KNOWN AMOUNTS OF CALCIUM AND STRONTIUM

Theoretical Ca ppm	Theoretical Sr ppm	Observed Ca ppm	Observed Sr ppm	Error in ppm. Ca	Error in ppm. Sr	Error in % Ca	Error in % Sr
25	1	23.5	1.0	−1.5	0.0	−6.0	0.0
50	1	48.5	1.0	−1.5	0.0	−3.0	0.0
40	5	37.0	4.8	−3.0	−0.2	−7.5	−4.0
25	5	23.0	4.9	−2.0	−0.1	−8.0	−2.0
200	10	198.5	9.8	−2.0	−0.2	−1.0	−2.0
50	10	50.0	10.0	0.0	0.0	0.0	0.0
50	2	48.0	2.0	−2.0	0.0	−4.0	0.0
40	2	39.0	2.3	−1.0	+0.3	−2.5	+1.5
				Average		−4.0	−0.81

TABLE III

Collected on	Fraction	Sample content Ca ppm	Added Ca ppm	Theoretical Ca ppm	Found Ca ppm	Error in
July 23, '55	1	4.1	60	64.1	65.3	+1.9
	2	8.2	60	68.2	68.0	−0.29
	3	4.0	50	54.0	55.4	+2.6
	6	9.3	20	29.3	29.3	+1.7
Aug. 27, '55	2	3.5	40	43.5	42.3	−2.8
	3	7.0	40	47.0	46.0	−2.1
Sept. 7, '55	2	1.5	40	41.5	41.0	−1.2
				Average		−0.02

Collected on	Fraction	Sample content Sr ppm	Added Sr ppm	Found Sr ppm	Error in ppm	Error in %
July 23, '55	1	5.8	5	11.0	+0.2	+2
	2	4.9	5	10.0	+0.1	+1
	4	5.5	6	11.7	+0.2	+2
				Average		+2

Samples have previously been condensed down to one-sixtieth of the original volumes. Consequently, values for calcium and strontium are sixty-times greater than those in the original samples.

The solution is made up to 50 ml. and ready for flame photometry of calcium.

Samples for strontium determination are prepared as follows: To a measured amount of sample water, a suitable amount of calcium chloride solution, 2 ml. of hydrochloric acid (1 : 1), 20 ml. of a saturated ammonium oxalate solution, 10 g. of urea and 2 drops of a methyl red solution are added successively. Then the solution is processed as indicated for the samples for calcium determination.

Flame Photometry.—Calcium is determined first by reading the emission intensity at about 5600 Å. Then the strontium emission is read at 4607 Å. The strontium content can be determined from the reading of the strontium emission and total calcium, calcium determined plus calcium added.

Accuracy of the Method.—The accuracy of the present method was tested in two different ways: a) The method was applied to a number of solutions containing chlorides of calcium and strontium of known composition. b) To rain water samples, the calcium or strontium content of which was previously known, certain amounts of calcium and storontium chlorides of definite concentration were added and determination was conducted.

As listed in Tables II and III, in test (a), error is from 0.0 to −8.0% with an average −4.0% for calcium and from +1.5 to −4.0% with an average −0.81% for strontium, while in test (b) it is from +2.6 to −2.8% with an average −0.02% for calcium and from +1 to +2% with an average +1.5% for strontium.

Interferences by Other Elements.—As previously mentioned, magnesium interferes considerably with both calcium and strontium. This is why we precipitate calcium and strontium in the presence of urea.

The presence of this substance secures the complete separation of calcium and strontium from magnesium. This caution is particularly essential when the method is applied to sea water.

Chemical Institute, Faculty of Science
Nagoya University, Nagoya

*Notes on the Geochemistry of Germanium**

By Hiroshi ONISHI

(Received April 7, 1956)

To Goldschmidt and Peters[1] we owe most of the present knowledge of the geochemistry of germanium. A value of 7 ppm. for the abundance of germanium in the lithosphere was reported by Goldschmidt[2,3]. This value is based on the content of a composite of shales in which germanium was found to be enriched. Goldschmidt and Peters showed that germanium replaces silicon and forms GeO_4 tetrahedra. Wickman[4] pointed out that, on the whole, germanium is preferably substituted for silicon in the least-linked silicate tetrahedra. Harris[5] found that germanium is enriched relative to silicon, in olivines (isolated tetrahedra), and pyroxenes (silicate chains), but is impoverished in feldspars and quartz (silicate networks). This confirms Wickman's supposition. In view of this new fact, it appeared to the present author that Goldschmidt and Peters' earlier observation indicating that silicic rocks are richer than subsilicic rocks in germanium, should be reexamined. This would lead to a further study on the germanium content of common igneous rocks (compare Fleischer[6]). Fortunately a sensitive and accurate photometric method for determination of germanium has now been made available.

The more pertinent abundance data for germanium are summarized in Table I. Goldschmidt and Peters' values were obtained by the spectrographic method having a sensitivity limit of about 1 ppm. Ge. This limit is not considered very sensitive. The spectrographic method of Preuss[7] involves fractional distillation of 1–3 g. samples. Harris used the spectrochemical determination after chemical concentration. His method had a sensitivity limit of 0.1 ppm. and the accuracy of ±10%. The results of the Noddacks[8,9] were obtained by an unspecified method. In the paper of the geochemistry of rhenium[10], they gave the germanium content of various geomaterials including meteorites. However, those values are not shown in Table I.

TABLE I
SUMMARY OF LITERATURE DATA ON ABUNDANCE OF GERMANIUM

Material	Ge, ppm.	Author
Igneous Rocks		
Igneous rocks, average	1	Noddacks (1930)[8]
Granites, average	3.5	Goldschmidt and Peters (1933)[1]
Composite of 14 German granites	3	Preuss (1940)[7]
Pitchstones, 3 samples	1.5, 1.4, 1.4	Harris (1954)[5]
Hypersthene-augite-dacite-pumice, Japan	1.7	Harris (1954)[5]
Andesite, New Zealand	1.4	Harris (1954)[5]
Nephelin syenites, average	2	Goldschmidt and Peters (1933)[1]
Basic plagioclase rocks, average	2	Goldschmidt and Peters (1933)[1]
Composite of 11 German gabbros	2	Preuss (1940)[7]
Greisen, average	35	Goldschmidt and Peters (1933)[1]
Sedimentary Rocks		
36 Shales, average	7	Goldschmidt and Peters (1933)[1]
Composite of 36 German shales	7	Preuss (1940)[7]
Red clay, Challenger Exp., Station 353	3.5	Goldschmidt and Peters (1933)[1]
Composite of 23 German sandstones	2	Preuss (1940)[7]
Meteorites		
Nickel-iron, average	500	Goldschmidt and Peters (1933)[1]
Troilite, average	40	Goldschmidt and Peters (1933)[1]
Meteorites, average	79	Goldschmidt (1937)[2]
Meteorites, average	55	Goldschmidt (1954)[3]
Chondrites, average	31	Noddacks (1934)[9]

* Presented at the 9th Annual Meeting of the Chemical Society of Japan in April, 1956.

1) V.M. Goldschmidt and C. Peters, *Nachr. Ges. Wis. Göttingen, Math.-physik. Kl.* IV, 1933, 141.

2) V.M. Goldschmidt, *Skr. Norske Videnskaps-Akad. Oslo, I. Mat.-naturv. Kl.*, No. 4. Geochemische Verteilungsgesetze der Elemente, IX (1937).

3) V.M. Goldschmidt, ed. by A. Muir, "Geochemistry", Oxford Univ. Press, London (1954), p. 379.

4) F. Wickman, *Geol. Foren. Stockh. Förh.*, 65, 371 (1943).

5) P.G. Harris, *Geochim. et Cosmochim. Acta*, 5, 185 (1954).

6) M. Fleischer, *Geol. Soc. Amer. Sp. Paper*, No. 62, 145 (1955).

7) E. Preuss. *Z. angew. Mineral.*, 3, 8 (1940).

8) I. Noddack and W. Noddack, *Naturw.*, 18, 757 (1930).

9) I. Noddack and W. Noddack, *Svensk. Kem. Tid.*, 46, 173 (1934).

10) I. Noddack and W. Noddack, *Z. physik. Chem.*, A154, 207 (1931).

Goldschmidt and Peters[11] found a strong enrichment of germanium in coals. Due to the growing importance of this element in the electrical industry, a few extensive studies on the occurrence of germanium in American[12] and Japanese coals[13] have recently been made. The germanium contents of coals are variable, ranging from a few parts per million to as much as several per cent in the ashes. It appears that there is a regional variation in the abundance of germanium. Occurrence of germanium in ore-minerals has been studied by Kimura and some other workers[14,15,16,17].

The present paper supplies data on the germanium content of the common igneous and sedimentary rocks, and of chondrites.

Analytical Method

For determination of germanium in silicate rocks, the photometric procedure described by Schneider and Sandell[18] was adopted with minor modifications. The method consists in decomposition of a 0.5 g. sample with sulfuric-nitric-hydrofluoric acid, extraction of germanium tetrachloride from 9 M hydrochloric acid solution of the residue, transfer of germanium to aqueous solution by shaking the carbon tetrachloride with water, and final photometric determination with phenylfluorone. Instead of gum arabic to disperse germanium-phenylfluorone complex, aqueous polyvinyl alcohol solution[19] was used. Absorbance measurements were made with a Hirama photoelectric colorimeter (517 mμ filter) in a 1 cm. cell. Recoveries of germanium were slightly low, and a correction of 10% was made. For 1 to 2 ppm. Ge the error should be within 20 to 10%.

Shale composites (0.4 g. each) were heated in an oven at 550°C[20] for about one hour to destory organic matter. The residue was then treated with sulfuric-nitric-hydrofluoric acid. To ensure the validity of this method, 3.0 μg. of Ge and 1 mg. of sodium chloride were added to a 0.50 g. shale sample (1.0 ppm. Ge) containing a considerable amount of organic matter, and after carrying out the above procedure, duplicate values of 7.8 and 7.8 ppm. Ge were obtained.

For determination of total germanium in chondrites, the sample (0.25 g.) was first treated with nitric and sulfuric acid and the solution was evaporated to slight fumes. The residue was treated with hydrofluoric acid and germanium extracted with carbon tetrachloride after elimination of hydrofluoric acid, followed by photometric determination.

Discussion

Igneous Rocks.—Table II–VI list the germanium content of igneous rocks arranged according to rock class. Silica contents of some silicic rocks are based on Shibata, Okada, and Hara's analyses[21]. A summary of igneous averages is given in Table VII. The frequency distribution of germanium in silicic, mafic, and ultramafic rocks is shown in Fig. 1.

TABLE II
GERMANIUM IN RHYOLITES AND GRANITIC ROCKS

	SiO_2, %	Ge ppm.	
Rhyolites			
Rhyolite, composite of 12 beach pebbles, 5 miles east of Grand Marais, Minn.		1.0	
Rhyolite, White Pine, Nevada		1.3	
Granitic Rocks			
Japan			
Quartz porphyry, Hatasa, Okumyo-mura, Gifu Prefecture		1.2	
Quartz porphyry, Hatasa, Okumyo-mura, Gifu Pref.		0.9	
Quartz porphyry, Hatasa, Okumyo-mura, Gifu Pref.		1.0	
Two mica-granite, Ouchi, Ishikawa-machi, Fukushima Pref.	73.89	1.3	
Granite, pink, Fusamata, Kawamata-machi, Fukushima Pref.	71.29	1.2	
Granite, Ono-shinmachi, Fukushima Pref.		1.0	
Granite, Soma-gun, Fukushima Pref.		1.4	
Granite, Soma-gun, Fukushima Pref.		1.5	
Granite, Tanakura-machi, Fukushima Pref.		1.0	
Granite, Tanakura-machi, Fukushima Pref.		1.3	
Granite, Higashishirakawa-gun, Fukushima Pref.		1.1	
Two mica-granite, Yamamoto, Nanae-mura, Ibaraki Pref.	72.82	1.3,	1.3
Two mica-granite, Hongo, Sanso-mura, Ibaraki Pref.	72.30	1.4	

11) V.M. Goldschmidt and C. Peters, *Nachr. Ges. Wis. Göttingen, Math.-physik. Kl.* IV, **1933**, 371.
12) T. Stadnichenko, K.J. Murata, P. Zubovic and E.L. Hufschmidt, *U.S. Geol. Survey Circ.*, 272 (1953). A considerably extensive bibliography is found there.
13) M. Inagaki, *J. Chem. Soc. Japan (Pure Chem. Sect.)* **74**, 19 (1953).
14) K. Kimura, T. Nakamura and T. Kushibe, ibid., **52**, 55 (1931).
15) K. Kimura and Y. Koyama, ibid., **57**, 1190 (1936).
16) K. Kimura, O. Nagashima, K. Saito, M. Shima and S. Nakai, ibid., **73**, 589 (1952).
17) E.H. Strickland, *Analyst*. **80**, 548 (1955).
18) W.A. Schneider, Jr. and E.B. Sandell, *Microchim. Acta*, **1954**, 263.
19) Y. Oka and T. Kanno, *J. Chem. Soc. Japan (Pure Chem. Sect.)* **76**, 874 (1955).
20) Cf. H. Almond, H.E. Crowe and C.E. Thompson, *U.S. Geol. Survey Bull.*, 1036-B (1955).
21) H. Shibata, S. Okada and K. Hara, *Sci. Repts. Tokyo Kyoiku Daigaku*, Sect. C. **3**, No. 22, 141-172 (1954).

	SiO_2, %	Ge, ppm.
Two mica-granite, Mito, Higashinaka-mura, Ibaraki Pref.	73.05	1.4
Two mica-granite, Kitanakayama, Nishiyamauchi-mura, Ibaraki Pref.	72.32	1.4
Biotite granite, Higashiiida, Amabiki-mura, Ibaraki Pref.	71.66	1.3
Biotite granite, Ogoto, Kitayamauchi-mura, Ibaraki Pref.	73.03	1.6
Hornblende biotite granite, Ashio-machi, Tochigi Pref.	67.68	1.1
Granite, Hotokezakikannon, Omachi-shi, Nagano Pref.	75.79	1.2
Hornblende biotite granite, Akazawa, Agematsu-machi, Nagano Pref.	71.27	1.2
Hornblende biotite granite, Haizawa, Agematsu-machi, Nagano Pref.	69.81	1.4
Granite, Kariyasutoge, Oyama-mura, Toyama Pref.	74.52	1.3
Granite, Shomyogawa, Tateyama, Toyama Pref.	65.08	1.2
Gneissic granite, Mizutani, Tateyama-mura, Toyama Pref.	69.84	0.7
Granodiorite, Tamanoyu, Ono-mura, Fukushima Pref.	62.86	1.2
Granodiorite, Ono-shinmachi, Fukushima Pref.		1.4
Granodiorite, Ono-shinmachi, Fukushima Pref.		1.4
Granodiorite, Ono-shinmachi, Fukushima Pref.		1.4
Granodiorite, Tanakuramachi, Fukushima Pref.		1.8
Granodiorite, Soma-gun, Fukushima Pref.		1.2
Granodiorite, Higashishirakawa-gun, Fukushima Pref.		1.2
Granodiorite, Higashishirakawa-gun, Fukushima Pref.		1.2
Granodiorite, Ishikawa-machi, Fukushima Pref.		1.4
Granodiorite, Senzai, Yoshihama-mura, Iwate Pref.	66.72	1.6
Granodiorite, Yokoishi, Yoshihama-mura, Iwate Pref.	65.18	1.0
Average		1.3
U.S.		
Granite, red, Lower Falls, Snake River, Kanabec Co., Minn.		1.4
Granite, grey, coarse-grained, Benton Co., Minn.		0.9
Granite, red, Stearns Co., Minn.		1.5
Hornblende granite, Freedhem, Minn.		1.1
Quartz monzonite, Warman, Minn.		1.0
Granite, near Pierz, Minn		1.0
Hornblende granite, Rockport, Mass.		1.8
Granite (standard G-1), Westerly, R.I.		0.9, 1.0
Average		1.2
Average of all		1.3

TABLE III

GERMANIUM IN INTERMEDIATE ROCKS

	SiO_2, %	Ge, ppm.
Japan		
Quartz diorite, Rajotoge, Yoshihama-mura, Iwate Pref.	61.94	1.6
Quartz diorite, Namiita, Okirai-mura, Iwate Pref.	55.96	1.4
Quartz diorite, composite of 7 samples, Miho, Yamakitamachi, Kanagawa Pref.		1.3
Diorite, Soma-gun, Fukushima Pref.		1.6
Diorite, Soma-gun, Fukushima Pref.		1.7
Diorite, Soma-gun, Fukushima Pref.		1.6
Diorite, Tanakura-machi, Fukushima Pref.		1.6
Diorite, Ono-shinmachi, Fukushima Pref.		1.2, 1.4
Diorite, Higashishirakawagun, Fukushima Pref.		1.6
Biotite-hornblende gabbro diorite, Kamioka-machi, Gifu Pref.		1.3
Average		1.5
U.S.		
Porphyritic syenite, Wausau, Wis.		2.0
Hornblende tonalite, medium texture, Freedhem, Minn.		0.9
Average of all		1.5

TABLE IV

GERMANIUM IN BASALTS AND DIABASES

	Ge, ppm.
Japan	
Basalt, Ajiro-machi, Shizuoka Prefecture	1.6
Basalt, Ajiro-machi, Shizuoka Pref.	1.7
Basalt (1951 lava) Miharayama, Oshima Volcano, Izu	1.7
Basalt, Tateyama, Toyama Pref.	1.0
Basalt, Tateyama, Toyama Pref.	1.3
Average	1.5

	Ge, ppm.
Localities outside Japan	
Diabase, Grand Marais, Minn.	1.4*
Basalt and diabase, composite of 4 samples, Minn.	1.2
Diabase (standard W-1), Fairfax Co., Va.	1.6, 1.6
Basalt, Columbia River (Nat. Bur. Standards sample no. 4978)	1.2
Triassic diabase (Nat. Bur. Standards sample no. 4984)	1.3
Trap, Deccan (Nat. Bur. Standards sample no. 4985)	1.4
Diabase porphyry, Mt. Etna, Sicily	1.1
Average	1.3
Average of all	1.3

* Triplicate values of 1.4, 1.4, and 1.4_5 have independently been obtained by El Wardani[33].

TABLE V

GERMANIUM IN GABBROS

	Ge, ppm.
Japan	
Gabbro, Higashishirakawa-gun, Fukushima Prefecture	1.3
Gabbro, Higashishirakawa-gun, Fukushima Pref.	0.9
Gabbro, Higashishirakawa-gun, Fukushima Pref.	1.3
Gabbro, Tanakura-machi, Fukushima Pref.	1.3
Gabbro, Miharu-machi, Fukushima Pref.	1.0
Gabbro, Miharu-machi, Fukushima Pref.	1.7
Gabbro, Soma-gun, Fukushima Pref.	1.4
Gabbro, Soma-gun, Fukushima Pref.	1.4
Olivine gabbro, Kamioka-machi, Gifu Pref.	0.9
Gabbro, olivine-bearing? Kamioka-machi, Gifu Pref.	0.9
Gabbro, olivine-free, Kamioka-machi, Gifu Pref.	0.8
Microgabbro, Kamioka-machi, Gifu Pref.	1.3
Average	1.2
Localities outside Japan	
Gabbro, Duluth, Minn., above cement plant	0.8
Gabbro, Duluth, Minn.	1.3
Gabbro, composite of 5 samples, Minn.	1.2
Olivine gabbro, Cripple Creek, Colo.	1.3
Hornblende gabbro, near Shelby, N. Car.	1.8
Hypersthene gabbro (Norite), near Sudbury, Ontario	1.1
Weighted average excluding the first two samples	1.3
Average of all	1.2

TABLE VI

GERMANIUM IN ULTRAMAFIC ROCKS

	Ge, ppm.
Japan	
Peridotite, Horoman, Hidaka, Hokkaido	0.9
Peridotite, Horoman, Hidaka, Hokkaido	1.0
Peridotite, Horoman, Hidaka, Hokkaido	0.8
Peridotite, Miharu-machi, Fukushima Prefecture	0.8
Peridotite, Ogawa-machi, Saitama Pref.	1.1
Cortlandite, Miharu-machi, Fukushima Pref.	1.6
Average	1.0
Localities outside Japan	
Dunite, Balsam, N. Car.	0.7
Dunite (Nat. Bur. Standards sample no. 4975)	1.0
Average	0.9
Average of all	1.0

TABLE VII

IGNEOUS AVERAGES

Rock (number of samples)	Range	Avg. Ge, ppm.
Granitic rocks (43)	0.7—1.8	1.3
Japanese (35)	0.7—1.8	1.3
U.S.A. (8)	0.9—1.8	1.2
Intermediate rocks (12)	0.9—2.0	1.5
Japanese (10)	1.3—1.7	1.5
Basalts and diabases (15)	1.0—1.7	1.3
Japanese (5)	1.0—1.7	1.5
Other localities (10)	1.1—1.6	1.3
Gabbros (20)	0.8—1.8	1.2
Japanese (12)	0.8—1.7	1.2
Other localities (8)	0.8—1.8	1.3
Ultramafic rocks (8)	0.7—1.6	1.0

The amounts and the distribution patterns are much the same for granitic rocks, basalts and diabases, and gabbros. The granitic average (1.3 ppm. Ge) does not differ from the basaltic and gabbroic averages (1.3 and 1.2 ppm.). This is in contrast with the finding of Goldschmidt and Peters showing a larger concentration of germanium in granitic rocks (3.5 ppm.) than plagioclase rocks (2 ppm.).

The average germanium content of the lithosphere probably lies in the range 1–2 ppm., and we may give the most reasonable figure as 1.5 ± 0.5 ppm. Ge. Although the samples studied were mostly from Japan, the same distribution patterns and a small dispersion in the germanium contents are observed for both Japanese and some other samples. Thus, for example, among the granitic and gabbroic rocks analyzed, there are a good number of samples from Fukushima Prefecture or Abu-

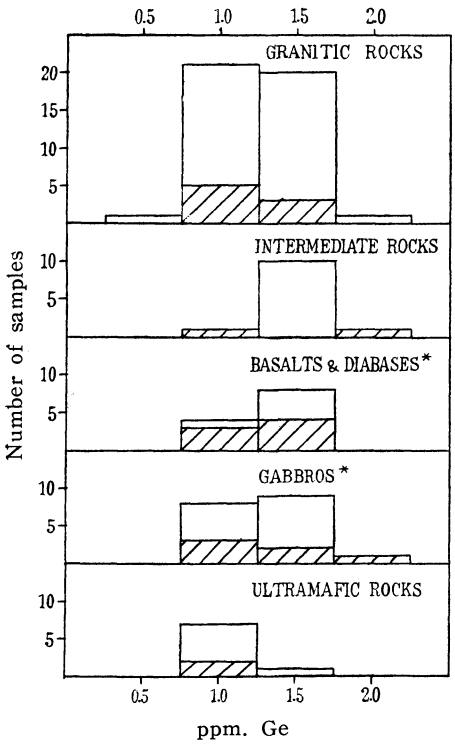

Fig. 1. Frequency distribution of germanium in igneous rocks.

▨ Outside Japan

* Minnesota composite taken as one sample

kuma Plateau. The average of 6 granites from this area is 1.2 ppm. compared to 1.2 ppm. as the average of 8 American granitic rocks. Nine granodiorites from Fukushima Prefecture gave an average of 1.2 ppm. Among 12 Japanese gabbro samples analyzed, 8 were from the same prefecture and an average of 1.3 ppm. is obtained for the latter samples. This value very favorably compares to the weighted average of 1.3 ppm. for 8 American and Canadian gabbros. Such an uniform distribution of germanium in igneous rocks (also compare Fig. 1) is the very basis of the new estimate of the terrestrial abundance of this element. Analysis of a larger number of samples from well-scattered areas of the globe is naturally desirable to get more exact averages. This will also serve as an inter-laboratory test of analyses.

The new igneous values are consistently lower than those of Goldschmidt and Peters and of Preuss. The reason for this discrepancy is not entirely evident: difference in the standardization could explain it to some extent, and some difference could be attributed to a lower limit of sensitivity of the spectrographic method. For the reason that will be discussed on **Sedimentory Rocks,** a possibility of regional variation may not be so great as one would suspect. As for intermediate rocks, two values obtained by Harris, i. e., 1.7 and 1.4 ppm., are just in the right range of the germanium content of this class of rocks obtained by the present author. Values for three pitchstones reported by Harris, i. e., 1.5, 1.4, and 1.4 ppm. and for rhyolites by the present author (Table II), seem to indicate that silicic volcanic rocks are not particularly high in germanium. This is opposite to the behavior of arsenic which shows a higher arsenic content in silicic volcanic rocks[22].

Goldschmidt's estimate in 1937[2] was based on the results of 12 igneous rocks and 13 sedimentary rocks, but several of the samples were composites. He found an average of 4 ppm. for igneous and 7 ppm. for sedimentary rocks but he preferred the latter for some reason as the abundance of germanium in the lithosphere. Recently Fleischer[6] stated that the Noddacks value for igneous rocks (1 ppm.) would probably be closer to the truth. He did not, however, mention the reason why he preferred Noddacks to Goldschmidt in the germanium abundance. The present data happen to confirm Fleischer's supposition.

Logarithms of the atomic abundances, expressed as parts per million atomic weight, of elements of atomic numbers 29 to 35 and 47 to 53 in igneous rocks are plotted in Fig. 2. The value for tellurium is quite uncertain. The data for selenium, silver, and iodine are not definitely established.

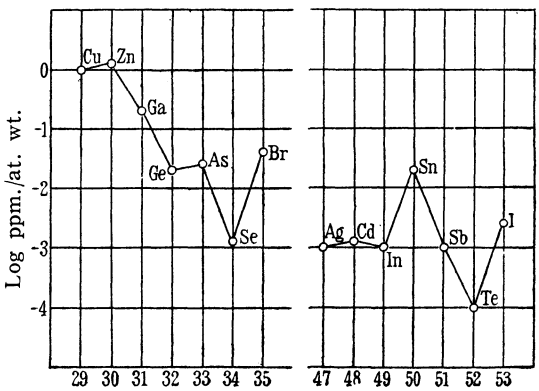

Fig. 2. Log of the atomic abundance, expressed as parts per million/atomic weight, of elements 29–35 and 47–53 in igneous rocks.

The average of 1.5 ppm. of germanium for igneous rocks arrived at above makes the

22) H. Onishi and E.B. Sandell, *Geochim. et Cosmochim. Acta*, 7, 1 (1955).

element definitely less abundant than gallium (15 ppm.), but comparable to arsenic (2 ppm.) in the upper lithosphere. The terrestrial abundances of germanium and tin (2–3 ppm.[23]) are much the same.

As already mentioned in the introductory part of this paper, germanium (using Ahrens' 1952 values for ionic radii[24], Ge^{4+} 0.53 Å) replaces silicon (0.42 Å). The valency of germanium in igneous rocks and magmas is usually quadrivalent, although, according to Ahrens[25], divalent germanium may apparently be found in some sulfide minerals that were formed at low oxidation potentials. Goldsmith[26] has synthesized and determined some of the crystal-chemical properties of Ge^{4+} substituted feldspars. Harris[5] studied the distribution of germanium among coexisting phases of partly glassy rocks such as pitchstone and andesite. Although his findings may not be applied to minerals formed at different stages of the crystallization of the different parent magmas, they deserve careful attention. His results showed that feldspar usually contained ~1 ppm. Ge, whereas olivines and pyroxenes 2–4 ppm. Thus a greater enrichment of germanium relative to silicon, takes place in the latter two minerals. Quartz may contain a fraction of a part per million of germanium, as one would infer from the presence of germanium in cherts and novaculites (0 to 3.0; average 0.4 ppm.)[27]. Also a few parts per million of germanium may be found in sandstones (Table VIII). The feldspar of igneous rocks probably accounts for one-half or more of the total germanium. However, the contribution of olivines and pyroxenes is also considerable, and this is probably the reason that germanium does not show any marked enrichment in a particular class of igneous rocks as shown by the present work.

For granitic rocks whose content of silica had been determined, no relation between germanium and silica was apparent.

In Fig. 3 the germanium contents of some igneous rocks are plotted against arsenic. The substitution of arsenic for silicon has already been indicated. As germanium behaves in the same way, a correlation between the two elements is not unexpected. A general tendency for germanium to rise with arsenic seems to exist, and it may be concluded that the process increasing the arsenic

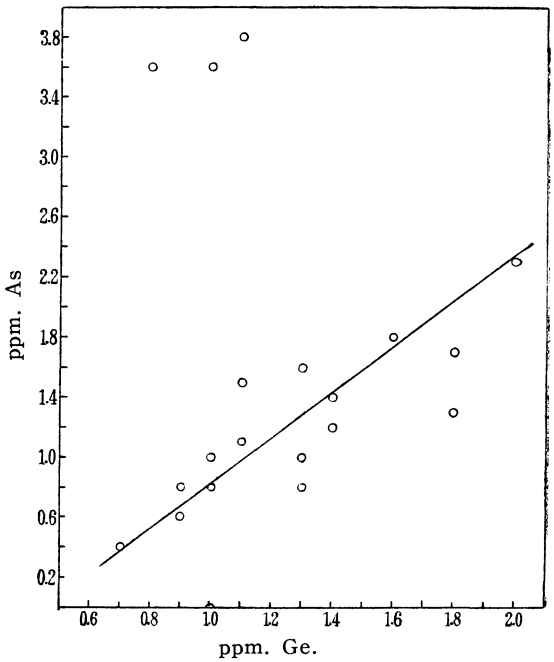

Fig. 3. Germanium as a function of arsenic in igneous rocks.

content of magmas also tends to increase the germanium content. Both germanium and arsenic are known to concentrate in the end stages of magmatic differentiation.

Replacement of iron (Fe^{3+} 0.64 Å) by germanium appears very probable since 1–3 ppm. Ge was found in magnetites[5]. The ionic radius of Al^{3+} (0.51 Å) suggests the possible substitution of germanium for aluminum. If substitutional disorder (Si–Al) in aluminosilicate is proved, this substitution of germanium for aluminum becomes a good possibility. This is, however, a mere speculation

TABLE VIII

GERMANIUM IN SEDIMENTARY ROCKS

	Ge, ppm.
Graywacke, Hatasa, Okumyo-mura, Gifu Prefecture	0.9, 0.9
Graywacke, Hatta, Hokuse-machi, Mie Prefecture	3.1, 3.5
Sandstone, Mitani-mura, Shiga Pref.	0.8, 0.8
Sandstone, Mitani-mura, Shiga Pref.	1.6, 1.5
Shale, Mitani-mura, Shiga Pref.	1.6, 1.6
Shale, Hatta, Hokuse-machi, Mie Pref.	1.7, 1.6
Shale, Hatta, Hokuse-machi, Mie Pref.	1.5, 1.4
Shale, Hatta, Hokuse-machi, Mie Pref.	1.6, 1.8
Composite of 14 Japanese Paleozoic shales (Minami)	1.6
Composite of 10 Japanese Mesozoic shales (Minami)	1.8
Composite of 36 European Paleozoic shales (Noll)	2.2

23) H. Onishi and E.B. Sandell, *Geochim. et Cosmochim. Acta*, To be published.
24) L.H. Ahrens, ibid., 2, 155 (1952).
25) L.H. Ahrens, ibid., 3, 1 (1953).
26) J.R. Goldsmith, *J. Geol.*, 58, 518 (1950).
27) J.A. Maxwell, Ph. D. Thesis, Univ. of Minnesota (1953).

unless a larger number of analyses of rock-forming minerals have been carried out and more pertinent information on the substitution has been obtained.

Sedimentary Rocks.—Tables VIII and IX list germanium values for sedimentary materials.

TABLE IX
GERMANIUM IN DEEP-SEA DEPOSITS

	Location		Depth, m	
Composite of red clays, Pacific Ocean	30°28.0'N	135°47.0'E	4363	Ge, ppm.
	15°10.0'	154°34.5'	5219	
	31°33.5'	136°20.5'	4096	1.6,
	13°39.5'	158°49.0'	5794	1.6*
Composite of red clays, Pacific Ocean	5°13.0'N	140°40.0'E	4884	
	9°25.5'	126°40.5'	5844	1.4,
	6°47.0'	139°27.0'	4293	1.6*
	6°43.0'	141°27.5'	4743	

* Most of the sodium chloride removed with water before hydrofluoric acid treatment.

The average of 4 shales, of which 3 are from Mie Prefecture and 1 from Shiga Prefecture, is 1.6 ppm. This figure is in good agreement with the weighted average of the two composites prepared by Minami[28] to represent 24 Japanese shales (1.7 ppm.). The composite of 36 European shales prepared by Noll[29] contained 2.2 ppm. The weighted average of the three composites above, based on 60 European and Japanese shales is 2.0 ppm. Here attention should be called to a difference in the results obtained by the previous workers and the present author. Goldschmidt and Peters[1], and Preuss[7] did not describe in detail the shale composites analyzed, but it appears that all three of the samples are the same. As shown in Table I, Goldschmidt and Peters reported 7 ppm. Ge or 0.001% GeO_2. Judging from the description of the analytical procedure they used, it is the impression of the present author that their value is rather approximate; the accuracy may well be 50% or more. However, Preuss' value of 7 ppm. Ge for 36 German shales is claimed to be obtained by a quantitative intensity measurement of the spectrogram. He mentions that the average error of ±50% was obtained for 10 determinations of germanium (as well as of other rare elements) in a shale sample. Considering this, the Preuss' value could be regarded as 7±4 ppm. or 3–11 ppm. Ge. In the present work, the procedure for shales was studied carefully, and, as mentioned in the *Analytical Method*, the recoveries were satisfactory. So the present figure of 2.2 ppm. could well be ±0.4 or 1.8–2.6 ppm. The agreement with Preuss' value is not very satisfactory, and the cause for this discrepancy may be sought elsewhere.

If we adopt the value of 7 ppm. Ge for European shale composite, the result is that it indicates that an extraordinary enrichment of germanium occurred in this sample (compare the data for Japanese shales and oceanic red clays). Of course it may be pointed out that too few shales have been examined in the present work to enable a satisfactory average to be established. Local concentration of germanium may be possible; two Chattanooga shales in which germanium-rich coals (average 470 ppm. in 4 samples) occurred, contained 8 and 18 ppm. Ge[30]. Further investigations of the germanium content of sedimentary rocks, particularly of shales, are very desirable.

The average germanium content of 2 pelagic red clay composites representing 8 individual samples from the Pacific Ocean, is 1.6 ppm. Antimony determination was already made on these composites[31]. A sample of deep-sea red clay contained 2 ppm. according to the analysis of J. A. Maxwell, Geological Survey of Canada[32]. El Wardani[33] has independently obtained the same value for the same sample. A value of 2 ppm. is thus indicated for red clays and this average is comparable to that of shales examined.

As a result of the above observations, it can be pointed out that shales and red clays tend to be rich in germanium compared to igneous rocks. This may be understandable from the fact that some germanium compounds are volatile at relatively low temperatures. Germanium is found in some waters of hot springs. In a mineral water of Senami Spring, Niigata Prefecture, Kuroda[34] found 0.03 mg. Ge per liter or 0.03 ppm. Data of germanium for sea water are scanty. El Wardani found 0.05 μg. Ge in a liter of sea water, corresponding to $\sim 10^{-5}$ ppm.[33] Arsenic is much more abundant in sea water (1–3 μg. As/l.[35,36]) than germanium. The escaping tendency of germanium is less than that of arsenic.

Chondrites.—Table X contains the chandrite data. The frequency distribution is shown

28) E. Minami, *Nachr. Ges. Wis. Göttingen, Math.-physik. Kl.* **IV**, N.F. **1**, 143 (1935).
29) W. Noll, *Chem. Erde*, 8, 537 (1934).
30) I.A. Breger and J.M. Schopf, *Geochim. et Cosmochim. Acta*, 7, 287 (1955).
31) H. Onishi and E.B. Sandell, ibid., 8, 213 (1955).
32) J. A. Maxwell, Private communication to E. B. Sandell.
33) S. A. El Wardani (Scripps Inst. Oceanography, Univ. of Calif.), Private communication to E.B. Sandell.
34) K. Kuroda, This Bulletin, **14**, 303 (1939).
35) A. A. Smales and B. D. Pate, *Analyst*, 77, 188 (1952).
36) K. Sugawara, Distribution of some minor bio-elements in western Pacific Waters, Regional Symposium on physical oceanography, Tokyo, October, 1955.

in Fig. 4. For the description of some samples, the readers are referred to Prior and Hey[37] or Onishi and Sandell[38].

TABLE X
GERMANIUM IN CHONDRITES

	Ge, ppm. Present work	El Wardani, analyst
Alamogordo, N. Mex.	10.3	
Arriba, Colo.	10.3	9.2*
Cope, Colo.	9.6	9.1*
Gladstone, N. Mex.	11.6	
Gruver, Texas	10.6	
Haven. Kans.	12.4	
Hesston, Kans.	9.6	
Hugoton, Kans.	9.6	
Kanzaki-gun, Saga Prefecture, Japan	10.6	
Kingfisher, Okla.	11.3	
Ladder Creek, Kans.	9.2, 9.2	6.1
Melrose, N. Mex.	10.0	9.4*
Miller, Kans.	12.4	
Morland, Kans.	10.6	
Oshima-gun, Kagoshima Pref., Japan	9.0	
Plainview, Texas	11.2	12.0
Potter, Neb.	11.9	
Roy, N. Mex.	11.2, 11.2	8.8
Average	10.6	
Composite I (Arriba, Beenham, Cope, Cotesfield, Morland, Plainview, Roy)	9.5, 10.0	10.6*
Composite II (Alamogordo, Estacado, Gladstone, Gruver, Kingfisher, Ladder Creek, Melrose)	11.7, 10.9	9.4*

* Average of duplicate analyses.

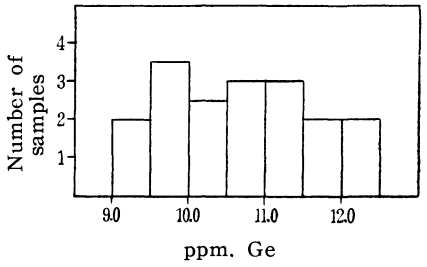

Fig. 4. Frequency distribution of germanium in chondrites.

El Wardani's[33] values were obtained by a photometric method with phenylfluorone after decomposing the sample with hydrofluoric acid only, followed by fusion of the residue with potassium pyrosulfate, and distillation of germanium tetrachloride. The agreement is generally good and this fact was already discussed from the standpoint of the present day trace analysis[39]. The worst agreement is found in the Ladder Creek chondrite which contains 6.1 ppm. (single analysis) according to El Wardani and 9.2, 9.2 ppm. (duplicate analyses) according to the author. For Composite I, a difference between the two analysts' values, taking an average respectively, is 8% with respect to the author's value. For Composite II, it is −17%. The average given by El Wardani for the two composites is 10.0 ppm. and by the author 10.5 ppm. The difference is only −5% which should, in the opinion of the author, be considered very satisfactory.

The average for 18 chondrites is 10.6 ppm. Ge, with a range from 9.0 to 12.4 ppm. The germanium content is uniform and it is probable that this average is not far from the truth. If we take the average for Haven, Hesston, Hugoton, Kanzaki, Miller, Oshima, and Potter chondrites, all of which are not included in either Composite I or II, a value of 10.8 ppm. is obtained and is comparable with 9.8 and 11.3 ppm. of those composites.

In the present work, no attempt was made to separate silicate, troilite, and metal phases of chondrites, or to determine germanium in these phases.

Some of the chondrite samples used in the present work are considerably weathered and the effect of this alteration on the gallium content was previously discussed[38]. We believed that no important change in the gallium content has occurred. In the case of germanium, no definite relation between the degreen of alteration and the germanium content is apparent. Thus, for example, the Kingfisher chondrite, which is the freshest in our collection, contains 11.3 ppm. Ge, as compared to 11.2 ppm. in the weathered Roy chondrite.

There seems to be no relation between the germanium and arsenic contents of chondrites, and this is in contrast with igneous rocks (see Fig. 3).

The new average germanium content of chondrites or approximate cosmic abundance (10.6 ppm. Ge) is much smaller than the values of 31 ppm. reported by the Noddacks[9] and of 55 ppm. by Goldschmidt[3]. The last value is based on the ratio 10 silicate phase : 2 metal : 1 troilite.

In Fig. 5 the meteoritic abundances of germanium, tin, and their neighbors of both even and odd atomic numbers are plotted. The

37) G. T. Prior and M. Hey, "Catalogue of Meteorites", 2nd ed., British Museum (Natural History), London (1953).

38) H. Onishi and E. B. Sandell, *Geochim. et Cosmochim. Acta* 9, 78 (1956).

39) H. Onishi, *Kagaku*, 26 306 (1956).

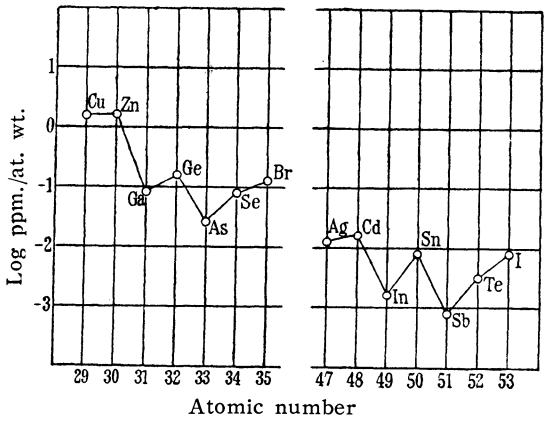

Fig. 5. Log of the atomic abundance, expressed as parts per million/atomic weight, of elements 29–35 and 47–53 in meteorites.

abundances of copper[40], gallium[38], arsenic[22], tin[23], and antimony[31] referred to chondrites. Other values are based on the Goldschmidt's ratio as representing the average of meteorites. Some of the values, e. g., bromine and iodine, are very uncertain. The value for tellurium is an estimate (0.5 ppm.) by the author.

If we adopt the Urey-Craig[41] average for silicon in chondrites, i. e., 18% Si, we obtain the weight ratio $Ge/Si=10.6/18\times10^4=5.9\times10^{-5}$ or the atomic ratio 2.3×10^{-5}.

Germanium (atomic number 32) is more abundant than gallium (A. N. 31) and arsenic (A. N. 33) if the respective contents are taken as 5.3 and 2 ppm. in chondrites.

40) J.M. Shreeve, Unpublished work, Univ. of Minnesota (1955).

41) H.C. Urey and H. Craig., *Geochim. et Cosmochim. Acta*, 4, 36 (1953).

Summary

Chondrites have uniform germanium contents: the average of 18 samples is 10.6 ppm. Ge, with the range 9.0–12.4 ppm.

The common igneous rocks do not differ greatly in germanium content as shown by the averages: granitic rocks 1.3 ppm., intermediate rocks 1.5 ppm., basalts and diabases 1.3 ppm., gabbros 1.2 ppm., and ultramafic rocks 1.0 ppm. The average for the lithosphere or the crustal rocks may be taken as 1.5±0.5 ppm. Ge.

Shales contain 2 ppm. Ge. Oceanic red clay also contains the similar amount. The germanium content of sedimentary materials seems to be somewhat higher than that of igneous rocks because of the possible escape of germanium in hydrothermal and volcanic emanations.

Special thanks are due Professor E. B. Sandell for generous cooperation in providing rock and meteorite samples and helpful suggestions. Dr. E. Minami kindly provided three composites of European and Japanese shales. Drs. S. S. Goldich, M. Gorai, H. Hamaguchi, and H. Shibata, and Messrs. R. Kuroda and S. Sato supplied various rock samples. Two Japanese meteorites were vigne through the courtesy of the Director, Geological Survey of Japan.

Government Industrial Research Institute, Nagoya

Spectrochemical Study of Microscopic Crystals. XII[1]. *Polarized Absorption Spectra of Cupric Complexes with Tropolone and Related Compounds*[2]

By Shoichiro YAMADA and Ryutaro TSUCHIDA

(Received April 10, 1956)

In the previous papers[3], the present authors studied the dichroism of planar quadri-coordinate complexes of platinum (II) and palladium (II), and induced the common rules on the dichroisms of these compounds. Besides those complexes of platinum and palladium, a number of cupric quadri-co-ordinate complexes are also known to possess planar configuration, for which a definite dichroism may be expected. In connection with the earlier studies on the planar complexes, it was supposed to be desirable to determine

1) Part XI of this series, S. Yamada and R. Tsuchida, This Bulletin, **29**, 421 (1956).

2) Presented in part at the sixth annual meeting of the Japan Chemical Society, Kyoto, April, 1953.

3) S. Yamada, H. Yoneda and R. Tsuchida, *J. Chem. Soc. Japan*, **69**, 145 (1948) (in Japanese); S. Yamada, *J. Am. Chem. Soc.*, **73**, 1182 (1951); S. Yamada and R. Tsuchida, This Bulletin, **26**, 489 (1953).

the dichroism of planar complexes of copper (II). As ligands we have taken up tropolone[4] and its derivative, which were kindly donated by Prof. T. Nozoe. In the study with compounds of tropolone and its derivative, it also seemed of great interest to make comparison of these metallic compounds with complexes of some β-diketones which bear resemblance to the former. In the present work, we have determined dichroisms of cupric complexes with tropolone, hinokitiol[5], acetylacetone and salicylaldehyde[6], all of these chelate groups co-ordinating to the metal through oxygen atoms, and the results have been discussed in relation to the above points.

Experimental

Materials.—Bis-(tropolonato)-copper(II).—The sample, which was kindly supplied by Professor T. Nozoe of Tohoku Univ., was recrystallized from alcohol. The green prismatic crystals belonging to the monoclinic system show an oblique extinction in the prism face. A marked dichroism was observed under the microscope. Measurement of the dichroism was made in the (110)-plane with polarized light vibrating along the directions of extinction the extinction angle being about 19.5° with reference to the *c*-axis.

Bis-(hinokitiolato)-copper (II).—The sample supplied by Prof. Nozoe was recrystallized from alcohol. The crystals obtained in green, monoclinic prisms show in the prism face a dichroism similar to that of the tropolonato-compound. Measurement of the dichroism was made in the prism face along the directions of extinction. The crystals exhibit an oblique extinction, the extinction angle being about 36° referred to the needle axis.

Bis-(acetylacetonato)-copper (II).—Was prepared from an aqueous solution of copper acetate and an alcoholic solution of acetylacetone[7]. Blue, monoclinic crystals of this compound, elongated along the *b*-axis, show a striking dichroism; they appear indigo with the electric vector along the *b*-axis, and greenish yellow with the electric vector perpendicular to the *b*-axis. The dichroism measurement was made with polarized light having its electric vector along the above two directions.

Bis-(*o*-formylphenolato)-copper (II).—Was prepared in green, monoclinic prisms according to the method of Tyson et al[8]. The crystals thus obtained exhibit a marked dichroism in the prism face; they appear yellow and brownish yellow, respectively, with the electric vector along and normal to the direction of elongation. The measurement was made with reference to the above two directions.

Measurements.—Quantitative dichroism measurements were made at room temperature in the region covering from 2400 to 7500 Å by Tsuchida-Kobayashi's microscopic method[9]. The symbol, α, represents absorption coefficient per mm. of a crystal.

Absorption spectrum in solution was determined with a Beckman DU quartz-spectrophotometer. ε represents extinction coefficient of the solution.

Results

Bis-(tropolonato)-copper (II).—The results of the measurements are shown in Fig. 1 and Table I. According to the X-ray analysis of

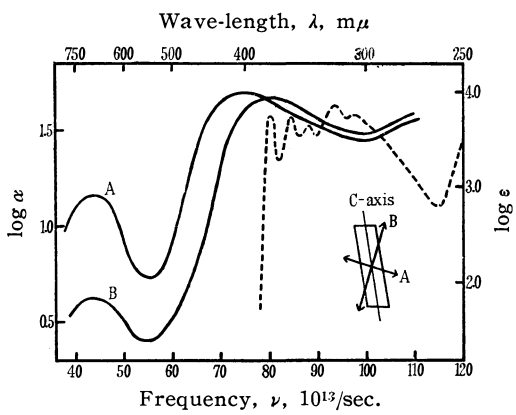

Fig. 1. Ultra-violet absorption spectra of bis-(tropolonato)-copper (II) and tropolone. The absorption spectrum of tropolone in hexane (dotted curve) is taken from J. W. Cook, A. R, Gibbs, R. A. Raphael and A. R. Somerville, *J. Chem. Soc.* **1951**, 503.

TABLE I
ABSORPTION MAXIMA OF BIS-(TROPOLONATO)-COPPER (II)

	ν, 10^{13}/sec.	log α	ν, 10^{13}/sec.	log α
A-abs	43.8	1.16	76	1.88
B-abs	44	0.71	81	1.88

the crystal structure by Robertson[10], a copper atom and four oxygen atoms around it form a square, the whole molecule containing the tropolone-rings being planar. The normal to the planes of the complexes makes an angle of about 26.5° with the *c*-axis. The X-ray analysis indicated that the A-absorption involves more ||-absorption of the molecule[11], and the B-absorption involves more ⊥-absorption (Fig. 1). The tropolonato-copper (II) complex in the crystalline state shows an absorption

4) Tropolone represents cycloheptatriene-2, 4, 6-one-1-ol.

6) Salicylaldehyde may be regarded as *o*-formylphenol. The latter is preferred, when it is necessary to stress that this is one of the phenolic compounds.

7) W. C. Fernelius, "Inorganic Syntheses", Vol. 2 (1946), p. 14.

8) G.N. Tyson, Jr. and S.C. Adams, *J. Am. Chem. Soc.*, **62**, 1228 (1940).

9) R. Tsuchida and M. Kobayashi, This Bulletin, **13**, 388 (1938); "The Colour and the Structure of Metallic Compounds", Zoshindo, Osaka (1944), p. 180 (in Japanese).

10) J.M. Robertson, *J. Chem. Soc.*, **1951**, 1223.

11) The ||- or ⊥-absorption represents absorption with polarized light having its electric vector along the plane of the complex or perpendicular to it, respectively.

band at about 44×10^{13}/sec. and another band at about 80×10^{13}/sec. and shorter wave-length. The former band (band A) may be considered as due to the copper atom in co-ordination with the ligand groups. The latter band may be due to the electronic transition in the ligand bound to the metal atom and should be designated as a specific band[12].

The following rules are obtained on the dichroism. (1) For the band A, the ||-absorption is remarkably hyperchromic to the ⊥-absorption, and (2) for the specific band, the ||-absorption is highly bathochromic to the ⊥-absorption.

Bis-(hinokitiolato)-copper (II).—The results of the measurements are shown in Fig. 2 and Table II. The compound shows a band

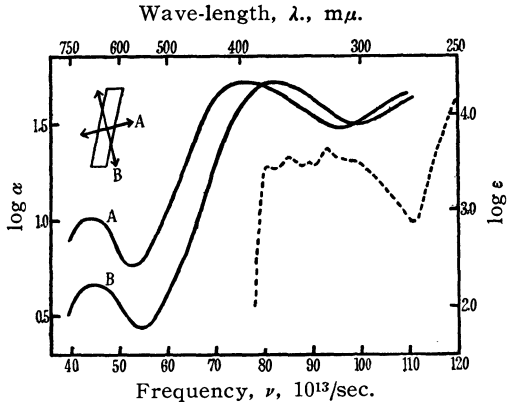

Fig. 2. Ultra-violet absorption spectra of bis-(hinokitiolato)-copper (II) and hinokitiol. The absorption spectrum, of hinokitiol in iso-octane (dotted curve) is taken from M. Tsuboi, This Bulletin, 25, 369 (1952).

TABLE II

ABSORPTION MAXIMA OF BIS-(HINOKITIOLATO)-COPPER (II)

	ν, 10^{13}/sec.	log α	ν, 10^{13}/sec.	log α
A-abs.	44.2	1.0	76	1.70
B-abs.	44	0.62	80	1.72

at about 44×10^{13}/sec. and the other band at about 80×10^{13}/sec. and shorter wave-length region. The crystal structure has not yet been determined. The dichroism of the compound, however, may be understood in a way similar to the case of the tropolonato-compound, assuming that the A-absorption involves the characteristics of the ||-absorption and the B-absorption involves those of the ⊥-absorption. On the basis of the assumption, we are led to the rules, the same as those of the tropolonato-compound.

12) About the specific band, see, for example, R. Tsuchida and M. Kobayashi, This Bulletin, 13, 476 (1938), etc.

Bis-(acetylacetonato)-copper (II).—The results of the measurements are shown in Fig. 3 and Table III. The analysis of the crystal

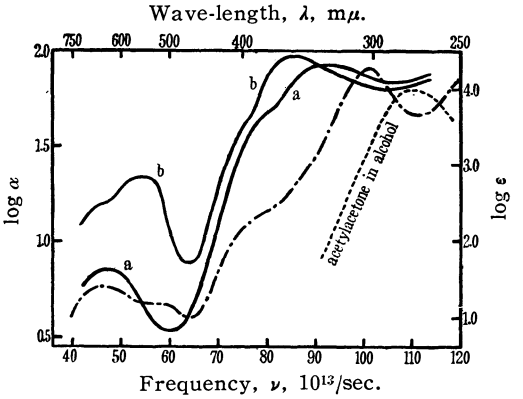

Fig. 3. Ultra-violet absorption spectra of bis-(acetylacetonato)-copper (II): ——— crystal; — — — chloroform solution. The absorption spectrum of acetylacetone in alcohol (------) is taken from P. Grossmann, *Z. physik. Chem.*, 109, 305 (1924).

TABLE III

ABSORPTION MAXIMA OF BIS-(ACETYLACETONATO)-COPPER (II)

	ν, 10^{13}/sec.	log α	ν, 10^{13}/sec.	log α
b-abs.	55.8	1.39	94	2.04
c-abs.	48	1.05	98	2.00

structure was performed by Koyama et al.[13], indicating that the planes of the complex molecules inclined by about 53.5° to the *b*-plane. It is seen from the X-ray study that the *a*-absorption, absorption with the electric vector along the *a*-axis, involves more ⊥-absorption, and the *b*-absorption, absorption with the electric vector along the *b*-axis, involves more ||-absorption. The crystal shows two absorption bands, one at about 50 to 55×10^{13}/sec. and the other in the region shorter than 70×10^{13}/sec. The band at shorter wave-length apparently corresponds with the specific band which is due to the electronic transition of the π-electron system in combination with the copper atom. From the result of the measurement, we obtain the following rules on the dichroism of the planar complex. (1) For the band A, the ||-absorption is greatly hyperchromic to the ⊥-absorption, the former being slightly hypsochromic to the latter, and (2) for the specific band, the absorption with the electric vector along the π-electron system is bathochromic to the absorption with the electric vector normal to the π-electron system.

13) H. Koyama, Y. Saito and H. Kuroya, *J. Inst. Polytech. Osaka City Univ.*, Vol. 4, No. 4, Series C, p. 43 (1953).

Bis-(*o*-formylphenolato)-copper (II). — The results of the measurements are shown in Fig. 4 and Table IV. The crystal is found to

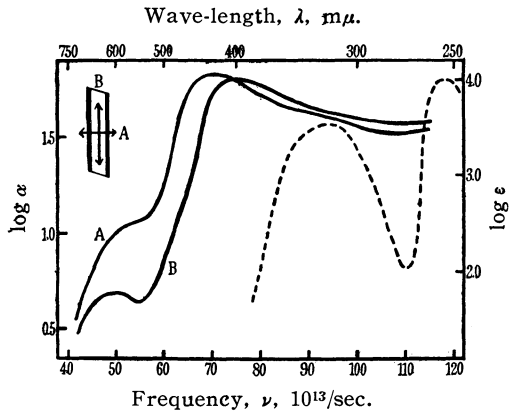

Fig. 4. Ultra-violet absorption spectra of bis-(*o*-formylphenolato)-copper (II). The absorption spectrum of *o*-formylphenol in hexane (dotted curve) is taken from R. A. Morton and A. L. Stubbs, *J. Chem. Soc.*, 1940, 1347.

TABLE IV

ABSORPTION MAXIMA OF BIS-(*o*-FORMYLPHENOLATO)-COPPER (II)

	ν, 10^{13}/sec.	log α	ν, 10^{13}/sec.	log α
A-abs.	51	1.01	69	1.82
B-abs.	51	0.70	73	1.84

show a band at about 50×10^{13}/sec. (band A) and another band at about 65×10^{13}/sec. and shorter wave-length. The latter band may be considered as due to the electronic transition in the *o*-formylphenolate ion co-ordinating to the copper atom, and should be designated as a specific band. The analysis of the crystal structure is not available as yet. Comparing the polarized absorption spectra of this compound with those of the other cupric complexs, however, we can readily assign the A- and B- absorption as representing the characteristics of the ||- and ⊥-absorption. Assuming the above assignment, the following relationships may be derived on the dichroism of the bis-(*o*-formylphenolato)-copper (II). (1) For the band A, the ||-absorption is greatly hyperchromic to the ⊥-absorption. (2) For the specific band, the ||-absorption is bathochromic to the ⊥-absorption.

Discussion of the Results

General Rules on the Polarized Absorption Spectra of the Cupric Complexes.—The planar complexes of copper (II) that have been examined in the present work are seen to show analogous absorption spectra and a quite similar type of dichroism. The four complexes exhibit two kinds of absorption bands, one in the visible region and the other in the ultra-violet.

The former (band A) may be considered as originating from the copper atom bound to the ligands. Reviewing the experimental data, the following rules which are common for the four cupric complexes may be derived for the band A. *The ||-absorption is much higher in intensity than the ⊥-absorption.* The same rule was also shown to hold for bis-(ethylenediamine)-copper (II) complexes[14] and bis-(dimethylglyoximato)-copper (II)[15]. In the previous papers[3], a similar relation on the dichroism was obtained with planar complexes of palladium (II) for the absorption band which was assumed to be due to the co-ordinate linkage between the metal and the ligands. The above rule on the dichroism implies that the electric moment responsible for the band in question is greater along the plane of the complex than that normal to the complex plane. This relationship seems to be readily understandable in a qualitative way. Thus, since the linkage lies in the plane of the complex, the electrons concerned with the linkage would be excited more readily with the electric vector along the plane of the complex than with the electric vector normal to the plane.

It is seen that with the four cupric complexes there are two types of dichroism for the band A. For the one, the ||- and ⊥-absorption show a band A at almost identical wave-lengths, and for the other, the ||- and ⊥-absorption show their band A at different wave-lengths. To the latter type, for example, belongs the acetylacetonato-complex. In the crystal of bis-(ethylenediamine)-copper (II) perchlorate also was observed a similar splitting of the band A, which was ascribed to the perturbations from the surrounding complex ions and anions[14]. According to the X-ray study, the closest distance between the copper atom and one CH group in the α-position of an adjacent molecule is 2.84 Å in the crystal of the acetylacetonato-complex, suggesting a kind of weak interaction between them. Therefore, the splitting of the band A in this compound might be ascribed mainly to the interaction between the *d*-electron of the copper atom in one molecule and the π-electron of the CH group in another in the crystalline state. Thus, the above interaction acting perpendicularly to the plane of the cupric complex is expected to give rise to the bathochromic shift with the ⊥-absorption.

14) S. Yamada and R. Tsuchida, This Bulletin, **29**, 289 (1956).
15) S. Yamada and R. Tsuchida, ibid., **27**, 156 (1954).

In connection with this, it also seems noteworthy that the absorption maximum for the band A of the acetylacetonato-copper (II) in the crystalline state is found at a wavelength considerably shorter than that in the solution. This fact suggests some bathochromic effect of the solvent molecules on the complex in solution. This effect may be due to close approach of the solvent molecules to the copper atom along the direction normal to the plane of the complex. The interaction between the complex molecules in the crystalline state might also be possible. The effect of the solvent molecules on the planar complexes, however, seems to be more probable, since the interaction between the complex molecules would be expected to cause bathochromic effect. This phenomenon would be similar to the bathochromic shift with the aqueous solution of bis-(ethylenediamine)-copper (II) complexes, where weak linkage of the solvent molecules to the copper atom was assumed in the direction along the normal to the plane of the complex[14].

The absorption band at the shorter wavelength may be considered as due to the characteristic absorption of the isolated ligands. It is seen that the characteristic absorption, which is exhibited by the isolated ligand in the ultra-violet region, is modified and displaced toward the longer wave-length when it is combined with the metal atom to form a complex molecule. As to the specific band of the ligand in the cupric complex, the present measurement shows (1) that *the absorption parallel to the π-electron system of the ligand is bathochromic to the absorption normal to the π-electron system*, and (2) that *the intensity is of almost equal magnitude for both the ||- and ⊥-absorption.*

For the isolated molecules of the ligands that have been treated in the present work, we may expect a dichroism which is similar to that for the benzene ring, since all of them involve a conjugated π-electron system. It was formerly established for the isolated benzene derivatives that the absorption parallel to the benzene ring is highly hyperchromic and slightly bathochromic to the absorption normal to the ring[16]. The above rule (1) seems to be similar to the relation derived for the isolated benzene derivatives. The polarization property of the ligand is retained in this respect, when the ligand combines with the metal. The rule (2), however, is quite different from that with the benzene derivatives or from what would be expected for the isolated π-electron systems. Thus, the ⊥-absorption which is forbidden in the isolated system of the ligand is seen to be allowed in forming the metallic complex. This change as to the polarization property of the specific band may be ascribed to the disturbance caused on the ligand when combining with the metal atom.

Absorption Spectra and Electronic Structure.—Comparison of the frequency at the maximum of the band A among the cupric complexes with different ligand ions gives the following hypsochromic order of the ligands: acetylacetone>salicylaldehyde>tropolone, hinokitiol. This order may be taken as one measure for the effect of the ligand on the electronic state about the copper. Thus, it is supposed that the effect of the ligand ion on the copper atom decreases in the above order.

The oxygen atoms directly attached to the metal atom would be greatly influenced by the neighbouring carbon atoms in the same ligand. According to Calvin et al.[17], who extensively studied stability constants of cupric complexes with a number of β-diketones, the most profound change within a ligand on its complex formation may be in the nature of the double bond between the two carbon atoms of the three-carbon systems forming the conjugated chain between the two oxygen atoms. They found a straightforward correlation between the stability constant of the cupric complexes and the nature of the double bond in the three-carbon systems of the conjugated chain. In those compounds which are treated in the present paper, the linkage between the oxygen and copper atom might involve, besides the ordinary σ-bond, some amount of additional π-binding which would be due to an overlap of atomic orbitals of the oxygen and copper atom. Thus, the chelate-ring system comprising the metal atom in the above type of compounds may be supposed to involve the conjugation of more or less unsaturated linkages, which would be somewhat analogous to that in the aromatic ring[17]. Going further on this assumption, the greater conjugation the many-carbon system between the two oxygen atoms would involve, the greater would be the contribution of the π-bond between the copper and oxygen atom, resulting in the stronger linkage between the metal and the ligand, which would yield

16) R. Tsuchida, M. Kobayashi and K. Nakamoto, *J. Chem. Soc. Japan*, **70**, 12 and 14 (1949) (in Japanese); K. Nakamoto, *J. Am. Chem. Soc.*, **74**, 390 (1952), etc.; G. Scheibe, S. Hartwig and H. Müller, *Z. Elektrochem.*, **49**, 372 (1943).

17) M. Calvin and K.W. Wilson, *J. Am. Chem Soc.*, **67**, 2003 (1945).

the more hypsochromic shift of the absorption band A[18].

Following the hypothesis[19] that tropolone is a vinylog of an enolized β-diketone, with the linkage of a small bond order between the carbon atoms 1 and 2 (Fig. 5), the seven-

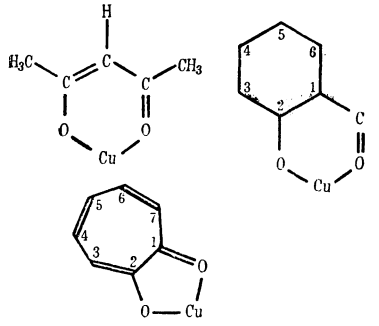

Fig. 5.

carbon system of tropolone might be assumed to have a structure similar to that of acetylacetone, involving considerable conjugation between the two oxygen atoms. The present measurement, however, indicates that with respect to the absorption band A, which is supposed to be closely connected with the linkage between the copper and the ligand, the tropolonato-copper complex is highly bathochromic to the acetylacetonato-copper. The wave-length difference between them seems to be so marked that it would be reasonable to suppose that the linkages around the copper atom in the tropolonato-complex are considerably different from those in the acetylacetonato-complex. That is, besides the contribution of the vinylog structure, we can not overlook the contribution in tropolone of a structure which involves linkage between carbon atoms 1 and 2 having a bond order considerably larger than a single bond. This assumption appears to be in agreement with the hypothesis that the tropolone ring involves some amount of aromaticity[20].

On the other hand, the present measurement also indicates that the cupric complex of salicylaldehyde shows its absorption band A at the shorter wave-length than the complex of tropolone, suggesting a stronger effect on the copper atom of salicylaldehyde than that of tropolone. Assuming for the compounds of the above type a similar criterion to that proposed by Calvin et al.[17], the stronger effect on the copper atom of salicylaldehyde seems to indicate a higher bond order of the carbon-to-carbon linkage (C_1—C_2) between the two oxygen atoms in salicylaldehyde than the corresponding C_1—C_2 linkage in tropolone (Fig. 5). This appears to be in agreement with the current concept on the structure of the tropolone ring.

When the ligand combines with a metal atom, the absorption of the ligand is seen to undergo some change or other according to the magnitude of the effect on the ligand. The magnitude of the change in the specific absorption band as compared with the original absorption of the isolated ligand may be taken roughly as one measure of the change in the electronic state of the ligand within the complex as compared with the free ligand. As the conjugation of the linkages would become greater within the chelate-ring involving the metal atom, the greater effect might be caused on the electronic state of the ligand and, in consequence, on its characteristic absorption. Thus, inspection of the previous data with the complexes in solution shows that the shift of the specific band of the metallic complex from the characteristic absorption of the free ligand molecule is smaller with the compound of tropolone than with the corresponding compound of acetylacetone and salicylaldehyde (Table V). This is parallel with the results described in the foregoing part of the present paper, leading to the same conclusion as that derived in the above.

TABLE V

WAVE-LENGTH SHIFT OF THE CHARACTERISTIC BAND OF THE LIGAND ON COMPLEX FORMATION WITH THE COPPER ATOM

Ligand	$\Delta\nu$, 10^{13}/sec.	ref.
Tropolone	1.2	(a), (b)
Salicylaldehyde	1.9	(c), (d)
Acetylacetone	8	(d), (e)

(a) J.W. Cook, A.R. Gibbs, R.A. Raphael and A.R. Somerville, *J. Chem. Soc.*, **1951**, 503.
(b) M. Tsuboi, This Bulletin. **25**, 369 (1952).
(c) R.A. Morton and A.L. Stubbs, *J. Chem. Soc.*, **1940**, 1347.
(d) K. Sone, *J. Am. Chem. Soc.*, **75**, 5207 (1953).
(e) P. Grossmann, *Z. physik. Chem.*, **109**, 305 (1924).

A similar frequency shift of the absorption band of the ligand may be expected in the infra-red spectra. Thus, the carbonyl stretching frequency of the free ligand molecule undergoes a shift to the lower frequency on its complex formation. As shown in Table VI, inspection of previous data seems to indicate that frequency shift is greatest for acetylacetone and smallest for tropolone. This is again coincident with the above hypsochromic order, giving another piece of

18) Such arguement is not strictly valid in every case, but may be applicable to those compounds which have a structure closely related to each other.
19) See, for example, W. von E. Doering and L.H. Knox, *J. Am. Chem. Soc.*, **74**, 5684 (1952), etc.
20) See, for example, T. Nozoe, *Proc, Japan Acad.*, **26**, 30 (1950), etc.

TABLE VI

FREQUENCY SHIFT OF THE C=O STRETCHING ON COMPLEX FORMATION

Compound	Free, cm^{-1}	Cu(II)-compd., cm^{-1}	ref.
Acetylacetone	1639–1538	1550–1562	a
Salicylaldehyde	1661	1600	b
Tropolone	1615	1510, 1595	c

(a) R.S. Rasmussen, D.D. Tunnicliff and R.R. Brattain, *J. Am. Chem. Soc.*, **71**, 1068 (1949); J.Le Comte, *Discuss. Faraday Soc.*, **9**, 125 (1950).
(b) I.M. Hunsberger, ibid , **72**, 5626 (1950).
(c) H.P. Koch, *J. Chem. Soc.*, **1951**, 512.

evidence for the conclusion on the electronic state of the ligands which has been reached in the former part of the present paper.

Summary

Polarized absorption spectra of cupric complexes with tropolone, hinokitiol, acetylacetone and salicylaldehyde have been determined in the visible and ultra-violet by Tsuchida-Kobayashi's microscopic method. The above compounds all exhibit two bands at about 40 to 55×10^{13}/sec. (band A) and at about 70×10^{13}/sec. or shorter wave-length (specific band). The following rules on the dichroism which are common for the above complexes, have been induced:

For the band A, the absorption parallel to the complex plane is highly hyperchromic to the absorption normal to the complex plane. For the specific band, the absorption parallel to the π-electron system is found considerably bathochromic to the absorption normal to the plane.

With different ligand ions, the wave-length of the band A of the cupric complexes have been compared, and the following hypsochromic order has been derived: acetylacetone> salicylaldehyde>tropolone, hinokitiol. The same order has been found for the wave-length shift of the specific band from the corresponding band of the free ligand.

The above results have been discussed in relation to the electronic state of the complexes and the ligands.

We thank Professor T. Nozoe and his collaborators for supplying us with the samples of the tropolonato- and hinokitiolato-complexes and drawing our attention to these compounds. We are also indebted to Professor M. Nakagawa for helpful discussions. The financial support of this work by the Education Ministry is gratefully aknowledged.

Department of Chemistry, Faculty of Science, Osaka University, Osaka

Determination of Nitrate Nitrogen by the Strong Phosphoric Acid-Iodic Acid Decomposition Method

By Shigeru OHASHI and Hiroshi MAKISHIMA

(Received April 24, 1956)

In the previous papers[1,2] one of the authors reported new methods for the determination of nitrogen in organic compounds by the strong phosphoric acid (SPA)-iodic acid decomposition. Organic compounds such as amines and azo-compounds or ammonium salts are decomposed by heating with a mixture of SPA and potassium iodate to liberate the nitrogen contained in them. By sending the liberated nitrogen with carbon dioxide into an azotometer, filled with potassium hydroxide solution, the nitrogen can be determined gas-volumetrically. The nitrogen in nitro or oxime compounds can also be determined by the SPA-iodic acid decomposition method after their reduction with a mixture of metallic iron powder and diluted sulfuric acid to the corresponding amines.

The purpose of the present investigation is to extend these methods to the determination of nitrogen in nitrates. Since nitrates or nitro compounds can not be directly decomposed to free nitrogen by the SPA-iodic acid decomposition method, nitrates should be converted into amines or ammonium salts prior to the decomposition.

A recent paper of T. Nakamura and F. Yamazoe[3] describing various methods for the determination of nitrate nitrogen in fertilizers concluded that the iron reduction method followed by the Kjeldahl distillation

1) S. Ohashi, This Bulletin, 28, 177 (1955).
2) S. Ohashi. This Bulletin, 28, 537 (1955).
3) T. Nakamura and F. Yamazoe, *The Bulletin of the National Institute of Agricultural Sciences* (Japan), Series B, No. 2, 1 (1953).

was the best. In the first place it was tried in the present investigation to combine the iron reduction method with the SPA-iodic acid decomposition method. However, when a small amount of iron was used, the authors obtained low values for nitrogen, due to incomplete reduction of nitrate. In the case of a large amount of iron, high values for nitrogen resulted, probably because some iron remained in the reaction medium and hydrogen was liberated during the decomposition with a mixture of SPA and potassium iodate. So it was difficult to find out the optimum amount of iron to be used.

It was then tried to combine the modified Gunning method[4] with the SPA-iodic acid decomposition method. The modified Gunning method involves three main steps as follows: (1) Solution of the nitrate in salicylic-sulfuric acid, for converting the nitrate into nitrosalicylic acid. (2) Treatment of the nitro compound with sodium thiosulfate to reduce it to an amino or ammonium compound. (3) The Kjeldahl digestion and distillation of the resulting compound. In this investigation the Kjeldahl digestion and distillation in the above mentioned steps were replaced by the SPA-iodic acid decomposition and statisfactory results were obtained.

Apparatus and Reagents

The apparatus used in the present experiment was almost the same as that described in the previous papers, but as shown in Fig. 1 a gas-safety bulb, filled with 42% aqueous solution of glycerine, was inserted between the reaction vessel and a Kipp's carbon dioxide generator in order to prevent a possible leak of the liberated nitrogen from the reaction vessel.

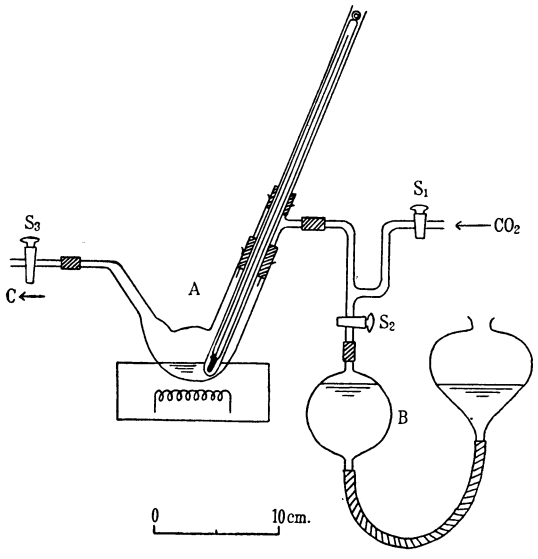

Fig. 1. Apparatus.
A: Reaction vessel B: Gas-safety bulb
C: Azotometer S_1–S_3: Stopcocks

The reagents were all of extra pure grade. The method for the preparation of strong phosphoric acid was described in the previous paper[1].

Results and Discussion

Since the decomposition process is carried out in a SPA medium, it seems to be convenient for the nitration process to be also done in the same medium. Therefore, at first, a mixture of salicylic acid and SPA was employed as a nitration reagent, but low results were given. Probably this may be due to the fact that salicylic acid is not easily dissolved in SPA. Using a common 89% orthophosphoric acid, also similar results were obtained. For this reason salicylic acid dissolved in concentrated sulfuric acid was used for the nitration. In the modified Gunning method the nitration is carried out by standing a reaction mixture for thirty minutes at room temperature. In the present study, however, according to the procedure suggested by W. E. Dickinson[5], the nitration was done by heating the reaction mixture for about fifteen seconds. For the reduction of the resulting nitrosalicylic acid, iron metal powder was tested as the reducing agent, but it was not favorable, as it required too much time and patience for the complete reaction. Thus, according to the general procedure, sodium thiosulfate was employed in its place. After examining several conditions for the determination of these facts, the following procedure was recommended.

Procedure.—Weigh a sample corresponding to about 6 to 12 mg. of NO_3 in a small weighing tube; place it in a reaction vessel and add 1.5 to 2.0 ml. of concentrated sulfuric acid containing 70 mg. of salicylic acid. Rotate the contents in the tip of a Bunsen burner for about fifteen seconds to dissolve all nitrate. To the still hot contents in the vessel add nearly 50 mg. of sodium thiosulfate and heat the contents with a small electric heater for four to five minutes until sufficient white fumes of sulfuric acid are produced. Add 5 ml. of strong phosphoric acid into the vessel. After completely cooling the contents, add 1.5 g. of potassium iodate to it. Now connect the reaction vessel with a carbon dioxide generator through the gas-safety bulb. After elevating the head of the liquid in the bulb slightly to the stopcock S_2, remove the air present in the vessel and connect it with an azotometer. Heat the mixture in the vessel with a small electric heater at 200 to 250°C and transfer the produced gas into the bulb. After the complete decomposition, transfer

4) H.C. Moore, *Ind. Eng. Chem.*, **12**, 669 (1920).

5) W.E. Dickinson, *Anal. Chem.*, **26**, 777 (1954).

the liberated nitrogen into the azotometer by sweeping it with carbon dioxide. From the volume of the nitrogen collected in the azotometer deduct the blank value (about 0.04 ml. in the authors' experiment) and calculate the percentage of the nitrogen.

The data obtained for potasium nitrate by means of this method were shown in Table I. The calculated value of nitrogen in the

TABLE I
DETERMINATION OF NITROGEN IN POTASSIUM NITRATE

Sample Weight mg.	N, Calcd. %	N, Found %	Deviation %
10.4	13.47	13.2	−0.3
12.3	〃	13.6	+0.1
17.1	〃	13.5	0.0
18.2	〃	13.5	0.0
18.8	〃	13.3	−0.2
19.8	〃	13.3	−0.2

Table was gravimetrically obtained by the nitron method. The accuracy for the results obtained is within ±2%. The time taken for an analysis is fifty to sixty minutes.

Since it was expected that this method can be effectively adopted to the analysis of nitrogenous fertilizers, some problems concerning this aspect were investigated. As shown in Table II, the presence of consider-

TABLE II
EFFECT OF SEVERAL SUBSTANCES ON DETERMINATION OF NITROGEN IN POTASSIUM NITRATE

KNO_3-Sample Weight mg.	Other Salts	mg.	N, Calcd. %	N, Found %	Deviation %
17.2	KCl	20	13.47	13.5	0.0
15.9	〃	30	〃	13.7	+0.2
15.7	〃	30	〃	13.4	−0.1
19.4	$FeSO_4$	20	〃	13.3	−0.2
18.6	$Fe_2(SO_4)_3$	20	〃	13.3	−0.2
19.1	〃	20	〃	13.2	−0.3
19.4	$CaCO_3$	20	〃	13.6	+0.1
18.5	〃	20	〃	13.2	−0.3

able amounts of chloride, ferrous and ferric iron, and calcium does not produce a serious error in the determination of nitrate nitrogen by this method. Of course a large amount of sulfate or phosphate has no injurious effect on this method. Nitrite can not be directly determined by this method. Therefore it seems that nitrite must be oxidized to nitrate prior to the nitration process.

When both nitrate and ammonium salt are present the total nitrogen can be determined by this method and only the ammonium nitrogen can be directly determined by the SPA-iodic acid decomposition method after expelling nitric acid by heating with SPA. When nitrate, ammonium salt, and urea are present together the total nitrogen and the sum of nitrogen in ammonium salt and urea can similarly be determined. These results are summarized in Table III and IV.

TABLE III
DETERMINATION OF NITROGEN IN POTASSIUM NITRATE AND AMMONIUM SULFATE

Sample Weight mg.	Total N		
	Calcd. %	Found %	Deviation %
20.0	17.17	17.2	0.0
〃	〃	17.0	−0.2
〃	〃	16.8	−0.4
〃	〃	17.4	+0.2
〃	〃	17.1	−0.1
Sample Weight mg.	**Ammonium N**		
	Calcd. %	Found %	Deviation %
20.0	10.44	10.4	0.0
〃	〃	10.3	−0.1
〃	〃	10.4	0.0
〃	〃	10.4	0.0
〃	〃	10.4	0.0

TABLE IV
DETERMINATION OF NITROGEN IN POTASSIUM NITRATE, AMMONIUM SULFATE, AND UREA

Sample Weight mg.	Total N		
	Calcd. %	Found %	Deviation %
15.7	27.92	27.2	−0.2
15.0	27.00	26.7	−0.3
15.9	28.12	27.8	−0.3
15.1	27.06	26.7	−0.4
Sample Weight mg.	**Ammonium N+Urea N**		
	Calcd. %	Found %	Deviation %
15.1	22.69	22.2	−0.5
15.4	23.08	23.4	+0.3
14.6	21.77	21.9	+0.1

Summary

(1) The strong phosphoric acid-iodic acid decomposition method for the determination of nitrogen in organic compounds, which was already reported, has been extended to the analysis of nitrate nitrogen.

(2) In a reaction vessel salicylic acid was nitrated by heating with the sample and concentrated sulfuric acid and the product was reduced by heating with sodium thiosulfate. The resulting mixture was decomposed by heating with a mixture of strong phosphoric

acid and potassium iodate. The liberated nitrogen was measured gas-volumetrically.

(3) In the presence of nitrate, ammonium salt, and urea, the total nitrogen and the nitrogen except nitrate could be determined by the strong phosphoric acid-iodic acid decomposition method, respectively.

Acknowledgments are made to Prof. T. Kiba for his interest and encouragement. The expense for the experiment has been defrayed from a grant given by the Ministry of Education, to which the authors' thanks are due.

Department of Chemistry, Faculty of Science, Kanazawa University
Kanazawa

Calculation on the Changes of Vibrational Frequencies due to Electronic Excitation in Several Organic Molecules

By Tosinobu ANNO*, Akira SADÔ and Ikuo MATUBARA

(Received April 4, 1956)

Introduction

In the vibrational analysis of the electronic spectrum it is important to know the correspondence between the vibrational frequencies in the ground electronic state and those in the excited state. This correspondence together with the Franck-Condon principle enables one to know about the change of the shape and dimension of the carrier molecule caused by an electronic excitation. This correspondence has hitherto been determined on the basis of the empirical facts found in similar molecules. To contribute a theoretical basis to this problem, a method will be proposed and will be applied to benzene, mesitylene, 1,3,5-trichlorobenzene and *p*-dichlorobenzene. The method is of the first approximation, as will be discussed later, but it can explain the frequency changes at least qualitatively.

Method of Calculation

The essential idea of the present method is that the bond-order is calculated by the empirical LCAO MO method for the two electronic states and the bond-length is deduced from the bond-order bond-length relation. Badger's relation[1,2] is used to calculate the stretching force constant, and the deformation force constant is deduced from a rather well established frequency. These force constants are then used to calculate the vibrational frequencies in the valence-force-field approximation.

Excepting the mesitylene molecule, the calculation of the orbital coefficients in the LCAO form was performed with the assumptions described elsewhere[3]. In the case of mesitylene, only the hyperconjugation perpendicular to the plane of the benzene ring was taken into account, assuming that the coulomb integral of the quasi H_3 "atom" is equal to the coulomb integral of the carbon atom in benzene[4], and that the resonance integral of $C{\equiv}H_3$ bond is equal to 4.83 times the resonance integral of the C–C bond in benzene[5]. The definition of the bond-order is the same as that of Coulson and Longuet-Higgins[6].

Bond-lengths were deduced from bond-orders with the help of Coulson's curve[7] for C–C bonds, taking into account the effect of hybridization[8]. For C–Cl bonds the order-length curve due to Anno and Sadô[3] was used with an appropriate modification which takes account of the effect of hybridization of carbon σ-atomic orbital only.

* Department of Chemistry, College of General Education, Kyushu University, Fukuoka.

T.A. is greatly indebted to the Dean of the Faculty of Science and Professor S. Imanishi for permitting him to continue his work in the Faculty.

1) R.M. Badger, *J. Chem. Phys.* **2**, 128 (1934).
2) R.M. Badger, *J. Chem. Phys.* **3**, 710 (1935).
3) T. Anno and A. Sadô, This Bulletin, **28**, 350 (1955).
4) R.S. Mulliken, C.A. Rieke and W.G. Brown, *J. Am. Chem. Soc.* **63**, 41 (1941).
5) Mulliken et al. (ref. (4)) took the resonance integral β^* of the $C{\equiv}H_3$ bond equal to 4.06 times the β_{CC} at $r = 1.33$ Å. Since β_{CC} in benzene ($r = 1.39$ Å) is 0.84 times β_{CC} at 1.33 Å according to Mulliken, we took $\beta^* = (4.06/0.84)\beta_{benzene} = 4.83\beta_{benzene}$.
6) C.A. Coulson and H. C. Longuet-Higgins, *Proc. Roy. Soc.* (London), **A191**, 39 (1947).
7) C.A. Coulson, *Proc. Roy. Soc.* (London) **A169**, 413 (1939).
8) C.A. Coulson, "Victor Henri Memorial Volume", Meson Desoer, Liège (1948), p. 15.

Badger's relation[1,2] of the following form was used to obtain the stretching force constant from the above-obtained values of bond-length:

$$r_e=(C/k_e)^{1/3}+d, \qquad (1)$$

where r_e and k_e are the equilibrium distance and the force constant of the bond, respectively, and C and d are constants. The physical meaning proposed by Badger[1] for d is that it represents the most approachable distance of the atom pair. It varies considerably from pair to pair. The meaning of C is not obvious. It remains rather constant as compaired with d. In fact Badger took it as a universal constant in the first paper of his series[1]. In Fig. 1 the inverse third power of the force constants of C–C bonds in several molecules are plotted against bond-lengths. In the same figure a line (*b*) is drawn through the point for benzene with the slope of $(1.86)^{1/3}$ (this is equal to the value of $C^{1/3}$ taken as a universal constant in Badger's first paper[1]) and it is seen that the line passes through the point for ethylene. If we draw straight lines parallel to the line *b* through points for acetylene and ethane, two lines *a* and *c* are obtained, which cut the r_e-axis at 0.717 and 0.798 Å, respectively, while the line *b* cuts the same axis at 0.765 Å. These values may be considered to represent three different *d*-values for C–C bond corresponding to three different states of hybridization of carbon atoms (*a*, *b*, *c* correspond to sp, sp^2, sp^3, respectively). Since Coulson[8] has shown that the carbon atom takes different covalent radii depending on its state of hybridization, it may be considered that this causes the change of the most approachable distance in the C–C bonds in the respective states of hybridization. If this is correct, the *d*-values for carbon atom pairs corresponding to sp, sp^2 and sp^3 hybridizations should have a sequence $d(\text{sp-sp})<d(\text{sp}^2\text{-sp}^2)<d(\text{sp}^3\text{-sp}^3)$. This is actually the case for lines *a*, *b* and *c* in Fig. 1. For this reason we assume that the relation (1) holds, where C is a universal constant but d may have different values depending upon the species and the states of hybridization of the participating atoms.

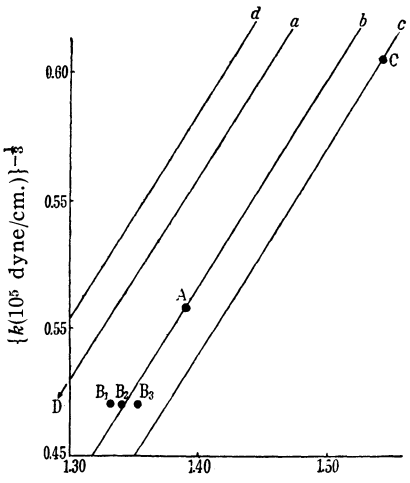

Fig. 1. Badger's rule for the C–C bonds.
a Drawn parallel to line *d* through the point for acetylene (not shown in the figure).
b Drawn parallel to line *d* through the point for benzene.
c Drawn parallel to line *d* through the point for ethane.
d From Badger's original paper (reference 1).

$$r=(1.86/k)^{\frac{1}{3}}+0.68$$

A: Benzene
(r=1.39 Å[a], k=7.61×10⁵ dyne/cm.[b]).
B_1: Ethylene
(r=1.331 Å[c], k=9.57×10⁵ dyne/cm.[d]).
B_2: Ethylene
(r=1.340 Å[e], k=9.57×10⁵ dyne/cm.[d]).
B_3: Ethylene
(r=1.353 Å[f], k=9.57×10⁵ dyne/cm.[d]).
C: Ethane
(r=1.543 Å[g], k=4.50×10⁵ dyne/cm.[h]).
D: Acetylene
(r=1.207 Å[i], k=15.80×10⁵ dyne/cm.[j]).

a V. Schomaker and L. Pauling, *J. Am. Chem. Soc.*, **61**, 1769 (1939).
b F.M. Garforth, C.K. Ingold and H.G. Pool, *J. Chem. Soc.*, **1948**, 491.
c H. W. Thompson, *Trans. Faraday Soc.*, **35**, 697 (1939).
d G. Herzberg, "Infrared and Raman Spectra of Polyatomic Molecules", D. Van Nostrand Co. Inc., New York (1945) p. 184.
e C.A.Coulson, "Victor Henri Memorial Volume", Meson Desoer, Liége, (1948) p. 15.
f W. S. Gallaway and E. F. Barker, *J. Chem. Phys.*, **10**, 88 (1942).
g G.H. Hansen and D. M. Dennison, *J. Chem. Phys.*, **20**, 313 (1952).
h Reference d p. 193.
i Reference d p. 398.
j Reference d p. 180.

In Fig. 2 the inverse third power of the force constants and the bond-lengths of the C–Cl bonds in chloroacetylene and methyl chloride are plotted as in Fig. 1 for C–C bonds. The straight lines *a* and *c* passing through the points for chloroacetylene and methyl chloride, respectively, are drawn with the slope of $1.86^{1/3}$ (see above). The line *a* gives a smaller *d*-value than the line *c*. This difference may result from the difference of the state of hybridization of the carbon atom. The state of hybridization of the carbon atom attached to the chlorine atom in chlorobenzenes is undoubtedly the intermediate of those in chloroacetylene and methyl chloride. Unfortunately, since we have neither the

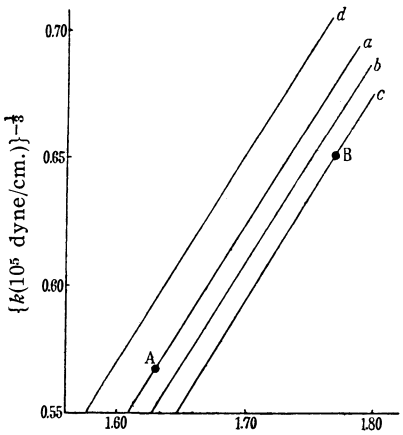

Fig. 2. Badger's rule for the C–Cl bonds.
a Drawn parallel to line *d* through the point for chloroacetylene.
b Drawn parallel to line *d* and at the middle of lines *a* and *c*.
c Drawn parallel to line *d* through the point for methyl chloride.
d From Badger's original paper (reference 1).

$$r=(1.86/k)^{\frac{1}{3}}+0.900.$$

A: Chloroacetylene (r=1.63 Åa, k=5.52×10⁵ dyne/cm.b).
B: Methyl chloride (r=1.77 Åa, k=3.64×10⁵ dyne/cm.c).

a Landolt-Börnstein, "Zahlenwerte und Funktionen", Springer, Berlin, (1951).
b W.S. Richardson and J.H. Goldstein, *J. Chem. Phys.*, 18, 1314 (1950).
c G. Herzberg, "Infrared and Raman Spectra of Polyatomic Molecules", D. Van Nostrand Co. Inc., New York (1945) p. 193.

precise knowledge of the hybridization of the carbon atoms in these molecules nor the quantitative knowledge about the variation of the *d*-values as a function of the state of hybridization, the line *b*, which we use throughout this paper, is drawn just in the middle of the lines *a* and *c*. Our conclusion may be little affected by the arbitrariness of drawing the line *b*, since we are concerned only with the change of vibrational frequencies in the two electronic states of a particular molecule, and not with the calculation of the absolute values of the vibrational frequency themselves.

Furthermore, we assume implicitly that the states of hybridization of the atoms are not affected by the electronic excitation. Briefly, we deduce the force constants from the calculated bond-lengths using the lines *b* of Figs. 1 and 2 for C–C and C–Cl bonds, respectively, both for the ground and the excited electronic states.

Bond-order, Bond-length and Bond-force-constant

The calculated values of bond-order, bond-length, and bond force-constant are shown in Tables I and II for the ground and the first excited states, respectively. Numberings of atoms are shown in Fig. 3. One thing should be mentioned in regard to the calculations for the first excited states of benzene, mesitylene and 1, 3, 5-trichlorobenzene. It can be shown that the first excited states of these molecules are accidentally degenerate and single configurations do not represent the excited states for these molecules even when the configurational interaction is neglected, because the wave functions corresponding to single configurations do not form the bases of the irreducible representations of the

TABLE I
CALCULATED VALUES OF BOND-ORDERS, BOND-LENGTHS, AND BOND-FORCE-CONSTANTS IN THE GROUND ELECTRONIC STATES

Molecule	Bond	Total bond-order	Bond-length (in Å)	Bond-force-constant (in 10⁵ dyne/cm.)
Benzene	C_1–C_2	1.667	1.390	7.61
Mesitylene	C_1–C_2	1.661	1.390	7.61
	C_1–C_1'	1.125	1.498	5.05
1, 3, 5-Trichlorobenzene	C_1–C_2	1.635	1.395	7.40
	C_1–Cl_1	1.320	1.687	4.68
p-Dichlorobenzene	C_1–C_2	1.633	1.395	7.45
	C_2–C_3	1.675	1.388	7.70
	C_1–Cl_1	1.298	1.691	4.60

TABLE II
CALCULATED VALUES OF BOND-ORDERS, BOND-LENGTHS, AND BOND-FORCE-CONSTANTS IN THE FIRST EXCITED STATES

Molecule	Bond	Total bond-order	Bond-length (in Å)	Bond-force-constant (in 10⁵ dyne/cm.)
Benzene	C_1–C_2	1.500	1.416	6.75
Mesitylene	C_1–C_2	1.497	1.415	6.79
	C_1–C_1'	1.138	1.496	5.08
1, 3, 5-Trichlorobenzene	C_1–C_2	1.523	1.413	6.90
	C_1–Cl_1	1.334	1.684	4.73
p-Dichlorobenzene	C_1–C_2	1.555	1.407	7.04
	C_2–C_3	1.481	1.418	6.68
	C_1–Cl_1	1.472	1.665	5.11

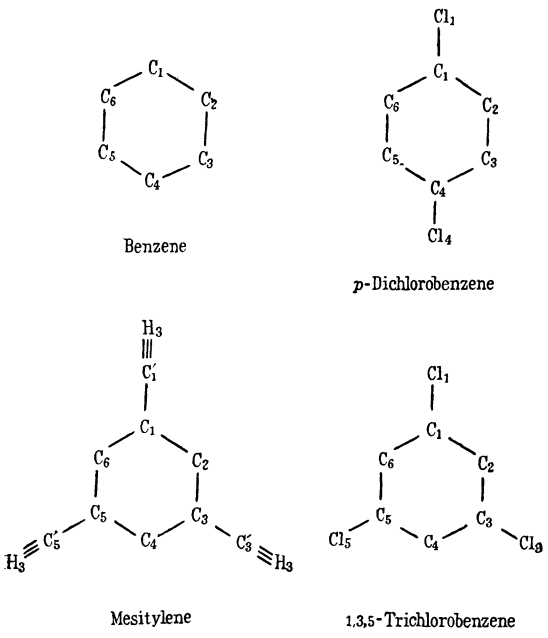

Fig. 3

point groups appropriate to these molecules. But it is easy to obtain, by linearly combining the configurational functions, the wave functions which do form the bases of the irreducible representations of the molecular point groups. These combinations involve only two configurational functions, which differ from each other in the assignment of two electrons so that the bond-orders for the states result only from superpositions of the participating configurations. Thus, the bond-order is found to be the same in the accidentally-degenerate first-excited states of particular one of these molecules.

Calculation of Vibrational Frequencies

In this paper we shall confine ourselves to the totally symmetrical skeleton vibrations since these appear more prominently in UV spectra for those molecules treated in the present paper than the other types of vibration.

Benzene.—For the benzene molecule the value of the C–C stretching force constant is only required to calculate the totally symmetrical skeleton vibrational frequency. The results are shown in Table III. Since the ground-state value is used to establish the line *b* in Fig. 1, the corresponding calculated value is in brackets. Comparison of the calculated values with the observed ones will be discussed later.

Mesitylene, 1, 3, 5-Trichlorobenzene and *p*-Dichlorobenzene.—In the case of the mesitylene molecule as well as other molecules than benzene, the totally symmetrical skeleton-vibrational frequencies are determined not only by bond-stretching force constants but also by bending force constants. These bending force constants come into the secular equation for each molecule as the combination of only one kind among them. So, one vibrational frequency for each molecule is sufficient to determine the value of the combination of bending force constants, and the other frequencies may be calculated. The results are shown in Table IV. The frequencies used for calculating deformation force constants are in brackets. The choice of the frequency from which the value of the deformation force constant was calculated was made on the basis of the following two conditions:

(i) Assignment of the frequency must be certain.

(ii) The corresponding vibrational mode must be mainly of deformation, in which case a large change in frequency yields only a small change in deduced deformation force constant, or a combination of such constants.

The first singlet-singlet absorption spectrum of mesitylene has been analyzed by Sponer and Stallcup[9]. There seems to be no question in correlating the 968- and 555-cm^{-1} frequencies in the upper state with the 997- and 575-cm^{-1} ground-state values, respectively. They obtained as an upper-state frequency 1300 cm^{-1} and correlated it with the observed Raman shift of 1299 cm^{-1} rather than the alternative one of 1378 cm^{-1}. The former correlation gives a frequency drop by -0.1%, while the latter gives a drop of 5.7%. Sponer and Stallcup preferred the former, commenting that it is not improbable for the corresponding vibrational frequencies in the two electronic states to have nearly

TABLE III

CALCULATED AND OBSERVED VALUES OF TOTALLY SYMMETRICAL SKELETON VIBRATIONAL FREQUENCY OF THE BENZENE MOLECULE

		Calculated	Observed[a]
Ground state (cm^{-1})	A_{1g}	(993)	992
	B_{2u}	937	923
Excited state (cm^{-1})	B_{1u}	937	965
	E_{1u}	937	—
	A_{1g}–B_{2u}	5.6	7.0
Drop(%)[b]	A_{1g}–B_{1u}	5.6	2.7
	A_{1g}–E_{1u}	5.6	—

a Taken from reference 14 and 15 in text.

b $\text{Drop}(\%) = \frac{\nu_{(\text{G.S.})} - \nu_{(\text{E.S.})}}{\nu_{(\text{G.S.})}} \times 100.$

9) H. Sponer and M. J. Stallcup, Ref. (8), p. 222.

TABLE IV

CALCULATED AND OBSERVED VALUES OF TOTALLY SYMMETRICAL SKELETON VIBRATIONAL FREQUENCY OF THE MESITYLENE, 1,3,5-TRICHLOROBENZENE, AND *p*-DICHLOROBENZENE MOLECULES (THE FORCE CONSTANTS USED IN CALCULATION ARE TAKEN FROM TABLE I AND II)

		Calculated			Observed[a]		
		G.S.(cm^{-1})	E.S.(cm^{-1})	Drop(%)[b]	G.S.(cm^{-1})	E.S.(cm^{-1})	Drop(%)[b]
Mesitylene	ν_1	1427	1422	0.4	1299	1300	−0.1
	ν_2	(997)	(968)	—	997	968	2.9
	ν_3	571	537	6.0	575	555	3.5
1,3,5-Trichlorobenzene	ν_1	1351	1332	1.4	1146	1122	2.1
	ν_2	(995)	(963)	—	995	963	3.2
	ν_3	365	360	1.4	375	369	1.6
p-Dichlorobenzene	ν_1	1675	1584	5.4	1589	1461/66	8.1/7.8
	ν_2	1186	1166	1.7	1102	1051	4.6
	ν_3	(755)	(725)	—	755	725	4.0
	ν_4	275	241	12.4	331	244	26.3

a a Taken from: mesitylene, reference 9; 1,3,5-$C_6H_3Cl_3$, reference 10, *p*-$C_6H_4Cl_2$, reference 11, in text.

b See footnote b in Table III.

the same values. According to our calculation the drop amounts to 0.4%, in favor of the correlation by Sponer and Stallcup.

The UV absorption spectrum of 1,3,5-trichlorobenzene was studied by Sponer and Hall[10]. In this case, the correlations of the 963- and 1122-cm^{-1} upper-state frequencies with the 995- and 1146-cm^{-1} ground-state values seem to be certain. The frequency difference of 369 cm^{-1} found in UV spectrum was correlated with the 375-cm^{-1} ground-state value with some reservations. This correlation gives only a small drop of 1.6%, which is not impossible according to Sponer and Hall. The present calculation shows this drop to be 1.4%.

The vibrational analysis of the longest wave length singlet-singlet absorption of *p*-dichlorobenzene was carried out by Anno and Matubara[11]. There can be no doubt in correlating 725 and 1051 cm^{-1} in the excited state with 755 and 1102 cm^{-1} in the ground state. It is reported there that the upper-state frequency corresponding to the 331-cm^{-1} ground-state value may be taken as 244 cm^{-1}, the 331-cm^{-1} frequency being considered as an alternative. The former choice gives a drop of 26.3%, while the latter would give no drop at all. The present calculation gives a drop of 12.4%, in favor of Anno and Matubara's analysis. To the remaining upper-state frequency 1461/66 cm^{-1} the ground-state frequency 1589 cm^{-1} may correspond. It is not certain which component of the band gives the fundamental frequency in the excited electronic state. This correlation gives a drop of 8.1/7.8%. The present calculation gives a drop of 5.4%.

Discussion

The calculated values of bond-order are naturally affected by the assumed values of the coulomb and resonance integrals. Anno and Sadô have recently found the best values of α_{Cl} and β_{CCl} by fitting the calculated shift of the UV spectrum of *p*-dichlorobenzene with experiment and the calculated value of the π-electron loss at the chlorine atom in vinyl chloride with quadrupole coupling data[12]. These values of α_{Cl} and β_{CCl} are also consistent with the experimental data for other chlorinated hydrocarbons. They have also found that the order-length relation holds as well on the basis of these values of α_{Cl} and β_{CCl}, and the relative calculation of C–Cl bond-length from the bond-order is little affected, whether we use these new values of α_{Cl} and β_{CCl} or whether we make the previously described assumption[3]. In order to show the effect of the assumed values of α_{Cl} and β_{CCl} on the changes of the vibrational frequencies of chlorinated benzenes, the calculated values of bond-order, bond-length and force constants for *p*-dichlorobenzene and 1,3,5-trichlorobenzene are listed in Table V. It may be seen in the table that the changes of the force constants for 1,3,5-trichlorobenzene are nearly the same as those given in

10) H. Sponer and M.B. Hall, Ref. (8), p. 211.

11) T. Anno and I. Matubara, *J. Chem. Phys.*, **23**, 796 (1955).

12) T. Anno and A. Sadô, To be published in *J. Chem. Phys.*, July (1956).

TABLE V

CALCULATED VALUES OF BOND-ORDERS, BOND-LENGTHS, AND BOND-FORCE-CONSTANTS FOR 1, 3, 5-TRICHLOROBENZENE AND *p*-DICHLOROBENZENE BASED ON α_{Cl} AND β_{CCl} DERIVED FROM EXPERIMENTAL DATA (SEE TEXT).

Molecule	Bond	Ground states			First excited states		
		Total bond-order	Bond-length (in Å)	Bond-force-constant (in 10^5 dyne/cm.)	Total bond-order	Bond-length (in Å)	Bond-force-constant (in 10^5 dyne/cm.)
1, 3, 5-Trichlorobenzene	C_1–C_2	1.626	1.396	7.42	1.548	1.408	7.02
	C_1–Cl_1	1.242	1.686	4.69	1.256	1.683	4.75
p-Dichlorobenzene	C_1–C_2	1.647	1.393	7.54	1.495	1.416	6.76
	C_2–C_3	1.670	1.388	7.72	1.515	1.413	6.87
	C_1–Cl_1	1.230	1.688	4.65	1.367	1.664	5.15

Tables I and II. As for *p*-dichlorobenzene the changes of the force constants are somewhat different from those listed in Tables I and II. Therefore we have calculated the vibrational frequencies of *p*-dichlorobenzene from the force constants given in Table V in the same manner as described previously. The results are given in Table VI. The calculated values of the changes of the frequency are in accordance with the values listed in Table IV at least qualitatively.

ing of different configurations are not found in the literature except for the ground A_{1g}– and the lowest E_{1u}–states of this molecule[13]. Therefore, we must be content with qualitative considerations. We hope to have another opportunity to discuss this effect more quantitatively.

Our calculated values of bond-orders for benzene are correct in so far as CI is neglected, and are independent of the method of calculation (e. g. simple LCAO MO, anti-

TABLE VI

CALCULATED AND OBSERVED VALUES OF TOTALLY SYMMETRICAL SKELETON VIBRATIONAL FREQUENCY OF *p*-DICHLOROBENZENE (THE STRETCHING FORCE CONSTANTS USED IN CALCULATION ARE TAKEN FROM TABLE V).

		Calculated			Observed[a]		
		G. S. (cm^{-1})	E. S. (cm^{-1})	Drop (%)[b]	G. S. (cm^{-1})	E. S. (cm^{-1})	Drop (%)[b]
p-Dichlorobenzene	ν_1	1677	1587	5.4	1589	1461/66	8.1/7.8
	ν_2	1190	1173	1.4	1102	1051	4.6
	ν_3	(755)	(725)	—	755	725	4.0
	ν_4	272	250	8.1	331	244	26.3

a Taken from reference 11 in text.
b See footnote b in Table III.

It is implicitly assumed in the present calculation that the molecules have planar configurations in both the electronic states. All molecules treated here have undoubtedly planar structures in their electronic ground states (treating each H_3 " atom " in mesitylene as a mass point). The vibrational analysis shows that these molecules seem also to be planar in their first excited electronic states, in which we are interested.

As to the effect of configurational interaction (CI) we are considering the case of the benzene molecule only, as for obvious reasons it is difficult at present to estimate such an effect in other molecules.

The effect of CI on the energy levels of the benzene molecule is well known. Unfortunately, however, the coefficients of mix-

TABLE VII

LOWER SINGLET LEVELS OF THE BENZENE MOLECULE CALCULATED WITH AND WITHOUT CONFIGURATIONAL INTERACTION (eV.).

Level	Roothaan and Parr[a]	Parr, Craig and Ross[b]	Observed[c]
$^1A_{1g}$	0.0	0.0	0.0
$^1B_{1u}$	7.3	9.0	6.0
$^1B_{2u}$	5.9	4.4	4.9
$^1E_{1u}$	9.8	9.9	7.0

a) Configurational interaction is neglected. All the integrals are included. (*J. Chem. Phys.*, **17**, 1001 (1949)).
b) Configurational interaction and all the integrals are included. (*J. Chem. Phys.*, **18**, 1561 (1950)).
c) Taken from Pariser and Parr, *J. Chem. Phys.*, **21**, 767 (1953).

13) C.W.L. Bevan and D.P. Craig, *Trans. Faraday Soc.*, **47**, 564 (1951). In this paper many-center integrals are neglected.

symmetrized products of molecular orbitals with or without many center integrals, etc.). However, CI produced by the higher energy configurations in which the C–C bonds have smaller bond-orders should decrease the bond-orders in the original configuration. It is to be noted that the bond-orders even in the ground state should more or less decrease. However, as can be seen in Table VII, the magnitudes of the energy changes produced by CI fit in the following sequence:

$$B_{2u}>A_{1g}\approx E_{1u}>B_{1u}.$$

If the same sequence applies to the bond-order changes, we can expect that for A_{1g}–B_{2u} or A_{1g}–B_{1u} transitions the bond-order decrease caused by the electronic excitation may be greater or smaller than when the CI is neglected, while for A_{1g}–E_{1u} transition it may be nearly the same, whether CI is considered or not. The same applies to the totally symmetrical ringvibrational frequency. Thus we can expect that the above-calculated value of 937 cm^{-1} should represent the upper and the lower limit for the vibrational frequency in the B_{1u}- and B_{2u}-state, respectively. The observed values are 923 and 965 cm^{-1} for the B_{2u}- and B_{1u}-state, respectively[14,15].

Errors due to Badger's relation appear to be small. As for the effect of d-values it may not be serious in calculating the change of the frequency caused by the electronic excitation as described above. The effect of C-values may have to be considered even for the calculation of the frequency change. According to Badger's second paper[2], this constant varies among atom pairs with the maximum deviation of 10%, which results in the error of 30% in the difference of the force constants. Therefore, the error in the frequency difference is estimated to be less than 20%.

Errors due to the valence-force-field (VFF) approximation are difficult to estimate. According to Wilson[16] the following equation holds:

$$\Lambda=L^{-1}GFL=L'FL, \qquad (2)$$

where Λ is a diagonal matrix whose diagonal elements are the characteristic roots of the secular equation $|GF-E\lambda|=0$. G is the inverse kinetic energy matrix and F is the force constant matrix. L is the transformation matrix defined by

$$R=LQ,$$

where R and Q represent the internal and normal coordinates, respectively, prime and reciprocal denoting the transpose and the inverse matrices, respectively. In the case of the symmetrical molecules, each symmetry type can be treated separately, and in such cases R represents the symmetry coordinate formed by an appropriate linear combination of the equivalent internal coordinates. Taking the ii element of Eq. (2) it follows that

$$\lambda_i=\sum_{k,m}(L')_{ik}F_{km}L_{mi}=\sum_{k,m}L_{ki}L_{mi}F_{km}. \qquad (2')$$

From this equation the first order change of λ_i produced by small changes of F_{km}'s is given by

$$\delta\lambda_i=\sum_{k,m}L_{ki}L_{mi}\delta F_{km}. \qquad (3)$$

Now, from Eqs. (2′) and (3) the relative change of λ_i is

$$\frac{\delta\lambda_i}{\lambda_i}=\frac{\sum_{k,m}L_{ki}L_{mi}\delta F_{km}}{\sum_{k,m}L_{ki}L_{mi}F_{km}}$$

$$=\frac{\sum_{k}L_{ki}L_{ki}\delta F_{kk}+\sum_{k,m\neq k}L_{ki}L_{mi}\delta F_{km}}{\sum_{k}L_{ki}L_{ki}F_{kk}+\sum_{k,m\neq k}L_{ki}L_{mi}F_{km}}. \qquad (4)$$

The use of the VFF approximation implies that in the last expression of Eq. (4) the second sums in the denominator and numerator can be neglected as compared with the corresponding first sums. In order to investigate the error due to the VFF approximation, four cases may be considered.

(i) If λ_i refers to the characteristic frequency of the stretching internal coordinate R_k, it holds that[17]

$$\lambda_i\approx(L_{ki})^2F_{kk}.$$

In general, for planar vibrations the magnitude and the change are greater for stretching force constants than those for deformation force constants and interaction constants[18]. Therefore,

$$\delta\lambda_i\approx(L_{ki})^2\delta F_{kk}.$$

Accordingly, the error due to the VFF approximation does not seem to be serious in this case.

(ii) If λ_i refers to the characteristic frequency of two (or more) stretching internal coordinates R_k and R_l, it holds that[17]

$$\lambda_i\approx(L_{ki})^2F_{kk}+(L_{li})^2F_{ll}+2(L_{ki}L_{li})F_{kl},$$

where the first and the second terms of the right hand side are of the same order of

14) H. Sponer, G. Nordheim, A.L. Sklar and E. Teller, *J. Chem. Phys.*, 7, 207 (1939).
15) G. Nordheim, H. Sponer and E. Teller, *J. Chem. Phys.*, 8, 455 (1940).
16) E.B. Wilson, Jr., *J. Chem. Phys.*, 7, 1047 (1939); 9, 76 (1941).
17) Y. Morino and K. Kuchitsu, *J. Chem. Phys.*, 20, 1809 (1952).
18) J. Duchesne, *J. Chem. Phys.*, 21, 548 (1953), 22, 1464 (1954), *Bull. Acad. Roy. Belg.*, 39, 697 (1953), *J. phys. radium*, 15, 211 (1954), *Acad. Roy. Belg., Classe sci. Mem. Collection in* 8°, 28, 3 (1955) and J. Duchesne and L. Burnelle, *J. Chem. Phys.* 21, 2005 (1953).

magnitude. From considerations similar to those in the previous case

$$\delta\lambda_i \approx (L_{ki})^2\delta F_{kk}+(L_{li})^2\delta F_{ll}+2(L_{ki}L_{li})\delta F_{kl}.$$

Taking into account the fact that the magnitude and the change are greater for stretching force constants than those for bond-bond interaction constants it follows that

$$\frac{\delta\lambda_i}{\lambda_i} \approx \frac{(L_{ki})^2\delta F_{kk}+(L_{li})^2\delta F_{ll}+2(L_{ki}L_{li})\delta F_{kl}}{(L_{ki})^2F_{kk}+(L_{li})^2F_{ll}+2(L_{ki}L_{li})F_{kl}}$$

$$\approx \frac{(L_{ki})^2\delta F_{kk}+(L_{li})^2\delta F_{ll}}{(L_{ki})^2F_{kk}+(L_{li})^2F_{ll}},$$

in which the relative error in the frequency change due to the second approximation may be of the same order of magnitude as the relative error due to the VFF approximation in the calculation of the absolute values of vibrational frequency.

(iii) If λ_i refers to the characteristic frequency of the deformation internal coordinate R_δ, it holds that[17]

$$\lambda_i \approx (L_{\delta i})^2F_{\delta\delta}.$$

In general, the magnitude and the change of the in-plane deformation force constants are small and are comparable with those of the interaction constants. Therefore, it is doubtful whether the following approximation holds fairly well:

$$\delta\lambda_i \approx (L_{\delta i})^2\delta F_{\delta\delta}.$$

In addition, in the method described in the present paper, various effects due to interaction constants are included in $F_{\delta\delta}$ when it is deduced form the experimental frequency. Furthermore, if we use this value of $F_{\delta\delta}$ in calculating another vibrational frequency the error included may be great, since the contributions from interaction constants to the latter frequency may be different from the contributions to the frequency from which $F_{\delta\delta}$ is calculated. Therefore, the error due to the VFF approximation is expected to be great in this case.

(iv) If λ_i refers to the characteristic frequency of the deformation (R_δ) and stretching (R_k) internal coordinates,

$$\lambda_i \approx (L_{\delta i})^2F_{\delta\delta}+(L_{ki})^2F_{kk}+2(L_{\delta i}L_{ki})F_{\delta k},$$

where the first and the second terms in the right hand side are nearly equal in magnitude. The error due to the VFF approximation is expected to be great also in this case on account of the error in $F_{\delta\delta}$ as described above.

Thus, it may be concluded that the use of the VFF approximation does not produce serious errors for the vibration whose mode is almost bond-stretching.

To summarize although the present approach to the problem of the changes of the vibrational frequencies in the course of the electronic excitation involves many sources of error, the results obtained are encouraging at least qualitatively. In other words, the present calculation cannot be expected to predict precisely the frequency changes in these molecules, but it is of some use in understanding or interpreting the observed frequency changes.

Finally, we express our sincere thanks to Professor S. Imanishi for his encouragement throughout this work and for his kindness in reading the manuscript.

Department of Chemistry, Faculty of Science, Kyushu University
Fukuoka

A Thermistor Method for the Determination of Velocity Coefficients of Vinyl Polymerization. I

By Hajime MIYAMA

(Received December 10, 1955)

Introduction

Various methods have been described for the measurement of the rate of vinyl polymerization. Dielectric constant[1] and refractive index[2] methods are suitable to follow rapidly the rate of exothermic polymerization in liquid-phase since these methods are sensitive to the slight rise in temperature during the reaction. However, these methods are applicable only with difficulty, therefore it is desirable to measure the small temperature rise with an easier operation. Thus recently the thermocouple method[3] was investigated by H. W. Melville et al. for the measurement of the rate of vinyl porymerization. Instead of using a thermocouple, the author used a bridge consisting of two thermistors, one of which was equipped at the center of a reaction vessel and the other was placed at the center of a standard vessel, to obtain better results from the point of view of sensitivity in temperature, adiabatic period of the system, response time of the instrument and saving the space of the reaction vessel.

This paper is concerned with the measurement of the ratio of the propagation constant to the termination constant for styrene polymerization which is catalyzed by 2, 2′-azobispropane. The data are compared with the values obtained by other methods.

Theoretical

Since the theory of this work is the same as that used in Melville's thermocouple method, the author describes briefly the outline of the theory. When the reaction vessel, which contains monomer M, is irradiated and photopolymerization takes place, the relationship between time t and fractional conversion $\Delta M/M$, is shown as follows.

$$\Delta M/M = k_p/k_t \ln \cosh (t/\tau) \qquad (1)$$

where k_p and k_t are the propagation and termination rate constants respectively and τ is the lifetime of the active species before they are removed by mutual termination. When t exceeds 3τ this relation becomes approximately linear.

$$\Delta M/M = k_p/k_t(t/\tau - \ln 2) \qquad (2)$$

The values of $\tau \ln 2$ and $k_p/k_t \times 1/\tau$ can be obtained from the interception of the time axis and the slope of this straight line. While the reaction remains adiabatic, the rise in temperature is directly proportional to the fractional conversion. Thus, provided that the heat of polymerization and the heat capacity of the system are known, the accurate values of k_p/k_t and τ can be obtained. Because of the lag in response of the instrument itself, however, the intercept does not represent $\tau \ln 2$, but the measured intercept X is given by

$$X = C + \tau \ln 2 \qquad (3)$$

where C is the lag in response of the instrument. From the kinetics of polymerization, the following formula can be obtained

$$\tau = k_p/k_t \times 1/V \qquad (4)$$

where V is the fractional rate of polymerization. From Eqs. (3) and (4)

$$X = C + k_p/k_t \times 1/\mathrm{V} \times \ln 2 \qquad (5)$$

Hence the plot of the measured interception X aginst the reciprocal of the rate $1/V$ is a straight line. The value of k_p/k_t depends only upon the slope of the line and therefore is independent of the response lag of the instrument, when this is of the same order with or less than the lifetime. But to use the theory described above, it is necessary to plot the logarithm of the light intensity $\log I$ against the logarithm of the fractional rate $\log V$ and to verify that the intensity exponent is 0.5 in this plot, as poved by Melville[3].

Experimental

The reaction vessel, shown in Fig. 1, made of transparent quartz and equipped with a thermistor is ca. 9 cc. in capacity. Its inside diameter is 38 mm., inside depth is 8 mm. and this vessel can be connected to the vacuum system by the soft-glass-quartz joint A. B and C are both softglass-quartz joints. This vessel can be cleaned easily after the reaction by removing the joints B and

1) C. M. Burnell, T. G. Majury and H. W. Melville, *Proc. Roy. Soc. London*, **A 205**, 309 (1951); T. G. Majury and Melville, ibid., **A 205**, 323 (1951).
2) N. grassie and H. W. Melville, ibid., **A 207**, 285 (1951).
3) W. I. Bengough and H. W. Melville, ibid., **225**, 331 (1954).

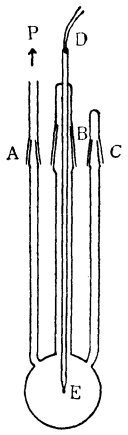

A, B, C; Softglass-quartz joints
D; Thermistor's lead wires
E; Thermistor
P; To vacuum

Fig. 1. Reaction vessel.

C. The lead-wires of thermistor are covered by very thin softglass tube which is sealed at the upper end of the joint B and the thermistor is placed at the center of the reaction vessel. One of such reaction vessels is used as a standard of temperature. Each thermistor, made by Ohizumi Factory, has the same characteristics shown in Fig. 2, of the temperature-resistance relation.

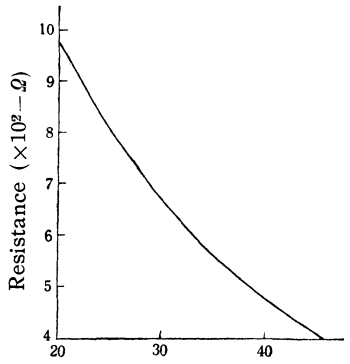

Fig. 2. Thermistor's charactestics.

A diagram of arrangement is shown in Fig. 3. In this figure, the oscillator A supplies the constant voltage 700 c/s sine waves to the bridge B and at the same time it is connected to the phase-discriminator of the amplifier C for detecting plus or minus sign of temperature difference. The bridge consists of two identical thermistors, X and S, two equally valuable resistance R, a variable resistance r and a variable condensor c. When two thermistors X and S are situated at the same temperature, the bridge can be balanced by varying the value or r and c. Then, if the temperature of S does not change but that of X changes, the balance of the bridge is broken up and the bridge supplies the output voltage e to the amplifier c. By a simple calculation, e is represented as follows.

$$e=(\Delta r/4r_0)E \qquad (6)$$

where E is the input voltage to the bridge, r_0 is the resistance value of thermistors and Δr is a

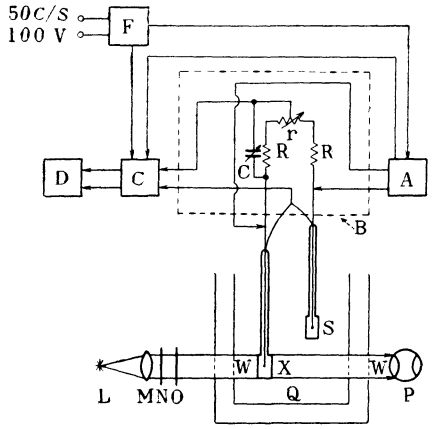

Fig. 3. Diagram of arrangement.
A; 700 c/s Oscillator B; Bridge
C; 700 c/s Amplifier
D; Penwriting-Oscillograph
F; Regulated power supply
L; Light-source M; Quartz lense
N; Shutter O; Filter
P; Photo-cell
Q; Double-thermostat W; Quatz-windows
X, S; Thermistors

resistance-change of one thermistor caused by the temperature change. When $E=2.0$ V is used $e=20\,\mu$V. for the temperature change of 0.001°C, provided that the resistance-change is ca. 4% for the temperature change of 1°C as shown in Fig. 2. The degree of amplification can be controlled from 1 to 1000 by gain-controller and multiplier of the amplifier. As to the amplifier, frequency is 700 c/s, gain is ca. 110 db and noise is ca. 1.5 μV. expressed in the same unit of the input signal. Therefore noise is neglegible for the temperature change of 0.001°C. The output from the amplifier is displayed on the galvanometer, the direct current resistance of which is 8 kΩ and amplitude per current is 15 mm./mA, of the pen-writing oscillograph D. Velocity of recording-paper can be varied in ten steps from 120 mm./sec. to 5 mm./min. The regulated power supply F is constructed so as to eliminate the outer noise and to stabilize the filament- and B-Voltage of the oscillator and the amplifier.

The source of light is a 400 watt high pressure mercury lamp (Japan Storage Battery Co. Type HL-400) fed from a constant voltage transformer. The light is passed through a quartz lens and then a Matsuda UVD_1 filter to obtain parallel and monochromatic (3660 Å) light. During the experiment the constancy of light is checked by a photocell 931 A.

Two vessels with thermistors are placed in a double water thermostat equipped with quartz-windows, which is regulated to ±0.001°C.

Commercial styrene is purified and distilled into the reaction vessel according to the method of Fujii[4].

2, 2'-Azobispropane was prepared by M. Shinichi Taira of Tokyo Metropolitan University and

4) Saburō Fujii, This Bulletin, 27, 216 (1954).

was used after distillation, b.p. 88.5°C, n_D^{23} 1.3890. In Fig. 4 is shown its absorption spectrum.

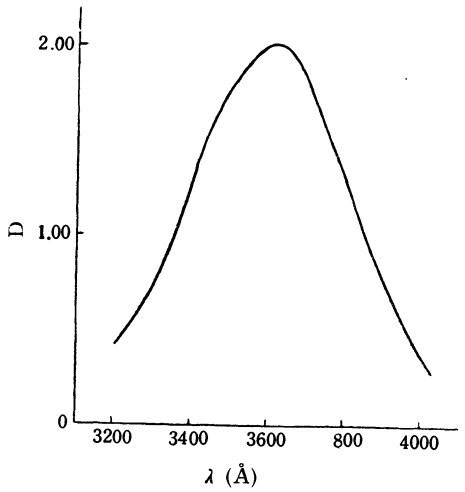

Fig. 4. Absorption spectrum of 2,2'-azobispropane at the concentration of 0.099 Mol./L in styrene.
D ; Optical density measured by Hitachi spectrophotometer EPB-U

The experimental procedure is as follows. The outputs of two thermistors are balanced by using a variable condensor c and resistance r of the bridge. A light through a lens and a filter UVD_1, irradiates the reaction vessel. At the same time, the time-mark is written on the recoreing-paper by an electric switch. After the reaction proceeds in a measurable amount, the shutter is closed and the time-mark of cutting-off light is recorded. The degree of amplification is adjusted so that the curve on the recording paper can be analyzed. This procedure is repeated until the results are reproducible.

Results

As a blank test, the reaction vessel which contained air or benzene but not monomer, was irradiated by light through a UVD_1 filter. The temperature-rise of the order of 10^{-3}°C was observed and this was supposed to be caused by the direct irradiation on the thermistor. Therfore a center of the outer surface of the reaction vessel was covered by a white-paint spot of ca. 5 mm. diameter to eliminate this effect by shutting out the direct irradiation on the thermistor. Then no temperature-rise was observed.

One of the curves of the recording-paper is shown in Fig. 5, in which A and B are the marks of opening shutting the and shutter respectively. This measurement was performed at 30°C, using 0.0202 mol./l. of 2,2'-azobispropane. Another vessel, used as a standard, was filled with benzene. Even if monomer

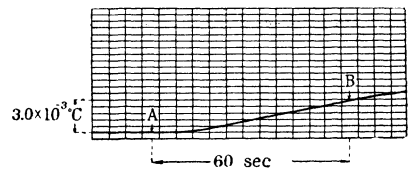

Fig. 5. A recorder trace of a typical experiment for the polymerization of styrene sensitized by 2,2'-azobispropane.

and sensitizer were placed in that vessel as well as in the reaction vessel, the curve was the same as that when only benzene was used. This means that the dark reaction is neglegible within the experimental error, compared with the light reaction. Accordingly all measurements were carried out under the condition that the standard cell was filled with benzene.

According to the theory equation (2) is true when t exceeds 3τ, but many measurements showed that this equation could be used when t exceeds approximately 1.5τ.

The necessary constants of styrene at 30°C are as follows[5].

Heat capacity	43.9 cal./mol.
Heat of polymerization	16.76 kcal./mol.

Therefore the relation between the conversion of monomer and the temperature-rise is

$$1\% = 3.82°C \qquad (7)$$

The relation between the temperature-rise of the reaction vessel and the amplitude of the oscillograph was checked experimentally at various temperature differences. The resistance-temperature curve of the thermistor as shown in Fig. 2 is not correctly lineart and therefore the amplitude-temperature-rise relation is not the same at different temperature-rise relation is not the same at different

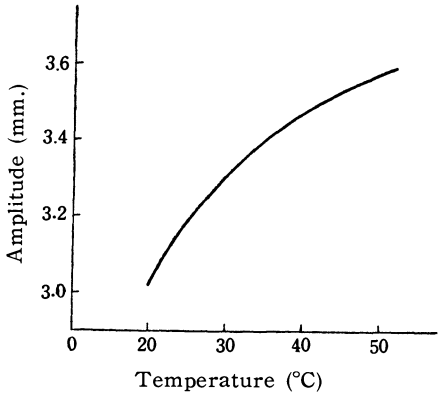

Fig. 6. The amplitude corresponding to the temperature difference of 0.001°C at maximum sensitivity.

5) Ray H. Boundy and Raymond F. Boyer, "Styrene", Reinhold, New York (1952), pp. 67, 68.

temperatures. Provided that the amplification is at its maximum sensitivity, the amplitude necessary to detect the temperature difference of 0.001°C is shown in Fig. 6. Therefore at 30°C, the amplitude of the recording paper is shown as follows.

$$1\,\text{mm.} = 3.0\times10^{-4}\text{°C} \qquad (8)$$

Since the amplitude can be read easily within the accuracy of 0.2 mm. on the recording paper, the sensitivity in temperature is 0.6×10^{-4}C. From Eqs. (7) and (8), the following relation can be obtained.

$$1\,\text{mm/s} = 0.785\times10^{-4}\%/\text{s} = 0.785\times10^{-6}/\text{s} \qquad (9)$$

To check this relation, the velocity measured by thermistor method was compared with the one measured dilatometrically. A dilatometer shown in Fig. 7, which was made from transparent quartz and of the same size as the

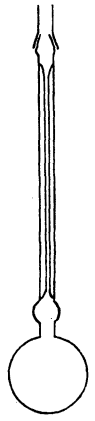

Fig. 7. Dilatometer.

reaction vessel shown in Fig. 1, was used. Under the same conditions, the values measured by the thermistor agreed with the one measured dilatometrically within the error of ±2%. Accordingly the value measured by thermistor method will be used without checking hereafter.

Various filters, of which the transparency factor is known, were used to change the light-intensity.

In Fig. 8 the relation between log I and log V is shown. From this line's slope, it can be shown that the exponent is 0.5 and therefore the theory already described is applicable.

The relation between $1/V$ and X is shown in Fig. 9. In Fig. 8 and Fig. 9, marks × and ○ are points obtained by using 0.0202 mol./l. and 0.0101 mol./l. of sensitizer respectively.

From the straight line's intercept in Fig. 9, it can be seen that instrument's lag in response is ca. 0.6 sec. This lag is possibly the thermistor's, because the maker of the thermistors gives ca. 0.5 sec. as the lag in response.

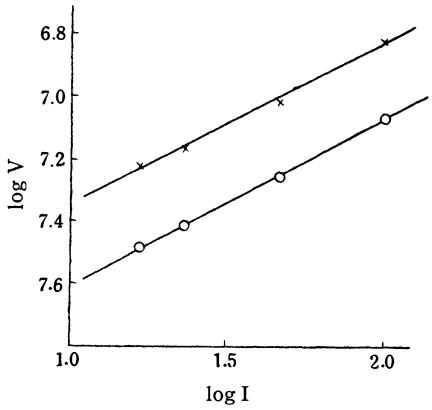

Fig. 8. The relation between log I and log V.

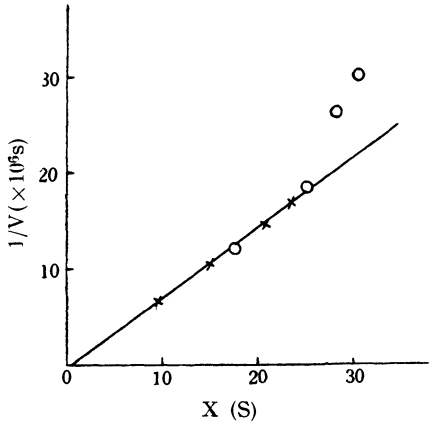

Fig. 9. The relation between X and 1/V.

The time period in which the reaction system remains adiabatic is about 70 sec., from the results of many measurements. One of these result is shown in Fig. 10. Beyond this period, the curve deviates from the straight line. As Melville showed experi-

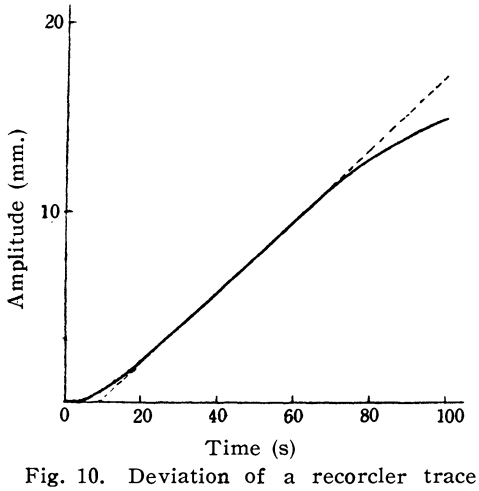

Fig. 10. Deviation of a recorcler trace from the straight line.

mentally the reaction, in which the lifetime is smaller than ca. 1/3 of this period, can be completely analyzed by using his theory. And Fig. 10 shows that the measurements, in which the lifetime is smaller than 25 sec., are all acceptable.

From the slope of Fig. 10, the value of k_p/k_t of styrene at 30°C is 2.02×10^{-6}.

Discussion

Compared with the thermocouple method, the results obtained are better in the points of sensitivity in temperature, adiabatic period of the system and instrument's lag in response. They are shown in Table I compared with the thermocouple method.

TABLE I
THE COMPARISON OF THIS METHOD WITH THE THERMOCOUPLE METHOD

	This method	Thermocouple method
Sensitivity in temperature	0.6×10^{-4}°C	2×10^{-4}°C
Adiabatic time period	70 sec. (9 cc. vessel)	60 sec. (15 cc. vessel)
Instrument's lag in response	0.6 sec.	1–3 sec.

The k_p/k_t value of styrene does not depend upon the concentration of sensitizer used. This value is reasonable in comparison with others obtained by a different method[6].

Summary

To measure the rate of vinyl polymerization, a thermistor method was devised and better results were obtained compared with the thermocouple method, in the points of sensitivity of temperature, adiabatic time period, instrument's lag in response and saving the space of the reaction vessel. The k_p/k_t value of styrene at 30°C obtained by this method was 2.02×10^{-6} and reasonable in comparison with other values obtained by different methods.

The auther wishes to express his hearty thanks to Dr. Momotato Suzuki of this Academy for his helpful advice and encouragement and to Mr. Shinichi Taira of Tokyo Metropolitan University for his kind proparation of 2, 2′-azobispropane.

Department of Chemistry, Defense Academy, Yokosuka

6) Other values are summarized in ref. 2).

A Thermistor Method for the Determination of Velocity Coefficients of Vinyl Polymerization. II

By Hajime MIYAMA

(Received January 11, 1956)

Introduction

In the 1st paper[1] of this series the author described a thermistor method for the measurement of the rate of vinyl polymerization and good results were obtained compared with the thermocouple method. According to this measurement, the k_p/k_t value of styrene at 30°C, when 2,2'-azobispropare used as photosensitizer, was 2.02×10^{-6}. However, this sensitizer was not very effective and the rate of polymerization was very slow especially when irradiation was weak. Thus the analysis of the curve of oscillograph was very difficult.

In this paper, α-azobisisobutyronitrile which is a very effective photosensitizer for vinyl polymerization is used. The measurement was fulfilled on styrene, vinyl acetate and methyl methacrylate at 30°C, 35°C and 40°C. And, from the value of k_p/k_t at various temperatures, the activation energy difference E_p-E_t of these monomers was obtained, where E_p was the activation energy of propagation process and E_t was the activation energy of termination process.

Experimental

The experimental apparatus and procedure are the same as those described in the previous paper.

The monomers were prepaped according to Fujii's meteod[2] as described in the first paper.

α-Azobisisobutyronitrile was a commercial product (Kanto Chemical Co. Inc.) and used after three recrystallizations from carbon tetrachloride.

1) H. Miyama, This Bulletin, 29, 711 (1956).

2) S. Fujii, This Bulletin, 27, 216 (1954); 27, 238 (1954).

In Fig. 1, its ultraviolet absorption spectrum is shown.

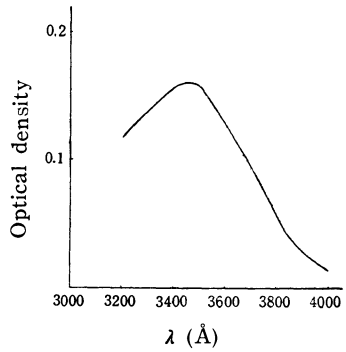

Fig. 1. Ultraviolet absorption Spectrum of α-azo-bisisobutyronitrile α-azolisisobutyronctrile at the concentration of 0.0122 mol./l. in CCl_4.

Results

Styrene.—As shown in Fig. 6 of the first paper, the amplitude of oscillograph corresponding to the temperature difference of 0.001°C is not the same at different temperatures. These values at 30°C, 35°C and 40°C obtained from that figure are as follows.

$$\begin{aligned} 1\text{ mm.} &= 3.00\times10^{-4}\text{°C at 30°C} \\ 1\text{ mm.} &= 2.94\times10^{-4}\text{°C at 35°C} \\ 1\text{ mm.} &= 2.88\times10^{-4}\text{°C at 40°C} \end{aligned} \quad (1)$$

Although heat capacity and heat of polymerization of styrene depend on the temperature, the values at 30°C are used, since the error caused by these values is small compared with the experimental error[3]. From the relation (1) and constants of styrene at 30°C, the following relations between amplitude-change per second and fractional rate of polymerization can be obtained.

$$\begin{aligned} 1\text{ mm./sec.} &= 0.785\times10^{-6}\text{/sec. at 30°C} \\ 1\text{ mm./sec.} &= 0.770\times10^{-6}\text{/sec. at 35°C} \\ 1\text{ mm./sec.} &= 0.755\times10^{-6}\text{/sec. at 40°C} \end{aligned} \quad (2)$$

In Fig. 2 a recorder trace of a typical experiment is shown, in which A and B are respectively the marks of lighting on and lighting off. This measurement was carried out at 30°C by using 0.0122 mol./l. of α-azoisobutyronitrile as a photosensitizer and other conditions were the same as those described for Fig. 5 of the first paper. From

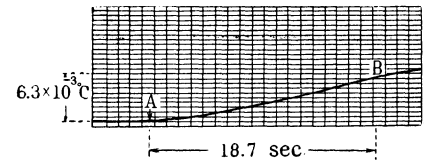

Fig. 2. A reconder trace of a typical experiment for the polymerization of styrene sensitized by α-azobisisobutyronitrile at 30°C.

Fig. 5 of the first paper and Fig. 2 it can be shown that the rate of polymerization photosensitized by 0.0122 mol./l. of α-azoisobutyronitrile is sixfold larger than the rate of polymerization photosensitized by 0.0202 mol./l. of 2,2′-azobispropane and thus the analysis of the curve can be more correctly preformed.

By varying the intensity of light, the relation between log I and log V at 30°C, 35°C and 40°C were obtained as shown in Fig. 3. From this

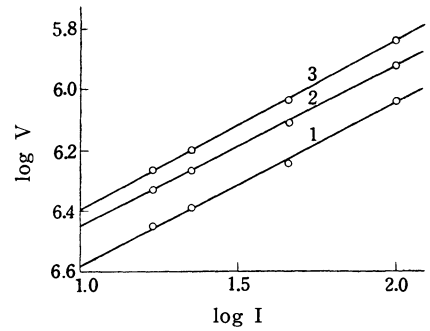

Fig. 3. Variation of the rate with the light intensity for styrene; Curve 1, at 30°C: Curve 2, at 35°C; Curve 3, af 40°C.

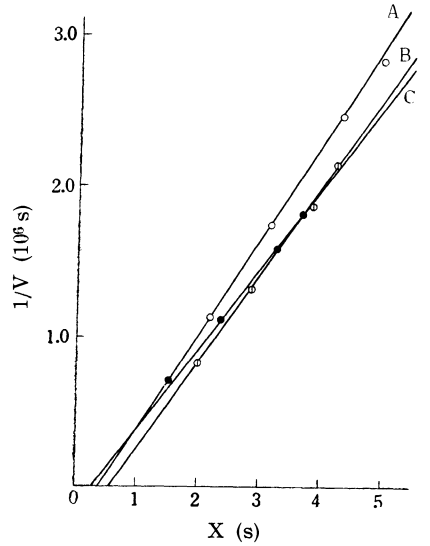

Fig. 4. Variation of the rate with the measured intercept for the polymerization of styrene.
○ Curve A, at 30°C; ◑ Curve B, at 35°C; ● Curve C, at 40°C.

3) Heat capacities and heat of polymerization of styrene at different temperatures are as follows[4].

Heat Capacity	Heat of Polymerization
30°C 43.9 cal./mol.	16.76 kcal./mol.
35°C 44.3 cal./mol.	16.84 kcal./mol.
40°C 44.6 cal./mol.	16.90 kcal./mol.

From these values and (1), the relations between the amplitude-change per second and the fractional rate can be obtained.

$$\begin{aligned} 1\text{ mm./sec.} &= 0.785\times10^{-6}\text{/sec. at 30°C} \\ 1\text{ mm./sec.} &= 0.775\times10^{-6}\text{/sec. at 35°C} \\ 1\text{ mm./sec.} &= 0.760\times10^{-6}\text{/sec. at 40°C} \end{aligned}$$

These Values coincide with (2) within the error of ca. ±0.3%, which is small compared with the usual experimental error.

4) Ray H. Boundy and Raymond F. Boyer; "Styrene", Reinhold, New York (1952), pp. 67, 68.

straight-line's slope, it can be shown that the exponent is 0.53 at 30°C, 0.53 at 35°C and 0.54 at 40°C. Therefore the theory described in the first paper is applicable.

The relation between $1/V$ and X is shown in Fig. 4 and from this straight-line's intercept the instrument's lag in response is 0.25–0.5 sec. This value coincides approximately with 0.6 sec. obtained in the first paper. From the slope of this line, the values k_p/k_t of styrene are 2.28×10^{-6} at 30°C, 2.50×10^{-6} at 35°C and 2.77×10^{-6} at 40°C.

Vinyl Acetate.—The rate of polymerization of vinyl acetate was ca. ninefold larger than that of styrene under the same conditions. Hence the sensitivity of the amplifier was lowered as follows.

$$\begin{aligned} &1\text{ mm.}=1.20\times10^{-3}\text{°C at 30°C}\\ &1\text{ mm.}=1.18\times10^{-3}\text{°C at 35°C}\\ &1\text{ mm.}=1.15\times10^{-3}\text{°C at 40°C} \end{aligned} \quad (4)$$

The necessary constants of vinyl acetate are as follows[5].

Heat capacity 40.5 cal./mol.
Heat of polymerization 21.3 kcal./mol.

From these values the relation between the conversion and the temperature-rise can be obtained.

$$1\% = 5.28\text{°C} \quad (4)$$

From (3) and (4) the following relations were obtained.

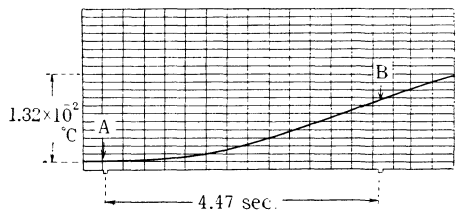

Fig. 5. A recorder trace of a typical experiment for the polymerization of vinyl acetate sensitized by α-azobisisbutyronitrile at 30°C.

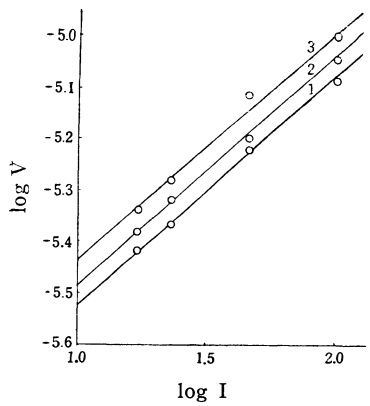

Fig. 6. Variation of the rate with the light intensity for the polymerization of vinyl acetate. Curve 1, at 30°C; Curve 2, at 35°C; Curve 3, at 40°C.

5) W.I. Bengough and H.W. Melville, *Proc. Roy. Soc.*, **A225**, 330 (1954).

$$\begin{aligned} &1\text{ mm./sec.}=0.228\times10^{-5}\text{/sec. at 30°C}\\ &1\text{ mm./sec.}=0.223\times10^{-5}\text{/sec. at 35°C}\\ &1\text{ mm./sec.}=0.218\times10^{-5}\text{/sec. at 40°C} \end{aligned} \quad (5)$$

In Figs. 5, 6 and 7, the exprimental results

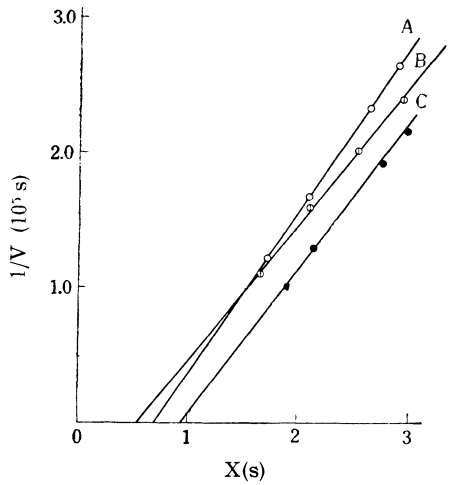

Fig. 7. Variation of the rate with the measused intercept for the polymerization of vinyl acetate.
○ Curve A, at 30°C; ① Curve B, at 35°C; ● Curve C, at 40°C.

obtained under the same conditions as in styrene are shown. From Fig. 7 the instrument's lag in respones is 0.5–0.9 sec. and the k_0/k_t values of vinyl acetate are 1.21×10^{-5} at 30°C, 1.34×10^{-5} at 35°C and 1.44×10^{-5} at 40°C.

Methyl Methacrylate.—The rate of polymerization of methyl methacrylate was ca. threefold larger than styrene under the same conditions. As the sensitivity of amplifier, (1) was used. The constants of methyl methacrylate used were as follows[5].

Heat capacity 49.0 cal./mol.
Heat of polymerization 13.0 kcal./mol.

From these values the relation between the conversion and the temperature-rise is

$$1\% = 2.65\text{°C} \quad (6)$$

From (1) and (6), the following relations were obtained.

$$\begin{aligned} &1\text{ mm./sec.}=1.132\times10^{-5}\text{/sec. at 30°C}\\ &1\text{ mm./sec.}=1.110\times10^{-5}\text{/sec. at 35°C}\\ &1\text{ mm./sec.}=1.078\times10^{-5}\text{/sec. at 40°C} \end{aligned} \quad (7)$$

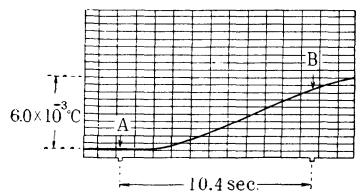

Fig. 8. A recorder trace of a typical experiment for the polymerization of Methyl Methacrylate sensitized by α-azobisisobutyronitrile at 30°C.

6) C.H. Bamford and Dewer, *Proc. Roy. Soc. London*, **A192**, 309 (1948).

In Figs. 8, 9 and 10, the experimental results are shown and the experimental condition is the same as in styrene and vinyl acetate. From Fig. 10 the instruments's lag is 0.5–0.6 sec. and k_p/k_t values of methyl methacrylate are 7.41×10^{-6} at 30°C, 8.08×10^{-6} at 35°C and 8.92×10^{-6} at 40°C.

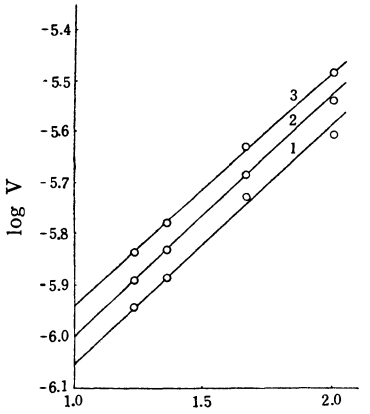

Fig. 9. Variation of the rate with the light intensity for the polymerization of methyl methacrylate. Curve 1, at 30°C; Curve 2, at 35°C; Curve 3, at 40°C.

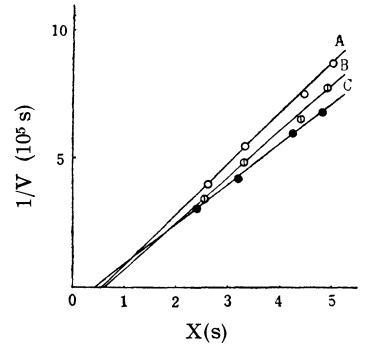

Fig. 10. Variation of the rate with the measured intercept for the polymerization of methyl methacrylate.
○ Curve A, at 30°C; ◑ Curve B, at 35°C; ● Curve C, at 40°C.

Discussion

From the k_p/k_t value at various temperatures, the difference between the activation energies E_p and E_t, where E_p and E_t are respectively the activation energy of propagation and termination processes, can be calculated. Thus the values of E_p-E_t are 3.71 kcal./mol., 3.25 kcal./mol. and 3.54 kcal./. mol. for styrene, vinyl acetate and methyl methacrylate respectively. Using these values and k_p/k_t values at values temperatures, the following equations can be obtained.

$$k_p/k_t=1.09\times10^{-3}\times e^{-3710/RT} \quad \text{for styrene}$$
$$k_p/k_t=2.72\times10^{-3}\times e^{-3250/RT} \quad \text{for vinyl acetate}$$
$$k_p/k_t=2.66\times10^{-3}\times e^{-3540/RT} \quad \text{for methyl methacrylate} \qquad (8)$$

These equations obtained by other workers are as follows.

$$k_p/k_t=3.33\times10^{-3}\times e^{-3700/RT} \quad \text{for styrene}^{6)}$$
$$k_p/k_t=5.34\times10^{-3}\times e^{-2080/RT} \quad \text{for vinyl acetat}^{7)}$$
$$k_p/k_t=3.78\times10^{-3}\times e^{-3470/RT} \quad \text{for methyl methacrylate}^{8)}$$

Using equations (8), the k_p/k_t values at 15°C can be obtained and they are compared with other worker's values in Table I, Table II and Table III.

Since the above results were, as described in the previous paper, obtained from measurements after the reaction system attained the stationary state and was then irradiated, the reaction in the dark is supposed to be canceled out. However heat-decomposition of α-azobisisobutyronitrile at higher temperature is considerable and accelerates the polymerization in the dark, hence the effect of

TABLE I
THE k_p/k_t VALUE OF STYRENE AT 15°C

Method	Sensitizer	$k_p/k_t\times10^6$	Ref.
Thermistor	Azobisisobutyronitrile	1.3	This work
Interferometer	Benzoyl Peroxide	2.0[9)]	Grassie & Melville (1951)
Sector	Benzoyl Perxide	3.6[9)]	Valentine & Melville (1950)
Sector	Azopropane	0.65[9)]	Matheson (1950)
Dilatometer	None	5.26[9)]	Burnett (1950)
Dielectric Constant	Azobisisobutyronitrile	0.68[9)]	Majury & Melville (1951)
Viscosity	None	5.3[9)]	Bamford & Dewer (1948)

7) M.S. Matheson, E.E. Auer, E.B. Bevilacpuer and E.T. Hart, *J. Am. Chem. Soc.*, **71**, 497 (1949).
8) ibid., **71**. 497 (1949).
9) N.G. Grassie and Melville, *Proc. Roy. Soc. London*, **A 207**, 285 (1951).
These values are summarized in this paper and corrected to 15°C assuming an activation energy of 4 kcal./mol. for the k_p/k_t term.
10) These values are summarized in ref. 5) and corrected to 15°C assuming an activation energy of 4.1 kcal./mol. for the k_p/k_t term.
11) These values are summarized in ref. 5) and corrected to 15°C assuming an activation energy of 3.7 kcal./mol. for the k_p/k_t term.

TABLE II

THE k_p/k_t VALUE OF VINYL ACETATE AT 15°C

Method	Sensitizer	$k_p/k_t \times 10^5$	Ref.
Thermistor	Azobisisobutyronitrle	0.92	Tgis work
Thermocouple	Azobiscyclohexanecarbonitrile	2.5[10]	Bengough & Melville (1954)
Refractometric	Azobisisobutyronitrile	2.0[10]	Grassi & Melville (1951)
Dielectric Constant	Azobisisobutyronitrile	0.35[10]	Majury & Melville (1951)
Sector	None	0.11[10]	Burnett & Melville (1947)
Sector	None	1.1[10]	Bartlett & Melville (1946)
Sector	Azobisisobutyronitrile	1.1[10]	Matheson, Bevilacqua, Auer, & Hart (1949)
Viscosity	None	1.9[10]	Dixqn-Lewis (1949)
Dilatometer	Azobiscyclohexanecarbonitrile	2.4[10]	Bengough (unpublished)
Sector	None	1.4[10]	Bartlett, Broadbent & Kwart (1950)

TABLE III

THE k_p/k_t VALUE OF METHYL METHACRYLATE AT 15°C

Method	Sensitizer	$k_p/k_t \times 10^6$	Ref.
Thermistor	Azobisisobutyronitrile	5.4	This work
Thermocouple	Azobiscyclohexanecarbonitrile	9.8[11]	Bengough Melville (1954)
Interferometer	None	6.1[11]	Grassie & Melville (1951)
Sector	None	3.8[11]	Mackay & Melville (1949)
Sector	Benzoine	8.9[11]	Chinmayanandam & Melville (1954)
Viscosity	None	20[11]	Bamford & Dewer (1948)
Sector	Bnnzoyl Peroxide	7.9[11]	Melville & Valentine (1950)

reaction in the dark must be taken in consideration. It is desirable, therefore, to use a photosensitizer which does not accelerate the reaction in the dark but the one in the light only.

Summary

The k_p/k_t value of styrene, vinyl acetate and methyl methacrylate was obtained by using thermistor method reported in the first paper of this series. Moreover from the k_p/k_t values at various temperatures, the activation energy difference between propagation and termination processes was calculated. They were 3.71, 3.25 and 3.54 kcal./mol. for styrene, vinyl acetat and methyl methacrylate respectively. The characteristics of this apparatus were almost the same as described in the first paper, although various monomers were used.

The author wishes to thank Dr. Momotaro Suzuki for his useful advice and encouragement.

Department of Chemistry, Defense Academy, Yokosuka

A Thermistor Method for the Determination of Velocity Coefficients of Vinyl Polymerization. III

By Hajime MIYAMA

(Received January 17, 1956)

Introduction

In the previous papers of this series[1] the author described, a thermistor method for the measurement of the rate of vinyl polymerization and obtained the values of k_p/k_t for styrene, vinyl acetate and methyl methacrylate in the initial stages of polymerization. As well as the thermocouple method, this method is not only applicable to the initial stages of polymerization, but can be used equally well for the study of the later stages when the reaction mixture becomes a viscous syrup or solid gel. Recently velocity coefficients for the later stages of the polymerization of vinyl acetate were evaluated by Melville and his co-worker with the use of a thermocouple[2].

In this paper, the author uses the thermistor method for studying the later stages of vinyl acetate polymerization. The monomer was photosensitized by the addition of 1,1'-azobiscyclohexanecarbonitrile, which is a better sensitizer than α-azobisisobutyronitrile, from the points of view of effectiveness and lack of accelaration of polymerization in the dark.

Theoretical

From the kinetics of polymerization[3], the fractional rate of polimerization is represented by equation (1).

$$V=-1/M.\ \mathrm{d}M/\mathrm{d}t=k_p(V_{init}/k_t)^{1/2} \qquad (1)$$

where k_p, k_t, V_{init}. and M are propagation constant, termination constant, velocity of of initiation and concentration of monomer respectively. Because V_{init}. of this equation is not varied by temperature-change in the photopolymerization, the difference between activation energy of propagation and the one half of activation energy of termination $E_p-1/2E_t$ can be obtained by measuring the variation of the fractional rate V with the temperature.

The lifetime of the active species τ is shown as follows.

$$\tau=(k_p/k_t)\times 1/V \qquad (2)$$

From Eqs (1) and (2) the following equation can be obtained.

$$\tau=(k_t\times V_{init})^{-1/2} \qquad (3)$$

Since V_{init} is not varied by the temperature-change in the photopolymerization, the activation energy of termination can be obtained by measuring the value τ at various temperatures.

An estimate of the extent of conversion can be obtained by the next formulas. Thus M of Eq. (1) is replaced by the initial concentration of monomer M_0,

$$V_0=-1/M_0\ \ \mathrm{d}M/\mathrm{d}t \qquad (4)$$

If the variation of V_0 against time t is measurable, M at any time t can be calculated according to the following equation.

$$M_0-M=M_0\int_{t_0}^{t}V_0\mathrm{d}t \qquad (5)$$

where t_0 is the initial time. Thus the extent of conversion φ is expressed as follows.

$$\varphi=(M_0-M)/M_0=\int_{t_0}^{t}V_0\mathrm{d}t \qquad (6)$$

Using the thermistor method, the value of V_0 can be obtained when specific heat of the system and heat of polymerization are known, as shown in the previous papers of this series. But the correct values of V_0 at various degrees of conversion are unknown, because the specific heat of the system varies with the extent of conversion. Approximately, the extent of conversion can be obtained by assuming that the specific heat does not change with conversion. Then using the specific heat at these values of conversion, the values of V_0 are corrected and therefore values of ρ are corrected. Repeating these procedures the correct values of V_0 and φ can be, obtained, although the extent of conversion cannot be measured directly and the specific heat of the system varies with the degree of conversion.

1) H. Miyama, This Bulletin, **29**, 711 (1956). H. Miyama, ibid., **29**, 715 (1656).
2) W.I. Bengough and H.W. Melville, *Proc. Roy. Soc.*, **230**, 429 (1955).
3) C.E.H. Bawn, "The Chemistry of High Polymers", London (1948), p. 68.

Experimental

The experimental apparatus and the preparation of vinyl acetate are the same as described in the previous papers[1]. 1,1'-azobiscyclohexanecarbonitrile was purified through recrystallization from ethanol and its ultraviolet absorption spectrum is shown in Fig. 1. The variation of the rate of

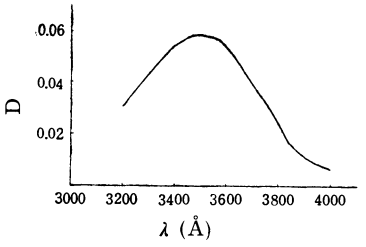

Fig. 1. Ultraviolet absorption spectrum of 0.003 mol./l. 1, 1'-azobiscyclohexanecarbonitrile in vinyl acetate.

polymerization and that of the lifetime with the intensity of irradiation was usually studied at 20°C. The temperature was then raised as rapidly as possible to other temperatures, and measurements of the rate and of the corresponding lifetime were performed. As soon as the necessary measurements had been done, the thermostat was cooled rapidly to 20°C. The rate and the lifetime at 20°C were then measured and compared with the values obtained before heating. The monomer was then polymerized to a further stage by continuous irradiation using an ultra high pressure mercury lamp. When the next arbitrary stage of the polymerization was attained, irradiation was discontinued and the sequence of measurement of rates and lifetimes was repeated. This procedure was repeated until the rate became so slow and the lifetime so great that accurate determination was impossible. The extent of conversion was obtained from the fractional velocity change with time, using Eq. (6). As specific heat of vinyl acetate, the next value[2] was used. (p. 2)

$$\text{Specific heat} = 0.470 - 0.081\,\varphi \qquad (7)$$

where φ is the extent of conversion.

Experimental Results

All measurements were carried out by using 0.003 mol./l. 1,1'−azobiscyclohexaecarbonitrile as photosensitizer.

The variation of velocity V_0 during continuous polymerization is shown in Fig. 2. Using Eq. (6), the variation of velocity V_0 with the extent of conversion is shown in Fig. 3. These values of V_0 and φ were corrected using the already described theory and specific heat (7). The first correction is shown by broken curves I in Fig. 2 and 3 and the second correction by broken curves II. In these figures, curves I and II are almost the same. To check these values of conversion the reaction mixture was dissolved in acetone; the polymer was precipitated by addition of methanol and weighted. The comparison is shown in Table I.

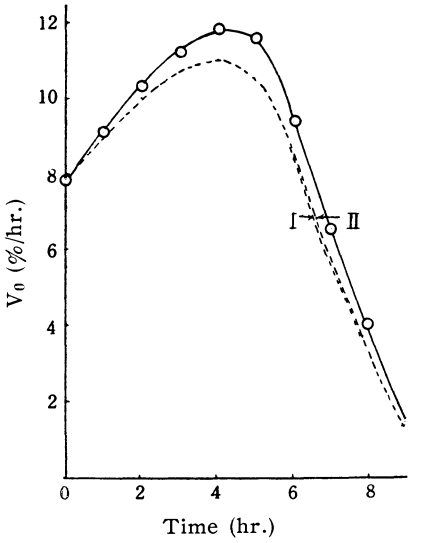

Fig. 2. Variation of the rate V_0 during the continuous polymerization at 20°C.

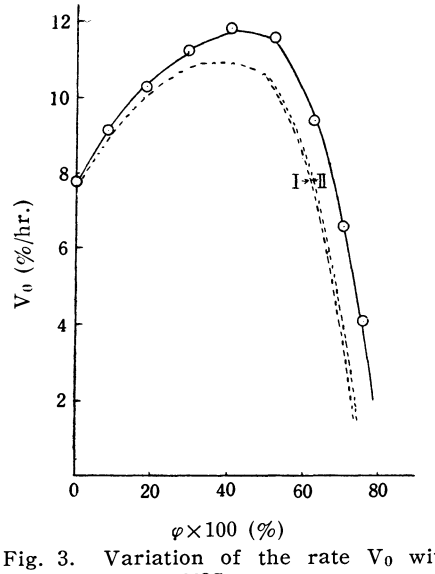

Fig. 3. Variation of the rate V_0 with conversion at 20°C.

TABLE I
COMPARISON OF CALCULATED CONVERSION WITH MEASURED ONE

Uncorr.	1st Corr.	2nd Corr.	Meas.
78.80%	73.60%	73.80%	75.20%

From these results it is seen that the first correction is good enough for use, within the experimental error. Therefore the first corrected values of V_0 and φ will be used hereafter.

The variation of the rate with intensity of irradiation at various stages of the reaction is shown in Fig. 4. From this figure, the exponent is 0.5 until 49.80% conversion. As polymerization proceeds over this conversion, the exponent exceeds 0.5, therefore the theory described in

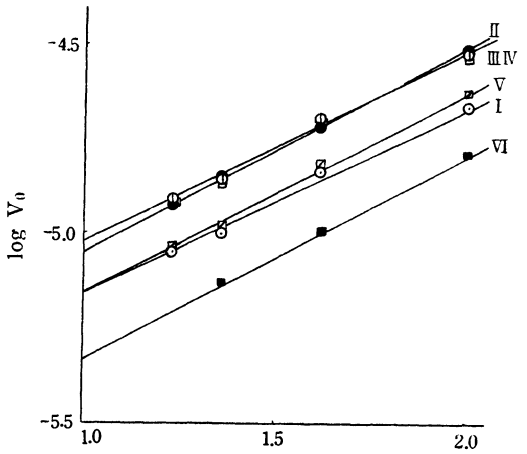

Fig. 4. Variation of the rate with the light intensity at 20°C, where V_0 is expressed in the unit of sec^{-1}.
○ Curve I, at 0% conversion; ◑ Curve II, at 28.15% conversion; ● Curve III, at 39.00% conversion; □ Curve IV, at 49.80% conversion; ◪ Curve V, at 59.30% conversion; ■ Curve VI, at 66.40% conversion.

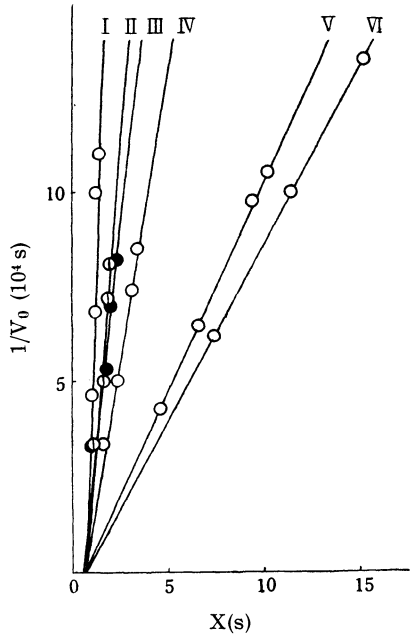

Fig. 5. Variation of the rate V_0 with the measured intercept at 20°C.
○ Curve I, at 0% conversion; ◑ Curve II, at 28.15% conversion; ● Curve III, at 39.00% conversion; ○ Curve IV, at 49.80% conversion; ○ Curve V, at 59.30% conversion; ○ Curve VI, at 66.43% conversion.

the first paper of this series cannot be applied correctly and the results at later stages are less accurate than those at initial stages.

The variation of the rate with the measured intercept X is shown in Fig. 5. From this intercept, the instrument's lag in response can be obtained and is 0.6–0.9 sec. From the slope of this line the values of k_p/k_t can be calculated. But at the conversion of 71.10%, the linearity between X and $1/V_0$ cannot be seen, because the lifetime becomes greater and velocity becomes slower. The values of V_0 and X at this conversion are shown in Table II.

TABLE II
VARIATION OF RATE AND LIFETIME WITH INTENSITY OF IRRADIATION AT 20°C AND AT 71.10% CONVERSION

Light Intensity	$V_0(s^{-1})$	$X(s)$	k_p/k_t
100	1.00×10^{-5}	14.5	20.0×10^{-5}
46	0.62×10^{-5}	19.7	19.0×10^{-5}
		Average	18.5×10^{-5}

The value of k_p/k_t in Table II is calculated by assuming that instrument's lag in response C in equation $X=C+(k_p/k_t)\times(1/V_0)\times\ln 2$ is 0.7 sec. The k_p/k_t value at various conversions is summarized in Table III.

TABLE III
THE VALUE OF k_p/k_t AT VARIOUS CONVERSION AT 20°C

Conversion (%)	$k_p/k_t\times10^{-5}$
0	1.08
28.15	2.02
39.00	2.72
49.80	4.78
59.30	13.1
66.40	16.3
71.10	18.5

The variation of rate V_0 with the extent of conversion at 30°C and 40°C is shown in Fig. 6.

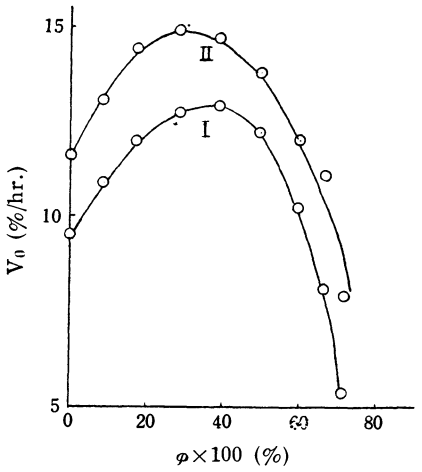

Fig. 6. Variation of the rate V_0 with conversion at 30°C and 40°C.
Curve I, at 30°C; Curve II, at 40°C.

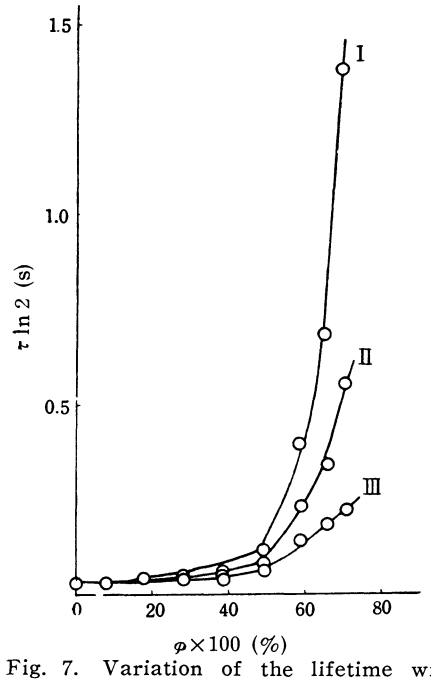

Fig. 7. Variation of the lifetime with conversion.
Curve I, at 20°C; Curve II, at 30°C; Curve III, at 40°C.

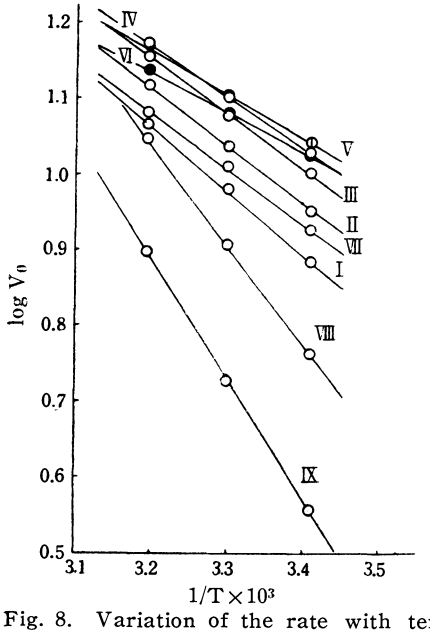

Fig. 8. Variation of the rate with temperature, where V_0 is expressed in the unit of %/hr.
Curve, I, at 0% conversion; Curve II, at 8.3% conversion; Curve III, at 17.8% conversion; Curve IV, at 28.15% conversion; ⓘ Curve V, at 39.00% conversion; ● Curve VI, at 49.80% conversion; Curve VII, at 59.30% conversion; Curve VIII, at 66.40% conversion; Curve IX, at 71.10% conversion.

where φ is the first corrected value. At these temperatures, the measurement of rate and lifetime at various light intensities was not carried out and the instrument's lag was unknown. But by using the lag at 20°C, the value of the lifetime was calculated according to the equation $X=C+\tau \ln 2$. The value of $\tau \ln 2$ at various conversions is shown in Fig. 7. The lifetime does not vary remarkably until 50% conversion is attained, but beyond this point it increases rapidly.

From Figs. 3 and 6 the variation of the rate with temperature can be obtained as shown in Fig. 8. And from Fig. 7 the variation of the lifetime with the temperature can be obtained as shown in Fig. 9.

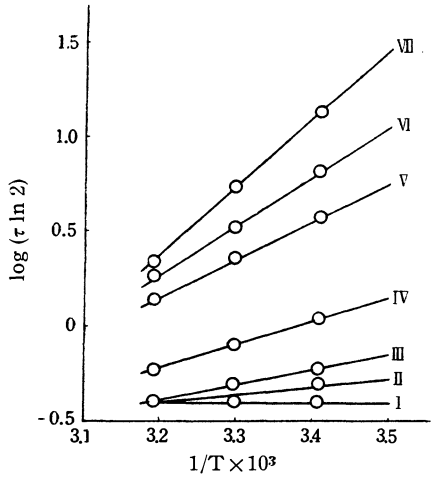

Fig. 9. Variation of the lifetime with temperature.
I, at 17.8% conversion; II, at 28.15% conversion; III, at 39.00% conversion IV, at 49.80% conversion; V, at 59.30% conversion; VI, at 66.40% conversion; VII, at 71.10% conversion.

Discussion

Because the value of k_p/k_t in Table III is calculated by using V_0 of Eq. (4), it is neccessary to correct these values by using the true fractional rate V. From Eqs. (1) and (4) V can be expressed as follows.

$$V=V_0\times(M_0/M)=V_0/(1-\varphi) \qquad (8)$$

Since $k_p/k_t=V\times\tau$, the true k_p/k_t values can be obtained through multiplication $1/(1-\varphi)$ by the values of Table III. These values are summarized in Table IV, comparing with Melville's results[2].

From both the results it is clear that the value of k_a/k_t increases gradually until 50% conversion and beyond this point increases rapidly. But the author's values are lower than the values obtained by Melville.

The overall activation energy $E_p-\frac{1}{2}E_t$ and activation energy of termination E_t are

obtained from figures 7 and 8 and compared with Melville's values[2] in Table V.

TABLE IV
THE CORRECTED VALUE OF k_p/k_t COMPARED WITH MELVILLE'S VALUE AT VARIOUS CONVERSIONS

Conversion	$k_p/k_t \times 10^5$	
%	This Work[a]	Thermocouple Method[b]
0	1.08	
4		3.72
23		10.2
28.15	2.82	
39.00	4.13	
46		22.1
49.80	9.55	
57		82.8
59.30	32.3	
65		75
66.40	48.6	
71.10	64.2	

a) This measurement was carried out at 20°C.
b) This measurement was carried out at 25°C.

TABLE V
THE VALUE OF $E_p - 1/2\ E_t$, E_t AND E_p AT VARIOUS CONVERSIONS, COMPARED WITH MELVILLE'S VALUE

Conversion	$E_p - \frac{1}{2} E_t$ (kcal./mol.)		E_t (kcal./mol.)		E_p (kcal./mol.)	
(%)	This Work	Melville	This Work	Melville	This Work	Melville
0	3.7		0		3.7	
4		4.2		<1		≥4.2
6		4.2		<1		≥4.2
8.3	3.4		0		3.4	
17.8	3.4		0		3.4	
20		4.0		—		≥4.0
23		3.5		1.4		4.2
28.15	2.8		2.2		3.9	
39.00	2.6		3.8		4.5	
46		1.9		3.4		3.6
49.80	2.5		5.6		5.3	
54		2.0		10.8		7.4
57		2.7		11.8		8.6
59.30	3.3		9.4		8.0	
65		>4.9		>13.0		>11.4
66.40	6.0		12.2		12.1	
71.10	7.2		16.8		15.6	
73		>6.7		>15.4		>14.4

Where E_p is calculated from $E_p - 1/2\ E_t$ and E_t. In both values, the overall energy of activation remains constant up to 20% conversion and then gradually decreases to a minimum value in the region of 50% conversion. It then increases rapidly beyond this region. The activation energy of termination is very low at the initial stages but it gradually increases at 20—30% conversion and then increases through the polymerization. On the other hand, the activation energy of propagation remains constant until 40—50% is reached and then increases very rapidly as further polymerization takes place.

Although differences between the author's and Melville's values are, to some extent, observed in Tables IV and V, the qualitative tendency coincides satisfactorily in spite of the differences of methods and temperature.

From these results, it seems that as the polymerization proceeds, increasing viscosity effects the termination process to slow down, but the effect of viscosity upon the propagation process is not so marked and becomes appreciable only at high conversions. But this conclusion must be proved by further study and in the next paper the author will describe the variation of k_p and k_t with the extent of polymerization.

Summary

The author used a thermistor method to study the later stages of polymerization of vinyl acetate, which was photosensitized with 1,1'-azobiscyclohexanecarbonitrile and obtained the variation of k_p/k_t, E_p and E_t with conversion.

From these results it was observed that the value of k_p/k_t increases gradually until about 50% conversion is reached and beyond this point increases rapidly. At the same time, the extent of conversion effects E_t in the region of 20—30% conversion, but the effect upon E_p is not so marked in these stages and becomes appreciable at high conversions.

The author wishes to express his hearty thanks to Dr. Momotaro Suzuki of this Academy for his helpful advice and encouragement and Mr. Shinichi Taira of Tokyo Metropolitan University for his kind supply of 1,1'-azobiscyclohexanecarbonitrile.

Department of Chemistry
Defense Academy
Yokosuka

The Reaction between Diphenylalkanes and Maleic Anhydride by the Friedel and Crafts Method

By Wataru KOGA

(Received April 25, 1956)

Introduction

It is a well-known fact that the Friedel and Crafts reaction between maleic anhydride and an aromatic compound results in the formation of a β-aroylacrylic acid. For example, benzene reacts with maleic anhydride to produce β-benzoylacrylic acid. In this case, an excess of maleic anhydride does not lead to the production of any detectable quantity of acids of the types, $C_6H_4(COCH=CHCOOH)_2$, $C_6H_3(COCH=CHCOOH)_3$, etc., nor can such products be obtained by the action of maleic anhydride on benzoylacrylic acid in any solvent with alminum chloride as catalyst[1]. This is also the case in the reaction between maleic anhydride and diphenyl[2]. This fact is illustrated as an E-effect of a carbonyl group by the electronic theory. Therefore, it is expected that the reaction between maleic anhydride and such a compound as one in which two benzene rings are separated by some methylene groups, e. g. diphenylmethane or bibenzyl, should result in substitution of each benzene ring by $-COCH=CHCOOH$ radicals. But some investigators[3] reported that the reaction between diphenylmethane and succinic anhydride, similarly to the reaction under consideration, gave only β-(*p*-benzyl) benzoyl propionic acid. On the other hand, there are some reports which support the first opinion. For instance, in addition to $C_6H_5-(CH_2)_n-C_6H_4COOH$ (n is 1 or 2), Liebermann[4], and Liebermann and Zsuffa[5] obtained $HOOCC_6H_4-(CH_2)_n-C_6H_4COOH$ (n is 1 or 2) by the reaction of diphenylmethane or bibenzyl and oxalyl chloride, and Duval[6] produced *p*-benzylacetophenone and *p*, *p*′-diacetyldiphenylmethane from diphenylmethane and acetyl chloride by the Friedel and Grafts reaction. But hitherto the reaction of diphenylalkanes and maleic anhydride has not been reported.

Now, in the present work the Friedel and Crafts reaction between diphenylmethane and bibenzyl, and maleic anhydride were studied, and diphenylmethane-4, 4′-di-γ-oxocrotonic acid and bibenzyl-4, 4′-di-γ-oxocrotonic acid were obtained respectively. The reduction of these compounds by zinc and acetic acid was examined and diphenylmethane-4, 4′-di-γ-oxobutyric acid and bibenzyl-4, 4′-di-γ-oxobutyric acid respectively were obtained. Furthermore these saturated ketoacids were reduced by a modified Clemmensen reduction method to diphenylmethane-4, 4′-dibutyric acid and bibenzyl-4, 4′-dibutyric acid, respectively.

Experimental Part

(1) Synthesis of Diphenylmethane and Bibenzyl.—a) Diphenylmethane was produced by the reaction between benzyl chloride and benzene in the presence of aluminium amalgam as catalyst according to the method of Hartman and Phillips[7]. The reaction product was purified by fractional distillation under reduced pressure and distillate boiling at 97–98°C/1.5 mmHg was collected. The yield was 49–54.6% of the theoretical amount.

b) Bibenzyl was produced by the reaction of 1, 2-dichloroethane with benzene in the presence of anhydrous aluminium chloride as catalyst according to the method described in "Organic Synthetic Chemistry"[8]. The reaction product was also purified by fractional distillation under reduced pressure and distillate boiling at 105–6°C/3 mmHg (m.p. 51–52°C) was collected. The yield was 66.2–74.6% of the theoretical amount.

(2) Diphenylmethane-4, 4′-di-γ-oxocrotonic acid.—The Friedel and Crafts condensation of maleic anhydride with various aromatic hydrocarbons was extensively studied by the use of such a solvent as carbon disulfide, nitrobenzene, and chlorinated hydrocarbons or aromatic hydrocarbon itself. It was found in the previous work[9] that 1, 2-dichloroethane gave the best result. So it was also used here as a solvent.

In a 1 l. four-necked, round-bottomed flask fitted with a mechanical stirrer, a reflux condenser, a dropping funnel, and a thermometer, were placed

1) M.T. Bogert and J.T. Ritter, *J. Am. Chem. Soc.*, **47**, 526 (1925).
2) H.G. Oddy, *J. Am. Chem. Soc.*, **45**, 2156 (1923).
3) J.W. Cook, A.M. Robinson and E.M. Roe, *J. Chem. Soc.*, **1939**, 266; L.F. Fieser, et al., *J. Am. Chem. Soc.*, **70**, 3201, Table C (1948).
4) C. Liebermann, *Ber.*, **45**, 1186 (1912).
5) C. Liebermann and M. Zsuffa, *Ber.*, **45**, 852 (1911).
6) M.H. Duval, *Bull. chim. soc.*, [4], **7**, 789 (1913).
7) W.W. Hartman and R. Philips, "Organic Syntheses, Coll. Vol.", John Wiley & Sons, Inc., New York, N.Y. (1943), II, p. 232.
8) R. Oda, "Organic Synthetic Chemistry", Kyoritsu-sha, Tokyo (1949), p. 92.
9) W. Koga, *J. Chem. Soc. Japan (Pure Chem. Sect.)* **76**, 1053 (1955).

49 g. (0.5 mol.) of maleic anhydride and 200 g. of dichloroethane. With cooling 105 g. of powdered, anhydrous aluminium chloride was added and stirred for about ten minutes, during which period most of the solid matter went into solution. Forty two grams (0.25 mol.) of diphenylmethane was then added slowly through a dropping funnel with efficient cooling and stirring. During this period the reaction mixture had to be kept below 3°C. After the addition had been completed, stirring was continued for about two hours at 5–6°C; at the end of this period the reaction mixture became very viscous and finally could not be stirred. The reaction mass was poured onto ice and hydrochloric acid and the solvent was removed by steam distillation. After cooling, the solid mass was collected and was dissolved in soda solution. The insoluble mass was filtered and the filtrate was acidified to Congo red by hydrochloric acid. The precipitated diphenylmethane-4, 4′-di-γ-oxocrotonic acid was filtered and washed with water. After drying for a day in vacuum desiccator, it weighed 42–53 g. (46–58% of the theoretical amount). It was purified by recrystallization from ethanol.

The purified acid is straw-yellow needles and melts at 255–6°C (from temperature at 220°C it turns from yellow to brown). It is soluble in hot alcohol and acetic acid but slightly in cold. It is practically insoluble in any other organic solvents or water.

Neutralization equivalent. Found: 304, 303. Calcd.: 308.

Anal. Found: C, 69.29; H, 4.36. Calcd. for $C_{21}H_{16}O_6$: C, 69.23; H, 4.40%.

Oxidation of this acid with alkaline permanganate gave colorlese crystals, which did not melt up to 300°C. The esterification of this acid in methanol gave colorless crystals which melted at 224–5°C (recrystallized from methyl ethyl ketone). This melting point agrees with that of dimethyl ester of benzophenone dicarboxylic acid-4, 4′ reported by Limplicht[10] and Staudinger[11] and analytical data is also in accordance with the calculated value as shown below.

Anal. Found: C, 68.45; H, 4.89. Calcd. for $C_{17}H_{14}O_5$: C, 68.46; H, 4.70%.

Furthermore alkaline fusion of the colorless acid melting above 300°C gave benzoic acid, m.p. 120°C, and terephthalic acid, identified as the methyl ester, m.p. 140–41°C; mixed m.p. 141–42°C.

Dimethyl ester of diphenylmethane-4, 4′-di-γ-oxocrotonic acid was made under the usual variety of conditions. The purified ester is a straw-yellow needle and melts at 128–128.5°C (recrystallized from methyl ethyl ketone).

Anal. Found: C, 70.38; H, 5.03. Calcd. for $C_{23}H_{20}O_6$: C, 70.41; H, 5.10%.

This colored isomeric ester (*trans*) rearranges slowly to the *cis*-isomer when its methyl ethyl ketone solution is exposed to sunlight for a few days. The *cis*-isomer is a colorless needle melting at 84–84.5°C.

(3) Bibenzyl-4, 4′-di-γ-oxocrotonic acid.—Bibenzyl-4, 4′-di-γ-oxocrotonic acid was produced similarly to diphenylmethane-4, 4′-di-γ-oxocrotonic acid. The yield was 56–69 g. (57.8–70.3% of the theoretical amount.)

This acid is practically insoluble in most organic solvents and water. So the purification is carried out in such a way that it was disssolved in soda solution and filtered and the filtrate was acidified by hydrochloric acid, or by the hydrolysis of the purified dimethyl ester of the acid by mineral acid.

The purified acid is a straw-yellow crystal and does not melt up to 300°C.

Nentralization equivalent. Found: 296, 292. Calcd.: 297.

Anal. Found: C, 69.89; H, 4.73. Calcd. for $C_{22}H_{18}O_6$: C, 69.84; H, 4.76%.

Oxidation of this acid with alkaline permanganate gave terephthalic acid, identified as the methyl ester, m.p. 140–41°C, mixed m.p. 141–42°C.

Dimethyl ester is formed in the same way as above. The purified ester is a straw-yellow needle melting at 137–8°C (recrystallized from methyl ethyl ketone).

Anal. Found: C, 70.88; H, 5.38. Calcd. for $C_{24}H_{22}O_6$: C, 70.94; H, 5.42%.

This colored isomer (*trnas*) also rearranges to the *cis*-isomer when its methyl ethyl ketone solution is exposed to sunlight for a few days. The *cis*-isomer is a colorless needle melting at 175.5–6.5°C.

(4) Diphenylmethane-4, 4′-di-γ-oxobutyric acid.—Ten grams of diphenylmethane-4, 4′-di-γ-oxocrotonic acid was suspended in 80 g. of acetic acid and to this was added a small portion of 15 g. of zinc dust with stirring After threee to four hours the reaction mixture became colorless; then it was poured in 1 l. of soda solution and dissolved. The insoluble mass was filtered and the filtrate was acidified with hydrochloric acid. The precipitated diphenylmethane-4, 4′-di-γ-oxobutyric acid was filtered and washed with water. After drying, it was purified by recrystallization from ethanol. The yield was 6.2–7.5 g. (61.3–74.3% for theoretical amount). The purified acid is a colorless needle melting at 224–5°C.

Anal. Found: C, 68.45; H, 5.56. Calcd. for $C_{21}H_{20}O_6$: C, 68.48; H, 5.43%.

Dimethyl ester is formed by refluxing methanol solution of the acid in the presence of concentrated sulfuric acid as catalyst. The purified ester (recrystallized from methanol) is a colorless thin plate and melts at 95°C.

Anal. Found: C, 69.23, H, 6.11. Calcd. for $C_{23}H_{24}O_6$: C, 69.70; H, 6.06%.

(5) Bibenzyl-4, 4′-di-γ-oxobutyric acid.—The reduction of the diphenylethane-4, 4′-di-γ-oxocrotonic acid was carried out in the same way as above. The yield was 5.5–7.6 g. (54.4–75.2% for theoretical amount). The purified acid is a colorless needle (recrystallized from a large amount of ethanol) and melts at 259–60°C.

10) H. Limpricht, *Ann.*, **312**, 97 (1900).
11) H. Staudinger and G.A.R. Kon, *Ann.*, **384**, 98 (1911).

Anal. Found: C, 69.06; H, 5.58. Calcd. for $C_{24}H_{22}O_6$: C, 69.11; H, 5.76%.

Dimethyl ester is formed by refluxing suspension of the acid in methanol in the presence of a small amount of concentrated sulfuric acid as catalyst. The purified ester (recrystallized from methyl ethyl ketone) is a colorless needle melting at 114.5°C.

Anal. Found: C, 70.40; H, 6.36. Calcd. for $C_{24}H_{26}O_6$: C, 70.24; H, 6.34%.

(6) Diphenylmethane-4, 4′-dibutyric acid and Bibenzyl-4, 4′-dibutyric acid.—The reduction of the carbonyl group of the above saturated keto acids according to Clemmensen's method or modified Martin-Clemmensen's method was unsuccessful, for these acids were insoluble in water, hydrochloric acid, or toluene. So the reduction was carried out according to Koelsch[12] who used ethanol as a solvent.

To the mixture of 45 cc. of ethanol, 45 cc. of concentrated hydrochloric acid, and amalgamated zinc, which was prepared from 15 g. of zinc dust and 1.5 g. of murcuric chloride, 5 g. of the acid, which should be reduced, was added and then was refluxed for one hour. A second portion of 45 cc. of concentrated hydrochloric acid was then added and refluxing was continued for six hours. The mixture was cooled and the solid mass was collected and dissolved in boilling 500 cc. of 5% aqueous sodium hydroxide. After filtration and acidification of the filtrate, the reduced acid was separated. It was purified recrystallization from ethanol.

Diphenylmethane-4, 4′-dibutyric acid.—The yield was 2.5–2.7 g. (54.1–58.4% for theoretical amount). Colorless needles, m.p. 199.5–200°C.

12) C.F. Koelsch, *J. Am. Chem. Soc.*, 55, 3885 (1933).

Anal. Found: C, 73.76; H, 6.97. Calcd. for $C_{21}H_{24}O_4$: C, 74.12; H, 7.06%.

Bibenzyl-4, 4′-dibutyric acid.—The yield was 2.2–2.5 g. (54.1–58.4% for theoretical amount). Colorless needles, m.p. 182–3°.

Anal. Found: C, 74.86; H, 7.44. Calcd. for $C_{22}H_{26}O_4$: C, 74.58; H, 7.36%.

Summary

(1) By the reaction of diphenylmethane and diphenylethane with maleic anhydride in the presence of aluminium chloride, diphenylmethane-4, 4′-di-γ-oxocrotonic acid and bibenzyl-4, 4′-di-γ-oxocrotonic acid were produced, respectively. And *cis* and *trans* isomers of dimethyl esters of these acids were prepared.

(2) By the reduction of the above two acids by zinc and acetic acid, diphenylmethane-4, 4′-di-γ-oxobutyric acid and bibenzyl-4, 4′-di-γ-oxobutyric acid were prepared.

(3) These saturated keto acids were reduced by amalgamated zinc in the mixture of ethanol and hydrochloric acid to diphenylmethane-4, 4′-dibutyric acid and diphenylethane-4, 4′-dibutyric acid.

The author wish to express his gratitude to Dr. Tomoyoshi Miura and Dr. Shiro Tsuruta for their helpful advice in performing these experiments.

Hitachi Research Laboratory, Hitachi Ltd., Hitachi

A New Method for Radiochemical Prospecting of Uranium Ore. I. Estimation of the Amount of Uranium

By Yūji YOKOYAMA

(Received April 2, 1956)

Introduction

The economic importance of uranium and thorium has been stimulating extensive investigations of terrestrial occurrence and distribution of these elements. One of the important parts of these investigations is prospecting for uranium and thorium ores.

For many years, radioactive survey with a Geiger-Müller counter has been extensively used for this purpose. Recently, the development of a scintillation counter has made it possible to prospect radioactive deposits by the airborne radioactive survey.

However, these methods are effective only for the cases in which a uranium deposit is cropping out on the surface of the ground, because gamma radiation from these elements can not penetrate thick layers of rocks and soils. Furthermore, it is considerably difficult to distinguish between uranium and thorium ores by these methods.

Therefore, practically there has been no method to prospect and evaluate an underground uranium deposit without a test boring of the ground. The aim in the present work is to establish a new radiochemical method in which naturally radioactive elements in natural waters are used as a kind of tracer for the purpose of estimating the amount and the depth of uranium layer under the ground.

It is well known that the uranium content of mineral waters is less than that of sea water, but radon and radium content of some mineral waters is much higher than that of sea water. (Table I)

TABLE I
RADIOACTIVE ELEMENTS IN NATURAL WATERS

	U (g./l.)	Ra (g./l.)	Rn (curie/l.)
Sea Water[1]	10^{-6}	10^{-13} to 10^{-14}	10^{-13}
Mineral Water[2]			
Hot Spring			
Arima	10^{-6} to 10^{-7}	10^{-10}	10^{-10}
Mineral Spring			
Masutomi	10^{-7} to 10^{-8}	10^{-11} to 10^{-12}	10^{-6} to 10^{-10}

The content of radon and radium in mineral waters could be explained as follows; mineral water passes through a uranium-rich layer under the ground, dissolving radon and radium which have greater solubility than their ancestors. Based on these facts, the author considered that the radiochemical studies of mineral waters can be used as a tool for prospecting a uranium-rich layer under the ground.

The Presence of Two Radioactive Strata

It has been suggested, in some of the previous reports[3], that there must be two radioactive strata under the ground of mineral springs. A deep stratum, which is probably related to the uranium or thorium ores, may be located at a depth of the order of several kilometers. This stratum is considered as a supplying zone of radium and its isotopes, such as thorium X, mesothorium 1 and actinium X, for mineral waters. The other radioactive stratum, which is considered to be the source of radon and thoron for mineral waters, is located very close to the surface of the earth at a depth from 10 to 50 meters below the ground.

When radium-containing mineral waters come close to the surface of the earth, deposition of the sinter deposits takes place, which is caused by the escape of carbon dioxide, contact with air, decrease in temperature etc. Then a part of radium and its isotopes is precipitated with sinter deposits.

The porous zones of the sinter deposits, which are as radioactive as ordinary radioactive minerals such as monazite, etc., are often found in the areas of radioactive springs. The radio activity of sinter deposits is mainly due to radium and its isotopes, and it is a very important fact that the uranium content of these deposits is much lower than the value expected from radium content. For example, the uranium content of sinter deposits from a mineral spring in Japan ranges from 0.004 to 0.05 p. p. m.[4] (both extremes for Masutomi Mineral Springs), whereas these sinter deposits contain about 10^{-10} g. Ra per gram.

The very low content of uranium in mineral waters and sinter deposits was apt to lead us to a faulty conclusion that there was probably no uranium-rich ore in the areas of radioactive springs of Japan. But the occurrence of a remarkably uraniumbearing layer is concluded by the author's present estimation.

Estimation of the Amount of Uranium Reserves

It is possible to estimate the amount of uranium, which occurs in a supplying zone of radium, by calculating the amount of supply of radium to mineral waters per second. The estimation may be carried out by two different ways.

In the first one, it is assumed that the atoms of radium, which are generated by the radioactive decay of uranium, are directly supplied into mineral waters.

The amount of radium, G_{Ra} which is generated from 1 g. of uranium per second, is calculated as follows.

$$G_{Ra} = \frac{226}{238}\lambda_U = 4.6\times10^{-18}\ \text{g./sec.} \qquad (1)$$

where λ_U is a decay constant of uranium and 226 and 238 are mass number of radium and uranium respectively.

On the other hand, the amount of radium,

1) F. Herneggar, *Anz. Akad. Wis. Wien*, **1**, 19 (1933), R.D. Evans, A.F. Kip and E.G. Moberg, *Am. J. Sci.*, **36**, 241 (1938), I. Iwasaki and T. Ishimori, *J. Chem. Soc. Japan*, **72**, 14 (1951), M. Nakanishi, This Bulletin, **24**, 36 (1951), E. Rona and W.D. Urry, *Am. J. Sci.*, **250**, 241 (1952).

2) T. Nakai, This Bulletin, **15**, 333 (1940), P.K. Kuroda and Y. Yokoyama, ibid., **22**, 34, 43 (1949), M. Nakanishi, ibid., **24**, 33 (1951), Y. Yokoyama, *J. Chem. Soc. Japan*, **76**, 558 (1955).

3) P.K. Kuroda and Y. Yokoyama, This Bulletin, **21**, 52, 58 (1948); **22**, 34, 43 (1949); *Anal. Chem.*, **26**, 1509 (1954); Y. Yokoyama, *J. Chem. Soc. Japan*, **70**, 399 (1949).

4) M. Nakanishi, This Bulletin, **24**, 33 (1951).

which is supplied into mineral waters per second, is $C_{Ra} \cdot F$, where C_{Ra} is the radium content of mineral waters (g./l.), and F is the amount of flow (l./sec.).

From the supplying rate of radium, therefore, one can expect that the following amount of uranium, W, is present in supply zone.

$$W=\frac{C_{Ra} \cdot F}{G_{Ra} \cdot K} \text{ g.} \quad (2)$$

where K is a dissolving coefficient of radium into mineral waters from uranium ore. In the case of perfect dissolving, the value of K is 1.00.

For example, in Hot Spring Arima, which has the highest radium content in Japan, C_{Ra} is 2×10^{-10} g./l. and F is 5 l./sec. Then one can obtain the following equation.

$$W=\frac{2\times10^{-10}\times5}{4.6\times10^{-18}\times K}=\frac{2\times10^{8}\text{g.}}{K}=\frac{200\text{ ton}}{K} \quad (3)$$

From the foregoing calculation, one might expect that 200 ton or 2,000 ton of uranium is present under the ground of Hot Spring Arima, on the assumption that K=1.00 or 0.10 respectively.

The exact value of K is unknown, but it may be not unreasonable to suppose that the value of K is of the order of 0.1. It was found by the present author that mineral waters contain usually a comparable amount of thorium X with mesothorium 1[5].

Table II

Isotopes of radium in mineral waters

Name of Spring		^{226}Ra 10^{-12} c./l.	^{224}Ra(Th X) 10^{-12} c./l.	^{228}Ra(MsTh I) 10^{-12} c./l.	^{225}Ra(Ac X) 10^{-12} c./l.	Th X/MsTh I
Arima	Shin-onsen	170±5	560±20	580±10	9±0.5	0.97±0.04
〃	Ariake-no-yu	170±7	310±10	380±20	9±0.9	0.82±0.05
Ikeda	No. 1	33±1	100±2	85±8	——	1.18±0.07
〃	No. 2	36±3	113±12	53±7	——	2.12±0.36
Masutomi	A 5	66±3	200±7	230±10	——	0.87±0.05
〃	B 7	24±1	66±2	240±1	1.3±0.1	3.6 ±0.1
Misasa	Misasa-kan	14±1	34±2	38±4	——	0.90±0.11
〃	Ōhashi-sotoyu	9±2	95±6	30±6	——	3.2 ±0.7
Tamagawa	Ōbuki	16±1	144±2	109±3	——	1.32±0.04
〃	Kobuki	24±0.5	160±6	131±2	——	1.22±0.05

Table III

Amount of uranium estimated by radiochemical method

Name of Spring	Pref.	Ra Content 10^{-12} g./l.	Amount of flow l./sec.	Ra Discharge 10^{-12} g./sec.	Amount of Uranium K=1.00 ton	Amount of Uranium K=0.10 ton
Springs with Ra Content $>10^{-11}$ g./l.						
Tamagawa	Akita	20	150	3,000	700	7,000
Arima	Hyōgo	300	5	1,000	200	2,000
Masutomi	Yamanashi	30	2	60	10	100
Matsunoyama	Niigata	15	4	60	10	100
Misasa	Tottori	15	3	45	10	100
Yugakae	Shimane	30	1	30	7	70
Ikeda	Shimane	40	0.25	10	2	20
Takarazuka	Hyōgo	25	0.4	10	2	20
Isobe	Gumma	15	0.3	5	1	10
Springs with Ra Content $\leq10^{-11}$ g./l.						
Onogawa	Yamagata	8	600	4,800	1,000	10,000
Toyotomi	Hokkaido	10	300	3,000	700	7,000
Yuzaki	Wakayama	8	15	120	30	300
Kawatana	Yamaguchi	10	8	80	20	200
Wakura	Ishikawa	5	10	50	10	100
Ōshio	Fukushima	4	3	12	3	30

5) Y Yokoyama, *J. Chem. Soc. Japan*, **76**, 558 (1955).

This fact indicates that the dissolving coefficient of radium and its isotopes is not very large. The reason can be explained as follows. If mesothorium 1 dissolves prefectly into mineral waters, it would be impossible to supply thorium X in mineral waters from supply zone. Because, in such case, no mesothorium 1 and its descendants (radiothorium and thorium X etc.) are present in supply zone.

Another method of calculation for the amount of uranium is as follows.

It is assumed that at first, uranium of supply zone is in radioactive equilibrium with radium, then mineral waters dissolve radium. The amount of radium, which is in equilibrium with 1 g. of uranium, is

$$E_{Ra} = \frac{\lambda_U \cdot 226}{\lambda_{Ra} \cdot 238} = 3.4 \times 10^{-7} \text{ g.} \qquad (4)$$

where λ_U and λ_{Ra} are decay constants of uranium and radium respectively.

During the time interval T second, the amount of radium brought to the surface of the earth by mineral waters is $C_{Ra} \cdot F \cdot T$(g.). From the total supplying amount of radium, therefore, one can expect that the following amount of uranium, W', is present in the supply zone.

$$W' = \frac{C_{Ra} \cdot F \cdot T}{E_{Ra} \cdot K'} \qquad (5)$$

where K' is a portion of radium, which is soluble in mineral waters, to total radium.

For example, on Hot Spring Arima, assuming $T=100$ year (3×10^9 sec.) and $T=1{,}000$ year (3×10^{10} sec.) we get

$$W' = \frac{2\times10^{-10}\times5\times3\times10^{9}\text{g.}}{3.4\times10^{-7}\times K'} = \frac{10 \text{ ton}}{K'}, \text{ for } T=100 \text{ year},$$

$$W' = \frac{2\times10^{-10}\times5\times3\times10^{10}\text{g.}}{3.4\times10^{-7}\times K'} = \frac{100 \text{ ton}}{K'}, \text{ for } T=1{,}000 \text{ year} \qquad (6)$$

The foregoing calculation shows that the value of W' in Eq. (6) becomes close to the value of W in Eq. (3) when the time interval T is as long as the order of the half life of radium (1622 years). Therefore these two calculating methods will give practically the same value, if issue of mineral waters continues during some long time in which a kind of equilibrium state takes place between leaching and supplying of radium. More general discussions about these points will be reported in future in detail. But it may be supposed that the times required for equilibrium will be shorter than the values expected from the half life of radium, because those times are determined not with physical half life but with actual half life in which geochemical half life by leaching effect is also considered.

Using Eq. (2), the author estimates the amount of uranium in the supplying zone of the main mineral springs, containing radium, in Japan. The results are shown in Table III. It must be noticed that the amount of uranium, calculated in this way, is not the weight of minerals but the weight of uranium metal only. In Table III, two values are shown for the amount of uranium, where K is supposed to be 1.00 and 0.10.

The largest amount of uranium ore in Japan, discovered in the past, is Suishō-yama at Ishikawa, Fukushima Pref. The amount of uranium reserves in Suishō-yama is estimated as about 1 to 2 ton as uranium metals, or 2,000 to 4,000 ton as minerals. The mean uranium content of ore is estimated as 0.05% in Suishō-yama.

It is found in Table III that the amounts of uranium in some mineral-spring areas estimated by the author, are very much higher than that of Suishō-yama.

Recently a new uranium deposit has been discovered at Ogamo Mine near the Hot Spring Misasa, which is one of the largest radioactive springs in Japan. This fact may support the author's opinion.

Summary

A radiochemical method for the prospecting and the estimation of the amount of uranium layer under the ground based upon the determination of radium in mineral waters, is described. Results show, 700 to 7,000 ton of uranium may occur in Hot Spring Tamagawa and 200 to 2,000 ton of uranium in Hot Spring Arima. The natural radioactive elements in mineral waters will give valuable information on the geological structures, especially the nature of the underground radioactive strata.

The authour expresses his hearty thanks to Prof. Kenjirō Kimura of the University of Tokyo for his kind guidance in the course of this study, to Prof. Masatake Kozaki of Yokohama National University, to Dr. Paul K. Kuroda of the University of Arkansas, to Dr. Nobufusa Saitō of the University of Tokyo and Dr. Jean Delloue of the Atomic Energy Committee of France for their valuable advice and encouragement.

Faculty of Liberal Arts and Education
Yokohama National University
Kamakura

The Adsorption of Water Vapor by Gelatin-Detergent Complexes

By Kunio TAMAKI and Bun-ichi TAMAMUSHI

(Received May 29, 1956)

In the previous investigation[1] on the interaction of gelatin with detergent anions or cations, we have found that hydrophobic complexes are formed between them under appropriate conditions. Observing the sedimentation velocity as well as the sedimentation volume in both cases of gelatin-detergent anion complex and gelatin-detergent cation complex, it has been found that the sedimentation velocity of the former complex is greater than that of the latter, while the sedimentation volume of the former is smaller than that of the latter. This suggests that there must be some difference in the hydrophobic nature of these two types of complexes. It is the purpose of this paper to detect such a difference by measuring the adsorption of water vapor by these two types of complexes.

Experimental

Materials.—Gelatin, sodium dodecyl sulfate and dodecyl ammonium chloride used in this experiment are the same samples as used in the previous work[1].

Samples for Adsorption Experiments.—The gelatin, purified by use of ion exchange resins, was precipitated by the addition of methanol to its aqueous solution, and the precipitate was dried in a vacuum desiccator. The detergent-gelatin complex was separated from the solution by centrifugation after the precipitate was formed, repeatedly washed with water and centrifugated, and then dried in a vacuum desiccator. The nitrogen content of the complex was determined by the Kjeldahl method. As the complex may be considered as a compound between gelatin molecule and dodecyl sulfate ion ($C_{12}H_{25}OSO_3^-$= 265.4) or dodecyl ammonium ion ($C_{12}H_{25}NH_3^+$= 186.3), the detergent content in the complex is calculated from the nitrogen percentage. The combined detergent, calculated in this way, was found to agree very well with that obtained by direct analysis in the previous investigation[1]. The data are given in Table I.

TABLE I

	Sample	pH of Solution	Nitrogen Content (%)	Detergent Content (mM/g. Gel.) Cal.	Detergent Content (mM/g. Gel.) Exp.	Gelatin Content (%)
No. 1	Pure Gelatin	4.8	16.26	0	0	100
2	Gelatin-Dodecyl	2.0	12.96	0.96	0.92	79.7
3	Sulfate Ion	3.6	13.80	0.67	0.68	84.9
4	Complex	4.0	14.70	0.40	0.40	90.4
5	Gelatin-Dodecyl	8.0	15.56	0.41	0.40	92.8
6	Ammonium Ion	9.3	15.20	0.65	0.63	89.2
7	Complex	10.6	14.80	0.94	0.98	85.0

Adsorption Experiment.—Adsorption experiment was carried out by the desiccator method similar to that adopted by H. Bull[2], who first studied in detail the adsorption of water vapor by several purified proteins. A definite quantity —between 0.5 g. and 0.9 g.—of each samples of complexes was taken in a weighing bottle, which was then placed in a desiccator containing sulfuric acid of a definite concentration. The desiccator was submerged in a thermostat maintained at 25±0.1°C. After the attainment of the equilibrium, the weighing bottle was weighed, and the density of the sulfuric acid was measured, from which the relative vapor pressure was calculated. The amount of the water vapor adsorbed by a given weight of protein was obtained from the increase in weight of the weighing bottle. In order to allow for the dilution effect of the added detergent, the amount of adsorbed water was calculated on the basis of protein portion.

According to Bull[2], it requires about two weeks for the attainment of equilibrium, but as Robinson[3], Benson et al[4]. have remarked, the equilibrium can be attained in a shorter time, if the adsorption takes place under diminished air pressure. In our experiment, it was sufficient, to wait under the pressure of 10−20 mmHg for about twentyfour hours.

Fig. 1 shows some of the isotherms obtained, one with a sample of pure gelatin and two with samples of different type complexes.

1) K. Tamaki and B. Tamamushi, This Bulletin, 28, 555 (1955).

2) H. Bull, *J. Am. Chem. Soc.*, **66**, 1499 (1944).

3) R.A. Robinson, *J. Chem. Soc.*, **1948**, 1083.

4) S.W. Benson, D.A. Ellis and R.W. Zwanzig, *J. Am. Chem. Soc.*, **72**, 2102 (1950).

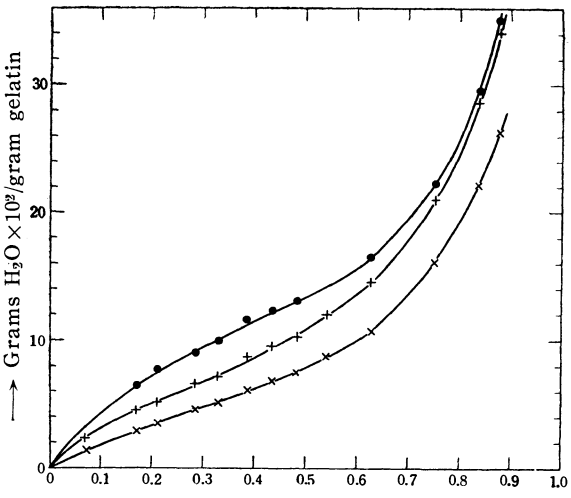

Fig. 1. Water vapor adsorption isotherms
·No. 1; ×No. 2; +No. 7

Discussion

As Fig. 1 indicates, the amount of water vapor adsorbed by gelatin is markedly reduced by the combination of detergent ion with it. However, the amount adsorbed by the gelatin-dodecyl sulfate ion complex is less than that by gelatin-dodecyl ammonium ion complex over the whole range of relative vapor pressures. From this fact, it is concluded that the former is more hydrophobic than the latter, which is in accord with the experimental results obtained in the measurement of sedimentation volume and sedimentation velocity. For both types of complexes, it was found that the complexes containing detergent in greater amount adsorb water vapor in less degree.

As has been reported by many investigators, adsorption isotherms of water vapor on proteins are generally S-shaped, and these are represented by the Brunauer-Emmett-Teller (B.E.T.) equation[5] in the range of relative vapor pressure from 0.05 to 0.5. The isotherms obtained in our experiment have been found too in accord with the B.E.T. theory as shown by Fig. 2. The amount of the first monolayer coverage V_m as well as the constant C in in the B.E.T. equation are listed in Table II.

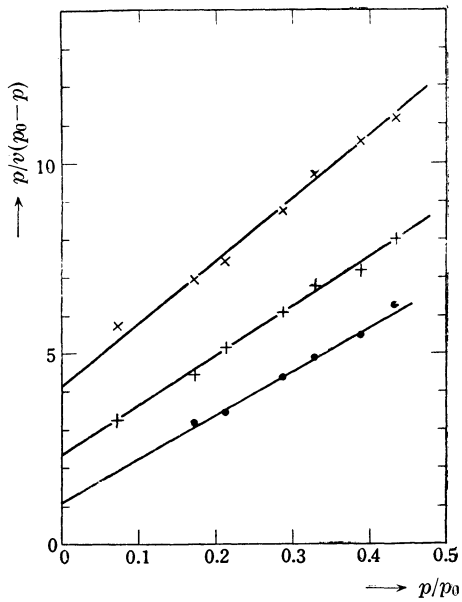

Fig. 2. B.E.T. plot.
·No. 1; ×No. 2; +No. 7

According to Dunford and Morrison[6], the isotherms obtained by Bull[2] are represented by the Harkins-Jura equation[7], while the isotherms obtained in our experiment do not obey that equation except the isotherm for pure gelatin.

Many workers have discussed the mechanism of the adsorption of water on proteins. Pauling[8] suggested that the amount of the first monolayer adsorption V_m could be interpreted in terms of the number of polar

TABLE II

	Sample	($g.H_2O$/g. Gel.) V_m	C	Decrease in V_m (mM/g. Gel.)	Detergent Combined (mM/g. Gel.)
No. 1	Pure Gelatin	0.0821	9.54		
2	Gelatin-Dodecyl	0.0493	4.85	1.82	0.96
3	Sulfate Ion	0.0503	5.73	1.76	0.67
4	Complex	0.0512	6.13	1.71	0.40
5	Gelatin-Dodecyl	0.0654	7.66	0.93	0.41
6	Ammonium Ion	0.0648	7.45	0.96	0.65
7	Complex	0.0632	7.00	1.05	0.94

5) S. Brunauer, P.H. Emmett and E. Teller, ibid., 60, 309 (1938).
6) H.B. Dunford and J.L. Morrison, *Can. J. Chem.*, 32, 558 (1954).
7) W.D. Harkins and G. Jura, *J. Am. Chem. Soc.*, 66, 1366 (1944).
8) L. Pauling, ibid., 67, 555 (1945).

amino-acid side-chains in protein molecules. Benson et al[4]. inferred from their experimental result that the adsorption of water vapor on proteins should be qualitatively different from that of non-polar gases such as nitrogen, and the adsorption of water would take place at specific sites on protein molecules. According to the work of Mellon, Korn and Hoover[9], a reduction in the amount of adsorption takes place over the whole range of relative vapor pressures, when the amino-groups of casein are benzoylated. By the B.E.T. treatment of the data, they have shown that the amount of reduction in V_m roughly correspnds to the amounts benzoylated on the protein molecule. On the other hand, Green and Ang[10] came to the conclusion, on the basis of their study of the adsorption of water vapor by acetyl derivatives of collagen and of silk fibroin, that the change in V_m caused by acetylation is independent of number the of acetyl groups introduced.

As indicated in Table II, there is a certain parallel correlation, but no stoichiometrically definite relation between the reduction in V_m and the amount of the combined detergent in our experimental data. For both complexes, the decrease in V_m is always greater than the amount of combined detergent.

9) E.F. Mellon, A.H. Korn and S.R. Hoover, ibid., 70, 3040 (1948).
10) R.W. Green and K.P. Ang, ibid., 75, 2733 (1953).

Summary

1. The adsorption of water vapor by gelatin-dodecyl sulfate ion complexes and gelatin-dodecyl ammonium ion complexes has been measured.
2. The adsorption of water vapor by both those kinds of complexes has been found to be less than that by pure gelatin.
3. The amount of adsorption on the gelatin-dodecyl sulfate ion complexes is always smaller than on the gelatin-dodecyl ammonium ion complexes, and this fact indicates that the former complexes are more hydrophobic than the latter.
4. The adsorption isotherms have been interpreted by the B.E.T. theory and the amount of the first monolayer adsorption has been calculated.
5. In both types of complexes, there is a certain parallel correlation but no stoichiometric relationship between the reduction in the amount of the first monolayer adsorption and the amount of combined detergent.

We should like to express our sincere thanks to Armour and Co., U.S.A. and Nezu Chemical Laboratory, Tokyo, for their kind supply of pure detergents.

Chemistry Department, College of General Education; and Institute of Science and Technology, The University of Tokyo, Tokyo

Dielectric Studies on Colloidal Solutions. II. The Behavior of Small Counter Ions in the Aqueous Solutions of the Hydrochlorides of Homologous Long-chain Amines

By Michio SHIRAI and Bun-ichi TAMAMUSHI

(Received June, 6, 1956)

In the previous work[1] of this series the high-frequency conductivity of aqueous solutions of paraffin-chain salts has been measured and the results have been interpreted in terms of the Debye-Falkenhagen's theory of strong electrolytes. The sudden rise of the high-frequency effect as well as the fall of the low-frequency equivalent conductivity of these solutions have been considered to be due to the electrostatic interaction between ionic micelles and small counter ions. It is, however, probable that some fraction of counter ions associate with the micelle, and consequently, the valence of the ionic micelle does not agree with the number of single ions contained in the micelle. The fraction of counter ions associated with the micelle has been estimated from the data of conductivity and transference number[2,3], from those of electro-

1) M. Shirai and B. Tamamushi, This Bulletin, **28**, 545 (1955).

2) G.S. Hartley, B. Collie and C. S. Samis, *Trans. Faraday Soc.*, **32**, 785 (1936).

3) A.P. Brady and D.J. Salley, *J. Am. Chem. Soc.*, **70**, 914 (1948).

motive force measurement[4], from those of self-diffusion coefficient[3], etc. Chandler and McBain[5] have recently estimated, based on the results of anomalous osmosis, that the effective charge on the micelle is only two or three, whereas Hartley and his collaborators[2] came to the conclusion that the micelles behave as polyvalent ions having a large number of effective charges.

In the present paper we discuss this problem on the basis of the experimental data of low-frequency and high-frequency conductivities, and those of transference number obtained for the hydrochlorides of homologous long-chain amines.

Experimental

Procedure.—The method and apparatus applied for the high-frequency conductivity measurement are the same as described in the previous paper[1].

The determination of transference number was carried out by the moving boundary method. The principle of that method was fully discussed by McInnes et al.[6], and the method suitable for the measurement of transference number of large radical-ions was developed by Hartley et al.[7] A brief outline of the method used in our present work is as follows. The micellar solution which is to be investigated acts as a following solution and potassium chloride solution is used as a leading one. The transference number of the following radical-ion, T_F, is determined by the concentration, C_L, and the transference number of the leading ion, T_L, and the concentration of the following radical-ion left behind the boundary, C_F, according to the following relation:

$$\frac{T_F}{C_F}=\frac{T_L}{C_L}$$

Thus, if C_F is determined, T_F is calculated by using the known values of C_L and T_L[8].

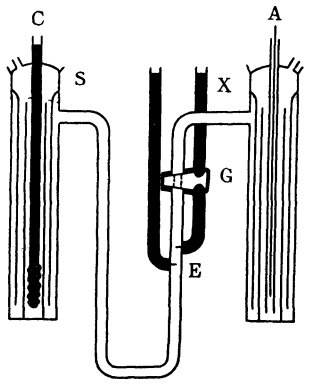

Fig. 1. Moving boundary apparatus.

The apparatus used is shown in Fig. 1. The initial boundary is formed at the position of the stopcock G. The platinum wire C immersed in a strong ferric chloride solution is used as the cathode, while the silver wire A serves as the anode. The electrodes must be nonpolarizable, which condition is fulfilled in this case. The part S of the vessel is filled with potassium chloride solution and the part X with the colloidal electrolyte solution which is to be investigated. After letting electric current flow for a few hours by connecting the apparatus in series with a constant current regulator, the concentration of the colloidal electrolyte solution left behind the boundary is determined by measuring its conductivity. This is performed by using the platinum electrodes E and the alternating-current bridge employing the frequency of 1000 cycle/sec. As it is difficult to measure the high-frequency conductivity at higher temperatures, all these measurements have been carried out at 30°C.

Materials.—Octyl-, decyl-, dodecyl-, tetradecyl-, and hexadecylamine hydrochlorides were prepared from the corresponding amines supplied by Armour & Co., U. S. A., by passing gaseous hydrogen chloride through their benzene solutions. The products were subjected to careful recrystallization from ethanol, and then they were dried in a vacuum desiccator over calcium chloride. All dissolution and dilution processes were carried out with conductivity water but no special precautions were taken to prevent access of carbon dioxide in the transference number measurement.

Results and Discussion

The experimental data of the equivatent conductivity at the frequency of 1000 cycle/sec. and the high-frequency effect at the frequency of 30 Mc./sec. for the electrolytes under investigation are tabulated in Table I, where the high-frequency effect denotes the increase of the equivalent conductivity at the applied high-frequency expressed in terms of the percentage as defined in the previous paper[1]. The measurement of the high-frequency conductivity was carried out only in the range of concentration shown in Table I, on account of the great increase of the conductance in higher concentrations.

The increase of equivalent conductivity at high-frequency is attributable to the relaxation effect of the ionic atmosphere surrounding the micelle ion, and therefore, that increase is expected to be the larger, the greater the electric charge of the micelle, and the smaller its radius. As is seen from Table I, dodecyl-, tetradecyl-, and hexadecylamine hydrochlorides show considerable increase of equivalent conductivity at high-frequency in spite of their large ionic

4) J.W. McBain and M.D. Betz, ibid., 57, 1909 (1935).
5) C. Chandler and J.W. McBain, *J. Phys. & Colloid Chem.*, 53, 930 (1949).
6) D.A. McInnes and L.G. Longsworth, *Chem. Reviews*, 11, 171 (1932).
7) G.S. Hartley, E. Drew and B. Collie, *Trans. Faraday Soc.*, 36, 648 (1934).
8) L.G. Longsworth, *J. Am. Chem. Soc.*, 54, 2741 (1932).

TABLE I

LOW-FREQUENCY CONDUCTIVITY AND HIGH-FREQUENCY EFFECT

Substance	Conc. (mole/1.)	Equivalent Conductivity at 1000 c./sec.	High-frequency Effect at 30 Mc./sec.
Octylamine	0.005	133	0
Hydrochloride	0.01	129	0
	0.02	120	0
	0.05	99	—
	0.1	85	—
	0.2	78.5	—
Decylamine	0.005	122	0
Hydrochloride	0.01	116	0
	0.02	108	0
	0.05	76	—
	0.1	64	—
	0.2	59	—
Dodecylamine	0.005	110	0
Hydrochloride	0.01	105	0
	0.02	75	4.2
	0.05	52	—
Tetradecylamine	0.002	107	0
Hydrochloride	0.005	102	0
	0.01	68	4.5
	0.02	48.5	6.6
Hexadecylamine	0.0001	102	0
Hydrochloride	0.001	100	0
	0.003	64	4.8
	0.005	40.4	8.6

micelles. This result can be accounted for only if the micelles behave themselves as polyvalent ions. In the case of octyl- and decylamine hydrochlorides the high-frequency effect is very small, and this fact can be considered to be due to the imperfect formation of micelles on account of the shortness of their paraffin-chains. Moreover, throughout all these electrolytes, the lower the low-frequency equivatent conductivity, the higher the high-frequency effect. This experimental fact is also in accord with the conclusion that the critical fall of equivalent conductivity is mainly due to the electrostatic interaction between large micelle ions and small counter ions, which has been inferred in the previous paper[1].

The results of transference number measurements are listed in Table II. The values of transference numbers shown in Table III are obtained from those in Table II by interpolation. For all the solutions under investigation, the transference number at an infinite dilution is about 0.2 or 0.3, but it rises very rapidly in the range where the total conductivity falls, and then tends towards a constant value. However, for the solutions of tetradecyl- and hexadecylamine hydrochlorides, the constant values could not be determined on account of their small solubilities. The mobility of each ion in the free state can be determined by using the value of the transference number and that of the equivalent conductivity at an infinite dilution, the result of calculation being shown in the last column of Table II. The mobility of chlorine ion at an infinite dilution for each solution is almost constant as is to be expected.

The critical rise of the transference number should come mainly from the association of counter ions to micelle ions. This association may take place mainly by electrical force in the low potential region around each micelle, because some other interactions, such as chemisorption or van der Waals adsorption, are unlikely to take place, taking into account the small effect of the nature of counter ions on the critical micelle concentration. The fact that the transference number reaches a nearly constant value with increasing concentration can be interpreted as follows: The fraction of counter ions which associate to the micelle will be governed by their

TABLE II

TRANSFERENCE NUMBER

Substance	Conc. (mole/1.)	Transference Number of Cation	Mobility at Infinite Dilution ($\times 10^4$ cm²/v.sec.)	
			Cation	Anion
Octylamie Hydrochloride	0.008	0.39	(5.6)	(8.8)
	0.0166	0.40		
	0.032	0.40		
	0.050	0.42		
	0.090	0.45		
Decylamine Hydrochloride	0.0068	0.34	(4.4)	(8.7)
	0.014	0.34		
	0.057	0.71		
	0.086	0.72		
Dedecylamine Hydrochloride	0.00053	0.26	(3.1)	(8.7)
	0.0053	0.26		
	0.0172	0.42		
	0.052	1.04		
	0.067	1.11		
	0.090	1.12		
Tetradecylamine Hydrochloride	0.00092	0.23	(2.5)	(8.7)
	0.0019	0.23		
	0.0033	0.27		
	0.018	1.12		
Hexadecylamine Hydrochloride	0.000074	0.181	(2.0)	(8.7)
	0.0014	0.34		
	0.0042	0.84		

TABLE III

TRANSFERENCE NUMBER AND RELATED QUANTITIES

Substance	Conc. (mole/1.)	Transference Number of Cation	Apparent Conductivity of		$C_{\pm}^{B}/C$
			Cation	Anion	
Octylamine Hydrochloride	0.005	0.39	51.9	81.1	—
	0.01	0.40	51.6	77.4	—
	0.02	0.39	50.4	69.6	—
	0.05	0.40	50.5	48.5	—
	0.1	0.45	52.7	32.3	—
Decylamine Hydrochloride	0.005	0.34	40.9	81.1	—
	0.01	0.34	39.8	76.2	—
	0.02	0.33	35.6	72.4	—
	0.05	0.60	45.6	30.4	0.23
	0.1	0.72	46.0	1.8	0.38
Deodcylamine Hydrochloride	0.005	0.26	28.6	81.4	—
	0.01	0.26	27.3	77.7	—
	0.02	0.50	37.5	37.5	0.31
	0.05	1.10	57.2	− 5.2	0.57
	0.1	1.12	44.8	− 4.8	0.66
Tetradecylamine Hydrochloride	0.002	0.22	23.6	83.4	—
	0.005	0.24	24.5	77.5	—
	0.01	0.65	44.2	23.8	0.38
	0.018	1.12	54.3	− 5.8	0.59
Hexadecylamine Hydrochloride	0.0001	0.18	18.4	83.6	—
	0.001	0.28	28.0	72.0	0.09
	0.003	0.59	37.8	26.2	0.46
	0.0042	0.84	33.9	6.5	0.65

concentration near its surface, and this must be greater than their concentration in bulk, and as the ratio of the former concentration to the latter is given by the Boltzmann-Poisson equation, the concentration of counter ions near the surface of the micelle will tend towards a constant value, and consequently, its transference number will tend towards a constant value as the bulk concentration increases. The greater-than-unity value of the transference number means, of course, that more chlorine ions are being carried towards the cathode than towards the anode.

In order to calculate the fraction of small ions bound to the micelle, some assumptions are necessary. It is first assumed, that the critical rise of the transference number arises only from the association of counter ions to the micelle. This assumption is equivatent to that of "square well potential" around the micelle. In the second place, it is assumed that, above the critical micelle concentration, the number of free cations is equal to the total number of cations existing in solution just before the critical micelle concentration. The second assumption will, however, have little effect on the result of the calculation except in the range near the critical micelle concentration. The equation obtained under these two assumptions is the same type as that obtained by Brady and Salley[3], which is expressed as follows:

$$\frac{C^B_-}{C}=1-\frac{\Lambda-(C^0_+/C)(T_-\Lambda+\Lambda^0_+)}{\Lambda^0_-+T_+\Lambda-(C^0_+/C)\Lambda^0}$$

where C, C^B_-, C^0_+ are the concentrations of total ions, bound anions, and free cations, respectively, and Λ, Λ^0, Λ^0_+, Λ^0_- denote the equivalent conductivity of total ions, total free ions, free cations, and free anions, respectively. T_+ and T_- are the transference number of the cation and the anion, respectively.

In Table III, calculated values of C^B_-/C are listed, together with the values of the apparent conductivities of the cation and the anion. It is shown here that at the concentration far above the critical micelle concentration, 60 or 70% of small ions are bound to the micelle. These bound ions can be considered to have no kinetic independence, and therefore, the valence of a micelle is about one third of the number of single molecules contained in a micelle. If we assume for dodecylamine hydrochloride the molecular weight determined by Debye[9] on the basis of his light scattering measurement, a micelle of this colloidal electrolyte is regarded to consist of 55 single molecules, so that it may possess an electrical charge of about 18 units.

If it is further assumed that the mobility of a free ion is not altered with increasing concentration; the mobility of the micelle ion of dodecylamine hydrochloride can be calculated by using the above mentioned data. The value thus obtained is 5.2×10^{-4} cm^2/v.sec., which is the same order of magnitude as simple ions. According to a simple consideration, the mobility of a micelle ion is proportional to its electric charge and is inversely proportional to the cubic root of the number of molecules composing it, so that the micelle is expected to have a greater mobility than that above obtained. In order to explain the above obtained value, it should be supposed that the mobility of a micelle ion is considerably reduced by the electrostatic interaction with small ions forming an ionic atmosphere.

From Tables I and III, it is suggested that, in the solution which has a large high-frequency effect, the micelle includes many associated counter ions as its kinetic unit, and consequently, has a compact structure. Generally, the greater the number of single ions forming a micelle, the greater the number of counter ions associated and the more compact the micelle structure. The association of counter ions, being probably an evidence for the electrostatic association in Bjerrum's sense[10], should play an important role in micelle formation, in such a way that it makes the polar heads of long-chain molecules forming a micelle less repulsive to each other.

Summary

The high-frequency and low-frequency equivalent conductivities and transference numbers for aqueous solutions of octyl-, decyl-, dodecyl-, tetradecyl-, and hexadecylamine hydrochlorides have been measured.

For the latter three solutions a considerable increase of the high-frequency concuctivity was observed, and for these three solutions it has been shown that the transference numbers of cations abruptly rise at the critical concentration for the micelle formation, and then tend towards a constant value.

These experimental facts have been accounted for from the electrostatic point of view of the micelle structure. It has been inferred from the experimental results that the counter ion association may be essential to the formation of the micelle.

We are grateful to Armour & Co., U.S.A. for the kind supply of the samples of the electrolytes used in our present work.

Chemistry Dept., College of General Education, and Institute of Science and Technonogy, The University of Tokyo, Tokyo

9) P. Debye, *J. Phys. & Colloid Chem.*, **53**, 1 (1949).

10) N. Bjerrum, *Erg. exakt. Naturwiss.*, **6**, 125 (1926).

Physical Properties and Crystal Structure of 1, 1, 1, 2-Tetrachloro-2-methylpropane

By Tsutomu KOIDE, Tsutomu ODA and Isamu NITTA*

(Received March 9, 1956)

Hexamethylethane and hexachloroethane are known to undergo phase transition, the transition points being −125°C for hexamethylethane[1] and 43°C and 71°C for hexachloroethane[2]. The high temperature modifications are characterized by relatively high melting points, 100.6°C and 185°C, respectively. These phases are also characterized by high volatility, high plasticity and optical isotropy. The X-ray study of these cubic modifications was made by C. D. West[3] and C. Finbak[4] and other investigators[5], who concluded that the molecules are in rotational motion in a rough sense. It seems of interest to examine what will occur in the phase just below the melting point of a hexa-substituted ethane of the type of $(CH_3)_xCl_{3-x}CC(CH_3)_{x'}Cl_{3-x'}$. We have carried out an X-ray diffraction study of 1, 1, 1, 2-tetrachloro-2-methylpropane, which was reported[6] to have high volatility and a relatively high melting point such as 169°C.

Experimental

Sample.—The sample used was prepared by the method of C. Willgerodt and F. Dürr[6] and a modified method by S. M. McElvain and C. L. Stevens[7]. In a flask with a reflux condenser 26 g. of purified chloretone was allowed to react with 60 g. of phosphorus pentachloride for twelve hours, the temperature of the water bath being kept at about 80°C. The reaction mixture was then cooled and the solidified excess of phosphorus pentachloride was filtered off. The solid was washed with benzene. The filtrates were subjected to fractional distillation. At the final stage the compound came out as solidified distillate. The solid thus obtained was pressed with filter paper to remove liquid impurities contained in it, and then refined by sublimation at a pressure of 30 mmHg.

Physical Properties.—It was observed that it melts at 173°C, and boils at almost the same temperature. The vapour of this solid is irritating to the eyes and nose. The solid is soft and shows plasticity, and we have found it to be optically isotropic. It sublimed readilly in a closed vessel to give well-formed rhombic prisms. These properties are very much like those of cubic hexamethylethane and cubic hexachloroethane. By suspending the crystals in a mixture of chloroform and carbon tetrachloride, the density of the solid was found to be 1.52 g./cc. at 10°C.

X-Ray Crystallographic Analysis.—As the solid is volatile, we used single crystals sealed in thin-walled glass capillary tubes. Such a sample was mounted on a goniometer-head of an X-ray camera. Using Cu radiation, we took Laue photographs and a group of 20° oscillation photographs over a range of 60° about [001] as the axis of rotation. Laue photographs taken with the X-ray beam parallel to [100], [110] and [111] showed holotesseral symmetry, and thus the point group of the crystal should be T_d-$\bar{4}3m$, O-43 or O_h-$m3m$. All spots appearing on the oscillation photographs were indexed satisfactorily by a cubic reciprocal lattice corresponding to $a=7.4$Å. All spots were extinguished except those for which $h+k+l=2n$. This classifies the crystal as being body-centered cubic. Thus the space group should be T_d^3-$I\bar{4}3m$, O^5-$I43$ or O_h^9-$Im3m$.

The density indicates the existence of two molecules in the unit cell, the calculated one 1.59 bing in agreement with the value mentioned above.

The apparent feature of the present X-ray data as well as such properties mentioned above lead us to imagine that this crystal will be isomorphous with cubic $C_2(CH_3)_6$ and cubic C_2Cl_3. Therefore we may also expect that this solid would undergo phase transition similar to those[1,2] of the hexa-substituted ethanes. In this respect we have carried out a differential thermal analysis.

Differential Thermal Analysis.—The apparatus used for the differential thermal analysis was almost the same as that previously reported by H. Chihara and S. Seki[8], so that only a brief account may be given here. As shown in Fig. 1, two thin-walled glass tubes are fitted separately in two drilled holes in a copper block A. One of the glass tubes contains NaCl as a standard

* Faculty of Science, Osaka University, Nakanoshima, Osaka.

1) G.S. Parks, H.M. Huffman and B. Thomas, *J. Am. Chem. Soc.*, **52**, 1032 (1930).

2) I. Nitta and S. Seki, *J. Chem. Soc. Japan*, **62**, 581 (1941); K.J. Ivin and F.S. Dainton, *Trans. Faraday Soc.*, **43**, 32 (1947); S. Seki and M. Momotani, This Bulletin, **23**, 30 (1950). See also O. Lehman, *Z. Krist.*, **1**, 106 (1877); ibid., **6**, 584 (1882).

3) C.D. West, *Z. Krist.*, **88**, 195 (1934).

4) C. Finbak, *Tids. Kiem. Bergv.*, **17**, No. 9, 2 (1937).

5) M. Atoji, T. Oda and T. Watanabé, *Acta Cryst.*, **6**, 868 (1953).

6) C. Willgerodt and F. Dürr, *Ber.*, **20**, 539 (1887).

7) S.M. McElvain and C.L. Stevens, *J. Am. Chem. Soc.*, **69**, 2667 (1947).

8) H. Chihara and S. Seki, This Bulletin, **26**, 88 (1953).

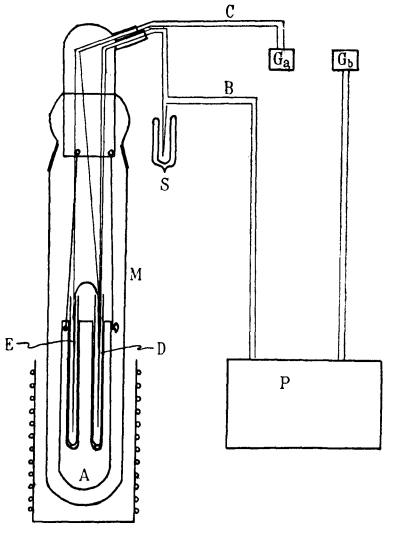

Fig. 1. A schematic diagram of the apparatus for differential thermal analysis.
D: a reference cell containing NaCl; E: a sample tube; Ga, Gb: galvanometers; M: a mantle; P: a potentiometer; S: the standard temperature (ice).

material and the other the sample to be investigated. B and C are copper constantan thermocouples for the measurement of the temperature of NaCl, operated with a cotentiometer, and of the temperature difference between NaCl and the sample, operated with a galvanometer and a lamp-scale.

We have observed the anomalous heat effect at −62.2°C when the sample was cooled starting at a room temperature, and at −39.7°C, when heated starting at the temperature of solid CO_2. One of the typical curves is given in Fig. 2.

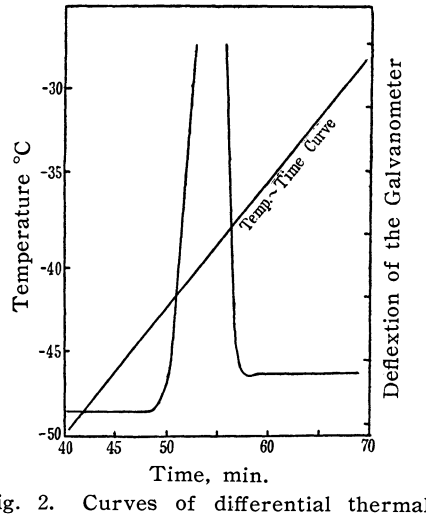

Fig. 2. Curves of differential thermal analysis of $Cl_3C{\cdot}C(CH_3)_2Cl$.

Discussion

Since there are two molecules in the unit cell with the body-centered translation, it is reasonable to place the centers of the molecules at the positions 0, 0, 0 and $\frac{1}{2}$, $\frac{1}{2}$, $\frac{1}{2}$, of which the symmetry should be T_d-$\bar{4}3m$, O-43 or O_h-$m3m$. On the other hand, as the rigid molecule of $Cl_3CC(CH_3)_2Cl$ can have at highest only one plane of symmetry which contains the central C–C bond axis, it becomes necessary to consider some statistical explanation of the structure, as is always so in plastic crystals[3,4,5,9]. In order that the statistical symmetry of the molecule be as high as T_d-$\bar{4}3m$ at 0, 0, 0 and $\frac{1}{2}$, $\frac{1}{2}$, $\frac{1}{2}$, the molecule should orientate its central C–C axis parallel to each one of the four body-diagonals statistically equally and at the same time laterally so that the C–C axis acquires a statistical symmetry of $3m$ at least. Such statistical symmetry can also be gained by a model of molecule in rotation about the C–C axis. In the cases of O^5-$I43$ and O_h^9-$Im3m$, it is necessary to add the antiparallel orientations of the polar C–C axis along the four body-diagonals, these directions having the symmetry of 3 or $3m$. It is also conceivable that the observed feature of X-ray diffraction can be explained by molecules in free spherical rotation. Which one of these possibilities is the case for the present statistical structure seems indiscernible from the consideration of intensity data, since the observable reflexions are few. However it may be said that the structure found for the present crystal is statistically analogous to those of the high temperature modifications of C_2Cl_6 and $C_2(CH_3)_6$.

The rapid decrease in intensity of the X-ray reflexions with increasing angle of scattering is evidently due to the disordered orientation of molecules in intense thermal motion. In accordance with these X-ray observations the crystal shows softness, plasticity, high volatility and relatively high melting point. The transformation observed at about −62.2°C may be attributed to a kind of order-disorder transition.

9) J. Timmermans, *J. Chim. Phys.*, **35**, 331 (1938); I. Nitta and T. Watanabé, This Bulletin, **13**, 28 (1938); T. Oda and T. Watanabé, *J. Chem. Soc. Japan*, **65**, 154 (1944); R.S. Schwartz, B. Post and I. Fankuchen *J. Am. Chem, Soc.*, **73**, 4490, 5113 (1951); T.B. Reed and W.N. Lipscomb, *Acta Cryst.*, **6**, 108 (1953); H.J. Backer and W G. Perdok, *Rec. Trav. Chim.*, **62**, 533 (1943).

Summary

1,1,1,2-Tetrachloro-2-methylpropane is cubic at room temperatures. X-ray date may be interpreted on the basis of a body-centered packing of molecules in disorder, orientational or rotational. The cube edge of the unit containing two molecules is $a=7.4$Å. The crystal undergoes transition at about -62.2°C, when cooled, and at -39.7°C, when heated starting at a lower temperature.

The authors are grateful to the Ministry of Education for the Research Encouragement Grant in aid of this work.

Chemical Laboratory, Osaka University of Liberal Arts and Education
Tennoji, Osaka

SHORT COMMUNICATIONS

Precipitation of Silica in the Presence of Aluminum

By Katsumi Goto

(Received December 12, 1955)

It is commonly received among geologists[1] that silica in river water is colloidal and precipitated by electrolytes in sea water as a result of coagulation. It was shown in our previous reports[2-4], that colloidal silica, unless its concentration is very high, can not be precipitated even in sea water, where colloidal silica rather depolymerizes into molecularly dispersed state, owing to the high solubility of silica.

On the other hand, molecularly dispersed silica is precipitated by the addition of a small amount of aluminum salt, which hydrolyses into aluminum hydroxide and coprecipitates the silica, as has been employed to remove silica from boiler-feed water[5,6].

Thus a considerable literature has grown up around the subject of precipitation of molecularly dispersed silica by aluminum hydroxide, but little is known about the precipitation of colloidal silica.

Experimental

To a solution of silica, a known amount of aluminum was added as acidic solution of $AlCl_3$ or $Al_2(SO_4)_3$. The hydrogen ion concentration was adjusted to a pH 4 to 11 by the addition of dilute NaOH solution. The resulting solutions were filtered after about thirty minutes and analysed for the concentration of residual silica. As a similar effect was observed with $Al_2(SO_4)_3$ as well as with $AlCl_3$, the results obtained with $Al_2(SO_4)_3$ are described below. The colloidal solution of silica was prepared from sodium silicate solution containing 20 g. SiO_2 per litre by the ion-exchange method[2] followed by aging for several months at pH about 8.

Figs. 1. and 2 show the effects of pH on the

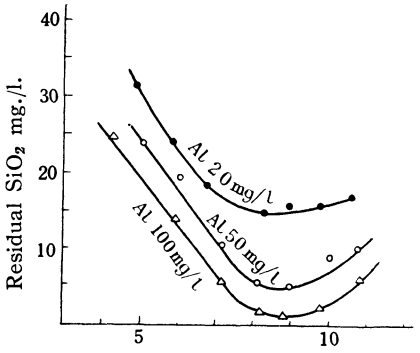

Fig. 1. Precipitation of molecularly dispersed silica. SiO_2 35 mg./l.

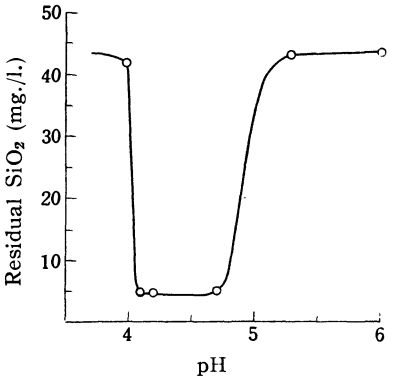

Fig. 2. Precipitation of colloidal silica SiO_2 45 mg./l., Al1 mg./l.

precipitation of molecularly dispersed silica as well as colloidal silica, by aluminum. It is interesting to note that the optimum pH for the precipitation of molecularly dispersed silica is about 9, while colloidal silica is precipitated most

effectively at pH about 4.5. Much smaller amount of aluminum is sufficient for the precipitation of colloidal silica compared with that for molecularly dispersed silica. One milligram of aluminum precipitates as much as 40 mg. of colloidal silica. This may be closely connected with the fact that colloidal silica has a electrophoretic mobility much greater than that of molecularly dispersed silica[2,7].

Colloidal silica can not be precipitated, in the case where the ratio of colloidal silica to aluminum exceeds a certain value, as will be seen in Fig. 3. Neither aluminum nor colloidal silica precipitates in this case.

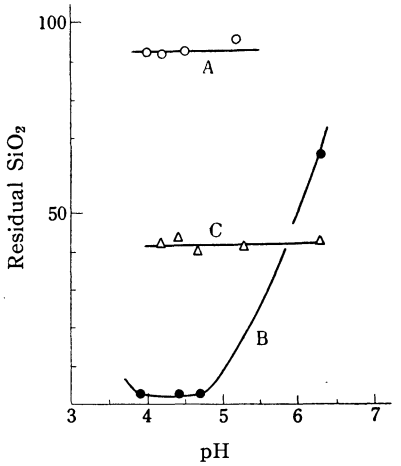

Fig. 3. Presipitation of colloidal silia.

A	SiO_2	92 mg./l.	Al	1 mg./l.
B	SiO_2	〃	Al	2 〃
C	SiO_2	43 mg./l.	Al	0.5 mg./l.

According to the results shown above, it is clear that a trace amount of aluminum plays an important role in the precipitation of silica, especially when the silica is colloidal. Biological sedimentation[1] of silica must also be taken into account, but at least in some cases, precipitation of colloidal silica by a trace amount of aluminum will successfully explain the sedimentation of silica in natural waters.

The author wishes to express his thanks to prof. Y. Uzumasa, Prof. G. Okamoto, Prof. I. Kayama, and Assist. prof. T. Okura for their invaluable advice and encouragement. The author is also indebted to T. Ogawa for carrying out a part of the experiments.

Faculty of Engineering, Hokkaido University, Sapporo

1) W.H. Twenhofel, "Principles of Sedimentation", McGraw-Hill (1950), p. 398.
2) K. Goto, T. Okura and I. Kayama, *Kagaku*, **23**, 428 (1953).
3) K. Goto, *J. Chem. Soc. Japan (Pure Chem. Sect.)*, **76**, 729 (1955).
4) K. Goto, ibid., **76**, 1364 (1955).
5) L.D. Betz, C.A. Noll and J.J. Maguire, *Ind. Eng. Chem.*, **32**, 1320 (1940).
6) G. Okamoto, T. Okura and N. Sudo, *J. Electrochem. Soc. Japan*, **19**, 289 (1951).
7) R.K. Iler, "The Colloid Chemistry of Silica and Silicate", Cornell Univ. Press (1955), p. 248.

Adiabatic Compressibility of Aqueous Solution. III. Egg Albumin

By Yutaka MIYAHARA

(Received March 12, 1956)

R. J. Urick[1] has pointed out empirically that the adiabatic compressibility of a suspensoid could be computed from the compressibilities of dispersed phase and dispersion medium. His treatment was based on the assumption that the compression of the suspension is the arithmetic sum of compressions of components. The extension of this idea to the hydrophilic colloids has been tried by the present author in a preliminary study on a starch sol[2].

In this paper the ultrasonic velocity in the aqueous solution of egg albumin was measured and the numerical value of the compressibility of the albumin molecule in the aqueous solution at its isoelectric point was estimated approximately. Along this line of the investigation, Jacobson[3] has determined the compressibilities of oxyhemoglobin, hemocyanin and serum albumin molecules.

The ultrasonic velocity was measured with an ultrasonic interferometer, the detailed description of which and the experimental procedures have been reported previously[4]. The frequency of the ultrasonics was 1090 KC and the measurement was made at 20.0°C.

The egg albumin used was prepared from the white of a fresh hen's egg by the usual procedure, using ammonium sulphate as a salting out agent. After recrystallizing several times, the electrolytes' impurities were removed by dialysis with redistilled water until no trace of ammonia was detected by the Nessler reagent. The concentration of the egg albumin in the solution was determined by the density measurement. The relation between density and concentration used here was obtained from the partial specific volume, numerical values of which had been given as 0.749 cc./g. by T. Svedberg et al.[5]

The experimental results of the measurements of the ultrasonic velocities and other related quantities are listed in Table I. The physical meaning of the notations here used was given in the previous paper[6].

The numerical value of K/x, the specific compression of the albumin solution at an infinite dilution, was calculated from the present data by using the method of least squares and is found to be -0.16.

To get the numerical value of the com-

TABLE I

No.	D_S/D_O	x	c/c_O	κ/κ_O	K
1	1.0034	0.0134	1.0022	0.9922	−0.0022
2	1.0005	0.0019	1.0003	0.9989	−0.0003
3	1.0062	0.0247	1.0041	0.9857	−0.0041
4	1.0045	0.0179	1.0031	0.9893	−0.0027
5	1.0030	0.0117	1.0019	0.9933	−0.0020
6	1.0025	0.0100	1.0019	0.9937	−0.0012
7	1.0032	0.0125	1.0024	0.9922	−0.0015
8	1.0027	0.0107	1.0017	0.9939	−0.0019
9	1.0026	0.0104	1.0016	0.9942	−0.0019
10	1.0005	0.0020	1.0003	0.9988	−0.0003

pressibility of the albumin molecule itself, we should estimate the effect of hydration on the compressibility of the solution. The necessary equation has already been given in the previous paper[6]. However, we have not obtained sufficient data for these terms, because we could not measure the hydration effect and compressibility separately. In the present investigation, the data of amino acid solutions were used for this purpose. As was shown in the previous paper[4], the hydration effect of amino acids is nearly independent of their species, and their numerical values are almost constant. The molar value, K_m ($=M\cdot K_h/x$, M being molecular weight) is about $6\cdot10$ on an average. In the albumin molecule, the radicals which give the dominant effects upon the compressibility of the solution by the hydration effect may be its ionized radicals only, and the effects of non-ionic groups could be neglected as in the case of amino acid solution. Further we assume here that the hydration effect of polar groups which are ionized perfectly in the solution at its isoelectric point is not greatly different from the effect of free amino acids in the solution. Of course this assumption should be subjected to further discussion. The number of pairs of ionized radicals in an albumin molecule at its isoelectric point could be determined from the data of potensiometric titration. The value adopted here is 9.10^{-4} gram equivalent per gram[7]. Using these data, the effect of hydration, K_h/x for albumin molecule is estimated as 0.05, about thirty per cent of K/x. That means that the deviation due to the above assumption produces not so much difference from the right value, if we expect just semi-quantitative discussion. The actual volume occupied by albumin molecule in the aqueous solution, which is necessary for the present purposes, was calculated as well from the specific volume obtained by Svedverg[5]. The value is $v_m=0.749\ x$ per one cc. solution.

The molecular compressibility of albumin molecule in the aqueous solution at its isoelectric point is then found to be 13.10^{-12} cgs. The values of oxyhemoglobin, hemocyanin and serum albumin were recalculated from Jacobson's data[3] by using the same procedure are 11, 17 and 11 cgs. respectively. These values are in the order of the compressibilities of organic molecular crystals and they are of reasonable magnitudes, considering that protein molecules have some special structures, not like artificial polymermolecules which stretch in the solution. The extension of the present survey is thought to deserve further investigation.

Chemical Institute, Faculty of Science
Nagoya University, Nagoya

1) R.J. Urick, *J. Applied Phys.*, 18, 983 (1947).
2) Y. Miyahara and H. Shiio, *J. Chem. Soc. Japan (Pure Chem. Sect.)*, 73, 1 (1953).
3) B. Jacobson, *Arkiv För Kemi.* 2, 177 (1950).
4) Y. Miyahara, *Bull. Chem. Soc. Japan*, 26, 390 (1953).
5) T. Svedberg and J.B. Nichols, *J. Am. Chem. Soc.*, 48. 3081 (1926).
6) Y. Miyahara, *Bull. Chem Soc. Japan*, 25, 326 (1952).
7) E.J. Cohn and J.T. Edsall, "Protein, Amino Acids and Peptides", (1943), p. 498.

*Studies on the Oxy-acid Phosphors. VI. Antimonate Phosphors**

By Yoshihide KOTERA, Tadao SEKINE and Michiko YONEMURA

(Received March 13, 1956)

Few reports have ever been published on the antimonate phosphors. K. H. Butler et al. reported the formation of calcium pyroantimonate during the preparation of calcium halophosphate phosphor, but he did not find any emission for this material[1]. R. Bernard and J. Janin observed recently the luminescence of calcium metaantimonate activated by manganese[2], and M. Tomono et al. reported the green luminescence of calcium metaantimonate activated by manganese[3], but the full details of their preparation, characteristics etc. remain still unknown.

In the preparation of antimonate phosphors, a commercially available pure grade of antimony chloride was used as one of the starting materials and purified by the process described in a previous paper[4]. As for the other starting materials, respective metallic salts were used, which were purified by the process described in another previous paper[5]. Their purity was established spectrographically. Purified antimony oxide and metallic oxide

TABLE I

THE OPTIMUM MIXING RATIO FOR THE PREPARATION OF ANTIMONATE PHOSPHORS

	Sb_2O_3 : (MO or $M(NO_3)_2$)	Firing Coditions
Ca antimonate	1 : 2.4 mol.	1100°C 2 hr.
Sr antimonate	1 : 2.2 mol.	1100°C 2 hr.
Ba antimonate	1 : 2.2 mol.	1100°C 2 hr.
Mg antimonate	1 : 4.8 mol.	1150°C 1 hr.
Zn antimonate	1 : 2.2 mol.	1100°C 1 hr.

or carbonate were mixed in an agate mortar in the molar ratio as shown in Table I and, if necessary, an appropriate salt was also added as an activator; then the mixture was fired for one to two hours at 1100°C in air.

5 weight % of NH_4NO_3 was added to the batch so as to increase the brightness[6].

The properties of antimonate phosphors are shown in Table II. The $Ca_2Sb_2O_7$: Bi phosphor gives the highest brightness among them, the spectral distribution of its emission under cathode-rays excitation being shown in Fig. 1. Data showing the X-ray diffraction pattern for $Ca_2Sb_2O_7$ are presented on Table III together with the results by K. H. Butler et al.[1].

TABLE II

THE EMISSIONS COLOURS OF ANTIMONATE PHOSPHORS

	3650 Å	2537 Å	Cathode rays
$Ca_2Sb_2O_7$	pink f	pink f	orange f
$Sr_2Sb_2O_7$	none	bluish white ff	none
$Ba_2Sb_2O_7$	none	white ff	none
$Mg_2Sb_2O_7$	none	none	orange ff
$Zn_2Sb_2O_7$	yellow ff	none	yellow ff
$Ca_2Sb_2O_7$: Bi	blue m	blue m	blue m
$Sr_2Sb_2O_7$: Bi	green f	green f	green f
$Mg_2Sb_2O_7$: Bi	green f	green f	none
$Zn_2Sb_2O_7$: Bi	green f	none	yellow f

m: medium, f: faint, ff: very faint

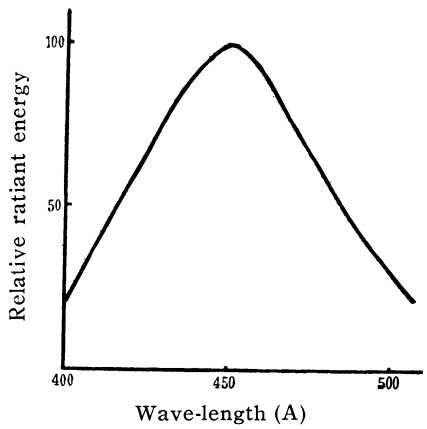

Fig. 1. Emission of $Ca_2Sb_2O_7$: Bi with cathode-rays excitation.

The formation of $Ca_2Sb_2O_7$ during the preparation of calcium halophosphate phosphors was verified by K. H. Butler et al. 's X-ray diffraction analysis. We found that various antimonates without any intentional activator are able to luminesce and give blue, green or yellow luminescence when bismuth is employed as an activator. The emission of samples without activators might be due to the activation by antimony itself, although such a possibility is not definitely ascertained. From the mixing molar ratio shown in Table I and the X-ray diffraction patterns in Table III, it is concluded that these phosphors are composed of pyroantimonate. The emissions of haloantimonates are expected from the

TABLE III

X-RAY DIFFRACTION PATTERN OF $Ca_2Sb_2O_7$ PHOSPHOR

Phosphor		$Ca_2Sb_2O_7$*		Phosphor		$Ca_2Sb_2O_7$*		Phosphor		Phosphor		Phosphor	
d	I	d	I	d	I	d	I	d	I	d	I	d	I
		10.05	0.4	2.58	s	2.607	0.6	1.72	w	1.435	w	1.141	m
6.05	m	5.97	0.7			2.551	0.4	1.70	w	1.400	w	1.127	vw
5.13	m	5.19	0.6	2.37	vw	2.351	0.1	1.66	vw	1.364	w	1.092	vw
4.51	w			2.31	m	2.290	0.1	1.64	vw	1.344	vw	1.085	vw
3.99	w					2.132	0.1	1.61	vw	1.299	m	1.066	m
3.62	m	3.633	0.5	2.09	vw	2.106	0.2	1.57	s	1.266	w	1.049	m
3.29	s			2.00	s	2.009	0.4	1.55	s	1.225	vw	1.041	w
3.03	w	3.105	0.4	1.85	w	1.867	0.4	1.53	m	1.204	vw	1.029	w
2.97	s	3.009	0.9	1.81	vs	1.824	1.0	1.499	m	1.175	vs	1.015	w
2.93	s	2.960	0.9	1.74	w			1.475	m	1.157	m	1.003	m

* Data by K.H. Butler et al.

In all columns "d" and "I" represent the interplanar spacing in Angstrom and its intensity respectively. The abbreviations in columns "I" mean:

vs: very strong. s: strong. m: medium. w: weak. vw: very weak.

fact, that the change of emission colour was observed when halide was employed as a flux, but their details are not yet investigated.

We wish to thank Dr. Shoji Makishima for the general discussion on the subject and the experimental work he and his associates have done.

Government Chemical Industrial Research Institute, Tokyo
Hatagaya-honmachi, Tokyo

* Read before the Seventh Annual Meeting of the Chemical Society of Japan 1954. Report V was published in This Bulletin.

1) K.H. Butler, M.J. Bergin and V.M.B. Hannaford, *J. Electrochem. Soc.*, **97**, 117 (1950).
2) R. Bernard and J. Janin, *Compt. rend.*, **237**, 798 (1953); **239**, 489 (1954); **240**, 614 (1955).
3) M. Tomono et al., Read before the Eighth Annual Meeting of the Chemical Society of Japan, 1955.
4) Y. Kotera and T. Sekine, *J. Electrochem. Soc.*, **102**, 390 (1955).
5) Y. Kotera and T. Sekine, This Bulletin, **27**, 13 (1954).
6) Y. Kotera and T. Sekine, *J. Chem. Soc. Japan (Ind. Sect.)* **54**, 625 (1951).

Lattice Constant of Digenite

By Tsuguyasu WADA

(Received June 19, 1956)

Digenite, $Cu_{1.8}S$, was first discovered by Buerger[1] in copper-sulfur system. The crystal structure of this phase is known as a cubic lattice of anti-fluorite type, in which half of the copper atoms are statistically distributed in the interstices of the sulfur atoms, forming so-called *averaged structure*[1,2]. Ramdohr[3] has thereafter discovered the naturally occurring mineral of this composition, and named it *Neodigenite*.

The Buerger's phase diagram of copper-sulfur system shows that the digenite phase has no range of solid solution at room temperature. However, some investigators[4] have maintained that this is not the case but that the digenite has some range of solid solution.

In this communication, the lattice constant of digenite at room temperature is measured using the samples of various compositions, and it is confirmed that the digenite has a range of solid solution.

The sample used was synthesized from electrolytic copper and thoroughly-distilled sulfur. The stoichiometric Cu_2S and CuS were first prepared by heat-treatment of copper and a corresponding amount of sulfur sealed in a vacuum Pyrex tube for about two hundred hours at 400°C. Then, these materials were mixed in appropriate ratio, sealed in vacuum, and heat-treated by the same procedure as above, with gradual cooling to the room temperature. Thus the samples of desired compositions were obtained.

X-ray powder photographs were obtained for these samples using Straumanis-type camera of 90 mm. diameter and $CuK\alpha$ radiation. The line of (551) (711) is very suitable to determine the lattice constant, since its Bragg angle for $CuK\alpha$ is about 81°, although its intensity is very weak. Sometimes, (440) line was measured by focusing backreflection camera and $FeK\alpha$ radiation. The Bragg angle of this case is about 80°. As the wave lengths of X-rays, the values of Siegbahn's table[5] were used.

In the Figure, the lattice constants observed are plotted against the composition, and it is shown that these vary from 5.554 to 5.544 kX with the increase of sulfur content. The accuracy for the measurement of the lattice constant is estimated to be ±0.001 kX, and that of the composition to be ±0.2 atomic percent of sulfur.

From this result, it is obvious that the digenite has a range of solid solution, though it is relatively narrow, at room temperature. The range seems to cover the compositions from 35.7 to 36.1 atomic percent of sulfur, but more sufficient experimental points are necessary to determine it precisely. The fact

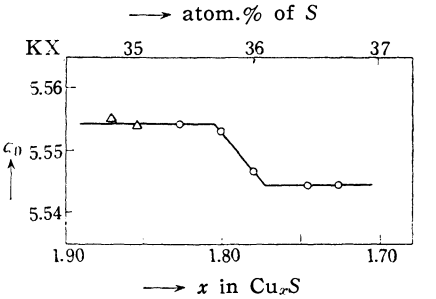

Fig. 1. Lattice constant of digenite.

that the lattice contracts when the atomic fraction of cation is decreased suggests that the variation of composition may be caused by the escape of cations from their lattice sites.

Department of Chemistry, Faculty of Science, Hokkaido University
Sapporo

1) N.W. Buerger, *J. Chem. Phys.*, 7, 1067 (1939); *Econ. Geol.*, 36, 19 (1941).
2) P. Rahlfs, *Z. phys. Chem.*, (B) 31, 157 (1936).
3) P. Ramdohr, *Z. prakt. Geol.*, 51, 1 (1943); *Chem. Abstr.*, 38, 4500 (1944).
4) L. Eisenmann, *Ann. Phys.*, 6. Folge, 10, 129 (1952).
5) M. Siegbahn, "Spektroscopie der Röntgenstrahlen". Berlin (1931).

Preparation of Carrier-Free Yttrium-90 by Paper Chromatography

By Toshiyasu KIBA, Shigeru OHASHI and Satoshi TADA

(Received April 24, 1956)

Although carrier-free yttrium-90 has been separated from strontium-90 by various methods[1], the authors have found that carrier-free yttrium-90 can be separated more simply and rapidly by paper chromatography than by other methods and the preliminary report of this investigation has been already published in this Bulletin[1]. The separation of yttrium-90 and strontium-90 by paper chromatography was also studied by H. Kamada and et al.[2], but they did not aim at the preparation of carrier-free yttrium-90. In this paper the detailed results of the study on the preparation of carrier-free yttrium-90 by this method and some types of behavior of yttrium on the paper are described.

Experimental

A mixture of strontium-90 and yttrium-90 was employed as a form of carrier-free nitrate in 0.3 N nitric acid. Yttrium oxide prepared by F. H. Spedding was converted into nitrate and was used as a carrier. The other reagents were all of extra pure grade.

A sample solution was placed at a point 3 cm. from one edge of the strip of the filter paper (Toyo No. 3, 2×40 cm.), allowed to dry in the air and then developed chromatographically by the ascending method. After the development, the paper strip was dried and cut off at an interval of 1 cm. Each piece of the paper strip was placed at the center of a sample pan and its radioactivity was measured with an end-window counter (Kobe Kogyo Corp.). All of the original positions of samples were in the middle of the pieces No. 0 and No. 1 of the histograms shown in the figures of the present paper.

Solvent and Developing Time

In the early work of this investigation a mixture of ethyl alcohol, butyl alcohol, and 10% aqueous solution of ammonium thiocyanate was used as a solvent, but subsequently it has been disclosed that butyl alcohol is not a substantial agent for the present purpose. Therefore a mixture of ethyl alcohol and 10% solution of ammonium thiocyanate was mainly employed as a solvent.

The dependence of the distribution of yttrium-90 and strontium-90 upon the ratio of ethyl alcohol and 10% solution of ammonium thiocyanate is illustrated in Fig. 1. A larger amount of thiocyanate solution gives a higher Rf value of strontium-90, while it also causes the upward diffusion

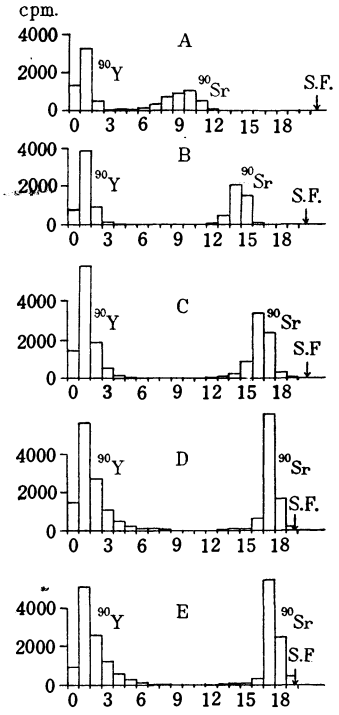

Fig. 1. Chromatograms of ^{90}Y and ^{90}Sr.
A. EtOH−10% NH_4SCN aq. (5:1).
B. 〃 〃 (5:2).
C. 〃 〃 (5:3).
D. 〃 〃 (5:4).
E. 〃 〃 (5:5).

of yttrium-90 and, on the other hand, a smaller amount of thiocyanate solution can hold yttrium-90 near the original position, but the Rf value of strontium-90 is lower. Therefore the solvent of the optimum composition is a mixture of 5 parts of ethyl alcohol and 2 or 3 parts of 10% solution of ammonium thiocyanate. When the ratio of ethyl alcohol and aqueous solution is fixed at 5 to 3, the concentration variation of thiocyanate in aqueous solution from 6 to 18% does not exert any remarkable influences on the distribution of yttrium-90 and strontium-90.

Ammonium thiocyanate can be replaced by potassium thiocyanate. When the ammonium salt of chloride or nitrate is used instead of thiocyanate, yttrium-90 can be similarly separated from

1) cf. T. Kiba, S. Ohashi and T. Minabe, This Bulletin, **28**, 444 (1955).

2) H. Kamada, et al., presented at the Meeting of The Japan Society for Analytical Chemistry in Tokyo, May 9, 1953.

strontium-90, but the Rf values of strontium-90 are relatively low. Ammonium sulfate does not provide a sharp separation of these nuclides. These results are shown in Fig. 2.

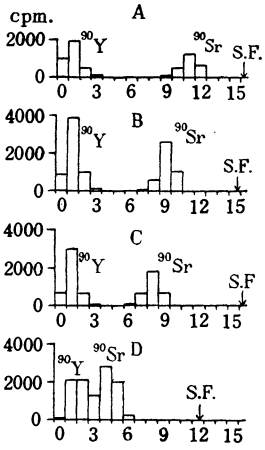

Nos. of Pieces of Paper Strip ⟶

Fig. 2. Chromatograms of ^{90}Y and ^{90}Sr.
A. EtOH−2 N (15%) NH_4SCNaq. (2:1).
B. 〃 −2 N NH_4NO_3aq. (2:1).
C. 〃 −2 N NH_4Cl aq. (2:1).
D. 〃 −1 N $(NH_4)_2SO_4$ aq. (1:1).

As it was supposed that strontium may have an affinity to combine with thiocyanate, some examinations about it were carried out by spectrophotometric and polarographic methods. However it was found at least that strontium does not form a stable complex with thiocyanate.

The minimum developing time required to separate completely yttrium-90 from strontium-90 is thirty minutes as shown in Fig. 3.

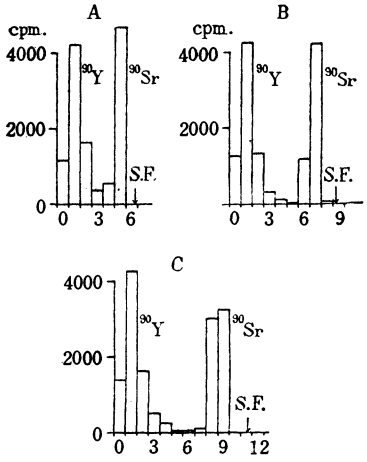

Nos. of Pieces of Paper Strip ⟶

Fig. 3. Chromatograms of ^{90}Y and ^{90}Sr.
Solvent: EtOH−10% NH_4SCN aq. (5:3).
A. Developing time 15 min.
B. 〃 30 min.
C. 〃 45 min.

Leaching of the Separated Yttrium-90

Although several methods were tried to leach the separated yttrium-90 from the paper strip, the following method was the best.

As shown in Fig. 4 the paper strip holding the

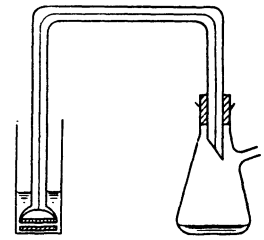

Fig. 4. Apparatus for leaching of ^{90}Y.

separated yttrium-90 was placed in a small glass tube with a flat bottom and 2 ml. of 3 N hydrochloric acid was added in it. After digesting the contents in the tube for a few minutes the solution was sucked up by means of a small filter stick. Repeating this procedure the results as shown in Table I were obtained.

TABLE I
LEACHING OF THE SEPARATED YTTRIUM-90

3 N HCl, ml.	Yield, %
2	96.3
4	98.8
6	98.4
8	99.2
10	99.7

By the use of 10 ml. of 3 N hydrochloric acid the separated yttrium-90 can be almost completely released from the paper.

Purity of the Separated Yttrium-90

The half-life of the separated yttrium-90 was estimated as sixty-two to sixty-four hours as fairly coinciding with the value of sixty-four hours in the recent literature[3].

However it was found that the separated yttrium-90 had a very small amount of radioactive impurity, and by the redevelopment of the separated yttrium-90 it was also confirmed that the impurity was due to strontium-90. The amount of strontium-90 as the impurity was estimated by measuring the remaining radioactivity after all of the initially existing yttrium-90 had practically disappeared. As shown in Table II the impurity, strontium-90, in the separated yttrium-90 was less than 0.1% at the moment of the separation. Even in the case of the development of thirty minutes there was only 0.024% of strontium-90.

Relation between the Distribution of Yttrium on the Paper and the Amount of Yttrium-Carrier

As described above, the carrier-free yttrium-90 is located near the original position on the paper,

3) M.L. Salutsky and H.W. Kirby, *Anal. Chem.*, **27**, 567 (1955).

TABLE II
THE IMPURITY OF THE SEPARATED YTTRIUM-90

Solvent Ratio	EtOH	5	—	5	5	5	5
	BuOH	—	5	—	—	—	—
	10% NH_4CNS aq.	2	2	3	4	3	3
Developing Time, hr.		3	3	3	3	1	0.5
Solvent Front, cm.		19.7	17.8	19.8	18.7	11.2	8.3
Initial Activity, cpm.		3922	5211	5872	5599	4405	4582
Activity after t Days, cpm.		4.4	6.7	5.1	0.3	3.2	2.2
t Days		62	62	104	104	103	103
^{90}Sr in Initial Activity, %		0.056	0.064	0.044	0.003	0.036	0.024

when it is developed with a solvent composed of 5 parts of ethyl alcohol and 2 or 3 parts of 10% solution of ammonium thiocyanate. However, if yttrium-carrier is added to carrier-free yttrium-90, its distribution on the paper is varied as indicated in Fig. 5. Namely, when the amount of

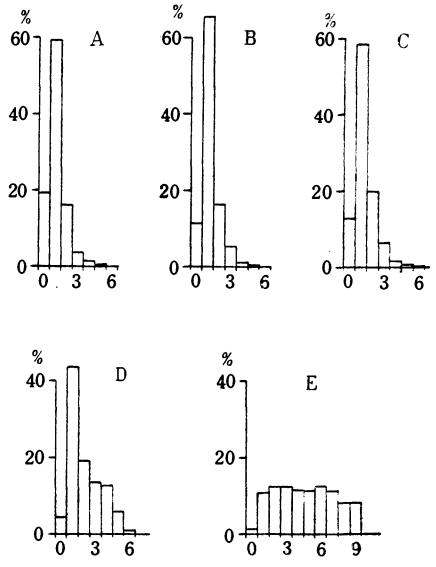

Fig. 5. Chromatograms of Y-carrier.
Solvent: EtOH−10% NH_4SCN aq (5 : 2).
Solvent front: 17.5−18.5 cm.
A. Y ca. 5×10^{-5} μg.
B. Y ca. 6×10^{-4} μg.
C. Y ca. 7×10^{-3} μg.
D. Y ca. 7×10^{-2} μg.
E. Y ca. 8×10^{-1} μg.

yttrium-carrier exceeds about 6×10^{-1} μg., yttrium goes gradually upward from the original position as the amount of its carrier increases. The similar behavior of lanthanum was observed by Y. Kitano[4]. On the other hand the Rf value of strontium-90 obtained by the development with the above mentioned solvent is kept constant, regardless of the presence of strontium-carrier.

If the amount of yttrium-carrier is fixed on 0.8 μg., its distribution on the paper is varied according to the developing time as illustrated in (A) to (E) of Fig. 6. In the case of 2.5 μg. of yttrium-carrier its distribution at ninety minutes is given in (F) of Fig. 6.

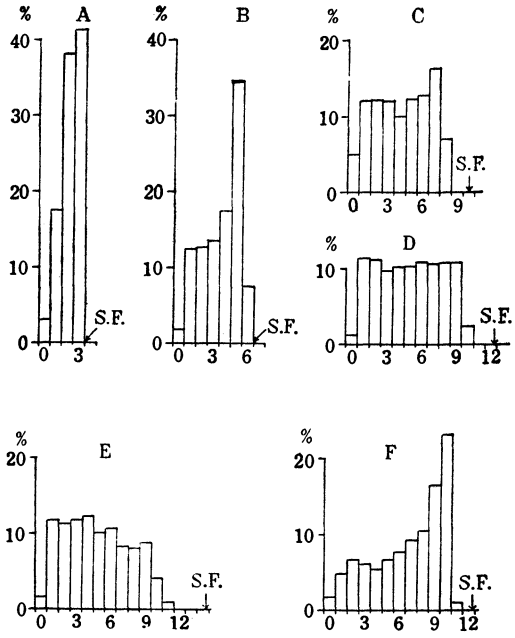

Fig. 6. Chromatograms of Y-carrier.
Solvent: EtOH−10% NH_4SCN aq. (5 : 2).
A. Y ca. 0.8 μg, developing time 15 min.
B. 〃 〃 30 min.
C. 〃 〃 60 min.
D. 〃 〃 90 min.
E. 〃 〃 120 min.
F. Y. ca. 2.5 μg. 〃 90 min.

These results may be explained by the assumption that yttrium is adsorbed on the paper and the adsorbable amount of the yttrium has a definite limit. The fact that the carrier-free yttrium-90 can be almost completely held near the original position may be due to its extremely small amount. If an amount of yttrium-carrier on a definite area of the paper exceeds the adsorbable amount, its excess part is accumulated at the top of its distribution pattern as shown in (B) or (F) of Fig. 6.

If a mixture of 5 parts of ethyl alcohol, 3 parts of 10% solution of ammonium thiocyanate, and

4) Y. Kitano, presented at the Symposium of The Japan Society for Analytical Chemistry in Osaka, May 3, 1955.

2 parts of 1 N hydrochloric acid is used as a solvent, yttrium gives a normal chromatographic spot with the Rf value of 0.79 regardless of the amount of yttrium-carrier, because the adsorption of yttrium on the paper is forbidden by the presence of hydrochloric acid.

Summary

(1) Carrier-free yttrium-90 can be separated rapidly and simply from strontium-90 by paper chromatography. The most suitable solvent is a mixture of ethyl alcohol and 10% solution of ammonium thiocyanate (5 : 3 or 5 : 2). The Rf value of carrier-free yttrium-90 is 0 and that of strontium is 0.7 to 0.8.

(2) Carrier-free yttrium-90 having a radiochemical purity more than 99.9% can be prepared within forty minutes.

(3) If yttrium-carrier is present, when it is developed with the above mentioned solvent, it is distributed upward from the original position on the paper. Its distribution pattern depends upon the amount of yttrium-carrier and the developing time and it may be caused by the adsorption of yttrium on the paper.

The expense of this investigation has been defrayed from a grant given by the Ministry of Education, to which the authors' thanks are due. The authors wish to thank Dr. T. Nakai and Mr. H. Natsume for supplying yttrium oxide prepared by Dr. F. H. Spedding of Iowa State College.

Department of Chemistry, Faculty of Science, Kanazawa University
Kanazawa

Lateral Order Distribution of Native Cellulose

By Yoshizo TSUDA and Sadataka MUKOYAMA

(Received April 8, 1956)

Introduction

Howsmon and Sisson[1] have discussed the characterization of lateral order distribution in cellulose fibers and suggested how to estimate it. Lately they showed[2] that the lateral order distribution in native cellulose fibers is characterized in the extent of lowering of the "level-off degree of polymerization" after swelling and hydrolysis.

Yurugi[3] and Maeda[4] found that the fractional dissolution in sodium hydroxide solutions of various concentrations after hydrolysis can be another method to estimate the lateral order distribution and they obtained many interesting results about regenerated cellulose fibers.

The present authors[5] have also shown the lateral order distribution in some regenerated cellulose fibers by making use of the method proposed by Yurugi and Maeda.

Every one of these methods is useful to obtain the lateral order distribution but the distributions obtained may be different from each other. So it is desirable to compare these methods and to seek the possible explanation in the phenomena observed.

In this paper the lateral order distributions in native cellulose fibers was obtained by various methods and they were compared with each other and the meaning of distribution was discussed.

Procedure

Cellulose Sample.—For this study the following three native cellulose samples were used:

(A) Cotton linters pulp, viscose grade, α-cellulose 98.3%, degree of polymerization 610.

(B) Sulfate wood pulp, viscose grade, α-cellulose 94.3%, degree of polymerization 690.

(C) Sulfite wood pulp, viscose grade, α-cellulose 93.8%, degree of polymerization 730.

The methods to obtain the lateral order distribution were as follows:

(1) The fractional dissolution in sodium hydroxide solutions of various concentrations after methanolysis,

(2) The measurement of the drop of the "level-off degree of polymerization",

1) J.A. Howsmon and W.A. Sisson, in Otto-Spurlin, "Cellulose and Cellulose Derivatives", Interscience, New York (1954), pp. 251-91.

2) O. A. Battista, S. Coppick, J.A. Howsmon, F.F. Morehead and W.A. Sisson, *Ind. Eng. Chem*, 48, 333 (1956).

3) T. Yurugi, *J. Soc. Chem. Ind., Japan*, 58, 27 (1955).

4) H. Maeda, *J. Soc. Textile Cellulose Ind. (Japan)*, 12, 6 (1956).

5) S. Mukoyama, *J. Soc. Textile Cellulose Ind. (Japan)*, 11, 772 (1955).

designated as *D.P.*, after swelling and hydrolysis,

(3) The moisture regain measurement after swelling.

(1) The Fractional Dissolution Method.—Methanolysis.—The purpose of methanolysis was to depolymerize the cellulose without accompanying the recrystallization which would be indispensable in an aqueous acid hydrolysis.

1 N hydrogen chloride in absolute methyl alcohol was used as a methanolysis reagent, which was prepared by blowing dry hydrogen chloride gas in dry absolute alcohol. The methanolysis was performed in an Ehrenmeyer flask in a thermostat kept at 50±0.1°C for forty-eight hours, 6 g. of bone-dry powdered sample being placed in about 250 ml. of reagent. After methanolysis, the sample was filtered, and washed with methyl alcohol until it became chloride-free and then it was dried.

Fractional Dissolution.—Every 0.2 g. of the methanolyzed samples was treated with 20 ml. of sodium hydroxide solutions of increasing concentrations and after being kept at 8±0.1°C for two hours the undissolved residues were filtered, washed with distilled water until the neutral reaction was obtained and dried at 105°C to constant weight.

Lateral Order Distribution.—Solubility Q was defined as follows:

$$Q=1-a\cdot m,$$

where a represents a fraction of residue at fractional dissolution and m a yield at methanolysis.

Summative mass-order relations were given by plotting Q versus increasing concentrations of sodium hydroxide. The lateral order distribution for the original sample was given by differentiating the mass-order curve.

(2) The *D. P.* Method. — Jörgensen[6,7] has pointed out that the *D.P.*'s of native cellulose fibers depend on the extent of preswelling by sodium hydroxide solutions. This phenomenon was applied by Battista et al.[2] to estimate the lateral order distribution of native cellulose fibers.

The powdered samples were swollen at 20°C for two hours in sodium hydroxide solutions of various concentrations and then excess solutions was drawn off, the residual sodium hydroxide was neutralized with N/2 acetic acid, washed acid-free with distilled water and then dried from methyl alcohol.

Acid hydrolysis was performed by boiling with 2.5 N hydrogen chloride solution for one and a half hours. Preliminary experiments show that the degree of polymerization of each sample attains to a constant level-off value by this procedure. The *D.P.* was measured using Cuprammonium solvent ($K_m=2\times10^3$).

To obtain the lateral order distribution curve the extent of drop in *D.P.* after swelling and hydrolysis was measured. The relative decrease in *D.P.* ($D.P._r$) is defined as follows:

$$D.P._r=\frac{(D.P.)_0-(D.P.)}{(D.P.)_0-(D.P.)_m},$$

where $(D.P.)_0$ and $(D.P.)_m$ denote the *D.P.* of unswollen sample and of completely mercerized sample respectively. Differential lateral order distribution curves were obtained by plotting $d(D.P._r)/d(NaOH)$ versus increasing concentrations of sodium hydroxide.

(3) The Moisture Regain Method.—Rånby[8], Jörgensen[7] and Mitchell[9] have shown the dependence of the moisture regain on the extent of preswelling of native cellulose samples by sodium hydroxide solutions. Sisson and Howsmon[1] suggested that this phenomenon is useful for lateral order measurement.

Samples preswollen in sodium hydroxide solutions of various concentrations were dried over conc. sulfuric acid solution and then transferred to a desiccator with 65 per cent relative humidity at 23°C (over saturated solution of sodium nitrite). When equilibrium at 65 per cent. R.H. was reached (seven days), the samples were weighed and then dried at 105°C to constant weight.

The water content (w) was calculated in per cent of the weight of the dry sample. From the water content w the relative increase in the water content w_r was calculated according to the following relation:

$$w_r=\frac{w-w_0}{w_m-w_0}$$

where w_0 and w_m denote the water contents of unswollen and completely mercerized samples respectively. Differential lateral order distribution was obtained by plotting $dw_r/d(NaOH)$ against increasing concentrations of sodium hydroxide.

Results

(1) The Fractional Dissolution Method.—The samples dissolved a little in the methanolysis reagent. The yield m and the degree of polymerization (*D.P.*) of the methanolyzed samples are collected in Table I.

TABLE I

THE YIELD m AND THE *D.P.* OF THE METHANOLYZED SAMPLE ARE AS FOLLOWS:

Samples	m (%)	*D.P.*
Linters pulp	98.3	150
Sulfate pulp	95.5	120
Sulfite pulp	96.5	140

As shown in Table I, the degree of polymerization of each sample after methanolysis reaches to the leveloff value which has been expected from preliminary experiments.

Summative mass-order curves are shown in Fig. 1 and the lateral order distributions are derived in Fig. 2 from these curves.

6) L. Jörgensen, *Acta Chem. Scand.*, **4**, 185 (1950).
7) L. Jörgensen and E. Ribi, *Nature*, **166**, 148 (1950).
8) B.G. Rånby, *Acta Chem. Scand.*, **6**, 101 (1952).
9) R.L. Mitchell, *Ind. Eng. Chem.*, **43**, 1786 (1951).

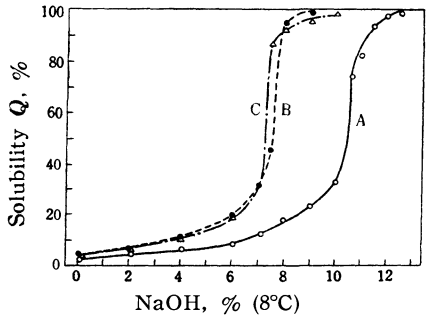

Fig. 1. Solubilities of methanolyzed native celluloses in sodium hydroxide of increasing concentrations.
(A) Cotton linters pulp.
(B) Sulfate wood pulp.
(C) Sulfite wood pulp.

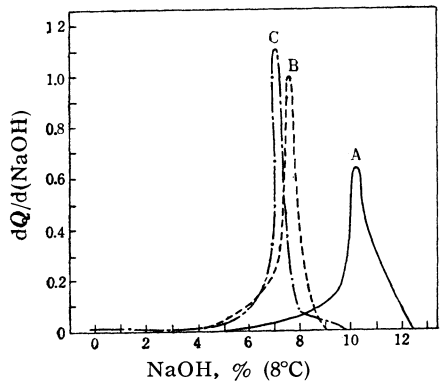

Fig. 2. Lateral order distribution curves obtained by the fractional dissolution method.

From Fig. 2 it will be seen that the linters pulp is more highly ordered relative to sulfate and sulfite pulp, but between the latter two no difference in their distribution is observed. Each of the distribution curves has a sharp peak, suggesting that the samples are mainly composed of crystalline regions of uniform perfection.

(2) **The *D.P.* Method.**—In Fig. 3 the *D.P.*'s after swelling and hydrolysis are plotted against increasing concentrations of sodium hydroxide. From these data the lateral order distribution curves are derived in Fig. 4.

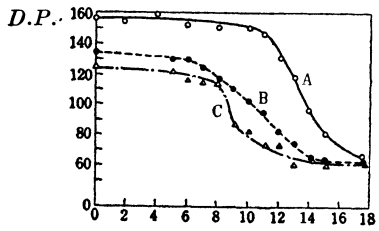

Fig. 3. Drop in *D.P.* with sodium hydroxide swelling.

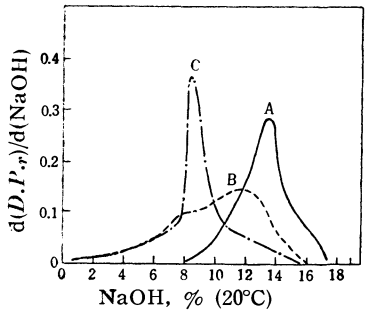

Fig. 4. Lateral order distribution curves obtained by the *D.P.* method.

As shown in Fig. 3, the *D.P.*'s of original pulps are in the range of 135 to 160, whereas mercerized pulps exhibit almost the same *D.P.*'s of about 65.

It is interesting to note that the lateral order distribution of sulfate pulp in Fig. 4 is different from that in Fig. 2. In Fig. 2 the distribution curve of sulfate pulp has a sharp peak of the same order as the sulfite pulp, whereas in Fig. 4 sulfate pulp has a broad distribution extending between the peaks of curve of sulfite pulp and that of linters pulp. In general the distribution curves in Fig. 4 are more flat than those in Fig. 2.

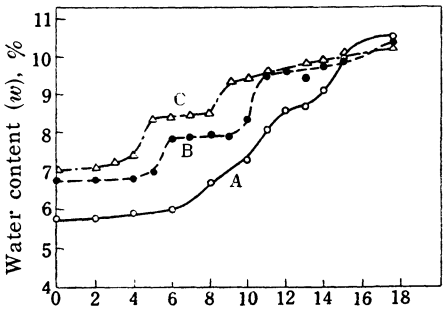

Fig. 5. Increase in moisture regain with sodium hydroxide swelling.

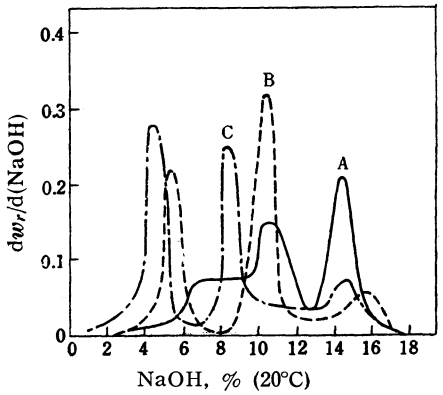

Fig. 6. Lateral order distribution curves obtained by the moisture regain method.

(3) **The Moisture Regain Method.** — In Fig. 5 water contents at 65 per cent R.H. for the preswollen samples are plotted against increasing concentrations of sodium hydroxide.

From these data the lateral order distribution is derived by the procedure described previously. They are shown in Fig. 6.

The distribution curves in Fig. 6 are different from those in Fig. 2 and Fig. 4; they have two peaks respectively, one of which is of lower order than the other which is of the same order as that in Fig. 4.

Discussion

As previously pointed out by Howsmon and Sisson[1], there are various methods to obtain the lateral order distribution of cellulose. In the present experiment the following methods were adopted: the fractional dissolution method, the *D.P.* method and the moisture regain method.

Among them the fractional dissolution method gives the most distinct distribution curve. In this method the samples were depolymerised before the alkali treatment, so that the solubilities of samples into sodium hydroxide solutions of various concentrations were determined simply by the degree of perfection of the separated crystalline regions.

In the other two methods the swelling in sodium hydroxide solution was performed in the original state, so that the swelling was restricted by many other morphological factors. These restrictions give rise to broadening of the distribution range as shown in the curve of sulfate pulp obtained by the *D.P.* method.

The difference between sulfate and sulfite pulps, which is the so-called "sulfate effect"[10], is observed in Fig. 4 and Fig. 6, but no difference in Fig. 2. This fact shows that the depolymerization before the alkali treatment reduces the higher resistance of sulfate pulp against the swelling in the aqueous sodium hydroxide solution. In other words, the lateral order of the crystalline regions in sulfate pulp is the same as that in sulfite pulp and some other morphological factors probably affect to increase the resistance of sulfate pulp against the swelling. Thus it is apparent that the "sulfate effect" is not due to the difference in the crystalline regions.

The crystallinities of sulfite wood pulp and cotton were found to be 65 and 70 per cent respectively by Hermans[11] from X-ray diffraction measurement. It is interesting to compare its result with the summative mass-order curves in Fig. 1. In Fig. 1, the concentrations of sodium hydroxide at which the solubility curves rise sharply are 7 per cent for sulfite pulp and 10 per cent for linters pulp, and the solubilities at these concentrations are the same value of about 30 per cent. This fact suggests that the crystallinity obtained by X-ray diffraction method shows the quantity of such uniform crystalline regions irrespective of their lateral orders. The difference between cotton linters pulp and wood pulp is considered to be remarkable in the crystalline regions as shown in Fig. 2; that is, the crystalline regions of wood cellulose are less perfect than those of cotton cellulose.

In Fig. 6 each of the distribution curves has two peaks, one of which appears at almost the same concentration of sodium hydroxide as that in Fig. 4, while the other occurs at lower concentration. To understand the meaning of these circumstances the mechanism of mercerization must be considered. Nukushina[12] has recently reported that the decrystallization precedes the phase transition when native cellulose fibers are treated with the alkali of increasing concentrations. The present authors have confirmed this fact with respect to linters pulp by making use of X-ray diffraction. In their experiment, linters pulp started to decrystallize at 10 per cent sodium hydroxide and to induce the phase transition at 13 per cent sodium hydroxide at 20°C. The lower ordered peak of the distribution curve of linters pulp may be attributed to this decrystallization, for the decrystallization in general gives rise to increase in moisture regain. The same line of argument will be possible with respect to wood pulps, too.

If these views are accepted, the conclusion may be drawn that the fractional dissolution method will be the best method to obtain the lateral order distribution of native cellulose fibers. Thus the following concept will be accepted; that is the native cellulose fibers consist of a large proportion of uniform crystalline regions separated by amorphous regions of fairly high order, and the crystalline regions in wood cellulose are less perfect than those in cotton cellulose.

Summary

To obtain the lateral order distribution of native cellulose fibers the fractional dissolution method, the *D.P.* method and the mois-

10) B.G. Rånby and H.F. Mark, *Svensk Papperstidning*, **10**, 374 (1955).

11) P.H. Hermans and A. Weidinger, *J. Polymer Sci.*, **4**, 135 (1949).

12) Y. Nukushina, *J. Soc. Textile Cellulose Ind. (Japan)*, **12**, 158 (1956).

ture regain method were adopted. Among these three methods the fractional dissolution method gives the most correct distribution. The other methods give somewhat different distribution curves, the meanings of which were discussed. The structural difference between wood pulp and linters pulp is due to the difference in the degrees of perfection of crystalline regions, whereas no difference between sulfate pulp and sulfite pulp is observed in their crystalline regions.

One might conclude that the fractional dissolution method is the best method to obtain the lateral order distribution in both native and regenerated cellulose fibers.

The authors are grateful to Dr. K. Hoshino for permitting this publication.

Research Department of
Toyo Rayon Co., Ltd.
Otsu, Shiga

The Studies on Micelles of Surfactants. I. The Phase in the interior of Micelles of Surfactants

By Hiroji SASAKI, Haruhiko OKUYAMA and Shūji SAITO

(Received March 24, 1956)

Introduction

It is well known that organic compounds with conjugated bonds show light absorption in the visible and ultraviolet regions. These bands characteristic for the conjugated system are called K[1] or π[2] bands, because π electrons are responsible for them. The intensity of π bands has the order of $\varepsilon=10000-20000$ and their maximum shifts towards red when solvents are changed from nonpolar to polar or the conjugated system becomes larger[3].

It is known too that so-called R bands[1] appear when hetero atoms which have n electrons (nonbonding electrons, i.e., lone pair) are conjugated to the planar conjugated organic system[4]. Afterwards R bands have been usually called n bands. The intensity of n bands has the order of $\varepsilon=10-1000$ and the position of them is always at the region of the longer wave length than that of π bands when the two kinds of bands appear in one system. N bands shift towards blue when solvents are changed from nonpolar to polar liquids which act as proton donor[5], but shift towards red if solvents act as proton accetor[5].

The definitions of both bands were given by Kasha[7]. We can readily distinguish the n band from the π band by their relative positions, intensities and shifts when solvents are changed.

The band which is characteristic of the benzenoid system and can not be observed in the aliphatic conjugated system is called B band. Its position and intensity are the media between the π and the n band ($\varepsilon=250-3000$). This band is caused by the vibration of the ring and has many fine structures[8].

It has been believed that the interior of micelles of surfactants is constructed by hydrocarbon but this fact is not yet experimentally determined. When the substances, which are insoluble or hardly soluble in water, are solubilized in the aq. surfactant solutions and their spectra are compared with those of the same substances in nonpolar solvents, and if there is no spectral change, we may safely draw the conclusion that the interior phase of surfactant-micelles is perfectly nonpolar. But if the spectral change is observed, we can say that the solubilizate molecules are under the influence of water molecules. If the latter case is observed it is our purpose to show whether some of those water molecules are contained in the micelles or not.

In our present work we have used azobenzene, Yellow OB (which have the π and the

1) A. Burawoy, *Ber.*, **63**, 3155 (1930).
2) H. L. McMurry, *J, Chem. Phys.*, **9**, 241 (1941). H.L. McMurry and R.S. Mulliken, *Proc. Nat Acad. Sci.* US. **26**, 312 (1940).
3) J.R. Platt, *J. Chem. Phys.*, **19**, 101 (1951).
4) R.S. Mulliken. *J. Chem. Phys.*, **3**, 564 (1935).
5) (a) H. McConnel, ibid., **20**, 700 (1952): (b) G.J. Brealey and M. Kasha, *J. Am. Chem. Soc.*, **77**, 4462 (1955).
6) S. Nagakura and H. Baba, *J. Am. Chem. Soc.*, **74**, 5693 (1952).
7) M. Kasha, *Disc. Faraday Soc.*, No. 9, 14 (1950).
8) F.O. Rice and E. Teller, "The Structure of Matter", John Wiley and Sons, Inc., New York (1949), p. 273.

n bands), anthracene and phenanthrene (which have the B and the π bands) as the solubilizates or the absorbers to study the phase of the micelle. These four absorbers are insoluble in aq. phase but soluble in various organic solvents and also solubilized in aq. surfactant solutions.

Materials and Experimental Methods

1) Samples.—Sodium dodecyl sulfate (SDS), offered by The Daiichi Seiyaku Co., was purified with ether and recrystallized from alcohol. Trimethyl dedecylammonium chloride (TMD), offered by The Nihon Yushi Co., was purified by the extraction with isopropyl alcohol. Nonionic surfactant Emulgen 120 (E120), (lauryl-polyethylene ether) offered by The Kaō Sekken Co., has been used with no purification except to remove the water by desiccation. Yellow OB and azobenzene, which are of chemical pure grade and consist mainly of trans type, have been used after being extracted several times with hexane. Anthracene and phenanthrene which are also chemical pure grade have been used after several extractions with benzene. As we need only the relative positions and intensities of the bands of these absorbers and not the absolute ones, the influences of minute impurities contained in these absorbers are thought to be negligible.

2) Methods.—The measurements of the absorption spectra have been carried out by the Beckman DU Spectro-photometer at the room temperature.

Results

1) Experiments with Azobenzene as the Solubilizate.—a) The Concentration Dependence of the Absorption Spectra of Azobenzene in the Nonpolar Solvent.—In Fig. 1 the absorption spectra of azobenzene in CCl_4 are shown. The absorption maximum at 320 mμ (curve I) is the π band which depends remarkably on the concentrations. The reason why the π band depends on the concentration comes from the nature of benzene ring responsible for producing the π band which is able to act as π acid and as π base[9]. The maximum at 445 mμ is the n band and its dependence on the concentration is very little, because the azo-group which is responsible for producing the n band acts only base and its electronic state is hardly affected by the association.

b) The Dependence of the Spectra on the Concentration of Azobenzene in the Aqueous Surfactant Solutions.—As the azobenzene molecules are thought to be equally distributed in every micelle in surfactant solutions, the change of the π band can not occur so long as the number of absorbent molecules does not exceed that of micelles. From the curve I, III, and IV in Fig. 2 it is seen, when the 10% aq. SDS solution is used, the spectral changes of azobenzene are little until its concentration exceeds about 10^{-4}M.

9) R.S. Mulliken, *J. Am. Chem. Soc.*, **74**, 811 (1952).

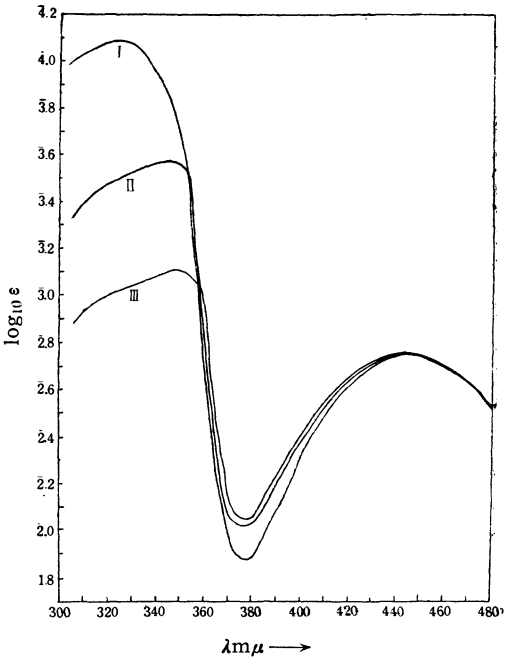

Fig. 1. Absorption spectra of azobenzene in CCl_4, measured three days after preparation. Concentration of azobenzene: I. 1.183×10^{-4}M. II. 1.183×10^{-3}M. III. 3.94×10^{-3}M/L.

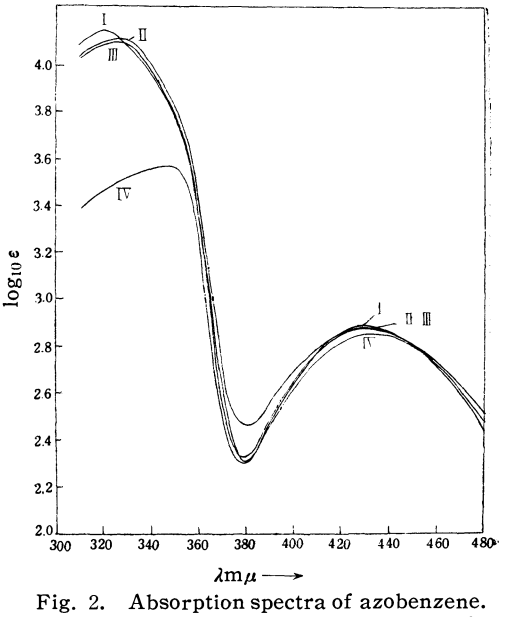

Fig. 2. Absorption spectra of azobenzene. Concentration of azobenzene: I. 2.283×10^{-5}, II and III. 2.283×10^{-4}, IV. 1.183×10^{-3}. Solvents: I. 10% SDS aq., II and III. 10% SDS+1.5% CCl_4 solubilized, IV. 10% SDS+2.5% CCl_4 solubilized. Reference: I. water, others. solvents. Measured 3 days (I and IV), 8 hours (II and III) after preparation.

Using this fact, it is thought possible to determine the number of micelles, accordingly* the number of surfactant molecules which form every micelle at the definite concentration. The details on this subject will be reported in our next paper.

c) The Scattering and Absorbing Effects by the Micelles.—In Fig. 2 the curve II and III are almost the same except that the intensity of the latter is a little less than that of the former. When we use the solvent (including aq. surfactant solutions) as the reference liquid we need not be concerned about the scattering and absorbing effects by the micelles[10].

d) The Time-dependence of the Intensity of the Bands.—In Fig. 3a it is seen that the

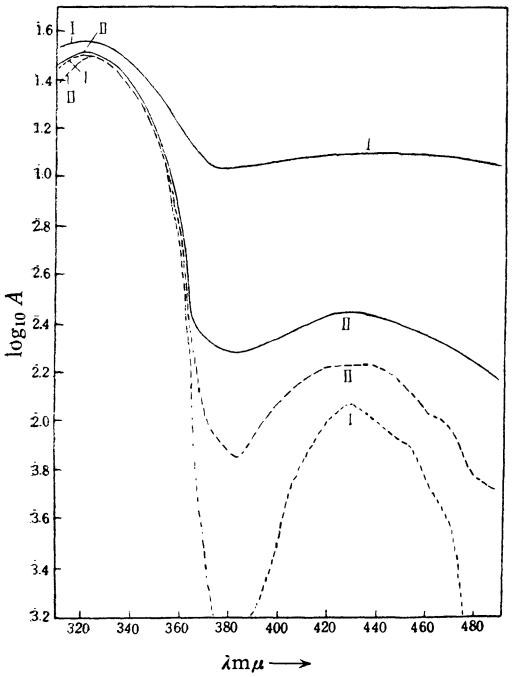

Fig. 3a. Absorption spectra of azobenzene. ——— Measured 8 hours, ---- measured 7 days after preparation. Concentration of azobenzene 2.278×10^{-5}M. b (the width of the cell)=1 cm. Solvents: I. 5% SDS aq., II. 10% SDS $A=(\log_{10})I_0/I$.

intensities of π bands decrease a little with time but the positions of their maxima do not alter. The intensities of the n bands (not the positions of maxima), however, depend markedly on time. This is, we suppose, because of the increasing amount of hydrogen-bonding between the azo-group and the water molecules. In Fig. 3a the solid curve (measured eight hours after preparation) I (5% SDS) has the higher intensity than that of the solid curve II (10%); this shows that in 5% SDS the n electrons of azo-group are much more perturbed at first by the water molecules than in 10% SDS. The broken curve (measured seven days after preparation) I (5% SDS) of Fig. 3a, on the contrary, has the lower intensity than that

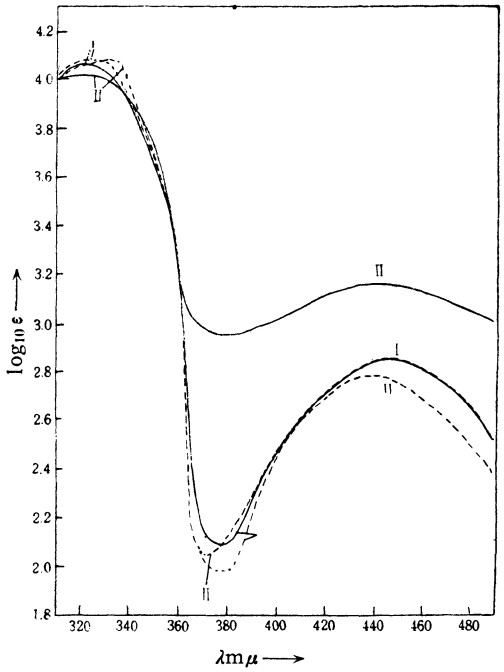

Fig. 3b. Absorption spectra of azobenzene 1.006×10^{-4} M/l. ——— Measured 8 hours, ---- measured 7 days after preparation. Solvents: I. CCl_4, II, C_2H_5OH.

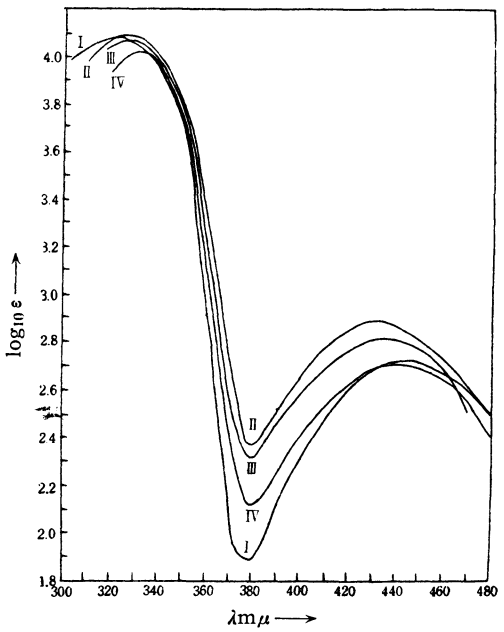

Fig. 4. Absorption spectra of azobenzene measured three days after preparation. Concentration of azobenzene 1.183×10^{-4} M. Solvents: I. CCl_4, II. 5% SDS, III. 5% TMD, IV. 2.5% E 120.

10) E. Freiver, W. Berndt and H. Toplak, *Angew. Chem.*, **67**, 69 (1955).

of the broken curve II (10%). This is because of the velocity of the hydrogen-bonding being greater in 5% SDS than in 10% SDS.

In alcohol the intensity of the n band also changes with time, and the effect of the association appears in the π band, but in a nonpolar liquid such as CCl_4 the n band is not affected and the lowering of the intensity of the π band is very little with time (Fig. 3b).

e) The Absorption Spectra of Azobenzene in Various Aqueous Surfactant Solutions.—In Fig. 4 it is seen, if we take the maxima in the CCl_4 solution as the standard, all the n bands shift towards blue and all the π bands shift towards red in aq. surfactant solutions, which show that the solubilizate molecules are in contact with water molecules as is the case of Fig. 3a.

f) The Dependence of Absorption Spectra of Azobenzene on the Concentration of Surfactants.—In Fig. 5a (measured eight hours after preparation) and 5b (seven days) it is seen that the spectra of azobenzene in aq. surfactant solutions deviate from that in CCl_4 in the order 5% SDS>10% SDS>5% SDS+1.2% CCl_4 solubilized.

2) Experiment with Yellow OB.—In the case of Yellow OB the degree of the shift of the π band is more marked. The maximum at 440 mμ in CCl_4 is the π band (Fig. 6a) which shifts towards red in the surfactant solutions. The n band is covered by this massive π band and can not be observed. The maximum at 350 mμ seems to correspond to the third maximum (about 260 mμ) of Benzeneazo-α-naphthalene (Fig. 6b), which makes the skeleton of Yellow OB, caused probably by

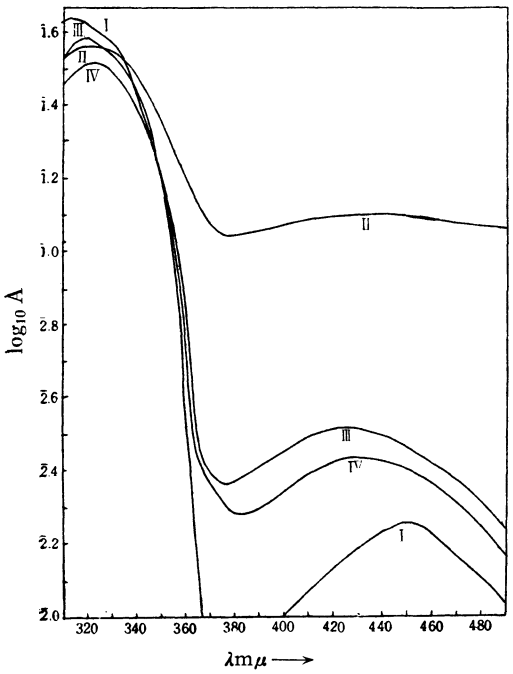

Fig. 5a. Absorption spectra of azobenzene measured 8 hours after preparation. Concentration of azobenzene is 2.278×10^{-5} M. b=1 cm. Solvents: I. CCl_4, II. 5% SDS, III. 5% SDS+1.2% CCl_4 solubilized, IV. 10% SDS.

$$A=\log_{10}\frac{I_0}{I}$$

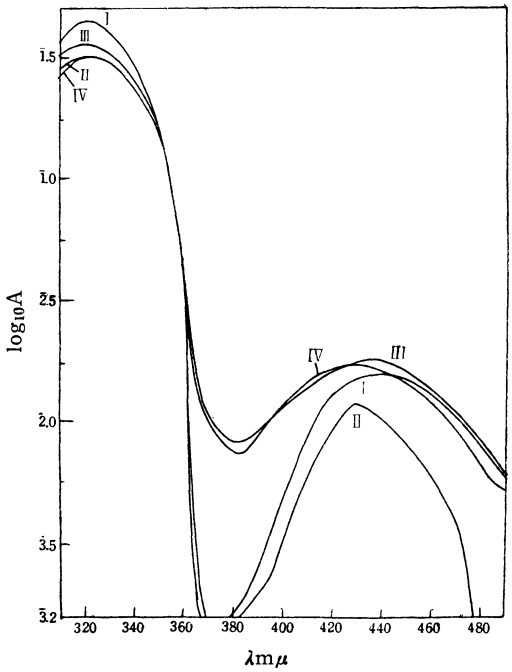

Fig. 5b. Absorption spectra of azobenzene measured 7 days after preparation. Concentration of azobenzene 2.278×10^{-5} M. b=1 cm. Solvents: I CCl_4, II. 5% SDS, III. 5% SDS+1.2% CCl_4 solubilized. IV. 10% SDS.

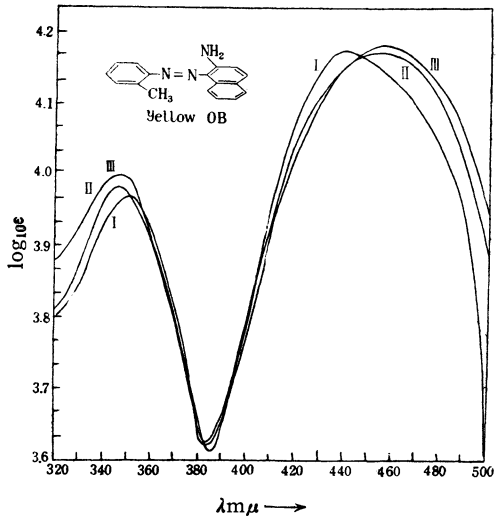

Fig. 6a. Absorption spectra of Yellow OB measured three days after preparation. Concentration of Yellow OB is 1.245×10^{-5} M. Solvents: I. CCl_4, II. 5% SDS, III. 5% TMD.

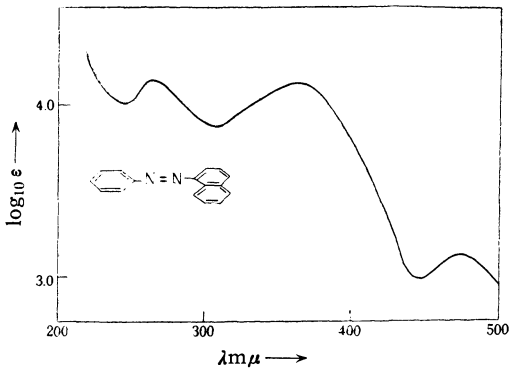

Fig. 6b. Absorption spectrum of benzene-azo-α-naphtharene from A. Burawoy, J. C. S., 1177 (1939).

the π-π^*second excited transition, and diffuses and shifts a little towards blue in the aq. surfactant solution.

(3) The Changes of B Bands of Anthracene in the Aqueous Surfactant Solutions.—In Fig. 7 are shown the B bands of anthracene in hexane,

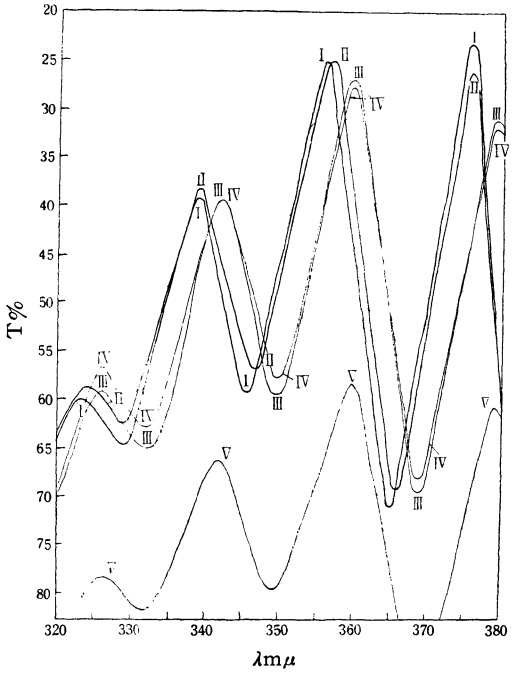

Fig. 7. Absorption spectra of anthracene. b=1 cm. $T=(I/I_0)\times100$. Measured one day after preparation. Concentration of anthracene=10^{-4} M/l. Solvents: I. Hexane, II. C_2H_5OH, III. 10% TMD+2% Hexane, IV. 1% TMD, V. 10% TMD.

alcohol and the aq. TMD solutions. The changes of the B bands in alcohol are not remarkable, but in the aq. TMD solutions they shift wholly towards red about 3 mμ and particularly in the 1% aq. TMD solution the marked intensity lowering occurs. The influence of the added hexane is also observed.

(4) The Changes of π Bands of Phenanthrene in the Aqueous Surfactant Solutions.—In Fig. 8 are shown the π bands of phenanthrene. In

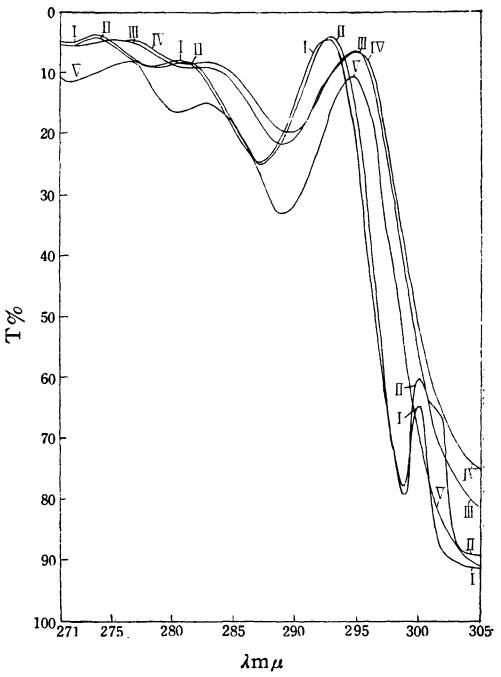

Fig. 8. Absorption spectra of phenanthrene. b=1 cm.. Measured one days after preparation. Concentration of phenanthrene=1.115×10^{-4} M/l.
Solvent: I. Hexane, II. C_2H_5OH, III. 10% TMD+2% Hexane solubilized. IV, 10% TMD, V. 1% TMD.

the aq. TMD solutions these π bands shift toward red 2–3 mμ; in 1% TMD the intensity lowering is also observed. As the result of the red shift of the π bands the maximum at 300 mμ, one of the B bands, disappears in the surfactant solutions.

Discussion

(1) From the changes of the absorption bands such as the time dependence and blue shift of the n band, the red shifts of the π and the B bands, it is apparent that the solubilizates are under the influences of some polar solvents.

(2) We suppose first that there is no water molecule in the micelle, and these spectral changes are caused by the longer-range electrostatic force in the water, and thus a solubilizate molecule and a water molecule are not in contact with each other.

This supposition is refuted by the consideration of the experiments of Foster[11]: he has shown that no spectral change occurs except when the functional group of the solute molecule and the solvent molecule,

11) L. S. Foster, *J. Am. Chem. Soc.*, **77**, 1417 (1955).

which has the ability to affect the electronic state of the former, are in contact with each other directly. Therefore it is sure that the solubilizate must be in contact with some polar molecules.

(3) We suppose next that there is no water molecule in the micelle but the polar groups of some surfactant molecules are contained in the micelle.

Such a random structure of the micelle is hardly acceptable.

(4) Next we suppose that there are no water molecules in the micelle but the solubilizate such as azobenzene and Yellow OB, which have azo or amino groups, are in the palisade and these groups of the solubilizate molecules are in contact with some water molecules.

But the changes of the π bands show that the benzene rings are also under the influence of water molecules. To explain this fact, the greater part of a solubilizate molecule is in the aq. phase and the lesser part of it is in the palisade. Such a situation is not conceivable. Especially in the case of anthracene and phenanthrene which have no hydrophilic group and are never solubilized in the palisade, there occur also similar spectral changes.

(5) When a small amount of the nonpolar organic liquid is added to the solubilized absorber systems, the spectral changes occur. The solubilized nonpolar liquid must be thought to drive the water molecules which are contained out of the micelle.

When the concentration of the surfactant is in creased, the spectral changes also becomes less. This is thought to show that the micelles become more compact with increasing concentration, and at the same time the number of the water molecules contained in the micelle decreases.

From the consideration discussed above we must conclude that some water molecules are contained in the micelle at least until 10% surfactant concentration.

(6) The reason why surfactant micelles contain some water molecules may easily be understood from the consideration of the fact that such a small volume as the interior of micelles are under the intense thermal agitation of the water molecules.

(7) Because of the fact that some water molecules are contained in the micelle, it is natural to think that in the initiation of the emulsion polymerization[12], the catalyser which is in the aq. phase diffuses into the inside of the micelle and activates the modifier or monomer molecule solubilized there.

Summary

From the spectral changes of the n, π, and B bands, it is concluded that the surfactant micelle, at least until 10% concentration, contains some water molecules.

The authors wish to express their sincere thanks to Prof. N. Sata for his advice and encouragement, and to The Kaō Sekken Co., The Daiichi Seiyaku Co. and The Nihon Yusi Co., for offering us the samples.

Department of Chemistry, Faculty of Science, Osaka University, Osaka

12) W.D. Harkins, "Physical Chemistry of Surface Films", Reinhold Publishing Co., New York (1952).

Interaction between Surface Active Agents and Proteins. III. Precipitation Curve of the System Sodium Dodecyl Sulfate-Egg Albumin at Various pH's and the Determination of the Concentration of Protein by the Titration Using Surfactant

By Koichiro AOKI*, Joji HORI and Keiko SAKURAI

(Received January 11, 1956)

Introduction

As described in Part I[1], we observed in the reaction of egg albumin and sodium dodecyl sulfate (SDS) in the acetate buffer solution at pH 4.2 that the amount of precipitate formed changed with the mixing ratio of egg albumin to SDS (albumin/SDS). In this reaction a large amount of white precipitate was formed when albumin was in excess, and the amount of precipitate decreased with an increase in the relative amount of SDS. Furthermore, there was no precipitate when the relative amount of SDS exceeded a certain mixing ratio. We drew a curve, named precipitation curve, by plotting the precipitation percentage against the mixing ratio albumin/SDS.

The present paper is a report of the precipitation curve when the pH of the buffer solution was lower than 4.2. In addition, we made a study of this curve when the neutral salt solution instead of the buffer solution was used.

Further, we investigated the possibility of a rapid determination of the concentration of the protein solution by the titration using surfactant solution, taking advantage of the above fact; namely, that the protein and surfactant react quantitatively.

Experimental

Materials.—SDS, egg albumin and horse serum albumin used in this study were obtained by the method described previously[1,2].

Precipitation Curve.—We determined the precipitation curve of the system egg albumin-SDS at pH's 4.2, 3.6, 3.1, and 2.3 and at constant ionic strength (μ) 0.30, using the same method as in Part I. Further we determined the precipitation curve of this system in the sodium chloride solution at μ 0.30, and the curve in distilled water.

Determination of Protein.—As is seen in Fig. 1, there is a precipitate when the concentration of SDS is below a certain mixing ratio of albumin/SDS, but no precipitate when the concentration of SDS exceeds this mixing ratio. We tried to titrate the protein solution by surfactant solution taking the point where the precipitate disappeard as the end point. When the concentration of one of the two, i.e., albumin or SDS, is known, the concentration of the other can be found by the titration. In this study definite amounts of protein solutions varying in concentration were titrated by SDS solution of known concentration. Plotting the volume (X cc.) of SDS used up to the end point of titration against the concentration (Y%) of albumin, a relation between these two quantities was found. Using this relation, the concentration of albumin solution, the value of which is unknown, can be found through the titration by SDS solution. Of course, by conducting this titration in the reverse way, the amount of SDS can be determined by the titration using protein solution.

Procedure of Titration.—Albumin solutions of known concentration were prepared using acetate buffer* of known pH and ionic strength, or using sodium chloride solution. The concentration of protein was first determined by the Kjeldahl method, and then this protein solution was successively diluted with the same medium in order to have a series of solutions varying in concentration.

SDS solution of a known concentration was prepared using the same medium as used in the preparation of albumin solution.

Taking exactly 2.00 cc. of the albumin solution of known concentration, 1.00% SDS solution was gradually added. The egg albumin solution turned turbid by the first drop of SDS. Continuing the titration, the turbidity increased, and then the precipitate appeared. On the further addition of SDS, the precipitate dissolved and a transparent solution was obtained. This was taken as the end point of the titration.

When the SDS solution was added to the serum albumin solution, no precipitate appeared until a few drops of SDS solution were added[1]. With the addition of SDS the precipitate first increased in amount and then disappeared in the same way as in the titration of egg albumin.

* Present temporary address: Department of Chemistry, Purdue University, Lafayette, Indiana, U.S.A.

1) K. Aoki and J. Hori, This Bulletin, 29, 104 (1956).

2) K. Aoki, H. Shimosato and Y. Kamino, *Bull. Nagoya City Univ.*, 1, 67 (1955).

Results

Precipitation Curves.—Fig. 1 shows precipitation curves of the system egg albumin-SDS at pH's 4.2, 3.6, 3.1, and 2.3 and at μ 0.30. In this figure we find that in the region of albumin excess plots are on the same line *ab* regardless of pH, while in the other region they lie on separate lines*. By use of plots on the curve *abc* in Fig. 1, we can calculate the number of SDS molecules which are bound to one molecule of egg albumin. The method of calculation is the same as described in Part I. The result is shown in Fig. 2.

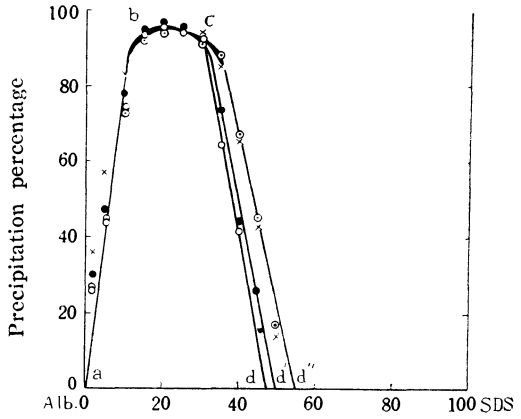

Fig. 1. Precipitation curves of the system egg albumin and sodium dodecyl sulfate in acetate buffer at 0.30 ionic strength. PH's are as follows; ○ 4.2, ● 3.6, ⊙ 3.1, and × 2.3.

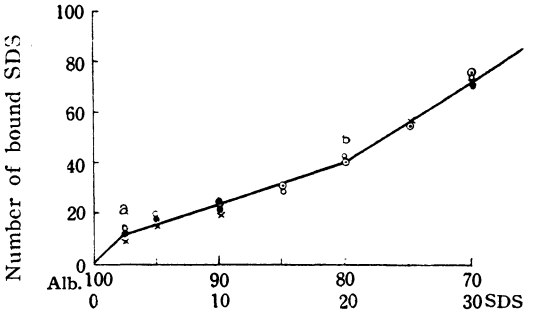

Fig. 2. Number of SDS molecules bound to one molecule of egg albumin. PH's are as follows; ○ 4.2, ● 3.6, ⊙ 3.1, and × 2.3.

Fig. 3 shows the precipitation curve of the system egg albumin-SDS in 0.30 N sodium chloride solution. Fig. 4 shows the precipitation curve of the same system in distilled water. As is shown there is a small precipitation curve even when distilled water is used. On the contrary, there is no precipitation curve in the system serum albumin-SDS when sodium chloride solution or distilled water is used.

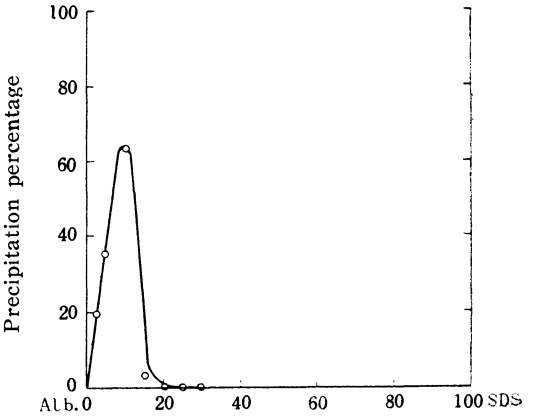

Fig. 3. Precipitation curve of the system egg albumin-SDS in 0.30 N sodium chloride solution.

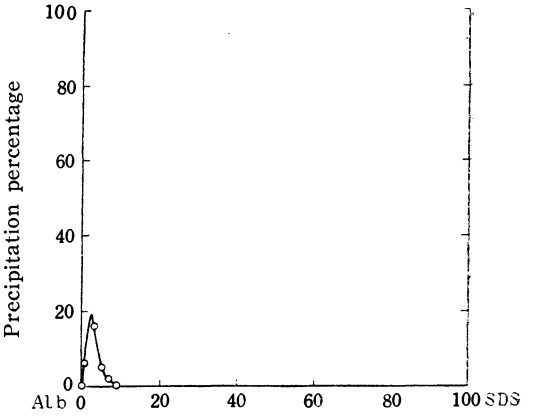

Fig. 4. Precipitation curve of the system egg albumin-SDS in distilled water.

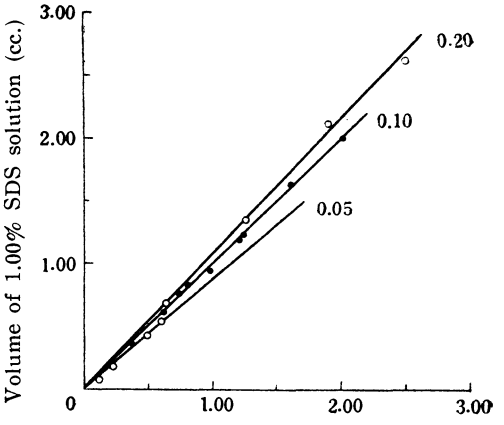

Fig. 5a. Titration of egg albumin by SDS in acetate buffer at pH 4.2 and ionic strengths 0.20, 0.10, and 0.05.

* This buffer was composed of hydrochloric acid and sodium acetate.

* Below pH 3.0 plots fall on a common line *cd''*.

Titration of Egg Albumin.—Some results obtained are shown in Figs. 5a, 5b, 5c and 6. Fig. 5a shows the result obtained at pH 4.2 and at three different ionic strengths. The abscissa represents the concentration of egg albumin used, and the ordinate represents the volume of the 1.00% SDS solution required to titrate 2.00 cc. of albumin solution. A linear relation was obtained between these two quantities. Slopes of these straight lines vary according to the ionic strength, and the lower the ionic strength the smaller the slope. At pH 3.6 and 3.1 also, straight lines having the same characteristics as those in Fig. 5a were obtained.

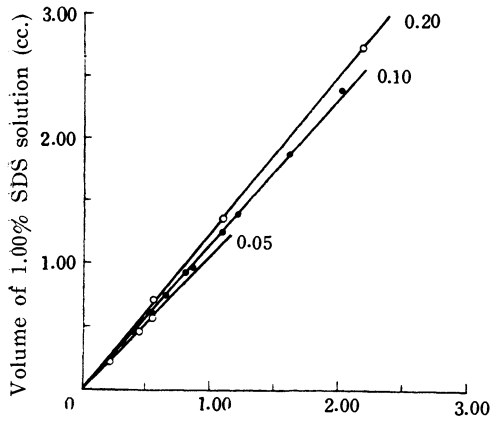

Fig. 5b. Titration of egg albumin by SDS in acetate buffer at pH 3.6 and ionic strengths 0.20, 0.10, and 0.05.

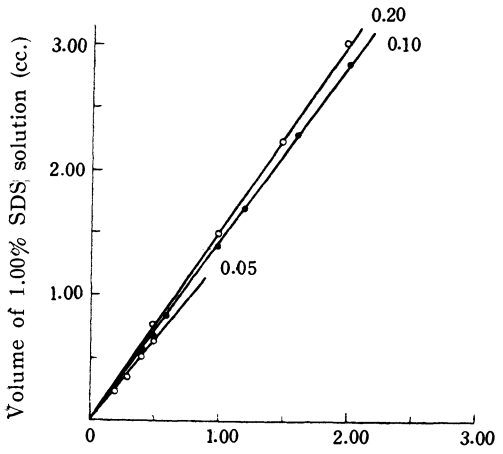

Fig. 5c. Titration of egg albumin by SDS in acetate buffer at pH 3.1 and ionic strength 0.20, 0.10, and 0.05.

Fig. 6 shows the results obtained when 0.50 N and 0.25 N sodium chloride solutions were used. In these cases also a linear relation was obtained, and the slope of the straight line varied with the concentration of sodium chloride. The pH of sodium chloride solution containing protein was 5.2.

As is seen in Fig. 4 there is a precipitation curve when distilled water is used. Therefore the titration of egg albumin in distilled water was thought possible; the results, however, were not satisfactory because the greater error accompanies the titration.

Titration of Serum Albumin.—The results at pH 4.2 is shown in Fig. 7.

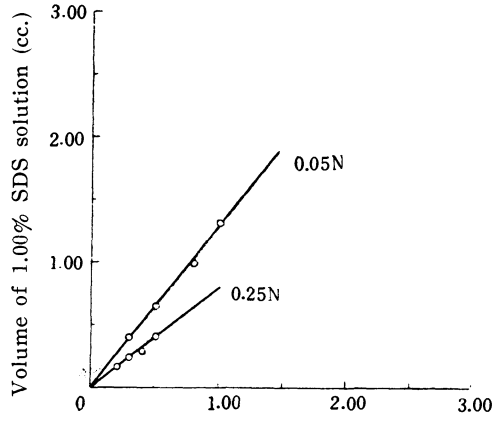

Fig. 6. Titration of egg albumin by SDS in sodium chloride solution.

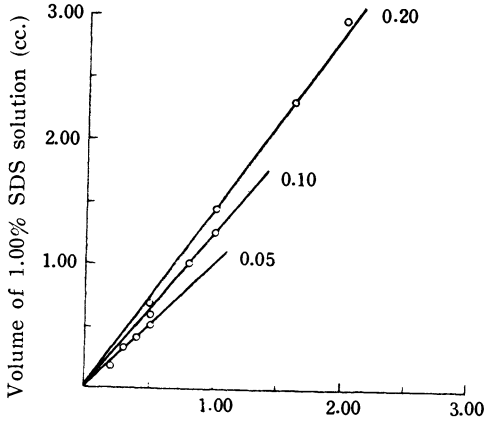

Fig. 7. Titration of horse serum albumin by SDS in acetate buffer solution at pH 4.2 and ionic strengths 0.20, 0.10, and 0.05.

Discussion

Precipitation Curve of Egg Albumin in Acetate Buffer.—Precipitation curves were found in the pH region between 4.2 and 2.3 and μ 0.30. Fig. 2, which is to be interpreted as described in Part I, shows that four series of plots fall near the same curve. This indicates that, regardless of pH, about forty molecules of SDS are bound to one molecule of egg albumin in the region of albumin

excess. As will be shown elsewhere[3], the number of positive charges on one egg albumin molecule should be constant and 42 for pH<6. The above result is considered to be an experimental verification of the fact that the number of positive charges on one egg albumin molecule is constant in this pH range.

Titration of Protein.—As was shown, the concentration of albumin is proportional to the volume of the 1.00% SDS solution required in the titration. The proportionality constant changes according to the conditions of the titration, i.e., pH and ionic strength of the buffer or the concentration of sodium chloride solution. As is seen in Figs. 5a, 5b, 5c, 6, and 7, the greater the ionic strength becomes at the same pH the more SDS is necessary. This fact is observed whether buffer or sodium chloride solution is used, for either egg albumin or serum albumin.

There is a limitation in the ionic strength of the medium to be used. When the ionic strength is too large, SDS does not dissolve completely, because of the limited solubility of surfactant due to the increase in the concentration of salt. When the ionic strength is too small, reproducible results cannot be obtained since the end point becomes somewhat obscure. The following are the media to be used; acetate buffer solution of an ionic strength between 0.50 and 0.05, or the sodium chloride solution of an ionic strength between 0.50 and 0.25. These values were found when the room temperature was about 20°C, and are affected by temperature.

When buffer solution is used, there is no limit of pH other than that the pH must be smaller than that of the isoelectric point of the protein*. It is interesting, however, that there was a precipitate in sodium chloride solution, although the pH of the egg albumin solution was 5.2 and was on the alkaline side of the isoelectric point of this protein. This is a difference in behavior observed between the buffer solution and the neutral salt solution.

Considering the results described above, it is concluded that a rapid determination of the concentration of the protein solution is possible. As is clear in Figs. 5a, 5b, 5c, 6 and 7, the accuracy of the titration using SDS is ±0.03 cc. In other words, the concentration of the protein is determined within an error of ±2%.

Difference between Egg Albumin and Serum Albumin.—Comparing the results of the titration by SDS, a difference is found between egg albumin and horse serum albumin. On horse serum albumin, no precipitate appeared until the addition of a few drops of SDS. But on egg albumin a precipitate occurred with the first drop. Therefore, egg albumin and serum albumin can be distinguished from each other by the titration using SDS.

When horse serum albumin and SDS were mixed in distilled water, there was no precipitate; this phenomenon agrees with the observation by Putnam and Neurath[4]. When egg albumin and SDS were mixed in distilled water, there was a little precipitate. This fact shows another difference between these two proteins.

Summary

(1) The precipitation curve of the system egg albumin-SDS was studied in the pH region between 4.2 and 2.3, and at constant ionic strength 0.30. It was found that the number of SDS molecules bound to one molecule of egg albumin is constant and this is considered to be a verification of the fact that the number of positive charges on one egg albumin molecule is constant in this pH region.

(2) A rapid determination of the protein concentration by the titration using SDS is possible within an error of ±2%.

(3) Egg albumin and horse serum albumin react in different ways with SDS in distilled water and in sodium chloride solution.

The authors wish to express their appreciation to Prof. Rempei Goto of Kyoto University for his encouragement during this study.

Chemical Laboratory
Nagoya City University
Nagoya

3) K. Aoki, unpublished.

* When the pH is lower than 2, egg albumin is gradually denatured.

4) F.W. Putnam and H. Neurath, *J. Am. Chem. Soc.*, **66**, 692 (1944).

Exchange Reaction between Deuterium and Ammonia on Synthetic Ammonia Catalysts Promoted Singly, Doubly, and Triply

By Hiroshi UCHIDA and Naoyuki TODO

(Received May 22, 1956)

Introduction

A few investigations[1,2,3] have been made on the exchange reaction between deuterium and ammonia over iron catalysts for ammonia synthesis. Every one of them, however, confined the kinetic measurement to only one kind of the catalyst and no relation of the catalytic activity in the exchange reaction to the one in the ammonia synthesis is available as yet.

The present paper deals with the rate in the exchange reaction on three catalysts promoted by alumina with or without potash or potash and lime. The results presented here are of particular interest in connection with the catalyst performance in the ammonia synthesis.

Experimental Procedure

The rate of exchange reaction between deuterium and ammonia was determined on three kinds of fused iron catalysts, which was accompanied by the determinations of their surface area and the fractions of the surface covered by potash and of iron surface. The catalytic activity for ammonia synthesis was also evaluated.

Catalyst.—Catalysts for ammonia synthesis which were promoted singly, doubly, and triply respectively were employed in this investigation. Their promoter-compositions were (5% Al_2O_3), (5% Al_2O_3, 1% K_2O), and (4% Al_2O_3, 1% CaO, 1% K_2O). These catalysts were specimens taken from respective batches prepared for our previous investigations[4,5].

Catalytic Activity of Ammonia Synthesis.—The catalyst should exhaustively be reduced to be used for the determinations of the activity and of the rate of exchange reaction, and this was achieved as follows. A quantity (10 g.) of the catalyst granules rauging from 1 to 2 mm. in diameter was placed in a catalyst container (A in Fig. 1), and was reduced at 500°C in a current of a gas mixture composed of hydrogen and nitrogen in a ratio of 3: 1, which was passed over the catalyst at a space velocity of 2000. At various intervals in the reduction, the temperature was lowered to 350°C. and the exit gas from the container was quantitatively analyzed for ammonia. The reduction was continued until no more increase in the ammonia concentration was observed after six hours of further reduction. Usually about one hundred hours were required for the completion.

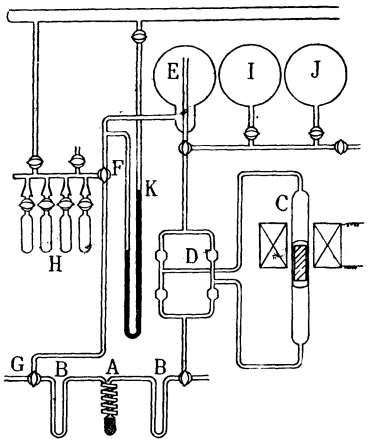

Fig. 1. Apparatus.

The ammonia concentration in the exit gas having passed over the catalyst at temperatures between 300° and 450°C at a space velocity of 2000 is employed as a measure of the activity of ammonia synthesis.

Rate of Exchange Reaction.—An apparatus similar to the one used by J. R. Gutmann[6] was employed for the determination of the rate. It is shown in Fig. 1. A catalyst container (A) is heated in an electric furnance and the catalyst is protected from contamination with the vapours of tap grease and mercury by U tubes (B, and B′) immersed in a melting chlorobenzene bath (−45°C). An all-glass electromagnetic pump (C, D) based on the design of J. Aman et al.[7] and having pumping capacity of 2.5 l/min. was used to prevent the effect of diffusion in gas phase on the rate. During the reaction, a part of the gas circulating successively through the container, a glass bulb (E, 11 in volume), and the pump, was withdrawn by a three-way cock (F) into a small bottle (H), which was then removed from the apparatus and connected to another apparatus equipped with a thermo-conductivity gauge. The samples of the gas were freed from the included

1) H.S. Taylor and J.C. Jungers, *J. Am. Chem. Soc.*, 57, 660 (1935).
2) S. Enomoto, *Shokubai* (*Catalysis*), 8, 47 (1952) (in Japanese).
3) J. Weber and K.J. Laidler, *J. Chem. Phys.*, 19, 1089 (1951).
4) H. Uchida and M. Kuraishi, This Bulletin, 28, 106 (1955).
5) H. Uchida and N. Todo, ibid., 29, 20 (1956).
6) J.R. Gutmann, *J. Phys. Chem.*, 57, 309 (1953).
7) J. Aman, L. Farkas et al., *J. Am. Chem. Soc.*, 70, 729 (1948).

ammonia by means of a liquid oxygen trap and then admitted into the gauge for the determination of the deuterium content. The gauge was kept at 0°C in a vigorously stirred mixture of ice and water, and the deuterium content could be determined to ±0.2% at a pressure of 20±0.05 mmHg adjusted by means of a leveling mercury reservoir and a cathetometer.

The deuterium was obtained by electrolysis from the heavy water supplied by Norsk Hydro-elektrisk Comp., by use of NaOD as electrolyte, and was purified by passing through a column of palladium asbestos and a liquid oxygen trap. A mixture of deuterium and hydrogen in a ratio of 1: 1 was used in the reaction. A mixing apparatus fitted with a manometer and a gas circulating pump was used to prepare the homogeneous mixture of deuterium and hydrogen, and mixture was then transferred into a reservoir (I) in Fig. 1, while ammonia was introduced into another one (J) after purification by drying over solid caustic potash and by fractional distillation in vacuo. From the reservoirs both the deuterium and the ammonia were introduced into the catalyst container to the desired composition by reading the pressures on a manometer (K).

The catalyst was degassed at 500°C till a high vacuum of 1×10^{-5} mmHg could be attained, and was then cooled down to the reaction temperature. After the admissions of the deuterium (50% D_2) and the ammonia, the circulating pump was started and the exchange reaction was followed by checking the deuterium content by analysis at definite time intervals.

Fractions of Surface Covered by Potash and of Iron Surface.—The fractions were determined according to the procedure by P. H. Emmett[8]. Nitrogen adsorption data were plotted according to the BET theory for obtaining the surface area, and the amount of carbon dioxide chemisorbed at −78°C was available for the determination of the fraction of the surface covered by potash, while the amount of carbon monoxide chemisorbed at −183°C was available for the determination of the fraction of the iron surface. In the latter case the amount at the pressure of 200 mmHg was employed for the determination, as the adsorbed amount remained constant independently of the increasing equilibrium pressure higher than this pressure*1.

Results

Catalytic Activity for Ammonia Synthesis.—The results are shown in Fig. 2. The triply promoted catalyst revealed a higher activity than any other and was followed by the doubly promoted one. Their activities are of the same order as those at a high pressure of 100 kg./cm² (refer to our previous papers[4,5]).

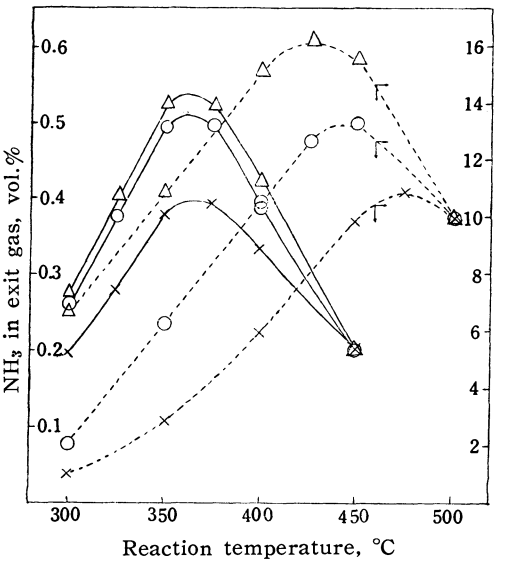

Fig. 2. Full line, results at a normal pressure at a S. V. of 2000: dotted line, results at 100 kg./cm² at a S. V. of 5000. ×, singly promoted catalyst, ○, doubly promoted catalyst, △, triply promoted catalyst.

Rate of Exchange Reaction.—The investigation was particularly concerned with establishing the relationship of the initial rate to the initial pressure of deuterium as well

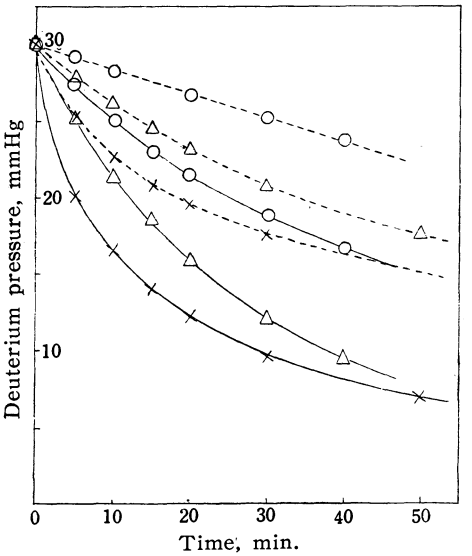

Fig. 3. Decrease in deuterium pressure with time.
Initial pressure of deuterium, 30 mmHg, initial pressure of ammonia, 120 mmHg.
Full line, results at 150°C: dotted line, results at 130°C.
×, singly promoted catalyst: ○, doubly promoted catalyst: △, triply promoted catalyst.

8) P.H. Emmett, "Structure and Properties of Solid Surfaces" (edited by R. Gomer and C.S. Smith) (1952), p. 428.

*1 The isotherm with the singly promoted catalyst, however, rose slightly with further increasing pressure.

as of ammonia. In this respect the measurement of the rate was carried out at a constant pressure of ammonia with varying pressures of deuterium and then at a constant pressure of deuterium with varying pressures of ammonia. The rates were measured at three different temperatures, 115°, 130°, and 150°C, on the three catalysts*2.

In each kinetic run the deuterium pressure vs. time curve was determined. The results for a particular series are plotted in Fig. 3. From the figure the initial rate was obtained graphically by drawing the initial tangent. Fig. 4 presents the initial rate as a function

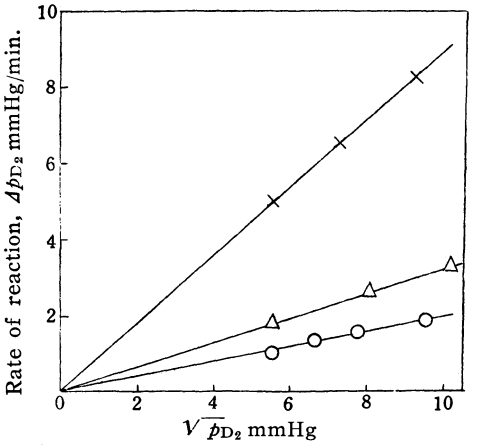

Fig. 4. Relation of reaction rate to square root of deuterium pressure.
Reaction temperature, 150°C, initial pressure of ammonia, 120 mmHg.
×, singly promoted catalyst: ○, doubly promoted catalyst: △, triply promoted catalyst.

of the square root of the initial deuterium pressure, at a constant ammonia pressure of 120 mmHg at 150°C. There is found a straight proportionality established between them, and the proportionality is also true with other series of runs at different temperatures.

The proportionality was found by A. Farkas[9] on an evaporated iron film, by J. Weber et al.[3] on a singly promoted iron catalyst, and also by J. Horiuti et al.[10] in the exchange reaction between nitrogen deuteride and hydrogen on nickel. On the other hand, J. R. Gutmann[6] and J. H. Singleton et al.[11] described the rate of first order with regard to deuterium pressure from their results obtained with the powders of iron and nickel and with an evaporated iron film respectively.

The rate was then determined at a constant pressure of deuterium (60 mmHg of 50% D_2), at 150°, 130°, and 115°C, with varying initial pressures of ammonia. The maximum and minimum ammonia pressures were 300 mm. and 30 mmHg respectively. The factors limiting the range of ammonia pressure were the vapour pressure of ammonia at −45°C, which was the temperature of U tubes (B, B′ in Fig. 1), and the accuracy of deuterium analysis in experiments where a high ratio of deuterium to ammonia resulted in too small a change of deuterium content for accurate determination.

The results are shown in Fig. 5 presenting

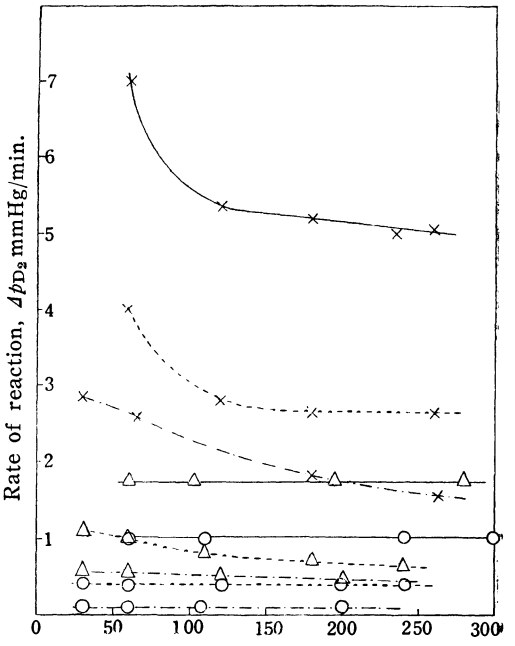

Fig. 5. Dependence of initial rate upon initial ammonia pressure.
Full line, results at 150°C: dotted line, results at 130°C: dotted and dashed line, results at 115°C.
×, singly promoted catalyst: ○, doubly promoted catalyst: △, triply promoted catalyst.

the initial rate as a function of the initial ammonia pressure*3. The initial rates on the doubly promoted catalyst, at the three different temperatures, persisted unchanged independently of the varying initial pressures,

*2 Immediately after the reduction, the catalyst slightly decomposed the ammonia in the exchange reaction at 150°C. From run to run the decomposition tended to diminish in extent and simultaneously the rate became lower. After three or four runs there could hardly be recognized any decomposition of ammonia and the runs became reproducible in respect of the rate.

9) A. Farkas, *Trans. Faraday Soc.*, **32**, 416 (1936).
10) J. Horiuti and N. Suzuki, *Shokubai*, **4**, 1 (1948).
11) J.H. Singleton, E.R. Roberts and E.R.S. Winter, *Trans. Faraday Soc.*, **47**, 1318 (1951).

*3 In the reaction with a low ammonia pressure of 30 mmHg, the rate at 115°C was too rapid to permit accurate measurement.

whereas the initial rate on the singly promoted one tended to decrease, at first, rapidly with the increasing initial ammonia pressure until it gradually approached a nearly constant value. At the high temperature of 150°C, the triply promoted catalyst was similar to the doubly promoted one in holding the initial rate constant; however, at the low temperatures of 130° and 115°C, it resembled the singly promoted one in revealing the decreasing rate with the increasing pressure of ammonia.

Our results observed with the doubly promoted catalyst are consistent with the rates observed by A. Farkas[9] on the evaporated iron film and by J. R. Gutmann[6] on the iron powder. Further, the kinetic results obtained by J. Weber et al.[3] with their singly promoted catalyst revealed a maximum of the rate at a certain ammonia pressure, from which the present results obtained with our singly promoted catalyst differed in giving the rate decreasing monotonously with the increasing initial ammonia pressure. The tendency found on the triply promoted catalyst coincides with the results obtained by J. H. Singleton et al.[11] on their evaporated iron film.

So far as the rate per 1 g. of catalyst is concerned, the rate is highest with the singly promoted catalyst, whereas it is lowest with the doubly promoted one.

Fractions of Surface Covered by Potash and of Iron Surface.—The results are listed in Table I. The catalysts have the surface

TABLE I

SURFACE AREA AND FRACTIONS OF SURFACE COVERED BY POTASH AND OF IRON SURFACE

Catalyst	Surface Area $m^2/g.$ Oxide	Fraction of Surface Covered by Potash	Fraction of Iron Surface
Singly Promoted Catalyst	16.4	0.01	0.51
Doubly Promoted Catalyst	14.2	0.46	0.24
Triply Promoted Catalyst	18.4	0.28	0.44

area descending in the order of the triply promoted, singly promoted, and doubly promoted catalysts, while the fraction of the surface covered by potash decreases in the order of the doubly promoted, triply promoted, and singly promoted catalysts. The larger the fraction of the surface covered by potash, the smaller is that of iron.

Discussion

Rate of Exchange Reaction.—J. R. Gutmann[6] and J. H. Singleton et al.[11] represented their experimental rates by equation (1), while J. Horiuti et al.[10] expressed the rate by equation (2), both equations being based on the consideration of the rates of zeroth order with respect to the ammonia pressure. On the other hand J. Weber et al.[3] interpreted their results obtained with their singly promoted catalyst by equation (3), assuming the reaction to take place between an adsorbed deuterium atom and an adsorbed ammonia molecule. In the last equation the rate attains to a maximum value at a certain pressure of ammonia.

$$r = kp_{D_2} \tag{1}$$

$$r = kp_{D_2}^{1/2} \tag{2}$$

$$r = kp_{NH_3}p_{D_2}^{1/2}/(1+ap_{NH_3}+bp_{D_2}^{1/2})^2 \tag{3}$$

In our present investigation the initial rate was found to be proportional to the square root of the initial deuterium pressure but to depend differently upon the initial ammonia pressure according to the kind of the catalyst. The experimental rate may then be expressed by the following equation (4)

$$r = kp_{D_2}^{1/2}/(1+ap_{NH_3}+bp_{D_2}^{1/2}) \tag{4}$$

The last term in the denominator may be ignored, since the relation observed between the initial rate and the square root of the initial deuterium pressure was linear. In the equation, a is an equilibrium adsorption constant of ammonia given by Langmuir's adsorption isotherm, and therefore takes different values according to the kind of the catalyst as well as the reaction temperature.

The equation suggests the rate to be based on the jump of dissociated deuterium atom from one site to another as the rate determining step, and to be retarded by the adsorption of ammonia on the surface more readily if the catalyst has the higher value of a.

Values of a may be predicted from the extent to which potash covers the surface, since the potash existing in the surface prevents the adsorption of ammonia. A larger value of a may thus reasonably be expected for the singly promoted catalyst whose surface is free from potash, whereas the extremely small one for the doubly promoted catalyst having the surface covered by potash to such an extent as a half of the total surface (refer to Table I), and this has appeared consistent qualitatively with the experimental rates for the singly promoted and doubly promoted catalysts. From the medium extent of the covering by potash found with the

triply promoted catalyst, a value of a smaller than that for the singly promoted catalyst but larger than that for the doubly promoted one is expected for the catalyst. This can explain both the rate remaining constant independently of the increasing initial ammonia pressure at high temperatures where the value is comparatively small and the rate decreasing with the increasing initial pressure of ammonia at low temperatures where the value becomes larger.

The apparent activation energies of the exchange reaction were obtained from Arrhenius plots of the rate constant k in equation (4), and are listed in Table II. The

TABLE II

APPARENT ACTIVATION ENERGY OF EXCHANGE REACTION

Catalyst	Apparent Activation Energy (kcal./mol.) at Initial Ammonia Pressure of		
	60	120	200 mmHg
Singly Promoted Catalyst	13.8	13.2	12.8
Doubly Promoted Catalyst	15.3	15.1	15.2
Triply Promoted Catalyst	14.2	14.1	14.1

energy for the singly promoted catalyst is smaller than any other, and this probably contributes to the higher activity in the exchange reaction. Whereas the energies for the doubly promoted catalyst and the triply promoted one persist unchange independently of the varying pressures of ammonia, the energy for the singly promoted one tends to decrease with the increasing initial pressure of ammonia. The decrease was once found by J. Weber et al.[3] on their singly promoted catalyst and also by J. H. Singleton et al.[11] on the evaporated iron film. No certain explanation of the tendency can be available as yet.

Relation of Activity for Exchange Reaction to Activity for Ammonia Synthesis.— Considering that the exchange reaction as well as the synthesis takes place on the iron surface of the catalyst, both rates measured per an equal quantity of the catalyst are divided, for the sake of comparison, by the surface area multiplied by the fraction of the iron surface ($s\times\alpha$ in Table III). The results are shown in Table III*4.

TABLE III

RATES OF EXCHANGE REACTION AND AMMONIA SYNTHESIS BASED ON A DEFINITE SURFACE AREA OF IRON

Catalyst	Initial Rate of Exchange Reaction ($r/s\times\alpha$)*, Δp_{D_2}/min.			Initial Rate of Ammonia Synthesis ($r'/s\times\alpha$)*, Δp_{NH_3}/min., 350°C
	150°	130°	115°C	
Singly Promoted Catalyst	0.616	0.257	0.022	$0.61\cdot10^2$
Doubly Promoted Catalyst	0.293	0.073	0.027	$2.36\cdot10^2$
Triply Promoted Catalyst	0.216	0.070	0.027	$1.15\cdot10^2$

* In $r/s\times\alpha$, r is the rate of the exchange reaction, s is the surface area of the catalyst, and α is the fraction of iron surface. The initial rate of ammonia synthesis (r') at 350°C was calculated with the aid of Temkin's equation at the low pressure.

The rates thus obtained of the exchange reaction at 150° and 130°C for the singly promoted catalyst are remarkably higher than the rates for the others, of which the rate for the doubly promoted catalyst is slightly higher than that for the triply promoted one*5. The comparison of the rate in the exchange reaction with the one in the ammonia synthesis, both being based on a definite extent of iron surface (refer to Table II), reveals no parallel relation existing between them: the singly promoted catalyst of the highest rate in the exchange reaction gives the lowest rate in the ammonia synthesis, while the doubly promoted catalyst with the highest rate in the latter gives the markedly low rate in the former.

As described by H. S. Taylor[1], the rate involved in the equation (4) can not be expected to determine the rate of ammonia synthesis, since the exchange reaction will proceed with great rapidity at the high temperatures obtaining in the ammonia synthesis. Usually the rate in the ammonia synthesis is considered to be determined by the rate of activated adsorption of nitrogen. This, in connection with the results in the preceding paragraph, reveals the fact that the catalyst surface rapidly adsorbing deute-

*4 As for the singly promoted catalyst, the rate at the ammonia pressure of 200 mmHg was employed for the calculation. No remarkable decrease of the rate was observed beyond this ammonia pressure.

*5 There has hardly ever been found any distinct difference between the activities for the exchange reaction at 115°C.

rium at the low temperatures slowly adsorbes nitrogen at the high temperatures. It, however, follows by no means that the surface is homogeneous, but it leads us to expect the surface as described by R. P. Eischens[12], which is rather heterogeneous, being divided into a few homogeneous portions. Either one of the portions will be predominant according to the promoter-composition.

Summary

The tendencies observed of the experimental rate (r) in the exchange reaction are represented by the following equation

$$r=kp_{D_2}^{1/2}/(1+ap_{NH_3}).$$

In the equation a is the equilibrium adsorption constant in Langmuir's isotherm. The value of a varies according to both the reaction temperature and the promoter-composition which causes different extents of the covering by potash on the surface after reduction.

The apparent activation energies in the exchange reaction are in a range of 15.3 to 12.8 kcal./mol. and the energy for the singly promoted catalyst is remakably smaller than the others. Whereas the energies for the doubly promoted and triply promoted catalysts persisted unchanged independently of the varying initial pressures of ammonia, the one for the singly promoted catalyst tended to decrease with the increasing initial pressure of ammonia.

The comparison of the rate in the exchange reaction with the one in ammonia synthesis, both being based on a definite extent of iron surface, reveals no parallel relation existing between them, namely the catalyst (the singly promoted catalyst) having the highest activity in the exchange reaction has a very low activity for the ammonia synthesis.

Government Chemical Industrial Research Institute, Tokyo

12) R. P. Eischens, *J. Am. Chem. Soc.*, **74**, 6167 (1952).

Magnetic Susceptibility of Erythrocruorin from the Blood of an Ark-Shell

By Masaji KUBO, Takehiro KOBAYASHI and Michihiko KISHITA

(Received May 23, 1956)

Since Pauling and Coryell[1] studied the magnetic properties of hemoglobin and oxyhemoglobin from bovine blood, it has become clear that a hemoglobin molecule undergoes a change in electronic structure on combination with oxygen molecules. The conversion of hemoglobin to oxyhemoglobin is accompanied by a change in the molecule from the paramagnetic to the diamagnetic condition and also the oxygen molecule, which in its free state is paramagnetic, is involved in the change of the magnetic condition. Following this, one of the present writers[2] carried out a similar investigation on another iron-containing respiratory pigment called hemerythrin. He found that the change from the paramagnetic to the diamagnetic condition on oxygenation is so profound that the effect of the combining of an oxygen molecule extends to all of the three iron atoms of a magnetic group in the molecule of hemerythrin. On the other hand, in hemoglobin, which combines with oxygen in the definite proportion of one molecule of oxygen per one atom of iron, the effect is naturally limited to a single iron atom.

The present investigation deals with erythrocruorin, another respiratory pigment containing ferroheme. It can be found in the blood and tissue fluids of invertebrates. Erythrocruorin (or hemoglobin) occurs even in the root nodules of certain legumes[3]. Although erythrocruorins bear resemblance to hemoglobins from vertebrates in many respects, these two types are by no means identical. As a class, the erythrocruorins have more acid isoelectric points than the hemoglobins. In some cases the protein is present in solution, but in others the pigment is found in cells. In the former, most of the erythrocruorins have very high molecular weights of the order of a million or more,

1) L. Pauling and C.D. Coryell, *Proc. Natl. Acad. Sci. U.S.*, **22**, 159 (1936); **22**, 210 (1936). C.D. Coryell, F. Stitt and L. Pauling, *J. Am. Chem. Soc.*, **59**, 633 (1937).

2) M. Kubo, This Bulletin, **26**, 244 (1953); *Monograph Series of Research Inst. Applied Electricity*, **5**, 37 (1955).

3) H. Kubo, *Acta Phytochim.* (Japan), **11**, 195 (1939).

and presumably contain a very large number of hemes. In view of these facts, it seemed worth while to make magnetic measurements on erythrocruorin and to compare the results with findings on hemoglobin. The probable reason why erythrocruorins have eluded magnetic investigation is that this respiratory pigment in any great amount is difficult to obtain, whereas measurement by a Gouy magnetic balance reguires a fairly large amount of sample solution. Fortunately an ark-shell known as *Anadara* (=*Arca*) *inflata* (Reeve) is commonly found at various places along the coast of Japan. Ample blood is obtainable from this shell-fish[4]. The present writers prepared a solution of erythrocruorin using the blood of this shell-fish and measured the magnetic susceptibility of the solution in both deoxygenated and oxygenated states. A control experiment was made on horse hemoglobin using the same apparatus and experimental technique.

Material

Anadara inflata (Reeve) used in the present experiment was procured in a fish market in Nagoya. Presumably the shell-fish were taken from a nearby bay. All precautions were taken in the preparation of erythrocruorin solution. The umbonal part of each shell was broken by a blow with the base of a glass bottle. Then the heart was carefully incised with the sharp point of a glass rod in order to let the blood flow into a beaker. These precautions were taken because the use of an iron hammer and a steel knife might possibly introduce ferromagnetic impurities into the sample. To remove the fragments of tissues, the blood was filtered through several layers of antiseptic gauze. When centrifuged, the dark red corpuscles settled as sediment on the bottom of the tube. To completely remove the plasma, the sediment was washed several times with 3 percent sodium chloride solution. After the solution was aerated for about one hour, it was left to stand in a refrigerator for 1–1.5 hours. Finally these blood cells were put into distilled water to subject them to hemolysis. Immediately before use, the stroma was removed by centrifuging. The clear solution which was pipetted out assumed a dark red color. Blood cells occupying approximately 25 cc. were obtained from about 4 kg. of this material.

Apparatus and Experimental Procedure

For the determination of magnetic susceptibility, a Gouy magnetic balance was used at room temperature (ca. 15°C) as described in a paper[5] by two of the present writers and their collaborators.

An erythrocruorin solution prepared in accordance with the foregoing procedure was in the state of practically complete oxygenation. For magnetic measurement, the solution was placed in a cell. In order to prepare a deoxygenated specimen, the air in a vessel which contained the solution (about 15 cc.*) was evacuated and nitrogen bubbled through alkaline pyrogallol solutions in advance was admitted into the vessel. The equilibration was repeated several times until deoxygenation was complete, as indicated by the red color of the solution becoming tinged with violet. Finally, the solution was transferred from the vessel into the cell which had been connected to the vessel by means of a rubber tube. The intrusion of air into the cell was prevented by keeping the pressure of nitrogen in the vessel higher than the atmospheric pressure.

It was of prime importance that in spite of repeated partial evacuation and equilibration with nitrogen, the concentration of the deoxygenated solution was the same as that of the oxygenated solution. Therefore use was made of nitrogen saturated with water. Moreover, the fact that no appreciable loss of water took place during manipulation was confirmed by carrying out measurements both on the original oxygenated solution and on the solution subjected to deoxygenation followed by oxygenation. The results of these two measurements were in good agreement with each other within the allowable limit of experimental errors.

Determination of Iron Content

The solution of erythrocruorin (4 cc.) was subjected to the wet-ashing procedure and the amount of iron brought into solution as an inorganic salt was determined colorimetrically by the use α,α'-dipyridyl. The method employed was essentially the same as those given by Eden and Green[6] and by Thorp[7]. A color comparison was made using a Coleman spectrophotometer with green light of wavelength 525 mμ. A blank test was carried out in exactly the same manner as above with an equal volume of water in place of the solution under investigation.

Hemoglobin Solution

Fresh horse blood was defibrinated and centrifuged. The sediment was washed six times with 0.85 percent solution of sodium chloride. The blood cells, after being aerated, were hemolysed with approximately a half volume of water. The hemoglobin solution was centrifuged before use. The experimental procedures for magnetic measurements and for iron content determination were the same as those employed for erythrocruorin solution.

Experimental Results and Discussion

The results are summarized in Table I.

The difference, $\kappa_{\text{deoxy.}}-\kappa_{\text{oxy.}}$, divided by the iron concentration and multiplied by the

* A single measurement required only about 3.5 cc. of solution.

4) T. Sato, *Z. vergleich. Physiol.*, **14**, 763 (1931).

5) M. Kondo, M. Kishita, M. Kimura and M. Kubo, This Bulletin, **29**, 305 (1956).

6) A. Eden and H.H. Green, *Biochem. J.*, **34**, 1202 (1940).

7) R.H. Thorp, *Biochem. J.*, **35**, 672 (1941).

atomic weight of iron yields the difference ($\chi_{deoxy.}-\chi_{oxy.}$) between the susceptibility of deoxygenated erythrocruorin (or hemoglobin) and that of oxygenated preparation per gram atom of iron, as given in Table I. The

TABLE I

MAGNETIC SUSCEPTIBILITIES, κ, PER UNIT VOLUME OF ERYTHROCRUORIN SOLUTION AND HEMOGLOBIN SOLUTION IN DEOXYGENATED AND OXYGENATED STATES

	Erythrocruorin	Hemoglobin
Deoxygenated	$-0.691_4\times10^{-6}$	$-0.599_1\times10^{-6}$
Oxygenated	$-0.724_0\times10^{-6}$	$-0.727_0\times10^{-6}$
Density	1.023 g./cc.	1.043 g./cc.
Iron Concentration	170.9 γ/cc.	558.1 γ/cc.
$\chi_{deoxy.}-\chi_{oxy.}$	0.01064cc./mole	0.01279cc./mole

difference between molecular susceptibilities is some simple multiple of $\Delta\chi$ depending upon how many atoms of iron are contained in a molecule. Let $\Delta\chi$ be used rather than the difference between molecular susceptibilities simply because this does not involve making an initial assumption on the molecular weight of erythrocruorin. The use of $\Delta\chi$ presupposes that the magnetic coupling between different hemes is inappreciable, or in other words that the different magnetic groups in a molecule are practically indepedent of each other as if they were located in separate molecules. This condition is satisfied to a fair degree of exactness for hemoglobin and presumably also for erythrocruorin.

The diamagnetic term is cancelled in the difference, $\Delta\chi$. Therefore assuming that all oxygen combining centers are alike, it holds that

$$\Delta\chi=\frac{N}{3kT}(\mu^2_{deoxy.}-\mu^2_{oxy.}).$$

Here N and k denote Avogadro number and Boltzmann constant respectively, T the absolute temperature, and μ the magnetic moment associated with a heme. There are good reasons[1] for believing that oxyhemoglobin contains no unpaired electrons, i.e., $\mu_{oxy.}=0$. This leads directly to $\mu=5.43$ Bohr magnetons per heme of deoxygenated horse hemoglobin, which value is in good agreement with 5.46 and 5.43 Bohr magnetons given respectively by Pauling and Coryell[1] for cow hemoglobin and by Taylor and Coryell[8] for horse hemoglobin. In the case of erythrocruorin, one has no *ad hoc* reason to assign any particular value to $\mu_{oxy.}$. The assumption that oxygenated erythrocruorin contains no unpaired electrons gives the minimum value of 4.96 Bohr magnetons or the magnetic moment of deoxygenated erythrocruorin. If some iron atoms were not affected by oxygenation, and/or if there were some unpaired electrons in the oxygenated erythrocruorin, the figure would be larger. Since it is known that molecules of all kinds of respiratory pigments heretofore investigated contain no unpaired electrons, let it be taken for granted that this assumption is adequate. This leads to the conclusion that

$$\mu_{deoxy.}=4.96 \text{ Bohr magnetons.}$$

This value corresponds closely to the presence of four unpaired electrons per heme and to the almost complete quenching of orbital moments because the resultant of the spin moments of four unpaired electrons has the theoretical value of 4.90 Bohr magnetons, neglecting contributions due to ordital moments. Although extracted from the blood of an invertebrate, the erythrocruorin under investigation must be regarded as being similar to hemoglobins from vertebrates at least with regard to its magnetic properties.

Recently Yagi[9] and his collaborators in the Chemical Department of Nagoya University succeeded in isolating this erythrocruorin in crystalline state. They found that the minimum molecular weight of this compound is equal to 19,000. The molecular weight is 73,000, as determined by Ui[9] in Tokyo University from the sedimentation equilibrium in an ultracentrifuge. Therefore one molecule contains four hemes, and the molecular weight is equal to 73,000~76,000. These facts also confirm the view that the erythrocruorin under investigation has something in common with vertebrate hemoglobins which have molecular weights close to 67,000.

Summary

The magnetic susceptibility of an aqueous solution of erythrocruorin from an ark-shell known as *Anadara inflata* (Reeve) was measured by a Gouy magnetic balance at 15°C in deoxygenated and in oxygenated state. On the plausible assumption that oxygenated erythrocruorin contains no unpaired electrons, the magnetic moment per one iron atom of this respiratory pigment in deoxygenated state was calculated to be equal to 4.96 Bohr magnetons. This corresponds closely to the presence of four unpaired electrons per heme and to almost complete quenching of orbital moments. For this reason, the erythrocruorin bears a remarkable

8) D.S. Taylor and C.D. Coryell, *J. Am. Chem. Soc.*, **60**, 1177 (1938).

9) Y. Yagi, T. Mishima, T. Tsujimura, K. Sato, F. Egami and N. Ui, *Compt. rend.; J. Biochem.* (Japan), to be published shortly.

resemblance to hemoglobins of vertebrates in so far as its magnetic properties are concerned.

We wish to express our appreciation to Prof. Sato and to Prof. Egami and his associates for their helpful advice in the preparation of materials. We thank the Ministry of Education for supporting this research.

Chemical Department
Faculty of Science
Nagoya University

Partial Methanolysis of the Mucilage of Chondrus Ocellatus Holmes[1]

By Choji ARAKI and Susumu HIRASE

(Received April 26, 1956)

The mucilage of *Chondrus ocellatus Holmes* closely resembles carrageenin, the mucilage of *Chondrus crispus*, in properties and chemical structure[2]. Both mucilages are the metallic salts of sulfate esters of polysaccharides containing D-galactose residues, which are connected through their positions 1 and 3[3]. The galactoside linkages were inferred to be of the α-type[3b,4]. Small amounts of L-galactose[5], D-glucose[6] and 2-keto-D-gluconic acid[7] were also reported to be present in one of the mucilages. Recently, O'Neil found the presence of an appreciable amount of 3,6-anhydro-D-galactose in the mucilage of *C. crispus*[8], using the mercaptolysis method which had been developed by the present authors in the investigation of agar[9]. The anhydro-sugar found is the enanthiomorph of that present in agar, and the result obtained by O'Neil was confirmed by Percival[10]. On the other hand, the present authors succeeded in the isolation of agarobiose dimethylacetal(4-*O*-β-D-galactopyranosyl-3,6-anhydro-L-galactose dimethylacetal) in a high yield by the partial methanolysis method from agar[11]. With this in mind, the method has been applied to the mucilage of *C. ocellatus*, and the results obtained are reported herein.

The mucilage has been prepared by extraction of *C. ocellatus Holmes* (*f. canaliculatus* Okam.) with hot water and precipitation of the extract with ethanol. The product showed a specific rotation $[\alpha]_D+54^\circ$ in water, and contained 24% sulfate. The partial methanolysis has been carried out in a manner similar to that used for agar[11]. After saponification the methanolysate was deionized with ion exchange resins. The acidic product, absorbed by the anion resin, was eluted from the resin and was isolated as a barium salt. The sole product obtained was barium monomethylsulfate arising from the sulfate residue present in the mucilage. The deionized methanolysate was separated by column chromatography, which led to the isolation of the following products in the yields indicated by weight percentages based on the deionized material: methyl D-galactoside(IV, 6%), 3,6-anhydro-D-galactose dimethylacetal (V, 5%), 4-*O*-β-D-galactopyranosyl-3,6-anhydro-D-galactose dimethylacetal (III, 68%) and methyl 4-*O*-β-D-galactopyranosyl-3,6-anhydro-β-D-galactoside (II, 5%).

4-*O*-β-D-Galactopyranosyl-3,6-anhydro-D-galactose dimethylacetal (III) could not be crystallized, but it was characterized as its crystalline hexa-acetate (VI) having the formula $C_{12}H_{14}O_9(COCH_3)_6(OCH_3)_2$. Saponification of the acetate regenerated the non-crystallizable dimethylacetal (III), which was then hydrolysed with a 0.02 N oxalic acid solution to give a reducing disaccharide (I). Its phenylosazone was prepared in a crystalline condi-

1) After this article had been submitted to be read at the 9th Annual Meeting (1956) of the Chemical Society of Japan, the authors saw O'Neil's report of the isolation of 4-O-β-D-galactopyranosyl-3,6-anhydro-D-galactose diethylmercaptal from the mercaptolysis product of carrageenin; A.N. O'Neil, *J. Am. Chem. Soc.*, 77, 6324 (1955).

2) T. Mori, *Advances in Carbohydrate Chemistry*, 8, 315 (1953).

3) a) T. Mori and T. Tsuchiya, *J. Agr. Chem. Soc. Japan*, 14, 585 (1941). b) R. Johnston and E.G.V. Percival, *J. Chem. Soc.*, 1950, 1994.

4) T. Mori and S. Fumoto, *J. Agr. Chem. Soc. Japan*, 23, 81 (1949).

5) C. Araki and K. Arai, Collected Papers for the Celebration of the 45th Anniversary of the Founding of Kyoto Technical College, 80 (1948).

6) A. Müther and B. Tollens, *Ber.*, 37, 298 (1904); P. Haas and B. Russell-Wells, *Biochem. J.*, 23, 425 (1929).

7) E.G. Yong and F.A.H. Rice, *J. Biol. Chem.*, 164, 35 (1946).

8) A.N. O'Neil, *J. Am. Chem. Soc.*, 77, 2837 (1955).

9) a) C. Araki and S. Hirase, This Bulletin, 26, 463 (1953). b) S. Hirase and C. Araki, ibid., 27, 105 (1954).

10) E.E. Percival, *Chem. & Ind.*, 1954, 1487.

11) C. Araki and S. Hirase, This Bulletin, 27, 109 (1954).

tion. The structure assignment to III has arisen for the following reasons. Methanolysis afforded methyl D-galactoside (IV) and 3,6-anhydro-D-galactose dimethylacetal (V), indicating that III is composed of D-galactose and 3,6-anhydro-D-galactose residues. On the other hand, the hexa-acetate (VI) was treated with dimethylsulfate and potassium hydroxide, and was further methylated with Purdie's reagents. When the resulting methylated dimethylacetal (VII) was subjected to methanolysis, there was obtained a mixture of methyl 2,3,4,6-tetra-*O*-methyl-D-galactoside (VIII) and 2,5-di-*O*-methyl-3,6-anhydro-D-galactose dimethylacetal (IX). The controlled hydrolysis converted only the latter product into the corresponding reducing sugar, from which the former product was separated by extraction with petroleum ether. Methyl 2,3,4,6-tetra-*O*-methyl-D-galactoside obtained was hydrolysed to give the corresponding reducing sugar, which was identified as its well known anilide. 2,5-Di-*O*-methyl-3,6-anhydro-D-galactose was oxidized with bromine water to give crystalline 2,5-di-*O*-methyl-3,6-anhydro-D-galactonic acid, the identity of which was established by comparison with its enanthiomorph previously obtained from methylated agarobiose derivatives[9b,12]. The amide was also prepared in a crystalline

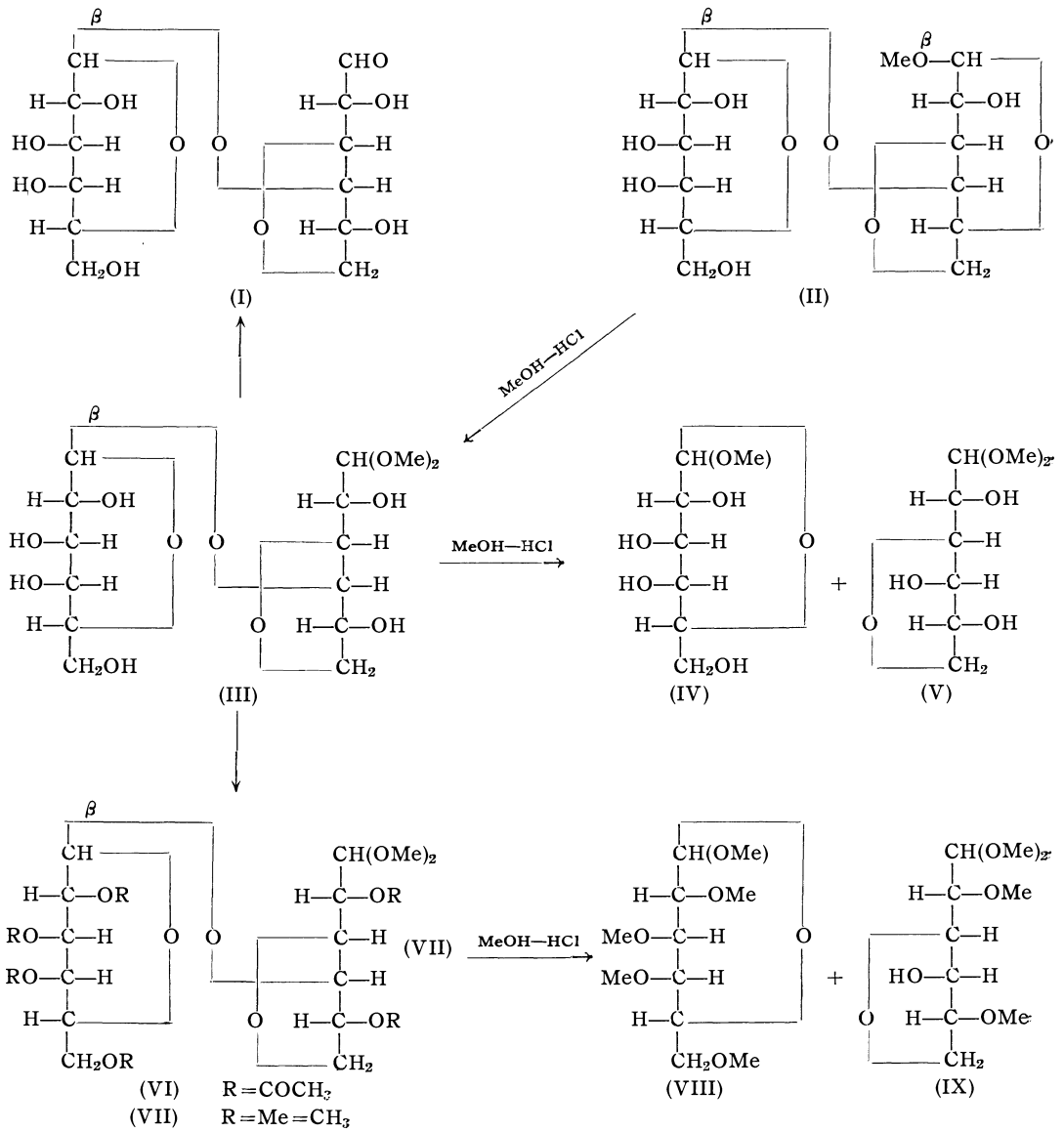

12) C. Araki, *J. Chem. Soc., Japan*, **65** 533, 627 (1944).

condition. This result has indicated that the D-galactose residue is glycosidically joined with the position 4 of the 3,6-anhydro-D-galactose residue. Moreover, from the low positive value of the specific rotation of III, it has been suggested that the galactoside linkage has the β-configuration, in disagreement with the inference so far drawn[3b,4].

Methyl 4-*O*-β-D-galactopyranosyl-3,6-anhydro-β-D-galactoside (II) was isolated as crystalline monohydrate, having the formula $C_{12}H_{19}O_9(OCH_3)$. On treatment with 0.5% methanolic hydrogen chloride for a short period, it afforded the foregoing dimethylacetal (III), in agreement with the structure (II) assigned. In addition, on the basis that the methyl glycoside (II) has a highly negative value of the specific rotation ($[\alpha]_D-78.6°$ in water), the β-configuration has been assigned to the methoxyl group.

From the high yield, in which the disaccharide (I) has been isolated as its dimethylacetal (III) and methyl glycoside (II), and also from the fact that D-galactose residues are connected by 1,3-linkages[3], it necessarily follows that the most part of the carbohydrate of the *Chondrus* mucilage employed is composed of such repeating units as are illustrated in the formula (X), the α-configuration being assigned to the 3,6-anhydro-D-galactoside linkages because of the positive value of the specific rotation of the mucilage.

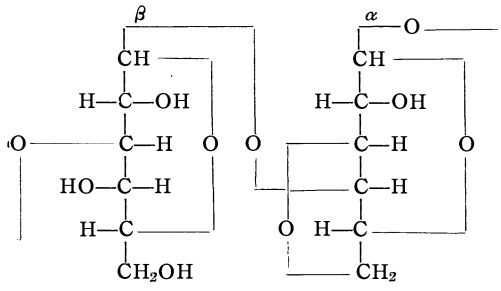

(X) Repeating Unit of the Carbohydrate of the *Chondrus* Mucilage.

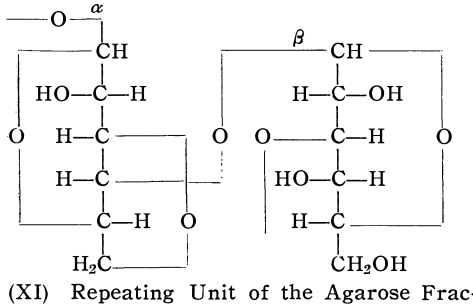

(XI) Repeating Unit of the Agarose Fraction of Agar[13]

The repeating unit (X) suggested above forms a novel contrast with that (XI) of the agarose fraction of agar[13], because they are of "half-antipode" with each other. Since the parent disaccharide of XI was isolated from agar and termed agarobiose[12], it is now suggested that the parent disaccharide (I) of X is conveniently named carrabiose. Accordingly, the dimethylacetal (III) and methyl glycoside (II) isolated in this work are respectively called carrabiose dimethylacetal and methyl β-carrabioside.

Last, it should be emphasized that further investigation is needed to establish the end group and the molecular shape as well as the disposition of sulfate groups of the mucilage.

Experimental

General Procedure.—Evaporation and concentration were carried out under reduced pressure below 40°. The Melting points are uncorrected. Specific rotations were measured in aqueous solutions unless otherwise stated. The paper chromatograms were irrigated with *n*-butanol-ethanol-water (4 : 1 : 2 by volume) in the ascending manner, and were sprayed with *o*-aminophenol reagent[14] unless otherwise stated.

Material.—The mucilage was extracted from sun-dried *C. ocellatus Holmes* (*f. canaliculatus* Okam.) (30 g.) with hot water (3 *l.*). After filtration through a Celite-bed, the extract was concentrated and precipitated by 95% ethanol. The product was obtained as fibres, which were then ground to powder; yield 15.8 g.; $[\alpha]_D^{15}+53.7°$ (*c*, 0.54); SO_4, 24.14; Ash, 17.34; SO_4 in ash, 7.25%, of the mucilage on the moisture-free basis, respectively.

Partial Methanolysis.—The mucilage (20.0 g., moisture 11.32%) was suspended in 0.5% methanolic hydrogen chloride (200 cc.). After being left overnight at room temperature, the suspension was heated under reflux for two hours and filtered. The filtrate was neutralized with silver carbonate, refiltered, and concentrated to a sirup (A). The insoluble material (5.2 g.), which had escaped the first methanolysis, was again subjected to methanolysis in a similar manner. An insoluble material (2.5 g.) and a sirup (B) were obtained, respectively.

The sirups A and B were combined, dissolved in a 0.3 N barium hydroxide solution (300 cc.), and saponified at 60° for two hours. Excess barium hydroxide was removed by neutralization with carbon dioxide and filtration, and the filtrate was concentrated to a sirup; yield 17.0 g.; $[\alpha]_D^7+17.7°$ (*c* 1.13). It was dissolved in water (200 cc.) and passed through a column of Amberlite IR-120 (200 cc.) to remove cations and then through a column of Amberlite IR-4B (250 cc.), where anions were absorbed. The resins were thoroughly washed with water, and the neutral effluent and

13) C. Araki, This Bulletin, **29**, 543 (1956).
14) S. Hirase, C. Araki and S. Nakanishi, This Bulletin, **26**, 183 (1953).

washings were combined and concentrated to a sirup; yield 9.0 g., $[\alpha]_D^9$+29.3°. Paper chromatographic examination revealed two distinct spots having respective R_f values 0.67 and 0.34.

Meanwhile, anions, which were retained by the IR-4B resin, were displaced from the resin by stirring it for fifteen minutes with excess 2 N sulfuric acid under ice-cooling. After filtration the resin was washed with water (1 *l.*). The combined filtrate and washings were immediately neutralized with saturated barium hydroxide solution and filtered. Evaporation gave crystals of barium monomethylsulfate dihydrates; yield 7.8 g. No evidence was obtained to suggest the presence of uronic acid derivatives and other organic acids.

Chromatography of the Deionized Methanolysate.—The deionized methanolysate (9.0 g.), dissolved in water (200 cc.), was placed on a column (5.0×26 cm.) of active carbon Shirasagi[15]-Celite (4:3 by weight), and developed successively with water, 5%, 10%, 15% and 30% ethanol at room temperature (10–12°), according to Whistler and Durso[16]. The effluent was grouped into six fractions containing polarimetrically and chromatographically identical materials. Table I shows the yields and properties of the fractions obtained.

Fraction I was rechromatographed on a column (2.5×30 cm.) of powdered filter paper, *n*-butanol-water (6:1 by volume) being used as a mobile phase until the components showing R_f values 0.67 and 0.34 were successively removed from the column. The column was then washed with 80% methanol (300 cc.). The eluates were separately evaporated to dryness, and three fractions Ia, Ib and Ic were obtained (Table II).

TABLE I

CHARCOAL CHROMATOGRAPHY OF THE DEIONIZED METHANOLYSATE OF THE CHONDRUS MUCILAGE

Fraction	Eluted by	Yield, g.	$[\alpha]_D$	R_f value
I	W (6 *l.*)	1.3	+64.9	0.34, 0.67
II	5%-E (0.7 *l.*)	0.7	+19.3	0.34, 0.67
III	5%-E (12 *l.*)	5.1	+18.1	0.34
IV	10%-E (6 *l.*)	0.6	−36.2	0.34
V	15%-E (5 *l.*)	0.4	+55.0	0.26
VI	30%-E (5 *l.*)	0.7	+60.0	0.18

W: water; E: ethanol.

TABLE II

RECHROMATOGRAPHY OF FRACTIONS I AND II

Fraction	Yield g.	$[\alpha]_D$	OCH_3%	R_f value
Ia	0.37	+26.0	28.2	0.67
Ib	0.36	+22.0	16.9	0.34
Ic	0.54	+105.0	15.8	0.31*
IIa	0.09	+27.0	28.6	0.67
IIb	0.61	+21.0	16.9	0.34

* The spot was located by a lead tetraacetate reagent[17].

15) Product of Takeda Pharmaceutical Industries, Ltd., Osaka.

16) R.L. Whistler and D.F. Durso, *J. Am. Chem. Soc.*, 72, 677 (1950).

17) J.G. Buchanan, C.A. Dekker and A.G. Long, *J. Chem. Soc.*, 1950, 3162.

Fraction II was also rechromatographed in the same way as above, giving two fractions IIa and IIb. In this case, the 80% methanolic eluate left no material on evaporation.

Fractions III and IV were chromatographically pure, and respectively treated in the manner described later. Fractions V and VI are not treated in this communication.

3, 6-Anhydro-D-galactose Dimethylacetal.—Data listed in Table II indicate that fractions Ia and IIa, obtained as colorless sirups, are 3, 6-anhydro-D-galactose dimethylacetal. It was hydrolysed with 0.02 N sulfuric acid in a boiling water bath for two hours, producing 3, 6-anhydro-D-galactose, $[\alpha]_D^0$+21.3° (*c*, 0.75), which was then converted into the diphenylhydrazone in the usual manner[18]; m.p. 153–155°; $[\alpha]_D^{14}$ + 34.5° (initial) ⟶ + 23.6° (after twenty-four hours, methanol, *c*, 0.55). Accepted values[18] for 3, 6-anhydro-D-galactose diphenylhydrazone are m.p. 154° and $[\alpha]_D$+23.9° (after twenty-four hours, methanol).

Anal. Found: C, 65.68; H, 6.25; N, 8.11. Calcd. for $C_{18}H_{20}O_4N_2$: C, 65.82; H, 6.14; N, 8.34%.

Methyl D-Galactoside.—Fraction Ic, a sirup, was a mixture of α- and β-forms of methyl D-galactoside, from which the α-form was crystallized as monohydrates from ethanol-ethyl acetate; yield 0.21 g., m.p. and mixed m.p. 109°; $[\alpha]_D^{10}$+175° (*c*, 1.00). The mother liquor was concentrated and subsequently hydrolysed with N sulfuric acid, affording D-galactose only; m.p. and mixed m.p. 165°; $[\alpha]_D^0$+80.4° (*c*, 0.51).

Methyl β-Carrabioside(II).—Fraction IV crystallized spontaneously. Recrystallization twice from ethanol-acetone afforded monohydrates of II; needles; m.p. 136-138°; $[\alpha]_D^9$−78.6° (*c*, 0.70).

Anal. Found: C, 43.56; H, 6.60; OCH_3, 8.76. Calcd. for $C_{12}H_{19}O_9(OCH_3)\cdot H_2O$: C, 43.81; H, 6.79; OCH_3, 8.70%.

It migrated at the same rate as carrabiose-dimethylacetal on a paper chromatogram. Since the fraction IV produced a single spot on a paper chromatogram, it has been considered that the fraction is a mixture composed of the dimethylacetal (0.18 g.) and the methyl glycoside (0.42 g.), the proportion being calculated from the values of a specific rotation.

Conversion of Methyl β-Carrabioside into the Dimethylacetal(III).—Methyl β-carrabioside monohydrate (0.15 g.) in 0.5% methanolic hydrogen chloride (15 cc.) was heated under reflux. The specific rotation of the solution was rapidly changed from the initial value −76° to a constant value +30° after thirty minutes. The solution was neutralized with silver carbonate, filtered and evaporated to dryness. Carrabiose dimethylacetal was obtained as an amorphous powder; yield 0.15 g., $[\alpha]_D^2$+26.4° (*c*, 0.34); OCH_3, found: 17.02%, (calcd. for $C_{12}H_{20}O_9\cdot(OCH_3)_2$: 16.74%).

18) C. Araki and K. Arai, Collected Papers for the Celebration of the 45th Anniversary of the Founding of Kyoto Technical College, 84 (1948).

For identification, the dimethylacetal was converted into its hexa-acetate, m. p. 147–149°, $[\alpha]_D^{16}$ −16.0° (benzene, *c*, 1.00). Its m. p. was not depressed on admixture with the sample described below.

Hexa-*O*-acetyl-carrabiose Dimethylacetal(VI). —Fractions Ib, IIb and III, having the same properties, were combined and purified by dissolution in absolute ethanol and filtration. Evaporation afforded carrabiose dimethylacetal in an amorphous condition; yield 6.0 g.; $[\alpha]_D^{10}$+19.0° (*c*, 1.00); OCH_3, found: 16.58 (calcd. for $C_{12}H_{20}O_9(OCH_3)_2$: 16.74%).

It was then dissolved in pyridine (30 cc.) and acetylated with acetic anhydride (60 cc.) at room temperature for two days. The reaction mixture was poured into ice-water with stirring, and the crystals deposited were filtered, washed with water, and dried in vacuo; yield 9.0 g. Two recrystallizations from ethanol-water gave pure needles of VI; m. p. 147–149°; $[\alpha]_D^{16}$ −16.3° (benzene, *c*, 1.23); ±0° (chloroform, *c*, 1.22).

Anal. Found: C, 50.42; H, 6.19; CH_3CO, 41.41; OCH_3, 9.92%; M. W. (Rast), 620. Calcd. for $C_{12}H_{14}O_9(CH_3CO)_6(OCH_3)_2$: C, 50.16; H, 6.15; CH_3CO, 41.49; OCH_3, 9.96%; M.W., 622.

Saponification of Hexa-*O*-acetyl-carrabiose Dimethylacetal.—The hexa-acetate (VI) (5.0 g.) was suspended in absolute methanol (20 cc.), and a sodium methoxide solution (5 cc.), prepared by dissolving metallic sodium (0.2 g.) in absolute methanol (25 cc.), was added. The crystals of the acetate were soon dissolved. After being left overnight, the solution was carefully neutralized with dilute acetic acid, deionized with ion exchange resins, and evaporated to dryness. Carrabiose dimethylacetal (III) was obtained as a hygroscopic amorphous powder, which could not be crystallized; yield 3.0 g.; $[\alpha]_D^{11}$ +25.0° (*c*, 1.32), +28.0° (methanol, *c*, 1.42); OCH_3, found: 16.69% (calcd. for $C_{12}H_{20}O_9(OCH_3)_2$: 16.74%). It migrated on a paper chromatogram at the same rate as agarobiose dimethylacetal (Rf, 0.34).

Carrabiose(I).—The dimethylacetal (1.0 g.), obtained by saponification of the acetate, was hydrolysed with a 0.02 N oxalic acid solution (50 cc.) in a boiling water bath until the optical rotation of the solution reached a constant value: $[\alpha]_D$ +25.0° (initial); +11.0° (0.5 and 1.0 hour); +12.5° (1.5 hour); +14.0° (2.0 and 2.5 hours). The solution was neutralized with calcium carbonate, filtered, and concentrated to a sirup, which was purified by dissolution in absolute methanol and filtration. Evaporation gave carrabiose as an amorphous material; yield 0.8 g., $[\alpha]_D^{11}$ +15.6° (an equilibrium value, *c*, 1.28). It slowly reduced a Fehling's solution at room temperature, showed a strong Seliwanoff's reaction, and restored the color to a Schiff's reagent. The last observation suggests that the sugar seems to exist in an aldehyde form.

Phenylosazone.—The above disaccharide (0.5 g.) was dissolved in water (10 cc.) and phenylhydrazine (0.5 g.) and 50% aqueous acetic acid (1 cc.) were added. The mixture was heated in a boiling water bath for thirty minutes, at which time oily precipitates were removed by decantation. Additional phenylhydrazine (0.3 g.) was added to the supernatant, and the solution was again heated for one and a half hours. On cooling it deposited yellow precipitates, which were filtered, washed with cold ethanol, and recrystallized three times from aqueous ethanol. The osazone was obtained as yellow needles in a poor yield; m. p. 216°; $[\alpha]_D^{10}$ +46.0° (no mutarotation) in pyridine-ethanol (2:3) (*c*, 0.50).

Anal. Found: N, 11.24. Calcd. for $C_{24}H_{30}O_8N_4$: N, 11.15%.

Methanolysis of Carrabiose Dimethylacetal. Carrabiose dimethylacetal (1.0 g.), obtained by saponification of the acetate, was dissolved in 3% methanolic hydrogen chloride (30 cc.) and the solution was boiled until the optical rotation of the solution reached a constant value after fifteen hours ($[\alpha]_D$ +30° ⟶ +70°). It was neutralized with silver carbonate, filtered and concentrated. The residual sirup (0.9 g.) was chromatographed on a column of powdered filter paper in a manner similar to the separation of the fraction I of the charcoal chromatography. The following two products were obtained and identified in the same manner as already described: 3,6-anhydro-D-galactose dimethylacetal (0.45 g.), $[\alpha]_D^{10}$ +29.7° (*c*, 0.64) and methyl α,β-D-galactoside (0.45 g.), $[\alpha]_D^{10}$ +100° (*c*, 0.50).

Hexa-*O*-methyl-carrabiose Dimethylacetal (VII).—The hexa-acetate (VI) (2.1 g.) in acetone-water (3:1, 20 cc.) was treated with dimethylsulfate (50 cc.) and a 30% potassium hydroxide solution (90 cc.) at 30° over two days. The product (1.5 g., OCH_3 47.2%), which was isolated by extraction with chloroform and subsequent evaporation of the extract, was further methylated with methyl iodide (20 g.) and silver oxide (10 g.) twice in the usual manner. VII was obtained as a slightly colored sirup; yield 1.4 g.; $[\alpha]_D^{11}$ +25.0° (*c*, 0.80), +6.9° (chloroform, *c*, 0.87); OCH_3, found: 53.67% (calcd. for $C_{12}H_{14}O_3(OCH_3)_8$: 54.63%).

Methanolysis of Hexa-*O*-methyl-carrabiose Dimethylacetal. — Hexa-*O*-methylcarrabiose dimethylacetal (1.3 g.) in 3% methanolic hydrogen chloride (30 cc.) was boiled for fifteen hours, when the optical rotation of the solution became constant ($[\alpha]_D$+17.5° → +75.0°). The solution was neutralized with silver carbonate, filtered and concentrated to a sirup; yield 1.3 g.; $[\alpha]_D^{10}$ +73.7° (*c*, 0.95). This sirup proved to be a mixture of methyl 2,3,4,6-tetra-*O*-methyl-D-galactoside (VIII) and 2,5-di-*O*-methyl-3,6-anhydro-D-galactose dimethylacetal(IX). The separation was effected by the selective hydrolysis and subsequent solvent fractionation as described below.

Methyl 2, 3, 4, 6-Tetra-*O*-methyl-D-galactoside (VIII). — The above mixture (1.3 g.) in a 0.02 N oxalic acid solution (20 cc.) was heated in a boiling water bath for two hours. With this

treatment, only the anhydro-sugar derivative(IX) was hydrolysed to give the corresponding reducing sugar. Then the solution was neutralized with calcium carbonate, filtered and evaporated to dryness. Extraction with warm petroleum ether followed by evaporation afforded VIII as a mobile sirup; yield 0.60 g.; n_D^{25} 1.4481; $[\alpha]_D^{10}$ +111.8° (*c*,1.10); OCH_3, found: 60.17% (calcd. for $C_6H_7O(OCH_3)_5$: 62.05%). The petroleum ether-insoluble residue was kept aside.

2, 3, 4, 6-Tetra-*O*-methyl-D-galactose. — The methylated galactoside (0.50 g.), obtained above, was hydrolysed with N-sulfuric acid for four hours in the usual manner. 2, 3, 4, 6-Tetra-*O*-methyl-D-galactose was obtained as a colorless sirup; yield 0.40 g.; n_D^{25} 1.4613; $[\alpha]_D^{10}$ +108.2° (an equilibrium value, *c*, 0.98); OCH_3, found: 52.28% (calcd. for $C_6H_8O_2(OCH_3)_4$: 52.56%.).

For identification, it was converted into an anilide in the usual manner; m.p. and mixed m.p. 193°; $[\alpha]_D^{10}$ −85.4° (acetone, an initial value, *c*, 0.41).

2, 5-Di-*O*-methyl-3, 6-anhydro-D-galactose. —The petroleum ether-insoluble residue, separated from VIII, was shown to be 2, 5-di-*O*-methyl-3, 6-anhydro-D-galactose on solvent removal; a colorless sirup; yield 0.55 g.: n_D^{25} 1.4758; $[\alpha]_D^{10}$ + 28.8° (an equilibrium value, *c*, 0.59); OCH_3, found: 33.08% (calcd. for $C_6H_8O_3(OCH_3)_2$: 32.60%). It reduced a cold Fehling's solution, showed a strong Seliwanoff's reaction, and restored the color to a Schiff's reagent.

2, 5-Di-*O*-methyl-3, 6-anhydro-D-galactonic Acid.—2, 5-Di-*O*-methyl-3, 6-anhydro-D-galactose (0.45 g.) in water (15 cc.) was oxidized with bromine (0.5 cc.) in the usual manner, affording 2, 5-di-*O*-methyl-3, 6-anhydro-D-galactonic acid (0.35g.), which was twice recrystallized from ethyl acetate; m.p. 161°; $[\alpha]_D^{10}$ +62.5° (*c*, 0.64). Recorded values for its enantiomorph are m. p. 161° and $[\alpha]_D$ −54.3°[12], −58.6°[9b] and −65°[19].

Anal. Found: C, 46.23; H, 6.67; OCH_3, 29.91. Calcd. for $C_6H_8O_4(OCH_3)_2$: C, 46.61; H, 6.84; OCH_3, 30.07%.

Amide: The acid obtained above was converted into the amide through its methyl ester in the usual manner; m. p. 172° (from methanol-ether); $[\alpha]_D^{10}$ +72.0° (*c*, 1.00). Recorded values for its enanthiomorh are m. p. 172°[12,9b] and 173°[20], and $[\alpha]_D$ −64.8°[12], −67.0°[20] and −75.7°[22].

Anal. Found: N, 6.55; OCH_3, 30.12. Calcd. for $C_8H_{15}O_5N$: N, 6.82; OCH_3, 30.22%.

Summary

1. The mucilage of *Chondrus ocellatus Holmes* has been investigated by the partial methanolysis method.

2. A new disaccharide, the structure of which is shown to be 4-*O*-β-D-galactopyranosyl-3, 6-anhydro-D-galactose, has been isolated in the form of its dimethylacetal and methyl β-glycoside in a good yield.

3. The disaccharide has been named carrabiose.

4. It has been suggested that 1→3′ linked carrabiose represents the repeating unit for the most part of the carbohydrate of the Chondrus mucilage.

The authours wish to express their hearty thanks to Mr. T. Ito for his assistance in this study and to Mr. K. Arai for the microanalysis.

Institute of Chemistry
Faculty of Industrial Arts
Kyoto Technical University
Matsugasaki, Kyoto

19) E.G.V. Percival and T.G.H. Thompson, *J. Chem. Soc.*, **1942**, 750.

20) W.G.M. Jones and S. Peat, *J. Chem. Soc.*, **1942**, 225.

Mikroanalyse mit Hilfe von Ionenaustauschharzen. VII. Über den Nachweis spurweise vorhandenes Eisens(III) mit drei Arten der Phenolderivate, d. h., Tiron, Sulfosalicylsäure und Chromotropsaurem Natrium[1]

Von Masatoshi FUJIMOTO

(Eingegangen am 24. April, 1956)

Einleitung

In neutraler oder schwach saurer wässeriger Lösung liefern die meisten Phenole mit Eisen-(III)salzen insbesondere mit Eisen(III)chlorid intensive Färbungen, die je nach der Natur des Phenols oft in ihren Tönen ganz verschieden sind. Beispielsweise ist es wohl schon lange bekannt, dass das Phenol oder die Salicylsäure durch Einwirkung des Eisen-(III)chlorides sich bedeutend charakteristisch violett färbt. Diese Färbungen rühren von der Bildung der Chelatverbindungen zwischen den Phenolen und Eisen(III)salzen her und dienen häufig zum Nachweis der betreffenden Phenole.

Bei der vorliegenden Mitteilung wurden folgende drei Sulfonsäurederivate der Phenole, nämlich, Tiron (Brenzkatechin-3, 5-disulfonsaures Natrium), (I), Sulfosalicylsäure, (II), und Chromotropsaures Natrium (1, 8-Dioxynaphthalin-3, 6-disulfonsaures Natrium), (III), als Vertreter solcher für den Nachweis des Eisens(III) anwendbaren Phenole ausgewählt:

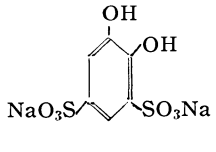

I.
farblos

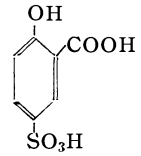

II.
farblos

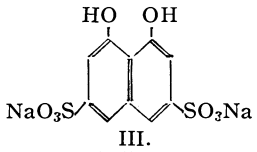

III.
hellgelb

Unter geeignetem pH-Wert von der Probelösung, geben die obenerwähnten Phenolderivate mit Eisen(III)salzen sehr stabile Chelatverbindungen, die nicht nur sich sehr intensiv färben, sondern auch sich stark an ihrer Sulfongruppe dissoziieren. Wenn man daher in die obige Lösung farblose Anionenaustauschharze eintaucht, so werden die obengenannten sich intensiv färbenden Chelatanionen stark in die Harzphase adsorbiert und infolgedessen färben sich diese Phase entschieden stärker als die Färbung der Lösungsphase:

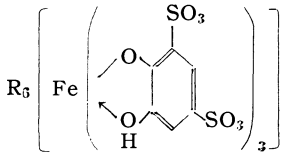

III.
violett

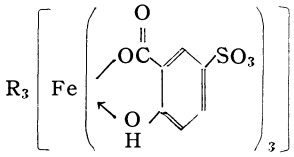

IV.
orange

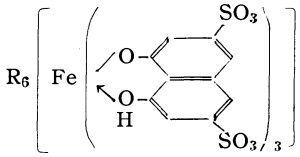

V.
grasgrün

Infolge der Zunahme des Anionenvolumens durch Chelatbildung, wird hierbei die Austauschselektivität für die Harze von den Chelatanionen im Vergleich mit der von den betreffenden Reagensanionen sichtlich grösser.

Man konnte daher durch einfache Anwendung starkbasischer Anionenaustauschharze eine ausserordentlich empfindliche sowie selektive Nachweismethode folgendermassen vollkommen feststellen, wobei durch ausführliche Gegenüberstellungen der genannten drei Arten der Reagenzien zahlreiche interessante Ergebnisse erhalten wurden.

Die in gegenwärtiger Untersuchung benutzten Anionenaustauschharze

Folgende vier Arten der Anionenaustauschharze wurden zum gegenwärtigen Zwecke verwandt:

Dowex 1-X1: Ein käufliches farbloses sowie starkbasisches Harz von quartärem Ammoniumtypus, das aus Styrol und Divinylbenzol dargestellt wird und dessen Divinylbenzolgehalt etwa einprozentig ist. Die Korngrösse ist ungefähr 50 Maschen von Tylerschem Normalsieb.

Dowex 1-X8: Ein ebenso starkbasisches und farbloses Harz wie Dowex 1-X1, dessen Divinylbenzolgehalt jedoch achtprozentig ist. Die Korngrösse ist 50 bis 100 Maschen.

1) Die sechste Mitteilung: M. Fujimoto, Dieses Bulletin, **29**, 600 (1956).

Amberlite XE-114: Ein hellgelbes mittelstarkbasisches Harz, dessen Korngrösse etwa 30 Maschen ist.

Amberlite IR-45: Ein hellgelbes schwachbasisches Harz, dessen Korngrösse ungefähr 50 Maschen ist.

Alle diese wurden vor dem Gebrauch durch zweimaliges Durchlaufen der 0.5 N Salzsäure und des destillierten Wassers in die RCl-Form völlig übergeführt.

Versuchsanordnung

Auf eine weisse Tüpfelplatte bringt man einige Körnchen des Anionenaustauschharzes sowie einen Tropfen der Reagenslösung, und rührt sie mit einem kleinen Glasstab völlig um. Nach einigen Minuten langem Stehen fügt man nacheinander einen Tropfen der Probelösung und, um den pH-Wert der Versuchslösung sowie der Harzphase am geeignetsten zu regulieren, einige Tropfen der Pufferlösung dazu. Mit Hilfe einer Lupe beobachtet man die in der Harzphase entstandene Färbung, die je nach dem ausgewählten Reagens charakteristisch ist.

Massflüssigkeit und Reagenzien

1. Massflüssigkeit.—Eine Reihe der Massflüssigkeiten von Eisen(III) wurde aus der 0.1 N-salzsauren Lösung des Eisen(III)chlorides, deren 1 ccm 10.00±0.03 mg von Eisen(III) enthielt,[2] durch Verdünnung mit extrareiner 0.1 N Salzsäure hergestellt.

2. Lösungen der Reagenzien.—Als Stammlösungen der extrareinen Reagenzien wurden die folgenden vorbereitet:

(1) Vierprozentige wässerige Lösung des Tirons.

(2) Vierprozentige wässerige Lösung der Sulfosalicylsäure.

(3) Einprozentige wässerige Lösung des Chromotropsauren Natriums.

3. Pufferlösungen[3].—Um die Wasserstoffionenaktivität von der Versuchslösung beliebig zu regulieren, wurden folgende drei Arten der Puffergemische angewandt:

(1) Eine Pufferlösung, deren pH-Wert genau 2.86 ist, wurde durch Versetzung der 0.2 M Natronlauge mit geringem Überschusse der 0.2 M wässerigen Lösung der Monochloressigsäure hergestellt.

(2) Eine Pufferlösung, deren pH-Wert genau 4.70 ist, wurde durch Versetzung der 1.0 M Essigsäure mit gleichem Teil der 1.0 M wässerigen Lösung des Ammoniumacetats hergestellt.

(3) Eine Pufferlösung, deren pH-Wert genau 9.9 ist, wurde durch Vermengung von 4 Teilen des 0.1 M Ammoniakwassers mit 1 Teil der 0.1 M wässerigen Lösung des Ammoniumchlorids hergestellt.

2) Die Menge des in der Massflüssigkeit vorhandenen Eisens(III) wurde gravimetrisch als Eisen(III)oxyd (Fe_2O_3) genau bestimmt.

3) Die pH-Werte der obengenannten Puffergemische wurden mit einer Glaselektrode gegen Kalomelelektrode durch Null-Methode potentiometrisch bestimmt.

Bestimmung der Bedingungen höchster Empfindlichkeit

Die Experimentalbedingungen höchster Empfindlichkeit wurden zuerst für Tiron besonders sorgfältig bestimmt, und danach wurden mit Hilfe von deren Resultaten die für Sulfosalicylsäure oder Chromotropsaures Natrium geeignetsten Bedingungen verhältnismässig einfach angeleitet. Die Resultate der so ausgeführten Untersuchungen werden wie unten gegeben:

(I) Tiron

Neuerdings haben Joe und Armstrong[4] vom Standpunkt der kolorimetrischen Bestimmung des Eisens(III) über die Chelatbildung zwischen Tiron und Eisen(III)salzen mitgeteilt, dass, wenn der pH-Wert von der Versuchslösung gegen 4.7 liegt, so färbt sich die Lösung deshalb am stärksten, weil beim genannten pH-Wert das betreffende Komplexgleichgewicht für die Bildung des Eisen(III)chelates am günstigsten liegt. Überdies handelt es sich darum, dass wegen grösseres Ionenvolumens die Diffusionsgeschwindigkeit genannter Chelatanionen entschieden niedriger werde. Daher hat der Verfasser erstens mit Dowex 1-X1 (RCl) und der Pufferlösung von pH 4.7 verschiedene Experimentalbedingungen miteinander näher verglichen. Die Resultate dafür stehen in Abb. 1[5] und Tabelle I:

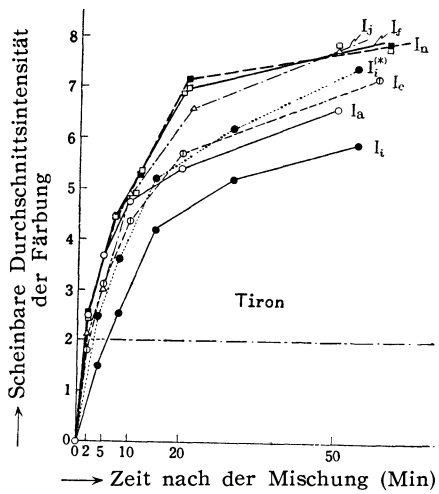

Abb. 1. Vergleichung unter verschiedenen Bedingungen, mit Dowex 1-X1 und einer Pufferlösung von pH 4.7, ausgeführter Versuche.

Betrachtet man aus der Ergebnisse dieser Gegenüberstellung, so wählt man das Verfahren „I_f" oder das „I_n" als das, unter gegebenem pH-Wert und mit Dowex 1-X1 (RCl), am besten geeignete Verfahren aus.

4) J.H. Joe und A.R. Armstrong, Economic Geology, 48, 282 (1953).

5) In bezug auf die in allen Abbildungen vorliegender Mitteilung angewandten halbquantitative Darstellungsweise der scheinbaren Durchschnittsintensität der Färbung von der Harzphase, vergleiche die dritte Mitteilung: M. Fujimoto, Dieses Bulletin, 29, 567 (1956).

TABELLE I

VERSCHIEDENE EXPERIMENTALBEDINGUNGEN VON ABB. 1

Nr. des Experiments	Zeichen der Kurve	Ordnung der Versetzung von Reagenzien und Probelösung 1.	2.	3.	4.	Bemerkungen über Verfahren und Resultate*
I_a	—○—	RCl**—Nadelspitzmenge***—(2 Tage****)—Probelsg.***** der 4proz. Lsg. des Tirons			Pufferlsg.******	*a*
I_c	--◐--	RCl—Nadelspitzmenge—(10 Min)—Probelsg. der 4proz. Lsg. des Tirons			Pufferlsg.	*a*
I_f	—□—	RCl 1 Tropfen der 0.1proz. Lsg. des Tirons	—(2 Min)—Probelsg.		Pufferlsg.	
I_i	—●—	RCl—Nadelspitzmenge—(4 Tage)—Probelsg. der 4proz. Lsg. des Tirons			Pufferlsg.	*b*
I_j	--△--	1 Tropfen der 0.1proz. Lsg. des Tirons	Probelsg.	Pufferlsg.—(3 Min)—RCl		
I_n	--■--	RCl 1 Tropen der 0.5proz. Lsg. des Tirons	—(2 Min)—Probelsg.		Pufferlsg	

**a*: Die Harzkörnchen wurden vorher im ganzen in die 4 prozentige Lösung des Tirons eingetaucht, um die Harze in die R-Tiron-Form überzuführen.

b: Die vorher in die R-Tiron-Form übergeführten Harzkörnchen wurden mit destilliertem Wasser völlig ausgewaschen.

** Bei vorliegender Tabelle bedeutet „RCl" Dowex 1-X1 von RCl-Form.

*** Hierbei wurden die in die Reagenslösung eingetauchten Harzkörnchen mit der Reagenslösung zusammen in eine Kapillarpipette aufgesogen. Diese wurde an ihrem oberen Ende mit dem Zeigefinger zugehalten und wurde dann an ihrer anderen Spitze auf die Vertiefung von der Tüpfelplatte leicht berührt. Durch solches Verfahren konnte man sehr leicht die Nadelspitzmenge der Reagenslösung mit den Harzkörnchen zusammen auf die Tüpfelplatte bringen. Die Nadelspitzmenge entspricht etwa 180 γ.

**** Zeitdauer nach dem Eintauchen der Harzkörnchen in die Reagenslösung.

***** Die hier benutzte Probelösung enthielt 0.2 γ von Eisen(III) (5 γ/ccm).

****** Der pH-Wert von der obengenannten Pufferlösung ist genau 4.70.

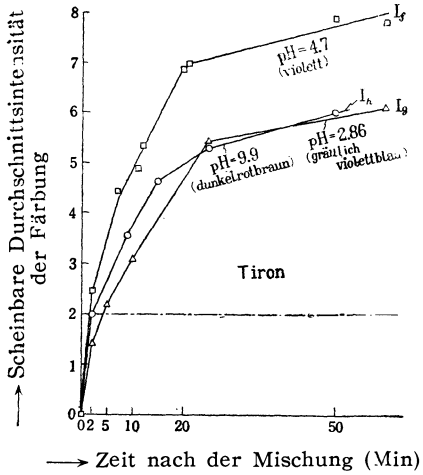

Abb. 2. Einfluss der Pufferlösung von verschiedenen pH-Werten auf die Resultate nach dem Verfahren „I_f" mit Dowex 1-X1 durchgeführter Versuche: Die in Klammer beschriebene ist die Färbung der Harzphase bei gegebenem pH-Werte.

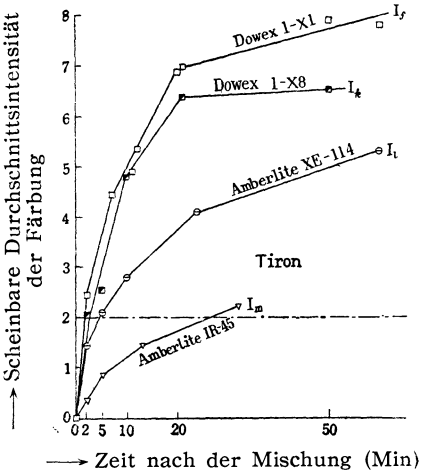

Abb. 3. Einfluss der Harzart auf die Resultate nach dem Verfahren „I_f", mit einer Pufferlösung von pH 4.7 ausgeführter Versuche.

Hierbei ist es besonders interessant, dass, wie man durch Vergleichung der Kurven „I_f" und der „I_j" leicht ersieht, die Differenz der Färb-

ungsintensität, die von der Ordnung der Versetzung des Harzes und Reagenslösung usw. hauptsächlich herrührt, nur geringfügig ist.

Zweitens hat der Verfasser versuchsweise die Einflüsse verschiedenartiger Faktoren, d.h., pH-Wert der Versuchslösung, Harzart, Konzentration der Reagenslösung, usw., gegenübergestellt. Die Ergebnisse dieser Versuche werden in Abbildungen 2, 3 und 4 zusammen dargestellt:

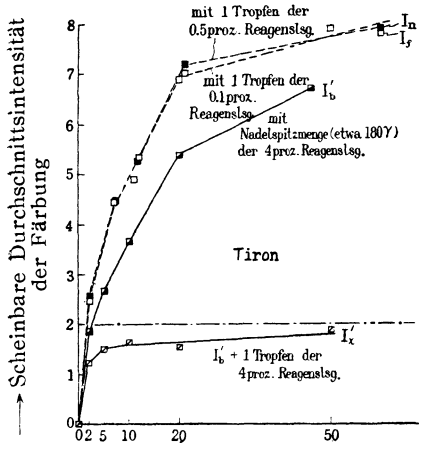

Abb. 4. Einfluss der Konzentration des Tirons auf die Färbungsintensität der Harzphase.

Abschliessend wird das Verfahren „I_f" (ebensowie das „I_n") als das für Tiron geeignetste Verfahren wie folgt vollkommen festgestellt:

„Man bringt auf eine weisse Tüpfelplatte einige Körnchen starkbasisches sowie niedrig vernetztes Anionenaustauschharzes von RCl-Form wie Dowex 1-X1 und einen Tropfen 0.1- bzw. 0.5 prozentiger wässeriger Lösung des Tirons, rührt sie mit einem kleinen Glasstab völlig um. Nach 2 oder 3 Minuten langem Stehen fügt man dazu nacheinander einen Tropfen der Probelösung und zwei oder drei Tropfen der Pufferlösung von pH 4.7, welche aus 1 Teil der 1.0 M Essigsäure und 1 Teil 1.0 M wässeriger Lösung des Ammoniumacetats hergestellt wird. Etwa 10 Min nach der Mischung beobachtet man mit einer Lupe eine violette Färbung, die am Rande oder über dem Ganze der Harzkörnchen entsteht".

(II) Sulfosalicylsäure

Zur Bestimmung der für vorliegendes Reagens am besten geeigneten Bedingungen wurden die im vorhergehenden Abschnitt gewonnenen Resultate mit Erfolg benutzt. Abb. 5 stellt die Gegenüberstellung der wesentlichen Experimentalbedingungen

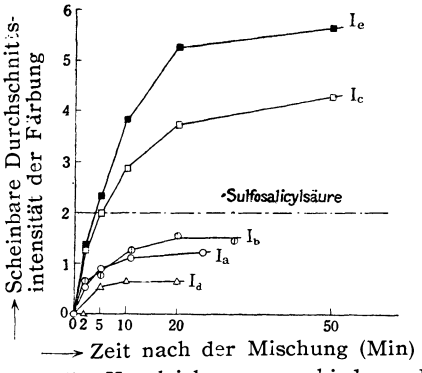

Abb. 5. Vergleichung verschiedener Experimentalbedingungen für Sulfosalicylsäure.

TABELLE II

VERSCHIEDENE EXPERIMENTALBEDINGUNGEN VON ABB. 5

Nr. des Experiments	Zeichen der Kurve	Ordnung der Versetzung von Reagenzien und Probelösung 1.	2.	3.	4.	Bemerkungen*
I_a	—○—	RCl**	1 Tropfen der 4proz. Lsg. der Sulfosalicylsäure	Probelsg.***	Pufferlsg. von pH 2.86	*a*
I_b	—◐—	RCl	1 Tropfen der 0.1proz. Lsg. der Sulfosalicylsäure	Probelsg.	Pufferlsg. von pH 2.86	*b*
I_c	—□—	RCl	1 Tropfen der 0.1proz. Lsg. der Sulfosalicylsäure	Probelsg.	Pufferlsg. von pH 4.70	*c*
I_d	—△—	RCl	1 Tropfen der 0.1proz. Lsg. der Sulfosalicylsäure	Probelsg.	Pufferlsg. von pH 9.9	*d*
I_e	—■—	RCl	1 Tropfen der 0.5proz. Lsg. der Sulfosalicylsäure	Probelsg.	Pufferlsg. von pH 4.70	*c*

*a: Die Oberfläche der Harzkörnchen trüben sich weiss.
b: Die Harzkörnchen färben sich sehr hell violettbraun.
c: Die Harzkörnchen färben sich hell bräunlich orange.
d: Die Harzkörnchen werden kaum gefärbt.
** RCl bedeutet hierbei Dowex 1-X1 von RCl-Form.
*** Die hier benutzte Probelösung enthielt 0.2 γ von Eisen(III) (5 γ/ccm)

dar, die man aus der für Tiron festgestellten Bedingungen leicht erwarten kann:

Von dieser Abbildung aus betrachtet, ist für Sulfosalicylsäure anzunehmen, den Nachweis mit Dowex 1-X1 (RCl), 0.5 prozentiger wässeriger Lösung des Reagens und der Pufferlösung von pH 4.7 auszuführen.

(III) Chromotropsaures Natrium

Da auch hierbei die für Tiron erhaltenen Ergebnisse zur Gegenüberstellung verschiedener Experimentalbedingungen anzuwenden ist, wurde das beste Verfahren, wie man in Abb. 6 wohl ersieht, verhältnismässig einfach festgestellt. Nämlich, die Anwendung von Dowex 1-X1 (RCl), 1prozentiger wässeriger Lösung des Reagens und dem Puffergemische von pH 4.7 ist wünschenswert.

Bestimmung der Erfassungsgrenze

Die Abbildungen 7, 8 und 9 zeigen den Färbungsverlauf der Harzphase, der unter den für die betreffenden Reagenzien am besten geeigneten Bedingungen für verschiedene Eisen(III)menge erhalten wurde:

Aus den obengenannten Kurven wurden die Erfassungsgrenze sowie die Grenzkonzentration für die betreffenden Reagenzien wie in der folgenden Tabelle festgestellt:

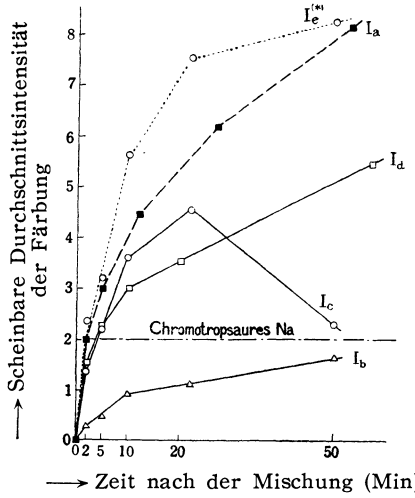

Abb. 6. Vergleichung verschiedener Experimentalbedingungen für Chromotropsaures Natrium.

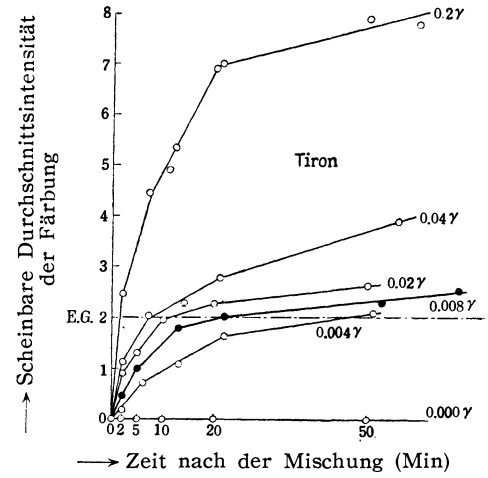

Abb. 7. Bestimmung der Erfassungsgrenze mit Tiron nach dem Verfahren „If" von Abb. 1.

TABELLE III

VERSCHIEDENE EXPERIMENTALBEDINGUNGEN VON ABB. 6

Nr. des Experiments	Zeichen der Kurve	Ordnung der Versetzung von Reagenzien und Probelösung 1.	2.	3.	4.	Bemerkungen*
I_a	--■--	RCl**	1 Tropfen der 1proz. Lsg. des Chromotropsauren Natriums	Probelsg.***	Pufferlsg. von pH 4.70	*a*
I_b	—△—	RCl	1 Tropfen der 1proz. Lsg. des Chromotropsauren Natriums	Probelsg.	Pufferlsg. von pH 2.86	*b*
I_c	—○—	RCl	1 Tropfen der 1proz. Lsg. des Chromotropsauren Natriums	Probelsg.	Pufferlsg. von pH 9.9	*c*
I_d	—□—	RCl	1 Tropfen der 0.1proz. Lsg. des Chromotropsauren Natriums	Probelsg.	Pufferlsg. von pH 4.70	*a*

a: Die Harzkörnchen färben sich dunkelgraugrün.

b: Die Harzkörnchen färben sich hell fleischfarben.

c: Die Harzkörnchen werden sehr intensiv braunviolett, wie man an der Kurve I_c(*) (mit dem Zeichen, --○--, gezeigt) sieht, gefärbt, aber wegen der stärkeren Dunkelrotfärbung vom Blindversuche nimmt die Nettunterscheidbarkeit der Färbung von den Harzkörnchen bis zur Kurve I_c ab.

** RCl bedeutet bei vorliegender Tabelle Dowex 1-X1 von RCl-Form.

*** Die hier benutzte Probelösung enthielt 0.2 γ von Eisen(III) (5 γ/ccm).

TABELLE IV

EINFLÜSSE DER BEGLEITSTOFFE

Begleitstoffe	benutzter Verbindungstypus	Reagens*	Färbung der Harzphase**	Menge der Begleitstoffe	Nachweisbare Eisen(III)-menge	Grenzverhältnis	Bemerkungen***
Ti(IV)	$TiOSO_4$	T.	tiefgelb	21 γ	0.8 γ	$1:2.6\times10$	*a*, Ti≦0.05proz.
		S.	zitronengelb	21 γ	0.8 γ	$1:2.6\times10$	*a*, Ti≦0.05proz.
		C.	scharlachrot	13 γ	2 γ	1:6.5	*a*, Ti≦0.03proz.
V(V)	NH_4VO_3	T.	gelb	64 γ	0.08 γ	$1:8\times10^2$	*b*, V≦0.2proz.
		S.	tiefgelb	64 γ	0.4 γ	$1:1.6\times10^2$	*a*, V≦0.2proz.
		C.	tiefbraun	40 γ	2 γ	$1:2\times10$	*a*, V≦0.1proz.
Cr(III)	$KCr(SO_4)_2$	T.	grünlich grau	360 γ	0.008 γ	$1:4.5\times10^4$	*a*
		S.	gräulich hellblau	200 γ	0.1 γ	$1:2\times10^3$	—
		C.	gräulich hellgrün	320 γ	0.04 γ	$1:8\times10^3$	*a*, *c*
Mn(II)	$MnSO_4$	T.	farblos	1.46 mg	0.008 γ	$1:1.8\times10^5$	—
		S.	farblos	1.2 mg	0.07 γ	$1:1.7\times10^4$	—
		C.	hellgelbbraun	900 γ	0.02 γ	$1:4.5\times10^4$	—
Co(II)	$Co(NO_3)_2$	T.	farblos	190 γ	0.008 γ	$1:2.4\times10^4$	*d*
		S.	farblos	155 γ	0.07 γ	$1:2.2\times10^3$	—
		C.	farblos	210 γ	0.02 γ	$1:1.1\times10^3$	*e*
Ni(II)	$NiCl_2$	T.	farblos	1.7 mg	0.008 γ	$1:2.1\times10^5$	—
		S.	farblos	1.2 mg	0.08 γ	$1:1.5\times10^4$	*e*
		C.	farblos	1.8 mg	0.02 γ	$1:9\times10^4$	—
Cu(II)	$CuSO_4$	T.	gelbgrün	720 γ	0.02 γ	$1:3.6\times10^4$	*a*
		S.	sehr hell gelb	570 γ	0.07 γ	$1:8\times10^3$	—
		C.	hellgrün	640 γ	0.04 γ	$1:1.6\times10^4$	*a*
Zn(II)	$ZnSO_4$	T.	farblos	320 γ	0.008 γ	$1:4\times10^4$	—
		S.	farblos	320 γ	0.04 γ	$1:8\times10^3$	—
		C.	farblos	300 γ	0.05 γ	$1:6\times10^3$	—
Cd(II)	$CdSO_4$	T.	farblos	365 γ	0.008 γ	$1:4.6\times10^4$	—
		S.	farblos	290 γ	0.07 γ	$1:4.2\times10^3$	—
		C.	hellbraun	230 γ	0.02 γ	$1:1.2\times10^4$	—
Hg(II)	$HgCl_2$	T.	weiss	1.2 mg	0.02 γ	$1:6\times10^4$	*f*
		S.	orangegelb	300 γ	0.16 γ	$1:1.9\times10^3$	—
		C.	weiss	300 γ	0.16 γ	$1:1.9\times10^3$	*f*
Cr(VI)	$K_2Cr_2O_7$	T.	hellgelb	3.2 γ	0.16 γ	$1:2\times10$	*a*, Cr≦0.01proz.
		S.	zitronengelb	2 γ	0.2 γ	$1:1\times10$	Cr≦0.005proz.
		C.	gelbbraun	2 γ	0.2 γ	$1:1\times10$	*a*, Cr≦0.005proz.
〃	〃 〃	T.	grün	320 γ	0.08 γ	$1:4\times10^3$	*a*, *g*
		S.	grün	400 γ	0.4 γ	$1:1\times10^3$	*g*
		C.	grün	200 γ	0.2 γ	$1:1\times10^3$	*a*, *c*, *g*
Mo(VI)	$(NH_4)_2MoO_4$	T.	orangegelb	2.4 γ	0.1 γ	$1:2.4\times10$	*a*, Mo≦0.006proz.
		S.	hellgelb	24 γ	0.1 γ	$1:2.4\times10^2$	Mo≦0.06proz.
		C.	tiefgelb	24 γ	0.1 γ	$1:2.4\times10^2$	*a*, Mo≦0.06proz.
W(VI)	Na_2WO_4	T.	sehr hell gelb	21 γ	0.1 γ	$1:2.1\times10^2$	*a*
		S.	grau	8.2 γ	0.16 γ	$1:5\times10$	—
		C.	chromgelb	82 γ	0.16 γ	$1:5\times10^2$	*a*
U(VI)	$UO_2(CH_3COO)_2$	T.	orangerot	56 γ	0.2 γ	$1:2.8\times10^2$	*a*, U≦0.015proz.
		S.	orange	90 γ	0.8 γ	$1:1.1\times10^2$	*a*, U≦0.03proz.
		C.	dunkelbraun	100 γ	0.4 γ	$1:2.5\times10^2$	*a*, U≦0.03proz.
Sb(III)	$SbCl_3$	T.	farblos	200 γ	2 γ	$1:1\times10^2$	—
		S.	farblos	320 γ	0.8 γ	$1:4\times10^2$	—
		C.	farblos	320 γ	0.8 γ	$1:4\times10^2$	—
Ge(IV)	GeO_2	T.	farblos	23 γ	0.008 γ	$1:3\times10^3$	—
		S.	farblos	23 γ	0.04 γ	$1:6\times10^2$	—
		C.	hellbraun	26 γ	0.02 γ	$1:1.3\times10^3$	*a*
Sn(IV)	$SnCl_4$	T.	farblos	170 γ	2 γ	$1:8.5\times10$	—
		S.	farblos	170 γ	2 γ	$1:8.5\times10$	—
		C.	bräunlich gelb	270 γ	0.8 γ	$1:3.4\times10^2$	*a*

Begleitstoffe	benutzter Verbindungstypus	Reagens*	Färbung der Harzphase**	Menge der Begleitstoffe	Nachweisbare Eisen(III)-menge	Grenzverhältnis	Bemerkungen***
Pb(II)	$Pb(NO_3)_2$	T.	farblos	2.2 mg	0.02 γ	$1:1.1\times10^5$	—
		S.	farblos	2.0 mg	0.04 γ	$1:5\times10^4$	—
		C.	sehr hell braun	2.2 mg	0.02 γ	$1:1.1\times10^5$	—
Ba(II)	$BaCl_2$	T.	farblos	320 γ	0.008 γ	$1:1.4\times10^4$	—
		S.	farblos	320 γ	0.04 γ	$1:8\times10^3$	—
		C.	hellbraun	200 γ	0.02 γ	$1:1\times10^4$	*a*
La(III)	$LaCl_3$****	T.	farblos	190 γ	0.008 γ	$1:2.4\times10^4$	—
		S.	farblos	190 γ	0.04 γ	$1:4.8\times10^3$	—
		C.	hellbraunrosa	210 γ	0.02 γ	$1:1.1\times10^4$	*a*
Al(III)	$AlCl_3$	T.	hell gräulich blau	76 γ	0.02 γ	$1:3.8\times10^3$	—
		S.	farblos	76 γ	0.1 γ	$1:7.6\times10^2$	—
		C.	violettrot	30 γ	0.16 γ	$1:1.9\times10^2$	*a*
Be(II)	$BeCl_2$	T.	farblos ?	160 γ	0.02 γ	$1:8\times10^3$	—
		S.	farblos	40 γ	0.16 γ	$1:2.5\times10^2$	—
		C.	rosa	40 γ	0.16 γ	$1:2.5\times10^2$	*a*
Mg(II)	$MgCl_2$	T.	farblos	140 γ	0.008 γ	$1:1.8\times10^4$	—
		S.	farblos	140 γ	0.04 γ	$1:3.5\times10^4$	—
		C.	hellbraun	155 γ	0.02 γ	$1:7.8\times10^3$	*a*
F^-	KF	T.	farblos	235 γ	0.02 γ	$1:1.2\times10^4$	—
		S.	farblos	52 γ	0.16 γ	$1:3.3\times10^2$	—
		C.	hellbraun	210 γ	0.04 γ	$1:5.3\times10^3$	*a*
HPO_4^{2-}	Na_2HPO_4	T.	farblos	7.7 mg	0.008 γ	$1:9.6\times10^5$	—
		S.	farblos	1.9 mg	0.16 γ	$1:1.2\times10^4$	—
		C.	dunkelrosa	7.7 mg	0.04 γ	$1:1.9\times10^5$	*a*
NO_2^-	$NaNO_2$	T.	zitronengelb	310 γ	0.04 γ	$1:7.8\times10^3$	*a*
		S.	farblos	310 γ	0.04 γ	$1:7.8\times10^3$	—
		C.	gelbocker bzw. tiefbraunrot	20 γ	0.1 γ	$1:2\times10^2$	*a*, $NO_2^-\leq0.05$proz.
Br_2	Bromwasser	T.	sehr hell gelb	290 γ	0.02 γ	$1:1.5\times10^4$	*a*
		S.	farblos	160 γ	0.1 γ	$1:1.6\times10^3$	*a*
		C.	schwarzrot	160 γ	0.1 γ	$1:1.6\times10^3$	*a*
H_2O_2	H_2O_2-wasser	T.	farblos	960 γ	0.008 γ	$1:1.2\times10^5$	—
		S.	farblos	960 γ	0.04 γ	$1:2.4\times10^4$	—
		C.	fleischfarben	1.1 mg	0.02 γ	$1:5.5\times10^4$	*a*
$C_2O_4^{2-}$	Oxalsaures Ammonium	T.	farblos	900 γ	0.02 γ	$1:4.5\times10^4$	—
		S.	farblos	250 γ	2 γ	$1:1.3\times10^2$	—
		C.	hellorangebraun	800 γ	0.04 γ	$1:2\times10^4$	*a*
$C_4H_4O_6^{2-}$	Seignettesalz	T.	grau	840 γ	0.04 γ	$1:2.1\times10^4$	*a*
		S.	farblos	530 γ	0.1 γ	$1:5.3\times10^3$	—
		C.	hellbraun	840 γ	0.04 γ	$1:2.1\times10^4$	*a*
$C_6H_5O_7^{3-}$	Zitronensaures Ammonium	T.	grau	1.25 mg	0.04 γ	$1:3.1\times10^4$	*a*
		S.	farblos	800 γ	2 γ	$1:4\times10^2$	—
		C.	hellbraun	800 γ	0.1 γ	$1:8\times10^3$	*a*

* T.=Tiron; S.=Sulfosalicylsäure; C.=Chromotropsaures Natrium.

** Diese bedeutet die Färbung der Harzphase von dem Falle, wo allein der betreffende Begleitstoff in der Versuchslösung vorhanden ist.

****a*: Nur dann, wenn der Nachweis mit einem Blindversuche nebeneinander ausgeführt wird, ist das betreffende Grenzverhältnis nutzbar.

b: Die Harzphase färbt sich schwarzgrau.

c: Mit Hilfe der am Rande der Harzkörnchen insbesondere stark entstehenden Grünfärbung wird die Anwesenheit des Eisens(III) bestätigt.

d: Infolge gleichartiges Farbentons zwischen der Harzphase und der Lösungsphase nimmt die Reaktionsempfindlichkeit beträchtlich ab.

e: Infolge des verschiedenen Farbentons der Harz- und Lösungsphase wird die Empfindlichkeit der Nachweisreaktion stark vergrössert.

f: Die Harzkörnchen trüben sich milchweiss.

g: Nach der Reduktion des Chromates zum Chrom(III)salze durch gelindes Erhitzen mit einigen Tropfen dreissigprozentiges Wasserstoffperoxydes und verdünnter Schwefelsäure wird der Nachweis ausgeführt.

**** Die hier benutzte Lanthanchloridprobe enthielt eine kleine Menge von Cer(III)-chlorid (Nach der Privatmitteilung von Herrn Y. Suzuki).

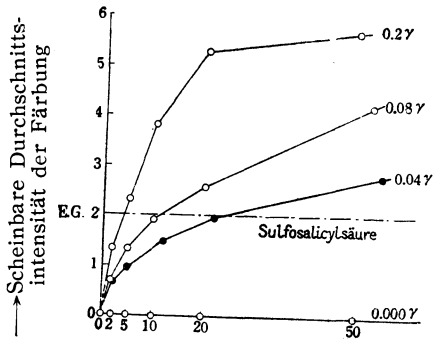

Abb. 8. Bestimmung der Erfassungsgrenze mit Sulfosalicylsäure nach dem Verfahren „I_e" von Abb. 5.

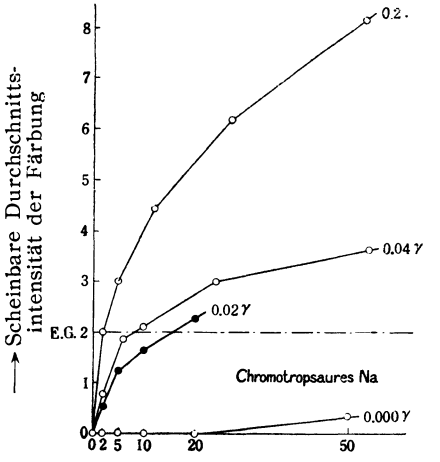

Abb. 9. Bestimmung der Erfassungsgrenze mit Chromotropsaurem Natrium nach dem Verfahren „I_a" von Abb. 6.

Reagens	Erfassungsgrenze	Grenzkonzentration
Tiron	0.008 γ	$1:5\times10^5$
Sulfosalicylsäure	0.04 γ	$1:1\times10^5$
Chromotropsaures Natrium	0.02 γ	$1:2\times10^5$

Einflüsse der Begleitstoffe

Die Einflüsse von fremden Ionen auf die vorliegenden drei Nachweisreaktionen wurden besonders ausführlich untersucht. Die Resultate der Untersuchungen werden in Tabelle IV zusammengefasst, worin die an einem beliebigen Begleitstoffe erhaltenen Ergebnisse auf einer Stelle gegenübergestellt werden, um drei Reagenzien miteinander direkt zu vergleichen:

Wie man aus der genannten Tabelle deutlich erkennt, stören alle Elemente ausser den mit dicker Linie umgebenen kaum den Nachweis.

Titan(IV)-, Antimon(III)-, Zinn(IV)- und Uranylsalze, sowie Vanadate, Chromate, Molybdate und Wolframate geben der Harzphase sehr intensive Färbungen, die die Nachweisreaktion des Eisens(III) beträchtlich stören.

Unter den obengenannten Ionen wurden nur die Chromate durch gelindes Erhitzen mit einigen Tropfen konzentriertes Wasserstoffperoxydes sowie verdünnter Schwefelsäure in die Chrom(III)-salze sehr leicht übergeführt, die den Nachweis kaum stören. Jedoch die Störung von Titan(IV)-, Antimon(III)-, Zinn(IV)- und Uranylsalzen konnte man nicht einfach beseitigen. Die Vanadate, Molybdate und Wolframate kann man vielleicht durch Anwendung von Mikrosäule des Anionenaustauschharzes[5] verhältnismässig einfach beseitigen.

Überdies ist es sehr bemerkenswert, dass solche Anionen wie Fluoride, Oxalate, Tartrate, Citrate usw., die gewöhnlich manche Farbenreaktionen von Eisen(III) stark stören und demnach zur Maskierung der Eisen(III)reaktionen häufig benutzt werden, die hier verzeichneten Nachweisreaktionen nur ein wenig stören.

Es ist übrigens auch interessant, dass das Chromotropsaure Natrium, wie es so genannt ist, unter gegebenen Bedingungen durch Einwirkung von grosser Anzahl der Elemente in die Harzphase verschiedenartige sehr charakteristische Färbungen liefert.

Zusammenfassung

1. Durch einfache Anwendung von farblosen starkbasischen Anionenaustauschharzen zu den Chelatbildungsreaktionen kann man verschiedenartige bedeutend empfindliche Nachweismethoden neu feststellen. Hier wird die Bildung der charakteristisch sich färbenden Chelatanionen, die die Eisen(III)salze durch Einwirkung der Phenolderivate, d. h., Tirons, Sulfosalicylsäure oder Chromotropsaures Natriums sich bilden lassen, als die geeigneten Beispiele dafür angewandt, und die ungewöhnlich ausgezeichneten Nachweismethoden für Eisen(III) werden vollkommen festgestellt.

2. Die Experimentalbedingungen höchster Empfindlichkeit werden durch gründliche Untersuchung über die verschiedenartigen Faktoren, z. B., Harzart, Konzentration der Reagenslösung, pH-Wert der Versuchslösung usw., fest bestimmt (vgl. den Abschnitt: „Tiron" von „Bestimmung der Bedingungen höchster Empfindlichkeit").

3. In bezug auf die Einflüsse von fremden Stoffen werden einunddreissig Arten der Ionen besonders ausführlich untersucht. Titan(IV)-, Antimon(III)-, Zinn(IV)- und Uranylsalzen, sowie Vanadate, Chromate, Molybdate und Wolframate stören beträchtlich den Nachweis. Übrigens ist es sehr bemerkenswert, dass solche Anionen wie Fluoride, Oxalate, Tartrate, Citrate usw., den Nachweis nur ein wenig stören.

Zu besonders herzlichem Dank ist der Verfasser Herrn Prof. Dr. E. Minami sowie den jüngeren Fachgenossen an seinem Laboratorium verpflichtet für zahlreiche wertvolle Ratschläge und freundlichste Anregungen über die vorliegende Untersuchung.

Laboratorium der analytischen Chemie, Chemisches Institut der wissenschaftlichen Fakultät, Tokyo Universität, Tokyo

6) Vgl. die fünfte Mitteilung: M. Fujimoto, Dieses Bulletin, 29, 595 (1956).

Addition of Trichlorosilane to Styrene, 2 Vinylpyridine, Allylcyanide and Octene-1[1]

By Shun'ichi NOZAKURA

(Received April 10, 1956)

It is a well-known fact that trichlorosilane is added to olefinic double bonds in the presence of radical catalysts such as organic peroxides or ultraviolet light. In the previous papers the author has reported that in addition to the typical radical catalysts, organic bases and nickel complex compounds could also effect the reaction. Thus, addition of trichlorosilane to acrylonitrile took place in the presence of organic bases (β-addition)[2] and of nickel complex compound (α-addition)[3]. The reaction between trichlorosilane and acetylene (or vinyltrichlorosilane)[4] was also catalysed by tetrapyridine nickel (II) chloride, and led to the formation of a mixture of two isomeric addition products, i. e., 1, 1- and 1-2-di (trichlorosilyl) ethanes.

The objectives of the work to be reported below are to study the effectiveness of such catalysts for the other vinyl compounds, and to establish the structures of the resulting addition products.

Styrene, 2-vinylpyridine, allylcyanide, octene-1 were tried as the representatives of vinyl compounds. All the addition reactions were carried out in sealed glass tubes. The reaction conditions and results are summarized in Table I.

Styrene.—Addition of trichlorosilane to styrene was attempted first by Burkhard[5] in the presence of peroxide, resulting in the formation of only a non-volatile telomeric product. Wagner and coworkers[6] succeded in the preparation of β-phenylethyltrichlorosilane by the reaction using platinized charcoal as the catalyst at 200°C.

In the present work, when trichlorosilane and styrene were heated at 160°C in the presence of pyridine, no addition product was obtained except for a non-volatile viscous polymer. But in the presence of tetrapyridine nickel chloride, about 30 percent of addition product was obtained accompanied with a considerable amount of non-volatile product. This non-volatile product may probably be a telomeric one taking into consideration the fact that it has a moderate chlorine content of 13 percent.

The phenylethyltrichlorosilane thus obtained was methylated by methylmagnesium bromide and distilled fractionally into two components. These are the isomers of phenylethyltrimethylsilane (Table II). Although the direct confirmation was not undertaken, the lower boiling isomer may be considered to be α-phenylethyltrimethylsilane by analogy

TABLE I

THE ADDITION REACTIONS BETWEEN TRICHLOROSILANE AND VINYL COMPOUNDS

	Styrene		2-Vinyl-pyridine	Allylcyanide			Octene-1		
$HSiCl_3$, g.	16.4	20.4	20.5	20.4	20.0	21.9	21.0	19.8	22.0
Vinyl Compound, g.	18.1	17.2	16.0	11.1	10.9	11.1	11.4	16.4	18.2
Catalyst, g.	C_5H_5N, 0.1	$NiCl_2 \cdot 4C_5H_5N$, 0.1	—	C_5H_5N, 0.2	$(C_2H_5)_3N$, 0.1	$NiCl_2 \cdot C_5H_5N$, 0.1	$NiCl_2 \cdot 4C_5H_5N$, 0.1	C_5H_5N, 0.1	$NiCl_2 \cdot 4C_5H_5N$, 0.1
Reaction Temp., °C	160	160	160	160	160	180–5	160	160	180
Reaction time, hr.	5.0	4.2	5.0	7.2	5.0	5.3	1.5	4.6	7.0
B. p. of the Product, °C (mmHg)	—	130–5 (40)	—	100–2 (27)	100–3 (26)	116–25 (41)	117–30 (41)	—	115–24 (24)
Yield, %[a]	0	30[b]	Farely good[c]	10	19	16	26	0	17

a) Yields are based on trichlorosilane used.
b) The chlorine content of the distillation residue was found to be 13%.
c) The reaction product was a crystalline mass and was methylated directly. M. p. (ca. 164°) and b. p. (ca. 190° at 24 mmHg) are measured with the sample obtained from the other run.

1) Paper VII in a series on the study of organosilicon compounds.
2) S. Nozakura and S. Konotsune, This Bulletin, **29**, 322 (1956).
3) S. Nozakura and S. Konotsune, ibid., **29**, 326 (1956).
4) S. Nozakura, ibid., **29**, 660 (1956).
5) C. A. Burkhard and R. H. Krieble, *J. Am. Chem. Soc.*, **69**, 2687 (1947).
6) Wagner et al., *Ind. Eng. Chem.*, **45**, 367 (1953).

TABLE II

PHYSICAL AND ANALYTICAL DATA OF THE METHYRATED ADDITION PRODUCTS

Compound	α-Trimethylsilylethylbenzene	β-Trimethylsilylethylbenzene	2-β-Trimethylsilylethylpyridine	β-Trimethylsilylbutyronitrile	γ-Trimethylsilylbutyronitrile	Trimethylsilyl-sec-octylsilane[a]	Trimethylsilyl-*n*-octylsilane
B. p., °C (mmHg)	103.0–4.5 (32)	112.0–2.2 (32)	106–7 (21)	91.0–2.5 (30)	97.0–8.0 (30)	99.0–100.0 (30)	107 (29)
d_4^{25}	0.8747	0.8603	0.8982	0.8326	0.8227	0.7667	0.7584
n_D^{25}	1.4958	1.4851	1.4843	1.4292	1.4258	1.4308	1.4241
C%, Found	74.13	74.44	—	—	—	71.37	70.62
Calcd.	74.09	74.09	—	—	—	70.86	70.86
H%, Found	10.12	10.12	—	—	—	13.38	13.79
Calcd.	10.18	10.18	—	—	—	14.05	14.05
N%, Found	—	—	8.09	9.67	9.47	—	—
Calcd.	—	—	7.82	9.92	9.02	—	—
Mol. Wt., Found	174	173	175	145	141	185	188
Calcd.	178.3	178.3	179.3	141.3	141.3	186.4	186.4
MR_D, Found	59.56	59.41	57.20	43.75	43.45	62.90	62.72
Calcd.	59.30	59.30	56.77	43.72	43.72	62.69	62.69

a) This sample is considered to be somewhat impure.

to the assignment of Wagner and coworkers, i. e., they assigned the lower boiling phenylethyltrichlorosilane to be α-isomer.

2-Vinylpyridine.—The addition reaction between trichlorosilane and 2-vinylpyridine took place very easily at about 160°C without the addition of any catalyst, but the product obtained is very difficult to be handled directly because of its high hygroscopicity. The product, pyridylethyltrichlorosilane, has a high melting point and it is probably due to an intermolecular attractive force exerted between silicon atoms and nitrogen atoms.

Pyridylethyltrichlorosilane is hydrolyzed by water giving a clear aqueous solution. When the solution is made alkaline by adding aqueous ammonia, an amorphous precipitate appears which is considered to be pyridylethylpolysiloxane. And this polysiloxane dissolved again in dilute hydrochloric acid.

The structure of the addition product was established by methylating it and comparing the resulting product with the sample which was synthesized by the other route from α-picoline in the following manner:

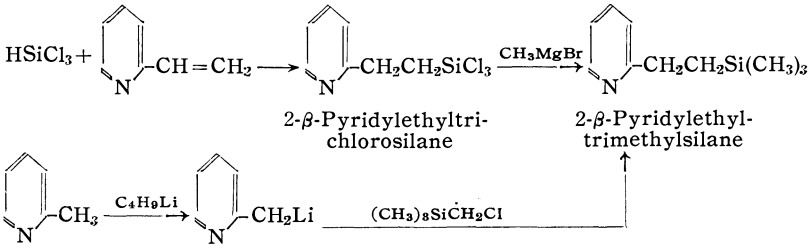

These two samples are proved to be identical in their infrared spectra, and moreover to give the same picrate.

The reaction in the presence of tetrapyridine nickel chloride was not attempted in this case.

Since the reactant itself is a base, the reaction should be base-catalyzed one just as the cyanoethylation of trichlorosilane catalyzed by bases[2].

Allylcyanide.—The reactivity of trichlorosilane for allylcyanide was rather low in the presence of organic bases. The product may possibly be either one of two isomers, β- and γ-trichlorosilylbutylonitrile, or a mixture of them. The acid amide which was derived from the product has the melting point of 95–6°C. The manners of conversion were as follows:

$$Cl_3SiCHCH_2CN \xrightarrow{CH_3MgBr} (CH_3)_3SiCHCH_2CN \xrightarrow{\text{aq. KOH}}$$
$$(CH_3)_3SiCHCH_2COOH \xrightarrow{SOCl_2} (CH_3)_3SiCHCH_2COCl$$
$$\xrightarrow{NH_3} (CH_3)SiCHCH_2CONH_2 \quad \text{m. p. } 95\text{–}6^\circ C$$

Since γ-trimethylsilylbutyric acid amide is known to have the melting point of 66.5–6.7°C.[5], the product here obtained must be

the other isomer, that is β-trichlorosilylbutyronitrile.

β-Trichlorosilylbutyronitrile gave on hydrolysis the corresponding polysiloxane, $NCCH_2CH(CH_3)SiO_{1.5}$.

In the presence of tetrapyridine nickel chloride, the yield of the addition product was somewhat higher than the corresponding one with the pyridine catalyst (Table I). However, the product showed a very wide range of boiling point, indicating that it contained more than one component. The product was methylated and fractionally distilled into two isomers (Table II). The structures of these isomers were established by converting them into the corresponding acid amides as follows and comparing them with the specimens formerly obtained by Sommer[7]:

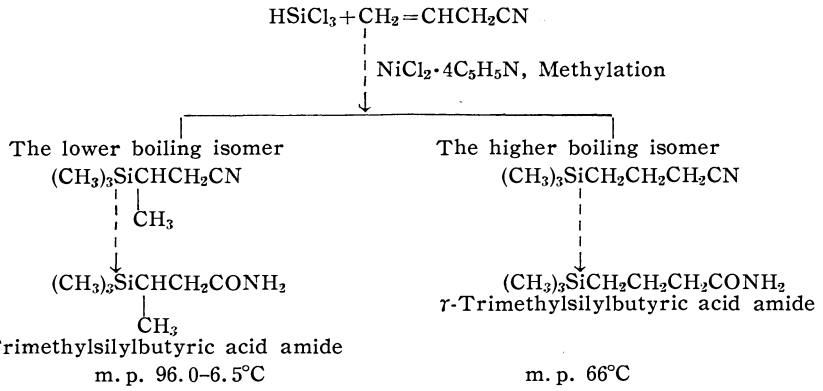

Thus, the melting point of the acid amide derived from the higher boiling isomer is in good agreement with that of γ-trimethylsilylbutyric acid amide reported by Sommer[7]. Therefore, it is concluded that the lower boiling alternative may be β-trimethylsilylbutyronitrile and the higher one may be γ-isomer.

Octene-1.—The reaction of trichlorosilane and octene-1 did not take place at all in the presence of catalytic amount of pyridine, but it took place to a small extent (17%) in the presence of tetrapyridine nickel chloride catalyst at 180°C (Table I). As the product obtained showed a rather wide range of boiling point, it was methylated as usual and was subjected to fractional distillation. Two isomers of trimethyloctylsilanes were isolated and their physical constants are listed in Table II. As the higher boiling one has the physical constants which coincide fairly well with those of *n*-octyltrimethylsilane described by Pietrusza and coworkers[8], the higher boiling one could be assigned to be *n*-octyltrimethylsilane. Although the lower boiling fraction is considered to be mainly composed of sec-octyltrimethylsilane, its purity is rather doubtful considering from its analytical data and infrared spectrum, which showed unexpected weak bands at 1622$^{-cm.}$ and 2116$^{-cm.}$. Further purification may be necessary.

General Conclusion.—The experimental results of all these additional experiments are summarized in Table III including the results of the previous paper. The following conclusions are deduced: (1) In the reactions between trichlorosilane and vinyl compounds, organic bases such as pyridine showed the catalytic action in some special cases (acrylonitrile, allylcyanide, and 2-vinylpyridine). 2-Vinylpyridine may be classified into this group because of its own basicity. The orientation of the addition could be well explained by the base-catalyzed ionic mechanism as follows:

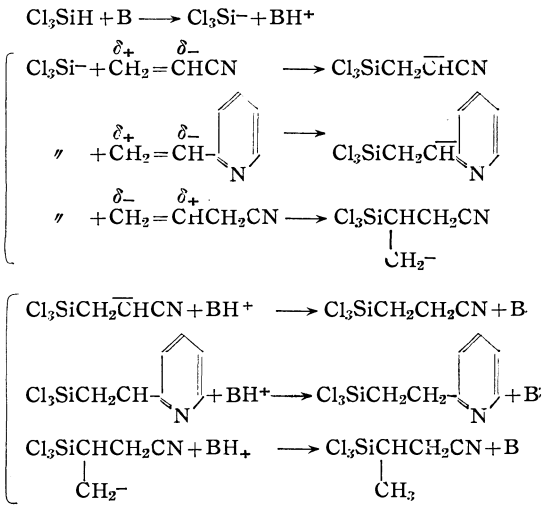

where B represents a base.

(2) Tetrapyridine nickel chloride showed the catalytic action for all the compounds

7) L.H. Sommer, U.S.P., 2, 610, 198, Sept. 9 (1952); *C.A.*, 47, 9346 b (1953).

8) E.W. Pietrusza et al., *J. Am. Chem. Soc.*, 70, 484 (1948).

TABLE III

ADDITION OF TRICHLOROSILANE TO VINYL COMPOUNDS IN THE PRESENCE OF PYRIDINE OR TETRAPYRIDINE NICKEL(II) CHLORIDE

Vinyl Compound	The Product in the Presence of Pyridine	The Product in the presence of $NiCl_2 \cdot 4C_5H_5N$
Acrylonitrile	$Cl_3SiCH_2CH_2CN$	$Cl_3SiCHCN$ $\quad\quad\quad

The product obtained from the reaction described in Table I was directly methylated as follows: the crystalline mass of the crude 2-β-trichlorosilylethylpyridine and 50 ml. of ether were placed in a three necked flask equipped with a mercury-sealed stirrer, a dropping funnel, and a reflux condenser which was connected to a calcium chloride tube. The ethereal solution of methylmagnesium bromide which was obtained from 13.2 g. of magnesium was dropped into it through the funnel within about forty minutes so as to keep the solution gently refluxing. And then the refluxing was continued for four hours. After cooling, the reaction mixture was treated with ice-water and an excess of hydrochloric acid. The aqueous layer was separated, and made alkaline by an excess of aqueous sodium hydroxide, and then subjected to steam distillation. The distillate was extracted with ether and the extract was dried with anhydrous sodium sulfate. After filtration, the ether solution was distilled, yielding 13.3 g. of 2-β-trimethylsilylethylpyridine, b. p. 106–7°C (21 mmHg). The overall yield calculated from trichlorosilane used was 49 percent. The analytical and physical data are given in Table II.

Its picrate melted at 89°C.

Anal. Found: N, 13.80; Si, 6.94. Calcd. for $C_{16}H_{20}N_4O_7Si$: N, 13.73; Si, 6.85%.

Its hydrochloride has the melting point of 102–3°C. and it was not analyzed because of its extreme hydroscopicity.

Synthesis of 2-β-Trimethylsilylethylpyridine from α-Picoline.—Into the benzene solution of butyllithium prepared from 2.0 g. of lithium, 9.3 g. of *n*-butylchloride, and 60 ml. of benzene, 9.3 g. of α-picoline was added dropwise at room temperature and let stand for forty minutes. Twelve grams of chloromethyltrimethylsilane was added to this reaction mixture, and it was let stand overnight. Then the mixture was treated with a solution of 20 ml. of water and 22 ml. of concentrated hydrochloric acid. The aqueous layer was separated, 14 g. of sodium hydroxide was added, and extracted with ether. After drying with anhydrous sodium sulfate, the ether solution was distilled, yielding 4.1 g. of 2-β-trimethylsilylethylpyridine, b. p. 105–7°C (21 mmHg). n_D^{25}, 1.4845.

Anal. Found: N, 7.99. Calcd. for $C_{10}H_{17}NSi$: N, 7.82%.

The identity of this compounds with the one derived from the addition product of trichlorosilane and 2-vinylpyridine was established through comparison of their infrared spectra.

Methylation of the Addition Product Obtained from the Reactions of Trichlorosilane and Allylcyanide in the Presence of Bases, and Conversion into the Corresponding Acid Amide.—The products of two runs were combined and redistilled to yield 5.5 g. of β-trichlorosilylbutyronitrile, b. p. 105.0–6.5°C (25 mmHg) (Found: Cl, 51.4. Calcd. for $C_4H_6NSiCl_3$: Cl, 52.5%).

A few drops of β-trichlorosilylbutyronitrile was poured onto a large excess of water. When the resulting solution was neutralized with aqueous ammonia, an amorphous precipitate of β-cyanopropylpolysiloxane appeared. It was filtered, washed with water, and dried over phosphorous pentoxide.

Anal. Found: Si, 23.0. Calcd. for $C_4H_3NO_{1.5}Si$: Si, 23.3%.

β-Trichlorosilylbutyronitrile (4.9 g.) was methylated in a usual manner by methylmagnesium bromide prepared from 2.0 g. of magnesium. In order to remove the impurity of ketone the methylated product was shaken with a saturated solution of sodium bisulfite, and then distilled, yielding 1.4 g. crude β-trimethylsilylbutyronitrile, b. p. 90–93°C (34.5 mmHg), (41%).

A mixture of 1.2 g. of β-trimethylsilylbutyronitrile, 5 ml. of aqueous 50 percent sodium hydroxide, and 5 ml. of alcohol was refluxed for twenteen hours. After cooling, alcohol was evaporated in reduced pressure, 10 ml. of water was added, and then extracted with ether to remove the unreacted nitrile. The remaining aqueous layer was then acidified with hydrochloric acid, and again extracted with ether. After drying with anhydrous sodium sulfate, the ether extract was distilled to yield 0.7 g. of β-trimethylsilylbutyric acid, b. p. 106–111°C (10.5 mmHg) (51%).

A mixture of 0.4 g. of β-trimethylsilylbutyric acid and 1.6 g. of thionyl chloride was gently refluxed for one hour. The excess of thionyl chloride was evaporated under reduced pressure. The residual oil was dissolved in 20 ml. of dry ether and saturated with dry ammonia under cooling with ice-water, and let stand for a short time. After filtration of the resulting ammonium chloride, the ether solution was evaporated to yield 0.3 g. of crude β-trimethylsilylbutyric acid amide, m. p. 93–4°C. Purification was carried out by recrystallization from petroleum benzine, m. p. 95–6°C.

Anal. Found: N, 8.68. Calcd. for $C_7H_{17}NOSi$: N, 8.79%.

The Product Obtained from the Reactions of Trichlorosilane and Allylcyanide in the Presence of Tetrapyridine Nickel Chloride.—The products of several runs (23.6 g.) were combined and methylated in the usual manner using 9.4 g. of magnesium. The methylated product was shaken with an aqueous saturated solution of sodium bisulfite, and then washed with water, dried with calcium chloride, and distilled through a Stedman column of about thirty theoretical plates. The following fractions were obtained under the pressure of 30 mmHg: (1) 87.5–91.0°, a few drops, (2) 91.0–2.5° 1.7 g., (3) 92.5–5.0°, 1.5 g., (4) 95.0–7.0°, 0.8 g., (5) 97.0–8.0°, 2.8 g., (6) residue, 3.5 g. Analytical and physical data of two main fractions (No. 2 and 5) are listed in Table II.

One gram of the fraction No. 2 (β-trimethylsilylbutyronitrile) was hydrolyzed in the same manner mentioned above, and yielded 0.5 g. of crude β-trimethylsilylbutyric acid, b. p. 108-115° (10 mmHg). The latter product was immediately treated with 2.0 g. of thionylchloride and then ammonia, yielding 0.5 g. of crude β-trimethylsilylbutyric acid amide. Recrystallization from a mixture of alcohol and water gave 0.3 g. of pure sample, m. p. 96.0–6.5°C.

Anal. Found: N, 8.47. Calcd for $C_7H_{17}NOSi$: N, 8.79%.

One and two tenth grams of fraction No. 5 (γ-trimethylsilylbutyronitrile) was treated in a similar manner, and gave 0.8 g. of γ-trimethylsilylbutyric acid (b. p. 115–7° (11 mmHg)) and then 0.5 g. of crude γ-trimethylsilylbutyric acid amide, m. p. 61.5–4.0°C. By recrystallization from *n*-heptane, the pure sample was obtained, m. p. 66.0°C.

Anal. Found: N, 8.96. Calcd. for $C_7H_{17}NOSi$: N, 8.79%.

The Product Obtained from the Reactions of Trichlorosilane and Octene-1.—The products of several runs (16.9 g.) were combined and methylated in the usual manner by methylmagnesium bromide prepared from 6.5 g. of magnesium. The methylated product was distilled through a Stedman column into the following fractions: (1) 96.0–9.0° (30 mm.), 0.4 g. (2) 99–100.0° (30 mm.), 1.7 g. (3) 100.0° (30 mm.)–103.0° (29 mm.), 2.1 g. (4) 103.0–107.° (29 mm.), 0.3 g. (5) 107° (29 mm.), 4.1 g.

Analytical and physical data of two main fractions (No. 2 and 5) are listed in Table II.

Summary

Addition reactions of trichlorosilane to styrene, 2-vinylpyridine, allylcyanide, and octene-1 were attempted in the presence of bases such as pyridine and in the presence of tetrapyridine nickel(II) chloride. The structures of the reaction products were established. In the presence of bases, trichlorosilane was added to 2-vinylpyridine and allylcyanide, yielding 2-β-trichlorosilylethylpyridine and β-trichlorosilylbutyronitrile, respectively. On the other hand, in the presence of tetrapyridine nickel chloride, the addition was effected for all the vinyl compounds examined. (2-vinylpyridine was not attempted.) In this case, however, the addition products proved to be composed of two position isomers, the occurrence of which was due to the difference in the orientation of addition, for each of the starting vinyl compounds.

The author is much indebted to Prof. S. Murahashi for his helpful suggestions, and to Mr. S. Konotsune for his help in the experiments. Appreciation is also expressed to Nihon Silicon Resin Co. for their kindness in supplying the trichlorosilane.

Department, of Chemistry Faculty of Science, Osaka University
Osaka

Studies on the Reduction Processes of Germanium Dioxide by Hydrogen

By Hideo BABA

(Received August 26, 1955)

Introduction

Two methods of obtaining a metallic germanium are known, namely the one is by the reduction of germanium tetrachloride with metallic zinc in gas phase[1] which is known as the duPont process, and the other by the reduction of germanium dioxide by hydrogen[1,2]. The latter process is superior to the former for obtaining a highly pure germanium because its product is less contaminated with impurities.

In general, the reaction between metal oxide and hydrogen have been well studied by many workers, but as there have been few papers on the reduction of germanium dioxide, we have made a study of this problem.

1) H.C. Torrey and C.A. Whitmer, "Crystal Rectifiers", McGrow-Hill (1948), Chap. 10.

2) A.P. Thompson and J.R. Musgrave, *J. of Metals*, **4**, 1132 (1952).

Experimental Procedure

A study of the rate of the reduction of germanium dioxide may be pursued by measuring the weight decrease of the oxide in hydrogen at intervals of the reduction. The measuring apparatus consists of a vertical quartz tube and a quartz spring balance suspended at one end of a rod in the tube. The rod can be moved vertically to bring a sample dish to the hot zone of the tube kept at a desired temperature. The decrease in weight of the oxide can be estimated by reading the shrinkage of the spring by means of a cathetometer.

The sensitivity of the spring balance is calibrated by weighing the weight of 0 to 500 mg. to determine the weight-elongation relationship. From the experiment, it was found that the relationship is shown by

$$W \text{ mg.} = 1.53 \times 10^2 \times l \text{ cm.}$$

Germanium dioxide has three crystal structures, i.e., tetragonal rutile type, hexagonal α-quartz type, and amorphous[3]. It was desirable to ex-

3) Otto H. Johnson, *Chem. Rev.*, **51**, 431 (1952).

amine the reduction process on each of the above three crystal types, but unfortunately tetragonal rutile type crystal could be prepared by neither heat treatment nor any other processes which might be expected. The samples are highly pure germanium dioxide made by "Otavi Meinen und Eisenbarn Gesellschaft", Germany, and the crystal structure was hexagonal α-quartz type by an X-Ray analysis.

The amorphous type structure was prepared by fusing the crystalline germanium dioxide.

Experimental Results

A known weight of hexagonal α-quartz type germanium dioxide was placed on the sample dish and the weight decrease was measured as the temperature increased at a constant velocity of 5.3°/min. in the hydrogen stream. Curves I and II in Fig. 1 show the temperature-time and weight decrease-time relationship respectively. These curves show that the reduction occurs at about 450°C.

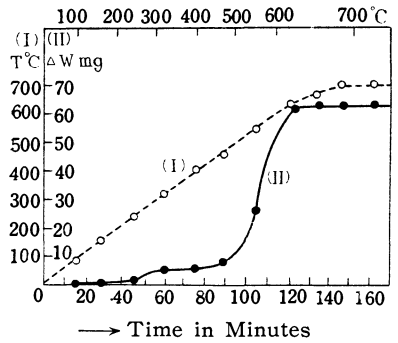

Fig. 1. Curve (I) Temperature-Time relationship. Curve (II) Weight decrease-Time relationship.

Hexagonal α-quartz Type Germanium Dioxide.—About 180 mg. of hexagonal α-quartz type germanium dioxide was placed in the apparatus and the absorbed water was removed by heating at 300°C for about thirty minutes in the stream of dry hydrogen, then the sample dish was pulled up above the heating zone and then it was pushed down to the heating zone of the furnace kept at a desired temperature. The reaction temperatures which we studied were 450, 500 and 600°C and the flow velocity of hydrogen was varied from 50 cc./min. to 210 cc./min. The results are shown in Fig. 2.

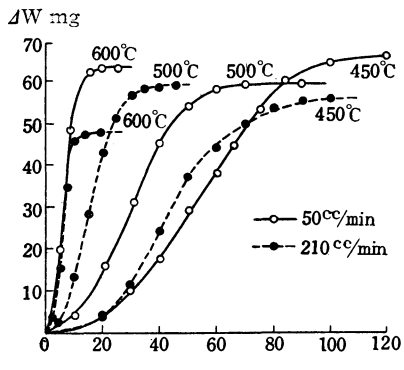

Fig. 2. Reaction curves with different temperature and hydrogen flow rate. (crystalline germanium dioxide)

Amorphous Germanium Dioxide.—*Preparation of Amorphous Germanium Dioxide.*—The hexagonal type germanium dioxide used in the previous experiment was melted at 1300°C and a glossy transparent mass was obtained which was shown to be amorphous by the X-ray analysis. This mass was crushed to the same size as the crystalline sample. The reaction curves are shown in Fig. 3. In the case of the amorphous sample the reaction type was represented by the first order reaction and showed no distinct induction period.

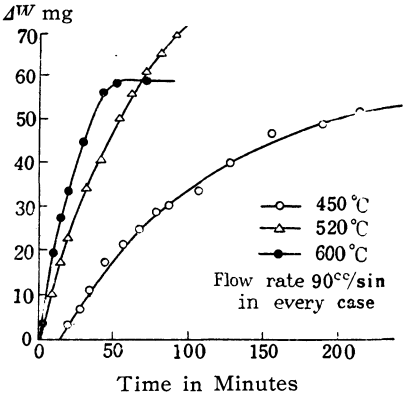

Fig. 3. Reaction curves with different temperatures. (amorphous germanium dioxide)

Consideration of the Results of the Experiment

a) Hexagonal α-quartz Type Germanium Dioxide.—This reaction has an autocatalytic phenomena as shown in Fig. 2 and the reaction velocity of this kind is ordinarily shown as follows[4].

$$dx/dt = Kx^n(a-x) \qquad (1)$$

x: product at a time t. a: initial amount. K: const. n: const.

The exponential factor n in (1) is a topochemical factor and is varied by the surface condition of solid phase and by the number of the reaction centers on the surface of the crystal, and can be determined by the following method.

Eq. (1) is differentiated by t.

$$d^2x/dt^2 = K\{(nx^{(n-1)}(a-x) - x^n\}$$

at the maximum of the reaction velocity curve

$$d^2x/dt^2 = 0 \text{ then, } nx^{(n-1)}(a-x) - x^n = 0$$

as $x \neq 0$ during the reaction,

4) K. Kawakita, *Proc. of Phys. Chem. Japan*, **14**, 79 (1940).

$$x=an/(n+1) \quad (2)$$

As the value of x at the maximum of dx/dt can be obtained from the experiment, the value of n can be determined. Relations between dx/dt and t can be obtained graphically from Fig. 2 and are shown in Fig. 4. Since time t at the maximum of dx/dt is

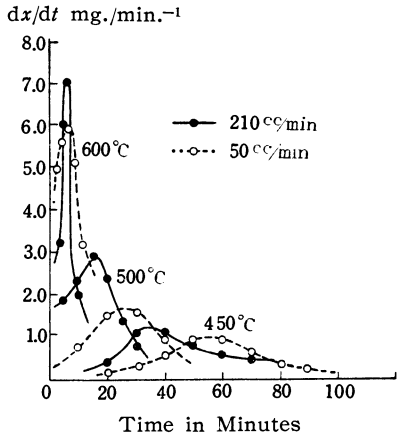

Fig. 4. Reaction velocity and time relationship at different temperatures.

determined from this figure, the corresponding value of x is found from Fig. 2. On the other hand, x at the completion of reaction, which equals a, is known from the experiment. The corresponding values are calculated by inserting these values in Eq. (2).

The values of n vary indefinitely from 0.4 to 2.2 corresponding to the reaction temperature and hydrogen flow rates. This is caused by the formation of reaction nuclei and their rate of propagation, which are concerned with the formation and evaporation of germanium monoxide. The faster the hydrogen flow rate, the more the evaporation of monoxide becomes appreciable as shown in Table I and the n values become more irregular. But in the case of 50 cc./min. because the formation of monoxide is limited, the n values become constant, independent of temperature and may be taken as unity as shown in Table II.

Table I

Deviation of weight decrease from calculated value

Temp. °C	Flow Rate cc./min.	Weight Decrease ΔW Calculated mg.	Weight Decrease ΔW Found mg.	Difference mg.	Percent of Deviation against Calculated Value
450	50	71.2	75.0	−3.8	−5.3
	210	54.7	60.0	−5.2	−9.5
600	50	62.2	64.0	−1.8	−2.8
	90	59.9	64.0	−4.1	−6.8
	210	45.7	52.0	−6.3	−13.7

Then Eq. (1) becomes rather simple and is shown by:

$$dx/dt=Kx(a-x).$$

Dissolving this differential equation

$$\ln x/(a-x)=aKt+C$$

when $\ln x/(a-x)$ is plotted against t, the inclination of the curve shows aK, from which K is obtained as shown in Fig. 5 and listed in Table II.

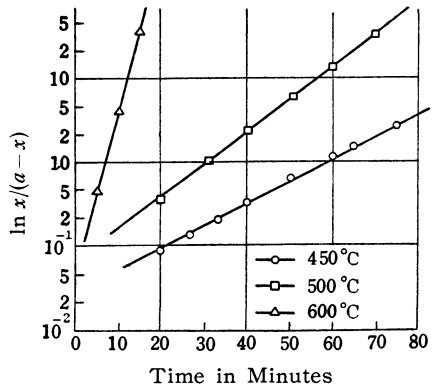

Fig. 5. Determination of reaction velocity constant k at flow velocity 50 cc/min.

From these data, the apparent activation energy is calculated and is found to be 18.3 kcal./mol. for the gas flowing velocity of 50 cc./min. as shown in Fig. 7.

Table II

n and K values corresponding with different tfmperatures at flow rate of 50 cc./min.

Reaction Temp. °C	n	K (min.$^{-1}$ mol.$^{-1}$)
450	0.80	11.7
500	1.22	21.7
600	1.13	105

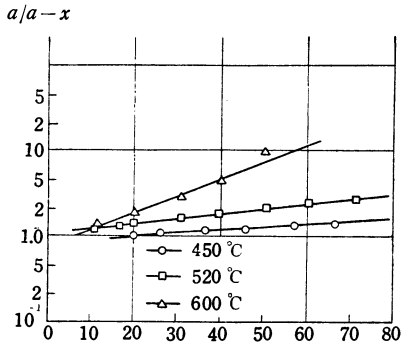

Fig. 6. Determination of reaction velocity constant k with different temperatures (amorphous germanium dioxide)

b) Reduction of Amorphous Germanium Dioxide.—In the case of crystalline germanium dioxide, the maximum of dx/dt exists at about one third of the whole reaction process, but in this case, the reaction velocity is represented by a rate equation of ordinary first order reaction. If dx/dt is plotted against t it is clear that it is corresponding to $n=0$ in Eq. (1) as is shown in Fig. 6.

In this case, the reaction equation is represented by

$$dx/dt=K(a-x) \text{ then, } \ln a/(a-x)=Kt.$$

From this equation we can obtain the values of K.

$$K\ (450°C)=0.0096\ \text{min.}^{-1}$$
$$K\ (520°C)=0.016\ \text{min.}^{-1}$$
$$K\ (600°C)=0.604\ \text{min.}^{-1}$$

From these values the apparent activation energy is shown to be 15.2 kcal./mol.

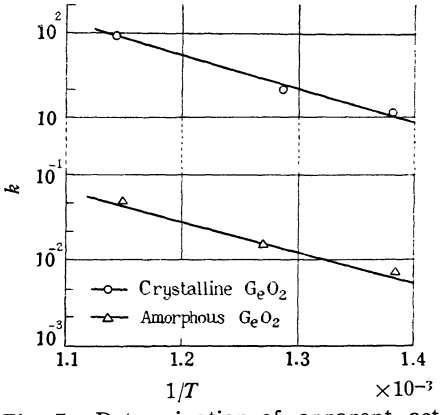

Fig. 7. Determination of apparent activation energy of reduction of crystalline and amorphous germanium dioxides.

The gas-solid reactions discussed above, are ordinarily considered to follow the following five steps and the slowest process among them determines the reaction velocity[5].

(1) Collision of hydrogen gas on the surface of germanium dioxide.
(2) Adsorption of hydrogen gas.
(3) Reaction on the surface.
(4) Desorption of products from the surface.
(5) Diffusion of products from surface to the gas phase.

Since the reaction process of (1) and (5) are diffusional ones, the observed activation energy must be very small, and judging from the observed activation energy, these processes will not play a predominant rôle in the whole reaction.

The process of (3) is rather complicated and the following four reactions must be considered[3,7,8,9].

(1) $GeO_2+2H_2=Ge+2H_2O$
(2) $GeO_2+H_2=GeO+H_2O$
(3) $GeO+H_2=Ge+H_2O$
(4) $Ge+GeO_2=2GeO$

The observed reaction rate will be the superposition of these four reactions.

Reaction (1) is the most common reduction reaction of metal oxide and the reactions (2) and (3) seem to be the transition steps of the reduction process. In the case of germanium dioxide, reactions of (2) and (3) can not be neglected, because the observed weight decrease in the reduction is greater than the calculated values from the initially weighed germanium dioxide according to reaction (1). This discrepancy can not be explained without considering the evaporation of germanium monoxide produced by the reaction (2). For this reason the formation of germanium monoxide will be genuine, but the period during which the evaporation of this material occurs is limited to the beginning of the reaction, and since the surface of the grain of germanium oxide is immediately covered with germanium metal by the reaction (3), further evaporation of monoxide is prevented by the germanium metal film. On the contrary, in the case of amorphous germanium dioxide, no more weight decrease is observed than that which was calculated and this fact seems to be owing to the difficulty of reaction (2) because of the different surface condition, and the fact that the reaction (1) will be the predominant process.

It is clear from Eq. 1 that the greater the value of n, the longer the induction period which should be observed, also that the value of n reprsents the surface conditions and the rate of propagation of reaction nuclei on the surface. The two different reaction types described above on crystalline and amorphous germanium oxides with hydrogen will be explained considering this factor n. This difference seemed to be caused by the differences of the surface conditions; namely that the crystalline germanium dioxide has many crystal edges which act as active centers. At the beginning, the reaction occurs from such points and the reaction propagates to other parts of the surface and thus the main reaction occurs after some induction period. During the induction period, the reaction (2)

5) N.F. Mott and R.W. Gurney, "Electronic processes in Ionic Crystals", Oxford at the Clarendon Press (1950), Chap. 8.

6) Les. Brawer, *Chem. Rev.*, 52, 1 (1953).
7) R.B. Bernstein and D. Cubicciotti, *J. Am. Chem. Soc.*, 73, 4112 (1951).
8) Meller. "Comprehensive treatise in Inorganic and Physical Chemistry", Vol. 7, p. 265.
9) W. Bues u. H.V. Wartenberg, *Z. f. anorg. u. allgem. Chem.*, 266, 281 (1951).

become appreciable. On the other hand, the surface of the amorphous germanium dioxide has a more uniform character point to point and has same chances of starting a reaction, so that a sufficient number of nuclei form at once at the beginning of the reaction and the main reaction occurs without occuring reaction (2).

Reaction (4) occurs on the contact surface during the reduction process between the germanium produced and the remaining germanium dioxide. But since this is solid-solid reaction, its velocity is small enough to be neglected in this case.

Conclusion

The reduction process of germanium dioxide and the hydrogen system were studied for the crystalline and amorphous germanium dioxides. In the case of the crystalline dioxide, the reduction process had autocatalytic action and its velocity was represented by the formula $dx/dt=Kx(a-x)$. On the other hand, in the case of amorphous germanium dioxide the process showed no distinct induction period and followed the first order reaction type. This difference seemed to be owing to the differences of surface conditions of crystalline and amorphous germanium dioxides and was well represented by the value of topochemical factor n in Eq. (1).

The activation energies of reduction process of crystalline and amorphous germanium dioxide were found to be 18.3 kcal./mol. and 15.2 kcal./mol. respectively. This reduction process seemed to be rather complicated, and we must consider some reactions belonging to the GeO_2-GeO-Ge system, but we treated the reaction under the assumption that the $GeO_2+2H_2=Ge+2H_2O$ was the main process as the first order approximation.

The author wishes to acknowledge the many helpful suggestions made by Dr. S. Yanagisawa who is a professor of chemistry at Keio University, and to thank Dr. Y. Takeda and Mr. T. Niimi for their encouragement during this work. The author also wishes to express his thanks to Mr. T. Igo who assisted in the experimental parts of this study and to Mr. R. Nii who made the X-ray analysis.

The Electrical Communication Laboratory
Nippon Telegraph and Telephone
Public Corporation, Tokyo

*Polarographic Studies of Metal Complexes. V. Ethylenediamine Complexes of Cadmium, Nickel and Zinc**

By Ken-ichi MORINAGA

(Received January 23, 1956)

Introduction

The complex salts hitherto studied by polarographic methods were mostly confined to the so-called polarographically reversible systems and there are found very few studies on the irreversible complex systems. In the previous papers[1], the author reported the polarographic behaviour of the ammonia complexes of cadmium, nickel and zinc. The polarographic reductions of the ethylenediamine complexes of these metals, in 0.1 N potassium nitrate medium with various concentrations of the complexing agent, were investigated in the present paper. While the reductions of nickel and zinc were irreversible, the reduction of cadmium complex was found to be reversible, and it was possible to determine the number of coordinated ligands and the overall complex formation constant for the cadmium complex, which existed in the solution under investigation. The attempt was also made to interpret the irreversible polarographic waves with the aid of the theoretical treatment of the current-voltage curves developed recently by Matsuda and Ayabe[2], and the number of ligands in the complex ions which participated in the electron transfer process could be determined. The forward rate constants of the electron transfer process could also be

* This paper was read at the 2nd Symposium on Polarography held on November 22, 1955 at Hiroshima University by the Chemical Society of Japan and the Electrochemical Society of Japan.

1) K. Morinaga, *J. Chem. Soc. Japan* (*Pure Chem. Sect.*), **75**, 627 (1954); **76**, 133, 136 (1955).

2) H. Matsuda and Y. Ayabe, This Bulletin, **29**, 134 (1956).

calculated using the known complex formation constants.

Experimental Part

The Heyrovsky-Shikata type polarograph with the circuit for extendable and adjustable e.m.f. was employed to record the enlarged polarograms, from which the half-wave potentials were determined by the log plot method. The span voltage applied to a potentiometer-drum was selected in the range of 0.24 to 0.60 v. The H-cell with a saturated calomel electrode was used, the internal resistance of which was found to be about 400 Ω. The reproducibility of the values for the half-wave potential was ± 1 mV. for cadmium and was ± 3 mV. for nickel and zinc. The capillary used had an m value of 2.11_9 mg./sec. and a drop time of 4.61 sec./drop at the mercury height of 68.5 cm., in distilled water with an open circuit. All polarographic measurements were carried out in a thermostat of 25.0±0.1°C.

The solutions of cadmium, nickel and zinc sulfates, and the 1 N stock solution of potassium nitrate used as a supporting electrolyte, were all prepared from reagent grade materials. The 2 and 4 M solutions of ethylenediamine were prepared by dilution of twice distilled reagent and was standardized with hydrochloric acid using B.P.B. as an indicator. The concentration of gelatine solution which was employed as a maximum suppressor, had considerable influence on the characteristics of the reduction waves for nickel as seen below; therefore the greatest care was taken with its preparation. The electrolytic solutions were prepared by adding the stock solutions of metal sulfates, potassium nitrate, ethylenediamine and lastly a fresh solution of 0.1% gelatine in a measuring flask. Oxygen was removed from the electrolytic solution by passing nitrogen gas through it for half an hour.

The Relation between E and log $(i/(i_l-i))$.— The waves were analyzed by the log plot method from the observed current i at the potential E of the dropping mercury electrode and the limiting current i_l. The reciprocal slope of cadmium waves was 31.6 mV. in average, as shown in Table II, and the reduction was reversible. Two examples of the plot of E against log $(i/(i_l-i))$ are illustrated in Fig. 1. The reciprocal slope of zinc waves was found to be 34.2 mV. and a little larger than the one expected for the reversible waves. For nickel waves a slight deviation from the linearity was observed, but five points which are gathered around the half-wave potential, gave a straight line, from which the reciprocal slope was estimated as a first approximation. It is probable that the deviation from the linearity may be partly due to an inappropriate concentration of gelatine, and partly due to an experimental error caused by a rather large span voltage applied to the potentiometer-drum*.

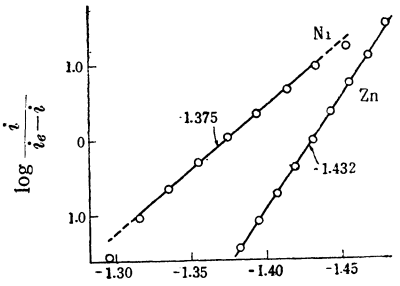

Fig. 1. Plot of E against log $(i/(i_l-i))$.
Concentration of ethylenediamine: 0.966 M for nickel and 1.05 M for zinc

The Dependence of the Limiting Currents on the Heights of Mercury Column. — The limiting currents were measured at various heights of mercury column. If the limiting current is diffusion-controlled, it should be proportional to the square root of the height of mercury column $H_{corr.}$, corrected for the back pressure. Data given in Table I indicate that the limiting currents are determined by a diffusion process for the reductions of these complex metal ions.

TABLE I
DEPENDENCE OF LIMITING CURRENTS ON HEIGHT OF MERCURY COLUMN

		Cd		Ni		Zn	
		0.5×10^{-3} M		0.6×10^{-3} M		0.46×10^{-3} M	
		0.15 M en		1.15 M en		1.05 M en	
		0.01% gel.		0.02% gel.		0.02% gel.	
$H_{corr.}$	$\sqrt{H_{corr.}}$	i_l	$i_l/\sqrt{H_{corr.}}$	i_l	$i_l/\sqrt{H_{corr.}}$	i_l	$i_l/\sqrt{H_{corr.}}$
(cm.)		(μA)		(μA)		(μA)	
68.5	8.28	3.61	0.436	3.52	0.425	2.98	0.360
64.5	8.03	3.51	0.437	3.40	0.423	2.88	0.359
60.5	7.78	3.41	0.438	3.31	0.425	2.80	0.360
56.5	7.52	3.30	0.439	3.19	0.424	2.72	0.362

Experimental Results

The Variation of the Half-wave Potential as a Function of the Ethylenediamine Concentration.—The characteristics of waves at various concentrations of ethylenediamine C_{en} are given in Tables II, III and IV.

The half-wave potentials for cadmium and zinc

* The log plot of nickel wave, shown in Fig. 1, appears to give a convex curve, but this is not always the case.

were independent of the concentrations of the depolarizers, as shown in Tables II and IV, and the reciprocal slopes remained constant in the concentration range of 0.1 to 2.5 M ethylenediamine.

The same was no longer the case for nickel. The reciprocal slope decreased with the increase of concentration of ethylenediamine. Moreover, the concentration of gelatine had considerable influence on the slope and the half-wave potential. At the lower concentration of gelatine, the slope was smaller and the half-wave potential was more positive.

TABLE II

VARIATION OF $(E_{1/2})_c$ AS A FUNCTION OF ETHYLENEDIAMINE CONCENTRATION 0.1 N KNO_3, 0.01% GELATINE, $m=2.12$ mg./sec., $t=4.12$ sec./drop., $H=68.5$ cm.

C_{en} (M)	log C_{en}	Concn. of Cadmium (10^{-3} M)	E/log$(i/(i_d-i))$ (mV.)	i_d (μA)	$-(E_{1/2})_c$ (V.vs.S.C.E.)
0		0.5	32	3.85	0.581
0.115	$\bar{1}$.061	0.5	32	3.65	0.845
0.154	$\bar{1}$.187	0.5	32	3.61	0.856
0.231	$\bar{1}$.363	0.5	31.5	3.59	0.873
0.308	$\bar{1}$.488	0.5	30	3.55	0.882
0.308	$\bar{1}$.488	0.2	32	1.43	0.884
0.308	$\bar{1}$.488	0.7	31	4.99	0.885
0.462	$\bar{1}$.665	0.5	32	3.51	0.902
0.616	$\bar{1}$.789	0.5	32	3.44	0.914
0.770	$\bar{1}$.886	0.5	31	3.39	0.922
0.866	$\bar{1}$.937	0.5	33	3.34	0.928
0.924	$\bar{1}$.965	0.5	31	3.30	0.930
1.15	0.061	0.5	31	3.26	0.940
1.44	0.158	0.5	33	3.15	0.950
1.79	0.253	0.5	31	3.07	0.960
2.02	0.305	0.5	31	2.94	0.967
2.31	0.363	0.5	31	2.84	0.974
2.60	0.415	0.5	32	2.75	0.980
2.89	0.460	0.5	32	2.66	0.987

TABLE III

VARIATION OF $(E_{1/2})_c$ AS A FUNCTION OF ETHYLENEDIAMINE CONCENTRATION 0.1 N KNO_3, $m=2.01$ mg./sec., $t=3.72$ sec./drop, $H=64.5$ cm.

C_{en} (M)	Concn. of Nickel (10^{-3} M)	Concn. of Gelatine (%)	E/log $(i/(i_d-i))$ (mV.)	i_d (μA)	$-(E_{1/2})_c$ (V.vs.S.C.E)
0	0.6			(4.01)	
0.146	0.6	0.013	78	3.86	1.327
0.146	0.6	0.020	90	3.77	1.351
0.219	0.6	0.020	82	3.73	1.353
0.292	0.6	0.015	72	3.77	1.342
0.292	0.6	0.016	74	3.73	1.346
0.292	0.6	0.020	80	3.69	1.355
0.365	0.6	0.020	76	3.67	1.358
0.438	0.6	0.016	70	3.69	1.353
0.438	0.6	0.020	74	3.64	1.361
0.584	0.6	0.020	70	3.60	1.365
0.730	0.6	0.020	67	3.54	1.369
0.876	0.6	0.020	63	3.50	1.373
0.966	0.6	0.020	60	3.47	1.375
0.966	0.4_2	0.020	55	2.46	1.370
0.966	0.2_4	0.020	52	1.42	1.363
1.21	0.6	0.020	59	3.37	1.381
1.45	0.6	0.020	56	3.31	1.385
1.69	0.6	0.020	54	3.20	1.391
1.93	0.6	0.020	52	3.12	1.394

TABLE IV

VARIATION OF $(E_{1/2})_c$ AS A FUNCTION OF ETHYLENEDIAMINE CONCENTRATION

0.1 N KNO_3, 0.02% Gelatine, m=2.01 mg./sec., t=3.65 sec./drop, H=64.5 cm.

C_{en} (M)	log C_{en}	Concn. of Zinc (10^{-3} M)	$E/\log(i/(i_d-i))$ (mV.)	i_d (μA)	$-(E_{1/2})_c$ (V.vs.S.C.E.)
0		0.46		(3.39)	
0.103	$\bar{1}$.013	0.46	34.5	3.26	1.356
0.154	$\bar{1}$.187	0.46	34.5	3.18	1.370
0.231	$\bar{1}$.363	0.46	34	3.14	1.383
0.308	$\bar{1}$.488	0.46	34	3.12	1.391
0.384	$\bar{1}$.585	0.46	34.5	3.10	1.399
0.461	$\bar{1}$.664	0.46	34	3.09	1.404
0.615	$\bar{1}$.789	0.46	34	3.01	1.413
0.769	$\bar{1}$.886	0.46	34.5	2.97	1.421
0.923	$\bar{1}$.965	0.46	34.5	2.92	1.426
1.05	0.020	0.46	34	2.88	1.432
1.05	0.020	0.55	34	3.43	1.434
1.05	0.020	0.27	33.5	1.72	1.431
1.31	0.117	0.46	34.5	2.80	1.440
1.57	0.196	0.46	34.5	2.69	1.446
1.83	0.263	0.46	34.5	2.61	1.452
2.10	0.321	0.46	34	2.53	1.458
2.36	0.372	0.46	34	2.41	1.463
2.62	0.418	0.46	34	2.36	1.466

The Viscosities of the Electolytic Solutions. —Diffusion currents i_d in each case decreased with the increase of concentration of ethylenediamine. The viscosities of the solutions η were measured with Ostwald viscometer, taking distilled water as a standard, and the observed diffusion currents were plotted against the inverse square root of the relative viscosities. As illustrated in Fig. 2, The product of the diffusion current and the square root of the viscosity remained constant at each concentration of ethylenediamine. Thus the decrease of the diffusion current was found to be due to the increase of the viscosities of the electrolytic solutions[3]. The extrapolated points

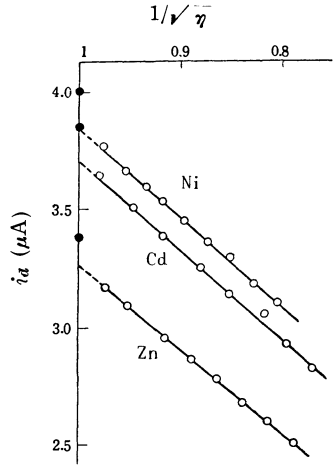

Fig. 2. Plot of i_d against $1/\sqrt{\eta}$.
The black circles represent the diffusion currents of the simple metal ions.

at relative viscosity of 1 may represent the apparent diffusion currents of the complex ions, comparable to those of the simple ions. So the square roots of the apparent polarographic diffusion coefficients of these complex metal ions may be estimated to be ca. 4% less than those of the simple metal ions*.

Discussion

Matsuda and Ayabe[2] have recently derived a general expression for the polarographic current-voltage curves of complex metal ions, by assuming that the net electrode reaction

$$MX_\nu^{(n-\nu b)+}+ne+Hg=M(Hg)+\nu X^{-b}$$

($\nu=N, N-1, \cdots\cdots, 1, 0$: N is the maximum number of ligands which can be combined)

take place according to the following scheme:

(1) dissociation and association processes

$$MX_\nu^{(n-\nu b)+}=MX_{\nu-1}^{[n-(\nu-1)b]+}+X^{-b}$$
($\nu=N, N-1, \cdots\cdots, p+1$)
$$MX_{\mu-1}^{[n-(\mu-1)b]+}+X^{-b}=MX_\mu^{(n-\mu b)+}$$
($\mu=p, p-1, \cdots\cdots, 1$)

(2) electron transfer process

$$MX_p^{(n-pb)+}+ne+Hg=M(Hg)+pX^{-b}$$

In the above equations M(Hg) represents the amalgam formed on the electrode surface and n is the number of electrons associated with the electrode reaction; X^{-b} represents the complexing agent and

3) I.M. Kolthoff and J.J. Lingane, "Polarography", Vol. I, Interscience Pub., New York, London (1952), p. 97.

* Usually the presence of gelatine causes the lowering of the limiting current, so the observed limiting current in the presence of gelatine is not the true diffusion current. But, in the meaning that the limiting current is diffusion-controlled, the apparent polarographic diffusion coefficient may be estimated from the observed diffusion current.

$MX_p^{(n-pb)+}$ represents the complex which participates in the electron transfer process, among various complex species $MX_\nu^{(n-\nu b)+}$ ($\nu=N, N-1, \cdots\cdots, 1, 0$) which exist in the bulk of the solution.

If the reaction rates of dissociation and association are sufficiently rapid, that is, the limiting current is diffusion-controlled, the wave for the reversible system may be expressed:

$$E=E_0-2.3\frac{RT}{nF}\log\frac{\sqrt{D}}{\sqrt{D_a}}-2.3\frac{RT}{nF}\log\frac{i}{i_d-i}$$
$$-2.3\frac{RT}{nF}\log\left\{1+\sum_{\nu=1}^{N}(C_X)^\nu\left(\prod_{\mu=1}^{\nu}k_\mu\right)\right\}. \quad (1)$$

The wave for the irreversible system may be expressed:

$$E^*=2.3\frac{RT}{\alpha nF}\left\{\log\frac{k_f^0}{\sqrt{D}}\sqrt{\tau}-0.049-\log\frac{i}{i_d-i}\right.$$
$$\left.-\log\left[\sum_{\nu=0}^{N}(C_X)^{\nu-p}\left(\prod_{\mu=0}^{\nu}k_\mu\right)\Big/\left(\prod_{\mu=1}^{n}k_\mu\right)\right]\right\}, \quad (2)$$

where E_0 is the standard potential for the reduction of the simple metal ion M^{n+} to the amalgam state; D and D_a are the diffusion coefficients of the complex metal ions $MX_\nu^{(n-\nu b)+}$ in the solution and of the metal atoms M(Hg) in the amalgam, respectively; C_X is the concentration of the complexing agent and k_μ is the successive formation constants defined by Bjerrum[4]; α is the transfer coefficient and τ is the drop time and k_f^0 is the forward (reduction) rate constant of the electron transfer process at the potential of the normal hydrogen electrode. (All activity coefficients are assumed to be equal to 1 in the above equations.)

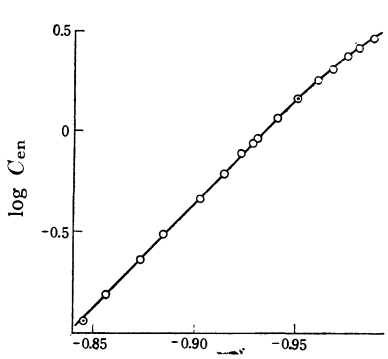

Fig. 3. Variation of $(E_{1/2})_c$ for cadmium as a function of log C_{en}.

* E in Eq. (2) is measured with reference to the normal hydrogen electrode.

4) J. Bjerrum, "Metal Ammine Formation in Aqueous Solution", P. Haase and Son, Copenhagen (1941), p. 20.

Cadmium Complexes.—In Fig. 3 the half-wave potentials are plotted against the logarithm of the concentrations of ethylenediamine. As the activity coefficients of ethylenediamine are unknown at the ionic strength of 0.1 (KNO_3), they are all assumed as equal to 1 in the following calculations. The values found are lying on the line:

$$(E_{1/2})_c=-0.934-0.096\log C_{en}$$

This system belongs to a reversible type and Eq. (1) can be used. From the above data it can be concluded that the complex ion $[Cd\ en_3]^{++}$ predominates in the concentration range of 0.1 to 2.0 M ethylenediamine and its formation constant is equal to $10^{12.01}$. This value is in good agreement with the value of $10^{12.18}$ determined polarographically by Douglas, Laitinen and Bailar[5].

Nickel Complexes.—The reduction of nickel is irreversible and we have attempted to interpret the waves by Eq. (2). When only the complex $MX_s^{(n-sb)+}$, which predominates in the bulk of the solution, dissociates very rapidly into the complex $MX_p^{(n-pb)+}$ in the vicinity of the electrode surface and the complex $MX_p^{(n-pb)+}$ is reduced irreversibly at the dropping electrode, Eq. (2) can be reduced to the more simple form:

$$E=2.3\frac{RT}{\alpha nF}\left\{\log\frac{k_f^0}{\sqrt{D}}\sqrt{\tau}-0.049-\log\frac{i}{i_d-i}\right.$$
$$\left.-\log\left[\left(\prod_{\mu=0}^{p}k_\mu\right)\Big/\left(\prod_{\mu=1}^{n}k_\mu\right)\right]-(S-p)\log C_X\right\} \quad (3)$$

Since the successive formation constants of nickel-ethylenediamine complexes[6] are $k_1=10^{7.52}$, $k_2=10^{5.28}$ and $k_3=10^{4.26}$, the overall stability constant $K_3(\equiv k_1k_2k_3=10^{18.06})$ is much larger than $K_2(\equiv k_1k_2=10^{13.80})$ or $K_1(\equiv k_1)$ and therefore the concentrations of the complexes $[Ni\ en_2]^{++}$ and $[Ni\ en]^{++}$ are negligibly small in comparison to that of the complex $[Ni\ en_3]^{++}$ in the concentration range of 0.1 to 2.0 M ethylenediamine. Thus S in Eq. (3) are equal to 3 in the present case.

If Eq. (3) is valid for the reduction of nickel complexes, the value of α can be estimated from the log plot shown in Fig. 1 and the value of $(3-p)$ can be obtained by plotting the half-wave potentials against the logarithm of the ethylenediamine concentrations. It is to be noted that the value of α is dependent on the concentration of ethylenediamine and it is not easy to determine $(3-p)$

5) B.E. Douglas, H.A. Laitinen and J.C. Bailar, *J. Am. Chem. Soc.*, 72, 2484 (1950).

6) A.E. Martell and M. Calvin, "Chemistry of the Metal Chelate Compounds", Prentice-Hall, New York (1952), p. 518, 519.

so definitely as in the nickel-ammonia system[2]. But, as shown in Fig. 4, the value of $(3-p)$ may be estimated as approximately equal to 1, that is, $p \simeq 2$. This value seems reasonable, considering the higher stability of the ethylenediamine complex than that of the ammonia complex, for which p was found to be equal to 2*. Thus the complex $[Ni\ en_3]^{++}$ in the solution may dissociate into the complex $[Ni\ en_2]^{++}$ in the vicinity of the electrode surface, and then it will be reduced at the dropping electrode.

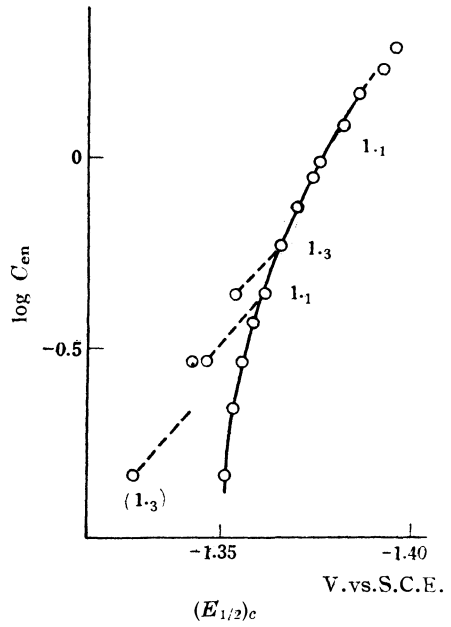

Fig. 4. Variation of $(E_{1/2})_c$ for nickel as a function of log C_{en}.

Figures of $1._1$, $1._3$ and $1._0$ represent values of $(S-p)$ at the reciprocal slopes of 74, 70 and 60 mV., respectively.

The forward rate constant of this electron transfer process can also be calculated by Eq. (3)**. The results are given in Table V. Since α depends on the concentration of ethylenediamine and gelatine, k_f^0 thus calculated no longer remains constant. The values of α greatly influence the calculated values of the rate constant. The relation between α and k_f^0 is not yet clear, but Table V shows that the larger α is, the smaller k_f^0 is. Moreover, the equal value for α gave the nearly consistent value for k_f^0 even at the different concentrations of ethylenediamine. This suggests that estimation of α from the log plot (Fig. 1) may be allowed as a first approximation. At the concentration of 1 M ethylenediamine, the values of α and k_f^0 may be close to 0.5 and $10^{-17.3}$ cm./sec., respectively**. For the ammonia complexes, the values $\alpha \simeq 0.7$ and $k_f^0 \simeq 10^{-16.8}$ cm./sec. were found in the solution of 1 M ammonia and 0.1 N KNO_3. Comparing these values, it seems that in the ethylenediamine system the transfer coefficient and the reduction rate constant of the electron transfer process at the normal hydrogen electrode are smaller than those in the ammonia system.

TABLE V
VALUES OF α AND k_f^0 FOR NICKEL
(in 0.1 N KNO_3)

C_{en} (M)	Concn. of Nickel (10^{-3} M)	Concn. of Gelatine (%)	α	$-\log k_f^0$ (k_f^0: cm./sec.)
0.146	0.6	0.020	0.33	$11._5$
0.146	0.6	0.013	0.38	$13._3$
0.219	0.6	0.020	0.36	$12._8$
0.292	0.6	0.020	0.37	$13._0$
0.292	0.6	0.016	0.40	$14._0$
0.292	0.6	0.015	0.41	$14._3$
0.365	0.6	0.020	0.39	$13._7$
0.438	0.6	0.020	0.40	$14._0$
0.438	0.6	0.016	0.42	$14._5$
0.584	0.6	0.020	0.42	$14._8$
0.730	0.6	0.020	0.44	$15._5$
0.876	0.6	0.020	0.47	$16._5$
0.966	0.6	0.020	0.49	$17._5$
0.966	0.4_2	0.020	0.54	$19._1$
0.966	0.2_4	0.020	0.57	$20._1$
1.21	0.6	0.020	0.50	$17._8$
1.45	0.6	0.020	0.53	$18._8$
1.69	0.6	0.020	0.55	$19._7$
1.93	0.6	0.020	0.57	$20._5$

Zinc Complexes.—This system belongs also to an irreversible type and Eq. (1) can not be used to interpret the waves[7]. The plot of $(E_{1/2})_c$ against log C_{en} are given in Fig. 5.

In the range of 0.1 to 2.0 M ethylenediamine α, taken from the log plot, remains constant to be equal to 0.86. Since the successive complex formation constants for zinc-ethylenediamine system[6] are $k_1=10^{5.71}$, $k_2=10^{4.33}$ and $k_3=10^{1.72}$, K_3 is larger than K_2 or

* Ethylenediamine is a bidentate group, while ammonia is a monodentate group. The successive formation constants for nickel-ammonia system are $k_1=10^{2.80}$, $k_2=10^{2.24}$, $k_3=10^{1.78}$, $k_4=10^{1.19}$, $k_5=10^{0.75}$ and $k_6=10^{0.04}$.

** The ratio of the diffusion current of the complex ion to that of the simple ion is taken from Tables III and IV. D may be calculated using this ratio and the diffusion coefficient of the simple ion at infinite dilution (0.69×10^{-5} cm.^{2}/sec. for nickel and 0.72×10^{-5} cm.^{2}/sec. for zinc).

** Since $\alpha \simeq 0.5$ is used in the calculation of the rate constant, the values given here may be allowed as approximate values, although it is found that the slope and the half-wave potential are dependent on the concentration of nickel.

7) C.J. Nyman, E.W. Murbach and G.B. Millard, *J. Am. Chem. Soc.*, 77. 4194 (1955).

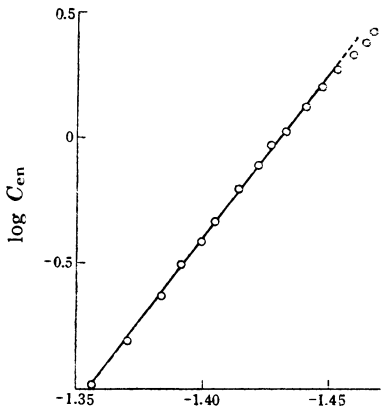

Fig. 5. Variation of $(E_{1/2})_c$ for zinc as a function of $\log C_{en}$.

K_1 and therefore the complex $[Zn\ en_3]^{++}$ predominates in the solution under investigation. So Eq. (3) can be used to interpret the waves. From the plot shown in Fig. 5 the value of $(3-p)$ is obtained as equal to 2.2, that is, $p \simeq 1$. Thus the complex $[Zn\ en_3]^{++}$ in the solution may dissociate into the complex $[Zn\ en]^{++}$ and then it will participate in the electron transfer process. The forward rate constant of the electron transfer process at the concentration of 1 M ethylenediamine can be calculated to be nearly equal to $10^{-31.2}$ cm./sec. The reduction rate constant of the electron transfer process at the equilibrium potential ($E_G = -0.930$ V. vs. N.H.E.*) can be obtained as $k_G \simeq 10^{-4.9}$ cm./sec. This value seems reasonable in comparison to the rate constant $k_G \simeq 10^{-2.4}$ cm./sec. for zinc ion in the solution of 1 M KCl found by Randles and Somerton[8], since the ethylenediamine complex is much more stable than the chloride complex.

* This value was estimated using $E_G = -0.762$ V. vs. N.H.E. for the reduction of simple zinc ion in 1 N KNO_3 and $K_1 = 10^{5.71}$.

8) J. E. B. Randles and K. W. Somerton, *Trans. Faraday Soc.*, **48**, 951 (1952).

Summary

1. The reduction of cadmium-ethylenediamine complexes is reversible. In the concentration range of 0.1 to 2.0 M ethylenediamine $[Cd\ en_3]^{++}$ predominates in the solution, of which complex formation constant is equal to $10^{12.01}$.

2. The reduction of nickel-ethylenediamine complexes is irreversible. With the aid of the theoretical treatment developed by Matsuda and Ayabe, it was found that at the concentration of 1 M ethylenediamine $[Ni\ en_2]^{++}$ participated in the electron transfer process with the forward rate constant nearly equal to $10^{-17.6}$ cm./sec. and the transfer coefficient nearly equal to 0.5.

3. The reduction of zinc-ethylenediamine complexes is irreversible. It was found that in the concentration range of 0.1 to 2.0 M ethylenediamine $[Zn\ en]^{++}$ participated in the electron transfer process with the forward rate constant nearly equal to $10^{-31.2}$ cm./sec. and the transfer coefficient equal to 0.86.

4. The decrease of the diffusion currents are due to the increase of the viscosities of the solutions. The apparent polarographic diffusion coefficients of these complex metal ions are ca. 8% smaller than those of the simple metal ions.

The author wishes to express his gratitude to Mr. M. Senda, Faculty of Agriculture, Kyoto University and to Mr. H. Matsuda, Government Chemical Industrial Research Institute, Tokyo, for their valuable suggestions.

Department of Industrial Chemistry
Nagoya Institute of Technology
Nagoya

Magnetic Susceptibilities of Coronene, Pentacene and Related Compounds

By Hideo AKAMATU and Yoshio MATSUNAGA

(Received May 1, 1956)

Introduction

In a previous paper[1] the magnetic susceptibilities and anisotropies of polycyclic aromatic compounds have been presented. In that paper, however, data on coronene and pentacene have not been included. Recently, good specimens of these compounds have kindly been provided by Dr. E. Clar of the University of Glasgow, who had synthesized them. We append here the data on these compounds with some related ones which have been re-examined.

Experimental and Results

The measurements of the magnetic susceptibility were made by the Gouy method, referring to the volume susceptibility of water as $-0.720\cdot10^{-6}$ at 20°C.

Coronene.—Coronene which has been provided by Dr. Clar consists of long yellow needle crystals.

The gram susceptibility, $-\chi\cdot10^{6}=0.810\pm0.003$ (in c.g.s. unit).

The mole susceptibility, $-\chi_M\cdot10^{6}=243.3$.

Pentacene.—The pentacene which has been provided by Dr. Clar is a deep bluish violet powder. After preliminary measurements had been made, the sample was sublimed in vacuum. The greater part of the sample was sublimed excepting a small amount of dark residue. In practice, however, this procedure had not much effect upon the result.

The gram susceptibility, $-\chi\cdot10^{6}=0.738\pm0.003$.

The mole susceptibility, $-\chi_M\cdot10^{6}=205.4$.

Anthracene and Tetracene.—Anthracene was synthesized starting from anthraquinone, and tetracene was obtained from Fulka. They were purified carefully in the usual manner.

Anthracene, $-\chi\cdot10^{6}=0.731\pm0.002$.

Tetracene, $-\chi\cdot10^{6}=0.736\pm0.002$.

Violanthrene.—The magnetic susceptibility of violanthrene has been re-examined, because there occured some doubt about the purity of the former specimen. Violanthrone was synthesized from benzanthrone, and reduced to violanthrene by zinc dust fusion after Clar. In this procedure, the so-called B-compound was carefully separated. The specimen was purified by sublimation in vacuum.

The gram susceptibility, $-\chi\cdot10^{6}=0.733\pm0.004$.

The mole susceptibility, $-\chi_M\cdot10^{6}=312.6$.

1) H. Akamatu and Y. Matsunaga, This Bulletin, **26**, 364 (1953).

Discussion

Let K_1, K_2 and K_3 be the principal mole susceptibilities of the molecule, where K_1 and K_2 are those in the plane of molecule and K_3 is that perpendicular to it. As presented in the previous paper, K_1 $(=K_2)$ is calculated by the empirical formula after Hazato[2],

$$K_1=\Sigma\chi(C=)+\Sigma\chi(H) \qquad (1)$$

where $\chi(C=)=-3.36\cdot10^{-6}$ and $\chi(H)=-2.93\cdot10^{-6}$. The diamagnetic anisotropy is given by

$$\Delta K=K_3-K_1=3(\chi_M-K_1) \qquad (2)$$

This results for coronene, $K_1=-115.8\cdot10^{-6}$, and $\Delta K=-383\cdot10^{-6}$.

Such an approximate calculation has, hitherto, been made because it is difficult to obtain single crystals large enough in size for the magnetic measurements.

For coronene, however, Rogers[3] has measured the magnetic anisotropy of a single crystal, and his results were,

$$X_1-X_2=180\cdot10^{-6},\quad X_1-X_3=210\cdot10^{-6},$$
$$X_2-X_3=30\cdot10^{-6},\text{ and }\Delta K=-390\cdot10^{-6},$$

where X_1, X_2 and X_3 are the principal mole susceptibilities of the crystal. However, the mean susceptibility has not been measured but was assumed to be $\chi_M=-220\cdot10^{-6}$ following Pascal's formula. This value is somewhat small from the present view. When we combine the observed value of χ_M $(=-243\cdot10^{-6})$ with his data of anisotropy, we obtain

$$-X_1\cdot10^{6}=113,\quad -X_2\cdot10^{6}=293,\quad\text{and}$$
$$-X_3\cdot10^{6}=323.$$

As coronene crystal belongs to monoclinic system, X_1 is equal to K_1[4]. Consequently, this value of X_1 (or K_1) as well as ΔK are in good agreement with the corresponding values which are obtained using equation (1).

Krishnan and Banerjee[5] have observed the mean susceptibilities and the anisotropies of single crystals of chrysene, pyrene and perylene. Their results are compared with the

2) H. Shiba and G. Hazato, This Bulletin, **22**, 92 (1949).

3) M.T. Rogers, *J. Am. Chem. Soc.*, **69**, 1506 (1947).

4) K. Lonsdale and K.S. Krishnan, *Proc. Roy. Soc., London*, **A156**, 597 (1936).

5) a. K.S. Krishnan and S. Banerjee, *Phil. Trans. Roy. Soc.*, **A234**, 265 (1935). b. S. Banerjee, *Z. Krist.*, **100**, 316 (1939).

corresponding ones which were calculated in accordance with the equation (1) using our own observed values of mean susceptibility.

Chrysene:	(K. & B.)	$-\chi_M\cdot10^5=160.7$,	$-K_1\cdot10^5=88.0$,	$-\Delta K\cdot10^5=218.$
	(A. & M.)	168.5,	95.6,	219.
Pyrene:	(K. & B.)	$-\chi_M\cdot10^5=154.9$,	$-K_1\cdot10^5=80.6$,	$-\Delta K\cdot10^5=223.$
	(A. & M.)	148.6,	83.1,	197.
Perylene:	(B.)	$-\chi_M\cdot10^5=159.6$,	$-K_1\cdot10^5=95.5$,	$-\Delta K\cdot10^5=192.$
	(A. & M.)	166.8,	102.4,	193.

They are in pretty good agreement with each other, therefore, an empirical formula such as equation (1) is a useful expression.

There is a little argument about the contribution of the number of aromatic rings to the diamagnetic anisotropy of the polycyclic hydrocarbon molecule. In the present case of coronene, $\Delta K/\Delta K_B=7.2$, where ΔK_B, the diamagnetic anisotropy of benzene, is $-54\cdot10^{-6}$. This value denotes approximately the number of aromatic rings in coronene molecule, whilst, the theoretical calculation by the molecular orbital method after London has been presented as

$\Delta K/\Delta K_B=9.796$ (when $S=0$),
and $\Delta K/\Delta K_B=10.13$ (when $S=0.25$),

where S is the overlap integral[6]. The present result reveals that these calculated values are too large.

Assuming $\Delta K=-(Ne^2/4mc^2)\sum_p\overline{r^2}$, where p is the number of π-electrons and other symbols are the usual ones, the average effective radius of the π-electron orbitals $\sqrt{\overline{r^2}}$ has been estimated. The result is $\sqrt{\overline{r^2}}=1.94$ Å for coronene. Such a quantity is assumed as measuring the delocalized character of π-electrons in a molecule and increases linearly with the number of π-electrons in a series of hydrocarbons. This is shown in Fig. 1. This figure includes also the re-examined value for violanthrene i.e., $\sqrt{\overline{r^2}}=1.74$ Å.

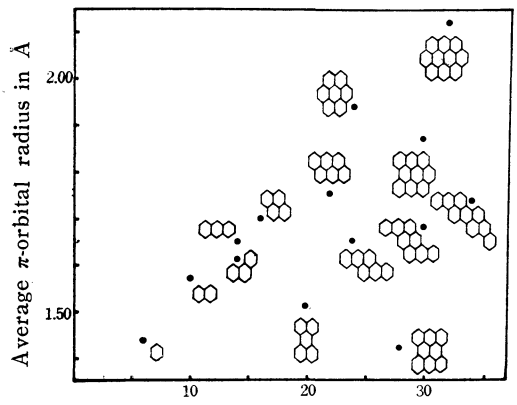

Fig. 1. $\sqrt{\overline{r^2}}$ is plotted against the number of carbon atoms.

The values of K_1, ΔK and $\sqrt{\overline{r^2}}$ have been estimated in a similar way by the empirical formula for pentacene and other polyacenes. The results are shown in Table I.

TABLE I

	$-\chi_M\cdot10^5$	$-K_1\cdot10^5$	$-\Delta K\cdot10^6$	$\sqrt{\overline{r^2}}$ (Å)
Naphthalene	92.2	57.0	106	1.57
Anthracene	130.3	76.3	162	1.65
Tetracene	168.0	95.6	217	1.69
Pentacene	205.4	114.9	272	1.71

The magnetic anisotropies of single crystals of these compounds have been presented, excepting pentacene, and the observed values are as follows,

Naphthalene[4]	$-K_1\cdot10^5=55.0$,	$-\Delta K\cdot10^5=114$
Anthracene[4]	69.2,	183
Tetracene[5b]	108.8,	154

In the case of tetracene, the discrepancy in ΔK is great. However, this does not mean that the correctness of the empirical calculation is destroyed. It is rather unnatural for ΔK of tetracene to be smaller than that of anthracene. The direct measurement of anisotropy of a single crystal does not give necessarily the correct value, because it demands a delicate technique.

From the present results, it is found that from naphthalene to pentacene the increment in ΔK is $-55\cdot10^{-6}$ per benzene ring, this value is equal to ΔK_B, therefore, the diamagnetic anisotropy increases proportionally with the number of benzene rings.

Meanwhile, the molecular orbital calculation for the diamagnetic anisotropies of these compounds have been presented as follows[7]-

ΔK(naphthalene)$/\Delta K_B=2.19(S=0)$, $2.22(S=0.25)$,
ΔK(anthracene)$/\Delta K_B=3.45(S=0)$, $3.53(S=0.25)$,
ΔK(tetracene)$/\Delta K_B=4.75(S=0)$, $4.88(S=0.25)$,
ΔK(pentacene)$/\Delta K_B=6.06(S=0)$, $6.26(S=0.25)$

6) R. McWeeny, *Proc. Phys. Soc.*, **A64**, 921 (1951); G. Berthier, M. Mayot, A. Pullman and B. Pullman, *J. phys. radium.*, **13**, 15 (1952).

7) R. McWeeny, *Pro. Phys. Soc.*, **A65**, 839 (1952).

The calculated values are again greater than the observed ones, and the discrepancy tends to be high the larger the molecule is.

The mole susceptibility of pentacene was presented before, that is, $-172 \cdot 10^{-6}$ by Müller[8] and $-183 \cdot 10^{-6}$ by Pacault[9]. These values are remarkably smaller than the presumed value from the number of benzene rings in this molecule. In consequence, it has been frequently assumed that in polyacene series the localization of π-electrons or even a paramagnetic contribution could take place when the molecule becomes larger. But it reveals, from the present results, that this is not the case. The diamagnetic anisotropy increases proportionally with the number of benzene rings, and this means, in the case of polyacene series, that the effective π-orbital radius becomes constant regardless of the number of aromatic rings, since the increment in the number of π-electrons is four per one benzene ring.

We are grateful to Dr. E. Clar who kindly provided us with his samples of coronene and pentacene. Violanthrene and anthracene were prepared by Mr. J. Aoki to whom our hearty thanks are due.

Department of Chemistry
Faculty of Science
The University of Tokyo
Tokyo

8) E. Müller and I. Müller-Rodloff, *Ann.*, **517**, 134 (1935).
9) A. Pacault and Ch. Marshalk, *Bull. soc. chim. France*, **19**, 141 (1952).

Internal Rotation in Amino Acids

By Michiro HAYASHI, Takehiko SHIMANOUCHI and San-ichiro MIZUSHIMA

(Received April 12, 1956)

Introduction

Several models of proteins have been presented[1-4]. They cannot differ much from one another in bond lengths and bond angles. The essential point in their difference lies in the manner of the chain-folding due to the internal rotation about single bonds contained in the polypeptide chain.

With regard to the equilibrium angles of internal rotation in amides and related compounds we have published many papers[5,6,7]. The work has been extended to the study of equilibrium angles in amino acids based on the data of the X-ray structure analysis. The references for these data are as follows:

DL-Norleucine (α-form); A. M. Mathieson, *Acta Cryst.*, **6**, 399 (1953).

DL-Methionine (α-form); A. M. Mathieson, *Acta Cryst.*, **5**, 332 (1952).

DL-Methionine (β-form); A. M. Mathieson, *Acta Cryst.*, **5**, 332 (1952).

Hydroxy-L-proline; J. Donohue, *Acta Cryst.*, **5**, 419 (1952).

DL-Serine: D. P. Shoemaker, R. E. Barieau, J. Donohue and Chia-Si Lu; *Acta Cryst.*, **6**, 241 (1953).

Glycyl-L-tyrosin hydrochloride; D.W. Smits and E. H. Wiebenga; *Acta Cryst.*, **6**, 531 (1953).

α-Glycine; G. Albrecht and R. B. Corey, *J. Am. Chem. Soc.*, **61**, 1087 (1939).

α-DL-Alanine; H. A. Levy and R. B. Corey, *J. Am. Chem. Soc.* **63**, 2095 (1941), J. Donohue, *J. Am. Chem. Soc.*, **72**, 949 (1950).

β-Glycylglycine; E. W. Hughes and W. J. Moore, *J. Am. Chem. Soc.*, **71**, 2618 (1949).

N-Acetylglycine; G. B. Carpenter and S. Donohue, *J. Am. Chem. Soc.* **72**, 2315 (1950).

LS-Threonine; D. P. Shoemaker, J. Donohue, V. Shoemaker and R. B. Corey, *J. Am. Chem. Soc.*, **72**, 2328 (1950).

DL-Glutamic acid hydrochloride; B. Dawson, *Acta Cryst.*, **6**, 81 (1953).

Glycyl-L-asparagine; R. A. Pasternak, L. Katz and R. Corey: *Acta Cryst.*, **7**, 225 (1954).

NN'-Diglycyl-L-cystine dihydrate; H. L. Yakel and E. W. Hughes, *Acta Cryst.*, **7**, 29 (1954).

D(−)-Isoleucine hydrochloride; J. Trommel and J. M. Bijvoet; *Acta Cryst.*, **7**, 703 (1954).

D(−)-Isoleucine hydrobromide: J. Trommel and J. M. Bijvoet; *Acta Cryst.*, **7**, 703 (1954).

L-Glutamine; W. Cochran and B. P. Penfold, *Acta Cryst.*, **5**, 644 (1952).

1) T. Shimanouchi and S. Mizushima, *Kagaku*, **17**, 24, 52 (1947); *Bull. Chem. Soc. Japan*, **21**, 1 (1948); S. Mizushima, Advances in Protein Chemistry IX.

2) H. Zahn, *Z. Naturforschung*, **2B**, 104 (1947).

3) E.J. Ambrose and W.E. Hanby, *Nature*, **163**, 483 (1949).

4) L. Pauling, R.B. Corey and H.R. Branson. *Proc. Natl. Acad. Sci. U.S.*, **37**, 205 (1951).

5) For the summary, see S. Mizushima, Structure of Molecules and Internal Rotation, Academic Press, New York (1954). See also ref. 1.

6) S. Mizushima, T. Shimanouchi, M. Tsuboi, et al., *J. Am. Chem. Soc.*, **72**, 3490 (1950); **73**, 1330 (1951); **74**, 270, 4639, 5550 (1952); **75**, 1863 (1953); **76**, 2479, 6003 (1954).

7) T. Shimanouchi and S. Mizushima, *J. Chem. Phys.*, **23**, 707 (1955).

L-Glutamic acid; S. Hirokawa, *Acta Cryst.*, 8, 637 (1955)*.

The Method of Calculation

In order to obtain equilibrium angles of internal rotation from the X-ray data, it is convenient to express the positions of atoms in rectangular coordinate systems.

The transformation from oblique coordinates to rectangular coordinates can be expressed as:

$$X=AU, \tag{1}$$

where X and U are unit vectors in the rectangular and oblique coordinates, respectively and A is a matrix:

$$A=\begin{pmatrix} a, & b\cos\gamma, & c\cos\beta \\ 0, & b\sin\gamma, & \frac{c}{\sin\gamma}(\cos\alpha-\cos\beta\cos\gamma) \\ 0, & 0, & \frac{c}{\sin\gamma}(\sin^2\gamma-\cos^2\alpha-\cos^2\beta+2\cos\alpha\cos\beta\cos\gamma) \end{pmatrix} \tag{2}$$

Here a, b, c are the lengths and α, β, γ, the angles of the unit cell in the oblique coordinate system.

The equilibrium angle θ of internal rotation about X_2–X_3 axis of the part X_1–X_2–X_3–X_4 is calculated as:

$$\cos\theta=\pm(\lambda\lambda'+\mu\mu'+\nu\nu'), \tag{3}$$

where λ, μ, ν and λ', μ', ν' are the direction cosines of the normals to the X_1–X_2–X_3 and X_2–X_3–X_4 planes, respectively.

The results of the calculation are listed in Tables I–VI. Table I refers to the

TABLE I

θ ABOUT THE C—C_α AXIS IN

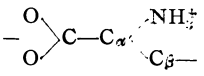

Compound	NH_3^+	C_β
α-DL-Norleucine	12.5°	− 71.5°
α-DL-Methionine	33.5	− 90
β-DL-Methionine	29.5	− 89
Hydroxy-L-proline	3	−114
DL-Serine	4	−126
α-Glycine	13	—
α-DL-Alanine	17	−104.5
Ls-Threonine	25	− 95
DL-Glutamic acid hydrochloride	37	− 90
D(−)-Isoleucine hydrochloride	6.5	138
D(−)-Isoleucine hydrobromide	14	−121
L-Glutamine	51	−113
L-Glutamic acid	43	77
L-Glutamic acid hydrochloride	18	100

internal rotation about the C—C_α axis in 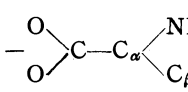 . The θ values of the NH_3^+ group lie in the range 0 to 37° and those of the C_β atom in the range −126° to −90° referred to the 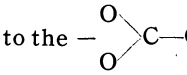 plane. An exception is made for D(−)-isoleucine hydrochloride with the θ value of 138°. By some reason the C_β atom and the NH_3^+ group are on the same side of the 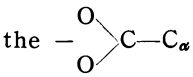 plane.

TABLE II

θ ABOUT THE C—C_α AXIS IN

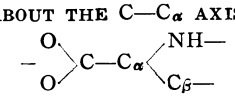

Compound	NH	C_β
β-Glycylglycine	0°	—
N-Acetylglycine	2.5	—
Glycyl-L-tyrosine hydrochloride	37	174.5
Glycyl-L-asparagine	63	173.5
NN′-Diglycyl-L-cystine dihydrate	73.5	175

Table II lists the θ values for the structure 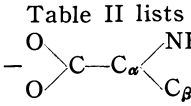 . Those for the stable positions of the —NH— group fall into two groups. One has the θ values almost equal to zero: i.e. the N atom lies close to the 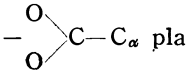 plane. In the other group the θ values lie in the range ca. 40° to 70°. This difference is due to the presence of the C_β atom in the latter group which makes the steric relation in the molecule quite different from that of the former group. It is to be noted that the C_β atom lies on the other side of the 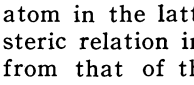 plane with respect to the N atom.

The θ values of the C_γ atom of the structure 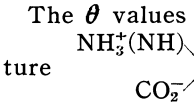 are shown in Table III. In some cases we have the OH group or S atom in place of the C_γ atom. The values lie in the three ranges, 50° to 80°, 180° to 160° and −80° to −60°. These correspond, respectively, to the *gauche, trans* and *gauche* positions with respect to C_α—CO_2^- and to the *gauche, gauche* and *trans* positions with respect to C_α—NH_3^+(NH). In other words, the stable positions are almost the same as those found in simple molecules such as ClH_2C—CH_2Cl.

* The author has calculated the equilibrium angles of internal rotation.

TABLE III

θ ABOUT THE $C_\alpha - C_\beta$ AXIS IN

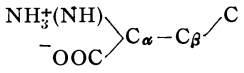

Compound	C_γ	Note
DL-Norleucine	178.5	
α-DL-Methionine	177	
β-DL-Methionine	179	
L$_S$-Threonine	177.5	OH in place of C_γ
DL-Glutamic acid hydrochloride	157	
Glycyl-L-asparagine	173.5	
D(-)-Isoleucine hydrochloride	160	
DL-Serine	53	OH in place of C_γ
D(−)-Isoleucine hydrochloride	79	
D(−)-Isoleucine hydrobromide	65	
L-Glutamine	54	
Glycyl-L-tyrosine hydrochloride	−80	
L$_S$-Threonine	−63	
NN′-Diglycyl-L-cystine dihydrate	−77.5	S in place of C_γ
D(−)-Isoleucine hydrobromide	−60	
L-Glutamic acid	180	

TABLE IV

θ ABOUT THE $C_\beta - C_\gamma$ AXIS IN

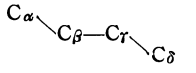

Compound	C_δ	Note
DL-Norleucine	179°	
α-DL-Methionine	177	S in place of C_δ
β-DL-Methionine	176.5	S in place of C_δ
D(−)-Isoleucine hydrochloride	172	
D(−)-Isoleucine hydrobromide	−69	
L-Glutamine	176	
L-Glutamic acid	90	
DL-Glutamic acid hydrochloride	180	

Table IV refers to the structure of $C_\alpha - C_\beta - C_\gamma - C_\delta$ which is similar to that of a segment of a normal paraffin molecule. This has been shown to be in the *trans* form (or the extended form) in the solid state[8]. As shown in this table, the C_δ atom is almost in the *trans* position with respect to the C_α atom except for D(−)-isoleucine hydrobromide.

Table V shows structure of NH—C—C—N^+, ‖ O including the similar structures with C in place of NH and with C or N in place of N^+. NH (or C) is in the *trans* position with respect to N^+ (or C or N).

Table VI refers to the structure of C—NH ‖ O —C—C. C=O is in the *trans* or the *gauche* position with respect to the C atom.

TABLE V

θ ABOUT THE C—C AXIS IN

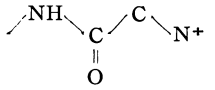

Compound	N(C)	Note
β-Glycylglycine	−146°	
Glycyl-L-asparagine	−172	
Glycyl-L-asparagine	−171	C in place of N^+
NN′-Diglycyl-L-cystine	−170.5	
L-Glutamine	−165	C in place of N^+

TABLE VI

θ ABOUT THE N—C AXIS IN

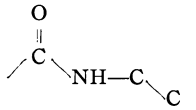

Compound	C	Note
Glycyl-L-tyrosine hydrochloride	177.5°	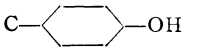
β-Glycylglycine	177.5	
N-Acetylglycine	180	
NN′-Diglycyl-L-cystine	154	CO_2^-
Glycyl-L-tyrosine hydrochloride	85	CO_2^-
NN′-Diglycyl-L-cystine dihydrate	62.5	CH_2

In addition to the axes of internal rotation mentioned above we have the C—S axis in the structure of C—C—S—C and the S—S axis in the structure of C—S—S—C. The θ values in the former in α and β forms of DL-Methionine are 80° and 170°, respectively and that of the latter in NN′-diglycyl-L-cystine dihydrate is 101°. It is to be noted that in the S—S axis the dominant factor in determining the θ value is the electronic clouds on the S atoms which are unsymmetrical about the S—S axis[9]. In other cases where the hindering of internal rotation mainly arises from the interaction between the rotating groups, the results obtained above for amino acids are compatible with our conclusion of the *trans* and *gauche* stable positions derived from the structure determination of many molecules containing the C—C, C—O and C—N axes[5,7]. The result obtained in the present work provides us with further information which would permit the reliable prediction of the structure of polypeptide chain.

Summary

Equibrium angles of internal rotation about single bonds in amino acids have been calculated based on the data of the X-ray structure analysis. The result was similar to that obtained so far for many molecules containing similar bonds

Chemical Laboratory, Faculty of Science
The University of Tokyo, Hongo
Tokyo

8) S. Mizushima and T. Shimanouchi, *J. Am. Chem. Soc.*, **71**, 1320 (1949).

9) Y. Morino and S. Mizushima, *Sci. Pap. Inst. Phys. Chem. Res., Tokyo*, **32**, 220 (1937).

Investigation on Mixed Complex. I. Spectrophotometric Study of Mixed Complexes Formed by Cupric Ion and Bidentate Ligands

By Sigeo KIDA

(Received January 27, 1956)

If two kinds of cupric complexes having bidentate ligands are dissolved to make a solution, the mixed complex is to be formed; e.g., bisethylenediamine copper nitrate and potassium bisoxalato cupriate are expected to react in an aqueous solution and reach the following equilibrium.

$$[Cu\ en_2]^{++}+[Cu\ ox_2]^{--} \rightleftarrows 2[Cu\ en\ ox]$$

(en=ethylenediamine, ox=oxalate ion)

This kind of equilibrium is expressed by the following general formula:

$$MA_2+MB_2 \rightleftarrows 2MAB \qquad (1)$$

$$Km=\frac{(MAB)^2}{(MA_2)(MB_2)} \qquad (2)$$

where, M is the metallic ion of the coordination number four, A and B are bidentate ligands. The reciprocal of Km corresponds to the dismutation constant introduced by Watters et al.[1]

If the bond energies of M–A and M–B are not altered in the two sides of this equilibrium, and there is no interaction between MAB, MA_2 and MB_2, three complex species would be distributed entirely statistically; in this condition Km is equal to 4*.

When the value of Km is found to be far from 4, we can conclude that the bond energies of M–A and M–B are affected by each other in the mixed complex.

The determination of Km makes it possible to draw the absorption curve of the mixed complex by using the measured extinction data of the parent complexes, and it will be interesting to examine the absorption curves of the mixed complex and its parent complexes.

However, there was no investigation on the mixed complexes of this kind, until the investigations were reported by Watters et al. in very recent years[1]. They succeeded in obtaining the formation constants of mixed complexes such as [Cu en P_2O_7]$^{--}$ and [Cu en ox], by using a newly devised "isosbestic method". The present author modified Watters' isosbestic method, and by this method obtained the values of Km and the absorption spectra of the following three mixed complexes, [Cu en ox], [Cu en aca]$^+$ and [Cu dgH aca], where aca and dgH denote acetylacetonate ion ($C_5H_7O_2^-$) and dimethylglyoximate ion ($C_4H_7O_2N_2^-$) respectively.

Determination of *Km*

From the equations (1) and (2) the following relations are derived.

$$Km=\frac{4x^2}{(c_1-x)(c_2-x)} \qquad (3)$$

$$x=\frac{D-\varepsilon_1 c_1-\varepsilon_2 c_2}{2\varepsilon_3-\varepsilon_2-\varepsilon_1}$$

$$D=\varepsilon_1(c_1-x)+\varepsilon_2(c_3-x)+2\varepsilon_3 x \qquad (4)$$

where c_1 and c_2 are concentrations of MA_2 and MB_2 respectively**, and ε_1, ε_2 and ε_3 are the molar extinction coefficients of MA_2, MB_2 and MAB respectively. D is the measured optical density $\left(\log\frac{I_0}{I}\right)$ of the solution in equilibrium. $2x$ is the concentration of the mixed complex. From the equation (4)

$$x=\frac{D-\varepsilon_1 c_1-\varepsilon_2 c_2}{2\varepsilon_3-\varepsilon_2-\varepsilon_1}$$

is obtained. In the case of $\varepsilon_3=m\varepsilon_1$

$$x=\frac{D-\varepsilon_1 c_1-\varepsilon_2 c_2}{\varepsilon_1(2m-1)-\varepsilon_2} \qquad (5)$$

As will be seen from the following examples,

1) R. De Witt and J. Watters, *J. Am. Chem. Soc.*, **76**, 3810 (1954). J.I. Watters, A. Aaron and J. Mason, ibid., **75**, 5212 (1953). J.I. Watters and E.D. Lougham, ibid., **75**, 4819 (1953).

* The statistical value of Km is found in the following way. Since, in this equilibrium, M exists always in combination with any one of pairs AA, BB and AB, instead of MAA, MBB and MAB. Let P_{AA}, P_{BB} and P_{AB} be the probabilities with which the pairs of AA, BB and AB are found, when two particles are picked out from the n particles of both A and B.

$$P_{AA}=P_{BB}=\frac{{}_nC_2}{{}_{2n}C_2}=\frac{n-1}{2(2n-1)}$$

$$P_{AB}=\frac{{}_nC_1\cdot{}_nC_1}{{}_{2n}C_2}=\frac{n}{2n-1}$$

$$\therefore \lim_{n\to\infty} P_{AA}=\lim_{n\to\infty} P_{BB}=\frac{1}{4}$$

$$\lim_{n\to\infty} P_{AB}=\frac{1}{2}$$

$$\therefore Km=\frac{(MAB)^2}{(MA_2)(MB_2)}=\frac{(\frac{1}{2}\times n)^2}{(\frac{1}{4}\times n)(\frac{1}{4}\times n)}=4$$

** c_1 and c_2 are concentrations of MA_2 and MB_2 respectively, when it is assumed that, in the mixed solution of MA_2 and MB_2, MAB is not formed at all. Hereafter such a concentration as the above mentioned will be called the "initial concentration" of MA_2 or MB_2.

the value of m is chosen for the convenience of the experiment (e. g., $m=1, 2, 3$ or 5.5 etc.); and the wavelength where ε_3 is equal to $m\varepsilon_1$ is found in the following procedure.

First, the optical densities of the solution containing MA_2 at the concentration c_0 are measured, and then those of the solution containing MA_2 and MB_2 at the initial concentrations c_0-c and c' are measured respectively. Provided that c and c' are very small compared to c_0, and the equilibrium is not much shifted towards the left side of the following equation, the relation of the concentrations may be considered to be:

$$\underset{(c_0-c-c')}{MA_2} + \underset{(0)}{MB_2} \rightleftarrows \underset{(2c')}{2MAB}$$

Therefore, the condition that the extinction curve of MA_2 (whose concentration is c_0) crosses with the extinction curve of the mixed solution at the wavelength where ε_3 is equal to $m\varepsilon_1$ is:

$$\varepsilon_1 c_0 = \varepsilon_1(c_0-c-c') + 2m\varepsilon_1 c'$$

or

$$c' = \frac{c}{2m-1} \qquad (6)$$

Accordingly, if the initial concentrations of MA_2 and MB_2 are chosen as c_0-c and $c/2m-1$ respectively, (where c is a small variable value—e. g., 5×10^{-5} or 1×10^{-4} etc.), the extinction curves of this mixed solution have the isosbestic point at $\varepsilon_3=m\varepsilon_1$. Thus, from the isosbestic point of these extinction curves, the wavelength where ε_3 is equal to $m\varepsilon_1$ is readily found. Then, at this wavelength extinction measurements are made on the mixed solution of the parent complexes in appropriate concentrations (see the curves of 6, 7 and 8 in Fig. 1 and Table I). From these data and the relations (2) and (4), Km is readily obtained.

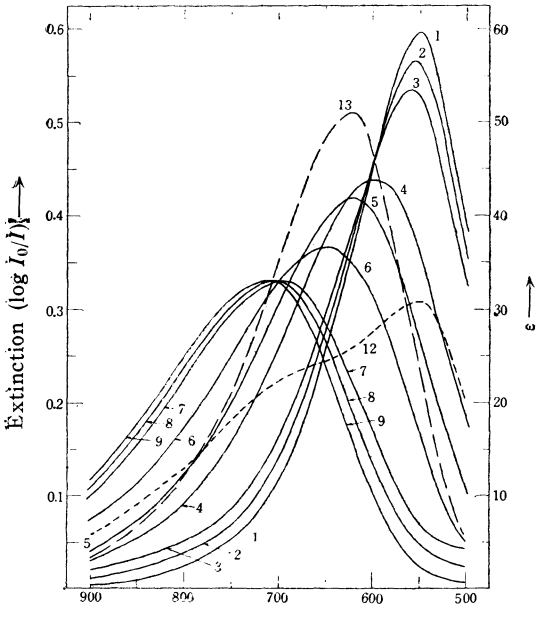

Fig. 1. (cf. Table I)

TABLE I

(cf. Figs. 1 and 2)

Curve	$c_1\times10^2$	$c_2\times10^2$
1	1	0
2	0.95	0.05
3	0.9	0.1
4	$\frac{2}{3}$	$\frac{1}{3}$
5	$\frac{1}{2}$	$\frac{1}{2}$
6	$\frac{1}{3}$	$\frac{2}{3}$
7	0.1	0.9
8	0.05	0.95
9	0	1
10	$0.05\times\frac{1}{3}$	0.95
11	$0.1\times\frac{1}{3}$	0.9
12	$\frac{\varepsilon_1+\varepsilon_2}{2}$	
13	extinction of [Cu en ox] (calcd.)	

c_1: initial concentration of $[Cu\ en_2]^{++}$
c_2: initial concentration of $[Cu\ ox_2]^{--}$

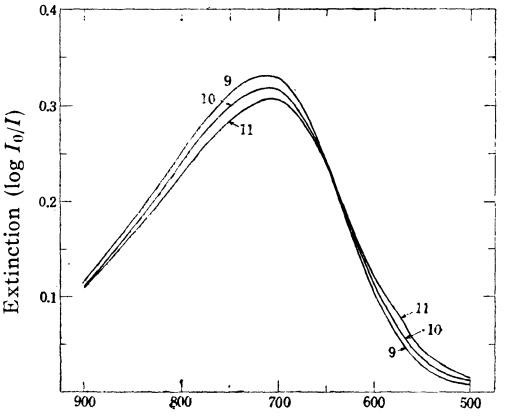

Fig. 2. (cf. Table I)

In the case of $\varepsilon_3=m\varepsilon_2$ the procedure of determining Km is quite similar to that above mentioned.

[Cu en ox]: The wavelength where ε_3 is equal to ε_1 was determined to be 600 mμ by curves 1, 2 and 3 in Fig. 1. The wavelength where ε_3 is equal to $2\varepsilon_1$ was determined to be 650 mμ by curves 9, 10 and 11 in Fig. 2. The wavelength where ε_3 is equal to ε_2 was determined to be 706 mμ by curves 7, 8 and 9 in Fig. 1. At these three wavelengths Km of

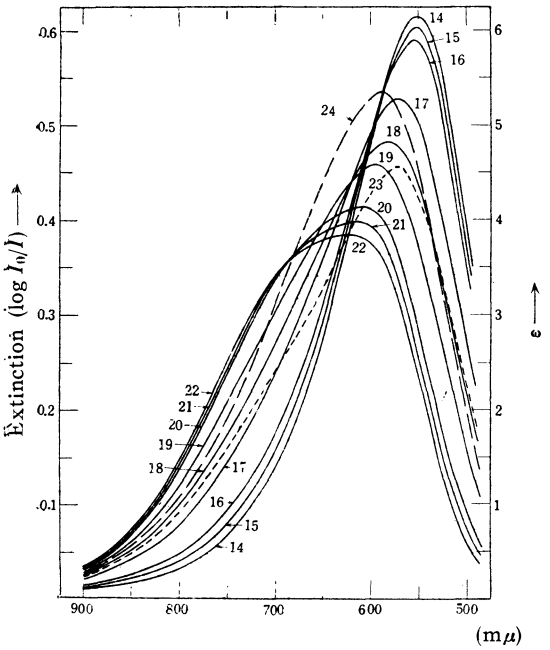

Fig. 3. (cf. Table II)

TABLE II
(cf. Fig. 3)

Curve	$c_1' \times 10^2$	$c_2' \times 10^2$
14	1	0
15	0.95	0.05
16	0.9	0.1
17	$\frac{2}{3}$	$\frac{1}{3}$
18	$\frac{1}{2}$	$\frac{1}{2}$
19	$\frac{1}{3}$	$\frac{2}{3}$
20	0.1	0.9
21	0.05	0.95
22	0	1
23	$\frac{\varepsilon_1' + \varepsilon_2'}{2}$	
24	extinction of [Cu en aca]$^+$ (calcd.)	

c_1': initial concentration of $[Cu\ en_2]^{++}$

c_2': initial concentration of $[Cu\ aca_2]$

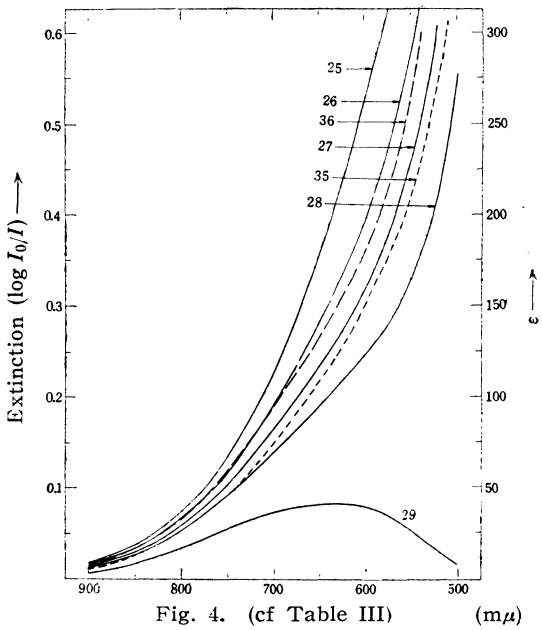

Fig. 4. (cf Table III)

TABLE III
(cf. Figs. 4, 5 and 6)

Curve	$c_1'' \times 10^2$	$c_2'' \times 10^2$
25	0.2	0
26	$0.2 \times \frac{2}{3}$	$0.2 \times \frac{1}{3}$
27	0.1	0.1
28	$0.2 \times \frac{1}{3}$	$0.2 \times \frac{2}{3}$
29	0	0.2
30	0	1
31	$0.05 \times \frac{1}{5}$	0.95
32	$0.1 \times \frac{1}{5}$	0.9
33	$0.05 \times \frac{1}{10}$	0.95
34	$0.1 \times \frac{1}{10}$	0.9
35	$\frac{\varepsilon_2'' + \varepsilon_1''}{2}$	
36	extinction of [Cu dgH aca] (calcd.)	

c_1'': initial concentration of $[Cu(dgH)_2]$

c_2'': initial concentration of $[Cu\ aca_2]$

[Cu en ox] was calculated according to (2) and (4) using the data of curves 1, 4, 5, 6 and 9 in Fig. 1. The results are given in Table V.

[Cu en aca]$^+$: The wavelength where ε_3 is equal to ε_1 was determined to be 588 mμ from curves 14, 15 and 16 in Fig. 3. The wavelength where ε_3 is equal to ε_2 was determined by curves 20, 21, and 22 in Fig. 3 to be 684 mμ. At these two wavelengths Km of [Cu en aca]$^+$ was calculated using the curves 14, 17, 18, 19 and 22 in Fig. 3 according to the method described above. The results are given in Table VI.

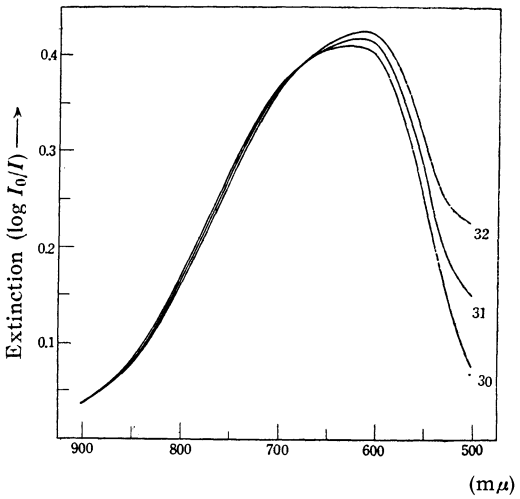

Fig. 5. (cf. Table III)

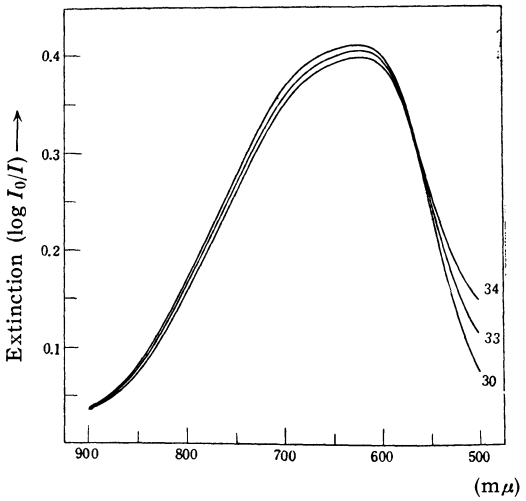

Fig. 6. (cf. Table III)

TABLE IV

RESULTS OF THE EXPERIMENTS ON THE EQUILIBRIUM $[Cu\ en_2]^{++}+[Cu\ ox_2]^{--} \rightleftarrows 2[Cuen\ ox]$, AT 20° IN AQUEOUS SOLUTION, IONIC STRENGTH WAS ADJUSTED TO 0.25 BY $NaNO_3$

Wavelength (mμ)	$c_1\times10^2$	$c_2\times10^2$	D	ε_1	ε_2	ε_3	log Km
600	$\frac{2}{3}$	$\frac{1}{3}$	0.440	45.8	10.3	ε_1	1.12
600	$\frac{1}{2}$	$\frac{1}{2}$	0.404	〃	〃	〃	1.38
600	$\frac{1}{3}$	$\frac{2}{3}$	0.315	〃	〃	〃	0.91
706	$\frac{2}{3}$	$\frac{1}{3}$	0.249	11.4	33.4	ε_2	1.12
706	$\frac{1}{2}$	$\frac{1}{2}$	0.291	〃	〃	〃	1.11
706	$\frac{1}{3}$	$\frac{2}{3}$	0.322	〃	〃	〃	1.05
650	$\frac{2}{3}$	$\frac{1}{3}$	0.379	26.2	23.9	$2\varepsilon_2$	1.05
650	$\frac{1}{2}$	$\frac{1}{2}$	0.395	〃	〃	〃	1.13
650	$\frac{1}{3}$	$\frac{2}{3}$	0.369	〃	〃	〃	1.03

Mean value of log Km=1.10

c_1, c_2: initial concentrations of [Cu en)$^{++}$ and [Cu ox]$^{--}$ respectively

D: optical bensity of the solution

ε_1, ε_2, ε_3: molar extinction coefficients of $[Cu\ en_2]^{++}$, $[Cu\ ox_2]^{--}$ and [Cu en ox] respectively

[Cu dgH aca]: The wavelength where ε_3 is equal to $3\varepsilon_1$ was determined to be 674 mμ from curves 30, 31 and in Fig. 5. The wavelength where ε_3 is equal to 5.5 ε_1 was determined to be 582 mμ from curves 30, 33 and 34 in Fig. 6. At these two wavelengths Km of [Cu dgH aca] was calculated using curves 25, 26, 27, 28 and 29 in Fig. 4. The results are given in Table VI.

TABLE V

RESULTS OF THE EXPERIMENTS ON THE EQUILIBRIUM, $[Cu\ en_2]^{++}+[Cu\ aca_2] \rightleftarrows 2[Cu\ en\ aca]^+$, AT 20° IN 75% DIOXANE SOLUTION WHICH CONTAINS $NaNO_3$ IN THE CONCENTRATION OF 0.1 M

Wavelength	$c_1' \times 10^2$	$c_2' \times 10^2$	D	ε_1'	ε_2'	ε_3'	$\log Km$
588	$\frac{2}{3}$	$\frac{1}{3}$	0.510	53.2	35.9	ε_1'	0.42
588	$\frac{1}{2}$	$\frac{1}{2}$	0.484	〃	〃	〃	0.40
588	$\frac{1}{3}$	$\frac{2}{3}$	0.452	〃	〃	〃	0.42
684	$\frac{2}{3}$	$\frac{1}{3}$	0.272	17.0	35.8	ε_2'	0.49
684	$\frac{1}{2}$	$\frac{1}{2}$	0.305	〃	〃	〃	0.39
684	$\frac{1}{3}$	$\frac{2}{3}$	0.334	〃	〃	〃	0.43

Mean value of $\log Km = 0.42$

c_1', c_2': initial concentrations of $[Cu\ en_2]^{++}$ and $[Cu\ aca_2]$, respectively

D: optical density of the solution

ε_1', ε_2', ε_3': molar extinction coefficients of $[Cu\ en_2]^{++}$, $[Cu\ aca_2]$ and $[Cu(en)\ aca]^+$ respectively

TABLE VI

RESULTS OF THE EXPERIMENTS ON THE EQUILIBRIUM, $[Cu(dgH)_2]+[Cu\ aca_2] \rightleftarrows 2[Cu\ dgH\ aca]$, AT 20° IN 50% DIOXANE AND 50% ETHYL ALCOHOL MIXTURE

Wavelength (mμ)	$c_1'' \times 10^3$	$c_2'' \times 10^3$	D	ε_1''	ε_2''	ε_3''	$\log Km$
582	$\frac{3}{4}$	$\frac{2}{3}$	0.446	302	36.0	$5.5\varepsilon_1''$	$\bar{1}.87$
582	1	1	0.368	〃	〃	〃	$\bar{1}.99$
582	$\frac{2}{3}$	$\frac{3}{4}$	0.269	〃	〃	〃	$\bar{1}.98$
674	$\frac{3}{4}$	$\frac{2}{3}$	0.235	143	38.0	$3\varepsilon_1''$	$\bar{1}.96$
674	1	1	0.198	〃	〃	〃	$\bar{1}.97$
674	$\frac{2}{3}$	$\frac{4}{3}$	0.165	〃	〃	〃	$\bar{1}.97$

Mean value of $\log Km = \bar{1}.96$

c_1'', c_2'': initial concentrations of $[Cu(dgH)_2]$ and $[Cu\ aca_2]$, respectively

D: optical density of the solution

ε_1'', ε_2'', ε_3'': molar extinction coefficient of $[Cu(dgH)_2]$, $[Cu\ aca_2]$ and $[Cu\ dgH\ aca]$ respectively

TABLE VII

THE VALUE OF $\log Km$

	$[Cu\ en\ P_2O_7]^{--}$	$[Cu\ en\ ox]$	$[Cu\ en\ aca]^+$	$[Cu\ dgH\ aca]$	Statistical Value
$\log Km$	1.70*	1.00*, 1.10	0.42	$\bar{1}.96$	0.60

* Data from the investigation of Watters and Lougham

Experimental

Apparatus.—All extinction measurements were made by the Beckman DU Spectrophotometer using 1 cm. quartz cells.

Materials.—[Cu en_2]$(NO_3)_2$ was prepared from copper nitrate and ethylenediamine, and purified by recrystallization from a mixture of water and alcohol. K_2[Cu ox_2] was obtained from cupric sulphate and potassium oxalate by heating them for a few hours on a steam bath, and purified by recrystallization from 0.1 M aqueous potassium oxalate solution. The crystal was heated in vacuum at 100°C., and desiccated over P_2O_5. [Cu aca_2] was prepared from cupric acetate and acetylacetone, and recrystallized from a mixture of benzene and chloroform. [Cu$(dgH)_2$] was prepared from equivalent amounts of cupric acetate, dimethylglyoxime and caustic soda, and it was recrystallized from alcohol.

All these complexes were analyzed for their copper contents by iodometric titration.

Solvent.—The solvent used for extinction measurements of [Cu en ox] was an aqueous solution of 0.01 M potassium oxalate. To this 0.17 M sodium nitrate was added to keep the ionic strength at about 0.25. Thus, solutions of 0.01 M [Cu en_2]$^{++}$ and [Cu ox_2]$^{--}$ were prepared by dissolving weighed amounts of each complex in this solvent. In the case of [Cu en aca]$^{+}$ the mixture of 75% dioxane and 25% water was used for the solvent, which contained sodium nitrate in the concentration of 0.1 M. The solvent used for determining Km of [Cu dgH aca] was the mixture of 50% absolute ethyl alcohol and 50% dioxane.

Results and Discussion

The determination of Km by the method used in this investigation is possible only when hydrolysis such as, $MA_2+2H_2O \rightleftarrows MA(H_2O)_2+A$, does not occur to a measureable extent. To fulfil this requirement, it is necessary that the concentration of $MA(H_2O)_2$ be lower than 0.1% of that of MA_2. Since the concentration of MA_2 used in this experiment is the magnitude of 10^{-2}, the concentrations of $MA(H_2O)_2$ and A must be lower than 10^{-5}. Accordingly, it is necessary that the second consecutive formation constant (k_2) of MA_2 be greater than 10^8.

According to the data of other studies[2], k_2 of [Cu en_2]$^{++}$ is $10^{9.05}$ and that of [Cu aca_2] is $10^{8.1}$. In both cases the above requirement is fulfilled.

As the formation constant of [Cu$(dgH)_2$] is not known, in the present experiment the extinction measurements were carried out in a water-free solvent in order to eliminate hydrolysis, though it is expected to be a considerably stable complex, from the analogy of the dimethylglyoxime complexes of other metals.

Since [Cu ox_2]$^{--}$ is not so stable as to make it possible to ignore hydrolysis, ($k_1k_2=10^{8.3}$)[3], potassium oxalate was added to the solvent in the concentration 0.01 M to remove the error due to hydrolysis. On the other hand, the error due to the following equilibrium may be caused by the addition of the oxalate ion;

$$[\text{Cu } en_2]^{++}+ox^{--} \rightleftarrows [\text{Cu en ox}]+en.$$

But the extinction measurements of the solution of [Cu en_2] $(NO_3)_2$ containing 0.01 M potassium oxalate showed that the results agreed well with those of solutions containing no oxalate ion within the experimental error. Therefore, the error due to the addition of oxalate can be ignored.

If Watters' isosbestic method is adopted, such elaborate considerations as have been made above are not necessary. In his method only the total concentration of copper is known (0.01 M), and the concentration of the complexes in the solution is to be determined by calculation using the extinction data. For example, the concentration of [Cu en_2]$^{++}$ can be determined by the following relation at the isosbestic point where ε_2 is equal to ε_3. Here ε_1. ε_2 and ε_3 mean the molar extinction coefficients of [Cu en_2]$^{++}$, [Cu ox_2]$^{--}$ and [Cu en ox] respectively.

$$(\text{Cu } en_2^{++})=\frac{e-0.01\varepsilon_2}{\varepsilon_1-\varepsilon_2} \qquad (7)$$

(where e is the extinction of the mixed solution).

While, in the present method, as the concentration of [Cu en_2]$^{++}$ etc. is determined by direct weighing, its experimental error will be smaller than that calculated from the extinction data, and at the same time, will not be magnified in the process of calculation. (In the process of calculation after (7) the experimental error may be multiplied several times.)

The values of log Km determined are given in Table V. It can readily be seen from the table that the order of the value of Km is

$$[\text{Cu } P_2O_7 \text{ en}]^{--} > [\text{Cu en ox}] > [\text{Cu en aca}]^{+} > [\text{Cu dgH aca}].$$

Watters and De Witt ascribed the variety of the value of Km to the difference of the mutual ionic repulsion of ligands from their data of [Cu P_2O_7 en]$^{--}$ and [Cu en ox]. The results of the present study also seem to support their suggestion. It is reasonable

2) G.A. Carlson, J.P. Mc Reynolds and F.H. Verhoek, *J. Am. Chem. Soc.*, **67**, 1334 (1945); M. Calvin and K.W. Wilson, ibid., **67**, 2003 (1945).

3) A.E. Martell and M. Calvin, "Chemistry of the Metal Chelate Compounds", (1952), p. 516.

TABLE VIII
COMPARISON OF THE ABSORPTION MAXIMUM OF THE MIXED COMPLEX WITH IT PARENT COMPLEXES

	ν_{max}	ε_{max}		ν_{max}	ε_{max}		ν_{max}	ε_{max}
$[Cu\ en_2]^{++}$	54.9 (55.1*)	59.8 (63.1*)	$[Cu\ en_2]^{++}$	54.5	61.4	$[Cu\ en_2]^{++}$	54.3*	63.0*
$[Cu\ ox_2]^{--}$	42.0 (42.3*)	33.2 (34.7*)	$[Cu\ aca_2]$	48.0	38.0	$[Cu(P_2O_7)_2]^{6-}$	40.6*	27.5*
Mean value	48.45 (48.7*)	46.5 (48.9*)	Mean value	51.25	49.85	Mean value	47.45*	45.25*
[Cu en ox]	48.5 (48.2*)	51.0 (49.8*)	[Cu en aca]$^+$	51.1	53.6	[Cu en P_2O_7]$^{--}$	47.5*	43.0*

$\nu_{max} \times 10^{13}$: the frequency of the absorption maximum (sec^{-1})
ε_{max}: molar extinction coefficient of the absorption maximum
* Data from the investigation of Watters and Lougham[1].

to consider that, in the case of [Cu en ox], electrical repulsion between ethylenediamine and oxalate ion is smaller than that between two oxalate ions, therefore, *Km* is greater than the statistical value. On the other hand in the case of [Cu en aca]$^+$ and its parent complexes, the contribution of electrical repulsion of the ligand to *Km* is negligibly small, so the value of *Km* of this complex is expected to be near the statistical value. But the found value is smaller than the expected value. This fact cannot be sufficiently explained by mere electric repulsion. For the complete interpretation further investigations will be necessary.

The absorption curves of the mixed complexes are shown with broken lines in Fig. 1, Fig. 3 and Fig. 4. These curves were determined from extinction data of parent complexes and the mixed solution, and *Km* by using the relations (3) and (4).

The absorption curve of the mixed complex is generally higher than the mean extinction curve of parent complexes which is shown with a dotted line in Fig. 1, 3 and 4. This is a very interesting fact for the investigation of the electronic state of metallic complexes, considering together the previous data[4,5,6] of aquo-ammine mixed complex of Cu(II), Ni(II), Cr(III) and Co(III) in which the similar relations are found.

The absorption maxima of the mixed complexes are shown in Table VIII. From these data, it is readily seen that the frequency of the maximum absorption of a mixed complex coincides with the mean value of the parent complexes. This fact is also interesting in consideration of the study of Shimura and Tsuchida[6], in which the shift of the frequency of the first absorption maximum of Co(III) ammine complexes was found to be proportional to the number of substituted ligands.

The detailed discussion of the absorption spectra of mixed complexes will be reported later.

Summary

The dismutation constants of the three mixed complexes [Cu en ox], [Cu en aca]$^+$ and [Cu dgH aca] were determined photometrically. The negative logarithms of their dismutation constants were found to be 1.10, 0.42 and $\bar{1}.96$ respectively.

By the use of determined, dismutation constants absorption spectra of these mixed complexes were found. The frequency of the absorption maximum was found to coincide with the mean value of the parent complexes. At the same time the absorption of the mixed complex is generally stronger than the mean absorption of the parent complexes.

The author wishes to express his sincere thanks to Prof. R. Tsuchida, Osaka University, for his kind advice and encouragement, and also to Prof. H Yoneda for helpful discussions. The extinction measurement was carried out in the laboratory of the Wakayama Medical College, and the author is very grateful to Prof. O. Nagai for the hospitality shown to him.

Department of Chemistry, Wakayama University, Sekido, Wakayama

4) J. Bjerrum "Metal Ammine Formation in Aqueous Solution", P. Haase and Son, Copenhagen (1941); R. Tsuchida, "The Colors and the Structure of Metallic Compounds", Zoshindo, Osaka (1948) (in Japanese).

5) J. Bjerrum, C.J. Ballhausen and C.K. Jorgensen, *Acta Chem. Scand.*, 8, 1275 (1954).

6) Y. Shimura and R. Tsuchida, This Bulletin, 28, 572 (1955).

Studies on Organic Reagents for the Colorimetric Analysis of Germanium. III.[1,2] *Colorimetric Determination of Germanium with a New Reagent*

By Kenjiro KIMURA and Masako ASADA

(Received April 18, 1956)

In the previous report[2], it was demonstrated that a new compound, 2,6,7-trihydroxy-9 [4'-dimethylaminophenyl]-fluorone (hereafter called "dimethylaminophenylfluorone"), is a suitable reagent for the colorimetric determination of germanium. In this paper, the authors describe a detailed procedure for the determination of germanium using this compound.

Experimental

As mentioned in the previous paper[2] dimethylaminophenylfluorone forms a soluble complex with germanium in ethanolic solution containing hydrochloric acid. In order to use this compound as a colorimetric reagent, it was necessary to explore favourable experimental conditions under which a stable germanium complex is formed with adequate absorption for colorimetry.

Reagents.—Standard germanium solutions: A series of solutions were prepared by the same procedure as described in the preceding paper[2].

One tenth per cent dimethylaminophenylfluorone solution (hereafter called "reagent solution"): One tenth gram of dimethylaminophenylfluorone was dissolved in a mixture of 80 ml. of ethanol and 5 ml. of 6 N hydrochloric acid. The resulting solution was diluted to 100 ml. with ethanol.

Effect of Acid Concentration on the Complex Formation.—Five milliliter portions of germanium standard solution were taken in 50-ml. measuring flasks. Then each solution was diluted to approximately 30-ml. with hydrochloric acid and water. The reagent was added to these solutions at room temperature. The final concentrations of hydrochloric acid and the reagent in these solutions ranged from 0.3 to 1.5 N and 0.006 to 0.020% by weight respectively. When the volume of the reagent solution to added was less than 10 ml., it was diluted to 10 ml. with ethanol before being mixed with germanium solution. After mixing, the solution was diluted to 50 ml. with water. The final solution contained 34.7 μg. of germanium. A reference solution was prepared by similar procedure without germanium. The results are shown in Fig. 1. It is clear from Fig. 1 that at acid concentrations over 0.6 N, the absorption of the complex decreases very slightly with the increase in acid concentration. At acid concentrations between 0.3 and 0.6 N, the absorption is almost constant.

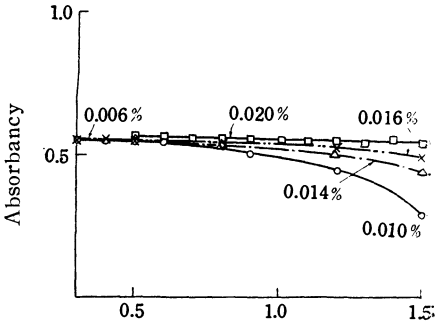

Fig. 1. Effect of Acid Concentration

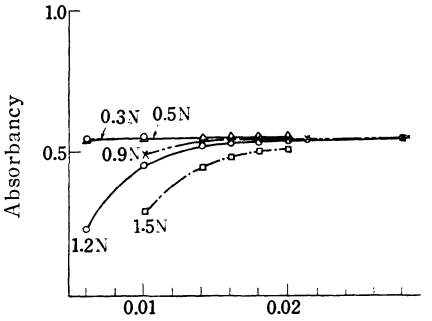

Fig. 2. Effect of Dimethylaminophenylfluorone Concentration

Effect of Reagent Concentration on the Complex Formation.—Test solutions were prepared by the same procedure as before and the effects of reagent concentrations were examined at hydrochloric acid concentrations between 0.3 N to 1.5 N. When the solutions contain more than 0.020% of dimethylaminophenylfluorone by weight, 0.15% reagent was used. The results of the measurements of the absorption are shown in Fig. 2. From Fig. 2 it is seen that the absorption remain almost unchanged in a 0.5 N acid solution, without regard to the change in the concentration of the reagent.

Effect of Time after the Addition of Reagent.—Five milliliters of a standard germanium solution was taken in a 50-ml. measuring flask. After the addition of 5 ml. of 6 N hydrochloric acid, it was diluted to approximately 30 ml. with water. The solution was cooled down to room tempera-

1) K. Kimura, K. Saito, M. Asada, This Bulletin, 29, 635 (1956).
2) K. Kimura, H. Sano, M. Asada, ibid., 29, 640 (1956).

ture, mixed with 10 ml. of 0.05% reagent solution and then diluted to a difinite volume with water. The reference solution was prepared by a similar procedure without germanium. After the solution was kept in running water for thirty minutes at 6°C, the absorbancy was measured at 510 and 520 mμ. The results are shown in Fig. 3. It seems that the development of color of the complex is complete in less than fifteen minutes after the addition of the reagent.

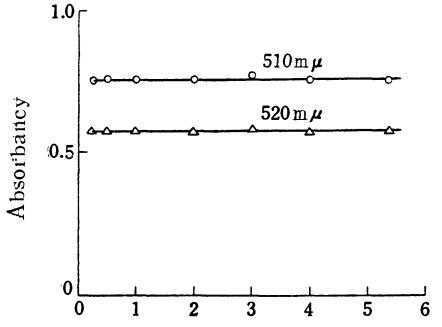

Fig. 3. Effect of Time

Effect of Temperature.—Test solutions were prepared by a similar method as described before. These solutions were allowed to stand for thirty minutes at various temperatures: 0°C, 6.0°C, 7.0°C, 17.3°C and 30.2°C. The absorption of these solutions was measured at 510 and 520 mμ. The results are shown in Fig. 4. It is clear that temperature has no effect on the absorption of the complex in a range 0° to 30.2°C. At 0°C, however, a slight precipitation of the reagent was observed after two hours since the solution was prepared. Hence, it is desirable to measure absorption within two hours after the reagent is added.

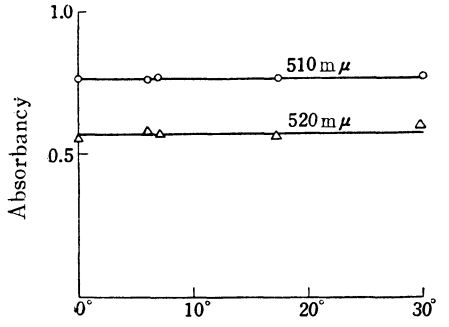

Fig. 4. Effect of Temperature

Effect of Germanium Concentration.—The experiment was carried out by a procedure simiar to that used for the experiment on the effect of temperature. In this case, germanium concentrations of the solutions ranged from 0.0278 to 1.25 μg. per ml. Each solution was introduced into a 50-ml. measuring flask and the volume was adjusted to 50 ml. Then the absorption of the solution was measured at 510 and 520 mμ, respectively, after the solution was kept standing for thirty minutes at temperature of about 17°C. The results were tabulated in Table I, and were also shown graphically in Fig. 5. The calculated values in Table I were obtained by using an empirical formula which was derived by the application of the method of least squares.

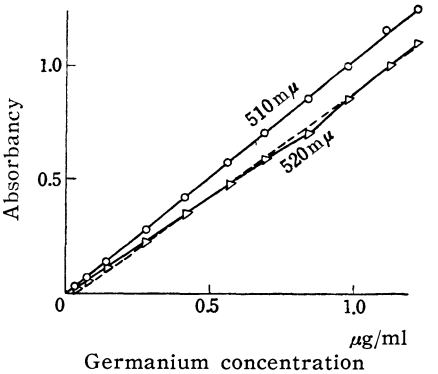

Germanium concentration
- - - Calculated value

Fig. 5. Calibration Curves

TABLE I
EFFECT OF GERMANIUM CONCENTRATION UPON EXTINCTION

Germanium Concentration in Solution (μg/ml.)	510 mμ			520 mμ		
	Drum Readings	Calculated Values ($\varepsilon^* = 1.024\,C^{**}$)	Difference	Drum Readings	Calculated Values ($\varepsilon^* = 0.911\,C^{**} - 0.003$)	Difference
0.0278	0.020	0.028	−0.008	0.008	−0.004	0.012
0.0694	0.070	0.071	−0.001	0.048	0.030	0.018
0.139	0.142	0.142	0	0.112	0.094	0.018
0.278	0.284	0.284	0	0.226	0.220	0.006
0.416	0.429	0.426	0.003	0.348	0.346	0.002
0.555	0.575	0.568	0.007	0.474	0.472	0.002
0.694	0.707	0.711	−0.005	0.585	0.599	−0.014
0.833	0.845	0.853	−0.008	0.695	0.726	−0.031
0.970	0.980	0.993	−0.003	0.860	0.851	0.009
1.11	1.163	1.137	0.026	0.992	0.978	0.014
1.25	1.28	1.280	0	1.178	1.106	0.072

* ε: extinction of the complex between germanium and the reagent
** C: concentration of germanium

From the results it is concluded that the values of extinction at 510 and 520 mμ can be used for the analysis in a range of germanium concentration from 0.05 to 1.2 p.p.m.

Reproducibility of the Extinction.—In order to check the reproducibility of the extinction of a solution containing germanium complex at a given concentration, experiments were repeated at certain intervals over a period of about one week. The experimental conditions were the same as before. The results were shown in Table II.

TABLE II
TEST ON THE REPRODUCIBILITY

Germanium Concentration (μg/ml)	Run # 1	# 2	# 3	# 4	# 5	# 6	# 7	Number of Measurement	Average Value	Probable Error of Observed Value
(1) Measured at 510 mμ										
0.276	0.267	0.256	0.272	0.265	0.274	0.284	0.271	7	$0.270 \pm 0.002_2$	0.006
0.690	0.687	0.699	0.690	0.674	0.690	0.707	0.700	7	$0.692 \pm 0.002_7$	0.007
0.966				0.980	0.982	0.980	1.000	4	$0.985 \pm 0.003_3$	
(2) Measured at 520 mμ										
0.276	0.208	0.200	0.224	0.218	0.218	0.226	0.225	7	$0.217 \pm 0.002_5$	0.007
0.690	0.571	0 579	0.576	0.590	0.589	0.585	0.590	7	$0.583 \pm 0.001_9$	0.006
0.966				0.860	0.862	0.860	0.860	4	$0.861 \pm 0.000_3$	

From these results, it is concluded that the reproducibility is satisfactory. But another series of experiments showed that the values slightly fluctuated when a different batch of reagent was used. In order to obtain a better reproducibility, the method for the purification of the reagent should be studied further.

Effect of Other Elements.—The following ions interfere with the colorimetric determination of germanium using this reagent, Sn^{4+}(1), Sb^{3+}(10), Zr^{4+}(100), Ce^{4+}(1), Fe^{3+}(10), MnO_4^{2-}(1). The numerical values in parentheses are maximum permissible ratios of interfering ions to germanium by weight. To eliminate the interference, the ratios of interfering ion to germanium in solution should be lower than these values. The wavelengths of absorption bands of these coloured compounds are similar to those of germanium complex.

In the presence of a small quantity of oxidizing agent, the reagent solution shows an absorption at a wavelength near 500 mμ; this colour and that of the complex disappear when the solution is boiled. A large quantity of oxidizing agent completely prevents the development of the colour of the germanium complex. It is likely that the reagent was decomposed by an oxidizing reagent.

When 50 mg. were present in 50 ml., the following ions failed to form any compound having absorption near 500 mμ. This amount is approximately one thausand times the weight of germanium in the solution.

Li^+, Na^+, K^+, Rb^+, Cs^+, NH_4^+, Mg^{2+}, Ca^{2+}, Sr^{2+}, Ba^{2+}, Zn^{2+}, Cd^{2+}, Cu^{2+}, Hg^{2+}, As^{3+}, Bi^{3+}, Pb^{2+}, Mn^{2+}, Fe^{2+}, Co^{2+}, Ni^{2+}, Al^{3+}, Ti^{4+}, Cl^-, I^-, SO_4^{2-}, NO_3^-, CH_3COO^-, PO_4^{3-}, $B_4O_7^{2-}$.

Interference may result from the presence of a very large quantity of these ions, because under a great ionic strength they are apt to cause precipitation of either the reagent or the germanium complex. The degree of precipitation depends on the temperature. In the presence of 4.4 g. of sodium chloride, no precipitate appeared at 30°C in 50 ml. of the solution containing germanium complex and the reagent, whereas some precipitates are formed on standing at 6°C for one hour, in the presence of only 1.8 g. of sodium chloride.

Recommended Procedure

A sample is exactly weighed, decomposed eigher with acid* or by fusion with alkali and extraction with hot water. After being cooled, it is transferred to a 300 ml. round bottomed flask. If there is any possibility of the presence of an oxidizing reagent in the solution, an adequate quantity of ferrous sulphate should be added. The resulting solution is diluted to 70 ml., to which 70 ml. of conc. hydrochloric acid is added and germanium is distilled. The distillate is collected in a receiver containing approximately 20 ml. of water. The distillation is continued until 50 ml. of the distillate are obtained. Then the distillate is transferred to a measuring flask and diluted to 100 ml. with water. The acid concentration of this solution is determined by titration with 3 N sodium hydroxide. An aliquot of the solution containing germanium in a range

* At the decomposition of the sample, hydrochioric acid and halide must not be present because germanium halide is easily formed and tends to escape from the solution.

from 3 to 60 μg is taken in a 50 ml. measuring flask and the acid concentration is adjusted to 0.5 N by adding either sodium hydroxide or hydrochloric acid. It is diluted to approximately 30 ml. with water and cooled down to room temperature. Ten ml. of 0.05% ethanol solution of dimethylaminophenylfluorone is added to the solution. Then the resulting solution is diluted to 50 ml. with water. A reference solution is similarly prepared without germanium. The extinction of the solution is measured at 510 and 520 mμ and the quantity of germanium is determined with the aid of calibration curves.

Conclusion

Although a new compound, dimethylaminophenylfluorone, is not a specific reagent for germanium, the colorimetric method using this compound is recommended because of its simplicity. The advantage of this method is very similar to that of phenylfluorone method. Germanium is separated from interfering ions by distillation and the resulting solution is subjected to colorimetric analysis. The disadvantage of the phenylfluorone method consists in the fact that the germanium complex is insoluble or only slightly soluble in water and in organic solvents. In this new method such a disadvantage is eliminated. Dimethylaminophenylfluorone forms a soluble complex with germanium in ethanolic solution containing hydrochloric acid. The colour of the complex is stable. The extinction can be measured more easily than in the case of the phenylfluorone method. The only disadvantage of this method is that the molar extinction coefficient of germanium complex can not be obtained because the extinction of the complex slightly fluctuates, when a different batch of the reagent is used.

Department of Chemistry, Faculty of Science, The University of Tokyo
Hongo, Tokyo

The Nature of the Urushibara Nickel Catalyst as Revealed by Electron Diffraction

By Yoshiyuki URUSHIBARA, Shigeto YAMAGUCHI and Michio KOBAYASHI

(Received July 3, 1956)

Nickel catalyst prepared by Urushibara and his coworkers[1] has been studied by electron diffraction. Electron waves of two energies, one relatively hard and another soft were alternately used here in order to investigate the surfaces of catalyst particles[2]. The harder electrons (wavelength, about 0.02 Å) were able to penetrate thick particles (thickness, about 5000 Å)[3]. On the other hand, the softer electrons (wavelength, about 0.05 Å) could graze only the surfaces of the particles.

Metallic nickel was deposited onto zinc dust from a nickel chloride solution. The composite powder of Zinc-Nickel was treated with an acetic acid solution in order to dissolve zinc *partially* and *appropriately*[1]. Ten grams of zinc dust and 3 cc. of distilled water were placed in a round flask of 10 cc. capacity and heated on a boiling waterbath. Ten cc. of an aqueous solution containing 4.04 g. of nickel chloride, $NiCl_2 \cdot 6H_2O$, were boiled and added to the zinc dust by means of a pipet, in a few seconds time accompanied by rapid stirring. The precipitate was collected on a glass filter by suction, washed with a small quantity of hot distilled water and quickly transferred into 160 cc. of 13% acetic acid. When the generation of hydrogen gas subsided, the product was filtered with a glass filter and washed with distilled water (50–60°C) and finally with alcohol.

A sample of the powder gave a diffraction pattern of Fig. 1 with the harder electrons (wavelength, 0.0284 Å). The positions and the intensities of the diffraction rings observed in Fig. 1 are illustrated in Fig. 2. In the diffraction pattern obtained, there are found diffraction rings corresponding to nickel, zinc oxide and zinc. The diffraction rings characteristic of nickel are quite diffuse, whereas those of zinc oxide and of zinc are comparatively sharp. It was impossible to observe nickel in this crystalline state by means of X-ray diffraction.

1) Y. Urushibara S. Nishimura and H. Uehara, This Bulletin, 28, 446 (1955).
2) S. Yamaguchi, *Z. phys. Chem. N. F.*, 7, 115 (1956).
3) S. Yamaguchi, *J. Appl. Phys.*, 25, 811 (1954).

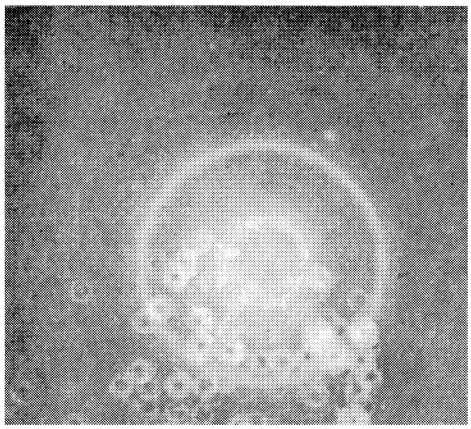

Fig. 1. An electron diffraction pattern of the Urushibara nickel catalyst.
The diffraction rings corresponding to nickel, zinc oxide and zinc. Nickel crystallites are very fine, whereas zinc and zinc oxide are granular. Wavelength, 0.0284 Å. Camera length, 495 mm. Positive enlarged 2.3 times.

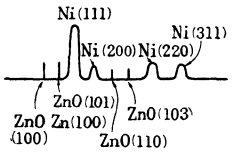

Fig. 2. Positions and the intensities of the diffraction rings are illustrated here.

The same spot in the specimen as in Fig. 1 was observed with the softer electrons (wavelength, 0.0490 Å). A diffraction pattern of Fig. 3 was then obtained. In Fig. 3, diffuseness of the rings from nickel seems to be greater than would be expected from the electron wavelength applied (0.0490 Å). This implies that the surfaces of the nickel particles are nearly amorphous. As a matter of fact, there is no indication of refraction in the diffraction rings of Fig. 3, as well

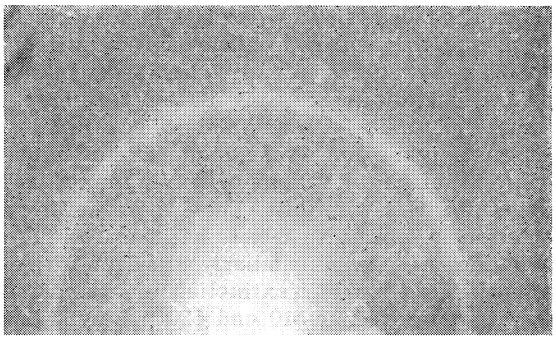

Fig. 3. Diffraction pattern from the same spot of the specimen as for Fig. 1.
Very diffuse rings from nickel are found. Wavelength, 0.0490 Å. Camera length, 495 mm. Positive enlarged 2.3 times.

those of Fig. 1. The nickel in the Urushibara catalyst thus exists in a state of *crystallites*, and is *not crystals*.

The Urushibara catalyst is composed of nickel, zinc and zinc oxide, as is demonstrated in Figs. 1 and 2. The coexistence of zinc, zinc oxide and nickel implies that zinc not only plays the part of a carrier, but also protects nickel from oxidation. This is because of galvanic relation between zinc and nickel (formation of local cells). As long as metallic zinc exists in the catalyst, nickel can survive as active centres. This is the case with the Raney nickel catalyst. Zinc found in the Urushibara catalyst corresponds to the aluminum of the Raney catalyst.

The authors wish to acknowledge gratefully the special grant extended by the Ministry of Education for the present study.

Department of Chemistry, Faculty of Science, The University of Tokyo ; Scientific Research Institute Ltd., Tokyo

Synthetic Studies of Dictamnine, an Alkaloid of Skimmia Repens, Nakai I. The Synthesis of Dictamnal

By Tadashi SATO and Masaki OHTA

(Received April 15, 1956)

The structure of dictamnine, an alkaloid of Skimmia repens, Nakai, was determined by Asahina to be 4-methoxy-[2,3-b]-furoquinoline (I)[1]. Since then some other alkaloids (kokusagine, etc.) have been isolated and shown to be of furoquinoline type by analogous methods to that used by Asahina[2]. Recently some experiments assuring these structures were reported[3], but in none has it been possible to show definitely the existence of the furan nucleus.

Synthetic studies of dictamnine were carried out by Asahina[4] and by Grundon[3b], but they could only obtain pseudodictamnine, an isomer of dictamnine. As an approach to the synthesis of dictamnine, we attempted to obtain quinolines, in which positions 2 and 4 are substituted by groups different from each other. Although we have not yet been able to finish the synthesis of dictamnine itself, dictamnal, which is a degradative product of dictamnine, was first synthesized and its structure was ascertained.

Starting from nor-dictamnal, we obtained a series of compounds (Fig. 1). As to these compounds, it was ambiguous whether the compounds obtained were of the type II or III.

This problem was solved spectroscopically, as shown below.

When nor-dictamnal (IV) was refluxed with phosphorus oxychloride, tetrachloro derivative V was obtained, accompanied by a small amount of trichloro derivative VI and a basic compound (m.p. 260°) whose structure has not been ascertained yet. The tetrachloro derivative (V) was unexpectedly stable, being unable to react with conc. sulfuric acid, aniline, phenylhydrazine, and alkali, but gave the trichloro derivative (VI) when refluxed in acetic acid. The trichloro derivative (VI) gave acetal VII by a reaction with sodium methoxide in methanol. Treatment of this acetal (VII) with 10% hydrochloric acid afforded aldehyde VIII quantitatively. This aldehyde (VIII) gave methoxy derivative IX when refluxed with sodium methoxide in methanol. This product (IX) has properties very close to those of dictamnal[1], the degradative product of dictamnine. Namely, it melts at 260°, is not easily soluble in most organic solvents, gives a phenylhydrazone of m.p. 228°, and gradually dissolves in aqueous alkali to a yellow solution. But we are not in possession of the natural dictamnal to compare it with. Tetrachloro derivative V gave acetal X by a reaction with sodium

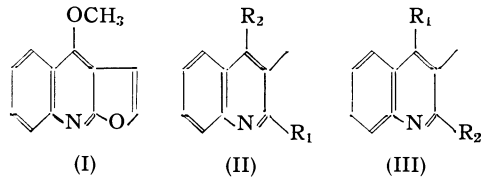

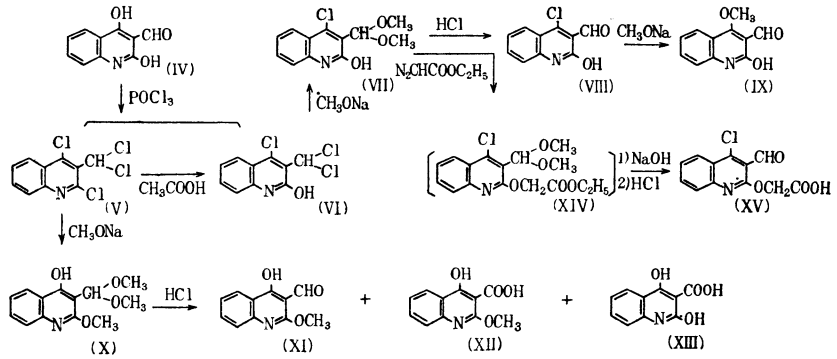

Fig. 1

1) T. Asahina, Y. Ohta and M. Inubuse, *Ber.*, **63**, 2045 (1930).

2) Y. Asahina and M. Inubuse, *Ber.*, **63**, 2052 (1930); R.J. Gell et al., *Austral. J. Chem.*, 8, 422 (1955).

3) (a) T. Ohta and Y. Mori, *Pharm. Bull.* **3**, 396 (1955). (b) M.F. Grundon, et al., *J. Chem. Soc.*, **1955**, 4284.

4) Y. Asahina and M. Inubuse, *Ber.*, **65**, 61 (1932).

methoxide in methanol. It was dissolved in dilute hydrochloric acid and, on neutralization with sodium hydroxide, gave a precipitate of aldehyde XI (m.p. 80°), an isomer of dictamnal. Some amounts of white crystals were obtained from the filtrate on standing for a long time. On fractional recrystallization from dilute methanol, two amphoteric substances were obtained (m.p. 110°, and m.p. 172–3°). These seem to be XII and XIII, respectively, but the melting point of XII is not identical with the reported one (225°)[1,*].

Ewing et al.[5] reported on the influence of the position of the substituent upon the spectra of monohydroxyquinolines. From their data one can say as a whole that hydroxyquinolines of α-naphthol type (4-, 5- and 8-) have only one maximum over 250 mμ (about 320 mμ) while β-naphthol types (2-, 3-, 6- and 7-) have two maxima in the same region (275 mμ and 330 mμ). Of these quinolines, 2- and 4-hydroxyquinolines can take keto-forms as well as phenol-forms. In practice the spectra of these two are unaffected in 1/100 N alkali, contrary to the practice of all the other derivatives. When the concentration of the alkali increases to 10%, the spectrum of 2-hydroxyquinoline shifts, while that of the 4-isomer is not affected even in the concentration of 50%. This fact shows that both of them exist as the keto-forms but the 2-isomer takes the phenol-form in alkali more easily than the 4-isomer. By making the solutions alkaline, all the curves of hydroxyquinolines of α-naphthol type shift, but, in case of β-type, it is characteristic that the short-wavelength absorption maximum flattens.

Keeping these data in mind we measured the ultraviolet spectra of the above mentioned compounds (VI–IX) (Figs. 2–5). The spectra of all these compounds are very similar to those of hydroxyquinolines of β-naphthol type, especially to that of 2-hydroxyquinoline. (Although the spectrum of dictamnal deviates a little from the others, it shows at least the same inclination.) It is to be noted here that the substituents at position 3 do not affect the spectra and the acidity of these quinolines is so strong as to cause the flattening of the short-wavelength absorption maxima even in the alkali concentration of 1/100 N and as not to be affected in acid concentration of 1/100 N. From these facts it can be concluded that all these compounds (VI–IX) are 2-hydroxyquinoline derivatives.

Contrary to the spectroscopic behaviors of the above mentioned compounds (VI–IX), the spectra of X and XI (Figs. 6 and 7) are not like those of β-naphthol types. They are affected in acid but not in alkali. Moreover, the spectra of both compounds are very different from each other in either neutral or alkaline solution, while they are similar in acid solution. It can be supposed from these facts that these compounds are 4-hydroxy derivatives and exist as the keto-

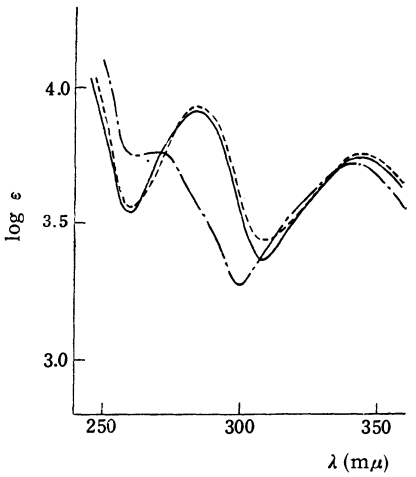

Fig. 2. 2-Hydroxy-3-dichloromethyl-4-chloroquinoline (VI).
—— neutral
····· acid
—·— alkali

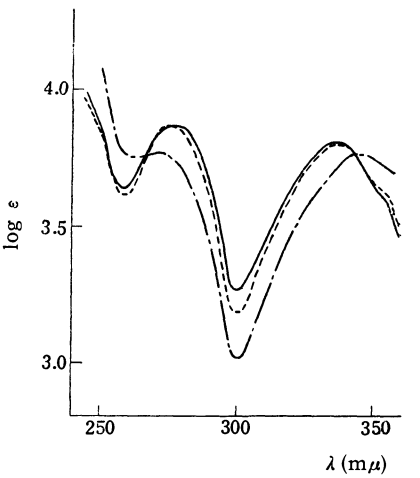

Fig. 3. 2-Hydroxy-3-dimethoxymethyl-4-chloroquinoline (VII).
—— neutral
····· acid
—·— alkali

* R.F.C. Brown reported that this value was not correct: *Austral. J. Chem.*, 7, 384 (1954).

5) G.W. Ewing and E.A. Steck, *J. Am. Chem. Soc.*, 68, 2181 (1946); ibid, 71, 238 (1949). cf. B. Witkop et al., *J. Am. Chem. Soc.*, 73, 2641 (1951).

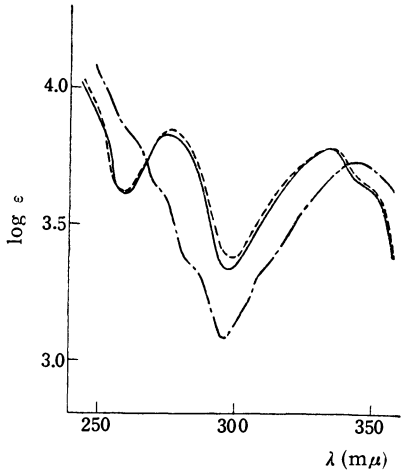

Fig. 4. 2-Hydroxy-3-formyl-4-chloroquinoline (VIII).
—— neutral ····· acid —·— alkali

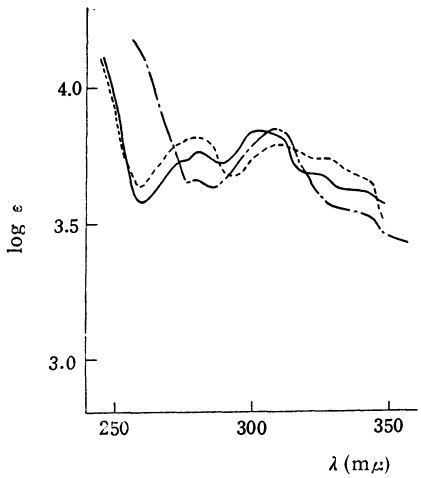

Fig. 5. 2-Hydroxy-3-formyl-4-methoxyquinoline (IX).
—— neutral ····· acid —·— alkali

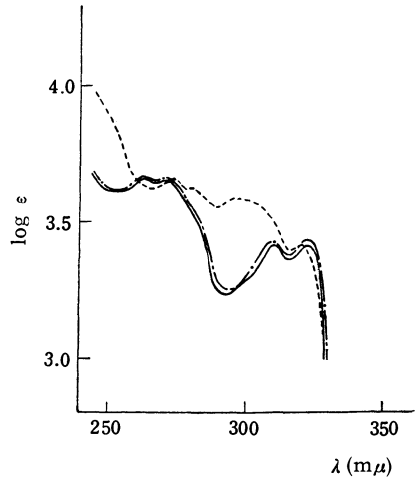

Fig. 6. 2-Methoxy-3-dimethoxymethyl-4-hydroxyquinoline (X).
—— neutral ····· acid —·— alkali

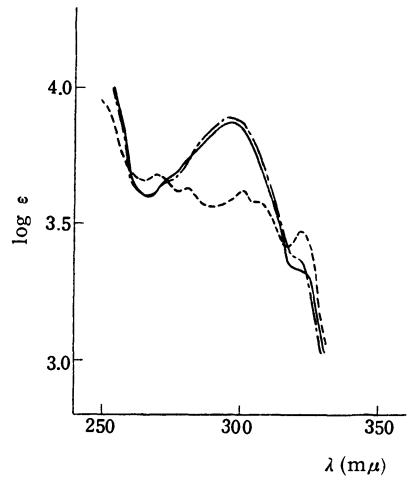

Fig. 7. 2-Methoxy-3-formyl-4-hydroxyquinoline (XI).
—— neutral ····· acid —·— alkali

forms. The extinct absorption maximum of XI at 297 mμ (log ε, 3.9) is supposed to be caused by the partial structure like XVI. Indeed, the other compounds having such structures (3-acyl-2,4-dihydroxyquinoline, XVII, and 3-acyl-4-hydroxycoumarin, XVIII) show strong absorption in the same region[6]. Acetal X lacking this structure, therefore, exhibits a very different spectrum. But, in acid solution, that is in protonated state, the enol-form (XX) is supposed to be more stable than the keto-form (XIX); so that the influence of the substituent at position 3 disappears and the spectra of X and XI become similar. Indeed, both the spectra in

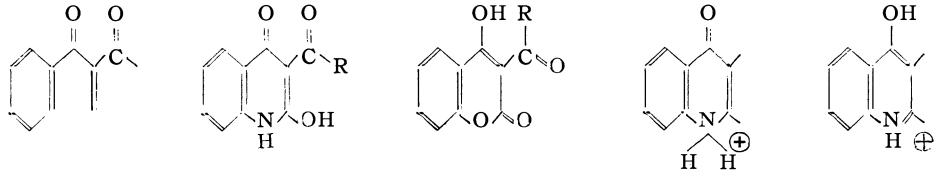

(XVI) (XVII) (XVIII) (XIX) (XX)

6) K. Tomita, *J. Pharm. Soc. Japan.* **71**, 1100 (1951).

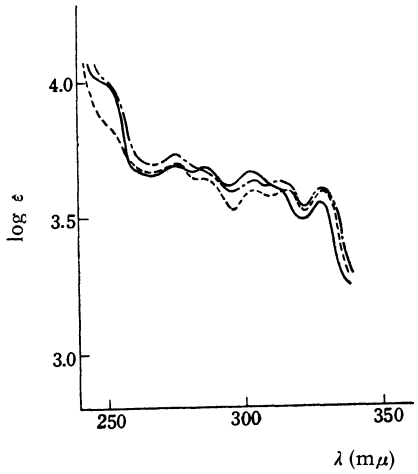

Fig. 8. 3-Formyl-4-chloroquinolyl-2-glycolic acid (XV).
—— neutral ····· acid –·— alkali

acid solution are very similar to that of XV (Fig. 8), which can take only an enol-form like XX.

In order to synthesize dictamnine, we tried to get a compound of the type XV. The previously mentioned acetal (VII) is fairly acidic and, when a sodium methoxide solution was added to its methanol solution, a sodium salt was obtained. From the aqueous solution of this sodium salt a precipitate, supposedly a silver salt, was obtained by the addition of aqueous silver nitrate. Its purification, however, was difficult. It was soluble in toluene and seemed to have reacted with ethyl bromoacetate, but the substance obtained from the reaction mixture was only the starting acetal (VII). The sodium salt, moreover, did not react with ethylene oxide. The acetal (VII) did not react with ethyl diazoacetate even at 160°, but it did at 110° in the presence of copper powder to give an oil which was supposed to be XIV[7]. This was directly hydrolysed by aqueous alkali and acidification with hydrochloric acid gave XV. The cyclization to make furan nucleus is being carried out at present.

Experimental

Absorption Spectra.—All spectra were measured with Beckman Quartz Spectrophotometer, Model DU.

Solvents.—(a) Neutral: Commercial methanol was once distilled. (b) Acid and alkaline: One cubic centimeter of tenth normal aqueous solutions of reagent grade hydrochloric acid (f=1.27) and sodium hydroxide (f=0.941) were diluted with methanol to 10 cc.

7) J. Maas et al., *Rec. trav. chim.*, **74**, 175 (1955).

2,4-Dichloro-3-dichloromethylquinoline (V). —Fifteen grams of nor-dictamnal (IV)[4] was refluxed with 110 cc. of phosphorus oxychloride for ninety minutes. The brown solution was gradually poured into crushed ice with constant stirring. After standing overnight, the separated crystals were collected. Yield 20 g. They were washed with 15% hydrochloric acid and the insoluble matter was recrystallized from dilute methanol. White needles, m.p. 125.5–6°. Yield 13 g.

Anal. Found: C, 42.25; H, 2.05; N, 5.31. Calcd. for $C_{10}H_5NCl_4$: C, 42.70; H, 1.78; N, 4.98%. From the mother liquor, a small amount of trichloro derivative VI was obtained (see below).

2-Hydroxy-3-dichloromethyl-4-chloroquinoline (VI).—Tetrachloro derivative V (5.5 g.) was refluxed with 30 cc. of glacial acetic acid for ninety minutes. Hydrogen chloride was soon evolved and crystals began to separate in one hour. After cooling the precipitate was collected and washed with acetic acid. It was fairly pure and used for the succeeding reactions without purification. Yield 3 g. The sample for analysis was obtained by recrystallization from glacial acetic acid. White needles, m.p. 253°.

Anal. Found: C, 46.31; H, 2.60; N, 6.02. Calcd. for $C_{10}H_5NOCl_3$: C, 45.63; H, 2.28; N, 5.34%.

2-Hydroxy-3-dimethoxymethyl-4-chloroquinoline (VII).—Four grams of crude substance VI was suspended in 40 cc. of methanol and 50 cc. of a sodium methylate solution, containing 1.5 g. of sodium, was added. The solid dissolved immediatety to give a yellow solution, but soon after, a white solid was deposited. After being refluxed for ninety minutes, the solid was collected, washed with methanol, and dissolved in hot water. After the insoluble matter was filtered off, aqueous ammonium chloride was added to the yellow filtrate to precipitate a white crystalline substance. It was fairly pure and used for succeeding reactions without purification. m.p. 163°. Yield 2 g. The sample for analysis was obtained by recrystallization from dilute methanol. m.p. 164–5°

Anal. Found: C, 56.11; H, 4.95; N, 5.23. Calcd. for $C_{12}H_{12}NO_3Cl$: C, 56.69; H, 4.74; N, 5.53%.

Sodium Salt of 2-Hydroxy-3-dimethoxymethyl-4-chloroquinoline.—To a hot solution of 1 g. of VII in 50 cc. of methanol, 40 cc. of a sodium methylate solution, containing 1.2 g. of sodium, was added. On cooling, white needles were obtained. m.p. over 250°. Yield 0.85 g. The substance was dissolved in hot water and on adding aqueous ammonium chloride, VII was recovered.

Anal. Found: N, 4.90, Calcd. for $C_{12}H_{11}NO_3ClNa$: N, 5.07%.

3-Formyl-4-chloroquinol-2-yl-glycolic Acid (XV).—Two grams of acetal VII was intimately mixed with 0.4 g. of copper powder, and 1 g. of ethyl diazoacetate was dropwise added during a period of forty-five minutes at 110–120°, with continuous stirring. The reaction mixture was kept at 130° for an additional fifteen minutes and cooled. To the brown paste a small amount of ether was added, and the unchanged starting material and

copper powder were filtered off and washed with ether. The filtrate and washings were combined and ether was evaporated. The residual oil was heated with 40 cc. of 10% aqueous sodium hydroxide at about 50° to complete solution. Acidification of the solution with hydrochloric acid gave a yellow oil which soon solidified. Recrystallization from benzene gave XV in light yellow needles melting at 162°.

Anal. Found: C, 54.23; H, 3.56; N, 5.65; Cl, 13.0. Calcd. for $C_{12}H_8NO_4Cl$: C, 54.13; H, 3.01; N, 5.26; Cl, 13.4%.

2-Hydroxy-3-formyl-4-chloroquinoline (VIII).—Acetal VII was suspended in a small amount of 10% aqueous hydrochloric acid and warmed for ten minutes. The insoluble matter was collected and recrystallized from methanol. Yellow needles, m.p. 268°.

Anal. Found: C, 57.95; H, 3.14; N, 6.92. Calcd. for $C_{10}H_6NO_2Cl$: C, 57.69; H, 2.89; N, 6.75%.

2-Hydroxy-3-formyl-4-chloroquinoline Phenylhydrazone.—Aldehyde VIII and phenylhydrazine were heated in methanol for thirty minutes. On cooling, the yellow needles were recrystallized from methanol, m.p. 233°.

Anal. Found: N, 13.92. Calcd. for $C_{13}H_{12}N_3OCl$: N, 14.09%.

2-Hydroxy-3-formyl-4-methoxyquinoline (dictamnal) (IX).—Two grams of aldehyde VIII were refluxed with 9 cc. of methanol and 9 cc. of a sodium methylate solution, containing 0.27 g. of sodium, for two hours. During this period the form of crystals changed. The light yellow solid was collected and washed with water. It was recrystallized from a large amount of methanol. White needles, m.p. 260°.

Anal. Found: C, 64.62; H, 4.56; N, 7.17. Calcd. for $C_{11}H_9NO_3$: C, 65.02; H, 4.46; N, 6.89%.

2-Hydroxy-3-formyl-4-methoxyquinoline Phenylhydrazone.—Aldehyde IX and phenylhydrazine were heated in methanol. Addition of water gave yellow needles. They were recrystallized from methanol, m.p. 228°.

Anal. Found: N, 14.28. Calcd. for $C_{17}H_{15}N_3O_2$: N, 14.33%.

2-Methoxy-3-dimethoxymethyl-4-hydroxyquinoline (X).—The tetrachloro derivative (V) (4.3 g.) and 60 cc. of a sodium methylate solution, containing 1.8 g. of sodium, were refluxed for ninety minutes. After standing overnight the solid was filtered off. The filtrate was concentrated in vacuo to about 40 cc., and water was added. The separated oil was taken up in ether, and the ethereal solution was evaporated. The residual oil soon solidified. A small amount of the solid was recrystallized from dilute methanol for analysis. White needles, m.p. 62–4°.

Anal. Found: C, 62.37; H, 6.27; N, 5.44. Calcd. for $C_{13}H_{15}NO_4$: C, 62.64; H, 6.07; N, 5.62%.

2-Methoxy-3-formyl-4-hydroxyquinoline (XI).—The crude acetal (X) was suspended in water and 18% aqueous hydrochloric acid was gradually added until all the solid was dissolved. The solution was warmed for some time and made alkaline with aqueous caustic soda. Repeated recrystallizations of the separated solid (A) from dilute methanol gave XI in white needles melting at 82–3°.

Anal. Found: C, 65.43; H, 4.81; N, 6.88. Calcd. for $C_{11}H_9NO_3$: C, 65.02; H, 4.46; N, 6.89%.

2-Methoxy-4-hydroxyquinoline-3-carboxylic Acid (XII).—The alkaline mother liquor, from which the solid (A) was removed in the above process, gave some amounts of crystals on standing for a few days. They were dissolved in water and the solution was neutralized with aqueous hydrochloric acid. An amphoteric substance was obtained. Recrystallization from dilute methanol gave XII in white needles melting at 110°. Soluble in aqueous sodium bicarbonate.

Anal. Found: C, 60.10; H, 4.02; N, 6.83. Calcd. for $C_{11}H_9NO_4$: C, 60.27; H, 4 14; N, 6.39%.

2,4-Dihydroxyquinoline-3-carboxylic Acid (XIII).—From the mother liquor in the above recrystallization process, white needles were obtained by adding water. Recrystallization from dilute methanol gave XIII in white needles melting at 172–3°. Soluble in aqueous sodium bicarbonate.

Anal. Found: C, 58.26; H, 3.30; N, 6.85. Calcd. for $C_{10}H_7NO_4$: C, 58.54; H, 3.44; N, 6.83%.

The authors are indebted to Mr. A. Kondo for the microanalyses.

Laboratory of Organic Chemistry
Tokyo Institute of Technology
Tokyo

A Synthesis of γ-Alkylbutyrolactones from Furfural and a Lower Group of Methyl Ketones

By Yoshio TERAI and Toyosuke TANAKA[1)]

(Received June 20, 1956)

Although γ-alkylbutyrolactones are a group of the most important of all the synthetic perfumes, the lactones are used only to a limited extent by the perfume industry. It seems likely that only two compounds–namely; γ-nonalactone (commonly known as coconut aldehyde) and γ-undecalactone (peach aldehyde) are practically manufactured[2)]. Their limited use is due to the lack of suitable raw materials. The authors have found that Clemmensen reduction of γ,ζ-dioxocarboxylic acid gave successfully γ-alkylbutyrolactone in excellent yield. γ,ζ-Dioxocarboxylic acid could be obtained by furan-ring opening of furfurylidene ketone, as the condensation product between furfural and methyl ketone. Thus this paper concerns a new method for preparation of γ-alkylbutyrolactones from furfural and a lower group of methyl ketones, as illustrated by the formulation described below.

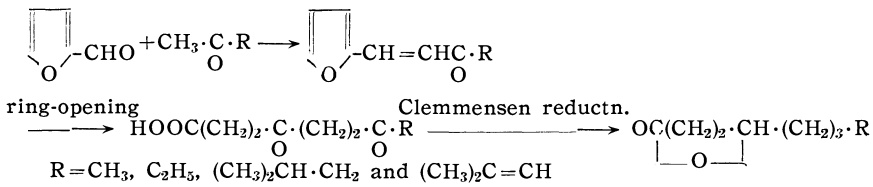

The condensation for furfurylidene ketone by aqueous sodium hydroxide was carried out between furfural and a series of acetone, methyl ethyl ketone, methyl isobutyl ketone and mesityl oxide by the usual procedure[3),4)], and corresponding furfurylidene ketones were obtained. In the reaction of furfural with mesityl oxide, of which some different results were reported by Surmin[5)], furfurylidene mesityl oxide (b. p. 128–132°/5 mm.) was distilled, accompanying furfurylidene acetone and difurfurylidene acetone as by-products. Surmin obtained exclusively amorphous furfurylidene mesityl oxide (m. p. 140–145°) without these by-products. The furfurylidene mesityl oxide gave, on furan-ring opening reaction, γ,ζ-dioxocaprylic acid which is identical with ring-cleavage product of furfurylidene acetone. This shows that the isopropylidene group in the ketone is broken down in acidic or alkali solution of an elevated temperature.

Hitherto γ,ζ-dioxocarboxylic acid has been synthesized by means of refluxing furfurylidene ketone in alcoholic hydrochloric acid for a comparatively short period with slight yield[6)]. We improved Hunsdiecker's method[7)] which was applied on ring-cleavage of furfurylidene acetone with good results. In our study furfurylidene ketone was added to refluxing solution of alcoholic hydrochloric acid for a period of sixty hours and corresponding γ,ζ-dioxocarboxylic acid was gained in steady and excellent yield.

Ohkawara[6)] and Grundmann et al.[8)] described that various reductions of ε-nitro-γ-oxocaproic acid, with an attempt to get ε-aminocaproic acid gave ε-amino-γ-oxocaproic acid, isoxazolylpropionic acid or γ-caprolactone instead of the required compounds. Taking into account these facts, we tried Clemmensen reduction on γ,ζ-dioxocarboxylic acid and, indeed, could obtain γ-alkylbutyrolactone in good yield. γ,ζ-Dioxocaprylic acid, γ,ζ-dioxopelargonic acid, and γ,ζ-dioxo-θ-methylcapric acid, were smoothly reduced to γ-octalactone, γ-nonalactone and θ-methyl-γ-

1) To whom inquiries concerning the paper should be directed. Saitama University, Urawa.

2) P.Z. Bedoukian, "Perfumery Synthetics and Isolates", D. Van Nostrand Co. Inc., New York, N.Y. (1951), p. 271.

3) H. Gilman and A.H. Blatt, "Organic Syntheses", Coll. Vol. I, John Wiley and Sons, Inc., New York, N.Y. (1948), p. 283.

4) H. Midorikawa, This Bulletin, 27, 149 (1954), ibid., 27, 210 (1954).

5) P.P. Surmin, *J. Gen. Chem.*, 5, 1642 (1935); *C.A.*, 30, 3430 (1936).

6) E.A. Kehrer and P. Igler, *Ber.*, 32, 1177 (1899), F.L. Breusch and E. Ulusoy, *Rev. faculté sci. univ. Istanbul*, 13 A, 51 (1948); *C. A.*, 42, 5850 (1948). M. Ohkawara, *J. Chem. Soc. Japan*, (*Ind. Chem. Sect.*), 56, 90 (1953).

7) H. Hunsdiecker, *Ber.*, 75, 447 (1942).

8) C. Grundmann and W. Ruske, *Ber.*, 86, 939 (1953).

decalactone in 76%, 73% and 66% respectively. The butyrolactones were identified by comparison of their hydrazides with those of authentic butyrolactones prepared by another method. θ-Methyl-γ-decalactone is a new compound and a liquid of strong odor, recalling that of cocos in a concentrated state and of peaches in a diluted state. It may be said to have greater odor value than γ-undecalactone.

Experimental

Condensation of Furfural with Methyl Ketones.—The condensation was carried out according to the well-established procedure of Midorikawa[3,4]. To a mixture of furfural and methyl ketone in water was at once added aqueous sodium hydroxide and the suspension was stirred for an hour as expected at a definite temperature. The reaction mixture was neutralized with acetic acid. The separated oily layer was subjected to distillation. The results are shown in Table I.

Furfurylidene mesityl oxide is a viscous and slightly yellowish liquid (yellow amorphous substance of m. p. 140–145° according to Surmin[5]) and does not easily show the formation of semicarbazone, hydrazone or bisulfite-addition product. B. p. 128–132° (5 mm).

Anal. Found: C, 74.47; H, 7.05. Calcd. for $C_{11}H_{12}O_2$: C, 74.97; H, 6.86%.

Ring-opening of Furfurylidene Ketones.—All runs were carried out according to the following general procedure. 30 g. of furfurylidene ketone dropped onto a refluxing mixture of 150 cc. of conc. hydrochloric acid and 300 cc. of methanol. The addition required sixty hours. After evaporating methanol and hydrochloric acid under reduced pressure, the crystallized residue was pressed on a porous plate. Once recrystallization from petrolether-ethyl acetate gave γ,ς-dioxocarboxylic acid as shown in Table II.

Clemmensen Reduction of γ,ς-Dioxocarboxylic Acids[9].—The general procedure of the reduction is illustrated as follows: A mixture

Table I

Ketone	Grams of Ketone	Furfural g.	aq. NaOH, 5%	10%	cc. 33%	Reactn. Temp., °C	Reactn. Time hr.	Condn. Product	B. p., °C	mm	Yield[a], %
Acetone	32	25	—	—	5	10–20	4	FA and DFA	95–96 181–184	6 4	66 28
Methyl Ethyl Ketone	50	25	—	25	—	60	1	FMEK	103–104	6	77
Methyl Isobutyl Ketone	50	25	18	—	—	60	2	FMIBK	116–117	5	80
Mesityl Oxide	50	25	16	—	—	60	1	FMSO, FA and DFA	128–132 95–96 181–184	5 6 4	17 16 —

a) Yield was based on furfural. FA refers to furfurylidene acetone, DFA to difurfurylidene acetone, FMEK to furfurylidene methyl ethyl ketone, FMIBK to furfurylidene methyl isobutyl ketone and FMSO to furfurylidene mesityl oxide.

Table II

Furfurylidene Ketone	Reactn. Time, hr.	Reactn. Product	M. p., °C	Yield, %	Carbon, % Found	Carbon, % Calcd.	Hydrogen, % Found	Hydrogen, % Calcd.
FA	60	γ,ς-Dioxocaprylic acid[a]	75–76[3]	50	55.85	55.80	7.22	7.03
FMEK	60	γ,ς-Dioxopelargonic acid	85–86[4]	24	58.07	58.05	7.55	7.58
FMIBK	60	γ,ς-Dioxo-θ-methyl capric acid	80[2,3]	32	61.70	61.66	8.34	8.47
FMSO	60	γ,ς-Dioxocaprylic acid[b]	75–76	30	—	—	—	—

a, b) The mixture melting point with a) and b) was not depressed.

Table III

γ,ς-Dioxocarboxylic Acid	Product	Hydrazide B. p., °C, mm	Yield, %	M. p., °C	Nitrogen, % Found	Nitrogen, % Calcd.
γ,ς-Dioxocaprylic Acid[10]	γ-Octalactone	102–105 5.5	76	79–80	16.21	16.08
γ,ς-Dioxopelargonic Acid[10]	γ-Nonalactone	126–127 8	73	84	14.73	14.88
γ,ς-Dioxo-θ-methylcapric Acid	θ-Methyl-γ-decalactone	120–122 2	70	96–97	12.96	12.96

Fractionation of condensation product of furfural with mesityl oxide gave furfurylidene acetone (b. p. 95–96°/6 mm.), furfurylidene mesityl oxide (b. p. 128–132°/5 mm.) and the last distillate (b. p. 181–184°/4 mm.) whose boiling point approximately corresponds to that of difurfurylidene acetone.

of 10 g. of γ,ς-dioxocarboxylic acid, 50 g. of amalgamated zinc, 40 cc. of water, 100 cc. of conc.

9) E. L. Martin", Organic Reactions", Vol. I, John Wiley and Sons, Inc., New York, N.Y. (1942), p. 162.

10) B. Rothstein, *Bull. soc. chim. France*, (5), 2, 80 (1935); ibid., (5), 2, 1936 (1935); E. E. Blaise and A. Koehler, ibid., (4), 7, 415 (1910).

hydrochloric acid and 50 cc. of toluene, was boiled vigorously for twenty-four hours. The three 25 cc. portions of conc. hydrochloric acid were added at six-hour intervals during the refluxing period. The toluene layer and ether extracts which were obtained by shaking the water layer, were combined, washed with sodium bicarbonate solution and then subjected to distillation. The results are listed in Table III.

A mixture melting point of hydrazide of γ-nonalactone obtained by Clemmensen reduction and that of authentic lactone[10] prepared by employing *n*-heptaldehyde and malonic acid, was not depressed.

θ-Methyl-γ-decalactone.—This lactone is a transparent liquid having a strong coco odor and is easily soluble in usual organic solvents. B. p. 121° (2 mm.), d_4^{20} 0.941, n_D^{20} 1.4500.

Anal. Found: C, 71.33; H, 11.00. Calcd. for $C_{11}H_{20}O_2$: C, 71.69; H, 10.94%. Saponification value, Found: 309. Calcd.: 304.

The authors wish to express their hearty thanks to Prof. T. Hoshino, Prof. Y. Iwakura and Mr. K. Nagakubo of Tokyo Institute of Technology, for their kind guidance throughout the present work, and also to Mr. A. Kondo for microanalyses.

Showa Perfumery Co. Ltd., Shibuya-ku
Tokyo and Chemical Department
Saitama University, Urawa

Mechanism of the Exchange Reaction of Oxygen Atoms between Gaseous Oxygen and Water Vapor Catalyzed by Calcium Oxide

By Sadahiro SAKATA and Noriyoshi MORITA

(Received April 23, 1956)

Introduction

In previous papers[1] where we studied the rate R of the exchange reaction of oxygen atoms between gaseous oxygen and water vapor from measurements of the rate of the isotopic exchange reaction of oxygen isotopes catalyzed by chromic oxide, we concluded that the rate R remains constant irrespective of the feed rate of the reacting gaseous mixture so long as it maintained a rate higher than about 30 cc./sec.·cm^2. In that case the rate of the exchange reaction should be controlled by some one or more of the surface processes, i. e. adsorption of reactants, chemical reaction on surface, and desorption of products. Then by observing the change in rate of the exchange reaction under various mixing molar ratios of the reacting gases $\alpha=O_2/H_2O$ and under the assumption that only one chemical step is rate controlling, we can examine the mechanism of the reaction by the method developed by Langmuir-Hinshelwood and later extended by Hougen[2]. The result obtained with chromic oxide catalyst was read at the 4th Symposium of Catalysis of the Chemical Society of Japan held in Sapporo on July 24, 1955[3]. Now, this method has been applied to the reaction catalyzed by calcium oxide and the results compared with that obtained with chromic oxide.

Experimental and Analytical Procedure

The experimental procedure was the same as described in the previous paper[1]. A quartz tube of 1.6 cm. inside diameter was used in a vertical position. The rate R, number of exchange per sec. per cc. of the reactor, was calculated by the following relation:

$$R=\frac{6.155\cdot10^{19}}{Z}\frac{\alpha}{(2\alpha+1)(\alpha+1)}F\{-\log(1-x)\} \quad (1)$$

Here x is the conversion, net fraction of the isotopic exchange reaction to equilibrium, F is the feed rate of the gaseous mixture in cc. (S.C.)/sec., and Z is the height of the catalyst bed in cm.

The calcium oxide catalyst was prepared from commercial calcium oxide of chemically pure grade. The blocks of calcium oxide were crushed to particles of 2–3 mm., and calcined at 850°C for four hours under oxygen gas flow.

As the foundation for analysis of experimental results, we assume, as has been done by many authors[4], that all adsorption sites on the catalyst

* The main part of this paper was presented at the 9th Annual Meeting of the Chemical Society of Japan on April 2, 1956, Kyoto.

1) S. Sakata and N. Morita, This Bulletin, **29**, 230 (1956); *Chem. Eng. (Japan)*, **19**, 64 (1955).

2) O.A. Hougen and K.M. Watson, *Ind. Eng. Chem.*, **35**, 529 (1943); "Chemical Process Principles", John Wiley & Sons, Inc., New York, N.Y. (1950).

3) S. Sakata and N. Morita, *Shokubai* Catalyst, **12**, 80 (1955).

4) O.A. Hougen and K.M. Watson, l.c.; H.F. Rase and R.S. Kirk, *Chem. Eng. Progr.*, **50**, 35 (1954).

surface behave similarly and that the interfacial activities of components of the reacting gaseous mixture are equal to their partial pressures in the bulk phase Then, (I) if we consider the case in which molecular adsorption of both reactants occur, the equilibrium concentrations of molecularly adsorbed oxygen and water on the surface, c_{O_2} and c_{H_2O}, and equilibrium concentration of vacant site on the surface, c_l, all in number of sites per unit mass of catalyst, can be expressed by

$$c_{O_2}=p_oK_oL/(1+p_oK_o+p_wK_w) \quad (2)$$

$$c_{H_2O}=p_wK_wL/(1+p_oK_o+p_wK_w) \quad (3)$$

$$c_l=L/(1+p_oK_o+p_wK_w) \quad (4)$$

where p_o is the partial pressure of oxygen in atm. and p_w the same of water, K_o is the adsorption equilibrium constant of oxygen in atm.$^{-1}$ and K_w the same of water, and L is the total number of active sites on the surface per unit mass of catalyst. During the exchange reaction the chemical concentration of reactants, i.e. p_o and p_w, do not change and therefore the values of c's remain constant. Consequently, (A) when the rate of molecular adsorption of oxygen controls the rate of the exchange reaction, it can be expressed by $R=kp_oc_l=kp_oL/(1+p_oK_o+p_wK_w)$, or $p_o/R=(1/kL)+(K_o/kL)p_o+(K_w/kL)p_w$, where k is the adsorption velocity constant for oxygen. Taking total pressure p_o+p_w as a unit pressure which is kept constant during a series of experiments, we can write $p_o=\alpha/(\alpha+1)$ and $p_w=1(\alpha+1)$. Then we obtain

$$\alpha/R=(a+b)\alpha+(a+c) \quad (5)$$

where a, b and c are positive constants and $a=1/kL$, $b=K_o/kL$ and $c=K_w/kL$. On the contrary, (B) when the rate of desorption of molecularly adsorbed oxygen is controlling, we obtain $R=kc_{O_2}=kp_oK_oL/(1+p_oK_o+p_wK_w)$, where, in this case, k is the desorption velocity constant for oxygen. Then we can write

$$\alpha/R=(a+b)\alpha+(a+c) \quad (6)$$

where a, b and c are positive constants different from those in Eq. (5) and $a=1/kK_oL$, $b=1/kL$ and $c=K_w/kK_oL$.

By the same reasoning we can obtain the following expression, (C, D) when adsorption or desorption of water is rate-controlling

$$1/R=(a+b)\alpha+(a+c) \quad (7)$$

Finally, (E) when the surface chemical reaction is controlling, R is proportional to the surface concentration of pairs of adsorbed oxygen and water molecules in adjacent positions. This concentration is equal to $sc_{O_2}c_{H_2O}/L$, where s is the number of equidistant active sites adjacent to each site. Therefore, $R=ksp_op_wK_oK_wL/(1+p_oK_o+p_wK_w)^2$, and by rearrangement we obtain

$$\sqrt{\alpha/R}=(a+b)\alpha+(a+c) \quad (8)$$

where. $a=1/\sqrt{ksK_oK_wL}$, $b=K_o/\sqrt{ksK_oK_wL}$ and $c=\sqrt{K_w/ksK_oL}$.

(II) When oxygen is adsorbed with dissociation, its equilibrium concentration c_O and that of water and of vacant sites c_{H_2O} and c_l are expressed by

$$c_O=L\sqrt{p_oK_o}/(1+\sqrt{p_oK_o}+p_wK_w) \quad (9)$$

$$c_{H_2O}=p_wK_wL/(1+\sqrt{p_oK_o}+p_wK_w) \quad (10)$$

$$c_l=L/(1+\sqrt{p_oK_o}+p_wK_w) \quad (11)$$

In order that oxygen molecules can be atomically adsorbed, dual adsorption sites are necessary and their concentration can be expressed by $c_{l_2}=sc_l^2/2L$. Therefore, (A) when the rate of adsorption of oxygen with dissociation controls the rate of the exchange reaction, we have the relation $R=kp_oc_{l_2}=(ksp_oL/2)/(1+\sqrt{p_oK_o}+p_wK_w)^2$, and then

$$\sqrt{\alpha(\alpha+1)/R}=a\alpha+b\sqrt{\alpha(\alpha+1)}+(a+c) \quad (12)$$

For the case (B) where the rate of recombination of atomically adsorbed oxygen to molecule is controlling we obtain the same expression as Eq. (12).

In the same way we can obtain the expressions (C, D) when adsorption or desorption of water is controlling

$$1/R=a\alpha+b\sqrt{\alpha(\alpha+1)}+(a+c) \quad (13)$$

and (E) when chemical reaction on the surface is controlling

$$\sqrt{\sqrt{\alpha(\alpha+1)}/R}=a\alpha+c\sqrt{\alpha(\alpha+1)}+(a+c) \quad (14)$$

(III) We have to consider adsorption of water vapor with dissociation. In this case the state of adsorption is HOl+Hl, where l indicates adsorption site. However, adsorption of hydrogen atom may occur at the oxygen atom on the surface of metallic oxide, and, therefore, as an additional assumption, we consider the state of adsorption to be HOl+HOl, both behaving similarly. Then we have the forms which are summarized in Table I for the relation between the rate of exchange reaction and the mixing ratio of reactants according as (A, B) adsorption or desorption of oxygen or (C, D) adsorption of water with dissociation or recombination or (E) chemical reaction on surfaces is rate-controlling.

(IV) We have also the cases where both oxygen and water are absorbed with dissociation and (A, B) adsorption of oxygen with dissociation or recombination or (C, D) adsorption of water with dissociation or recombination or (E) some one of the surface chemical reactions is rate-controlling.

The equations from these postulated mechanisms are summarized in Table I. By comparing these forms with experimental results we can select one or more of them as the probable mechanism. We can consider mechanisms other than those listed in Table I such as when one reactant in the gaseous phase reacts with another adsorbed reactant. However, we have excluded these mechanisms because for an exchange reaction to take place, there is a necessary step of dissociation which needs much more activation energy than the collision of molecules on the catalyst surface. It is a fact that most of the observed rates of exchange reaction are less than one-millionth of the collision number of the gaseous reactant on the other surface of the catalyst.

TABLE I

SUMMARY OF EQUATIONS FROM POSTULATED MECHANISMS

Mechanism		Equation	Values of Constants		
			a	b	c
I	A	$\alpha/R=(a+b)\alpha+(a+c)$	$1/kL$	K_o/kL	K_w/kL
	B	$\alpha/R=(a+b)\alpha+(a+c)$	$1/kLK_o$	$1/kL$	K_w/kLK_o
	C	$1/R=(a+b)\alpha+(a+c)$	$1/kL$	K_o/kL	K_w/kL
	D	$1/R=(a+b)\alpha+(a+c)$	$1/kLK_w$	K_o/kLK_w	$1/kL$
	E	$\sqrt{\alpha/R}=(a+b)\alpha+(a+c)$	$1/\sqrt{ksLK_oK_w}$	$K_o/\sqrt{ksLK_oK_w}$	$\sqrt{K_w/ksLK_o}$
II	A	$\sqrt{\alpha(\alpha+1)}/R=a\alpha+b\sqrt{\alpha(\alpha+1)}+(a+c)$	$\sqrt{2/ksL}$	$\sqrt{2K_o/ksL}$	$K_w\sqrt{2/ksL}$
	B	$\sqrt{\alpha(\alpha+1)}/R=a\alpha+b\sqrt{\alpha(\alpha+1)}+(a+c)$	$\sqrt{2/ksLK_o}$	$\sqrt{2/ksL}$	$K_w\sqrt{2/ksLK_o}$
	C	$1/R=a\alpha+b\sqrt{\alpha(\alpha+1)}+(a+c)$	$1/kL$	$\sqrt{K_o/kL}$	K_w/kL
	D	$1/R=a\alpha+b\sqrt{\alpha(\alpha+1)}+(a+c)$	$1/kLK_w$	$\sqrt{K_o/kLK_w}$	$1/kL$
	E	$\sqrt{\sqrt{\alpha(\alpha+1)}/R}=a\alpha+b\sqrt{\alpha(\alpha+1)}+(a+c)$	$\sqrt{1/ksL\sqrt{K_oK_w}}$	$\sqrt{\sqrt{K_o}/ksLK_w}$	$\sqrt{K_w/ksL\sqrt{K_o}}$
III	A	$\alpha/R=(a+b)\alpha+c\sqrt{\alpha+1}+a$	$1/kL$	K_o/kL	$\sqrt{K_w}/kL$
	B	$\alpha/R=(a+b)\alpha+c\sqrt{\alpha+1}+a$	$1/kLK_o$	$1/kL$	$\sqrt{K_w}/kLK_o$
	C	$\sqrt{1/R}=a\sqrt{\alpha+1}+b\alpha/\sqrt{\alpha+1}+c$	$\sqrt{2/ksL}$	$K_o\sqrt{2/ksL}$	$\sqrt{2K_w/ksL}$
	D	$\sqrt{1/R}=a\sqrt{\alpha+1}+b\alpha/\sqrt{\alpha+1}+c$	$\sqrt{2/ksLK_w}$	$K_o\sqrt{2/ksLK_w}$	$\sqrt{2/ksL}$
	E	$\sqrt{\alpha\sqrt{\alpha+1}/R}=(a+b)\alpha+c\sqrt{\alpha+1}+a$	$\sqrt{1/ksLK_o\sqrt{K_w}}$	$\sqrt{K_o/ksL\sqrt{K_w}}$	$\sqrt{\sqrt{K_w}/ksLK_o}$
IV	A	$\sqrt{\alpha/R}=a\sqrt{\alpha+1}+b\sqrt{\alpha}+c$	$\sqrt{2/ksL}$	$\sqrt{2K_o/ksL}$	$\sqrt{2K_w/ksL}$
	B	$\sqrt{\alpha/R}=a\sqrt{\alpha+1}+b\sqrt{\alpha}+c$	$\sqrt{2/ksLK_o}$	$\sqrt{2/ksL}$	$\sqrt{2K_w/ksLK_o}$
	C	$\sqrt{1/R}=a\sqrt{\alpha+1}+b\sqrt{\alpha}+c$	$\sqrt{2/ksL}$	$\sqrt{2K_o/ksL}$	$\sqrt{2K_w/ksL}$
	D	$\sqrt{1/R}=a\sqrt{\alpha+1}+b\sqrt{\alpha}+c$	$\sqrt{2/ksLK_w}$	$\sqrt{2K_o/ksLK_w}$	$\sqrt{2/ksL}$
	E	$\sqrt{\sqrt{\alpha}/R}=a\sqrt{\alpha+1}+b\sqrt{\alpha}+c$	$\sqrt{1/ksL\sqrt{K_oK_w}}$	$\sqrt{\sqrt{K_o}/ksL\sqrt{K_w}}$	$\sqrt{\sqrt{K_w}/ksL\sqrt{K_o}}$

Experimental Results and Discussion

The results obtained are tabulated in Table II. For comparison, the results obtained with chromic oxide catalyst are also included in the table. In both cases, for the lower values of α, the rate R increases with the increase in α, and for the higher values of α the rate remains almost constant irrespective of the values of α. The main differences are the lower activity and the more gradual approach to a constant value of R of calcium oxide as compared with chromic oxide. Those facts indicate that we can examine the mechanism of the exchange reaction catalyzed by calcium oxide by the same course as that of chromic oxide except for the point that the relative importance of adsorption equilibrium constants K_o and K_w may be different for both catalysts.

For selection of the probable mechanism, Hougen recommended that the constants of the equations for the various proposed mechanisms be determined, i.e. a, b and c, which must be positive, by use of the method of least squares. However, as for every one of the equations from the postulated mechanisms of groups II and IV there were two nearly parallel terms, so the probable errors of the constants which were determined by

TABLE II

Calcium Oxide			Chromic Oxide		
Temperature=743°C			Temperature=521°C		
F=28.9 cc./sec.·cm²			F=30.1 cc./sec.·cm²		
Average Total Pressure=769 mmHg			Average Total Pressure=783 mmHg		
Exp. No.	α	$R\times10^{-18}$ atoms/sec.·cc.	Exp. No.	α	$R\times10^{-18}$ atoms/sec.·cc.
1418	0.553	4.74	1304	0.050	2.38
1411	0.571	5.01	1303	0.080	2.75
1414	1.142	6.21	1302	0.082	2.64
1420	1.951	6.52	1211	0.336	2.86
1410	2.010	6.84	1204	0.410	4.09
1419	3.63	7.60	1307	0.495	3.38
1412	4.60	9.37	1107	0.842	4.44
1413	5.56	8.75	1105	0.926	4.75
1417	7.67	8.80	1104	0.966	4.75
1415	10.40	8.82	1210	1.231	3.91
			1202	1.337	4.11
Temperature=700°C			1109	2.094	4.63
F=29.9 cc./sec.·cm²			1102	2.222	4.81
1502	0.536	2.35	1106	2.876	4.99
1505	1.079	3.02	1201	3.30	5.43
1501	2.040	3.56	1108	3.86	4.56
1509	2.153	3.24	1103	4.14	4.67
1507	3.78	3.96	1203	8.78	5.20
1503	4.70	4.02	1301	13.12	5.01
1504	6.43	4.41			
1508	8.29	4.44			
1506	10.52	4.38			

the method of least squares were considerable. Therefore, we examined the mechanisms graphically.

First, the mechanisms in which adsorption or desorption of water is rate controlling, i.e. all of C's and D's can be excluded. In these mechanisms $1/R$ must be increased with the increase in α which is inconsistent with the experimental results.

The mechanisms of group I can be examined by plotting values of left-hand terms of the equations against α. In Fig. 1, curves I-E are the relations of $\sqrt{\alpha/R}$ vs. α. They

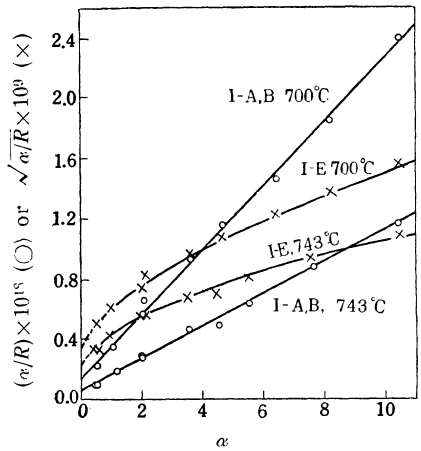

Fig. 1. Mechanisms I-A, B and I-E.

do not indicate linear relation and the mechanism I-E can not be applied. The relation α/R vs. α is practically linear as shown by lines I-A, B in Fig. 1, and the mechanisms I-A and I-B must be reserved as probable mechanisms. We will consider these mechanisms again later.

The right-hand side of each equation for the mechanisms of groups II, III and IV has two variable terms. We scrutinize these mechanisms by plotting two variables separately against the values of the left-hand terms and testing the possibility of constructing a linear combination with positive coefficients from these two curves to gain linear relation. Fig. 2 to Fig. 7 are such plottings. In examining these plottings we notice the further facts that the value of the left-hand side of each equation extrapolated to $\alpha=0$ gives $a+c$ and that the inclination of the curves for mechanisms of groups II and IV converge to $a+b$ for high values of α.

By such criterions we can easily exclude the mechanisms of II-E, III-A, B and III-E. In Fig 3 which represents the relation for mechanism II-E, both of the curves for α and $\sqrt{\alpha(\alpha+1)}$ vs. $\sqrt{\sqrt{\alpha(\alpha+1)}/R}$ are concave and can not gain combination to give linearity. In Fig. 4 for mechanisms III-A, B the relation of α vs. α/R is almost linear but $\sqrt{\alpha+1}$ vs. α/R is convex and their combination can be linear only when the values of

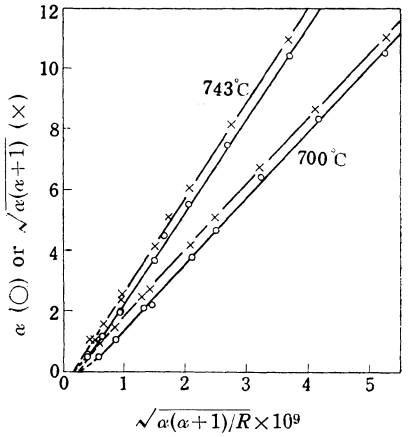

Fig. 2. Mechanisms II-A, B.

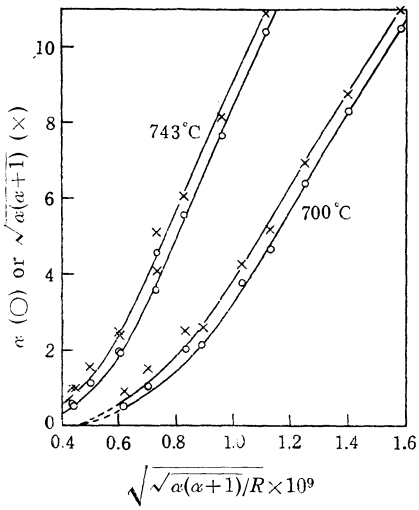

Fig. 3. Mechanism II-E.

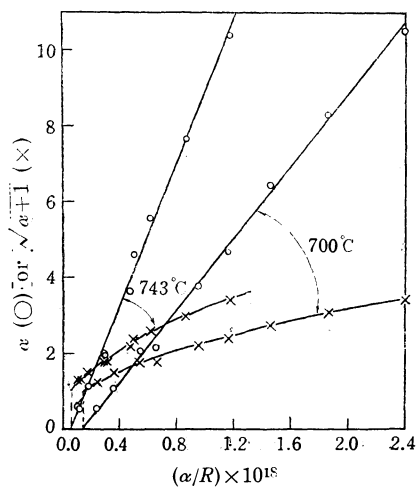

Fig. 4. Mechanisms III-A, B.

c are very small, and then this is the same as the mechanisms I-A, B. For mechanism III-E only $\sqrt{\alpha+1}$ vs. $\sqrt{\alpha\sqrt{\alpha+1}/R}$ is linear as shown in Fig. 5. To select this mechanism, a and b must be very small and then both of the extrapolated values of abscissa at $\alpha=0$ and the inclination of the straight line must be nearly equal to c. This is not the case. The abscissa values at $\alpha=0$ are less than 0.3×10^{-9} compared with the inclinations of the lines which are about 1×10^{-9}.

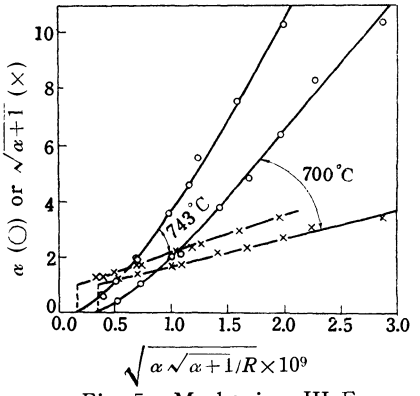

Fig. 5. Mechanism III-E.

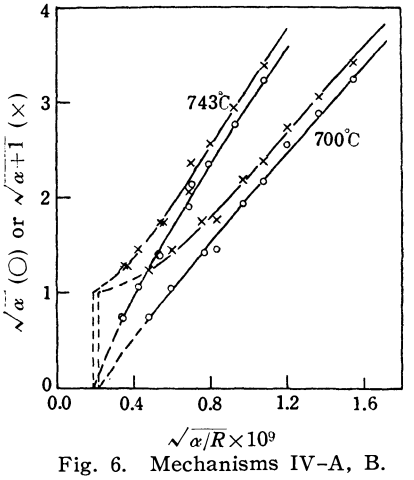

Fig. 6. Mechanisms IV-A, B.

For all other mechanisms we can not state exactly from Figs. 2, 6 and 7 their applicability or non-applicability. Therefore, we first evaluated the constants a, b and c for each mechanism by applying the two criterions noted above for the determination of $a+b$ and $a+c$ and using a pair of values on the pair of smoothed curves. And then we examined the propriety of these constants to the mechanism. Evaluated values are tabulated in Table III. For comparison, values of constants for the exchange reaction with chromic oxide catalyst are also included. Values of K_o were calculated from a and b, and K_w's from a and c. The apparent activation energies E for calcium oxide catalyst were calculated from pairs of values of a obtained at two temperatures, assuming constants values for L and s.

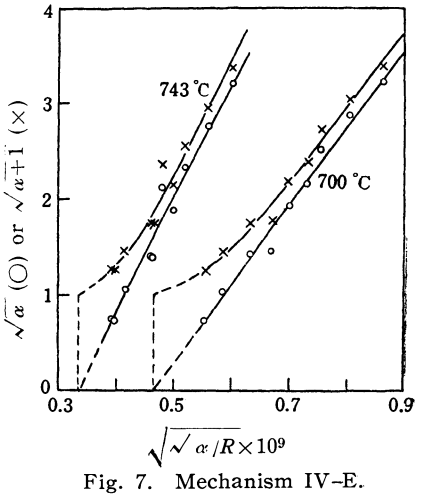

Fig. 7. Mechanism IV-E.

TABLE III
EVALUATED VALUES OF CONSTANTS

Mechanism	Catalyst	Temp. °C	$a+b$ $\times10^9$	$a+c$ $\times10^9$	a $\times10^9$	b $\times10^9$	c $\times10^9$	K_o	K_w	E kcal.
II A, B	Calcium Oxide	743	0.321	0.156	0.061	0.260	0.095	18.2	1.56	33
	〃	700	0.460	0.250	0.088	0.372	0.162	17.9	3.40	
	Chromic Oxide	521	0.439	0.112	0.094	0.345	0.018	13.5	0.19	
IV A, B	Calcium Oxide	743	0.317	0.194	0.165	0.152	0.029	0.8_5	0.03_1	7.4
	〃	700	0.458	0.213	0.179	0.279	0.034	2.4_3	0.03_6	
	Chromic Oxide	521	0.437	0.071	0.050	0.378	0.021	60.0	0.16	
IV E	Calcium Oxide	743	0.092	0.335	0.038	0.054	0.397	2.0_2	109	22
	〃	700	0.134	0.465	0.050	0.084	0.415	2.8_1	69	
	Chromic Oxide	521	0.117×10^{18}	0.270×10^{18}	negative	—	—	—	—	
I A, B	Calcium Oxide	743	0.105	0.065						
	〃	700	0.212	0.145						
	Chromic Oxide	521	0.204	0.040						

Taken from the criterion that a, b and c must be positive, all the mechanisms in Table III, except IV-E for chromic oxide, are applicable. However, mechanism IV-E for calcium oxide may also be excluded because such a mechanism, where both reactants are adsorbed with dissociation and where surface chemical reaction controls the over-all rate, seems incomprehensible for the exchange reaction of atoms. As far as mechanisms I-A, B are concerned we can not determine the values of a, b and c, uniquely. However, in contrast to mechanisms group IV, mechanisms of group I, where only molecular adsorption occurs, may also be improbable for exchange reaction of atoms. Thus mechanisms II-A, B and IV-A, B remain as acceptable.

From preliminary experiments where we measured changes of R with temperature by calcium oxide catalyst to find adequate range of temperature for further resarches, we obtained activation energy of 30.6 kcal./mol. between 697°C and 740°C. In this respect mechanisms II-A, B are most comprehensible. We could not find adequate data concerning adsorption of oxygen or water vapor by calcium oxide. The equilibrium data[5] of dissociation of CaO_2 and $Ca(OH)_2$ give heat of dissociation of 4-11 kcal./mol. for CaO_2 and 25-43 kcal./mol. for $Ca(OH)_2$. Heat of activation must be greater than these and the mechanisms IV-A, B seem more improbable than mechanisms II-A, B. Values of K_o and K_w of mechanisms II-A, B seem reasonable. For these mechanisms K_o is equal to $c_O^2/p_o c_l^2$ and K_w is equal to $c_{H_2O}/p_w c_l$. Then $c_{H_2O}/c_O = p_w K_w/\sqrt{p_o K_o}$. The evaluated values of c_{H_2O}/c_O at $p_o = p_w = 1/2$ are 0.26 for 743°C and 0.57 for 700°C for calcium oxide catalyst and 0.037 for chromic oxide catalyst. Thus the remarkable difference between calcium oxide catalyst and chromic oxide catalyst is the much stronger adsorption of water by the former.

In an earlier paper[6] dealing with exchange reaction of oxygen atoms between gaseous oxygen and water vapor by oxide catalysts of metals belonging to the even series of the first long period of the periodic table of elements we concluded that the exchange reaction catalyzed by calcium oxide would be controlled by adsorption or desorption of water vapor. This conclusion seems inconsistent with the present results. However, earlier researches were done under much lower temperatures than those of the present, and the relative dominating effect of adsorption of oxygen and water vapor for the rate may differ by temperature as can be seen by the great difference of the heat of adsorption between oxygen and water. It can be expected that the rate of adsorption or desorption of water will become the controlling factor in the over-all rate of the exchange reaction by minimizing the concentration of water vapor, i. e. by greater values of α, much more than has been done in these experiments.

5) "International Critical Tables", Vol. VII, p. 294 (1930).

6) N. Morita, H. Tanaka and T. Titani, This Bulletin, 14, 9 (1939).

Summary

Employing a high-feed rate of reacting gaseous reactants where the rate of reaction did not depend upon the feed rate, measurements of the dependence of the exchange reaction rate of oxygen atoms between gaseous oxygen and water vapor catalyzed by calcium oxide on the mixing molar ratio of reacting gases were made, and the results analyzed by the method of Hougen. The most probable among twenty postulated mechanisms is mechanism II-A where oxygen is adsorbed with dissociation and the rate of dissociative adsorption of oxygen is rate-controlling or II-B where oxygen is adsorbed with dissociation and the recombination of adsorbed oxygen atoms to desorption is rate-controlling. According to these mechanisms, the activation energy of adsorption of oxygen with dissociation or recombination to desorption is about 33 kcal./mol., which is in good agreement with the activation energy 30.6 kcal./mol. for the over-all rate of exchange reaction.

This conclusion is compared to the results obtained with chromic oxide catalyst. The result which was described in an earlier paper is also discussed.

Department of Chemical Engineering,
Faculty of Engineering,
Nagoya University,
Nagoya

Heats of Dilution of Polyvinylalcohol Solutions. II

By Kazuo AMAYA and Ryoichi FUJISHIRO

(Received June 27, 1956)

Introduction

In the previous paper[1] we measured the heats of dilution of aqueous solution of polyvinylalcohol and found that the value of the interaction parameter is about −3 cal./cc., which is too small compared with that of ethylalcohol-water solution (−40 cal./cc.) and indicates considerable inter-segmental associations of polyvinylalcohol.

In order to make a further study about these facts, we measured the heats of mixing for the 1,3- or 1,4-butanediol and water system, and the heats of dilution for the polyvinyl-alcohol of different acetyl radical content and water systems.

These butanediols may be regarded as dimer molecules of polyvinylalcohol and it is expected that they play an important role as intermediate molecules between ethylalcohol and polyvinylalcohol. As the polyvinylalcohol has been thought to have a large number of inter-segmental hydrogen bondings, it is supposed that if a portion of hydroxyl radicals is substituted with acetyl ones, the formation of inter-segmental hydrogen bondings may be disturbed and there may occur some changes in the interaction parameter.

Experimental

The apparatus used was already described in the previous paper. Commercial 1,3- and 1,4-butanediol* were dehydrated under the pressure of about 1 mmHg for long time and then distilled with a long column under the reduced pressure.

Polyvinylalcohol samples** of the degree of polymerization 1200 were supplied by the Laboratory of the Mitsubishi Rayon Campany and the acetyl contents of these samples were 0.4, 7.8, 15.6 and 19.4 mol.% respectively.

Results and Discussion

The heats evolved, when the butanediol and water were mixed and then the solution was diluted successively with water or butanediol, were measured at 25°C. By integrating these heats evolved by mixing or dilution, the heats of mixing at various concentrations were obtained and are shown in Table I and II.

TABLE I

HEATS OF MIXING OF 1,3-BUTANEDIOL AND WATER

Weight of Diol, g.	Weight of Water, g.	Heat Evolved, cal.	$-\Delta H$, cal. / Unit Mole Solution	Unit Mole Fraction
1.973	16.130	52.6	56.1	0.046
1.973	8.131	45.7	92.3	0.088
1.973	4.125	36.5	134	0.161
1.973	2.061	24.4	154	0.277
1.921	2.045	25.7	165	0.273
3.884	2.045	30.0	150	0.432
7.711	2.045	34.3	120	0.601
1.748	11.96	44.7	63.3	0.055
1.748	5.982	39.6	106	0.104
1.748	3.988	34.9	134	0.149
1.748	1.994	24.2	162	0.259
1.970	1.994	25.1	162	0.282
3.980	1.994	30.4	153	0.442
5.990	1.994	32.3	133	0.544

TABLE II

HEATS OF MIXING OF 1,4-BUTANEDIOL AND WATER

Weight of Diol, g.	Weight of Water, g.	Heat Evolved, cal.	$-\Delta H$, cal. / Unit Mole Solution	Unit Mole Fraction
2.004	17.58	44.1	43.2	0.044
2.004	8.194	40.0	80.1	0.089
2.004	4.134	32.0	117	0.162
2.004	2.058	22.3	140	0.280
1.961	2.006	23.1	149	0.281
3.965	2.006	29.2	147	0.441
7.990	2.006	35.5	123	0.614

The accuracy of the measurement was not so satisfactory, because the butanediols are highly viscous and adhere to the wall of the mixing vessel. The accuracy may be estimated from the two measurements at nearly the same concentration (about 0.5 volume fraction), one with water in the inside bulb and butanediols in the outside bulb and the other the reverse.

As ethylalcohol and butanediol may be regarded as a monomer- and dimer-unit of polyvinylalcohol respectively, by considering the butanediol as two unit molecules the heats of mixing per unit mole of solution (which means that the number of water molecules

1) K. Amaya and R. Fujishiro. This Bulletin 29, 361 (1956).

* We wish to thank Mr. T. Wakabayashi of the Nippon Yushi Company for supplying these butanediols.

** We are indebted to Dr. H. Suyama of the Mitsubishi Rayon Company for these samples.

plus two times the number of butanediol molecules is equal to the Avogadro number) are calculated from the above data and plotted in Fig. 1 against the unit mole fraction

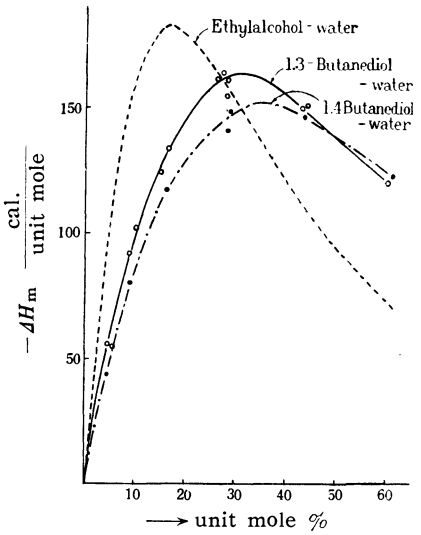

Fig. 1

of butanediol. For the sake of comparison, the heats of mixing per mole of the ethylalcohol-water solution[2] at the same temperature are shown in the same figure.

The remarkable features which appeared in this figure are the lowering of the maximum of the curve and the shift of the maximum position to the higher concentration of butanediol. The former may be easily explained as the intra-molecular association of the two hydroxyl groups of the butanediol molecule which decreases the apparent interaction of the butanediol with the solvent molecule. The magnitude of lowering of the maximum is more in 1,4-butanediol than in 1,3-butanediol and this is consistent with the fact that 1,4-butanediol is apt to form the intra-molecular hydrogen bonding from the steric standpoint in comparison with 1,4-butanediol.

Generally the maximum in the heats of mixing per unit volume of mixture of two kinds of normal liquids where there is no specific interaction will be at the equi-volume concentration. In the mixture where the two normal liquids have the same molecular volume, the maximum in the heats of mixing per mole of the mixture will be at the equi-molar concentration. But in the mixture of two normal liquids having different molecular volumes, the maximum in the heats of mixing per mole of the mixture will be shifted to the $(\sqrt{x}-1)/(x-1)$ mole fraction, where x is the ratio of molecular volume of the two liquids.

In a case when one or both liquids have specific groups of interaction, the position of the maximum may shift more or less from the normal value $(\sqrt{x}-1)/(x-1)$. Ethylalcohol-water system is such a typical example and the maximum shifts to a lower value of the mol. fraction of ethylalcohol such as 0.18, to be compared with the nomal value 0.36 calculated by using $x=3$ for this system.

In the butanediol-water systems the observed values of the maximum point are 0.30 and 0.35 for 1,3- and 1,4-butanediol respectively, and these values are compared with the normal one 0.40 which is evaluated by using the value 2.4 for the ratio of molecular volume of monomer-unit of both butanediols to that of water.

Hence it is shown that the maximum point approaches considerably to a normal one for both butanediol-water systems compared with that for the ethylalcohol-water system.

It may be supposed to be natural that this will be due to the intra-molecular association of butanediol which decreases the specific interaction power per unit molecule.

From the fact above mentioned, the more the number of units in a molecule, the smaller the magnitude of the maximum for the solution containing the molecule and the more the maximum point may approach to the normal value.

This indicates a remarkable lowering of the heats of mixing and thus a remarkable decrease of the magnitude of the interaction parameter in the polyvinylalcohol-water solution.

In order to get the quantitative explanation, the conventional interaction parameter which is the quantity per cc. of solution, is evaluated and plotted in Fig. 2 against the

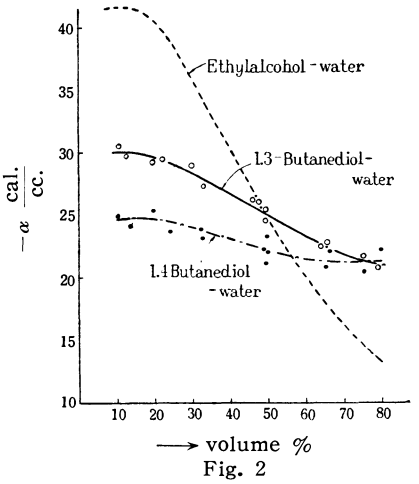

Fig. 2

2) E. Bose, *Z. physik. Chem.*, 58, 587 (1907).

volume fraction of ethylalcohol or butanediols respectively. Here the equation used for the evaluation of the interaction parameter is the following van Laar's,

$$\Delta H_m = \alpha V v_o v_r$$

where v_o, v_r are the volume fractions of solvent (water) and ethylalcohol or butanediols respectively, V the total volume of the solution, ΔH_m the heats of mixing of such solution and α the interaction parameter per cc.

In Fig. 2 it is found that in the ethylalcohol-water system the value of $-\alpha$ decreases sharply as the volume concentration of ethylalcohol increases, but not in the butanediol-water one. In the previous paper it was in the volume fraction less than 0.2 where the heats of dilution of polyvinylalcohol solution were measured.

In the same concentration range, the value of α of the ethylalcohol solution is -40 cal./cc. and those of the 1,3- and 1,4-butanediol solutions are -30 and -25 cal./cc. respectively.

A large decrease in magnitude of the interaction parameter is seen in transfer from monomer to dimer.

Such a decrease may probably be expected successively as the molecules become larger. Thus it may stand to reason that in the polyvinylalcohol solution the value of α has such small value as -3 cal./cc.

The heats of dilution of polyvinylalcohol which contains different acetyl contents were also measured and shown in Table III.

TABLE III

HEATS OF DILUTION OF POLYVINYLALCOHOL WITH DIFFERENT ACETYL CONTENT

Acetyl Content Mole %	Before Dilution: Volume of Solution cc.	Before Dilution: Volume Fraction of P.V.A.	Volume of Water Added cc.	Heat Evolved, cal.	$-\alpha$ cal./cc.
0.4	9.00	0.099	10	0.145	3.1
0.4	9.51	0.109	10	0.177	3.0
7.8	9.57	0.077	10	0.167	5.7
7.8	8.57	0.077	10	0.151	5.5
15.6	9.91	0.052	10	0.040	2.9
15.6	9.94	0.052	10	0.041	3.0
19.4	9.86	0.038	10	0.017	2.4
19.4	9.94	0.038	10	0.015	2.1

By use of the van Laar equation, the values of the interaction parameter are calculated. The order of magnitude of α is found to be in good agreement with that of the previous paper. These values of α are plotted in Fig. 3 against the acetyl content in the polyvinylalcohol.

In Fig. 3 the absolute value of the parameter α seems to show maximum between 0 to 10 mole % of acetyl radicals.

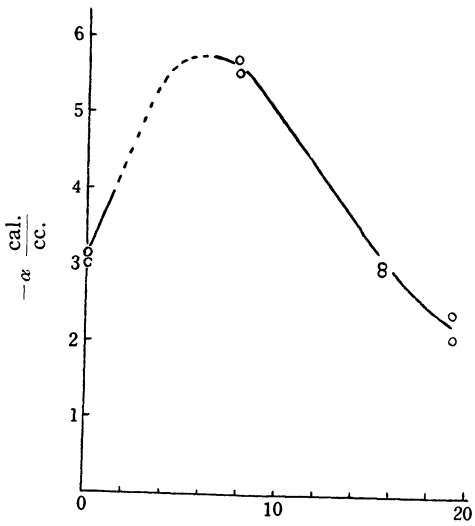

Mole % of acetyl radical

Fig. 3

If some of hydroxyl radicals in the polyvinylalcohol are substituted by acetyl ones, two main effects may appear.

First, as it is supposed that there is no strong interaction between acetyl group and water molecule, these interactions may be repulsive and decrease the absolute value of α. Secondly, the substitution of hydroxyl radical with acetyl will disturb intra-molecular or inter-segmental hydrogen bonding in the polyvinylalcohol and consequently increase the hydroxyl radicals which do not form hydrogen bonding with each other. This means the increase of the absolute value of α.

Thus, these two effects may change the value of α in the reverse way as the acetyl content increases.

But it will be supposed that the effect of disturbing hydrogen bonding by substitution is considerable in the small acetyl content and saturated in the more concentrated fraction, while the interaction between acetyl radical and water increases linearly with acetyl content.

Consequently, in the small acetyl content the effect of disturbing inter-segmental hydrogen bonds is predominant compared with the first, and the absolute value of the interaction parameter may increase as the acetyl content increases.

But in the range of larger acetyl content the second effect may exceed the first.

So, it will be reasonable to assume that the absolute value of α increases at first, passes through a maximum and decreases as the acetyl content increases.

Summary

Heats of mixing of 1, 4- and 1, 3-butandiols with water and heats of dilution of polyvinylalcohol of different acetyl contents were measured.

The results obtained for the two butanediols and water system were compared with the results for ethylalcohol-water system and for polyvinylalcohol-water system (reported in the previous paper) and it was found that the apparent interaction parameter of these substances with water decreases and becomes more normal as the degree of polymerization becomes larger. The interaction parameter for polyvinylalcohol of different acetyl content with water first increases and then (through max.) decreases as the content of acetyl radical increases.

All these results are consistently explained from the standpoint of intra-molecular or inter-segmental association.

We would like to express our gratitude to Professor Y. Morino of Tokyo University and Professor A. Kotera of Tokyo University of Education for their kind encouragement and discussions throughout the work.

Department of Chemistry, Faculty of Science, Kobe University, Kobe

Mikroanalyse mit Hilfe von Ionenaustauschharzen. VIII. Über den Nachweis geringer Menge des Titans(IV) mit Wasserstoffperoxyd[1]

Von Masatoshi FUJIMOTO

(Eingegangen am 15. Juni, 1956)

Einleitung

Eine charakteristische Gelbfärbung, die die saure wässerige Lösung der Titan(IV)-salze mit dem Wasserstoffperoxyd gibt, ist schon lange gern zur kolorimetrischen Bestimmung geringer Menge des Titans(IV) angewandt[2], da die genannte Färbung für Titan(IV) sehr empfindlich und spezifisch, und auch dauerhaft ist. Früher hielt man die obengenannte stark sich färbende Verbindung für ein Komplexsalz mit dem Anion, $\left[\mathrm{Ti}\begin{smallmatrix}\diagup\mathrm{O}\\ \vdots\\ \diagdown\mathrm{O}\end{smallmatrix}(\mathrm{SO_4})_2\right]^{2-}$[3], aber diese Ansicht wurde von K. F. Jahr[4] wie folgt umgeändert; nämlich; in der sauren wässerigen Lösung, ohne Beziehung auf die angewandte Säureart, ergibt sich das Komplexgleichgewicht zwischen den Titan(IV)salzen und dem Wasserstoffperoxyd wie folgt:

$$(\mathrm{TiO\cdot aq})^{2+} + \mathrm{H_2O_2} \rightleftharpoons (\mathrm{Ti}\begin{smallmatrix}\diagup\mathrm{O}\\ \vdots\\ \diagdown\mathrm{O}\end{smallmatrix}\cdot\mathrm{aq})^{2+} + \mathrm{H_2O}.$$

I. farblos — II. intensiv gelb

Aus der Tatsache, dass die genannte sich färbende Verbindung von Kationenaustauschharz stark adsorbiert wird, wobei die Harzphase sich entschieden stärker als die Aussenlösung färbt, kann die Ansicht, dass das intensiv gelbe Titan(IV)wasserstoffperoxydkomplex als eine Kationenart wie II. vorliege, sehr einfach geprüft werden.

Im folgenden konnte der Verfasser durch Anwendung von den farblosen starksauren Kationenaustauschharzen zur obengenannten Farbenreaktion eine für Titan(IV) sehr empfindliche Nachweismethode neu feststellen.

Die in der vorliegenden Untersuchung benutzten Ionenaustauschharze

Hierbei wurden die folgenden aus Styrol und Divinylbenzol dargestellten farblosen bzw. hellgelben starksauren Kationenaustauschharze von verschiedenen Vernetzungsgraden angewandt:

„1proz. DVB"[5]: Ein farbloses starksaures Harz von Sulfonsäuretypus, dessen Divinylbenzolgehalt einprozentig ist[5]. Die Korngrösse ist ungefähr 30 Maschen von Tylerschem Normalsieb.

„20proz. DVB"[5]: Ein starksaures und

1) Die siebente Mitteilung: M. Fujimoto, Dieses Bulletin **29**, 776 (1956).

2) Vgl. E.B. Sandell, „Colorimetric Determination of Traces of Metals," 2. Aufl., 1950, New York, S. 572ff.

3) Z.B., vgl. H. Remy, „Lehrbuch der Anorganischen Chemie," II. Band. 7. Aufl., 1954, Leipzig, S. 60, sowie F. Feigl, „Spot Tests. I. Inorganic Applications." 4. engl. Aufl., übersetzt von R.E. Oesper, 1954, Amsterdam, S. 186.

4) Vgl. H. J. Emeléus und J. S. Anderson, „Modern Aspects of Inorganic Chemistry," 2. Aufl., 1952, London, S. 375 (ausgezogen aus K.F. Jahr, „Peroxy compounds," FIAT Rev. German Sci. 1939-1946, Inorganic Chemistry Pt. III, 1948, 170).

5) In bezug auf die abgekürzte Schreibweise wie „1 proz. DVB" usw., vergleiche die sechste Mitteilung: M. Fujimoto, Dieses Bulletin **29**, 600 (1956).

hellgelbes Harz von Sulfonsäuretypus, dessen Divinylbenzolgehalt zwanzigprozentig ist[5]. Die Korngrösse ist ungefähr 50 Maschen.

Dowex 50W-X8: Ein käufliches farbloses und starksaures Harz von Sulfonsäuretypus, dessen Divinylbenzolgehalt etwa achtprozentig ist. Die Korngrösse ist 50 bis 100 Maschen.

Dowex 50W-X12: Ein ebenso käufliches farbloses starksaures Harz wie Dowex 50W-X8, dessen Divinylbenzolgehalt etwa zwölfprozentig ist. Die Korngrösse ist 50 bis 100 Maschen.

Alle diese Harze wurden vor dem Gebrauch durch zweimaliges Durchlaufen der 2 N Salzsäure sowie des destillierten Wassers in die HR-Form vollständig übergeführt.

Versuchsanordnung

Man bringt auf eine weisse Tüpfelplatte nacheinander einige Körnchen farbloses sowie starksaures Kationenaustauschharzes von HR-Form, je einen Tropfen saurer wässeriger Probelösung und verdünnter Lösung des Wasserstoffperoxydes, und rührt sie danach mit einem kleinen Glasstab gründlich um. Nach einigen Minuten langem Stehen, beobachtet man mit einer Lupe eine in der Harzphase entstandene Gelbfärbung.

Massflüssigkeit

Zum gegenwärtigen Zwecke wurde eine saure Stammlösung des Titanylsulfates, $TiOSO_4$, woraus eine Reihe der Massflüssigkeiten des Titans(IV) hergestellt wurde, folgenderweise dargestellt[7]:

„In einem kleinen Porzellantiegel versetzt man eine bestimmte Menge des extrareinen Titan-(IV)dioxydes, TiO_2, welches vorher in einem Luftbad bei 110°C bis zum konstanten Gewicht getrocknet wurde, mit einer etwa zehnfachen Menge des extrareinen Kaliumbisulfates. Man erhitzt danach dieses Gemisch anfangs sehr schwach, dann immer stärker bis zum Glühen Das Gemisch schmilzt allmählich, und nach einigen Minuten braust es stark auf, und geht schliesslich in eine homogene Schmelze über. Man kühlt diese Schmelze vollkommen ab, und zieht das hier gebildete weisse Klümpchen mit je etwa 10 ccm heisser verdünnter Schwefelsäure wieder und wieder aus. Schliesslich verdünnt man die so ausgezogene klare Lösung des Titanylsulfates mit destilliertem Wasser genau bis zum bestimmten Volumen".

Der Titan(IV)gehalt von der genannten Stammlösung wurde aus der Menge des anfänglich angewandten Titan(IV)dioxydes mit genügender Genauigkeit umgekehrt ausgerechnet. Sie beträgt 4.13 mg /ccm.

Bestimmung der Bedingungen höchster Empfindlichkeit[8]

1. Einfluss der Harzart.—Wie man in Abb. 1 deutlich ersieht, wird die Färbung der Harzphase

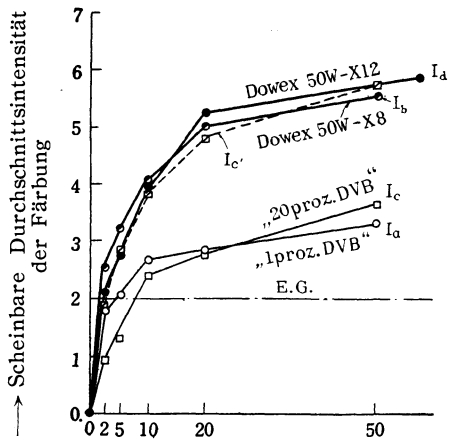

Abb. 1. Einfluss der Harzart.

durch Differenz von Vernetzungsgrad des Harzes beeinflusst, von dem die Festionenkonzentration der Harzphase abhängig ist. Aus Rücksicht auf die Unterscheidbarkeit des Farbentons der Harzphase gegen Blindversuch wurde Dowex 50W-X8 als die meist geeignete Harzprobe angewandt.

2. Einfluss der Konzentration des Wasserstoffperoxydes.—Abb. 2 stellt die Abhängigkeit

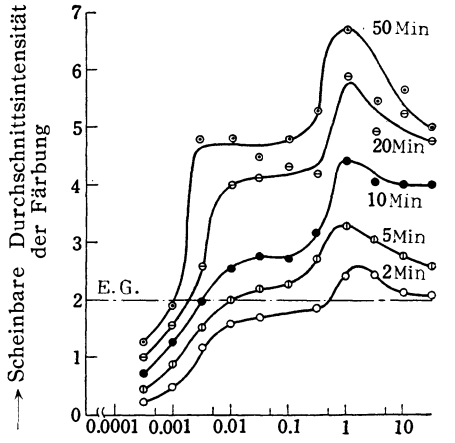

Abb. 2. Einfluss der Wasserstoffperoxydkonzentration auf die scheinbare Färbungsintensität.

der scheinbaren Intensität der Färbung, die die Harzphase annimmt, von der Konzentration hinzugefügter Wasserstoffperoxydlösung dar. Bemerkenswert ist dabei, dass unter selbst so niedriger Konzentration an Wasserstoffperoxyd wie 0.01-Prozent bereits eine beinahe genügend starke Gelbfärbung auf der Harzphase entsteht, und zwar, dass diese Färbung bis zu so hoher

6) Die hier angewandten zwei Harzproben wurden von Herrn Prof. Dr. A. Kawamura an der Landwirtschaftlichen und Technischen Universität zu Tokyo nach dem Verfahren K.W. Peppers kürzlich dargestellt.

7) Vgl. J.W. Mellor und H.V. Thompson, „A Treatise on Quantitative Inorganic Analysis," 2. Aufl., 1938, London, S. 191, S. 736.

8) In bezug auf die in allen Abbildungen gegenwärtiger Mitteilung angewandte halbquantitative Darstellungsweise der scheinbaren Durchschnittsintensität der Färbung von der Harzphase, vergleiche die dritte Mitteilung: M. Fujimoto, Dieses Bulletin 29, 567 (1956).

Konzentration an Wasserstoffperoxyd wie Dreissigprozent fast unverändert intensiv auftritt. In folgender Versuche wurde 1prozentige Lösung des Wasserstoffperoxydes, in Betracht des Verlaufes genannter Kurven, als die geeignetste Konzentration ausgewählt.

3. Einfluss der Konzentration der Neutralsalze.—Weil die an der genannten gelben Färbung sich beteiligte Substanz, wie es in der obigen Formulierung beschrieben wird, ein Kation von verhältnismässig kleinem Volumen ist, ist es wahrscheinlich, dass das betreffende Austauschgleichgewicht mit steigender Konzentration der in der Aussenlösung befindlichen Kationen für das genannte gelbe Kation sich nachteilig verschiebt und die Färbung der Harzphase infolgedessen beträchtlich geschwächt wird.

Die Kurven von Abb. 3 stellen die Einflüsse

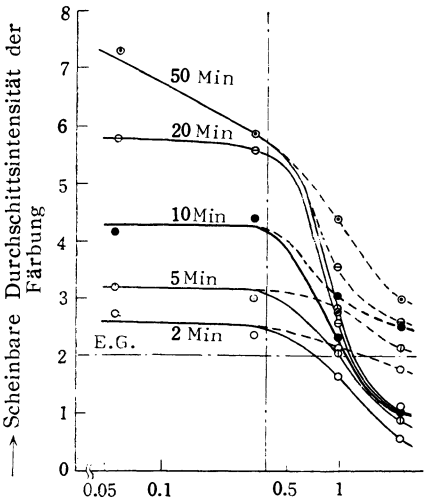

Abb. 3. Einfluss der Neutralsalzkonzentration von der Probelösung.

der Konzentration des Natriumsulfates, das diesmal als Vertreter der Neutralsalze ausgewählt wurde, auf die scheinbare Färbungsintensität der Harzphase im beliebigen Zeitpunkt nach der Mischung dar. Wie aus dem Verlauf genannter Kurven zu ersehen ist, sinkt die Färbungsintensität der Harzphase dann mit der Konzentration des Natriumsulfates stark ab, wenn diese höher als 0.4 N steigt. Dieses rasche Herabsinken der Gelbfärbung der Harzphase kann man durch Verdünnung der Probelösung mit destilliertem Wasser bis zu einem gewissen Grade vermindern. Die gestrichelten Kurven in der genannnten Abbildung stellen die Resultate dar, wo man anfangs die betreffende Probelösung durch Zusatz von fünf Tropfen destilliertes Wassers verdünnt und danach mit drei Tropfen 1prozentiger Lösung des Wasserstoffperoxydes versetzt. Dabei wird klar gezeigt, dass die Austauschselektivität der sich färbenden Komplexperoxyverbindung durch einfache Verdünnung der Aussenlösung beträchtlich zunimmt.

4. Einfluss der Konzentration der Schwefelsäure.—Da es wahrscheinlich ist, dass die Schwefelsäurekonzentration von der Probelösung auf das betreffende Komplexgleichgewicht beträchtlich einwirkt, wurde eine Reihe der Experimente mit den Probelösungen, in denen die Schwefelsäure von verschiedenen Konzentrationen enthalten waren, ausgeführt.

Die Resultate dieser Versuche stehen in Abb. 4.

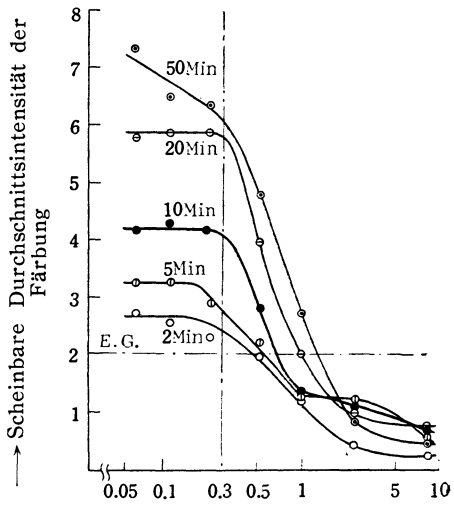

Abb. 4. Einfluss der Schwefelsäurekonzentration von der Probelösung auf die Durchschnittsfärbungsintensität.

Hierbei ist es auch wünschenswert, die Konzentration der Schwefelsäure niedriger als 0.3 N zu halten.

5. Einfluss der Säureart.—Um zu zeigen, welchen Einfluss die Sorte der benutzten Säure auf die scheinbare Intensität der Gelbfärbung der Harzphase ausübt, wurde eine Reihe von Versuchen mit verschiedenartigen starken Mineralsäuren, die zu beinahe gleicher Konzentration reguliert wurden, durchgeführt. Die hierbei zur Untersuchung benutzten Mineralsäuren waren Salz-, Schwefel-, Salpeter-, Phosphor- und Perchlorsäuren.

Die scheinbare Durchschnittsintensität der Färbung der Harzphase wird nach folgender Reihenfolge schwächer (Abb. 5):

$$HClO_4 > HCl > H_2SO_4 > HNO_3 \gg H_3PO_4.$$

Vor allem befördert dabei Perchlorsäure die Färbung der Harzphase. Dagegen beschädigt die Anwendung der Phosphorsäure auffallend die Empfindlichkeit der genannten Farbenreaktion.

6. Bedingungen höchster Empfindlichkeit.—Aus dem obenerwähnten zusammengefasst, so wurde das folgende Verfahren als das am besten geeignete ausgewählt:

„Auf eine weisse Tüpfelplatte bringt man nacheinander einige Körnchen farbloses Kationenaustauschharzes „1proz. DVB" von HR-Form, einen Tropfen der sauren Probelösung, deren Anionenkonzentration vorher niedriger als 0.4 N reguliert wurde, und einen Tropfen der 0.2 N Säure, wie Schwefel-, Salz- oder Perchlorsäuren. Man rührt dieses Gemisch mit einem

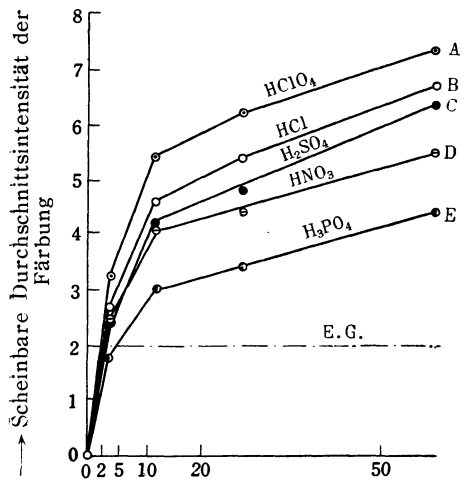

Abb. 5. Einfluss der Säureart.

Experimentalbedingungen:—

0.03 N H_2SO_4, { A: 0.105 N $HClO_4$, B: 0.103 N HCl, C: 0.100 N H_2SO_4, D: 0.107 N HNO_3, E: 0.112 N H_3PO_4 },

+2.5 γTi/0.08 ccm,

+H_2O_2: 1proz. Lsg (0.04 cm)

Glasstäbchen vollständig um und fügt noch einen Tropfen 1prozentiger Lösung des Wasserstoffperoxydes dazu. Etwa zehn Minuten nach der Mischung beobachtet man mit einer Lupe zwanzigfacher Vergrösserung eine in der Harzphase entstandene intensive Gelbfärbung".

Bestimmung der Erfassungsgrenze

Durch Anwendung des obenerwähnten empfindlichsten Verfahrens wurde die Erfassungsgrenze des Nachweises eindeutig bestimmt. Aus dem Verlaufe der in Abb. 6 beschriebenen Kurven

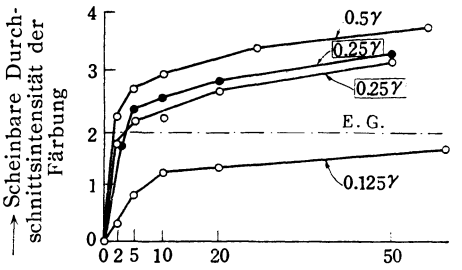

Abb. 6. Bestimmung der Erfassungsgrenze.
—○— Ohne hinzugefügte Säure:
—●— Nach dem Zusatze von 1 Tropfen der 0.2 N Perchlorsäure:

TABELLE I

EINFLÜSSE DER BEGLEITSTOFFE

Begleitstoffe	benutzter Verbindungstypus	Menge der Begleitstoffe	Nachweisbare Titan(IV)menge	Grenzverhältnis	Bemerkungen*
V(V)	NH_4VO_3	360 γ	0.25 γ	$1:1.3\times10^3$	*a*, *b*
Cr(III)	$KCr(SO_4)_2$	40 γ	1.26 γ	$1:3.2\times10$	Cr≦0.2proz.
Mn(II)	$MnSO_4$	200 γ	1.25 γ	$1:1.6\times10^2$	——
Fe(III)	$FeCl_3$	32 γ	0.5 γ	$1:6.4\times10$	Fe≦0.1proz.
〃 〃	〃 〃	930 γ	0.25 γ	$1:3.7\times10^3$	*c*
Co(II)	$CoCl_2$	230 γ	1.25 γ	$1:1.8\times10^2$	*d*
Ni(II)	$NiCl_2$	200 γ	1.25 γ	$1:1.6\times10^2$	*d*
Cu(II)	$CuSO_4$	70 γ	0.25 γ	$1:2.8\times10^2$	*d*, Cu≦0.2proz.
Zn(II)	$ZnSO_4$	320 γ	0.5 γ	$1:6.4\times10^2$	——
Cr(VI)	$K_2Cr_2O_7$	3.2 γ	0.25 γ	$1:1.3\times10$	Cr≦0.01proz.
〃 〃	〃 〃	320 γ	0.5 γ	$1:6.4\times10^2$	*e*
Mo(VI)	$(NH_4)_2MoO_4$	435 γ	0.25 γ	$1:1.8\times10^3$	——
W(VI)	Na_2WO_4	330 γ	0.5 γ	$1:6.6\times10^2$	*d*
U(VI)	$UO_2(CH_3COO)_2$	360 γ	0.25 γ	$1:1.4\times10^3$	*d*
Ge(IV)	GeO_2	26 γ	0.25 γ	$1:1\times10^2$	——
Sn(IV)	$SnCl_4$	300 γ	0.25 γ	$1:1.2\times10^3$	——
F^-	KF	16.4 γ	2 γ	1:8	*b*, F^-≦0.1proz.
〃	〃	53 γ	0.5 γ	$1:1.1\times10^2$	*b*,*f*, F^-≦0.5proz.
NO_2^-	$NaNO_2$	350 γ	0.25 γ	$1:1.4\times10^3$	——
PO_4^{3-}(HPO_4^{2-})	Na_2HPO_4	850 γ	0.25 γ	$1:3.4\times10^3$	——

*a: Die Harzkörnchen färben sich einen Moment braun, aber entfärben sich nach etwa fünf Minuten vollkommen.
b: 10proz. Lösung des Wasserstoffperoxydes wurde angewandt.
c: Nach dem Zusatze von verdünnter Phosphorsäure wurde der Nachweis durchgeführt.
d: Neben einem Blindversuche wurde erst die Anwesenheit des Titans(IV) nachgewiesen.
e: Nach der Beseitigung der Bichromationen durch eine Mikroharzsäule von Dowex 1-X8 (RCl-Form) wurde der Nachweis ausgeführt.[9]
f: Um die Störung des Fluorides zu beseitigen, wurde vorher ein Tropfen verdünnter salzsaurer Lösung des Berylliumchlorides zur Versuchslösung gefügt.

9) M. Fujimoto, Diese Bulletin, **29**, 595 (1956).

wurde die Erfassungsgrenze 0.25 γ Titan(IV) unter Grenzkonzentration $1:1.6\times10^5$ bei gegenwärtiger Nachweisreaktion festgestellt.

Einflüsse der Begleitstoffe

Die Resultate der Experimente werden gesamt in Tabelle I kurz erläutert:

Zusammenfassung

1. Durch Anwendung der niedrig vernetzten starksauren und farblosen Kationenaustauschharze steigt die Empfindlichkeit der Titan(IV)-Wasserstoffperoxydreaktion merklich an.
2. Die empfindlichsten Experimentalbedingungen werden durch eingehende Untersuchung über Einflüsse verschiedenartiger Faktoren, wie Harzart, Konzentration des Wasserstoffperoxydes, der Schwefelsäure und der Neutralsalze, und Säureart, vollkommen festgestellt.
3. Die Einflüsse der Begleitstoffe werden genau untersucht und verschiedene Massregeln gegen ihre Störung werden auch genommen (vgl. Tabelle I).

Der Verfasser möchte Herrn Prof. Dr. E. Minami für seine freundlichen Anregungen zur vorliegenden Untersuchung seinen herzlichsten Dank aussprechen.

Für die Harzproben, „1proz. DVB“ und „20proz. DVB,“ ist der Verfasser Herrn Prof. Dr. A. Kawamura an der Landwirtschaftlichen und Technischen Universität zu Tokyo zu grossem Dank verpflichtet.

Laboratorium der analytischen Chemie
Chemisches Institut der wissenschaftlichen Fakultät, Tokyo Universität, Tokyo

Voltammetry of Nitrite at the Stationary and Rotated Platinum-Wire Electrodes

By Nobuyuki TANAKA and Kiyoko KATO

(Received June 22, 1956)

The oxidation-reduction of nitrite-nitrate system has been investigated from the electrochemical standpoint[1]. Most of these investigations, however, were limited to the measurement and the discussion of equilibrium potentials of the system, but gave little information of the mechanism of the electrode reaction. Recently K. Vetter[2] studied the subject from the standpoint of electrode kinetics and proposed a mechanism for the electrode processes at the platinum electrode. He assumed the following steps:

$$H^+ + NO_3^- \rightleftarrows HNO_3 \quad (1)$$

$$HNO_3 + HNO_2 \rightleftarrows N_2O_4 + H_2O \quad (2)$$

$$N_2O_4 \rightleftarrows 2NO_2 \quad (3)$$

$$NO_2 + e^- \rightleftarrows NO_2^- \quad (4)$$

$$NO_2^- + H^+ \rightleftarrows HNO_2 \quad (5)$$

and concluded that the reactions given in eqs. (2) and (4) must be rate-determining. Although his interpretation seemed fairly satisfactory as far as his experimental conditions were concerned, his data were restricted only to those obtained in nitric acid of more than 1 M in concentration.

Since his method was quite different from the conventional voltammetry, the investigation of the oxidation of nitrite at the platinum electrode was carried out from the voltammetric standpoint and has been presented in the present paper. From the theoretical consideration of observed current-voltage curves, the assumptions proposed by Vetter for the oxidation-reduction of nitrite-nitrate system have been verified in the solution with and without nitrate or nitric acid. The method was also applied to the determination of a minute quantity of nitrite in potassium nitrate with a good result.

Experimental

Apparatus.—A manual polarograph[3] was used for the measurement of current-voltage curves. The current was measured in terms of the iR drop across the 10,000 ohm precision fixed resistance in series with the electrolysis cell by means of potentiometer, or measured directly with

1) R. Ihle, *Z. physik. Chem.*, **19**, 577 (1896); W.C. Moore, *J. Am. Chem. Soc.*, **35**, 333 (1913); H. Pick, *Z. Elektrochem. angew. physik. Chem.*, **26**, 183 (1920); **28**, 56 (1922); A. Klemenc and E. Hayek, *Z. anorg. allgem. Chem.*, **186**, 181 (1930); H. Bode, ibid., **195**, 201 (1931); R.G. Monk and H.J.T. Ellingham, *J. Chem. Soc.* (*London*), **1935**, 125.

2) K. Vetter, *Z. physik. Chem.*, **194**, 199 (1950).

3) I. M. Kolthoff and J. J. Lingane, "Polarography", Interscience Publishers, New York (1952) Vol. I, p. 297.

a galvanometer. Potentials were referred to a saturated caromel electrode (S. C. E). All experiments were carried out in a thermostat of 25.00±0.05°C. All current-voltage curves are corrected for the residual current.

Two platinum-wire electrodes of 0.6 mm. in diameter and approximately 5 mm. in length were used. One was used for the stationary electrode, which had 0.1033 cm^2 of geometrical surface area and gave a steady state diffusion current of 4.35 μ amp./millimole/l. for the oxidation of potassium ferrocyanide in deaerated 0.1 M potassium chloride solution. The other, which had 0.0944 cm^2 of geometrical surface area, was used for the rotated electrode. Being rotated at 650 r. p. m., it yielded diffusion currents of 9.90 μ amp./millimole/l. for the oxidation of ferrous ion in deaerated 0.1 M hydrochloric acid, and also 10.00 μ amp./millmole/l. for the reduction of ferric ion in the same medium.

Reagents.—A standard solution of nitrite was prepared by dissolving recrystallized potassium nitrite in distilled water free from oxygen, the concentration of which was determined volumetrically with the standardized solutions of potassium permanganate and sodium oxalate[4].

Pretreatment of Electrode.—The electrodes were treated in hot 10 M nitric acid for ten minutes and washed thoroughly with distilled water. Then, the electrodes were polarized at 0 volt vs. S. C. E. in the supporting electrolyte to eliminate the oxide film which might have formed on the surface upon the treatment with nitric acid[5].

Results

With Stationary Electrode.—Current-voltage curves were obtained with the stationary electrode in supporting electrolytes of pH between 0 and 9 in the absence of oxygen by measuring from negative to positive potentials. Typical examples obtained with 0.960×10^{-3} M potassium nitrite are given in Fig. 1. The half-wave potentials and the limiting currents are indicated in Table I. In the solutions of pH 0 to 3, the half-wave potentials were found to shift to more negative potentials by some 60 mV. with the increase of unit pH. At higher pH's, they tend to be independent of pH and approach to a limiting value. This fact, however, could not be clearly recognized, because the current-voltage curves were gradually drawn out with increasing pH of solutions. This may be attributed to the formation of the oxide film on the surface of platinum[5]. The potentials of the oxide film formation shift to negative potentials by 60 mV. with the increase of unit pH[5], whereas those of nitrite waves remain constant in solutions of higher pH.

The oxide film formation also accounts for the difficulty in the measurement of limiting current. Even in 1 M nitric acid the limiting current plateau

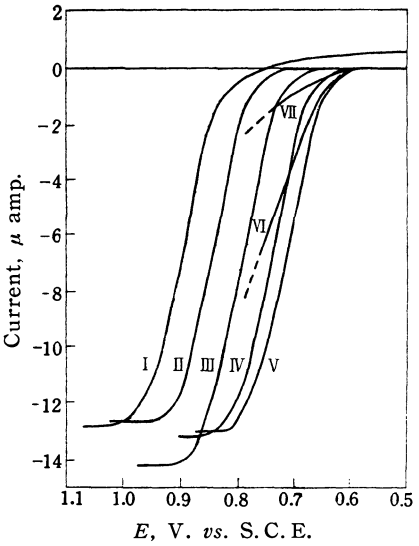

Fig. 1. Current-voltage curves of 0.960×10^{-3} M potassium nitrite obtained with the sationary electrode, being measured from negative to positive potentials in supporting electrolytes: I, 1 M HNO_3; II, 0.1 M HNO_3; III, 0.01 M NHO_3+0.09 M KNO_3; IV, citric acid-phosphate buffer of pH 3; V, acetate buffer of 4.75; VI, citric acid-phosphate buffer of pH 6 and VII, 0.05 M borax of pH 9.23.

TABLE I

ANODIC LIMITING CURRENTS AND HALF-WAVE POTENTIALS OF 0.960×10^{-3} M POTASSIUM NITRITE IN VARIOUS SUPPORTING ELECTROLYTES MEASURED WITH THE STATIONARY PLATINUM-WIRE ELECTRODE

Supporting Electrolyte	pH	i_l, μ amp.	$E_{1/2}$, V. vs. S. C. E.
1 M HNO_3	0	−12.80	0.892
0.5 M HNO_3+0.5 N H_2SO_4	0	−13.50	0.885
0.1 M HNO_3+0.9 N H_2SO_4	0	−12.08	0.877
0.1 M HNO_3	1	−12.70	0.841
0.1 N H_2SO_4	1	−11.26	0.836
0.01 M HNO_3+0.09 M KNO_3	2	−14.14	0.786
Citric acid-phosphate buffer	3	−13.13	0.725
Acetate buffer	4.75	−13.0	0.719
Citric acid-phosphate buffer	6	−12.6	0.746

appeared at the potentials where the electrode surface can be oxidized. Although this difficulty was encountered, an almost linear relation was obtained between the limiting current and the concentration of nitrite added, as given in Fig. 2, which was obtained in 1 M nitric acid.

If it is assumed that the limiting current is controlled by the rate of diffusion of nitrite, it is possible to calculate the number of electrons involved in the electrode reaction, n, by the relation[5],

4) I. M. Kolthoff and E. B. Sandell, "Textbook of Quantitative Inorganic Analysis", The MacMillan Co., New York (1952), p. 573.

5) I. M. Kolthoff and Nobuyuki Tanaka, *Anal. Chem.*, **26**, 632 (1954).

6) H. A. Laitinen and I. M. Kolthoff, *J. Phys. Chem.*, **45**, 1061 (1941).

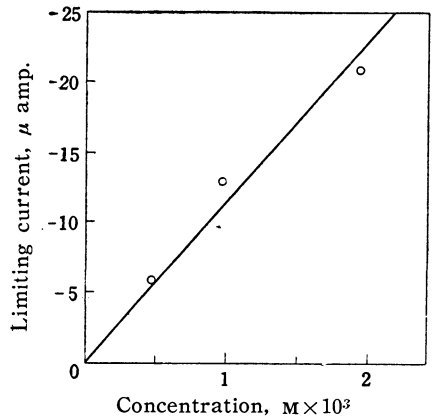

Fig. 2. Relation between limiting current and concentration of potassium nitrite in 1 M nitric acid measured with the stationary electrode.

$$i_d = \frac{AD}{l} nFC, \qquad (6)$$

where i_d represents the diffusion current, A, the surface area of the electrode, D, the diffusion coefficient, l, the effective thickness of diffusion layer, C, the concentration of the oxidizable or reducible substance and F, the Faraday constant. The diffusion coefficients of nitrite and ferrocyanide were calculated to be 1.92×10^{-5} and 0.74×10^{-5} cm²/sec., respectively, from the equivalent conductance at infinite dilution at 25°C. The diffusion current of nitrite was determined approximately 13 μ amp./millimole/l. averaging those obtained in various conditions, while that of ferrocyanide was 4.35 μ amp./millimole/l. in 0.1 M potassium chloride at the same electrode. Introducing those values into eq. (6) and assuming the identity of the effective thickness of diffusion layer for both electrode reactions[5], the number of electrons involved in the oxidation of nitrite was calculated to be approximately unity, from which electrode process of the oxidation of nitrite could be concluded as a one-electron reaction.

With Rotated Electrode.—Current-voltage curves were also obtained with the rotated electrode in supporting electrolytes of various pH's. Typical examples obtained with 0.960×10^{-4} M potassium nitrite are reproduced in Fig. 3, and the results are tabulated in Table II. A proportionality was found between the limiting current and the concentration as shown in Fig. 4.

TABLE II

ANODIC LIMITING CURRENTS AND HALF-WAVE POTENTIALS OF 0.960×10^{-4} M POTASSIUM NITRITE IN VARIOUS SUPPORTING ELECTROLYTES MEASURED WITH THE ROTATED PLATINUM-WIRE ELECTRODE AT THE RATE OF 650 R.P.M.

Supporting Electrolyte	pH	i_l, μ amp.	$E_{1/2}$, V. *vs.* S.C.E.
0.1 M HNO_3	1	−3.35	0.860
0.01 M HNO_3 + 0.09 M KNO_3	2	−3.36	0.810
Citric acid-phosphate buffer	3	−3.59	0.752
Acetate buffer	4.75	−4	—

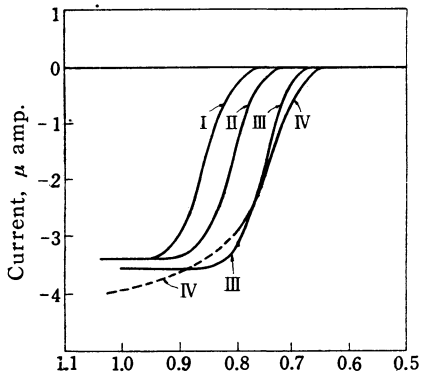

Fig. 3. Current-voltage curves of 0.960×10^{-4} M potassium nitrite obtained with the rotated platinum electrode at the rate of 650 r.p.m., being measured from negative to positive potentials in supporting electrolytes: I, 0.1 M HNO_3; II, 0.01 M HNO_3 + 0.09 M KNO_3; III, citric acid-phosphate buffer of pH 3 and IV, acetate buffer of pH 4.75.

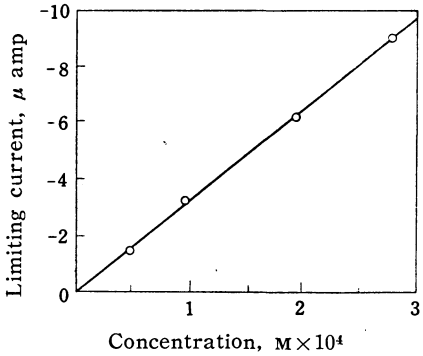

Fig. 4. Relation between limiting current and concentration of potassium nitrite in 0.1 N sulfuric acid measured with the rotated electrode at the rate of 650 r.p.m.

Discussion

The net reaction of oxidation-reduction of nitrite-nitrate system is represented as,

$$NO_2^- + H_2O \rightleftarrows NO_3^- + 2H^+ + 2e^-. \qquad (7)$$

The value of limiting current, however, suggested that the oxidation of nitrite at the platinum electrode must be a one-electron reaction. This can not be accounted for by eq. (7), but agrees with the findings by Vetter[2]. According to his proposal, the following reaction mechanism was set down:

$$HNO_2 \rightleftarrows H^+ + NO_2^-, \quad K_{HNO_2} = 4.5\times10^{-4} \qquad (8)$$

$$NO_2 + e^- \rightleftarrows NO_2^-, \quad E_0 = 0.650 \text{ V. } vs. \text{ S.C.E.} \qquad (9)$$

$$2NO_2 \rightleftarrows N_2O_4, \quad K_2 = 8.79 \qquad (10)$$

$$N_2O_4+H_2O \rightleftarrows H^+ + NO_3^- + HNO_2, \quad K_1=2.82\times10^4 \qquad (11)$$

where K_{HNO_2} is the dissociation constant of nitrous acid[7], K_2 and K_1 are the equilibrium constants of eqs. (10) and (11), respectively, and E_0 is the standard oxidation-reduction potential of $NO_2-NO_2^-$ system. The values of K_2, K_1 and E_0 were calculated from data given by Latimer[7].

In the electrode reactions represented with eqs. (8) to (11) the following conditions are considered:

(i) Nitrous acid and nitrite are in equilibrium at the surface of electrode according to eq. (8).

(ii) The potentials of oxidation of nitrite or nitrous acid are determined by the reaction given in eq. (9).

(iii) NO_2 formed by the oxidation of nitrite is in equilibrium with N_2O_4 at the surface of electrode according to eq. (10).

(iv) The reaction given in eq. (11) proceeds so slowly that the reproduction of nitrous acid at the surface of electrode can be neglected.

The reduction potential of reaction of eq. (8) is expressed with,

$$E=E_0+0.059\log\frac{[NO_2]}{[NO_2^-]}, \qquad (12)$$

where, for simplicity, the concentration is employed rather than activity. If the sum of nitrous acid (i. e., potassium nitrite added) is represented with $\sum[HNO_2]$, the concentration of nitrite is given by

$$[NO_2^-]=\sum[HNO_2]\Big/\left\{1+\frac{[H^+]}{K_{HNO_2}}\right\}. \qquad (13)$$

Introducing eq. (13) into eq. (12), the equation,

$$E=E_0+0.059\log\left\{1+\frac{[H^+]}{K_{HNO_2}}\right\}\frac{[NO_2]}{\sum[HNO_2]}, \qquad (14)$$

is obtained. As NO_2 is in equilibrium with N_2O_4 at the surface of electrode, the following relations must be fulfilled when b mole/l. of total nitrite, $\sum[HNO_2]$, is oxidized at the electrode surface:

$$[NO_2]+2[N_2O_4]=b,$$
$$[N_2O_4]/[NO_2]^2=K_2,$$

then,

$$[NO_2]^2+\frac{[NO_2]}{2K_2}-\frac{b}{2K_2}=0. \qquad (15)$$

The concentration of NO_2 calculated from eq. (15) would be introduced into eq. (14). When either nitrate or nitric acid is contained in the supporting electrolyte, some amounts of NO_2 and N_2O_4 which are formed by the reverse reactions of eqs. (10) and (9) may yield a reduction wave. This was proved from the current-voltage curve obtained in 1 M nitric acid, which gives a cathodic current as shown in Fig. 1. (Curve I in Fig. 1).

The consideration of the effect of nitric acid makes it possible to derive an equation for the composite wave of the oxidation-reduction of NO_2-NO_2^- system. If the total nitrite added, $\sum[HNO_2]$, is written as a, the concentration of nitrous acid $[HNO_2]$ is given by

$$[HNO_2]=a\Big/\left\{1+\frac{K_{HNO_2}}{[H^+]}\right\}. \qquad (16)$$

In the electrolytic solution, HNO_2, NO_3^-, N_2O_4 and NO_2 are considered to be in equilibrium. Under the present conditions the concentration of N_2O_4 which is in equilibrium with NO_2 is negligibly small compared with that of NO_2 so that $\{2[NO_2]+[N_2O_4]\}$ equals approximately $2[NO_2]$. When x mole/l. of the total nitrite added (a) decreases to form N_2O_4 or NO_2 in equilibrium condition, the concentration of NO_2 is approximately equal to $2x$ mole/l., that is,

$$[NO_2]\fallingdotseq 2x, \qquad (17)$$

and the total nitrite unchanged is equal to $(a-x)$ mole/l. Introducing these quantities into the product of equilibrium constants K_1 and K_2,

$$K_1K_2=\frac{[H^+][NO_3^-][HNO_2]}{[NO_2]^2}=\frac{[H^+][NO_3^-](a-x)}{(2x)^2\left\{1+\frac{K_{HNO_2}}{[H^+]}\right\}},$$

then

$$x^2+\frac{[H^+][NO_3^-]x}{4K_1K_2\left\{1+\frac{K_{HNO_2}}{[H^+]}\right\}}-\frac{[H^+][NO_3^-]a}{4K_1K_1\left\{1+\frac{K_{HNO_2}}{[H^+]}\right\}}=0 \qquad (18)$$

are obtained.

Eq. (14) is now considered as a general formula of experssing the electrode potential of NO_2-NO_2^- system, if the values of $[HNO_2]$ and $[NO_2]$ therein are corrected for x, the latter being calculated from eq. (18). When neither nitrate nor nitric acid is contained in the supproting electrolyte, x becomes practially zero. Taking 0.960×10^{-3} M for a, the values for $E-E_0$ in eq. (14) were calculated at the point where the anodic current reaches one-tenth of the limiting current, i. e., $i=1/10\ i_l$, and where the concentration of the total nitrite $\{[NO_2^-]+[HNO_2]\}$ at the surface of electrode equals $9/10(a-x)$ and that of $\{2[NO_2]+[N_2O_4]\}$, $1/10\{(a-x)+2x\}$. These values are given in Table III. Introducing the potentials obtained experimentally at the point where $i=1/10\ i_l$ on the anodic

7) W. M. Latimer, "Oxidation Potentials", Prentice-Hall, Inc., New York (1952), pp. 90-92.

TABLE III

STANDARD ELECTRODE POTENTIALS OF 0.960×10^{-3} M POTASSIUM NITRITE IN VARIOUS SUPPORTING ELECTROLYTES CALCULATED BY EQUATION (14)

Supporting Electrolyte	pH	$E-E_0$, V.	$E_{obs.}$, V. *vs.* S.C.E.	E_0, V. *vs.* S.C.E.
1 M HNO_3	0	0.154	0.839	0.685
0.1 M HNO_3	1	0.084	0.784	0.700
0.01 M HNO_3 + 0.09 M KNO_3	2	0.025	0.730	0.705
Citric acid-phosphate buffer	3	−0.026	0.682	0.708
Acetate buffer	4.75	−0.055	0.650	0.705
Citric acid-phosphate buffer	6	−0.056	0.663	(0.719)
			Mean,	0.701

part of the current-voltage curve, the values for E_0 were calculated as given in the last column of Table III. A constancy in E_0 values obtained in various supporting electrolytes apparently shows the electrode processes given in eqs. (8) to (11) correct.

A further confirmation of the electrode processes was attained in the comparison of current-voltage curves observed and those calculated theoretically. The potential values, E, at various points on the current-voltage curves were calculated at pH 0 and 2 with eqs. (14) and (18). For the values for E_0, +0.70 V. *vs.* S. C. E. was employed. The limiting current of theoretical curves is assumed to equal that of the observed one. A fair agreement between theoretical and observed curves is clearly seen in Fig. 5. The deviation of the experimental curve from the theoretical one is rather remarkable in the cathodic part of the current voltage curve. This has not been clearly understood, but may be due to other slow reactions involved.

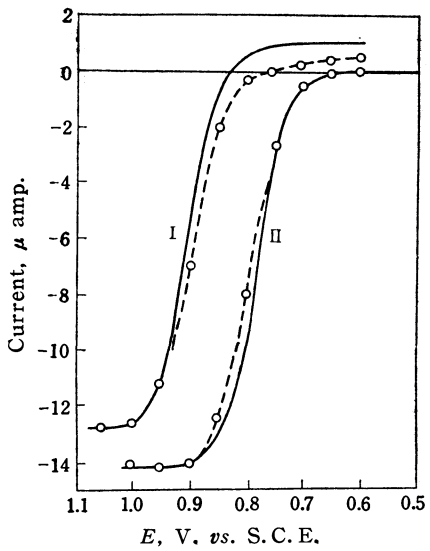

Fig. 5. Theoretical and observed current-voltage curves of 0.960×10^{-3} M potassium nitrite in supporting electrolytes: I, 1 M HNO_3 and II, 0.01 M HNO_3 + 0.09 M KNO_3. Solid lines indicate the theoretical curves and dotted lines, the observed ones obtained with stationary electrode.

It is predicted, from eq. (14), that at higher pH's the electrode potentials become independent of pH, because $\left\{1+\frac{[H^+]}{K_{HNO_2}}\right\}$ approaches to 1 with increasing pH of the solution. The half-wave potentials were calculated from eq. (14) with +0.70 V. *vs.* S. C. E. for E_0, which are plotted with pH as given in Fig. 6. A good agreement between the observed and calculated curves is clearly seen.

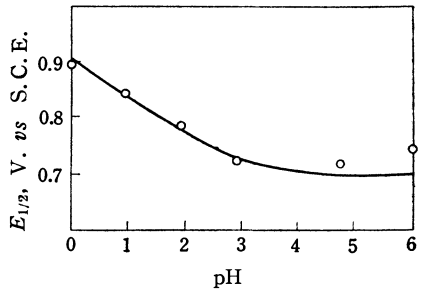

Fig. 6. Relation between the half-wave potential of anodic wave of 0.960×10^{-3} M potassium nitrite and pH of the solution: ○ indicate the experimental value observed with the stationary electrode.

In this calculation as well as in the calculation of the theoretical current-voltage curve, the value of +0.70 V. *vs.* S. C. E. was employed for E_0, which deviates by some 0.05 V. from the standard oxidation-reduction potential calculated with values given by Latimer[7]. The reason of deviation, however, has not been completely explained. The use of concentration instead of activity in the calculation could account for only a small part of the deviation. Some type of irreversibility seems to be involved in the electrode processes of the oxidation of nitrite.

When the electrode was rotated, the values of i_d/C for the anodic wave increased, whereas the slope of the current-voltage curves remained unchanged. S. S. Lord, Jr. and L. B. Rogers[8] stated, in their paper, that, if the electrode reaction is activation-controlled in nature, the value of i_d/C markedly increases and the current-voltage curve is drawn out when the electrode is rotated,

8) S. S. Lord, Jr. and L. B. Rogers, *Anal. Chem.*, **26**, 284 (1954).

while the rotation of the electrode gives only a small increase of i_d/C and also little influence to the slope of the current-voltage curve, if the electrode reaction is kinetic in nature. Since this criterion, however, has not been verified, no discussion should be presented here from this standpoint.

Analytical Application

The experimental result, that the limiting currents of the anodic wave obtained with the rotated electrode are proportional to the concentration of nitrite present, was applied to the determination of potassium nitrite contained in commercial potassium nitrate as impurity. A current-voltage curve of 1 M potassium nitrate was measured with the rotated electrode at the rate of 650 r. p. m. from negative to positive potentials. A small oxidation wave of nitrite was observed at +0.65 V. *vs.* S. C. E. to more positive potentials, the limiting current being 0.25 μ amp. measured at +0.95 V.

The measurement was also made in the same condition but after the addition of 0.960×10^{-5} M potassium nitrite with the limiting current of 0.62 μ amp. From the ratio of two values, the content of nitrite in potassium nitrate was calculated to be $0.0005_5\%$ as potassium nitrate.

The authors thank the Ministry of Education for the financial support to this research.

Department of Chemistry, Faculty of Science, Tohoku University, Sendai

SHORT COMMUNICATIONS

Extraction of Tellurium with Dithizone

By Hisao MABUCHI

(Received June 26, 1956)

Although various metal-dithizone complexes have so far been studied and effectively used for the extraction or the colorimetric determination of metals, dithizone complex of tellurium has not been reported. Recently, ion exchange resin study of tellurium by Y. Sasaki[1] proved that in a dilute hydrochloric acid solution tellurium (IV) can exist as positively charged ion ($TeO(OH)^+$ or $Te(OH)_3^+$). From the fact that polonium, a homologue of tellurium, combines with dithizone to form a complex, it is expected that positively charged tellurium, when shaken with a dithizone solution, may form a dithizone complex, which is extractable from the aqueous solution into an organic layer.

To confirm the presence of such a complex of tellurium, the following experiments were carried out by the present author.

(I) Extraction of Tellurium.—As a tracer, carrier-free radioactive tellurium (chiefly Te-129 and Te-129 m) was prepared from fission products with cation and anion exchange resins*,[1].

The extraction of carrier-free radioactive tellurium from hydrochloric acid solution was carried out with 1.8×10^{-3} M dithizone in carbon tetrachloride. Fig. 1 shows the relationship between the percentage of extraction and the pH of the aqueous solution used. The latter was adjusted with hydrochloric acid and ammonium hydroxide.

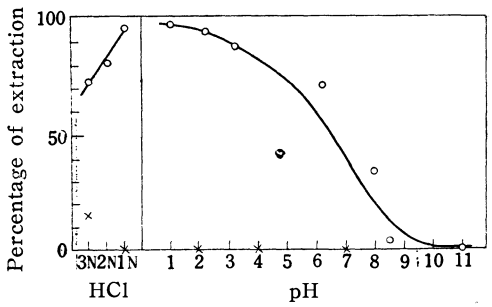

Fig. 1. Extraction of carrier-free tellurium with dithizone carbon tetrachloride solution.
○, extraction with dithizone carbon tetrachloride solution (1.8×10^{-3} M)
×, extraction with carbon tetrachloride volume of organic phase: 2 ml; volume of aqueous phase: 10 ml

From Fig. 1, it can be seen that tellurium is extracted to some extent with carbon tetrachloride solution of dithizone, but not with carbon tetrachloride over the pH range investigated. (the percentage of extraction from 3 N hydrochloric acid exceptionally amounts to 14%.)

Then 0.5 N hydrochloric acid solutions containing various quantities of tellurium from 10^{-5} to 1 mg. were prepared and the extraction was tried

with 0.6×10^{-3} M dithizone carbon tetrachloride solution. The results obtained are shown in Fig. 2. The percentage of extraction is plotted as a function of the quantity of tellurium used.

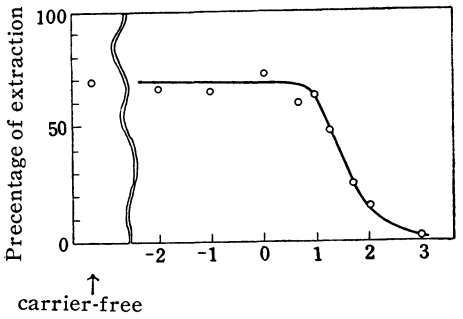

Fig. 2 Extraction of macro-scale tellurium with dithizone carbon tetrachloride solution (0.6×10^{-3} M) volume of organic phase: 2 ml; volume of aqueous phase: 10 ml.

(II) Color of the Dithizone Solution Containing Tellurium.—The author observed that the green color of carbon tetrachloride solution of dithizone turns yellowish green in the presence of tellurium. Spectrophotometric measurement showed that the residual green color is probably due to uncomplexed dithizone. It was also observed that dithizone complex of tellurium has a maximum absorption at 430 mμ.

(III) Volatility of the Extracted Compound.—K. Kimura and the present author[2] previously reported that polonium dithizonate sublimes at a temperature around 120°C. Similar behavior was observed with the extracted compound of carrier-free tellurium. This indicates the similarity of the complex of tellurium to that of polonium.

These experiments described above led the author to the conclusion that tellurium (IV) forms a complex with dithizon. The study of this complex is now in progress; its detail will be reported in a separate paper.

The author wishes to thank Professor K. Kimura and Dr. N. Saito for valuable advice, and also Mr. Y. Sasaki for the preparation of the sample and helpful discussions.

Department of Chemistry, Faculty of Science, The University of Tokyo, Tokyo

* The author owes the preparation entirely to Mr. Y. Sasaki.

1) Y. Sasaki, *Japan Analyst*, 4, 637 (1955).
2) K. Kimura, and H. Mabuchi, This Bulletin, 28, 535 (1955).

Nuclear Magnetic Resonance of High Polymers (Phase Transition of P. V. A. Fibers)

By Kōji TANAKA, Kyōzō YAMAGATA and Shigeyoshi KITTAKA

(Recived march 19, 1956)

It is known that P. V. A. has a phase transition of the second order between about 60°C and 120°C[1], but the mechanism of the transition is not clear. In this connection, the line shape of the proton resonance in P. V. A. has been studied as the function of temperature.

The samples used were P. V. A. fibers "Mewlon" prepared by Dai Nippon Spinning Co. Ltd. in the following way: saponified vinylacetate, P. V. A., was spun through a solution of a mixture of zinc sulphate and glaubesalt. After washing with methanol, these fibers were sealed in an evacuated glass tube.

We have used the usual apparatus, composed of an autodyne oscillator, a lock-in-amplifier and a recorder as shown in Fig. 1, and the field intensity is about 3000 gauss.

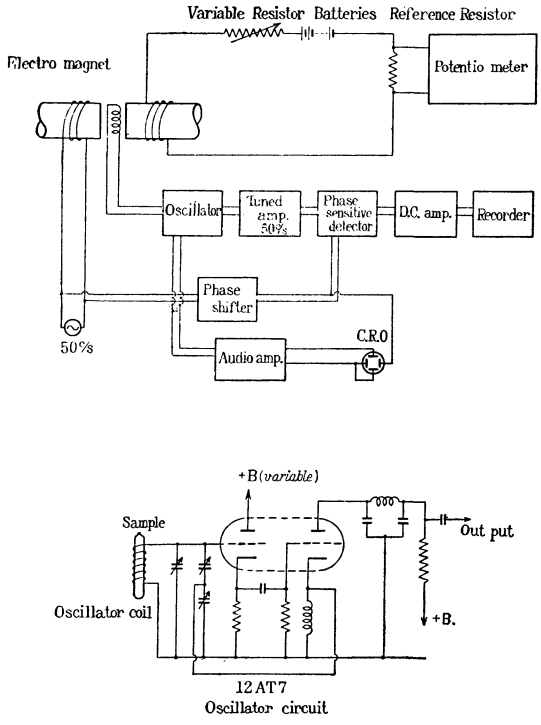

Fig. 1

Some of the experimental results of the line shape are shown in Fig. 2. Both the line width and the second moment were

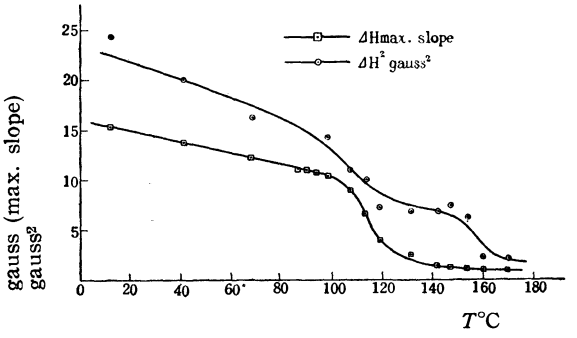

Fig. 3

shown in Fig. 3 as the function of temperature. The derivative curves of proton resonance at 48°, 84° and 94°C may be interpreted to be composed of two parts; one is at the center and very narrow in width and the other very broad. The central component becomes more sharp and intense with temperature. The broad part becomes narrower with temperature and disappears at about 170°C. The values of the experimental second moment decrease gradually with rise of temperature. The gradual narrowing of the width and the experimental second moment are attributed to the development of thermal motions including rotations and oscillations of the protons.[2]

The central peaks of the curves may be assumed to be due to the thermal motion of the water molecule adsorbed by the sample.

The results of more detailed considerations on the effect of crystallization on the phase transition and the appearance of the central peaks will be published later.

The authors wish to express their appreciation to Prof. Masatami Takeda for his kind discussion on our works.

Tokyo College of Science, Tokyo

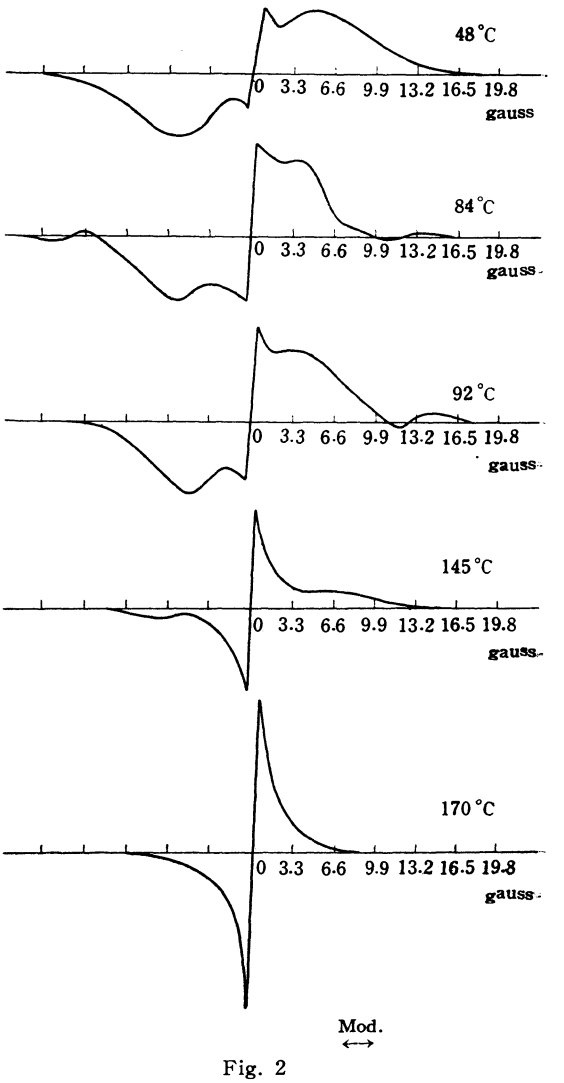

Fig. 2

1) Y. Yano, *J. Chem. Soc. Japan*, **73**, 708 (1952).
2) W. P. Slichter, *J. Appl. Physics*, **26**, 1099 (1955).

Spectrophotometric Determination of Beryllium with Eriochrome Cyanine R

By Shunji UMEMOTO

(Received June 11, 1956)

For the colorimetric determination of beryllium with organic reagents, various reagents have been used. The following reagents are known; *p*-nitrobenzeneazoorcinol[1,2,3,4,5], quinalizarin[6,7,8,9] curcumin[2,10], alkanin[11,12], naphthazarin[11,12], naphthacrome green G[13] aluminon[14,15,16], quinizarine-2-sulfonic acid[17,18,19], acetylacetone[20], sulfo-salicylic acid[21], sodium salt of chlorophenol-azo-dioxynaphthalene disulfonic acid[22], 8-hydroxyquinaldine[23] solochrome cyanine[24], benzene-2-arsonic acid-(1-azo-2)-1, 8-dioxynaphthalene-3, 6-disulfonic acid[25], solochrome brilliant blue B (sodium salt of sulfo-dichloro-hydroxy-dimethyl fuchson dicarboxylic acid[26] etc.. Beryllium fails to give a specific color change on a reaction with these reagents; but in general some other ions including iron, aluminum, alkali earth metals and rare earth metals give color change. Therefore, on their application, any of the above mentioned reagents is to be chosen according to the purpose. The method here proposed also seems possible of utilization for some purpose.

Introduction

The color reaction of the following three organic reagents of a similar structure with beryllium was examined at pH 1.42–11.0.

To 2 ml. of the buffer solution, 2 drops of metal solutions containing 50 p. p. m. metals

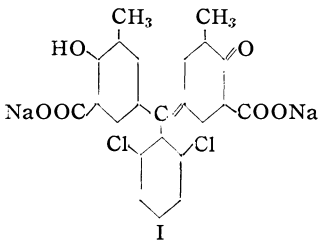

I

Sodium salt of dichloro-hydroxy-dimethyl fuchson dicarboxylic acid

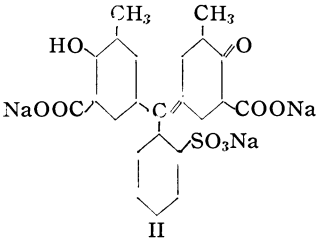

II

Sodium salt of sulfo-hydroxy-dimethyl fuchson dicarboxylic acid (Eriochrome cyanine R)

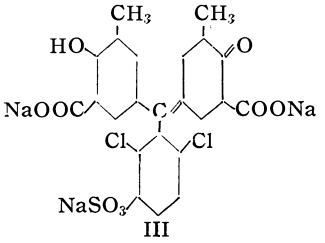

III

Sodium salt of sulfo-dichloro-hydroxy-dimethyl fuchson dicarboxylic acid (Solochrome brilliant blue B)

1) F.A. Vinci, *Anal. Chem.*, **25**, 1580 (1953).
2) T. Furuhata, *Repts. Sci. Research Inst.* (Tokyo), **26**, 15 (1950).
3) A. S. Komarovskii and N. S. Poluektov, *Mikrochemie*, **14**, 315 (1934).
4) L.W. Neidrach, A.M. Mitchell and C. J. Rodden, Natl. Nuclear Energy Ser., Div. VIII, **1**, Anal. Chem. Manhattan Project, 350 (1950).
5) W. Stross and G.H. Osborn, *J. Soc. Chem. Ind.*, **63**, 249 (1644).
6) M. Bose, *J. Indian Chem. Soc., Ind. & News Ed.*, **14**, 61 (1951).
7) G. Charlot, *Anal. Chim. Acta*, **1**, 218 (1947).
8) H.Z. Fischer, *Z. anal. Chem.*, **73**, 54 (1928).
9) T. Furuhata, *Repts. Sci. Research Inst. (Tokyo)*, **26**, 9 (1950).
10) I.M. Kolthoff, *J. Am. Chem. Soc.*, **50**, 393 (1928).
11) T.Y. Toribara and A.L. Underwood, *Anal. Chem.*, **21**, 1352 (1949).
12) A.L. Underwood and W.F. Neuman, ibid, 1348 (1949).
13) W.N. Aldridge and H.G. Liddell, *Analyst*, **73**, 607 (1948).
14) H. Goto and Y. Kakita, *Sci. Repts, Research Insts. Tôhoku Univ.*, **5**, 163 (1953).
15) G.E. Kosel and W.F. Neuman, *Anal. Chem.*, **22**, 936 (1950).
16) C.L. Luke and M. E. Campbell, ibib, **24**, 1056 (1952).
17) M.W. Cucci, W.F. Neuman and B.J. Mulryan, *U.S. Atomic Energy Commission*, AECD-**1990** (1948).
18) M.W. Cucci, W. F. Neuman and B. J. Mulryan, *Anal. Chem.*, **21**, 1358 (1949).
19) F. Hyslop, E. D. Palmes, Wm. C. Alford, A.R. Monaco and L.T. Fairhall, *Natl. Inst. Health Bull.*, **181**, 49 (1943).
20) J.A. Adam, E. Booth and J.D.H. Strickland, *Anal. Chim. Acta*, **6**, 462 (1952).
21) H.V. Meek and C. V. Banks, *Anal. Chem.*, **22**, 1512 (1950).
22) T. Furuhata, *Repts. Sci. Research Inst. (Tokyo)*, **26**, 139 (1950).
23) K. Motojima, This Bulletin, **29**, 71 (1956).
24) C.H. Wood and H. Isherwood, *Metallurgia*, **39**, 321 (1949).
25) V.I. Kuznetsov, *J. Anal. Chem. U.S.S.R.*, **10**, 276 (1955).
26) J.H. Wood, *Mikrochim. Acta*, **1955**, 11.

and 2 drops of 0.1% reagent solution were added. After three hours the color change was observed. For the pH ranges of 1.42–5.2, 7.0–9.2 and 9.2–11.0, the following buffer solutions were used respectively; hydrochloric acid–sodium acetate, hydrochloric acid-barbital and borax–sodium carbonate. In a buffered solution, pH 9.2, the color is yellow for all three blanks (water), and in the presence of beryllium, the color changes to brownish red (I), pinkish red (II) and dark reddish brown (III) respectively. Titanium changes the color of I to brownish yellow. But the same amounts of alminum, iron (ferric and ferrous), titanium (with II and III), copper, thorium and zirconium do not give any color change. The same amounts of calcium, magnesium, manganese and uranium ($(UO_2)^{2+}$) also fail to give any color change to II. In the other buffered solution, beryllium gives a color change, but fails to give a specific color change on reaction with these reagents as in pH 9.2.

Concerning eriochrome cyanine R[27] and solochrome brilliant blue B[25], their application to spectrophotometric determination has been already suggested.

Apparatus

Light absorption was measured against water by means of Shimadzu photoelectric spectrophotometer with 10 mm. absorption cells.

Reagents

Distilled Water.—Redistilled water is obtained by using a water distilling apparatus made of quartz.

Standard Beryllium Solution.—In 5 ml. of concentrated sulfuric acid, 0.1417 g. of beryllium oxide is dissolved. The resulting solution is transferred to a 500 ml. measuring flask containing about 100 ml. of water and is diluted to volume. This solution contains 0.1022 mg. of beryllium per ml.

0.05M Borax Buffer Solution.—In 1000 ml. of distilled water, 19.10 g. of borax are dissolved.

5% Potassium Sodium Tartrate Solution.—In 1000 ml. of distilled water, 50 g. of potassium sodium tartrate are dissolved.

Dye Solutions.—In 1000 ml of distilled water, 1, 3 or 5 g. of dyes are dissolved. The solutions thus obtained contain 0.1, 0.3 or 0.5% of dyes. Dye solutions should not be stored for more than one week.

Absorption Spectra

Absorption spectra of the reagents I, II and III, and of the complexes formed with beryllium are respectively presented in Figs. 1, 2 and 3. These curves were measured in buffered solutions of pH 9.2. The blank solution was prepared by mixing 20 ml. of 0.05 M borax solution with 1 ml. of water and 1 (I) or 2 ml. (II, III) of 0.1% reagent solution, whilst for the preparation of the complex solution 1 ml. of beryllium solution (50 micrograms of beryllium) was used in place of water. The solutions were made to stand for three hours at room temperature before the light absorption was measured.

Inspection of the curves shows that the reagent II is the most desirable for the spectrophotometric determination and that a wave length of 527 mμ gives the greatest difference in light absorption between the blank and the complex of reagent II, eriochrome cyanine R.

Therefore, the following experiments were carried out only with eriochrome cyanine R.

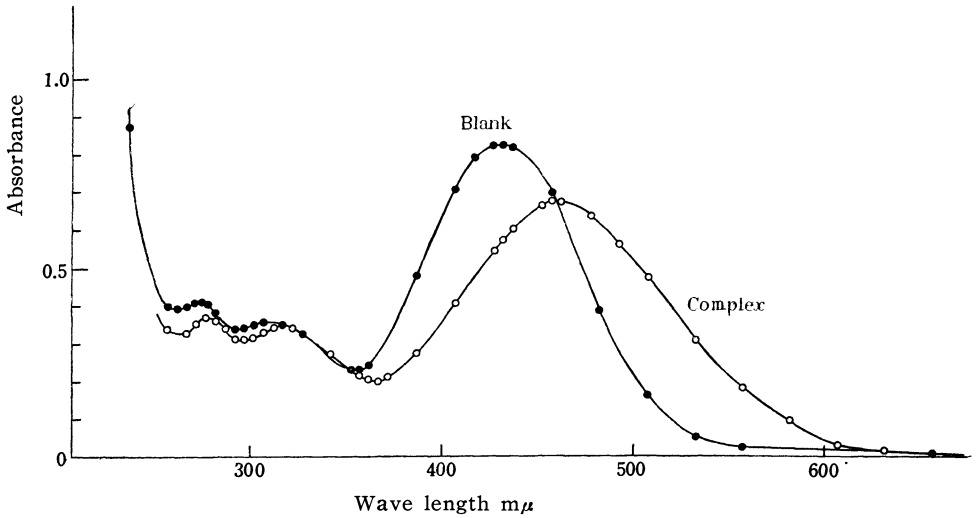

Fig. 1. Absorption spectra of reagent I and its complex.

27) T.Y. Toribara and R.E. Sherman. *Anal. Chem.*, 25, 1594 (1953).

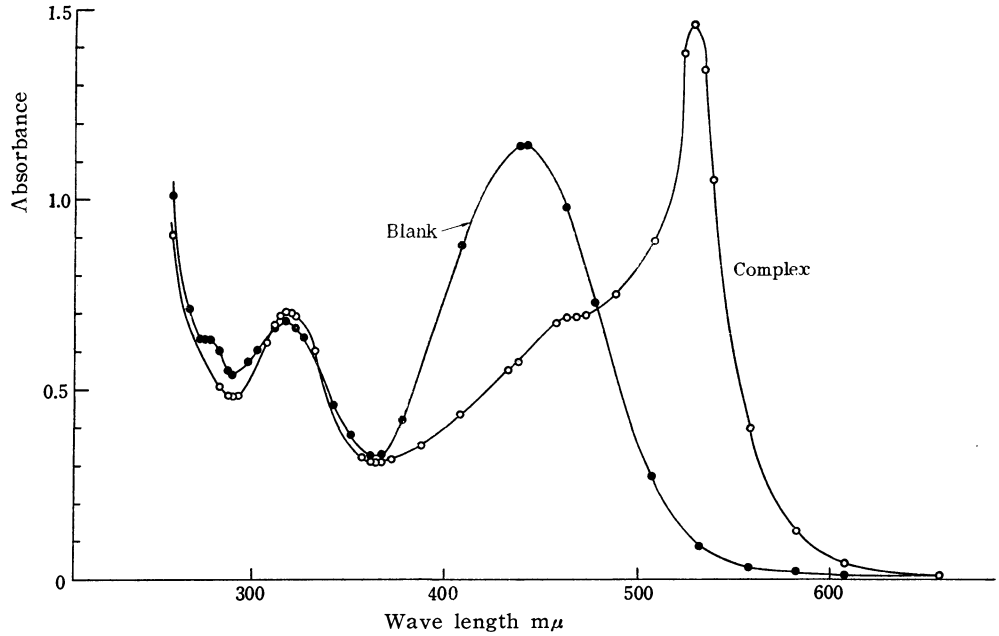

Fig. 2. Absorption spectra of reagent II and its complex.

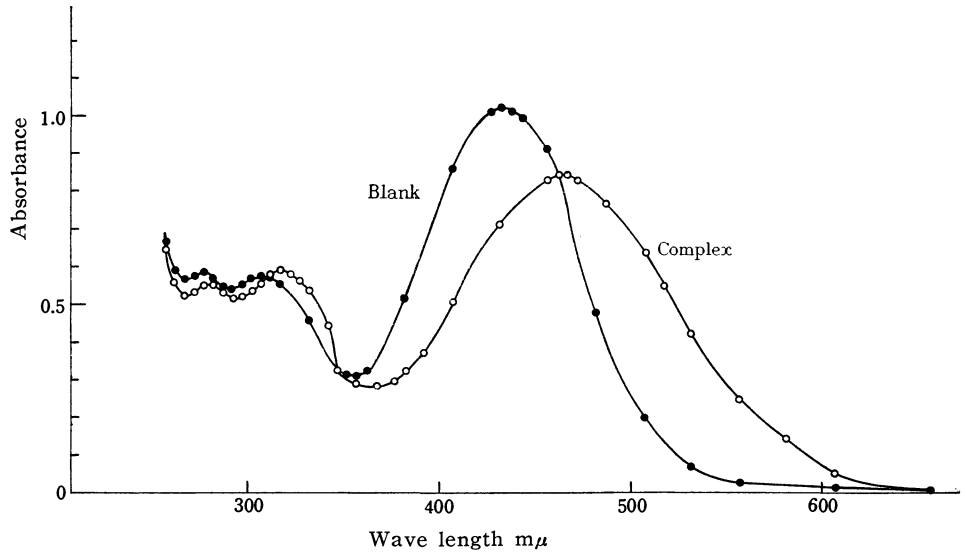

Fig. 3. Absorption spectra of reagent III and its complex.

Effect of Temperature and Time

In general, the organic reagents and beryllium may react slowly in an alkaline medium and at a low temperature. Consequently the effect of temperature and time of standing on the color change was studied.

Five ml. of beryllium solution and 100 ml. of 0.05 M borax solution were mixed, and made to stand for one hour in an ice box or in an air bath, its temperature being controlled. Five ml. of 0.1% eriochrome cyanine R solution were added. Light absorption at 527 mμ was measured ten, twenty and thirty minutes, one, two, three, five, eight, twenty-four and forty-eight hours after the development of the color for aliquots of the beryllium solutions of various concentrations. The results are presented in Table I and II and also in Fig. 4.

From these results, the color intensity was found to be dependent on the temperature and on the time after color development. At a lower temperature, color intensity is high but develops slow, but at a higher temperature, color intensity is low but develops fast. Therefore, the temperature has to be strictly controlled and the mesure-

TABLE I

EFFECT OF TEMPERATURE AND STANDING TIME

Temperature °C	Concentration of Beryllium Solution Mixed with Borax Solution p. p. m.	Standing Time									
		10min.	20min.	30min.	1 hr.	2 hr.	3 hr.	5 hr.	8 hr.	24 hr.	48 hr.
0	25	34.2	39.9	43.4	51.0	65.1	75.1	88.3	97.9	100	98.6
	20	37.8	41.3	44.6	52.9	66.2	74.5	89.1	100	100	100
	15	47.0	50.1	53.1	60.5	69.6	78.7	90.6	99.7	99.5	100
	10	58.9	63.1	63.7	70.3	76.7	83.3	92.5	99.6	98.9	100
	5	79.9	80.8	83.0	87.9	89.7	92.4	96.0	98.2	97.3	100
	0	90.9	96.1	92.2	94.8	98.7	100	96.1	97.4	97.4	97.4
15	25	39.7	66.8	73.4	89.0	94.3	100	100	100	87.7	82.7
	20	61.8	71.2	76.9	87.1	93.3	99.9	100	99.9	88.5	84.1
	15	72.7	80.2	83.5	92.7	97.3	100	100	100	94.0	89.3
	10	86.6	88.3	90.4	96.8	99.1	100	99.4	100	97.1	94.8
	5	90.9	93.9	94.4	97.0	98.5	100	98.0	99.0	94.4	92.9
	0	97.1	92.9	94.3	100	100	100	100	100	95.7	100
25	25	92.2	99.4	99.9	99.7	98.7	99.3	100	99.0	91.3	77.3
	20	89.6	100	98.0	98.7	98.2	97.7	97.3	97.5	91.0	89.6
	15	93.5	99.3	100	98.6	98.6	98.8	99.3	98.8	93.3	92.3
	10	97.7	100	100	100	98.0	99.3	99.7	99.7	96.7	93.0
	5	91.9	99.5	100	98.4	98.9	100	99.5	99.5	94.1	91.4
	0	87.2	87.2	93.6	97.4	94.9	93.6	94.9	92.3	100	97.4
50	25	99.3	98.5	97.6	98.2	97.5	98.4	100	98.5	71.8	65.4
	20	98.9	98.7	99.3	99.6	99.8	100	100	99.1	77.3	72.6
	15	99.2	100	97.2	98.1	97.8	96.7	95.0	96.7	87.3	82.3
	10	96.3	98.1	98.9	100	98.1	98.9	100	100	93.7	92.6
	5	94.1	97.1	96.5	95.9	100	97.1	98.8	100	94.1	89.4
	0	89.5	89.5	96.1	100	97.4	96.1	97.4	94.7	98.7	98.7

Figures shown are the percentages of light absorptions for the maximum light absorption of the solutions which contained same amount of beryllium and were kept at the same temperatures.

TABLE II

ANALYSIS OF VARIANCE

Source of Variation		Degrees of Freedom	Sum of Squares	Mean Square
Main Effects	Temperature (T)	3	9,681.15	3,227.05**
	Time (H)	9	7,217.42	801.94**
	Concentration (C)	5	3,930.46	786.09**
2-Factor Interactions	T×H	27	16,846.31	623.94**
	C×H	45	2,052.73	45.62**
	T×C	15	4,018.36	267.89**
3-Factor Interaction	T×H×C	135	3,097.32	22.94
Total		239	46,843.45	

** Highly significant * Significant

TABLE III

EFFECT OF DYE CONCENTRATION AND TARTRATE

Figures are the readings of the photometer

	20 ml. 0.05M Borax				10 ml. 0.05M Borax +10 ml. 5% Tartrate			
	Concentration of Beryllium Solutions Added p. p. m.*							
	0	3	7	10	0	3	7	10
0.1% Eriochrome Cyanine R	0.090	0.152	0.234	0.314	0.092	0.152	0.223	0.273
0.3% Eriochrome Cyanine R	0.267	0.393	0.593	0.769	0.273	0.423	0.609	0.755
0.5% Eriochrome Cyanine R	0.442	0.616	0.880	1.10_0	0.452	0.663	0.947	1.15_3

* Beryllium content of the solutions, the light absorptions of which were measured is 1/22 of these figures.

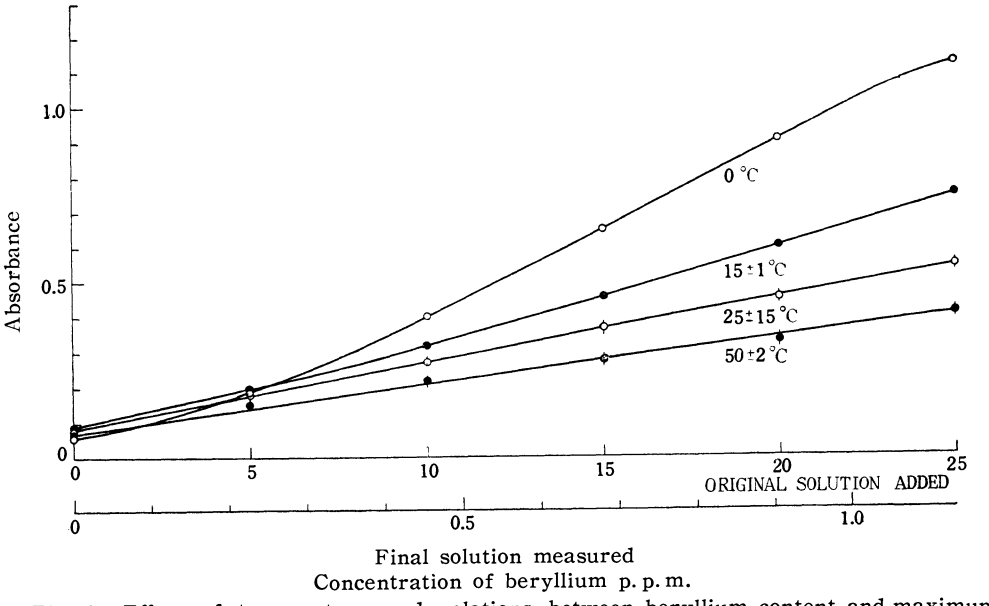

Fig. 4. Effect of temperature and relations between beryllium content and maximum light absorption.

ment of the maximum absorption has to be made at an adequate time after color development.

For an easier control, it seems convenient to select the temperature at 15–30°C and the measuring time in accordance with the temperature.

Effect of Dye Concentration and Tartrate

At pH 9.2, various metals are precipitated; when these elements are present in a large amount, beryllium is coprecipitated and the color change of eriochrome cyanine R by beryllium is inhibited. To avoid this, the presence of potassium sodium tartrate is desirable.

To determine the effect of potassium sodium tartrate and of the concentration of eriochrome cyanine R solution, 0.1, 0.3 and 0.5% eriochrome cyanine R solutions, 3 p. p. m., 7 p. p. m. and 10 p. p. m. of beryllium solutions and 5% potassium sodium tartrate in 0.05 M borax solution were used respectively. One ml. of beryllium solution and 10 ml. of tartrate solution were mixed and 10 ml. of 0.05 M borax solution were added. After standing for one hour in an air bath of 15°C (±1°C), 1 ml. of eriochrome cyanine R solution was added. After four hours, light absorptions were measured at 527 mμ. The results are shown in Table III and IV and in Fig. 5.

The larger the quantity of eriochrome cyanine R, the more intensive is the color (see the inclination of the curve in Fig. 5). Since, however, the light absorption of the blank should not be too high for an accurate determination, the concentration of eriochrome cyanine R cannot be higher than 0.5%.

As the results of presence of tartrate, the relations between the beryllium concentration and the light absorption of the complex holds linear. Moreover, the rate of increase in light absorption with increase in the concentration of eriochrome cyanine R is greater in the presence of tartrate than in its absence.

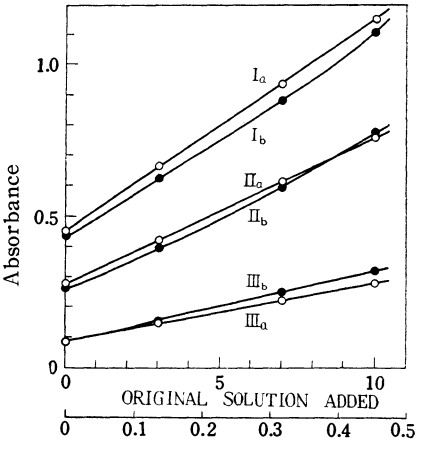

Fig. 5. Effect of dye concentration and tartrate.

Ia: 0.5% dye solution, presence of tartrate
Ib: 0.5% dye solution, absence of tartrate
IIa: 0.3% dye solution, presence of tartrate
IIb: 0.3% dye solution, absence of tartrate
IIIa: 0.1% dye solution, presence of tartrate
IIIb: 0.1% dye solution, absence of tartrate

TABLE IV
ANALYSIS OF VARIANCE

Source of Variation		Degrees of Freedom	Sum of Squares	Mean Square
Main Effects	Concentration of Dye (D)	2	1,397,195	698,597.5**
	Concentration of Beryllium (B)	3	728,133	242,711.0**
	Tartrate (T)	1	1,135	1,135.0**
2-Factor Interactions	D×B	6	135,318	22,553.0**
	T×D	2	3,274	1,637.0
	B×T	3	771	257.0
3-Factor Interaction	D×B×T	6	1,220	203.3
Total		23	2,267,046	

** Highly significant * Significant

Thus, the addition of tartrate gives many benefits for an accurate determination.

For the most sensitive condition at 15°C, i.e. for the application of 0.5% eriochrome cyanine R and the presence of tartrate, the calibration curve for beryllium is shown in Fig. 6.

ing 3 p.p.m. of beryllium and various amounts of a metal or of an anion were prepared. One ml. of a metal or anion solution and 10 ml. of 5% potassium sodium tartrate solution were mixed with 10 ml. of 0.05M borax solution, and set aside for one hour at 15°C. One ml. of 0.5% eriochrome

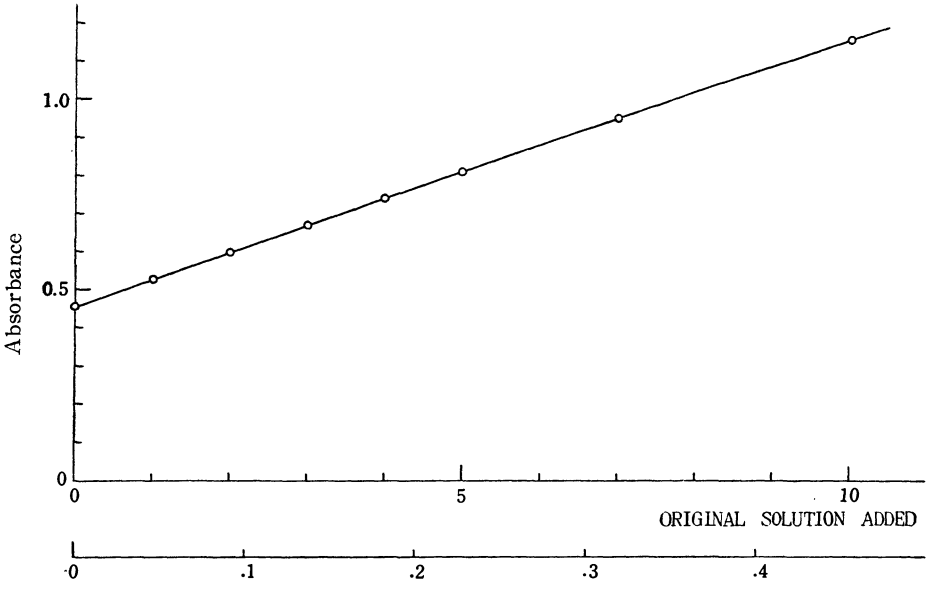

Final solution measured
Concentration of beryllium p.p.m

Fig. 6. Calibration curve of beryllium.
(15°C, presence of tartrate, 0.5% eriochrome cyanine *R* solution)

Effect of Metals and Anions

It has already been mentioned that small amounts of various metals fail to give any color change to eriochrome cynine R in a medium of 0.05 M borax solution, pH 9.2. In the presence of tartrate, however, many metal ions can be held in solution and are expected to give color change of the dye.

In order to disclose the limit of interference of various metals and anions with the color development of beryllium, one series of solutions containcyanine R solution was added, and the light absorption at 527 mμ was measured after four hours. The limit and mode of interference of various metals and anions were shown in Table V.

When a dilute solution of eriochrome cynine R was used, the limit of interference of each metal or anion became greater and the color change caused by beryllium smaller. An example is shown in Table VI and VII (c.f. Table V). Experimental conditions were the same as in the case of the above experiment except for the use of 0.1% dye solution instead of 0.5%.

TABLE V
INTERFERENCE LIMIT OF METALS AND ANIONS

Metal or Anion	Compound	Interference Limit: For the Metal or Anion Solutions Mixed with Tartrate Solution	Interference Limit: For the Final Solutions, Light Absorption of which were measured p. p. m.†	Mode of Interference
Fe^{3+}	Ferric chloride	250	12	Color enhancement
Al^{3+}	Alum	250	12	ditto
Ti^{4+}	Titanium sulfate	>300	>14	—
Mg^{2+}	Magnesium sulfate	250	12	Color inhibition
Ca^{2+}	Calcium chloride	700	32	ditto
Th^{4+}	Thorium nitrate	2000	91	ditto
Fe^{2+}	Ferrous ammonium sulfate	—*	—*	—
$(ZrO)^{2+}$	Zirconium oxychloride	100	4.5	Color inhibition
$(UO_2)^{2+}$	Uranyl acetate	>1000	>45	—
SiO_3^{2-}	Sodium silicate	300	14	Color inhibition
F^-	Sodium fluoride	1000	45	ditto
PO_4^{3-}	Potassium phosphate, monobasic	3000	136	ditto

* For standing, Fe^{2+} is oxidized to Fe^{3+}, and same figure was obtained as Fe^{3+}.
† The concentration of beryllium was 0.17 p. p. m. in this experiment.

TABLE VI
EFFECT OF METAL IONS

One milliliter of 20 p. p. m. beryllium solution containing various amounts of metals and 10 ml. of tartrate solution were mixed and added 10 ml. of 0.05M borax solution. After standing for one hour at 15°C, 1 ml. of 0.1% eriochrome cyanine R solution is added and after four hours light absorption of the solution was measured. Figures of light absorptions are as follows.

Concentration of Iron p. p. m.*	Concentration of Titanium p. p. m.* 0 — Concentration of Aluminum p. p. m. 0	200	1000	Concentration of Titanium p. p. m.* 50 — Concentration of Aluminum p. p. m. 0	200	1000
0	0.441	0.453	0.446	0.452	0.452	0.451
200	0.446	0.447	0.448	0.449	0.453	0.445
1000	0.456	0.459	0.451	0.452	0.442	0.447

* These concentrations are the concentration of the metal solutions mixed with tartrate. For the final solutions, these concentrations must be devided by 22.

Discussion

In the case of the determination of beryllium using eriochrome cyanine R, temperature, standing time, concentration of the dye solution, the presence of tartrate, and the concentration of various other ions are the factors which regulate the accuracy, precision and reproducibility.

Above all, the concentration of dye solution should be as high as possible. When it is high, one of the beneficial effects of tartrate, increase in color intensity, is promoted.

Concerning further advantages brought about by tartrate, it makes the working curve linear and prevents the coprecipitation of beryllium with metal ions such as iron, aluminum, calcium and magnesium. Thus, the addition of tartrate is essential.

Temperature is also an important factor; at a lower temperature the color intensity is

TABLE VII
ANALYSIS OF VARIANCE

Source of Variation		Degrees of Freedom	Sum of Squares	Mean Square
Main Effects	(Ti)	1	1.39	1.39
	(Fe)	2	31.45	15.73
	(Al)	2	24.11	12.06
2-Factor Interactions	(Ti)×(Fe)	2	141.44	70.72
	(Fe)×(Al)	4	46.22	11.56
	(Al)×(Ti)	2	44.11	22.06
3-Factor Interaction	(Ti)×(Fe)×(Al)	4	75.56	18.89
Total		17	364.28	

** Highly significant * Significant

higher, but to get maximum light absorption it requires a long time to obtain it and the temperature control is difficult; at a higher temperature standing time for obtaining the maximum light absorption is shorter but the resulting color intensity is lower, the temperature control being also difficult.

Consequently, temperature of 15–30°C will also be recommended from these respects. The interfering cations and anions should not be present with beryllium over the interference limit. The latter is a function of the concentration of the dye solution as mentioned above.

The following procedure is recommended.

One ml. of the sample solution containing from 1 to 10 micrograms of beryllium and 10 ml. of 5% potassium sodium tartrate solution are mixed with 10 ml. of 0.05M borax solution. After standing for one hour at 15°C, 1 ml. of 0.5% eriochrome cyanine R solution is added. After three hours the light absorption of the colored solution is measured at 527 mμ. With the aid of the calibration curve, the amounts of beryllium can be determined (see Table V and Fig. 6).

To a dilute solution of beryllium containing from 0.05 to 0.5 milligram Be per liter, the following procedure is applied. Into a 25 ml. measuring flask, 0.5 g. of potassium sodium tartrate is taken and 20 ml. of the sample solution are poured. After dissolution of tartrate, 0.191 g. of borax is added, dissolved and the whole diluted to 25 ml. After being kept for one hour at 15°C, 1 ml. of 0.5% eriochrome cyanine R solution is added and the light absorption is measured at 527 mμ after four hours. In this case, the calibration curve must be used, which is prepared by the same procedure for a standard beryllium solution.

In any case, when an interfering substance is present in greater quantity than the interfering limit, its amount has to be diminished below the interfering limit.

The author wishes to thank Professor Kenjiro Kimura and Nobufusa Saito of the University of Tokyo for their kind guidance and encouragement, Mr. Shunichi Soma for his kind supply of information, and Mr. Kenji Umemoto for his assistance with a part of the experiment.

Balneological Laboratory, Okayama University, Misasa Hot Springs Tottori Prefecture

Study on the Molecular Structure of Bisacetylacetone-Copper(II) by Electron Diffraction[1]

By Shuzo SHIBATA and Kôzô SONE*

(Received June 27, 1956)

Although the structures and properties of metallic chelate compounds have attracted considerable attention of many recent investigators, the number of compounds whose molecular structures have been accurately determined by X-rays seems to be rather limited on account of their highly complicated crystal structures. However, it is well known that some of these compounds can readily be vaporized. Therefore, it is possible to apply the gas electron diffraction method to the determination of their molecular structures. The present paper deals with the study on the molecular structure of copper chelate of acetylacetone by this method.

The structure of copper acetylacetonate is of interest, particularly, in respect to the question whether the configuration of four oxygen atoms relative to the divalent copper atom is square or tetrahedral, from the point of view of the metallic chelate chemistry. Such a problem has not yet been completely clarified in spite of many earlier investigations, e.g. X-ray analysis[2], dipole moment[3] and infra-red absorption[4] measurements. Our present electron diffraction study was intended to obtain such information, and directly clarified the fact that the chelate possesses a square planar configuration with

1) Presented at Symposium on the metallic complex compounds held on November 13, 1951.

* Present address: Aichi College of Liberal Arts, Higashiku, Nagoya.

2) E. G. Cox and K. C. Webster, *J. Chem. Soc.*, **1935**, 731.

3) A. E. Finn, G. C. Hampson, and L. E. Sutton, *J. Chem. Soc.*, **1938**, 1254.

4) e.g. J. Lecomte, *Discussions Faraday Soc.*, **1950**, 125.

Cu-O distance equal to 1.95 Å. Our results were in good agreement with the recent X-ray investigations[5,6].

Experimental

The sample was prepared by the reaction of aqueous cupric acetate solution with acetylacetone. It was recrystallized from alcohol. The sample was evaporated at about 170°C in a high temperature nozzle and was led into a vacuum chamber to interfere with an electron beam of about 0.06 Å in wave length. The diffraction photographs were taken in the usual way[7]. The camera length was about 11 cm.

Analysis

Measurements were made visually of the q values and the intensities of maxima and minima below $q=70$ in the photographs. Only the intensity of the 14th maximum could be measured. The measured q values are listed in Table I.

TABLE I
OBSERVED AND CALCULATED q VALUES OF THE MAXIMA AND MINIMA

Max.	Min.	$q_{obs.}$	q_c(Model C)	$q_c/q_{obs.}$[a]
	2	7.56	7.6	(1.005)
2		10.05	10.2	1.015
3		14.61	14.7	1.006
4		17.82	17.4	(0.976)
5		21.05	21.0	0.998
6		24.83	23.6	(0.950)
7		29.18	29.6	1.014
8		33.71	33.5	0.994*
9		37.85	36.9	(0.975)
10		43.32	43.3	1.000*
11		52.06	52.2	1.003*
12		57.29	56.4	0.984
13		62.77	62.0	0.988
Average of $q_c/q_{obs.}$				1.000
Average Deviation				0.007

a) The values in parentheses were omitted in calculating the average and values marked with asterisk were given double weight.

The positions of the minima except the 2nd were not measured because of the highly short period of the halos. Curve V_1 in Fig. 3 shows the visual curve which was drawn so as to reproduce the feature of halos and to have the intensities corresponding to the following formula.

$$I(q)=\sum_{i\neq j}(Z_iZ_j/r_{ij})\sin(\pi qr_{ij}/10)$$

Here notations have their usual significances. However, the accurate measurement of intensity in the region of small q values is considerably difficult on account of the intense background of photographs; hence it is probable that the inaccuracy of intensity measurement introduces errors into the radial distribution curve. Therefore the intensity of the first visual curve in this region was corrected by the preliminary theoretical intensity curves in a way described below. The R.D. curve was calculated from the visual curve by use of the formula

$$rD(r)=\sum_i I(q_i)\exp(-aq_i^2)\sin(\pi q_i r/10),$$

where the constant a was chosen so that $\exp(-aq_i^2)=0.1$ for the last term ($q_i=65$). In this case, the unobservable part of q below 7 which is shown by a dotted curve in V_1 in Fig. 3 was appropriately estimated from the feature of the theoretical intensity curve. The R.D. curve thus obtained is shown by R.D. 1 in Fig. 1. The interatomic distances obtained from this

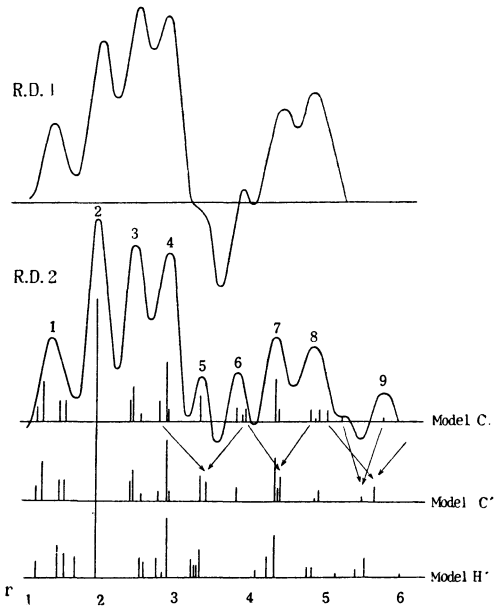

Fig. 1. The radial distribution curves of copper acetylacetonate.
The vertical bars in R.D. 2 indicate all atomic distances (below 6 Å) calculated for model C (square planar), model C' (rectangular twisted) and model H' (tetrahedral).

curve are given in Table 2 with assignments to these distances. It must be mentioned here that the following assumption was made throughout the present analysis; the ligand is planar and possesses D_{2h} symmetry. Using the values obtained for the interatomic distances, especially, Cu-O_1**, Cu-C_1, Cu-C_2, and Cu-C_4, preliminary theoretical intensity curves were calculated for various reasonable models. Then, it can be seen that these models*** did not seriously change the

5) E. A. Shugam, *Doklady Akad. Nauk S.S.S.R.* **81**, 853 (1951); *Chem. Abst.*, **46**, 3894 (1952).
6) H. Koyama, Y. Saito and H. Kuroya, *Journal of the Institute of Polytechnics, Osaka City University*, **4**, No. 1, Series C., 43 (1953).
7) e.g. L. O. Brockway, *Rev. Mod. Phys.*, 8, 231 (1936).

** The notation "Cu-O_1" also means Cu-O_1', Cu-O_2 and Cu-O_2'. In the case of other atomic pairs the situation is the same as in the Cu-O_1 by the above assumption.
*** A twisted model is also taken into consideration together with a planar model.

TABLE II
THE POSITIONS AND THE ASSIGNMENTS OF THE PEAKS IN THE R.D. CURVES

Peak	Distance Å R.D. 1	R.D. 2	Assignment[a]
1	1.34	1.34	$C_1O_1(3)$ $C_1C_2(2)$ $C_1C_4(2)$ CH(1)
2	1.97	1.95	*CuO*$_1$(10)
3	2.44	2.41	$C_2O_1(2)$ $C_4O_1(2)$ $C_2C_4(1)$
4	2.84	2.87	*CuC*$_1$(5) O_1O_2, $O_1O_{2'}$*(2) $O_1C_3(1)$
5	3.25	3.32	*CuC*$_2$(2)
6	3.82	3.80	C_1C_5*(1) $O_1C_{3'}(1)$
7	4.32	4.30	*CuC*$_4$(3) $O_1C_5(1)$
8	4.80	4.81	$O_1C_{1'}$*(1) $O_1C_{2'}(1)$ $O_1C_{5'}(1)$
9		5.72	$C_1C_{1'}$

a) These assignments correspond to the most probable model C. Numbers in parentheses show approximately the relative magnitudes of the ratio Z_iZ_j/r_{ij}. Here the atomic pairs contributing predominantly to each peak are listed. Also the italicized atomic distances are assumed in the calculation of the intensity curves. The bond distances marked with asterisks vary depending on the configuration of the molecule.

intensities for small q values, and therefore the features of these curves can be used to modify the intensity of the first visual curve for small q values (below about 15). The visual curve thus corrected is shown by V_2 in Fig. 3. For example, it was found that the height of the 2nd maximum and the depths of the 2nd and 3rd minima were overestimated in the first visual curve.

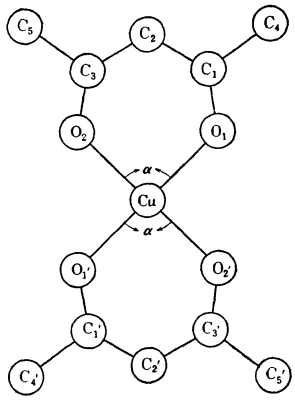

Fig. 2. The shape of the best model and the numbering of atoms.

The corrected R.D. curve was further calculated from the second visual curve in the same way as before, and is shown by R.D. 2 in Fig. 1. This curve is almost non-negative, and this fact is a desirable feature in general. Table II lists the positions and assignments of peaks in its curve. The 2nd, 4th, 5th and 7th peaks are definitely assigned to the Cu-O_1, Cu-C_1, Cu-C_2 and Cu-C_4 atomic pairs, respectively, since these peaks are taken as single or nearly single peaks because of their great scattering powers, so these distances seem to be probably correct. If the structures of the ligands are assumed as mentioned above, the geometrical consideration of the 3rd peak (assigned to C_2-O_1, C_4-O_1 and C_2-C_4) with the above four distances leads to the value of $\angle O_1CuO_2(\angle\alpha)$ nearly equal to 90°. Furthermore, the complete structure of the ligand is probably estimated with use of the 6th peak (C_1-C_5); thus the structure of ligand of the square model C is selected as the most probable model. Thus the structure of the molecule is determined by the configuration dependent on the angle between two ligand planes. Therefore, to determine particularly whether the configuration of molecule is coplanar (model C) or rectangular (model C'), computed radial distributions for each model were compared with the observed one. The vertical bars under the R.D. 2 in Fig. 1 show the interatomic distances for each model and the heights of the bars are drawn proportional to Z_iZ_j/r_{ij} of the respective atomic pairs. Oblique arrows in this figure show the corresponding atomic pairs by the change of the molecular configuration. The comparison of the two computed radial distributions with the observed one leads to the fact that the planar model is superior to the rectangular twisted model, because in the latter the areas of the 5th, 6th, 7th and 8th peaks are not in quantitative accordance with the sum of the heights of the bars. This fact will be made clear by the comparison of both theoretical intensity curves with the observed curve as described later.

Furthermore, a large number of theoretical intensity curves were calculated for various molecular models in order to check the acceptability of the most probable model C mentioned above and to determine the molecular structure in more detail. However, on account of the many parameters involved a complete analysis on the molecular structure of copper acetylacetonate would be a very laborious task. Therefore this analysis was carried out by means of the following assumptions: Cu-O_1, Cu-C_1, Cu-C_2, and Cu-C_4 distances are 1.95 Å, 2.87 Å, 3.32 Å and 4.30 Å, respectively, which are the most probable values obtained from R.D. method. Then other parameters determining the structure are $\angle\alpha$, C_1-C_2, and C_1-C_4 for the ligands, and the configuration of the molecule dependent on the angle between the two ligand planes. The values of the parameters $\angle\alpha$ and C_1-C_2 were taken over the range from 80° to 110° and from 1.33 Å to 1.62 Å respectively, and the position of the C_4 atom was taken in such a way that the C_1-C_4 bond nearly bisects $\angle O_1C_1C_2$. In regard to the configuration of molecule, a coplanar and a rectangular form (including a tetrahedral form) are taken into account. A number of intensity curves were calculated for these carefully selected models with various values for the above parameters and were compared with the observed one. These intensity curves contain the contributions from all the atomic pairs, the pairs pertaining to hydrogen being ignored except H-C bondings.

Some of the calculated intensity curves are

depicted in Fig. 3. The corresponding models are listed in Table III. The relative positions

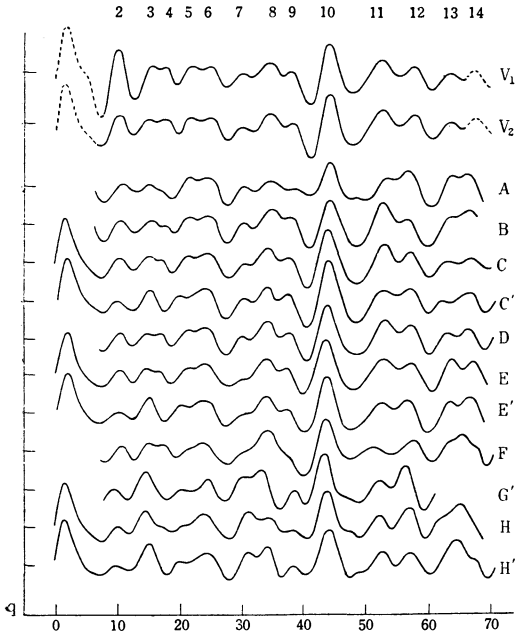

Fig. 3. Visual and theoretical intensity curves.

$\angle\alpha$. Curves B and E are satisfactory. Curves C and D are more satisfactory. Curve F is unsatisfactory because of the feature of the 9th maximum (depressed to an unacceptable extent) and the relative heights and the positions of the 11th and 12th maxima, and this model provides the upper limit of $\angle\alpha$. Model H*****, a planar model with $\angle\alpha$ equal to a tetrahedral angle, is very unsatisfactory because it requires that the heights of the 3rd and 6th maxima and especially the features of the 7th, 8th and 9th maxima disagree with observations. If the molecule takes a configuration with one ligand plane at a right angle to the plane of the other ligand, such as in models C', E', G' and H' (the latter two are tetrahadral), the features of the 3rd and 4th (disappearing) maxima and position of 5th maximum disagree remarkably with those of the visual curve as seen in Fig. 3, so that these twisted models (including the tetrahedral) are rejected. This conclusion was also confirmed by the computed R.D. as shown by C' and H' (tetrahedral) in Fig. 1. If the molecule would take the twisted form, the 5th and 7th peaks in the observed R.D. should be larger and the 6th and 8th peaks should be smaller. After all, the general qualitative appearance of the photographs is well reproduced by the square planar model. A quantitative comparison of the q values of maxima calculated for the best model C with the observed one is shown in Table I. The discrepancies in the positions

TABLE III

THE MODELS OF THE THEORETICAL INTENSITY CURVES SHOWN IN FIG. 3

Model	$\angle$OCuO	C_1-C_2, Å	C_1-O_1, Å	C_1-C_4, Å	Configuration*
A	80°	1.33	1.15	1.55	Coplanar
B	90°	1.33	1.28	1.55	,, (Square form)
C	90°	1.46	1.21	1.51	,, (,,)
C'	,,	,,	,,	,,	Rectangular
D	90°	1.46	1.21	1.56	Coplanar (Square form)
E	93°	1.46	1.25	1.56	,,
E'	,,	,,	,,	,,	Rectangular
F	98°	1.45	1.32	1 51	Coplanar
G'	110°	1.46	1.50	1.51	Rectangular (Nearly tetrahedral form)
H	110°	1.62	1.40	1.50	Coplanar
H'	,,	,,	,,	,,	Rectangular (Nearly tetrahedral form)

* The configuration is determined by the twisted angle between two ligand planes.

and features of maxima and minima of these curves will be compared with those of the visual curve as follows. Curve A is unsatisfactory since the 8th maximum is low and since the 10th minimum is shallow, and since the 11th maximum is lower than the 12th maximum. If the value of $\angle\alpha$ is smaller than 80°, the intensity curves cannot be obtained in agreement with the observed one in regard to the points mentioned above, even though various values of other parameters**** were used. Therefore model A provides the lower limit of

**** In general the feature of intensity curves are not seriously sensitive to the parameters $C_1 \cdot C_2$ and $C_1 \cdot C_4$.

of the 4th, 6th and 9th are presumably due to errors in the measurement, errors of this type being rather common. Also it must be mentioned that although the effect of molecular vibration was taken into account, it did not seriously affect the positions and the features of maxima and minima for q value below 65.

From the analysis described above, the molecular structure of copper acetylacetonate was

***** The models with $\angle\alpha$ equal to a tetrahedral angle seems to be unresonable since the ligand require unreasonably long $C_1 \cdot C_2$ or $C_1 \cdot O_1$ distances from the previous assumption.

determined as follows: Cu-O_1=1.95 Å, Cu-C_1=2.87 Å, Cu-C_2=3.32 Å and Cu-C_4=4.30 Å, (These values were obtained from the R.D. method and the correctness of these values were checked by the calculations of the theoretical intensity curves.), $\angle O_1CuO_2=90\pm10°$, and planar configuration. The latter two are more important conclusions. On the basis of the present photographs it is not possible to make any definite statements as to the distances of C_1-C_2, C_1-O_1 and C_1-C_4 on account of the complexity of the chelate, but for these distances the following average values are obtained from the acceptable models: 1.42 Å, 1.25 Å and 1.55 Å, respectively.

Discussion

Our gas electron diffraction study lead to the conclusion that copper acetylacetonate has a square coplanar configuration with Cu-O distance equal to 1.95 Å.

The result that this chelate takes a square coplanar configuration agrees with the earlier indication of Cox and Webster[2] and also with the recent data of Shugam[5] and Koyama et al.[6] (The $\angle O_1CuO_2$ was determined to be 93° by Shugam and 87.5° by Koyama et al., respectively.) The fact that the chelate forms the square coplanar (not tetrahedral) configuration seems to be due to the fact that an unpaired electron in the 3d orbital of Cu (II) is promoted to the 4p orbital so that Cu (II) constructs dsp^2 hybrid orbitals which have higher bond strengths than sp^3 hybrid orbitals, as suggested by Pauling[8]. Also in this case the conjugation between $d\pi$ orbital of Cu atom and $p\pi$ orbitals of the ligand atoms may highly strengthen the Cu-O bonds, so that this configuration will become more stable.

The observed value of the Cu-O distance was 1.95 Å. It is in good agreement with the sum of the covalent radius of oxygen (0.66 Å) and the metallic radius[8] of copper with a coordination number of 12 (1.28 Å), but is much smaller than the sum (2.4 Å) of ionic radii****** of the two atoms. This supports the evidence of covalent bond character of Cu-O bond. The Cu-O distances in various molecules hitherto reported are: 1.95 Å for cupric oxide[9], 2.01 Å for $CuCl_2\cdot 2H_2O$[9], 1.97 Å for $K_2CuCl_4\cdot 2H_2O$ and $(NH_4)_2CuCl_4\cdot 2H_2O$[9], 1.98 Å and 2.01 Å (mean values) for two types of Cu atoms of malachite[10], 1.98 Å for bandylite[11], 2.03 Å for copper proline dihydrate[12], and 1.91 Å and 1.96 Å (mean values) for copper acetylacetonate (by Shugam and Koyama et al., respectively). The observed Cu-O distance agrees fairly well with these values, but better with that of cupric oxide than with others. This seems to be due probably to the fact that in cupric oxide Cu (II) takes a square coplanar configuration with four covalent Cu-O bonds as in a free molecule of copper acetylacetonate, rather than a distorted octahedral configuration as found in other examples mentioned above. Consequently the observed Cu-O distance of 1.95 Å corresponds to the covalent radius 1.29 Å for Cu (II) in square configuration with coordination number of 4, in contrast with the known radius[8], 1.35 Å in tetrahedral configuration.

The authors express their deep appreciation to Prof. M. Kubo and Dr. M. Kimura for their valuable advice and also to the Ministry of Education for supporting this research.

Department of Chemistry
Faculty of Science
Nagoya University
Chikusa, Nagoya

8) L. Pauling, "Nature of the Chemical Bond", Cornell University Press, New York (1939).

****** Pauling's univalent ionic radii were used after the correction for the ionic valence and coordination number.

9) Ref. 8). R. W. G. Wyckoff, "Crystal Structures", Vol. I, Interscience Publishers, Inc., New York (1948). ibid., (Vol. II) (1951).

10) A. F. Wells, *Acta Cryst.*, **4**, 200 (1951).

11) R. L. Collin, *Acta Cryst.*, **4**, 204 (1951).

12) A. McL. Mathieson and H. K. Walsh, *Acta Cryst.*, **5**, 599 (1952).

*Measurement of Solubilities of Sparingly Soluble Liquids in Water and Aqueous Detergent Solution Using Non-ionic Surfactant**

By Makoto HAYASHI** and Tsunetaka SASAKI

(Received June 26, 1956)

Introduction

During the past few years, numerous studies were reported with regard to the solubilization of various substances into the aqueous solutions of surface active agents. But in the region of concentration below cmc., little is known as to the behavior of solutes in solution. To know such characteristics of the surface active agents in aqueous solution, particularly their interactions with the solutes, it is necessary to begin with the determination of the solubility of solutes in water as well as in aqueous solutions of detergents, since we have unfortunately no reliable data available up to the present. This lack of correct data may come partly from the roughness of the method itself, and partly from the fact that the sparingly soluble substances usually show a tendency to be dispersed as colloidal particles, which make obscure the true solubility determination. Formerly, one of the present authors also determined the solubility of iso-amyl alcohol in water taking account of this fact[1]. In the present paper we determined the solubility of iso-amyl alcohol, *n*-butyl alcohol and benzene in water, making use of the influence on solubility of these substances produced by the addition of non-ionic surfactant, Tween 80.

Experiment

(a) Materials.—The surfactant used in this experiment was a kind of non-ionic surfactant, Tween 80, of Atlas Powder Co., which was kept in vacuum until a constant weight was attained.

For the purification of iso-amyl alcohol and *n*-butyl alcohol, they were boiled with a concentrated sodium hydroxide solution, washed with water, dried with anhydrous potassium carbonate and distilled over calcium oxide. Distillation was repeated over calcium metal, and the fractions distilled at 131°C for the former and 118°C for the latter were collected. Benzene was purified by the ordinary method, that is, it was shaken repeatedly with concentrated sulfuric acid, boiled with mercuric oxide, recrystallized several times and distilled over sodium metal.

(b) Principle and Apparatus.—A definite amount of iso-amyl alcohol is added to a varying amount of Tween 80 solution of known concentration in the cylindrical tube with a well-ground stopper. The mixture is then shaken vigorously, and is stood in the thermostat for about fifteen minutes. If the alcohol concentration is higher than its solubilization limit, the system becomes turbid due to emulsification. The turbidity decreases and finally disappears with an increasing amount of Tween 80 solution added. The diagram is drawn between the turbidity and the concentration (wt. %) of iso-amyl alcohol in the mixture taking the concentration of Tween 80 constant as shown in Fig. 1. From these curves

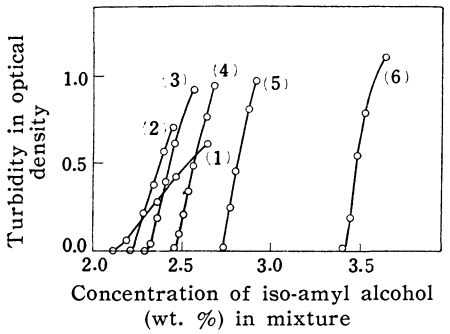

Fig. 1. Relation between turbidity and iso-amyl alcohol concentration in Tween 80 solution of concentration: (1) 0.0998%, (2) 0.228%, (3) 0.52%, (4) 1.046%, (5) 2.00%, (6) 3.86%.

we can estimate the limit of solubilization by extrapolating the linear parts of these curves to zero turbidity. The values of solubilization thus obtained are plotted against the concentration of Tween 80, which is shown as f(c) in Fig. 2. In this figure the point A represents the solubility of iso-amyl alcohol in pure water which is determined as follows. The saturate solution of iso-amyl alcohol in water is prepared and is titrated using Tween 80 solution of the concentration corresponding to the point C in Fig. 2. Hereby, turbidity increases, passes through a maximum, and then decreases gradually, when plotted against the concentration of Tween 80 added, as in Fig. 3. The decreasing portion of the curve is linear. From the extrapolation of this portion to zero turbidity, we can obtain the concentration of Tween 80 (D) required just to dissolve alcohol, which in turn corresponds to the ordinate of the

* This work was presented at the Symposium of Colloid Chemistry, held at Osaka, in November 13, 1954.

** Present address, Kassui Women's Junior College, Higashi Yamate-machi, Nagasaki.

1) S. Mitsui and T. Sasaki, *J. Chem. Soc. Japan*, **63**, 1766 (1942).

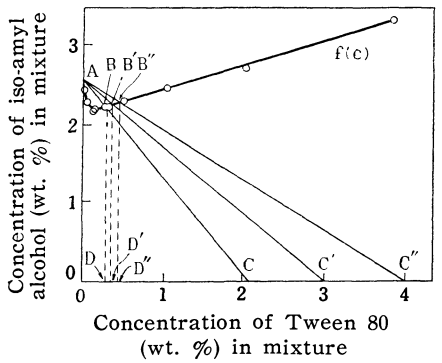

Fig. 2. Solubility of iso-amyl alcohol in aqueous Tween 80 solution. Concentration of Tween 80 in aqueous solution: C=2.061%, C′=2.988%, C″=3.99%; D=0.272%, D′=0.346%, D″=0.436%; A, Saturate solution of iso-amyl alcohol in water; B, B′, B″, End point of titration of saturate solution A.

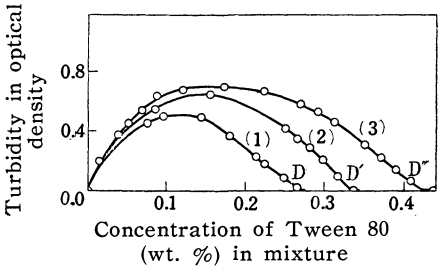

Fig. 3. Turbidities of saturate iso-amyl alcohol solution when titrated with aqueous Tween 80 solution. Concentration of Tween 80 solution used: (1) 2.061%, (2) 2.988%, (3) 3.99%.

point of intersection (B) made by the curve f(c) and the straight line AC in Fig. 2. Inversely, the point B can be determined from D and f(c); thus we can determine the point A, namely the solubility of iso-amyl alcohol, by extrapolating the straight line BC. The turbidity was measured by the photocell type photometer, and expressed in terms of the optical density of transmitted light. The monochromatic light (550 mμ) from a 50 watt lamp with an interference filter was used as a light source.

The temperature of the cell containing solution was regulated within 30.1±0.1°C by the thermostatted water circulating through a water mantle surrounding it.

(c) Experimental Procedure and Results.— For the determination of f(c) of iso-amyl alcohol, about 0.7 g. of it was accurately weighed and mixed with known weight (about 20 g.) of Tween 80 solution of the concentration from 0.0998 to 3.86%. For the determination of the steeply inclined portion of f(c) near the point A, aqueous iso-amyl alcohol was usen instead of pure alcohol. For the preparation of saturate solution, about 7 g. of iso-amyl alcohol and about 200 cc. of water were well shaken together at a temperature lower than that of the measurement (30.1°C), and then stood in the thermostat for about twenty-four hours. After the excess solute particles cleared up, a transparent saturate solution was obtained which was taken out from the bottom of the vessel by a siphon. A known amount of this solution (about 20 g.) was titrated with Tween 80 solution corresponding to C(2.061%), C′(2.988%) and C″(3.99%) as indicated in Fig. 2, under the constant temperature (30.1°C). The points D, D′ and D″ were thus obtained and the corresponding points B, B′ and B″ were found on f(c) of Fig. 2. The extrapolation of the straight lines BC, B′C′ and B″C″ gave nearly the same values of solubility corresponding to the point A in Fig. 2, which were also listed in Table I.

The solubility of *n*-butyl alcohol could be obtained similarly.

In the case of benzene, however, the above method could not be applied directly as the turbidity plotted aginst the concentration of benzene was not linear as shown in Fig. 4. This fact made the extrapolation inaccurate. In this case, however, the addition of ethyl alcohol enabled us to overcome this difficulty. Fig. 5 shows the opacity curve of benzene emulsion using the ethyl alcohol solution of Tween 80 (1.67%) instead of Tween 80 alone as the solubilizer. Further procedures were the same as in the case of iso-amyl

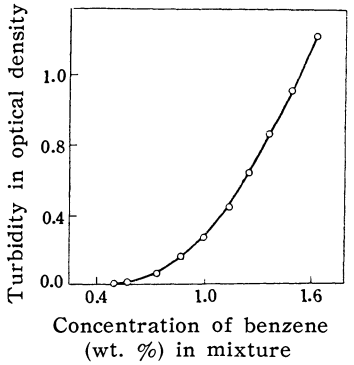

Fig. 4. Relation between turbidity and benzene concentration in 1.07% Tween 80 aqueous solution.

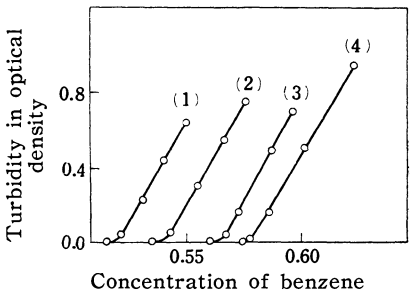

Fig. 5. Relation between turbidity and benzene concentration in aqueous solution of Tween 80-ethyl alcohol mixture. Concentration of 1.67% Tween 80-ethyl alcohol mixture in total mixture: (1) 25.8%, (2) 26.8%, (3) 28.0%, (4) 28.6%.

alcohol. The curve g(c) was thus obtained and shown in Fig. 6.

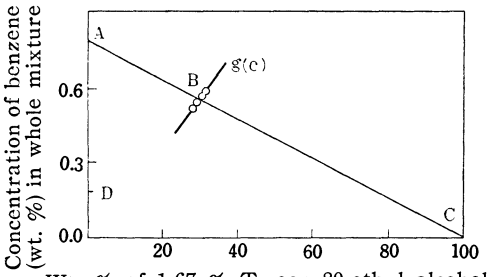

Fig. 6. Solubility of benzene in aqueous solution of Tween 80-ethyl alcohol mixture.
A, Heterogeneous benzene-water mixture obtained by the addition of benzene to the saturate solution
B, End point of titration of heterogeneous system A
C, 1.67% alcohol solution of Tween 80
D, Saturate solution of benzene in water

The saturate solution of benzene expressed as D in Fig. 6 was prepared by the same method as iso-amyl alcohol except for the temperature of shaking being higher than that of the measurement. Actually 0.5244 g. of benzene was added to 92.9926 g. of the saturate solution thus obtained, so as to bring the system in favorable conditions for titration. The point A in Fig. 6 represents the composition of the heterogeneous system thus obtained which was titrated with the solution C, namely 1.67% alcohol solution of Tween 80 containing no water. Now, the titration easily went on just as in the case of iso-amyl alcohol and the point A was obtained similarly. From the composition of A, the solubility of benzene in water could be obtained by subtracting the excess concentration of benzene added to the saturate solution. Solubility data for *n*-butyl alcohol and benzene were also listed in Table I.

TABLE I

Substance	Temperature	Solubility in Water (wt. %)		Reference	
Iso-amyl alcohol	30.1°C	2.587 2.565 2.577	2.57±0.01	2.56 2.31	(30°C)[5] (29°C)[6]
Benzene	20.0°C	0.137		0.179	(25°C)[2]
	25.0°C	0.180		0.174	(25°C)[3]
				0.1865	(25°C)[4]
n-Butyl alcohol	30.0°C	7.01		7.08	(30°C)[7]

2) R. L. Bohn and W. F. Claussen, *J. Am. Chem. Soc.*, **73**, 1571 (1951).
3) L. J. Andrews and R. M. Keefer, *J. Am. Chem. Soc.*, **71**, 3645 (1949).
4) Landolt-Börnstein, "Physikalische-Chemisch Tabellen", IIIA, 667 (1935).
5) I. A. Kablukov and V. T. Malischeva, *J. Am. Chem. Soc.*, **47**, 1553 (1925).
6) F. Fontein, *Z. physik. Chem.*, **73**, 212 (1910).
7) Int. Crit. Table, III, p. 388 (1928).

Discussion

As shown in the earlier part of this paper, we proposed a new method of determining a sparlingly soluble solute in water. This method offers advantages in that the process of preparing a saturate solution and that of the determination of a saturate concentration were separated, whereas in other methods such as the determination of the amount of a solute added to a solvent before the turbidity appears, the above two processes are not separated from each other, so the errors are inevitably introduced due to the inaccuracy of the judgement of saturation, especially in the case where the solute shows a tendency to be dispersed colloidally. The accuracy of our method is satisfactory compared with that of the other method as shown in Table I. We should like further to draw attention to the curve f(c) in Fig. 2 which shows a distinct minimum in solubility of iso-amyl alcohol in Tween 80 solution. Such a behavior is interesting in relation to the mechanism of surfactant in solution from the standpoint of solubilizate versus surfactant interaction. But we need further study for a more precise discussion.

Summary

1. The solubility of iso-amyl alcohol, *n*-butyl alcohol and benzene were determined by the titration using the surfactant, Tween 80.

2. In the case of iso-amyl alcohol and *n*-butyl alcohol, the relation between the turbidity and the quantity of solute in surfactant solution is linear, and the solubility limits are both lower than the solubilities in pure water in the dilute region of the surfactant. This makes the determination of their solubility easy and accurate both in pure water and aqueous solution of the detergent.

3. The above method cannot be applied directly for the determination of the solubility of benzene. Ethyl alcohol–Tween 80 mixture is used instead of Tween 80 to overcome this difficulty.

4. The solubilities obtained by this method are accurate enough compared with other methods, in the case of iso-amyl alcohol and *n*-butyl alcohol, possible error being estimated to be 0.4%. In benzene, the error is somewhat larger, but is in good agreement with the values of the literature.

Chemical Institute, College of Arts and Sciences, Chiba University, Chiba and Department of Chemistry, Faculty of Science, Tokyo Metropolitan University, Tokyo

A New Spectrophotometric Method for the Determination of Small Amounts of Chloride Using the Mercuric Thiocyanate Method

By Iwaji IWASAKI, Satori UTSUMI, Ken HAGINO and Takejiro OZAWA

(Received February 28, 1956)

Introduction

A more rapid and accurate method for the determination of a very small amount of chloride ion in natural waters such as rain water, river waters, etc., has been desired.

An indirect colorimetric determination of chloride using solid silver chromate and diphenylcarbazide has been reported[1]. A small amount of chloride can also be estimated by the effect on suppression of reaction of mercuric ion with diphenylcarbazide or diphenylcarbazone[2]. K. Kuroda and E. B. Sandell[3] have studied a photometric method for the determination of chloride which is based on the formation of a colloidal suspension of silver sulfide by treatment of the ammoniacal solution of silver chloride with sulfide. Recently, chloride ion has been determined colorimetrically after exchanging for iodate ion with granular silver iodate in a column[4].

In the previous paper[5], the authors presented a new rapid colorimetric method for the determination of low concentrations of chloride using a very slightly ionizing mercuric thiocyanate solution and an iron alum solution. Chloride ion reacts with $Hg(SCN)_2$ to form $HgCl_2$, $HgCl_4^{2-}$, and SCN^-, which gives a reddish-orange color with ferric ion in nitric acid solution. The orange color of ferric thiocyanate ($FeSCN^{2+}$) formed in the solution is determined colorimetrically. The colored solution obtained has an absorption maximum at 460 mμ, and this colored substance is not extracted with ethyl ether[6]. The calibration curves (absorbance-concentration curves) do not show a linear relationship with the concentrations of chloride.

Lately we have found that the calibration curves of chloride conform to Beer's law at concentrations up to 50 p. p. m. when dioxane is used in the determination of chloride by the mercuric thiocyanate method. This improved spectrophotometric method for the determination of chloride, which is satisfactory for the range of 0.05–80 p. p. m. of chloride, is described in this report.

Experiments and Discussion

Reagents.—*Standard chloride solution* (1,000 p. p. m. Cl^-): 2.103 g. of potassium chloride (guaranteed reagent) was dissolved in 1 l. of distilled water. Solutions of suitable concentrations were prepared by diluting this stock solution.

Potassium Thiocyanate Solution.—About 10 g. of potassium thiocyanate (guaranteed reagent) was dissolved in 1 l. of water. This solution (about 0.1 M) was then standardized by the Volhard's method. Solutions of suitable concentrations were prepared by diluting this standard solution.

Solid Mercuric Thiocyanate.—When a potassium thiocyanate solution is added, drop by drop, to a mercuric nitrate solution containing nitric acid, using iron alum as an indicator, white crystalline $Hg(SCN)_2$ is precipitated. This precipitate is filtered off through a glass filter, and washed with cold water, and then dried in the air. Utilizing this procedure, solid mercuric thiocyanate was prepared. (This compound is stable for a long time.)

1,4-Dioxane (b.p. 102°C, m. p. 11.3°C, Dielectric const. 2.1).—Dioxane (guaranteed reagent) was used after being purified. Purification was accomplished by distilling with an adequate amount of metallic sodium, and collecting at 102°C.

*Mercuric thiocyanate solution (A)** was prepared by dissolving 100 mg. of mercuric thiocyanate in 100 cc. of a mixed solvent consisting of 9 volumes of dioxane and 1 volume of absolute ethyl alcohol. The freezing point of this mixed solvent was about 4°C. Mercuric thiocyanate solution (B) was prepared by dissolving 100 mg. of mercuric thiocyanate in 100 cc. of a mixed solvent consisting of 2 volumes of dioxane and 1 volume of alcohol. Mercuric thiocyanate solution (C)[5] was prepared by dissolving 300 mg. of mercuric thiocyanate in 100 cc. of alcohol. All these mercuric thiocyanate solutions mentioned above were stable.

1) F.D. and C.T. Snell, "Colorimetric Methods of Analysis", (1949) Vol. II, p. 715; K. Imai, *J. Japan Biochem. Soc.*, 20, 147 (1948).

2) Yu. Yu. Luré and Z. V. Nikoraeva, *Zavodskaya Lab.*, 12, 161 (1946); *C. A.*, 40, 7070 (1946); S.M. Drachev and F.I. Ginzburg, *J. Applied Chem. (U.S.S.R.)*, 11, 879 (1938); F. E. Clark, *Anal. Chem.*, 22, 553 (1950).

3) K, Kuroda and F.B. Sandell, *Anal. Chem.*, 22, 1144 (1950).

4) J.L. Lambert, S.K. Yasuda, *Anal. Chem.*, 27, 444 (1955).

5) I. Iwasaki, S. Utsumi and T. Ozawa, This Bulletin, 25, 226 (1952). S. Utsumi, *J. Chem. Soc. Japan (Pure Chem. Sect.)*, 73, 835, 838 (1952).

6) I. Iwasaki and H. Shimojima, ibid., 76, 749 (1955). H.S. Frank and R.L. Oswalt, *J. Am. Chem. Soc.*, 69, 1321 (1947).

* Mercuric thiocyanate is difficultly soluble in cold water and dioxane, but more soluble in ethyl alcohol.

Iron alum solution (A) was prepared by dissolving 8 g. of ferric ammonium sulfate (guaranteed reagent) in 100 cc. of 6 N nitric acid, free from chloride. Iron alum solution (B) was prepared by dissolving 6 g. of ferric ammonium sulfate in 100 cc. of 6 N nitric acid. Iron alum was used as a reagent of ferric ion, because it is easily obtained in the purely crystallized state, free from chloride, whereas ferric nitrate is hygroscopic and often contains chloride.

Apparatus.—Absorption measurements were carried out with a Beckman Model DU spectrophotometer using 10 mm. cells at 460 mμ.

Effect of Dioxane.—The influence of the addition of dioxane upon the colorimetric determination of chloride by the mercuric thiocyanate method was studied. Results obtained are shown in Fig. 1, in which line (I) corresponds to the calibration curve of chloride obtained by the former method[5] reported previously. The experiments were carried out under the following conditions: 10 cc. of the sample solution were pipetted into a test tube equipped with a glass stopper. Then 2 cc. of iron alum solution (B) and 1 cc. of mercuric thiocyanate solution (C) were added. The absorbances were plotted against the concentrations of chloride at 20°C, ten minutes after mixing.

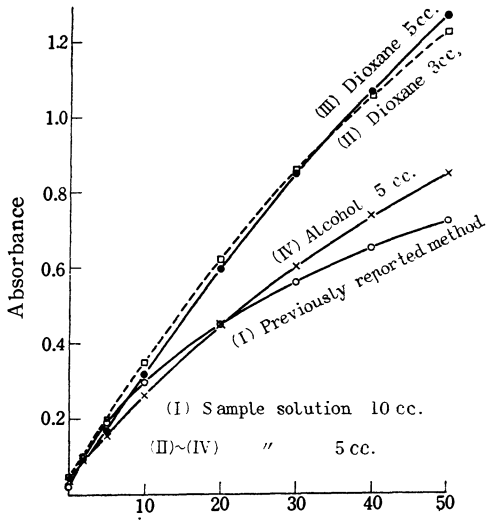

Fig. 1. Absorbance-concentration curves and effect of dioxane and alcohol at 460 mμ, 20°C.

As will be seen in Fig. 1, the calibration curve (I) was not linear with respect to the concentrations of chloride. When 2 cc. of iron alum solution (B), 1 cc. of mercuric thiocyanate solution (C) and then 3 cc. of dioxane were added to 5 cc. of the sample solution, the absorbance- concentration curve shown in the broken line (II) was obtained. When 5 cc. of dioxane, and ethyl alcohol were added respectively instead of 3 cc. of dioxane, the calibration curves corresponding to line (III) and (IV) respectively were obtained.

In this mercuric thiocyanate method, it is clear that the intensity of the color obtained is markedly affected by the addition of dioxane, but not of alcohol. The calibration curve of line (III) can be seen to conform nearly to Beer's law. After preliminary experiments the authors established a new spectrophotometric method available for the determination of chloride over the range of 0.05 to 80 p. p. m. of chloride.

Determination for a Range of 3 to 80 p.p.m. of Chloride.—Procedure (A).—To 2.5 cc. of the sample solution, 1 cc. of iron alum solution (A) and 3 cc. of mercuric thiocyanate solution (A) were added. The absorption measurements were carried out with a Beckman Model DU spectrophotometer using 10 mm. cells ten minutes after mixing.

Absorption Spectral Curves.—The absorption of the colored solutions (blank test, 10 and 30 p. p. m. Cl^-) was measured over the range of 390–600 mμ; absorbance was plotted against wave length in Fig. 2, in which there is one absorption maximum at 460 mμ. In addition, the solution has an absorption below 430 mμ, owing to the formation of a yellow ferric sulfate complex ion.

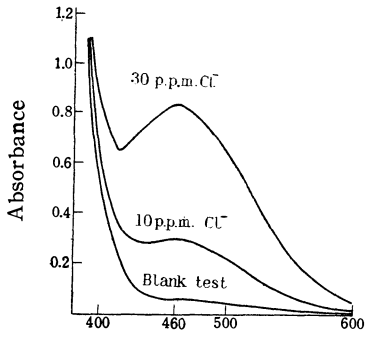

Fig. 2. Absorption Curves.

Time of Standing and Stability of Color.—Constant absorbance values of colored solutions (blank test, 10 and 30 p. p. m. Cl^-) were obtained after then minutes at room temperature (about 10°C). The color of the solution was stable. The results obtained are shown in Table I.

TABLE I

TIME OF STANDING AND STABILITY OF COLOR AT ABOUT 10°C

Time	Absorbance		
	Blank test	10 p. p. m. Cl^-	30 p. p. m. Cl^-
2 min.	0.065	0.285	0.824
3 〃	0.055	0.280	0.810
4 〃	0.051	0.275	0.801
5 〃	0.050	0.272	0.799
10 〃	0.050	0.272	0.791
15 〃	0.050	0.272	0.791
1 hr.	0.050	0.273	0.793
3 〃	0.050	0.272	0.793

Calibration Curves and Effect of Temperature.—The calibration curves shown in Fig. 3 were prepared by the Procedure (A) mentioned

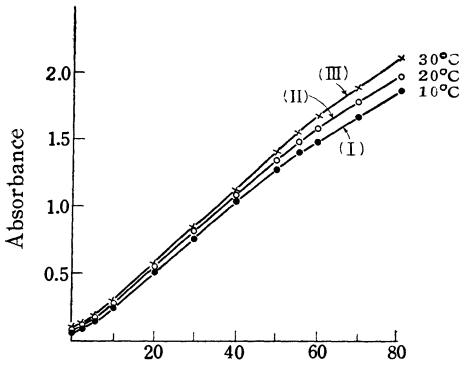

Concentration of chloride P. P. M.

Fig. 3. Calibration curves and effect of temperature, at 460 mμ.

above using standard chloride solutions of known concentrations at 10°, 20° and 30°C. As will be seen in Fig. 3, the calibration curves show good agreement with Beer's law over the concentration range of 2–50 p. p. m. of chloride. But, for the concentrations higher than 50 p. p. m. of chloride, and lower than 2 p. p. m., the calibration curves do not show linear relation-ships, curving very slightly as shown in Fig. 3.

Since absorbance is considerably affected by temperature, as shown in Fig. 3, it is necessary to measure the absorbance under the same conditions of temperature in order to determine the concentration of chloride with good accuracy by this method. For the determination of concentrations lower than 3 p. p. m. Cl^-, the Procedure (B) described later in this report should be used.

A faintly colored blank solution was obtained when redistilled water was treated. The absorbance of the blank test was small, but constant, and was probably due to the dissociation of mercuric thiocyanate. The calibration curves shown in Fig. 3 were reproducible within ±1% for the range of 5–80 p. p. m. Cl^-.

Effect of the Reagent Concentrations.—The absorbance was affected by the amounts of mercuric thiocyanate solution and the concentrations of iron alum reagents. The experimental results obtained are shown in Fig. 4, in which line (I) corresponds to the calibration curve for line (II) in Fig. 3, and lines (II) and (III) show the experimental results obtained under the following conditions: for line (II), to 2.5 cc. of sample solution, 1 cc. of iron alum solution (B) and 3 cc. of mercuric thiocyanate solution (A) were added; for line (III), to 2.5 cc. of sample solution, 1 cc. of iron alum solution (A) and 2.5 cc. of mercuric thiocyanate solution (A) were added.

As will be seen in Fig. 4, it is necessary to use 3 cc. of mercuric thiocyanate solution (A) for 2.5 cc. of the sample solutions. On the other hand, when the amount of iron alum is increased, the color obtained is deeper, as in the case reported previously[5].

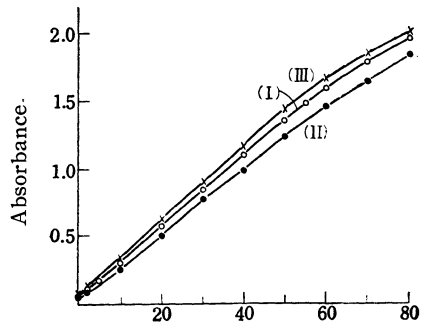

Concentration of chloride P. P. M.

Fig. 4. Absorbance-concentration curves. Effect of the reagent concentration at 460 mμ. 20°C.

(I) $Hg(SCN)_2$ Soln. (A) 3 cc.
Fe-Alum Soln. (A) 1 cc.
(II) $Hg(SCN)_2$ Soln. (A) 3 cc.
Fe-Alum Soln. (B) 1 cc.
(III) $Hg(SCN)_2$ Soln. (A) 2.5 cc
Fe-Alum Soln. (A) 1 cc.

In this method the color intensity was slightly affected by the concentration of nitric acid. The effect of the concentration of nitric acid in iron alum reagent on this colorimetric method was observed in the presence of 30 p. p. m. of chloride at 15°C. The results obtained are shown in Table II.

TABLE II

EFFECT OF THE CONCENTRATION OF NITRIC ACID

Concns. of HNO_3 (N)	5	5.5	6	6.5	7
Absorbance	0.760	0.788	0.815	0.836	0.860

When the concentration of nitric acid was increased, the reddish-orange color became deeper.

Color Reaction.—In order to explain this color reaction some experiments were carried out. The results obtained are shown in Fig. 5, in which the line (I) corresponds to the calibration curve (II) in Fig. 3, and the other lines are obtained under the following conditions: for broken line (II), to 2.5 cc. of standard thiocyanate solutions of known concentrations, 1 cc. of iron alum solu-

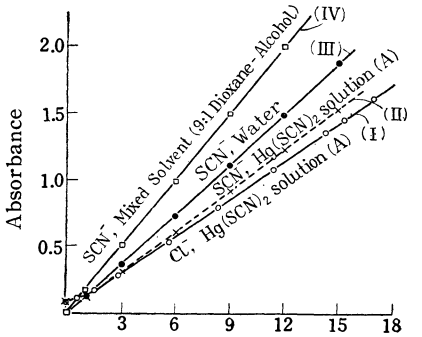

Concentration of Cl^- or SCN^- 10^{-4} M

Fig. 5. Absorbance-concentration curves. Equilibrium of the color reaction.

tion (A) and 3 cc. of mercuric thiocyanate solution (A) were added; for line (III), to 2.5 cc. of the thiocyanate solution 3 cc. of distilled water and 1 cc. of iron alum solution (A) were added; and for line (IV), to 2.5 cc. of the thiocyanate solution, 1 cc. of iron alum solution (A) and 3 cc. of mixed solvents consisting of 9 volumes of dioxane and 1 volume of alcohol were added. The absorbances were plotted against the concentrations in 10^{-4} moles per liter at 20°C.

The calibration curve for chloride (line (I)) falls approximately along the calibration curve for thiocyanate (line (II)) containing the same amounts of mercuric thiocyanate solution. This fact indicates that the following reaction takes place from left to right almost completely.

$$2Cl^- + Hg(SCN)_2 \rightleftarrows HgCl_2 + 2SCN^-$$

The liberated SCN^- reacts with Fe^{3+} to give a reddish-orange color, as follows:

$$SCN^- + Fe^{3+} \rightleftarrows FeSCN^{2+}$$

The fact that the orange color of ferric thiocyanate formed in the solution becomes stronger in the presence of dioxane seems to indicate that the equilibrium of the above equation is largely shifted from left to right (lines (III) and (IV)). On the other hand, the difference between line (II) and (IV) seems to be due to the formation of mercuric thiocyanate complex ion[7] as follows:

$$n\,SCN^- + Hg(SCN)_2 \rightleftarrows [Hg(SCN)_{2+n}]^{n-}$$

Determination for a Range of 0.05 to 5 p.p.m. of Chloride.—The determination of lower concentrations of chloride was carried out by the following Procedure (B).

Procedure (B). Five cubic centimetres of the sample solution were pipetted into a test tube equipped with a glass stopper. Then 1 cc. of iron alum solution (A) and 1.5 cc. of mercuric thiocyanate solution (B) were added.

Calibration Curves and Effect of Temperature.—The calibration curves, (I) and (II) in Fig. 6, were prepared by Procedure (B) described above using standard chloride solutions of known concentrations at 15°C and 25°C respectively. Line (III) corresponds to the calibration curve obtained by the previously reported method[5] at 15°C (i.e., to 10 cc. of the sample solution, 2 cc. of iron alum solution (B) and 1 cc. of mercuric thiocyanate solution (C) were added). These calibration curves in Fig. 6 show good agreement with Beer's law over the range 0.05–3 p.p.m. of chloride.

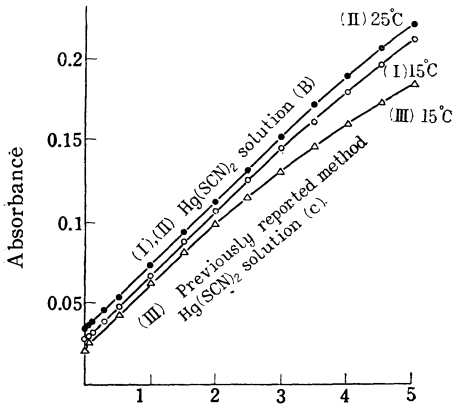

Concentration of chloride, P. P. M.

Fig. 6. Calibration curves for the lower range of chloride (I—II).

These curves were affected slightly by temperature as will be seen in Fig. 6. The absorbance of the blank test was very small, but constant. The lowest concentration of the standard solution whose color could be distinguished from that of the blank test was 0.05 p.p.m. Cl^- (1.4×10^{-3} M). The calibration curves shown in Fig. 6 were reproducible within ±0.05 p.p.m. Cl^-. In this method a better result will be obtained by the use of 100 mm. cells instead of 10 mm. cells. Especially in the determination of lower concentrations of chloride, the operator must be properly careful of contamination from outside.

Effect of Various Ions.—Bromide, iodide, cyanide, sulfide and thiosulfate react with $Hg(SCN)_2$ solution to liberate SCN^- ion, which gives a reddish-orange color with ferric ion in the same way as chloride[8], even in this improved method. Among the substances which interfere intrinsically with this method, sulfide, thiosulfate, cyanide, and thiocyanate are destroyed by heating with hydrogen peroxide in alkaline solution[9].

The effect of various ions except the interfering ions described above on this method (Procedure A) was examined in the presence of 30 p.p.m. Cl^- and blank test. Some of the results obtained are given in Table III.

TABLE III

EFFECT OF IONS ON PROCEDURE (A) AT 15°C

Substance	Concentration	Absorbance	
None	p.p.m. 0	Blank test 0.053, 0.053	30 p.p.m. Cl^- 0.815, 0.813
$NaNO_3$	85,000 (1 M)	0.070	0.907
〃	8,500 (0.1 M)	0.053	0.818
SO_4^{2-}	5,000	0.052	0.738
〃	500	0.053	0.813
H_2O_2	1,000 (0.1%)	0.053	0.813
PO_4^{3-}	100	0.048	0.772
〃	10	0.053	0.815
F^-	100	0.052	0.793
〃	10	0.053	0.807
Ca^{2+}	1,000	0.053	0.818
Al^{3+}	1,000	0.053	0.815
Cu^{2+}	100	0.053	0.813
Ba^{2+}	100	0.053	0.818
Cr^{3+}	100	0.053	0.815
Fe^{3+}	100	0.054	0.821

7) F. Gallais and J. Mounier, *Compt. rend.*, **223**, 722, 790 (1946).

8) S. Utsumi, *J. Chem. Soc. Japan (Pure Chem. Sect.)*, **73**, 889 (1952); ibid., **74**, 32, 301 (1953).

9) S. Utsumi, ibid., **74**, 608 (1953); I. Iwasaki, S. Utsumi and T. Ozawa, This report was presented at a symposium of the Japan Soc. for Anal. Chem. May, 1953.

Substance	Concentration	Absorbance	
None	p. p. m.	Blank test	30 p. p. m. Cl^-
	0	0.053, 0.053	0.815, 0.813
Fe^{2+}	100	0.053	0.818
Ni^{2+}	100	0.052	0.813
Co^{2+}	100	0.053	0.815
SO_3^{2-}	100	0.053	0.813
NO_2^-	100	0.053	0.815
ClO_4^-	100	0.053	0.815
ClO_3^-	100	0.052	0.813
BrO_3^-	100	0.777	1.523
〃	10	0.103	0.903
IO_3^-	100	0.053	0.886
〃	10	0.053	0.815
$[Fe(CN)_6]^{4-}$	10	0.255	0.824
〃	1	0.063	0.815
$[Fe(CN)_6]^{3-}$	10	0.130	0.830
〃	1	0.060	0.815

The experimental results are summarized as follows:

(1) Na^+, K^+, Mg^{2+}, Ca^{2+}, Al^{3+}, acetate and silicate (calculated as SiO_2) ions have no effect even when found to be of the magnitude of 1,000 p. p. m.

(2) Cu^{2+}, Sr^{2+}, Ba^{2+}, Zn^{2+}, Cd^{2+}, Pb^{2+}, Ti^{4+}, Ce^{3+}, Th^{4+}, Bi^{3+}, Cr^{3+}, Mn^{2+}, Fe^{3+}, Fe^{2+}, Ni^{2+}, Co^{2+}, SO_3^{2-}, AsO_4^{3-}, BO_2^- and $C_2O_4^{2-}$ ions do not interfere when the concentration is as high as 100 p. p. m. Since a precipitate is formed in the case of barium, it should be centrifuged off in order to remove it. The color of Cu^{2+}, Cr^{3+}, Ni^{2+} and Co^{2+} ions is negligible up to 100 p. p. m. in this method.

(3) Sodium nitrate** does not interfere when present even in the amount of 0.1 M (8,500 p. p. m.); but at a very large concentration higher results are obtained.

(4) 500 p. p. m. of sulfate do not interfere; but 5,000 p. p. m. give lower results probably due to the reaction with ferric ion.

(5) 10 p. p. m. of fluoride and phosphate do not interfere; but 100 p. p. m. give lower results probably owing to the formation of complex ion with ferric ion.

(6) The presence of nitrite at the concentration of 100 p. p. m. does not interfere at 15°C, but at 30°C a slight interference is observed.

(7) Hydrogen peroxide does not interfere at 0.1% (1,000 p. p. m.).

(8) 100 p. p. m. of chlorate and perchlorate, and 10 p. p. m. of iodate do not interfere; but 10 p. p. m. of bromate and 100 p. p. m. of iodate give higher results.

(9) Ferrocyanide and ferricyanide interfere when present in small amounts.

** For the determination of chloride in silicate rocks, large amounts of sodium nitrate are formed[10].

As mentioned above, interfering substances are few. Bromide, iodide, cyanide, thiocyanate, sulfide, thiosulfate, bromate, ferrocyanide and ferricyanide interfere; but they are not usually present in natural waters in such concentrations as would give a serious error. This rapid and accurate spectrophotometric method for the determination of a small amount of chloride can possibly be applied widely to the determination of chloride in rocks[10], natural waters[11] and metals[12].

Summary

A new spectrophotometric method suitable for the determination of a small amount of chloride using iron alum solution in nitric acid solution, and mercuric thiocyanate solution in a mixture of dioxane and alcohol solution has been established.

The calibration curves conform to Beer's law at concentrations up to 50 p. p. m. of chloride. The calibration curves are reproducible within ±1% for the range of 5–80 p. p. m. Cl^- (Procedure A), and within ±0.05 p. p. m. for the range of 0.05–5 p. p. m. Cl^- (Procedure B). As the calibration curves are affected by temperature, it is necessary to measure the absorbance always under the same conditions of temperature in order to achieve good accuracy.

The colored solution is stable. A very small volume of the sample solution such as 5 cc. or 2.5 cc. is good enough for the determination. Interfering substances are few, because this method is carried out in acid medium. Br^-, I^-, CN^-, SCN^-, S^{2-}, $S_2O_3^{2-}$, BrO_3^-, $[Fe(CN)_6]^{4-}$ and $[Fe(CN)_6]^{3-}$ interfere, but usually they are not present in natural waters in concentrations that would give a serious error.

This simple method is suitable for rapid determinations, because it is unnecessary to control pH or filter the precipitate. It is suggested that this method can be widely applied to the determination of chloride in waters, rocks, etc.

Laboratory of Analytical Chemistry and Geochemistry, Tokyo Institute of Technology, Tokyo

10) I. Iwasaki, T. Katsura and N. Sakato, *J. Chem. Soc. Japan (Pure Chem. Sect.)*, **76**, 1116 (1955).

11) I. Iwasaki, T. Nitta and T. Tarutani, ibid., **74**, 1003 (1953).

12) I. Iwasaki, T. Tashiro and T. Ozawa, *Japan Analyst*, 5, 275 (1956).

Molecular Structure Investigations by Electron Diffraction Method. II. The Molecular Structure of Ethylene Chlorohydrin

By Mashio YAMAHA

(Received December 7, 1955)

Introduction

Many physico-chemical investigations such as the dipole moment measurements by C. T. Zahn[1], I. Watanabe[2], the spectroscopic studies by Kohlrauch and Ypsilanti[3], R. M. Badger[4,5], S. Mizushima et al[6,7] have shown that the ethylene chlorohydrin molecule in the gaseous state consists of two rotational isomers. Badger[5] investigated the temperature variation of the infrared and Raman spectra in relation to the intramolecular hydrogen, bonding and established the fact that, in the gaseous state, at room temperature, the molecule consists of a *trans* form and another stable one. Watanabe concluded that the latter stable form of this molecule is one for which the rotational angle φ (see Fig. 1) is $0\sim60°$.

However, the interatomic distances, C–C, C–O, C–Cl, Cl″···O etc., cannot be determined directly by measurement of dipole moments or other spectroscopic methods. Recently, O. Bastiansen[8] determined them directly by means of an electron diffraction method using a rotating sector, as follows: C–C=1.54; C–Cl=1.76; C–O=1.43; and O″···Cl=3.17 Å. Consequently, the *gauche* form of this molecule is characterized by $\varphi=74°$.

In the discussion of the molecular structure of ethyl alcohol by M. Kimura[9], the interatomic distance C–O in this molecule was considered greater than in the case of the normal covalent bond, namely, 1.42 Å. In this report, the author has investigated the molecular parameters of ethylene chlorohydrin, and has also tried to investigate, if possible, the height of the potential barrier of internal rotation, including hydrogen bonding, in this molecule.

Experimental Procedure

(1) *Sample.* — The commercial reagent of ethylene chlorohydrin, colored slightly yellowish, after dehydrated sodium sulphate had been immersed in it for many days, was distilled several times with a flask having a 5–10 cm. long rectifying column. The colorless viscous distillate (b. p. 128°–128.5°C) was obtained for the experiment.

(2) Details of the apparatus and methods of measurement are omitted, because they are the same as in our previous report[10].

Apparatus: Hot cathode, vertical type.
Camera length: 91 to 110 mm.
Wave length: 0.053–0.056 Å

The sample was spurted from the nozzle at room temperature, 25°–35°C.

The diffraction pattern thus obtained is comparatively indistinct and yet eleven diffracted

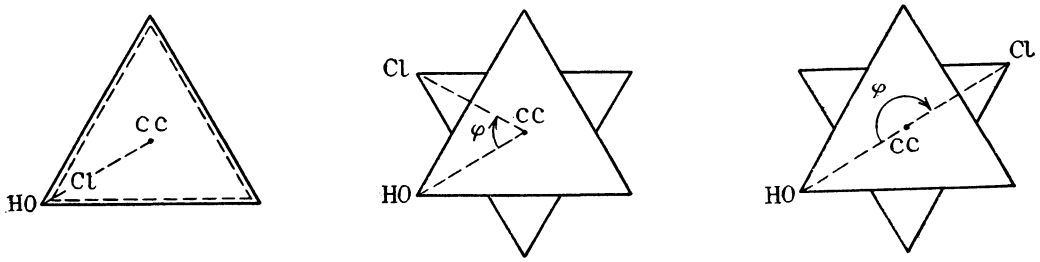

Cis form $\varphi=0°$ *Gauche* form $\varphi=60°$ *Trans* form $\varphi=180°$

Fig. 1. Schematic models showing the rotational angle φ about the C-C bond for ethylene chlorohydrin molecule.

1) C.T. Zahn, *Trans. Acad. Soc.*, **30**, 804 (1934).
2) I. Watanabe, *Riken Iho* (in Japanese), **20**, 838 (1941).
3) K.W. Kohlrauch and G.P. Ypsilanti, *Z. Physik. Chem.*, **B 29**, 274 (1935).
4) R.M. Badger and S.H. Baner, *J. Chem. Phys.*, **4**, 711 (1936).
5) L.R. Zumwalt and R.M. Badger, *J. Chem. Phys.*, **7**, 87 (1939); *J. Am. Chem. Soc.*, **62**, 305 (1940).
6) S. Mizushima, Y. Morino and T. Kubota, This Bulletin, **14**, 15 (1939).
7) S. Mizushima, Y. Morino and S. Nakamura, *Sci. Papers I.P.C.R.*, **37**, 205 (1940).
8) O. Bastiansen, *Acta Chem. Scand.*, **3**, 415 (1949).
9) M. Kimura, *J. Chem. Soc. Japan* (in Japanese), **71**, 18 (1950).
10) T. Yuzawa and M. Yamaha, This Bulletin, **26** (No. 8), 414 (1953).

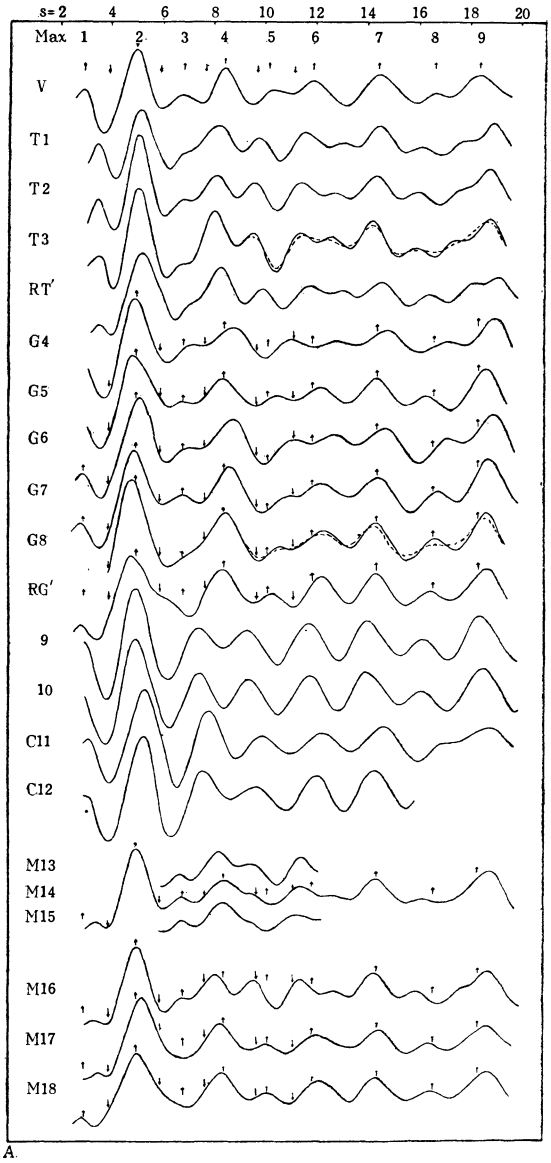

Fig. 2. Visual (V) and theoretical intensity curves for ethylene chlorohydrin molecule. (cf. Table I and II). (The curves are shown in the s-scale).

halos have been measured by means of a visual method up to the limit of $q<80$. The measured *s-values* (or *q-values*) of the maxima and minima are shown in Table I, and the visual intensity curves shown at the top of Figs. 2 and 3.

Molecular Models

In constructing the assumed molecular models, the combinations of various molecular parameters have been considered and are given in Table II. First, the models were divided into several groups according to the rotational equilibrium positions about the

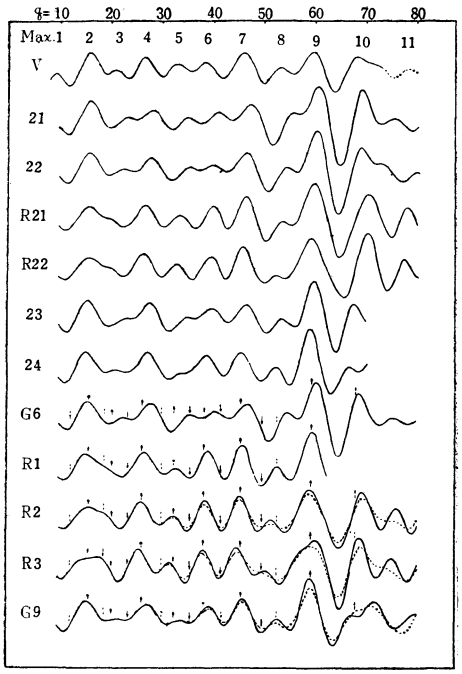

Fig. 3. Visual (V) and theoretical intensity curves for ethylene chlorohydrin molecule. (cf. Table II). (The curves are shown in the q-scale).

C-C bond: that is, the groups of *trans*, *gauche* and *cis* forms including the slight variations of φ close to each form (see Fig. 1). In each groups, the interatomic distance C–O was varied from 1.43 to 1.49 Å, and the valence angles $\angle$CCCl and $\angle$CCO were varied within the range 109.5° to 112°, assuming C–H=1.09 and C–C=1.54 Å. Then assuming the other parameters inclusive of the several combinations of bond lengths, bond angles and rotational angle φ to be constant, the mixtures of *trans* and *gauche* forms were considered (see Fig. 2). Subsequently, the bond length C–C was varied from 1.50 to 1.58 Å. Finally, in better models, the rotational angle φ was varied from 60° to 80° (see Fig. 3).

Intensity Curves

The theoretical intensity curves corresponding to the models mentioned above as calculated by the use of the well-known Pauling formula are given in Fig. 2:

$$I(s)=k\sum_{i}\sum_{j}Z_iZ_j\cdot\sin(sr_{ij})/sr_{ij},$$

where $s=(4\pi\sin\theta/2)/\lambda$; θ, the scattering angle: λ, the wave length; and r_{ij}, the interatomic distance between atoms i and j, and those as calculated by the use of Pauling-Schomaker formula in Fig. 3:

TABLE I

LIST OF MOLECULAR MODELS AND ASSUMED CORRESPONDING MOLECULAR CONSTANTS

(cf. Fig. 2) Other assumed constants: C-C=1.54 Å, C-H=1.10 Å, ∠CCH=109.5°

Groups	Models	(φ°)	∠CCO°	∠CCCl°	C-O (Å)	O″···Cl (Å)
Trans	T1	180	109.5	109.5	1.43	
	T2	〃	112	112	1.43	
	T3	〃	109.5	112	1.49	
	RT′	150	109.5	112	1.46	3.93
Gauche	G4	60	109.5	109.5	1.43	
	G5	〃	112	112	1.43	
	G6	〃	109.5	109.5	1.46	3.03
	G7	〃	109.5	112	1.46	3.09
	G8	〃	109.5	112	1.49	
	RG′	70	109.5	112	1.46	3.15
Forms of $0<\varphi<60°$	9	30	109.5	112	1.43	
	10	15	112	112	1.43	
Cis	C11	0	109.5	109.5	1.43	
	C12	0	112	112	1.43	

TABLE II

LIST OF MOLECULAR MODELS AND ASSUMED CORRESPONDING MOLECULAR CONSTANTS, SHOWING THE PROPORTION OF COEXISTENCE OF TWO DIFFERENT ISOMERS (cf. Fig. 2)

Models	Components of Two Isomer Types	Proportion %	C-O (Å)	∠CCO°	∠CCCl°
M13	*Trans* and *Gauche*	75:25	1.43	109.5	112
M14	〃 〃	50:50	〃	〃	〃
M15	〃 〃	25:75	〃	〃	〃
M16	〃 〃	50:50	1.43	112	112
M17	*Trans* (RT′) and *Gauche* (RG′)	20:80	1.46	109.5	112
M18	〃 〃	50:50	〃	〃	〃

TABLE III

LIST OF MOLECULAR MODELS AND ASSUMED CORRESPONDING MOLECULAR CONSTANTS, SHOWING THE VARIATIONS OF OTHER CONSTANTS φ AND C-C AS COMPARED WITH TABLES I AND II

Other assumed constants: C-O=1.46 Å, C-H=1.10 Å, ∠CCH=109.5°

Models	(φ°)	∠CCO°	∠CCCl°	C-C (Å)	O″...Cl (Å)	q/q_{obs}	Mean dev.
21	60	109.5	109.5	1.50	3.01		
22	60	〃	112	〃	3.05		
R21	70	〃	109.5	〃	3.12		
R22	70	〃	112	〃	3.17		
23	60	〃	109.5	1.58	3.07		
24	60	〃	112	〃	3.14		
G6	60	109.5	109.5	1.54	3.03	1.015	0.020
R1	70	〃	112	〃	3.15	1.001	0.023
R2	75	〃	〃	〃	3.22	0.995	0.009
R3	80	〃	〃	〃	3.28	0.988	0.013
G9	60	112	〃	〃	3.13	1.005	0.023

$$I(q)=k\sum_i\sum_j(Z_iZ_j/r_{ij})\sin(\pi qr_{ij}/10)\cdot\exp(-b_{ij}q^2),$$

where $q=10s/\pi$; and b_{ij}, the temperature factor.

The values of b_{ij}'s are shown in Table V. As regards the factor relating to the interatomic distance $O''\cdots Cl_{gauche}$, whose contribution to

TABLE IV
OBSERVED *s* AND *q-values* AND CALCULATED q/q_{obs} VALUES FOR BEST MOLECULAR MODELS

Max.	Min.	s_{obs}	q_{obs}	q/q_{obs} R1	q/q_{obs} R2
1		(2.93)	(9.23)		
	2′	(3.91)	(12.33)		
2		5.00	15.84	0.953	1.007
	3′	(5.92)	(18.84)	—	—
3		6.83	20.44	0.952	—
	4′	7.70	23.63		
4		(8.42)	(26.22)	1.022	0.995
	5′	9.72	30.06	1.021	0.988
5		10.15	32.31	1.018	0.994
	6′	11.17	35.56	1.004	0.984
6		11.90	38.32	1.019	1.007
	7′		41.66	1.020	1.005
7		(14.42)	45.59	1.005	0.995
	8′		49.67	1.001	0.995
8		(16.67)	52.73	0.998	0.979
9		18.39	59.28	1.004	0.995
		Mean average:		1.001_4	0.995_0
		Mean deviation:		0.023	0.009

the intensity relations is large, the calculation was made according to the method of J. Karle[11] in consideration of the effect of the hindered rotation about the C-C bond. The details are dealt with in a later section.

To the curves T3, G8, R2, R3 and G9, the dotted curves, in which temperature factors were taken into account, are added in Figs. 2 and 3 (see later).

Selection of the Best Model

The theoretical intensity curves of different groups which correspond to the structure of *trans*, *gauche* and *cis* forms are compared with the visual intensity curve V.

(1) In the case of *cis* form, the maximum which corresponds to the minor max. 3 of curve V does not appear and the intensity curve becomes almost sinusoidal up to $s \approx 14$.

In successive variations of the rotational angle φ up to $\varphi = 30°$ from this *cis* position, the *s-value* of each maximum or minimum varies slightly, and the intensity curves still show simple sinusoidal features. This intensity relation is different from the actual measurement (curve V), so that the *cis* group, including the model with $\varphi = 0°$–$30°$, must be rejected.

(2) In comparing cases of the *trans* and *gauche* forms, three maxima appear between max. 4 and max. 7 in the case of the *trans* form, but two maxima appear in the case of the *gauche* form. In the case of the *trans* form, max. 3 accompanies max. 4, but in the visual curve, max. 3 seems to accompany max. 2. In this respect, the intensity relations of the visual curve are similar to those of the *gauche* form.

(3) Special attention was paid to the curves in the *gauche* group, which seem preferable for the present. The *s-values* vary slightly when the valence angle ∠CCCl is changed from tetrahedral to 112°. The *s-values* of max. 4 and max. 7 agree most closely with those of the visual curve when this angle is taken to be 112°.

Further, even when the valence angle ∠CCO is varied from tetrahedral to 112°, the variation of *s-values* is not distinct, because it seems to be obscured by the resultant intensity relation due to the variation of the O″···Cl distance and other distances.

(4) As the C–O distance is extended from 1.43 to 1.49 Å, max. 3 acquires a shelf-like feature, approaches max. 4, and almost disappears as shown in curve G8. Furthermore, the *s-value* for each maximum does not coincide with the actual measurement.

The above-mentioned discussion cannot be made independently in regard to the variations of each parameter. Since no satisfactory result has been obtained thus far as shown in Fig. 2, cases wherein the *trans* and *gauche* forms coexist and cases wherein C–C=1.50 and C−C=1.58 Å have been examined (see Figs. 2 and 3).

(5) The curves in which the *trans* and *gauche* forms are mixed are M13∼M18 of Fig. 2 (see Table II).

The result does not necessarily coincide with the actual measurement, but it shows better agreement. Recently S. Mizushima and collaborators confirmed the co-existence of rotational isomers through the analyses of Raman- and infrared spectra, and our result coincides with theirs in general. The visual intensity curve is close to that of the *gauche* form; so that, in view of the ratio of mixing at room temperature, the *gauche* form may be considered predominant.

(6) Good results have been obtained by taking the co-existence of the *trans* and *gauche* forms into consideration, but, on account of the intensity relation of max. 5 and max. 6 in the actual measurement, the models were not sufficient. Therefore, assuming tentatively that the *trans* and *gauche* forms do not co-exist, that is, that the molecule exists in only one form, further investigations have been made in cases of $\varphi = 70°$, 75°, 80°, and 150° (Fig. 3—the curves G6, R1, R2, R3, G9).

11) J. Karle, *J. Chem. Phys.* **15**, 202 (1947).

Upon varying φ from 70° to 80°, the shelf-like feature appears in max. 2 and 3, but this intensity relation is not apparent in the actual measurement. Max. 5 shifts towards a smaller *s-value* than in the case of the *gauche* form, so as to coincide with the visual curve. This tendency is similar to cases of C–C=1.50 Å, φ=70° (see curves R21 and R22).

O. Bastiansen reported that the rotational angle φ of the *gauche* form has been determined to be 74°. In our investigation, the curve φ=75° seems to show very excellent agreement with the actual measurement (see curve R2 in Fig. 3).

(7) In the cases of C–C=1.50 and 1.58 Å, the curves 21 to 24 of the *gauche* form are shown in Fig. 3. Their intensity relations are mostly not different from those of the *gauche* form in Fig. 2, but the *q-value* of each maximum or minimum changes appreciably. By assuming φ=70°, the *s-values* (*q-values*) of max. 3 and max. 5 and their intensity relations are in better agreement than by assuming the *gauche* form (φ=60°).

Radial Distribution Curve

The radial distribution curve has been calculated by using the following formula:

$$rD(r)=\sum_{q=1}^{q=\max} I(q)\cdot\sin(\pi qr/10)\cdot\exp(-aq^2),$$

where the a is determined to be $\exp(-aq_{\max}^2)=0.1$, $q_{\max}$ being the largest *q-value* observed (about $q_{\max}=80$) in the actual measurement. For the numerical function $I(q)$, the visual intensity curve has been used.

Each maximum (peak) of radial distribution curve (Fig. 4) is interpreted as follows:

1.46 Å=C–O, 1.76 Å=C–Cl,
2.75 Å=C′···Cl, 3.10 Å=O″···Cl_{gauche}.

Maxima other than the above-mentioned are considered to be the superpositions of maxima of corresponding interatomic distances, and they are difficult to separate individually. Further, a maximum, though not sufficiently distinct, appears close to r=3.90 Å, which is supposed to be due to the co-existence of a *trans* form.

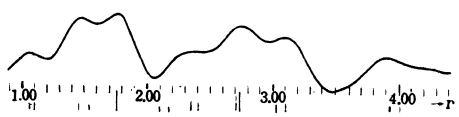

Fig. 4. Radial distribution curve for ethylene chlorohydrin molecule.
The interatomic distance corresponding to each peak is shown under the curve.

The distance which corresponds to the O″···Cl in this *trans*-form seems slightly shorter than the calculated O″···Cl_{trans} (about 4.13 Å). If this distance is considered for the moment to be correct, the following three conditions can be given;

(1) Angle $\varphi<180°$,
(2) Valence angles ∠CCO, and ∠CCCl may be smaller than 112°,
(3) Bond length C–C<1.54 Å.

Calculation of Temperature Dependence Affecting the Intensity Curves

According to the report by J. Karle, in the case of the XY_2C–CY_2X type molecule, the contribution of each atom pair X″···X to the intensity curve is represented by the following formula, in which the variation of the following intensity relation caused by the restricted rotation about the C–C single bond in the vicinity of the "*gauche*" form is taken into consideration:

$$(\cos\Theta)^{1/2}\sin[\tau_1-(\gamma^2\tau_1\cdot\sin^2\Theta/4\beta)+\Theta/2]\times\exp[-\gamma^2\tau_1\cos^2\Theta/4b^2]/\tau_1, \quad (1)$$

where: than $\Theta=\beta\tau_1/b^2$,

$\beta=C_2/[8(C_1-C_2/2)]-3[C_2/(C_1-C_2/2)]^2/32$,
$b^2=\alpha\tanh(h\nu/2kT)$, $\nu=\sigma(V_0/2I)^{1/2}/2\pi$,
$\tau_1=s(C_1-C_2/2)^{1/2}$, $\alpha^2=2\sigma^2\pi^2IV_0/h^2$,
$\sigma=3$,
$I=\sum mr^2=I_1I_2/(I_1+I_2)$,
$\gamma=\sqrt{3}C_2/[4(C_1-C_2/2)]$,
$C_1=(l_1^2+l_2^2)/2$,
$C_2=(l_1^2-l_2^2)/2$, $s=(4\pi\sin\theta/2)/\lambda$*,

and where V_0 is the assumed potential barrier of the hindered rotation about C–C bond. In the case of the ethylene chlorohydrin molecule, V_0 includes the potential

TABLE V
APPROXIMATE TEMPERATURE FACTORS USED FOR EACH ATOM PAIR EXCEPT THAT OF O′′···Cl (For the factor $\exp(-b_{ij}q^2)$ in pauling-schomaker formula

Atom Pairs	r_{ij}(Å)	$(\pi^2/200)<l_{ij}^2>_{av.}$	b_{ij} (used)
C–H	1.10	0.00030	0.00015
C–O	1.43–1.49	0.000145	0
C–C	1.50–1.58	0.000148	0
C–Cl	1.74–1.80	0.000139	0
O′···H	(2.10)	0.00041	0.00026
C′···H	(2.17)	0.00037	0.00022
Cl′···H	(2.35)	0.00053	0.00037
C′···O	(2.44)	0.00022	0.00007
C′···Cl	2.67–2.78	0.00022	0.00007
O″···H_g			0.0008**
O″···H_t			0.0006**
Cl″···H_g			0.0006**
Cl″···H_t			0.0004**

** Roughly assumed values.

TABLE VI

NUMERCIAL VALUES IN FORMULA (1) RELATING TO THE ESTIMATED HINDERED-ROTATIONAL POTENTIAL BARRIER V_0 CORRESPONDING TO THE ATOM PAIR $O''\cdots Cl_{gauche}$ FOR ETHYLENE CHLOROHYDRIN (C–Cl=1.77 Å assumed)

V_0 kcal./mol.	τ_1	γ^2	$\gamma^2/4b^2$	C–O (Å)	∠CCO°	∠CCCl°
3	3.0943 s	0.0439_3	0.00098_7	1.48	109.5	112
5	〃	〃	0.00059_4	〃	〃	〃
10	〃	〃	0.00030_3	〃	〃	〃
20	〃	〃	0.00014_3	〃	〃	〃
3	3.0789 s	0.0408_4	0.00091_8	1.43	〃	〃
10	〃	〃	0.00028_2	〃	〃	〃

energy of hydrogen bonding. (In other words, it includes, in the *gauche* form, the portion of the potential energy caused by the hydrogen bond O–H···Cl.) l_1 is the largest interatomic distance of X''···X (i.e. at the *trans* position) and l_2 the smallest (i.e. at the *cis* position). I_1 and I_2 are the moments of inertia of the atoms X's (that is, atoms O and Cl in our case respectively) around the axis C–C, h is Planck's constant and k is Boltzmann's constant. The computed values τ_1, γ^2 and $\gamma^2/4b^2$ in the case of the ethylene chlorohydrin molecule are shown in Table VI with the assumed values V_0, C–O (Å), ∠CCO° and ∠CCCl°.

Strictly speaking, however, this formula is originally to be applied to the case in which two X-atoms are the same, for instance, the case of 1,2-dichloroethane molecule, which has a threefold symmetry axis, namely $\sigma=3$. When the restricted rotation of this molecular type becomes infinitesimal, that is, the molecule is assumed to be rigid, the formula (1) approaches the form:

$$(\sin sl_{ij})/sl_{ij}. \qquad (2)^*$$

In the strict calculation of the contribution of intensity variations made by the restricted rotation, all atomic distances whose variations contribute to the intensity variations should be taken into account (that is, the distances assigned to the form Y''···Y, Y''···X). Because the two X atoms are O and Cl in our case, that is, not identical, and also because similar calculation regarding the other interatomic distances Cl''···H, O''···H, and H''···H etc., whose contributions may be appreciable but have actually been neglected, the approximation resulting from the application of this principle proposed by J. Karle may be considered comparatively rough for our case of the ethylene chlorohydrin molecule.

* Since the τ_1 in the formula (1) corresponds to sl_{ij} of the formula (2), the part of $(\cos\Theta)^{1/2}\cdot\sin(\cdots\cdots)$ in the former approaches $(\sin sl_{ij})/sl_{ij}$ and the part of the exponential approaches 1 in the latter.

Assuming the approximations in our case to be admissible, the contributions have been calculated for the cases in which V_0 is chosen as 3, 5, 10 and 20 kcal./mol. It has been found that V_0 is about 10 kcal./mol. or more as a result of the comparisons of the observed intensity relations. The dotted lines on the curves T3, G8, G9, R2 have been calculated for the presumed V_0 value. If the value V_0 is assumed to be $V_0<10$ kcal./mol., the curves become of a very much more damped form in the range $q>50$, and it would become impossible to observe clearly the maxima which can actually be detected in this range of our experiment.

Discussion and Summary of Results

From the above considerations, the intensity curves RG', R1, R2, R21, R22, M17 and M18 seem to be nearly satisfactory, and thus the final results of the molecular structure of ethylene chlorohydrin have been obtained as follows:

C–O=1.46 Å±0.02 Å, O''···Cl=3.20 Å±0.06 Å,
∠CCCl=111°±2°, ∠CCO=110°±2°.

The stable form of the internal rotation about the C–C bond seems to be nearly a *gauche* form, that is, the exact position $\varphi=75°$ is regarded as the most reasonable one from the overall intensity relation of diffracted pattern.

These results are considered to agree with those from the electron diffraction method using a rotating sector by O. Bastiansen[8] and also with those from the dipole moment measurement[2].

From the analysis of the radial distribution curve and of the intensity curves, the *gauche* ($\varphi=75°$) and *trans* forms might be supposed to co-exist, and this has been confirmed from the spectroscopic results, but the proportion of these co-existing forms has not been determined from our study.

The fact that the *gauche* form is predominant at room temperature is thought to be caused by the formation of the intramolecular

hydrogen bond[12]. The potential V_0 of the internal hindered rotation including the contribution of the hydrogen bond is presumed to be approximately from 7 to 10 kcal./mol. or more, as judged from the examination of the approximate calculation and of the degree of damping of the experimental intensity curve.

It would be very interesting, but hardly possible, to determine V_0 precisely by an experimental method other than the electron diffraction. Even by the electron diffraction method (using the visual method), it is very difficult to confirm precisely the height of the potential barrier of internal hindered rotation to which the intramolecular hydrogen bond contributes, because the variation of the intensity relation is not so obvious as to allow conclusions in the order of several kcal. per mol.

The author would like to express his gratitude to Professor Y. Morino of the Faculty of Science, Tokyo University, Professor A. Kotera of this University and Assistant Professor M. Kimura of Nagoya University for their very kind guidance, advice and discussions throughout this work.

Chemical Institute, Faculty of Science
Tokyo University of Education
Ootsuka, Tokyo

12) S. Mizushima, T. Shimanouchi, T. Miyazawa, K. Abe and M. Yasumi, *J. Chem. Phys.*, **19**, 1477 (1951), *J. Am. Chem. Soc.* **74**, 1378 (1952). L.P. Kuhn, "The Hydrogen Bond. I. Intra- and Intermolecular Hydrogen Bonds in Alcohols", *J. Am. Chem. Soc.*, **74**, 2492 (1952).

Molecular Structure Investigations by Electron Diffraction Method. III. The Molecular Structure of Ethylene Fluorohydrin

By Masato IGARASHI and Mashio YAMAHA

(Received December 7, 1955)

Introduction

In regard to the molecular structure of ethylene chlorohydrin, many investigations were made as mentioned in the previous report[1]. From electron diffraction studies of this molecule, it was concluded that the structure having the rotational angle $\varphi=75°$ about the C–C bond is predominant at room temperature.

A few structural investigations of ethylene fluorohydrin molecule have been made[2]. In this report the structure has been investigated in relation to the rotationally stable form of this molecule including the problem of intramolecular hydrogen bonding. Moreover, the problem of the bond length C–F of fluorine-substituted compounds is very interesting, and this problem has also been taken into consideration.

Experimental Procedures

(1) Sample.—The ethylene fluorohydrin has been synthesized according to F. W. Hoffmann's method[3].

122.5 g. potassium fluoride (previously dried by heating and powdered) is mixed with 112 g. dried ethylene glycol and 45.5 g. diethylene glycol in a flask, and then heated with continuous stirring at a temperature about 175°–185°C, while 114.5 g. ethylene chlorohydrin is being gradually dropped into the flask. The addition of the chlorohydrin takes about 2.5 hours. Gaseous evaporate is distilled out through a rectifying column filled with small glass balls, the temperature at the top of the column being held constant at 100°C.

Finally, air is blown into the reaction product in the flask, and the distillate is completely distilled. Sodium fluoride is added to the distillate, and the ethylene fluorohydrin thus produced is collected by distillation at a temperature between 95°–105°C (boiling point). As traces of water mixed in the fluorohydrin cannot be removed by distillation, the product is left with dehydrated Glauber's salt (sodium sulfate anhydride) for many days for dehydration before final distillation.

(2) Photograph of Diffracted Pattern.—The apparatus of electron diffraction is the same as that described in the previous report[5], and a horizontal type camera having a camera length of 130 mm. was also used.

Generally the halos of this pattern are lacking in sharpness and are comparatively diffused. Eight diffracted halos have been measured

1) M. Yamaha, This Bulletin publised 29, 865 (1956).
2) For Example, H. D. Cowan, M. Herman, et al., "Raman spectra of single fluorine compounds", *Ind. chim. belge.*, 16, 86 (1951).
3) F. W. Hoffmann, *J. Am. Chem. Soc.*, 70, 2596 (1948).
4) M. Kimura, *J. Chem. Soc. Japan* (in Japanese), 71, 18 (1950).
5) T. Yuzawa and M. Yamaha, This Bulletin, 26, 414 (1953).

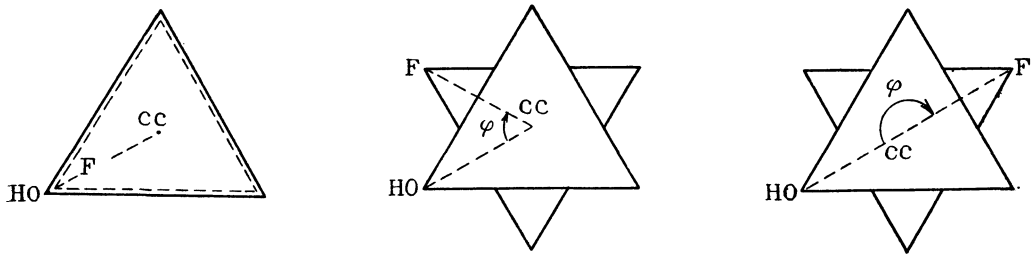

Cis Form $\varphi=0°$ | *Gauche* Form $\varphi=60°$ | *Trans* Form $\varphi=180°$

Fig. 1. Schematic models showing the rotational angle φ about the C–C bond for ethylene fluorohydrin molecule.

TABLE I

THE MOLECULAR MODELS AND CORRESPONDING ASSUMED MOLECULAR CONSTANTS

(cf. Fig. 2)

Groups	Models	C–O (Å)	C–F (Å)	∠CCO°	∠CCF°	O″···F (Å)
Trans	T1	1.43	1.36	109.5	107	3.58
	T2	1.48	1.40	109.5	112	3.71
Gauche	G3	1.43	1.36	109.5	107	2.75
	G4	1.45	1.36	108	109.5	2.75 (C–C=1.50
	G5	1.45	1.36	109.5	109.5	2.77 (C–C=1.50
	G6	1.45	1.33	109.5	109.5	2.80
	G7	1.48	1.40	109.5	107	2.80
Form of $\varphi=30°$	8	1.43	1.36	109.5	107	
Cis	C9	1.43	1.36	109.5	107	2.42
	C10	1.48	1.40	109.5	112	2.56

visually, up to the limit of the range $q<75$ from about 20 photographed plates.

The measured *q-values* of the maxima and minima are shown in Table III, and the visual intensity curve is shown at the top of Fig. 2.

Molecular Models and Theoretical Curves

(1) The theoretical intensity curves for the assumed molecular models have been calculated by the use of the well-known Pauling-Schomaker formula:

$$I(q)=k\sum_i\sum_j(Z_iZ_j/r_{ij})\cdot\sin(\pi qr_{ij}/10)\cdot\exp(-b'_{ij}q^2),$$

where Z_i is the atomic number of the atom i. Z_H is assumed to 1.25.

$q=10\,s/\pi$, $s=(4\pi\sin\theta/2)/\lambda$, θ: the scattering angle,

r_{ij}: the distance between the ith and jth atoms,

λ: the wave length of the electron beam used,

b'_{ij}: the temperature factor for the atom pair i–j.

(2) The assumed molecular models corresponding to the theoretical intensity curves in Figs. 2 and 3 are tabulated in Tables I and II. In constructing the models, the bond distance C–H=1.09 Å and the angle ∠CCH=109.5° are assumed.

The models are divided into several groups according to the rotational equilibrium positions about the C–C bond, that is, the *trans*, *gauche*, the form of $\varphi=30°$ and *cis* groups (see Fig. 1). Secondly, in each group, the bond length C–O varies from 1.43 to 1.48 Å, C–F from 1.33 to 1.40 Å, and ∠CCF from 107° to 112°. Thirdly, in the case of the *gauche* group, the angle φ varies from 30° to 75°. In this case, the other parameters are assumed to be C–C=1.54, C–O=1.43, C–F=1.36 Å and ∠CCF=∠CCO=109.5°.

The value b_{ij}'s used for each atom-pair are shown in Table VI.

TABLE II

THE MOLECULAR MODELS AND CORRESPONDING ASSUMED MOLECULAR CONSTANTS IN REGARD TO THE VARIATION OF ANGLE φ

C–C=1.54 Å, C–O=1.43 Å, C–F=1.36 Å and ∠CCF=∠CCO=109.5 are assumed constantly

Models	φ°	O″...F(Å)
A	75	2.94
B	68	2.88
C	60	2.80
D	45	2.67
E	38	2.62
F	30	2.56

TABLE III

OBSERVED q-VALUES AND CALCULATED q/q_{obs}. VALUES FOR THE BETTER MOLECULAR MODELS

Max.	Min.	q_{obs}	q/q_{obs} G4	G5	B	C
1		(10.87)	(0.892)	—	—	—
	2′	(14.37)	(0.905)	—	(0.891)	(0.898)
2		18.99	0.995	1.006	0.995	0.979
	3′	24.80	1.008	0.980	0.996	1.008
3		29.39	1.034	1.028	1.014	1.044
	4′	33.39	(1.045)	—	0.994	—
4		36.09	1.006	—	0.975	—
	5′	39.56	1.001	0.996	0.998	1.001
5		44.17	0.998	0.994	0.988	1.003
	6′	49.82	0.974	0.965	0.959	0.976
6		52.88	0.970	0.953	0.957	0.978
	7′	56.18	0.970	0.961	0.968	0.981
7		60.19	0.990	0.985	0.995	0.995
	8′	65.58	1.016	1.016	1.019	0.988
8		70.20	1.019	1.010	1.004	0.957
Mean Average:			0.998_4	0.990_4	0.989_4	0.991_8
Mean sq. deviation:			0.019	0.023	0.019	0.022

(3) The radial distribution curve

$$rD(r)=\sum_{q=1}^{q=\max} I(q)\cdot\sin(\pi qr/10)\cdot\exp(-aq^2)$$

is calculated by using the best visual intensity curve V for the function $I(q)$, where the value a is determined to be $\exp(-aq^2_{\max})=0.1$, $q_{\max}$ being about 75.

Comparisons of the Intensity Curves and the Selection of the Best Model

From the comparison of the visual and theoretical intensity curves as shown in Fig. 2 and from the analysis of the radical distribution curve as shown in Fig. 4, the characteristic features for the selection of the best model are specified as follows:

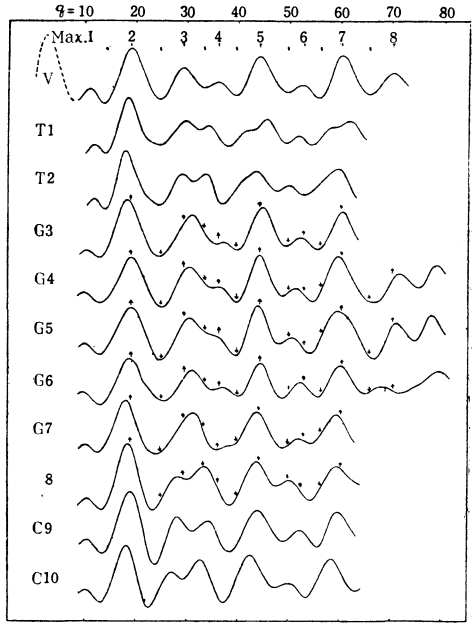

Fig. 2. Visual (V) and theoretical intensity curves for ethylene fluorohydrin molecule. (cf. Table I).

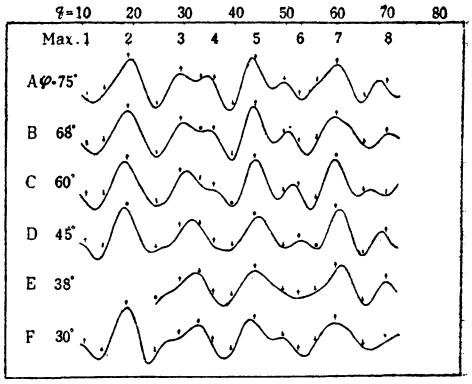

Fig. 3. Theoretical intensity curves showing the variations of models according to the changes of angle φ. (cf. Table II).

TABLE IV

THE DISTANCE O″···F *gauche* IN RELATION TO OTHER MOLECULAR CONSTANTS

C-C (Å)	C-O (Å)	C-F (Å)	∠CCO°	∠CCF°	O″···F (Å)	Models
1.54	1.43	1.36	109.5	109.5	2.75	G3
1.50	1.45	1.36	108	109.5	2.75	G4
1.54	1.43	1.40	109.5	107	2.77	
1.50	1.45	1.36	109.5	109.5	2.77	G5
1.54	1.48	1.36	109.5	107	2.78	
1.54	1.43	1.36	109.5	109.5	2.80	C
1.54	1.45	1.33	109.5	109.5	2.80	G6
1.54	1.48	1.40	109.5	107	2.80	G7
1.54	1.43	1.36	109.5	112	2.84	
1.54	1.43	1.40	109.5	112	2.87	
1.54	1.48	1.36	109.5	112	2.87	
1.54	1.48	1.40	109.5	112	2.89	

TABLE V

THE LIST OF MOLECULAR CONSTANTS OF FLUORINE-SUBSTITUTED COMPOUNDS

Molecules	C-C (Å)	C-F (Å)	C-Cl (Å)	Other Parameters	References
CCl_3F		1.40			6), 7)
$CHCl_2F$		1.40	1.76		6)
CCl_2F_2		1.35	1.74	$\angle FCF = 108°48'$	6), 7)
CH_3F		1.332			8)
CHF_2		1.39 (1.384)			9)
$CClF_3$		1.328	1.740	$\angle FCF = 108°$, $\angle FCF = 110°$	10)
CF_3-COOH		1.36			11)
CH_3-CCl_2F		1.40	1.78	$\angle CCF = 109.5°$, $\angle CCCl = 111°$	12)
CH_3-$CClF_2$		1.37	1.77	$\angle CCF = \angle CCCl = 111°$, $\angle FCF = \angle FCCl = 108°$	12)
CH_3-COF		1.41			13)
CH_3-CF_3	1.45	1.33		$\angle FCF = 108.5°$	14)
	1.53	1.36		$\angle CCF = 112°$, $\angle FCF = 107°$	12)
	1.54	1.33			15)
CF_3-CF_3	1.45 (±0.06)				16)
($CClF_2$-$CClF_2$)	1.45 (ass.)	1.33	1.74		17)

(1) Comparison of each group corresponding to the *trans*, *gauche* and *cis* forms of molecular models.

a) The curves corresponding to the *trans* and *cis* groups are comparatively similar in shape, but the *q-values* of each maximum or minimum are different from one another. Further, the intensity relations of max. 3 and max. 4 differ slightly from one another, and also the shapes of max. 5 and max. 7 are broad with the shelf-like feature in the *trans* form.

b) Max. 3 and the accompanying shelf-like max. 4 are characteristic of the *gauche* group. These features are slightly different from those of the other groups.

So far as the considerations of these features, as compared with those of the visual curve, are concerned, the curves of the *gauche* group appear to be in best agreement (see Fig. 2, curves G4 and G5, and section (4)).

(2) In the *gauche* form, the variation of the O″···F distance, depending upon the variations of the parameters C-O, C-F and $\angle$CCF, is listed in Table IV, (not all of the corresponding curves are shown in Figs. 2 and 3).

The variation of the intensity relation of each curve is not so clear as to determine each allowable range of the respective parameters C-O, C-F and $\angle$CCF independently. However, from the analysis of the radial distribution curve, the distance O″···F seems to be in the vicinity of the value $r = 2.81$ Å (see (4)). The intensity curves for which O″···F is about 2.81 Å are generally satisfactory.

The curve G6, having a smaller distance C-F = 1.33 Å, is hardly satisfactory, because the *q-values* of max. 3, max. 4 and max. 8 clearly show disagreement with those of the visual curve.

(3) When the rotational angle φ is varied from 30° to 75°, the smaller the angle φ becomes, the more max. 3 shifts toward larger *q-values*, accompanied by the disappearance of the shelf-like max. 4 and the later appearance of a small shelf-like maximum at about the position of max. 3 in the visual curve.

Up to a point, the larger the angle φ becomes, the more the intensity relations of all the maxima and minima agree with that of the measured visual curve; but when $\varphi = 75°$, the features of max. 3, max. 4 and max. 7 become similar to those of the *trans* form, that is, max. 4 approaches max. 3, max. 7 becomes broader with a small shelf, and the *q-values* of each maximum shift slightly from those of the visual curve.

6) L. O. Brockway, *J. Phys. Chem.*, **41**, 185, 747 (1937).
7) J. Wouters and M. de Hemptinne, *Nature* (London), **141**, 412 (1938).
8) V. Schomaker and D.P. Stevenson, *J. Am. Chem. Soc.*, **63**, 37 (1941), W. Gordy, J.W. Simmons and A.G. Smith, *Phys. Rev.*, 74, 243 (1948) (Microwave Spectra).
9) S.N. Chosh, R. Trambarulo and W. Gordy, *J. Chem. Phys.*, **20**, 605 (1952) (Microwave Spectra).
10) D.K. Coles and R.H. Hughes, *Phys. Rev.*, **76**, 858 (1949). (Microwave Spectra).
11) J. Karle and L.O. Brockway, *J. Am. Chem. Soc.*, **66**, 574 (1944).
12) R.A. Spurr and W. Shand (private communication to L. Pauling and V. Schomaker).
13) H.A. Skinner, Thesis (Oxford).
14) L.O. Brockway, J.H. Secrist and F. Lucht, Am. Chem. Soc. Meeting, Buffalo, N. Y.
15) W.F. Edgell, *J. Chem. Phys.*, **16**, 1002 (1948) (Microwave Spectra).
16) See, J.R. Nielsen and C.M. Richards, *J. Chem. Phys.*, **16**, 67 (1948).
17) M. Iwasaki, S. Nagase and R. Kojima, *J. Chem. Phys.*, **22**, 959 (1954) (Letter).

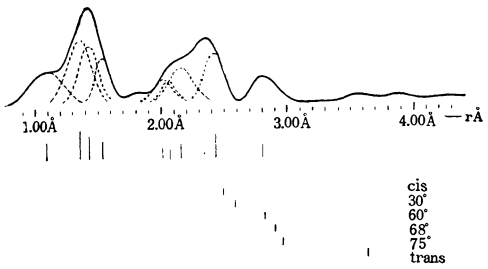

Fig. 4. Radial distribution curve for ethylene fluorohydrin molecule.
Under the curve, the interatomic distance corresponding to each peak is shown by the short line.
O″···F distance which corresponds to the variation of rotational angle φ from 0° (*cis*) to 180° (*trans*) is also shown in due order under the corresponding position of the curve. (cf. Tables I and II).

The model which has the rotational angle about $\varphi=60°$–$70°$ (see Fig. 3, B and C) seems to be the best.

(4) When attention is paid to the radial distribution curve (Fig. 4), two broad peaks appear in the range of $r<2.6$ Å, each of the peaks being the superposition of several interatomic distances: that is, one corresponds to the peaks of the distances C–F, C–O and C–C, and the other to those of F′···H, O′···H and C′...O, etc. However, all the broad peaks cannot be analyzed accurately as peaks of respective component distances.

For the present purpose, particular peaks corresponding to the assumed interatomic distances (for example, C–H, C–F, C–O, C–C, F′···H, O′···H, C′···O, etc.) are indicated by dotted lines on the distribution curve (Fig. 4).

It is expected that the comparatively large peak corresponding to the distance C′···O which is related to the angle ∠CCO and the length C–C appears at the point about $r=$ 2.4 Å. On the distribution curve, there seems to be a corresponding peak at the point $r=$ 2.38 Å. The distance 2.38 Å seems to be slightly smaller than 2.44 Å, the normal distance of C′···O.

The shortening of this distance can be interpreted in two ways: the angle ∠CCO may be slightly smaller than 109.5° (nearly 108°), or the distance C–C may be about 1.50 Å*, in both cases the distance C–O being assumed to be 1.45 Å.

The intensity curves G4 and G5 correspond to the models which have the distance C–C= 1.50 Å. G4, having ∠CCO=108°, and G5, having ∠CCO=109.5°, coincide better with the visual curve than the others in the *gauche* group.

(5) On the radial distribution curve, the peak corresponding to the distance O″···F appears distinctly at about $r=2.81$ Å, and this distance agrees rather well with the O″···F distance of the *gauche* form.

In the cases of C–C=1.50 Å mentioned above (G4, G5), the O″···F distance seems to be slightly smaller than the value 2.81 Å. As a result, the cases of $\varphi>60°$, that is, those which allow slightly longer O″···F, are considered. Upon comparing the curves of the group of the *gauche* form with B and C, the curves B and C are seen to coincide fairly well with the visual one with respect to the intensity relations and *q-values*.

(6) No peak corresponding to the *trans* distance of O″···F appears in the presumable r range in the radial distribution curve, and therefore the *trans* and *gauche* isomers of this molecule hardly seem to co-exist.

(7) In the curves A to F in Fig. 3, the effects of temperature factors are taken into account (as tabulated in Table VI). However, since the characteristic features of these curves appear to change very little, these factors are not considered in further details.

Discussion and Summary of Results

From the preceding considerations, the intensity curves G4, G5, B and C seem to be regarded as satisfactory, and the final results of the molecular structure of ethylene fluorohydrin have been obtained as follows:

C–O=1.45 Å±0.02 Å O″···F=2.82 Å±0.03 Å,
C–C=1.50 Å~1.55 Å ∠CCF=109°±2°,
C–F=1.35 Å~1.40 Å ∠CCO=109.5°±2°.

Through many other investigations, that is, the results of ethylene chlorohydrin[1], ethyl alcohol[4], and isopropyl alcohol[5], the same conclusion has been reached as regards the bond distance C–O=1.45 Å.

According to many structural investigations of fluorine-substituted compounds, the slightly shorter distances C–C<1.54 Å and C–F= 1.36 Å~1.40 Å seem to be satisfactory (see Table V).

TABLE VI
APPROXIMATE TEMPERATURE FACTORS b'_{ij} USED IN CALCULATIONS

$b'_{ij}=0$	for C–C,
$b'_{ij}=-0.00016$	for C–O, C–F, C′···O, C′···F and C″···F,
$b'_{ij}=-0.00030$	for C′···H, O′···H, F′···H, O″···H and F″···H.

* In the investigations flourine-substituted compounds, it has often been observed tha. the distance c-c is slightly smaller than the normal covalent distance 1.54Å (see Table V).

In regard to paraffines in which two or more hydrogen atoms have been substituted by fluorine atoms, a smaller value of distance C–F>1.35 Å has often been found, but the distance C–F<1.35 Å seems adequate in the case of this molecule.

In the case of ethylene chlorohydrin, it was concluded that the *gauche* and the *trans* forms co-exist, but a similar conclusion can not be reached in the present compound. From the analysis of the radial distribution curve, it is concluded that there is almost certainly one form of this molecule at room temperature. That is, the ethylene fluorohydrin molecule is of the *gauche* form (φ= 60°–70°), and is considered to form the intramolecular hydrogen bond. This is a reasonable interpretation by virtue of the fact that hydrogen bonding of the type O–H···F seems to be stronger than that of the type O–H···Cl[18]: even in the case of ethylene chlorohydrin, the *gauche* from seems to be predominant at room temperature.

The author wishes to express his deep gratitude to the late Professor H. Oosaka of this University and to Professor Y. Morino of Tokyo University, for their kind advice throughout this work.

Chemical Institute, Faculty of Science
Tokyo University of Education
Ootsuka, Tokyo

18) L. Pauling, "The Nature of the Chemical Bond", p. 284; "Hydrogen Bond", Cornell Univ. Press (1940).

Molecular Structure Investigations by Electron Diffraction Method. IV. The Molecular Structures of α, γ-Dichlorohydrin and Ethylene Cyanohydrin

By Mashio YAMAHA

(Received December 7, 1955)

Introduction

The molecular structure of ethylene chlorohydrin has been surveyed by S. Mizushima[1-4] by means of infra-red and Raman spectra studies in regard to the problems of energy and entropy differences between the two intramolecular rotational isomers, i.e., the *trans* and the *gauche* forms of this molecule.

According to the surveys by O. Bastiansen[5] and by the author[6] using an electron diffraction method, a considerable fraction of the molecules in the gaseous state exist in the *gauche* form, in which the intramolecular hydrogen bond is formed between the O and Cl atoms. Previously, Zumwalt and Badger[7], by using infra-red spectroscopic data, established the fact that each of the ethylene chloro-, bromo- and iodo-hydrin, and α,γ-dichlorohydrin molecules, all of which have -O-H radicals, forms an intramolecular hydrogen bond between the oxygen and halogen atoms. Since the publication of the previous report[6], surveys have been continued on the molecular structures of α,γ-dichlorohydrin (1, 3-dichloropropanol (2)) and ethylene cyanohydrin (Hydracrylonitrile) by using the visual electron diffraction method. As to the structure of ethylene cyanohydrin, the molecule does not seem to form the intramolecular hydrogen bond, and the question, in what stable position the molecule exists in a gaseous state, has been examined.

Experimental Procedure

1) Apparatus. — The electron diffraction apparatus of the vertical, hot cathode type was described in the previous publication[8] (camera length: 91 mm. and 101 mm.).

The samples are viscous liquids and they show high boiling points. They were spurted from the high temperature nozzle having a nichrome-wire heating device.

2) Samples.—*α, γ-Dichlorohydrin.*—A commercial sample was purified by distillation under reduced pressure (boiling point: 87°C/35 mmHg).

1) S. Mizushima, Y. Morino and T. Kubota, *Bull. Chem. Soc. Japan*, **14**, 15 (1939).
2) S. Mizushima, Y. Morino and S. Nakamura, *Sci. Paper I.P.C.R.*, **37**, 205 (1940).
3) S. Mizushima et al., *J. Chem. Phys.*, **19**, 1477 (1951).
4) S. Mizushima et al., *J. Am. Chem. Soc.*, **74**, 1378 (1952).
5) O. Bastiansen, *Acta Chim. Scand.*, **3**, 415 (1949).
6) M. Yamaha, This Bulletin, 29, 865 (1956).
7) L.R. Zumwalt and R.M. Badger, *J. Am. Chem. Soc.*, **62**, 305 (1940); *J. Chem. Phys.*, **7**, 87 (1939).
8) T. Yuzawa and M. Yamaha, This Bulletin, **28**, 414 (1953).

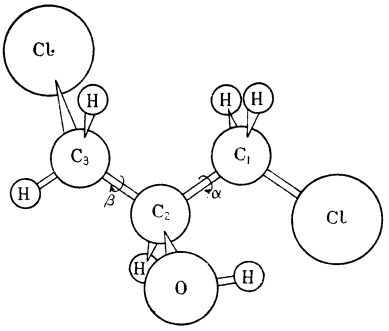

α, γ-Dichlorohydrin

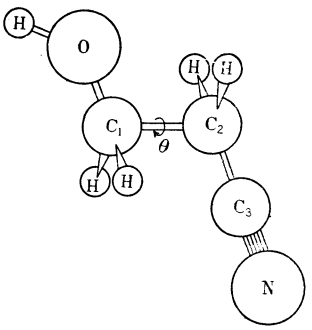

Ethylene Cyanohydrin

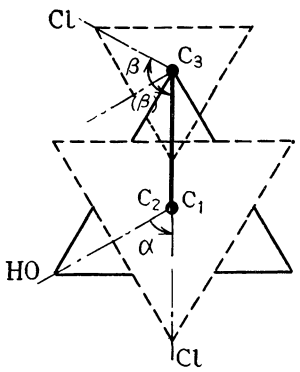

$\alpha=60°$
$\beta=-60°$ (or $\beta'=\mp 60°$)
(cf. curve G or H)

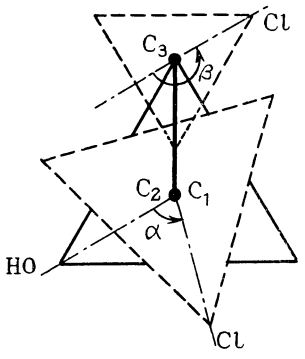

$\alpha=75°$
$\beta=180°$
(cf. curve N)

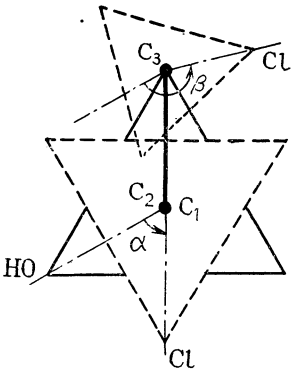

$\alpha=60°$
$\beta=165°$
(cf. curve K)

α, γ-Dichlorohydrin

Fig. 1. Schematic models which show the relative atomic configulations for α, γ-dichlorohydrin and ethylene cyanohydrin molecules.

The relative position between O and two Cl atoms of each form varying according to the internal rotation about C-C bonds, is also shown at the lower position for the dichlorohydrin molecule.

TABLE I

THE LIST OF MOLECULAR MODELS AND CORRESPONDING MOLECULAR PARAMETERS OF α, γ-DICHLOROHYDRIN

Models	∠CCC°	∠CCCl°	α°	β°	C–Cl	C′′···Cl$_g$	C′′···Cl$_t$	O′′···Cl$_g$	O′′···Cl$_t$	Cl′′′···Cl
A	109.5	109.5	60	180	1.77	3.08	4.09	3.03	4.01	4.52
B	〃	112	〃	〃	〃	3.13	4.12	3.09	4.03	4.76
C	112	〃	〃	〃	〃	3.17	4.14	〃	〃	4.73
D	109.5	109.5	〃	150	〃	2.77	4.09	3.03	3.93	4.49
E	〃	112	〃	〃	〃	2.84	4.12	3.09	3.96	4.56
F	〃	109.5	〃	120	〃	3.78	4.09	3.03	3.71	4.93
G	〃	〃	〃	+60	〃		〃	〃		5.40
H	112	112	〃	−60	〃	3.17	4.14	3.09		4.81
I	〃	〃	45	180	〃	3.13	4.13	2.93	4.03	4.80
J	〃	〃	60	〃	1.75	3.17	4.12	3.08	4.01	4.70
K	109.5	〃	〃	165	1.77	2.97	〃	3.09	4.03	4.66
L(=B)	〃	〃	〃	180	〃	3.13	〃	〃	〃	4.76
M	〃	〃	〃	195	〃	3.31	〃	〃	〃	4.90
N	〃	〃	75	180	〃	3.13	4.10	3.22	〃	4.60
O	〃	109.5	60	〃	1.80	3.09	4.12	3.05	〃	〃

TABLE II

THE LIST OF MOLECULAR MODELS AND CORRESPONDING MOLECULAR PARAMETERS OF ETHYLENE CYANOHYDRIN

Models	∠CCC°	θ°	C_1–C_2	C_2–C_3	C≡N (Å)	O″···C (Å)	O‴···N (Å)
A	109.5	180	1.54	1.54	1.16	3.79	4.88
B	〃	〃	〃	1.50	〃	3.76	4.85
C	112	〃	〃	〃	〃	3.78	4.86
D	109.5	〃	1.52	1.46	1.20	3.70	4.83
E	〃	〃	〃	1.42	1.16	3.67	4.76
F	〃	60	1.54	1.50	〃	2.88	3.63
G	112	〃	〃	〃	〃	2.93	3.70
H	109.5	〃	1.52	1.46	1.20	2.84	3.62
I	〃	0	1.54	1.50	1.16	2.52	3.13
J	112	〃	〃	〃	〃	2.59	3.21

Ethylene Cyanohydrin.—A sample synthesized from ethylene bromohydrin by Mr. Kubouchi of the Electrical Communication Laboratory has been used (boiling point: 108°/12 mmHg).

3) Electron Diffraction Patterns. — The maxima and minima of diffracted halos appearing on photographic plates have been measured visually. For dichlorohydrin, nine distinct halos have been observed in the range of $q<80$ in addition to several faint or indistinct halos. For ethylene cyanohydrin, eight halos including weak and indistinct ones have been observed in the range of $q<60$. Measured *q-values* of maxima and minima are shown in Tables IV and V, and visual intensity curves are shown at the top of Figs. 2 and 4, followed by the theoretical intensity curves.

4) Theoretical Intensity Curves and Radial Distribution Curves.—The theoretical intensity curves have been calculated by using the following well-known Pauling-Schomaker formula;

$$I(q)=k\sum_i\sum_j (nZ_iZ_j/r_{ij})\cdot\sin(\pi qr_{ij}/10)\cdot\exp(-b'_{ij}q^2),$$

where, $q=10\,s/\pi$; $s=(4\pi\sin\theta/2)/\lambda$; θ, the scattering angle and λ, the wave length of the beam.

The molecular parameters which are used in the construction of models are listed in Table I for dichlorohydrin and in Table II for cyanohydrin (cf. Fig. 1).

For dichlorohydrin, the temperature factors b'_{ij}, whose values are suggested from the case of

TABLE III

TEMPERATURE FACTORS b'_{ij} FOR THE CALCULATION OF INTENSITY CURVES OF α,γ-DICHLOROHYDRIN MOLECULE

Atompairs	b'_{ij}
C–H	0.00015
C–O	0
C–C	0
C–Cl	0
C′···H	0.00022
C′···O	0.00008
C′···C	0.00017
C′···Cl	0.00008
Cl′···H	0.00040
C″···Cl_g	0.00050
Cl″···O_g	0.00040
C″···Cl_t	0.00040
Cl″···O_t	0.00033
Cl‴···Cl	0.00070

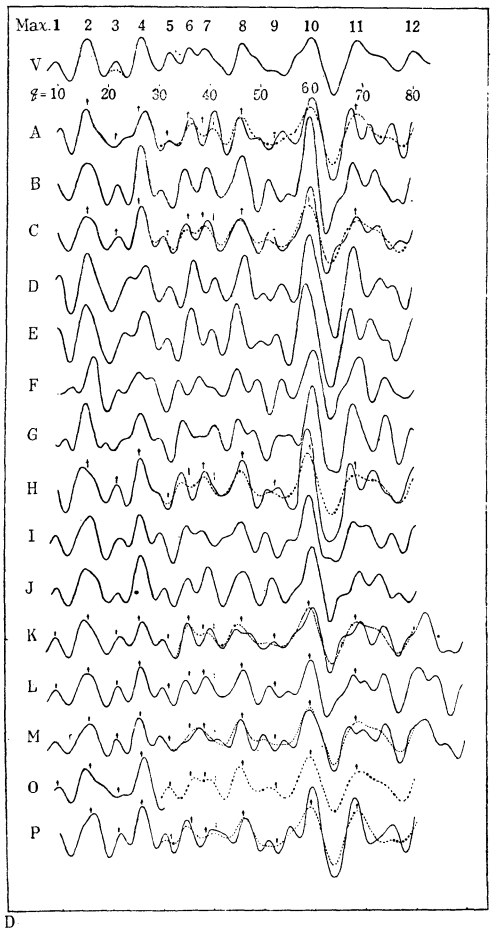

D

Fig. 2. Visual (V) and theoretical intensity curves for dichlorohydrin molecule.
Dotted curves correspond to the curves in which the temperature factors for each atomic distance as shown in Table III are taken into consideration.

ethylene chlorohydrin[9] and are listed in Table III, are taken into consideration, the corresponding curves being shown by dotted curves in Fig. 2.

For ethylene cyanohydrin, the temperature factors are ignored in the approximate calculation, since the observed intensity curve extends to $q<60$.

Also the radial distribution curves using the visual intensity curves have been calculated by means of the following formula;

$$rD(r)=\sum_{q=1}^{q=\max} I(q)\cdot\sin(\pi qr/10)\cdot\exp(-aq^2).$$

and are shown in Figs. 3 and 5.

5) Analyses of Intensity Curves and Radial Distribution Curves.—a) α,γ-**Dichlorohydrin.**— In constructing the molecular models, the following parameters are assumed (i), and varied in the ranges (ii):

(i) C-C=1.54 Å, C-O=1.45 Å, C-H=1.10 Å ($Z_H=1.2$),

(ii) C-Cl=1.75 Å~1.80 Å, ∠CCC=109.5°~112°, ∠CCCl=109.5°~112°.

TABLE IV

OBSERVED *q-values* AND CALCULATED q/q_{obs} VALUES FOR BETTER MOLECULAR MODELS OF α,γ-DICHLOROHYDRIN

Max.	Min.	q_{obs}	q/q_{obs} N	C	O
2		16.07	0.996	0.989	0.989
	3′	(19.70)	—	0.990	0.990
3		21.54	(1.040)	1.003	1.010
	4′	23.47	0.997	1.010	0.999
4		26.12	1.015	0.999	0.995
5		31.70	0.987	0.962	0.962
6		35.90	1.008	0.987	0.972
7		(38.72–40.93)			
		(39.82)	1.008	(0.989)	0.997
8		46.41	0.978	0.989	0.991
9		(52.85)	(0.967)	0.973	—
10		59.68	0.995	0.999	0.994
11		68.53	1.008	1.007	0.998
Mean deviation:			0.999_1	0.991_4	0.990_3
Mean sq. average deviation:			0.011_2	0.012_5	0.012_6

9) For molecules having C≡N triple bond, the distance C≡N seems reasonably to be 1.16Å; that is, for example, for methyl cyanide, $CH_3-C\equiv N$,
C≡N=1.16Å by L.O. Brockway, *J. Am. Chem. Soc.*, **58**, 2516 (1936).
C≡N=1.16Å and C–C=1.49Å by L Pauling et al., *J. Am. Chem. Soc.*, **61**, 927 (1939).
$r_{C\equiv N}$=1.157Å (HCN),
1.163Å (Cl–CN),
1.160Å (Br–CN),
1.159Å (I–CN), by means of microwave spectra by W.J.O. Thomas, *J. Chem. Phys.*, **19**, 1162 (1951),
for Acrylonitrile $CH_2=CH^*-C\equiv N$
$C^*-C=1.44$Å and C≡N=1.16Å.
by T. Saito, reported in the Ann. Meeting of the Chem. Soc. Japan, (1954), April.

TABLE V

OBSERVED *q-values* AND CALCULATED q/q_{obs} VALUES FOR THE BEST MODEL OF ETHYLENE CYANOHYDRIN

Max.	q_{obs}	q/q_{obs} E
(shelf)	13.14	0.989
2	18.00	1.014
(shelf)	21.78	1.010
3	25.86	1.025
4	30.68	0.999
5	34.13	1.002
6	40.40~	0.990
	43.78	0.984
7	49.22	(1.034)
8	55.73~	1.005
	59.00	1.012
Mean deviation:		1.003
Mean sq. average deviation:		0.012_2

In this case, since the molecule has a complicated structure, the values of parameters are confined to the narrower range of variation referring to the values of ethylene chlorohydrin previously determined. It was established that considerable fraction of the ethylene chlorohydrin molecules have the structure of *gauche* form, that is, the structure in which the intramolecular hydrogen bond is formed between Cl and O atoms even at room temperature, the rotational angle α of *gaucke* form being about 75°.

The dichlorohydrin molecule has two O···Cl atom pairs, the combinations of two rotational equilibrium angles α and β (see Fig. 1) around the two C-C bonds being taken up as shown in the fourth and fifth columns of Table I, in which atomic distances and valence angles corresponding to each model are listed.

The ranges of variations of angles α and β are as follows*:

α=45°, 60° (*gauche*), 75°.

$\beta=\pm60°$ (*gauche*), 120°, 150°, 165°, 180° (*trans*) and 195°.

(1) As the angles ∠CCC and ∠CCCl are varied from 109.5° to 112°, the *q-values* of maxima 5, 6 and 7 decrease slightly. The intensity relations of maxima 2, 3 and 4, and those in the range $45<q<60$ differ from one another in the curves A, B and C. Also, in the curves D and E, the *q-values* of maxima 4, 5, 6, 7, 8 and 9 decrease according to the similar variation of parameters. The intensity relations and *q-valus* of the models having both 112° of angles ∠CCC and ∠CCCl are clearly different from those of the visual curve.

(2) As the C-Cl distances are changed from 1.75 Å to 1.80 Å, the *q-values* of the maxima and minima change slightly, and the height of maximum 7 becomes lower. However, the intensity relations and *q-values* of maxima 5, 6 and 7 for

* In the combinations of angles α and β, obviously, a model having $\alpha=60°$, $\beta=180°$ and one having $\alpha=180°$, $\beta=60°$, are equivalent.

both models J and P are unsatisfactory, although model O seems better.

(3) If one of the two O···Cl pairs forms the intramolecular hydrogen bond, i.e. with the angle $\alpha \approx 60°$, the other O···Cl pair seems unable to form another hydrogen bond, and consequently the rotational angle $\beta = \pm 60°$ seems inadequate. This fact is made clear from the comparisons of the curves G ($\alpha = 60°$, $\beta = 60°$) and H ($\alpha = 60°$, $\beta = -60°$) with the curves A, B and C, each of which has the combination of $\alpha = 60°$, and $\beta = 180°$.

In the curves G and H, maximum 5 accompanies maximum 4 and shows shelf-like feature, especially in the curve G, the intensity relation seems clearly different from that of the visual one, and also the maxima 6 and 7 shift inward for curve H.

(4) Assuming one O···Cl pair is in a position of $\alpha = 60°$, the relative position of the other O···Cl pair is examined by varying the angle $\beta = 120°$, 150°, 165°, 180° and 195°. In the curves D and E ($\beta = 150°$), maximum 3 accompanies maximum 4 with a shelf-like feature. The curve F ($\beta = 120°$) illustrates the extreme feature in which both maxima 3 and 5 come together with maximum 4 and show deterioration. In the curve M ($\beta = 195°$), the maxima 3, 4, 5 and 8 shift inward, and maxima 6 and 7 seem to become one maximum. In the curves K and L, the intensity relations and the positions of maxima of over-all q-range become better and nearly adequate, but maximum 5 is situated at a smaller *q-value* than the visual curve, in which minimum 5′ seems to be deeper than minimum 6′ and maximum 5 comes comparatively near maximum 6.

(5) In the case of ethylene chlorohydrin, the rotational angle α relating to one O′′···Cl atom pair in the vicinity of *gauche* position was shown to be 75°. Consequently, in the case of this molecule, the combination of $\alpha = 75°$ and $\beta = 180°$ is considered as shown in the curve N. The intensity relations for the entire q-range, except maximum 3, and the *q-values* of the maxima and minima of this curve coincide with those of the visual curve.

(6) The radial distribution curve (Fig. 3) computed by using the experimental intensity curve has been analyzed into various corresponding peaks, and several peaks corresponding to the distances of atom pairs are as follows:

Peak A : 1.15 Å = C-H (a little longer)
B : = C-O and C-C
C : 1.77 Å = C-Cl
D : = O′···H and C′···H
E : = Cl′···H, C′···O, C′···C
F : 2.71 Å = C′···Cl
G : = C′′···Cl, O′′···Cl (in the vicinity of the *gauche* position)
H : = C′′···Cl, O′···Cl (in the vicinity of the *trans* position)
I : 4.45 Å~4.70 Å = Cl′′′···Cl.

The superposed peaks E, G and H can not be clearly separated into the component peaks (corresponding distances), but the corresponding distances of the better models resulting from the selection of intensity curves are fairly consistent with those in the radial distribution curve. That is, two rotationally stable positions of O′′···Cl atom pairs are probable $\alpha = 60°$–$75°$ and $\beta = 165°$–$180°$. The corresponding O′′···Cl, and C′′···Cl distances in these cases are shown under the corresponding peaks G and H by small rectangles whose respective widths show the allowances according to the slight variations of bond distances and angles (see Table I). The existence of a peak of 4.45 Å–4.70 Å corresponding to the Cl′′′···Cl distance also seems to show adequately the relative position of the two Cl atoms (see column 11 in Table I).

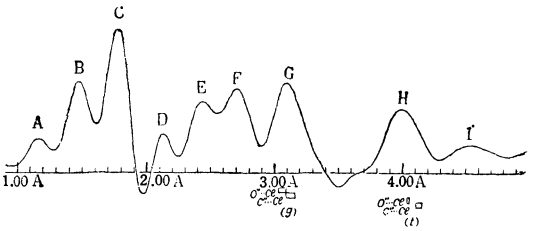

Fig. 3. Radial distribution curve for dichlorohydrin molecule.

Under the curves, the O′′...Cl and C′′... Cl interatomic distances corresponding to the relative positions in the *gauche* (g) and the *trans* (t) forms respectively are shown with small squares.

O′′···Cl$_g$ 3.04~3.09 (Å)
C′′···Cl$_g$ 3.09~3.16 (Å)
O′′···Cl$_t$ 4.03~4.05 (Å)
C′···Cl$_t$ 4.10~4.15 (Å)

In considering the conclusions in the previous report on ethylene chlorohydrin, that is, the values C-Cl = 1.77 Å, C-O = 1.45 Å, ∠CCC = 109.5° and ∠CCCl = 112° with the assumed C-C = 1.54 Å, the model of dichlorohydrin molecule having the rotational angles $\alpha = 75°$ and $\beta = 180°$ is reasonable (cf. curve N).

b) Ethylene Cyanohydrin.—In constructing molecular models, the following parameters are assumed (i), and varied in the ranges (ii):

(i) C-O = 1.45 Å, C-H = 1.10 Å ($Z_H = 1.2$), C≡N = 1.16 Å[9] and ∠CCO = 109.5°,
(ii) C_1-C_2 = 1.52 Å–1.54 Å, C_2-C_3 = 1.42 Å–1.54 Å and $\angle C_1C_2C_3 = 109.5°$–112°.

The list of models with molecular parameters is shown in Table II, and corresponding theoretical intensity curves in Fig. 4.

Regarding the relative position of -C≡N and -OH radicals, representated by the rotational angle θ, the models are classified into three groups, the *trans* group ($\theta = 180°$, curves from A to E), the *gauche* group ($\theta = 60°$, curves from F to H) and the *cis* group ($\theta = 0°$, curves I and J).

In comparing the intensity relations and *q-values* of maxima and minima of the visual and theoretical intensity curves, the better models are selected by means of the following view-points of analysis;

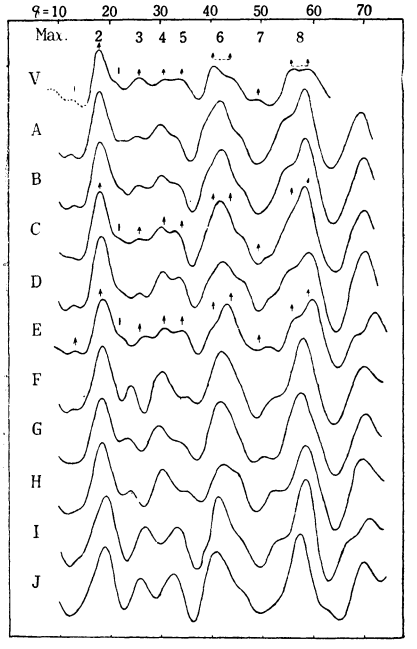

Fig. 4. Visual (V) and theoretical intensity curve for ethylene cyanohydrin molecule.

(1) The *trans*-, *gauche*- and *cis*-forms change clearly in the features of intensity relations as shown in Fig. 4. That is, the maxima 2 and 6 remain almost unchanged throughout the curves; the variation of intensity between maxima 3 and 5 is relatively small in the curves of the *trans*-group (A to E). For the *gauche* group (F to H), both maximum 3 and minimum 4′ shift inward and maximum 4 becomes higher; however, these features do not coincide with those of the visual curve. In the range of $20<q<40$ in the curves I and J (the *cis* group), the simply sinusoidal features differ distinctly from the visual one. The characteristic features of the visual curve are a very low shelf ($q\approx21.8$) accompanying maximum 2 and a slowly-varying intensity between maxima 3, 4 and 5 (i.e. (a) slightly separated low maximum 3 and (b) adjacent maxima 4 and 5 near each other having almost equal heights). These features seem to coincide fairly well with those of the curves in the *trans* group, especially with those of curves E (see later).

(2) From the analysis of the radial distribution curve as shown later, the molecule could be regarded as belonging to the *trans* group, and the C_1–C_2 and C_2–C_3 distances and $\angle C_1C_2C_3$ angles are examined on this assumption.

The C_2–C_3 distance nearest to the triple bond of C≡N can be considered to be short, and the variations of C_2–C_3 distance are compared with one another as: C_2–C_3=1.50 Å (curve B and C), 1.46 Å (curve D) and 1.42 Å (curve E). The case of the angle $\angle C_1C_2C_3=112°$ as shown in the curve C (cf. curve G in the *gauche* form and curve J in the *cis* form having $\angle C_1C_2C_3=112°$) is also compared. In each case, the intensity relation of maxima from 3 to 5 slightly changes, and the heights of maxima 4 and 5 are nearly equal in the visual curve. The curves B, C and D seem comparatively good. The intensity relation of curve E seems the best, although the maxima of curve E shift slightly outward from those of the visual curve in the entire q-range. In spite of the intensity relation of maxima from 3 to 5 being comparatively diffused, it can be safely said, though not conclusively, that the C_2–C_3 distance is slightly shorter than 1.54 Å.

(3) A somewhat obscure and diffuse experimental intensity curve of ethylene cyanohydrin has been obtained up to $q\approx60$, because the sample is a viscous and less volatile liquid having high boiling temperature. Despite this, a radial distribution curve, curve RD1 has been computed with some uncertainty as shown in Fig. 5. From the curve, the corresponding atom pairs and distances between each peak are analyzed as follows:

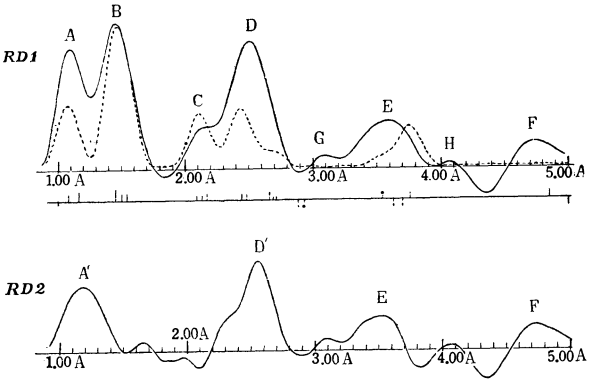

Fig. 5. Radial Distribution curves for ethylene cyanohydrin molecule.
*RD*1, total radial distribution curve. *RD*2, the curve which shows the residual curve produced by the subtraction of the area under the hypothetical partial *RD* curve (as shown by the dotted curve) from the area under the *RD*1 curve.

A: C-H, C≡N,
B: C_1-C_2, C_2-C_3 C-O,
C: C'···H, O'···H,
D: C'···O (≈2.40 Å), C'···C (2.43 Å~2.55 Å),
O''···H (≈2.70 Å), C'···N (2.66 Å~2.70 Å),
E: C''···N (3.48 Å~3.55 Å),
C''...O_{trans} (3.30 Å~3.79 Å),
F: O'''...N_{trans} (4.83 Å~4.88 Å).

Each of these analyzed values seems to agree fairly well with each corresponding parameter of the better models. In particular, the *trans*-form seems acceptable as regards the rotational equilibrium position around the C_1-C_2 bond. That is, the peak F (4.70 Å-4.80 Å) does not appear in the cases other than the *trans* form: for example, if the *gauche* formexists, the peak corresponding to O''···O_{gauche}≈2.85 Å~2.95 Å will appear, but not in RD1. It is not clear, however, whether or not the two rotational isomers may coexist. The distances other than O'''···N_{trans} (peak F) cannot be determined separately from the curve RD1, since the other peaks appear to be the combinations of two or more peaks. From consideration of the intensity curves, the dotted curve which is the hypothetical radial distribution curve of the following eight distances on RD1, is computed;

C-H=1.08 Å, C-O=1.45 Å, C_1-C_2=1.54 Å*,
C'···H=2.17 Å**, C'···O=2.44 Å**,
C''···O_{trans}=3.76 Å**, O''···H_{gauche}=2.69 Å**,
N'···H=3.55 Å**.

In consequence of the subtraction of the area under the dotted curve from that of RD1, the peaks other than those corresponding to eight distances mentioned above appear in the curve RD2.

The new distribution curve RD2 is analyzed with some uncertainty as follows:

A': The peaks corresponding to the distances C≡N and C_2-C_3 should appear, but could hardly be separated.
D': 2.56 Å=C_2'···N,
E': 3.45 Å~3.60 Å=C''···N,
from this value the angle ∠$C_1C_2C_3$ could not be decided conclusively.

The intensity curve E, which is computed in consideration of the results of radial distribution curve, seems to be the most acceptable one, except the shape of maximum 6 and the slight disagreements of all *q-values*. The structure of ethylene cyanohydrin could not be determined more fully, because only insufficient diffracted patterns were obtained.

Results and Discussions

1) α,γ-Dichlorohydrin.—From the intensity and radial distribution curves, the following results are obtained:

C-Cl=1.76 Å-1.80 Å, ∠CCC=109.5°±1.5°,
∠CCCl=111°±1.5°,
α=70°±10°, β=180°±10°.

The results of α, γ-dichlorohydrin seem sufficiently acceptable in comparison with those of ethylene chlorohydrin.

One of the two O''···Cl atom pairs is in the *gauche* position and the other *trans* at room temperature, because probably intramolecular hydrogen bond can only be formed in one or the other set of O''···Cl atom pairs.

2) Ethylene Cyanohydrin.—

C_2-C_3=(1.48 Å±0.04 Å)<C_1-C_2
θ=180° (The stable form of rotation about C_1-C_2 bond is of *trans*.)

Upon consideration of the present results, the C_2-C_3 bond neighboring the triple bond C≡N seems to be comparatively short. In the series of bonds -C_2-C_3≡N, the N atom is capable of becoming a weak "proton-acceptor", while the C_3 atom does not have this capacity. However, it is probably difficult to form the intramolecular hydrogen bond O-H···N in this molecule because of the longer distance of the O···N atom pair and of the repulsive force between the O···C_3 atom pair in the *cis* form (i. e. O···N_{cis}=3.20Å and O···$C_{3,cis}$=2.60Å). Consequently, the molecule exists almost in the *trans* form in the gaseous state, and the coexistence of another isomer forming the intramolecular hydrogen bond can not be confirmed.

Summary of Results

The molecular structures of α, γ-dichlorohydrin and ethylene cyanohydrin in the gaseous state were investigated by a visual electron diffraction method. The results obtained from the analyses of intensity curves and radial distribution curves are as follows:

α, γ-Dichlorohydrin (1, 3-dichloropropanol (2))

Assumption: C-C=1.54 Å, C-O=1.45 Å, and C-H=1.10 Å and ∠CCH=∠CCO=109.5°.
Results: C-Cl=1.78 Å±0.02 Å, ∠CCC=109.5°±1.5° and ∠CCCl=111°±1.5°.
Stable rotational position: α=70°±10°, β=180°±10°.

Ethylene Cyanohydrin

Assumption: C-H=1.10 Å, C_1-C_2=1.52 Å-1.54 Å, C≡N=1.16 Å, ∠CCH=10.95°, ∠$C_1C_2C_3$=109.5°-112°
Results: C_2-C_3=(1.48 Å±0.04 Å)<C_1-C_2.
Stable rotational position: θ=180° (*trans* form).

* In order to obtain the peak corresponding to C_2~C_3, the value of C_1-C_2 is assumed.

** These values should be varied functionally with the angle ∠$C_1C_2C_3$, but the values are assumed in the first approximation.

The author wishes to express his deep gratitude to Mr. Y. Kubouchi of the Electrical Communication Laboratory for having kindly offered the useful sample of ethylene cyanohydrin, and to Professor A. Kotera of this University, and Dr. S. Nagakura of the Scientific and Technical Laboratory, Tokyo University, for their valuable discussions throughout this work.

Chemical Institute, Faculty of Science
Tokyo University of Education
Ootsuka Tokyo

Studies on the Synthesis of Metal Complexes. I. Synthesis of an Ammine-carbonato Series of Cobalt (III) Complexes*

By Motoshichi MORI, Muraji SHIBATA, Eishin KYUNO and Tomohiko ADACHI

(Received April 30, 1956)

It has been well known that in the presence of alkali bicarbonates cobaltous salts such as chloride and sulfate give green coloration by the action of hydrogen peroxide on the aquous solution, and this reaction has been used for the iodometric or colorimetric determination of cobalt by several workers[1,2].

On the other hand, this reaction product has been regarded as tricarbonatocobalt (III) anion, $[Co(CO_3)_3]^{3-}$, from measurement of the absorption spectrum[2] or chemical analysis of a derivative with hexamminecobalt (III) cation, $[Co(NH_3)_6][Co(CO_3)_3]$[3].

The present study was first directed to the isolation of the complex salt and the determination of its chemical formula and then turned to the synthesis of cobalt (III) complexes belonging to an ammine-carbonato series. All the objects were attained with success.

Experimental

Synthesis—1) Potassium Tricarbonatocobaltate (III), $K_3[Co(CO_3)_3]\cdot 3H_2O$.—Twenty grams of $KHCO_3$ was mixed with 20 cc. of water and the mixture was cooled in an ice-bath. In a separate beaker 10 g. of $CoCl_2\cdot 6H_2O$ was dissolved in 10 cc. of water and 5 cc. of 30% H_2O_2 was added to this solution. This was added to the $KHCO_3$ solution drop by drop with stirring, allowing about an hour for the operation. The green solution obtained was quickly filtered by suction, and the clear filtrate was again cooled and kept in a dark place. When about 15 cc. of alcohol was added to the filtrate, crystals began to appear, but they were contaminated with bicarbonate. The precipitates, therefore, were filtered off and the filtrate was again kept in a dark place at nearly 0°C. Then a little more alcohol was added to the filtrate, and the solution was allowed to stand until the deposition of crystals ceased, which took more than half an hour. The crystals were collected on a glass filter, washed with alcohol and then by ether, and stored in a brown bottle. The yield was 13.5 g. The solid was soluble in water containing potassium bicarbonate, but suffered decomposition by pure water, yielding the hydrous oxide.

Some care had to be exercised in isolating this complex. If the addition of the $CoCl_2$-H_2O_2 mixture was too rapid it brought about precipitation of cobaltic hydroxide, while if too much alcohol was added, it caused co-precipitation of other salts such as potassium chloride.

2) Blue Variety of Potassium Dicarbonatodiamminecobaltate (III), Blue-$K[Co(NH_3)_2(CO_3)_2]\cdot H_2O$.—To the clear green solution, prepared from $KHCO_3$ and CoCl-H_2O_2 mixture as described in 1), was added 5 g. of ammonium carbonate and the mixture was warmed on a water-bath until the green color of the solution changed into blue, which took about ten minutes. At the end of this period the vessel containing the warm solution was immediately dipped in the ice-bath in order to stop further progress of the reaction and to effect crystallization of the product. After the removal by filtration of the first crop of crystals another crop could be obtained from the residual solution by gradual addition of alcohol. These crops were collected together, recrystallized from water and washed with pure alcohol. Total yield, about 7 g.

3) Violet Variety of Potassium Dicarbonatodiamminecobaltate (III), Violet-$K[Co(NH_3)_2(CO_3)_2]\cdot H_2O$.—The green solution containing 5 g. of ammonium carbonate was heated on the water-bath until the color of the solution turned into blue and finally violet. Then the solution was

* Presented at the 9th Annual Meeting of the Chemical Society of Japan, Kyoto, April 2, 1956.

1) H.A. Laitinen and L.W. Burdett, *Anal. Chem.*, 23, 1268 (1951).

2) M. Mori and M. Shibata, *J. Chem. Soc. Japan*, 75, 1046 (1954).

3) T.P. McCutcheon and W.J. Schuele, *J. Am. Chem. Soc.*, 75, 1845 (1953).

cooled rapidly and a large amount of alcohol was added to it, and the whole was allowed to stand for some time. The violet precipitate was collected and dissolved in a little cold water to remove impurities as residues, and then the complex sought for was reprecipitated from the solution by the addition of alcohol. After repeating this procedure, the product was washed with alcohol and ether in turn and finally dried in a vacuum desiccator over sulfuric acid. Thus about one gram of violet powder was obtained. The complex was hygroscopic and very readily soluble in water.

TABLE I

A FLOW SHEET OF SYNTHESIS OF AMMINE-CARBONATO Co(III) COMPLEXES

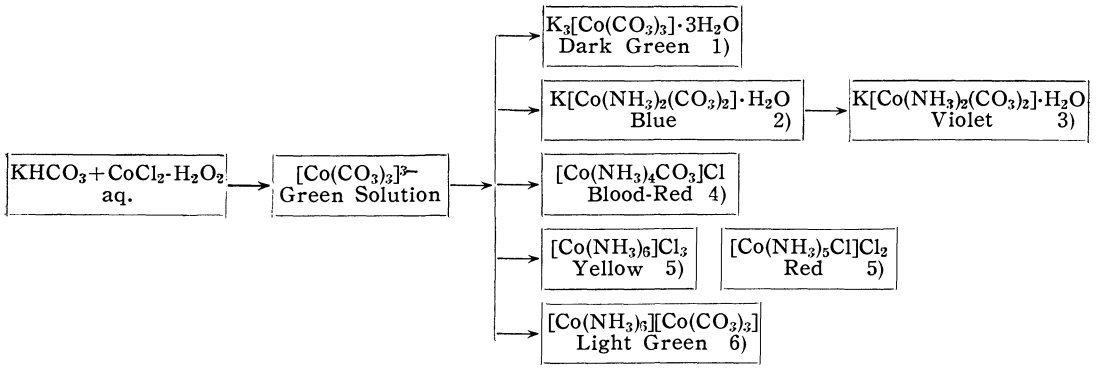

4) Carbonatotetramminecobalt (III) Chloride, $[Co(NH_3)_4CO_3]Cl$.—To the green solution were added 15 g. of ammonium carbonate and 30 cc. of conc. ammonia and the mixture was boiled on the water-bath until the color of the solution became blood-red. At the end of this heating the liquid was poured into an evaporating dish and concentrated to a small volume with the addition of a small amount of ammonium carbonate. On adding alcohol, the complex was precipitated, the yield being about 9 g.

5) Hexamminecobalt (III) Chloride and Chloropentammine Cobalt (III) Chloride, $[Co(NH_3)_6]Cl_3$ and $[Co(NH_3)_5Cl]Cl_2$.—Thirty grams of ammonium chloride, 40 cc. of conc. ammonia and 2 g. of active charcoal were introduced into the green solution and the mixture was boiled until its color became reddish-brown (about thirty minutes). In this case, a reflux condenser was used to avoid the escape of ammonia from the solution. After filtering and cooling, conc. hydrochloric acid was gradually added to the filtrate, until a yellow precipitate separated out. The purification of the product was effected by the usual method for this complex. Yield, about 4 g.

On evaporating the mother liquor, chloropentamminecobalt (III) chloride was obtained as a by-product.

6) Hexamminecbalt (III) Tricarbonatocobaltate (III), $[Co(NH_3)_6][Co(CO_3)_3]$.—This compound was quantitatively precipitated from the green solution by the addition of solid hexamminecobalt (III) chloride. The compound appeared as light-green powder. It was extremely insoluble in water, alcohol and acetone and was very stable against day-light.

All the complexes described above are shown in the accompanying flow sheet (Table I).

Analysis.—Determination of chemical formulas was carried out for the complexes obtained in 1), 2), 3) and 6). The other complexes were identified by their characteristic properties such as precipitation reaction and absorption spectrum.

Water of crystallization was determined from the loss of weight of the product at 100–130°C by means of a Shimazu Thermano Balance and the fact nothing but water of crystallization has been removed was confirmed by re-dissolving the dehydrated sample in water.

When the dehydrated sample was heated with gradual elevation of temperature up to 300°C, all of the ammonia molecules and part of the carbonate ions attached to the central cobalt atom were expelled from the sample, and the remainder consisted of potassium carbonate and an oxide of cobalt (perhaps, Co_2O_3). The reaction may be represented as follows:

$$2K_3[Co(CO_3)_3] \longrightarrow 3K_2CO_3 + Co_2O_3 + 3CO_2\uparrow$$

$$2K[Co(NH_3)_2(CO_3)_2] \longrightarrow K_2CO_3 + Co_2O_3 + 4NH_3\uparrow + 3CO_2\uparrow$$

$$[Co(NH_3)_6][Co(CO_3)_3] \longrightarrow Co_2O_3 + 6NH_3\uparrow + 3CO_2\uparrow$$

The quantity of ammonia and carbondioxide expelled was estimated from the observed loss of weight. The potassium carbonate was alkalimetrically estimated after the residue was extracted with hot water and the cobalt content was iodometrically determined after the oxide in the residue was dissolved with hot sulfuric acid.

To confirm the validity of the above methods, direct analysis of ammonia and carbondioxide was also carried out.

Absorption Spectra.—The absorption spectra of the above complexes in aqueous solution were measured with a Beckman Model DU Spectrophotometer using a cell 1.0 cm. in thickness.

Results and Discussion

The results of thermal decomposition are shown in Fig. 1 and all the numerical values

TABLE II
ANALYTICAL RESULTS

(amounts in %)

Complexes	H_2O		$CO_2+(NH_3)$		K_2CO_3		Co		CO_2*		NH_3*	
	calcd.	obs.	calcd.	obs.	calcd.	obs.	calcd.	obs.	calcd.	obs.	calcd.	obs.
$K_3[Co(CO_3)_3]\cdot 3H_2O$	13.5	13.2	16.1	15.5	50.4	45.0	14.4	14.9	44.6	46.9	—	—
Blue-$K[Co(NH_3)_2(CO_3)_2]\cdot H_2O$	6.7	6.6	36.7	35.9	25.6	23.5	21.6	22.1	—	—	12.6	12.5
Violet-$K[Co(NH_3)_2(CO_3)_2]\cdot H_2O$	6.7	6.5	36.7	36.0	25.6	23.5	21.6	20.6	—	—	12.6	13.8
$[Co(NH_3)_6][Co(CO_3)_3]$	—	—	58.5	58.0	—	—	29.5	28.0	—	—	—	—

* direct determination

TABLE III
ABSORPTION MAXIMA AND log ε

Complexes	ν_1	log ε_1	ν_2	log ε_2	ν_3 ($10^{13}\cdot sec^{-1}$)	log ε_3
$K_3[Co(CO_3)_3]$	46.5	2.19	68.1	2.22	117.6	3.97
$K_3[Co(C_2O_4)_3]$	49.5	2.09	70.8	2.19	122.4	4.42
Blue-$K[Co(NH_3)_2(CO_3)_2]$	52.2	2.14	76.8	2.40	126.6	4.14
Violet-$K[Co(NH_3)_2(CO_3)_2]$	55.5	1.80	80.2	2.04	128.1	4.30
$NH_4[Co(NH_3)_2(C_2O_4)_2]$	54.0	1.95	82.4	2.10	129.3	3.24
Na[Coedta]	55.6	2.48	78.9	2.33	133.3	4.34

are given in Table II. These data seem to justify the assignment of such chemical formulae as $K_3[Co(CO_3)_3]\cdot 3H_2O$, blue- and violet-$K[Co(NH_3)_2(CO_3)_2]\cdot H_2O$ and $[Co(NH_3)_6][CoCO_3)_3]$ to our compounds. Additional evidence of the validity of these formulae exists in the absorptiometric data (Fig. 2 and Table III). Thus, the absorption curve of $K_3[Co(CO_3)_3]$ is similar to that of $K_3[Co(C_2O_4)_3]$, and that of violet-$K[Co[NH_3)_2(CO_3)_2]$ to those of $NH_4[Co(NH_3)_2(C_2O_4)_2]$ and K[Coedta].

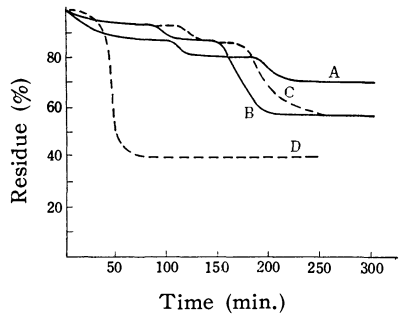

Fig. 1. Thermal decomposition of complexes at 100-300°C.
A. $K_3[Co(CO_3)_3]\cdot 3H_2O$
B. Blue-$K[Co(NH_3)_2(CO_3)_2]\cdot H_2O$
C. Violet-$K[Co(NH_3)_2(CO_3)_2]\cdot H_2O$
D. $[Co(NH_3)_6][Co(CO_3)_3]$

$K_3[Co(CO_3)_3]\cdot 3H_2O$.—The exact formula for this complex had not been determined before. According to reference[1], Job assigned to it the formula K_3CoO_3, Durrant considered it to be $(KCO_2\text{-}O)_2\text{-}Co\text{-}O\text{-}Co\text{-}(O\text{-}O_2CK)_2$ and Duval called it cobalt (III) tricarbonatocobaltiate, $Co[Co(CO_3)_3]$. None of these formulas, however, correctly represents the constitution of the pure substances obtained by the present workers.

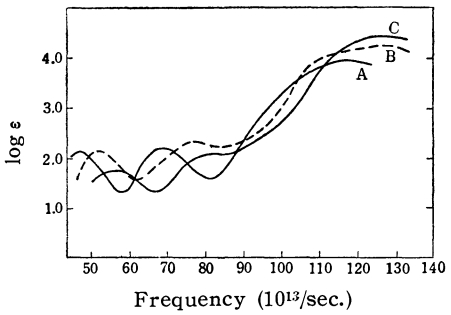

Fig. 2. Absorption spectra of:
A. $K_3[Co(CO_3)_3]$
B. Blue-$K[Co(NH_3)_2(CO_3)_2]$
C. Violet-$K[Co(NH_3)_2(CO_3)_2]$.

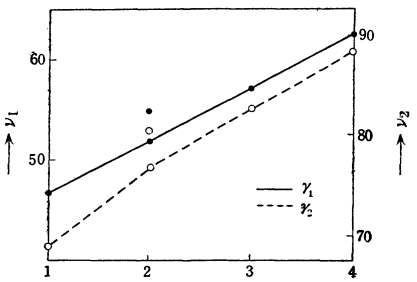

Fig. 3. Frequency positions of the ammine-carbonato Co(III) complexes.
1. $[Co(CO_3)_3]^{3-}$ 2. $[Co(NH_3)_2(CO_3)_2]^-$
3. $[Co(NH_3)_4CO_3]^+$ 4. $[Co(NH_3)_6]^{3+}$

From the results of analysis and because of the absorption spectrum of this complex, it is reasonable to give it *tris*-structure. The difficulty of isolating this complex in the pure state will be appreciated by considering the fact that trioxalatocobaltate (III) easily decomposes in day-light. In order to draw a final conclusion, however, it is necessary to resolve the complex into the antipodes. In fact, attempts were carried out by using *l*-strychnine and *d-tris*-(ethylenediamine)-cobalt (III) ion. In both cases, green precipitates were fractionally obtained from the original solution of the complex. But, since decomposition of the complex took place during the process of removing the precipitants, the optical rotation of the fractionated complex was not measured. Further studies will be carried out.

Blue- and Violet-K[Co(NH_3)$_2$(CO_3)$_2$]·H_2O.—Now, it is important to determine the configuration of these stereoisomers. Provided that a bifunctional group such as carbonate ion can span only *cis*-positions and that no intramolecular change of configuration occurs during the reaction of ammonium salt on tricarbonatocobaltate, the blue compound formed at an earlier stage of the reaction must be *cis*-form, while violet one formed through blue complex is regarded as *trans*-form. Studies of the resolution of both complexes may shed light on this problem.

Absorption Spectra.—The frequency values for the first and second bands of a series of ammine-carbonato complexes are plotted in Fig. 3. From the diagram, it is seen that the values of the first band lie on a single line except for one of violet complex. On the other hand, such a linearity can not exist among the frequencies of the second band. It should be added that the violet complex has the absorption maximum at the same frequency as EDTA-Co (III) complex as indicated in Table III.

Synthesis.—Our methods in which green tris-cobaltate is used as starting material, have the advantage of simplicity. For example, carbonatotetramminecobalt (III) salt, which is useful for the synthesis of various complexes, is prepared by the successive substitution of carbonate ions with ammonia groups without atmospheric oxidation, and hexamminecobalt (III) salt is also prepared by further substitution in the presence of active charcoal. It has also been observed that the cobalt (III) complexes belonging to an ethylenediamine-carbonato series is synthesized in the same way, and this will be reported later.

Summary

A green compound is isolated from the concentrated solution obtained by the action of hydrogen peroxide on cobalt (II) ions in the presence of potassium bicarbonate, and the formula $K_3[Co(CO_3)_3]\cdot 3H_2O$ is assigned to it on the basis of the analysis of the solid and of the absorption spectrum of the solution.

A series of ammine-carbonatocobalt (III) complexes, $K_3[Co(CO_3)_3]\cdot 3H_2O$, blue (perhaps, *cis*)- and violet(perhaps, *trans*)-$K[Co(NH_3)_2(CO_3)_2]\cdot H_2O$, $[Co(NH_3)_4CO_3]Cl$ and $[Co(NH_3)_6]Cl_3$, are synthesized from the abovementioned green solution by means of successive substitution of carbonate ions by ammonia groups. Hexamminecobalt (III) tricarbonatocobaltate, $[Co(NH_3)_6]$ $[Co(CO_3)_3]$, is also obtained by adding a hexamminecobalt (III) salt to the green solution of tricarbonato-complex. Three complexes, $K_3[Co(CO_3)_3]\cdot 3H_2O$ and blue- and violet-$K[Co(NH_3)_2(CO_3)_2]\cdot H_2O$, are probably to be regarded as new complexes and may be identified by their absorption spectra.

Department of Chemistry, Faculty of Science, Kanazawa University
Kanazawa

Studies on the Synthesis of Metal Complexes. II. Synthesis and Absorption Spectra of Hydrogen Ethylenediaminetetraacetato-cobaltate (III) and Sodium-hydrogen Chloro-ethylenediaminetetraacetato-cobaltate (III)*

By Motoshichi MORI, Muraji SHIBATA, Eishin KYUNO and Hiroshi NAKAJIMA

(Received April 30, 1956)

The common cobalt (III) complex in which ethylenediaminetetraacetic acid is hexadentate was first prepared by Brintzinger, Thiele and Mueller[1], and nitro-(ethylenediaminetetraacetato)-cobaltate (III) and bromo-(ethylenediaminetetraacetato-cobaltate (III) were later synthesized by Schwarzenbach[2]. Hereafter, ethylenediaminetetraacetic acid, quadrivalent ethylenediaminetetraacetate anion and tervalent anion will be denoted by EDTA, edta and edtaH respectively.

In the present study, free acid of the common complex, H[Coedta]·$4H_2O$ and sodium salt of the chloro-complex, Na[Co(Cl) (edtaH)]·$2H_2O$ were newly synthesized, and absorption spectra of all Co(III)-EDTA complexes including older ones were also measured. The geometrical configuration of the complexes is also discussed in this paper.

Experimental

Synthesis of H[Coedta]·$4H_2O$.—Ten grams of EDTA(edtaH_4) and about the same amount of freshly prepared cobaltic hydroxide were introduced into 200 cc. of water, and the mixture was heated on a water-bath for about one hour until the completion of the reaction. After cooling, the solution was filtered and then the filtrate was poured into a column of cation exchanger Amberlite IR-120 which had been converted into H-form. By this operation the alkali ions contained in the cobaltic hydroxide were completely removed. The solution passing through the exchanger was collected and then concentrated by means of vacuum distillation. On cooling the residual solution in an ice-bath, crystals were deposited, which were filtered by suction and recrystallized from the aqueous solution by adding dil. hydrochloric acid in the cold. Yield, about 65%

Anal. Found: H_2O, 17.1; Co, 14.30. Calcd.: H_2O, 17.0; Co, 14.15%.

The crystals obtained were deep lavender in color like the common complex, Na[Coedta]·$4H_2O$, but less soluble than the latter. The pH of a 10^{-3} M aqueous solution was found to be 2.80.

Synthesis of Na[Co(Cl) (edtaH)]·$2H_2O$.—This compound was prepared as blue crystals by the following method. To a conc. solution prepared by dissolving 10 g. of Na[Co(edta)]·$4H_2O$ in water was added 40 cc. of conc. hydrochloric acid, and the solution was evaporated nearly to dryness on a water-bath. After cooling, the blue residue was washed several times with a little water until the washings did not show any reddish-violet color. By this treatment the unchanged salt, Na[Co(edta)], was removed from the complex aimed at. The remainder was dissolved in water containing a small amount of sodium acetate, and then pure alcohol was added to this solution until blue crystals separated out. They were dissolved again in water containing sodium acetate and then recrystallized by adding dil. hydrochloric acid to the cooled solution. Yield, about 45%.

Anal. Found: H_2O, 8.0; Co, 13.08; Cl, 10.0%. Calcd: H_2O, 7.95; Co, 13.02; Cl, 7.84%.

The complex was readily soluble in water containing an acetate and was converted to the common complex when the aqueous solution was heated for a long time or some silver nitrate or an acid was added to it. The pH of a 10^{-3} M aqueous solution was found to be 2.91.

The same complex was synthesized alternatively by using Na[Co(Br) (edtaH)]·$2H_2O$ or Na[Co(NO_2) (edtaH)]·H_2O in place of Na[Coedta]·$4H_2O$. Free acid of the chloro-complex, H[Co(Cl) (edtaH]·$2H_2O$ was prepared by using H[Coedta]·$4H_2O$ in place of Na[Coedta]·$4H_2O$. It came in blue crystals like the sodium salt and the yield was about 50%.

Formation of Blue Co-EDTA Complex.—To an alkaline solution of EDTA prepared by dissolving the disodium salt (Na_2H_2edta·$2H_2O$) in dil. aqueous solution of sodium hydroxide, an aqueous solution of cobalt sulfate was added and the mixture was inserted in an ice-bath. On adding 10% solution of hydrogene peroxide, the reaction mixture changed from pink to blue in color. Attempts to isolate crystals from this solution ended in failure. This blue solution was very unstable and was converted to the violet solution of common complex with elevation of temperature or by acidification of the solution.

Other Complexes.—Na[Coedta]·$4H_2O$, Na[Co(NO_2) (edtaH)]·H_2O and Na[Co(Br) (edtaH)]·$2H_2O$ were synthesized by the methods reported by Schwarzenbach[2].

* Presented at the 9th Annual Meeting of the Chemical Society of Japan, Kyoto, April 2, 1956.

1) H. Brintzinger, H. Thiele and U. Mueller, *Z. anorg. Chem.*, **251**, 285 (1943).

2) G. Schwarzenbach, *Helv. Chim. Acta*, **32**, 839 (1949).

Analysis.—The water of crystallization was determined from the loss of weight of samples at 130°C by means of a Shimazu Thermano Balance, and it was also found that the samples could be dehydrated by the drying with no change in their chemical properties. The cobalt contents were iodometrically determined for samples treated by bisulfate fusion. The chlorine content was determined by Volhard's method.

Measurement.—The visible and ultraviolet absorption spectra were measured by using a Beckman Model DU Spectrophotometer, and the infrared absorption spectrum, by a Hilger Model 800 Recording Spectrophotometer. Potentiometric titration was carried out by a Shimazu Model MT-3 Electronic Titrimeter.

Results and Discussion

The titration curves of the complexes and the infrared spectrum of chloro-complex are shown in Fig. 1 and Fig. 2 respectively. All the absorption curves of the aqueous solution of the complexes are shown in Figs. 3 and 4, and their absorption maxima are given in Table I.

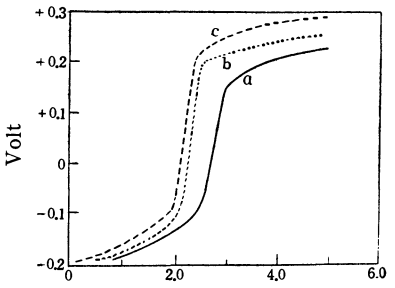

Fig. 1. Titration curves of 10^{-3} M complexes (20 cc) with 10^{-2} N sodium hydroxide.
a. $H[Coedta]\cdot 4H_2O$
b. $Na[Co(Cl)(edtaH)]\cdot 2H_2O$
c. $Na[Co(NO_2)(edtaH)]\cdot H_2O$

TABLE I
ABSORPTION MAXIMA OF Co (III)-EDTA COMPLEXES

Complexes	First Band ν_1	First Band log ε_1	Second Band ν_2	Second Band log ε_2	Third Band ν_3	Third Band log ε_3	Specific Band ν_s	Specific Band log ε_s
Common complex $Na[Coedta]\cdot 4H_2O$	55.9	2.51	78.5	2.34	132.16	4.34	—	—
Blue Complex [Coedta]⁻ ?..	51.7	2.47	77.9	2.37	135.14	4.25	—	—
Free Acid of Common Complex $H[Coedta]\cdot 4H_2O$	55.9	2.55	78.5	2.38	133.33	4.45	—	—
Nitro-Complex $Na[Co(NO_2)(edtaH)]\cdot H_2O$.....	53.0 60.6	2.03 2.33	—	—	120.00 133.33	4.26 4.26	88.24	3.52
Bromo-complex $Na[Co(Br)(edtaH)]\cdot 2H_2O$.....	50.9	2.37	75.0 ?	2.39	111.11 130.43	4.18 4.22	—	—
Chloro-complex $Na[Co(Cl)(edtaH)]\cdot 2H_2O$.....	51.3	2.38	74.6	2.31	111.52 132.74	4.18 4.43	—	—

Chemical Formulae of the Synthesized Compounds.—As will be seen in Fig. 1, the titration curve of our chloro-complex is very similar to that of the nitro-complex, and both complexes act as monobasic acids. A like behavior is observed in the free acid of common complex. Further, the two carbonyl bands shown by the infrared spectrum of the chloro-complex are strong evidence for the existence of a free carboxyl group in the coordination sphere of the complex (Fig. 2). The stronger band, which appears at 1610 cm^{-1}, is attributed to the presence of coordinated carboxyl groups. The weaker band, at 1724 cm^{-1}, is associated with the free carboxyl group. Incidentally, the bands for corresponding bromo-complex appear at 1628 cm^{-1} and 1723 cm^{-1} [3]. Thus, in view of the information obtained from the chemical analysis, titration and infrared spectrum measurement, it is reasonable to give our compounds such formulae as given in the experimental section.

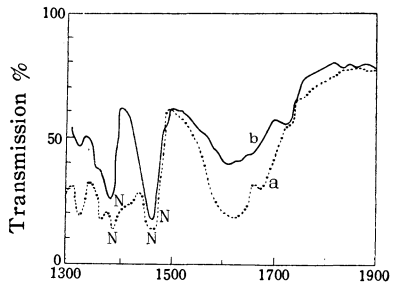

Fig. 2. Infrared absorption spectra of:
a. $Na_2H_2edta\cdot 2H_2O$
b. $Na[Co(Cl)(edtaH)]\cdot 2H_2O$
N. Nujol.

3) D.H. Bush and J.C. Bailar, *J. Am. Chem. Soc.*, 75, 4574 (1953).

Absorption Spectra of [Coedta] and Blue Co-EDTA Species.—Although the absorption spectrum of the common violet complex had already been measured by Y. Shimura and R. Tsuchida[4], the present workers made new measurements to investigate the pH effect on the absorption spectrum. As is seen in Fig. 3, the absorption curves of buffer solutions prepared in the pH range 2 to 4 are exactly identical with that of an aqueous solution, while those of alkaline solution prepared in the pH range 8 to 10 are different, and further the variation of the optical density shows appreciable deviation from that predicted by Beer's law.

The blue-Co-EDTA complex species described in the experimental section may be identical with the blue complex species regarded as hydroxo-complex, $[Co(OH)(edtaH)]^-$, by Schwarzenbach[2]. The absorption curve of this complex is given in the same figure (Fig. 3d). Discussion of the configuration of species will be given later.

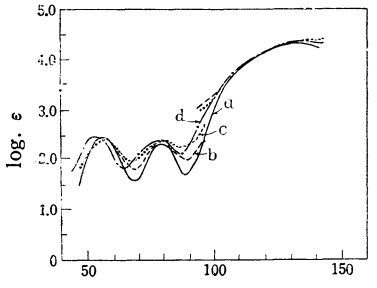

Frequency, 10^{13}/sec.

Fig. 3. Absorption spectra of $[Coedta]^-$:
a. in aqueous sol. (pH 6.9), acid sols. (pH>2).
b. in pH 9.5.
c. in pH 10.3.
d. blue Co-EDTA complex species.

Absorption Spectra of [Co(X) (edtaH)].—Although the absorption spectra of nitro-and bromo-complex had already been measured by Y. Shimura and R. Tsuchida*, the same thing was attempted by the present workers in relation to the chloro-complex. As is seen in Fig. 4, the absorption curves of bromo- and chloro-complex are similar to each other in appearance, and the maxima of the first and second bands both show a bathochromical shift from the corresponding maxima of the common complex. A little difference between the two, however, is clearly to be seen from Table I, that is, the maximum of the first band for the bromo-complex is shifted to a slightly longer wave-length than that for chloro-complex. The reason for these bathochromic effects of the ligands may be explained by the familiar empirical rule that the bromide and chloride ions are more bathochromic ligands than the oxalate ion, and the bromide ion is slightly more bathochromic than the chloride ion as ligand. The same relation probably holds for the second set of bands, but it is still uncertain since the absorption curve of bromo-complex does not show a well-defined maximum in the second band.

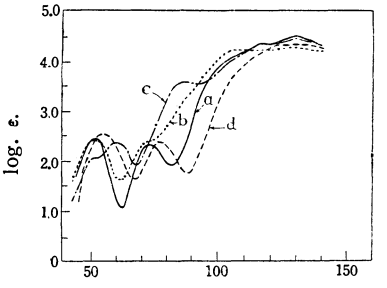

Frequency, 10^{13}/sec.

Fig. 4. Absorption spectra of:
a. $Na[Co(Cl)(edtaH)]\cdot 2H_2O$
b. $Na[Co(Br)(edtaH)]\cdot 2H_2O$
c. $Na[Co(NO_2)(edtaH)]\cdot H_2O$
d. $Na[Coedta]\cdot 4H_2O$.

As is seen in the same figure, the first band of nitro-complex clearly splits into two components, and this interesting fact will be reported shortly by other workers*. Inspection of the absorption spectra in the ultraviolet region reveals the interesting fact that there are two absorption maxima in the region. For nitro-complex they appear at 120.00 ($\times 10^{13}$/sec.) and 133.33, for bromo-complex, at 111.11 and 130.43, and for chloro-complex, at 111.52 and 132.74 (Table I). In contrast, the common complex shows a single maximum at 132.16. Accordingly, the appearance of two maxima in the longer wave-lengths may be attributed to the entrance of ligand X into the coordination sphere.

Configuration of the Complexes.—Now, we are in a position to discuss the configuration of the complexes. So far as the absorption spectrum of the blue Co-EDTA complex is concerned, the maximum of the first band is shifted bathochromically to a considerable degree as is seen in Fig. 3d. If the complex in question is hydroxo- or aquo-complex including ethylenediaminetetraacetate anion as a pentadentate ligand, the absorption maximum will be shifted hypsochromically from the maximum of common complex according to the empirical rule of "spectrochemical series". Therefore we regard this blue

4) Y. Shimura and R. Tsuchida, This Bulletin, 28, 572 (1955).

* Private information from Dr. Y. Shimura.

complex as a modification of Co(III)-EDTA complexes in which ethylenediaminetetraacetate anion acts as a hexadentate ligand.

In a previous paper[5], the authors reported the synthesis of a blue and a violet variety of $K[Co(NH_3)_2(CO_3)_2]\cdot H_2O$ and assumed *cis*-form for the former and *trans*-form for the latter. Comparison of the absorption spectra of these complexes with those of the complexes obtained in the present work showed that the maxima of the first and second bands of the two blue complexes occupied similar positions and that the same thing was true about the two violet complexes (for blue Co (III)-EDTA; 51.7 ($\times 10^{13}$/sec.), 77.9; for blue-$[Co(NH_3)_2(CO_3)_2]$, 52.2, 76.8; for violet-[Coedta], 55.9, 78.5; for violet-$[Co(NH_3)_2(CO_3)_2]$, 55.5, 80.2).

By this analogy of the absorption maxima, therefore, it may be assumed that the blue complex has one configuration in which the two nitrogen atoms span in *cis*-positions of octahedron and the violet common complex has another configuration in which the two nitrogen atoms span in *trans*-positions. Of course, the regular octahedron will suffer considerable distortion in the latter configuration. Such hypothesis about the configuration of the common complex, however, gives us a convenient explanation for the origin of the absorption band in the ultraviolet region. Provided that the absorption band in the ultraviolet region—"the third band"—is due to negative ions coordinated in trans-positions, the appearance of two maxima in the absorption spectra of [Co(X) (edtaH)] can be understood by taking into consideration such configuration as is indicated in Fig. 5.

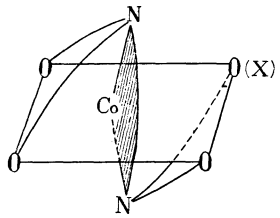

Fig. 5. Assumed configuration.

The present discussion of the configuration of "hexadentate" and "pentadentate" complexes is based on the assumption that the blue Co(III)-EDTA complex is a modification of "hexadentate" complex in spite of our failure to isolate this complex. Furthermore the dimentional restriction of the EDTA molecule makes it appear unnatural that the nitrogen atoms should span in trans-positions. Consequently, further studies must be carried out.

5) M. Mori, M. Shibata, E. Kyuno and T. Adachi, This Bulletin, **29**, 883 (1956).

Summary

Two new compounds, $H[Coedta]\cdot 4H_2O$ and $Na[Co(Cl)(edtaH)]\cdot 2H_2O$ were synthesized, and their chemical formulae were confirmed by means of potentiometric titration and by examination of the infrared spectrum.

The absorption spectrum of $Na[Coedta]\cdot 4H_2O$ in solution was measured to investigate the pH effect. The absorption curves in acid solutions (pH>2) were wholly identical with that in aqueous solution of the salt, but those of alkaline solutions (pH<10) were not identical and further showed deviation from Beer's law.

The absorption curves of $Na[Co(NO_2)(edtaH)]\cdot H_2O$, $Na[Co(Br)(edtaH)]\cdot 2H_2O$ and $Na[Co(Cl)(edtaH)]\cdot 2H_2O$ were also measured. The first band for the chloro-complex and that for the bromo-complex occupied the similar position and shifted bathochromically as compared with the corresponding maximum for the common complex [Coedta]. These results may be explained on the basis of the so-called "spectrochemical series". The absorption spectra of the complexes [Co(X) (edtaH)] were found to have two absorption maxima in the ultraviolet region. This phenomenon may be attributed to the "trans effect" of negative ions.

By oxidation of an alkaline solution containing cobaltous and edta ions with hydrogen peroxide, a blue complex was produced. Although an attempt to isolate it ended in failure, existence of cobalt (III) complex containing hexadentate EDTA was assumed on the basis of the absorption spectrum.

The authors wish to express their sincere thanks to professor K. Yamazaki of Nagoya University for the measurement of the infrared spectra, and to Dr. Y. Shimura of Osaka University for his helpful advice.

Department of Chemistry, Faculty of Science, Kanazawa University
Kanazawa

By-products of Acrylonitrile Synthesis from Acetylene and Hydrocyanic Acid. II. Amines Obtained by Hydrogenation of Nitriles

By Shiro MORIMOTO

(Received April 21, 1956)

Introduction

In the previous paper[1], the presence of propionitrile, benzonitrile and naphthalene was confirmed and that of five olefinic nitriles, i. e., 1-cyanobutadiene, 2-cyanobutadiene, 1-cyanohexatriene, 2-cyanohexatriene, 3-cyanohexatriene, was suggested in the neutral by-products of acrylonitrile synthesis from acetylene and hydrocyanic acid.

The present paper deals with the comfirmation of these suggestions by means of the identification of the amines which were produced by the hydrogenation of the above mentioned by-products.

Results and Discussion

The neutral by-products of acrylonitrile synthesis were hydrogenated with Raney nickel. The hydrogenation products were divided into two parts, neutral and basic. The basic part was fractionated by distillation through a Stedman-type column. The results obtained are shown in Figs. 1 and 2. Thus the two constant boiling fractions were obtained, i. e., A–2 (b. p. 77–78.5°C) and A–7 (b. p. 103–106°C).

A–2 was treated with phenylisothiocyanate, resulting in the formation of crystals which melted at 61–61.5°C and were identified to be N, N′-*n*-butylphenylthiourea after a mixed melting point test. Treatment of A–7 with

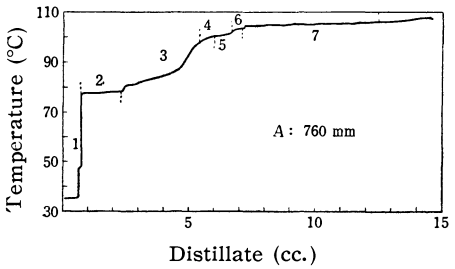

Fig. 1. Distillation curve of A-fractions.

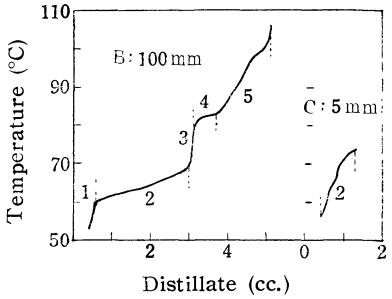

Fig. 2. Distillation curves of B- and C-fractions.

phenylisothiocyanate also gave crystals which melted at 62–63°C. The crystals were identified to be N, N′-*n*-amylphenylthiourea because the mixed melting point showed no depression. So it was confirmed that A–2 and A–7 contained *n*-butylamine and *n*-amylamine, respectively.

The paperchromatograms of hydrochlorides of A–3, A–4, B–2, B–4, B–5 and C–2 showed the presence of butylamines, amylamines, di-propylamine, heptylamines and benzylamine. But this method was not able to separate isomers mutually, i. e., 2-methylbufyl- from *n*-amyl-amine; 2-methylhexyl- and 2-ethylamyl- from *n*-heptyl-amine.

By the chromatography of N-2, 4-dinitrophenylamines (DNP-amines) on the column of cation exchanger the author[2] had already succeeded in separating isomers, i. e., DNP-isopropyl- from DNP-*n*-propyl-amine; DNP-isobutyl- from DNP-*n*-butyl-amine.

By the column-chromatography of DNP-derivatives of A–4, B–4, B–5 and C–2, the presence of *n*-butyl-, 2-methylbutyl-, *n*-amyl-, di-*n*-propyl-, benzyl- and *n*-heptyl-amines and two other primary heptylamines than *n*-heptylamine could be confirmed.

The amines which may be obtained by the hydrogenation of the above mentioned nitriles are as follows:

1) S. Morimoto, This Bulletin, 29, 450 (1956).

2) T. Seki and S. Morimoto, *J. Chm. Soc. Japan* (*Pure Chem. Sect.*), 77, 1124 (1956).

$CH_2=CH-CN,\ CH_3-CH_2-CN \longrightarrow CH_3\cdot CH_2\cdot CH_2-NH_2,\ CH_3\cdot CH_2\cdot CH_2-NH-CH_2\cdot CH_2\cdot CH_3$

$CH_2=CH-CH=CH-CN \longrightarrow CH_3\cdot CH_2\cdot CH_2\cdot CH_2\cdot CH_2-NH_2$

$CH_2=CH-C(CN)=CH_2 \longrightarrow CH_3\cdot CH_2\cdot CH(CH_3)\cdot CH_2-NH_2$

$CH_2=CH-CH=CH-CH=CH-CN \longrightarrow CH_3\cdot CH_2\cdot CH_2\cdot CH_2\cdot CH_2\cdot CH_2\cdot CH_2-NH_2$

$CH_2=CH-CH=CH-C(CN)=CH_2 \longrightarrow CH_3\cdot CH_2\cdot CH_2\cdot CH_2\cdot CH(CH_3)\cdot CH_2-NH_2$

$CH_2=CH-CH=C(CN)-CH=CH_2 \longrightarrow CH_3\cdot CH_2\cdot CH_2\cdot CH(C_2H_5)\cdot CH_2-NH_2$

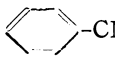

$\longrightarrow$
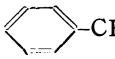

The two primary heptylamines other than *n*-heptylamine are possibly 2-methylhexyl- and 2-ethylamyl-amines which may be obtained from 2-cyanohexatriene and 3-cyanohexatriene, respectively.

These facts confirmed the suggestions described in the previous paper. The presence of *n*-butylamine may be explained by the formation of allylcyanide, since the formation of acetonitrile from acetylene and hydrocyanic acid was confirmed in the author's other experiment[3].

Experimental

1. Catalytic Hydrogenation of the Neutral By-products.—The neutral part[1] (109 g.) of by-products which were obtained as the intermediate distillation fraction between acrylonitrile and succinodinitrile was hydrogenated with Raney nickel under the condition shown in Table I.

TABLE I

HYDROGENATION OF THE NEUTRAL BY-PRODUCTS OF ACRYLONITRILE SYNTHESIS

Inhalt of stainless steel autoclave, 330 cc.

Expt. No.	Starting material g.	Catalyst (Alloy) g.	Press. atm.	Temp. °C	Time min.	Hydrogen absorbed mol.	Prod. g.
1	29	5	80–20	130	220	0.90	27
2	80	5	86–18	120	326	1.95	79

TABLE II

FRACTIONAL DISTILLATION OF BASIC HYDROGENATION PRODUCTS

No.	Temp. °C	Distillate cc.	No.	Temp. °C	Distillate cc.
A-Fractions (760 mmHg)			B-Fractions (100 mmHg)		
1	35–47.5	0.7	1	45–59.8	0.6
2	77–78.5	1.6	2	59.9–69.0	2.4
3	79–97.2	3.1	3	69–69.5	0.1
4	97.2–100	0.6	4	77–82.8	0.6
5	100–102	0.7	5	83.4–104.7	1.4
6	102–103	0.4			
7	103–106	5.4	C-Fractions (5 mmHg)		
8	106–107	2.2	1	–56.7	0.4
			2	58–73.5	0.9
			3	74	

The hydrogenation products (106 g.) were dissolved in the same amount of ether and treated with aq. hydrochloric acid solution, resulting in the separation of 11.2 cc. (containing ether and water) of the neutral part and 51 cc. (containing ether and water) of the basic part.

This basic part (51 cc.) was fractionated by distillation through a Stedman-type column (with stainless steel net; plate number 14–18) under different pressures successively: A, 760 mmHg; B, 100 mmHg; C, 5 mmHg: and the results are shown in Table II.

2. N,N'-Alkylphenylthiourea.—To 0.5 cc. of the constant boiling fraction A-2 (b. p. 77–78.5°C), 1 cc. of phenylisothiocyanate was added (exothermic) to form a very viscous liquid. After an addition of petroleum ether, the mixture was allowed to stand for several days to form crystals. These crystals were filtered and melted at 61–61.5°C, after recrystallization from benzene and petroleum ether. Yield 0.1 g. These crystals mixed with N,N'-*n*-butylphenylthiourea (m. p. 65 °C[4]) melted at 62.5–63°C, showing no melting point depression.

Anal. Found: C, 63.71; H, 7.46; N, 13.21. Calcd. for $C_{11}H_{16}N_2S$: C, 63.42; H, 7.74; N, 13.44%.

From the mixture of 0.5 cc. of the constant boiling fraction A-7 (b. p. 103–106°C) and 1 cc. of phenylisothiocyanate, 0.1 g. of crystals were obtained, and melted at 62–63°C. These crystals mixed with N,N'-*n*-amylphenylthiourea (m. p. 68–69°C[4]) melted at 65–68°C, showing no melting point depression.

Anal. Found: C, 65.04; H, 8.13; N, 12.53. Calcd. for $C_{12}H_{18}N_2S$: C, 64.81; H, 8.16; N, 12.60%.

3. Paperchromatography of Amine Hydrochlorides.—The paperchromatograms of hydrochlorides of A-3, A-4, B-2, B-4, B-5 and C-2 are shown in Fig. 3.

4. Chromatographic Separation of DNP-Amines on the Column of Cation Exchange Resin.—The aqueous solution of hydrochloride of A-4, B-4, B-5 or C-2 (5–10 cc., containing 0.3–4.0 mg.), the same amount of acetone, 1 cc. of acetone solution of 1-fluoro-2,4-dinitrobenzene

3) S. Morimoto, To be published.

4) Otterbacher and Whitmore, *J. Am. Chem. Soc.*, 51, 1909 (1929).

TABLE III

MELTING POINTS AND ANALYTICAL RESULTS OF DNP-AMINES

DNP-Amine	Melting point Found °C	Literat. °C	Analytical results (%) Found C	H	N	Calcd. C	H	N
-benzyl-	115–6	115–6[5] 126[5']	57.30	4.78	15.75	57.14	4.06	15.38
-*n*-heptyl-	22–3	20[6]	55.64	6.61	15.33	55.50	6.81	14.94

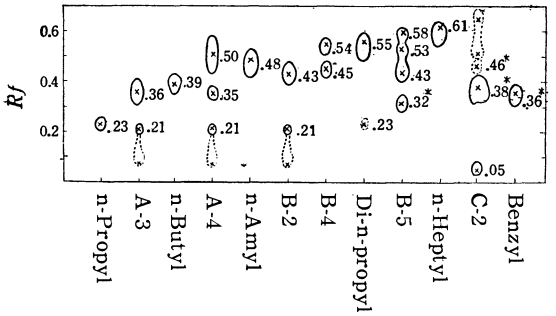

Fig. 3. Paperchromatograms of hydrochlorides of amines.
Developer, Butanol satuarated with water.
*yellow→purple

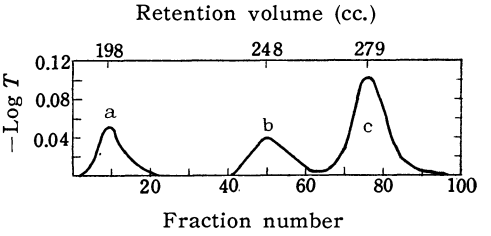

Fig. 4. Elution curve of DNP-A-4 one fraction=1.2 cc.

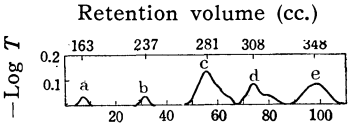

Fig. 5. Elution curve of DNP-B-4 one fraction=1.7 cc.

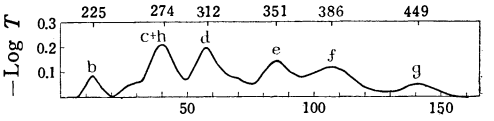

Fig. 6. Elution curve of DNP-B-5 one fraction=1.75 cc.

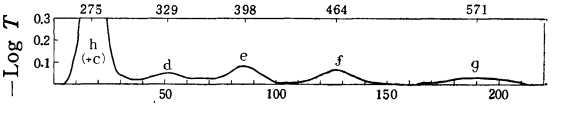

Fig. 7. Elution curve of DNP-C-2 one fraction=1.7 cc.

(FDNB) containing 0.02 g./cc.) and 1 cc. of 2% aqueous sodium bicarbonate solution were mixed and shaken for four hours. Then 1 cc. of aqueous solution of glycine and sodium carbonate (containing 0.008 g. glycine and 0.02 g. sodium carbonate per cc.) was added to the mixture and the resulting mixture was shaken for two more hours. After acetone was evaporated off under reduced pressure, the reaction mixture was extracted with ether three times. From the ether solution, ether was evaporated off under reduced pressure. The residue was dissolved in ten cc. of the mixed solvent (tetrahydrofuran, methylethylketone and water, 4:3:13). Two cc. of the solution was charged on the column (9×400 mm.) of cation exchanger, Amberlite IRC 50 (H-type), and developed with the same solvent.

An ultraviolet spectrophotometer was used to detect and estimate DNP-amines in effluents, taking advantage of the characteristic ultraviolet absorption at 360 mμ. The elution curves are shown in Figs. 4–7. The peaks a, b, c, d, g and h in these figures were identified to be those of DNP-*n*-butyl-, DNP-2-methylbutyl-, DNP-*n*-amyl-, DNP-di-*n*-propyl, DNP-*n*-heptyl- and DNP-benzylamines, by compareing with those of the standard samples, respectively. The peaks e and f are considered to be those of DNP-derivatives of two other primary heptylamines than *n*-heptylamine on the basis of their retention volumes.

5. Preparations of the Standard Samples of DNP-Amines.—N-2, 4-Dinitrophenyl-2-methylbutylamine.—To 30 cc. of aqueous solution containing 0.3 g. of 2-methylbutylamine hydrochloride and 0.6 g. of sodium bicarbonate, 35 cc. of alcoholic (or acetone) solution containing 0.5 g. of FDNB was added and allowed to stand over night in a refrigerator. The oil separated by decantation from the supernatant was dissolved in 30 cc. of alcohol (or acetone). To the solution, 16 cc. of water was added and allowed to stand over night to form 0.35 g. of crystals. The crystals were recrystallized from 25 cc. of alcohol (or acetone) and 11 cc. of water to form 0.3 g. of crystals which melted at 47.3–48°C.

Anal. Found: C, 52.10; H, 5.87; N, 16.87. Calcd. for $C_{11}H_{15}N_3O_4$: C, 52.17; H, 5.97; N, 16.59%. This substance has not been reported in literature up to this time.

5) A. Mulder, *Rec. trav. chim. Pay-Bas*, **25**, 111 (1906): H.J. Backer, ibid., **70**, 92 (1951).
5') G.T. Morgan, *J. Chem. Soc.*, **1915**, **107**, 1307.
6) E.J. Van der Kam, *Rec. trav. chim. Pay-Bas*, **45**, 722 (1926).

By the same way, DNP-benzylamine and DNP-*n*-heptylamine were prepared. Their melting points and analytical results are shown in Table III.

The reaction products of di-*n*-propylamine with FDNB did not solidify by the same way. But the sample showed an unique chromatographic band on the column except for DNP-*n*-propylamine. Thus the sample was employed as a qualitative standard.

The preparations of DNP-derivatives of *n*-propyl-, *n*-butyl- and *n*-amyl-amine were reported in the author's other paper[2].

Summary

The basic substances were obtained from the hydrogenation products of the neutral by-products of acrylonitrile synthesis from acetylene and hydrocyanic acid. They were fractionated by distillation through a Stedman-type column. *n*-Butylamine and *n*-amylamine were isolated and identified as derivatives of phenylthiourea. On the basis of chromatograms, i.e., the paperchromatograms of hydrochlorides of amines and chromatograms of N-2,4-dinitrophenyl-derivatives on the column of cation exchanger, the presence of seven amines, i.e., *n*-propyl-, *n*-butyl-, 2-methylbutyl-, *n*-amyl-, di-*n*-propyl-, *n*-heptyl- and benzyl-amines was confirmed and that of two primary heptylamines other than *n*-heptylamine, i.e., 2-methylhexyl- and 2-ethylamyl-amines, was suggested.

Heartfelt thanks are to be returned to Professors Shiro Akabori and Shunsuke Murahashi of Osake University for their kind instruction and suggestions; and to Kazuo Adachi and Masamichi Miura for their helpful technical assistance.

Department of Chemistry, Faculty of Science, Osaka University, Osaka

Spectrochemical Study of Microscopic Crystals. XIII[1]. *The Structure of Wolffram's Red Salt,* $Pt(NH_2 \cdot C_2H_5)_4Cl_3 \cdot 2H_2O$ *and a Related Compound*[2]

By Shoichiro YAMADA and Ryutaro TSUCHIDA

(Received July 11, 1956)

Formerly the present authors studied the polarized absorption spectra of those compounds involving apparently tervalent platinum or palladium which display extraordinarily deep colours[1,3]. It was found in the earlier studies[3] that some of the above compounds have chains consisting of platium or palladium atoms in different oxidation states connected through halide ions and that the formation of the chains gives rise to a characteristic charge transfer absorption polarized along the chains. Wolffram's red salt, $Pt(EA)_4Cl_3 \cdot 2H_2O$[4], which contains a platinum atom in an apparently tervalent state, may be supposed to belong to a similar type of compound[3]. This compound was first synthesized by Wolffram[5], who obtained the red crystals of this compound by oxidizing an aqueous solution of tetrakis-(ethylamine)-platinum(II) chloride, $Pt(EA)_4Cl_2$, with hydrogen peroxide. Much later Reihlen and Flohr[6] considered the compound as containing divalent and quadrivalent platinum atoms, and ascribed the unusually deep colour of the compound to a special structure of the crystal lattice, which, however, was not explained at all. On the contrary, Drew and Tress[7] attempted to explain the deep colour of this compound on the assumption that the compound might involve a tervalent platinum atom. Establishing the diamagnetism of this compound, Jensen showed that the compound did not involve the platinum in the tervalent state. The deep colour of this compound, however, was still left unexplained[8].

The present work was undertaken in order to explain the color of Wolffram's salt and a related compound in relation to the structure and the probable aid in the comprehension of the charge transfer spectra.

1) Part XII of this series. S. Yamada and R. Tsuchida, This Bulletin, **29**, 694 (1956).
2) Presented in part before the ninth annual meeting of the Japan Chemical Society, Kyoto, April 2nd, 1956.
3) R. Tsuchida and S. Yamada, *Nature*, **174**, 1064 (1954); This Bulletin, **29**, 421 (1956).
4) The notation, A, denotes a molecule of ethylamine.
5) H. Wolffram, Dissertation Königsberg, 1900.
6) H. Reihlen and E. Flohr, *Ber.*, **67**, 2010 (1934).
7) H. D. K. Drew and H. J. Tress, *J. Chem. Soc.*, **1935**, 1244.
8) K. A Jensen, *Z. anorg. allgem, Chem.*, **229**, 252 (1936).

Experimental

Materials.—Tetratkis-(ethylamine)-platinum(II) chloride dihydrate was prepared according to the method of Reihlen and Flohr[5] as colourless crystals. The absorption spectrum was determined with the aqueous solution.

Dichloro-tetrakis-(ethylamine)-platinum(IV) chloride dihydrate was prepared by the method of Reihlen and Flohr[5] in pale-yellow crystals. The crystals of the compound are quite stable in the dark, but undergo decomposition on irradiation of ultra-violet light to form a red compound. The aqueous solution of the compound is rather stable in the light. The absorption spectrum was determined in an aqueous solution.

Wolffram's red salt, $Pt(ethylamine)_4Cl_2 \cdot 2H_2O$, was obtained by the method of Reihlen and Flohr[5] from $[Pt(EA)_4]Cl_2$ and $[Pt(EA)_4Cl_2]Cl_2$. Red crystals of the compound thus obtained show a striking dichroism; they are dark-red with polarized light having its electric vector along the needle axis and almost colourless with polarized light having its electric vector normal to the needle axis. The measurement of the dichroism was carried out along the above two directions.

Tribromo-tetrakis-(ethylamine)-platinum dihydrate, $Pt(EA)_4Br_3 \cdot 2H_2O$, was obtained by the method of Reihlen and Flohr from Wolffram's red salt. Green crystals thus obtained show a striking dichroism; they are dark-green with polarized light having its electric vector along the needle axis, and pale yellow with the electric vector normal to the needle axis. The measurement of the polarized absorption spectra was carried out in these two directions.

Dibromo-tetrakis-(ethylamine)-platinum (IV) bromide, $[Pt(EA)_4Br_2]Br_2$, was prepared in orange, crystalline powder by treating an aqueous solution of $[Pt(EA)_4]Cl_2$ with an excess of hydrogen peroxide and concentrated hydrobromic acid. The absorption spectrum was determined in an aqueous solution.

Measurement.—Quantitative measurements of absorption spectra of the crystals were made by Tsuchida—Kobayashi's microscopic method[9] with polarized light in the regions covering 2400 to 7500 Å. The notation, α, represents the absorption coefficient per mm. of a crystal. The *c*- and *a*-absorption denotes absorption with the electric vector parallel and normal to the needle axis, respectively.

Absorption spectra in solution were determined with a Beckman DU quartz-spectrophotometer. The symbol, ε represents a molar extinction coefficient.

Results and Discussion

Structure of Wolffram's Red Salt.—It seems to be obvious that Wolffram's salt, $Pt(EA)_4Cl_3 \cdot 2H_2O$, contains platinum atoms in bi- and quadri-valent states, but not the tervalent state, since the compound in its crystalline state proved to be diamagnetic[8]. The compound is obtained when evaporating a mixed solution of $[Pt(EA)_4]Cl_2$ and $[Pt(EA)_4Cl_2]Cl_2$. The red crystals of the compound dissolve in water to give a colourless solution from which the red crystals of the original compound separate out on cooling. All these facts indicate that Wolffram's salt may be formulated as $[Pt(EA)_4][Pt(EA)_4Cl_2]Cl_4 \cdot 4H_2O$.

Polarized absorption spectra of Wolffram's red salt in the crystalline state and absorption spectra of the component complexes in aqueous solution have been determined in the visible and ultra-violet region, and are shown in Fig. 1. It is seen from the curves that

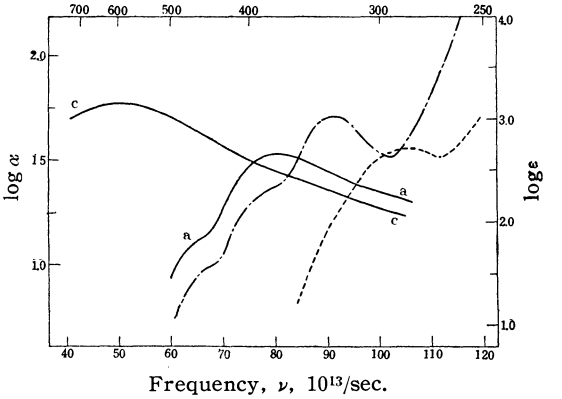

Fig. 1. Absorption spectra of $[Pt(EA)_4][Pt(EA)_4Cl_2]Cl_4 \cdot 4H_2O$ in the crystalline state (———), $[Pt(EA)_4]Cl_2$ in solution (- - - -) and $[Pt(EA)_4Cl_2]Cl_2$ in solution (·—·—).

$[Pt(EA)_4]Cl_2$ or $[Pt(EA)_4Cl_2]Cl_2$ does not show absorption in the visible region, only the tail of the latter absorption extending into the end of the visible region. Comparison of the absorption spectra of Wolffram's salt with those of the component complexes indicates that Wolffram's salt shows to the long wavelength side a new absorption band which is not observed with either of the component complexes alone. This fact implies that the component complexes in the crystal of Wolffram's salt undergo some great effect which does not exist in either of the component complexes alone. The nature of the effect may be judged from the polarization property of the new band at the long wavelength. The present measurement shows that the absorption occurs only with the electric vector along the needle axis, and does not with the electric vector normal to the needle axis. This relationship may be readily understood on the assumption that Wolffram's salt involves infinite chains consisting of the com-

9) R. Tsuchida and M. Kobayashi, "The Colours and the Structures of Metallic Compounds," Zōshindo, Osaka (1944), p. 180; This Bulletin, 13, 619 (1938).

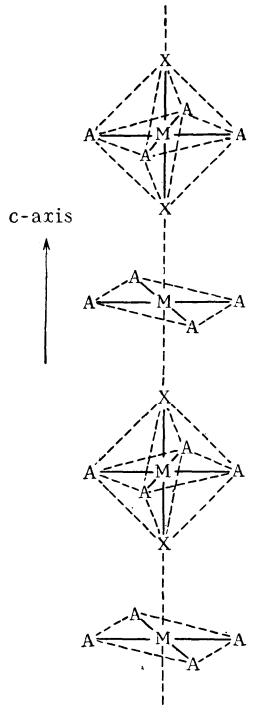

Fig. 2. Chain structure in the crystals of Wolffram's red salt and a related compound having the empirical formula, $Pt(EA)_4X_3 \cdot 2H_2O$.

ponent complexes arranged so that they are piled one just above another along the needle axis (Fig. 2).

In our former studies on the compounds of apparently tervalent platinum and palladium which display unusually deep colours, it was shown that some of those compounds involve infinite chains consisting of the metal atoms in two different oxidation states connected through halogen atoms, and that the chains give rise to a new kind of absorption polarized along the chains. This is quite similar to the relationships which are obtained with Wolffram's salt in the present work. Thus we are led to the conclusion that *the extraordinarily deep colour of Wolffram's salt in the crystalline state is due to the structure containing the infinite chains*, ---Cl—Pt^{IV}—Cl---Pt^{II}---Cl—Pt^{IV}—Cl---.

The new absorption observed with Wolffram's red salt at the longer wave-length, which has been assumed to be originated from the infinite chains, as shown above, may be considered as due to a charge transfer along the chains.

It was concluded in our former researches[3] that the crystal of [Pt en Cl_2][Pt en Cl_4][10], which has an unusually deep colour as compared with the colours of its component complexes, involves similar chains of ---Cl—Pt^{IV}—Cl---Pt^{II}---Cl—Pt^{IV}—Cl---, along which the crystals show a characteristic charge transfer band at about 59×10^{13}/sec. Wolffram's salt involving similar chains shows a charge transfer band at about 58×10^{13}/sec. Comparing the two compounds, the platinum atoms are co-ordinated through chloride ions and/or nitrogen atoms in both the compounds, and the difference between the two may be expected to be rather small, as far as the electronic state along the infinite chains is concerned. In fact, the charge transfer absorption characteristic of the infinite chains are observed at about the same wave-length. This also seems to support the above assumption of the chain structure.

It was formerly proposed that the compounds with apparently tervalent platinum and palladium which are dealt with in the present and former papers of this series might be dinuclear complexes of such a type as are represented by (1)[11]:

$$\left[A_4Pt^{II}\begin{matrix}X\\X\end{matrix}Pt^{IV}A_4\right]^{4+} \rightleftharpoons \left[A_4Pt^{IV}\begin{matrix}X\\X\end{matrix}Pt^{II}A_4\right]^{4+}. \qquad (1)$$

The evidence for this view, however, seems to be very insufficient. Since bivalent platinum usually assumes planar co-ordination, the supposed 6-co-ordination of the bivalent platinum is unusual. It may be impossible to suppose that the bivalent platinum should take octahedral 6-co-ordination which is equivalent to the octahedral co-ordination around the quadrivalent platinum so that the above resonance (1) might be allowed. The spectroscopic studies into polynuclear complexes, which will be reported elsewhere[12], indicate that the dibridged polynuclear complexes in general do not show their absorption in the wave-length regions much longer than the related monomeric compounds. Nor do they show any charge transfer band of the above sort. All these considerations, together with the X-ray structure analysis of a similar compound of tervalent platinum, $Pt(NH_3)_2Br_3$,

10) The notation, en, denotes a molecule of ethylenediamine.

11) See, for example, N. V. Sidgwick, "The Chemical Elements and Their Compounds. Vol. II". Oxford Univ. Press, London (1952). p. 1605, etc.

12) The work is concerned with halogen-bridged complexes: R. Tsuchida and S. Yamada, To be submitted soon.

seem to support our view that the appearance of a new absorption band at the long wave-length and the remarkable polarization of this new band along the *c*-axis in the crystal of Wolffram's red salt may be explained by the assumption of the infinite chains much better than by the model of the dinuclear complex.

In the coure of the present study, we have found that the crystal of $[Pt(EA)_4Cl_2]Cl_2 \cdot 2H_2O$ undergoes photo-decomposition with ultra-violet light. Thus on evaporating spontaneously an aqueous solution of $[Pt(EA)_4Cl_2]Cl_2$ in a sunny room, a small amount of Wolffram's salt is formed besides the crystals of the original compound. The compound, however, is quite stable to the visible light. On irradiating the crystal with a powerful tungsten lamp at a close distance, no decomposition has been observed. On the contrary, when the crystal was put into the light beam from the iron arc, photo-decomposition was found to take place in a few minutes, the crystal beginning to turn red. Observed under the microscope, red spots are formed here and there in the crystal, the spots getting larger and the number of the spots increasing. The red spots might possibly be due to the photo-reduction of the compound, followed by formation of the chain structure, which would be similar to Wolffram's salt. Thus we suppose the main change might be what follows:

$$[Pt(EA)_4Cl_2]^{2+} \xrightarrow{h\nu} [Pt(EA)_4]^{2+} + Cl_2. \quad (2)$$

This change seems to be rather incomplete in an aqueous solution. After the aqueous solution of the compound is exposed to the sun for scores of hours, the absorption spectrum is found to be slightly different from the absorption of the original compound before the irradiation. Thus the absorption at 76.8×10^{13}/sec. diminishes its intensity. This may be explained as due to the decomposition of $[Pt(EA)_4Cl_2]^{2+}$ and subsequent formation of the $[Pt(EA)_4]^{2+}$ ion, since the former has an absorption band at this wave-length whereas the latter shows no absorption at the same wave-length. A rough estimation indicates that about twenty percent of the original compound has undergone the photo-reduction after the exposure of the solution to the sun for about one hundred hours.

It was suggested in the former papers[3] that the formation of the infinite chains as assumed for Wolffram's salt would stabilize some complex radicals which would other-wise be rather unstable. In fact, the complex ion, $[Pt(EA)_4Cl_2]^{2+}$, in the crystal of Wolffram's salt is far more stable to the photo-decomposition than in the crystal of dichloro-tetrakis-(ethylamine)-platinum (IV) chloride. Thus Wolffram's salt does not undergo any change after irradiation with the iron arc for many hours. In the crystal of Wolffram's salt, the approach of the chloride ion in $[Pt(EA)_4Cl_2]^{2+}$ to the platinum(II) ion of an adjacent complex radical may partly diminish the negative charge on the chloride ion, suppressing the charge transfer from the chloride to the platinum(IV) ion, which is the reaction represented by (2). This also is an example of the stabilization of the otherwise unstable complex ions due to their incorporation into the chain structure[3].

There is known a similar type of compounds, such as $Pt(NH_3)pyCl_3$[13], $Pt(NH_3)(EA)Br_3$ and $Pt(NH_3)(EA)Cl_3$[14]. These compounds, which contain apparently tervalent platinum and show quite deep colours, may be believed to have a chain structure similar to that of Wolffram's salt. The unusually deep colour of those compounds may probably be due to the infinite chains in the crystalline state.

Structure of Reihlen's Green Salt.—On adding potassium bromide to a luke-warm, aqueous solution of Wolffram's salt, there are formed slender, green needles[6,15], which have an empirical formula, $Pt(EA)_4Br_3 \cdot 2H_2O$, analogous to that of Wolffram's red salt. Just as in the case of Wolffram's red salt, the crystals of the compound, Reihlen's green salt, dissolve in water to give an orangish-yellow solution, from which the green crystals of the original compound separate out on cooling. From these facts, it is supposed that this compound in the crystalline state may involve a structure similar to that of Wolffram's red salt, being formulated as $[Pt(EA)_4][Pt(EA)_4Br_2]Br_4 \cdot 4H_2O$.

Polarized absorption spectra of this compound have been determined, and shown in Fig. 3. It is seen from this measurement that this compound in the crystalline state shows to the long wave-length side a new absorption band, which may not be observed with the component complex ions alone. This shows that the complex ions in this crystal are subject to some effect. The present measurement also indicates that the new absorption band at the long wave length occurs only with the electric vector along the needle-axis, and not with the electric vector normal to the needle-axis. These re-

13) H. D. K. Drew, F. W. Pinkard, W. Wardlaw and E. G. Cox, *J Chem. Soc.*, **1932**, 1004. The symbol, py, denotes a molecule of pyridine.

14) S. M. Jörgensen, *J. prakt, Chem.*, 33, 489 (1886), etc.

15) The green compound is referred to tentatively as Reihlen's green salt in the present paper.

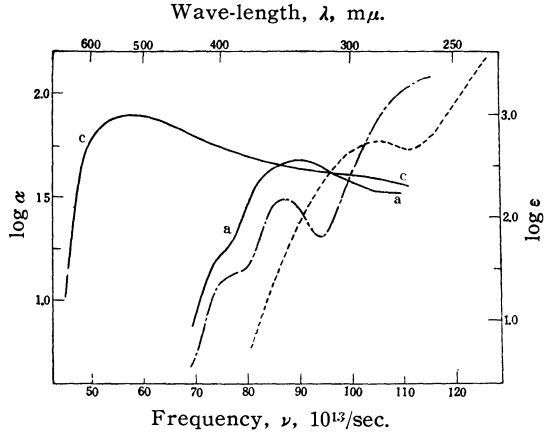

Fig. 3. Absorption spectra of $[Pt(EA)_4][Pt(EA)_4Br_2]Br_4 \cdot 4H_2O$ in the crystalline state (———), $[Pt(EA)_4]Cl_2$ in solution (- - - -) and $[Pt(EA)_4Br_2]Br_2$ in solution (·—·—).

lationships, which are quite similar to those obtained with Wolffram's red salt, may be understood if we assume that the crystal of this compound involves a structure similar to Wolffram's red salt. Thus we are led to the presumption that the compound in the crystalline state contains infinite chains of ---Br—Pt^{IV}—Br---Pt^{II}---Br—Pt^{IV}—Br---. The absorption at about 51×10^{13}/sec. may possibly be due to the charge transfer along the infinite chains. It is concluded that *the deep colour of this compound is due to the formation of the infinite chains which are similar to those in the crystal of Wolffram's red salt.*

Charge Transfer Spectra.—It has been shown in the above discussion that the compounds with infinite chains of the above kind exhibit in the long wave-length regions charge transfer spectra which are polarized along the chains. Reviewing the data so far obtained, the following relationships on the charge transfer spectra may be derived. (1) *The charge transfer spectrum seems to be unrelated to the spectrum of both the components alone.* (2) *The spectrum is rather intense and broad.* (3) *The spectrum is strongly polarized along the infinite chains. That is, the spectrum is observed only with the electric vector along the infinite chains.*

These relationships are found to be consistent with the theory of the charge transfer spectra recently developed by Mulliken[16].

It is to be noted that the absorption normal to the infinite chains has in the long wave-length a shape similar to the superposition of the absorption spectra of the component complexes in solution. This fact seems to indicate that the absorption normal to the infinite chains may be more closely related to the linkages in the complex radicals.

Comparing the two compounds dealt with in the present work, it is seen that Reihlen's green salt shows its charge transfer band in the longer wave-length regions than the chlorine analogue, Wolffram's red salt. The difference in the wave-length of the charge transfer band between the two is found to be nearly equal to the difference in the ionization potential between the chlorine and bromine. This may also be explained on the basis of the assumption that the charge transfer takes place from the halide to platinum(II) ions.

Summary

Polarized absorption spectra of Wolffram's red salt, $Pt(EA)_4Cl_3 \cdot 2H_2O$, and a related compound, $Pt(EA)_4Br_3 \cdot 2H_2O$, EA being ethylamine, have been determined by Tsuchida-Kobayashi's microscopic method in the regions covering from 2400 to 7500 Å.

Both the compounds, which are supposed to be formulated by $[Pt(EA)_4][Pt(EA)_4X_2]X_4 \cdot 4H_2O$, have been found to show an absorption band that has not been observed with either of the components alone. Moreover, this band is strongly polarized along the needle axis. These relationships may be understood on the assumption that the crystals of these compounds involve infinite chains of ---X—Pt^{IV}—X---Pt^{II}---X—Pt^{IV}—X--- along the needle axis, X being chlorine or bromine.

The new absorption at the longer wave-length may be considered as a charge transfer band along the infinite chains as assumed above.

The present authors are indebted to Mr. H. Nakamura for assistance in the experimental work. The work reported here was supported by the grant in aid of the ministry of Education.

Department of Chemistry, Faculty of Science, Osaka University, Osaka

16) R. S. Mulliken, *J. Am. Chem. Soc.*, **72**, 600 (1950); **74**, 811 (1952). *J. Phys. Chem.*, **56**, 801 (1952).

Irreversible Photobleaching of the Solution of Fluorescent Dyes. II. Photobleaching of the Alcoholic Solution of Eosine in Vacuo

By Masashi IMAMURA and Masao KOIZUMI

(Received July 9, 1956)

Introduction

In the first paper of this series[1] kinetic studies on the photobleaching of eosine, erythrosine and uranine in aqueous solutions in the presence of oxygen were reported and some probable schemes were proposed for the primary processes of the reaction. In that paper the notable fact was found that the addition of ethyl alcohol to the aqueous solution of eosine caused a marked retardation on the rate of aerobic photobleaching. Thus in the mixture of water and ethyl alcohol 7: 3 in volume, the rate became practically negligible and in the pure alcoholic solution there was no photobleaching observed. But another remarkable fact then found was that if such solutions are deaerated, considerable rapid photobleaching takes place in contrast to the pure aqueous solution which shows no such photobleaching in vacuo at all.

Though it appears that the vacuum photobleaching (in alcohol) and the aerobic photobleaching (in aqueous solution) will proceed by different mechanisms, it is interesting to study about the primary processes of the former and about the retarding effect of oxygen. Moreover, it is not unexpected that the information obtained therefrom may be helpful for the further attack on the primary processes of the aerobic photobleaching in the pure aqueous solution.

The purpose of the present paper is to report some results obtained using methyl, ethyl, isopropyl and *n*-butyl alcohol as solvents and to make some discussions on the mechanism of the reaction.

Experimental

Procedure.—Eosine and the arrangements for irradiation were the same as those described previously[1,2]. Methanol, ethanol, isopropanol and *n*-butanol were purified by the method similar to that employed in the preceding paper for ethanol. Stock solutions of eosine in these alcohols were prepared at concentration of 10^{-3} mol./l. These solutions were diluted to the concentration of 10^{-5} mol./l. and were deaerated with much caution in view of the high solubility of oxygen in alcohols. The procedure was as follows. The solution was put into one of two ampoules attached to a reaction cell and was evacuated under cooling with use of a mercury diffusion pump. Then the alcohol was distilled into another ampoule and evacuated again. These processes were repeated four to six times.

Irradiated alcoholic solution of eosine in vacuo did not show any shift of the absorption maxima as compared with the initial solution, and the almost perfect absorption curve in visible region declined monotonously as the bleaching went on. Hence the change of the concentration of eosine could be followed by a photomultiplier and an interference filter in exactly the same way as described already[1,2].

Experiments were made on the oxygen effect on the rate, with use of the apparatus schematically shown in Fig. 1. At first, complete deaeration was accomplished by repeated vacuum distillation between E and F. Then a definite small amount of oxygen was taken between A and B manometrically and it was expanded to the right hand side of B, in which the solution F was being cooled with dry ice. (The volume of these two parts had been determined previously.) The oxygen pressure after expansion could easily be calculated. After C was fused off, oxygen was dissolved at room temperature into the solution, which was then poured into the cell, and D was fused off. Of course all the manipulations were made in the dark. The amount of oxygen in a reaction cell was calculated, employing the value

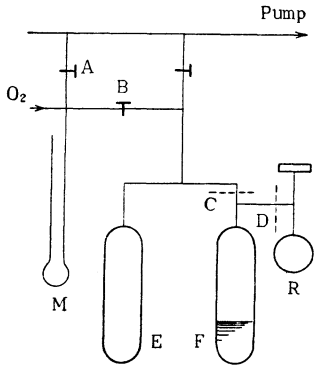

Fig. 1. Schematic diagram of the apparatus. M: manometer; R: reaction cell.

1) M. Imamura and M. Koizumi, This Bulletin, 28, 117 (1955).

2) M. Imamura, *J. Inst. Polytech. Osaka City Univ.*, **6**, No. 1, Series C, 85 (1956).

of 0.14 as a Bunsen coefficient[3] for pure ethanol. and taking into account the volume of the solution and that of the gaseous phase.

Results

1. Photobleaching of the Alcoholic Solutions in Vacuo.—Investigations were carried out at 20°C with a filter Matsuda VG1. The intensity of light was varied with blackened metallic nets.

The rate of bleaching was relatively great compared with that of aerobic aqueous solution. Some examples of the bleaching curve are shown in Fig. 2, which includes a curve for the aerobic photobleaching of the aqueous solution for comparison. Absorption spectra of the irradiated solution are compared with the original one in Fig. 3.

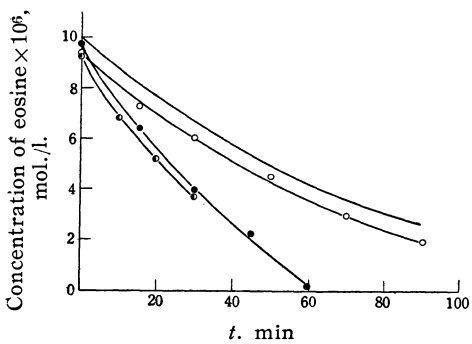

Fig. 2. Fading curves of eosine in vacuo at 20°C.

Full line: in aerobic aqueous solution, $I_0=1.74\times10^{16}$ $h\bar{\nu}$/cm². sec.; ○: in methanol, $I_0=1.18\times10^{15}$ $h\mu$/cm². sec., ●: in ethanol, $I_0=1.41\times10^{16}$, ◐: in isopropanol, $I_0=1.18\times10^{15}$. In all cases $d=15$ mm.

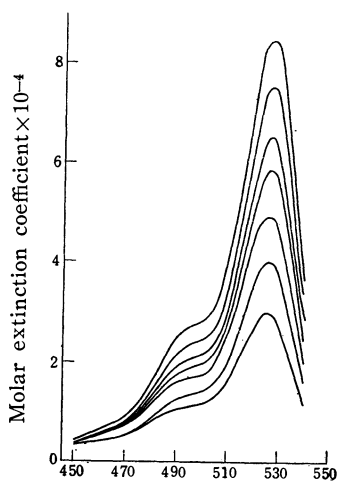

Fig. 3. Absorption spectra of irradiated eosine in EtOH in vacuo. At 34°C.

As anticipated from these figures, the experimental results obtained for every sort of alcohol except *n*-butanol could be represented satisfactorily by the same rate formula as that proposed in the previous paper[1].

$$-\frac{dc}{dt}=\frac{k}{d}I_0(1-e^{-\alpha cd})\times1000^* \quad (1)$$

$$S\equiv\ln(1-e^{-\alpha c_0 d})-\ln(1-e^{-\alpha cd})+\alpha d(c_0-c)=1000k\alpha I_0 t \quad (2)$$

where c and c_0 are the concentrations of dye in mol./l. at time $t=t$ and $t=0$, α the mean molar absorption coefficient, d the thickness of the solution in cm., I_0 the intensity of light in moles per cm² per sec., and k is the usual overall rate constant and is also considered as a quantum yield of bleaching. Mean molar absorption coefficients of eosine (α's) in methanol, ethanol, isopropanol were determined by a thermopile to be 4.8×10^4, 6.6×10^4, 6.1×10^4 and 5.2×10^4, respectively.

Some examples of the application of eq. (2) to the experimental results are shown in Fig. 4 and

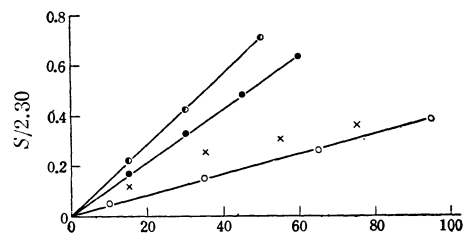

Fig. 4. Dependence of the left-hand side of eq. (2) divided with 2.30 (S/2.30) on irradiation time t. At 20°C.

○: in methanol, $I_0=0.69\times10^{16}$ $h\bar{\nu}$/².cm sec.; ●: in ethanol, $I_0=0.83\times10^{16}$; ◐: in isopropanol, $I_0=0.69\times10^{16}$; ×: in *n*-butanol, $I_0=0.68\times10^{16}$.

TABLE I

QUANTUM YIELDS FOR PHOTOBLEACHING OF EOSINE IN MeOH, EtOH, AND i-PrOH AT 20°C

(k for aerobic photobleaching in aqueous solution is 1.8×10^4.)

Solvent	$I_0\times10^{15}$ $h\bar{\nu}$/cm² sec.	$k\times10^4$	Solvent	$I_0\times10^{15}$ $h\bar{\nu}$/cm² sec	$k\times10^4$
MeOH	0.69	5.3	EtOH	0.74	6.4
〃	〃	2.7	〃	0.83	4.4
〃	〃	4.0	〃	〃	4.6
〃	1.18	3.8	〃	1.25	5.4
〃	〃	3.7	〃	1.41	4.5
〃	〃	2.9	〃	〃	9.0
Average		(3.7)	Average		(5.6)
EtOH	0.35	4.2	*i*-PrOH	0.69	3.9
〃	0.39	4.3	〃	〃	7.4
〃	〃	4.5	〃	〃	7.8
〃	0.62	10.3	〃	1.18	4.6
〃	0.66	4.9	〃	〃	5.6
〃	〃	4.6	〃	〃	5.9
〃	0.74	6.4	Average		(5.9)
〃	0.83	4.4			

3) "International Critical Table", McGraw Hill, New York (1929), 3, p. 262.

the values of k's calculated are summarized in Table I. Though it is certain that eq. (1) can be applied to ethanol, methanol, and isopropanol, some fluctuations exist among the k-values of different runs. It may perhaps be due to the slight difference of the pretreatment of alcohols in view of the existence of the very sensitive effect of a trace of oxygen described below. In spite of these fluctuations, it is evident that the order of the rate of photobleaching in vacuo is MeOH< EtOH<i-PrOH. From the measurements made on the quantum yield of the ethanolic solution of eosine at various temperatures, it was found that the activation energy for the reaction in ethanol in vacuo was computed as 5 ± 1 kcal./mol., which is about the same as that obtained for aerobic aqueous solution of eosine[1].

As to the reaction products, qualitative tests of aldehyde and acid were applied to the vacuum distillate from the irradiated ethanolic solution of eosine.

Acidity was examined by a glass electrode pH meter and also by the spectroscopic measurements with some ordinary pH indicators. There was no change observed in pH.

Aldehyde, on the other hand, could be detected by every test employed, i.e., by Tollen's reagent (NH_3—$AgNO_3$ solution), by Schiff's reagent (reduced p-fuchsine solution) and by the method which utilized the catalytic action of aldehyde on the oxidation of p-phenylene diamin by hydrogen peroxide[4].

2. Effect of Small Amounts of Oxygen on the Photobleaching of Alcoholic Solution.—As mentioned above, aerobic pure alcoholic solution of eosine did not show any photobleaching. When a very small amount of oxygen was added to the completely evacuated solution, the photobleaching did not take place for a certain period which was almost proportional to the amounts of added oxygen, but after this induction period, the reaction began to proceed abruptly and with almost the same rate as that in the completely evacuated solutions.

Results are shown in Fig. 5, in which the number depicted along each curve is the oxygen pressure (mmHg) in the gaseous phase of a cell.

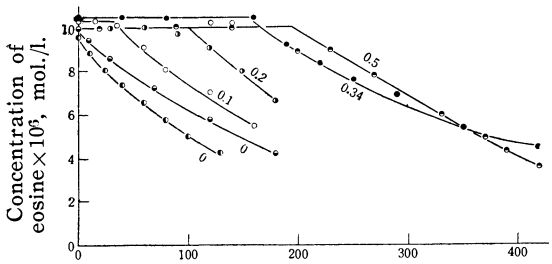

Fig. 5. Fading curves of eosine in EtOH in the presence of various amounts of oxygen. At 27°C.
The number depicted along each line is the oxygen pressure in mmHg. in the gaseous phase of a cell.

From the above results, there scarcely remains any doubt that a small amount of oxygen inhibits the photobleaching of eosine and this inhibiting action comes to its end when oxygen is used up by some unknown reaction. Thus it must be interpreted that during the induction period some photosensitized oxidation reaction is going on by virtue of eosine as a photosensitizer. As such a photosensitized oxidation, there will be no other possibility than that of the oxidation of alcohol to acid or aldehyde. Hence several tests for aldehyde and acid were tried for the irradiated aerobic alcoholic solution of eosine. The result was that the formation of aldehyde could not be detected by Tollens' and by Schiff's reagents, while the formation of acid was definitely established from the facts that reduction of pH could be observed by means of a glass electrode pH meter and by usual indicators spectroscopically.

Aldehyde would perhaps be oxidized to acid if it were produced, which was ascertained by an independent test that a small amount of aldehyde added to the aerobic alcohol solution was quickly converted to acid by irradiation. The acid formed would probably be acetic acid, but could not be identified because of its small quantity.

Another product confirmed in the irradiated aerobic alcoholic solution was hydrogen peroxide; it was detected by iodometry in nitrogen atmosphere and by titanium trichloride.

Assuming that the existing oxygen is exhausted during the induction period, the quantum yield for the photochemical disapperance of oxygen (γ) could be calculated from the data shown in Fig. 5. The ratio of γ to k (the quantum yield of photobleaching of eosine) is tabulated in Table II, which shows that the ratio is almost constant, independent of the quantity of oxygen; the value is about 3.

Table II
The ratio of γ to k

P_{O_2} (mmHg)	O_2 (10^{-3} mol.)	t_{ind} (min.)	γ/k
0.1	4.2	31	3.5
0.2	8.4	100	2.4
0.3	14.6	160	3.1
0.5	21.4	200	3.3
		Average	(3.1)

Discussion

Since the photobleaching of eosine in the evacuated alcoholic solution is accompanied by the production of aldehyde, it can be concluded that its primary process is the dehydrogenation of alcohol by the excited dye, most certainly in the triplet state;

$$D^t + RH \longrightarrow DH\cdot + R\cdot, \qquad \text{(i)}$$

where D^t is the excited dye in the triplet state, RH is alcohol, DH· a semiquinone-type intermediate and R· a radical from alcohol. The process (i) can also be considered as an

4) F. Feigl, "Spot Tests", Elsevier (1954), Vol. II, p. 146.

essential step of the photobleaching if one assumes, as is probable, that DH· is colorless or almost colorless. This is consistent with the experimental result that the rate of photobleaching depends only on the amounts of light absorbed; moreover, the fact that the rate increases in the order, MeOH<EtOH <i-PrOH, coincides nicely with the general trend of hydrogen releasing power of R· as observed, for example, in the oxidation of alcohol with Fenton's reagent[5]. Thus there scarcely remains any doubt about the primary process of the photobleaching in vacuo.

Turning to the inhibiting action of oxygen, although it is certain that oxygen oxidizes alcohol to acid by virtue of the excited dye, which acts as a sensitizer, there are two alternative mechanisms conceivable in respect to the step in which oxygen takes part. The one is

$$\begin{aligned} D^t+RH &\longrightarrow DH\cdot+R\cdot \quad (a) \\ DH\cdot+O_2 &\longrightarrow D+HO_2\cdot \quad (b) \end{aligned} \qquad (ii)$$

and the other is

$$\begin{aligned} D^t+O_2 &\longrightarrow D^t\cdots O_2 \quad (a) \\ D^t\cdots O_2+RH &\longrightarrow D+R\cdot+HO_2\cdot \quad (b) \end{aligned} \qquad (iii)$$

In general, two processes may occur simultaneously, but in the case of ethyl alcohol, the former is considered to be the principal process for the following reason.

As seen from Table II, the duration of the induction period during which photobleaching is completely suppressed, is roughly proportional to the amount of oxygen, and it reaches thirty minutes by the existence of as little oxygen as 4×10^{-8} mol., which corresponds to the oxygen concentration of 8×10^{-7} mol./l. in the solution. Thus it is almost certain that 10^{-8} mol./l. of oxygen or less is enough to completely prevent photobleaching.

This requires quite a long lifetime for the intermediate which is attacked by oxygen; it is estimated to be not less than 10^{-2}–10^{-3} sec. by the analogous argument performed in the previous paper[1]. Hence if the reactions (iii) are to occur, the lifetime of the triplet state must be of the same order. But in the case of the aerobic photobleaching in the aqueous solution, the lifetime of D^t is estimated to be 10^{-6} sec. or so if the reaction goes by (iii)**. Thus the process (iii) can be denied unless one recognizes a very unprobable assumption that the lifetime of the triplet state differs markedly in water and in ethyl alcohol.

Next, let us consider the processes which follow the reaction (ii). There were some investigations published on the photoöxidation of alcohols sensitized by some substances such as azo-compounds[6], benzoquinone[7] and benzophenone[8]. In particular, a recent work of Bolland and Cooper[9], on the photoöxidation of ethanol by anthraquinone 2,6-disodiumsulfonate as a sensitizer afforded some detailed mechanism of the reaction. Applying it to our case it was really found, as shown below, that our experimental results concerning the reaction products and particularly the fact that the ratio r/k is about 3 can all be explained satisfactorily.

For the photobleaching in vacuo, the mechanism in question can be written as follows:

$$D \xrightarrow{h\nu} D^* \qquad (iv)$$

$$D^* \longrightarrow D^t \qquad (v)$$

$$D^t+RH \longrightarrow DH\cdot+R\cdot \quad (vi)\ (\text{same as (i)})$$

$$DH\cdot+DH\cdot \longrightarrow DH_2+D \qquad (vii)$$

$$DH_2 \longrightarrow \cdots \text{products} \qquad (viii)$$

$$R\cdot+R\cdot \longrightarrow RH+\text{aldehyde} \qquad (ix)$$

In this scheme, (vi) is the main step of photobleaching and DH· has the lifetime of 10^{-2}–10^{-3} sec. as stated above. On the other hand, D is regenerated according to (vii). Hence the k-value experimentally obtained is just one half of the rate constant for the formation of DH· by (vi).

When oxygen is present, the following reactions[10] would occur producing hydrogen peroxide and acetic acid and regenerating the original dye molecule. (Aldehyde produced by (xiv) will be further oxidized to acid).

$$R\cdot+O_2 \longrightarrow RO_2\cdot \qquad (x)$$

$$DH\cdot+O_2 \longrightarrow D+HO_2\cdot \qquad (xi)$$

$$RO_2\cdot+RO_2\cdot \longrightarrow 2\text{Acid}+H_2O_2 \qquad (xii)$$

$$HO_2\cdot+HO_2\cdot \longrightarrow H_2O_2+O_2 \qquad (xiii)$$

$$RO_2\cdot+HO_2\cdot \longrightarrow H_2O_2+\text{Aldehyde}+O_2 \qquad (xiv)$$

As regards the last three steps, the following three cases are possible:

5) J.H. Merz and W.A. Waters, *Faraday Soc. Discussion*, 2, 179 (1947); W.A. Waters, "The Chemistry of Free Radicals", Oxford (1946), p. 247.

* The rate formula $dc/dt=kI_0(1-e^{-\alpha cd})$ (3) written in the previous paper[1] must be corrected as above since all the evaluated values of k in that paper were the quantum yields and did not correspond to k in eq. (3). All the results and discussions given in it, however, are not affected by this modification.

** The proof that the primary process of the aerobic photobleaching of eosine in the aqueous solution is really $D^t+O_2 \rightarrow D^t\cdots O_2$ will be concluded in the next paper. Cf. G. Oster and A.H. Adelman, *J. Am. Chem. Soc.*, 78, 913 (1956).

6) B.E. Blaisdell, *J. Soc. Dyers & Colourists*, 65, 618 (1949).

7) A. Berthoud and D. Parret, *Helv. Chim. Acta*, 17, 694 (1934).

8) H.L.J. Bäckström, *The Suedberg (Mem. Vol.)*, 1944, 45; *C. A.*, 39, 1105 (1945); A. Berthoud, *Helv. Chim. Acta*, 16, 592 (1933).

9) J.L. Bolland and H.R. Cooper, *Proc. Roy. Soc. (London)*, 225, 405 (1954).

10) For the rapid reaction of radical R· with oxygen, see, for example, J. R. McNesby and C. A. Heller, Jr., *Chem. Rev.*, 54, 342 (1954).

(a) only (xii) and (xiii) take place;

(b) only (xiv) takes place;

(c) all the three processes take place simultaneously.

According to the above scheme the result, $\gamma/k=3$, can be accounted for as follows. For each DH· produced by (vi), two oxygen molecules are consumed in (x) and (xi), but in (xiii) and (xiv) one is regenerated. The total consumption of oxygen for one molecule of DH· thus becomes 3/2 for all the above three cases:

(a) $2-1/2=3/2$;

(b) $2-1+1/2=3/2$ (since 1/2 O_2 is necessary for the further oxidation of aldehyde);

(c) 3/2 (superposition of (a) and (b)).

In vacuo, on the other hand, for one DH· produced by (vi) 1/2 D should disappear since the process (vii) regenerates one D from two DH·.

Thus the ratio of the quantum yield for the oxygen consumption to that for the photobleaching should be $(3/2)/(1/2)=3$, which agrees very satisfactorily with the experimental values in Table II.

Here it is to be noted that from the above argument, the decomposition of dye through the interaction between DH· and R· can be practically neglected, for γ/k must otherwise be less than 3. Another fact to be added is that the reaction,

$$D^t+O_2 \longrightarrow D^t\cdots O_2,$$

is neglected in the above argument. But even if this reaction partially takes part, the products and the quantitative relation between γ and k are not affected, because, in this case, it is only necessary to replace (xi) by

$$D^t\cdots O_2+RH \longrightarrow D+R\cdot+HO_2\cdot \qquad (xv)$$

without any alterations for the succeeding steps.

Summary

Photobleaching of eosine in methanol, ethanol, isopropanol and *n*-butanol in vacuo was investigated and it was concluded that the primary process is the dehydrogenation of alcohols by the metastable excited eosine molecule. In the presence of oxygen, the photobleaching is suppressed completely, but the sensitized photoöxidation of alcohol takes place.

When a small amount of oxygen is added to the evacuated alcoholic solution of eosine, the induction period appears, after which the photobleaching proceeds with almost the same rate as that in the evacuated state. Both the quantum yield for the consumption of oxygen during the induction period (γ) and that of the photobleaching in vacuo (k) were determined and the ratio γ/k was found to be ca. 3. This result and the reaction products detected (aldehyde in vacuo, acid and hydrogen peroxide in the presence of oxygen) were satisfactorily explained by the mechanism proposed by Bolland and Cooper. Further results somewhat important from the general standpoint of photobleaching of dye are:

(1) The lifetime of the intermediate to be attacked by oxygen (which is most probably DH·) is not less than 10^{-2}–10^{-3} sec.

(2) The quantum yield for the primary process of the photobleaching $D \rightarrow D^* \rightarrow D^t(+RH) \rightarrow DH\cdot(+R\cdot)$ in pure ethanol is ca. 10×10^{-4} at 20°C.

(3) In pure ethanolic solution, the decomposition of dye by the interaction between DH· and R· practically does not occur.

The cost of the present research has been partly defrayed from the Scientific Research Grant from the Ministry of Education.

Institute of Polytechnics
Osaka City University
Osaka

*Reaction of Hydrogen Peroxide with Titanium (IV) at Different pH Values**

By Motoshichi MORI, Muraji SHIBATA, Eishin KYUNO and Syu ITO

(Received May 21, 1956)

Titanium (IV) gives the well-known orange coloration by the action of hydrogen peroxide on an acidified solution, and the production of color has been shown by Jahr and his co-workers[1] to be due to the $(TiO_2 \cdot aq)^{2+}$ ion. On the other hand a yellow compound is formed when ammoniacal hydrogen peroxide is added to a solution of a titanyl salt, and this compound has been regarded by Schwarz and Giese[2] as ortho-pertitanic acid, $Ti(OH)_3(OOH)$. Recently, Babko and Valkova[3] found that the orange color in an acidified solution faded away with the decreasing of the acidity and assumed the existence of different ion-species in solutions with different pH values.

pH below 3, $Ti^{4+}+H_2O_2 \rightleftarrows Ti(H_2O_2)^{4+}$ (orange)

pH 3–6, $Ti^{4+}+H_2O_2 \rightleftarrows Ti(HO_2)^{3+}+H^+$ or (colorless)

$Ti^{4+}\ \ H_2O_2 \rightleftarrows Ti(O_2)^{2+}+2H^+$

We have carried out a series of experiments with a view to finding out whether this assumption is correct.

Early in this work, our attention was attracted by a noteworthy fact that at least four different ion-species exist in solutions whose pH range 1 to 13. The first species, orange in color, appears in solutions of high acidity (pH<2), the second, the bright yellow kind, in solutions of lower acidity (pH 3–6), the third, the pale yellow kind, in slightly alkaline solutions (pH<9), and the fourth, which is colorless, exists in more strongly basic solutions (pH>10). Proceeding with our experiments we obtained various kinds of information about the behavior of these ions, and also devised a new method of volumetric analysis of titanium.

Experimental

Materials.—Stock solution of titanyl sulfate was prepared by carbonate-fusion and acid-digestion of titanium dioxide free from iron. Other reagents used were of analytical grade.

Measurement.—A Beckman Model DU Spectrophotometer and an Ito Spectrophotometer were used to obtain the absorptiometric data and all the measurements were made in matched 1.0 cm. cells. The Molar extinction coefficient was calculated from the titanium content of the solution.

Adjustment of pH was made with a buffer solution and the measurement of pH was made with a Mitamura pH meter. The content of structural water in the solid sample was estimated from the loss of weight of the sample by drying at 400°C by using a Shimazu Thermano Balance. The titanium content was determined by the usual gravimetric or colorimetric method depending upon the sample taken. Active oxygen was volumetrically estimated by using a standard permanganate solution. Molar ratio of hydrogen peroxide to titanium in colored solution was determined by the method of continuous variation. The analysis of the sulfate ion was made gravimetrically and that of potassium ion, alkalimetrically.

Results and Discussion

Appearances of Different Species of Ion with Changes of pH.—When an aliquot of the yellowish solution obtained by neutralizing titanyl sulfate solution with potassium carbonate and then adding a few drops of hydrogen peroxide was introduced into each of a number of buffer solutions, the resulting mixtures showed different colors ranging from orange to colorlessness according to the pH of each solution. The optical density of the colors was measured at 415 mμ, and the values were plotted against the pH (Fig. 1). The curve has its first point of inflexion in the range of pH 1 to 2, its second in that of pH 6 to 7 and the third, which is not so clear as the others, near pH 9. This information indicates the probability that there are at least four different ion-species, each of which exists in solutions having pH value within a certain range. Additional evidence for this was obtained through the measurement of absorption spectra of the solutions (Fig. 2). As shown in Fig. 2 the maximum on each absorption curve is shifted to the short wavelength side with increase of pH. Namely, the species arising from solutions with pH 1.5, 4.2 and 8.6 show the absorption maximum at 400, 330 and 313 mμ respectively. This may be attributed to co-ordination binding

* Presented at the Symposium on Co-ordination Compound, Osaka, October 29, 1955.

1) H. J. Emeleus and J. S. Anderson, "Modern Aspects of Inorganic Chemistry", D. Van Nostrand Co., Inc., N.Y., (1952), p. 375.

2) Schwarz und Giese, *Z. anorg. Chem.*, **176**, 209 (1928).

3) *C. A.*, **42**, 44836 (1948).

of the peroxide ion, O_2^{2-}, with the titanium ion since a certain μ-peroxo-cobalt (III) complex has a similar maximum at 330 mμ[4]. In a strongly alkalified solution (pH 13.0), the absorption band lies in far shorter region and has no maximum. This may be considered to be due to weaker co-ordination binding of the peroxide ion. Thus, it may be said that at least four different species exist separately in specified pH regions (i. e. pH<2, 3–6, 7–9 and 10<pH). Hereafter these species will be denoted by "A", "B", "C" and "D" respectively.

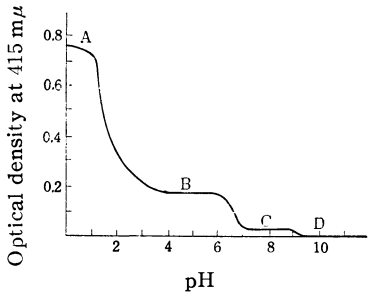

Fig. 1. Light absorption of the Ti(IV)-H_2O_2 system vs. pH. Concentration of Ti, approximately 1×10^{-3} mol./l.

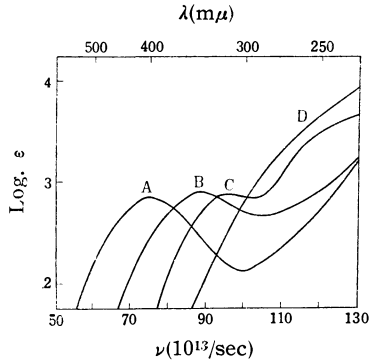

Fig. 2. Absorption spectra of various species.
A. at pH 1.5 B. at pH 4.2
C. at pH 8.6 D. at pH 13.0

Types of Behavior and Formulas.—In order to determine the chemical compositions of "B" and "C", continuous variation studies were carried out, and the results are shown in Fig. 3. In both species, titanium appears to combine with only one molecule of hydrogen peroxide. By the way, it has been well known that in highly acidified solutions they react in the one-to-one molar proportion[5].

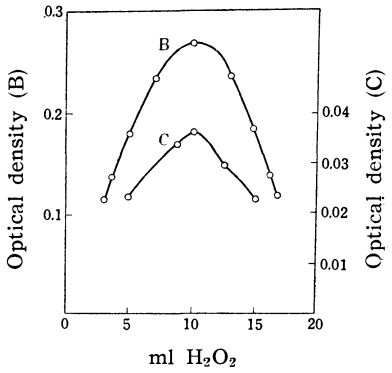

Fig. 3. Curves for graphical determination of ratio of H_2O_2 to Ti (λ=415 mμ). Concentrations of $TiOSO_4$ and H_2O_2, 7.2×10^{-3} M. Total volume, 20 ml.

Further experiments were conducted to isolate solids from the solutions containing each species of ions. Addition of a large amount of alcohol resulted in precipitation of solids. Namely, in the presence of potassium sulfate an orange-colored solid was isolated from the solution containing "A", and a yellow solid, from the solution containing "B". From solutions containing "C" and "D" a pale yellow and a white compound were isolated respectively in the absence of sulfate. After being washed with water, alcohol and finally ether, each precipitate was dried over sulfuric acid and kept for analyses. For convenience' sake they are denoted by A_1, B_1, C_1 and D_1. A_1 and D_1 were easily soluble, B_1 was slightly soluble in water, but C_1 was insoluble in water. All the solids were soluble in mineral acids. C_1 was stable at room temperature but B_1 underwent gradual decomposition. A_1 and D_1 were hygroscopic. Molar ratios of the various components to titanium were as follows.

For A_1: O, 1; H_2O, 3; SO_4, 2; K, 2; assumed composition, $K_2O\cdot TiO_3\cdot 2SO_3\cdot 3H_2O$. For B_1: O, 1; H_2O, 2.5; SO_4, 2.5; K, 4; $4K_2O\cdot Ti_2O_5\cdot 5SO_3\cdot 5H_2O$. For C_1: O, 1; H_2O, 2; $TiO_3\cdot 2H_2O$. For D_1: O, 2; H_2O, 1; K, 2; $K_2O\cdot TiO_4\cdot H_2O$.

On standing at room temperature the solution containing "A" acquired no turbidity, but pale yellow precipitates appeared in the solution containing "C" after standing for a little while, and on standing for several days the solutions containing "B" and "D" yielded a bright yellow and a pale yellow precipitate respectively. On heating them to about 70°C, however, the precipitation was quickly completed. After being washed with water, alcohol and ether, they were dried over sulfuric acid and kept in a vacuum desiccator for analysis. These are denoted

4) S. Yamada, Y. Shimura and R. Tsuchida, This Bulletin, **26**, 72 (1953).
5) Y. Shaeppi and W.D. Treadwell, *Helv. Chim. Acta*, **31**, 577 (1948).

by B_2, C_2 and D_2. All the precipitates were insoluble in water and soluble in 3 N sulfuric acid. The analytical results were as follows.

For B_2: O, 0.9; H_2O, 1; assumed composition $TiO_3 \cdot H_2O$. For C_2 and D_2: O, 0.5; H_2O, 1; assumed composition, $Ti_2O_5 \cdot 2H_2O$.

Now, we are in a position to discuss the reactions taking place in solutions consisting of the titanium (IV)-hydrogen peroxide system. In addition to the absorptiometric and analytical results, the types of behavior of the species toward ion-exchangers are also useful for this discussion. Namely, "A" and "B" were held on a cation exchanger in Na-form (i. e. positively charged) and "D" was held on an anion exchanger in Cl-form (i. e. negatively charged), but "C" passed through both exchangers (i. e. uncharged). Thus, assuming that the co-ordination number of tetravalent titanium is four and that a hydrogen peroxide molecule can unite with the central ion through co-ordination linkage, the reactions involved may be represented as follows:

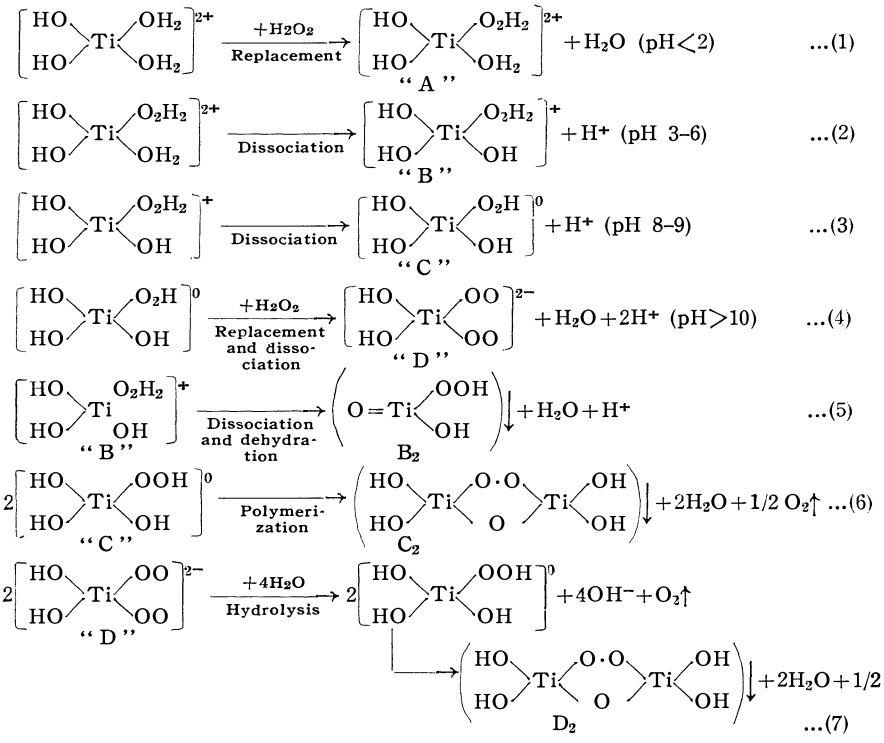

Among the hypothetical formulae, $[Ti(OH)_2(H_2O)(H_2O_2)]^{2+}$ is substantially identical with $(TiO_2 \cdot aq)^{2+}$, and its double salt $K_2SO_4 \cdot [Ti(OH)_2(H_2O)(H_2O_2)]SO_4$ is also identical with $K_2(TiO_2)(SO_4)_2 \cdot 3H_2O$[1]. The chemical formulae of B_1, C_1 and D_1 are presumed to be $4K_2SO_4 \cdot [Ti(OH)_3(H_2O_2)]_2SO_4$, $[Ti(OH)_3(O_2H)]$ and $K_2[Ti(OH)_2(O_2)_2]$ respectively.

Furthermore, the precipitation reactions taking place during the standing or heating of the solutions, may be represented by the following equations.

New Volumetric Analysis of Titanium

Procedure.—By means of a pipet, transfer a 10 ml. portion of the sample solution containing about 10 mg. of titanium (IV) to each of 300-ml. Erlenmeyer flasks, dilute them to about 150 ml. with distilled water and then add a saturated solution of potassium bicarbonate until each solution becomes alkaline and a white precipitate appears. Carefully add a few drops of 30% hydrogen peroxide; then the precipitate will be redissolved and the solution will become yellowish in color. Stand them on a water-bath in the neighborhood of 80°C until effervescence ceases (about two hours). During the time a pale yellow precipitate will separate out. Cool the contents to room temperature and dissolve the precipitate by adding about 50 ml. of 6 N sulfuric acid and standing the mixture about half an hour. Finally, titrate each of the orange-colored solutions with a 0.1 N permanganate solution by using a microburette. One ml of the 0.1 N solution corresponds to 0.00479 g. of titanium.

Discussion

Some of the results obtained by the procedure described above are given in Table I, which clearly shows that the procedure is

TABLE I

ANALYSIS OF TITANIUM

Expt. No.	0.1 N $KMnO_4$ (f=0.9763) ml.	Ti Found mg.	Ti Present mg.	Expt. No.	0.1 N $KMnO_4$ (f=0.9763) ml.	Ti Found mg.	Ti Present mg.
1	1.630	7.62	7.48	6	10.02	46.84	48.15
2	1.610	7.53	〃	7	10.54	49.27	〃
3	1.605	7.50	〃	8	10.19	47.64	〃
4	1.625	7.60	〃	9	10.40	48.62	〃
5	1.610	7.53	〃	10	11.30	52.83	〃

suited for the determination of titanium in quantities of the order of 10 mg. This method is based on the fact that when an alkaline solution containing a titanyl salt and hydrogen peroxide is heated, a pale yellow compound is formed in which the molar ratio of active oxygen to titanium is one to two. (Reaction (6)). By being dissolved with sulfuric acid, this compound decomposes into two components;

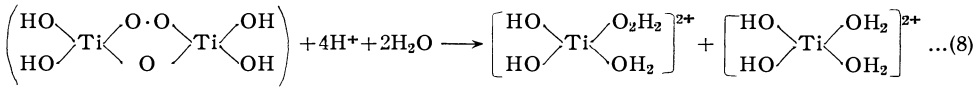

Accordingly, it may be said that the reaction of hydrogen peroxide with a permanganate is applied to this method. Incomplete removal of the oxygen produced by reaction (6) and further decomposition of $[Ti(OH)_2(H_2O)(H_2O_2)]^{2+}$ into the hydrous oxide may interfere with the accuracy of the analysis and long and gentle heating on a water-bath and dissolution of the precipitates without heating should be resorted to in order to avoid these sources of error.

Summary

Reaction of hydrogen peroxide with titanium(IV) has been investigated over the range of pH 0 to 13. Below pH 2 this reaction gives orange-colored ion-species, $[Ti(OH)_2(H_2O)(H_2O_2)]^{2+}$ or $(TiO_2 \cdot aq)^{2+}$. In the range of pH 3 to 6 formation of a yellow species is observed and its chemical formula is presumed to be $[Ti(OH)_3(H_2O_2)]^{+}$. Existence of a species different from the above is indicated by the pale yellow color observed in the region of pH 7 to 9. This species is very unstable unless a large excess of hydrogen peroxide is present, and its chemical formula is presumed to be $[Ti(OH)_3(OOH)]^{0}$. At higher pH values (10<pH), the reaction mixture is colorless, and presumably contains $[Ti(OH)_2(O_2)_2]^{2-}$. All the tentative formulae of these species are based on the composition of isolated salts, the absorption spectra of the solutions etc. A solution containing $[Ti(OH)_2(H_2O)(H_2O_2)]^{2+}$ remains unchanged but a solution containing $[Ti(OH)_3(H_2O_2)]^{+}$ gives a yellow precipitate TiO(OH)(OOH), and one containing $[Ti(OH)_3(OOH)]^{0}$ or $[Ti(OH)_2(O_2)_2]^{2-}$ gives a pale yellow compound

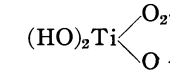

at room temperature or more quickly when heated on a water-bath. The precipitation reaction of

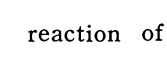

is taken advantage of in a new volumetric analysis suited for determination of titanium in quantities of the order of 10 mg.

Department of Chemistry, Faculty of Science, Kanazawa University
Kanazawa

A Kinetic Study of the Reaction of Substituted Benzyl Chlorides with Tertiary Amines

By Teruaki MUKAIYAMA and Hiromi TANAKA

(Received June 21, 1956)

Introduction

The kinetics of the bimolecular nucleophilic substitution of benzyl chlorides have been studied by many workers[1-9]. In a single stage process considered for the bimolecular substitution, bond formation between the central carbon atom and a nucleophilic reagent occurs simultaneously with bond fission between the central carbon atom and the halogen atom. The bond fission should be facilitated by electron releasing groups; however, the approach of the nucleophilic reagent, which is necessary for the bond formation is almost certain to be hindered by these substituents. The net result is a different effect and the polar effects of the substituents on the S_{N_2} reaction can not be clear cut. In addition to the polar effect, the steric effect and the solvent effect to be considered in the reaction mechanism multiplies the difficulty for explaining the factors which determine the reactivity.

In the present experiment, the kinetics of the reaction of substituted benzyl chlorides with tertiary amines in benzyl alcohol solvent were studied in order to investigate the polar and the steric effects in the S_{N_2} reaction by using the tertiary amines with bulky substituents as nucleophilic reagents.

Experimental

Materials.—Melting points, boiling points and literature references for benzyl chlorides, amines and benzyl alcohol are listed in Table I.

TABLE I

	M. p. or B. p. (°C)	Reference
Solvent		
Benzyl alcohol	112/20	
Amines		
Tri-*n*-butylamine	116/42	
Dimethylaminoethanol	135	
Diethylaminoethanol	42～44/8	
Diisopropylaminoethanol	104/39	(a)
Diisobutylaminoethanol	84/9	(a)
Di-*n*-butylaminoethanol	99/10.5	(b)
Benzyl chlorides		
H	69～70/17	
o-NO_2	[48]	(c)
p-NO_2	[71]	
o-Cl	94/10	
p-Cl	68/3	
o-CN	[60]	(d)
p-CN	[79]	(d)
o-CH_3	86～88/16	(e)
p-CH_3	63～65/5	(f)

a) Einhorn, Fiedler and Uhlfelder, *Ann.*, **371**, 145 (1909).
b) Kamm, Adams and Volwieler, U.S. Patent, 1,358, 750.
c) L. Vanino, "Handbuch der Präparativen Chemie", Bände II, 459.
d) C. Barkenbus and J.B. Holtzchaw, *J. Am. Chem. Soc.*, **47**, 2191 (1925).
e) I. Smith and L.J. Spillane, *J. Am. Chem. Soc.*, **62**, 2640 (1940).
f) M.G. Darzens and M.M. Delépine, *Compt. rend.*, **208**, 818 (1939).

Procedure.—In each run, 1 ml. of 0.1 N benzyl alcohol solutions of benzyl chlorides and amines were mixed into a 20 ml. reaction tube having a ground stopper. At appropriate intervals of time the reaction tubes placed in a thermostat were taken out and the reaction was stopped by rapid cooling with ice water. Then, the reaction mixture was washed out with 10 ml. of methanol and the chlorine ion formed was determined by titration with 0.01 N silver nitrate (Mohr's method). The temperature control was accurate to ±0.03° within the temperature ranges between 25°C–135°C.

The second order rate constant was calculated by equation 1

$$k_2 = \frac{1}{t} \cdot \frac{x}{a(a-x)} \qquad (1)$$

where k_2 is the second order rate constant; t, the time in seconds; x, the amount of chlorine ion.

1) D.H. Peacock, *J. Chem. Soc.*, 1924, 1975; 1925, 2177.
2) P.P. Krichenko and V. Opotsky, *Ber.* 59B, 2131 (1926).
3) H. Mc Combie, H.A. Scarborouch and F.P. Smith, *J. Chem. Soc.*, 1927, 802.
4) B.V. Tronov and A.I. Gershevich, *C. A.*, 22, 3397 (1928).
5) G.M. Bennett and B. Jones, *J. Chem. Soc.*, 1935, 1815.
6) S.C.J. Olivier and A. Ph. Weber, *Rec. trav. chim. Pay-Bas*, 53, 869, 899 (1934).
7) V.A. Hol'tsshmidt and N. K. Vorobev, *J. Phys. Chem.*, 13, 473 (1939).
8) J.W. Baker and W.S. Nathan, *J. Chem. Soc.*, 1933, 1128; 1934, 987; 1935, 519, 1840, 1844, 1847; 1936, 236.
9) C.W.L. Bevan, E. D. Hughes and C. K. Ingold, *Nature*, 171, 301 (1953).

formed at time t; a, the initial concentration of both benzyl chlorides and tertiary amines. As an example of a typical run, the reactions of benzyl chloride with diethylaminoethanol at the temperature between 55°C–95°C are shown in Fig. 1.

The rate constants of the reaction of benzyl chlorides with amines are shown in Table II.

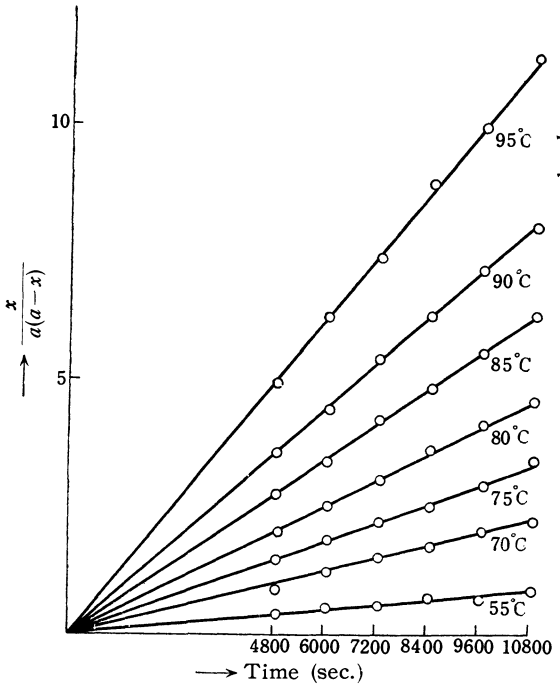

Fig. 1. Second order plots for the reaction of benzyl chloride with diethylaminoethanol.

The activation energies of the reactions were obtained from the linear relationship between log k and reciprocal absolute temperature. Typical runs are shown in Fig. 2. The rate constants, the activation energies and the entropies of activation obtained in this study are listed in Table III.

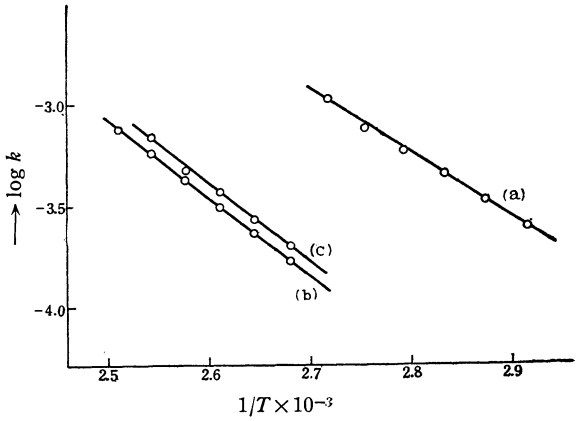

Fig. 2. The reaction of benzyl chloride with amines: the plot of log k against $1/T$. (a) diethylaminoethanol, (b) diisopropylaminoethanol, (c) diisobutylaminoethanol.

Results and Discussion

The experimental results listed in Table II are noted from the two different viewpoints, i. e. the effects of the substituents of amines (a) and those of benzyl chlorides (b), as follows.

TABLE II

THE RATE CONSTANTS OF THE REACTION OF BENZYL CHLORIDES WITH TERTIARY AMINES

$k_2 \times 10^4$ (mol.$^{-1}$·l.·sec.$^{-1}$), t(°C)

1) The reaction of benzyl chloride with amines.

t	k_2	t	k_2
(Dimethylaminoethanol)		(Diethylaminoethanol)	
25.0	2.21	55.0	0.824
30.0	3.26	70.0	2.09
35.0	4.74	75.0	3.40
40.0	6.84	80.0	4.57
		85.0	5.79
		90.0	7.43
		95.0	10.8
(Diisopropylamino-ethanol)		(Diisobutylamino-ethanol)	
100.0	1.66	95.0	1.39
105.0	2.31	100.0	2.01
110.0	3.10	105.0	2.70
115.0	4.21	110.0	3.44
120.0	5.67	115.0	4.66
125.0	7.55	120.0	7.02
(Di-*n*-butylaminoethanol)		(Tri-*n*-butylamine)	
80.0	2.44	80.0	0.622
85.0	3.24	85.0	0.834
90.0	4.23	90.0	1.11
95.0	5.52	95.0	1.46
100.0	7.48	100.0	1.93
120.0	21.22	105.0	2.36

2) The reaction of *o*-methylbenzyl chloride with amines.

(Dimethylaminoethanol)		(Diethylaminoethanol)	
25.0	2.68	60.0	1.29
30.0	4.10	65.0	1.83
35.0	5.99	70.0	2.59
40.0	9.00	75.0	3.56
		80.0	4.83
		85.0	6.50
(Diisopropylamino-ethanol)		(Diisobutylamino-ethanol)	
75.0	0.80	80.0	1.20
80.0	1.14	85.0	1.73
85.0	1.58	90.0	2.47
90.0	2.10	95.0	3.41
95.0	3.03	100.0	4.76
100.0	4.15	105.0	6.62

t	k_2	t	k_2
(Di-*n*-butylaminoethanol		(Tri-*n*-butylamine)	
75.0	2.21	54.5	0.740
80.0	3.02	60.0	1.16
85.0	4.05	65.0	1.67
90.0	5.81	70.0	2.67
95.0	7.85	75.0	3.40
100.0	10.55	80.0	5.04

3) The reaction of *p*-methylbenzyl chloride with amines.

(Dimethylaminoethanol)		(Diethylaminoethanol)	
20.0	2.85	60.0	2.40
25.0	4.27	65.0	3.44
30.0	6.46	70.0	4.96
35.0	9.77	75.0	6.66
		80.0	9.91
		85.0	13.5
(Diisopropylamino-ethanol)		(Diisobutylamino-ethanol)	
80.0	1.61	80.0	1.69
85.0	2.34	85.0	2.47
90.0	3.35	90.0	3.59
95.0	4.95	95.0	5.49
100.0	7.23	100.0	8.02
105.0	10.49	105.0	11.65
(Di-*n*-butylaminoethanol)		(Tri-*n*-butylamine)	
60.0	1.50	50.0	1.20
65.0	2.11	55.0	2.06
70.0	2.88	60.0	2.54
75.0	3.85	65.0	3.93
78.0	4.65	70.0	4.95
83.0	6.33	75.0	6.94

4) The reaction of *o*-chlorobenzyl chloride with amines.

(Dimethylaminoethanol)		(Diethylaminothanol)	
35.0	2.25	80.0	1.14
40.0	3.33	90.0	2.24
45.0	4.82	100.0	4.11
50.0	7.10	105.0	5.49
(Diisopropylamino-ethanol)		(Diisobutylamino-ethanol)	
110.0	0.870	110.0	1.36
115.0	1.18	115.0	1.72
120.0	1.52	120.0	2.27
125.0	2.07	125.0	2.98
130.0	2.76	130.0	3.99
135.0	3.67	135.0	5.05
(Di-*n*-butylaminoethanol)		(Tri-*n*-butylamine)	
95.0	1.76	85.5	3.45
100.0	2.33	90.0	4.17
105.0	2.80	95.0	4.89
115.0	4.65	100.0	7.06
120.0	5.99	105.0	8.66
125.0	8.21	110.0	11.3

5) The reaction of *p*-chlorobenzyl chloride with amines.

t	k_2	t	k_2
(Dimethylaminoethanol)		(Diethylaminoethanol)	
30.0	2.83	75.0	2.47
35.0	4.01	80.0	3.33
40.0	5.91	90.0	5.70
45.0	8.41	95.0	7.91
		100.0	11.25
(Diisopropylamino-ethanol)		(Diisobutylamino-ethanol)	
105.0	1.43	105.0	1.76
110.0	1.91	110.0	2.38
115.0	2.60	115.0	3.19
120.0	3.45	120.0	4.40
125.0	4.61	125.0	5.75
(Di-*n*-butylaminoethanol)		(Tri-*n*-butylamine)	
85.0	2.26	85.5	6.15
90.0	3.00	90.0	7.96
95.0	4.02	95.0	10.3
100.0	5.30	100.0	14.3
105.0	6.78	105.0	18.1
		110.0	22.2

6) The reaction of *o*-cyanobenzyl chloride with amines.

(Dimethylaminoethanol)		(Diethylaminoethanol)	
40.0	2.00	90.0	1.27
45.0	3.03	95.0	1.71
50.0	4.43	100.0	2.32
55.0	6.38	105.0	3.01
		110.0	3.82
(Diisopropylamino-ethanol)		(Diisobutylamino-ethanol)	
125.0	0.840	110.0	0.810
130.0	1.14	115.0	0.93
135.0	1.48	120.0	1.04
140.0	2.13	130.0	1.91
145.0	2.97	135.0	2.39
		140.0	3.01
		145.0	3.78
(Di-*n*-butylaminoethanol)		(Tri-*n*-butylamine)	
100.0	1.19	90.0	2.10
105.0	1.61	95.0	2.69
110.0	2.09	100.0	3.70
115.0	2.71	105.0	4.68
120.0	3.28	110.0	5.93
125.0	3.97	115.0	7.27

7) The reaction of *p*-cyanobenzyl chloride with amines.

(Dimethylaminoethanol)		(Diethylaminoethanol)	
40.0	2.58	90.0	2.26
45.0	3.94	95.0	3.02
50.0	5.75	100.0	3.99
55.0	8.21	105.0	5.32
		109.8	6.70

t	k_2	t	k_2
(Diisopropylamino ethanol)		(Diisobutylamino-ethanol)	
110.0	0.660	110.0	0.580
115.0	0.810	120.0	0.890
120.0	1.13	130.0	1.52
130.0	1.80	135.0	1.99
135.0	2.40	140.0	2.65
140.0	3.00	145.0	3.54
145.0	3.78		
(Di-*n*-butylaminoethanol)		(Tri-*n*-butylamine)	
100.0	1.80	90.0	2.86
105.0	2.35	95.0	3.63
110.0	3.10	100.0	4.81
115.0	4.11	105.0	6.42
120.0	5.00	110.0	7.93
		115.0	9.53

8) The reaction of *o*-nitrobenzyl chloride with amines.

(Tri-*n*-butylamine)	
105.0	3.66
110.0	4.75
115.0	6.34
120.0	8.38
125.1	11.3

9) The reaction of *p*-nitrobenzyl chloride with amines.

t	k_2	t	k_2
(Dimethylaminoethanol)		(Diethylaminoethanol)	
40.0	2.56	95.0	3.28
45.0	3.67	100.0	4.32
50.0	5.33	105.0	5.49
55.0	7.37	110.0	6.79
		115.0	8.79
(Di-*n*-butylaminoethanol)		(Tri-*n*-butylamine)	
90.0	0.810	105.0	6.10
100.0	1.54	110.0	7.97
105.0	2.08	115.0	10.1
110.0	2.61	120.0	11.8
115.0	3.77	125.1	14.9
120.0	6.15	130.0	18.1

TABLE III

THE SUMMARY OF RATE CONSTANTS ($k_2 \times 10^4$ mol.$^{-1}$·l.·sec.$^{-1}$ at 105°C), THE ACTIVATION ENERGIES (E kcal.) AND THE ENTROPIES OF ACTIVATION ($\Delta S^{\neq}$ e. u.)

Amines	Dimethylaminoethanol			Diethylaminoethanol		
Benzyl chlorides	k_2	E	$\Delta S^{\neq}$	k_2	E	$\Delta S^{\neq}$
H	32.3	14.0	−28.8	19.2	15.5	−30.5
o-CH_3	596	15.2	−24.4	24.0	15.3	−30.9
p-CH_3	740	14.4	−25.7	46.0	16.7	−25.6
o-Cl	21.4	15.1	−26.7	5.52	15.9	−31.9
p-Cl	27.9	13.9	−29.4	13.6	14.9	−32.7
o-CN	7.38	16.0	−26.5	3.05	16.0	−32.8
p-CN	8.63	15.5	−27.5	5.32	15.6	−32.8
o-NO_2						
p-NO_2	6.56	14.4	−30.9	5.55	14.7	−35.1
	Diisopropylaminoethanol			Diisobutylaminoethanol		
H	2.30	17.8	−28.5	2.70	18.5	−26.4
o-CH_3	5.59	16.7	−29.7	6.58	18.1	−25.8
p-CH_3	9.57	18.9	−23.0	11.5	20.6	−18.0
o-Cl	0.650	17.4	−32.2	0.100	16.7	−33.2
p-Cl	1.43	17.4	−30.7	1.76	17.8	−29.1
o-CN	0.212	20.4	−26.5	0.526	15.5	−37.7
p-CN	0.459	16.9	−34.2	0.348	18.0	−31.9
o-NO_2						
p-NO_2						
	Di-*n*-butylaminoethanol			Tri-*n*-butylamine		
H	9.68	14.6	−34.2	2.36	14.1	−33.6
o-CH_3	14.3	16.5	−28.4	22.9	16.6	−27.2
p-CH_3	13.0	14.6	−33.6	41.3	16.2	−31.7
o-Cl	2.90	14.0	−38.3	0.866	15.2	−32.8
p-Cl	6.98	15.1	−33.6	1.81	15.1	−33.2
o-CN	1.59	15.9	−38.9	0.506	14.2	−41.2
p-CN	2.38	15.1	−35.7	0.642	14.1	−40.9
o-NO_2				0.370	16.1	−32.1
p-NO_2	2.07	17.2	−30.4	0.600	13.2	−38.8

I—a) The rate constants of the reaction of amines with benzyl chlorides at 105°C increase in the following order,

diisopropylaminoethanol, diisobutylaminoethanol≪di-*n*-butylaminoethanol, tri-*n*-butylamine, diethylaminoethanol≪dimethylaminoethanol.

As noted in the above sequence, dimethylaminoethanol reacts much faster than the other amines and amines with normal alkyl groups react faster than those with branched alkyl groups. I—b) The rate constants of benzyl chlorides with amines at 105°C increase in the following order,

$$p\text{-}CH_3 > o\text{-}CH_3 > H > p\text{-}Cl > o\text{-}Cl > p\text{-}CN > o\text{-}CN > p\text{-}NO_2 > o\text{-}NO_2 .$$

The rates of reaction decrease by introducing the electron attracting groups and the *para* derivatives react faster than the corresponding *ortho* derivatives.

II—a) The activation energies for amines increase in the following order,

dimethylaminoethanol, diethylaminoethanol, di-*n*-butylaminoethanol, tri-*n*-butylamine≪diisopropylaminoethanol, diisobutylaminoethanol.

Amines with the branched alkyl groups, such as isopropyl and isobutyl groups, require more energy than amines with normal alkyl groups, such as methyl, ethyl and *n*-butyl groups. The activation energies required for the latter four amines are nearly equal.

II—b) The activation energies for benzyl chlorides do not show the characteristic variation of the substituents as found in the rate constant, in which regular sequences are shown according to their polar effects.

The following relations are found for *ortho* and *para* derivatives of benzyl chlorides according to the nature of the attacking amines. *Ortho* derivatives require more energy of activation than *para* derivatives in the reaction with four amines with normal alkyl groups and the reversed order is found in the reaction with amines with branched alkyl groups.

III—a) The entropies of activation for amines increase in the following order,

tri-*n*-butylamine, di-*n*-butylaminoethanol, diethylaminoethanol<diisobutylaminoethanol, diisopropylaminoethanol<dimethylaminoethanol.

The entropy of activation for dimethylaminoethanol is less negative than the other amines. The slow rates of amines with normal alkyl groups, such as ethyl and *n*-butyl groups, which require the nearly equal energies of activation with dimethylaminoethanol are attributed to the more negative entropies of activation.

III—b) The linear relationship between the activation energy and the entropy of activation could not be found for benzyl chlorides; however, the results show a combined increase in the activation energy and decrease in the entropy of activation. Benzyl chlorides with electron attracting groups show more negative entropy of activation than those with the electron releasing groups.

Ortho derivatives show more negative entropy of activation than *para* derivatives in the reaction with amines with branched alkyl groups and the reversed relation is found in the reaction with the other four amines.

The single stage process is considered for the bimolecular nucleophilic substitution and, in the transition state, by the approach of the nucleophilic reagent, the bond formation occurs simultaneously with bond fission, in which chlorine atom ionizes by the interaction of the solvent molecule.

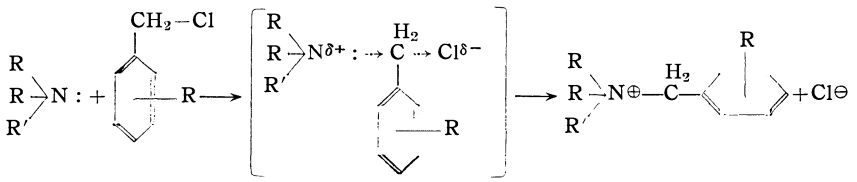

Assuming the above mechanism for the reaction, the effects of the substituents of amines are considered as follows. The electron density of the nitrogen atom in amines increases from methyl to *n*-butyl by an inductive effect, which is favorable for bond formation, but, the frontal strain considered in the transition state increases by the same sequence, which is unfavorable for the reaction. The simple explanation becomes difficult because of these two opposing effects, i.e., polar effect and steric effect; however, the results that amines with bulky substituents always require 2–3 kcal. more activation energy than the other four amines may be due to the increased F-strain considered in the transition state.

As shown in II—b), the relative order of activation energies for *ortho* and *para* derivatives of benzyl chlorides are changed by the nature of the attacking amines. The lower activation energies for the reaction of

ortho derivatives with bulky amines may be explained by assuming the increased F-strain between *ortho* derivatives and the amines with bulky groups in the transition state, which causes the dissociation of chlorine atoms more readily.

The activation energies for the reaction of benzyl chlorides with electron attracting groups or electron releasing groups are nearly equal. These results may be due to the two opposing effects which are considered in the single stage process, namely the ionization of chlorine atom facilitated by the electron releasing groups and the approach of amine molecule to the central carbon atom retarded by the same substituents.

As shown in III—a), the entropy of activation for dimethylaminoethanol is less negative than the other four amines studied. This may be explained by assuming the solvation of amines, e. g. the interaction of protonic solvent with amines, in the ground state, which must be lost in the transition state. Dimethylaminoethanol solvates more than the other amines in which solvation is hindered by the increased B-strain due to their bulky substituents. Therefore, the entropies of activation for the latter amines are more negative than dimethylaminoethanol.

The results shown in III—b) are explained by a similar consideration in which the differences of the entropies of activation in the benzyl chloride series depend on the degree of solvation in their ground state. The solvation of benzyl chlorides to the chlorine atom by the protonic solvent, in the ground state, increases by introducing the electron releasing group, such as methyl group, but, in the transition state, the solvent interaction with the ionizing chlorine atom is nearly the same irrespective of the nature of their substituents. Therefore, the more negative entropies of activation of benzyl chlorides with electron attracting groups are expected.

In bimolecular nucleophilic substitution, the polar effects are not clearly shown as mentioned above, but, it can be concluded that the steric effect and the solvent effect play an important role for the reaction.

Summary

(1) The rate constants, the activation energies and the entropies of activation of the reaction of benzyl chlorides with tertiary amines in benzyl alcohol were determined.

(2) In the single stage process for the bimolecular nucleophilic substitution, the polar effects of the substituents are not clearly shown.

(3) Both steric and solvent effects play important roles on the reaction studied in this experiment.

The authors wish to express their hearty thanks to Prof. Toshio Hoshino for his encouragement and to Mr. Tsuyoshi Nakamura and Mr. Keiki Shibata for their help during the course of this experiment.

Department of Physics and Chemistry
Gakushuin University, Mejiro
Toshima-ku, Tokyo

Irreversible Photobleaching of the Solution of Fluorescent Dyes. III. Photoreaction of Eosine in the Aqueous Alcoholic Solutions under Evacuated State

By Masashi IMAMURA and Masao KOIZUMI

(Received July 9, 1956)

Introduction

In the preceding paper[1], the vacuum photobleaching of eosine in pure methanol, ethanol and isopropanol was investigated, and it was found that the absorption spectra decline steadily without any shift and that the rate depends only on the light absorbed.

Now as a natural extension of our research, the effect of water added on the vacuum photobleaching was examined, and a remarkable result was obtained; this was that the addition of water does cause a gradual displacement of the absorption spectra towards shorter wavelengths in the course of reaction and at the same time the solution becomes more and more fluorescent. The reaction is completely irreversible and the strongly fluo-

1) M. Imamura and M. Koizumi, This Bulletin, 29, 900 (1956).

rescent product is very stable. Analyzing the absorption spectra carefully, this ultimate product was definitely confirmed to be uranine.

Kinetic studies were also undertaken, and from the results obtained, a conclusion was given as to the primary process of the aerobic photobleaching of eosine in the aqueous solution, which had remained undecided in the first paper[2] of this series.

Experimental Procedures and Results

1. Photobleaching in the Aqueous Alcoholic Solutions.—Materials were the same as before[1,2]. Concentrated aqueous solution of eosine was diluted with water and ethanol to a desired concentration of alcohol, the resulting concentration of eosine being kept constant as 10^{-5} mol./l.

Evacuation was done under repeated cooling with dry ice and melting for several times with the use of a mercury diffusion pump. Reaction was carried out in a cylindrical glass cell to which a cuvett (path length: 1 cm.) for Beckman spectrophotometer was attached. Evacuated samples were irradiated with a tungsten lamp and Matsuda color filter VG1 as before.

At some minutes' intervals the cell was taken out of a thermostat and the absorption spectra were measured by Beckman spectrophotometer model DU.

An example of a series of measurements is shown in Fig. 1. From Fig. 1, it is seen that the

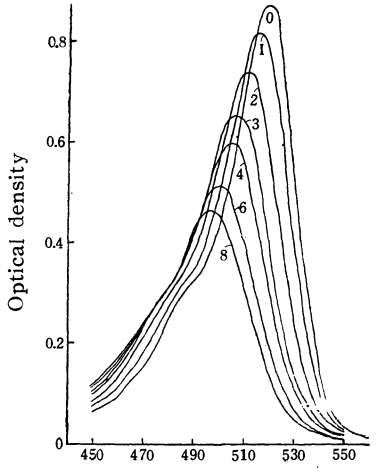

Fig. 1. Absorption spectra of the irradiated eosine in 10 vol. % EtOH solution in vacuo.
No.'s depicted indicate the order of measurement.

optical density gradually decreases and, at the same time, absorption maximum is displaced towards shorter wavelengths; the irradiated solution becomes more greenly fluorescent than the initial solution.

2. Analysis of the Absorption Spectra.—Although a gradual shift of the absorption maximum was observed during the reaction, its limiting position in every case was in the neighborhood of 490 mμ. Since the above results strongly suggest the formation of a coloring product from eosine, identification of the product was attempted from the analysis of absorption spectra. The method is essentially the same as reported by Blaisdell[3].

At various wavelengths, the ratio of the optical density of each irradiated solution to that of the initial solution was calculated, and the value of the minimum ratio was decided. For all the curves tried, the minimum points fell alike between 530 and 540 mμ. Minimum ratios thus obtained may be considered as relative measures of the concentration of eosine remaining.

Multiplying these values to the optical densities of the initial solution at each wavelength, the absorption curves could be drawn which may approximately be considered as the curves of eosine remaining in solution at each time.

Substracting these curves from the absorption curves of the original solutions, one can get the curves which may be attributed to intermediate products.

An example of such curves obtained is given in Fig. 2. It is seen from Fig. 2 that with decreasing concentration of eosine, optical density

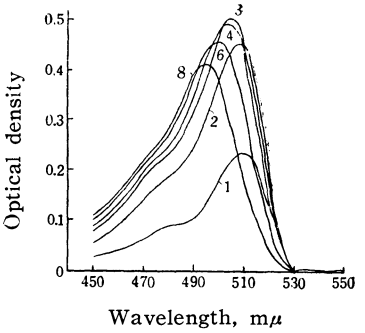

Fig. 2. Absorption spectra of the intermediates produced in 10 vol. % EtOH solution in vacuo.
No.'s depicted indicate the order of measurement. (cf. Fig. 1).

of the products increases moderately at the beginning, then more and more slowly, and at last begins to decrease very slowly. At the same time the position of the maximum is gradually displaced towards 490 mμ, where the displacement comes to a halt.

3. Identification of an Ultimate Intermediate Product.—The coloring product intermediately produced by the irradiation of the aqueous alcoholic solution of eosine has a strong green fluorescence and has its absorption maximum near 490 mμ as mentioned above.

From these facts, it seemed very plausible to suspect that this product would be fluoresceine-Na

2) M. Imamura and M. Koizumi, This Bulletin, 28, 117 (1955).

3) B. E. Blaisdell, *J. Soc. Dyers & Colourists*, 65, 619 (1949).

(uranine) (II) which is a debrominated product of eosine (I).

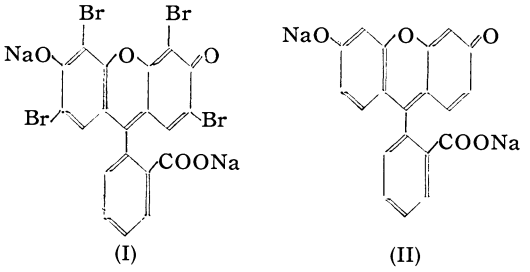

To confirm this conjecture, the following methods were adopted.

(*a*) *Comparison of Absorption Spectra.*—If the coloring material were uranine as supposed, then the separated absorption curves in the final stage of reaction should be the same as that of uranine, or of uranine which is partly photobleached in vacuo in the same aqueous alcoholic solution. Uranine in alcoholic or in aqueous alcoholic solution also decolorizes in vacuo, but no shift of spectrum such as for eosine is observed.

The comparison of the separated curves with that of uranine partly photobleached in vacuo is shown in Fig. 3. In Fig. 3 suitable normalization

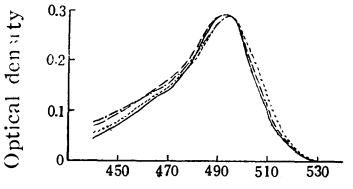

Fig. 3. Comparison of the absorption spectra.

———: Uranine partly photobleached in 10 vol. % EtOH solution;
- - - -: Separated curve for 5 vol. % EtOH solution;
·····: For 10 vol. % EtOH solution;
·—·—: For 20 vol. % EtOH solution;
(normalized at 495 mμ)

is done to make all the curves coincide at 495 mμ.

Absorption curves of an ultimate intermediate were measured in vacuo for the solutions in which the concentrations of alcohol were 5, 10 and 20 vol. per cent while the uranine partly photobleached was also measured in vacuo for 10 vol. per cent alcoholic solution. Agreement of all curves is satisfactory in view of the approximate nature of the analytical procedures.

(*b*) *Bromination.*—It is known that fluoresceine can easily be brominated by bromine into tetrabromofluoresceine[4,5]. In fact, uranine in aqueous alcoholic solution could be converted to eosine by adding few amounts of bromine and of sodium hydroxide. Hence similar bromination was applied to the 10 vol. per cent alcoholic solution in which eosine had almost completely disappeared in vacuo and the products were examined spectroscopically. The result is illustrated in Fig. 4.

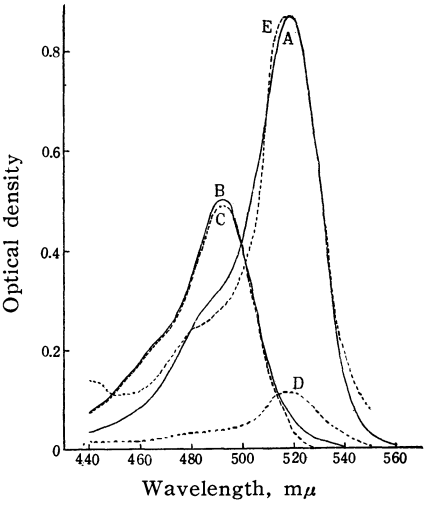

Fig. 4. Bromination of the intermediate. See sec. 3-b of procedures and results.

Curve A in Fig. 4 is an initial absorption curve of eosine in 10 vol. per cent alcoholic solution, B is the one after almost complete photobleaching of eosine in vacuo. Applying the analytical method mentioned in Sec. 2 to curve B, the resulting curve for intermediate is C. One drop of bromine and of concentrated sodium hydroxide solution were added to the irradiated solution of 10 ml.; then yellow color with strong green fluorescence instantly became reddish with weak fluorescence. Curve D indicates this color change. Levelling the curve D up to A at 520 mμ, the resultant is E.

If the intermediate, which is supposed to be uranine (curve C), be converted quantitatively to eosine by bromination, the maximum optical density of the curve D must be higher than the maximum optical density of the curve C*. The reason why the curve D is lower than the curve C in the present case, may plausibly be attributed to the simultaneous oxidative decomposition of uranine by bromine. When compared with the curve A, there scarcely remains any doubt that the curve E represents the absorption curve of eosine, although in the shorter wavelength region discrepancy is appreciable; this discrepancy may be due to the decomposition products.

(*c*) *Photobleaching of Uranine in Vacuo.*—When uranine in aqueous alcoholic solution was irradiated in vacuo under the same conditions as for eosine, it bleached in the same way but with a very slow rate and without any shift of its spectrum.

This behavior is qualitatively similar to that of the ultimate intermediate in eosine solution which was shown in Fig. 2.

From the facts mentioned above it can be concluded that the intermediate produced in the course of photobleaching reaction of eosine in aqueous alcoholic solution in vacuo is the debrominated eosine, that is, uranine.

* Maximum molar extinction coefficient of uranine is lower than that of eosine in aqueous or alcoholic solution.

4) K. Venkataraman, "The Chemistry of Synthetic Dyes", (1952) II, p. 747.

5) G. Schultz, "Farbstofftabellen", Leipzig (1931), I-2, p. 374.

4. Rate of the Conversion of Eosine.—The real rate of disappearance of eosine can be found by the method described in Sec. 2. It seems very natural to expect that the rate thus obtained be expressed, if I_{abs} is the light absorbed and is expressed in mol. per 1. per sec., by the following equation:

$$-\frac{dc}{dt}=kI_{abs}, \tag{1}$$

since, as reported already[1], the photobleaching of eosine both in aerobic aqueous solution and in deaerated alcoholic solution obeys the following formula which is only a different form of Eq. (1).

$$-\frac{dc}{dt}=k\frac{I_0}{d}(1-e^{-\alpha cd})\times 1000. \tag{2}$$

It is to be noted, however, that in the present case there are more than two light absorbing species, eosine and intermediates, because the transmission of the filter covered the main absorption regions of them all. Hence, I_{abs} in Eq. (1) must be put as the portion of light actually absorbed by eosine, and this must be calculated as an integrated sum over the necessary wavelength regions, since the inner filter effect of the intermediates depends on the wavelength λ. Taking into account this fact, Eq. (1) is to be written as follows:

$$-\frac{dc_1}{dt}=1000k\int_{\lambda_1}^{\lambda_2} I_{0\lambda}\frac{\varepsilon_{1\lambda}c_1}{D_\lambda}(1-10^{-D_\lambda})d\lambda, \tag{3}$$

where $\varepsilon_{1\lambda}$, D_λ and $I_{0\lambda}$ are the molar extinction coefficient of eosine, the optical density of the solution and the incident light intensity all at λ, respectively. In making the computation of Eq. (3), values of $I_{0\lambda}$'s are necessary and these can be given as follows:

$$I_{0\lambda}=L_\lambda T_{f\lambda}=L_{\lambda max}T_{f\lambda}f_\lambda, \tag{4}$$

where,

L_λ: the light intensity per unit band of wavelength for a light source at λ,

$T_{f\lambda}$: transmission of the filter at λ.

f_λ: the intensity distribution fraction of the light source at λ.

Then I_0, the light intensity, is expressed as follows

$$I_0=\int_{\lambda_1}^{\lambda_2} I_{0\lambda}d\lambda=\int_{\lambda_1}^{\lambda_2} L_\lambda T_{f\lambda}d\lambda=L_{\lambda max}\int_{\lambda_1}^{\lambda_2} f_\lambda T_{f\lambda}d\lambda. \tag{5}$$

From Eqs. (3), (4) and (5),

$$-\frac{dc_1}{dt}=1000kI_0\frac{\int_{\lambda_1}^{\lambda_2} f_\lambda T_{f\lambda}\frac{\varepsilon_{1\lambda}c_1}{D_\lambda}(1-10^{-D_\lambda})d\lambda}{\int_{\lambda_1}^{\lambda_2} f_\lambda T f_\lambda d\lambda} \tag{6}$$

$$=1000kI_0f_{abs}.$$

f_λ's were calculated assuming that the temperature of the light source was 2500°K,[6] which gave just the same value of the mean molar absorption coefficient, α, of pure eosine as that determined experimentally by a thermopile.

The values of f_{abs} were calculated at several points of each run using the value of D_λ of the solution. The rate of the disappearance of eosine at the corresponding time-point was determined directly from the concentration-time curve, and dividing this by $1000I_0f_{abs}$, one could get the value of k. Values of k, which ought to be constant if Eq. (1) holds, are plotted against f_{abs}. Some examples are shown in Fig. 5. The constancy of k does not hold except for the solution in which alcohol concentration is high. In general, k decreases more and more as the reaction proceeds, in other words, as the quantity of coloring intermediate increases. But in the earlier stage of the reaction k does not change practically.

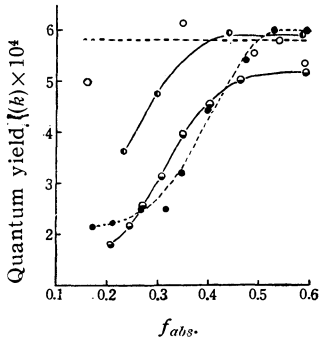

Fig. 5. Variation of the quantum yield with f_{abs}.
◒: 10 vol. %; ●: 20 vol. %;
◐: 50 vol. %; ○: 90 vol. %.

Although the above calculations are not altogether free from any ambiguity, there is no doubt about the general tendency that k-values decrease with the accumulation of the intermediate. Hence it was attempted to make clear some reasons for this behavior.

Supposedly Eq. (1) holds in the present case. One possible reason for this decrease might be the non-homogeneity of the irradiated solution; under the condition of non-stirring, intermediate coloring substances will become concentrated in the front part of the solution and this may cause a larger filter effect than that under the homogeneous condition which was assumed in the above calculation.

If this be the case, it should be possible to make this effect smaller with proper choice of experimental conditions. Some experiments were conducted for this purpose. Thus the initial concentration of eosine selected was half that of the ordinary one using another cell of 10 mm. path length (5 mm. shorter than ordinary cells) and the measurements of absorption spectra were made at shorter intervals. But the result is that there was no noticeable difference.

Another conceivable reason is some sort of retarding effect of the reaction products on the rate of photobleaching of eosine. The following experiments were conducted to examine this possibility. A definite amount of uranine was added previously to the pure ethanol solution of eosine and the rate of the photobleaching of the latter was measured by the usual method. It was definitely established by several experiments that

6) A. N. Lowan and G. Blanch, *J. Opt. Soc. Am.*, **30**, 79 (1940).

the addition of uranine causes a marked retarding effect and that the effect increases greatly with the increase of added uranine. Some results are shown in Table I, where k values are calculated by the method analogous to that stated above, taking the filter effect of uranine into account.

TABLE I

QUANTUM YIELDS FOR THE VACUUM PHOTOBLEACHING OF EOSINE IN EtOH IN THE PRESENCE OF URANINE

$I_0=1.4\times10^{15}h\bar{\nu}$/cm². sec. 27°C

Conc. $\times10^5$mol./l.		Quantum Yield, $k\times10^4$
Eosine	Uranine	
10.0	—	6.0
10.0	2.5	3.4
10.0	5.0	1.0
10.0	10.0	0.5

From the above tests it is certain that the decrease of k is mainly due to the retarding effect of intermediates including uranine, although it is impossible, in the present stage of investigation, to interpret the matter quantitatively on the basis of the above data, in view of the facts that the experimental conditions of the above tests differ from those in the ethanol-water solutions which contain some other unknown intermediate products preceding final uranine production.

Thus the k-value extrapolated to t=0 can be accepted as a true one. Plotting the quantum yield thus obtained, against the concentration of ethanol, a curve is obtained which is shown in Fig. 6. As seen from Fig. 6, the quantum yield increases with increasing concentration of ethanol up to ca. 20 vol. per cent and then it becomes constant, the value being the same as that obtained in pure ethanol in vacuo.

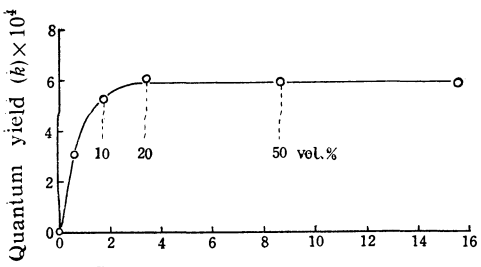

Fig. 6. Variation of the quantum yield with the concentration of EtOH.

Discussion

1. First the reliability of the evaluation of k-values and of the interpretation of the absorption spectra of intermediates will be discussed briefly. There is some suspicion that Blaisdell's method by which the minimum ratio of the optical density of the irradiated solution to that of the original one was taken for a measure of the concentration of the remaining eosine, might have given a smaller value than the real one, in view of the fact that the absorption curve of the intermediate is superposed on that of eosine in the whole range of wavelengths. But the superposition is negligible in the longer wavelength region above 530 mμ and the minimum ratio is exactly between 530 and 540 mμ without a single exception. Furthermore, the k-values in Fig. 6 are obtained from the initial rate which is scarcely affected by the reaction products. From these facts it is considered that the evaluation of k-values is very reliable.

As to the absorption spectra of the intermediates, there is no doubt that they are related only to the reaction products which are specific in the water-alcohol mixture. For, although there is another type of reaction which takes place in pure alcohol, the product of this reaction gives only a very small absorption band near ultraviolet and this band can not affect the present band even if the reaction of the latter type participates in wateralcohol mixture. Hence, the interpretation of the intermediates is considered to be fairly trustworthy.

2. From the fact that the quantum yield, k, is independent of the concentration of ethanol above 20 vol. per cent, it can be concluded that the primary processes in water-alcohol mixture are just the same as those in pure alcohol. They are

$$D \xrightarrow{h\nu} D^* \longrightarrow D^t \qquad \text{(i)}$$

$$D^t + RH \longrightarrow DH\cdot + R\cdot, \qquad \text{(ii)}$$

where D^t is eosine in the triplet state, RH is alcohol, and DH· is a colorless or almost colorless semiquinoid radical. This conclusion is further supported by the following preliminary experiments. Thus, similar experiments using methanol- and isopropanol-water mixtures were attempted and analogous spectral shifts due to the production of coloring intermediates were observed, the extent of which was less in methanol and was nearly equal or a little greater in isopropanol than in ethanol. This order is exactly the same as for the rate of photobleaching in pure alcohols as reported already[1], and the result is quite reasonable if the two types of reaction proceed via the common primary processes.

It is significant that water molecules act as retarders only below 20 vol. per cent of alcohol. This result shows evidently a strong reactivity of ethanol with D^t, while the reaction of water with D^t is negligible, if it exist, at least when the content of alcohol exceeds ca 20 vol. per cent.

The production of uranine can be interpreted as a result of further interaction of

DH· with water.

3. On the basis of the above results concerning the variation of k with the concentration of ethanol, a definite conclusion can be drawn about the primary processes of the aerobic photobleaching of eosine in aqueous solution which remained undecided in the first paper[2] of this series. The two schemes then proposed were

$$D^t + O_2 \longrightarrow D\cdots O_2 \xrightarrow{H_2O} \cdots\cdots \text{prod.} \quad \text{(iii)}$$

$$D^t + H_2O \longrightarrow D\cdots HOH \xrightarrow{O_2} \cdots\cdots \text{prod.} \quad \text{(iv)}$$

and it can now be said that the former is suitable. The reason for it is as follows. As reported previously[2], ethanol causes a marked retardation on the aerobic photobleaching, but, at the concentration of ethanol of 20 vol. per cent there is observed photobleaching to some extent with a quantum yield about 1/5 of that in the pure aqueous solution. Hence if aerobic photobleaching in the aqueous solution goes via (iv), water ought to show a retarding effect just as great or greater than this value on the photobleaching in vacuo. But the present investigation shows that it is not the case.

Thus it can be concluded that the primary process in the aerobic photobleaching in the pure aqueous solution is (iii), in which D^t primarily reacts with oxygen molecule to form a labile complex, $D\cdots O_2$. It is to be noted, however, that the data for k-values are rather few and it is desirable to accumulate them or to find some other facts in support of this mechanism. Further confirmations and somewhat quantitative discussions will be given in the next paper.

4. Though the detailed mechanism of the uranine-producing reaction is not yet clear, it is certain that uranine is not directly formed from eosine but is formed via some preceding intermediates, may be dibromo-compound, in view of the fact that the absorption for intermediates (Fig. 2) shows a gradual displacement of their maxima towards shorter wavelengths.

When the quantity of intermediates produced per unit quantity of decomposed eosine is evaluated from the absorption data and is plotted against time, then it is found from the value extrapolated to time zero that the reaction which produces coloring materials decreases with increasing concentration of alcohol. The molar extinction coefficient of the intermediates can be estimated to be roughly 10^5 from the data for the solution of low alcohol content. Hence, in the region of low concentration of alcohol (~20 vol. per cent), the principal reaction is an uranine-producing one, while, with rising concentration of ethanol, the reaction in pure ethanol becomes predominant.

It is to be added here that, according to our supplementary experiments, an uranine-producing reaction is sensitive to pH; the addition of a very small amount of acetic acid causes no shift of spectrum. Further, in the case of erythrosine, uranine is not so much produced as in the case of eosine under analogous conditions.

At any rate, the reaction of this type seems to be exceedingly curious from the standpoint of organic reactions and may be worthy of further research from this point of view, as well as from the view point of photochemistry.

Summary

The photoreaction of eosine has been studied in ethanol-water mixture in vacuo. Irradiated solution showed a gradual spectral shift towards shorter wavelengths. Analyzing the spectra and applying the chemical method, it was found that the spectral shift is due to the production of uranine.

The rate of disappearance of eosine increases with rising concentration of ethanol until 20 vol. per cent, at which it reaches its maximum and constant value, which is the same as that in pure ethanol.

The primary processes of the aerobic photobleaching of eosine in aqueous solution were discussed and it was concluded that the process must be

$$D^t + O_2 \longrightarrow D\cdots O_2 \xrightarrow{H_2O} \cdots \text{prod.} \quad \text{(iii)}$$

The cost of the present research has been partly defrayed from the Scientific Research Grant from the Ministry of Education.

Institute of Polytechnics
Osaka City University
Osaka

*Partition Equilibrium of Cumene Hydroperoxide between Water and Cumene**

By Shigehiko YAMADA and Tokio KATŌ

(Received May 17, 1956)

In the "cumene process", the hydroperoxide (CHP) is sometimes obliged to come in contact with water chiefly because the latter is the general stabilizer to thermal decomposition of CHP in the oxidate. The contact is operated during and after the hydroperoxidation, where dissolution of CHP in the water phase cannot be neglected. In this relation, studies on the partition equilibrium of CHP between water and cumene seem to contribute to the solution of the problem, so the partition constant K and its dependence on the temperature and CHP concentration were investigated. We can find no description of such an investigation in the literature up to the present, though CHP is said to be insoluble in water[1].

Experimental

Apparatus and Sample.—Thermostat adjusted to ±1°C, and conical flasks of 200 cc. and 500 cc. with tight stoppers were used.

Cumene was prepared by alkylation of benzene with propylene in the presence of 90% sulfuric acid at 20~30°C. The fraction of the mixture after washing with concentrated sulfuric acid and 25% aqueous sodium hydroxide for more than 10 times, had b. p. 151~3°C.

CHP was prepared by the liquid phase oxidation of the cumene with oxygen gas at 128~132°C. The sodium salt was precipitated by shaking the steam-stripped oxidate with 25% aqueous sodium hydroxide, filtering off, washing with petroleum benzine, and dissolving in water. The solution was acidified with carbon dioxide, the oily layer extracted with petroleum ether, dried over anhydrous sodium sulfate, filtered and concentrated at 50~70°C under 1~3 mmHg pressure. The clear residue was found to contain 99% be weight of CHP by iodometry.

Method.—Several solutions, varying in concentration of CHP in the cumene were prepared in the flasks. Distilled water was added to the same volume as that of the oil and they were settled for a certain time after being subjected to vigorous shakings every 10~15 min. Volumes of samples employed for analysis were 1 or 5 cc. for the oily layer and 20 or 25 cc. for the aqueous layer according to the concentration of CHP in solution.

Each group of four samples was brought side by side in the thermostat for 2.5 hr. at 10, 20, 35, 50°C, and served for analysis.

Determination of Partition Constants.—We assume that v_1 is the volume (cc) of N/10 aqueous sodium thiosulfate consumed for 5 cc. of oily layer, v_2 that for 25 cc. of water, and c_1, c_2 moles of CHP per litre in the oily and aqueous layer respectively. Then the partition constant $K(t)$ at t°C is shown as follows.

$$K = c_2/c_1 = 0.2\, v_2/v_1$$

Results are given in Table I.

TABLE I

PARTITION CONSTANTS AT SEVERAL TEMPERATURES

t (± 1°C)	v_1 (cc.)	v_2 (cc.)	K ($\times 10^2$)
10	9.46	1.75	3.7
	9.56	1.82	3.8
	19.70	3.12	3.2
	36.20	6.38	3.5
20	4.30	0.64	3.0
	9.10	1.48	3.3
	19.18	2.48	2.6
	32.45	4.00	2.5
35	5.40	0.62	2.3
	11.43	1.28	2.2
	23.03	2.32	2.0
	44.68	4.50	2.0
50	6.10	0.51	1.7
	11.40	1.10	1 9
	21.76	2.05	1.9
	39.73	3.37	1.7

The Time Required for the Equilibrium.—Some samples in Table I were further taken to determine K under the settling time of 1.5 hr., which however gave approximately the same value, as in the case of Table I. The following data show the variation of CHP concentration with the settling time. In these cases the temperature was subjected to the fluctuation ranging from 7 to 15°C and the shaking time of 10~15 min. was not exactly maintained.

A and B in Table II are the volume (cc.) of thiosulfate solution required for titrating 5 cc. of aqueous layer of the system, composed of 200 cc. of distilled water and 200 cc. of 15~20% CHP solution, prepared from pure CHP and the steam-stripped oxidate of cumene respectively.

* Presented at the 9th Annual Meeting of the Chemical Society of Japan held in Kyōto, April, 1956.

1) H. Hock and S. Lang, *Ber.*, 77, 259 (1944).

TABLE II

VARIATION OF CHP CONCENTRATION IN THE AQUEOUS LAYER WITH TIME AS EXPRESSED BY CC. OF THIOSULFATE SOLUTION

	10 min.	2 hr.	4 hr.	6 hr.	1 week
A	0.54	0.92	0.59	0.56	0.69
B	0.52	0.74	0.39	0.59	0.65

Data for the Practical Oxidate.—A similar method was applied for the practical oxidate of cumene prepared as mentioned above. Results are given in Table III.

TABLE III

PARTITION CONSTANT FOR THE PRACTICAL OXIDATE AT 10°C

v_1'	v_2'	K ($\times 10^2$)
6.18	1.25	1.0_1
12.70	2.41	0.9_5
24.40	4.75	0.9_7

v_1', v_2' are volumes for 1 cc. and 20 cc.

$K = 0.05\, v_2'/v_1'$

Discussion

Concentration and Temperature Dependence of Equilibrium Constant K.— Constancy of K regardless of the change of CHP concentration at each temperature seems to be affirmed within the limits of experimental error, while its dependence on the temperature is shown in Table IV and Fig. 1.

TABLE IV

ARITHMETIC MEAN OF CONSTANT, $\bar{K}$ AT EACH TEMPERATURE

t (±1°C)	$\bar{K}$ ($\times 10^2$)
10	3.6
20	2.9
35	2.1
50	1.8

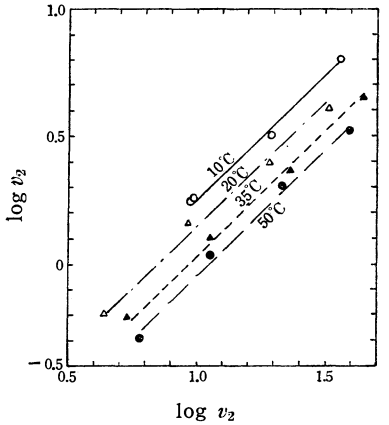

Fig. 1. Relation between log v_1 and log v_2.

Linear relation between log $\bar{K}$ and reciprocal of absolute temperature shown in Fig. 2. suggests that it will satisfy the following thermodynamic formula,

$$\ln K_2/K_1 = -Q/R\cdot(1/T_1 - 1/T_2),$$

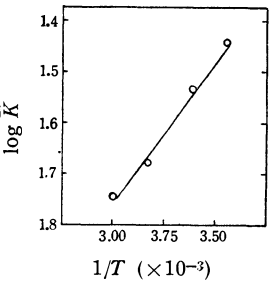

Fig. 2. Relation between log $\bar{K}$ and $1/T$.

where, R is the gas constant, and Q, the heat of transference of 1 mol. of CHP from cumene solution into water under the equilibrium condition. Thus, Q was determined as 3.16 kcal./mol. Accordingly, equilibrium constant K approximately satisfied the following formula,

$$K = 1.3_4 \times 10^{-4} e^{1580/T}$$

Other Problems.—From data in Table II the equilibrium is supposed to be established within two hours under these conditions. Further, values of K for the practical oxidate appear remarkably smaller than those for pure CHP series. A similar tendency was also observed in other practical cases which may presumably be explained as the influence due to the side products of the hydroperoxidation.

Summary

The partition equilibrium was investigated in relation to the steam-blowing and stripping, during and after the hydroperoxidation of cumene, and the following results were obtained.

1. Equilibrium constant K does not depend on the concentration of CHP within the limit of experimental error, but it depends on the temperature.

2. The partition constant, K approximately satisfies the following formula,

$$K = 1.3_4 \times 10^{-4} e^{1580/T}.$$

3. The heat of transference of 1 mol. of cumene hydroperoxide from cumene solution into water under the equilibrium condition, was determined as 3.16 k cal./mol.

This article is a part of the investigations of the cumene process which have been studied by many members of Tōkai Electrode Mfg. Co. The authors are grateful to them and wish to express their thanks to Dr. H. Sobue, professor of Tokyo University, for his valuable suggestions and discussions, to Mr. M. Nomaguchi, the chief of our laboratory for his instructive advice and encouragement, and to the authorities of Tōkai Electrode Mfg. Co. for the publication of this work.

Technical Research Laboratory
Tōkai Electrode Mfg. Co.
Fujisawa

*Antioxygenic Activity of α- and β-Glycerophosphoric Acids**

By Chieko URAKAMI, Yoshiko KAKUTANI and Hirotomo OKURA

(Received June 24, 1956)

Introduction

Since Bollmann[1] discovered antioxygenic activity of crude lecithin, a number of other investigators[2] have reported similar findings. However, Hilditch[3] found that purified lecithin did not show any antioxygenic activity in the autoxidized esters of the distilled fatty acids of olive oil. For the study of relations of molecular structures of phosphatides to antioxygenic activity, their hydrolysis products have been investigated by a number of workers. Olcott and Mattill[4] reported that cephalin among other phosphatides had the strongest activity and suggested that the phosphoryl group in the molecule has some relation to the activity. Strohecker, et al.[5] obtained the result that only choline among other hydrolytic products of cephaline was active against oils of plant origin, whereas Dutton, Olcott, and Mattill[6] observed that the phosphoryl residue in the cephalin or lecithin molecules possessed activity. Altman[7] reported that phosphatides, choline and amino acids were effective in rubber latex. Recently, Desneulle et al.[8] have found that the phosphatidyl choline which has been obtained from eggs did not possess antioxygenic activity in the methyl esters of sunflower seed oil fatty acids but the phosphatidic acids obtained on treating the phosphatidyl choline with phosphatase prepared from carrots exerted the activity. Calkin[9] proposed the theory that cephaline with one free hydroxyl gorup should show some activity but lecithin which has no free hydroxyl group in its molecule should have no activity.

It is conceivable that nothing definite has been established as to the relation of molecular structures of the phosphatides to antioxygeninc activity. It is, however, reasonable to assume that the phosphoryl group in these molecules would possess the activity since a number of organic esters of phosphoric acid[10] are known to be antioxygenic to fat-containing materials.

The confusing results[3,5,6] on the phosphatidic acids may be due to difference in composition of the hydrolysis products with respect to the α and β-structures of the glycerophosphoric acids, since the isomerization of the phosphoryl group has been found to occur in either acid or alkaline hydrolysis[11], to a greater extent with the former. Therefore, we have called our attention to the relation of the structural difference of the phosphatidic acid, to antioxygenic activity and, as a preliminary work, studied α and β-glycerophosphoric acids, relatively stable hydrolysis products of the phosphatides, in purified oleic acid.

Conditions for autoxidation were selected so that least kinds and amounts of by-products would be produced during autoxidation, as demonstrated by Swern, et al.[12] As the rate of oxidation of oleic acid is slow compared to that of methyl oleate, we chose 50°C for the temperature of autoxidation and compared activities of the glycerophosphoric acids with that of phosphoric acid in an early stage, up to peroxide value of about 10 mM per 100 g. of the acid. It was found that the α-compound was just as active as orthophosphoric acid but the β-isomer did not have any activity.

We have also investigated recovery of the water soluble glycerophosphoric acids during autoxidation to obtain some clue as to mechanism involved in the antioxygenic activity. Preliminary results showed that the recovery of the water soluble gryceropho-sphoric acids from the autoxidized oleic acid

* Presented in part at the 9th Annual Meeting of The Chem. Soc., Japan, April, 1956.

1) H. Bollmann. *U. S. Pat* 1, 575, 529 (1926).

2) G. I. Evans, *Ind. Eng. Chem..*, 27, 399 (1935); H. N. Holmes, R. E. Corbet and R. A. Ragatz, ibid., 28, 133 (1936); M. R. Sahasrabudhe, *J. Sci. Ind. Research*, 12B 63 (1953); H. J. Lips, *Food in Canada*, 12, No. 6, 9, 12 16 (1952).

3) T. P. Hilditch and S. Paul, *J. Soc. Chem, Ind* , 58, 21 (1939).

4) H. S. Olcott and H. A. Mattill, *Oil and Soap*, 13, 98 (1936).

5) R. Strohecker, W. Diemair and K. Reuland, *Z. Untersuch. Lebensm.*, 79, 23 (1940).

6) H. J. Dutton, H. S. Olcott, and H. A. Mattill, *J. Am. Oil Chemists' Soc.*, 26, 441 (1949).

7) R. F. A. Altman, *Trans. Inst. Rubber Ind.*, 23, 179 (1947).

8) P. Desneulle, R. Massoni and O. Benoit-Micaelli, *Bull. Soc. chim. France*, 1953, 595.

9) V. P. Calkins, *J. Am. Chem. Soc.*, 69, 384 (1947).

10) H. R. Kraybill and B. W. Beadle, *U. S. Pat.*, 2, 521, 856.

11) E. Baer and M. Kates, *J. Biol. Chem.*, 185, 615 (1950); E. Baer, H. C. Stancer and I. A. Korman, ibid., 200, 251 (1953).

12) H. B. Knight, J. E. Coleman and D. Swern *J. Am. Oil Chemists' Soc.*, 28, 498 (1951); ibid., 32, 135 (1955); D. H. Saunders, C. Ricciuti and D. Swern, ibid., 32, 79 (1955).

was very small, implying that a larger amount is associated with the fatty acid.

Experimental

Oleic Acid.—"Tokusei olein NTA 34" of the Nihon Yushi K. K.[13] was purified by recrystallization from acetone at low temperatures[14], first at −5° to remove stearic and other saturated acids present and then at −53° to removed linoleic and other highly unsaturated acids. The solvent was removed from the acetone solution containing chiefly oleic acid and the residue distilled three times. The sample thus prepared had the following constants: B.p., 220°/7 mm.and 221°/8 mm (220°/7 mm.).; Iodine number, 89.10 (89.9); Neutralization value, 199.7 (198.8); n_D^{20}, 1.4599, (1.4585, 1.4599). The figures given in the parentheses are those calculated or found in the literature.

Orthophosphoric Acid.—Analytical reagent (85%) of Mallinckrodt Chemical Works, U. S. A. was used. It was dehydrated in a vacuum desiccator over calcium chloride and then taken up in absolute alcohol. Its concentration was determined by Burmaster's method[15]. For the determination of absorption coefficients, Shimazu Model DF-11 with the filter no. 634 and 5 mm. cell were employed.

α-Glycerophosphoric Acid.—The barium ion of barium α-glycero-Phosphate[15] was removed in the form of sulfate by treating with 0.1 N sulfuric acid (adjusted to pH 1.5), followed by repeated washing with alcohol. The alcoholic solution was concentrated to 3 cc. in volume and the concentrate analyzed according to Burmaster's method. Analysis of 1 cc. of the alcoholic concentrate: inorganic P, 0.000 mg.; α-glycerophosphoric acid, 10.656 mg.; the β-isomer, 0.500 mg.

β-Glycerophosphoric Acid.—Sodium β-glycerophosphate suspended in alcohol was treated with 0.1N alcoholic HCl (adjusted to pH 1.5), the mixture concentrated under reduced pressure, and the residue washed several times with alcohol to remove the sodium chloride precipitated. The process was repeated several times to remove as much of the sodium chloride as possible, and the final alcoholic solution concentrated to give 3 cc. in volume. Analysis of 1 cc. of the solution: inorganic P, 0.000 mg.; α-glycerophosphoric acid, 0.600 mg.; the β-isomer, 20.960 mg.

Autoxidation of Oleic Acid.—After adding a sufficient amount of an alcoholic solution of the compound under consideration to 14 g. of oleic acid, the alcohol was removed at less than 40°C under reduced pressure and nitrogen atomosphere. The concentration of the compound in oleic acid was kept at 0.1%. The sample thus prepared was autoxidized at 50°C by passing purified air at a rate of 3l. per min. through a sintered glass funnel (a medium sized pore) without the sleeve. Aliquots were removed at intervals (into a weighing bottle containing 1–2 drops of a 0.05% solution of hydroquinone in isopropanol) and their peroxide values were determined according to Volz-Gortner's method[17], using 0.005N solution of sodium thiosulfate. The titration was carried out by using a 1 or 2 cc. pipette provided with a large injection needle at the tip end with the aid or rubber tubing and a long rubber tubing attached to a syringe at the other end. By manipulating the syringe, one cc. was cut into 70 drops, The method gave more accurate results than those obtained by using the microburette sold on the market. The error of average deviation involved was found to be 2% with peroxide values up to 1.5mM/100 g, 0.1% with 9 mM/100 g, and 0.5–1% for the intermediate values.

Recovery Test.—An aliquot of 0.1 cc. was removed at intervals during the autoxidation, weighed accurately, and dissolved in 2 cc. of ether. The ether solution was washed four times with 1 cc. portions of fresh water. The washing were combined, made up to a known volume and analyzed for the recovery of the glycerophosphoric acids. Blank tests were carried out in exactly the same manner with β-glycerophosphoric acid in non-autoxidized oleic acid.

Results

The effect of alcohol used as a solvent was observed, as shown in Tables I and II, higher peroxide values were obtained with the sample treated with alcohol. The results obtained with orthophosphoric acid, α and β-glycerophosphoric acids are shown in Tables III, IV and V, respectively. The maximum error

TABLE I

AUTOXIDATION OF OLEIC ACID AT 50°C

Time hr.	Peroxide Value m. mol./100 g.	Amount of Air Passed, Kl.
6.5	1.32±0.02	0.85
11.8	2.23±0.02	1.67
22.1	4.25±0.09	3.43
26.8	5.30±0.11	4.20
34.4	6.88±0.02	5.38
47.9	9.53±0.02*	7.68

* The determination was carried out 6 hr. after removing the sample from the autoxidation chamber.

TABLE II

AUTOXIDATION OF OLEIC ACID WITH TRACE OF ALCOHOL AT 50°C

Time hr.	Peroxide Value m. mol./100 g.	Amount of Air Passed, Kl.
5.9	1.56±0.02	0.95
18.4	4.00±0.06	3.15
23.0	5.01±0.02	3.86
28.1	6.20±0.04	4.66
43.8	9.70±0.04	7.28

13) We thank the Nihon Yushi K. K. Kenkyu-sho for the supply of the sample.

14) D. K. Kolb and J. B. Brown, *J. Am. Oil Chemists' Soc.*, **32**, 357 (1955).

15) C. F. Burmaster, *J. Biol. Chem.*, **164**, 233 (1946).

16) C. Urakami and Y. Kakutani, *Repts. Sci. Living*, Osaka City Univ., Series D. No. 1, 3 (1953).

17) F. E Volz and W. A. Gortner, *J. Am. Oil Chemists' Soc.*, **24**, 417 (1947).

involved in the rates of aeration of the samples were found to be 5% but the rates were very close to each other in the samples containing α and β-glycerophosphoric acids.

TABLE III
AUTOXIDATION OF OLEIC ACID IN THE PRESENCE OF H_3PO_4 AT 50°C

Time hr.	Peroxide Value m. mol./100 g.	Amount of Air Passed, Kl.
5.8	0.73±0.02	0.75
20.6	1.84±0.04	3.02
30.2	2.72±0.02	4.05
44.7	4.44±0.07	6.48
53.2	5.60±0.04	7.90

TABLE IV
AUTOXIDATION OF OLEIC ACID IN THE PRESENCE OF α-GLYCEROPHOSPHORIC ACID AT 50°C

Time hr.	Peroxide Value m. mol./100 g.	Amount of Air Passed, Kl.
6.0	0.69±0.01	1.00
19.1	1.20±0.01	3.33
29.0	1.97±0.01	4.95
43.6	4.27±0.08	7.51
51.6	5.50±0.00	8.81

As shown in Tables IV and V, there is a distinct difference in antioxygenic activity between the two isomers, α-glycerophosphoric acid has the activity somewhat better than phosphoric acid while the β-isomer has no activity at all. The peroxide values for the latter are somewhat higher than those of

TABLE V
AUTOXIDATION OF OLEIC ACID IN THE PRESENCE OF β-GLYCEROPHOSPHORIC ACID AT 50°C

Time hr.	Peroxide Value m. mol./100 g.	Amount of Air Passed, Kl.
5.4	1.93±0.02	1.00
20.0	4.65±0.04	3.52
29.5	6.55±0.07	5.05
43.2	8.98±0.07	7.43
50.5	10.2 ±0.1	8.61

oleic acid alone but close to those of the blank run made with the addition of alcohol.

Recovery of water soluble β-glycerophosphoric acid from unautoxidized oleic acid was found to be 95%. However, there was a sharp drop in recovery of both α and β-glycerophosphoric acids from autoxidized oleic acid, 21–35% and 2–8%, respectively, as shown in Tables VI and VII. As the autoxidation progressed, a small amount of the α compound was detected in the β-sample.

Discussion

It has been demonstrated that α-glycerophosphoric acid has antioxygenic activity comparable to that of orthophosphoric acid in purified oleic acid but the β-isomer has no activity. According to Baer et al.[11] and Long and Maguire[18], alkaline or acid hydrolysis of the naturally occurring phosphatides results in migration of the phosphoryl radical. Consequently, the samples of glycero-

TABLE VI
RECOVERY OF α-GLYCEROPHOSPHORIC ACID FROM AUTOXIDIZED OLEIC ACID

Aliquot g.	Time of autoxidation, hr.	Absorbance* P			Microgram P				The Acids/0.2 g. Sample, μg.			Total recovery %
		H_3PO_4	α	Total	H_3PO_4	α	Total	β	α	β	H_3PO_4	
25 μl**		0.003	0.38	0.39	0.00	24.0	24.9	0.9	106.6 (96.4)	3.7 (3.4)		100
0.2408	29.0		0.113			6.9			63.6 (26.9)			
0.2421	〃			0.115			7.0			0.6 (0.25)		27.2
0.1907	43.4	0.008										
0.1899	〃		0.111			6.75			79.9 (33.8)			
0.1889	〃			0.115			7.0			2.3 (1.0)		34.8
0.2148	51.4	0.010			0.05						0.52 (0.2)	
0.1978	〃		0.062			3.5			39.3 (16.6)			
0.2164	〃			0.082			4.9			11.0 (4.7)		21.2

* The values were obtained by subtracting absorbance of blank from that of sample.
** Analysis of the alcoholic solution added to oleic acid. The figures in the parentheses are per cent recovery of the respective acid.

18) C. Long and M. F. Maguire, *Biochem. J.*, 54, 612 (1953).

TABLE VII

RECOVERY OF β-GLYCEROPHOSPHORIC ACID FROM AUTOXIDIZED OLEIC ACID

Aliquot g.	Time of Autoxidation, hr.	Absorbance* P			Microgram P			The Acid/0.2 g. Sample, μg.		Total recovery %
		H_3PO_4	α	Total	H_3PO_4	α	Tatal	α	β	
10 μl**		0.004	0.017	0.295		0.50	18.88	5.8	218.5 (97.4)	100
0.2382	19.6		0.007							
0.2368	〃			0.037			1.83		17.07	7.6
0.2164	29.3		0.010			0.05		0.51 (0.2)		
0.2269	〃			0.037			1.83		17.40 (7.8)	8.0
0.1027	43.1	0.00								
0.2110	〃		0.010			0.05		0.52 (0.2)		
0.2125	〃			0.022			0.86		8.36 (3.7)	4.0
0.2070	50.3	0.00								
0.2146	〃		0.010			0.05		0.25 (0.2)		
0.2206	〃			0.018			0.55		4.82 (2.2)	2.4

* The values were obtained by subtracting absorbance of blank from that of sample.
** Analysis of the alcoholic solution added to oleic acid. The figures in the parentheses are per cent recovery of the respective acid.

phosphoric acids or the hydrolysates of phosphatides studied earlier for their antioxygenic activity might have been a mixture of the isomers in various proportions and this might have been responsible for the confusing results found in the literature.

Concerning mechanisms of antioxygenic activity of orthophosphoric acid, Quackenbush[19] reported that at a higher temperature phosphoric acid reacted with the peroxides of lard to give an oil soluble polymer-like substance. On the other hand, Calkin[9] suggested that the activated oleic acid adsorbs phosphoric acid molecules to form an ester-like intermediate, which on dissipating its energy disintergrates into the original substances, oleic acid and phosphoric acid. Our preliminary results in the recovery of the glycerophosphoric acids indicate that they are either adsorbed on the oleic acid molecules or transformed into some kind of oil soluble products. Further investigation on this point is of great interest and we are extending the study.

Faculty of Science of Living, Osaka City University, Osaka

19) F. W. Quackenbush and O. S. Privett, *J. Am. Oil Chemists' Soc.*, **31**, 225 (1954).

Metal Chelate Compounds with Higher Rings. I. The Preparations and Some Properties of Copper(II) Complexes of ω-Aminocarboxylic Acids

By Akitsugu NAKAHARA, Jinsai HIDAKA and Ryutaro TSUCHIDA

(Received July 21, 1956)

Introduction

It is well-known that chelation in metal chelate compounds is most favoured when the functional groups are in the 1, 4 or 1, 5 positions.

In fact, relatively few chelate rings containing more than six atoms have been prepared from bidentate compounds. But the formation of larger rings does not always seem to be difficult if the preparation is carried out in non-aqueous media such as alcohol, ether, or chloroform. Recently Pfeiffer[1,2], for instance, has succeeded in preparing 7-, 8-, and 9-membered rings by the reaction of tetra-, penta-, and hexa-methylenediamine, respectively, with some metal salts in organic solvents. In the case of dicarboxylic acid complexes, there have also been reported some other complexes containing 7- and 8-membered rings[3,4,5]. Those increasing examples of higher rings have led us to perform the further systematic researches of metal chelate compounds with higher rings. The chief purpose of this series of work is to establish experimental data concerning the relation between the stability and ring sizes.

First of all, we picked up copper(II) complexes of ω-aminocarboxylic acids which contain carbon atoms from C_2 to C_6, getting two new examples of higher rings and one new type of amino acid complex. They are copper(II) complexes of γ-aminobutyric*- and δ-aminovaleric-acid, and of ε-aminocaproic acid, respectively. This paper describes the preparations and some properties of those three new compounds with some discussion on their stabilities.

Experimental

General Method of Preparation.—Two methods were adopted for preparing copper(II) complexes of ω-aminocarboxylic acids. The one was a heterogeneous reaction, (**A**), of a ligand with copper(II) perchlorate in an organic solvent, while the other was a homogeneous reaction, (**B**), making use of the action of an overwhelming amount of a ligand in an aqueous solution. The product obtained by the method (**A**) necessitated to be recrystallized from a mixed solution of alcohol and water containing a large amount of the ligand. Therefore, the difference between the two methods was rather slight. When the preparation was performed on a small scale, however, the method (**A**) seemed to have much advantage over (**B**).

Preparation of Bis-(γ-aminobutyrato)-copper(II), $[Cu(NH_2(CH_2)_3COO)_2]\cdot 2H_2O$.—The method (**A**) was applied to prepare this compound. To a suspension of 4 g. of γ-aminobutyric acid in chloroform, was added 3.5 g. of copper(II) perchlorate hexahydrate. The heterogeneous mixture was shaken vigorously till the light blue of the copper(II) perchlorate changed to deep blue or violet. To complete the reaction the mixture was preserved overnight. The viscous product was freed from chloroform by blowing dry air on it after decantation. Then the crude product was dissolved in a small quantity of water, and the resulting solution was filtered quickly. A large amount of alcohol was added carefully to the clear deep blue filtrate. Within a few days fine crystals of $[Cu(NH_2(CH_2)_3COO)_2]\cdot 2H_2O$ were obtained. The yield of the reaction was almost quantitative, and the compound was pure enough at least for spectrochemical studies. The results of the analyses were as follows.

Anal. Found: C, 31.54; H, 6.49; N, 9.29; H_2O, 11.55. Calcd. for $[Cu(NH_2(CH_2)_3COO)_2]\cdot 2H_2O$: C. 31.57: H, 6.56: N, 9.21: H_2O, 11.84%.

Preparation of Bis-(δ-aminovalerato)-copper (II), $[Cu(NH_2(CH_2)_4COO)_2]$.—This compound was prepared by the method (**A**). In this case, however, there was provided twice the quantity of the ligand in mole ratio for the complex formation, since it was assumed that the complex might have less stability compared with bis-(γ-aminobutyrato)-copper(II). Other procedures for preparation were the same as those described above.

Anal. Found: C, 40.54; H, 7.09; N, 9.13. Calcd. for $[Cu(NH_2(CH_2)_4COO)_2]$: C, 40.60; H, 6.76; N, 9.47%.

Preparation of Tetrakis-(ε-carboxyamylamine)-copper(II) Perchlorate, $[Cu(NH_2(CH_2)_5COOH)_4](ClO_4)_2$.—To prepare this compound the method (**B**) was adopted as well as (**A**). Copper(II)

1) P. Pfeiffer, E. Schmitz and A. Böhm. *Z. anorg. allg. Chem.*, **270**, 287 (1952).
2) P. Pfeiffer, *Naturwiss.*, **35**, 190 (1948).
3) J. C. Duff, *J. Chem. Soc.*, **119**, 385, 1982 (1921); **123**, 560 (1923).
4) T.S. Price and S.A. Brazier, ibid., **107**, 1367 (1915).
5) T. S. Price and J. C. Duff, ibid., **117**, 1071 (1920).
* Although there are some descriptions of the complex formation of bis-(γ-aminobutyrato)-copper (II), the compound has never been isolated in the crystalline state up to date.

perchlorate hexahydrate was added to an aqueous solution which contained an over-whelming amount of ε-aminocarboxylic acid. After filtration of the deep blue solution, beautiful violet crystals were obtained. Within a couple of hours the deposition of the complex ended. The yield of the reaction was almost quantitative. The analyses of the compound were as follows.

Anal. Found: C, 36.52; H, 6.52; N, 7.02; Cu, 7.87; Cl, 9.39. Calcd. for $[Cu(NH_2(CH_2)_5COOH)_4](ClO_4)_2$: C, 36.62; H, 6.62; N, 7.12; Cu, 8.08; Cl, 9.01%.

The compound prepared by the method (**B**) was ascertained to be identical with that obtained by the method (**A**). However, (**B**) was much more convenient than (**A**), when the preparation was carried out on a large scale.

Preparation of Bis-(glycinato)-copper(II), $[Cu(NH_2CH_2COO)_2]\cdot H_2O$, and Bis-(β-alaninato)-copper(II), $[Cu(NH_2(CH_2)_2COO)_2]\cdot 6H_2O$.—Although there are some known methods, the above described method, (**A**), was also applied for preparing these two complexes. It was confirmed that there was no difference between the known and the present method.

Syntheses of the Ligands.—The synthesis of δ-aminovaleric acid was carried out by the method of Wallach[6] as shown in the following scheme:

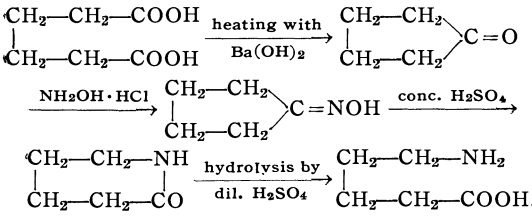

γ-Aminobutyric acid was obtained from pyrrolidone according to the direction of Tafel et al.[7] ε-aminocaproic acid was derived from caprolactam by heating with dilute hydrochloric acid[8].

Preparation of Bis-(hexamethylenediamine)-copper(II) Perchlorate, $[Cu(NH_2(CH_2)_6NH_2)_2](ClO_4)_2$.—The preparation of this compound was reinvestigated in order to clarify the ambiguity concerning the purity of the compound obtained by Pfeiffer[1]. Analytical values showed a good agreement with each other as follows: Pfeiffer's analyses (crude substance): Cu, 12.74; N, 11.34. Analysis in this work (pure crystal): N, 11.09. Calcd. for $[Cu(NH_2(CH_2)_6NH_2)_2](ClO_4)_2$: Cu, 12.85; N, 11.32%.

The recrystallization of Pfeiffer's crude substance was performed in the same way as that used in the preparation of bis-(γ-aminobutyrato)-copper(II).

Properties of the Three Amino Acid Complexes.—The crystal of bis-(γ-aminobutyrato)-copper(II) is very small and prismatic, and shows a remarkable dichroism on the prism face, that is, deep violet and almost colourless. Tetrakis-(ε-carboxyamylamine)-copper(II) perchlorate also shows a clear dichroism on the well-developed face of the acicular crystal, that is, violet and blue. In the case of bis-(δ-aminovalerato)-copper(II), no optical properties were observed cleary because the crystal was extremely small. All the three compounds are stable in the crystalline state but quite unstable in water, and decompose over 180°C.

It is impossible to get the 0.01 M-solution of bis-(γ-aminobutyrato)-copper(II) on account of its decomposition even in an aqueous solution containing 0.08 M of the ligand. In water containing over 1.5 M of the ligand, however, clear solutions of the complex are obtainable without any detectable decomposition. δ-Aminovalerato-complex resembles the γ-aminobutyrato-complex in many respects, but the former is still more unstable in water than the latter. Although the three complexes show different colours from one another in the crystalline state, it is impossible to discriminate one from the others when they are dissolved in water with a large amount of the respective ligand. With respect to their infrared spectra, only the ε-aminocaproic acid complex shows a widely different curve, suggesting a different type of structure[9].

Results and Discussion

In this work three new complexes were obtained as shown in the experimental part. They were bis-(γ-aminobutyrato)-copper(II), bis-(δ-aminovalerato)-copper(II) and tetrakis-(ε-carboxyamylamine)-copper(II) perchlorate. As is clear from the analytical values of those compounds the former two complexes must be metal chelate compounds of the bis-(glycinato)-copper(II) type in structure. (Fig. 1). On the other hand, the last complex must have a structure which corresponds to an amminederivative complex, containing four unidentate ligands, as is seen in Fig. 2.

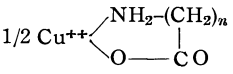

Fig. 1. Chelate-type.

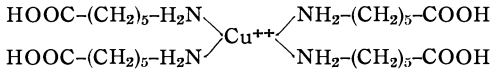

Fig. 2. Unidentate-type.

It is of interest to notice here that the stabilities of copper(II) complexes of ω-amino acids in aqueous solution decrease with an increasing length of the ligands. For example, bis-(glycinato)-copper(II) is so stable that it is quite easy to recrystallize the complex from a hot aqueous solution, while, in the case of bis-(β-alaninato)-copper(II), it is difficult to recrystallize the complex from a hot solution without any detectable decomposition. The comparison of the stabilities of β-alaninato- and γ-aminobutyrato-complex is

6) O. Wallach, *Ann.*, **312**, 179 (1900).
7) J. Tafel and M. Stern, *Ber.*, **33**, 2230 (1900).
8) J. C. Eck, Org. Syn., **17**, 7 (1937).
9) To be submitted later.

the same as that of glycinato- and β-alaninato-complex, that is, the former is less unstable than the latter. This tendency is well-observed in the comparison of γ-aminobutyrato- and δ-aminovalerato-complex, too.

Judging from this tendency, it may be supposed that ε-aminocaproato-complex would be extremely unstable, if it would coördinate to a copper atom as a chelate ligand. In fact, ε-aminocaproic acid does not behave as a chelate ligand but coördinates to a copper atom as an unidentate ligand, as was already shown in the preceding section.

Thus, we may conclude that 8-ring is the highest ring for the formation of metal chelate compounds, so far as the copper(II) complexes of ω-aminocarboxylic acids are concerned. On the other hand, Pfeiffer has succeeded in preparing a 9-membered ring by the reaction of hexamethylenediamine with copper(II) perchlorate according to the same method*. This indicates directly that hexamethylenediamine is more favoured than ε-aminocaproic acid in forming the chelate ring. In other words, those bidentate ligands which have two nitrogen atoms in the functional end groups can form more stable copper(II) chelate compounds than can those having one nitrogen and one oxygen atom. With respect to the ligand, ε-aminocaproic acid, there are two possible ways in coördinating to a copper atom as an unidentate ligand. The one corresponds to the case in which the nitrogen attaches directly to the copper atom, and the other the case in which the oxygen plays the part of the donor atom. In the present case, however, the former is more likely than the latter in many respects. For example, the color of the complex quite resembles that of the ammine-complex. Spectroscopic studies also support the above interpretation, and show the presence of free carboxyl groups[9]. Therefore, the structure of the copper(II) complex of ε-aminocaproic acid should coincide with that shown in Fig. 2, and the nomenclature of the complex should be "tetrakis-(ε-carboxyamylamine)-copper(II) perchlorate" taking the copper-nitrogen linkage into consideration. *In consequence, we reach a conclusion that nitrogen has a greater affinity than oxygen for copper.* In the case of chromium(III) complexes with amino acids[10], oxygen seems to be more favoured than nitrogen in uniting with chromium contrary to the case with copper.

* Pfeiffer's 9-membered ring seemed to be unreliable, since the reaction product obtained by heterogeneous reaction had not been recrystallized. According to our reinvestigation, however, the analytical value of the pure crystal which was obtained by the present authors showed a good agreement with that of Pfeiffer's product.

The Relation between Chelate Formation and Ring Sizes.—As is clear from the above described facts the greater the separation of the carboxyl and amino groups the less the tendency for chelate formation. In an aqueous solution, therefore, it is considered to be difficult to obtain a metal chelate compound which has a larger ring on account of the strong solvolytic aquation[11,12,13,14]. In this respect, the heterogeneous reaction method adopted in this work is quite suitable for the study of the metal chelate compounds with higher ring, since there are very few interrupting factors in the reaction system. But yet the 9-membered ring was too unstable to be included in this work. In connexion with this fact, it seems to be desirable to afford some elucidation concerning the reason why the stablities of metal chelate compounds decrease with an increasing number of ring members.

Firstly, we propose steric effects. With very few exceptions the recognized examples of steric influences on stability are based on qualitative observations which usually involve formation or non-formation of the metal complexes. In the present case, however, that is not the way to consider the subject, since it is clear through the examinations of models that there is hardly expected any remarkable difference between the steric condition of δ-aminovalerato-chelate and that of ε-aminocaproato-chelate. Judging from their lactam forms, the amino and carboxyl groups in the free molecules of δ-amino- and ε-aminocarboxylic acid are accessible to each other without any serious distortion. Therefore, it seems to be easy for both the ligands to arrange their functional groups about a central metal atom so that the respective metal chelate complex can be formed. Such being the case, the stability of higher rings is not fully explained from the standpoint of the steric effect, though it is considered to be a very important factor.

Secondly, electronic influences induced with the separation of the two functional groups probably play another important role for the chelate formation. According to the work of Ley[15], the acidity of ω-aminocarboxylic acid decreases with an increasing distance between carboxyl and amino groups, and there is the opposite inclination with respect-

10) R. W. Green and K. P. Ang, *J. Am. Chem. Soc.*, 77, 5482 (1955).
11) A. Werner, *Ber.*, **40**, 15 (1907).
12) L. Tschugaeff, ibid., **39**, 3190 (1906); *J. Prakt. Chem.*, [2] **75**. 159 (1907).
13) P. Pfeiffer and M. Haimann, *Ber.*, **36**, 1063 (1903).
14) P. Pfeiffer and E. Lübbe, *J. prakt. Chem.*, [2] **136**, 321 (1933).
15) H. Ley, *Ber.*, **42**, 354 (1909).

to the basicity. Thus, it is quite natural to expect a different affinity for a metal with the separation of the two functional groups.

It may be considered that the stability of higher chelate rings is mainly influenced by the above two factors. Probably accumulations of slight steric constraints and electronic influences may prevent the ε-aminocaproic acid from the chelate formation with copper. We are continuing the study of the stability of higher chelate rings from another point of view.

Summary

Three new compounds, bis-(γ-aminobutyrato)-copper(II), bis-(δ-aminovalerato)-copper (II), and tetrakis-(ε-carboxyamylamine)-coppe(II) perchlorate, have been prepared. The first and the second compound belong to the bis-(glycinato)-copper(II) type, having a 7- and 8-membered ring, respectively. The last compound has a structure of ammine-derivative complex. In all cases preparations were carried out in non-aqueous media such as ether and chloroform.

It has been concluded that the 8-membered ring is the highest ring for the formation of metal chelate compounds, so far as the copper(II) complexes of ω-aminocarboxylic acids are concerned.

Stability of higher chelate rings was considered as the functions of steric constraints and electronic influences which may be induced with the separation of the two functional groups.

The authors are grateful to Mr. Y. Kinoshita of the Toyo Rayon Co. and Mr. H. Sekiguchi of Osaka University for supplying part of the samples used in this work. This investigation was supported by a grant from the Ministry of Education.

Department of Chemistry, Faculty of Science, Osaka University, Osaka

Action of Emulsifier upon the Copolymerization of Acrylonitrile and Styrene

By Moriya UCHIDA and Hideo NAGAO

(Received June 21, 1956)

Introduction

The mechanism of emulsion polymerizations of water-insoluble monomers as styrene and isoprene has been shown by Harkins[1] and Smith[2]. However, the mechanism of emulsion polymerizations of water-soluble monomers as acrylonitrile seems to be different from that of styrene and isoprene. It has been known that the polymerization rate of acrylonitrile in water increases as the polymer forms[3]. It appears to be due to diffusion and adsorption of monomer to polymer precipitated in water[4]. It has been known that in heterogeneous polymerization the loci of polymer propagation reaction are the polymers adsorpted with monomers and the appearance of this polymerization looks like that of emulsion polymerization. It was already reported that the compositions of emulsion copolymers of water-soluble monomer as acrylonitrile and water-insoluble monomer as vinylidenechloride depended on the concentrations of emulsifier used in copolymerization[5]. The reactivity of acrylonitrile and styrene in emulsion copolymerization was studied by Fordyce and Chapin[6] and Smith[7]. Although they proved that the composition of formed copolymer depended on the composition of oil phase, the action of emulsifier has not been cleared up yet. In the present paper, in the first place, some observations in emulsifier-free copolymerization, and then the action of anionic emulsifier upon the rate of polymerization, the degree of polymerization and the composition of formed copolymer are given.

1) W. D. Harkins, *J. Am. Chem. Soc.*, **69**, 1428 (1947).
2) W. V. Smith and R. H. Ewart, *J. Chem. Phys.*, **16**, 592 (1948),
3) P. J. Flory, "Principles of Polymer Chemistry", Cornell University Press (1953), p. 208.
4) H. Nagao, M. Uchida and T. Yamaguchi, *J. Chem. Soc. Japan* (in Japanese) **59**, 695 (1956).
5) H. Nagao, M. Uchida and T. Yamaguchi, *J. Chem. Soc. Japan*, in press.
6) R. G. Fordyce and E. C. Chapin, *J. Am. Chem. Soc.*, **69**, 581 (1947).
7) W. V. Smith, *J. Am. Chem.Soc.*, **70**, 2177 (1948).

Experimental

Acrylonitrile (AN).—Redistilled American Cyanamid Co. material was used for all experiments.

Styrene Monomer (St).—Redistilled commercial material was employed.

Emulsifier (Sodium Dodecyl Sulfate).—Recrystallized Kao Soap Co. material was used.

Polymerization Procedure.—A stirred 1-liter, four-necked-fiask placed in a water bath maintained at 45±0.1°C was charged by the additions of the required emulsifier aqueous solution and monomers. The air in the flask was purged by the introduction of nitrogen. Then the catalyst (potassium persulfate) 0.8 weight % and the reductant (sodium bisulfite) 0.8 weight % were added after the flask had attained thermal equilibrium. These weight % concentrations were based on total monomers. The mixer of the flask was rotated at 300 revolution per minute. The latex was coagulated in water or in a calcium chloride solution which contained hydroquinone as an inhibitor. Conversion data were based on total solid determinations. η_{sp}/c was measured in 2 g./l. dimethylformamide solution at 25°C. The combined acrylonitrile in copolymer was determined by Kjeldahl analysis.

Results and Discussion

(1) Rate of Polymerization in Emulsifier-free Copolymerization

The mixture of water-soluble monomer as acrylonitrile and water-insoluble monomer as styrene in the presence of suitable water-soluble redox initiating reagents is capable of undergoing copolymerization in water without the assistance of emulsifying agents. The relation between conversion and polymerization times is shown in Fig. 1.

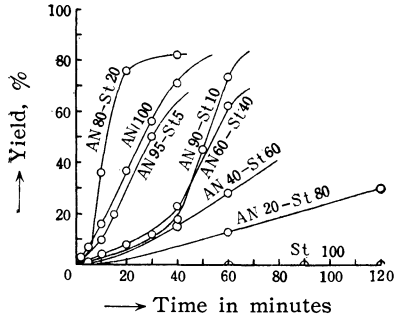

Fig. 1. Rate of polymerization of acrylonitrile and styrene in aqueous solution.

The rate of polymerization was very slow in only styrene and became faster as the mixture of monomer contained much acrylonitrile. The polymerization of water-insoluble monomer as styrene without soap or with a very small amount of soap was very slow, and the degree of polymerization of the formed polymer was low[8]. The water-soluble monomer as acrylonitrile was absorbed remarkably in the initial polymer in water[4], so that the rate of polymerization would be fast and the degree of polymerization of the formed polymer would be high even if the emulsifier was not used. The difference of the property as above existed between the two monomers used. The copolymerization rate of these monomers was dependent upon the average water-solubility of their mixture. It has been known that the rate of polymerization is roughly proportional to the solubility of the monomer in water in case of polymerization of water-soluble momomer such as methyl-methacrylate, vinylacetate or acrylonitrile[8]. Consequently, the solubilized amount of monomer in water must depend on the rate of polymerization. Whitby, Gross, Miller and Costanza[9] found that the addition of a small amount of acrylonitrile in copolymerization of styrene and butadiene accelerated the rate of reaction and the polymerization rate of styrene containing 5–10% methacrylonitrile was faster than that of only styrene.

It has been known that the initiation of polymerization occurs in water phase in these polymerization systems. When a layer of styrene is placed on a column of a dilute potassium persulfate solution in water and the system is allowed to stand for several days, the aqueous phase slowly becomes cloudy. If substances with greater solubility in water, e.g., methacrylic ester, vinyl acetate or acrylonitrile, are used, the cloudiness appears much more rapidly although the area of the interface is the same as before. Moreover, if a small amount of an inhibitor is added to monomer phase, the course of the polymerization in the aqueous phase is not noticeably affected; if, however, the same amount is added to the aqueous phase, the appearance of the cloudiness is considerably delayed.

This is an indication that at least the formation of active nuclei takes place in the aqueous phase.

Fryling and Harrington[10] observed that, in the case of the layer polymerization of acrylonitrile on top of an aqueous potassium persulfate solution, the aqueous phase remains clear and transparent for a distance of about five millimeters below the interface, indicating that no polymer is actually being formed at

8) W. P. Hohenstein and H. Mark, *J. Polymer Sci.*, **1**, 549 (1946).
9) G. S. Whitby, M. D. Gross, J. R. Miller and A. J. Costanza, *J. Polymer Sci.*, **16**, 549 (1955).
10) C. F. Fryling and E. W. Harrington, *Ind. Eng. Chem.*, **36**, 114 (1944).

the interface itself but that the dissolved monomer is the principal center for the formation of polymer. Moreover, the active center produced by interaction of monomer and potassium persulfate in water, can grow in the aqueous phase without being in any direct contact with liquid monomer and the adsorption rate of monomer to active center is greater than the consumption rate of monomer as we reported[4], so the propagation reaction seems to occur in the polymer adsorpted monomer.

It has been found that the polymer of water-insoluble monomer as styrene was slowly formed in the aqueous phase outside of the droplet by the observation of the behavior of small droplets of styrene in aqueous solutions of peroxides under the microscope[8]. The interface between monomer and aqueous solution of catalyst seems not to be appropriate locus for the initiation and propagation of polymer. Consequently, it is thought that the initiation of polymer occurs also in aqueous phase in copolymerization of acrylonitrile and styrene, and is remarkable because of the increase of active centers in water as the amount of acrylonitrile is great in the mixture of monomer so that the rate of polymerization increases.

At the same time the reactivity of monomers must also be taken into account. The monomer reactivity ratios in the copolymerization of acrylonitrile and styrene were the following[11].

r_1 (Styrene)	r_2 (Acrylonitrile)	
0.41±0.08	0.04±0.04	60°C

Consequently, the rate of addition of acrylonitrile to styrene radical is faster than that to acrylonitrile radical, and the rate of addition of styrene to acrylonitrile radical is faster than that to styrene radical. The rate of propagation reaction must be maximum in the mixture of equal molecules of monomers according to the above-mentioned concept.

This concept will be applied to the copolymerization of acrylonitrile (r_1, 0.91±0.10) and vinylidenechloride (r_2, 0.34±0.10). It has been reported that the maximum rate of polymerization related to the compositions of monomer mixtures appears in the mixture of almost equal molecules of acrylonitrile and vinylidene chloride[5]. Accordingly the maximum of the rate in the emulsifier-free copolymerization of acrylonitrile and styrene seems to be due to the effect of monomer reactivity which overlapped the effect of average water-solubility of the mixture of monomer and appears in the acrylonitrile richer composition.

11) F. M. Lewis, F. R. Mayo and W. F. Hulse, *J. Am. Chem. Soc.*, 67, 1701 (1945).

(2) Rate of Polymerization in Emulsion Copolymerization

The results of emulsion copolymerization rate which used emulsifier 0, 0.1, 0.2, 0.4, 0.6, 1.0, 1.5 weight % to total monomer are given in Figs. 2, 3, 4, 5, 6, 7, 8 and 9.

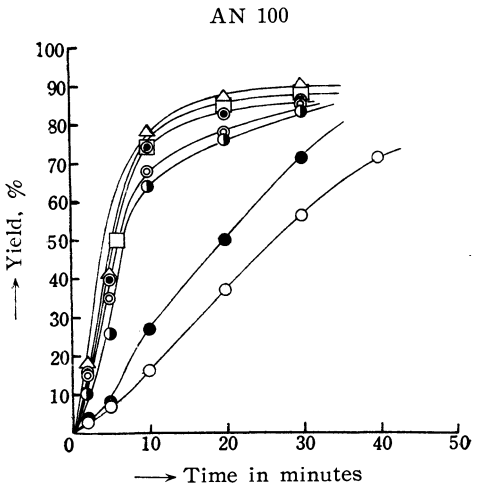

Fig. 2. Rate of emulsion polymerization, No. 1.

Emulsifier (to Total Monomers)
□ 1.5% △ 1.0% ⊙ 0.6%
◎ 0.4% ◑ 0.2% ● 0.1%
○ 0%

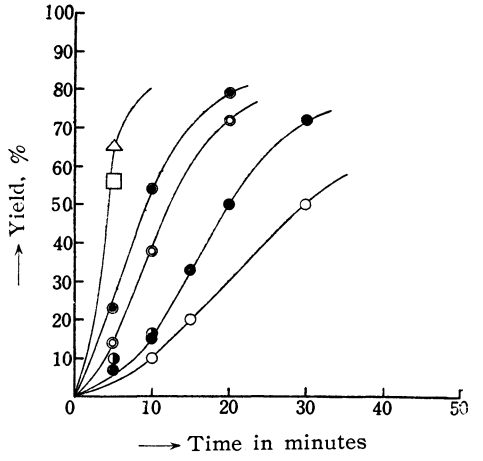

Fig. 3. Rate of emulsion polymerization, No. 2.

Emulsifier (to Total Monomers)
□ 1.5% △ 1.0% ⊙ 0.6%
◎ 0.4% ◑ 0.2% ● 0.1%
○ 0%

AN 90–St 10

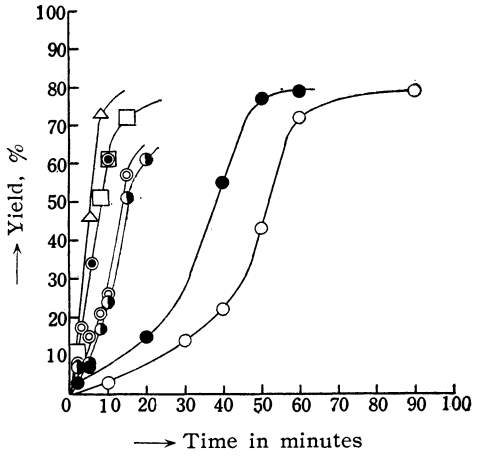

Fig. 4. Rate of emulsion polymerization, No. 3.
Emulsifier (to Total Monomers)
□ 1.5% △ 1.0% ⊙ 0.6%
◎ 0.4% ◑ 0.2% ● 0.1%
○ 0%

AN 80–St 20

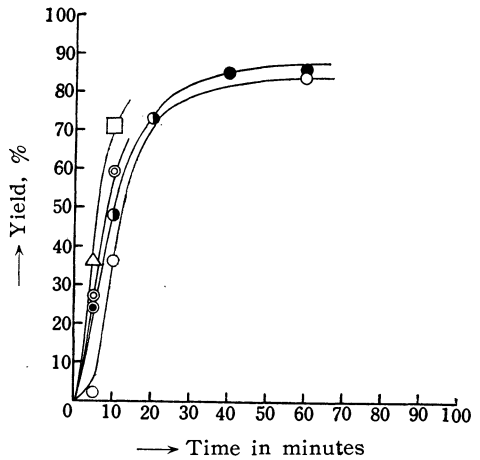

Fig. 5. Rate of emulsion polymerization, No. 4.
Emulsifier (to Total Monomers)
□ 1.5% △ 1.0% ⊙ 0.6%
◎ 0.4% ◑ 0.2% ● 0.1%
○ 0%

The situation changes significantly if soap solutions are used instead of pure water. Hess and his co-workers[12,13,14] found the presence of lamellar soap micelles from the observation of the diffraction of X rays by soap solutions. The increase of average distance of adjacent lamellae due to solubilization of hydrocarbon was observed by McBain and

AN 60–St 40

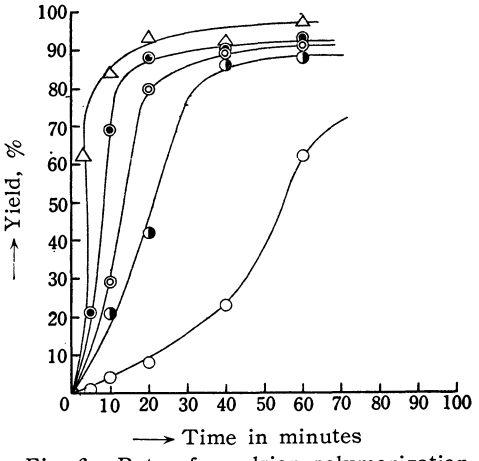

Fig. 6. Rate of emulsion polymerization, No. 5.
Emulsifier (to Total Monomers)
△ 1.0% ⊙ 0.6% ◎ 0.4%
◑ 0.2% ● 0.1% ○ 0.0%

AN 40–St 60

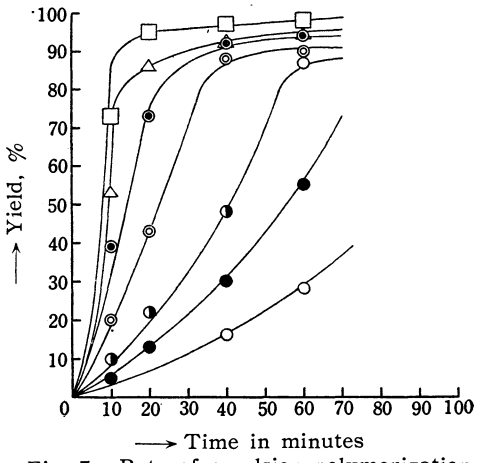

Fig. 7. Rate of emulsion polymerization, No. 6.
Emulsifier (to Total Monomers)
□ 1.5% △ 1.0% ⊙ 0.6%
◎ 0.4% ◑ 0.2% ● 0.1%
○ 0%

Harkins[15–20]. The water-soluble initiator is allowed free-diffusion and the formation of active center seems to occur mainly in micelles for these micelles contained monomer

12) K. Hess and J. Gundermenn, *Ber.*, **70**, 1800 (1937).
13) K. Hess and W. Philippoff, *Ber.*, **70**, 1808 (1937).
14) K. Hess, W. Philippoff and H. Kiessig, *Naturwissenschaften*, **26**, 184 (1938).
15) J. W. McBain, *Trans. Faraday Soc.*, **9**, 99 (1913).
16) W. D. Harkins, R. W. Mattoon and M. L. Corrin, *J. Am. Chem. Soc.*, **68**, 220 (1946); *J. Colloid Sci.*, **1**, 105 (1946).
17) J. W. McBain, "Advance in Colloid Science" Interscience Publishers, Inc., New York, N. Y. (1942), Vol. 1, p. 124.
18) W. D. Harkins, *J. Chem. Phys.*, **13**, 381 (1945).
19) W. D. Harkins, *J. Chem. Phys.*, **14**, 47 (1946).
20) W. D. Harkins and R. S. Stearns, *J. Chem. Phys.*, **14**, 215 (1946).

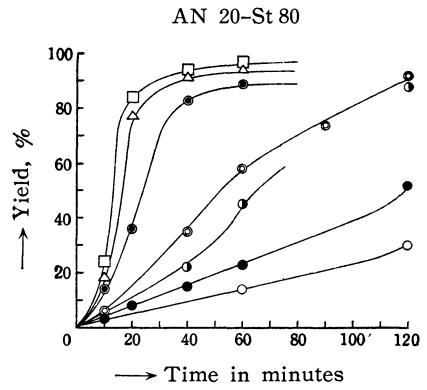

Fig. 8. Rate of emulsion polymerization, No. 7.
Emulsifier (to Total Monomers)
□ 1.5% △ 1.0% ⊙ 0.6%
◎ 0.4% ◑ 0.2% ● 0.1%
○ 0%

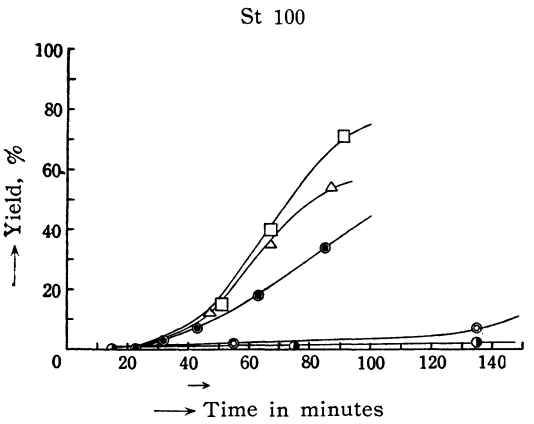

Fig. 9. Rate of emulsion polymerization, No. 8.
Emulsifier (to Total Monomers)
□ 1.5% △ 1.0% ⊙ 0.6%
◎ 0.4% ◑ 0.2%

and swelled by water in the soap concentrations of our polymerization systems as Fikentscher[21] and Hohenstein[22] have shown. The rate of polymerization increased as the emulsifier was used much, for the formation of an active center in a micelle increased as above mentioned. Moreover, it seemed to depend upon the average water-solubility of mixture of monomers, for it increased as the mixture contained much acrylonitrile. If the initiation occurs by the interaction between the radical of catalyst and monomers solubilized in micelles, according to Harkins' theory, the reaction rate will vigorously increase in the critical micelle concentration of emulsifier. The critical micelle concentration of Sodium Dodecyl Sulfate used as emulsifier has been known to be 0.05–0.2% aqueous solution[23,24]. It has been known that the critical micelle concentration becomes low by the addition of polar organic materials[25], so that 0.1–1.0 weight % (to total monomer) solution of emulsifier corresponds to about 0.01–0.15 weight % aqueous solution, that is to say, critical micelle concentration. In fact, the increase of reaction rate was found in this concentration range. The rate of polymerization seems also to depend upon the average water-solubility of monomer mixture, for it depends upon the solubilized volume of monomer in emulsion polymerization. Accordingly, it increases as the mixture of monomers contains much acrylonitrile having good ability of solubilization[26].

The rates of polymerization shown in about 40% conversion in various system are given in Table I.

TABLE I
RATE OF POLYMERIZATION (%/min.)

Amount of Emulsifier % to Total Monomer	Acrylonitrile mol. % in Monomer Mixture							
	100	95	90	80	60	40	20	0
1.5	16	16	9.0	7.1	—	7.0	5.0	1.7
1.0	19	16	9.0	7.1	9.0	5.0	4.2	1.2
0.6	14	6.0	7.0	—	8.1	3.5	3.2	0.7
0.4	12	4.8	6.0	6.8	4.8	2.2	1.1	0.3
0.2	8.6	—	5.0	6.6	2.9	1.4	0.6	0.02
0.1	2.4	3.5	3.0	6.1	—	1.2	0.4	0.01
0	2.0	2.1	2.8	6.1	2.0	0.7	0.3	0.0

Its maximum appeared in the composition of acrylonitrile 80 mol. % and styrene 20 mol. %. This seems to depend upon the effect of the monomer reactivity which overlapped that of the average water-solubility of monomer mixture as above described. The rate of acrylonitrile rich polymerization shows maximum in the concentration nearly 1% (to total monomer) of emulsifier. The emulsifier acts less upon the polymerization of water-soluble monomer than that of water-insoluble monomer, for the initiation of water-soluble monomer is easy even in emulsifier-free polymerization. It appears to be the cause of rate maximum related to emulsifier aqueous concentration that the monomer solubilized in water makes critical micelle concentration lower and in more high concentration of emulsifier the radical diffusion into micelle

21) H. Fikentscher, *Angew. Chem.*, **51**, 433 (1934).
22) W. Hohenstein, S. Siggia and H. Mark, *India Rubber World*, **111**, 173 (1944).
23) R. Goto, "Outlook of High Polymer", Association of High Polymer Chemistry, Kyoto, Japan (1951), Vol. 5, p. 47.
24) K. A. Wright, A. D. Abbott, V, Sivertz and H. V. Tartar, *J. Am. Chem. Soc.*, **61**, 549 (1939).
25) K. Schinoda, *J. Phys. Chem.*, 58, 1136 (1954).
26) S. Okamura and T. Motoyama, *J. Chem. Soc. Japan*, **57**, 930 (1954).

becomes difficult due to the fact that the wall of micelle is thick or the solubilized amount of monomers decrease because of the excess of emulsifier[27]. Consequently, the maximum will easily appear in the polymerization of acrylonitrile rich monomer mixtures.

(3) Degree of Polymerization

The relations between ηsp/c and conversion are given in Figs. 10, 11, 12, 13 and 14.

AN 95–St 5

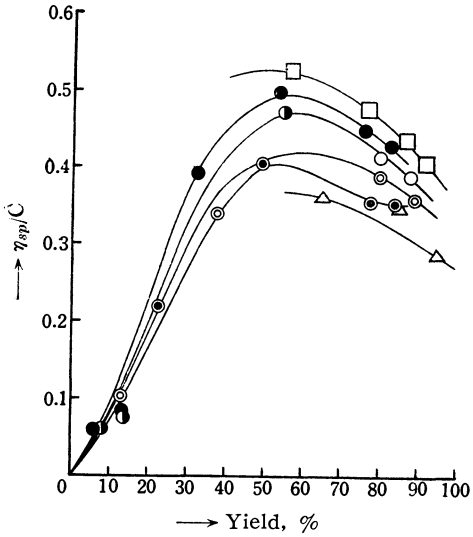

Fig. 10. η_{sp}/C vs. yield of copolymer, No. 1.
Emulsifier (to Total Monomers)
□ 1.5% △ 1.0% ⊙ 0.6%
◎ 0.4% ◑ 0.2% ● 0.1%

AN 80–St 20

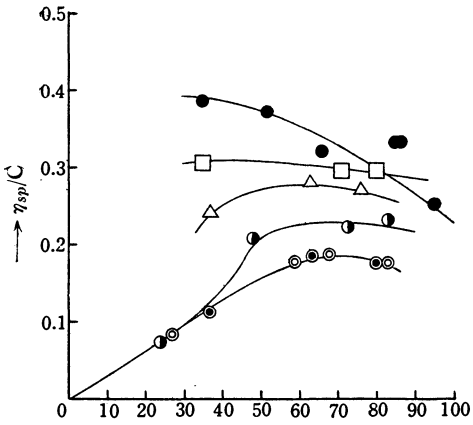

Fig. 11. η_{sp}/C vs. yield of copolymer, No. 2.
Emulsifier (to Total Monomers)
□ 1.5% △ 1.0% ⊙ 0.6%
◎ 0.4% ◑ 0.2% ● 0.1%

27) K. Kanamaru et al., *J. Chem. Soc. Japan*, 58, 221 (1955).

AN 60–St 40

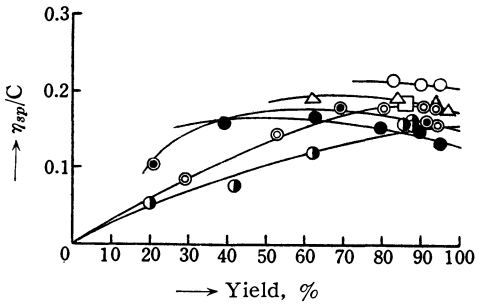

Fig. 12. η_{sp}/C vs. yield of copolymer, No. 3.
Emulsifier (to Total Monomers)
□ 1.5% △ 1.0% ⊙ 0.6% ◎ 0.4%
◑ 0.2% ● 0.1% ○ 0%

AN 40–St 60

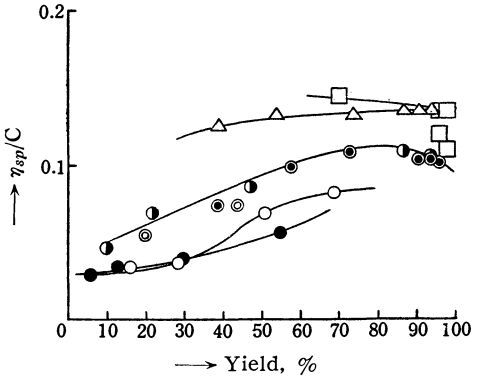

Fig. 13. η_{sp}/C vs. yield of copolymer, No. 4.
Emulsifier (to Total Monomers)
□ 1.5% △ 1.0% ⊙ 0.6% ◎ 0.4%
◑ 0.2% ● 0.1% ○ 0%

AN 20–St 80

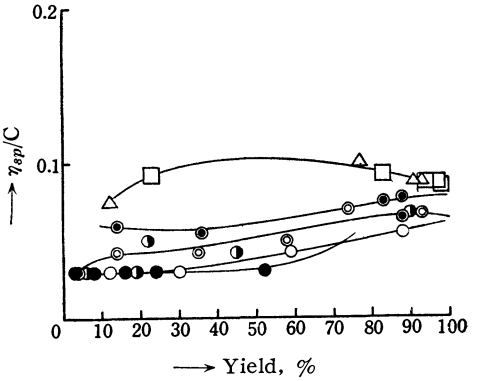

Fig. 14. η_{sp}/C vs. yield of copolymer, No. 5.
Emulsifier (to Total Monomers)
□ 1.5% △ 1.0% ⊙ 0.6% ◎ 0.4%
◑ 0.2% ● 0.1% ○ 0%

In the polymerization of styrene rich monomer ηsp/c increases with much using of

emulsifier and is proportional to the tendency of polymerization rate and it seems that the increase of the active center also brings the increase of the degree of polymerization according to its rate. However, $\eta sp/c$ in the polymerization of the monomer containing acrylonitrile decreases, shows the minimum and increases as the concentration of emulsifier becomes thick. The used amounts of emulsifier when $\eta sp/c$ becomes minimum are given in the following Table.

TABLE II

The Composition of Monomer Mixture		The Amount of Emulsifier Minimunized $\eta sp/c$
Acrylonitrile (mol. %)	Styrene (mol. %)	(weight %)
0	100	0
20	80	0.1
40	60	0.1
60	40	0.2
80	20	0.4-0.6
95	5	1.0
100	0	1.0

It has been known that the initiation of styrene occurs in micelle, so the increase of emulsifier brings the increase of polymerization rate due to the increase of active center and the increase of the degree of polymerization due to the decrease of termination. But the diffusion of water-soluble monomer as acrylonitrile in water is very faster than that of styrene, so that the degree of polymerization of monomers containing acrylonitrile becomes high even in emulsifier-free polymerization. The second radical can be more easy to diffuse into polymer swelled by water and to combines with polymer radical as the concentration of emulsifier becomes thick, so that the polymerization degree of formed polymer becomes low. In thicker concentration, the diffusion of the second radical may be hindered by the thick wall of emulsifier, so that the degree of polymerization seems to be large. In any case, the degree of polymerization of formed polymer depends upon the state of water in micelles and the affinity between monomer, polymer, emulsifier and radical due to the water-solubility of monomer. $\eta sp/c$ decreased as the monomer mixture contained much acrylonitrile. It has been known that the relation between $\eta sp/c$ and the degree of polymerization varies with the composition of the copolymer, but $\eta sp/c$ of copolymer becomes great even in the same molecular weight as the used solvent becomes poor solvent to copolymer as Maeda, Kawai and Yamaguchi[28] mentioned in regard to the copolymer of vinylchloride and vinylacetate. Dimethylformamide which is used for the measurement of $\eta sp/c$ in this paper is a good solvent for the copolymers containing much acrylonitrile unit in their structure. Consequently, the degree of polymerization becomes greater because of the increase of the solubilized amount of monomer due to its containing richer acrylonitrile.

28) K. Maeda et al., *J. Chem. Soc. Japan*, 58, 502 (1955).

(4) Composition of Copolymer on the Process of Polymerization

The compositions of copolymers formed in various conversions are given in Figs. 15, 16 and 17.

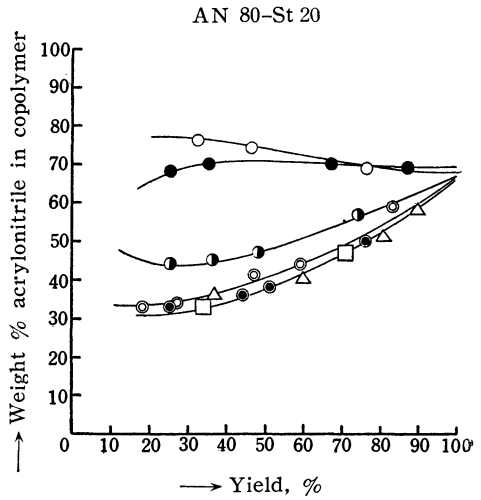

Fig. 15. Variation of copolymer composition with yield, No. 1.
Emulsifier (to Total Monomers)
□ 1.5% △ 1.0% ⊙ 0.6% ◎ 0.4%
◑ 0.2% ● 0.1% ○ 0%

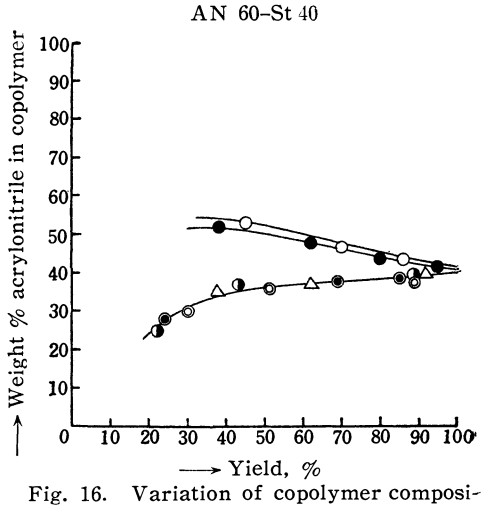

Fig. 16. Variation of copolymer composition with yield, No. 2.
Emulsifier (to Total Monomers)
△ 1.0% ⊙ 0.6% ◎ 0.4%
◑ 0.2% ● 0.1% ○ 0%

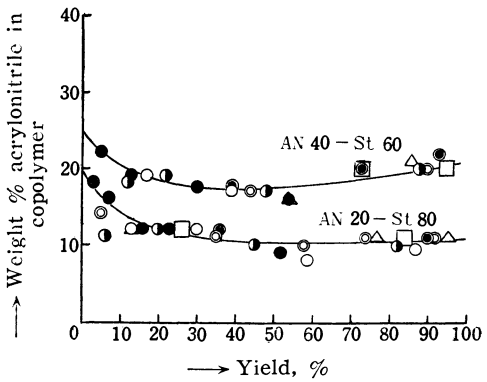

Fig. 17. Variation of copolymer composition with yield, No. 3.
Emulsifier (to Total Monomers)
□ 1.5% △ 1.0% ⊙ 0.6%
◎ 0.4% ◑ 0.2% ● 0.1%
○ 0%

It has been reported that in emulsion copolymerization of acrylonitrile and vinylidene chloride, the compositions of formed copolymers depended upon the concentration of emulsifier used and the copolymer produced in low concentration of emulsifier contained much acrylonitrile[5,29].

The same phenomena were observed in the copolymerization of acrylonitrile and styrene. It is supposed that the water-solubility of monomer depends upon the compositions of copolymer, for these copolymerizations are those of water-soluble monomer and water insoluble monomer. The variation of the composition is especially great in the copolymerization of almost equal weight water-soluble and water-insoluble monomer.

29) H. Nagao, M. Uchida and T. Yamaguchi, *J. Chem. Soc. Japan*, in press.

Conclusion

From the copolymerization of acrylonitrile and styrene done in emulsion and suspension, the following facts were found.

1. The polymerization rate becomes fast as the mixture of monomer contains much acrylonitrile and reaches the maximum in the mixture of acrylonitrile 80 mol.% and styrene 20 mol.%.

2. The polymerization rate becomes generally fast as the concentration of emulsifier becomes thick; however, it is maximum at about 1.0 weight % emulsifier (to total monomer) in the copolymerization of monomers containing above 80 mol.% acrylonitrile.

3. η sp/c becomes great as the mixture of monomers contains much acrylonitrile.

4. η sp/c becomes small, reaches the minimum and then becomes great as the concentration of emulsifier becomes thick.

The concentration of emulsifier giving η sp/c minimum becoms thick as the mixture of monomers contains much acrylonitrile.

5. The composition of copolymer depends upon the concentration of emulsifier and it contains less acrylonitrile as the concentration becomes thick.

Research Institute of Teikoku Rayon Co. Ltd., Iwakuni

*Some Optical Properties of Zinc Sulfide Phosphors Doubly Activated with Copper and Manganese**

By Shigeo SHIONOYA

(Received July 14, 1956)

Introduction

The sensitized luminescence in doubly activated phosphors has been one of the most interesting problems in the field of solid-state luminescence in recent years. In these phosphors two kinds of activating impurity, called "sensitizer" and "activator", are incorporated. The activator is sensitized to emit luminescence as a result of the absorption of excitation energy by the sensitizer and of the subsequent radiationless transfer of this energy from the sensitizer, in such a spectral region that the activator has no appreciable absorption band unless the sensitizer is incorporated. In most cases the sensitizer causes also the luminescence of its own, so that these phosphors show two

* A part of this work was read at the Symposium on Photochemistry held by the Chemical Society of Japan on Sept. 25, 1954, and at the 8th Annual Meeting of this Society on Apr. 1, 1955, and was briefly reported in *J. Chem. Phys.* **23**, 1173, 1976 (1955).

kinds of emission band.

Generally, the sensitizer is an atom or ion of heavy metals such as lead, thallium, copper, antimony and other metals, while the activator is an ion of transition metals such as manganese and samarium. Manganese incorporated as a divalent ion is most popular as the activator, and known to be apt to show a strong luminescence by sensitization because the optical transition involved which leads to the luminescence is a forbidden one[1].

The sensitized phosphors recently developed and investigated are confined almost entirely to non-photoconductive phosphors such as $CaSiO_3$:(Pb+Mn)[2,3,4], $Ca_3(PO_4)_2$:(Ce+Mn)[4,5], $3Ca_3(PO_4)_2$-$Ca(Cl, F)_2$:(Sb+Mn)[6], and CaF_2:(Ce+Mn)[7]. On the other hand, the investigation for photoconductive ones such as the sulfide type are rather few except those by Makishima[8] for calcium sulfide type, CaS:(Bi+Sm), CaS:(Pb+Sm), CaS:(Bi+Mn) and others, and those by the author[9] for self and manganese-activated zinc sulfide.

The theory of sensitization mechanism has been developed by Botden[5] and more fundamentally by Dexter[10], and it was concluded that the resonance transfer of excitation energy from sensitizer to activator is responsible for the sensitization process in non-photoconductive phosphors. However, in photoconductive phosphors the possibility of sensitization due to the mechanism which will be described below may be also taken into consideration, namely the mechanism by the transfer of photoelectrons through the conduction band simultaneously accompanied by the migration of holes through the filled band[11,12,13].

The present work was undertaken in order to investigate the sensitization process in photoconductive phosphors and to discuss the mechanism by which the process is governed. Zinc sulfide doubly activated with copper and manganese was taken up as an example to be investigated, and its optical properties, the emission, absorption and excitation spectra, thermoluminescences and photoconductivities, were measured. This phosphor seems to be suitable for the present purpose, since zinc sulfide singly activated with copper and that with manganese are both very familiar and their properties are well-known. The results presented below will show that in this phosphor, manganese emission is really sensitized by copper incorporated as a sensitizer, and that some interesting phenomena characteristic of sensitized luminescence take place.

Experimental

1 Preparation of the Samples.—The preparation of the samples was carried out according to the method currently used. Several series of the samples were prepared, in which the copper concentration was fixed to be constant, 3×10^{-5}g./g.ZnS*, and the manganese concentration was varied from zero to 3×10^{-3}g./g.ZnS. These were fired at 1200°C for one hour in air with the flux of sodium or potassium chloride (0.02–0.05g./g.ZnS). Each series was fired at one time so as to keep the firing condition completely constant.

2 Emission.—As is well konwn, copper-activated zinc sulfide phosphor and that which is manganese- activated show the yellow green and orange luminescence, respectively. A series of the doubly activated ones with a constant copper concentration and varying manganese concentrations shows the luminescence with colors varying from yellow green to orange with the increase of manganese concentrations under 3650Å excitation.

The exmission spectra were measured under 3650Å excitation at room temperature with a glass monochromator of constant deviation type and a photomultiplier, RCA 931A or 1P21. The excitation source was a high pressure mercury discharge lamp, Matsuda SHL-100, with a Matsuda UV-D1 filter. The output of the photomultiplier was further amplified with either of two kinds of high sensitive amplifier, a *dc* or *ac* amplifier. The *dc* amplifier was constructed by using a vacuum tube 954 operating as an electrometer tube[14]. The current amplification was about 80–100db. In the case of the *ac* amplifier, the light emitted by the phosphor was interrupted and modulated to 200cps by means of a rotating sector set just before the entrance slit of the monochromator, and the *ac* output of the photomultiplier was amplified with the *ac* amplifier tuned to this frequency, the design of which follows closely to the one devised by Yamada et al[15]. The gain of the *ac* amplifier was almost the same as that of the *dc* amplifier. The spectral sensitivity of the photomultiplier set just behind the exit slit was determined by

1) C. C. Klick, *Brit. J. Appl. Phys.*, Sup. No. 4 ("Luminescence"), 74 (1955).
2) J.B. Merril and J.H. Schulman, *J. Opt. Soc. Am.*, 38, 471 (1948).
3) J. H. Schulman, R. J. Ginther and C. C. Klick, *J. Electrochem. Soc.*, 97, 123 (1950).
4) Th. P.J. Botden and F.A. Kröger, *Physica*, 18. 553 (1948).
5) Th. P.J. Botden, *Philips Res. Rep.*, 7, 197 (1952).
6) H.G. Jenkins, A.H. McKeag and P.W. Ranby, *J. Electrochem. Soc.*, 96, 1 (1949).
7) R.J. Ginther, *J. Electrochem. Soc.*, 101, 248 (1954).
8) S. Makishima, Doctral Thesis (1945).
9) S. Shionoya, *Bull. Fac. Eng.*, Yokohama Natl. Univ. 3, 97 (1954).
10) D.L. Dexter, *J. Chem. Phys.*, 21, 836 (1953).
11) N.F. Mott and R.W. Gurney, "Electronic Processes in Ionic Crystals", (1940), p. 207.
12) M. Schön, *Z. Phys.*, 119, 463 (1942).
13) H.A. Klasens, W. Ramsden and C. Quantie, *J. Opt. Soc. Am.*, 38, 60 (1948).

* Concentrations of activating impurities are given in weight ratios, g./g.ZnS, throughout this paper.
14) H. Matsuda and K. Ogata, *J. Appl. Phys. Japan*, 20, 229 (1951).
15) M. Yamada, K. Mitsuhashi and K. Akagi, *Tech. J. Japan Broadcasting Corp.*, 13, 29 (1953).

measuring the emission spectrum of a tungsten-incandescent lamp having the approved true temperature, including not only the spectral sensitivity of the photomultiplier itself but also the variation of the dispersion of the monochromator with wavelength and the absorption by glass.

Some typical results are shown in Fig. 1. The

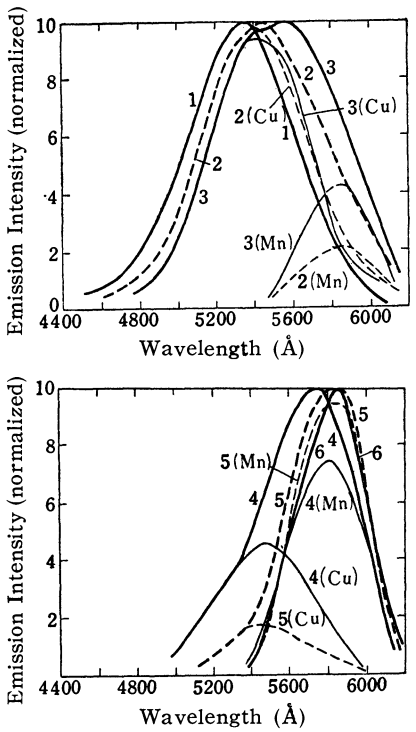

Fig. 1. Emission spectra of (1) ZnS:Cu and (2)-(6) ZnS:(Cu+Mn) under 3650 Å excitation. The Mn concentrations are (2) 2×10^{-4}, (3) 4×10^{-4}, (4) 8×10^{-4}, (5) 1.5×10^{-3} and (6) 3×10^{-3}. The Cu concentration is always 3×10^{-5} for all of the samples in this paper.

emission of manganese increases with the increase of its concentration, the emission of the copper decreasing simultaneously. Because of the overlap of the copper band with the manganese band, the samples showing both the copper and manganese emissions have broad bands, which are divided graphically into the copper and manganese bands as shown in the figure. The samples containing less than 1×10^{-4} manganese show the manganese emissions scarcely observable, those containing $2\text{-}8\times10^{-4}$ show distinctly both the copper and manganese emissions and those containing more than 1.5×10^{-3} show the predominant manganese emissions, while the copper emissions almost disappear. These concentrations of manganese are varied slightly by the firing conditions.

The emission peaks of copper and manganese are located at 5350-5450Å and about 5850Å, respectively, both being almost unchanged from those of the case where each of them is singly incorporated[16]. The copper peak has a tendency to shift slightly towards longer wavelength with the increase of manganese concentration. The reason for this effect is considered to be that since manganese is incorporated substitutionally into zinc sulfide, forming a solid solution[17] and causing the expansion of the lattice, the forbidden gap of the host lattice is made smaller, and then the energy of the copper emission becomes smaller.

3 Absorption. — The measurements of absorption were made by measuring the diffuse reflectivity from a layer of phosphor with an effectively infinite thickness. A Hitachi's quartz monochromator of Littrow type and an integrating sphere, which was set behind the exit slit, were used. The excitation source was a tungsten incandescent lamp. The intensity of the reflected light was measured with a photomultiplier, 1P28, attached to the *dc* amplifier mentioned above, and the reflectivity was determined as the ratio to that of magnesium oxide powder. An ultraviolet transmitting filter, Corning No. 9863 or Matsuda V-V1, was inserted between the integrating sphere and the photomultiplier so as to separate the reflected light from the luminescence, in the spectral region 3200–4800Å where the incident light excites the phosphor.

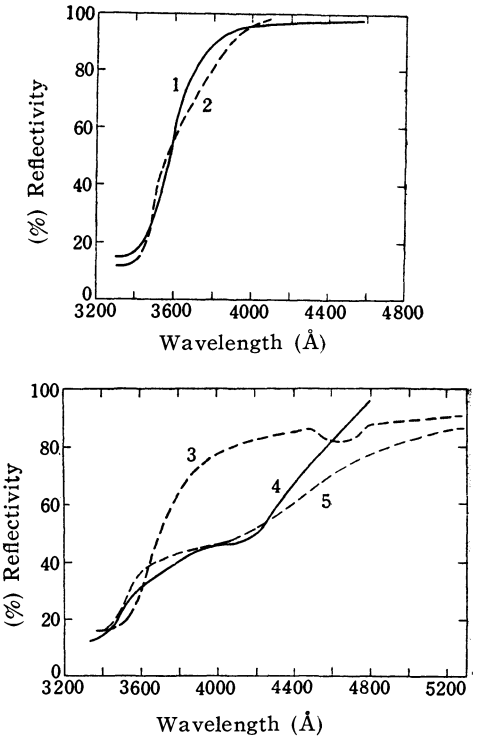

Fig. 2. Reflection spectra of (1) ZnS unfired, (2) ZnS fired without any activating impurities, (3) ZnS:Mn (Mn: 1×10^{-2}), (4) ZnS:Cu and (5) ZnS:(Cu+Mn) (Mn: 8×10^{-4}).

16) R.H. Bube, *Phys. Rev.*, **90**, 70 (1953).
17) F.A. Kröger, *Z. Krist.*, **100**, 543 (1939).

Results of reflection spectra at room temperature are shown in Fig. 2, including those for ZnS unfired, ZnS fired without activating impurities and ZnS : Mn (Cu not in corporated). The long wavelength threshold of the fundamental absorption of zinc sulfide host crystal is located at about 3400Å which is nearly in agreement with the value reported by Piper[18] for single crystals of zinc sulfide. In the long wavelength region beyond the fundamental absorption, the absorption bands due to copper and manganese appear. The copper band seems to be located from 3600 to 4200Å. The manganese band has a small peak at 4600–4700Å.

4 Excitation. — The excitation spectra were measured with the same quartz monochromator and the excitation source as used in the case of absorption. The phosphor sample was coated uniformly on a glass plate in a thin layer of the thickness, 2.5mg./cm², by means of the sedimentation method, and was set just behind the exit slit. The intensity of the emission was measured through suitable filters with the photomultiplier, 1P21, set behind the plate of the phosphor, the output photocurrent being amplified by the *dc* amplifier. The copper and manganese emissions were isolated from each other with filters, namely Matsuda V-Y1 plus V-B2 for copper and V-O2 or V-R3 for manganese.

Results at room temperature are shown in Fig. 3, including those for ZnS : Mn (Cu not incorporated). All of the samples have a strong excitation peak near 3400Å. This corresponds to the

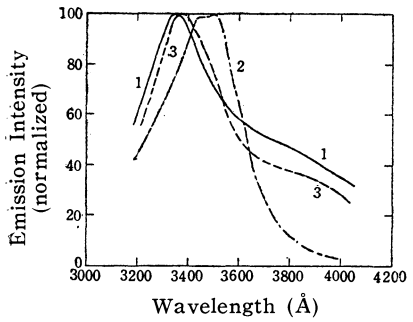

Fig. 3. Excitation spectra for (1) Cu emission of ZnS : Cu, (2) Mn emission of ZnS : Mn (Mn : 1×10^{-2}) and (3) Mn emission of ZnS : (Cu+Mn) (Mn : 8×10^{-4}).

fundamental absorption edge of the host crystal as seen at a glance by comparing it with the reflection spectra, so that this peak is regarded as the one due to the absorption of the host crystal. ZnS : Cu has, in addition, the broad excitation band the peak of which seems to be located at about 3800Å. This band is regarded as the one due to the absorption of copper impurity by comparing it with reflection spectra. These results are nearly in agreement with those of Bube[16]. While manganese in ZnS : Mn has only the excitation band due to the host crystal, manganese in ZnS : (Cu+Mn) has, in addition, the excitation band regarded as the one due to copper. It is no doubt obvious that this additional band is attributed to the absorption of copper, since its shape is very similar to that for copper in ZnS : Cu. This result shows that manganese emission is really sensitized by copper behaving as a sensitizer.

According to Bube[16], the excitation spectrum of manganese in ZnS : Mn shows, in addition to the host excitation band, four excitation peaks due to the forbidden transition within Mn^{+2} ion itself in the wavelength region 3900–5100Å, namely 3980, 4320, 4770 and 5060Å peaks. However, they were not found in the present phosphors, and this fact seems to be probably due to the effect of impurity, especially oxygen.

As thus found, ZnS : (Cu+Mn) has two kinds of excitation band, one due to the host crystal and the other due to the copper sensitizer. Then a new problem arises whether the emission spectra are different under the host or copper excitation. As the excitation source to be used for these excitations, an ordinary 100 W. tungsten incandescent lamp was used, selecting only the necessary wavelength region for each of these excitations with suitable filters; namely Matsuda UV-D1 plus nickel sulfate solution filter (the concentration: $NiSO_4\cdot7H_2O$, 100g./*l.*; the optical path: 5 cm) for the host xcitation, and Matsuda UV-D1 plus V-B2 for the copper excitation. The transmission spectra of these filters are shown in Fig. 4. Since this

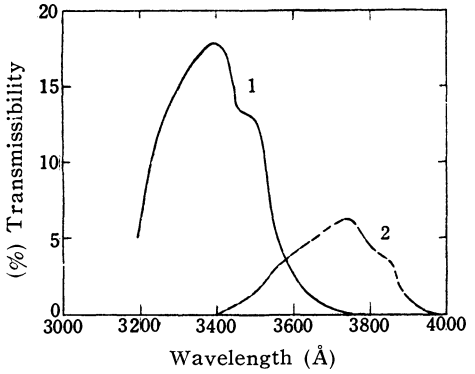

Fig. 4. Transmission spectra of filters for (1) the host and (2) Cu excitations.

excitation source was too weak to measure the emission spectra, only the ratios of the emission peak intensities of manganese to those of copper, *R*, were determined by separating these two kinds of emissions with filters.

It was found that the values of the ratios under the host excitation, R_{host}'s, are about 1.2 times R_{3650}'s for all the phosphors, while R_{Cu}'s are about 0.8 times R_{3650}'s. It may be suggested that the excitation energy absorbed by the host crystal is shared between copper and manganese in proportion to their capture cross sections under the host excitation, whereas under the copper excitation a part of the excitation energy absorbed by copper is transferred to manganese. This results shows that the transfer probability from copper to manganese is rather small as compared with the probability that manganese captures the

18) W.W. Piper, *Phys. Rev.*, **92**, 23 (1953).

host absorbed energy. R_{3650}'s shows the intermediate values between R_{host}'s and R_{Cu}'s, since 3650 Å line lies just at a middle position between the two excitation peaks, and consequently causes the both kinds of excitation.

5 Thermoluminescence.—The thermoluminescence for both the copper and manganese emissions after both the host and copper excitations were measured with a specially designed Dewar vessel shown in Fig. 5, using liquid air as

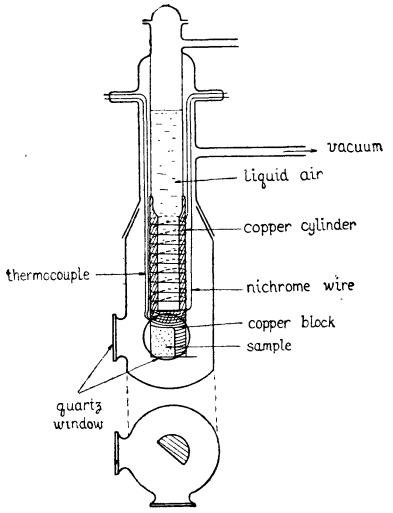

Fig. 5. An apparatus for the thermoluminescence measurement.

a coolant. The phosphors were coated with distilled water on an aluminum plate, which was attached to the copper block. The excitation source was the same as mentioned just above, the tungsten incandescent lamp with filters. The phosphors were excited up to the saturated emission intensities at a liquid air temperature, and then heated by means of nichrome wire with a constant rate, 0.22°K/sec., after allowing the emission to decay for six minutes, detecting the glow intensities with the photomultiplier attached to the *ac* amplifier mentioned in Sec. 2. The copper and manganese emissions were isolated from each other with filters.

Examples of the results are shown in Fig. 6. Every phosphor shows the main glow peak in the temperature range 230–300°K. Low temperature peaks associated with shallow traps were not found, because the emissions were allowed to decay for six minutes after the ceasing of the excitation. In ZnS: Cu, the glow curves for the copper emission after the host and copper excitations are similar to each other, showing main glow peaks at about 240°K. On the other hand, in ZnS: (Cu +Mn) (Mn: 8×10^{-4}) with the copper and manganese emissions which are both distinct, the glow curves for the copper and manganese emissions after the copper excitation are very similar to each other having the main glow peaks at 265°K, whereas those after the host excitation are remarkably different from each other, the main glow peaks

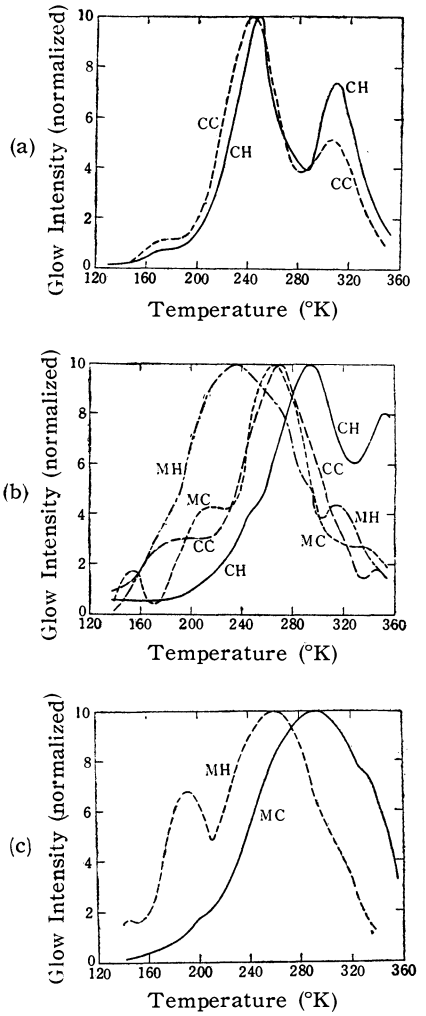

Fig. 6. Glow curve of (a) ZuS: Cu, (b) ZnS: (Cu+Mn) (Mn: 8×10^{-4}) and (c) ZnS: (Cu+Mn) (Mn: 3×10^{-3}).
CH: Cu glow after the host excitation
CC: Cu glow after the Cu excitation
MH: Mn glow after the host excitation
MC: Mn glow after the Cu excitation

being at 295°K for the copper emission and at 235°K for the manganese emission. This result should be strongly noticed in connection with the sensitization mechanism. Also in ZnS: (Cu+Mn) (Mn: 3×10^{-3}) with the predominant manganese emission, the two manganese glow curves are different depending on either the host or copper excitation.

Analyses for the main glow peaks were carried out in the usual manner. The thermoluminescence is produced when the trapped electrons are released by the thermal energy and recombine with the holes in the ground states of the luminescence centers. In the photoconductive phosphors such as zinc sulfide, it is suggested that this process is governed by the bimolecular

mechanism. However, Randall and Wilkins[19,20] found that the phosphorescence and thermoluminescence in the sulfide type phosphors can be explained by the monomolecular mechanism rather than by the bimolecular one. Also, Williams and Eyring[21] established fairly conclusively that the rate-determining process for the glow emission of ZnS: Cu is predominantly monomolecular, based on the analysis of the shape of the glow curve. The reason for these results appears to be that the number of electrons escaping from traps is much smaller than the number of holes in luminescence centers, and so the thermoluminescence process is determined by the rate at which electrons escape from traps, or in other words that the time necessary for the release of electrons from traps is much larger than that during which electrons stay in the conduction band. Furthermore, the effect of the retrapping of thermally released electrons should be also taken into consideration in the photoconductive phosphors. However, Randall and Wilkins[19,20] showed that the retrapping is a negligible process during luminescence, although an empty luminescence center and an empty electron trap have similar cross-sections for electron capture.

Therefore, the analyses were done assuming the monomolecular kinetics and the negligible retrapping. The distribution of trap depth was also ignored. In the case of the monomolecular kinetics, the intensity of the glow emission, I, is given by

$$I=-\alpha \mathrm{d}n/\mathrm{d}t=akn, \tag{1}$$

where n is the number of electrons in the trap at any instant and k is the specific rate constant for the thermal release of trapped electrons. The rate constant is expressed by

$$k=s\exp(-E/kT), \tag{2}$$

where s is the frequency factor and E is the activation energy, i.e. the trap depth. Integrating Eq. (1),

$$n=n_0\exp\left(-\int_{t_0}^{t}k\mathrm{d}t\right) \tag{3}$$

where n_0 is the number of electrons in the trap at time t_0. Introducing the heating rate, $\beta=\mathrm{d}T/\mathrm{d}t$,

$$n=n_0\exp\left(-\frac{1}{\beta}\int_{T_0}^{T}k\mathrm{d}T\right). \tag{4}$$

The emmission intensity is given by inserting Eq. (4) into Eq. (1),

$$I=\alpha n_0 k\exp\left(-\frac{1}{\beta}\int_{T_0}^{T}k\mathrm{d}T\right). \tag{5}$$

From Eq. (4),

$$k=\frac{\mathrm{d}}{\mathrm{d}T}\left[-\beta\ln\frac{n}{n_0}\right]=\beta\frac{\mathrm{d}}{\mathrm{d}T}\left[-\ln\left(1-\frac{n_0-n}{n_0}\right)\right]. \tag{6}$$

Assuming that the number of trapped electrons which undergo radiationless transition is negligible, n_0 and (n_0-n) can be expressed in terms of the light sums, i.e.

$$n_0=\frac{1}{\alpha\beta}\int_{T_0}^{\infty}I\,\mathrm{d}T \quad \text{and} \quad n_0-n=\frac{1}{\alpha\beta}\int_{T_0}^{T}I\,\mathrm{d}T. \tag{7}$$

Hence, the rate constant is given as a function of observables,

$$k=\beta\frac{\mathrm{d}}{\mathrm{d}T}\left[-\ln\left(1-\frac{\int_{T_0}^{T}I\,\mathrm{d}T}{\int_{T_0}^{\infty}I\,\mathrm{d}T}\right)\right]. \tag{8}$$

With this equation both the frequency factor and activation energy can be calculated, although absolute intensities are not observed.

In Table I, The calculated values for the main peaks of the glow curves shown in Fig. 6 are given. The trap depth for the copper main peaks are 0.21–0.23 e.V., irrespective of either the host or copper excitation. The frequency factors for these are made a bit smaller by the incorporation of manganese. The trap depth for the manganese main peak of ZnS: (Cu+Mn)(Mn: 8×10^{-4}) after the copper excitation shows a similar value to that for copper, whereas that after the host excitation shows a considerably different value from that for copper, namely, a smaller one 0.15 e.V., as expected from the results of Fig. 6. Similarly for ZnS: (Cu+Mn) (Mn: 3×10^{-3}), the manganese trap depth after the host excitation is smaller than that after the copper excitation, although both show smaller values than those for ZnS: (Cu+Mn)(Mn: 8×10^{-4}). This effect of trap shallowing by the increased concentration of manganese appears to be caused by the same reason as suggested for the effect that the copper emission peak shifts towards a longer wavelength with the increase of manganese concentration.

TABLE I

TRAP DEPTHS AND FREQUENCY FACTORS FOR THE MAIN PEAKS OF THE GLOW CURVES

Phosphor	Emission	Excitation	Trap Depth e.V.	Frequency Factor (sec^{-1})
ZnS: Cu	Cu	host	0.23	4×10^{2}
		Cu	0.23	6×10^{2}
ZnS: (Cu+Mn) (Mn: 8×10^{-4})	Cu	host	0.21	2×10
		Cu	0.21	6×10
	Mn	host	0.15	1×10
		Cu	0.23	2×10^{2}
ZnS: (Cu+Mn) (Mn: 3×10^{-3})	Mn	host	0.14	2
		Cu	0.18	7

19) J.T. Randall and M.H.F. Wilkins, *Proc. Roy. Soc.* (London), **A184**, 347, 365, 390 (1945).

20) G.F.J. Garlick, "Luminescent Materials", Oxford Press (1949), Chap. II.

21) F.E. Willams and H. Eyring, *J. Chem. Phys.*, **15**, 289 (1947).

The values of Table I are characterized by the unusually low values of frequency factors, resulting from the fact that the width of the main glow peaks are rather broad. The neglect of trap depth distribution seems predominantly responsible for this result. If the trap depth were not a single one, but had a distribution, or two or more traps which could not be resolved by the heating rate used were involved, the broad glow peak would result, which would give the apparent low value of the frequency factor by the analysis on the assumption of the single trap depth. The ignoring of the effect of the retrapping can be also considered as the cause of the low frequency factor. It was shown by Randall and Wilkins[19,20] that when retrapping is present the half-width of the peak for the same values of trap depth and frequency factor becomes much larger. Therefore, if retrapping were involved, it would give the apparent low value of the frequency factor similarly to the trap depth distribution.

The aforementioned results may be reasonably explained by the following inference, if an assumption is made that two kinks of main traps are involved in these phosphors, the deep one associated with copper and the shallow one associated with manganese, as indicated in Fig. 8 in Discussion 2. Under the copper excitation, the freed electron from the copper center enters only into the copper associated trap, and the thermal release from it is the rate-determining step for both of the copper and manganese main glow peaks. On the other hand, under the host excitation, the freed electron from the host lattice enters, probably through the conduction band, into either of the copper and manganese associated traps, and the thermal release from either of them is the rate-determining step for each of the copper and manganese main glow peaks. On the nature of these traps nothing can be discussed here from only this experiment.

6 Photoconductivity.—Only a preliminary experiment was done on the photoconductivity. Cells were made by packing the phosphor powder between a conductive glass and an aluminum plate in the thickness of 1mm. Photocurrents induced by applying *dc* electric field of 280V./cm. under 3650Å excitation were detected by means of a sensitive amplifier constructed with a Matsuda UX-54 vacuum tube and a galvanometer.

In Fig. 7 the relative photoconductive response of a series of ZnS: (Cu+Mn) with a constant copper concentration and varying manganese concentrations are given as the function of manganese concentrations. The response of the samples with higher manganese concentrations are by far smaller than those with lower concentrations. Comparing this with the results of emission spectra, it is shown that the photoconductive response changes abruptly to the smaller value at the manganese concentration at which the manganese emission becomes distinct.

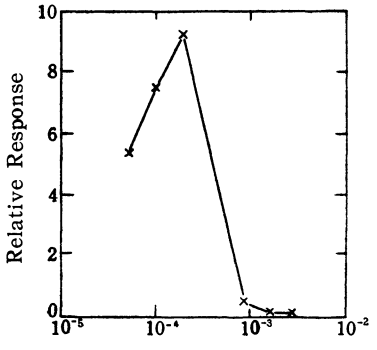

Fig. 7. The relative photoconductive response of a series of ZnS: (Cu+Mn) as the function of the manganese concentration.

Discussion

1 The Range of Energy Transfer from Copper to Manganese.—As mentioned in Experimental 4, the manganese emission in zinc sulfide phosphor is really sensitized by copper behaving as a sensitizer. In other words, a part of the excitation energy absorbed by copper is transferred to manganese to give rise to its emission. The extent of the range surrounding the sensitizer where this energy transfer takes place can be estimated from the relation between the concentrations and luminescent intensities of the sensitizer and activator, based on the assumption that they are distributed at random over the whole lattice sites[9].

Defining z as the number of lattice sites (substitutional or interstitial, or both) surrounding a given sensitizer, it is assumed that if any one of these z sites is occupied by an activator the sensitization can take place with the probability of unity, but that if none of them is occupied by an activator the emission of the sensitizer itself is caused. Then, the mole fraction of the sensitizer incapable of the sensitization and responsible for its own emission is given by

$$C_s(1-C_a)^z, \tag{9}$$

where C_s and C_a are the mole fraction of the sensitizer and activator, respectively. Therefore, the mole fraction of the sensitizer capable of the sensitization, which corresponds to the mole fraction of the activator to be sensitized, is given by

$$C_s[1-(1-C_a)^z]. \tag{10}$$

Under the excitation by the sensitizer absorption, the emission of both the sensitizer and activator are caused only by the light absorption of the sensitizer. Accordingly, the ratio of the number of the quanta emitted by the activator, N_a, to that emitted by the sensitizer, N_s, is expressed by the ratio of Eq. (10) to (9), i. e.

$$B=\frac{N_a}{N_s}=\frac{1-(1-C_a)^z}{(1-C_a)^z}=\frac{1}{(1-C_a)^z}-1 \tag{11}$$

This equation holds if only the following

three conditions are satisfied; the first is that no transfer of the excitation energy between the sensitizers takes place, the second is that the concentrations of both the sensitizer and activator are so low that we may permit the concentration quenching of luminescences among themselves to be neglected, and the third is that the radiationless transition of excitation energy does not occur. It is known[22,23] that for both copper and manganese in zinc sulfide the temperatures at which the radiationless transition begins to occur are higher than room temperature. Then, the value of z is calculated by

$$z=-\frac{\log(B+1)}{\log(1-C_a)}. \qquad (12)$$

The values of B can be estimated by the shapes of the emission bands and the peak intensities for the sensitizer and activator.

In Table II, the values of z calculated for a series of ZnS : (Cu+Mn) with a fixed copper concentration and varied manganese concentrations under the copper excitation are given. The sensitization is shown to take place over the range of 400–500 lattice sites.

TABLE II

THE CALCULATION OF THE VALUES OF z FOR ZnS : (Cu+Mn) UNDER THE COPPER EXCITATION

R: The ratio of the peak intensity of manganese to that of copper.

B: The ratio of the number of quanta emitted by manganese to that emitted by copper.

Mn conc. (g./g.ZnS)	R	B	z	
1×10^{-4}	0.13	0.095	500	Mean 440
2×10^{-4}	0.18	0.13	360	
4×10^{-4}	0.37	0.28	350	
8×10^{-4}	1.3	0.96	470	
1.5×10^{-3}	4.3	3.2	530	

The values of z were already estimated for several non-photoconductive phosphors, such as $CaSiO_3$: (Pb+Mn)[3,9], $Ca_3(PO_4)_2$: (Ce+Mn)[5], and CaF_2 : (Ce+Mn)[7]. All of them lie between 10 and 70. The one calculated here for ZnS : (Cu+Mn) is characterized by a value one order of magnitude larger than these.

2 Sensitization Mechanism.—In the photoconductive phosphors two kinds of sensitization mechanism, the resonance transfer and the photoelectron transfer, are suggested as the possible mechanisms, as already mentioned in Discussion 1.

Dexter[10] has developed a quantum-mechanical theory of the sensitized luminescence due to the resonance transfer in non-photoconductive phosphors. He has calculated the probability of the energy transfer by the following mechanisms, i.e. the overlapping of the electric dipole fields of sensitizer and activator, the overlapping of the dipole field of sensitizer with the quadrupole field of activator, and the exchange effect, and has concluded that these mechanisms will give rise to the sensitization of about 10^3–10^4, 10^2 and 30 lattice sites surrounding each sensitizer in typical systems.

The energy levels of doubly ionized manganese in the gaseous state are ^6S, ^4G, ^4P, ^4D and ^4F starting with the lowest term[24]. Based on the experimental results of magnetic susceptibility change accompanying the optical excitation for ZnF_2 : Mn[25] and ZnS : Mn[26] and on the comparision of the excitation spectra of phosphors containing manganese with the energy levels in the gaseous state[27], it is indicated[1] that the excited state leading to the luminescence of divalent manganese has four of the 3d electrons with parallel spins and one anti-parallel, while the ground state has all electrons with parallel spins. The luminescence may be suggested to correspond to $^4G\rightarrow{}^6S$ transition.

Although it seems difficult to determine whether the dipole-quadrupole or the exchange transfer is responsible for the sensitized luminescence of divalent manganese in non-photoconductive phosphors, the experimentally derived values of z for these phosphors agree with the theoretical one for the exchange transfer, giving a suggestion that this transfer might be the case. The value of z for ZnS : (Cu+Mn) here calculated is too large to assume the exchange transfer, and still large even for the dipole-quadrupole transfer. This result seems to preclude these mechanisms. However, this value is the one calculated from the assumption that sensitizers and activators are distributed at random, so that the true value might be much smaller if they had a tendency to approach to each other in the host crystal.

Manganese will be distributed at random, since it is incorporated substitutionally forming a solid solution, but copper would not be so. The author has shown[28] in the

22) G.F.J. Garlick and A.F. Gibson, *J. Opt. Soc. Am.*, **39**, 935 (1949).

23) S. Makishima, J. Yamauchi, T. Mukaibo and S. Shionoya, *Ann. Rept. Eng. Res. Inst.*, Fac. Eng., Univ. Tokyo, No. 9, 33 (1951).

24) M.A. Catalan and O. Garciái-Riquelme, "Atomic Energy Levels", National Bureau of Standards, Washington (1952), Vol. 2, Circular 647.

25) P.D. Johnson and F.E. Williams, *J. Chem. Phys.*, **17**, 435 (1949).

26) K. Oshima and H. Nagano, *J. Chem Phys.*, **23** 1473 (1955).

27) C.C. Klick and J.H. Schulman, *J. Opt. Soc. Am.*, **42**, 910 (1952).

28) S. Shionoya and K. Kikuchi, *J. Chem. Soc. Japan, (Pure, Chem. Sect.)*, **77**, 291 (1956).

study of the diffusion of copper into zinc sulfide crystal that copper seems to diffuse, not through the perfect lattice, but along the internal surface, grain boundary or dislocation line. Diemer[29] has studied light patterns in electroluminescent zinc sulfide single crystals activated by the diffusion of copper, and shown that at temperatures a little above room temperature copper diffuses into the bulk of the crystal along certain imperfections which are supposed to be screw dislocations. Therefore, it is likely that copper incorporated as an activating impurity is situated at the vicinity of crystal imperfections. Substitutionally incorporated manganese will give rise to a small disturbance of lattice. Hence, the above assumption that copper and manganese have a tendency to approach to each other might be rather reasonable.

According to Bube[16] zinc sulfide activated with copper shows a photoconductivity by the absorption of copper as well as by the host absorption. Therefore, there is a possibility that the sensitization by photoelectron transfer may occur. This mechanism is shown schematically in Fig. 8. As a result of the

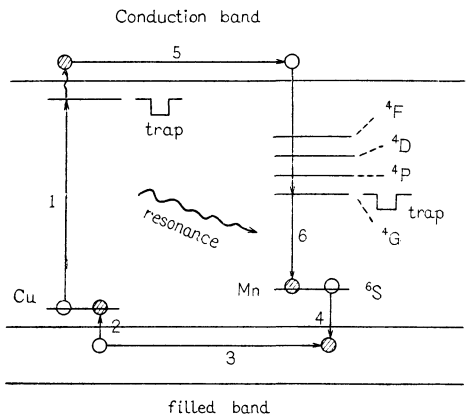

Fig. 8. An energy level diagram for ZnS: (Cu+Mn).

excitation of the copper sensitizer, the electron is raised directly or thermally into the conduction band (process 1). The hole left in the ground state of the sensitizer is released thermally (2), migrates through the lattice (3), and is trapped at the ground state of the manganese activator (4). The electron in the conduction band is transferred to the excited state of the activator (5), and then recombines with the hole producing the luminescence of the activator (6).

For the occurrence of this mechanism, it is needed that the thermal energy for the process 2 is supplied, and that the hole in the filled band has an appreciable mobility. This thermal energy will be so little, the order of 10^{-1} e. V. or less, as to be easily supplied, because the energy for the process 1 is 3.3 e. V. (3800 Å) and that for the host absorption which corresponds to the band gap is 3.6 e. V. (3400 Å). Nothing is yet known for the mobility of holes in zinc sulfide. It was shown in the measurement of thermoelectric effect[22] and in the study of the modulation of luminescence by an *ac* electric field[30] that the dominant charge carriers in zinc sulfide are electrons, and not holes. If the hole mobility were very small, the sensitization by photoelectron transfer mechanism would not occur with an appreciable probability.

In the continuation of this study, it was examined whether heavy metals other than copper which are capable of having luminescence of their own caused by allowed transitions when incorporated in zinc sulfide can act as effective sensitizers for divalent manganese[31]. The results of the study were that lead can sensitize manganese whereas silver or bismuth cannot. This gives a suggestion for the sensitization mechanism. Silver in zinc sulfide is known[16] to show a photoconductivity by the absorption of its own likewise to copper. Also in the case of lead or bismuth the sameness may be expected. If the photoelectron transfer mechanism is the case, any sensitizer which has a photoconductivity in its own absorption band should alway be able to sensitize manganese although the sensitization probability may vary with the kinds of sensitizer used. The above fact that silver and bismuth cannot sensitize manganese at all seems to argue against this mechanism. Thus it appears reasonable to conclude tentatively in the present situation that the resonance transfer rather than the photoelectron transfer is the predominant mechanism. The different behavior of silver and bismuth from that of copper and lead might be attributed to the difference of the electronic state between these two groups.

The results of thermoluminescence are considered to be favorable to the resonance transfer mechanism. If it is assumed that the manganese thermoluminescence after the copper excitation is caused by the photoelectron transfer, it would show the same glow curve as after the host excitation, since

29) G. Diemer, *Philips Res. Rept.*, **10**, 194 (1955).

30) R.E. Halsted, *Phys. Rev.*, **99**, 1897 (1955).

31) S. Shionoya and K. Amano, *J. Chem. Phys.*, **25**, 380 (1056).

electrons raised into the conduction band seem to behave irrespectively of their history, whether they have originated from the host crystal or the coppzer sensitizer. Therefore this assumption appears inconsistent with the experimental results. On the assumption of the resonance transfer, however, the experimental results that the thermoluminescence of copper and manganese after the copper excitation are very similar to each other may be reasonably understood.

The results of photoconductivity measurement might also present a support for the occurrence of sensitized luminescence by the resonance transfer. As mentioned in Experimental 6 the photoconductive response for ZnS : (Cu+Mn) decreases with the increase of the manganese concentration. The similar experiment was done for ZnS : (Ag+Mn), but such an effect was not observed. This difference between copper and manganese seems to be correlated with the different behavior as a sensitizer between them. This effect in the case of copper is explained as follows if the resonance transfer is assumed. The life-time of the excited electron of copper sensitizer, which, it is considered, gives rise to photoconductivity owing to the thermal excitation, will be made shorter by the sensitization of manganese, so that the photoconductive response should becomes smaller with the increase of manganese concentrations.

A tentatively determined energy level diagram for ZnS : (Cu+Mn) is given in Fig. 8. As already mentioned in Experimental 4 manganese in ZnS : Mn has four excitation peaks due to the forbidden transitions within Mn^{+2} ion, i.e. 5060, 4770, 4320 and 3980 Å peaks, which were found by Bube[16]. They are considered to correspond to the excitation from ^6S ground state to ^4G, ^4P, ^4D and ^4F excited states, respectively. Since the energy of the manganese ground level is not yet determined, its position is written arbitrarily. If the resonance transfer is responsible for the sensitized luminescence, the overlap of the emission band of sensitizer with the excitation band of activator is required essentially, and the sensitization probability is proportional to this overlap[10]. Since the emission peak of copper is located at 5350–5450 Å, the excitation energy will be transferred directly to ^4G state of manganese, the lowest excited state from which the luminescence is emitted.

Summary

Optical properties of ZnS : (Cu+Mn) phosphors have been extensively studied with the purpose to investigate the phenomena of sensitized luminescence in photoconductive phosphors. Spectra of emission, absorption and excitation, thermoluminescence and photoconductivity were measured. It was confirmed from the measurement of excitation spectra that the manganese emission is really sensitized by copper behaving as a sensitizer. Some interesting phenomena ascribed to this sensitization were found in the measurements of thermoluminescence and photoconductivity. The mechanism of the sensitization was discussed exhaustively. It appears reasonable to conclude tentatively in the present situation that the resonance transfer rather than the photoelectron transfer is the predominant mechanism.

The author would like to express his thanks to Prof. S. Makishima, University of Tokyo, Dr. Y. Kotera, Government Chemical Industrial Research Institute, Tokyo, and Assist. Prof. K. Oshima, University of Tokyo, for their encouragement and discussions, and to Mr. S. Kamiya*, Mr. W. Ichise** and Mr. K. Amano of this laboratory for their assistance in the experimental works.

A Part of the expense of this study was defrayed by the Grant in Aid of the Ministry of Education for Scientific Research.

Department of Electrochemistry, Faculty of Engineering, Yokohama National University, Minami-ku, Yokohama

* At present: Matsushita Electronics Ind. Co.
** At present: Tokyo Shibaura Electric Co.

SHORT COMMUNICATIONS

New Photometric Method for Determining Thallium with Rhodamine B

By Hiroshi Onishi

(Received July 17, 1956)

A satisfactory color or fluorescence reagent for thallium is lacking. The photometric methods available at the present time are either indirect or insensitive. A procedure for detecting traces of thallium with rhodamine B has recently been described by Feigl and his coworkers[1]. It does not appear, however, that a quantitative method based on this reaction has been reported. The difficulty in developing the method was ascribed by MacNulty and Woollard[2] to the instability of the higher valency compounds of thallium. According to them, no oxidizing agent has been found that will consistently retain thallium in a higher valency state until the complex with rhodamine B is formed and extracted.

The present author has found that the oxidation of univalent thallium to trivalent with bromine is a satisfactory method preparatory to rhodamine B-benzene extraction. The absorbance-concentration curve shown in Fig. 1 was obtained by the following procedure: Take 0, 2, 4, 6 and 8 μg. of thallium (as Tl_2SO_4) into beakers respectively, add 5.0 ml. of 2.0 N hydrochloric acid and 0.5 ml. of saturated bromine water. Heat near the boiling point and keep heating until immediately after the color due to bromine has disappeared. Cool to room temperature, transfer the solution to a 10-ml. volumetric flask and dilute to the mark with 2.0 N hydrochloric acid. Transfer the solution to a separatory funnel, add 1.0 ml. of 0.20% (w/v) aqueous rhodamine B solution and mix. Add 10.0 ml. of pure benzene and shake for one minute. When the two phases have separated, drain off the aqueous phase, transfer and centrifuge the benzene phase until a clear solution has been obtained. Measure the absorbance of the benzene extract at 560 mμ.

Absorbance is proportional to thallium concentration in the range 0.1 to at least 1 p.p.m. (based on the amount of thallium present originally in the aqueous phase). At 560 mμ the molar extinction coefficient is about 87,000, or 0.0023 μg. Tl/cm^2 corresponding to log $I_0/I=0.001$. Thus the method appears to offer a good basis for the photometric determination of traces of thallium. Details of the study will be published later.

Government Industrial Research Institute, Nagoya

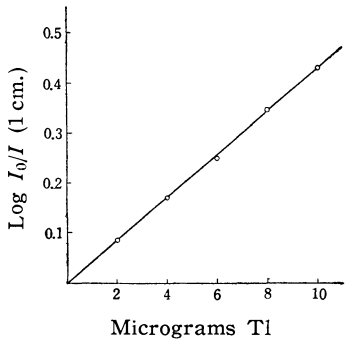

Fig. 1. Absorbance-concentration curve of thallium. Hitachi spectrophotometer, EPB-U, 560 mμ, temperature 18–26°C.

1) F. Feigl, V. Gentil and D. Goldstein, *Anal. Chim. Acta*, **9**, 393 (1953).
2) B. J. MacNulty and L. D. Wollard, ibid., **13**, 154 (1955).

Trennung von Metalkomplexisomerien mit Ionenaustauscher. II. Über Dichloro-bis-äthylendiamin-kobalt (III)- und Dirhodanato-bis-äthylendiamin-kobalt (III)-ionen*

Von Motoshichi MORI, Muraji SHIBATA und Masatoshi NANASAWA

(Eingegangen am 30. April 1956)

Wir forschten in diesem Versuche das Verhalten der Komplexisomerie gegen Ionenaustauscher und ihre Trennung auszuführen. Wir veröffentlichten schon über sogenannte Flavo- und Croseo-kobaltsalze[1] und berichten hier über *cis*-, *trans*-Dichloro-bis-athylendiamin-kobalt (III)-chlorid und *cis*-, *trans*-Dirhodanato-bis-athylendiamin-kobalt (III)-chlorid.

Experimenteller Teil

Herstellung von Komplexsalzen.—*cis*-, *trans*-$[Coen_2Cl_2]Cl$ und *trans*-$[Coen_2(CNS)_2]Cl$ wurden nach der Literatur[2] dargestellt, während *cis*-$[Coen_2(CNS)_2]Cl$ auf unsere Weise hergestellt wurde.

Fünf Gramme $[Coen_2CO_3]Cl \cdot H_2O$ wurden in Wasser von 50 ccm gelöst und darin 4 g KCNS zugegeben. Nachdem das Gemisch mit Essigsäure angesäuert wurde, wurde es konzentriert, um das rohe Salz zu gewinnen. Die Reinigung geschah durch Lösen in verd. Salzsäure und dann noch einmal in Wasser.

Wir vergewisserten uns, dass alle diese Komplexsalze durch Messung ihrer Absorptionsspektra unvermischt sind. Die Salzlösungen wurden zu einer etwa 10^{-2} M Konzentration zubereitet und als Probelösungen gebraucht.

Durchführung der Elutionsversuche.—Als Austauschmaterial war der Kationenaustauscher Amberlit IR 120 in der Na-Form verwendet. Neun Gramme davon wurden mit Wasser in eine Säule von 1.5 cm Durchmesser und 30 cm Höhe eingefüllt. Je 5 cm der oben gezeigten Probelösung wurden darauf einzeln oder gemischt gegeben. Nachdem die Säule mit Wasser genug gewaschen wurde, wurde 0.5 M Natriumchloridlösung (f = 1.012) weiter als Eluierungsmittel eingegossen. Die ausfliessende Lösung, die eine Durchflussgeschwindigkeit von 1 ccm in 3.5 Minuten einhält, wurde je 10 cm mit Hilfe von automatischem Fraktionierkollektor gesammelt.

Die Erkennung von *cis*- oder *trans*-Ionen wurde bei ihren Maximalwellenlängen durch Messung der Extinktion von einzelner Fraktion ausgeführt. D.h. die Wellenlängen 535 mμ und 615 mμ sind zur Unterscheidung der *cis*-, *trans*-$[Coen_2Cl_2]^+$, und die 490 mμ und 505 mμ zu der von *cis*-, *trans*-$[Coen_2(CNS)_2]^+$ benutzt worden.

Messungen der Adsorptionsmenge von Komplexionen an Austauschern.—Zwanzig Kubikzentimeter der von 10^{-2} M zu 10^{-4} M präparierten Lösung wurden in die Erlenmeyerflasche, worin 100 mg Austauscher sind, eingeleitet. Sie wurde drei Stunden im auf 25°C gehaltenen Thermostat gestellt und oft gerührt. Die Lösung wurde vom Adsorbense abgetrennt und ihre Extinktion bei Maximalwellenlänge gemessen. Die Extinktion der ohne Adsorbens gestellten Lösung wurde auch gleich gemessen. Durch die Differenz von beiden Extinktionen rechnete man die Adsorptionsmenge im mM an 100 mg Austauscher.

Zu den alleinigen Lichtabsorptionsmessungen wurde Beckman DU Typus Spektrophotometer mit der 1.00 cm Küvette benutzt.

Ergebnisse

Tabelle I und Abb. 1 zeigen das Ergebnis, das nach der obigen Weise infolge der Trennung der gemischten Lösung von *cis*-, *trans*-$[Coen_2Cl_2]^+$ gewonnen wurde. Bei der einzelnen Lösung sowohl als auch der Gemischten strömte jedes Komplexion mit dem gleichen Verhältnis aus.

Es begann nämlich das *trans*-Ion in der Fraktionsnummer 6 zu erscheinen und zeigte das Konzentrationsmaximum in der Nummer 7, wurde aber in der Nummer 10 kaum nachgewiesen. Das *cis*-Ion begann in der Nummer 10 zu erscheinen und zeigte das Maximum in der Nr. 12.

Die gleiche Erscheinung wurde auch über *cis*-, *trans*-$[Coen_2(CNS)_2]^+$ beobachtet (Siehe Tabelle II und Abb. 2). Bei dem *trans*-Ion erscheint das Maximum der Konzentrationsverteilung in der Nr. 5, bei dem *cis*-Ion in der Nr. 14. Es wurde beobachtet, dass dieses Ion im ganzen langsam ausströmt. Das *cis*-Ion strömte mit voller Wirkung als 2 M Natriumchlorid Lösung statt der 0.5 M Lösung abgetropft wurde, sofort nachdem das *trans*-Ion fast schloss.

Tabelle III und Abb. 3 zeigen das Ergebnis der Trennung von *cis*-, *trans*-$[Coen_2(NO_2)_2]^+$. Wir versuchten schon mit Austauscher von NH_4-Form über dieselben[1], aber wir wieder holten es um ihre Trennung zu vergleichen. Das *trans*- Ion zeigt hier in der Fraktionsnummer 6 seine maximale Verteilung und *cis*-Ion in der N1 17.

* Dies wurde auf der 9ten Generalversammlung der Chemischen Gesellschaft vou Japan vorgetragen, am 2. April, 1956, in Kyoto.

1) M. Mori, M. Shibata und J. Azami, *J. Chem. Soc. Japan*, **76**, 1003 (1955).

2) T. Inoue, "Synthetische anorganische Chemie (Mukikagaku-Seizo-Jikken)", Shokabo, Tokyo, 1946.

TABELLE I

TRENNUNG EINES GEMISCHES VON *cis*- UND *trans*-$[Coen_2Cl_2]^+$

Fraktion Nr.	E_{535}	E_{615}	E_{615}/E_{535}
5	0	0	—
6	0.010	0.056	5.60
7	0.030	0.166	5.53
8	0.030	0.165	5.50
9	0.016	0.084	5.25
10	0.050	0.024	0.48
11	0.114	0.039	0.37
12	0.155	0.047	0.30
13	0.133	0.040	0.30
14	0.087	0.029	0.33
15	0.048	0.015	0.31
16	0.030	0.010	0.33
17	0.019	0.006	0.31
18	0.008	0.003	0.37

TABELLE II

TRENNUNG EINES GEMISCHES VON *cis*- UND *trans*-$[Coen_2(CNS)_2]^+$

Fraktion Nr.	E_{490}	E_{505}	E_{505}/E_{490}
2	0	0	—
3	0.031	0.036	1.16
4	0.200	0.229	1.15
5	0.362	0.410	1.13
6	0.328	0.370	1.13
7	0.216	0.246	1.14
8	0.123	0.138	1.12
9	0.076	0.086	1.13
10	0.051	0.050	1.02
11	0.100	0.090	0.90
12	0.125	0.112	0.89
13	0.132	0.119	0.90
14	0.140	0.125	0.89
15	0.135	0.122	0.90
16	0.130	0.114	0.88
17	0.120	0.106	0.88
18	0.109	0.100	0.91
19	0.082	0.073	0.89
20	0.072	0.063	0.87
21	0.065	0.060	0.92
22	0.056	0.050	0.89
23	0.037	0.034	0.91
24	0.020	0.018	0.90
25	0.009	0.008	0.88

TABELLE III

TRENNUNG EINES GEMISCHES VON *cis*- UND *trans*-$[Coen_2(NO_2)_2]^+$

Fraktion Nr.	E_{324}	E_{340}	E_{340}/E_{324}
3	0	0	—
4	0.149	0.190	1.28
5	2.519	3.245	1.29
6	6.468	8.360	1.29
7	4.455	5.742	1.29
8	1.276	1.606	1.26
9	0.216	0.269	1.25
10	0.100	0.125	1.25
11	0.092	0.090	0.97
12	0.342	0.265	0.77
13	1.034	0.803	0.77
14	2.090	1.595	0.76
15	3.432	2.640	0.76
16	3.938	3.003	0.76
17	3.982	3.025	0.76
18	3.377	2.574	0.76
19	2.970	2.255	0.75
20	1.980	1.540	0.77
21	1.463	1.122	0.76
22	0.815	0.633	0.77
23	0.513	0.395	0.76
24	0.268	0.206	0.76
25	0.125	0.095	0.76
26	0.055	0.043	0.78

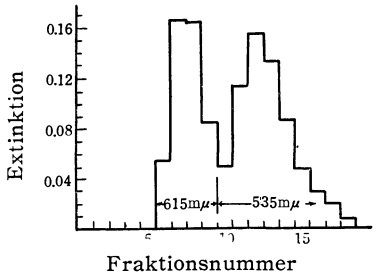

Abb. 1. Trennung eines Gemisches von *cis*-und *trans*-$[Coen_2Cl_2]^+$.

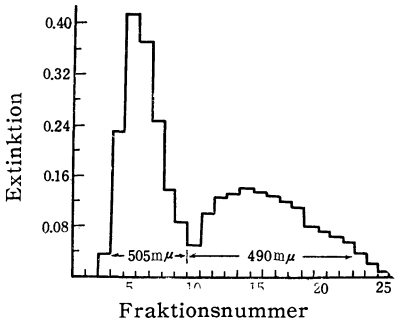

Abb. 2. Trennung eines Gemisches von *cis*-und *trans*-$[Coen_2(CNS)_2]^+$.

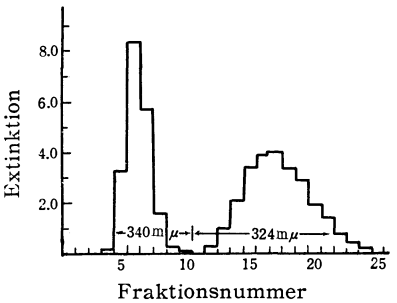

Abb. 3. Trennung eines Gemisches von *cis*-und *trans*-$[Coen_2(NO_2)_2]^+$.

Die über Adsorption der Komplexionen an Austauscher gewonenen Ergebnisse werden in Tabellen IV und V gezeigt. Hierbei bezeichnet C_o die Anfangskonzentration, C_s die Gleichgewichtskonzentration der Komplexionen, m die Menge des Austauschers und C_r die adsorbierte Menge an 100 mg Austauscher. K_d ist der nachstehend definierte Verteilungskoeffizient.

$$K_d = \frac{\text{adsorbierte Menge (mM) pro 1 meq. } H^+\text{-wertiger Austauscher (250 mg)}}{\text{Gleichgewichtskonzentration (mM/l)}}$$

$$= \frac{C_r}{C_s} \times 2.50$$

Diese Ergebnisse werden auch in Abb. 4 graphish zusammengestellt. Auf der Abszisse wird die Gleichgewichtskonzentration und auf der Ordinate der Verteilungskoeffizient logarithmisch aufgetragen.

TABELLE IV

ADSORPTION VON *cis-* UND *trans-* $[Coen_2(CNS)_2]Cl$ AN AUSTAUSCHER

(250 mg Austauscher, 1 meq. H^+)

C_o (mM/l)	C_s (mM/l)	C_r (mM/100 mg)	m (mg)	K_d	E_{505}/E_{490}
cis-					
7.66	0.95	0.064	209.4	0.16	0.90
3.06	0.49	0.050	103.0	0.26	0.88
1.55	0.19	0.027	101.1	0.35	0.90
0.77	0.09	0.013	101.5	0.36	0.86
0.15	0.02	0.003	100.8	0.37	0.85
trans-					
10.16	2.23	0.078	203.9	0.08	1.14
4.06	1.10	0.057	103.9	0.12	1.13
2.03	0.47	0.031	100.7	0.16	1.14
1.02	0.23	0.015	100.4	0.16	1.14
0.20	0.04	0.003	102.6	0.18	1.09

TABELLE V

ADSORPTION VON *cis-* UND *trans-* $[Coen_2(NO_2)_2]Cl$ AN AUSTAUSCHER

C_o (mM/l)	C_s (mM/l)	C_r (mM/100 mg)	m (mg)	K_d	E_{340}/E_{324}
cis-					
10.44	0.93	0.092	206.5	0.24	0.74
4.18	0.53	0.073	100.4	0.34	0.76
2.09	0.24	0.037	100.9	0.38	0.75
1.04	0.10	0.018	101.2	0.45	0.76
0.42	0.04	0.007	101.0	0.43	0.75
trans-					
10.80	2.37	0.083	203.8	0.08	1.25
4.32	1.00	0.065	100.9	0.16	1.27
2.16	0.42	0.033	104.6	0.19	1.21
1.08	0.20	0.018	100.9	0.22	1.23
0.43	0.07	0.007	101.5	0.25	1.26

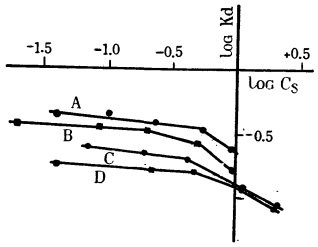

Abb. 4. Adsorption von Komplexionen an Austauscher.
A *cis*-$[Coen_2(NO_2)_2]^+$
B *cis*-$[Coen_2(CNS)_2]^+$
C *trans*-$[Coen_2(NO_2)_2]^+$
D *trans*-$[Coen_2(CNS)_2]^+$

Die über *cis-*, *trans*-$[Coen_2Cl_2]^+$ gemessenen Ergebnisse werden nicht in Abb. 4 zusammengestellt, da diese Komplexe teilweise zu den Aquokomplexe übergingen.

Diskussion

E. L. King und R. R. Walter[3] haben schon gefunden, dass *trans*-$[Co(NH_3)_4(NO_2)_2]^+$ als *cis*-$[Co(NH_3)_4(NO_2)_2]^+$ schneller ausfliessen, und wir[1] bestätigten auch dies über $[Co(NH_3)_4(NO_2)_2]^+$ und $[Coen_2(NO_2)_2]^+$. Aus diesen Tatsachen und den hier gewonnenen Ergebnisses entsteht wahrscheinlich ein empirisches Gesetz, nach dem *trans*-Form als *cis*-Form bei $[CoA_4X_2]^+$ oder $[Co(a\text{-}a)_2X_2]^+$ schneller ausfliesst. Es dünkt uns, dass solcher Unterschied in der Affinität zum Austauscher in dem Unterschiede der von Säureradikal X produzierten Dipolmomenten begründet ist.

Die Affinität zum Austauscher entsteht aus der Differenz von Ligande X sowohl unter denselben *cis*-Formen als auch unter denselben *trans*-Formen. Nach unseren Versuchen nimmt die Affinität zum Austauscher bei *trans*-Formen in der Reihenfolge $[Coen_2Cl_2]^+ > [Coen_2(NO_2)_2]^+ > [Coen_2(CNS)_2]^+$, bei *cis*-Formen $[Coen_2(NO_2)_2]^+ > [Coen_2(CNS)_2]^+ > [Coen_2Cl_2]^+$ ab. Dass die beiden Reihenfolgen nicht übereinstimmen, so meinen wir, ist der Unterschied des herrschenden Faktors zur Affinität. Wir müssen die objektiven Komplexsalze noch mehr vermehren und versuchen, um den Faktor zu erforschen.

Wir stellten oft fest, dass *cis-*, *trans*-Form sich einander in fen hergestellten Komplexsalzen mischen. In solchem Falle kann diese Weise als eine Weise bequem benutzen, die die Reinheit der Komplexsalzen einfach anerkennen kann.

Zusammenfassung

Wir machten Versuche über Trennung von

3) E. L. King und R. R. Walter, *J. Am. Chem. Soc.*, **74**, 4471 (1952).

cis- und *trans*-Form der drei Isomerien—$[Coen_2Cl_2]Cl$, $[Coen_2(CNS)_2]Cl$ und $[Coen_2(NO_2)_2]Cl$—, benutzten dabei als Austauscher den Kationenaustauscher Amberlit IR 120 in der Na-Form und als Elutionsmittel die 0.5 M Natriumchlorid Lösung und gewannen somit die folgenden Ergebnisse.

1) *Trans*-Form floss immer als *cis*-Form der entsprechenden Komplexsalze schneller aus und wurde fast ganz unter dieser experimentalen Bedingung getrennt (Durchflussgeschwindigkeit 1 cm/3.5 Min).

2) Unter *trans*-Komplexen ist die leichte Elution die nachstehende Reihenfolge:

$[Coen_2(CNS)_2]^+ > [Coen_2(NO_2)_2]^+ > [Coen_2Cl_2]^+$.

Diese Reihenfolge widerspricht nicht den vom Experiment der Adsorption an Austauscher gewonnenen Ergebnisse. Unter *cis*-Komplexen:

$[Coen_2Cl_2]^+ > [Coen_2(CNS)_2]^+ > [Coen_2(NO_2)_2]^+$.

3) Wenn wir dieses mit der über *cis*-, *trans*-$[Co(NH_3)_4(NO_2)_2]^+$ schon veröffentlichten Ergebnissen betrachten, denken wir, dass *trans*-Form als *cis*-Form bei Isomerien von Typus $[CoA_4X_2]^+$ oder $[Co(a\text{-}a)_2X_2]^+$ schneller ausfliesse.

Für die Unterstützung dieser Arbeit sind wir der Stiftung für synthetische wissenschaftliche Forschung am Unterrichtsministerium zu Dank verpflichtet.

Chemisches Laboratorium der wissenschaftlichen Fakultät, Kanazawa Universität, Kanazawa

The Solubility of Silver Bromate in Tetrahydrofuran-Water Mixed Solvents

By Ei KOIZUMI and Hiroshi MIYAMOTO

(Received June 29, 1956)

Introduction

In the previous reports regarding the investigation of the relation between solubilities of inorganic salt and dielectric constants of solvents, the solubilities of silver bromate in dioxane- and sucrose-water mixed solvents were described[1,2]. In the present work, the solubility of silver bromate in tetrahydrofuran-water mixed solvents which have a wide range of dielectric constant dependent on the composition was measured at 20°, 25° and 30°C. These data were examined using the theoretical formula[3] concerning the solubility of sparingly soluble salt and the dielectric constant of the solvent.

With regard to the investigations which use tetrahydrofuran as the solvent, few reports have appead so far. The physical properties of the tetrahydrofuran-water system have been studied by Erva[4] and Yoshioka et al.[5] Likewise, the solubility of silver bromate in this mixed solvent has not yet been measured.

1) E. Koizumi and H. Miyamoto, *J. Chem. Soc. Japan (Pure Chem. Sect.)*, **75**, 1302 (1954).
2) E. Koizumi and H. Miyamoto, *J. Chem. Soc. Japan (Pure Chem. Sect.)*, **77**, 193 (1956).
3) E. Koizumi, *J. Chem. Soc. Japan*, **68**, 19 (1947).
4) J. Erva, *Suomen Kemistilehti*, **28B**, 131 (1955). —By *C. A.*, **50**, 6171 (1956).
5) T. Yoshioka and M. Taniyama, *J. Chem. Soc. Japan (Ind. Chem. Sect.)*, **57**, 747 (1954).

Experimental

(1) Preparation of Solute and Solvent.—The silver bromate was prepared from the dilute solution of silver nitrate and potassium bromate by the infinite dilution method. The precipitates were recrystallized from boiling conductivity water by the modified Reedy's method[6], and stocked in the vacuum.

After the inhibitor was removed, the tetrahydrofuran (from Badische Anilin und Sodafabrik A. G.) was purified twice by fractional distillation in a special rectifier with threefold reflux tube (30 cm. in length) and glass spiral (25 cm. in length) in its inner tube. The fraction boiling at 64.5°–65.5°C was used for the present experiment. From the density determination at 25°C using a Sprengel type pycnometer, this fraction was found to have a purity of 99.15% (wt.), when calculated after Critchfield's empirical equation assuming water to be the only impurity. This grade of purity was sufficient for the present purpose.

Eleven tetrahydrofuran-water mixed solvents were prepared from the purified tetrahydrofuran mentioned above and the conductivity water (1×10^{-6} mho at 20°C), the concentrations of which are ranging from zero to 64.232 per cent by weight of tetrahydrofuran.

(2) Determination of the Solubility of Silver Bromate.—The mixed solvent and excess solute were placed in shaking bottles made of quartz, and sealed. The bottles were rotated in thermostats regulated within ±0.02°C of 20°, 25° and 30°C,

6) J. H. Reedy. *J. Am. Chem. Soc.*, **43**, 1440 (1921).

respectively. These bottles were slowly rotated for seventy-two hours, which were sufficient to give the saturated solutions.

The solubility of silver bromate was determined volumetrically from the total silver ion using dichlorofluorescein as the indicator. To the sample to be determined was added a definite excess of sodium chloride solution (0.050 mol./l.), then the sodium chloride remaining was determined by titration with 0.025 mol./l. silver nitrate solution.

Results and Discussions

(1) Results.—The solubilities of silver bromate and other values are shown in Tables I, II, III and IV. The observed solubilities

TABLE I

SOLUBILITY OF SILVER BROMATE IN TETRAHYDROFURAN-WATER MIXED SOLVENT AT 20°C

T. H. F. %(wt.)	Density	Dielectric Constant	Solubility $S\times10^3$	Solubility $S'\times10^4$	$\log S+3$	$1/D\times100$
0.	0.9982	80.37	7.28	2.62	0.8621	1.244
3.347	0.9966	78.18	6.34	2.35	0.8021	1.279
6.769	0.9952	75.88	5.72	2.18	0.7574	1.318
12.645	0.9936	71.87	4.73	1.89	0.6749	1.391
18.770	0.9909	67.39	3.97	1.68	0.5988	1.484
24.471	0.9880	62.93	3.39	1.51	0.5302	1.589
29.208	0.9853	59.12	2.93	1.37	0.4669	1.691
35.670	0.9801	52.74	2.51	1.26	0.3997	1.896
43.537	0.9719	46.78	1.90	1.05	0.2788	2.138
54.513	0.9595	37.48	1.34	0.85	0.1271	2.668
64.232	0.9461	29.71	0.99	0.73	$\bar{1}$.9956	3.366

TABLE II

SOLUBILITY OF SILVER BROMATE IN TETRAHYDROFURAN-WATER MIXED SOLVENT AT 25°C

T. H. F. %(wt.)	Density	Dielectric Constant	Solubility $S\times10^3$	Solubility $S'\times10^4$	$\log S+3$	$1/D\times100$
0.	0.9971	78.54	8.59	3.09	0.9340	1.273
3.347	0.9954	76.34	7.62	2.83	0.8820	1.310
6.769	0.9938	74.00	6.83	2.61	0.8344	1.351
12.645	0.9912	69.92	5.81	2.33	0.7642	1.430
18.770	0.9886	65.56	4.88	2.07	0.6884	1.525
24.471	0.9846	61.09	4.23	1.90	0.6263	1.637
29.208	0.9808	57.24	3.67	1.72	0.5647	1.747
35.670	0.9750	50.98	2.90	1.46	0.4624	1.962
43.537	0.9669	45.25	2.31	1.28	0.3636	2.210
54.513	0.9593	36.28	1.53	0.98	0.1847	2.756
64.232	0.9408	28.72	1.13	0.83	0.0531	3.482

TABLE III

SOLUBILITY OF SILVER BROMATE IN TETRAHYDROFURAN-WATER MIXED SOLVENT AT 30°C

T. H. F. %(wt.)	Density	Dielectric Constant	Solubility $S\times10^3$	Solubility $S'\times10^4$	$\log S+3$	$1/D\times100$
0.	0.9957	76.73	10.02	3.59	1.0009	1.303
3.347	0.9937	74.58	8.99	3.34	0.9538	1.341
6.769	0.9921	72.34	8.08	3.09	0.9074	1.382
12.645	0.9893	68.34	6.82	2.74	0.8338	1.463
18.770	0.9860	63.95	5.62	2.39	0.7497	1.564
24.471	0.9821	59.56	4.79	2.15	0.6803	1.679
29.208	0.9780	55.85	4.12	1.94	0.6149	1.791
35.670	0.9727	49.70	3.28	1.66	0.5159	2.012
43.537	0.9640	44.01	2.55	1.42	0.4065	2.272
54.513	0.9498	35.18	1.77	1.14	0.2480	2.843
64.232	0.9361	28.00	1.43	1.10	0.1553	3.571

TABLE IV

SOLVATION RADIUS OF SILVER BROMATE IN TETRAHYDROFURAN-WATER MIXED SOLVENT

T. H. F. %(wt.)	20°C		25°C		30°C	
	$A\times10^8$	$B\times10^8$	$A\times10^8$	$B\times10^8$	$A\times10^8$	$B\times10^8$
3.347	0.773	0.758	0.789	0.774	0.968	0.956
6.769	0.907	0.895	0.988	0.975	1.024	1.013
12.645	0.994	0.983	1.148	1.141	1.154	1.148
18.770	1.135	1.128	1.251	1.248	1.246	1.242
24.471	1.296	1.294	1.433	1.438	1.400	1.403
29.208	1.165	1.166	1.549	1.559	1.503	1.510
35.670	1.743	1.745	1.755	1.777	1.910	1.932
43.537	1.878	1.899	1.966	1.997	2.265	2.302
54.513	2.354	2.402	2.354	2.405	2.390	2.447
64.232	2.463	2.541	2.949	3.050	3.076	3.208

of silver bromate in tetrahydrofuran-water mixed solvents at 20°, 25° and 30°C are listed in the fourth column ($S\times10^3$ mol./l.) and in the fifth column ($S'\times10^4$ mole fraction) of Table I, II and III, respectively. The probable error of observed solubility is $\pm0.02\times10^{-3}$ mol./l. Further, the observed densities of the tetrahydrofuran-water system are given in the second column of Tables I and III. The densities listed in Table II were obtained by applying Critchfield's experimental equation. The probable error of the observed density is $\pm0.9\times10^{-5}$g./cc. The dielectric constants (D) at 20°, 25° and 30°C are those from the data of Critchfield[7].

(2) The Relation between the Solubility and the Dielectric Constant.—The relation between the solubility (S) and the dielectric constant (D) is shown graphically in Figs. 1 and 2. In Fig. 2, these curves are approximated by straight lines in the region of higher dielectric constant (about 60–80), in the range of concentration smaller than about twenty per cent by weight of tetrahydrofuran, while in the whole range of concentration we can see the smoothly continuous curves.

When the concentration of tetrahydrofuran

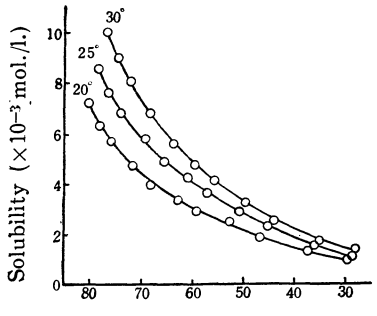

Fig. 1. Relation between solubility and dielectric constant.

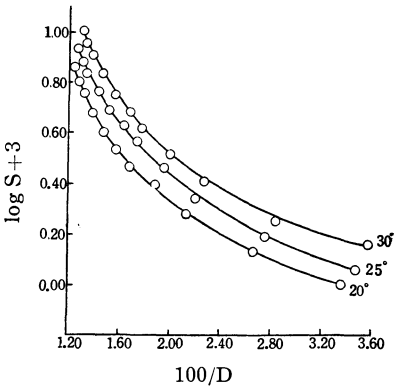

Fig. 2. Relation between logarithm of solubility and reciprocal of dielectric constant.

in solution is relatively low, and provided that the molecular association of the solvent does not exist, the relation between the observed solubility and the dielectric constant of solvent was expressed by the following theoretical equation (I)[3]

$$ln\frac{C_0}{C_1}=\frac{Z^2\varepsilon^2}{2RTr_s}N\left(\frac{1}{D_1}-\frac{1}{D_0}\right)-\frac{Z^2\varepsilon^2}{2kT}\sqrt{\frac{8\pi NZ^2\varepsilon^2}{10^3kT}}\left(\frac{C_1^{\frac{1}{2}}}{D_1^{\frac{3}{2}}}-\frac{C_0^{\frac{1}{2}}}{D_0^{\frac{3}{2}}}\right) \quad (I)$$

where N, R, T, Z, k and ε are the Roschmidt number, gas constant, absolute temperature, valency, Boltzman number, and electric elementary quantum, respectively, C_0 and D_0 are the solubility of the solute in water and the dielectric constant of water, C_1 and D_1 are the solubility of the solute in tetrahydrofuran-water mixed solvents and the dielectric constant of these solvents.

In the equation, as C_0 and D_0 are constant at constant temperature, assuming the solvation radius r_s being constant, neglecting the second term as it is very small compared with the first, the logarithm of solubility of the electrolyte should be reciprocally proportional

7) F. E. Critchfield, J. A. Gibson and J. L. Hall, *J. Am. Chem. Soc.*, **75**, 6044 (1953).

to the dielectric constant. The theoretical equation (I) agrees almost exactly with the experimental results shown in Fig. 2 in the region of higher dielectric constant.

On the other hand, no linear relation was found in the wide range of the dielectric constant of concentrated tetrahydrofuran-water mixed solvents. Undoubtedly, the equation (I) is in such a case incorrect due to the approximations adopted in its theoretical treatment. Since the equation was derived to investigate the relation between the solubility of sparingly soluble salt and the dielectric constant of the solvent, it is not satisfactory for this investigation.

Generally speaking, the solubility of the inorganic salt does not merely depend upon the dielectric constant of the solvent, but it may also depend on the chemical constitution of the solvent. Thus, in a more improved treatment, the intermolecular reaction of the solvent (tetrahydrofuran) and water should be considered. Also to know the effect of polarization of the solubility of inorganic salt in the mixed solvents, the dipole moment of the solvent should be taken into account. Further investigations are necessary in regard to these point.

(3) **Calculation of Solvation Radius.**—The solvation radius (r_s) of silver bromate in these mixed solvents, was calculated by using values of observed solubility. The solvation radius is about 1 Å at each temperature in the solvent of high water concentration. These are listed in Table IV, the values in column (A) were calculated by the equation (I), the values in column (B) by the equation without the second term of the equation (I). The effect of the second term increases with the decrease of the dielectric constant, in a non-linear range of curve in Fig. 2. The solvation radius of this solvent is smaller than in the case of any other previous reports[1,2].

Summary

To investigate the relation between the solubility of inorganic salts and the dielectric constants of solvents, the solubility of silver bromate in tetrahydrofuran-water mixed solvent was determined at 20°, 25° and 30°C, respectively. The logarithm of solubility is almost reciprocally proportional to the dielectric constant of the solvent in the region of the higher dielectric constant. But no linear relation was found in that of the lower dielectric constant of tetrahydrofuran-water mixed solvent.

Also, the solvation radius of silver bromate was calculated applying the above-mentioned data. The solvation radius is about 1 Å at each temperature.

Department of Chemistry, Faculty of Liberal Arts, Ibaraki University
Mito

Hydroformylation and Hydrogenation of Methylacrylate in Presence of Dicobalt Octacarbonyl or Iron Pentacarbonyl. Dependence of Reaction Rate on Partial Pressures of Carbon Monoxide and Hydrogen

By Hiroshi UCHIDA and Kenichiro BANDO

(Received July 26, 1956)

Introduction

In the presence of dicobalt octacarbonyl, ethylacrylate can readily be hydroformylated to β-carbethoxypropionaldehyde. The reaction was once investigated by H. Adkins et al.[1] and thereafter in greater detail by K. Ohashi et al.[2] More recently G. Natta[3] made a study on the hydroformylation of cyclohexene and obtained the remarkable result that the ratio of carbon monoxide to hydrogen in a gas mixture has a considerable influence upon the reaction rate. In this study the hydroformylation of methylacrylate has therefore been conducted by paying special attention to the effect of the gas composition on the rate.

In contrast to dicobalt octacarbonyl, iron pentacarbonyl was generally thought to be ineffective for the hydroformylation. Recently the effect of iron pentacarbonyl upon the isomerization of olefin due to the migration of a double bond-effect which is similar to that of dicobalt octacarbonyl, was however

1) H. Adkins and G. Kresek, *J. Am. Chem. Soc.*, **71**, 3051 (1949).
2) K. Ohashi and S. Suzuki, *J. Chem. Soc. Japan (Ind. Chem. Sec.)*, **56**, 792 (1952), (in Japanese).
3) G. Natta, *Brennstoff-Chem.*, **36**, 176 (1955).

found by A. Asinger et al.[4], so far as the carbon monoxide pressure was comparatively low. The present paper also deals with the reaction that has been made between methylacrylate and gaseous mixtures comprising carbon monoxide and hydrogen in the presence of iron pentacarbonyl, with the expectation that some effect of the carbonyl on the reaction may appear.

Experimental Procedure

In the presence of dicobalt octacarbonyl or iron pentacarbonyl, the reaction between a gaseous mixture of carbon monoxide and hydrogen and a quantity of methylacrylate was conducted in an autoclave (1 l. in volume) of shaking type, at a constant pressure at a fixed temperature. The carbonyls were used for the reaction after they were dissolved in benzene. The rate of the reaction was estimated by the pressure decrease in a high pressure gas storage (1.6 l. capacity) from which the gas was continuously introduced into the autoclave in order that during the reaction the initial pressure in the autoclave might be maintained at the reaction temperature.

Since the use ratio of carbon monoxide to hydrogen in the reaction of hydroformylation was 1:1, the continuous supply of gaseous mixture comprising equal volumes of carbon monoxide and hydrogen into the autoclave causes scarcely any change of gas composition compared with the orginal gas composition in the autoclave. In this way a constant ratio of carbon monoxide to hydrogen of the gaseous mixture in the autoclave was kept throughout the reaction.

As for the reaction with dicobalt octacarbonyl, a reaction temperature of 110°C was preferred, at which the reaction proceeded with a measurable rate. At temperatures (100–104°C), a little lower than 110°C, the slow absorption of gas had already begun to take place. During this period of slow absorption, the gas was supplied from the gas storage into the autoclave up to the pressure which would be expected by steadily increasing temperature up to 110°C if there no absorption. The temperature rise from 100 to 110°C usually required about eight minutes. Once the temperature arrived at 110°C, both the temperature and the pressure were kept constant during further progress of the reaction.

β-carbmethoxypropionaldehyde could not be obtained in a yield as expected theoretically from the amount of gases absorbed in the reaction, and the maximum yield atained to only 80% of the theoretical*.

Dicobalt octacarbonyl was prepared according to the procedure by I. Wender et al.[5]: namely a slurry of 30 g. cobalt (II) carbonate in 200 cc. of petroleum-ether was treated with water-gas under a pressure of 200 kg./cm² in 1 l autoclave at 150°C for two hours, and the petroleum-ether solution of the carbonyl was cooled in dry ice for a short period of time, whereupon the crystalline dicobalt octacarbonyl separated. The crystallite was stored under the high pressure of carbon monoxide in a steel vessel, and a quantity of it was dissolved in 100 cc. of benzene immediately before use. Methylacrylate was supplied by the Toa Gosei Company and was 98% in purity. It was used without any further purification.

The reaction with iron pentacarbonyl was first conducted under conditions identical with those for dicobalt octacarbonyl, but it appeared soon that another kind of reaction took place, as will be described later. Iron pentacarbonyl was manufactured as was reported by one of the authors of this paper et al.[6] previously.

Results

Hydroformylation of Methylacrylate in Presence of Dicobalt Octacarbonyl.—The reaction was first carried out at a fixed partial pressure of hydrogen with different partial pressures of carbon monoxide, and then at a fixed partial pressure of the latter with different partial pressures of the former.

In Fig. 1 are shown the results obtained in a series of the experiments carried out at a constant pressure of hydrogen with different partial pressures of carbon monoxide, using 92 g. of methylacrylate and 1.72 g. of dicobalt octacarbonyl in 100 cc. of benzene. Three curves in the figure reveal the pressure decrease in the gas storage

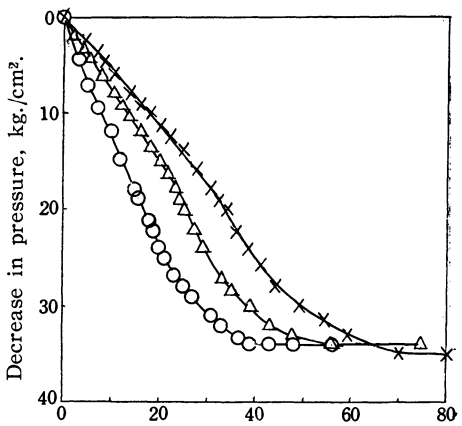

Every experiment was conducted at 110°C under a constant hydrogen pressure (97 kg./cm².), with different carbon monoxide pressures of 21 (—○—), 52 (—△—), and 99 kg./cm². (—×—) respectively.

Fig. 1. Decrease in pressure of gas storage with time.

4) A. Asinger and O. Berg, *Ber.*, **88**, 445 (1955).

* The aldehyde was determined according to the procedure by H. Adkins et al.[1] Even though the distillation was made, after an addition of a small quantity of hydroquinone, at as low a pressure and as rapidly as was possible, it seemed difficult to isolate aldehyde without a considerable loss.

5) I. Wender, H. Greenfield and M. Orchin, *J. Am. Chem. Soc.*, **73**, 2659 (1951).

6) H. Uchida and T. Minegishi, *Rpt. Govt. Chem. Ind. Res. Inst. Tokyo*, **45**, 1 (1950).

with time. A linear relation of the pressure decreae to time is observed during a time interval between the ten-minute and thirty-minute periods from the beginning of the reaction, and the slopes of the straight line give the rate of the reaction.

The dependence of the rate upon the partial pressure of carbon monoxide is given by curve A in Fig. 2. The rate attains the maximum value

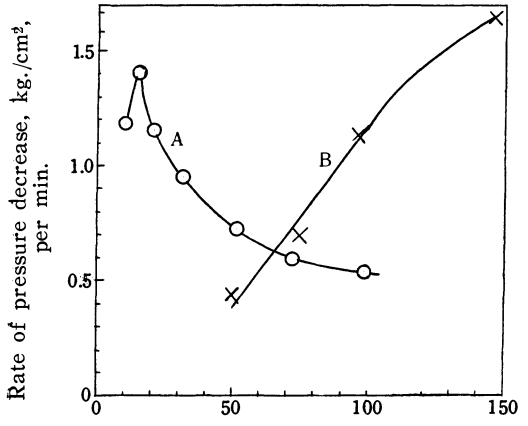

Partial pressure of carbon monoxide or hydrogen, kg./cm².

A: hydrogen partial pressure, 97 kg./cm².

B: carbon monoxide partial pressure, 21 kg./cm².

Fig. 2. Relation of rate of hydroformylation to partial pressure of carbon monoxide (A) or hydrogen (B).

at a carbon monoxide pressure of 15 kg./cm³. At a lower carbon monoxide pressure of 11 kg./cm² the absorption of the gas remained incomplete, proceeding to only half the theoretically available extent and part of the carbonyl was found to decompose into precipitates of a composition which is unclarified as yet. At the carbon monoxide pressure higher than 15 kg./cm² the hydroformylation** proceeded to completion because of the absorption of the theoretical amount of the gas, but the absorption took place rather slowly. In this case any decomposition of the carbonyl was hardly recognized after the reaction.

Curve B in Fig. 2 reveals the rate as a function of the hydrogen partial pressure at a fixed partial pressure of carbon monoxide. At hydrogen pressures higher than 75 kg./cm², the gas was absorbed in an amount just necessary for the hydroformylation of methylacrylate; however, at the lower pressures it was absorbed in only half the theoretical amount. In the former case the carbonyl persisted unchanged during the reaction, whereas in the latter case part of the carbonyl underwent decomposition. The high pressure of hydrogen has thus proved to be a requisite for the carbonyl to remain undecomposed in the reaction.

** Hydrogenation of β-carbmethoxypropionaldehyde as well as of methylacrylate seemed not to take place, as hydrogen was absorbed in an amount equal in mole to that of carbon monoxide.

The tendencies presented here agree with the results obtained by G. Natta on the hydroformylation of cyclohexene.

A. R. Martin[7] proposed a rate equation for the case of hydroformylation of di-isobutene,

$$\text{initial rate} = a p_{H_2} / (b p_{H_2} + c p_{CO}) \cdot [CO_2(CO)_8][C_8H_{16}]$$

where a, b, and c are constants. According to the equation the initial rate tends to decrease always with the rising carbon monoxide pressure. The tendency is in agreement with the present results obtained in a range of high carbon monoxide pressures, but is not so with those in a range of low pressures. In the latter case the carbonyl has been found to decompose during the reaction, and this is probably the reason why the rate begins to diminish again in this range. As for the dependence of the rate upon hydrogen pressure the equation suggests that, when b is not much greater than c, the rate tends to increase rather proportionally with the hydrogen pressure and then more slowly with the further increasing pressure. This is also consistent with the present results.

Hydrogenation of Methylacrylate in Presence of Iron Pentacarbonyl.—In the presence of iron pentacarbonyl, no reaction between methylacrylate and a gaseous mixture composed of carbon monoxide and hydrogen proceeded at 110°C, but at the higher temperature of 160°C the absorption of gas was found to take place if carbon monoxide partial pressure remained considerably low. Of the two gaseous reactants only hydrogen was absorbed to such an extent that, at the maximum absorption, the absorbed hydrogen amounted to one mole for one mole of methylacrylate, whereas the carbon monoxide was absorbed in extremely small amounts (0.03–0.04 mol.).

No absorption of hydrogen was observed in the reactions, either in the presence or absence of carbon monoxide conducted with iron catalysts such as the reduced one from iron oxide and the other one produced by thermal decomposition of iron pentacarbonyl.

The product of the reaction was confirmed as methylpropionate***.

In order to see the effect of the partial pressure of an individual gaseous component on the reaction rate, the reaction was conducted at a fixed hydrogen pressure with varying carbon monoxide pressures and with varying hydrogen

7) A. R. Martin, *Chem. and Ind.*, **1536** (1954).

*** The confirmation was made as follows. Since the boiling temperatures of methylpropionate and benzene differed too little to permit the separation from each other by distillation, the synthesis of the product for the confirmation was carried out without any addition of benzene. In this case the hydrogen absorption proceeded to only three quaters of the theoretical extent. About 70% of the product distilled out at 78—80°C, leaving a higher boiling residue of polymerized products of methylacrylate. After the distillate had been freed from iron pentacarbonyl by adding mercuric chloride together with aceton and water, 70% of the distillate distilled out again at 79—79.5°C which corresponded to the b.p. of methylpropionate. The second distillate has a saponification value of 630. It contains a minute quantity (1%) of methylacrylate as determined according to the procedure by D.W. Beesing et al. using dodecanethiol (*Anal. Chem.*, **21**, 1073 (1949)).

pressures without an addition of carbon monoxide. During the reaction only hydrogen, but not a mixture of carban monoxide and hydrogen, was introduced into the autoclave from the gas storage. After the reaction without carbon monoxide the gaseous product contained about one per cent of carbon monoxide.

The initial rate obtainable from the initial tangent drawn to the curves for the pressure in the gas storage during the reaction vs. time is given in Fig. 3 as functions of carbon monoxide and hydrogen pressures respectively****. The reduction of

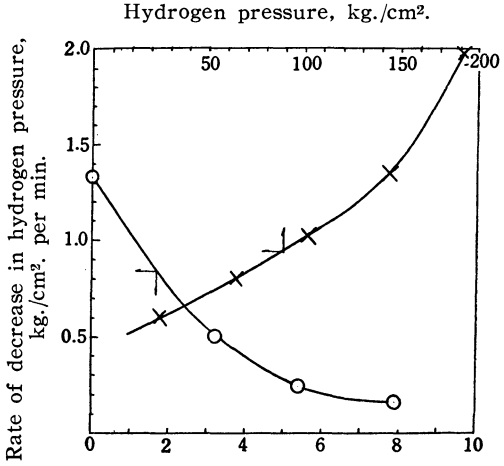

Raw meterials: 92 methylacrylate and 10 g. iron pentacarbonyl in 100 cc. of benzene.

—○—: under a hydrogen partial pressure of 155 kg./cm².

—×—: in the absence of carbon monoxide.

Fig. 3. Relation of rate of hydrogenation to partial pressure of carbon monoxide or hydrogen pressure.

**** In this series of experiments the absorption of gas at the temperature lower than 160°C was small and hence the initial tangent served for the representation of the initial rate.

methylacrylate by hydrogen takes place even in the presence of carbon monoxide at a pressure of 8 kg./cm². The lower the carbon monoxide pressure is, the higher the rate is; and the higher the hydrogen pressure is, the more rapidly the reaction proceeds.

M. Orchin[8] stated that although ethylacrylate could be hydroformylated in the presence of dicobalt octacarbonyl it could not be reduced. The present results show that methylacrylate can be reduced in the presence of iron pentacarbonyl.

Summary

Hydroformylation of methylacrylate in the presence of dicobalt octacarbonyl was investigated by paying a special attention to the effect of varying ratios of carbon monoxide to hydrogen on the rate. The rate attains the maximum value at a certain partial pressure of carbon monoxide, and increases with the increasing partial pressure of hydrogen. The tendencies agree with the results obtained by G. Natta on the hydroformylation of cyclohexene. The rate equation proposed by A. R. Martin with respect to the rate of hydroformylation of di-isobutene can represent the tendencies observed in the present results.

In the presence of iron pentacarbonyl, methylacrylate has been found to be reduced to methylpropionate under high pressure of hydrogen containing carbon monoxide. The reduction becomes more difficult with the increasing partial pressure of carbon monoxide, but was made catalytically neither by an iron catalyst reduced from iron oxide nor by the one produced by the thermal decomposition of iron pentacarbonyl.

Government Chemical Industrial Research Institute, Tokyo

8) M. Orchin, *Advances in Catalysis*, 5, 391 (1953).

Tie Line Correlation for Ternary Liquid Equilibria

By Kiyoharu ISHIDA

(Received April 9, 1956)

Since only a few tie lines have been experimentally determined in most systems described in the literature, several methods of interpolating and extrapolating such data over the entire range of composition have been devised. Except for the graphical methods[1,2], they are expected to give a straight line from the appropriate plot of conjugate values at equilibrium. Most of these are related to the systems which comprise two miscible pairs of liquids and one partially miscible pair (type 1), while only a few methods[3,4,5]

1) "International Critical Tables", McGraw-Hill Book Company, Inc., New York (1928), Vol. III, p. 398.
T.K. Sherwood, "Absorption and Extraction", McGraw-Hill Book Company, Inc., New York (1937), p. 242.
A. V. Brancker, T. G. Hunter and A. W. Nash, *Ind. Eng. Chem., Anal. Ed.*, **12**, 35 (1940).

2) D. B. Hand, *J. Phys. Chem.*, **34**, 1961 (1930).

3) K. A. Varteressian and M. R. Fenske, *Ind. Eng. Chem.*, **29**, 270 (1937).

4) T. F. Brown, ibid., **40**, 103 (1948).

5) J. B. Conway and J. B. Philip, ibid., **45**, 1083 (1953).

have been proposed to the systems which comprise two partially miscible pairs of liquids and one miscible pair (type 2).

It seems that no useful method applicable to both types has ever been proposed, thus, the method useful for type 1 does not always give satisfactory results when applied to type 2 and vice versa[6,7]. Since it is evident that both types may interchange with each other with changing temperatures, the useful method applicable for both types is desirable, if it is possible.

The upper critical solution temperature in the binary system containing toluene and liquid ammonia was found to be −7.4°C by the measurement of mutual solubilities of this system. Therefore, the equilibrium for the system *n*-heptane-toluene-liquid ammonia at the temperatures below −7.5°C involves two pairs of partially miscible liquids, and the binodal curve of the system at −7.5°C touches the side of the triangle which represents the binary mixture of toluene and liquid ammonia. It is considered that the methods resulting in a straight line for the tie-line data at the critical solution temperature of one pair of binary systems are generally applicable to systems for both types.

In the present study, the system *n*-heptane-toluene-liquid ammonia has been investigated at −7.5° and −15°C to determine whether the previous methods for obtaining the straight line correlation were applicable to both types independent of temperature.

Experimental Procedure and Results

The equilibrium data for the ternary system and mutual solubilities of toluene and liquid ammonia at the temperatures of −10°, −15° and −20°C were determined by the same way as described in the previous paper[8]. Alcohol cooled by dry ice in the Dewar vessel of large capacity was used as a constant temperature bath, and the desired temperature could be maintained within the range of ±0.1°C throughout the experiment. In order to minimize the change of temperature, thermal insulating tubes were used by means of which alcohol was made to circulate around the bottle containing the system. The heterogeneous liquid layers were separated and analysed after the saturation equilibrium was attained. The mutual solubilities of toluene and liquid ammonia at temperatures near the critical solution temperature were determined by noting the miscibility temperatures of mixtures of known composition. In these cases, the vapor pressure of a saturated solution at that temperature was determined experimentally, and the necessary correction for the composition of liquid components was estimated using the vapor pressure data and the volume of the vapor space.

The experimental data for the binary system toluene-liquid ammonia are given in Table I and the equilibrium data for the ternary system are given in Table II and shown in Fig. 1 and 2. In

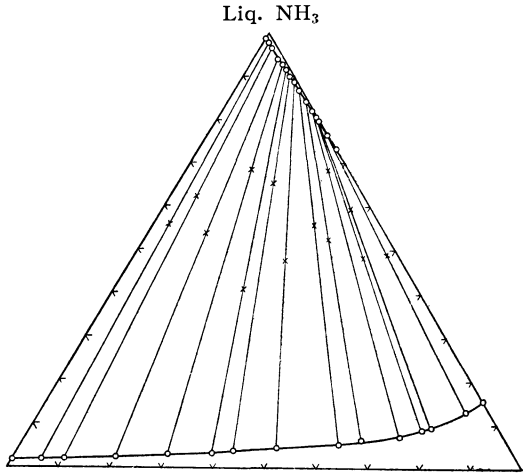

Fig. 1. System *n*-Heptane-Toluene-Liq. NH_3 at −15°C, wt. %.

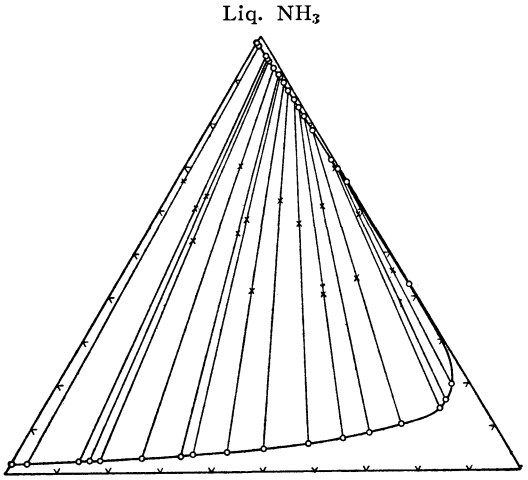

Fig. 2. System *n*-Heptane-Toluene-Liq. NH_3 at −7.5°C, wt. %.

TABLE I

SOLUBILITY DATA FOR THE SYSTEM TOLUENE AND LIQ. NH_3

Temperature °C	Wt. % NH_3 in NH_3 rich Layer	Wt. % NH_3 in Toluene rich Layer
−10	64.4	20.2
−15	73.2	15.3
−20	78.6	12.4

Cloud Point, °C	Wt. % NH_3 in Solution
−8.0	29.3
−7.6	35.9
−7.4	39.6
−7.4	41.1
−7.5	46.0
−7.8	54.4
−7.8	56.1
−8.3	59.7

6) C. E. Dryden, ibid., 35, 492 (1943).
7) D. DeB. Darwent and C. A. Winkler, *J. Phys. Chem.*, 47, 442 (1943).
8) K. Ishida, *J. Chem. Soc. Japan* (Ind. Chem. Sect.,) 56, 469 (1953).

TABLE II

EQUILIBRIUM DATA FOR THE SYSTEM *n*-HEPTANE-TOLUENE-LIQUID AMMONIA

Total Mixture		Hydrocarbon Layer		Solvent Layer	
Toluene Wt. % (Solvent-free Basis)	NH_3 Wt. %	NH_3 Wt. %	Toluene Wt. % in the Raff. (Solvent-free Basis)	NH_3 Wt. %	Toluene Wt. % in the Ext. (Solvent-free Basis)
	At −15.0°C				
0.0	—	1.7	0.0	98.8	0.0
6.8	56.0	1.8	5.7	97.7	43.5[a]
13.3	62.4	2.0	10.3	96.4	59.5[a]
24.2	53.8	2.4	20.3	93.9	75.0
39.8	68.4	3.1	30.7	92.7	85.0
42.6	41.2	3.4	39.5	91.6	88.8
52.9	65.3	4.0	43.6	89.9	89.9
56.9	47.5	4.6	52.7	88.6	93.0
70.5	55.7	5.4	65.2	86.7	95.1
75.0	52.5	6.5	70.0	84.2	96.1
86.1	68.2	7.1	78.2	82.0	97.7
86.1	48.1	8.8	83.4	80.6	98.3
90.0	59.5	9.3	85.4	79.7	98.3
96.0	49.1	12.9	94.8	76.6	99.0
100.0	—	15.3	100.0	73.2	100.0
	At −7.5°C				
0.0	—	2.2	0.0	98.5	0.0
4.0	67.0	2.2	2.9	97.7	25.4[a]
17.7	60.6	2.7	13.3	95.3	72.1[a]
21.0	63.5	2.8	15.3	94.7	74.6[a]
21.5	53.0	2.8	17.5	94.3	77.0[a]
36.5	70.3	3.3	25.7	92.6	83.8[a]
39.7	54.9	3.7	33.4	90.9	87.7[a]
43.2	58.0	4.1	35.8	90.6	89.0
46.8	41.4	4.6	42.6	89.2	91.0
59.6	62.2	5.3	50.1	87.6	92.6
66.8	56.9	6.4	59.3	85.5	94.1
69.7	40.5	7.5	66.6	83.7	95.3
80.0	61.0	8.8	72.6	81.5	96.0
82.7	44.1	10.5	79.9	78.4	97.0
96.6	69.5	14.1	90.0	71.5	97.9
95.7	58.9	16.0	92.3	69.2	98.4
96.6	45.8	19.7	95.6	66.1	99.0
100.0	—	42.5[b]	100.0	42.5[b]	100.0
	At 0.0°C				
0.0	—	2.7	0.0	98.2	0.0
15.4	68.3	3.4	9.8	95.5	76.0
15.4	47.8	3.6	12.2	94.8	79.0
19.5	44.3	3.7	16.3	93.9	83.0
37.9	68.9	4.1	25.3	91.3	87.5
37.9	54.4	4.7	30.2	90.2	88.5
47.4	61.3	5.0	36.7	88.3	89.8
53.7	61.2	5.6	42.1	86.0	90.1
47.4	34.2	5.9	43.4	84.9	90.5
53.7	36.3	6.7	49.8	83.8	91.3
74.0	61.8	8.2	60.4	79.9	92.9
74.0	39.9	10.8	70.3	76.3	93.7
84.3	61.0	12.2	75.2	74.2	94.7
84.3	31.2	15.8	82.8	66.7	95.2

Total Mixture		Hydrocarbon Layer		Solvent Layer	
Toluene Wt. % (Solvent-free Basis)	NH_3 Wt. %	NH_3 Wt. %	Toluene Wt. % in the Raff. (Solvent-free Basis)	NH_3 Wt. %	Toluene Wt. % in the Ext. (Solvent-free Basis)
91.0	48.2	20.9	87.9	62.3	95.4
91.0	35.4	23.9	90.2	58.2	95.6
93.7	45.1	29.5	92.2	52.6	95.4
Plait Point[c]		45.4	94.8	45.4	94.8
	At 20.0°C				
0.0	—	4.8	0.0	96.9	0.0
8.7	48.3	5.4	6.6	93.8	41.1
19.5	40.1	6.6	16.4	89.7	61.7
28.4	67.1	6.6	17.3	89.3	62.5
29.5	50.3	7.4	22.8	86.4	69.1
29.5	44.0	7.5	24.2	86.0	71.2
37.9	62.1	7.7	25.4	85.6	71.9
49.1	64.0	9.0	32.3	81.6	75.6
37.9	35.1	9.1	33.6	81.5	76.3
49.1	35.0	11.8	44.4	75.8	79.4
59.4	49.3	13.4	49.3	72.3	80.3
59.4	39.2	15.3	53.6	69.4	81.0
70.7	56.3	16.8	56.7	67.2	80.6
70.7	43.4	22.7	64.5	57.8	78.9
74.1	43.3	30.8	69.6	47.5	76.4
Plait Point[c]		43.4	75.0	43.4	75.0

a) This value was calculated from the concentrations of ammonia in both layers and the compositions of the total mixture and raffinate.

b) The upper critical solution temperature for the binary mixtures of toluene and liquid ammonia is −7.4°C. But, since in the equilibrium temperature the change of temperature within ±0.1°C was inevitable, the composition at the critical point were estimated to be the same as the solubility of toluene at −7.5°C.

c) The plait point was estimated according to Treybal et al.[9]

addition to the data at −15° and −7.5°C, the equilibrium data at the temperatures of 0° and 20°C for this ternary system are also given in Table II for convenience of discussion, as these data have not been presented in the previous paper[8]. It is found that in the neighborhood of the critical solution temperature for the binary mixtures of toluene and liquid ammonia, the selectivity[10] of liquid ammonia for toluene which is defined by the difference between the concentration of the solute in the extract, free from the solvent, and the corresponding concentration in the raffinate, is almost unaffected with the change of temperature at the higher concentrations of toluene, but at the lower concentrations of toluene its selectivity increases as the temperature rises to about 0°C. The effect of temperature on the selectivity will be discussed in the later paper.

Discussion

It has already been found that the Hand plot[2] and the Othmer-Tobias plot[11] give a straight line for the data at 20° and 0°C[8], but these plots were unsatisfactory for the data at −7.5° and −15°C, showing the curvature at the higher concentrations of toluene. This can be shown more conveniently by using a notation where E is the solute distributed between the substantially immiscible diluent R and solvent S, and the suffix r and s represent the concentration in the raffinate and the extract layer, respectively. It is clear that good results cannot be obtained for the systems of type 2 by these methods, because the values on the one hand give the definite values in all concentrations of the solute, while, the values on the other hand become infinite at $R=0$ on these coordinates, where a plot of conjugate values of Es/Ss against Er/Rr or $(1-Ss)/Ss$ against $(1-Rr)/Rr$ is made on double logarithmic coordinates.

Brown plot[4] of conjugate values of Rr/Ss against Rr made on arithmetic coordinates, which has been found to be applicable for the systems of type 2, gave lines of considerable curvature for the present data. Both methods of Conway and Philip[5] plotting the conjugate values of log Ss against Rr and Varteressian and Fenske[3] in which the equa-

9) R. E. Treybal, L. D. Weber and J. F. Daley, *Ind. Eng. Chem.*, 38, 817 (1946).

10) K. Ishida, *Sience Repts. Research Inst. Tohoku Univ.*, Ser. A, 5, 377 (1953); *C. A.*, 48, 9045h (1954).

11) D. F. Othmer and P. E. Tobias, ibid., 34, 693 (1942).

tion of distribution ratio may be represented by hyperbola and a straight line results from a plot of Es/Er against Es in the systems of type 2, did not give good results showing large curvature at higher concentrations of toluene.

No satisfactory method giving a straight line by the simple plot for the present data was found in many other previous methods in which a plot of conjugate values of Ss/Rr against Ss proposing by Bachman[12], Smith plot[13] of conjugate values of log (Es/Er) against log Es, Campbell plot[14] of log Es against log Er at equilibrium, and a plot of log $(1-Es)/Es$ against log $(1-Er)/Er$ by Major and Swenson[15] were included.

Of these methods just described, coordinates by Othmer and Tobias and Conway and Philip indicated a relatively good straight line except for the higher concentration of toluene.

The method by Dryden[6] which correlates the concentrations of the solute at equilibrium phases on the solvent free basis, namely a plot of conjugate values of $\{Er/(Er+Rr)\}/\{Es/(Es+Rs)\}$ against $Er/(Er+Rr)$, showed goood results for the data at the temperatures of $-15°$, $-7.5°$ and 0°C, but was unsatisfactroy for the data at 20°C, since the relative distribution ratio was not always constant, as he pointed out.

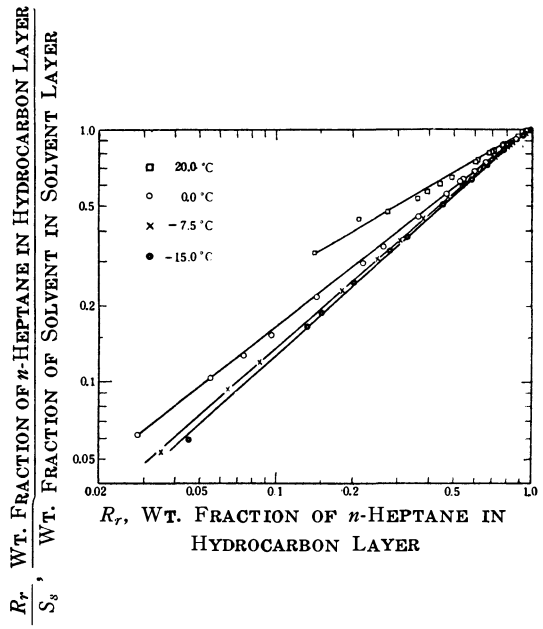

Fig. 3. Plot on logarithmic coordinates of R_r/S_s against R_r for the system *n*-Heptane-Toluene-Liq. NH_3.

12) I. Bachman, ibid., Anal. Ed. **12**, 38 (1940).
13) A. S. Smith. ibid., **42**. 1206 (1950).
14) J. A. Campbell, ibid., **36**, 1158 (1944).
15) C. J. Major and O. J. Swenson, ibid., **38**, 834 (1946).

Tests of these methods for the system *n*-hexane-methylcyclopentane-aniline[7], which is another system investigated at several temperatures neighbouring the critical solution temperature for the binary mixtures of the solute and the solvent, indicated the same results as the present data.

The author has found that a straight line results from a plot of log (Rr/Ss) against log Rr at equilibrium, where Ss is the fraction of the solvent in the solvent phase and Rr is the fraction of the diluent in the diluent phase. Plots by this method for the present data at the various temperatures are shown in Fig. 3, and for the system of *n*-hexane-methylcyclopentane-aniline[7] in Fig. 4. In Fig. 4, plots for the systems using liquid ammonia as a solvent are also included. It is clear that satisfactory results are obtained not only for the systems of type 2, but also type 1. In Fig. 5, several systems investigated by various

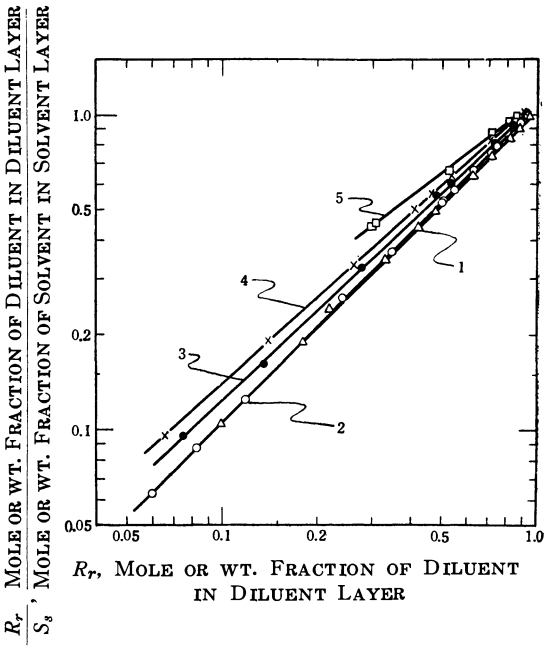

Fig. 4. Plot on logarithmic coordinates R_r/S_s against R_r for the systems *n*-Hexane-Methylcyclopentane-Aniline (3, 4, 5), *n*-Hexane-Cyclohexane-Liq. NH_3 (2) and *n*-Heptane-Octene-1-Liq. NH_3 (1).

Number	System R	System E	System S	Temperature, °C	Reference
1	*n*-Heptane	Octene-1-Liq.	NH_3, wt. fraction.	20.0	(16)
2	*n*-Hexane	Cyclohexane-Liq.	NH_3, wt. fraction.	20.0	(16)
3	*n*-Hexane	Methylcyclopentane	Aniline, mole fraction.	25.0	(7)
4	*n*-Hexane	Methylcyclopentane	Aniline, mole fraction.	34.5	(7)
5	*n*-Hexane	Methylcyclopentane	Aniline, mole fraction.	45.0	(7)

16) K. Ishida, *J. Chem. Soc. Japan*, (Ind. Chem. Sect.,) **57**, 479 (1954).

workers are plotted and plots for systems having the distribution ratio greater than unity are shown in Fig. 6. These systems were selected at random. Among the systems represented by two straight lines changing their slopes, the system water-isopropanol-benzene and the system *n*-heptane-pyridine-liquid ammonia are the instances, in which curves or two straight lines having different slopes have also been obtained by the other methods.

Although plots for all systems do not always give a straight line, the plotted data fall on straight lines almost within their probable experimental accuracy, and especially for the systems containing two pairs of partially miscible liquids fair straight lines are obtained.

The straight lines can be represented by equations of the form

$$\log (Rr/Ss)=n \log Rr+m \quad (1)$$

If the value of n is near unity, letting $m=\log m'$, it follows approximately,

$$Rr/Ss=m'Rr \quad (2)$$

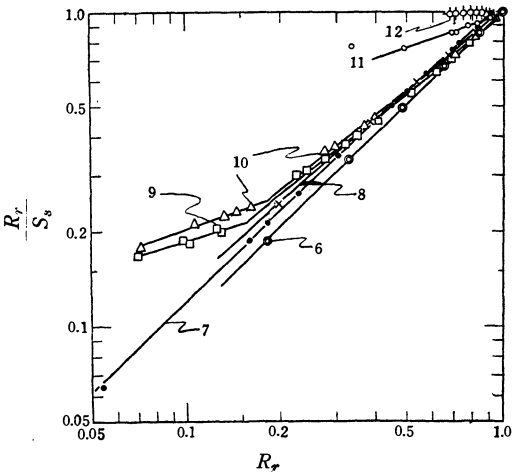

Fig. 5. Plot on logarithmic coordinates of R_r/S_s against R_r for systems of various investigators.

Number	System R	E	S	Temperature, °C	Reference
6	Toluene-	Aniline-	Water	25	(17)
7	*n*-Heptane-	Methylcyclohexane-	Aniline	25.0	(3)
8	1,1,2-Trichloroethane-	Methyl ethyl Ketone-	Water	25	(18)
9	Water-	Acetic acid-	Toluene	25	(19)
10	Water-	Acetic acid-	Benzene	25	(2)
11	Water-	Acetaldehyde-	Toluene	17	(20)
12	Water-	Acetic acid-	Furfural	26.7	(21)

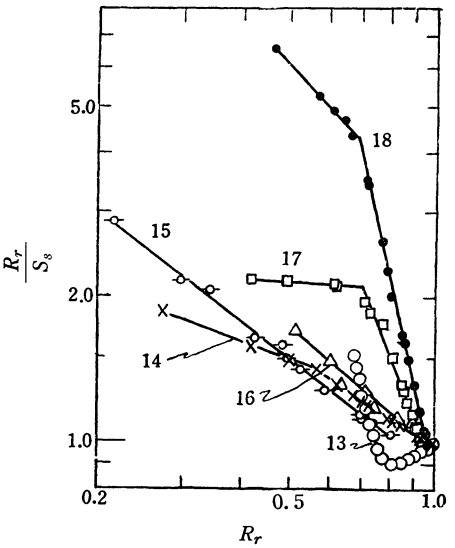

Fig. 6. Plot on logarithmic coordinate of R_r/S_s against R_r for systems having distribution ratio more than unity. (except for No. 16)

Number	System R	E	S	Temperature, °C	Reference
13	Water-	Isopropanol-	Benzene	25.0	(22)
14	Water-	Acetone-	1,1,2-Trichloroethane	25.0	(10)
15	Water-	Dioxane-	Benzene	25.0	(23)
16	Water-	Methanol-	Butanol	0.0	(24)
17	*n*-Heptane-	Pyridine-	Liq. NH_3	20.0	(25)
18	*n*-Heptane-	Pyridine-	Liq. NH_3	0.0	(25)

The method represented by equation 2 is that of Brown[4], of course. Therefore, it is possible to say that the author's method is Brown's generalized. In this plot, it is clear from equation 1 that a straight line will be obtained by using mole fraction on values of Rr and Ss, as well as weight fraction.

In equation 1, m is estimated from the mutual solubilities of R and S. When the same components are used for the diluent and the solvent, there is another possibility that the distribution ratio of the various solutes distributed between the diluent and the solvent can be compared by the values of slope n at the same temperature, since the value of m becomes constant, and distribution curves of the various solutes are given by lines which have various slopes and converge to a point representing the value of m.

If the value of n does not equal unity in equation 1 in all cases, equation 3 can be followed.

$$\log (Ss/Rr)=\{n/(n-1)\} \log Ss+m/(n-1) \quad (3)$$

17) J. C. Smith and R. E. Drexel, *Ind. Eng. Chem.*, **37**, 601 (1945).
18) M. Newman, C. B. Hayworth and R. E. Treybal, ibid., **41**, 2039 (1949).
19) R. M. Woodman, *J. Phys. Chem.*, **30**, 1283 (1926).
20) D. F. Othmer and P. E. Tobias, *Ind. Eng. Chem.*, **34**, 690 (1942).
21) A. E. Skrzec and N. F. Murphy, ibid., **46**, 2245 (1954).
22) A. L. Olsen and E. R. Washburn, *J. Am. Chem. Soc.*, **57**, 303 (1935).
23) R. J. Berndt and C. C. Lynch, ibid., **66**, 282 (1944).
24) A. J. Mueller, L. I. Pugsley and J. B. Ferguson, *J. Phys. Chem.*, **35**, 1314 (1931).
25) K. Ishida, *Bull. Chem. Res. Inst. Non-Aqueous Sol.*, Tohoku Univ., **3**, 109 (1953).

Therefore, it is possible to consider that the author's method is the modification of the Bachman plot, and a plot using equation 3 is also possible. However, the application of equation 3 for the systems containing the formation of two pairs of partially miscible liquids gives lines of curvature which approach the definite values at the infinite, since the value of n in these systems almost equals unity.

It is interesting that the method of Othmer and Tobias and the method presented in this paper are introduced by modifying the method of Bachman.

Summary

The various methods for obtaining straight lines were examined for the tie-line data investigated at several temperatures near the critical solution temperature for binary mixtures of the solute and the solvent, and the following results were obtained.

1. The Hand plot and the Othmer and Tobias plot which are useful for the systems containing one partially miscible pair are unsatisfactory for the systems containing two partially miscible pairs.

2. The method proposed by Brown and the method by Conway and Philip which have been said to be applicable for the systems containing the formation of two pairs of partially miscible liquids do not give good results for the systems at temperatures near the critical solution temperature for binary mixtures of the solute and the solvent.

3. If a plot is made of the logarithm of the ratio of the concentration of the diluent in the diluent phase to the concentration of the solvent in the solvent phase against the logarithm of the concentration of the diluent in the diluent phase, a straight line will be obtained not only for systems containing two partially miscible pairs, but also for systems containing one partially miscible pair.

The experimental expenses were defrayed by the scientific research fund of the Educational Department, to which the author's thanks are due.

The Chemical Research Institute of Non-Aqueous Solutions, Tohoku University, Sendai

Non-Newtonian Viscosity of Dilute High Polymer Solutions. II. Measurements on Polystyrene Fractions in Toluene*

By Toshiaki KUROIWA

(Received September 9, 1956)

Introduction

During recent years it has been recognized by several investigators that the non-Newtonian behavior of polymer solutions can no longer be ignored in the evaluation of the intrinsic viscosity (limiting viscosity number), $[\eta]$, in some cases. As the result, various investigators[1-8] have recently examined the shear-rate dependence of viscosity of dilute polymer solutions and some have proposed the methods of extrapolating the viscosity data to the limit of zero rate of shear.

Most of the empirical equations[9-12] that have been proposed to express the shear dependence of $[\eta]$ or reduced viscosity, η_{sp}/c, show the velocity gradient entering to the first power. For example, Fox, Fox and Flory[9] have proposed the empirical relationship:

$$\ln \eta_{sp} = [\ln \eta_{sp}]_0 - (\phi/100)q, \qquad (1)$$

where $[\ln \eta_{sp}]_0$ is the value of $\ln \eta_{sp}$ at zero rate of shear, ϕ is a constant which is independent of concentration in a given solvent, and q denotes the velocity gradient. These equations are in marked disagreement with the prediction of the theory of Kuhn and Kuhn[13] according to which $[\eta]$ should decrease

* Presented at the 9-th Annual Meeting of the Chemical Society of Japan held in Tokyo, April, 1956.

1) P. Alexander and K. A. Stacey, *Trans. Faraday Soc.*, **51**, 299 (1955).
2) J. Schurz, *Makromol. Chem.*, **12**, 127 (1954).
3) M. A. Golub, *J. Polymer Sci.*, **18**, 27, 156 (1955).
4) F. Patat and J. Hartmann, *Makromol. Chem.*, **18/19**, 422 (1956).
5) T. Hotta, *Chem. High Polymers*, **12**, 276 (1955).
6) M. A. Golub, *J. Phys. Chem.*, **60**, 431 (1956).
7) T. Kuroiwa, This bulletin, **29**, 164 (1956).
8) See also the literatures cited in the previous paper (7) 1—16), 20) for this subject.
9) T. G. Fox, Jr., J. C. Fox and P. J. Flory, *J. Am. Chem. Soc.*, **73**, 1901 (1951).
10) H. T. Hall and R. M. Fuoss, ibid., **73**, 265 (1951).
11) G. de Wind and J. J. Hermans, *Rec. trav. Chim. Pay-Bas*, **70**, 521 (1951).
12) S. Newman, L. Loeb and C. M. Conrad, *J. Polymer Sci.*, **10**, 463 (1953).
13) W. Kuhn and H. Kuhn, *Helv. Chim. Acta*, **28**, 1533 (1945).

initially with q^2, and accordingly $[\eta]$ vs. q curve should have horizontal tangent at $q=0$.

Kuhn and Kuhn[13] have suggested that the non-Newtonian character of polymer solution depends on the ease with which the chain molecule is deformed. Thus for a fairly rigid molecule, since the orientation of the chain molecule in the direction of flow increases as the gradient field increases and since the frictional resistance of the chain decreases with increasing orientation, $[\eta]$ decreases with increasing q. For a completely flexible or soft molecule, on the other hand, which can change its shape in flow and become stretched in the gradient field, $[\eta]$ is independent on q because of the complete compensation of stretching and orientation effects.

The viscous resistance which must be overcome by a force, which tends to change the end-to-end distance of a molecule, consists not only of the usual resistance of the surrounding medium but also of an additional resistivity-the inner viscosity of Kuhn and Kuhn-which is inherent in the molecular chain.

The resistance force due to the inner viscosity, K_2, can be written as follows:

$$K_2=-B\mathrm{d}h/\mathrm{d}t, \tag{2}$$

where h is the end-to-end distance of the molecule, and B may be called "the coefficient of stiffness" of the chain.

These authors have deduced for the limiting case of $B\gg\lambda\eta_0 L$ the following expression[14]:

$$[\eta]_q/[\eta]_0=1-2\xi^2+\frac{473}{16}\xi^4-\cdots\cdots \tag{3}$$

where

$$\xi=q\bar{h}_0^2/16\,D_{\mathrm{rot}}, \tag{3'}$$

and L is the so-called hydrodynamic length, i.e., the fully extended legnth of the chain, η_0 is the solvent viscosity and λ a numerical factor which is approximately equal to $3\pi/16$, $[\eta]_q$ is the intrinsic viscosity at a shear rate q and $[\eta]_0$ is the one at $q=0$, D_{rot} represents the rotational diffusion constant of the chain in the solution and $\bar{h}_0^2$ is the mean square end-to-end distance of the chain at rest. Moreover, it has been shown that the approximate value of ξ for a given polymer can be evaluated according to the equation:

$$\xi=[\eta]_0M\cdot10^3\eta_0q/mRT \tag{4}$$

where M and m are the molecular weight (MW) of the polymer and the monomer, respectively.

14) Kuhn and Kuhn treated the problem only in the two-dimensional motion on the xy-plane. The three dimensional treatment will change the numerical factors but not affect the functional dependence.

Real polymer chains are neither quite stiff nor completely soft, and the dependence of $[\eta]$ on q should lie somewhere between these limiting cases. Furthermore, according to the theory[15], B decreases with MW as $1/M$ owing to the increase of the number of links where a rotation can take place. Hence the shear rate effect should become progressively less pronounced with increasing MW, and this means that $[\eta]_q/[\eta]_0$ vs. ξ curve for real polymer should approach to $[\eta]_q/[\eta]_0=1$ (for $B\ll\lambda\eta_0L$) with increasing MW and to the curve according to Eq. (3) with decreasing MW[16].

In order to determine whether the increase in viscosity persists up to the region of very low rates of shear in accordance with the proposed empirical relations such as Eq. (1) or it vanishes in a range of small q as has been demanded by the theory, most of the existing data are of little avail because they are concerned only with regions of rather high q. It is worthy of notice that a few recent works[1,7,17] in which the measurements have been extended down to very low q appear to show the quadratic dependence of viscocity on q and thus to support the above-mentioned theory[18].

In the present paper the results of measurements on the shear dependences of several polystyrene fractions in toluene are presented and the effect of non-Newtonian behavior on the evaluation of $[\eta]$ and Huggins' slope constant k' are discussed from these data and some remarks are made as to $[\eta]$-MW relationship and the effect of polydispersity of polymer on the shear dependence of viscosity. Finally, a comparison is made between the above-mentioned theory and the results of the present investigation on the basis of $[\eta]_q/[\eta]_0$ vs. ξ relation.

Experimental

The original polystyrene was prepared by polymerizing the pure monomer at 60°C. The procedures for purification of the monomer and for polymerization of the monomer were described in the previous paper[7].

15) W. Kuhn and H. Kuhn, *Helv. Chim. Acta*, **29**, 609 (1946).

16) Of course, in a simple $[\eta]_q/[\eta]_0$ vs. q plot, such a tendency cannot be expected and the variation of $[\eta]_q/[\eta]_0$ with q is larger, the larger the MW is, as has been pointed out several investigators.

17) E. Wada, *J. Sci. Res. Inst.*, **47**, 159 (1953); *J. Polymer Sci.*, **14**, 305 (1954).

18) On the other hand, non-vanishing increase of viscosity at very small q was found to be real for some polymers. From this fact, Schurz has considered that the shear dependence is mainly caused by molecular interactions (formation of temporary structure), and that the contributions of the single molecules only play a role of minor importance. See the literature 19) for the further details.

19) J. Schurz, *Makromol. Chem.*, **10**, 194 (1953).

The fractionation of the polymer was carried out by precipitating the polymer from a mixture: polystyrene-methylethylketone-n-butanol. Methylethylketone was slowly evaporated at constant temperature by suction until precipitation began. The mixture was then heated until the precipitate redissolved and was allowed to stand overnight, after which time a fraction reprecipitated to gel at the original temperature. A fraction separated from the mixture was then dissolved in benzene to make up about 1% solution and reprecipitated in a large excess of methanol. This precipitate was washed with methanol and dried by pumping in vacuum at about 70°C for six hours. 22 fractions were obtained in this way[20].

Molecular weight (*MW*) of the original polymer (*UF*) and the fractions used in this study were determined by light scattering measurements of toluene solutions of these samples[21] and are listed below together with the viscosity data obtained by an Ostwald viscometer.

fraction	$MW\times10^{-4}$	$[\eta]$ (100 cc./g.) in toluene at 30°C	k'
F- 4	410	5.49	0.39
F-10	308	4.53	0.37
F-16	194	3.27	0.34
F-20	100	2.07	0.38
UF	283	4.01	0.33

The apparatus used in this work consists of a manostat system, a manometer and a horizontal viscometer. These were already described in detail in the previous paper[7] together with the experimental procedure employed, and are not repeated here.

The maximum rate of shear at the wall of the capillary was calculated by the equation[22]:

$$q=4Q/\pi R^3 t\times(1-1/4t\times \mathrm{d}(Pt)/\mathrm{d}P), \qquad (5)$$

and the relative viscosity, η_r, which corresponds to the above value of q was evaluated by the equation[22]:

$$\eta_r=t/t_0\times(1-1/4t\times \mathrm{d}(Pt)/\mathrm{d}P)^{-1}, \qquad (6)$$

where R is the radius of the capillary, P is the driving pressure and t and t_0 are the efflux times for a given volume, Q, of the solution and the solvent, respectively.

Results and Discussion

Figs. 1 and 2 show the products of applied pressure and efflux time, Pt, for these fractions, measured at several concentrations at 25°C, plotted against P, where t is the efflux time for unit volume of flow (Pt is nearly proportional to η_r). On casual inspection, the more concentrated the solution, the larger the shear dependence of viscosity. An examination of these results, however, reveals that

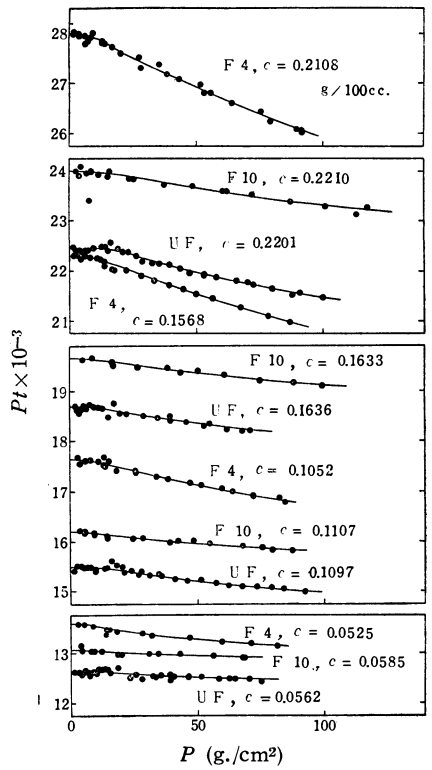

Fig. 1. Product of applied pressure and efflux time for unit volume of flow, Pt vs. applied pressure, P for F 4, F 10 and UF, measured at several concentrations at 25°C by a horizontal viscometer No. 1 (R=0.01440 cm, L=30.3 cm).

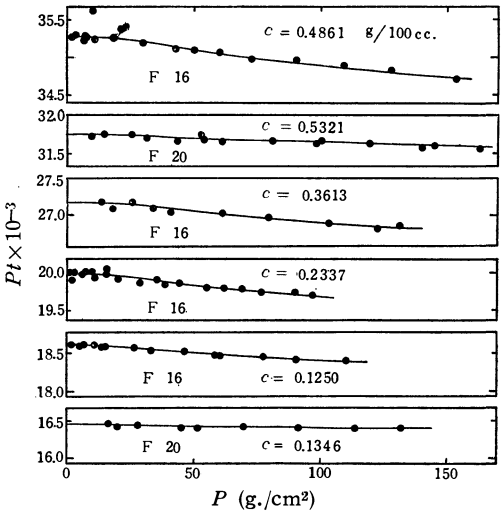

Fig. 2. Product of applied pressure and efflux time for unit volume of flow, Pt vs. applied pressure, P for F 16 and F 20 measured at 25°C. Results for F 16, c=0.1250 and F 20 were obtained by a horizontal viscometer No. 2 (R=0.01362 cm, L=30.1 cm) and the other by a horizontal viscometer No. 1.

20) Details of these procedures were described already in the *Annual Reports of Fiber Science Research Institute* (*Osaka University*), No. 9, p. 30 (1956), by K. Kawahara of this laboratory.

21) This author is indebted to T. Oyama and K. Kawahara of this laboratory for these measurements. Details of these will be published in near future.

22) T. Hotta, *Reports of Laboratory of High Polymer Research, Nagoya University*, No. 3, 22 (1951).

MW of the polymer has the most pronounced effect on degree of shear dependence; for example, the shear effect is quite small in the case of F 20 even when concentration is as high as 0.53%, but it is fairly large for F 4 even when concentration is ten times smaller than that of the solution of F 20.

It may be seem from these figures that these curves have horizontal tangents at the origin instead of showing sharp rises in the neighborhood of zero pressure, although this is somewhat ambiguous for the fractions of low MW owing to the rather large scattering of points in this region. Breadth of initial horizontal part seems to be roughly independent on concentration for a given fraction and it extends toward a high pressure as MW of fraction decreases. The tendency for solution viscosity to be constant at low pressures may be found also in Fig. 3, which

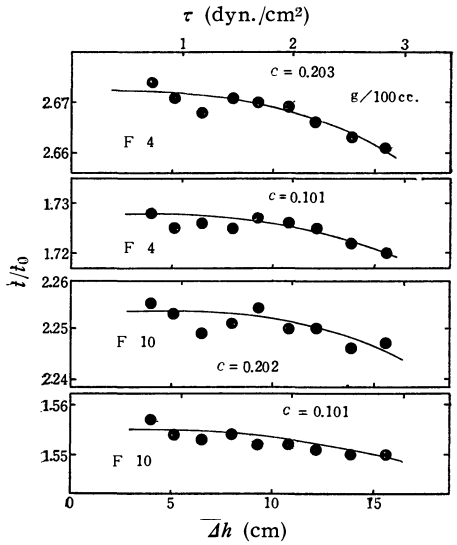

Fig. 3. Ratio of efflux times of solution and solvent, t/t_0, measured at 35°C by a multi-bulb viscometer (see foot-note (23)). $\overline{\Delta h}$ denotes the mean pressure head of the viscometer. For the upper abscissa, τ, see Eq. (7).

shows ratios of efflux times of solution and solvent measured by a specially designed multi-bulb viscometer[23] which is essentially similar to that designed by Schurz[2] as a function of the mean pressure head of the viscometer.

Included in Fig. 1 are the results obtained previously for UF, of which a description was already given in the earlier paper[7]. It is interesting to note that these solutions of UF exhibits the more pronounced shear dependences than the solutions of F 10 despite the fact that the average MW of F 10 is somewhat higher than that of UF and the concentration range covered by these two are approximately equal to each other. The characteristic feature of Pt vs. P relation also seems to be somewhat different between these two. This can be presumably ascribed to the presence of high MW components in UF. In this connection, it is very attractive to compare the shear dependences of viscosities of several solutions at the same concentration, the solute polymers of which are comparable to each other in average MW but different in patterns of MW distribution.

The results of measurements on two kinds of mixtures of two fractions and on single fractions are illustrated in Fig. 4, as Pt vs. P plots and these samples measured are tabulated in Table I. From these results, it

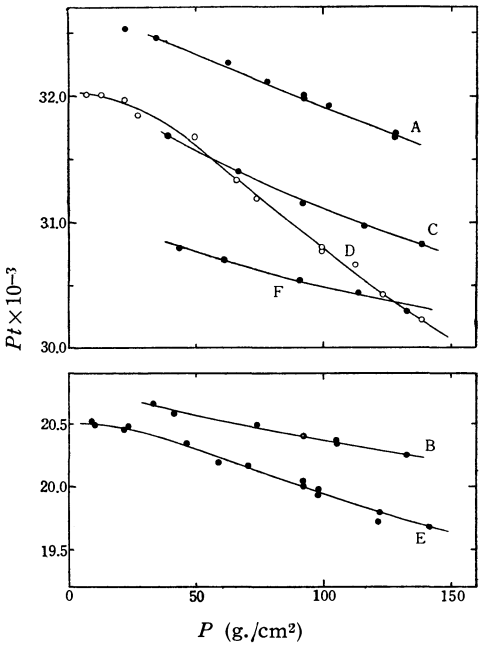

Fig. 4. Product of applied pressure and efflux time for unit volume of flow, Pt vs. applied pressure, P for the solutions shown in Table I, measured at 30°C by the viscometer No. 2 (see foot-note of Fig. 2). For A, B, C etc., see the last column of Table I.

seems that the shear effect should be considered dependent on patterns of MW distribution and is markedly affected by the presence of high MW components in the polymer mixture. This means that it might be possible to find somewhat smaller shear dependences of polystyrens fractions than those found in the present investigation if better fractionated samples were used, and so too quantitatively distinct interpretation of the present

23) The design of the viscometer (R=0.0131 cm, L= 30 cm) and results for the other solutions obtained by the viscometer will be published in this bulletin in near future.

TABLE I

SAMPLES USED IN THE MEASUREMENTS RESULTS OF WHICH ARE SHOWN IN FIG. 3

Sample	Component, Weight%	$[\eta]^a$	Concentration in g./100 cc.	
F- 12	——	3.98	0.3022	A
			0.1510	B
MF-1	F 8 ($[\eta]^a$=4.91), 36.2	3.86[b]	0.3022	C
	F 16 ($[\eta]^a$=3.27), 63.8	(calc'd)		
MF-2	F 4 ($[\eta]^a$=5.49), 52.2	3.85[b]	0.3022	D
	F 20 ($[\eta]^a$=2.07), 47.8	(calc'd)	0.1512	E
F- 13	——	3.76	0.3022	F

a measured by an Ostwald viscometer in toluene at 30°C.

b calculated from $[\eta]$ of each component assuming contribution of components to the viscosity of mixture by their weight fractions.

results must be abandoned.

For each of these solutions, η_r was calculated as a function of q by the use of Eqs. (5) and (6) from the results in Figs. 1 and 2, and from the data for the dimensions of the viscometer. A typical set of η_r vs. q curves for F 4 is shown in Fig. 5. Values of η_{sp}/c were interpolated from these η_r vs. q relations at various q and plotted against the concentration for F 4 and F 10 as shown in Fig. 6.

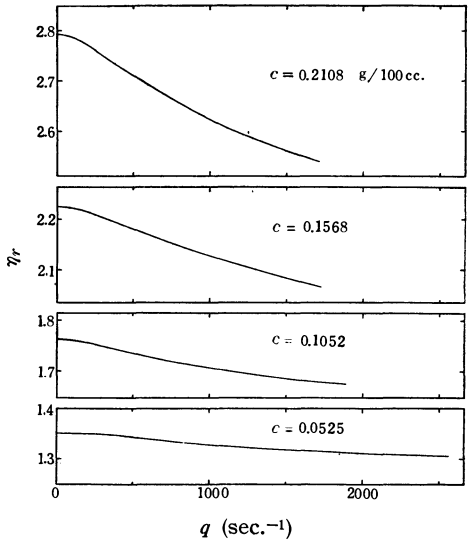

Fig. 5. Relative viscosity, η_r, vs. shear-rate, q, for F 4.

In the usual viscometry carried out by the ordinary Ostwald-type viscometer, measurements are made at constant shearing *stress* rather than at constant q by operating the viscometer at a standard driving pressure[24]. Moreover, it is customary to calculate η_r according to $\eta_r=t/t_0$ which is only the apparent η_r owing to the neglect of the second term in the bracket of Eq. (6). Accordingly, it is

24) Strictly speaking, driving pressure is not constant owing to small differences of densities amongst solutions and solvent.

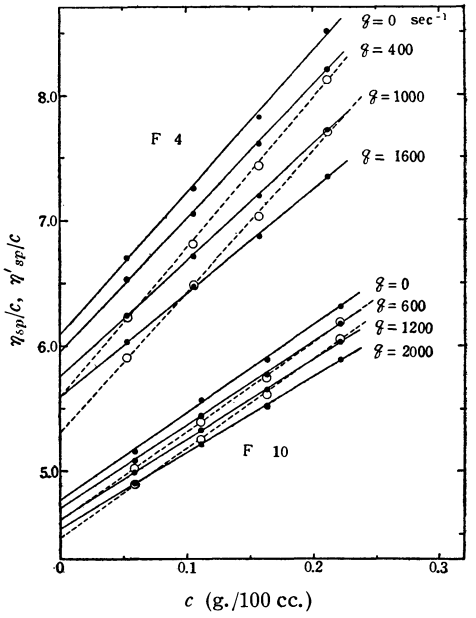

Fig. 6. Iso-shear η_{sp}/c vs. c (—●—) and iso-stress η_{sp}'/c vs. c (- - -○- - -) for F 4 and F 10. The upper iso-stress curve for each fraction is for τ=9.4 dyn./cm² and the lower for τ=18.8 dyn./cm².

pertinent to find η_{sp}/c vs. c relation at constant stress using $\eta_r'=(Pt)/(Pt)_0$ at constant P in order to see the influences of non-Newtonian behavior on the results of the usual viscometry. Some of these curves thus obtained, η_{sr}'/c vs. c, are inserted in Fig. 6 for the convenience of comparison, where shearing stress τ was calculated by the equation:

$$\tau=PR/2L \qquad (7)$$

which is the expression for the maximum stress at the capillary wall.

It can be seen from Fig. 6 that the tangent of iso-stress η_{sp}'/c vs. c curve is always larger than that of iso-shear η_{sp}/c vs. c curve. This means that Huggins' constant k' evaluated

from the data of the usual viscometry is generally greater than that from iso-shear η_{sp}/c vs. c relation except when τ is zero when the shear effect is appreciable. This is merely the natural consequence of the fact that q increases as the concentration of solution is decreased owing to the decrease in viscosity when τ is kept constant.

$[\eta]_q$ and $[\eta]_\tau$, obtained by linear extrapolation of these η_{sp}/c vs. c and η_{sp}'/c vs. c relations respectively to $c=0$, are shown in Fig. 7 as a function of q and τ, respectively.

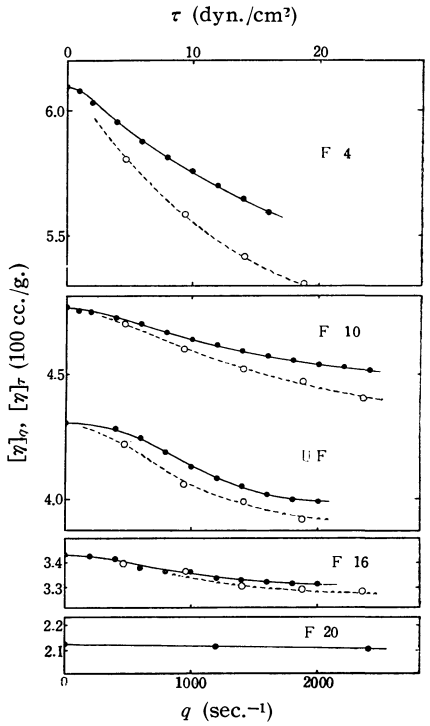

Fig. 7. $[\eta]_q$ vs. q (—●—) and $[\eta]_\tau$ vs. τ (- - -○- - -). For the upper abscissa, τ, see Eq. (7).

It can be easily shown[2] that the dependence of shear-viscosity relation on MW distribution cannot take place if the shear dependence of viscosity is proportional to the first power of MW. Thus the existence of the effect of MW distribution on shear dependence such as has been noted above suggests a non-linear dependence of shear effect on MW, and in fact this seems to be brought out in Fig. 8, which shows $[\eta]_q-[\eta]_0$ and $[\eta]_\tau-[\eta]_0$ as a function of MW for a few values of q and τ.

k'_q and k'_τ, obtained from the slopes of η_{sp}/c vs. c and η'_{sp}/c vs. c curves divided by the square of each intersept, respectively, appear plotted against q and τ, respectively in Fig. 9. Although the uncertainty of k' value is large owing to the sensitiveness of k' to the experimental error, it may be safely concluded

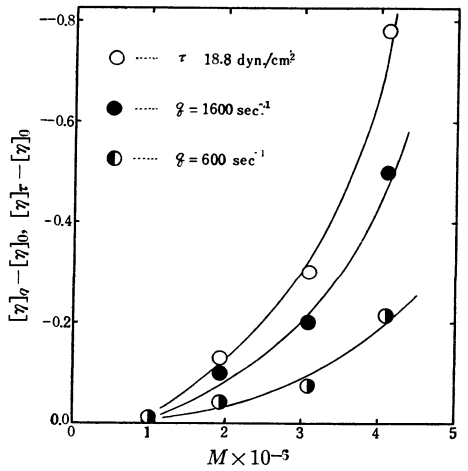

Fig. 8. $[\eta]_q-[\eta]_0$ vs. MW and $[\eta]_\tau-[\eta]_0$ vs. MW.

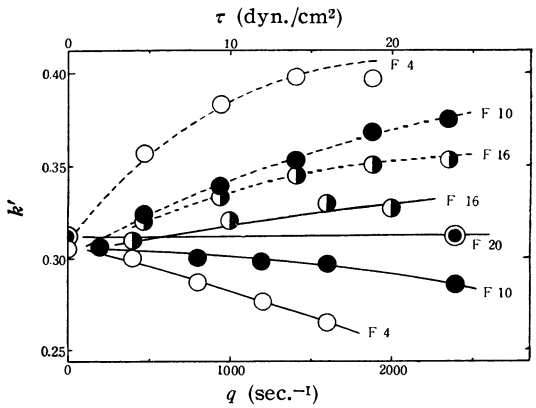

Fig. 9. k'_q vs. q and k'_τ vs. τ. For the upper abscissa, τ, see Eq. (7).

that k'_q decreases to some extent with increasing q while k'_τ increases rather rapidly with increasing τ. A small increase of k'_q with q for F 16 may simply reflect the experimental error. Fig. 10 shows k'_q and k'_τ at some values of q and τ as a function of $[\eta]_0$. It is interesting to note that $k'_{q=0}$ $(=k'_{\tau=0})$ seems to be independent on MW,

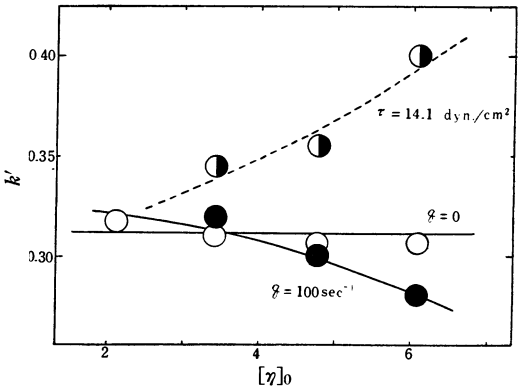

Fig. 10. k'_q vs. $[\eta]_0$ and k'_τ vs. $[\eta]_0$.

while k'_q at finite q decreases slowly and k'_τ at finite τ remarkably increases as MW is increased.

The relations between $[\eta]_\tau$ and MW are shown in log-log plot for $\tau=(q=)0$ and for $\tau=18.8$ dyn./cm^2 in Fig. 11. For the present case, reliable determinations of K and α in $[\eta]=KM^\alpha$ as a function of τ may be hampered by the small number of fractions measured and by the possible effect of MW distribution on shear dependence of $[\eta]$ mentioned above. These results of Fig. 11 may be sufficient only to get a rough idea of the relation between α and τ. The tangents of these two lines drawn in Fig. 11 are 0.74 and

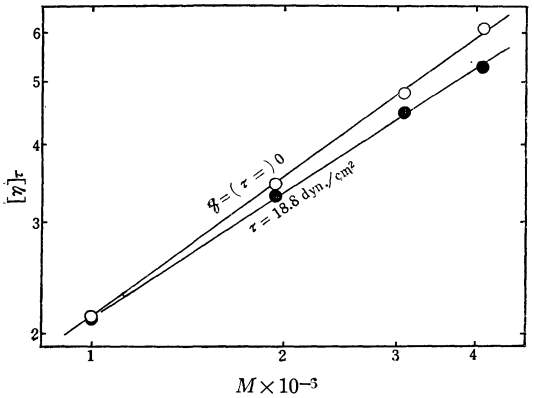

Fig. 11. $\log[\eta]_\tau$ vs. $\log M$.

0.66, respectively.

Turning to the comparison with the theory, $[\eta]_q/[\eta]_0$ of these fractions are plotted against ξ, which was calculated for each fraction by the use of Eq. (4) putting $m=104$ and $\eta_0=0.552\times10^{-2}$ poise, as shown in Fig. 12. The theoretical dependence of $[\eta]_q/[\eta]_0$ for $B\gg\lambda\eta_0L$ as given by Eq. (3) is represented by the broken line in Fig. 12.

As may be seen from Fig. 12, the tendency for $[\eta]_q/[\eta]_0$ vs. ξ relation to approach to the theoretical curve for $B\gg\lambda\eta_0L$ with decreasing MW of the polymer cannot be observed for the present case, which is not in line with what would be expected from the theory of Kuhn and Kuhn mentioned above. This should not seem, however, to be regarded as a conflict with the theory.

Kuhn and Kuhn[25] have suggested on the

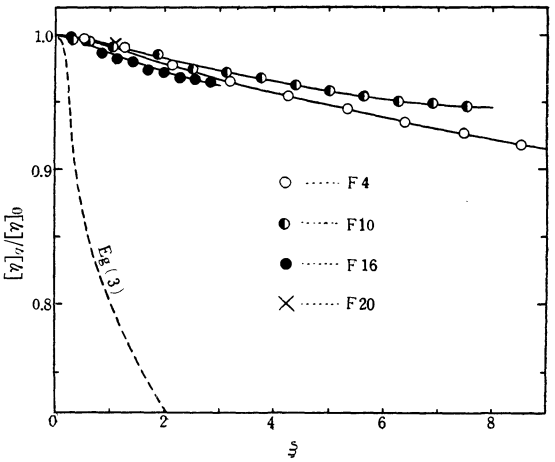

Fig. 12. $[\eta]_q/[\eta]_0$ vs. ξ for the fractions.

basis of the results of streambirefringence measurements by Signer and Gross, that the inner viscosity of a polystyrene molecule is fairly small already at MW of 44×10^4. And in this region of such high MW as have been studied in this work, the inner viscosity may be significantly small as would be expected from the theoretical relation $B\propto1/M$. The same information regarding the stiffness of the polymer molecule may be obtained from the fact that all the experimental curves lie near to the curve $[\eta]_q/[\eta]_0=1$ being apart from the theoretical curves in Fig. 12.

The apparent disaccord with the theory may be merely due to the fact that the further decrease in B with increasing MW from the order of 100×10^4 to higher values can cause only an indistinguishable change in $[\eta]_q/[\eta]_0$ vs. ξ relation within experimental error.

It appears that, in order to make a more critical test of the theory, the similar measurements should be made in the range of lower MW and over a wider range of q or on polymer of more stiff nature.

This author should like to express his gratitude to Prof. S. Murahashi and Prof. S. Akabori of this university for their kind encouragements and to Prof. W. Kuhn of the University of Basel for his kind instruction and information.

The financial asistance of the Tekkōsha Company is also gratefully acknowleged.

Department of Chemistry, Faculty of Science, Osaka University, Osaka

25) W. Kuhn and H. Kuhn, *Ergeb. exakt. Naturwiss.*, **25**, 8 (1951).

Magnetochemical Study of Nitroso Compounds

By Yoshio MATSUNAGA

(Received July 16, 1956)

Introduction

Since the early investigation of Pascal[1], little attention has been paid to the magnitude of diamagnetic susceptibility of nitroso compounds. Pascal treated the nitroso group as equivalent to the carbonyl group, and assigned +3.46[2] for the constant of the oxygen atom in the former group. But his value was supported by measurements on three compounds only, namely nitrosobenzene, N-nitrosopiperidine, and N-nitrosodiethylamine. Since nitroso compounds show deep color and a tendency to form dimer, some authors[3] proposed a triplet structure to the nitroso group. Although Wilson[4] found nitrosobenzene and *p*-nitrosodimethylaniline to be diamagnetic and did not accept the above-mentioned suggestion, he did not give any value of susceptibility of these two compounds. Farquharson[5] examined the susceptibility of nitrosobenzene, as a solid, as a melt and as a solute in benzene and acetic acid. His results showed that this compound is less diamagnetic in a molten or dissolved state than in a solid state.

It seems of interest to measure the susceptibility of some nitroso compounds, both in solid and dissolved states, in order to test the validity of Pascal's constant for the oxygen atom in the nitroso group, and to throw further light on the extraordinary change of diamagnetism found by Farquharson.

Experimental

Materials.—Nitrosobenzene[6], recrystallized from ethanol, m.p. 66–67°C. *p*-Nitrosotoluene[7], from ethanol, m.p. 48.5–49.5°C. *p*-Nitrosodimethylaniline[8], from petroleum ether, m.p. 87.5–88°C. *p*-Nitrosodimethylaniline hydrochloride[8], prepared from purified free base and hydrochloric acid, m.p. 177°C (decomp.). *p*-Nitrosodiethylaniline[9], from petroleum ether, m.p. 87.5°C. *p*-Nitrosonitrobenzene[10] from ethanol, 119–120°C. *m*-Nitrosonitrobenzene[10], from ethanol, m.p. 89–90°C. 2-Methyl-2-nitrosopropane, provided by Dr. F. Iimura, used without further purification. N-Nitrosodiethylamine[11], b.p. 170–170.5°C/756 mmHg. n_D=1.4412 at 13.0°C. N-Nitrosodiphenylamine[12], from ligroin, m.p. 68.5–69.5°C. *p*-Benzoquinone[13], sublimed in vacuum, m.p. 114°C. *p*-Nitrosophenol[14], from toluene, m.p. 124°C (decomp.). α-Naphthoquinone[15], sublimed in vacuum, m.p. 124°C. α-Nitro-α-naphthol[16], from ethanol, m.p. 190°C (decomp.). β-Naphthoquinone, commercial product, used without further purification, m.p. 125–130°C (decomp.). β-Nitroso-α-naphthol[16], from ethanol, m.p. 146–148°C (decomp.). α-Nitroso-β-naphthol[17], from ligroin, m.p. 109°C.

Magnetic Measurement.—The measurements were carried out by the Gouy method as previously described[18], using two specimen tubes, a small one (ca, 0.32 cc.) for solid specimens and a large one (ca. 1.20 cc.) for liquids. For some compounds, the susceptibility was also determined by measuring the susceptibility of the solution, and assuming that the additivity law holds for the constituents of the solution. The following solvents were used for this purpose, acetic acid ($\chi=-0.534$), dioxan (−0.570), toluene (−0.716), and concentrated hydrochloric acid (−0.675).

Results and Discussion

In Table I are presented molecular weight, and specific and molar susceptibilities for the specimens of C- and N-nitroso compounds measured, together with the values calculated by Pascal's constants for the molar susceptibility. In the cases of C-nitroso compound, the observed values of molar susceptibility are in serious disagreement with the calculated ones. For the estimation of constant of the oxygen atom in nitroso group, Pascal used nitrosobenzene alone as an example of this series of compounds, and his value is appreciably less diamagnetic than those presented by Farquharson and by us, therefore the calculated values for C-nitroso compounds have no meaning except for the convenience of the following discussion.

1) P. Pascal, *Bull. soc. chim. France*, **9**, 336 (1911).
2) Susceptibility values have been multiplied by 10^6 throughout this paper.
3) L. Pauling, *J. Am. Chem. Soc.*, **53**, 3225 (1931) and references cited there.
4) E. B. Wilson Jr., ibid., **56**, 747 (1934).
5) J. Farquharson, *Trans. Faraday Soc.*, **32**, 219 (1936).
6) "Organic Syntheses", (1945), **25**, 80.
7) E. Bamberger and A. Rising, *Ann.*, **316**, 257 (1901).
8) A. Baeyer and H. Caro. *Ber.*, **7**, 963 (1874).
9) "Organic Syntheses", Coll. Vol., (1943) **2**, 223.
10) E. Bamberger and R. Hübner, *Ber.*, **36**, 3803 (1903).
11) A. Geuther, *Ann.*, **128**, 151 (1863).
12) E. Fischer' ibid., **190**, 67 (1878).
13) "Organic Syntheses", Coll. Vol., (1948) **1**, 482.
14) J. L. Bridge, *Ann.*, **277**, 79 (1893).
15) C. E. Groves, *J. Chem. Soc.*, **26**, 209 (1873).
16) R. Henriques and M. Ilinski, *Ber.*, **18**, 704 (1885).
17) "Organic Syntheses", Coll. Vol. (1948) **1**, 411.
18) H. Akamatu and Y. Matsunaga, This Bulletin, **26**, 364 (1953).

TABLE I
DIAMAGNETIC SUSCEPTIBILITIES OF NITROSO COMPOUNDS

Substance	M.w.	Suscept. ($-\chi$)	Molar Suscept. ($-\chi_M$)		
			Obs.	Calcd.	Lit
Nitrosobenzene	107	0.552	59.1	54.2	55.0[1] 60.2[5]
p-Nitrosotoluene	121	0.582	70.4	66.1	—
p-Nitrosodimethylaniline	150	0.489	73.3	86.4	—
p-Nitrosodiethylaniline	178	0.520	92.6	110.1	—
p-Nitrosonitrobenzene	152	0.433	65.8	60.5	—
m-Nitrosonitrobenzene	152	0.434	66.0	60.5	—
N-Nitrosodiethylamine	102	0.581	59.3	61.0	60.6[1]
N-Nitrosodiphenylamine	198	0.559	110.7	111.9	—

As it is well known that nitrosobenzene exists as dimeric form in the solid state, the calculated molar susceptibility must be computed for this structure. But the structure of dimeric nitrosobenzene has not been determined yet. Ingold and Piggott[19] and Pauling[3] suggested the structure (I) containing the nitrogen-oxygen ring which is analogous to that of dimeric nitric oxide[20]. On the other hand, the chemical evidence favors the structure in which nitrogen atoms are bound together, and Stewart[21] and Hammick[22] proposed the structures (II) and (III) respectively.

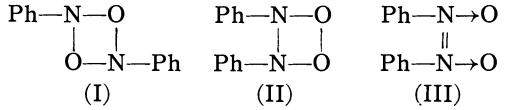

(I) (II) (III)

The same apparent molar susceptibility is computed by Pascal's law to be -58.2 or -60.2 for the structures (I) and (II), using the constitutional correction constant for four-membered carbon ring $+3.05$[23] or $+1.1$[24] instead of the unknown one for nitrogen-oxygen ring. For the structure (III), -59.2 is estimated from the observed value for azobenzene -105.3[25] with the aid of the system of Gray and Cruickshank[26]. All of these calculated molar susceptibilities are in good agreement with the observed one, and we cannot decide the most probable one among these three structures. The differences between the observed and calculated molar susceptibilities of *p*-nitrosotoluene, and *m*- and *p*-nitrosonitrobenzenes can be interpreted similarly, but those of *p*-nitrosodialkylanilines, which are less diamagnetic than the calculated values in contrast with the above-mentioned cases, must be considered further.

In the dissolved state, nitrosobenzene and its derivatives are blue or green, and cryoscopic data[22] show that they exist mainly as monomeric form. As *p*-nitrosodialkylanilines are green even in the solid state, they have certainly the nitroso group which is chromophoric, and the depression of diamagetism may be attributed to this distinctive character. With the purpose of confirming this view we examined the susceptibility of the solution, and the values of these compounds were calculated by the direct application of Wiedemann's additivity law. The results are in Table II, with the calculated molar susceptibilities given by Pascal's constant for nitroso group.

It should be noted that the observed molar susceptibilities are from 10 to 18 units less diamagnetic than the calculated values in all of the C-nitroso compound. The depression is also found in nitrosobutane, and we thus conclude that this depression is attributed to the presence of nitroso group attached to a carbon atom, and its magnitude is affected by the conjugation with aromatic nucleus and the other substituents. Consequently, the magnetic contribution of the nitroso group as a whole in these compounds is paramagnetic of the order of 10 units. In the cases of the N-nitroso compound, the molar susceptibility does not depend on the states, i.e. solid, liquid and dissolved, and they agree with the calculated values within the accuracy of measurements and estimations. From the magnetic standpoint, it is apparent that the nitroso group attached to a nitrogen atom is unlike that attached to a carbon atom.

The paramagnetic contribution of the nitroso group found here is very weak, if we compare it with that found in the substance with a permanent magnetic moment.

19) C. K. Ingold and H. A. Piggott, *J. Chem. Soc.*, **125**, 168 (1924).
20) W. J. Dulmage, E. A. Meyers and W. N. Lipscomb, *J. Chem. Phys.*, **19**, 1432 (1951).
21) Cited in reference 3.
22) D. Ll. Hammick, *J. Chem. Soc.*, **1931**, 3105.
23) J. Farquharson and M. V. C. Sastri, *Trans. Faraday Soc.*, **33**, 1474 (1937).
24) P. Pascal, *Compt. rend.*, **181**, 656 (1925).
25) Y. Matsunaga, This Bulletin, **29**, 308 (1956).
26) F. W. Gray and J. H. Cruickshank, *Trans. Faraday Soc.*, **31**, 1491 (1935).

TABLE II

DIAMAGNETIC SUSCEPTIBILITIES OF NITROSO COMPOUNDS IN THE DISSOLVED STATE

Solute	Solvents*	No. of Detn.	Suscept. ($-\chi$)	Molar Suscept. ($-\chi_M$) Obs.	Calcd.
Nitrosobenzene	A	3	0.372		
	T	2	0.393	41.0	54.2
p-Nitrosotoluene	D	1	0.440		
	T	1	0.435	53.0	66.1
p-Nitrosodimethylaniline	T	2	0.490	73.5	86.4
p-Nitrosodiethylaniline	T	2	0.691	92.4	110.1
2-Methyl-2-nitrosopropane (Nitrosobutane)	D	1	0.489	42.5	52.5
N-Nitrosodiethylamine	D	1	0.569		
	T	1	0.587	59.0	61.0
N-Nitrosodiphenylamine	D	1	0.545		
	T	1	0.566	110	111.9

* A: acetic acid. D: dioxan. T: toluene.

Therefore, if we assume that the apparent difference is due to the partial compensation of diamagnetism by the paramagnetic contribution of triplet state, the molecule may be excited at the rate of the order of one thousandth. This assumption seems to be improbable for the following two reasons. In the first place, the excitation energy expected from the magnetic data is about 7 kcal. mol.$^{-1}$, and this is only one fifth of that suggested from the spectroscopic data[27]. In the second, the state of the substance may somewhat affect the magnitude of the excitation energy, and also the apparent paramagnetic contribution of the nitroso group. But *p*-nitrosodialkylanilines do not show such a tendency[28]. In another explanation of the contribution of the nitroso group, we must consult Van Vleck's equation[29] for the molar susceptibility of a polyatomic molecule with no resultant electron spin moment, namely,

$$\chi_M = -\frac{Ne^2}{6mc^2}\sum r^2 + \frac{2}{3}N\sum_{n'\neq n}\frac{|m^0(n';n)|^2}{h\nu(n';n)}$$

where $m^0(n';n)$ is a non-diagonal element of the matrix for the angular momentum of the system, $\nu(n';n)$ is the frequency corresponding to $n';n$ transition, and the other terms have their usual physical significance. If the second term is dominant in the nitroso group, the magnetic contribution of this group as a whole may be feebly paramagnetic and independent of temperature. Such examples are not rare in inorganic compounds, but in organic compounds, the second term is usually smaller than the first one, and the case found here is very striking. However, we wish to emphasize that there is no essential difference between diamagnetism and temperature-independent paramagnetism, and the sign of the susceptibility depends only on the magnitude of these two terms.

TABLE III

DIAMAGNETIC SUSCEPTIBILITIES OF QUINONES AND THEIR MONOXIMES

Substance*	M. w.	Suscept. ($-\chi$)	Molar Suscept. ($-\chi_M$) Obs.	Diff**	Lit.
p-Benzoquinone	108	0.355	38.4	—	41.3[30], 40.0[31], 38.2[32], 34.4[33]
p-Nitrosophenol	123	0.412	50.7	12.3	50.3[31]
α-Naphthoquinone	158	0.465	73.5	—	73.8[21], 73.0[33],
α-Nitroso-α-naphthol	173	0.530	91.8	18.3	—
β-Naphthoquinone	158	0.430	67.9	—	—
β-Nitroso-α-naphthol	173	0.478	82.7	14.8	—
α-Nitroso-β-naphthol	173	0.485	83.9	16.0	—

* Monoximes are indicated by the name of isomeric nitrosophenol.

** Monoxime (obs.) −Quinone (obs.).

27) G. N. Lewis and M. Kasha, *J. Am. Chem. Soc.*, **67**, 994 (1945).

28) The validity of this assumption was completely denied. According to Dr. I. Miyashita, Hokkaido University, *p*-nitrosodialkylanilines do not show paramagnetic absorption (private communication).

29) J. H. Van Vleck, "Theory of Electric and Magnetic Susceptibilities", Oxford University Press, Oxford (1932), p. 275.

30) P. Pascal, *Bull. soc. chim. France*, **9**, 177 (1911).

31) K. S. Krishnan and S. Banerjee, *Phil. Trans. Roy. Soc.*, **A234**, 265 (1935).

32) H. Mikhail and F. G. Baddar, *J. Chem. Soc.*, **1944**, 590.

33) E. D. Bergmann et al., *J. chim. phys.*, **49**, 474 (1952).

Pascal concluded that nitrosophenol exists as quinone monoxime in the crystal, comparing its molar susceptibility to the calculated value using his own constants. However, as already shown, owing to the paramagnetic contribution of nitroso group it seems to be difficult to decide whether the magnitude of molar susceptibility favors the quinone monoxime form. We measured also some of quinone monoxime, and the values are compared with those of the parent quinones. The results are presented in Table III. The values of the molar susceptibility increment associated with the transition $>C=O \rightarrow >C=N-OH$ markedly depend on the nature of the rest of the molecule, and they are more diamagnetic than those found in the aliphatic series which were reported as from 7.4 to 11.7 units[34]. Hence it appears that the oxime group cannot localize π-electrons in the aromatic nucleus so strongly as carbonyl group, and the evaluation of the molar susceptibility of quinone monoxime by a set of constants is difficult.

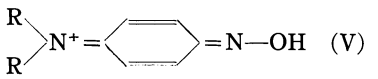

The possible other structure is (V), in which the hydrogen ion is attached to the oxygen atom in the nitroso group. The expected values for this stucture are somewhat obscure, because the most similar compound the susceptibility of which is known is quinone monoxime, and the substitution of carbonyl group by $>C=NR_2$ may affect the degree of localization of aromatic electrons. If the transition $>C=O \rightarrow >C=NR_2$ does not affect the magnetic contribution of aromatic electrons, the value B_1 may be expected, and if the delocalization occurs in this transition again to a similar extent to that found in the transition from quinone to its monoxime, the value B_2 may be expected. The observed values are in the expected ranges, and seem to be consistent with the structure (V).

Summary

The magnetic susceptibility of nine nitroso compounds, as solids and as solutes, were measured by the Gouy method. The constant for the nitroso group attached to a carbon atom was found to be paramagnetic of the order of 10 units. The author suggested that the second term in Van Vleck's equation for the diamagnetism of a molecule is dominant in this case. Some quinones and their monoximes were also measured, and it appeared that the ability of the oxime group to localize aromatic electrons is less than that of the carbonyl group. In addition, the structure of nitrosodialkylaniline hydrochloride was discussed from the magnetic standpoint.

TABLE IV

DIAMAGNETIC SUSCEPTIBILITIES OF *p*-NITROSODIALKYLANILINE HYDROCHLORIDES

Ion	Obs. (Molar Suscept. $(-\chi_M)$)	Calcd.			
		A_1	A_2	B_1	B_2
p-Nitrosodimethylaniline+H^+	79.9*	73.9	93.0	77.0	82.7
p-Nitrosodiethylaniline+H^+	101**	93.2	116.7	100.7	106.4

* Hydrochloride (103.3) −Chloride ion (23.4)[35].

** Apparent susceptibility of free base in hydrochloric acid solution.

Nitrosodialkylanilines form the salts with inorganic acids, and the color change from green to yellow suggests the disappearence of the distinctive nature of the nitroso group. In order to elucidate the structure of the cation, we examined their susceptibilities measuring the susceptibility of the crystalline salt or the hydrochloric acid solution. The observed values shown in Table IV will be compared with the calculated values of some of the models of the cation. The value A_1 is for the monomeric anilinium ion (IV), and the value A_2 for the dimer. However, the former computed on the basis of the observed susceptibility for the free base is too small and the latter given by Pascal's law is too large.

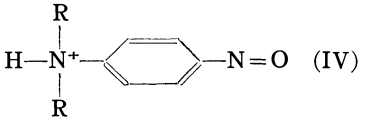

The author wishes to express his hearty thanks to Prof. H. Akamatu for his kind direction, and to the late Dr. F. Iimura for a sample of nitrosobutane. The cost of this study has been defrayed from the Grant in Aid for Scientific Research from the Ministry of Education, to which the author's thanks are also due.

Department of Chemistry, Faculty of Science, The University of Tokyo
Tokyo

34) C. M. French and D. Harrison, *J. Chem. Soc.*, 1955, 3513.

35) V. C. G. Trew, *Trans. Faraday Soc.*, 37 476 (1941).

The Action of Hydrogen Bromide and Oxygen on Various Ethenoid Compounds. II[1]

By Makoto TAKAHASI

(Received August 9, 1956)

The mechanism of the reactions of the mixture of hydrogen bromide and oxygen with various ethenoid compound has been studied by many workers, and its main character has been elucidated as follows:

(1) $\rangle C=C\langle + O_2 + HBr \longrightarrow Br\cdot$ (initiation)

(2) $\rangle C=C\langle + Br\cdot \longrightarrow \rangle \underset{\cdot}{C}-C(Br)\langle$ (propagation)

(3) $\rangle \underset{\cdot}{C}-C(Br)\langle + O_2 \longrightarrow \rangle C(O_2\cdot)-C(Br)\langle$ (propagation)

(4) $\rangle C(O_2\cdot)-C(Br)\langle + HBr \longrightarrow \rangle C(HO_2)-C(Br)\langle + Br\cdot$ (propagation)

(5) $\rangle C(HO_2)-C(Br)\langle + HBr \longrightarrow$ inert product $+ Br\cdot$ (propagation)

(6) $Br\cdot + Br\cdot \longrightarrow Br_2$ (termination)

(7) $\rangle \underset{\cdot}{C}-C(Br)\langle + Br\cdot \longrightarrow \rangle C(Br)-C(Br)\langle$ (termination)

Although the mechanism of the abnormal addition of hydrogen bromide to ethenoid compounds has been established by several workers, the oxidation reaction of ethenoid compounds with oxygen in the presence of hydrogen bromide has not yet been completely elucidated. The mechanism represented above involves several problems to be solved:

(1) The initiation process has been assumed to start by the interaction of an ethenoid compound with hydrogen bromide and oxygen, but it does not mean that a triple collision takes place actually. The process may be composed of at least two steps, but it is not yet determined whether oxygen reacts first with the ethenoid compound and then with hydrogen bromide or vice versa. Consideration of the autoxidation reaction of ethenoid compounds (in the absence of hydrogen bromide) leads to an assumption that oxygen reacts first with the ethenoid compound. But the mechanism of the initiation reaction of autoxidation itself is not clearly known in spite of many discussions. L. Bateman[2] pointed out that the direct olefin-oxygen reaction is so slow that it cannot be hoped that examination of the oxidation product may provide any information on any non-hydroperoxide initiation in the absence of a large amount of inhibitors. The situation, however, is here a little different, because many olefins investigated by the present author have no α-methylene group, so that the oxygen molecule acts on π-electrons of the double bond. Moreover, if the initiation reaction and the propagation reaction give different kinds of products (and the latter a large amount), they may be distinguished by an appropriate analytical method. It is also possible that the ethenoid compound reacts first with hydrogen bromide to form a loose molecular complex, because hydrogen bromide increases the solubility of ethenoid compounds in solvents such as benzene and carbon tetrachloride and there is certain evidence for the formation of complex compounds from aromatic compounds and hydrogen chloride[3].

The formation of small amounts of carbon dioxide and diphenylbromomethane in the reaction of diphenylethylene with hydrogen bromide and oxygen appears to be helpful to the elucidation of the reaction of ethenoid compounds with hydrogen bromide and oxygen. The three following ways of explanation may be possible for the mechanism of the formation of carbon dioxide and diphenylbromomethane. (a) Carbon dioxide and diphenylbromomethane may be formed by an initiation reaction, but not by a propagation reaction. If it is the case, oxygen acts first on the β-carbon atom of diphenylethylene to give $Ph_2\underset{\cdot}{C}-CH_2(O_2\cdot)$ rather than on the α-carbon atom to give $Ph-C(O_2\cdot)-\underset{\cdot}{C}H_2$, and the reaction proceeds in the following way:

1) Part I, This Bulletin, **29**, 625 (1956).

2) L. Bateman, *Quart. Rev.* VIII, 147, (1954).

3) H. C. Brown and J. D. Brady, *J. Am. Chem. Soc.*, **74**, 3572 (1952).

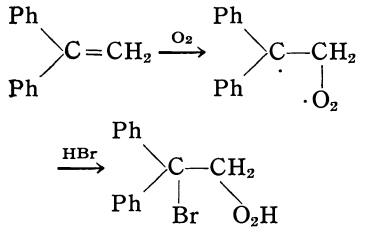

The bromohydroperoxide may decompose to carbon dioxide and diphenylbromomethane through a not yet characterized process in the presence of oxygen and hydrogen bromide. (b) The products are produced by the initiation process as above. But the olefin may form an intermediate complex with oxygen*, and then the complex reacts with hydrogen bromide:

$$Ph_2C=CH_2 \xrightarrow{O_2} O_2\text{-Complex} \xrightarrow{HBr} Ph_2C(Br)-CH_2(O_2H)$$

(c) An alternative assumption might be that these products were produced by a propagation reaction, but it is probably far from the fact because diphenylethylene adds the bromine atom at the β-carbon atom more rapidly than at the α-carbon atom due to the stability of $Ph_2\dot{C}-CH_2Br$ greater than that of $Ph_2BrC-\dot{C}H_2$. The formation of ω-bromoacetophenone and a phenolic compound in relatively large amounts in the reaction may be explained by assuming a propagation reaction as follows:

$$Ph_2C=CH_2 \xrightarrow{Br\cdot} Ph_2\dot{C}-CH_2Br$$

$$\xrightarrow{O_2} Ph_2C(\cdot O_2)-CH_2Br \xrightarrow{HBr} Ph_2C(HO_2)-CH_2Br$$

$$\longrightarrow PhC(=O)-CH_2Br + PhOH.$$

The author considers that the assumptions (a) and (b) are more probable than (c). The decomposition of hydroperoxides (e.g. $Ph_2C(HO_2)-CH_2Br$) by hydrogen bromide has not been studied in detail until the present, but it may probably proceed through an acid catalysed mechanism, as suggested by F. F. Rust and W. E. Vaughan[4]. The formation of phenolic substances from diphenylethylene and from styrene is explained by this mechanism.

(2) It is impossible to establish completely the scheme of the propagation, chain transfer and termination reactions from the result of the yield of the final products, because the velocity constants of the following most probable competitive processes have not yet been estimated in any case:

(1) $\dot{C}-CH_2Br + O_2 \xrightarrow{K_{O_2}} C(\cdot O_2)-CH_2Br$

(2) $\dot{C}-CH_2Br + HBr \xrightarrow{K_{HBr}} C(H)-CH_2Br + Br\cdot$

(3) $\dot{C}-CH_2Br + Br\cdot \xrightarrow{K_{Br\cdot}} C(Br)-CH_2Br$

(4) $\dot{C}-CH_2Br + Br_2 \xrightarrow{K_{Br_2}} C(Br)-CH_2Br + Br\cdot$

(5) $\dot{C}-CH_2Br + \cdot OH \xrightarrow{K_{OH\cdot}} C(HO)-CH_2Br$

Generally. the velocity constants of the recombination reactions of the free radical with the bromine atom (3) and with the free hydroxyl radical (5) may be far greater than those of the reactions of the free radical with molecular oxygen (1), with hydrogen bromide (2), and with bromine molecule (4), unless some steric effect modifies the velocity constants, but the concentrations of the bromine atom and of the free hydroxyl radical may be far smaller than those of oxygen, hydrogen bromide and molecular bromine. Although atropic acid gives a large amount of α-hydroxy-β-bromohydratropic acid, it is improbable from the reason stated below that the product is yielded by the reaction of free radical $Ph\dot{C}(COOH)-CH_2Br$ with free hydroxyl radical. A comparison of the velocity constants of the reactions (1), (2) and (3) is also impossible now. It seems probable that the reactivity of the free radical with hydrogen bromide depends upon the stability of the free radical, and that the velocity constant K_{O_2} is in general greater than K_{HBr}, considering that many compounds such as cinnamic acid, atropic acid, and diphenylethylene, which give free radicals stabilized by conjugation, give various oxygenated compounds but not hydrogen bromide adducts in spite of the presence of a large amount of hydrogen bromide. The comparison of the velocity constants K_{O_2} and K_{HBr} has an important meaning in considering the reaction mechanism discussed here. It is known that the bromine addition reaction of cinnamic acid is inhibited by the presence of oxygen,

* There is an indication that aromatic compounds form complex compounds with oxygen. D. F. Evans, *J. Chem. Soc.*, 1953, 345.

4) R. R. Rust and W. E. Vaughan, *Ind. Eng. Chem.*, **41**., 2595 (1949).

but the inhibition seems not to be serious according to our experiment described in the next paper.

In the previous paper[1] the author emphasized the significance of the material balance in order to discuss the reaction mechanism. Unfortunately, in many cases of the reactions discussed by the author such as those of crotonic acid, diphenylethylene and stilbene, the reaction mixtures are composed of several compounds, which are relatively labile to chromatography, recrystallization and distillation, so that the establishment of the material balance is unsuccessful. Fortunately, in the reaction of atropic acid with hydrogen bromide and oxygen, α-hydroxy-β-bromohydratropic acid (the determination of the structure of the acid is described in the experimental part) was obtained in about 77 mole percent yield of atropic acid. In addition to this a very small amount of ω,ω-dibromoacetophenone and carbon dioxide and bromine were obtained. These products may be derived by the initiation reaction or a side reaction, but the details of the mechanism is not clear. Atropic acid which gives neither a hydrogen bromide adduct nor atropic acid dibromide is clearly distinguished from cinnamic acid giving more than fifty mole percent of cinnamic acid dibromide and about 25 mole percent of ω-bromoacetophenone under the same conditions. If α-hydroxy-β-bromohydratropic acid was formed by the following process,

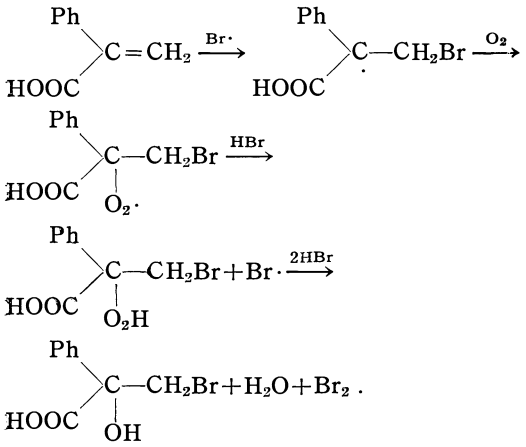

bromine should be produced in moles equal to α-hydroxy-β-bromohydratropic acid, but actually only a small amount of free bromine, no appreciable amount of water, and no atropic acid dibromide is found in the reaction products. The necessary condition in considering the reaction mechanism is that the atom which adds first to double bond should attack the β-carbon atom of atropic acid, but not the α-carbon atom, because of the greater stability of the free radical formed. Then the following may be a possible mechanism, which involves no cyclic chain propagation:

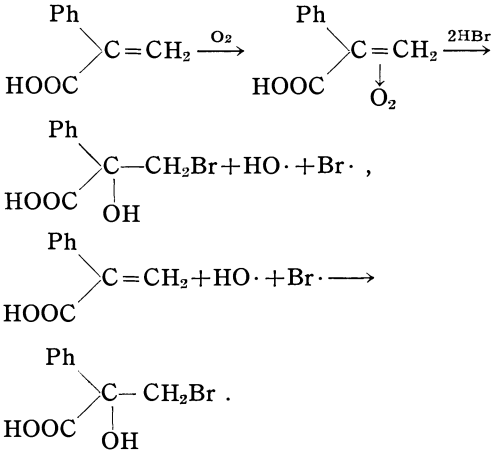

The problem, however, will be left unsolved until a kinetic study of these reactions is possible.

G. Merling[5] asserted, that atropic acid gave β-bromohydratropic acid with hydrobromic acid, while α-bromohydratropic acid was obtained when dry hydrogen bromide was passed through a benzene solution of atropic acid. If such a reversal of the direction of addition of hydrogen bromide to atropic acid should take place, it could not be explained on the grounds of the formation of the more stable free radical in the of reaction of bromine atom with the olefinic compound, because

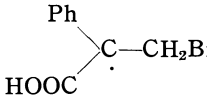

the radical would be more

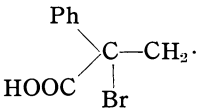

stable than the other radical

The author investigated the addition of hydrogen bromide to atropic acid both under oxydant and anti-oxydant conditions, but no reversal was observed.

Experimental

Materials.—Hydrogen bromide and oxygen were prepared and purified as described in the previous paper[1]. Diphenylethylene was prepared from bromobenzene and ethyl acetate according to Org. Syntheses[3], b. p. 123–5°C/mmHg, $n_D^{19.0}$ 1.6084, $n_D^{9.6°}$ 1.6135. Atropic acid was prepared by the hydrolysis of acetophenone cyanohydrin and recrystallized from benzene, m. p. 106°C. Styrene, a

5) G. Merling, *Ann.*, **209**, 1 (1881).
6) "Organic Syntheses", Collective Vol. I, John Wiley & Sons, Inc., p. 221.

commercial product, was washed with alkaline water, dried with calcium chloride and distilled under reduced pressure with a fractionation column.

Reaction of Diphenylethylene with Hydrogen Bromide and Oxygen.—The mixture of hydrogen bromide and oxygen was passed into a solution of diphenylethylene in benzene or in carbon tetrachloride for several hours. The results of experiments under various conditions are summarized in Table I and details will be described below. a) Identification of diphenylbromomethane. The reaction mixture of Exp. 1. was washed with water, and dried with anhydrous sodium sulfate. When benzene was removed by distillation, a light yellow oil was obtained. The oil was heated with a few ml. of water in a sealed tube at 150°C for about four hours. After cooling, the sealed tube was opened, and a mixture of an oil and a crystalline mass was obtained. The crystalline mass was separated and recrystallized from petroleum ether, m. p. 120°C. It contained no bromine and was identified as dibenzhydrylether $((C_6H_5)_2CH)_2O$ by a mixed melting point. The authentic dibenzhydrylether was synthesized from diphenylbromomethane by heating it with water in the same way. An attempted separation of diphenylbromomethane itself in Expt. 6 by distillation under reduced pressure was rendered unsuccessful by the presence of a large amount of unchanged diphenylethylene. b) Identification of ω-bromoacetophenone. In Expt. 5 the oil was kept in an electric refrigerator, giving a mixture of an oil and a crystalline mass. The crystalline mass was separated on a glassfilter, and weighed about 0.4 g., m. p. 52°C., and it was identified as ω-bromoacetophenone, by a mixed melting point and by the preparation of 2, 4-dinitrophenylhydrazone, m. p. 214–216°C. d) Identification of phenol. When the reaction mixture was shaken with water or alkaline water, and a bromine-potassium bromide solution was added to the aqueous extract, tribromophenol was precipitated. Furthermore, when the alkaline extract was saturated with carbon dioxide and extracted with ether, about 2 g. of a phenolic oil were obtained. From the oil about 1.45 g. of phenyl benzoate was obtained by treating it with benzoyl chloride (Expt. 7). Unfortunately, the separation of these products from the reaction mixture of one experiment using 10 g. of diphenylethylene was unsuccessful. When 10 g. of diphenylethylene were used, the feature of the reaction was a little different. (Expt. 6 and 7) The amount of carbon dioxide was nearly in the same order. When the carbon tetrachloride solution was shaken with 1 N NaOH solution once and with 100 ml. of distilled water dried with anhydrous sodium sulfate, and distilled under reduced pressure, it gave the three following fractions, b.p. 82–85°C/0.9 mmHg, and 100°C/1 mmHg and the residue. The first fraction ($n_D^{9.5°}$ 1.6182) contained no bromine and was found to be mainly composed of unchanged diphenylethylene, ($n_D^{9.5°}$ 1.6135). The second fraction solidified and was recrystallized from petroleum ether, m. p. 38°C.

Anal. Found: Br, 30.9. Calcd. for $(C_6H_5)_2CCHBr$: Br, 30.9%.

These results suggest that a large amount of diphenylethylene does not react with the mixture of hydrogen bromide and oxygen due to the accumulation of a phenolic substance in the reaction mixture. β-Bromodiphenylethylene may be derived from α, β-dibromodiphenylethane during distillation, for the latter is very sensitive to heat.

Reaction of Atropic Acid with Hydrogen Bromide and Oxygen.—Experimental results are summarized in Table II. Expt. 59 was carried out as following: Atropic acid (5 g., 0.034 mol.) was dissolved in 50 ml. of carbon tetrachloride and the mixture of hydrogen bromide and oxygen was passed into the solution for 300 min. at room temperature. The solution turned red during the reaction. It was kept over-night in an electric refrigerator, giving 2 g. of a crystalline mass, which was recrystallized from benzene to colorless crystals, m. p. 115°C. The substance was acidic, and found to be α-hydroxy-β-bromohydratopic acid as described below.

The carbon tetrachloride solution was washed twice with distilled water, and the aqueous solution was extracted with ether. The ethereal extract gave about 2 g. of the same acid, m. p.

TABLE I

THE REACTION OF DIPHENYLETHYLENE WITH HYDROGEN BROMIDE AND OXYGEN

No.	Diphenylethylene g. (mol.)	Solvent ml.	Reagents	Time Min.	Products: CO_2 mm. mol.	Ph_2CHBr	$PhCOCH_2Br$	PhOH mm. mol.	Ph_2CBrCH_2Br	$Ph_2C=CH_2$
1	2(0.011)	Benzene 70	$HBr+O_2$	180	0.9	+	Not investigated	Not investigated	?	?
2	2	〃 30	〃	70	0.7		Purification unsuccessful			
3	2	〃 30	〃	105	0.8	+	?	?	?	?
5	3.51(0.0195)	〃 40	〃	100	0.6	?	?	5	?	+
6	10(0.0056)	CCl_4 70	〃	215	0.6	?	?	6	?	+
7	10	〃 70	〃	360	0.8	?	?	7	+	+

"?" Means that its existence was not ascertained, but it is most probable.
"+" Means that its existence was ascertained qualitatively.
"−" Means that its absence was ascertained.

TABLE II

THE REACTION OF ATROPIC ACID WITH HYDROGEN BROMIDE AND OXYGEN

No.	Atropic Acid, g. mol.	Solvent, ml.	Reagent	Reaction Time Min.	Products: CO_2 mm mol.	Br_2 mm mol.	$PhCCH_2Br$ (HOOC, OH) mm mol.	$PhCHCH_2Br$ (HOOC) mm mol.	$PhCOCHBr_2$
48	1	CCl_4 30	$HBr+O_2$	230	1.3				
52	1.5 (0.01)	〃 30	N_2 HBr	60 290	None			6.5	
53	1.5	〃 30	Benzoyl Peroxide, 30 mg. HBr	295	〃			5.7	
55	5.00 (0.034)	〃 50	$HBr+O_2$	325	5.3	1.45	18		+
58	〃	〃 50	〃	300	3.5		19		+
59	〃	〃 50	〃	300	3.4	0.25	25		+
56	0.2	Benzene 20	(O_2 for a short time) HBr	180	—	—	—	Oily product	
57	0.2	〃 30	HBr Catechol 10 mg.	195	—	—	—	+	

115°C. The carbon tetrachloride solution was then shaken twice with 50 ml. of 1 N aqueous sodium hydroxide, and the alkaline solution was acidified with hydrochloric acid and extracted with ether. The ethereal extract gave about 0.9 g. of the same acid. Thus about 6.1 g. (0.026 mol. as calculated for α-hydroxy-β-bromohydratropic acid) of the acid, m. p. 115°C, was obtained from 5 g. (0.034 mol.) of atropic acid. The carbon tetrachloride solution was then dried with anhydrous sodium sulfate, and evaporated under reduced pressure, when a small amount of a precipitate and 0.94 g. of an oil were left. The oil (0.78 g. of the oil in ethyl alcohol) and 2,4-dinitrophenylhydrazine gave a precipitate weighing 0.377 g. It was separated into parts soluble and insoluble in hot chloroform. The former was a yellow crystalline substance, which melted at 178–180°C after one recrystallization from chloroform.

Anal. Found: C, 38.27; H, 2.51; N, 12.7; Br, 33.5. Calcd. for $C_{14}H_{10}O_4Br_2$: C, 36.71; H, 2.20; N, 12.2; Br, 34.9%.

The latter was an orange crystal, insoluble in any solvents available, contained no bromine, and melted at about 200°C. Its amount was very small, so that its identification was unsuccessful. ω,ω-Dibromoacetophenone itself also gave two species of products with 2,4-dinitrophenylhydrazine, which appeared to be the same substances as those obtained above. The 2,4-dinitrophenylhydrazone, m. p. 178–180°C was identified with the 2,4-dinitrophenylhydrazone of ω,ω-dibromoacetophenone by mixed melting point and by comparison of their infrared spectra as shown in Fig. 1 and 2, although the analytical results did not give a good agreement as 2,4-dinitrophenylhydrazone of ω,ω-dibromoacetophenone $C_{14}H_{10}O_4Br_2$, because the amount of the sample was so small that it could not be repeatedly recrystallized.

The acid, m. p. 115°C, had a neutralization equivalent of 244, and its composition was as follows:

Anal. Found: C, 44.9; H, 3.92; Br, 32.0. Calcd. for $C_9H_9O_3Br$: C, 44.1; H, 3.67; Br, 32.3%.

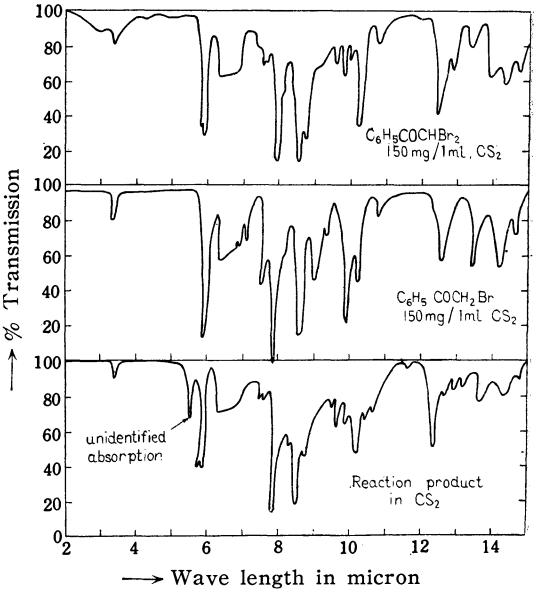

Fig. 1. Infrared spectra of two ketones and of reaction products (Expt. 59).

This indicates that the acid is either α-hydroxy-β-bromo- or α-bromo-β-hydroxyhydratropic acid. The positions of the hydroxyl group and the bromine atom were determined as follows: Infrared spectrum of the acid appeared to be similar to that of atrolactic acid as shown in Fig. 3. Treatment of the acid with Fenton reagent gave no carbonyl compound. An attempted synthesis of the acid by the reaction of atropic acid with hypobromic acid resulted in the formation of only a polymeric substance containing no bromine. However, when it was brought to reaction with lead tetracetate, it gave ω-bomoacetophenone, which resulted from the oxidative scission of α-hydroxy-β-bromohydratropic acid, because it was reported that[7], when an α-hydroxycarboxylic acid is treated with lead tetracetate, it gives a carbonyl

7) H. Oeda, This Bulletin, 9, 8 (1934).

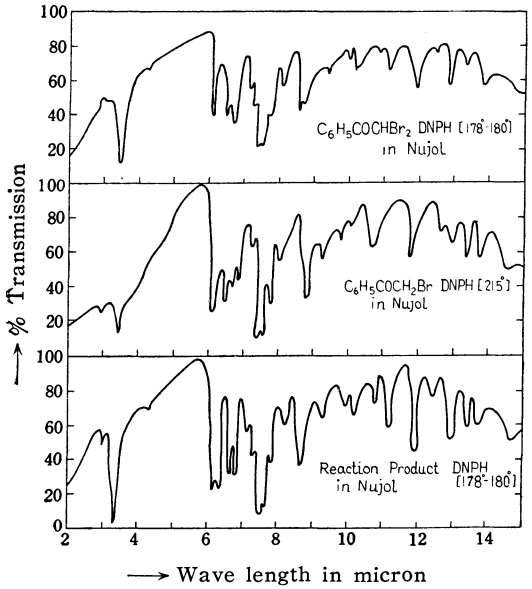

Fig. 2. Infrared spectra of 2, 4-dinitrophenylhydrazones (DNPH) of two ketones and of reaction products (Exp. 59).

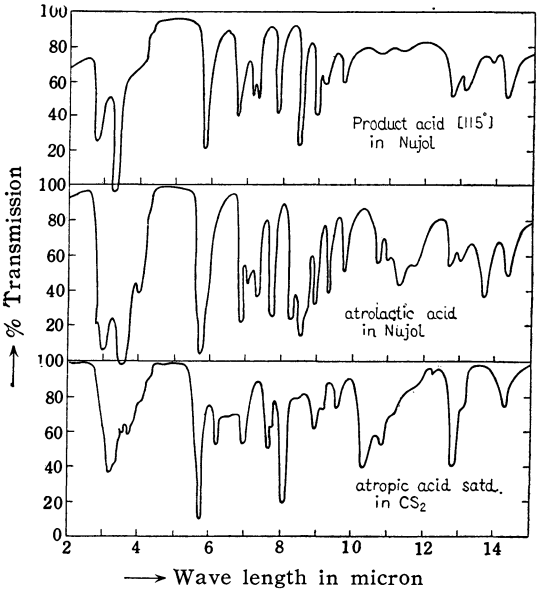

Fig. 3. Infrared spectra of α-hydroxy-β-bromohydratropic acid, atrolactic acid, and atropic acid.

compound and carbon dioxide as follows:

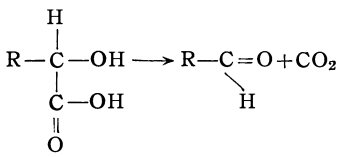

A mixture of 0.236 g. of $Pb(AcO)_4$ and 0.245 g. of the acid, m. p. 115°C, in 3 ml. of benzene was heated at 60–65°C. for 1.5 hr. After it was assured with a KI solution that no unchanged $Pb(AcO)_4$ remained, the yellow precipitate was filtered off. From the benzene solution a highly irritating oil was obtained on removing benzene by distillation. The oil partly solidified when it was kept in a cold place, but, as the amount was very small, the whole was brought to reaction with 2, 4-dinitrophenylhydrazine, giving an orange-colored precipitate. It was recrystallized from chloroform, m. p. 215°C.

Anal. Found: Br, 20.7. Calcd. for 2, 4-dinitrophenylhydrazone of ω-bromoacetophenone, $C_{14}H_{11}N_4O_4Br$: 21.7%.

A mixed melting point showed it was 2, 4-ninitrophenylhydrazone of ω-bromoacetophenone. From these results it was concluded that the acid was α-hydroxy-β-bromohydratropic acid, $C_6H_5C(CH_2Br)(OH)COOH$. This acid did not react with Fenton reagent, probably because of the absence of hydrogen atom at the hydroxylated carbon atom.

Addition of Hydrogen Bromide to Atropic Acid.—In 30 ml. of carbon tetrachloride 1.5 g. of atropic acid was dissolved, and hydrogen bromide was passed into the solution for 290 min. after sweeping the solution by nitrogen. A very small amount of a precipitate was obtained, which did not dissolve in various solvents and melted at 220°C. It contained no bromine and it may be a dimer of atropic acid. The solution was washed twice with distilled water, dried with anhydrous sodium sulfate, and evaporated, giving 1.5 g. of a crystalline substance, which was recrystallized from carbon disulfide, m. p. 96°C.

Anal. Found: Br, 34.1. Calcd. for $C_9H_{10}O_2Br$: Br, 34.9%.

By a mixed melting point, it was found to be β-bromohydratropic acid (Expt. 52.)

Addition of Hydrogen Bromide to Atropic Acid in the Presence of Benzoyl Peroxide.—Into a solution of 1.5 g. of atropic acid and 0.030 g. of benzoyl peroxide in 30 ml. of carbon tetrachloride hydrogen bromide was passed for 300 min. at the room temperature. By the same treatment as described above β-bromohydratropic acid was identified by a mixed melting point (Expt. 53).

The Reaction of Styrene with Hydrogen Bromide and Oxygen.—The mixture of hydrogen bromide and oxygen was passed into a solution of 10.0 g. (0.096 mol.) of styrene in 60 ml. of carbon tetrachloride for 240 min. at 20°C. The amount of carbon dioxide was 0.144 g. as barium carbonate (0.00073 mol.), and the water used to absorb waste hydrogen bromide gave a positive test with Schiff reagent, suggesting the presence of formaldehyde, although its identification was not successful. The carbon tetrachloride solution was washed with 120 ml. of 1 N NaOH, then with 60 ml. of water, and dried with anhydrous sodium sulfate. The alkaline solution was saturated with carbon dioxide, and extracted with ether. The ethereal solution gave a phenolic substance, but its identification was unsuccessful. The neutral oil obtained from the carbon tetrachloride solution was distilled under reduced pressure. The first fraction, which distilled at 58–60°C/3 mmHg weighed about 1.6 g., and was identified as α-bromoethylbenzene, by comparing the refractive index of

the oil ($n_D^{12.0}$ 1.5642) with that of an authentic specimen ($n_D^{12.0}$ 1.5636). The second fraction distilled at 108–110°C/3 mmHg and about 2.3 g. of the distillate solidified and showed a melting point 65°C.

Anal. Found: Br, 61.1. Calcd. for styrene dibromide, $C_8H_8Br_2$: Br, 60.7%. The total amount of styrene dibromide obtained in crystals in this experiment was not less than 4.8 g. (2.3+1.8+0.7). Supposedly the oil separated from the solid styrene dibromide contained yet styrene dibromide. The characteristic feature of the reaction was that a phenolic substance, styrene dibromide, and carbon dioxide were produced. The formation of the phenolic substance may be accompanied by the production of formaldehyde and carbon dioxide. Detailed investigation of the reaction mechanism of styrene with hydrogen bromide and oxygen will be made in future.

Summary

(1) The reaction of diphenylethylene, atropic acid, and styrene with the mixture of hydrogen bromide and oxygen were studied. In the case of diphenylethylene, diphenylbromomethane, ω-bromoacetophenone, diphenylethylene dibromide, phenol and carbon dioxide were obtained as reaction products. A reaction mechanism was proposed to explain how these compounds were produced.

(2) In the case of atropic acid, a large amount of α-hydroxy-β-bromohydratopic acid and a small amount of ω,ω-dibromoacetophenone and of carbon dioxide were obtained. A consideration on the mechanism of the formation of these products was given on the basis of the identified products and their semiquantitative estimation.

(3) Addition of hydrogen bromide to atropic was carried out under various conditions. No reversal of the direction of addition of hydrogen bromide was observed contrary to the previous reference.

(4) The reaction of styrene with the mixture of hydrogen bromide and oxygen added an example yielding a phenolic substance in the reaction.

Tne author wishes to express his hearty thanks to Prof. Y. Urushibara and Prof. O. Simamura for their kind guidance and encouragement throughout this work. The author is indebted to Dr. S. Tanaka for the infrared spectra measurement and their interpretation.

Department of Chemistry
College of General Education
The University of Tokyo

Studies on Antibiotics and Related Substances. III. Oxazolidines Derived from Some α-Hydroxy Schiff Bases and a Synthesis of DL-*threo*-*1-p-Nitrophenyl-2-amino-1, 3-propanediol**

By Tetsuo SUAMI and Sumio UMEZAWA

(Received June 28, 1956)

The present authors[1] previously reported that the reduction of *threo*-β-phenylserine[2] ethyl ester[3–6] by Raney nickel catalyst resulted in the formation of a new compound $C_{16}H_{17}NO_2$ (I), m. p. 138–139°C, which gave an N-acetyl oxazolidine derivative (II), m. p. 148–148.5°C, on acetylation with acetic anhydride at room temperature. II was led to DL-*threo*-1-*p*-nitrophenyl-2-amino-1, 3-propanediol by a synthetic route.

The present paper describes further investigations on the constitutions of I and II and also the synthesis of DL-chloramphenicol[7] from II in details.

The failure of II to hydrolyze under Kunz's conditions[8] demonstrated that II was an N-acetyl derivative. Consequently, the authors had assumed I to be an oxazolidine derivative. To establish the differentiation between oxazolidines and isomeric Schiff bases, the infrared and ultraviolet spectra of I and II

* Presented in part before the Division of Organic Chemistry at the Annual Meeting of the Chemical Society of Japan, Tokyo, April 2, 1955. Previous papers: This Bulletin, 27, 477 (1954); 29, 417 (1956).

1) S. Umezawa and T. Suami, This Bulletin, 27, 477 (1954).

2) E. Erlenmeyer, Jr., *Ber.*, 25, 3445 (1892).

3) G. Carrara and G. Weitnauer, *Gazz. chim. ital.*, 79, 856 (1949).

4) E. D. Bergmann, H. Bendas and W. Taub, *J. Chem. Soc.*, 1951, 2673.

5) G. W. Moersch, U. S., 2,538,792 (1951).

6) K. N. F. Shaw and S. W. Fox, *J. Am. Chem. Soc.*, 75, 3420 (1953).

7) J. Controulis, M. C. Rebstock and H. M. Crooks, Jr,, *J. Am. Chem. Soc.*, 71, 2463 (1949).

8) A. Kunz aud C. S. Hudson, *J. Am. Chem. Soc.*, 48, 1982 (1926).

were measured. Infrared spectrum of I (Fig. 1) showed the presence of C=N bond in 1642 cm^{-1}, while II (acetylated product) showed no band in the absorption region of the C=N double bond and showed the triplet at 1089, 1168 and 1212 cm^{-1}, very likely because of the O—C—N system in the expected oxazolidine system[4], was found.

For the corresponding *p*-nitro derivatives (III and IV) of I and II, the infrared spectra were studied (Fig. 1). As was expected, DL-*threo*-1-*p*-nitrophenyl-2-benzylideneamino-1, 3-propanediol (III) prepared by the condensation of DL-*threo*-1-*p*-nitrophenyl-2-amino-1, 3-propanediol with benzaldehyde showed the presence of C=N bond in 1631 cm^{-1}, while the acetylated product (IV) of III showed no band in the absorption region of the C=N bond and showed the triplet at 1099, 1172 and 1217 cm^{-1} [4].

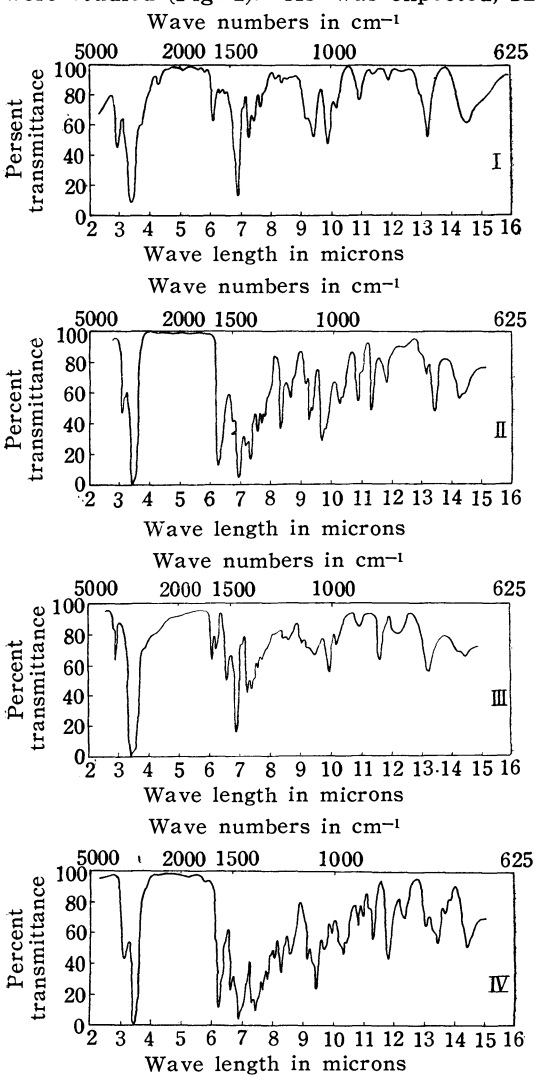

Fig. 1. Infrared absorption spectra of Schiff bases and corresponding oxazolidine compounds (in Nujol).
I) DL-*threo*-1-Phenyl-2-benzylideneamino-1, 3-propanediol.
II) DL-*threo*-N-Acetyl-2-phenyl-4-(α-hydroxybenzyl)oxazolidine.
III) DL-*threo*-1-*p*-Nitrophenyl-2-benzylideneamino-1, 3-propanediol.
IV) DL-*threo*-N-Acetyl-2-phenyl-4-(α-hydroxy-*p*-nitrobenzyl)oxazolidine.

In addition, the ultraviolet absorption spectra of I, II, III and IV were measured. As the ultraviolet absorption spectra of the Schiff base of ethyl *p*-nitrophenylserinate and its acetylated product had been reported by Bergmann et al.[9], DL-*threo*-1-phenyl-2-amino-1, 3-propanediol and DL-*threo*-1-*p*-nitrophenyl-2-amino-1, 3-propanediol were condensed with *p*-nitrobenzaldehyde to give the Schiff bases (I′, III′) respectively which were further acetylated with acetic anhydride to give N-acetyl oxazolidine derivatives (II′, IV′).

Absorption maxima of these derivatives are recorded in Table I. The melting points, analyses and yields are given in Tables II and III.

DL-*threo*-1-*p*-Nitrophenyl-2-(*p*-nitrobenzylidene)amino-1, 3-propanediol (III′) possessed an absorption maximum (λ 2680 Å, log ε 4.29) similar to that reported for the Schiff base of ethyl *p*-nitrophenylserinate (λ 2700 Å, log ε 4.39)[9]. Correspondingly, the acetylated product (IV′) of III′ possessed a maximum (λ 2670 Å, log ε 4.34) similar to that of the acetylated product of the Schiff base of ethyl *p*-nitrophenylserinate (λ 2655 Å, log ε 4.35)[9].

Acetylated product of the Schiff base obtained from DL-*threo*-1-phenyl-2-amino-1, 3-propanediol and benzaldehyde showed three maxima (2520, 2580 and 2640 Å).

The condensation products of DL-*threo*-1-phenyl-2-amino-1, 3-propanediol and DL-*threo*-1-*p*-nitrophenyl-2-amino-1, 3-propanediol with *o*-nitro and *m*-nitrobenzaldehyde were further prepared and then acetylated to give oxazolidine derivatives, which failed to hydrolyze under Kunz's conditions[8]. The melting points, analyses and yields of these products are given in Table II and III.

Two isomeric structures—one with the oxazolidine ring containing the oxygen of the primary alcohol and the other with the oxazolidine ring containing the oxygen of the secondary alcohol—were expected for the acetylated product II which was prepared from the Schiff base I.

Considering the fact that II was not further acetylated on standing with acetic anhydride for three hours at room tempera-

9) E. D. Bergmann, H. Bendas and Ch. Resnick, *J. Chem. Soc.*, 1953, 2564.

TABLE I

ULTRAVIOLET ABSORPTION MAXIMA OF SCHIFF BASES AND N-ACETYL OXAZOLIDINE DERIVATIVES

Derivatives	Wave Lengths and Intensities of Maxima (in Chloroform)	
	$\lambda_{max.}$ (Å)	log $\varepsilon_{max.}$
I	2510	3.59
II	2580	2.68
III***	2760	4.14
IV	2680	4.30
I'**	2660	4.16
II'*	—	—
III'	2680	4.29
IV'	2670	4.34

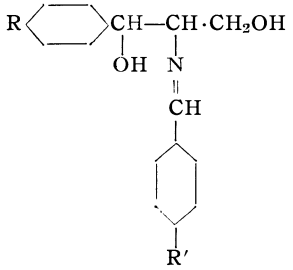

I R=H, R'=H
III R=NO_2, R'=H
I' R=H, R'=NO_2
III' R=NO_2, R'=NO_2

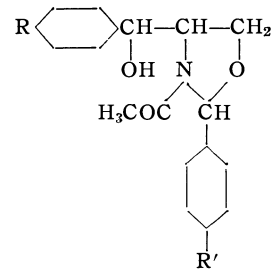

II R=H, R'=H
IV R=NO_2, R'=H
II' R=H, R'=NO_2
IV' R=NO_2, R'=NO_2

* This derivative did not crystallize.

** This derivative was reported recently by S. Umezawa et al.[10]

*** This derivative was reported by Iliceto et al.[11]

ture, while DL-*threo*-1-phenyl-2-amino-1, 3-propanediol was acetylated by acetic anhydride in half an hour at room temperature to yield DL-*threo*-1-phenyl-2-acetamido-3-acetoxy-1-propanol[12], II was considered to be of the former structure combined with the oxygen of the primary alcohol.

Recently, two analogous cases were reported. McCasland et al.[13] demonstrated that the condensation product of 2-amino-cyclohexanol and benzaldehyde had the structure

TABLE II

CONDENSATION PRODUCTS OF AMINOALCOHOLS AND ALDEHYDES (SCHIFF BASES)

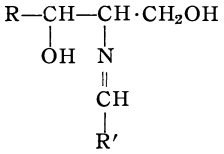

R	R'	Formula	M. p., °C	Yield, %	Carbon, %		Hydrogen, %		Nitrogen, %	
					Calcd.	Found	Calcd.	Found	Calcd.	Found
Phenyl	Phenyl	$C_{16}H_{17}NO_2$	138–139	78.6	—	—	—	—	—	—
Phenyl	*o*-Nitrophenyl	$C_{16}H_{16}N_2O_4$	122–123	50.1	—	—	—	—	9.33	9.17
Phenyl	*m*-Nitrophenyl	$C_{16}H_{16}N_2O_4$	98–99	11.1	—	—	—	—	9.33	9.45
p-Nitrophenyl	Phenyl	$C_{16}H_{16}N_2O_4$	158–159*	77.5	63.99	64.24	5.37	5.33	—	—
p-Nitrophenyl	*o*-Nitrophenyl	$C_{16}H_{15}N_3O_6$	140–141**	55.3	—	—	—	—	12.17	11.97
p-Nitrophenyl	*m*-Nitrophenyl	$C_{16}H_{15}N_3O_6$	135–136.5	49.2	—	—	—	—	12.17	12.52
p-Nitrophenyl	*p*-Nitrophenyl	$C_{16}H_{15}N_3O_6$	173–174	55.3	—	—	—	—	12.17	12.32

* M. p. reported by Iliceto et al.[11] was 155–156°C.

** M. p. reported by Iliceto et al.[11] was 144–146°C.

10) T. Suami, I. Uchida and S. Umezawa, This Bulletin, 29, 417 (195).

11) A. Iliceto and E. Scoffone, *Gazz. chim. ital.*, 81, 133 (1951).

12) L. M. Long and H. D. Troutman, *J. Am. Chem. Soc.*, 71, 2469 (1949).

13) G. E. McCasland and E. C. Horswill, *J. Am. Chem. Soc.*, 73, 3923 (1951).

TABLE III
ACETYLATION PRODUCTS OF SCHIFF BASES (OXAZOLIDINE DERIVATIVES)

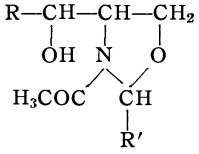

R	R′	Formula	M. p., °C	Yield, %	Carbon, %		Hydrogen, %		Nitrogen, %	
					Calcd.	Found	Calcd.	Found	Calcd.	Found
Phenyl	Phenyl	$C_{18}H_{19}NO_3$	148–148.5	42.9	72.70	72.97	6.44	6.49	4.71	4.64
p-Nitrophenyl	Phenyl	$C_{18}H_{18}N_2O_5$	178–180	35.1	63.15	63.25	5.30	5.31	—	—
p-Nitrophenyl	*o*-Nitrophenyl	$C_{18}H_{17}N_3O_7$	242–244	53.5	—	—	—	—	10.85	10.98
p-Nitrophenyl	*m*-Nitrophenyl	$C_{18}H_{17}N_3O_7$	202–203.5	53.5	—	—	—	—	10.85	10.40
p-Nitrophenyl	*p*-Nitrophenyl	$C_{18}H_{17}N_3O_7$	170–171	62.4	—	—	—	—	10.85	11.12

of a Schiff base, while its N-benzoyl derivative had that of oxazolidine. As mentioned above, Bergmann et al.[9] also described that the condensation products of the *threo* and *erythro*-forms of *p*-nitrophenylserine ethyl ester with *p*-nitrobenzaldehyde had the structures of Schiff bases and acetylation converted them into diastereoisomeric oxazolidines.

It is of interest to extend the observation that the acetylation of the Schiff bases of β-phenylserinol and its derivatives converted them into oxazolidine compounds.

Schiff base I was easily hydrolyzed on warming with 0.95N hydrochloric acid at 60°C for one hour, to give DL-*threo*-1-phenyl-2-amino-1, 3-propanediol and benzaldehyde.

It is interesting that the rate of catalytic reduction of the C=N bond in Schiff base I was very slow and practically stopped after the reduction of the ester group. In this regard, Goldberg and Nace[14] reported recently on the selected reduction of the unsaturated Schiff base system C=C—C=N.

Starting from the above described DL-*threo*-N-acetyl-2-phenyl-4-(α-hydroxybenzyl) oxazolidine II, DL-chloramphenicol[7], an important antibiotic found by scientists of Parke, Davis and Company, was synthesized through the route described below. Further acetylation of II with acetic anhydride in pyridine gave a viscous product (V), which, on nitration with mixed acid under dry ice-cooling for thirty minutes and then ice-cooling for thirty minutes, and finally at 15°C for thirty minutes, gave a viscous product containing a small amount of crystals. The latter, after recrystallization, appeared to be the diacetyl derivative of 2-(*m*-nitrophenyl)-4-(α-hydroxy-*p*-nitrobenzyl)oxazolidine (VI), m. p. 192–193°C. The diacetyl derivative gave one mole of acetic acid on hydrolysis under Kunz's conditions[8], demonstrating that VI is an N, O-diacetyl oxazolidine compound. VI gave *m*-nitrobenzaldehyde on refluxing with 4.5 N hydrochloric acid.

The crude, viscous-oily, nitration product containing VI mainly, was refluxed with 3 N hydrochloric acid for three hours and the reaction solution was concentrated by evaporation under reduced pressure, followed by pH adjustment with 5 N sodium hydroxide

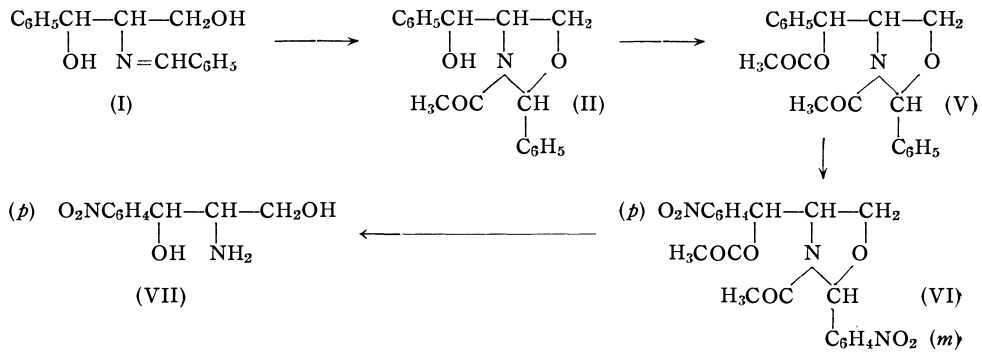

14) E. P. Goldberg and H. R. Nace, *J. Am. Chem. Soc.*, **77**, 359 (1955).

to 10, to give DL-*threo*-1-*p*-nitrophenyl-2-amino-1, 3-propanediol (VII) melting at 143.5–145°C, which did not depress the melting point of an authentic sample obtained by the synthetic route from *p*-nitroacetophenone[15].

VII was acylated with dichloroacetamide to yield DL-chloramphenicol.

Experimental

Reduction of DL-*threo*-Phenylserine Ethyl Ester with Raney Nickel Catalyst.—DL-*threo*-1-Phenyl-2-benzylideneamino-1, 3-propanediol (I).—Ten grams of DL-*threo*-phenylserine ethyl ester[3-6] was dissolved in 50 cc. of absolute ethanol and reduced in an autoclave for six hours, at 50–60°C under 110 atms. H_2 with 17 g. of Raney nickel W-4[16]. After standing overnight, the catalyst was filtered off and the solvent was removed under reduced pressure to yield a pale yellow oily residue. After it was settled in a desiccator overnight, colorless crystals appeared in it. The crystals were collected and washed with ether to yield 2.5 g. (41.0%) of colorless crystals. They were recrystallized twice from ethanol. Colorless plates, m.p. 138–139°C.

Anal. Found: C, 75.26; H, 6.74; N, 5.53. Calcd. for $C_{16}H_{17}NO_2$: C, 75.27; H, 6.71; N, 5.49%.

Infrared (Fig. 1) and ultraviolet absorption spectra (Table I) were measured.

2.0 g. of I was hydrolyzed for one hour with 10 cc. of 0.95 N hydrochloric acid at 60°C. Benzaldehyde which separated on the solution was extracted with ether, and the aqueous layer was concentrated at 40°C under reduced pressure. The residue was redissolved in 5 cc. of cold water. After an excess of potassium carbonate was added to the solution, it was extracted five times with ethyl acetate. The combined ethyl acetate solution was dried over anhydrous sodium sulfate and concentrated under reduced pressure to yield 1.0 g. (76.4%) of a pale yellow oil. This oil crystallized on standing at room temperature with two drops of ethyl acetate. The crystals were recrystallized twice from ethyl acetate. Yield, 0.59 g. (45.1%). Colorless crystals, m.p. 87–88°C. They did not depress the melting point of an authentic sample of DL-*threo*-1-phenyl-2-amino-1, 3-propanediol obtained by the method of Controulis et al.[7].

Acetylation of DL-*threo*-1-Phenyl-2-benzylideneamino-1, 3-propanediol.—DL-*threo*-N-Acetyl-2-phenyl-4-(α-hydroxybenzyl) oxazolidine (II).—2.0g. of DL-*threo*-1-phenyl-2-benzylideneamino-1, 3-propanediol (I) was added to 4.0 cc. of acetic anhydride with agitation at room temperature. The colorless crystals which appeared immediately were collected and washed with ether to yield 1.9 g. of the crude product melting at 145–146°C (81.5%). This was recrystallized twice from methanol to yield 1.0 g. (42.9%) of colorless crystals melting at 148–148.5°C. This product was not further acetylated on standing with ten volumes of acetic anhydride for three hours at room temperature. This failed to hydrolyze under Kunz's conditions[8].

Anal. Found: C, 72.97; H, 6.49; N, 4.64. Calcd. for $C_{18}H_{19}NO_3$: C, 72.70; H, 6.44; N, 4.71%.

Infrared (Fig. 1) and ultraviolet absorption spectra (Table I) were measured.

Condensation of DL-*threo*-1-Phenyl-2-amino-1, 3-propanediol and DL-*threo*-1-*p*-Nitrophenyl-2-amino-1, 3-propanediol with Benzaldehyde, *o*-, *m*- and *p*-Nitrobenzaldehyde.—DL-*threo*-1-Phenyl-2-benzylideneamino-1, 3-propanediol (I) and other Schiff bases were all prepared by essentially the same procedure.

DL-*threo*-1-Phenyl-2-benzylideneamino-1, 3-propanediol (I).—1.0 g. of DL-*threo*-1-phenyl-2-amino-1, 3-propanediol was added to a mixture of 0.7 g. of freshly distilled benzaldehyde and a small quantity of ethyl acetate. After the mixture was stirred at room temperature for fifteen minutes, ethyl acetate was removed in vacuo. The residual solid was washed with ether to obtain 1.5 g. (98.2%) of a colorless powder melting at 133–135°C.

It was recrystallized twice from ethanol. Yield, 1.2 g. (78.6%). Colorless crystals, m. p. 138–139°. They did not depress the melting point of the sample of I obtained by the reduction of DL-*threo*-phenylserine ethy ester with Raney nickel catalyst.

DL-*threo*-1-Phenyl-2-(*o*-nitrobenzylidene) amino-1, 3-propanediol was purified by recrystallization from acetone, DL-*threo*-1-*p*-nitrophenyl-2-(*m*-nitrobenzylidene) amino-1, 3-propanediol and DL-*threo*-1-*p*-nitrophenyl-2-(*p*-nitrobenzylidene)amino-1, 3-propanediol were purified by recrystallization from methanol, whereas, DL-*threo*-1-phenyl-2-(*m*-nitrobenzylidene)amino-1, 3-propanediol was not purified. The melting points, analyses and yields are given in Table II.

Acetylation of the Above Described Schiff Bases.—Acetylation products of DL-*threo*-1-phenyl-2-(*o*-nitrobenzylidene)amino-1, 3-propanediol and DL-*threo*-1-phenyl-2-(*p*-nitrobenzylidene)amino-1, 3-propanediol[10] failed to crystallize. The following four products were obtained as crystals.

Acetylated products (oxazolidine derivatives) were all prepared by essentially the same procedure as that of DL-*threo*-N-acetyl-2-phenyl-4-(α-hydroxybenzyl)oxazolidine (II), but DL-*threo*-N-acetyl-2-phenyl-4-(α-hydroxy-*p*-nitrobenzyl) oxazolidine was prepared by the following procedure.

DL-*threo*-N-Acetyl-2-phenyl-4-(α-hydroxy-*p*-nitrobenzyl)oxazolidine (IV).—0.5 g. of III was added to 2.0 cc. of acetic anhydride. After standing at room temperature for two hours, the reaction solution was diluted with water, neutralized with sodium bicarbonate, and extracted with ethyl acetate. The ethyl acetate solution was dried over anhydrous sodium sulfate, and evaporated under reduced pressure to yield 0.5 g. of a pale yellow oily residue. It was dissolved in a small quantity of ether and added to an equal volume of petroleum ether. After standing overnight in a refrigerator, 0.3 g. (52.6%) of colorless crystals were obtained and recrystallized from acetone. Yield, 0.2 g. (35.1%). Colorless crystals, m.p. 178–180°C.

Anal. Found: C, 63.25; H, 5.31. Calcd. for $C_{18}H_{18}N_2O_5$: C, 63.15; H, 5.30%.

This failed to hydrolyze under Kunz's condi-

15) L. M. Long and H. D. Troutman, *J. Am. Chem. Soc.*, **71**, 2473 (1949).

16) A. A. Pavlic and H. Adkins, *J. Am. Chem. Soc.*, **68**, 1471 (1946).

tions[8]. Infrared (Fig. 1) and ultraviolet absorption spectra (Table I) were measured.

DL-*threo*-N-Acetyl-2-(*o*-nitrophenyl)-4-(α-hydroxy-*p*-nitrobenzyl)oxazolidine and DL-*threo*-N-acetyl-2-(*m*-nitrophenyl)-4-(α-hydroxy-*p*-nitrobenzyl)oxazolidine were purified by recrystallization from acetone. DL-*threo*-N-Acetyl-2-(*p*-nitrophenyl)-4-(α-hydroxy-*p*-nitrobenzyl)oxazolidine (IV') was purified by recrystallization from acetone-petroleum ether. The melting points, analyses and yields are given in Table III.

Synthesis of DL-Chloramphenicol from II.—DL-*threo*-N, O-Diacetyl-2-phenyl-4-(α-hydroxybenzyl) oxazolidine (V).—5.5 g. of II was dissolved in 14.0 cc. of dry pyridine and 8.0 cc. of acetic anhydride. After standing at room temperature for forty-eight hours, the solution was poured into ice water. The mixture was extracted with ethyl acetate and the ethyl acetate solution was washed with 0.5N hydrochloric acid, 1% sodium carbonate solution, and water. Then the ethyl acetate solution was concentrated in vacuo and 6.4 g. of a yellow viscous oil was obtained.

DL-*threo*-N, O-Diacetyl-2-(*m*-nitrophenyl)-4-(α-hydroxy-*p*-nitrobenzyl)oxazolidine (VI).—6.4 g. of V was added to 30 cc. of a 1:1 mixture of nitric acid (d. 1.38) and sulfuric acid (d. 1.84) with dry ice cooling and vigorous shaking. After thirty minutes, the reaction flask was transferred to an ice bath for thirty minutes, and then kept at room temperature for thirty minutes. The solution was quenched on 200 g. of ice and immediately neutralized with sodium bicarbonate. The product was extracted five times with ethyl acetate and the combined ethyl acetate solution was washed with cold water, dried over anhydrous sodium sulfate, and concentrated under reduced pressure to yield 8.0 g. (98.8%) of a pale yellow viscous product. The crude product was added to absolute acetone to yield 0.97 g. (12.0%) of colorless crystals melting at 192–193°C.

Anal. Found: C, 55.45; H, 4.24; N, 9.44; O-acetyl, 11.0. Calcd. for $C_{20}H_{19}N_3O_8$: C, 55.94; H, 4.46; N, 9.79; O-acetyl 10.0%.

This product gave one mole of acetic acid on hydrolysis under Kunz's conditions[8].

0.5 g. of these crystals were refluxed for four hours with 18 cc. of 4.5 N hydrochloric acid and then settled at room temperature overnight. Pale yellow needles melting at 56–57°C appeared in the solution and they did not depress the melting point of an authentic sample of *m*-nitrobenzaldehyde.

The solution remaining after the Kunz's determination for O-acetyl was evaporated under reduced pressure to remove acetone. The colorless crystals which precipitated in the solution were collected and washed with water. The crystals melted at 201–203°C and did not depress the melting point of DL-*threo*-N-acetyl-2-(*m*-nitrophenyl)-4-(α-hydroxy-*p*-nitrobenzyl)oxazolidine.

DL-*threo*-1-*p*-Nitrophenyl-2-amino-1, 3-propanediol (VII).—7.2 g. of crude VI was refluxed for three hours with 80 cc. of 3 N hydrochloric acid. The solution was washed with ether to remove an oily precipitate of nitrobenzaldehyde and concentrated under reduced pressure. The residue was dissolved in 5 cc. of cold water and the pH of the solution was adjusted to 10 with 5 N sodium hydroxide with ice cooling. After standing overnight in a refrigerator, 1.75 g. (49.2%) of the crude base melting at 129–133°C was obtained. The base was repeatedly recrystallized from hot water to yield pale yellow crystals melting at 143.5–145°C which did not depress the melting point of an authentic sample obtained by the method of Long et al.[15]

DL-*threo*-1-*p*-Nitrophenyl-2-dichloroacetamido-1, 3-propanediol.—2.0 g. of VII was finely mixed with 1.2 g. of dichloroacetamide, and the mixture was heated on a boiling water bath for three hours, and dissolved in ethyl acetate. The solution was filtered, washed with 0.5 N hydrochloric acid to remove the unreacted free base and then with water, dried over anhydrous sodium sulfate, passed through a short chromatographic column of 10 g. alumina to remove the coloring matter and then evaporated under reduced pressure to yield 2.3 g. of a crystalline residue melting at 128–137°C. It was recrystallized from ethylene dichloride and washed with ether. Pale yellow crystals, m.p. 147–149°C. Yield, 1.2 g. (39.1%). The product was further recrystallized from ethyl acetate-petroleum ether to yield colorless crystals melting at 149–150°C, which did not depress the melting point of an authentic sample obtained by the method of Long et al.[15]

One mg. of these crystals was equivalent to 512 γ of natural chloramphenicol[17] by the cup assay method (test organism E.coli).

Summary

1) When Erlenmeyer's β-phenylserine ethyl ester was reduced with Raney nickel catalyst, DL-*threo*-1-phenyl-2-benzylideneamino-1, 3-propanediol (a Schiff base) was obtained as a main product. The structure was demonstrated by means of its infrared and ultraviolet absorption spectra.

2) It was found that DL-*threo*-1-phenyl-2-benzylideneamino-1, 3-propanediol gave DL-*threo*-N-acetyl-2-phenyl-4-(α-hydroxybenzyl) oxazolidine on acetylation with acetic anhydride.

3) The condensation products of DL-*threo*-1-phenyl-2-amino-1, 3-propanediol and DL-*threo*-1-*p*-nitrophenyl-2-amino-1, 3-propanediol with benzaldehyde, *o*-, *m*- and *p*-nitrobenzaldehyde were prepared and acetylated to give corresponding oxazolidine derivatives, which failed to hydrolyze under Kunz's conditions. Infrared and ultraviolet absorption spectra of some of these compounds were observed. Acetylated derivatives failed to show the characteristic absorption of $\rangle C=N-$ bond in the 1660–1610 cm^{-1} region.

17) J. Ehrlich, Q.R. Bartz, R.M. Smith and D.A. Joslyn, *Science*, **106**, 417 (1947).

4) DL-Chloramphenicol was synthesized from DL-*threo*-N-acetyl-2-phenyl-4-(α-hydroxybenzyl)oxazolidine.

The authors thank Dr. K. Kuratani for the measurement of the infrared spectra, and Mr. S. Nakada for elementary analyses.

Department of Applied Chemistry
Faculty of Engineering
Keio University, Tokyo

Constituents of the Mucilage of Gloiopeltis Furcata

By Susumu HIRASE, Choji ARAKI and Toshiya ITŌ

(Received September 11, 1956)

Certain species of the *Gloiopeltis* family of *Rhodophyceae* contain a water-soluble mucilage, which on dissolution in water forms a highly viscous solution. It is widely used in this country as a sizing agent for silk textiles and as a thickening agent for mortar and plaster. The mucilage is a metallic salt of the sulfate ester of a polysaccharide, which on acid hydrolysis produces chiefly D-galactose together with a small amount of L-arabinose and L-fucose[1,2]. But there has also been reported the presence of a considerable amount of an unidentified constituent showing a Seliwanoff's ketose reaction[1,2]. On the other hand, it is established that agar-agar contains 3, 6-anhydro-L-galactose as well as D-galactose as the chief constituent[3], and that carrageenin contains an enanthiomorph of the anhydro-sugar present in agar in addition to D-galactose[4,5]. Both agar and carrageenin also contain a small amount of L-galactose[5,6]. Since 3, 6-anhydro-galactose shows a distinct Seliwanoff's reaction, it is most probable that the unidentified constituent of the *Gloiopeltis* mucilage is 3, 6-anhydro-galactose. This has been proved to be the case as reported herein, and the anhydro-sugar has been shown to be of the L-series. In addition, the presence of a small amount of L-galactose has also been confirmed.

The mucilage used in this study was extracted from commercial "sheet Funori", which is prepared from *Gloiopeltis furcata* by conglutinating the plant bodies with each other by means of their own mucilage. The mucilage extracted has a specific rotation, $[\alpha]_D^{15} = -20.6°$, in water and contains 18.5% of sulfate. It was then subjected to complete methanolysis. After an appropriate treatment the methanolysate was separated by column chromatography into 3, 6-anhydro-L-galactose dimethylacetal and a mixture of methyl D- and L-galactoside. The former product was hydrolysed to give a reducing sugar, which was then identified as its phenylosazone. The latter mixture was further separated into crystalline methyl α-D-galactoside and a residual syrup, which on hydrolysis gave rise to a mixture of D- and L-galactose. Then D-galactose was removed therefrom as much as possible by crystallization, and the residue was treated with ethylmercaptan and concentrated hydrochloric acid. L-Galactose was isolated in the form of crystalline DL-galactose diethylmercaptal, which was further identified as its penta-acetate. The yields of the products have indicated that the *Gloiopeltis* mucilage used contains 3, 6-anhydro-L-galactose, D-galactose and L-galactose in the approximate ratio of 8 : 12 : 1.

Experimental

Evaporation and concentration were carried out under reduced pressure below 40°. Specific rotations were measured in aqueous solutions unless otherwise stated. The melting points are uncorrected.

Material.—Twenty grams of commercial sheet of *Gloiopeltis furcata* was extracted with water (2 l.) in a boiling water bath for two hours. After filtration through a bed of Celite-active carbon, the extract was concentrated and precipitated with 95% ethanol. The product, collected and pressed in a cotton sack, was dehydrated with absolute ethanol and then ether, air-dried and finally ground to powder; yield 6.5 g. (moisture 9.33%); $[\alpha]_D^{15} = -20.6°$ (c 0.63); found: ash, 13.14%; SO_4 total, 18.48%; SO_4 in ash, 6.84%, of the mucilage, respectively, on the moisture-free basis.

1) K. Kawakami, *J. Soc. Chem. Ind. Japan*, **13**, 341 (1910).
2) E. Takahashi, *J. Coll. Agr. Hokkaido Imp. Univ.*, **8**, 183 (1920).
3) f. i. see C. Araki, This Bulletin, **29**, 543 (1956).
4) C. Araki and S. Hirase, ibid, **29**, 991 (1956); A. N. O'Neil, *J. Am. Chem. Soc.*, **77**, 2837, 6324 (1955).
5) E. E. Percival, *Chemistry & Industry*, **1954**, 1487.
6) C. Araki and K. Arai, Collection of Treatises in Commemoration of 45th Anniversary of Kyoto Technical College, p. 80 (1948).

Methanolysis.—The mucilage (1.50 g., moisture 9.33%) in 3% methanolic hydrogen chloride (20 cc.) was heated under reflux for twenty-five hours. The resulting solution was neutralized with silver carbonate, filtered and concentrated to a syrup, which was then treated with 0.3N-barium hydroxide solution (20 cc.) at 60° for two hours. Excess barium hydroxide was removed by neutralization with carbon dioxide and filtration, and the filtrate was concentrated to a syrup. It was dissolved in water and deionized by passing the solution through columns of Amberlite IR-120 and IR-4B resins in succession, the resins being subsequently washed with water. The effluent and washings were combined and concentrated to a syrup; yield 0.779 g. (57.3% of the mucilage); $[\alpha]_D^{24}=+46.9°$ (*c* 0.64). Paper chromatographic examination, using *n*-butanol-ethanol-water (4:1:2 by volume) as a solvent and *o*-aminophenol reagent[7] as a spraying reagent, indicated the presence of 3,6-anhydro-galactose dimethylacetal (R_f 0.67[8]).

Chromatographic Separation.—The deionized methanolysate (0.754 g.) obtained above was chromatographed on a column (2.5×30 cm.) of powdered filter paper, *n*-butanol-water (6:1) being used as a developer until the effluent showed no longer a spot of 3,6-anhydro-galactose dimethylacetal on a paper chromatogram. Then the column was developed with 80% aqueous methanol (300 cc.). Butanolic and methanolic effluents were separately evaporated to dryness, giving 3,6-anhydro-L-galactose dimethylacetal and a mixture of methyl D- and L-galactoside, respectively, in yields of 0.290 g. and 0.456 g. Since L-galactose amounts to 7.9% of total galactose as described later, 3,6-anhydro-L-galactose, D-galactose and L-galactose are in the molar ratio 7.6:11.6:1.

3,6-Anhydro-L-galactose Dimethylacetal.—3,6-Anhydro-L-galactose dimethylacetal above obtained was a colorless syrup, which was further purified by dissolution in dry acetone followed by filtration and subsequent evaporation; $[\alpha]_D^{27}=-25.9°$ (*c* 0.80); OCH_3, found: 27.73% (calcd. for $C_8H_{16}O_6$: 29.81%). It showed a distinct Seliwanoff's ketose reaction.

3,6-Anhydro-L-galactose.—The above dimethylacetal (0.3 g.) was hydrolysed with 0.02N-sulfuric acid (10 cc.) in a boiling water bath for two hours. The solution was neutralized with barium carbonate, filtered and concentrated to dryness, when 3,6-anhydro-L-galactose was obtained as a syrup (0.2 g.). It reduced a Fehling's solution at room temperature.

Phenylosazone: The sugar above obtained was converted to its phenylosazone by reaction with phenylhydrazine in the presence of dilute acetic acid in the usual manner. The osazone was twice recrystallized from ethanol-water (2:1), forming yellow needles; m.p. 217°; $[\alpha]_D^{30}=-65.9°$ (an initial value, pyridine-methanol (2:3), *c* 0.44) → −52.3° (an equilibrium value). Reported values[9] are m.p. 217° and $[\alpha]_D=-52.8°$ (an equilibrium value, pyridine-methanol). Admixture with an authentic sample showed no depression of the melting point.

Methyl α-D-Galactoside.—When the mixture of methyl D- and L-galactoside, obtained from the methanolic effluent of chromatography, was dissolved in ethanol and kept in a refrigerator, methyl α-D-galactoside was deposited as its monohydrate; yield 0.191 g. It was recrystallized from ethanol, giving prisms; m.p. 94–98°, not depressed on admixture with an authentic sample; $[\alpha]_D^{12}=+175°$ (*c* 1.00); OCH_3, found: 14.63% (calcd. for $C_7H_{14}O_6\cdot H_2O$: 14.61%).

D-Galactose.—The mother liquor, separated from crystals of methyl α-D-galactoside monohydrate, was concentrated to a syrup (0.262 g.), which was then subjected to hydrolysis with N-sulfuric acid (5 cc.) in a boiling water bath for four hours. The product (0.239 g.), isolated in the usual manner, was crystallized from methanol, affording D-galactose; yield 0.107 g. The recrystallized sample melted at 164–165° and had a specific rotation $[\alpha]_D^{27}=+80.8°$ (an equilibrium value, *c* 0.73). Mixed melting point determination showed no depression.

DL-Galactose Diethylmercaptal.—The mother liquor, separated from crystals of D-galactose, was concentrated to a syrup (0.123 g.), which was then combined with two other batches. The resulting mixture was extracted with boiling absolute ethanol. On cooling the extract gave crystals (0.10 g.) melting at 140–144° and having a specific rotation, $[\alpha]_D^{28}=+32.5°$ (an equilibrium value, *c* 0.80). The value of the specific rotation indicates that the crystals are a mixture of D-galactose and L-galactose, the former predominating. The filtered mother liquor was concentrated to a syrup (0.20 g.), $[\alpha]_D^{27}=+4.6°$ (an equilibrium value, *c* 0.65). It showed on a paper chromatogram a single spot corresponding to galactose. This observation and the low value of a specific rotation may show that the above-mentioned syrup is nearly pure DL-galactose. Then, on being calculated for a single batch, the yield (0.067 g.) of DL-galactose amounts to 15.8% of the whole galactose, and hence that of L-galactose is 7.9%.

For conclusive identification, the syrupy DL-galactose above obtained was converted to its diethylmercaptal as follows. The syrup (0.20 g.) was dissolved in concentrated hydrochloric acid ($d=1.20$, 2 cc.), and ethylmercaptan (2 cc.) was added. After being vigorously shaken for fifteen minutes under ice-cooling, the reaction mixture was diluted with ice-water, immediately neutralized with excess lead carbonate, filtered and concentrated to dryness. The residue was extracted with boiling acetone. On evaporation the extract afforded DL-galactose diethylmercaptal melting at 121-124°; yield 0.18 g. A pure compound was obtained on recrystallization from acetone; m.p. 126-127°; $[\alpha]_D^{28}=\pm0°$ (*c* 0.80); SC_2H_5[10], found: 42.80% (calcd. for

7) S. Hirase, C. Araki and S. Nakanishi, This Bulletin, **26**, 183 (1953).
8) C. Araki and S. Hirase, ibid., **27**, 109 (1954).
9) C. Araki, *J. Chem. Soc. Japan*, **65**, 725 (1944).
10) S. Hirase and C. Araki, This Bulletin, **28**, 481 (1955).

$C_{10}H_{22}O_5S_2$: 42.68%). The values previously reported by two of the present authors[11] are m.p. 126-127° and $[\alpha]_D = \pm 0°$. The admixture of an authentic sample showed no depression of the melting point.

For further identification, the diethylmercaptal was converted to its penta-acetate by acetylation with acetic anhydride and pyridine. The acetate obtained was recrystallized from aqueous methanol; m.p. 112–113°; $[\alpha]_D^{18} = \pm 0°$ (chloroform, *c* 0.75). Reported values are m.p. 112-113° and $[\alpha]_D = \pm 0°$ (chloroform). Admixture with an authentic sample showed no depression of the melting point.

Summary

1. The mucilage of *Gloiopeltis furcata* has been investigated by the complete methanolysis method.

2. 3, 6-Anhydro-L-galactose dimethylacetal and methyl D-galactoside have been isolated from the methanolysate. In addition, L-galactose has also been isolated in the form of the crystalline DL-galactose diethylmercaptal.

3. The yields of the isolates have indicated that the mucilage used contains 3, 6-anhydro-L-galactose, D-galactose and L-galactose in the approximate molar ratio of 8 : 12 : 1.

One of the authors (S. H.) of the present report is obliged for a Grant in Aid for the Miscellaneous Scientific Research from the Department of Education for the year 1956–1957.

Institute of Chemistry, Faculty of Industrial Arts, Kyoto Technical University, Matsugasaki, Kyoto

11) C. Araki and S. Hirase, This Bulletin,, **26**, 463 (1953).

Studies on Antibiotics and Related Substances. IV. Synthesis of* DL-*threo*-β-*Cyclohexylserine and* DL-*threo*-2-*Dichloroacetamido*-1-*cyclohexylpropane*-1,3-*diol*

By Sumio UMEZAWA and Yoshihisa OGUMA

(Received August 23, 1956)

Synthesis of DL-*threo*-β-cyclohexylserine and its Derivatives.— In earlier papers[1] the reduction of E. Erlenmeyer's phenylserine[2] with Raney nickel catalyst in ethanol was found to yield DL-*threo*-2-benzylideneamino-1-phenylpropane-1, 3-diol (a Schiff base) as the main product. The present paper records the result of the reduction of the N-acetyl ester of phenylserine.

When ethyl DL-*threo*-N-acetyl-β-phenylserinate (I) was reduced with hydrogen over Raney nickel catalyst in ethanol, the product was ethyl DL-*threo*-N-acetyl-β-cyclohexylserinate (II) melting at 94–95°C. Hydrolysis of the N-acetyl derivative (II) by refluxing in dilute hydrochloric acid was followed by concentration of the solution *in vacuo* and subsequent neutralization to pH 6.8 with sodium hydroxide yielding crystalline DL-β-cyclohexylserine (III) melting at 231°C (dec.).

Confirmation of the structure of β-cyclohexylserine (III) was obtained in the following ways. III was oxidized by sodium periodate to give 62% crude yield of cyclohexanealdehyde, which was identified as the 2,4-dinitrophenylhydrazone and did not depress the melting point of an authentic sample of 2,4-dinitrophenylhydrazone of cyclohexanealdehyde prepared by hydrolysis and decarboxylation of ethyl cyclohexylglycidate[3]. The N-acetylcyclohexylserinate(II) was further acetylated with acetic anhydride in the presence of pyridine to yield ethyl N, O-diacetyl-β-cyclohexylserinate, m.p. 115.5–116.5°C, which, on hydrolysis under Kunz's conditions[4] (for O-acyl group), liberated two moles of carboxylic acid. As anticipated, ethyl N-acetylcyclohexylserinate liberated one mole of carboxylic acid under the same conditions. Thus, the presence of the cyclohexyl group and that of contiguous hydroxyl and amino groups in β-cyclohexylserine (III) were ascertained.

Since it is well established that the configuration of Erlenmeyer's phenylserine, the starting material, is of the *threo* configuration, it is necessary for III to be DL-*threo*-β-cyclohexylserine.

* Presented before the Division of Organic Chemistry at the Annual Meeting of the Chemical Society of Japan, at Kyoto University, April 3, 1956. Previous papers of this series: This Bulletin, 27, 477 (1954); 29, 417 (1956); 29, 979 (1956).

1) S. Umezawa and T. Suami, This Bulletin, 27, 477 (1954); T. Suami, and S. Umezawa, ibid., 29, 979 (1956).

2) E. Erlenmeyer, *Ber.*, 25, 3445 (1892).

3) G. Darzens, *Compt. rend.*, 142, 214 (1906).

4) A. Kunz and C. S. Hudson, *J. Am. Chem. Soc.*, 48, 1982 (1926); M. L. Wolfrom, M. Königsberg and S. Stolzberg, ibid., 58, 409 (1936).

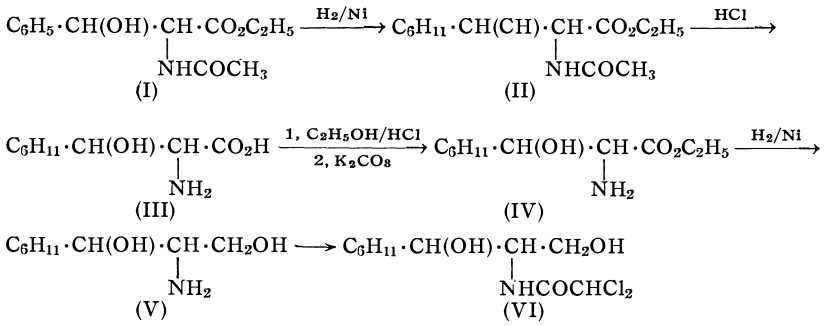

Synthesis of DL-*threo*-2-Dichloroacetamido-1-cyclohexylpropane-1, 3-diol.—The derivatives of 2-aminopropane-1, 3-diol have received considerable attention in recent years as analogues of chloramphenicol, an important antibiotic found by scientists of Parke, Davis and Company[5]. Ashley and Davis[6] recently synthesized an isomer of 2-amino-1-cyclohexylpropane-1, 3-diol by reduction of 2-nitro-1-cyclohexylpropane-1, 3-diol which was obtained by condensation of cyclohexanealdehyde with β-nitroethanol in the presence of sodium methoxide. The dichloroacetyl derivative of this isomer of 2-amino-1-cyclohexylpropane-1, 3-diol had no antibacterial activity and it was likely that this isomer is of the *erythro* configuration.

It became of interest to us to convert the ethyl ester of the above-mentioned β-cyclohexylserine (III) into the corresponding aminoalcohol. Ethyl DL-*threo*-β-cyclohexylserinate (IV), m. p. 60–61°C, was readily prepared from the above-mentioned β-cyclohexylserine (III) by the Fischer-Speier method. The catalytic reduction* of IV with hydrogen over Raney nickel catalyst at 150 kg./cm² and 100°C for 4.5 hours gave DL-*threo*-2-amino-1-cyclohexylpropane-1, 3-diol(V), m.p. 112–113°C. Acylation of V by refluxing with methyl dichloroacetate gave DL-*threo*-2-dichloroacetamido-1-cyclohexylpropane-1, 3-diol (VI), m. p. 167–168°C. It has now been found that, though the chloramphenicol analogue possesses the *threo* configuration, it shows no significant antibacterial activity.

Experimental

Ethyl DL-*threo*-N-Acetyl-β-phenylserinate(I).—Ethyl DL-*threo*-phenylserinate was prepared by treatment of Erlenmeyer's phenylserine in absolute ethanol with dry hydrogen chloride followed by liberating the aminoester by rendering alkaline with potassium carbonate, as reported by G. Carrara and G. Weitnauer[7]. The compound was very hygroscopic and decomposed upon prolonged standing.

With the aid of gentle warming, 6.0 g. of ethyl DL-*threo*-β-phenylserinate was dissolved in 6 cc. of glacial acetic acid and 2.8 cc. of acetic anhydride was added with stirring. The ethyl DL-*threo*-N-acetyl-β-phenylserinate separated as a crystalline mass and was filtered after keeping for thirty minutes, and then washed well with ether and water. The yield was 6.8 g. (91.8%) and m. p. 175–176°C. The compound was almost insoluble in ether and acetone, soluble in hot ethyl acetate and ethanol. Recrystallization from ethanol failed to raise the melting point.

Anal. Found: N, 5.52. Calcd. for $C_{13}H_{17}O_4N$: N, 5.57%.

Ethyl DL-*threo*-N-Acetyl-β-cyclohexylserinate (II).—A solution of 6.0 g. of ethyl DL-*threo*-N-acetyl-β-phenylserinate (I) in 150 cc. of absolute ethanol was shaken with 10 g. of Raney nickel catalyst[8] at 50–60°C and 130 kg./cm² for sixteen hours. The content was filtered to remove the catalyst and the solvent was removed *in vacuo*. The oily residue was dissolved in 25 cc. of ether and the solution was diluted with an equal volume of petroleumether, whereupon there separated a crystalline precipitate, which was collected after standing overnight; yield 5.3 g. (86.8%) and m. p. 83–88°C. Two recrystallizations from ether afforded 1.5 g. of pure ethyl DL-*threo*-N-acetyl-β-cyclohexylserinate (II) melting at 94–95°C. The compound liberated one mole of carboxylic acid on hydrolysis under Kunz's conditions[4].

Anal. Found: C, 60.96; H, 8.81; N, 5.65; saponification equivalent*, 275. Calcd. for $C_{13}H_{23}O_4N$: C, 60.68; H, 8.95; N, 5.44%; saponification equivalent*, 257.

DL-*threo*-β-Cyclohexylserine (III).—A mixture of 0.8 g. of ethyl DL-*threo*-N-acetyl-β-cyclohexylserinate in 16 cc. of 5% hydrochloric acid was refluxed for 2.5 hr. The solution was evaporated *in vacuo* to dryness and the resulting solid was dissolved in 10 cc. of water and the solution was neutralized to pH 6.8 by addition of 5 N sodium hydroxide. After standing overnight the cry-

5) J. Ehrlich. Q. R. Bartz, R. M. Smith and A. A. Joslyn, *Science*, **106**, 417 (1947); J. Controulis, M. C. Rebstock and H. M. Crooks, Jr., *J. Am. Chem. Soc.*, **71**, 2463 (1949), and later papers.

6) N. J. Ashley and M. Davis, *J. Chem. Soc.*, **1952**, 63.

* When this reduction was carried out at 50°C and 150 kg./cm² for seven hours, the original aminoester was recovered in a high yield.

7) G. Carrara and G. Weitnauer, *Gazz. chim. ital.*, **79**, 856 (1949); *C. A.* **44**, 7268 (1650).

8) Organic Syntheses, **21**, 15 (1940).

* Saponified under Kunz's conditions.

stalline precipitate was separated from the solution; yield 0.42 g. (72.5%) and m. p. 223°C (dec,) Two recrystallizations from distilled water gave 0.22 g. of pure DL-*threo*-β-cyclohexylserine, m. p. 231°C (dec.).

Anal. Found: C, 57.50; H, 9.38; N, 7.18. Calcd. for $C_9H_{17}O_3N$: C, 57.73; H, 9.15; N, 7.48%.

Ethyl DL-*threo*-N, O-Diacetyl-β-cyclohexylserinate.—A mixture of 0.52 g. of ethyl DL-*threo*-N-acetyl-β-cyclohexylserinate (II), 3.0 cc. of acetic anhydride and 2 cc. of pyridine was allowed to stand overnight at room temperature. The solution was poured into about 20 cc. of ice water with stirring. After standing for 2.5 hr., a yield of 0.40 g. of crude ethyl DL-*threo*-N, O-diacetyl-β-cyclohexylserinate was collected, m. p. 113.5–114.5°C. Purification for analysis was accomplished by dissolving the product in ether with subsequent addition of petroleum ether; yield 0.16 g. and m. p. 115.5–116.5°C. The N, O-diacetyl ester liberated two moles of carboxylic acid on hydrolysis under Kunz's conditions[4], indicating the presence of an O-acetyl and a carbethoxyl group.

Anal. Found: C, 60.13; H, 8.19; N, 4,96; O-acetyl, 13.8%. Calcd. for $C_{15}H_{25}O_5N$: C, 60.18; H, 8.35; N, 4.68; O-acetyl, 14.4%.

Periodate Oxidation of DL-*threo*-β-Cyclohexylserine.—A solution of 0.65 g. of sodium periodate hydrate in 25 cc. of distilled water containing ten drops of 6 N sulfuric acid was added with stirring to a solution of 0.5 g. of DL-*threo*-β-cyclohexylserine (III) in 15 cc. of distilled water containing five drops of 6 N sulfuric acid and warmed to about 40°C. After about thirty minutes the solution gave off the characteristic smell of an aldehyde. After standing overnight the reaction mixture was extracted four times with 15 cc. of ether. The pale-yellow ethereal extract was washed in turn with 5 cc. of 1% sodium carbonate solution and 5 cc. of distilled water and dried with anhydrous sodium sulfate. Removal of ether afforded 0.18 g. (62%) of crude hexahydrobenzaldehyde.

The crude hexahydrobenzaldehyde was dissolved in 1 cc. of ethanol and distilled water was added until the solution became just turbid. Again, ethanol was added until the mixture just clarified. To the solution were added 0.2 g. of semicarbazide hydrochloride and 0.3 g. of sodium acetate. The mixture was warmed for several minutes and allowed to stand overnight at room temperature. Concentration *in vacuo* gave 0.12 g. (44%) of crude semicarbazone, m. p. 168.5–170°C. After two recrystallizations from distilled water pure hexahydrobenzaldehyde semicarbazone, m. p. 172–173°C, was obtained, undepressed on admixture with the authentic sample prepared by decarboxylation of cyclohexylglycidic acid, as described below.

To a solution of 4.0 g. of sodium hydroxide in 11.5 cc. of distilled water was added 9.5 g. of ethyl cyclohexylglycidate[3] and the mixture was stirred for 6.5 hr. at 45–50°C. After standing overnight the reaction mixture was acidified with 6 N hydrochloric acid using Congo Red as indicator and then steamdistilled for about 4.5 hr. Extraction with benzene followed by vacuum distillation gave 10 g. of hexahydrobenzaldehyde, b. p. 56°C/24 mm. The semicarbazone melted at 171–172°C after recrystallization from distilled water.

Ethyl DL-*threo*-β-Cyclohexylserinate (IV).—A solution of 6.3 g. of DL-*threo*-β-cyclohexylserine (III) in 65 cc. of absolute ethanol was saturated with dry hydrogen chloride and allowed to stand overnight. Concentration *in vacuo* left an oily product, which was dissolved in 35 cc. of distilled water, washed twice with 10 cc. of ethyl acetate and rendered alkaline by addition of solid potassium carbonate. Extraction with ethyl acetate followed by removal of the solvent *in vacuo* gave 6.37 g. (86.5%) of crude ethyl DL-*threo*-β-cyclohexylserinate which could not be crystallized on prolonged standing. The crude ester was used in subsequent reduction without further purification.

However, it was found that the aminoester forms a crystalline oxalate and this furnishes a method of purifing and crystallizing the aminoester.

A sample of 0.4 g. of the crystalline oxalate prepared as described below was dissolved in 8 cc. of distilled water and rendered alkaline to pH 10 with potassium carbonate and extracted five times with 8 cc. of ethyl acetate, which were combined and dried with anhydrous sodium sulfate. Removal of the solvent *in vacuo* left a syrup which crystallized after standing overnight; yield 0.31 g. and m. p. 47–52°C. Four recrystallizations from petroleumether gave 0.09 g. of pure ethyl DL-*threo*-β-cyclohexylserinate, m. p. 60–61°C.

Anal. Found: N, 6.55. Calcd. for $C_{11}H_{21}O_3N$: N, 6.51%.

Oxalate of IV.—A solution of 0.11 g. of oxalic acid hydrate in 1 cc. of absolute ethanol was added to a solution of 0.15 g. of the crude syrup of ethyl DL-*threo*-β-cyclohexylserinate (IV) in 0.5 cc. of absolute ethanol. After addition of ether followed by stirring, the mixture was allowed to stand for two hours at room temperature. Colorless minute crystals which separated, were collected and washed with ether; yield 0.12 g. and m. p. 182–185°C (dec.). Recrystallizations from ethanol-water mixture (7:3) gave the oxalate of ethyl DL-*threo*-β-cyclohexylserinate (IV), $C_6H_{11}CH(OH)\cdot CHNH_2\cdot CO_2C_2H_5\cdot 1/2(COOH)_2$, m. p. 181–181.5°C (dec.).

Anal. Found: N, 5.57. Calcd. for $C_{12}H_{22}O_5N$: N, 5.38%.

DL-*threo*-2-Amino-1-cyclohexylpropane-1, 3-diol (V).—A solution of 2.83 g. of ethyl DL-*threo*-β-cyclohexylserinate (a crude syrup) in 50 cc. of absolute ethanol was hydrogenated over 4 g. of Raney nickel catalyst[8] at 95–100°C for 4.5 hr. under an initial pressure of 130 kg./cm². The catalyst was removed by filtration. The filtrate was concentrated *in vacuo* to about a fifth of its bulk, filtered from a small amount of solid impurity and the filtrate was again concentrated to give 2.97 g. of an oily product, which deposited a crystalline solid on standing overnight. Three recrystallizations from ethyl acetate gave colorless needles of DL-*threo*-2-amino-1-cyclohexylpropane-1, 3-diol; yield 0.32 g. (12.3%) and m. p. 112–113°C.

Anal. Found: C, 62.40; H, 10.89; N, 7.87. Calcd. for $C_9H_{19}O_2N$: C, 62.39; H, 11.05; N, 8.09%.

DL-*threo*-2-Dichloroacetamido-1-cyclohexylpropane-1,3-diol (VI).—A mixture of 0.13 g. of DL-

threo-2-amino-1-cyclohexylpropane-1, 3-diol (V) and 1.5 cc. of methyl dichloroacetate was refluxed for two hours. Removal of excess of the ester left 0.08 g. of a pale-green syrup. Washing with petroleum-ether and addition of ethyl acetate gave 0.03 g. (14%) of DL-*threo*-2-dichloroacetamido-1-cyclohexylpropane-1, 3-diol, m. p. 167–168°.

Anal. Found: N, 4.54. Calcd. for $C_{11}H_{19}O_3NCl_2$: N, 4.92%C.

The chloramphenicol analogue showed no significant antibacterial activity (test organism E. coli).

Summary

(1) When the N-acetyl ethyl ester of Erlenmeyer's phenylserine was reduced with hydrogen over Raney nickel catalyst, ethyl DL-*threo*-N-acetyl-β-cyclohexylserinate was obtained in crude yields as high as 86.8 %. Subsequent hydrolysis with dilute hydrochloric acid afforded DL-*threo*-β-cyclohexylserine, which gave hexahydrobenzaldehyde by periodate oxidation.

(2) Raney nickel reduction of ethyl DL-*threo*-β-cyclohexyl-serinate afforded DL-*threo*-2-amino-1-cyclohexylpropane-1, 3-diol. The aminoalcohol was converted into DL-*threo*-2-dichloroacetamido-1-cyclohexylpropane-1, 3-diol, a chloramphenicol analogue.

The authors are indebted to Mr. S. Nakada of this Laboratory for the microanalytical data.

Department of Applied Chemistry
Engineering Faculty of Keio
University, Tokyo

*Studies on Azeotropic Mixtures. I. General Considerations**

By Toshio YOSHIMOTO and Yo-ichiro MASHIKO

(Received July 13, 1956)

Introduction

In 1900 Zawidzki[1] showed in his pioneering study on the liquid solutions that non-ideal binary solutions could be classified into two types with positive and negative deviations from Raoult's law. He also showed that when the two components of such solution had sufficiently equal vapor pressures, the positive type yielded a maximum point and the negative one a minimum point in the vapor pressure-composition curve. These points are called azeotropic points and the solutions are said, at such points, to form azeotropes or azeotropic mixtures. It is well known that the liquid phase of an azeotrope may be transformed to the vapor phase without changing the composition of any of these phases. This is a condition of practical importance, since it limits the possibility of separation by fractional distillation.

Recently Prigogine[2] has investigated azeotropic phenomenon assuming the solution to be regular. In this paper we will treat the same phenomenon along his line but from a more explicit standpoint of molecular interaction, with the aim of comparing the azeotrope-forming power of a number of solutions.

Our assumption is that an azeotropic mixture can be regarded as a strictly regular solution[3] near its boiling point, which can be treated with the quasi-crystalline model, introducing explicit representation for interaction energy of component molecules. Component molecules of the azeotropic mixture are usually more or less polar or non-spherically shaped and at a lower temperature they are prevented by their dipoles or shapes from executing free rotation. Thus it is by no means a good approximation to assume that they constitute a strictly regular solution, i.e., solution with spherical molecules of sufficiently equal size and of weak interaction energy. However, near its boiling point, the rotations of component molecules will become free enough to allow them to be regarded as constituting a strictly regular solution. Thus, near the boiling point, though all molecules distributed on each site of the quasi-crystalline lattice may not be always executing completely free rotation, their dipole or other figure axes are considered to orient at random.

The above assumption seems to be too crude to interpret the azeotropic phenomenon quantitatively, but some successes obtained in this paper suggest that we are not far from the right way. It may be mentioned that we have some suggestions[4] to interpret

* Presented at the 9th Annual Meeting of the Chemical Society of Japan held in Kyoto, April, 1956.

1) J. V. Zawidzki, *Z. physik. Chem.*, 35, 129 (1900).

2) I. Prigogine and R. Defay, "Chemical Thermodynamics", Translated by D. H. Everett, Longmans (1954), chapt. XXVIII.

3) E. A. Guggenheim, "Mixture", Oxford (1952), chapt. IV.

4) R. S. Halford, *J. Chem. Phys.*, 8, 496 (1940); K. S. Pitzer, *J. Chem. Phys.*, 7, 583 (1939).

the deviation from Trouton's or Hildebrand's constant of real pure liquids by similar assumptions.

Derivation of Basic Formula for an Azeotropic Mixture

In the following study we will restrict our consideration to the binary solution. The molar Helmholtz free energy of pure components 1 and 2 is

$$\Delta_m F = RT(x_1 \ln x_1 + x_2 \ln x_2) + N x_1 x_2 w. \quad (1)$$

Here, x_i is the mole fraction of component $i (i=1, 2)$, T the absolute temperature, N the Avogadro number and R the gas constant. The equation is the zeroth approximation (treatment of random mixing) of the quasi-chemical treatment of strictly regular solution developed by Guggenheim[3] and it will be shown later that the approximation is quite reasonable within the range considered, so that we do not need further higher terms. w is a quantity determining the non-ideality of the solution and is called molecular interchange energy. We will give its explicit form in terms of the absolute average potential energy ε of the pair of molecules:

$$w = \frac{z}{2}(\varepsilon_{11} + \varepsilon_{22} - 2\varepsilon_{12}). \quad (2)$$

z denotes the average number of nearest neighbors of a given molecule, i.e., the coordination number of the molecule on the quasi-lattice. In making a single exchange of molecule between liquid 1 and 2, we destory z 1-1 and z 2-2 pairs and form $2z$ 1-2 pairs of nearest neighbors, and the increase of potential energy is $2w$.

Denoting μ_i and γ_i the chemical potential and the activity coefficient of the ith component and the superscript o referring to the pure component, we obtain the chemical potentials from equation (1) by a usual procedure,

$$\mu_1 - \mu_1^0 = RT \ln x_1 + N x_2^2 w, \quad (3)$$

$$\mu_2 - \mu_2^0 = RT \ln x_2 + N x_1^2 w. \quad (4)$$

Further from the definition of the activity coefficient, we have

$$\mu_1 - \mu_1^0 = RT \ln x_1 \gamma_1, \quad (5)$$

$$\mu_2 - \mu_2^0 = RT \ln x_2 \gamma_2. \quad (6)$$

From these equations, we get

$$\ln \gamma_1 = \frac{Nw}{RT} x_2^2, \quad (7)$$

$$\ln \gamma_2 = \frac{Nw}{RT} x_1^2. \quad (8)$$

These are Hildebrand's relations for the regular solution and Nw corresponds to his constant B[5].

We will now turn to the equilibrium between the vapor and the liquid phase of binary azeotropic mixture[6]. In equilibrium state the chemical potentials of component i in both phases are equal:

$$\mu_i = \mu_{i'},$$

where

$$\mu_i = \mu_i^0 + RT \ln x_i \gamma_i, \quad (9)$$

$$\mu_{i'} = \mu_i^{0'} + RT \ln x_{i'} \gamma_{i'}. \quad (10)$$

In these equations a single prime refers to the vapor phase and no prime to the liquid one. Thus we obtain

$$\ln \frac{x_{i'} \gamma_{i'}}{x_i \gamma_i} = -\frac{\mu_i^{0'} - \mu_i^0}{RT}. \quad (11)$$

As the activity coefficient is the function of temperature and pressure, we obtain the following equation by considering an infinitesimal increment of the chemical potential in going from the liquid to the vapor phase,

$$\begin{aligned} \delta\left(\ln \frac{x_{i'} \gamma_{i'}}{x_i \gamma_i}\right) &= \left\{\frac{\partial\left(-\frac{\mu_i^{0'} - \mu_i^0}{RT}\right)}{\partial T}\right\}_p dT \\ &\quad + \left\{\frac{\partial\left(-\frac{\mu_i^0 - \mu_i^0}{RT}\right)}{\partial p}\right\}_T dp \\ &= -\frac{\Delta_v H_i^0}{RT^2} dT - \frac{\Delta_v V_i^0}{RT} dp, \end{aligned} \quad (12)$$

since

$$\left\{\frac{\partial(\mu_i/T)}{\partial T}\right\}_p = -\frac{H_i}{T^2} \quad (13)$$

and

$$\left(\frac{\partial \mu_i}{\partial p}\right)_T = V_i. \quad (14)$$

Here, $\Delta_v H_i^0$ is the molar heat of vaporization and $\Delta_v V_i^0$ the molar volume change of vaporization of ith pure component. We integrate the equation from an initial state T_i^0, p_i^0, $x_i^0 = 1$, $x_i^{0'} = 1$, $\gamma_i^0 = 1$, $\gamma_i^{0'} = 1$, corresponding to the vapor-liquid equilibrium of the pure component i, to a final equilibrium state (azeotropic point) T^a, p^a, x_i, $x_{i'}$, γ_i, $\gamma_{i'}$, so that

$$\ln \frac{x_{i'} \gamma_{i'}}{x_i \gamma_i} = \int_{T_i^0}^{T^a} \frac{\Delta_v H_i^0}{RT^2} dT - \frac{1}{RT} \int_{p_i^0}^{p^a} \Delta_v V_i^0 dp. \quad (15)$$

5) J. H. Hildebrand and R. L. Scott, "The Solubility of Non-electrolytes", Reinhold (1950), 121.
6) I. Prigogine and R. Defay, op. cit,, chapt. XVIII.

An azeotrope is formed when, in a closed system, the mass of one of the phases increases at the expense of the others without changing the composition. When the equilibrium is attained from, the definition of azeotrope formation, we have a condition as follows:

$$x_i = x_{i'}. \tag{16}$$

At a constant pressure (1 atm.) we have to consider only the first term of the right hand of equation (15). For most practical cases, it is sufficiently accurate to assume the heat of vaporization to be independent of temperature in the range considered and the vapor to be perfact ($\gamma_{i'}=1$), so we have

$$\ln \gamma_i = \frac{\Delta_v H_i^0}{RT_i^0}\frac{T_i^0-T^a}{T^a} = \frac{\Delta_v S_i^0}{R}\frac{T_i^0-T^a}{T^a}, \tag{17}$$

where $\Delta_v S_i^0$ is the molar entropy of vaporization of ith pure component. At a constant temperature T^a, we have, again taking the vapor to be perfect and neglecting the liquid volume compared with vapor one $\Delta_v V_i^0 = V_i^{0'} - V_i^0 \simeq V_i^{0'} \simeq RT^a/p$),

$$\gamma_i = p^a/p_i^0. \tag{18}$$

Thus we can combine equations (17) and (18) with (7) and (8) at the azeotropic point to obtain final equations for the azeotropic mixture.

At constant pressure ($p=1$ atm.) we have

$$\Delta_v S_1^0(T_1^0-T^a) = Nwx_2^2, \tag{19}$$

and

$$\Delta_v S_2^0(T_2^0-T^a) = Nwx_1^2. \tag{20}$$

At constant temperature T^a we have

$$RT^a \ln (p^a/p_1^0) = Nwx_2^2, \tag{21}$$

and

$$RT^a \ln (p^a/p_2^0) = Nwx_1^2. \tag{22}$$

Entirely the same equations as those from (19) to (22) can be derived from the final equations given by Prigogine[7] except that he has not retained Nw (α in his equations in an explicit form (2) in his further discussion of azeotropic mixtures. In the following discussion we will mainly use the equations (19) and (20), since most of the azeotropic data are investigated under constant pressure (1 atm.).

Here, it should be mentioned that if we take higher terms in the quasi-chemical treatment, we have, instead of equations (19) and (20),

$$\Delta_v S_1^0(T_1^0-T^a) = Nwx_2^2\left\{1+\frac{2x_1(x_1-x_2)}{2!}\left(\frac{2w}{zkT^a}\right) + \frac{2x_1(x_1-x_2)(1-6x_2+6x_2^2)}{3!}\left(\frac{2w}{zkT^a}\right)^2+\cdots\right\} \tag{23}$$

and

$$\Delta_v S_2^0(T_2^0-T^a) = Nwx_1^2\left\{1-\frac{2x_2(x_1-x_2)}{2!}\left(\frac{2w}{zkT^a}\right) - \frac{2x_2(x_1-x_2)(1-6x_2+6x_2^2)}{3!}\left(\frac{2w}{zkT^a}\right)^2-\cdots\right\}, \tag{24}$$

where k is Boltzmann's constant.

In the quasi-chemical approximation[8] w/kT cannot for example, exceed 2.301 for a body-centered cubic lattice, $z=8$, or 2.188 for a face-centered cubic lattice, $z=12$, without phase separation. Thus within the range $1>x_2\geq\frac{1}{2}$ in (23) and the range $1>x_1\geq\frac{1}{2}$ in (24), even the second term of the series cannot exceed 0.072 or 0.046 for the respective lattice, the higher terms being much smaller. Therefore, as far as we take the data from these ranges or their vicinity it will be sufficiently accurate to leave only the first terms as we did, but as x_2 approaches 0 in (23) and x_1 approaches 0 in (24) the error of the above approximation will be considerable. As the first step, however, we will start with the approximate equations (19) and (20) to compare the azeotrope-forming power of a number of azeotropic mixtures.

Azeotrope-forming Power and Condition for Azeotrope Formation

It is of interest for our purpose to see whether an azeotrope is of a maximum or minimum type according to the sign of w, and how the magnitude of w determines the range of boiling points or vapor pressures of pure components allowable in azeotrope formation.

If w is positive in sign we have the minimum azeotrope with T_1^0, $T_2^0 > T^a$ from equations (19) and (20) or positive azeotrope with $p^a > p_1^0$, p_2^0 from equation (21) and (22). If w is negative we have the maximum azeotrope with T_1^0, $T_2^0 < T^a$ or negative azeotrope with $p^a < p_1^0$, p_2^0 conversely.

For an azeotrope to have existence in homogeneous solution, x_i must lie between 0 and 1. Therefore as conditions of azeotrope existence we can readily derive from equations (19) and (20) or (21) and (22),

$$-\frac{Nw}{\Delta_v S_2^0} \leq T_1^0 - T_2^0 \leq \frac{Nw}{\Delta_v S_1^0} \tag{25}$$

7) I. Prigogine and R. Defay op. cit., p. 455 (28.25), (28.22).

8) E. A. Guggenheim, op. cit., p. 41.

or $$-\frac{Nw}{RT^a}\leq\ln(P_1^0/P_2^0)\leq\frac{Nw}{RT^a} \quad (26)$$

respectively.

Equation (26) is also derived by Prigogine[9]. The equality in equation (25) will give maximum and minimum boiling temperatures of pure component 1. Between these temperatures various kinds of component 1 are allowed to form azeotropes with a fixed component 2. Thus w is considered as a measure of the azeotropeforming power of solutions. The larger the value of w, the more different boiling points the component 1 and 2 can have in azeotrope formation.

Discussion

For the discussion of various kinds of azeotropic mixtures it is appropriate to group them into four classes* as shown in Tables I–IV, according to the following different types of intermolecular forces: (1) force between non-polar molecules (dispersion effect): (2) force between permanent dipoles (dipole-dipole interaction): (3) force between a permanent dipole and an induced dipole (dipole-induced dipole interaction). For simplicity, we will involve in the type (2) the attraction due to hydrogen bonding that is essentially electrostatic. Among these types the second appears to have the most important effect on azeotrope formation.

(a) Dispersion Force Solutions

London[10] derived for the absolute value of an attractive potential between 1 and 2 molecule

$$\epsilon_{12}=-\frac{3\alpha_1\alpha_2}{2r_{12}^3}\frac{h\nu_{01}\cdot h\nu_{02}}{h\nu_{01}+h\nu_{02}}, \quad (27)$$

where h is Planck's constant, α_i the polarizability of the ith molecule and $h\nu_{0i}$ is the energy closely related to the ionization potential of the i-th molecule. In the model under consideration the distances between all molecules may be taken as nearly equal:

$$r_{11}=r_{12}=r_{22}=r.$$

Equations (2) and (27) can now be used to obtain

$$w=\frac{3}{2}\frac{z}{2}\frac{h}{r^6}\left\{\frac{\nu_{01}\alpha_1^2}{2}+\frac{\nu_{02}\alpha_2^2}{2}-2\frac{\nu_{01}\cdot\nu_{02}}{\nu_{01}+\nu_{02}}\alpha_1\alpha_2\right\}.$$

Noting that

$$\frac{\nu_{01}\cdot\nu_{02}}{\nu_{01}+\nu_{02}}\leq\frac{\sqrt{\nu_{01}\cdot\nu_{02}}}{2},$$

we conclude that

$$w\geq\frac{3}{2}\frac{z}{2}\frac{h}{r^6}\left\{\frac{\nu_{01}\alpha_1^2}{2}+\frac{\nu_{02}\alpha_2^2}{2}-\sqrt{\nu_{01}\cdot\nu_{02}}\,\alpha_1\alpha_2\right\}. \quad (28)$$

Thus we see that if the interactions are caused solely by dispersion force we must always have

$$w\geq 0$$

and so azeotropes, if any, are always minimum. Examples are found in azeotropes between two different types of hydrocarbons, i.e. aromatics-paraffins and aromatics-naphthens. Another examples are azeotropes between non-polar liquids and paraffinic or naphthenic hydrocarbons. Some of them (No. 1 to 5 for the former, 6 for the latter examples) are listed in Table I together with their calculated w values. Here we see that values of w calculated from equation (19) or (20) show agreement as a whole.

(b) Solutions Involving Addition Compounds

We shall have an "addition compound" in a case where the potential energies ϵ_{11} and ϵ_{22} are of the same order of magnitude, while,

$$\epsilon_{12}\gg\epsilon_{11},\ \epsilon_{22},$$

and so

$$w<0.$$

We thus have maximum type azeotropes in this case. It appears reasonable to attribute these intermolecular forces mainly to the dipole interaction due to hydrogen bonding between components 1 and 2, but here we will not proceed further to the quantitative discussion as in the case of free molecules because of the inapplicability of simple Boltzmann's statistics. A number of instances are found in azeotropes between polyhalogen compounds and the compounds involving donor atoms such as esters, ketones, aldehydes, ethers and acetals. Examples are listed in Table II.

(c) Solutions Involving Associations in Non-polar Solvents

In this class ϵ_{22} is far more important than ϵ_{11} and ϵ_{12}, where ϵ_{22} is considered to be due mainly to dipole-dipole, ϵ_{11} to dispersion effect and ϵ_{12} to dipole-induced dipole interactions. The ϵ_{22} is frequently due to strong hydrogen bonding. That is,

$$\epsilon_{22}\gg\epsilon_{12}>\epsilon_{11}$$

and so

$$w>0.$$

We thus have minimum type azeotropes. Examples are listed in Table III.

(d) Solutions Involving Associations in Polar Solvents

In a way similar to class (c) ϵ_{22} is greater

9) I. Prigogine and R. Defay, op. cit., p. 465 (28.50).

* Similar classification was given by I. Prigogine and R. Defay, op. cit., p. 385ff.

10) F. London, *Trans. Faraday Soc.*, **33**, 19 (1937), *J. Phys. Chem.*, **46**, 305 (1942).

than ε_{12} or ε_{11}, but the differences between them are not so great as in class (c), the difference between ε_{11} and ε_{12} being smaller than that between ε_{22} and ε_{12}:

$$\varepsilon_{22}>\varepsilon_{12},\ \varepsilon_{22}>\varepsilon_{11},\ (\varepsilon_{22}-\varepsilon_{12})>\varepsilon_{11}-\varepsilon_{12},$$

so still we have

$$w>0.$$

Here all ε's are considered to be due to a certain extent to dipole interaction (or hydrogen bonding). Thus azeotropes are minimum, but their extents are not so great as in the class (c), with a few exceptions. Examples are given in Table IV.

TABLE I

AZEOTROPIC DATA OF CLASS (a)

No.	Component 2	Component 1	T_2^0 (°C)	T_1^0 (°C)	T^a (°C)	x_2[a] (mole fraction)	$\Delta_v S_1^{0b}$ $\left(\frac{\text{cal}}{M°C}\right)$	$\Delta_v S_1^{0b}$ $\left(\frac{\text{cal}}{M°C}\right)$	Nw_1 $\left(\frac{\text{kcal}}{M}\right)$	Nw_2 $\left(\frac{\text{kcal}}{M}\right)$
1	Benzene	2,2-Dimethylpentane	80.15	79.1	75.85	0.526	(20.3)	20.8	0.24	0.40
2	Benzene	2,4-Dimethylpentane	80.15	80.8	76.7	0.536	(20.3)	20.8	0.40	0.48
3	Benzene	Cyclohexane	80.15	80.6	77.7	0.537	20.4	20.8	0.20	0.24
4	Toluene	2,3,4-Trimethylpentane	110.7	113.5	109.5	0.615	(20.3)	20.8	0.19	0.20
5	Toluene	*cis-trans-cis*-1,2,4-trimethylcyclopentene	110.7	109.3	107.4	0.439	(20.3)	20.8	0.24	0.24
6	Carbon disulfide	Cyclopentane	46.25	49.4	44.0	0.652	(20.3)	20.0	0.25	0.37

Azeotropic data are taken from Horsely's "Azeotropic Data" published in 1956 by the American Chemical Society except for butanethiol (R.L. Denyer, F.A. Fidler and R.A. Lowry, *Ind. Eng Chem.*, **41**, 2727 (1949).

a) Mole fractions calculated from wt. % in Horsely's data.

b) Values taken from "International Critical Table", Vol. V (1929).

Values enclosed in parentheses are those presumed from similar substances.

TABLE II

AZEOTROPIC DATA OF CLASS (b)

No.	Component 2	Component 1	T_2^0 (°C)	T_1^0 (°C)	T^a (°C)	x_2[a] (mole fraction)	$\Delta_v S_1^{0b}$ $\left(\frac{\text{cal}}{M°C}\right)$	$\Delta_v S_2^{0b}$ $\left(\frac{\text{cal}}{M°C}\right)$	Nw_1 $\left(\frac{\text{kcal}}{M}\right)$	Nw_2 $\left(\frac{\text{kcal}}{M}\right)$
1	Trichloromethane	2-Propanone	61.2	56.10	64.43	0.640	22.0	21.0	−0.45	−0.52
2	Bromodichloromethane	2-Butanone	90.2	79.6	90.85	0.790	21.7	(21.0)	−0.39	−0.31
3	Bromodichloromethane	3-Methyl-2-butanone	90.2	95.4	97.2	0.348	(21.0)	(21.0)	−0.31	−0.35
4	Bromodichloromethane	Propyl Ethanonate	90.2	101.6	102.3	0.207	21.9	(21.0)	−0.36	−0.40
5	Bromodichloromethane	Methyl Carbonate	90.2	90.35	91.95	0.499	21.8	(21.0)	−0.14	−0.15
6	Trichloroethylene	Diethoxymethane	86.9	87.9	89.2	0.477	(21.7)	21.0	−0.12	−0.18

TABLE III

AZEOTROPIC DATA OF CLASS (c)

No.	Component 2	Component 1	T_2^0 (°C)	T_1^0 (°C)	T^a (°C)	x_2[a] (mole fraction)	$\Delta_v S_1^{0b}$ $\left(\frac{\text{cal}}{M°C}\right)$	$\Delta_v S_2^{0b}$ $\left(\frac{\text{cal}}{M°C}\right)$	Nw_1 $\left(\frac{\text{kcal}}{M}\right)$	Nw_2 $\left(\frac{\text{kcal}}{M}\right)$
1	Trichloromethane	2,3-Dimethylbutane	61.2	58.0	55.5	0.391	(20.3)	21.0	0.33	0.32
2	Acetonitrile	Carbon tetrachloride	81.6	76.75	75.3	0.434	20.4	20.2	1.26	1.04
3	Acetonitrile	Benzene	81.6	80.1	73	0.494	20.8	20.2	0.61	0.68
4	Nitromethane	Toluene	101.2	110.75	96.5	0.648	20.8	22.1	0.71	0.84

No.	Component 2	Component 1	T_2^0 (°C)	T_1^0 (°C)	T^a (°C)	x_2[a] (mole fraction)	$\Delta_v S_1^{0b}$ $\left(\frac{\text{cal}}{M°C}\right)$	$\Delta_v S_1^{0b}$ $\left(\frac{\text{cal}}{M°C}\right)$	Nw_1 $\left(\frac{\text{kcal}}{M}\right)$	Nw_2 $\left(\frac{\text{kcal}}{M}\right)$
5	Nitromethane	Cyclohexane	101.2	80.75	70.2	0.349	20.4	22.1	1.76	1.62
6	Nitromethane	Heptane	101.2	98.4	80.2	0.492	20.6	22.1	1.55	1.79
7	Butanethiol	Heptane	98.58	98.40	95.45	0.520	20.6	(23.4)	0.23	0.32
8	Butanethiol	Methylcyclohexane	98.58	101.05	97.0	0.603	20.2	(23.4)	0.22	0.23
9	Phenol	Indene	182.2	183.0	177.8	0.523	(20.3)	(22)	0.39	0.43
10	1,2-Benzenediol	2-Methylnaphthalene	245.9	241.15	233.25	0.431	(20.3)	(22.5)	0.86	0.88
11	1,3-Benzenediol	2-Methylnaphthalene	281.4	241.15	240.05	0.131	(20.3)	(23.5)	1.30	1.29

TABLE IV
AZEOTROPIC DATA OF CLASS (d)

No.	Component 2	Component 1	T_2^0 (°C)	T_1^0 (°C)	T^a (°C)	x_2[a] (mole fraction)	$\Delta_v S_1^{0b}$ $\left(\frac{\text{cal}}{M°C}\right)$	$\Delta_v S_2^{0b}$ $\left(\frac{\text{cal}}{M°C}\right)$	Nw_1 $\left(\frac{\text{kcal}}{M}\right)$	Nw_2 $\left(\frac{\text{kcal}}{M}\right)$
1	Acetonitrile	Methyl Propanoate	81.6	79.85	76.2	0.479	21.9	20.2	0.35	0.40
2	Acetonitrile	Propyl methanoate	81.6	80.85	76.5	0.513	22.0	20.2	0.36	0.44
3	Acetonitrile	1-Chlorobutane	81.6	78.5	67.2	0.526	(20.7)	20.2	0.85	1.29
4	Acetonitrile	1-Chloro-2-methylpropane	81.6	68.85	62.0	0.360	(20.7)	20.2	1.09	0.97
5	Nitromethane	1-Bromobutane	101.2	101.5	90.0	0.691	(20.7)	22.1	0.50	2.60
6	Nitromethane	1-Bromo-2-methylpropane	101.2	91.4	84.0	0.536	(20.7)	22.1	0.53	1.77
7	Nitromethane	2-Iodopropane	101.2	89.45	82.0	0.579	(20.7)	22.1	0.46	2.40
8	Nitromethane	2-Pentanone	101.2	102.35	99.15	0.643	(21)	22.1	0.16	0.36
9	Nitromethane	3-Pentanone	101.2	102.05	99.1	0.633	20.9	22.1	0.16	0.34
10	Nitromethane	Ethyl Propanoate	101.2	99.1	96.0	0.474	22.0	22.1	0.31	0.42
11	Nitromethane	Methyl Butanoate	101.2	102.65	97.95	0.627	21.7	22.1	0.26	0.52
12	Nitromethane	Propyl Ethanoate	101.2	101.6	97.6	0.578	21.9	22.1	0.26	0.45
13	1,2-Benzendiol	1,4-Dibromobenzene	245.9	220.25	218.15	0.192	(21.3)	(22.5)	1.21	0.96
14	1,2-Benzendiol	1-Chloronaphthalene	245.9	262.7	241.0	0.680	(21.3)	(22.5)	1.00	1.08

In the above classifications all ε's in each type of solution of course involve more or less attractive energy due to dispersion effect.

So far we have considered the azeotropic mixtures on the basis of the fairly simple model proposed. Apparently it is not satisfactory for quantitative discussions, since the values of w_1 and w_2 calculated from equations (19) and (20), respectively, do not agree so well with each other, though they show rough coincidences. The cause of considerable disagreements in No. 1 and 6 of Table I is uncertain and will be left to further study. It is mentioned, however, that this disagreement may be partly due to the approximation we used on the one hand and to the errors introduced in experimental data on the other hand. In the class (d) solution such a disagreement is remarkable and in most cases $w_1 < w_2$. This will give a measure of the deviation of activity coefficients from regular solutions.

It is of great interest to see how w's change with varying pairs of component molecules in connection with the azeotrope-forming power of solutions. In general the decreasing order of azeotrope-forming power are (c), (d), (a) in minimum type azeotropes.

Summary

The general expression for the azeotrope-forming power of binary solution has been derived and the conditions for azeotrope existence presented. The quasi-crystalline model has been adopted for the solution, which is assumed to be a strictly regular solution at an azetropic point and an explicit representation for interaction energy of component molecules introduced.

Azeotropic mixtures have been grouped into four classes according to the type of molecular interaction and the azeotrope-forming power (molecular interchange energy) has been calculated and discussed.

Government Chemical Industrial Research Institute, Tokyo

An Anomalous Catalytic Activity of Reduced Silver

By Kozo HIROTA and Yasushi KOBAYASHI

(Received August 3, 1956)

Introduction

Though metallic silver is often used an oxidation catalyst, its activity does not seem clarified yet in spite of its simple structure as compared to that of defect catalysts. In the course of our study[1,2] on the isotopic exchange reaction between heavy oxygen and carbon dioxide, $O^*_{ads.} + CO_2 \rightleftarrows O_{ads.} + COO^*$, we were obliged to conclude that even when the silver catalyst is reduced at 300°C for five hours before each run, there remain some chemical species containing oxygen which can exchange with the gaseous one. As the experiment was carried out under the partial pressure of oxygen of about 70 mmHg, the formation of silver oxide is improbable from the view point of thermodynamics[3]. On the other hand, as the exchangeable oxygen was found to exist in so great an amount that it is of comparable order of magnitude to that which was monomolecularly adsorbed[4], it was presumed that they may remain as an occluded state in the layers very close to the surface (subsurface) rather than as the adsorbed state on the surface. Both sorts of oxygen-containing species may probably be oxygen atoms, as assumed in the present paper and also by other researchers[5,6] in which, however, only the adsorbed state was considered.

The present research was begun in order to support the above presumption with experimental facts, studying the behaviour of oxygen adsorbed by the silver catalyst in detail, with special regard to the method of reduction of the catalyst. To meet the object, the exchange reaction between adsorbed oxygen and carbon dioxide was utilized as well as the reaction between adsorbed oxygen and carbon monoxide, $O_{ads.} + CO \longrightarrow CO_2$, which can easily occur even at room temperature[5].

Experimental

The catalyst (10.0 g.) was newly prepared by reducing the silver oxide with a flow of hydrogen gas at 300°C, similarly as in the previous reports[1,2]. Preparation of the silver oxide was different only in the procedure that, instead of ammonium hydroxide, it was precipitated by barium hydroxide as done Benton et al.[7]. The precipitated silver oxide was washed with distilled water free from carbon dioxide, until no barium ion was detected in the filtrate. It was found that this catalyst has a normal lattice distance 4.086 Å, as compared to the values in the tables*. The catalyst was reduced again in each run before the experiments at 250°C or 275°C to minimize the possible sintering of the catalyst.

The apparatus is shown in Fig. 1, its wall was made of hard glass, the reaction tube was 119 ±1 cc. (NTP) and the catalyst was spread on the wall of the tube a few millimeters in thickness. The temperature of the furnace was kept constant within ±1°C for a few hours and within ±5°C for a few days by the use of an automatic controlling device.

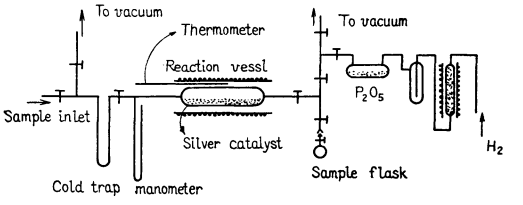

Fig. 1. Schematic diagram of the apparatus

The heavy oxygen (OO*) used was prepared in our laboratory by a thermal diffusion column, its molar isotopic concentration being 2.58%. The abundance ratios of OO^*/O_2 and COO^*/CO_2 were determined mass-spectrometrically. The accuracy of one determination of the abundance ratio was ±0.05%.

1) H. Mori, K. Hirota and Y. Kobayashi, This Bulletin, 28, 532 (1955).
2) H. Mori, Y. Kobayashi and K. Hirota, *Shokubai*, 12, 34 (1955).
3) A. F. Benton and R. P. Bell *J. Am. Chem. Soc.*, 56, 501 (1934).
4) Y. Kobayashi, K. Hirota and T. Otaki, unpublished.
5) D. Garvin, *J. Am. Chem. Soc.*, 76, 1581 (1954).
6) cf. T. Titani et al., *J. Chem. Soc. Japan*, 55, 13, 224, 305 (1934).
7) A. F. Benton and L. C. Drake, *J. Am. Chem. Soc.*, 54, 2186 (1932); 56, 255 (1934).
* Landolt-Börnstein, 6. Aufl., 4.077s KX (25°C); Natl. Bur. St., 4.086$_2$Å.

TABLE I

EXPERIMENTAL RESULTS (Reaction Temperature: 200°C)

No. of Runs	Time of the 1st Outgassing (hr.)	Press. before the Reduction (mmHg)	Reduction Time (hr.)	Time of the 2nd Outgassing (hr.)	Initial Gas and Press. (mmHg)	OO*, CO* or COO* % in the Gas	OO* or COO* % in Gas after the Reaction (Time in hr.)		
I.	Experiment I			(Reduction Temperature 250°C)					
1	—	$\sim 10^{-5}$	8	4	O_2 76	2.58	2.36 (1/3)	2.08 (1)	1.82 (25)
2	3	2×10^{-4}	10	5	O_2 82	2.58	2.58 (0.5)	2.44 (16.5)	
3	5.5	1×10^{-4}	18	4	CO_2 24	0.40	0.92 (3)	—	
4	3.5	5×10^{-5}	40(7)	4	O_2 73	2.58	—	2.41 (18)	
II.	Experiment II			(Reduction Temperature: 275°C)					
5	5.5	1×10^{-5}	65(16)	6	O_2 61	2.58	2.58 (3)	2.46 (18)	
6	4	3×10^{-5}	—	—	CO_2 29	0.40	0.87 (3)	0.98 (20)	
7	24	$\sim 10^{-4}$	18(3)	4	O_2 91	2.58	2.58 (3)	2.48 (44)	
8	5	$\sim 10^{-5}$	18(3)	5	CO_2 70	0.40	0.46 (3)	0.43 (19)	
9	4	$\sim 10^{-5}$	18.5(3)	5.5	CO 58	0.20	0.20 (3)	0.20 (20)	
10	5	$\sim 10^{-5}$	18(3)	5	O_2 50	0.40	0.68 (3)	0.92 (20)	

N. B.

Pressure of the second outgassing need not be described, because it reached to 10^{-6} mmHg within a few minutes. The first outgassing of No. 5 was carried out at 250°C. Numerals in parentheses in the fourth column designate the time of reduction by flowing hydrogen gas.

Results

All the experiment which is shown in Table I was performed, in the order of the number of runs, and can be divided into I and II.

The first experiment (I) was done, in order to confirm the conclusion reported already that some chemical species containing oxygen atoms remain in the catalyst even after the reduction by hydrogen. Hereafter this sort of oxygen will be called the residual oxygen, the existence of which was really shown by the reduction at 250°C, as will be described.

By the decrease of concentration of heavy oxygen in the gas (No. 1) eight hours' contact of hydrogen was insufficient to remove all the residual oxygen, while by the repeated treatment of heavy oxygen these kinds of oxygen were fairly replaced by the heavy ones (No. 2). This catalyst was then treated by normal carbon dioxide in the next run (No. 3), by which the possible exchange effect with heavy oxygen charged in the catalyst was observed. The dilution of the heavy oxygen which ought to be brought about by this procedure was confirmed by the next run (No. 4). In this run, notwithstanding the fact that the catalyst was reduced for forty hours, for seven of which hydrogen gas was allowed to flow over the catalyst the decrease of heavy oxygen concentration was observed to the degree equivalent to the dilution which occurred in No. 3. It seems that because of the process of severer reduction, the object, to charge the catalyst with heavy oxygen, was practically attained by only one run.

As the existence of oxygen in the catalyst even after the reduction at 250°C was shown by the above experiment, the second experiment (II) was carried out, in order to investigate its nature in detial, i.e., presumption in the former report. In the present series of runs, the reduction and degassing temperatures were raised from 250°C to 275°C, so as to remove the oxygen occluded as much as possible.

In the run next to No. 4, heavy oxygen was again diluted (No. 5), when it was brought into contact with the catalyst, probably because of a severer condition than in Exp. I. Then if the catalyst was only degassed and not reduced before the introduction of carbon dioxide, the exchange effect was observed as in No. 3, suggesting that exchangeable oxygen remains on the surface (No. 6). However, if the catalyst was reduced (No. 7) and was again brought into contact with carbon dioxide (No. 8), it seemed that the above oxygen had been removed, because in this run, the isotopic composition of the carbon dioxide did not change practically. Moreover, it was found in No. 9 that carbon monoxide neither exchanges nor reacts with the residual oxygen as shown by the constancy of its isotopic composition and its pressure. However, the possible suspicion that heavy oxygen might already be removed completely was rejected by making normal oxygen contact with the catalyst (No. 10); i.e., heavy oxygen still remained in the catalyst after the

repeated reduction process before the commencement of three runs (No. 8, 9 and 10).

Discussion

Now, the above result will be discussed in more details. First, if it is assumed that the concentration of the residual oxygen in the catalyst is 2.48% (No. 7) and that an equilibrium is realized between normal oxygen and the residual heavy oxygen after twenty hours of contact (No. 10), giving 0.92% as the concentration of the latter, the total amount of oxygen per gram-catalyst remaining in the catalyst, if expressed by gaseous volume (NTP), will be given by

$$69\text{ cc.}\times\frac{0.92-0.40}{2.48-0.92}\times\frac{50(\text{cm.})}{760(\text{cm.})\times 10.0\text{ g.}}$$
$$=0.15_1\text{ cc./g.-cat.} \qquad (A)$$

considering that the gaseous volume in the tube at 200°C corresponds to 69 cc. (=119 ×273/473) at NTP, and neglecting the effect of isotopic separation.

According to our adsorption measurement[4], the amount of oxygen monomolecularly adsorbed on the surface is 0.069 cc./g.-catalyst at 200°C, so the numeral obtained in (A) is twice as large as the present one. Second, by the similar reasoning as the above, the volume (NTP) of oxygen remaining after the evacuation will be estimated by the data of No. 6 and 7 as follows:

$$69\text{ cc.}\times\frac{0.98-0.40}{2.48-0.98}\times\frac{29(\text{cm.})}{760(\text{cm.})\times 10.0\text{ g.}}$$
$$=0.10_2\text{ cc./g.-cat.} \qquad (B)$$

It is found that the amount of exchangeable oxygen is smaller in this case but larger than that absorbed on the surface, suggesting that most of the exchange reaction seems to proceed between the normally adsorbed oxygen and carbon dioxide.

Thus it is made clear that metallic silver, though easily reducible, retains oxygen atoms firmly even when the reduction was performed carefully. Though the existence of non-removable oxygen was already reported by Benton and Bell[3], it can be shown by the present investigation that such oxygen in the catalyst is not restricted to one kind of state. It may exist as an adsorbed state on the surface, but also as a state more firmly bound, e.g., in the subsurface rather than to the adsorption to a special part of the surface. Because, by the curious behavior shown in No. 8, 9 and 10, most firmly bound oxygen ("residual oxygen") can neither exchange with carbon dioxide nor react with carbon monoxide, but, contrary to our expectation, it can exchange with gaseous oxygen.

The above behaviour can be explained analogously by the scheme proposed by Garner et al.[8], in the case when cuprous oxide is in contact with oxygen; i.e., when oxygen is brought into contact with the silver surface, silver atoms on the surface will migrate so as to cover some of the oxygen atoms, and the oxygen atoms thus covered will exchange with the residual oxygen atoms. On the other hand, as both carbon dioxide and carbon monoxide are slightly adsorbed to silver, probably to such a degree as one-hundredth of oxygen[4] even if they are adsorbed such migration cannot occur in case of contact with these gases. It is natural, therefore, that the exchange reaction was not observed in No. 8 and 9. However, the process of migration will not continue infinitely into the silver bulk-phase, as can be expected for the thermodynamical reason. This is actually realized by the fact that the amount of adsorbed oxygen remains to the degree, corresponding to one or two layers. However, as the isotopic effect in adsorption equilibrium is not taken into consideration the quantitative discussion on this matter will not be developed further.

Conclusion

From the different catalytic behaviour of reduced silver against carbon dioxide, carbon monoxide and oxygen, it may be concluded that the silver retains a special kind of "residual oxygen" firmly after it is brought into contact with oxygen, even at above the temperature region, at which the dissociation of silver oxide would begin.

A part of the expense for the experiment has been defrayed from a grant given by the Ministry of Education, to which the author's thanks are due.

Department of Chemistry, Faculty of Science, Osaka University
Nakanoshima, Osaka City

8) W. F. Garner, F. S. Stone and P. F. Tiley, *Proc. Roy. Soc.*, **A211**, 472 (1952).

SHORT COMMUNICATIONS

An X-ray Study on Thiacyclohexane

By Seiichi KONDO

(Received June 18, 1956)

McCullough and his collaborators[1] reported that thiacyclohexane (pentamethylene sulphide) has three modifications in the solid state and the molal entropy of fusion is 2.002 cal./deg. A chair form having the point group symmetry Cs is suggested for the molecule from the infrared and Raman spectroscopy.

The highest temperature modification of this crystal, stable between the transition point, 240.02°K, and the melting point, 292.25°K, is found to be optically isotropic and shows plastic behavior. These facts, together with the very low value of molal entropy of fusion, suggest that this modification falls into the category of plastic crystal.

The dipole moment of this molecule is estimated to be about 1.7 D. U., assuming the bond moment of C–S to be 1.4 D. U., (obtained from the dipole moments of diethyl and diphenyl sulphides[2,3]), and the valence angle C–S–C, 105°[1,4]. It is of interest to see that the physical properties of this compound in the highest temperature modification such as the entropy of fusion, plasticity and isotropy are quite similar to those of the non-polar compound cyclohexane[5], in spite of the difference in the molecular symmetry and polarity, which would give rise to different types of intermolecular correlation in the solid state. Furthermore, another related compound pentamethylene oxide having the molecular form analogous to that of thiacyclohexane does not seem to give plastic crystals. It would be because of the difference between the electronegativity of oxygen and sulphur atoms. The highest temperature modification has been studied by means of X-rays.

(A) The material used for this investigation was prepared and purified by the American Petroleum Institute research project 48 at the Laramie Station of U. S. Bureau of Mines, Wyoming. The material received was claimed to be 99.92% pure. It was again purified by drying and sublimation and was sealed in a thin wall capillary made of borosilicate glass. Single crystals can be grown very easily in a capillary by slow cooling of the melt. It is likely to occur that the [110] direction of the crystal lies nearly parallel to the capillary axis.

Laue, rotation, and oscilation photographs were taken with filtered Cu Kα and Mo Kα X-rays, at 14°C.

(B) The symmetry of the crystal is determined as face centered cubic with four molecules in the unit cell. The six Bragg reflection spectra observed are indexed as 111, 200, 220, 311, 222 and 331. The lattice constant is found to be 8.69±0.02 A at 14°C. With this value, the density of the crystal is calculated to be 1.036, which seems to be reasonable compared with the measured value, 0.985, of the liquid at 21°C. The spectral intensities are much like those of other plastic crystals such as trimethylacetic acid[6].

Considered from the standpont of the crystal and molecular symmetry, molecules will be in highly disordered orientation, including some sort of rotational motion, keeping presumably the center of the mass of the molecule fixed at the lattice site. We have observed very pronounced X-ray diffuse scattering. Spot-like diffuse scattering is appearing on Laue photographs, the intensity of which is strongest around the reciprocal lattice points 200 and 111, and there are also weaker ones around 100. The general appearance of those diffuse scatterings are very similar to those of other plastic crystals like cyclohexane[5].

From these observations we conclude that the highest temperature modification of thiacyclohexane belongs to the plastic crystal.

The author is very grateful to Professor Tsutomu Oda for his valuable discussions and to Dr. J. P. McCullough of the Thermodynamic Laboratory, Bartlesville, Ohio, of U. S. Bureau of Mines for the supply of the material and useful discussions.

Laboratory of Physical Chemistry, Osaka University of Liberal Arts and Education

1) J. P. McCullough, H. L. Finke, W. N. Hubbard, W.D. Good, R. E. Pennington, J. P. Messerly and Guy Waddington, *J. Am. Chem. Soc.*, **76**, 2661 (1954).
2) M. Kubo, *Sci. Papers Inst. Phys-Chem. Research* (Tokyo), **29**, 122 (1936).
3) G. C. Hampson, R. H. Farmer and L. E. Sutton, *Proc. Roy. Soc.* (London), **A143**, 147
4) S. Kondo, To be published.
5) T. Oda, *X-rays*, 5, 26 (1948).
6) Y. Namba and T. Oda, Unpublished data.